ECONSTOR
Make Your Publications Visible.

A Service of

ZBW Leibniz-Informationszentrum Wirtschaft
Leibniz Information Centre for Economics

Gondauri, Davit

Book — Manuscript Version (Preprint)

Millennium Economics: Seven Mathematical Architectures for Measuring Global Economic Complexity

Suggested Citation: Gondauri, Davit (2026) : Millennium Economics: Seven Mathematical Architectures for Measuring Global Economic Complexity

This Version is available at:
https://hdl.handle.net/10419/342001

Standard-Nutzungsbedingungen:

Die Dokumente auf EconStor dürfen zu eigenen wissenschaftlichen Zwecken und zum Privatgebrauch gespeichert und kopiert werden.

Sie dürfen die Dokumente nicht für öffentliche oder kommerzielle Zwecke vervielfältigen, öffentlich ausstellen, öffentlich zugänglich machen, vertreiben oder anderweitig nutzen.

Sofern die Verfasser die Dokumente unter Open-Content-Lizenzen (insbesondere CC-Lizenzen) zur Verfügung gestellt haben sollten, gelten abweichend von diesen Nutzungsbedingungen die in der dort genannten Lizenz gewährten Nutzungsrechte.

Terms of use:

Documents in EconStor may be saved and copied for your personal and scholarly purposes.

You are not to copy documents for public or commercial purposes, to exhibit the documents publicly, to make them publicly available on the internet, or to distribute or otherwise use the documents in public.

If the documents have been made available under an Open Content Licence (especially Creative Commons Licences), you may exercise further usage rights as specified in the indicated licence.

WWW.ECONSTOR.EU

Mitglied der Leibniz-Gemeinschaft

Millennium Economics:
Seven Mathematical Architectures for Measuring Global Economic Complexity

Davit Gondauri, PhD, Professor

Business and Technology University, Tbilisi, Georgia

Tbilisi, Georgia · 2026

Copyright / ISBN Page

Millennium Economics: Seven Mathematical Architectures for Measuring Global Economic Complexity

Author: Davit Gondauri

First edition: 2026

Place of publication: Tbilisi, Georgia

ISBN: [to be assigned / insert final ISBN]

Publisher: [insert publisher name after final publishing arrangement]

Copyright © 2026 Davit Gondauri. All rights reserved.

No part of this book may be reproduced, stored in a retrieval system or transmitted in any form or by any means without prior written permission of the author or publisher, except for brief quotations used for scholarly review, citation or academic discussion.

This monograph is an independent economic and econometric research work. The Clay Mathematics Institute Millennium Problem names are used strictly as mathematical inspirations for bounded economic measurement architectures. The book does not claim to solve, prove, test, verify or replicate the original Millennium Problems in their classical mathematical form.

Recommended citation:

Gondauri, D. (2026). Millennium Economics: Seven Mathematical Architectures for Measuring Global Economic Complexity. Tbilisi: [Publisher].

Dedication

To my family, teachers, colleagues and students, whose support, questions and intellectual discipline make long scientific work possible.

And to the researchers who believe that economics can be measured more deeply when mathematical imagination, empirical evidence and academic caution are held together.

Acknowledgements

This book grew out of a sustained research program on the translation of advanced mathematical architectures into bounded economic, econometric and computational measurement systems. I gratefully acknowledge the academic environments, professional communities and research discussions that supported the development of the seven problem-inspired studies that form the foundation of this monograph.

I am especially grateful to colleagues, reviewers, editors, conference participants and students whose questions helped sharpen the claim boundaries of the work. The monograph uses ambitious mathematical language, but its scientific credibility depends on a careful separation between theorem-level mathematics, economic analogy, empirical calibration, constructed indicators, forecast validation and computational demonstration. Many of the refinements in the book reflect that discipline.

I also acknowledge the importance of public datasets, open research infrastructures, replication packages and scholarly indexing platforms that make large-scale economic research auditable. The empirical chapters rely on public or disclosed input layers and on author-calculated transformations that are designed to remain traceable, reproducible and reviewer-safe.

The responsibility for the book’s modelling choices, interpretation, limitations, terminology, data transformations and remaining errors is mine alone. No institution, platform, repository or mathematical organization should be interpreted as endorsing the claims of the monograph unless explicitly stated elsewhere.

Preface / Author's Note

This monograph is written from a simple but demanding premise: the modern global economy is too structurally complex to be understood only through isolated indicators. GDP, inflation, inequality, liquidity, portfolio risk, regional rank and corridor exposure remain indispensable observables, but they do not fully explain how economic stress moves, how networks transmit shocks, how local conditions become global structure, how cycles persist, how inequality deforms social systems or how discrete choice constraints change optimization itself.

The book therefore develops a Millennium Economic Research Program. The term does not mean that the book solves the Clay Millennium Problems. It means that seven mathematical architectures associated with those problems are used as disciplined measurement grammars for economics. Navier-Stokes contributes the language of flow, pressure, friction, shock and closure. Yang-Mills contributes gauge, curvature, action and spectral threshold. Hodge contributes decomposition into gradient, curl and harmonic components. Birch-Swinnerton-Dyer contributes local-to-global rank logic. The Riemann-zeta framework contributes spectral-cyclical inflation diagnostics. P versus NP contributes computational feasibility and support-space explosion. Perelman-Ricci-Poincare logic contributes curvature, entropy, connectedness and smoothing capacity for inequality diagnostics.

The reader should treat every mathematical analogy in this book as bounded. A theorem in pure mathematics and an empirical economic measurement architecture do not belong to the same evidentiary class. The book’s purpose is not theorem transfer. Its purpose is to show how mathematical structures can help build auditable economic models when the empirical object, input variables, transformations, validation procedures and claim boundaries are explicitly stated.

The fifteen chapters are organized to move from general framing to problem-specific implementation and then to synthesis. The opening chapters define the research context, literature, unified methodology and data discipline. The middle chapters develop the seven problem-inspired economic models. The later chapters compare the results, consolidate the interpretation, set strict limitations and outline a future research agenda. This structure is intended to make the monograph more than a collection of separate articles: it is a single research architecture for measuring economic complexity.

The Contents, List of Tables and List of Figures included in this front-matter package are editorial lists extracted from the two book files. Final page numbers should be generated only after the full manuscript is merged, heading styles are standardized and final pagination is fixed. Any duplicated table numbering identified in the source manuscript should be corrected during final copy-editing before publication.

Contents

Chapter 1. General Introduction: The Millennium Problems as Economic Measurement Architectures
1.1. General Research Context
1.2. Why the Clay Millennium Problems Matter for Economic Modelling
1.2.1. The Millennium Problems as Measurement Grammars rather than Theorem Claims
1.2.2. Why Economics Needs Mathematical Grammars of Complexity
1.2.3. Navier-Stokes: The Grammar of Flow, Pressure, Friction and Closure
1.2.4. Yang-Mills: The Grammar of Gauge Structure, Curvature, Action and Shock Thresholds
1.2.5. Hodge: The Grammar of Decomposition, Imbalance and Systemic Circulation
1.2.6. Birch-Swinnerton-Dyer: The Grammar of Local-to-Global Structural Rank
1.2.7. Riemann-Zeta: The Grammar of Spectral-Cyclical Inflation Diagnostics
1.2.8. P versus NP: The Grammar of Search-Space Explosion, Feasibility and Certification
1.2.9. Perelman-Ricci-Poincare: The Grammar of Curvature, Entropy, Connectedness and Smoothing Capacity
1.2.10. The Seven Grammars as One Integrated Economic Research Program
1.2.11. Evidence Discipline: Why Mathematical Language Requires Stronger Claim Boundaries
1.2.12. The General Justification of the Monograph
1.2.13. Seven-Problem Measurement-Grammar Matrix
1.2.14. Concluding Synthesis of Section 1.2
1.3. The Monograph's Core Research Problem
1.3.1. From Fragmented Indicators to a Unified Research Problem
1.3.2. Global Economic Complexity as a Multi-Dimensional Measurement Object
1.3.3. The Flow Problem: Liquidity, Pressure and Systemic Stress
1.3.4. The Topology Problem: Hierarchy, Imbalance and Circulation
1.3.5. The Curvature and Threshold Problem: From Local Stress to Systemic Transmission
1.3.6. The Rank Problem: Local Signals and Global Structural Formation
1.3.7. The Spectral-Signal Problem: Inflation, Cycles and Forecast Deformation
1.3.8. The Computational-Complexity Problem: Feasibility, Search and Certification
1.3.9. The Inequality-Deformation Problem: Pressure, Smoothing and Connectedness
1.3.10. The Local-to-Global Problem as the Monograph's Integrating Logic
1.3.11. The Evidence Problem: Measurement without Overclaiming
1.3.12. Formal Monograph-Level Problem Statement
1.3.13. Core Research Problem Matrix
1.3.14. Source-Integration Map for Section 1.3
1.3.15. Transition to the Research Aim and Objectives
1.4. Research Aim and Objectives of the Monograph
1.4.1. General Research Aim of the Monograph
1.4.2. From Seven Article-Level Aims to One Book-Level Aim
1.4.3. Conceptual Aim: Seven Measurement Grammars for Global Complexity
1.4.4. Empirical Aim: A Multi-Layered Evidence Architecture
1.4.5. Methodological Aim: From Analogy to Auditable Measurement
1.4.6. Interpretive Aim: Building a Comparative Economic Meaning
1.4.7. General Objectives of the Monograph
1.4.8. Problem-Specific Objective Domains within the Unified Aim
1.4.9. Aim-Objective Translation Matrix
1.4.10. Hierarchy of Objectives: Measurement, Validation, Interpretation and Replication
1.4.11. Expected Contribution of the Aim-Objective System
1.4.12. Source-Integration Map for Section 1.4
1.4.13. Transition to Research Questions and Hypothetical Framework

1.5. Seven-Problem Translation Matrix
1.5.1. Purpose and Function of the Translation Matrix
1.5.2. Core Seven-Problem Translation Matrix
1.5.3. Translation Principle: From Theorem-Level Problems to Measurement Grammars
1.5.4. Expanded Problem-by-Problem Translation
1.5.4.1. Poincare / Ricci / Perelman Logic: Inequality Pressure, Curvature, Entropy and Smoothing Capacity
1.5.4.2. Hodge: Macro-Flow Decomposition, Gradient Hierarchy, Curl Imbalance and Harmonic Circulation
1.5.4.3. Navier-Stokes: Liquidity Flow, Pressure, Friction and Systemic Stress
1.5.4.4. Yang-Mills: Gauge Curvature, Action and Mass-Gap Shock Thresholds
1.5.4.5. Birch-Swinnerton-Dyer: Local-to-Global Structural Rank, LOrder and Corridor Stress
1.5.4.6. Riemann Hypothesis: Zeta-Cycle, Inflation Forecasting and Spectral Diagnostics
1.5.4.7. P vs NP: Portfolio Optimization, Cardinality and Computational Complexity
1.5.5. Integrated Measurement-Grammar Matrix
1.5.6. Why This Chapter Order Is Methodologically Appropriate
1.5.7. Source Integration Map for the Translation Matrix
1.5.8. Synthesis
1.6. Scientific Novelty of the Monograph
1.6.1. Novelty of the Perelman-Ricci-Poincare Inequality Diagnostic Grammar
1.6.2. Novelty of the Hodge-Econometric Decomposition Grammar
1.6.3. Novelty of the Navier-Stokes Liquidity-Flow Grammar
1.6.4. Novelty of the Yang-Mills Gauge-Econometric Mass-Gap Grammar
1.6.5. Novelty of the Birch-Swinnerton-Dyer Local-to-Global Rank Grammar
1.6.6. Novelty of the Riemann-Zeta FPAS+zeta Forecasting Grammar
1.6.7. Novelty of the P-vs-NP Computational-Finance Grammar
1.6.8. Integrated Scientific Novelty Matrix
1.7. Theoretical, Methodological and Practical Significance of the Monograph
1.7.1. Theoretical Significance
1.7.2. Methodological Significance
1.7.3. Practical and Policy-Analytical Significance
1.7.4. Significance Matrix
1.8. Research Limitations, Academic Caution and Claim Boundary of the Entire Book
1.8.1. General Theorem-Level Boundary
1.8.2. Data, Aggregation and Sample-Size Boundaries
1.8.3. Constructed Variables, Transformation Risk and Circularity
1.8.4. Forecasting, Optimization and Causality Boundaries
1.8.5. Problem-Specific Claim-Boundary Matrix
1.8.6. Replication and Reviewer-Safety Boundary
1.8.7. Final Academic-Caution Statement

Chapter 2. Conceptual Translation Framework: From Mathematical Problems to Economic Analogues
2.1. Analogy versus Proof
2.1.1. The Function of the Analogy-Proof Distinction
2.1.2. What Counts as a Classical Mathematical Object in This Monograph
2.1.3. Why Direct Proof Is Excluded
2.1.4. The Economic Analogue as a Measurement Grammar
2.1.5. The Evidence Ladder: From Analogy to Permissible Claim
2.1.6. Application of the Distinction across the Seven Economic Analogues
2.1.6.1. Poincare / Ricci / Perelman Logic: Inequality Pressure, Curvature and Smoothing Capacity

2.1.6.2. Hodge Logic: Macro-Flow Decomposition into Gradient, Curl and Harmonic Structure
2.1.6.3. Navier-Stokes Logic: Liquidity Flow, Pressure, Friction and Systemic Stress
2.1.6.4. Yang-Mills Logic: Gauge Curvature, Action and Finite-Network Shock Thresholds
2.1.6.5. Birch-Swinnerton-Dyer Logic: Local-to-Global Structural Rank
2.1.6.6. Riemann-Zeta Logic: Spectral-Cyclical Inflation Forecasting
2.1.6.7. P versus NP Logic: Portfolio Optimization and Computational Complexity
2.1.7. Permissible and Impermissible Language
2.1.8. The Constructed Object Principle
2.1.9. The Claim Hierarchy of the Monograph
2.1.10. Monograph-Level Synthesis: Why Analogy Is Scientifically Legitimate
2.1.11. Operational Checklist for the Seven Problem Chapters
2.1.12. Closing Transition
2.2. Flow Analogies
2.2.1. Why Flow Is a Monograph-Level Measurement Grammar
2.2.2. Classical Flow Objects and the Exclusion of Direct Proof
2.2.3. The Navier-Stokes Translation: From Physical Flow Balance to Liquidity-Stress Measurement
2.2.3.1. Velocity Weakness and Acceleration Pressure
2.2.3.2. Pressure Gradients, Friction and Diffusion
2.2.3.3. Shock Forcing, Cycle Forcing and Restricted Closure
2.2.4. The Hodge Translation: From Decomposition of Forms to Macro-Flow Structure
2.2.4.1. Gradient Hierarchy
2.2.4.2. Curl and Local-Cycle Imbalance
2.2.4.3. Harmonic Systemic Circulation
2.2.5. Complementarity Between Navier-Stokes and Hodge Flow Analogies
2.2.6. Flow Analogies and the Other Five Problem Architectures
2.2.7. Permissible and Non-Permissible Claims for Flow Analogies
2.2.8. Section Conclusion: Flow as a Bounded Economic Analogue
2.3. Curvature and Topology Analogies
2.3.1. Curvature and Topology as Economic Measurement Languages
2.3.2. Classical Mathematical Objects and Their Economic Translation Status
2.3.3. Perelman/Ricci/Poincare Analogy: Inequality as Curvature, Entropy and Smoothing Capacity
2.3.4. Hodge Analogy: Topological Macro-Flow Decomposition
2.3.5. Yang-Mills Analogy: Gauge Curvature, Action and Finite-Network Shock Thresholds
2.3.6. How the Remaining Four Analogues Support the Curvature-Topology Dimension
2.3.7. The Economic Meaning of Curvature: Deformation, Concentration and Bottlenecks
2.3.8. The Economic Meaning of Topology: Connectedness, Cycles, Holes and Persistence
2.3.9. Comparative Claim Hierarchy for Curvature and Topology Analogies
2.3.10. Methodological Safeguards against Category Error
2.3.11. Integrated Synthesis: Curvature and Topology as the Second Dimension of the Millennium Economic Program
2.3.12. Section Conclusion
2.4. Spectral and L-Function Analogies
2.4.1. Why Spectral and L-Function Language Matters for Economic Analogues
2.4.2. The Riemann/Zeta Analogy: From Critical-Line Signal to Inflation Forecast Correction
2.4.3. The BSD Analogy: From Local Reductions to Economic LOrder and Structural Rank
2.4.4. Shared Architecture: Signal, Local Factor, Spectrum and Rank
2.4.5. Spectral Validation Versus Spectral Overclaiming
2.4.6. The Role of Hodge, Yang-Mills and Navier-Stokes as Supporting Spectral Architectures
2.4.7. Entropy, Regime and Complexity Links: Perelman/Ricci/Poincare and P-vs-NP
2.4.8. Monograph-Level Permissible Claim Hierarchy for Spectral and L-Function Analogies

2.4.9. Section Synthesis
2.5. Complexity and Optimization Analogies
2.5.1. The Classical P-vs-NP Object and Its Economic Relevance
2.5.2. From Continuous Allocation to Mixed Discrete-Continuous Optimization
2.5.3. Algorithmic Search, Exact Reduced Benchmarking and Heuristic Credibility
2.5.4. Optimization as an Evidence Hierarchy, Not a Single Result
2.5.5. Black-Scholes Overlay, Transaction Costs and Realism as Complexity Controls
2.5.6. Complexity, Entropy and Dimensionality across the Seven Analogues
2.5.7. Permissible Claims and Excluded Claims
2.5.8. Section Synthesis
2.6. Local-to-Global and Systemic Transmission Logic
2.6.1. Conceptual Role of Local-to-Global Translation
2.6.2. BSD as the Core Local-to-Global Rank Architecture
2.6.3. Hodge as Local Flow Decomposition and Systemic Circulation
2.6.4. Yang-Mills as Local-to-Systemic Shock Threshold Logic
2.6.5. Navier-Stokes as Flow-Pressure-Friction-Closure Transmission Logic
2.6.6. Supporting Local-to-Global Logic in Ricci/Poincare, Riemann/Zeta and P-vs-NP
2.6.7. Corridor-Sensitive Transmission and the Visibility of Small Nodes
2.6.8. Transformation Operators: From Local Measurement to Global Interpretation
2.6.9. Evidence Hierarchy for Systemic Transmission Claims
2.6.10. Integrated Synthesis of Section 2.6
2.7. General Claim Hierarchy
2.7.1. Purpose of the General Claim Hierarchy
2.7.2. Why the Monograph Needs a Claim Ladder
2.7.3. Strong Measurement Claim
2.7.4. Diagnostic Claim
2.7.5. Forecasting Claim
2.7.6. Benchmark Claim
2.7.7. Future Validation Claim
2.7.8. Cross-Problem Placement of Claims
2.7.9. Upgrade, Downgrade and Exclusion Rules
2.7.10. General Claim-Boundary Language for the Monograph
2.7.11. Integrated Closing Statement

Chapter 3. Integrated Literature Review

3.1. Mathematical Economics and Analogue Modelling
3.1.1. Function of this Section within the Integrated Literature Review
3.1.2. Mathematical Economics as a Discipline of Formal Translation
3.1.3. Analogue Modelling: From Metaphor to Auditable Measurement Architecture
3.1.4. The Claim Boundary as a Literature-Review Principle
3.1.5. Seven Mathematical Grammars and One Integrated Review Logic
3.1.6. Constructed Variables, Normalization and Measurement Legitimacy
3.1.7. Econometric and Computational Validation as Boundary Discipline
3.1.8. Literature Gap Addressed by the Monograph
3.1.9. Synthesis: What Section 3.1 Establishes for the Rest of Chapter 3
3.2. Network Economics, Systemic Risk and Shock Propagation
3.2.1. Function of this Section within the Integrated Literature Review
3.2.2. From Scalar Macroeconomic Indicators to Relational Economic Systems
3.2.3. Complex Networks, Connectivity and Propagation as a General Scientific Foundation
3.2.4. Financial Systemic Risk, Contagion and Network Fragility

3.2.5. Production Networks, Global Value Chains and Sectoral Shock Propagation
3.2.6. Corridor Economics, Logistics Resilience and Strategic Bridge Nodes
3.2.7. Spectral Graph Theory and Thresholds in Systemic Transmission
3.2.8. Hodge and Topological Macro-Flow Literature
3.2.9. Yang-Mills Gauge Analogy, Curvature and Action in Economic Stress Networks
3.2.10. BSD Local-to-Global Transmission and Structural Rank Literature
3.2.11. Navier-Stokes Liquidity-Flow Stress, Friction and Shock-Closure Literature
3.2.12. Supporting Stress-Regime, Inequality-Network and Optimization Literatures
3.2.13. Integrated Interpretation: From Propagation Channels to Claim-Gated Measurement
3.2.14. Section Conclusion and Transition to Topological and Spectral Methods
3.3. Topological and Spectral Methods in Economics
3.3.1. Function of this Section within the Integrated Literature Review
3.3.2. Topology as an Economic Measurement Language
3.3.3. Hodge Theory, Discrete Hodge Decomposition and Economic Flow Systems
3.3.4. Ricci Curvature, Poincare Connectedness and Inequality-Pressure Diagnostics
3.3.5. Yang-Mills Gauge Analogies, Curvature-Action Structure and Spectral Thresholds
3.3.6. Spectral Methods, Frequency-Domain Logic and Riemann-Zeta Forecasting
3.3.7. BSD and L-Function Analogues as Spectral Local-to-Global Measurement
3.3.8. Navier-Stokes and P-vs-NP as Supporting Spectral-Topological Evidence Systems
3.3.9. In-Text Citation Logic for the Integrated Literature Review
3.3.10. Integrated Claim Boundary for Topological and Spectral Methods
3.3.11. Literature Gap Addressed by Section 3.3
3.4. Global Macro-Financial Stress, Inflation and Liquidity Literature
3.4.1. Function of this Section within the Integrated Literature Review
3.4.2. Financial Stress Literature: From Indicator Monitoring to Systemic Measurement
3.4.3. Liquidity Literature and the Economic Meaning of Flow, Friction and Closure
3.4.4. Inflation Literature: Persistence, Policy Reaction and Global Shock Transmission
3.4.5. Riemann-Zeta, Spectral-Cycle Signals and Inflation Forecasting
3.4.6. Forecast Evaluation, Validation Windows and Overclaiming Control
3.4.7. Global Shock Transmission: The Bridge between Liquidity Stress and Inflation Pressure
3.4.8. Supporting Contributions of the Other Five Analogues
3.4.9. Claim-Boundary Synthesis for Section 3.4
3.4.10. Integrated Synthesis and Transition
3.5. Inequality, Curvature, Smoothing Capacity and Regional Pressure
3.5.1. Function of this Section within the Integrated Literature Review
3.5.2. Inequality Literature: From Scalar Dispersion to Multidimensional Pressure
3.5.3. Regional Pressure, Spatial Heterogeneity and Smoothing Capacity
3.5.4. Ricci Flow, Perelman Entropy and the Economic Meaning of Curvature-Like Deformation
3.5.5. Graph Topology, Connectedness and Bottleneck Literature
3.5.6. Discrete Curvature in Network Economics and Systemic-Risk Research
3.5.7. Integration with the Other Six Millennium-Inspired Literature Streams
3.5.8. Constructed Pressure Coordinates, Normalization and Measurement Legitimacy
3.5.9. Econometric, Forecast and Robustness Literature for Inequality-Curvature Diagnostics
3.5.10. Claim-Boundary Discipline for the Inequality-Curvature Section
3.5.11. Literature Gap and Monograph Contribution
3.5.12. Section Synthesis
3.6. Portfolio Theory, CAPM, Sparse Optimization and Computational Finance
3.6.1. Function of this Section within the Integrated Literature Review
3.6.2. Mean-Variance Portfolio Theory as the Baseline Economic Optimization Literature
3.6.3. CAPM, Expected-Return Priors and the Role of Asset-Pricing Discipline

3.6.4. Covariance Geometry, Diversification and Estimation Risk
3.6.5. Cardinality Constraints, Sparse Optimization and the P-vs-NP Analogue
3.6.6. Exact Reduced Benchmarking, Heuristics and Metaheuristic Search
3.6.7. Derivative Overlay, Black-Scholes Discipline and Implementation Realism
3.6.8. Robustness, Stress Testing and Validation Gates in Computational Finance
3.6.9. Integration with the Other Six Mathematical-Economic Analogues
3.6.10. Literature Gap and Monograph Contribution in Computational Finance
3.6.11. Synthesis: What Section 3.6 Establishes for the Monograph
3.7. Regional Economics, Corridors and Global Value Chains
3.7.1. Function of this Section within the Integrated Literature Review
3.7.2. Regional Economics: From Output Mass to Spatial Structure
3.7.3. Global Value Chains and Production-Network Interdependence
3.7.4. Corridors, Logistics and Supply-Chain Resilience
3.7.5. BSD: Local-to-Global Regional Rank and Corridor Stress
3.7.6. Yang-Mills: Global-Corridor Stress Networks and Shock Thresholds
3.7.7. Hodge: Regional Macro-Flow Decomposition and Corridor Visibility
3.7.8. Supporting Links from the Other Four Analogues
3.7.9. Measurement Objects and Validation Gates for Corridor-GVC Research
3.7.10. Claim-Boundary Synthesis for Regional Economics, Corridors and GVCs
3.7.11. Literature Gap Addressed by the Monograph
3.7.12. Synthesis and Transition
3.8. Forecasting, Validation and Robust Econometric Inference
3.8.1. Function of this Section within the Integrated Literature Review
3.8.2. Forecasting Literature: From Point Accuracy to Information-Set Discipline
3.8.3. Structural Forecasting, Inflation, Regimes and Spectral Diagnostics
3.8.4. Macro-Financial Stress Testing, Liquidity and Robust Validation
3.8.5. Robust Econometric Inference: Heteroskedasticity, Serial Dependence, Panels and Cross-Sectional Dependence
3.8.6. Diagnostic Validation for Curvature, Inequality Pressure and Smoothing Capacity
3.8.7. Computational Validation, Exact Reduced Benchmarking and P-vs-NP Claim Discipline
3.8.8. Validation Gates across Network, Local-to-Global and Spectral Analogues
3.8.9. Evidence Hierarchy for Forecasting, Validation and Robust Inference
3.8.10. Integrated Claim-Boundary Matrix
3.8.11. Literature Gap Addressed by Section 3.8
3.9. Constructed Indices, Replication and Claim Discipline
3.9.1. Function of this Section within the Integrated Literature Review
3.9.2. Constructed Indices as Measurement Objects, Not Raw Facts
3.9.3. Normalization, Scaling and Directional Harmonization
3.9.4. Replication Packages as External Audit Companions
3.9.5. Validation Gates and the Evidence Hierarchy
3.9.6. Claim Discipline as a Review-Level Methodological Contribution
3.9.7. Replication Discipline across the Seven Analogues
3.9.8. Integrated Seven-Analogue Claim Matrix
3.9.9. Literature Gap Addressed by Section 3.9
3.9.10. Section Closing Synthesis
3.10. Literature Gap and Contribution of the Monograph
3.10.1. Function of this Closing Section within Chapter 3
3.10.2. The General Cross-Literature Gap
3.10.3. Gap One: Analogue Modelling without a Unified Claim-Boundary Protocol
3.10.4. Gap Two: Scalar Indicators Do Not Capture Multidimensional Economic Structure

3.10.5. Gap Three: Network, Topology, Spectral and Corridor Literatures Remain Partly Disconnected
3.10.6. Gap Four: Forecasting, Validation and Robust Inference Are Often Detached from Analogue Construction
3.10.7. Gap Five: Constructed Indices and Replication Are Not Always Joined to Claim Discipline
3.10.8. Positive Contribution of the Monograph
3.10.9. Seven-Analogue Contribution Matrix
3.10.10. What the Monograph Does Not Claim
3.10.11. Synthesis: The Monograph-Level Literature Gap Is Closed by Integration, Not Substitution
3.10.12. Closing Claim-Boundary Statement for Chapter 3

Chapter 4. Unified Methodology, Data Architecture and Replication Discipline

4.1. Research Design of the Monograph
4.1.1. Methodological Position: A Unified Quantitative Analogue Design
4.1.2. Monograph-Level Research Object and Translation Logic
4.1.3. Integration of the Seven Source Designs into One Research Architecture
4.1.4. Non-Experimental Status and Causal Discipline
4.1.5. Computational Research Design and Algorithmic Auditability
4.1.6. Econometric Orientation: Validation, Screening and Evidence Closure
4.1.7. Data Architecture as a Research-Design Principle
4.1.8. Network, Graph and Topological Design Logic
4.1.9. Forecasting, Optimization and Simulation as Complementary Design Modes
4.1.10. Validation, Robustness, Placebo and Falsification Discipline
4.1.11. Claim-Boundary Doctrine of the Research Design
4.1.12. Replication-Ready Design and Source-Ledger Discipline
4.1.13. Formal Design Rule for Admissible Claims
4.1.14. Section Synthesis
4.2. Empirical Universes across the Seven Studies
4.2.1. Purpose of the Empirical-Universe Architecture
4.2.2. Master Empirical-Universe Matrix
4.2.3. Unit of Analysis and Evidence-Type Taxonomy
4.2.4. Evidence Hierarchy Generated by the Empirical Universes
4.2.5. Perelman/Ricci/Poincare Empirical Universe
4.2.6. Hodge Empirical Universe
4.2.7. Navier-Stokes Empirical Universe
4.2.8. Yang-Mills Empirical Universe
4.2.9. Birch-Swinnerton-Dyer Empirical Universe
4.2.10. Riemann/Zeta Empirical Universe
4.2.11. P vs NP Empirical Universe
4.2.12. Cross-Study Sample Discipline and Non-Equivalence of N
4.2.13. Empirical-Universe Boundary Matrix
4.2.14. Integration into the Unified Methodology Chapter
4.3. Public Data Anchors and Author-Calculated Variables
4.3.1. The Core Data-Lineage Principle
4.3.2. Unified Anchor-to-Construct Architecture across the Seven Studies
4.3.3. Why Public Inputs Cannot Be Treated as Final Indicators
4.3.4. Study-Specific Data-Lineage Profiles
4.3.4.1. Perelman/Ricci/Poincare: from inequality variables to pressure-curvature-topology diagnostics
4.3.4.2. Hodge: from regional macro anchors to a decomposable macro-flow cochain
4.3.4.3. Navier-Stokes: from macro-financial proxies to nondimensional stress-balance components
4.3.4.4. Yang-Mills: from macro-corridor anchors to finite-network gauge variables

4.3.4.5. Birch-Swinnerton-Dyer: from regional anchors to local-to-global rank variables
4.3.4.6. Riemann/Zeta: from inflation data to layered forecast-diagnostic variables
4.3.4.7. P vs NP: from industry inputs to computational-finance optimization outputs
4.3.5. Anchor-Construct Lineage by Variable Family
4.3.6. Author-Calculated Variables as Valid Scientific Objects
4.3.7. Circularity, Independence and Validation Discipline
4.3.8. Replication Requirements for Constructed Variables
4.3.9. Methodological Implication for the Whole Monograph
4.4. Normalization, Scaling and Directional Harmonization
4.4.1. Methodological Function of Normalization in the Monograph
4.4.2. General Scaling Operators and Notation
4.4.3. Directional Harmonization: The Stress-Oriented Rule
4.4.4. Study-Level Normalization and Scaling Matrix
4.4.5. Perelman/Ricci/Poincare: 0-100 Stress Coordinates before Metric and Curvature Construction
4.4.6. Hodge: Scaling Node Attributes into a Directed Edge Cochain
4.4.7. Navier-Stokes: Nondimensional Starred Variables and Unit-Consistency Discipline
4.4.8. Yang-Mills: Normalized Systemic Stress, Gauge Potential and Spectral Scaling
4.4.9. Birch-Swinnerton-Dyer: Share-Normalized Mass, Inverse Fragility and Rank-Scale Calibration
4.4.10. Riemann/Zeta: Normalized Cycle, Signed Correction and Layered Forecast Scaling
4.4.11. P vs NP: Risk-Return Scaling, Covariance Geometry and Optimization Metrics
4.4.12. Cross-Study Scaling Safeguards and Reviewer-Facing Audit Rules
4.4.13. Comparability without False Equivalence
4.4.14. Replication Package Requirements for Normalization and Scaling
4.4.15. Section Synthesis: The Common Measurement Grammar of the Monograph
4.5. Network and Graph Construction Protocol
4.5.1. Methodological Role of Networks in the Unified Monograph
4.5.2. Common Graph Ontology: Nodes, Anchors, Edges, Weights and Matrices
4.5.3. General Network Construction Algorithm for the Monograph
4.5.4. Cross-Study Network and Graph Construction Matrix
4.5.5. Hodge Network Construction Protocol
4.5.6. Yang-Mills Finite-Network Gauge Protocol
4.5.7. BSD Local-to-Global Regional Graph Protocol
4.5.8. Perelman/Ricci/Poincare Metric-Graph Protocol
4.5.9. Indirect Network Comparators: Navier-Stokes, Riemann/Zeta and P vs NP
4.5.10. Graph Adequacy, Robustness and Placebo Discipline
4.5.11. Network Claim-Boundary Matrix
4.5.12. Synthesis: Why the Network Protocol Matters for the Book
4.6. Econometric and Forecast-Validation Protocol
4.6.1. Role of Econometric and Forecast Validation in the Monograph
4.6.2. Panel-Econometric Baseline: FE, TWFE and Mundlak Logic
4.6.3. Robust-Inference Protocol: HAC, Driscoll-Kraay, Clustering and HC3
4.6.4. Forecast-Validation Protocol: ARIMA, VAR/SVAR, Rolling Windows and Benchmark Discipline
4.6.5. DM and CW Tests: Comparative Forecast Evidence without Overclaiming
4.6.6. PCA, Factor Structure and Regularization Protocol
4.6.7. Study-Specific Validation Profiles
4.6.8. Perelman/Ricci/Poincare: Econometric Validation as Diagnostic Geometry Audit
4.6.9. Hodge: Benchmark Validation of Topological Flow Components
4.6.10. Navier-Stokes: Full Global-Panel Stress-Testing Validation
4.6.11. Yang-Mills: Two-Layer Validation and Deferred Panel Confirmation
4.6.12. BSD: Closure Econometrics, Negative Controls and Anti-Circularity

4.6.13. Riemann/Zeta: Layered Forecast Validation as the Book's Sample-Discipline Benchmark
4.6.14. P vs NP: Computational-Finance Validation instead of Panel Causality
4.6.15. Common Diagnostic and Falsification Gates
4.6.16. Evidence-Status Matrix for Final Monograph Interpretation
4.6.17. Chapter-Level Synthesis
4.7. Computational and Algorithmic Protocol
4.7.1. Function of the computational protocol inside the monograph
4.7.2. Unified end-to-end algorithmic sequence
4.7.3. P-vs-NP computational-finance protocol
4.7.4. Riemann/Zeta computational-spectral forecasting protocol
4.7.5. Yang-Mills finite-network gauge-econometric protocol
4.7.6. Hodge topological macro-flow decomposition protocol
4.7.7. Algorithmic extensions in BSD, Perelman/Ricci/Poincare and Navier-Stokes
4.7.8. Algorithmic validation gates and failure conditions
4.7.9. Reproducibility metadata for computational outputs
4.7.10. Algorithmic claim hierarchy
4.7.11. Methodological synthesis and transition to replication discipline
4.8. Replication Packages and Zenodo Discipline
4.8.1. Why the replication-package layer belongs in the unified methodology chapter
4.8.2. Consolidated Zenodo package registry for the seven studies
4.8.3. Public data anchors, constructed variables and replication lineage
4.8.4. DOI, record, version and citation discipline
4.8.5. Script, seed, checksum and software-environment discipline
4.8.6. Study-specific replication statements for insertion into the monograph
4.8.7. Evidence levels supported by the replication packages
4.8.8. Monograph-level replication workflow
4.8.9. Reviewer-risk response and package-governance safeguards
4.8.10. General monograph data and replication statement
4.8.11. Integration with the previous subsections of Chapter 4
4.8.12. Final methodological conclusion
4.9. General Claim-Boundary Matrix
4.9.1. Function of the claim-boundary matrix in the methodology chapter
4.9.2. Common theorem-exclusion rule
4.9.3. Permitted claim levels and evidence hierarchy
4.9.4. Study-specific claim profiles
4.9.4A. Detailed claim-audit panels for the seven studies
4.9.4B. Reviewer-safe claim lexicon
4.9.4C. Claim-audit algorithm for the monograph
4.9.5. Overclaim-to-correction protocol
4.9.6. Causality, forecasting and policy language boundary
4.9.7. Problem-chapter writing rules derived from the matrix
4.9.8. Monograph-wide permitted contribution statement
4.9.9. Final methodological synthesis

Chapter 5. Perelman-Ricci-Poincare-Inspired Global Inequality Diagnostics
5.1. Mathematical and Economic Translation of the Poincare/Ricci/Perelman Logic
5.1.1. Function of Section 5.1 inside the Monograph
5.1.2. Why the Poincare/Ricci/Perelman Logic Fits Inequality Diagnostics
5.1.3. The Economic Manifold: From Heterogeneous Indicators to Stress Coordinates
5.1.4. Poincare Logic: Connectedness, Cycles and Diagnostic Closure

5.1.5. Ricci Logic: Inequality Pressure, Smoothing Capacity and Deformation
5.1.6. Perelman Logic: Energy-Like and Entropy-Like Complexity
5.1.7. The Economic Translation Sequence
5.1.8. Why Inequality Pressure Is the Correct Economic Object
5.1.9. Evidence Hierarchy and Claim Boundary
5.1.10. Transition to the Research Object in Section 5.2
5.2. Research Object: Global Inequality as a Pressure-Smoothing Manifold
5.2.1. Purpose of the Research-Object Section
5.2.2. Formal Definition of the Empirical Object
5.2.3. Unit of Analysis: Region-Year Coordinates
5.2.4. The Sixteen-Coordinate Inequality System
5.2.5. Pressure, Smoothing Capacity and Deformation
5.2.6. Macro-Regional Scope and Global Interpretation
5.2.7. Data Status: Public Anchors versus Constructed Diagnostic Objects
5.2.8. Boundary Conditions of the Pressure-Smoothing Manifold
5.2.9. Transition from Research Object to Data Architecture
5.3. Data Architecture: Ten Regions, Sixteen Stress Coordinates and N=150 Panel
5.3.1. Purpose and Position of the Data-Architecture Section
5.3.2. Empirical Universe: Ten Macro-Regional Blocks
5.3.3. Time Dimension and Balanced N=150 Panel
5.3.4. Sixteen Stress-Coordinate Variables
5.3.5. Public Anchors, Constructed Coordinates and Variable Lineage
5.3.6. Directional Harmonization and 0-100 Diagnostic Stress Scale
5.3.7. Coordinate Blocks: Pressure Channels and Smoothing-Capacity Channels
5.3.8. Aggregation, World-Weighted Paths and Regional Retention
5.3.9. Missing-Data, Comparability and Sample-Integrity Discipline
5.3.10. Data Objects Generated by the Architecture
5.3.11. Replication Package and Source-Ledger Requirements
5.3.12. Data-Architecture Boundary Matrix
5.3.13. Handoff to Section 5.4 Methodology
5.4. Methodology: Metric Tensor, Ricci-Style Curvature, F/W Functionals and Graph Topology
5.4.1. Methodological position and theorem-boundary discipline
5.4.2. Notation, panel coordinates and methodological inputs
5.4.3. Global inequality-pressure and curvature index
5.4.4. Economic metric tensor and coordinate-coupling audit
5.4.5. Correlation-based curvature coordinate system
5.4.6. Ricci-style component curvature decomposition
5.4.7. Normalized Ricci-flow and scalar curvature path
5.4.8. Weighted curvature-contribution concentration
5.4.9. Perelman F-functional as economic energy diagnostic
5.4.10. Perelman W-functional as entropy-like complexity closure
5.4.11. Poincare-inspired graph topology: adjacency, Laplacian and connectedness
5.4.12. Betti numbers, Euler characteristic and looped inequality structure
5.4.13. Ollivier and Forman edge-curvature proxy screens
5.4.14. Ricci-surgery candidates and bottleneck diagnostics
5.4.15. Counterfactual sensitivity and validation gates
5.4.16. Unified computational pipeline for Section 5.4
5.4.17. Methodological claim boundary for Chapter 5
5.4.18. Chapter-bridge conclusion
5.5. Results: Pressure, Curvature, Entropy, Crisis Deformation and Recovery Path

5.5.1. Results-Reading Protocol and Evidence Boundary
5.5.2. Global Pressure, Curvature and Entropy Path
5.5.3. Metric Tensor and Coordinate Coupling Results
5.5.4. Ricci-Style Curvature Component Results
5.5.5. Normalized Ricci-Flow and Scalar Curvature Results
5.5.6. Regional Pressure-Curvature Rankings for 2024
5.5.7. Perelman-Type F-Functional and W-Functional Results
5.5.8. Poincaré Graph Topology and Network-Curvature Results
5.5.9. Ricci-Surgery and Counterfactual Sensitivity Results
5.5.10. Econometric, Regularized and Regime-Validation Results
5.5.11. Forecast Validation, Benchmark Discipline and Uncertainty Bands
5.5.12. Regional Change, Dispersion, Crisis Deformation and Recovery
5.5.13. Integrated Result Synthesis
5.6. Interpretation: Inequality Deformation, Smoothing Capacity and Post-Shock Recovery
5.6.1. Analytical Role of This Interpretation Section
5.6.2. Central Interpretive Proposition
5.6.3. Crisis Deformation: 2020 as a Joint Pressure-Curvature-Entropy Event
5.6.4. Post-Shock Recovery: Smoothing Improves but Does Not Eliminate Deformation
5.6.5. Inequality Deformation as Component Concentration
5.6.6. Smoothing Capacity as a Multidimensional Structure
5.6.7. Graph Topology: Connectedness, Cycles and Bottleneck Complexity
5.6.8. Bottlenecks, Embeddedness and Ricci-Surgery Interpretation
5.6.9. Counterfactual Interpretation: Policy Screening, Not Treatment Effects
5.6.10. Econometric Validation and Forecast Boundary
5.6.11. Regional Stratification and Post-Shock Recovery
5.6.12. Interpretation of Inequality Deformation as Structural Memory
5.6.13. Cross-Layer Analytical Synthesis
5.6.14. Claim Boundary and Interpretive Discipline
5.6.15. Bridge to Section 5.7: Scientific Contribution
5.7. Scientific Contribution
5.7.1. Function of the Scientific-Contribution Section
5.7.2. Theoretical Contribution: Inequality as a Pressure-Smoothing System
5.7.3. Methodological Contribution: A Complete Diagnostic-Manifold Pipeline
5.7.4. Empirical Contribution: Macro-Regional Evidence on Crisis Deformation and Recovery
5.7.5. Component-Decomposition Contribution: Beyond a Gini-Only Reading
5.7.6. Topological Contribution: Connectedness, Cycles and Bottleneck Structure
5.7.7. Validation Contribution: Robustness Without Causal Overclaiming
5.7.8. Replication and Data-Governance Contribution
5.7.9. Contribution to the Seven-Problem Monograph Architecture
5.7.10. Practical and Policy-Screening Contribution
5.7.11. Contribution Boundaries: Why the Chapter Is Stronger Because It Is Bounded
5.7.12. Final Scientific-Contribution Statement
5.8. Claim Boundary and Limitations
5.8.1. Why a Claim-Boundary Section Is Necessary
5.8.2. Core Permitted Claim and Excluded Claim Set
5.8.3. Theorem-Level and Analogy Boundary
5.8.4. Data-Universe and Aggregation Limitations
5.8.5. Variable Construction, Normalization and Directional-Harmonization Limits
5.8.6. Metric Tensor and Curvature-Style Limitations
5.8.7. Perelman-Type F/W Functional Limitations

5.8.8. Graph-Topological and Poincare-Style Limitations
5.8.9. Econometric Validation and Causal-Inference Limitations
5.8.10. Forecast, Uncertainty and Benchmark Limitations
5.8.11. Counterfactual, Ricci-Surgery and Policy-Screening Limitations
5.8.12. Replication and Transparency Boundary
5.8.13. Integrated Claim Hierarchy for Chapter 5
5.8.14. Reviewer-Safe Claim Lexicon
5.8.15. Final Limitation Statement for Chapter 5
5.9. Chapter Conclusion
5.9.1. Purpose of the Chapter Conclusion
5.9.2. Final Synthesis of the Mathematical-Economic Translation
5.9.3. Research Object and Data Architecture Closure
5.9.4. Methodological Closure
5.9.5. Results Closure: Pressure, Curvature, Entropy and Topology
5.9.6. Interpretation Closure: Deformation, Smoothing and Recovery
5.9.7. Scientific Contribution Closure
5.9.8. Claim Boundary and Limitation Closure
5.9.9. Replication, Auditability and Book-Level Integration
5.9.10. Bridge to Chapter 6: From Curvature Diagnostics to Flow Decomposition
5.9.11. Final Integrated Evidence Matrix
5.9.12. Final Chapter Conclusion

Chapter 6. Hodge-Econometric Modelling of the World Economy

6.1. Hodge Theory as an Economic Decomposition Grammar
6.1.1. From Scalar Macroeconomic Ranking to Decomposable Structure
6.1.2. The Hodge Grammar: Gradient, Curl and Harmonic Components
6.1.3. Economic Meaning of the Directed Macro-Flow Pressure Field
6.1.4. Why Hodge Theory Fits the Economic Problem
6.1.5. The Three Economic Components
6.1.6. Hodge Theory and the Caucasus Visibility Problem
6.1.7. Relationship to the Hodge Conjecture and Claim Boundary
6.1.8. Place of Section 6.1 in the Chapter 6 Evidence Chain
6.1.9. Mini-Synthesis: The Hodge-Econometric Grammar in One Statement
6.2. Research Object: The World Economy as a Regional Macro-Flow Network
6.2.1. Formal Definition of the Research Object
6.2.2. Unit of Analysis: Global Region Rather than Country
6.2.3. The World Anchor as Normalization Device, Not as a Competing Node
6.2.4. The Caucasus as a Corridor-Sensitive Research-Object Choice
6.2.5. Regional Macro-Flow Network as a Node-Edge-Pressure Object
6.2.6. Public Data Inputs and Author-Calculated Research Variables
6.2.7. Research Questions Embedded in the Object
6.2.8. Boundary Conditions of the Research Object
6.2.9. Link to Data Construction and Hodge Decomposition
6.2.10. Section Synthesis
6.3. Data and Network Construction: World Anchor, Ten Regional Nodes and Caucasus Visibility
6.3.1. Public Anchor Layer and Constructed Hodge Layer
6.3.2. The World Anchor as Normalization Device, Not Regional Node
6.3.3. Ten Regional Nodes and the Closed Macro-Regional Universe
6.3.4. Caucasus Visibility as a Design Principle
6.3.5. Network Construction from Regional Anchors

6.3.6. Network Adequacy: Connectedness, Density and Cycles
6.3.7. From Undirected Connectivity to Directed Macro-Flow Pressure
6.3.8. Data and Network Construction Algorithm
6.3.9. Replication and Source-Ledger Discipline
6.3.10. Boundary Conditions for Interpreting the Constructed Network
6.3.11. Bridge to Section 6.4
6.4. Methodology: Directed Edge Pressure and Discrete Hodge Decomposition
6.4.1. Methodological Object: An Edge Cochain, Not a GDP Ranking
6.4.2. Standardized Regional Pressure Potential
6.4.3. Directed Macro-Flow Pressure on Edges
6.4.4. Incidence Matrices and Orientation Convention
6.4.5. Weighted Hodge Decomposition
6.4.6. Gradient Hierarchy as the Regional Ranking Layer
6.4.7. Curl-Based Local Imbalance on Regional Triangles
6.4.8. Harmonic Component and Systemic Circulation
6.4.9. Hodge Energy Decomposition and Component Shares
6.4.10. Regional Indices Derived from Hodge Components
6.4.11. Spectral and Higher-Order Hodge-Laplacian Validation
6.4.12. Algorithm 6.4A: Directed Pressure and Weighted Hodge Decomposition
6.4.13. Numerical Verification and Acceptance Criteria
6.4.14. Claim Boundary of the Methodology
6.4.15. Transition to Section 6.5
6.5. Results: Gradient Hierarchy, Curl Imbalance and Harmonic Circulation
6.5.1. Empirical Anchor: The Regional System Being Decomposed
6.5.2. Network Topology: Connected and Cycle-Rich Regional Graph
6.5.3. Hodge Energy Decomposition of Regional Macro-Flow Pressure
6.5.4. Gradient Hierarchy: Directed Pressure Is Not GDP Ranking
6.5.5. Curl Imbalance: Local-Cycle Pressure Around Regional Triangles
6.5.6. Harmonic Circulation: Residual Systemic Flow After Hierarchy and Curl
6.5.7. Resilience and Tail Risk Derived from Hodge Components
6.5.8. Higher-Order Hodge-Laplacian and Simplicial Closure
6.5.9. Multilayer Structure, SVD Evidence and Shock-Response Dynamics
6.5.10. Econometric, Machine-Learning and Persistent-Homology Results
6.5.11. Integrated Evidence Map and Result Synthesis
6.5.12. Result Boundary: What Section 6.5 Establishes and What It Does Not Establish
6.6. Interpretation: Why the World Economy Is Not Reducible to GDP Mass
6.6.1. From Economic Mass to Economic Organization
6.6.2. The Hodge Decomposition as the Main Non-Reducibility Evidence
6.6.3. Why the Gradient Hierarchy Is Not a GDP Ranking
6.6.4. Curl Imbalance: Local Cycles That GDP Tables Cannot Show
6.6.5. Harmonic Circulation: The Systemic Residual Beyond Hierarchy and Local Imbalance
6.6.6. Resilience and Tail Risk: Stability Is Not the Same as Size
6.6.7. Network Topology: Why the Graph Matters Before the Decomposition
6.6.8. Higher-Order Topology: Local Closure and Residual Circulation
6.6.9. The Caucasus: Corridor Visibility Without Output Exaggeration
6.6.10. Econometric and Validation Reading: Structural Evidence, Not Final Causality
6.6.11. Why GDP Remains Necessary but Not Sufficient
6.6.12. Policy and Strategic Meaning of the Interpretation
6.6.13. Theoretical Implication: A Topological Reading of the World Economy
6.6.14. Interpretation Boundaries

6.6.15. Transition to Robustness, Machine Learning and Persistent-Homology Validation
6.7. Robustness, Machine Learning and Persistent-Homology Validation
6.7.1. Purpose of the Validation Layer
6.7.2. Validation Logic and Evidence-Closure Formula
6.7.3. Robust Econometric Validation: Baseline Informativeness
6.7.4. Identification and Endogeneity-Screen Logic
6.7.5. Threshold, Quantile, Regime and Tail-Risk Robustness
6.7.6. Bayesian Approximation and Posterior Caution
6.7.7. Robustness and Placebo Validation
6.7.8. Machine-Learning Forecast Validation
6.7.9. Leakage-Control and Fold-Level Audit Discipline
6.7.10. Persistent-Homology Validation of Cycle Stability
6.7.11. Integrated Evidence Map
6.7.12. Replication and Zenodo-Linked Audit Requirements
6.7.13. Validation of the Caucasus as a Corridor-Sensitive Node
6.7.14. Validation Gate and Final Claim Classification
6.7.15. Section Conclusion: What the Validation Layer Establishes
6.8. Chapter Conclusion
6.8.1. Final research synthesis
6.8.2. Methodological conclusion: from macro indicators to a decomposable cochain
6.8.3. Empirical conclusion: a connected and cycle-rich regional topology
6.8.4. Hodge-theoretic conclusion: hierarchy is dominant but incomplete
6.8.5. Regional conclusion: GDP mass, resilience and risk do not collapse into one rank
6.8.6. Caucasus conclusion: visibility without output inflation
6.8.7. Validation conclusion: robust, predictive and topological evidence as benchmark support
6.8.8. Scientific contribution of the completed Hodge chapter
6.8.9. Claim boundary and limitation closure
6.8.10. Replication agenda: from regional prototype to full international Hodge model
6.8.11. Transition to Chapter 7: from Hodge flow topology to Navier-Stokes liquidity-flow stress
6.8.12. Final chapter conclusion

Chapter 7. Navier-Stokes-Inspired Global Liquidity-Flow and Systemic-Stress Modelling
7.1. Navier-Stokes Logic and the Economic Flow Analogy
7.1.1. Function of this Section within the Monograph
7.1.2. Why a Flow Analogy is Needed for Global Macro-Financial Stress
7.1.3. Classical Navier-Stokes Grammar and the Translation Boundary
7.1.4. Liquidity Velocity as Economic Flow Capacity
7.1.5. Liquidity Acceleration and the Stress of Changing Flow Conditions
7.1.6. Pressure Gradients as Macro-Financial Stress Direction
7.1.7. Friction and Diffusion: From Viscosity to Credit and Liquidity Impediments
7.1.8. Stochastic Forcing and Event-Shock Transmission
7.1.9. GDP-Cycle Forcing and Fourier Macro-Dynamic Logic
7.1.10. Restricted epsilon(t) Closure as Hidden Adjustment, Not a Free Residual
7.1.11. Nondimensionalization and Directional Harmonization
7.1.12. Economic Meaning of the Stress-Balance Components
7.1.13. From Indicator Collection to Balance Architecture
7.1.14. Global Liquidity-Flow Stress as a Country-Year Field
7.1.15. Why Liquidity Resilience Must be Read with Systemic Stress
7.1.16. Relationship to Rolling Validation, Benchmarks and External Targets
7.1.17. Monographic Integration with the Other Six Problem Chapters

7.1.18. Claim Boundary for the Economic Flow Analogy
7.1.19. Section Synthesis
7.2. Research Object: Global Liquidity, Pressure, Friction and Closure
7.2.1. Definition of the Research Object
7.2.2. Liquidity as an Economic Flow Capacity
7.2.3. Pressure as a Macro-Financial Gradient
7.2.4. Friction as Impaired Liquidity Transmission
7.2.5. Closure as Restricted Hidden Adjustment
7.2.6. Systemic Stress and Liquidity Resilience as Paired Diagnostic Fields
7.2.7. Formal Object Notation
7.2.8. Boundary between Raw Inputs, Public Anchors and Constructed Objects
7.2.9. Country, World, Macro-Regional and Validation Layers
7.2.10. Position of Chapter 7.2 within the Seven-Problem Monograph
7.2.11. Claim Boundary of the Research Object
7.2.12. Synthesis: Why the Research Object Matters
7.3. Data Architecture: 100-Country Panel, World Anchor and Macro-Regional Layers
7.3.1. Purpose of the Data Architecture
7.3.2. Empirical Universe and Observation Geometry
7.3.3. Country-Year Panel as the Main Econometric Layer
7.3.4. World Aggregate Anchor and Normalization Logic
7.3.5. Macro-Regional Layers and Corridor-Sensitive Interpretation
7.3.6. Variable Lineage: From Raw Inputs to Nondimensional Components
7.3.7. Preprocessing Discipline: Comparability before Modelling
7.3.8. Directional Harmonization and Nondimensional Scaling
7.3.9. Closure-State Variables and Restricted Epsilon Data
7.3.10. Rolling Validation, Benchmark Data and External Targets
7.3.11. Alignment with the Seven-Problem Monograph Data Architecture
7.3.12. Replication Package, Metadata and Formula-Audit Contract
7.3.13. Data Limitations and Claim-Boundary Discipline
7.3.14. Chapter 7.3 Conclusion
7.4. Methodology: Nondimensional Stress Balance, ε(t) Closure and Validation Design
7.4.1. Methodological orientation
7.4.2. Nondimensionalization and direction harmonization
7.4.3. Stress and liquidity-resilience construction
7.4.4. Navier-Stokes-inspired nondimensional stress balance
7.4.5. Restricted ε(t) closure methodology
7.4.6. Fourier GDP-cycle forcing and leakage-control discipline
7.4.7. Rolling validation and benchmark comparison
7.4.8. Panel fixed effects and robust-inference specification
7.4.9. External-target validation, robustness and residual diagnostics
7.4.10. Monte Carlo uncertainty and policy counterfactual design
7.4.11. Integration with the seven-problem methodology of the monograph
7.4.12. Replication algorithm for Chapter 7.4
7.4.13. Methodological claim-boundary protocol
7.4.14. Methodological synthesis
7.5. Results: Systemic Stress, Liquidity Resilience, Rolling Forecasts and Benchmarks
7.5.1. Results Architecture and Evidence-Status Logic
7.5.2. Global Systemic-Stress and Liquidity-Resilience Results
7.5.3. Rolling One-Year-Ahead Validation Results, 2017-2024
7.5.4. Benchmark Comparison: ARIMA, VAR, GARCH and Composite-Index Baselines

7.5.5. Panel Fixed-Effects Stress-Channel Results
7.5.6. Macro-Regional Stress Rankings and Dominant Liquidity-Flow Mechanisms
7.5.7. Equation-Balance and ε(t) Closure Results
7.5.8. Robustness, Panel Diagnostics and Inference Stability
7.5.9. External-Target Validation and Residual Stability
7.5.10. Policy-Counterfactual Result Preview and Link to Section 7.7
7.5.11. Position of the Results inside the Seven-Problem Monograph
7.5.12. Results Synthesis and Transition to Interpretation
7.6. Interpretation: Liquidity-Flow Weakness, Pressure Gradients and Systemic Vulnerability
7.6.1. From Results to Interpretation: Why Chapter 7 Is More Than a Stress Index
7.6.2. Liquidity-Flow Weakness as the First Vulnerability Mechanism
7.6.3. Pressure Gradients: Why Stress Is Directional Rather Than Merely High
7.6.4. Friction, Diffusion and the Meaning of Financial Viscosity
7.6.5. Restricted ε(t): Hidden Adjustment Without Residual Overclaiming
7.6.6. Systemic Vulnerability as a Balance Between Stress and Absorption Capacity
7.6.7. Interpreting Rolling Forecasts and Benchmarks Without Forecast Overclaiming
7.6.8. Macro-Regional Heterogeneity: Why the Same Stress Score Can Mean Different Things
7.6.9. External Validation and Circularity Control
7.6.10. Policy Interpretation: Diagnostic Guidance, Not Mechanical Prescription
7.6.11. Integration with the Seven-Problem Monograph
7.6.12. Claim Discipline: What the Interpretation Can and Cannot Say
7.6.13. Section Conclusion
7.7. Monte Carlo, Policy Counterfactuals and External Validation
7.7.1. Why the Validation-Scenario Layer Is Necessary
7.7.2. Monte Carlo Uncertainty as a Probability Layer
7.7.3. Reported Scenario Medians and High-Stress Probabilities
7.7.4. Policy Counterfactuals: From Stress Decomposition to Scenario Interpretation
7.7.5. External Validation: Target Families, Classification Metrics and Plausibility
7.7.6. External Validation Is Not Causal Identification
7.7.7. Monte Carlo and Counterfactual Results as Macroprudential Stress-Testing Tools
7.7.8. Relationship with the Restricted epsilon(t) Closure
7.7.9. Cross-Problem Alignment: Why Section 7.7 Belongs in the Monograph
7.7.10. Reviewer-Safety Matrix for Section 7.7
7.7.11. Integrated Interpretation of the Monte Carlo and Policy Results
7.7.12. Section Conclusion
7.8. Chapter Conclusion and Claim Boundary
7.8.1. Purpose of the Chapter-Level Conclusion
7.8.2. What Chapter 7 Establishes
7.8.3. Final Methodological Conclusion: Nondimensional Discipline
7.8.4. Final Modelling Conclusion: Restricted epsilon(t) Closure
7.8.5. Final Empirical Conclusion: Systemic Stress and Liquidity Resilience
7.8.6. Final Forecasting Conclusion: Rolling Validation and Benchmarks
7.8.7. Final Policy Conclusion: Counterfactual Usefulness without Policy Determinism
7.8.8. External Validation and Robustness: Final Interpretation
7.8.9. Contribution of Chapter 7 to the Seven-Problem Monograph
7.8.10. Final Claim Boundary
7.8.11. Limitations and Academic Caution
7.8.12. Data, Replication and Reproducibility Closure
7.8.13. Final Integrated Conclusion of Chapter 7
7.8.14. Transition to the Comparative Synthesis of the Monograph

Chapter 8. Yang-Mills Economic Mass Gap in Global and Corridor Flow Networks

8.1. Yang-Mills Gauge Logic and the Economic Mass-Gap Analogy
- 8.1.1. Function of the Section within the Monograph
- 8.1.2. From Yang-Mills Gauge Logic to Economic Measurement Grammar
- 8.1.3. Economic Field Representation: Nodes, Edges, Stress and Corridor Exposure
- 8.1.4. Gauge Potential and Orientation Discipline
- 8.1.5. Curvature, Action and Non-Neutralized Stress Circulation
- 8.1.6. Mass-Gap Analogy as a Finite-Network Spectral Threshold
- 8.1.7. Relation to the Other Millennium-Inspired Economic Models
- 8.1.8. Evidence Hierarchy and Reviewer-Safe Claim Boundary
- 8.1.9. Section Synthesis
- 8.1.10. Formal Propositions for the Economic Analogue
- 8.1.11. Why the Chapter Is More Than Network Centrality
- 8.1.12. Why the Chapter Is More Than a Regression Model
- 8.1.13. Conceptual Questions Answered by Each Construct
- 8.1.14. Transition from Conceptual Analogy to Empirical Chapter Design

8.2. Research Object: Global-Corridor Stress Network
- 8.2.1. Purpose of the Research-Object Section
- 8.2.2. Formal Definition of the Global-Corridor Stress Network
- 8.2.3. Node Universe: World Anchor and Ten Regional/Corridor Nodes
- 8.2.4. Why the Object Is a Stress Network Rather Than a GDP Ranking
- 8.2.5. Edge Universe: Twenty-Seven Weighted Corridor Relations
- 8.2.6. Layer A and Layer B Evidence Status
- 8.2.7. Public Anchors versus Author-Calculated Analytical Objects
- 8.2.8. Stress-Field Components and Node-Level Measurement Logic
- 8.2.9. Corridor Role of the Caucasus, Central Asia and Middle Corridor Interfaces
- 8.2.10. Research Object as Input to Gauge Potential, Curvature, Action and Laplacian
- 8.2.11. Validation Pathway and Non-Overclaiming Rules
- 8.2.12. Cross-Chapter Integration with the Seven Millennium Economic Models
- 8.2.13. Section Synthesis

8.3. Data Architecture: Ten Nodes, Twenty-Seven Edges and Layered Evidence Status
- 8.3.1. Role of Data Architecture inside Chapter 8
- 8.3.2. Source Ledger and Public-Data Anchor Layer
- 8.3.3. Node Codebook: World Anchor and Ten Regional/Corridor Nodes
- 8.3.4. Raw-to-Normalized Stress-Field Construction
- 8.3.5. Twenty-Seven-Edge Graph Layer and Corridor Coding
- 8.3.6. Matrix Layer: Adjacency, Stress-Weighted Adjacency, Degree and Laplacian
- 8.3.7. Benchmark Parameters and Audit Rules
- 8.3.8. Output Data Objects: Gauge, Curvature, Action, Mass Gap, EMGI and BridgeStress
- 8.3.9. Layer A Evidence Status: Completed Finite-Network Benchmark
- 8.3.10. Layer B Evidence Status: 100-Country by 15-Year Validation Pathway
- 8.3.11. Replication Manifest, Versioning and File-Hash Discipline
- 8.3.12. Cross-Seven-Problem Data-Architecture Alignment
- 8.3.13. Reviewer-Risk Controls and Non-Overclaiming Rules
- 8.3.14. Section Synthesis

8.4. Methodology: Gauge Potential, Curvature, Action and Stress Laplacian
- 8.4.1. Methodological Purpose and Results-to-Method Closure
- 8.4.2. Empirical Objects, Operators and Notation Discipline
- 8.4.3. Stress-Field Construction as the Scalar Source of the Gauge System
- 8.4.4. Corridor-Weighted Graph and Stress-Weighted Adjacency Matrix

8.4.5. Economic Gauge Potential and Orientation Discipline
8.4.6. Field Strength, Triangular Curvature and Curvature Exposure
8.4.7. Yang-Mills Economic Action and Stress-Energy Decomposition
8.4.8. Stress Laplacian and Finite-Network Economic Mass Gap
8.4.9. Robustness, Filtering and Placebo Discipline
8.4.10. Shock Propagation and Threshold Compression Method
8.4.11. EMGI, Fragility and BridgeStress as Post-Spectral Indices
8.4.12. Algorithmic Replication Sequence
8.4.13. Cross-Chapter Methodological Integration
8.4.14. Methodological Limitations and Claim Boundary
8.4.15. Subsection Conclusion
8.5. Results: Positive Finite-Network Mass Gap, EMGI, Fragility and BridgeStress
8.5.0. Executive Result Statement
8.5.1. Reading Rule for the Results Chapter
8.5.2. Positive Finite-Network Mass Gap: Spectral Benchmark
8.5.3. Robustness Across Filtered Graph Specifications
8.5.4. Monte Carlo Uncertainty Audit
8.5.5. Curvature Cycles and Yang-Mills Economic Action
8.5.6. Regional Curvature Exposure and Action-Layer Decomposition
8.5.7. Economic Mass Gap Index: Local Protection and Structural Fragility
8.5.8. EMGI Component Audit and Reproducibility
8.5.9. EMGI Ranking and Systemic Fragility Classes
8.5.10. BridgeStress: Corridor Strategic Exposure Beyond GDP Mass
8.5.11. Shock Scenarios: Threshold Compression and Action Expansion
8.5.12. Scenario Interpretation Matrix
8.5.13. Shock Propagation by Origin Node
8.5.14. Local-to-Systemic Transition Threshold
8.5.15. Integration with the Seven-Problem Monograph
8.5.16. Integrated Result Synthesis
8.5.17. Result Claim Boundary
8.5.18. Replication and Reviewer Checklist for the Results Chapter
8.5.19. Conclusion
8.6. Interpretation: Systemic Shock Thresholds and Corridor Exposure
8.6.0. Executive Interpretive Synthesis
8.6.1. Interpretation of the Positive Finite-Network Mass Gap
8.6.2. From Local Stress to Systemic Shock Thresholds
8.6.3. Corridor Exposure Is Not GDP Mass
8.6.4. EMGI and Fragility as Local Protection Diagnostics
8.6.5. BridgeStress and the Middle Corridor Reading
8.6.6. Curvature, Action Concentration and Corridor Exposure
8.6.7. Shock Scenarios: How the Threshold Is Compressed
8.6.8. Correlation Evidence and Why It Remains Diagnostic
8.6.9. Integration with the Other Six Millennium-Inspired Economic Chapters
8.6.10. Policy, Corridor and Research Implications
8.6.11. Evidence Gate: What the Interpretation Establishes and What It Does Not
8.6.12. Section Conclusion
8.7. Scenario Simulations and Local-to-Systemic Transition
8.7.1. Analytical Purpose: Moving from Static Mass Gap to Shock Transition
8.7.2. Scenario Equations and Recalculation Rules
8.7.3. Baseline Boundary Before Shock Injection

8.7.4. Threshold Compression: The Core Local-to-Systemic Result
8.7.5. Action Amplification and Stress-Energy Concentration
8.7.6. EMGI Deterioration and Fragility Transmission
8.7.7. Scenario-Specific Interpretive Readings
8.7.8. Shock Propagation by Origin Node
8.7.9. Corridor-Specific Local-to-Systemic Mechanism
8.7.10. Transition Regime Classification
8.7.11. Integration with the Seven-Problem Monograph
8.7.12. Evidence Status and Claim Boundary
8.7.13. Replication Checklist for Scenario Simulations
8.7.14. Section Conclusion
8.8. N=1,500 Validation Pathway and Claim Boundary
8.8.1. Why the N = 1,500 layer is necessary
8.8.2. From Layer A to Layer B: benchmark evidence versus panel evidence
8.8.3. Country-year variable ledger and anti-circularity discipline
8.8.4. Panel model system: from benchmark diagnostics to robust validation
8.8.5. Validation gates and evidentiary decision rules
8.8.6. Claim boundary: what the chapter may say now and what it must reserve
8.8.7. Reviewer-risk response and scientific caution
8.8.8. Replication closure and Zenodo-linked audit pathway
8.8.9. Position of the Yang-Mills validation pathway inside the seven-problem monograph
8.8.10. Final synthesis of Section 8.8
8.9. Chapter Conclusion
8.9.1. Final Synthesis of the Chapter
8.9.2. What the Chapter Establishes
8.9.3. Interpretation of the Positive Economic Mass Gap
8.9.4. Closing Formula Map
8.9.5. EMGI, Fragility and BridgeStress Conclusions
8.9.6. Scenario Simulations and Local-to-Systemic Transition
8.9.7. Evidence Hierarchy and Claim Discipline
8.9.8. Position inside the Seven-Problem Monograph
8.9.9. Validation Pathway after the Chapter Conclusion
8.9.10. Limitations, Reviewer-Safety and Scientific Contribution
8.9.11. Final Chapter Conclusion

Chapter 9. Birch-Swinnerton-Dyer Economic Local-to-Global Structural Rank Model
9.1. BSD Logic and Economic Local-to-Global Translation
9.1.1. Why Chapter 9 Begins with Local-to-Global Translation
9.1.2. The Classical BSD Logic as a Local-to-Global Grammar
9.1.3. The Economic Problem: Rank Is Not Reducible to Output Mass
9.1.4. Defining Local and Global in the Economic BSD Analogue
9.1.5. The Measurement Chain from Public Anchors to LOrder
9.1.6. Finite-State Reductions as Economic Regime Logic
9.1.7. Economic L-Function, LOrder and Structural Rank
9.1.8. Corridor Stress as the Economic Meaning of Local-to-Global Transmission
9.1.9. Position of BSD within the Seven-Problem Monograph
9.1.10. Claim Boundary: What Chapter 9.1 Authorizes and What It Does Not
9.1.11. Transition to the Remaining Chapter 9 Sections
9.1.12. Section Conclusion
9.2. Research Object: Regional Structural Rank Formation under Corridor Stress

9.2.1. Position of the Research Object inside Chapter 9
9.2.2. Empirical Object: World Anchor and Ten Regional/Corridor Nodes
9.2.3. Rank-Formation Object: Structural Rank Is Not GDP Rank
9.2.4. Corridor-Stress Object: Why Regional Rank Forms under Transmission Pressure
9.2.5. Local-to-Global Object: From Regional State to Structural Rank
9.2.6. Formal Definition of the Research Object
9.2.7. Public Anchors, Author-Calculated Objects and Lineage Discipline
9.2.8. Research Questions Assigned to the Research Object
9.2.9. Alignment with the Seven-Problem Monograph Architecture
9.2.10. Evidence Status and Claim Boundary of the Research Object
9.2.11. Subsection Synthesis: What 9.2 Establishes for the Rest of Chapter 9
9.3. Data Architecture: World Anchor, Ten Regional/Corridor Nodes and N = 150 Closure Layer
9.3.1. Function of the Data Architecture in Chapter 9
9.3.2. World Anchor and Ten Regional/Corridor Nodes
9.3.3. Regional Node Taxonomy and Corridor Logic
9.3.4. N = 150 Regional-Year Closure Layer
9.3.5. Public Source Families and Variable Lineage
9.3.6. Public Anchors versus Author-Calculated BSD Objects
9.3.7. Normalization, Directional Harmonization and Stress Coordinates
9.3.8. Stress Components as Data Architecture, Not Final Results
9.3.9. Graph and Corridor Data Layer
9.3.10. Closure Diagnostics and Evidence-Gate Requirements
9.3.11. Replication Package, Seeds, Hashes and Audit Trail
9.3.12. Cross-Problem Data-Architecture Alignment
9.3.13. Claim Boundary of the Data Architecture
9.3.14. Section Synthesis
9.4. Methodology: Economic Curve Coefficients, Discriminants and Finite-State Reductions
9.4.1. Methodological Position of the Subsection
9.4.2. Regional Economic State Vector and Variable Lineage
9.4.3. Economic Curve Coefficients and the Cubic Analogue
9.4.4. Economic Discriminant and Non-Degeneracy Audit
9.4.5. Finite-State Local Reductions: q-Bases as Economic Discretization
9.4.6. Trace Analogues and Local Signal Extraction
9.4.7. Algorithmic Procedure for Coefficients, Discriminants and Reductions
9.4.8. Boundary Between Subsection 9.4 and Subsection 9.5
9.4.9. Alignment with the Seven-Problem Monograph Methodology
9.4.10. Claim-Boundary Protocol for the Methodology
9.4.11. Replication Checklist for Subsection 9.4
9.4.12. Subsection Summary
9.5. Economic L-Function, Euler Factors, LOrder and Structural Rank
9.5.1. Position of the L-Function Layer inside Chapter 9
9.5.2. From Regional Trace Analogues to Economic Euler Factors
9.5.3. Economic Euler Factors and the Product Construction
9.5.4. The Economic L-Function near s = 1
9.5.5. LOrder as a Normalized Order-of-Behavior Measure
9.5.6. Structural Rank: Productive, Hodge-Flow, Network and Agentic Components
9.5.7. Calibrated Correspondence between LOrder and Structural Rank
9.5.8. q-Base Sensitivity, Placebo Logic and Anti-Circularity Implications
9.5.9. Cross-Problem Alignment within the Seven-Analogue Monograph
9.5.10. Algorithmic Workflow and Replication Requirements

9.5.11. Section-Level Claim Boundary
9.5.12. Transition to Section 9.6
9.6. Results: LOrder-Rank Correspondence, BridgeStress, Regulator, Tamagawa-Type Friction and Torsion
9.6.1. Results Architecture and Reading Rule
9.6.2. Structural-Rank Component Results
9.6.3. LOrder-Rank Correspondence Results
9.6.4. Economic Regulator Analogue: Rank Support and Absorption Capacity
9.6.5. Tamagawa-Type Friction Results
9.6.6. Economic Torsion: Locked Capacity and Non-Productive Circularity
9.6.7. BridgeStress and Corridor-Rank Leverage
9.6.8. Corridor-Function Interpretation Layer
9.6.9. Scenario Threshold Compression and Action Concentration
9.6.10. Integrated Results Synthesis and Cross-Problem Position
9.6.11. Section-Level Claim Boundary
9.7. Interpretation: How Local Regional Signals Inform Global Structural Rank, Friction and Torsion
9.7.1. Interpretation Problem and Reading Rule
9.7.2. From Local Regional Signals to Global Structural Rank
9.7.3. Interpreting LOrder-Rank Correspondence
9.7.4. Regulator as Rank-Support Capacity
9.7.5. Tamagawa-Type Friction and Torsion as Rank-Conversion Barriers
9.7.6. BridgeStress and the Visibility of Corridor Nodes
9.7.7. Regional Signal Profiles and Multidimensional Interpretation
9.7.8. Local Shock Signals, Threshold Compression and Global Vulnerability
9.7.9. Interpretation within the Seven-Problem Monograph Architecture
9.7.10. What the Local-to-Global Interpretation Explains and What It Does Not Explain
9.7.11. Final Interpretive Synthesis
9.8. Robustness, Anti-Circularity, Placebo and Claim Hierarchy
9.8.1. Robust-Inference and Small-Cluster Discipline
9.8.2. Variable Lineage and Anti-Circularity
9.8.3. Practical Equivalence, Bland-Altman Agreement and Rank-Scale Error
9.8.4. Leave-One-Block, Out-of-Sample and Sensitivity Validation
9.8.5. Placebo, Negative Controls and Falsification Logic
9.8.6. Replication Closure, Source Ledger and Reviewer-Risk Response
9.8.7. Final Claim Hierarchy of the Robustness Layer
9.8.8. Cross-Problem Robustness Alignment inside the Monograph
9.9. Chapter Conclusion
9.9.1. What the Chapter Establishes
9.9.2. What the Chapter Does Not Establish
9.9.3. Final Evidence and Claim-Boundary Statement
9.9.4. Contribution to the Monograph
9.9.5. Transition to the Next Chapter

Chapter 10. Riemann-Zeta FPAS+ζ Inflation Forecasting
10.1. Riemann-Zeta Logic and the Economic Spectral-Signal Analogy
10.1.1. Position of the Riemann-Zeta Chapter inside the Monograph
10.1.2. From the Classical Zeta Object to an Economic Signal Grammar
10.1.3. Why Inflation Forecasting Requires a Spectral-Signal Layer
10.1.4. Layered Validation as the Scientific Discipline of the Analogy
10.1.5. The FPAS+ζ Correction Gate
10.1.6. Crisis Resonance and Zeta-Deformation Logic

10.1.7. Claim Boundary: Strong Forecast-Diagnostic Architecture without Theorem Overclaiming
10.1.8. Integration with the Seven-Problem Monograph
10.1.9. Reviewer-Safety Logic for the Opening Subsection
10.1.10. Transition to Chapter 10.2
10.2. Research Object: Global Inflation as a Layered Macro-Financial Pressure System
10.2.1. Position of the Research Object inside Chapter 10
10.2.2. Global Inflation as a Layered Macro-Financial Pressure System
10.2.3. Layered Empirical Universe and Sample-Discipline Logic
10.2.4. Target Variable, Forecast Objects and Diagnostic Objects
10.2.5. Benchmark Result Context for the Research Object
10.2.6. Data Status, Replication Object and Manuscript Closure
10.2.7. Evidence-Status Hierarchy: What the Object Can and Cannot Support
10.2.8. Research Questions Reframed for the Book Chapter
10.2.9. Cross-Chapter Integration with the Seven-Problem Monograph
10.2.10. Reviewer-Risk Controls Embedded in the Research Object
10.2.11. Section Synthesis
10.3. Data Architecture: Annual, Quarterly and Monthly Validation Layers
10.3.1. Purpose of the Data Architecture
10.3.2. Layer Separation as Sample-Discipline
10.3.3. Target Variable, Forecast Objects and Diagnostic Objects
10.3.4. Public-Anchor Layer versus Author-Calculated Layer
10.3.5. Annual Validation Layers
10.3.6. Quarterly and Monthly Evidence Layers
10.3.7. Replication Package and Traceability Discipline
10.3.8. Cross-Seven-Problem Data Alignment
10.3.9. Data-Architecture Closure Statement
10.4. Methodology: FPAS Baseline, ζ-Cycle, τ Argument and Correction Gate
10.4.1. Methodological Objective
10.4.2. Normalization and Composite Pressure Index
10.4.3. FPAS Baseline Forecast
10.4.4. Nonlinear τ Argument
10.4.5. Critical-Line Zeta Evaluation and Real-Valued ζ-Cycle
10.4.6. Alpha-Calibrated Correction Gate
10.4.7. Alpha Calibration and Overfitting Controls
10.4.8. Forecast Construction Algorithm
10.4.9. Methodology-to-Results Alignment
10.4.10. Evidence Gate and Claim Boundary
10.4.11. Section Conclusion
10.5. Forecast-Evaluation Protocol: RMSE, MAE, sMAPE, MZ, DM, CW and Rolling Validation
10.5.1. Forecast objects and residual sign convention
10.5.2. Loss metrics: RMSE, MAE and sMAPE
10.5.3. Rolling no-look-ahead validation
10.5.4. Mincer-Zarnowitz calibration and forecast-encompassing gates
10.5.5. Diebold-Mariano and Clark-West benchmark-comparison tests
10.5.6. Protocol-level decision gate
10.6. Results: FPAS+zeta versus FPAS and ARIMA across Validation Layers
10.6.1. Main annual N = 55 forecast accuracy results
10.6.2. Annual robustness N = 45 results
10.6.3. Crisis-era N = 20 comparison results
10.6.4. Cross-layer stability and alpha overfitting controls

10.6.5. Formal validation-test results
10.6.6. Quarterly N = 100 and monthly N = 240 validation evidence
10.6.7. Integrated result synthesis
10.6.8. Cross-seven-problem methodological connection
10.6.9. Final subsection conclusion
10.7. Interpretation: Crisis Resonance, Zeta-Deformation and Inflation-Cycle Diagnostics
10.8. Spectral, HMM, Markov-Switching and Robustness Evidence
10.9. Chapter Conclusion and Claim Boundary

Chapter 11. P-vs-NP-Inspired Robust Portfolio Optimization
11.1. P vs NP Logic and the Economic Meaning of Computational Complexity
11.1.1. Why computational complexity belongs in an economic monograph
11.1.2. From theorem-level P versus NP to bounded economic analogy
11.1.3. Support-space explosion as an economic measurement object
11.1.4. Economic complexity versus mathematical theorem proof
11.1.5. Why Chapter 11 completes the seven-problem architecture
11.2. Research Object: Cardinality-Constrained Portfolio Optimization
11.2.1. Definition of the research object
11.2.2. The empirical universe: fixed industry portfolios, not ex-post selection
11.2.3. The formal optimization object
11.2.4. Research-object boundaries: what is inside and outside the chapter
11.2.5. Evidence architecture and transition to later sections
11.2.6. Section-level conclusion
11.3. Data Architecture: Damodaran Industry Universe, CAPM Priors and Covariance Geometry
11.3.1. Empirical universe and source-vintage discipline
11.3.2. Data status: public inputs versus author-constructed objects
11.3.3. CAPM prior and expected-return construction
11.3.4. Covariance geometry and market-mode concentration
11.3.5. Replication status and data-package logic
11.4. Methodology: Support-Space Explosion, Greedy Search, Monte Carlo, GA and Exact Benchmarking
11.4.1. Methodological system and evidence vector
11.4.2. Support-space explosion and P-vs-NP operationalization
11.4.3. Baseline sparse Sharpe maximization
11.4.4. Greedy search methodology
11.4.5. Monte Carlo support sampling
11.4.6. Genetic algorithm and continuous reoptimization
11.4.7. Exact reduced benchmark and optimality-gap measurement
11.4.8. Full-universe search coverage and no-global-certificate rule
11.4.9. Algorithmic comparison and runtime discipline
11.4.10. Boundary between exactness, approximation and interpretability
11.4.11. Section-level synthesis
11.5. Black-Scholes Overlay, Transaction Costs, Stress Scenarios and Robustness Gates
11.5.1. Transaction-cost and turnover realism
11.5.2. Black-Scholes derivative-overlay protocol
11.5.3. Local delta validation and option-limit boundary
11.5.4. Baseline versus option-augmented portfolio check
11.5.5. Stress scenarios and crisis-regime interpretation
11.5.6. Falsification and robustness-gate closure
11.6. Results: Best-Found Portfolios, K-Grid, Exact Reduced Benchmark and Algorithmic Comparison
11.6.1. Baseline K=10 best-found portfolio evidence

11.6.2. K-grid and cardinality-sensitive results
11.6.3. Exact reduced benchmark and full-universe coverage boundary
11.6.4. Algorithmic comparison and continuous reoptimization
11.6.5. Statistical inference and descriptive effect-size status
11.6.6. Risk contribution, robustness results and integrated strategy ranking
11.6.7. Results-closure and claim boundary
11.6.8. Section-level synthesis
11.7. Interpretation: What Computational Finance Shows and What It Cannot Certify
11.7.1. Interpretation of support-space explosion as economic complexity
11.7.2. Interpretation of algorithmic comparison: convergence, not certification
11.7.3. Interpretation of covariance dependence and risk-model conditionality
11.7.4. Interpretation of derivative overlay: leverage discipline rather than free performance
11.7.5. What computational finance shows in this chapter
11.8. Claim Boundary: No P != NP Proof, No Certified n = 94 Global Optimum, No Realized-Return Dominance
11.8.1. Why no P != NP proof is claimed
11.8.2. Why no certified n = 94 global optimum is claimed
11.8.3. Why no realized-return dominance is claimed
11.9. Chapter Conclusion
11.9.1. Final permissible claim of Chapter 11
11.9.2. Contribution to the monograph as a whole
11.9.3. Closing statement

Chapter 12. Comparative Results across the Seven Millennium Economic Models

12.1. Comparative Empirical Universe
12.1.1. Why sample heterogeneity is methodologically necessary
12.1.2. Panel evidence versus benchmark evidence
12.1.3. Forecast layers versus computational support spaces
12.1.4. Comparative empirical implication
12.2. Comparative Mathematical Object
12.2.1. Curvature and smoothing as inequality diagnostics
12.2.2. Hodge decomposition as macro-flow organization
12.2.3. Navier-Stokes and Yang-Mills as stress-transmission grammars
12.2.4. BSD, Riemann/Zeta and P vs NP as information, forecasting and decision grammars
12.3. Comparative Validation Strength
12.3.1. The strongest panel claim: Navier-Stokes
12.3.2. The strongest forecast claim: Riemann/Zeta
12.3.3. The strongest computational claim: P vs NP
12.3.4. Benchmark, calibration and finite-network claims
12.3.5. Why claim-boundary discipline is a comparative result
12.4. Cross-Problem Results Matrix
12.4.1. Ricci/Poincare result in the comparative matrix
12.4.2. Hodge result in the comparative matrix
12.4.3. Navier-Stokes result in the comparative matrix
12.4.4. Yang-Mills result in the comparative matrix
12.4.5. BSD result in the comparative matrix
12.4.6. Riemann/Zeta result in the comparative matrix
12.4.7. P vs NP result in the comparative matrix
12.4.8. Integrated result of Chapter 12

Chapter 13. Unified Interpretation: The Millennium Economic Research Program

13.0. Integrative Premise: From Seven Analogues to One Research Program
13.1. Flow Dimension: Navier-Stokes and Hodge
13.2. Curvature and Topological Deformation Dimension: Ricci/Poincare, Yang-Mills and Hodge
13.3. Local-to-Global Rank Dimension: Birch-Swinnerton-Dyer
13.4. Spectral-Cyclical Forecast Dimension: Riemann/Zeta
13.5. Computational-Decision Dimension: P vs NP
13.6. Unified Contribution to Economic Science
13.7. Cross-Dimensional Coupling: Why the Five Dimensions Cannot Be Separated
13.8. What the Chapter Establishes and What It Excludes
13.9. Final Theoretical Synthesis

Chapter 14. Limitations, Claim Boundaries and Reviewer-Safety Matrix

14.1. What the Book Does Not Claim
14.2. Analogy, Calibration and Measurement
14.3. Constructed Variables and Circularity Risk
14.4. Sample-Size Boundaries
14.5. Forecasting and Optimization Boundaries
14.6. Evidence-Level Matrix
14.7. Reviewer-Safety Matrix: Likely Objections and Direct Responses
14.8. Model-by-Model Claim Boundary
14.9. Data, Replication and Version-Control Boundaries
14.10. Econometric Identification and Causality Boundaries
14.11. Claim-Language Protocol for the Final Monograph
14.12. Chapter Conclusion: Why Boundary Discipline Strengthens the Book

Chapter 15. General Conclusion and Future Research Agenda

15.1. Return to the General Aim of the Monograph
15.2. Summary of the Seven Economic Analogues
15.3. Main Scientific Contribution
15.4. Theoretical Contribution
15.5. Methodological Contribution
15.6. Empirical and Practical Contribution
15.7. Future Research: Country Panels, Dyadic Flows, Sectoral Systems, Firm-Level Extensions
15.8. Final Conclusion

Appendices A-I

Appendix A. Perelman-Ricci-Poincare Data, Variables and Extended Tables

Appendix B. Hodge Network Matrices and Decomposition Outputs

Appendix C. Navier-Stokes Stress-Balance Variables and Forecast Diagnostics

Appendix D. Yang-Mills Gauge Matrices, Curvature and Spectral Tests

Appendix E. BSD Finite-State, Euler-Factor and LOrder Tables

Appendix F. Riemann-Zeta Annual, Quarterly and Monthly Validation Outputs

Appendix G. P vs NP Portfolio Search, Exact Enumeration and Robustness Tables

Appendix H. Unified Claim-Boundary and Replication Manifest

Appendix I. Full Zenodo/Data Package Registry

Extraction and Deduplication Audit

References

List of Tables

Editorial note: page numbers should be generated after the full manuscript is merged, final styles are applied and the manuscript is paginated. Entries marked with [A]/[B] indicate duplicate numbering present in the source manuscript and should be reconciled during final copy-editing.

Chapter 1

Table 1.2. Monograph-level translation matrix: why each Clay problem matters for economic modelling
Table 1.3. Seven operational research sub-problems, empirical architectures and admissible claim levels
Table 1.4. Unified monograph aim and objectives across the seven source manuscripts
Table 1.5.1. Core structural map of the monograph
Table 1.5.3. Source-manuscript integration in the seven-problem translation matrix

Chapter 2

Table 2.1.1. Analogy-proof evidence ladder for the monograph
Table 2.1.2. Safe language rule for theorem-inspired economic analogues
Table 2.1.3. Minimum translation checklist for each problem chapter
Table 2.2.1. Flow logic across the seven economic analogues
Table 2.2.2. Classical object, translation boundary and economic analogue in the two flow chapters
Table 2.2.3. Navier-Stokes economic translation map
Table 2.2.4. Hodge economic translation map
Table 2.2.5. Comparative role of the two primary flow analogies
Table 2.2.6. Claim hierarchy for the flow analogies
Table 2.3.1. Curvature and topology translation map across the seven economic analogues
Table 2.3.2. Primary curvature-topology objects and direct-proof exclusion
Table 2.3.3. Perelman/Ricci/Poincare economic translation chain
Table 2.3.4. Hodge topology and decomposition safeguards
Table 2.3.5. Yang-Mills finite-network translation and claim gates
Table 2.3.6. Supporting roles of the non-primary analogues in curvature-topology reasoning
Table 2.3.8. Topological concepts and economic interpretation rules
Table 2.3.9. Claim hierarchy for curvature and topology analogies
Table 2.3.10. Category-error prevention matrix
Table 2.4.1. Spectral and L-function translation architecture across the seven economic analogues
Table 2.4.2. Riemann/zeta translation sequence and claim discipline
Table 2.4.3. BSD local-to-global L-function translation sequence
Table 2.4.4. Comparative spectral roles of the seven problem chapters
Table 2.4.5. Overclaiming risks and monograph-level safeguards
Table 2.4.6. Final permissible claim hierarchy for Section 2.4
Table 2.5.1. Complexity and optimization translation map across the monograph
Table 2.5.2. From mathematical complexity to economic optimization evidence
Table 2.5.3. Optimization analogies beyond the P-vs-NP chapter
Table 2.5.4. Distinguishing types of complexity in the seven-problem monograph
Table 2.5.5. Final claim hierarchy for complexity and optimization analogies
Table 2.6.1. Local-to-global and systemic-transmission map across the seven economic analogues
Table 2.6.2. BSD local-to-global transformation chain
Table 2.6.3. Systemic-transmission mechanisms and evidence gates
Table 2.6.4. Transformation operators and methodological safeguards
Table 2.6.5. Claim hierarchy for local-to-global and systemic-transmission logic
Table 2.7.1. Core claim hierarchy used in the monograph
Table 2.7.2. Strong measurement claims across the seven economic analogues

Table 2.7.3. Diagnostic claim taxonomy
Table 2.7.4. Forecasting claim discipline
Table 2.7.5. Benchmark claim matrix
Table 2.7.6. Future validation claims and required evidence
Table 2.7.7. Seven-problem claim placement
Table 2.7.8. Upgrade, downgrade and exclusion rules
Table 2.7.9. General reviewer-safety matrix

Chapter 3

Table 3.1. Integrated source-literature transfer map for Section 3.1. Source synthesis: Hamilton (1982), Perelman (2002), Hodge (1952), Leray (1934), Yang and Mills (1954), Birch and Swinnerton-Dyer (1965), Riemann (1859), Cook (1971), Karp (1972), and Gondauri (2026a-g)
Table 3.2. From weak analogy to admissible mathematical-economic analogue. Source synthesis: Box (1976), Morgan and Morrison (1999), OECD and JRC (2008), Saltelli et al. (2008), and Gondauri (2026a-g)
Table 3.3. Claim-boundary synthesis across the seven mathematical-economic analogues. Source synthesis: the seven source manuscripts and their claim-boundary literature (Gondauri, 2026a-g)
Table 3.4. Mathematical grammars and their economic modelling functions. Source synthesis: Leray (1934), Hodge (1952), Hamilton (1982), Yang and Mills (1954), Birch and Swinnerton-Dyer (1965), Riemann (1859), Cook (1971), Karp (1972), and Gondauri (2026a-g)
Table 3.5. Validation gates required by analogue modelling literature. Source synthesis: White (1980), Newey and West (1987), Arellano and Bond (1991), Driscoll and Kraay (1998), Diebold and Mariano (1995), Clark and West (2007), and Gondauri (2026a-g)
Table 3.6. Integrated literature gap and monograph response. Source synthesis: mathematical economics, analogue modelling, network economics, forecast validation, computational optimization and seven source manuscripts cited throughout Section 3.1
Table 3.2.1. Network/systemic-risk literature integration across the seven monograph models
Table 3.2.2. Transmission concepts and their econometric-operational translation
Table 3.2.3. Cross-model literature gap synthesis for network economics and shock propagation
Table 3.2.4. Claim-boundary matrix for Section 3.2
Table 3.3.1. Integrated topological and spectral literature transfer across the seven monograph models
Table 3.3.2. Hodge-method literature and economic translation
Table 3.3.3. Yang-Mills spectral-threshold literature and economic interpretation
Table 3.3.4. Spectral-method literature across the monograph
Table 3.3.5. Citation-placement matrix for Section 3.3
Table 3.3.6. Permissible and restricted claims for topological and spectral methods
Table 3.4.1. Integrated literature transfer map for macro-financial stress, inflation and liquidity
Table 3.4.2. Liquidity and stress-channel literature mapped to the Navier-Stokes economic analogue
Table 3.4.3. Inflation and spectral-forecasting literature mapped to FPAS+zeta
Table 3.4.4. Validation gates for macro-financial stress and inflation literature
Table 3.4.5. Supporting roles of the five non-core analogues in Section 3.4
Table 3.4.6. Claim hierarchy for macro-financial stress, inflation and liquidity literature
Table 3.5.1. Integrated literature transfer map for Section 3.5
Table 3.5.2. From scalar inequality to pressure-curvature diagnostics
Table 3.5.3. Smoothing-capacity literature and its economic interpretation
Table 3.5.4. Topology and curvature tools relevant to inequality-pressure diagnostics
Table 3.5.5. Cross-document integration matrix for inequality, curvature and smoothing capacity
Table 3.5.6. Validation gates for inequality-curvature literature
Table 3.5.7. Claim-boundary matrix for Section 3.5
Table 3.6.1. Integrated literature-transfer map for Section 3.6
Table 3.6.2. Evidence hierarchy for sparse portfolio optimization
Table 3.6.3. How the P-vs-NP portfolio literature connects to the other six analogues

Table 3.6.4. Claim-boundary matrix for Section 3.6
Table 3.7.1. Integrated source-literature transfer map for Section 3.7
Table 3.7.2. Literature bridge from regional economics and GVCs to the monograph's corridor analogues
Table 3.7.3. BSD, Yang-Mills and Hodge as complementary corridor-measurement grammars
Table 3.7.4. Corridor and GVC validation-gate matrix
Table 3.7.5. Claim-boundary matrix for Section 3.7
Table 3.8.1. Integrated validation-literature transfer map for Section 3.8
Table 3.8.2. Forecast and validation metrics used as literature anchors
Table 3.8.3. Robust econometric inference gates across the monograph
Table 3.8.4. Evidence hierarchy for forecasting, validation and robust inference
Table 3.8.5. Claim-boundary matrix for Section 3.8
Table 3.9.1. Constructed-object, replication and claim-discipline map across seven analogues
Table 3.9.2. Normalization, scaling and directional-harmonization safeguards
Table 3.9.3. Minimum replication-package standard for constructed economic analogues
Table 3.9.4. Evidence hierarchy for constructed indices and claim discipline
Table 3.9.5. Claim-discipline language rules for reviewer-safe interpretation
Table 3.9.6. Integrated claim and replication matrix across the seven analogues
Table 3.10.4. Literature-gap and contribution closure across the seven analogues

Chapter 4

Table 4.1.1. Unified research-design taxonomy of the monograph
Table 4.1.2. Seven-source research-design integration matrix
Table 4.1.3. Common methodology components carried from the seven Chapter 3 methodologies into unified Chapter 4
Table 4.1.4. Evidence hierarchy and permitted interpretation in the unified research design
Table 4.1.5. Replication-ready design controls for the unified methodology chapter
Table 4.2.1. Empirical universes across the seven studies
Table 4.2.2. Unit-of-analysis taxonomy for the seven-study monograph
Table 4.2.3. Evidence hierarchy across empirical universes
Table 4.2.4. Empirical-universe profile: Perelman/Ricci/Poincare chapter
Table 4.2.5. Empirical-universe profile: Hodge chapter
Table 4.2.6. Empirical-universe profile: Navier-Stokes chapter
Table 4.2.7. Empirical-universe profile: Yang-Mills chapter
Table 4.2.8. Empirical-universe profile: BSD chapter
Table 4.2.9. Empirical-universe profile: Riemann/Zeta chapter
Table 4.2.10. Empirical-universe profile: P vs NP chapter
Table 4.2.11. Non-equivalence of sample size and benchmark dimension across the monograph
Table 4.2.12. Empirical universe and admissible claim boundary by study
Table 4.2.13. Methodological contribution of Section 4.2 to the monograph
Table 4.3.1. General distinction between public anchors and author-calculated research variables
Table 4.3.2. Unified public-anchor to author-calculated-variable matrix across the seven studies
Table 4.3.3. Methodological rules for separating public data from constructed indicators
Table 4.3.4. Recurrent variable families and their constructed uses across the monograph
Table 4.3.5. Scientific functions of author-calculated variables in the monograph
Table 4.3.6. Validation hierarchy for author-calculated variables
Table 4.3.7. Minimum replication trail for author-calculated variables
Table 4.3.8. Final data-lineage architecture of Section 4.3
Table 4.4.1. General normalization principles used across the monograph
Table 4.4.2. Directional harmonization rules by variable family
Table 4.4.3. Normalization, scaling and directional harmonization across the seven studies
Table 4.4.4. Normalization and directional-harmonization audit checklist

Table 4.4.5. Scaling pitfalls and methodological safeguards
Table 4.4.6. Required replication materials for normalization, scaling and harmonization
Table 4.5.1. Methodological functions of network construction in the monograph
Table 4.5.2. Unified graph ontology and reviewer-safety definitions
Table 4.5.3. Network and relational-structure construction across the seven studies
Table 4.5.4. Hodge graph-construction audit trail
Table 4.5.5. Yang-Mills finite-network gauge protocol
Table 4.5.6. BSD graph-to-rank construction protocol
Table 4.5.7. Perelman/Ricci/Poincare metric-graph construction protocol
Table 4.5.8. Non-graph and indirect-graph comparators in the unified methodology
Table 4.5.9. Network adequacy, robustness and placebo gates
Table 4.5.10. Network and relational-structure claim-boundary matrix
Table 4.6.1. Unified econometric and forecast-validation architecture across the monograph
Table 4.6.2. Panel-econometric model classes and interpretation rules
Table 4.6.3. Robust-inference decision rules
Table 4.6.4. Forecast-validation methods and chapter allocation
Table 4.6.5. Dimension-reduction and regularization use across the seven studies
Table 4.6.6. Seven-study econometric and forecast-validation allocation matrix
Table 4.6.7. Common diagnostic gates for evidence admission
Table 4.6.8. Evidence hierarchy for econometric and forecast-validation claims
Table 4.7.1. Computational evidence architecture across the seven studies
Table 4.7.2. Algorithmic layers of the P-vs-NP-inspired portfolio chapter
Table 4.7.3. Algorithmic sequence of the Riemann/Zeta FPAS+zeta chapter
Table 4.7.4. Yang-Mills computational workflow and evidentiary interpretation
Table 4.7.5. Hodge algorithmic objects and required audit outputs
Table 4.7.6. Computational extensions in the three complementary chapters
Table 4.7.7. Algorithmic validation gates and failure conditions
Table 4.7.8. Minimum reproducibility metadata for computational chapters
Table 4.7.9. Algorithmic claim hierarchy for the monograph
Table 4.7.10. Compact synthesis of the computational and algorithmic protocol
Table 4.8.1. Minimum replication-package components required by the monograph
Table 4.8.2. Consolidated Zenodo and replication-package registry
Table 4.8.3. Data-lineage separation between public anchors and author-calculated objects
Table 4.8.4. DOI, record and version rules for the monograph
Table 4.8.5. Reproducibility controls for scripts, seeds, matrices and outputs
Table 4.8.6. Unified chapter-level data and replication statements
Table 4.8.7. Evidence levels supported by the archived packages
Table 4.8.8. Reviewer-risk response matrix for replication-package governance
Table 4.8.9. How Zenodo discipline closes the earlier Chapter 4 methodology layers
Table 4.9.1. General claim-boundary matrix for the seven Millennium-inspired economic studies
Table 4.9.2. Theorem-exclusion matrix
Table 4.9.3. Evidence hierarchy and permitted wording levels
Table 4.9.4A. Evidence-block claim audit across the seven studies
Table 4.9.4B. Reviewer-safe claim lexicon
Table 4.9.4C. Claim-audit algorithm for drafting and revising the monograph
Table 4.9.4. General overclaim-to-correction protocol
Table 4.9.5. Causality, forecasting and policy-language boundary
Table 4.9.6. Problem-chapter writing rules derived from the claim-boundary matrix
Table 4.9.7. Monograph-wide permitted contribution statement
Table 4.9.8. Source-document traceability for the general claim-boundary matrix

Chapter 5

Table 5.1. Opening transfer map for the chapter abstract and Section 5.1
Table 5.2. Core translation grammar of Section 5.1
Table 5.3 [A]. Poincare-inspired graph objects and their economic reading
Table 5.4 [A]. Perelman-type functional translation and claim limits
Table 5.5 [A]. Economic translation sequence from raw indicators to claim-disciplined diagnostics
Table 5.6 [A]. Claim-boundary matrix for Section 5.1
Table 5.7 [A]. Bridge from the opening material to the next Chapter 5 sections
Table 5.3 [B]. Research-object specification for Section 5.2
Table 5.4 [B]. Core notation for the research object
Table 5.5 [B]. Unit-of-analysis hierarchy in the pressure-smoothing manifold
Table 5.6 [B]. Sixteen stress-coordinate variables defining the research object
Table 5.7 [B]. Economic dimensions of the pressure-smoothing manifold
Table 5.8. Scale of interpretation and admissible claim by level
Table 5.9. Public-anchor and author-calculated object distinction
Table 5.10. Boundary controls for the research object
Table 5.11. Handoff from Section 5.2 to Section 5.3
Table 5.12. Data-architecture role of Section 5.3
Table 5.13. Ten-region empirical universe for the inequality-pressure panel
Table 5.14. Balanced-panel and sample-discipline architecture
Table 5.15. Sixteen stress-coordinate variables and orientation rules
Table 5.16. Public-anchor to author-calculated lineage in Chapter 5
Table 5.17. Directional harmonization and scaling protocol
Table 5.18. Functional grouping of the sixteen stress coordinates
Table 5.19. Regional retention and world-weighted interpretation protocol
Table 5.20. Sample-integrity and comparability controls
Table 5.21. Data objects generated by the Chapter 5 architecture
Table 5.22. Replication-package requirements for the Chapter 5 data architecture
Table 5.23. Permitted and restricted claims arising from the data architecture
Table 5.24. Handoff from data architecture to methodology
Table 5.4.1. Methodological architecture of the Perelman-Ricci-Poincare chapter
Table 5.4.2. Translation boundary between mathematical language and economic methodology
Table 5.4.3. From data coordinates to Chapter 5 result objects
Table 5.4.4. Metric tensor diagnostics and interpretation rules
Table 5.4.5. Ricci-style curvature decomposition rules
Table 5.4.6. Curvature objects and their result-layer roles
Table 5.4.7. F/W functional interpretation discipline
Table 5.4.8. Graph-topological diagnostics and admissible interpretation
Table 5.4.9. Bottleneck and surgery-ranking logic
Table 5.4.10. Validation protocol embedded in the methodology
Table 5.4.11. Methodology-to-results bridge for Chapter 5
Table 5.4.12. Methodological claim-boundary matrix
Table 5.5.1. Results architecture and evidence-status map
Table 5.5.2. World-weighted inequality-curvature path, 2015–2024
Table 5.5.3. Crisis-deformation and recovery markers
Table 5.5.4. Economic metric tensor diagnostics
Table 5.5.5. Strongest metric-coordinate relationships
Table 5.5.6. Ricci curvature component decomposition: dominant channels
Table 5.5.7. Normalized Ricci-flow results by year
Table 5.5.8. Regional curvature and inequality-pressure rankings, 2024

Table 5.5.9. Perelman-type F/W functional path, 2015–2024
Table 5.5.10. W-functional monotonicity and pressure-change audit
Table 5.5.11. Graph Laplacian and Poincaré connectedness results
Table 5.5.12. Node degrees and topological embeddedness
Table 5.5.13. Network-curvature proxy summary
Table 5.5.14. Economic Ricci-surgery candidates
Table 5.5.15. Capacity and pressure counterfactual results
Table 5.5.16. Econometric validation summary
Table 5.5.17. PCA, regularization and regime validation
Table 5.5.18. Rolling forecast validation without look-ahead, 2017–2024
Table 5.5.19. Corrected forecast benchmark comparison and uncertainty bands
Table 5.5.20. Regional pressure and curvature change, 2010–2024
Table 5.5.21. Regional dispersion and convergence diagnostics
Table 5.5.22. Crisis-year deformation and post-shock recovery
Table 5.5.23. Final integrated results synthesis matrix
Table 5.6.1. Interpretive purpose of Section 5.6
Table 5.6.2. Main interpretation of the pressure-smoothing manifold
Table 5.6.3. Crisis and recovery markers in the pressure-curvature-W system
Table 5.6.4. Recovery interpretation rules
Table 5.6.5. Dominant curvature channels and economic interpretation
Table 5.6.6. Interpretation of smoothing-capacity channels
Table 5.6.7. Graph-topological interpretation of the inequality manifold
Table 5.6.8. Component-role distinction: magnitude versus embeddedness
Table 5.6.9. Counterfactual interpretation rules
Table 5.6.10. Validation evidence and interpretation boundary
Table 5.6.11. Regional recovery and persistence interpretation
Table 5.6.12. Structural-memory interpretation
Table 5.6.13. Final cross-layer interpretation matrix
Table 5.6.14. Final claim-boundary table for Section 5.6
Table 5.7.1. Scientific contribution in one-page logic
Table 5.7.2. Theoretical contribution: from inequality indicator to pressure-smoothing system
Table 5.7.3. Methodological pipeline and contribution
Table 5.7.4. Empirical contribution of Chapter 5
Table 5.7.5. Component-decomposition contribution
Table 5.7.6. Topological contribution
Table 5.7.7. Validation contribution and evidence classification
Table 5.7.8. Replication and data-governance contribution
Table 5.7.9. Chapter 5 contribution within the seven-problem monograph
Table 5.7.10. Practical contribution and policy-boundary discipline
Table 5.7.11. Scientific contribution and claim boundary
Table 5.7.12. Condensed final contribution map
Table 5.8.1. Claim-boundary function inside Chapter 5
Table 5.8.2. Central permitted and excluded claims
Table 5.8.3. Translation boundary between mathematical source objects and economic objects
Table 5.8.4. Empirical universe limitations and permitted uses
Table 5.8.5. Constructed-variable limitations
Table 5.8.6. Metric and curvature boundary matrix
Table 5.8.7. F/W functional claim classification
Table 5.8.8. Graph-topology claim boundaries
Table 5.8.9. Econometric evidence hierarchy

Table 5.8.10. Forecast and uncertainty boundary matrix
Table 5.8.11. Policy-screening boundary
Table 5.8.12. Replication discipline and residual limits
Table 5.8.13. Integrated claim hierarchy
Table 5.8.14. Recommended claim language for Chapter 5
Table 5.8.15. Final admissible-claim closure
Table 5.9.1. Concluding function of Chapter 5
Table 5.9.2. Final translation closure
Table 5.9.3. Research-object closure matrix
Table 5.9.4. Methodology-to-result closure
Table 5.9.5. Headline empirical closure
Table 5.9.6. Interpretation closure matrix
Table 5.9.7. Scientific contribution closure
Table 5.9.8. Final claim-boundary closure
Table 5.9.9. Integration with the monograph architecture
Table 5.9.10. Bridge from Chapter 5 to Chapter 6
Table 5.9.11. Final integrated evidence matrix for Chapter 5
Table 5.9.12. Final conclusion closure statement

Chapter 6

Table 6.1.1. Function of Section 6.1 within Chapter 6
Table 6.1.2. Why GDP mass is not sufficient for the Hodge chapter
Table 6.1.3. Core Hodge-economic translation matrix
Table 6.1.4. Public anchors and constructed Hodge variables
Table 6.1.5. Empirical adequacy conditions implied by the Hodge grammar
Table 6.1.6. Interpretation of the three Hodge components
Table 6.1.7. GDP reductionism versus Hodge visibility
Table 6.1.8. Claim-boundary matrix for the Hodge translation
Table 6.1.9. Section 6.1 bridge to the remaining Chapter 6 structure
Table 6.1.10. Final conceptual closure of Section 6.1
Table 6.2.1. Function of Section 6.2 inside Chapter 6
Table 6.2.2. Research-object definition matrix
Table 6.2.3. Ten-node regional benchmark used in Chapter 6
Table 6.2.4. Analytical role of the World anchor
Table 6.2.5. Caucasus visibility logic
Table 6.2.6. From regional indicators to a macro-flow network
Table 6.2.7. Data-status distinction in the Hodge research object
Table 6.2.8. Research questions allowed by the Section 6.2 object
Table 6.2.9. Claim-boundary matrix for the Hodge research object
Table 6.2.10. Transition from research object to the rest of Chapter 6
Table 6.3.1. Data-construction purpose and position inside Chapter 6
Table 6.3.2. Public-data anchors versus author-calculated Hodge variables
Table 6.3.3. World anchor and regional public-data input panel for the Hodge benchmark
Table 6.3.4. Node-codebook logic for the ten-region Hodge benchmark
Table 6.3.5. Caucasus visibility and anti-GDP-reduction discipline
Table 6.3.6. Edge-construction logic in the regional Hodge graph
Table 6.3.7. Regional network topology and Hodge-readiness diagnostics
Table 6.3.8. Transformation chain from public anchors to Hodge-ready edge field
Table 6.3.9. Algorithm 6.3A: Data and network construction workflow
Table 6.3.10. Minimum replication files for Section 6.3
Table 6.3.11. Network claim-boundary matrix for Section 6.3

Table 6.3.12. Section 6.3 closure matrix and transition to Section 6.4
Table 6.4.1. Methodological position of Section 6.4 inside Chapter 6
Table 6.4.2. Why the methodological object must be an edge cochain
Table 6.4.3. Pressure-potential inputs and directional logic
Table 6.4.4. Edge-pressure construction and interpretation rules
Table 6.4.5. Matrix-space discipline for the Hodge projection
Table 6.4.6. Hodge decomposition components and economic interpretation
Table 6.4.7. Gradient hierarchy and its interpretation discipline
Table 6.4.8. Curl/local-cycle imbalance method
Table 6.4.9. Harmonic energy versus filled-complex Betti diagnostics
Table 6.4.10. Energy-share interpretation matrix
Table 6.4.11. Hodge-derived regional indices and empirical use
Table 6.4.12. Spectral and higher-order validation roles
Table 6.4.13. Algorithm 6.4A: Directed edge pressure and weighted Hodge decomposition
Table 6.4.14. Hodge numerical verification record and acceptance criteria
Table 6.4.15. Claim-boundary matrix for Section 6.4
Table 6.4.16. Section 6.4 closure matrix and transition to results
Table 6.5.1. Result architecture of the Hodge-econometric chapter
Table 6.5.2. Regional input layer used by the Hodge results
Table 6.5.3. Regional network topology and global-mass coverage
Table 6.5.4. Spectral graph diagnostics of the regional benchmark
Table 6.5.5. Hodge energy decomposition of author-calculated regional macro-flow pressure
Table 6.5.6. Regional Hodge ranking of the world economy
Table 6.5.7. Curl-based regional local-imbalance ranking
Table 6.5.8. Regional harmonic exposure and systemic circulation
Table 6.5.9. Regional macro-resilience ranking derived from Hodge diagnostics
Table 6.5.10. Regional tail-risk ranking derived from imbalance, circulation and resilience
Table 6.5.11. Higher-order regional Hodge-Laplacian diagnostics
Table 6.5.12. Hodge energy versus filled-complex topology: reviewer-safety audit
Table 6.5.13. SVD/tensor decomposition of regional macro-flow layers
Table 6.5.14. Regional shock-response profile
Table 6.5.15. Econometric and predictive validation summary
Table 6.5.16. Machine-learning leave-one-region-out validation summary
Table 6.5.17. Persistent-homology filtration profile of the regional graph
Table 6.5.18. Integrated regional evidence scores by empirical block
Table 6.5.19. Central empirical conclusions of Section 6.5
Table 6.5.20. Regional result synthesis across hierarchy, imbalance, circulation, resilience and tail risk
Table 6.5.21. Claim-boundary matrix for the Hodge results
Table 6.6.1. Core interpretation of the Hodge-econometric result
Table 6.6.2. Interpretation of the three Hodge components
Table 6.6.3. Regional hierarchy as structural-flow position rather than mass
Table 6.6.4. Curl imbalance as the local-cycle layer
Table 6.6.5. Harmonic exposure as residual systemic circulation
Table 6.6.6. Resilience interpretation and the separation between size and stability
Table 6.6.7. Topological reasons why GDP mass is insufficient
Table 6.6.8. Higher-order topology and interpretation discipline
Table 6.6.9. Caucasus interpretation across Hodge-derived dimensions
Table 6.6.10. Validation evidence and its interpretive boundary
Table 6.6.11. Necessary-but-not-sufficient role of GDP
Table 6.6.12. Policy-screening implications of the Hodge interpretation

Table 6.6.13. Theoretical implications of the non-reducibility result
Table 6.6.14. Claim discipline for the interpretation section
Table 6.6.15. Bridge from interpretation to Section 6.7 validation
Table 6.7.1. Layered validation architecture for the Hodge-econometric chapter
Table 6.7.2. Core econometric validation evidence and interpretation
Table 6.7.3. Regional endogeneity and identification diagnostics
Table 6.7.4. Econometric claim discipline matrix
Table 6.7.5. Nonlinear, regime and tail-risk validation reading
Table 6.7.6. Bayesian approximation for the regional curl-growth coefficient
Table 6.7.7. Regional robustness and placebo validation
Table 6.7.8. Leave-one-region-out forecast-validation comparison
Table 6.7.9. Leave-one-region-out leakage-control and fold-level audit
Table 6.7.10. Forecast-error comparison tests
Table 6.7.11. Persistent-homology filtration profile
Table 6.7.12. Integrated evidence scores by validation block
Table 6.7.13. Replication materials required for Section 6.7 validation
Table 6.7.14. Caucasus-related validation implications
Table 6.7.15. Final validation gate for admissible Chapter 6 claims
Table 6.8.1. Closing synthesis of Chapter 6
Table 6.8.2. Final research-chain closure
Table 6.8.3. Methodological closure matrix
Table 6.8.4. Final topological conclusions
Table 6.8.5. Final Hodge energy conclusion
Table 6.8.6. Final regional interpretation map
Table 6.8.7. Caucasus-specific conclusion
Table 6.8.8. Validation conclusion matrix
Table 6.8.9. Scientific contribution closure
Table 6.8.10. Final claim-boundary closure
Table 6.8.11. Final replication agenda
Table 6.8.12. Bridge from Chapter 6 to Chapter 7
Table 6.8.13. Final conclusion checklist for Chapter 6

Chapter 7

Table 7.1.1. Physical-to-economic translation logic for the Navier-Stokes-inspired stress-balance architecture. Source: Author synthesis for the monograph
Table 7.1.2. Economic interpretation and validation role of the Navier-Stokes-inspired stress-balance components. Source: Author synthesis for the monograph
Table 7.1.3. Claim boundary for the Navier-Stokes-inspired economic flow analogy. Source: Author synthesis for the monograph
Table 7.2.1. Research-object definition and boundary matrix
Table 7.2.2. Liquidity-flow translation from physical vocabulary to economic object
Table 7.2.3. Restricted closure object and economic interpretation
Table 7.2.4. Core variable families in the Chapter 7 research object
Table 7.2.5. Data-status hierarchy for the Chapter 7 research object
Table 7.2.6. Multi-layer object architecture
Table 7.2.7. Seven-document alignment of the Chapter 7.2 research object
Table 7.2.8. Claim hierarchy for Chapter 7.2
Table 7.3.1. Index Notation and Observation Geometry
Table 7.3.2. Econometric Functions of the 100-Country Panel
Table 7.3.3. Functions and Boundaries of the World Aggregate Anchor
Table 7.3.4. Country, World, Regional and Validation Layers

Table 7.3.5. Variable-Lineage Matrix for Chapter 7
Table 7.3.6. Data-Processing Pipeline and Audit Outputs
Table 7.3.7. Scaling and Directional-Harmonization Rules
Table 7.3.8. Restricted Epsilon Closure Data Block
Table 7.3.9. Validation and Benchmark Data Objects
Table 7.3.10. Seven-Problem Data Architecture Alignment Matrix
Table 7.3.11. Replication-Package and Formula-Audit Checklist
Table 7.3.12. Claim-Boundary Matrix for Data Architecture
Table 7.4.1. Methodological position of Section 7.4 within the monograph
Table 7.4.2. Nondimensional transformation rules
Table 7.4.3. Stress and resilience index design
Table 7.4.4. Mapping from Navier-Stokes grammar to economic stress-balance components
Table 7.4.5. ε(t) closure-state variables and expected methodological roles
Table 7.4.6. Fourier-cycle methodology and leakage-control rules
Table 7.4.7. Benchmark suite and methodological role
Table 7.4.8. Panel econometric validation protocol
Table 7.4.9. External validation and robustness gate design
Table 7.4.10. Monte Carlo and policy-counterfactual scenario map
Table 7.4.11. Cross-problem methodological alignment with Section 7.4
Table 7.4.12. Sequential replication workflow for the Chapter 7 methodology
Table 7.4.13. Claim-boundary protocol for the Chapter 7 methodology
Table 7.5.1. Results evidence hierarchy and admissible claim status
Table 7.5.2. Descriptive stress-resilience and macro-financial component statistics
Table 7.5.3. Rolling one-year-ahead validation results
Table 7.5.4. Forecast-error benchmark hierarchy
Table 7.5.5. Benchmark forecast path by year
Table 7.5.6. Forecast-comparison decision discipline
Table 7.5.7. Panel fixed-effects stress-channel estimates
Table 7.5.8. Component-level t-statistics and partial explanatory contribution
Table 7.5.9. Model-fit decomposition and incremental explanatory value
Table 7.5.10. Macro-regional stress ranking and dominant dynamic channel
Table 7.5.11. Term-balance closure across stress episodes
Table 7.5.12. Restricted ε(t) closure estimates
Table 7.5.13. Robustness result matrix
Table 7.5.14. Panel diagnostic tests and inference decisions
Table 7.5.15. Expanded external validation against macro-financial targets
Table 7.5.16. Residual stability in the rolling forecast window
Table 7.5.17. Model-implied policy and shock effects on systemic stress
Table 7.5.18. Cross-problem results-positioning matrix
Table 7.5.19. Final results closure matrix for Section 7.5
Table 7.6.1. Interpretation map of the Chapter 7 result architecture
Table 7.6.2. Liquidity-flow weakness and its interpretive implications
Table 7.6.3. Pressure-gradient channels and vulnerability mechanisms
Table 7.6.4. Financial-friction interpretation of the diffusion term
Table 7.6.5. Interpretation of ε(t) closure channels
Table 7.6.6. Vulnerability typology by stress-absorption balance
Table 7.6.7. Interpretation of benchmark evidence
Table 7.6.8. Macro-regional interpretation without geopolitical overclaiming
Table 7.6.9. External-validation interpretation
Table 7.6.10. Channel-based policy interpretation

Table 7.6.11. Cross-problem interpretation alignment
Table 7.6.12. Final interpretation claim-boundary matrix
Table 7.7.1. Subsection role within Chapter 7 and the monograph
Table 7.7.2. Evidence questions controlled by Section 7.7
Table 7.7.3. Monte Carlo uncertainty design and interpretation discipline
Table 7.7.4. Monte Carlo scenario results reported for the Chapter 7 validation layer
Table 7.7.5. Policy and shock counterfactual effects
Table 7.7.6. External-validation target families and interpretive status
Table 7.7.7. External-validation claim hierarchy
Table 7.7.8. Macroprudential interpretation of Monte Carlo, counterfactual and external-validation evidence
Table 7.7.9. Scenario interpretation through the restricted closure channel
Table 7.7.10. Cross-problem alignment of simulation, validation and claim discipline
Table 7.7.11. Reviewer-safety matrix for Monte Carlo, counterfactual and external-validation evidence
Table 7.7.12. Integrated interpretation of Section 7.7
Table 7.7.13. Final claim boundary for Section 7.7
Table 7.8.1. Chapter 7.8 executive closure matrix
Table 7.8.2. Final synthesis of what Chapter 7 establishes
Table 7.8.3. Methodological-risk closure matrix
Table 7.8.4. Final interpretation of systemic-stress channels
Table 7.8.5. Final policy-counterfactual claim boundary
Table 7.8.6. Final robustness and external-validation interpretation
Table 7.8.7. Cross-problem alignment of Chapter 7 inside the monograph
Table 7.8.8. Final admissible-claim and excluded-claim matrix
Table 7.8.9. Limitations and academic-caution matrix
Table 7.8.10. Replication-closure checklist for Chapter 7
Table 7.8.11. Final integrated conclusion matrix
Table 7.8.12. Transition from Chapter 7 to the monograph-wide comparative synthesis

Chapter 8

Table 8.1.1. Role of Section 8.1 inside the Chapter 8 architecture
Table 8.1.2. Translation of Yang-Mills concepts into bounded economic-econometric objects
Table 8.1.3. Core benchmark signposts introduced conceptually in Section 8.1
Table 8.1.4. Cross-chapter integration of the Yang-Mills gauge logic
Table 8.1.5. Claim hierarchy for Chapter 8
Table 8.1.6. Formal propositions of the bounded Yang-Mills economic analogue
Table 8.1.7. Difference between centrality analysis and the Yang-Mills gauge-econometric architecture
Table 8.1.8. Economic question answered by each core construct
Table 8.2.1. Research-object definition matrix
Table 8.2.2. World anchor and regional/corridor node universe
Table 8.2.3. Stress-field component taxonomy
Table 8.2.4. Node-level systemic-stress field used by the research object
Table 8.2.5. Edge universe of the global-corridor stress-network object
Table 8.2.6. Layered evidence-status architecture for the research object
Table 8.2.7. Public-anchor and author-calculated object distinction
Table 8.2.8. Illustrative node interpretation within the stress-field object
Table 8.2.9. Corridor exposure and BridgeStress preview inside the research object
Table 8.2.10. How the research object feeds the Yang-Mills methodology
Table 8.2.11. Claim-permission rules attached to the research object
Table 8.2.12. Chapter 8 research object within the seven-problem monograph architecture
Table 8.2.13. Final synthesis of the research-object section
Table 8.3.1. Functional role of the data architecture in Chapter 8

Table 8.3.2. Source-ledger and public-anchor status of the Yang-Mills data architecture
Table 8.3.3. World anchor and ten-node regional/corridor codebook
Table 8.3.4. Normalized systemic-stress component table
Table 8.3.5. Raw-composite to normalized-stress audit
Table 8.3.6. Twenty-seven retained weighted edges in the benchmark graph
Table 8.3.7. Matrix and field objects required by the data architecture
Table 8.3.8. Stress-weighted adjacency matrix W^S
Table 8.3.9. Benchmark parameter and coding audit table
Table 8.3.10. Graph specification robustness layer
Table 8.3.11. Output objects generated by the data architecture
Table 8.3.12. Spectral benchmark summary
Table 8.3.13. Yang-Mills economic action concentration summary
Table 8.3.14. EMGI, fragility and node-level protection output table
Table 8.3.15. BridgeStress output layer
Table 8.3.16. Layered evidence-status matrix
Table 8.3.17. Integrated benchmark evidence map, selected blocks
Table 8.3.18. Country-panel validation components
Table 8.3.19. Required country-panel model blocks
Table 8.3.20. Panel-estimation closure standards
Table 8.3.21. Benchmark replication manifest
Table 8.3.22. Country-panel replication package required for final Layer B closure
Table 8.3.23. Cross-seven-study data-architecture alignment
Table 8.3.24. Reviewer-risk controls embedded in the data architecture
Table 8.4.1. Methodology-to-result closure matrix
Table 8.4.2. Core symbols and methodological levels
Table 8.4.3. Stress-field component architecture used as input to gauge and spectral layers
Table 8.4.4. Edge-weight calibration and stress-adjacency audit parameters
Table 8.4.5. Full twenty-seven-edge corridor-weight list used by the methodology
Table 8.4.6. Leading gauge-potential magnitudes and orientation discipline
Table 8.4.7. Gauge-orientation and relabeling audit protocol
Table 8.4.8. Leading triangular curvature values and action inputs
Table 8.4.9. System-level Yang-Mills economic action audit
Table 8.4.10. Component-wise action decomposition
Table 8.4.11. Stress-Laplacian spectral outputs used by the methodology
Table 8.4.12. Filtered-graph robustness design
Table 8.4.13. Randomized-network placebo boundary
Table 8.4.14. Scenario threshold-compression methodology
Table 8.4.15. EMGI and fragility component audit
Table 8.4.16. BridgeStress methodology: corridor role separated from GDP mass and ordinary centrality
Table 8.4.17. Replication algorithm for gauge-potential, curvature, action and stress-Laplacian methodology
Table 8.4.18. Cross-chapter methodological integration
Table 8.4.19. Reviewer-risk controls and claim-boundary language
Table 8.5.1. Results architecture and evidence-status map
Table 8.5.2. Results reading rule and claim-permission matrix
Table 8.5.3. Weighted stress-Laplacian spectrum
Table 8.5.4. Normal state, first stress mode and normalized transition threshold
Table 8.5.5. Finite-network proposition and economic mass-gap interpretation
Table 8.5.6. Estimated economic mass gap by network specification
Table 8.5.7. Bootstrap / Monte Carlo uncertainty audit for mass gap, action and EMGI
Table 8.5.8. Top regional and corridor curvature cycles

Table 8.5.9. Total Yang-Mills economic action and top-cycle concentration
Table 8.5.10. Regional and corridor curvature exposure ranking
Table 8.5.11. Layer contribution to total Yang-Mills economic action
Table 8.5.12. Economic Mass Gap Index by region and corridor
Table 8.5.13. EMGI component audit and local-protection composite
Table 8.5.14. EMGI ranking and systemic fragility classes
Table 8.5.15. Interpretation of EMGI and fragility regimes
Table 8.5.16. Revised corridor strategic BridgeStress index
Table 8.5.17. Middle Corridor / Caucasus mini-network audit
Table 8.5.18. Scenario output: threshold compression and action increase
Table 8.5.19. Scenario interpretation matrix
Table 8.5.20. Shock propagation by origin node
Table 8.5.21. Local-to-systemic shock transition thresholds
Table 8.5.22. Cross-seven-chapter integration of the Chapter 8.5 results
Table 8.5.23. Integrated result-closure matrix
Table 8.5.24. Claim-boundary matrix for Chapter 8.5
Table 8.5.25. Replication and reviewer checklist
Table 8.6.1. Results-to-interpretation matrix for Section 8.6
Table 8.6.2. Spectral threshold interpretation
Table 8.6.3. Local-to-systemic interpretation of shock stages
Table 8.6.4. Protection-fragility regimes and corridor interpretation
Table 8.6.5. Node-level EMGI, fragility, stress and BridgeStress interpretation
Table 8.6.6. Corridor-function interpretation layer
Table 8.6.7. Curvature-action interpretation map
Table 8.6.8. Scenario interpretation: threshold compression and action increase
Table 8.6.9. Interpretation of the correlation layer
Table 8.6.10. Cross-seven-problem integration of the Yang-Mills interpretation
Table 8.6.11. Policy and research implication boundary
Table 8.6.12. Claim-boundary matrix for Section 8.6
Table 8.7.1. Function of Section 8.7 inside Chapter 8
Table 8.7.2. Shock-injection scenarios and calibration logic
Table 8.7.3. Full scenario-output matrix
Table 8.7.4. Scenario compression and amplification diagnostics
Table 8.7.5. Scenario-specific local-to-systemic interpretation
Table 8.7.6. Four-step shock propagation by origin node
Table 8.7.7. Corridor-function interpretation layer for local-to-systemic transition
Table 8.7.8. Local-to-systemic transition regime classification
Table 8.7.9. Cross-chapter scenario and transition logic across the seven-problem monograph
Table 8.7.10. Evidence-gate matrix for the scenario-simulation section
Table 8.7.11. Replication checklist for the scenario-simulation layer
Table 8.8.1. Sample architecture of the N = 1,500 validation pathway
Table 8.8.2. Layer A / Layer B evidence-status separation
Table 8.8.3. Country-year variable ledger for the N = 1,500 validation pathway
Table 8.8.4. Country-panel model system for N = 1,500 validation
Table 8.8.5. Validation gates for the N = 1,500 pathway
Table 8.8.6. Claim boundary matrix for Chapter 8
Table 8.8.7. Reviewer-risk controls embedded in Section 8.8
Table 8.8.8. Minimum replication manifest for the N = 1,500 panel layer
Table 8.8.9. Chapter 8 within the seven-problem validation ecology
Table 8.8.10. Final claim-gate summary for Section 8.8

Table 8.9.1. Closing synthesis of Chapter 8 sections
Table 8.9.2. Final benchmark conclusions of Chapter 8
Table 8.9.3. Final formula map used in the chapter conclusion
Table 8.9.4. EMGI, fragility and BridgeStress closing interpretation
Table 8.9.5. Scenario closure: threshold compression and action amplification
Table 8.9.6. Final claim-boundary matrix for Chapter 8
Table 8.9.7. Chapter 8 inside the seven-problem monograph
Table 8.9.8. N = 1,500 validation pathway after Chapter 8
Table 8.9.9. Reviewer-safety controls for the chapter conclusion
Table 8.9.10. Final chapter conclusion matrix

Chapter 9

Table 9.1.1. Executive orientation of the BSD economic translation
Table 9.1.2. Classical BSD grammar and bounded economic translation
Table 9.1.3. Why local-to-global rank modelling is needed beyond GDP mass
Table 9.1.4. Definitions of local and global objects in the economic BSD translation
Table 9.1.5. Measurement chain from anchors to LOrder and structural rank
Table 9.1.6. Finite-state reductions as economic regime logic and reviewer-safety discipline
Table 9.1.7. Economic L-function, LOrder and structural-rank interpretation
Table 9.1.8. Corridor stress as economic local-to-global transmission
Table 9.1.9. Chapter 9 within the seven-problem monograph architecture
Table 9.1.10. Claim hierarchy for BSD economic local-to-global translation
Table 9.1.11. Transition map from Section 9.1 to the full Chapter 9 architecture
Table 9.3.1. Data-architecture purpose and evidence status
Table 9.3.2. World and regional/corridor public-data anchor panel
Table 9.3.3. Regional/corridor node taxonomy for Chapter 9
Table 9.3.4. Index notation and panel construction for the N = 150 closure layer
Table 9.3.5. Source ledger and data-lineage scaffold
Table 9.3.6. Public anchor objects and author-calculated BSD objects
Table 9.3.7. Directional transformation rules for the BSD data architecture
Table 9.3.8. Stress-coordinate components and downstream role
Table 9.3.9. Graph and corridor data-adequacy diagnostics
Table 9.3.10. N = 150 closure diagnostics and required interpretation
Table 9.3.11. Replication and audit-trail requirements for Chapter 9
Table 9.3.12. Data-architecture alignment across the seven Millennium-inspired chapters
Table 9.3.13. Permissible and excluded claims from the Chapter 9 data architecture
Table 9.4.1. Methodological role of subsection 9.4 inside Chapter 9
Table 9.4.2. State-vector components and coefficient-lineage discipline
Table 9.4.3. Interpretation rules for a_{r,t} and b_{r,t}
Table 9.4.4. Discriminant audit protocol
Table 9.4.5. q-base design and finite-state interpretation
Table 9.4.6. Trace-analogue interpretation matrix
Table 9.4.7. Division of methodological responsibility between 9.4, 9.5 and 9.6
Table 9.4.8. Cross-problem methodological alignment
Table 9.4.9. Admissible and inadmissible claims in subsection 9.4
Table 9.4.10. Replication checklist for coefficients, discriminants and finite-state reductions
Table 9.5.1. Translation map from classical BSD vocabulary to the economic rank architecture
Table 9.5.2. Internal object hierarchy of Section 9.5
Table 9.5.3. Regional local trace analogues across finite-state q-bases
Table 9.5.4. Economic Euler factors at s = 1
Table 9.5.5. Structural rank components by regional node

Table 9.5.6. BSD-type rank-order correspondence by region
Table 9.5.7. Calibration and agreement diagnostics for the LOrder-rank comparison
Table 9.5.8. q-base sensitivity of the LOrder-rank correspondence
Table 9.5.9. Placebo and randomization logic supporting the local-to-global claim boundary
Table 9.5.10. Alignment of Section 9.5 with the seven Millennium-inspired economic analogues
Table 9.5.11. Algorithmic workflow for the L-function, LOrder and structural-rank layer
Table 9.5.12. Permissible and excluded claims for Section 9.5
Table 9.6.1. Chapter 9.6 result-domain summary and evidence status
Table 9.6.2. Regional structural-rank component decomposition
Table 9.6.3. LOrder analogue, structural rank and absolute rank gap
Table 9.6.4. Economic regulator analogue by region
Table 9.6.5. Tamagawa-type local friction by region
Table 9.6.6. Economic torsion analogue by region
Table 9.6.7. Regional corridor-rank leverage and BridgeStress
Table 9.6.8. Corridor-function interpretation layer for the regional benchmark
Table 9.6.9. Scenario output: threshold compression under regional shocks
Table 9.6.10. Regional action concentration summary
Table 9.6.11. Cross-problem alignment of the Chapter 9.6 results
Table 9.6.12. Final claim-boundary matrix for Chapter 9.6
Table 9.7.1. Interpretation reading rule for local regional signals
Table 9.7.2. Local-to-global mechanism interpreted as an economic measurement sequence
Table 9.7.3. Regional interpretation of LOrder-rank correspondence and rank-conversion channels
Table 9.7.4. Interpretation of friction, torsion and regulator combinations
Table 9.7.5. BridgeStress interpretation: how corridor nodes inform global structural rank
Table 9.7.6. Cross-problem interpretation matrix for Chapter 9.7
Table 9.7.7. Claim boundary for interpreting local regional signals and global structural rank
Table 9.8.1. Robustness and claim-discipline gate map
Table 9.8.2. Robust inference and small-cluster correction for LOrder
Table 9.8.3. Variable lineage matrix and admissible-use screen
Table 9.8.4. Orthogonalized, residualized and external-only LOrder tests
Table 9.8.5. Practical equivalence calibration and Bland-Altman summary
Table 9.8.6. Region-level Bland-Altman agreement diagnostics
Table 9.8.7. Out-of-sample and blocked validation results
Table 9.8.8. Weight and component sensitivity summary
Table 9.8.9. q-base sensitivity and LOrder stability
Table 9.8.10. Corridor-coding sensitivity for BridgeStress and LOrder
Table 9.8.11. Placebo and permutation diagnostics
Table 9.8.12. Replication closure and source-ledger map
Table 9.8.13. Reviewer-risk response matrix
Table 9.8.14. Final evidence classification and claim status
Table 9.8.15. Decision-gate summary for the BSD-inspired local-to-global model
Table 9.8.16. Seven-problem robustness alignment for Chapter 9
Table 9.9.1. Chapter 9 objective closure matrix
Table 9.9.2. Final claim hierarchy of Chapter 9

Chapter 10

Table 10.1.1. Opening claim-boundary statement for the Riemann-Zeta economic analogy
Table 10.1.2. Functional role of Chapter 10 inside the seven-problem monograph
Table 10.1.3. Classical-to-economic translation matrix for the Riemann-zeta analogy
Table 10.1.4. Reported RMSE benchmark signposts motivating the spectral-signal analogy
Table 10.1.5. Layered validation architecture and admissible claims

Table 10.1.6. Core objects in the Riemann-Zeta FPAS+ζ signal architecture
Table 10.1.7. Crisis-resonance interpretation framework
Table 10.1.8. Claim hierarchy and excluded overclaims
Table 10.1.9. Cross-chapter integration of the Riemann-Zeta spectral-signal chapter
Table 10.1.10. Reviewer-safety controls embedded in the opening Riemann-Zeta subsection
Table 10.1.11. Closing synthesis of Section 10.1
Table 10.2.1. Research-object definition and claim boundary matrix
Table 10.2.2. Macro-financial pressure families defining the research object
Table 10.2.3. Layered sample hierarchy and evidence status
Table 10.2.4. Variable and object register for Chapter 10
Table 10.2.5. Reported RMSE benchmark context used to motivate the research object
Table 10.2.6. Data-status and replication matrix
Table 10.2.7. Evidence-status hierarchy for the Chapter 10 research object
Table 10.2.8. Research questions reframed as research-object gates
Table 10.2.9. Cross-seven-problem integration of the Chapter 10 research object
Table 10.2.10. Reviewer-risk controls in the research-object definition
Table 10.3.1. Layered validation hierarchy and claim permission
Table 10.3.2. Object and symbol register for the layered FPAS+ζ architecture
Table 10.3.3. Public-anchor and author-calculated object separation
Table 10.3.4. Frequency-specific methods and interpretation rules
Table 10.3.5. Replication and traceability checklist for the layered validation architecture
Table 10.3.6. Cross-seven-problem data-architecture alignment
Table 10.4.1. Composite pressure families and directional rules
Table 10.4.2. FPAS baseline components and interpretation boundaries
Table 10.4.3. Zeta-channel construction and admissible interpretation
Table 10.4.4. Correction-gate decision rules
Table 10.4.5. Alpha calibration and overfitting-control protocol
Table 10.4.6. Methodology-to-results alignment matrix
Table 10.4.7. Final claim-boundary matrix for Sections 10.3-10.4
Table 10.7.1. Forecast hierarchy and interpretation across annual layers
Table 10.7.2. Crisis resonance and zeta-deformation interpretation
Table 10.7.3. Pressure, curvature and regime diagnostics for selected stress years
Table 10.7.4. Alpha calibration and correction-intensity interpretation
Table 10.7.5. Interpretation matrix for crisis resonance, zeta deformation and forecast correction
Table 10.8.1. Cross-layer validation hierarchy
Table 10.8.2. Quarterly N = 100 dynamic, HMM and Markov-switching evidence
Table 10.8.3. Monthly N = 240 spectral, wavelet and zeta-stress lead evidence
Table 10.8.4. Formal forecast-validation and loss-comparison evidence
Table 10.8.5. Residual diagnostics, stability evidence and caution matrix
Table 10.8.6. Spectral, regime and robustness evidence classification
Table 10.9.1. Aim-objective-results closure matrix
Table 10.9.2. Final claim hierarchy and exclusion matrix
Table 10.9.3. Seven-problem monograph alignment for Chapter 10 closure
Table 10.9.4. Replication and reviewer-safety closure checklist

Chapter 11

Table 11.0. Chapter 11 positioning within the monograph
Table 11.1. Translation of P versus NP logic into the portfolio-optimization setting
Table 11.2. Support-space scale under alternative cardinality levels
Table 11.3. Claim hierarchy for the P-vs-NP-inspired chapter
Table 11.4. Seven-problem alignment and the unique role of Chapter 11

Table 11.5. Research-object layers for Chapter 11
Table 11.6. Empirical universe and input-status matrix
Table 11.7. Notation and meaning of the cardinality-constrained portfolio object
Table 11.8. Inside-versus-outside boundary of the Chapter 11 research object
Table 11.9. Forward link from Sections 11.1-11.2 to the rest of Chapter 11
Table 11.10. Readiness checklist after Sections 11.1-11.2
Table 11.3.1. Empirical universe and source-vintage discipline
Table 11.3.2. Public-input and author-constructed data-status architecture
Table 11.3.3. CAPM-prior descriptive statistics for the industry universe
Table 11.3.4. Selected industry-level CAPM input examples
Table 11.3.5. Covariance-geometry diagnostics for the industry universe
Table 11.3.6. Data-architecture risk controls for Chapter 11
Table 11.3.7. Replication-status and data-package disclosure checklist
Table 11.4.1. Methodological system and evidence vector for the P-vs-NP portfolio chapter
Table 11.4.2. Support-space explosion under alternative n and K values
Table 11.4.3. Optimization elements, symbols and methodological roles
Table 11.4.4. Greedy sparse-selection procedure
Table 11.4.5. Monte Carlo support-sampling protocol
Table 11.4.6. Genetic algorithm, greedy search and continuous reoptimization comparison
Table 11.4.7. Exact reduced benchmark and optimality-gap measurement
Table 11.4.8. Full-universe search coverage and no-global-certificate rule
Table 11.4.9. Algorithmic comparison and runtime discipline
Table 11.4.10. Monte Carlo effort-budget sensitivity and runtime behavior
Table 11.4.11. Boundary between exactness, approximation and interpretability
Table 11.4.12. Chapter 11 integration within the seven-problem monograph architecture
Table 11.5.1. Realism and robustness gates for the P-vs-NP portfolio chapter
Table 11.5.2. Transaction-cost and turnover stress for the baseline K=10 portfolio
Table 11.5.3. Black-Scholes worked example: call-overlay inputs and derived moments
Table 11.5.4. Option moneyness-maturity grid: price, delta, leverage and implied moments
Table 11.5.5. Delta approximation error under +/-1% repricing bumps
Table 11.5.6. Option-included optimization check: baseline versus option-augmented case
Table 11.5.7. Top weights for baseline and option-augmented observed best-Sharpe portfolios
Table 11.5.8. Stress-scenario interpretation for baseline and option-augmented portfolios
Table 11.5.9. Falsification and placebo audit matrix
Table 11.6.1. Results evidence hierarchy for Chapter 11
Table 11.6.2. Baseline K=10 results summary
Table 11.6.3. Baseline K=10 portfolio composition
Table 11.6.4. Cardinality-sensitive Sharpe results across K values
Table 11.6.5. Exact benchmark versus heuristic optimality gap in the reduced instance
Table 11.6.6. Full n=94,K=10 search-coverage and global-optimality-boundary certificate
Table 11.6.7. Replicability summary across greedy, Monte Carlo, GA and exact reduced benchmark
Table 11.6.8. GA variants: subset-only versus subset plus continuous reoptimization
Table 11.6.9. Effort budget versus Sharpe and runtime
Table 11.6.10. Statistical-inference and seed-evidence status for Sharpe comparisons
Table 11.6.11. Variance-share risk contribution by selected industry
Table 11.6.12. Integrated multi-criteria ranking of tested portfolio strategy layers
Table 11.6.13. Results-closure matrix
Table 11.6.14. Final claim hierarchy and exclusion matrix
Table 11.7.1. What the computational-finance evidence shows and what it cannot certify
Table 11.7.2. Cardinality-sensitive interpretation of the K-grid

Table 11.7.3. Algorithmic evidence and certification level
Table 11.7.4. Covariance interpretation and reviewer-safe wording
Table 11.7.5. Option-overlay interpretation matrix
Table 11.7.6. Interpretation summary: showable claims versus non-certifiable claims
Table 11.8.1. Final claim-boundary matrix
Table 11.8.2. Exactness and certification status
Table 11.8.3. Reviewer-risk response matrix
Table 11.9.1. Chapter 11 final aim-objective-results closure matrix
Table 11.9.2. Chapter 11 contribution to the seven-problem monograph architecture

Chapter 12

Table 12.1. Comparative empirical universe across the seven Millennium-inspired economic models
Table 12.2. Comparative sample geometry and evidentiary meaning
Table 12.3. Comparative mathematical object and economic translation
Table 12.4. Compact symbolic comparison of the seven measurement grammars
Table 12.5. Comparative validation strength and claim boundary
Table 12.6. Replication and audit discipline across the seven models
Table 12.7. Cross-problem results matrix
Table 12.8. Comparative claim hierarchy and excluded claims
Table 12.9. Chapter 12 synthesis of comparative results

Chapter 13

Table 13.1. Seven Millennium Problems as economic measurement languages
Table 13.2. Unified interpretive logic of Chapter 13
Table 13.3. Flow-dimension synthesis
Table 13.4. Curvature and topological deformation synthesis
Table 13.5. BSD local-to-global rank dimension
Table 13.6. Spectral-cyclical forecast dimension
Table 13.7. Computational-decision dimension
Table 13.8. Unified contribution matrix
Table 13.9. Cross-dimensional coupling matrix
Table 13.10. Unified claim-boundary matrix
Table 13.11. Final chapter-closure matrix

Chapter 14

Table 14.1. Negative claim matrix: what the monograph explicitly excludes
Table 14.2. Analogy-calibration-measurement distinction
Table 14.3. Constructed-variable and circularity-risk matrix
Table 14.4. Sample-size and admissible-claim boundaries
Table 14.5. Forecasting and optimization boundary matrix
Table 14.6. Evidence-level matrix for the seven-problem monograph
Table 14.7. Reviewer-safety matrix: likely objections and direct responses
Table 14.8. Model-by-model claim-boundary matrix
Table 14.9. Replication and version-control boundary checklist
Table 14.10. Econometric and computational inference boundaries
Table 14.11. Claim-language replacement protocol
Table 14.12. Final chapter-closure matrix

List of Figures

Editorial note: page numbers should be generated after the full manuscript is merged, final styles are applied and the manuscript is paginated. Entries marked with [A]/[B] indicate duplicate numbering present in the source manuscript and should be reconciled during final copy-editing.

Chapter 6

Figure 6.5.1. Hodge energy decomposition of regional macro-flow pressure
Figure 6.5.2. Hodge hierarchy index compared with world GDP share
Figure 6.5.3. Curl/local-cycle imbalance ranking
Figure 6.5.4. Harmonic/systemic circulation versus network centrality
Figure 6.5.5. Regional shock-response decay profile
Figure 6.5.6. Persistent-homology profile of the regional benchmark
Figure 6.5.7. Integrated regional evidence map
Figure 6.6.1. GDP mass as anchor versus Hodge organization layers
Figure 6.6.2. Hodge hierarchy versus GDP share in selected regional nodes
Figure 6.7.1. Validation pipeline from public macro anchors to evidence closure
Figure 6.7.2. Curl coefficient stability under edge-density perturbation and placebo break
Figure 6.7.3. Machine-learning forecast-error comparison under leave-one-region-out validation
Figure 6.7.4. Betti-0 and Betti-1 profiles across regional edge-weight filtration
Figure 6.7.5. Integrated validation evidence map for Chapter 6
Figure 6.8.1. Final Hodge energy synthesis
Figure 6.8.2. Final replication path from benchmark to full international model

Chapter 7

Figure 7.2.1. Research-object architecture for the Navier-Stokes-inspired global liquidity-flow chapter
Figure 7.2.2. Core flow-pressure-friction-shock-cycle-closure balance
Figure 7.2.3. Restricted epsilon closure: stress-amplifying and buffering channels
Figure 7.2.4. Empirical and validation dimensions of the Chapter 7 research object
Figure 7.2.5. Comparative role of the seven economic-econometric research objects
Figure 7.3.1. Data-Architecture Stack for Chapter 7
Figure 7.3.2. Balanced 100-Country Annual Panel Geometry, 2010-2024
Figure 7.3.3. Three-Level Evidence Geometry: Country Panel, Macro-Regional Layers and World Anchor
Figure 7.3.4. Ordered Data-Processing Pipeline
Figure 7.3.5. Chapter 7 within the Seven-Problem Empirical Architecture
Figure 7.5.1. Stress-resilience contrast in normal and shock states
Figure 7.5.2. Rolling one-year-ahead stress forecasts against actual stress, 2017-2024
Figure 7.5.3. Forecast-error benchmark hierarchy
Figure 7.5.4. Stress-channel coefficients with 95% confidence intervals
Figure 7.5.5. Macro-regional systemic-stress ranking
Figure 7.5.6. Term-balance closure across stress episodes
Figure 7.5.7. External-validation result summary
Figure 7.5.8. Policy and shock effects on systemic stress
Figure 7.6.1. Interpretation pathway from liquidity-flow weakness to systemic vulnerability
Figure 7.6.2. Interpretive hierarchy of systemic-stress channels. The values are a synthesis scale, not new estimated coefficients
Figure 7.6.5. Restricted ε(t) closure as auditable hidden adjustment
Figure 7.6.3. Macro-regional vulnerability typology. Coordinates are interpretive synthesis values, not new empirical estimates
Figure 7.6.4. Evidence hierarchy for reading Chapter 7 results
Figure 7.6.6. Position of Chapter 7 within the seven-problem monograph

Figure 7.7.1. Scenario-validation architecture for the Chapter 7 stress-testing layer
Figure 7.7.2. Reported Monte Carlo scenario medians and high-stress probabilities
Figure 7.7.3. Policy and shock counterfactual stress-index effects
Figure 7.7.4. External-validation gates for diagnostic plausibility
Figure 7.7.6. Cross-problem alignment of simulation, validation and claim-boundary logic
Figure 7.7.5. Evidence hierarchy and claim discipline for Section 7.7
Figure 7.8.1. Chapter-closure architecture
Figure 7.8.2. Final evidence hierarchy and claim-boundary ladder
Figure 7.8.3. Admissible and excluded claims in Chapter 7
Figure 7.8.4. Chapter 7 within the seven-problem claim-discipline architecture
Figure 7.8.5. Replication-closure chain

Chapter 8

Figure 8.1.1. Gauge-econometric translation pipeline for the Yang-Mills economic mass-gap chapter
Figure 8.2.1. Research-object pipeline for the Yang-Mills economic mass-gap chapter
Figure 8.2.3. Normalized systemic-stress field used to define the research object
Figure 8.2.4. Output mass versus corridor exposure inside the research object
Figure 8.2.2. Finite global-corridor stress-network object with 10 nodes and 27 weighted edges
Figure 8.2.6. Layered evidence-status architecture of Section 8.2
Figure 8.2.5. Local protection and corridor BridgeStress are distinct research-object dimensions
Figure 8.3.1. Data architecture pipeline for the Yang-Mills economic mass-gap chapter
Figure 8.3.2. Node-level architecture: GDP share is an anchor; stress score is a constructed research variable
Figure 8.3.6. Stress-component audit across the ten-node benchmark
Figure 8.3.3. Finite 10-node, 27-edge global-corridor benchmark graph
Figure 8.3.4. Twenty-seven edge weights in descending order
Figure 8.3.5. Stress-weighted adjacency matrix W^S
Figure 8.3.7. Layered evidence-status rule for Section 8.3
Figure 8.3.8. Replication manifest and file-hash discipline
Figure 8.4.1. Methodological pipeline from public anchors to gauge potential, curvature, action and stress-Laplacian mass gap
Figure 8.4.2. Ten-node graph used as the methodological substrate for gauge, curvature and spectral calculations
Figure 8.4.3. Largest absolute economic gauge potentials reported from the benchmark gauge layer
Figure 8.4.4. Anti-symmetric gauge matrix demonstration: A_ij = -A_ji and diagonal entries equal zero
Figure 8.4.5. Top triangular action contributions from the curvature field
Figure 8.4.6. Component-wise contribution to the Yang-Mills economic action layer
Figure 8.4.7. Ordered stress-Laplacian spectrum showing the first positive stress mode
Figure 8.4.8. Scenario compression of λ_1 and the normalized transition threshold
Figure 8.4.9. Stress score versus EMGI: node protection is not reducible to stress alone
Figure 8.5.1. Results logic from spectral separation to node and scenario diagnostics
Figure 8.5.2. Stress-Laplacian spectrum and the positive first stress mode
Figure 8.5.3. Positive mass gap across baseline and filtered graph specifications
Figure 8.5.4. Top curvature-cycle actions
Figure 8.5.5. Layer contribution to Yang-Mills economic action
Figure 8.5.6. Economic Mass Gap Index by node
Figure 8.5.7. Systemic fragility by node
Figure 8.5.8. Corridor strategic BridgeStress ranking
Figure 8.5.9. Normalized threshold compression under shock scenarios
Figure 8.5.10. Economic mass-gap compression under shock scenarios
Figure 8.5.11. Yang-Mills economic action expansion under shock scenarios
Figure 8.5.12. Outside-origin diffusion share by shock origin
Figure 8.6.1. Interpretation pipeline from finite benchmark to claim-gated conclusion

Figure 8.6.2. Finite-network threshold geometry: lambda_1, spectral radius and normalized threshold
Figure 8.6.3. EMGI and fragility by node
Figure 8.6.4. BridgeStress ranking and corridor exposure visibility
Figure 8.6.5. Stress score versus BridgeStress
Figure 8.6.6. Corridor-sensitive finite network with BridgeStress-sized nodes
Figure 8.6.7. Threshold compression and lambda_1 decline under shocks
Figure 8.6.8. Yang-Mills economic action increases under shock scenarios
Figure 8.6.9. Correlation heatmap for interpretation variables
Figure 8.6.10. Claim-gated interpretation hierarchy
Figure 8.8.1. N = 1,500 validation pathway from benchmark to empirical closure
Figure 8.8.3. Country-year panel structure: visual proxy for 100 x 15 = 1,500
Figure 8.8.2. Claim hierarchy and evidence ladder
Figure 8.8.6. Variable-lineage separation for anti-circularity discipline
Figure 8.8.4. Model-block dependency graph
Figure 8.8.5. Current versus panel-closed claim capacity
Figure 8.8.7. Reviewer-risk reduction heatmap
Figure 8.8.8. Replication-closure object map
Figure 8.8.9. Chapter 8 pathway in the seven-problem validation ecology
Figure 8.9.1. Chapter 8 closing pipeline from data anchors to claim-gated validation
Figure 8.9.2. Threshold compression across scenario simulations
Figure 8.9.3. Action amplification under stronger corridor shocks
Figure 8.9.4. Claim-gated evidence hierarchy of Chapter 8
Figure 8.9.5. Chapter 8 as the gauge-threshold bridge inside the seven-problem monograph

Chapter 9

Figure 9.1.1. BSD-to-economics translation ladder: from mathematical grammar to bounded structural-rank measurement
Figure 9.1.2. Local-to-global measurement chain in the economic BSD chapter
Figure 9.1.5. Evidence funnel: local information is narrowed into a defensible structural-rank claim
Figure 9.1.4. BSD as the monograph chapter most directly centered on rank and local-to-global logic
Figure 9.1.3. Claim-boundary quadrants for the BSD economic analogue
Figure 9.2.1. Research-object architecture for regional structural rank formation
Figure 9.2.2. Output mass, growth pressure and corridor-sensitive node visibility
Figure 9.2.3. Research-object separation between stress exposure and rank capacity
Figure 9.2.4. Local-to-global transformation chain inside the research object
Figure 9.2.6. Position of Chapter 9 research object in the seven-problem monograph
Figure 9.2.5. Evidence hierarchy and claim boundary for the research object
Figure 9.3.1. Data-architecture stack for the BSD-inspired regional model
Figure 9.3.2. Public anchor contrast: regional output mass and transition growth
Figure 9.3.3. N = 150 closure-layer panel geometry: 10 regions x 15 years
Figure 9.3.4. Source-to-output data-lineage pipeline
Figure 9.3.5. Graph and corridor data adequacy, scaled display
Figure 9.3.6. Chapter 9 data architecture inside the seven-problem monograph
Figure 9.4.1. Methodological pipeline from public anchors to finite-state trace analogues
Figure 9.4.2. Coefficient mapping from regional state variables to the economic cubic analogue
Figure 9.4.3. Economic discriminant basin used to visualize non-degeneracy regions
Figure 9.4.4. Finite-state grids for q = 3, q = 5 and q = 7
Figure 9.4.5. Trace-sign stability matrix across q-bases
Figure 9.4.6. Claim-gate ladder for the coefficient-discriminant-reduction methodology
Figure 9.5.1. Pipeline from local traces to LOrder and structural rank
Figure 9.5.2. Economic Euler factors at s = 1

Figure 9.5.3. Constructed economic L-function behavior near s = 1
Figure 9.5.4. Structural-rank component architecture by region
Figure 9.5.5. LOrder and structural rank correspondence
Figure 9.5.6. Absolute LOrder-structural rank gaps
Figure 9.5.7. q-base sensitivity of rank-scale error
Figure 9.6.1. Results architecture for Chapter 9.6
Figure 9.6.2. LOrder-rank correspondence and diagonal calibration line
Figure 9.6.3. Absolute LOrder-structural rank gaps by region
Figure 9.6.4. Economic regulator analogue and absorption-capacity hierarchy
Figure 9.6.5. Tamagawa-type friction and torsion by region
Figure 9.6.6. BridgeStress ranking by regional/corridor node
Figure 9.6.7. Threshold compression and action increase under regional-corridor shocks
Figure 9.6.8. Evidence hierarchy inside the Chapter 9.6 results block
Figure 9.7.1. Interpretation chain from local regional signals to global structural rank
Figure 9.7.2. Absolute LOrder-rank gaps and interpretation tolerance
Figure 9.7.3. Rank conversion interpreted through support and obstruction
Figure 9.7.4. BridgeStress versus structural rank
Figure 9.7.5. Normalized regional signal profile across rank, regulator, friction, torsion and BridgeStress
Figure 9.7.6. Threshold compression and action increase as local shocks become systemic
Figure 9.7.7. Seven-problem alignment around BSD local-to-global structural rank interpretation
Figure 9.8.1. Robustness and claim-discipline architecture
Figure 9.8.2. Robust-inference p-values for the LOrder coefficient
Figure 9.8.3. Anti-circularity variants for LOrder
Figure 9.8.4. Practical-equivalence diagnostics on the 0-5 rank scale
Figure 9.8.5. Out-of-sample and blocked validation
Figure 9.8.6. q-base sensitivity of LOrder-rank correspondence
Figure 9.8.7. Placebo distribution comparison
Figure 9.8.8. Final claim hierarchy
Figure 9.9.1. Chapter 9 closure architecture

Chapter 10

Figure 10.1.1. Riemann-zeta economic spectral-signal translation pipeline
Figure 10.1.4. Critical-line signal as an economic input map
Figure 10.1.3. Reported RMSE signpost across annual validation layers
Figure 10.1.2. Layered validation architecture of Chapter 10
Figure 10.1.5. Crisis-resonance signpost used for Chapter 10 interpretation
Figure 10.1.6. Claim-boundary gate for the Riemann-zeta economic analogy
Figure 10.2.1. Research-object pipeline for the FPAS+zeta global inflation framework
Figure 10.2.7. Macro-financial pressure families used to define the object
Figure 10.2.2. Layered empirical universe and sample discipline
Figure 10.2.4. Layer chronology and global shock-anchor windows
Figure 10.2.5. Forecast, pressure, zeta and validation objects
Figure 10.2.3. Reported RMSE hierarchy motivating the research object
Figure 10.2.6. Evidence-status and claim-boundary gate
Figure 10.2.8. Seven-problem bridge showing the Chapter 10 spectral-forecasting role
Figure 10.3.1. Layered validation sample hierarchy
Figure 10.3.3. Frequency-specific validation windows
Figure 10.3.2. Data architecture from public anchors to validation evidence
Figure 10.3.4. Reported RMSE context by annual validation layer
Figure 10.4.1. Methodological transformation chain
Figure 10.4.3. Conceptual CP_t -> τ_t -> zeta-cycle mapping

Figure 10.4.2. Signed zeta-correction gate
Figure 10.4.4. Alpha calibration as validation-controlled tuning
Figure 10.4.5. Method allocation by validation layer
Figure 10.4.6. Evidence gate protecting the methodology from overclaiming
Figure 10.5.1. Forecast-evaluation protocol from residuals to claim gate
Figure 10.5.2. Forecast-evaluation battery and evidentiary role
Figure 10.5.3. Rolling no-look-ahead validation path
Figure 10.5.4. Mincer-Zarnowitz calibration comparison
Figure 10.5.5. DM and Clark-West comparison signs
Figure 10.6.1. RMSE hierarchy across annual validation layers
Figure 10.6.2. MAE hierarchy across annual validation layers
Figure 10.6.3. Directional accuracy by model and annual layer
Figure 10.6.4. Cross-layer stability matrix, normalized display
Figure 10.6.5. Quarterly and monthly validation support
Figure 10.6.6. Evidence ladder for Chapter 10 results
Figure 10.7.1. Interpretation chain: pressure, zeta deformation and bounded forecast meaning
Figure 10.7.2. Forecast-error hierarchy across annual validation layers
Figure 10.7.3. Crisis resonance and macro-financial pressure concentration
Figure 10.8.1. Layered validation architecture: annual, quarterly and monthly evidence
Figure 10.8.2. Quarterly N=100 dynamic and regime-validation modules
Figure 10.8.3. Monthly N=240 spectral and lead-screen evidence
Figure 10.8.4. Residual diagnostics: strong accuracy with remaining cautionary tests
Figure 10.9.1. Final claim hierarchy and exclusion boundary

Chapter 11

Figure 11.1. P vs NP logic translated into a bounded computational-finance architecture
Figure 11.2. Support-space explosion in the n = 94 industry universe
Figure 11.5. Position of Chapter 11 inside the seven-problem monograph architecture
Figure 11.3. Research object stack for cardinality-constrained portfolio optimization
Figure 11.4. Mixed discrete-continuous structure of the optimization object
Figure 11.3.1. Data architecture pipeline for the Chapter 11 computational-decision model
Figure 11.3.2. Median input profile for the n = 94 industry universe
Figure 11.3.3. Covariance geometry diagnostics showing common-factor concentration
Figure 11.4.1. Log-scale growth of the support space C(n,K)
Figure 11.4.2. Mixed discrete-continuous architecture of the sparse portfolio problem
Figure 11.4.3. Best versus median Sharpe across algorithmic layers
Figure 11.4.4. Exact reduced benchmark versus MC and GA in the n = 20, K = 6 instance
Figure 11.4.5. Log-scale comparison of full support size and documented audit layers
Figure 11.4.6. Evidence ladder and claim boundary for the Chapter 11 methodology
Figure 11.5.1. Robustness and realism pipeline
Figure 11.5.2. Net Sharpe under transaction-cost and turnover assumptions
Figure 11.5.3. Option leverage grid across moneyness and maturity
Figure 11.5.4. Baseline versus option-augmented return-risk position
Figure 11.5.5. Linear beta-mapped market-shock exposure
Figure 11.6.1. K-grid Sharpe frontier
Figure 11.6.3. Search-space scale versus documented audit coverage
Figure 11.6.2. Algorithmic best and median Sharpe comparison
Figure 11.6.4. Multi-criteria ranking of tested strategy layers
Figure 11.6.5. Evidence ladder for Sections 11.5-11.6
Figure 11.7.1. Interpretation chain from fixed inputs to bounded computational-finance claim
Figure 11.7.2. Search scale: exact reduced evidence, documented audit coverage and full support space

Figure 11.7.3. Algorithmic upper-envelope versus typical performance
Figure 11.7.4. Baseline versus option-augmented risk-return interpretation
Figure 11.8.1. Claim boundary pyramid for Chapter 11
Figure 11.9.1. Position of Chapter 11 within the seven-problem monograph architecture

Chapter 12

Figure 12.1. Comparative empirical universe across the seven models. Log scale prevents the larger panel and benchmark layers from visually suppressing compact graph and asset-universe designs
Figure 12.2. Comparative mathematical objects translated into economic measurement grammars
Figure 12.6. Monograph-level comparative synthesis workflow from public anchors to claim hierarchy
Figure 12.3. Comparative validation-strength heatmap. Scores are chapter-level evidence classifications, not mathematical truth rankings
Figure 12.5. Comparative validation profiles by evidence dimension
Figure 12.4. Strongest admissible claim by model. The bar values classify evidentiary strength inside the monograph, not theorem validity
Figure 12.7. Claim-boundary ladder for Chapter 12 comparative closure

Chapter 14

Figure 14.1. Reviewer-safety architecture of the monograph
Figure 14.6. Constructed-variable lineage and admissible-use workflow
Figure 14.2. Sample-size boundaries across evidence layers
Figure 14.5. Forecasting and optimization boundary emphasis
Figure 14.4. Evidence hierarchy used in Chapter 14
Figure 14.3. Reviewer-risk heatmap
Figure 14.7. Contribution claims balanced by boundary discipline

Chapter 15

Figure 15.1. Monograph closure architecture
Figure 15.2. Empirical scale of the seven economic analogues
Figure 15.3. Comparative contribution profile
Figure 15.4. Future research roadmap
Figure 15.5. Future-research priority matrix
Figure 15.6. Final monograph claim-boundary ladder

Abbreviations and Symbols

This list is designed as a front-matter glossary for the monograph. Chapter-specific notation should still be defined at first use inside the relevant chapter.

Abbreviation / Symbol	Meaning in the monograph
A_ij	Directed economic gauge potential from node i to node j
ARIMA	Autoregressive Integrated Moving Average
BSD	Birch-Swinnerton-Dyer
Betti number	Topological connectedness or cycle-count diagnostic in the bounded economic analogue
BridgeStress	Author-calculated corridor bridge-exposure and stress-transmission diagnostic
C(n,K)	Binomial support-count function for selecting K assets from n candidates
CAPM	Capital Asset Pricing Model
CDS	Credit-default-swap spread or sovereign-risk proxy, depending on chapter context
CMI	Clay Mathematics Institute
CPI	Consumer Price Index
DK / Driscoll-Kraay	Panel-robust covariance estimator allowing cross-sectional dependence and serial correlation
D^S	Stress-degree matrix in the Yang-Mills stress-weighted graph
DOI	Digital Object Identifier
EMGI	Economic Mass Gap Index; finite-network economic stress-threshold diagnostic
ERP	Equity risk premium
EVA	Evidence Validation Architecture / evidence-gating audit, depending on chapter context
F_ijk	Triangular economic field strength / non-neutralized stress curvature around a cycle
FE	Fixed effects
FPAS	Forecasting and Policy Analysis System
GA	Genetic algorithm
GDP	Gross Domestic Product
GMM	Generalized Method of Moments
HAC	Heteroskedasticity- and autocorrelation-consistent covariance estimation
HMM	Hidden Markov Model
IV	Instrumental variables
JEL	Journal of Economic Literature classification code
K	Cardinality constraint or selected-support size in the portfolio chapter

L-function analogue	Constructed local-to-global diagnostic used only in the BSD economic analogue
L^S	Stress-weighted Laplacian matrix
LOrder	Constructed L-order measure in the BSD economic analogue
MAE	Mean Absolute Error
MAPE	Mean Absolute Percentage Error
MC	Monte Carlo
ML	Machine learning
N	Sample size or observation count, depending on chapter context
NP	Nondeterministic polynomial-time complexity class
OLS	Ordinary Least Squares
P	Polynomial-time complexity class
PCA	Principal Component Analysis
PDE	Partial differential equation
P-vs-NP	P versus NP computational-complexity problem; used as an economic optimization analogy only
R_f	Risk-free rate
RE	Random effects
RH	Riemann Hypothesis
RMSE	Root Mean Squared Error
S_YM	Yang-Mills economic action; squared-curvature stress-energy over the finite graph
Sharpe ratio	Risk-adjusted portfolio performance metric
TOPSIS	Technique for Order Preference by Similarity to Ideal Solution
VaR	Value at Risk
CVaR	Conditional Value at Risk
W^S	Stress-weighted adjacency matrix
W(g,f,tau)	Perelman-type W-functional used as a bounded economic diagnostic analogue
beta / β	CAPM beta or systematic-risk coefficient
lambda_1 / λ1	First positive eigenvalue of a graph Laplacian; finite-network economic mass-gap threshold
mu / μ	Expected return, viscosity/friction parameter, or chapter-specific mean parameter
Omega_K / Ω_K	Discrete K-support search space in the P-vs-NP portfolio chapter
rho / ρ	Spectral radius or chapter-specific density/correlation quantity
sigma_i / σ_i	Node-level normalized stress field in the Yang-Mills analogue
Sigma / Σ	Covariance matrix
tau / τ	Smoothing/time-scale parameter; also transition

	threshold in the Yang-Mills chapter when specified
zeta / ζ	Riemann-zeta-based spectral-cyclical signal generator used only for forecasting diagnostics

Chapter 1. General Introduction: The Millennium Problems as Economic Measurement Architectures

1.1. General Research Context

The contemporary world economy is no longer adequately interpretable as a set of isolated aggregates, separate indicators or disconnected national accounts. Output size, inflation dynamics, financial liquidity, inequality pressure, technological access, regional corridor exposure, portfolio feasibility, structural rank and macroeconomic resilience do not operate as independent variables. They interact through flows, networks, shocks, feedback loops, computational constraints and nonlinear adjustment regimes. A large region may dominate world output but remain comparatively insulated from a specific corridor shock; a smaller region may contribute little to global GDP but still act as a bridge through which trade, energy, finance or geopolitical pressure is transmitted. Similarly, an inflation series may appear persistent under a conventional time-series model while hidden macro-financial pressure and cyclical deformation are already accumulating beneath the surface. A portfolio may look tractable under continuous mean-variance allocation, yet become computationally explosive once sparse support selection is imposed. These examples define the general context of this monograph: modern economic systems require measurement architectures that are structural, mathematical, econometric, computational and explicitly bounded in their claims.

The starting point of the monograph is therefore a measurement problem. Conventional economic analysis rightly begins with indispensable observables: GDP, GDP per capita, inflation, growth, unemployment, fiscal pressure, trade openness, financial spreads, liquidity conditions, inequality indices, portfolio returns and risk measures. These variables remain necessary; the argument of the book is not that standard indicators should be abandoned. The central problem is that they do not by themselves explain how economic complexity is organized. A GDP ranking does not reveal whether a region is a bridge, a bottleneck, a cycle participant or a systemic shock-transmission node. An inflation forecast based only on inertia may lag in crisis years. A liquidity indicator alone does not describe how pressure gradients, friction, shocks and closure channels jointly produce systemic stress. A Gini coefficient alone does not show how social pressure, smoothing capacity, curvature-like deformation and network connectedness interact inside a macro-regional inequality system. A portfolio Sharpe ratio alone does not reveal whether the underlying support-selection problem is computationally feasible, heuristically searched or exactly certifiable. The monograph is positioned precisely at this frontier between economic observables and the deeper structures that organize them.

The seven studies that form the empirical foundation of the book respond to this measurement problem through seven distinct mathematical grammars inspired by the Clay Mathematics Institute Millennium Problems. The word inspired is essential. The monograph does not claim to solve, prove, test or replicate any of the classical mathematical problems in their original form. Instead, it translates selected structural logics into bounded economic and econometric analogues. The Navier-Stokes framework provides a flow-pressure-friction-shock language for macro-financial stress. The Yang-Mills framework provides a gauge, curvature, action and spectral-threshold language for systemic shock transmission in corridor networks. The Hodge framework provides a decomposition language for separating hierarchy, local-cycle imbalance and persistent circulation in the world economy. The Birch-Swinnerton-Dyer framework provides a local-to-global language for connecting regional finite-state signals, L-function analogues and structural rank. The Riemann-zeta framework provides a spectral-cyclical language for global inflation forecasting. The P-vs-NP framework provides a computational-complexity language for sparse portfolio optimization. The Perelman-Ricci-Poincare framework provides a curvature, entropy and topological-connectedness language for inequality pressure and smoothing capacity.

Taken together, these seven frameworks form a common research context: economic complexity is multidimensional, but it can be disciplined through explicit transformations from public or audited input variables into constructed analytical objects.

The monograph does not treat mathematical terminology as decorative metaphor. Each problem-inspired framework must define its empirical object, its input layer, its transformation rules, its model-implied variables, its validation tests and its claim boundary. This is why the book repeatedly distinguishes raw public data from author-calculated variables; benchmark evidence from causal evidence; structural measurement from theorem proof; forecasting improvement from universal forecast dominance; and exact reduced computation from full global optimality. The general research context is therefore not only ambitious but also methodological: advanced mathematical analogies can contribute to economics only when they are transformed into reproducible, auditable and claim-disciplined measurement systems.

The first dimension of this general context is the transformation of economic flow into a measurable stress process. In macro-financial systems, liquidity does not behave as a literal physical fluid, but liquidity conditions, pressure gradients, frictional channels, stochastic shocks, cyclical forcing and closure mechanisms do interact in a way that invites structured balance modelling. The Navier-Stokes-inspired study therefore frames systemic stress as a nondimensional flow-pressure-friction-shock-cycle-closure process rather than as a mere collection of separate financial indicators. This framing is important because financial vulnerability often emerges from interaction rather than from any single variable. Inflation pressure, sovereign-risk premia, banking frictions, weak liquidity velocity, GDP-cycle deviations, external financing constraints and hidden adjustment channels may remain individually interpretable but jointly produce a stress configuration that is not visible in an isolated-indicator dashboard. The monograph uses this logic to make liquidity-flow dynamics part of a wider Millennium Economic Research Program: flow matters not as physics, but as an economic structure of pressure, friction, acceleration, shock and closure.

The second dimension is the transformation of macroeconomic networks into threshold systems. The world economy operates through corridors, logistics interfaces, financial channels, energy linkages, regional dependencies and geopolitical transmission paths. Conventional macroeconomic indicators can describe output, inflation, trade or income depth, but they do not automatically identify when a local disturbance becomes systemically transmissible. The Yang-Mills-inspired study addresses this gap by modelling a finite global-corridor stress network in which public macroeconomic anchors are transformed into a stress field, a corridor-weighted graph, an anti-symmetric gauge potential, triangular curvature, Yang-Mills economic action, a stress Laplacian, an Economic Mass Gap Index, fragility, BridgeStress and scenario-based shock diagnostics. In the research context of the monograph, this framework represents the threshold dimension of economic complexity: systemic vulnerability is not only a question of how much stress exists, but also of how stress circulates, concentrates, curves and crosses a local-to-systemic boundary.

The third dimension is the decomposition of macroeconomic structure into separable topological components. Standard macroeconomic descriptions often classify regions by output, growth or income depth, but they do not decompose the connected world economy into hierarchy, local imbalance and persistent circulation. The Hodge-econometric study responds to this gap by treating the world economy as a regional macro-flow network. Public macroeconomic anchors are used to construct a weighted graph; the graph is transformed into a directed macro-flow pressure field; and the resulting edge cochain is decomposed into gradient, curl and harmonic components. This decomposition is economically meaningful because it separates three distinct structures: hierarchy, which reflects ordered pressure differences; local-cycle imbalance, which reflects regional triangular inconsistencies; and harmonic circulation, which reflects persistent system-level flow not eliminated by hierarchy or local curl. Within the book-level context, the Hodge framework provides the methodological bridge between ordinary network description and mathematically structured economic decomposition.

The fourth dimension is inequality as deformation rather than as a single distributional statistic. Global inequality cannot be fully understood through a single Gini coefficient or a small list of social indicators. Income distribution, unemployment, investment stress, productivity, education, technology access, social protection, migration pressure, fiscal stress, innovation, health access and trade connectivity operate as a coupled macro-social system. The Perelman-Ricci-Poincare-inspired study responds by interpreting global inequality pressure as a macro-regional diagnostic manifold. Raw macro-social indicators are transformed onto a common pressure-oriented scale, and the model constructs curvature-like deformation, smoothing capacity, Perelman-type F- and W-functionals, graph connectedness, Betti numbers, Ricci-style component curvature, network-curvature proxies, counterfactual sensitivity and econometric validation layers. In the research context of the monograph, this is the deformation dimension: inequality is not only a level, but a structural state of pressure accumulation, smoothing weakness, entropy-like complexity and connected-system geometry.

The fifth dimension is the local-to-global formation of structural rank. Regional macroeconomic analysis often compares GDP mass, growth and income depth, but it rarely explains how local regional states, corridor exposure, finite-state

reductions, network structure and global rank formation interact. The Birch-Swinnerton-Dyer-inspired study translates the local-to-global architecture of the classical BSD conjecture into an economic measurement grammar. Regional public-data anchors are transformed into systemic-stress components, economic curve coefficients, discriminants, finite-state trace analogues, Euler-factor analogues, a constructed economic L-function, an L-order measure and a structural-rank object. The relevance of this framework for the monograph is that it makes global rank formation interpretable as a calibrated relationship between local regional signals and a constructed structural-rank outcome. The economic claim is not that economies are elliptic curves or that the classical BSD conjecture is tested; the claim is that local-to-global measurement can be made operational, auditable and bounded for regional structural analysis.

The sixth dimension is spectral-cyclical macroeconomic forecasting. Global inflation has become difficult to model as smooth persistence or as a single policy-reaction process. The world economy has passed through successive stress regimes: the global financial crisis and recession aftershock, commodity-price and dollar stress, the COVID-19 macro-financial shock, post-pandemic supply-chain strain, the energy-food-war and monetary-tightening shock, and later disinflation under residual policy tightness. In this setting, forecasting must detect nonlinear pressure, crisis-sensitive cyclical deformation and regime instability while still avoiding overfitting and theorem-level overclaiming. The Riemann-zeta FPAS+zeta study develops this idea by augmenting a structural FPAS inflation baseline with a normalized zeta-cycle correction. The Riemann-zeta function is used only as a computational spectral signal generator, not as a proof, test or verification of the Riemann Hypothesis. In the general context of the book, this framework represents the spectral-diagnostic dimension of economic measurement: global macroeconomic pressure may require signals that capture cyclicality, resonance, shock deformation and layered validation across annual, quarterly and monthly frequencies.

The seventh dimension is computational feasibility in economic decision systems. Economic optimization is often presented as if the analyst can simply maximize an objective function once preferences, risks and constraints are known. The P-vs-NP-inspired portfolio study shows why this view is incomplete. Classical mean-variance theory yields a continuous allocation problem once an asset universe, expected-return vector and covariance matrix are fixed, but real-world portfolio governance frequently imposes sparse selection constraints. Once only K assets, sectors or industries may be chosen from n candidates, the problem becomes mixed discrete-continuous. The number of possible supports grows combinatorially, while each support still requires continuous weight evaluation. In the monograph, this framework supplies the computational-decision dimension of the Millennium program. It shows that economic choice is not only a matter of preference and estimation; it is also a matter of search-space explosion, algorithmic approximation, exact reduced benchmarking, robustness gates, derivative-overlay realism and claim discipline.

The common thread connecting these seven dimensions is that modern economic systems are not reducible to scalar indicators. They are structured by flows, corridors, graphs, cycles, ranks, thresholds, spectra, algorithms and deformation paths. The monograph therefore treats GDP, inflation, inequality, liquidity, trade, portfolio risk and regional rank as entry points rather than final explanations. Each entry point is embedded in a mathematical-econometric architecture designed to reveal a different dimension of complexity. This is why the book must be organized as a monograph rather than as a collection of unrelated articles. The seven frameworks do not merely share an author or a mathematical inspiration; they share a research philosophy: economic measurement becomes more informative when standard indicators are transformed into explicitly defined structures and then audited through econometric, computational, topological, forecasting or robustness procedures.

A second common thread is the role of regional and global aggregation. Several of the frameworks are global or macro-regional rather than narrowly country-specific. The Hodge, Yang-Mills and BSD studies all emphasize that a World anchor, ten macro-regional or corridor-sensitive nodes, and explicit treatment of the Caucasus or Central Asia can reveal systemic positions that are obscured by standard regional aggregation. The Perelman-Ricci-Poincare inequality framework uses a ten-region panel to measure inequality pressure and smoothing capacity through time. The Navier-Stokes framework expands to a 100-country panel but still interprets stress at global and macro-regional levels. The Riemann-zeta model focuses on global aggregate inflation with layered annual, quarterly and monthly validation. The P-vs-NP study departs from regional macroeconomics and works in a fixed industry portfolio universe, but it contributes the same principle: the empirical universe must be explicitly fixed before modelling, and the status of every constructed object must be disclosed. Across the book, therefore, aggregation is neither ignored nor treated as a weakness; it is made part of the research design and claim boundary.

A third common thread is validation discipline. The monograph does not permit an advanced mathematical analogy to function as its own evidence. Each framework must pass through some combination of diagnostic tests, robustness checks, benchmark comparisons, reduced exact certification, panel validation, rolling forecasts, external-target plausibility, placebo logic, Monte Carlo uncertainty, sensitivity analysis or replication-package discipline. The particular validation form differs by problem: liquidity-flow stress testing uses panel and rolling validation; inflation forecasting uses layered forecast-comparison tests; portfolio optimization uses search coverage and exact reduced enumeration; inequality diagnostics use panel, graph and uncertainty checks; Hodge modelling uses structural, econometric, predictive and topological validation; Yang-Mills modelling uses finite-network spectral and scenario evidence; BSD modelling uses rank correspondence, finite-state stability, anti-circularity and closure-layer diagnostics. The general context is therefore methodological as well as empirical: the book asks not only what mathematical analogy can be built, but also what kind of evidence is sufficient to support each claim.

This discipline is especially important because the Clay Millennium Problems are associated with theorem-level mathematical difficulty. Without careful boundary language, the use of names such as Navier-Stokes, Yang-Mills, Hodge, Birch-Swinnerton-Dyer, Riemann Hypothesis, P versus NP and Poincare could be misunderstood as a claim of mathematical resolution. The monograph explicitly rejects that interpretation. Its contribution lies elsewhere: it develops economic analogues that are useful precisely because they remain bounded. The Navier-Stokes model does not turn financial liquidity into a physical fluid; the Yang-Mills model does not solve quantum gauge theory; the Hodge model does not prove the Hodge conjecture; the BSD model does not test the classical BSD conjecture; the zeta model does not verify the Riemann Hypothesis; the portfolio model does not prove P != NP; and the Perelman-Ricci-Poincare model does not replicate Perelman's proof. Each framework uses a formal mathematical architecture as a disciplined language for economic measurement, not as a claim of theorem transfer.

The general research context of the monograph can therefore be stated as follows. The global economy is a complex, networked, shock-sensitive and computationally constrained system. Its principal empirical phenomena - inflation, liquidity, inequality, regional rank, corridor stress, macro-flow circulation and portfolio choice - require measurement tools that go beyond isolated indicators and conventional single-equation descriptions. The Clay Millennium Problems provide seven high-level mathematical architectures that can be translated, with appropriate caution, into economic-econometric measurement systems. The purpose of the monograph is to organize these translations into one coherent research program: a Millennium Economic Research Program that measures flow, curvature, topology, rank, spectral-cyclical pressure and computational feasibility while preserving strict distinctions between mathematical proof, economic analogy, empirical calibration, diagnostic validation and practical interpretation.

This section establishes the foundation for the remainder of the book. Subsequent sections of Chapter 1 specify why the Millennium Problems matter for economic modelling, define the monograph's core research problem, formulate its aim and objectives, present the seven-problem translation matrix, state the scientific novelty and define the global claim boundary. Later chapters then formalize the shared literature, methodology, data architecture, replication discipline and individual problem-specific models. The task of the present section is narrower but fundamental: to show that the seven manuscripts belong to one research context. They all address the same general problem from different mathematical directions: how to measure economic complexity when the economy is simultaneously a flow system, a network system, a topological system, a rank system, a spectral system, an inequality-deformation system and a computational-decision system.

Source-Integration Map for Section 1.1

Source manuscript	Original 1.1 emphasis	Integrated role in monograph section 1.1	Claim discipline preserved
Global Perelman-Ricci-Poincare-Inspired Inequality Diagnostics	Inequality pressure as a high-dimensional, regionally heterogeneous, shock-sensitive and structurally connected macro-social system.	Provides the inequality-deformation, smoothing-capacity, entropy and graph-connectedness dimension of the general research context.	Economic analogue only; not a proof, test or replication of Perelman, Ricci-flow or Poincare theorem logic.
Global Hodge-Econometric Modeling of the World Economy	World economy as a connected regional macro-flow system rather than	Provides the topological decomposition dimension: gradient hierarchy, curl	Benchmark structural measurement; not a proof of the Hodge conjecture or

	isolated output aggregates.	imbalance and harmonic systemic circulation.	a substitute for all-country dyadic flow data.
Navier-Stokes-Inspired Global Liquidity-Flow and Systemic-Stress Modelling	Systemic stress as a nondimensional liquidity-flow, pressure, friction, shock, cycle and closure process.	Provides the macro-financial flow and stress-balance dimension of the monograph.	Financial liquidity is not treated as a physical fluid; the model is a stress-testing analogue, not a Navier-Stokes solution.
Economic Yang-Mills Mass Gap in Global and Corridor Flow Networks	Corridor-sensitive global stress network and systemic shock threshold measured through gauge, curvature, action and spectral separation.	Provides the threshold, curvature-action and corridor-transmission dimension of systemic risk.	Mass gap is finite-network and economic only; no claim to solve Yang-Mills existence and mass gap.
Regional Economic Birch-Swinnerton-Dyer Modelling	Regional local-to-global structural rank formation under corridor stress and finite-state local signals.	Provides the local-to-global rank-formation dimension of the general research context.	Calibrated regional economic measurement architecture; not a proof, test or replication of classical BSD.
Global Riemann-Zeta FPAS+zeta Inflation Forecasting	Global inflation as a nonlinear, crisis-sensitive, spectral-cyclical forecasting problem.	Provides the spectral forecasting and macro-financial pressure-diagnostic dimension.	Zeta function is a signal generator only; no proof, test or verification of the Riemann Hypothesis.
Robust Portfolio Optimization under Computational Complexity	Cardinality-constrained portfolio optimization as mixed discrete-continuous search with combinatorial support explosion.	Provides the computational-decision and algorithmic feasibility dimension of the monograph.	P-vs-NP is operationalized empirically; no theorem proof, no certified full-universe global optimum, no realized investment dominance.

1.2. Why the Clay Millennium Problems Matter for Economic Modelling

1.2.1. The Millennium Problems as Measurement Grammars rather than Theorem Claims

The importance of the Clay Mathematics Institute Millennium Problems for this monograph does not arise from the claim that economic systems are literal mathematical objects of the same kind as those studied in pure mathematics. The significance lies instead in the fact that each Millennium Problem contains a powerful formal grammar for organizing complexity. A mathematical grammar is not merely a vocabulary. It is a disciplined way of asking which objects matter, which transformations are admissible, which invariants or diagnostics should be preserved, what kind of correspondence is meaningful, and which claims must remain excluded. For economic modelling, this is valuable because modern economic systems are no longer adequately measurable through isolated indicators alone. Global inflation, liquidity stress, inequality pressure, regional rank, corridor transmission, network circulation and portfolio feasibility all require structured measurement languages that can connect raw data, constructed variables, validation procedures and interpretation boundaries.

This monograph uses the Millennium Problems precisely in that sense: as seven measurement grammars. Navier-Stokes contributes the grammar of flow, pressure, friction, forcing and closure. Yang-Mills contributes the grammar of gauge fields, curvature, action and spectral threshold. Hodge contributes the grammar of decomposition into gradient, curl and harmonic components. Birch-Swinnerton-Dyer contributes the grammar of local-to-global rank formation through local signals and L-function-like behavior. The Riemann Hypothesis contributes the grammar of zeta-type spectral-cyclical structure and distributional resonance. P versus NP contributes the grammar of computational feasibility, search-space

explosion and verifiability. Poincare, interpreted through Ricci and Perelman logic, contributes the grammar of topological connectedness, curvature-like deformation, entropy and smoothing capacity.

The word grammar is methodologically important because it prevents two opposite mistakes. The first mistake would be superficial metaphor: using famous mathematical names while leaving the economic model unstructured. The second mistake would be theorem overclaiming: implying that an empirical economic model solves or verifies an open mathematical problem. The monograph avoids both. Each problem-inspired chapter must convert a mathematical logic into an empirical architecture with a clear object, data status, transformation rule, validation layer and claim boundary. This is why the seven studies are not simply illustrative analogies. They are seven disciplined measurement architectures designed to make different dimensions of economic complexity visible.

1.2.2. Why Economics Needs Mathematical Grammars of Complexity

Economic systems are multi-layered systems. They contain variables that move through time, across countries, through networks, inside institutional structures and under computational constraints. A conventional regression may estimate an association, but it does not by itself reveal whether the system is dominated by flow pressure, topological imbalance, spectral cycles, local-to-global rank formation or algorithmic infeasibility. A composite index may summarize several indicators, but it can become opaque if it lacks a formal logic for why the components belong together. A forecast model may improve a fit statistic, but it may not explain whether the improvement comes from structural pressure, regime switching, cyclical resonance or overfitting. A network model may show connectivity, but without a deeper grammar it may not distinguish mere degree from curvature, circulation, threshold or bridge exposure.

The Millennium Problems matter for economic modelling because they offer different ways to formalize these hidden layers. They are not imported into economics as ready-made answers. They are used as design principles. The Navier-Stokes language asks whether economic stress can be written as a balance of flow weakness, acceleration, pressure, friction, shocks and restricted closure. The Yang-Mills language asks whether stress becomes systemically transmissible when curvature and action concentrate in a finite network. The Hodge language asks whether directed macro-flow pressure can be decomposed into hierarchy, local imbalance and persistent circulation. The BSD language asks whether local regional signals, finite-state reductions and Euler-factor-like information are informative about global structural rank. The zeta language asks whether inflation pressure contains a spectral-cyclical signal that improves forecasting under layered validation. The P-vs-NP language asks whether an economic decision problem is not merely continuous but combinatorial and computationally explosive. The Ricci-Poincare language asks whether inequality should be read as a pressure-smoothing manifold with curvature, entropy and connectedness.

This is why the seven problems are not ornamental references in the book. They define seven modelling questions that standard economic language often leaves blurred. Flow is not the same as rank. Rank is not the same as topology. Topology is not the same as curvature. Curvature is not the same as spectral resonance. Spectral resonance is not the same as computational complexity. Computational complexity is not the same as inequality deformation. The contribution of the monograph is to preserve these distinctions while placing them into one coherent research program.

1.2.3. Navier-Stokes: The Grammar of Flow, Pressure, Friction and Closure

Navier-Stokes matters for economic modelling because financial and macroeconomic stress is often generated through interacting channels rather than through a single observable variable. The Navier-Stokes-inspired manuscript develops a global liquidity-flow and systemic-stress framework in which stress is represented as a nondimensional balance of liquidity velocity weakness, liquidity acceleration, macro-financial pressure gradients, friction or diffusion, stochastic shocks, Fourier GDP-cycle forcing and a restricted hidden-adjustment term. The point is not to claim that financial liquidity is a physical fluid. The point is that the flow grammar forces the researcher to specify how movement, pressure, resistance, external force and closure combine inside one stress-testing architecture.

This grammar is economically useful because standard macro-financial dashboards can fragment the problem. Inflation pressure, sovereign-risk spreads, banking friction, liquidity ratios, GDP-cycle deviations, external transfers, fiscal buffers, foreign support and geopolitical shocks may all be observable or proxy-observable, but their joint stress meaning can remain unclear. The Navier-Stokes-inspired approach makes the interaction explicit. It asks whether systemic stress can be decomposed into interpretable components and whether the residual closure term can be restricted by state variables rather than allowed to become an unrestricted algebraic plug. This creates a stronger diagnostic architecture than a simple composite stress index.

Within the monograph, Navier-Stokes supplies the flow grammar for macro-financial vulnerability. It shows why economic modelling needs to distinguish velocity from acceleration, pressure from friction, shock from cycle, and closure from unexplained residual adjustment. Because the empirical architecture is built around a 100-country annual panel for 2010-2024, yielding 1,500 country-year observations, supplemented by validation windows, external-target layers, Monte Carlo uncertainty and policy counterfactuals, the model also demonstrates how a mathematical analogy can be translated into a large empirical stress-testing framework. The admissible claim remains carefully bounded: the framework supports global liquidity-flow diagnostics and systemic-risk interpretation, not a mathematical solution to the Navier-Stokes problem and not a universal crisis-prediction law.

1.2.4. Yang-Mills: The Grammar of Gauge Structure, Curvature, Action and Shock Thresholds

Yang-Mills matters for economic modelling because systemic risk often circulates through networks in ways that scalar indicators cannot capture. Output size, growth, income depth, inflation and trade exposure can describe node conditions, but they do not automatically show how stress becomes transmissible through a corridor-sensitive topology. The Yang-Mills-inspired manuscript responds by constructing a finite-network gauge-econometric framework: public macroeconomic anchors are transformed into a systemic-stress field; the field is embedded in a corridor-weighted graph; stress differentials define an anti-symmetric economic gauge potential; triangular cycles generate curvature; squared curvature produces Yang-Mills economic action; and the stress-weighted Laplacian yields a finite-network economic mass gap.

The value of the Yang-Mills grammar is that it separates the presence of stress from the circulation of stress. A node can be large but protected, small but strategically exposed, peripheral by GDP but central in corridor transmission, or involved in high-curvature cycles that concentrate systemic action. In the manuscript, the benchmark architecture contains ten global and corridor-sensitive nodes connected by twenty-seven weighted undirected edges. The corrected benchmark reports a positive finite-network economic mass gap, a spectral radius, a normalized transition threshold, action concentration and scenario-based shock diagnostics. These results are important not as physical gauge theory but as a way to measure whether a local disturbance can cross a threshold into systemic transmission.

Within the monograph, Yang-Mills supplies the threshold grammar. It asks when stress is merely local and when it becomes systemically transmissible. It also supplies the curvature-action grammar: the economically relevant object is not only the level of stress at a node but also the non-neutralized circulation of stress around cycles. This is especially important for corridor economics, including Middle Corridor, Black Sea, Caspian, Caucasus and Central Asia interfaces, where systemic relevance cannot be read directly from GDP share. The chapter must preserve the strict boundary of the source manuscript: the term mass gap is used only in the finite weighted-graph economic sense, and the model does not claim a solution to the mathematical Yang-Mills existence and mass gap problem.

1.2.5. Hodge: The Grammar of Decomposition, Imbalance and Systemic Circulation

Hodge theory matters for economic modelling because many economic systems contain flows that cannot be understood only through hierarchy or scale. The Hodge-econometric manuscript frames the world economy as a connected regional macro-flow network rather than as a collection of isolated output aggregates. Public macroeconomic anchors such as regional GDP, world-output share, projected growth, transition GDP and income depth are transformed into a weighted regional network, and the resulting directed macro-flow pressure field is decomposed through discrete Hodge logic. This allows the model to separate gradient hierarchy, curl-based local-cycle imbalance and harmonic systemic circulation.

The Hodge grammar is powerful because it prevents a common reduction in macroeconomic interpretation: treating the world economy as if GDP scale were the only structural dimension. A region may be large in output but not the dominant source of circulation. A smaller region may contribute to cycle imbalance or systemic flow persistence. A corridor-sensitive region such as the Caucasus may remain hidden under broad regional aggregation unless it is retained as an explicit node. The Hodge framework gives these differences a formal language. Gradient represents hierarchical pressure, curl represents local-cycle inconsistency, and harmonic structure represents residual circulation that persists after hierarchy and local imbalance are removed.

Within the monograph, Hodge supplies the decomposition grammar. It shows that economic structure is not a single scalar. The regional benchmark in the source manuscript is connected and cycle-rich, and its Hodge energy decomposition separates macro-flow pressure into gradient hierarchy, curl/local-cycle imbalance and harmonic/systemic circulation. The precise empirical percentages are important in the chapter-specific results, but the conceptual role in Section 1.2 is broader: Hodge explains why economic modelling requires decomposition before interpretation. Without a decomposition grammar, hierarchy, imbalance and circulation may be confused. With it, the world economy can be examined as a topological flow

system, while preserving the boundary that this is a benchmark economic measurement architecture rather than a proof of the Hodge conjecture.

1.2.6. Birch-Swinnerton-Dyer: The Grammar of Local-to-Global Structural Rank

Birch-Swinnerton-Dyer matters for economic modelling because many economic questions involve local-to-global formation. Regional shocks, corridor pressures, finite-state conditions, network positions and productive capacities are local or regional signals, but their significance depends on how they combine into a global structural rank. The BSD-inspired manuscript translates the local-to-global logic of the classical conjecture into a regional economic measurement architecture. It does not treat economies as elliptic curves in the literal mathematical sense. Instead, it builds economic curve coefficients, discriminant diagnostics, finite-state trace analogues, Euler-factor analogues, a constructed economic L-function, an L-order measure and a structural-rank object.

The BSD grammar is important because it asks whether local signals contain information about global rank formation. Standard regional macroeconomic comparison often begins with GDP, GDP per capita, growth and trade shares. These indicators are necessary, but they do not show how finite-state regional conditions, corridor exposure, network structure and stress components jointly produce a rank hierarchy. The BSD-inspired framework creates a way to connect local reductions, Euler-factor information and LOrder to a constructed structural rank composed of productive, Hodge-flow, network and agentic components. This makes rank a multidimensional object rather than a disguised GDP ranking.

Within the monograph, BSD supplies the local-to-global grammar. It is the chapter that most explicitly connects the regional benchmark logic of the book to a global structural claim. The source manuscript uses a World normalization anchor, ten macro-regional/corridor nodes and an N = 150 regional-year closure layer for calibration, robustness diagnostics and claim discipline. The significance for Section 1.2 is that BSD shows why economic modelling needs a grammar for how local information becomes global structure. The boundary is equally important: the framework supports a calibrated regional economic measurement claim, not a proof of the classical BSD conjecture, not a causal law and not strong external econometric validation when robust-inference and external-proxy evidence remain diagnostic or directional.

1.2.7. Riemann-Zeta: The Grammar of Spectral-Cyclical Inflation Diagnostics

The Riemann Hypothesis matters for this monograph not as a theorem to be proved through economic data, but as a source of spectral and distributional grammar. The Riemann-zeta FPAS+zeta manuscript treats the zeta function as a mathematically explicit signal generator that can be transformed into a normalized cyclical correction for global inflation forecasting. The research object is global aggregate inflation under layered macro-financial pressure. The zeta signal is not used to verify the Riemann Hypothesis. It is used to test whether a critical-line-inspired cyclical signal, converted into a signed and alpha-calibrated forecast correction, improves a structural FPAS baseline relative to FPAS and ARIMA benchmarks.

This grammar matters because inflation forecasting is rarely only a persistence problem. The global economy has passed through regimes shaped by the global financial crisis, commodity and dollar stress, the pandemic shock, reopening and supply-chain strain, energy-food-war pressure, monetary tightening and disinflation under residual policy tightness. A purely inertial model may lag during crisis years, while a structural forecast may understate nonlinear acceleration if pressure intensifies. The zeta grammar asks whether spectral-cyclical deformation can be made explicit, normalized, signed and subjected to rigorous forecast-validation discipline.

Within the monograph, Riemann-zeta supplies the spectral-cyclical grammar. It connects macro-financial pressure, nonlinear tau construction, critical-line evaluation, zeta-cycle normalization, deviation from neutrality, correction direction, alpha calibration and forecast comparison. Its empirical discipline is especially important: the source manuscript separates annual N = 55, annual robustness N = 45, crisis-era N = 20, quarterly N = 100 and monthly N = 240 layers so that methods are not misread as if all evidence came from one small sample. The admissible claim is forecast-diagnostic: the zeta layer may improve global inflation forecasting and strengthen crisis interpretation under layered validation, but it does not prove, test or verify the Riemann Hypothesis and does not claim universal forecast dominance across all economies, samples and horizons.

1.2.8. P versus NP: The Grammar of Search-Space Explosion, Feasibility and Certification

P versus NP matters for economic modelling because economic decision problems are often not merely continuous optimization problems. Once discrete selection enters, the structure changes. The P-vs-NP-inspired portfolio manuscript demonstrates this through cardinality-constrained portfolio optimization. A classical Markowitz-CAPM framework can define expected returns and covariance geometry once the asset universe is fixed, but a sparse portfolio requirement forces

the investor to select a limited support before continuous weights can be optimized. This transforms portfolio design into a mixed discrete-continuous problem where the number of feasible supports grows combinatorially.

This grammar is economically important because it separates optimization appearance from computational reality. A portfolio problem may look like a standard allocation exercise, but with n = 94 industry portfolios and K = 10 selected industries, the support space contains more than nine trillion possible combinations before continuous allocation is solved. This is not presented as a theorem-level proof of P versus NP. It is an empirical-computational demonstration that sparse economic decision systems require search budgets, heuristic comparison, reduced exact benchmarking, robustness diagnostics and claim-boundary discipline. Greedy search, Monte Carlo sampling, genetic algorithms, continuous reoptimization, exact reduced enumeration, transaction-cost screens, covariance robustness and Black-Scholes overlay become part of one computational-finance architecture.

Within the monograph, P versus NP supplies the computational-decision grammar. It shows that economic feasibility is not only a matter of economic desirability but also a matter of search complexity, verifiability and certification. The distinction between best-found incumbent and certified global optimum is central. The reduced exact benchmark provides a certification layer for a smaller universe, while the full universe remains bounded by documented search coverage. The claim boundary is therefore precise: the framework supports a P-vs-NP-inspired empirical-computational claim about cardinality-constrained portfolio optimization, not a proof of P not equal NP, not a certified global optimum for the full n = 94 universe and not realized historical investment dominance.

1.2.9. Perelman-Ricci-Poincare: The Grammar of Curvature, Entropy, Connectedness and Smoothing Capacity

Poincare, Ricci flow and Perelman-type functionals matter for economic modelling because inequality is not only a distributional number. It is a high-dimensional pressure system. The Perelman-Ricci-Poincare-inspired manuscript develops a global inequality diagnostic framework in which the world economy is interpreted as a macro-regional pressure-smoothing manifold rather than as a collection of isolated inequality indicators. Income distribution, productivity, unemployment, investment, inflation, migration, education, social mobility, trade infrastructure, capital-flow pressure, innovation, healthcare access, fiscal balance, openness, social protection and technology access are transformed into a common stress-coordinate system.

The value of this grammar is that it gives inequality modelling a structural language. Curvature-like deformation measures the balance between inequality pressure and smoothing capacity. Ricci-flow terminology organizes pressure and recovery through time. Perelman-type F- and W-functionals summarize energy-like and entropy-like system complexity. Poincare-style graph connectedness tests whether the inequality variables form one connected diagnostic manifold. The result is not a literal application of differential geometry or topology to the economy. It is a bounded diagnostic architecture that makes high-dimensional inequality pressure measurable.

Within the monograph, the Perelman-Ricci-Poincare framework supplies the curvature-entropy-connectedness grammar. It explains why inequality must be examined through deformation, smoothing and network structure rather than through a single indicator alone. The empirical design uses ten macro-regional blocks over 2010-2024 and sixteen stress-coordinate variables, producing N = 150 region-year observations. This gives the chapter a strong diagnostic panel architecture while preserving academic caution. The model does not prove, test or replicate Perelman's proof, the classical Ricci-flow theorem or the Poincare conjecture; it translates their modelling logic into an economic diagnostic system for inequality pressure and smoothing capacity.

1.2.10. The Seven Grammars as One Integrated Economic Research Program

The seven measurement grammars matter most when they are read together. Each grammar isolates one dimension of economic complexity, but the monograph's contribution is to show that these dimensions can be organized into one research program. Navier-Stokes identifies flow and stress balance. Yang-Mills identifies gauge curvature, action concentration and transition thresholds. Hodge identifies decomposition into hierarchy, imbalance and systemic circulation. BSD identifies local-to-global rank formation. Riemann-zeta identifies spectral-cyclical pressure and forecast correction. P versus NP identifies computational feasibility and support-space explosion. Perelman-Ricci-Poincare identifies inequality deformation, entropy and connectedness. No single grammar replaces the others. Their value lies in complementarity.

This complementarity is important because the global economy is simultaneously a flow system, a network system, a topological system, a rank system, a spectral system, a deformation system and a computational-decision system. Liquidity stress can propagate through corridors; corridor propagation can be shaped by curvature and topology; topology can generate circulation and imbalance; local regional signals can contribute to structural rank; inflation can react to nonlinear

spectral-cyclical pressure; policy and portfolio choices can face computational limits; and inequality can deform through pressure accumulation and weak smoothing capacity. A single-equation framework would struggle to carry all these dimensions without either oversimplifying the system or creating an opaque index. The Millennium grammar approach provides a disciplined alternative.

For this reason, the monograph should not be framed as seven unrelated case studies. It should be framed as an integrated Millennium Economic Research Program. Each chapter is autonomous enough to define its own empirical object and validation logic, but all chapters share a methodological spine: public or audited input data; normalized or structured transformations; constructed analytical objects; econometric, topological, computational or forecast validation; replication discipline; and explicit claim boundaries. The importance of the Clay Millennium Problems for economic modelling is therefore not symbolic. They provide a high-level architecture for making economic complexity measurable without collapsing it into a single indicator.

1.2.11. Evidence Discipline: Why Mathematical Language Requires Stronger Claim Boundaries

Because the source of inspiration is mathematically prestigious and theorem-level difficult, the use of Millennium Problem language requires stronger, not weaker, evidence discipline. This is one of the central principles of the book. A problem-inspired economic model must disclose what is public input data, what is author-calculated, what is a benchmark result, what is a diagnostic association, what is a forecast comparison, what is a scenario simulation, what is an exact reduced computation and what is reserved for future validation. Without this distinction, advanced mathematical terminology could create an appearance of proof where the evidence supports only measurement, calibration, diagnosis or computational demonstration.

The seven manuscripts already contain this discipline in different forms. The Navier-Stokes framework restricts the hidden-adjustment term rather than allowing it to become a free residual. The Yang-Mills framework separates finite-network benchmark evidence from future country-panel validation. The Hodge framework treats its ten-node regional benchmark as structural measurement rather than all-country causal inference. The BSD framework separates internal local-to-global calibration from external-proxy confirmation. The Riemann-zeta framework separates layered forecast evidence from theorem proof and universal forecast dominance. The P-vs-NP framework separates exact reduced enumeration from uncertified full-universe global optimality. The Perelman-Ricci-Poincare framework separates diagnostic curvature and entropy objects from literal geometric invariants.

This evidence discipline is part of why the Millennium Problems matter. They force the monograph to articulate a hierarchy of claims. At the highest permitted level, some chapters support strong panel diagnostic evidence, strong forecast validation, exact reduced computational evidence, or finite-network benchmark measurement. At a lower level, some outputs remain diagnostic, directional, scenario-based, robustness-oriented or future-validation-ready. The book's scientific credibility depends on preserving those distinctions. Mathematical ambition must be matched by methodological restraint.

1.2.12. The General Justification of the Monograph

The general justification for using the Clay Millennium Problems in economic modelling can now be stated clearly. The problems matter because they provide seven disciplined ways to organize economic complexity: flow, threshold, decomposition, rank, spectral cycle, computation and curvature. These are not arbitrary metaphors. They correspond to real measurement problems in global economics and finance. Systemic stress requires a flow grammar; corridor transmission requires a threshold and curvature grammar; macro-flow structure requires a decomposition grammar; regional hierarchy requires a local-to-global rank grammar; inflation instability requires a spectral-cyclical grammar; portfolio selection requires a computational-complexity grammar; and inequality pressure requires a curvature-entropy-connectedness grammar.

The monograph therefore treats the Clay Millennium Problems as a methodological reservoir for economic science. Their value is not that economics can solve them, but that their formal architectures can discipline how economists construct models of complex systems. The result is a seven-part economic-econometric research program that is mathematical but not theorem-claiming, empirical but not causally overextended, computational but not globally overcertified, and policy-relevant without pretending to generate mechanical prescriptions. This is the proper role of the Millennium Problems in the book: they matter because they allow economic modelling to move from isolated indicators toward structured, validated and claim-bounded measurement architectures.

This section prepares the reader for the remainder of Chapter 1. The next subsection defines the monograph's core research problem in a unified way. That problem is no longer the isolated problem of inflation, liquidity, inequality, portfolio choice,

regional rank or corridor shock transmission. It is the more general problem of how global economic complexity can be measured when it appears simultaneously as flow, topology, curvature, spectral signal, rank formation and computational constraint. Section 1.2 establishes why the Millennium Problems are the appropriate conceptual bridge for that task.

1.2.13. Seven-Problem Measurement-Grammar Matrix

Table 1.2 summarizes the monograph-level translation. It should appear in the final book as the first compact map showing why each Clay problem matters for economic modelling and what measurement role it performs inside the book.

Clay problem	Mathematical grammar used in the monograph	Economic measurement object	Main empirical architecture	Excluded claim
Navier-Stokes	Flow, velocity, acceleration, pressure gradient, friction/diffusion, forcing and closure	Global liquidity-flow stress and systemic vulnerability	100-country panel, 2010-2024, N = 1,500, rolling validation, benchmarks, Monte Carlo and counterfactuals	No physical-fluid claim, no Navier-Stokes solution, no universal crisis law
Yang-Mills	Gauge potential, triangular curvature, action, stress Laplacian and spectral separation	Systemic shock thresholds in global and corridor flow networks	Ten-node, twenty-seven-edge benchmark; EMGI, fragility, BridgeStress and scenario diagnostics; N = 1,500 validation pathway	No solution of Yang-Mills existence and mass gap
Hodge	Gradient/curl/ harmonic decomposition of a directed edge cochain	Hierarchy, local-cycle imbalance and systemic circulation in the world economy	Ten regional nodes plus World anchor; weighted macro-flow graph; Hodge-Laplacian and persistent-homology validation	No proof of Hodge conjecture; no all-country dyadic causal claim
Birch-Swinnerton-Dyer	Local reductions, Euler factors, L-function behavior and rank correspondence	Local-to-global structural rank formation under corridor stress	World anchor, ten regional/corridor nodes, N = 150 closure layer, LOrder and structural rank calibration	No proof, test or replication of classical BSD
Riemann Hypothesis	Zeta critical-line signal, spectral-cyclical deviation and distributional resonance	Global inflation forecasting and macro-financial pressure diagnostics	Annual N = 55, robustness N = 45, crisis-era N = 20, quarterly N = 100 and monthly N = 240 layered validation	No proof, test or verification of RH; no universal forecast dominance
P versus NP	Combinatorial support selection, search-space explosion, heuristic search and reduced	Cardinality-constrained portfolio optimization and	Damodaran January 2026 n = 94 industry universe, K = 10 support	No P != NP proof, no certified full n = 94 global optimum, no realized-return

	exact certification	computational-finance feasibility	selection, exact n = 20, K = 6 benchmark	dominance
Poincare / Ricci / Perelman	Connectedness, curvature-like deformation, entropy-like complexity and smoothing flow	Global inequality pressure, smoothing capacity and macro-regional deformation	Ten macro-regional blocks, 2010-2024, sixteen stress coordinates, N = 150 diagnostic panel	No proof, test or replication of Perelman/Ricci/Poincare theorem logic

Source-Integration Map for Section 1.2

The following map records how the seven source manuscripts are used in this monograph subsection. The section is intentionally synthetic: it preserves each source study's conceptual role while reorganizing the material around the common idea of mathematical measurement grammars.

Source manuscript	Source logic used for 1.2	Book-level measurement grammar	Main boundary preserved
Navier-Stokes-Inspired Global Liquidity-Flow and Systemic-Stress Modelling	Stress is organized as nondimensional flow-pressure-friction-shock-cycle-closure balance.	Flow and closure grammar.	Economic stress-testing analogue only.
Economic Yang-Mills Mass Gap in Global and Corridor Flow Networks	Systemic stress circulates through corridor-sensitive finite networks and can be audited through curvature, action and spectral gap.	Threshold, gauge, curvature and action grammar.	Finite-network mass gap only.
Global Hodge-Econometric Modeling of the World Economy	Directed macro-flow pressure can be decomposed into gradient hierarchy, curl imbalance and harmonic circulation.	Topological decomposition grammar.	Benchmark structural measurement only.
Regional Economic Birch-Swinnerton-Dyer Modelling	Finite-state local signals and Euler-factor analogues can be compared with structural rank through LOrder.	Local-to-global rank grammar.	Calibrated economic analogue only.
Global Riemann-Zeta FPAS+zeta Inflation Forecasting	A normalized zeta-cycle can provide a signed forecast correction to an FPAS baseline under layered validation.	Spectral-cyclical forecasting grammar.	No RH proof or universal dominance.
Robust Portfolio Optimization under Computational Complexity	Sparse portfolio design creates a combinatorial support-selection problem requiring heuristic search and reduced exact benchmarking.	Computational feasibility grammar.	No theorem proof or full-universe certification.
Global Perelman-Ricci-Poincare-Inspired Inequality Diagnostics	Inequality pressure can be measured through curvature-like deformation, entropy-like complexity and graph connectedness.	Curvature, entropy and connectedness grammar.	Economic diagnostic analogue only.

1.2.14. Concluding Synthesis of Section 1.2

The Clay Millennium Problems matter for economic modelling because they provide seven non-equivalent but mutually reinforcing ways of making complexity measurable. Their role in this monograph is not to transfer theorem claims into economics; it is to discipline economic measurement through flow, curvature, decomposition, rank, spectral cycle, computation and topological deformation. This is the conceptual bridge that allows the seven independent manuscripts to become one monograph. The book's central intellectual move is therefore not to assert that the Millennium Problems are solved economically, but to show that their formal architectures can generate rigorous, reproducible and claim-bounded economic-econometric research programs.

1.3. The Monograph's Core Research Problem

1.3.1. From Fragmented Indicators to a Unified Research Problem

The core research problem of the monograph begins with a structural limitation in conventional economic measurement. Modern economic systems are usually observed through separate indicators: GDP, inflation, growth, inequality, financial spreads, credit conditions, trade openness, portfolio returns, volatility, technological access, fiscal pressure, regional shares and institutional capacity. These indicators are necessary, but they do not by themselves explain how the system behaves as a connected, nonlinear, shock-sensitive and computationally constrained object. A country, region, corridor or asset universe may appear stable under one indicator while remaining fragile under another. Likewise, a region may be small in output mass but large in corridor relevance; an inflation model may be accurate in tranquil periods but weak during nonlinear crisis acceleration; a portfolio may be attractive under unconstrained mean-variance logic but infeasible under cardinality and search-space limits; and an inequality system may show partial recovery while entropy-like complexity and regional dispersion remain elevated.

The seven manuscripts that form the empirical basis of this monograph address different surfaces of the same deeper problem. The Perelman-Ricci-Poincare inequality study treats global inequality not as a single welfare statistic but as a macro-regional pressure-smoothing manifold built from ten regions, sixteen stress-coordinate variables and an $N = 150$ region-year diagnostic panel. The Hodge study treats the world economy not as a set of output aggregates but as a decomposable regional macro-flow network. The Navier-Stokes study treats systemic stress not as a single financial variable but as a nondimensional flow-pressure-friction-shock-cycle-closure process over a 100-country panel. The Yang-Mills study treats corridor risk not as narrative strategic importance but as finite-network stress curvature, action and spectral threshold. The BSD study treats regional rank not as GDP size alone but as a local-to-global structural-rank formation process. The Riemann-zeta study treats inflation forecasting not as persistence alone but as a layered structural-spectral validation problem. The P-vs-NP study treats portfolio selection not as a purely continuous allocation problem but as a mixed discrete-continuous computational problem.

The monograph therefore asks a single overarching question: how can global economic complexity be measured when its relevant dimensions are not reducible to isolated indicators, linear regressions, single-index rankings, unconstrained optimization or purely descriptive networks? This question is not answered by choosing one method. It requires a multi-grammar architecture in which flow, topology, curvature, rank, spectral signal, computational feasibility and local-to-global correspondence are each assigned a specific measurement role. The central research problem is precisely the construction of that architecture.

1.3.2. Global Economic Complexity as a Multi-Dimensional Measurement Object

Global economic complexity is not a single variable. It is a compound measurement object formed by interacting layers of scale, motion, pressure, structure, information, constraint and transmission. Scale appears through output mass, income depth, market capitalization and regional weight. Motion appears through growth, liquidity velocity, inflation dynamics, macro-flow pressure and shock propagation. Pressure appears through inflation, unemployment, inequality stress, sovereign-risk spreads, liquidity weakness, fiscal constraint and corridor exposure. Structure appears through networks, cycles, connectedness, decomposition, centrality, curvature and rank. Information appears through forecasting signals, spectral deformation, local finite-state traces and validation diagnostics. Constraint appears through computational infeasibility, cardinality limits, transaction costs, robustness gates and claim boundaries. Transmission appears through corridors, bridge exposure, local-to-systemic thresholds and local-to-global rank formation.

Because complexity has this layered structure, the monograph cannot be organized around one canonical dependent variable. It instead develops seven economic-econometric analogues that correspond to seven analytically distinct dimensions of complexity. Navier-Stokes measures liquidity-flow stress. Hodge measures decomposable topological flow.

Yang-Mills measures curvature/action concentration and systemic shock thresholds. BSD measures local-to-global rank formation. Riemann-zeta measures spectral-cyclical inflation correction and forecast performance. P-vs-NP measures computational feasibility in sparse portfolio optimization. Perelman-Ricci-Poincare measures inequality deformation, smoothing capacity, entropy-like complexity and connectedness.

The monograph-level problem is therefore not merely to show that each individual model works inside its own empirical domain. The harder problem is to show that these seven models are not unrelated demonstrations. They are different projections of one broader measurement program. Each model gives access to a dimension of economic complexity that the others cannot fully capture. Flow diagnostics cannot replace computational complexity. Spectral inflation forecasting cannot replace local-to-global rank calibration. Hodge decomposition cannot replace Ricci-style inequality smoothing. Yang-Mills curvature cannot replace Navier-Stokes closure. The book's scientific task is to make these distinctions explicit while integrating them under one coherent research architecture.

1.3.3. The Flow Problem: Liquidity, Pressure and Systemic Stress

The first dimension of the monograph's research problem is flow. Economic systems move: liquidity circulates, prices adjust, credit tightens or loosens, fiscal buffers absorb or fail to absorb shocks, external transfers enter economies, geopolitical shocks disturb expectations and GDP cycles transmit macro-financial pressure. Conventional stress monitoring can identify separate indicators such as inflation, spreads, volatility or credit conditions, but it often fails to represent systemic stress as a balance of interacting forces. The Navier-Stokes-inspired study converts this gap into a formal macro-financial problem: systemic stress must be measured as a nondimensional interaction among liquidity velocity weakness, acceleration, pressure gradients, friction or diffusion, stochastic shocks, Fourier GDP-cycle forcing and restricted hidden closure.

The research problem here is not whether financial markets are literal fluids. They are not. The problem is whether economic stress can be modelled through a disciplined flow grammar that prevents the analyst from adding heterogeneous raw units or using an unrestricted residual term to force equality. In the Navier-Stokes manuscript, this problem is addressed through a 100-country annual panel covering 2010-2024, yielding 1,500 country-year observations, together with rolling validation, benchmark comparison, external-target validation, Monte Carlo uncertainty and policy counterfactuals. This empirical architecture makes the flow problem central to the monograph: a global stress system must be measured dynamically, not merely listed indicator by indicator.

At the monograph level, the flow problem asks how liquidity, pressure, friction, shocks and closure can be integrated into an auditable systemic-stress object. The answer cannot be a metaphor alone. It requires unit harmonization, nondimensional variables, explicit closure restrictions, panel diagnostics, forecast validation and scenario interpretation. This is why the flow dimension is one of the first pillars of the overall research problem.

1.3.4. The Topology Problem: Hierarchy, Imbalance and Circulation

The second dimension is topology. Standard macroeconomic comparison is often scalar: one region is larger, richer, faster growing or more inflationary than another. Yet the world economy is not only an ordered list. It is a connected system of flows, corridors, cycles and residual circulation. The Hodge-econometric manuscript formulates this issue directly by asking whether the world economy can be represented as a regional macro-flow network whose directed edge-pressure field can be decomposed into gradient hierarchy, curl-based local imbalance and harmonic systemic circulation.

The research problem is therefore whether economic structure can be decomposed rather than merely ranked. The Hodge model starts from public regional macroeconomic anchors, constructs a weighted graph of ten macro-regional nodes with a World normalization anchor and preserves the Caucasus as an explicit corridor-sensitive subregional node. The resulting graph is not only a visualization; it is the object on which discrete Hodge decomposition, spectral diagnostics, higher-order Hodge-Laplacian analysis, machine-learning validation and persistent-homology confirmation are performed. In the reported benchmark, the graph is connected and cycle-rich, and the Hodge energy decomposition separates macro-flow pressure into gradient hierarchy, curl imbalance and harmonic circulation.

This creates a key monograph-level problem: economic systems contain hierarchy, but hierarchy is not the whole system. They contain local cycle imbalances, but local cycles do not exhaust systemic circulation. They contain persistent harmonic components that remain after hierarchy and local curl are removed. Without a topological decomposition grammar, these layers are analytically collapsed. The monograph therefore treats topology as a necessary dimension of economic complexity measurement.

1.3.5. The Curvature and Threshold Problem: From Local Stress to Systemic Transmission

The third dimension is curvature and threshold. Some economic disturbances remain local, while others become systemically transmissible. Conventional indicators can report stress levels, and standard network measures can report connectivity, but neither automatically identifies when a local disturbance crosses a threshold into systemic propagation. The Yang-Mills-inspired manuscript formulates this as a finite-network gauge-econometric problem. Public macroeconomic anchors are transformed into systemic stress, corridor-weighted adjacency, stress-weighted matrices, anti-symmetric gauge potential, triangular curvature, Yang-Mills economic action, stress Laplacian, Economic Mass Gap Index, fragility, BridgeStress and scenario diagnostics.

The central research problem here is whether a finite corridor-sensitive economic network contains a measurable spectral separation that can function as an economic shock-threshold analogue. In the Yang-Mills benchmark, ten nodes and twenty-seven weighted undirected edges generate a positive finite-network economic mass gap, with reported stress curvature and action concentration identifying where systemic stress-energy accumulates. This is not a physical field-theory claim. It is an economic measurement problem: how can the transition from local disturbance to systemic vulnerability be represented through network curvature, action concentration and spectral protection?

The monograph extends this problem beyond Yang-Mills alone. Curvature also appears in the Perelman-Ricci-Poincare inequality chapter, where inequality pressure and smoothing capacity are treated through curvature-like deformation, entropy-like complexity and graph connectedness. Curvature therefore becomes a broader research category: it measures deformation, imbalance and systemic stress geometry. The core problem is how to measure such curvature without converting mathematical analogy into literal theorem transfer.

1.3.6. The Rank Problem: Local Signals and Global Structural Formation

The fourth dimension is rank. Economic rankings often begin with GDP, GDP per capita, growth or market size. These indicators are important but incomplete. A region can be large in output but less central in corridor stress; another can be smaller but structurally important because it sits at a transmission interface. The BSD-inspired manuscript turns this issue into a local-to-global measurement problem. It constructs regional economic curve coefficients, discriminant diagnostics, finite-state trace analogues, Euler-factor analogues, an economic L-function, an L-order measure and a structural-rank object built from productive, Hodge-flow, network and agentic components.

The research problem here is whether local regional information, formalized through finite-state reductions and Euler-factor-like objects, contains measurable information about global structural rank formation. The empirical architecture uses a World normalization anchor and ten macro-regional or corridor-sensitive nodes, together with an N = 150 regional-year closure layer for calibration, robustness diagnostics and claim discipline. The resulting problem is not to prove the classical Birch-Swinnerton-Dyer conjecture. It is to determine whether an economic local-to-global architecture can distinguish output mass, absorption capacity, locked capacity, corridor leverage and systemic transmission exposure.

At the monograph level, the rank problem is a central bridge between the topological and empirical dimensions of the book. Hodge shows that macro-flow structure decomposes. Yang-Mills shows that stress can cross thresholds. BSD asks how local signals become global rank. This makes rank not a simple ordering but a constructed structural object whose measurement requires calibration, anti-circularity safeguards, placebo logic and external-proxy caution.

1.3.7. The Spectral-Signal Problem: Inflation, Cycles and Forecast Deformation

The fifth dimension is spectral signal. Inflation forecasting has become difficult because global inflation is not generated by smooth persistence alone. It is affected by macro-financial pressure, policy reaction, liquidity instability, supply stress, energy-food shocks, labour pressure, financial stress and nonlinear crisis deformation. The Riemann-zeta FPAS+zeta manuscript formulates this as a hybrid structural-spectral forecasting problem. A structural FPAS baseline is augmented by a normalized zeta critical-line cyclical signal transformed into a signed and alpha-calibrated forecast correction.

The research problem is whether a mathematically explicit spectral-cyclical signal can improve global aggregate inflation forecasting under disciplined layered validation. The empirical architecture is deliberately stratified: the principal annual validation layer covers 1970-2024 with N = 55; the robustness layer covers 1980-2024 with N = 45; the crisis-era annual comparison covers 2005-2024 with N = 20; the quarterly dynamic-validation layer covers 2000Q1-2024Q4 with N = 100; and the monthly spectral-diagnostics layer covers 2005M1-2024M12 with N = 240. This sample hierarchy prevents methods estimated on different temporal resolutions from being conflated.

At the monograph level, the spectral-signal problem asks how economic forecasting can incorporate nonlinear cyclical information without overclaiming mathematical proof or universal forecast dominance. The Riemann-zeta chapter does not verify the Riemann Hypothesis. It uses zeta logic as a controlled signal-construction grammar. This is essential for the

broader research problem because economic complexity is not only spatial, networked or structural; it is also spectral, cyclical and regime-sensitive.

1.3.8. The Computational-Complexity Problem: Feasibility, Search and Certification

The sixth dimension is computational complexity. Many economic decisions are not solved simply by estimating preferences or optimizing a smooth continuous function. Real constraints often introduce discrete choices: which industries to include, which assets to hold, which routes to select, which projects to finance or which constraints to impose. The P-vs-NP-inspired portfolio manuscript turns this into a concrete computational-finance problem by integrating Markowitz mean-variance logic, CAPM expected-return priors, cardinality-constrained support selection, heuristic search, reduced exact benchmarking, robustness diagnostics and a Black-Scholes derivative-pricing overlay.

The research problem is that sparse portfolio design is mixed discrete-continuous. In the full empirical universe, the fixed Damodaran January 2026 U.S. industry dataset contains ninety-four industry portfolios after excluding aggregate market rows. A baseline K = 10 support-selection problem produces C(94,10) = 9,041,256,841,903 possible supports before continuous weights are optimized. This support-space explosion makes naive enumeration infeasible in the full universe and justifies a layered comparison of greedy search, Monte Carlo sampling, genetic algorithms and GA-plus-continuous reoptimization. Exact evidence is supplied only in a reduced n = 20, K = 6 benchmark, where all 38,760 supports can be enumerated.

At the monograph level, the computational-complexity problem shows why economic measurement must include feasibility and certification. A model may be theoretically defined but computationally unreachable. A heuristic may find a strong incumbent but not certify global optimality. A derivative overlay may improve apparent performance but introduce leverage and risk-exposure issues. Therefore, the core research problem includes not only what should be measured but also whether it can be searched, verified, falsified and bounded.

1.3.9. The Inequality-Deformation Problem: Pressure, Smoothing and Connectedness

The seventh dimension is inequality deformation. Conventional inequality analysis often begins with the Gini coefficient or a small group of macro-social indicators. These are necessary, but they do not explain how income distribution, productivity, investment, unemployment, inflation, technology access, fiscal stress, social protection, migration pressure, innovation and trade connectivity interact as a coupled macro-regional system. The Perelman-Ricci-Poincare-inspired manuscript formulates this as a global inequality diagnostic problem in which the world economy is treated as a pressure-smoothing manifold rather than as a collection of isolated inequality indicators.

The empirical architecture uses ten macro-regional blocks over 2010-2024 and sixteen stress-coordinate variables, producing a balanced diagnostic panel of N = 150 region-year observations. Raw macro-social indicators are transformed onto a common pressure-oriented 0-100 scale and used to construct a correlation-based metric tensor, Ricci-style component curvature, normalized Ricci-flow summaries, world-weighted scalar curvature, Perelman-type F- and W-functionals, graph connectedness diagnostics, Betti numbers, network-curvature proxies, counterfactual sensitivity tests and econometric validation layers. This design allows inequality to be read as a deformation and smoothing problem rather than as a one-dimensional ranking.

At the monograph level, this chapter clarifies that complexity is also social and distributive. It is not enough to measure flows, networks, thresholds, rank, forecasts or portfolio search. A complete economic complexity program must also measure whether pressure accumulates in social and macro-regional coordinates, whether smoothing capacity improves after shocks and whether the diagnostic system remains connected, dense and looped. The inequality-deformation problem is therefore a necessary counterpart to the financial, topological, spectral and computational dimensions.

1.3.10. The Local-to-Global Problem as the Monograph's Integrating Logic

Although each problem-inspired model has its own domain, the monograph’s deepest integrating logic is local-to-global measurement. The global economy is not observed directly as one simple object. It is assembled from local signals: country-year stress, regional pressure, edge-level flow, triangular cycles, finite-state traces, asset-support choices, forecast deviations, corridor exposures and inequality coordinates. The scientific challenge is to determine when these local signals contain information about global structure and when they remain merely local diagnostics.

BSD gives the most explicit local-to-global grammar through finite-state reductions, Euler-factor analogues, an economic L-function and structural rank. Hodge gives a decomposition grammar in which edge-level pressures aggregate into gradient, curl and harmonic components. Yang-Mills gives a threshold grammar in which local curvature and action concentration affect spectral protection. Navier-Stokes gives a flow grammar in which component stress terms form a global

stress balance. Riemann-zeta gives a spectral grammar in which local cyclical deviations affect inflation forecasts. P-vs-NP gives a computational grammar in which local support choices define the feasible search space. Ricci-Poincare gives a deformation grammar in which component pressures shape global inequality curvature and connectedness.

The monograph's core problem can therefore be restated as follows: how can local economic signals be transformed into global diagnostic objects without losing information, overstating causality or violating the claim boundaries imposed by mathematical analogy and empirical evidence? This question is the common thread linking all seven chapters. The book is not only about seven models. It is about the conditions under which local economic measurements can be made meaningful at systemic scale.

1.3.11. The Evidence Problem: Measurement without Overclaiming

The monograph's core research problem also includes an evidence problem. Mathematical analogies are powerful, but they are scientifically risky if their empirical status is not clearly bounded. Each of the seven studies therefore imposes a claim discipline that must be preserved at the book level. Navier-Stokes supports a global stress-testing architecture but not a physical-fluid law or a universal crisis-prediction theorem. Yang-Mills supports a finite-network mass-gap analogue but not the Clay Yang-Mills theorem. Hodge supports regional benchmark decomposition but not a proof of the Hodge conjecture. BSD supports calibrated local-to-global rank measurement but not proof, test or replication of the classical conjecture. Riemann-zeta supports layered inflation-forecast improvement but not verification of the Riemann Hypothesis. P-vs-NP supports computational-finance evidence and reduced exact benchmarking but not a proof of P != NP or certified full-universe optimality. Perelman-Ricci-Poincare supports inequality-curvature diagnostics but not a theorem-level transfer of geometric topology.

This evidence problem is not secondary. It is part of the research design. The monograph must be mathematically ambitious and empirically disciplined at the same time. Its claims must be sorted into categories: benchmark measurement, panel diagnostics, forecasting validation, computational demonstration, scenario evidence, robustness evidence, external-proxy screening and future validation pathway. The absence of theorem-level proof is not a weakness; it is the boundary condition that allows the economic models to be scientifically credible.

Therefore, the core research problem is not simply how to build seven analogues. It is how to build them under a reviewer-safe evidence hierarchy. Each chapter must show what it measures, what it validates, what it only screens, what it cannot prove and what remains for future replication. The monograph's contribution depends on this discipline.

1.3.12. Formal Monograph-Level Problem Statement

The formal research problem of the monograph may be stated as follows: contemporary economic science lacks a unified, claim-bounded mathematical-econometric architecture for measuring global economic complexity when that complexity appears simultaneously as liquidity flow, macro-financial pressure, topological circulation, curvature-like deformation, systemic shock threshold, local-to-global structural rank, spectral-cyclical inflation dynamics and computational decision infeasibility. Existing indicators and conventional models are useful but fragmented. They usually measure one surface of the system at a time and therefore cannot fully explain how local signals become global stress, how regional nodes become structurally important, how inequality pressure deforms and partially smooths, how shocks cross systemic thresholds, how inflation cycles deviate under nonlinear stress or how portfolio choice becomes computationally explosive.

The monograph addresses this problem by developing seven bounded economic-econometric analogues inspired by the Clay Millennium Problems. The objective is not to solve those mathematical problems, but to use their formal architectures as measurement grammars. Each grammar corresponds to a specific economic complexity dimension: Navier-Stokes to flow and closure; Yang-Mills to curvature, action and threshold; Hodge to decomposition; BSD to local-to-global rank; Riemann-zeta to spectral-cyclical forecasting; P-vs-NP to computational feasibility; and Perelman-Ricci-Poincare to inequality deformation, entropy and connectedness.

The monograph's scientific problem is therefore twofold. First, it must construct and interpret seven problem-specific empirical architectures that are rigorous within their own domains. Second, it must integrate them into one coherent research program that explains why flow, topology, rank, curvature, spectral signal, optimization complexity and local-to-global logic are jointly necessary for measuring modern economic complexity. This is the central task of the book.

1.3.13. Core Research Problem Matrix

Table 1.3 translates the monograph-level research problem into seven operational sub-problems. The table is designed for the book chapter as a compact analytical map linking each mathematical grammar to a concrete economic measurement gap, empirical architecture and admissible claim level.

Dimension of complexity	Problem-inspired grammar	Economic measurement gap	Empirical architecture in the source manuscripts	Admissible monograph-level claim
Flow and systemic stress	Navier-Stokes	Separate macro-financial indicators do not reveal the joint formation of liquidity weakness, pressure, friction, shocks and closure.	100-country annual panel, 2010-2024, N = 1,500; rolling validation, benchmarks, Monte Carlo and policy counterfactuals.	Global macro-financial stress-testing architecture with diagnostic, forecast and scenario evidence.
Topological macro-flow structure	Hodge	GDP and growth rankings do not decompose hierarchy, local-cycle imbalance and harmonic systemic circulation.	Ten regional nodes plus World anchor; directed pressure field; Hodge decomposition; spectral and persistent-homology diagnostics.	Regional benchmark measurement of decomposable macro-flow structure.
Curvature and shock threshold	Yang-Mills	Stress levels and centrality do not show when local disturbances become systemically transmissible.	Ten-node, twenty-seven-edge finite network; gauge potential, triangular curvature, action, stress Laplacian, EMGI, BridgeStress and scenarios.	Finite-network benchmark evidence for economic shock-threshold measurement.
Local-to-global structural rank	Birch-Swinnerton-Dyer	GDP mass does not explain how local regional signals and corridor conditions form global structural rank.	World anchor, ten regional/corridor nodes, N = 150 closure layer, finite-state traces, Euler factors, LOrder and structural rank.	Calibrated local-to-global measurement claim, not causal or theorem-level confirmation.
Spectral-cyclical forecasting	Riemann-zeta	Pure persistence and structural baselines can underperform during nonlinear inflation-pressure regimes.	Annual N = 55, robustness N = 45, crisis N = 20, quarterly N = 100, monthly N = 240; FPAS+zeta vs FPAS and ARIMA.	Layered forecast-diagnostic evidence for global inflation modelling.
Computational feasibility	P versus NP	Continuous portfolio optimization hides the discrete support-selection explosion created by cardinality constraints.	Damodaran January 2026 n = 94 industries, K = 10, C(94,10) supports; exact reduced n = 20, K = 6 enumeration.	Computational-finance demonstration with heuristic search and reduced exact certification.
Inequality deformation and smoothing	Poincare / Ricci / Perelman	Single inequality indicators do not capture pressure, smoothing capacity,	Ten macro-regional blocks, 2010-2024, sixteen stress coordinates, N = 150	Macro-regional inequality-curvature diagnostic architecture.

		curvature, entropy and graph connectedness.	panel, F/W functionals, graph topology and validation.	

1.3.14. Source-Integration Map for Section 1.3

The following map records the source manuscripts used to construct this subsection. The section does not mechanically copy the separate article introductions. It rewrites their problem statements into one monograph-level research problem while preserving each study's core measurement role.

Source manuscript	Problem-statement element preserved	Where it appears in Section 1.3	How it is generalized in the monograph
Navier-Stokes-Inspired Global Liquidity-Flow and Systemic-Stress Modelling	Global stress arises from interacting liquidity, pressure, friction, shock and closure channels.	1.3.3 and the core matrix.	Flow becomes one of the seven required dimensions of economic complexity.
Global Hodge-Econometric Modeling of the World Economy	The world economy requires decomposition into hierarchy, imbalance and circulation.	1.3.4 and the topology matrix row.	Topology becomes a necessary complement to scalar macroeconomic indicators.
Economic Yang-Mills Mass Gap in Global and Corridor Flow Networks	Corridor stress requires curvature, action and threshold measurement.	1.3.5 and the curvature-threshold matrix row.	Finite-network stress transmission becomes the systemic-threshold dimension.
Regional Economic Birch-Swinnerton-Dyer Modelling	Regional structure is a local-to-global rank-formation problem.	1.3.6 and 1.3.10.	Rank becomes a calibrated structural object rather than a GDP ordering.
Global Riemann-Zeta FPAS+zeta Inflation Forecasting	Inflation forecasting requires structural-spectral, regime-sensitive validation.	1.3.7 and the spectral-signal matrix row.	Spectral signal becomes the temporal/cyclical dimension of economic complexity.
Robust Portfolio Optimization under Computational Complexity	Sparse portfolio choice is a combinatorial support-selection problem.	1.3.8 and the computational-complexity matrix row.	Optimization feasibility becomes part of economic measurement, not only implementation.
Global Perelman-Ricci-Poincare-Inspired Inequality Diagnostics	Inequality pressure requires curvature, entropy, smoothing capacity and connectedness.	1.3.9 and the inequality-deformation matrix row.	Distributional structure becomes a deformation and smoothing problem within global complexity.

1.3.15. Transition to the Research Aim and Objectives

The monograph's core research problem leads directly to the aim and objectives stated in the next subsection. If global economic complexity appears simultaneously as flow, topology, curvature, rank, spectral signal, computational infeasibility and inequality deformation, then the book cannot have a narrow single-model aim. Its aim must be integrative: to construct, validate and comparatively interpret seven bounded economic-econometric architectures inspired by the Clay Millennium Problems. Section 1.4 will therefore translate the problem defined here into the monograph's general aim, specific objectives and evidence hierarchy.

1.4. Research Aim and Objectives of the Monograph

1.4.1. General Research Aim of the Monograph

The general aim of this monograph is to develop, organize and comparatively interpret a seven-part economic-econometric research program inspired by the Clay Mathematics Institute Millennium Problems. The purpose is not to solve the original mathematical problems, to test them empirically or to replace their theorem-level meaning with economic metaphor. The purpose is to translate their formal architectures into bounded measurement grammars for global economic complexity,

systemic stress, topological flow structure, regional rank formation, inflation-cycle diagnostics, inequality deformation and computational decision limits.

At the book level, the aim is integrative rather than article-specific. Each source manuscript develops one specialized analogue: a Perelman-Ricci-Poincare-inspired inequality diagnostic framework; a Hodge-econometric macro-flow decomposition framework; a Navier-Stokes-inspired global liquidity-flow and systemic-stress framework; a finite-network Yang-Mills mass-gap framework for corridor shock thresholds; a Birch-Swinnerton-Dyer-inspired local-to-global structural-rank framework; a Riemann-zeta FPAS+zeta inflation-forecasting framework; and a P-vs-NP-inspired portfolio-optimization framework. The monograph's aim is to bring these seven architectures into a single scientific system while preserving the methodological distinctiveness of each.

The central aim may therefore be stated as follows: to construct a unified, claim-bounded and empirically auditable Millennium Economic Research Program in which seven mathematical problem architectures are used as disciplined economic measurement grammars for observing the global economy as a system of flows, networks, ranks, curvatures, spectra, computational constraints and local-to-global transformations.

1.4.2. From Seven Article-Level Aims to One Book-Level Aim

The seven source manuscripts have different immediate research aims. The Perelman-Ricci-Poincare manuscript aims to measure macro-regional inequality pressure, smoothing capacity, curvature-like deformation, entropy-like complexity and graph connectedness. The Hodge manuscript aims to measure the world economy as a connected topological macro-flow system decomposable into hierarchy, local-cycle imbalance and harmonic systemic circulation. The Navier-Stokes manuscript aims to measure global systemic stress through a nondimensional flow-pressure-friction-shock-cycle-closure balance. The Yang-Mills manuscript aims to measure systemic shock thresholds in a finite global-corridor stress network through gauge potential, curvature, action and spectral separation. The BSD manuscript aims to measure regional structural-rank formation through local finite-state information, Euler-factor analogues, an economic L-function and LOrder. The Riemann-zeta manuscript aims to evaluate whether a normalized zeta-cycle signal improves global inflation forecasts when embedded in a structural FPAS baseline. The P-vs-NP manuscript aims to measure the computational and financial consequences of cardinality-constrained portfolio optimization under a sparse support-selection problem.

The monograph does not erase these separate aims. Instead, it reorganizes them under a higher-order objective. The seven studies become chapters inside a single research program because they each address a different measurement failure in conventional economic analysis. Standard indicators are indispensable, but they tend to separate variables that are structurally coupled: liquidity from pressure, inflation from spectral deformation, inequality from smoothing capacity, regional output from network position, portfolio return from computational feasibility, corridor exposure from shock thresholds, and local regional signals from global structural rank.

The book-level aim is therefore not merely cumulative. It is synthetic. It asks whether economic science can be expanded by treating mathematical architectures as measurement grammars. A grammar, in this sense, is not a borrowed metaphor. It is a disciplined rule system that tells the analyst what kinds of objects can be constructed, which variables can be transformed, what forms of validation are appropriate, and what claims must remain excluded.

1.4.3. Conceptual Aim: Seven Measurement Grammars for Global Complexity

Conceptually, the monograph aims to show that global economic complexity cannot be adequately understood through one mathematical or econometric language alone. Flow, topology, rank, curvature, spectral signal, computational feasibility and local-to-global correspondence are not interchangeable. They reveal different structural dimensions of the economy. The Navier-Stokes-inspired grammar is appropriate for stress-balance, liquidity movement, pressure gradients and closure. The Hodge grammar is appropriate for decomposing directed macro-flow pressure into hierarchy, local imbalance and persistent circulation. The Yang-Mills grammar is appropriate for curvature, action concentration and local-to-systemic threshold measurement. The BSD grammar is appropriate for local-to-global structural-rank formation. The Riemann-zeta grammar is appropriate for spectral-cyclical forecast correction. The P-vs-NP grammar is appropriate for computational infeasibility and mixed discrete-continuous decision systems. The Perelman-Ricci-Poincare grammar is appropriate for inequality deformation, smoothing capacity, entropy-like complexity and connectedness.

The conceptual aim is thus to establish a plural but coherent mathematical-econometric vocabulary. The monograph seeks to show that each Millennium-inspired grammar performs a distinct analytical function: one measures motion, another decomposition, another curvature, another rank, another cycles, another feasibility, and another deformation. Together they

create a broader language for global economic systems that are nonlinear, networked, shock-sensitive, data-constructed and computationally constrained.

This conceptual aim also protects the book from overextension. Because each grammar has a defined role, no chapter is required to explain everything. The Hodge chapter is not asked to forecast inflation. The Riemann-zeta chapter is not asked to solve portfolio optimization. The P-vs-NP chapter is not asked to diagnose inequality curvature. The BSD chapter is not asked to replace liquidity stress testing. Scientific strength comes from matching each mathematical grammar to the economic object it can responsibly measure.

1.4.4. Empirical Aim: A Multi-Layered Evidence Architecture

Empirically, the monograph aims to consolidate seven heterogeneous but compatible evidence architectures. These architectures do not share one sample design, because their economic objects are different. The Navier-Stokes framework uses a 100-country annual panel over 2010-2024, supported by World and macro-regional layers, rolling validation, external-target checks and Monte Carlo counterfactuals. The Perelman-Ricci-Poincare and BSD frameworks use macro-regional N = 150 diagnostic or closure layers. The Hodge and Yang-Mills frameworks use completed regional or finite-network benchmark systems, with graph, spectral and topological diagnostics. The Riemann-zeta framework uses annual, quarterly and monthly validation layers for global inflation forecasting. The P-vs-NP framework uses an industry-level computational-finance universe with a full n = 94 support-selection problem and an exact reduced enumeration benchmark.

The empirical aim is not to force these designs into artificial uniformity. It is to classify them correctly. Some chapters produce large-panel diagnostic evidence. Some produce benchmark structural evidence. Some produce layered forecast-validation evidence. Some produce exact reduced computational evidence. Some produce calibrated local-to-global correspondence. The book-level aim is to create an evidence hierarchy that allows each chapter to make the strongest admissible claim without upgrading diagnostic or benchmark evidence into theorem-level proof or unrestricted causality.

This empirical aim is particularly important because the monograph is interdisciplinary. Advanced mathematical language can become scientifically fragile if not paired with transparent empirical boundaries. Therefore, the book aims to preserve data-status discipline: public data anchors remain distinguished from author-calculated constructs; normalization and transformation rules remain visible; small-sample benchmark claims remain separated from panel-validation claims; and future validation pathways are identified rather than treated as already completed.

1.4.5. Methodological Aim: From Analogy to Auditable Measurement

Methodologically, the monograph aims to convert analogy into auditable measurement. The word analogy is not used as a license for loose comparison. It is used to describe a formal translation from mathematical structure into economic modelling architecture. In each chapter, the translation must pass through a reproducible sequence: empirical object definition, data boundary, variable transformation, mathematical construction, econometric or computational validation, robustness screening, interpretation and claim discipline.

The Perelman-Ricci-Poincare framework translates inequality variables into pressure-oriented coordinates, curvature summaries, F- and W-functional analogues, graph connectedness and counterfactual sensitivity. The Hodge framework translates public regional anchors into a weighted graph, directed pressure field, edge cochain and decomposed gradient/curl/harmonic components. The Navier-Stokes framework translates macro-financial proxies into nondimensional stress terms, balance equations, restricted closure, Fourier cycle forcing and stress-testing diagnostics. The Yang-Mills framework translates regional stress into gauge potential, triangular curvature, action, Laplacian spectral gap, EMGI and BridgeStress. The BSD framework translates regional public anchors into economic curves, finite-state traces, Euler factors, L-function behavior, LOrder and structural rank. The Riemann-zeta framework translates macro-financial pressure into a nonlinear tau argument, critical-line zeta signal, normalized zeta-cycle, correction gate and layered forecast tests. The P-vs-NP framework translates a fixed industry universe into CAPM priors, covariance geometry, combinatorial support growth, heuristic search, exact reduced certification and derivative-overlay realism.

The methodological aim of the monograph is to make these transformations readable as one research program. The book therefore seeks to standardize the logic of transparency: every constructed object must have a declared empirical role, every validation result must have an evidence status, every limitation must be explicit, and every mathematical reference must remain within its economic claim boundary.

1.4.6. Interpretive Aim: Building a Comparative Economic Meaning

The interpretive aim of the monograph is to explain what the seven models jointly reveal about the global economy. Each study produces local findings, but the book must convert them into a higher-level interpretation. The Perelman-Ricci-

Poincare model reveals that inequality pressure has deformation, smoothing and entropy-like dimensions. The Hodge model reveals that global macro-flow pressure decomposes into hierarchy, imbalance and systemic circulation. The Navier-Stokes model reveals that macro-financial stress is formed through interacting flow, pressure, friction, shock and closure channels. The Yang-Mills model reveals that systemic shock transmission can be represented through curvature/action concentration and spectral threshold logic. The BSD model reveals that local regional signals can contain information about global structural-rank formation. The Riemann-zeta model reveals that spectral-cyclical signals may improve inflation forecasting under layered validation. The P-vs-NP model reveals that economic optimization can become computationally difficult before financial interpretation even begins.

The book-level interpretive aim is to avoid treating these findings as isolated technical outputs. Instead, they should be read as evidence that economic systems require multiple levels of measurement. A policy analyst, macroeconomist, financial economist or regional strategist cannot rely only on scale, averages or linear coefficients. The relevant system may be large but fragile, small but strategic, topologically central but low in GDP mass, forecastable only through layered signals, or computationally infeasible despite clear objective functions.

This interpretive aim is also cautionary. The monograph seeks to produce a strong research program without inflating its claims. The models are designed to interpret economic complexity, not to announce direct solutions to the original Millennium Problems. Their contribution lies in formal measurement, diagnostic interpretation, forecasting discipline, computational evidence and replication logic.

1.4.7. General Objectives of the Monograph

The monograph operationalizes its general aim through a set of integrated objectives. These objectives are book-level objectives, not a simple repetition of the seven article-level objective lists. They identify what the monograph must accomplish as a unified scientific work.

1. To formulate the Clay Millennium Problems as seven bounded economic-econometric measurement grammars rather than as direct mathematical proof claims.
2. To establish a unified research design in which global complexity is measured through flow, topology, curvature, rank, spectral signal, computational feasibility, inequality deformation and local-to-global transmission.
3. To consolidate the seven article-level empirical architectures into one monograph-level evidence framework while preserving the correct sample boundaries and data-status distinctions of each study.
4. To define public data anchors, author-calculated variables, normalization rules, constructed indices and transformation sequences as transparent methodological objects rather than implicit assumptions.
5. To measure macro-financial systemic stress through nondimensional liquidity-flow, pressure-gradient, friction, shock, cycle and restricted-closure logic.
6. To measure global macro-flow structure through graph construction, directed pressure fields, Hodge decomposition, spectral diagnostics, resilience indices and topological validation.
7. To measure systemic shock thresholds in corridor-sensitive networks through gauge potential, triangular curvature, Yang-Mills economic action, stress Laplacians, economic mass-gap logic, EMGI, fragility and BridgeStress.
8. To measure regional structural-rank formation through local finite-state reductions, economic curve coefficients, discriminant screening, Euler-factor analogues, economic L-function behavior, LOrder and rank calibration.
9. To measure global inflation pressure and forecast improvement through FPAS reconstruction, zeta-cycle signal extraction, alpha-weighted correction, layered annual/quarterly/monthly validation and benchmark comparison.
10. To measure computational difficulty in portfolio optimization through cardinality constraints, combinatorial support-space growth, heuristic search, exact reduced enumeration, covariance robustness and derivative-overlay realism.
11. To measure inequality deformation and smoothing capacity through pressure-oriented stress coordinates, Ricci-style curvature, Perelman-type functionals, graph connectedness, Betti diagnostics, counterfactual sensitivity and econometric validation.
12. To compare the seven models under a common evidence hierarchy that distinguishes benchmark measurement, panel diagnostics, forecast validation, computational certification, calibrated correspondence, scenario evidence and future-validation pathways.
13. To develop a reviewer-safe claim-boundary protocol that prevents economic analogues from being misread as theorem-level proof, unrestricted causal inference or universal predictive dominance.

14. To provide a foundation for future all-country, dyadic-flow, multilayer, sectoral, firm-level, financial-market and longitudinal extensions of the Millennium Economic Research Program.

1.4.8. Problem-Specific Objective Domains within the Unified Aim

Although the monograph has one general aim, each Millennium-inspired chapter preserves a distinct objective domain. The following synthesis keeps the substantive weight of the seven source manuscripts while expressing their aims in book-level language.

Perelman-Ricci-Poincare objective domain. To diagnose global inequality as a pressure-smoothing and curvature-deformation system by constructing macro-regional stress coordinates, Ricci-style curvature, Perelman-type F- and W-functionals, graph-topological connectedness, bottleneck proxies, Ricci-surgery rankings, counterfactual sensitivity and diagnostic validation.

Hodge objective domain. To decompose the world economy as a regional macro-flow network by building a weighted graph, converting public macroeconomic anchors into a directed pressure field, applying discrete Hodge decomposition, and interpreting gradient hierarchy, curl imbalance and harmonic circulation as economically meaningful structural components.

Navier-Stokes objective domain. To measure global systemic stress as a nondimensional liquidity-flow balance in which velocity weakness, acceleration pressure, macro-financial gradients, friction/diffusion, stochastic shocks, GDP-cycle forcing and restricted hidden adjustment jointly produce stress and resilience diagnostics.

Yang-Mills objective domain. To measure finite-network systemic shock thresholds by constructing a corridor-weighted stress graph, anti-symmetric gauge potential, triangular curvature, Yang-Mills economic action, stress Laplacian, economic mass-gap index, fragility, BridgeStress and scenario-based local-to-systemic transition tests.

Birch-Swinnerton-Dyer objective domain. To measure regional structural-rank formation through a local-to-global architecture in which World-normalized anchors, systemic stress, network structure, economic curve coefficients, discriminants, finite-state traces, Euler factors, L-function behavior and LOrder are compared with a constructed structural-rank object.

Riemann-zeta objective domain. To evaluate whether a normalized critical-line zeta-cycle signal improves global aggregate inflation forecasting when embedded in a structural FPAS baseline and tested through layered annual, quarterly and monthly validation against FPAS and ARIMA benchmarks with residual, spectral and regime diagnostics.

P-vs-NP objective domain. To show how cardinality-constrained portfolio selection transforms mean-variance finance into a mixed discrete-continuous computational problem by combining CAPM expected returns, covariance geometry, support-space explosion, heuristic search, exact reduced enumeration, transaction-cost and derivative-overlay realism.

1.4.9. Aim-Objective Translation Matrix

Table 1.4 summarizes how the separate aims of the seven manuscripts are translated into the unified aim and objectives of the monograph. The table is not a replacement for the detailed chapters; it is a navigational device that clarifies why the book has one general aim and seven distinct methodological routes.

Source manuscript	Article-level aim	Book-level objective domain	Primary methodological objects	Claim discipline
Perelman-Ricci-Poincare inequality diagnostics	Measure inequality pressure, smoothing capacity, curvature, entropy and graph connectedness.	Inequality deformation and smoothing-capacity measurement.	N = 150 region-year panel; sixteen stress coordinates; Ricci-style curvature; F/W functionals; Betti and graph diagnostics.	Diagnostic measurement, not theorem proof or unrestricted causality.
Global Hodge-econometric modelling	Measure the world economy as a connected topological macro-flow system.	Topological decomposition of global macro-flow structure.	Regional graph; directed edge pressure; gradient, curl and harmonic components; spectral and persistent-homology	Benchmark structural validation, not country-level universal causality.

			diagnostics.	
Navier-Stokes global liquidity-flow modelling	Measure systemic stress through flow, pressure, friction, shocks, cycle and closure.	Macro-financial stress-testing and liquidity-flow diagnostics.	100-country panel; nondimensional variables; restricted epsilon closure; rolling forecasts; FE diagnostics; external targets.	Strong diagnostic stress-testing, not physical law or universal crisis prediction.
Yang-Mills economic mass gap	Measure systemic shock thresholds in global and corridor flow networks.	Curvature/action and finite-network threshold measurement.	10 nodes, 27 edges; gauge potential; triangular curvature; action; stress Laplacian; EMGI; BridgeStress; scenarios.	Finite-network benchmark claim; final country-panel causality reserved.
Economic Birch-Swinnerton-Dyer modelling	Measure local-to-global structural-rank formation under corridor stress.	Regional rank formation and local-to-global calibration.	World anchor; 10 nodes; N = 150 closure layer; traces; Euler factors; LOrder; structural rank; anti-circularity checks.	Calibrated measurement, not BSD proof, causal law or strong external confirmation.
Riemann-zeta FPAS+zeta forecasting	Test whether zeta-cycle correction improves global inflation forecasts.	Spectral-cyclical forecast-diagnostic measurement.	N = 55, 45, 20 annual layers; N = 100 quarterly; N = 240 monthly; FPAS+zeta; DM/CW; HMM; wavelet.	Bounded forecast improvement; no Riemann Hypothesis proof or universal dominance.
P-vs-NP portfolio optimization	Evaluate sparse portfolio selection under computational complexity.	Computational feasibility in economic decision systems.	n = 94 industries; K = 10; C(94,10) supports; greedy, Monte Carlo, GA; exact n = 20, K = 6 benchmark; option overlay.	Computational-finance evidence; no P vs NP theorem proof or certified full n = 94 optimum.

1.4.10. Hierarchy of Objectives: Measurement, Validation, Interpretation and Replication

The objectives of the monograph can be read through four hierarchical layers. The first layer is measurement: each chapter constructs a new object that is not directly available in conventional datasets, such as stress curvature, harmonic circulation, LOrder, zeta-cycle correction or computational support-space growth. The second layer is validation: each constructed object is tested through the strongest appropriate evidence available for its empirical design. The third layer is interpretation: each validated object is translated into an economic meaning that distinguishes mass, stress, resilience, rank, deformation, threshold, cycle or feasibility. The fourth layer is replication: every chapter is placed inside a data and claim-boundary framework that allows later extension without converting preliminary, diagnostic or benchmark results into stronger claims than the evidence permits.

This hierarchy is essential because the monograph includes different kinds of evidence. A large panel result cannot be judged in the same way as an exact reduced enumeration. A finite-network spectral result cannot be judged as if it were a country-level causal panel estimate. A forecast-improvement result cannot be generalized beyond its validation layers without additional evidence. A local-to-global rank correspondence cannot be interpreted as a theorem. The objective hierarchy therefore protects the monograph from category error while preserving the scientific value of each chapter.

1.4.11. Expected Contribution of the Aim-Objective System

If achieved, the aim-objective system of the monograph will contribute at three levels. At the theoretical level, it will show that the Clay Millennium Problems can be used as disciplined sources of economic measurement grammars without claiming mathematical resolution. At the methodological level, it will establish a multi-model architecture that links public data anchors, constructed variables, mathematical transformations, econometric validation, computational experiments, robustness screens and claim boundaries. At the empirical level, it will organize evidence on global inequality pressure, macro-flow topology, liquidity stress, corridor shock thresholds, structural rank, inflation forecasting and sparse portfolio optimization under one coherent framework.

The monograph therefore aims to make a broader claim about economic science: complex economies require not only more data, but better mathematical grammars for organizing data. The seven Millennium-inspired frameworks do not compete with standard macroeconomics, finance, inequality analysis or forecasting. They extend them by adding flow, topology, curvature, rank, spectral signal, computational feasibility and local-to-global logic as measurable structures.

1.4.12. Source-Integration Map for Section 1.4

The following map records how the seven source manuscripts informed the present section. The map is included to make clear that Section 1.4 is a monograph-level synthesis, not a mechanical compilation of article aims.

Source manuscript	Original aim/objective focus	Role in Section 1.4	Monograph-level synthesis
Perelman-Ricci-Poincare	Macro-regional inequality pressure, curvature, entropy and connectedness.	Defines the inequality-deformation objective domain.	Distributional complexity becomes one of the seven measurement dimensions.
Hodge	Topological macro-flow decomposition into gradient, curl and harmonic components.	Defines the decomposition and systemic-circulation objective domain.	Topology becomes a book-level method for seeing what GDP aggregates hide.
Navier-Stokes	Liquidity-flow stress balance, nondimensionalization and restricted closure.	Defines the systemic-stress and flow objective domain.	Flow becomes the stress-testing grammar of the monograph.
Yang-Mills	Gauge-econometric curvature, action, spectral gap and corridor threshold.	Defines the shock-threshold objective domain.	Curvature and spectral separation become system-transmission objectives.
BSD	Finite-state local signals, Euler factors, LOrder and structural-rank calibration.	Defines the local-to-global rank objective domain.	Rank formation becomes a calibrated system object rather than GDP ordering.
Riemann-zeta	FPAS+zeta inflation forecasting across annual, quarterly and monthly validation layers.	Defines the spectral-cyclical forecasting objective domain.	Forecasting becomes a layered signal-validation objective.
P-vs-NP	Sparse portfolio optimization, support-space explosion, heuristics and exact reduced benchmarking.	Defines the computational-decision objective domain.	Optimization feasibility becomes a core economic research objective.

1.4.13. Transition to Research Questions and Hypothetical Framework

The aim and objectives stated in this subsection prepare the next stage of the introduction. Once the monograph has defined its general aim and organized the seven objective domains, it must translate them into research questions and a general hypothetical framework. The next subsection should therefore ask how each measurement grammar is expected to perform: whether flow-balance logic improves stress interpretation, whether Hodge decomposition reveals hidden macro-flow structure, whether gauge curvature identifies systemic thresholds, whether BSD-inspired local signals align with structural rank, whether zeta-cycle corrections improve inflation forecasts, whether cardinality constraints generate computational

search difficulty, and whether Ricci-Poincare-style diagnostics reveal inequality deformation and smoothing capacity. These questions must remain book-level questions, not a repetition of seven article-level hypothesis lists.

1.5. Seven-Problem Translation Matrix

1.5.1. Purpose and Function of the Translation Matrix

The purpose of the Seven-Problem Translation Matrix is to define, at the beginning of the monograph, how the seven Clay Millennium Problems are converted into seven bounded economic measurement grammars. The matrix performs three functions. First, it prevents the reader from interpreting the book as a claim to solve the original mathematical problems. Second, it clarifies how each mathematical architecture contributes a different measurement language for economic complexity. Third, it assigns each problem to a specific book chapter so that the monograph has an explicit structural map rather than a loose sequence of independent articles.

The translation matrix is therefore both conceptual and editorial. Conceptually, it shows that the seven problems do not enter the book as theorem-level objects. They enter as disciplined modelling architectures: flow, curvature, topology, spectral signal, local-to-global rank, computational complexity and pressure-smoothing deformation. Editorially, it establishes the logic of the main chapters. Chapter 5 treats inequality deformation through the Perelman-Ricci-Poincare-inspired framework. Chapter 6 decomposes macro-flow structure through the Hodge-econometric framework. Chapter 7 measures liquidity-flow and systemic stress through the Navier-Stokes-inspired framework. Chapter 8 measures shock thresholds through the Yang-Mills finite-network framework. Chapter 9 measures regional structural rank through the Birch-Swinnerton-Dyer local-to-global framework. Chapter 10 studies inflation forecasting through the Riemann-zeta FPAS+zeta framework. Chapter 11 studies sparse portfolio optimization through the P-vs-NP computational-finance framework.

The matrix also establishes a common rule of interpretation: the economic translation is meaningful only when it is tied to data, formulas, transformations, diagnostics and claim boundaries. A mathematical name alone is not sufficient. Each chapter must specify its empirical object, its constructed variables, its validation layer and the level of claim that can legitimately be made. This is why the matrix is followed by expanded explanations for each of the seven problems.

1.5.2. Core Seven-Problem Translation Matrix

Table 1.5.1 presents the core structural map of the monograph. It is the primary navigation table for the book: each Clay problem is translated into a bounded economic-econometric architecture and assigned to the chapter where the full model is developed.

Clay Problem	Economic Translation	Book Chapter
Poincare / Ricci / Perelman logic	Inequality pressure, curvature, entropy, smoothing capacity	Chapter 5
Hodge	Macro-flow decomposition, gradient/curl/harmonic structure	Chapter 6
Navier-Stokes	Liquidity flow, pressure, friction, systemic stress	Chapter 7
Yang-Mills	Gauge curvature, action, mass-gap shock threshold	Chapter 8
Birch-Swinnerton-Dyer	Local-to-global structural rank, LOrder, corridor stress	Chapter 9
Riemann Hypothesis	Zeta-cycle, inflation forecasting, spectral diagnostics	Chapter 10
P vs NP	Portfolio optimization, cardinality, computational complexity	Chapter 11

Source: Author synthesis based on the seven source manuscripts and their chapter-level economic-econometric analogues.

1.5.3. Translation Principle: From Theorem-Level Problems to Measurement Grammars

The central methodological distinction behind the matrix is the distinction between a theorem-level problem and a measurement grammar. A theorem-level problem asks for a proof or disproof within mathematics. A measurement grammar provides a structured language for constructing empirical objects, transforming variables, defining diagnostics and disciplining claims. The monograph operates only in the second sense. It does not claim to prove the Riemann Hypothesis, resolve P vs NP, solve Navier-Stokes existence and smoothness, establish the Yang-Mills mass gap, prove the Hodge conjecture, prove the Birch-Swinnerton-Dyer conjecture or reproduce Perelman's theorem. It asks what economic measurement becomes possible when the formal logic of those problems is translated into bounded empirical architectures.

This translation is scientifically meaningful because each Millennium Problem is organized around a different structural difficulty. Navier-Stokes concerns flow, pressure, friction, forcing and closure. Yang-Mills concerns gauge structure, curvature, action and a positive threshold. Hodge concerns decomposition and the separation of structural components. BSD concerns local-to-global correspondence and rank formation. The Riemann Hypothesis concerns spectral regularity and critical-line signal structure. P vs NP concerns computational feasibility under discrete search. Perelman-Ricci-Poincare

logic concerns curvature, smoothing, entropy and connectedness. These are not interchangeable metaphors; they are distinct measurement grammars that allow the global economy to be studied through different dimensions of complexity.

For this reason, the matrix is not a mere table of analogies. It is a research-design device. It defines the role of each mathematical architecture in the book, assigns each to an empirical domain, and determines the kind of evidence that can be reported. Flow models require stress and pressure diagnostics. Topological decomposition requires graph construction and component separation. Rank models require calibration and local-to-global comparison. Spectral forecasting requires layered validation and benchmark tests. Complexity models require support-space growth, algorithmic search and exact reduced benchmarking. Curvature models require pressure coordinates, smoothing capacity and graph-topological connectedness.

1.5.4. Expanded Problem-by-Problem Translation

The following subsections expand the matrix into a substantive chapter map. Each block identifies the mathematical grammar, the economic translation, the empirical object, the main measurement outputs and the claim boundary that must govern the corresponding book chapter.

1.5.4.1. Poincare / Ricci / Perelman Logic: Inequality Pressure, Curvature, Entropy and Smoothing Capacity

The Poincare / Ricci / Perelman-inspired chapter translates the language of curvature, smoothing and topological connectedness into a global inequality diagnostic architecture. The economic object is not a literal differentiable manifold. It is a macro-regional pressure-smoothing system in which inequality, productivity, unemployment, investment, inflation, migration, education, social mobility, logistics, capital-flow pressure, innovation, health, fiscal pressure, openness, social protection and technology access are transformed into a common diagnostic stress-coordinate system.

This grammar is appropriate because inequality is not only a distributional statistic. It is also a deformation process. A region can display moderate inequality on one indicator while being structurally vulnerable through productivity stress, weak investment, technology-access gaps, fiscal pressure or insufficient smoothing capacity. The Perelman-Ricci-Poincare chapter therefore treats inequality as a connected pressure field rather than as a single Gini coefficient. Ricci-style curvature measures deformation; Perelman-type F and W functionals summarize energy-like and entropy-like system states; graph connectedness and Betti diagnostics test whether the inequality variables form one connected diagnostic structure.

In the book architecture, this chapter comes first among the seven models because it establishes the macro-social and structural deformation dimension of the research program. It shows why economic complexity has to be measured not only through output, finance and forecasting, but also through inequality pressure and recovery capacity. Its claim is diagnostic and measurement-oriented: it does not prove Poincare topology or Ricci-flow mathematics; it constructs a bounded global inequality measurement grammar.

1.5.4.2. Hodge: Macro-Flow Decomposition, Gradient Hierarchy, Curl Imbalance and Harmonic Circulation

The Hodge chapter translates the logic of decomposition into a regional macro-flow framework. The economic object is a weighted, directed and topologically decomposable macro-flow network of the world economy. Public macroeconomic anchors such as regional GDP, world-output share, projected growth, transition GDP and income depth are not treated as final indicators. They are transformed into a directed edge-pressure field on a regional graph and then decomposed into distinct structural components.

The Hodge grammar matters because the world economy is not reducible to aggregate scale. A large region may dominate output while not fully explaining systemic circulation; a smaller corridor-sensitive node may have limited GDP mass while remaining important for network flow, resilience and shock transmission. The decomposition separates gradient hierarchy, curl-based local-cycle imbalance and harmonic systemic circulation. This creates a measurement structure in which hierarchy, imbalance and persistent circulation can be observed jointly rather than collapsed into a single index.

In the book, the Hodge model follows the inequality-curvature chapter because it shifts the analysis from pressure-smoothing deformation to topological flow decomposition. It provides the book's core decomposition grammar: when the economy is represented as a network, the analyst must ask which part of the observed pressure is hierarchical, which part circulates around local cycles and which part persists as systemic harmonic circulation. Its claim is structural and benchmark-validating, not theorem-level proof of the Hodge conjecture.

1.5.4.3. Navier-Stokes: Liquidity Flow, Pressure, Friction and Systemic Stress

The Navier-Stokes chapter translates the structural logic of flow, velocity, pressure gradient, friction or diffusion, forcing and closure into a nondimensional macro-financial stress-testing framework. The empirical object is a global macro-

financial system represented through a 100-country annual panel for 2010-2024, supported by world and macro-regional layers, rolling validation, external-target checks, Monte Carlo uncertainty and policy counterfactuals.

The Navier-Stokes grammar is necessary because systemic stress is not generated by isolated financial indicators. Inflation pressure, sovereign-risk premia, liquidity weakness, external financing constraints, credit conditions, GDP-cycle movement, stochastic shocks and hidden adjustment interact jointly. A conventional composite index may aggregate these components, but it does not by itself impose a flow-pressure-friction-shock-cycle-closure structure. The Navier-Stokes translation provides this structure while keeping all variables nondimensional and empirically auditable.

In the book, this chapter becomes the main liquidity-flow and macro-financial stress-testing grammar. It turns the global economy into a diagnostic balance system: stress forms when liquidity velocity weakens, pressure gradients rise, friction/diffusion increases, shocks enter the system, cycles amplify instability and the restricted closure term absorbs only state-dependent observable or proxy-observable adjustment. Its claim is strong as a diagnostic stress-testing architecture, but it is not a physical fluid model and does not solve the mathematical Navier-Stokes problem.

1.5.4.4. Yang-Mills: Gauge Curvature, Action and Mass-Gap Shock Thresholds

The Yang-Mills chapter translates gauge, curvature, action and mass-gap logic into a finite-network model of systemic shock thresholds. The economic object is a corridor-sensitive stress network with ten nodes and twenty-seven weighted undirected edges. Public macroeconomic anchors are transformed into normalized systemic stress, corridor-weighted adjacency, stress-weighted adjacency, anti-symmetric gauge potential, triangular curvature, Yang-Mills economic action, stress Laplacian, Economic Mass Gap Index, fragility, BridgeStress and scenario outputs.

This grammar matters because a global-corridor economy can absorb some disturbances locally while transmitting others systemically. Conventional macroeconomic variables describe levels of output, growth, inflation or trade exposure, but they do not identify when local stress crosses a network threshold. A finite-network mass gap, interpreted as the first positive eigenvalue of a stress-weighted graph Laplacian, provides a bounded way to represent this threshold without making any claim about physical field theory.

In the book, the Yang-Mills chapter is placed after Navier-Stokes because it moves from stress formation to systemic threshold. Navier-Stokes asks how stress forms through flow, pressure, friction and closure. Yang-Mills asks how stress circulates through network curvature and when the network retains or loses spectral protection. Its claim is a finite-network benchmark claim: the economic mass gap is a graph-theoretic threshold measure, not a solution to the Clay Yang-Mills existence and mass-gap problem.

1.5.4.5. Birch-Swinnerton-Dyer: Local-to-Global Structural Rank, LOrder and Corridor Stress

The Birch-Swinnerton-Dyer chapter translates local-to-global rank logic into a regional structural-rank measurement framework. The economic object is a World-normalized macro-regional/corridor system in which public-data anchors are transformed into systemic-stress components, network structure, economic curve coefficients, discriminant diagnostics, finite-state trace analogues, Euler-factor analogues, an economic L-function, LOrder and a structural-rank object.

The BSD grammar is essential for the book because it addresses a problem not solved by flow, curvature or decomposition alone: how local regional signals become informative about global structural rank. In the economic translation, local reductions are not arithmetic reductions over finite fields. They are finite-state regional regimes used to represent discretized local economic conditions. Euler factors and L-function behavior become a disciplined measurement language for comparing local information with a constructed global rank.

In the book, this chapter functions as the local-to-global synthesis point. It links regional macroeconomic anchors, corridor exposure, finite-state information and structural rank. It also incorporates regulator, Tamagawa-type friction, torsion, BridgeStress, scenario-threshold and action-concentration diagnostics. Its claim is calibrated measurement: local regional signals and Euler-factor information may be informative about structural rank under the specified analogue, but this does not prove, test or replicate the classical BSD conjecture.

1.5.4.6. Riemann Hypothesis: Zeta-Cycle, Inflation Forecasting and Spectral Diagnostics

The Riemann-zeta chapter translates critical-line signal structure into a bounded global inflation forecasting architecture. The economic object is global aggregate inflation observed through layered annual, quarterly and monthly validation samples. A structural FPAS baseline is augmented by a normalized zeta-cycle signal constructed from a nonlinear macro-financial tau argument and converted into an alpha-weighted forecast correction.

This grammar matters because inflation is not only a persistence process. It can be influenced by macro-financial pressure, supply stress, liquidity instability, policy reaction, crisis regimes and nonlinear cyclical deformation. The Riemann-zeta

signal is not used as a theorem-level object. It is used as an explicit computational cycle generator that can be normalized, signed, calibrated and tested against forecast benchmarks such as FPAS and ARIMA.

In the book, this chapter provides the spectral and forecasting grammar of the Millennium Economic Research Program. It is methodologically distinct because its central evidence is layered forecast validation: annual validation, annual robustness, crisis-era comparison, quarterly dynamic validation and monthly spectral diagnostics. Its claim is bounded forecast improvement and diagnostic informativeness. It does not verify or test the Riemann Hypothesis and does not claim universal forecast dominance across all economies, samples and horizons.

1.5.4.7. P vs NP: Portfolio Optimization, Cardinality and Computational Complexity

The P-vs-NP chapter translates computational-complexity logic into a cardinality-constrained portfolio-optimization framework. The economic object is a sparse portfolio selection problem built on a fixed U.S. industry universe. CAPM-implied expected returns, covariance geometry, correlation structure, eigenvalue diagnostics, support-space growth, heuristic search, exact reduced benchmarking, robustness tests and a Black-Scholes derivative-pricing overlay are combined into one computational-finance architecture.

This grammar matters because many economic decisions are not purely continuous. Once a portfolio must select a limited number of industries, the optimization problem becomes mixed discrete-continuous: the analyst must select a support set and then allocate weights. The combinatorial support space grows as C(n,K), and the full n = 94, K = 10 universe generates 9,041,256,841,903 possible supports before continuous weights are optimized. This makes the economic meaning of computational difficulty visible without making any theorem-level claim about P vs NP.

In the book, this chapter closes the seven-problem sequence because it shifts the research program from measurement of global systems to decision feasibility under computational limits. It shows that even when expected returns, covariance and constraints are specified, the economic decision system may be bounded by search-space explosion. Its claim is empirical-computational: it provides best-found full-universe incumbents, heuristic comparisons and exact reduced enumeration, but it does not prove P != NP, certify the full n = 94 global optimum or establish realized historical investment dominance.

1.5.5. Integrated Measurement-Grammar Matrix

The expanded translation can be summarized more technically through the measurement-grammar matrix below. This matrix identifies how each chapter converts inputs into constructed objects, outputs and evidence claims.

Chapter	Measurement grammar	Empirical input layer	Constructed objects	Main output / claim level
5	Curvature, entropy and connectedness	Ten macro-regions, 2010-2024, sixteen stress-coordinate variables	Pressure scale, Ricci-style curvature, F/W functionals, graph topology, Betti diagnostics	Global inequality deformation and smoothing-capacity diagnostics
6	Topological flow decomposition	World anchor, ten regional nodes, public macroeconomic anchors	Weighted graph, directed edge pressure, gradient/curl/harmonic components, resilience and tail-risk indices	Regional macro-flow structure is decomposable beyond GDP mass
7	Flow-pressure-friction-closure balance	100 countries, 2010-2024, macro-financial stress proxies	Nondimensional stress components, restricted epsilon closure, resilience, rolling forecasts, counterfactuals	Global liquidity-flow stress-testing architecture
8	Gauge curvature and spectral threshold	Ten nodes, twenty-seven weighted edges, corridor stress variables	Gauge potential, triangular curvature, action, stress Laplacian, EMGI, BridgeStress	Finite-network shock threshold and corridor exposure
9	Local-to-global structural rank	World anchor, ten regional/corridor nodes, N = 150 closure layer	Economic curves, traces, Euler factors, L-function, LOrder, structural rank	Calibrated local-to-global rank correspondence

10	Spectral-cyclical forecast correction	Annual N = 55/45/20, quarterly N = 100, monthly N = 240	FPAS baseline, zeta-cycle, tau argument, alpha correction, spectral diagnostics	Bounded improvement in global inflation forecasting
11	Computational-complexity decision grammar	Damodaran January 2026 industry universe, n = 94, K = 10	Support-space growth, heuristic search, exact reduced enumeration, covariance and option-overlay robustness	Computational feasibility and sparse portfolio optimization discipline

Source: Author synthesis. The table defines the measurement grammar of each book chapter rather than claiming mathematical solution status.

1.5.6. Why This Chapter Order Is Methodologically Appropriate

The order of Chapters 5-11 is not arbitrary. The sequence moves from macro-social deformation to topological decomposition, from flow stress to shock thresholds, from local-to-global rank to spectral forecasting, and finally to computational decision feasibility. This order helps the reader move from system measurement to decision complexity.

Chapter 5 begins with inequality pressure because it establishes the macro-social deformation problem that motivates the broader research program. Chapter 6 then introduces decomposition, showing how global macro-flow structure can be separated into hierarchy, imbalance and circulation. Chapter 7 moves from structural decomposition to dynamic stress formation in liquidity-flow systems. Chapter 8 then asks how stress becomes systemically transmissible through curvature, action and spectral threshold. Chapter 9 shifts from transmission to rank formation, using local-to-global logic to connect regional signals with structural rank. Chapter 10 turns to spectral-cyclical forecasting, showing how a mathematical signal can improve inflation diagnostics under layered validation. Chapter 11 closes the sequence by examining the computational limits of economic decision-making, where the problem is no longer only measurement but feasible search under combinatorial explosion.

This ordering gives the monograph a coherent intellectual trajectory. It begins with global inequality and structural pressure, passes through topology, flow, threshold and rank, then moves toward forecasting and optimization. The result is a book-level research program rather than a set of disconnected applications.

1.5.7. Source Integration Map for the Translation Matrix

Table 1.5.3 identifies how the seven source manuscripts feed into the translation matrix. The purpose is to make clear that the matrix is grounded in the actual research documents and not imposed externally after the fact.

Book chapter	**Source manuscript**	**Main source elements used in the matrix**
Chapter 5	Global Perelman-Ricci-Poincare-Inspired Inequality Diagnostics	Inequality pressure, smoothing capacity, Ricci-style curvature, Perelman F/W functionals, graph connectedness, N = 150 panel, academic caution.
Chapter 6	Global Hodge-Econometric Modeling of the World Economy	World anchor, ten-node regional graph, Caucasus visibility, directed pressure field, Hodge decomposition, gradient/curl/harmonic energy, persistent homology.
Chapter 7	Navier-Stokes-Inspired Global Liquidity-Flow and Systemic-Stress Modelling	100-country panel, nondimensional stress balance, velocity/pressure/friction/shock/cycle/closure logic, rolling validation, benchmark comparison, policy counterfactuals.
Chapter 8	Economic Yang-Mills Mass Gap in Global and Corridor Flow Networks	Ten-node, twenty-seven-edge finite network, gauge potential, triangular curvature, Yang-Mills action, stress Laplacian, positive finite-network mass gap, EMGI, BridgeStress.
Chapter 9	Regional Economic Birch-Swinnerton-Dyer Modelling	World normalization anchor, regional/corridor nodes, finite-state traces, Euler factors, economic L-function, LOrder, structural rank, N = 150 closure layer.
Chapter 10	Global Riemann-Zeta FPAS+zeta Inflation Forecasting	FPAS baseline, zeta-cycle, tau argument, alpha correction, annual/quarterly/monthly layered validation, RMSE/MAE/sMAPE, DM/CW, HMM and spectral diagnostics.

Chapter 11	Robust Portfolio Optimization under Computational Complexity	Damodaran industry universe, CAPM priors, covariance geometry, C(94,10), greedy/Monte Carlo/GA search, exact reduced benchmark, Black-Scholes overlay, claim boundary.

1.5.8. Synthesis

The Seven-Problem Translation Matrix is the structural hinge of the monograph. It translates seven mathematical problem architectures into seven economic-econometric chapters while preserving the distinction between analogy and proof. Its role is to make the book intelligible as a unified research program before the reader enters the technical chapters.

The matrix shows that the seven problems are not used as ornamental references. Each one supplies a specific measurement grammar: Perelman-Ricci-Poincare logic measures inequality deformation and smoothing; Hodge measures decomposition of macro-flow; Navier-Stokes measures liquidity-flow stress; Yang-Mills measures curvature and shock thresholds; BSD measures local-to-global rank formation; Riemann-zeta measures spectral-cyclical inflation diagnostics; and P vs NP measures computational feasibility in portfolio decision systems.

Taken together, these translations support the central claim of the monograph: the Clay Millennium Problems are not solved here, but their formal architectures can be converted into a rigorous, reproducible and claim-bounded economic measurement program. The matrix therefore becomes the roadmap for Chapters 5-11 and the foundation for the comparative synthesis that follows later in the book.

1.6. Scientific Novelty of the Monograph

The scientific novelty of this monograph does not lie in attaching famous mathematical names to economic models. Its originality lies in the construction of a unified seven-part economic-econometric measurement program in which the formal architectures of the Clay Millennium Problems are translated into disciplined, auditable and claim-bounded systems for measuring global economic complexity. The monograph does not treat the seven mathematical problems as decorative metaphors. It treats them as seven distinct measurement grammars: flow, curvature, topology, decomposition, local-to-global rank, spectral-cyclical signal extraction and computational feasibility.

Across the seven source studies, the central methodological innovation is that mathematical structures are not imported as theorem-level claims. They are reconstructed as economic objects with defined inputs, transformations, algorithms, validation tests and evidence boundaries. The result is a monograph that moves beyond ordinary analogy. It creates a layered research architecture in which public macroeconomic anchors, author-calculated variables, normalized stress coordinates, network matrices, decomposition outputs, spectral signals, optimization searches, robustness diagnostics and replication packages are organized under one integrated scientific framework.

The novelty is therefore cumulative. Each chapter contributes a separate modelling grammar, but the book contributes the higher-order synthesis: an economic research program in which complex global systems are measured not only through scalar indicators such as GDP, inflation, inequality, portfolio returns or trade exposure, but through structured objects such as pressure fields, graph cochains, gauge potentials, curvature measures, L-order analogues, zeta-cycle corrections and combinatorial search spaces. This is the essential monograph-level contribution.

1.6.1. Novelty of the Perelman-Ricci-Poincare Inequality Diagnostic Grammar

The Perelman-Ricci-Poincare-inspired component contributes a curvature, entropy and connectedness grammar for global inequality diagnostics. Its novelty is the transformation of inequality analysis from a single-indicator or small-variable framework into a macro-regional diagnostic manifold. Instead of treating the Gini coefficient or labour-market stress as isolated indicators, the model converts sixteen macro-social variables into pressure-oriented stress coordinates and uses them to construct a metric-tensor-like diagnostic space, Ricci-style component curvature, Perelman-type F- and W-functional objects, graph Laplacian connectedness, Betti numbers, network-curvature proxies, counterfactual sensitivity tests and econometric validation layers.

This is a major conceptual advance because it reframes global inequality as a pressure-smoothing system. The novelty is not the claim that economies literally obey Ricci flow or that the Poincare conjecture is empirically tested. The novelty is that curvature-like deformation, smoothing capacity, entropy-like complexity and graph connectedness become measurable economic diagnostics. In this grammar, inequality is not only a distributional state; it is a deformation process generated by investment pressure, productivity gaps, technology access, unemployment, fiscal pressure, social protection and regional topology. The contribution is strongest as a diagnostic measurement framework for crisis deformation, partial recovery and structural smoothing capacity.

1.6.2. Novelty of the Hodge-Econometric Decomposition Grammar

The Hodge-econometric component contributes a decomposition grammar for the world economy. Its novelty is the conversion of public macroeconomic anchors into a weighted regional graph, then into a directed macro-flow pressure cochain, and finally into decomposed gradient, curl and harmonic components. This makes it possible to distinguish regional hierarchy, local-cycle imbalance and persistent systemic circulation inside one empirical architecture.

The contribution is not limited to a graph visualization. The Hodge study builds an integrated pipeline: public data are transformed into a graph; the graph carries a directed edge field; the edge field is decomposed; the components are converted into hierarchy, imbalance, circulation, resilience and tail-risk indices; and those indices are evaluated through econometric diagnostics, robustness checks, machine-learning validation and persistent homology. This is scientifically novel because it allows the world economy to be studied as a topological macro-flow system rather than as a set of isolated output aggregates.

1.6.3. Novelty of the Navier-Stokes Liquidity-Flow Grammar

The Navier-Stokes-inspired component contributes a flow-balance grammar for macro-financial stress. Its novelty is the construction of a nondimensional stress-testing architecture in which systemic stress is decomposed into liquidity-flow weakness, acceleration, pressure gradients, friction or diffusion, stochastic shocks, Fourier GDP-cycle forcing and a restricted hidden-adjustment term. The framework is mathematically structured, econometrically audited and scientifically bounded.

The novelty is not that financial liquidity is described as a physical fluid. The novelty is that each term in the Navier-Stokes-inspired balance receives a defined economic interpretation, a normalization rule, a validation route and a claim boundary. The model therefore avoids the two main dangers of ambitious analogue research: uncontrolled metaphor and residual plug construction. By restricting epsilon(t), reporting residual imbalance, comparing ARIMA/VAR/GARCH and composite-index benchmarks, validating against external targets, running fixed effects, perturbation robustness, Monte Carlo simulation and policy counterfactuals, the chapter provides a full stress-testing system rather than a single stress index.

1.6.4. Novelty of the Yang-Mills Gauge-Econometric Mass-Gap Grammar

The Yang-Mills component contributes a gauge, curvature and threshold grammar for global and corridor flow networks. Its novelty is the operationalization of an Economic Yang-Mills Mass Gap as a finite-network spectral threshold. Public macroeconomic anchors and corridor-sensitive weights are transformed into a normalized systemic-stress field, a corridor-weighted graph, a stress-weighted adjacency matrix, an anti-symmetric economic gauge potential, triangular curvature, Yang-Mills economic action, a stress Laplacian, EMGI, fragility, BridgeStress and scenario-based shock diagnostics.

This grammar is important because it separates scalar output mass from systemic transmissibility. In conventional macroeconomic comparison, a large region may dominate GDP while a smaller corridor region remains hidden. In the Yang-Mills framework, stress vulnerability is produced by interaction among macroeconomic pressure, network position, corridor exposure, curvature participation, local protection and resilience. The scientific novelty is the creation of a finite-network gauge-econometric architecture that can measure systemic shock thresholds without claiming a physical Yang-Mills theorem or final causal country-panel validation.

1.6.5. Novelty of the Birch-Swinnerton-Dyer Local-to-Global Rank Grammar

The BSD-inspired component contributes a local-to-global structural-rank grammar. Its novelty is the construction of a regional economic measurement architecture in which public macro-regional anchors are transformed into systemic stress components, weighted regional-network structure, economic curve coefficients, discriminant diagnostics, finite-state trace analogues, Euler-factor analogues, a constructed economic L-function, an L-order measure and a structural-rank object.

The distinctive contribution is that structural rank is not equated with GDP size. It is built from productive depth, Hodge-flow information, network position, agentic capacity, resilience, fragility and corridor exposure. Local regional states are then converted into finite-state reductions, q-base traces, Euler-factor analogues and LOrder measures whose behavior is compared with structural rank. The novelty is the disciplined local-to-global measurement chain, not a claim to prove the classical Birch-Swinnerton-Dyer conjecture. The framework adds a rigorous anti-overclaiming architecture through discriminant audits, q-base sensitivity, Bland-Altman logic, equivalence checks, negative controls, circularity screens, out-of-sample validation and placebo distributions.

1.6.6. Novelty of the Riemann-Zeta FPAS+zeta Forecasting Grammar

The Riemann-Zeta component contributes a spectral-cyclical forecasting grammar for global inflation. Its novelty is the transformation of a critical-line Riemann-zeta signal into a bounded, normalized and empirically testable macro-financial forecast correction. The zeta layer is not presented as a proof or test of the Riemann Hypothesis. It is used as a

mathematically explicit signal generator whose real-valued cycle, deviation from neutrality and alpha-calibrated correction are evaluated against FPAS and ARIMA benchmarks.

The most important methodological novelty is the layered validation architecture. The headline annual result is assigned to the N=55 layer, stability to N=45, crisis-era interpretation to N=20, dynamic validation to quarterly N=100 and spectral diagnostics to monthly N=240. This prevents the model from relying on a compact crisis-era window alone. The signed correction gate is also novel because the zeta term does not mechanically add a permanent premium to the baseline; it changes direction with the zeta deviation and macro-financial pressure state. The integration of Mincer-Zarnowitz calibration, forecast encompassing, Diebold-Mariano and Clark-West tests, HMM/Markov-switching regimes, Fourier, wavelet and spectral-entropy diagnostics turns the chapter into a disciplined forecast-diagnostic architecture rather than a high-fit annual exercise.

1.6.7. Novelty of the P-vs-NP Computational-Finance Grammar

The P-vs-NP component contributes a computational-decision grammar for portfolio optimization. Its novelty is the empirical operationalization of computational complexity through a cardinality-constrained portfolio-selection problem. The model does not attempt to prove P=NP or P!=NP. Instead, it shows how combinatorial support-space growth, CAPM-implied expected returns, covariance geometry, heuristic search, exact reduced benchmarking, derivative overlays, transaction costs, stress scenarios and falsification gates can be combined in one reproducible computational-finance architecture.

The chapter is scientifically novel because it makes computational difficulty visible in an economically meaningful setting. The full industry universe contains n=94 candidate portfolios and the baseline K=10 sparse-selection problem creates 9,041,256,841,903 possible supports before continuous weights are optimized. This combinatorial explosion motivates greedy search, Monte Carlo sampling, genetic algorithms, GA-plus-continuous reoptimization and exact reduced enumeration in a smaller n=20, K=6 universe. The key contribution is claim-bounded computational evidence: best-found full-universe incumbents are reported as incumbents under documented search coverage, while exact certification is reserved for the reduced benchmark.

1.6.8. Integrated Scientific Novelty Matrix

Millennium grammar	Economic object	Main novelty	Primary evidence type	Claim level
Perelman/Ricci/Poincare	Global inequality pressure	Curvature, entropy and graph-topological diagnostic manifold	N=150 macro-regional panel and topology validation	Diagnostic measurement
Hodge	World macro-flow topology	Gradient/curl/harmonic decomposition of a regional edge cochain	10-node benchmark with econometric, ML and persistence checks	Structural benchmark
Navier-Stokes	Global liquidity-flow stress	Nondimensional flow-pressure-friction-shock-closure balance	100-country, 2010-2024 panel with rolling validation	Macro-financial stress-testing
Yang-Mills	Corridor shock thresholds	Gauge potential, curvature/action and finite-network mass gap	10-node, 27-edge benchmark plus N=1,500 pathway	Finite-network benchmark
BSD	Structural rank formation	Finite-state local reductions, LOrder and rank calibration	N=150 closure with placebo and anti-circularity checks	Calibrated local-to-global measurement
Riemann-Zeta	Global inflation forecasting	Signed zeta-cycle correction integrated	Annual, quarterly and monthly layered	Bounded forecast-diagnostic claim

		with FPAS	validation	
P vs NP	Sparse portfolio selection	Combinatorial support search with exact reduced certification	n=94 full universe and n=20 exact benchmark	Computational-finance demonstration

1.7. Theoretical, Methodological and Practical Significance of the Monograph

Section 1.7 should not be a second novelty section and should not repeat the claim-boundary section. Its correct role is to explain why the novelty matters. In the final monograph, Section 1.7 should therefore be titled Theoretical, Methodological and Practical Significance of the Monograph. This placement is consistent with the internal architecture of several source manuscripts, where scientific novelty is followed by theoretical, methodological and practical significance before limitations and academic caution.

The theoretical significance of the monograph is that it expands the language of economic analysis from scalar indicators to structured mathematical-economic objects. The world economy, global inequality, systemic liquidity, corridor stress, structural rank, inflation cycles and portfolio choice are not treated as isolated empirical problems. They are interpreted as flow systems, topological networks, curvature fields, local-to-global rank architectures, spectral-cycle processes and computational decision systems. This creates a broader conceptual vocabulary for economic science.

The methodological significance is that the book converts these conceptual vocabularies into reproducible measurement pipelines. Each model begins with defined data inputs, applies explicit transformations, constructs mathematical-economic objects, generates results, tests robustness, separates evidence levels and states claim boundaries. The result is not a set of disconnected analogies, but a research architecture in which formal mathematics, econometrics, computation, validation and academic caution are jointly organized.

The practical significance lies in the diagnostic capacity of the seven models. The monograph can support systemic-risk monitoring, inflation-forecast interpretation, inequality-pressure analysis, regional-corridor diagnostics, portfolio-governance audits, shock-threshold evaluation and macroeconomic resilience assessment. Its practical use is not mechanical prediction or policy prescription. Its value is to provide structured maps of where stress forms, how shocks circulate, which nodes transmit pressure, where rank emerges, when forecasts require nonlinear correction and where optimization complexity limits certifiable decision-making.

1.7.1. Theoretical Significance

At the theoretical level, the monograph challenges the sufficiency of economic measurement systems based only on aggregate scale, linear association or single-index comparison. It does not reject conventional indicators; GDP, inflation, inequality, returns, risk and growth remain indispensable anchors. However, it argues that such indicators become more informative when embedded in a structured architecture that measures flows, decomposition, curvature, spectral movement, rank formation and computational feasibility.

This theoretical contribution is especially important for global and regional economics. A small corridor node can be structurally relevant despite low GDP mass; a high-output region can be exposed to shock propagation despite apparent scale; an inflation baseline can fail during nonlinear global stress; and a portfolio can look efficient while remaining computationally uncertified or covariance-fragile. The book provides theoretical language for these situations by translating mathematical grammars into economic measurement systems.

1.7.2. Methodological Significance

At the methodological level, the monograph shows how complex analogue modelling can remain scientifically disciplined. Each chapter uses explicit transformation rules rather than loose metaphor. The Hodge chapter constructs incidence matrices and decomposes a directed edge field. The Yang-Mills chapter builds adjacency matrices, gauge potentials, curvature and a stress Laplacian. The BSD chapter maps regional variables into coefficients, finite-state traces and LOrder. The Navier-Stokes chapter builds nondimensional stress balances and restricted closure. The Riemann-Zeta chapter assigns methods to annual, quarterly and monthly layers. The P-vs-NP chapter separates heuristic search from exact reduced enumeration. The Ricci/Poincare chapter separates pressure coordinates, curvature diagnostics, topology and forecast boundaries.

The methodological significance therefore lies in auditability. The book treats formulas, data provenance, normalization, model construction, robustness checks, placebo logic, external screening and replication packages as part of the scientific argument. This is a high-value contribution because mathematical-economic models are vulnerable to reviewer criticism

when their transformations are not transparent. The monograph directly addresses that risk by making claim discipline a methodological component rather than an afterthought.

1.7.3. Practical and Policy-Analytical Significance

The practical significance is diagnostic, not prescriptive. The monograph does not claim to provide mechanical policy rules or universal forecasting laws. Instead, it provides tools for interpreting complex economic states. The Navier-Stokes model can map systemic stress channels. The Riemann-Zeta model can identify when a structural inflation baseline under-reacts to nonlinear pressure. The Yang-Mills model can distinguish corridor shock transmissibility from GDP mass. The Hodge model can identify hierarchy, local imbalance and systemic circulation. The BSD model can interpret structural rank formation under local-to-global constraints. The Ricci/Poincare model can diagnose inequality deformation and smoothing capacity. The P-vs-NP model can guide portfolio audit and model-governance decisions under combinatorial complexity.

For institutions, this means the monograph can support stress dashboards, regional resilience analysis, corridor-risk monitoring, inflation-forecast diagnostics, inequality pressure mapping, portfolio-model validation and replication-oriented research design. The contribution is strongest when used as a structured diagnostic framework rather than as a deterministic decision engine.

1.7.4. Significance Matrix

Problem grammar	Theoretical significance	Methodological significance	Practical significance	Non-overclaiming rule
Ricci/Poincare	Inequality as deformation and smoothing system	Curvature, entropy and topology diagnostics	Inequality pressure and recovery mapping	Not a geometric theorem proof
Hodge	Economy as decomposable macro-flow topology	Edge cochain and Hodge decomposition	Resilience, imbalance and circulation diagnostics	Benchmark, not full causal world model
Navier-Stokes	Liquidity stress as flow-pressure-friction balance	Nondimensional panel stress-testing pipeline	Macroprudential stress and policy-scenario interpretation	Not a physical fluid law
Yang-Mills	Stress as gauge-curvature-threshold network	Finite-network spectral mass-gap construction	Corridor shock-threshold monitoring	Not Clay Yang-Mills proof
BSD	Structural rank as local-to-global formation	LOrder, traces, Euler-factor analogues and rank calibration	Corridor and rank vulnerability interpretation	Not classical BSD proof
Riemann-Zeta	Inflation as pressure-cycle and spectral process	Layered FPAS+zeta validation	Shock-year forecast correction diagnostics	Not RH proof or universal dominance
P vs NP	Economic choice as computationally constrained support selection	Heuristic search plus exact reduced benchmark	Portfolio governance and model audit	Not P-vs-NP theorem proof

1.8. Research Limitations, Academic Caution and Claim Boundary of the Entire Book

Section 1.8 should absorb and expand the previously drafted Claim Boundary of the Entire Book. It should combine all seven studies limitations and academic-caution principles into one strict monograph-level reviewer-safety framework. The correct purpose of Section 1.8 is to make the scientific perimeter of the book unambiguous: the monograph does not solve the Clay Millennium Problems; it develops economic-econometric analogues inspired by their formal structures.

This limitation is not a rhetorical disclaimer added at the end of the introduction. It is a methodological condition of the entire book. Each model is permitted to make only the claim supported by its data, transformations and validation architecture. A finite-network spectral gap is not a proof of the Yang-Mills mass gap. A zeta-cycle correction is not a proof or test of the Riemann Hypothesis. A cardinality-constrained portfolio search is not a proof about P vs NP. A local-to-global rank analogue is not a proof of BSD. A Hodge decomposition of macro-flow pressure is not a proof of the Hodge conjecture. A Ricci/Poincare-inspired inequality manifold is not a proof of a topological theorem. A Navier-Stokes-inspired stress balance is not a solution to the Navier-Stokes existence and smoothness problem.

1.8.1. General Theorem-Level Boundary

The first limitation is conceptual. The book uses the Clay Millennium Problems as formal modelling grammars, not as theorem-level objects to be solved through economic data. No chapter claims a mathematical proof, disproof, empirical verification or theorem-level approximation of the original problems. The admissible claims are economic, econometric, computational, diagnostic, benchmark, forecasting or calibration claims. This boundary must be stated at the beginning of the monograph because it protects the entire work from the most predictable reviewer objection.

The correct reading is therefore analogue-based. The book asks whether mathematical structures can help organize economic measurement. It does not ask whether global macroeconomic data can prove number-theoretic, topological, PDE, gauge-theoretic or computational-complexity theorems. This distinction allows the work to be ambitious without being scientifically overextended.

1.8.2. Data, Aggregation and Sample-Size Boundaries

The second limitation concerns empirical scale and aggregation. Several chapters use macro-regional benchmark designs. Hodge, Yang-Mills and BSD rely heavily on ten-node or ten-region architectures, while Perelman/Ricci/Poincare and BSD use N=150 region-year closure layers. These designs are appropriate for structural measurement, local-to-global calibration, finite-network topology and proof-of-concept validation, but they are not equivalent to full country-level causal panels or observed transaction matrices.

The Navier-Stokes chapter has a larger 100-country, 2010-2024 panel and therefore supports stronger macro-financial stress-testing claims, but even there the evidence remains diagnostic rather than causal. The Riemann-Zeta chapter uses a layered annual, quarterly and monthly validation hierarchy, but forecast superiority remains bounded by sample, horizon and benchmark design. The P-vs-NP chapter has exact reduced enumeration only in the n=20, K=6 benchmark; the full n=94, K=10 universe is not exhaustively enumerated. These boundaries must be preserved in the final book.

1.8.3. Constructed Variables, Transformation Risk and Circularity

The third limitation concerns constructed variables. Many of the monograph objects are author-calculated: stress scores, curvature measures, Hodge components, gauge potentials, LOrder, structural rank, EMGI, BridgeStress, zeta corrections and portfolio search outputs. This is not a defect. Constructed variables are necessary for mathematical-economic measurement. However, their scientific validity depends on transparent source ledgers, formula disclosure, normalization rules, sensitivity tests, robustness checks, variable-lineage controls and replication packages.

The BSD framework is especially sensitive to circularity because LOrder and structural rank can share input families unless lineage is carefully separated. The Hodge and Yang-Mills chapters depend on graph-construction choices. The Ricci/Poincare chapter depends on stress-coordinate orientation. The Navier-Stokes chapter depends on nondimensionalization and closure restrictions. The Riemann-Zeta chapter depends on alpha calibration and layered validation. The P-vs-NP chapter depends on covariance assumptions and search coverage. The monograph must treat these design choices as auditable modelling decisions rather than hidden assumptions.

1.8.4. Forecasting, Optimization and Causality Boundaries

The fourth limitation concerns claims about forecasting, optimization and causality. A strong forecast result is not a universal law. A strong benchmark result is not a causal mechanism. A best-found optimization result is not necessarily a certified global optimum. A positive coefficient under diagnostic regression is not proof of structural causality. The book therefore classifies forecast evidence, computational evidence, benchmark evidence, calibration evidence and econometric association evidence separately.

The Riemann-Zeta chapter may claim bounded forecast improvement under its layered validation architecture, but not universal dominance across all economies, samples or horizons. The P-vs-NP chapter may claim computational-finance evidence under documented search coverage, but not a theorem about complexity classes or certified optimality in the full universe. The Yang-Mills and Hodge chapters may claim benchmark measurement and structural diagnostics, but not final

country-panel causal validation. The BSD chapter may claim calibrated structured agreement, but not classical BSD proof or strong external econometric confirmation. The Navier-Stokes chapter may claim stress-testing usefulness, but not a physical liquidity law or unconditional crisis-prediction rule.

1.8.5. Problem-Specific Claim-Boundary Matrix

Problem grammar	What the book may claim	What it may not claim	Main evidence boundary	Academic-caution device
Ricci/Poincare	A diagnostic architecture for inequality pressure, curvature, entropy and connectedness	Proof, test or replication of Perelman/Ricci/Poincare theorems	Macro-regional N=150 diagnostic panel and constructed stress coordinates	Benchmark forecasting and theorem-proof rejection
Hodge	A regional Hodge-econometric decomposition of macro-flow pressure	Proof of the Hodge conjecture or final causal model of the world economy	Ten-node regional benchmark with graph-construction sensitivity	Small-N benchmark and replication-path discipline
Navier-Stokes	A nondimensional macro-financial stress-testing balance	Physical fluid law, viscosity estimate or Navier-Stokes solution	100-country panel but diagnostic, not causal	Restricted epsilon(t), benchmark comparison and validation-window language
Yang-Mills	A finite-network spectral shock-threshold benchmark	Mathematical Yang-Mills mass-gap solution or final causal country-panel evidence	Ten-node, 27-edge benchmark with N=1,500 pathway pending	Evidence hierarchy: pass, partial, caution and future validation
BSD	Calibrated local-to-global structural-rank measurement	Classical BSD proof, arithmetic L-function estimation or algebraic rank identification	N=150 closure and directional external screening	Anti-circularity, placebo, q-sensitivity and claim-gate matrix
Riemann-Zeta	Bounded global inflation forecast improvement and spectral diagnostics	Riemann Hypothesis proof/test or universal forecast dominance	N=55/N=45/N=20/N=100/N=240 layered design	Rolling validation, DM/CW tests, residual and regime diagnostics
P vs NP	Computational-finance architecture for sparse portfolio selection	P vs NP theorem proof, certified full n=94 optimum or realized return dominance	Best-found full universe and exact reduced benchmark only	Search-coverage reporting, covariance sensitivity and falsification

				gates

1.8.6. Replication and Reviewer-Safety Boundary

The fifth limitation concerns replication status. The source studies are strengthened by Zenodo data and replication packages, source ledgers, formulas, algorithms, output files and checksums. However, the monograph must still treat replication as a structured audit requirement. The Word manuscript is the interpretive and methodological exposition; the replication packages are the external audit companions. Where a chapter includes a future panel architecture, the book must not write as if the future estimation layer has already supplied final causal evidence.

The reviewer-safety principle is simple: the book is strongest when it distinguishes what has been demonstrated, what is diagnostic, what is benchmark-level, what is forecast-level, what is computationally best-found, what is exact only in a reduced universe and what remains future work. This classification does not weaken the monograph. It makes the scientific ambition credible.

1.8.7. Final Academic-Caution Statement

The final academic-caution statement of the monograph should be explicit. This book does not solve the Clay Millennium Problems. It does not offer theorem-level proof, physical-law identification, number-theoretic verification, universal forecast dominance, unrestricted causality or fully certified global optimization. Its contribution is different: it constructs seven disciplined economic-econometric analogues that translate the formal grammars of the Millennium Problems into auditable systems for measuring global complexity, systemic stress, structural rank, inequality deformation, inflation cycles, corridor shock thresholds and computational decision limits.

Within that boundary, the book makes a substantial scientific contribution. It shows that mathematical structures can enrich economic measurement when they are translated carefully, validated empirically, bounded explicitly and replicated transparently. The limitation is therefore also the strength: the monograph is not a theorem-claiming text; it is a claim-disciplined research program for mathematical economics, applied econometrics and global complexity measurement.

Chapter 2. Conceptual Translation Framework: From Mathematical Problems to Economic Analogues

2.1. Analogy versus Proof

This section establishes the conceptual rule that governs the whole monograph: a mathematical theorem is not the same object as an economic model. The Clay Millennium Problems enter the book not as claims to mathematical resolution, but as disciplined architectures for economic measurement. Their value for the monograph lies in the formal grammars they offer - flow, curvature, topology, spectral threshold, local-to-global rank, spectral-cycle diagnostics and computational complexity - not in any assertion that the corresponding pure mathematical problems have been solved, tested or replicated inside economic data.

The distinction is not a minor disclaimer. It is the central methodological safeguard of the book. Without it, the use of terms such as Ricci flow, Hodge decomposition, Navier-Stokes balance, Yang-Mills mass gap, Birch-Swinnerton-Dyer rank, Riemann zeta signal and P versus NP could be misread as theorem-level mathematical ambition. With the distinction made explicit, those terms become bounded modelling instruments: each is converted into a specified economic object, connected to data transformations, audited by validation layers and interpreted only at the level supported by the empirical design.

The monograph therefore works between two unacceptable extremes. The first extreme is overclaiming: treating an economic-econometric construction as if it proved an open theorem in mathematics. The second extreme is underclaiming: treating any mathematical vocabulary in economics as a mere metaphor because it does not solve the original theorem. The correct position is more precise. The models are not theorem proofs, but they are also not decorative metaphors. They are formal analogues whose scientific content depends on transparent translation rules, reproducible data construction, diagnostic validation and strict limits on inference.

In this sense, Chapter 2 functions as the translation constitution of the monograph. Chapter 1 states the book-level claim boundary; Chapter 2 explains how such a boundary operates conceptually. Section 2.1 begins with the most basic rule: analogy can organize a model, but proof belongs to the discipline in which the theorem is formulated. Economic evidence may validate an economic analogue. It cannot prove a theorem about smooth three-dimensional fluid equations, algebraic cycles, quantum gauge fields, elliptic curves, zeta zeros or formal complexity classes.

2.1.1. The Function of the Analogy-Proof Distinction

The analogy-proof distinction performs four functions in the monograph. First, it protects the mathematical integrity of the Clay problems. These problems are theorem-level questions located in pure mathematics, mathematical physics or theoretical computer science. They have formal definitions, proof standards and disciplinary criteria that cannot be replaced by empirical modelling. A regression coefficient, a network statistic, a spectral graph value, a forecast improvement or a portfolio search result does not become a proof simply because it uses terminology inspired by a theorem.

Second, the distinction protects the economic integrity of the monograph. The book does not need to prove a Millennium Problem in order to make a contribution to economics. Its contribution is to show that selected mathematical architectures can be translated into auditable measurement systems for the world economy. That contribution is methodological and empirical. It concerns how to measure systemic stress, inequality deformation, flow decomposition, structural rank, shock thresholds, inflation cycles and computational feasibility under complex economic conditions.

Third, the distinction defines the admissible evidentiary level. Economic analogues may be assessed through internal consistency, formula transparency, data provenance, calibration stability, robustness checks, rolling validation, benchmark comparison, placebo logic, reduced exact certification, finite-network spectral diagnostics and replication packages. These forms of evidence can support a strong economic modelling claim. They do not establish theorem-level truth in the originating mathematical domain.

Fourth, the distinction gives the monograph a unified voice. The seven source manuscripts use different empirical objects and methods, but they all obey the same rule: the mathematical object is translated, not proved. The Perelman-Ricci-Poincare chapter translates curvature and topology into inequality diagnostics; the Hodge chapter translates decomposition logic into macro-flow structure; the Navier-Stokes chapter translates flow balance into liquidity-stress testing; the Yang-Mills chapter translates gauge curvature and spectral separation into shock-threshold measurement; the BSD chapter translates local-to-global rank logic into regional structural-rank calibration; the Riemann chapter translates zeta-cycle construction into inflation forecasting; and the P-vs-NP chapter translates complexity logic into sparse portfolio selection.

Because all seven chapters share this rule, the book becomes a monograph rather than a compilation of separate articles. The shared principle is not that the models are identical. They are not. The shared principle is that each model converts a theorem-associated mathematical grammar into a bounded economic analogue, then limits the final claim to what the constructed analogue and empirical evidence can support.

2.1.2. What Counts as a Classical Mathematical Object in This Monograph

A classical mathematical object, as the term is used in this chapter, is the original formal object associated with the corresponding Millennium Problem or theorem-level mathematical architecture. It is not the economic variable later created by the author. It is the object as understood within its own mathematical discipline: a three-dimensional incompressible fluid equation, a gauge field and mass gap, an algebraic-geometric Hodge class, an elliptic-curve L-function and rank relation, the distribution of zeta zeros, a topological statement about simply connected three-manifolds, or a formal relation between complexity classes.

The classical object carries proof obligations that are not empirical in the ordinary econometric sense. To resolve Navier-Stokes existence and smoothness, one would need a proof about solutions of the partial differential equations under the required conditions. To resolve Yang-Mills existence and mass gap, one would need a mathematical construction and proof in quantum gauge theory. To resolve the Hodge conjecture, one would need a proof concerning algebraic cycles and Hodge classes. To resolve BSD, one would need a theorem linking the analytic behavior of the L-function and algebraic rank. To resolve the Riemann Hypothesis, one would need a proof about the location of non-trivial zeros. To resolve P versus NP, one would need a proof about formal complexity classes. None of these proof obligations can be discharged by economic data.

This does not mean that mathematical objects are irrelevant for economic science. On the contrary, the formal structure of a mathematical object can inspire powerful economic measurement. The key is to identify which component of the mathematical architecture is transferable as a modelling grammar and which component remains non-transferable as a theorem claim. In this monograph, the transferable components are structural: flow balance, decomposition, curvature, spectral separation, local-to-global aggregation, zeta-type cyclical signal construction and combinatorial search. The non-transferable component is the proof of the original mathematical theorem.

The term classical is therefore used to prevent category confusion. A classical Hodge object is not the same as a macroeconomic edge cochain. A classical Navier-Stokes equation is not the same as a nondimensional financial-stress

balance. A classical zeta function is not the same as an alpha-calibrated inflation correction. A classical elliptic curve is not the same as an economic curve coefficient system. The economic versions may be formally motivated, computationally specified and empirically meaningful, but they remain constructed measurement objects.

2.1.3. Why Direct Proof Is Excluded

Direct proof is excluded for disciplinary, logical and empirical reasons. The disciplinary reason is that the Clay problems belong to mathematics, mathematical physics and theoretical computer science. Their resolution requires proof within those disciplines. The fact that an economic system can be represented through a network, a flow, a rank object, a spectral signal or a combinatorial search space does not shift the proof standard of the original problem into economics.

The logical reason is that the domains are not identical. A financial liquidity variable is not a fluid velocity field. A systemic-stress graph is not a quantum gauge field. A regional structural-rank object is not the rank of rational points on an elliptic curve. A discrete macro-flow decomposition is not a proof about algebraic cycles. A zeta-cycle forecast component is not a statement about all non-trivial zeros of the Riemann zeta function. A portfolio support-selection problem is not the formal P versus NP problem. Because the domains differ, a result in one domain cannot automatically prove a proposition in the other.

The empirical reason is that the data architecture of the monograph is constructed for economic measurement, not for theorem verification. The source manuscripts use country-year panels, macro-regional benchmarks, finite weighted graphs, forecast-validation layers, public-data anchors, author-calculated indices, algorithmic search budgets and robustness diagnostics. These are appropriate for econometric and computational-economic inference. They are not mathematical proof devices for open problems.

This exclusion also prevents an important methodological error: confusing analogy with identity. Analogy says that two structures share a useful formal resemblance. Identity says that they are the same object. The monograph uses analogy, not identity. It states that liquidity stress can be organized by flow-pressure-friction logic; it does not state that liquidity is physically identical to a viscous fluid. It states that regional finite-state signals can be aggregated through BSD-inspired local-to-global logic; it does not state that regions are elliptic curves or that q-bases are literal primes. It states that zeta-type signals can be normalized into forecast corrections; it does not state that inflation data verifies the Riemann Hypothesis.

For these reasons, every chapter must contain a proof-exclusion clause. The clause is not a sign of weakness. It is a sign of scientific control. A model that clearly states what it cannot claim is more credible than a model that allows the reader to infer a theorem-level conclusion from empirical diagnostics. In this monograph, the proof-exclusion clause enables stronger economic claims because it prevents those claims from being contaminated by impossible mathematical overreach.

2.1.4. The Economic Analogue as a Measurement Grammar

An economic analogue is the result of a controlled translation from a mathematical architecture into an economic measurement system. It does not reproduce the theorem. It extracts a structural grammar from the theorem-associated domain and applies that grammar to economic data. In the monograph, the word grammar is used deliberately. A grammar defines how objects are formed, how relations are organized and what statements can be made. It does not guarantee the truth of every sentence; it supplies a disciplined language in which meaningful sentences can be constructed.

The translation process has four steps. The first step identifies the mathematical source architecture. For example, Navier-Stokes supplies flow, acceleration, pressure, diffusion and forcing; Hodge theory supplies decomposition into gradient, curl and harmonic components; BSD supplies local-to-global rank logic; P versus NP supplies a distinction between feasible verification and combinatorial search difficulty. The second step selects the economic object to be measured: liquidity stress, macro-flow pressure, structural rank, inflation dynamics, systemic shock threshold, inequality deformation or sparse portfolio choice.

The third step defines transformation rules. Raw economic variables rarely have the units, direction or structure needed for direct combination. The source manuscripts therefore use normalization, stress-orientation, nondimensionalization, finite-state discretization, graph construction, covariance modelling, CAPM calibration, zeta-cycle normalization, pressure scaling, curvature proxies, spectral Laplacians and algorithmic search layers. These transformations are where analogy becomes methodology. They prevent the model from relying on decorative terminology alone.

The fourth step defines permissible inference. A model may claim internal consistency if its constructed objects behave coherently under the stated rules. It may claim diagnostic usefulness if the constructed indicators reveal interpretable structure. It may claim forecast improvement inside a specified validation design. It may claim computational difficulty for a concrete search instance. It may claim finite-network spectral separation in a specified graph. It may claim calibrated local-

to-global correspondence between regional signals and structural rank. It may not claim theorem proof unless the original mathematical theorem has actually been proved by valid mathematical means.

The economic analogue is therefore neither arbitrary nor absolute. It is not arbitrary because the transformation is formalized and auditable. It is not absolute because the claim remains conditional on the model design, data construction, sample, validation strategy and assumptions. This conditionality is especially important for a monograph that uses seven ambitious mathematical names. The names give the book intellectual architecture; the claim boundaries give it scientific credibility.

2.1.5. The Evidence Ladder: From Analogy to Permissible Claim

The monograph uses an evidence ladder to separate weak analogy from strong economic evidence. The lowest level is conceptual resemblance: a mathematical structure appears relevant to an economic phenomenon. This level is not enough for scientific contribution. A statement such as 'the economy is like a fluid' or 'inflation has cycles' is insufficient unless it is converted into operational variables and testable diagnostics.

The second level is formal translation. At this level the model specifies economic variables, transformations, matrices, functions, indices, objective functions or algorithms. A Navier-Stokes-inspired model must define its velocity, pressure, friction, shock and closure terms. A Hodge-econometric model must define its graph, edge cochain and decomposition. A BSD-inspired model must define local states, trace analogues, Euler factors, an L-function analogue and structural rank. Without these definitions, the analogy remains literary rather than scientific.

The third level is empirical calibration. The model must be populated with data or a clearly specified benchmark. Public anchors and author-calculated variables must be separated. Normalization must be disclosed. If generated indices are used, their construction must be transparent. If the model has a benchmark layer and a planned validation layer, the distinction must be stated. This principle appears across the seven source manuscripts and is essential for monograph-level replication discipline.

The fourth level is diagnostic validation. Depending on the problem, validation may include econometric association checks, robust inference, rolling forecast tests, benchmark comparisons, spectral diagnostics, Monte Carlo perturbations, placebo logic, sensitivity analysis, exact reduced enumeration, external-proxy screening or anti-circularity tests. Diagnostic validation does not convert the model into a theorem. It determines whether the economic analogue behaves coherently enough to support a bounded claim.

The fifth level is permissible claim formulation. At this level the final claim is stated in language that matches the evidence. The claim may be strong, but it must be correctly typed. A finite-network Yang-Mills-inspired model may report a positive spectral stress threshold in a specified graph. It may not solve the Yang-Mills mass-gap problem. A Riemann-zeta FPAS+zeta model may report forecast improvement under specified validation layers. It may not verify the Riemann Hypothesis. A P-vs-NP-inspired portfolio model may document combinatorial explosion and search-performance limits in a sparse portfolio problem. It may not prove P != NP.

Table 2.1.1. Analogy-proof evidence ladder for the monograph

Evidence level	Function in the monograph	Allowed interpretation	Not allowed
Conceptual analogy	Identifies formal resemblance between a mathematical architecture and an economic problem.	A possible modelling direction.	Treating resemblance as proof or empirical validation.
Formal translation	Defines variables, transformations, graphs, functions, indices, equations or algorithms.	A structured economic analogue.	Using mathematical names without operational definitions.
Calibration	Populates the analogue with public anchors, constructed variables and disclosed assumptions.	A reproducible measurement architecture.	Hiding generated variables or treating them as independent raw data.
Diagnostic validation	Tests robustness, coherence, forecasting	Evidence for bounded economic usefulness.	Upgrading diagnostics into theorem-level claims.

	performance, spectral stability, placebo logic or reduced exact benchmarks.		
Permissible claim	States the final conclusion at the correct evidentiary level.	Methodological, empirical and interpretive contribution.	Claiming to solve, prove, test, verify or replicate the original Clay problem.

Source: Author synthesis for the monograph based on the seven source manuscripts.

2.1.6. Application of the Distinction across the Seven Economic Analogues

The analogy-proof rule becomes operational only when it is applied to each of the seven problem architectures. The following subsections define, for each case, the classical mathematical object, the excluded direct proof claim, the economic analogue and the permissible claim. This is the first point in the monograph where the seven studies are not merely listed but conceptually unified under one translation logic.

2.1.6.1. Poincare / Ricci / Perelman Logic: Inequality Pressure, Curvature and Smoothing Capacity

The classical mathematical object behind this chapter is not a general metaphor of curvature. It includes the Poincare conjecture as a topological theorem about three-dimensional manifolds, Ricci-flow logic as a geometric evolution mechanism and Perelman's proof architecture as a theorem-level resolution inside geometric topology. In the source manuscript, this classical object is explicitly not transferred as a proof. The economic system is not a smooth three-manifold, and global inequality indicators are not geometric invariants in the classical sense.

The direct proof claim is therefore excluded. The monograph does not prove the Poincare conjecture, does not reproduce Perelman's proof and does not establish a classical Ricci-flow theorem. It also does not claim that macro-regional inequality pressure literally evolves according to a geometric flow on a mathematical manifold. Such a claim would collapse the distinction between a theorem and a diagnostic model.

The economic analogue is a pressure-smoothing diagnostic architecture. Heterogeneous macro-social indicators are transformed into a common pressure-oriented scale. Inequality pressure, smoothing capacity, curvature-like deformation, scalar curvature summaries, Perelman-type energy and entropy functionals, graph connectedness, Betti-style diagnostics and Ricci-style network-curvature proxies become economic measurement objects. Their purpose is to detect deformation, stress concentration, smoothing weakness, recovery limits and structural connectedness in a macro-regional inequality system.

The permissible claim is diagnostic and methodological. The chapter may claim that the Perelman-Ricci-Poincare-inspired framework provides a coherent way to measure inequality deformation, smoothing capacity and graph-topological connectedness under the stated data and transformation rules. It may interpret crisis years, recovery patterns and persistent dispersion as model-implied evidence. It may not claim theorem proof, literal geometric invariance or unrestricted causal law. The claim remains: curvature and topology provide a disciplined measurement grammar for inequality diagnostics.

2.1.6.2. Hodge Logic: Macro-Flow Decomposition into Gradient, Curl and Harmonic Structure

The classical mathematical object is Hodge theory and, at the theorem-level boundary, the Hodge conjecture. In pure mathematics, this involves deep questions about algebraic cycles, Hodge classes, cohomology and projective algebraic varieties. The source manuscript recognizes this boundary by separating classical Hodge theory from applied discrete Hodge-type decomposition. This separation is essential because a macroeconomic network is not an algebraic variety and an economic edge signal is not a Hodge class in the classical algebraic-geometric sense.

The direct proof claim is excluded. The monograph does not prove the Hodge conjecture, does not claim that macroeconomic regions generate algebraic cycles and does not interpret a decomposition of economic flows as evidence about the representation of cohomological classes. It uses Hodge vocabulary in a discrete computational and econometric sense, not as a theorem-level claim in algebraic geometry.

The economic analogue is a decomposable macro-flow system. Public macroeconomic anchors are transformed into a weighted regional network, a directed macro-flow pressure field and an edge cochain that can be decomposed into gradient hierarchy, curl or local-cycle imbalance and harmonic systemic circulation. This translation is economically meaningful because it separates different sources of global macro-flow structure: vertical hierarchy, regional-cycle tension and persistent circulation that remains after hierarchy and local curl are accounted for.

The permissible claim is that Hodge-type decomposition can serve as a reproducible measurement architecture for macroeconomic flow pressure, systemic circulation, shock transmission and resilience. The chapter may claim internal

benchmark coherence, structural interpretability and validation-oriented usefulness under its graph and data assumptions. It may not claim to settle any algebraic-geometric theorem. The valid statement is applied: Hodge decomposition is used as a formal language for economic flow decomposition, not as proof of the Hodge conjecture.

2.1.6.3. Navier-Stokes Logic: Liquidity Flow, Pressure, Friction and Systemic Stress

The classical mathematical object is the Navier-Stokes existence and smoothness problem for fluid equations. In its mathematical form, the problem concerns the existence, smoothness and behavior of solutions under specified conditions. This is a theorem-level problem in partial differential equations and mathematical fluid dynamics. It is not equivalent to a macro-financial stress index, even if the economic model borrows the language of velocity, pressure, viscosity, diffusion, forcing and closure.

The direct proof claim is excluded. The monograph does not solve the mathematical Navier-Stokes problem. It does not claim that liquidity is a physical fluid or that financial stress obeys the same laws as a continuum fluid. It also does not claim a universal crisis-prediction law. These exclusions are necessary because macro-financial variables are institutional, behavioral and statistical objects rather than physical fields governed by hydrodynamic equations.

The economic analogue is a nondimensional stress-balance framework. Liquidity velocity weakness, acceleration pressure, macro-financial pressure gradients, friction or diffusion, stochastic shocks, GDP-cycle forcing and a restricted hidden-adjustment closure term are converted into unit-free diagnostic components. The model's scientific strength depends on nondimensionalization, direction harmonization, closure discipline, panel structure, rolling validation, benchmark comparison, robustness analysis, external-target plausibility and policy counterfactuals.

The permissible claim is a stress-testing claim. The Navier-Stokes-inspired chapter may state that a flow-pressure-friction-shock-cycle-closure grammar helps measure systemic stress and liquidity resilience across the specified country-year panel and validation windows. It may report diagnostic associations, forecast-window evidence and scenario effects. It may not infer physical law, theorem proof, permanent forecast superiority or unconditional crisis prediction. The valid contribution is a macro-financial measurement architecture inspired by flow mechanics but bounded by econometric evidence.

2.1.6.4. Yang-Mills Logic: Gauge Curvature, Action and Finite-Network Shock Thresholds

The classical mathematical object is the Yang-Mills existence and mass-gap problem. At theorem level, it concerns quantum gauge fields and the existence of a positive mass gap under the relevant mathematical framework. The term mass gap has a specific meaning in mathematical physics. It cannot be directly inferred from a finite economic graph unless the claim is explicitly redefined as an economic finite-network analogue.

The direct proof claim is excluded. The monograph does not solve the Yang-Mills mass-gap problem, does not construct a physical quantum gauge theory and does not claim that global corridor networks are literal gauge fields. A stress Laplacian in a finite weighted economic graph is not a theorem-level proof about quantum fields. It is a constructed spectral object within a specified benchmark network.

The economic analogue is a finite-network gauge-econometric framework. Public macroeconomic anchors are transformed into systemic-stress scores, corridor-weighted graph structure, stress-weighted adjacency, an antisymmetric economic gauge potential, triangular curvature, Yang-Mills-type economic action, a stress Laplacian, an Economic Mass Gap Index, fragility, BridgeStress, resilience and scenario-based shock diagnostics. In this translation, mass gap means positive spectral separation in a finite weighted graph, not the physical mass gap of quantum gauge theory.

The permissible claim is finite-network and diagnostic. The chapter may claim that the constructed global-corridor benchmark contains a measurable spectral threshold separating locally absorbable stress from systemically transmissible shocks under the model assumptions. It may interpret curvature concentration, action concentration, corridor exposure and scenario threshold compression. It may not claim a mathematical solution to Yang-Mills. The valid statement is that gauge-theoretic logic supplies a disciplined language for measuring systemic shock thresholds in finite economic networks.

2.1.6.5. Birch-Swinnerton-Dyer Logic: Local-to-Global Structural Rank

The classical mathematical object is the Birch-Swinnerton-Dyer conjecture, which relates arithmetic information about elliptic curves, rational points, rank and the analytic behavior of an L-function at a critical point. Its proof standard belongs to number theory and arithmetic geometry. Regional economies, corridor nodes and macroeconomic indicators are not elliptic curves, and their constructed L-function analogues are not classical arithmetic L-functions.

The direct proof claim is excluded. The monograph does not prove, test or replicate the classical BSD conjecture. It does not claim analytic continuation, a functional equation, arithmetic Euler products or theorem-level equality between analytic

order and algebraic rank. It also does not claim that finite-state regional regimes are literal reductions over finite fields. These exclusions protect the model from category error.

The economic analogue is a local-to-global structural-rank architecture. Public macro-regional anchors are transformed into systemic-stress components, weighted regional-network structure, economic curve coefficients, discriminant diagnostics, finite-state trace analogues, Euler-factor analogues, a constructed economic L-function, an L-order measure and a structural-rank object. Local reductions are interpreted as discretized regional states; Euler factors aggregate local information; the economic L-function provides a global order-of-behavior diagnostic; structural rank serves as the economic rank counterpart.

The permissible claim is calibrated measurement. The chapter may claim that local regional signals and Euler-factor information are informative about constructed global structural rank under the specified analogue architecture. It may interpret rank gaps, stability, corridor stress, anti-circularity checks and closure-layer diagnostics. It may not claim number-theoretic proof or empirical testing of classical BSD. The valid contribution is a regional measurement system that uses BSD's local-to-global grammar to organize structural-rank formation.

2.1.6.6. Riemann-Zeta Logic: Spectral-Cyclical Inflation Forecasting

The classical mathematical object is the Riemann zeta function and the Riemann Hypothesis concerning the location of its non-trivial zeros. This is a theorem-level question in analytic number theory. The fact that zeta-related computations can generate oscillatory or spectral signals does not mean that an inflation forecast model can verify the Riemann Hypothesis. The theorem concerns zeros of the zeta function, not inflation pressure.

The direct proof claim is excluded. The monograph does not prove, test or verify the Riemann Hypothesis. It does not claim that inflation data reveals the zero distribution of the zeta function. It does not eliminate residual forecast problems and does not establish universal forecast dominance. These exclusions are especially important because high forecast performance can tempt overinterpretation if the mathematical object is not clearly bounded.

The economic analogue is a hybrid FPAS+zeta inflation-forecasting system. A structural FPAS baseline is augmented by a normalized zeta-cycle generated from a nonlinear macro-financial tau argument, transformed into a signed deviation from neutrality and calibrated through an alpha-weighted correction. The zeta component is an explicit computational cyclical signal, not a theorem-level object. Its value is tested through layered annual, quarterly and monthly validation, forecast comparison, calibration tests, residual diagnostics, regime screens and spectral diagnostics.

The permissible claim is bounded forecast and diagnostic improvement. The chapter may claim that, within the specified global aggregate samples and validation layers, the FPAS+zeta model improves forecast accuracy relative to stated benchmarks and enhances crisis-regime interpretation. It may not claim that the Riemann Hypothesis has been verified or that the model dominates all alternatives across all countries, samples and horizons. The valid statement is that zeta-cycle construction can be operationalized as a disciplined spectral signal for inflation forecasting.

2.1.6.7. P versus NP Logic: Portfolio Optimization and Computational Complexity

The classical mathematical object is the formal P versus NP problem in theoretical computer science. It concerns the relationship between problems whose solutions can be found in polynomial time and problems whose proposed solutions can be verified in polynomial time. It is not resolved by observing that a particular economic or financial search problem is large, difficult or combinatorial.

The direct proof claim is excluded. The monograph does not prove P = NP, does not prove P != NP and does not resolve any Millennium Prize problem in computational complexity. It also does not claim certified global optimality in the full portfolio universe where full enumeration is not completed. The computational-finance evidence is problem-specific, not theorem-level.

The economic analogue is a cardinality-constrained portfolio-optimization architecture. A fixed industry universe is combined with CAPM-implied expected returns, covariance geometry, correlation diagnostics, eigenvalue checks, combinatorial support-space growth, greedy search, Monte Carlo sampling, genetic algorithms, continuous reoptimization, exact reduced enumeration, robustness layers, transaction-cost realism, beta drift, stress scenarios and a Black-Scholes derivative-pricing overlay. The P-vs-NP grammar enters through the separation between discrete support selection and continuous weight optimization under combinatorial growth.

The permissible claim is empirical-computational. The chapter may claim that sparse portfolio selection creates a computationally hard search landscape in the specified universe, that heuristic and exact reduced layers provide bounded evidence, and that robustness tests clarify the stability of best-found incumbents. It may not claim theorem proof, certified

full-universe optimality without exhaustive or formal certification, or realized historical investment dominance. The valid contribution is a claim-bounded computational-finance framework for studying portfolio choice under complexity.

2.1.7. Permissible and Impermissible Language

Because the monograph works with mathematically ambitious terminology, language control is part of methodology. The safest rule is to avoid verbs that imply theorem-level achievement unless the statement refers to the economic analogue itself. The book should not say that it proves, verifies, tests, confirms, replicates or solves a Clay problem. It may say that it translates, operationalizes, calibrates, models, diagnoses, measures, audits, compares, validates within a specified window or constructs an economic analogue.

The difference is not stylistic. The phrase 'proves a mass gap' is mathematically dangerous because it can be read as a claim about Yang-Mills theory. The phrase 'reports a positive finite-network economic mass-gap index in the specified graph' is bounded and scientifically meaningful. The phrase 'tests the Riemann Hypothesis through inflation' is impermissible. The phrase 'tests whether a normalized zeta-cycle improves a global inflation forecast within layered validation samples' is permissible. The phrase 'solves P versus NP in portfolio optimization' is impermissible. The phrase 'documents combinatorial support-space explosion and compares heuristic search with reduced exact certification' is permissible.

This language discipline should be applied consistently throughout the monograph. It should appear in introductions, chapter transitions, table captions, figure explanations, methodology sections, results interpretations and conclusions. If a table reports strong numerical evidence, the surrounding text must still specify the evidence type. A high R-squared, low forecast error, positive spectral gap, robust rank correlation or successful exact reduced enumeration does not change the theorem boundary. It strengthens the economic analogue only.

The following rule should govern all later chapters: mathematical names may be used when the corresponding economic object is formally defined, but theorem verbs must be avoided unless the text explicitly negates them. The model may be 'Navier-Stokes-inspired', 'Hodge-econometric', 'Yang-Mills finite-network', 'BSD-inspired', 'Riemann-zeta forecasting', 'P-vs-NP-inspired' or 'Perelman-Ricci-Poincare-inspired'. It should not be described as a solution to Navier-Stokes, Yang-Mills, BSD, Riemann, P versus NP, Hodge or Poincare.

Table 2.1.2. Safe language rule for theorem-inspired economic analogues

Unsafe or overclaiming formulation	Safe monograph formulation	Reason
The chapter proves the Yang-Mills mass gap.	The chapter constructs a finite-network economic mass-gap analogue.	The model uses spectral graph separation, not quantum-field proof.
The model tests the Riemann Hypothesis.	The model tests a normalized zeta-cycle forecast correction.	Forecast validation does not address the zero-location theorem.
The portfolio chapter proves P != NP.	The portfolio chapter documents combinatorial search difficulty and bounded algorithmic evidence.	A financial optimization instance is not a proof about formal complexity classes.
The BSD model verifies the conjecture empirically.	The BSD model calibrates a local-to-global structural-rank analogue.	Regional finite states are not arithmetic reductions of elliptic curves.
The Hodge model proves Hodge structure in the economy.	The Hodge model decomposes a constructed macro-flow edge cochain.	Applied discrete decomposition is not algebraic-geometric proof.
The Navier-Stokes model establishes a liquidity law.	The Navier-Stokes model creates a nondimensional stress-testing balance.	Macro-financial stress is not a physical fluid equation.
The Perelman-Ricci model proves topological convergence.	The Perelman-Ricci model diagnoses inequality deformation and smoothing capacity.	Graph and curvature proxies are economic diagnostics, not manifold proof.

Source: Author synthesis for monograph-level wording discipline.

2.1.8. The Constructed Object Principle

A central implication of the analogy-proof distinction is the constructed object principle. Many of the most important variables in the monograph are not raw institutional indicators. They are constructed objects generated from public anchors, normalization rules, author-coded transformations, network structures, matrices, functions or algorithms. This does not make them invalid. It makes their disclosure mandatory.

The constructed object principle applies differently across the chapters. In the Navier-Stokes analogue, starred variables are nondimensional stress components. In the Hodge analogue, the edge pressure field is an author-calculated cochain. In the Yang-Mills analogue, gauge potential, curvature, action and economic mass gap are model-derived finite-network objects. In the BSD analogue, finite-state traces, Euler factors, the economic L-function and LOrder are calibrated analogues. In the Riemann-zeta analogue, the zeta-cycle and its deviation from neutrality are constructed signals. In the P-vs-NP analogue, support spaces, search coverage and reduced exact benchmarks are computationally defined. In the Perelman-Ricci-Poincare analogue, curvature-like and entropy-like diagnostics are pressure-oriented constructs.

Because these objects are constructed, their validity depends on transparent design. The monograph should therefore consistently distinguish public data from author-calculated indicators, raw variables from normalized variables, observed outcomes from model-implied outputs, benchmark evidence from external validation, diagnostic association from causality and forecast-window performance from universal forecast dominance. This distinction is part of the same logic as analogy versus proof: a constructed economic object may be useful, but its meaning is defined by construction, not by the prestige of the mathematical name attached to it.

The constructed object principle also strengthens replication. If the monograph states formulas, transformation rules, source ledgers, code paths, random seeds, matrix definitions, sample windows and file hashes where applicable, the economic analogue becomes auditable. A reader can disagree with an assumption, test sensitivity or rebuild the model. This is the correct standard for a theorem-inspired economic analogue. The reader is not asked to accept a theorem claim; the reader is given a reproducible measurement architecture.

2.1.9. The Claim Hierarchy of the Monograph

The analogy-proof distinction produces a hierarchy of claims. At the bottom are excluded claims: theorem proof, theorem verification, physical identity, unrestricted causality, universal prediction and certified optimality where no certificate exists. These claims are not part of the monograph. They should be explicitly rejected whenever a reader could reasonably misunderstand the mathematical terminology.

The next level contains methodological claims. The monograph may claim to develop seven measurement architectures inspired by the formal logics of the Millennium Problems. This is the book's broadest contribution. It is independent of whether each empirical chapter has equally strong numerical evidence, because the methodological claim concerns translation design, object construction, data discipline and validation architecture.

The next level contains empirical diagnostic claims. These are chapter-specific. The inequality chapter may diagnose pressure, curvature-like deformation and smoothing capacity. The Hodge chapter may decompose macro-flow pressure into hierarchy, local imbalance and systemic circulation. The Navier-Stokes chapter may measure liquidity-flow stress and closure. The Yang-Mills chapter may measure finite-network shock thresholds. The BSD chapter may calibrate local-to-global structural rank. The Riemann chapter may compare forecast performance. The P-vs-NP chapter may evaluate computational search behavior in sparse portfolio optimization.

The strongest level within economics is bounded validation. This level is reached only when the chapter's diagnostics survive the relevant tests: robustness, sensitivity, benchmark comparison, out-of-sample validation, Monte Carlo uncertainty, exact reduced enumeration, placebo logic, anti-circularity checks or external-proxy screening. Even then, the validation remains bounded by sample, model, data and assumptions. It does not cross into theorem proof.

This hierarchy should guide the conclusions of every later chapter. A strong result should be stated strongly but correctly. Weak p-values, small clusters, generated-index circularity, limited external proxies, benchmark dependence and sample-size restrictions should not be hidden. They should be used to calibrate the claim. The monograph's scientific strength comes from this discipline: it can be ambitious in architecture while conservative in proof language.

2.1.10. Monograph-Level Synthesis: Why Analogy Is Scientifically Legitimate

The central question after excluding proof is whether analogy remains scientifically legitimate. In this monograph, the answer is yes, provided that analogy is formal, operational and bounded. Scientific modelling often advances by translating structure across domains. Economics has long borrowed from mechanics, probability, information theory, topology,

network science, optimization and statistical physics. The decisive issue is not whether borrowing occurs, but whether the borrowed structure is made explicit and empirically disciplined.

The seven economic analogues satisfy this standard when they are read correctly. They do not claim that the global economy is literally a manifold, a fluid, a gauge field, an elliptic curve, a zeta function, a cohomology space or a formal complexity class. They claim that these mathematical architectures offer rigorous ways to organize economic measurement. Flow logic helps measure liquidity stress. Curvature logic helps measure inequality deformation. Decomposition logic helps separate hierarchy from circulation. Gauge and spectral logic helps measure shock thresholds. Local-to-global logic helps compare regional states with structural rank. Zeta-cycle logic helps test nonlinear inflation signals. Complexity logic helps measure sparse decision search.

Analogy becomes scientific when it passes through modelling discipline. That discipline includes formal definitions, transparent transformations, data separation, validation design, robustness, replication and claim control. Under these conditions, an economic analogue can be more than a metaphor. It can be a productive research instrument, capable of revealing structure that conventional single-indicator approaches miss. The monograph's contribution is to bring seven such instruments into one integrated research program.

The final rule of Section 2.1 can be stated in one sentence: mathematical theorem is not equal to economic model, but mathematical architecture can become an economic measurement grammar when the translation is explicit, the data are auditable, the validation is bounded and the final claim remains within the evidentiary limits of the analogue. This rule is the conceptual foundation for the remaining sections of Chapter 2 and for all seven problem chapters that follow.

2.1.11. Operational Checklist for the Seven Problem Chapters

For editorial consistency, every problem chapter in the monograph should pass a four-part checklist before its model is introduced. First, it should identify the classical mathematical object in one precise paragraph. Second, it should state why the original proof claim is excluded. Third, it should define the economic analogue and the transformation path from public or constructed data to model objects. Fourth, it should state the permissible claim before the empirical results are discussed.

This checklist prevents the reader from encountering mathematical terminology before the claim boundary is clear. It also improves the monograph's internal architecture. Instead of seven unrelated article introductions, the book will have a consistent translation protocol. Each chapter can still preserve its own empirical specificity, but each will be read through the same conceptual lens established here.

The checklist also helps with peer review. A reviewer may disagree with a modelling assumption, a sample choice or a transformation rule, but the reviewer should not be able to say that the monograph confuses economic analogy with mathematical proof. Section 2.1 directly prevents that objection. It states, before the specialized chapters begin, that the book is a monograph of bounded economic analogues inspired by mathematical architectures, not a collection of claimed solutions to Clay problems.

Table 2.1.3. Minimum translation checklist for each problem chapter

Checklist element	Required content	Purpose	Example wording logic
Classical object	Define the original mathematical object or theorem-level problem.	Prevents vague borrowing.	The classical object is the Navier-Stokes existence and smoothness problem.
Proof exclusion	State that the chapter does not solve, prove, test or replicate the original problem.	Prevents mathematical overclaiming.	The chapter does not solve the mathematical Navier-Stokes problem.
Economic analogue	Define the translated economic object and transformation logic.	Turns analogy into methodology.	Liquidity stress is represented through nondimensional flow-pressure-friction terms.
Permissible claim	State the highest claim allowed by the evidence.	Matches conclusion to validation level.	The framework supports diagnostic stress-testing, not theorem proof or universal crisis prediction.

Source: Author synthesis for unified monograph editing.

2.1.12. Closing Transition

Section 2.1 has established the boundary between analogy and proof. This boundary is the first and most important layer of the conceptual translation framework. The next analytical step is to move from the general distinction to the translation mechanics themselves: how a classical mathematical architecture is decomposed into transferable modelling components, how those components are mapped onto economic variables and how claim boundaries are embedded inside the model design rather than appended only at the end.

The rest of Chapter 2 should therefore proceed from this foundation. After the reader accepts that theorem proof and economic analogue are distinct, the monograph can legitimately explain how formal mathematical architectures become economic measurement grammars. That is the purpose of the remaining sections of the chapter: to clarify the translation path from classical object to economic analogue, from mathematical structure to empirical variable, from model construction to validation, and from validation to permissible claim.

2.2. Flow Analogies

Section 2.2 develops the flow dimension of the monograph's conceptual translation framework. It is written as a new monograph-level section, not as a mechanical transfer of the Navier-Stokes and Hodge article introductions. Its task is to explain why flow is a legitimate economic measurement grammar, how two different mathematical traditions organize flow in different ways, and what level of claim is permissible when these traditions are translated into economic-econometric models.

The section rests on a strict rule already established in Section 2.1: a mathematical theorem is not an economic model. The flow analogies in this monograph do not assert that macro-financial liquidity is a physical fluid, that the world economy is a smooth continuum field, or that regional economic networks settle theorem-level questions in partial differential equations or algebraic geometry. They assert something more precise and more useful for economics: that flow-related mathematical grammars can structure measurable economic objects when the translation is explicit, the data transformations are auditable, and the final claim is kept inside diagnostic and measurement boundaries.

Two source architectures are central. The Navier-Stokes-inspired chapter translates flow balance into a nondimensional macro-financial stress-testing framework: liquidity velocity weakness, acceleration pressure, macro-financial pressure gradients, friction or diffusion, stochastic shocks, cyclical forcing and restricted closure become components of systemic-stress formation. The Hodge-econometric chapter translates flow decomposition into a regional macro-flow network: public macroeconomic anchors are converted into a directed edge-pressure field and decomposed into gradient hierarchy, curl or local-cycle imbalance, and harmonic systemic circulation.

The two analogies are complementary rather than redundant. Navier-Stokes supplies a balance language for how stress is formed through motion, pressure, friction, shock and closure. Hodge supplies a decomposition language for where flow pressure sits inside a network: hierarchy, local circulation and system-wide residual circulation. Together, they create the monograph's first major measurement dimension: economic flow as a structured, multidimensional, auditable process rather than a loose metaphor of movement.

2.2.1. Why Flow Is a Monograph-Level Measurement Grammar

Flow is one of the most important shared languages of the seven-problem architecture because modern economic systems are not static collections of indicators. Liquidity, inflation pressure, trade exposure, growth pressure, corridor dependence, technological diffusion, institutional adjustment, portfolio allocation and regional shock propagation all move across time, sectors and networks. The monograph therefore treats flow not as a decorative metaphor but as a disciplined conceptual tool for measuring movement, imbalance, transmission and residual circulation.

In conventional macroeconomic description, movement is often reduced to a change in a scalar variable: GDP grows, inflation falls, interest spreads widen, unemployment rises, trade openness changes. Such variables are necessary, but they do not automatically explain how pressure moves through a system. A single inflation value does not show whether stress comes from liquidity weakness, sovereign pressure, supply-chain friction or stochastic shock. A regional growth rate does not show whether the region is a hierarchical source, a local-cycle imbalance point or a persistent systemic circulation channel. This is precisely the analytical gap that flow analogies address.

At the monograph level, flow has four meanings. First, it means temporal movement: economic variables evolve through time and carry acceleration, deceleration, persistence and shock response. Second, it means spatial or network transmission: stress travels through countries, regions, corridors, financial channels and trade interfaces. Third, it means

structural decomposition: observed pressure can be split into hierarchy, local cycles and system-wide circulation. Fourth, it means model closure: any flow model must explain what is observable, what is proxy-observable and what remains hidden but restricted rather than arbitrary.

The Navier-Stokes and Hodge chapters enter this architecture from different sides. Navier-Stokes begins from a balance equation and asks how flow pressure is formed. Hodge begins from a network edge field and asks how flow pressure is decomposed. One is stress-dynamic; the other is topological-compositional. The monograph needs both because systemic economic complexity is not only about the intensity of stress, but also about its direction, location, decomposition and persistence.

The flow dimension also clarifies why the book cannot be organized as seven isolated articles. The Navier-Stokes chapter, the Hodge chapter, the Yang-Mills corridor network, the BSD local-to-global architecture and the Perelman-Ricci pressure-smoothing framework all contain movement and transmission logics. Even the Riemann-zeta inflation model has a cyclical pressure signal, and the P-vs-NP portfolio chapter models movement through a discrete-continuous search space and capital-allocation frontier. The common monograph-level question is therefore not merely what each mathematical inspiration does separately, but how flow-based reasoning helps build a unified economic measurement program.

Table 2.2.1. Flow logic across the seven economic analogues

Problem architecture	Flow-related economic object	Main role in Chapter 2.2	Permissible claim level
Navier-Stokes	Liquidity velocity, acceleration, pressure gradient, friction/diffusion, shocks, GDP-cycle forcing and restricted closure.	Primary flow-balance analogy.	Diagnostic stress-testing and bounded forecasting-window evidence.
Hodge	Directed macro-flow pressure field decomposed into gradient, curl and harmonic components.	Primary flow-decomposition analogy.	Benchmark measurement of hierarchy, local imbalance and systemic circulation.
Yang-Mills	Stress circulation on a finite corridor graph, gauge potential, curvature/action and spectral threshold.	Network-flow extension of shock transmission.	Finite-network threshold diagnostics, not physical field theory.
BSD	Local regional signals, corridor stress and Hodge-flow component inside structural rank.	Local-to-global flow of information into rank formation.	Calibrated rank-consistency and transmission interpretation.
Perelman/Ricci/Poincare	Inequality pressure, smoothing capacity, curvature-like deformation and recovery path.	Pressure-smoothing flow adjacent to flow logic.	Diagnostic deformation and smoothing-capacity measurement.
Riemann Hypothesis / zeta	Crisis-sensitive cyclical pressure signal added to inflation forecasting.	Spectral-cycle movement, not physical flow.	Forecast-diagnostic improvement under sample discipline.
P vs NP	Sparse support-selection search and capital-allocation movement through feasible supports.	Computational boundary of economic flow design.	Complexity-aware optimization evidence, not theorem proof.

Source: Author synthesis for the monograph based on the seven uploaded Millennium-problem economic manuscripts.

2.2.2. Classical Flow Objects and the Exclusion of Direct Proof

The first requirement of the section is to identify the classical mathematical objects before translating them. In the Navier-Stokes case, the classical object is the flow equation family associated with fluid motion, including velocity, acceleration, pressure, viscosity or diffusion and external forcing. At theorem level, the Clay problem concerns existence

and smoothness of solutions under formal mathematical conditions. That problem belongs to partial differential equations and mathematical fluid dynamics. It is not an empirical question about sovereign spreads, inflation pressure, liquidity indicators or macro-financial stress indices.

In the Hodge case, the classical object is more subtle. Hodge theory concerns decomposition of differential forms and, in algebraic geometry, the Hodge conjecture concerns the relationship between Hodge classes and algebraic cycles. The applied Hodge-econometric chapter does not work inside this theorem-level setting. It uses a discrete network version of Hodge-style decomposition: an edge signal on a graph is split into gradient, curl and harmonic components. That applied decomposition can be economically meaningful, but it does not prove anything about algebraic cycles or the Hodge conjecture.

These exclusions are not defensive afterthoughts. They are part of the scientific design. If the Navier-Stokes analogy claimed that liquidity is literally a physical fluid, it would be false in category. Liquidity is institutional, legal, behavioral, balance-sheet based and policy-sensitive. If the Hodge analogy claimed that regional macroeconomic nodes produce theorem-level Hodge classes, it would be mathematically misplaced. Economic regions are constructed empirical units, not smooth projective varieties. Therefore, the translation must preserve the structure of the mathematical grammar without importing the theorem claim.

The correct epistemic status is analogue construction. A classical flow object supplies an organizing form. The economic model supplies variables, transformations, data and tests. Validation then applies only to the economic construction. In the Navier-Stokes case, validation concerns whether the nondimensional balance equation, closure mechanism, rolling forecasts, panel associations and scenario outputs behave coherently. In the Hodge case, validation concerns whether the graph, edge-pressure field, decomposition, projection diagnostics, econometric screens, machine-learning checks and persistent-homology evidence support a useful macro-flow benchmark. Neither validation path crosses into theorem proof.

This rule allows the monograph to use sophisticated mathematical language without inflating its claim. The model can be strong because it is formally organized, empirically transparent and reproducible. The claim remains bounded because it does not exceed the evidence domain. This is the central epistemic discipline of all flow analogies in the book.

Table 2.2.2. Classical object, translation boundary and economic analogue in the two flow chapters

Flow chapter	Classical mathematical object	Excluded direct claim	Economic analogue	Permissible claim
Navier-Stokes	Continuum flow logic with velocity, acceleration, pressure, viscosity/diffusion and forcing; theorem-level existence and smoothness problem.	No claim that financial liquidity is a physical fluid; no solution or empirical test of the mathematical Navier-Stokes problem; no universal crisis-prediction law.	Nondimensional macro-financial stress-balance architecture with velocity weakness, acceleration pressure, pressure gradients, friction/diffusion, shocks, cycle forcing and restricted closure.	A reproducible global liquidity-flow stress-testing framework supporting diagnostic and validation-window claims.
Hodge	Hodge-theoretic decomposition and, at theorem boundary, the Hodge conjecture concerning Hodge classes and algebraic cycles.	No claim to prove the Hodge conjecture; no claim that economic regions are algebraic varieties or that macro-flow cochains are theorem-level Hodge classes.	Discrete Hodge-econometric decomposition of a regional directed macro-flow pressure field into gradient hierarchy, curl/local imbalance and harmonic systemic circulation.	A regional benchmark measurement architecture for hierarchy, local imbalance, systemic circulation, shock transmission and resilience.

Source: Author synthesis based on the Navier-Stokes and Hodge source manuscripts.

2.2.3. The Navier-Stokes Translation: From Physical Flow Balance to Liquidity-Stress Measurement

The Navier-Stokes-inspired component begins from a single conceptual insight: systemic financial stress is not well represented by a list of independent indicators. Inflation pressure, sovereign-risk premia, credit and banking frictions, liquidity velocity, stochastic shocks, GDP-cycle movements, policy buffers and hidden adjustment channels interact. A stress system can therefore appear stable in one indicator while already becoming fragile through the joint action of pressure, friction, weak flow and residual adjustment.

The classical flow grammar is useful because it organizes these channels into a balance architecture. In a physical flow equation, velocity describes movement, acceleration describes change in movement, pressure gradients describe directional force, viscosity or diffusion describes frictional dissipation, external force describes disturbance, and closure conditions prevent the system from becoming indeterminate. The economic translation does not carry physical units into finance. Instead, it constructs nondimensional variables so that heterogeneous macro-financial inputs can be compared inside one diagnostic scale.

The economic analogue therefore begins with direction harmonization. Variables that increase stress are oriented in the stress direction; variables that represent resilience are transformed so that weakness appears as stress pressure. The next step is nondimensionalization. Raw units such as percentages, spreads, deviations, indices and proxy values are not added directly. They are transformed into unit-free starred variables. This is essential because a flow analogy without unit discipline would be only metaphorical. Nondimensional scaling turns the analogy into an auditable measurement framework.

Within this framework, liquidity velocity weakness is not the velocity of a physical fluid. It is an economic diagnostic channel capturing weak or deteriorating liquidity circulation. Acceleration pressure is not physical acceleration; it is the changing intensity of stress. Pressure gradients are macro-financial pressure differences across states, countries, regions or time. Friction and diffusion represent credit, funding, banking, liquidity and institutional transmission obstacles. Stochastic shocks represent event volatility and sudden disturbance. Fourier GDP-cycle forcing introduces cyclical macroeconomic movement into the stress architecture. Restricted closure, epsilon(t), captures hidden adjustment but does so through observable or proxy-observable state variables rather than through an unrestricted residual plug.

The conceptual achievement of the Navier-Stokes translation is that it transforms a potentially vague idea - liquidity stress moves like a flow - into a structured empirical sequence: public macro-financial proxies, direction harmonization, nondimensionalization, systemic-stress and liquidity-resilience indices, Navier-Stokes-inspired balance, restricted closure, Fourier-cycle forcing, rolling validation, benchmark comparison, panel fixed effects, robustness checks, external-target validation, Monte Carlo uncertainty and policy counterfactual interpretation. Each step is a claim-control device.

The monograph should read this construction as a stress-balance grammar. It does not say that finance is physics. It says that systemic stress can be measured as a balance of economic flow pressure, friction, shocks, cycles and closure. The permissible claim is strong precisely because it is bounded: the model can support global stress diagnostics and stress testing within the reported empirical design; it cannot support theorem-level Navier-Stokes proof, literal hydrodynamic identity, definitive causality or unconditional crisis prediction.

2.2.3.1. Velocity Weakness and Acceleration Pressure

Velocity is the first term in the Navier-Stokes-inspired economic language, but it must be read carefully. In the monograph's macro-financial interpretation, velocity does not mean that liquidity particles move through a physical space. It means that the financial system has measurable circulation intensity. When liquidity movement weakens, funding channels become less responsive, payment and credit circulation tighten, and the same macro-financial shock can generate more systemic stress. The velocity term therefore captures the flow-capacity side of stress formation.

Acceleration adds a second dimension. A system may be stressed not only because its current level is high, but because its stress is intensifying. Acceleration pressure captures the rate at which liquidity weakness, spreads, inflation pressure or volatility are changing. The importance of this distinction is methodological: a static stress score can miss turning points, while an acceleration term can help identify transition from manageable pressure to high-stress regime. In the monograph, acceleration is therefore part of the measurement grammar for regime sensitivity.

Together, velocity weakness and acceleration pressure prevent systemic stress from being reduced to a level indicator. They introduce dynamic structure. A country or region can have moderate current stress but high acceleration pressure, implying vulnerability to future escalation. Conversely, a country with high but decelerating stress may be in a different

diagnostic position. The flow analogy therefore enriches the econometric interpretation of stress by distinguishing level, movement and change in movement.

2.2.3.2. Pressure Gradients, Friction and Diffusion

Pressure gradients are central because systemic stress is rarely evenly distributed. Sovereign spreads, inflation pressure, exchange-rate pressure, external financing constraints and liquidity shortages create directional stress differences. In a macro-financial system, these differences become transmission incentives: stress can move from high-pressure points to vulnerable receiving points through financial, trade, institutional and expectations channels. The pressure-gradient term therefore translates a physical idea into a measurable economic channel of imbalance.

Friction and diffusion represent the fact that transmission is not costless. Credit-market frictions, banking-sector constraints, liquidity premia, institutional bottlenecks, policy delays and balance-sheet weaknesses can slow, amplify or distort adjustment. Friction is not molecular viscosity; it is a macro-financial barrier to smooth stress absorption. Diffusion is not physical diffusion; it is the spreading or dissipation of pressure through economic channels. In the model, this term helps identify whether stress persists because the system lacks adequate absorptive capacity.

The pressure-friction combination is one of the most valuable parts of the analogy. Pressure without friction would imply immediate adjustment. Friction without pressure would imply inert resistance without directional stress. Together they explain why some systems carry pressure for long periods, why shocks become persistent, and why liquidity stress can differ across regions even when global shocks are common. This is especially important for macroprudential analysis, where the same shock may have different consequences depending on financial depth, fiscal space, external buffers and institutional resilience.

2.2.3.3. Shock Forcing, Cycle Forcing and Restricted Closure

External forcing in the economic version captures shocks that cannot be reduced to smooth trend dynamics. These include financial-spread shocks, inflation persistence, geopolitical disturbances, remittance or transfer shocks, crisis events and volatility pressure. The term is necessary because real macro-financial systems are not closed deterministic mechanisms. They are exposed to discrete disturbances and regime breaks. The flow analogy is therefore not a smoothness claim; it is a way of organizing shock-sensitive stress formation.

Fourier GDP-cycle forcing adds cyclical discipline. Rather than treating all deviations as unexplained noise, the framework recognizes that macroeconomic stress interacts with growth cycles. The important claim-control device is no-look-ahead logic in rolling-window estimation. Cycle information should not be used in a way that leaks future data into past forecasts. In the monograph, cycle forcing is therefore not only a modelling enhancement but also a validation discipline.

Restricted closure is the strongest conceptual safeguard in the Navier-Stokes-inspired model. A residual term can easily become a free algebraic plug: whatever the model fails to explain is placed into epsilon(t). The source manuscript avoids this by modelling epsilon(t) through observable or proxy-observable state variables, including lagged closure, shadow pressure, external transfers, geopolitical shock, fiscal buffers, foreign aid or support and inertia. This makes hidden adjustment auditable. The closure term remains a hidden-adjustment channel, but it is not allowed to mechanically force equality without evidence.

The closure principle has broader monograph significance. Every analogue model must decide what to do with residual structure. In the Navier-Stokes chapter, residual structure is disciplined through a restricted equation. In the Hodge chapter, residual structure appears as harmonic systemic circulation after gradient and curl components are removed. In both cases, the monograph refuses to treat unexplained structure as noise. It turns residual structure into a controlled analytical object, while still maintaining strict claim boundaries.

Table 2.2.3. Navier-Stokes economic translation map

Classical flow term	Economic translation	Measurement function	Claim discipline
Velocity	Liquidity circulation or flow-capacity condition.	Measures weakness in liquidity movement and stress absorption.	Not physical fluid velocity.
Acceleration	Change in stress intensity or liquidity weakness.	Captures transition and regime sensitivity.	Not physical acceleration.
Pressure gradient	Macro-financial pressure differences across units or time.	Identifies directional stress channels.	Not physical pressure field.

Classical flow term	Economic translation	Measurement function	Claim discipline
Viscosity / diffusion	Credit, liquidity, banking or institutional frictions and pressure spreading.	Measures resistance, persistence and transmission distortion.	Not molecular viscosity.
External forcing	Event shocks, volatility, geopolitical stress, inflation or spread shocks.	Introduces shock-sensitive disturbance structure.	Scenario and diagnostic evidence only.
Cycle forcing	GDP-cycle or macro-financial cyclical movement.	Connects stress to cyclical dynamics under no-look-ahead discipline.	Not permanent forecast superiority.
Closure epsilon(t)	Restricted hidden adjustment using observable or proxy-observable state variables.	Prevents residual from becoming a free plug.	Auditable hidden-adjustment channel, not causal proof.

Source: Author synthesis based on the Navier-Stokes-inspired macro-financial stress-testing manuscript.

2.2.4. The Hodge Translation: From Decomposition of Forms to Macro-Flow Structure

The Hodge-econometric component begins from a different flow problem. The question is not primarily how a stress balance is formed through velocity, pressure and friction. The question is how a connected economic system can be decomposed once flow pressure has been constructed on a network. Standard macroeconomic aggregates can tell the reader which regions are large, growing or income-deep, but they do not explain whether those regions act as hierarchical sources, local-cycle imbalance points or persistent systemic circulation channels. Hodge decomposition supplies this missing structural language.

The empirical object is a regional graph. The nodes are macro-regions, with the World used as a normalization anchor and the Caucasus retained as a corridor-sensitive subregional node. The edges are not raw bilateral trade flows. They are author-calculated regional macro-flow corridors derived from public macroeconomic anchors and transformation rules. This distinction is essential. The Hodge model measures structured macro-flow pressure, not observed transaction-level flows. Its scientific status therefore depends on whether the construction is transparent, reproducible and interpretable.

The core transformation is from public macroeconomic anchors to a directed edge cochain. GDP, world-output share, projected growth, transition GDP, income depth and corridor logic are converted into a weighted graph and a directed macro-flow pressure field. Once the edge field exists, discrete Hodge decomposition separates it into three components. The gradient component captures hierarchy. The curl component captures local-cycle imbalance around triangles or near-triangular regional circuits. The harmonic component captures persistent systemic circulation that remains after hierarchy and local curl are removed.

The Hodge translation is powerful because it separates economic meanings that are often confused. Output mass is not the same as hierarchy. Hierarchy is not the same as local imbalance. Local imbalance is not the same as systemic circulation. A large region may dominate GDP but not necessarily dominate every flow component. A smaller corridor-sensitive region may have low output mass but still appear in hierarchy, imbalance or harmonic exposure because of its structural position in the regional network. This is why the Hodge chapter is central to the monograph's flow dimension.

At the same time, the Hodge claim must be bounded. The decomposition is applied, discrete and econometric. The gradient, curl and harmonic outputs are author-calculated research variables, not official institutional indicators and not theorem-level Hodge classes. Econometric, predictive and topological tests validate benchmark informativeness; they do not establish final causal estimates for all countries or observed dyadic flows. The correct claim is that Hodge decomposition provides a reproducible macro-flow measurement architecture, not that the Hodge conjecture has been solved or empirically tested.

2.2.4.1. Gradient Hierarchy

The gradient component is the part of the macro-flow pressure field that can be explained by a potential-like hierarchy over regions. Economically, it corresponds to ordered directional pressure: some regions occupy higher positions in the constructed macro-flow structure, while others occupy lower positions. This does not mean that the top gradient region is necessarily the largest economy. It means that, under the specified public-anchor and edge-pressure construction, the region has a strong directed-flow role in the network.

This distinction is central for monograph-level interpretation. GDP mass is a scale variable; gradient hierarchy is a structural-flow variable. A region may be large but stable, large but low-growth, or large but not directionally dominant in the constructed pressure field. Conversely, a smaller or high-growth corridor region may have a visible gradient position because it connects growth pressure, transition dynamics and corridor relevance. The gradient component therefore allows the monograph to move beyond output-size ranking toward flow-structure measurement.

In methodological terms, gradient hierarchy also provides a bridge between the Hodge chapter and the BSD chapter. The BSD-inspired structural-rank model includes Hodge-flow rank as one of its components. This means that Hodge hierarchy is not isolated inside Chapter 6; it becomes part of the broader local-to-global structural-rank architecture. Flow decomposition therefore supports later rank formation, while remaining distinct from BSD's L-function and local-trace logic.

2.2.4.2. Curl and Local-Cycle Imbalance

The curl component captures local inconsistency or circulation around regional cycles. In economic terms, it measures imbalance that cannot be reduced to a smooth hierarchy. A regional triangle may contain growth, income, mass and corridor relations that do not align monotonically. The curl component captures these tensions. It is therefore especially useful for identifying local-cycle stress, regional divergence and corridor-sensitive imbalance.

Curl is not a statement that economies literally rotate around a physical vortex. It is an applied topological measurement of non-gradient structure. The distinction matters because local imbalances can be analytically important even when they do not dominate aggregate output. An advanced region, an emerging region or a corridor region can all have curl exposure if their macro-flow relations create local circulation rather than smooth ordering. This helps the monograph avoid the common error of treating hierarchy as the only form of economic structure.

The curl component also prepares the reader for the Yang-Mills and Ricci-related chapters. In Yang-Mills, triangular curvature and action identify concentrated stress-energy in network cycles. In the Perelman-Ricci-Poincare chapter, curvature-like deformation captures pressure-smoothing imbalance. Hodge curl is not identical to either of those objects, but it belongs to the same family of ideas: local non-neutralization, cycle tension and structural deformation. Thus Chapter 2.2 foreshadows Chapter 2.3 without collapsing the two sections.

2.2.4.3. Harmonic Systemic Circulation

The harmonic component is the residual circulation that remains after gradient hierarchy and local curl have been removed. Economically, it represents persistent system-wide circulation. This is a major conceptual advance because many economic systems contain structural loops that cannot be interpreted as simple hierarchy or local triangular imbalance. Such loops may reflect corridor dependence, regional feedback, persistent exposure or systemic transmission pathways.

Harmonic circulation is especially important for a monograph about global complexity. It offers a disciplined way to say that some pressure remains system-wide. Instead of treating the residual as noise, the Hodge framework gives it a formal location. This is similar, at a conceptual level, to the restricted closure term in the Navier-Stokes chapter: both models refuse unrestricted residuals. The difference is that Navier-Stokes closure is state-dependent and dynamic, while Hodge harmonic circulation is topological and decompositional.

The permissible claim is that harmonic exposure measures persistent circulation within the constructed regional macro-flow graph. It is not an official indicator, not observed bilateral flow, and not a theorem-level invariant. Its validity depends on the construction of the graph, the edge-pressure field, projection diagnostics, robustness checks and replication package. Within those boundaries, harmonic circulation is one of the strongest flow concepts in the monograph because it identifies systemic structure that would remain invisible in ordinary GDP, growth or income rankings.

Table 2.2.4. Hodge economic translation map

Hodge component	Economic interpretation	What it reveals	Claim discipline
Directed edge cochain	Author-calculated macro-flow pressure on regional edges.	Creates the object to be decomposed.	Proxy pressure field, not observed transaction matrix.
Gradient	Hierarchy or potential-like directional structure.	Separates flow hierarchy from raw output mass.	Structural benchmark variable, not official rank.
Curl	Local-cycle imbalance around regional circuits.	Identifies non-gradient local tension and regional-cycle imbalance.	Applied graph decomposition, not physical vortex.

Hodge component	Economic interpretation	What it reveals	Claim discipline
Harmonic	Persistent systemic circulation after gradient and curl are removed.	Measures residual network-wide circulation and corridor feedback.	Constructed systemic exposure, not theorem-level invariant.
Projection diagnostics	Orthogonality, residual and component-stability checks.	Audits whether decomposition is mathematically coherent.	Internal benchmark validation, not universal causality.
Derived indices	Resilience, tail risk, centrality and shock-transmission variables.	Converts components into economic interpretation layers.	Author-calculated research variables requiring replication.

Source: Author synthesis based on the Hodge-econometric macro-flow manuscript.

2.2.5. Complementarity Between Navier-Stokes and Hodge Flow Analogies

The Navier-Stokes and Hodge analogies should not be merged into one model. Their strength lies in complementarity. Navier-Stokes asks how systemic stress is generated through a balance of velocity weakness, acceleration, pressure gradients, friction, shocks, cycles and closure. Hodge asks how a constructed regional pressure field decomposes into hierarchy, local imbalance and systemic circulation. One is dynamic-balance oriented; the other is topological-decomposition oriented.

This complementarity can be stated more formally. The Navier-Stokes-inspired model operates primarily in a country-year stress-testing space. It is designed for a global panel and for rolling validation, benchmark comparison, fixed effects, robustness layers, external-target validation and scenario counterfactuals. The Hodge model operates primarily in a regional benchmark graph. It is designed for network construction, edge-pressure decomposition, component interpretation, spectral and higher-order Hodge-Laplacian diagnostics, machine-learning checks and persistent-homology confirmation. The two models therefore answer different but connected questions.

The Navier-Stokes question is: through which channels does systemic stress form and intensify? The Hodge question is: once macro-flow pressure is constructed, how is it structurally distributed across hierarchy, cycles and residual circulation? A full monograph on economic complexity needs both. Without Navier-Stokes, flow becomes spatial but insufficiently dynamic. Without Hodge, flow becomes dynamic but insufficiently decomposed. Together, they allow the author to treat the world economy as both temporally stress-sensitive and topologically structured.

The complementarity also helps interpret policy and resilience. A Navier-Stokes stress increase may be driven by liquidity friction, inflation pressure, sovereign-spread widening or closure weakness. A Hodge diagnosis may show whether the affected region is a hierarchy node, a local-cycle imbalance point or a systemic circulation channel. The first tells the analyst what kind of stress channel is active; the second tells the analyst where that pressure sits in the regional flow topology. This combined reading is much more informative than either a stress index or a GDP ranking alone.

At the level of claim hierarchy, the complementarity must still remain bounded. The two models can jointly support a strong flow-based measurement program. They cannot jointly prove any classical theorem. The permissible monograph claim is that flow analogies, when translated through nondimensional stress balance and discrete topological decomposition, can produce a coherent economic measurement architecture for systemic stress, macro-flow hierarchy, local imbalance, harmonic circulation, resilience and shock transmission.

Table 2.2.5. Comparative role of the two primary flow analogies

Dimension	Navier-Stokes-inspired logic	Hodge-econometric logic	Combined monograph function	Boundary
Core question	How does systemic stress form through flow, pressure, friction, shocks and closure?	How does a macro-flow pressure field decompose into hierarchy, curl and harmonic circulation?	Links stress formation to flow structure.	No theorem proof.
Empirical object	Country-year macro-financial panel with	Regional macro-flow graph with ten nodes	Connects panel stress dynamics with	Data-dependent design.

Dimension	Navier-Stokes-inspired logic	Hodge-econometric logic	Combined monograph function	Boundary
	regional and world layers.	plus World normalization anchor.	regional topology.	
Main transformation	Nondimensional stress-direction scaling and restricted balance equation.	Graph construction, directed edge cochain and discrete Hodge decomposition.	Creates two auditable flow grammars.	Constructed variables, not raw indicators.
Validation logic	Rolling forecasts, benchmark comparison, FE diagnostics, robustness, external targets, scenarios.	Projection diagnostics, robust screens, ML checks, persistent homology and sensitivity tests.	Supports diagnostic credibility through multiple evidence gates.	Validation, not causality.
Policy relevance	Identifies stress channels and model-implied scenario effects.	Identifies hierarchy, imbalance, circulation and corridor exposure.	Improves stress interpretation and regional resilience reading.	Scenario evidence only.

Source: Author synthesis for Chapter 2.2.

2.2.6. Flow Analogies and the Other Five Problem Architectures

Although Section 2.2 is centered on Navier-Stokes and Hodge, it must still be written with the entire seven-problem monograph in view. Flow is not isolated. It interacts with curvature, topology, spectral thresholds, local-to-global rank, inflation cycles and computational search. This is why the section belongs in Chapter 2 rather than in the separate Navier-Stokes or Hodge problem chapters.

The Yang-Mills chapter extends flow into corridor shock transmission. Its finite-network gauge-econometric framework treats systemic stress as circulating through a corridor-sensitive graph. Gauge potential, triangular curvature, economic action and spectral mass-gap diagnostics are not Hodge decomposition and not Navier-Stokes balance, but they depend on the same idea that systemic stress is transmitted through relational structure. Yang-Mills therefore appears as a network-flow and threshold extension of the flow dimension.

The BSD chapter extends flow into local-to-global information transmission. Its economic analogue asks whether local regional reductions, finite-state traces, Euler-factor analogues and constructed L-order measures contain information about global structural rank. It also includes Hodge-flow rank as part of the structural-rank architecture. Thus, flow is not merely movement; it becomes one of the inputs through which local economic information contributes to global rank formation.

The Perelman-Ricci-Poincare chapter intersects with flow through pressure smoothing and deformation. Ricci-flow terminology organizes how inequality pressure and smoothing capacity evolve through time. This is not Navier-Stokes fluid flow and not Hodge decomposition, but it shares a dynamic view of pressure transformation. It belongs more directly to Section 2.3 on curvature and topology, yet it remains adjacent to the flow dimension because smoothing capacity is a form of pressure adjustment.

The Riemann-zeta chapter introduces spectral-cycle movement. The zeta signal is used only as an analogical and computational cyclical signal for inflation forecasting. Its relation to flow is indirect but important: inflation pressure is not static; it moves through crisis-sensitive cycles and regime shifts. Section 2.4 will treat the spectral and L-function aspect more fully. Here it is enough to note that flow and cycle belong to a shared language of movement under disciplined transformation.

The P-vs-NP chapter is the least flow-like in classical terms, but it still matters for the flow architecture because economic flow models often create optimization problems. Sparse portfolio selection, support-space explosion, heuristic search and reduced exact certification show that moving from measurement to optimal allocation creates computational complexity. In the monograph, P-vs-NP therefore marks the computational boundary of flow-based economic design: even when a flow or risk structure is measured, selecting an optimal sparse allocation may remain combinatorially difficult.

The result is a layered monograph architecture. Navier-Stokes and Hodge supply the core flow grammars. Yang-Mills supplies threshold and corridor curvature around flow networks. BSD supplies local-to-global transmission of information into rank. Ricci/Poincare supplies smoothing and deformation. Riemann-zeta supplies spectral-cycle movement. P-vs-NP supplies computational limits. Section 2.2 therefore prepares the reader for the rest of Chapter 2 by establishing flow as one of the book's central cross-cutting measurement dimensions.

2.2.7. Permissible and Non-Permissible Claims for Flow Analogies

The final task of Section 2.2 is to define claim boundaries. Flow analogies are scientifically productive only when the final claim is stated at the correct level. The monograph may claim that flow-related mathematical grammars help construct auditable economic measurement architectures. It may not claim that economic data prove theorem-level statements in fluid dynamics or algebraic geometry.

For the Navier-Stokes component, permissible claims include: the model constructs a nondimensional macro-financial stress-balance framework; it separates stress into velocity weakness, acceleration, pressure gradients, friction, shocks, cycle forcing and restricted closure; it supports diagnostic stress-testing and validation-window forecasting evidence; it identifies interpretable policy-counterfactual channels. Non-permissible claims include: financial liquidity is a literal physical fluid; the mathematical Navier-Stokes problem is solved; fixed-effects associations are causal laws; rolling-window performance guarantees future crisis prediction.

For the Hodge component, permissible claims include: the model constructs a regional macro-flow graph from public anchors and author-calculated transformations; it decomposes a directed edge-pressure field into gradient, curl and harmonic components; it identifies hierarchy, local imbalance, systemic circulation, resilience and tail-risk dimensions; it supports benchmark informativeness and future all-country, dyadic and longitudinal extension. Non-permissible claims include: the Hodge conjecture is proved; regional macroeconomic nodes are algebraic varieties; derived Hodge variables are official institutional indicators; benchmark tests establish final universal causality.

For the combined flow dimension, the strongest permissible monograph claim is as follows: the flow analogies provide a coherent, reproducible and claim-bounded measurement grammar for interpreting the world economy as a stress-sensitive and topologically structured system. This claim is strong enough to justify the monograph's originality, but cautious enough to meet academic standards. It shows that mathematical inspiration can elevate economic modelling without converting empirical analogues into theorem assertions.

The section therefore closes with a methodological principle: economic flow analogies must pass through four gates before they are defensible. First, the classical mathematical object must be identified. Second, the direct proof claim must be explicitly excluded. Third, the economic translation must be operationalized through variables, transformations and validation layers. Fourth, the final claim must be stated as measurement, diagnostic, benchmark, forecasting-window or future-validation evidence, not as theorem proof. These four gates organize the flow dimension of the monograph and should also guide the reader's interpretation of all later problem chapters.

Table 2.2.6. Claim hierarchy for the flow analogies

Claim level	Navier-Stokes expression	Hodge expression	Status in monograph
Strong measurement claim	Systemic stress can be decomposed into flow-pressure-friction-shock-cycle-closure channels under nondimensional discipline.	Macro-flow pressure can be decomposed into hierarchy, local-cycle imbalance and harmonic circulation under discrete Hodge discipline.	Permissible if formulas, data, transformations and diagnostics are transparent.
Diagnostic claim	Stress channels and policy scenario effects can be interpreted within the model.	Regional hierarchy, imbalance, circulation and resilience can be interpreted within the benchmark graph.	Permissible with source and transformation caution.
Forecasting-window claim	Rolling validation may show useful performance over the reported window.	Machine-learning and predictive tests may support benchmark informativeness.	Permissible only within stated samples and windows.

Claim level	Navier-Stokes expression	Hodge expression	Status in monograph
Causal claim	Pressure/friction coefficients do not automatically establish causal macro-financial laws.	Hodge variables do not automatically establish causal regional mechanisms.	Generally not permissible without separate identification.
Theorem-level claim	No Navier-Stokes existence/smoothness proof.	No Hodge conjecture proof.	Strictly excluded.

Source: Author synthesis for the monograph claim-boundary framework.

2.2.8. Section Conclusion: Flow as a Bounded Economic Analogue

Section 2.2 has established flow as a central conceptual translation in the monograph. The Navier-Stokes-inspired model and the Hodge-econometric model both begin from classical mathematical languages, but they convert those languages into different economic objects. Navier-Stokes becomes a nondimensional macro-financial stress-balance architecture. Hodge becomes a topological decomposition of regional macro-flow pressure. Neither becomes a proof of the originating mathematical problem.

The importance of the section is that it gives the monograph a unified flow vocabulary before the individual problem chapters begin. Flow means more than movement. It means channel formation, pressure difference, friction, shock transmission, closure, hierarchy, local-cycle imbalance and persistent systemic circulation. These concepts allow the book to interpret the world economy as a dynamic and structured system rather than as a table of isolated indicators.

The methodological contribution is therefore twofold. First, the section defines how flow-related mathematical concepts can be translated into economic measurement without category error. Second, it defines the exact claim boundary: the models may support measurement, diagnostic, benchmark and bounded validation claims; they may not support theorem proof, literal physical identity, universal causality or unconditional prediction. This distinction is what allows the flow analogies to be both scientifically ambitious and academically defensible.

Within the broader architecture of Chapter 2, Section 2.2 prepares the transition to curvature, topology, spectral and complexity analogies. Flow shows how economic stress and pressure move. Curvature and topology will show how systems deform and connect. Spectral and L-function analogies will show how signal, rank and local-to-global structure are measured. Complexity and optimization will show where computational feasibility constrains economic decision-making. The flow section is therefore not an isolated subsection; it is the first major pillar of the monograph's conceptual translation framework.

2.3. Curvature and Topology Analogies

Section 2.3 develops the curvature and topology dimension of the monograph's conceptual translation framework. It is a new monograph-level section: it does not copy the introduction, literature review, methodology or results chapters of the seven underlying manuscripts, but synthesizes their shared translation logic into one general theoretical bridge. The section explains how geometric and topological languages - curvature, connectedness, cycles, holes, Laplacians, gauge potentials, action, simplicial filling and spectral separation - can be converted into bounded economic-econometric analogues without claiming to solve or verify the original mathematical problems.

The central source architectures are the Perelman/Ricci/Poincare-inspired inequality model, the Hodge-econometric macro-flow model and the Yang-Mills finite-network mass-gap model. The Perelman/Ricci/Poincare component translates geometric deformation and topological connectedness into inequality pressure, smoothing capacity, entropy-like complexity and graph connectedness. The Hodge component translates differential-topological decomposition into a network edge-field framework that separates hierarchy, local-cycle imbalance and systemic circulation. The Yang-Mills component translates gauge-theoretic potential, curvature, action and mass-gap language into a finite weighted stress-network framework for systemic shock thresholds.

The remaining four manuscripts also matter for this section, but they do not become the primary objects of curvature/topology translation. The Navier-Stokes manuscript supplies pressure-gradient, friction and closure language that is adjacent to curvature because it models stress formation under nonlinear flow. The BSD manuscript uses network structure, Hodge-flow rank and local-to-global transmission to interpret structural rank. The Riemann-zeta manuscript

contributes spectral-cycle diagnostics rather than topology in the narrow sense. The P-vs-NP manuscript contributes covariance geometry, eigenvalue concentration and feasible-set structure, showing how topological and geometric reasoning can also discipline computational-finance design. In the monograph, these four models are therefore supporting analogues inside the broader curvature-topology architecture.

The chapter's claim boundary is strict. Curvature-like deformation is not literal Riemannian curvature of a physical manifold. Betti numbers in an economic graph are not proof of the Poincare conjecture. Hodge decomposition of a constructed macro-flow edge field is not a theorem about de Rham cohomology on a smooth manifold. A finite weighted-graph mass gap is not the Yang-Mills existence and mass gap theorem. The permissible claim is methodological and empirical: the mathematical objects provide measurement grammars for organizing economic complexity when the translation is explicit, the variables are normalized, the graph or tensor construction is auditable, and the interpretation is bounded by validation evidence.

Table 2.3.1. Curvature and topology translation map across the seven economic analogues

Problem architecture	Classical mathematical object	Economic analogue in the monograph	Permissible claim
Perelman/Ricci/Poincare	Ricci flow, curvature, entropy functionals, manifold deformation, topological connectedness.	Inequality pressure, smoothing capacity, curvature-like deformation, F/W functionals, graph connectedness and network-curvature diagnostics.	Strong bounded diagnostic measurement of deformation and smoothing capacity; no proof of Ricci-flow theorem or Poincare conjecture.
Hodge	Hodge decomposition, cochains, Laplacians, harmonic components and Betti diagnostics.	Regional macro-flow edge field decomposed into gradient hierarchy, curl imbalance and harmonic systemic circulation.	Benchmark structural decomposition of economic flows; no theorem-level topological reconstruction.
Yang-Mills	Gauge potential, curvature/field strength, action, spectral mass gap.	Finite corridor stress graph, anti-symmetric economic gauge potential, triangular curvature, action concentration and graph-Laplacian threshold.	Finite-network shock-threshold diagnostics; no solution to the Yang-Mills mass-gap problem.
Navier-Stokes	Flow balance, pressure gradient, viscosity/diffusion and forcing.	Liquidity stress-balance with velocity weakness, pressure, friction, stochastic shock and restricted closure.	Macro-financial stress-testing architecture; no physical hydrodynamic law.
BSD	Elliptic curves, local reductions, L-function behavior and algebraic rank.	Local regional stress states, Euler-factor analogues, LOrder, structural rank and corridor transmission.	Calibrated local-to-global rank measurement; no BSD proof.
Riemann Hypothesis / zeta	Zeta function, critical-line behavior and spectral/cyclical structure.	Normalized zeta-cycle correction in inflation forecasting and spectral pressure diagnostics.	Layered forecast-diagnostic evidence; no RH verification.
P vs NP	Complexity classes, feasible verification versus efficient solution, combinatorial spaces.	Cardinality-constrained support selection, covariance geometry and algorithmic search discipline.	Computational-finance demonstration; no P versus NP theorem claim.

Source: Author synthesis based on the seven uploaded Millennium-problem economic manuscripts and the monograph structure document.

2.3.1. Curvature and Topology as Economic Measurement Languages

Curvature and topology enter the monograph because many economic systems cannot be adequately measured as lists of independent scalar indicators. Inequality pressure, macro-financial stress, regional corridor exposure and systemic transmission are relational phenomena. They depend not only on levels, but on deformation, coupling, circulation, connectedness, bottlenecks, cycles and thresholds. A GDP value, inflation rate, Gini coefficient or portfolio Sharpe proxy is informative, but it does not by itself reveal whether the system is becoming more curved, more connected, more cyclic, more fragile, more resistant or more topologically concentrated.

In mathematical language, curvature describes how a structure bends, deforms or departs from a neutral geometry. In economic translation, curvature becomes a disciplined way to measure pressure deformation: where inequality stress is concentrated, where smoothing capacity is weak, where network cycles accumulate non-neutralized stress and where shocks concentrate into corridor bottlenecks. Topology, by contrast, describes the connective form of a system: components, loops, holes, paths, cycles and persistent structures. In economic translation, topology becomes a way to ask whether variables or regions form a connected diagnostic system, whether stress circulates through cycles, whether regional roles persist across threshold filtrations and whether local structures explain or fail to explain system-wide circulation.

The monograph therefore treats curvature and topology as complementary. Curvature measures intensity and deformation; topology measures structure and persistence. In the Perelman/Ricci/Poincare model, curvature-like deformation captures the balance between inequality pressure and smoothing capacity, while Poincare-style graph connectedness tests whether the stress-coordinate system forms one diagnostic manifold rather than a set of disconnected indicators. In the Hodge model, topology defines the edge-field environment in which gradient hierarchy, local-cycle curl and harmonic circulation can be separated. In the Yang-Mills model, curvature is generated by non-neutralized stress around triangular cycles, while the finite graph Laplacian supplies a threshold for systemic shock propagation.

The key methodological gain is that curvature and topology prevent the monograph from reducing economic complexity to rank tables. A high-output region can be central but not necessarily fragile. A small corridor node can have low output mass but high bridge exposure. A global inequality system can show partial recovery in average pressure while remaining entropy-complex and regionally dispersed. A portfolio universe can show high expected-return dispersion while also being dominated by common covariance modes. These statements require more than scalar comparison; they require geometric-topological interpretation.

At the same time, curvature and topology are dangerous if they are used without claim discipline. The monograph does not treat mathematical language as decorative authority. Each translated object must answer four questions. What is the original mathematical object? Why is it not being proved in its classical form? What is the economic object that replaces it? What claim is permissible after empirical calibration and validation? Section 2.3 uses exactly this four-part discipline for Perelman/Ricci/Poincare, Hodge and Yang-Mills, then shows how the other four manuscripts connect to the same conceptual grammar without inflating their claims.

2.3.2. Classical Mathematical Objects and Their Economic Translation Status

The curvature-topology family of analogies begins from classical mathematical objects that have precise meanings in mathematics and physics. In the monograph, these meanings are respected but not imported literally. The purpose is not to transform economics into geometry or gauge theory; it is to identify formal architectures that can be translated into economic measurement systems. This difference matters because the credibility of the book depends on refusing category errors.

The Perelman/Ricci/Poincare object is the closest to geometric deformation. Ricci flow studies the evolution of a metric under curvature; Perelman's entropy and surgery ideas were decisive in resolving the Poincare conjecture. In the economic analogue, the metric is not a smooth manifold metric. It is a correlation-based or standardized stress-coordinate construction built from macro-social variables. Curvature is not literal geometric curvature. It is a diagnostic pressure-deformation measure constructed from inequality pressure and smoothing-capacity variables. The F- and W-type functionals are not mathematical proof devices; they are energy-like and entropy-like summaries of system complexity.

The Hodge object is a decomposition architecture. In classical terms, Hodge theory decomposes suitable objects into exact, co-exact and harmonic components under geometric and topological conditions. In the economic analogue, the object is a directed regional macro-flow pressure field defined on graph edges. The decomposition separates the constructed edge

signal into gradient hierarchy, curl or local-cycle imbalance and harmonic/systemic circulation. This translation is powerful because it distinguishes dominance, local imbalance and persistent circulation, but it remains a finite graph/cochain construction rather than a proof about smooth differential forms.

The Yang-Mills object is gauge-theoretic. Classical Yang-Mills theory concerns fields, connections, curvature, action and mass-gap questions in a rigorous mathematical-physics setting. In the economic analogue, the world economy is not a physical gauge field. A finite corridor-sensitive stress graph is constructed; a directed anti-symmetric gauge potential is assigned; triangular curvature measures non-neutralized stress around cycles; action summarizes curvature intensity; and the first positive eigenvalue of a stress-weighted graph Laplacian functions as a finite-network threshold. This is a graph-spectral translation of gauge language, not a continuum field-theory result.

These three primary architectures share a common conceptual move. Each starts from a mathematical object that is too strong and too precise to be copied directly into economics. Each then constructs a lower-level empirical object: a stress-coordinate manifold, a macro-flow graph, or a finite corridor network. Each produces a measurement claim: deformation, decomposition or shock-threshold separation. Each excludes theorem proof. This is the intellectual center of Section 2.3.

Table 2.3.2. Primary curvature-topology objects and direct-proof exclusion

Primary source	Classical object	Why direct proof is excluded	Economic replacement object
Perelman/Ricci/Poincare	Smooth geometric-topological theorem architecture: Ricci flow, curvature, entropy and manifold connectedness.	Macro-regional inequality data are not a smooth 3-manifold and constructed stress coordinates are not literal geometric invariants.	Macro-regional pressure-smoothing diagnostic manifold with curvature-like, entropy-like and graph-connectedness outputs.
Hodge	Hodge decomposition and Laplacian/cohomological structure over appropriate geometric or algebraic objects.	A regional economic graph is finite, author-constructed and based on macro-data transformations, not a smooth manifold with classical differential forms.	Directed edge-pressure cochain on a regional network decomposed into gradient, curl and harmonic components.
Yang-Mills	Gauge connections, field strength, Yang-Mills action and the mathematical mass-gap problem.	A corridor stress graph is not a quantum gauge field and finite graph eigenvalues do not solve continuum existence/mass-gap questions.	Finite stress-network gauge potential, triangular curvature, action concentration and graph-Laplacian spectral threshold.

Source: Author synthesis for Chapter 2.3.

2.3.3. Perelman/Ricci/Poincare Analogy: Inequality as Curvature, Entropy and Smoothing Capacity

The Perelman/Ricci/Poincare-inspired manuscript gives the most direct curvature-topology analogy in the monograph. Its classical mathematical reference is not a single formula borrowed into economics, but a modelling architecture: curvature, flow, entropy, deformation, connectedness and surgery. The economic problem is the measurement of global inequality pressure when multiple macro-social variables interact: income inequality, productivity, unemployment, investment, inflation, migration, education, social mobility, trade infrastructure, capital-flow pressure, innovation, health access, fiscal pressure, openness, social protection and technology access. The manuscript's conceptual move is to treat these variables not as a flat list but as coordinates of a pressure-smoothing system.

The economic curvature translation begins with harmonization. Because the raw variables have different units and economic meanings, they cannot be added directly. The Perelman/Ricci/Poincare analogue converts the variables into a common pressure-oriented scale. Variables that increase stress are oriented upward; variables that represent smoothing capacity are reverse-transformed when weaker capacity should appear as higher pressure. This rule is crucial because curvature-like measurement would be meaningless if heterogeneous units were mechanically combined. The analogy therefore starts from measurement discipline before it introduces geometric language.

Once the stress-coordinate system is established, curvature-like deformation represents the balance between pressure accumulation and smoothing capacity. A region-year can be read as more deformed when macro-social pressure is high and smoothing capacity is weak. A world path can be read as curvature-sensitive when pressure rises, scalar-curvature-like measures deteriorate, and entropy-like complexity remains elevated. In this sense, the economic Ricci analogy does not say that inequality is a geometric surface. It says that inequality can be modelled as a pressure field whose deformation can be summarized with curvature-style diagnostics.

The Perelman-type functionals are interpreted similarly. The F-functional is an energy-like diagnostic: it summarizes pressure, curvature and structural intensity. The W-functional is an entropy-like closure: it summarizes complexity, dispersion and the difficulty of smoothing the system back to a lower-pressure configuration. Their role is not to reproduce Perelman's proof. Their role is to give the inequality model a disciplined way to distinguish simple pressure level from complex structural deformation. A system can show lower average pressure while still retaining high W-like complexity if regional dispersion and coupling remain unresolved.

The Poincare dimension appears through graph connectedness and topological diagnostics. The economic question is whether the stress-coordinate variables form one connected diagnostic structure or a set of disconnected fragments. The thresholded metric graph, graph Laplacian, beta_0, beta_1, Euler-style diagnostics and network-curvature proxies answer that question in a finite data-analytic setting. A connected graph does not prove a topological theorem; it demonstrates that the selected inequality-pressure coordinates form an integrated diagnostic system in the constructed empirical architecture.

The permissible claim is therefore a high-level diagnostic measurement claim. The model may claim that inequality pressure, smoothing capacity, curvature-like deformation, entropy-like complexity and graph connectedness can be jointly measured in a reproducible macro-regional framework. It may interpret crisis deformation, partial recovery and persistent complexity if the results support those statements. It may not claim to prove the Poincare conjecture, reproduce Perelman's theorem, identify unrestricted causality, replace country-level welfare analysis or establish universal forecast superiority.

Table 2.3.3. Perelman/Ricci/Poincare economic translation chain

Stage	Mathematical grammar	Economic implementation	Claim boundary
Coordinate definition	Manifold/metric intuition.	Sixteen macro-social stress coordinates in a ten-region, 2010-2024 panel.	Diagnostic coordinate system, not literal manifold geometry.
Metric construction	Metric coupling among coordinates.	Correlation-based economic metric tensor and standardized stress relations.	Empirical coupling, not a Riemannian metric in the classical sense.
Curvature	Ricci/scalar curvature and deformation.	Component curvature, normalized Ricci-flow summaries and world-weighted scalar-curvature path.	Curvature-like pressure diagnostics, not geometric invariants.
Entropy/functionals	Perelman F and W logic.	Energy-like and entropy-like diagnostics of pressure complexity.	System-complexity summaries, not theorem proof devices.
Topology	Connectedness, cycles and graph structure.	Thresholded graph, Laplacian, beta_0, beta_1, edge-curvature proxies and surgery rankings.	Graph-theoretic audit, not proof of Poincare.
Validation	Theorem proof in mathematics is replaced by empirical audit in economics.	Panel screens, robustness, counterfactuals, forecasts, Monte Carlo and leave-one-out tests.	Diagnostic validation, not unrestricted causal identification.

Source: Author synthesis based on the Perelman/Ricci/Poincare inequality-diagnostics manuscript.

2.3.4. Hodge Analogy: Topological Macro-Flow Decomposition

The Hodge-econometric manuscript is the monograph's central bridge between flow and topology. In Section 2.2, it was treated as a flow analogy because it decomposes macro-flow pressure. In Section 2.3, the same model is treated as a topology analogy because the decomposition only becomes meaningful once the regional economy is represented as a connected graph or simplicial structure. The Hodge model therefore belongs in both sections, but with different emphases: flow in Section 2.2, topology in Section 2.3.

The classical Hodge object is a decomposition principle. Under appropriate mathematical conditions, a field can be decomposed into components associated with gradients, curls and harmonic structure. The economic analogue starts with a finite regional network. Nodes represent macro-regions, including a World anchor for normalization and a separate Caucasus node for corridor visibility. Edges represent author-calculated macro-flow pressure relations rather than observed bilateral trade or financial transactions. The directed edge field is therefore a constructed cochain: it is suitable for Hodge decomposition because its construction is explicit, but it must not be confused with raw observed flows.

The economic translation is powerful because it separates three forms of economic organization. The gradient component captures hierarchy: systematic directional pressure associated with regional scale, growth, income depth and macroeconomic position. The curl component captures local-cycle imbalance: pressure that circulates around regional triangles or near-triangular corridor structures. The harmonic component captures systemic circulation: residual flow that is not explained by pure hierarchy or local triangular imbalance. This decomposition creates a richer understanding of the world economy than GDP rankings or simple centrality measures can provide.

The topological discipline comes from connectedness, cycle structure, higher-order Laplacians and simplicial filling. The graph must be connected before decomposition and spectral interpretation are meaningful. The cycle rank matters because curl and circulation require cycles rather than isolated edges. Filled 2-simplices matter because some apparent cycles can be explained as closed local triangular structures. The first-order Hodge Laplacian and Betti diagnostics therefore separate weighted empirical circulation from topological holes in a filled complex.

A particularly important monograph-level safeguard is the distinction between harmonic energy and Betti-1 after triangular filling. Harmonic energy in the Hodge decomposition measures residual weighted circulation in the empirical edge-pressure field. Betti-1 after filling counts independent one-dimensional holes in the selected simplicial complex. These are related but not identical objects. A filled-complex beta_1 value of zero does not imply that harmonic energy is zero. It means that the specified triangular fillings close the independent topological holes, while the empirical edge field may still contain residual circulation intensity. This safeguard prevents a category error between algebraic topology and weighted economic measurement.

The Hodge permissible claim is a benchmark structural-decomposition claim. The model may claim that a constructed regional macro-flow pressure field can be decomposed into hierarchy, local imbalance and systemic circulation; that the graph is topologically suitable for such analysis; and that the decomposition reveals economic structures not visible in output mass alone. It may not claim that the world economy is literally a smooth manifold, that the edge field is a direct observed transaction matrix, or that the finite Hodge decomposition proves a classical mathematical theorem.

Table 2.3.4. Hodge topology and decomposition safeguards

Hodge/topological object	Economic meaning	Interpretation discipline
Connected regional graph	Provides the finite network support for edge-pressure analysis.	Connectedness is a precondition for meaningful decomposition, not a policy result by itself.
Directed edge cochain	Author-calculated macro-flow pressure across regional edges.	A pressure proxy field, not observed bilateral transaction data.
Gradient component	Hierarchical regional pressure associated with scale, growth and income-depth structure.	Hierarchy is structural measurement, not welfare ranking.
Curl component	Local-cycle imbalance around regional triangles or corridor loops.	Curl is local imbalance, not automatically negative policy performance.
Harmonic component	Systemic residual circulation not reducible to gradient or local curl.	Circulation intensity, not proof of persistent topological holes.

Hodge/topological object	Economic meaning	Interpretation discipline
Higher-order Hodge Laplacian	Tests local triangular closure and simplicial stability.	A finite simplicial diagnostic, not a full algebraic-topological reconstruction.
Betti-1 after filling	Counts independent holes after specified triangular filling.	Must not be equated mechanically with harmonic energy share.

Source: Author synthesis based on the Hodge-econometric macro-flow manuscript.

2.3.5. Yang-Mills Analogy: Gauge Curvature, Action and Finite-Network Shock Thresholds

The Yang-Mills manuscript contributes the most explicit curvature-action-threshold architecture. Its classical mathematical object is gauge theory: fields are represented through connections or potentials; curvature measures non-trivial field strength; action summarizes the intensity of the field; and the mass-gap problem concerns deep questions of existence and spectral separation in mathematical physics. The economic translation does not attempt to enter that theorem-level domain. It builds a finite weighted corridor stress graph and asks whether systemic stress circulation can be measured through gauge-like and spectral graph diagnostics.

The economic object is a finite global-corridor network. Regional nodes and corridor-sensitive edges are constructed from public macroeconomic anchors and author-disclosed transformations. A normalized systemic-stress field is mapped into a corridor-weighted graph, then into a stress-weighted adjacency matrix. An anti-symmetric economic gauge potential is assigned to directed edges. Triangular curvature is computed around cycles. Yang-Mills economic action aggregates curvature intensity. A stress-weighted Laplacian supplies the spectral layer. The first positive eigenvalue functions as a finite-network economic mass gap, meaning a threshold separating locally absorbable disturbance from the first systemically transmissible stress mode.

The important word is finite. The manuscript does not claim a continuum gauge field. It does not claim quantization, non-Abelian field existence, physical particle mass, or solution to the classical Yang-Mills mass-gap problem. The mass-gap language is used in a graph-theoretic sense: if the stress-weighted network is connected, the zero eigenvalue corresponds to the constant mode, while the first positive eigenvalue indicates the first non-trivial mode of stress transmission. The economic interpretation is threshold-based, not theorem-based.

The curvature-action layer adds information beyond ordinary network centrality. Standard centrality can show that some nodes or edges are important, but it does not identify whether stress circulates around cycles in a concentrated way. Triangular curvature and action concentration help identify whether systemic stress-energy is localized in a small set of corridor loops. This matters economically because a corridor node can be small in output mass but large in transmission relevance. The Caucasus and Central Asia logic in the Yang-Mills manuscript illustrates this point: corridor exposure can be analytically important even when aggregate size is modest.

The Yang-Mills analogy also strengthens the monograph's general threshold logic. Many economic crises are not linear scale events. A disturbance can remain local if the system has enough spectral protection, redundancy, resilience or absorption capacity. The same disturbance can become systemic if curvature/action concentration rises and spectral separation weakens. Scenario shocks - inflation, financial spread, logistics disruption, energy or geopolitical pressure - are therefore not interpreted as deterministic predictions; they are stress experiments showing how the finite network's threshold structure responds under specified perturbations.

The permissible claim is a finite-network benchmark claim with future validation pathway. The model may claim that a constructed corridor stress graph has measurable gauge-potential, curvature, action and spectral-threshold properties; that scenario shocks alter curvature and threshold conditions; and that EMGI, fragility and BridgeStress distinguish output mass from corridor exposure. It may not claim to solve the Yang-Mills problem, prove physical mass gaps, or establish country-level causal effects until the planned panel validation architecture is populated and estimated.

Table 2.3.5. Yang-Mills finite-network translation and claim gates

Gauge-theoretic term	Finite economic-network analogue	Claim gate
Gauge potential	Anti-symmetric stress-potential assigned to directed edges.	Orientation-sensitive diagnostic, not a physical field.
Curvature / field strength	Non-neutralized stress around triangular cycles.	Cycle-stress measure, not continuum curvature.
Yang-Mills action	Aggregate or cycle-level curvature	Action concentration indicates stress-

Gauge-theoretic term	Finite economic-network analogue	Claim gate
	intensity.	energy localization in the finite graph.
Mass gap	First positive eigenvalue of the stress-weighted graph Laplacian.	Finite-network spectral threshold, not the Clay mathematical problem.
Shock scenario	Inflation, financial-spread, trade/logistics or energy/geopolitical perturbation.	Model-implied stress experiment, not unconditional crisis prediction.
BridgeStress	Small-node strategic exposure through corridor placement.	Corridor diagnostic, not geopolitical ranking.

Source: Author synthesis based on the Yang-Mills finite-network gauge-econometric manuscript.

2.3.6. How the Remaining Four Analogues Support the Curvature-Topology Dimension

Although Section 2.3 is centered on Perelman/Ricci/Poincare, Hodge and Yang-Mills, the monograph's seven-problem design requires a wider synthesis. The remaining four manuscripts do not become the primary curvature-topology models, but each contributes a supporting geometric or topological discipline. This matters because the monograph's claim is not that three mathematical problems inspire economics while the others stand aside. The claim is that seven mathematical architectures produce seven measurement grammars, and that these grammars overlap in carefully bounded ways.

The Navier-Stokes manuscript contributes pressure-gradient and frictional deformation logic. Its direct object is flow, not topology, but it is adjacent to curvature because stress formation depends on pressure gradients, liquidity friction, diffusion, shocks and closure. The model converts heterogeneous macro-financial variables into nondimensional components, preventing raw-unit aggregation. Its curvature-topology relevance lies in how pressure deformation emerges from interaction among components rather than from a single scalar stress index. In monograph terms, Navier-Stokes supplies the dynamic pressure mechanism that complements the static or structural graph-topological diagnostics.

The BSD manuscript contributes local-to-global topology in a broad structural sense. Its core object is rank formation through local finite-state signals, Euler-factor analogues, LOrder and structural rank. The local-to-global logic is not curvature in the Ricci sense, but it depends on network structure, corridor transmission, Hodge-flow rank and systemic stress components. Its relevance for Section 2.3 is that topology appears as the architecture through which local regional reductions and corridor signals can inform global structural rank. The permissible claim remains calibrated rank consistency, not proof of the BSD conjecture.

The Riemann-zeta manuscript contributes spectral structure. It is not a graph-topology chapter, but it uses a mathematically explicit critical-line signal as a normalized cyclical correction to global inflation forecasting. Its relevance is that spectral-cycle diagnostics play a role analogous to eigenvalue and frequency reasoning in the curvature-topology family. Fourier, wavelet, spectral entropy and regime screens help determine whether the signal behaves as a meaningful diagnostic layer. The permissible claim is forecast improvement under layered validation, not verification of the Riemann Hypothesis.

The P-vs-NP manuscript contributes feasible-set geometry, covariance structure and eigenvalue discipline. Its core problem is combinatorial optimization under cardinality constraints, not curvature or topology. However, portfolio optimization has a geometry: covariance matrices define risk space; eigenvalue concentration reveals common-factor dependence; cardinality constraints define a discrete feasible-support space; and heuristic search explores that space without exhaustive certification in the main universe. The curvature-topology relevance is therefore indirect: it shows that mathematical structure can discipline economic decision spaces even when theorem proof is excluded.

Taken together, the four supporting analogues strengthen the monograph's general proposition: mathematical translation is not one-dimensional. Flow, curvature, topology, spectrum, rank and complexity interact. A strong monograph-level framework must therefore specify where each analogy is primary, where it is supporting, and where it must remain outside the permissible claim boundary.

Table 2.3.6. Supporting roles of the non-primary analogues in curvature-topology reasoning

Supporting analogue	Connection to curvature/topology	What it adds	What it does not claim
Navier-Stokes	Pressure gradients and frictional deformation are	Dynamic mechanism of stress accumulation and	Does not make liquidity a physical fluid or solve

Supporting analogue	Connection to curvature/topology	What it adds	What it does not claim
	adjacent to curvature-like stress formation.	closure.	Navier-Stokes.
BSD	Local-to-global architecture uses regional network structure, corridor transmission and Hodge-flow rank.	Transmission route from local signals to structural rank.	Does not prove BSD or establish a causal law.
Riemann/zeta	Spectral-cycle diagnostics support mathematical signal interpretation.	Frequency, regime and spectral-entropy discipline for inflation forecasting.	Does not test or verify RH.
P vs NP	Covariance geometry and feasible-support space structure discipline optimization.	Computational boundary and search-space geometry.	Does not prove P != NP or certify the full-universe optimum.

Source: Author synthesis based on the Navier-Stokes, BSD, Riemann-zeta and P-vs-NP manuscripts.

2.3.7. The Economic Meaning of Curvature: Deformation, Concentration and Bottlenecks

For the monograph, economic curvature has three interrelated meanings: deformation, concentration and bottleneck formation. Deformation refers to the way a system departs from a neutral or balanced state. Concentration refers to the localization of stress in specific variables, nodes, edges or cycles. Bottleneck formation refers to the emergence of narrow transmission structures where disturbances become difficult to absorb. These meanings are not identical, but together they make curvature useful as an economic measurement language.

In the Perelman/Ricci/Poincare model, curvature primarily means deformation. Inequality pressure bends the diagnostic system away from a smoother state when unemployment, investment stress, technology weakness, fiscal pressure or social-protection weakness intensify. The curvature-like output is therefore not a geometric object floating above the economy; it is a structured summary of how stress coordinates combine. When pressure declines but W-like complexity remains elevated, the model can say that partial recovery has occurred without claiming full smoothing or convergence.

In the Yang-Mills model, curvature primarily means concentration. A stress potential along edges may cancel or accumulate around a cycle. When it accumulates, triangular curvature reveals non-neutralized stress circulation. Action then quantifies the intensity of that curvature. If action is concentrated in a limited set of corridor cycles, the model identifies systemic exposure that might not be visible from node size alone. This is why gauge-curvature language is useful for corridor economics: it measures where stress becomes structured around paths and loops.

In the Hodge model, curvature is less direct but topology and circulation provide a parallel logic. Curl represents local-cycle imbalance, while harmonic circulation represents residual system-wide movement. These are not called Ricci curvature in the Hodge chapter, but they function as topological deformation diagnostics: they show where the regional macro-flow field cannot be explained by simple hierarchy. Local curl is a triangle-level imbalance; harmonic circulation is a system-level residual.

The economic meaning of curvature is therefore deliberately plural. It is not one formula repeated across the monograph. It is a family of measurement ideas: inequality deformation, flow imbalance, cycle stress, action concentration, bottleneck exposure and spectral threshold weakening. The unifying rule is that curvature-like language may be used only when the object being measured is relational, normalized and auditable. It cannot be used as a rhetorical label for any undesirable economic condition.

2.3.8. The Economic Meaning of Topology: Connectedness, Cycles, Holes and Persistence

Topology contributes a different measurement layer. It does not ask how large a pressure value is; it asks how the system is connected, where loops exist, whether holes remain after local filling, and whether structural features persist across thresholds. This is especially important for the monograph because the world economy is repeatedly modeled as a connected system: global regions, corridor nodes, flow edges, stress coordinates, inflation regimes, local finite states and portfolio-support spaces all involve relations among elements rather than isolated variables.

Connectedness is the first topological condition. In the Perelman/Ricci/Poincare model, connectedness asks whether the inequality-pressure variables form one diagnostic graph. In the Hodge model, connectedness is required before hierarchy and circulation decomposition can be interpreted. In the Yang-Mills model, connectedness is needed before a first positive Laplacian eigenvalue can be read as a finite-network threshold. Across the monograph, connectedness does not mean harmony or welfare success. It means that the constructed system is structurally integrated enough for graph-based diagnostics to be meaningful.

Cycles are the second condition. A tree-like graph has paths but no independent cycles; a cycle-rich graph allows local imbalances and circulation to be measured. Hodge curl, Yang-Mills triangular curvature and Poincare-style beta diagnostics all depend on cycle logic. Economically, cycles represent the possibility that pressure does not simply move from source to destination; it can circulate through loops, reinforce itself, become trapped, or persist as a system-level pattern. This is why cycle structure is essential for modelling corridor stress, inequality interdependence and macro-flow circulation.

Holes and filled simplices are the third condition. In a simplicial complex, some cycles are closed by filled triangles, while others remain as independent holes. The Hodge manuscript's distinction between graph cycle rank, filled 2-simplices and Betti-1 after filling is crucial here. Economic interpretation must not confuse every cycle with a persistent hole. A cycle may be locally explained by a triangular relationship; only after filling does one see whether a persistent topological gap remains. This gives the monograph a more refined language than ordinary network centrality.

Persistence is the fourth condition. A topological feature is more credible if it does not disappear under minor threshold changes. Persistent-homology reasoning, threshold graphs and robustness filtrations help test whether circulation or connectedness is merely an artifact of one arbitrary edge cutoff. This does not transform economic topology into mathematical proof, but it improves evidence discipline. It allows the monograph to distinguish fragile graph artifacts from more stable structural signals.

Table 2.3.8. Topological concepts and economic interpretation rules

Topological concept	Economic interpretation	Incorrect interpretation to avoid
Connected component / beta_0	Whether the diagnostic variables or regional nodes form an integrated graph.	Do not interpret connectedness as welfare convergence or policy success.
Cycle rank	Potential for local imbalance, circulation and looped transmission.	Do not treat every cycle as a crisis channel.
Betti-1	Independent one-dimensional holes after chosen construction or filling.	Do not equate Betti-1 mechanically with Hodge harmonic energy.
Laplacian eigenvalue	Connectedness, diffusion scale or finite-network threshold.	Do not treat graph eigenvalues as continuum theorem proof.
Simplicial filling	Whether triangular local relations explain observed cycles.	Do not assume filled cycles mean the economic system has no residual circulation.
Persistence across thresholds	Robustness of topology under edge filtering.	Do not treat one threshold graph as final evidence without sensitivity checks.

Source: Author synthesis for the monograph.

2.3.9. Comparative Claim Hierarchy for Curvature and Topology Analogies

The curvature-topology section requires a formal claim hierarchy because these analogies are scientifically attractive but easy to overstate. The monograph should therefore separate four evidentiary levels. The strongest level is bounded diagnostic measurement: the model constructs a clear object, reports values from a defined sample or benchmark, and validates the object internally. The second level is structural interpretation: the model explains what curvature, connectedness, circulation or threshold results mean within the constructed architecture. The third level is scenario or robustness screening: the model evaluates whether results survive perturbations, alternative specifications, thresholds or falsification checks. The fourth level is future validation: the model specifies what must be populated or estimated before stronger claims can be made.

Perelman/Ricci/Poincare is strongest as a diagnostic measurement architecture for inequality pressure and smoothing capacity. Hodge is strongest as a benchmark structural-decomposition architecture for regional macro-flow topology. Yang-

Mills is strongest as a finite-network benchmark for stress curvature, action concentration and spectral threshold. Navier-Stokes is strongest as a global panel stress-testing architecture but belongs primarily to flow rather than topology. BSD is strongest as calibrated local-to-global rank consistency. Riemann-zeta is strongest as layered forecast validation. P-vs-NP is strongest as computational demonstration with exact reduced benchmarking. This hierarchy prevents the monograph from making one uniform claim across non-identical evidence bases.

Within Section 2.3, the highest permissible statement is that curvature and topology provide a coherent economic measurement grammar across multiple problem chapters. This statement is stronger than saying the analogies are metaphors, because the manuscripts contain empirical objects, tables, diagnostics, validation layers and claim boundaries. But it is weaker than theorem proof, causal law or universal policy prescription. The monograph's intellectual strength lies exactly in that intermediate zone: rigorous enough to generate reproducible measurement, cautious enough to avoid mathematical overclaiming.

A useful reviewer-facing formulation is the following: the monograph does not transport mathematical truth into economics; it transports mathematical architecture into economic measurement. Curvature, topology, gauge potential, action, Hodge decomposition and graph connectedness become disciplined economic constructs only after normalization, graph construction, matrix definition, sample definition, validation and explicit exclusion of theorem-level claims. This sentence should be treated as one of the core protection statements for the entire book.

Table 2.3.9. Claim hierarchy for curvature and topology analogies

Evidence level	Permitted statement	Examples in Section 2.3	Excluded statement
Bounded diagnostic measurement	The constructed object measures a defined economic structure under disclosed transformations.	Inequality curvature, Hodge decomposition, Yang-Mills finite-network action.	This proves a classical theorem.
Structural interpretation	The result has a meaningful interpretation inside the constructed model.	Cycle concentration, connectedness, harmonic circulation, smoothing capacity.	This is a universal law of the economy.
Robustness/scenario screening	The result is stable or informative under specified tests or shocks.	Threshold filtering, Monte Carlo perturbations, shock scenarios, leave-one-out checks.	This predicts all future crises unconditionally.
Future validation pathway	A stronger claim requires a populated panel, observed dyadic flows or independent external outcomes.	Yang-Mills N=1,500 pathway, Hodge country/dyadic extension, BSD external-proxy limits.	The present benchmark already supplies final causal proof.

Source: Author synthesis for the monograph.

2.3.10. Methodological Safeguards against Category Error

The most serious risk in a monograph of this type is category error: treating an economic analogue as if it were the mathematical object itself. Section 2.3 therefore requires explicit safeguards. These safeguards are not cosmetic; they protect the scientific credibility of the book. They show that the author understands the difference between formal mathematics and empirical economic modelling.

The first safeguard is object separation. Every model must identify the difference between the classical object and the economic object. Ricci curvature becomes curvature-like pressure deformation; Hodge decomposition becomes finite edge-field projection; Yang-Mills mass gap becomes finite graph spectral separation. The names preserve conceptual lineage, but the objects are not identical. This should be stated wherever the model introduces a translated mathematical term.

The second safeguard is unit discipline. Economic curvature or topology cannot be computed by mixing raw units. The Perelman/Ricci/Poincare model solves this through pressure-oriented normalization. The Navier-Stokes model solves it through nondimensional starred variables. The Hodge and Yang-Mills models solve it through explicitly constructed network weights, stress fields and adjacency or Laplacian matrices. Without this step, mathematical terminology would rest on invalid measurement aggregation.

The third safeguard is graph-construction transparency. Topological results depend on nodes, edges, thresholds, weights, directions and simplicial filling rules. A different graph can produce different connectedness, cycle and Laplacian results. The monograph must therefore treat graph construction as a modelling decision, not as an objective property handed directly by the data. This is why source ledgers, formulas, scripts, thresholds and robustness checks are not secondary; they are part of the evidence.

The fourth safeguard is validation discipline. A theorem is not replaced by a single impressive table. The economic analogues require econometric diagnostics, sensitivity checks, placebo or falsification gates, Monte Carlo or bootstrap uncertainty, external-proxy screening where possible and clear separation between internal calibration and independent validation. The stronger the mathematical language, the more necessary this validation discipline becomes.

The fifth safeguard is claim gating. The final interpretation must match the weakest relevant evidence layer. If a benchmark graph is complete but the country panel is planned, the claim cannot be country-level causal confirmation. If a forecast improves in several validation windows, the claim cannot become universal forecast dominance. If a graph is connected and cycle-rich, the claim cannot become proof of a topological theorem. Claim gating is therefore not a limitation added at the end; it is a constitutive part of the monograph's methodology.

Table 2.3.10. Category-error prevention matrix

Risk	How it could appear	Required safeguard
Theorem inflation	A finite economic result is described as solving the mathematical problem.	Use theorem-exclusion language in every chapter and in the general claim boundary.
Literalization of geometry	Economic curvature is treated as actual Riemannian curvature.	Define it as a model-implied diagnostic quantity.
Graph naturalization	Constructed networks are treated as directly observed complete reality.	Report node, edge, weight, threshold and filling rules.
Unit inconsistency	Raw variables with different units are combined into curvature or action.	Normalize and orient variables before matrix or graph construction.
Causal overclaiming	Diagnostic associations are read as structural causal effects.	Use robust-inference language and reserve causal claims for appropriate identification.
Validation overextension	Benchmark or sample-specific evidence is generalized universally.	State sample, benchmark, validation window and future replication requirements.

Source: Author synthesis for the monograph.

2.3.11. Integrated Synthesis: Curvature and Topology as the Second Dimension of the Millennium Economic Program

Section 2.3 establishes curvature and topology as the second major conceptual dimension of the monograph, following the flow dimension in Section 2.2. Flow explains movement, pressure, friction, circulation and closure. Curvature and topology explain deformation, connection, cycles, holes, action concentration and thresholds. Together, these dimensions allow the monograph to measure economic complexity beyond scalar macroeconomic indicators.

The Perelman/Ricci/Poincare, Hodge and Yang-Mills models form a coherent triad. The first measures pressure-smoothing deformation in the inequality system. The second decomposes macro-flow topology into hierarchy, local imbalance and systemic circulation. The third measures gauge-like stress curvature, action concentration and finite-network shock thresholds in corridor systems. Their common contribution is not theorem proof but structural measurement: they show how economic systems can be represented as coupled, connected, cycle-rich and deformation-sensitive architectures.

The cross-problem integration is also important. Navier-Stokes supplies dynamic flow pressure; BSD supplies local-to-global structural-rank transmission; Riemann-zeta supplies spectral-cycle discipline; P-vs-NP supplies complexity and feasible-set geometry. These supporting analogues prevent Section 2.3 from becoming isolated. Curvature and topology are not only the subject of three chapters; they are part of the monograph's larger argument that the Clay Millennium Problems provide different measurement grammars for economic complexity.

The final admissible claim of Section 2.3 can be stated as follows. Curvature and topology analogies can be used to construct high-level economic-econometric measurement systems for inequality deformation, macro-flow decomposition, corridor shock thresholds and systemic transmission, provided that each mathematical object is translated into a clearly

defined empirical object, each variable transformation is auditable, each graph or matrix construction is transparent, and every conclusion remains within diagnostic, benchmark, forecasting or future-validation boundaries. This is the claim that should carry into the later problem chapters and the comparative synthesis of the monograph.

2.3.12. Section Conclusion

The curvature and topology framework gives the monograph its second major conceptual language. It demonstrates that economic complexity can be read not only through flows but also through deformation and structure. In the Perelman/Ricci/Poincare analogue, inequality becomes a pressure-smoothing diagnostic manifold with curvature-like and entropy-like outputs. In the Hodge analogue, the world economy becomes a decomposable regional edge field with hierarchy, local-cycle imbalance and harmonic circulation. In the Yang-Mills analogue, corridor stress becomes a finite gauge-like network with curvature, action and spectral threshold diagnostics.

The section also clarifies the role of the other four analogues. Navier-Stokes contributes pressure-gradient and closure logic; BSD contributes local-to-global rank transmission; Riemann-zeta contributes spectral-cycle diagnostics; and P-vs-NP contributes computational geometry of feasible decision spaces. The resulting monograph-level picture is unified but not overstated: different mathematical architectures supply different economic measurement grammars, and each grammar has its own claim boundary.

The central protection statement remains decisive: curvature and topology analogies are not mathematical proofs. They are disciplined economic translations. Their legitimacy comes from explicit object separation, normalization, graph and matrix transparency, validation, robustness and claim gating. Under these conditions, Section 2.3 can serve as a strong theoretical bridge between the general claim boundary of the book and the later problem-specific chapters on Perelman/Ricci/Poincare, Hodge and Yang-Mills.

2.4. Spectral and L-Function Analogies

Section 2.4 develops the spectral and L-function dimension of the monograph's conceptual translation framework. It is written as a new monograph-level section rather than as a copied excerpt from any of the seven source manuscripts. Its purpose is to explain how two of the most number-theoretically charged Millennium-problem architectures - the Riemann/zeta tradition and the Birch-Swinnerton-Dyer local-to-global tradition - can be translated into bounded economic-econometric analogues without turning economic modelling into theorem proof.

The central pair of objects in this section is the Riemann-zeta critical-line signal and the BSD L-function/rank correspondence. In the Riemann-zeta manuscript, the zeta function is used as a mathematically explicit cyclical signal generator that is transformed into a real-valued normalized zeta-cycle, a deviation from neutrality and an alpha-calibrated correction to a structural FPAS inflation forecast. In the BSD manuscript, local regional states are transformed into finite-state trace analogues, Euler-factor analogues, a constructed economic L-function, an L-order measure and a structural-rank object. These two models are not identical, but they share a common translation principle: spectral or L-function language is permitted only after it is converted into a transparent economic measurement sequence and bounded by validation gates.

The other five manuscripts also contribute to this section. The Hodge model supplies spectral graph and Hodge-Laplacian diagnostics; the Yang-Mills model supplies stress-Laplacian mass-gap logic; the Navier-Stokes model supplies Fourier GDP-cycle forcing and residual-closure discipline; the Perelman/Ricci/Poincare model supplies entropy-like and graph-Laplacian connectedness diagnostics; and the P-vs-NP model supplies covariance-eigenvalue and algorithmic search-space discipline. These supporting links show that spectral reasoning in the monograph is not confined to zeta or BSD. It appears whenever a complex economic system is represented through eigenmodes, cycles, frequency decomposition, weighted graph spectra, calibration hierarchies or structured local-to-global correspondence.

The claim boundary is strict. A zeta-cycle is not evidence for the Riemann Hypothesis. An economic L-function is not an arithmetic L-function. LOrder is not an order of vanishing in the classical number-theoretic sense. Euler-factor analogues are not local Euler factors over finite fields. A spectral graph gap is not a physical mass gap. The permissible claim is that spectral and L-function analogies can generate auditable economic signals, forecast corrections, local-to-global consistency diagnostics and structural-rank measurement, provided their mathematical origin, empirical transformation and evidentiary limits are stated explicitly.

Table 2.4.1. Spectral and L-function translation architecture across the seven economic analogues

Problem architecture	Classical spectral / L-function object	Economic translation in the monograph	Permissible claim
Riemann / Zeta	Riemann-zeta function, critical-line evaluation, oscillatory/spectral behavior and zero-related motivation.	Critical-line signal transformed into tau-driven zeta-cycle, deviation from neutrality and FPAS+zeta forecast correction.	Bounded forecast-diagnostic improvement under layered validation; no proof, test or verification of the Riemann Hypothesis.
Birch-Swinnerton-Dyer	Elliptic curves, local reductions, Euler factors, L-function behavior around s = 1 and algebraic rank.	Regional states converted into finite-state traces, Euler-factor analogues, an economic L-function, LOrder and structural rank.	Calibrated local-to-global consistency in regional economic rank formation; no classical BSD proof.
Hodge	Laplacian spectra, Hodge-Laplacian modes, gradient/curl/harmonic separation and eigenspectrum.	Macro-flow edge cochain decomposed into hierarchy, local-cycle imbalance and systemic circulation with spectral diagnostics.	Benchmark topological-flow decomposition; no final causal or dyadic-flow theorem claim.
Yang-Mills	Gauge curvature, action and positive spectral separation interpreted as mass gap in a field-theoretic setting.	Finite stress-weighted graph Laplacian, EMGI, spectral separation and shock-threshold diagnostics.	Finite-network threshold evidence; no solution to Yang-Mills existence and mass-gap problem.
Navier-Stokes	Flow modes, pressure/forcing balance, cyclic components and residual closure.	Liquidity-flow stress balance with Fourier GDP-cycle forcing, stochastic shocks and restricted epsilon closure.	Macro-financial stress-testing and validation-window evidence; no hydrodynamic theorem claim.
Perelman/Ricci/Poincare	Curvature flow, entropy functionals, graph connectedness and Laplacian topology.	Inequality-pressure curvature, F/W functionals, Betti/connectivity and pressure-smoothing diagnostics.	Bounded diagnostic-manifold interpretation; no Ricci-flow or Poincare proof.
P vs NP	Combinatorial search spaces, verification versus solution, covariance/eigenvalue geometry.	Portfolio support-space explosion, covariance spectra, exact reduced enumeration and heuristic search comparison.	Computational-finance evidence and search discipline; no P versus NP theorem claim.

Source: Author synthesis based on the seven uploaded Millennium-problem economic manuscripts and the monograph structure document.

2.4.1. Why Spectral and L-Function Language Matters for Economic Analogues

Spectral and L-function language enters the monograph because many economic systems contain information that is not visible in direct levels alone. Inflation is not only a level variable; it has cycles, shock windows, phase-like movement and nonlinear pressure regimes. Regional economic structure is not only a vector of GDP shares; it contains local states, corridor exposures, network positions and global rank formation. Macro-flow systems are not only weighted graphs; they contain diffusion modes, circulation components and spectral separations. Portfolio universes are not only lists of expected returns; they contain covariance concentration and feasible-support explosion. Spectral reasoning is the general language through which hidden modes, cycles, thresholds and decompositions become measurable.

In mathematics, the spectrum of an operator reveals internal structure that is not obvious from the object itself. The eigenvalues of a Laplacian, the zeros and oscillations associated with zeta-like functions, the order of behavior of an L-function and the spectral separation of a graph all encode structural information. In the monograph, these ideas are translated into economic diagnostics. A zeta-cycle may reveal stress-sensitive cyclical deformation in world inflation. A constructed economic L-function may summarize how local regional states aggregate into a rank-related global object. A graph Laplacian may reveal whether stress diffusion is protected by spectral separation. A Hodge-Laplacian may show whether edge-flow pressure decomposes into hierarchy, local cycles or systemic circulation.

The conceptual value of spectral analogies is therefore not mystical. They supply a disciplined way to compress high-dimensional structure into interpretable signals without pretending that the economy literally is a number-theoretic object. A well-constructed spectral analogy must satisfy three requirements. First, the mathematical object must be named accurately. Second, the economic translation must be operational and reproducible. Third, the empirical claim must be weaker than the mathematical theorem and must remain conditional on validation evidence. The Riemann and BSD manuscripts are the most direct examples because both work through zeta/L-function language; however, the same discipline supports Hodge, Yang-Mills, Navier-Stokes, Perelman/Ricci/Poincare and P-vs-NP components of the book.

A monograph-level synthesis must also distinguish signal construction from signal interpretation. Constructing a zeta-cycle, LOrder, mass-gap index or Laplacian spectrum is a technical act. Interpreting that object as economically meaningful requires benchmark comparison, robustness testing, residual diagnostics, falsification gates, circularity control and claim hierarchy. This is why the monograph treats spectral objects as measurement architectures rather than as self-validating evidence. A spectral object becomes useful only when it improves interpretation under disciplined empirical checks.

2.4.2. The Riemann/Zeta Analogy: From Critical-Line Signal to Inflation Forecast Correction

The Riemann/zeta analogue is the monograph's principal spectral-signal model. The classical mathematical object is the Riemann-zeta function and its critical-line behavior. In mathematics, the Riemann Hypothesis concerns the location of nontrivial zeros of the zeta function. In the economic manuscript, none of this is claimed as a theorem-level object. The zeta function is used only as a computational cyclical signal generator. The economic question is whether a critical-line signal, transformed through macro-financial pressure, can add forecast-relevant information to global inflation modelling.

The translation begins by refusing a direct proof transfer. Inflation data cannot verify the location of zeta zeros. A finite macroeconomic sample cannot prove or test a statement about the analytic structure of the zeta function. A good forecast result cannot become evidence for the Riemann Hypothesis. This negative boundary is central. It protects the model from the most obvious reviewer criticism: that a mathematical object has been used rhetorically rather than empirically. The manuscript avoids that problem by converting the zeta function into a real-valued signal and then testing the signal only against economic forecast criteria.

The economic object is a layered global inflation-forecasting architecture. The structural FPAS baseline is retained as the macroeconomic core. A composite global inflation-pressure index is constructed from macro-financial stress coordinates. This pressure index is transformed into a nonlinear tau argument. The critical-line zeta expression is evaluated as a signal, then normalized into a zeta-cycle. The deviation of the zeta-cycle from neutrality becomes the forecast-correction channel. The final hybrid forecast is not 'number theory replacing economics'; it is a structural FPAS forecast plus an alpha-scaled zeta-cycle correction.

At monograph level, this model contributes a clear example of permissible spectral translation. The admissible claim is not that the zeta function causes inflation, nor that the Riemann Hypothesis is empirically supported. The admissible claim is that a normalized critical-line signal, when embedded in a structural macro-financial forecasting baseline and checked across annual, quarterly and monthly validation layers, can improve the forecast hierarchy and identify crisis-sensitive cyclical deformation. This is a forecast-diagnostic claim, not a theorem claim.

The source manuscript is particularly important because it separates validation layers. The principal annual layer covers 1970-2024 with N = 55; the annual robustness layer covers 1980-2024 with N = 45; a compact crisis-era annual window covers 2005-2024 with N = 20; quarterly dynamic validation covers 2000Q1-2024Q4 with N = 100; and monthly spectral diagnostics cover 2005M1-2024M12 with N = 240. This layered structure matters because it prevents the zeta correction from being judged only on a compact high-fit window. The monograph should preserve this logic: spectral evidence is meaningful only when compact-sample overfitting is demoted and broader validation layers remain visible.

The zeta component also clarifies how a spectral object can be economically interpretable. Crisis years such as 2008, 2020 and 2022 are not treated as metaphysical zeta events. They are treated as macro-financial stress windows in which the

zeta-cycle, composite pressure and regime diagnostics align. The interpretation is therefore one of diagnostic alignment. A zeta deformation that coincides with known inflation-stress regimes can support a cyclical interpretation, but it cannot be upgraded into causal proof.

$$\hat{\pi}^{Z}_t = \hat{\pi}^{F}_t + \alpha * \lambda_{\zeta} * d_t$$

Monograph-level reading: the hybrid forecast is a structural FPAS baseline plus a bounded zeta-cycle correction. The correction is admissible only after normalization, alpha calibration, benchmark comparison and residual diagnostics.

Table 2.4.2. Riemann/zeta translation sequence and claim discipline

Translation step	Technical role	Economic interpretation	Claim boundary
Composite pressure CP_t	Aggregates macro-financial stress coordinates.	Defines the inflation-pressure environment.	Constructed index, not an official global policy variable.
Nonlinear tau argument tau_t	Maps macro-pressure into zeta evaluation input.	Converts economic pressure into spectral-signal coordinate.	Parameterization choice requiring sensitivity checks.
Critical-line signal zeta(1/2 + i tau_t)	Generates mathematically explicit oscillatory information.	Supplies potential cyclical signal.	Not a RH proof, test or verification.
Normalized zeta-cycle zeta_t	Transforms complex output into real-valued diagnostic cycle.	Makes the signal usable in forecasting.	A constructed signal, not a theorem-level invariant.
Deviation d_t	Measures distance from neutral zeta-cycle level.	Determines direction and magnitude of correction.	Correction signal requires benchmark validation.
FPAS+zeta forecast	Adds alpha-scaled zeta correction to FPAS baseline.	Tests whether spectral information improves forecast accuracy.	Bounded forecast improvement only; no universal dominance.
Spectral/regime diagnostics	Uses wavelet, spectral entropy, HMM/Markov screens and residual tests.	Checks cyclical alignment and overfitting risk.	Diagnostic support only; not deterministic crisis prediction.

2.4.3. The BSD Analogy: From Local Reductions to Economic LOrder and Structural Rank

The BSD analogue is the monograph's principal L-function and local-to-global model. The classical mathematical object is the Birch-Swinnerton-Dyer framework linking elliptic curves, local reductions, Euler products, L-function behavior near s = 1 and algebraic rank. In the economic manuscript, this architecture is not imported as number theory. It is translated into a regional macroeconomic measurement system in which local regional states, corridor exposure and finite-state reductions are used to construct an economic L-function analogue and an L-order measure that can be compared with structural economic rank.

The direct proof boundary is especially important here. A regional economy is not an elliptic curve. Regional stress states are not reductions over finite fields. Economic Euler factors are not arithmetic Euler factors. Economic LOrder is not the order of vanishing of a classical L-function. Structural rank is not Mordell-Weil rank. Because of these category differences, the BSD chapter cannot claim to prove, test or replicate the BSD conjecture. It can only claim that the BSD local-to-global architecture offers a disciplined grammar for measuring whether local regional information contains structured information about global economic rank formation.

The translation sequence is more elaborate than the zeta forecast sequence because BSD logic is inherently local-to-global. The model begins with a World-normalized regional anchor panel. Regional macroeconomic variables are normalized and transformed into systemic stress, fragility, transition momentum and corridor exposure. These states are embedded in a weighted regional graph. Regional variables are mapped into economic curve coefficients, and non-degeneracy is checked through discriminant logic. Finite-state local traces are then computed over selected q-bases. These traces are aggregated into Euler-factor analogues. The Euler-factor structure is used to build an economic L-function around s = 1. From this behavior the model derives LOrder, which is compared with a structural-rank object composed of productive, Hodge-flow, network and agentic dimensions.

The value of this translation is that it gives the monograph a rank-formation language that is stronger than GDP comparison but weaker than theorem proof. GDP mass alone cannot explain corridor leverage, local stress states, network position, absorption capacity or locked capacity. The BSD analogue organizes these dimensions into a local-to-global chain. The result is not a single index but a measurement architecture: local finite-state regimes are treated as economic reductions; Euler factors summarize local information; the constructed L-function aggregates local signals; LOrder summarizes behavior; structural rank supplies the global comparison object; and robustness gates determine the claim level.

The permissible claim is calibrated local-to-global consistency. The strongest defensible statement is that, within the constructed regional system and its N = 150 closure architecture, local finite-state information and Euler-factor analogues are informative about structural-rank formation. This does not imply causal law, theorem-level equality or strong independent external validation where robust-inference p-values are weak or external-proxy signs are mixed. The chapter's decision-gate logic is therefore not a secondary detail. It is the mechanism that keeps the BSD analogy scientifically admissible.

The monograph should emphasize that BSD is one of the most important bridge chapters because it connects several earlier analogies. The structural-rank object includes Hodge-flow rank; the corridor-stress and BridgeStress logic links to Yang-Mills and Navier-Stokes; the L-function construction links to Riemann/zeta spectral logic; the finite-state reduction and q-grid sensitivity link to computational and robustness discipline; and the claim-boundary hierarchy links back to the general analogy-versus-proof principle in Section 2.1.

Local states -> traces a_q -> Euler-factor analogues -> L_E(s) -> LOrder -> structural rank

Monograph-level reading: the BSD-inspired chain is a measurement architecture for local-to-global rank formation, not a number-theoretic proof chain.

Table 2.4.3. BSD local-to-global L-function translation sequence

BSD-inspired layer	Economic construction	Analytical role	Restricted interpretation
World-normalized anchor panel	GDP mass, world share, growth, transition GDP, income depth and system role.	Defines the regional coordinate system.	Not a country ranking or complete macro database.
Stress/corridor transformation	Systemic stress, fragility, transition momentum and corridor exposure.	Turns public anchors into local-state inputs.	Derived variables require audit and source disclosure.
Economic curve coefficients	Regional states mapped into coefficient objects with discriminant screening.	Creates non-degenerate analogue objects.	Not literal elliptic curves over number fields.
Finite-state reductions	q-base regional trace analogues under selected finite-state regimes.	Represents local regional behavior.	Not arithmetic reduction over finite fields.
Euler-factor analogues	Aggregated local traces translated into local factor behavior.	Builds local-to-global bridge.	Not classical Euler factors.
Economic L-function	Constructed L-function behavior around s = 1.	Aggregates local information into global signal.	Not an arithmetic L-function.
LOrder	Order-of-behavior measure derived from constructed L-function.	Compared with structural rank.	Not classical order of vanishing.
Structural rank	Productive, Hodge-flow, network and agentic rank components.	Global rank object for calibration.	Constructed measurement object, not welfare or algebraic rank.
Closure diagnostics	N = 150 panel checks, robust inference, circularity	Determines final evidence level.	Diagnostic consistency, not causal proof.

BSD-inspired layer	Economic construction	Analytical role	Restricted interpretation
	screens, placebo and sensitivity tests.		

2.4.4. Shared Architecture: Signal, Local Factor, Spectrum and Rank

Riemann/zeta and BSD differ in empirical purpose. The zeta model is a forecast-diagnostic architecture for global inflation. The BSD model is a local-to-global structural-rank architecture for regional economic systems. Yet they share a common four-part structure: a mathematical signal source, an economic transformation, a validation layer and a claim boundary. The zeta model begins from a critical-line signal and ends in a forecast correction. The BSD model begins from local reductions and ends in LOrder-structural-rank correspondence. In both cases, the mathematical object is valuable only after it is transformed into a measurable economic signal and tested against a non-identical economic target.

The shared architecture also explains why the monograph should not isolate Riemann and BSD from the rest of the book. Hodge decomposition supplies the internal macro-flow component used inside structural rank. Yang-Mills mass-gap logic supplies a spectral-threshold interpretation for stress transmission. Navier-Stokes supplies cycle and closure discipline in macro-financial stress testing. Perelman/Ricci/Poincare supplies entropy and graph-topology diagnostics. P-vs-NP supplies the computational warning that an apparently clear mathematical problem can become infeasible when the discrete support space explodes. Together, these models show that spectral and L-function analogies are part of a broader measurement programme, not separate mathematical decorations.

A useful monograph-level statement is therefore this: spectral objects convert hidden economic structure into observable diagnostic modes; L-function analogues convert local information into global rank-related behavior. The zeta-cycle is a spectral correction mode. The economic L-function is a local-to-global aggregation device. The Hodge-Laplacian spectrum verifies diffusion and circulation structure. The Yang-Mills stress-Laplacian gap measures systemic shock threshold. The Navier-Stokes Fourier term captures cyclical forcing. The Perelman W-functional captures entropy-like complexity. The P-vs-NP covariance spectrum evaluates risk concentration. Each object has a different purpose, but all belong to the same translation family because all use formal mathematical structure to discipline economic interpretation.

The important methodological distinction is between explanatory analogy and evidentiary upgrade. A spectral object may improve measurement, but it does not automatically establish causation. A local-to-global analogy may reveal rank consistency, but it does not establish theorem equivalence. A positive graph spectral gap may indicate threshold protection in a finite network, but it does not prove a field-theoretic mass gap. A forecast improvement may show useful information, but it does not prove universal dominance across all countries, horizons or regimes. This is why the monograph consistently uses the language of bounded analogues, diagnostic evidence, calibration, robustness and decision gates.

Table 2.4.4. Comparative spectral roles of the seven problem chapters

Chapter/problem	Main spectral or L-function role	Economic target	Main safeguard
Riemann/zeta	Critical-line zeta-cycle, wavelet/spectral entropy and regime screens.	Global inflation forecast correction and pressure-cycle interpretation.	Layered N = 55, 45, 20, 100 and 240 validation; residual caveats.
BSD	Euler-factor analogues, constructed L-function and LOrder.	Local-to-global structural rank formation under corridor stress.	N = 150 closure, circularity screens, external-proxy demotion and placebo logic.
Hodge	Weighted Laplacian, Hodge-Laplacian and eigenspectrum.	Macro-flow decomposition into hierarchy, imbalance and circulation.	Benchmark interpretation only; future all-country/dyadic replication required.
Yang-Mills	Stress-weighted Laplacian spectral separation.	Systemic shock threshold and finite-network mass-gap index.	Finite graph only; country-panel causal claims reserved.
Navier-Stokes	Fourier GDP-cycle forcing and validation-window forecasting.	Liquidity-flow systemic stress and restricted closure.	Nondimensional scaling and restricted epsilon equation.

Chapter/problem	Main spectral or L-function role	Economic target	Main safeguard
Perelman/Ricci/Poincare	Graph Laplacian connectedness, Betti diagnostics and entropy-like W functional.	Inequality pressure, smoothing capacity and diagnostic manifold structure.	Constructed curvature/topology objects, not literal invariants.
P vs NP	Covariance eigenvalue diagnostics and support-space complexity.	Robust portfolio search under cardinality constraints.	Exact reduced enumeration only; full-universe optimum not certified.

2.4.5. Spectral Validation Versus Spectral Overclaiming

Spectral validation is powerful because it can reveal whether a constructed signal behaves coherently across frequencies, regimes, eigenmodes or local-to-global mappings. However, spectral validation is also prone to overclaiming. A visually compelling cycle can be overfit. A high correlation between LOrder and structural rank can be mechanically inflated if variables share lineage. A graph spectral gap can be sensitive to edge weighting. A covariance eigenvalue pattern can reflect modelling assumptions rather than market truth. Therefore, Section 2.4 must give special attention to the difference between validation and overclaiming.

In the Riemann/zeta model, overclaiming is controlled through layered validation. The N = 20 crisis-era annual window is informative but demoted; the principal claim relies on broader annual, robustness, quarterly and monthly layers. Forecast comparisons are made against FPAS and ARIMA. Rolling no-look-ahead validation, Mincer-Zarnowitz calibration, forecast-encompassing tests, Diebold-Mariano and Clark-West comparisons, residual diagnostics, HMM/Markov-switching regimes, Fourier/wavelet coherence and spectral-entropy screens all operate as gates. The monograph should read these gates as a protection against visual-fit storytelling.

In the BSD model, overclaiming is controlled through local-to-global closure discipline. LOrder and structural rank are compared through gaps, MAE, RMSE, Spearman correlation, calibration and Bland-Altman audits, but this is not enough by itself. The manuscript adds high-R2 audits, variable-lineage analysis, residualized LOrder, external-only diagnostics, negative controls, robust inference, circularity tests, out-of-sample validation, sensitivity analysis and permutation placebo logic. This is necessary because LOrder and structural rank are both constructed objects. Their relationship must be defended against circularity, not merely reported.

The supporting chapters reinforce the same principle. Hodge spectral diagnostics are internal benchmark checks rather than observed dyadic-flow validation. Yang-Mills spectral separation is a finite-network threshold, not a physical theorem. Navier-Stokes cycle terms and rolling forecasts are validation-window evidence, not permanent crisis-prediction dominance. Perelman/Ricci/Poincare forecast and graph diagnostics are bounded by AR(1) and uncertainty discipline. P-vs-NP exact enumeration is available only in the reduced benchmark, while the full n = 94 universe remains best-found rather than globally certified. Across the monograph, spectral evidence is never allowed to become self-certifying.

A useful editorial rule follows. When a spectral or L-function object appears in the book, the surrounding text must state three things: what the object measures, what it does not measure and what validation gate supports its use. For example, the zeta-cycle measures a normalized cyclical correction; it does not measure truth of RH; it is supported only by layered forecast validation. LOrder measures order-of-behavior in a constructed regional L-function; it does not measure classical order of vanishing; it is supported by calibration and closure diagnostics. The mass-gap index measures finite weighted-graph spectral separation; it does not solve Yang-Mills; it is supported by robustness across graph filters and perturbation tests.

Table 2.4.5. Overclaiming risks and monograph-level safeguards

Risk	Where it appears	Why it matters	Required safeguard
Theorem inflation	Riemann, BSD, Yang-Mills and P vs NP analogies.	Economic results may be mistaken for mathematical proof.	Explicit statement that models are analogues, not theorem solutions.
Visual spectral fit	Zeta cycles, wavelet coherence, Fourier terms.	Cyclical graphs can look persuasive even when overfit.	Rolling validation, benchmark comparison and residual diagnostics.
Circular rank construction	BSD LOrder and structural	Constructed variables may	Variable-lineage audit,

Risk	Where it appears	Why it matters	Required safeguard
	rank.	share inputs.	residualization and external-only checks.
Edge-weight sensitivity	Hodge and Yang-Mills graph spectra.	Spectral gaps and cycles depend on graph construction.	Graph-filter robustness, perturbation tests and source-ledger disclosure.
Small-sample overstatement	Regional benchmark chapters and compact windows.	Few nodes or short windows can inflate confidence.	Claim demotion, bootstrap/Monte Carlo bands and future replication pathway.
Causal upgrade	All seven analogues.	Diagnostic association may be misread as causality.	Use diagnostic wording unless identification design supports causal language.

2.4.6. The Role of Hodge, Yang-Mills and Navier-Stokes as Supporting Spectral Architectures

Although Section 2.4 is centered on Riemann/zeta and BSD, three other chapters supply essential spectral support: Hodge, Yang-Mills and Navier-Stokes. Their function is to show that spectral reasoning is a general measurement language across the monograph, not an isolated number-theoretic feature. These chapters also help the reader understand why zeta and L-function analogies are admissible: they are part of a broader pattern in which formal mathematical tools are converted into transparent economic diagnostics.

The Hodge chapter uses spectral graph diagnostics to verify connectedness and diffusion structure in a regional macro-flow network. The weighted Laplacian summarizes how shocks can spread across the network, while Hodge-Laplacian diagnostics distinguish local curl from harmonic circulation after economically meaningful triangular filling. This gives the monograph a spectral-topological foundation for macro-flow decomposition. The Hodge contribution is especially important for the BSD chapter because structural rank includes a Hodge-flow component. In other words, the BSD LOrder-rank comparison is not only a GDP-rank exercise; it includes topological macro-flow information developed in the Hodge architecture.

The Yang-Mills chapter uses a stress-weighted graph Laplacian to define a finite-network economic mass gap. The word mass gap is restricted to the first positive spectral separation of a finite weighted graph. This is not a physical gauge-theory result, but it is a meaningful economic threshold: if spectral separation is positive and robust, local stress may require a measurable threshold before becoming systemically transmissible. This supports Section 2.4 because it shows a second way of translating spectral structure into economic meaning: not as a zeta-cycle forecast correction, but as a shock-propagation threshold.

The Navier-Stokes chapter contributes spectral logic through cycle and forcing terms. Its macro-financial stress-balance framework includes Fourier GDP-cycle forcing, stochastic shocks and a restricted hidden-adjustment term. This is not an L-function object, but it is a spectral/cyclical object in the broader sense: cyclical macroeconomic modes enter the stress-balance equation and are tested through rolling validation and benchmark comparisons. This supports the zeta chapter because both treat global macroeconomic pressure as partly cyclical and nonlinear, while preserving different model architectures.

Together these supporting chapters make Section 2.4 stronger. Riemann/zeta supplies the explicit spectral signal; BSD supplies the L-function local-to-global structure; Hodge supplies graph-Laplacian and Hodge-Laplacian decomposition; Yang-Mills supplies spectral threshold logic; Navier-Stokes supplies cycle forcing and closure discipline. The book's conceptual framework therefore becomes internally coherent: spectral objects are used whenever hidden modes, thresholds, cycles or local-to-global behavior cannot be captured by scalar indicators alone.

2.4.7. Entropy, Regime and Complexity Links: Perelman/Ricci/Poincare and P-vs-NP

Perelman/Ricci/Poincare and P-vs-NP are not L-function chapters, but they complete the spectral-complexity environment of the monograph. The Perelman/Ricci/Poincare model uses F- and W-type functionals, graph connectedness, Betti diagnostics, Laplacian connectedness and entropy-like complexity to interpret global inequality pressure. These objects do not behave like zeta or BSD L-functions, but they share the same idea that complex economic systems contain structured information beyond scalar averages. In the inequality model, W-functional complexity and graph topology prevent the reader from interpreting partial pressure recovery as full convergence.

The P-vs-NP chapter contributes a different form of spectral-complexity discipline. Its main object is cardinality-constrained portfolio optimization under computational complexity, not spectral number theory. Yet covariance geometry and eigenvalue concentration matter because they determine the risk structure of the portfolio universe. A high expected-return asset universe can still be dominated by common-factor covariance modes; a search process can identify a best-found incumbent without certifying the global optimum. The chapter therefore extends Section 2.4's general lesson: mathematical structure improves economic measurement only when it is matched with computational and evidentiary boundaries.

These two supporting chapters are also useful editorially. Perelman/Ricci/Poincare reminds the reader that entropy and topology are diagnostic, not proof. P-vs-NP reminds the reader that mathematical hardness and empirical search are not the same thing as theorem resolution. When the monograph later discusses zeta cycles and economic L-functions, these lessons will help prevent overreading. A spectral signal can be useful without being metaphysical; a local-to-global construction can be informative without being theorem-level; a high-performance algorithm can be valuable without being globally certified.

Therefore, Section 2.4 should be read as a bridge between number-theoretic analogies and the broader monograph methodology. Riemann and BSD are central, but their legitimacy is reinforced by the fact that all seven manuscripts share the same discipline: mathematical objects become economic analogues only through operational translation, validation and claim restriction.

2.4.8. Monograph-Level Permissible Claim Hierarchy for Spectral and L-Function Analogies

The final task of Section 2.4 is to establish a claim hierarchy for spectral and L-function analogies. This hierarchy will protect the monograph from two opposite errors. The first error is underclaiming: treating the mathematical analogies as merely decorative metaphors and failing to recognize their methodological contribution. The second error is overclaiming: presenting constructed economic signals as if they were mathematical proofs or universal laws. The correct position lies between these extremes.

At the strongest permissible level, the monograph may claim reproducible measurement architecture. The zeta and BSD models both provide auditable pipelines from inputs to constructed signals, validation outputs and decision gates. The zeta pipeline links macro-financial pressure to tau, zeta-cycle, deviation, correction and forecast comparison. The BSD pipeline links regional anchors to stress states, finite-state traces, Euler-factor analogues, economic L-function behavior, LOrder and structural rank. These are legitimate methodological contributions.

At the second level, the monograph may claim calibrated diagnostic informativeness. The zeta signal may be described as improving the reported global inflation forecast hierarchy under layered validation. The BSD LOrder may be described as informative about structural rank inside the N = 150 regional-year calibration and screening architecture. Hodge, Yang-Mills, Navier-Stokes, Perelman/Ricci/Poincare and P-vs-NP may be described as supplying supporting spectral, topological, cyclical, entropy or computational diagnostics. These are strong empirical claims, but they remain conditional and bounded.

At the third level, the monograph may claim conceptual synthesis. The seven problem chapters jointly show how flow, curvature, topology, spectral signals, local-to-global rank and computational complexity can be translated into economic measurement grammars. This is the central monographic contribution. The book is not merely a collection of seven papers; it is a unified framework for converting mathematical problem architectures into economic-econometric analogues.

The monograph may not claim theorem solution, direct mathematical proof, universal causality, global forecast dominance, complete residual elimination, certified full-universe optimization where only heuristic search was performed, or strong external validation where evidence is weak. These restrictions are not weaknesses. They are the conditions that make the analogical programme academically defensible.

Table 2.4.6. Final permissible claim hierarchy for Section 2.4

Claim level	Allowed wording	Examples	Forbidden upgrade
Level 1: architecture	The model constructs a reproducible spectral or L-function-inspired measurement pipeline.	Zeta-cycle pipeline; BSD finite-state/Euler-factor/LOrder pipeline.	Do not call the pipeline a proof of RH or BSD.
Level 2: diagnostic informativeness	The constructed signal is informative under stated validation layers.	FPAS+zeta forecast improvement; LOrder-rank calibration.	Do not claim universal causality or theorem equality.
Level 3: bounded empirical	The model improves	N = 55, 45, 20, 100, 240	Do not generalize to all

Claim level	Allowed wording	Examples	Forbidden upgrade
performance	selected benchmarks in stated samples or passes robustness gates.	validation; N = 150 BSD closure.	economies, horizons or datasets.
Level 4: conceptual synthesis	The monograph shows how spectral and L-function grammars enrich economic measurement.	Hidden cycles, local-to-global rank, graph spectra, shock thresholds.	Do not present analogy as mathematical identity.
Level 5: restricted non-claims	The book explicitly refuses theorem-level, causal and universal claims.	No RH proof; no BSD proof; no physical mass-gap solution; no P vs NP resolution.	Do not soften the restriction in abstracts, conclusions or promotional summaries.

2.4.9. Section Synthesis

Section 2.4 establishes the spectral and L-function core of the monograph's conceptual translation framework. Riemann/zeta and BSD are the central cases because they directly use zeta-cycle and L-function language. The Riemann/zeta component translates critical-line signal behavior into a normalized cyclical correction for global inflation forecasting. The BSD component translates local regional states into finite-state traces, Euler-factor analogues, an economic L-function, LOrder and structural-rank calibration. Both models are explicitly bounded: zeta is not used to prove or test the Riemann Hypothesis, and BSD is not used to prove or test the classical Birch-Swinnerton-Dyer conjecture.

The section also shows why the remaining five manuscripts are necessary for a monograph-level synthesis. Hodge provides spectral graph and Hodge-Laplacian diagnostics; Yang-Mills provides finite-network spectral-threshold logic; Navier-Stokes provides cyclical forcing and closure discipline; Perelman/Ricci/Poincare provides entropy and graph-topology diagnostics; and P-vs-NP provides covariance-eigenvalue and computational search-space discipline. These supporting elements prevent Section 2.4 from becoming only a number-theory discussion. They make it part of a broader economic measurement architecture.

The main scientific message is that spectral and L-function analogies are permissible when they are operational, auditable and bounded. They are not permissible when they are used as rhetorical shortcuts to mathematical prestige. The monograph's contribution is therefore not to solve Millennium Problems, but to show how their formal architectures can discipline economic modelling: cycles can become forecast corrections, local factors can become rank signals, spectra can become shock thresholds, and eigenmodes can become validation objects. Each step remains an economic analogue, not a mathematical proof.

2.5. Complexity and Optimization Analogies

Section 2.5 develops the complexity and optimization dimension of the monograph's conceptual translation framework. It is written as a new monograph-level section rather than as a mechanical extraction from the seven manuscripts. Its primary mathematical source is the P versus NP problem, while its primary economic embodiment is the cardinality-constrained portfolio-optimization architecture. The section explains how computational difficulty, sparse selection, mixed discrete-continuous search, heuristic approximation, exact reduced benchmarking, robustness gates and final claim discipline become an economic-econometric analogue of complexity without becoming a proof of the P versus NP problem.

The core proposition is simple but methodologically powerful: economic decision systems are often not difficult because the continuous model is conceptually unclear; they become difficult because discrete choices must be made before continuous optimization can proceed. In the P-vs-NP portfolio manuscript, the economic problem is not merely to allocate weights across assets. It is first to choose a sparse support of K industries out of n candidates and only then to optimize weights under risk, return, covariance, transaction-cost, stress and derivative-overlay constraints. This transforms a familiar mean-variance problem into an operationally difficult search problem.

The section is therefore positioned between mathematical complexity theory and empirical finance. The classical P versus NP problem asks whether every problem whose solution can be verified efficiently can also be solved efficiently. The monograph does not translate this theorem-level question directly into economics. Instead, it treats the P-vs-NP architecture as a measurement grammar for problems in which verification, search and certification differ sharply. A proposed portfolio

can be evaluated, stress-tested and reproduced, but that does not mean the global optimum over all possible supports has been certified. This distinction - evaluation is not exhaustive solution - is the conceptual core of the economic analogue.

Although P vs NP is the leading object in this section, all seven manuscripts contribute to the broader complexity logic. Navier-Stokes introduces restricted closure and stress-testing under multiple interacting components; Hodge introduces topological decomposition of complex macro-flow systems; Yang-Mills introduces spectral-threshold diagnostics and scenario stress under network curvature; BSD introduces local-to-global rank calibration and circularity safeguards; Riemann/Zeta introduces layered forecast validation and spectral signal discipline; Perelman/Ricci/Poincare introduces entropy-like complexity, curvature concentration and non-monotonicity audits. The common idea is that complex economic systems require auditable layers rather than single-statistic declarations.

The claim boundary is strict. The monograph may claim that cardinality-constrained portfolio optimization operationalizes computational complexity in a concrete financial workflow. It may claim that a fixed n = 94 industry universe with K = 10 generates a combinatorial support space of 9,041,256,841,903 possible supports before continuous weight optimization. It may claim that heuristic search can be disciplined through exact reduced enumeration, robustness diagnostics and falsification gates. It may not claim to prove P not equal NP, certify the full n = 94 global optimum, or establish realized historical investment dominance.

Table 2.5.1. Complexity and optimization translation map across the monograph

Model	Classical or formal object	Economic complexity translation	Permissible claim
P vs NP	Efficient solvability versus efficient verification; combinatorial growth; computational hardness.	Cardinality-constrained portfolio optimization with binary support variables, continuous weights, C(n,K) support growth, heuristic search and exact reduced benchmarking.	Strong empirical-computational demonstration of sparse portfolio search; no theorem proof and no certified full-universe optimum.
Navier-Stokes	Nonlinear flow balance with velocity, acceleration, pressure, diffusion, forcing and closure.	Stress-balance system in which liquidity weakness, pressure, friction, shocks, Fourier cycles and restricted hidden adjustment must be jointly optimized and audited.	Diagnostic stress-testing and scenario interpretation; no hydrodynamic law and no universal crisis-prediction theorem.
Hodge	Decomposition of flows into gradient, curl and harmonic components on a topological structure.	Complex macro-flow system decomposed into hierarchy, local-cycle imbalance and systemic circulation; complexity is reduced by decomposition rather than by oversimplification.	Benchmark structural decomposition; no claim that economic flows are literal differential forms.
Yang-Mills	Gauge curvature, action and mass-gap logic in mathematical physics.	Network stress curvature, action concentration, spectral separation and shock-threshold diagnostics in a finite weighted graph.	Finite-network threshold evidence; no solution to the Yang-Mills existence and mass gap problem.
BSD	Elliptic curves, local reductions, Euler factors, L-functions and rank.	Local-to-global rank calibration, finite-state trace analogues, constructed economic L-function, LOrder and	Calibrated local-to-global consistency; no proof or empirical test of the BSD conjecture.

Model	Classical or formal object	Economic complexity translation	Permissible claim
		structural-rank comparison.	
Riemann/Zeta	Riemann-zeta function, critical-line structure and spectral/cyclical behaviour.	Normalized zeta-cycle used as a signed forecast correction and spectral diagnostic in global inflation forecasting.	Layered forecast-validation claim; no proof, test or verification of the Riemann Hypothesis.
Perelman/Ricci/Poincare	Ricci flow, curvature, entropy functionals and topological connectedness.	Inequality pressure, smoothing capacity, curvature-like deformation, entropy-like complexity and graph connectedness.	High-level diagnostic measurement claim; no proof of geometric or topological theorems.

2.5.1. The Classical P-vs-NP Object and Its Economic Relevance

The classical P versus NP problem belongs to theoretical computer science and mathematical logic, not to portfolio management. In its formal setting, the problem concerns classes of decision problems. Problems in P can be solved in polynomial time by a deterministic algorithm. Problems in NP have candidate solutions that can be verified in polynomial time. The open question is whether efficient verification implies efficient solution. A theorem-level answer would require a rigorous mathematical proof about computational classes, reductions, machines and complexity bounds. Nothing in the economic manuscripts attempts such a proof.

The relevance of P vs NP for the monograph lies in the asymmetry between search and verification. In many economic contexts a proposed solution can be checked more easily than it can be found. A proposed sparse portfolio can be evaluated by computing expected return, variance, Sharpe ratio, beta, risk contribution, transaction cost effect and derivative-overlay exposure. However, verifying the properties of one candidate portfolio is not the same as searching all possible candidate portfolios and certifying the best one. The same conceptual asymmetry appears in model selection, scenario design, policy counterfactual ranking, network threshold identification and local-to-global structural-rank calibration.

The P-vs-NP portfolio manuscript operationalizes this asymmetry through support selection. If n assets are available and exactly K must be selected, the number of discrete supports is given by the binomial coefficient. Each support is only the beginning of the problem, because weights still have to be assigned, covariance has to be evaluated and constraints have to be respected. The problem is therefore mixed discrete-continuous: binary variables decide inclusion, and continuous variables decide allocation. This mixed structure is what makes the P-vs-NP analogy economically meaningful.

In the fixed Damodaran January 2026 industry universe, the study reports n = 94 industries after excluding aggregate market rows. The baseline sparse-selection problem imposes K = 10, producing 9,041,256,841,903 possible supports before continuous weight optimization. This number is not presented as a theorem about P vs NP. It is an empirical-computational magnitude that demonstrates why naive exhaustive enumeration is not a practical main-universe research strategy. The analogue is therefore operational: the monograph studies how computational complexity appears inside a real financial modelling workflow.

$$C(n,K) = n! / [K!(n-K)!]$$

The binomial coefficient measures the number of possible K-element supports from an n-asset universe. In the P-vs-NP economic analogue, C(n,K) is used as a transparent measure of support-space growth, not as a proof of theorem-level computational hardness.

$$C(94,10) = 9{,}041{,}256{,}841{,}903$$

The reported main-universe magnitude shows operational search-space explosion in the fixed industry dataset. It motivates heuristic search, exact reduced benchmarking and careful claim boundaries.

2.5.2. From Continuous Allocation to Mixed Discrete-Continuous Optimization

Classical Markowitz mean-variance theory is already mathematically structured, but in its simplest form it is a continuous allocation problem. Given a return vector and covariance matrix, the investor chooses weights. Once cardinality is introduced, the structure changes. The model must decide which assets are included and then how much capital each selected asset receives. The resulting problem cannot be understood as a routine continuous optimization exercise, because the support set itself is an object of search.

The monograph treats this transformation as the economic analogue of computational-complexity escalation. The continuous layer remains essential: expected returns are CAPM-implied priors, covariance geometry governs risk, and Sharpe ratio or related objectives define risk-adjusted performance. But the discrete support-selection layer changes the epistemic status of the result. A best-found incumbent can be strong, reproducible and economically meaningful without being a certified global optimum over all possible supports.

This distinction is the reviewer-safety core of the P-vs-NP manuscript. The study can report greedy, Monte Carlo, genetic algorithm and GA-plus-continuous reoptimization results. It can compare their performance across common metrics. It can enumerate a reduced n = 20, K = 6 benchmark and use it as an exact reference layer. It can use robustness tests to evaluate covariance alternatives, risk-free-rate and equity-risk-premium perturbations, weight caps, transaction costs, beta drift, stress scenarios and derivative overlays. It cannot convert these empirical-computational steps into a theorem about P and NP.

The broader monograph uses this logic beyond portfolio optimization. In Navier-Stokes, the stress balance is not difficult because each component is impossible to compute; it is difficult because pressure, friction, shocks, cycles and restricted closure interact. In Hodge, the system is complex because hierarchy, curl and harmonic circulation coexist. In Yang-Mills, network stress becomes complex because curvature, action concentration and spectral separation interact with shock scenarios. In BSD, local-to-global rank formation becomes complex because local signals, Euler-factor analogues, LOrder and structural rank are linked but not identical. P vs NP gives the monograph a formal vocabulary for this family of problems: complex economic measurement is often a layered search and validation problem rather than a single closed-form computation.

$$\text{maximize } S(w,z) = (w'\mu - R_f) / \sqrt{w'\Sigma w}, \text{ subject to } \sum_i z_i = K,\ w_i = 0 \text{ if } z_i = 0$$

This stylized expression captures the mixed nature of the sparse portfolio problem: z_i is the binary inclusion decision, w_i is the continuous portfolio weight, μ is the expected-return vector and Σ is the covariance matrix. The expression is conceptual and monograph-level; detailed specifications remain in the P-vs-NP problem chapter.

Table 2.5.2. From mathematical complexity to economic optimization evidence

Translation step	Formal meaning	Economic operation	Evidence gate
Search space	The set of all candidate supports or configurations grows combinatorially.	Compute C(n,K), define the asset universe before optimization and document support-space scale.	Report n, K, C(n,K), input vintage and exclusion rules.
Verification	A candidate solution can be checked against objective and constraints.	Evaluate one portfolio by return, risk, Sharpe, beta, weights, risk contribution and stress exposure.	Candidate-level audit, not global-optimality proof.
Exact solution layer	Full enumeration or solver certificate can certify a reduced instance.	Enumerate all supports only where the instance is computationally manageable, such as n = 20, K = 6.	Reduced exact benchmark; supports algorithmic credibility but does not certify the full universe.
Heuristic search	Algorithms explore a subset of a large search space.	Use greedy, Monte Carlo, GA and reoptimization layers under common evaluation criteria.	Document search budget, incumbent quality, stability and approximation behaviour.
Robustness	A solution should not be an artefact of one parameterization.	Test covariance alternatives, Rf/ERP perturbations, transaction costs, beta drift, stress cases and option overlays.	Admissible only if interpretation survives economically meaningful perturbations.
Claim discipline	Computational evidence has boundaries.	Separate best-found incumbent, exact reduced	Final claim hierarchy and exclusion matrix.

Translation step	Formal meaning	Economic operation	Evidence gate
		result, derivative realism and excluded theorem claims.	

2.5.3. Algorithmic Search, Exact Reduced Benchmarking and Heuristic Credibility

The methodological contribution of the P-vs-NP economic analogue does not come from using a heuristic algorithm alone. Heuristics are common in applied optimization. The contribution comes from placing heuristic search inside an evidence architecture that acknowledges what has and has not been certified. Greedy search provides a deterministic or rule-based baseline. Monte Carlo sampling provides stochastic coverage of the support space. Genetic algorithms provide structured recombination and selection. GA-plus-continuous reoptimization connects the discrete support layer back to the continuous allocation layer.

Exact reduced benchmarking plays a special role. A reduced universe does not solve the full universe, but it provides a laboratory in which the behaviour of the heuristic layer can be audited against a known exhaustive result. In the P-vs-NP manuscript, the n = 20, K = 6 benchmark enumerates all 38,760 supports. This layer functions as a credibility check. If a heuristic cannot perform well where the exact answer is known, its use in the larger n = 94 universe would be less persuasive. If it performs well in the reduced benchmark, it gains evidentiary support, but not full certification for the main universe.

This approach is important for the monograph as a whole because it formalizes the difference between benchmark validation and universal proof. The Riemann/Zeta manuscript uses layered annual, quarterly and monthly validation rather than one in-sample fit. The Navier-Stokes manuscript uses rolling validation, external-target checks and Monte Carlo counterfactuals rather than a universal crisis law. The Yang-Mills manuscript uses finite-network spectral robustness rather than a continuum field-theory proof. The Perelman/Ricci/Poincare manuscript uses monotonicity audits and graph diagnostics rather than theorem transfer. The same epistemic pattern appears everywhere: evidence becomes credible when it is layered, falsifiable and bounded.

The algorithmic section also clarifies the role of replication. In a computational-complexity analogue, reproducibility is not merely a formatting requirement. It is part of the evidence. Input files, calibration constants, random seeds or search budgets, output tables, formula audits, data dictionaries and checksums are needed because the reader must be able to distinguish the empirical object from the algorithmic search procedure. Without replication structure, a best-found portfolio is only an assertion. With replication structure, it becomes an auditable computational result.

2.5.4. Optimization as an Evidence Hierarchy, Not a Single Result

The strongest feature of the P-vs-NP analogue is that it refuses to treat an optimization output as a final scientific conclusion. A portfolio result is meaningful only after the chain that produced it has been examined. The input universe must be fixed. The expected-return layer must be defined. The covariance model must be audited. The support-space scale must be measured. The algorithms must be compared. The reduced benchmark must be interpreted properly. Transaction costs and derivative overlays must be handled without leverage illusion. The final claim must distinguish what is supported, what is suggestive and what is excluded.

This evidence hierarchy is central to the monograph's general methodology. The seven models do not produce seven isolated numerical claims. They produce seven kinds of measurement architecture. Flow models require balance and closure. Curvature models require deformation and smoothing-capacity interpretation. Spectral models require signal normalization and benchmark comparison. Local-to-global models require variable-lineage and circularity checks. Complexity models require search-space measurement and certification boundaries. The complexity section therefore supplies a methodological discipline that can be reused across the entire book.

Optimization also has a broader economic meaning. In the portfolio chapter, optimization is explicit: choose a sparse support and allocate weights. In Navier-Stokes, optimization is implicit in stress reduction and policy-counterfactual interpretation. In Hodge, it appears as the search for a decomposition that preserves hierarchy, cycle imbalance and harmonic circulation. In Yang-Mills, it appears as the identification of shock thresholds and action-concentration nodes. In BSD, it appears as calibration between local signals and structural rank. In Riemann/Zeta, it appears as forecast correction and error reduction. In Perelman/Ricci/Poincare, it appears as smoothing-capacity improvement and pressure reduction. The P-vs-NP language makes this common optimization structure visible.

At the same time, the monograph avoids an important category error. Optimization does not imply policy optimality, welfare optimality or theorem optimality. A sparse portfolio may be best-found under model-implied CAPM priors, but that

does not prove realized investment dominance. A stress-reduction scenario may improve a model-implied index, but that does not prove an unconditional policy multiplier. A forecast model may outperform benchmarks in reported validation layers, but that does not prove universal forecast dominance. The complexity section therefore strengthens the entire claim-boundary system of the book.

Table 2.5.3. Optimization analogies beyond the P-vs-NP chapter

Model	Optimization or search element	What is being optimized or disciplined	Excluded overclaim
Navier-Stokes	Stress-balance calibration, restricted residual closure, rolling validation and policy counterfactuals.	Systemic-stress interpretation under pressure, friction, shocks, cycles and resilience buffers.	No universal crisis-prediction law and no physical-fluid identity.
Hodge	Graph construction and decomposition into gradient, curl and harmonic components.	A structurally meaningful representation of hierarchy, local imbalance and systemic circulation.	No claim that the regional economy is a literal smooth manifold or exact differential-form system.
Yang-Mills	Network threshold diagnostics and scenario shock comparisons.	Identification of spectral protection, fragility, BridgeStress and action concentration in a finite graph.	No continuum gauge-theory proof and no mathematical mass-gap solution.
BSD	Calibration between finite-state local signals, LOrder and structural rank.	Local-to-global measurement consistency and rank-order correspondence under claim discipline.	No proof of BSD and no independent causal validation when circularity risk remains.
Riemann/Zeta	Alpha-calibrated forecast correction and layered model comparison.	Reduction of forecast error relative to FPAS and ARIMA inside defined validation layers.	No Riemann Hypothesis proof and no universal forecast superiority.
Perelman/Ricci/Poincare	Pressure-smoothing diagnostics, curvature contribution rankings and counterfactual sensitivity.	Identification of deformation, entropy-like complexity and smoothing-capacity bottlenecks.	No theorem-level monotonicity, no unrestricted causality and no country-level welfare ranking.
P vs NP	Sparse support selection and continuous weight optimization.	Best-found portfolio evidence, heuristic credibility and exact reduced benchmarking.	No proof of P not equal NP and no certified full n = 94 global optimum.

2.5.5. Black-Scholes Overlay, Transaction Costs and Realism as Complexity Controls

The derivative-pricing overlay in the P-vs-NP manuscript plays a crucial conceptual role in the monograph. It shows that optimization must not be allowed to exploit leverage, optionality or modelling artefacts as if they were free performance. The Black-Scholes layer demonstrates how option value, delta exposure, leverage-adjusted beta and volatility can be incorporated into the portfolio architecture, but it also imposes a claim boundary: derivative overlay is an additional risk-adjusted structure, not a shortcut to unconditional improvement.

Transaction costs and implementation frictions perform a similar function. A portfolio that looks attractive before costs may weaken after turnover, spreads, liquidity constraints or implementation frictions are introduced. The monograph therefore interprets costs as complexity controls. They prevent the optimization exercise from becoming an abstract maximum detached from market implementation. This is consistent with the larger book, where every mathematical translation is filtered through empirical auditability.

The realism layer also clarifies why computational finance is more than an algorithmic exercise. A purely combinatorial search could identify a high objective value under a narrow specification. A scientific monograph must ask whether that value survives covariance perturbation, risk-premium changes, beta drift, stress scenarios, derivative leverage adjustment and falsification gates. Complexity is therefore not only the number of possible supports; it is also the number of economically meaningful ways in which an apparent optimum can fail.

This insight connects back to the other six models. Navier-Stokes uses restricted epsilon closure to prevent residuals from becoming an unrestricted plug. BSD uses variable-lineage and residualized diagnostics to control circularity. Riemann/Zeta uses no-look-ahead validation and benchmark comparison to control overfit. Perelman/Ricci/Poincare uses monotonicity audits to prevent theorem importation. Yang-Mills uses finite-network boundaries and future panel separation to prevent mass-gap overclaiming. Hodge uses benchmark and topological validation to distinguish decomposition from causal proof. The P-vs-NP realism layer is therefore part of a shared monograph-wide anti-overclaiming grammar.

2.5.6. Complexity, Entropy and Dimensionality across the Seven Analogues

The word complexity has several meanings across the monograph. In the P-vs-NP chapter, it is computational: the support space grows combinatorially and the search problem becomes difficult. In Perelman/Ricci/Poincare, complexity is entropy-like: the W-functional summarizes pressure-curvature deformation and the persistence of systemic stress after shocks. In Hodge, complexity is structural: hierarchy, local-cycle imbalance and harmonic circulation coexist. In Yang-Mills, complexity is network-curvature concentration: systemic stress-energy is concentrated in cycles and thresholds. In BSD, complexity is local-to-global: regional signals must be mapped into structural rank. In Riemann/Zeta, complexity is spectral-cyclical: inflation pressure interacts with nonlinear zeta-cycle deviations and shock regimes. In Navier-Stokes, complexity is flow-balance interaction: velocity weakness, pressure, friction, shocks and closure variables combine.

This multiplicity is not a weakness. It is exactly why the monograph requires a conceptual translation chapter. The seven Millennium-inspired models do not reduce economic complexity to one metric. They provide seven mathematical-econometric languages for different forms of complexity. P vs NP contributes the computational-decision language: when feasible configurations multiply rapidly, the analyst must separate search, verification, approximation, exact certification, robustness and final claim status.

The economic value of the P-vs-NP analogue is therefore not that it borrows prestige from an open mathematical problem. Its value is that it imposes a precise discipline on economic optimization claims. It asks: what is the search space; what is the candidate; what is the objective; what is the verification method; what is the exact benchmark; what is only heuristic; what is robust; what is economically realistic; what is explicitly excluded? These questions are transferable beyond portfolio finance and become part of the monograph's general methodological contribution.

Table 2.5.4. Distinguishing types of complexity in the seven-problem monograph

Complexity type	Primary model	Economic meaning	Validation discipline
Computational-decision complexity	P vs NP	Large support spaces, mixed discrete-continuous search and asymmetric search versus verification.	Exact reduced benchmark, heuristic comparison, search-coverage reporting and claim hierarchy.
Flow-interaction complexity	Navier-Stokes	Liquidity, pressure, friction, stochastic shocks, Fourier cycles and restricted closure interact.	Rolling validation, external targets, residual checks, Monte Carlo and policy counterfactuals.
Topological-decomposition complexity	Hodge	A macro-flow system contains hierarchy, local imbalance and persistent circulation.	Hodge energy decomposition, graph adequacy, Hodge-Laplacian diagnostics and benchmark interpretation.
Gauge-network threshold complexity	Yang-Mills	Stress curvature and action concentration define local-to-systemic shock thresholds.	Finite graph spectrum, perturbation tests, scenario compression and future panel boundary.
Local-to-global rank	BSD	Local finite-state signals	LOrder comparison, rank

Complexity type	Primary model	Economic meaning	Validation discipline
complexity		must be calibrated against global structural rank.	gaps, placebo logic, external-proxy screening and circularity controls.
Spectral-cyclical complexity	Riemann/Zeta	Inflation pressure has nonlinear spectral and shock-regime components.	Layered annual/quarterly/monthly validation, benchmark comparison and no-look-ahead testing.
Curvature-entropy complexity	Perelman/Ricci/Poincare	Inequality pressure and smoothing capacity produce deformation and entropy-like persistence.	N = 150 diagnostic panel, graph connectedness, monotonicity audit and bounded forecast uncertainty.

2.5.7. Permissible Claims and Excluded Claims

The permissible claim of Section 2.5 is a strong but bounded computational-econometric claim. The monograph may state that the P-vs-NP-inspired framework provides a transparent and reproducible way to study cardinality-constrained portfolio optimization under CAPM priors, covariance geometry, sparse support selection, heuristic search, exact reduced enumeration, robustness diagnostics, derivative-overlay realism and final claim discipline. This is a substantive contribution to computational finance and to the monograph's broader analogue programme.

The section may also claim that computational-complexity reasoning improves the interpretation of economic modelling. It forces the researcher to avoid confusing a candidate result with a certified optimum, an exact reduced benchmark with a full-universe proof, a model-implied incumbent with realized investment dominance, or a financial optimization result with a theorem about P and NP. This claim is not modest in intellectual ambition, but it is modest in proof status. It is methodological and empirical, not theorem-level.

The explicitly excluded claims are equally important. The monograph does not prove P = NP or P not equal NP. It does not show that the full n = 94, K = 10 industry universe has been exhaustively solved. It does not claim that genetic algorithms or Monte Carlo methods guarantee global optimality in the main universe. It does not claim that CAPM-implied expected returns are realized returns. It does not claim that the Black-Scholes overlay produces unconditional free performance. It does not claim that any model-implied portfolio universally dominates all real-world strategies.

The reviewer-safe formulation is therefore the following: P-vs-NP logic is translated into economics as a disciplined architecture for measuring and auditing computational difficulty in sparse portfolio selection. The admissible output is a reproducible empirical-computational demonstration with exact reduced benchmarking and robustness gates. The inadmissible output would be a theorem claim, a global-optimality certificate without full proof, or a realized-performance claim without the relevant empirical evidence.

Table 2.5.5. Final claim hierarchy for complexity and optimization analogies

Claim level	Admissible statement	Evidence basis	Boundary
Strong computational-finance claim	Cardinality-constrained portfolio optimization is a mixed discrete-continuous search problem with operational support-space explosion.	Binary support variables, continuous weights, C(94,10) scale and documented search architecture.	Empirical-computational claim only; not theorem proof.
Strong benchmark claim	Heuristic search can be audited through exact reduced enumeration and algorithmic comparison.	Reduced n = 20, K = 6 full enumeration and search-layer comparison.	Reduced benchmark supports credibility; it does not certify the full n = 94 optimum.
Robustness claim	Portfolio interpretation must survive covariance, Rf/ERP, cost, beta, stress	Sensitivity, stress and realism gates.	Robust model-implied evidence; not realized investment dominance.

Claim level	Admissible statement	Evidence basis	Boundary
	and derivative-overlay diagnostics.		
Monograph-level methodological claim	Complex economic models require layered search, verification, calibration, robustness and claim boundaries.	Cross-model synthesis across all seven analogues.	Conceptual-methodological contribution; not a universal theory of all economic complexity.
Excluded theorem claim	The study proves P not equal NP or resolves the formal P-vs-NP problem.	No theorem-proof apparatus is provided or claimed.	Explicitly outside scope.
Excluded global-optimality claim	The full n = 94, K = 10 global optimum is certified.	Full enumeration or solver certificate is not reported for the main universe.	Explicitly outside scope.
Excluded performance claim	The optimized portfolio universally beats real-world strategies.	The return layer is CAPM-implied, not a realized-return dominance test.	Explicitly outside scope.

2.5.8. Section Synthesis

Complexity and optimization analogies give the monograph its computational-decision dimension. The P-vs-NP-inspired portfolio chapter is the central source because it converts the abstract distinction between search and verification into a concrete empirical-finance setting. The selection of K industries from n candidates creates a support-space explosion; each support then requires continuous evaluation; heuristic results require benchmarking; derivative and transaction-cost layers require realism; and final conclusions require explicit exclusion of theorem proof, full global-optimality certification and realized investment dominance.

The section also shows why the P-vs-NP logic belongs in Chapter 2 rather than only in the later portfolio problem chapter. At the monograph level, P vs NP provides a general warning: economic complexity cannot be reduced to attractive numerical outputs. A result is scientifically credible only when the path from input definition to candidate search, validation, robustness and claim classification is visible. This warning applies to every model in the book, from Navier-Stokes stress testing to Riemann/Zeta forecasting, from Yang-Mills network thresholds to BSD rank calibration.

The final conceptual conclusion is that the monograph does not use the Millennium Problems as decorative metaphors. It uses them as bounded measurement grammars. P vs NP contributes the grammar of computational difficulty, sparse decision-making, search-space growth, heuristic discipline and certification limits. Its permissible claim is strong: it demonstrates how computational-complexity logic can organize a high-level economic optimization architecture. Its forbidden claim is equally clear: it does not solve, prove, test or replicate the formal P versus NP problem.

2.6. Local-to-Global and Systemic Transmission Logic

Section 2.6 defines the local-to-global and systemic-transmission logic of the monograph. It is a new conceptual section written for the book, not a direct transfer of one article chapter. Its core function is to explain how the seven Millennium-inspired economic analogues convert local signals, regional states, corridor pressures, network relations, stress thresholds and validation gates into global measurement objects. The primary models are Birch-Swinnerton-Dyer, Hodge, Yang-Mills and Navier-Stokes, while Perelman/Ricci/Poincare, Riemann/Zeta and P-vs-NP supply supporting logic for deformation, spectral validation and computational decision discipline.

The phrase local-to-global has a precise meaning in this monograph. It does not mean that a local empirical observation automatically proves a global economic law. It means that local units - regions, edges, cycles, stress components, finite-state regimes, shock amplitudes, liquidity channels or forecast residuals - are transformed through explicit operators into global diagnostic objects. The scientific value of the monograph lies in the transparency of those operators: each model states what counts as a local signal, how it is normalized or discretized, how it is aggregated or transmitted, what global object is produced, and what claim boundary prevents overinterpretation.

Systemic transmission is the applied counterpart of local-to-global translation. In conventional macroeconomic description, GDP, inflation, growth, inequality, trade and volatility are often read as separate indicators. In the monograph,

these indicators become inputs into networks, flows, curvature structures, spectral thresholds, rank objects and forecast layers. A local disturbance becomes analytically important only when it can travel through the constructed system: through a corridor, a pressure gradient, a curl cycle, a harmonic circulation component, a spectral Laplacian mode, an Euler-factor product, a stress-balance closure term or an optimization constraint.

The strongest local-to-global design is found in the BSD-inspired manuscript. There, World-normalized public anchors are transformed into systemic stress, network structure, economic curve coefficients, finite-state trace analogues, Euler-factor analogues, a constructed economic L-function, LOrder and structural rank. The strongest systemic-transmission design is shared by Hodge, Yang-Mills and Navier-Stokes. Hodge decomposes macro-flow pressure into hierarchy, local imbalance and persistent circulation. Yang-Mills represents corridor stress as a finite gauge-curvature network with a local-to-systemic shock threshold. Navier-Stokes represents systemic stress as a nondimensional balance of flow weakness, pressure, friction, stochastic forcing, cycle effects and restricted closure.

The monograph therefore uses local-to-global logic as a disciplined measurement grammar. It does not claim that the economy is an elliptic curve, a physical gauge field, a fluid or a manifold. It claims that these formal architectures help define structured economic diagnostics: where a local signal comes from, how it propagates, when it becomes systemic, how it changes global rank or stress, and which validation gate limits the permissible interpretation.

Table 2.6.1. Local-to-global and systemic-transmission map across the seven economic analogues

Model	Local object	Transmission operator	Global object	Permissible claim
BSD	Regional finite-state reductions, trace analogues, stress and corridor states.	Euler-factor product, constructed economic L-function and LOrder-rank comparison.	Structural rank, corridor stress and local-to-global consistency.	Local regional signals are informative about constructed global structural rank; no proof or test of classical BSD.
Hodge	Directed regional edge-pressure values and local cycles.	Discrete Hodge projection into gradient, curl and harmonic components.	Hierarchy, local imbalance, systemic circulation, resilience and tail risk.	Macro-flow pressure is decomposable in the benchmark network; no final country-level causal claim.
Yang-Mills	Node stress, edge gauge potentials, triangular curvature and shock amplitude.	Stress-weighted Laplacian, spectral separation and threshold comparison.	Finite-network mass gap, EMGI, BridgeStress and local-to-systemic transition.	Shocks above the normalized threshold become systemically transmissible in the benchmark; no physical Yang-Mills theorem claim.
Navier-Stokes	Liquidity weakness, acceleration, pressure gradients, friction, shocks and closure states.	Nondimensional stress-balance equation with restricted epsilon(t) closure.	Global systemic-stress index, resilience, rolling validation and counterfactual stress paths.	Macro-financial stress can be measured as a flow-pressure-friction-shock system; no hydrodynamic identity or universal crisis law.
Perelman/Ricci/ Poincare	Region-year inequality pressure coordinates and	Curvature-like deformation, smoothing-capacity	World pressure-curvature path, entropy-like	Global inequality deformation can be diagnosed; no

Model	Local object	Transmission operator	Global object	Permissible claim
	stress variables.	and graph connectedness diagnostics.	complexity and inequality manifold connectedness.	transfer of geometric theorem proof.
Riemann/Zeta	Zeta-cycle deviations, macro-financial tau argument and pressure states.	Spectral correction, alpha calibration and layered forecast validation.	FPAS+zeta inflation forecast and spectral-regime diagnostics.	Zeta signal may improve forecast diagnostics under validation layers; no Riemann Hypothesis proof or verification.
P vs NP	Candidate supports, asset weights, covariance states, search paths and robustness gates.	Heuristic search, exact reduced enumeration and falsification logic.	Best-found sparse portfolio evidence and computational-optimization discipline.	Search difficulty is empirically demonstrated; no P-vs-NP theorem result or full-universe optimum certificate.

2.6.1. Conceptual Role of Local-to-Global Translation

The local-to-global relation is the most general methodological bridge in the monograph. It allows the seven economic analogues to move beyond static description without becoming mathematically overclaimed. Local information is never treated as self-evidently global. It must pass through a defined transformation chain. A regional stress score is not yet a systemic rank. An edge pressure is not yet a global circulation pattern. A shock amplitude is not yet a systemic crisis. A liquidity friction term is not yet a global stress path. A trace value is not yet a rank object. The monograph insists that every transition must be explicit.

The first condition is local definition. Each model must state the unit at which information is first observed or constructed. In BSD this unit is a finite-state regional trace; in Hodge it is an edge-flow pressure value; in Yang-Mills it is a node or triangle-level stress-curvature object; in Navier-Stokes it is a normalized component of liquidity-flow stress; in Ricci/Poincare it is a region-year stress coordinate; in Riemann/Zeta it is a time-specific spectral deviation; in P-vs-NP it is a candidate support or feasible portfolio state. Without a defined local object, local-to-global language becomes metaphorical.

The second condition is transformation discipline. The local signal must be normalized, discretized, projected, multiplied, decomposed, thresholded, forecast-corrected or optimized through a stated method. This is where the monograph separates formal analogy from vague inspiration. The local-to-global claim does not come from the name of a Clay problem. It comes from the auditable chain that converts input anchors into constructed objects.

The third condition is global object construction. A global object can be a structural-rank measure, a systemic-circulation component, a spectral threshold, a stress index, an entropy path, a forecast hierarchy or a best-found optimization incumbent. It is global because it summarizes relations across the system, not because it is universal or theorem-level. This distinction is central to the claim boundary of the book.

The fourth condition is evidence gating. Local-to-global coherence is accepted only within the evidence level supported by the model: internal calibration, benchmark decomposition, scenario threshold, forecast validation, robust association, external-proxy screening or future validation pathway. The permissible claim depends not only on the elegance of the analogy, but on the strength and independence of the evidence.

Local signal -> transformation operator -> global diagnostic object -> evidence gate -> permissible claim

This generic chain governs Section 2.6. It states that local observations do not become global conclusions automatically. They become global diagnostic objects only after passing through explicit transformations and evidence boundaries.

2.6.2. BSD as the Core Local-to-Global Rank Architecture

The BSD-inspired manuscript gives the monograph its most direct local-to-global grammar. In the classical Birch-Swinnerton-Dyer setting, the conceptual architecture links local arithmetic information, L-function behaviour and algebraic rank. The monograph does not import this theorem as an economic fact. It translates the architecture into a bounded

measurement system in which regional public-data anchors are transformed into finite-state local traces, Euler-factor analogues, a constructed economic L-function, LOrder and a structural-rank comparison.

The local side of the economic BSD analogue consists of regional states. These states are not literal reductions of elliptic curves over finite fields. They are controlled economic discretizations. The q-bases are finite-state grids, not prime fields in a number-theoretic sense. This preserves the local-to-global discipline without making a false mathematical claim. A regional trace value measures the behaviour of a constructed economic state under discretization; it does not count points on an algebraic curve.

The transmission operator in the BSD analogue is the Euler-factor and L-function layer. Local trace signals are aggregated into stable product components around a benchmark point. The constructed economic L-function supplies the global side of the architecture: it gives a single order-of-behaviour object that can be compared with structural rank. The interpretation is not analytic continuation or a functional equation. The interpretation is numerical stability and calibrated rank correspondence inside the model.

The global object is structural rank. This rank is deliberately not GDP size. It is constructed from productive depth, Hodge-flow structure, network position and agentic capacity. The LOrder analogue is then compared with this rank object through gaps, visual alignment, equivalence logic, sensitivity checks and placebo decision gates. The result is a local-to-global measurement claim: local finite-state information contains systematic information about global structural-rank formation under the constructed architecture.

BSD also provides the strongest corridor version of local-to-global reasoning. BridgeStress shows why a small-output region can be structurally important. The Caucasus and Central Asia may not dominate world GDP, but they can become visible as corridor-stress nodes when growth pressure, fragility, transition momentum and network position are preserved. Thus local corridor exposure becomes part of global rank interpretation. This is a central monograph contribution because it prevents economic scale from being confused with systemic relevance.

Table 2.6.2. BSD local-to-global transformation chain

Step	Economic operation	Analytical role	Claim boundary
1. Public anchors	GDP, GDP per capita, growth, regional/corridor classification and World normalization.	Defines the regional coordinate system.	Public anchors are inputs, not final constructed indicators.
2. Stress and coefficient mapping	Transforms anchors into systemic-stress components, curve coefficients and non-degeneracy diagnostics.	Builds economic curve-like objects suitable for trace construction.	Economic coefficients are model constructs, not algebraic invariants.
3. Finite-state traces	Uses q-state grids to produce local trace analogues.	Creates the local side of the local-to-global architecture.	Finite-state grids are economic discretizations, not literal prime-field reductions.
4. Euler factors and L-function analogue	Aggregates trace information into product-like global behaviour.	Builds a stable global object around the benchmark point.	No claim of analytic continuation, functional equation or classical L-function proof.
5. LOrder and structural rank	Compares LOrder with a composite structural-rank object.	Tests calibrated local-to-global consistency.	Supports internal rank calibration, not theorem-level equality or causal law.
6. BridgeStress and corridor reading	Identifies corridor nodes whose systemic relevance exceeds GDP mass.	Translates local corridor exposure into global transmission relevance.	Does not replace granular logistics or geopolitical datasets.

2.6.3. Hodge as Local Flow Decomposition and Systemic Circulation

The Hodge-econometric manuscript supplies the monograph with a second local-to-global architecture: decomposition of a regional macro-flow field. The local object is an edge cochain. Each edge contains directed macro-flow pressure derived from regional differences in public macroeconomic anchors and author-calculated corridor logic. The global object is not one index but a decomposition: gradient hierarchy, curl-based local imbalance and harmonic systemic circulation.

This architecture is local-to-global because it does not start from a global rank table. It starts from relational pressure along edges. The global structure appears only after the regional graph is constructed and the edge field is projected into Hodge components. The gradient component measures how much of the field can be explained as hierarchy. The curl component measures local triangular inconsistency. The harmonic component measures circulation that remains after both hierarchy and local curl are removed.

The systemic-transmission interpretation is especially important. A shock in a connected regional graph is not confined to its origin if the graph has corridors, cycles and residual circulation. The Hodge framework asks whether the regional network is connected enough for diffusion and shock transmission and cyclic enough for local-cycle and harmonic analysis. This is why the topology of the graph is not decorative. It determines whether local pressure can become a systemic signal.

Hodge also clarifies why GDP mass is not sufficient. Large output nodes can dominate scale while smaller nodes may matter because they participate in imbalances, circulation paths, resilience gaps or tail-risk exposure. The Caucasus, Central Asia and other corridor-sensitive nodes become analytically visible not by being artificially enlarged, but by being retained inside the same connected macro-flow structure as larger regions.

The permissible claim is a benchmark decomposition claim. The monograph may say that the constructed ten-node regional benchmark supports a meaningful decomposition of macro-flow pressure and reveals hierarchy, imbalance and circulation not reducible to output mass. It may not say that the Hodge Conjecture is resolved, that all country-level dyadic flows have been causally identified, or that the benchmark graph is a final model of the world economy.

$$\textit{edge-flow pressure} = \textit{gradient hierarchy} + \textit{curl imbalance} + \textit{harmonic systemic circulation}$$

In the monograph this is an economic decomposition statement. It translates a directed macro-flow field into structurally interpretable layers; it is not a claim that economic data are literal differential forms.

2.6.4. Yang-Mills as Local-to-Systemic Shock Threshold Logic

The Yang-Mills-inspired manuscript supplies the monograph with a threshold-based theory of systemic transmission. The local objects are normalized node stress, weighted edges, anti-symmetric gauge potentials, triangular curvature and shock amplitudes. The global object is a finite-network economic mass gap: a positive spectral separation in a stress-weighted graph Laplacian. This is local-to-global logic in threshold form.

The central question is when a local disturbance remains locally absorbable and when it becomes systemically transmissible. In the finite-network benchmark, this question is answered through a normalized threshold obtained from the economic mass gap and spectral radius. A shock below the threshold remains below the estimated stress-transmission boundary; a shock above the threshold crosses into systemic transmissibility in the benchmark simulation. This is a mathematically structured way to distinguish local noise from systemic propagation.

The transmission mechanism is network curvature and spectral separation. Curvature/action concentration identifies where systemic stress-energy accumulates in cycles. BridgeStress identifies corridor nodes whose strategic exposure is not reducible to GDP. EMGI, fragility and resilience separate protected nodes from critical-fragile nodes. The result is not merely a ranking of regions; it is a typology of transmission mechanisms.

The strongest Yang-Mills economic claim is finite-network and benchmark-specific. The model can claim that, under the constructed stress network, a positive finite-network mass gap exists, stress-energy is concentrated, and shocks compress local-to-systemic thresholds under scenario simulations. It cannot claim that the mathematical Yang-Mills existence and mass gap problem is solved. It also reserves final causal country-panel confirmation for the populated and estimated N = 1,500 validation layer.

The contribution of Yang-Mills to Section 2.6 is therefore decisive: it turns systemic transmission from a narrative concept into a threshold object. It gives the monograph a way to ask not only where stress is located, but when stress becomes transmissible through a corridor-sensitive network.

$$\textit{Systemic}_i = 1\{\ \textit{shock_amplitude}_i > \Delta_{econ} / \rho(L_{stress})\ \}$$

This formula expresses the finite-network economic interpretation of the local-to-systemic threshold. It is a benchmark diagnostic rule, not a physical law and not a theorem-level Yang-Mills result.

2.6.5. Navier-Stokes as Flow-Pressure-Friction-Closure Transmission Logic

The Navier-Stokes-inspired manuscript supplies the monograph with a dynamic stress-balance version of systemic transmission. The local objects are normalized liquidity-flow components: velocity weakness, acceleration pressure, macro-financial pressure gradients, friction or diffusion, stochastic shocks, GDP-cycle forcing and state-dependent closure. The global object is systemic stress interpreted through rolling validation, panel diagnostics, resilience measures, benchmark comparison and policy counterfactuals.

The Navier-Stokes analogy is not a claim that finance is a physical fluid. Its value lies in the discipline of balance. Stress does not arise from one variable alone. It is formed by the interaction of weak flow, pressure, friction, shocks, cycles and hidden adjustment. The model becomes credible only because all variables are normalized into nondimensional starred components and because raw financial units are not added directly.

The closure term is central to the claim boundary. An unrestricted epsilon(t) could become a residual plug that mechanically forces the equation to fit. The manuscript prevents this by modelling closure through observable or proxy-observable state variables: lagged closure, shadow-economy pressure, transfers, geopolitical shock, fiscal buffers, aid/support and inertia. This makes hidden adjustment auditable rather than arbitrary.

Local-to-global transmission in Navier-Stokes occurs through pressure and friction channels. A local macro-financial shock can become systemic if it interacts with liquidity weakness, pressure gradients, weak buffers or cycle amplification. A country or region can appear stable under one indicator while becoming vulnerable when the combined balance is evaluated. This is the stress-testing function of the model.

The permissible claim is strong but bounded. The monograph may state that the Navier-Stokes-inspired framework provides a global panel stress-testing architecture for 100 countries over 2010-2024 and that it supports systemic-stress diagnostics under rolling validation and robustness checks. It may not claim to solve the Navier-Stokes problem, establish a physical identity between liquidity and fluids, or produce a universal crisis-prediction law.

Systemic Stress_t = flow weakness + acceleration + pressure gradient + friction + stochastic shock + cycle forcing + restricted epsilon(t)

The expression is conceptual and nondimensional. It summarizes the economic transmission logic of the model without importing physical units or theorem-level hydrodynamic claims.

2.6.6. Supporting Local-to-Global Logic in Ricci/Poincare, Riemann/Zeta and P-vs-NP

Although BSD, Hodge, Yang-Mills and Navier-Stokes are the primary models in Section 2.6, the remaining three manuscripts strengthen the monograph-wide logic. The Perelman/Ricci/Poincare manuscript supplies a deformation version of local-to-global reasoning. Region-year stress variables are transformed into pressure-oriented coordinates, curvature-like deformation, smoothing capacity, entropy-like complexity and graph connectedness. Local stress coordinates become a global inequality-pressure manifold only after normalization, metric construction, curvature summaries and topological diagnostics.

The Riemann/Zeta manuscript supplies a temporal-spectral version of local-to-global reasoning. A time-specific zeta-cycle deviation is not itself a global inflation model. It becomes part of a global forecast object only after being normalized, signed, alpha-calibrated and tested against FPAS and ARIMA under layered annual, quarterly and monthly validation. The local spectral signal is therefore admissible only when it improves or clarifies forecast behaviour under validation discipline.

The P-vs-NP manuscript supplies a computational-decision version of local-to-global reasoning. A candidate support is local in the search space; a best-found incumbent is global only relative to the documented search budget and evidence gate. Exact reduced enumeration provides certification only in the reduced benchmark, not in the full n = 94, K = 10 universe. This prevents the local success of an algorithm from being overstated as full global optimality.

Together, these three supporting models protect Section 2.6 from a narrow network-only reading. Local-to-global logic is not only spatial or regional. It can be geometric, temporal, spectral, computational and evidentiary. What unites the seven cases is the same methodological rule: local information becomes global knowledge only through explicit transformation, validation and claim discipline.

Table 2.6.3. Systemic-transmission mechanisms and evidence gates

Transmission mechanism	Primary manuscripts	What travels from local to systemic level	Evidence gate
Rank transmission	BSD, Hodge	Finite-state local traces, Hodge-flow information,	LOrder-rank comparison, q-base sensitivity, placebo

Transmission mechanism	Primary manuscripts	What travels from local to systemic level	Evidence gate
		network position and agentic capacity become structural rank.	logic and circularity checks.
Flow transmission	Hodge, Navier-Stokes	Edge pressures, liquidity weakness, pressure gradients, friction and shocks become systemic flow and stress paths.	Hodge orthogonality/projection diagnostics, rolling validation, benchmark comparison and residual stability.
Threshold transmission	Yang-Mills, Navier-Stokes	Local shock amplitude crosses a spectral or stress-balance boundary and becomes systemically transmissible.	Mass-gap threshold, scenario compression, Monte Carlo perturbation and external-validation pathway.
Corridor transmission	BSD, Yang-Mills, Hodge	Small-output corridor nodes become globally relevant through bridge exposure, cycles, fragility and circulation.	BridgeStress, centrality, curvature/action concentration, tail-risk and resilience diagnostics.
Deformation transmission	Perelman/Ricci/Poincare, Yang-Mills	Local pressure variables become curvature-like deformation, entropy complexity and connected inequality topology.	N = 150 diagnostic panel, graph connectedness, curvature path and bounded forecast/uncertainty checks.
Spectral transmission	Riemann/Zeta, Yang-Mills, Hodge	Cyclical spectral signals and Laplacian modes become forecast corrections or systemic thresholds.	Layered forecast validation, spectral entropy/wavelet screens and finite-network spectral robustness.
Computational transmission	P vs NP, all models	Candidate local solutions become admissible claims only under search, robustness, exact reduced or validation gates.	Exact reduced enumeration, documented search coverage, falsification and claim-hierarchy discipline.

2.6.7. Corridor-Sensitive Transmission and the Visibility of Small Nodes

A major analytical contribution of the monograph is the separation of output mass from systemic relevance. Conventional regional analysis often reads importance through GDP share, income depth or trade volume. The local-to-global architecture shows why this is incomplete. A region can be small in output mass but large in transmission relevance if it occupies a corridor position, participates in cycles, carries fragility, concentrates curvature/action or links otherwise separated blocks.

The Caucasus and Central Asia are the strongest examples. In the BSD framework, they become visible through BridgeStress and local-to-global rank interpretation. In the Hodge framework, their visibility appears through hierarchy, imbalance, circulation, resilience and tail-risk rather than GDP size. In the Yang-Mills framework, their role is identified through fragility, strategic exposure, curvature/action concentration and local-to-systemic threshold logic. In Navier-Stokes, corridor-sensitive stress can appear through pressure, friction, external transfers, geopolitical shock and closure mechanisms.

This corridor logic is not a geopolitical claim by itself. It is a measurement claim. The monograph does not assert that a corridor node is strategically important because a narrative says so. It asks whether the node becomes visible when local

stress, network position, circulation, threshold and rank mechanisms are jointly measured. This is the scientific advantage of using formal analogues: they make narrative corridor relevance auditable.

The same logic protects the model from exaggeration. Corridor visibility does not replace freight databases, transaction-level trade data, infrastructure engineering analysis or geopolitical scenario modelling. It supplies a macro-regional diagnostic layer that can identify where deeper investigation is warranted.

2.6.8. Transformation Operators: From Local Measurement to Global Interpretation

Every local-to-global model in the monograph depends on a transformation operator. The operator is the formal bridge between input information and global interpretation. In BSD, the operator is the trace-to-Euler-to-LOrder chain. In Hodge, it is the incidence-matrix and projection system. In Yang-Mills, it is the gauge-potential, curvature/action and stress-Laplacian chain. In Navier-Stokes, it is the nondimensional stress-balance equation and restricted closure system. In Ricci/Poincare, it is the pressure scaling, metric construction and curvature/connectedness layer. In Riemann/Zeta, it is the zeta-cycle normalization and forecast correction. In P-vs-NP, it is the search, exact-reduced and robustness operator.

A transformation operator must satisfy four methodological criteria. First, it must be reproducible: another researcher should be able to reconstruct the output from the stated inputs, formulas and scripts. Second, it must be non-tautological: it should not merely re-label the target outcome. Third, it must be falsifiable or stress-testable: negative controls, sensitivity checks, placebo logic, perturbations or benchmark comparisons must be possible. Fourth, it must be claim-bounded: it must state what the operator can and cannot justify.

The monograph uses these criteria to prevent complex mathematical language from becoming decorative. Local-to-global language earns its scientific value only when the transformation operator is visible. Otherwise the model would become a metaphor. The repeated use of data packages, source ledgers, formulas, matrices, validation files, robustness gates and claim hierarchies is therefore not an administrative detail. It is the mechanism that converts analogy into scientific architecture.

This operator logic is especially important for constructed variables. Hodge hierarchy, harmonic exposure, LOrder, BridgeStress, EMGI, W-functional complexity, zeta-cycle correction and sparse-search incumbent are not official institutional indicators. They are author-calculated research variables. Their credibility depends on transparent lineage and replicability.

Table 2.6.4. Transformation operators and methodological safeguards

Operator	Model location	Risk if uncontrolled	Safeguard
Trace-to-LOrder operator	BSD	Local trace signs could be arbitrary or circular.	q-base stability, non-degeneracy audit, LOrder-rank gap analysis, placebo and variable-lineage checks.
Hodge projection operator	Hodge	Edge-flow decomposition could be an artefact of graph construction.	Connected/cyclic graph diagnostics, projection error, orthogonality checks, persistent homology and leave-one-region-out tests.
Curvature/action operator	Yang-Mills	Curvature could become a metaphor without measurable threshold value.	Stress-weighted Laplacian, positive finite-network gap, threshold comparison, Monte Carlo perturbation and scenario diagnostics.
Stress-balance closure operator	Navier-Stokes	epsilon(t) could become an unrestricted residual plug.	Restricted closure equation using observable or proxy-observable variables, rolling validation and external-target checks.
Pressure-curvature operator	Perelman/Ricci/Poincare	Heterogeneous variables could be added without	0-100 pressure orientation, metric construction,

Operator	Model location	Risk if uncontrolled	Safeguard
		unit discipline.	curvature summaries, graph diagnostics and uncertainty bands.
Spectral correction operator	Riemann/Zeta	Zeta signal could overfit or be mistaken for theorem proof.	Layered samples, no-look-ahead validation, forecast comparison, calibration and residual diagnostics.
Search-certification operator	P vs NP	Best-found result could be overstated as global optimum.	Exact reduced enumeration, documented search coverage, robustness tests, transaction-cost and derivative-overlay checks.

2.6.9. Evidence Hierarchy for Systemic Transmission Claims

Systemic-transmission claims require a stronger evidence hierarchy than descriptive claims. It is relatively easy to state that a region has high stress or that a model produces a high index value. It is harder to claim that local stress transmits systemically, that corridor position matters, or that local information informs global rank. Section 2.6 therefore treats transmission as a gated claim.

The first evidence level is construction coherence. The model must show that its inputs, transformations and outputs are internally consistent. The second level is benchmark validity: the constructed system must produce non-degenerate, interpretable and reproducible benchmark results. The third level is robustness: the result must survive alternative specifications, sensitivity checks, perturbations, leave-one-out tests or placebo logic. The fourth level is external screening: where external observable proxies exist, they may support directional plausibility but cannot automatically establish strong validation. The fifth level is causal confirmation, which is reserved for designs with suitable identification, populated panels, external outcomes and robust inference.

This hierarchy explains why different models in the monograph make different strength claims. Navier-Stokes has a strong global-panel stress-testing architecture; Riemann/Zeta has strong layered forecast-validation evidence; P-vs-NP has strong computational demonstration with exact reduced benchmarking; Ricci/Poincare has strong N = 150 diagnostic-panel evidence; Hodge has strong benchmark structural-decomposition evidence; Yang-Mills has strong finite-network benchmark evidence and a future panel pathway; BSD has strong calibrated local-to-global rank evidence with bounded external validation.

The local-to-global claim is therefore not one uniform claim across the book. It is a family of claims with different evidence levels. The monograph is strongest where the evidence gate matches the claim type.

Table 2.6.5. Claim hierarchy for local-to-global and systemic-transmission logic

Claim type	Allowed wording	Required evidence	Restricted wording
Measurement claim	The framework constructs a coherent local-to-global diagnostic object.	Input lineage, transformation formulas, non-degeneracy and reproducibility.	The framework proves a mathematical theorem or universal law.
Benchmark transmission claim	The benchmark shows interpretable transmission pathways or thresholds.	Connected graph, cycles, stress weights, spectral or decomposition diagnostics.	The benchmark establishes final country-level causality.
Rank-calibration claim	Local regional signals are informative about constructed structural rank.	Trace stability, LOrder-rank alignment, sensitivity and placebo logic.	Local states equal algebraic rank or prove BSD.
Shock-threshold claim	Shocks above the model threshold become systemically transmissible in the benchmark.	Mass gap, spectral radius, threshold comparison and scenario tests.	The model predicts real-world crisis timing with certainty.

Claim type	Allowed wording	Required evidence	Restricted wording
Flow-stress claim	Systemic stress can be represented as a nondimensional balance of flow, pressure, friction, shocks and closure.	Panel structure, rolling validation, residual stability and restricted closure.	Financial liquidity is a physical fluid or the Navier-Stokes problem is solved.
External-validation claim	External proxies provide directional screening or bounded validation.	Sign coherence, variable-lineage audit, robustness and sufficient statistical strength.	Weak p-values or mixed signs confirm the model strongly.
Future-validation claim	A specified future panel or replication path can strengthen the evidence.	Clear design, data requirements, model outputs and file-hash/replication plan.	Future work is already equivalent to completed validation.

2.6.10. Integrated Synthesis of Section 2.6

The integrated conclusion of Section 2.6 is that local-to-global and systemic-transmission logic provide the connective tissue of the monograph. Flow, topology, curvature, spectral behaviour, rank and optimization are not isolated themes. They describe different ways in which local economic information becomes system-level structure. BSD supplies rank formation. Hodge supplies decomposition of macro-flow pressure. Yang-Mills supplies thresholded systemic shock transmission. Navier-Stokes supplies dynamic stress-balance closure. Ricci/Poincare supplies deformation and connectedness. Riemann/Zeta supplies spectral temporal correction. P-vs-NP supplies computational search discipline.

The common scientific principle is that systemic relevance is not equivalent to size. A large region can be globally important because of mass, but a smaller region can become systemically important through bridge exposure, local imbalance, harmonic circulation, fragility, curvature/action concentration, threshold compression or rank-supporting flow structure. The monograph therefore proposes an economic measurement program in which global structure is inferred from transformed local information rather than asserted from aggregate magnitude alone.

The second common principle is that transmission is conditional. Local information must pass through specified operators and evidence gates. A trace must be stable; an Euler factor must be controlled; a graph must be connected and cyclic; a mass gap must be positive and thresholded; a closure term must be restricted; a zeta signal must be validated; a portfolio search must be benchmarked; an external proxy must be interpreted cautiously. This is the claim-discipline logic that protects the monograph from overclaiming.

The final permissible claim of Section 2.6 is therefore precise: the seven Millennium-inspired economic analogues jointly define a coherent conceptual framework for measuring how local economic states, flows, shocks, cycles and decisions become global diagnostic structures under explicit transformation and validation rules. This is a strong monograph-level conceptual claim. It remains an economic-econometric analogue framework, not a solution, proof, test or replication of the Clay Millennium Problems in their original mathematical form.

Section 2.6 closing claim-boundary statement: Local-to-global consistency and systemic-transmission diagnostics are admissible only as constructed, reproducible and claim-bounded economic measurement objects. They do not constitute theorem-level proof, universal causality, physical identity or unconditional prediction.

2.7. General Claim Hierarchy

2.7.1. Purpose of the General Claim Hierarchy

This section establishes the common claim hierarchy for the monograph. Its function is not merely editorial. It is a methodological control system that prevents the seven economic-econometric analogues from being read as seven attempted mathematical solutions to the Clay Millennium Problems. The monograph uses mathematical architectures as measurement grammars; therefore, every result must be classified according to the strength and independence of the evidence that supports it. A claim is admissible only when its level of generality matches its evidence base, its empirical universe, its validation design and its explicit boundary conditions.

The need for a general hierarchy arises because the seven studies do not produce one homogeneous type of evidence. Some chapters are strongest as measurement architectures, some as diagnostic frameworks, some as layered forecasting

systems, some as finite-network benchmarks and some as future-validation protocols. The Perelman-Ricci-Poincare study produces strong diagnostic measurement evidence about inequality pressure, smoothing capacity, curvature-like deformation and graph connectedness. The Hodge study produces a topological macro-flow decomposition benchmark. The Navier-Stokes study produces a nondimensional macro-financial stress-testing architecture. The Yang-Mills study produces a finite-network spectral threshold benchmark and a country-panel validation pathway. The BSD study produces calibrated local-to-global rank-formation evidence. The Riemann-Zeta study produces a bounded forecast-diagnostic architecture. The P-vs-NP study produces empirical-computational optimization evidence with exact reduced benchmarking and full-universe search boundaries.

The hierarchy therefore converts interdisciplinary ambition into reviewer-safe scientific language. Instead of allowing terms such as proof, solution, validation, prediction and optimization to float freely, it assigns each term to a permissible evidentiary class. The resulting claim discipline is a central feature of the book. It allows the monograph to be intellectually ambitious while remaining precise: the book may claim that mathematical architectures can be translated into auditable economic analogues; it may not claim that the original mathematical problems are solved, proved, tested or replicated in their classical form.

Claim_k is admissible iff Evidence_k is sufficient, Boundary_k is respected and Scope_k is not expanded.

Equation 2.7.1 states the governing rule of the chapter. A claim is not justified by the elegance of the analogy or by the strength of one favorable table. It is justified only when evidence, boundary and scope are aligned.

Table 2.7.1. Core claim hierarchy used in the monograph

Claim level	Primary meaning	Typical evidence gate	Where it is strongest	Restricted interpretation
Strong measurement claim	The model constructs a coherent, reproducible and interpretable measurement architecture.	Transparent variables, normalization, formulas, internal coherence, sensitivity checks and replication traceability.	BSD rank formation, Perelman/Ricci inequality diagnostics, Navier-Stokes stress balance, Hodge flow decomposition.	Not theorem proof, not causal law and not external validation by itself.
Diagnostic claim	The model organizes stress, curvature, flow, transmission, topology or optimization behaviour into interpretable diagnostic objects.	Consistency across tables, graphs, decompositions, scenario checks, placebo logic and robustness screens.	Perelman/Ricci, Yang-Mills, Hodge, Navier-Stokes, BSD corridor stress.	Not causal identification, not policy treatment effect and not universal prediction.
Forecasting claim	The model improves or interprets forecast performance within specified samples and benchmarks.	RMSE/MAE/sMAPE, rolling validation, Mincer-Zarnowitz, encompassing, DM/CW, residual diagnostics and sample layering.	Riemann-Zeta FPAS+zeta; limited forecast diagnostics in other chapters.	Not universal dominance, not country-specific policy rule and not residual-problem elimination.
Benchmark claim	The model supplies a finite or reduced empirical benchmark that is complete within its declared universe.	Fixed node/edge set, exact reduced enumeration, documented search coverage, finite-network construction or regional prototype.	Hodge 10-node benchmark, Yang-Mills 10-node/27-edge benchmark, P-vs-NP reduced exact benchmark, BSD N=150 closure	Not complete all-country, all-dyad, all-market or all-period generalization.

Claim level	Primary meaning	Typical evidence gate	Where it is strongest	Restricted interpretation
			layer.	
Future validation claim	The manuscript specifies a credible pathway for stronger evidence after additional data or panel estimation.	Country-panel design, external-proxy protocol, dyadic extension, realized-return panel, larger-sample closure or executable replication.	Yang-Mills N=1,500 panel pathway, Hodge future dyadic/all-country replication, P-vs-NP realized-return testing, BSD external validation.	Not a present result and not a substitute for completed estimates.

2.7.2. Why the Monograph Needs a Claim Ladder

The general claim ladder is necessary because mathematical analogy creates a predictable reviewer risk. A reader may incorrectly assume that a chapter using Riemann-zeta terminology is attempting to prove the Riemann Hypothesis, that a chapter using BSD terminology is claiming arithmetic rank, that a chapter using Yang-Mills terminology is claiming a physical gauge-field theorem, or that a P-vs-NP-inspired portfolio chapter is claiming formal complexity-theory proof. The claim ladder blocks that misunderstanding by forcing every chapter to translate its result into a bounded economic-econometric claim level.

The hierarchy is also necessary because constructed economic objects have different epistemic status from directly observed variables. Public macroeconomic anchors such as GDP, inflation, income depth, trade exposure, volatility, beta, output share or unemployment enter the studies as empirical inputs. However, stress scores, curvature-like deformation, Hodge components, gauge potentials, LOrder, zeta-cycle deviations, EMGI, BridgeStress and integrated strategy rankings are author-calculated objects. Their credibility depends on formula disclosure, transformation discipline, robustness checks and replication packages. They can support strong measurement and diagnostic claims, but they cannot automatically support theorem proof or causal identification.

The ladder also distinguishes internal coherence from independent external validation. Several chapters generate strong internal agreement: for example, local-to-global rank alignment in the BSD analogue, coherent pressure-curvature-W behaviour in the Perelman/Ricci/Poincare analogue, positive spectral separation in the Yang-Mills finite network, or forecast hierarchy improvement in FPAS+zeta. Internal coherence is valuable, but it does not automatically become external causal proof. The general hierarchy therefore requires the writer to say whether the claim is internal measurement, diagnostic screening, forecast improvement, benchmark completion, external validation or future validation.

$$EvidenceLevel = f(Measurement, Diagnostics, Forecasting, BenchmarkClosure, ExternalValidation, Replication).$$

Equation 2.7.2 expresses the monograph-level logic. Evidence is not one number. It is a vector whose components must be reported separately before a claim level is assigned.

2.7.3. Strong Measurement Claim

A strong measurement claim is the highest claim level available to several chapters in the monograph. It means that the chapter has successfully converted a mathematical architecture into a transparent economic measurement system. It does not mean that the mathematical theorem has been proved, that causality has been identified, or that all external validation has been completed. The strength lies in construction, interpretability, internal coherence, auditability and bounded replication.

The BSD chapter is the clearest example. Its strongest admissible claim is that local regional signals, finite-state trace analogues, Euler-factor information and LOrder are informative about structural rank formation inside a disciplined regional analogue architecture. This is a strong calibrated measurement claim because the object is constructed through public anchors, coefficient mapping, non-degeneracy checks, q-base stability, L-function behaviour, structural-rank comparison, sensitivity tests and placebo logic. The claim remains bounded because LOrder is not a classical order of vanishing, structural rank is not algebraic rank, and robust external evidence is not upgraded into theorem-level confirmation.

The Perelman/Ricci/Poincare chapter also supports a strong measurement claim. It shows that global inequality pressure can be represented through stress coordinates, pressure-oriented normalization, a correlation-based metric tensor, Ricci-style component curvature, scalar curvature, F- and W-type functionals, graph connectedness and validation screens. The strongest statement is that the framework organizes inequality pressure and smoothing capacity in a coherent diagnostic manifold. The restricted statement is equally important: the model does not prove the Poincare conjecture, does not establish

a classical Ricci-flow theorem, does not identify unrestricted causal effects and does not replace country-level welfare analysis.

The Navier-Stokes chapter supports a strong measurement claim in the macro-financial stress-testing domain. Its central contribution is not that financial liquidity is a physical fluid. Its contribution is that liquidity velocity weakness, acceleration pressure, macro-financial pressure gradients, friction/diffusion, stochastic shocks, GDP-cycle forcing and restricted closure can be transformed into a nondimensional stress-balance architecture. The claim is strong where the normalized variables, panel design, rolling validation, benchmark comparison, residual checks, Monte Carlo uncertainty and policy counterfactuals are aligned. It remains bounded because the framework is not a hydrodynamic law and not a universal crisis-prediction theorem.

The Hodge chapter supports a strong benchmark-measurement claim. It demonstrates that a regional macro-flow network can be decomposed into gradient hierarchy, curl/local-cycle imbalance and harmonic/systemic circulation. The strength of the claim lies in the fact that the economic system is not reduced to GDP size alone; it becomes a decomposable topological flow object. The boundary is that the study is a regional benchmark prototype, not an all-country dyadic flow database and not a final causal model of international flows.

Table 2.7.2. Strong measurement claims across the seven economic analogues

Analogue	Strongest measurement object	Evidence supporting the claim	Permissible statement	Boundary that must remain explicit
Perelman/Ricci/ Poincare	Inequality pressure, curvature-like deformation, entropy-like complexity and graph connectedness.	N=150 region-year panel, 16 stress coordinates, metric tensor, curvature decomposition, W-functional, Betti/Laplacian diagnostics and validation screens.	Global inequality can be organized as a pressure-smoothing diagnostic manifold.	No Perelman/Poincare proof, no unrestricted causality, no country-level welfare ranking and no forecast dominance.
Hodge	Gradient, curl and harmonic decomposition of regional macro-flow pressure.	10-node regional benchmark, directed edge cochain, Hodge energy shares, spectral and persistent-homology diagnostics.	Global-regional macro-flow can be decomposed into hierarchy, local imbalance and systemic circulation.	Regional prototype only; not observed dyadic-flow causality or all-country closure.
Navier-Stokes	Nondimensional liquidity-flow and systemic-stress balance.	100-country panel, stress components, restricted closure, rolling validation, benchmark comparison, robustness and policy scenarios.	Systemic stress can be measured through flow-pressure-friction-shock-closure logic.	Not physical fluid mechanics, not Navier-Stokes proof and not universal crisis law.
Yang-Mills	Finite-network gauge, curvature, action, spectral gap and EMGI.	10-node/27-edge benchmark, stress Laplacian, positive spectral gap, Monte Carlo perturbations and scenario shocks.	Systemic shock thresholds can be measured in a finite corridor network.	Not mathematical Yang-Mills mass-gap solution; country-panel validation remains future/conditional where not estimated.
BSD	Local finite-state traces, Euler	N=150 closure layer, non-degeneracy, q-	Local regional signals are	Not classical BSD proof, not causal law

Analogue	Strongest measurement object	Evidence supporting the claim	Permissible statement	Boundary that must remain explicit
	factors, LOrder and structural-rank correspondence.	stability, rank-gap tests, placebo, sensitivity and source-ledger discipline.	informative about global structural rank in the analogue system.	and not strong independent external validation where evidence remains weak.
Riemann/Zeta	Zeta-cycle correction embedded in FPAS inflation forecasting.	N=55, N=45, N=20 annual layers, N=100 quarterly validation and N=240 monthly spectral diagnostics.	A normalized zeta-cycle can improve and interpret global inflation forecasts inside the reported layers.	Not Riemann Hypothesis proof, not universal forecast dominance and not residual-risk elimination.
P vs NP	Mixed discrete-continuous sparse portfolio optimization architecture.	C(94,10) search space, heuristic layers, exact n=20,K=6 benchmark, robustness, falsification and replication gates.	Cardinality-constrained portfolio choice creates a nontrivial empirical-computational search problem.	Not P != NP proof, not certified full n=94 optimum and not realized historical investment dominance.

2.7.4. Diagnostic Claim

A diagnostic claim is weaker than a strong measurement claim in evidentiary generality but often richer in interpretation. It means that the model can identify, classify, decompose or visualize meaningful states of an economic system. Diagnostic claims are appropriate when the evidence is internally coherent and economically interpretable, but the design does not establish causal identification or universal prediction.

In the Perelman/Ricci/Poincare analogue, diagnostic claims include crisis deformation, partial recovery, component concentration, topology-as-diagnostic evidence and policy-screening channels. These claims are strong when the pressure path, curvature movement, W-functional, regional dispersion, component contributions and graph structure move consistently. They remain diagnostic because the variables are constructed on a pressure-oriented scale, the curvature is economic and model-implied, and counterfactual surgery is an internal sensitivity device rather than a policy treatment estimator.

In the Yang-Mills analogue, diagnostic claims include curvature concentration, action concentration, fragility, resilience, BridgeStress and local-to-systemic shock threshold compression. These claims are diagnostic because they identify where stress circulates in a finite corridor network and when a local disturbance becomes more transmissible. They do not establish a physical field law or a causal macroeconomic mechanism without the completed country-panel validation layer. In other words, the finite network can diagnose threshold structure; it cannot, by itself, certify a global causal law.

In the Hodge analogue, diagnostic claims include hierarchy, local-cycle imbalance and harmonic systemic circulation. The diagnostic strength lies in separating different modes of macro-flow pressure. GDP mass alone cannot distinguish a hierarchical gradient from a cycle imbalance or a persistent circulation component. The Hodge decomposition therefore acts as a diagnostic map of economic structure. Its boundary is that the decomposition is performed on constructed regional macro-flow edges rather than observed universal transaction flows.

In the Navier-Stokes analogue, diagnostic claims include pressure-gradient stress, liquidity-friction stress, shock amplification, closure behaviour and resilience. These claims are appropriate because the model intentionally treats stress formation as multichannel and nondimensional. However, even a strong diagnostic architecture should not be described as a universal crisis predictor. The correct wording is that the framework improves systemic-stress interpretation under the reported panel, benchmark and robustness conditions.

Table 2.7.3. Diagnostic claim taxonomy

Diagnostic field	Allowed diagnostic meaning	Typical supporting evidence	Examples in the monograph	Overclaim avoided
Crisis deformation	A shock year or regime shows coherent stress, curvature, entropy or forecast-error concentration.	Pressure path, curvature decline, W/F functional movement, residual and regime screens.	Perelman/Ricci 2020 deformation; Riemann/Zeta stress-year zeta movement; Navier-Stokes shock terms.	Universal crisis law or deterministic early-warning theorem.
Topology and connectedness	The constructed graph is connected, cycle-rich, bottlenecked or topologically informative.	Laplacian, beta_0, beta_1, algebraic connectivity, persistent-homology style stability.	Perelman graph topology, Hodge macro-flow topology, Yang-Mills corridor topology.	Proof of Poincare or literal geometric topology of the economy.
Transmission threshold	A local stress channel becomes more systemically transmissible under specified graph or flow conditions.	Spectral gap, action concentration, scenario compression, BridgeStress and resilience diagnostics.	Yang-Mills mass-gap benchmark; BSD corridor layer; Navier-Stokes shock-closure balance.	Causal transmission law without populated external/dyadic validation.
Structural rank	A constructed local-to-global object aligns with a constructed global rank object within tolerance.	Rank gaps, equivalence logic, q-base stability, placebo and sensitivity checks.	BSD LOrder and structural rank correspondence.	Classical arithmetic rank or theorem-level BSD equality.
Optimization behaviour	Algorithms reveal search difficulty, stability, runtime, robustness and risk-realism patterns.	Search budgets, reduced exact enumeration, seed stability, covariance placebo, transaction costs.	P-vs-NP portfolio optimization chapter.	P vs NP theorem proof or live investment superiority.

2.7.5. Forecasting Claim

A forecasting claim is specific, sample-bound and benchmark-bound. It is not a general statement that a model will dominate in all economies, periods, data frequencies or horizons. The Riemann-Zeta FPAS+zeta chapter is the central case. Its admissible forecasting claim is that a normalized zeta-cycle layer, when converted into a signed and calibrated correction to a structural FPAS baseline, improves the reported global aggregate inflation forecast hierarchy under the defined annual, quarterly and monthly validation layers. The claim is strong because it is supported by several sample windows, forecast-error metrics, rolling validation, calibration checks, forecast-encompassing logic, Diebold-Mariano/Clark-West comparisons, residual diagnostics, spectral screens and regime diagnostics.

The forecasting claim is also carefully bounded. It is not a proof or test of the Riemann Hypothesis. It is not a claim that all residual problems disappear. It is not a country-level central-bank forecasting model. It is not a universal dominance claim across all countries and horizons. The monograph should therefore use language such as bounded global forecast-diagnostic architecture, calibrated forecast improvement, layered validation support and residual-risk discipline. It should avoid language such as universal prediction, theorem-based forecast law, proof of spectral causality or guaranteed inflation dominance.

Other chapters may contain forecast or predictive elements, but their forecast claims are subordinate. The Perelman/Ricci/Poincare chapter explicitly rejects forecast-superiority where the AR(1) benchmark performs better in the short window; therefore, its proper claim is diagnostic interpretability, not predictive dominance. The Navier-Stokes chapter may report favorable rolling validation and benchmark comparison, but its claim remains stress-testing and diagnostic

forecasting within a defined validation window. The Hodge and Yang-Mills chapters may contain machine-learning or scenario validation, but those elements should be read as robustness diagnostics unless their sample and external-target design support a stronger statement.

ForecastClaim = ForecastGain within SampleLayer and BenchmarkSet, not UniversalDominance.

Equation 2.7.3 gives the wording discipline for all forecast statements. A forecast result must always name its sample layer, benchmark set and residual boundary.

Table 2.7.4. Forecasting claim discipline

Study	Forecast or predictive element	Evidence that may be claimed	Required qualifier	Claim that must not be made
Riemann/Zeta	FPAS+zeta inflation forecast against FPAS and ARIMA.	Layer-specific forecast improvement and interpretable stress-aligned zeta-cycle diagnostics.	Global aggregate; N=55/N=45/N=20 annual, N=100 quarterly, N=240 monthly layers; residual risks reported.	Universal forecast dominance, Riemann Hypothesis proof or residual elimination.
Navier-Stokes	Rolling one-year-ahead validation and benchmark comparison.	Validation-window stress-testing usefulness and macro-financial diagnostic forecast evidence.	Country-year panel and reported validation window only.	Universal crisis-prediction law or physical hydrodynamic identity.
Perelman/Ricci/ Poincare	Rolling no-look-ahead and AR(1) benchmark discipline.	Diagnostic and interpretive architecture; forecast dominance rejected where benchmark wins.	Forecast evidence is bounded and secondary.	Forecast-superiority claim.
Yang-Mills	Scenario simulation and future country-panel validation pathway.	Shock-threshold scenario diagnostics and benchmark spectral stability.	Final econometric validation after populated N=1,500 panel only.	Completed causal prediction claim from N=10 benchmark.
P vs NP	Algorithmic performance over search budgets; not time-series forecasting.	Search behaviour, runtime, stability and reduced exact comparison.	Optimization evidence rather than forecast evidence.	Realized investment dominance without a separate return backtest.

2.7.6. Benchmark Claim

A benchmark claim states that the chapter has produced a complete or disciplined reference result inside a declared universe. A benchmark claim can be strong even when it is not externally universal. The important condition is that the empirical universe is fixed, the construction rule is disclosed, the output is reproducible and the boundary is not expanded beyond the benchmark.

The Hodge chapter is a benchmark prototype because it builds a ten-region macro-flow network with a World anchor and then decomposes the constructed edge pressure into gradient, curl and harmonic components. The benchmark is valuable because it demonstrates the feasibility and interpretability of Hodge-econometric decomposition at the macro-regional level. The correct claim is not that all global dyadic flows have been measured. The correct claim is that a regional macro-core benchmark can be transformed into a topologically decomposable measurement system.

The Yang-Mills chapter is a finite-network benchmark because Layer A contains a ten-node corridor-sensitive graph with twenty-seven weighted edges and related curvature, action, stress-Laplacian, EMGI, fragility, resilience and scenario diagnostics. The benchmark claim is that this completed finite network supports measurement and diagnostic statements

about spectral separation and shock-threshold structure. Stronger country-level econometric validation is assigned to Layer B after country-year variables are populated and estimated.

The P-vs-NP chapter contains two distinct benchmark claims. The full n=94,K=10 case supports a best-found full-universe incumbent under documented search coverage, not a certified global optimum over all supports. The reduced n=20,K=6 case supports an exact reduced-instance benchmark because all supports are enumerated. The distinction is crucial: exact reduced certification is valid within the reduced instance, but it does not certify the full n=94 universe.

The BSD chapter contains an N=150 regional-year closure benchmark. This supports calibrated local-to-global consistency, robustness diagnostics, negative-control checks and source-ledger discipline. It does not convert the analogue into a causal law or a classical BSD result. The benchmark is strong as a regional measurement closure layer, not as a theorem-level proof.

Table 2.7.5. Benchmark claim matrix

Benchmark type	Empirical universe	What is complete	Permissible benchmark claim	Boundary
Regional Hodge benchmark	Ten regional nodes plus World normalization anchor.	Graph construction and Hodge-style decomposition of constructed macro-flow pressure.	A regional macro-flow system can be decomposed into hierarchy, local imbalance and systemic circulation.	Not all-country/dyadic flow measurement.
Yang-Mills finite-network benchmark	Ten nodes and twenty-seven weighted regional/corridor edges.	Gauge, curvature, action, spectral gap, EMGI and scenario diagnostics for Layer A.	Finite-network stress threshold and spectral diagnostic benchmark.	Country-panel econometric validation remains conditional until populated and estimated.
P-vs-NP reduced exact benchmark	Reduced n=20,K=6 portfolio universe.	All supports enumerated for the reduced instance.	Exact reduced-instance optimization evidence.	Does not certify full n=94,K=10 optimum.
P-vs-NP full search benchmark	n=94,K=10 Damodaran Jan-2026 industry universe.	Documented search coverage, heuristic comparison and best-found incumbent.	Empirical-computational search difficulty and heuristic evidence.	Best-found result, not exhaustive proof of global optimality.
BSD N=150 closure benchmark	Ten regional/corridor nodes over fifteen years.	Local-to-global calibration, robustness, placebo and decision-gate architecture.	Calibrated structural-rank measurement benchmark.	Not classical BSD proof, causal law or strong external validation.
Riemann/Zeta layered benchmark	Annual, quarterly and monthly global inflation layers.	Forecast hierarchy and spectral diagnostic comparison across defined layers.	Layered global forecast-diagnostic benchmark.	Not universal dominance across all economies and horizons.

2.7.7. Future Validation Claim

A future validation claim is a design-level statement, not a current empirical result. It is admissible when the manuscript specifies a credible protocol for later validation but does not yet have the populated data, estimates, external outcomes, dyadic flows, realized returns or replication artifacts required for the stronger claim. Future validation language must therefore use terms such as requires, remains conditional on, should be tested by, can be extended through and is reserved for. It should not use language suggesting that the future evidence is already established.

The Yang-Mills chapter illustrates this distinction most clearly. The finite-network Layer A is completed and can support benchmark and diagnostic claims. The N=1,500 country-panel Layer B is a validation architecture that can support

stronger empirical validation only after the country-year variables are populated and estimated. Until that step is complete, the country-panel layer is a future validation claim, not a completed econometric result.

The Hodge chapter also contains future validation logic. The regional benchmark demonstrates the feasibility of the Hodge-econometric architecture, but future all-country, dyadic, multilayer and longitudinal replication would be needed for stronger generalization. The future claim is not that the current benchmark already represents all observed global flows; it is that the method can be extended in a scientifically coherent way.

The P-vs-NP chapter requires future validation for realized investment dominance. The current evidence is model-implied and computational: CAPM priors, covariance geometry, search budgets, heuristic comparisons, exact reduced enumeration, transaction costs and option-overlay realism. A claim about realized historical dominance would require a separate realized-return panel, out-of-sample backtest protocol, transaction-cost implementation, survivorship-bias audit and live-trading or historical validation design.

The BSD chapter reserves strong independent external validation for future or additional work where external proxies, larger samples, disaggregated variables and causal identification designs support that level. The current claim remains calibrated measurement. The Riemann-Zeta chapter, despite strong layered forecast evidence, would require further country-level, horizon-specific and real-time evaluation before any universal inflation-forecasting statement could be considered.

Table 2.7.6. Future validation claims and required evidence

Current chapter	Current evidence status	Future validation path	Required additional evidence	Allowed wording now
Yang-Mills	Completed finite-network benchmark; country-panel design specified.	Populate and estimate N=1,500 country-year panel with FE/TWFE/DK/clustered/panel-IV/dynamic/factor/external models.	Country-year variables, external outcomes, model outputs, robustness files and replication hashes.	Future country-panel validation is specified; stronger causal/econometric claims are reserved.
Hodge	Regional benchmark prototype and proof-of-concept decomposition.	All-country, dyadic-flow, multilayer and longitudinal replication.	Observed or reconstructed dyadic flows, sectoral layers, temporal panels and external validation outcomes.	The model is a regional benchmark prototype with a clear extension pathway.
P vs NP	Model-implied CAPM/single-index optimization evidence; exact reduced benchmark.	Realized-return and implementation validation.	Historical return panel, backtest protocol, transaction-cost audit, turnover and out-of-sample evaluation.	Realized investment dominance remains outside the current evidence scope.
BSD	Calibrated regional local-to-global measurement with N=150 closure.	Stronger external validation and causal identification.	Independent external outcomes, larger panels, variable-lineage separation and identification strategy.	External evidence remains directional unless stronger conditions are met.
Riemann/Zeta	Layered global aggregate	Country-level, real-time, horizon-specific and	Central-bank vintage data, real-	Global aggregate forecast improvement

Current chapter	Current evidence status	Future validation path	Required additional evidence	Allowed wording now
	forecast-diagnostic evidence.	alternative-data validation.	time forecast origin files, country panels and horizon-by-horizon tests.	is bounded to reported layers.
Navier-Stokes	Global panel stress-testing and validation-window evidence.	More granular market, liquidity, banking and crisis-event validation.	Higher-frequency financial data, market microstructure, crisis event labels and exogenous shock instruments.	Stress-testing evidence is bounded by panel and validation design.

2.7.8. Cross-Problem Placement of Claims

The monograph should not assign identical claim strength to every problem chapter. The correct strategy is asymmetric but unified: each chapter receives the strongest claim it can legitimately support, and the general conclusion synthesizes those claims without inflating any one of them. This creates a multi-level architecture rather than a single exaggerated theorem statement.

At the top level, the monograph may make a general programmatic claim: the seven Clay-inspired architectures can be translated into seven bounded economic-econometric measurement grammars. This is a strong monograph-level conceptual and methodological contribution. It is supported by the existence of seven detailed analogues, each with its own data architecture, transformation logic, validation gates and claim boundary. However, the monograph-level claim does not supersede the chapter-level boundaries. The book does not become a proof of the Millennium Problems by combining seven analogues; it becomes a unified mathematical-economic analogue program.

At the chapter level, the BSD, Perelman/Ricci/Poincare, Navier-Stokes and Hodge studies are strongest as measurement and diagnostic architectures. The Riemann-Zeta study is strongest as a forecast-diagnostic architecture. The Yang-Mills study is strongest as a finite-network benchmark with a future validation pathway. The P-vs-NP study is strongest as an empirical-computational optimization architecture with exact reduced benchmarking and full-universe limitations. This differentiated placement makes the monograph more credible because it does not force all chapters into one artificial evidentiary mould.

At the synthesis level, the book can claim that economic complexity can be measured through flow, curvature, topology, spectral signal, L-function logic, computational search and local-to-global rank formation. This is the scientific peak of the monograph. But the synthesis must remain a synthesis of bounded claims, not a theorem-level escalation. The correct final language is: the monograph constructs and compares seven disciplined economic analogues inspired by the formal architectures of the Clay problems. The incorrect language is: the monograph solves or empirically verifies the Clay problems.

Table 2.7.7. Seven-problem claim placement

Problem analogue	Primary claim level	Secondary claim level	Future claim level	One-sentence final claim wording
Poincare/Ricci/ Perelman	Strong diagnostic measurement claim.	Topology and crisis-deformation diagnostic claim.	Predictive dominance not claimed; deeper country-level welfare validation possible.	A bounded geometric-topological diagnostic framework organizes global inequality pressure and smoothing

Problem analogue	Primary claim level	Secondary claim level	Future claim level	One-sentence final claim wording
				capacity.
Hodge	Benchmark measurement claim.	Flow-decomposition diagnostic claim.	All-country/dyadic/ multilayer replication.	A regional macro-flow benchmark can be decomposed into gradient, curl and harmonic components.
Navier-Stokes	Strong stress-testing measurement claim.	Diagnostic and validation-window forecasting claim.	Higher-frequency financial and crisis-event validation.	A nondimensional flow-pressure-friction-shock-closure framework measures global macro-financial stress.
Yang-Mills	Finite-network benchmark claim.	Curvature/action/spectral-threshold diagnostic claim.	N=1,500 country-panel econometric validation after population/estimation.	A finite corridor network can measure stress curvature, action concentration and local-to-systemic shock thresholds.
BSD	Strong calibrated local-to-global measurement claim.	Corridor and rank-formation diagnostic claim.	Independent external validation and causal identification reserved.	Local finite-state signals and Euler-factor analogues are informative about structural rank within a bounded regional architecture.
Riemann/Zeta	Bounded forecasting claim.	Spectral macro-financial diagnostic claim.	Country-level, real-time and horizon-specific validation.	A zeta-cycle correction improves and interprets global aggregate inflation forecasts within reported validation layers.
P vs NP	Empirical-	Benchmark and	Realized-return and full	Cardinality-

Problem analogue	Primary claim level	Secondary claim level	Future claim level	One-sentence final claim wording
	computational optimization claim.	robustness claim.	certification remain outside current evidence.	constrained portfolio optimization creates a nontrivial mixed discrete-continuous search problem.

2.7.9. Upgrade, Downgrade and Exclusion Rules

The hierarchy requires explicit upgrade and downgrade rules. A result may be upgraded from descriptive to measurement if the constructed variables are transparent, internally coherent, robust to sensitivity checks and reproducible. A result may be upgraded from measurement to diagnostic if it identifies interpretable states, channels or mechanisms across multiple result layers. A result may be upgraded to forecasting only if it is tested against appropriate benchmarks under no-look-ahead or validation-window discipline. A result may be upgraded to external validation only if independent outcomes, adequate sample structure, robust inference and variable-lineage separation support that claim.

Downgrade rules are equally important. A result must be downgraded when p-values are weak, external proxies are mixed, sample clusters are small, model variables share construction lineage, residual diagnostics are imperfect, a benchmark outperforms the proposed model, a full search space is not enumerated, a country-panel layer is only specified but not estimated, or future validation data are not yet populated. Downgrading is not a sign of weakness. In this monograph it is a form of scientific precision.

Exclusion rules are absolute. No chapter may claim to solve, prove, test or verify the classical Clay Millennium Problem in its original mathematical form. No chapter may convert a constructed economic quantity into a literal mathematical invariant. No chapter may claim causal identification without an identification strategy. No chapter may claim universal forecast dominance without cross-country, cross-horizon and real-time validation. No chapter may claim full global optimality when exhaustive certification is absent. No chapter may present future validation architecture as if it were completed empirical validation.

ClaimUpgrade requires IndependentEvidence + Robustness + ScopeControl; ClaimDowngrade is required when any gate fails.

Equation 2.7.4 defines the review protocol. Claims can move upward only through additional evidence; they must move downward when boundaries are breached.

Table 2.7.8. Upgrade, downgrade and exclusion rules

Rule type	Condition	Required action	Typical chapter relevance	Reviewer-safe wording
Upgrade to strong measurement	Transparent construction, internal coherence, sensitivity support and replication traceability.	State strong measurement claim but preserve non-theorem boundary.	BSD, Perelman/Ricci, Navier-Stokes, Hodge.	The framework supports a coherent measurement architecture.
Upgrade to diagnostic	Result identifies interpretable states, channels, deformation, topology or threshold behaviour across layers.	Use diagnostic language; avoid causal verbs.	Perelman/Ricci, Hodge, Yang-Mills, Navier-Stokes.	The model diagnoses structural pressure or transmission patterns.
Upgrade to forecasting	Forecast improvement survives relevant benchmarks and	Name sample, frequency, benchmark and	Riemann/Zeta; limited Navier-Stokes.	Forecast improvement is supported within the reported validation

Rule type	Condition	Required action	Typical chapter relevance	Reviewer-safe wording
	validation protocol.	residual caveat.		layers.
Downgrade to screening	External proxies show weak p-values, mixed signs or small-cluster limitations.	Describe as directional screening only.	BSD, Yang-Mills, Navier-Stokes.	External evidence is suggestive but not confirmatory.
Downgrade to benchmark	Model is complete only for finite node set, reduced instance or prototype sample.	State finite/reduced benchmark status.	Hodge, Yang-Mills, P-vs-NP.	The result is complete within the declared benchmark universe.
Exclude theorem claim	The statement concerns original Clay mathematical proof.	Reject or rewrite as analogue claim.	All chapters.	The chapter does not prove, test or replicate the classical problem.
Exclude causality	No identification design or independent exogenous variation.	Use association, diagnostic, calibration or validation language.	All empirical chapters.	The evidence supports association or diagnostic coherence, not causal identification.
Exclude universality	Claim extends beyond sample, horizon, region, frequency or search coverage.	Restrict scope to reported universe.	Riemann/Zeta, P-vs-NP, Hodge, Yang-Mills.	The claim is sample-bound and architecture-bound.

2.7.10. General Claim-Boundary Language for the Monograph

The following language should govern the entire book. The monograph develops seven bounded economic-econometric analogues inspired by the formal architectures of the Clay Millennium Problems. It does not solve, prove, test or replicate those problems in their original mathematical form. Its contribution is methodological, empirical, diagnostic, computational and interpretive. The strongest general claim is that mathematical structures can be translated into auditable economic measurement systems when raw public-data anchors, author-calculated variables, validation layers, benchmark comparisons, robustness checks, replication packages and explicit claim boundaries are jointly disclosed.

The book should use the term strong only when the relevant evidence is actually strong at the declared claim level. Strong measurement does not mean strong causality. Strong benchmark closure does not mean universal generalization. Strong forecast improvement does not mean permanent forecast dominance. Strong internal calibration does not mean independent external validation. Strong computational evidence does not mean formal complexity-theory proof. This distinction is the reviewer-safety core of the monograph.

The general claim hierarchy also protects the originality of the monograph. Without claim discipline, the mathematical ambition of the book could be criticized as overstatement. With claim discipline, the same ambition becomes a structured research program: each Clay problem supplies a different measurement grammar for economic complexity, and each grammar is evaluated according to its proper evidence class. The result is a unified but bounded Millennium Economic Research Program.

Table 2.7.9. General reviewer-safety matrix

Potential reviewer concern	Risk if not controlled	Monograph-level response	Where the response is implemented	Final safe wording
Does the book claim to solve the Clay problems?	The entire project may be rejected as theorem overclaiming.	State repeatedly that the book develops bounded economic analogues only.	Front matter, Chapter 1, Chapter 2, Chapter 14 and every problem chapter.	The monograph does not solve, prove, test or replicate the Clay problems in their original form.
Are economic	Analogy may be	Define all objects as	Methodology and	The variables are

Potential reviewer concern	Risk if not controlled	Monograph-level response	Where the response is implemented	Final safe wording
variables literal mathematical objects?	misread as identity.	constructed economic measurements, proxies or diagnostics.	conceptual translation chapters.	economic analogues, not literal invariants.
Are results causal?	Associations and calibrations may be overstated.	Separate measurement, diagnostic association, screening and causal identification.	Claim hierarchy tables and interpretation chapters.	The evidence is diagnostic/associational unless an identification design supports causality.
Are forecasts universally dominant?	Forecast claims may exceed sample evidence.	Assign forecast claims to named samples, frequencies and benchmarks.	Riemann/Zeta and forecast-related sections.	Forecast improvement is bounded by the reported validation layers.
Are small benchmarks generalized too far?	N=10 or reduced-instance results may be overstated.	Label finite-network, regional and reduced instances as benchmarks.	Hodge, Yang-Mills and P-vs-NP chapters.	The result is complete within the declared benchmark, not universal.
Are future panels treated as completed evidence?	Protocol may be confused with result.	Classify as future validation until variables are populated and estimates produced.	Yang-Mills, Hodge, BSD and P-vs-NP extension paths.	Stronger validation is reserved for future completed data and estimates.

2.7.11. Integrated Closing Statement

The claim hierarchy developed in this section completes the conceptual translation framework of Chapter 2. Sections 2.1 through 2.6 explained how mathematical objects become economic analogues through flow, curvature, topology, spectral signal, L-function logic, optimization complexity and local-to-global transmission. Section 2.7 now specifies how those analogues may speak scientifically. The answer is precise: they may speak as measurement architectures, diagnostic systems, bounded forecast models, finite or reduced benchmarks and future validation protocols. They may not speak as theorem proofs, causal laws, universal forecast machines, certified global optima or completed external validations where the evidence does not support those claims.

This final distinction is not a rhetorical safeguard added at the end. It is part of the scientific method of the monograph. Every chapter is designed to transform mathematical grammar into economic measurement while preventing the translation from becoming an overclaim. For that reason, the general claim hierarchy should remain visible throughout the book: in the front matter, in the introduction, in the integrated methodology, in each problem chapter, in the comparative synthesis, and especially in the final limitations and reviewer-safety matrix.

The monograph-level conclusion of Chapter 2 is therefore high but bounded. The seven Clay-inspired economic analogues jointly establish a mathematical-econometric research program for measuring economic complexity. They show how global stress, inequality deformation, macro-flow structure, corridor transmission, spectral cycles, local-to-global rank formation and computational search can be organized in one systematic architecture. The admissible claim is not that mathematics has been solved by economics. The admissible claim is that deep mathematical architectures can discipline economic measurement when analogy, evidence, validation and boundary are kept in exact alignment.

3.1. Mathematical Economics and Analogue Modelling

Integrated Review of Claim-Boundary Literature and Mathematical-Economic Translation across Seven Millennium-Inspired Models

3.1.1. Function of this Section within the Integrated Literature Review

This section opens the integrated literature review by consolidating the common theoretical and methodological foundation of the seven Millennium-inspired economic studies. It replaces seven separate article-level literature-review openings with one monographic review of mathematical economics, analogue modelling and claim-boundary discipline. The purpose is not to repeat the Chapter 2 conceptual translation framework. Chapter 2 defined the internal translation logic of the monograph. Section 3.1 now positions that logic within the wider literature: mathematical economics, structural modelling, applied analogy, constructed indices, network and topological measurement, spectral signal construction, computational optimization and robust empirical validation (Samuelson, 1947; Arrow and Debreu, 1954; Debreu, 1959; Morgan and Morrison, 1999; Gondauri, 2026a-g).

The unifying premise is that modern economics has long used mathematical structures not merely to decorate economic language, but to formalize mechanisms, constraints, equilibrium concepts, stability conditions, measurement systems and inference protocols. This view is consistent with the core tradition of mathematical economics, where formal representation is treated as an analytic device for equilibrium, optimization and comparative statics rather than as a literal identity between the economy and the mathematical domain (Samuelson, 1947; Arrow and Debreu, 1954; Debreu, 1959; Koopmans, 1957). However, a monograph based on the Clay Millennium Problems requires a stronger version of this discipline. The mathematical objects behind the seven problems are deep theorem-level or conjectural objects in analysis, topology, geometry, number theory, gauge theory and computational complexity; therefore, the literature review must distinguish mathematical origin from economic use and must restrict every analogue to bounded measurement, diagnostic, forecasting, benchmark or computational claims (Hamilton, 1982; Perelman, 2002; Deligne, 1974; Yang and Mills, 1954; Birch and Swinnerton-Dyer, 1965; Riemann, 1859; Cook, 1971; Karp, 1972; Gondauri, 2026a-g).

The source articles already contain this discipline separately. The Hodge study frames its literature review around Hodge theory, discrete Hodge decomposition, graph signal processing, topological signal processing, network science, international macroeconomics and validation literature (Hodge, 1952; Jiang et al., 2011; Schaub et al., 2020; Edelsbrunner and Harer, 2010; Gondauri, 2026b). The Yang-Mills study organizes prior work around complex networks, systemic risk, input-output and corridor networks, spectral graph theory, gauge analogies and econometric validation (Yang and Mills, 1954; Watts and Strogatz, 1998; Barabasi and Albert, 1999; Fiedler, 1973; Acemoglu et al., 2012; Elliott et al., 2014; Gondauri, 2026d). The Navier-Stokes study combines fluid-mechanics foundations with liquidity, systemic-risk, forecasting, panel-econometric and stress-testing literatures (Leray, 1934; Caffarelli et al., 1982; Brunnermeier and Pedersen, 2009; Adrian and Brunnermeier, 2016; Diebold and Mariano, 1995; Gondauri, 2026c). The BSD study links local-to-global number theory with network, structural-rank, corridor and panel-diagnostic literatures (Birch and Swinnerton-Dyer, 1965; Gross and Zagier, 1986; Silverman, 1986; Hausmann and Hidalgo, 2011; Gondauri, 2026e). The Riemann-Zeta study links critical-line signal foundations with structural inflation forecasting and spectral validation (Riemann, 1859; Titchmarsh, 1986; Keating and Snaith, 2000; Stock and Watson, 1999; Hyndman and Koehler, 2006; Gondauri, 2026f). The P-vs-NP study links portfolio theory, covariance modelling, sparse optimization, computational complexity, metaheuristics, Monte Carlo benchmarking and implementation realism (Markowitz, 1952; Sharpe, 1964; Black and Scholes, 1973; Cook, 1971; Karp, 1972; Garey and Johnson, 1979; Deb et al., 2002; Gondauri, 2026g). The Perelman-Ricci-Poincare study links Ricci flow, entropy, graph topology, inequality measurement and econometric validation (Hamilton, 1982; Perelman, 2002; Forman, 2003; Ollivier, 2009; Sen, 1997; Gondauri, 2026a). Section 3.1 synthesizes these streams into one methodological literature base.

Table 3.1. Integrated source-literature transfer map for Section 3.1. Source synthesis: Hamilton (1982), Perelman (2002), Hodge (1952), Leray (1934), Yang and Mills (1954), Birch and Swinnerton-Dyer (1965), Riemann (1859), Cook (1971), Karp (1972), and Gondauri (2026a-g).

Source model	Literature review material merged into Section 3.1	Role in mathematical economics and analogue modelling
Perelman/Ricci/ Poincare inequality diagnostics	Geometric analysis, Ricci flow, Perelman-type entropy, graph topology, inequality measurement, smoothing capacity and	Defines diagnostic-manifold logic: economic pressure may be represented through curvature-like deformation, entropy-like

Source model	Literature review material merged into Section 3.1	Role in mathematical economics and analogue modelling
	validation literature.	complexity and graph connectedness, but not as a proof of geometric/topological theorems.
Hodge macro-flow decomposition	Pure Hodge theory, discrete Hodge theory, Hodge Laplacians, graph/topological signal processing, persistent homology, networks, international macroeconomics and validation literature.	Defines decomposition logic: a regional edge-flow can be separated into hierarchy, local-cycle imbalance and systemic circulation, while the Hodge Conjecture remains outside the economic claim.
Navier-Stokes liquidity-flow stress modelling	Flow-balance foundations, liquidity and market microstructure, systemic risk, financial-stress indices, forecasting, panel econometrics and composite-index validation.	Defines nondimensional stress-balance logic: velocity weakness, pressure, friction, shocks, cycles and closure can be measured as macro-financial channels without treating liquidity as physical fluid.
Yang-Mills finite-network mass-gap benchmark	Complex networks, financial contagion, GVC and corridor networks, spectral graph theory, Hodge/simplicial methods, gauge analogies and econometric validation.	Defines threshold logic: gauge potential, curvature, action and spectral separation can become finite-network stress diagnostics without solving the Yang-Mills mass-gap problem.
BSD regional local-to-global rank model	BSD and elliptic-curve local-to-global mathematics, L-functions, network science, Hodge/topology, economic complexity, corridor transmission and robust panel diagnostics.	Defines local-to-global logic: finite-state regional traces, Euler-factor analogues and economic LOrder can measure structural-rank formation without estimating an arithmetic L-function.
Riemann-Zeta FPAS+zeta forecasting	Zeta/critical-line foundations, structural inflation forecasting, global shock transmission, forecast evaluation, time-series dynamics, regime-switching, spectral diagnostics and residual testing.	Defines spectral-signal logic: a critical-line inspired zeta-cycle can supply a calibrated forecast correction without testing or verifying the Riemann Hypothesis.
P-vs-NP computational portfolio optimization	Portfolio theory, CAPM, covariance geometry, cardinality-constrained optimization, computational complexity, metaheuristics, Monte Carlo and exact reduced benchmarking.	Defines computational-complexity logic: sparse support selection operationalizes combinatorial difficulty without proving P != NP or certifying full-universe optimality.

3.1.2. Mathematical Economics as a Discipline of Formal Translation

The first literature foundation is mathematical economics itself. From equilibrium theory, fixed-point methods, convex analysis, stochastic processes and dynamic optimization to econometrics, game theory and asset pricing, economics has repeatedly advanced by translating conceptual problems into formal objects (Samuelson, 1947; Arrow and Debreu, 1954; Debreu, 1959; Koopmans, 1957; Stokey et al., 1989). This does not mean that the economy is identical to the mathematical domain from which a tool is borrowed. Rather, mathematical economics operates through disciplined representation: a price vector becomes useful because it organizes scarcity and substitution; a covariance matrix becomes useful because it measures dependence and portfolio risk; and a graph becomes useful because it represents relations, exposures and propagation paths (Markowitz, 1952; Sharpe, 1964; Newman, 2010; Jackson, 2008).

This distinction is crucial for the present monograph. The seven mathematical architectures are not inserted into economics as decorative analogies. They are used as measurement grammars: Navier-Stokes supplies a grammar for flow, pressure, friction and closure; Hodge supplies a grammar for decomposing edge flows into hierarchy, local imbalance and circulation; Perelman/Ricci/Poincare supplies a grammar for pressure smoothing, curvature-like deformation, entropy and connectedness; Yang-Mills supplies a grammar for edge potentials, curvature, action and shock thresholds; BSD supplies a grammar for local-to-global rank formation; Riemann/Zeta supplies a grammar for nonlinear spectral-cycle signals; and P-vs-NP supplies a grammar for computational search, support-space explosion and bounded algorithmic evidence (Leray,

1934; Hodge, 1952; Hamilton, 1982; Yang and Mills, 1954; Birch and Swinnerton-Dyer, 1965; Riemann, 1859; Cook, 1971; Karp, 1972; Gondauri, 2026a-g).

The literature therefore supports a two-sided argument. On one side, formal modelling is indispensable because the economic systems studied in the monograph cannot be understood through scalar indicators alone: GDP, inflation, volatility, inequality and portfolio returns remain necessary anchors, but each is insufficient when the research object is interdependence, stress propagation, cycle structure, local-to-global rank or combinatorial search (Acemoglu et al., 2012; Elliott et al., 2014; Adrian and Brunnermeier, 2016; Hausmann and Hidalgo, 2011; Markowitz, 1952). On the other side, formal modelling must remain bounded because mathematical structure can easily produce an illusion of proof. The monograph therefore adopts a standard principle of applied modelling: a model is an organized measurement claim under specified assumptions, not an automatic transfer of truth from the source mathematics (Box, 1976; Morgan and Morrison, 1999; Lucas, 1976).

ClassicalObject_k -> TranslationOperator_k -> EconomicAnalogue_k -> ValidationGate_k -> PermissibleClaim_k

This schematic summarizes the literature-based logic of the monograph. Each mathematical object enters the economic model only through a defined translation operator, a constructed economic analogue, a validation gate and a bounded claim class; this sequence follows the modelling tradition in which abstraction is scientifically admissible only when its assumptions, domain, observables and inferential limits are made explicit (Box, 1976; Morgan and Morrison, 1999; OECD and JRC, 2008; Gondauri, 2026a-g).

3.1.3. Analogue Modelling: From Metaphor to Auditable Measurement Architecture

The analogue-modelling literature relevant to this monograph is not satisfied by resemblance. A weak analogy says that one system looks like another; a scientific analogue is stronger because it identifies a structural correspondence, defines which elements are transferred, specifies which elements are not transferred, constructs measurable variables and subjects the result to empirical or computational audit (Hesse, 1966; Morgan and Morrison, 1999; Box, 1976). The seven studies follow this stronger path. They do not merely state that liquidity is like a fluid, inequality is like curvature, networks are like gauge fields, inflation cycles resemble zeta oscillations or portfolios display complexity. Each study builds a transformation sequence from raw or public-data anchors into normalized objects, matrices, graphs, cochains, functions, search spaces, indices, diagnostics, robustness checks and claim hierarchies (OECD and JRC, 2008; Saltelli et al., 2008; Gondauri, 2026a-g).

This is why the source literature reviews repeatedly use protocol language. The Navier-Stokes review identifies fluid regularity and flow-balance concepts only insofar as they justify nondimensional stress components (Leray, 1934; Caffarelli et al., 1982; Gondauri, 2026c). The Hodge review selects pure Hodge theory to define origin and discrete Hodge/topological signal processing to define computability (Hodge, 1952; Jiang et al., 2011; Schaub et al., 2020; Gondauri, 2026b). The Yang-Mills review draws on gauge and spectral graph language to build a finite-network shock-threshold architecture (Yang and Mills, 1954; Fiedler, 1973; Chung, 1997; Gondauri, 2026d). The BSD review extracts local-to-global logic, trace analogues, Euler factors and L-function ordering as economic measurement devices (Birch and Swinnerton-Dyer, 1965; Gross and Zagier, 1986; Silverman, 1986; Gondauri, 2026e). The Riemann-Zeta review uses critical-line signal construction as a bounded cyclical correction layer (Riemann, 1859; Titchmarsh, 1986; Keating and Snaith, 2000; Gondauri, 2026f). The P-vs-NP review turns cardinality constraints into an empirical-computational environment where exact reduced benchmarking and heuristic search can be compared (Cook, 1971; Karp, 1972; Garey and Johnson, 1979; Deb et al., 2002; Gondauri, 2026g). The Perelman/Ricci/Poincare review uses curvature, entropy and graph connectedness as diagnostic tools for inequality pressure and smoothing capacity (Hamilton, 1982; Perelman, 2002; Forman, 2003; Ollivier, 2009; Gondauri, 2026a).

The literature base therefore justifies a general rule for Chapter 3: analogy becomes admissible only after it becomes auditable. An analogy is auditable when it has explicit inputs, transformations, mathematical or computational definitions, validation tests, falsification or placebo logic, replication materials and a defined claim boundary. Without these elements, a mathematical analogy remains rhetorical; with these elements, it becomes a formal research architecture capable of producing bounded scientific claims (Box, 1976; OECD and JRC, 2008; Saltelli et al., 2008; Driscoll and Kraay, 1998; Diebold and Mariano, 1995; Gondauri, 2026a-g).

Table 3.2. From weak analogy to admissible mathematical-economic analogue. Source synthesis: Box (1976), Morgan and Morrison (1999), OECD and JRC (2008), Saltelli et al. (2008), and Gondauri (2026a-g).

Criterion	Weak or inadmissible analogy	Admissible monograph-level analogue
Object definition	Uses a mathematical term without defining what economic object it measures.	Defines the economic object: stress field, flow cochain, curvature score, LOrder, zeta-cycle, support set or rank analogue.
Unit discipline	Adds heterogeneous variables because the metaphor seems intuitive.	Uses normalization, direction harmonization, nondimensionalization, scaling, indexing or matrix construction before aggregation.
Scope control	Treats similarity as proof or transfers theorem status into economics.	States that theorem proof, physical identity and unrestricted causality are excluded.
Validation	Reports a constructed value without benchmark, robustness or diagnostic audit.	Uses rolling validation, fixed effects, robust inference, Monte Carlo, placebo tests, sensitivity checks, exact reduced enumeration or external screening where appropriate.
Replication	Relies on narrative description of a complex construction.	Provides formula, algorithm, source, data-package, matrix, seed, checksum or reproducibility discipline.
Claim level	Claims solution, law, universal prediction or certified optimality.	Claims measurement, diagnostic, forecast-window improvement, benchmark evidence or future validation design according to the evidence level.

3.1.4. The Claim Boundary as a Literature-Review Principle

A distinctive feature of the seven source literature reviews is that the claim boundary is not left to the conclusion alone. It is embedded in the review logic itself. This is methodologically important because a literature review defines not only what has been studied, but also what prior literature authorizes the present manuscript to claim. The reviewed mathematical literature authorizes formal language only within its correct domain; the reviewed economic and econometric literature authorizes empirical interpretation only within the design, sample, identification and validation limits (Lucas, 1976; White, 1980; Newey and West, 1987; Driscoll and Kraay, 1998; Morgan and Morrison, 1999). Consequently, the integrated review must classify each claim before the reader reaches the results chapters.

For the Perelman/Ricci/Poincare framework, the review authorizes curvature-like and entropy-like diagnostics for inequality pressure, but not theorem proof, unrestricted causal identification or country-level welfare ranking (Hamilton, 1982; Perelman, 2002; Sen, 1997; Gondauri, 2026a). For the Hodge framework, the review authorizes edge-flow decomposition and topological validation, but not a claim about algebraic varieties or Hodge cycles (Hodge, 1952; Jiang et al., 2011; Schaub et al., 2020; Gondauri, 2026b). For the Navier-Stokes framework, the review authorizes flow-balance stress interpretation, but not physical hydrodynamics or a universal crisis-prediction theorem (Leray, 1934; Caffarelli et al., 1982; Adrian and Brunnermeier, 2016; Gondauri, 2026c). For the Yang-Mills framework, the review authorizes finite-network spectral thresholds, gauge potential and curvature-action diagnostics, but not a solution to the Yang-Mills existence and mass-gap problem (Yang and Mills, 1954; Fiedler, 1973; Chung, 1997; Gondauri, 2026d). For the BSD framework, the review authorizes local-to-global regional measurement and LOrder-structural-rank comparison, but not classical BSD proof, arithmetic L-function estimation or algebraic rank identification (Birch and Swinnerton-Dyer, 1965; Gross and Zagier, 1986; Silverman, 1986; Gondauri, 2026e). For the Riemann-Zeta framework, the review authorizes a critical-line inspired cyclical signal and layered forecast validation, but not verification of the Riemann Hypothesis or universal forecast dominance (Riemann, 1859; Titchmarsh, 1986; Keating and Snaith, 2000; Gondauri, 2026f). For the P-vs-NP framework, the review authorizes empirical-computational complexity analysis, but not proof of P != NP, certified full-universe optimality or realized historical investment dominance (Cook, 1971; Karp, 1972; Garey and Johnson, 1979; Gondauri, 2026g).

This integrated claim-boundary approach is not a defensive afterthought. It is a positive scholarly contribution because it shows how high-level mathematics can enter economics without collapsing into either overclaiming or superficial metaphor. The literature review therefore performs a gatekeeping function: it accepts mathematical inspiration, rejects theorem transfer, accepts constructed measurement, rejects ontological identity, accepts validation-window evidence and

rejects universal law unless identification and replication conditions justify it (Box, 1976; Lucas, 1976; Morgan and Morrison, 1999; OECD and JRC, 2008; Gondauri, 2026a-g).

Table 3.3. Claim-boundary synthesis across the seven mathematical-economic analogues. Source synthesis: the seven source manuscripts and their claim-boundary literature (Gondauri, 2026a-g).

Analogue	Permissible literature-supported claim	Restricted or excluded claim
Perelman/Ricci/ Poincare	A diagnostic measurement architecture can organize global inequality pressure, smoothing capacity, curvature-like deformation, entropy-like complexity and graph connectedness.	No proof/test/replication of Perelman's proof, Ricci-flow theorem or Poincare conjecture; no unrestricted causal welfare law.
Hodge	A directed macro-flow pressure field can be decomposed into gradient hierarchy, curl/local imbalance and harmonic/systemic circulation under a specified graph construction.	No solution of the Hodge Conjecture; no claim that macro-regions are algebraic varieties or that Hodge classes are economically estimated.
Navier-Stokes	Global systemic stress can be measured as a nondimensional flow-pressure-friction-shock-cycle-closure process.	No claim that liquidity is a physical fluid; no solution to the classical Navier-Stokes problem; no universal crisis-prediction theorem.
Yang-Mills	A finite stress-weighted corridor network can support gauge-potential, curvature, action and spectral mass-gap threshold diagnostics.	No physical Yang-Mills field, no solution to the mathematical mass-gap problem, no final country-panel causal claim before N = 1,500 validation.
BSD	Regional finite-state signals and Euler-factor analogues can be informative about structural rank under calibrated local-to-global measurement logic.	No proof or empirical test of classical BSD; no arithmetic L-function; no algebraic rank of rational points.
Riemann/Zeta	A normalized zeta-cycle can be tested as a signed nonlinear correction to structural global inflation forecasting under layered validation.	No proof/test/verification of the Riemann Hypothesis; no universal inflation law or unrestricted forecast superiority.
P-vs-NP	Cardinality-constrained portfolio selection can be studied as a mixed discrete-continuous empirical-computational optimization problem.	No proof of P != NP; no certified full-universe optimum without exhaustive certificate; no realized historical trading dominance.

3.1.5. Seven Mathematical Grammars and One Integrated Review Logic

The seven source reviews do not contribute identical types of literature. Their integration requires classification by mathematical grammar. A grammar is a formal way of organizing economic evidence. Flow grammar organizes movement, pressure and friction; curvature grammar organizes deformation and smoothing; topological grammar organizes connectedness, cycles and holes; spectral grammar organizes thresholds, frequencies and eigenmodes; local-to-global grammar organizes how local signals aggregate into rank or systemic structure; complexity grammar organizes search spaces, computational feasibility and approximation evidence; and claim-boundary grammar organizes what each evidence class permits the author to say (Leray, 1934; Hodge, 1952; Hamilton, 1982; Yang and Mills, 1954; Birch and Swinnerton-Dyer, 1965; Riemann, 1859; Cook, 1971; Karp, 1972; Gondauri, 2026a-g).

The monograph needs these grammars because global economic systems are multidimensional. A scalar variable cannot distinguish whether stress is caused by pressure gradients, topology, local-cycle imbalance, spectral threshold compression, weak smoothing capacity, rank mismatch or computational constraint. The literature confirms that different mathematical traditions provide different diagnostic lenses: Ricci-flow and Perelman-type entropy frame deformation and smoothing; Hodge decomposition separates hierarchy, curl and harmonic circulation; Navier-Stokes flow balance organizes velocity, pressure, friction and forcing; Yang-Mills and spectral-graph theory organize curvature/action and threshold separation; BSD and L-function theory organize local-to-global rank logic; Riemann-zeta and random matrix methods organize spectral-cycle signals; and computational complexity frames combinatorial search (Hamilton, 1982; Perelman,

2002; Jiang et al., 2011; Leray, 1934; Yang and Mills, 1954; Fiedler, 1973; Birch and Swinnerton-Dyer, 1965; Keating and Snaith, 2000; Cook, 1971; Karp, 1972).

This grammar-based classification allows the integrated literature review to avoid repetition. Instead of treating each article as an isolated bibliography, Chapter 3 classifies literatures by function. The same network literature may support Hodge, Yang-Mills and BSD, but it does different work in each: in Hodge it supports graph-based flow decomposition; in Yang-Mills it supports finite-network stress transmission and mass-gap threshold logic; and in BSD it supports structural-rank and corridor-stress interpretation (Watts and Strogatz, 1998; Barabasi and Albert, 1999; Newman, 2010; Jackson, 2008; Gondauri, 2026b, 2026d, 2026e). Similarly, robust inference literature supports all seven studies, but its role changes across forecasting, algorithmic, rank-calibration, stress-testing and diagnostic frameworks (White, 1980; Newey and West, 1987; Driscoll and Kraay, 1998; Diebold and Mariano, 1995; Clark and West, 2007).

Table 3.4. Mathematical grammars and their economic modelling functions. Source synthesis: Leray (1934), Hodge (1952), Hamilton (1982), Yang and Mills (1954), Birch and Swinnerton-Dyer (1965), Riemann (1859), Cook (1971), Karp (1972), and Gondauri (2026a-g).

Mathematical grammar	Main source chapters	Economic modelling function in the monograph
Flow grammar	Navier-Stokes, Hodge, Yang-Mills	Converts economic relations into directed or channel-based flow structures: liquidity weakness, macro-flow pressure, corridor transmission and stress propagation.
Curvature grammar	Perelman/Ricci/Poincare, Yang-Mills, Hodge	Measures deformation, bottlenecks, cycle stress and structural distortion rather than only levels or averages.
Topology grammar	Hodge, Perelman/Ricci/Poincare, Yang-Mills	Identifies connectedness, cycles, graph closure, Laplacian structure, Betti-style diagnostics and higher-order interdependence.
Spectral grammar	Riemann/Zeta, Yang-Mills, Hodge, BSD	Uses eigenvalues, frequency-domain signals, zeta cycles, L-function analogues and spectral thresholds as validation or measurement objects.
Local-to-global grammar	BSD, Hodge, Yang-Mills, Navier-Stokes	Explains how local finite-state signals, local imbalance, corridor shocks and pressure channels become system-level rank or stress outcomes.
Complexity grammar	P-vs-NP, Riemann/Zeta, Yang-Mills	Defines search-space explosion, algorithmic feasibility, computational signal construction, simulation burden and reproducibility gates.
Claim-boundary grammar	All seven	Maps every result to an admissible claim level: measurement, diagnostic, forecast-window, benchmark or future-validation claim.

3.1.6. Constructed Variables, Normalization and Measurement Legitimacy

A second integrated literature issue is the legitimacy of constructed variables. Each source manuscript transforms raw inputs into author-calculated objects: pressure coordinates, stress fields, macro-flow cochains, curvature scores, LOrder, zeta-cycle deviations, support spaces, algorithmic incumbents, EMGI, BridgeStress, fragility, resilience or closure terms. The literature on composite indicators, index construction and applied econometrics permits such construction only under transparency: a constructed variable is not inferior to a raw variable merely because it is derived, but it becomes scientifically weak when data lineage, transformation rule, scaling convention and validation status are unclear (OECD and JRC, 2008; Saltelli et al., 2008; Saisana et al., 2005; White, 1980; Gondauri, 2026a-g).

The seven studies address this by separating public or fixed input anchors from derived analytical objects. The Navier-Stokes framework distinguishes raw macro-financial proxies from nondimensional starred variables; the Perelman/Ricci/Poincare framework transforms heterogeneous macro-social variables into a common pressure-oriented 0-100 coordinate system; the Hodge framework separates public regional macroeconomic anchors from author-calculated directed macro-flow pressure; the Yang-Mills framework separates public macroeconomic anchors from normalized systemic stress, gauge potential, curvature, action and mass-gap diagnostics; the BSD framework separates public regional anchors from coefficient maps, finite-state trace analogues, Euler-factor analogues and LOrder; the Riemann-Zeta

framework separates observed inflation and FPAS baseline forecasts from the normalized zeta-cycle and signed correction; and the P-vs-NP framework separates fixed industry inputs and CAPM priors from search-space enumeration, heuristic incumbents and option-overlay diagnostics (Gondauri, 2026a-g). This public-anchor/constructed-object distinction is consistent with composite-indicator and replication literature, where transformation transparency is a condition of interpretability (OECD and JRC, 2008; Saltelli et al., 2008).

The literature-review implication is that the monograph should not apologize for constructed variables; it should make them auditable. Constructed variables are appropriate when they solve a measurement problem that raw variables cannot solve: topology, curvature, rank formation, systemic circulation, shock threshold, spectral correction or computational search. Their claim status, however, must remain proportional to their independence and validation. A constructed index can support measurement and diagnostic claims; it cannot automatically support causal identification. A spectral correction can support forecast-window improvement; it cannot automatically support universal prediction. A best-found computational incumbent can support optimization evidence under disclosed search coverage; it cannot automatically certify global optimality (Lucas, 1976; Box, 1976; Diebold and Mariano, 1995; Clark and West, 2007; Garey and Johnson, 1979; Gondauri, 2026a-g).

InputAnchor -> Normalization -> ConstructedObject -> DiagnosticTest -> ClaimClass

The common construction pipeline transforms raw or public anchors into auditable objects only after scale discipline, model definition and validation controls have been applied. This is the same methodological logic that underlies composite-index construction, robust econometric inference, forecast evaluation and computational benchmarking (OECD and JRC, 2008; Saltelli et al., 2008; White, 1980; Newey and West, 1987; Diebold and Mariano, 1995; Deb et al., 2002).

3.1.7. Econometric and Computational Validation as Boundary Discipline

The integrated literature also shows that mathematical analogy alone cannot close an economic argument. Validation is the mechanism by which analogy is forced to become evidence. The source reviews repeatedly draw on robust inference, fixed effects, dynamic panels, forecast evaluation, residual tests, Monte Carlo uncertainty, placebo logic, negative controls, sensitivity analysis, equivalence checks, reduced exact enumeration, machine-learning validation and external-proxy screening. These tools are not interchangeable, but they share the same function: they determine how strong a claim may be (White, 1980; Newey and West, 1987; Driscoll and Kraay, 1998; Arellano and Bond, 1991; Diebold and Mariano, 1995; Clark and West, 2007; Hyndman and Koehler, 2006; Saltelli et al., 2008).

In the Navier-Stokes model, rolling validation, benchmark comparison, fixed effects, external-target validation, residual tests and Monte Carlo counterfactuals prevent the flow-balance analogy from becoming a universal crisis-prediction claim (Diebold and Mariano, 1995; Adrian and Brunnermeier, 2016; Gondauri, 2026c). In the Riemann-Zeta model, RMSE/MAE/sMAPE hierarchies, rolling no-look-ahead validation, Mincer-Zarnowitz calibration, Diebold-Mariano and Clark-West tests, regime screens and residual diagnostics determine whether the zeta-cycle improves forecasting in the reported layers (Diebold and Mariano, 1995; Clark and West, 2007; Hyndman and Koehler, 2006; Gondauri, 2026f). In the BSD model, rank gaps, equivalence logic, agreement diagnostics, negative controls, circularity tests, out-of-sample validation, external-proxy screening and permutation placebo logic determine whether the local-to-global claim is internal, directional or externally supported (Gross and Zagier, 1986; Silverman, 1986; Driscoll and Kraay, 1998; Gondauri, 2026e). In the P-vs-NP model, exact reduced enumeration, heuristic comparison, covariance alternatives, transaction costs, beta drift and search-coverage reporting determine whether a result is best-found, benchmark-certified or uncertified (Markowitz, 1952; Sharpe, 1964; Cook, 1971; Karp, 1972; Deb et al., 2002; Gondauri, 2026g). In the Hodge, Perelman/Ricci/Poincare and Yang-Mills models, topology, spectral diagnostics, robustness, edge-curvature and simulation evidence determine whether constructed structures are coherent measurement objects rather than decorative mathematics (Hamilton, 1982; Jiang et al., 2011; Schaub et al., 2020; Fiedler, 1973; Gondauri, 2026a, 2026b, 2026d).

This literature-based validation discipline should guide the entire Chapter 3. The integrated review must not treat econometrics as a final decoration after mathematics. It must treat validation as a constitutive part of analogue modelling. In this monograph, a mathematical-economic analogue has three layers: a translation layer, a measurement layer and a validation layer. Without validation, the model remains conceptually interesting but scientifically underbounded; with validation, the model becomes publishable because its strongest claim can be stated precisely and its restricted claims can be excluded explicitly (Box, 1976; Morgan and Morrison, 1999; White, 1980; Driscoll and Kraay, 1998; OECD and JRC, 2008; Gondauri, 2026a-g).

Table 3.5. Validation gates required by analogue modelling literature. Source synthesis: White (1980), Newey and West (1987), Arellano and Bond (1991), Driscoll and Kraay (1998), Diebold and Mariano (1995), Clark and West (2007), and Gondauri (2026a-g).

Gate	Purpose	Examples across the seven models
Conceptual gate	Ensures the source mathematical object is translated structurally, not literally.	No physical liquidity fluid; no macroeconomic algebraic variety; no arithmetic L-function; no theorem-level zeta or P-vs-NP claim.
Scale gate	Prevents raw-unit inconsistency and unsupported aggregation.	Nondimensional stress terms; 0-100 pressure coordinates; normalized zeta-cycle; CAPM priors; region-weighted anchors.
Topology/network gate	Checks whether the constructed graph or network is adequate for decomposition, curvature, spectral or propagation claims.	Connected regional graph, cycle structure, Laplacian diagnostics, stress-weighted adjacency, Hodge-Laplacian and persistent homology checks.
Econometric gate	Determines whether associations are diagnostic, robust, directional or causal.	FE/TWFE, HAC/HC, Driscoll-Kraay, residual diagnostics, cross-sectional dependence, negative controls and external-proxy screening.
Forecast gate	Determines whether predictive improvement is restricted to reported validation layers.	FPAS+zeta versus FPAS/ARIMA; rolling no-look-ahead; MZ, DM and CW tests; AR(1) benchmark discipline.
Computational gate	Determines whether optimization evidence is exact, approximate, heuristic or merely illustrative.	C(n,K), exact reduced enumeration, greedy/MC/GA comparison, runtime scaling, seed stability and search-coverage reports.
Replication gate	Makes the constructed object reproducible and reviewable.	Data packages, formulas, matrices, source ledgers, seeds, checksums, method tables and final claim matrices.

3.1.8. Literature Gap Addressed by the Monograph

The merged review reveals a large cross-disciplinary gap. Existing literatures are strong within their own domains, but they rarely combine formal mathematical architectures, economic measurement, systemic transmission, forecast validation, computational optimization, replication discipline and claim hierarchy in one integrated programme. Network economics explains interdependence but does not by itself define Hodge decomposition, gauge curvature, LOrder or zeta-cycle correction (Watts and Strogatz, 1998; Barabasi and Albert, 1999; Jackson, 2008; Newman, 2010). Mathematical physics and topology define curvature, flow, gauge, spectral and topological objects but do not directly supply macroeconomic variables, public-data anchors or panel validation (Hamilton, 1982; Perelman, 2002; Hodge, 1952; Yang and Mills, 1954). Forecasting literature supplies performance tests but does not define local-to-global structural rank (Diebold and Mariano, 1995; Clark and West, 2007; Hyndman and Koehler, 2006). Portfolio optimization literature supplies sparse search and complexity tools but does not address macro-systemic flow or curvature (Markowitz, 1952; Sharpe, 1964; Cook, 1971; Karp, 1972). BSD and zeta literatures define profound number-theoretic structures but do not provide economic measurement systems (Birch and Swinnerton-Dyer, 1965; Riemann, 1859).

The contribution of the monograph is therefore not that it invents each underlying mathematical, economic or econometric tradition. Its contribution is integrative and architectural. It asks whether seven different mathematical grammars can be converted into seven bounded, auditable economic-econometric analogues under one consistent claim-boundary regime. This is different from writing seven unrelated papers: the monograph builds a comparative research programme in which flow, topology, curvature, spectral signal, local-to-global rank, computational complexity and validation discipline become complementary measurement languages for global economic complexity (Morgan and Morrison, 1999; OECD and JRC, 2008; Gondauri, 2026a-g).

This gap is especially important because economic systems increasingly exhibit features that scalar indicators do not capture well: corridor exposure, nonlinear shocks, systemic circulation, high-dimensional inequality pressure, spectral-cycle behaviour, combinatorial choice and stress-threshold compression. The literature supports each component separately, from network propagation and systemic risk to forecast evaluation and sparse optimization; the monograph contributes by showing how to integrate them without overstating the result (Acemoglu et al., 2012; Elliott et al., 2014; Adrian and

Brunnermeier, 2016; Diebold and Mariano, 1995; Markowitz, 1952; Garey and Johnson, 1979). Its strongest general claim is not that the Clay Millennium Problems are solved economically. Its strongest claim is that the formal architectures associated with these problems can generate transparent, reproducible and claim-bounded economic measurement systems (Gondauri, 2026a-g).

Table 3.6. Integrated literature gap and monograph response. Source synthesis: mathematical economics, analogue modelling, network economics, forecast validation, computational optimization and seven source manuscripts cited throughout Section 3.1.

Existing literature strength	Remaining gap	Monograph response in Section 3.1 and subsequent Chapter 3 sections
Mathematical economics formalizes economic objects through equilibrium, optimization, stochastic and econometric structures.	It rarely systematizes claim boundaries for transferring unsolved Millennium-level architectures into economics.	Defines mathematical analogy as translation plus validation plus claim hierarchy.
Network economics and systemic-risk literature explain interdependence and propagation.	They do not automatically define curvature, Hodge decomposition, gauge action, LOrder or zeta-cycle corrections.	Uses network literature as a base for flow, topology, local-to-global and shock-threshold analogues.
Topological and spectral methods provide powerful tools for graphs, cycles, Laplacians, persistence and signal processing.	They are often methodologically separate from macroeconomic anchors, replication packages and econometric validation.	Converts topological/spectral tools into auditable macroeconomic measurement systems.
Forecasting and econometric literatures provide validation tests, residual diagnostics and robust inference.	They do not by themselves create mathematical-economic analogues or determine theorem-transfer boundaries.	Treats validation as the gate that classifies claims into measurement, diagnostic, forecasting, benchmark or future-validation categories.
Computational finance and optimization literatures address sparse search, heuristics and exact benchmarking.	They can overstate algorithmic success without explicit proof/global-optimality boundaries.	Uses exact reduced enumeration and search-coverage reporting to keep P-vs-NP-inspired claims bounded.
Inequality, regional, corridor and macro-financial literatures provide substantive economic interpretation.	They are often disconnected from high-level mathematical grammars of curvature, flow, topology and spectral structure.	Unifies substantive economic objects with formal analogues under a monographic review architecture.

3.1.9. Synthesis: What Section 3.1 Establishes for the Rest of Chapter 3

Section 3.1 establishes the methodological foundation for the rest of the integrated literature review. It shows that the seven source literature reviews should not remain separate because they share a common epistemic structure. Each uses a high-level mathematical object as an economic measurement grammar; each separates mathematical origin from economic use; each constructs derived variables or formal objects from public or fixed input anchors; each requires validation gates; and each produces a bounded claim rather than a theorem-level solution (Box, 1976; Morgan and Morrison, 1999; OECD and JRC, 2008; Gondauri, 2026a-g). The remaining sections of Chapter 3 can therefore proceed by substantive domain rather than by source document: network economics and systemic transmission; topology and spectral methods; macro-financial stress and inflation; inequality and smoothing capacity; portfolio optimization and computational finance; regional corridors and GVCs; validation and robust inference; constructed indices and replication discipline; and the final literature gap of the monograph.

The section also establishes the reviewer-facing defense of the monograph. A reader may reasonably ask whether the book is attempting to solve the Clay Millennium Problems. The answer, grounded in the literature, is no. A reader may also ask whether the book is merely using famous mathematical names rhetorically. The answer is also no. The integrated review shows that each analogue is built through explicit modelling pipelines, public or fixed data anchors, mathematical

definitions, diagnostic checks, robustness controls and claim-boundary rules (Lucas, 1976; Box, 1976; Morgan and Morrison, 1999; OECD and JRC, 2008; Gondauri, 2026a-g).

This conclusion is the bridge from Chapter 2 to the rest of Chapter 3. Chapter 2 explained how the translations work internally. Section 3.1 now shows why those translations are legitimate within the literature of mathematical economics and applied analogue modelling. The following review sections will deepen the substantive evidence base for the specific domains: networks, topology, spectral methods, liquidity, inflation, inequality, computational finance, corridors, validation and replication (Arrow and Debreu, 1954; Debreu, 1959; Morgan and Morrison, 1999; Gondauri, 2026a-g).

Section closing claim-boundary statement.

The integrated literature supports the monograph as a high-level mathematical-economic measurement programme. It permits strong claims about disciplined translation, auditable measurement, diagnostic architecture, bounded forecasting, finite-network benchmarking, sparse optimization evidence and future validation design. It does not permit claims of theorem proof, physical identity, unrestricted causal law, universal forecast superiority, certified global portfolio optimality or complete external validation where the evidence does not support those conclusions (Box, 1976; Lucas, 1976; Diebold and Mariano, 1995; Clark and West, 2007; Garey and Johnson, 1979; Gondauri, 2026a-g).

3.2. Network Economics, Systemic Risk and Shock Propagation

3.2.1. Function of this Section within the Integrated Literature Review

This section integrates the literatures on network economics, systemic risk and shock propagation that support the monograph's treatment of the world economy as a connected, corridor-sensitive and stress-transmitting system. It does not reproduce four separate literature reviews from the Yang-Mills, Hodge, BSD and Navier-Stokes manuscripts. Instead, it consolidates their shared intellectual field: complex networks, financial contagion, production and trade networks, corridor economics, supply-chain resilience, spectral thresholds, topological decomposition, gauge-inspired curvature, liquidity-flow stress testing and robust econometric validation (Watts & Strogatz, 1998; Newman, 2003; Jackson, 2008; Acemoglu et al., 2012).

The organizing proposition is that contemporary economic risk cannot be fully understood through scalar variables alone. GDP, inflation, debt, trade shares, liquidity indicators and regional growth rates remain necessary, but they do not by themselves identify the pathways through which shocks travel. A small region may be economically modest in output mass but topologically central in a corridor. A large region may dominate aggregate scale while remaining less exposed to a specific propagation channel. A financial system may appear stable in isolated balance-sheet ratios while being vulnerable through common liquidity pressure, funding interdependence or network cascades. The literature reviewed here supplies the scientific foundation for moving from isolated indicators to relational measurement systems (Allen & Gale, 2000; Eisenberg & Noe, 2001; Acharya & Pedersen, 2005; Adrian & Brunnermeier, 2016).

Within the monograph, Section 3.2 performs a bridging function. Section 3.1 established mathematical economics and analogue modelling as a general epistemic basis. Section 3.2 now narrows the review to economic systems in which nodes, edges, flows, shocks, thresholds and feedback loops become the primary analytical objects. The subsection is especially aligned with four problem chapters: Yang-Mills for finite-network stress thresholds; Hodge for macro-flow decomposition into hierarchy, local imbalance and systemic circulation; BSD for local-to-global structural-rank transmission and corridor stress; and Navier-Stokes for liquidity-flow pressure, friction, shocks and restricted closure. The Perelman/Ricci/Poincare, Riemann/Zeta and P-vs-NP studies are integrated as supporting fields because inequality deformation, inflation stress regimes and portfolio-complexity risk all depend on propagation, network dependence or stress amplification (Jiang et al., 2011; Schaub et al., 2020; Yang & Mills, 1954; Leray, 1934).

Table 3.2.1. Network/systemic-risk literature integration across the seven monograph models

Model block	Primary network/systemic-risk function	Literature role in Section 3.2	Claim boundary
Yang-Mills	Finite stress network, gauge potential, curvature/action and spectral mass-gap threshold.	Connects complex networks, financial contagion, corridor systems, spectral graph theory and gauge analogies into a shock-threshold literature.	Finite-network benchmark and diagnostic threshold; not physical Yang-Mills proof or final causal

Model block	Primary network/systemic-risk function	Literature role in Section 3.2	Claim boundary
			panel evidence.
Hodge	Directed macro-flow pressure and decomposition into hierarchy, curl imbalance and harmonic circulation.	Connects network economics, topological signal processing, Hodge decomposition, persistent homology and macro-resilience literature.	Benchmark structural decomposition; not observed dyadic transaction flow or final causal estimate.
BSD	Local regional signals, finite-state trace analogues, economic LOrder, structural rank and corridor transmission.	Connects local-to-global measurement, regional networks, corridor economics, systemic-risk propagation and panel closure diagnostics.	Calibrated internal local-to-global consistency; not BSD proof or causal law.
Navier-Stokes	Liquidity-flow stress balance, pressure gradients, friction/diffusion, stochastic shocks, cycle forcing and restricted closure.	Connects liquidity literature, systemic risk, macro-financial stress testing, forecasting and robust panel econometrics.	Stress-testing and diagnostic association; not physical fluid mechanics or universal crisis-prediction law.
Perelman/Ricci/ Poincare	Inequality pressure, smoothing capacity, curvature-like deformation and graph connectedness.	Supports the idea that macro-social pressure systems are coupled, connected and shock-sensitive.	Diagnostic manifold; not theorem-level geometry or unrestricted causality.
Riemann/Zeta	Global inflation pressure, stress regimes, spectral diagnostics and nonlinear cyclical deformation.	Supports the regime and shock-cycle literature that explains why stress propagation can be temporal and spectral, not only spatial.	Bounded forecast-diagnostic claim; not Riemann Hypothesis evidence.
P vs NP	Portfolio risk, covariance dependence, sparse support selection and stress-scenario realism.	Shows that financial network exposure and optimization risk are also constrained by computational search and robustness gates.	Empirical-computational demonstration; not proof of P != NP or certified full-universe optimum.

3.2.2. From Scalar Macroeconomic Indicators to Relational Economic Systems

A central literature shift underlying this monograph is the transition from scalar macroeconomic comparison to relational economic measurement. Traditional macroeconomic analysis often begins with country or regional aggregates: GDP, GDP per capita, inflation, trade openness, fiscal balance, credit growth, sovereign spreads, unemployment and investment rates. These variables provide indispensable information about scale, pressure and capacity. Yet they remain incomplete when the research question concerns systemic transmission. A shock is not only a value of a variable; it is also a movement through an architecture. Whether a disturbance remains local or becomes systemic depends on exposure, connectivity, substitutability, centrality, network topology, balance-sheet interdependence, corridor position and the strength of propagation channels (Jackson, 2008; Newman, 2003; Acemoglu et al., 2012; Carvalho, 2014).

The network-economics literature responds to this limitation by representing economic agents, firms, banks, sectors, regions or countries as nodes connected by edges. Edges may represent trade flows, input-output dependencies, financial exposures, payment obligations, supply-chain links, ownership relations, corridor routes, information channels or constructed pressure differentials. This relational turn is important because it changes the unit of inference. In a scalar model, the analyst compares magnitudes. In a network model, the analyst studies position, transmission, cycles, bottlenecks,

connectivity, communities, hubs, fragility, cascade conditions and resilience. A node can be systemically important because of its location even when its own scalar mass is moderate (Watts & Strogatz, 1998; Barabasi & Albert, 1999; Newman, 2003; Jackson, 2008).

The monograph uses this shift differently across its seven models. The Hodge model constructs a directed macro-flow pressure field rather than relying on GDP rankings. The Yang-Mills model constructs a finite stress-weighted corridor graph and asks whether the graph has a positive threshold separating local absorption from systemic transmission. The BSD model treats local regional signals and finite-state economic reductions as informative about global structural rank. The Navier-Stokes model treats macro-financial stress as a flow-pressure-friction-shock process rather than as a list of independent risk indicators. The Perelman/Ricci/Poincare model treats inequality variables as a coupled pressure-smoothing manifold. The Riemann/Zeta model treats inflation pressure as layered, cyclical and shock-sensitive. The P-vs-NP model treats portfolio construction as a mixed discrete-continuous optimization process embedded in covariance geometry and stress scenarios (Jiang et al., 2011; Schaub et al., 2020; Fiedler, 1973; Chung, 1997).

This integrated position is consistent with foundational network research on complex systems, small-world structure, scale-free connectivity, graph centrality, clustering and diffusion. Such literature does not provide an economic model by itself; it supplies an architecture for seeing why relationships matter. Economic network studies then translate that architecture into concrete mechanisms: interbank contagion, production bottlenecks, global value-chain propagation, regional transport corridors, liquidity spirals and financial-stress spillovers. Section 3.2 therefore reviews the literature not as background decoration but as the theoretical justification for the monograph's core object: a world economy that is measurable as a set of connected stress, flow, rank and shock-transmission structures (Allen & Gale, 2000; Acemoglu et al., 2015; Brunnermeier & Pedersen, 2009; Gai & Kapadia, 2010).

3.2.3. Complex Networks, Connectivity and Propagation as a General Scientific Foundation

The general literature on complex networks supplies the first pillar of this review. Watts and Strogatz's small-world model, Barabasi and Albert's preferential-attachment model, Newman's synthesis of network structure and Jackson's economic-network framework collectively show that systems may be neither random collections nor simple hierarchies. They can combine local clustering with short global paths, concentration of connectivity in hubs, community structure, weighted relations and heterogeneous centrality. For economics, the significance is straightforward: the structure of connections can determine the reach and speed of shocks independently of the size of the initial disturbance (Watts & Strogatz, 1998; Barabasi & Albert, 1999; Newman, 2003; Jackson, 2008).

This insight is essential for systemic-risk analysis. A small initial shock may remain local if the network is modular, redundant and well-buffered. The same shock may spread widely if it reaches a hub, bridge, highly leveraged counterparty, non-substitutable input, logistics chokepoint or liquidity-stressed corridor. Connectivity is therefore not automatically stabilizing. Dense networks can provide diversification and risk sharing, but they can also provide multiple propagation paths. Sparse networks can limit contagion, but they can also create critical bottlenecks. Network economics must therefore analyze not only how many links exist, but what kinds of links they are, how weighted they are, whether they form cycles, whether they create bridge exposure, and whether shocks can be absorbed or amplified (Gai & Kapadia, 2010; Acemoglu et al., 2015; Battiston et al., 2012).

The Yang-Mills and Hodge chapters use this literature most directly. In the Yang-Mills model, a finite graph with ten global and corridor-sensitive nodes becomes the benchmark architecture for calculating stress-weighted adjacency, gauge potential, triangular curvature, action and spectral separation. In the Hodge model, a weighted regional network is transformed into an edge cochain whose decomposition separates hierarchy from curl imbalance and harmonic systemic circulation. The BSD model uses network structure as part of its regional local-to-global rank architecture; the Navier-Stokes model uses network and systemic-risk literature to interpret liquidity-flow stress channels and macro-financial shock propagation. In all four cases, network structure is not a decorative metaphor. It is the bridge between observed or constructed inputs and systemic interpretation (Yang & Mills, 1954; Wilson, 1974; Jiang et al., 2011; Schaub et al., 2020).

The literature also clarifies why network models require validation discipline. Graph measures can be visually persuasive but empirically weak if they are not tied to clear input definitions, reproducible edge construction, robustness checks and inferential boundaries. Centrality, density, clustering, transitivity, algebraic connectivity, spectral radius and community structure are meaningful only if the node set, edge weights and transformation rules are declared. This is why the monograph repeatedly separates public data anchors from author-calculated network objects. A network index is not

automatically an official economic fact; it is a constructed measurement object requiring replication, sensitivity analysis and claim-boundary discipline (Fiedler, 1973; Chung, 1997; von Luxburg, 2007; Carlsson, 2009).

3.2.4. Financial Systemic Risk, Contagion and Network Fragility

The financial systemic-risk literature constitutes the second pillar. Research on financial contagion, clearing networks, interbank obligations, systemic capital shortfall, CoVaR, DebtRank, liquidity commonality and leverage amplification demonstrates that modern financial systems cannot be understood through the standalone risk of each institution or country. The risk contribution of an institution depends on who is exposed to it, how liabilities are distributed, whether fire sales affect common asset prices, whether funding liquidity dries up simultaneously, and whether one failure imposes balance-sheet pressure on others (Allen & Gale, 2000; Eisenberg & Noe, 2001; Gai & Kapadia, 2010; Battiston et al., 2012).

Allen and Gale, Eisenberg and Noe, Adrian and Brunnermeier, Acharya and Pedersen, Brunnermeier and Pedersen, Acemoglu, Ozdaglar and Tahbaz-Salehi, Battiston and colleagues, and related systemic-risk researchers provide the analytical logic for the monograph's shock-propagation language. The common conclusion is that systemic risk is not simply high volatility, high debt or high inflation. It is a condition in which interdependence, common exposure, liquidity constraints and feedback loops make local stress capable of producing broader instability. This directly supports the Yang-Mills concept of a local-to-systemic transition threshold and the Navier-Stokes concept of a pressure-friction-shock stress balance (Allen & Gale, 2000; Eisenberg & Noe, 2001; Adrian & Brunnermeier, 2016; Battiston et al., 2012).

The Navier-Stokes framework draws particularly heavily on liquidity and systemic-risk traditions. Market liquidity, funding liquidity, commonality in liquidity, sovereign spreads, crisis regimes and macroprudential stress indicators form the empirical background for interpreting liquidity velocity weakness, pressure gradients, friction/diffusion and external shocks. The key methodological contribution is not the assertion that finance is fluid mechanics. Rather, the literature justifies the view that liquidity pressure behaves as a coupled system: weak flow, pressure gradients and friction can interact in ways that produce systemic vulnerability (Acharya & Pedersen, 2005; Brunnermeier & Pedersen, 2009; Adrian & Brunnermeier, 2016).

The Yang-Mills framework uses systemic-risk literature to sharpen the idea of threshold. Financial contagion studies show that a system can change regime when exposure, leverage or connectivity crosses a critical level. The monograph's finite-network mass-gap analogy formalizes this intuition through spectral separation: below a benchmark threshold, shocks are interpreted as locally absorbable; above it, they become systemically transmissible. The claim remains bounded because the threshold is calculated within a finite stress-weighted benchmark graph, not as a universal law of financial contagion. The literature justifies the analogy but does not remove the need for robustness checks, scenario simulations and future panel validation (Acemoglu et al., 2015; Gai & Kapadia, 2010; Battiston et al., 2012; Fiedler, 1973).

3.2.5. Production Networks, Global Value Chains and Sectoral Shock Propagation

Production-network and global-value-chain literature provides a third major foundation for Section 3.2. Input-output linkages, supply chains, vertical specialization and firm-level production networks show that macroeconomic shocks can originate from microeconomic or sectoral disturbances. Acemoglu, Carvalho, Ozdaglar and Tahbaz-Salehi, Gabaix, Carvalho, Caliendo and Parro, Costinot and Rodriguez-Clare and related trade-network literatures demonstrate that aggregate fluctuations may emerge from networked production, not only from aggregate demand or aggregate supply shocks (Acemoglu et al., 2012; Gabaix, 2011; Carvalho, 2014; Carvalho & Tahbaz-Salehi, 2019).

This literature matters for the monograph because it legitimizes the transition from macro aggregates to structural propagation channels. If production networks transmit idiosyncratic shocks through supplier-customer chains, then regional and corridor networks can transmit macroeconomic stress through logistics, trade, energy, finance and policy channels. The logic is parallel even when the data object differs. Input-output models often use sector-by-sector transaction matrices; the monograph's Yang-Mills, Hodge and BSD chapters often use regional public anchors and author-constructed corridor weights. The shared conceptual point is that economic structure is relational and that aggregate outcomes may depend on the topology of relations (Acemoglu et al., 2012; Carvalho, 2014; Antras & Chor, 2013; Costinot & Rodriguez-Clare, 2014).

Production-network literature also helps distinguish output mass from structural importance. A large sector or region may dominate aggregate output, but a smaller sector or corridor can be essential if it occupies a non-substitutable position. This distinction supports the monograph's repeated treatment of the Caucasus, Central Asia, corridor routes and bridge nodes. Their relevance is not based on claiming output equivalence with major macro-regions; it is based on the idea that propagation role may differ from scale. The Hodge model captures this through hierarchy, imbalance and harmonic circulation; the Yang-Mills model through BridgeStress, fragility and threshold compression; the BSD model through

corridor exposure and local-to-global rank signals (Carvalho & Tahbaz-Salehi, 2019; Caliendo & Parro, 2015; Christopher & Peck, 2004).

A further lesson from production-network research concerns heterogeneity. The same shock can have different consequences depending on the structure it enters. A supply-chain shock, financial-spread shock, energy/geopolitical shock or logistics disturbance will not propagate uniformly across regions. It will interact with trade dependence, substitution possibilities, network redundancy, income depth, resilience buffers and policy capacity. For this reason, the monograph does not treat shocks as scalar impulses only. It treats them as structured disturbances whose systemic effect must be measured through networks, flows, thresholds and validation gates (Gabaix, 2011; Acemoglu et al., 2012; Tang, 2006; Sheffi, 2005).

3.2.6. Corridor Economics, Logistics Resilience and Strategic Bridge Nodes

Corridor economics and supply-chain resilience supply the fourth pillar. Transport corridors, port systems, energy routes, rail and maritime interfaces, border crossings, chokepoints and regional logistics hubs create forms of systemic relevance that are not visible in GDP tables. The literature on supply-chain disruption, resilience, survivability, redundancy, route vulnerability and logistics performance shows that a corridor can be strategically important because it concentrates routes, connects otherwise separated markets, or offers substitute capacity during geopolitical disruption (Christopher & Peck, 2004; Sheffi, 2005; Tang, 2006; Antras & Chor, 2013).

This literature is central to the Yang-Mills, BSD and Hodge parts of the monograph. The Yang-Mills model explicitly treats global and corridor-sensitive nodes as a stress network. Its BridgeStress logic separates corridor strategic exposure from pure centrality or output mass. The BSD model incorporates corridor stress into a local-to-global structural-rank architecture. The Hodge model retains the Caucasus as an explicit subregional node to prevent corridor-sensitive structure from disappearing inside broader regional aggregates. These choices reflect a common literature gap: many trade and macroeconomic models recognize geography, infrastructure and market access, but fewer combine corridor exposure with topological stress measures, spectral thresholds, local-to-global rank diagnostics and econometric claim gates (Christopher & Peck, 2004; Sheffi, 2005; Tang, 2006; Caliendo & Parro, 2015).

The corridor literature also changes how the monograph interprets small regions. A small node can be negligible in output share but material in route vulnerability, shock transmission, energy interface, logistics substitution or strategic resilience. This is not an argument for exaggerating its economic mass. It is an argument for measuring a different object: positional exposure. In a corridor-sensitive framework, a bridge node may amplify or absorb stress because of where it sits. That role can be evaluated through BridgeStress, centrality, local-cycle imbalance, harmonic circulation, stress thresholds, scenario shocks and robustness screens (Costinot & Rodriguez-Clare, 2014; Antras & Chor, 2013; Carvalho & Tahbaz-Salehi, 2019).

This section therefore treats corridor economics not as a regional-policy side topic but as a systemic-risk literature. When a trade/logistics or geopolitical shock occurs, the question is not only which economies are large, but which routes, interfaces and bridges convert disturbance into wider stress. The monograph's methodological novelty lies in linking this corridor literature to mathematical-economic analogues: Hodge decomposition for flow structure, Yang-Mills gauge curvature for stress concentration, BSD local-to-global logic for rank formation and Navier-Stokes stress balance for liquidity-pressure dynamics (Sheffi, 2005; Tang, 2006; Christopher & Peck, 2004).

3.2.7. Spectral Graph Theory and Thresholds in Systemic Transmission

Spectral graph theory provides the mathematical language through which connectivity can be translated into threshold, stability and diffusion concepts. The graph Laplacian, algebraic connectivity, spectral radius, eigenvalue separation, sparsification and diffusion dynamics allow researchers to move beyond visual network description. In economic applications, spectral methods help identify whether a system is connected, how quickly shocks diffuse, whether bottlenecks exist, whether communities are weakly tied and whether a first positive mode can be interpreted as a transition threshold (Fiedler, 1973; Chung, 1997; von Luxburg, 2007).

The Yang-Mills chapter makes spectral logic explicit by defining the economic mass gap as the first positive eigenvalue of a stress-weighted graph Laplacian in a finite weighted network. This spectral separation becomes the benchmark measure of local-to-systemic transition. The Hodge chapter uses spectral and higher-order Hodge-Laplacian diagnostics as part of its topological macro-flow architecture. The Perelman/Ricci/Poincare chapter uses graph Laplacian connectedness and Betti diagnostics to test whether the inequality system forms a connected diagnostic manifold. The Riemann/Zeta chapter extends spectral thinking into time-series and frequency-domain diagnostics by using Fourier, wavelet and spectral-entropy screens.

Across the monograph, spectral language therefore becomes a cross-domain evidence gate: it translates connectedness, cycles, thresholds and regimes into measurable objects (Fiedler, 1973; Chung, 1997; Yang & Mills, 1954; Wilson, 1974).

The literature also warns against overinterpretation. A spectral gap in a graph is not automatically a causal shock threshold in the world economy. It depends on node construction, edge weighting, normalization, data quality and model purpose. Therefore, the monograph treats spectral outputs as benchmark or diagnostic evidence unless supported by independent validation layers. This is especially important in the Yang-Mills chapter: the finite-network mass gap is meaningful within the declared graph, but stronger causal country-panel claims require the specified N = 1,500 validation architecture. Likewise, Hodge and Perelman spectral/topological diagnostics support structural interpretation, not theorem proof or universal causality (von Luxburg, 2007; Carlsson, 2009; Ghrist, 2008).

Table 3.2.2. Transmission concepts and their econometric-operational translation

Transmission concept	Relevant literature family	Operational translation in the monograph	Main model location
Connectivity	Complex networks; spectral graph theory; systemic risk.	Graph connectedness, density, degree, transitivity, algebraic connectivity and edge-weight adequacy.	Hodge, Yang-Mills, Perelman/Ricci/Poincare, BSD.
Contagion	Financial networks; interbank clearing; CoVaR; DebtRank; liquidity spirals.	Local disturbance becomes systemically transmissible through exposure, stress, leverage, friction or common channels.	Navier-Stokes, Yang-Mills, P-vs-NP.
Corridor exposure	Trade networks; global value chains; logistics resilience; route vulnerability.	BridgeStress, corridor weights, scenario shocks and small-node strategic exposure.	Yang-Mills, BSD, Hodge.
Flow decomposition	Discrete Hodge theory; topological signal processing; graph flows.	Gradient hierarchy, curl imbalance and harmonic systemic circulation.	Hodge; also supports BSD and Yang-Mills.
Shock threshold	Spectral graph theory; systemic risk; stress testing.	First positive stress-Laplacian mode or threshold compression under scenarios.	Yang-Mills; supported by Navier-Stokes.
Stress balance	Liquidity risk; macroprudential stress testing; flow-balance analogies.	Velocity weakness, pressure gradients, friction/diffusion, shocks, cycles and restricted closure.	Navier-Stokes.
Local-to-global rank formation	BSD local-to-global mathematics; regional economics; economic complexity.	Finite-state regional traces, Euler-factor analogues, economic LOrder and structural rank.	BSD; supported by Hodge and Yang-Mills.
Regime transmission	Inflation forecasting; Markov switching; crisis regimes; spectral diagnostics.	Stress-regime identification, shock anchors, zeta-cycle deviations and forecast validation layers.	Riemann/Zeta; supports Navier-Stokes.

3.2.8. Hodge and Topological Macro-Flow Literature

The Hodge literature provides one of the most important conceptual innovations for network economics: it allows flows on edges to be decomposed into structurally distinct components. In a graph or simplicial setting, a directed edge signal can contain a gradient component, a curl component and a harmonic component. Translated into economic language, this supports the distinction between hierarchy, local-cycle imbalance and persistent systemic circulation. The Hodge model in the monograph uses this logic to show that the world economy is not reducible to GDP hierarchy alone. It contains local imbalances and residual circulation patterns that remain after hierarchy is removed (Hodge, 1941; Jiang et al., 2011; Schaub et al., 2020).

The literature on combinatorial Hodge theory, statistical ranking, graph flows, topological signal processing and higher-order networks is particularly relevant because economic networks often contain cycles. A cycle is not simply redundant geometry. It may indicate local imbalance, circular trade pressure, regional feedback, corridor dependence, arbitrage-like structural tension or persistent residual circulation. Standard node centrality does not fully capture this. Hodge decomposition allows the analyst to ask whether observed or constructed edge pressure is mostly hierarchical, locally circular or systemically persistent (Jiang et al., 2011; Schaub et al., 2020; Ghrist, 2008; Carlsson, 2009).

In the monograph, this logic supports both direct and indirect uses. Directly, the Hodge chapter constructs a regional macro-flow pressure field and decomposes it into gradient, curl and harmonic components. Indirectly, the Hodge logic supports the BSD structural-rank construction by allowing Hodge-flow rank to become one component of structural rank. It supports Yang-Mills by clarifying why triangular curvature and action concentrate stress in cycles rather than merely on nodes. It also supports the corridor interpretation of small nodes, because a small region can have nonzero circulation or local imbalance even if its output mass is limited (Jiang et al., 2011; Schaub et al., 2020).

The Hodge literature also contributes to validation discipline. A decomposed flow is meaningful only if the projection is reproducible, orthogonality conditions are audited, residuals are checked and robustness tests show that the decomposition does not collapse under reasonable perturbation. The Hodge manuscript therefore uses econometric, predictive and topological tests as internal benchmark-validation diagnostics rather than final causal estimates. In the integrated literature review, this becomes a broader rule: network decomposition is a powerful measurement architecture, but it must be accompanied by explicit data status, validation status and claim status (Jiang et al., 2011; Schaub et al., 2020; Carlsson, 2009).

3.2.9. Yang-Mills Gauge Analogy, Curvature and Action in Economic Stress Networks

The Yang-Mills part of the literature review occupies the intersection of network science, spectral graph theory, systemic risk and gauge-theoretic analogy. In physical mathematics, Yang-Mills theory involves gauge fields, curvature, action and mass-gap questions. The monograph does not transfer the physical theorem into economics. Instead, it uses the structural grammar of gauge potential, curvature and action to measure stress concentration on a finite economic network. The analytical question becomes economic: can a finite corridor-sensitive stress graph produce a reproducible threshold separating locally absorbable from systemically transmissible shocks? (Yang & Mills, 1954; Wilson, 1974; Fiedler, 1973; Chung, 1997)

Gauge-theoretic language is useful because systemic stress often has directional and relational properties. A stress difference between two nodes is not only a scalar gap; it can be interpreted as a directed edge potential. When edge potentials form triangles or cycles, their inconsistency or circulation can be interpreted as curvature-like stress. Aggregating curvature over cycles produces action-like concentration. The economic meaning is not physical field energy; it is the concentration of systemic stress in a limited set of network cycles. This supports a more refined literature position than simple centrality: a node or corridor can matter not only because it is connected, but because it participates in high-curvature stress cycles (Yang & Mills, 1954; Wilson, 1974; Battiston et al., 2012; Fiedler, 1973).

The Yang-Mills chapter's literature review identifies a gap that Section 3.2 adopts for the monograph: network science explains connectivity and cascades; financial systemic-risk literature explains contagion; input-output and GVC literature explains production propagation; corridor literature explains logistics vulnerability; spectral graph theory explains thresholds; gauge theory explains curvature/action language; econometrics supplies validation discipline. No single literature combines all of these into a finite-network gauge-econometric architecture. The monograph's contribution is therefore synthetic and methodological rather than theorem-solving (Acemoglu et al., 2015; Carvalho & Tahbaz-Salehi, 2019; Christopher & Peck, 2004; Schaub et al., 2020).

This also explains the importance of claim hierarchy. The finite-network mass gap may be strong benchmark evidence if it is positive, interpretable and robust under graph filtering and Monte Carlo perturbation. It becomes stronger if scenario simulations show coherent threshold compression under inflation, financial-spread, trade/logistics or geopolitical shocks. However, it remains a benchmark and diagnostic claim until the country-year validation layer is populated and estimated. The literature supports the threshold analogy; it does not license universal causal inference (Yang & Mills, 1954; Wilson, 1974; Chung, 1997; von Luxburg, 2007).

3.2.10. BSD Local-to-Global Transmission and Structural Rank Literature

The BSD literature enters Section 3.2 through local-to-global transmission rather than through network theory alone. In its classical mathematical setting, BSD connects local arithmetic data and L-function behavior to global rank on an elliptic

curve. The economic analogue in the monograph asks whether local regional states, represented through stress, corridor exposure, finite-state reductions and trace/Euler-factor analogues, contain measurable information about global structural economic rank. This is a local-to-global transmission question: how do local conditions aggregate into global structure? (Birch & Swinnerton-Dyer, 1965; Wiles, 1995; Gross & Zagier, 1986; Kolyvagin, 1990)

The BSD literature review is deliberately interdisciplinary. It includes local-to-global number theory, but it also includes network science, Hodge/topological decomposition, regional economics, corridor transmission, economic complexity, productivity and robust panel validation. This combination is necessary because the economic object is not an elliptic curve. It is a regional world-economy measurement system in which public macro-regional anchors are transformed into systemic stress, weighted network structure, economic curve coefficients, finite-state traces, Euler factors, economic L-function behavior, LOrder and structural rank. The network literature supplies the transmission architecture; the local-to-global literature supplies the measurement grammar; econometrics supplies the claim gate (Birch & Swinnerton-Dyer, 1965; Wiles, 1995; Acemoglu et al., 2012; Jackson, 2008).

The BSD chapter is especially important for integrating corridor economics into rank formation. Corridor exposure and BridgeStress are not merely supplementary variables; they affect how local regional signals enter the global structural-rank interpretation. This allows the monograph to review systemic-risk and regional-transmission literatures as part of a broader rank problem. A region is not ranked only by GDP. It may obtain structural rank through productive depth, network position, Hodge-flow exposure, agentic capacity, corridor leverage and stress absorption. Local stress and local network position therefore become information about global structural formation (Costinot & Rodriguez-Clare, 2014; Caliendo & Parro, 2015; Christopher & Peck, 2004; Sheffi, 2005).

The literature gap is clear: systemic-risk research explains contagion but usually not BSD-style rank correspondence; regional economics explains market access and corridors but often not local-to-global trace logic; economic-complexity literature explains productive capabilities but does not generate Euler-factor analogues or LOrder; econometric literature explains validation but not the substantive mathematical-economic architecture. The BSD chapter fills this gap by assigning a strong calibrated measurement claim while refusing theorem-level proof, causal law or strong external validation when the evidence is only directional (Birch & Swinnerton-Dyer, 1965; Acemoglu et al., 2015; Jiang et al., 2011; Rosenbaum, 1987).

3.2.11. Navier-Stokes Liquidity-Flow Stress, Friction and Shock-Closure Literature

The Navier-Stokes component brings macro-financial stress testing into the network and shock-propagation review. Its literature foundation includes flow-balance mathematics, liquidity risk, market microstructure, systemic-risk finance, financial-stress indices, macroprudential policy, forecasting, robust panel econometrics, composite-index construction and external validation. The central claim is not that money or credit are physical fluids. Rather, the flow-balance literature provides a structured grammar: velocity, acceleration, pressure gradient, friction or diffusion, external forcing and closure (Leray, 1934; Caffarelli et al., 1982; Kato, 1984; Constantin & Fefferman, 1993).

Liquidity-risk and systemic-risk literatures justify this grammar economically. Liquidity can weaken, funding constraints can tighten, spreads can widen, balance-sheet pressures can propagate, volatility can increase and common exposure can amplify shocks. The Navier-Stokes-inspired model translates these ideas into a nondimensional stress-balance system. Heterogeneous raw variables are not added directly; they are transformed into unit-free stress-direction components. A restricted closure term prevents the residual from becoming a free algebraic plug. Rolling validation, benchmark comparison, fixed effects, robustness checks, external-target validation, Monte Carlo uncertainty and policy counterfactuals supply the evidence discipline (Acharya & Pedersen, 2005; Brunnermeier & Pedersen, 2009; Adrian & Brunnermeier, 2016; Acemoglu et al., 2015).

Within Section 3.2, the Navier-Stokes literature plays two roles. First, it explains systemic stress as an interaction among flow weakness, pressure, friction and shock. This complements Yang-Mills threshold logic by showing the channels through which stress accumulates before crossing a threshold. Second, it provides an empirical panel-stress-testing counterpart to the regional benchmark models. While Hodge and Yang-Mills begin from regional/corridor networks, the Navier-Stokes model uses a 100-country annual panel and a World aggregate anchor to audit stress-channel associations across a wider global design. This strengthens the monograph's literature position by showing that systemic transmission can be studied both through finite benchmark networks and broader panel stress-testing architectures (Diebold & Mariano, 1995; Clark & West, 2007; Arellano, 1987; Driscoll & Kraay, 1998).

The same caution applies: the literature supports a high but bounded claim. The model can support global systemic-stress diagnostics and stress testing within the reported empirical design. It cannot claim literal hydrodynamic identity,

theorem-level PDE proof, definitive causality or universal crisis prediction. In the integrated literature review, this becomes an exemplar of responsible analogy: mathematical structure is used to organize measurement, not to replace economic inference (Leray, 1934; Brunnermeier & Pedersen, 2009; Diebold & Mariano, 1995).

3.2.12. Supporting Stress-Regime, Inequality-Network and Optimization Literatures

Although Section 3.2 is centered on Yang-Mills, Hodge, BSD and Navier-Stokes, the other three models also contribute to the network and systemic-risk review. The Perelman/Ricci/Poincare model contributes a coupled pressure-smoothing view of inequality. Its sixteen-variable diagnostic system treats inequality, productivity, unemployment, investment, inflation, migration, education, mobility, logistics, capital flows, innovation, health, fiscal pressure, openness, social protection and technology access as a connected macro-social pressure manifold. This supports the broader claim that systemic deformation may arise from multi-channel coupling rather than one indicator alone (Hamilton, 1982; Perelman, 2002; Forman, 2003; Ollivier, 2009).

The Riemann/Zeta inflation-forecasting model contributes temporal and spectral stress-regime logic. Global inflation shocks do not merely increase a scalar variable. They occur in regimes, crisis clusters and nonlinear pressure cycles. The zeta-cycle layer, Fourier/wavelet diagnostics, Markov-switching screens and forecast-validation architecture support a temporal analogue of propagation: stress transmits through time, policy reaction, liquidity instability, supply pressure and financial conditions. Thus, the Riemann/Zeta literature enriches Section 3.2 by showing that shock propagation is both network-spatial and dynamic-temporal (Riemann, 1859; Hardy, 1914; Diebold & Mariano, 1995; Clark & West, 2007).

The P-vs-NP portfolio-optimization model contributes a computational-risk perspective. Portfolio risk is not only about expected return and volatility; it is also about support selection, covariance dependence, search-space explosion, heuristic reliability, stress scenarios and robustness under frictions. Sparse portfolio selection creates a mixed discrete-continuous optimization problem. The literature on computational finance, cardinality constraints, metaheuristics, covariance modelling and derivative overlays therefore shows that systemic exposure can arise from the interaction between risk geometry and computational tractability. This does not make the P-vs-NP chapter a network-systemic-risk chapter in the same sense as Yang-Mills or Hodge, but it adds an essential reviewer-safe point: robustness and search discipline are themselves part of systemic financial modelling (Markowitz, 1952; Sharpe, 1964; Black & Scholes, 1973; Karp, 1972).

Table 3.2.3. Cross-model literature gap synthesis for network economics and shock propagation

Literature stream	What prior literature explains well	What remains incomplete for this monograph	Monograph response
Complex networks	Connectivity, centrality, communities, cascades, weighted paths and multilayer relations.	Does not by itself convert macroeconomic stress into calibrated economic thresholds or rank objects.	Combines graph construction with Hodge decomposition, Yang-Mills stress thresholds and BSD local-to-global rank.
Financial systemic risk	Interbank contagion, liquidity spirals, CoVaR, DebtRank, clearing networks and common exposures.	Often focuses on financial institutions rather than global corridor, regional rank and macro-flow topology.	Extends systemic-risk logic to corridor stress, liquidity-flow panels, benchmark networks and stress scenarios.
Production and GVC networks	Input-output propagation, sectoral shocks, value-chain dependence and micro-to-macro amplification.	Usually lacks gauge-curvature, spectral mass-gap, Hodge-flow or BSD-style LOrder interpretation.	Uses GVC/corridor logic as the economic substrate for flow, threshold and local-to-global models.
Corridor and supply-chain resilience	Disruption, route vulnerability, substitutability, logistics resilience and chokepoints.	Often lacks formal topological decomposition, spectral thresholds and robust claim hierarchy.	Introduces BridgeStress, corridor weights, scenario threshold compression and subregional visibility.
Spectral and topological methods	Connectivity, algebraic separation, cycles, persistence and higher-order structure.	Mathematical tools are often not fully integrated into macro-corridor econometrics.	Embeds Laplacians, Hodge projections, Betti diagnostics and spectral thresholds inside economic

Literature stream	What prior literature explains well	What remains incomplete for this monograph	Monograph response
			measurement pipelines.
Econometric validation	Robust inference, panel diagnostics, sensitivity analysis, forecast validation and falsification logic.	Econometrics alone does not define the substantive network object or mathematical analogy.	Uses validation gates after network construction to separate measurement, diagnostics, forecasting and causal restraint.

3.2.13. Integrated Interpretation: From Propagation Channels to Claim-Gated Measurement

The literature reviewed in Section 3.2 supports a coherent integrated interpretation: systemic transmission is a structural phenomenon. It is not reducible to a single shock, a single variable, a single regression coefficient or a single centrality score. Transmission emerges when local stress interacts with network position, flow pressure, friction, corridor exposure, financial interdependence, production linkages, cycle structure, spectral separation, resilience buffers and validation constraints. The monograph's distinctive contribution is to formalize this insight across seven different Millennium-inspired economic analogues (Newman, 2003; Jackson, 2008; Acemoglu et al., 2015; Carvalho & Tahbaz-Salehi, 2019).

The four core models of this section each answer a different propagation question. Hodge asks: how can macro-flow pressure be decomposed into hierarchy, local imbalance and systemic circulation? Yang-Mills asks: when does stress in a finite corridor network cross a measurable threshold from local absorption to systemic transmission? BSD asks: do local regional reductions and Euler-factor-like signals contain information about global structural rank? Navier-Stokes asks: how do liquidity weakness, pressure gradients, friction, stochastic shocks, cycles and closure combine into systemic stress? Together, these models transform the network literature into a monographic architecture for measuring economic propagation (Jiang et al., 2011; Schaub et al., 2020; Yang & Mills, 1954; Birch & Swinnerton-Dyer, 1965; Leray, 1934).

The supporting models complete the architecture. Perelman/Ricci/Poincare shows that inequality pressure is coupled, connected and deformation-sensitive. Riemann/Zeta shows that macro-financial pressure also has regime, spectral and forecast-validation dimensions. P-vs-NP shows that financial risk modelling must confront computational complexity, heuristic search, covariance geometry and robustness gates. These perspectives prevent Section 3.2 from becoming a narrow network-science review. It becomes an integrated literature review of systemic economic structure (Hamilton, 1982; Perelman, 2002; Riemann, 1859; Karp, 1972).

The claim hierarchy follows directly from this literature. Strong benchmark evidence is permitted when the network object is constructed transparently, the result is reproducible, and robustness tests support it. Strong measurement evidence is permitted when constructed variables produce coherent internal diagnostics and are bounded by lineage and validation rules. Diagnostic association is permitted when econometric tests support signs or relationships without causal identification. Forecasting claims are permitted only within declared validation windows and benchmark comparisons. Future validation claims are permitted only as specified pathways, not as completed evidence. This claim-gated structure is one of the monograph's main methodological contributions (Bland & Altman, 1986; Rosenbaum, 1987; Lipsitch et al., 2010; Imai et al., 2010).

3.2.14. Section Conclusion and Transition to Topological and Spectral Methods

Section 3.2 has integrated the literatures required to treat the world economy as a connected system of networks, flows, corridors and shock-propagation channels. The review shows that the monograph is not built on isolated mathematical metaphors. It is grounded in a large interdisciplinary literature on complex networks, financial contagion, production networks, corridor resilience, spectral thresholds, topological decomposition, liquidity stress testing, macro-financial regimes and econometric validation. The strongest conclusion is that network structure changes economic interpretation: size matters, but position, flow, threshold, corridor exposure, resilience and validation status also matter (Watts & Strogatz, 1998; Acemoglu et al., 2015; Jiang et al., 2011; Brunnermeier & Pedersen, 2009).

The review also defines what the monograph adds. Existing literatures explain many components of systemic transmission, but they rarely combine them into one claim-disciplined mathematical-economic architecture. The monograph does so through seven analogues: Hodge decomposes flow, Yang-Mills measures threshold and curvature/action, BSD connects local regional signals to structural rank, Navier-Stokes measures liquidity-flow stress, Perelman/Ricci/Poincare measures pressure-smoothing deformation, Riemann/Zeta measures spectral inflation regimes, and P-vs-NP measures computational risk in sparse optimization. This integrated review therefore prepares the next subsection, 3.3, where

topological and spectral methods are examined more directly as formal economic measurement tools (Yang & Mills, 1954; Birch & Swinnerton-Dyer, 1965; Leray, 1934; Riemann, 1859; Karp, 1972).

Table 3.2.4. Claim-boundary matrix for Section 3.2

Claim type	Allowed formulation in this literature-review section	Forbidden overclaim	Evidence gate
Network measurement claim	Economic systems can be represented as constructed networks when nodes, edges, weights and transformations are disclosed.	The network is the economy itself or an official institutional flow matrix.	Data lineage, edge construction, sensitivity checks and replication package.
Systemic-risk diagnostic claim	Stress propagation can be interpreted through connectedness, exposure, liquidity pressure and shock channels.	Diagnostic association proves unrestricted causality.	Robust inference, external validation, placebo/falsification and bounded wording.
Finite-threshold claim	A finite stress-weighted graph may have an interpretable spectral threshold inside the benchmark.	The threshold is a universal law or a proof of a mathematical Millennium problem.	Spectral calculation, graph filtering, Monte Carlo perturbation and scenario coherence.
Flow-decomposition claim	Directed macro-flow pressure can be decomposed into hierarchy, local imbalance and systemic circulation.	The decomposition equals observed dyadic trade or financial transactions.	Projection audit, residual check, robustness tests and topological validation.
Local-to-global claim	Local regional signals may be informative about constructed global structural rank.	Economic results prove BSD or establish causal global rank law.	Rank-gap, agreement, negative control, residualization and external-screening gates.
Stress-testing claim	Liquidity-flow, pressure, friction and shock variables can support a bounded macro-financial stress-testing architecture.	The model is a physical fluid law or unconditional crisis predictor.	Nondimensionalization, panel diagnostics, rolling validation and counterfactual uncertainty.

3.3. Topological and Spectral Methods in Economics

Integrated Review of Hodge, Ricci/Poincare, Yang-Mills, Riemann-Zeta and Supporting Millennium-Inspired Economic Analogues

3.3.1. Function of this Section within the Integrated Literature Review

This section integrates the literature on topological and spectral methods in economics as it supports the monograph's use of Hodge decomposition, Ricci/Poincare graph diagnostics, Yang-Mills finite-network curvature and Riemann-Zeta spectral-cycle forecasting. The section does not present four separate article-level reviews. It constructs one unified literature review in which topology, graph Laplacians, curvature, homology, spectral thresholds, frequency-domain signals, zeta-cycle construction, network validation and claim-boundary discipline are treated as one methodological field of economic measurement (Gondauri, 2026a, 2026b, 2026d, 2026f).

The rationale for this integration is methodological. Modern economic systems are not only collections of scalar indicators; they are structured objects with connectivity, direction, cycles, bottlenecks, eigenmodes, shock paths, latent regimes and nonlinear oscillations. Network economics and systemic-risk literature already show that topology matters for propagation and amplification (Allen and Gale, 2000; Haldane and May, 2011; Acemoglu et al., 2012; Elliott, Golub and Jackson, 2014). Topological data analysis, graph signal processing and spectral graph theory add a further layer: they make it possible to measure connectedness, cycles, harmonic residuals, curvature-like distortion, spectral separation and persistent structure rather than only node-level size or pairwise correlation (Chung, 1997; Ghrist, 2008; Carlsson, 2009; Shuman et al., 2013; Ortega et al., 2018).

The main source blocks are Hodge, Ricci/Poincare, Yang-Mills and Riemann/Zeta. Hodge supplies the language of decomposable edge flows. Ricci/Poincare supplies curvature, smoothing, entropy and connectedness language. Yang-Mills supplies gauge potential, curvature, action and finite-network spectral threshold language. Riemann/Zeta supplies spectral-cycle and critical-line signal language. The remaining three source models also enter the section: BSD through L-function and local-to-global spectral ordering, Navier-Stokes through Fourier GDP-cycle forcing and flow-pressure dynamics, and P-vs-NP through covariance eigenstructure, algorithmic search and complexity-validation gates (Gondauri, 2026c, 2026e, 2026g).

Table 3.3.1. Integrated topological and spectral literature transfer across the seven monograph models

Source model	Topological/spectral object	Economic function in the monograph	Primary claim boundary
Hodge	Graph, edge cochain, Hodge Laplacian, gradient/curl/harmonic decomposition and persistent-homology checks.	Measures macro-flow hierarchy, local-cycle imbalance, harmonic systemic circulation, shock exposure and resilience.	Economic flow decomposition only; no Hodge Conjecture claim.
Perelman/Ricci/ Poincare	Metric tensor analogue, Ricci-style component curvature, Perelman F/W functionals, graph connectedness, Betti diagnostics and edge-curvature proxies.	Measures inequality pressure, smoothing capacity, deformation, entropy-like complexity and connected macro-social structure.	Diagnostic curvature/topology only; no proof/test/replication of Perelman, Ricci flow or Poincare.
Yang-Mills	Gauge potential, triangular curvature, Yang-Mills action, stress Laplacian, spectral radius and finite-network mass-gap index.	Measures stress circulation, action concentration, shock threshold and corridor fragility in a finite weighted network.	Finite weighted-graph benchmark only; no physical gauge field or mathematical mass-gap proof.
Riemann/Zeta	Critical-line inspired zeta-cycle, normalized spectral signal, zeta deviation, spectral entropy, Fourier and wavelet screens.	Adds nonlinear spectral-cycle correction and crisis-regime diagnostics to global inflation forecasting.	Forecast-diagnostic signal only; no Riemann Hypothesis proof, test or verification.
BSD	Finite-state traces, Euler-factor analogues, constructed economic L-function and LOrder.	Connects local regional signals with global structural rank through local-to-global spectral ordering logic.	Calibrated economic L-function analogue; no arithmetic BSD claim.
Navier-Stokes	Flow-pressure-friction balance with Fourier cycle forcing and restricted closure.	Connects temporal cycles, liquidity pressure and systemic stress propagation.	Nondimensional stress-testing analogue; no hydrodynamic identity.
P-vs-NP	Covariance eigenstructure, combinatorial search space, exact reduced enumeration and heuristic search diagnostics.	Links spectral risk geometry with optimization complexity and validation status.	Empirical-computational optimization claim only; no P vs NP proof.

Source: Author synthesis based on the seven source manuscripts and the integrated topological, spectral, network and econometric literature (Gondauri, 2026a-g).

3.3.2. Topology as an Economic Measurement Language

Topology enters economics when the relevant object is relational structure rather than isolated magnitude. In a purely scalar view, a region is described by GDP, growth, inflation, inequality or credit conditions. In a topological view, a region is also described by its position in a network: its edges, cycles, bridges, connected components, bottlenecks and higher-order interactions. This shift is consistent with network economics, input-output propagation and systemic-risk literature, where aggregate outcomes depend not only on shocks at individual nodes but also on the structure through which those shocks move (Acemoglu et al., 2012; Acemoglu, Ozdaglar and Tahbaz-Salehi, 2015; Gai and Kapadia, 2010; Battiston et al., 2012).

For the monograph, topology performs three roles. First, it defines connectedness: whether the constructed economic system is one system or a set of disconnected pieces. Second, it defines circulation and cycles: whether stress, flow or imbalance is locally trapped, globally transmitted or harmonically persistent. Third, it defines robustness: whether a graph remains structurally meaningful under thresholding, perturbation, alternative edge construction or validation checks. These roles are central to the Hodge, Perelman/Ricci/Poincare and Yang-Mills models, and they also support BSD local-to-global rank logic and Navier-Stokes systemic-stress propagation (Gondauri, 2026a, 2026b, 2026c, 2026d, 2026e).

The topological-data-analysis literature provides the general methodological base for such measurement. Persistent homology and related tools were developed to identify stable shape features in data, including connected components, loops and higher-dimensional voids under changing thresholds (Edelsbrunner, Letscher and Zomorodian, 2002; Zomorodian and Carlsson, 2005; Ghrist, 2008; Carlsson, 2009; Edelsbrunner and Harer, 2010). In economics, the transfer must be bounded. A Betti number or persistence barcode does not prove that an economy has a literal geometric shape. It provides a diagnostic summary of the constructed relational object under a specified graph, metric or filtration (Gondauri, 2026a, 2026b).

$$EconomicTopology_t = (Nodes_t, Edges_t, Weights_t, Cycles_t, SpectralDiagnostics_t, ValidationGate_t)$$

The monograph treats topology as an auditable measurement architecture. A topological claim requires node definition, edge construction, weighting, cycle or component diagnostics, spectral checks and validation gates.

3.3.3. Hodge Theory, Discrete Hodge Decomposition and Economic Flow Systems

Hodge theory originally provides a deep bridge between geometry, topology and harmonic analysis. In its classical setting, it relates differential forms, cohomology classes and harmonic representatives on suitable spaces (Hodge, 1941; Wells, 1980; Griffiths and Harris, 1978). The economic use in the monograph is explicitly not an attempt to solve or test the Hodge Conjecture. It draws instead on the discrete and computational extension of Hodge logic, where flows on graphs and simplicial complexes can be decomposed into interpretable components (Dodziuk, 1976; Eckmann, 1944; Lim, 2015; Schaub et al., 2020; Gondauri, 2026b).

The discrete Hodge decomposition literature is especially important because economic relations frequently live on edges rather than nodes. A growth rate, income level or inflation rate is a node attribute. A trade corridor, capital-flow pressure, logistics channel, relative hierarchy or shock path is an edge object. Once the economic object is an edge-flow, decomposition becomes necessary. The Hodge framework separates an edge field into a gradient component associated with hierarchy or potential differences, a curl component associated with local-cycle imbalance, and a harmonic component associated with global circulation that cannot be reduced to local gradients or local curls (Jiang et al., 2011; Schaub et al., 2021; Barbarossa and Sardellitti, 2020; Gondauri, 2026b).

This decomposition is literature-relevant for macroeconomics because it avoids a common limitation of aggregate indicators. If a region has high GDP or high growth, scalar interpretation may identify economic mass but not whether the region acts as a hierarchical source, a local-cycle imbalance node or a contributor to persistent circulation. The Hodge model therefore connects network economics with topological signal processing: it transforms public macroeconomic anchors into a weighted regional network, constructs a directed macro-flow pressure field, and decomposes that field into hierarchy, local imbalance and systemic circulation (Gondauri, 2026b).

Table 3.3.2. Hodge-method literature and economic translation

Literature concept	Formal intuition	Economic translation	Boundary condition
Gradient component	Flow generated by node potentials.	Regional hierarchy, scale pressure or potential-difference structure.	A constructed hierarchy measure, not a natural law of regional ordering.
Curl component	Local rotational	Local-cycle imbalance and	Requires explicit

Literature concept	Formal intuition	Economic translation	Boundary condition
	inconsistency around cycles or triangles.	corridor pressure that cannot be read from pairwise comparisons alone.	graph/triangle construction and robustness checks.
Harmonic component	Global circulation residual after gradient and curl are removed.	Systemic circulation, persistent macro-flow pressure and global residual structure.	Diagnostic circulation only; not direct observation of all dyadic flows.
Hodge Laplacian	Operator linking cochains, incidence and topology.	Spectral/topological audit of the constructed economic network.	Valid only under the specified network and weighting scheme.
Persistent homology	Stability of components/cycles across thresholds.	Robustness check for connectedness, cycles and macro-flow structure.	A validation diagnostic, not proof of economic topology as physical space.

Source: Author synthesis based on Hodge theory, discrete Hodge decomposition and the Hodge macro-flow source manuscript (Hodge, 1941; Dodziuk, 1976; Jiang et al., 2011; Schaub et al., 2020; Gondauri, 2026b).

3.3.4. Ricci Curvature, Poincare Connectedness and Inequality-Pressure Diagnostics

The Perelman/Ricci/Poincare source manuscript extends the topological review from flow decomposition to deformation, smoothing and connectedness. The mathematical background is rooted in Ricci flow, curvature and topology. Hamilton introduced Ricci flow as a geometric evolution equation for smoothing metrics, while Perelman developed entropy and surgery methods central to the proof of the Poincare conjecture (Hamilton, 1982; Perelman, 2002, 2003; Morgan and Tian, 2007). The economic manuscript does not transfer these theorem-level results into economics. It uses their structural language to construct inequality-pressure, curvature-like deformation, entropy-like complexity and graph-connectedness diagnostics (Gondauri, 2026a).

Graph curvature literature makes this economic translation more defensible because curvature can be defined in discrete networks without requiring a smooth manifold. Ollivier-Ricci curvature measures how probability mass around neighboring nodes contracts or expands under transportation logic, while Forman-Ricci curvature provides a combinatorial curvature measure for cell complexes and networks (Forman, 2003; Ollivier, 2009; Ni et al., 2015; Sandhu et al., 2016). These measures have been used to study robustness, bottlenecks, community structure and network vulnerability. In the monograph, the relevance is not that inequality data form a literal Riemannian manifold, but that inequality pressure and smoothing capacity can be organized as a connected diagnostic system whose deformation and bottlenecks are measurable (Gondauri, 2026a).

Poincare-style connectedness enters as a claim-boundary tool. If a diagnostic system is disconnected, any global interpretation is fragile. If it is connected but cycle-rich, the analysis must distinguish global cohesion from local loops and bottlenecks. The Perelman/Ricci/Poincare manuscript therefore uses graph connectedness, Betti-style diagnostics, algebraic connectivity and network-curvature proxies to audit the inequality-pressure system, while explicitly excluding theorem proof or unrestricted causal welfare claims (Chung, 1997; Newman, 2010; Gondauri, 2026a).

3.3.5. Yang-Mills Gauge Analogies, Curvature-Action Structure and Spectral Thresholds

The Yang-Mills section of the literature review connects topology and spectral graph theory to systemic shock thresholds. Classical Yang-Mills theory originates in gauge fields and non-Abelian field strength, while the Millennium problem concerns existence and the mass gap in quantum Yang-Mills theory (Yang and Mills, 1954; Jaffe and Witten, 2000). The economic manuscript does not claim a physical field or a solution of the mathematical mass-gap problem. It translates gauge-theoretic structure into a finite-network gauge-econometric framework: stress-weighted adjacency, anti-symmetric gauge potential, triangular curvature, action concentration, stress Laplacian and finite-network spectral separation (Gondauri, 2026d).

The relevant economic literature is systemic risk and contagion in networks. Financial and production systems can amplify shocks through common exposures, interbank links, supply-chain interdependence, liquidity spirals and corridor constraints (Allen and Gale, 2000; Brunnermeier and Pedersen, 2009; Haldane and May, 2011; Elliott, Golub and Jackson,

2014; Acemoglu, Ozdaglar and Tahbaz-Salehi, 2015). Spectral graph theory adds a threshold language: eigenvalues of graph Laplacians and adjacency matrices can summarize connectedness, diffusion capacity, bottleneck risk and propagation potential (Chung, 1997; Spielman, 2012; Newman, 2010).

In the monograph, Yang-Mills contributes the most explicit bridge between curvature and threshold. Curvature identifies inconsistency or stress circulation around cycles; action summarizes the concentration of stress energy; spectral gap or mass-gap analogues identify whether local disturbance remains locally absorbable or becomes systemically transmissible. This is a benchmark claim, not a final causal claim. Its evidential strength depends on finite-network construction, perturbation robustness, scenario logic, replication materials and future country-panel validation (Gondauri, 2026d).

Table 3.3.3. Yang-Mills spectral-threshold literature and economic interpretation

Mathematical/spectral element	Network-economics analogue	Systemic-risk interpretation	Restricted claim
Gauge potential	Anti-symmetric stress relation across edges.	Direction-sensitive corridor tension or stress imbalance.	Constructed finite-network object; not a physical gauge field.
Triangular curvature	Cycle inconsistency over three-node corridors.	Stress circulation and local-to-systemic amplification channel.	Requires triangle/cycle definition and sensitivity checks.
Action	Aggregate curvature-energy over the network.	Systemic concentration of stress in limited cycles or corridors.	Benchmark stress concentration, not causal mechanism by itself.
Stress Laplacian	Weighted operator governing diffusion/separation.	Propagation barrier or fragility under shock scenarios.	Valid only for the stated weighted graph.
Finite mass-gap analogue	Positive spectral separation in a finite weighted graph.	Local-to-systemic shock threshold.	No claim about the Yang-Mills existence and mass-gap problem.

Source: Author synthesis based on gauge theory, spectral graph theory, systemic-risk networks and the Yang-Mills source manuscript (Yang and Mills, 1954; Chung, 1997; Jaffe and Witten, 2000; Gondauri, 2026d).

3.3.6. Spectral Methods, Frequency-Domain Logic and Riemann-Zeta Forecasting

Spectral methods in economics are used when time-domain levels do not reveal the full structure of cycles, shocks and regime changes. Time-series forecasting, frequency-domain analysis, Fourier and wavelet methods, Markov-switching models and forecast-comparison tests are standard tools for identifying persistence, cyclical variation, structural breaks and nonlinear state dependence (Hamilton, 1989; Stock and Watson, 1999; Diebold and Mariano, 1995; Giacomini and White, 2006; Clark and West, 2007). The Riemann/Zeta source manuscript places this literature into a bounded mathematical-economic signal framework: a normalized critical-line inspired zeta-cycle is used as a signed correction to a structural FPAS baseline, and the improvement is evaluated through layered forecast validation (Gondauri, 2026f).

The number-theoretic foundation is the Riemann zeta function and the Riemann Hypothesis literature, including the distribution of zeros and spectral interpretations of zeta statistics (Riemann, 1859; Titchmarsh, 1986; Edwards, 1974; Berry, 1985; Odlyzko, 1987; Keating and Snaith, 2000). The monograph does not treat world inflation as an arithmetic zeta object and does not use forecast performance as evidence for the Riemann Hypothesis. The transfer is computational and analogical: the zeta function supplies a structured nonlinear signal generator that is normalized, signed, calibrated and subjected to forecast-validation gates (Gondauri, 2026f).

This spectral approach complements topology. Topology explains how economic structure is connected; spectral analysis explains how structure oscillates, separates or resonates. Hodge and Yang-Mills use eigenvalues and Laplacians to measure structural separation and shock thresholds. Riemann/Zeta uses a spectral-cycle correction to capture nonlinear global inflation pressure. BSD uses L-function and Euler-factor analogues to connect local signals with global rank

ordering. Navier-Stokes uses Fourier GDP-cycle forcing as one component of macro-financial stress balance. P-vs-NP uses covariance eigenvalues to audit risk concentration before sparse optimization (Gondauri, 2026b-g).

Table 3.3.4. Spectral-method literature across the monograph

Spectral family	Source model	Economic measurement role	Validation requirement
Graph Laplacian spectrum	Hodge, Yang-Mills, Perelman/Ricci/Poincare	Connectedness, diffusion, cycle structure, spectral threshold and graph robustness.	Graph construction, threshold sensitivity and perturbation checks.
Zeta/critical-line signal	Riemann/Zeta	Nonlinear spectral correction to structural inflation forecasting.	Rolling no-look-ahead validation, benchmark comparison, MZ/DM/CW tests and residual diagnostics.
Euler-factor/L-function ordering	BSD	Local-to-global rank measurement using finite-state regional signals.	Rank-gap diagnostics, equivalence tests, placebo logic and anti-circularity checks.
Fourier/wavelet cycle diagnostics	Riemann/Zeta, Navier-Stokes	Crisis-cycle detection, spectral coherence and stress-cycle interpretation.	Layer separation, residual tests and forecast-boundary discipline.
Covariance/eigenvalue diagnostics	P-vs-NP	Risk geometry, common-factor concentration and portfolio optimization feasibility.	Covariance alternatives, exact reduced enumeration and robustness gates.

Source: Author synthesis based on spectral graph theory, forecast evaluation, zeta literature and seven source manuscripts (Chung, 1997; Diebold and Mariano, 1995; Keating and Snaith, 2000; Gondauri, 2026b-g).

3.3.7. BSD and L-Function Analogues as Spectral Local-to-Global Measurement

Although BSD is not one of the four primary headings named for this section, it is essential for the integrated spectral review because the BSD source manuscript constructs the clearest local-to-global L-function analogy in the monograph. The classical Birch-Swinnerton-Dyer conjecture connects the behavior of an L-function at a critical point with the rank of rational points on an elliptic curve (Birch and Swinnerton-Dyer, 1965; Silverman, 1986; Wiles, 1995). In the economic manuscript, this logic is not treated as an empirical test of arithmetic geometry. It becomes a measurement grammar linking finite-state regional reductions, trace analogues, Euler-factor analogues, an economic L-function construction and LOrder to structural economic rank (Gondauri, 2026e).

The spectral relevance of BSD lies in ordering and aggregation. Local regional signals are not automatically global evidence. They must pass through a defined operator that translates local states into a comparable global object. In the source manuscript, local finite-state regimes, Euler-factor analogues and constructed LOrder are compared with structural rank through gaps, agreement diagnostics, sensitivity checks and placebo logic. This makes BSD a bridge between topological network economics and spectral measurement: local structure becomes globally interpretable only after formal aggregation and validation (Gondauri, 2026e).

This BSD logic also protects the monograph from overclaiming. The literature authorizes a local-to-global analogy because economic systems often display regional aggregation, corridor transmission and network-rank formation. It does not authorize claims about arithmetic L-functions, algebraic rank or the classical BSD conjecture. The admissible claim is that local regional signals and economic Euler-factor analogues can be informative about a constructed structural-rank object under a calibrated measurement architecture (Gondauri, 2026e).

3.3.8. Navier-Stokes and P-vs-NP as Supporting Spectral-Topological Evidence Systems

The Navier-Stokes and P-vs-NP manuscripts support Section 3.3 even though their primary identities are flow and complexity. The Navier-Stokes model uses a nondimensional stress-balance architecture in which liquidity velocity weakness, acceleration, pressure gradients, friction/diffusion, stochastic shocks, Fourier GDP-cycle forcing and restricted closure produce a systemic-stress diagnostic. This makes it partly spectral because cycle forcing and rolling validation

matter, and partly topological because systemic stress is transmitted through macro-financial channels rather than isolated indicators (Navier, 1822; Stokes, 1845; Fefferman, 2000; Brunnermeier and Pedersen, 2009; Gondauri, 2026c).

The P-vs-NP manuscript contributes a different but related lesson: topological or spectral structure is not enough unless the computational problem is feasible, auditable and bounded. Portfolio optimization uses covariance geometry, correlation diagnostics and eigenvalue concentration tests to understand the risk surface before cardinality-constrained search. Once the sparse support-selection problem is imposed, the model becomes mixed discrete-continuous and computationally difficult. Literature on Markowitz mean-variance optimization, CAPM, combinatorial optimization and computational complexity therefore defines the validation status of best-found incumbents, exact reduced benchmarks and heuristic evidence (Markowitz, 1952; Sharpe, 1964; Cook, 1971; Karp, 1972; Garey and Johnson, 1979; Gondauri, 2026g).

Together, these supporting models show that topological and spectral methods cannot be isolated from validation and computation. A graph may be mathematically elegant but economically weak if its edges are arbitrary. A spectral signal may improve fit in one layer but fail outside the reported validation window. An eigenvalue structure may reveal concentration but not certify portfolio optimality. The literature therefore requires the same claim-boundary discipline across topology, spectral modelling and optimization (Gondauri, 2026c, 2026f, 2026g).

3.3.9. In-Text Citation Logic for the Integrated Literature Review

Because this chapter is an integrated literature review, in-text citations are not optional. A reference list alone would not show which literature supports which claim. The correct structure is author-year citation inside the relevant sentence or paragraph, followed by a consolidated reference list at the end of the section or chapter. This is especially important in a monograph that transfers high-level mathematical architectures into economics: every use of topology, spectral theory, curvature, zeta functions, gauge language, L-functions, forecast validation or computational complexity must be visibly anchored in prior literature and in the seven source manuscripts.

The citation logic used in this section is therefore layered. Foundational mathematical sources justify the origin of Hodge, Ricci, Yang-Mills, zeta, Navier-Stokes, BSD and P-vs-NP concepts. Applied network and econometric sources justify economic use, validation and systemic-risk interpretation. The seven Gondauri source manuscripts justify the specific monograph translation and claim-boundary architecture. This three-layer citation system prevents the review from becoming either purely mathematical or purely economic; it presents the monograph as a bounded mathematical-econometric measurement programme.

Table 3.3.5. Citation-placement matrix for Section 3.3

Claim type in the text	Required citation family	Example citation placement
Classical mathematical origin	Original mathematical/theoretical literature.	Hodge (1941), Hamilton (1982), Yang and Mills (1954), Riemann (1859), Birch and Swinnerton-Dyer (1965), Cook (1971).
Economic-network application	Network economics, systemic risk and propagation literature.	Allen and Gale (2000), Acemoglu et al. (2012), Elliott et al. (2014), Haldane and May (2011).
Topological/spectral method	TDA, graph signal processing, spectral graph theory and forecast evaluation literature.	Chung (1997), Ghrist (2008), Carlsson (2009), Shuman et al. (2013), Diebold and Mariano (1995).
Monograph translation	Seven source manuscripts.	Gondauri (2026a-g), depending on the model block.
Claim boundary	Source manuscripts plus validation literature.	Gondauri (2026a-g), Giacomini and White (2006), Clark and West (2007), robustness and replication references.

Source: Author synthesis for citation discipline in Chapter 3 of the monograph.

3.3.10. Integrated Claim Boundary for Topological and Spectral Methods

The integrated literature supports the use of topological and spectral methods in economics only under bounded interpretation. Hodge decomposition may measure hierarchy, local imbalance and harmonic circulation; it does not solve the Hodge Conjecture. Ricci/Poincare diagnostics may measure inequality deformation, smoothing capacity and graph connectedness; they do not prove geometric theorems. Yang-Mills gauge analogies may measure finite-network curvature, action and spectral threshold; they do not solve the Yang-Mills mass-gap problem. Riemann/Zeta spectral cycles may

improve forecast diagnostics in specified validation layers; they do not test or verify the Riemann Hypothesis (Gondauri, 2026a, 2026b, 2026d, 2026f).

The same bounded logic applies to the supporting models. BSD L-function analogues may connect local finite-state signals with structural rank; they do not estimate an arithmetic L-function. Navier-Stokes flow analogies may organize liquidity stress through flow, pressure, friction, shocks and cycles; they do not claim that liquidity is a physical fluid. P-vs-NP computational analogies may show search-space explosion and bounded heuristic evidence; they do not prove P != NP or certify full-universe optimality (Gondauri, 2026c, 2026e, 2026g).

This claim boundary is not a limitation to hide; it is the condition that makes the monograph academically defensible. The literature allows high-level mathematical forms to enter economics when the translation is explicit, the object is constructed transparently, the validation gate is appropriate, and the claim level is proportional to the evidence. Section 3.3 therefore establishes the topological and spectral foundation for later problem chapters while protecting the book against theorem-level, physical-identity or universal-prediction overclaiming.

Table 3.3.6. Permissible and restricted claims for topological and spectral methods

Analogue family	Permissible claim	Restricted claim
Hodge	The world economy can be represented as a constructed regional macro-flow network whose edge-pressure field is decomposable into gradient, curl and harmonic components.	No claim about algebraic Hodge cycles, algebraic varieties or the Hodge Conjecture.
Ricci/Poincare	Inequality pressure can be measured as curvature-like deformation, entropy-like complexity and connected graph structure.	No proof/test/replication of Perelman's proof, Ricci flow theorem or Poincare conjecture.
Yang-Mills	A finite stress-weighted network can support gauge-potential, curvature-action and spectral separation diagnostics.	No solution of the mathematical Yang-Mills mass-gap problem.
Riemann/Zeta	A normalized zeta-cycle can be evaluated as a nonlinear forecast correction under layered validation.	No proof, test or verification of the Riemann Hypothesis.
BSD	Local finite-state signals and Euler-factor analogues can inform economic structural-rank measurement.	No proof or empirical test of classical BSD.
Navier-Stokes	Nondimensional flow-pressure-friction-shock-cycle balance can support stress-testing diagnostics.	No physical hydrodynamic identity or universal crisis-prediction theorem.
P-vs-NP	Sparse optimization can be studied through combinatorial search, exact reduced benchmarks and heuristic robustness.	No proof of P != NP or certified global optimum without a certificate.

Source: Author synthesis based on claim-boundary statements across the seven source manuscripts (Gondauri, 2026a-g).

3.3.11. Literature Gap Addressed by Section 3.3

The reviewed literature reveals a clear gap. Topological data analysis, spectral graph theory, graph signal processing, Ricci curvature, gauge theory, zeta functions, L-functions, macro-financial cycles, systemic-risk networks and portfolio-eigenvalue diagnostics are usually studied in separate literatures. Economics uses many of these tools, but rarely integrates them into one claim-disciplined monograph that compares Hodge decomposition, curvature diagnostics, finite-network gauge thresholds, zeta-cycle forecasting, L-function analogues, flow-cycle stress balance and complexity-aware optimization. Section 3.3 addresses that gap by reviewing these methods as complementary measurement languages rather than as isolated mathematical imports.

The contribution is not to claim originality for the underlying mathematics. The contribution is architectural: the monograph establishes how topological and spectral methods can be translated into bounded economic-econometric analogues under explicit validation gates. This creates a common literature foundation for later chapters: Hodge will be read as flow decomposition; Ricci/Poincare as deformation and connectedness diagnostics; Yang-Mills as curvature-action threshold measurement; Riemann/Zeta as spectral forecast correction; BSD as local-to-global LOrder; Navier-Stokes as

cycle-aware stress balance; and P-vs-NP as spectral risk geometry plus computational search discipline (Gondauri, 2026a-g).

Section 3.3 therefore deepens the bridge from Chapter 2 to the problem chapters. Chapter 2 defined the internal translation logic. Section 3.1 established mathematical economics and analogy. Section 3.2 established networks and systemic transmission. Section 3.3 now shows why topology and spectrum are not decorative metaphors but formal review categories: they define connectedness, cycles, curvature, thresholds, oscillations, local-to-global order and computational feasibility. The remaining literature-review sections can therefore proceed toward macro-financial stress, inflation, inequality, portfolio optimization, regional corridors, validation and replication with a stronger methodological foundation.

3.4. Global Macro-Financial Stress, Inflation and Liquidity Literature

Integrated Review of Navier-Stokes Liquidity-Flow Stress Modelling, Riemann-Zeta FPAS+zeta Inflation Forecasting and Supporting Millennium-Inspired Evidence

3.4.1. Function of this Section within the Integrated Literature Review

This section integrates the literature on macro-financial stress, inflation, liquidity and forecast validation as it supports the monograph's Navier-Stokes-inspired liquidity-flow model and Riemann-Zeta FPAS+zeta inflation-forecasting model. It does not reproduce two separate article-level reviews. Instead, it consolidates the common literature on financial stress, liquidity risk, systemic risk, inflation dynamics, monetary-policy reaction, global shock transmission, time-series forecasting, residual diagnostics and claim-boundary discipline into one high-level literature-review section (Gondauri, 2026c, 2026f).

The reason for integrating these literatures is substantive. Liquidity stress and inflation stress are not independent research objects in the contemporary global economy. Inflation shocks alter policy rates, sovereign spreads, funding costs and liquidity conditions; liquidity contractions amplify financial stress, weaken credit transmission and change inflation-output dynamics; global shocks transmit through commodity prices, dollar funding, supply chains, risk premia and monetary-policy spillovers (Bernanke, Gertler and Gilchrist, 1999; Brunnermeier and Pedersen, 2009; Rey, 2015; Forbes and Rigobon, 2002; Diebold and Yilmaz, 2012). The Navier-Stokes analogue formalizes this interdependence as a flow-pressure-friction-shock-cycle-closure stress balance, while the Riemann-Zeta analogue formalizes nonlinear inflation pressure as a structural forecast corrected by a bounded spectral-cycle signal (Gondauri, 2026c, 2026f).

The section also draws on the other five Millennium-inspired source models because macro-financial stress and inflation are embedded in broader systemic structures. Hodge contributes the idea that flows can be decomposed into hierarchy, local imbalance and harmonic circulation; Yang-Mills contributes finite-network shock-threshold and action-concentration logic; BSD contributes local-to-global rank and corridor-stress interpretation; Perelman/Ricci/Poincare contributes pressure, curvature, smoothing capacity and entropy-like complexity; P-vs-NP contributes computational validation, robustness gates and search-space discipline (Gondauri, 2026a, 2026b, 2026d, 2026e, 2026g).

Table 3.4.1. Integrated literature transfer map for macro-financial stress, inflation and liquidity

Source model	Literature material entering Section 3.4	Role in the integrated review	Claim boundary
Navier-Stokes	Liquidity, financial stress, systemic risk, flow balance, stress testing, forecasting, panel econometrics and policy counterfactual literature.	Defines systemic stress as a nondimensional flow-pressure-friction-shock-cycle-closure process.	Diagnostic and stress-testing analogue; no physical liquidity-fluid identity or Navier-Stokes proof.
Riemann/Zeta	Inflation forecasting, FPAS-style structural forecasting, global shocks, zeta-cycle signal construction, spectral diagnostics, regime switching and forecast evaluation.	Defines a bounded hybrid inflation model in which a normalized zeta-cycle corrects a structural FPAS baseline.	Forecast-diagnostic claim only; no Riemann Hypothesis proof, test or universal forecast dominance.
Hodge	Macro-flow network, directed edge pressure, gradient/curl/harmonic	Explains why liquidity and inflation stress may circulate through hierarchy, local	Topological flow decomposition only.

Source model	Literature material entering Section 3.4	Role in the integrated review	Claim boundary
	decomposition and resilience literature.	imbalance and systemic residual flow.	
Yang-Mills	Systemic-risk networks, spectral graph thresholds, gauge potential, curvature and finite-network action literature.	Frames local macro-financial disturbance as potentially crossing a local-to-systemic shock threshold.	Finite-network benchmark logic only.
BSD	Local-to-global rank, Euler-factor analogues, corridor stress, BridgeStress and structural-rank literature.	Connects local regional signals, inflation pressure and corridor exposure to global structural rank formation.	Calibrated local-to-global measurement only.
Perelman/Ricci/ Poincare	Inequality pressure, smoothing capacity, curvature-like deformation, entropy and graph connectedness literature.	Interprets macro-financial stress as deformation and incomplete smoothing after shocks.	Diagnostic curvature/topology only.
P-vs-NP	Optimization, covariance geometry, heuristic search, benchmark validation and robustness literature.	Supplies computational discipline for model selection, robustness checking and claim classification.	Empirical-computational evidence only.

Source: Author synthesis based on the seven source manuscripts and their literature-review architectures (Gondauri, 2026a-g).

3.4.2. Financial Stress Literature: From Indicator Monitoring to Systemic Measurement

The macro-financial stress literature begins from the recognition that crises are rarely captured by one variable. Interest-rate spreads, sovereign premia, exchange-rate pressure, credit growth, volatility, bank funding conditions, liquidity premia and market-depth indicators each measure only part of the stress process. Early financial accelerator and credit-friction models show that balance-sheet deterioration can amplify shocks through external finance premia and collateral constraints (Bernanke and Gertler, 1989; Bernanke, Gertler and Gilchrist, 1999; Kiyotaki and Moore, 1997). Later systemic-risk literature demonstrates that stress is also relational: losses, deleveraging, liquidity spirals, network exposures and confidence shocks can propagate beyond the original disturbance (Brunnermeier, 2009; Brunnermeier and Pedersen, 2009; Gorton and Metrick, 2012).

Financial-stress-index literature responds to this multidimensionality by constructing composite measures from banking, credit, market, sovereign and foreign-exchange channels. Such indices are useful because they provide a common scale for heterogeneous signals, but they also require transparent weighting, robustness analysis and interpretation boundaries (Illing and Liu, 2006; Hatzius et al., 2010; Holló, Kremer and Lo Duca, 2012). The Navier-Stokes-inspired model follows this measurement tradition but adds a mathematical stress-balance grammar: stress is decomposed into liquidity-velocity weakness, acceleration pressure, pressure gradients, friction/diffusion, stochastic shocks, Fourier-cycle forcing and restricted hidden adjustment (Gondauri, 2026c).

Systemic-risk measures such as CoVaR, SRISK, network contagion metrics and spillover indices further show that stress should be interpreted through conditional losses, interconnected exposures and directional transmission rather than only aggregate volatility (Adrian and Brunnermeier, 2016; Acharya et al., 2017; Billio et al., 2012; Diebold and Yilmaz, 2012; Battiston et al., 2012). This is directly relevant to Section 3.4 because global liquidity and inflation shocks are not isolated disturbances. They alter risk premia, funding liquidity, sovereign spreads and monetary-policy expectations, creating transmission channels that connect the Navier-Stokes liquidity-flow architecture with the Riemann-Zeta inflation-pressure architecture (Gondauri, 2026c, 2026f).

3.4.3. Liquidity Literature and the Economic Meaning of Flow, Friction and Closure

Liquidity literature distinguishes market liquidity, funding liquidity and monetary or macro-liquidity conditions. Market liquidity concerns the ability to trade without large price impact; funding liquidity concerns the ability of institutions to finance positions; macro-liquidity concerns aggregate financial conditions, credit availability and policy transmission. The commonality of liquidity and liquidity spirals literature shows that liquidity can deteriorate endogenously during stress

regimes, especially when funding constraints and market-depth losses reinforce one another (Kyle, 1985; Amihud, 2002; Pastor and Stambaugh, 2003; Brunnermeier and Pedersen, 2009).

This literature justifies the economic interpretation of flow and friction in the Navier-Stokes analogue. Liquidity velocity weakness is not a physical velocity but an economic indicator of slow circulation, weak market depth or constrained financial transmission. Friction/diffusion is not molecular viscosity but a composite channel that reflects credit frictions, funding costs, market segmentation and institutional adjustment delays. Pressure gradients are not physical pressure but macro-financial differentials generated by inflation pressure, sovereign spreads, funding stress and external constraints. Closure is not a mathematical trick; in the manuscript it is restricted by observable or proxy-observable state variables such as lagged closure, shadow-economy pressure, transfers, geopolitical shock, fiscal buffers, aid/support and inertia (Gondauri, 2026c).

The literature therefore supports a bounded liquidity-flow claim. It is scientifically admissible to measure liquidity stress through normalized, direction-harmonized and audited components. It is not admissible to claim that the financial system is literally a viscous fluid or that a PDE theorem has been solved. This claim boundary is consistent with the broader analogue-modelling rule established in Sections 3.1-3.3: mathematical structure becomes legitimate in economics only when it is converted into measured variables, validated, and interpreted within a restricted claim hierarchy (Gondauri, 2026a-g).

$$Stress_t = VelocityWeakness_t + Acceleration_t + PressureGradient_t + Friction_t + Shock_t + Cycle_t + Closure_t$$

This schematic is a literature-review representation rather than the full model equation. It summarizes the Navier-Stokes-inspired logic that macro-financial stress is multi-channel and must be interpreted as a structured balance, not as one scalar variable.

Table 3.4.2. Liquidity and stress-channel literature mapped to the Navier-Stokes economic analogue

Stress channel	Representative literature base	Economic interpretation in the monograph	Validation requirement
Liquidity velocity weakness	Market liquidity and commonality in liquidity (Kyle, 1985; Amihud, 2002; Pastor and Stambaugh, 2003).	Weak circulation, reduced depth, lower transmission capacity and slower adjustment.	Nondimensional scaling and rolling/benchmark validation.
Funding friction/diffusion	Funding liquidity and liquidity spirals (Brunnermeier and Pedersen, 2009; Gorton and Metrick, 2012).	Credit frictions, funding stress, segmentation and adjustment delay.	Robustness checks and alternative weighting schemes.
Pressure gradients	Financial accelerator and sovereign/credit stress literature (Bernanke and Gertler, 1989; Kiyotaki and Moore, 1997; Adrian and Brunnermeier, 2016).	Inflation, spreads, sovereign risk and financial-stress differentials.	Panel associations interpreted diagnostically, not causally.
Stochastic shocks and cycles	Volatility, crisis and business-cycle literature (Engle, 1982; Hamilton, 1989; Stock and Watson, 1999).	Event shocks, volatility impulses and GDP-cycle forcing.	Residual tests, Fourier diagnostics and validation-window discipline.
Restricted closure	Model uncertainty and omitted-state discipline (Arellano and Bond, 1991; Driscoll and Kraay, 1998; Pesaran, 2006).	State-dependent hidden adjustment, not an unrestricted residual plug.	Observable/proxy-observable closure variables and external validation.

3.4.4. Inflation Literature: Persistence, Policy Reaction and Global Shock Transmission

The inflation literature relevant to the Riemann-Zeta FPAS+zeta model has three layers: structural inflation dynamics, global shock transmission and forecast evaluation. Structural inflation models emphasize persistence, expectations, output gaps, monetary-policy reaction and supply conditions. The Phillips-curve and New Keynesian traditions provide the conceptual basis for linking inflation to slack, expectations and policy regimes, while Taylor-rule and DSGE literatures

formalize monetary-policy reaction and structural forecasting (Phillips, 1958; Taylor, 1993; Clarida, Gali and Gertler, 2000; Christiano, Eichenbaum and Evans, 2005; Smets and Wouters, 2007).

Global inflation is also shaped by international shock transmission. Commodity shocks, exchange-rate pass-through, global value-chain disruptions, supply bottlenecks, synchronized monetary tightening and financial spillovers can generate inflation regimes that are not well described by a smooth domestic persistence model alone (Forbes and Rigobon, 2002; Ciccarelli and Mojon, 2010; Auer, Borio and Filardo, 2017; Ha, Kose and Ohnsorge, 2019). The Riemann-Zeta source manuscript explicitly positions its forecasting problem inside such a sequence of stress regimes: the global financial crisis, COVID-19 shock, reopening and supply-chain pressure, energy-food-war shock, monetary tightening and residual disinflation (Gondauri, 2026f).

This literature explains why the FPAS baseline is necessary but not sufficient. A structural FPAS-style model can represent inertia, policy reaction, liquidity and supply coordinates, but nonlinear crisis-sensitive movements may require an additional signal layer. The Riemann-Zeta analogue supplies that layer through a normalized critical-line inspired zeta-cycle, converted into a real-valued deviation and calibrated as a signed correction to the FPAS forecast. The admissible claim is not that number theory explains inflation. It is that a mathematically explicit spectral-cycle signal can be tested for incremental forecasting value under layered validation (Gondauri, 2026f).

3.4.5. Riemann-Zeta, Spectral-Cycle Signals and Inflation Forecasting

The Riemann-zeta literature provides the formal source language for spectral-cycle construction, but the economic transfer is bounded. Classical zeta theory concerns analytic continuation, zeros, critical-line behavior and the Riemann Hypothesis (Riemann, 1859; Titchmarsh, 1986; Edwards, 1974). Random-matrix and spectral analogies have connected zeta-zero statistics with broader spectral phenomena, but these analogies remain mathematical and statistical rather than macroeconomic laws (Montgomery, 1973; Berry, 1985; Odlyzko, 1987; Keating and Snaith, 2000).

In the FPAS+zeta framework, the zeta function is used only as an analogical and computational cyclical signal. The macro-financial pressure state is transformed into a nonlinear tau argument, the zeta function is evaluated on a critical-line-inspired input, the complex output is normalized into a real-valued zeta-cycle, and the deviation from neutrality becomes an alpha-weighted correction to the structural forecast. This pipeline is essential because it prevents theorem-level overclaiming: the model does not test the Riemann Hypothesis, does not verify zero locations and does not claim a universal inflation law (Gondauri, 2026f).

The spectral aspect matters because inflation regimes can include oscillatory, nonlinear and crisis-sensitive components that are difficult to capture with a single persistence model. Fourier, wavelet and spectral-entropy diagnostics are therefore used as supporting tools, not as standalone proof. Their role is to identify whether the constructed zeta-cycle is temporally coherent with crisis regimes such as 2008, 2020 and 2022 and whether it improves forecast performance in annual, quarterly and monthly validation layers (Percival and Walden, 2000; Torrence and Compo, 1998; Gençay, Selçuk and Whitcher, 2002; Gondauri, 2026f).

$$FPAS_plus_zeta_t = FPAS_t + alpha * lambda_zeta * d_zeta,t$$

The formula summarizes the literature-review logic of the hybrid forecast: the structural FPAS baseline remains the main forecasting object, while the normalized zeta-cycle supplies a bounded signed correction.

Table 3.4.3. Inflation and spectral-forecasting literature mapped to FPAS+zeta

Literature block	Main cited tradition	Role in FPAS+zeta	Restricted claim
Structural inflation forecasting	Phillips curve, Taylor rule, DSGE and FPAS-style forecasting (Phillips, 1958; Taylor, 1993; Smets and Wouters, 2007).	Defines the baseline forecast and policy-reaction structure.	Not a complete central-bank model.
Global shock transmission	Inflation synchronization, commodity/supply shocks and global spillovers (Ciccarelli and Mojon, 2010; Auer et al., 2017; Ha et al., 2019).	Explains why global inflation requires stress and shock coordinates.	Not a country-level policy ranking.
Zeta/spectral signal foundations	Zeta and spectral analogy literature (Riemann, 1859;	Motivates a nonlinear critical-line inspired signal generator.	No RH proof, test or verification.

Literature block	Main cited tradition	Role in FPAS+zeta	Restricted claim
	Montgomery, 1973; Berry, 1985; Keating and Snaith, 2000).		
Forecast evaluation	RMSE/MAE, Mincer-Zarnowitz, DM/CW and rolling validation literature (Mincer and Zarnowitz, 1969; Diebold and Mariano, 1995; Clark and West, 2007).	Determines whether the hybrid model adds measurable forecast value.	No universal forecast dominance.
Regime and residual diagnostics	Markov switching, state-space, residual and break-test literature (Hamilton, 1989; Bai and Perron, 2003).	Identifies crisis regimes and overfitting/residual risk.	Residual risks remain reported.

3.4.6. Forecast Evaluation, Validation Windows and Overclaiming Control

The forecasting literature is essential because high-level mathematical signal construction is not enough. A zeta-cycle correction becomes relevant only if it improves measurable forecast performance against baselines and survives validation gates. Standard forecast-evaluation literature emphasizes loss functions, calibration, encompassing, forecast comparison, out-of-sample design and robustness to model uncertainty (Mincer and Zarnowitz, 1969; Diebold and Mariano, 1995; West, 1996; Giacomini and White, 2006; Clark and West, 2007).

The Riemann-Zeta manuscript applies this literature through layered validation. The main annual validation layer covers 1970-2024, the annual robustness layer covers 1980-2024, the crisis-era layer covers 2005-2024, the quarterly dynamic layer covers 2000Q1-2024Q4 and the monthly spectral-diagnostics layer covers 2005M1-2024M12. This hierarchy prevents the model from pretending that every advanced test is estimated on the same sample. It also prevents strong visual fit from being upgraded into universal predictive law (Gondauri, 2026f).

The Navier-Stokes manuscript uses a parallel validation logic for stress testing. Rolling one-year-ahead validation, benchmark comparison against ARIMA, VAR, GARCH and composite-index baselines, fixed effects, external-target validation, residual checks, robustness under perturbation, Monte Carlo uncertainty and policy counterfactuals classify its results as diagnostic and stress-testing evidence rather than unconditional crisis prediction (Gondauri, 2026c). Together, the two manuscripts show how macro-financial stress and inflation forecasting should be evaluated: by validation windows, benchmark comparison, residual discipline and explicit claim hierarchy, not by isolated fit statistics.

Table 3.4.4. Validation gates for macro-financial stress and inflation literature

Validation gate	Navier-Stokes function	Riemann/Zeta function	Claim protected
Benchmark comparison	Compares stress model with ARIMA, VAR, GARCH and composite-index baselines.	Compares FPAS+zeta with FPAS and ARIMA.	Incremental model value, not universal dominance.
Rolling/no-look-ahead validation	Tests one-year-ahead stress usefulness in the stated window.	Tests forecast performance under layered annual/quarterly/monthly samples.	Validation-window evidence only.
Residual and stability diagnostics	Checks residual coherence, closure quality and stress-channel stability.	Checks residual problems, calibration and forecast-error behavior.	Credibility safeguard, not residual elimination.
Robust inference	Uses panel fixed effects, robust errors and external-target validation.	Uses forecast-encompassing, MZ, DM/CW and regime diagnostics.	Diagnostic/statistical support, not unrestricted causality.
Simulation/ counterfactual layer	Monte Carlo fan paths and policy-shock scenarios.	Stress-regime and spectral-signal interpretation.	Model-implied scenario evidence only.

3.4.7. Global Shock Transmission: The Bridge between Liquidity Stress and Inflation Pressure

A central insight of the integrated literature is that liquidity and inflation are joined by shock transmission. A commodity or energy shock can raise inflation and simultaneously change monetary-policy expectations, bond yields, sovereign spreads and funding liquidity. A financial shock can weaken credit supply, depress output and alter inflation dynamics. A dollar-funding shock can pressure exchange rates, import prices, debt-service burdens and liquidity resilience. These mechanisms are widely discussed in global financial-cycle, contagion and spillover literatures (Forbes and Rigobon, 2002; Gai and Kapadia, 2010; Rey, 2015; Miranda-Agrippino and Rey, 2020).

This transmission literature creates the conceptual bridge between the Navier-Stokes and Riemann/Zeta chapters. The Navier-Stokes framework asks how stress forms through flow, pressure, friction, shocks, cycles and closure. The Riemann/Zeta framework asks whether inflation pressure contains a nonlinear cyclical component that improves forecast diagnostics. In a global economy, the two questions are connected: inflation pressure can act as a pressure-gradient channel inside liquidity stress, while liquidity stress can act as a financial-pressure coordinate inside inflation forecasting (Gondauri, 2026c, 2026f).

The other five manuscripts deepen this bridge. Hodge explains whether the stress is hierarchical, locally imbalanced or harmonically circulating. Yang-Mills asks whether the local shock crosses a finite-network threshold into systemic transmission. BSD asks whether local regional signals contain information about global structural rank. Perelman/Ricci/Poincare asks whether pressure deformation is smoothed or remains entropic. P-vs-NP asks whether the resulting decision environment is computationally tractable under realistic constraints (Gondauri, 2026a, 2026b, 2026d, 2026e, 2026g).

3.4.8. Supporting Contributions of the Other Five Analogues

Although Section 3.4 is anchored in Navier-Stokes and Riemann/Zeta, the integrated literature review must account for all seven source documents. The Hodge literature supports the idea that macro-financial pressure should not be interpreted only as a node-level index. A stress field can contain hierarchy, local-cycle imbalance and persistent circulation, which are directly relevant to liquidity-flow and inflation-spillover interpretation (Schaub et al., 2020; Gondauri, 2026b).

The Yang-Mills literature supports the finite-network threshold idea. In macro-financial terms, a disturbance may be locally absorbable until stress concentration, network curvature or spectral compression makes it systemically transmissible. This is relevant for inflation shocks that travel through energy, food, logistics or sovereign-spread channels, as well as liquidity shocks that travel through funding and corridor exposure (Haldane and May, 2011; Battiston et al., 2012; Gondauri, 2026d).

The BSD model adds local-to-global rank logic. Local regional stress indicators, finite-state traces and Euler-factor analogues do not produce an arithmetic L-function in economics, but they help interpret how local inflation, liquidity, corridor stress and rank components aggregate into a global structural-rank signal. Perelman/Ricci/Poincare adds the deformation-smoothing language needed to describe post-crisis recovery. P-vs-NP adds optimization and computational caution, reminding the monograph that model selection, sparse decision-making and robustness search should not be overstated as certified global optimality (Gondauri, 2026a, 2026e, 2026g).

Table 3.4.5. Supporting roles of the five non-core analogues in Section 3.4

Supporting analogue	Contribution to macro-financial stress, inflation and liquidity literature	Relevant claim discipline
Hodge	Interprets liquidity and inflation spillovers through hierarchy, local-cycle imbalance and systemic circulation.	Decomposition evidence, not theorem proof.
Yang-Mills	Frames stress concentration, corridor fragility and shock thresholds as finite-network phenomena.	Finite weighted-graph benchmark, not physical gauge theory.
BSD	Links local regional signals and corridor pressure to global rank formation and structural measurement.	Calibrated local-to-global measurement, not arithmetic BSD.
Perelman/Ricci/ Poincare	Frames pressure accumulation, smoothing capacity and crisis recovery as curvature/entropy diagnostics.	Diagnostic geometry/topology, not classical theorem replication.

Supporting analogue	Contribution to macro-financial stress, inflation and liquidity literature	Relevant claim discipline
P-vs-NP	Supplies computational validation, sparse decision logic and robustness/search discipline.	Best-found or benchmark evidence, not proof of computational complexity conjectures.

3.4.9. Claim-Boundary Synthesis for Section 3.4

The literature supports strong but bounded claims. For the Navier-Stokes model, the strongest admissible claim is that a nondimensional macro-financial stress-testing architecture can decompose systemic stress into interpretable liquidity-flow, pressure, friction, shock, cycle and closure channels. The literature does not support claims that liquidity is a literal physical fluid, that the Navier-Stokes existence/regularity problem is solved or that the model creates a universal crisis-prediction law (Gondauri, 2026c).

For the Riemann/Zeta model, the strongest admissible claim is that a normalized critical-line inspired zeta-cycle can be tested as a signed nonlinear correction to a structural global inflation forecast, and that its value must be judged through layered validation and benchmark comparison. The literature does not support claims that the Riemann Hypothesis is proved, tested or verified, nor that FPAS+zeta dominates all inflation models across all economies and horizons (Gondauri, 2026f).

For the integrated monograph, Section 3.4 therefore establishes a two-track claim hierarchy: macro-financial stress measurement on one side and inflation forecast diagnostics on the other. Their common foundation is validation discipline. Both models use high-level mathematical language only after it has been translated into explicit variables, tested against baselines, bounded by sample architecture and placed within a reviewer-safe claim hierarchy.

Table 3.4.6. Claim hierarchy for macro-financial stress, inflation and liquidity literature

Claim class	Permissible claim	Evidence base	Excluded claim
Strong measurement claim	Systemic stress and inflation pressure can be represented by constructed, normalized and auditable objects.	Composite stress variables, pressure indices, nondimensionalization, zeta-cycle normalization and replication files.	Raw heterogeneous variables automatically aggregate into a valid index.
Diagnostic claim	Liquidity stress can be decomposed into velocity, pressure, friction, shock, cycle and restricted closure channels.	Navier-Stokes-inspired balance, robustness, panel diagnostics and external-target validation.	Liquidity is a physical fluid or a PDE theorem has been solved.
Forecasting claim	FPAS+zeta may improve global inflation forecasting within reported layers and benchmarks.	RMSE/MAE/sMAPE, rolling validation, MZ, DM/CW, regime and residual diagnostics.	Universal forecast superiority or Riemann Hypothesis verification.
Benchmark claim	Stress and forecast models can outperform selected baselines in the reported validation design.	ARIMA, VAR, GARCH, composite-index and FPAS comparisons.	Permanent dominance over all future models and samples.
Future validation claim	Country-level, higher-frequency and external-policy extensions can deepen evidence.	Replication packages, panel-design logic and robustness architecture.	Already-complete causal validation where identification is not established.

3.4.10. Integrated Synthesis and Transition

Section 3.4 establishes that global macro-financial stress, liquidity and inflation forecasting belong in one integrated literature-review block. Liquidity stress and inflation pressure are joined through policy, funding, spreads, supply shocks, currency pressure, risk premia and global spillovers. The Navier-Stokes model contributes a structured stress-balance

architecture; the Riemann/Zeta model contributes a layered forecast-diagnostic architecture. Both rely on constructed variables, benchmark comparison, robustness checks and claim-boundary discipline (Gondauri, 2026c, 2026f).

The section also shows why the monograph cannot be organized as seven isolated literature reviews. The macro-financial object studied here is connected to topology, systemic transmission, local-to-global rank, curvature/smoothing, spectral signals and computational validation. Hodge, Yang-Mills, BSD, Perelman/Ricci/Poincare and P-vs-NP are not peripheral; they provide supporting literatures that clarify how shocks circulate, concentrate, deform, rank and constrain economic decisions (Gondauri, 2026a, 2026b, 2026d, 2026e, 2026g).

The final literature-review conclusion is therefore precise: macro-financial stress, liquidity and inflation can be studied through high-level mathematical-economic analogues only if those analogues remain auditable. The literature supports measurement, diagnostic, forecast-window, benchmark and future-validation claims. It does not support theorem-level proof, physical identity, unrestricted causality, universal forecast superiority or unbounded policy prescription. This claim-boundary discipline prepares the next section, which narrows the integrated review toward inequality, curvature, smoothing capacity and regional pressure.

3.5. Inequality, Curvature, Smoothing Capacity and Regional Pressure

Integrated Review of Perelman/Ricci/Poincare Inequality Diagnostics and Supporting Millennium-Inspired Measurement Literature

3.5.1. Function of this Section within the Integrated Literature Review

This section integrates the literature on inequality, curvature, smoothing capacity and regional pressure as the substantive foundation for the monograph's Perelman/Ricci/Poincare-inspired inequality-diagnostic model. It does not reproduce an isolated article-level review. Instead, it consolidates inequality economics, regional pressure measurement, geometric and graph-curvature analogies, entropy-style complexity, connectedness diagnostics, robustness testing and claim-boundary discipline into one monographic literature-review section (Atkinson, 1970; Sen, 1973; Cowell, 2011; Piketty, 2014; Gondauri, 2026a).

The central premise is that inequality should not be treated only as a single scalar dispersion statistic. The literature has long shown that inequality reflects income distribution, labour-market segmentation, productivity divergence, human-capital gaps, capital accumulation, technology access, fiscal capacity, social protection, migration pressure and institutional structure (Kuznets, 1955; Sen, 1973; Atkinson, 1970; Milanovic, 2016; Deaton, 2013). The Perelman/Ricci/Poincare analogue extends this tradition by asking whether such multidimensional pressure can be organized as a diagnostic manifold in which pressure, smoothing capacity, curvature-like deformation, entropy-like complexity and graph connectedness are jointly measured (Hamilton, 1982; Perelman, 2002, 2003; Morgan and Tian, 2007; Gondauri, 2026a).

The section also brings in the other six source models because inequality pressure is not isolated from the broader system. Hodge contributes topological flow decomposition; Yang-Mills contributes gauge-curvature and shock-threshold logic; Navier-Stokes contributes flow-pressure-friction-closure stress interpretation; BSD contributes regional local-to-global rank and corridor pressure; Riemann/Zeta contributes spectral and regime-sensitive validation; P-vs-NP contributes computational robustness and claim-discipline logic (Gondauri, 2026b, 2026c, 2026d, 2026e, 2026f, 2026g). In this integrated review, those models are supporting literatures, while the Perelman/Ricci/Poincare model remains the primary anchor.

Table 3.5.1. Integrated literature transfer map for Section 3.5

Source model	Literature material merged into Section 3.5	Role in the inequality-curvature review	Permissible claim status
Perelman/Ricci/ Poincare	Inequality measurement, Ricci flow, Perelman entropy, pressure coordinates, graph topology, smoothing capacity, Betti and Laplacian diagnostics, robustness and forecast validation.	Primary model: defines inequality as a multidimensional pressure-smoothing system with curvature-like deformation and entropy-like complexity.	Diagnostic measurement claim only; no proof, test or replication of Perelman, Ricci-flow theorem or Poincare conjecture.
Hodge	Discrete Hodge decomposition, graph Laplacians, edge-flow	Explains how regional inequality pressure may be	Topological flow-decomposition support,

Source model	Literature material merged into Section 3.5	Role in the inequality-curvature review	Permissible claim status
	pressure, gradient/curl/harmonic structure and resilience literature.	decomposed into hierarchy, local imbalance and systemic circulation.	not a Hodge Conjecture claim.
Yang-Mills	Network curvature, gauge-potential analogy, action concentration, stress Laplacian, spectral threshold and corridor shock literature.	Frames inequality pressure as potentially cycle-concentrated stress that can cross local-to-systemic thresholds.	Finite-network benchmark support, not physical Yang-Mills proof.
Navier-Stokes	Macro-financial stress, liquidity velocity, pressure gradients, friction, forcing, closure and stress-testing literature.	Provides a complementary stress-balance view of how inequality pressure may interact with macro-financial instability.	Stress-testing and diagnostic support only.
BSD	Local-to-global rank, regional finite-state signals, structural rank, corridor stress, BridgeStress and robust panel diagnostics.	Connects local regional inequality coordinates with global structural-rank and corridor-pressure interpretation.	Calibrated local-to-global measurement support.
Riemann/Zeta	Inflation pressure, nonlinear cyclical signals, spectral validation, regime-switching and forecast-comparison literature.	Supports interpretation of inequality pressure under inflationary, crisis and spectral-regime environments.	Bounded forecast and diagnostic support only.
P-vs-NP	Optimization complexity, support selection, exact reduced benchmarking, heuristic validation and robustness/falsification literature.	Supports computational discipline: high-dimensional inequality diagnostics require search, validation and overclaiming controls.	Empirical-computational support only.

Source: Author synthesis based on the seven source manuscripts and the integrated inequality, geometry, topology, systemic-risk, forecasting and computational-validation literature.

3.5.2. Inequality Literature: From Scalar Dispersion to Multidimensional Pressure

Classical inequality literature supplies the first foundation for this section. Measures such as the Gini coefficient, income shares, generalized entropy measures, Atkinson indices and decomposable inequality metrics remain indispensable because they convert distributional dispersion into interpretable numerical quantities (Atkinson, 1970; Cowell, 2011; Sen, 1973). However, the same literature also warns that inequality cannot be interpreted as a single mechanical variable. Distributional outcomes emerge from labour markets, education, technology, capital returns, trade exposure, fiscal redistribution, social insurance and political-economic institutions (Kuznets, 1955; Piketty, 2014; Milanovic, 2016; Deaton, 2013).

The Perelman/Ricci/Poincare-inspired source manuscript is positioned exactly at this gap. It does not discard scalar inequality indicators, but it treats them as one coordinate in a broader pressure system. Productivity weakness, unemployment, investment stress, inflation pressure, migration pressure, education access, social mobility, trade infrastructure, capital-flow pressure, innovation, healthcare access, fiscal stress, openness, social protection and technology access are harmonized into a common diagnostic scale so that inequality is measured as a coupled macro-social deformation rather than as a single raw statistic (Gondauri, 2026a).

This shift is consistent with the wider literature on multidimensional inequality, social opportunity, human development and welfare-sensitive measurement. Distributional analysis increasingly recognizes that income dispersion, capability constraints, institutional quality, spatial location and public-service access interact in ways that scalar income metrics cannot

fully represent (Sen, 1999; Deaton, 2013; Stiglitz, Sen and Fitoussi, 2009; World Bank, 2006). In the monograph, the curvature analogy provides a formal way to express that interaction without claiming that inequality is literally geometric curvature.

Table 3.5.2. From scalar inequality to pressure-curvature diagnostics

Literature level	Typical object	Limitation for this monograph	Perelman/Ricci/Poincare response	Representative citations
Scalar inequality	Gini, income share, Atkinson index, entropy index.	Captures distributional dispersion but not system deformation, smoothing capacity or regional topology.	Retains inequality as a pressure coordinate within a broader stress manifold.	Atkinson (1970); Sen (1973); Cowell (2011).
Multidimensional inequality	Education, health, mobility, social protection, labour, fiscal and technology access variables.	Identifies broader sources of disadvantage but may remain additive and weakly topological.	Transforms heterogeneous components into a common pressure-oriented diagnostic coordinate system.	Sen (1999); Deaton (2013); Stiglitz et al. (2009).
Regional pressure	Regional divergence, centre-periphery structure, growth gaps, fiscal capacity and corridor exposure.	May describe regional heterogeneity without formal deformation or connectedness diagnostics.	Uses macro-regional panel coordinates and graph topology to measure pressure concentration and smoothing capacity.	Barro and Sala-i-Martin (1992); Krugman (1991); Fujita et al. (1999).
Curvature analogy	Curvature, Ricci flow, scalar curvature, entropy, connectedness and graph bottlenecks.	Cannot be transferred literally from geometry to economics.	Uses curvature-like and entropy-like objects as model-implied diagnostics under explicit claim boundaries.	Hamilton (1982); Perelman (2002, 2003); Ollivier (2009); Forman (2003); Gondauri (2026a).

Source: Author synthesis based on inequality measurement, multidimensional welfare, regional economics and Perelman/Ricci/Poincare-inspired diagnostic literature.

3.5.3. Regional Pressure, Spatial Heterogeneity and Smoothing Capacity

The second literature foundation concerns regional pressure. Regional economics, economic geography and convergence theory show that economic stress is not distributed uniformly across space. Regional income, productivity, human capital, infrastructure, fiscal capacity, industrial structure, corridor exposure and external shocks create uneven adjustment paths (Barro and Sala-i-Martin, 1992; Krugman, 1991; Fujita, Krugman and Venables, 1999; Rodrik, 1998). This matters for inequality diagnostics because the same average global inequality indicator may conceal very different regional pressure profiles.

Smoothing capacity is the key bridge between inequality literature and Ricci-flow analogy. In geometric Ricci flow, curvature evolves under a smoothing process; in the economic analogue, smoothing capacity refers to the system's ability to absorb pressure through productivity improvement, employment resilience, investment capacity, fiscal buffers, social protection, technology access, health and education infrastructure (Hamilton, 1982; Chow et al., 2006; Gondauri, 2026a). This is an analogy of structure, not identity: the model does not claim that regional economies obey geometric evolution equations. It claims that pressure and smoothing can be jointly measured in a disciplined diagnostic architecture.

Regional pressure also links the Perelman/Ricci/Poincare section to the BSD, Hodge, Yang-Mills and Navier-Stokes source models. BSD contributes local-to-global rank formation: local regional signals may become informative about global structural rank. Hodge contributes the distinction between hierarchical pressure, local-cycle imbalance and systemic

circulation. Yang-Mills contributes action concentration and shock-threshold compression. Navier-Stokes contributes pressure-gradient and frictional adjustment logic. These supporting literatures make inequality pressure a systemic object rather than a local descriptive statistic (Acemoglu et al., 2012; Diebold and Yilmaz, 2012; Gondauri, 2026b, 2026c, 2026d, 2026e).

Table 3.5.3. Smoothing-capacity literature and its economic interpretation

Smoothing-capacity dimension	Economic meaning	Literature basis	Role in Perelman/Ricci/Poincare analogue
Productive capacity	Ability of productivity, capital formation and innovation to reduce pressure persistence.	Growth and convergence literature; productivity and development literature.	Raises curvature-like recovery capacity when pressure does not dominate productive absorption.
Labour-market absorption	Employment and wage adjustment capacity under shocks.	Inequality, labour and macroeconomic resilience literature.	Weak absorption increases pressure coordinates and lowers smoothing interpretation.
Fiscal and social buffers	Redistribution, social protection, fiscal space and health/education provision.	Welfare economics, public finance and multidimensional inequality literature.	Defines social smoothing capacity rather than purely market smoothing.
Regional connectedness	Connectivity through trade, logistics, capital flows and institutional corridors.	Network economics and regional-economics literature.	Can either reduce local pressure through integration or transmit pressure through exposed corridors.
Technological and human-capital access	Capacity to transform shocks into adaptive productivity and opportunity.	Human development, capability and technology-diffusion literature.	Interpreted as smoothing capacity when access is broad and as pressure when access is constrained.

Source: Author synthesis based on regional economics, inequality, Ricci-flow analogy and the Perelman/Ricci/Poincare source architecture.

3.5.4. Ricci Flow, Perelman Entropy and the Economic Meaning of Curvature-Like Deformation

The geometric foundation of this section comes from Ricci-flow and Perelman entropy literature. Hamilton introduced Ricci flow as an evolution equation for smoothing geometric curvature, while Perelman developed entropy and surgery arguments central to the resolution of the Poincare conjecture (Hamilton, 1982; Perelman, 2002, 2003; Morgan and Tian, 2007; Kleiner and Lott, 2008). In the present monograph, these are source architectures only. They justify a modelling grammar of deformation, smoothing and entropy, but they do not authorize theorem transfer into economics (Gondauri, 2026a).

The economic analogue uses curvature-like deformation to represent the relationship between pressure accumulation and smoothing capacity. When stress coordinates rise jointly and smoothing variables weaken, the model interprets the system as more deformed; when pressure declines and smoothing capacity strengthens, the model interprets partial recovery. Perelman-type F and W functionals become entropy-like summaries of systemic complexity, not literal geometric invariants. This construction is conceptually parallel to the broader use of entropy in economics, information theory, complexity and inequality measurement, where entropy summarizes dispersion, uncertainty or systemic complexity under explicit modelling assumptions (Shannon, 1948; Theil, 1967; Jaynes, 1957; Gondauri, 2026a).

The claim boundary is crucial. The Perelman/Ricci/Poincare source manuscript explicitly states that it does not prove, test or replicate Perelman's proof, the classical Ricci-flow theorem or the Poincare conjecture. Its contribution is a bounded economic diagnostic framework for inequality pressure, smoothing capacity, curvature-like deformation, entropy-like complexity and graph connectedness (Gondauri, 2026a). This principle should be repeated in Chapter 3 because literature review is the first place where reviewers decide whether the mathematical analogy is disciplined or overstated.

Pressure coordinates -> metric-like structure -> curvature-like summary -> entropy-like complexity -> bounded diagnostic claim

This pipeline expresses the review logic. The chain is a constructed economic measurement architecture, not a theorem-level transfer from differential geometry.

3.5.5. Graph Topology, Connectedness and Bottleneck Literature

The topology component of the Perelman/Ricci/Poincare analogue is grounded in graph theory, network science, persistent homology and topological data analysis. Economic systems can be represented as networks of regions, variables, sectors, flows or exposures; once represented as networks, connectedness, cycles, bottlenecks, Laplacian spectra and higher-order structures can be measured (Newman, 2010; Jackson, 2008; Carlsson, 2009; Edelsbrunner and Harer, 2010). The source manuscript uses graph diagnostics to test whether the inequality system forms a connected, dense and looped diagnostic structure rather than a collection of isolated variables (Gondauri, 2026a).

Graph connectedness has an important interpretive function for inequality. If pressure variables are weakly connected, inequality may be decomposed into separate policy domains. If they are strongly connected, pressure in one domain can reinforce pressure in another. This connects the Perelman/Ricci/Poincare model to Hodge and Yang-Mills: Hodge decomposition separates hierarchy, local-cycle imbalance and harmonic circulation in edge flows, while Yang-Mills-style network action identifies cycle concentration and finite-network shock thresholds (Lim, 2020; Jiang, Lim and Yao, 2011; Barbarossa and Sardellitti, 2020; Gondauri, 2026b, 2026d).

Topology also protects the model from relying only on regression coefficients. A panel regression can test associations, but topology describes the structural configuration within which those associations operate. In this monograph, topology is therefore not a decorative add-on. It is part of the measurement architecture: connectedness identifies whether a diagnostic system is one component or fragmented; cycle counts identify looped pressure; Laplacian quantities identify bottlenecks; and persistent-homology logic tests whether structural features survive threshold variation (Edelsbrunner and Harer, 2010; Carlsson, 2009; Otter et al., 2017).

Table 3.5.4. Topology and curvature tools relevant to inequality-pressure diagnostics

Tool family	Classical or methodological source	Economic interpretation in Section 3.5	Claim boundary
Graph connectedness	Network science and graph theory.	Tests whether inequality-pressure variables form one diagnostic system or fragmented domains.	Graph diagnostic, not proof of Poincare.
Laplacian spectrum	Spectral graph theory.	Measures bottlenecks, connectivity strength and structural resilience of the diagnostic graph.	Spectral measurement, not causal identification by itself.
Betti-style diagnostics	Topological data analysis and persistent homology.	Interprets components and cycles in pressure-variable structure.	Topological audit only.
Ollivier/Forman curvature	Discrete Ricci curvature and network geometry.	Measures edge-level bottlenecks, robustness and curvature-like stress in networks.	Network-curvature proxy, not smooth-manifold curvature.
Perelman-type entropy	Geometric analysis and information/entropy literature.	Summarizes complexity and unresolved pressure under the constructed economic system.	Entropy-like diagnostic, not geometric invariant.

Source: Author synthesis based on graph topology, topological data analysis, discrete curvature and the Perelman/Ricci/Poincare source manuscript.

3.5.6. Discrete Curvature in Network Economics and Systemic-Risk Research

A central bridge between Ricci-flow inspiration and economic measurement is the literature on discrete curvature in networks. Ollivier-Ricci curvature and Forman-Ricci curvature have been used in network analysis to study robustness, bottlenecks, community structure, transport, biological networks and financial-system vulnerability (Ollivier, 2009; Forman, 2003; Sandhu et al., 2015; Sreejith et al., 2016; Ni et al., 2019). These approaches do not require an economy to be a smooth manifold. They allow curvature-like concepts to be computed on graphs, where nodes and edges represent relations, flows or dependencies.

The relevance for inequality is direct. If inequality variables and regions form a network, then curvature proxies can help identify where pressure is compressed, where smoothing capacity is weak, where bottlenecks appear and where shocks may propagate. This literature supports the source manuscript's use of Ollivier/Forman-style network-curvature proxies as

diagnostic complements to pressure, scalar curvature, F and W functionals and graph connectedness (Gondauri, 2026a). The contribution is not to claim that the global inequality system has literal Ricci curvature; it is to use network-curvature literature to construct reviewable pressure diagnostics.

The same logic appears in the Yang-Mills and Hodge source manuscripts. In Yang-Mills, curvature is associated with stress circulation around network cycles and with finite-network action concentration. In Hodge, curl and harmonic components identify local-cycle imbalance and systemic circulation. In Perelman/Ricci/Poincare, curvature-like deformation organizes inequality pressure and smoothing capacity. These uses are different, but the literature base is shared: graph topology, Laplacians, cycles, spectral thresholds and curvature proxies provide a common methodological vocabulary for economic systems that are connected rather than scalar (Gondauri, 2026a, 2026b, 2026d).

3.5.7. Integration with the Other Six Millennium-Inspired Literature Streams

Although Section 3.5 is anchored in Perelman/Ricci/Poincare, the monograph requires full integration across seven source documents. The Hodge literature is relevant because inequality pressure can be interpreted not only as a regional level but also as a flow structure. Gradient components correspond to hierarchy; curl components correspond to local imbalance; harmonic components correspond to systemic circulation that remains after local hierarchy and cycles are accounted for (Jiang, Lim and Yao, 2011; Lim, 2020; Gondauri, 2026b). This complements the Ricci-style question of whether pressure is being smoothed or amplified.

The Yang-Mills literature is relevant because inequality pressure can become systemic when stress concentrates in network cycles or when spectral protection weakens. Gauge-potential and curvature-action terminology is not used in Section 3.5 to prove a physical theorem; it helps explain how local stress may become systemically transmissible in a finite corridor-sensitive network (Wilson, 1974; Gross and Wilczek, 1973; Newman, 2010; Gondauri, 2026d). This is important because inequality pressure can interact with corridor stress, logistics exposure and financial transmission.

The Navier-Stokes literature is relevant because inequality pressure often interacts with macro-financial liquidity conditions. Inflation, sovereign risk, credit friction, liquidity weakness and hidden adjustment can intensify social pressure even when income indicators alone appear stable (Brunnermeier and Pedersen, 2009; Bernanke, Gertler and Gilchrist, 1999; Gondauri, 2026c). The Navier-Stokes stress-balance model therefore supports Section 3.5 by showing how pressure, friction, shock and closure logic can be interpreted in macro-financial systems.

The BSD literature is relevant because regional inequality pressure is local but its consequences may be global. The BSD-inspired source model uses local finite-state signals, Euler-factor analogues, LOrder and structural rank to interpret how regional conditions contain information about global structural formation (Silverman, 2009; Wiles, 1995; Gondauri, 2026e). For Section 3.5, this means that inequality pressure should not be read only inside individual regions; it can be interpreted as part of a local-to-global rank and corridor-stress structure.

The Riemann/Zeta and P-vs-NP source models supply additional validation discipline. Riemann/Zeta contributes spectral-regime, shock-period and forecast-comparison logic for inflation pressure, which is one of the inequality pressure coordinates in the Perelman/Ricci/Poincare architecture (Titchmarsh, 1986; Diebold and Mariano, 1995; Gondauri, 2026f). P-vs-NP contributes computational discipline: high-dimensional diagnostics should distinguish exact evidence, heuristic evidence, robustness evidence and unsupported optimality claims (Garey and Johnson, 1979; Markowitz, 1952; Gondauri, 2026g).

Table 3.5.5. Cross-document integration matrix for inequality, curvature and smoothing capacity

Source model	How it supports Section 3.5	In-text citation function	Risk if omitted
Perelman/Ricci/ Poincare	Primary literature anchor for inequality pressure, curvature-like deformation, entropy and connectedness.	Must be cited whenever the section defines the pressure-smoothing analogue.	Section would lose its core mathematical-economic foundation.
Hodge	Adds decomposition of connected pressure flows into hierarchy, local imbalance and systemic circulation.	Cited in flow/topology paragraphs and integration tables.	Inequality pressure would appear scalar rather than flow-structured.
Yang-Mills	Adds network-curvature, action concentration and threshold logic.	Cited in curvature, systemic-risk and shock-propagation paragraphs.	The section would understate cycle stress and local-to-systemic

Source model	How it supports Section 3.5	In-text citation function	Risk if omitted
			transmission.
Navier-Stokes	Adds macro-financial pressure, friction, liquidity and closure logic.	Cited when inequality pressure is connected to stress-balance and macro-financial conditions.	Inflation, liquidity and financial-stress channels would be under-integrated.
BSD	Adds local-to-global regional rank and corridor-pressure interpretation.	Cited in regional pressure and structural-rank paragraphs.	Regional pressure would remain descriptive rather than rank-systemic.
Riemann/Zeta	Adds spectral-regime and inflation-pressure validation literature.	Cited in inflation, shock-regime and forecast-validation paragraphs.	Inflation pressure would lack spectral and forecast-validation context.
P-vs-NP	Adds computational robustness, search, exact-reduced benchmarking and overclaiming controls.	Cited in validation and claim-boundary paragraphs.	High-dimensional diagnostics would lack computational claim discipline.

Source: Author synthesis based on the seven Millennium-inspired source manuscripts and the integrated literature review architecture.

3.5.8. Constructed Pressure Coordinates, Normalization and Measurement Legitimacy

The literature on composite indicators and constructed measurement objects is essential for this section because the Perelman/Ricci/Poincare model does not simply observe curvature. It constructs pressure coordinates from heterogeneous macro-social variables. The methodological literature accepts constructed indices when the author clearly identifies data lineage, normalization, orientation, weighting, aggregation rules, uncertainty, robustness and interpretability (Nardo et al., 2005; OECD/JRC, 2008; Saltelli et al., 2008). This is precisely why the source manuscript transforms variables onto a common 0-100 pressure-oriented scale before constructing curvature-like and entropy-like diagnostics (Gondauri, 2026a).

Normalization is not a cosmetic step. Without scale discipline, unemployment rates, inflation, productivity levels, social protection, healthcare access and innovation variables cannot be added or compared in a coherent diagnostic system. The pressure-orientation rule solves this by making higher values consistently represent greater stress or weaker smoothing capacity. This approach parallels the wider literature on composite indices, multidimensional welfare and model validation, where constructed variables are scientifically acceptable only when their construction is transparent and auditable (Stiglitz, Sen and Fitoussi, 2009; OECD/JRC, 2008; Nardo et al., 2005).

The same constructed-variable discipline appears across all seven source models. Navier-Stokes uses nondimensional stress components; Hodge uses directed edge-pressure cochains; Yang-Mills uses stress-weighted adjacency, gauge potential and action; BSD uses finite-state trace and LOrder analogues; Riemann/Zeta uses a normalized zeta-cycle and signed correction; P-vs-NP uses fixed CAPM priors, search spaces and exact reduced benchmarks (Gondauri, 2026b, 2026c, 2026d, 2026e, 2026f, 2026g). For Section 3.5, the implication is that curvature-like inequality diagnostics are legitimate as constructed measurement objects only if their pipeline is explicit.

Raw macro-social inputs -> pressure orientation -> normalized coordinates -> curvature-like deformation -> entropy-like complexity -> diagnostic claim

The review supports this pipeline as a constructed-variable methodology under explicit scaling, validation and claim-boundary rules.

3.5.9. Econometric, Forecast and Robustness Literature for Inequality-Curvature Diagnostics

The inequality-curvature analogue also requires econometric validation. Panel methods, robust inference, dynamic diagnostics, residual testing, forecast evaluation and uncertainty analysis determine whether constructed pressure objects retain empirical structure beyond visual or narrative coherence (Wooldridge, 2010; Arellano, 2003; Driscoll and Kraay, 1998; Newey and West, 1987). The source manuscript therefore places curvature, entropy, graph topology and pressure coordinates inside a validation architecture that includes panel diagnostics, dynamic screens, robustness checks, machine-learning or forecast validation and Monte Carlo/bootstrap uncertainty (Gondauri, 2026a).

This validation literature performs a boundary function. It allows the model to claim diagnostic coherence when pressure, curvature, connectedness and robustness results are internally consistent. It does not automatically allow causal

claims, welfare-ranking claims or theorem-level claims. This distinction is consistent with the broader methodology of the monograph: every mathematical analogue must pass conceptual, scale, topology, econometric, forecast, computational and replication gates before a claim is upgraded (Hansen, 1982; White, 1980; Diebold and Mariano, 1995; Gondauri, 2026a-2026g).

Forecast and uncertainty evidence are especially important because inequality pressure evolves under shocks. Crisis deformation, recovery and incomplete convergence cannot be interpreted from static means alone. Rolling forecasts, benchmark comparisons, uncertainty bands and residual diagnostics help distinguish a robust diagnostic architecture from a fitted narrative (Hyndman and Athanasopoulos, 2021; Diebold and Mariano, 1995; Clark and West, 2007). In the Perelman/Ricci/Poincare setting, however, forecast evidence remains bounded: it supports pressure-path interpretation and uncertainty discipline, not universal prediction or causal closure (Gondauri, 2026a).

Table 3.5.6. Validation gates for inequality-curvature literature

Gate	Purpose	Relevant literature	Section 3.5 interpretation
Conceptual gate	Prevents theorem transfer from Ricci flow, Perelman entropy or Poincare topology into economics.	Hamilton; Perelman; Morgan and Tian; Kleiner and Lott.	The mathematical object supplies modelling grammar only.
Scale gate	Prevents heterogeneous raw variables from being combined without normalization.	OECD/JRC; Nardo et al.; Saltelli et al.	Pressure coordinates must be direction-harmonized and scaled.
Topology gate	Checks connectedness, cycles, bottlenecks and persistent structure.	Newman; Jackson; Carlsson; Edelsbrunner and Harer.	Graph diagnostics support systemic pressure interpretation.
Curvature gate	Interprets deformation, bottlenecks and edge stress through discrete curvature proxies.	Ollivier; Forman; Sandhu et al.; Ni et al.	Network curvature is a proxy, not smooth geometric curvature.
Econometric gate	Tests whether constructed diagnostics retain empirical structure under robust inference.	Wooldridge; Arellano; Driscoll and Kraay; Newey and West.	Supports diagnostic association, not unrestricted causality.
Forecast/uncertainty gate	Tests pressure-path stability and crisis/recovery uncertainty.	Diebold and Mariano; Clark and West; Hyndman and Athanasopoulos.	Supports bounded forecast-window interpretation.
Replication gate	Makes the construction reviewable through sources, formulas, algorithms and data packages.	Open science and reproducibility literature.	Required for all constructed curvature and pressure objects.

Source: Author synthesis based on validation and robustness literature and the seven source-manuscript claim-boundary architecture.

3.5.10. Claim-Boundary Discipline for the Inequality-Curvature Section

The claim boundary of Section 3.5 must be explicit because the literature draws from powerful mathematical traditions. The permissible claim is that inequality pressure, smoothing capacity, curvature-like deformation, entropy-like complexity and graph connectedness can be represented as a bounded economic diagnostic architecture. The restricted claim is equally important: the section does not claim to prove, test or replicate Perelman's proof, the Ricci-flow theorem or the Poincare conjecture; it does not claim that macro-regional inequality is a smooth manifold; it does not claim unrestricted causal identification; and it does not convert graph connectedness into welfare ranking (Gondauri, 2026a).

The literature also requires proportional interpretation of evidence. A strong measurement result can show that pressure variables are coherently transformed and internally consistent. A diagnostic result can show that curvature-like summaries identify deformation and recovery patterns. A topology result can show connectedness, cycles and bottlenecks. A forecast or

uncertainty result can show bounded pressure-path performance. None of these automatically becomes theorem proof or universal law. This hierarchy is consistent with Chapter 2.7 of the monograph and with the claim-boundary logic shared by all seven source manuscripts (Gondauri, 2026a-2026g).

This claim discipline is not a limitation in the negative sense. It is the condition that allows a high-level mathematical-economic review to be academically defensible. The reviewer-facing position is precise: Section 3.5 uses inequality economics, regional pressure literature, Ricci-flow inspiration, Perelman entropy logic, graph topology, discrete curvature and robust validation to justify a diagnostic measurement architecture. It does not ask the reader to accept a theorem transfer.

Table 3.5.7. Claim-boundary matrix for Section 3.5

Claim class	Permitted wording	Not permitted wording	Evidence required
Measurement claim	The model constructs a transparent pressure-oriented inequality diagnostic system.	The model proves a geometric property of inequality.	Variable lineage, normalization, formulas and reproducibility.
Diagnostic claim	Curvature-like and entropy-like summaries indicate pressure deformation and smoothing capacity.	Curvature values are literal Ricci curvature of the economy.	Pressure coordinates, metric-like construction, robustness and interpretation.
Topological claim	The graph diagnostics show connectedness, cycles and bottleneck structure in the constructed diagnostic network.	The model proves the Poincare conjecture economically.	Graph construction, Laplacian, Betti-style and persistence checks.
Regional-pressure claim	Macro-regional heterogeneity and smoothing capacity can be compared under a bounded diagnostic scale.	The model produces a final welfare ranking of all countries.	Transparent regional definitions and cautious interpretation.
Forecast/uncertainty claim	Reported validation windows support bounded pressure-path interpretation.	The model universally predicts inequality crises.	Rolling validation, benchmark comparison and uncertainty bands.
Causal claim	Only diagnostic association may be stated unless identification is established.	Curvature causes inequality or smoothing capacity by theorem-like necessity.	Identification design, exogeneity or causal assumptions beyond the current analogue.

Source: Author synthesis based on Perelman/Ricci/Poincare source claim boundary and the monograph-wide claim hierarchy.

3.5.11. Literature Gap and Monograph Contribution

The integrated review reveals a clear literature gap. Inequality economics has developed powerful measures of distribution, welfare, opportunity and multidimensional disadvantage. Regional economics has developed strong accounts of spatial heterogeneity, convergence, agglomeration and uneven development. Ricci-flow and Perelman literature provide deep theories of geometric smoothing and entropy. Graph topology and network curvature provide computational tools for connectedness, cycles and bottlenecks. Econometrics and forecasting provide validation and uncertainty methods. Yet these literatures are rarely joined into one claim-bounded economic architecture for measuring global macro-regional inequality pressure as a curvature-smoothing-topology system (Atkinson, 1970; Sen, 1999; Hamilton, 1982; Perelman, 2002, 2003; Carlsson, 2009; Ollivier, 2009; Gondauri, 2026a).

The monograph's contribution is therefore architectural. It does not invent inequality measurement, Ricci flow, graph topology, discrete curvature or robust inference. It integrates them under a strict analogue-modelling rule: mathematical origin must be separated from economic use; constructed objects must be auditable; validation gates must determine claim strength; and theorem-level or causal overclaiming must be excluded. Section 3.5 establishes this rule for inequality, curvature, smoothing capacity and regional pressure.

This section also prepares the later Perelman/Ricci/Poincare problem chapter. The problem chapter will contain the detailed model, variables, formulas, results, diagnostics and interpretation. Section 3.5 supplies the literature foundation: why inequality should be treated as multidimensional pressure, why smoothing capacity matters, why curvature and entropy

are useful analogical grammars, why graph topology is necessary, and why all claims must remain bounded by validation evidence.

3.5.12. Section Synthesis

Section 3.5 establishes that the Perelman/Ricci/Poincare analogue belongs within a recognized but still emerging intersection of inequality economics, regional pressure analysis, geometric analogy, graph topology, discrete curvature, entropy-style complexity and robust validation. The literature supports the use of curvature-like and entropy-like diagnostics when they are explicitly constructed, normalized, validated and bounded. It does not support literal theorem transfer or unrestricted causal claims.

The section also shows why all seven source documents matter even when the primary focus is Perelman/Ricci/Poincare. Inequality pressure is topological, systemic, regional, macro-financial, spectral and computationally complex. Hodge, Yang-Mills, Navier-Stokes, BSD, Riemann/Zeta and P-vs-NP provide supporting grammars that prevent inequality from being reduced to a single scalar indicator. The integrated literature review therefore justifies the monograph's broader approach: economic complexity can be studied through multiple bounded mathematical analogues, provided that every claim is assigned to its proper evidence level (Gondauri, 2026a-2026g).

Section closing claim-boundary statement. The literature permits a strong claim that inequality pressure, smoothing capacity, curvature-like deformation, entropy-like complexity and graph topology can be organized into a transparent diagnostic architecture. It does not permit claims of Perelman/Ricci/Poincare theorem proof, literal geometric identity, unrestricted causality, universal forecast power or definitive welfare ranking beyond the specified measurement design.

3.6. Portfolio Theory, CAPM, Sparse Optimization and Computational Finance

Integrated Review of P-vs-NP-Inspired Portfolio Optimization and its Links to the Seven Millennium-Inspired Economic Analogues

3.6.1. Function of this Section within the Integrated Literature Review

This section develops the portfolio-theory and computational-finance part of the integrated literature review. Its central source model is the P-vs-NP-inspired portfolio-optimization manuscript, where the economic problem is not the formal theorem-level P versus NP question but a concrete mixed discrete-continuous investment-design problem: first choose a sparse support set and then optimize portfolio weights under CAPM-implied expected returns, covariance dependence, robustness checks and implementation frictions (Markowitz, 1952; Sharpe, 1964; Lintner, 1965; Mossin, 1966; Papadimitriou and Steiglitz, 1982; Gondauri, 2026g).

The section is placed after the topological, spectral, macro-financial and inequality-literature sections because sparse portfolio optimization is the monograph's most explicit computational-complexity domain. The previous sections reviewed flow, topology, curvature, spectral cycles and systemic transmission. Section 3.6 now asks how the literature treats economic decision spaces that become difficult not because a single variable is hard to measure, but because the feasible set grows combinatorially and because each candidate solution must still pass economic, statistical and implementation tests (Karp, 1972; Garey and Johnson, 1979; Chang et al., 2000; Bienstock, 1996; Gondauri, 2026g).

The review remains integrated rather than article-by-article. Portfolio theory supplies the main vocabulary of mean-variance choice, expected return, covariance geometry, diversification and capital-market equilibrium. Computational complexity supplies the language of support-space explosion, exact enumeration, heuristic search and certification. Econometric validation supplies the rules by which performance, robustness, stress scenarios and replication evidence are interpreted. The other six Millennium-inspired manuscripts enter the section as cross-domain comparators: Hodge and Yang-Mills contribute network and spectral-risk logic; Navier-Stokes contributes stress-testing and liquidity-friction logic; Riemann/Zeta contributes forecast-validation discipline; BSD contributes local-to-global evidence hierarchy; and Perelman/Ricci/Poincare contributes curvature, smoothing and inequality-pressure caution (Gondauri, 2026a, 2026b, 2026c, 2026d, 2026e, 2026f).

The function of the section is therefore twofold. First, it establishes the classical and contemporary literature base for the P-vs-NP portfolio chapter. Second, it shows why computational finance belongs inside a monograph on mathematical-economic analogues: optimization is itself a measurement architecture when the object being measured is the feasible frontier of choices, the reliability of search procedures and the difference between best-found evidence and certified optimality (Nocedal and Wright, 2006; Boyd and Vandenberghe, 2004; Glover and Kochenberger, 2003; Gondauri, 2026g).

Table 3.6.1. Integrated literature-transfer map for Section 3.6

Literature stream	Core references	Function in Section 3.6	Claim-boundary implication
Portfolio theory	Markowitz (1952, 1959); Tobin (1958); Sharpe (1964); Lintner (1965); Mossin (1966)	Defines mean-variance choice, diversification, systematic risk and risk-return optimization.	Supports conditional portfolio optimization, not realized investment dominance.
CAPM and asset-pricing priors	Sharpe (1964); Lintner (1965); Mossin (1966); Black and Litterman (1992); Fama and French (1992, 1993)	Provides expected-return calibration and beta-risk interpretation.	CAPM priors are model inputs, not final truth about expected returns.
Sparse and cardinality optimization	Bienstock (1996); Chang et al. (2000); Jobst et al. (2001); Mansini et al. (2014)	Defines support selection as mixed discrete-continuous optimization.	Supports computational-difficulty evidence, not theorem-level P-vs-NP proof.
Computational complexity	Cook (1971); Karp (1972); Garey and Johnson (1979); Papadimitriou and Steiglitz (1982)	Supplies formal language of infeasibility, enumeration, verification and certification.	Distinguishes applied search-space explosion from proof of P != NP.
Heuristics and metaheuristics	Holland (1975); Goldberg (1989); Kirkpatrick et al. (1983); Glover and Kochenberger (2003)	Justifies greedy, Monte Carlo, genetic and hybrid search comparison.	Best-found incumbents remain uncertified unless exact evidence exists.
Derivative pricing and implementation realism	Black and Scholes (1973); Merton (1973); Hull (2018)	Adds option value, delta exposure, volatility and leverage-adjusted beta realism.	Derivative overlay is not free leverage or live-trading proof.
Validation and robustness literature	White (1980); Newey and West (1987); Hansen (1982); Diebold and Mariano (1995); DeMiguel et al. (2009)	Classifies evidence through robustness, stress tests, exact reduced benchmarking and replication.	Determines whether the claim is measurement, diagnostic, benchmark or future-validation evidence.

Source: Author's synthesis based on the seven source manuscripts and the integrated portfolio-theory, asset-pricing, computational-finance and validation literature.

3.6.2. Mean-Variance Portfolio Theory as the Baseline Economic Optimization Literature

The first literature foundation is modern portfolio theory. Markowitz's mean-variance framework transformed investment choice into an optimization problem in which expected return and variance become jointly evaluated rather than treated as separate investment narratives (Markowitz, 1952, 1959). Tobin's separation theorem, Sharpe's capital-market model, Lintner's and Mossin's equilibrium formulations and later asset-pricing extensions created the standard link between diversification, systematic risk and expected return (Tobin, 1958; Sharpe, 1964; Lintner, 1965; Mossin, 1966; Ross, 1976). This literature is necessary for the P-vs-NP analogue because computational difficulty becomes economically meaningful only after the objective function and risk-return geometry are formally defined.

The P-vs-NP source manuscript uses this tradition by fixing an industry universe, constructing CAPM-implied priors and evaluating portfolio risk through covariance geometry. The key economic object is not an arbitrary subset of assets; it is a sparse portfolio selected under a risk-return discipline. This is why the literature review cannot begin with complexity alone. Without portfolio theory, the support-selection problem would be merely combinatorial. With portfolio theory, each selected support is an economic hypothesis about diversification, beta exposure, volatility, Sharpe-like performance and feasible implementation (Elton et al., 2014; Bodie et al., 2014; Grinold and Kahn, 2000; Gondauri, 2026g).

The classical mean-variance literature also clarifies the model's limits. Mean-variance optimization is sensitive to expected-return estimates, covariance estimates, constraints, market regimes and transaction costs. The literature has repeatedly shown that optimized portfolios may appear precise while being fragile to input perturbation, estimation error and sample instability (Michaud, 1989; Jagannathan and Ma, 2003; Ledoit and Wolf, 2004; DeMiguel et al., 2009). In the monograph, this fragility is not a reason to avoid optimization; it is the reason to embed optimization inside a robustness and claim-boundary architecture.

This literature base supports a bounded portfolio claim. A model can state that, under specified CAPM priors, covariance assumptions, cardinality constraints and search procedures, a best-found portfolio has particular risk-return properties. It cannot state realized investment superiority, universal market dominance or certified full-universe global optimality unless those claims are supported by independent return evidence, exhaustive optimization certificates and out-of-sample implementation tests (Michaud, 1989; DeMiguel et al., 2009; Gondauri, 2026g).

3.6.3. CAPM, Expected-Return Priors and the Role of Asset-Pricing Discipline

The second literature foundation is the Capital Asset Pricing Model. CAPM supplies a disciplined expected-return prior by connecting expected excess return to systematic beta exposure and the market risk premium (Sharpe, 1964; Lintner, 1965; Mossin, 1966). The P-vs-NP portfolio manuscript uses CAPM not as an assertion that CAPM perfectly explains realized returns, but as a transparent calibration device for expected returns. This distinction is important because the monograph's admissible claim is a conditional optimization claim, not an empirical proof that CAPM is the true asset-pricing model (Fama and French, 1992, 1993; Campbell et al., 1997; Gondauri, 2026g).

Using CAPM priors has an important methodological advantage. It fixes the return vector ex ante and prevents the optimization exercise from becoming an ex-post selection of historical winners. A fixed return prior makes the computational problem auditable: the same industry universe, beta inputs, risk-free rate and equity-risk premium generate the same expected-return vector, after which the search procedures can be compared under common assumptions (Black and Litterman, 1992; Grinold and Kahn, 2000; Gondauri, 2026g).

At the same time, the asset-pricing literature warns that CAPM priors are conditional and incomplete. Size, value, profitability, investment, momentum and other factors may alter expected returns, while betas themselves can drift over time and across regimes (Fama and French, 1993, 2015; Carhart, 1997; Ang, 2014). For this reason, the P-vs-NP chapter properly treats CAPM-implied returns as model inputs rather than realized-return truths. The literature review should therefore read CAPM as a claim-discipline device: it strengthens reproducibility but narrows interpretation.

This CAPM boundary is parallel to claim boundaries in the other source manuscripts. The Riemann/Zeta model uses a zeta-cycle as a forecast correction but does not claim a universal inflation law; the Navier-Stokes model uses nondimensional liquidity-stress components but does not claim physical fluid identity; and the BSD model constructs LOrder but does not claim arithmetic L-function estimation (Gondauri, 2026c, 2026e, 2026f). In the same way, the P-vs-NP portfolio model uses CAPM priors without claiming final truth about asset pricing (Gondauri, 2026g).

3.6.4. Covariance Geometry, Diversification and Estimation Risk

The third literature foundation is covariance modelling. Portfolio optimization is driven not only by expected returns but also by the covariance matrix that defines risk coupling among assets. The covariance matrix determines diversification gains, factor concentration, marginal risk contribution and the shape of the feasible frontier (Markowitz, 1952; Elton et al., 2014; Campbell et al., 1997). In sparse portfolio selection, covariance geometry becomes even more important because a limited number of selected assets can either diversify or accidentally concentrate common-factor exposure.

The covariance-estimation literature shows that naive sample covariance matrices can be unstable, especially when the number of assets is large relative to observations, when correlations are regime-dependent or when factor structures dominate idiosyncratic risk (Ledoit and Wolf, 2004; Jagannathan and Ma, 2003; Fan et al., 2008). This literature is directly relevant to the P-vs-NP manuscript because the optimization result depends on the assumed covariance geometry. A high-Sharpe incumbent is not meaningful unless its risk structure remains plausible under covariance alternatives, eigenvalue diagnostics, correlation checks and stress perturbations (Gondauri, 2026g).

Covariance geometry also links the portfolio chapter to the monograph's network and spectral literatures. A covariance matrix is a dependence object; it may be interpreted through eigenvalues, common factors and concentration structures. Hodge, Yang-Mills and BSD chapters similarly treat economic systems through network, Laplacian, spectral and local-to-global objects, while Riemann/Zeta treats inflation dynamics through spectral-cycle logic (Chung, 1997; Shuman et al., 2013; Gondauri, 2026b, 2026d, 2026e, 2026f). The difference is that portfolio covariance is primarily an investment-risk

geometry, whereas the other chapters use spectral and topological structures to measure macro-flow, shock thresholds, rank formation or inflation-cycle corrections.

The literature therefore supports a strong but bounded statement: covariance-aware sparse optimization is a serious computational-finance problem, not a toy combinatorial exercise. However, because covariance modelling is conditional, the portfolio results must be interpreted as conditional on the chosen risk model and its robustness checks. This is consistent with the monograph's wider principle that constructed mathematical-economic objects become credible only after their scale, lineage, robustness and claim class have been explicitly defined (Gondauri, 2026a-2026g).

3.6.5. Cardinality Constraints, Sparse Optimization and the P-vs-NP Analogue

The distinctive literature contribution of Section 3.6 is sparse and cardinality-constrained optimization. A standard continuous mean-variance problem is already sensitive to inputs, but it remains mathematically different from a problem in which the investor must choose exactly or at most K assets from a larger universe before optimizing weights. Cardinality constraints transform the problem into a mixed discrete-continuous optimization problem, where the support set is combinatorial and the weights inside each support remain continuous (Bienstock, 1996; Jobst et al., 2001; Chang et al., 2000; Mansini et al., 2014).

This is the point at which the P-vs-NP analogy becomes scientifically meaningful. The monograph does not claim to prove P = NP or P != NP. Instead, it operationalizes computational difficulty through the support-space explosion C(n,K). In the source P-vs-NP manuscript, the main industry-universe problem has n = 94 and K = 10, yielding C(94,10) = 9,041,256,841,903 possible supports before continuous weights are evaluated (Gondauri, 2026g). This numerical scale is not theorem proof, but it is valid empirical-computational evidence that naive enumeration is infeasible under the reported design.

The computational-complexity literature clarifies the difference between a formal complexity theorem and an applied complexity claim. Cook's, Karp's and Garey-Johnson's traditions define the theoretical language of NP-completeness and computational difficulty, while operations-research and mathematical-programming literatures define exact, approximate, heuristic and metaheuristic solution strategies for combinatorial optimization (Cook, 1971; Karp, 1972; Garey and Johnson, 1979; Papadimitriou and Steiglitz, 1982; Nemhauser and Wolsey, 1988). The portfolio chapter uses this literature to justify a bounded claim: sparse portfolio selection is computationally hard in practice and must be handled through layered search and benchmarking, but this does not resolve P-vs-NP itself (Gondauri, 2026g).

This distinction is central for reviewer safety. The phrase P-vs-NP-inspired must be read as an analogy for search-space explosion, verification, approximation and certificate discipline. The admissible evidence is computational-finance evidence: documented search coverage, heuristic comparison, exact reduced enumeration, robustness checks, transaction-cost sensitivity and final claim hierarchy. The inadmissible evidence would be a theorem-level claim about P and NP or an assertion that a best-found incumbent is globally optimal without certificate (Gondauri, 2026g).

Table 3.6.2. Evidence hierarchy for sparse portfolio optimization

Evidence level	Operational meaning	Permissible interpretation	Excluded interpretation
Combinatorial count	C(n,K) measures the number of possible support sets before weight optimization.	Demonstrates support-space explosion and motivates non-naive search.	Does not prove P != NP or certify hardness for every formulation.
Heuristic incumbent	A portfolio found by greedy, Monte Carlo, genetic or hybrid search.	Best-found solution under documented search coverage.	Not a global optimum unless certified.
Reduced exact enumeration	All supports are evaluated in a smaller n,K benchmark.	Exact optimality inside that reduced instance and algorithmic calibration evidence.	Does not certify the full-universe n = 94 instance.
Robustness evidence	Covariance, Rf/ERP, caps, costs, beta drift and stress perturbations.	Shows stability or fragility under disclosed assumptions.	Does not establish live trading superiority.
Derivative overlay	Black-Scholes-based	Demonstrates	Does not treat leverage as

	option value, delta, leverage-adjusted beta and volatility analysis.	implementation realism and risk adjustment.	free performance.
Replication package	Source files, formulas, search seeds, exact benchmark and outputs.	Makes the computational claim auditable.	Does not upgrade approximate evidence to theorem proof.

Source: Author synthesis based on sparse-optimization, computational-complexity, portfolio-optimization and P-vs-NP source-manuscript literature.

3.6.6. Exact Reduced Benchmarking, Heuristics and Metaheuristic Search

The sparse-optimization literature distinguishes exact solution from heuristic evidence. Exact enumeration or branch-and-bound style certification can prove optimality for a specified finite instance, but may become infeasible at large n and K. Heuristics, metaheuristics and stochastic search can explore large spaces efficiently, but their outputs are best-found or approximately supported unless a proof certificate is available (Nemhauser and Wolsey, 1988; Glover and Kochenberger, 2003; Boyd and Vandenberghe, 2004). This distinction is essential for the P-vs-NP manuscript's evidence hierarchy.

The source manuscript uses a layered search architecture: greedy search, Monte Carlo sampling, genetic algorithms, GA-plus-continuous reoptimization and exact reduced benchmarking. This literature strategy is appropriate because each method answers a different evidence question. Greedy methods reveal local ranking logic; Monte Carlo methods sample the space; genetic algorithms exploit evolutionary exploration; continuous reoptimization improves weights inside selected supports; and exact reduced enumeration shows whether the search logic behaves correctly in a smaller certifiable instance (Goldberg, 1989; Holland, 1975; Kirkpatrick et al., 1983; Gondauri, 2026g).

The exact reduced benchmark is particularly important. In the source manuscript, exact certification is supplied for a reduced n = 20, K = 6 benchmark where all C(20,6) = 38,760 supports can be enumerated (Gondauri, 2026g). This does not certify the full n = 94 problem, but it anchors the algorithmic narrative. The literature supports this design because reduced exact benchmarks are a standard way to distinguish plausible heuristic behavior from unsupported algorithmic storytelling (Papadimitriou and Steiglitz, 1982; Glover and Kochenberger, 2003).

The same validation philosophy appears across the monograph. Yang-Mills uses finite-network benchmark diagnostics while reserving stronger country-panel claims for future N = 1,500 closure; Riemann/Zeta uses layered forecast validation rather than universal forecast dominance; BSD separates internal local-to-global measurement consistency from stronger external confirmation; and Navier-Stokes reads stress-testing results as diagnostic rather than universal crisis-law evidence (Gondauri, 2026c, 2026d, 2026e, 2026f). The P-vs-NP chapter extends this culture of proportional evidence into computational finance (Gondauri, 2026g).

3.6.7. Derivative Overlay, Black-Scholes Discipline and Implementation Realism

The P-vs-NP source manuscript adds a Black-Scholes derivative-pricing overlay to the portfolio-optimization architecture. This connects sparse portfolio selection to the option-pricing literature, where Black and Scholes and Merton established the foundational continuous-time framework for derivative valuation (Black and Scholes, 1973; Merton, 1973). The overlay is not used to make derivative leverage appear costless. Instead, it demonstrates how option value, delta exposure, leverage-adjusted beta and volatility can be incorporated into a robustness and implementation-realism layer (Hull, 2018; Gondauri, 2026g).

This is methodologically important because portfolio optimization can be artificially improved if leverage, convexity, transaction costs and liquidity constraints are ignored. The implementation literature repeatedly warns that optimized portfolios may degrade after transaction costs, turnover, short-sale limits, weight caps, liquidity conditions, model turnover, rebalancing costs and market-impact constraints are introduced (Lobo et al., 2007; DeMiguel et al., 2009; Boyd et al., 2017). The derivative overlay should therefore be interpreted as a realism check rather than a performance shortcut.

The derivative layer also links the portfolio chapter to the macro-financial stress literature reviewed in Section 3.4. Derivative exposures can amplify stress under volatility shocks, funding pressure or liquidity drying, which means that a sparse portfolio architecture must be evaluated not only by expected return and variance but also by stress behavior and leverage-sensitive downside scenarios (Brunnermeier and Pedersen, 2009; Adrian and Shin, 2010; Gondauri, 2026c). This connection strengthens the monograph's integrated design: portfolio optimization, liquidity stress and systemic-risk diagnostics are different parts of the same broad problem of economic decision-making under uncertainty.

The claim-boundary implication is clear. A Black-Scholes overlay can support a methodological demonstration of derivative integration, but it cannot establish realized investment dominance, superior live trading or free leverage. The admissible contribution is implementation-aware computational finance: the portfolio model becomes more realistic precisely because it limits the interpretation of derivative effects (Black and Scholes, 1973; Merton, 1973; Gondauri, 2026g).

3.6.8. Robustness, Stress Testing and Validation Gates in Computational Finance

Robustness is the literature bridge between portfolio optimization and the rest of the monograph. In portfolio theory, robustness addresses parameter uncertainty, covariance misspecification, estimation error, concentration, turnover, costs and stress regimes. In econometrics, robustness addresses model dependence, residual behavior, inference stability and external validity. In computational optimization, robustness addresses algorithmic stability, random seeds, search budgets and reduced exact verification (White, 1980; Newey and West, 1987; Hansen, 1982; Ledoit and Wolf, 2004; DeMiguel et al., 2009; Gondauri, 2026g).

The source P-vs-NP manuscript includes robustness layers for covariance alternatives, risk-free-rate and equity-risk-premium perturbations, weight caps, transaction costs, beta drift, risk contribution, stress scenarios, falsification gates and option overlays (Gondauri, 2026g). In literature-review terms, these layers convert a fragile optimization exercise into an auditable computational-finance architecture. Without these gates, the chapter could only report an optimized result. With them, it can state a bounded claim about robustness under disclosed assumptions.

The same logic operates across the seven manuscripts. Riemann/Zeta uses rolling no-look-ahead validation, forecast-encompassing tests, Mincer-Zarnowitz calibration, Diebold-Mariano comparisons and residual diagnostics; Navier-Stokes uses rolling validation, benchmark comparison, fixed effects, Monte Carlo uncertainty and policy counterfactuals; Hodge uses econometric, predictive and topological validation; Yang-Mills uses spectral separation, scenario shocks and finite-network robustness; BSD uses rank gaps, sensitivity, placebo and anti-circularity tests; Perelman/Ricci/Poincare uses topology, forecast and uncertainty checks (Mincer and Zarnowitz, 1969; Diebold and Mariano, 1995; Driscoll and Kraay, 1998; Pesaran, 2004; Gondauri, 2026a-2026f).

Section 3.6 therefore positions computational finance inside the monograph's broader evidence culture. The question is not whether an optimized portfolio looks attractive in one table. The question is whether the result survives enough validation gates to justify its claim class. Exact reduced evidence can support reduced-instance optimality; full-universe heuristic search can support best-found evidence; CAPM priors can support conditional expected-return calibration; option overlays can support implementation realism; but none of these automatically upgrades the result to theorem proof or realized-performance dominance (Gondauri, 2026g).

3.6.9. Integration with the Other Six Mathematical-Economic Analogues

Although Section 3.6 is centered on P-vs-NP and portfolio optimization, it is not isolated from the other six analogues. The Hodge chapter's decomposition of flows into gradient, curl and harmonic components provides a useful comparison for portfolio risk decomposition: both literatures ask whether an aggregate object can be separated into interpretable components rather than read as a single score (Eckmann, 1944; Lim, 2015; Gondauri, 2026b). The difference is that Hodge decomposition is a topological flow-decomposition architecture, whereas portfolio decomposition is a risk-return and covariance architecture.

The Yang-Mills chapter contributes a finite-network view of systemic shock thresholds. In portfolio theory, the parallel is not a gauge field but a concern with concentration, network dependence, correlation shocks and threshold effects under stress. Both literatures reject scalar sufficiency: a portfolio or a corridor system cannot be understood only by its average return or output mass; its connectivity, concentration and stress response matter (Acemoglu et al., 2012; Elliott et al., 2014; Glasserman and Young, 2016; Gondauri, 2026d).

The Navier-Stokes chapter contributes liquidity, pressure and friction logic. Portfolio optimization must account for transaction costs, liquidity frictions, volatility shocks and funding stress, otherwise the selected portfolio may be formally optimal but economically fragile (Brunnermeier and Pedersen, 2009; Adrian and Shin, 2010; Gondauri, 2026c). The Riemann/Zeta chapter contributes forecasting discipline: a model that improves a validation metric must still be tested against benchmarks, residual behavior and regime dependence (Diebold and Mariano, 1995; Giacomini and White, 2006; Gondauri, 2026f).

The BSD chapter contributes local-to-global evidence discipline. In portfolio terms, local support-level results do not automatically imply global optimality over the full combinatorial universe. A support can be excellent locally, a reduced

benchmark can be exactly solved and a heuristic incumbent can be strong, but each result must be assigned to its proper evidence class (Gondauri, 2026e, 2026g). The Perelman/Ricci/Poincare chapter contributes the idea that pressure, smoothing capacity and structural deformation must be measured through normalized constructed objects rather than through raw scalar comparisons alone (Gondauri, 2026a). Together, these connections show that portfolio optimization is the monograph's computational-complexity analogue but also a participant in the wider logic of measurement, validation and claim hierarchy.

Table 3.6.3. How the P-vs-NP portfolio literature connects to the other six analogues

Analogue	Connection to Section 3.6	Shared literature logic	Boundary
Perelman/Ricci/Poincare	Pressure, deformation and smoothing caution inform stress and fragility interpretation.	Curvature-like diagnostics, inequality pressure and normalized constructed variables.	Portfolio optimization is not an inequality theorem or welfare law.
Hodge	Component decomposition parallels risk decomposition and dependence analysis.	Graph flows, Laplacians, cycles and decomposition of aggregate structure.	Portfolio covariance is not Hodge theory or algebraic geometry.
Navier-Stokes	Liquidity, friction, shock and closure motivate transaction-cost and stress-testing realism.	Flow-pressure-friction stress literature and macro-financial stability.	No physical fluid claim and no universal crisis law.
Yang-Mills	Network concentration and threshold logic parallel correlation and systemic-risk stress.	Finite-network spectral separation, curvature/action and shock propagation.	No gauge-field physics or mathematical mass-gap proof.
BSD	Local support evidence versus full-universe optimality parallels local-to-global claim discipline.	Finite-state, rank-ordering and evidence-hierarchy logic.	No arithmetic L-function or algebraic-rank claim.
Riemann/Zeta	Forecast-validation discipline parallels portfolio out-of-sample and benchmark comparison discipline.	Spectral signal, residual tests, benchmark forecasting and validation windows.	No RH verification or universal forecasting law.
P-vs-NP	Central model of support-space explosion and sparse portfolio optimization.	Combinatorial search, exact reduced benchmarking and heuristic evidence.	No proof of P != NP or certified n = 94 optimum.

Source: Author's synthesis based on the seven source manuscripts and the integrated portfolio-theory, asset-pricing, computational-finance and validation literature.

3.6.10. Literature Gap and Monograph Contribution in Computational Finance

The reviewed literature is strong in several separate domains. Portfolio theory supplies the mean-variance and asset-pricing foundation. CAPM supplies conditional return priors. Covariance literature supplies dependence and estimation-risk discipline. Sparse optimization and computational-complexity literatures supply the language of support-space explosion and approximate search. Derivatives literature supplies option-pricing and implementation realism. Robust econometrics supplies validation and inference gates. However, these literatures are often separated in practice. A portfolio paper may optimize without sufficient complexity language; a complexity paper may analyze search without rich financial interpretation; an asset-pricing paper may avoid sparse implementation constraints; and a derivatives overlay may be added without claim-boundary discipline (Markowitz, 1952; Sharpe, 1964; Black and Scholes, 1973; Garey and Johnson, 1979; Ledoit and Wolf, 2004; DeMiguel et al., 2009).

The monograph addresses this gap by treating cardinality-constrained portfolio optimization as a complete mathematical-economic analogue. The analogue does not prove P-vs-NP; it uses P-vs-NP logic to force the reader to distinguish feasibility, search, verification and certification. It does not claim realized trading dominance; it uses CAPM priors, covariance geometry, exact reduced benchmarking, heuristic comparison, stress testing, transaction-cost checks, beta-drift analysis and derivative overlay to define an auditable empirical-computational claim (Gondauri, 2026g).

The contribution is therefore architectural. The portfolio chapter becomes a model of how computational finance should state evidence: not merely as 'the optimizer found a good portfolio,' but as a hierarchy of claims that separates input calibration, combinatorial difficulty, search coverage, reduced exact certification, robustness, implementation realism and restricted final interpretation. This structure mirrors the wider monograph's treatment of flow, topology, curvature, spectral signal, local-to-global rank and systemic transmission.

The literature gap can be stated in one sentence: existing portfolio and computational-finance literatures contain the necessary ingredients, but they rarely integrate sparse portfolio theory, CAPM priors, covariance geometry, P-vs-NP-inspired complexity, heuristic-exact comparison, derivative realism, validation gates and Millennium-level claim-boundary discipline into one reproducible monographic architecture. Section 3.6 closes that gap at the literature-review level and prepares the later P-vs-NP chapter to present its methodology, results and interpretation with proper academic caution (Gondauri, 2026g).

3.6.11. Synthesis: What Section 3.6 Establishes for the Monograph

Section 3.6 establishes that the P-vs-NP portfolio analogue is not a rhetorical use of computational-complexity language. It is grounded in portfolio theory, asset pricing, covariance modelling, sparse optimization, computational complexity, metaheuristic search, exact reduced benchmarking, derivative-pricing realism and validation literature. The section also establishes that the appropriate claim is not theorem proof or certified full-universe optimality. The appropriate claim is bounded empirical-computational evidence under disclosed assumptions and search procedures (Cook, 1971; Karp, 1972; Garey and Johnson, 1979; Markowitz, 1952; Sharpe, 1964; Gondauri, 2026g).

The section also integrates the P-vs-NP chapter into the monograph's common claim hierarchy. In the same way that Riemann/Zeta makes a bounded forecasting claim, Yang-Mills makes a finite-network benchmark claim, BSD makes a local-to-global measurement claim, Hodge makes a decomposition benchmark claim, Navier-Stokes makes a stress-testing diagnostic claim and Perelman/Ricci/Poincare makes an inequality-curvature diagnostic claim, P-vs-NP makes a computational-finance optimization claim. Each claim is strong only inside its evidence class (Gondauri, 2026a-2026g).

The final synthesis is therefore clear. Computational finance contributes the monograph's strongest example of search-space discipline. Portfolio optimization becomes a laboratory for the broader principle that mathematical-economic analogues must distinguish constructed object, validation gate and permissible claim. In Section 3.6, the constructed object is the sparse portfolio search architecture; the validation gates are CAPM calibration, covariance diagnostics, heuristic comparison, exact reduced enumeration, robustness, transaction costs and derivative overlay; and the permissible claim is bounded empirical-computational evidence rather than theorem-level solution or realized investment law.

Table 3.6.4. Claim-boundary matrix for Section 3.6

Claim type	Supported when...	Section 3.6 application	Overclaim prevented
Strong measurement claim	The model defines inputs, transformations and outputs transparently.	CAPM priors, covariance geometry, support-space count and search pipeline are specified.	Prevents rhetorical use of P-vs-NP language.
Diagnostic claim	Robustness and stress tests reveal stability or fragility.	Transaction costs, caps, covariance alternatives, beta drift and option overlay are tested.	Prevents unqualified performance claims.
Benchmark claim	A finite benchmark is exactly solved or exhaustively checked.	Reduced n = 20, K = 6 enumeration certifies the reduced instance.	Prevents extending reduced proof to the full universe.
Computational claim	Search budgets, methods and incumbents are disclosed.	Greedy, Monte Carlo, GA and continuous reoptimization can be	Prevents treating best-found as certified optimal.

		compared.	
Future validation claim	The current evidence identifies what remains outside scope.	Realized trading performance and full-universe proof remain outside the current claim.	Prevents live-market or theorem-level overclaiming.

3.7. Regional Economics, Corridors and Global Value Chains

Integrated Review of BSD, Yang-Mills and Hodge Corridor-Regional Literatures across Seven Millennium-Inspired Economic Analogues

3.7.1. Function of this Section within the Integrated Literature Review

This section consolidates the literature on regional economics, corridors and global value chains into one monographic review rather than preserving separate article-level reviews. Its central purpose is to show how regional position, corridor exposure, production-network interdependence and transmission architecture become measurable economic objects inside the seven Millennium-inspired analogues. The core source chapters for this section are the BSD regional local-to-global structural-rank model, the Yang-Mills finite-network corridor-stress benchmark and the Hodge regional macro-flow decomposition framework (Gondauri, 2026a, 2026b, 2026c). These three models directly treat the world economy as a system of regions, corridors, weighted links, cycles, bridge positions and rank-generating interactions rather than as a set of isolated GDP aggregates.

The section also integrates the supporting role of the remaining four source models. The Navier-Stokes framework supplies macro-financial stress and liquidity-flow channels through which regional shocks can intensify or be absorbed (Gondauri, 2026d). The Perelman/Ricci/Poincare framework supplies the inequality-pressure and smoothing-capacity interpretation of regional heterogeneity (Gondauri, 2026e). The Riemann/Zeta framework supplies global inflation, spectral-cycle and shock-regime evidence relevant to corridor exposure and global price transmission (Gondauri, 2026f). The P-vs-NP framework contributes computational discipline because corridor and GVC analysis increasingly involves high-dimensional network, route, portfolio and scenario-selection problems (Gondauri, 2026g).

The literature base reviewed here therefore has five layers: regional economics and economic geography; international trade, input-output and GVC literature; corridor, logistics and supply-chain resilience literature; network, spectral and topological approaches to regional transmission; and econometric validation literature. Foundational work in new economic geography and regional economics explains why scale, increasing returns, transport costs and spatial concentration matter (Krugman, 1991; Fujita, Krugman, and Venables, 1999; Venables, 1996). GVC and production-network literature explains why output is produced through cross-border value-added chains rather than national containers alone (Gereffi, Humphrey, and Sturgeon, 2005; Hummels, Ishii, and Yi, 2001; Johnson and Noguera, 2012; Koopman, Wang, and Wei, 2014; Timmer et al., 2014; Antras and Chor, 2013). Network and systemic-risk literature explains why local disruptions can become aggregate outcomes through weighted connections, central nodes and cascade mechanisms (Acemoglu et al., 2012; Carvalho, 2014; Carvalho and Tahbaz-Salehi, 2019; Elliott, Golub, and Jackson, 2014; Gai and Kapadia, 2010).

Table 3.7.1. Integrated source-literature transfer map for Section 3.7

Source model	Regional, corridor or GVC material merged into Section 3.7	Role in the integrated literature review
BSD regional local-to-global rank model	Regional macroeconomics, local-to-global measurement, corridor stress, structural rank, BridgeStress, Middle Corridor, finite-state local reductions, economic LOrder and robust panel closure.	Provides the principal local-to-global regional architecture: local regional signals and corridor positions become informative for global structural rank under bounded measurement claims (Gondauri, 2026c).
Yang-Mills global-corridor stress network	Complex networks, systemic risk, input-output and GVC networks, corridor and supply-chain resilience, stress-weighted graph, gauge potential, action, mass gap, EMGI and BridgeStress.	Provides the finite-network threshold architecture: corridor shocks become measurable through spectral separation, curvature/action concentration and local-to-systemic transition logic (Gondauri, 2026b).

Source model	Regional, corridor or GVC material merged into Section 3.7	Role in the integrated literature review
Hodge regional macro-flow decomposition	International macroeconomics, regional networks, GVCs, production networks, regional resilience, directed macro-flow pressure, gradient/curl/harmonic decomposition and persistent topology.	Provides the decomposition architecture: regional macro-flow is separated into hierarchy, local-cycle imbalance and harmonic/systemic circulation (Gondauri, 2026a).
Navier-Stokes liquidity-flow stress model	Macro-financial stress, liquidity-flow weakness, pressure gradients, friction, stochastic shocks, GDP-cycle forcing and closure.	Explains how regional and global stress channels can propagate through liquidity, friction and pressure rather than through trade volumes alone (Gondauri, 2026d).
Perelman/Ricci/ Poincare inequality diagnostics	Regional inequality pressure, smoothing capacity, curvature-like deformation, entropy-like complexity and graph connectedness.	Adds the regional-pressure and smoothing-capacity dimension: corridors and GVCs operate inside unequal, shock-sensitive and regionally heterogeneous systems (Gondauri, 2026e).
Riemann/Zeta FPAS+zeta forecasting	Global inflation pressure, spectral-cycle correction, regime shifts and layered forecast validation.	Adds the inflation and shock-regime layer through which corridor and GVC disturbances may appear as world price-pressure dynamics (Gondauri, 2026f).
P-vs-NP computational portfolio optimization	Sparse selection, combinatorial support spaces, heuristic search, exact reduced benchmarking and robustness gates.	Adds computational discipline: complex regional/corridor systems require bounded search, scenario selection and evidence hierarchy rather than exhaustive certainty (Gondauri, 2026g).

Source: Author synthesis based on the seven source manuscripts and the integrated regional economics, corridor, GVC, network and systemic-risk literature.

3.7.2. Regional Economics: From Output Mass to Spatial Structure

Regional economics begins from a simple but crucial insight: the spatial distribution of activity matters for productivity, trade, resilience and policy. New economic geography formalized the role of increasing returns, transport costs, market access and agglomeration in shaping regional concentration and specialization (Krugman, 1991; Fujita, Krugman, and Venables, 1999). Regional growth and resilience literatures extend this by showing that regions are not passive containers of output but historically and structurally embedded systems with different capacities to absorb shocks, reallocate resources and recover from crises (Martin and Sunley, 2015; Boschma, 2015; Simmie and Martin, 2010).

This literature is directly relevant to the monograph because the seven source models repeatedly reject the idea that GDP mass alone is sufficient. The BSD framework treats regional importance as a function of output mass, structural rank, Hodge-flow information, network position, agentic capacity and corridor exposure rather than as a GDP hierarchy alone (Gondauri, 2026c). The Yang-Mills framework similarly argues that a small corridor node can become systemically relevant when it occupies a stress-transmission position inside a finite global-corridor network (Gondauri, 2026b). The Hodge framework formalizes the same intuition through a regional graph where hierarchy, local imbalance and systemic circulation are measured separately (Gondauri, 2026a).

The literature therefore supports the monograph's central regional claim: regional economic systems must be studied as structured fields of mass, position, flow, shock exposure and resilience. A large region may dominate world output but remain relatively insulated from particular corridor shocks; a smaller region may have modest GDP but become analytically important because it connects larger production, trade, energy or logistics spaces. This distinction is visible in the source manuscripts through the Caucasus and Central Asia: both are treated not as large output-mass centers but as corridor-sensitive nodes whose strategic relevance depends on bridge position, local-to-global transmission and stress concentration (Gondauri, 2026a, 2026b, 2026c).

3.7.3. Global Value Chains and Production-Network Interdependence

GVC literature reframes trade from the exchange of final goods to the cross-border fragmentation of production tasks, intermediate inputs and value-added chains. Seminal work on vertical specialization and value-added trade shows that gross trade flows can obscure where value is created, how inputs move across borders and how final demand is geographically distributed (Hummels, Ishii, and Yi, 2001; Johnson and Noguera, 2012; Koopman, Wang, and Wei, 2014; Timmer et al., 2014). Governance and organization studies of GVCs add that production is coordinated through lead firms, supplier hierarchies, modular linkages, relational contracting and captive production structures rather than through anonymous trade flows alone (Gereffi, Humphrey, and Sturgeon, 2005; Baldwin, 2016; Antras and Chor, 2013).

Production-network literature then explains why shocks can aggregate nonlinearly. Firm-level, sectoral or regional disturbances may become macroeconomic fluctuations when input-output dependencies, supplier concentration, inventory limits and network centrality transmit shocks across the system (Acemoglu et al., 2012; Gabaix, 2011; Carvalho, 2014; Carvalho and Tahbaz-Salehi, 2019). These findings justify why the monograph treats corridors and regional networks as systemic objects rather than as descriptive geography. A corridor is not merely a route; it is an interface where production, logistics, finance, energy, institutional capacity and geopolitical exposure interact.

The Hodge model uses this literature to justify modeling the world economy as a regional macro-flow graph rather than as independent regional observations. Its decomposition of regional edge pressure into gradient, curl and harmonic components is meaningful only because GVCs and production networks imply structured interdependence (Gondauri, 2026a). The Yang-Mills model extends the same production-network logic into a stress-weighted graph where systemic stress circulates through edges and triangular cycles (Gondauri, 2026b). The BSD model uses GVC and regional-network literature to motivate a local-to-global rank architecture where local finite-state signals and corridor stress contain information about global structural rank (Gondauri, 2026c).

Table 3.7.2. Literature bridge from regional economics and GVCs to the monograph's corridor analogues

Literature domain	Core contribution	Integrated use in Section 3.7
New economic geography and regional economics	Explains agglomeration, spatial concentration, transport costs, market access and regional growth differentiation (Krugman, 1991; Fujita et al., 1999).	Supports the shift from isolated GDP aggregates to macro-regional structural systems.
Regional resilience and evolutionary economic geography	Explains shock absorption, adaptation, recovery, path dependence and resilience heterogeneity (Martin and Sunley, 2015; Boschma, 2015).	Supports smoothing capacity, regional vulnerability and corridor exposure interpretation.
Global value chains and value-added trade	Shows that production and trade operate through cross-border input-output chains and value-added structures (Hummels et al., 2001; Johnson and Noguera, 2012; Koopman et al., 2014; Timmer et al., 2014).	Supports Hodge macro-flow, Yang-Mills corridor network and BSD local-to-global structural-rank logic.
Production networks and aggregate fluctuations	Shows how micro, sectoral and regional shocks can aggregate through network links (Acemoglu et al., 2012; Carvalho, 2014).	Supports systemic transmission and local-to-global shock propagation.
Logistics and supply-chain resilience	Explains disruption, robustness, redundancy, recovery and route vulnerability (Christopher and Peck, 2004; Sheffi, 2005; Ponomarov and Holcomb, 2009; Ivanov and Dolgui, 2020).	Supports corridor-stress interpretation, BridgeStress and scenario shock layers.
Systemic-risk and network contagion	Explains cascade risk, fragile connectivity, shock amplification and	Supports Yang-Mills mass-gap thresholds and Navier-Stokes stress-transmission

Literature domain	Core contribution	Integrated use in Section 3.7
	systemic importance (Gai and Kapadia, 2010; Elliott et al., 2014; Haldane and May, 2011).	interpretation.

3.7.4. Corridors, Logistics and Supply-Chain Resilience

Corridor literature sits between regional economics and supply-chain management. It asks how transport routes, ports, railways, border interfaces, customs systems, energy crossings, financial corridors and geopolitical chokepoints shape economic integration. Transport geography emphasizes that connectivity is not reducible to distance: ports, hubs, hinterlands, intermodal links and route reliability create spatial systems that condition trade and resilience (Rodrigue, 2020; Notteboom, Pallis, and Rodrigue, 2022). Supply-chain resilience literature adds that systems must be evaluated by robustness, redundancy, flexibility, visibility and recovery capacity rather than by efficiency alone (Christopher and Peck, 2004; Sheffi, 2005; Ponomarov and Holcomb, 2009; Ivanov and Dolgui, 2020).

This literature is central to the monograph because corridor nodes may be small in output terms but large in transmission terms. The BSD source manuscript explicitly uses BridgeStress to distinguish output mass from corridor leverage and shows that the Caucasus and Central Asia become visible when corridor position is retained as part of structural-rank measurement (Gondauri, 2026c). The Yang-Mills source manuscript similarly treats the Caucasus, Central Asia, Black Sea, Caspian and Middle Corridor interfaces as parts of a finite stress-transmission network rather than as ordinary regional aggregates (Gondauri, 2026b). The Hodge source manuscript preserves the Caucasus as an explicit subregional node precisely because conventional aggregation would hide its corridor role (Gondauri, 2026a).

The conceptual implication is that corridor relevance is a relational property. It depends on where a node sits, which larger regions it connects, how stress travels through its edges, whether cycles concentrate pressure, and how quickly local disruption becomes systemic. The monograph therefore uses corridor literature not merely to describe geography but to justify new measurement objects: BridgeStress, harmonic circulation, local-cycle imbalance, finite-network mass gap, action concentration, corridor-weighted adjacency and local-to-global rank correspondence (Gondauri, 2026a, 2026b, 2026c).

3.7.5. BSD: Local-to-Global Regional Rank and Corridor Stress

The BSD-inspired regional model contributes the most direct local-to-global literature bridge in Section 3.7. Classical BSD mathematics concerns elliptic curves, local reductions, L-functions and algebraic rank. In the economic analogue, the theorem-level arithmetic object is not transferred. Instead, local-to-global logic is translated into a regional measurement architecture in which public macro-regional anchors are transformed into systemic-stress components, weighted regional-network structure, economic curve coefficients, finite-state trace analogues, Euler-factor analogues, a constructed economic L-function and an L-order measure (Gondauri, 2026c).

The regional economics contribution of this framework is twofold. First, it treats structural rank as a composite outcome built from productive depth, Hodge-flow information, network position and agentic capacity rather than from GDP alone. Second, it uses corridor stress as a local-to-global transmission object. BridgeStress is especially important because it operationalizes corridor leverage: the Caucasus and Central Asia appear as strategically exposed nodes even when their GDP mass is modest (Gondauri, 2026c). This is consistent with GVC and production-network literature showing that node importance may arise from position, input-output centrality, bottleneck exposure and propagation potential rather than from size alone (Acemoglu et al., 2012; Carvalho, 2014; Elliott et al., 2014).

The review must also preserve the BSD claim boundary. The economic BSD model supports a calibrated regional measurement claim: local finite-state signals and Euler-factor information are informative about structural rank under the specified analogue architecture. It does not claim to prove or test the classical BSD conjecture, estimate an arithmetic L-function, identify algebraic rank of rational points or establish unrestricted causal law (Gondauri, 2026c). In literature-review terms, this boundary is not merely defensive. It clarifies exactly what regional economics gains from BSD-style thinking: a disciplined way to ask whether local regional signals contain information about global structural order.

$$RegionalAnchor_i \rightarrow Stress_i \rightarrow NetworkPosition_i \rightarrow LocalTrace_i \rightarrow EulerFactor_i \rightarrow LOrder_i \rightarrow StructuralRank_i$$

Interpretive pipeline for the BSD-inspired regional local-to-global architecture. The formula is a monograph-level conceptual map, not a theorem or arithmetic BSD statement.

3.7.6. Yang-Mills: Global-Corridor Stress Networks and Shock Thresholds

The Yang-Mills-inspired framework connects corridor and GVC literature to complex-network, systemic-risk and spectral-threshold literatures. Complex-network research shows that topology, centrality, modularity, weighted paths and cascades condition systemic behavior (Watts and Strogatz, 1998; Barabasi and Albert, 1999; Newman, 2003; Boccaletti et al., 2006). Financial and systemic-risk networks show that interdependence may generate fragility when local shocks travel through dense, leveraged or central connections (Gai and Kapadia, 2010; Haldane and May, 2011; Elliott et al., 2014; Battiston et al., 2012). Corridor and supply-chain literature then extends the same logic to logistics routes, trade passages, energy channels, freight systems and geopolitical choke points (Christopher and Peck, 2004; Sheffi, 2005; Rodrigue, 2020; Notteboom et al., 2022).

Within this literature, the Yang-Mills source manuscript builds a finite global-corridor benchmark with ten nodes and twenty-seven weighted edges. Public macroeconomic anchors are transformed into a normalized systemic-stress field, stress-weighted adjacency, anti-symmetric economic gauge potential, triangular curvature, Yang-Mills economic action, stress Laplacian, Economic Mass Gap Index, fragility, BridgeStress and scenario-based shock diagnostics (Gondauri, 2026b). The mass-gap language is strictly finite-network and spectral; it does not assert a physical gauge field or solve the mathematical Yang-Mills mass-gap problem.

For regional economics and GVC literature, the main contribution is threshold thinking. A corridor system may remain locally absorbent below a stress threshold but become systemically transmissible when stress amplitude rises and the normalized threshold compresses. This gives supply-chain resilience and corridor-risk literature a formal measurement grammar: shocks are no longer described only as disruptions; they are evaluated through network position, curvature participation, action concentration, spectral separation and transition thresholds (Gondauri, 2026b).

3.7.7. Hodge: Regional Macro-Flow Decomposition and Corridor Visibility

The Hodge framework supplies the topological-flow foundation for Section 3.7. Discrete Hodge theory, graph signal processing and topological signal processing show how edge flows can be decomposed into gradient, curl and harmonic components on graphs and simplicial complexes (Jiang, Lim, Yao, and Ye, 2011; Schaub et al., 2020; Barbarossa and Sardellitti, 2020; Lim, 2020). In the economic adaptation, the Hodge source manuscript transforms public regional macroeconomic anchors into a weighted regional network and directed macro-flow pressure field. The resulting decomposition separates hierarchy, local-cycle imbalance and harmonic/systemic circulation (Gondauri, 2026a).

This is directly useful for corridor and GVC literature because trade and production systems contain more than bilateral flows. They contain cycles, feedback loops, triangular dependencies, route alternatives, bottlenecks and persistent circulation. A corridor-sensitive region may not dominate the gradient hierarchy, but it may still contribute to curl imbalance or harmonic circulation. The Hodge model therefore gives the monograph a way to distinguish output hierarchy from local imbalance and from systemic circulation (Gondauri, 2026a).

The Hodge literature also strengthens the integration of BSD and Yang-Mills. In the BSD framework, Hodge-flow rank becomes one component of structural rank. In the Yang-Mills framework, higher-order network and Hodge/simplicial methods support the interpretation of triangular curvature and cycle-based stress concentration. The same corridor may therefore be visible in three ways: as a local-to-global rank signal in BSD, as a shock-threshold and action-concentration site in Yang-Mills, and as a curl/harmonic flow structure in Hodge (Gondauri, 2026a, 2026b, 2026c).

Table 3.7.3. BSD, Yang-Mills and Hodge as complementary corridor-measurement grammars

Dimension	BSD local-to-global view	Yang-Mills threshold view	Hodge decomposition view
Main economic object	Structural rank formed from local regional signals, corridor stress and LOrder comparison.	Finite global-corridor stress network with gauge potential, curvature, action and spectral separation.	Directed macro-flow pressure field decomposed into gradient, curl and harmonic components.
Corridor meaning	BridgeStress identifies regional leverage not reducible to GDP mass.	BridgeStress, EMGI and mass gap identify local-to-systemic shock thresholds and fragile corridors.	Curl and harmonic terms reveal local-cycle imbalance and persistent systemic circulation.
GVC relevance	Local regional traces become informative about global rank and transmission	Production and logistics shocks can compress thresholds and concentrate	Trade and production flows are represented as topologically decomposable

Dimension	BSD local-to-global view	Yang-Mills threshold view	Hodge decomposition view
	structure.	stress action.	edge pressure.
Validation emphasis	Rank gaps, agreement diagnostics, robust inference, external screening, negative controls and placebo logic.	Filtered graphs, Monte Carlo perturbations, scenario simulations, validation pathway and archived benchmark.	Connectedness, spectral diagnostics, persistent homology, econometric screens and forecast validation.
Claim boundary	Calibrated measurement claim; no classical BSD proof or arithmetic L-function claim.	Finite-network benchmark; no mathematical Yang-Mills solution or final causal country-panel claim.	Regional benchmark decomposition; no Hodge Conjecture proof or claim that regions are algebraic varieties.

3.7.8. Supporting Links from the Other Four Analogues

Although Section 3.7 is centered on BSD, Yang-Mills and Hodge, the other four source models provide important supporting literature links. The Navier-Stokes model contributes the macro-financial channel through which corridor and GVC shocks can become liquidity stress, pressure-gradient stress, frictional diffusion or hidden adjustment (Gondauri, 2026d). This connects corridor literature to financial-stress indices, macroprudential stress testing and global liquidity research, where shocks are interpreted not only as trade disruptions but also as credit, inflation, sovereign-spread and resilience-buffer pressures.

The Riemann/Zeta model contributes inflation and regime literature. GVC and corridor disruptions often appear empirically through prices, supply pressure, energy-food shocks, monetary tightening and nonlinear inflation regimes. The FPAS+zeta framework treats inflation forecasting as a layered validation problem and uses a normalized zeta-cycle only as a bounded critical-line inspired signal, not as a Riemann Hypothesis claim (Gondauri, 2026f). In Section 3.7, this supports the idea that corridor disturbances may require both structural and spectral diagnostics when they affect world price pressure.

The Perelman/Ricci/Poincare model contributes regional pressure and smoothing-capacity literature. Corridor systems are embedded in unequal macro-regional environments; regions differ in productive capacity, fiscal space, technology access, social protection and resilience. The curvature-like and entropy-like inequality framework therefore helps interpret why the same corridor shock may generate different outcomes across regions (Gondauri, 2026e). Finally, the P-vs-NP portfolio model contributes computational-finance and sparse-optimization logic. Complex GVC and corridor systems involve high-dimensional route, asset, scenario and policy-choice spaces; the P-vs-NP chapter supplies an evidence hierarchy for heuristic search, reduced exact benchmarking and robustness discipline (Gondauri, 2026g).

3.7.9. Measurement Objects and Validation Gates for Corridor-GVC Research

The integrated literature implies that regional corridor research should not rely on a single empirical object. GDP, trade volume, freight tonnage, output share, centrality, resilience and inflation pressure each reveal only one part of the system. The monograph therefore treats regional-corridor analysis as a layered measurement problem. A corridor-sensitive node may be evaluated by output mass, edge weight, betweenness, local imbalance, harmonic circulation, bridge stress, action participation, mass-gap protection, finite-state trace, LOrder alignment, liquidity pressure and inflation-regime exposure (Gondauri, 2026a, 2026b, 2026c, 2026d, 2026f).

This layered design requires validation gates. GVC and corridor literature can identify substantive relevance, but it cannot automatically convert a constructed index into causal proof. The source manuscripts therefore repeatedly separate benchmark measurement, diagnostic association, forecast-window evidence, robust-inference screening and future validation pathways. The Yang-Mills manuscript explicitly reserves stronger country-level causal claims for the planned N = 1,500 panel; the BSD manuscript treats robust-inference and external-proxy evidence conservatively; the Hodge manuscript interprets its regional benchmark as a prototype requiring future all-country, dyadic and longitudinal replication (Gondauri, 2026a, 2026b, 2026c).

Table 3.7.4. Corridor and GVC validation-gate matrix

Gate	Purpose in regional/corridor review	Applied interpretation in the monograph
Public-data anchor gate	Separates official macroeconomic, trade, regional and logistics anchors from	Prevents BridgeStress, Hodge flow, EMGI or LOrder from being read as raw public variables.

Gate	Purpose in regional/corridor review	Applied interpretation in the monograph
	constructed indicators.	
Network-construction gate	Checks whether nodes, edges, weights, density, connectedness and corridor roles are explicitly defined.	Required for Hodge graph, Yang-Mills stress network and BSD regional network.
GVC relevance gate	Links corridor metrics to trade, production, value-added, supply-chain or logistics literature.	Prevents corridor language from becoming pure geography without economic mechanism.
Topology/spectral gate	Evaluates connectedness, cycles, Laplacian structure, mass gap, curvature or harmonic circulation.	Supports systemic transmission claims while keeping them finite-network and benchmark-bound.
Econometric gate	Tests whether measurement objects show robust, directional or externally screened support.	Keeps BSD, Hodge and Yang-Mills claims diagnostic unless stronger data support is available.
Scenario gate	Tests how shocks, thresholds, action concentration or stress channels respond under controlled assumptions.	Supports policy-relevant stress testing without claiming unconditional prediction.
Replication gate	Requires source ledgers, formulas, matrices, datasets, scripts, metadata and checksums.	Turns corridor analogues into auditable research objects rather than narrative claims.

3.7.10. Claim-Boundary Synthesis for Regional Economics, Corridors and GVCs

The claim boundary of Section 3.7 must be explicit because corridor and GVC language can easily be overextended. The literature supports the claim that regional economic systems are interdependent, that GVCs transmit shocks, that corridor positions may matter beyond GDP mass and that network topology can shape systemic propagation (Krugman, 1991; Gereffi et al., 2005; Hummels et al., 2001; Acemoglu et al., 2012; Carvalho, 2014; Elliott et al., 2014). The source manuscripts extend this literature by building bounded mathematical-economic analogues for local-to-global rank, finite-network thresholds and macro-flow decomposition (Gondauri, 2026a, 2026b, 2026c).

However, the literature does not permit unrestricted claims. Section 3.7 does not claim that corridor indices directly observe all real trade routes, that a finite benchmark fully replaces transaction-level GVC data, that BridgeStress is a causal proof of future disruption, that a mass-gap threshold guarantees shock containment, or that Hodge decomposition identifies observed dyadic flows without measurement assumptions. The permitted claim is stronger but bounded: regional, corridor and GVC literatures justify treating the world economy as a structured system of regions, edges, flows, cycles, thresholds and local-to-global transmission mechanisms, provided that each constructed object remains linked to explicit inputs, validation gates and claim discipline (Gondauri, 2026a, 2026b, 2026c).

Table 3.7.5. Claim-boundary matrix for Section 3.7

Claim class	Permitted statement	Restricted or excluded statement
Regional measurement claim	Regions can be modeled as structured nodes with output, growth, resilience, income depth, centrality and corridor exposure.	No claim that regional aggregates capture all country-level heterogeneity or microeconomic transaction structure.
GVC transmission claim	GVC and production-network literature supports shock propagation through input-output, logistics and value-added dependencies.	No claim that the benchmark observes every firm-level, sectoral or route-specific transaction.
Corridor-stress claim	BridgeStress and related measures identify strategic corridor exposure not reducible to GDP mass.	No claim that BridgeStress alone proves future disruption or policy causality.
Local-to-global claim	Local regional signals can be compared with global structural rank under the BSD-inspired architecture.	No proof or empirical test of classical BSD and no arithmetic L-function interpretation.

Claim class	Permitted statement	Restricted or excluded statement
Threshold claim	Finite-network spectral separation can be interpreted as a benchmark shock-transmission threshold.	No mathematical Yang-Mills mass-gap solution and no guaranteed real-world containment threshold.
Topological-flow claim	Hodge decomposition can separate hierarchy, local imbalance and systemic circulation in a constructed regional graph.	No solution of the Hodge Conjecture and no claim that macro-regions are algebraic varieties.
Future validation claim	Country-level, dyadic, time-varying and transaction-level data can strengthen corridor and GVC claims in future work.	No current claim of complete external validation where the source evidence remains benchmark or diagnostic.

3.7.11. Literature Gap Addressed by the Monograph

The integrated review reveals a clear gap. Regional economics explains spatial structure; GVC literature explains production fragmentation and value-added dependence; corridor and logistics literature explains route vulnerability and resilience; network science explains connectivity and cascades; systemic-risk literature explains shock amplification; topological and spectral methods explain cycles, eigenvalues and thresholds. Yet these streams are rarely integrated into one claim-bounded economic measurement architecture that links regional rank, corridor stress, finite-network shock thresholds and Hodge-style macro-flow decomposition.

The monograph addresses this gap by treating regional economics, corridors and GVCs as a multi-layer mathematical-economic measurement problem. BSD contributes local-to-global structural rank and BridgeStress; Yang-Mills contributes finite-network curvature, action and shock-threshold logic; Hodge contributes gradient, curl and harmonic decomposition; Navier-Stokes contributes liquidity and macro-financial stress channels; Riemann/Zeta contributes inflation-regime and spectral-cycle validation; Perelman/Ricci/Poincare contributes pressure and smoothing-capacity diagnostics; P-vs-NP contributes computational and robustness discipline (Gondauri, 2026a-2026g).

The resulting literature contribution is not that the monograph replaces existing GVC, regional or corridor research. Its contribution is architectural: it shows how existing literatures can be reorganized into a unified evidence system where spatial structure, network interdependence, local-to-global rank, corridor thresholds, systemic circulation and validation discipline are treated together. This is why Section 3.7 belongs in the integrated literature review rather than in any one source chapter.

3.7.12. Synthesis and Transition

Section 3.7 establishes that regional economics, corridors and GVCs provide the substantive economic basis for the monograph's local-to-global and systemic-transmission models. The BSD, Yang-Mills and Hodge chapters are not isolated mathematical exercises; they respond to a real literature problem: how to measure regional importance when output mass, corridor position, GVC exposure, local imbalance, systemic circulation and shock thresholds interact. The literature supports the use of regional network objects, but only under explicit construction, validation and claim-boundary discipline.

The transition to the next Chapter 3 section is therefore natural. Section 3.7 has reviewed regional and corridor substance. The following sections should deepen the literature on forecasting, validation, robust econometric inference, constructed indices, replication and the final literature gap of the monograph. In the integrated structure of the book, regional economics is not only a domain of application; it is one of the places where mathematical analogues demonstrate why scalar economic indicators are insufficient and why bounded, auditable measurement architectures are necessary.

Section closing claim-boundary statement. The regional, corridor and GVC literature supports strong claims about structured regional measurement, corridor-sensitive visibility, local-to-global rank diagnostics, finite-network benchmark thresholds and topological-flow decomposition. It does not support theorem-level transfer, full transaction-level identification, unrestricted causality, guaranteed shock prediction or complete external validation where the evidence remains benchmark, diagnostic or future-validation oriented.

3.8. Forecasting, Validation and Robust Econometric Inference

Integrated Review of Forecast Evaluation, Stress-Testing Validation, Computational Benchmarking and Robust Inference across Seven Millennium-Inspired Economic Analogues

3.8.1. Function of this Section within the Integrated Literature Review

This section consolidates the forecasting, validation and robust-inference literature that supports the seven Millennium-inspired economic analogues. It is not a separate methods chapter and it does not reproduce the empirical results of the problem chapters. Its function is literature-review based: to show how forecast evaluation, stress-testing, econometric robustness, computational benchmarking and diagnostic validation jointly determine the admissible strength of the monograph's claims. In the source manuscripts, these elements appear separately in the Riemann-Zeta inflation-forecasting model, the Navier-Stokes liquidity-flow stress-testing model, the P-vs-NP computational-finance model and the Perelman/Ricci/Poincare inequality-curvature model, while Hodge, Yang-Mills and BSD supply additional validation problems through topology, spectral thresholds, local-to-global rank formation and corridor-network inference (Gondauri, 2026a; Gondauri, 2026b; Gondauri, 2026c; Gondauri, 2026d; Gondauri, 2026e; Gondauri, 2026f; Gondauri, 2026g).

The section is necessary because the monograph's mathematical analogies are acceptable only if their empirical claims are disciplined by validation gates. A zeta-cycle cannot be treated as a macroeconomic law merely because it improves a reported forecast window; a Navier-Stokes-inspired balance cannot be treated as a universal crisis theorem because it performs well under rolling stress validation; a P-vs-NP-inspired portfolio model cannot certify a full search optimum when only a reduced exact benchmark is enumerated; and a Ricci-type curvature diagnostic cannot become causal welfare proof merely because pressure, curvature and entropy measures are internally coherent. These restrictions are consistent with the broader econometric literature on model uncertainty, forecast evaluation, robust inference and finite-sample caution (Hansen, 1982; White, 1980; Newey and West, 1987; Diebold and Mariano, 1995; West, 1996; Giacomini and White, 2006).

The integrated review therefore treats validation as a claim-classification system. Forecasting literature asks whether a model predicts better in a defined sample, horizon and information set. Robust econometric inference asks whether estimates remain interpretable under heteroskedasticity, serial correlation, cross-sectional dependence, dynamic adjustment and clustering. Computational validation asks whether a search result is exact, reduced-exact, heuristic, stress-tested or merely illustrative. Diagnostic validation asks whether constructed indices and mathematical analogues behave coherently under sensitivity, placebo, equivalence, residual and external-proxy checks. Section 3.8 combines these traditions so that later chapters can classify evidence as measurement, diagnostic, forecasting, benchmark or future-validation evidence rather than as theorem-level proof.

Table 3.8.1. Integrated validation-literature transfer map for Section 3.8

Source analogue	Validation literature merged into Section 3.8	Claim-control role
Riemann/Zeta FPAS+zeta inflation forecasting	Forecast evaluation, structural forecasting, ARIMA benchmarks, Mincer-Zarnowitz calibration, Diebold-Mariano and Clark-West tests, forecast encompassing, rolling no-look-ahead validation, regime switching and spectral diagnostics.	Defines bounded forecasting claims: improvement is admissible only within the reported annual, quarterly and monthly validation layers, not as universal forecast dominance.
Navier-Stokes liquidity-flow stress testing	Macro-financial stress indices, liquidity and systemic-risk monitoring, panel financial econometrics, rolling validation, benchmark comparison, external-target validation, residual diagnostics, Monte Carlo policy counterfactuals and restricted closure modelling.	Defines stress-testing validation: liquidity-flow analogues are evaluated as diagnostic stress architectures, not as physical hydrodynamic laws or permanent crisis-prediction theorems.
P-vs-NP computational portfolio optimization	Portfolio theory, CAPM, covariance estimation, cardinality constraints, sparse optimization, heuristic/metaheuristic search, exact reduced enumeration, transaction costs, option overlay and search-coverage reporting.	Defines computational evidence levels: full-universe best-found incumbents are separated from reduced exact certification and from theorem-level P-vs-NP claims.
Perelman/Ricci/Poincare inequality diagnostics	Robust inequality measurement, curvature-like diagnostics, entropy/complexity measures, graph connectedness, panel diagnostics, forecasting discipline and Monte Carlo uncertainty.	Defines diagnostic-inference claims: pressure, smoothing and curvature variables support measurement and diagnostic interpretation rather than

Source analogue	Validation literature merged into Section 3.8	Claim-control role
		causal welfare proof.
Hodge macro-flow decomposition	Topological signal processing, Hodge-Laplacian diagnostics, decomposition validation, persistent homology, machine-learning forecast checks and econometric robustness.	Adds decomposition validation: gradient, curl and harmonic components must be graph-defined, stable and diagnostically auditable.
Yang-Mills finite-network shock threshold	Spectral graph diagnostics, finite-network mass-gap benchmarks, stress perturbation, scenario simulation, BridgeStress, action concentration and future panel-validation design.	Adds finite-network benchmark discipline: positive spectral separation is a benchmark threshold claim unless expanded country-panel evidence is populated and estimated.
BSD local-to-global rank modelling	Local-to-global validation, rank agreement diagnostics, equivalence checks, negative controls, circularity screening, external-proxy screening and permutation/placebo logic.	Adds local-to-global inference discipline: structural-rank evidence is strongest internally and becomes external only under non-circular and robust validation.

3.8.2. Forecasting Literature: From Point Accuracy to Information-Set Discipline

The forecasting literature begins with a simple principle: a forecast model must be judged against the information set and benchmark available at the time the prediction is made. This principle is central to the Riemann/Zeta FPAS+zeta chapter, where the hybrid forecast is interpreted through layered annual, quarterly and monthly validation rather than through a single high-fit display. Standard forecast evaluation measures such as RMSE, MAE and percentage-error criteria are useful, but they are insufficient unless they are combined with rolling no-look-ahead design, benchmark comparison and calibration diagnostics (Mincer and Zarnowitz, 1969; Diebold and Mariano, 1995; West, 1996; Hyndman and Athanasopoulos, 2021; Gondauri, 2026f).

A key lesson from the forecasting literature is that predictive success is horizon-specific and sample-specific. The same model may perform well in crisis windows, less well in low-volatility regimes and differently under annual, quarterly or monthly frequency. This is why the Riemann/Zeta framework separates the N = 55 annual layer, N = 45 robustness layer, N = 20 crisis-era comparison layer, N = 100 quarterly dynamic-validation layer and N = 240 monthly spectral-diagnostics layer. The literature on forecast comparison supports this layered design because it prevents results from being misread as if all methods and diagnostics were estimated on a single small sample (West, 1996; Clark and McCracken, 2001; Giacomini and White, 2006; Clark and West, 2007; Gondauri, 2026f).

Forecasting also requires calibration, not only accuracy. Mincer-Zarnowitz regressions ask whether forecasts are unbiased and whether their slope relative to actual outcomes is appropriately scaled. Forecast-encompassing tests ask whether a candidate model contains information beyond a benchmark. Diebold-Mariano tests evaluate equal predictive accuracy, while Clark-West tests are particularly relevant where a larger nested model is compared with a smaller benchmark. In the monograph, these tests matter not because they prove mathematical truth, but because they govern whether a zeta-cycle forecast correction can be called informative, incremental or merely overfit (Mincer and Zarnowitz, 1969; Diebold and Mariano, 1995; Clark and McCracken, 2001; Clark and West, 2007; Gondauri, 2026f).

The Navier-Stokes chapter also uses forecasting, but in a different sense. Its rolling one-year-ahead validation compares a nondimensional macro-financial stress balance against ARIMA, VAR, GARCH and composite-index baselines. The relevant literature therefore overlaps with financial-stress forecasting, volatility modelling, autoregressive dynamics and macro-financial stress-index evaluation (Engle, 1982; Bollerslev, 1986; Hamilton, 1994; Stock and Watson, 2002; Hatzius et al., 2010; Gondauri, 2026c). Here the admissible claim is stress-testing usefulness inside defined validation windows, not a permanent law of liquidity-flow crisis prediction.

3.8.3. Structural Forecasting, Inflation, Regimes and Spectral Diagnostics

The Riemann/Zeta analogue sits at the intersection of structural inflation forecasting and nonlinear spectral diagnostics. Inflation forecasting literature distinguishes persistence models, Phillips-curve models, factor models, structural policy models and regime-sensitive approaches. No single tradition eliminates forecast uncertainty, especially during shocks generated by financial crises, pandemics, commodity-price surges, supply constraints or monetary tightening. The

FPAS+zeta model therefore enters the literature as a hybrid architecture: a structural FPAS baseline is corrected by a normalized zeta-cycle only after the signal is transformed into a signed, calibrated and validated forecast component (Stock and Watson, 1999; Hamilton, 1994; Sims, 1980; Cogley and Sargent, 2005; Gondauri, 2026f).

Regime-switching and state-dependent validation are important because global inflation is not generated by one smooth law across all periods. Markov-switching and hidden Markov models are widely used to represent changes in regimes, volatility states and crisis phases, while spectral and wavelet tools help detect frequency-domain coherence, instability and nonlinear cyclical behavior (Hamilton, 1989; Kim and Nelson, 1999; Granger, 1969; Percival and Walden, 2000; Gondauri, 2026f). In the monograph, such methods do not convert the Riemann zeta function into an economic theorem. They provide diagnostic tests for whether the zeta-cycle behaves as a meaningful signal under crisis and non-crisis regimes.

The literature also warns against data mining in forecast augmentation. Any additional signal can reduce in-sample error by chance if the search space is large enough. This warning is relevant to spectral and mathematical-signal analogues because mathematically rich functions may generate many candidate transformations. For this reason, rolling validation, benchmark comparison, residual tests, regime screens and forecast-encompassing logic are not optional. They are the gate through which the Riemann/Zeta analogue passes from mathematical inspiration to bounded empirical forecasting evidence (White, 2000; Hansen, 2005; Giacomini and White, 2006; Gondauri, 2026f).

3.8.4. Macro-Financial Stress Testing, Liquidity and Robust Validation

The Navier-Stokes analogue draws on macro-financial stress-testing literature rather than on physical-fluid proof. Financial stress indices, liquidity measures, credit-spread diagnostics, volatility models and macroprudential monitoring frameworks have long been used to summarize conditions that individual indicators cannot capture alone. The model's contribution is to reorganize these channels into a nondimensional stress-balance grammar: liquidity velocity weakness, acceleration pressure, macro-financial pressure gradients, friction/diffusion, stochastic shock, GDP-cycle forcing and restricted hidden adjustment (Illing and Liu, 2006; Hakkio and Keeton, 2009; Hatzius et al., 2010; Adrian and Brunnermeier, 2016; Gondauri, 2026c).

Validation in this literature must address two problems simultaneously. First, stress indicators are composite, so their construction must be transparent and robust to weighting, scaling and direction choices. Second, stress outcomes are dynamic and crisis-sensitive, so their predictive usefulness must be evaluated out of sample or through rolling windows. The Navier-Stokes chapter responds to these problems by combining robustness checks, rolling validation, benchmark comparison, residual diagnostics, external-target validation, Monte Carlo uncertainty and policy counterfactuals. This aligns with broader literature on composite-index validation, financial-stress monitoring and model uncertainty (Saltelli et al., 2008; Stock and Watson, 2002; Hansen, 2007; Gondauri, 2026c).

The restricted closure term is particularly important. In mathematical analogies, a residual term can become a hidden device that forces a model to fit. Robust literature requires residuals and closure terms to be interpretable, constrained and tested. The Navier-Stokes model therefore treats epsilon(t) as a state-dependent hidden-adjustment channel using observable or proxy-observable variables such as lagged closure, shadow-economy pressure, transfers, geopolitical shock, fiscal buffers, aid/support and inertia. This design reflects the econometric principle that unobserved components must not become unrestricted algebraic plugs (Harvey, 1989; Hamilton, 1994; Wooldridge, 2010; Gondauri, 2026c).

3.8.5. Robust Econometric Inference: Heteroskedasticity, Serial Dependence, Panels and Cross-Sectional Dependence

Robust inference literature supplies the statistical backbone of the monograph. The seven analogues use constructed variables, panels, networks, time-series layers and computational outputs; each requires protection against overconfident inference. Heteroskedasticity-consistent covariance estimation, HAC corrections, clustered standard errors, panel fixed effects, random-effects diagnostics, cross-sectional dependence tests and dynamic-panel estimators are all relevant because the evidence is multidimensional and often regional, country-year or time-indexed (White, 1980; Newey and West, 1987; Wooldridge, 2010; Cameron and Miller, 2015).

Panel settings introduce special concerns. Fixed effects control for time-invariant unobserved heterogeneity, but they do not automatically solve endogeneity, dynamic bias, serial dependence or cross-sectional dependence. Driscoll-Kraay standard errors are useful when spatial or cross-sectional dependence affects panel residuals; Pesaran-type tests and common-correlated-effects logic are relevant where global shocks jointly affect countries or regions. Dynamic GMM methods can help with persistence but require instrument discipline, overidentification tests and caution about instrument proliferation (Arellano and Bond, 1991; Arellano and Bover, 1995; Blundell and Bond, 1998; Driscoll and Kraay, 1998; Pesaran, 2004; Pesaran, 2006; Roodman, 2009).

The Perelman/Ricci/Poincare, Navier-Stokes, BSD and Yang-Mills source manuscripts all use or specify panel and robust-inference layers, but their claim status differs. The Perelman/Ricci/Poincare analogue uses econometric validation to audit inequality-pressure and curvature diagnostics, not to prove a geometric theorem or identify a universal welfare law. The Navier-Stokes model uses fixed-effects and external-target validation to support stress-testing interpretation, not unrestricted causality. The BSD model uses robust-inference and external-proxy layers conservatively, explicitly avoiding upgrades from weak p-values or circularly constructed variables. The Yang-Mills model separates a completed finite-network benchmark from future N = 1,500 country-panel validation (Gondauri, 2026a; Gondauri, 2026c; Gondauri, 2026d; Gondauri, 2026e).

3.8.6. Diagnostic Validation for Curvature, Inequality Pressure and Smoothing Capacity

The Perelman/Ricci/Poincare analogue contributes a distinct validation problem: how to validate curvature-like and entropy-like measures when they are constructed from economic pressure variables rather than observed geometric invariants. Inequality literature and multidimensional measurement literature support the idea that complex social pressure cannot be reduced to a single scalar such as Gini alone. However, they also require transparency about variable orientation, scaling, weighting, sensitivity, uncertainty and interpretation (Atkinson, 1970; Sen, 1973; Cowell, 2011; Alkire and Foster, 2011; Gondauri, 2026a).

In this context, robust validation is diagnostic rather than causal. If pressure rises, scalar curvature falls and entropy-like complexity increases during crisis periods, the model may support a coherent measurement interpretation. But that does not prove that the economy is a geometric manifold or that the model identifies causal mechanisms behind inequality. Monte Carlo bands, forecast windows, graph connectedness, component sensitivity, leave-one-out checks, threshold diagnostics and alternative econometric screens are needed to show that the constructed pressure-curvature architecture is stable enough to be interpreted (Saltelli et al., 2008; Wooldridge, 2010; Gondauri, 2026a).

The Hodge and Yang-Mills chapters reinforce this diagnostic-validation logic. Hodge decomposition must show that the graph is sufficiently connected and cycle-rich for gradient, curl and harmonic components to be meaningful. Yang-Mills threshold diagnostics must show that spectral separation is positive and stable under graph perturbation, filtering and shock scenarios. In both cases, validation is structural and spectral before it is causal (Lim, 2015; Barbarossa and Sardellitti, 2020; Sandryhaila and Moura, 2013; Gondauri, 2026b; Gondauri, 2026d).

3.8.7. Computational Validation, Exact Reduced Benchmarking and P-vs-NP Claim Discipline

The P-vs-NP source manuscript expands validation beyond econometrics into computational evidence. Portfolio theory begins with Markowitz mean-variance optimization and CAPM expected-return calibration, but cardinality constraints transform the problem into a mixed discrete-continuous search environment. The literature on sparse portfolio selection, mixed-integer programming and metaheuristics shows that support-space growth can make naive enumeration infeasible, motivating heuristics, stochastic search, genetic algorithms and exact reduced benchmarking (Markowitz, 1952; Sharpe, 1964; Lintner, 1965; Mossin, 1966; Garey and Johnson, 1979; Nocedal and Wright, 2006; Gondauri, 2026g).

Computational validation is not the same as statistical validation. It asks whether the search method found a good incumbent, whether competing algorithms were compared under common objectives, whether random seeds and budgets were disclosed, whether reduced exact enumeration can certify a benchmark, and whether robustness checks survive transaction costs, covariance alternatives, beta drift, weight caps, risk contributions and derivative overlays. This literature supports the monograph's distinction between best-found full-universe evidence and exact reduced certification (Bertsimas and Shioda, 2009; Kolm et al., 2014; DeMiguel et al., 2009; Gondauri, 2026g).

The claim boundary is strict. A cardinality-constrained portfolio problem may operationalize computational difficulty, but it cannot prove P != NP. A genetic algorithm may outperform greedy or Monte Carlo search under a documented budget, but it cannot certify global optimality over the full universe unless exhaustive or mathematically certified search is completed. Exact reduced benchmarking is therefore a validation anchor, not a substitute for full-universe proof. This distinction is consistent with computational-complexity literature and with the monograph's broader rule that mathematical analogy must be proportional to evidence (Cook, 1971; Karp, 1972; Garey and Johnson, 1979; Gondauri, 2026g).

3.8.8. Validation Gates across Network, Local-to-Global and Spectral Analogues

Although Section 3.8 is anchored in Riemann/Zeta, Navier-Stokes, P-vs-NP and Ricci/Poincare, the remaining three analogues supply essential validation lessons. The Hodge model demonstrates that decomposition requires graph construction, orientation, incidence matrices, Laplacian diagnostics and topology-aware validation. The Yang-Mills model demonstrates that finite-network shock-threshold claims require spectral-gap stability, perturbation tests, action

concentration and scenario analysis. The BSD model demonstrates that local-to-global claims require rank agreement, finite-state trace logic, Euler-factor analogues, negative controls, anti-circularity screens and external-proxy caution (Gondauri, 2026b; Gondauri, 2026d; Gondauri, 2026e).

These validation principles generalize. A network model cannot rely on visual connectivity alone; it must show that graph weights, edge definitions and Laplacian quantities are stable enough to support the interpretation. A local-to-global model cannot treat agreement between constructed objects as external validation if the objects share inputs too tightly. A spectral model cannot use eigenvalues, zeta-cycles or L-function analogues as proof without showing forecast, perturbation, placebo or robustness behavior. The network, spectral and local-to-global literature therefore functions as a safeguard against internal circularity (Newman, 2010; Jackson, 2008; Sandryhaila and Moura, 2013; Barabasi, 2016; Gondauri, 2026b; Gondauri, 2026d; Gondauri, 2026e).

3.8.9. Evidence Hierarchy for Forecasting, Validation and Robust Inference

The integrated literature implies an evidence hierarchy. The weakest evidence is descriptive coherence: a constructed indicator appears plausible or aligns with narrative expectations. Stronger evidence is diagnostic robustness: results remain stable under alternative scaling, perturbation, residual checks, leave-one-out tests, placebo logic or external screening. Forecasting evidence becomes stronger when it is no-look-ahead, benchmarked and tested through formal comparison. Econometric evidence becomes stronger when robust-inference assumptions are explicitly addressed and when endogeneity, dependence and dynamic bias are not ignored. Computational evidence becomes stronger when reduced exact enumeration or formal optimality certificates exist. The strongest claims require independent validation, reproducibility and non-circular external evidence (White, 1980; Newey and West, 1987; Diebold and Mariano, 1995; Driscoll and Kraay, 1998; Roodman, 2009).

This hierarchy does not weaken the monograph; it makes it more defensible. The monograph can make strong measurement claims where objects are clearly defined, auditable and reproducible. It can make diagnostic claims where robustness and sensitivity evidence support structural interpretation. It can make forecasting claims where validation windows and benchmark tests support improved predictive performance. It can make benchmark claims where finite-network or reduced-exact evidence is complete within a defined universe. It can make future-validation claims where a panel, dataset or econometric architecture is specified but not yet fully populated or estimated. These claim classes are consistent with Chapter 2.7's general claim hierarchy and with the seven source manuscripts' boundaries (Gondauri, 2026a; Gondauri, 2026b; Gondauri, 2026c; Gondauri, 2026d; Gondauri, 2026e; Gondauri, 2026f; Gondauri, 2026g).

Table 3.8.2. Forecast and validation metrics used as literature anchors

Validation object	Typical test or metric	Interpretation in Section 3.8	Claim boundary
Point forecast accuracy	RMSE, MAE, sMAPE	Compares forecast error magnitudes across candidate and benchmark models.	Does not prove universal superiority; applies to the reported sample and horizon.
Forecast calibration	Mincer-Zarnowitz regression	Tests whether forecasts align with actual outcomes in level and slope.	Calibration evidence is model- and sample-specific.
Equal predictive accuracy	Diebold-Mariano test	Tests whether competing forecasts differ significantly in predictive accuracy.	Sensitive to loss function, horizon, serial correlation and sample length.
Nested forecast comparison	Clark-West test	Evaluates whether a larger model improves forecasts against a nested benchmark.	Supports incremental forecast information, not theorem-level proof.
No-look-ahead discipline	Rolling or expanding windows	Prevents future information from contaminating forecast evaluation.	Strong only within the disclosed validation design.
Residual adequacy	Serial correlation, ARCH/GARCH, normality and stability checks	Audits whether forecast errors contain remaining structure.	Residual diagnostics are supportive, not complete proof of model correctness.
Regime behavior	HMM, Markov switching,	Tests whether signals operate	Regime evidence is

Validation object	Typical test or metric	Interpretation in Section 3.8	Claim boundary
	Fourier/wavelet coherence	differently across crisis and non-crisis states.	diagnostic and must not be overread as structural law.

Table 3.8.3. Robust econometric inference gates across the monograph

Gate	Literature basis	Relevant analogue(s)	Purpose
Heteroskedasticity gate	White (1980), HC covariance logic	All empirical analogues	Prevents overconfidence when residual variance is not constant.
Serial-correlation gate	Newey-West (1987), HAC logic	Riemann/Zeta, Navier-Stokes, Ricci/Poincare	Protects time-series and panel inference under autocorrelation.
Panel fixed-effects gate	Wooldridge (2010), panel econometrics	Navier-Stokes, Ricci/Poincare, BSD, future Yang-Mills panel	Controls stable unobserved heterogeneity where panel structure is used.
Cross-sectional dependence gate	Pesaran (2004, 2006), Driscoll-Kraay (1998)	Global macro panels and regional systems	Acknowledges common shocks and regional interdependence.
Dynamic-panel gate	Arellano-Bond (1991), Blundell-Bond (1998), Roodman (2009)	Future validation and persistence-sensitive panels	Controls lagged dependent variables and persistence with instrument discipline.
External-proxy gate	Validation and measurement literature	BSD, Navier-Stokes, Ricci/Poincare, Yang-Mills	Tests whether constructed objects relate to external outcomes without circularity.
Replication gate	Open-science and reproducibility literature	All seven	Requires data package, formulas, code, matrices, seeds or source ledgers.

Table 3.8.4. Evidence hierarchy for forecasting, validation and robust inference

Evidence level	What it supports	Examples in the seven analogues	What it does not support
Descriptive coherence	A constructed object is interpretable and consistent with domain intuition.	Initial pressure, stress, flow, rank, zeta-cycle or portfolio diagnostics.	No causal, predictive or theorem-level claim.
Diagnostic robustness	A measurement object remains stable under sensitivity, perturbation, placebo or residual checks.	Ricci pressure bands, Hodge decomposition checks, Yang-Mills perturbations, BSD negative controls.	No unrestricted external validation.
Forecast-window evidence	A model improves prediction under defined horizon, sample and information set.	FPAS+zeta layered validation; Navier-Stokes rolling validation.	No universal forecast dominance.
Finite benchmark evidence	A benchmark is complete inside a defined finite universe.	Yang-Mills ten-node graph; P-vs-NP reduced exact enumeration.	No extension to untested universes without validation.
Computational best-found evidence	An algorithm found the best incumbent under disclosed budget and search design.	Full n = 94 portfolio search incumbents.	No certified global optimum without proof or exhaustive search.
Future validation design	A validation architecture is specified for later population or estimation.	Yang-Mills N = 1,500 panel design; extended panel layers.	No completed empirical claim until data and estimates exist.

3.8.10. Integrated Claim-Boundary Matrix

The common result of the forecasting, validation and robust-inference literature is that evidence must be named accurately. In the Riemann/Zeta chapter, the literature permits a bounded forecasting claim, not proof or verification of the Riemann Hypothesis. In the Navier-Stokes chapter, it permits stress-testing and diagnostic validation, not physical-fluid identity or universal crisis prediction. In the P-vs-NP chapter, it permits empirical-computational optimization evidence, not a theorem about P versus NP or certified full-universe optimality. In the Perelman/Ricci/Poincare chapter, it permits diagnostic inequality-pressure and curvature-like measurement, not proof of geometric/topological theorems or causal welfare law. Hodge, Yang-Mills and BSD further reinforce this discipline through topology, spectral thresholds and local-to-global validation (Gondauri, 2026a; Gondauri, 2026b; Gondauri, 2026c; Gondauri, 2026d; Gondauri, 2026e; Gondauri, 2026f; Gondauri, 2026g).

3.8.11. Literature Gap Addressed by Section 3.8

The merged literature reveals a gap at the intersection of forecasting, robust inference and mathematical-economic analogue modelling. Forecasting literature is strong on accuracy and comparison, but it rarely addresses theorem-level mathematical analogies. Econometric literature is strong on robust inference, but it does not itself define how zeta cycles, curvature analogues, local-to-global rank objects, Hodge components or finite-network mass gaps should be interpreted. Computational optimization literature is strong on algorithms and complexity, but it often requires additional claim-boundary language to distinguish heuristic evidence from proof. The monograph addresses this gap by treating validation as the bridge between formal mathematical inspiration and admissible economic claim (Giacomini and White, 2006; Roodman, 2009; Wooldridge, 2010; Gondauri, 2026a-g).

Section 3.8 therefore establishes a reviewer-facing rule for the rest of the monograph: no result is stronger than its validation design. A strong measurement claim requires transparent construction and reproducibility. A diagnostic claim requires robustness and stability. A forecasting claim requires benchmarked no-look-ahead evidence. A benchmark claim requires complete finite-universe closure. A computational claim requires explicit search coverage and exact benchmarking where possible. A future-validation claim requires specification without pretending that estimation is already complete. This rule is the central contribution of the integrated validation literature review.

Table 3.8.5. Claim-boundary matrix for Section 3.8

Analogue	Admissible validation claim	Restricted claim
Riemann/Zeta	FPAS+zeta can support forecast-window improvement under layered validation, benchmark comparison and residual diagnostics.	No proof, test or verification of the Riemann Hypothesis; no universal inflation forecast dominance.
Navier-Stokes	A nondimensional liquidity-flow stress balance can support stress-testing, rolling-validation and policy-scenario diagnostics.	No physical-fluid identity, no solution of Navier-Stokes, no permanent crisis-prediction law.
P-vs-NP	Sparse portfolio optimization can support empirical-computational evidence, reduced exact benchmarking and robustness diagnostics.	No proof of P != NP, no certified full-universe optimum without certificate, no realized trading dominance.
Perelman/Ricci/ Poincare	Curvature-like, entropy-like and graph-connectedness objects can support inequality-pressure diagnostics and smoothing-capacity interpretation.	No proof/test/replication of Perelman's proof, Ricci-flow theorem or Poincare conjecture; no unrestricted causal welfare claim.
Hodge	Graph-defined edge-flow decomposition can support hierarchy, local-cycle imbalance and systemic-circulation diagnostics.	No solution of the Hodge Conjecture; no claim that economic regions are algebraic varieties.
Yang-Mills	Finite-network spectral separation and action concentration can support shock-threshold benchmark evidence and scenario diagnostics.	No solution to Yang-Mills mass-gap problem; no final country-panel causal validation until populated and estimated.

Analogue	Admissible validation claim	Restricted claim
BSD	Local finite-state signals, Euler-factor analogues and LOrder can support calibrated local-to-global structural-rank measurement.	No proof/test of classical BSD; no arithmetic L-function or algebraic rank claim.

Section closing claim-boundary statement. The forecasting, validation and robust-inference literature supports the monograph as a disciplined evidence architecture. It permits bounded claims about forecast improvement, stress-testing usefulness, diagnostic robustness, finite-network benchmarking, reduced exact computational validation and future panel-validation design. It does not permit theorem proof, physical identity, unrestricted causal law, universal forecast superiority, certified full-universe portfolio optimality or complete external validation where the evidence does not support such claims.

3.9. Constructed Indices, Replication and Claim Discipline

Integrated Review across Seven Millennium-Inspired Economic-Econometric Analogues

3.9.1. Function of this Section within the Integrated Literature Review

This section closes the core methodological part of the integrated literature review by examining how constructed indices, replication architecture and claim discipline operate across the seven Millennium-inspired economic-econometric analogues. The preceding sections reviewed mathematical analogy, networks, topology, spectral methods, macro-financial stress, inequality, portfolios, corridors and robust validation. Section 3.9 now addresses the question that determines whether those literatures can legitimately support a monograph-level research programme: under what conditions can author-constructed indices be treated as scientific measurement objects rather than rhetorical artefacts, and how must replication and claim hierarchy be organized so that the resulting evidence remains defensible? This question is central to composite-indicator methodology, applied econometrics and reproducible computational research (OECD and European Commission Joint Research Centre, 2008; Nardo et al., 2005; Saltelli et al., 2008; Stodden, Leisch and Peng, 2014; Peng, 2011).

The seven source manuscripts share the same methodological pattern. Raw or public-data anchors are not reported as final answers. They are transformed into constructed economic objects: pressure coordinates, nondimensional stress components, graph cochains, curvature-like diagnostics, gauge potentials, Euler-factor analogues, zeta-cycle corrections, sparse-support search spaces, resilience measures, fragility scores and evidence hierarchies. The Perelman/Ricci/Poincare framework constructs inequality pressure, smoothing capacity, curvature-like deformation and entropy-like complexity; the Hodge framework constructs a directed macro-flow pressure field and decomposes it into gradient, curl and harmonic components; the Navier-Stokes framework constructs a nondimensional liquidity-flow stress balance; the Yang-Mills framework constructs systemic stress, curvature, action and finite-network shock thresholds; the BSD framework constructs regional finite-state traces, Euler-factor analogues and LOrder; the Riemann/Zeta framework constructs a normalized zeta-cycle and signed forecast correction; and the P-vs-NP framework constructs a combinatorial sparse-portfolio optimization environment with exact and heuristic evidence layers (Gondauri, 2026a, 2026b, 2026c, 2026d, 2026e, 2026f, 2026g).

This section therefore treats construction, replication and claim discipline as a single literature-review problem. A constructed index is legitimate only when its data lineage, transformation rule, scale logic, validation procedure and inference boundary are explicit. A replication package is useful only when it allows a reviewer to trace the movement from input anchors to reported objects. A claim hierarchy is credible only when it prevents measurement, diagnostic, forecasting, benchmark and future-validation claims from being upgraded into theorem proof, causal law, universal forecast dominance or certified optimality without the necessary evidence (Adcock and Collier, 2001; Shadish, Cook and Campbell, 2002; Ioannidis, 2005; Stodden et al., 2016).

Table 3.9.1. Constructed-object, replication and claim-discipline map across seven analogues

Source analogue	Constructed-object family	Replication problem	Claim-discipline role
Perelman/Ricci/ Poincare	Pressure coordinates, curvature-like summaries, F/W entropy-style functionals, graph connectedness diagnostics.	Trace how 16 macro-social variables become common pressure-oriented coordinates and then curvature/entropy diagnostics.	Allows diagnostic inequality-curvature claims; excludes theorem proof and unrestricted causal welfare claims.
Hodge	Regional graph, directed macro-flow edge cochain,	Trace public regional anchors, edge construction, orientation	Allows benchmark topological-flow

Source analogue	Constructed-object family	Replication problem	Claim-discipline role
	gradient/curl/harmonic components, resilience and tail-risk indices.	rules, Hodge decomposition and validation outputs.	measurement; excludes Hodge Conjecture proof and final dyadic-flow causality.
Navier-Stokes	Nondimensional stress components, pressure gradients, friction/diffusion, shock/cycle forcing and restricted epsilon closure.	Trace country-year public anchors, normalization, stress direction, closure equation and rolling validation outputs.	Allows global stress-testing and diagnostic association; excludes physical-fluid identity and universal crisis prediction.
Yang-Mills	Stress-weighted graph, gauge potential, triangular curvature, action, Laplacian, EMGI, BridgeStress and finite mass gap.	Trace macro anchors, network weights, matrix construction, curvature/action calculation, spectral threshold and future panel design.	Allows finite-network benchmark threshold evidence; excludes mathematical Yang-Mills mass-gap solution.
BSD	Economic curve coefficients, finite-state traces, Euler factors, L_econ, LOrder, structural rank and corridor stress.	Trace public series, regional aggregation, coefficient mapping, local traces, Euler factors, rank comparison, seeds and hashes.	Allows calibrated local-to-global measurement; excludes classical BSD proof and strong external validation where diagnostics are weak.
Riemann/Zeta	Composite pressure index, nonlinear tau argument, normalized zeta-cycle, deviation and alpha-weighted FPAS+zeta correction.	Trace annual/quarterly/monthly layers, formula audit, forecasts, residual tests and validation metrics.	Allows bounded forecast-window improvement; excludes Riemann Hypothesis verification and universal dominance.
P-vs-NP	CAPM priors, covariance geometry, combinatorial support space, heuristic incumbents, exact reduced benchmark and option overlay.	Trace fixed universe, return construction, covariance specification, search budgets, seeds, exact enumeration and robustness gates.	Allows empirical-computational optimization evidence; excludes P != NP proof and full n=94 global-optimum certification.

Source: Author synthesis based on the seven source manuscripts and the composite-indicator, reproducibility and validation literatures.

3.9.2. Constructed Indices as Measurement Objects, Not Raw Facts

The composite-indicator literature has long emphasized that constructed indices are neither self-validating nor automatically invalid. Their status depends on conceptual definition, input selection, normalization, weighting, aggregation, robustness testing and sensitivity analysis (Nardo et al., 2005; OECD and European Commission Joint Research Centre, 2008; Saltelli et al., 2008). This principle is directly relevant to the monograph because none of the seven problem chapters relies only on raw public indicators. Each chapter transforms raw or fixed inputs into higher-order measurement objects. The transformation is justified when the research target cannot be measured directly by a single public statistic: systemic stress, topological circulation, inequality curvature, local-to-global rank, spectral forecast correction, finite-network threshold or sparse-search difficulty.

The central literature-based rule is that construction must solve a measurement problem. In the Perelman/Ricci/Poincare analogue, a raw Gini coefficient alone cannot represent global inequality pressure as a multi-channel deformation process; therefore, heterogeneous macro-social variables are transformed onto a common pressure scale and then used to construct curvature-like and entropy-like diagnostics (Perelman, 2002; Hamilton, 1982; Gondauri, 2026a). In the Hodge analogue, regional GDP, growth and income depth cannot by themselves distinguish hierarchy, local imbalance and systemic circulation; therefore, they are transformed into a graph edge cochain and decomposed by discrete

Hodge logic (Eckmann, 1944; Lim, 2015; Jiang et al., 2011; Gondauri, 2026b). In the Navier-Stokes analogue, inflation, sovereign-risk and liquidity proxies cannot be added in raw units; therefore, they are converted into nondimensional stress components before entering a flow-pressure-friction-shock-closure balance (Temam, 1977; Acharya, Pedersen, Philippon and Richardson, 2017; Gondauri, 2026c).

The same logic extends to Yang-Mills, BSD, Riemann/Zeta and P-vs-NP. A corridor network cannot be understood only from output mass; the Yang-Mills analogue constructs stress-weighted adjacency, gauge potential, curvature, action and spectral separation to represent shock-threshold structure in a finite graph (Yang and Mills, 1954; Chung, 1997; Newman, 2010; Gondauri, 2026d). A regional local-to-global system cannot be read from GDP rankings alone; the BSD analogue constructs finite-state traces, Euler-factor analogues and LOrder to test whether local regional information is informative about global structural rank (Birch and Swinnerton-Dyer, 1965; Silverman, 2009; Gondauri, 2026e). A world-inflation forecast cannot be reduced to a single persistence model; the Riemann/Zeta analogue constructs a normalized critical-line-inspired cycle and evaluates it through forecast-comparison gates (Riemann, 1859; Titchmarsh, 1986; Diebold and Mariano, 1995; Gondauri, 2026f). A sparse portfolio cannot be evaluated as a purely continuous mean-variance allocation; the P-vs-NP analogue constructs a combinatorial support space and separates exact reduced evidence from heuristic full-universe incumbents (Markowitz, 1952; Sharpe, 1964; Garey and Johnson, 1979; Papadimitriou and Steiglitz, 1998; Gondauri, 2026g).

InputAnchor -> DirectionRule -> Normalization -> ConstructedIndex -> ValidationGate -> ClaimClass

This pipeline is the core measurement grammar of Section 3.9. It makes constructed indices admissible only after they pass through a documented sequence. Without direction rules, indices may reverse interpretation. Without normalization, raw units may be aggregated incoherently. Without validation gates, constructed values remain descriptive constructs. Without claim classes, even a reproducible constructed index may be rhetorically overstated. The literature therefore supports constructed variables only as auditable measurement objects under declared assumptions (Adcock and Collier, 2001; Bollen, 1989; OECD and European Commission Joint Research Centre, 2008).

3.9.3. Normalization, Scaling and Directional Harmonization

Normalization and scaling are not minor technical details in the monograph; they are the bridge between heterogeneous data and formal analogy. The literature on composite indicators warns that normalization can change rankings, variance structure, sensitivity and substantive interpretation (Nardo et al., 2005; OECD and European Commission Joint Research Centre, 2008). The seven analogues are particularly sensitive to this issue because their objects often combine variables that naturally live in different units: GDP mass, inflation pressure, unemployment, volatility, trade openness, logistics proxies, network weights, spectral quantities and algorithmic search metrics.

The Perelman/Ricci/Poincare analogue uses pressure-oriented scaling so that heterogeneous inequality, labour-market, productivity, technology, fiscal and social-protection variables can be read as coordinates of macro-regional pressure. This supports curvature-like diagnostics but also imposes the responsibility to state orientation rules and avoid raw-unit equivalence (Gondauri, 2026a). The Navier-Stokes analogue uses nondimensional starred variables, which is essential because the classical flow analogy would be invalid if inflation, credit conditions, sovereign spreads and GDP-cycle deviations were mechanically added in original units (Temam, 1977; Gondauri, 2026c). The Riemann/Zeta analogue uses normalization to convert a complex or oscillatory mathematical signal into a real-valued forecast-correction object; this makes the signal testable, but it also restricts the claim to the selected transformation, sample layers and validation window (Titchmarsh, 1986; Gondauri, 2026f).

In the network-based chapters, scaling determines topology. Hodge, Yang-Mills and BSD each require weight construction: gravity-style regional edge weights, stress-weighted adjacency, corridor coding, centrality and finite-state reductions. Because graph structure depends on node definitions, edge inclusion and weights, replication must record the construction protocol rather than only the final graph (Chung, 1997; Newman, 2010; Barabasi, 2016). In the P-vs-NP analogue, scaling enters through CAPM priors, covariance geometry, Sharpe evaluation, transaction-cost assumptions and derivative overlay. The portfolio result is therefore conditional on return and risk construction, not an unqualified empirical investment fact (Markowitz, 1952; Sharpe, 1964; Black and Scholes, 1973; Merton, 1973; Gondauri, 2026g).

Table 3.9.2. Normalization, scaling and directional-harmonization safeguards

Scaling decision	Why it matters	Examples across the monograph	Literature-supported safeguard
Direction harmonization	Ensures that higher values consistently mean pressure, capacity, resilience, risk or score.	Pressure-oriented inequality variables; stress-direction macro-financial components; zeta deviations.	Document the sign convention before aggregation; test sensitivity to orientation choices.

Scaling decision	Why it matters	Examples across the monograph	Literature-supported safeguard
Unit-free scaling	Prevents raw GDP, inflation, volatility and network weights from being summed incoherently.	0-100 pressure coordinates; nondimensional starred Navier-Stokes variables; normalized zeta-cycle.	Use transparent normalization and report how scaling affects rankings or diagnostics.
Weight construction	Determines whether an index reflects theory, data variance, equal weighting or author-coded structure.	Regional graphs, corridor weights, composite stress indices, CAPM priors.	Justify weights, report alternatives and avoid causal claims from constructed weights alone.
Graph thresholds	Can create or remove cycles, connectedness and spectral gaps.	Hodge graph, Yang-Mills stress graph, Perelman/Poincare correlation graph, BSD regional network.	Report graph adequacy, robustness and sensitivity to edge rules.
Algorithmic scaling	Affects search coverage, runtime and feasible support comparison.	P-vs-NP C(n,K), exact reduced benchmark, Monte Carlo/GA search budgets.	Separate exact certification from best-found heuristic evidence.

Source: Author synthesis based on composite-indicator, network-methods and computational-validation literatures.

3.9.4. Replication Packages as External Audit Companions

Reproducibility is now a central part of scientific credibility, especially in empirical economics, computational modelling and complex data pipelines (Peng, 2011; Stodden, Leisch and Peng, 2014; Stodden et al., 2016). The seven source manuscripts treat replication not merely as a final data-availability sentence but as an evidentiary device. The BSD manuscript explicitly records public input series, World Bank API patterns, aggregation rules, author-calculated BSD objects, seeds, hashes and a Zenodo data and replication package with DOI 10.5281/zenodo.20796984 (Gondauri, 2026e). The Riemann/Zeta manuscript similarly links annual, quarterly and monthly validation layers to a Zenodo replication package with DOI 10.5281/zenodo.20852478, including structured workbooks, reported tables, formula-audit files and supporting documentation (Gondauri, 2026f).

This replication logic should govern the entire monograph. A Word manuscript is an interpretive artifact; it explains the theoretical background, methodology, results and claim hierarchy. A replication package is an audit artifact; it stores raw or extracted inputs, transformation rules, scripts, matrices, seeds, outputs, checksums, version information and formula catalogues. The literature on reproducible research emphasizes that a published result should be traceable from input to output, particularly when the analysis involves computational transformations that are difficult to reconstruct from prose alone (Gentleman and Lang, 2007; Peng, 2011; Stodden et al., 2016).

The monograph therefore requires a general replication standard: each constructed index must be accompanied by a source ledger, transformation map, software or formula record, random-seed record when applicable, output-hash record where feasible, and claim-class note. This does not require every chapter to have the same empirical scale. The Hodge chapter may be a benchmark regional topology; Yang-Mills may be a finite-network benchmark with a future N=1,500 pathway; Navier-Stokes may have a completed N=1,500 macro-financial panel; BSD may use an N=150 closure layer; Riemann/Zeta may use layered annual, quarterly and monthly validation; P-vs-NP may combine a full n=94 heuristic universe with exact n=20 certification; Perelman/Ricci/Poincare may use an N=150 macro-regional diagnostic panel. What must be common is not sample size, but auditability (Gondauri, 2026a-g).

Table 3.9.3. Minimum replication-package standard for constructed economic analogues

Replication element	Minimum content	Why it matters for claim discipline
Source ledger	Source family, variable name, extraction date, transformation rule, aggregation rule and output use.	Prevents public anchors and author-derived objects from being confused.
Formula catalogue	All index formulas, matrix definitions, graph rules, forecast equations and optimization criteria.	Makes constructed indices reviewable rather than narrative black boxes.
Data-layer separation	Raw inputs, normalized inputs, constructed objects, validation outputs and final tables	Allows reviewers to identify where interpretation enters the pipeline.

Replication element	Minimum content	Why it matters for claim discipline
	stored separately.	
Seeds and stochastic controls	Seeds for Monte Carlo, bootstrap, permutation, heuristic search and simulation layers.	Distinguishes reproducible computational evidence from irreproducible random output.
Output hashes	Cryptographic or file-version identifiers for core CSV, workbook, matrix or result artifacts.	Supports version control and prevents undocumented replacement of results.
Validation scripts or workbooks	Code/workbooks that reproduce forecast metrics, regression tables, graph diagnostics or optimization outputs.	Links results to executable audit evidence rather than manuscript assertion.
Claim-class note	Classification of each output as measurement, diagnostic, forecasting, benchmark or future-validation evidence.	Prevents a valid constructed value from being overinterpreted as proof, causality or universal law.

Source: Author synthesis based on reproducible-research literature and the replication architecture of the seven source manuscripts.

3.9.5. Validation Gates and the Evidence Hierarchy

The validation literature is essential because constructed indices can be internally coherent and still empirically weak if they are not tested against alternatives, benchmarks or falsification gates. Robust econometric inference, forecast evaluation, sensitivity analysis, placebo logic, negative controls, cross-validation and exact benchmarking all serve the same epistemic function: they determine how far a claim may travel (White, 1980; Newey and West, 1987; Diebold and Mariano, 1995; Driscoll and Kraay, 1998; Clark and West, 2007; Saltelli et al., 2008). Section 3.9 therefore treats validation as a claim-classifier rather than as a decorative appendix.

Across the seven source manuscripts, validation appears in different forms because the empirical objects differ. In the Riemann/Zeta chapter, forecast validation uses RMSE, MAE, sMAPE, rolling no-look-ahead logic, Mincer-Zarnowitz calibration, encompassing tests, Diebold-Mariano and Clark-West comparisons, residual diagnostics and spectral/regime screens (Mincer and Zarnowitz, 1969; Diebold and Mariano, 1995; Clark and West, 2007; Gondauri, 2026f). In the Navier-Stokes chapter, validation uses rolling windows, benchmark comparison, fixed effects, external-target validation, residual stability, Monte Carlo uncertainty and policy counterfactuals to keep the stress-testing claim bounded (Acharya et al., 2017; Gondauri, 2026c). In the P-vs-NP chapter, validation uses exact reduced enumeration, search-coverage reporting, heuristic comparison and robustness to distinguish exact certification from best-found incumbents (Garey and Johnson, 1979; Papadimitriou and Steiglitz, 1998; Gondauri, 2026g).

In the topology and network chapters, validation tests whether the constructed mathematical object is suitable for the diagnostic task. Hodge uses graph connectedness, cycle structure, Hodge-Laplacian diagnostics, econometric tests, predictive checks and persistent homology as benchmark validation rather than full causal proof (Ghrist, 2008; Edelsbrunner and Harer, 2010; Gondauri, 2026b). Yang-Mills uses spectral separation, curvature/action concentration, scenario simulations, perturbation robustness and a future country-panel validation design to prevent the finite-network mass gap from being misread as a theorem-level result (Chung, 1997; Newman, 2010; Gondauri, 2026d). BSD uses rank-gap logic, calibration agreement, placebo, sensitivity, external-proxy screening and reproducibility notes to classify the evidence as calibrated measurement rather than causal law or classical BSD proof (Silverman, 2009; Gondauri, 2026e). Perelman/Ricci/Poincare uses panel diagnostics, graph topology, Monte Carlo uncertainty, forecast discipline and stress-coordinate sensitivity to keep inequality-curvature claims diagnostic and bounded (Hamilton, 1982; Perelman, 2002; Gondauri, 2026a).

Table 3.9.4. Evidence hierarchy for constructed indices and claim discipline

Evidence class	Validation gate	Claim allowed	Claim not allowed
Measurement construction	Explicit definition, normalization, source ledger and formula catalogue.	The constructed object is transparent and reproducible under its assumptions.	The object is a raw fact, theorem or causal truth.
Diagnostic association	Robust regressions, sensitivity checks, residual diagnostics, graph adequacy or external	The object has empirical diagnostic content.	Unrestricted causal identification or policy law.

Evidence class	Validation gate	Claim allowed	Claim not allowed
	screening.		
Forecasting evidence	Rolling no-look-ahead validation, benchmark comparison, calibration tests and residual screens.	Forecast-window improvement under reported samples and horizons.	Universal forecast superiority or residual-problem elimination.
Benchmark topology/network evidence	Connectedness, cycles, spectral gaps, perturbations, persistent homology or finite-network simulations.	The finite constructed network is suitable for benchmark interpretation.	Full country-level causal confirmation or physical theorem transfer.
Computational evidence	Exact reduced enumeration, heuristic comparison, seeds, runtime/search coverage and robustness.	Best-found or benchmark-certified computational evidence according to search class.	P != NP proof or uncertified full-universe global optimality.
Future validation design	Pre-specified all-country, dyadic, multilayer, external-proxy or dynamic-panel extension.	The framework identifies what must be validated next.	Present evidence already proves the future claim.

Source: Author synthesis based on robust-inference, forecast-evaluation, computational-validation and claim-boundary literatures.

3.9.6. Claim Discipline as a Review-Level Methodological Contribution

The integrated literature review shows that claim discipline is not merely a defensive response to reviewer criticism. It is a positive methodological contribution. In conventional empirical work, the risk is often that a statistically significant coefficient is overstated as causality. In the present monograph, the risk is broader: a mathematical analogy may be overstated as theorem proof; a constructed index may be overstated as raw measurement; a forecast improvement may be overstated as universal prediction; a finite-network spectral gap may be overstated as a physical mass gap; a heuristic optimization result may be overstated as certified global optimality. The literature on validity, causal inference, robust statistics and reproducible research supports explicit claim classification as the appropriate response (Shadish, Cook and Campbell, 2002; Ioannidis, 2005; Angrist and Pischke, 2009; Stodden et al., 2016).

This is especially important for the seven Millennium-inspired analogues because the source mathematical problems have theorem-level prestige. The monograph must therefore prevent prestige transfer. The existence of a classical mathematical object does not raise the evidence level of an economic analogue. Only the economic construction, data architecture, validation gates and replication discipline determine the economic claim. Thus, the Hodge chapter may claim a decomposable macro-flow benchmark, not a solution to the Hodge Conjecture. The Yang-Mills chapter may claim finite-network spectral separation, not the Yang-Mills mass-gap theorem. The BSD chapter may claim calibrated local-to-global regional measurement, not classical BSD proof. The Riemann/Zeta chapter may claim bounded forecast improvement, not RH verification. The P-vs-NP chapter may claim empirical-computational evidence, not complexity-theory proof. The Navier-Stokes chapter may claim stress-testing architecture, not physical hydrodynamic law. The Perelman/Ricci/Poincare chapter may claim inequality-curvature diagnostics, not theorem-level geometry or topology (Gondauri, 2026a-g).

The review implication is that Chapter 3 must cite literature in two ways. First, it must cite domain literatures: composite indicators, network science, topology, spectral methods, forecast evaluation, portfolio theory and robust econometrics. Second, it must cite the seven source manuscripts as monograph-specific evidence architectures. The first group authorizes methods; the second group shows how those methods are bounded inside the present research programme. Both are necessary. A literature review that cites only external methodology would understate the monograph-specific architecture; a review that cites only the author's source manuscripts would not sufficiently ground the work in the wider academic tradition.

Table 3.9.5. Claim-discipline language rules for reviewer-safe interpretation

Potential overclaim	Correct claim class	Required language in the monograph
The model solves a Clay Millennium Problem.	Excluded claim.	The model is an economic-econometric analogue inspired by the formal architecture; it does not solve, prove, test or replicate the classical problem.
The constructed index is a raw objective fact.	Measurement claim.	The index is an author-constructed measurement object derived from declared inputs, transformations and validation

Potential overclaim	Correct claim class	Required language in the monograph
		gates.
The regression proves causality.	Diagnostic or causal claim depending on design.	Coefficients are interpreted as diagnostic associations unless identification, instruments, panel design and robustness justify stronger causal language.
The forecast will dominate in all samples.	Forecasting claim.	Forecast improvement is bounded to the reported sample layers, horizons and benchmark set.
The finite-network mass gap is a mathematical mass gap.	Benchmark claim.	The mass gap is a finite weighted-graph spectral separation used as an economic shock-threshold diagnostic.
The heuristic portfolio is globally optimal.	Computational claim.	The full-universe result is a best-found incumbent unless exhaustive or certified global optimization evidence is supplied.
Future validation is already completed.	Future validation claim.	The manuscript specifies the validation pathway; the stronger claim is reserved for populated and estimated future layers.

Source: Author synthesis based on the monograph claim-boundary standard and the seven source manuscripts.

3.9.7. Replication Discipline across the Seven Analogues

The replication requirement differs by analogue, but the discipline is common. A replication package for Perelman/Ricci/Poincare must document the 10-region, 2010-2024, 16-variable stress-coordinate panel, pressure scaling, curvature-like calculations, graph topology, uncertainty and validation outputs (Gondauri, 2026a). A Hodge replication package must document regional nodes, World anchor use, public macro anchors, edge weights, directed pressure construction, Hodge decomposition, spectral diagnostics and persistent-homology checks (Gondauri, 2026b). A Navier-Stokes package must document the 100-country, 2010-2024 panel, nondimensional stress variables, closure equation, rolling validation, benchmarks, Monte Carlo and policy-counterfactual outputs (Gondauri, 2026c).

A Yang-Mills replication package must document the ten-node, twenty-seven-edge benchmark, systemic-stress normalization, adjacency and stress-weighted matrices, gauge potential, triangular curvature, action, Laplacian, spectral mass-gap calculation, scenario shocks and the planned N=1,500 validation architecture (Gondauri, 2026d). A BSD replication package must document public series, regional aggregation, economic curve coefficients, local finite-state traces, Euler factors, L-function analogue, LOrder, structural rank, seeds, hashes and the Zenodo data package with DOI 10.5281/zenodo.20796984 (Gondauri, 2026e). A Riemann/Zeta package must document the N=55, N=45, N=20, N=100 and N=240 validation layers, FPAS baseline, tau argument, normalized zeta-cycle, alpha calibration, forecast outputs, residual diagnostics and the Zenodo package with DOI 10.5281/zenodo.20852478 (Gondauri, 2026f). A P-vs-NP package must document the fixed n=94 industry universe, CAPM priors, covariance alternatives, C(94,10) support space, heuristic search budgets, exact C(20,6) reduced benchmark, seeds, transaction-cost and derivative-overlay robustness (Gondauri, 2026g).

These requirements support a monograph-wide replication principle: no constructed claim should appear in the final manuscript unless the reader can identify its input source, transformation rule, validation status and claim level. This principle should carry forward into Chapter 4, where the unified methodology, data architecture and replication discipline will convert the literature-review standard into an operational protocol. Section 3.9 therefore functions as the literature bridge between the conceptual review and the technical methodology chapter.

3.9.8. Integrated Seven-Analogue Claim Matrix

Table 3.9.6. Integrated claim and replication matrix across the seven analogues

Analogue	Strongest permitted claim	Main replication anchor	Main restriction
Perelman/Ricci/ Poincare	Diagnostic measurement of inequality pressure, curvature-like deformation, smoothing capacity and graph connectedness.	Stress-coordinate panel, curvature/entropy formulas, graph diagnostics, uncertainty and validation outputs.	No theorem proof; no unrestricted welfare-causal law.
Hodge	Benchmark decomposition of regional macro-flow into gradient hierarchy, curl	Regional graph, edge cochain, decomposition code/formulas, component indices and topology-	No Hodge Conjecture solution; no final dyadic-flow

Analogue	Strongest permitted claim	Main replication anchor	Main restriction
	imbalance and harmonic/systemic circulation.	validation outputs.	causality.
Navier-Stokes	Global macro-financial stress can be measured through nondimensional flow-pressure-friction-shock-cycle-closure logic.	Country-year panel, normalized variables, closure equation, rolling validation, benchmark and Monte Carlo outputs.	No physical liquidity fluid; no universal crisis-prediction theorem.
Yang-Mills	Finite stress-weighted corridor network exhibits benchmark spectral threshold and curvature/action diagnostics.	Node/edge file, stress matrix, gauge potential, curvature/action calculations, Laplacian and perturbation/scenario files.	No mathematical Yang-Mills mass-gap solution; stronger panel claims reserved for N=1,500 closure.
BSD	Local regional signals and Euler-factor analogues are informative about structural rank under calibrated measurement logic.	Source ledger, regional aggregation, finite-state traces, Euler factors, LOrder, seeds, hashes and DOI 10.5281/zenodo.20796984.	No classical BSD proof; no strong external validation where evidence remains directional.
Riemann/Zeta	Zeta-cycle correction improves reported global-inflation forecasts in bounded validation layers.	Annual/quarterly/monthly workbooks, formula audit, forecast metrics, residual tests and DOI 10.5281/zenodo.20852478.	No RH verification; no universal forecast dominance.
P-vs-NP	Sparse portfolio selection can be analyzed as a reproducible empirical-computational complexity problem.	Fixed input universe, CAPM priors, covariance files, search logs, seeds, exact reduced enumeration and robustness outputs.	No P != NP proof; no uncertified full n=94 global optimality or realized investment dominance.

Source: Author synthesis based on the seven source manuscripts and the integrated literature-review claim hierarchy.

3.9.9. Literature Gap Addressed by Section 3.9

The literature reviewed in this section reveals a gap that is different from the gap addressed by any single problem chapter. Composite-indicator literature provides guidance on normalization and weighting, but it does not by itself address theorem-level mathematical analogies. Reproducible-research literature provides transparency standards, but it does not decide which economic claims are permissible for Hodge, Yang-Mills, BSD, zeta or P-vs-NP analogues. Robust econometrics and forecast evaluation define inference gates, but they do not automatically integrate topology, spectral methods, computational finance and regional corridors. The monograph contributes by combining these literatures into one claim-disciplined architecture.

This gap is especially important because the monograph is not a conventional empirical collection. It links seven different mathematical grammars to seven economic measurement systems. Such a programme would be vulnerable if it lacked a unified index-construction and replication standard. Section 3.9 supplies that standard at the literature-review level. It argues that constructed indices are acceptable when they are conceptually justified, normalized, replicable and validated; replication packages are necessary when transformations are too complex to be audited through prose alone; and claim discipline is the mechanism that prevents mathematical prestige, high fit, spectral separation, forecast improvement or heuristic performance from being overstated.

The strongest conclusion of Section 3.9 is therefore not only that each chapter has a data or replication component. The stronger conclusion is that replication and claim hierarchy are themselves part of the scientific contribution. The monograph's credibility depends on showing not only what each analogue measures, but also how each object is constructed, how it can be checked, what evidence class it belongs to and what it cannot claim. This is the bridge from the literature review to Chapter 4, where the monograph's unified methodology and replication discipline must be formalized.

3.9.10. Section Closing Synthesis

Section 3.9 establishes a general literature-supported principle for the monograph: every constructed index must be matched with a replication path and every empirical result must be matched with a claim class. The seven Millennium-inspired analogues do not become scientifically stronger by borrowing famous mathematical names. They become stronger when their constructed objects are transparent, their transformations are reproducible, their validation gates are explicit and their claims are limited to what the evidence can support. This principle connects composite-indicator methodology, reproducible research, robust econometric inference, network and topological validation, forecast evaluation and computational benchmarking into one reviewer-safe architecture (OECD and European Commission Joint Research Centre, 2008; Saltelli et al., 2008; Peng, 2011; Stodden et al., 2016).

The section also defines the standard for the rest of the book. Chapter 4 should convert this literature-review logic into a unified methodology: empirical universes, public-data anchors, author-calculated variables, normalization, graph construction, econometric validation, computational protocols, replication packages and claim-boundary matrices. The problem chapters should then apply that standard individually. The final monograph should therefore be read as a high-level mathematical-economic measurement programme, not as a claim to solve, prove, test or replicate the Clay Millennium Problems in their original mathematical form.

3.10. Literature Gap and Contribution of the Monograph

Integrated Review Closure across the Seven Millennium-Inspired Economic-Econometric Analogues

3.10.1. Function of this Closing Section within Chapter 3

Section 3.10 closes the integrated literature review by converting the preceding thematic review into a single literature-gap and contribution statement. The purpose is not to repeat the seven article-level research gaps separately. The purpose is to identify what is still missing when mathematical economics, systemic-risk networks, topological and spectral methods, macro-financial stress testing, inflation forecasting, inequality diagnostics, computational finance, regional corridor economics, constructed-index methodology and robust validation are considered together. In this sense, the section performs the same monographic function that a concluding review chapter performs in a research book: it states what the literature already knows, what it does not yet integrate, and what this monograph adds (Samuelson, 1947; Arrow and Debreu, 1954; Debreu, 1959; Lucas, 1976; Manski, 2007).

The seven source manuscripts already formulate bounded contributions inside their own domains. The Perelman/Ricci/Poincare manuscript identifies a gap between scalar inequality measurement and geometric-topological pressure diagnostics (Gondauri, 2026a). The Hodge manuscript identifies a gap between macroeconomic regional indicators and decomposable flow topology (Gondauri, 2026b). The Navier-Stokes manuscript identifies a gap between separate financial-stress indicators and a nondimensional liquidity-flow stress-balance architecture (Gondauri, 2026c). The Yang-Mills manuscript identifies a gap between network systemic-risk literature and finite-network gauge-curvature shock-threshold measurement (Gondauri, 2026d). The BSD manuscript identifies a gap between regional macroeconomics and local-to-global structural-rank logic (Gondauri, 2026e). The Riemann/Zeta manuscript identifies a gap between inflation forecasting and mathematically explicit spectral-cycle correction (Gondauri, 2026f). The P-vs-NP manuscript identifies a gap between portfolio optimization, sparse support selection and explicit computational-complexity claim discipline (Gondauri, 2026g).

The monograph-level gap is larger than any one of these seven gaps. Existing literatures are strong inside their own domains, but they rarely combine formal mathematical architectures, economic measurement, systemic transmission, forecast validation, computational optimization, replication discipline and claim hierarchy in one coherent programme (OECD/JRC, 2008; Saltelli et al., 2008; Imbens and Rubin, 2015; Nosek et al., 2015; Christensen and Miguel, 2018). The contribution of the monograph is therefore integrative and architectural. It converts seven high-level mathematical grammars into bounded, auditable economic-econometric analogues while explicitly refusing theorem-level proof, physical identity, unrestricted causality, universal forecast superiority and uncertified global optimality.

3.10.2. The General Cross-Literature Gap

The first cross-literature gap is fragmentation. Mathematical economics provides a long tradition of formal representation, equilibrium analysis, optimization and dynamic modelling, but it does not normally address how unsolved Millennium-level architectures should be translated into economics with explicit claim boundaries (Samuelson, 1947; Arrow and Debreu, 1954; Debreu, 1959; Koopmans, 1957; Stokey et al., 1989). Network economics and systemic-risk research explain interdependence, cascades, production networks and shock propagation, but they do not by themselves define Hodge

decomposition, gauge curvature, economic mass-gap thresholds, LOrder or zeta-cycle correction (Gabaix, 2011; Acemoglu et al., 2012; Haldane and May, 2011; Elliott et al., 2014; Carvalho, 2014).

The second gap is scalar reduction. GDP, inflation, inequality indices, liquidity ratios, risk premia, portfolio Sharpe ratios and regional output shares remain necessary anchors, but the reviewed literature increasingly shows that global economic systems are generated through higher-dimensional interaction, propagation, regime shifts, network position, resilience, tail risk and computational constraint (Timmer et al., 2014; Koopman et al., 2014; Baldwin and Lopez-Gonzalez, 2015; Adrian and Brunnermeier, 2016; Brownlees and Engle, 2017). The monograph therefore treats scalar indicators as input anchors rather than as sufficient representations of system structure (Gondauri, 2026b; Gondauri, 2026c; Gondauri, 2026e).

The third gap is methodological separation. Topological methods, spectral graph theory, persistent homology and graph signal processing provide rigorous tools for connectedness, cycles, Laplacians, eigenvalues and higher-order relations, but they are often methodologically separate from macroeconomic data architecture and econometric validation (Chung, 1997; Ghrist, 2008; Edelsbrunner and Harer, 2010; Shuman et al., 2013; Schaub et al., 2021). Forecast evaluation and robust econometric inference provide validation gates, but they do not by themselves generate mathematical-economic analogues or determine theorem-transfer boundaries (White, 1980; Newey and West, 1987; Driscoll and Kraay, 1998; Diebold and Mariano, 1995; Clark and West, 2007).

The fourth gap is claim discipline. Many interdisciplinary models fail either by overclaiming the mathematical analogy or by weakening the analogy into metaphor. The source manuscripts show the alternative: analogy becomes scientifically admissible when it is translated through data lineage, normalization, constructed objects, validation gates, replication files and restricted claim classes (Gondauri, 2026a; Gondauri, 2026b; Gondauri, 2026c; Gondauri, 2026d; Gondauri, 2026e; Gondauri, 2026f; Gondauri, 2026g).

Existing literature domain	What it explains well	Remaining monograph-level gap
Mathematical economics and formal modelling	Equilibrium, optimization, dynamic systems, stochastic modelling, econometric representation and formal abstraction.	Does not provide a unified protocol for bounded economic translation of unsolved Millennium-level mathematical architectures.
Network economics and systemic risk	Interdependence, cascades, contagion, input-output propagation, systemic importance and production-network amplification.	Does not by itself integrate Hodge decomposition, gauge curvature, finite-network mass gap, corridor rank and zeta-cycle forecasting.
Topology and spectral methods	Connectedness, Laplacians, eigenvalues, cycles, persistent structure, graph signals and higher-order relations.	Often remains separated from macroeconomic anchors, constructed-index audit, robust inference and claim hierarchy.
Forecasting and robust econometrics	Forecast accuracy, residual diagnostics, robust covariance, rolling validation, structural breaks and benchmark comparison.	Does not define mathematical analogues or decide whether evidence supports measurement, diagnostic, benchmark or theorem-level claims.
Portfolio optimization and computational finance	Risk-return allocation, CAPM priors, covariance geometry, sparse optimization, mixed-integer search and derivative realism.	Often separates algorithmic output from exact reduced benchmarking, search-coverage disclosure and global-optimality boundaries.
Regional, corridor and GVC literature	Value-added trade, corridor exposure, supply-chain disruption, regional resilience and transmission channels.	Does not fully define local-to-global structural rank or finite-network shock-threshold analogues under one reproducible architecture.

3.10.3. Gap One: Analogue Modelling without a Unified Claim-Boundary Protocol

A major gap in interdisciplinary mathematical economics is that analogies are frequently justified conceptually but not governed by a full claim-boundary protocol. Classical mathematical economics distinguishes models from reality, but the problem becomes sharper when the source object is a Millennium-level conjecture, theorem or regularity problem (Samuelson, 1947; Debreu, 1959; Lucas, 1976). The present monograph requires more than the ordinary claim that

mathematics is useful in economics. It requires a rule that the mathematical origin, the economic translation, the constructed measurement object, the validation gate and the permissible claim must be explicitly separated.

This gap is visible across all seven domains. Curvature, topology, flow, gauge action, L-functions, zeta signals and computational complexity can easily sound stronger than the evidence permits if the claim boundary is not explicit. The seven source manuscripts respond by excluding theorem proof at the outset: the Perelman/Ricci/Poincare analogue does not prove Perelman's theorem or the Poincare conjecture; the Hodge analogue does not solve the Hodge Conjecture; the Navier-Stokes analogue does not solve the Navier-Stokes problem; the Yang-Mills analogue does not solve the Yang-Mills mass-gap problem; the BSD analogue does not prove or test BSD; the Riemann/Zeta analogue does not verify the Riemann Hypothesis; and the P-vs-NP analogue does not prove P != NP (Gondauri, 2026a; Gondauri, 2026b; Gondauri, 2026c; Gondauri, 2026d; Gondauri, 2026e; Gondauri, 2026f; Gondauri, 2026g).

The monograph contributes a general claim-boundary protocol. It treats analogy as a scientific operation only when the economic analogue is auditable, the validation gate is specified, the replication materials are disclosed and the final claim is classified as measurement, diagnostic, forecasting, benchmark, computational or future-validation evidence. This is a methodological contribution because it shows how high-level mathematics can enter economics without becoming rhetorical borrowing or theorem overclaiming.

3.10.4. Gap Two: Scalar Indicators Do Not Capture Multidimensional Economic Structure

The second gap concerns the dominance of scalar measurement. The literature contains mature scalar measures of output, inflation, inequality, volatility, liquidity, risk and portfolio performance. Yet the global economy increasingly behaves as a multidimensional system in which scale, pressure, network position, cycle structure, resilience, stress propagation and computational feasibility interact (Gabaix, 2011; Acemoglu et al., 2012; Carvalho, 2014; Timmer et al., 2014). Scalar indicators remain necessary, but they often fail to distinguish whether a region is large because of output mass, structurally important because of corridor position, vulnerable because of weak smoothing capacity, fragile because of network threshold compression or difficult to optimize because of combinatorial search space.

The seven analogues address this gap by converting scalar anchors into structured objects. Perelman/Ricci/Poincare converts inequality and macro-social variables into pressure coordinates, curvature-like deformation and entropy-like complexity (Gondauri, 2026a). Hodge converts regional macro anchors into a directed edge-flow that can be decomposed into gradient, curl and harmonic components (Gondauri, 2026b). Navier-Stokes converts macro-financial variables into nondimensional flow-pressure-friction-shock-cycle-closure components (Gondauri, 2026c). Yang-Mills converts macro-corridor anchors into a stress-weighted graph, gauge potential, triangular curvature, action and spectral separation (Gondauri, 2026d). BSD converts regional anchors into finite-state traces, Euler-factor analogues, LOrder and structural rank (Gondauri, 2026e). Riemann/Zeta converts macro-financial pressure into a nonlinear zeta-cycle forecast correction (Gondauri, 2026f). P-vs-NP converts industry-level financial inputs into a sparse support-selection and optimization evidence architecture (Gondauri, 2026g).

The contribution of the monograph is not the rejection of scalar indicators. It is the systematic demonstration that scalar indicators can become input anchors inside richer measurement architectures. This is crucial for reviewer safety: the monograph does not replace GDP, inflation, Gini, beta, volatility or Sharpe ratios; it repositions them inside flow, topology, curvature, spectral, local-to-global and complexity grammars.

Scalar anchor	Monograph transformation	Contribution to literature gap
GDP, growth and regional share	Regional network, corridor exposure, structural rank, LOrder and local-to-global measurement.	Moves regional economics beyond output-size ranking toward systemic position and rank formation.
Inflation and macro-financial pressure	FPAS baseline, zeta-cycle correction, stress regimes and validation hierarchy.	Links structural forecasting with mathematical signal construction and benchmark discipline.
Inequality and social pressure variables	Pressure coordinates, curvature-like deformation, smoothing capacity and graph topology.	Moves inequality review from scalar distribution to pressure-smoothing diagnostic architecture.
Liquidity, spreads and financial stress proxies	Nondimensional flow-pressure-friction-shock-cycle-closure balance.	Integrates separate financial-stress indicators into an auditable stress-balance model.
Beta, volatility and portfolio returns	CAPM priors, covariance geometry, cardinality search, heuristic/exact	Connects asset-pricing literature with computational-complexity evidence and

Scalar anchor	Monograph transformation	Contribution to literature gap
	benchmarking and derivative overlay.	claim boundaries.

3.10.5. Gap Three: Network, Topology, Spectral and Corridor Literatures Remain Partly Disconnected

The third gap is the incomplete integration of network, topology, spectral and corridor literatures. Network economics and systemic-risk research show that connectivity, centrality, cascades and exposure matter for propagation (Haldane and May, 2011; Acemoglu et al., 2012; Elliott et al., 2014; Battiston et al., 2012). GVC and production-network research show that value-added trade, sectoral linkages and supply-chain organization shape shock transmission (Koopman et al., 2014; Timmer et al., 2014; Baldwin and Lopez-Gonzalez, 2015; Antras and Chor, 2022). Spectral graph and topological research provide mathematical tools for connectedness, algebraic connectivity, Hodge Laplacians, persistence and higher-order cycles (Chung, 1997; Edelsbrunner and Harer, 2010; Shuman et al., 2013; Schaub et al., 2021). Yet these literatures are rarely unified in a regional macroeconomic architecture that also includes claim-boundary and replication discipline.

The monograph's contribution is to show how these literatures can be connected through the seven analogues. Hodge supplies decomposable macro-flow topology; Yang-Mills supplies finite-network curvature, action and shock-threshold logic; BSD supplies local-to-global structural rank and corridor-stress interpretation; Navier-Stokes supplies stress-flow closure; Perelman/Ricci/Poincare supplies curvature-like pressure and connectedness logic; Riemann/Zeta supplies spectral-cycle forecasting; and P-vs-NP supplies computational feasibility and search discipline (Gondauri, 2026a-g). The contribution is not that one model absorbs all others. It is that each model occupies a specific role within a wider network-spectral-topological measurement programme.

This is especially important for corridor economics. A corridor node may be small in GDP but large in systemic exposure. Standard regional ranking can miss this. The BSD, Yang-Mills and Hodge analogues jointly address the gap: BSD interprets local regional states and corridor stress as information about global structural rank; Yang-Mills asks whether a local disturbance crosses a finite-network spectral threshold; Hodge asks whether a region contributes to hierarchy, local-cycle imbalance or systemic circulation (Gondauri, 2026b; Gondauri, 2026d; Gondauri, 2026e).

3.10.6. Gap Four: Forecasting, Validation and Robust Inference Are Often Detached from Analogue Construction

The fourth gap is validation separation. Forecasting literature offers strong tools for benchmark comparison, calibration, residual diagnostics and no-look-ahead evaluation, while robust econometrics offers tools for heteroskedasticity, autocorrelation, panel dependence, robust covariance and identification caution (White, 1980; Newey and West, 1987; Driscoll and Kraay, 1998; Diebold and Mariano, 1995; Clark and West, 2007; Pesaran, 2006). However, these tools often enter applied work after the modelling object has already been constructed. In the monograph, validation is not an appendix to analogy; it is a condition of admissibility.

The Riemann/Zeta model is the clearest forecasting case: it can claim only bounded forecast-diagnostic evidence where FPAS+zeta improves reported validation-window performance against FPAS and ARIMA and survives rolling, calibration and residual screens (Gondauri, 2026f). The Navier-Stokes model uses rolling validation, benchmark comparison, panel fixed effects, external-target validation, residual diagnostics and Monte Carlo counterfactuals to prevent the liquidity-flow analogy from becoming a universal crisis-prediction law (Gondauri, 2026c). The P-vs-NP model uses reduced exact enumeration and search-coverage disclosure to prevent heuristic portfolio output from being misread as certified global optimality (Gondauri, 2026g). The Perelman/Ricci/Poincare model treats forecasts and counterfactuals as bounded diagnostics, not causal multipliers or universal prediction claims (Gondauri, 2026a).

The contribution of the monograph is therefore a validation-centered analogue methodology. Each mathematical-economic object must pass the relevant gate: scale gate, topology gate, econometric gate, forecast gate, computational gate, replication gate and final claim gate. This directly addresses a literature weakness: sophisticated models may be mathematically elegant but inferentially underbounded if validation and claim classification are not built into the design.

Evidence type	Literature basis	Monograph contribution
Forecasting evidence	Forecast comparison, rolling validation, calibration, encompassing and residual diagnostics.	Classifies FPAS+zeta and related predictive results as bounded validation-window evidence, not universal forecasting law.
Robust econometric evidence	HC/HAC covariance, panel robustness, cross-sectional dependence, factor and diagnostic inference.	Treats coefficients and associations as diagnostic unless identification supports stronger claims.
Computational evidence	Complexity theory, mixed-integer optimization, metaheuristics and exact	Separates best-found incumbents, exact reduced certificates and uncertified full-

Evidence type	Literature basis	Monograph contribution
	enumeration.	universe optima.
Network/topological evidence	Laplacians, Hodge decomposition, connectivity, Betti structure, persistence and spectral thresholds.	Interprets graph results as constructed measurement evidence, not as theorem proof or ontological identity.
Replication evidence	Open science, computational reproducibility, data packages, formulas, scripts and source ledgers.	Makes every constructed object reviewable by requiring source-data lineage, transformation disclosure and claim matrices.

3.10.7. Gap Five: Constructed Indices and Replication Are Not Always Joined to Claim Discipline

The fifth gap concerns constructed indices and reproducibility. Composite indicators, normalized scores, stress indices and model-implied objects are standard in economics and policy research, but their credibility depends on transparent construction, sensitivity analysis, data lineage and replication (Nardo et al., 2005; OECD/JRC, 2008; Saltelli et al., 2008). The source manuscripts repeatedly build constructed objects: pressure coordinates, Hodge-flow components, nondimensional stress terms, gauge potentials, EMGI, BridgeStress, LOrder, zeta-cycle deviations, sparse support sets and option-overlay diagnostics (Gondauri, 2026a-g). These objects are legitimate only if they are auditable.

The monograph contributes by turning replication into part of the literature argument itself. The relevant question is not only whether a constructed index is intuitive. The question is whether its inputs, normalization, directionality, formulas, matrices, scripts, robustness gates, sensitivity rules and claim restrictions are disclosed. This is aligned with the broader reproducibility movement in economics and computational science, where data packages, code availability, pre-analysis clarity and transparent workflow design are increasingly treated as credibility conditions rather than optional supplements (Buckheit and Donoho, 1995; Peng, 2011; Nosek et al., 2015; Christensen and Miguel, 2018).

This is why the monograph's contribution is methodological as much as empirical. It does not merely report seven sets of constructed results. It proposes a general replication discipline for Millennium-inspired economic analogues: every constructed object must be tied to an input anchor, a transformation rule, a validation gate and a permissible claim. This closes a common gap in interdisciplinary work, where complex constructs may appear impressive but remain difficult for reviewers to audit.

3.10.8. Positive Contribution of the Monograph

The positive contribution of the monograph can be stated in one sentence: it develops a unified, reproducible and claim-bounded research programme that translates seven formal mathematical architectures into seven economic-econometric measurement systems. This contribution is not a claim of solving the Clay Millennium Problems in economics. It is a claim that their formal architectures can organize distinct economic measurement problems: inequality deformation, macro-flow decomposition, liquidity stress, corridor shock thresholds, local-to-global structural rank, inflation spectral cycles and sparse portfolio optimization.

The first contribution is conceptual. The monograph defines a general theory of mathematical-economic translation: classical object -> translation operator -> economic analogue -> validation gate -> permissible claim. This framework advances the literature by making analogy auditable rather than rhetorical (Samuelson, 1947; Debreu, 1959; Manski, 2007).

The second contribution is methodological. The monograph organizes seven mathematical grammars - flow, curvature, topology, spectral signal, local-to-global rank, computational complexity and claim discipline - into one monographic review and methodology architecture. This is different from a collection of seven papers because it identifies cross-model principles that recur across all applications (Gondauri, 2026a-g).

The third contribution is empirical-architectural. Each analogue is tied to public or fixed data anchors, constructed variables, formulas, matrices, algorithms, robustness checks and replication materials. The contribution is not only to propose an idea, but to convert that idea into an auditable measurement architecture. This gives the monograph a higher evidentiary status than a purely conceptual analogy while preserving academic caution.

The fourth contribution is reviewer-safety and claim hierarchy. The monograph establishes explicit rules for strong measurement claims, diagnostic claims, forecasting claims, benchmark claims and future-validation claims. This contribution is important because the scientific value of a high-level analogy depends not only on what it reveals, but also on what it refuses to claim.

Contribution layer	What the monograph adds	Primary supporting analogues
Conceptual contribution	A general translation framework that separates mathematical origin, economic analogue,	All seven analogues.

Contribution layer	What the monograph adds	Primary supporting analogues
	validation gate and permissible claim.	
Measurement contribution	Structured transformation of scalar anchors into pressure fields, flow cochains, curvature scores, LOrder, zeta-cycles and sparse supports.	Perelman/Ricci/Poincare; Hodge; Navier-Stokes; BSD; Riemann/Zeta; P-vs-NP.
Network/systemic contribution	A unified literature bridge between systemic risk, corridor exposure, topology, spectral thresholds and local-to-global transmission.	Hodge; Yang-Mills; BSD; Navier-Stokes.
Forecasting/validation contribution	Forecast-window evidence and robust inference treated as claim gates rather than post-hoc checks.	Riemann/Zeta; Navier-Stokes; P-vs-NP; Perelman/Ricci/Poincare.
Replication contribution	Data lineage, formulas, source ledgers, matrices, scripts, sensitivity tests and claim matrices become part of the scientific contribution.	All seven analogues.
Claim-discipline contribution	The book systematically distinguishes theorem proof from bounded economic measurement, diagnostic, benchmark and future-validation claims.	All seven analogues.

3.10.9. Seven-Analogue Contribution Matrix

Table 3.10.4 summarizes how the literature gap and contribution are closed across the seven analogues. The table is intentionally monographic: it does not reproduce seven separate literature reviews, but classifies each analogue by the missing link it addresses and the bounded contribution it makes.

Analogue	Literature gap closed by the monograph	Bounded contribution
Perelman/Ricci/ Poincare	Inequality and macro-pressure literatures often remain scalar, decompositional or policy-specific rather than geometric-topological.	Constructs a diagnostic manifold for inequality pressure, smoothing capacity, curvature-like deformation, entropy-like complexity and graph connectedness.
Hodge	Regional macroeconomics and network economics rarely decompose macro-flow into hierarchy, local-cycle imbalance and systemic circulation.	Builds a Hodge-econometric decomposition architecture for regional macro-flow and topological validation.
Navier-Stokes	Liquidity and stress literatures often treat stress indicators separately rather than through flow-pressure-friction-shock closure.	Develops a nondimensional global liquidity-flow and systemic-stress balance with rolling validation and bounded stress-testing claims.
Yang-Mills	Systemic-risk and corridor literatures often lack a finite-network spectral threshold and gauge-curvature-action representation.	Constructs a finite-network gauge-econometric benchmark for shock thresholds, curvature, action, EMGI and BridgeStress.
BSD	Regional economics and GVC literatures rarely link local finite-state signals to global structural rank through local-to-global logic.	Creates a calibrated BSD-inspired local-to-global measurement architecture using finite-state traces, Euler-factor analogues, LOrder and structural rank.
Riemann/Zeta	Inflation forecasting rarely integrates structural FPAS logic with mathematically explicit critical-line spectral-cycle correction.	Constructs and validates a bounded FPAS+zeta global inflation forecast-diagnostic architecture.
P-vs-NP	Portfolio theory, CAPM, sparse optimization and metaheuristics are often not integrated with explicit complexity and	Builds a P-vs-NP-inspired computational-finance design with sparse support selection, search-space measurement, heuristics, exact

Analogue	Literature gap closed by the monograph	Bounded contribution
	claim-boundary discipline.	reduced benchmarking and robustness gates.

3.10.10. What the Monograph Does Not Claim

The contribution of the monograph is strengthened by its exclusions. It does not claim to solve, prove, test or replicate the Clay Millennium Problems in their original mathematical form. It does not claim that financial liquidity is a physical fluid, that macro-regions are algebraic varieties, that an economic L-function is an arithmetic L-function, that a zeta-cycle verifies the Riemann Hypothesis, that a finite-network mass gap solves Yang-Mills theory, or that sparse portfolio optimization proves P != NP (Gondauri, 2026a-g).

The monograph also does not claim unrestricted causal law. Robust associations, benchmark coherence, internal calibration, forecast-window improvement, finite-network spectral separation and best-found optimization incumbents are not treated as causal identification unless the design supports such interpretation (Angrist and Pischke, 2009; Imbens and Rubin, 2015; Manski, 2007). This limitation is essential for scientific credibility. It prevents the monograph from overstating model-implied structures as universal empirical laws.

Finally, the monograph does not claim complete external validation where the evidence is not yet complete. Some layers are fully populated benchmark architectures; some are diagnostic closure layers; some are future validation architectures. The contribution is therefore tiered. The book offers strong measurement and diagnostic architecture where the evidence is internally closed, bounded forecasting where validation windows support it, benchmark claims where benchmark data are complete, and future-validation claims where full country-level or dyadic empirical closure remains a research agenda.

Claim category	Allowed in the monograph	Not allowed
Mathematical claim	Use of formal architectures as economic measurement grammars.	Theorem proof, Clay-problem solution, physical identity or number-theoretic verification.
Measurement claim	Auditable construction of pressure, flow, curvature, spectral, rank, stress and optimization objects.	Claim that constructed indices are raw observables or causal laws.
Diagnostic claim	Interpretation of stress, deformation, imbalance, resilience, threshold compression and rank mismatch.	Universal welfare, policy or crisis law without identification.
Forecasting claim	Validation-window forecast improvement and benchmark comparison where reported tests support it.	Universal forecast dominance across all samples, horizons and economies.
Computational claim	Search-space measurement, heuristic comparison and exact reduced benchmarking.	Certified full-universe global optimality without exhaustive certificate or proof.
Future-validation claim	Clear agenda for country-level, dyadic, longitudinal or external-proxy validation.	Treating planned validation as already completed evidence.

3.10.11. Synthesis: The Monograph-Level Literature Gap Is Closed by Integration, Not Substitution

The literature gap is closed not by substituting one field for another, but by integration. The monograph does not replace inequality economics with Ricci flow, macro-finance with Navier-Stokes, regional economics with BSD, inflation forecasting with zeta theory or portfolio theory with P-vs-NP. Instead, it converts each mathematical architecture into a bounded measurement grammar that expands what can be measured, decomposed, validated and claimed.

This integrated position is the final contribution of Chapter 3. Mathematical economics provides the formal tradition; network and systemic-risk literature provides interdependence; topology and spectral methods provide higher-order structure; macro-financial and inflation literatures provide stress and forecast targets; inequality literature provides pressure and smoothing targets; portfolio theory provides optimization targets; regional and GVC literature provides corridor and transmission targets; econometric and replication literatures provide validation discipline. The monograph contributes by aligning all of these traditions under one architecture and one claim hierarchy.

The next chapter should therefore proceed from literature to methodology. Chapter 4 can specify the unified methodology, data architecture and replication discipline because Chapter 3 has already established the literature justification for every

required element: formal translation, constructed indicators, normalization, network and spectral objects, forecast validation, robust inference, exact/computational benchmarking, source-ledger discipline and final claim classification.

3.10.12. Closing Claim-Boundary Statement for Chapter 3

The integrated literature review supports the monograph as a high-level mathematical-economic measurement programme. It authorizes disciplined translation, constructed measurement, diagnostic architecture, bounded forecasting, finite-network benchmarking, sparse optimization evidence, replication discipline and future validation design. It does not authorize theorem proof, physical identity, unrestricted causal law, universal forecast superiority, certified full-universe portfolio optimality or completed external validation where such evidence has not been produced. This is the central literature-based defense of the monograph: seven Millennium-inspired mathematical architectures can be converted into seven bounded economic-econometric analogues, but their scientific value depends on explicit translation, validation and claim discipline.

Chapter 4. Unified Methodology, Data Architecture and Replication Discipline

4.1. Research Design of the Monograph

Quantitative, non-experimental, computational, econometric and validation-oriented design

This section establishes the research-design core of the monograph. Its role is not to repeat the seven separate methodology chapters in sequence, but to convert their common methodological logic into one unified technical architecture. The monograph is designed as a quantitative, non-experimental, computational, econometric and validation-oriented study of seven economic analogues inspired by the Clay Millennium Problems. Each analogue translates a formal mathematical grammar into an empirically bounded economic measurement system, and each system is governed by the same discipline: public-data anchoring, explicit transformation rules, author-calculated variables, normalization, validation, robustness, placebo screening, claim-boundary control and replication-package transparency.

The chapter therefore functions as the technical spine of the book. It defines how evidence can be admitted, how constructed variables may be interpreted, how mathematical analogies are protected from theorem-level overclaiming, and how the seven problem-specific empirical architectures can be read as parts of one monograph rather than as a mechanical collection of seven papers. The research design is unified because the object of inquiry is unified: the book studies whether global economic complexity can be measured through seven complementary structural grammars - curvature and smoothing, flow decomposition, liquidity balance, gauge curvature and spectral separation, local-to-global rank, spectral forecasting, and computational optimization.

The section is deliberately placed before the detailed data-architecture subsections of Chapter 4. Subsections 4.2-4.9 will later specify empirical universes, public data anchors, normalization, graph construction, econometric validation, computational protocols, replication packages and claim-boundary matrices. Section 4.1 provides the prior design logic that makes those later subsections coherent. It answers the methodological question: what kind of research is this monograph, what kind of evidence does it generate, and what kinds of claims does it permit?

4.1.1. Methodological Position: A Unified Quantitative Analogue Design

The monograph adopts a unified quantitative analogue design. In methodological terms, the book is not a purely theoretical mathematics manuscript, not a historical essay, not a policy narrative and not a conventional single-model econometric article. It is a structured research programme in applied mathematical economics in which seven distinct mathematical architectures are transformed into bounded economic-econometric measurement systems. The word "analogue" is central. It means that the book uses the formal grammar of each Millennium Problem as a modelling inspiration, while refusing to identify the economic construction with the original mathematical problem itself.

This design choice solves a central scientific problem. The Clay Millennium Problems are theorem-level mathematical problems. Their original objects - smooth manifolds, elliptic curves, gauge fields, Navier-Stokes equations, zeta zeros, Hodge classes and computational complexity classes - cannot be empirically proven or disproven by macroeconomic data. However, their formal architectures can be used as disciplined measurement grammars. The monograph uses this possibility. It asks how economic systems can be measured when they exhibit curvature-like deformation, decomposable flow, pressure-friction balance, network curvature, local-to-global rank formation, spectral-cycle forecasting and combinatorial search complexity.

The research design is quantitative because every chapter ultimately works with measurable variables, constructed indices, matrices, panels, graphs, simulations, forecast errors, optimization results or validation diagnostics. Even when the motivating object is conceptual, the operational object is numerical. Inequality pressure is converted into stress coordinates;

global macro-flow is converted into a directed edge field; liquidity stress is converted into nondimensional balance components; corridor stress is converted into graph curvature and spectral separation; regional rank is converted into structural-rank and L-order analogues; inflation cycles are converted into forecast signals; and sparse portfolio selection is converted into a documented computational search space.

The research design is non-experimental because none of the seven studies manipulates real economies, countries, regions, prices or policies under controlled laboratory or randomized conditions. The empirical material consists of public macroeconomic anchors, author-calculated transformations, benchmark networks, panel structures, forecast layers, simulation layers and computational optimization experiments. Identification is therefore not experimental identification. The evidentiary standard is instead diagnostic, computational, comparative and validation-based.

The research design is computational because the central objects cannot be produced by simple tabulation. They require algorithmic construction: matrix normalization, graph creation, edge-weight calibration, stress-field construction, Hodge projection, Laplacian spectra, curvature/action calculation, local finite-state reductions, zeta-signal generation, rolling forecast validation, Monte Carlo perturbation, genetic search, exact reduced enumeration and replication manifests. Computation is not auxiliary; it is part of the research object. The book therefore treats algorithms, software settings, seeds, search budgets, formulas and output files as methodological evidence.

The research design is econometric because constructed variables are not accepted solely because they are mathematically elegant. They are audited through panel regressions, fixed-effects screens, robust-inference procedures, rolling forecasts, benchmark comparisons, residual diagnostics, factor models, regularization, threshold tests, external-proxy checks, placebo outcomes and falsification gates. The econometric role is not to convert every analogue into a causal law. Its function is to test whether the constructed measurement objects retain empirical structure under alternative diagnostic procedures.

Finally, the research design is validation-oriented because the strongest contribution of the monograph is not a theorem claim but an evidence-governed measurement architecture. The book repeatedly distinguishes construction from validation, internal calibration from external confirmation, diagnostic association from causality, and model-implied scenario output from unconditional prediction. This validation orientation is the main reviewer-safety device of the monograph.

Equation (4.1.1). For each analogue p in P = {Ricci-Poincare, Hodge, Navier-Stokes, Yang-Mills, BSD, Riemann-Zeta, P-vs-NP}, the research design is R_p = {A_p, X_p, Z_p, M_p, V_p, B_p, Q_p}, where A_p denotes public anchors, X_p raw or benchmark inputs, Z_p normalized or constructed variables, M_p the mathematical-computational model, V_p validation layers, B_p claim boundaries and Q_p replication controls.

Equation (4.1.1) formalizes the monograph-level design. The expression is not a substantive economic law. It is a methodological rule: every chapter must disclose the public input layer, the transformation layer, the model layer, the validation layer, the boundary layer and the replication layer. A result is admissible only when it can be traced through all six layers.

Table 4.1.1. Unified research-design taxonomy of the monograph

Design attribute	Operational meaning in the monograph	Methodological function
Quantitative	Variables, matrices, panels, graphs, forecasts, simulations and optimization outputs are numerically specified.	Prevents the book from remaining at the level of metaphor or qualitative analogy.
Non-experimental	No randomized intervention or controlled manipulation of real economies is performed.	Requires diagnostic rather than experimental causal interpretation.
Computational	Main objects are generated through explicit algorithms, matrix operations, graph construction, spectral diagnostics and search routines.	Makes algorithm disclosure and replication packages part of the evidence base.
Econometric	Constructed objects are audited through regression, robust inference, forecast comparison, validation	Prevents mathematical construction from being treated as empirical confirmation by itself.

	screens and falsification logic.	
Validation-oriented	Every chapter contains internal checks, robustness layers, placebo or falsification screens and claim boundaries.	Creates a disciplined hierarchy of admissible claims.
Analogue-based	The Clay problem is used as a measurement grammar rather than as an object literally solved or tested by economic data.	Separates economic contribution from theorem-level overclaiming.

Source: Author synthesis based on the seven methodology chapters and the monograph design architecture.

4.1.2. Monograph-Level Research Object and Translation Logic

The monograph-level research object is global economic complexity interpreted through seven bounded mathematical-economic measurement grammars. The object is not a single country, a single region, a single asset universe or a single macroeconomic indicator. It is the broader problem of how economic systems form structure under multiple dimensions: inequality pressure, macro-flow hierarchy, liquidity stress, corridor shock transmission, regional rank formation, inflation-cycle deformation and combinatorial portfolio choice. The seven chapters are therefore not independent islands. They are seven views of the same methodological question: how can economic structure be measured when linear aggregates are insufficient?

The translation logic of the monograph follows three rules. First, the mathematical object must be reduced to a structural economic function. A Ricci-flow language becomes a way of measuring pressure and smoothing capacity; Hodge theory becomes a way of separating hierarchy, local imbalance and systemic circulation; Navier-Stokes balance becomes a way of organizing liquidity velocity, pressure, friction, shock and closure; Yang-Mills gauge language becomes a way of measuring corridor curvature and spectral shock thresholds; BSD local-to-global logic becomes a way of constructing regional rank analogues; Riemann-zeta cyclicality becomes a way of generating a bounded forecast signal; and P-vs-NP complexity becomes a way of studying sparse portfolio support selection under combinatorial explosion.

Second, the translation must be operational. A conceptual analogy becomes research only when it produces variables, matrices, panels, networks, forecasts, search spaces or validation objects that can be independently inspected. For example, the Perelman-Ricci-Poincare chapter does not merely speak about curvature; it constructs a macro-regional pressure-smoothing diagnostic system from ten regions, annual observations and sixteen stress-coordinate variables. The Hodge chapter does not merely mention decomposition; it builds a regional macro-flow graph and decomposes a directed edge field. The P-vs-NP chapter does not merely invoke complexity; it fixes an industry universe, imposes cardinality and documents the scale of the discrete support space.

Third, the translation must be bounded. A constructed economic curvature is not a literal geometric invariant. A finite weighted-graph mass gap is not the mathematical Yang-Mills mass gap. A zeta-cycle signal is not a proof of the Riemann Hypothesis. A sparse portfolio search problem is not a proof of P != NP. The design therefore treats mathematical inspiration as a modelling grammar, not as a theorem claim. This boundary is not a limitation added after the fact; it is built into the research design.

At the monograph level, this produces a consistent methodological pipeline. Each source study begins from a public or fixed empirical anchor, transforms it into a problem-specific constructed object, evaluates that object through a mathematical-computational architecture, audits the result through validation and robustness layers, and then restricts the final interpretation through a claim boundary. The same pipeline is used even when the empirical universe differs across chapters. This is why a macro-regional inequality panel, a ten-node Hodge graph, a 100-country liquidity panel, a finite corridor gauge network, a regional BSD closure layer, a layered inflation-forecasting system and a 94-industry optimization universe can belong to one book.

The translation is also comparative. The seven mathematical grammars are not competing explanations of the same variable. They measure different structural dimensions of economic complexity. The design therefore avoids a forced single-index synthesis at this stage. Instead, it establishes comparability at the level of research protocol: public-data anchors, constructed variables, normalized scales, validation gates, replication files and claim-boundary rules.

4.1.3. Integration of the Seven Source Designs into One Research Architecture

The seven source studies differ in empirical universe, mathematical language and validation method, but their research designs are compatible. Each is quantitative; each is built around a bounded analogue; each separates source data from constructed indicators; each includes a validation or robustness layer; and each contains a claim-boundary statement. The purpose of Section 4.1 is to make that shared architecture explicit before the book moves into problem-specific chapters.

The Perelman-Ricci-Poincare design is a diagnostic-manifold design for macro-regional inequality pressure. Its object is the interaction of stress coordinates, smoothing capacity, curvature-like deformation, entropy-like complexity and graph connectedness. It is a macro-regional panel design rather than a theorem-level topology claim. The methodological contribution is the conversion of heterogeneous inequality-related indicators into a common diagnostic pressure system and the auditing of that system through curvature, topology, econometric and forecast-validation screens.

The Hodge design is a topological macro-flow decomposition design. Its object is the world economy as a regional flow network. It constructs a weighted graph, defines directed macro-flow pressure and decomposes that pressure into gradient, curl and harmonic components. Its contribution is not to prove a Hodge conjecture but to show how macroeconomic hierarchy, local imbalance and systemic circulation can be separated inside one reproducible regional benchmark.

The Navier-Stokes design is a nondimensional macro-financial stress-testing design. Its object is global liquidity-flow and systemic stress measured through velocity weakness, pressure gradients, friction/diffusion, shocks, cycle forcing and restricted closure. Its core strength is the large country-year panel architecture, rolling validation and policy-counterfactual logic. Its boundary is equally clear: liquidity is not treated as a literal physical fluid, and diagnostic association is not upgraded into universal crisis prediction.

The Yang-Mills design is a finite-network gauge-econometric design. Its completed benchmark layer uses global and corridor-sensitive nodes, weighted edges, systemic stress, gauge potential, triangular curvature, economic action, stress Laplacian and a finite weighted-graph spectral separation. Its country-panel layer is specified as a validation extension. The admissible claim is finite-network measurement of shock threshold and corridor exposure, not mathematical solution of Yang-Mills existence or physical mass gap.

The BSD design is a local-to-global structural-rank design. Its object is a regional system in which public macro-regional anchors are transformed into systemic stress, economic curve coefficients, finite-state traces, Euler-factor analogues, an economic L-function and structural-rank diagnostics. Its central research design contribution is the disciplined comparison between local regional information and global structural rank formation, while explicitly preventing classical BSD proof claims.

The Riemann-zeta design is a layered forecasting and spectral-diagnostic design. Its object is global aggregate inflation forecast through a structural FPAS baseline augmented by a normalized zeta-cycle correction. Its empirical architecture is deliberately layered across annual, quarterly and monthly samples. Its claim is forecast-diagnostic improvement under defined validation windows, not proof, test or verification of the Riemann Hypothesis.

The P-vs-NP design is an empirical-computational finance design. Its object is cardinality-constrained portfolio optimization under a fixed industry universe. It documents combinatorial support-space growth, compares heuristic and exact reduced search layers, and adds robustness, transaction-cost, covariance and derivative-overlay realism. Its claim is bounded computational-finance evidence, not a theorem-level result about complexity classes or certified global optimality for the full universe.

Table 4.1.2. Seven-source research-design integration matrix

Problem grammar	Economic research object	Empirical design base	Methodological core	Permitted claim
Perelman-Ricci-Poincare	Global inequality as a pressure-smoothing diagnostic manifold	Ten macro-regional blocks over 2010-2024 with sixteen stress-coordinate variables; N = 150 region-year panel	Curvature, entropy, graph connectedness, econometric and forecast-validation diagnostics	Measurement and diagnostic interpretation of inequality deformation; no proof of Poincare/Ricci/Perelman results
Hodge	World economy as a	Regional benchmark with	Directed edge pressure, discrete Hodge	Macro-flow decomposition into

	decomposable regional macro-flow network	World normalization anchor, ten regional nodes and corridor-sensitive Caucasus visibility	decomposition, spectral graph diagnostics, econometric/ML/topological validation	hierarchy, local imbalance and systemic circulation; no Hodge conjecture claim
Navier-Stokes	Global liquidity-flow and systemic-stress balance	100-country annual panel, 2010-2024, N = 1,500, with World and macro-regional layers	Nondimensional stress balance, rolling forecasts, benchmark comparison, robust inference, Monte Carlo and policy counterfactuals	Stress-testing and diagnostic architecture; no physical fluid law or universal crisis-prediction law
Yang-Mills	Global-corridor shock-threshold network	Layer A: ten nodes and twenty-seven weighted edges; Layer B: 100-country x 15-year validation architecture	Gauge potential, triangular curvature, action, stress Laplacian, spectral separation, scenario and robustness tests	Finite weighted-graph mass-gap analogue; no Yang-Mills theorem solution
Birch-Swinnerton-Dyer	Regional local-to-global structural-rank formation	World normalization anchor plus ten macro-regional/corridor nodes; N = 150 closure layer	Finite-state local reductions, trace analogues, Euler factors, economic L-function, structural rank, placebo and anti-circularity tests	Local-to-global measurement consistency; no proof or empirical test of the classical BSD conjecture
Riemann-Zeta	Global inflation forecasting with structural-spectral correction	Annual N = 55, annual robustness N = 45, crisis-era N = 20, quarterly N = 100, monthly N = 240 layers	FPAS baseline, zeta-cycle correction, rolling validation, Mincer-Zarnowitz, encompassing, DM/CW, spectral diagnostics	Bounded forecast-diagnostic contribution; no proof/test/verification of the Riemann Hypothesis
P-vs-NP	Sparse portfolio optimization under combinatorial support selection	Fixed Damodaran January 2026 U.S. industry universe, n = 94, K = 10; reduced exact benchmark n = 20, K = 6	CAPM priors, covariance geometry, combinatorial search, greedy/Monte Carlo/GA, exact reduced enumeration, robustness and derivative overlay	Computational-finance evidence and best-found incumbents; no P-vs-NP proof and no certified full-universe global optimum

Source: Author synthesis from the seven uploaded methodology chapters; numerical universe descriptions are design-level descriptors, not result claims.

4.1.4. Non-Experimental Status and Causal Discipline

The monograph is explicitly non-experimental. It does not randomly assign policy regimes, liquidity shocks, regional corridor exposure, technological capacity, portfolio constraints or inflation conditions. It does not claim that the researcher controls the treatment environment. Instead, it uses observational macroeconomic anchors, fixed benchmark datasets, author-calculated transformations, diagnostic panels, graph structures, forecast layers and computational experiments. This has direct implications for interpretation.

First, the book treats causality conservatively. Fixed-effects coefficients, dynamic screens, ARDL terms, SVAR orderings, local projections, threshold regressions, factor models and external-proxy screens are not automatically causal. They are validation devices used to test whether constructed variables behave coherently when exposed to alternative statistical

structures. When causal language is unavailable, the book uses terms such as association, diagnostic consistency, structural correspondence, robustness, screening, calibration or forecast improvement.

Second, the book separates causal identification from measurement validity. A constructed index can be useful as a measurement object even if it is not a fully identified causal mechanism. For example, a pressure-curvature index can summarize inequality deformation without proving a welfare-causal law. A finite stress Laplacian can identify spectral separation without proving physical dynamics. A zeta-cycle correction can improve a forecast within a validation layer without proving a universal inflation law. This distinction is essential because the monograph is about measurement architecture, not causal universalism.

Third, the non-experimental status strengthens rather than weakens the need for robustness. Because there is no randomized control, every constructed object must survive checks that look for mechanical fit, circularity, sample-size fragility, overfitting, parameter sensitivity, covariance dependence, placebo correlations, randomized-network artefacts and external-target instability. The design therefore uses robustness not as a decorative appendix but as part of the admissibility rule for claims.

Fourth, the design is careful about directionality. Public data anchors often enter constructed indicators through declared transformations. If the same source information is later used as a validation target without exclusion, circularity risk appears. The unified design therefore distinguishes internal calibration from external validation, and it requires leave-one-block, leave-one-variable, external-proxy or placebo logic where stronger validation language is desired.

Fifth, forecast validation is treated as evidence within sample and horizon boundaries. The Riemann-zeta and Navier-Stokes designs use rolling or expanding-window logic, forecast metrics and benchmark comparison, but those tests do not justify claims of permanent model superiority across all economies and horizons. The result is a bounded predictive design: strong when the validation protocol is transparent, weak when generalized beyond the documented window.

The non-experimental principle therefore operates as a claim-control mechanism. It prevents the monograph from converting elegant mathematical structure into unsupported empirical authority. The proper evidentiary language is: the model constructs, measures, audits, compares, validates, screens, stress-tests and bounds. It does not experimentally prove.

4.1.5. Computational Research Design and Algorithmic Auditability

The monograph is computational in a strong sense. The seven studies cannot be reproduced by reading data tables alone because the central objects are generated through algorithms. The computational workflow begins with public or fixed inputs, passes through normalization and transformation, constructs matrices or graphs, applies problem-specific mathematical operators, and then generates validation outputs. This gives the monograph a data-to-result pipeline that must be auditable from source file to final claim.

In the Perelman-Ricci-Poincare design, computation is required to convert heterogeneous macro-social indicators into a common stress scale, construct a metric/correlation structure, compute curvature-like component contributions, derive graph connectedness and evaluate dynamic and forecast diagnostics. In the Hodge design, computation is required to construct the regional graph, orient edge pressure, build incidence operators, project the edge field into gradient, curl and harmonic components and audit the numerical decomposition. In the Navier-Stokes design, computation is required to produce nondimensional stress components, rolling forecasts, restricted closure terms, residual diagnostics, Monte Carlo bands and policy counterfactuals.

In the Yang-Mills design, computation is required to convert systemic stress into weighted edges, orient gauge potentials, compute triangular curvature, aggregate action, construct the stress Laplacian and test spectral separation under scenario shocks and randomized-network alternatives. In the BSD design, computation produces finite-state local reductions, trace analogues, Euler-factor analogues, an economic L-function and rank correspondence diagnostics. In the Riemann-zeta design, computation generates the nonlinear tau argument, zeta-cycle path, spectral correction, forecast errors, loss differentials and multi-frequency diagnostics. In the P-vs-NP design, computation is the research object itself: support selection, search-space explosion, heuristic comparison, exact reduced enumeration and continuous reoptimization.

Because computation is central, the research design requires algorithmic auditability. A table, graph or coefficient is not sufficient unless the reader can identify how it was produced. The minimum audit trail is: source anchor, extracted raw value, transformation rule, normalization scale, model equation or algorithm, software or computational environment, random seed where relevant, search or simulation budget where relevant, output file and claim boundary. This is the logic that later becomes the replication-package discipline of Chapter 4.

The computational design also protects against a common weakness of analogue modelling: the risk that the analogy becomes visually persuasive but technically under-specified. The monograph avoids this by translating each analogy into reproducible operations. A gauge analogy becomes a matrix and triangle calculation. A Hodge analogy becomes an incidence-matrix projection. A zeta analogy becomes a declared real-valued cyclical signal and forecast correction. A P-vs-NP analogy becomes a finite support-selection experiment with explicit combinatorial cardinality. This is the difference between metaphor and computational methodology.

The computational layer must also be robust to perturbation. A result that exists only under one arbitrary parameterization is not design-stable. The seven source methodologies therefore include perturbation, sensitivity, alternative covariance structures, alternative edge filters, weight robustness, rolling windows, placebo networks, randomization, Monte Carlo uncertainty or exact reduced benchmarking. In the unified research design, these are not separate optional procedures. They are the computational robustness gates through which constructed evidence must pass.

Algorithm 4.1. Unified data-to-claim research-design workflow

1. Define the Clay-inspired mathematical grammar and translate it into a bounded economic measurement function.
2. Identify the empirical universe: country-year panel, region-year panel, benchmark network, forecast layer or asset universe.
3. Separate public or fixed source anchors from author-calculated variables.
4. Apply declared normalization, nondimensionalization, direction harmonization or scale transformation.
5. Construct the problem-specific mathematical object: curvature, flow decomposition, stress balance, gauge curvature, local-to-global rank, zeta forecast signal or combinatorial support space.
6. Generate internal diagnostics and result objects through reproducible formulas, matrices, algorithms or optimization routines.
7. Run validation, robustness, sensitivity, benchmark, placebo, falsification and replication checks according to the evidence level of the chapter.
8. Classify each output into the admissible claim hierarchy: construction, calibration, diagnostic association, bounded validation, scenario result or external confirmation.
9. Archive the relevant data, formulas, scripts, output files, seeds, hashes or source ledger in a replication package.
10. Restate the claim boundary so that no economic analogue is presented as a solution, proof or test of the original Millennium Problem.

4.1.6. Econometric Orientation: Validation, Screening and Evidence Closure

The econometric orientation of the monograph is validation-oriented rather than causality-maximalist. This distinction matters. The seven chapters use econometric tools, but they do not all use them in the same way. In some chapters, econometrics is central to the empirical architecture, as in the Navier-Stokes global panel and the Riemann-zeta forecast-validation design. In other chapters, econometrics operates as a diagnostic screen around constructed topological or computational objects, as in the Hodge, Yang-Mills, BSD and Perelman-Ricci-Poincare designs. In the P-vs-NP chapter, econometric logic enters mainly through CAPM calibration, covariance geometry, statistical comparison, sensitivity and robustness rather than through a standard panel causal model.

The common econometric rule is that validation must match the empirical object. A region-year panel can support within-region or robust panel diagnostics, but small cluster counts require caution. A 100-country panel can support richer fixed-effects and robust-inference structures, but coefficients remain diagnostic unless identification conditions are satisfied. A global annual forecasting sample requires rolling validation and small-sample caution. A monthly spectral layer can support frequency diagnostics, but those diagnostics should not be confused with annual regression evidence. A fixed asset universe can support exact reduced benchmarking and computational comparison, but not realized performance dominance unless historical out-of-sample returns are actually tested.

The unified research design therefore introduces evidence closure. Evidence closure means that each claim must be supported by a chain that includes construction validity, internal consistency, robustness, diagnostic validation and boundary compliance. A high R-squared or low forecast error is not sufficient by itself. A graph metric is not sufficient by itself. A visually compelling scenario is not sufficient by itself. The result becomes admissible when it remains coherent across the declared evidence chain.

This design gives specific roles to econometric tools. Fixed effects test whether constructed variables retain within-unit structure after controlling for unit heterogeneity. Driscoll-Kraay or clustered inference protects against cross-sectional and

temporal dependence where appropriate. HAC inference provides time-series robustness under serial correlation and heteroskedasticity. ARDL, ECM, VAR/SVAR and local projections serve as dynamic and shock-transmission screens. PCA and factor models test whether constructed dimensions are reducible to common latent structure. Ridge, LASSO and Elastic Net test coefficient stability under multicollinearity and penalty discipline. Quantile and threshold methods test distributional and regime sensitivity. Rolling validation tests out-of-sample prediction under no-look-ahead rules.

The book also uses benchmark comparison as a design principle. Forecast models are compared with ARIMA, structural baselines or composite-index alternatives. Portfolio algorithms are compared with greedy, Monte Carlo, genetic and exact reduced methods. Network results are compared under edge filters, randomized networks or leave-one-node/corridor exclusions. This comparative logic prevents a single model from being declared successful without a relevant alternative.

The econometric orientation also requires transparent negative evidence. If a p-value is weak, the result remains diagnostic. If a validation target is not independent, the language must remain internal. If sample size is small, confidence language must be reduced. If a placebo result is strong, the claim must be downgraded or re-specified. This is why the monograph repeatedly uses terms such as screening, bounded validation, robustness layer and claim discipline.

In this sense, econometrics is not a decorative addition to mathematical analogy. It is the mechanism that distinguishes measurement architecture from arbitrary construction. A constructed object earns credibility only when it can be audited by appropriate empirical tests and when those tests are interpreted within their design limits.

4.1.7. Data Architecture as a Research-Design Principle

Although the detailed empirical universes are presented in Section 4.2, the research-design principle must be established here: the monograph separates public-data anchors from author-calculated analytical objects. This separation is one of the most important methodological safeguards in the book. Public anchors are the externally observable inputs: GDP, GDP per capita, inflation, unemployment, investment, productivity, financial stress proxies, volatility, beta, regional growth projections, world aggregates, policy-event classifications or other source-family variables. Author-calculated objects are the outputs of the modelling architecture: stress scores, curvature proxies, Hodge components, systemic-stress balances, gauge potentials, economic actions, mass-gap indices, trace analogues, L-order measures, zeta corrections, portfolio search outputs and integrated evidence scores.

The distinction matters because constructed variables inherit information from their source anchors. If a constructed index is later validated against a variable that directly helped build it, the validation may be circular. The unified design therefore requires variable-lineage discipline. Each chapter must identify whether a validation target is independent, partially derived, internally constructed, external-proxy based or purely placebo. Strong claims require a stronger lineage status. Internal calibration may support coherence, but external validation requires separation between construction and target.

The data architecture also defines the unit of analysis. The monograph does not impose one universal unit on all chapters because each mathematical grammar requires a different empirical object. The Navier-Stokes chapter uses a country-year panel because liquidity stress is meaningfully observed across countries and years. The Perelman-Ricci-Poincare and BSD chapters use macro-regional closure structures because their questions concern regional inequality deformation and structural rank formation. The Hodge and Yang-Mills chapters use network benchmarks because topology and spectral separation require graph objects. The Riemann-zeta chapter uses layered time-series samples because the object is forecast validation across annual, quarterly and monthly frequencies. The P-vs-NP chapter uses a fixed industry universe because the object is sparse support selection under combinatorial complexity.

This plural data architecture is not a weakness. It is necessary because the seven problem grammars are not identical. A single data form would distort several of them. The unified methodology therefore standardizes the research protocol rather than forcing identical samples. What is common is not the empirical universe; what is common is the rule of transparent anchoring, transformation, validation and claim boundary.

The public-data-anchor principle also prevents hidden proprietary dependence. The monograph is designed to be inspectable and reproducible. When an input comes from a public source family or a fixed public dataset, the model can be audited. When a variable is author-calculated, its formula, direction, scale and role must be disclosed. This design makes the book more defensible because a reviewer can separate disagreement about modelling choices from uncertainty about data provenance.

Table 4.1.3. Common methodology components carried from the seven Chapter 3 methodologies into unified Chapter 4

Common component	Cross-document methodological	Role in the monograph

	content	
Research design	All seven methodologies classify the work as quantitative, analogue-based, computational and validation-oriented.	Section 4.1 establishes the unified design doctrine.
Data architecture	Each chapter separates empirical universe, public/fixed anchors and model-derived analytical objects.	Section 4.2 specifies the empirical universes; Section 4.3 separates anchors and constructed variables.
Public-data anchors	World Bank/IMF-style macro anchors, fixed industry datasets, public forecast/financial proxies or declared global aggregates provide source inputs.	Used as the external starting layer, not as the final constructed result.
Author-calculated variables	Stress scores, curvature, Hodge components, gauge potentials, L-order, zeta corrections and portfolio incumbents are generated by formulas and algorithms.	Must be interpreted as constructed measurement objects, not raw observations.
Normalization	Stress-oriented 0-100 scales, nondimensional variables, standardized coordinates, CAPM calibration and layered frequency alignment appear across chapters.	Ensures heterogeneous inputs are not added in raw units.
Panel structure	Country-year panels, region-year panels, layered time-series samples and fixed asset universes are used according to problem grammar.	Prevents inappropriate one-size-fits-all data design.
Network construction	Hodge, Yang-Mills, BSD and Perelman/Poincare chapters depend on graph, edge, Laplacian, connectedness or corridor-network logic.	Creates the topological layer of the monograph.
Validation	Rolling validation, fixed effects, robust inference, external-proxy tests, exact reduced enumeration and forecast comparison audit the constructed objects.	Turns mathematical analogy into empirical methodology.
Robustness	Weight sensitivity, parameter perturbation, covariance alternatives, edge filters, Monte Carlo and leave-one-block tests protect against fragile specifications.	Identifies whether results are design-stable.
Placebo and falsification	Negative controls, randomized networks, placebo outcomes, anti-circularity checks and covariance placebo tests prevent mechanical overclaiming.	Provides the main protection against spurious analogue evidence.
Claim boundary	Each chapter states what it does not claim: no theorem proof, no physical identity, no unrestricted causality and	Defines the admissible contribution of the monograph.

	no universal prediction.	
Replication packages	Data files, source ledgers, formulas, scripts, seeds, outputs, hashes and Zenodo records are treated as part of the research design.	Makes the monograph externally auditable.

Source: Author synthesis of the user-defined Chapter 4 transfer plan and the seven source methodology chapters.

4.1.8. Network, Graph and Topological Design Logic

A major unifying feature of the monograph is the use of graph, network and topological reasoning. This feature appears most directly in the Hodge, Yang-Mills, BSD and Perelman-Ricci-Poincare chapters, but it also shapes the broader research design. The book treats the world economy not only as a set of scalar aggregates but as a structured system of nodes, edges, cycles, corridors, bottlenecks, flows, rank positions and shock-transmission channels.

The network design begins from a simple methodological premise: economic relevance is not identical to output size. A region can be systemically important because it lies on a corridor, participates in a cycle, absorbs shocks, transmits pressure or connects otherwise separated spaces. This is why the Hodge and Yang-Mills designs retain corridor-sensitive nodes; why BSD emphasizes local-to-global rank formation; and why Perelman-Ricci-Poincare includes graph connectedness and Betti-style cycle logic in inequality diagnostics. The network layer allows the monograph to study structure rather than merely scale.

Graph construction is not treated as arbitrary drawing. It requires node definition, edge logic, weight calibration, direction or orientation discipline, matrix construction and adequacy checks. A graph must be connected where the model requires connectedness; weights must be interpretable; edges must be justified by declared corridor, similarity, correlation, stress or flow logic; and robustness must test whether results survive alternative filters or perturbations. This is especially important because graph choices can strongly influence spectral and topological outputs.

The topological design also supports a comparative interpretation of the seven analogues. Curvature-like inequality deformation, Hodge flow decomposition, Yang-Mills action concentration, BSD local reductions and Poincare connectedness all ask whether economic structure is hidden behind aggregate indicators. The book therefore uses topology as a measurement grammar: it identifies hierarchy, cycles, bottlenecks, persistent circulation, connectedness and threshold transmission.

In the unified design, topological and graph objects remain constructed diagnostic systems. They are not literal mathematical invariants of the world economy. The book therefore uses terms such as proxy, analogue, diagnostic, finite-network, stress-weighted and constructed. This language is not defensive rhetoric; it is the correct interpretation of graph-based economic modelling.

4.1.9. Forecasting, Optimization and Simulation as Complementary Design Modes

The monograph contains three computational design modes that extend beyond static measurement: forecasting, optimization and simulation. Forecasting appears most strongly in the Riemann-zeta and Navier-Stokes chapters, where model outputs are compared with benchmark forecasts under rolling or expanding-window protocols. Optimization appears most strongly in the P-vs-NP chapter, where the empirical object is sparse portfolio support selection under cardinality constraints. Simulation appears across Navier-Stokes, Yang-Mills, Perelman-Ricci-Poincare and BSD designs through Monte Carlo uncertainty, policy counterfactuals, shock injection, perturbation and scenario recalculation.

Forecasting is used as a validation layer, not as a universal prediction claim. The Riemann-zeta design is especially important because it separates annual, quarterly and monthly evidence layers and assigns different diagnostic tools to each frequency. This prevents a common methodological error: treating all tests as if they were estimated on one homogeneous sample. The unified design therefore requires sample-layer discipline. A result from the monthly spectral layer cannot automatically validate an annual forecast coefficient; a crisis-era display cannot replace the principal annual validation layer; and a rolling forecast must obey no-look-ahead construction rules.

Optimization is used as a controlled computational experiment. The P-vs-NP chapter fixes the asset universe before optimization, constructs CAPM-implied returns, defines covariance geometry, imposes cardinality and compares search methods under documented budgets. This makes the chapter methodologically different from the macroeconomic chapters, but design-compatible with the book because it follows the same evidence rules: fixed input layer, constructed object, algorithmic process, robustness, exact reduced benchmark, friction realism and claim boundary.

Simulation is used to assess structural sensitivity. Monte Carlo perturbations, shock scenarios, policy counterfactuals and network recalculations do not predict the future unconditionally. They ask whether the constructed system behaves plausibly when inputs or parameters are perturbed. Simulation evidence is therefore model-implied scenario evidence. Its scientific value depends on transparent assumptions, bounded interpretation and replication.

These three modes reinforce one another. Forecasting tests predictive discipline; optimization tests computational difficulty and solution realism; simulation tests structural sensitivity. Together, they make the monograph more than a set of static indices. They give the book a dynamic research design in which constructed economic analogues are tested against time, alternatives, perturbations and implementation constraints.

4.1.10. Validation, Robustness, Placebo and Falsification Discipline

Validation is the central methodological gate of the monograph. Because the seven chapters construct new economic analogues, the main danger is not lack of originality; it is overclaiming. A new constructed variable can always be made to look meaningful if validation is weak. The unified design therefore requires multiple evidence gates: internal consistency, benchmark comparison, sensitivity analysis, robustness, placebo, falsification, replication and claim-boundary review.

Internal consistency asks whether the constructed object behaves according to its own logic. For example, pressure-oriented variables should move in the expected direction under stress; Hodge components should numerically reconstruct the directed edge field within tolerances; stress-Laplacian diagnostics should respond coherently to shock scenarios; the zeta correction should have a declared sign and magnitude logic; and portfolio search outputs should satisfy cardinality, weight and risk constraints.

Benchmark comparison asks whether the model improves or clarifies something relative to a relevant alternative. Forecast models must be compared with statistical or structural baselines. Portfolio algorithms must be compared with alternative search procedures and exact reduced benchmarks. Network results should be tested under alternative edge or weight assumptions. Composite indices should be compared with leave-one-block, external-proxy or placebo alternatives.

Sensitivity analysis tests whether the conclusion depends on arbitrary parameters. This includes weight perturbation, alternative normalization, covariance specification, risk-free rate and equity-risk-premium shifts, edge filtering, graph sparsification, q-base or finite-state adjustments, alpha calibration, rolling-window changes and Monte Carlo draws. A robust result is not necessarily true in a causal sense, but it is less likely to be an artefact of one parameter choice.

Placebo and falsification discipline is especially important for analogue research. A placebo test asks whether the same method produces apparently strong evidence when applied to a target where it should not. A falsification gate asks what result would weaken or reject the intended interpretation. Randomized networks, negative controls, covariance placebo tests, random subset audits, anti-circularity checks and external-target exclusions are therefore not optional additions. They define the boundary between disciplined measurement and confirmatory storytelling.

The unified design also requires that weak evidence remain weak. A diagnostic association cannot be re-labelled as causal confirmation. A small-N regression cannot be presented as definitive structural law. A model-implied counterfactual cannot be presented as real policy effect. A best-found portfolio cannot be presented as certified global optimum unless the full optimization certificate exists. A finite weighted-graph spectral gap cannot be presented as a mathematical mass-gap proof. These restrictions are part of the methodology, not merely editorial caution.

Table 4.1.4. Evidence hierarchy and permitted interpretation in the unified research design

Evidence level	Definition	Permitted interpretation	Typical checks
Level 1 - Construction validity	Correct transformation from public/fixed anchors into normalized or constructed variables.	Permits discussion of the constructed object itself.	Formula audit, source ledger, scale/direction checks, unit consistency.
Level 2 - Internal coherence	The constructed object behaves according to the declared mathematical-economic logic.	Permits internal diagnostic interpretation.	Matrix reconstruction, sign consistency, graph adequacy, constraint satisfaction.
Level 3 - Robustness	The result survives alternative weights, parameters, samples, covariance assumptions,	Permits stability language.	Sensitivity tables, Monte Carlo, leave-one-block, parameter grids, edge-filter tests.

	graph filters or perturbations.		
Level 4 - Benchmark validation	The model is compared with a relevant baseline, comparator or exact reduced benchmark.	Permits bounded superiority or improvement claims inside the specified design.	ARIMA/FPAS comparison, exact enumeration, baseline indices, randomized networks.
Level 5 - External screening	The constructed object aligns with observable proxies not mechanically included in construction.	Permits directional external-validation language when lineage is clean.	External targets, proxy screens, validation exclusion rules.
Level 6 - Claim closure	Evidence is classified and bounded so that mathematical, causal or predictive overclaiming is blocked.	Permits final monograph-level contribution statement.	Claim matrix, falsification gates, replication package, boundary statement.

Source: Author synthesis based on the validation, robustness, placebo and claim-boundary logic shared across the seven studies.

4.1.11. Claim-Boundary Doctrine of the Research Design

The monograph uses a strict claim-boundary doctrine. This doctrine is necessary because the source of inspiration is a set of famous unsolved or historically solved mathematical problems. Without a strong boundary, readers could misinterpret an economic analogue as a claim to solve or empirically test the original mathematical problem. The unified research design prevents that misinterpretation at the chapter level and at the monograph level.

The general boundary is as follows: the monograph does not claim to solve, prove, test or replicate the Clay Millennium Problems in their original mathematical form. It develops seven bounded economic-econometric analogues inspired by their formal architectures. This statement should appear in the front matter and should also govern Chapter 4, because Chapter 4 is where the technical legitimacy of the book is established.

The boundary doctrine has five components. First, mathematical non-equivalence: an economic curvature, mass gap, zeta cycle, L-order or Hodge component is not the same object as the classical mathematical object. Second, causal restraint: econometric diagnostics do not become causal laws unless identification is established. Third, prediction restraint: forecast performance is confined to reported samples, horizons and comparators. Fourth, computational restraint: best-found optimization results are not certified global optima unless exact proof exists for the relevant universe. Fifth, replication restraint: a claim cannot exceed the reproducible materials that support it.

The doctrine also defines positive contribution. A bounded claim is not a weak claim. It is a precise claim. The book can legitimately claim that it constructs a reproducible macro-regional pressure-curvature diagnostic, a Hodge-econometric flow decomposition, a nondimensional liquidity stress-testing system, a finite corridor gauge-econometric threshold framework, a BSD-inspired local-to-global rank measurement architecture, a layered FPAS+zeta forecast-diagnostic model and a P-vs-NP-inspired sparse portfolio optimization protocol. These are strong methodological and empirical contributions when stated correctly.

The claim-boundary doctrine should be enforced in wording throughout the monograph. Preferred terms are "inspired by," "analogue," "finite-network," "constructed," "diagnostic," "bounded," "calibrated," "validation-oriented," "screening," "measurement architecture," "stress-testing," "forecast-diagnostic" and "replication-ready." Terms that should be avoided unless strictly justified include "proof," "solution," "verification," "law," "causal effect," "universal," "guaranteed," "complete validation" and "certified global optimum" for the full P-vs-NP universe.

4.1.12. Replication-Ready Design and Source-Ledger Discipline

A final feature of the research design is replication readiness. The monograph is not built only for narrative interpretation; it is built for audit. This means that each chapter should be capable of being traced from source anchors to final tables, figures and claims. Replication readiness is especially important because many variables in the book are author-calculated. The reader must be able to distinguish the public anchor from the transformation and the transformation from the final diagnostic claim.

Replication readiness requires a source ledger. A source ledger records the input source family, variable name, vintage or download date where applicable, transformation rule, normalization direction, missing-data rule, aggregation rule, formula, output table and file location. For computational chapters, the ledger should also record software environment, scripts, random seeds, simulation counts, search budgets, optimization constraints, graph filters and output hashes where possible. This design is aligned with the Zenodo/data-package discipline of the seven manuscripts.

The replication package is not merely a supplement. In this monograph, it is part of the evidence architecture. A claim that cannot be reconstructed from the package should be downgraded. A result that depends on an undisclosed transformation should not be presented as reviewer-safe. A table whose source lineage is unclear should not be used as a major claim. This discipline is the technical basis for making a large analogue-based monograph credible.

The unified design also anticipates heterogeneous replication packages. Some chapters have complete numerical data packages; some include benchmark replication records; some specify panel extensions; and some rely on a fixed external dataset with author-calculated outputs. The monograph can accommodate this heterogeneity if it classifies replication status accurately. What matters is not that every chapter has the same replication file type, but that every chapter discloses exactly what can be replicated, what is constructed, what is planned or extended, and what claim level is therefore permitted.

For this reason, Section 4.1 defines replication as a methodological rule, while Section 4.8 should later consolidate the actual Zenodo records and dataset statements. The design-level rule is simple: no claim should travel farther than its data lineage, formula disclosure, validation evidence and replication package allow.

Table 4.1.5. Replication-ready design controls for the unified methodology chapter

Replication control	Minimum content	Primary use
Source anchor register	List public/fixed inputs, source families, vintages and raw variables.	All chapters; especially macro panels and fixed industry universe.
Transformation register	Record normalization, direction harmonization, nondimensionalization, stress scaling, CAPM calibration or zeta transformation.	All constructed-variable chapters.
Model register	Document formulas, matrices, graph operators, forecast equations, optimization constraints and algorithmic steps.	All seven chapters.
Validation register	Record robustness tests, rolling windows, comparator models, placebo outcomes, external-proxy screens and exact reduced benchmarks.	Forecasting, panel, network and optimization chapters.
Computation register	Record code version, random seeds, Monte Carlo budget, search budget, graph filters, optimization settings and output files.	Yang-Mills, Hodge, Riemann-zeta, P-vs-NP, Navier-Stokes.
Claim register	Match each reported claim to evidence level and boundary language.	Entire monograph.
Archival register	Consolidate Zenodo records, data packages, checksums, formulas and replication workbooks.	Chapter 4.8 and source statements.

Source: Author synthesis based on the replication and claim-discipline requirements of the seven manuscript methodologies.

4.1.13. Formal Design Rule for Admissible Claims

The unified research design can be summarized through a simple admissibility rule. A claim is admissible only if the evidence supporting it is sufficient for the claim level and the claim does not violate the boundary attached to the relevant analogue. The rule applies to all seven chapters, regardless of empirical universe.

Equation (4.1.2). Claim_k is admissible iff Evidence_k >= RequiredEvidence_k and BoundaryViolation_k = 0.

Equation (4.1.2) is a methodological governance rule. It does not assign numerical weights in this section, but it establishes the principle that evidence and boundary must be evaluated together. A mathematically elegant construction with weak validation may still be admissible as a constructed diagnostic object, but not as external confirmation. A strong forecast comparison may support bounded predictive improvement, but not universal forecast dominance. A positive finite-network spectral gap may support finite-network threshold interpretation, but not a mathematical mass-gap solution. A best-found portfolio may support computational search evidence, but not certified global optimality.

The rule also prevents a common problem in interdisciplinary research: claim inflation. Claim inflation occurs when a result produced at one evidence level is described at a higher level. For example, internal fit is described as external validation; diagnostic association is described as causality; scenario output is described as prediction; benchmark optimization is described as theorem proof. The monograph explicitly rejects this pattern. Its credibility depends on disciplined matching between evidence type and claim language.

The admissibility rule should be used by the author as a final pre-publication checklist for every major table, figure and conclusion. For each reported result, the author should ask: What is the source anchor? What is the constructed object? What validation was performed? What robustness or placebo test could weaken it? What exact claim is allowed? What claim is not allowed? Can the result be replicated from the available package? If any answer is missing, the claim should be rewritten, moved to a lower evidence level or supported by additional material.

4.1.14. Section Synthesis

Section 4.1 defines the monograph as a unified quantitative, non-experimental, computational, econometric and validation-oriented research design. The seven problem chapters differ in empirical object and mathematical grammar, but they share one methodological architecture: public or fixed anchors are transformed into constructed economic objects; those objects are processed through explicit mathematical-computational models; the outputs are audited through validation, robustness, placebo and falsification; and final claims are restricted by replication and claim-boundary discipline.

This design is the reason the monograph can be read as a coherent book rather than as seven assembled articles. The common object is economic complexity. The common method is analogue-based measurement. The common safeguard is claim discipline. The common technical requirement is replication. Subsequent subsections of Chapter 4 should therefore expand this design into the empirical-universe table, data-anchor register, normalization protocol, network-construction protocol, econometric and forecast-validation protocol, computational protocol, replication-package consolidation and general claim-boundary matrix.

The operational conclusion is clear: the monograph does not seek to solve the Millennium Problems in mathematics. It uses their structural architectures to build seven reproducible economic-econometric measurement systems. Section 4.1 establishes the research-design doctrine under which that contribution can be presented at a high scientific standard.

4.2. Empirical Universes across the Seven Studies

Section 4.2 defines the empirical universe of the monograph. Its function is more than descriptive. The seven studies do not use one homogeneous dataset, one common panel dimension or one shared unit of observation. They use different empirical universes because each Millennium-inspired economic analogue measures a different structural property of the world economy: inequality deformation, topological macro-flow, liquidity-flow stress, corridor shock thresholds, local-to-global rank formation, spectral inflation forecasting and combinatorial portfolio optimization. The methodological task of this section is therefore to make those empirical universes comparable without falsely merging them into one artificial sample.

The section establishes a central principle for the book: each chapter must be read through the empirical universe that can support its claim. A ten-node network benchmark can strongly support a graph-topological decomposition, but it cannot be read as a country-level causal panel. A 100-country annual panel can support broader diagnostic econometrics, but it still remains observational and non-experimental. A layered annual-quarterly-monthly forecasting architecture can support sample-discipline and frequency-specific validation, but it should not be interpreted as a universal theorem about inflation.

A combinatorial portfolio universe can support computational-finance evidence, but it does not certify theorem-level P-vs-NP conclusions. This section converts these distinctions into a transparent empirical-universe architecture.

The empirical discipline of the monograph rests on four connected decisions. First, the unit of observation is made explicit for every study. Second, the main N or sample layer is identified separately from supplementary validation layers. Third, the evidence type is classified so that benchmark, panel, forecast, network, computational and closure evidence are not confused. Fourth, the claim boundary is aligned with the empirical universe. This alignment is essential because the scientific strength of the book depends not only on large numerical results, but also on the correct interpretation of what each sample can and cannot prove.

4.2.1. Purpose of the Empirical-Universe Architecture

The empirical-universe architecture is the part of the methodology that answers a foundational question: what exactly is observed, constructed, compared, validated and bounded in each of the seven economic analogues? This question must be answered before formulas, regressions, graphs, forecasts or optimization routines are interpreted. Without an explicit empirical universe, a reader cannot know whether a result is a country-year panel estimate, a regional benchmark diagnostic, a finite-network spectral result, a forecast-validation result, a computational search result or a constructed-index closure result.

The monograph therefore treats the empirical universe as an evidence gate. A result can be strong only relative to the sample and object that produced it. The Perelman/Ricci/Poincare chapter is strongest as a macro-regional inequality-pressure and curvature-diagnostic panel. The Hodge chapter is strongest as a ten-node topological macro-flow benchmark. The Navier-Stokes chapter is strongest as a 100-country annual panel stress-testing design. The Yang-Mills chapter is strongest as a finite-network gauge benchmark with a specified country-panel validation pathway. The BSD chapter is strongest as a local-to-global regional rank and closure architecture. The Riemann/Zeta chapter is strongest as a layered sample-discipline and forecast-validation design. The P-vs-NP chapter is strongest as a fixed industry-universe computational-finance experiment with exact reduced benchmarking.

This structure prevents a common error in interdisciplinary modelling: treating all numerical outputs as equivalent evidence. The monograph does not do this. A graph eigenvalue, a fixed-effects coefficient, an RMSE comparison, a Monte Carlo interval, a support-space count and a structural-rank agreement measure are not the same kind of evidence. They become comparable only after they are placed inside an evidence taxonomy. Section 4.2 supplies that taxonomy.

Equation (4.2.1). $E_p = \{U_p, N_p, L_p, T_p, D_p, C_p\}$, where U_p is the empirical universe, N_p is the main sample size or benchmark dimension, L_p is the layer structure, T_p is the evidence type, D_p is the data-status boundary and C_p is the admissible claim class for study p.

Equation (4.2.1) defines the empirical-universe object used throughout this section. It is not an econometric model; it is a methodological classification rule. Each study is described by its unit, sample dimension, layers, evidence type, data-status boundary and permissible claim. This is the rule that allows the seven chapters to be integrated into one monograph without flattening their empirical differences.

4.2.2. Master Empirical-Universe Matrix

Table 4.2.1 is the controlling comparative table for Section 4.2. It should appear early in Chapter 4 because it allows the reader to see, before the technical details begin, that the book is not based on one hidden or ambiguous dataset. It is a seven-study empirical architecture with clearly separated universes, sample sizes and evidence types.

Table 4.2.1. Empirical universes across the seven studies

Study	Empirical universe	Main N / sample	Main evidence type
Perelman/Ricci/Poincare	10 macro-regional blocks observed over 2010-2024 with sixteen pressure-oriented stress-coordinate variables.	N = 150 region-year observations; 2015-2024 harmonized pressure-curvature path used for main world path; full 2010-2024 retained for topology, entropy, regional change and recovery diagnostics.	Inequality-curvature diagnostics; pressure-smoothing manifold; Ricci-style curvature; Perelman F/W functionals; graph-topological connectedness; bounded econometric validation.
Hodge	World normalization anchor plus ten regional	10-node regional benchmark; connected	Hodge decomposition of regional macro-flow

	nodes, including the Caucasus as an explicit corridor-sensitive subregional node.	graph with 27 weighted edges; benchmark evidence rather than all-country panel evidence.	pressure into gradient hierarchy, curl/local-cycle imbalance and harmonic/systemic circulation; topological and predictive benchmark validation.
Navier-Stokes	100-country annual macro-financial panel for 2010-2024, complemented by World aggregate, macro-regional aggregation, quarterly robustness layer, rolling validation windows and external-target validation.	N = 1,500 country-year observations as the main evidence base; rolling one-year-ahead validation over 2017-2024; additional robustness and scenario layers.	Macro-financial stress-testing; nondimensional flow-pressure-friction-shock-cycle-closure balance; fixed-effects diagnostics; rolling forecast validation; robustness, external validation, Monte Carlo and policy counterfactuals.
Yang-Mills	Completed finite global-corridor stress network with ten global/corridor-sensitive regional nodes and twenty-seven weighted undirected edges; planned 100-country by 15-year validation architecture.	Benchmark network layer plus N = 1,500 country-year validation pathway; current benchmark populated, panel pathway specified for future numerical closure.	Finite-network gauge-econometric mass-gap/network-threshold evidence; stress Laplacian, triangular curvature, Yang-Mills economic action, EMGI, fragility, BridgeStress, scenario diagnostics and panel-ready validation design.
Birch-Swinnerton-Dyer	World normalization anchor plus ten macro-regional/corridor nodes: EAP, NAM, EUR, LAC, SAS, MENA, SSA, OCE, CAS and CAU.	N = 150 regional-year closure layer built from ten regional nodes over fifteen years; substantive regional/corridor benchmark plus panel-based closure architecture.	Local-to-global structural-rank evidence; economic curve coefficients, local traces, Euler-factor analogues, economic L-function, LOrder, structural rank, corridor stress and claim-discipline diagnostics.
Riemann/Zeta	World aggregate inflation-forecasting system with annual, quarterly and monthly validation layers.	N = 55 for 1970-2024 principal annual layer; N = 45 for 1980-2024 robustness layer; N = 20 for 2005-2024 crisis-era comparison; N = 100 for 2000Q1-2024Q4 quarterly dynamic layer; N = 240 for 2005M1-2024M12 monthly spectral layer.	Inflation forecast validation; FPAS baseline plus normalized zeta-cycle correction; RMSE/MAE/sMAPE comparison; rolling no-look-ahead validation; Mincer-Zarnowitz, encompassing, Diebold-Mariano/Clark-West, residual, regime and spectral diagnostics.
P vs NP	Fixed Damodaran January	Full universe: n = 94, K =	Computational-finance

	2026 U.S. industry universe after excluding aggregate market rows; 94 industry portfolios with beta, volatility, firm count and CAPM-implied expected-return inputs.	10 with C(94,10) = 9,041,256,841,903 possible supports; exact reduced benchmark: n = 20, K = 6 with C(20,6) = 38,760 supports enumerated.	optimization evidence; cardinality-constrained Markowitz-CAPM sparse selection; heuristic search, Monte Carlo, genetic algorithms, GA reoptimization, exact reduced enumeration, robustness and derivative-overlay discipline.

Source: Author synthesis based on the seven source manuscripts and the monograph-level methodology architecture.

The table should be interpreted as a methodological map rather than as a ranking of studies by sample size. A larger N does not automatically mean a stronger claim if the research question requires a finite network, a spectral graph, a forecast layer or a computational support space. The correct criterion is fit between empirical universe and evidence type. The Perelman/Ricci/Poincare and BSD chapters both use N = 150 closure structures, but their objects differ: one measures inequality-pressure curvature; the other measures local-to-global structural rank. The Navier-Stokes and Yang-Mills chapters both reference N = 1,500 structures, but the first uses the country-year panel as a main evidence base, whereas the second treats it as a specified validation pathway beyond the populated benchmark. The Riemann/Zeta chapter has the most explicit sample-discipline structure because it assigns different validation tools to annual, quarterly and monthly layers. The P-vs-NP chapter does not use an econometric time panel at all; its main sample discipline is combinatorial.

4.2.3. Unit of Analysis and Evidence-Type Taxonomy

The seven studies use different units of analysis. This is methodologically necessary. A curvature-diagnostic inequality model requires region-year stress coordinates. A Hodge model requires nodes, edges and a directed edge cochain. A liquidity-flow stress test requires country-year macro-financial observations. A Yang-Mills gauge network requires nodes, edges, cycles and a stress Laplacian. A BSD local-to-global model requires regional nodes, local-state traces and a structural-rank comparison. A zeta-forecasting model requires time-indexed global inflation layers. A P-vs-NP portfolio model requires assets, supports and optimization weights. These are not interchangeable units.

Table 4.2.2. Unit-of-analysis taxonomy for the seven-study monograph

Unit type	Primary studies	Operational definition	Evidence generated
Region-year coordinate	Perelman/Ricci/Poincare; BSD closure layer	Region r observed over year t.	Panel-style diagnostics, fixed-effects screening, robustness, closure and sensitivity.
Regional node	Hodge; Yang-Mills; BSD	Macro-region or corridor-sensitive node used as a structural component of the world economy.	Network topology, centrality, rank, spectral and corridor-exposure measurement.
World anchor	Hodge; BSD; Navier-Stokes; Riemann/Zeta	Global normalization or aggregate reference, not always an ordinary competing observation.	Scale consistency, normalization, global benchmark or target aggregate.
Country-year observation	Navier-Stokes; Yang-Mills validation pathway	Country i observed in year t.	Main diagnostic econometrics for Navier-Stokes; future stronger validation for Yang-Mills.
Edge/cycle object	Hodge; Yang-Mills; BSD network layer	Weighted relation between nodes or triangular/cyclic structure.	Flow decomposition, gauge potential, curvature, action, spectral separation and local-to-global transmission.

Time-layer observation	Riemann/Zeta	Annual, quarterly or monthly observation assigned to a specific validation task.	Forecast accuracy, dynamic validation, spectral diagnostics and regime analysis.
Asset/support object	P vs NP	Industry portfolio i, selected support S and continuous weight vector w_S.	Combinatorial search, exact reduced enumeration, heuristic validation and optimization robustness.

Source: Author synthesis based on the empirical-universe and methodology descriptions of the seven studies.

The taxonomy clarifies why the monograph cannot be reduced to a single panel database. It is a multi-object empirical architecture. Some objects are observations in the conventional econometric sense; others are graph objects, time-frequency layers, forecast targets or computational search spaces. The methodological unity of the book is therefore not supplied by identical data form. It is supplied by identical discipline: explicit universe, explicit transformation, explicit validation and explicit claim boundary.

This distinction also helps the reader interpret N. In panel econometrics, N usually refers to observations. In network analysis, N may refer to nodes; in optimization, the relevant scale may be the combinatorial number of supports rather than the number of assets. In the Riemann/Zeta chapter, N changes by frequency and validation layer. Therefore, Section 4.2 treats N as a sample-discipline descriptor, not as a single universal measure of evidence.

4.2.4. Evidence Hierarchy Generated by the Empirical Universes

The empirical universes generate different evidence classes. The monograph uses a hierarchy rather than a flat evidence language. Benchmark evidence is appropriate when a complete network or structured object is constructed and audited. Panel evidence is appropriate when country-year or region-year variation supports diagnostic econometrics. Forecast evidence is appropriate when the target is predictive performance over time. Computational evidence is appropriate when the research question concerns search-space growth, algorithmic performance and exact reduced comparison. Closure evidence is appropriate when the model uses additional tests to prevent overclaiming.

Table 4.2.3. Evidence hierarchy across empirical universes

Evidence class	Main chapters	Definition	Permitted interpretation
Benchmark evidence	Hodge; Yang-Mills; BSD regional core	A complete structured empirical object is built and audited.	Strong for decomposition, graph topology, spectral diagnostics and structural-rank calibration within the specified benchmark.
Panel diagnostic evidence	Perelman/Ricci/Poincare; Navier-Stokes; BSD closure; Yang-Mills future pathway	Region-year or country-year observations allow fixed-effects, robust inference or closure diagnostics.	Supports association, robustness and stress-channel interpretation; not automatic causal proof.
Forecast-validation evidence	Riemann/Zeta; Navier-Stokes rolling layer; Perelman forecasting layer	Observed time sequence is divided into validation windows or frequency layers.	Supports predictive usefulness inside defined horizons and samples; not universal forecast superiority.
Network/spectral evidence	Hodge; Yang-Mills; BSD; Perelman graph layer	Graph, Laplacian, connectedness, cycles, eigenvalues or curvature proxies are computed.	Supports topology, connectivity, spectral separation or curvature measurement inside the constructed graph.
Computational-search evidence	P vs NP	Large discrete support space is searched by heuristic and exact reduced	Supports bounded computational-finance claims; not theorem proof

		methods.	or full-universe global-optimum certification.
Scenario/Monte Carlo evidence	Navier-Stokes; Yang-Mills; Perelman; P vs NP robustness	Perturbations, stress scenarios or simulated paths test fragility.	Supports uncertainty, sensitivity and conditional interpretation; not unconditional prediction.
Replication/claim-boundary evidence	All seven studies	External packages, formulas, tables, code logic, source ledgers and decision gates document reproducibility.	Supports auditability and disciplined interpretation rather than unrestricted generalization.

Source: Author synthesis based on the methodology and claim-boundary logic of the seven studies.

The hierarchy is important because it allows a result to be strong without being overstated. For example, the Yang-Mills chapter can strongly claim a positive finite-network spectral separation in its populated benchmark, while still reserving stronger causal country-level claims for the planned N = 1,500 panel. The Riemann/Zeta chapter can strongly report layered forecast improvements across its stated samples, while still excluding Riemann Hypothesis proof and universal forecast dominance. The P-vs-NP chapter can strongly document combinatorial support-space explosion and exact reduced enumeration, while still excluding a full n = 94 global-optimality certificate.

4.2.5. Perelman/Ricci/Poincare Empirical Universe

The Perelman/Ricci/Poincare chapter uses a macro-regional inequality-pressure universe. Its empirical object is a global diagnostic manifold made from ten macro-regional blocks observed annually over 2010-2024 and measured through sixteen stress-coordinate variables. The resulting balanced panel contains N = 150 region-year observations. This empirical universe is appropriate because the research question is not country-level welfare ranking, but the measurement of global inequality pressure, smoothing capacity, curvature-like deformation, entropy-like complexity and graph connectedness.

The unit of observation is the region-year coordinate. Each region-year is not treated as a raw welfare outcome alone; it is transformed into part of a pressure-oriented diagnostic manifold. The sixteen variables include inequality, productivity, unemployment, investment, inflation, migration, education, mobility, logistics or trade infrastructure, capital-flow pressure, innovation, health, fiscal deficit, openness, social protection and technology access. Heterogeneous raw units are not added directly. They are transformed onto a common 0-100 pressure-oriented scale so that higher scores represent higher stress or weaker smoothing capacity after directional harmonization.

The main evidence type is inequality-curvature diagnostics. The chapter constructs a pressure index, correlation-based metric tensor, Ricci-style component curvature, scalar curvature, Perelman-type F and W functionals, graph Laplacian connectedness, Betti numbers, edge-curvature proxies, Ricci-surgery rankings, counterfactual sensitivity tests and econometric validation layers. Its N = 150 panel supplies diagnostic closure and dynamic context, while the graph-topology layer tests whether the stress-coordinate system forms a connected and cycle-rich diagnostic structure.

Table 4.2.4. Empirical-universe profile: Perelman/Ricci/Poincare chapter

Dimension	Specification
Empirical object	Global macro-regional inequality system interpreted as a pressure-smoothing diagnostic manifold.
Unit of analysis	Region-year coordinate across ten macro-regional blocks.
Main period	2010-2024 annual panel; 2015-2024 harmonized path used for main pressure-curvature reporting.
Main N	N = 150 region-year observations.
Variable structure	Sixteen pressure-oriented stress coordinates transformed onto a common 0-100 scale.
Main evidence type	Inequality-pressure, Ricci-style curvature, F/W functionals, graph topology, econometric screens and Monte Carlo/forecast discipline.
Claim boundary	Diagnostic measurement and bounded validation; not proof of Poincare, not literal Ricci-flow theorem transfer

	and not unrestricted causality.

Source: Author synthesis based on the Perelman/Ricci/Poincare methodology and results architecture.

The strength of this empirical universe is its internal measurement coherence. The panel is large enough to support region-year descriptive statistics, pressure paths, curvature decomposition and diagnostic econometric screens. It is also small and aggregated enough to require caution. The monograph therefore classifies this chapter as a macro-regional diagnostic panel, not as a country-level welfare study and not as theorem-level geometric evidence.

4.2.6. Hodge Empirical Universe

The Hodge chapter uses a regional benchmark universe rather than a conventional country-year panel. Its empirical object is the world economy represented as a weighted, directed and topologically decomposable macro-flow network. The model contains a World normalization anchor and ten regional nodes: East Asia and Pacific, North America, Europe, Latin America and Caribbean, South Asia, Middle East and North Africa, Sub-Saharan Africa, Oceania, Central Asia and the Caucasus. The Caucasus is retained as an explicit corridor-sensitive subregional node so that its structural position is not hidden inside broader aggregates.

The Hodge empirical universe is a 10-node regional benchmark with 27 weighted edges. This network is not an observed bilateral transaction matrix. It is an author-calculated macro-flow pressure graph derived from public macroeconomic anchors such as regional GDP, world-output share, projected growth, transition GDP and income depth. The main evidence type is topological macro-flow decomposition. The study transforms standard macroeconomic anchors into a directed edge cochain and decomposes it into gradient, curl and harmonic components.

This design is appropriate for the Hodge analogy because Hodge decomposition requires a structured graph with edges and cycles. A conventional country ranking would not produce the required edge-cochain object. The empirical universe is therefore intentionally benchmark-based. Its strength is structural completeness at the regional macro-core level: it covers the world through major regions, preserves corridor visibility, produces a connected cycle-rich graph and supports decomposition, spectral diagnostics, robust econometric checks, machine-learning forecast validation and persistent-homology confirmation.

Table 4.2.5. Empirical-universe profile: Hodge chapter

Dimension	Specification
Empirical object	World economy as a regional topological macro-flow network.
Unit of analysis	Regional nodes, weighted edges, directed edge pressure and decomposable cochain.
World anchor	Used for normalization, scale consistency and global benchmarking; not treated as an ordinary Hodge edge-field node.
Main sample	10-node regional benchmark with 27 weighted edges.
Main evidence type	Discrete Hodge decomposition into gradient hierarchy, curl/local-cycle imbalance and harmonic/systemic circulation.
Validation layers	Spectral connectivity, higher-order Hodge-Laplacian diagnostics, robust econometric screens, ML validation and persistent homology.
Claim boundary	Benchmark structural measurement; not final causal estimates for all countries or observed dyadic flows.

Source: Author synthesis based on the Hodge-econometric methodology and regional benchmark architecture.

The Hodge chapter therefore represents the monograph's clearest example of a benchmark network universe. Its N is not a time-panel N; it is a structural benchmark dimension. The reader should evaluate it by graph completeness, connectedness, cycle adequacy, decomposition validity and replication transparency rather than by the standards of a large-N panel regression alone.

4.2.7. Navier-Stokes Empirical Universe

The Navier-Stokes chapter supplies the largest conventional panel evidence base in the monograph. Its empirical design is centered on a 100-country annual macro-financial panel observed over 2010-2024, yielding N = 1,500 country-year

observations. This is the main econometric layer of the chapter and must be included in the monograph-level empirical-universe table as the principal evidence base for the Navier-Stokes-inspired macro-financial stress-testing framework.

The empirical universe is broader than the country-year panel alone. It is supplemented by a World aggregate anchor, macro-regional aggregation, a quarterly robustness layer, rolling validation windows and external-target validation layers. These supplementary layers allow the model to be interpreted at multiple levels: country-year stress dynamics, macro-regional pressure and friction patterns, global aggregate context, rolling forecast performance, robustness under alternative proxies and external plausibility screening.

The main evidence type is nondimensional macro-financial stress testing. Raw macro-financial indicators are not added in their original units. Inflation, sovereign-risk proxies, liquidity/friction indicators, GDP-cycle deviations, event-volatility measures, resilience buffers and closure-state variables are direction-harmonized, nondimensionalized and interpreted as unit-free starred stress or resilience components. This preprocessing rule is central because it keeps the Navier-Stokes analogy methodologically defensible: the model borrows the structural logic of flow, pressure, friction, shock, cycle and closure without claiming literal hydrodynamic identity.

Table 4.2.6. Empirical-universe profile: Navier-Stokes chapter

Dimension	Specification
Empirical object	Global macro-financial system interpreted through liquidity-flow and systemic-stress measurement.
Main unit of analysis	Country-year observation.
Main sample	100 countries observed annually from 2010 to 2024.
Main N	N = 1,500 country-year observations.
Supplementary layers	World aggregate anchor, macro-regional aggregation, quarterly robustness, rolling validation windows and external-target validation.
Main evidence type	Nondimensional flow-pressure-friction-shock-cycle-closure stress testing; fixed-effects diagnostics; rolling benchmark comparison; robustness and policy counterfactuals.
Claim boundary	Global diagnostic stress-testing evidence; not physical hydrodynamic proof, not randomized causality and not universal crisis-prediction law.

Source: Author synthesis based on the Navier-Stokes empirical universe, observation structure and validation architecture.

The Navier-Stokes empirical universe is important for the monograph because it demonstrates that the unified methodology is not limited to small benchmark networks. It also supports a large observational panel with fixed effects, stress-channel estimation, rolling validation, benchmark comparison, residual diagnostics, external validation, Monte Carlo uncertainty and policy counterfactuals. At the same time, the chapter remains observational and diagnostic. The N = 1,500 panel strengthens empirical assessment but does not convert the analogy into a physical law or a causal experimental result.

4.2.8. Yang-Mills Empirical Universe

The Yang-Mills chapter uses a deliberately two-layered empirical universe. Layer A is a completed finite-network benchmark composed of ten global and corridor-sensitive regional nodes connected by twenty-seven weighted undirected edges. Layer B is a planned 100-country by 15-year validation architecture, producing a potential N = 1,500 country-year panel once the country-year variables are populated and estimated. This distinction must be preserved in the monograph because the benchmark is completed, while the stronger country-panel evidence remains a validation pathway rather than a finalized empirical result.

The benchmark universe is designed for finite-network gauge-econometric measurement. Public macroeconomic anchors are transformed into a normalized systemic-stress field, corridor-weighted graph, stress-weighted adjacency matrix, anti-symmetric gauge potential, triangular curvature, Yang-Mills economic action, stress Laplacian, Economic Mass Gap Index, fragility, BridgeStress and shock scenarios. The main evidence type is therefore not a country-level regression but a finite-network threshold measurement: whether a stress-weighted corridor network contains positive spectral separation and how shocks affect that threshold.

The N = 1,500 pathway has a different status. It is not the current benchmark evidence; it is the empirical architecture required for stronger country-level validation. It specifies fixed effects, two-way fixed effects, Driscoll-Kraay, clustered inference, dynamic panels, panel-IV, factor models and external-validation models once the data are populated. In the monograph table, this must be written as benchmark + N = 1,500 pathway, not as if both layers had the same evidence status.

Table 4.2.7. Empirical-universe profile: Yang-Mills chapter

Dimension	Specification
Empirical object	Finite global-corridor systemic-stress network constructed from public macroeconomic anchors and corridor transformations.
Completed layer	Ten global/corridor-sensitive regional nodes and twenty-seven weighted undirected edges.
Constructed objects	Systemic stress, corridor weights, gauge potential, triangular curvature, action, stress Laplacian, mass gap, EMGI, fragility, BridgeStress and scenarios.
Validation pathway	Planned 100-country by 15-year country-year structure, yielding N = 1,500 once populated and estimated.
Main evidence type	Finite-network mass-gap/network-threshold evidence and corridor shock-transmission diagnostics.
Current evidence status	Benchmark populated and auditable; country-panel validation specified but not yet numerically closed.
Claim boundary	Finite weighted-graph economic mass-gap interpretation; not solution of the mathematical Yang-Mills existence and mass gap problem; stronger causal claims reserved for panel closure.

Source: Author synthesis based on the Yang-Mills finite-network and panel-validation architecture.

This two-layer distinction is one of the strongest examples of claim discipline in the monograph. The chapter reports strong finite-network benchmark evidence where the data are populated and reproducible. It does not prematurely upgrade the planned country-year architecture into completed causal validation. This is exactly how the monograph should handle staged empirical universes: completed benchmark evidence is interpreted as benchmark evidence; planned validation evidence is identified as panel-ready but not yet final.

4.2.9. Birch-Swinnerton-Dyer Empirical Universe

The BSD chapter uses a World-normalized regional/corridor universe. The empirical object consists of the World anchor and ten macro-regional or corridor-sensitive nodes: East Asia and Pacific, North America, Europe, Latin America and Caribbean, South Asia, Middle East and North Africa, Sub-Saharan Africa, Oceania, Central Asia and the Caucasus. The World row is a normalization anchor, not a competing regional node in the rank hierarchy. This distinction is essential because the chapter is not a country-ranking or simple regional-output exercise; it is a local-to-global structural-rank measurement architecture.

The chapter has two empirical levels. The first is the substantive regional/corridor benchmark, where public macro-regional anchors are transformed into systemic-stress components, weighted regional-network structure, economic curve coefficients, discriminant diagnostics, finite-state trace analogues, Euler-factor analogues, economic L-function behavior and L-order measurement. The second is the N = 150 regional-year closure layer, built from ten regional nodes over fifteen years. This closure layer is used for calibration, robustness diagnostics, external-proxy screening, negative controls, anti-circularity tests, equivalence logic, out-of-sample validation and permutation evidence.

The main evidence type is local-to-global structural-rank evidence. The BSD analogue tests whether local regional signals and Euler-factor information are informative about a constructed global structural-rank object. The evidence is strongest as calibrated local-to-global consistency. It does not become a proof of the classical BSD conjecture, a causal regional law or strong external econometric validation when robust p-values and external proxies remain limited.

Table 4.2.8. Empirical-universe profile: BSD chapter

Dimension	Specification
Empirical object	World-normalized regional/corridor system interpreted

	through a BSD-inspired local-to-global measurement framework.
Regional node set	Ten macro-regional/corridor nodes: EAP, NAM, EUR, LAC, SAS, MENA, SSA, OCE, CAS and CAU.
World anchor	Global GDP, growth and income-depth reference used for normalization; not a competing node in the rank hierarchy.
Main N / sample	N = 150 regional-year closure layer from ten regions over fifteen years.
Constructed objects	Stress, fragility, corridor exposure, coefficient maps, local traces, Euler factors, economic L-function, LOrder and structural rank.
Main evidence type	Local-to-global structural rank, rank agreement, corridor stress, scenario diagnostics and closure tests.
Claim boundary	Calibrated regional measurement and internal consistency; not proof or empirical test of classical BSD and not unrestricted causal confirmation.

Source: Author synthesis based on the regional BSD-inspired local-to-global methodology and closure architecture.

The BSD universe is methodologically important because it demonstrates how a small number of regional nodes can still produce a rich empirical architecture when the purpose is local-to-global measurement rather than country-level causal inference. The N = 150 closure layer adds empirical discipline, but the strongest claim remains calibrated measurement consistency. This is the appropriate claim level for a constructed local-to-global analogue.

4.2.10. Riemann/Zeta Empirical Universe

The Riemann/Zeta chapter provides the most explicit sample-discipline architecture in the monograph. Its empirical object is the global aggregate inflation-forecasting system. Unlike the regional benchmark chapters, this chapter is organized around time-frequency validation layers. The principal annual validation layer covers 1970-2024 with N = 55. The annual robustness layer covers 1980-2024 with N = 45. The compact crisis-era annual comparison layer covers 2005-2024 with N = 20. The quarterly dynamic-validation layer covers 2000Q1-2024Q4 with N = 100. The monthly spectral-diagnostics layer covers 2005M1-2024M12 with N = 240.

This layered structure should be emphasized in the book because it is a model example of sample discipline. The chapter does not pretend that every advanced validation procedure is estimated on the same small annual sample. Instead, each method is assigned to the frequency and sample length that can support it. Principal annual forecast-accuracy claims are attached to the N = 55 layer. Robustness is attached to the N = 45 layer. Crisis-era illustration is attached to the N = 20 layer. Dynamic validation is assigned to the quarterly N = 100 layer. Fourier, wavelet, spectral entropy and zeta-stress lead diagnostics are assigned to the monthly N = 240 layer.

The main evidence type is inflation forecast validation. The model starts from a structural FPAS baseline and augments it with a normalized Riemann-zeta critical-line cyclical signal transformed into a signed and alpha-calibrated forecast correction. Forecast performance is evaluated against FPAS and ARIMA through RMSE, MAE, sMAPE, rolling no-look-ahead validation, Mincer-Zarnowitz calibration, forecast-encompassing tests, Diebold-Mariano and Clark-West comparisons, residual diagnostics, HMM or Markov-switching regimes, Fourier/wavelet coherence and spectral-entropy screens.

Table 4.2.9. Empirical-universe profile: Riemann/Zeta chapter

Dimension	Specification
Empirical object	Global aggregate inflation-forecasting system interpreted through structural FPAS and normalized zeta-cycle correction.
Principal annual layer	1970-2024, N = 55; main annual forecast-accuracy claim.
Annual robustness layer	1980-2024, N = 45; robustness and stability check.
Crisis-era comparison layer	2005-2024, N = 20; compact crisis-era annual comparison and display.

Quarterly dynamic layer	2000Q1-2024Q4, N = 100; dynamic validation tools.
Monthly spectral layer	2005M1-2024M12, N = 240; Fourier, wavelet, spectral entropy and zeta-stress lead diagnostics.
Main evidence type	Forecast validation, benchmark comparison, regime diagnostics, residual checks and spectral screens.
Claim boundary	Bounded global forecast-diagnostic claim; not proof/test of Riemann Hypothesis, not unrestricted causality and not universal forecast dominance.

Source: Author synthesis based on the FPAS+zeta layered validation architecture.

The Riemann/Zeta empirical universe should be presented in Chapter 4 as the strongest example of cross-frequency sample discipline. It shows how a complex mathematical signal can be evaluated without allowing visual fit, compact-sample success or high in-sample accuracy to become an overclaim. The admissible claim is not that zeta mathematics solves inflation. The admissible claim is that a normalized zeta-cycle signal, under the stated layers and validation tests, improves and enriches the reported global aggregate inflation forecast architecture.

4.2.11. P vs NP Empirical Universe

The P vs NP chapter uses a computational-finance universe rather than a macroeconomic time panel. Its empirical object is a fixed Damodaran January 2026 U.S. industry dataset containing 94 industry portfolios after aggregate market rows are excluded. Each industry is characterized by firm count, levered beta, annual equity volatility, CAPM-implied expected return and a CAPM Sharpe proxy. The baseline calibration uses a risk-free rate of 3.97 percent and an equity risk premium of 4.23 percent.

The key empirical scale is not only n = 94. The core evidence scale is the cardinality-constrained support space. The baseline sparse-selection problem imposes K = 10, producing C(94,10) = 9,041,256,841,903 possible industry supports before continuous weights are optimized. This support-space explosion is the operational P-vs-NP-inspired object in the study. It shows why full naive enumeration is infeasible in the main universe and why heuristic search, Monte Carlo sampling, genetic algorithms, GA-plus-continuous reoptimization, runtime reporting and claim-boundary discipline are required.

Exact evidence is supplied through a reduced n = 20, K = 6 benchmark, where all C(20,6) = 38,760 supports can be enumerated. This exact reduced benchmark is critical because it separates two kinds of evidence. The full n = 94, K = 10 universe supports documented search coverage and best-found incumbents, but not certified global optimality. The reduced n = 20, K = 6 universe supplies exact enumeration evidence, but only for the reduced instance. This distinction is one of the most important claim-boundary devices in the chapter.

Table 4.2.10. Empirical-universe profile: P vs NP chapter

Dimension	Specification
Empirical object	Cardinality-constrained portfolio-optimization system interpreted through a P-vs-NP-inspired computational-finance lens.
Input universe	94 U.S. industry portfolios from the Damodaran January 2026 dataset after aggregate market rows are excluded.
Calibration inputs	Risk-free rate = 3.97 percent; equity risk premium = 4.23 percent; CAPM-implied returns generated from beta.
Full support-space scale	n = 94, K = 10; C(94,10) = 9,041,256,841,903 possible supports before continuous weight optimization.
Exact reduced benchmark	n = 20, K = 6; C(20,6) = 38,760 supports fully enumerated.
Main evidence type	Computational-finance optimization: greedy search, Monte Carlo, genetic algorithms, GA reoptimization, exact reduced enumeration, robustness, frictions and derivative overlay.
Claim boundary	Best-found full-universe incumbent and bounded computational evidence; not proof of P != NP, not full n = 94 global-optimum certification and not realized

	investment dominance.

Source: Author synthesis based on the P-vs-NP-inspired portfolio-optimization data audit and computational design.

The P vs NP chapter expands the meaning of empirical universe in the monograph. Here the decisive empirical object is not temporal observation but computational search space. The data are fixed before optimization, and the methodological discipline lies in search-space disclosure, algorithm comparison, exact reduced benchmarking, covariance robustness, transaction-cost realism, derivative-overlay caution and final claim hierarchy. This is why the chapter belongs in the unified methodology even though it does not resemble a standard macroeconomic panel.

4.2.12. Cross-Study Sample Discipline and Non-Equivalence of N

A major methodological contribution of this section is the rejection of mechanical N-comparison. The monograph contains N = 150 region-year panels, a 10-node benchmark, an N = 1,500 country-year panel, a benchmark plus N = 1,500 pathway, layered time samples of N = 55, 45, 20, 100 and 240, and a combinatorial universe with C(94,10) possible supports. These are different empirical scales and they should not be ranked on one linear axis.

The correct comparison is claim-fit. A 10-node Hodge benchmark is appropriate if the claim is that a constructed regional graph is connected, cycle-rich and decomposable into gradient, curl and harmonic components. An N = 1,500 Navier-Stokes panel is appropriate if the claim is that global macro-financial stress channels can be audited through country-year diagnostic econometrics and rolling validation. A layered Riemann/Zeta design is appropriate if the claim is forecast improvement under annual, quarterly and monthly validation. A C(94,10) support space is appropriate if the claim is computational complexity in sparse portfolio selection. In each case, the empirical universe is judged by its match to the research question.

Table 4.2.11. Non-equivalence of sample size and benchmark dimension across the monograph

Meaning of N	Primary use	Interpretation	Methodological consequence
N as observations	Perelman/Ricci/Poincare, Navier-Stokes, BSD closure, Riemann/Zeta time layers	Counts region-year, country-year or time observations.	Useful for panel, forecast and closure diagnostics.
N as nodes	Hodge, Yang-Mills, BSD node set	Counts regions or corridor nodes in a graph.	Useful for topology, network structure, Hodge decomposition, gauge curvature and rank objects.
N as validation pathway	Yang-Mills	Specifies a planned country-year panel not yet equivalent to completed benchmark evidence.	Must be reported as pathway rather than completed empirical confirmation.
N as frequency-specific layer	Riemann/Zeta	Different N values correspond to annual, quarterly and monthly layers.	Prevents assigning advanced diagnostics to the wrong sample frequency.
N as combinatorial support space	P vs NP	The relevant scale is C(n,K), not only the number of input assets.	Captures search-space explosion and motivates heuristic/exact reduced comparison.

Source: Author synthesis based on the monograph-level empirical-universe architecture.

This non-equivalence of N is especially important for reviewers. Without it, a reader might mistakenly criticize a benchmark network for not being a large country panel, or mistakenly treat a planned panel pathway as already completed evidence, or mistakenly compare combinatorial search scale with time-series sample size. Section 4.2 prevents those errors by making the empirical meaning of N explicit in every chapter.

4.2.13. Empirical-Universe Boundary Matrix

The final role of Section 4.2 is to align each empirical universe with its claim boundary. The boundary is not a defensive sentence at the end of the chapter. It is a methodological rule derived from the empirical universe itself. The following matrix defines what each universe can support and what it cannot support.

Table 4.2.12. Empirical universe and admissible claim boundary by study

Study	What the empirical universe can support	What the empirical universe cannot support
Perelman/Ricci/Poincare	Supports global macro-regional inequality-pressure, curvature, entropy, connectedness, sensitivity and bounded validation diagnostics.	Does not support proof of Poincare/Ricci/Perelman results, literal geometric invariants or unrestricted causal welfare claims.
Hodge	Supports regional macro-flow topology, Hodge decomposition, hierarchy/curl/harmonic interpretation and benchmark validation.	Does not support final country-level causality, observed dyadic-flow claims or theorem-level Hodge conjecture claims.
Navier-Stokes	Supports global macro-financial stress-testing, country-year diagnostic econometrics, rolling validation, robustness and policy-counterfactual scenarios.	Does not support physical liquidity-fluid identity, randomized causality or universal crisis-prediction law.
Yang-Mills	Supports finite-network stress curvature, action, positive spectral separation, EMGI, BridgeStress and scenario-threshold diagnostics in the populated benchmark.	Does not support mathematical Yang-Mills mass-gap solution or completed country-level causal validation until N = 1,500 panel is populated and estimated.
BSD	Supports calibrated local-to-global regional structural-rank consistency, corridor stress and N = 150 closure diagnostics.	Does not support classical BSD proof, causal regional law or strong external validation when proxy results remain directional.
Riemann/Zeta	Supports layered global inflation forecast-validation and spectral/regime diagnostic interpretation under stated annual, quarterly and monthly samples.	Does not support Riemann Hypothesis proof/test, unrestricted causality, residual elimination or universal forecast dominance.
P vs NP	Supports bounded computational-finance evidence on sparse portfolio selection, support-space explosion, heuristic search and exact reduced benchmarking.	Does not support P != NP proof, full n = 94 certified global optimum or realized historical investment dominance.

Source: Author synthesis based on the seven claim-boundary and data-status statements.

This boundary matrix should be retained in the final book because it is a direct answer to the most likely methodological objection: whether the monograph overextends mathematical analogies beyond their empirical support. The matrix shows that each claim is bounded by its own universe. The book is strong precisely because it does not need to claim more than its evidence can support.

4.2.14. Integration into the Unified Methodology Chapter

Section 4.2 prepares the remainder of Chapter 4. Once the empirical universes are defined, the following subsections can proceed in a disciplined order. Section 4.3 can distinguish public-data anchors from author-calculated variables. Section 4.4 can define normalization, scaling and directional harmonization without ambiguity. Section 4.5 can explain network and graph construction only for the studies that actually require graph objects. Section 4.6 can classify econometric and forecast-validation protocols by evidence type. Section 4.7 can discuss computational and algorithmic protocols where the relevant empirical object is a search space or constructed signal. Section 4.8 can consolidate replication packages. Section 4.9 can build the general claim-boundary matrix.

The empirical-universe architecture therefore acts as the data spine of the monograph. It tells the reader where each result comes from, what it measures, what level of validation it receives and what interpretive boundary governs it. This is essential because the book intentionally combines regional panels, graph benchmarks, country-year panels, time-frequency forecast layers and computational optimization universes. Without Section 4.2, Chapter 4 would risk becoming a list of methods. With Section 4.2, it becomes a coherent methodology chapter.

The final methodological conclusion is that the seven empirical universes are heterogeneous but not inconsistent. Their heterogeneity is the correct response to the heterogeneity of the underlying economic problems. Inequality curvature, macro-flow decomposition, liquidity stress, corridor shock thresholds, local-to-global rank formation, inflation forecasting and sparse portfolio optimization require different empirical objects. The monograph unifies them not by forcing one dataset onto all seven studies, but by enforcing one research discipline across all of them: explicit universe, transparent transformation, appropriate validation, bounded interpretation and reproducible replication.

Table 4.2.13. Methodological contribution of Section 4.2 to the monograph

Contribution	How Section 4.2 operationalizes it	Why it matters
Empirical transparency	Every chapter states its empirical universe before interpreting technical results.	Prevents hidden sample ambiguity.
Sample discipline	Different N values are treated as evidence-specific rather than mechanically comparable.	Prevents false cross-chapter ranking by sample size alone.
Evidence alignment	Benchmark, panel, forecast, network and computational evidence are classified separately.	Prevents graph outputs, regressions, forecasts and optimization results from being conflated.
Boundary discipline	Each claim boundary follows from the empirical universe that supports it.	Prevents theorem-level or causal overclaiming.
Monograph integration	Heterogeneous empirical universes are integrated by common methodological rules.	Turns seven studies into one coherent book architecture.

Source: Author synthesis for the unified methodology chapter.

4.3. Public Data Anchors and Author-Calculated Variables

This section defines the data-lineage discipline of the monograph. Across the seven Millennium-problem-inspired economic studies, official or public datasets serve as empirical anchors, not as finished analytical outcomes. The central rule is simple but methodologically decisive: official/public data are not identical to the final constructed indicators. GDP, inflation, unemployment, trade openness, beta, volatility, growth projections, fiscal variables or institutional source-family series enter the architecture as observed or publicly reproducible inputs. Curvature, pressure, Hodge components, mass-gap indices, L-order analogues, FPAS+zeta corrections, computational search outputs and robustness scores are author-calculated research variables generated by a disclosed transformation pipeline.

The distinction protects the monograph from two common methodological errors. The first error would be to present constructed mathematical-econometric objects as if they were official institutional statistics. The second would be to dismiss constructed indicators merely because they are not directly published by an external agency. The proper position is intermediate and scientific: constructed variables are admissible when their public anchors, formulas, normalization rules, algorithms, code, sample boundaries and replication packages are transparent.

Accordingly, this section specifies how the seven studies convert public-data anchors into author-calculated variables, how the constructed variables should be interpreted, and which claim boundary must accompany each transformation. It provides the technical bridge between the empirical-universe table in Section 4.2 and the normalization, network, econometric, computational and replication protocols developed in later sections of Chapter 4.

4.3.1. The Core Data-Lineage Principle

The monograph uses a layered data architecture rather than a flat variable list. Each study begins with an input layer consisting of public, official, institutional or reproducibly disclosed data. These inputs are then passed through author-

defined transformation rules. The outputs become constructed research variables. These constructed variables are not invalid because they are calculated by the author; they are valid only to the degree that the transformation is traceable, auditable and claim-bounded.

The general data-lineage equation may be summarized as follows:

Public anchor x -> harmonized input x^H -> normalized/scaled object x^N -> model-specific constructed variable z -> validated diagnostic output y.

This sequence establishes that the official/public input is the provenance layer, while the final indicator is the measurement layer. A World Bank GDP value, an IMF growth projection, a Damodaran beta, or a global inflation series is therefore not itself a Ricci curvature, Hodge harmonic component, Yang-Mills action, BSD LOrder, FPAS+zeta forecast or portfolio search certificate. Those final objects are produced by explicit modelling choices and must be interpreted as research constructs.

Table 4.3.1. General distinction between public anchors and author-calculated research variables

Layer	Definition	Function in the monograph	Claim discipline
Public or official data anchor	Observed, institutional, externally published or reproducibly disclosed input series; examples include GDP, inflation, unemployment, trade openness, GDP per capita, beta, volatility, risk-free rate and equity risk premium.	Provides empirical grounding; fixes scale, sample and source provenance.	May be cited as input evidence, but cannot by itself prove the constructed analogue.
Author harmonization	Reclassification, regional aggregation, window selection, direction alignment, missing-value treatment and time/sample matching.	Makes heterogeneous inputs comparable across regions, countries, industries or time layers.	Must be disclosed because harmonization can affect results.
Author normalization or nondimensionalization	0-100 scaling, stress orientation, min-max transformation, unit-free starred variables, or layer-specific standardization.	Prevents raw units from being added directly and allows mathematical/econometric operations on comparable scales.	A normalized variable is no longer a raw official statistic.
Author-calculated intermediate variable	Composite pressure, stress, transition GDP, corridor exposure, network weight, cochain, tau argument, covariance matrix or support space.	Connects public anchors to the specific mathematical analogue.	Requires formula, parameter and replication disclosure.
Author-calculated final indicator	Curvature, entropy, Hodge component, mass-gap index, EMGI, LOrder, structural rank, FPAS+zeta forecast, Sharpe incumbent or exact reduced benchmark.	Produces the study-specific result and interpretation object.	May support bounded measurement, validation or computational claims, not theorem-level proof or unrestricted causality.

4.3.2. Unified Anchor-to-Construct Architecture across the Seven Studies

The seven studies differ in mathematical inspiration and empirical universe, but their data architecture follows the same methodological grammar. First, each study identifies a public-anchor layer. Second, it constructs a transformation layer. Third, it produces analogue-specific variables. Fourth, it subjects the constructed objects to validation, robustness, placebo or replication checks. This common structure is what allows the seven manuscripts to be converted into one monograph rather than seven disconnected articles.

Table 4.3.2. Unified public-anchor to author-calculated-variable matrix across the seven studies

Study	Public-data anchors	Transformation layer	Author-calculated variables	Admissible claim boundary
Perelman/Ricci/Poincare	Macro-regional inequality and stress-coordinate inputs: Gini/income distribution, productivity, unemployment, investment, inflation, migration, education, social mobility, logistics/trade infrastructure, capital-flow pressure, innovation, healthcare access, fiscal deficit, trade openness, social protection and technology access.	Pressure orientation; 0-100 stress-coordinate conversion; correlation-based metric tensor; component curvature mapping; world-weighted aggregation.	Global pressure, Ricci-style component curvature, scalar curvature, Perelman-type F-functional and W-functional, graph Laplacian connectedness, Betti diagnostics, Ollivier/Forman proxies, surgery rankings, counterfactual sensitivity and Monte Carlo bands.	Inequality-curvature diagnostics; not literal Ricci-flow theorem, not Poincare proof and not unrestricted welfare causality.
Hodge	Regional GDP, world-output share, projected growth, transition GDP, GDP per capita, World anchor and author-preserved Caucasus corridor node.	Regional aggregation; graph construction; edge weighting; anti-symmetric directed macro-flow pressure construction from output share, growth, income depth, mass-growth interaction and corridor logic.	Directed 1-cochain, gradient hierarchy, curl/local-cycle imbalance, harmonic/systemic circulation, energy shares, centrality, resilience, tail risk, shock diffusion and persistent-homology diagnostics.	Topological macro-flow benchmark; not an official flow matrix and not final country-level causal identification.
Navier-Stokes	100-country macro-financial public/proxy inputs: inflation, sovereign-risk proxies, liquidity/friction indicators, credit/banking	Direction harmonization; nondimensional scaling into starred unit-free variables; stress/resilience construction; restricted closure-	Liquidity velocity weakness, acceleration pressure, pressure gradient, friction/diffusion, stochastic shock, GDP-cycle forcing, restricted epsilon(t), systemic-stress index, resilience index, rolling forecasts, benchmark	Macro-financial stress-testing evidence; not literal hydrodynamics, not Navier-Stokes solution and not universal crisis-

	proxies, GDP-cycle deviations, event-volatility measures, resilience buffers, transfers, geopolitical shock proxies, aid/support and closure-state variables.	state modelling; Fourier cycle extraction.	comparisons, Monte Carlo and policy counterfactuals.	prediction law.
Yang-Mills	GDP mass, world-output share, GDP per capita, projected growth, transition GDP, trade/openness proxies, inflation/price-pressure proxies and author-coded corridor exposure.	0-100 anchor normalization; corridor weighting; finite network construction with 10 nodes and 27 edges; stress-weighted adjacency and Laplacian construction.	Systemic-stress field, gauge potential A_ij, triangular curvature F_ijk, Yang-Mills economic action, finite-network mass gap, EMGI, fragility, BridgeStress, resilience, shock scenarios and panel-extension variables.	Finite weighted-graph gauge-econometric benchmark; not continuum gauge field, not mathematical Yang-Mills proof and not final causal panel evidence until country-year closure is populated.
Birch-Swinnerton-Dyer	World anchor, regional GDP, GDP per capita, growth projections, transition GDP, inflation, trade openness/logistics proxies and regional/corridor node definitions.	Regional aggregation; normalization; systemic-stress construction; corridor coding; coefficient mapping; local finite-state trace construction; Euler-factor analogue construction; N=150 closure panel.	Economic curve coefficients, discriminants, finite-state traces, Euler-factor analogues, economic L-function, LOrder, structural rank, regulator/friction/torsion analogues, BridgeStress and local-to-global rank diagnostics.	Calibrated local-to-global structural-rank measurement; not BSD proof, not literal elliptic-curve arithmetic and not independent causal validation where variable lineage overlaps.
Riemann/Zeta	World aggregate inflation and macro-financial forecasting inputs across annual, quarterly and monthly layers; inflation, growth, unemployment, policy, liquidity,	Layered-sample discipline; composite pressure construction; nonlinear tau argument; zeta critical-line computation; real-valued zeta-	Composite pressure CP_t, tau_t, normalized zeta-cycle, zeta deviation, zeta correction, FPAS baseline, FPAS+zeta forecast, forecast-error metrics, MZ/encompassing/DM/CW tests, HMM/regime and spectral diagnostics.	Forecast-diagnostic validation; not Riemann Hypothesis proof, not causal theorem and not universal forecast dominance

	financial and supply-stress coordinates.	cycle normalization; alpha calibration against FPAS baseline.		across all economies, samples and horizons.
P vs NP	Damodaran January 2026 U.S. industry beta and volatility dataset; 94 industries after aggregate exclusions; firm counts, levered beta, annual volatility, risk-free rate and equity risk premium.	Data audit; CAPM expected-return construction; Sharpe proxy construction; single-index covariance and correlation geometry; combinatorial support-space enumeration; heuristic search and exact reduced benchmark.	CAPM-implied returns, covariance matrix, eigenvalue diagnostics, C(94,10), greedy/Monte Carlo/GA/GA+continuous incumbents, exact C(20,6) benchmark, robustness/stress/friction tests and Black-Scholes overlay variables.	Computational-finance optimization evidence; not proof of P != NP, not certified global optimum for n=94 and not realized historical trading-performance evidence.

4.3.3. Why Public Inputs Cannot Be Treated as Final Indicators

The conceptual separation between input and constructed indicator is especially important in a monograph that translates mathematical architectures into economic measurement systems. Each Clay-inspired economic analogue uses public data to make the model empirically grounded. However, the mathematical object appears only after transformation. A public inflation series may help construct FPAS pressure, zeta-cycle deviations or Navier-Stokes pressure terms, but the published inflation rate is not itself a zeta signal or a liquidity-flow pressure gradient. A GDP value may help define mass exposure, transition scale or network weights, but GDP is not itself a Yang-Mills action, Hodge harmonic residual or BSD structural rank.

This principle has three consequences. First, every constructed variable must be described as an author-calculated variable. Second, every constructed variable must be traceable from public anchors through formula, algorithm and output table. Third, every validation test must respect lineage dependence: if a dependent variable and an explanatory variable are derived from overlapping inputs, the result is calibration or internal consistency evidence rather than independent external validation.

Table 4.3.3. Methodological rules for separating public data from constructed indicators

Rule	Operational meaning	Reviewer-safety function
Provenance rule	Every final variable must have a visible ancestry: source family, raw input, transformation, formula, algorithm and output table.	Prevents unexplained indices from entering the monograph as black-box indicators.
Non-equivalence rule	A constructed indicator must not be described as an official World Bank, IMF, Damodaran, central-bank or institutional statistic unless the institution actually publishes that indicator.	Protects scientific credibility and avoids misattribution.
Lineage-dependence rule	Variables generated from overlapping public anchors cannot automatically validate one another as independent evidence.	Controls circularity risk, especially in BSD, Hodge, Yang-Mills, Ricci and composite-index layers.
Scale-consistency rule	Raw units cannot be added or compared directly unless they are normalized, nondimensionalized or otherwise transformed onto a common scale.	Protects Navier-Stokes, Ricci, Yang-Mills and composite pressure models from unit inconsistency.
Claim-boundary rule	The stronger the constructed variable, the more	Prevents theorem-level, causal and

	explicit the boundary must be: measurement, diagnostic, validation, screening, scenario or causal claim.	forecast-dominance overclaims.
Replication rule	Constructed variables must be accompanied by data dictionaries, formula registers, scripts, seeds, hashes or Zenodo packages where available.	Makes author-calculated indicators auditable rather than merely asserted.

4.3.4. Study-Specific Data-Lineage Profiles

4.3.4.1. Perelman/Ricci/Poincare: from inequality variables to pressure-curvature-topology diagnostics

The Perelman/Ricci/Poincare study begins from public macro-social and inequality-related input families, but its final objects are not public inequality statistics. The raw variables are heterogeneous: some describe distributional pressure, some productive capacity, some labour-market stress, some technology access, some fiscal or trade pressure, and some smoothing capacity. The methodological move is to orient these variables toward a common stress interpretation and transform them onto a 0-100 scale. Only after this harmonization can the model construct an economic diagnostic manifold.

The author-calculated layer then produces a correlation-based metric tensor, Ricci-style component curvature, scalar curvature, normalized Ricci-flow summaries, Perelman-type F- and W-functionals, graph Laplacian connectedness, Betti numbers, edge-curvature proxies, surgery rankings, counterfactuals and uncertainty bands. None of these variables should be represented as raw official statistics. Their legitimacy comes from the disclosed mapping from public inputs into pressure coordinates and from the validation battery applied after construction.

- Public-anchor role: supplies observable macro-social coordinates for a global inequality-pressure system.
- Author-calculated role: converts those coordinates into curvature, entropy and topology diagnostics.
- Claim boundary: supports bounded inequality-curvature measurement and validation, not a proof of Ricci flow, Perelman theorem or the Poincare conjecture.

4.3.4.2. Hodge: from regional macro anchors to a decomposable macro-flow cochain

The Hodge study is one of the clearest examples of the input-output distinction. GDP, world share, projected growth, transition GDP and income depth remain public or source-family-aligned macroeconomic anchors. They do not directly measure hierarchy, curl imbalance or harmonic circulation. Those Hodge components appear only after the author constructs a weighted regional graph, defines edge orientation and computes an anti-symmetric directed pressure field.

The Hodge cochain is therefore a proxy macro-flow pressure object. It is not an observed bilateral trade matrix, input-output table, financial-flow matrix or logistics-transaction database. The public anchors keep the model empirically grounded, while the directed cochain and the Hodge decomposition create the mathematical-econometric measurement layer. This is why Hodge hierarchy, curl imbalance, harmonic exposure, resilience and tail risk must be described as author-calculated research variables.

- Public-anchor role: defines node mass, growth momentum, transition scale and income depth.
- Author-calculated role: transforms node attributes into weighted edges, directed pressure, Hodge decomposition and derived indices.
- Claim boundary: supports regional benchmark topology and structural measurement, not final country-level causal inference or observed dyadic-flow confirmation.

4.3.4.3. Navier-Stokes: from macro-financial proxies to nondimensional stress-balance components

The Navier-Stokes study has the strongest need for scale discipline because its analogy is based on a balance among flow, pressure, friction, shocks, cycle and closure. The public-anchor layer contains heterogeneous macro-financial proxies: inflation, sovereign-risk indicators, liquidity and friction variables, credit or banking proxies, growth-cycle deviations, event-volatility measures, buffers, transfer variables, aid/support and closure-state variables. These variables cannot be added in raw form.

The author-calculated layer resolves this by direction harmonization and nondimensionalization. Variables enter the model as starred, unit-free components. Systemic stress is then decomposed into liquidity velocity weakness, liquidity acceleration, pressure gradients, friction/diffusion effects, stochastic shocks, Fourier GDP-cycle forcing and a restricted hidden-adjustment term epsilon(t). The restricted closure term is crucial: epsilon(t) is not a free residual used to force equality; it is a state-dependent hidden-adjustment channel constructed from observable or proxy-observable variables.

- Public-anchor role: supplies macro-financial conditions for the 100-country, 2010-2024 evidence base.

- Author-calculated role: creates nondimensional stress/resilience components and a flow-pressure-friction-shock-cycle-closure balance.
- Claim boundary: supports stress-testing, rolling validation, external screening and scenario interpretation, not literal financial hydrodynamics or universal crisis prediction.

4.3.4.4. Yang-Mills: from macro-corridor anchors to finite-network gauge variables

The Yang-Mills study begins from public macroeconomic anchor families and a disclosed author-coded corridor layer. GDP mass, output share, GDP per capita, growth projections, transition GDP, trade/openness and inflation proxies define the observable part of the system. Corridor exposure is partly author-coded because corridor relevance cannot be recovered mechanically from GDP alone. This author-coded layer must remain transparent because it influences edge weights, bridge exposure and stress transmission.

The final Yang-Mills variables are produced after the finite network is built. The model creates a normalized stress field, corridor-weighted adjacency matrix, stress-weighted graph, anti-symmetric gauge potential, triangular curvature, Yang-Mills economic action, stress Laplacian, finite-network mass gap, EMGI, fragility, BridgeStress, resilience and shock scenarios. These objects are not official indicators. They are finite weighted-graph variables whose evidentiary status depends on matrix disclosure, formula transparency, robustness tests, placebo checks and replication-package availability.

- Public-anchor role: provides mass, income, growth, openness and price-pressure coordinates for nodes.
- Author-calculated role: builds stress, gauge, curvature, action, mass-gap and bridge-risk variables on a finite graph.
- Claim boundary: permits finite-network benchmark and diagnostic claims; stronger causal claims require populated N=1,500 panel closure.

4.3.4.5. Birch-Swinnerton-Dyer: from regional anchors to local-to-global rank variables

The BSD-inspired study explicitly separates public anchors from derived analytical objects. World GDP, regional GDP, GDP per capita, growth projections, transition GDP, inflation, trade openness, logistics and corridor-proxy inputs define the regional coordinate system. The World row is used as a normalization anchor, not as a competing regional observation. The ten regional or corridor-sensitive nodes are then used to construct a local-to-global economic measurement framework.

The author-calculated layer transforms the anchors into stress components, corridor exposure, economic curve coefficients, discriminants, finite-state local trace analogues, Euler-factor analogues, an economic L-function, LOrder, structural rank, regulator/friction/torsion analogues and BridgeStress. Because many of these variables share upstream inputs, the study must treat internal calibration as internal local-to-global consistency rather than independent causal validation. External proxies may serve as directional screens, but they cannot automatically prove the mechanism if p-values, signs or variable lineage do not support a stronger claim.

- Public-anchor role: fixes the World-normalized regional economic coordinate system.
- Author-calculated role: generates local finite-state, L-function, LOrder and structural-rank objects.
- Claim boundary: supports calibrated local-to-global measurement, not classical BSD proof, analytic rank proof or independent causal law.

4.3.4.6. Riemann/Zeta: from inflation data to layered forecast-diagnostic variables

The Riemann/Zeta study uses public or reproducible macro-financial time-series anchors as the empirical basis for a layered forecast-validation design. Actual global inflation is the target variable. The FPAS baseline uses inflation inertia, pressure, policy, liquidity, financial and supply coordinates. The zeta layer is not a public inflation series and not a theorem-level mathematical result. It is an author-calculated cyclical signal: the model builds a nonlinear macro-financial tau argument, evaluates the zeta function on the critical-line analogue, converts the complex output into a normalized real-valued zeta cycle and then computes a signed deviation from neutrality.

The final FPAS+zeta forecast is author-calculated as a calibrated correction to the FPAS baseline. Forecast evidence is therefore interpreted only through the layered validation architecture: annual N=55 principal layer, annual N=45 robustness layer, N=20 crisis-era comparison layer, N=100 quarterly dynamic layer and N=240 monthly spectral layer. This layered discipline prevents compact-sample overclaiming and keeps advanced tools assigned to the appropriate frequency layer.

- Public-anchor role: supplies inflation and macro-financial time-series inputs for annual, quarterly and monthly validation.

- Author-calculated role: constructs composite pressure, tau, zeta-cycle deviation, alpha-calibrated correction and FPAS+zeta forecast.
- Claim boundary: supports bounded forecast-diagnostic improvement evidence, not Riemann Hypothesis proof or universal forecast dominance.

4.3.4.7. P vs NP: from industry inputs to computational-finance optimization outputs

The P vs NP study uses a fixed empirical-finance input vintage: the Damodaran January 2026 U.S. industry dataset after excluding aggregate market rows. The public or externally disclosed anchor layer consists of industry beta, volatility, firm count and related input attributes, together with the selected risk-free rate and equity risk premium used for CAPM construction. These are not yet optimal portfolios. They are audited inputs.

The author-calculated layer constructs expected returns, Sharpe proxies, covariance geometry, correlation diagnostics, eigenvalue concentration, combinatorial support-space size, heuristic search incumbents, exact reduced benchmark results, robustness diagnostics, transaction-cost tests, beta drift, stress scenarios and Black-Scholes overlay variables. The combinatorial quantity C(94,10) is a support-space measure, not a proof of P != NP. The exact C(20,6) benchmark provides certification only for the reduced instance. The full n=94, K=10 result remains a best-found incumbent under documented search coverage unless a complete solver certificate is supplied.

- Public-anchor role: fixes the industry universe and raw financial inputs before optimization.
- Author-calculated role: creates CAPM returns, covariance geometry, search outputs, robustness tests and option-overlay diagnostics.
- Claim boundary: supports bounded computational-finance evidence, not theorem proof, certified full-universe global optimality or realized trading dominance.

4.3.5. Anchor-Construct Lineage by Variable Family

A variable-family view is useful because the same public inputs recur across several studies but produce different constructed objects. GDP may become mass exposure in Yang-Mills, node scale in Hodge, normalization anchor in BSD or regional context in Perelman/Ricci/Poincare. Inflation may become a pressure coordinate in Ricci, a macro-financial pressure term in Navier-Stokes, a scenario input in Yang-Mills, an external proxy in BSD and the target variable in Riemann/Zeta. The same input does not have the same evidentiary meaning in every model.

Table 4.3.4. Recurrent variable families and their constructed uses across the monograph

Variable family	Main studies using it	Constructed uses	Interpretive caution
GDP / output mass	Hodge, Yang-Mills, BSD, Perelman/Ricci/Poincare, Navier-Stokes regional interpretation	Node mass, world share, transition GDP, regional scale, network weight, structural-rank coordinate	GDP remains official or public; graph weight, stress contribution, rank contribution or action concentration are author-calculated.
GDP per capita / income depth	Hodge, Yang-Mills, BSD, Perelman/Ricci/Poincare	Income-depth pressure, fragility, resilience, node capacity or smoothing-capacity component	Income depth is an anchor; resilience or fragility is a model-derived object.
Projected growth / transition growth	Hodge, Yang-Mills, BSD, Navier-Stokes	Transition GDP, momentum, pressure differential, resilience and local-to-global rank information	Projection is an input; transition pressure and rank implications are constructed.
Inflation / price pressure	Perelman/Ricci/Poincare, Navier-Stokes, Yang-Mills, BSD, Riemann/Zeta	Stress coordinate, pressure gradient, scenario shock, external proxy, target variable and forecast-evaluation object	Inflation may be both target and input depending on study; constructed corrections must be distinguished from actual inflation.
Trade openness / logistics / corridor exposure	Hodge, Yang-Mills, BSD, Perelman/Ricci/Poincare	Edge weights, corridor coding, BridgeStress, finite-state signals, external-proxy screens and network role	Observed openness is not the same as corridor centrality or bridge stress.
Financial-market	P vs NP, Navier-Stokes,	CAPM expected returns,	Risk-free rate, ERP, beta and

parameters	Riemann/Zeta	covariance geometry, friction terms, financial-pressure coordinates, stress validation	volatility are inputs; optimized portfolios and stress-balance outputs are constructed.
Mathematical signal or analogue objects	All studies, in different forms	Curvature, cochain, gauge potential, L-function analogue, zeta-cycle, combinatorial support space	These are not public data; they are author-calculated formal objects requiring claim-boundary discipline.

4.3.6. Author-Calculated Variables as Valid Scientific Objects

The monograph should not apologize for using author-calculated variables. Modern econometric and computational research routinely constructs indices, latent variables, factors, predicted values, residual diagnostics, risk measures, simulated scenarios and algorithmic outputs. The decisive issue is not whether a variable is author-calculated. The decisive issue is whether the construction is transparent, replicable and properly bounded.

In this monograph, author-calculated variables have four legitimate functions. First, they translate public macroeconomic anchors into mathematical measurement grammars. Second, they make otherwise hidden structures visible: curvature, circulation, bridge stress, local-to-global rank, nonlinear zeta-cycle deformation or search-space explosion. Third, they provide testable objects for validation, robustness and placebo checks. Fourth, they impose claim discipline by requiring the author to state exactly what the constructed object can and cannot prove.

Table 4.3.5. Scientific functions of author-calculated variables in the monograph

Function	Definition	Examples
Measurement function	Creates a variable that captures a system property not directly published as official data.	Hodge harmonic circulation, Yang-Mills EMGI, BSD LOrder, Perelman W-functional.
Translation function	Converts a mathematical architecture into an economic analogue while preserving empirical anchoring.	Ricci-style curvature, gauge potential, local trace analogue, zeta-cycle correction.
Validation function	Allows formal testing against benchmarks, robustness layers, external screens or exact reduced cases.	Rolling forecast errors, placebo graphs, negative controls, exact C(20,6) enumeration.
Diagnostic function	Organizes interpretation into pressure, resilience, fragility, rank, shock threshold or optimization difficulty.	Navier-Stokes stress balance, BridgeStress, portfolio support-space growth.
Replication function	Forces disclosure of formulas, code, seeds, data dictionaries and output hashes.	Zenodo packages, formula registers, source logs, checksum materials.

4.3.7. Circularity, Independence and Validation Discipline

The most important statistical risk in a constructed-variable monograph is circularity. Circularity occurs when two variables appear to validate each other even though both are derived from the same or heavily overlapping inputs. This risk does not invalidate the research, but it changes the evidentiary label. If LOrder and structural rank share upstream GDP, growth, resilience or network components, their high agreement supports calibrated local-to-global consistency, not independent external validation. If EMGI and fragility are mechanically related, their association cannot be interpreted as independent causal evidence. If FPAS+zeta is tuned on one layer, its credibility depends on no-look-ahead validation, robustness windows and independent benchmark comparison.

Therefore, the monograph adopts three levels of validation: internal consistency, external directional screening and independent validation. Internal consistency checks whether the constructed architecture behaves coherently according to its own formulas. External directional screening compares constructed variables with observable proxy families, while admitting that statistical strength may be limited. Independent validation requires external outcomes, temporal ordering, robustness, non-overlapping lineage and reproducible estimation files. This hierarchy should be used consistently in all seven problem chapters.

Table 4.3.6. Validation hierarchy for author-calculated variables

Validation level	Definition	Examples in the monograph	Admissible interpretation

Internal calibration / consistency	Constructed variables are compared within the same model architecture.	Rank-LOrder agreement; curvature-pressure coherence; Hodge energy decomposition; EMGI-fragility structure.	May support methodological coherence and calibrated measurement, not independent causal validation.
External directional screening	Constructed indicators are compared with observable proxies such as inflation, trade, growth, financial or logistics outcomes.	BSD external proxies; Yang-Mills corridor plausibility; Navier-Stokes external-target tests.	May support plausibility if signs and robustness align; weak p-values remain weak.
Independent validation	Constructed variables predict or explain outcomes with distinct lineage, temporal ordering and robust inference.	Populated country-year panels, no-look-ahead forecast windows, external outcomes, exact reduced optimization benchmarks.	Can support stronger empirical language only when sample, inference and replication files are sufficient.

4.3.8. Replication Requirements for Constructed Variables

A constructed variable becomes scientifically defensible when an independent reader can reconstruct it. For this reason, the monograph treats replication as part of the data architecture rather than as a final administrative appendix. Each author-calculated object must be linked to a minimum replication trail: public-anchor list, extraction or source-family note, raw-input file, harmonization rule, normalization formula, construction formula, code or pseudo-code, output table, validation table and claim-boundary statement.

The replication standard does not require every variable to come from the same source type. The Perelman/Ricci/Poincare and Navier-Stokes studies rely on broader macro-social and macro-financial panels. Hodge, Yang-Mills and BSD use regional network and corridor transformations. Riemann/Zeta uses layered annual, quarterly and monthly time-series architecture. P vs NP uses a fixed financial dataset and algorithmic search files. The common requirement is not identical data origin; it is transparent source-to-construct traceability.

Table 4.3.7. Minimum replication trail for author-calculated variables

Replication component	Required content	Relevant studies
Raw anchor register	Public source family, indicator names, vintage, sample period, node/country/industry universe and access note.	All seven studies.
Harmonization file	Regional aggregation, exclusions, direction alignment, frequency conversion, window selection or industry filtering.	Hodge, BSD, Yang-Mills, Riemann/Zeta, P vs NP.
Normalization register	0-100 scale, nondimensional starred variables, standardization, min-max limits or layer-specific scaling.	Perelman/Ricci/Poincare, Navier-Stokes, Yang-Mills, BSD, Riemann/Zeta.
Formula catalogue	Every constructed variable expressed by formula, algorithm or reproducible pseudo-code.	Curvature, cochains, gauge variables, LOrder, zeta correction, portfolio objective.
Output audit tables	Tables matching manuscript-reported values, including intermediate and final variables.	All final problem chapters.
Validation and placebo files	Robustness, placebo, sensitivity, no-look-ahead, exact benchmark or external-target outputs.	All seven studies, with method-specific content.
Version-control and hashes	Seeds, timestamps, checksums, DOI/Zenodo package or equivalent archival trail.	Especially Yang-Mills, BSD, Riemann/Zeta, Navier-Stokes and P vs NP.

4.3.9. Methodological Implication for the Whole Monograph

The public-anchor/author-calculated-variable distinction is not a minor technical note. It is the methodological hinge of the entire monograph. The book does not merely collect public macroeconomic tables. It builds seven disciplined

economic analogues from public-data anchors and author-calculated transformations. This is exactly why Chapter 4 must precede the seven problem chapters: readers must understand the data-lineage protocol before interpreting curvature, Hodge decomposition, liquidity-flow stress, gauge action, structural rank, zeta-cycle forecasting or computational portfolio optimization.

The correct reading of the monograph is therefore layered. Public data provide empirical anchoring. Author transformations create the model-specific mathematical-econometric objects. Validation and robustness determine how much confidence those objects deserve. Claim boundaries determine what the author may legitimately say. Replication packages make the entire chain auditable.

This structure also gives the monograph its scientific defensibility. It neither hides behind raw data nor overstates constructed indicators as official truth. Instead, it presents a transparent architecture in which each constructed variable is named, traced, tested and bounded. The final claim is correspondingly high but disciplined: the seven studies demonstrate that Millennium-problem-inspired mathematical grammars can be translated into reproducible economic-econometric measurement systems, provided that public anchors, author-calculated variables, validation layers and claim boundaries remain sharply separated.

Table 4.3.8. Final data-lineage architecture of Section 4.3

Layer	Object	Function	Main caution
Input	Public/official/reproducible anchors	Empirical grounding; source provenance	Source reliability, vintage, coverage and sample boundaries.
Transformation	Author harmonization, normalization and model mapping	Creates comparability and mathematical usability	Formula disclosure, scale discipline and parameter transparency.
Constructed indicator	Curvature, cochain, stress, gauge, rank, zeta correction or optimization output	Generates the substantive result	Must not be mislabeled as official data.
Validation	Robustness, placebo, external screening, forecast test, exact benchmark or panel evidence	Determines evidence strength	Internal consistency is not the same as independent validation.
Claim boundary	Measurement, diagnostic, forecast, scenario, computational or causal language	Controls interpretation	No theorem proof, no universal law and no unsupported causality.
Replication	Data package, formula catalogue, script, seed, hash and output audit	Enables independent reconstruction	Unreplicated constructed variables remain weaker.

4.4. Normalization, Scaling and Directional Harmonization

This section defines the common measurement grammar through which heterogeneous empirical inputs in the monograph are converted into comparable, auditable and claim-bounded analytical variables. The seven studies do not use identical raw data, identical sample structures or identical mathematical analogues. Some are macro-regional panel diagnostics, some are finite-network benchmarks, one is a global panel stress-testing design, one is a layered forecast-validation architecture, and one is an empirical-computational portfolio-optimization design. Nevertheless, they share a central methodological discipline: raw official or public inputs are not directly interpreted as final evidence. They are first aligned, scaled, directionally harmonized and transformed into author-calculated research variables whose evidentiary status is explicitly bounded.

The purpose of this normalization layer is therefore twofold. First, it prevents raw-unit confusion: GDP, GDP per capita, inflation, unemployment, sovereign-spread proxies, liquidity variables, firm counts, beta, volatility, zeta-cycle values, graph weights and curvature/action quantities cannot be added or compared unless their measurement scales have been explicitly defined. Second, it prevents claim inflation: a normalized stress score, a nondimensional starred variable, a Hodge cochain, a zeta correction or a CAPM-Sharpe proxy is a constructed research object, not an official statistic and not theorem-level

evidence. The monograph treats these variables as transparent analytical instruments whose construction, orientation and validation must be auditable.

4.4.1. Methodological Function of Normalization in the Monograph

Normalization is the bridge between public-data anchoring and mathematical-econometric modelling. In the monograph, each Clay-inspired economic analogue begins with observable or publicly anchored quantities, but the research claim is made only after those quantities are transformed into a common model scale. The transformation is not cosmetic. It determines whether a variable is interpreted as pressure, capacity, resilience, rank support, fragility, cycle deviation, curvature contribution, risk or optimization performance.

The normalization protocol is especially important because the seven studies translate different mathematical architectures into economics. The Perelman/Ricci/Poincare study needs a common pressure-oriented coordinate system before constructing metric, curvature and entropy-like quantities. The Hodge study needs a directed edge-pressure field before decomposition into gradient, curl and harmonic components. The Navier-Stokes study needs nondimensional starred variables before pressure, friction, shock, cycle and closure terms can appear in one stress-balance equation. The Yang-Mills and BSD studies need min-max and corridor-sensitive stress transformations before finite-network curvature, action, local-to-global rank or mass-gap claims can be interpreted. The Riemann/Zeta study needs normalized pressure and zeta-cycle variables before the zeta term can become a signed forecast correction. The P vs NP study needs risk-return and covariance scaling rather than a universal 0-100 stress scale, because its empirical object is not an inequality or systemic-stress field but a sparse portfolio-optimization universe.

Table 4.4.1. General normalization principles used across the monograph

Principle	Operational meaning	Methodological purpose
Raw-unit discipline	Heterogeneous inputs are not added in their original units.	Prevents GDP, inflation, volatility, network weights and zeta signals from being treated as commensurable without transformation.
Scale discipline	Variables are converted to a defined model scale: 0-100, unit-free starred variables, standardized coordinates, signed deviations, or risk-return ratios.	Makes the measurement procedure reproducible and interpretable.
Direction discipline	Every variable is oriented so that its sign has a consistent economic meaning.	Higher values can mean higher stress, higher resilience, stronger rank support or higher objective value, depending on the declared family.
Lineage discipline	Public inputs and author-calculated outputs are separated.	Prevents constructed variables from being misrepresented as official data.
Validation discipline	Normalized variables are tested through robustness, sensitivity, placebo, forecast or econometric checks.	Prevents a transformation from becoming an unsupported numerical artefact.
Claim discipline	The transformation defines the level of permissible inference.	A normalized analogue supports measurement and diagnostics, not proof of the original Millennium Problem.

Source: Author synthesis for the monograph based on the seven study methodologies and data-architecture chapters.

4.4.2. General Scaling Operators and Notation

The monograph uses a small set of recurring transformation operators. They are not always applied identically, because each problem chapter has its own empirical object, but they supply the common technical vocabulary for Chapter 4. The most frequent operator is min-max scaling onto a bounded 0-100 interval. This transformation is suitable when the research object is a cross-sectional or panel-based diagnostic score and when the lower and upper empirical anchors are explicitly reported.

(4.4.1) $N(x_{it}) = 100 * (x_{it} - \min(x)) / (\max(x) - \min(x))$.

(4.4.2) $N_R(x_{rt}) = 100 * (x_{rt} - \min_R x_{rt}) / (\max_R x_{rt} - \min_R x_{rt})$, where the comparison set is the regional universe R at the relevant time or benchmark layer.

(4.4.3) $F(x_{it}) = 100 - N(x_{it})$, applied when lower raw values imply higher fragility, vulnerability or stress.

(4.4.4) X*_itk = Scale(X_itk), where the asterisk denotes a unit-free, model-scale variable after direction harmonization and nondimensionalization.

(4.4.5) Z(x_it) = (x_it - mean(x)) / sd(x), used where standardized coordinates, correlation geometry, robustness or metric construction require mean-zero scaling.

(4.4.6) R(x_it) = (x_it - median(x)) / IQR(x), used as a robust-scaling alternative when outliers or heavy-tailed stress channels may distort min-max or z-score transformations.

(4.4.7) d_t = zeta_t - zeta_bar, c^zeta_t = alpha * lambda_zeta * d_t, where the signed zeta deviation is converted into a calibrated forecast correction.

(4.4.8) Sharpe_i = (mu_i - R_f) / sigma_i, where CAPM-implied return and volatility are placed into a risk-adjusted scale rather than a 0-100 stress scale.

Equations (4.4.1)-(4.4.8) define the shared measurement language. Min-max scaling is appropriate where the research requires bounded comparability; inverse normalization is appropriate where high raw capacity reduces stress; starred nondimensional variables are appropriate where different macro-financial units are combined in one stress-balance equation; z-score and robust scaling support metric, covariance and robustness diagnostics; signed zeta deviations support forecast correction; and Sharpe-style ratios support the P vs NP portfolio-optimization chapter.

4.4.3. Directional Harmonization: The Stress-Oriented Rule

Directional harmonization is the procedure through which variables with opposite economic meanings are converted into a common interpretive direction. Without this step, a model could mistakenly add a high-resilience variable to a high-stress variable and treat both as if they increased systemic vulnerability. The monograph therefore requires every transformed component to carry a declared direction: stress-increasing, resilience-increasing, rank-supporting, fragility-increasing, forecast-correcting or optimization-improving.

The most common rule is the stress-oriented convention: after transformation, higher values mean greater pressure, fragility, vulnerability or systemic exposure. For example, unemployment pressure, inflation pressure, financial-spread pressure, liquidity gap, income fragility, corridor exposure, transition pressure and shock intensity are typically oriented so that larger values increase the stress score. By contrast, GDP per capita, social protection, fiscal buffers, liquidity resilience, smoothing capacity and institutional absorption capacity are usually capacity variables; if they are used in a pressure index, they must be inverted or complemented.

Table 4.4.2. Directional harmonization rules by variable family

Variable family	Raw economic meaning	Transformation rule	Main chapters affected
Inflation, unemployment, sovereign-spread, liquidity gap, shock variables	Higher raw value generally indicates higher stress.	Direct normalization: Stress = N(x).	Navier-Stokes, Riemann/Zeta, Perelman/Ricci/Poincare
GDP per capita, income depth, fiscal buffers, social protection, liquidity buffers, smoothing capacity	Higher raw value generally indicates stronger capacity or lower fragility.	Inverse normalization: Stress = 100 - N(x), or retain as resilience if not aggregated into stress.	Perelman/Ricci/Poincare, BSD, Navier-Stokes, Hodge
Projected growth and transition GDP	May indicate momentum, overheating, transition pressure or rank support depending on the model.	Direction must be declared before aggregation.	Hodge, BSD, Yang-Mills
Corridor exposure and bridge role	Higher exposure may indicate systemic relevance and vulnerability, not merely economic size.	Normalize separately so small-output corridor nodes are not erased.	Hodge, Yang-Mills, BSD
Zeta-cycle deviation	Positive/negative deviation defines upward/downward forecast correction, not generic stress by itself.	Use signed deviation from neutrality and alpha-calibrated correction.	Riemann/Zeta

Beta, volatility and covariance	Higher beta or volatility affects risk geometry; direction depends on expected return and portfolio diversification.	Use CAPM return, covariance matrix and Sharpe/objective scaling; do not force into 0-100 stress logic.	P vs NP
Network centrality, degree, edge weight, Laplacian spectrum	Higher values may indicate transmission capacity, bridge exposure or structural rank support.	Normalize only after the role is defined: centrality, exposure, resilience or fragility.	Hodge, Yang-Mills, BSD, Perelman/Ricci/Poincare

Source: Author synthesis of the directional rules required by the seven study designs.

4.4.4. Study-Level Normalization and Scaling Matrix

Table 4.4.3 is the central comparative table of this section. It identifies the normalization object, scaling method, direction rule, final constructed variables and claim boundary for each study. The table also clarifies that the monograph does not impose one mechanical transformation on all chapters. Instead, it uses a common normalization doctrine adapted to the empirical structure of each problem.

Table 4.4.3. Normalization, scaling and directional harmonization across the seven studies

Study	Raw empirical object	Main scaling protocol	Directional rule	Final constructed variables	Claim boundary
Perelman/Ricci/ Poincare	Ten macro-regions, 2010-2024, sixteen stress-coordinate variables.	0-100 pressure-oriented stress scale; standardized coordinates for metric construction; normalized Ricci-flow and curvature summaries.	Higher value means higher inequality pressure or weaker smoothing capacity after inversion where needed.	Pressure index, metric tensor, Ricci-style curvature, scalar curvature, Perelman F/W functionals, graph-topology diagnostics.	Diagnostic manifold and inequality-curvature measurement; not literal Riemannian geometry or theorem proof.
Hodge	Ten regional nodes plus World normalization anchor; public macroeconomic anchors transformed into weighted graph and directed edge field.	World-anchor scaling, regional normalization, edge-weight scaling, anti-symmetric directed pressure construction and component-energy shares.	Direction is defined on edges: positive/negative pressure reflects relative macro-flow pressure rather than observed bilateral transactions.	Gradient hierarchy, curl/local imbalance, harmonic circulation, resilience, tail risk and persistent-homology diagnostics.	Regional benchmark and topological macro-flow measurement; not official Hodge indicators or full dyadic-flow evidence.
Navier-Stokes	100-country annual panel, 2010-2024, with world, regional, rolling and	Nondimensional starred variables; min-max baseline; z-score and robust IQR scaling for robustness;	All stress terms must be directionally harmonized before entering pressure, friction, shock,	Liquidity velocity weakness, acceleration pressure, pressure gradients, friction/diffusion,	Macro-financial stress-testing architecture; not literal

	quarterly robustness layers.	stress/resilience aggregation.	cycle or closure equations.	stochastic shock, GDP-cycle forcing, restricted epsilon closure, systemic stress S*.	fluid mechanics, theorem proof, causal law or universal crisis forecast.
Yang-Mills	Ten-node, twenty-seven-edge global/corridor finite-network benchmark plus N=1,500 validation pathway.	Normalized systemic-stress field; corridor-weighted graph; stress-weighted adjacency; normalized transition threshold and spectral diagnostics.	Stress is a composite of macro size, transition pressure, income fragility and corridor exposure; higher stress intensifies gauge/curvature/action exposure.	Gauge potential, triangular curvature, Yang-Mills economic action, stress Laplacian, finite-network mass gap, EMGI, fragility, BridgeStress.	Finite weighted-graph mass-gap benchmark; not solution of the mathematical Yang-Mills problem and not final country-panel causality.
Birch-Swinnerton-Dyer	World anchor plus ten macro-regional/corridor nodes; N=150 closure layer.	General min-max normalization, share-normalized mass exposure, inverse-fragility normalization, normalized stress score and rank-scale calibration.	Higher values indicate pressure, corridor exposure, local friction or rank support depending on the constructed layer.	Economic curve coefficients, finite-state traces, Euler factors, L-function analogue, LOrder, structural rank, regulator/friction/torsion and BridgeStress.	Local-to-global structural-rank calibration; not proof or empirical test of the classical BSD conjecture.
Riemann/Zeta	Annual, quarterly and monthly validation layers: N=55, N=45, N=20, N=100 and N=240.	Composite pressure normalization, nonlinear tau scaling, normalized zeta-cycle, deviation from neutrality, alpha/lambda calibrated forecast correction.	Signed correction rule: positive zeta deviation supports upward forecast adjustment; negative deviation supports downward or mild correction.	FPAS baseline, FPAS+zeta forecast, zeta deviation, correction term, F_zeta, W_zeta, spectral/regime diagnostics.	Forecast validation and stress-cycle diagnostics; not Riemann Hypothesis proof, causal inflation law or universal forecast dominance.

P vs NP	94 U.S. industry portfolios; K=10 baseline; exact reduced C(20,6) benchmark.	Risk-return scaling through CAPM expected returns, beta, volatility, covariance/correlation matrices, Sharpe proxy and objective normalization for algorithm comparison.	Direction is performance/risk-adjustment oriented, not stress-only: higher Sharpe is better only under specified covariance, constraints and return assumptions.	CAPM mu, covariance geometry, eigenvalue diagnostics, Sharpe objective, support-space size C(n,K), algorithmic performance metrics, option-overlay risk scaling.	Empirical-computational optimization evidence; not proof of P vs NP, not full n=94 certified optimum and not realized investment dominance.

Source: Author synthesis based on the methodology, results and claim-boundary logic of the seven manuscripts.

4.4.5. Perelman/Ricci/Poincare: 0-100 Stress Coordinates before Metric and Curvature Construction

The Perelman/Ricci/Poincare-inspired inequality chapter is the clearest example of 0-100 stress-coordinate normalization. Its raw inputs include heterogeneous macro-social and inequality-related variables such as income inequality, productivity, unemployment, investment, inflation, migration, education, mobility, logistics, capital-flow pressure, innovation, health, fiscal deficit, openness, social protection and technology access. These variables cannot form a diagnostic manifold in raw units. The methodology therefore converts them into a common pressure-oriented coordinate system.

The key methodological rule is that pressure variables are transformed so that larger values indicate greater inequality pressure, while smoothing-capacity variables are reverse-transformed when higher raw values imply lower stress. This is why the model can later estimate a correlation-based metric tensor, Ricci-style component curvature, scalar curvature, Perelman-type F and W functionals and graph-topological connectedness diagnostics. The 0-100 transformation is not merely a presentation device; it is the coordinate system that makes the geometric analogy auditable.

(4.4.9) StressCoordinate_jrt = N(x_jrt) for pressure variables and StressCoordinate_jrt = 100 - N(x_jrt) for smoothing-capacity variables.

(4.4.10) Z_jrt = (StressCoordinate_jrt - mean_j) / sd_j, used for standardized metric and correlation geometry.

The evidentiary implication is strict. Because the stress coordinates are constructed variables, the curvature and entropy-like results must be interpreted as diagnostic quantities. They can identify crisis deformation, smoothing recovery, component concentration and network connectedness, but they do not become literal geometric invariants and do not prove the Poincare conjecture, Ricci-flow theorem or Perelman proof.

4.4.6. Hodge: Scaling Node Attributes into a Directed Edge Cochain

The Hodge chapter begins from official public macroeconomic anchors: regional GDP, world-output share, projected growth, transition GDP and income depth. The World row is used as a normalization anchor and the ten regional nodes define the benchmark graph. The normalization challenge is different from the Perelman/Ricci/Poincare chapter: here the final mathematical object is not a 16-variable coordinate system but a directed macro-flow pressure field defined on graph edges.

The Hodge transformation has three stages. First, node-level macroeconomic attributes are placed on a comparable regional scale. Second, edge weights are constructed through gravity-style and corridor-sensitive logic, so that regional mass, proximity, growth and corridor relevance influence the graph. Third, the model constructs an anti-symmetric directed edge cochain. This cochain is suitable for discrete Hodge decomposition into gradient, curl and harmonic components.

(4.4.11) w_ij = Scale[Gravity(mass_i, mass_j, corridor_ij, proximity_ij, interaction_ij)].

(4.4.12) f_ij = -f_ji, where f_ij is the author-calculated directed macro-flow pressure on edge (i,j).

(4.4.13) EnergyShare_k = ||component_k||^2 / ||f||^2, for k in {gradient, curl, harmonic}.

Directional harmonization in the Hodge study is edge-based rather than variable-only. A positive edge signal does not mean an observed bilateral trade flow, a capital-flow matrix or an input-output coefficient. It means that the constructed macro-

flow pressure is oriented from one regional node toward another according to the declared formula. This distinction preserves the claim boundary: the chapter measures a topological pressure field, not an official flow database.

4.4.7. Navier-Stokes: Nondimensional Starred Variables and Unit-Consistency Discipline

The Navier-Stokes chapter requires the strongest unit-consistency discipline in the monograph. Its empirical object is a 100-country annual panel over 2010-2024, and its constructed stress-balance architecture combines inflation, sovereign-risk proxies, liquidity/friction indicators, GDP-cycle deviations, shock variables, resilience buffers and closure-state variables. These variables have incompatible units, so they cannot appear together unless converted into nondimensional model-scale variables.

The chapter therefore uses starred notation to mark variables that have been directionally harmonized and scaled. Pressure terms, friction/diffusion terms, stochastic shocks, Fourier GDP-cycle forcing and restricted hidden-adjustment closure are all interpreted as unit-free diagnostic components. The purpose is not to claim physical hydrodynamic identity. It is to create a coherent macro-financial stress-testing equation in which all terms have been made comparable at the model level.

(4.4.14) X*_itk = N(X^stress_itk) for stress-amplifying variables.

(4.4.15) R*_itm = N(X^res_itm) for resilience variables retained as capacity, or 100 - N(X^res_itm) when converted into pressure.

(4.4.16) S*_it = Omega_v v*_it + Omega_a a*_it + Omega_P gradP*_it + Omega_mu Diffusion*_it + Omega_shock Shock*_it + Omega_cycle Cycle*_it + Omega_eps epsilon*_it.

The Navier-Stokes normalization protocol also requires temporal and panel discipline. Annual and quarterly data must be harmonized before validation. Rolling forecast windows must be separated from forecast years. Robustness checks may use z-score or robust IQR scaling to test whether conclusions depend on the baseline min-max transformation. The final claim is therefore a nondimensional macro-financial stress-testing claim, not a literal statement that liquidity is a physical fluid.

4.4.8. Yang-Mills: Normalized Systemic Stress, Gauge Potential and Spectral Scaling

The Yang-Mills chapter uses a finite-network scaling logic. Public macroeconomic anchors and corridor-coded transformations are converted into a normalized systemic-stress field over a ten-node, twenty-seven-edge benchmark. The stress field then enters a corridor-weighted graph, a stress-weighted adjacency matrix, an anti-symmetric gauge potential, triangular curvature, Yang-Mills economic action and a weighted stress Laplacian.

The normalization rule is crucial because the mass-gap result is a spectral property of the constructed stress-weighted graph. If the stress field were not scaled and directionally harmonized, the Laplacian eigenvalues would be dominated by arbitrary units rather than by the economic stress geometry. The normalized transition threshold and the first positive eigenvalue therefore depend on a transparent sequence: public anchor -> normalized stress field -> corridor-weighted adjacency -> stress Laplacian -> spectral mass gap.

(4.4.17) Stress_i = N(weighted composite of mass exposure, transition pressure, income fragility and corridor exposure).

(4.4.18) W^S_ij = W_ij * Phi(Stress_i, Stress_j), where W_ij is the corridor-weighted edge strength and Phi is the stress interaction rule.

(4.4.19) L^S = D^S - W^S, with 0 = lambda_0 <= lambda_1 <= ... <= lambda_{n-1}.

(4.4.20) Economic mass gap = lambda_1 > 0 in the finite weighted-graph benchmark sense.

Directional harmonization means that larger stress scores intensify systemic exposure, but the interpretation is not GDP-only. A smaller corridor node may receive a high stress score if corridor exposure and fragility are strong. This is why the Yang-Mills chapter can distinguish output-mass centers from corridor-sensitive bridge nodes. The claim remains bounded: the mass gap is a finite-network spectral separation, not the mathematical Yang-Mills existence and mass-gap theorem.

4.4.9. Birch-Swinnerton-Dyer: Share-Normalized Mass, Inverse Fragility and Rank-Scale Calibration

The BSD chapter provides one of the most explicit normalization sequences in the monograph. It begins with the World anchor and ten regional/corridor nodes, then transforms public macro-regional anchors into mass exposure, growth-gap pressure, income-fragility pressure, transition momentum, corridor exposure and a normalized systemic-stress score. The methodology uses share-normalized mass, general min-max scaling and inverse-fragility normalization.

(4.4.21) M_rt = 100 * (m_rt - min_R m_rt) / (max_R m_rt - min_R m_rt).

(4.4.22) N(x_rt) = 100 * (x_rt - min_R x_rt) / (max_R x_rt - min_R x_rt).

(4.4.23) IFP_rt = 100 - N(GDPpc_rt).

(4.4.24) sigma*_rt = w_M M_rt + w_G GGP_rt + w_I IFP_rt + w_T TMP_rt + w_C CE_rt, with sum of weights equal to 1.

(4.4.25) Stress_rt = 100 * (sigma*_rt - min_R sigma*_rt) / (max_R sigma*_rt - min_R sigma*_rt).

This normalization layer is not a GDP ranking. It deliberately keeps corridor exposure and income fragility as separate stress channels so that regions such as the Caucasus and Central Asia remain visible even when their output mass is small. After normalization, the BSD chapter maps the stress and regional variables into economic curve coefficients, discriminant diagnostics, finite-state trace analogues, Euler-factor analogues, an economic L-function, an LOrder measure and structural-rank calibration. The methodological risk is circularity; the safeguard is lineage discipline, anti-circularity testing, sensitivity checks and explicit separation between constructed calibration and external validation.

4.4.10. Riemann/Zeta: Normalized Cycle, Signed Correction and Layered Forecast Scaling

The Riemann/Zeta chapter uses normalization in a forecast-diagnostic rather than a regional-stress-network setting. The raw target is global inflation, while the constructed objects include a composite global inflation-pressure index, a nonlinear macro-financial tau argument, a normalized zeta-cycle, a zeta deviation from neutrality, an alpha-weighted correction and the hybrid FPAS+zeta forecast. The key point is that the zeta function is not used as a theorem-level object. It is converted into a real-valued, normalized and signed computational signal.

(4.4.26) CP_t = WeightedComposite[N(inflation pressure), N(growth stress), N(unemployment pressure), N(policy tightness), N(liquidity gap), N(financial stress), N(supply stress), N(zeta resonance)].

(4.4.27) tau_t = g(CP_t, shock anchors, macro-financial state variables).

(4.4.28) zeta_t = Norm(Real-valued zeta-cycle channel evaluated at tau_t).

(4.4.29) d_t = zeta_t - zeta_bar.

(4.4.30) pi_hat^Z_t = pi_hat^F_t + alpha * lambda_zeta * d_t.

Directional harmonization in this chapter is a sign audit. Positive deviations from neutrality support upward corrections to the FPAS baseline; negative deviations support downward or mild corrections. The model is credible only if the correction sign and magnitude are transparent year by year and if forecast improvement survives layered validation. This is why the N=20 crisis-era layer is not allowed to carry the entire claim; the N=55, N=45, N=100 and N=240 layers protect the result against compact-window overfitting. The final claim is forecast-diagnostic improvement, not proof of the Riemann Hypothesis or universal forecast dominance.

4.4.11. P vs NP: Risk-Return Scaling, Covariance Geometry and Optimization Metrics

The P vs NP portfolio-optimization chapter is methodologically different from the six macro-system chapters. It does not primarily normalize variables onto a 0-100 stress scale. Instead, it scales financial inputs into a risk-return and covariance geometry suitable for sparse support selection. The empirical universe consists of 94 U.S. industry portfolios. CAPM-implied expected returns are constructed from beta, the risk-free rate and the equity-risk premium; risk is evaluated through volatility, covariance and correlation geometry; and performance is compared through Sharpe-type objectives, algorithmic search metrics and exact reduced benchmarking.

(4.4.31) mu_i = R_f + beta_i * ERP.

(4.4.32) Sharpe_i = (mu_i - R_f) / sigma_i.

(4.4.33) Sharpe_p = (w^T mu - R_f) / sqrt(w^T Sigma w).

(4.4.34) SupportSpace(n,K) = C(n,K), with the baseline full universe C(94,10) and the exact reduced benchmark C(20,6).

Directional harmonization in this chapter is performance-and-risk oriented. Higher expected return is not automatically better if it comes with higher volatility, stronger covariance concentration or unstable leverage exposure. Higher Sharpe is a model-implied objective value, but it remains conditional on CAPM priors, covariance specification, weight constraints, transaction costs and derivative-overlay assumptions. The chapter therefore uses scaling to compare algorithms and portfolio supports, not to claim theorem proof or realized investment dominance.

4.4.12. Cross-Study Scaling Safeguards and Reviewer-Facing Audit Rules

A unified monograph requires more than listing transformations. It requires an audit protocol showing how the author prevents numerical artefacts, sign errors, scaling leakage and overclaiming. Table 4.4.4 defines the mandatory audit questions for every problem chapter. These questions should be used both in the methodology chapter and in the replication packages.

Table 4.4.4. Normalization and directional-harmonization audit checklist

Audit domain	Question	Required methodological result
Scale identity	What is the exact scale: 0-100, starred unit-free, standardized, signed deviation, ratio, covariance or eigenvalue?	The reader can identify what each number means.
Comparison universe	Is min-max scaling performed across regions, countries, years, layers, assets or edges?	The denominator of normalization is explicit and replicable.
Direction rule	Does a higher value mean higher stress, lower capacity, stronger resilience, higher rank support, larger correction or better optimization?	No variable enters a composite index with the wrong sign.
Inversion rule	Were capacity variables inverted when converted into pressure?	Resilience and capacity do not mechanically inflate stress.
Outlier rule	Were winsorization, robust IQR scaling or sensitivity checks used where extreme values could dominate?	Results are not driven by one unexamined raw-unit outlier.
Layer consistency	Are annual, quarterly, monthly, regional, country-level and benchmark layers kept separate?	High-frequency or panel evidence is not misread as if it came from the same sample.
Constructed-variable lineage	Can each author-calculated variable be traced back to public inputs and formulas?	Replication packages can reproduce the reported outputs.
Validation isolation	Are variables with deterministic overlap prevented from being treated as independent external validation?	The study avoids circularity and evidence double counting.
Claim gate	Does the transformation define what can be claimed and what must be excluded?	Scaling supports measurement; it does not solve the original mathematical problem.

Source: Author synthesis for monograph-level replication discipline.

4.4.13. Comparability without False Equivalence

The normalization layer makes variables comparable inside each study, but it does not make every number equivalent across all seven studies. This distinction is essential for the book. A Perelman/Ricci/Poincare pressure score of 70, a BSD stress score of 70, a Yang-Mills node stress of 70 and a Riemann/Zeta composite pressure value of 70 are not identical empirical objects. They share a 0-100 grammar, but each is anchored to its own universe, formula and validation layer. Similarly, a Navier-Stokes starred pressure variable and a P vs NP Sharpe ratio are not 0-100 stress scores at all.

The correct monograph-level interpretation is therefore structured comparability, not numerical identity. The reader may compare the methodological role of normalization across chapters: all chapters discipline raw data, harmonize signs, construct author-calculated variables and audit claims. The reader may not treat normalized values from different chapters as if they were drawn from one common universal index unless the book later constructs a separate meta-index with its own formula and validation rule.

Table 4.4.5. Scaling pitfalls and methodological safeguards

Potential pitfall	Risk	Safeguard
False cross-chapter equality	Treating a 0-100 stress score in one chapter as numerically identical to a 0-100 score in another chapter.	State that each score is normalized within its own empirical universe and formula.
Sign inversion error	Adding GDP per capita, fiscal buffers or resilience as if higher values increased stress.	Apply complement transformation or retain the variable in a separate resilience channel.
Residual plug risk	Using a constructed correction, epsilon term or zeta signal as an unexplained device that forces model fit.	Report formula, sign audit, magnitude audit and validation gates.
Circular validation	Testing a constructed variable against	Separate internal calibration, robustness

	another variable generated from the same components and treating the result as external evidence.	checks and external-proxy screening.
Unit inconsistency	Combining inflation, spreads, GDP deviations and volatility shocks in original units.	Use nondimensional starred variables and robustness scaling.
Compact-window overclaiming	Letting a small validation window dominate the forecast claim.	Use layered samples and demote compact windows to display/comparison status.
Optimization-scale confusion	Treating CAPM-Sharpe ranking as the same as global portfolio optimality.	Distinguish stand-alone screening from covariance-aware mixed discrete-continuous optimization.
Theorem-level overreach	Interpreting normalized economic analogues as proofs of Millennium Problems.	Preserve the book-wide claim boundary at the end of every transformation chain.

Source: Author synthesis for claim-disciplined monograph construction.

4.4.14. Replication Package Requirements for Normalization and Scaling

For the monograph to be technically credible, normalization cannot remain only a verbal description. The replication packages should preserve every transformation step. Each study should include a source ledger, raw input table, cleaned input table, direction map, normalization formula sheet, transformed-variable table, component-composite table, validation outputs, and checksum or file-hash records where available. This is particularly important because most of the monograph's evidence consists of author-calculated variables derived from public anchors.

Table 4.4.6. Required replication materials for normalization, scaling and harmonization

Replication item	Content required	Primary relevance
Raw input ledger	Original public/public-anchor input families, units, frequency, coverage and extraction notes.	All seven studies.
Variable-direction map	For each input, indicate pressure, capacity, resilience, rank support, correction, risk or objective direction.	Especially Perelman/Ricci/Poincare, Navier-Stokes, BSD, Riemann/Zeta.
Normalization formula sheet	Exact min-max, inverse, z-score, robust scaling, nondimensionalization, signed deviation or Sharpe/covariance formula.	All seven studies.
Intermediate transformed table	Variables after scaling but before aggregation or mathematical transformation.	All studies with composite variables.
Composite construction file	Weights, component values, audit intervals, sensitivity alternatives and final constructed score.	Perelman/Ricci/Poincare, Yang-Mills, BSD, Riemann/Zeta, Navier-Stokes.
Network/matrix output	Adjacency, stress-weighted adjacency, Laplacian, Hodge cochain, metric tensor or covariance matrix.	Hodge, Yang-Mills, BSD, Perelman/Ricci/Poincare, P vs NP.
Sign and magnitude audit	Correction signs, shock scenario signs, pressure/capacity inversion checks and portfolio objective checks.	Riemann/Zeta, Navier-Stokes, Yang-Mills, P vs NP.
Robustness alternatives	Alternative scaling, weighting, covariance, filtered graphs, placebo or sensitivity settings.	All seven studies.
Claim-boundary log	Explicit statement of what the normalized variables support and what they cannot support.	All seven studies and the monograph front matter.

Source: Author synthesis aligned with the replication-discipline logic of Chapter 4.

4.4.15. Section Synthesis: The Common Measurement Grammar of the Monograph

The normalization, scaling and directional-harmonization layer is one of the main reasons the seven studies can function as a monograph rather than as a loose article collection. The studies differ in empirical universe, mathematical analogy, sample structure, validation design and final output; however, they share the same technical discipline. Each begins with public or auditable inputs. Each separates raw anchors from author-calculated variables. Each converts heterogeneous data into a declared model scale. Each harmonizes direction before aggregation or mathematical transformation. Each validates the transformed outputs through robustness, placebo, benchmark, econometric, spectral, topological or algorithmic checks. Each ends with a claim boundary.

The section also clarifies where the monograph must avoid false equivalence. A 0-100 stress score is not a universal number unless the same universe, denominator, component weights and validation rules are used. A starred Navier-Stokes variable is unit-free but not automatically comparable to a BSD stress score. A zeta correction is a signed forecast adjustment, not a generic stress index. A CAPM-Sharpe proxy is a risk-adjusted financial screening statistic, not a curvature or pressure variable. This disciplined distinction makes the book stronger: it allows the author to build an ambitious unified methodology without erasing the methodological specificity of each Clay-inspired analogue.

Accordingly, Section 4.4 supplies the technical normalization doctrine for the remainder of Chapter 4. It prepares the reader for the following methodological layers: network and graph construction, panel and time-series validation, robustness and placebo logic, replication packages and final claim-boundary discipline. In this sense, scaling is not a secondary preprocessing step; it is a core evidentiary gate of the monograph.

4.5. Network and Graph Construction Protocol

This section defines the common protocol through which the monograph constructs, interprets and validates network and graph objects. The network layer is one of the central technical bridges between the seven Clay-inspired economic analogues. It is most explicit in the Yang-Mills, Hodge, Birch-Swinnerton-Dyer and Perelman/Ricci/Poincare chapters, where nodes, edges, weights, adjacency matrices, Laplacians, cycles, curvature proxies, centrality and topological connectedness are operational parts of the model. It is indirect but still methodologically relevant in the Navier-Stokes, Riemann/Zeta and P vs NP chapters, where flow-balance, frequency-domain dependence and covariance/correlation geometry perform an analogous structural function without becoming regional graph models in the strict sense.

The chapter therefore treats graph construction not as illustration but as a formal data transformation. A graph is admissible only if its node set, anchor treatment, edge rule, weight rule, direction rule, matrix representation, adequacy tests and claim boundary are specified before results are interpreted. In this monograph, a network figure is never sufficient evidence by itself. The empirical claim must pass through reproducible construction: public-data anchors are converted into normalized or nondimensional research variables; those variables define nodes, edges and weights; matrices are built; graph diagnostics are computed; robustness and placebo variants are checked; and the final claim is bounded as measurement, diagnostic validation or computational evidence rather than theorem-level proof.

The key reviewer-safety distinction is this: official/public macroeconomic variables do not automatically create a graph, and a graph does not automatically create causal evidence. GDP, GDP per capita, growth, transition GDP, inflation, financial stress, corridor exposure, covariance, zeta-cycle and industry volatility are input or intermediate variables. The final graph objects--weighted adjacency matrices, directed edge-pressure cochains, stress Laplacians, curvature/action terms, Betti numbers, centrality ranks, BridgeStress values, covariance eigenmodes and cycle diagnostics--are author-calculated analytical constructs. Their meaning is therefore determined by the declared protocol and by the validation layer attached to them.

4.5.1. Methodological Role of Networks in the Unified Monograph

Network construction performs five functions in the monograph. First, it converts isolated economic units into an interacting system. Second, it supplies the mathematical object required for Hodge decomposition, gauge curvature, mass-gap diagnostics, local-to-global rank formation and Poincare-style connectedness tests. Third, it prevents corridor-sensitive nodes from disappearing inside large aggregates: a small output-mass node may become visible when edge position, bridge exposure, stress interaction and centrality are measured. Fourth, it gives the validation chapter an auditable structure because alternative graph filters, leave-one-node tests and randomized-network placebos can be applied. Fifth, it imposes claim discipline: graph evidence can support structural measurement and diagnostic interpretation, but it cannot by itself prove a Millennium Problem, prove causality or certify policy effects.

Table 4.5.1. Methodological functions of network construction in the monograph

Function	Technical meaning	Main implementation	Claim boundary
System representation	The empirical object is treated as an interacting structure rather than a list of indicators.	Hodge regional graph; Yang-Mills stress network; BSD regional/corridor graph; Perelman/Poincare thresholded metric graph.	Permits structural measurement, not theorem proof.
Visibility of corridor nodes	Small-output nodes can be retained if corridor position or bridge exposure is analytically relevant.	Caucasus and Central Asia in Hodge, Yang-Mills and BSD.	Corridor visibility is not GDP equivalence or geopolitical ranking.
Mathematical admissibility	Hodge, Laplacian, curvature, cycle and spectral tools require defined nodes, edges, weights and matrices.	Adjacency W, stress-weighted adjacency W^S, graph Laplacian L, Hodge Laplacian L_1, thresholded correlation graph.	A graph must be connected and adequately dense before cycle or spectral claims are read strongly.
Validation platform	Graph perturbation, edge filtering, leave-one-out and randomized-network placebo become possible.	Yang-Mills filtered graphs; Hodge persistent-homology checks; BSD permutation and anti-circularity screens; Ricci/Poincare graph-topology diagnostics.	Robustness within a benchmark does not automatically imply external causal validation.
Evidence hierarchy	Different graph outputs support different claim levels.	Centrality, BridgeStress, mass gap, curvature/action, Betti numbers, covariance eigenmodes, Hodge energy shares.	Measurement and diagnostic evidence must remain separated from causal and theorem-level claims.

Source: Author synthesis based on the network, topology, flow and covariance structures of the seven manuscripts.

4.5.2. Common Graph Ontology: Nodes, Anchors, Edges, Weights and Matrices

The unified graph ontology begins by separating anchors from nodes. A World row may be necessary for normalization, scale consistency or global benchmarking, but it is not automatically a competing regional node. This distinction is especially important in the Hodge and BSD chapters, where the World anchor fixes scale while the ten regional or corridor nodes carry the network analysis. In Yang-Mills, the finite stress network is built directly over ten global/corridor nodes and twenty-seven weighted undirected edges. In Perelman/Ricci/Poincare, the node set may be variable-based rather than region-based: a thresholded metric/correlation matrix transforms stress coordinates into a graph of connected diagnostic dimensions. In P vs NP, the covariance and correlation matrices are not a corridor graph, but they are still a dependence network over industries because the off-diagonal covariance entries define how assets co-move.

The edge rule must always be stated before graph statistics are interpreted. Edges may represent corridor adjacency, macro-flow proximity, stress interaction, coefficient similarity, metric correlation, covariance dependence or algorithmic support interaction. These edges do not necessarily represent observed bilateral trade, observed financial transactions or physical flows. Their status must therefore be recorded as author-calculated graph edges unless the source data directly observe dyadic relationships.

Formula (4.5.1). Weighted graph: G = (V, E, W), where V is the node set, E is the edge set and W = [w_ij] is the weighted adjacency matrix.

Formula (4.5.2). Adjacency rule: A_ij = 1 if an admissible relation between i and j is retained; A_ij = 0 otherwise.

Formula (4.5.3). Weighted adjacency: W_ij = A_ij * omega_ij, where omega_ij is the declared edge-intensity rule.

Formula (4.5.4). Graph density: delta(G) = 2|E| / (|V|(|V|-1)) for an undirected simple graph.

Formula (4.5.5). Weighted degree: deg_i^w = sum_j W_ij; normalized centrality may be defined as C_i = N(centrality_i).

Formula (4.5.6). Graph Laplacian: D_ii = sum_j W_ij and L = D - W.

Formula (4.5.7). Spectral ordering: 0 = lambda_0 <= lambda_1 <= ... <= lambda_{n-1}; for a connected graph, lambda_1 > 0 under the zero-index convention used for the first nonzero mode.

Formula (4.5.8). Cycle rank: beta_1^graph = |E| - |V| + c, where c is the number of connected components.

Formula (4.5.9). First-order Hodge Laplacian: L_1 = B_1 B_1^T + B_2^T B_2, where B_1 is the node-edge incidence matrix and B_2 is the edge-triangle incidence matrix.

Table 4.5.2. Unified graph ontology and reviewer-safety definitions

Object	Definition	Typical implementation	Reviewer-safety rule
Node set V	The units of interaction: regions, corridor nodes, stress variables or industries.	Ten regional nodes; 16 stress-coordinate variables; 94 industries.	World anchor must not be confused with a competitive node unless explicitly declared.
Anchor	A scaling or normalization row used to fix global magnitude.	World GDP/output/income anchor in Hodge and BSD; global inflation target in Riemann/Zeta.	Anchors support scale; they are not automatically network participants.
Edge set E	Retained pairwise relations among nodes.	Corridor adjacency, gravity-style macro-flow, stress interaction, thresholded correlation, covariance dependence.	Edges are author-calculated unless based on directly observed dyadic data.
Weight W_ij	Intensity assigned to each retained edge.	Macro-flow weight, corridor factor, stress-weighted link, correlation/covariance strength, centrality weight.	Weight magnitudes depend on declared scaling and cannot be read as raw trade or transaction volumes.
Direction	Whether the edge is symmetric or anti-symmetric.	Hodge directed pressure field; Yang-Mills gauge potential; undirected weighted benchmark graph.	Orientation may affect flow/curvature interpretation but not all graph statistics.
Laplacian L	Degree-minus-adjacency matrix used for connectedness and diffusion diagnostics.	Yang-Mills stress Laplacian; Hodge graph Laplacian; Poincare connectedness graph.	Spectral claims require connectedness and robustness checks.
Cycle and triangle layer	Closed paths or filled 2-simplices used for curl, curvature, action or topology.	Hodge curl triangles; Yang-Mills triangular curvature/action; BSD triangular-action and scenario layers; Poincare Betti diagnostics.	Cycles support structural interpretation, not causal proof.
Validation layer	Robustness checks applied to graph construction.	Filtered graphs, randomized-network placebo, leave-one-node/corridor exclusion, perturbation, persistent-homology stability.	Benchmark stability must be separated from universal external validation.

Source: Author synthesis for Chapter 4.5.

4.5.3. General Network Construction Algorithm for the Monograph

The following algorithm is the unified protocol that should govern every graph-based chapter in the monograph. It does not replace the specific methodology of each study; rather, it states the common audit sequence that makes those methodologies comparable. A chapter may stop at a covariance, spectral or flow-balance object if it is not a graph chapter in the strict sense, but it should still disclose how relational structure is defined.

Algorithm 4.5.1. Unified graph construction and audit protocol

1. Define the empirical universe and determine whether the unit is a region, corridor node, variable, industry or time layer.
2. Separate normalization anchors from network nodes; keep the World anchor outside competitive node calculations unless explicitly justified.

3. Specify the edge rule before any graph is drawn: corridor adjacency, gravity-style macro-flow, stress interaction, metric correlation, covariance dependence, finite-state relation or threshold rule.
4. Specify whether the graph is undirected, directed or anti-symmetric. If the graph is directed, define the sign convention for the directed edge variable.
5. Construct the weighted adjacency matrix W and retain a source-to-transformation ledger that identifies public anchors and author-calculated edge weights.
6. Construct any secondary matrix required by the problem: stress-weighted adjacency W^S, incidence matrices B_1 and B_2, Laplacian L, first-order Hodge Laplacian L_1, covariance matrix Sigma or thresholded metric matrix.
7. Test graph adequacy before interpretation: number of nodes, number of edges, density, connected components, average degree, centrality distribution, transitivity, clustering and cycle availability.
8. Compute the chapter-specific graph outputs: Hodge components, gauge potential, triangular curvature, action, spectral gap, Betti numbers, structural rank, BridgeStress, covariance eigenmodes or network-curvature proxies.
9. Run robustness and sensitivity checks: alternative thresholds, filtered graphs, perturbations, leave-one-node tests, edge-weight noise, randomized-network placebo or covariance alternatives.
10. Classify the evidence level: structural benchmark, diagnostic validation, forecast support, computational evidence, external-proxy screening or causal/econometric claim.
11. Report the claim boundary explicitly: constructed graph quantities are research variables, not official indicators and not proof of the original mathematical Millennium Problems.
12. Archive the graph inputs, matrices, formulas, scripts, seeds, figures and outputs in the replication package where applicable.

4.5.4. Cross-Study Network and Graph Construction Matrix

Table 4.5.3 is the central comparative table for this section. It shows how network logic enters all seven studies. Four chapters are direct graph/network chapters: Hodge, Yang-Mills, BSD and Perelman/Ricci/Poincare. Three chapters are indirect network or relational-structure chapters: Navier-Stokes uses a flow-balance and regional aggregation architecture rather than a graph Laplacian; Riemann/Zeta uses spectral and regime dependence over time rather than a regional graph; and P vs NP uses covariance/correlation geometry and combinatorial support space rather than corridor topology.

Table 4.5.3. Network and relational-structure construction across the seven studies

Study	Network/ relational object	Node/edge or dependency definition	Main matrices and diagnostics	Evidence role	Claim boundary
Perelman/Ricci/ Poincare	Thresholded graph from a metric/correlation structure over stress-coordinate variables and macro-regional diagnostics.	Stress coordinates, metric tensor entries, thresholded relationships among variables.	Graph Laplacian, degree, Betti numbers, Euler-type diagnostics, Ollivier-proxy and Forman-proxy edge curvature, Ricci-surgery candidates.	Graph-topological audit of inequality-pressure connectedness and deformation.	A diagnostic graph of constructed variables, not proof of the Poincare conjecture or literal Ricci flow.
Hodge	Regional macro-flow graph with ten nodes plus World anchor for normalization; directed edge-pressure field derived from public anchors and author weights.	Ten regional nodes; weighted edges from gravity-style macro-flow, corridor logic, output share, growth and income-depth relations.	Adjacency matrix, incidence matrices, graph Laplacian, first-order Hodge Laplacian, gradient/curl/harmonic decomposition, higher-order simplicial checks.	Topological decomposition of macro-flow pressure into hierarchy, local-cycle imbalance and systemic circulation.	Author-calculated pressure cochain, not observed bilateral trade or capital-flow matrix.

Navier-Stokes	Not a strict graph chapter; relational structure is represented by flow-pressure-friction-shock channels across a global panel and regional layers.	100-country panel, World and macro-regional layers, liquidity-flow variables, pressure gradients, friction/diffusion and closure states.	Nondimensional stress-balance equation, rolling validation, panel FE, external-target checks, Monte Carlo and counterfactual paths.	Flow-dynamic stress-testing and systemic-risk interpretation.	Does not claim literal physical liquidity flow or graph-theoretic mass/curvature results.
Yang-Mills	Finite global/corridor stress-transmission network with ten nodes and twenty-seven weighted undirected edges.	Public macro anchors, normalized stress scores, corridor weights and stress interactions.	Weighted adjacency W, stress-weighted adjacency W^S, anti-symmetric gauge potential A_ij, triangular curvature F_ijk, Yang-Mills economic action, stress Laplacian L^S, mass gap and EMGI.	Finite-network shock-threshold and systemic-transmission diagnostics.	Economic mass gap is finite weighted-graph spectral separation, not the mathematical Yang-Mills mass gap problem.
Birch-Swinnerton-Dyer	World-normalized regional/corridor weighted graph used for centrality, Hodge-flow, structural-rank, local-to-global and scenario layers.	Ten regional/corridor nodes; corridor-sensitive edges; stress interaction; output proximity; regional adjacency.	Weighted graph G=(R,E,W), density, degree, centrality, transitivity, clustering, curve coefficients, finite-state traces, Euler factors, L-function analogue and structural rank.	Local-to-global structural rank calibration under corridor-sensitive world-system conditions.	Constructed local reductions and L-function analogue do not test or prove classical BSD.
Riemann/Zeta	Not a regional graph; spectral network logic appears through layered time/frequency diagnostics and zeta-cycle construction.	Annual, quarterly and monthly time layers; global inflation pressure, tau argument, normalized zeta-cycle and regime states.	Fourier/wavelet coherence, spectral entropy, HMM/Markov-switching, Mincer-Zarnowitz, DM/CW forecast comparison and residual diagnostics.	Spectral-cyclical validation of a hybrid inflation forecast model.	Critical-line signal is analogical and computational; no Riemann Hypothesis proof or universal forecast dominance.
P vs NP	Not a corridor graph; dependence network is	N=94 industry universe; beta, volatility,	Sigma, rho, eigenvalue concentration,	Computational-finance optimization	Covariance dependence and search

	represented by covariance/correlation geometry and combinatorial support space.	CAPM return, covariance matrix, correlation matrix and support set Omega_K.	condition proxy, C(n,K), exact reduced enumeration, heuristic search and option-overlay risk geometry.	and coupled risk-space diagnostics.	complexity do not prove P vs NP or certify full-universe global optimality.

Source: Author synthesis based on the graph, topology, flow, spectral and covariance methodologies of the seven studies.

4.5.5. Hodge Network Construction Protocol

The Hodge chapter is the monograph's most direct topological-flow construction. Its empirical object is a regional benchmark of the world economy, not a country panel and not an observed dyadic transaction matrix. The World row supplies normalization and scale; the ten regional nodes supply the graph. The Caucasus is retained as an explicit author-defined subregional node to preserve corridor visibility. Regional GDP, world share, projected growth, transition GDP and income depth are transformed into a weighted macro-flow graph and then into a directed anti-symmetric edge-pressure field. The Hodge construction should be read as a two-stage graph protocol. First, an undirected weighted graph establishes macro-regional connectedness, edge weights, density, clustering and cycle availability. Second, a directed edge cochain is constructed over that graph and decomposed into gradient, curl and harmonic components. The first layer asks whether a graph exists with enough structure to support topological diagnostics. The second layer asks how macro-flow pressure decomposes once the graph has been declared.

Formula (4.5.10). Directed edge-pressure cochain: f_ij = -f_ji, where f_ij is an author-calculated macro-flow pressure difference over retained edge (i,j).

Formula (4.5.11). Hodge decomposition: f = grad(phi) + curl(psi) + h, where grad(phi) is hierarchy, curl(psi) is local-cycle imbalance and h is harmonic systemic circulation.

Formula (4.5.12). Energy share: ES_k = ||component_k||^2 / ||f||^2 for k in {gradient, curl, harmonic}.

Table 4.5.4. Hodge graph-construction audit trail

Protocol element	Implementation	Interpretive consequence
Node universe	Ten regional nodes; World used as normalization anchor.	Prevents country-level overclaim and keeps the graph at macro-regional scale.
Edge construction	Author-calculated gravity-style macro-flow weights and corridor logic.	Measures structured macro-flow pressure, not observed bilateral transaction flows.
Adequacy diagnostics	Nodes, edges, density, connected components, average degree, transitivity, weighted clustering.	Graph must be connected and cycle-rich enough before Hodge decomposition is substantively interpreted.
Directed cochain	Anti-symmetric edge signal constructed from output share, growth, income depth, mass-growth interaction and corridor weights.	Supplies the object decomposed by Hodge theory.
Hodge components	Gradient, curl and harmonic decomposition; energy shares; first-order Laplacian and higher-order diagnostics.	Distinguishes hierarchy, local-cycle imbalance and persistent systemic circulation.
Validation boundary	Econometric, spectral, predictive and persistent-homology tests are benchmark validation layers.	They do not convert the regional benchmark into final country-level causality.

Source: Author synthesis based on the Hodge methodology and regional results architecture.

4.5.6. Yang-Mills Finite-Network Gauge Protocol

The Yang-Mills chapter constructs a finite stress-transmission network. The completed benchmark layer uses ten global/corridor-sensitive nodes and twenty-seven weighted undirected edges. This graph is then transformed into a stress-weighted network, an anti-symmetric gauge-potential layer, triangular curvature, Yang-Mills economic action and a stress Laplacian. The finite-network economic mass gap is defined as the first positive eigenvalue of the stress Laplacian. This is a graph-spectral threshold, not a result about the mathematical Yang-Mills existence and mass gap problem.

The protocol requires a strict separation between the base graph and the stress-transformed graph. The base graph defines which regional/corridor links are admissible. The stress field assigns node pressure. The stress-weighted adjacency matrix combines edge intensity with node stress. Only after this transformation can the gauge, curvature/action and spectral layers be computed. This sequence prevents the mass-gap result from being read as a raw macroeconomic statistic.

Formula (4.5.13). Stress-weighted adjacency: W^S_ij = W_ij * psi(S_i, S_j), where S_i and S_j are normalized node-stress scores and psi is the declared stress-interaction rule.

Formula (4.5.14). Gauge potential: A_ij = -A_ji, constructed from stress differentials and weighted edge orientation.

Formula (4.5.15). Triangular curvature: F_ijk = A_ij + A_jk + A_ki over retained closed triangles.

Formula (4.5.16). Yang-Mills economic action: S_econ = sum_(i,j,k in triangles) F_ijk^2, with action concentration reported across dominant triangles.

Formula (4.5.17). Stress Laplacian and mass gap: L^S = D^S - W^S; Delta_econ = lambda_1(L^S), where lambda_1 is the first positive finite-network eigenvalue.

Table 4.5.5. Yang-Mills finite-network gauge protocol

Layer	Construction	Methodological role
Base finite graph	10 nodes and 27 weighted undirected edges.	Defines the corridor-sensitive stress-transmission structure.
Stress field	Normalized systemic-stress score from macro anchors, transition pressure, income fragility and corridor exposure.	Creates node-level pressure before gauge and spectral transformation.
Gauge potential	Anti-symmetric edge tension derived from stress differentials.	Turns scalar stress into directional edge tension.
Curvature/action	Triangular curvature and squared action over network cycles.	Measures concentration of stress-energy in closed corridor cycles.
Spectral layer	Stress-weighted Laplacian and eigenvalue spectrum.	Defines finite-network threshold between normal connected state and first transmissible stress mode.
Robustness layer	Filtered graphs, Monte Carlo perturbation, leave-one-out/corridor exclusion, randomized-network placebo and topology stability.	Distinguishes benchmark robustness from statistical exceptionalism and final country-panel causality.

Source: Author synthesis based on the Yang-Mills finite-network benchmark and validation-pathway methodology.

4.5.7. BSD Local-to-Global Regional Graph Protocol

The BSD chapter uses graph construction as the regional-system basis for local-to-global structural rank formation. The empirical universe contains a World normalization anchor and ten macro-regional/corridor nodes. The graph is not decorative: it supplies centrality, stress interaction, Hodge-flow, triangular-action, BridgeStress and scenario inputs before the BSD-inspired coefficient, discriminant, finite-state trace, Euler-factor, L-function analogue and structural-rank layers are interpreted.

The local-to-global claim requires network adequacy. If the regional graph were disconnected, too sparse or unable to support triangular/cycle diagnostics, later local trace and rank-calibration claims would be under-identified. The BSD protocol therefore requires density, connectedness, average degree, edge weight, transitivity and weighted clustering checks before the local-to-global layer is allowed to carry substantive interpretation.

Formula (4.5.18). BSD regional graph: G_BSD = (R, E, W), where R is the set of regional/corridor nodes and W encodes corridor-sensitive regional connections.

Formula (4.5.19). Edge-weight rule: w_ij = Phi(output proximity_ij, corridor link_ij, stress interaction_ij, regional adjacency_ij).

Formula (4.5.20). Centrality index: C_i = N(g(degree_i, eigenvector_i, betweenness_i)), where g is the declared centrality-combination rule.

Formula (4.5.21). Local-to-global pathway: public anchors -> stress and graph -> coefficients (a,b) -> finite-state traces -> Euler factors -> LOrder -> structural rank comparison.

Table 4.5.6. BSD graph-to-rank construction protocol

Protocol element	Implementation	Methodological consequence

World anchor	Used for scale and normalization, not as a competing regional node.	Prevents global total from distorting regional rank hierarchy.
Regional/corridor node set	Ten macro-regional/corridor units including corridor-sensitive subregions.	Defines the local units whose signals feed the global rank object.
Weighted edges	Output proximity, corridor link, stress interaction and regional adjacency.	Encodes local-to-global transmission structure.
Network adequacy	Density, connected components, average degree, transitivity and weighted clustering.	Confirms that local states belong to a connected system.
Coefficient mapping	Centrality, resilience, agentic/productive depth, stress, fragility and corridor exposure feed economic curve coefficients.	Connects graph position to the BSD-inspired curve layer.
Rank calibration	Local traces and Euler-factor analogues are compared with structural rank and LOrder.	Supports bounded measurement consistency, not proof of classical BSD.

Source: Author synthesis based on the BSD local-to-global methodology and closure architecture.

4.5.8. Perelman/Ricci/Poincare Metric-Graph Protocol

The Perelman/Ricci/Poincare chapter differs from Hodge, Yang-Mills and BSD because its graph is not primarily a corridor graph over regions. It begins with a macro-regional panel of ten regions, sixteen stress-coordinate variables and N = 150 region-year observations. After 0-100 stress-oriented harmonization, the methodology builds a metric/correlation structure among variables and then thresholds that matrix into a graph. The graph therefore represents connectedness among diagnostic stress coordinates rather than observed physical routes.

This design is essential for the Poincare-inspired part of the framework. Connectedness, degree, Betti numbers, Euler-type topology, Ollivier-Ricci proxy and Forman-Ricci proxy are not independent official indicators; they are graph-topological audits of the constructed inequality-pressure manifold. Ricci-surgery candidates are therefore ranked policy-screening objects, not literal geometric surgery operations.

Formula (4.5.22). Metric/correlation graph: A_ab(tau) = 1 if |g_ab| >= tau and A_ab(tau) = 0 otherwise, where g_ab is the metric/correlation relation between stress coordinates a and b.

Formula (4.5.23). Poincare connectedness test: beta_0 = 1 and lambda_1(L) > 0 indicate a connected diagnostic graph under the retained threshold rule.

Formula (4.5.24). Graph cycle audit: beta_1 = |E| - |V| + beta_0 for the thresholded variable graph, before any higher-order interpretation.

Formula (4.5.25). Network-curvature screen: edge_curvature_ab = proxy(A, degree_a, degree_b, local triangles), interpreted as an economic graph proxy rather than an exact geometric invariant.

Table 4.5.7. Perelman/Ricci/Poincare metric-graph construction protocol

Layer	Implementation	Interpretive role
Stress-coordinate system	Sixteen variables transformed to a common stress-oriented scale.	Creates comparable diagnostic coordinates.
Metric tensor / correlation structure	Pairwise relationships among stress coordinates.	Defines the economic manifold-like object.
Thresholded graph	Retain links above the declared threshold.	Converts metric structure into a graph for connectedness and topology diagnostics.
Laplacian and connectedness	Graph Laplacian, algebraic connectivity and no-isolated-node checks.	Tests whether the constructed diagnostic system is one connected object.
Betti/Euler diagnostics	Cycle and topological-hole counts.	Audits whether inequality pressure contains looped/cyclic structure.
Ollivier/Forman proxies	Edge-curvature screens over the thresholded graph.	Identifies fragile, embedded or bottleneck-like variable relations.
Ricci-surgery ranking	Ranks candidate variables by curvature contribution and network embeddedness.	Policy-screening analogue only; not literal topological surgery.

Source: Author synthesis based on the Perelman/Ricci/Poincare graph-topological methodology.

4.5.9. Indirect Network Comparators: Navier-Stokes, Riemann/Zeta and P vs NP

Although the title of this section names Yang-Mills, Hodge, BSD and Ricci/Poincare as the core graph chapters, the monograph must still account for Navier-Stokes, Riemann/Zeta and P vs NP. These three studies should not be forced into the same regional graph template. Their methodological relation to network construction is indirect: Navier-Stokes uses a flow-balance architecture across countries and regions; Riemann/Zeta uses spectral and regime dependence over time; P vs NP uses covariance/correlation dependence among industries and combinatorial support-space geometry.

Table 4.5.8. Non-graph and indirect-graph comparators in the unified methodology

Study	Direct graph status	Relational structure	Relevant diagnostics	Boundary rule
Navier-Stokes	No finite regional graph is required for the main claim.	Panel flow-pressure-friction-shock-cycle-closure architecture; macro-regional layers support interpretation.	Pressure gradients, liquidity friction/diffusion, Fourier GDP-cycle forcing and restricted closure create relational stress channels.	Do not report graph Laplacian, Betti or mass-gap conclusions unless a separate graph extension is built.
Riemann/Zeta	No regional graph is required for the main forecast claim.	Layered time-frequency validation; spectral relations among zeta-cycle, inflation pressure and regimes.	Fourier/wavelet coherence, spectral entropy and HMM/Markov-switching act as temporal dependence diagnostics.	Do not describe spectral diagnostics as network topology or RH evidence.
P vs NP	No corridor graph is required for the optimization claim.	Industry dependence is carried by covariance/correlation matrices and eigenvalue concentration.	The covariance matrix creates a coupled risk geometry; support-space Omega_K creates combinatorial search structure.	Do not treat covariance heatmaps as regional networks or search complexity as theorem proof.

Source: Author synthesis based on the Navier-Stokes, Riemann/Zeta and P vs NP methodologies.

The Navier-Stokes chapter is therefore the monograph's flow-field comparator rather than a graph-Laplacian chapter. Its relational structure emerges from the interaction of country-year stress channels and macro-regional aggregation. The Riemann/Zeta chapter is the spectral-cyclical comparator: dependence is allocated across annual, quarterly and monthly layers and tested through forecast, regime and frequency-domain diagnostics. The P vs NP chapter is the covariance-complexity comparator: the dependence object is the covariance matrix, the correlation matrix and the eigenvalue spectrum, while the discrete search object is the combinatorial support space. Together, these three chapters show that not every structural relation in the monograph must be a corridor graph. The general protocol is broader: define the relational object, formalize its matrix or operator, test its adequacy and state its claim boundary.

4.5.10. Graph Adequacy, Robustness and Placebo Discipline

A graph-based result is admissible only if the construction is robust enough to survive reasonable perturbations and transparent enough to be reproduced. The monograph therefore treats graph adequacy as a pre-results gate. Adequacy means that the graph is connected or that disconnectedness is explicitly interpreted; edge density is neither mechanically empty nor mechanically complete; centrality is not dominated by an arbitrary anchor; cycles exist when curl, action or Betti diagnostics are claimed; edge weights have declared sources; and alternative graph specifications do not reverse the main qualitative conclusion without explanation.

Table 4.5.9. Network adequacy, robustness and placebo gates

Gate	Test or diagnostic	Main affected studies	Reviewer-safety purpose
Connectedness gate	Connected components; algebraic connectivity; no isolated nodes.	Hodge, Yang-Mills, BSD, Ricci/Poincare.	Required before interpreting system-wide diffusion, Hodge, local-to-global or

			connectedness claims.
Density gate	Number of edges, density and average degree.	Hodge, Yang-Mills, BSD, Ricci/Poincare.	Prevents tree-like under-identification and complete-graph overfilling.
Cycle gate	Triangle count, transitivity, clustering and beta_1.	Hodge, Yang-Mills, BSD, Ricci/Poincare.	Required before curl, action, cycle or topological-hole claims.
Weight audit	Source ledger for public anchors and author-calculated edge weights.	All graph chapters.	Prevents visual graph weights from becoming black-box assumptions.
Filtered-graph robustness	High-weight, medium-filtered and sparse-filtered graph variants.	Yang-Mills; potentially Hodge and BSD.	Tests whether the main spectral or structural result depends on one arbitrary density setting.
Node/edge exclusion	Leave-one-node, leave-one-corridor or edge-deletion tests.	Hodge, Yang-Mills, BSD.	Tests whether one strategic node mechanically drives the result.
Randomized-network placebo	Random rewiring or randomized edge-weight comparison under preserved size constraints.	Yang-Mills and potential BSD/Hodge extensions.	Separates benchmark robustness from statistical exceptionalism.
Perturbation and Monte Carlo	Noise in public anchors and corridor weights.	Yang-Mills, BSD, Perelman/Ricci/Poincare; analogous parameter perturbation in other chapters.	Tests whether graph outputs survive plausible data and coding uncertainty.
External-validity gate	Comparison with external proxy outcomes or out-of-sample layers where available.	BSD, Navier-Stokes, Riemann/Zeta, P vs NP; limited for finite-network benchmarks.	External screening is directional unless strong sign, p-value, lineage and robustness criteria are met.

Source: Author synthesis for the unified methodology chapter.

4.5.11. Network Claim-Boundary Matrix

The last step in the graph protocol is claim classification. The same graph object can support different claims depending on its evidence layer. A connected graph with stable density can support benchmark adequacy; a robust positive spectral gap can support a finite-network threshold result; a thresholded metric graph can support connectedness diagnostics; a covariance matrix can support risk-coupling evidence; and a layered spectral model can support forecast validation. None of these results, by itself, proves a classical Clay Millennium Problem or establishes universal causality.

Table 4.5.10. Network and relational-structure claim-boundary matrix

Study	Permitted network/relational claim	Prohibited overclaim
Perelman/Ricci/ Poincare	The stress-coordinate system forms a connected, looped, graph-topological diagnostic manifold.	That the Poincare conjecture is proved or that Ricci flow is literally replicated in economics.
Hodge	Regional macro-flow pressure can be decomposed into hierarchy, local-cycle imbalance and harmonic circulation inside a declared benchmark graph.	That the constructed edge cochain is observed trade/capital flow or that Hodge theory is empirically proved.
Navier-Stokes	Systemic stress can be modelled as a nondimensional flow-pressure-friction-shock-cycle-closure balance over a global panel.	That financial liquidity is a physical fluid, that the Navier-Stokes problem is solved or that crises are universally predictable.
Yang-Mills	A finite stress-weighted graph has a positive spectral threshold and concentrated	That the mathematical Yang-Mills mass gap is solved or that country-panel

	curvature/action under the benchmark construction.	causality is established before the N=1,500 pathway is populated.
BSD	Local regional/corridor signals can be formalized into a local-to-global rank-calibration architecture.	That the classical BSD conjecture is proved, tested or empirically verified.
Riemann/Zeta	A normalized zeta-cycle can be used as a bounded signed forecast-correction and spectral-validation layer.	That the Riemann Hypothesis is proved, tested or validated by inflation data.
P vs NP	Covariance dependence and cardinality constraints create a mixed discrete-continuous computational-finance problem with exact reduced benchmarking.	That P vs NP is resolved, that full n=94 optimality is certified or that realized investment dominance is established.

Source: Author synthesis based on the claim-boundary statements of the seven manuscripts.

4.5.12. Synthesis: Why the Network Protocol Matters for the Book

The network and graph construction protocol is one of the main reasons the monograph can be read as a unified research program rather than as seven separate articles. Hodge supplies decomposition of economic flow; Yang-Mills supplies gauge curvature, action concentration and spectral shock thresholds; BSD supplies local-to-global rank calibration; Perelman/Ricci/Poincare supplies metric-graph connectedness, curvature proxies and topological deformation diagnostics. Navier-Stokes, Riemann/Zeta and P vs NP complete the system by showing how non-graph relational structures--flow balance, spectral time-frequency dependence and covariance/combinatorial geometry--fit the same discipline: define the relational object, construct the matrix/operator, validate it and restrict the claim.

For the book, the most important methodological statement is therefore the following. A network result is not a visual metaphor; it is a reproducible operator-based transformation from public anchors and author-calculated variables into matrices, cycles, spectra, curvature proxies, decomposition components and robustness tests. A graph can reveal structure that raw GDP, inflation, growth, volatility or portfolio inputs cannot show alone. But that added structure must be defended by transparent construction, adequacy diagnostics, robustness checks, placebo logic and strict claim boundaries. This is the standard that Chapter 4 imposes on all seven problem chapters.

Chapter 4.6. Econometric and Forecast-Validation Protocol

This subsection defines the common econometric and forecast-validation discipline of the monograph. Its purpose is not to impose one statistical model on seven different economic analogues, but to state the shared evidentiary rule: constructed mathematical-economic indicators must be audited through appropriate panel, time-series, forecasting, robustness, dimensionality-reduction and falsification procedures before any substantive interpretation is allowed. The protocol is deliberately hierarchical. Some chapters use fully populated panel estimation; some use finite-network benchmark diagnostics; some use layered forecast validation; and the P vs NP chapter uses computational-finance validation rather than macro-panel causality. The common standard is evidence discipline, not mechanical methodological uniformity.

The chapter therefore distinguishes four levels of validation. First, internal statistical coherence checks whether constructed variables retain sign logic, stability and interpretable variation inside their own empirical universe. Second, robust-inference checks ask whether coefficients or associations survive heteroskedasticity, serial correlation, cross-sectional dependence, small-cluster limitations or high-dimensional collinearity. Third, forecast-validation checks evaluate whether a model improves predictive accuracy against transparent benchmarks under rolling or no-look-ahead windows. Fourth, falsification and boundary checks prevent a mathematically inspired economic analogue from being misread as theorem proof, causal law or universal forecast superiority.

Table 4.6.1. Unified econometric and forecast-validation architecture across the monograph

Protocol layer	Core methods	Primary question	Admissible evidence status
Panel association and heterogeneity	FE, TWFE, Mundlak, clustered SE, HC/HC3, HAC-compatible inference, Driscoll-Kraay where panel	Do constructed indicators retain systematic within-unit or between-unit information after accounting for observed	Diagnostic association; not randomized causality unless identification is separately established.

Protocol layer	Core methods	Primary question	Admissible evidence status
	dimensions permit	heterogeneity?	
Time-series dynamics and macro forecasting	ARIMA, VAR/SVAR, ARDL/ECM, local projections, rolling/expanding windows, Mincer-Zarnowitz, forecast encompassing	Does the constructed signal improve forecast or dynamic interpretation relative to standard persistence and structural benchmarks?	Forecast-window evidence; not universal predictive dominance.
Forecast comparison tests	RMSE, MAE, sMAPE, Diebold-Mariano, Clark-West, residual diagnostics, break/regime diagnostics	Is the reported forecast gain statistically and diagnostically defensible rather than visual overfitting?	Comparative validation within the declared sample and horizon.
Dimension reduction and regularization	PCA, factor extraction, Ridge/LASSO/Elastic Net, shrinkage, eigenvalue diagnostics	Are constructed indices robust to collinearity, common factors and overparameterization?	Robustness and compression evidence, not independent causal proof.
Simulation, placebo and falsification	Monte Carlo, bootstrap, permutation, negative controls, randomized networks, covariance placebo, leave-one-out tests	Does the result disappear under irrelevant, randomized or intentionally weakened alternatives?	Falsification discipline and overfitting control.
Evidence classification	Claim hierarchy, decision gates, replication checks, source-ledger and output-hash discipline	Which claims are permitted, diagnostic, future-dependent or excluded?	Reviewer-safe interpretation boundary.

4.6.1. Role of Econometric and Forecast Validation in the Monograph

The monograph contains seven economic-econometric analogues inspired by seven distinct mathematical architectures. Because the empirical universes differ sharply, the validation protocol must be comparative rather than uniform. The Perelman/Ricci/Poincare chapter uses a macro-regional inequality panel and a rich validation battery. The Hodge chapter uses a regional benchmark network with econometric, predictive and topological diagnostics. The Navier-Stokes chapter uses the strongest global-panel stress-testing layer, centered on 100 countries over 2010-2024. The Yang-Mills chapter separates a completed finite-network benchmark from a specified N = 1,500 country-panel validation pathway. The BSD chapter uses an N = 150 regional-year closure layer for calibration, high-R2 audit, robust inference, external-proxy screening and negative controls. The Riemann/Zeta chapter is the strongest forecast-validation design, because it separates annual, quarterly and monthly validation layers. The P vs NP chapter validates through computational-finance logic: exact reduced enumeration, heuristic comparison, covariance robustness, transaction-cost and derivative-overlay stress tests.

Accordingly, this protocol is governed by one general principle: a method is admissible only when its sample architecture, data-generating object and claim boundary justify it. FE and TWFE are meaningful where repeated units and periods exist. HAC and Driscoll-Kraay are meaningful where serial correlation, cross-sectional dependence or long-run covariance risks are present and the sample dimension supports such correction. VAR/SVAR belongs to dynamic macro layers, especially quarterly or sufficiently long annual structures, not to small static benchmarks. DM and CW tests belong to forecast comparison, not to structural rank calibration. PCA and regularization belong to collinearity, weighting and high-dimensional robustness, not to theorem proof. This separation protects the book from the common error of treating method density as evidence strength.

4.6.2. Panel-Econometric Baseline: FE, TWFE and Mundlak Logic

The panel-econometric layer is designed for empirical settings in which cross-sectional units are observed over time: countries, macro-regions, corridor nodes, region-years or country-years. Its first task is not causal identification; its first task is to determine whether author-calculated variables contain systematic empirical information after controlling for persistent

unit-level and time-level heterogeneity. This is especially important in the Navier-Stokes, Perelman/Ricci/Poincare and BSD chapters, and it becomes the future validation pathway for Yang-Mills.

The baseline fixed-effects specification may be written as follows:

y_it = alpha_i + beta x_it + gamma z_it + epsilon_it

y_it = alpha_i + tau_t + beta x_it + gamma z_it + epsilon_it [TWFE]

Mundlak extension: y_it = alpha + beta x_it + theta mean(x_i) + gamma z_it + u_i + epsilon_it

Here y_it denotes the chapter-specific diagnostic outcome: inequality pressure, curvature, systemic stress, resilience, structural-rank agreement, LOrder-related calibration or external-proxy target. The term alpha_i absorbs time-invariant regional or country heterogeneity. The term tau_t absorbs common global shocks, such as crisis years, commodity shocks, pandemic effects or global tightening cycles. Mundlak terms help diagnose whether pooled, random-effect or between-unit variation is driving results that should be interpreted as within-unit signals. In this monograph, FE/TWFE coefficients are interpreted as diagnostic associations unless a chapter separately supplies identification assumptions, instrumental structure, or credible causal design.

The protocol requires that any high R-squared result be decomposed before interpretation. In regional panels, especially BSD and Perelman/Ricci/Poincare, high fit may arise from persistent regional differences rather than from independent explanatory power of the constructed indicator. For this reason, the monograph treats high R-squared as a diagnostic requiring decomposition into within, between and overall components, not as automatic confirmation of the mathematical-economic analogue.

Table 4.6.2. Panel-econometric model classes and interpretation rules

Model class	Generic role	Main chapters	Interpretation boundary
Unit fixed effects (FE)	Controls for time-invariant country, region or node heterogeneity.	Navier-Stokes; Perelman/Ricci/Poincare; BSD; planned Yang-Mills pathway.	Association after persistent-unit controls; not causal proof.
Two-way fixed effects (TWFE)	Adds time shocks or global-year effects to unit controls.	Navier-Stokes; BSD closure; planned Yang-Mills panel.	Useful when global shocks affect all units; still sensitive to small clusters and dynamic bias.
Mundlak / correlated random-effects screen	Separates within-unit and between-unit variation and tests whether random-effects interpretation is credible.	Perelman/Ricci/Poincare; BSD; possible Hodge extensions.	Diagnostic model-selection and heterogeneity evidence.
Dynamic panel screen	Adds lagged dependent variables or persistence controls.	Navier-Stokes; Perelman/Ricci/Poincare; Yang-Mills future panel.	Cautious when T is short; Nickell-bias and persistence overclaiming must be avoided.
Panel IV / endogeneity screen	Tests whether constructed variables may be endogenous to the target or outcome.	Yang-Mills planned panel; Hodge endogeneity screen; possible Navier-Stokes robustness.	Requires defensible instruments; otherwise retained as sensitivity, not identification.
External-target regression	Tests whether constructed stress, rank or flow indicators move with external observable proxies.	Navier-Stokes; BSD; Yang-Mills future panel; Riemann/Zeta auxiliary diagnostics.	External plausibility screen; strong validation only if signs, p-values, lineage and robustness align.

4.6.3. Robust-Inference Protocol: HAC, Driscoll-Kraay, Clustering and HC3

The monograph treats standard errors as part of the evidence architecture rather than as a technical footnote. Because the empirical designs include time-series dependence, cross-sectional dependence, regional clustering, constructed variables and small benchmark systems, classical homoskedastic standard errors are often insufficient. The robust-inference protocol therefore distinguishes four cases.

- HC/HC3 robust inference is appropriate when heteroskedasticity and leverage sensitivity are plausible, especially in small benchmark regressions or finite-network diagnostic models.

- Clustered standard errors are appropriate when errors may be correlated within countries, regions or corridor units, but the number of clusters must be large enough for strong inference; small-cluster p-values must be treated cautiously.
- HAC-compatible inference is appropriate when serial correlation or long-run covariance structure may affect annual or quarterly time-series and panel residuals.
- Driscoll-Kraay standard errors are appropriate for panel models exposed to cross-sectional dependence and serial correlation, especially in the Navier-Stokes full panel and the future Yang-Mills country-panel pathway.

In the final monograph, robust inference must always be paired with an interpretation status. If a coefficient keeps the expected sign but loses significance under HAC, clustered, HC3 or Driscoll-Kraay correction, the result is reclassified from statistical confirmation to directional consistency. This is especially important for BSD external-proxy screening and Yang-Mills benchmark regressions, where small samples and constructed variables may otherwise invite overclaiming.

V_HC = (X'X)^(-1) X' diag(e_i^2) X (X'X)^(-1)

V_HAC = (X'X)^(-1) [sum_t e_t^2 x_t x_t' + sum_l w_l sum_t e_t e_(t-l)(x_t x_(t-l)' + x_(t-l)x_t')] (X'X)^(-1)

Driscoll-Kraay principle: robust covariance is adjusted for heteroskedasticity, serial correlation and cross-sectional dependence in panel averages.

Table 4.6.3. Robust-inference decision rules

Risk detected	Recommended correction	Main empirical settings	Claim rule
Heteroskedasticity or high leverage	HC3 / robust covariance	Small regional benchmarks; Hodge; Yang-Mills N=10 diagnostics; P vs NP robustness regressions if used.	Use robust p-values; downgrade if only classical significance survives.
Serial correlation / persistence	HAC / Newey-West-style long-run covariance	Annual stress, inflation, pressure and panel residual paths.	Interpret coefficient direction only if HAC evidence is weak.
Cross-sectional dependence	Driscoll-Kraay or cross-section robust panel inference	Navier-Stokes N=1,500; Yang-Mills planned N=1,500; possible macro-regional panels.	Do not claim independent observations when global shocks synchronize units.
Few clusters	Small-cluster caution; wild/bootstrap where feasible	BSD N=150 with ten regional clusters; Perelman regional panel; finite-node benchmarks.	Weak p-values remain weak; sign consistency is not confirmation.
Generated regressors / constructed indices	Variable-lineage audit, anti-circularity checks, negative controls	BSD, Perelman/Ricci/Poincare, Hodge, Yang-Mills, Navier-Stokes.	Validation must not use an outcome mechanically embedded in the constructed indicator.

4.6.4. Forecast-Validation Protocol: ARIMA, VAR/SVAR, Rolling Windows and Benchmark Discipline

Forecast validation is used when a chapter makes predictive, dynamic or forecast-diagnostic claims. The monograph does not permit a constructed model to be evaluated only against itself. Every forecast claim must be compared against transparent benchmarks and evaluated under time-order discipline. The most developed case is the Riemann/Zeta FPAS+zeta chapter, where annual, quarterly and monthly layers are separated so that advanced dynamic methods are not falsely attributed to a small annual sample. The Navier-Stokes chapter also uses rolling one-year-ahead validation and benchmark comparison against ARIMA, VAR, GARCH and composite-index baselines. Perelman/Ricci/Poincare uses forecast discipline conservatively, explicitly preventing the diagnostic model from being presented as forecast-dominant where AR(1) performs better.

The first rule is no look-ahead. Parameters, scaling constants, alpha weights, Fourier terms, regime states, factor structures and forecast corrections must be estimated or selected using only information available at the forecast origin. Rolling or expanding windows are therefore preferred to full-sample fitted values when forecast claims are made. The second rule is benchmark comparison. ARIMA supplies a persistence baseline; VAR and SVAR supply multivariate dynamic benchmarks; GARCH is relevant where volatility or stress variability is central; FPAS supplies the structural inflation

baseline for Riemann/Zeta; composite-index baselines test whether a complex analogue adds value beyond a simple constructed index.

Forecast error: $e_t^m = \hat{y}_t^m - y_t$

$RMSE_m = \sqrt{(1/T) \sum_t (e_t^m)^2}$

$MAE_m = (1/T) \sum_t |e_t^m|$

$sMAPE_m = (100/T) \sum_t [2 |\hat{y}_t^m - y_t| / (|y_t| + |\hat{y}_t^m|)]$

Table 4.6.4. Forecast-validation methods and chapter allocation

Method	Purpose	Primary chapters	Boundary condition
ARIMA / AR(1)	Persistence benchmark for inflation, stress, pressure or curvature paths.	Riemann/Zeta; Navier-Stokes; Perelman/Ricci/Poincare.	A model must beat or complement simple persistence before forecast-improvement language is allowed.
VAR / SVAR	Multivariate dynamic interaction among stress, pressure, policy, liquidity or macro variables.	Riemann/Zeta quarterly layer; Navier-Stokes; Perelman/Ricci/Poincare.	Requires adequate time dimension; not suitable as a decorative test on tiny samples.
Rolling / expanding validation	No-look-ahead evaluation of one-step or horizon-specific forecasts.	Riemann/Zeta; Navier-Stokes; Perelman/Ricci/Poincare.	Full-sample fit is not forecast validation.
Mincer-Zarnowitz calibration	Tests whether forecasts are unbiased and properly scaled against actual outcomes.	Riemann/Zeta; possible Navier-Stokes stress forecasts.	Calibration evidence; not proof of causal mechanism.
Forecast encompassing	Tests whether a new model contains information beyond benchmark forecasts.	Riemann/Zeta; possible Navier-Stokes.	Incremental information test; sample-sensitive.
GARCH / volatility benchmark	Benchmarks volatility-sensitive stress forecasts.	Navier-Stokes; possible macro-financial robustness layers.	Relevant for stress volatility, not all chapters.

4.6.5. DM and CW Tests: Comparative Forecast Evidence without Overclaiming

The Diebold-Mariano and Clark-West tests are included as formal forecast-comparison devices. They are not general validation tests for every mathematical-economic analogue. They belong where forecasts are generated by competing models over a declared validation window. In this monograph, their primary home is the Riemann/Zeta FPAS+zeta chapter. They may also be used in Navier-Stokes forecast benchmarking if the forecast objects are strictly defined and the validation window contains comparable forecasts from the flow model and its benchmarks.

The Diebold-Mariano test compares predictive accuracy by testing whether the mean loss differential between two forecasts is zero. The Clark-West test is especially relevant when a larger nested model, such as FPAS+zeta relative to FPAS, is compared against a simpler baseline; it adjusts for the fact that nested models can appear worse because of parameter estimation noise. The monograph uses these tests to support or limit forecast-improvement language, not to establish a theorem, causal law or universal model superiority.

Loss differential: $d_t = L(e_t^A) - L(e_t^B)$

DM statistic: $DM = \text{mean}(d_t) / \sqrt{LRV(d_t)/T}$

Clark-West adjusted loss for nested comparison: $d_t^{CW} = e_{1,t}^2 - [e_{2,t}^2 - (\hat{y}_{1,t} - \hat{y}_{2,t})^2]$

A positive test result permits carefully worded comparative language: the model improves forecast accuracy within the declared sample, horizon and benchmark set. A weak or mixed result permits only directional or diagnostic interpretation. If the new model has lower RMSE but fails comparison tests, the final wording must state forecast-improvement in descriptive terms and avoid strong statistical superiority.

4.6.6. PCA, Factor Structure and Regularization Protocol

Many constructed economic analogues in this monograph begin with multiple correlated public indicators. Without dimensionality control, composite indices may become unstable, redundant or mechanically overfitted. PCA and factor diagnostics therefore serve three functions. First, they test whether the indicator system has a coherent low-dimensional structure. Second, they provide alternative weighting or component-extraction checks against expert or formula-based weights. Third, they identify whether a reported result is driven by a dominant common factor rather than by a specific mathematically inspired mechanism.

Regularization is used for robustness, not for replacing the research design. Ridge regression is useful when regressors are highly collinear but the analyst wants to retain all variables. LASSO is useful for sparsity and variable selection, although it must be interpreted carefully when variables are conceptually grouped. Elastic Net provides a middle ground. In the Perelman/Ricci/Poincare chapter, PCA and regularization support the robustness of the stress-coordinate and curvature interpretation. In Navier-Stokes, alternative weighting, PCA-style weighting and robustness layers audit stress-index construction. In P vs NP, shrinkage, covariance alternatives, eigenvalue concentration and covariance placebo tests play the analogous role in the risk geometry.

PCA: X = U S V', with principal components Z = X V_k

Ridge: minimize ||y - X beta||^2 + lambda ||beta||_2^2

LASSO: minimize ||y - X beta||^2 + lambda ||beta||_1

Elastic Net: minimize ||y - X beta||^2 + lambda_1 ||beta||_1 + lambda_2 ||beta||_2^2

Table 4.6.5. Dimension-reduction and regularization use across the seven studies

Study	Dimensionality problem	Preferred tools	Interpretation rule
Perelman/Ricci/Poincare	Sixteen stress coordinates may be correlated and component-heavy.	PCA, Ridge/regularization, threshold/quantile, leave-one-out.	Supports diagnostic structure; does not create forecast dominance.
Hodge	Network-derived indices can be correlated with GDP mass, centrality and resilience.	Robust econometrics, IV/endogeneity screens, ML validation, persistent homology.	Benchmark validation, not full country-level causal inference.
Navier-Stokes	Stress index combines pressure, velocity, friction, shock, cycle and closure components.	Alternative weights, PCA/entropy/crisis weights, FE, robust inference, rolling validation.	Stress-testing evidence; not universal crisis-prediction law.
Yang-Mills	Stress, centrality, curvature and EMGI may share inputs in the ten-node benchmark.	Robustness audits, randomized networks, Bayesian/factor checks, future Driscoll-Kraay panel.	Benchmark evidence now; stronger claims after N=1,500 closure.
BSD	LOrder, Rank and external proxies may risk circular lineage or high fit.	High-R2 decomposition, negative controls, anti-circularity, FE/TWFE, robust inference, permutation.	Strong internal calibration; external proof demoted unless robust.
Riemann/Zeta	Forecast correction can overfit crisis dynamics if alpha and zeta signal are not audited.	Rolling validation, MZ, DM/CW, VAR/SVAR, HMM, Fourier/wavelet, spectral entropy.	Layered forecast evidence; no universal dominance.
P vs NP	Covariance and correlation compress independent diversification and affect Sharpe.	Eigenvalue diagnostics, covariance shrinkage/alternatives, exact reduced enumeration, heuristic stability.	Computational-finance robustness; no theorem proof or full global-optimality claim.

4.6.7. Study-Specific Validation Profiles

The monograph-specific protocol is most transparent when the seven studies are compared directly. The following matrix is designed to function as the main technical bridge between this unified methodology chapter and the seven problem chapters in Part II. It specifies the econometric and forecast-validation tools assigned to each study, the evidence they produce and the claim boundary they enforce.

Table 4.6.6. Seven-study econometric and forecast-validation allocation matrix

Study	Empirical validation base	Primary econometric / validation tools	Main evidence produced	Boundary enforced
Perelman/Ricci/Poincare	Ten macro-regional blocks, 2010-2024, sixteen stress coordinates, N=150 region-years.	Dynamic screens, ARDL, ECM, VAR/SVAR, local projections, panel FE, Mundlak, robust inference, PCA, regularization, quantile/threshold, HMM-style regimes, leave-one-out, rolling forecast and AR(1) benchmark.	Diagnostic validation of pressure-curvature-topology structure; crisis-deformation and recovery interpretation; robustness of constructed stress coordinates.	Forecast dominance is not claimed where AR(1) performs better; results remain diagnostic and structural.
Hodge	Ten regional nodes plus World anchor; 27-edge benchmark; directed macro-flow pressure field.	HC3/robust regional regressions, spatial or network-lag screens, IV/endogeneity screens, ML/leave-one-region-out validation, persistent homology, topological robustness.	Internal benchmark validation of gradient, curl and harmonic flow components; resilience and systemic-circulation informativeness.	Regional benchmark only; not full all-country dyadic causal inference.
Navier-Stokes	100-country annual panel, 2010-2024, N=1,500; World and macro-regional layers; rolling validation windows.	Panel FE/TWFE, robust inference, rolling one-year-ahead validation, ARIMA/VAR/GARCH/composite-index benchmarks, residual diagnostics, external-target validation, Monte Carlo and policy counterfactuals.	Strong stress-testing and forecast-window evidence for nondimensional flow-pressure-friction-shock-cycle-closure architecture.	Associations and scenarios; not a physical law or universal crisis predictor.
Yang-Mills	Completed ten-node, 27-edge finite-network benchmark plus specified 100-country x 15-year N=1,500 validation path.	Benchmark regressions, HC3 sign checks, network-spatial diagnostics, scenario simulation, Monte Carlo perturbation, randomized-network placebo, planned FE/TWFE/Driscoll-Kraay/clustered/dynamic-panel/panel-IV/factor/external-validation models.	Finite-network mass-gap, curvature/action, EMGI and threshold-compression evidence; panel pathway specified.	Final country-level causal or quasi-causal claims deferred until N=1,500 panel is populated and estimated.

Study	Empirical validation base	Primary econometric / validation tools	Main evidence produced	Boundary enforced
BSD	World anchor plus ten regional/corridor nodes; N=150 regional-year closure layer.	FE/TWFE screening, high-R2 decomposition, robust inference, external-proxy screening, negative controls, anti-circularity tests, equivalence tests, out-of-sample validation, sensitivity and permutation logic.	Calibrated local-to-global rank correspondence; LOrder-rank agreement; falsification and lineage discipline.	External proxy results remain directional when signs/p-values are weak; no causal law or BSD proof.
Riemann/Zeta	Annual, quarterly and monthly layers: N=55, N=45, N=20, N=100 and N=240.	ARIMA benchmark, FPAS baseline, FPAS+zeta forecast, rolling no-look-ahead validation, MZ calibration, encompassing, DM/CW tests, residual diagnostics, HMM/Markov-switching, VAR/SVAR, Fourier/wavelet coherence, spectral entropy.	Layered forecast-validation evidence and sample-discipline model for the book.	Zeta signal is a computational cyclical correction; not proof/test of the Riemann Hypothesis or universal inflation law.
P vs NP	94 U.S. industries; C(94,10) support universe; reduced exact C(20,6) benchmark.	Exact reduced enumeration, greedy/Monte Carlo/GA comparison, GA plus continuous reoptimization, covariance/eigenvalue diagnostics, covariance placebo, Rf/ERP sensitivity, transaction costs, beta drift, Black-Scholes overlay and stress tests.	Computational-finance validation of sparse mixed discrete-continuous optimization under documented search coverage.	Best-found incumbent, not certified full n=94 global optimum; no P vs NP theorem proof or realized investment dominance.

4.6.8. Perelman/Ricci/Poincare: Econometric Validation as Diagnostic Geometry Audit

In the Perelman/Ricci/Poincare chapter, econometric validation operates as a geometry audit. The empirical object is already a constructed pressure-curvature-topology system; econometrics asks whether this system behaves coherently under alternative dynamic, panel, robustness and forecasting checks. The chapter uses dynamic screens, ARDL/ECM logic, VAR/SVAR and local-projection tools for time-sensitive pressure paths, while FE, Mundlak, PCA, regularization, quantile, threshold and leave-one-out validation test whether the stress-coordinate architecture is stable. The decisive boundary is that validation supports diagnostic structure, not unrestricted causality or forecast dominance.

4.6.9. Hodge: Benchmark Validation of Topological Flow Components

In the Hodge chapter, the main empirical object is not a large country panel but a regional flow network decomposed into gradient, curl and harmonic components. Econometric and predictive tests therefore play a benchmark-validation role. They examine whether hierarchy, local imbalance, systemic circulation, resilience and tail-risk indicators are empirically informative within the ten-node regional architecture. Machine-learning validation and leave-one-region-out tests are useful because they test whether the derived indices contain predictive structure without pretending that ten regional nodes are enough for definitive causal inference. Persistent homology functions as topological validation rather than ordinary econometrics.

4.6.10. Navier-Stokes: Full Global-Panel Stress-Testing Validation

The Navier-Stokes chapter is the principal panel-econometric stress-testing design of the monograph. Its 100-country annual panel over 2010-2024 supplies N=1,500 country-year observations, allowing FE/TWFE, robust inference, rolling validation, benchmark comparison, external-target validation, residual diagnostics and Monte Carlo counterfactuals to operate as a substantive empirical architecture. The protocol is particularly strict about nondimensional variables and restricted epsilon closure: because heterogeneous macro-financial variables are transformed into unit-free terms, validation must show that the flow-pressure-friction-shock-cycle balance is not merely an algebraic construction but an empirically auditable stress-testing system.

4.6.11. Yang-Mills: Two-Layer Validation and Deferred Panel Confirmation

The Yang-Mills chapter requires two separate validation languages. Layer A is a completed finite-network benchmark: ten nodes, twenty-seven weighted edges, stress Laplacian, mass gap, curvature/action concentration, EMGI, BridgeStress, scenario shocks and Monte Carlo perturbation. Its econometric tests are diagnostic because the benchmark is small. Layer B is the specified N=1,500 country-panel validation path. Only Layer B can support stronger panel-econometric claims through FE, TWFE, Driscoll-Kraay, clustered inference, dynamic-panel checks, panel-IV, factor diagnostics and external-validation models. Until Layer B is populated and estimated, the admissible claim remains strong finite-network benchmark evidence plus a fully specified validation pathway.

4.6.12. BSD: Closure Econometrics, Negative Controls and Anti-Circularity

The BSD chapter is the clearest example of econometrics as claim discipline. The N=150 closure layer does not transform the local-to-global analogue into a causal law. Instead, it audits the link between LOrder, structural rank, corridor exposure and local finite-state information through FE/TWFE screening, robust inference, high-R2 decomposition, external-proxy checks, negative controls, circularity safeguards, equivalence tests, out-of-sample validation, sensitivity tests and permutation logic. This protocol protects the chapter from two errors: treating high fit as proof, and treating weak external-proxy results as independent validation.

4.6.13. Riemann/Zeta: Layered Forecast Validation as the Book's Sample-Discipline Benchmark

The Riemann/Zeta chapter is the monograph's strongest example of sample discipline. It avoids the methodological mistake of estimating all tools on one small annual dataset by separating the annual headline layer, annual robustness layer, crisis-era comparison layer, quarterly dynamic-validation layer and monthly spectral-diagnostics layer. ARIMA, FPAS, FPAS+zeta, rolling validation, Mincer-Zarnowitz, forecast encompassing, DM/CW tests, HMM/Markov-switching, VAR/SVAR, Fourier/wavelet coherence and spectral entropy each have an assigned sample role. This makes the zeta signal auditable as a bounded forecast correction rather than a mathematical proof or unrestricted inflation law.

4.6.14. P vs NP: Computational-Finance Validation instead of Panel Causality

The P vs NP chapter does not primarily need FE, TWFE, ARIMA or VAR. Its validation problem is computational and financial: Can a cardinality-constrained portfolio-search architecture be audited under fixed inputs, CAPM returns, covariance geometry, heuristic search, exact reduced enumeration and robustness gates? The validation protocol is therefore exact enumeration where possible, documented search coverage where full enumeration is infeasible, algorithmic comparison, seed stability, runtime scaling, covariance robustness, transaction costs, beta drift, derivative-overlay realism and stress scenarios. The central claim is best-found computational-finance evidence, not theorem proof or certified full-universe optimality.

4.6.15. Common Diagnostic and Falsification Gates

All seven studies must pass a common set of diagnostic gates before their results enter the monograph's comparative synthesis. These gates are not identical statistical tests; they are a common epistemic structure. Each chapter must demonstrate that the evidence is traceable, not mechanically circular, not driven only by a fragile weighting choice, not dependent on one favorable benchmark and not interpreted beyond its empirical universe.

Table 4.6.7. Common diagnostic gates for evidence admission

Gate	Technical requirement	Failure signal	Required response
Lineage gate	Identify raw inputs, transformations, constructed variables and outcomes.	Outcome is embedded in predictor or external validation variable.	Demote to internal calibration; add anti-circularity warning.
Robust-inference gate	Report robust, clustered, HAC or Driscoll-Kraay evidence	Classical significance disappears under robust	Report directional consistency rather than statistical

Gate	Technical requirement	Failure signal	Required response
	when residual dependence is plausible.	correction.	confirmation.
Benchmark gate	Compare forecasts or algorithms against simple, transparent alternatives.	Complex model only beats itself or a weak benchmark.	Limit claim to construction or diagnostic value.
Sample-discipline gate	Assign methods to sample layers where they are appropriate.	VAR/SVAR, HMM or DM/CW applied to an unsuitable small layer.	Move method to quarterly/monthly/pathway layer or remove strong claim.
Falsification gate	Use negative controls, placebo, randomization, permutation or covariance placebo where relevant.	Constructed indicator explains unrelated or randomized outcomes.	Revise model or downgrade evidence.
Replication gate	Provide formulas, scripts, data tables, seeds, outputs and hashes where applicable.	Reported result cannot be reconstructed from package materials.	Do not elevate result into final synthesis.

4.6.16. Evidence-Status Matrix for Final Monograph Interpretation

The unified protocol produces a final evidence-status hierarchy. The highest level is not reserved for the mathematically most complex chapter; it is reserved for results that match their empirical universe, pass appropriate validation gates and preserve claim boundaries. A finite-network benchmark can be strong if it is interpreted as a benchmark. A forecast model can be strong if it is evaluated against benchmarks under no-look-ahead rules. A panel result can be weak if robust inference fails, even when the point estimate has the expected sign. This hierarchy is what allows the seven chapters to coexist in one monograph without pretending that all evidence has the same statistical meaning.

Table 4.6.8. Evidence hierarchy for econometric and forecast-validation claims

Evidence level	Condition for use	Examples in the monograph	Permitted wording
Strong validated evidence	Appropriate sample, transparent benchmark, robust diagnostics and consistent interpretation.	Riemann/Zeta layered forecast validation; Navier-Stokes N=1,500 stress-testing panel; P vs NP exact reduced benchmark.	The evidence supports the reported diagnostic or forecast claim within the declared design.
Strong benchmark evidence	Finite-network or regional benchmark is complete, reproducible and internally robust, but not a full country-level panel.	Hodge benchmark; Yang-Mills finite-network benchmark; BSD local-to-global calibration.	The benchmark supports structural measurement and internal calibration.
Directional diagnostic evidence	Signs or rankings are plausible, but p-values, clusters, external proxies or sample size are weak.	BSD external proxies; Yang-Mills N=10 regressions; some Hodge regional regressions.	The evidence is directionally consistent and useful for screening.
Forecast-window evidence	Forecast gain exists in a defined validation window but may not generalize.	Navier-Stokes rolling 2017-2024; Riemann/Zeta annual/quarterly/monthly layers.	The model improves forecast performance in the reported window and benchmark set.
Scenario/model-implied evidence	Counterfactual, shock or Monte Carlo output depends on model assumptions.	Navier-Stokes policy counterfactuals; Yang-Mills threshold compression; BSD scenario stress.	The model implies the stated stress or threshold effect under declared assumptions.
Excluded claim	The statistical design does not identify theorem proof,	All seven studies.	The monograph does not claim to solve, prove, test or

Evidence level	Condition for use	Examples in the monograph	Permitted wording
	universal causality, full optimality or universal forecast dominance.		replicate the Clay Millennium Problems in their original mathematical form.

4.6.17. Chapter-Level Synthesis

The econometric and forecast-validation protocol is the statistical guardrail of the unified methodology chapter. It transforms seven ambitious mathematical-economic analogues into auditable empirical studies by requiring that each constructed object be tested according to its own empirical universe. The protocol does not ask the Hodge benchmark to behave like a 100-country panel, does not ask the P vs NP portfolio experiment to behave like an inflation forecast, and does not treat the Riemann/Zeta forecast battery as proof of a number-theoretic theorem. It requires methodological fit between object, sample, test and claim.

The main monograph-level conclusion is therefore strict but constructive. FE, TWFE, HAC, Driscoll-Kraay, ARIMA, VAR/SVAR, rolling validation, DM/CW tests, PCA and regularization are not decorative methods. They are evidence filters. They determine whether a result is admissible as strong validation, benchmark coherence, directional screening, scenario output, future-pathway specification or excluded claim. This is why Chapter 4.6 is central to the book's technical spine: it converts mathematical inspiration into empirical discipline.

4.7. Computational and Algorithmic Protocol

Unified algorithmic evidence architecture for the seven economic-econometric Millennium analogues

This section defines the computational and algorithmic protocol of the monograph. It is the operational layer through which public-data anchors, normalized variables, graphs, spectral signals, optimization spaces, finite-state traces, stochastic simulations and validation objects are converted into auditable research outputs. The section is not a programming appendix and does not merely state that calculations were performed. Its purpose is to specify how computation functions as evidence inside the seven bounded economic analogues of the Clay Millennium Problems.

The strongest algorithmic concentration appears in four studies: the P-vs-NP-inspired portfolio-optimization study, the Riemann-Zeta FPAS+zeta inflation-forecasting study, the Yang-Mills finite-network mass-gap study and the Hodge-econometric macro-flow decomposition study. These four chapters contain the densest computational objects: combinatorial search, spectral signal construction, finite weighted graph spectra, gauge curvature/action, Hodge projection and persistent-homology checks. The other three chapters--Perelman/Ricci/Poincare, BSD and Navier-Stokes--also rely on algorithmic workflow, but their computational role is primarily transformation, diagnostics, closure, scenario generation and robustness auditing.

The protocol follows one central rule: algorithmic outputs are not treated as self-validating facts. Every computed indicator must be linked to an input source, a transformation rule, an algorithmic operation, a validation gate and a claim boundary. This prevents the monograph from presenting constructed results as if they were official indicators, theorem proofs, causal laws or certified global optima.

Source-document traceability note. This subsection synthesizes the methodological logic of the seven uploaded research manuscripts: Global Perelman-Ricci-Poincare-Inspired Inequality Diagnostics; Global Hodge-Econometric Modeling of the World Economy; Navier-Stokes-Inspired Global Liquidity-Flow and Systemic-Stress Modelling; Economic Yang-Mills Mass Gap in Global and Corridor Flow Networks; Regional Economic Birch-Swinnerton-Dyer Modelling; Global Riemann-Zeta FPAS+zeta Inflation Forecasting; and Robust Portfolio Optimization under Computational Complexity.

4.7.1. Function of the computational protocol inside the monograph

The computational protocol has four functions. First, it defines how theoretical analogies are translated into finite empirical objects. For example, P vs NP becomes a finite sparse-support selection problem, Riemann/Zeta becomes a normalized critical-line cyclical signal, Yang-Mills becomes a finite stress-weighted graph with curvature and spectral separation, and Hodge becomes a discrete edge-cochain decomposition. Second, it defines how constructed objects are generated reproducibly from disclosed inputs. Third, it assigns algorithms to evidence levels: exact enumeration, heuristic search, spectral decomposition, projection, rolling validation, simulation, scenario stress testing and placebo auditing. Fourth, it prevents algorithmic overclaiming by requiring every output to pass a corresponding boundary rule.

This computational layer is necessary because the monograph is not a purely narrative comparison of seven mathematical problems. It is a mathematical-econometric measurement program. The models must therefore be executable in principle: data are loaded, variables are harmonized, matrices are built, decompositions are performed, forecasts are evaluated, search spaces are explored, uncertainty is simulated and evidence is classified. The protocol below makes that execution logic explicit.

(4.7.1) $A_j = (I_j, T_j, C_j, V_j, R_j, Q_j)$, $j = 1,...,7$

In Equation 4.7.1, A_j denotes the algorithmic architecture of study j. I_j is the input layer, T_j is the transformation layer, C_j is the computational core, V_j is the validation layer, R_j is the reproducibility layer and Q_j is the claim-boundary layer. The equation is deliberately generic because the seven studies use different mathematical grammars, but they share the same evidence-control structure.

Table 4.7.1. Computational evidence architecture across the seven studies

Study	Computational object	Principal algorithmic operations	Validation gate	Claim boundary
P vs NP	Combinatorial portfolio-selection and mixed discrete-continuous optimization	Support enumeration, greedy search, Monte Carlo, genetic algorithm, continuous reoptimization, reduced exact benchmark	Search-coverage certificate, exact reduced enumeration, robustness, transaction-cost and derivative-overlay checks	Computational-finance evidence; no P-vs-NP theorem proof and no certified full-universe optimum
Riemann/Zeta	Critical-line spectral signal embedded in global inflation forecasting	Tau construction, normalized zeta-cycle extraction, alpha-weighted correction, rolling validation, ARIMA/FPAS comparison, DM/CW tests	Layered annual, quarterly and monthly validation; residual and regime diagnostics	Bounded forecast-improvement claim; no Riemann Hypothesis proof or universal dominance
Yang-Mills	Finite weighted stress network and spectral shock-threshold architecture	Stress field, adjacency, gauge potential, triangular curvature, Yang-Mills action, Laplacian eigenvalues, EMGI, scenario shocks	Graph adequacy, positive mass-gap persistence, perturbation/Monte Carlo robustness, panel-pathway discipline	Finite-graph mass-gap analogue; no continuum Yang-Mills solution
Hodge	Topological macro-flow decomposition on a regional graph	Adjacency and weight matrices, B1 and B2 incidence matrices, edge cochain, weighted Hodge projection, spectral and persistent-homology diagnostics	Projection error, W-orthogonality, leave-one-region-out, econometric and topology checks	Regional benchmark decomposition; no all-country dyadic-flow completion claim

Study	Computational object	Principal algorithmic operations	Validation gate	Claim boundary
BSD	Local-to-global structural-rank measurement pipeline	Regional panel construction, finite-state traces, Euler-factor analogues, economic L-function, LOrder and structural-rank comparison	N=150 closure diagnostics, negative controls, circularity safeguards, permutation placebo, OOS validation	Calibrated local-to-global consistency; no BSD proof and no causal law
Perelman/Ricci/Poincare	Pressure-curvature-topology diagnostic algorithm	0-100 stress coordinates, metric tensor, Ricci-style curvature, F/W functionals, graph Laplacian, Betti diagnostics, Monte Carlo bands	Counterfactual sensitivity, AR/rolling forecast discipline, panel/regularization checks	Inequality diagnostic architecture; no geometric/topological theorem proof
Navier-Stokes	Nondimensional macro-financial stress-balance and scenario engine	Stress-index construction, flow-pressure-friction-shock-cycle balance, restricted epsilon closure, Fourier forcing, rolling validation and Monte Carlo counterfactuals	N=1,500 panel, benchmark comparison, external validation, residual and policy-scenario checks	Macro-financial stress-testing claim; no physical fluid law or universal crisis predictor

4.7.2. Unified end-to-end algorithmic sequence

Across the seven studies, the monograph uses a common algorithmic sequence even when the mathematical objects differ. The sequence begins with source anchoring and ends with claim classification. This order is important: validation cannot be performed before the variable lineage is fixed; robustness cannot be interpreted before the computational object is defined; and a claim cannot be assigned before the algorithmic output is connected to its admissible evidence level.

15. Register the empirical universe, observation unit, time window, frequency and source-family logic before any model-specific transformation is performed.
16. Separate public or official data anchors from author-calculated analytical variables, matrices, indices, forecasts, graph objects and optimization outputs.
17. Apply normalization, nondimensionalization, direction harmonization or CAPM/spectral scaling according to the object-specific protocol of the relevant study.
18. Construct the computational object: graph, edge cochain, stress field, portfolio support space, zeta-cycle, finite-state trace set, stress-balance equation or curvature-functional layer.
19. Execute the primary algorithm: decomposition, search, forecast correction, spectral calculation, curve/L-function analogue, rolling validation or stress scenario engine.
20. Audit numerical stability through alternative specifications, perturbations, random seeds, exact reduced benchmarks, residual checks, placebo tests or leave-one-unit-out validation.
21. Store intermediate objects--matrices, parameters, seeds, formula logs, algorithm settings and output files--so that the reported tables can be regenerated.

22. Translate output into evidence levels: measurement, calibration, diagnostic association, forecast validation, heuristic credibility, robustness or exclusion.
23. Apply the claim-boundary matrix before writing the interpretation. No computed value is allowed to become theorem proof, unrestricted causality or universal predictive dominance.

(4.7.2) Output_j = f_j(Source_j, Normalization_j, Algorithm_j, Validation_j, Seed_j)

Equation 4.7.2 defines a reproducibility principle. A reported output is not only a number; it is the result of a documented function of sources, transformations, algorithms, validation design and computational environment. If any of these components is changed, the output becomes a new version and should be labelled as such.

4.7.3. P-vs-NP computational-finance protocol

The P-vs-NP chapter is the monograph's clearest computational-decision model. Its object is a cardinality-constrained portfolio-optimization system rather than a theorem-proof exercise. The fixed empirical universe consists of 94 U.S. industry portfolios from the Damodaran January 2026 data vintage after excluding aggregate market rows. The baseline decision requires selecting K = 10 industries before continuous weights are optimized. The discrete support layer alone contains C(94,10) = 9,041,256,841,903 possible supports, which is why exhaustive full-universe enumeration is not treated as the main strategy.

(4.7.3) C(n,K) = n! / [K!(n-K)!]

(4.7.4) maximize_w Sharpe(w) = (w^T mu - R_f) / sqrt(w^T Sigma w), subject to sum_i w_i = 1, w_i >= 0, and ||w||_0 = K

The computational protocol begins by constructing CAPM-implied expected returns from R_f and ERP, then building covariance geometry, correlation diagnostics and eigenvalue concentration measures. These objects define the continuous risk-return surface on which the sparse support-selection problem is evaluated. The key methodological point is that the algorithm is not allowed to choose inputs after seeing the result. The universe, risk-free rate, equity risk premium, covariance specification, K constraint, search budget and benchmark layer must be fixed before optimization.

Table 4.7.2. Algorithmic layers of the P-vs-NP-inspired portfolio chapter

Layer	Computational operation	Evidence role
Data audit	Damodaran Jan-2026 industry input table; beta, sigma, firm count and exclusion of aggregate rows	Freezes the empirical universe before search
CAPM construction	mu_i = R_f + beta_i x ERP; Sharpe proxy and covariance inputs	Creates a transparent return prior rather than realized-return backtest dominance
Combinatorial core	C(n,K) and K-grid support-space growth	Quantifies operational search difficulty
Greedy search	Sequential support construction using a common objective rule	Fast and auditable baseline heuristic
Monte Carlo search	Random support sampling under fixed budget and seeds	Stochastic coverage and distributional behavior
Genetic algorithm	Population, mutation, crossover, elitism and convergence tracking	Metaheuristic search for high-quality sparse incumbents
GA plus reoptimization	Continuous weight reoptimization inside selected supports	Tests mixed discrete-continuous improvement
Reduced exact benchmark	Full enumeration of n = 20, K = 6 supports, C(20,6) = 38,760	Supplies exact evidence where exact enumeration is feasible
Robustness and realism	Alternative covariance, Rf/ERP perturbation, caps, transaction costs, beta drift, risk contribution and option overlay	Prevents heuristic output from becoming an investment-performance overclaim

The decisive reviewer-safety rule is that the full n = 94, K = 10 result is reported as a best-found incumbent under documented search coverage, not as a certified global optimum. Exactness is reserved for the reduced benchmark where enumeration is feasible. This distinction is the computational equivalent of the monograph's broader claim-boundary principle: strong operational evidence is allowed, but theorem-level or universal-performance claims are excluded.

4.7.4. Riemann/Zeta computational-spectral forecasting protocol

The Riemann/Zeta chapter is algorithmic in a different way. Its computation does not search a portfolio support space; it constructs a spectral-cyclical signal and embeds that signal inside a forecast-validation architecture. The Riemann-zeta function is used as an analogical critical-line signal generator. The empirical claim is not that the Riemann Hypothesis is proved, tested or verified. The claim is whether a normalized zeta-cycle, once signed and calibrated, improves global aggregate inflation forecasting relative to FPAS and ARIMA benchmarks under layered validation.

(4.7.5) d_t = zeta_t - zeta_bar

(4.7.6) pi_hat^Z_t = pi_hat^F_t + alpha * lambda_zeta * d_t

The computational sequence is layered. The annual 1970-2024 layer supplies the headline N = 55 forecast-accuracy evidence. The 1980-2024 layer supplies annual robustness with N = 45. The 2005-2024 layer supplies compact crisis-era comparison with N = 20. The 2000Q1-2024Q4 quarterly layer supplies dynamic validation with N = 100, while the 2005M1-2024M12 monthly layer supplies spectral diagnostics with N = 240. The algorithmic discipline is that each method is assigned to the frequency and sample size appropriate for it; advanced spectral and regime tools are not treated as if they all came from the same small annual sample.

Table 4.7.3. Algorithmic sequence of the Riemann/Zeta FPAS+zeta chapter

Step	Computational operation	Evidence function
1. Build pressure input	Construct the composite global inflation-pressure index CP_t from macro-financial components	Defines the macro-financial state that drives tau
2. Construct tau	Map pressure, policy, liquidity, financial and supply stress into the nonlinear argument tau_t	Creates the argument for the critical-line signal
3. Evaluate zeta signal	Generate the critical-line zeta-cycle and normalize it into a real-valued series zeta_t	Turns mathematical signal language into a bounded economic diagnostic
4. Apply correction gate	Compute d_t = zeta_t - zeta_bar and pi_hat^Z_t = pi_hat^F_t + alpha lambda_zeta d_t	Adds signed and calibrated spectral correction to FPAS
5. Compare forecasts	Evaluate FPAS+zeta, FPAS and ARIMA using RMSE, MAE and sMAPE	Tests incremental forecast value
6. Validate dynamically	Use rolling/no-look-ahead validation, Mincer-Zarnowitz, encompassing, DM and CW tests	Protects against visual-fit and in-sample overclaiming
7. Audit regimes and spectra	Run HMM/Markov-switching, Fourier, wavelet and spectral-entropy diagnostics	Tests whether signal behavior aligns with crisis and cycle structure
8. Classify claim	Report bounded global forecast-diagnostic evidence	Excludes Riemann Hypothesis proof and universal forecast dominance

This is the monograph's strongest example of sample-discipline. It prevents the common methodological error of presenting all validation procedures as if they had the same sample basis. Forecast accuracy, dynamic validation, spectral diagnostics and regime classification are separated into appropriate layers, and the claim is written only at the level jointly supported by those layers.

4.7.5. Yang-Mills finite-network gauge-econometric protocol

The Yang-Mills chapter converts public macroeconomic anchors and corridor coding into a finite stress-weighted graph. Its computational object is not a physical field and not a continuum Yang-Mills system. It is a ten-node, twenty-seven-edge benchmark network in which systemic stress is transformed into edge weights, gauge potentials, triangular curvature, action concentration and Laplacian spectral separation. The mass-gap language is therefore confined to the first positive eigenvalue of a finite weighted stress Laplacian.

(4.7.7) L = D - W

(4.7.8) lambda_1 = first positive eigenvalue of L

(4.7.9) A_YM = sum_{triangles} ||F_ijk||^2

The algorithm begins by selecting the regional/corridor node set and retained edges. It then constructs a normalized systemic-stress field and converts the graph into an adjacency matrix, a corridor-weighted matrix and a stress-weighted matrix. The anti-symmetric gauge potential records directional stress differentials. Triangular cycles are used to compute curvature-like field strength, and the Yang-Mills economic action summarizes the concentration of stress-energy across cycles. The stress Laplacian then yields the finite-network spectral threshold. Scenario shocks and perturbation tests examine whether the threshold remains positive and how it compresses under inflation, financial-spread, trade/logistics and energy/geopolitical stress scenarios.

Table 4.7.4. Yang-Mills computational workflow and evidentiary interpretation

Algorithmic component	Operation	Interpretive role
Node and edge registration	Ten-node global/corridor benchmark and 27 retained weighted edges	Fixes finite graph universe
Stress-field construction	Normalize output, growth, income, corridor and vulnerability anchors into stress scores	Converts public anchors into a model-scale stress field
Matrix construction	Adjacency A, corridor weights, stress-weighted W and degree matrix D	Creates the linear-algebraic object for graph diagnostics
Gauge potential	Anti-symmetric potential from directional stress differentials	Encodes stress-direction imbalance
Curvature/action	Triangular curvature F_ijk and action A_YM	Measures non-neutralized cycle stress and concentration
Spectral threshold	Stress Laplacian L and first positive eigenvalue lambda_1	Defines finite-network mass-gap analogue
Scenario engine	Inflation, spread, logistics and geopolitical shock perturbations	Tests threshold compression and fragility
Panel pathway	Planned N = 1,500 country-year validation architecture	Separates benchmark evidence from future causal/panel claims

The reviewer-safety rule is strict: a positive finite-network lambda_1 supports a benchmark spectral-separation claim inside the constructed graph, not the physical Yang-Mills existence and mass-gap theorem. The benchmark can be strong, reproducible and informative while remaining explicitly finite, constructed and economic.

4.7.6. Hodge topological macro-flow decomposition protocol

The Hodge chapter is the monograph's core decomposition algorithm. It transforms a regional macroeconomic network into a directed edge cochain and decomposes that edge field into gradient hierarchy, curl/local-cycle imbalance and harmonic/systemic circulation. This protocol is computational because Hodge decomposition requires incidence matrices, weighted inner products, projection operators, orthogonality checks and residual diagnostics. It is also interpretive because the resulting components become regional hierarchy, imbalance, circulation, resilience and tail-risk variables.

(4.7.10) y = y_G + y_C + h_M + r

(4.7.11) <y_G, y_C>_W approx 0; <y_G, h_M>_W approx 0; <y_C, h_M>_W approx 0

Here y is the directed macro-flow pressure edge cochain; y_G is the gradient component generated by node potentials; y_C is the curl component generated by local cycles; h_M is the harmonic or systemic-circulation component; and r is the numerical residual. The projection is credible only if residual magnitude and weighted orthogonality diagnostics are reported. Without those diagnostics, the decomposition would become a narrative classification rather than an auditable topological calculation.

Table 4.7.5. Hodge algorithmic objects and required audit outputs

Object	Computational definition	Evidence role
Regional graph input	World anchor plus ten regional nodes, retained edge list, adjacency and row-normalized matrices	Defines the graph on which flow pressure is measured
Pressure cochain	Directed macro-flow pressure y_ij from public anchors and corridor weighting	Creates the edge-level object to be decomposed
Incidence matrices	B1 edge-node incidence and B2 triangle-edge incidence matrices	Defines gradient and curl operators
Weighted projection	Hodge decomposition under W-weighted inner product	Separates hierarchy, local imbalance and harmonic circulation
Component indices	phi_i, imbalance I_i, systemic circulation C_i, resilience R_i and tail-risk TR_i	Converts topological outputs into economic indicators
Diagnostics	Rank, projection error, W-orthogonality, spectral and simplicial checks	Audits numerical validity of the decomposition
Validation	Econometrics, machine learning, leave-one-region-out and persistent homology	Tests whether constructed components carry empirical structure
Replication	Regional input table, edge list, matrices, decomposition outputs and scripts	Makes the computational result reproducible

The Hodge protocol therefore supplies a central monograph-wide lesson: a constructed topological indicator is credible only when the matrix objects and projection diagnostics are available. The final Hodge variables are not official macroeconomic indicators; they are author-calculated decomposition outputs that must be reproduced from the input table, edge list, incidence matrices, weights and projection code.

4.7.7. Algorithmic extensions in BSD, Perelman/Ricci/Poincare and Navier-Stokes

Although this subsection's title foregrounds P vs NP, Riemann/Zeta, Yang-Mills and Hodge, the remaining three studies also contain important computational protocols. Their role is different: BSD uses local-to-global trace computation, Perelman/Ricci/Poincare uses pressure-curvature and topology algorithms, and Navier-Stokes uses stress-balance, Fourier, rolling-validation and simulation engines.

The BSD chapter uses the most explicit local-to-global algorithm among the non-primary computational chapters. It begins from a World-normalized regional anchor panel, constructs systemic stress and corridor exposure, embeds regions in a weighted network, maps regional variables into economic curve coefficients, verifies non-degeneracy, computes finite-state local traces for q = 2, 3, 5, 7 and 11, aggregates traces into Euler-factor analogues, constructs an economic L-function around s = 1, derives LOrder and compares it with a structural-rank object built from productive, Hodge-flow, network and agentic components. This is not an arithmetic BSD proof; it is an economic finite-state analogue with N = 150 closure diagnostics and explicit circularity safeguards.

The Perelman/Ricci/Poincare chapter uses a pressure-curvature-topology algorithm. Heterogeneous macro-social variables are transformed into 0-100 stress coordinates, standardized into a metric/correlation structure, decomposed into Ricci-style component curvature, summarized through scalar curvature, and then combined with Perelman-type F and W functionals. A graph-topological layer computes connectedness, algebraic connectivity, Betti numbers and edge-curvature proxies. Counterfactual sensitivity, panel validation, regularization, leave-one-out logic and Monte Carlo/bootstrap bands then prevent the pressure-curvature path from becoming an unsupported visual story.

The Navier-Stokes chapter uses a nondimensional stress-balance algorithm. Raw macro-financial variables are direction-harmonized and transformed into unit-free starred components. Systemic stress is then decomposed into liquidity velocity weakness, acceleration, pressure gradients, friction/diffusion, stochastic shocks, Fourier GDP-cycle forcing and a restricted hidden-adjustment term epsilon(t). The computational protocol includes weighting robustness, rolling forecasts, benchmark comparison against conventional time-series models, panel fixed effects, external-target validation, perturbation tests, Monte Carlo uncertainty and policy counterfactuals. The restricted epsilon(t) rule is especially important because it prevents residual closure from becoming an unrestricted algebraic plug.

Table 4.7.6. Computational extensions in the three complementary chapters

Chapter	Algorithmic core	Main computed outputs	Boundary rule
BSD	Finite-state local-to-global algorithm	q-state traces, Euler factors, L-function analogue, LOrder and structural-rank gap audit	Do not interpret local traces as literal finite-field arithmetic reductions
Perelman/Ricci/Poincare	Curvature-functional and graph-topology algorithm	Metric tensor, Ricci-style curvature, F/W functionals, graph Laplacian, Betti diagnostics, counterfactuals, Monte Carlo	Do not import theorem-level monotonicity, Ricci-flow or Poincare proof claims
Navier-Stokes	Nondimensional stress-balance and simulation algorithm	Starred variables, stress-balance equation, restricted epsilon closure, Fourier forcing, rolling validation and scenario simulation	Do not treat liquidity as literal physical fluid or stress scenarios as guaranteed forecasts

4.7.8. Algorithmic validation gates and failure conditions

The monograph treats computation as valid only when it passes appropriate validation gates. The gate differs by algorithm. A genetic algorithm requires seed, budget and benchmark disclosure; a zeta-cycle forecast requires no-look-ahead validation and forecast-comparison tests; a Laplacian mass gap requires graph connectedness and sensitivity to edge-weight perturbation; a Hodge decomposition requires projection-error and orthogonality audits; a local-to-global rank algorithm requires circularity screening; and a stress-balance model requires residual and external-target diagnostics.

Table 4.7.7. Algorithmic validation gates and failure conditions

Gate	Primary chapters	Pass condition	Failure condition
Input closure gate	All studies	Data vintage, source family, unit, frequency, region/country/industry universe and exclusion rules fixed before modelling	Post-hoc universe revision or undocumented source substitution
Transformation gate	Perelman, Hodge, Navier-Stokes, Yang-Mills, BSD, Riemann/Zeta	Normalization, direction harmonization and derived-variable formulas disclosed	Raw-unit addition, hidden sign changes or undocumented scaling
Exactness gate	P vs NP	Exact enumeration only where feasible, e.g., reduced n = 20, K = 6 benchmark	Calling a best-found full-universe incumbent a certified global optimum
Spectral gate	Yang-Mills, Hodge, Riemann/Zeta, Perelman	Connectedness, eigenvalue interpretation, spectral-diagnostic placement and stability checks	Treating finite spectra as theorem proof or universal causal mechanism
Projection gate	Hodge	Residual norm and W-orthogonality diagnostics reported	Publishing decomposition components without projection diagnostics
Forecast gate	Riemann/Zeta, Navier-Stokes, Perelman	Rolling/no-look-ahead validation, benchmarks, MZ/encompassing/DM/CW where appropriate	Claiming universal forecast dominance from in-sample fit
Simulation gate	Navier-Stokes, Yang-Mills, Perelman, BSD	Monte Carlo/perturbation seed, parameter range, scenario rule and output bands disclosed	Treating model scenarios as guaranteed future outcomes

Gate	Primary chapters	Pass condition	Failure condition
Circularity gate	BSD, constructed-index chapters	Variable-lineage screen, residualization, negative controls or external-only tests	Using overlapping constructed variables as independent confirmation
Replication gate	All studies	Formula catalogue, scripts, seeds, matrices, output tables and checksums included in package	Non-reproducible black-box computation
Claim gate	All studies	Permitted and excluded claims listed before interpretation	Theorem proof, unrestricted causality or policy certainty asserted without evidence

These gates are not optional appendices. They are part of the chapter-level evidence system. A computed object becomes scientifically usable only after its gate has been applied. This is especially important because the monograph uses high-level mathematical terminology. The stronger the mathematical analogy, the stricter the computational audit must be.

4.7.9. Reproducibility metadata for computational outputs

Every computational chapter should include a minimal reproducibility record. The record does not need to expose private working files, but it must allow the reported output to be audited and regenerated from public inputs and archived replication materials. The reproducibility metadata should include data version, source ledger, transformation rules, matrix files, algorithm parameters, random seeds, software environment, output filenames and hashes.

(4.7.12) R_k = (source_ledger_k, formula_k, script_k, seed_k, parameter_k, output_hash_k, version_k)

Table 4.7.8. Minimum reproducibility metadata for computational chapters

Metadata item	Required content	Scientific function
Data version	Study title, dataset vintage, record DOI, data-release date and file version	Prevents silent version drift
Source ledger	Source family, variable name, extraction rule, aggregation rule, transformation and output use	Connects outputs to inputs
Formula catalogue	Named equations for every constructed variable, matrix, index, forecast, score and scenario	Prevents black-box indicator creation
Algorithm settings	Search budget, population size, mutation rate, rolling window, number of draws, filtering rule, q-set or alpha grid	Makes computation auditable
Random seeds	Fixed seeds for Monte Carlo, bootstrap, permutation, GA initialization and stochastic validation	Supports deterministic replication of stochastic procedures
Intermediate matrices	Adjacency, weight, incidence, covariance, Laplacian, projection and normalization matrices	Allows verification of computed objects
Software environment	Language, package versions, operating system and hardware notes where runtime matters	Supports repeatability and explains runtime differences
Output hashes	Hashes for exported tables, figures, workbooks, scripts or result files	Protects file integrity
Claim log	Permitted claim, excluded claim and evidence source for each major table/figure	Prevents interpretation drift

The P-vs-NP chapter requires especially detailed computational metadata because random search and genetic algorithms are sensitive to seeds, budgets and implementation details. The Hodge and Yang-Mills chapters require matrix metadata

because decomposition and spectral results depend on adjacency, incidence and weight structures. The Riemann/Zeta chapter requires formula-audit metadata because small changes in normalization, alpha calibration, tau construction or correction sign can materially affect forecast outputs. BSD, Perelman/Ricci/Poincare and Navier-Stokes require lineage metadata because their constructed indices and scenario outputs are derived from multiple transformed components.

4.7.10. Algorithmic claim hierarchy

The final algorithmic protocol is a hierarchy of claims. The monograph is allowed to claim that the algorithms create transparent, reproducible and empirically useful economic-econometric analogues. It is not allowed to claim theorem proof, unconditional causality, universal forecast superiority, certified full-universe optimality or guaranteed policy impact unless the relevant evidence actually exists. This hierarchy should be carried into the interpretation chapters and the final claim-boundary matrix of the book.

Table 4.7.9. Algorithmic claim hierarchy for the monograph

Claim type	Status	Applicable chapter(s)
Algorithm was implemented on a fixed and disclosed empirical universe	Allowed if the data vintage, unit, source family and exclusions are documented	All chapters
Constructed variables are reproducible from disclosed inputs and formulas	Allowed if source ledger, formulas, scripts and replication package are available	All chapters
Heuristic search produces credible high-quality incumbents	Allowed if search coverage, seed/budget records and reduced exact benchmarks support it	P vs NP
FPAS+zeta improves the reported global forecast hierarchy	Allowed inside the stated annual, quarterly and monthly validation layers	Riemann/Zeta
A finite weighted graph has positive spectral separation	Allowed as finite-network evidence after connectedness and robustness checks	Yang-Mills
Hodge components decompose regional macro-flow pressure	Allowed if projection and orthogonality diagnostics are reported	Hodge
Local finite-state signals contain calibrated information about structural rank	Allowed inside the BSD-inspired regional analogue with circularity controls	BSD
Stress/curvature/flow/scenario algorithms support diagnostic interpretation	Allowed when robustness, residual and uncertainty checks are reported	Perelman/Ricci/Poincare and Navier-Stokes
The monograph solves, proves, tests or replicates the Clay Millennium Problems	Not allowed under any chapter	All chapters
A computed result establishes unrestricted causality or universal policy certainty	Not allowed unless a separate identification design supports it; not claimed here	All chapters

4.7.11. Methodological synthesis and transition to replication discipline

The computational protocol completes the operational side of the unified methodology. Sections 4.1-4.6 established research design, empirical universes, public-data anchors, normalization, graph construction and econometric/forecast-validation rules. Section 4.7 adds the execution layer: how the seven analogues are calculated, decomposed, searched, simulated, validated and bounded. This layer is indispensable because a monograph built on mathematical-econometric analogues must be reproducible at the level of formulas and algorithms, not only persuasive at the level of narrative.

The section also clarifies why computation does not weaken academic caution. On the contrary, computation makes caution measurable. It requires source ledgers, matrices, algorithm settings, seeds, validation tests, uncertainty bands and output hashes. It also forces the author to separate exact evidence from heuristic evidence, forecast improvement from universal dominance, finite graph spectra from theorem proof, and constructed-index coherence from causal identification.

The next subsection, 4.8, should therefore move naturally from computational protocol to replication-package and Zenodo discipline. If computation is the operational engine of the monograph, replication is the external audit mechanism. Together, they allow the book to make a strong scientific contribution while retaining strict claim boundaries.

Table 4.7.10. Compact synthesis of the computational and algorithmic protocol

Protocol item	Monograph-level requirement
Primary computational chapters	P vs NP; Riemann/Zeta; Yang-Mills; Hodge
Complementary computational chapters	BSD; Perelman/Ricci/Poincare; Navier-Stokes
Core algorithmic families	Combinatorial search; metaheuristics; exact reduced enumeration; zeta-signal construction; Hodge projection; graph Laplacian spectra; gauge curvature/action; finite-state traces; stress-balance simulation; Monte Carlo; rolling validation
Required audit artifacts	Data ledger; formula catalogue; matrices; scripts; seeds; search budgets; rolling windows; scenario parameters; output hashes; claim log
Excluded interpretations	Clay theorem proof; unrestricted causality; certified n=94 global optimum; universal forecast dominance; literal physical liquidity; continuum Yang-Mills mass gap; country-level policy certainty

In final terms, Section 4.7 defines computation as a disciplined evidentiary bridge. It links the seven mathematical inspirations to finite, auditable economic objects; it converts those objects into reproducible algorithmic workflows; and it establishes the conditions under which computed outputs may be interpreted scientifically. The result is a methodological standard that is sufficiently technical for a monograph-scale research program and sufficiently cautious to prevent mathematical, econometric or computational overclaiming.

4.8. Replication Packages and Zenodo Discipline

This section consolidates the seven Zenodo and data-availability statements into one monograph-level replication discipline. Its purpose is not merely bibliographic. The section defines how each study separates manuscript exposition from external audit material; how official public anchors are transformed into author-calculated research variables; how formulas, scripts, tables, figures, metadata, checksums and source ledgers should be preserved; and how the reader should cite the corresponding data and replication package when reproducing or checking any chapter of the monograph.

The central methodological rule is that the Word manuscript and the Zenodo record perform different functions. The manuscript explains the conceptual translation, model structure, economic interpretation and claim boundary. The Zenodo record preserves the replication artifact: input ledgers, normalized files, author-calculated outputs, tables, algorithms, scripts, software notes, metadata, checksums and citation files. The monograph should therefore treat each Zenodo package as a versioned research object, not as an informal storage location.

A second rule is equally important: a deposited package does not automatically escalate the scientific claim. Replication material strengthens transparency and auditability, but it does not turn an economic analogue into a mathematical proof, a diagnostic association into causality, a benchmark into a full country-level validation, or a heuristic search result into a certified global optimum. Zenodo discipline supports evidence classification; it does not replace methodological caution.

Source-document traceability note. This subsection synthesizes the data-availability and replication-package statements of the seven uploaded manuscripts: Perelman/Ricci/Poincare, Hodge, Navier-Stokes, Yang-Mills, Birch-Swinnerton-Dyer, Riemann/Zeta and P vs NP. Public repository details were also checked for the visible Zenodo records where available during document preparation.

4.8.1. Why the replication-package layer belongs in the unified methodology chapter

The seven studies are mathematically ambitious and empirically constructed. They use public-data anchors, normalization, author-calculated variables, graph objects, spectral calculations, forecast outputs, portfolio search procedures, curvature analogues, local-to-global rank measures and robustness layers. Without a unified replication package protocol, readers may confuse three different evidentiary layers: official data inputs, author-calculated analytical objects and manuscript-reported interpretations. The replication-package layer prevents this confusion by making the entire transformation chain externally inspectable.

The replication architecture also has a monographic function. A book composed from seven independently archived studies should not repeat seven unrelated data-availability statements without synthesis. Instead, Chapter 4 should provide one general doctrine and then list each package as a chapter-specific audit companion. This makes the book stronger than a bundle of articles: each problem chapter keeps its own empirical identity, while the methodology chapter defines one shared data-governance standard.

(4.8.1) $R_j = (S_j, A_j, T_j, O_j, M_j, H_j, C_j), \quad j = 1,...,7$

In Equation 4.8.1, R_j denotes the replication package of study j. S_j is the source-ledger component, A_j is the public-anchor component, T_j is the transformation and formula component, O_j is the output-table and figure component, M_j is the metadata and citation component, H_j is the hash/checksum component and C_j is the claim-boundary component. A package is methodologically complete only when all seven elements are identifiable.

Table 4.8.1. Minimum replication-package components required by the monograph

Component	Required content	Methodological purpose
Source ledger	Names source families, extraction dates, variable codes, public-anchor logic and any author-coded steps.	Prevents undocumented data provenance.
Transformation formulas	Records normalization, scaling, stress orientation, graph construction, forecast correction, covariance construction or rank-calibration formulas.	Separates public input data from author-calculated indicators.
Output tables and figures	Preserves reported numerical results, table exports, figure inputs and machine-readable outputs.	Allows table-level traceability and numerical audit.
Scripts and algorithms	Stores executable or pseudo-executable code, algorithm registry, search budgets, seeds and workflow steps.	Makes computation reproducible rather than narrative.
Metadata and citation files	Includes DOI/record metadata, README, data dictionary, CITATION.cff or equivalent citation record.	Turns the dataset into a citable research artifact.
Checksums and verification files	Records hashes, manifests, random seeds, QA checks or verification notes.	Protects against silent file drift and undocumented revision.
Claim boundary note	States what the package supports and what it does not support.	Prevents replication material from being misread as theorem proof or causal confirmation.

4.8.2. Consolidated Zenodo package registry for the seven studies

Table 4.8.2 is the central registry table for this subsection. It unifies the seven data and replication statements and should be retained in the monograph because it gives the reader a single audit map across the entire project. The table distinguishes DOI-based records from record-URL statements where the uploaded manuscript statement used the Zenodo record URL format. In the final book-production stage, all records should be cross-checked one more time against the live Zenodo metadata page and the exact citation string should be harmonized in the References section.

Table 4.8.2. Consolidated Zenodo and replication-package registry

Study	Package title / data statement	DOI or Zenodo record status	Main archived contents	Evidence boundary supported by the package
Perelman/Ricci/ Poincare	Data and Replication Package for "Global Perelman-Ricci-	10.5281/ zenodo.20844900; record 20844900	Excel replication workbook; methodology equations; algorithmic registry; variable definitions; table/figure metadata; results tables; QA checks; data dictionary; file manifest; citation metadata; license	Supports the N=150 macro-regional inequality-pressure, curvature, topology, validation and uncertainty

Study	Package title / data statement	DOI or Zenodo record status	Main archived contents	Evidence boundary supported by the package
	Poincare-Inspired Inequality Diagnostics: Curvature, Entropy and Graph-Topological Modelling of Macro-Regional Pressure and Smoothing Capacity"		documentation.	diagnostics; does not support theorem-level Perelman/Ricci/Poincare proof.
Hodge	Replication Package for "Global Hodge-Econometric Modeling of the World Economy: A Regional Benchmark Prototype for Topological Flow Decomposition, Systemic Circulation, Shock Transmission, and Macroeconomic Resilience"	10.5281/zenodo.20774659; record 20774659	Regional input table; ten-node codebook; 27-edge list; normalized adjacency matrices; corridor weights; B1/B2 incidence matrices; Hodge decomposition outputs; orthogonality and projection-error diagnostics; econometric scripts; leave-one-region-out audit; persistent-homology files; README/citation/license/software notes.	Supports the regional benchmark Hodge decomposition and validation audit; does not complete all-country dyadic or longitudinal replication by itself.
Navier-Stokes	Navier-Stokes-Inspired Global Liquidity-Flow and Systemic-	10.5281/zenodo.20835729; record 20835729	Reported empirical tables; extracted numerical outputs; formula catalogue; figure files; references with DOI links; metadata; source ledger; verification files; checksum records; structured workbook covering stress construction, epsilon	Supports the reported macro-financial stress-testing and N=1,500 panel evidence architecture; does not establish literal

Study	Package title / data statement	DOI or Zenodo record status	Main archived contents	Evidence boundary supported by the package
	Stress Modelling: Data and Replication Package for a Nondimensional Macro-Financial Stress-Testing Framework		closure, rolling validation, benchmarks, fixed effects, robustness, Monte Carlo and policy counterfactuals.	fluid dynamics, theorem proof or universal crisis prediction.
Yang-Mills	Dataset and Replication Package for "Economic Yang-Mills Mass Gap in Global and Corridor Flow Networks: A Finite-Network Gauge-Econometric Framework for Measuring Systemic Shock Thresholds"	10.5281/ zenodo.20786199; record 20786199	Finite-network benchmark data; extracted manuscript tables; formula and algorithm registers; core parameter files; DOI reference records; recalculated Laplacian and spectral-output files; metadata; file manifest; reproducibility audit script; files supporting the documented N=1,500 validation architecture.	Supports the ten-node finite-network benchmark and validation pathway; does not claim final country-panel causal estimates or mathematical Yang-Mills solution.
Birch-Swinnerton-Dyer	Regional Economic Birch-Swinnerton-Dyer Modelling: Data and Replication Package for a Local-to-Global Framework	10.5281/ zenodo.20796984; record 20796984	Extracted tables; core result CSV files; formula and argument catalogues; algorithm catalogue; Chapter 4 subsection catalogue; figure catalogue and embedded figures; source ledger; Zenodo metadata; CITATION.cff; data dictionary; validation reports; SHA-256 checksums; reproducibility scripts.	Supports the regional BSD-inspired local-to-global structural-rank architecture; does not prove BSD, establish causal law or convert weak external-proxy evidence into strong validation.

Study	Package title / data statement	DOI or Zenodo record status	Main archived contents	Evidence boundary supported by the package
	of Structural Rank Formation, Corridor Stress and World-Economy Calibration			
Riemann/Zeta	Data and Replication Package for "Global Riemann-Zeta FPAS+zeta Inflation Forecasting: Layered Annual, Quarterly and Monthly Validation of a Hybrid Global Macroeconomic Model"	10.5281/zenodo.20852478; record 20852478	Structured replication workbook; manuscript-reported tables; formula-audit files; annual, quarterly and monthly validation materials for N=55, N=45, N=20, N=100 and N=240; supporting documentation for forecast accuracy and spectral diagnostics.	Supports layered inflation forecast validation; does not prove/test the Riemann Hypothesis or establish universal forecast dominance.
P vs NP	Dataset Package for Robust Portfolio Optimization under Computational Complexity: A P-vs-NP-Inspired Markowitz-CAPM Framework with Cardinality Constraints	Zenodo record 20922272; DOI string should be cited from final Zenodo metadata if required by publisher style	Master Excel workbook; long-format table exports; extracted numerical registry; table index; figure index; equation register; data dictionary; README files; metadata files; checksum materials; Damodaran January 2026 input layer and author-calculated CAPM/covariance/search/robustness/option-overlay diagnostics.	Supports model-implied computational-finance replication; does not provide realized historical trading performance, certified full n=94 global optimum or proof of P != NP.

Study	Package title / data statement	DOI or Zenodo record status	Main archived contents	Evidence boundary supported by the package
	and Black-Scholes Derivative-Pricing Overlay			

4.8.3. Public data anchors, constructed variables and replication lineage

The monograph must maintain a strict lineage rule: public or official data are source anchors, not the final evidence objects. The final indicators are author-calculated variables generated through disclosed transformations. A Zenodo package must therefore preserve both the anchor information and the transformation path. This is especially important because the seven studies use terms such as curvature, mass gap, Hodge flow, LOrder, zeta correction, systemic stress and portfolio optimum. None of these are official variables. They are constructed research objects and must be reproducible from the package.

(4.8.2) X^{constructed}_{j,k} = f_{j,k}(X^{public}_{j}, W_j, N_j, G_j, A_j, heta_j)

Equation 4.8.2 states the data-lineage principle. A constructed variable X is generated from public inputs, weighting rules, normalization rules, graph or matrix structure, algorithmic operations and parameter choices. The replication package should make each component visible. If any component is missing, the result may still be readable, but it is not fully auditable.

Table 4.8.3. Data-lineage separation between public anchors and author-calculated objects

Study	Public/source anchor layer	Author-calculated layer	Replication-package trace
Perelman/Ricci/Poincare	Public macro-social regional indicators	0-100 pressure scale, metric tensor, Ricci-style curvature, F/W functionals, graph topology	Workbook, equations, results tables, QA and metadata
Hodge	Regional GDP, share, growth, transition GDP and income-depth anchors	Network matrices, edge cochain, gradient/curl/harmonic Hodge components, resilience and risk indices	Input table, 27-edge list, B1/B2 matrices, decomposition files and scripts
Navier-Stokes	Macro-financial, risk, liquidity, shock, cycle and resilience proxies	Nondimensional starred variables, stress-balance outputs, restricted epsilon closure, Monte Carlo and policy scenarios	Structured workbook, formula catalogue, verification and checksum records
Yang-Mills	GDP mass, world share, growth, income depth, corridor codes and stress proxies	Gauge potential, curvature, action, Laplacian, mass gap, EMGI, BridgeStress and scenario diagnostics	Benchmark data, matrices, spectrum files, algorithm registers and audit script
BSD	World-normalized regional macroeconomic and corridor anchors	Finite-state traces, Euler factors, L_econ, LOrder, structural rank, regulator/friction/torsion objects	CSV files, formula/argument catalogues, scripts, SHA-256 checks and validation reports
Riemann/Zeta	World inflation and macro-financial pressure inputs across	Composite pressure, tau, normalized zeta cycle, zeta correction, FPAS+zeta forecast	Replication workbook, table outputs, formula audit and layered

Study	Public/source anchor layer	Author-calculated layer	Replication-package trace
	annual/quarterly/monthly layers	and loss differentials	validation files
P vs NP	Damodaran January 2026 industry beta/volatility data and calibration constants	CAPM returns, covariance geometry, support-space enumeration, GA/Monte Carlo outputs, option overlay and robustness results	Excel workbook, numerical registry, table/figure/equation indexes, metadata and checksums

4.8.4. DOI, record, version and citation discipline

A Zenodo record should be cited as a dataset or replication package, not as an ordinary webpage. The preferred citation line should include author, year, package title, version if available, resource type, repository and DOI. When the manuscript source gives only a Zenodo record URL, the monograph should either cite the record URL exactly or verify the DOI on the Zenodo metadata page before inserting a DOI resolver link. This prevents accidental citation of a guessed DOI and protects the final bibliography from metadata inconsistency.

Version discipline is especially important for this book because several chapters are being revised from article form into monograph form. A Zenodo package is tied to a manuscript version. If the monograph later changes formulas, tables, data definitions or numerical results, the corresponding package must either be updated as a new version or explicitly described as supporting the earlier article version. The book should not silently rely on an article-level package for a substantially revised book-level calculation unless the package also contains the book-level replication files.

(4.8.3) Citation_j = (Author, Year, Title_j, Version_j, Repository, DOI_j/Record_j, Access/Metadata status)

Equation 4.8.3 defines the minimum citation tuple. For publication, the exact punctuation can follow APA, Chicago, journal style or publisher house style, but the content fields should remain stable.

Table 4.8.4. DOI, record and version rules for the monograph

Citation issue	Required treatment	Application
DOI record	Use DOI resolver citation and include record number if useful.	Perelman, Hodge, Navier-Stokes, Yang-Mills, BSD, Riemann/Zeta.
Record-URL statement	Use the Zenodo record URL and verify DOI before converting to DOI format.	P vs NP source statement gives record 20922272.
Version field	Include Version v1 or later version where the record states it.	Navier-Stokes, Yang-Mills and Riemann/Zeta source statements specify v1; other packages should follow their metadata.
Package title	Do not shorten the package title so severely that the dataset becomes hard to identify.	All seven records.
Chapter-linking	In the monograph bibliography, group the seven data packages with the chapter to which each belongs.	References and General Data and Replication Statement.
Update trigger	If book-level calculations differ materially from article-level calculations, issue a new package version or a monograph-level consolidated package.	All seven chapters.

4.8.5. Script, seed, checksum and software-environment discipline

The strongest replication packages do more than archive tables. They preserve the mechanisms by which the tables were generated. This is why the monograph should define script, seed, checksum and software-environment discipline as a general rule. Randomized procedures such as Monte Carlo perturbations, genetic algorithms, bootstrap uncertainty, permutation placebo tests and stochastic scenario engines require seed disclosure. Deterministic matrix calculations such as

Hodge decomposition, Laplacian spectra, covariance construction and Euler-factor analogues require formula and matrix disclosure. Forecast comparisons require data splits, rolling-window definitions and loss-function definitions. Portfolio search requires search budgets and exact reduced-enumeration records.

(4.8.4) $H(F_j) = SHA256(bytes(F_j))$

(4.8.5) $Replicate(Result) = g(SourceLedger, Formulas, Scripts, Seeds, Environment, Inputs)$

Equations 4.8.4 and 4.8.5 summarize the audit logic. A file hash allows the reported artifact to be checked for identity. A replication function states that results should be reproducible from the source ledger, formulas, scripts, seeds, software environment and inputs. If only a final table is archived, the evidence remains transparent but not fully executable. If the table, script, formula, seed and input ledger are all archived, the evidence becomes much stronger.

Table 4.8.5. Reproducibility controls for scripts, seeds, matrices and outputs

Control item	Where it matters most	Required action
Random seeds	Monte Carlo, bootstrap, permutation placebo, genetic algorithm and stochastic simulation procedures.	Record seed values and which routine used each seed.
Search budgets	P vs NP Monte Carlo/GA/search coverage and exact reduced benchmark.	Record iterations, population sizes, K-grid rules, support counts and runtime notes.
Matrix objects	Hodge B1/B2 matrices; Yang-Mills adjacency/Laplacian; BSD graph and trace files; covariance matrices in P vs NP.	Archive matrices in machine-readable form.
Forecast splits	Riemann/Zeta and Navier-Stokes rolling validation windows and benchmark comparisons.	Record training window, forecast horizon, benchmark model and loss function.
Formula catalogue	All constructed variables: curvature, F/W, mass gap, LOrder, stress balance, zeta correction, Sharpe and option overlay.	Archive formulas or scripts and map each to manuscript equations.
Checksums	Final datasets, panels, result tables, matrix files and script outputs.	Use SHA-256 or another explicitly named algorithm.
Software environment	Python/R/Stata/Excel version, package dependencies and operating environment if relevant.	Document enough detail for independent rerun or audit.

4.8.6. Study-specific replication statements for insertion into the monograph

The following statements can be used as chapter-level data notes or adapted for the general data and replication statement in the front matter. They are written in a unified style while preserving the identity of each original package.

Table 4.8.6. Unified chapter-level data and replication statements

Chapter / study	Monograph-ready statement
Perelman/Ricci/Poincare	The data and replication package for the Perelman-Ricci-Poincare-inspired inequality diagnostics chapter is archived on Zenodo as a dataset supporting the N=150 macro-regional pressure, curvature, graph-topology, validation and uncertainty architecture. DOI: 10.5281/zenodo.20844900; record: https://zenodo.org/records/20844900.
Hodge	The replication package for the Hodge-econometric macro-flow chapter is archived on Zenodo and contains the regional input table, ten-node codebook, 27-edge list, incidence matrices, Hodge decomposition outputs, projection/orthogonality diagnostics, econometric scripts and topology files. DOI: 10.5281/zenodo.20774659; record: https://zenodo.org/records/20774659.
Navier-Stokes	The data and replication package for the Navier-Stokes-inspired macro-financial stress-testing

Chapter / study	Monograph-ready statement
	chapter is archived on Zenodo and supports the reported empirical tables, formula catalogue, figure files, source ledger, checksum records, N=1,500 panel evidence architecture, rolling validation, benchmark comparison, robustness, Monte Carlo and policy-counterfactual layers. DOI: 10.5281/zenodo.20835729; record: https://zenodo.org/records/20835729.
Yang-Mills	The finite-network dataset and replication package for the Yang-Mills-inspired mass-gap chapter is archived on Zenodo and supports the ten-node benchmark, corridor-stress network, gauge-curvature/action calculations, Laplacian spectrum, mass-gap diagnostics and documented N=1,500 validation architecture. DOI: 10.5281/zenodo.20786199; record: https://zenodo.org/records/20786199.
BSD	The regional BSD-inspired data and replication package is archived on Zenodo and documents the source ledger, regional aggregation, finite-state traces, Euler-factor analogues, economic L-function, LOrder, structural rank, validation reports, checksums and reproducibility scripts. DOI: 10.5281/zenodo.20796984; record: https://zenodo.org/records/20796984.
Riemann/Zeta	The Riemann-Zeta FPAS+zeta replication package is archived on Zenodo and supports the reported annual, quarterly and monthly layered validation architecture, including N=55, N=45, N=20, N=100 and N=240 outputs, formula audit and forecast-validation tables. DOI: 10.5281/zenodo.20852478; record: https://zenodo.org/records/20852478.
P vs NP	The P-vs-NP-inspired portfolio-optimization dataset package is archived on Zenodo record 20922272 and contains the master Excel workbook, long-format tables, numerical registry, table/figure/equation indexes, data dictionary, README files, metadata and checksum materials supporting the Damodaran January 2026, CAPM, covariance, search-space, robustness and option-overlay diagnostics. Record: https://zenodo.org/records/20922272.

4.8.7. Evidence levels supported by the replication packages

Replication packages make the evidence inspectable, but the level of evidence differs across studies. Some packages support a completed benchmark; some support a fully reported validation architecture; some support a planned or pathway validation layer; some support a model-implied computational experiment rather than realized historical evidence. The book should classify these levels explicitly.

(4.8.6) ClaimLevel_j = min(ModelEvidence_j, ReplicationClosure_j, ExternalValidation_j, BoundaryRule_j)

Equation 4.8.6 expresses the no-escalation rule. The final claim level cannot exceed the weakest required evidence gate. For example, a strong Zenodo package cannot turn a planned N=1,500 panel into final country-level causal evidence; a documented heuristic search cannot become a certified full-universe optimum; and a well-structured zeta-cycle replication package cannot become a Riemann Hypothesis proof.

Table 4.8.7. Evidence levels supported by the archived packages

Evidence level	Meaning	Main applications
Completed reported-results package	Reported tables, formulas and outputs are archived for the manuscript version.	Perelman/Ricci/Poincare; Riemann/Zeta; P vs NP; BSD; Navier-Stokes.
Completed finite-network benchmark package	Network matrices, spectral outputs and benchmark diagnostic results are archived.	Yang-Mills; Hodge.
Validation pathway package	A future or specified larger validation architecture is documented, but final estimates are bounded or conditional.	Yang-Mills N=1,500 pathway; Hodge future dyadic/country-level extensions.
Model-implied computational package	Outputs reproduce computational or model-implied evidence, not realized historical	P vs NP; Riemann/Zeta; scenario/counterfactual parts of Navier-

Evidence level	Meaning	Main applications
	performance.	Stokes.
External audit companion	Package enables reviewers to trace the manuscript but does not replace source institutions or raw official repositories.	All seven studies.

4.8.8. Monograph-level replication workflow

The monograph should give readers a practical workflow for replication. The workflow below can be presented as the common rule for all seven chapters. It is intentionally conservative: it requires the reader to identify the relevant chapter package, inspect the README and data dictionary, map each table to an output file, reproduce constructed variables from the formulas, check hashes or file manifests where available and only then evaluate the claim boundary.

24. Identify the problem chapter and the corresponding Zenodo data or replication package from Table 4.8.2.
25. Read the package README, citation file, data dictionary and file manifest before opening result tables.
26. Locate the public-source anchor files or source ledger and confirm the extraction and aggregation logic used in the chapter.
27. Locate the transformation formulas, scripts or algorithm registry that convert public anchors into author-calculated variables.
28. Reproduce or inspect the main constructed objects: normalized stress scales, matrices, decompositions, spectra, forecasts, ranks, search outputs or scenario tables.
29. Compare reproduced outputs with the manuscript-reported tables and figures using the package table index or numerical registry.
30. Check random seeds, search budgets, validation windows, software notes and checksums where the package provides them.
31. Read the claim-boundary statement for the chapter and do not upgrade the result beyond the evidence supported by the package and the manuscript.

(4.8.7) ReplicationPass = 1{Inputs matched} x 1{Formulas matched} x 1{Outputs matched} x 1{Boundary respected}

Equation 4.8.7 defines a strict replication pass. A result is not replication-safe if the outputs match but the inputs are undocumented, or if the numerical result can be reproduced only by violating the stated claim boundary.

4.8.9. Reviewer-risk response and package-governance safeguards

The consolidated Zenodo discipline directly responds to predictable reviewer risks. These include missing data lineage, confusion between official indicators and constructed indices, excessive dependence on black-box computation, uncontrolled version drift, undocumented randomization, incomplete formula disclosure, and overclaiming. Table 4.8.8 maps these risks to the safeguards that should be retained in the monograph.

Table 4.8.8. Reviewer-risk response matrix for replication-package governance

Reviewer risk	Safeguard	Where applied
Official data confused with constructed indicators	Maintain public-anchor versus author-calculated distinction in every data statement.	All seven packages.
Zenodo package treated as proof of correctness	State that replication improves auditability but does not escalate theorem, causality or optimum claims.	General claim boundary and each chapter.
Version drift between article and book	Update package version or state which manuscript version is supported.	All chapter conversions.
Missing formula-to-table mapping	Use formula catalogue, equation register, table index and numerical registry.	Perelman, Riemann/Zeta, P vs NP, Yang-Mills, BSD.
Undocumented stochastic computation	Record seeds, Monte Carlo budgets, bootstrap/permutation settings and GA/search parameters.	P vs NP, BSD, Yang-Mills, Navier-Stokes, Perelman.

Reviewer risk	Safeguard	Where applied
Matrix or graph objects not reproducible	Archive adjacency, incidence, Laplacian, covariance, edge-list and spectral-output files.	Hodge, Yang-Mills, BSD, P vs NP.
Validation methods misread as stronger than they are	Separate benchmark validation, diagnostic association, rolling forecast evidence and planned validation pathways.	All seven, especially Yang-Mills and Riemann/Zeta.
Publisher bibliography inconsistency	Use a single package-citation style and verify DOI/record metadata before final submission.	References and data-availability section.

4.8.10. General monograph data and replication statement

The following unified statement can be placed in the front matter of the book or at the end of Chapter 4, with the chapter-specific package registry retained as Table 4.8.2.

> **General Data and Replication Statement.** The empirical materials supporting this monograph are organized through seven chapter-specific data and replication packages archived on Zenodo or identified by Zenodo record. These packages document the public-data anchors, author-calculated variables, methodological formulas, algorithms, result tables, figures, matrices, scripts, metadata, file manifests, checksums and citation materials required to audit the reported economic-econometric analogues. The packages should be cited as independent dataset or replication-package records and read together with the corresponding manuscript chapters. Public-source data remain attributable to their original institutional sources; the Zenodo packages document the author-calculated transformations and reported research outputs. The packages support transparency, reproducibility checking and methodological audit. They do not imply proof of the original Clay Millennium Problems, unrestricted causal identification, universal forecast dominance, certified global optimality or theorem-level mathematical resolution.

4.8.11. Integration with the previous subsections of Chapter 4

This subsection closes the methodological chain developed from Sections 4.1 to 4.7. Section 4.1 defined the monograph as quantitative, non-experimental, computational, econometric and validation-oriented. Section 4.2 classified the empirical universes. Section 4.3 separated public data anchors from author-calculated variables. Section 4.4 defined normalization and directional harmonization. Section 4.5 established network and graph construction. Section 4.6 defined econometric and forecast validation. Section 4.7 specified computational and algorithmic evidence. Section 4.8 now makes those procedures auditable through Zenodo and replication-package discipline.

For that reason, Section 4.8 is not a secondary administrative appendix. It is a methodological closure layer. It shows that the book can make ambitious analogue claims while still allowing readers to trace the data lineage, reproduce the constructed objects, inspect the validation steps and understand the evidence boundary of each chapter.

Table 4.8.9. How Zenodo discipline closes the earlier Chapter 4 methodology layers

Earlier subsection	Replication-package closure function
4.1 Research design	Replication packages preserve the design choices and evidence hierarchy.
4.2 Empirical universes	Packages identify sample, unit, frequency, observation count and validation layer.
4.3 Public anchors and calculated variables	Packages separate official inputs from author-generated outputs.
4.4 Normalization and scaling	Packages store formulas and normalized files used for stress, spectral or risk scaling.
4.5 Network and graph protocol	Packages archive edge lists, matrices, Laplacians, incidence matrices and graph diagnostics.
4.6 Econometric/forecast validation	Packages preserve rolling windows, loss metrics, models, residual diagnostics and robustness tests.
4.7 Computational protocol	Packages document algorithms, search budgets, scripts, seeds, simulations and computation-specific outputs.

4.8.12. Final methodological conclusion

The unified replication-package protocol is a central part of the monograph's scientific discipline. It transforms the seven studies from isolated article-level data notes into a single transparent research infrastructure. Each package has its own empirical object and claim boundary, but together they establish a common standard: every constructed economic analogue must be supported by source documentation, formulas, algorithms, outputs, metadata and citation discipline.

The strongest contribution of this subsection is evidentiary. It does not add a new empirical result; it defines the conditions under which the existing results can be audited. It therefore strengthens the credibility of the whole book. The reader can see which packages support completed benchmark evidence, which support layered forecast validation, which document a validation pathway, which preserve model-implied computational-finance outputs and which contain checksums, scripts or matrix files for deeper reproduction.

The final claim is precise: the seven Zenodo/data packages provide an external audit foundation for the monograph's economic-econometric analogues of the Millennium Problems. They support reproducibility, transparency, table-level traceability and methodological review. They do not convert the monograph into a proof of any Clay Millennium Problem and do not remove the need for cautious interpretation, especially where evidence remains diagnostic, benchmark-specific, planned, model-implied or non-causal.

4.9. General Claim-Boundary Matrix

This section consolidates the claim-boundary logic of the seven Millennium-inspired economic studies into a single monograph-level control matrix. Its purpose is not merely editorial. It is a technical reviewer-safety device: it fixes, before the problem chapters begin, what each study is allowed to claim, what it is not allowed to claim, what type of evidence supports the permitted claim, and what language must be avoided when the evidence remains diagnostic, benchmark-based, calibrated, forecast-specific or computational rather than theorem-level or causal.

The central boundary is common to the entire monograph: the book does not claim to solve, prove, test or replicate the Clay Millennium Problems in their original mathematical form. It develops seven bounded economic-econometric analogues inspired by their formal architectures. Each analogue has its own empirical universe, constructed variables, validation layer, replication package and admissible evidence status. The claim-boundary matrix below converts this principle into a chapter-by-chapter rule.

The matrix is especially important because the monograph uses powerful mathematical terms: Ricci flow, Perelman entropy, Poincare topology, Hodge decomposition, Navier-Stokes flow, Yang-Mills mass gap, Birch-Swinnerton-Dyer local-to-global logic, Riemann zeta signals and P versus NP complexity. These terms are used as measurement grammars, not as declarations that the mathematical Millennium Problems have been resolved. The safest scientific reading is therefore strong but bounded: the monograph contributes a mathematical-econometric analogue programme for economic complexity measurement.

Source-document traceability note. This section synthesizes the claim-boundary, evidence-status, limitations and final claim-hierarchy statements from the seven uploaded manuscripts and the monograph-structure memorandum.

4.9.1. Function of the claim-boundary matrix in the methodology chapter

In an ordinary empirical paper, claim boundaries are often placed near the conclusion. In this monograph, they must appear in the methodology chapter because the methodological architecture itself depends on analogy discipline. The claim boundary determines how formulas, networks, regressions, forecasts and optimization outputs may be interpreted. It prevents a strong model-implied result from being upgraded into a theorem, a calibrated correspondence from being upgraded into causality, or a benchmark simulation from being upgraded into universal predictive law.

The seven studies differ in evidence strength. Navier-Stokes has a large global country-year panel and stress-testing validation. Riemann/Zeta has the strongest layered forecast-validation architecture. P vs NP has the strongest computational exactness discipline because it combines a very large full-universe search space with a reduced exact enumeration benchmark. Yang-Mills, Hodge and BSD are structurally strong benchmark architectures, while Perelman/Ricci/Poincare uses a balanced regional diagnostic panel. The claim-boundary matrix does not flatten these differences. It assigns a permitted claim to each evidence type.

$$\text{Claim}_{j,c} \text{ is admissible only if } \text{Support}_{j,c}=1, \text{Boundary}_{j,c}=1 \text{ and } \text{Exclusion}_{j,c}=0. \quad (4.9.1)$$

Equation 4.9.1 states the governing rule. For study j and claim c, a claim is admissible only when the relevant evidence layer supports it, the language remains inside the study boundary, and the claim is not part of the excluded set. The rule applies to every table, figure, regression coefficient, graph diagnostic, forecast comparison, algorithmic result and final chapter conclusion.

Table 4.9.1. General claim-boundary matrix for the seven Millennium-inspired economic studies

Study	Permitted monograph claim	Evidence layer supporting the claim	Explicitly excluded claim	Final claim level
Perelman/Ricci/Poincare	Inequality pressure, smoothing capacity, curvature-like deformation, entropy-like complexity and graph-topological connectedness can be measured inside a macro-regional diagnostic architecture.	N=150 region-year diagnostic panel; 0-100 stress-coordinate system; curvature, functionals, graph topology, econometric and robustness diagnostics.	Proof/test/replication of Perelman proof, Ricci-flow theorem or Poincare conjecture; literal geometric invariants; unrestricted causality; country-level welfare replacement; universal forecast superiority.	High-level diagnostic measurement claim.
Hodge	The regional world economy can be represented as a connected macro-flow graph whose directed pressure cochain can be decomposed into hierarchy, local imbalance and systemic circulation.	Ten-node regional benchmark plus World anchor; weighted graph; incidence/cochain construction; gradient-curl-harmonic decomposition; econometric, predictive and topological diagnostics.	Proof of the Hodge Conjecture; claim that regions are algebraic varieties; observed dyadic-flow substitution; final all-country causality; claim that official institutions publish Hodge economic indicators.	Structural measurement and decomposition claim.
Navier-Stokes	Global liquidity-flow and systemic stress can be organized as a nondimensional pressure-friction-shock-cycle-closure stress-testing architecture.	100-country annual panel, 2010-2024, N=1,500; nondimensional starred variables; rolling validation; benchmark comparison; FE/robust inference; external validation; Monte Carlo and policy counterfactuals.	Financial liquidity as literal physical fluid; Navier-Stokes theorem-level PDE result; universal crisis forecast law; definitive causality; unconditional policy certainty.	Global macro-financial diagnostic and stress-testing claim.
Yang-Mills	A finite stress-weighted corridor network can exhibit a positive finite-graph spectral separation that functions as an economic mass-gap threshold for systemic shock transmission.	Completed ten-node, twenty-seven-edge benchmark; stress field, gauge potential, triangular curvature, action, Laplacian, EMGI, BridgeStress, scenario diagnostics; N=1,500 panel pathway reserved for later closure.	Solution to the mathematical Yang-Mills existence and mass gap problem; physical gauge-field identity; final causal country-panel confirmation before the N=1,500 layer is populated and estimated.	Finite-network threshold and benchmark-reproducibility claim.
Birch-Swinnerton-Dyer	Local regional finite-state signals, Euler-	World anchor plus ten regional/corridor nodes;	Proof/test/replication of the classical BSD	Calibrated local-to-global

Study	Permitted monograph claim	Evidence layer supporting the claim	Explicitly excluded claim	Final claim level
	factor analogues and an L-order measure contain calibrated information about global structural-rank formation.	N=150 closure layer; rank-gap diagnostics; agreement, sensitivity, placebo, anti-circularity and external-proxy screening.	conjecture; literal arithmetic reductions over finite fields; causal econometric law; strong external validation where robust-inference evidence remains weak.	structural-rank claim.
Riemann/Zeta	A normalized Riemann-zeta critical-line cyclical signal can improve and diagnose global aggregate inflation forecasts when embedded in an FPAS baseline and tested through layered validation.	Annual N=55, annual robustness N=45, crisis-era N=20, quarterly N=100 and monthly N=240 validation layers; RMSE/MAE/sMAPE, rolling validation, MZ, encompassing, DM/CW, HMM, spectral diagnostics.	Proof, test or verification of the Riemann Hypothesis; zeta signal as causal theorem; residual-problem elimination; universal forecast dominance across all economies, samples and horizons.	Bounded global forecast-diagnostic claim.
P vs NP	Cardinality-constrained portfolio optimization creates a nontrivial mixed discrete-continuous computational-finance problem whose heuristic results can be audited against exact reduced benchmarking.	Damodaran January 2026 n=94 industry universe; C(94,10) support space; greedy, Monte Carlo, GA and reoptimization; exact reduced n=20, K=6 enumeration with C(20,6)=38,760; robustness and option overlay.	Proof of P != NP or P = NP; certified global optimum for full n=94, K=10 instance; realized historical investment dominance; derivative leverage as free performance.	Empirical-computational optimization claim.

4.9.2. Common theorem-exclusion rule

The first common rule is the theorem-exclusion rule. None of the seven studies is framed as a proof, disproof, empirical test or verification of the original Clay Millennium Problem. The monograph is therefore not a mathematical proof monograph. It is a methodological monograph that uses mathematical architectures as economic measurement languages. This distinction must be kept in every abstract, introduction, methodology, results interpretation, conclusion and public-data statement.

(4.9.2) Mathematical reference -> economic analogue, not mathematical resolution.

Equation 4.9.2 is the translation rule. The mathematical reference supplies formal architecture: flow, curvature, topology, rank, spectral signal, local-to-global structure or computational complexity. The economic analogue supplies empirical measurement: stress, resilience, corridor exposure, inflation forecasting, structural rank, network thresholds or portfolio search. The arrow is not reversible. An economic analogue cannot be read back as a theorem-level statement about the original mathematical object.

Table 4.9.2. Theorem-exclusion matrix

Study	Original mathematical problem	Economic use in the monograph	Excluded theorem-level language
Perelman/Ricci/Poincare	Perelman proof, Ricci-flow theorem and Poincare conjecture	Inequality-pressure manifold, curvature-like deformation and graph connectedness	No geometric/topological theorem proof or literal manifold claim.
Hodge	Hodge Conjecture and Hodge classes/algebraic cycles	Discrete Hodge decomposition of a finite regional macro-flow cochain	No claim that economic regions are algebraic varieties or that economic cycles are algebraic cycles.
Navier-Stokes	Navier-Stokes existence/smoothness problem	Nondimensional macro-financial stress-balance analogy	No physical-fluid identity and no PDE theorem claim.
Yang-Mills	Yang-Mills existence and mass gap	Finite weighted-graph spectral separation and stress-threshold analogy	No physical gauge-field proof and no Clay mass-gap solution.
BSD	Birch-Swinnerton-Dyer conjecture	Regional local-to-global rank measurement using economic traces, Euler factors and L-order	No arithmetic proof, no literal elliptic-curve rank theorem and no theorem-level validation.
Riemann/Zeta	Riemann Hypothesis	Normalized zeta-cycle used as a forecast correction and spectral diagnostic	No RH proof, test or verification.
P vs NP	P versus NP problem	Cardinality-constrained portfolio search as empirical-computational complexity demonstration	No proof of P != NP, P = NP or certified full n=94 optimality.

4.9.3. Permitted claim levels and evidence hierarchy

The second common rule is the evidence-level rule. The same wording cannot be used for all chapters because the evidence layers differ. A populated 100-country panel, a layered forecast-validation design, an exact reduced enumeration, a ten-node graph benchmark and a regional N=150 closure layer do not support identical claims. The monograph should therefore classify claims using a hierarchy: measurement construction, benchmark diagnostic evidence, calibrated correspondence, forecast validation, computational demonstration, association evidence and causal exclusion.

Table 4.9.3. Evidence hierarchy and permitted wording levels

Evidence level	Definition	Typical location in this monograph	Permitted wording
Level 1: Analogue construction	The object is formally defined and reproducibly constructed.	All seven chapters.	May claim methodological construction; may not claim empirical dominance.
Level 2: Internal measurement consistency	Constructed indicators behave coherently under formulas, decompositions, rankings or diagnostics.	Perelman/Ricci/Poincare, Hodge, Yang-Mills, BSD, P vs NP.	May claim internal consistency; may not claim external causality.

Evidence level	Definition	Typical location in this monograph	Permitted wording
Level 3: Benchmark evidence	A finite benchmark, regional universe or exact reduced instance is fully reported.	Hodge, Yang-Mills, BSD, P vs NP, Perelman/Ricci/Poincare.	May claim benchmark validity under design assumptions.
Level 4: Forecast-validation evidence	Out-of-sample or rolling forecast performance is compared with benchmarks.	Riemann/Zeta, Navier-Stokes, Perelman/Ricci/Poincare where bounded.	May claim validation-window performance; may not claim universal forecasting superiority.
Level 5: Panel association evidence	FE, TWFE, robust inference or panel diagnostics support directional or association patterns.	Navier-Stokes, BSD, Perelman/Ricci/Poincare, planned Yang-Mills layer.	May claim diagnostic association; may not claim identification without causal design.
Level 6: Exact or certified evidence	Exact reduced enumeration or complete matrix/spectral computation is disclosed.	P vs NP reduced benchmark; Yang-Mills finite graph; Hodge decomposition.	May claim exactness only for the specified finite/reduced object.
Level 7: Causal/theorem proof	Requires identification design or mathematical proof.	Not claimed by any chapter.	Explicitly excluded throughout the monograph.

4.9.4. Study-specific claim profiles

The central matrix gives the compact result. The following profiles provide the interpretive detail that should guide the later problem chapters. Each profile has three parts: strongest admissible claim, claim-supporting evidence and prohibited escalation. This structure should be reused in the final paragraphs of Chapters 5 through 11 and again in the monograph-wide synthesis.

Perelman/Ricci/Poincare

The admissible claim is a diagnostic-measurement claim about global inequality pressure. The chapter may say that the model organizes inequality pressure, smoothing capacity, curvature-like deformation, entropy-like complexity and graph-topological connectedness in a coherent macro-regional framework. It may also say that the N=150 region-year panel and the validation layers support bounded diagnostic interpretation. It may not say that the study proves Perelman, Ricci flow or Poincare results, identifies unrestricted causal effects, replaces country-level welfare analysis or establishes universal forecast superiority.

Hodge

The admissible claim is a structural-decomposition claim. The chapter may say that public regional macroeconomic anchors can be transformed into a finite regional graph, a directed macro-flow pressure field and a decomposable edge cochain. It may interpret gradient hierarchy, curl/local-cycle imbalance and harmonic/systemic circulation as author-calculated Hodge-econometric indicators. It may not claim to solve the Hodge Conjecture, identify economic regions as algebraic varieties, substitute an observed dyadic transaction matrix, or close all causal and forecasting questions from a ten-node benchmark.

Navier-Stokes

The admissible claim is a global macro-financial stress-testing claim. The chapter may say that systemic stress can be organized through nondimensional liquidity velocity, acceleration, pressure gradients, friction/diffusion, shock, Fourier-cycle forcing and restricted hidden adjustment. Because the design uses a 100-country, 2010-2024, N=1,500 panel, rolling validation, benchmark models, robust inference, external-target validation, Monte Carlo uncertainty and policy counterfactuals, it may support a high stress-diagnostic interpretation. It may not say that liquidity is a physical fluid, that the Navier-Stokes mathematical problem is solved, or that the model is a universal crisis-prediction law.

Yang-Mills

The admissible claim is a finite-network threshold claim. The chapter may say that a completed ten-node, twenty-seven-edge stress-weighted corridor benchmark generates reproducible gauge-potential, curvature, action, Laplacian, EMGI, BridgeStress and scenario-threshold diagnostics, including a positive finite-network economic mass-gap indicator. It may not claim a physical Yang-Mills mass gap proof, a final country-level causal result, or a completed N=1,500 panel validation before that layer is populated, estimated and archived.

Birch-Swinnerton-Dyer

The admissible claim is a calibrated local-to-global structural-rank claim. The chapter may say that finite-state regional signals, Euler-factor analogues, L-function behavior and an L-order measure contain measurable information about structural economic rank under the specified regional/corridor architecture. It may rely on N=150 closure diagnostics, rank-gap agreement, sensitivity checks, placebo logic and anti-circularity gates. It may not claim proof of BSD, literal arithmetic reductions over finite fields, causal econometric law or strong external validation where robust p-values and external proxies remain weak or directional.

Riemann/Zeta

The admissible claim is a bounded global forecast-diagnostic claim. The chapter may say that the FPAS+zeta framework improves global aggregate inflation forecasting within the reported annual, quarterly and monthly validation layers and that the normalized zeta-cycle is diagnostically aligned with global stress years. It may not claim that the Riemann Hypothesis is proven, tested or verified, that the zeta signal is causal, that residual problems are eliminated, or that the model universally dominates in every economy, sample and horizon.

P vs NP

The admissible claim is an empirical-computational optimization claim. The chapter may say that cardinality-constrained portfolio optimization creates a mixed discrete-continuous search problem in a fixed Damodaran January 2026 n=94 industry universe; that C(94,10) demonstrates support-space explosion; that greedy, Monte Carlo, GA and reoptimization layers can be compared; and that the reduced n=20, K=6 enumeration gives exact benchmark evidence for that reduced instance. It may not claim to prove P != NP, certify the full n=94 global optimum or establish realized historical investment dominance.

4.9.4A. Detailed claim-audit panels for the seven studies

The compact permitted-claim matrix must be operationalized at the level of evidence blocks. Each study contains several evidence layers, and each layer has a different admissible claim. A diagnostic panel, a graph decomposition, a finite-network eigenvalue, a forecast-comparison test and a reduced exact enumeration do not authorize identical language. The following audit panels specify what each major evidence block can and cannot support.

Table 4.9.4A. Evidence-block claim audit across the seven studies

Study	Evidence block	Permitted statement	Forbidden escalation
Perelman/Ricci/Poincare	Pressure-curvature path and scalar curvature	May identify crisis deformation and partial recovery in the harmonized window.	May not claim literal Ricci curvature or theorem-level monotonicity.
Perelman/Ricci/Poincare	Graph topology, Betti and Laplacian diagnostics	May claim connected diagnostic topology and cycle-rich inequality structure.	May not claim proof of the Poincare conjecture.
Perelman/Ricci/Poincare	Econometric and forecast screens	May claim diagnostic association and bounded validation.	May not claim causal policy effects or universal forecast superiority.
Hodge	Gradient component	May interpret hierarchy in the constructed macro-flow pressure field.	May not reduce the whole world economy to GDP hierarchy alone.
Hodge	Curl component	May interpret local-cycle imbalance and corridor inconsistency.	May not claim direct observed transaction-flow measurement.

Study	Evidence block	Permitted statement	Forbidden escalation
Hodge	Harmonic component	May interpret systemic residual circulation in the finite graph.	May not claim full global dyadic circulation without all-country/dyadic replication.
Navier-Stokes	Nondimensional balance equation	May organize stress through velocity, acceleration, pressure, friction, shock, cycle and closure channels.	May not imply literal hydrodynamic law.
Navier-Stokes	Rolling validation and benchmark comparison	May claim reported validation-window diagnostic usefulness.	May not claim permanent crisis-prediction dominance.
Navier-Stokes	FE and external validation	May claim coherent diagnostic associations under controls.	May not claim definitive causal identification.
Yang-Mills	Stress Laplacian and finite mass gap	May claim finite-network spectral separation in the constructed benchmark.	May not claim Clay/Yang-Mills theorem proof.
Yang-Mills	Gauge potential, curvature and action	May claim stress-curvature/action concentration inside the finite network.	May not claim physical gauge field or quantum field identity.
Yang-Mills	N=1,500 validation pathway	May claim specified future panel-validation architecture.	May not report final country-panel causality before estimation.
BSD	Finite-state traces and Euler factors	May claim local regional signals are informative under the constructed analogue.	May not claim literal finite-field arithmetic reductions.
BSD	LOrder and structural rank	May claim calibrated local-to-global rank consistency.	May not claim exact equality, theorem proof or causal rank law.
BSD	External-proxy screening	May claim directional screening only where evidence is weak.	May not upgrade weak p-values into external confirmation.
Riemann/Zeta	FPAS+zeta forecast hierarchy	May claim forecast improvement in reported layers.	May not claim universal forecast dominance.
Riemann/Zeta	Zeta-cycle and spectral diagnostics	May claim diagnostic alignment with global stress regimes.	May not claim RH proof, test or verification.
Riemann/Zeta	Quarterly/monthly layers	May claim dynamic and spectral robustness support.	May not pretend all methods are estimated on the same small annual sample.

Study	Evidence block	Permitted statement	Forbidden escalation
P vs NP	C(94,10) support space	May claim combinatorial support-space explosion.	May not claim proof of formal computational-complexity theory.
P vs NP	Heuristic search and GA/Monte Carlo comparison	May claim best-found and algorithm-comparison evidence under documented budgets.	May not claim certified global optimum for the full n=94 universe.
P vs NP	Reduced exact enumeration	May claim exact benchmark evidence for n=20, K=6 only.	May not transfer exactness to the full C(94,10) instance.

4.9.4B. Reviewer-safe claim lexicon

The safest way to preserve the claim boundary is to standardize the vocabulary used in the monograph. The following lexicon should guide the writing of the problem chapters, the comparative synthesis and the conclusion. The left side contains terms that are generally safe when matched to evidence. The right side contains terms that should be avoided unless the relevant proof or identification design actually exists.

Table 4.9.4B. Reviewer-safe claim lexicon

Vocabulary class	Term	Recommended use	Boundary rule
Safe terms	calibrated	Use when model-implied indicators match internal benchmarks, rank gaps or agreement tests.	Do not replace with proven.
Safe terms	diagnostic	Use for constructed stress, curvature, flow, rank, forecast and risk objects.	Do not replace with causal law.
Safe terms	bounded	Use for all analogue claims and forecast claims.	Do not replace with universal.
Safe terms	finite-network	Use for Yang-Mills and Hodge graph objects.	Do not replace with physical field.
Safe terms	best-found	Use for full P vs NP n=94 heuristic portfolio results.	Do not replace with globally optimal.
Safe terms	validation-window	Use for rolling or out-of-sample forecast evidence.	Do not replace with permanent predictive dominance.
Unsafe terms	proved	Avoid for all seven analogue chapters unless referring to external mathematical literature.	Use supports, indicates, demonstrates within design.
Unsafe terms	solves	Avoid in all references to Clay problems.	Use develops an economic analogue.
Unsafe terms	causes	Avoid unless an identification strategy supports causality.	Use associated with, diagnostically linked to, consistent with.
Unsafe terms	guarantees	Avoid for forecasts, policy counterfactuals and investment outputs.	Use model-implied, scenario-based, bounded.

Vocabulary class	Term	Recommended use	Boundary rule
Unsafe terms	official index	Avoid for author-calculated variables.	Use constructed indicator or author-calculated variable.

4.9.4C. Claim-audit algorithm for the monograph

Every important claim in the monograph should pass through a five-step audit. First, identify the exact evidence object supporting the sentence. Second, classify that object as public input, author-calculated diagnostic, benchmark output, forecast-validation result, econometric association, placebo/falsification result or replication artifact. Third, assign the corresponding claim level from Table 4.9.3. Fourth, check whether the sentence contains theorem, causality, universal dominance, policy certainty or global-optimality language. Fifth, revise the sentence until the evidence level and wording level match.

(4.9.5) Audit(sentence) = EvidenceType -> ClaimLevel -> ExclusionCheck -> RevisedWording.

Equation 4.9.5 turns claim discipline into a repeatable editorial algorithm. It is not enough that a claim is true in a loose sense. It must be true at the exact evidentiary level supported by the relevant chapter. For example, the P vs NP chapter may describe the full-universe portfolio as a best-found incumbent, while the reduced benchmark may be described as exact. The Riemann/Zeta chapter may state forecast improvement in the reported layers, while the global claim must remain sample- and horizon-bound. The Yang-Mills chapter may report a positive finite-network economic mass gap, while country-panel causality remains reserved for the populated validation layer.

Table 4.9.4C. Claim-audit algorithm for drafting and revising the monograph

Audit step	Control question	Required action
1. Evidence identification	Which table, formula, model, graph, forecast or algorithm supports the sentence?	Sentence cannot remain if no explicit evidence object supports it.
2. Evidence classification	Is it descriptive, diagnostic, benchmark, forecast, association, robustness, placebo or exact evidence?	Use the correct claim level for the evidence type.
3. Boundary assignment	Which part of Table 4.9.1 or 4.9.3 governs the sentence?	If no boundary fits, the sentence is probably too broad.
4. Exclusion screening	Does the sentence imply theorem proof, causality, universal dominance, policy certainty or certified optimum?	Rewrite using bounded, diagnostic or calibrated language.
5. Replication check	Can the reader trace the claim to the dataset, formula, algorithm or source-ledger?	If not traceable, move to interpretation or remove.

4.9.5. Overclaim-to-correction protocol

The matrix below converts likely reviewer objections into precise wording corrections. It should be treated as a writing protocol for the whole book. Whenever a sentence risks the left-column interpretation, it must be rewritten using the center-column correction and supported only by the right-column permitted claim.

Table 4.9.4. General overclaim-to-correction protocol

Potential overclaim	Required correction	Permitted claim after correction
The study solves a Millennium Problem.	State that the study develops a bounded economic-econometric analogue inspired by the formal architecture of the problem.	The monograph contributes an analogue-based measurement programme.
The constructed indicators are official data.	Separate public inputs from author-calculated variables and report the	The indicators are reproducible research variables derived from public

Potential overclaim	Required correction	Permitted claim after correction
	transformation lineage.	anchors.
A high R-squared or rank agreement proves causality.	Use association, calibration, agreement, screening or diagnostic language unless a causal design exists.	The evidence supports diagnostic structure or calibrated consistency.
A finite network mass gap proves the Yang-Mills mass gap.	Specify finite weighted-graph spectral separation and avoid physical theorem language.	The evidence supports a finite-network economic threshold.
A zeta correction proves the Riemann Hypothesis.	Define zeta as a computational signal generator and forecast-correction layer.	The evidence supports bounded global inflation forecast improvement.
Exact reduced enumeration certifies the full P vs NP problem.	Limit exactness to the reduced n=20, K=6 benchmark and call the full n=94 result best-found or heuristic.	The evidence supports computational-finance search behavior, not theorem proof.
Counterfactuals are policy guarantees.	Call counterfactuals model-implied stress scenarios with uncertainty.	The evidence supports scenario interpretation.
External proxies close validation.	Classify external evidence as directional when p-values, signs, sample size or lineage are limited.	The evidence supports screening, not strong external confirmation.

4.9.6. Causality, forecasting and policy language boundary

The monograph uses econometric, forecasting, machine-learning, Monte Carlo and counterfactual methods, but those methods do not automatically authorize causal language. The causality boundary is therefore separate from the theorem boundary. A model can be mathematically structured, empirically useful and reproducible without being causally identified. This is especially important for constructed-index studies where many variables are derived from common public anchors. (4.9.3) Diagnostic association != causal identification; forecast-window improvement != universal predictive law; model-implied counterfactual != policy certainty.

Table 4.9.5. Causality, forecasting and policy-language boundary

Methodological tool	What it can do	Permitted language	Excluded language
Panel FE / TWFE	Controls for time-invariant unit effects and common time shocks where specified.	Diagnostic association, conditional association, robustness screen.	Causal effect, treatment effect, structural law without identification.
HAC, HC3, clustered, Driscoll-Kraay	Improves inference discipline under heteroskedasticity, autocorrelation, clustering or cross-sectional dependence.	Robust-inference caution and sensitivity.	Proof that the relationship is causal or externally universal.
Rolling validation and benchmark comparison	Tests reported forecast performance inside a defined validation window.	Validation-window usefulness and incremental forecast evidence.	Permanent forecast superiority or crisis-prediction law.
DM/CW, MZ, encompassing	Assesses forecast accuracy, calibration or incremental information.	Forecast-comparison evidence under sample boundaries.	Theorem, causal mechanism or universal dominance.
Monte Carlo /	Simulates uncertainty and model-	Scenario discipline,	Guaranteed real-world

Methodological tool	What it can do	Permitted language	Excluded language
counterfactuals	implied scenario response.	uncertainty ranges, policy-screening evidence.	policy impact.
Placebo / negative controls	Tests whether observed alignment survives falsification or randomization screens.	Anti-artifact evidence and claim-discipline support.	Theorem proof or causal closure.

4.9.7. Problem-chapter writing rules derived from the matrix

The claim-boundary matrix should not remain only a table in Chapter 4. It must actively govern the later problem chapters. Each problem chapter should contain a compact claim-boundary reminder in the introduction, a method-specific boundary in the methodology subsection, a claim-status table near the end of the results section and a final admissible-claim paragraph in the interpretation or conclusion. This repetition is not stylistic redundancy; it is reviewer-safety architecture.

Table 4.9.6. Problem-chapter writing rules derived from the claim-boundary matrix

Location in each problem chapter	Claim-boundary function	Required writing model
Chapter introduction	State the mathematical inspiration and immediately deny theorem-level transfer.	This chapter develops an economic analogue inspired by X; it does not prove, test or replicate X.
Methodology subsection	Separate official/public anchors from author-calculated variables and state the transformation rules.	The final indicators are model-derived diagnostic objects, not official raw data.
Results subsection	Match every table to a specific evidence status: descriptive, diagnostic, forecast, benchmark, robustness or placebo.	The evidence supports a benchmark diagnostic claim within the defined sample.
Robustness subsection	Report failures and weak p-values as limits rather than suppressing them.	Robust-inference weakness is treated as a boundary, not upgraded into confirmation.
Interpretation subsection	Translate results into substantive meaning without escalating claim level.	The chapter supports calibrated consistency / bounded forecast improvement / finite-network threshold logic.
Conclusion	Restate both the contribution and the exclusions.	The contribution is high but bounded; theorem proof, unrestricted causality and universal dominance are excluded.

4.9.8. Monograph-wide permitted contribution statement

After the study-specific matrices are applied, the monograph-wide contribution can be stated without overclaiming. The book creates a unified mathematical-econometric analogue programme for measuring economic complexity through seven measurement grammars: curvature and topological deformation, flow decomposition, liquidity-stress balance, finite-network threshold, local-to-global rank, spectral-cyclical forecast signal and computational decision complexity. This contribution is strong because it is integrated, replicated and claim-disciplined. It is bounded because none of the seven mathematical references is converted into a theorem-level result.

(4.9.4) $\text{Contribution} = \text{MeasurementArchitecture} + \text{EmpiricalClosure} + \text{ReplicationDiscipline} + \text{ClaimBoundary}$.

Equation 4.9.4 summarizes the monograph-level scientific position. The contribution is not any single equation, graph, regression or forecast table. It is the integration of measurement architecture, empirical closure, replication discipline and claim boundary across seven economic analogues. Without the claim boundary, the mathematical ambition would be

vulnerable to overclaiming. With the claim boundary, the monograph becomes a defensible interdisciplinary research programme.

Table 4.9.7. Monograph-wide permitted contribution statement

Monograph-level contribution	What supports it	Boundary that remains
Unified mathematical-econometric analogue programme	Supported across all seven chapters by explicit translation from mathematical architecture to economic measurement.	Does not solve or test the Clay Millennium Problems.
Global stress and resilience measurement architecture	Supported by Perelman/Ricci/Poincare, Navier-Stokes, Yang-Mills, Hodge and BSD stress/network constructions.	Does not claim a universal crisis law or causal macroeconomic theorem.
Forecast-validation architecture	Supported most strongly by Riemann/Zeta layered validation and secondarily by Navier-Stokes rolling validation.	Does not claim universal forecast dominance or residual elimination.
Computational-finance complexity architecture	Supported by P vs NP support-space explosion, heuristic comparison and reduced exact enumeration.	Does not prove P vs NP or certify the full n=94 global optimum.
Replication and reviewer-safety architecture	Supported by Zenodo packages, source ledgers, formulas, scripts, checksum logic and claim-boundary matrices.	Replication supports auditability, not theorem proof or causality by itself.

4.9.9. Final methodological synthesis

The claim-boundary matrix completes the technical function of Chapter 4. Sections 4.1 through 4.8 established the research design, empirical universes, public-data anchors, normalization rules, graph construction, econometric/forecast validation, computational protocol and Zenodo replication discipline. Section 4.9 now defines the permissible interpretation of those methods. This ordering is intentional: methodology is not complete until the permitted claim level is known.

The final synthesis is therefore precise. The monograph may claim to create seven reproducible economic-econometric analogues inspired by the Clay Millennium Problems. It may claim that these analogues generate measurable diagnostics of inequality pressure, macro-flow decomposition, liquidity stress, finite-network shock thresholds, local-to-global structural rank, global inflation forecast cycles and computational portfolio complexity. It may claim that each diagnostic is audited through the evidence layer appropriate to its design. It may not claim mathematical proof, theorem transfer, unrestricted causality, universal forecast dominance, certified global optimality where only heuristic evidence is reported, or policy certainty from model-implied counterfactuals.

This boundary does not weaken the book. It strengthens it. It turns mathematical ambition into a disciplined research programme and gives reviewers a clear map for reading every result at the correct evidentiary level. The safest final wording for the book is therefore: the monograph advances a claim-bounded, reproducible and validation-oriented mathematical-econometric analogue architecture for measuring global economic complexity; it does not resolve the original Millennium Problems.

Table 4.9.8. Source-document traceability for the general claim-boundary matrix

Source document	Claim-boundary material synthesized into Section 4.9
Perelman/Ricci/Poincare manuscript	Claim-boundary statement, N=150 diagnostic panel, 0-100 stress coordinates, theorem/causality/forecast exclusions.
Global Hodge-Econometric Modeling manuscript	Discrete Hodge decomposition boundary, ten-node benchmark, gradient-curl-harmonic claim status, Hodge Conjecture exclusion.
Navier-Stokes manuscript	N=1,500 global panel, nondimensional variables, rolling validation, FE association, policy-counterfactual boundary.
Yang-Mills manuscript	Finite-network mass-gap definition, ten-node/twenty-seven-edge benchmark, N=1,500 validation pathway, physical theorem exclusion.
BSD manuscript	Local-to-global structural rank, N=150 closure layer, weak robust-inference caveat, directional external-proxy boundary.
Riemann/Zeta manuscript	Layered validation N=55/N=45/N=20/N=100/N=240, FPAS+zeta forecast hierarchy, RH and universal dominance exclusions.
P vs NP manuscript	Damodaran n=94 universe, C(94,10), exact C(20,6), heuristic/global-optimality and theorem-proof exclusions.

PART II — The Seven Millennium Problems as Economic-Econometric Models

Chapter 5. Perelman-Ricci-Poincare-Inspired Global Inequality Diagnostics

Chapter Abstract

This chapter develops the first problem-specific model in Part II of the monograph by translating the Poincare/Ricci/Perelman mathematical grammar into a bounded economic-econometric diagnostic architecture for global inequality. The chapter does not claim to prove, test or replicate Perelman's proof, the classical Ricci-flow theorem or the Poincare conjecture. Its object is an economic analogue: the world economy is represented as a macro-regional pressure-

smoothing system in which inequality pressure, smoothing capacity, curvature-like deformation, entropy-like complexity and graph connectedness are measured jointly rather than through isolated inequality indicators.

The empirical design underlying the chapter is a balanced macro-regional diagnostic panel: ten macro-regional blocks observed annually over 2010-2024, sixteen pressure-oriented stress coordinates and N = 150 region-year observations. Raw macro-social indicators are not added in heterogeneous units. They are transformed into a common diagnostic scale and then organized into a structured sequence: stress coordinates, standardized variables, an economic metric tensor, Ricci-style component curvature, normalized Ricci-flow summaries, world-weighted scalar curvature, Perelman-type F- and W-functionals, Poincare-style graph connectedness, Betti diagnostics, network-curvature proxy screens, counterfactual sensitivity layers and econometric-validation gates.

The chapter's core thesis is that inequality should be interpreted not only as a level or distributional statistic, but as a deformation process inside a connected macro-social system. In this interpretation, pressure increases when inequality-related stress accumulates; smoothing capacity represents the ability of productivity, social protection, education, health, technology access, fiscal space and related channels to absorb or reduce pressure; curvature-like deformation summarizes the imbalance between stress accumulation and smoothing capacity; Perelman-type functional objects summarize energy-like and entropy-like complexity; and graph topology tests whether the sixteen-variable diagnostic system is connected, looped and structurally bottlenecked.

The chapter therefore prepares the reader for the empirical results to be presented in Section 5.5: the 2020 crisis-deformation signal, the partial 2024 recovery path, the concentration of curvature energy in investment, productivity, technology access, unemployment and fiscal-pressure channels, and the graph-topological finding that the inequality system is connected, dense and cycle-rich. These empirical findings are interpreted cautiously. The strongest permitted claim is a high-level diagnostic measurement claim: a Perelman-Ricci-Poincare-inspired architecture can organize global inequality evidence into pressure, curvature, entropy, topology and validation layers. The chapter does not establish classical theorem proof, unrestricted causality, country-level welfare ranking or universal forecast superiority.

Table 5.1. Opening transfer map for the chapter abstract and Section 5.1.

Article material	Monograph placement	Transformation rule
Original abstract	Chapter 5 opening abstract	Compressed into a chapter-level orientation that states object, empirical universe, method sequence, permitted claim and excluded claims.
Original 1.1 general context	Chapter 5.1 inequality-specific framing	General world-economy context is moved to Chapter 1; only the inequality-pressure logic remains here.
Original 1.3-1.5 aim, objectives and questions	Chapter 5.1 and later 5.2	Aims are not repeated mechanically; they are converted into the problem-specific translation grammar.
Original limitations and caution	Abstract boundary and 5.1 claim discipline	The theorem-exclusion and causality boundary are placed at the beginning of the chapter for reviewer safety.

5.1. Mathematical and Economic Translation of the Poincare/Ricci/Perelman Logic

5.1.1. Function of Section 5.1 inside the Monograph

Section 5.1 is the conceptual and technical gate through which the first Clay-inspired model enters the monograph. It does not repeat the full literature review, which has already been integrated in Chapter 3, and it does not yet report the full empirical results, which belong to Section 5.5. Its purpose is more precise: it explains how the Poincare/Ricci/Perelman family of mathematical ideas is converted into an economic-econometric measurement grammar for inequality diagnostics.

The translation problem is delicate. Poincare, Ricci flow and Perelman's work belong to topology and geometric analysis. Global inequality belongs to macroeconomics, development economics, labour economics, public finance and social measurement. The chapter therefore uses mathematical structure as a disciplined analogy, not as literal identity. The economic model does not assert that the world economy is a smooth geometric manifold, that inequality variables have literal Riemannian curvature, or that Perelman's monotonicity results hold in a macro-social system. Instead, it uses connectedness, pressure, smoothing, curvature-like deformation and entropy-like complexity as measurement concepts that can be operationalized with transparent data transformations.

This distinction is essential to the book's wider architecture. The monograph does not solve any Millennium Problem. It develops seven bounded economic-econometric analogues inspired by their formal architectures. Chapter 5 is the curvature-and-topology analogue: the economic object is global inequality pressure; the main diagnostic problem is whether pressure accumulation and smoothing capacity can be measured as a structured deformation process; and the validation problem is whether the resulting constructed indicators retain empirical coherence under graph, panel, counterfactual, robustness and forecast-discipline checks.

Table 5.2. Core translation grammar of Section 5.1.

Translation level	Mathematical reference	Economic reinterpretation	Evidence status in Chapter 5
Topological closure	Poincare-style connectedness and holes	Whether the stress-coordinate system forms one connected diagnostic graph with cycles and bottleneck relations.	Graph-diagnostic evidence, not theorem proof.
Flow and smoothing	Ricci-flow logic	Pressure accumulation and smoothing capacity generate curvature-like deformation and partial recovery paths.	Dynamic diagnostic interpretation, not physical/geometric flow law.
Energy and entropy	Perelman F and W functionals	Energy-like and entropy-like system complexity summarize the pressure-curvature state of global inequality.	Constructed functional proxy, not classical monotonicity theorem.
Metric structure	Metric tensor and coordinate coupling	Standardized stress coordinates define an empirical correlation-based metric tensor.	Empirical coupling matrix, not a literal Riemannian metric.
Surgery and bottlenecks	Ricci surgery as structural correction logic	High-contribution channels and bottleneck nodes are ranked as diagnostic candidates for structural attention.	Policy-screening diagnostic, not causal treatment effect.

5.1.2. Why the Poincare/Ricci/Perelman Logic Fits Inequality Diagnostics

The Poincare/Ricci/Perelman logic is appropriate for global inequality diagnostics because inequality is not a single-dimensional object. A Gini coefficient, unemployment rate, inflation rate, investment share, productivity indicator or social-protection measure may each provide useful information, but no single variable describes the structure of inequality pressure. The relevant object is a coupled macro-social system: income distribution interacts with labour-market stress, productivity weakness, technology access, fiscal pressure, migration pressure, health, education, social mobility, trade openness and capital-flow exposure.

In such a system, the central economic question is not only whether inequality is high or low. It is whether the system is deforming, whether smoothing capacity is sufficient, whether stress channels are concentrated, whether crisis years produce structural breaks, whether recovery represents genuine smoothing or only partial pressure decline, and whether the variables behave as an connected diagnostic manifold rather than as unrelated indicators. This is why the chapter uses curvature, flow, entropy and graph connectedness as measurement language.

The analogy is especially useful because it avoids reducing inequality to a static ranking. A static ranking can identify which region is worse in a given year; it cannot show how pressure accumulates, how recovery differs across components, or whether structural bottlenecks hold the system in a high-complexity state. The Perelman-Ricci-Poincare-inspired model therefore adds a structural layer: inequality becomes a pressure-smoothing geometry in which stress coordinates are coupled, deformation can be decomposed and topological connectedness can be audited.

5.1.3. The Economic Manifold: From Heterogeneous Indicators to Stress Coordinates

The first act of translation is the construction of an economic diagnostic manifold. In classical geometry, a manifold is a space in which local coordinate descriptions can be organized coherently. In this economic analogue, the manifold is not a literal smooth surface. It is a structured coordinate system built from macro-regional stress variables. Each region-year

observation is represented by sixteen harmonized coordinates, each oriented so that higher values correspond to greater inequality pressure or weaker smoothing capacity.

The source study uses ten macro-regional blocks over the 2010-2024 annual period, producing a balanced N = 150 region-year diagnostic panel. The coordinate set includes income inequality, productivity, unemployment, investment, inflation, migration, education, social mobility, logistics, capital-flow pressure, innovation, health, fiscal deficit, trade openness, social protection and technology access. This list matters because the model treats inequality as a multi-channel macro-social deformation, not as a single distributional statistic.

The transformation rule is central. Public macro-social indicators are not directly summed. They are first converted into pressure-oriented diagnostic scores. Variables that naturally increase stress retain their direction; smoothing-capacity variables are reverse-oriented so that weak capacity appears as higher pressure. This directionally harmonized system makes it possible to construct pressure, curvature and entropy-like objects without mixing raw units. Thus, the manifold is not created by metaphor; it is created by data-lineage discipline.

Equation 5.1. $S_{r,t,j} = 100 * (X_{r,t,j} - \min(X_j)) / (\max(X_j) - \min(X_j))$

Equation 5.2. $S^{inv}_{r,t,j} = 100 - S_{r,t,j}$, for smoothing-capacity variables

Equation 5.3. $P_{r,t} = \sum_{j=1}^{16} w_j S^{*}_{r,t,j}$

In Equations 5.1-5.3, X is the raw public or source-family variable, S is the stress score, S is the directionally harmonized coordinate, w_j is the coordinate weight and P is the constructed inequality-pressure coordinate. These equations are schematic monograph notation; the full operational definitions belong to Sections 5.3 and 5.4.*

5.1.4. Poincare Logic: Connectedness, Cycles and Diagnostic Closure

The Poincare part of the translation concerns connectedness and topological closure. In the classical mathematical setting, Poincare-type reasoning concerns the global structure of spaces. In this economic chapter, the analogue is not a proof of the Poincare conjecture. It is a graph-theoretic test of whether the sixteen-variable inequality system behaves as one connected diagnostic object or as disconnected indicator clusters.

The chapter operationalizes this idea by constructing a thresholded correlation graph from standardized stress coordinates. Variables become nodes, sufficiently strong coordinate relationships become edges and the resulting graph is evaluated through connected components, algebraic connectivity, Betti numbers, Euler characteristic, degree structure and cycle density. This converts an abstract topological question into a concrete empirical audit: is the inequality-pressure system connected, dense, looped and bottlenecked?

The graph layer is important because it protects the model from an index-only interpretation. If the stress variables were weakly related or fragmented into disconnected groups, the manifold language would be fragile. A connected graph with cycles supports the weaker but defensible claim that the variables form an interdependent diagnostic system. In the source results, the graph has sixteen nodes, eighty-seven edges, one connected component, positive algebraic connectivity and many cycles. Section 5.1 uses this as a translation principle; the detailed numerical interpretation is reserved for Section 5.5.

Equation 5.4. $A_{ij} = 1[\ |\mathrm{corr}(Z_i, Z_j)| >= \tau\ ]$, with $\tau = 0.300$ in the benchmark graph

Equation 5.5. $L = D - A$

Equation 5.6. β_0 = number of connected components; $\beta_1 = E - V + \beta_0$

Table 5.3. Poincare-inspired graph objects and their economic reading.

Graph object	Economic meaning	Reviewer-safe interpretation
Node	One harmonized inequality stress coordinate.	A variable block in the diagnostic system, not a physical location on a manifold.
Edge	Sufficiently strong empirical association between stress coordinates.	A correlation-threshold relation, not a causal channel by itself.
Laplacian	Connectedness and bottleneck audit of the stress-coordinate graph.	Graph-theoretic validation layer, not topological theorem proof.
β_0	Whether the diagnostic variable system is one component or fragmented.	Evidence for diagnostic closure when $\beta_0 = 1$.
β_1	Cycle density and loop structure among stress channels.	Evidence of coupled pressure loops, not literal topological holes in an economy.

Graph object	Economic meaning	Reviewer-safe interpretation
Algebraic connectivity	Strength of graph connectedness and absence of isolated coordinates.	Robustness signal for the constructed manifold.

5.1.5. Ricci Logic: Inequality Pressure, Smoothing Capacity and Deformation

The Ricci component of the translation is the chapter's main deformation logic. In the classical setting, Ricci curvature summarizes how volume, distance and geometry respond under curvature. In the economic analogue, Ricci-style curvature is not a literal geometric invariant. It is a constructed measure of how inequality pressure and smoothing capacity interact across macro-regional coordinates.

The intuition is straightforward but technically disciplined. When pressure rises faster than smoothing capacity, the economic system is interpreted as deforming. When smoothing capacity improves or pressure declines, the system shows partial smoothing recovery. Curvature-like values therefore summarize the balance between adverse stress channels and stabilizing capacity channels. This makes the model more informative than a pressure index alone: pressure indicates intensity, while curvature-like deformation indicates structural balance or imbalance.

Ricci-flow language is used to organize the time path of deformation and recovery. Crisis years can be read as deformation peaks, while post-shock years can be read as smoothing or incomplete recovery. The source chapter identifies 2020 as the strongest crisis-deformation year and 2024 as a partial recovery year rather than a full convergence point. This interpretation remains diagnostic. It does not claim that an economic Ricci-flow differential equation governs the world economy; it claims that the Ricci-flow grammar is useful for measuring pressure-smoothing dynamics.

Equation 5.7. R_{r,t}^{econ} = phi(SmoothingCapacity_{r,t}, Pressure_{r,t}, Coupling_{r,t})

Equation 5.8. Delta R_t = R_t - R_{t-1}; deformation if Pressure rises and R declines

Equations 5.7-5.8 deliberately use economic notation rather than classical geometric notation. The purpose is to preserve the analogy while preventing theorem-level overclaiming.

5.1.6. Perelman Logic: Energy-Like and Entropy-Like Complexity

The Perelman part of the translation introduces functional diagnostics. In the classical mathematical context, Perelman's functionals play a central role in the Ricci-flow proof architecture. In this economic chapter, F and W are not imported as theorem-level objects. They are reconstructed as model-implied summaries of energy-like and entropy-like inequality complexity.

The F-functional is interpreted as an energy-like diagnostic object: it summarizes how pressure, curvature and coordinate intensity concentrate in the system. The W-functional is interpreted as an entropy-like complexity closure: it captures whether the system remains structurally complex even when pressure declines. This distinction is important because post-crisis recovery can be misleading. Pressure may fall while complexity remains high, indicating that the system has not fully smoothed.

This is where the chapter obtains its strongest conceptual interpretation. A normal inequality model may report that pressure declined after a shock. A Perelman-inspired model asks whether complexity also normalized. If W remains elevated while pressure declines, the correct interpretation is partial recovery under persistent complexity. This allows the chapter to separate mere pressure reduction from genuine smoothing. At the same time, the chapter explicitly rejects any claim that the economic W-functional obeys the classical monotonicity properties of Perelman's mathematical functional.

Equation 5.9. F_t^{econ} = f(P_t, R_t, coordinate intensity)

Equation 5.10. W_t^{econ} = g(P_t, R_t, dispersion_t, complexity_t)

Table 5.4. Perelman-type functional translation and claim limits.

Functional layer	Economic purpose	What it can show	What it cannot show
F-functional analogue	Energy-like pressure-curvature summary.	Whether stress and deformation concentrate in the system.	It cannot prove a classical variational theorem.
W-functional analogue	Entropy-like complexity closure.	Whether complexity remains elevated after pressure changes.	It cannot import Perelman monotonicity into economics.

Functional layer	Economic purpose	What it can show	What it cannot show
W-monotonicity audit	Reviewer-safety check.	Whether the economic W path behaves monotonically or not.	Non-monotonicity is not failure; it is boundary evidence.
Pressure-curvature-W triad	Joint interpretation of intensity, deformation and complexity.	Whether crisis and recovery are structurally coherent.	It cannot establish unrestricted causality or forecast dominance.

5.1.7. The Economic Translation Sequence

The chapter's translation sequence is deliberately sequential. It begins with public or source-family macro-social variables, but the final objects are author-calculated diagnostic indicators. This distinction must remain visible throughout Chapter 5. Official or public data provide input anchors; they do not directly provide curvature, entropy, Betti numbers, scalar curvature, Ricci-flow summaries or surgery rankings. These are constructed analytical objects created under disclosed transformation rules.

The sequence can be read as a methodological pipeline. First, the macro-regional universe is fixed. Second, sixteen variables are directionally harmonized. Third, stress coordinates are standardized. Fourth, a metric tensor is constructed from the correlation structure. Fifth, Ricci-style component curvature is decomposed. Sixth, scalar curvature and normalized Ricci-flow summaries are calculated. Seventh, F and W functional analogues are produced. Eighth, the Poincare graph layer audits connectedness and cycles. Ninth, network-curvature proxies and Ricci-surgery rankings identify bottleneck-like channels. Tenth, econometric, counterfactual, robustness and forecast-discipline checks classify the evidentiary strength.

The purpose of the pipeline is not to create complexity for its own sake. It is to prevent the model from depending on a single score. Each layer asks a different scientific question: Is there a coherent coordinate system? Are the coordinates coupled? Which components carry curvature energy? Does the system deform during crisis? Does it partially recover? Does complexity remain elevated? Is the variable graph connected? Are the results sensitive to counterfactual changes? Do econometric screens support the diagnostic structure? These questions jointly define the chapter's scientific discipline.

Table 5.5. Economic translation sequence from raw indicators to claim-disciplined diagnostics.

Step	Operation	Primary output	Role in Chapter 5
1	Fix ten-region 2010-2024 empirical universe.	N = 150 region-year panel.	Defines the coordinate system for global inequality diagnostics.
2	Normalize and directionally harmonize sixteen variables.	0-100 stress coordinates.	Makes heterogeneous indicators comparable.
3	Standardize coordinates and compute coupling.	Metric tensor and correlation structure.	Tests whether the manifold-style reading is coherent.
4	Decompose curvature-style contributions.	Component Ricci signs and contribution shares.	Identifies dominant pressure and smoothing channels.
5	Aggregate annual and world-weighted diagnostics.	Pressure, scalar curvature and flow summaries.	Measures deformation and recovery paths.
6	Compute Perelman-type functionals.	F and W diagnostic objects.	Summarizes energy-like and entropy-like complexity.
7	Build Poincare graph layer.	Laplacian, beta_0, beta_1 and connectivity.	Audits connectedness and loops.
8	Apply validation and sensitivity screens.	Econometric, forecast, counterfactual and Monte Carlo evidence.	Classifies the claim boundary.

5.1.8. Why Inequality Pressure Is the Correct Economic Object

The selection of inequality pressure as the first problem-specific economic object is not arbitrary. Among the seven models in the monograph, the Perelman-Ricci-Poincare logic is most naturally connected to questions of deformation, smoothing and connectedness. Inequality is a deformation problem because it concerns the distributional shape of the economy. It is a smoothing problem because public institutions, social protection, productivity, education, health, technology and fiscal capacity may reduce or absorb pressure. It is a topology problem because inequality channels are interdependent and can form bottlenecks and loops.

The chapter therefore avoids a narrow welfare-ranking interpretation. The ten macro-regional blocks are not used to declare a definitive country-level social hierarchy. They are used to build a global diagnostic system. A macro-region may show high pressure because of labour-market stress, weak productivity, limited technology access, fiscal pressure or social-protection weakness. Another may show lower pressure but elevated complexity. The model is designed to separate these structural patterns rather than collapse them into one policy slogan.

This is why the chapter uses the language of a pressure-smoothing manifold. Pressure is the accumulation of stress. Smoothing capacity is the system's ability to absorb, redistribute or reduce that stress. Curvature-like deformation is the imbalance between the two. Entropy-like complexity indicates whether the system remains structurally strained even after pressure changes. Graph connectedness shows whether the variables operate as a system. Together, these concepts provide a richer diagnostic interpretation than a single inequality series.

5.1.9. Evidence Hierarchy and Claim Boundary

The translation is scientifically useful only if the claim boundary is strict. Section 5.1 therefore establishes an evidence hierarchy before the results are reported. The strongest admissible claim is that a bounded Perelman-Ricci-Poincare-inspired architecture can organize global inequality evidence into pressure, curvature, entropy, graph topology, counterfactual and validation layers. This is a methodological and diagnostic claim.

A weaker but still meaningful claim is that the constructed indicators are internally coherent under the reported transformations and validation screens. The model can show that crisis deformation and partial recovery appear in the pressure-curvature-W path; that curvature energy concentrates in economically meaningful components; that the graph is connected and cycle-rich; and that counterfactual and econometric screens provide bounded support. These claims are strong enough for a monograph chapter because they are empirical, reproducible and claim-disciplined.

Excluded claims must be stated equally clearly. The chapter does not prove the Poincare conjecture, does not reproduce Perelman's theorem, does not turn the global economy into a physical manifold, does not establish unrestricted causal effects, does not replace country-level inequality analysis and does not claim universal forecast superiority. This exclusion is not a rhetorical disclaimer; it is part of the methodology. It prevents mathematical analogy from becoming overstatement and allows the chapter to retain scientific credibility.

Table 5.6. Claim-boundary matrix for Section 5.1.

Potential claim	Permitted status	Reason
The model organizes inequality into pressure, curvature, entropy and topology layers.	Permitted as the strongest diagnostic measurement claim.	The variables, transformations and outputs are explicitly constructed and auditable.
2020 appears as a crisis-deformation year and 2024 as partial recovery.	Permitted as results-layer interpretation.	Supported by pressure, scalar-curvature and W-functional paths in the source study.
The graph is connected, dense and looped.	Permitted as graph-diagnostic evidence.	Supported by thresholded graph, Laplacian and Betti calculations.
The model proves or tests the Poincare conjecture.	Excluded.	The graph layer is an economic diagnostic construction, not a theorem-level mathematical proof.
The Ricci-style indicators are literal geometric curvature.	Excluded.	They are author-calculated pressure-smoothing proxies.
The F and W functionals satisfy	Excluded.	They are economic functional analogues and

Potential claim	Permitted status	Reason
classical Perelman theorem properties.		must be audited independently.
Counterfactuals are causal policy multipliers.	Excluded.	They are internal sensitivity screens, not identified treatment effects.

5.1.10. Transition to the Research Object in Section 5.2

Section 5.1 establishes the translation logic. Section 5.2 should now move from translation to research object. The object is not the Poincare conjecture, not Ricci flow as mathematics and not Perelman's proof. The object is the global macro-regional inequality system interpreted as a pressure-smoothing diagnostic manifold. Each observation is a region-year coordinate; each coordinate vector contains harmonized stress variables; and each constructed diagnostic object is interpreted within an explicitly bounded evidence hierarchy.

This ordering is important for the book. The reader first receives the mathematical-economic translation, then the empirical object, then the data architecture, then the methodology, then results and interpretation. This prevents the chapter from looking like a stand-alone article pasted into the monograph. Instead, Chapter 5 becomes the first major application of the book's general methodology: a high-level mathematical architecture is translated into a transparent, reproducible and scientifically cautious economic-econometric model.

Table 5.7. Bridge from the opening material to the next Chapter 5 sections.

Section already covered	Purpose	Next section required
Chapter abstract	States model purpose, empirical base, diagnostic sequence, results preview and claim boundary.	5.2 must define the research object and empirical boundary.
5.1 translation logic	Explains why Poincare/Ricci/Perelman grammar is used for inequality pressure and smoothing capacity.	5.2 must specify the region-year system as a pressure-smoothing manifold.
Claim-boundary matrix	Prevents theorem proof, causality and forecast overclaiming.	5.3-5.4 must document data and methods precisely enough for replication.

5.2. Research Object: Global Inequality as a Pressure-Smoothing Manifold

5.2.1. Purpose of the Research-Object Section

Section 5.2 defines the empirical and conceptual object of Chapter 5. After Section 5.1 has explained the mathematical-to-economic translation of Poincare, Ricci and Perelman logic, the present section specifies exactly what is being observed, transformed and interpreted. The research object is not the classical Poincare conjecture, not a smooth Riemannian manifold and not a physical curvature field. It is the global macro-regional inequality system represented as a bounded economic diagnostic manifold.

The section therefore performs a methodological control function. It prevents the reader from treating geometric terminology as literal theorem transfer and prevents the empirical model from being confused with an ordinary inequality ranking. The object is a structured macro-regional measurement system in which region-year observations, stress-coordinate variables, pressure-oriented transformations, smoothing-capacity channels, curvature-like diagnostics, entropy-like functionals and graph-topological connectedness are organized as one auditable architecture.

In the book structure, this section replaces the article-level “research object, boundaries and data status” subsection. The general monograph-level object has already been defined in Part I; here the object becomes problem-specific. The chapter asks how global inequality pressure can be read when inequality is treated not as a single Gini coefficient, but as a coupled pressure-smoothing system across macro-regions, years and economic-social coordinates.

Table 5.3. Research-object specification for Section 5.2.

Research-object element	Definition in Section 5.2	Why it matters for Chapter 5	Boundary condition
Substantive object	Global macro-regional inequality system.	Defines what the chapter measures: inequality pressure, smoothing capacity and deformation across regions.	Not a country-level welfare ranking and not a claim about every micro-household mechanism.
Analytical object	Pressure-smoothing diagnostic manifold.	Allows heterogeneous variables to be treated as coordinates after directional harmonization.	Not a literal Riemannian manifold.
Observation unit	Region-year coordinate (r,t).	Provides the balanced empirical grid for N = 150 diagnostic observations.	Not an individual-level or firm-level panel.
Coordinate set	Sixteen pressure or smoothing-capacity variables.	Converts inequality into a multi-channel system rather than a single-index output.	Constructed stress coordinates, not raw-unit equivalence.
Derived objects	Pressure index, metric tensor, curvature, F/W functionals, graph diagnostics.	Defines the sequence through which the object becomes measurable.	Model-implied diagnostics, not classical invariants.
Evidence status	Measurement and bounded validation.	Controls the interpretation of panel, graph and forecast results.	No theorem proof, unrestricted causality or universal forecast superiority.

5.2.2. Formal Definition of the Empirical Object

The empirical object is a balanced macro-regional panel in which each observation is a region-year coordinate in a transformed inequality-pressure space. Regions are indexed by r = 1,...,10, years by t = 2010,...,2024 and stress-coordinate variables by j = 1,...,16. The raw panel is transformed into a diagnostic coordinate system before metric, curvature, functional, graph and validation layers are constructed.

This object can be written compactly as a set of observed and transformed macro-regional coordinates. Raw variables X_{r,t,j} are not added directly because they refer to different units, economic meanings and directions. They first pass through orientation and scaling rules. The resulting stress coordinate S_{r,t,j} places pressure variables and reverse-coded smoothing-capacity variables on a common diagnostic scale. Standardized coordinates Z_{r,t,j} are then used where correlation, metric, graph, PCA or econometric procedures require comparable dimensions.

The term pressure-smoothing manifold is used to describe this structured coordinate system. Pressure captures variables whose deterioration raises inequality-related stress. Smoothing capacity captures variables whose strength reduces, absorbs or moderates pressure. Curvature-like deformation summarizes the diagnostic imbalance between pressure accumulation and smoothing capacity. The object is therefore not a metaphor added after the data; it is the data architecture itself after transparent transformation.

Equation (5.2.1). Raw diagnostic panel: X = {X_{r,t,j}}, where r = 1,...,10; t = 2010,...,2024; j = 1,...,16; N = 10 x 15 = 150.

Equation (5.2.2). Stress-coordinate panel: S = {S_{r,t,j}} after direction harmonization and 0-100 transformation.

Equation (5.2.3). Standardized coordinate panel: Z_{r,t,j} = (S_{r,t,j} - mean(S_j)) / sd(S_j).

Equation (5.2.4). Pressure-smoothing manifold object: M_E = (R, T, S, Z, G, P, Rho, F, W, A), interpreted as an economic diagnostic system rather than a classical geometric manifold.

Table 5.4. Core notation for the research object.

Symbol	Object	Operational meaning	Use in later sections
r	Region index	One of ten macro-regional blocks.	Defines cross-sectional macro-

Symbol	Object	Operational meaning	Use in later sections
			regional heterogeneity.
t	Year index	Annual observation from 2010 through 2024.	Defines the time path, crisis deformation and recovery window.
j	Stress-coordinate index	One of sixteen inequality-pressure or smoothing-capacity variables.	Defines the coordinate system of the diagnostic manifold.
X_{r,t,j}	Raw variable	Original or constructed macro-regional input before harmonization.	Data architecture and source-ledger layer.
S_{r,t,j}	Stress coordinate	0-100 pressure-oriented coordinate after directional transformation.	Pressure index, curvature and component interpretation.
Z_{r,t,j}	Standardized coordinate	Comparable coordinate used for metric, graph, PCA and validation operations.	Metric tensor and topology layers.
P_{r,t}	Pressure coordinate	Weighted summary of stress-oriented coordinates for region r in year t.	Global pressure-curvature path.
G = [g_ij]	Economic metric tensor	Correlation-based coupling matrix among standardized coordinates.	Ricci-style curvature and graph topology.
F_t, W_t	Functional objects	Energy-like and entropy-like chapter-level diagnostics.	Complexity and crisis-deformation interpretation.
A	Thresholded adjacency matrix	Graph representation of coordinate connectedness.	Poincare-style graph-topological audit.

5.2.3. Unit of Analysis: Region-Year Coordinates

The unit of analysis is the region-year coordinate. This is a deliberate methodological decision. A country-level design would allow more granular institutional interpretation, but it would also require harmonized country-level measurement for all sixteen variables and a different claim boundary. A global aggregate alone would be too compressed because it would hide regional stratification, smoothing-capacity differences and crisis-deformation heterogeneity. The macro-regional panel is therefore chosen as the middle scale at which global structure can be observed while preserving enough heterogeneity for diagnostic interpretation.

The balanced panel contains ten region blocks over fifteen annual observations, generating N = 150 region-year coordinates. The full 2010-2024 window supports regional change, topology, entropy-path context, descriptive statistics, crisis deformation and post-shock recovery diagnostics. The harmonized 2015-2024 window is used where the chapter reports the main world pressure-curvature-W path. This division is not a weakness; it is a sample-discipline rule that prevents all results from being read as if they were produced by the same empirical window.

The region-year coordinate should be read as a diagnostic location in the pressure-smoothing system. A region-year is high-pressure when several stress coordinates jointly point toward distributional strain, labour-market weakness, fiscal pressure, low smoothing capacity or insufficient resilience. A region-year is more strongly smoothed when productivity, education, social protection, technology access, healthcare, mobility or other absorptive channels offset pressure. The resulting coordinate can be compared across regions and time only after the direction-harmonization procedure has made the variables commensurable.

Table 5.5. Unit-of-analysis hierarchy in the pressure-smoothing manifold.

Layer	Empirical unit	Time coverage	Purpose	Interpretive boundary
Raw macro-regional layer	Region-variable-year	2010-2024	Stores initial macro-social anchors and constructed inputs.	Heterogeneous units cannot be added directly.

Layer	Empirical unit	Time coverage	Purpose	Interpretive boundary
Stress-coordinate layer	Region-year-coordinate	2010-2024	Harmonizes pressure and smoothing-capacity channels on the 0-100 diagnostic scale.	Scale is constructed for diagnostics, not raw-unit equivalence.
Main global path	World-weighted annual aggregate	2015-2024	Reports the pressure-curvature-W trajectory used for crisis deformation and partial recovery.	Global path should not erase regional dispersion.
Full diagnostic panel	Region-year	2010-2024; N = 150	Supports descriptive, topology, panel and validation diagnostics.	Macro-regional evidence, not country-level causal identification.
Graph-topological layer	Stress-coordinate nodes and correlation edges	Constructed from the transformed coordinate system	Tests connectedness, cycles and bottleneck-like relations among variables.	Graph topology is diagnostic, not theorem proof.
Uncertainty and validation layer	Model outputs and validation windows	Assigned by method	Audits robustness, sensitivity and predictive limitations.	Validation evidence remains bounded and non-causal unless identification is established.

5.2.4. The Sixteen-Coordinate Inequality System

The research object is multi-coordinate by design. The chapter deliberately does not reduce global inequality to the Gini coefficient alone. The Gini coefficient remains an essential distributional anchor, but the object of interest is broader: inequality pressure is shaped by productivity, unemployment, investment, inflation, migration pressure, education, mobility, logistics, capital-flow pressure, innovation, health, fiscal deficit, openness, social protection and technology access. These variables represent pressure channels and smoothing-capacity channels that interact inside the same diagnostic architecture.

The distinction between pressure variables and smoothing-capacity variables is essential. A pressure variable is interpreted so that a higher value means greater inequality-related stress. A smoothing-capacity variable is interpreted in reverse: stronger capacity lowers stress, so weak capacity is transformed into higher stress. This is the central reason the research object can be called pressure-smoothing. The model does not claim that all variables have the same economic meaning. It claims that after explicit orientation and scaling, they can be read as coordinates of a common diagnostic stress space.

The resulting sixteen-coordinate structure gives the chapter three advantages. First, it provides an integrated inequality object rather than a single outcome. Second, it allows curvature-like deformation to be decomposed by component. Third, it allows graph topology to examine whether the inequality system is connected, dense, cycle-rich or bottlenecked. These advantages would be unavailable if the chapter used only one scalar inequality indicator.

Table 5.6. Sixteen stress-coordinate variables defining the research object.

Variable block	Symbol	Role in pressure-smoothing manifold	Stress-orientation rule
Income inequality	GINI	Pressure anchor	Higher Gini raises distributional pressure.
Productivity	PROD	Smoothing-capacity channel	Lower productive capacity is transformed into higher stress.
Unemployment	UNEMP	Pressure channel	Higher unemployment raises labour-market stress.
Investment rate	INV	Smoothing/capital-formation	Lower or fragile investment is transformed into

Variable block	Symbol	Role in pressure-smoothing manifold	Stress-orientation rule
		channel	higher stress.
Inflation	INFL	Pressure channel	Higher price pressure raises stress.
Migration pressure	MIGR	Pressure channel	Higher demographic/external mobility pressure raises stress.
Education	EDU	Smoothing-capacity channel	Lower human-capital capacity is transformed into higher stress.
Social mobility	MOB	Smoothing-capacity channel	Lower mobility is transformed into higher stress.
Trade infrastructure	LOG	Smoothing/corridor-capacity channel	Weaker logistics and trade infrastructure are transformed into higher stress.
Capital-flow pressure	CAP	Pressure channel	Higher external-finance pressure raises stress.
Innovation activity	INNOV	Smoothing-capacity channel	Lower innovation capacity is transformed into higher stress.
Healthcare access	HEALTH	Smoothing-capacity channel	Lower health-system access is transformed into higher stress.
Fiscal deficit	FISC	Pressure channel	Higher fiscal-pressure deficit raises stress.
Trade openness	OPEN	Smoothing/integration channel	Lower or fragile openness is transformed into higher stress.
Social protection	SP	Smoothing-capacity channel	Lower redistribution and resilience capacity are transformed into higher stress.
Technology access	TECH	Smoothing-capacity channel	Lower digital and technology access is transformed into higher stress.

5.2.5. Pressure, Smoothing Capacity and Deformation

The first substantive dimension of the object is inequality pressure. Pressure is not restricted to one inequality coefficient. It is the composite diagnostic condition produced by distributional inequality, labour-market pressure, price pressure, migration pressure, capital-flow pressure, fiscal pressure and weak capacity channels after all variables have been oriented toward stress. In this chapter, pressure therefore measures the accumulation of inequality-related strain in the macro-regional system.

The second dimension is smoothing capacity. Smoothing capacity refers to the ability of the macro-social system to absorb, moderate or reduce pressure. Productivity, education, innovation, healthcare access, social protection, technology access, trade infrastructure, mobility and capital formation are not treated as decorative controls. They are the economic channels through which pressure can be smoothed. When those channels weaken, they enter the diagnostic manifold as stress rather than as benign capacity.

The third dimension is curvature-like deformation. In the economic analogue, deformation means that pressure and smoothing capacity are not balanced. A region-year can be interpreted as more deformed when pressure coordinates intensify or when smoothing-capacity channels are insufficient to absorb them. Conversely, partial recovery occurs when pressure declines and scalar curvature improves, even if entropy-like complexity and regional dispersion remain visible. This is why the research object is not only static; it is a dynamic pressure-smoothing field over region-year coordinates.

Equation (5.2.5). Regional pressure coordinate: $P_{r,t} = \sum_j v_j S_{r,t,j}$, with v_j denoting declared coordinate weights.

Equation (5.2.6). World-weighted pressure path: P_t = sum_r w_{r,t} P_{r,t}, where w_{r,t} denotes macro-regional aggregation weight.
Equation (5.2.7). Curvature-style deformation coordinate: R_{r,t} = Phi(P_{r,t}, C_{r,t}), where C_{r,t} denotes smoothing-capacity information and Phi is a disclosed diagnostic transformation.
Equation (5.2.8). Entropy-like complexity state: W_t = Psi(P_t, R_t, dispersion_t, auxiliary controls), interpreted as a model-implied functional object.

Table 5.7. Economic dimensions of the pressure-smoothing manifold.

Object dimension	Economic meaning	Main variable families	Later model output
Pressure accumulation	Stress formation from inequality, labour, inflation, migration, fiscal and external-pressure channels.	GINI, UNEMP, INFL, MIGR, CAP, FISC plus capacity weakness after reverse transformation.	Global pressure path, regional pressure ranking and counterfactual shock effects.
Smoothing capacity	Absorptive or resilience channels that reduce or moderate pressure when strong.	PROD, INV, EDU, MOB, LOG, INNOV, HEALTH, OPEN, SP, TECH.	Curvature balance, recovery path and Ricci-surgery candidate interpretation.
Curvature-like deformation	Diagnostic imbalance between pressure accumulation and smoothing capacity.	Pressure vector and transformed capacity vector.	Ricci-style component curvature and scalar curvature.
Entropy-like complexity	Residual systemic complexity after pressure and curvature are jointly summarized.	Pressure, scalar curvature, dispersion and functional terms.	Perelman-type F and W functionals.
Graph connectedness	Whether the sixteen-coordinate system forms one connected, looped and bottlenecked diagnostic structure.	Standardized stress-coordinate correlations.	Graph Laplacian, algebraic connectivity, Betti numbers and edge-curvature proxies.

5.2.6. Macro-Regional Scope and Global Interpretation

The macro-regional scope is central to the research object. The chapter is not designed as a country ranking and should not be read as a country-level welfare table. Its purpose is to diagnose global inequality structure at the level where regional pressure, smoothing capacity and systemic deformation can be compared without collapsing the world economy into a single aggregate. Macro-regional aggregation is therefore a scale choice, not a shortcut around country-level evidence.
The global interpretation has two levels. The region-level panel preserves heterogeneity: some regions may carry stronger pressure, weaker smoothing capacity or more persistent deformation. The world-weighted path summarizes the system-level pressure-curvature-W trajectory, especially over the harmonized reporting window. The two levels should be read together. A global decline in pressure can coexist with persistent regional dispersion; a rise in curvature can indicate partial recovery without implying convergence; and elevated W-functional complexity can show that system complexity remains high even when headline pressure improves.
This scale logic protects the chapter from two opposite errors. The first error would be excessive aggregation: presenting one world inequality line and ignoring regional variation. The second error would be excessive disaggregation: treating regional rankings as country-level welfare verdicts. The pressure-smoothing manifold uses the macro-regional scale because the chapter is concerned with global structure, not household microdistribution or national policy attribution.

Table 5.8. Scale of interpretation and admissible claim by level.

Interpretive level	What is observed	What can be claimed	What cannot be claimed
Global path	World-weighted pressure, curvature and functional trajectory.	The global system displays deformation and recovery patterns under the constructed	Universal prediction or proof of theorem-level monotonicity.

Interpretive level	What is observed	What can be claimed	What cannot be claimed
		diagnostics.	
Macro-regional heterogeneity	Regional differences in pressure and smoothing capacity.	Some regional blocks occupy higher or lower diagnostic-pressure positions.	Country-level welfare ranking or household-distribution inference.
Component structure	Contribution of variable blocks to curvature-like deformation.	Curvature energy is concentrated in economically interpretable channels.	Direct causal treatment effects of a single policy variable.
Network topology	Connectedness and cycles among stress-coordinate variables.	The inequality-coordinate system is structurally connected under the defined threshold.	Proof of the Poincare conjecture or literal topological classification of the economy.
Validation evidence	Econometric, robustness, sensitivity and forecast screens.	Constructed diagnostics retain bounded empirical coherence.	Unrestricted causality or permanent forecast superiority.

5.2.7. Data Status: Public Anchors versus Constructed Diagnostic Objects

The research object requires strict separation between public or externally anchored macro-social inputs and final constructed diagnostic indicators. Public-data anchors provide the empirical starting point, but they are not the final analytical objects of Chapter 5. The final objects are author-calculated variables generated through harmonization, scaling, weighting, standardization, metric construction, curvature mapping, functional construction, graph thresholding, counterfactual simulation and validation routines.

This distinction is necessary because the chapter uses a constructed-index and analogue-modelling architecture. If a raw variable has official or public status, that status does not automatically transfer to the derived pressure coordinate, curvature coordinate, W-functional or graph topology. Those outputs are reproducible only if the transformation rules, variable dictionary, normalization logic, formulas, weights, thresholds, seeds and replication files are disclosed. The research object is therefore as much a data-lineage object as an economic object.

The strongest data-status claim is transparency and reproducibility, not raw official identity. The chapter can claim that its public anchors and author-calculated transformations create an auditable diagnostic manifold. It should not claim that constructed curvature or entropy values are official statistics. They are model-implied diagnostic quantities whose credibility depends on clear formula disclosure, robust checks and bounded interpretation.

Table 5.9. Public-anchor and author-calculated object distinction.

Data layer	Examples in Chapter 5	Status	Rule for interpretation
Public or source-anchor layer	Macro-regional inequality, productivity, unemployment, investment, inflation, education, health, technology and related inputs.	Input evidence.	Used as empirical anchors before transformation.
Harmonized stress-coordinate layer	0-100 pressure-oriented S_{r,t,j} variables.	Author-calculated diagnostic scale.	Comparable only within the declared transformation system.
Standardized coordinate layer	Z_{r,t,j} values.	Author-calculated statistical scale.	Used for metric tensor, graph, PCA and validation procedures.
Metric and curvature layer	g_ij, Ricci-style component curvature and scalar curvature.	Model-implied diagnostic objects.	Interpreted as pressure-smoothing structure, not literal geometry.

Data layer	Examples in Chapter 5	Status	Rule for interpretation
Functional layer	Perelman-type F and W functionals.	Model-implied energy/entropy analogues.	Used to interpret complexity, not classical monotonicity.
Topology layer	Adjacency, Laplacian, Betti and edge-curvature proxies.	Graph-theoretic diagnostic objects.	Used for connectedness and bottleneck interpretation, not theorem proof.
Replication layer	Zenodo package, formulas, metadata, tables and QA checks.	External audit companion.	Supports reproducibility of reported calculations and claim discipline.

5.2.8. Boundary Conditions of the Pressure-Smoothing Manifold

The pressure-smoothing manifold is bounded by five scientific conditions. First, it is an economic analogue rather than a theorem-level transfer of differential geometry or topology. Second, constructed curvature, F-functional, W-functional, Betti, degree, edge-curvature, forecast and Monte Carlo values are model-implied diagnostic quantities rather than literal geometric invariants. Third, the results support measurement and diagnostic interpretation rather than unrestricted causal estimation. Fourth, macro-regional aggregation is useful for global structure but cannot replace country-specific welfare analysis. Fifth, forecast evidence is treated as bounded validation rather than forecast-superiority proof.

These boundary conditions should be stated inside the research-object section because they determine the meaning of every later result. A high pressure value indicates a constructed diagnostic state, not an official welfare verdict. A negative curvature-like component indicates stress dominance or weak smoothing under the model specification, not physical curvature. A connected graph indicates that the coordinate system is empirically coupled at the selected threshold, not that an economic analogue has become a mathematical theorem. A counterfactual result indicates internal sign consistency under the model, not a policy treatment effect.

The boundary logic also protects the book-level project. Chapter 5 is one of seven Millennium-inspired economic analogues. Its credibility depends on demonstrating that the analogy is disciplined, auditable and scientifically cautious. The research object is therefore deliberately narrower than a general theory of inequality and broader than a single inequality indicator. It is a diagnostic architecture for measuring global inequality pressure, smoothing capacity, deformation, complexity and connectedness under explicit claim limits.

Table 5.10. Boundary controls for the research object.

Potential over-reading	Correct boundary statement	Reason the boundary matters
The economy is a literal Riemannian manifold.	The model constructs an economic diagnostic manifold from transformed macro-regional coordinates.	Prevents false theorem transfer and category error.
Curvature is a literal geometric invariant.	Curvature-like values are model-implied pressure-smoothing diagnostics.	Keeps the result interpretable as economics, not geometry.
Macro-regional ranks are country welfare rankings.	The chapter measures macro-regional diagnostic pressure, not country-level welfare.	Avoids unsupported policy or distributional claims.
Panel validation proves causality.	Econometric layers support bounded validation and association evidence.	Protects the study from identification overclaiming.
F/W functionals inherit Perelman monotonicity.	F and W are economic functional analogues and must be audited empirically.	Prevents importing classical mathematical properties into constructed data.
Rolling forecast performance proves forecast dominance.	Forecast evidence is bounded and benchmark disciplined.	Maintains credibility where AR(1) benchmark performance

Potential over-reading	Correct boundary statement	Reason the boundary matters
		is stronger over a short window.

5.2.9. Transition from Research Object to Data Architecture

Section 5.2 has established the object to be measured: a global macro-regional inequality system represented as a pressure-smoothing manifold. The next section, 5.3, must therefore move from object definition to data architecture. It should specify the ten-region empirical universe, the sixteen stress-coordinate variables, the 2010-2024 annual panel, the N = 150 region-year structure, the harmonized 2015-2024 reporting path and the public-anchor versus author-calculated data lineage.

This transition is important because a research object is only credible when its empirical construction is visible. The pressure-smoothing manifold becomes measurable only after the data architecture identifies variables, scale, orientation, source status, aggregation rules and transformation steps. Section 5.3 should therefore not repeat the conceptual explanation of curvature and topology; it should document the empirical coordinate system from which the metric tensor, curvature values, functional objects and graph topology are later computed.

The chapter sequence is now controlled. Section 5.1 provided the mathematical-economic translation. Section 5.2 defined the research object and its boundaries. Section 5.3 will define the data architecture. Section 5.4 will specify the methodology. Section 5.5 will report results. Section 5.6 will interpret the evidence. Sections 5.7-5.9 will state contribution, limitations and the chapter conclusion.

Table 5.11. Handoff from Section 5.2 to Section 5.3.

From Section 5.2	To Section 5.3	Operational handoff
Research object defined as pressure-smoothing manifold.	Data architecture defines the panel and coordinate dictionary.	Turn conceptual object into empirical grid.
Region-year unit identified.	Ten macro-regional blocks and 2010-2024 coverage must be documented.	Turn unit of analysis into sample design.
Sixteen coordinates introduced.	Variable dictionary, symbols and stress orientation must be formalized.	Turn variable concept into reproducible input map.
Public anchor versus constructed output separated.	Source lineage and transformation rules must be shown.	Turn data status into auditability.
Claim boundaries declared.	Data limitations and sample boundaries must be attached to the architecture.	Turn caution into reviewer-safe empirical design.

Section 5.2 Synthesis

The research object of Chapter 5 is the global macro-regional inequality system represented as a pressure-smoothing diagnostic manifold. It is built from ten macro-regional blocks, fifteen annual observations from 2010 through 2024, sixteen stress-coordinate variables and a balanced N = 150 diagnostic panel. The object is macro-regional, multi-coordinate, transformed, auditable and claim-bounded.

Its core analytical meaning is that inequality is not only a distributional level. It is a pressure process shaped by stress accumulation and smoothing-capacity weakness. The manifold language is justified only because the model constructs a coordinate system, a metric coupling structure, curvature-like deformation objects, Perelman-type functionals and graph-topological diagnostics. The same language is bounded because none of those objects is a literal mathematical invariant or theorem-level proof.

This section therefore gives Chapter 5 its empirical and conceptual foundation. It defines what is measured, how it is positioned, what its evidence status is, and what it cannot claim. With the research object fixed, the chapter can now proceed to the data architecture, methodology, results and interpretation without ambiguity about the status of the Perelman-Ricci-Poincare-inspired economic analogue.

Source trace: This section synthesizes and rewrites the source manuscript sections on research object, boundaries, data status, objectives, methodology notation and conclusion-on-object. Numerical values appearing here are restricted to the research-object and sample architecture level; full results are reserved for Section 5.5.

5.3. Data Architecture: Ten Regions, Sixteen Stress Coordinates and N=150 Panel

5.3.1. Purpose and Position of the Data-Architecture Section

Section 5.3 converts the research object defined in Section 5.2 into an auditable data architecture. The chapter is built on a balanced macro-regional diagnostic panel: ten region blocks, fifteen annual observations from 2010 through 2024, and sixteen stress-coordinate variables. The resulting empirical base is N = 150 region-year observations before the sixteen-dimensional coordinate layer is used for normalization, standardization, metric construction, curvature decomposition, Perelman-type functional calculation, graph topology and validation screens.

The purpose of this section is not to report final results. Its purpose is to make the empirical construction transparent before the methodology is introduced in Section 5.4. The reader must be able to see which units enter the chapter, how the annual panel is organized, why heterogeneous variables are not added in raw form, how pressure and smoothing-capacity variables are directionally harmonized, and how the resulting coordinate system becomes a legitimate input for the geometric-topological analogue.

The data architecture is therefore a scientific safeguard. It prevents the model from appearing as a purely rhetorical use of Ricci, Perelman or Poincare terminology. The architecture shows that the chapter begins with observable macro-social information, applies declared transformations, creates author-calculated stress coordinates and then uses those coordinates in an explicitly bounded diagnostic framework. Official or public data status belongs to the input layer; the final pressure, curvature, entropy and graph indicators are constructed research objects.

Table 5.12. Data-architecture role of Section 5.3.

Architectural layer	Operational content	Role in Chapter 5	Boundary condition
Empirical unit	Region-year coordinate, indexed by r and t.	Defines the balanced diagnostic panel.	Not a country-level welfare observation.
Regional universe	Ten macro-regional blocks.	Preserves global structure while retaining regional heterogeneity.	Macro-regional aggregation cannot replace country analysis.
Time window	Annual observations, 2010-2024.	Supports crisis deformation and recovery-path interpretation.	Short T limits unrestricted dynamic claims.
Coordinate layer	Sixteen stress-coordinate variables.	Converts inequality into a multi-channel pressure-smoothing system.	Constructed coordinates are not official indicators.
Transformation layer	0-100 stress orientation and standardization.	Makes heterogeneous units comparable for metric and graph construction.	Scale equivalence is diagnostic, not raw-unit equivalence.
Replication layer	Zenodo data and replication package, DOI 10.5281/zenodo.20844900.	Provides audit trail for variables, formulas and outputs.	Replication package supports transparency, not theorem proof.

5.3.2. Empirical Universe: Ten Macro-Regional Blocks

The first layer of the data architecture is the regional universe. Chapter 5 is global in scope but does not estimate a country-level welfare model. It uses ten macro-regional blocks as the empirical coordinate system for inequality pressure and smoothing capacity. This level of aggregation is appropriate for a monograph chapter whose purpose is to model systemic inequality deformation rather than to rank countries or make micro-level welfare claims.

The macro-regional design allows inequality to be interpreted as a structured global system. Regional blocks can differ in distributional inequality, labour-market pressure, technology access, fiscal stress, social protection and resilience. A single world aggregate would hide these differences; a fully country-level design would require a different source architecture and a different claim boundary. The ten-region design therefore operates as a middle-level diagnostic architecture between world aggregation and country-level econometrics.

The ten regions should be treated as empirical coordinates rather than as political rankings. Each region enters the model because it represents a macro-social position in the world inequality system. The architecture is designed to ask whether

inequality pressure and smoothing capacity form a connected, measurable and dynamically interpretable diagnostic manifold across global regions.

Table 5.13. Ten-region empirical universe for the inequality-pressure panel.

Code	Macro-regional block	Analytical function in Chapter 5	Interpretive boundary
EAP	East Asia and Pacific	Large output and technology-production region; relevant for productivity, technology access, trade and demographic-pressure channels.	Macro-regional coordinate, not a single country proxy.
NAM	North America	High-income and high-capacity region; important for comparative smoothing-capacity benchmarks.	Regional block, not a country-specific welfare claim.
EUR	Europe	Institutionally dense and social-protection-intensive region; relevant for smoothing-capacity interpretation.	Macro-regional coordinate with internal heterogeneity.
LAC	Latin America and Caribbean	Distributional and social-mobility channel; relevant for inequality-pressure interpretation.	Regional average does not replace country-level distribution analysis.
SAS	South Asia	High demographic and development-pressure region; relevant for labour, education and technology-access channels.	Macro-region; within-region variation remains outside the chapter scope.
MENA	Middle East and North Africa	Macro-financial, fiscal, migration and external-pressure region.	Regional coordinate, not geopolitical ranking.
SSA	Sub-Saharan Africa	High development and smoothing-capacity challenge region; relevant for education, healthcare, productivity and technology access.	Diagnostic region-level object, not country welfare verdict.
OCE	Oceania	High-income and geographically distinct macro-region; useful for income-depth and capacity comparison.	Small regional mass does not imply analytical exclusion.
CAS	Central Asia	Transition and connectivity-sensitive macro-region; relevant for capacity, openness and pressure interpretation.	Regional diagnostic coordinate.
CAU	Caucasus	Explicit subregional/corridor-sensitive block retained to avoid invisibility inside wider aggregations.	Author-defined subregional block; claim is diagnostic and bounded.

5.3.3. Time Dimension and Balanced N=150 Panel

The second layer is the time structure. The panel covers fifteen annual observations from 2010 through 2024. With ten regions and fifteen years, the main diagnostic base is N = 10 x 15 = 150 region-year observations. The annual structure is appropriate because most macro-social variables in the chapter are available, interpretable or harmonizable at annual frequency.

The full 2010-2024 window provides the longitudinal context for regional change, topology, descriptive statistics, entropy-path interpretation, crisis deformation and post-shock recovery diagnostics. Within this full window, the harmonized 2015-2024 period is used in the source study for the main world pressure-curvature path and the interpretation of the 2020 crisis deformation and the 2024 partial recovery signal. The separation between full-panel context and harmonized reporting window is an important sample-discipline device.

The N = 150 panel does not imply that every later test has unrestricted inferential power. The number of region clusters is ten and the annual time dimension is short. Consequently, the chapter treats panel evidence, forecast screens, graph topology

and robustness as bounded diagnostic evidence. The data architecture is strong for measurement and internal validation, but it is not a license for unrestricted causality or theorem-level claims.

Equation (5.3.1). Region set: $R = \{r_1, ..., r_{10}\}$.

Equation (5.3.2). Time set: $T = \{2010, 2011, ..., 2024\}$, with $|T| = 15$.

Equation (5.3.3). Main diagnostic panel size: $N = |R| \times |T| = 10 \times 15 = 150$.

Equation (5.3.4). Full raw coordinate array: $X = \{X_{r,t,j}: r \in R, t \in T, j = 1,...,16\}$.

Table 5.14. Balanced-panel and sample-discipline architecture.

Panel element	Value / definition	Reason for inclusion	Claim implication
Regions	10 macro-regional blocks.	Captures global inequality structure with regional heterogeneity.	Supports macro-regional diagnostics only.
Years	2010-2024 annual observations.	Captures pre-crisis, crisis and recovery dynamics.	Annual frequency limits high-frequency claims.
Main N	150 region-year observations.	Provides balanced panel base for diagnostic calculations.	N is sufficient for measurement architecture, not unrestricted causality.
Coordinate count	16 variables per region-year.	Represents inequality pressure and smoothing capacity as a multi-channel system.	Coordinates are constructed and normalized.
Full coordinate cells	10 x 15 x 16 = 2,400 raw/normalized coordinate cells before derived objects.	Defines the underlying measurement grid.	Coordinate cells are inputs to constructed objects, not independent theorem evidence.
Harmonized results window	2015-2024 for main pressure-curvature path.	Improves comparability for core world-path interpretation.	Window-specific results should be labelled as such.

5.3.4. Sixteen Stress-Coordinate Variables

The third layer is the sixteen-variable coordinate system. The chapter deliberately avoids treating inequality as a single Gini coefficient. The Gini variable remains the distributional anchor, but global inequality pressure is wider than distributional dispersion alone. It also includes productivity weakness, labour-market stress, investment fragility, price pressure, migration pressure, education weakness, social-mobility constraint, logistics weakness, capital-flow pressure, innovation weakness, healthcare weakness, fiscal stress, openness fragility, social-protection weakness and technology-access weakness.

The variables are divided into pressure coordinates and smoothing-capacity coordinates. Pressure coordinates are those for which a higher raw value generally indicates higher stress. Smoothing-capacity coordinates are beneficial-capacity variables; their weakness is converted into stress through reverse transformation. This directional harmonization is the central data-architecture rule because it allows all transformed variables to have one interpretation: higher stress means higher inequality pressure or weaker smoothing capacity.

The use of sixteen coordinates creates a data architecture capable of supporting metric-tensor construction and graph topology. A one-variable inequality model can describe a level. A sixteen-coordinate model can describe structural coupling, component concentration, pressure deformation, smoothing weakness and the connectedness of the inequality system.

Table 5.15. Sixteen stress-coordinate variables and orientation rules.

No.	Symbol	Variable block	Coordinate class	Stress-orientation rule
1	GINI	Income inequality / distributional dispersion	Pressure	Higher value raises pressure.
2	PROD	Productivity / productive capacity	Smoothing capacity	Lower capacity is reversed into higher stress.

No.	Symbol	Variable block	Coordinate class	Stress-orientation rule
3	UNEMP	Unemployment / labour-market pressure	Pressure	Higher value raises pressure.
4	INV	Investment rate / capital formation	Smoothing capacity	Lower or fragile investment is reversed into higher stress.
5	INFL	Inflation / price pressure	Pressure	Higher value raises pressure.
6	MIGR	Migration pressure / demographic-external pressure	Pressure	Higher pressure raises stress.
7	EDU	Education / human-capital smoothing	Smoothing capacity	Lower education capacity is reversed into higher stress.
8	MOB	Social mobility / intergenerational mobility	Smoothing capacity	Lower mobility is reversed into higher stress.
9	LOG	Trade infrastructure / logistics capacity	Smoothing capacity	Lower capacity is reversed into higher stress.
10	CAP	Capital-flow pressure / external-finance stress	Pressure	Higher pressure raises stress.
11	INNOV	Innovation activity / technology-production capacity	Smoothing capacity	Lower innovation capacity is reversed into higher stress.
12	HEALTH	Healthcare access / health-system smoothing	Smoothing capacity	Lower access is reversed into higher stress.
13	FISC	Fiscal deficit / fiscal-pressure coordinate	Pressure	Higher deficit pressure raises stress.
14	OPEN	Trade openness / external integration	Smoothing capacity	Lower or fragile openness is reversed into higher stress.
15	SP	Social protection / redistribution and resilience	Smoothing capacity	Lower protection is reversed into higher stress.
16	TECH	Technology access / digital access capacity	Smoothing capacity	Lower access is reversed into higher stress.

5.3.5. Public Anchors, Constructed Coordinates and Variable Lineage

The data architecture separates three layers: public or externally anchored inputs, author-harmonized regional variables and final author-calculated diagnostic objects. This distinction is essential for scientific credibility. A raw indicator may be publicly sourced, but the transformed stress coordinate is not an official institutional statistic. It is a research variable created through direction harmonization and scaling. Curvature, F-functional, W-functional, graph connectivity and Monte Carlo outputs are still further removed from public raw data because they are generated by model-specific transformations.

The correct interpretation is therefore lineage-based. The chapter can claim that the final diagnostics are traceable to public or transparent input anchors and disclosed transformations. It cannot claim that the final curvature or entropy values are themselves official variables. This lineage discipline also protects later econometric validation. When variables share construction lineage, the chapter treats internal fit as diagnostic structure, not as independent causal confirmation.

Each coordinate must therefore carry a metadata record: variable name, symbol, raw source or source-family logic, region-year coverage, raw direction, transformed direction, normalization rule, missing-data rule, and the derived objects that use it. Without this metadata, the chapter would not satisfy replication discipline.

Table 5.16. Public-anchor to author-calculated lineage in Chapter 5.

Lineage layer	Examples in Chapter 5	Transformation status	Evidence status
Public / external anchor	Raw macro-social indicators such as inequality, unemployment, inflation, education, health, technology access, fiscal and trade indicators.	Observed or externally anchored input before harmonization.	Input evidence only.
Author regional harmonization	Mapping raw series into ten region-year coordinates.	Aggregation, alignment, imputation/documentation where needed.	Transparent construction layer.
Stress-coordinate transformation	S_{r,t,j} on a common 0-100 pressure scale.	Direction harmonization and min-max scaling.	Author-calculated research variable.
Standardized coordinate layer	Z_{r,t,j}.	Mean-centering and standard-deviation scaling for metric/PCA/econometric use.	Analytical input to metric and validation steps.
Derived geometric-topological objects	Metric tensor, curvature, F/W functionals, graph Laplacian, Betti numbers.	Model-specific calculations from stress coordinates.	Diagnostic evidence, not official statistics.
Validation outputs	Panel, ARDL, VAR, PCA, regularization, rolling and Monte Carlo outputs.	Tests and uncertainty screens applied to constructed variables.	Bounded validation, not unrestricted causality.

5.3.6. Directional Harmonization and 0-100 Diagnostic Stress Scale

The core transformation rule is that all coordinates are converted into a common pressure-oriented scale. For pressure variables, high raw values already mean high stress; the transformation maps the raw value to a 0-100 scale in the ordinary direction. For smoothing-capacity variables, high raw values usually mean stronger capacity and lower stress; the transformation therefore reverses the direction so that weak capacity becomes high stress. This makes the coordinate system coherent before variables are combined or correlated.

The 0-100 scale does not claim raw-unit equivalence. A score of 70 in inflation stress and a score of 70 in technology-access stress do not mean that inflation and technology are the same economic object. They mean that each variable has been placed on a comparable diagnostic intensity scale within its own observed range and direction. This is sufficient for diagnostic geometry, but it must not be misread as literal unit identity.

After 0-100 stress scaling, standardized coordinates are used for metric, PCA, graph and validation layers. Standardization prevents variables with different dispersion from mechanically dominating correlation-based structures. The sequence is therefore raw data -> direction classification -> stress scaling -> standardization -> model-derived objects.

Equation (5.3.5). Pressure-variable stress score: S_{r,t,j} = 100 * (X_{r,t,j} - min_j X) / (max_j X - min_j X).

Equation (5.3.6). Smoothing-capacity stress score: S_{r,t,j} = 100 * (max_j X - X_{r,t,j}) / (max_j X - min_j X).

Equation (5.3.7). Standardized coordinate: Z_{r,t,j} = (S_{r,t,j} - mean(S_j)) / sd(S_j).

Equation (5.3.8). Coordinate interpretation rule: higher S_{r,t,j} means higher pressure or weaker smoothing capacity for every j.

Table 5.17. Directional harmonization and scaling protocol.

Transformation step	Input	Output	Why it is required	Risk if omitted
Direction classification	Raw variables X_{r,t,j}.	Pressure or smoothing-capacity class.	Prevents signs from being mixed.	Beneficial capacity could be incorrectly read as higher stress.
Min-max stress scaling	Direction-classified	0-100 stress coordinates	Creates common diagnostic range.	Raw units would be added or compared incoherently.

Transformation step	Input	Output	Why it is required	Risk if omitted
	variables.	S_{r,t,j}.		
Reverse transformation	Beneficial capacity variables.	Weak capacity expressed as high stress.	Aligns smoothing weakness with pressure logic.	Education, health or technology strength could be misread as stress.
Standardization	0-100 coordinates.	Z_{r,t,j}.	Supports metric tensor, PCA and regression stability.	Variables with large dispersion could dominate.
Metadata recording	All transformed variables.	Reproducible data lineage.	Makes replication and audit possible.	Derived values would become opaque.

5.3.7. Coordinate Blocks: Pressure Channels and Smoothing-Capacity Channels

The sixteen variables can be organized into two broad functional families. The first family consists of pressure channels: variables that directly increase inequality-related stress when they intensify. These include distributional inequality, unemployment, inflation, migration pressure, capital-flow pressure and fiscal pressure. The second family consists of smoothing-capacity channels: variables whose strength helps absorb or reduce inequality pressure, but whose weakness becomes a source of stress. These include productivity, investment, education, mobility, logistics, innovation, healthcare, openness, social protection and technology access.

This distinction is important because the Perelman-Ricci-Poincare analogue is not only about the level of pressure. It is about the balance between pressure accumulation and smoothing capacity. Curvature-like deformation becomes meaningful only because pressure and smoothing capacity can be compared within one harmonized coordinate architecture.

The data architecture therefore anticipates the later curvature decomposition. If investment, productivity, technology access, unemployment and fiscal pressure dominate curvature-energy contribution in the results, that finding is interpretable because the coordinate blocks are known in advance. The model does not search for meaning after the fact; it defines the data grammar before estimating or reporting results.

Table 5.18. Functional grouping of the sixteen stress coordinates.

Coordinate family	Included variables	Economic meaning	Later methodological use
Distributional anchor	GINI.	Baseline inequality-pressure coordinate.	Enters pressure index, metric tensor and component interpretation.
Labour and price pressure	UNEMP, INFL.	Labour-market and price-level stress.	Supports crisis-deformation and recovery-path interpretation.
External and fiscal pressure	MIGR, CAP, FISC.	Demographic, capital-flow and fiscal-pressure channels.	Contributes to pressure index, curvature and sensitivity screens.
Productive and investment capacity	PROD, INV.	Capacity to generate income, productivity and capital formation.	Reverse-transformed into stress when weak or fragile.
Human and social capacity	EDU, MOB, HEALTH, SP.	Human capital, mobility, health-system access and redistribution capacity.	Supports smoothing-capacity and policy-screen interpretation.
Innovation, technology and connectivity capacity	INNOV, TECH, LOG, OPEN.	Innovation, technology access, logistics and external integration.	Feeds metric coupling, graph topology and counterfactual sensitivity.

5.3.8. Aggregation, World-Weighted Paths and Regional Retention

The data architecture has both regional and world-weighted levels. Region-level observations are retained because the central object is heterogeneous macro-regional pressure. At the same time, world-weighted summaries are needed to interpret the global pressure-curvature-W path. The architecture therefore does not collapse the panel into one world series, nor does it treat regional observations as isolated country-like cases.

World-weighted aggregation is used when the chapter interprets global pressure, scalar curvature and Perelman-type functionals over time. Regional retention is used when the chapter interprets heterogeneity, component differences, graph topology, regional recovery and post-shock dispersion. This dual level is necessary because a pressure-smoothing manifold has both local coordinates and system-level summaries.

The weighting layer must be disclosed because weights can alter global-path interpretation. A large output or population region may affect the world-weighted path more than a smaller region. The chapter therefore treats world-weighted measures as system summaries and region-level measures as heterogeneity diagnostics. Neither level is allowed to erase the other.

Equation (5.3.9). Regional composite pressure: $P_{r,t} = \sum_{j=1}^{16} v_j S_{r,t,j}$, where v_j are declared coordinate weights.

Equation (5.3.10). World-weighted pressure path: $P_t^W = \sum_{r=1}^{10} \omega_{r,t} P_{r,t}$, with $\sum_r \omega_{r,t} = 1$.

Equation (5.3.11). Regional dispersion: $D_t = \sqrt{[(1/10) * \sum_{r=1}^{10} (P_{r,t} - \text{mean}_r P_{r,t})^2]}$.

Equation (5.3.12). Heterogeneity-preservation rule: report P_t^W jointly with regional $P_{r,t}$ or D_t when interpreting system pressure.

Table 5.19. Regional retention and world-weighted interpretation protocol.

Analytical level	Data object	Purpose	Interpretive risk	Control rule
Region-year level	$P_{r,t}$, $S_{r,t,j}$, $Z_{r,t,j}$.	Preserves macro-regional heterogeneity.	May be misread as country-level welfare ranking.	State macro-regional boundary.
World-weighted annual level	P_t^W, scalar curvature path, W-functional path.	Summarizes system-wide pressure and deformation.	May hide regional dispersion.	Report dispersion and regional context.
Component level	Variable-specific curvature and contribution shares.	Identifies structural channels carrying pressure or smoothing weakness.	May be overread as causal channel proof.	Interpret as diagnostic contribution.
Graph-topology level	Thresholded metric graph, Laplacian, Betti numbers.	Tests connectedness and cycle structure among coordinates.	May be mistaken for topological theorem proof.	Define as graph audit only.
Validation level	Panel, dynamic, PCA, regularized and forecast screens.	Audits robustness and structure.	May be overstated as unrestricted econometric validation.	Use bounded validation language.

5.3.9. Missing-Data, Comparability and Sample-Integrity Discipline

A data architecture of this type requires explicit sample-integrity discipline. The panel is designed as a balanced $N = 150$ region-year structure. If a raw series is missing, substituted, interpolated or proxy-transformed, the transformation must be documented in the source ledger. The validity of the final diagnostic objects depends not only on formulas but also on whether each input coordinate has a traceable lineage.

Comparability is a more important standard than mechanical data volume. A larger dataset with inconsistent variable meanings would not improve the model. The chapter therefore prioritizes aligned region-year coordinates, common stress orientation, transparent scaling and declared transformation rules. The data architecture should make every later table reproducible from the same input matrix.

The appropriate claim is therefore balanced-panel diagnostic closure. The chapter can claim that the $N = 150$ architecture is sufficient for a coherent macro-regional measurement system. It cannot claim that the panel eliminates all source uncertainty, aggregation bias, within-region heterogeneity or short-time-dimension limitations.

Table 5.20. Sample-integrity and comparability controls.

Integrity issue	Potential problem	Required discipline	Permitted interpretation
Missing raw value	Breaks balanced region-year matrix.	Document source, proxy, interpolation or exclusion rule in source ledger.	Panel remains auditable only if rule is disclosed.
Different units	Variables cannot be added directly.	Normalize and orient to stress scale before combination.	0-100 comparability is diagnostic, not raw-unit equivalence.
Different direction	Good outcomes and bad outcomes may have opposite signs.	Classify pressure versus smoothing capacity and reverse beneficial variables.	Higher transformed value always means more stress.
Regional aggregation	Within-region heterogeneity is hidden.	State macro-regional claim boundary.	Supports global-regional diagnostics, not country welfare rankings.
Short annual T	Dynamic inference has limited power.	Use bounded validation and robustness language.	Supports diagnostic association, not unrestricted causality.
Constructed-index circularity	Derived objects may share input lineage.	Track variable lineage and separate internal calibration from external validation.	Internal coherence is not independent causal evidence.

5.3.10. Data Objects Generated by the Architecture

The data architecture produces several classes of objects. The first class is the raw regional panel X. The second class is the stress-coordinate panel S. The third class is the standardized coordinate panel Z. The fourth class consists of model-derived geometry and topology objects: the metric tensor, curvature vectors, scalar-curvature path, F-functional, W-functional, graph Laplacian, algebraic connectivity and Betti-number diagnostics. The fifth class consists of validation and uncertainty outputs.

This hierarchy matters because it prevents the reader from confusing data inputs with results. The N = 150 panel is an empirical base; the 16 x 16 metric tensor is a constructed coupling object; curvature is a diagnostic transformation; the F/W functionals are economic analogue summaries; graph connectedness is a topological audit; validation models are evidence screens. Each layer inherits information from the previous layer but also adds author-specified transformation logic.

The architecture is therefore reproducible only if each generated object is stored, named and traceable. The data package should contain raw or source-ledger information, transformed stress files, standardized coordinate files, weight files, metric matrices, graph inputs, functional outputs, validation outputs, uncertainty simulations and README metadata. This is why Zenodo discipline belongs to the data architecture rather than only to the final replication statement.

Table 5.21. Data objects generated by the Chapter 5 architecture.

Generated object	Notation / file logic	Derived from	Used for	Evidence status
Raw panel	X_{r,t,j}.	Public / external anchors and author regional harmonization.	Initial empirical coordinate matrix.	Input evidence.
Stress panel	S_{r,t,j}.	Directional harmonization and 0-100 scaling.	Pressure and smoothing-capacity measurement.	Author-calculated diagnostic input.
Standardized panel	Z_{r,t,j}.	Mean and dispersion normalization of stress coordinates.	Metric tensor, PCA and regression screens.	Analytical input.
Metric tensor	G or correlation-	Standardized coordinate	Curvature and graph-	Constructed

Generated object	Notation / file logic	Derived from	Used for	Evidence status
	based 16 x 16 matrix.	correlations.	topology construction.	coupling object.
Curvature layer	Component curvature and scalar curvature.	Metric/stress/weight transformations.	Deformation and recovery diagnostics.	Model-implied diagnostic object.
Functional layer	F_t and W_t.	Pressure, curvature, dispersion and auxiliary terms.	Energy-like and entropy-like system summaries.	Economic analogue object.
Graph layer	Laplacian, beta_0, lambda_2, beta_1.	Thresholded metric tensor / coordinate graph.	Connectedness and cycle audit.	Graph diagnostic evidence.
Validation layer	Panel, ARDL, VAR, PCA, regularization, rolling and Monte Carlo outputs.	Constructed data and validation specifications.	Robustness and uncertainty interpretation.	Bounded validation evidence.

5.3.11. Replication Package and Source-Ledger Requirements

The source manuscript states that the complete data and replication package for the Perelman-Ricci-Poincare-inspired inequality framework is deposited on Zenodo with DOI 10.5281/zenodo.20844900. In the monograph chapter, this statement should be used as a formal replication anchor rather than as a decorative data-availability note. The replication package should be understood as the external audit companion to the chapter.

The replication package should allow an independent reader to reconstruct the transformation chain from public anchors to final diagnostic outputs. At minimum, the audit trail should identify source families, region mapping, variable definitions, raw or extracted inputs, stress-normalization rules, standardized coordinate files, metric-tensor construction, curvature and functional formulas, graph thresholds, validation scripts, random seeds, output tables, figures and checksums where available.

This replication discipline directly supports claim boundary. The chapter is unusual because it translates high-level mathematical ideas into an economic diagnostic architecture. The best defense against overclaiming is not to weaken the model; it is to make each transformation reproducible and to classify every output by evidence status.

Table 5.22. Replication-package requirements for the Chapter 5 data architecture.

Replication item	Required content	Why it matters for Section 5.3
Source ledger	Raw indicator source families, extraction dates, region mapping and variable definitions.	Documents the input layer before author transformations.
Region-year panel file	Ten regions, 2010-2024, sixteen raw or harmonized variables.	Recreates the N = 150 empirical base.
Orientation table	Pressure/smoothing-capacity classification for each coordinate.	Prevents sign ambiguity.
Stress-normalization output	0-100 S_{r,t,j} values and formulas.	Recreates the diagnostic coordinate system.
Standardized coordinate output	Z_{r,t,j} values.	Feeds the metric tensor, PCA and validation layers.
Weights and aggregation files	World-weighting and component-weight rules.	Recreates world pressure and scalar-curvature paths.

Replication item	Required content	Why it matters for Section 5.3
Metric and graph inputs	Correlation matrix, threshold rules, graph adjacency and Laplacian inputs.	Supports graph-topological reproducibility.
Derived-output files	Curvature, F/W functionals, Betti, Monte Carlo and validation outputs.	Links data architecture to Sections 5.4-5.6.
README and metadata	Software environment, file descriptions, citation text, checksums and version notes.	Makes the package externally auditable.

5.3.12. Data-Architecture Boundary Matrix

The final function of Section 5.3 is to define what the data architecture permits and what it does not permit. The architecture supports a strong claim that global inequality can be represented as a multi-coordinate macro-regional diagnostic system. It supports a strong claim that heterogeneous variables are transformed through a transparent, pressure-oriented scale. It supports a bounded claim that the resulting diagnostic manifold can be used for curvature, entropy, topology and validation analysis. It does not support theorem proof, literal geometric invariance, unrestricted causality, country-level welfare ranking or universal forecast superiority.

Table 5.23. Permitted and restricted claims arising from the data architecture.

Data-architecture claim	Permitted status	Reason	Restricted claim
Ten-region macro-regional panel is coherent.	Permitted.	The design fixes a complete global-regional coordinate system.	Does not rank countries.
N = 150 provides diagnostic panel closure.	Permitted with boundary.	Ten regions x fifteen years supplies balanced measurement base.	Does not create large-cluster causal identification.
Sixteen-variable structure captures inequality pressure beyond Gini.	Permitted.	Pressure and smoothing-capacity coordinates are explicitly defined.	Does not prove all inequality mechanisms.
0-100 stress scale makes variables comparable for diagnostic use.	Permitted.	Direction and scale are harmonized before modeling.	Does not imply raw-unit equivalence.
Constructed curvature, F/W and graph objects are auditable.	Permitted if formulas and files are disclosed.	Replication package and source ledger support transformation audit.	Does not make these objects official statistics.
Validation layers can support bounded structure claims.	Permitted with caution.	Panel, PCA, regularization and forecast screens audit robustness.	Does not establish unrestricted causality or forecast dominance.
Perelman/Ricci/Poincare mathematical problem is solved or tested.	Explicitly not permitted.	The architecture is an economic analogue.	No theorem-level claim.

5.3.13. Handoff to Section 5.4 Methodology

Section 5.3 establishes the empirical material that Section 5.4 will transform into methodology. The ten-region, sixteen-coordinate, N = 150 panel is now fixed. The variables have been classified by orientation. Raw and constructed objects have been separated. Scaling and standardization have been specified. Replication and source-ledger requirements have been defined. The next step is to explain the actual methodology: metric tensor construction, Ricci-style curvature, normalized Ricci-flow summaries, Perelman-type F/W functionals and graph-topological diagnostics.

This handoff is important because Section 5.4 should not need to re-justify the empirical universe. It can begin from an already audited data architecture and focus on the transformation of the coordinate system into geometric, functional, graph

and validation objects. The monograph structure is therefore sequential: translation in 5.1, research object in 5.2, data architecture in 5.3, methodology in 5.4, results in 5.5 and interpretation in 5.6.

Table 5.24. Handoff from data architecture to methodology.

Section 5.3 output	Section 5.4 methodological use
Ten macro-regional blocks.	Defines r-index for regional pressure, scalar curvature and regional comparison.
Annual 2010-2024 panel, N = 150.	Defines panel base for diagnostic, dynamic and robustness specifications.
Sixteen stress-coordinate variables.	Defines j-index for metric tensor, curvature decomposition and graph nodes.
0-100 stress scaling.	Provides comparable diagnostic coordinates before metric and functional construction.
Standardized coordinate matrix Z.	Feeds correlation-based metric tensor, PCA and regularization screens.
World-weighting and regional-retention logic.	Supports world pressure-curvature-W path and regional heterogeneity interpretation.
Replication package and source ledger.	Provides audit trail for formulas, tables, scripts and output objects.

Section 5.3 Synthesis

The data architecture of Chapter 5 is a balanced macro-regional diagnostic system. It contains ten region blocks, fifteen annual observations, sixteen stress-coordinate variables and N = 150 region-year observations. Its scientific strength is not raw sample size alone, but the disciplined transformation of heterogeneous macro-social indicators into a coherent pressure-oriented coordinate system.

The central methodological rule is that raw public or external data are not the final diagnostic indicators. Public anchors enter the model as source material. The final analytical objects - stress coordinates, standardized coordinates, metric tensor, curvature-like deformation, F/W functionals, graph topology and validation outputs - are author-calculated research variables. Their credibility depends on transformation disclosure, source lineage, replication-package discipline and claim-boundary language.

With this architecture fixed, the chapter can proceed to Section 5.4. The methodology can now legitimately construct a metric tensor, Ricci-style curvature, normalized Ricci-flow summaries, Perelman-type functionals and graph-topological diagnostics because the underlying data system has already been defined, scaled, oriented and bounded.

Source trace: This section synthesizes the Perelman-Ricci-Poincare source manuscript sections on research object, data status, objectives, methodology notation, stress-coordinate definitions, normalization logic and replication-package statement. It also follows the monograph-level structure in which Chapter 5.3 is assigned to data architecture and Chapter 5.4 is reserved for methodology. No theorem-level claim is made or implied.

5.4. Methodology: Metric Tensor, Ricci-Style Curvature, F/W Functionals and Graph Topology

This section specifies the methodological core of Chapter 5. The purpose is to transform the empirical object defined in Sections 5.2-5.3 - ten macro-regional blocks, sixteen pressure-oriented coordinates and a balanced N = 150 region-year diagnostic panel - into a reproducible pressure-curvature-topology architecture. The methodology is intentionally mathematical, econometric, computational and validation-oriented, but it is not theorem-proving. Perelman, Ricci-flow and Poincare terminology is used as a disciplined modelling grammar for inequality pressure, smoothing capacity, curvature-like deformation, entropy-like complexity and graph connectedness.

The section should be read as the technical bridge between data architecture and results. It explains how raw and harmonized macro-social variables become a standardized diagnostic coordinate system; how the coordinate system becomes a 16 x 16 empirical metric tensor; how curvature-style component scores, scalar curvature, F-functional and W-functional diagnostics are constructed; how the Poincare-inspired graph layer tests connectedness, loops and bottlenecks; and how these objects are validated without overstating them as causal laws, literal geometric invariants or classical theorem transfers.

Table 5.4.1. Methodological architecture of the Perelman-Ricci-Poincare chapter

Layer	Object constructed	Core operation	Admissible evidence status
Input layer	X_{r,t,j}: ten regions, 2010-2024, sixteen variables	Collect, classify and harmonize macro-social coordinates	Public/author-constructed input layer
Stress layer	S_{r,t,j}: 0-100 pressure-oriented coordinates	Min-max scaling and inverse transformation for smoothing capacity	Comparable diagnostic stress scale
Coordinate layer	Z_{r,t,j}: standardized coordinates	Center and divide by standard deviation	Metric, PCA, graph and validation-ready coordinate system
Metric layer	G = [g_ij]_{16 x 16}	Correlation-based empirical coupling matrix	Diagnostic manifold proxy, not literal Riemannian geometry
Curvature layer	rho_j, m_j, R_{r,t}, R_t	Neutral-midpoint Ricci-style signs and alpha-weighted contributions	Curvature-like inequality deformation measure
Functional layer	F_t and W_t	Energy-like and entropy-like aggregation with pressure potential	System complexity diagnostics, not theorem-level monotonicity
Topology layer	A, L, lambda_2, beta_0, beta_1, chi	Thresholded graph, Laplacian, Betti and Euler diagnostics	Graph connectedness and cycle evidence, not Poincare proof
Validation layer	Lagged screens, FE/FD, Mundlak, PCA, regularization, quantile/threshold, rolling, AR(1), Monte Carlo	Anti-circularity and robustness checks	Bounded validation and uncertainty discipline

5.4.1. Methodological position and theorem-boundary discipline

The methodology begins from an analogue boundary. In the classical mathematical setting, Ricci flow, Perelman functionals and Poincare topology refer to geometric objects with strict formal meaning. In this chapter, those ideas are not imported as theorem-level claims. They are translated into an economic measurement architecture: stress coordinates play the role of manifold coordinates; the correlation matrix plays the role of an empirical metric tensor; component stress signs play the role of curvature-like deformation; F and W functionals summarize energy-like and entropy-like inequality complexity; and a thresholded graph tests whether the stress-coordinate system behaves as a connected diagnostic manifold.

This distinction protects the chapter from category error. The model is not claiming that global inequality is a literal smooth manifold, that Ricci-flow equations are solved in their original differential-geometric form, or that the Poincare conjecture is empirically tested. The permitted claim is narrower and stronger: a macro-regional inequality system can be transformed into an auditable pressure-smoothing diagnostic architecture whose metric, curvature, functional and graph-topological layers are internally reproducible and empirically interpretable.

Table 5.4.2. Translation boundary between mathematical language and economic methodology

Mathematical language	Economic translation in Chapter 5	Methodological output	Excluded overclaim
Manifold	High-dimensional inequality diagnostic space	Sixteen standardized stress coordinates over region-year observations	The world economy is not treated as a literal smooth manifold
Metric tensor	Empirical coordinate-coupling matrix	G = corr(Z_i, Z_j), with eigenvalue and mean-coupling audits	Correlation is not geometric proof
Ricci curvature	Pressure-smoothing balance by component	rho_j, m_j, absolute contribution shares and annual curvature	Curvature scores are not physical or differential-

Mathematical language	Economic translation in Chapter 5	Methodological output	Excluded overclaim
		summaries	geometric curvature
Ricci flow	Time-varying pressure-smoothing movement	Normalized annual curvature and crisis/recovery paths	No literal solution of the Ricci-flow PDE
Perelman F-functional	Energy-like stress-curvature diagnostic	Curvature plus pressure-gradient potential	No theorem-level energy identity
Perelman W-functional	Entropy-like complexity closure	Scale-adjusted pressure-curvature-potential complexity index	No imported monotonicity theorem
Poincare connectedness	Graph-topological connectedness of inequality coordinates	Laplacian, algebraic connectivity, beta_0, beta_1 and Euler diagnostics	No proof or empirical verification of the Poincare conjecture

5.4.2. Notation, panel coordinates and methodological inputs

The methodology operates on a balanced macro-regional panel. Each observation is a region-year coordinate in the diagnostic space. Regions are indexed by r = 1,...,10; years are indexed by t = 2010,...,2024; and stress-coordinate variables are indexed by j = 1,...,16. The N = 150 region-year structure provides enough cross-regional and temporal variation to construct diagnostic panels, graph objects and validation screens, while the 2015-2024 harmonized window is reserved for the main world pressure-curvature path where required by the results architecture.

Equation (5.4.1). X = {X_{r,t,j}}, r = 1,...,10; t = 2010,...,2024; j = 1,...,16; N = 10 x 15 = 150.

Components: X_{r,t,j} denotes the raw or harmonized value of coordinate j for region r in year t.

Interpretation discipline: The panel is a diagnostic coordinate system, not an unrestricted causal identification design.

Equation (5.4.2). S_{r,t,j} = 100 * (X_{r,t,j} - min(X_j)) / (max(X_j) - min(X_j)) for pressure variables.

Components: S_{r,t,j} is the pressure-oriented 0-100 stress score.

Interpretation discipline: A higher value must always indicate higher pressure or weaker smoothing capacity.

Equation (5.4.3). S_{r,t,j} = 100 * (max(X_j) - X_{r,t,j}) / (max(X_j) - min(X_j)) for smoothing-capacity variables.

Components: This inverse rule is applied when a higher raw value is beneficial.

Interpretation discipline: Raw variables are not directly additive; they first have to share the same diagnostic direction.

Equation (5.4.4). Z_{r,t,j} = (S_{r,t,j} - mean(S_j)) / sd(S_j).

Components: Z is the standardized stress-coordinate used for metric, PCA, graph and validation layers.

Interpretation discipline: Standardization makes coupling comparable across heterogeneous macro-social coordinates.

5.4.3. Global inequality-pressure and curvature index

The first constructed object is the global inequality-pressure path. It aggregates the sixteen pressure-oriented stress coordinates into a regional pressure score and then into a world-weighted annual pressure score. The same architecture creates a curvature-like smoothing score. The purpose is not to forecast inequality mechanically but to build a common diagnostic path that can later be compared with scalar curvature, W-functional complexity, Gini, unemployment and inflation.

Equation (5.4.5). P_{r,t} = sum_j v_j S_{r,t,j}; P_t = sum_r w_{r,t} P_{r,t}.

Components: v_j denotes the coordinate weight; w_{r,t} denotes the macro-regional aggregation weight.

Interpretation discipline: P_t is a world-weighted diagnostic pressure path, not an official inequality statistic.

Equation (5.4.6). R_{r,t} = lambda_R sum_j alpha_j rho_{r,t,j}; R_t = sum_r w_{r,t} R_{r,t}.

Components: alpha_j denotes structural relevance; rho_{r,t,j} is the Ricci-style component sign or score.

Interpretation discipline: R_t is a curvature-like smoothing/deformation diagnostic, not literal scalar curvature.

Equation (5.4.7). Y_t = [P_t, R_t, W_t, GINI_t, UNEMP_t, INFL_t].

Components: Y_t is the global diagnostic vector reported in the results chapter.

Interpretation discipline: The vector combines constructed and observable/proxy-observable indicators and must be interpreted with lineage discipline.

Table 5.4.3. From data coordinates to Chapter 5 result objects

Construction stage	Input used	Methodological operation	Result object
Pressure construction	Sixteen 0-100 stress coordinates	Weighted aggregation across coordinates and regions	Global and regional pressure scores
Curvature construction	Pressure/smoothing signs and alpha weights	Neutral-midpoint Ricci-style transformation	Component curvature and scalar curvature
Functional construction	Pressure potential, curvature and scale parameter	F/W functional analogues	Energy-like and entropy-like complexity diagnostics
Graph construction	16 x 16 metric tensor	Thresholded adjacency and Laplacian	Connectedness, degree, Betti and loop diagnostics
Validation construction	Lagged panel/time-series and robustness designs	Anti-circularity tests and benchmark comparison	Bounded measurement-validation evidence

5.4.4. Economic metric tensor and coordinate-coupling audit

The metric tensor is the central bridge between the data architecture and the geometric analogy. The sixteen standardized stress coordinates are treated as the coordinate axes of the economic diagnostic space. The element g_ij is defined as the empirical correlation between coordinates i and j over the region-year panel. In this design, the tensor is a reproducible coupling matrix: it shows which inequality-pressure and smoothing-capacity channels move together after harmonization, but it does not claim to be a literal Riemannian metric.

Equation (5.4.8). g_{ij} = corr(Z_i, Z_j), G = [g_{ij}]_{16 x 16}.

Components: G is the 16 x 16 empirical metric tensor built from standardized stress coordinates.

Interpretation discipline: Correlation-based metric logic identifies empirical coupling, not direction of causality.

Equation (5.4.9). trace(G) = sum_j g_{jj}; lambda_min(G) >= 0.

Components: The trace equals the number of standardized coordinates under unit self-correlation; lambda_min checks positive-semidefinite behavior.

Interpretation discipline: The eigenvalue audit is a numerical consistency check, not a theorem of geometry.

Equation (5.4.10). MeanCoupling = (2 / (k(k - 1))) * sum_{i<j} |g_{ij}|, k = 16.

Components: MeanCoupling summarizes average off-diagonal dependence in the metric tensor.

Interpretation discipline: High coupling supports the manifold-style interpretation but must not be upgraded into causal connectedness.

Table 5.4.4. Metric tensor diagnostics and interpretation rules

Diagnostic	Formula or rule	What it measures	Interpretation boundary
Diagonal entries	g_jj = 1 after standardization	Self-correlation of each stress coordinate	Identity convention, not substantive result
Off-diagonal entries	g_ij = corr(Z_i, Z_j)	Pairwise synchronized movement between coordinates	Association, not causation
Absolute coupling	|g_ij|	Strength of coordinate co-movement regardless of sign	Useful for graph thresholds but direction needs separate interpretation
Trace	trace(G) = sum g_jj	Dimensional closure of the standardized system	Numerical audit
Minimum eigenvalue	lambda_min(G)	Near-collinearity and positive-semidefinite consistency	Reviewer-safety check, not geometric proof
Mean off-diagonal coupling	Average |g_ij| for i < j	Overall density of coordinate relationships	Supports diagnostic manifold language if coupling is non-trivial

5.4.5. Correlation-based curvature coordinate system

Before component curvature is calculated, the strongest metric-coordinate relationships are extracted from the off-diagonal entries of G. This step maps the internal structure of the diagnostic manifold. It identifies which variables behave as synchronized pressure/smoothing blocks and which pairs may become edges in the graph-topological layer. The operation is deliberately non-causal: high absolute coupling indicates coordinated movement inside the transformed diagnostic system, not causal transmission from one variable to another.

Equation (5.4.11). C_{ij} = |g_{ij}| for i != j; TopPairs = sort_desc({(i,j,C_{ij}) : i < j}).

Components: C_{ij} is the absolute metric-coupling score.

Interpretation discipline: TopPairs are used for structural mapping, graph interpretation and component discussions, not for causal ordering.

5.4.6. Ricci-style component curvature decomposition

The Ricci-style component layer translates stress orientation into curvature-like signs. Each coordinate is centered around the neutral midpoint of the 0-100 scale. If the mean stress of a coordinate is above 50, the coordinate is treated as pressure-dominant and receives negative Ricci-style pressure. If it is below 50 after harmonization, it is interpreted as relatively smoothing-dominant. Alpha weights then express the methodological relevance of each coordinate in the curvature decomposition.

Equation (5.4.12). rho_j = (50 - mean(S_j)) / 50.

Components: rho_j is the neutral-midpoint Ricci-style sign for coordinate j.

Interpretation discipline: The midpoint rule converts the 0-100 stress scale into a bounded curvature-style diagnostic.

Equation (5.4.13). m_j = alpha_j rho_j.

Components: m_j is the alpha-weighted curvature contribution score.

Interpretation discipline: Alpha weights should be disclosed and treated as methodological weights rather than estimated causal effects.

Equation (5.4.14). abs_share_j = 100 * |m_j| / sum_l |m_l|.

Components: abs_share_j is the percentage contribution of component j to total absolute curvature energy.

Interpretation discipline: Contribution concentration is a diagnostic ranking, not a welfare multiplier.

Table 5.4.5. Ricci-style curvature decomposition rules

Component status	Condition	Curvature meaning	Allowed interpretation
Pressure-dominant coordinate	mean(S_j) > 50	rho_j < 0 after midpoint transformation	The coordinate contributes to inequality deformation
Smoothing-dominant coordinate	mean(S_j) < 50	rho_j > 0 after midpoint transformation	The coordinate contributes to smoothing capacity
Neutral coordinate	mean(S_j) approximately 50	rho_j approximately 0	The coordinate is balanced on the diagnostic scale
High curvature-energy coordinate	High |m_j| or high abs_share_j	Large role in the curvature decomposition	Component is structurally important inside the model
Low curvature-energy coordinate	Low |m_j| or low abs_share_j	Limited role in the curvature decomposition	Component remains in the panel but does not dominate curvature energy

5.4.7. Normalized Ricci-flow and scalar curvature path

The normalized Ricci-flow layer does not solve the classical Ricci-flow equation. It transforms component curvature into annual regional and world-weighted distributions. The term flow is used because the diagnostic path evolves over time: pressure can accumulate, smoothing capacity can weaken or recover, and curvature-like deformation can intensify or soften across annual slices. The scalar curvature path then condenses the multi-component regional curvature field into a world-weighted annual object.

Equation (5.4.15). R^{norm}_{r,t} = lambda_t sum_j alpha_j rho_{r,t,j}.

Components: R^{norm}_{r,t} is the normalized regional curvature score.

Interpretation discipline: lambda_t stabilizes diagnostic scaling; it is not a physical flow parameter.

Equation (5.4.16). AnnualSummary_t(R) = {mean_r(R_{r,t}), median_r(R_{r,t}), min_r(R_{r,t}), max_r(R_{r,t})}.

Components: Annual summaries describe the cross-regional distribution of curvature states.

Interpretation discipline: Distributional summaries prevent a single world average from hiding regional dispersion.

Equation (5.4.17). R_t = sum_r w_{r,t} R^{norm}_{r,t}.

Components: R_t is the world-weighted scalar-curvature proxy.

Interpretation discipline: It is a constructed economic scalar-curvature diagnostic.

Equation (5.4.18). sign_cov = sign(cov(P_t, R_t)); expected crisis-window sign is negative.

Components: The inversion audit checks whether higher pressure corresponds to lower smoothing curvature.

Interpretation discipline: This is a co-movement audit; causal interpretation requires lagged validation.

5.4.8. Weighted curvature-contribution concentration

The weighted contribution step asks whether curvature energy is concentrated in a small set of coordinates or widely distributed across the sixteen-variable system. This matters for interpretation: if a few coordinates dominate, the chapter can identify specific inequality-deformation channels; if contributions are diffuse, the chapter must emphasize systemic pressure rather than component concentration. The dominance rule compares observed contribution shares with a uniform benchmark.

Equation (5.4.19). Share(A) = sum_{j in A} abs_share_j.

Components: A is a subset of coordinates, such as investment, productivity, technology, unemployment and fiscal pressure.

Interpretation discipline: Subset contribution supports component-concentration interpretation only when the subset materially exceeds its uniform share.

Equation (5.4.20). Dominance if Share(A) materially exceeds |A| / k under uniform contribution, with k = 16.

Components: The uniform benchmark for one coordinate is 1/16 of total contribution.

Interpretation discipline: Dominance is a diagnostic concentration rule, not a causal decomposition theorem.

Table 5.4.6. Curvature objects and their result-layer roles

Curvature object	Primary formula	Result layer it supports	Reviewer-safe interpretation
Component sign	rho_j = (50 - mean(S_j))/50	Component Ricci-style decomposition	Pressure versus smoothing orientation
Weighted component score	m_j = alpha_j rho_j	Curvature contribution ranking	Structural contribution inside the index
Absolute contribution share	abs_share_j = 100 |m_j| / sum |m_l|	Weighted curvature-contribution decomposition	Concentration of curvature energy
Regional curvature	R^{norm}_{r,t}	Annual regional curvature distributions	Regional pressure-smoothing state
Scalar curvature	R_t = sum w R^{norm}	World pressure-curvature path	Global deformation/recovery signal
Inversion audit	sign(cov(P_t, R_t))	Crisis-deformation interpretation	Co-movement evidence, not causal proof

5.4.9. Perelman F-functional as economic energy diagnostic

The F-functional layer adds a pressure-potential term to the curvature architecture. In the economic analogue, the potential f_{r,t} is a normalized pressure concentration measure. A region with relatively high pressure in a given year has a higher potential; sharper cross-regional pressure differences raise the gradient component. The resulting F_t object is an energy-like diagnostic: it asks whether pressure and curvature are arranged in a way that indicates systemic inequality energy.

Equation (5.4.21). f_{r,t} = (P_{r,t} - min_r P_{r,t}) / (max_r P_{r,t} - min_r P_{r,t} + epsilon).

Components: f_{r,t} is the normalized pressure potential in the annual regional slice.

Interpretation discipline: epsilon prevents division by zero; f is an economic potential, not a geometric density function.

Equation (5.4.22). F_t = c_F + lambda_F sum_r w_{r,t} [R^+_{r,t} + ||grad_G f_{r,t}||^2] exp(-f_{r,t}).

Components: F_t combines positive curvature contribution and pressure-gradient intensity under a weighted exponential potential.

Interpretation discipline: F_t is scaled for diagnostic comparability and is not a literal Perelman integral.

The economic F-functional is therefore interpreted as a stress-energy screen. It becomes large when regional pressure differences are meaningful and when curvature-like conditions suggest strong deformation or concentrated stress. Its value is most important when read jointly with global pressure and W-functional complexity rather than in isolation.

5.4.10. Perelman W-functional as entropy-like complexity closure

The W-functional layer extends the energy diagnostic into an entropy-like complexity measure. It introduces a scale parameter tau_t and a transformed density u_{r,t}. The purpose is to summarize the complexity of the inequality manifold after pressure, curvature, potential and scale are jointly considered. Because this is an economic analogue, the chapter explicitly rejects the automatic importation of Perelman monotonicity into the macro-social system.

Equation (5.4.23). u_{r,t} = (4*pi*tau_t)^(-k/2) exp(-f_{r,t}), k = 16.

Components: u_{r,t} is the scale-adjusted pressure-potential density.

Interpretation discipline: u is a diagnostic weighting device, not a probability law derived from heat-kernel geometry.

Equation (5.4.24). W_t = c_W + lambda_W sum_r w_{r,t} [tau_t(R_{r,t} + ||grad_G f_{r,t}||^2) + f_{r,t} - k] u_{r,t}.

Components: W_t is the entropy-like complexity closure for year t.

Interpretation discipline: W_t is a model-implied complexity diagnostic, not a theorem-level entropy quantity.

Equation (5.4.25). dW_t = W_t - W_{t-1}; dP_t = P_t - P_{t-1}; M_t = 1[dW_t >= 0].

Components: The monotonicity audit records increases and decreases in W rather than imposing monotonicity.

Interpretation discipline: The audit prevents classical monotonicity from being overclaimed in an economic setting.

Table 5.4.7. F/W functional interpretation discipline

Functional layer	Economic role	Main inputs	What the chapter may claim	What the chapter may not claim
F-functional	Energy-like stress-curvature diagnostic	Curvature, pressure potential and gradient intensity	The model measures stress-energy concentration in inequality space	It proves or replicates Perelman F-functional results
W-functional	Entropy-like complexity closure	Scale parameter, curvature, gradient intensity, potential and density term	The model measures systemic inequality complexity and crisis sensitivity	It imports classical W-monotonicity as a theorem
Monotonicity audit	Annual complexity-variation screen	dW_t and dP_t	The model reports whether complexity rises or falls in each year	The model assumes W must always increase or decrease
Joint reading	Pressure-curvature-entropy interpretation	P_t, R_t, F_t, W_t	Crisis deformation and partial recovery can be diagnosed jointly	A single functional value is sufficient for all interpretation

5.4.11. Poincare-inspired graph topology: adjacency, Laplacian and connectedness

The Poincare-inspired layer converts the metric tensor into a graph. The nodes are the sixteen stress coordinates, and edges are included when absolute metric coupling exceeds a disclosed threshold. In the source methodology, theta = 0.300 is used as the benchmark threshold. The graph tests whether the inequality variables form a connected diagnostic structure and whether the structure is dense, looped or bottlenecked. This is a graph-theoretic audit of the economic manifold, not a topological proof.

Equation (5.4.26). A_{ij} = 1[|g_{ij}| >= theta] for i != j; A_{ii} = 0; theta = 0.300.

Components: A is the thresholded adjacency matrix derived from the empirical metric tensor.

Interpretation discipline: The threshold must be disclosed and treated as a modelling choice subject to sensitivity analysis.

Equation (5.4.27). D_{ii} = sum_j A_{ij}; L = D - A.

Components: D is the degree matrix and L is the unweighted graph Laplacian.

Interpretation discipline: The Laplacian tests graph structure among variables, not geographic or physical distance.

Equation (5.4.28). lambda_2(L) > 0 implies one connected graph component.

Components: lambda_2 is algebraic connectivity.

Interpretation discipline: A connected graph supports manifold-style diagnostic coherence, not theorem proof.

Equation (5.4.29). degree_i = sum_j A_{ij}; min_i degree_i >= 1 is the no-isolated-node condition.

Components: degree_i counts how many stress-coordinate edges connect to node i.

Interpretation discipline: Degree is network embeddedness, not causal importance.

5.4.12. Betti numbers, Euler characteristic and looped inequality structure

Connectedness is not sufficient for a topological reading. The graph may be a simple tree, a dense looped structure, or a bottlenecked system with concentrated transmission channels. The Betti diagnostics convert the thresholded graph into a compact topological summary. beta_0 counts connected components; beta_1 counts independent cycles in the graph skeleton; Euler characteristic and cycle density indicate whether the network is tree-like or loop-rich. In economic terms, loops represent repeated pressure-smoothing transmission channels among inequality variables.

Equation (5.4.30). beta_0 = number of connected components.

Components: beta_0 = 1 means the graph is connected.

Interpretation discipline: This is graph connectedness, not Poincare proof.

Equation (5.4.31). beta_1 = E - V + beta_0.

Components: E is the number of graph edges and V is the number of variable nodes.

Interpretation discipline: beta_1 counts independent graph cycles under the selected threshold.

Equation (5.4.32). chi = V - E; CycleDensity = beta_1 / E.

Components: chi is the Euler characteristic of the graph skeleton; CycleDensity normalizes loop abundance by edge count.

Interpretation discipline: These are graph-topological diagnostics of the constructed metric graph.

Table 5.4.8. Graph-topological diagnostics and admissible interpretation

Graph diagnostic	Definition	Economic meaning	Interpretation boundary
Adjacency matrix A	A_ij = 1 when |g_ij| >= theta	Defines which stress coordinates are linked in the metric graph	Depends on threshold choice
Degree	Number of incident edges	Variable embeddedness in inequality network	Centrality, not causal effect
Laplacian L	L = D - A	Connectedness and spectral structure	Graph object, not geometric Laplace-Beltrami operator
Algebraic connectivity	lambda_2(L)	Whether the variable graph is connected	Diagnostic connectedness, not theorem proof
beta_0	Number of connected components	Global coordination of the coordinate system	Does not prove classical topology
beta_1	E - V + beta_0	Independent cycles/loops among variables	Cycles indicate repeated diagnostic channels, not literal holes in an economy
Euler characteristic	chi = V - E	Tree-like versus loop-rich graph structure	Threshold-dependent topology

5.4.13. Ollivier and Forman edge-curvature proxy screens

The graph layer is extended through edge-curvature proxies. The Ollivier-style proxy is implemented as a practical screen for fragile edges rather than as a full optimal-transport curvature calculation. It combines edge weight, local clustering and

degree imbalance. The Forman-style proxy complements it by penalizing highly embedded edges. Together, these two screens help locate relationships that are present in the inequality network but potentially fragile or bottlenecked.

Equation (5.4.33). w_{ij} = |g_{ij}| for A_{ij} = 1.

Components: w_{ij} is the absolute metric-coupling weight assigned to an observed graph edge.

Interpretation discipline: Weights are derived from the empirical metric tensor.

Equation (5.4.34). OR_proxy_{ij} = scale[w_{ij} C_{ij} / (1 + |degree_i - degree_j|)].

Components: C_{ij} is a common-neighborhood or clustering adjustment.

Interpretation discipline: This is an Ollivier-inspired screen, not a full optimal-transport curvature estimate.

Equation (5.4.35). FR_proxy_{ij} = 4 + w_{ij} - degree_i - degree_j.

Components: FR_proxy penalizes edges attached to highly connected nodes.

Interpretation discipline: More negative values indicate embedded bottleneck candidates, not welfare losses.

5.4.14. Ricci-surgery candidates and bottleneck diagnostics

The Ricci-surgery layer converts curvature contribution and network embeddedness into a ranked diagnostic priority index. The term surgery is used analogically. It does not prescribe policy intervention and does not estimate treatment effects. It identifies components whose curvature contribution, network degree and pressure-dominant sign make them important for structural attention inside the inequality diagnostic manifold.

Equation (5.4.36). Surg_j = rank_score(|m_j|, abs_share_j, degree_j, I(m_j < 0)).

Components: The implemented score combines curvature magnitude, contribution share, graph embeddedness and pressure-dominant sign.

Interpretation discipline: The score is an internal diagnostic ranking, not a causal policy multiplier.

Equation (5.4.37). Priority_j = High if Surg_j >= q_0.70; Medium if q_0.35 <= Surg_j < q_0.70; Low otherwise.

Components: Quantile thresholds classify surgery candidates.

Interpretation discipline: Priority labels are methodological screens that guide interpretation, not policy mandates.

Table 5.4.9. Bottleneck and surgery-ranking logic

Ranking input	Why it matters	High-risk/priority signal	Claim boundary
Absolute curvature magnitude |m_j|	Shows component deformation strength	Large absolute score	Internal model contribution only
Contribution share abs_share_j	Shows concentration of curvature energy	Large share relative to uniform benchmark	Not causal decomposition
Degree_i	Shows network embeddedness	High degree or strong neighborhood involvement	Centrality, not intervention effect
Pressure-dominant sign I(m_j < 0)	Shows adverse stress orientation	Negative Ricci-style score	Diagnostic stress signal
Ollivier proxy	Shows fragile local edge structure	Low OR_proxy	Proxy screen, not transport curvature theorem
Forman proxy	Shows embedded bottleneck tendency	More negative FR_proxy	Proxy screen, not direct welfare bottleneck

5.4.15. Counterfactual sensitivity and validation gates

Although the main purpose of Section 5.4 is to define the metric-curvature-functional-topology machinery, the methodology also requires validation gates. Counterfactual sensitivity tests whether the constructed system responds in the expected direction when smoothing-capacity variables improve or adverse pressure variables intensify. Econometric validation tests whether the diagnostic variables retain structure under lagged, panel, robustness, regularization and forecast-benchmark designs. These gates prevent the framework from becoming a purely decorative mathematical analogy.

Equation (5.4.38). P_t^{cf}(delta_A) = P_t - eta_A delta_A + phi_A curvature_feedback(delta_A).

Components: A_t summarizes technology/innovation smoothing capacity.

Interpretation discipline: The result is internal model sensitivity, not a causal technology multiplier.

Equation (5.4.39). P_t^{cf}(delta_SP) = P_t - eta_SP delta_SP + phi_SP curvature_feedback(delta_SP).

Components: Social protection is treated as a smoothing-capacity coordinate.

Interpretation discipline: The result tests sign coherence of the diagnostic architecture.

Equation (5.4.40). P_t^{cf}(delta_U, delta_PI) = P_t + eta_U delta_U + eta_PI delta_PI + eta_UPI delta_U delta_PI.

Components: Unemployment and inflation are adverse pressure variables.

Interpretation discipline: Signed perturbations identify pressure sensitivity, not structural policy effects.

Table 5.4.10. Validation protocol embedded in the methodology

Validation block	Core specification or test	Purpose	Boundary
Dynamic pressure screen	Delta P_t on lagged pressure, smoothing curvature and macro-social changes	Avoids current-year mechanical reconstruction	Short annual sample; diagnostic only
ARDL/ECM target screen	Raw Gini as target with lagged macro-social predictors	Reduces circularity by using a non-identical target	Directional association only
VAR/SVAR and local projections	Lagged shock-transmission screens	Tests sign/persistence of pressure and smoothing channels	Not fully identified structural shocks
FE/FD panel models	Regional fixed effects and first differences over N = 150	Uses panel variation beyond a short world series	Only ten clusters; cautious inference
Mundlak diagnostic	Within and between-region predictor structure	Separates regional positioning from within movement	Diagnostic decomposition
PCA and regularization	PCA, Ridge, LASSO, Elastic Net	Tests dimensional structure and overfit discipline	Robustness screen
Quantile/threshold/regime screens	Heterogeneity across inequality or technology regimes	Checks nonlinear diagnostic behavior	Regime evidence, not causal law
Rolling/AR(1)/Monte Carlo	No-look-ahead validation, benchmark comparison, uncertainty bands	Defines predictive limits and uncertainty	No universal forecast superiority

5.4.16. Unified computational pipeline for Section 5.4

The methodology is best understood as a deterministic computational pipeline from public-data anchors and author-harmonized variables to final diagnostic objects. Each step has an output that feeds the next step. This one-to-one alignment is crucial for replication: a reader should be able to trace a result in Section 5.5 back to the exact metric, curvature, functional or graph operation that generated it.

32. Construct the N = 150 region-year panel from ten macro-regional blocks, 2010-2024, and sixteen stress-coordinate variables.
33. Classify each variable as pressure-oriented or smoothing-capacity-oriented and transform all coordinates onto the 0-100 stress scale.
34. Standardize the stress coordinates to produce Z_{r,t,j}, the coordinate system for metric, topology, PCA and validation layers.
35. Build the 16 x 16 metric tensor G from pairwise correlations among standardized coordinates and audit trace, eigenvalues and mean coupling.
36. Extract the strongest coordinate relationships from absolute off-diagonal metric entries to identify empirical blocks.
37. Compute Ricci-style component signs, alpha-weighted curvature scores and absolute contribution shares.
38. Aggregate regional and world-weighted normalized curvature, scalar curvature, F-functional and W-functional diagnostics.
39. Convert the metric tensor into a thresholded graph and calculate adjacency, degree, Laplacian, algebraic connectivity, Betti numbers, Euler characteristic and cycle density.
40. Compute Ollivier-style and Forman-style edge-curvature proxies and rank Ricci-surgery candidates.

41. Run counterfactual sensitivity, lagged validation, panel robustness, regularization, regime screens, rolling forecasts, benchmark comparison and Monte Carlo uncertainty.
42. Separate permitted diagnostic measurement claims from excluded theorem-proof, unrestricted-causality and universal-forecast-superiority claims.

Table 5.4.11. Methodology-to-results bridge for Chapter 5

Section 5.4 method	Main result object in Section 5.5	Interpretive role in Section 5.6	Scientific contribution later in Chapter 5
Stress normalization and standardized coordinates	Descriptive stress-coordinate panel and global pressure path	Shows that heterogeneous variables can be compared on one pressure-oriented scale	Transparent inequality-diagnostic data architecture
Metric tensor G	16 x 16 coordinate-coupling matrix and eigenvalue audit	Shows whether stress/smoothing variables form a coupled system	Empirical diagnostic-manifold construction
Ricci-style curvature decomposition	Component signs and contribution shares	Identifies deformation channels and smoothing channels	Curvature-like decomposition of global inequality pressure
Scalar curvature path	Annual world and regional curvature values	Interprets crisis deformation and recovery	Pressure-smoothing measurement over time
F-functional	Energy-like stress-curvature path	Measures pressure-gradient and curvature energy	Perelman-inspired energy diagnostic
W-functional	Entropy-like complexity path and monotonicity audit	Interprets systemic complexity, crisis peaks and residual post-shock dispersion	Claim-bounded entropy-style closure
Graph topology	lambda_2, beta_0, beta_1, degree and Euler diagnostics	Shows connected, looped or bottlenecked inequality structure	Poincare-inspired graph connectedness audit
Edge curvature and surgery ranking	Ollivier/Forman proxies and priority list	Identifies fragile links and bottleneck channels	Network-curvature-informed diagnostic prioritization
Validation protocol	Lagged, panel, robustness, forecast and uncertainty evidence	Prevents mechanical or overfit interpretation	Reviewer-safe evidence hierarchy

5.4.17. Methodological claim boundary for Chapter 5

The methodology supports a strong diagnostic measurement claim: it can translate global macro-regional inequality indicators into a reproducible pressure-curvature-topology system. It also supports bounded validation claims when results remain coherent under lagged regressions, panel screens, robustness estimators, regularization, threshold tests, rolling forecasts, benchmark comparisons and uncertainty simulations. However, the chapter must not state or imply that it proves the Poincare conjecture, verifies Perelman theory, solves Ricci flow on the economy, estimates unrestricted causal effects, or delivers universal forecast dominance.

Table 5.4.12. Methodological claim-boundary matrix

Methodological object	Permitted claim	Prohibited claim	Safe wording for the book chapter
Metric tensor	The sixteen coordinates form an empirically coupled diagnostic system	The metric is a literal Riemannian metric	Correlation-based economic metric tensor
Ricci-style curvature	Pressure and smoothing capacity can be summarized as curvature-like deformation	The model estimates true geometric curvature	Ricci-style economic curvature diagnostic
Normalized Ricci-flow	Annual curvature states show	The classical Ricci-flow PDE	Normalized curvature-

Methodological object	Permitted claim	Prohibited claim	Safe wording for the book chapter
	deformation and recovery movement	is solved	flow analogue
F-functional	The model measures energy-like pressure-curvature concentration	Perelman F-functional is replicated mathematically	Perelman-type economic F-functional
W-functional	The model measures entropy-like complexity and crisis sensitivity	Classical W-monotonicity is proven or required	Perelman-type W-functional entropy closure
Graph Laplacian and Betti diagnostics	The stress-coordinate network is connected, dense or looped under a threshold	Poincare conjecture is tested or proven	Poincare-inspired graph-topological audit
Counterfactual sensitivity	The model responds coherently to signed perturbations	The effects are causal policy multipliers	Internal model sensitivity
Econometric and forecast validation	Validation supports diagnostic usefulness within boundaries	The model provides unrestricted causality or universal forecast superiority	Bounded validation and claim discipline

5.4.18. Chapter-bridge conclusion

Section 5.4 establishes the complete technical mechanism through which Chapter 5 moves from data to results. The methodology begins with pressure-oriented normalization and standardized coordinates; constructs a metric tensor as the empirical coupling structure of the inequality manifold; derives Ricci-style curvature, normalized flow and scalar curvature; builds F-functional and W-functional diagnostics for energy-like and entropy-like complexity; converts the metric tensor into a graph to test connectedness and cycles; and adds edge-curvature, surgery, counterfactual and validation gates. The next section can therefore report pressure, curvature, entropy, crisis-deformation and recovery results without reintroducing the full technical machinery.

5.5. Results: Pressure, Curvature, Entropy, Crisis Deformation and Recovery Path

5.5.1. Results-Reading Protocol and Evidence Boundary

This section reports the empirical outputs of the Perelman–Ricci–Poincaré-inspired inequality framework. The results are not presented as a mathematical proof, theorem test or literal computation of geometric invariants. They are reported as diagnostic economic quantities constructed from ten macro-regional blocks, sixteen pressure-oriented stress coordinates and a balanced 2010–2024 region-year panel. The results therefore answer a measurement question: whether global inequality pressure can be organized into interpretable pressure, curvature, entropy, graph-topological, counterfactual, validation and recovery layers.

The results sequence follows the methodology established in Section 5.4. Raw public indicators are transformed into stress coordinates; standardized coordinates define the correlation-based economic metric tensor; the tensor and pressure coordinates generate Ricci-style component curvature; world-weighted aggregation produces scalar curvature; Perelman-type F and W functionals summarize energy-like and entropy-like system states; and thresholded metric relationships generate Poincaré-style connectedness, Betti and network-curvature diagnostics. The validation blocks then test whether these constructed quantities remain meaningful under counterfactual, econometric, regularized, rolling forecast and uncertainty procedures.

$P_{r,t} \rightarrow Z_{r,t,j} \rightarrow g_{ij} \rightarrow$ Ricci-style component curvature $\rightarrow R_t \rightarrow F_t, W_t \rightarrow G(A), L, \beta_0, \beta_1 \rightarrow$ validation gates

Table 5.5.1. Results architecture and evidence-status map

Result layer	Primary object	Main numerical evidence	Permitted interpretation
Global path	Pressure, scalar curvature, W	2020: pressure 38.079, curvature 6.216, W	Crisis deformation and partial recovery, not causal

Result layer	Primary object	Main numerical evidence	Permitted interpretation
		508.023; 2024: pressure 30.314, curvature 10.264, W 488.759	proof
Metric tensor	16 × 16 correlation-based tensor	Trace 16.000; mean off-diagonal |corr| 0.547; maximum |corr| 0.978	Coupled diagnostic coordinate system
Ricci-style decomposition	Component contribution shares	Top five components ≈ 69.951 percentage points of absolute contribution	Curvature energy is structurally concentrated
Perelman functionals	F-functional and W-functional	F peaks at 27.039 in 2020; W peaks at 508.023 in 2020	Energy-like and entropy-like diagnostic response
Graph topology	Thresholded component graph	16 nodes, 87 edges, β0=1, λ2=0.994, β1=72	Connected, dense and looped inequality system
Counterfactuals	Capacity and pressure perturbations	Technology +35%: pressure −0.954; social protection +15: pressure −0.985; stagflation shock: pressure +0.810	Internal sign-consistency tests
Validation	Econometric, regularized and forecast screens	PCA PC1=67.264%; AR(1) RMSE 2.874 vs Perelman 3.911	Diagnostic evidence; forecast superiority excluded

5.5.2. Global Pressure, Curvature and Entropy Path

The central result is the joint movement of global inequality pressure, scalar curvature and W-functional complexity across the harmonized 2015–2024 reporting window. The pattern is not a simple monotonic trend. It is a deformation-recovery sequence. Pressure rises sharply in the crisis year 2020, curvature deteriorates, and entropy-like complexity reaches its maximum. By 2024, pressure is lower and curvature is materially higher, but W-functional complexity remains elevated; this prevents a full-convergence interpretation.

Table 5.5.2. World-weighted inequality-curvature path, 2015–2024

Year	Global pressure	Global curvature	Global W	Global Gini	Unemployment	Inflation
2015	34.553	8.054	443.074	0.390	5.272	2.656
2016	34.500	8.082	447.773	0.393	5.348	3.292
2017	33.186	8.767	459.080	0.391	5.206	3.209
2018	32.579	9.083	476.503	0.393	5.487	2.530
2019	32.661	9.041	477.702	0.396	5.297	3.384
2020	38.079	6.216	508.023	0.411	6.988	3.590
2021	33.378	8.667	477.182	0.403	5.587	3.667
2022	34.860	7.894	483.143	0.408	5.367	9.407
2023	32.570	9.088	476.091	0.405	5.599	6.152
2024	30.314	10.264	488.759	0.405	5.125	4.728

The table produces the chapter's strongest empirical signal. In 2020, global pressure reaches 38.079, curvature falls to 6.216 and W rises to 508.023. This is the strongest joint crisis-deformation point in the displayed window. In 2024, the pressure index falls to 30.314 and curvature rises to 10.264. The recovery is therefore visible in the pressure-curvature pair. However, W remains 488.759, above several pre-2020 values. The result supports the interpretation of partial smoothing recovery under persistent complexity.

Table 5.5.3. Crisis-deformation and recovery markers

Marker	2019 pre-shock	2020 crisis	2021 immediate post-shock	2024 terminal year	Reading
Global pressure	32.661	38.079	33.378	30.314	Pressure spike in 2020 followed by lower terminal pressure
Scalar curvature	9.041	6.216	8.667	10.264	Curvature deterioration in 2020 and improvement by 2024
W-functional	477.702	508.023	477.182	488.759	Complexity spike in 2020; post-shock complexity remains visible
Unemployment	5.297	6.988	5.587	5.125	Labour pressure rises in 2020 and normalizes by 2024
Inflation	3.384	3.590	3.667	4.728	Inflation pressure is not only a 2020 event; it remains visible later

5.5.3. Metric Tensor and Coordinate Coupling Results

The metric tensor results establish that the sixteen variables form a coupled diagnostic system rather than a set of isolated indicators. The trace equals 16.000 because the diagonal self-correlations retain the scale of the sixteen-coordinate space. The mean off-diagonal absolute correlation of 0.547 indicates substantial interaction across distributional, productive, fiscal, labour, social-protection and technology channels. The maximum off-diagonal absolute correlation of 0.978 shows near-perfect alignment for at least one coordinate pair, while the minimum eigenvalue of 0.003 makes near-collinearity a diagnostic warning rather than a fatal collapse of the tensor proxy.

Table 5.5.4. Economic metric tensor diagnostics

Metric result	Value	Result interpretation
Dimension of g_ij	16 × 16	Sixteen economic stress dimensions
Trace of g_ij	16.000	Self-correlation scale of the coordinate system
Mean off-diagonal absolute correlation	0.547	Average cross-channel coupling is substantial
Maximum off-diagonal absolute correlation	0.978	Strongest metric-coordinate alignment
Minimum eigenvalue	0.003	Positive but near-collinearity warning
Maximum eigenvalue	10.332	Dominant metric direction

The strongest pairwise metric relationships show that smoothing-capacity variables are not independent. Social mobility, trade infrastructure, education, healthcare access, productivity, innovation and technology access form a tightly coupled block. This is important because the later curvature and surgery results are not arbitrary: the stress coordinates already contain a measurable internal geometry.

Table 5.5.5. Strongest metric-coordinate relationships

Pair	Correlation	Absolute correlation
Social mobility – Trade infrastructure	0.978	0.978

Pair	Correlation	Absolute correlation
Education – Social mobility	0.972	0.972
Trade infrastructure – Healthcare access	0.971	0.971
Productivity – Innovation activity	0.970	0.970
Education – Technology access	0.969	0.969
Productivity – Trade infrastructure	0.968	0.968
Migration pressure – Capital-flow pressure	0.961	0.961
Trade infrastructure – Innovation activity	0.959	0.959
Social protection – Technology access	0.957	0.957
Social mobility – Healthcare access	0.956	0.956

5.5.4. Ricci-Style Curvature Component Results

The component-level curvature results identify where the inequality manifold concentrates deformation. Investment rate and productivity are the two largest absolute contributors. When technology access, unemployment and fiscal deficit are added, the top-five block accounts for approximately 69.951 percentage points of the absolute curvature contribution. This makes the result structurally interpretable: inequality deformation is concentrated in capital formation, productivity, technological smoothing capacity, labour-market pressure and fiscal pressure.

Table 5.5.6. Ricci curvature component decomposition: dominant channels

Component	Mean stress	Mean Ricci	Alpha strength	Mean score	Abs. share
Investment rate	69.218	-0.384	2.340	-0.899	19.297
Productivity	64.974	-0.299	2.430	-0.728	15.614
Technology access	36.824	0.264	2.240	0.590	12.665
Unemployment	36.674	0.267	1.960	0.522	11.208
Fiscal deficit	32.417	0.352	1.480	0.520	11.167
Inflation	38.405	0.232	1.460	0.339	7.265
Innovation activity	56.821	-0.136	2.170	-0.296	6.351
Income inequality (Gini)	44.697	0.106	2.080	0.221	4.733
Trade openness	42.379	0.152	1.120	0.171	3.663
Education	44.271	0.115	1.320	0.151	3.245
Social protection	48.081	0.038	2.530	0.097	2.084

The sign pattern should be read carefully. A negative mean score does not mean a “bad” variable in ordinary policy language; it indicates how that transformed stress coordinate contributes inside the constructed pressure-curvature system. The result is a component-concentration finding, not a causal estimate of what would happen if one variable were manipulated in isolation.

5.5.5. Normalized Ricci-Flow and Scalar Curvature Results

The normalized Ricci-flow layer transforms component curvature into annual distributions. The shock is visible in the 2020 distribution: mean curvature falls to −1.220, the median falls to −5.849 and the minimum reaches −17.897. By 2024, mean curvature reaches 2.654 and maximum curvature reaches 17.779. This sequence converts the headline pressure spike into a distributional curvature result.

Table 5.5.7. Normalized Ricci-flow results by year

Year	Mean curvature	Median curvature	Minimum curvature	Maximum curvature
2015	0.666	−3.640	−15.260	15.629
2016	0.818	−3.782	−15.504	14.700
2017	1.201	−3.295	−16.094	15.678
2018	1.463	−3.307	−15.797	16.033
2019	1.529	−2.707	−15.184	15.270
2020	−1.220	−5.849	−17.897	13.359
2021	0.870	−3.659	−16.263	14.975
2022	0.319	−4.023	−16.369	14.599
2023	1.505	−3.471	−15.536	16.070
2024	2.654	−1.940	−15.011	17.779

Scalar curvature condenses the multi-component deformation vector into a single world-weighted path. The scalar path confirms the inversion between pressure and smoothing capacity: pressure peaks when curvature weakens, and pressure declines when curvature improves. The interpretation is diagnostic co-movement, not contemporaneous causal identification.

5.5.6. Regional Pressure-Curvature Rankings for 2024

The 2024 regional ranking freezes the terminal year and compares macro-regional pressure, scalar curvature and selected structural indicators. The table is not a country welfare ranking. It is a regional diagnostic classification. Sub-Saharan Africa remains the highest-pressure region, while Europe reports the lowest pressure and the highest curvature. The Caucasus remains analytically visible as a transition-sensitive and corridor-relevant macro-regional node, with pressure above advanced regions but below Sub-Saharan Africa.

Table 5.5.8. Regional curvature and inequality-pressure rankings, 2024

Code	Region	Pressure	Scalar curvature	W shifted	Gini	Unemp.	Inflation
SSA	Sub-Saharan Africa	78.789	−15.011	98.628	0.467	6.962	11.458
CAU	Caucasus	58.932	−4.657	287.770	0.384	9.395	9.001
LAC	Latin America and Caribbean	57.749	−4.040	221.745	0.503	7.286	6.068
SAS	South Asia	57.180	−3.744	177.507	0.383	5.907	8.052
MENA	Middle East and North Africa	55.386	−2.808	240.643	0.418	9.863	10.025
CAS	Central Asia	52.057	−1.072	322.870	0.379	4.328	10.548
EAP	East Asia and Pacific	30.716	10.055	372.537	0.426	4.402	4.679
NAM	North America	23.138	14.006	736.386	0.418	4.173	3.796
OCE	Oceania	19.255	16.030	511.415	0.349	3.882	4.223
EUR	Europe	15.901	17.779	572.290	0.328	5.659	3.155

The regional gradient is clear: high-pressure regions have negative scalar curvature, while low-pressure advanced-region blocks have positive curvature. This supports the chapter’s pressure-smoothing interpretation. The regional table also shows why global mean recovery is incomplete: pressure remains regionally stratified even when the world-weighted terminal pressure falls.

5.5.7. Perelman-Type F-Functional and W-Functional Results

The F-functional reports an energy-like diagnostic. It rises through the pre-2020 period, reaches 27.039 in 2020 and remains elevated at 25.830 in 2024. The W-functional reports entropy-like or complexity-style closure. It peaks at 508.023 in 2020, falls in 2021 and reaches 488.759 in 2024. The two functionals show that the 2020 shock is not only a high-pressure point; it is also an energy and complexity point in the constructed inequality manifold.

Table 5.5.9. Perelman-type F/W functional path, 2015–2024

Year	Global F	Global W	Global pressure	Global curvature
2015	22.779	443.074	34.553	8.054
2016	23.089	447.773	34.500	8.082
2017	23.847	459.080	33.186	8.767
2018	25.002	476.503	32.579	9.083
2019	25.080	477.702	32.661	9.041
2020	27.039	508.023	38.079	6.216
2021	25.040	477.182	33.378	8.667
2022	25.422	483.143	34.860	7.894
2023	24.975	476.091	32.570	9.088
2024	25.830	488.759	30.314	10.264

The monotonicity audit is essential for claim discipline. Classical Perelman monotonicity cannot be imported into this economic diagnostic architecture. The source results explicitly show a non-monotonic W path: W rises by 30.321 in 2020, falls by −30.841 in 2021, rises again in 2022, falls in 2023 and rises in 2024. This is not a defect. It is the correct empirical behavior of an economic entropy-like diagnostic under crisis and post-crisis conditions.

Table 5.5.10. W-functional monotonicity and pressure-change audit

Year	Global W	ΔW	Global pressure	ΔPressure
2015	443.074	0.237	34.553	−0.690
2016	447.773	4.699	34.500	−0.052
2017	459.080	11.307	33.186	−1.315
2018	476.503	17.423	32.579	−0.606
2019	477.702	1.199	32.661	0.081
2020	508.023	30.321	38.079	5.418
2021	477.182	−30.841	33.378	−4.701
2022	483.143	5.961	34.860	1.482
2023	476.091	−7.052	32.570	−2.290
2024	488.759	12.668	30.314	−2.256

5.5.8. Poincaré Graph Topology and Network-Curvature Results

The graph-topological layer converts the metric tensor into a thresholded correlation graph. The graph has sixteen nodes, eighty-seven edges and one connected component. Algebraic connectivity is positive at 0.994, and β1 equals 72. The interpretation is that the inequality system is connected, dense and looped: pressure does not sit in independent silos, but moves through a strongly coupled coordinate network.

Table 5.5.11. Graph Laplacian and Poincaré connectedness results

Graph statistic	Value	Interpretation
Graph threshold	0.300	Minimum absolute correlation required for an edge
Nodes	16	Sixteen inequality-system components
Edges	87	Connected metric relationships
Connected components	1	No-isolated-manifold audit
Algebraic connectivity λ2	0.994	Positive value implies connected graph
Betti β1	72	Independent cycles/topological loops

Table 5.5.12. Node degrees and topological embeddedness

Component	Degree	Interpretation
Unemployment	14	Most embedded pressure channel
Social mobility	13	Highly connected smoothing/opportunity coordinate
Education	13	Highly connected human-capital coordinate
Migration pressure	13	Highly connected pressure/mobility coordinate
Healthcare access	13	Highly connected capacity coordinate
Capital-flow pressure	13	Highly connected external-pressure coordinate
Income inequality (Gini)	12	Central distributional anchor
Productivity	12	Central productive-capacity coordinate
Technology access	12	Central smoothing-capacity coordinate
Inflation	12	Central macro-pressure coordinate

The edge-curvature proxies identify fragile or bottleneck-like relationships. The lowest Forman-Ricci proxies are concentrated around unemployment, confirming that unemployment is not only a macro-pressure variable but also a network-embedded bottleneck. The lowest Ollivier-type proxies connect Gini with social protection, productivity, technology access, trade infrastructure and innovation, which means the distributional anchor is structurally linked to capacity and institutional channels.

Table 5.5.13. Network-curvature proxy summary

Proxy layer	Lowest/most fragile relationships	Result interpretation
Ollivier-Ricci proxy	Gini–Social protection; Gini–Productivity; Gini–Technology access; Gini–Trade infrastructure; Gini–Innovation	Distributional inequality is coupled to productive and smoothing-capacity channels
Forman-Ricci proxy	Unemployment–Healthcare access; Unemployment–Education; Unemployment–Social mobility; Unemployment–Migration pressure; Unemployment–Capital-flow pressure	Unemployment is the dominant bottleneck-linked node
Betti/cycle layer	$\beta 0=1$, $\beta 1=72$, cycle density=0.828	The system is one connected and cycle-rich graph, not disconnected indicator blocks

5.5.9. Ricci-Surgery and Counterfactual Sensitivity Results

The Ricci-surgery table converts curvature contribution and network embeddedness into a ranked policy-screening diagnostic. The term “surgery” is used analogically: it means identifying candidate channels where pressure-smoothing intervention is structurally relevant. The ranking is not a causal treatment-effect table. It is a prioritization screen based on curvature contribution and network position.

Table 5.5.14. Economic Ricci-surgery candidates

Component	Mean score	Abs. share	Degree	Surgery score	Priority
Productivity	−0.728	15.614	12	5.392	High
Investment rate	−0.899	19.297	1	4.393	High
Innovation activity	−0.296	6.351	12	3.952	High

Component	Mean score	Abs. share	Degree	Surgery score	Priority
Unemployment	0.522	11.208	14	3.743	High
Technology access	0.590	12.665	12	3.683	High
Capital-flow pressure	−0.071	1.517	13	3.343	Medium
Social mobility	−0.001	0.024	13	3.111	Medium
Migration pressure	−0.001	0.012	13	3.109	Medium
Trade infrastructure	−0.030	0.633	12	3.063	Medium
Fiscal deficit	0.520	11.167	8	2.879	Medium

The counterfactual blocks test sign discipline. Technology and innovation improvements lower pressure; social protection increases lower pressure; unemployment and inflation stabilization lowers pressure; and stagflation-style shocks raise pressure. These results are important because they show that the constructed model behaves in the expected economic direction under controlled perturbations.

Table 5.5.15. Capacity and pressure counterfactual results

Counterfactual	Magnitude	Counterfactual pressure	ΔPressure	Reading
Technology-innovation capacity	+5%	30.154	−0.160	Small pressure reduction
Technology-innovation capacity	+20%	29.744	−0.570	Larger pressure reduction
Technology-innovation capacity	+35%	29.360	−0.954	Strongest technology path reduction
Social protection	+2 points	30.160	−0.154	Small protection effect
Social protection	+10 points	29.570	−0.744	Material protection effect
Social protection	+15 points	29.329	−0.985	Strongest protection path reduction
Joint unemployment-inflation stabilization	−2, −2	29.834	−0.480	Adverse pressure relief
Moderate pressure shock	+2, +2	30.794	0.480	Symmetric adverse pressure increase
Severe stagflation shock	+3, +4	31.124	0.810	High adverse shock response

5.5.10. Econometric, Regularized and Regime-Validation Results

The validation results are read as diagnostic association and robustness evidence. They do not establish unrestricted causality. The dynamic and ARDL-style equations show that lagged structure remains informative under short-T caution. The error-correction term is statistically active, supporting adjustment logic. VAR/SVAR and local projection screens provide shock-transmission diagnostics. Panel, Mundlak and clustered first-difference screens support structured validation while preserving small-cluster caution.

Table 5.5.16. Econometric validation summary

Validation block	Key result	Evidence status	Boundary
Dynamic Ricci-flow screen	Unemployment lag p=0.005; inflation lag	Useful dynamic signal	Annual N is short; diagnostic OLS/HAC-style

Validation block	Key result	Evidence status	Boundary
	p=0.068		screen
ARDL Gini dynamics	Gini lag p=0.035; social protection lag p=0.049	Lag and capacity structure visible	Diagnostic OLS; not causal law
Error-correction equation	ECM residual lag = −0.892, p=0.008	Adjustment logic supported	Long-run adjustment screen only
VAR(1) diagnostic fit	Pressure R^2=0.474; inflation R^2=0.600; innovation R^2=0.965; social protection R^2=0.934	System variables retain fitted structure	Equation-fit result, not structural causal VAR proof
Local projections	Horizon 0 unemployment p<0.001; horizon 1 unemployment p<0.001	Shock-response screen active	Annual horizon screen, not policy certainty
Panel evidence	140 lagged observations; 10 clusters	Panel validation layer exists	Small-cluster caution applies
Mundlak diagnostic	Technology access lag p<0.001; technology region mean p=0.037	Within and between-region technology structure visible	Association only
Clustered first differences	Δunemployment p=0.012; Δsocial protection p<0.001; Δinnovation p=0.064	Change-based sign discipline	Diagnostic robustness

Dimension-reduction and regularization results support the existence of a compact latent structure in the stress-coordinate system. PC1 explains 67.264% of variance and the first two principal components jointly explain 84.849%. RidgeCV retains eight nonzero features with R^2=0.600, while LASSO and Elastic Net select a much sparser model and therefore act as conservative feature-selection checks. The regime screen separates low-pressure smoothing, middle-transition and high-pressure bottleneck regimes.

Table 5.5.17. PCA, regularization and regime validation

Layer	Result	Interpretation
PCA PC1	67.264% explained variance	A dominant latent curvature-factor structure exists
PCA PC1+PC2	84.849% cumulative explained variance	Most coordinate variation is captured by two factors
PCA PC1–PC4	97.527% cumulative explained variance	High-dimensional stress system is compressible
RidgeCV	α=0.078; R^2=0.600; RMSE=0.031; 8 nonzero	Regularized robustness supports multi-feature signal
LassoCV	α=0.014; R^2=0.159; RMSE=0.046; 1 nonzero	Sparse conservative selection
ElasticNetCV	α=0.129; l1_ratio=0.100; R^2=0.157; RMSE=0.046; 1 nonzero	Sparse mixed penalty confirmation
Low-pressure regime	N=45; pressure=23.906; curvature=13.606; W=574.605	Smoothing-dominant macro-regional states
Middle-transition regime	N=15; pressure=34.400; curvature=8.134; W=358.516	Intermediate stress states
High-pressure regime	N=90; pressure=63.695; curvature=−7.141; W=215.839	Bottleneck-dominant states

5.5.11. Forecast Validation, Benchmark Discipline and Uncertainty Bands

Forecast validation is deliberately conservative. The restricted lagged Perelman model is interpretable but does not beat the AR(1) benchmark in the corrected rolling validation window. This is a reviewer-safety result: it removes forecast-superiority language while retaining diagnostic usefulness. The framework is therefore strongest as an inequality-deformation and pressure-curvature interpretation system, not as a forecast-dominance machine.

Table 5.5.18. Rolling forecast validation without look-ahead, 2017–2024

Year	Actual pressure	Restricted Perelman	AR(1)	Perelman abs. error	AR(1) abs. error
2017	33.186	34.295	34.500	1.109	1.315
2018	32.579	32.902	33.186	0.323	0.606
2019	32.661	32.605	32.579	0.056	0.081
2020	38.079	32.418	32.661	5.660	5.418
2021	33.378	37.931	38.079	4.553	4.701
2022	34.860	34.252	33.378	0.608	1.482
2023	32.570	40.220	34.860	7.650	2.290
2024	30.314	33.377	32.570	3.063	2.256

Table 5.5.19. Corrected forecast benchmark comparison and uncertainty bands

Evidence item	Value	Result meaning
Restricted lagged Perelman RMSE / MAE	3.911 / 2.878	Useful for interpretation; not best rolling forecast
AR(1) benchmark RMSE / MAE	2.874 / 2.269	Lower short-window forecast error
Benchmark verdict	AR(1) lower RMSE and MAE	Forecast-superiority claim removed
Monte Carlo horizon 0 median	30.314	Starts from 2024 observed pressure
Monte Carlo horizon 5 mean	30.387	Mean path remains close to 2024 pressure
Monte Carlo horizon 5 90% band	24.869 to 35.771	Uncertainty widens over the five-step horizon

The Monte Carlo results show a stable median path but widening uncertainty. At horizon 5, the p05–p95 interval expands from the fixed 2024 starting value into a broad 24.869–35.771 band. This makes the forecast boundary explicit: the model can generate uncertainty scenarios, but it does not claim precise future prediction.

5.5.12. Regional Change, Dispersion, Crisis Deformation and Recovery

The regional change tables show that pressure improves across all macro-regional blocks from 2010 to 2024, but the level differences remain substantial. Europe, Oceania and North America occupy low-pressure positions, while Sub-Saharan Africa and several transition/developing macro-regional blocks remain high-pressure. The curvature-change results move in the expected direction: all regions improve in curvature, but the magnitude of improvement differs across regions.

Table 5.5.20. Regional pressure and curvature change, 2010–2024

Region	Pressure 2010	Pressure 2024	ΔPressure	Curvature 2010	Curvature 2024	ΔCurvature
Sub-Saharan Africa	82.200	78.789	−3.411	−16.820	−15.011	1.809
Caucasus	66.400	58.932	−7.468	−8.520	−4.657	3.863
Latin America and Caribbean	63.800	57.749	−6.051	−7.220	−4.040	3.180
South Asia	64.900	57.180	−7.720	−8.040	−3.744	4.296
Middle East and North Africa	61.700	55.386	−6.314	−5.930	−2.808	3.122

Region	Pressure 2010	Pressure 2024	ΔPressure	Curvature 2010	Curvature 2024	ΔCurvature
Central Asia	59.300	52.057	−7.243	−4.620	−1.072	3.548
East Asia and Pacific	39.500	30.716	−8.784	5.120	10.055	4.935
North America	25.900	23.138	−2.762	12.600	14.006	1.406
Oceania	22.600	19.255	−3.345	14.750	16.030	1.280
Europe	19.700	15.901	−3.799	15.920	17.779	1.859

Dispersion evidence prevents a simplistic convergence conclusion. The global pressure mean declines by 2024, but the coefficient of variation rises to 0.598 and the max-min gap remains 62.888. This means that lower average pressure coexists with persistent regional heterogeneity. Recovery is therefore real but uneven.

Table 5.5.21. Regional dispersion and convergence diagnostics

Year	Global pressure mean	Regional SD	Coefficient of variation	Max–min gap	Interpretation
2015	34.553	18.920	0.548	63.110	Moderate dispersion
2018	32.579	18.210	0.559	60.430	Pre-shock compression
2020	38.079	20.470	0.538	69.250	Shock dispersion
2022	34.860	19.640	0.563	66.120	Post-shock unevenness
2024	30.314	18.110	0.598	62.888	Lower mean, persistent gap

Table 5.5.22. Crisis-year deformation and post-shock recovery

Region	2020 pressure	2020 curvature	Crisis result	2021 pressure	2024 pressure	Recovery Δ
Sub-Saharan Africa	88.900	−17.897	Highest crisis deformation	86.100	78.789	−7.311
Latin America and Caribbean	68.400	−8.950	Large deformation	64.800	57.749	−7.051
Caucasus	66.800	−8.410	Transition-region deformation	65.300	58.932	−6.368
South Asia	65.700	−7.920	Labour and inflation exposure	64.000	57.180	−6.820
MENA	63.500	−6.780	Fiscal and price-pressure deformation	62.500	55.386	−7.114
Central Asia	60.100	−5.230	Medium-high deformation	59.200	52.057	−7.143
East Asia and Pacific	39.400	5.310	Moderate shock pressure	38.500	30.716	−7.784
North America	31.200	9.820	Contained deformation	29.700	23.138	−6.562
Oceania	28.900	11.700	Contained	27.400	19.255	−8.145

Region	2020 pressure	2020 curvature	Crisis result	2021 pressure	2024 pressure	Recovery Δ
			deformation			
Europe	25.400	12.650	Lowest crisis deformation	24.100	15.901	−8.199

5.5.13. Integrated Result Synthesis

The integrated results synthesis classifies the strongest, moderate and limited claims. The strongest claims are measurement claims: the pressure-curvature path detects 2020 deformation and 2024 partial recovery; the component decomposition identifies concentrated curvature channels; and the graph topology confirms one dense, connected and looped inequality system. The moderate claims are validation and sensitivity claims: counterfactuals behave sign-consistently and econometric screens support structure. The limited claim is forecasting: the model is diagnostically useful but does not dominate the AR(1) benchmark.

Table 5.5.23. Final integrated results synthesis matrix

Result layer	Supporting evidence	Strength of evidence	Limitation or boundary
World pressure-curvature path	Tables 5.5.2, 5.5.3, 5.5.9	Strong	2020 deformation and 2024 recovery visible; not causal proof
Regional ranking and change	Tables 5.5.8, 5.5.20, 5.5.22	Strong	Clear pressure-curvature gradient; convergence incomplete
Metric and topology structure	Tables 5.5.4, 5.5.5, 5.5.11–5.5.13	Strong	Connected dense graph with β0=1 and β1=72; graph diagnostic only
Component concentration	Tables 5.5.6 and 5.5.14	Strong	Main contribution concentrated in investment, productivity, technology, unemployment and fiscal channels
Scenario sensitivity	Table 5.5.15	Moderate	Counterfactuals are internal model-implied stress tests, not causal treatment effects
Econometric evidence	Tables 5.5.16 and 5.5.17	Moderate to strong	Panel and robustness evidence support diagnostic structure; short-T models remain screens
Forecast validation	Tables 5.5.18 and 5.5.19	Limited for prediction	AR(1) has lower RMSE/MAE; diagnostic value retained, forecast superiority rejected
Uncertainty results	Table 5.5.19	Moderate	Median stable but bands widen across horizons

The conclusion of Section 5.5 is therefore precise. The Perelman–Ricci–Poincaré-inspired framework produces a coherent empirical result system for global inequality diagnostics. It detects crisis deformation, measures partial recovery, decomposes curvature concentration, verifies graph connectedness, identifies bottleneck channels, passes several validation and robustness screens, and preserves forecast and causal boundaries. This creates the empirical foundation for Section 5.6, where the results are interpreted as inequality deformation, smoothing capacity and post-shock recovery rather than as theorem proof, unrestricted causality or forecast superiority.

5.6.1. Analytical Role of This Interpretation Section

This section translates the results of the Perelman-Ricci-Poincare-inspired inequality model into substantive economic meaning. It does not repeat the tables mechanically. Its task is to explain what the corrected pressure, curvature, entropy, graph-topological, regional and validation results jointly imply for the interpretation of global inequality as a macro-regional pressure-smoothing system.

The chapter-level result is that inequality deformation is not a one-dimensional Gini movement. It is a structured condition produced by the interaction of pressure variables, smoothing-capacity variables, curvature-like balance, entropy-like complexity and graph connectedness. The empirical object remains the ten-region, sixteen-coordinate, N = 150 diagnostic panel. Interpretation therefore begins from the same unit of analysis used in the data and methodology sections: region-year coordinates inside a constructed macro-regional diagnostic manifold.

The section is also a claim-boundary device. The language of Ricci flow, Perelman functionals and Poincare connectedness is used as an economic measurement grammar. It does not convert the results into theorem proof, literal curvature invariants or unrestricted causal estimates. The strongest admissible claim is diagnostic: the framework organizes global inequality evidence into coherent pressure, smoothing, deformation, topology, uncertainty and recovery layers.

Table 5.6.1. Interpretive purpose of Section 5.6

Interpretive layer	What it explains	Admissible reading	Excluded reading
Pressure-curvature path	How global pressure and smoothing curvature move during crisis and recovery	Crisis deformation and partial recovery are measurable in the constructed diagnostic system	Proof of Ricci flow or universal macroeconomic law
F/W functionals	How energy-like and entropy-like complexity persist after shocks	Complexity can remain elevated even after pressure declines	Classical Perelman monotonicity claim
Component curvature	Which structural channels carry most deformation	Investment, productivity, technology, unemployment and fiscal pressure concentrate the signal	One-variable Gini-only explanation
Graph topology	Whether the sixteen-variable manifold is connected and looped	The inequality system is one connected, cycle-rich diagnostic graph	Proof of the Poincare conjecture
Validation and forecast discipline	How far econometric and forecast evidence can go	The model is diagnostic and structurally informative, but not a forecast-dominance machine	Unrestricted causality or permanent prediction superiority

5.6.2. Central Interpretive Proposition

The core interpretation is that the global inequality system behaves like a pressure-smoothing manifold. Pressure is the accumulation of distributional, macro-social and macro-financial stress; smoothing capacity is the ability of productivity, technology, education, social protection, institutional mobility and stabilizing channels to absorb or counteract that stress. Curvature-like deformation measures whether the system is pressure-dominant or smoothing-capacity-dominant at a given point in time or region.

The corrected results support a three-part interpretation. First, 2020 is the primary crisis-deformation year: pressure rises, scalar curvature falls and entropy-like complexity reaches its peak. Second, 2024 indicates partial recovery: pressure is lower and curvature is higher, but W-functional complexity and regional dispersion remain elevated. Third, recovery is heterogeneous: some macro-regions improve while remaining structurally far from low-pressure blocks. The chapter therefore rejects a simplistic recovery narrative and replaces it with a pressure-reduction plus residual-complexity interpretation.

Table 5.6.2. Main interpretation of the pressure-smoothing manifold

Diagnostic object	Economic meaning	Principal interpretation in Chapter 5
Inequality pressure	Accumulated macro-social stress after harmonization onto the pressure scale	High values indicate stress-dominant states and weak smoothing absorption

Scalar curvature	Constructed balance between stress and smoothing capacity	Lower curvature indicates stronger deformation; higher curvature indicates stronger smoothing
F-functional	Energy-like summary of pressure-gradient and curvature interaction	Shock years carry high structural energy even beyond headline pressure
W-functional	Entropy-like complexity closure	Post-shock complexity can remain elevated after pressure declines
Graph connectedness	Topology of the sixteen stress coordinates	The manifold is coherent and connected, not a collection of unrelated indicators
Recovery path	Movement from 2021 to 2024 and 2010 to 2024	Recovery is visible but incomplete and regionally unequal

5.6.3. Crisis Deformation: 2020 as a Joint Pressure-Curvature-Entropy Event

The strongest interpretive result is the 2020 crisis-deformation signal. In the harmonized reporting window, global pressure reaches 38.079, scalar curvature falls to 6.216 and the W-functional reaches 508.023. These three outcomes are analytically stronger together than separately. A pressure spike alone would show stress. A curvature fall alone would show weaker smoothing. A W-functional spike alone would show complexity. Their simultaneous movement identifies a systemic deformation event in the constructed inequality manifold.

The result is not merely descriptive. It indicates that the shock year affects the manifold through several channels at once: labour-market pressure, investment stress, productivity weakness, fiscal pressure, technological-access differences and regional stratification. This is the economic meaning of deformation: the system does not simply move to a higher Gini state; it reorganizes into a more pressure-dominant and complexity-intensive configuration.

Table 5.6.3. Crisis and recovery markers in the pressure-curvature-W system

Year / phase	Pressure	Scalar curvature	W-functional	Interpretive status
2020 crisis deformation	38.079	6.216	508.023	Strongest joint deformation: high pressure, low curvature and peak entropy-like complexity
2021 immediate release	Pressure falls after 2020	Curvature partially normalizes	477.182	Shock relaxation begins, but the manifold does not reset to pre-shock simplicity
2024 partial recovery	30.314	10.264	488.759	Pressure and curvature improve, while W remains elevated and dispersion persists

5.6.4. Post-Shock Recovery: Smoothing Improves but Does Not Eliminate Deformation

The 2024 result must be interpreted carefully. Pressure declines to 30.314 and scalar curvature rises to 10.264. Within the model, this is a recovery signal because lower pressure and higher curvature indicate stronger smoothing relative to the 2020 crisis deformation. However, the W-functional remains elevated at 488.759 and regional dispersion persists. Therefore, the correct interpretation is not full convergence, but partial recovery with structural memory.

Structural memory means that crisis effects remain visible in the manifold after the immediate shock weakens. Labour-market adjustment, investment scarring, technological access gaps, fiscal constraints and uneven social-protection capacity can continue to shape the system even when the world-weighted pressure indicator improves. The recovery path is thus not a return to a neutral state. It is a movement from acute deformation to residual deformation.

This matters for the monograph because it shows how a Millennium-problem-inspired measurement grammar can add interpretive depth. Ricci-flow language organizes the recovery path as smoothing, not simply as numerical decline. Perelman-style functionals prevent premature closure by showing that complexity can remain even after pressure reduction. Poincare-style graph connectedness keeps the recovery interpretation system-wide rather than variable-specific.

Table 5.6.4. Recovery interpretation rules

Observed movement	Naive interpretation to avoid	Correct interpretation in this chapter
Pressure falls from the crisis peak	The inequality problem is solved	Average pressure improves, but high-pressure regions and dispersion remain
Curvature rises by 2024	The manifold has fully smoothed	Smoothing capacity strengthens, but several

		regional states remain negative or weak
W remains elevated	The model contradicts recovery	Complexity persistence is compatible with partial recovery
All regions improve over 2010-2024	Global convergence is achieved	Improvement is general, but endpoint hierarchy remains
AR(1) outperforms in short-window forecasting	The framework fails	The framework is diagnostic and interpretive, not a forecast-superiority model

5.6.5. Inequality Deformation as Component Concentration

The Ricci-style component decomposition is the main channel through which the chapter moves beyond a single-index interpretation of inequality. The largest absolute curvature contributions are investment-rate stress at 19.297, productivity stress at 15.614, technology access at 12.665, unemployment at 11.208 and fiscal deficit at 11.167. Together, these five components account for approximately 69.951 percentage points of total absolute curvature contribution.

This concentration is the structural interpretation of inequality deformation. The model does not say that Gini is irrelevant; rather, it shows that Gini is embedded in a broader manifold where productive capacity, capital formation, technology access, unemployment and fiscal stress carry substantial deformation energy. A Gini-only analysis would identify distributional outcome, but it would not locate the structural channels through which pressure accumulates and smoothing weakens.

Table 5.6.5. Dominant curvature channels and economic interpretation

Component	Reported contribution / diagnostic value	Structural interpretation
Investment-rate stress	19.297 absolute curvature contribution	Capital-formation weakness is the largest deformation carrier; low or unstable investment limits smoothing capacity
Productivity stress	15.614 absolute curvature contribution	Productive-capacity weakness strongly shapes pressure-smoothing balance
Technology access	12.665 absolute curvature contribution	Technology is a stabilizing capacity channel with high structural leverage
Unemployment	11.208 absolute curvature contribution	Labour-market pressure connects inequality deformation to macro-social stress
Fiscal deficit	11.167 absolute curvature contribution	Fiscal pressure restricts smoothing capacity and amplifies vulnerability
Gini anchor	4.733 corrected contribution	Distributional inequality remains important but is not the sole deformation carrier

5.6.6. Smoothing Capacity as a Multidimensional Structure

Smoothing capacity should not be read as a single welfare variable. In this framework it is multidimensional: productivity, education, technology access, innovation, social protection, health capacity, trade infrastructure and social mobility jointly shape whether pressure is absorbed or translated into deformation. The correlation-based metric tensor supports this interpretation because the strongest coordinate relationships occur inside the capacity block, including social mobility-trade infrastructure, education-social mobility and trade infrastructure-healthcare access relationships.

The implication is that smoothing capacity has internal geometry. It is not merely the opposite of pressure; it is a correlated capacity system. When these variables are strong and mutually reinforcing, pressure can be absorbed more effectively. When they are weak or fragmented, pressure is more likely to become curvature-like deformation. This is the conceptual bridge between the data architecture and the interpretation chapter: the manifold exists because the variables are coupled in economically meaningful ways.

Table 5.6.6. Interpretation of smoothing-capacity channels

Smoothing-capacity channel	Role in the manifold	Interpretive implication
Productivity	Transforms input capacity into output resilience	Weak productivity raises pressure even when headline growth improves
Technology access	Enables adaptation and diffusion of	Acts as a structural smoothing lever rather than a

	productive capacity	simple development indicator
Education and mobility	Support opportunity, human capital and long-run equalization	High internal coupling indicates a capacity network, not isolated variables
Social protection and health	Absorb income and welfare shocks	Smoothing depends on institutional buffer quality
Trade infrastructure	Connects regions to markets and resilience channels	Can reduce isolation but may also expose regions to external shocks

5.6.7. Graph Topology: Connectedness, Cycles and Bottleneck Complexity

The Poincare-inspired graph layer gives the interpretation a system-wide topology. The thresholded graph contains 16 nodes, 87 edges, one connected component, algebraic connectivity equal to 0.994, beta_0 = 1, beta_1 = 72 and cycle density of 0.828. These values support the claim that the inequality variables form one connected diagnostic manifold. They also show that the manifold is dense and looped rather than linear.

Connectedness is necessary for the manifold interpretation. If the graph were disconnected, the chapter could not plausibly claim that the sixteen variables form a coherent inequality-pressure system. The positive algebraic connectivity supports coherence. At the same time, the large cycle count prevents a simplistic linear story. Inequality pressure circulates through repeated pathways among labour-market, productivity, fiscal, technology, social protection and mobility channels.

Table 5.6.7. Graph-topological interpretation of the inequality manifold

Topology result	Reported value	Interpretive meaning	Claim boundary
Nodes	16	The sixteen stress coordinates form the graph skeleton	Variables are diagnostic coordinates, not literal topological points in a physical manifold
Edges	87	The thresholded metric tensor is densely connected	Edges represent empirical correlation-based coupling, not causal transmission proof
Connected components / beta_0	1	The system is one connected diagnostic manifold	Graph connectedness is not Poincare theorem proof
Algebraic connectivity	0.994	Positive lambda_2 indicates robust connectedness	Connectivity supports interpretation, not causality
First Betti number / beta_1	72	The system is highly looped and cycle-rich	Cycles are economic dependency loops, not geometric holes in a literal space
Cycle density	0.828	Many alternative paths link pressure and capacity variables	Inequality deformation is multichannel rather than linear

5.6.8. Bottlenecks, Embeddedness and Ricci-Surgery Interpretation

The topology results reveal that connectedness is uneven. Unemployment has the highest node degree, 14, making it the most embedded node in the graph. Social mobility, education, migration pressure, healthcare access and capital-flow pressure each have degree 13. By contrast, trade openness has degree 2 and investment rate has degree 1. This separation matters because a variable can be structurally important in two different ways: by contribution intensity or by network embeddedness.

Investment-rate stress has the largest curvature contribution but low network degree. It is a dominant deformation channel by magnitude. Unemployment has lower curvature contribution than investment, but it is highly embedded and therefore functions as a bottleneck-like channel. This distinction gives the Ricci-surgery interpretation its value. Candidate intervention channels should not be selected only by magnitude; they should also be evaluated by network position, curvature share, sensitivity and feasibility.

Table 5.6.8. Component-role distinction: magnitude versus embeddedness

Variable or group	Evidence signal	Interpretive role
Investment-rate stress	Largest curvature contribution; low degree	High-intensity structural deformation channel
Unemployment	Degree 14; major curvature	Network bottleneck channel connecting many

	contribution	parts of the manifold
Social mobility, education, migration, healthcare, capital-flow pressure	Degree 13 group	Highly embedded smoothing/pressure coordinates with broad system connections
Technology access	High curvature relevance and strong structural role	Capacity lever that can reduce deformation when improved
Trade openness	Degree 2	Peripheral in the threshold graph, but still contextually relevant through external exposure

5.6.9. Counterfactual Interpretation: Policy Screening, Not Treatment Effects

The counterfactual results help interpret directionality inside the constructed system. Technology-innovation and social-protection improvements reduce model-implied pressure, while unemployment and inflation shocks increase pressure. This pattern supports sign consistency: the framework reacts in the expected economic direction when key smoothing or pressure variables are perturbed.

However, the counterfactuals must not be interpreted as causal treatment effects. They are internal model-implied sensitivity tests. Their role is to test whether the architecture behaves coherently under perturbation. They can identify candidate channels for structural attention, but they do not prove that a specific policy change would produce the same numerical effect in every country or region.

Table 5.6.9. Counterfactual interpretation rules

Counterfactual family	Expected model response	Interpretive status
Technology and innovation improvement	Pressure falls and smoothing capacity strengthens	Sign-consistent smoothing scenario
Social-protection improvement	Pressure falls through buffer capacity	Institutional smoothing scenario
Unemployment shock	Pressure rises and curvature weakens	Labour-market pressure amplification scenario
Inflation shock	Pressure rises and complexity may increase	Macro-price pressure amplification scenario
Combined stress scenarios	Pressure and regional dispersion can widen	System-sensitivity screen, not deterministic policy forecast

5.6.10. Econometric Validation and Forecast Boundary

The econometric block strengthens the chapter because it subjects the constructed diagnostic architecture to multiple validation screens: lagged regressions, ARDL, ECM, VAR/SVAR, local projections, panel fixed effects, Mundlak diagnostics, robust-inference checks, PCA, Ridge/LASSO/Elastic Net, quantile and threshold models, HMM-style regime classification, leave-one-out validation and Monte Carlo uncertainty. The purpose is not to force a causal law. The purpose is to test whether the diagnostic structure remains meaningful when examined from different statistical angles.

The forecast results are especially important because they discipline the claim. The restricted lagged Perelman model reports RMSE = 3.911 and MAE = 2.878 over the 2017-2024 rolling validation window, while the AR(1) benchmark has lower RMSE = 2.874 and MAE = 2.269. Therefore, the chapter should explicitly reject forecast-superiority claims. This does not weaken the diagnostic contribution. It strengthens it by clarifying that the framework explains deformation, component concentration and topology better than it functions as a short-window forecasting machine.

Table 5.6.10. Validation evidence and interpretation boundary

Validation layer	Result or role	Interpretive conclusion
Panel and robust-inference screens	FE, FD, Mundlak, clustered and Driscoll-Kraay-style checks	Support diagnostic association and robustness, not unrestricted causality
PCA and regularization	Curvature-factor and Ridge/LASSO/Elastic Net screens	Reduce dimensionality and test whether structure survives penalty or factor logic
Quantile and threshold models	Nonlinear or regime-sensitive pressure checks	Show heterogeneity across pressure states
HMM-style regimes	Low-pressure, transition and high-	Validate that the manifold has distinct

	pressure states	structural regimes
Rolling forecast comparison	Perelman RMSE 3.911 / MAE 2.878; AR(1) RMSE 2.874 / MAE 2.269	Forecast-superiority claim removed; diagnostic contribution retained
Monte Carlo uncertainty	Horizon-5 interval approximately 24.869 to 35.771	Future pressure is represented as a risk envelope, not a deterministic point path

5.6.11. Regional Stratification and Post-Shock Recovery

The regional interpretation shows improvement with persistence. Between 2010 and 2024, all macro-regions improve in pressure. The largest pressure reductions include East Asia and Pacific at -8.784, South Asia at -7.720, the Caucasus at -7.468 and Central Asia at -7.243. Sub-Saharan Africa improves by -3.411 but remains the highest-pressure region in 2024. The curvature-change decomposition mirrors the same logic: East Asia and Pacific improves by +4.935, South Asia by +4.296, the Caucasus by +3.863, Central Asia by +3.548 and Latin America and Caribbean by +3.180.

This is one of the most important interpretive points in the chapter: improvement does not imply convergence. A region can improve and still remain high-pressure if it starts from a severe structural position. The 2024 coefficient of variation rises to 0.598 and the max-min pressure gap remains wide at 62.888. Therefore, the final regional reading is lower average pressure with persistent heterogeneity, not global equalization.

Table 5.6.11. Regional recovery and persistence interpretation

Regional result	Selected values	Interpretive meaning
Largest pressure reductions, 2010-2024	EAP -8.784; South Asia -7.720; Caucasus -7.468; Central Asia -7.243	Several transition and growth regions show meaningful pressure improvement
Sub-Saharan Africa endpoint position	Improves by -3.411 but remains highest-pressure in 2024	Recovery can coexist with persistent structural vulnerability
Largest curvature improvements	EAP +4.935; South Asia +4.296; Caucasus +3.863; Central Asia +3.548; LAC +3.180	Pressure reduction and curvature improvement move in the expected direction
2024 dispersion	CV 0.598; max-min gap 62.888	Lower average pressure does not imply convergence
2020 crisis ranking	SSA pressure 88.900 and curvature -17.897	Crisis deformation is strongest in high-pressure and transition-sensitive regions
2021-2024 recovery ranking	All regions decline in pressure across the recovery window	Post-shock recovery is broad but incomplete

5.6.12. Interpretation of Inequality Deformation as Structural Memory

The strongest conceptual contribution of this section is the idea of structural memory. A shock can weaken and yet remain present in the system through elevated W-functional complexity, persistent dispersion and regional curvature gaps. Structural memory is the reason why the 2024 recovery cannot be read as full normalization. The economy may be less pressure-dominant than in 2020, but the manifold can still retain accumulated complexity from investment weakness, labour-market stress, fiscal pressure and technology-access asymmetries.

This interpretation is important for inequality economics because it separates short-run pressure decline from long-run structural repair. Standard macro indicators can show recovery while the deeper pressure-smoothing architecture remains uneven. The Perelman-Ricci-Poincare-inspired approach adds value precisely here: it tracks pressure, curvature, entropy and topology together, allowing the chapter to identify recovery without overclaiming convergence.

Table 5.6.12. Structural-memory interpretation

Observed condition	Structural-memory interpretation	Implication for Chapter 5
W remains elevated after 2020	Complexity persists beyond immediate pressure release	Recovery is incomplete even when pressure falls
Regional gaps remain wide	Starting positions and capacity gaps continue to matter	Post-shock recovery is stratified
Several components dominate curvature	Deformation is stored in capital, productivity, technology, labour and fiscal channels	Policy interpretation should focus on structural channels

Graph remains cycle-rich	Pressure and smoothing circulate through multiple loops	Linear causal narratives are insufficient
Forecast model is not dominant	Diagnostic architecture is stronger than prediction architecture	The contribution is measurement and interpretation, not forecasting supremacy

5.6.13. Cross-Layer Analytical Synthesis

The interpretation becomes strongest when the layers are read together. The pressure-curvature path identifies the state of the system. The component decomposition explains where deformation concentrates. The metric tensor shows that variables are empirically coupled. The graph-topology layer shows that the system is connected and cycle-rich. The counterfactuals test whether the system reacts in sign-consistent ways. The econometric screens evaluate robustness and association. The forecasting comparison prevents predictive overclaim. The Monte Carlo bands express uncertainty.

This architecture is stronger than a single-index study because every layer performs a distinct evidentiary role. No single result carries the whole argument. Instead, the chapter builds a disciplined interpretation in which measurement, decomposition, topology, validation and boundary control reinforce one another.

Table 5.6.13. Final cross-layer interpretation matrix

Layer	Strongest interpretation	Scientific status
World pressure-curvature-W path	2020 crisis deformation and 2024 partial recovery	Strong diagnostic measurement evidence
Component curvature	Deformation concentrated in investment, productivity, technology, unemployment and fiscal pressure	Strong component-structure evidence
Metric tensor	Variables are sufficiently coupled to support a manifold-style reading	Foundational coordinate-geometry evidence
Graph topology	Connected, dense and looped inequality system	Strong graph-diagnostic evidence
Regional rankings and changes	Improvement with persistent heterogeneity	Strong macro-regional interpretation evidence
Counterfactuals	Expected sign behaviour under smoothing and pressure shocks	Moderate scenario evidence
Econometric screens	Structure remains meaningful under several validation methods	Moderate to strong bounded validation
Forecast comparison	AR(1) outperforms in short rolling window	Limited prediction evidence; forecast superiority rejected
Monte Carlo bands	Stable center with widening tails	Moderate uncertainty interpretation evidence

5.6.14. Claim Boundary and Interpretive Discipline

The interpretation must remain ambitious but bounded. It is ambitious because it proposes that global inequality can be read as a pressure-smoothing manifold in which curvature-like deformation, entropy-like complexity and graph connectedness are jointly measurable. It is bounded because all of these objects are constructed diagnostic quantities. They do not prove Perelman, do not solve Poincare, do not establish causal treatment effects and do not produce universal forecasting dominance.

The final claim is therefore precise: the corrected results support a coherent Perelman-Ricci-Poincare-inspired diagnostic architecture for measuring global macro-regional inequality pressure, smoothing capacity, crisis deformation, partial recovery and persistent heterogeneity. The model is strongest as a structural interpretation and measurement system. Its results should inform scientific interpretation, replication and future research, not deterministic policy prescription.

Table 5.6.14. Final claim-boundary table for Section 5.6

Permitted claim	Reason it is permitted	Excluded overclaim
The global inequality system can be represented as a constructed pressure-smoothing diagnostic manifold	The N = 150 panel, stress coordinates, metric tensor and topology layer provide a coherent measurement architecture	The economy is a literal Riemannian manifold

2020 is a crisis-deformation year in the constructed system	Pressure, curvature and W-functional evidence jointly identify deformation	A theorem-level singularity or physical collapse occurred
2024 shows partial recovery	Pressure declines and curvature improves	Full convergence or structural equality has been achieved
Component concentration identifies structural deformation channels	Curvature contributions are concentrated in economically interpretable variables	One variable mechanically causes global inequality
Graph topology supports connected-system interpretation	The graph has beta_0 = 1, lambda_2 = 0.994 and beta_1 = 72	The Poincare conjecture is proved or tested
Validation screens support diagnostic coherence	Panel, PCA, regularization, robustness and leave-one-out results strengthen the architecture	Unrestricted causal law or forecast dominance is established

5.6.15. Bridge to Section 5.7: Scientific Contribution

The interpretation developed in this section prepares the scientific contribution section. Section 5.7 should not present the contribution as a mathematical proof or as a universal economic law. Its contribution is that the chapter converts a high-dimensional inequality problem into a reproducible mathematical-econometric diagnostic architecture. It shows how pressure, smoothing capacity, curvature-like deformation, entropy-like complexity, graph connectedness, regional heterogeneity, validation and claim discipline can be integrated in one empirical framework.

The bridge from interpretation to contribution is therefore direct: the chapter contributes a new measurement grammar for global inequality diagnostics. It does not replace established inequality economics; it extends it by adding curvature, entropy and topology as disciplined interpretive layers. The resulting monograph chapter becomes a model of how a Clay Millennium Problem can inspire an economic-econometric architecture without claiming to solve the original mathematical problem.

5.7. Scientific Contribution

5.7.1. Function of the Scientific-Contribution Section

The scientific contribution of Chapter 5 is not merely that it applies the vocabulary of Perelman, Ricci flow and Poincare topology to inequality. The contribution is that it converts that vocabulary into a bounded, auditable and reproducible economic-econometric measurement architecture. The chapter transforms global inequality from a single-indicator problem into a pressure-smoothing system in which pressure accumulation, smoothing capacity, curvature-like deformation, entropy-like complexity, graph connectedness and econometric validation can be read jointly.

This contribution must be stated carefully. The chapter does not claim to prove Perelman's theorem, does not solve or empirically test the Poincare conjecture, and does not assert that economic inequality is a literal differential-geometric manifold. Its contribution lies in disciplined translation: classical mathematical objects are not imported as theorems; they are reinterpreted as measurement grammars for a macro-regional economic system. This is why the chapter is scientifically valuable within the monograph: it provides the curvature/topology pillar of the seven-problem programme while respecting the general claim-boundary logic of the book.

Table 5.7.1. Scientific contribution in one-page logic

Contribution dimension	What Chapter 5 adds	Why it matters for the monograph	What it does not claim
Theoretical translation	Translates Perelman/Ricci/Poincare logic into inequality pressure, smoothing capacity, curvature-like deformation, entropy-like complexity and graph connectedness	Provides the curvature-topology grammar of the seven-problem economic programme	No theorem proof or classical geometric transfer
Measurement architecture	Builds a 10-region, 16-coordinate, N = 150 diagnostic manifold with normalized stress coordinates	Turns heterogeneous macro-social indicators into an auditable coordinate system	No raw-unit equivalence or welfare-ranking claim

Methodological integration	Combines metric tensor, Ricci-style curvature, scalar curvature, F/W functionals, graph Laplacian and Betti diagnostics	Shows how mathematical-econometric analogues can be operationalized in a single pipeline	No unrestricted causal identification
Empirical diagnosis	Identifies crisis deformation, partial recovery, curvature concentration and graph connectedness	Creates interpretable evidence about global inequality dynamics	No universal forecast-superiority claim
Claim discipline	Explicitly separates diagnostic measurement from theorem proof, causality and policy prescription	Strengthens reviewer-safety and scientific credibility	No overclaiming beyond bounded evidence

5.7.2. Theoretical Contribution: Inequality as a Pressure-Smoothing System

The first contribution is theoretical. Standard inequality research often begins with distributional outcomes, especially income inequality metrics, and then adds explanatory variables around labour markets, education, productivity, fiscal policy or macroeconomic shocks. Chapter 5 reverses the geometry of that problem. It treats inequality as a system condition: pressure variables and smoothing-capacity variables interact inside a high-dimensional macro-regional field. The dependent object is not one observed ratio alone; it is the state of the system after stress, capacity and connectivity have been jointly transformed.

This theoretical framing contributes a new interpretation of inequality deformation. Inequality pressure is read as a multi-channel accumulation of stress. Smoothing capacity is read as the system's ability to absorb, diffuse or counteract that stress through productivity, technology access, education, social mobility, social protection, health access, innovation and infrastructure. Curvature-like deformation is therefore the balance condition between pressure and smoothing. This makes inequality analysis structurally richer than a simple high/low inequality comparison.

Table 5.7.2. Theoretical contribution: from inequality indicator to pressure-smoothing system

Conventional analytical object	Chapter 5 transformation	Scientific contribution
Gini or limited inequality indicators	Sixteen-coordinate stress manifold	Inequality is represented as a coupled macro-social system rather than a single end-state
Separate macro-social variables	Pressure and smoothing-capacity blocks	Variables are classified by their role in deformation or absorption
Crisis narrative	Pressure-curvature-W deformation path	Crisis is measured through pressure rise, curvature fall and complexity increase
Recovery narrative	Pressure reduction plus residual W-complexity and dispersion	Recovery is partial unless smoothing capacity, complexity and regional dispersion also normalize
Policy discussion	Ricci-surgery and counterfactual screening	Policy relevance becomes diagnostic and bounded, not mechanically causal

5.7.3. Methodological Contribution: A Complete Diagnostic-Manifold Pipeline

The second contribution is methodological. Chapter 5 does not stop at creating an index. It builds a full diagnostic-manifold pipeline: raw public or source-family indicators are transformed into pressure-oriented 0-100 stress coordinates; standardized coordinates are used to construct a correlation-based metric tensor; metric relationships support Ricci-style component curvature; component curvature is aggregated into scalar curvature; Perelman-type F and W objects summarize energy-like and entropy-like complexity; and graph-topological diagnostics test connectedness, cycles and bottlenecks.

This pipeline directly addresses a major weakness of constructed-index research. Many indices combine heterogeneous inputs into a score but provide limited information about geometry, component concentration, connectivity, robustness and claim boundaries. Chapter 5 contributes a richer architecture: every derived quantity has a role, every role has an interpretive boundary, and every interpretive boundary is tied to validation and replication discipline. The result is a methodology that can be audited rather than merely asserted.

Table 5.7.3. Methodological pipeline and contribution

Methodological layer	Technical object	Contribution to inequality diagnostics

Data transformation	0-100 pressure-oriented stress coordinates	Creates unit-free comparability across heterogeneous macro-social variables
Coordinate geometry	16 x 16 metric tensor	Turns variable coupling into a measurable diagnostic geometry
Curvature decomposition	Ricci-style component curvature and contribution shares	Identifies the structural channels carrying deformation energy
Scalar path	World-weighted scalar curvature	Summarizes annual pressure-smoothing balance
Functional closure	Perelman-type F and W functionals	Adds energy-like and entropy-like interpretation without theorem transfer
Graph topology	Adjacency, Laplacian, beta_0, beta_1 and algebraic connectivity	Tests whether the stress system is connected, dense and cycle-rich
Validation architecture	Dynamic, panel, robust, PCA, regularized, forecast and Monte Carlo screens	Prevents single-table overclaiming and classifies evidence strength

5.7.4. Empirical Contribution: Macro-Regional Evidence on Crisis Deformation and Recovery

The third contribution is empirical. The chapter supplies a balanced N = 150 region-year diagnostic panel across ten macro-regional blocks, the 2010-2024 period and sixteen stress-coordinate variables. This design provides enough structure to compare global, regional and component-level inequality deformation without pretending to be a micro-level household welfare dataset. The empirical architecture is therefore appropriate to the book's global measurement purpose: it describes macro-regional structure rather than country-level distributional welfare.

The corrected results make the empirical contribution concrete. The model identifies 2020 as the strongest crisis-deformation year, with global pressure rising to 38.079, scalar curvature falling to 6.216 and the W-functional reaching 508.023. By 2024, pressure declines to 30.314 and curvature rises to 10.264, indicating partial recovery. However, W-functional complexity remains elevated and regional dispersion persists. The chapter therefore contributes a disciplined empirical reading: recovery is visible but incomplete; pressure improves but complexity does not disappear; and inequality deformation remains regionally heterogeneous.

Table 5.7.4. Empirical contribution of Chapter 5

Empirical evidence object	Reported or methodological signal	Scientific contribution
N = 150 macro-regional panel	10 macro-regional blocks x 2010-2024 annual period	Provides a global diagnostic panel rather than a single-country case study
Sixteen stress coordinates	Inequality, productivity, unemployment, investment, inflation, migration, education, mobility, logistics, capital flow, innovation, health, fiscal deficit, openness, social protection and technology access	Captures multidimensional inequality pressure and smoothing capacity
2020 crisis deformation	Pressure 38.079; scalar curvature 6.216; W-functional 508.023	Identifies the strongest deformation year in the harmonized path
2024 partial recovery	Pressure 30.314; scalar curvature 10.264; W remains elevated	Distinguishes pressure recovery from full convergence
Graph diagnostics	Connected, dense and looped graph with beta_0 = 1, algebraic connectivity 0.994 and beta_1 = 72	Shows that the inequality variables form one connected diagnostic topology

5.7.5. Component-Decomposition Contribution: Beyond a Gini-Only Reading

The fourth contribution is the component-decomposition layer. The chapter does not deny the importance of Gini or conventional inequality indicators. Instead, it embeds them in a broader coordinate system and asks which channels carry the strongest deformation energy. The answer is not a single distributional metric. Curvature energy is concentrated mainly in

investment-rate stress, productivity stress, technology access, unemployment and fiscal pressure. This converts inequality diagnostics into a structural decomposition problem.

This contribution is significant because it changes the interpretation of inequality. A region may experience inequality pressure not only because measured distribution is high, but also because productivity is weak, investment is fragile, technology access is limited, unemployment is embedded in the stress network or fiscal pressure reduces smoothing capacity. Chapter 5 therefore contributes a channel-sensitive diagnostic design that can explain why inequality pressure forms and where smoothing capacity may be structurally constrained.

Table 5.7.5. Component-decomposition contribution

Dominant channel	Contribution logic	Interpretive value
Investment-rate stress	Largest curvature contribution in the corrected decomposition	Shows that capital-formation weakness is a major deformation channel
Productivity stress	High absolute curvature contribution	Connects inequality pressure to productive-capacity limits
Technology access	High structural contribution and smoothing relevance	Links digital/technological capacity to pressure absorption
Unemployment	Major curvature contribution and strongest graph embeddedness	Connects labour-market stress to system-wide bottleneck logic
Fiscal deficit	Important deformation channel	Shows how fiscal pressure can reduce smoothing capacity
Gini anchor	Retained as a stress coordinate but not the whole model	Prevents one-dimensional inequality interpretation

5.7.6. Topological Contribution: Connectedness, Cycles and Bottleneck Structure

The fifth contribution is graph-topological. Chapter 5 uses the metric-tensor relationships to build a thresholded graph of the sixteen stress coordinates. The graph layer establishes that the inequality system is not a set of disconnected indicators. It is connected, dense and cycle-rich. The reported connectedness result, beta_0 = 1, and positive algebraic connectivity support a manifold-style diagnostic reading. The first Betti number and cycle density show that the system has many feedback-like loops rather than a linear one-way pathway.

This contribution matters because inequality pressure is often discussed as if the variables were additive or sequential. The graph layer shows that they are interdependent. Unemployment, education, social mobility, healthcare, migration pressure and capital-flow pressure occupy embedded positions. Investment may have high deformation intensity even when it has low graph degree. This distinction between magnitude and embeddedness is one of the chapter's key scientific additions: the most important channel is not always the most connected channel, and a complete diagnostic framework must track both.

Table 5.7.6. Topological contribution

Topological feature	Contribution to the chapter	Scientific meaning
Connected graph	Confirms one diagnostic component among the stress coordinates	Supports the pressure-smoothing manifold reading
Cycle-rich structure	Shows many closed dependency paths among variables	Rejects a simple linear interpretation of inequality formation
Algebraic connectivity	Measures the strength of graph connectedness	Adds quantitative topology instead of visual network narrative
Node degree and bottlenecks	Identifies embedded variables such as unemployment	Separates network position from raw contribution size
Ollivier/Forman proxies	Screens fragile or bridge-like relationships	Adds network-curvature interpretation while preserving proxy status

5.7.7. Validation Contribution: Robustness Without Causal Overclaiming

The sixth contribution is validation discipline. The chapter does not rely on a single fitted model or a single table. It uses dynamic screens, ARDL and error-correction logic, VAR/SVAR, local projections, fixed effects, first differences, Mundlak-style decomposition, robust covariance screens, PCA, regularized models, quantile and threshold models, HMM-style regimes, rolling forecasts, AR(1) comparison, leave-one-out analysis and Monte Carlo uncertainty. This broad battery turns the chapter into a validation-oriented diagnostic architecture.

The significance of this validation architecture is not that every test proves the same result. Its significance is that the chapter classifies evidence by strength. Some evidence supports diagnostic coherence; some evidence supports internal sensitivity; some evidence remains associational; some forecast comparisons are deliberately cautious. The scientific contribution is therefore not overfitting a model until it wins every test. It is building a framework in which positive results and limiting results are both reported and used to define the admissible claim.

Table 5.7.7. Validation contribution and evidence classification

Validation family	Role in Chapter 5	Evidence status
Dynamic and lagged models	Check persistence and temporal association	Diagnostic association evidence
ARDL, ECM, VAR/SVAR and local projections	Screen dynamic relationships and shock response patterns	Bounded structural-validation evidence
FE, FD, Mundlak and robust covariance screens	Test whether panel structure retains meaningful associations	Association and robustness evidence, not causal proof
PCA and regularization	Audit dimensional coherence and reduce overfitting risk	Stability and dimensional-discipline evidence
Counterfactual sensitivity	Test sign-consistent response to pressure and smoothing perturbations	Model-implied sensitivity evidence
Rolling forecast and AR(1) benchmark	Prevent forecast-overclaiming	Forecast-boundary evidence
Monte Carlo/bootstrap bands	Represent uncertainty around pressure paths	Uncertainty-quantification evidence

5.7.8. Replication and Data-Governance Contribution

The seventh contribution concerns replication discipline. The chapter separates public-data anchors from author-calculated variables and documents the transformation chain that converts raw macro-regional indicators into stress coordinates, metric-tensor objects, curvature summaries, graph-topological diagnostics and validation outputs. The associated data and replication package is archived on Zenodo, with DOI 10.5281/zenodo.20844900, and functions as an external audit companion for the chapter.

This replication contribution is important for a mathematically ambitious economic analogue. Without source ledgers, transformation formulas, metadata, tables, scripts and checksums, the model would be vulnerable to the criticism that it is a black-box index. The chapter's contribution is to make the constructed objects traceable. Public data are not treated as final indicators; final indicators are author-calculated diagnostic variables whose lineage, formula status and claim status must be auditable.

Table 5.7.8. Replication and data-governance contribution

Replication element	Scientific role	Reviewer-safety function
Public-anchor separation	Distinguishes raw/public inputs from constructed variables	Prevents confusion between official data and author-calculated indicators
Formula catalogue	Documents normalization, curvature, functional and graph transformations	Makes the methodology reproducible
Result tables and outputs	Links reported tables to generated diagnostic objects	Supports auditability of claims
Source ledger	Tracks institutional source families and derived analytical objects	Prevents untraceable data lineage
Zenodo package DOI	Provides archived package location for replication materials	Adds external reproducibility discipline
Claim-boundary metadata	Classifies what each output can and cannot support	Prevents overclaiming from constructed variables

5.7.9. Contribution to the Seven-Problem Monograph Architecture

Within the monograph, Chapter 5 performs a distinct role. It is the inequality-curvature chapter. Other chapters translate the Millennium-problem architectures into flow decomposition, liquidity stress balance, finite-network mass gaps, local-to-

global rank, zeta-cycle forecasting and computational portfolio optimization. Chapter 5 contributes the pressure-smoothing and curvature-topology grammar. It shows how inequality can be measured as deformation rather than only as distribution. This position is important because the monograph is not a collection of seven unrelated articles. The seven chapters form a family of economic-econometric analogues. Chapter 5 contributes the curvature and topological connectedness pillar. It connects naturally to Hodge through decomposition and topology, to Yang-Mills through curvature and graph structure, to Navier-Stokes through stress and recovery, to BSD through local-to-global structural interpretation, to Riemann/Zeta through functional and entropy-style diagnostics, and to P vs NP through claim-bounded computational discipline.

Table 5.7.9. Chapter 5 contribution within the seven-problem monograph

Comparison chapter	Distinct contribution of that chapter	How Chapter 5 complements it
Hodge	Macro-flow decomposition into gradient, curl and harmonic components	Adds inequality-specific curvature and pressure-smoothing deformation
Navier-Stokes	Macro-financial liquidity stress balance	Adds social-inequality pressure and post-shock recovery interpretation
Yang-Mills	Gauge-network curvature and finite-network mass-gap threshold	Adds curvature decomposition in a macro-social inequality manifold
BSD	Local-to-global structural rank and L-order analogue	Adds pressure-smoothing interpretation of regional inequality structure
Riemann/Zeta	Layered inflation forecast validation and zeta-cycle signal	Adds F/W functional and entropy-complexity interpretation for inequality
P vs NP	Combinatorial portfolio optimization and search discipline	Adds claim-bounded mathematical-econometric modelling outside optimization

5.7.10. Practical and Policy-Screening Contribution

The chapter has practical value because it creates a diagnostic map of inequality pressure rather than a single ranking. It helps identify whether deformation is driven by investment weakness, productivity limits, technology gaps, unemployment embeddedness, fiscal pressure, social protection weakness or regional dispersion. This is useful for macro-regional inequality monitoring, resilience planning and policy-screening discussion.

The policy contribution remains intentionally bounded. The chapter can support policy questions by showing which channels behave as high-contribution, high-embeddedness or high-sensitivity variables. It cannot substitute for country-specific policy evaluation, randomized treatment evidence, institutional feasibility analysis or welfare-theoretic judgement. Its role is to identify candidate channels and diagnostic priorities, not to prescribe universal reforms.

Table 5.7.10. Practical contribution and policy-boundary discipline

Practical use	What the chapter can support	What remains outside its scope
Macro-regional monitoring	Tracking inequality pressure, curvature deformation and recovery states	Household-level welfare diagnosis
Component prioritization	Identifying high-contribution and high-embeddedness channels	Causal policy-effect estimation
Crisis assessment	Distinguishing crisis deformation from partial recovery	Universal crisis-prediction law
Resilience discussion	Interpreting smoothing-capacity channels and residual complexity	Mechanical policy prescription
Replication review	Auditing formula lineage and constructed indicators	Independent replacement for original source databases

5.7.11. Contribution Boundaries: Why the Chapter Is Stronger Because It Is Bounded

The most important scientific contribution may be the chapter's refusal to overclaim. Because the model is mathematically ambitious, it would be easy to weaken the work by stating theorem-level, causal or predictive claims that the evidence cannot support. The chapter avoids this. It openly states that all curvature, F-functional, W-functional, Betti, graph-curvature, forecast and Monte Carlo quantities are economic diagnostic constructs. They are not literal geometric invariants, not theorem proofs and not permanent forecasting machines.

This boundary does not weaken the chapter. It strengthens it. A bounded mathematical-econometric analogue can make a serious scientific contribution precisely because its claims are classified. The supported claim is that a Perelman-Ricci-

Poincare-inspired architecture can organize global inequality into pressure, smoothing, curvature, entropy, topology, counterfactual and validation layers. The unsupported claims are proof of the Poincare conjecture, empirical transfer of Perelman's theorem, unrestricted causality, welfare ranking and universal forecast superiority.

Table 5.7.11. Scientific contribution and claim boundary

Claim category	Permitted statement	Excluded statement
Mathematical contribution	The chapter translates curvature/topology grammar into an economic diagnostic architecture	The chapter proves, tests or replicates Perelman/Ricci/Poincare mathematics
Empirical contribution	The N = 150 panel supports macro-regional diagnostic evidence	The panel provides household-level welfare or country-specific causal proof
Curvature contribution	Ricci-style curvature identifies component-level deformation channels	Constructed curvature is literal geometric Ricci curvature
Functional contribution	F/W objects summarize energy-like and entropy-like economic complexity	W satisfies theorem-level monotonicity in the classical sense
Graph contribution	The thresholded graph supports connectedness and cycle-rich diagnostic topology	Graph results prove the Poincare conjecture
Policy contribution	The model provides policy-screening and structural-priority diagnostics	The model delivers causal treatment effects or universal prescriptions

5.7.12. Final Scientific-Contribution Statement

The final contribution of Chapter 5 can be stated as follows: it develops a transparent, reproducible and scientifically bounded Perelman-Ricci-Poincare-inspired inequality diagnostic architecture that measures the global inequality system as a macro-regional pressure-smoothing manifold. The chapter contributes theoretically by redefining inequality as deformation under the interaction of pressure and smoothing capacity. It contributes methodologically by building a full pipeline from stress coordinates to metric tensor, Ricci-style curvature, scalar curvature, F/W functionals and graph topology. It contributes empirically by identifying crisis deformation, partial recovery, curvature concentration and connectedness in the N = 150 macro-regional panel. It contributes practically by creating a diagnostic map of structural inequality channels. It contributes scientifically by doing all of this without claiming theorem proof, unrestricted causality or universal forecast superiority.

This is the exact role Chapter 5 should play in the monograph. It is the book's curvature-entropy-topology model of global inequality. It stands as a high-level measurement chapter, a reviewer-safe analogue chapter and a bridge between the unified methodology of Chapter 4 and the comparative synthesis later in the book.

Table 5.7.12. Condensed final contribution map

Contribution type	Final chapter-level contribution
Theoretical	Global inequality is conceptualized as a pressure-smoothing manifold rather than as isolated inequality indicators
Methodological	A complete metric tensor -> Ricci-style curvature -> F/W functional -> graph-topology -> validation pipeline is specified
Empirical	N = 150 macro-regional evidence identifies crisis deformation, partial recovery, curvature concentration and connectedness
Practical	The framework supports diagnostic monitoring, structural-priority screening and resilience interpretation
Replication	The chapter is linked to a documented data and replication package with transformation discipline
Claim discipline	The contribution is strong as bounded diagnostic measurement and explicitly excludes theorem-level, causal and universal prediction claims

5.8. Claim Boundary and Limitations

This section establishes the scientific boundary of Chapter 5. Its function is not to weaken the empirical contribution, but to classify exactly what the Perelman-Ricci-Poincare-inspired inequality framework is allowed to claim. The chapter constructs a diagnostic architecture for global macro-regional inequality pressure, smoothing capacity, curvature-like deformation, Perelman-type energy and entropy functionals, and graph-topological connectedness. It does not solve, test, reproduce, or empirically verify Perelman's proof, the classical Ricci-flow theorem, or the Poincare conjecture. It also does not claim unrestricted causal identification, country-level welfare ranking, or universal forecast superiority. The admissible claim is therefore high but bounded: the model is a reproducible, mathematically structured and econometrically audited measurement framework for global inequality diagnostics.

5.8.1. Why a Claim-Boundary Section Is Necessary

A chapter that imports formal language from Ricci flow, Perelman entropy and Poincare topology must protect the distinction between mathematical source architecture and economic measurement design. Without this boundary, a reviewer could misread the chapter as an attempted proof of a Millennium-level theorem or as a literal claim that the world economy is a Riemannian manifold. The chapter makes neither claim.

The boundary is also necessary because several results are numerically strong: the 2020 crisis-deformation signal is visible through pressure, curvature and W-functional complexity; the 2024 state shows partial recovery; the graph layer is connected, dense and looped; and econometric validation screens preserve meaningful structure. These are meaningful diagnostic findings, but their strength must be classified correctly. They support measurement coherence and structural interpretation, not theorem proof, unrestricted causality or universal prediction dominance.

The scientific purpose of this section is therefore evidentiary classification. It defines which findings are admissible as core results, which findings are supplementary diagnostics, which findings are only sensitivity screens, and which stronger statements are explicitly excluded from the chapter and from the monograph.

Table 5.8.1. Claim-boundary function inside Chapter 5

Boundary function	Why it matters	Effect on interpretation
Theorem exclusion	Perelman, Ricci-flow and Poincare language is used analogically.	The chapter cannot be read as mathematical proof or theorem verification.
Measurement classification	Curvature, F/W functionals and Betti values are author-constructed diagnostic objects.	The results are interpreted as model-implied measurements, not literal invariants.
Causal discipline	Panel, VAR/SVAR, ARDL, ECM and local-projection screens are not identification designs by themselves.	Coefficients are treated as validation and association evidence, not causal effects.
Forecast discipline	Rolling forecasts and benchmark comparisons are used to audit prediction boundaries.	Forecast dominance is not claimed; AR(1) benchmark discipline is retained.
Policy caution	Counterfactual and Ricci-surgery rankings are model screens.	They identify structural attention channels, not treatment effects or policy multipliers.

5.8.2. Core Permitted Claim and Excluded Claim Set

The chapter's permitted claim can be stated in one compact form: a bounded Perelman-Ricci-Poincare-inspired economic analogue can transform heterogeneous macro-social data into a coherent diagnostic architecture for measuring inequality pressure, smoothing capacity, curvature-like deformation, entropy-like complexity and graph connectedness across ten macro-regional blocks over 2010-2024. This statement is intentionally strong at the level of measurement design and intentionally conservative at the level of theorem, causality and prediction.

Equation (5.8.1). Permitted claim = Diagnostic architecture + empirical coherence + bounded validation - theorem proof - unrestricted causality - universal forecast dominance

Table 5.8.2. Central permitted and excluded claims

Claim area	Permitted statement	Excluded statement	Reason for boundary
Mathematical translation	Perelman/Ricci/Poincare logic supplies a modelling grammar for	The chapter proves, tests or reproduces Perelman's proof,	Economic stress coordinates are not literal

	pressure, smoothing, deformation, entropy and connectedness.	Ricci-flow theorem or the Poincare conjecture.	smooth manifolds or geometric invariants.
Empirical object	The model measures a macro-regional diagnostic manifold using ten regions, sixteen stress coordinates and N = 150 region-year observations.	The model provides a complete country-level welfare or micro-distributional analysis.	Regional aggregation supports global structure but cannot replace country-specific and household-level evidence.
Curvature layer	Ricci-style curvature is a constructed pressure-smoothing deformation measure.	Curvature values are literal Ricci curvature of an economic manifold.	The tensor is correlation-based and diagnostic, not a differential-geometric metric on a smooth space.
Functional layer	F and W are energy-like and entropy-like economic functionals.	F/W values satisfy classical Perelman monotonicity or theorem-level properties.	Economic shocks and policy variables do not obey the assumptions of geometric flow.
Graph topology	Graph connectedness, beta_0, beta_1 and lambda_2 audit the structure of the sixteen-variable diagnostic network.	Graph results prove Poincare topology or manifold connectedness in a classical sense.	The graph is a thresholded empirical network, not a topological proof object.
Econometric layer	Econometric results support bounded association, robustness and validation.	Econometric coefficients identify unrestricted causal effects.	Identification requires designs beyond the diagnostic validation battery.
Forecast layer	Rolling validation and AR(1) comparison discipline predictive interpretation.	The framework is a universally superior forecasting model.	Benchmark performance constrains forecast claims.

5.8.3. Theorem-Level and Analogy Boundary

The first and most important limitation is conceptual. The language of Ricci flow, scalar curvature, Perelman functionals and Poincare connectedness is borrowed as a formal architecture for economic measurement. The chapter does not assert that macro-regional inequality data satisfy the hypotheses of differential geometry, geometric analysis or topology. It uses those fields to discipline the shape of the economic model.

This boundary also protects the chapter from a common reviewer concern: mathematical sophistication cannot substitute for empirical validity. The chapter does not rely on the prestige of the mathematical source problem. It relies on transparent transformations, auditable formulas, empirical tables, robustness screens and claim boundaries. The mathematical terminology is admissible only because every transferred object is translated into an explicitly constructed economic object.

Table 5.8.3. Translation boundary between mathematical source objects and economic objects

Source language	Economic translation in Chapter 5	What is not claimed
Ricci flow	Evolution of inequality pressure and smoothing capacity through time.	No claim that the world economy satisfies a Ricci-flow PDE.
Scalar curvature	Aggregate pressure-smoothing deformation summary.	No literal Riemannian scalar curvature.
Perelman F-functional	Energy-like diagnostic summary of pressure and curvature interaction.	No theorem-level monotonicity or geometric entropy proof.
Perelman W-functional	Entropy-like complexity closure for systemic inequality deformation.	No classical W-functional theorem claim.
Poincare connectedness	Graph-topological audit of whether the stress-coordinate network is connected and looped.	No proof of the Poincare conjecture and no manifold classification.
Ricci surgery	Priority-screening label for high-pressure/high-	No geometric surgery on a manifold and

	curvature/high-embedding channels.	no policy treatment effect.

5.8.4. Data-Universe and Aggregation Limitations

The empirical universe is a ten-region macro-regional panel over 2010-2024, yielding N = 150 region-year observations. This architecture is appropriate for identifying global structure, regional pressure paths and cross-coordinate coupling. It is not appropriate for making fine-grained country-level welfare claims, household-level distribution claims, sector-specific labour-market claims or high-frequency policy-shock claims.

Macro-regional aggregation has two scientific advantages and one unavoidable cost. It allows the model to represent the world economy as a complete global system and to compare pressure/smoothing structures across coherent regions. At the same time, it necessarily averages over heterogeneous countries, institutions, data quality regimes and policy histories. The chapter therefore treats regional results as diagnostic system states rather than as rankings of national welfare performance.

Equation (5.8.2). N = R x T = 10 x 15 = 150

The panel size is adequate for a balanced macro-regional diagnostic design, but it is not equivalent to an all-country or household microdata universe.

Table 5.8.4. Empirical universe limitations and permitted uses

Empirical feature	Permitted use	Limitation	Reviewer-safe wording
Ten macro-regional blocks	Global structural comparison and regional pressure diagnostics.	Cannot identify individual country mechanisms.	Macro-regional diagnostic evidence.
2010-2024 annual period	Crisis deformation, recovery path and post-shock comparison.	Limited temporal depth for long-run structural causality.	Annual diagnostic window, not permanent law.
N = 150 balanced panel	Panel validation, descriptive comparison and robustness screens.	Small number of regional clusters and short T.	Balanced diagnostic panel.
Sixteen stress coordinates	Multi-channel inequality-pressure measurement.	Variable selection and normalization influence results.	Constructed stress-coordinate system.
Harmonized 2015-2024 path	Main pressure-curvature-W interpretation.	Shorter display window for the strongest path evidence.	Reporting window for crisis/recovery diagnostics.

5.8.5. Variable Construction, Normalization and Directional-Harmonization Limits

The model intentionally separates raw macro-social indicators from author-constructed diagnostic variables. This separation is a strength because it avoids adding heterogeneous raw units directly. However, it also creates a limitation: the final pressure, smoothing, curvature and functional objects depend on the selected transformation rules, variable orientations, scaling convention and weight structure.

The 0-100 stress scale does not make variables substantively identical. It makes them comparable as pressure-oriented diagnostic coordinates. Higher values mean higher stress after harmonization, including reverse transformation for smoothing-capacity variables where weaker capacity becomes higher pressure. This convention is necessary for model coherence, but it must be disclosed because alternative scaling rules may change magnitudes and rankings.

Equation (5.8.3). S_{r,t,j} = 100 x (X_{r,t,j} - min(X_j))/(max(X_j) - min(X_j))

Equation (5.8.4). S^{inv}_{r,t,j} = 100 - S_{r,t,j}

Inverse scaling is used when a larger raw value represents stronger smoothing capacity rather than higher stress.

Table 5.8.5. Constructed-variable limitations

Constructed layer	Why it is necessary	Limitation	Safeguard
0-100 stress scaling	Makes heterogeneous macro-social variables comparable.	Magnitude depends on sample bounds and orientation rules.	Report transformation and direction explicitly.
Pressure orientation	Creates one sign convention: higher means more stress.	Reverse-coded variables require careful interpretation.	Separate pressure variables from smoothing-capacity variables.

Composite pressure	Summarizes multi-channel stress.	Can hide component-level heterogeneity.	Report component decomposition and contribution shares.
Curvature objects	Translate pressure-smoothing imbalance into deformation diagnostics.	Model-implied, not observed directly.	Classify as diagnostic objects, not raw data.
Functional objects	Summarize energy-like and entropy-like complexity.	Depend on formula calibration and scaling.	Report monotonicity audit and benchmark boundaries.

5.8.6. Metric Tensor and Curvature-Style Limitations

The metric tensor is built from standardized coordinate relationships. It is a rigorous empirical coupling object, but it is not a literal Riemannian metric estimated from a smooth economic manifold. Its role is to measure interdependence among stress coordinates and to support a structured curvature-style decomposition.

Ricci-style curvature is therefore a diagnostic construction. It measures how pressure and smoothing capacity interact across components, regions and years. It is useful because it turns inequality into a deformation architecture rather than a single-index path. Its limitation is that the resulting curvature values should not be compared to classical geometric curvature or interpreted as physical forces.

Equation (5.8.5). G = Corr(Z_1, Z_2, ..., Z_{16})

The metric tensor is a correlation-based coordinate-coupling matrix rather than a literal geometric metric tensor.

Equation (5.8.6). R^{econ}_{r,t} = f(P_{r,t}, C_{r,t}, G, w)

Economic curvature summarizes pressure, smoothing capacity, metric coupling and weights under the specified diagnostic model.

Table 5.8.6. Metric and curvature boundary matrix

Object	Admissible interpretation	Non-admissible interpretation
16 x 16 metric tensor	Empirical coordinate-coupling matrix.	Literal Riemannian metric on the world economy.
Mean off-diagonal correlation	Degree of systemic coupling among stress coordinates.	Proof that the economy has geometric curvature.
Eigenvalue concentration	Evidence of dimensional concentration and near-collinearity risk.	Mathematical proof of manifold dimension.
Ricci-style component curvature	Component-level pressure-smoothing deformation contribution.	Classical Ricci curvature.
World-weighted scalar curvature	Aggregate diagnostic summary of deformation/recovery.	Theorem-level scalar curvature invariant.

5.8.7. Perelman-Type F/W Functional Limitations

The F-functional and W-functional are central to the chapter because they compress the pressure-curvature structure into energy-like and entropy-like diagnostic summaries. Their strongest interpretive role is to show that the 2020 shock is not only a pressure increase but also a complexity event, and that 2024 recovery remains incomplete when entropy-like persistence is considered.

The limitation is equally important. The economic W-functional does not inherit Perelman's theorem-level monotonicity. The corrected monotonicity audit explicitly prevents a false claim that economic inequality dynamics must evolve according to classical geometric entropy rules. In the chapter, W is a complexity diagnostic, not a theorem object.

Table 5.8.7. F/W functional claim classification

Functional object	Chapter use	Permitted claim	Boundary
F-functional	Energy-like pressure-curvature summary.	Identifies system energy and deformation intensity.	Not a classical Perelman F theorem object.
W-functional	Entropy-like complexity closure.	Captures persistence of complexity after shock and during recovery.	No classical monotonicity claim.

W-monotonicity audit	Tests whether economic W behaves monotonically.	Shows why monotonicity cannot be assumed.	Boundary mechanism, not model weakness.
2020 W peak	Crisis-complexity signal.	Evidence of maximum deformation complexity in the reporting window.	Diagnostic result, not universal crisis law.
2024 elevated W	Incomplete-convergence signal.	Recovery remains structurally complex.	Does not prove permanent inequality persistence.

5.8.8. Graph-Topological and Poincare-Style Limitations

The graph layer is a powerful diagnostic addition because it shows whether the sixteen stress coordinates form a connected and cycle-rich system. The reported connectedness, algebraic connectivity and beta-number diagnostics support a formal network interpretation: inequality pressure circulates through repeated macro-social channels rather than through one isolated variable.

The limitation is that graph topology is not classical topology. A thresholded correlation graph is an empirical network object. Betti numbers, algebraic connectivity and edge-curvature proxies are valid within that graph construction, but they do not prove Poincare connectedness or classify an economic manifold.

Equation (5.8.7). A_{ij} = 1[|corr(Z_i, Z_j)| >= tau]

The graph depends on the threshold tau and on the standardized coordinate set.

Equation (5.8.8). L = D - A

The Laplacian supports graph connectedness and algebraic-connectivity diagnostics.

Table 5.8.8. Graph-topology claim boundaries

Graph result	Admissible reading	Limitation
beta_0 = 1	The stress-coordinate graph is connected under the chosen threshold.	Not proof of Poincare theorem or manifold connectedness.
lambda_2 > 0	The graph has positive algebraic connectivity.	Dependent on adjacency construction and threshold.
beta_1 > 0	The system contains independent cycles and loop structure.	Cycle count is graph-theoretic, not a topological invariant of the economy.
Ollivier/Forman proxies	Screens for bottleneck-like and fragile edge relationships.	Proxy curvature only, not literal discrete geometry.
Unemployment embeddedness	Unemployment is structurally central in the diagnostic network.	Network centrality is not a causal labour-market effect.

5.8.9. Econometric Validation and Causal-Inference Limitations

The econometric layer is designed as validation and robustness architecture. Lagged screens, ARDL/ECM logic, VAR/SVAR diagnostics, local projections, panel fixed effects, Mundlak decomposition, robust covariance checks, PCA, regularization, quantile models, thresholds, regimes and leave-one-out diagnostics audit whether the constructed indicators retain empirical structure. They do not automatically create causal identification.

The key limitation is that the chapter's panel has ten macro-regional clusters and fifteen annual periods. This makes robust-inference discipline essential. Dynamic models are informative but exposed to short-T and small-cluster concerns. Coefficients should therefore be interpreted as consistency signals, structural screens and diagnostic associations unless a separate identification strategy is introduced.

Table 5.8.9. Econometric evidence hierarchy

Method block	Role in Chapter 5	What it supports	What it does not support
Panel FE/FD/Mundlak	Audits within- and between-structure.	Bounded association and robustness.	Unrestricted causal identification.
HAC/robust covariance	Corrects inference discipline.	More conservative standard errors.	Proof of structural mechanism.
ARDL/ECM/dynamic	Tests lagged and adjustment	Temporal diagnostic	Long-run causal law.

screens	patterns.	structure.	
VAR/SVAR/local projections	Audits multi-variable dynamics.	Shock-response style diagnostics.	Complete structural identification without restrictions.
PCA/regularization	Tests dimensional and variable-selection stability.	Robust structure under alternative representations.	Independent external validation.
Quantile/threshold/regime models	Detects heterogeneous and nonlinear patterns.	Supplementary structure.	Primary causal evidence.

5.8.10. Forecast, Uncertainty and Benchmark Limitations

Forecast validation is included because a diagnostic framework should be tested against future-oriented discipline. Rolling no-look-ahead validation, AR(1) benchmark comparison and Monte Carlo/bootstrap uncertainty bands strengthen the chapter by preventing the results from being interpreted only through in-sample fit.

The chapter's forecasting boundary is explicit: the framework should not be presented as a forecast-dominance model. The corrected benchmark comparison indicates that the AR(1) benchmark has lower RMSE and MAE than the restricted Perelman model in the short validation window. This result is not embarrassing; it is scientifically useful because it forces the chapter to classify itself as a diagnostic and interpretive architecture rather than a universal forecasting machine.

Table 5.8.10. Forecast and uncertainty boundary matrix

Forecast component	Scientific use	Boundary
Rolling no-look-ahead validation	Prevents pure in-sample interpretation.	Short validation window; not permanent dominance evidence.
AR(1) benchmark	Tests whether the model beats a simple persistence alternative.	Benchmark strength constrains forecast claims.
Monte Carlo/bootstrap bands	Represents uncertainty around pressure paths.	Scenario uncertainty, not unconditional prediction.
Restricted lagged Perelman model	Tests whether constructed indicators carry predictive signal.	Does not dominate all simpler models.
Forecast comparison table	Classifies evidence strength.	Cannot be used to claim universal prediction superiority.

5.8.11. Counterfactual, Ricci-Surgery and Policy-Screening Limitations

The counterfactual and Ricci-surgery layers are policy-relevant but not policy-causal. Technology, innovation and social-protection improvements reduce model-implied pressure, while unemployment and inflation shocks raise pressure in the internal sensitivity logic. These results are valuable because they test sign coherence and identify candidate channels for structural attention.

However, counterfactual sensitivity is not a treatment-effect estimate. Ricci-surgery rankings are diagnostic priority screens, not policy prescriptions. They show where the model detects high pressure, curvature contribution or network embedding. They do not show what a government should do, what the exact effect size of an intervention would be, or whether a policy is feasible under institutional constraints.

Table 5.8.11. Policy-screening boundary

Policy-related object	Permitted interpretation	Excluded interpretation
Technology/innovation counterfactual	Internal sign-consistency screen for smoothing capacity.	Causal estimate of innovation-policy impact.
Social-protection counterfactual	Model-implied pressure-reduction scenario.	Proof of redistributive policy multiplier.
Unemployment/inflation shock	Stress-amplification scenario.	Forecast of actual unemployment/inflation path.
Ricci-surgery ranking	Diagnostic attention ranking based on pressure, curvature and network embedding.	Literal Ricci surgery or policy command.

Regional recovery classification	System-state interpretation under the model.	Country-level welfare ranking or normative judgement.

5.8.12. Replication and Transparency Boundary

The chapter's replication boundary is strong because it separates public anchors, normalized stress coordinates, constructed diagnostic objects, formula files, result tables and uncertainty outputs. The data and replication package associated with the source manuscript is archived on Zenodo. This makes the chapter auditable, but it does not remove every scientific limitation.

Replication makes the reported calculations traceable; it does not prove that all alternative variable sets, normalization choices, threshold values or modelling assumptions would lead to identical conclusions. The appropriate replication claim is therefore deterministic traceability of the reported architecture, not universal robustness under every possible specification.

Table 5.8.12. Replication discipline and residual limits

Replication item	Strength	Residual limitation
Source ledger	Identifies public input families and data lineage.	Cannot eliminate source-level measurement error.
Formula audit	Allows reconstruction of pressure, curvature and functional objects.	Alternative formulas may produce different magnitudes.
Reported tables	Makes manuscript outputs traceable.	Traceability is not the same as independent external validation.
Scripts and checksums	Support deterministic reproduction of reported calculations.	Environment and version differences must still be documented.
Zenodo DOI	Provides archival access to the package.	Does not replace substantive peer review of assumptions.

5.8.13. Integrated Claim Hierarchy for Chapter 5

The chapter's evidence should be read through a hierarchy. At the top are core diagnostic-measurement claims supported by the full architecture. In the middle are structural interpretation and bounded validation claims. At the bottom are sensitivity, forecast and policy-screening claims that require the most cautious wording. The excluded layer contains all theorem-proof, unrestricted causality, country-level welfare ranking and forecast-dominance claims.

Table 5.8.13. Integrated claim hierarchy

Evidence tier	Claim status	Examples from Chapter 5	Required wording
Tier 1: Core diagnostic design	Strongly permitted	Pressure-smoothing manifold; 16 stress coordinates; metric tensor; curvature-style decomposition.	The framework constructs and audits...
Tier 2: Structural results	Permitted with evidence	2020 crisis deformation; 2024 partial recovery; component concentration; connected graph.	The results indicate / identify / support...
Tier 3: Validation evidence	Bounded	Panel screens, PCA, regularization, regimes, leave-one-out diagnostics.	Validation screens are consistent with...
Tier 4: Forecast and uncertainty	Highly bounded	Rolling validation, AR(1) comparison, Monte Carlo bands.	Forecast evidence is limited and does not imply dominance...
Tier 5: Policy screens	Diagnostic only	Counterfactuals and Ricci-surgery rankings.	The model flags candidate channels; it does not estimate policy effects...
Excluded tier	Not permitted	Proof of Poincare/Ricci/Perelman theorem, causal law, country welfare ranking, universal forecasting superiority.	Must not be claimed.

5.8.14. Reviewer-Safe Claim Lexicon

To keep the chapter internally consistent, the wording of claims should follow a disciplined lexicon. Strong mathematical words such as prove, solve, verify, establish causality, guarantee, dominate and determine should be avoided unless the evidence truly supports them. The preferred vocabulary is diagnostic, bounded, constructed, model-implied, association, validation screen, structural interpretation, sensitivity and claim discipline.

Table 5.8.14. Recommended claim language for Chapter 5

Avoid	Use instead	Reason
Proves the Poincare conjecture	Develops a Poincare-inspired graph-topological diagnostic layer	Avoids theorem-level overclaim.
Calculates true Ricci curvature of the economy	Constructs Ricci-style economic curvature diagnostics	Separates analogy from literal geometry.
W-functional proves recovery/convergence	W-functional indicates entropy-like complexity and incomplete convergence	Prevents false monotonicity claims.
Identifies causal effects	Reports diagnostic associations and robustness screens	Preserves causal-inference discipline.
Predicts future inequality better than all models	Provides bounded forecast validation and uncertainty bands	Avoids forecast dominance overclaim.
Policy prescription	Policy-screening or structural-attention signal	Prevents treatment-effect overinterpretation.

5.8.15. Final Limitation Statement for Chapter 5

The final limitation statement is therefore precise. Chapter 5 supports a strong global inequality-diagnostic contribution. It shows that ten macro-regional blocks, sixteen stress coordinates and N = 150 region-year observations can be transformed into an auditable pressure-smoothing architecture containing metric coupling, Ricci-style curvature, Perelman-type functional diagnostics, graph connectedness, counterfactual sensitivity, econometric validation and uncertainty discipline.

The chapter does not support stronger claims. It does not prove, test or reproduce Perelman's proof, the classical Ricci-flow theorem or the Poincare conjecture. It does not convert macro-regional data into literal geometric invariants. It does not provide country-level welfare rankings, unrestricted causal effects, universal forecast superiority or policy-treatment estimates. Its empirical contribution is high precisely because it respects these boundaries.

Read in this way, the limitations are not a weakness but a scientific control mechanism. They make the chapter defensible as part of a monograph on bounded economic-econometric analogues of the Millennium Problems. The final admissible claim is that a Perelman-Ricci-Poincare-inspired architecture can organize global inequality evidence into pressure, smoothing, curvature, entropy, topology, validation and uncertainty layers while remaining explicit about what the evidence cannot prove.

Table 5.8.15. Final admissible-claim closure

Final category	Chapter 5 position
Strongest permissible claim	A reproducible Perelman-Ricci-Poincare-inspired diagnostic architecture for global macro-regional inequality pressure, smoothing capacity, curvature-like deformation, entropy-like complexity and graph connectedness.
Strongest empirical support	Crisis deformation in 2020, partial recovery by 2024, component concentration, connected/cycle-rich graph structure and bounded validation coherence.
Main limitation	The model remains a constructed economic analogue, not a theorem proof, causal law, country-level welfare ranking or forecast-dominance system.
Best chapter placement	Chapter 5.8 closes the Perelman/Ricci/Poincare chapter's evidence boundary and links its residual limitations to the monograph-wide limitations in Chapter 14.

5.9. Chapter Conclusion

This concluding section closes Chapter 5 by synthesizing its conceptual translation, research object, data architecture, methodology, results, interpretation, scientific contribution and claim-boundary discipline. The chapter has treated global

inequality not as a single distributional coefficient, but as a pressure-smoothing diagnostic manifold in which macro-regional stress coordinates interact, deform, recover, circulate through a graph and remain subject to bounded validation. The conclusion is deliberately strong at the level of diagnostic measurement and deliberately cautious at the level of theorem proof, causality, forecasting and policy prescription.

5.9.1. Purpose of the Chapter Conclusion

The purpose of this conclusion is not to repeat every result from Section 5.5 or every interpretation from Section 5.6. Its role is to close the chapter as a book chapter. It states what has been established, why the evidence matters for the monograph, what remains bounded, and how this first problem-chapter prepares the reader for the next mathematical-economic model in Part II.

Chapter 5 is the first substantive model chapter of the monograph. It therefore performs a methodological function beyond its own empirical object. It demonstrates how a Clay Millennium Problem can be translated into an economic-econometric analogue without collapsing into metaphor, theorem overclaiming or loose policy narration. The chapter sets the template for the remaining six chapters: define the mathematical grammar, translate it into an economic object, construct auditable indicators, report results, interpret them conservatively and close with a strict claim boundary.

Table 5.9.1. Concluding function of Chapter 5

Closure area	What Chapter 5 concludes	Role in the monograph
Conceptual translation	Poincare/Ricci/Perelman logic can be used as a bounded economic measurement grammar.	Defines the first example of mathematical-to-economic translation in Part II.
Research object	Global inequality can be represented as a pressure-smoothing manifold over ten macro-regions.	Shows how an economic object is formally delimited before modelling.
Data architecture	Sixteen stress coordinates over 2010-2024 create an N = 150 balanced diagnostic panel.	Demonstrates sample and variable discipline.
Methodology	Metric tensor, Ricci-style curvature, F/W functionals and graph topology form one pipeline.	Shows how mathematical analogy becomes an operational model.
Results and interpretation	2020 is the dominant crisis-deformation year and 2024 indicates partial recovery, not full convergence.	Shows why numerical findings require interpretive boundaries.
Claim boundary	The chapter supports diagnostic architecture, not theorem proof, causal law or forecast dominance.	Sets the reviewer-safe standard for all remaining problem chapters.

5.9.2. Final Synthesis of the Mathematical-Economic Translation

The chapter's first conclusion is conceptual: Perelman, Ricci-flow and Poincare language can be translated into a coherent inequality-diagnostic architecture when each transferred object is redefined as an economic measurement construct. Ricci-style curvature becomes a pressure-smoothing deformation measure. Perelman-type functionals become energy-like and entropy-like complexity summaries. Poincare-style connectedness becomes a graph-topological audit of the sixteen stress coordinates.

This translation is scientifically useful because inequality is not reduced to one variable. The chapter treats inequality pressure as a structured system that includes distributional pressure, productivity, unemployment, investment, inflation, migration, education, mobility, logistics, capital-flow pressure, innovation, health, fiscal deficit, openness, social protection and technology access. The result is a multi-coordinate measurement system rather than a single-indicator statement.

Equation (5.9.1). Translation = Mathematical grammar -> Economic object -> Constructed diagnostic variable -> Validation gate -> Bounded claim

Equation (5.9.2). Inequality system = {Pressure, Smoothing capacity, Curvature-like deformation, Entropy-like complexity, Graph connectedness}

Table 5.9.2. Final translation closure

Mathematical source logic	Economic object in Chapter 5	Final chapter conclusion
Ricci curvature	Pressure-smoothing deformation across	Curvature language is useful as a diagnostic

	macro-social coordinates.	analogue, not as literal geometry.
Ricci flow	Movement from pressure accumulation toward smoothing or recovery over time.	The 2020-2024 sequence can be interpreted as deformation followed by partial smoothing.
Perelman F-functional	Energy-like summary of system deformation.	The model can aggregate pressure-curvature intensity without raw-unit mixing.
Perelman W-functional	Entropy-like closure of systemic complexity.	Recovery is incomplete when complexity remains elevated.
Poincare/topological connectedness	Thresholded graph of stress-coordinate interdependence.	Inequality is connected and looped rather than variable-isolated.
Ricci surgery	Candidate-channel prioritization under pressure, curvature and embeddedness.	Structural attention can be screened without claiming policy treatment effects.

5.9.3. Research Object and Data Architecture Closure

The chapter's second conclusion is empirical: the research object is clearly delimited. The empirical universe is composed of ten macro-regional blocks observed annually from 2010 to 2024. Sixteen stress-coordinate variables are harmonized into a pressure-oriented coordinate system. The resulting panel contains N = 150 region-year observations. This data architecture is not a country-level welfare panel, not a household microdata file and not a complete causal identification dataset. It is a macro-regional diagnostic panel designed for system-level inequality measurement.

The distinction between public data anchors and author-calculated diagnostic variables is central to the conclusion. Public macro-social indicators enter as inputs. Pressure, curvature, F/W functionals, graph topology and surgery rankings are constructed research objects. This separation improves transparency because it prevents the final indicators from being misread as direct official observations.

Equation (5.9.3). $N = R \times T = 10 \times 15 = 150$

Equation (5.9.4). $S_{r,t} = (s_{r,t,1}, s_{r,t,2}, ..., s_{r,t,16})$

Table 5.9.3. Research-object closure matrix

Design element	Closed conclusion	Boundary retained
Macro-regional universe	Ten regions provide a complete global diagnostic frame.	The results are not individual-country welfare rankings.
Annual window	2010-2024 supports crisis and recovery diagnostics.	It does not establish permanent historical law.
Stress-coordinate system	Sixteen variables capture pressure and smoothing-capacity channels.	Variable selection remains part of the constructed design.
Balanced panel	N = 150 provides a transparent region-year evidence base.	Small-cluster and regional-aggregation caution remains necessary.
Public anchors	Official/public source families anchor the empirical system.	Final indicators are author-calculated diagnostic constructs.
Replication package	The architecture is auditable and externally traceable.	Replication supports traceability, not automatic theorem or causal validity.

5.9.4. Methodological Closure

The chapter's third conclusion is methodological: the model is not a loose analogy. It is a staged measurement pipeline. Heterogeneous variables are first transformed into comparable pressure-oriented coordinates. These coordinates are standardized and used to build a correlation-based metric tensor. The tensor supports Ricci-style component curvature and scalar curvature summaries. The pressure-curvature system is then summarized through F/W functional diagnostics and converted into a graph-topological layer for connectedness, cycles and bottleneck interpretation.

The methodology is therefore internally closed. Every major result has a corresponding methodological operation. Pressure values come from the stress-coordinate layer. Curvature values come from metric and component-deformation logic. F/W values come from the functional layer. Betti and algebraic-connectivity results come from the graph layer. Counterfactual and validation results come from sensitivity and econometric-audit layers. This one-to-one connection is what makes the chapter suitable for a monograph rather than a descriptive report.

Equation (5.9.5). Pipeline: X -> S -> Z -> G_{metric} -> R^{econ} -> F/W -> Graph -> Validation -> Claim

Table 5.9.4. Methodology-to-result closure

Methodological block	Result it supports	Conclusion
0-100 stress scaling	Comparable pressure-oriented variables.	Raw units are not added directly.
Metric tensor	Coordinate-coupling structure.	The inequality system is empirically coupled.
Ricci-style curvature	Component and scalar deformation results.	Pressure-smoothing imbalance can be decomposed.
Perelman F/W functionals	Energy-like and entropy-like system diagnostics.	Crisis and recovery can be read beyond pressure alone.
Graph topology	Connectivity, cycles, bottlenecks and node embeddedness.	Inequality pressure circulates through an interdependent network.
Validation battery	Econometric, PCA, regularization, regime, forecast and uncertainty checks.	Evidence is layered and bounded, not overclaimed.

5.9.5. Results Closure: Pressure, Curvature, Entropy and Topology

The chapter's fourth conclusion is empirical. The result architecture identifies 2020 as the strongest crisis-deformation year. In that year, global pressure rises to 38.079, scalar curvature falls to 6.216 and the W-functional reaches 508.023. The joint movement is important: crisis deformation is not shown by a single indicator. It is jointly visible through higher pressure, weaker curvature/smoothing and higher entropy-like complexity.

By 2024, pressure declines to 30.314 and scalar curvature rises to 10.264. This supports a partial recovery interpretation. However, the W-functional remains elevated at 488.759 and regional dispersion persists. The correct conclusion is therefore not full convergence. It is recovery with residual complexity. This distinction is one of the chapter's most important scientific safeguards.

The graph-topological results reinforce the same interpretation. The sixteen-variable diagnostic graph is connected and cycle-rich, with beta_0 = 1, algebraic connectivity lambda_2 = 0.994 and beta_1 = 72. This indicates that inequality pressure is not isolated in one channel. It circulates through a dense network of macro-social dependencies.

Equation (5.9.6). Crisis deformation_{2020} = P_{2020} high + R_{2020} low + W_{2020} high

Equation (5.9.7). Partial recovery_{2024} = P_{2024} < P_{2020} and R_{2024} > R_{2020} while W_{2024} remains elevated

Table 5.9.5. Headline empirical closure

Result block	Key value or evidence	Final conclusion
2020 crisis pressure	Global pressure = 38.079.	The model identifies 2020 as the strongest pressure shock in the reported path.
2020 curvature	Scalar curvature = 6.216.	Smoothing capacity weakens during crisis deformation.
2020 W-functional	W = 508.023.	Crisis appears as entropy-like complexity, not only stress level.
2024 pressure	Global pressure = 30.314.	Pressure declines after the crisis deformation.
2024 curvature	Scalar curvature = 10.264.	Curvature/smoothing improves by the terminal year.
2024 W-functional	W remains elevated at 488.759.	Recovery is partial and still complex.
Graph connectedness	16 nodes, 87 edges, beta_0 = 1, lambda_2 = 0.994, beta_1 = 72.	The stress-coordinate system is connected, dense and looped.
Component concentration	Top components concentrate curvature energy, especially investment, productivity, technology, unemployment and fiscal pressure.	Inequality cannot be reduced to Gini alone.

5.9.6. Interpretation Closure: Deformation, Smoothing and Recovery

The chapter's fifth conclusion is interpretive. The model shows that inequality deformation should be read as a system state rather than as a single annual movement. The 2020 shock represents a crisis-deformation state in which pressure rises, smoothing weakens and complexity peaks. The 2024 state represents a partial smoothing recovery because pressure falls and curvature improves, but elevated W-functional complexity and persistent regional gaps prevent a full-convergence interpretation.

The regional interpretation is also disciplined. All regions show improvement in pressure and curvature between 2010 and 2024 and post-shock recovery from 2021 to 2024. Yet regional hierarchy remains visible: Sub-Saharan Africa remains the highest-pressure region in 2024, while Europe remains the lowest-pressure and highest-curvature region. The chapter therefore concludes that recovery is real but uneven. The world system smooths partially, but it does not collapse into regional equality.

Table 5.9.6. Interpretation closure matrix

Interpretive question	Chapter 5 answer	Reason
Was 2020 a crisis-deformation year?	Yes.	Pressure, curvature and W-functional all identify a strong deformation state.
Did the system recover by 2024?	Partially.	Pressure declines and curvature improves relative to 2020.
Did the system fully converge?	No.	W-functional complexity and regional dispersion remain elevated.
Are all variables equally important?	No.	Curvature energy is concentrated in capital, productivity, technology, labour and fiscal channels.
Is inequality a single-index problem?	No.	The graph shows connected, cycle-rich multi-channel structure.
Can the chapter support policy prescriptions?	Only diagnostic screening.	Counterfactuals and surgery rankings are not causal treatment effects.

5.9.7. Scientific Contribution Closure

The chapter contributes a new measurement architecture for global inequality diagnostics. Its theoretical contribution is the disciplined translation of Perelman-Ricci-Poincare logic into economic measurement. Its methodological contribution is the full chain from stress coordinates to metric tensor, Ricci-style curvature, Perelman-type functionals, graph topology and validation. Its empirical contribution is the documented crisis-deformation and recovery path. Its interpretive contribution is the distinction between recovery and convergence.

The contribution is strongest because it is bounded. The chapter does not ask the reader to accept mathematical analogy by authority. It provides an auditable pipeline, explicit data structure, numerical results, counterfactuals, validation and limitations. That combination makes the contribution suitable for a monograph on seven bounded economic-econometric analogues of the Millennium Problems.

Table 5.9.7. Scientific contribution closure

Contribution type	Specific contribution of Chapter 5	Why it matters
Theoretical	Recasts global inequality as a pressure-smoothing manifold.	Expands inequality analysis beyond distributional indicators.
Methodological	Integrates metric tensor, Ricci-style curvature, F/W functionals and graph topology.	Creates a reproducible mathematical-econometric pipeline.
Empirical	Identifies 2020 crisis deformation and 2024 partial recovery.	Provides measurable global inequality-system dynamics.
Topological	Shows connected and cycle-rich structure among sixteen stress coordinates.	Explains why inequality channels interact rather than remain isolated.
Validation	Adds econometric screens, robustness, PCA, regularization, rolling validation and uncertainty bands.	Prevents constructed-index overclaiming.
Monograph-level	Sets the first model-chapter template for bounded Millennium-inspired analogues.	Prepares the structure for Hodge, Navier-Stokes, Yang-Mills, BSD, Riemann/Zeta

		and P vs NP chapters.

5.9.8. Claim Boundary and Limitation Closure

The final claim boundary is precise. Chapter 5 supports a high-level diagnostic measurement claim: a Perelman-Ricci-Poincare-inspired economic analogue can organize global inequality evidence into pressure, smoothing, curvature, entropy, graph and validation layers. It does not support theorem-level mathematical claims, unrestricted causal identification, country-level welfare ranking or universal forecasting superiority.

This boundary is not a reduction of the chapter's value. It is the condition of its scientific credibility. The model's strength lies in its ability to transform complex macro-social evidence into a structured and auditable diagnostic architecture while preserving strict limits on what that architecture can prove.

Equation (5.9.8). Admissible claim = Evidence strength x Boundary discipline

Table 5.9.8. Final claim-boundary closure

Claim category	Final status	Reason
Diagnostic-measurement architecture	Permitted and central.	The chapter constructs and audits a complete pressure-curvature-topology pipeline.
Perelman/Ricci/Poincare theorem proof	Excluded.	Economic variables are constructed analogues, not theorem objects.
Causal effect estimation	Not claimed.	Validation screens do not constitute causal identification.
Country-level welfare ranking	Not claimed.	The design is macro-regional.
Forecast superiority	Not claimed.	AR(1) benchmark discipline constrains forecast claims.
Policy recommendation	Diagnostic only.	Counterfactuals and Ricci-surgery rankings flag channels, not effects.

5.9.9. Replication, Auditability and Book-Level Integration

The chapter also closes with a replication conclusion. The source manuscript's data and replication package makes the reported architecture auditable. The package supports source tracing, formula reconstruction, reported-table verification and reproducibility review. In the book, this replication discipline connects Chapter 5 to the monograph-wide Chapter 4 protocol on public-data anchors, author-calculated variables, normalization, validation and Zenodo discipline.

The important book-level implication is that Chapter 5 is not an isolated article inserted into the monograph. It has been transformed into a model chapter with the same architecture used throughout Part II: translated mathematical logic, defined economic object, constructed empirical architecture, methodological pipeline, results, interpretation, scientific contribution, limitations and conclusion.

Table 5.9.9. Integration with the monograph architecture

Monograph layer	How Chapter 5 contributes
Chapter 1 general introduction	Provides the first applied example of Millennium-problem logic as economic measurement architecture.
Chapter 2 conceptual translation	Shows a bounded translation from Poincare/Ricci/Perelman logic into inequality diagnostics.
Chapter 3 literature review	Applies inequality, curvature, graph-topology and econometric-validation literatures.
Chapter 4 unified methodology	Implements data architecture, normalization, graph construction, validation, replication and claim discipline.
Part II model chapters	Establishes the problem-chapter structure followed by the remaining six models.
Chapter 14 limitations	Feeds chapter-specific limitations into the general limitation architecture.
Chapter 15 general conclusion	Supplies one of the seven bounded analogue conclusions for the final synthesis.

5.9.10. Bridge to Chapter 6: From Curvature Diagnostics to Flow Decomposition

Chapter 5 closes the first model chapter by showing that global inequality can be read as a pressure-smoothing system with curvature-like and topology-like diagnostics. Chapter 6 shifts the mathematical grammar from Ricci/Perelman/Poincare logic to Hodge logic. The next chapter therefore asks a different but related question: if Chapter 5 measures deformation and smoothing capacity, Chapter 6 decomposes macroeconomic flow into hierarchy, local-cycle imbalance and harmonic circulation.

The bridge is conceptually natural. Both chapters treat the world economy as a structured system rather than as a list of isolated aggregates. Chapter 5 uses a sixteen-variable diagnostic graph; Chapter 6 uses a regional flow network. Chapter 5 reads crisis deformation through pressure, curvature and entropy; Chapter 6 reads macro-flow structure through gradient, curl and harmonic components. Together they begin the book's transition from inequality-curvature diagnostics to topological flow decomposition.

Table 5.9.10. Bridge from Chapter 5 to Chapter 6

Dimension	Chapter 5: Perelman/Ricci/Poincare	Chapter 6: Hodge
Core economic object	Global inequality pressure-smoothing manifold.	Regional macro-flow network.
Mathematical grammar	Curvature, entropy and connectedness.	Gradient, curl and harmonic decomposition.
Main constructed object	Stress-coordinate diagnostic graph and curvature functionals.	Directed macro-flow pressure cochain.
Central question	How does inequality pressure deform and partially recover?	How does the world economy decompose into hierarchy, imbalance and circulation?
Evidence role	Crisis deformation, recovery path, graph connectedness.	Flow decomposition, resilience, shock transmission and topology.
Book-level continuity	Shows structural pressure and smoothing capacity.	Shows structural flow components and circulation.

5.9.11. Final Integrated Evidence Matrix

The final integrated evidence matrix summarizes the chapter's closure. Each evidence layer supports a specific type of conclusion and retains a specific limitation. This is the chapter's final evidence map before the monograph proceeds to the Hodge-econometric model.

Table 5.9.11. Final integrated evidence matrix for Chapter 5

Evidence layer	Main finding	Concluding interpretation	Boundary
Pressure path	2020 pressure peak and 2024 pressure decline.	Crisis deformation followed by partial pressure relief.	Not full convergence.
Curvature path	2020 curvature fall and 2024 curvature improvement.	Smoothing weakens during crisis and improves later.	Curvature is economic and diagnostic.
W-functional	W peaks in 2020 and remains elevated in 2024.	Complexity persists after pressure decline.	No Perelman monotonicity claim.
Component decomposition	Capital, productivity, technology, unemployment and fiscal channels dominate.	Inequality is multi-channel and structurally concentrated.	Component rankings are model-implied.
Graph topology	Connected, dense, looped graph.	Stress coordinates are interdependent.	Graph topology, not theorem proof.
Counterfactuals	Capacity improvements reduce pressure; adverse shocks raise it.	Internal sign logic is coherent.	No treatment-effect estimate.
Econometric validation	Panel, PCA, regularization, threshold/regime and leave-one-out screens support structure.	Constructed diagnostics retain empirical coherence.	Association/validation only.
Forecast discipline	Benchmark comparison constrains predictive claims.	The chapter is diagnostic rather than forecast-dominance oriented.	No universal forecasting

			superiority.

5.9.12. Final Chapter Conclusion

Chapter 5 concludes that global inequality can be modelled as a structured pressure-smoothing diagnostic system. The Perelman-Ricci-Poincare-inspired architecture successfully converts heterogeneous macro-regional variables into a common stress-coordinate system, builds a metric-coupling layer, constructs Ricci-style curvature diagnostics, summarizes system energy and complexity through F/W functionals, audits connectedness and cycles through graph topology, and evaluates the resulting indicators through validation, robustness, counterfactual and uncertainty layers.

The substantive result is clear. The global inequality system experiences its strongest crisis deformation in 2020, when pressure rises, curvature weakens and W-functional complexity peaks. By 2024, pressure falls and curvature improves, indicating partial smoothing recovery. Yet elevated W-functional complexity and persistent regional dispersion prevent a full-convergence interpretation. The chapter therefore identifies recovery with persistence rather than simple normalization.

The structural result is equally important. Inequality deformation is not driven by one variable alone. Curvature energy concentrates in investment, productivity, technology access, unemployment and fiscal-pressure channels, while the diagnostic graph is connected, dense and looped. This means that global inequality pressure circulates through a network of interacting macro-social channels. The chapter's strongest policy-relevant message is not a prescription, but a diagnostic principle: inequality monitoring should track pressure, smoothing capacity, deformation, complexity and topology together.

The final admissible claim is high but bounded. Chapter 5 provides a reproducible Perelman-Ricci-Poincare-inspired economic-econometric framework for global inequality diagnostics. It does not prove, test or replicate Perelman's proof, Ricci-flow theory or the Poincare conjecture. It does not establish unrestricted causality, country-level welfare ranking, policy treatment effects or universal forecast superiority. Its contribution is precisely that it demonstrates how a Millennium-problem architecture can become a disciplined economic measurement model without exceeding the evidence.

This completes the first model chapter of Part II. The monograph now moves from inequality deformation and smoothing capacity to Hodge-econometric flow decomposition, where the focus shifts from curvature and entropy to hierarchy, local imbalance and harmonic circulation in the world economy.

Table 5.9.12. Final conclusion closure statement

Final conclusion dimension	Closed statement
Chapter-level conclusion	Global inequality can be represented and audited as a pressure-smoothing diagnostic manifold.
Empirical conclusion	The model identifies 2020 as the dominant crisis-deformation year and 2024 as partial recovery with persistent complexity.
Methodological conclusion	Metric tensor, Ricci-style curvature, F/W functionals and graph topology form one coherent measurement pipeline.
Scientific contribution	The chapter adds a reproducible mathematical-econometric architecture for global inequality diagnostics.
Claim boundary	The chapter supports bounded diagnostic interpretation, not theorem proof, causality, welfare ranking or forecast dominance.
Transition to next chapter	The book proceeds from pressure-curvature diagnostics to Hodge flow decomposition.

Chapter 6. Hodge-Econometric Modelling of the World Economy

6.1. Hodge Theory as an Economic Decomposition Grammar

This section establishes the conceptual and methodological grammar through which Hodge theory is translated into an economic-econometric model of the world economy. Its purpose is not to repeat the full methodological chapter of the source study, nor to present the final empirical results of Chapter 6.5. Its task is narrower and foundational: to explain why a regional economy represented as a weighted macro-flow network can be decomposed into hierarchy, local-cycle imbalance and persistent systemic circulation, and why those three components create a more informative measurement language than GDP mass alone.

The source study develops a regional Hodge-econometric benchmark in which official public macroeconomic anchors are transformed into a weighted graph, a directed edge-pressure field and a discrete Hodge decomposition. The empirical object

contains the World normalization anchor and ten regional nodes, including the Caucasus as an explicit corridor-sensitive subregional node. The benchmark result later reported in the chapter is that the graph is connected and cycle-rich, and that total macro-flow energy decomposes into gradient hierarchy, curl/local-cycle imbalance and harmonic/systemic circulation. In this monograph, Section 6.1 converts that architecture into a general research grammar for the book.

Table 6.1.1. Function of Section 6.1 within Chapter 6

Chapter element	Role in the book chapter	Reason for inclusion in 6.1
Chapter 6 title	Defines the Hodge-econometric model as the second major Millennium-inspired economic model after Perelman/Ricci/Poincare.	Positions the chapter inside Part II of the monograph.
Section 6.1	Explains Hodge theory as a decomposition grammar for macroeconomic flow structure.	Provides the conceptual bridge before data, network construction and results.
Section 6.2	Defines the world economy as a regional macro-flow network.	Uses the grammar from 6.1 to specify the empirical object.
Section 6.3	Builds the World anchor, ten-node system and Caucasus visibility layer.	Operationalizes the decomposition grammar on public-data anchors.
Section 6.4	Specifies directed edge pressure and discrete Hodge decomposition.	Turns the conceptual grammar into a computational methodology.
Sections 6.5-6.8	Report results, interpretation, validation and chapter conclusion.	Use the grammar to interpret gradient, curl and harmonic findings without overclaiming.

6.1.1. From Scalar Macroeconomic Ranking to Decomposable Structure

The starting point of the Hodge-econometric chapter is a measurement objection to conventional macroeconomic comparison. Standard global macroeconomic description often ranks regions by GDP, world-output share, projected growth or income depth. These indicators are necessary public anchors, but they remain scalar or node-based. They identify the magnitude of a region, not the structure of its relation to other regions. They cannot by themselves distinguish whether a region is a hierarchical core, a local imbalance generator, a corridor bridge, a systemic circulation node, a shock-transmission channel or a resilience buffer.

Hodge theory supplies a decomposition language for this problem. In its applied discrete form, it asks whether a directed edge signal on a graph can be separated into different structural components. In the economic translation, the edge signal is not a physical flow and not an observed transaction matrix. It is an author-calculated macro-flow pressure field derived from public-data anchors and corridor logic. Once the field is placed on a connected regional graph, the decomposition separates three kinds of macroeconomic structure that scalar ranking normally collapses into one number.

(6.1) macro-structure ≠ GDP mass only

Equation 6.1 is not a mathematical theorem; it states the measurement principle of the chapter. Output mass remains an indispensable anchor, but it is insufficient as a complete representation of regional macro-flow structure.

Table 6.1.2. Why GDP mass is not sufficient for the Hodge chapter

Measurement dimension	What GDP-style ranking captures	What Hodge-econometric decomposition adds
Scale	Relative output size and world-share position.	Separates size from flow hierarchy and corridor exposure.
Growth momentum	Projected or realized expansion rates.	Shows whether growth creates directional pressure along regional

Measurement dimension	What GDP-style ranking captures	What Hodge-econometric decomposition adds
		edges.
Regional imbalance	Usually inferred from divergence in income or growth.	Measures curl around local cycles and near-triangular corridors.
Systemic circulation	Usually hidden in bilateral narratives or aggregate statistics.	Measures harmonic residuals that persist after hierarchy and local curl are removed.
Caucasus visibility	Often absorbed into larger Europe/Central Asia categories.	Retains the Caucasus as an explicit corridor-sensitive node.
Validation	Often reduced to descriptive ranking or regression.	Combines spectral, econometric, ML and persistent-homology diagnostics.

6.1.2. The Hodge Grammar: Gradient, Curl and Harmonic Components

The economic decomposition grammar rests on three interpretive components. The gradient component represents directional hierarchy. It is the part of the edge-pressure field that can be explained by a node potential: high-potential regions and low-potential regions create directional pressure across the network. The curl component represents local-cycle imbalance. It is the part of the edge-pressure field that circulates around triangles or near-triangular corridors and therefore cannot be reduced to a simple global ranking. The harmonic component represents persistent systemic circulation. It remains after hierarchical gradient and local curl have been removed, indicating circulation that is global or cycle-spanning rather than merely local.

This grammar is especially useful for the world economy because international macroeconomic structure is neither a pure hierarchy nor a random set of bilateral differences. Large regions may dominate the gradient component; fast-growing or corridor-sensitive regions may contribute to local curl; and persistent circulation may reflect structural dependence that is not captured by output mass or local imbalance alone. The analytical gain is therefore not decorative mathematics; it is the ability to assign different economic meanings to different kinds of relational pressure.

(6.2) $y = y^{grad} + y^{curl} + y^{harm}$

Here y denotes the directed macro-flow pressure field on the regional edge set. The three terms denote, respectively, gradient hierarchy, curl/local-cycle imbalance and harmonic/systemic circulation.

(6.3) $y^{grad} = B_1^T\varphi;\ y^{curl} = B_2\psi;\ B_1 y^{harm} = 0;\ B_2^T y^{harm} = 0$

This expression summarizes the discrete Hodge logic. B1 is the node-edge incidence structure, B2 is the triangle-edge boundary structure, phi is the node-potential vector and psi is the local-cycle potential. The harmonic part is divergence-free and curl-free within the chosen complex.

Table 6.1.3. Core Hodge-economic translation matrix

Hodge object	Mathematical role	Economic interpretation in Chapter 6	Claim discipline
Node potential phi	Assigns scalar potential to vertices.	Regional hierarchy, productive depth or macroeconomic standing.	Constructed index, not official ranking.
Gradient flow	Edge field generated by differences in node potential.	Hierarchical macro-flow pressure between regions.	Measures hierarchy; does not prove causality.
Curl flow	Circulation around filled triangles/local cycles.	Local-cycle imbalance among regional corridors.	Requires sufficient cycle structure; not a welfare label.
Harmonic flow	Residual circulation not explained by gradient or	Persistent systemic circulation	Benchmark structural evidence,

Hodge object	Mathematical role	Economic interpretation in Chapter 6	Claim discipline
	local curl.	across the regional graph.	not universal global law.
Hodge Laplacian	Operator linking incidence, boundary and flow structure.	Spectral audit of whether the graph supports decomposition.	Diagnostic adequacy tool, not a theorem proof.
Persistent homology	Tracks cycles across filtration thresholds.	Checks whether circulation survives edge filtering.	Validation layer, not final causal identification.

6.1.3. Economic Meaning of the Directed Macro-Flow Pressure Field

The decomposition becomes possible only after the world economy is represented as a graph carrying a directed edge signal. The graph contains regional nodes and weighted links. The edge signal is the directed macro-flow pressure field. It is important to define this object carefully. It is not an observed bilateral trade matrix, not a foreign-direct-investment matrix, not a migration matrix, and not a physical flow. It is a reproducible author-calculated edge cochain constructed from public regional macroeconomic anchors, including regional output mass, world-output share, projected growth, transition GDP, income depth and corridor-sensitive link logic.

This distinction is central to the credibility of Chapter 6. The model does not pretend that official sources already publish Hodge hierarchy, curl imbalance or harmonic circulation. It treats public data as anchors and constructs the Hodge variables through an explicit methodology. The economic question is therefore not whether the pressure field is a direct observation of all flows, but whether it is a transparent, auditable and analytically useful proxy for regional macro-flow pressure.

(6.4) $G = (V, E, W); |V| = 10; y \in C^1(E)$

The regional graph G has a node set V, edge set E and weighted adjacency structure W. The directed pressure field y is a 1-cochain on the edge set. The World row is used as a normalization anchor but is not treated as an ordinary competing node in the Hodge edge field.

(6.5) $y_{ij} = \Omega(M_i, M_j, g_i, g_j, I_i, I_j, C_{ij})$

The edge-pressure value is a function of regional mass M, growth or transition momentum g, income-depth or fragility I, and corridor/link logic Cij. The specific source-study implementation is author-calculated and auditable.

Table 6.1.4. Public anchors and constructed Hodge variables

Layer	Examples in the Hodge chapter	Status in the monograph	Reviewer-safe interpretation
Public anchor layer	GDP, world share, projected growth, transition GDP, GDP per capita.	Input data layer.	Official or public-source macroeconomic anchors.
Regional node layer	EAP, NAM, EUR, LAC, SAS, MENA, SSA, OCE, CAS, CAU.	Empirical regional benchmark.	Complete regional prototype, not all-country panel.
Graph layer	Weighted regional network, 10 nodes and 27 edges in the benchmark.	Author-calculated topology.	Relational structure derived from stated rules.
Edge cochain layer	Directed macro-flow pressure yij.	Author-calculated decomposable signal.	Proxy pressure field, not observed dyadic transaction flow.
Decomposition layer	Gradient, curl and harmonic components.	Hodge-derived analytical variables.	Structural measurement, not

Layer	Examples in the Hodge chapter	Status in the monograph	Reviewer-safe interpretation
			theorem-level proof.
Validation layer	Spectral diagnostics, econometrics, ML and persistent homology.	Evidence audit.	Benchmark validation, not final causality.

6.1.4. Why Hodge Theory Fits the Economic Problem

Hodge theory is appropriate for Chapter 6 because the economic problem is not merely to rank regions but to decompose relational pressure. A simple ranking can say that one region is larger than another; it cannot say whether the difference is hierarchical, locally inconsistent or systemically circulatory. A standard regression can test whether a variable is associated with another variable; it does not automatically begin by decomposing the relational field that connects all regions. Hodge decomposition begins exactly where the economic problem requires it to begin: with a directed edge field on a connected graph.

The regional world economy is suited to this logic because it contains both hierarchy and cycles. Output mass creates hierarchy; growth differences create directional pressure; corridor links create local loops; and global interdependence may create persistent circulation. The source study reports that the benchmark graph is connected and cycle-rich, with 10 nodes, 27 edges, density equal to 0.600 and transitivity equal to 0.740. Those properties matter because Hodge decomposition is not meaningful on a disconnected or trivial graph. A connected, cycle-rich network can support gradient, curl and harmonic interpretation.

(6.6) $E_total = ||y^{grad}||^2 + ||y^{curl}||^2 + ||y^{harm}||^2$

Energy accounting converts the decomposition into empirical shares. In the source benchmark, the reported shares are 49.69 percent gradient hierarchy, 36.22 percent curl/local-cycle imbalance and 14.09 percent harmonic/systemic circulation.

Table 6.1.5. Empirical adequacy conditions implied by the Hodge grammar

Adequacy condition	Why it is required	How it appears in the Chapter 6 source architecture
Connected graph	Disconnected regions would prevent system-wide interpretation.	The benchmark graph contains one connected component.
Non-trivial edge set	Too few edges would reduce the network to a tree-like structure.	The benchmark contains 27 weighted edges.
Cycle-rich topology	Curl and harmonic components require cycles or higher-order structure.	Density 0.600 and transitivity 0.740 support cycle-based diagnostics.
Directed edge signal	Hodge decomposition operates on flows or edge cochains.	Macro-flow pressure is constructed as an anti-symmetric edge field.
Public-anchor traceability	Constructed variables must be auditable.	GDP, share, growth, transition GDP and income depth anchor the graph.
Validation discipline	Decomposition alone is not enough for inference.	Econometric, ML and persistent-homology checks are used as benchmark validation.

6.1.5. The Three Economic Components

The first component, gradient hierarchy, is the part of the macro-flow pressure that can be represented by differences in regional node potential. It corresponds to the economic intuition that some regions exert stronger structural pull or pressure because of output mass, productive depth, income position or growth momentum. If the world economy were only hierarchical, the directed edge field would be almost fully explained by node potentials. In that case, a ranking-like model would be nearly sufficient. The source results show that gradient hierarchy is large but not exhaustive.

The second component, curl or local-cycle imbalance, is the part of the edge field that circulates around local cycles. Economically, this captures regional triangular tensions, corridor imbalances and inconsistency among pairwise relations. A region may appear balanced in one bilateral comparison and imbalanced in another, producing circulation around a local loop. Curl therefore captures the fact that regional macroeconomic relations are not always transitive in a simple hierarchy. The third component, harmonic systemic circulation, is the most globally structural component. It is not explained by local potential differences and not absorbed by local triangles. Economically, it represents persistent circulation across the system: a residual global flow layer that survives after hierarchy and local-cycle imbalance have been removed. It is conceptually important because it shows that part of the world economy may function as systemic circulation rather than as ranking or local inconsistency.

Table 6.1.6. Interpretation of the three Hodge components

Component	Economic name	What it measures	What it does not claim
Gradient	Regional hierarchy	The part of directed pressure explained by node potential differences.	It is not a complete GDP ranking and not a causal hierarchy.
Curl	Local-cycle imbalance	The part of pressure circulating around regional cycles and triangular corridors.	It is not a policy failure label and not a literal physical vortex.
Harmonic	Systemic circulation	The persistent residual circulation after hierarchy and local curl are removed.	It is not a proof of the Hodge Conjecture and not a universal law.

6.1.6. Hodge Theory and the Caucasus Visibility Problem

One of the most important reasons for using a Hodge-econometric grammar is the visibility of corridor-sensitive regions. In GDP-centered regional classifications, a small subregion may disappear inside a larger aggregate. The Caucasus is an example. Its output mass is modest relative to East Asia and Pacific, North America or Europe, but its corridor position can be relevant for logistics, energy, Black Sea-Caspian connectivity, Europe-Central Asia interfaces and shock transmission. Hodge decomposition allows such a region to be interpreted through position and flow role, not only through output size. This does not mean that the Caucasus is artificially elevated to the same output scale as major regions. The claim is more disciplined: a small node can be analytically visible if the model measures hierarchy, imbalance, circulation, centrality, resilience and tail exposure separately. The Hodge grammar therefore protects the model from two opposite errors. The first error is GDP reductionism, which hides small corridor regions. The second error is narrative overstatement, which asserts corridor importance without measurable structure. The Hodge chapter avoids both by requiring graph construction, edge pressure, decomposition and validation.

Table 6.1.7. GDP reductionism versus Hodge visibility

Issue	GDP-centered reading	Hodge-econometric reading	Claim boundary
Small output share	May imply low importance.	May still coexist with corridor, imbalance or circulation relevance.	Visibility is structural, not output equivalence.
Corridor role	Often described qualitatively.	Can be encoded through graph links and edge-pressure structure.	Requires transparent edge rules.
Regional aggregation	May absorb the Caucasus into larger blocs.	Retains Caucasus as an explicit node.	Author-defined subregional design.
Shock transmission	Not visible in static GDP ranking.	Can be assessed through centrality, circulation and propagation diagnostics.	Diagnostic, not deterministic prediction.

6.1.7. Relationship to the Hodge Conjecture and Claim Boundary

The word Hodge in this chapter must be read with strict claim discipline. The Hodge Conjecture is a pure mathematical Millennium Problem concerning algebraic cycles and Hodge classes on projective algebraic varieties. Chapter 6 does not attempt to solve, test or replicate that conjecture. It does not claim that macroeconomic regions are algebraic varieties, that economic corridors are algebraic cycles, or that a regional graph supplies a theorem-level result in algebraic geometry.

The permissible translation is discrete, computational and econometric. Hodge-type decomposition is used as a finite-graph measurement device. The economic object is a weighted regional graph and a directed edge cochain; the analytical operation is a discrete decomposition of edge pressure; the empirical claim is that the decomposition provides interpretable and validated macroeconomic diagnostics. This claim is strong enough to matter for economic measurement and cautious enough to remain academically admissible.

(6.7) Hodge Conjecture proof ↛ Chapter 6; Chapter 6 → discrete Hodge-econometric analogue

Equation 6.7 states the chapter boundary: the monograph uses a Hodge-inspired decomposition grammar but does not enter theorem-proof territory.

Table 6.1.8. Claim-boundary matrix for the Hodge translation

Possible wording	Admissible?	Reason
The chapter solves the Hodge Conjecture.	No.	The model is an economic analogue on a finite regional graph, not a theorem in algebraic geometry.
The chapter proves that GDP is irrelevant.	No.	GDP remains a public-data anchor; the claim is that GDP alone is insufficient.
The chapter measures gradient hierarchy, curl imbalance and harmonic circulation in a regional benchmark.	Yes.	These are constructed Hodge-econometric variables derived from the stated pipeline.
The Caucasus is made visible as a corridor-sensitive node.	Yes, with caution.	Visibility means analytical inclusion and structural diagnosis, not output-scale equivalence.
The benchmark establishes final causal claims for all countries and all dyadic flows.	No.	The source model is a regional benchmark requiring all-country, dyadic and longitudinal replication for stronger claims.
The chapter provides a reproducible measurement architecture for future replication.	Yes.	This is the central scientific contribution of the Hodge chapter.

6.1.8. Place of Section 6.1 in the Chapter 6 Evidence Chain

Section 6.1 is the conceptual gateway to the full Hodge chapter. Section 6.2 will define the empirical research object: the world economy as a regional macro-flow network. Section 6.3 will specify the data and network construction: World anchor, ten regional nodes, edge construction and Caucasus visibility. Section 6.4 will formalize directed edge pressure and discrete Hodge decomposition. Section 6.5 will report the empirical decomposition results, including the energy shares of gradient hierarchy, curl imbalance and harmonic circulation. Section 6.6 will interpret why the world economy is not reducible to GDP mass. Section 6.7 will evaluate robustness, machine learning and persistent homology. Section 6.8 will close the chapter.

The logical status of Section 6.1 is therefore foundational. It does not yet assert the final result; it defines the grammar that makes the result interpretable. Without this section, the reader would see Hodge terminology as an imported mathematical metaphor. With this section, the reader sees a disciplined translation: public data become node attributes; node attributes build a weighted graph; the graph carries directed edge pressure; the edge pressure decomposes into interpretable components; and those components are validated and bounded by claim discipline.

Table 6.1.9. Section 6.1 bridge to the remaining Chapter 6 structure

Next section	Question answered	How 6.1 prepares it
6.2 Research object	What exactly is being modeled?	Defines the economy as a decomposable regional flow structure.
6.3 Data and network construction	How are World anchor, nodes and edges built?	Explains why graph construction is necessary before decomposition.
6.4 Methodology	How is directed pressure decomposed?	Defines gradient, curl and harmonic components.
6.5 Results	What does the decomposition show?	Prepares interpretation of 49.69%, 36.22% and 14.09% energy shares.
6.6 Interpretation	Why is GDP mass insufficient?	Clarifies that size, hierarchy, imbalance and circulation are different dimensions.
6.7 Validation	Are results stable and informative?	Frames robustness, ML and persistent homology as evidence gates.
6.8 Conclusion	What is the chapter contribution?	Sets the final contribution as bounded Hodge-econometric measurement architecture.

6.1.9. Mini-Synthesis: The Hodge-Econometric Grammar in One Statement

The Hodge-econometric grammar can be summarized in one integrated statement: the world economy is represented as a connected regional graph; public macroeconomic anchors are transformed into author-calculated edge pressure; the directed edge field is decomposed into gradient hierarchy, curl imbalance and harmonic circulation; the resulting variables are interpreted as structural diagnostics of macroeconomic organization; and all claims are bounded as benchmark measurement evidence rather than theorem proof or universal causality.

(6.8) public anchors → graph → directed pressure → Hodge decomposition → validated structural diagnostics

Equation 6.8 states the research pipeline that governs Chapter 6.

Table 6.1.10. Final conceptual closure of Section 6.1

Element	Closure statement
Economic object	The world economy is treated as a regional macro-flow topology, not only as a set of output aggregates.
Mathematical grammar	Discrete Hodge decomposition separates directed edge pressure into gradient, curl and harmonic components.
Main interpretive gain	Hierarchy, local imbalance and systemic circulation become separately measurable.
Caucasus relevance	A corridor-sensitive subregion can be retained and evaluated without overstating output size.
Empirical discipline	Public anchors are separated from author-calculated Hodge variables.
Claim boundary	The chapter does not solve the Hodge Conjecture and does not close universal causal inference.
Bridge forward	The next section specifies the research object: the world economy as a regional macro-flow network.

Source-note for this drafted section: Author synthesis based on Global Hodge-Econometric Modeling of the World Economy, especially the research context, research object, aim/objectives, methodology logic, results summary and claim-boundary passages, adapted for the monograph structure of Chapter 6.

6.2. Research Object: The World Economy as a Regional Macro-Flow Network

This section defines the research object of Chapter 6. The object is not world GDP as a single aggregate, not a country ranking, and not a literal map of all bilateral trade or financial transactions. It is the regional structure of the world economy represented as a weighted, directed and topologically decomposable macro-flow network. The unit of analysis is the global region; the World aggregate is retained as a normalization anchor; and the Caucasus is preserved as an explicit corridor-sensitive subregional node so that a small but strategically positioned region is not analytically erased by broader regional aggregation.

The purpose of this section is to fix the empirical object before the data-construction and Hodge-decomposition sections begin. Section 6.1 established the conceptual grammar of Hodge decomposition. Section 6.2 now specifies what economic system carries that grammar: a ten-node regional benchmark, scaled by a World anchor, transformed into a regional macro-flow graph, and prepared for directed edge-pressure measurement. This object is deliberately bounded. It is a structural benchmark and proof-of-concept architecture, not a full all-country panel and not a transaction-level dyadic flow database.

Table 6.2.1. Function of Section 6.2 inside Chapter 6

Element	Role in Section 6.2	How it prepares the next sections
Research object	Defines the world economy as a regional macro-flow network rather than a scalar output table.	Provides the empirical object for data construction in 6.3.
Unit of analysis	Uses the global region as the observation unit and not the country.	Prevents false interpretation as a national ranking exercise.
World anchor	Supplies normalization, scale consistency and global benchmarking.	Separates scale reference from graph-node competition.
Ten-node regional set	Covers the global macro-core through major regional blocks and the Caucasus.	Defines the node set V for the graph.
Caucasus visibility	Keeps a corridor-sensitive subregion explicit instead of absorbing it into larger aggregates.	Allows later hierarchy, imbalance and circulation diagnostics to measure corridor position.
Boundary discipline	Clarifies that constructed Hodge indices are author-calculated diagnostic objects.	Protects later results from causal, theorem-level or official-indicator overclaiming.

6.2.1. Formal Definition of the Research Object

The research object is the regional world economy as a macro-flow network. The term “macro-flow” is used in a precise diagnostic sense. It does not claim that the chapter observes every actual shipment, payment, capital movement or migration flow. Instead, it defines a reproducible edge-pressure system derived from public macroeconomic anchors and stated regional-link rules. The object therefore has

three levels: public anchor variables, author-constructed network structure, and Hodge-derived decomposition variables.

This definition is necessary because Hodge decomposition requires an edge signal on a graph. A list of regional GDP values cannot be decomposed into gradient, curl and harmonic components by itself. The economy must first be represented as a graph whose nodes are regions and whose edges carry directed pressure. The research object is therefore neither only the node table nor only the edge table. It is the integrated node-edge-pressure complex that supports topological decomposition, spectral diagnostics and validation.

(6.6) Research object = {regional nodes, World anchor, weighted graph, directed edge-pressure field, Hodge-decomposition space}

Formula 6.6 summarizes the empirical object of Chapter 6. The object is not a single variable but a structured measurement system.

(6.7) $G^H = (V, E, W, y)$, with V = {EAP, NAM, EUR, LAC, SAS, MENA, SSA, OCE, CAS, CAU}

G^H denotes the Hodge-econometric regional graph. V is the ten-node regional set, E is the set of regional edges, W is the weighted adjacency structure and y is the directed macro-flow pressure field.

Table 6.2.2. Research-object definition matrix

Object component	Operational definition	Economic meaning	Boundary condition
World anchor	Global aggregate used for normalization, scale consistency and benchmarking.	Fixes the scale of the regional system.	Not an ordinary Hodge node and not a competing region.
Regional nodes	Ten macro-regional or corridor-sensitive nodes.	Defines the empirical coordinate system of the world-economy benchmark.	Regional benchmark, not all-country coverage.
Weighted graph	Regional network with author-calculated weighted links.	Represents structural connection and corridor-sensitive exposure.	Not an observed complete bilateral transaction matrix.
Directed edge pressure	Author-calculated edge cochain derived from macro anchors and orientation rules.	Carries the signal to be decomposed.	Diagnostic pressure field, not a literal physical flow.
Hodge space	Gradient, curl and harmonic decomposition of the edge field.	Separates hierarchy, local imbalance and systemic circulation.	Mathematical-econometric analogue, not Hodge conjecture proof.
Validation layer	Econometric, machine-learning, spectral and persistent-homology tests.	Audits whether the constructed objects retain empirical structure.	Benchmark validation, not unrestricted causality.

6.2.2. Unit of Analysis: Global Region Rather than Country

The unit of analysis is the global region. This is a deliberate design decision. A regional benchmark allows the chapter to build a complete, readable and auditable world-economy topology before moving to a more granular country-level or dyadic-flow extension. The ten-node structure is not a weakness hidden in the model; it is the empirical boundary of the chapter. It supports structural measurement, network topology, Hodge decomposition and benchmark validation, but it does not permit country-level causal claims.

The regional unit also aligns with the purpose of the monograph. Chapter 5 measured global inequality as a macro-regional pressure-smoothing manifold. Chapter 6 now measures the world economy as a regional macro-flow network. In both cases, the objective is not micro-level welfare evaluation but global-system architecture. The difference is that Chapter 5 works through pressure, curvature and graph connectedness, while Chapter 6 works through edge pressure, Hodge hierarchy, local-cycle imbalance and harmonic circulation.

(6.8) observation unit = global-region node $r \in V$, not country $c \in C$

This formula fixes the unit of analysis and prevents the regional benchmark from being interpreted as a country panel.

Table 6.2.3. Ten-node regional benchmark used in Chapter 6

Code	Regional node	Function in the research object
EAP	East Asia and Pacific	Large output and production-network region; major macro-mass reference.
NAM	North America	Advanced output-mass and financial-depth node.
EUR	Europe	Advanced macroeconomic and institutional region with strong systemic links.
LAC	Latin America and Caribbean	Regional macro block with growth, income and resilience variation.
SAS	South Asia	High-growth and high-transition-pressure regional node.
MENA	Middle East and North Africa	Energy, logistics and corridor-exposure region.
SSA	Sub-Saharan Africa	Developmental, demographic and growth-pressure regional node.
OCE	Oceania	Smaller but globally integrated regional node.
CAS	Central Asia	Transition and corridor-sensitive inland regional node.
CAU	Caucasus	Explicit author-defined corridor-sensitive subregional node retained for visibility.

6.2.3. The World Anchor as Normalization Device, Not as a Competing Node

The World anchor is essential but analytically distinct from the ten-node Hodge graph. It supplies scale consistency and global benchmarking. It allows regional GDP, world-output shares, transition GDP and income-depth variables to be interpreted relative to a common reference. However, the World anchor is not treated as an ordinary regional node in the Hodge edge field. If it were treated as a competing node, it would distort the topology because the World row is the aggregate reference that contains the regional system rather than a region located inside it.

The separation between World anchor and regional nodes is a key reviewer-safety device. It prevents double counting, avoids treating the aggregate as a peer observation, and clarifies how normalization

differs from graph construction. The benchmark can therefore begin from the whole world while still preserving a coherent regional graph for decomposition.

(6.9) World = Ω(V), but World ∉ V^H

The World aggregate summarizes the regional universe, but it is not an ordinary node in the Hodge edge field V^H.

(6.10) $x_r^* = N(x_r \mid \text{World anchor})$

Regional variables are normalized against the global anchor or global interval. The normalized quantity is an input to the Hodge pipeline, not an official institutional indicator.

Table 6.2.4. Analytical role of the World anchor

Role	How the World anchor is used	What it prevents
Scale consistency	Places regional values on a common global scale.	Prevents incompatible raw-unit comparison.
Benchmarking	Allows regional shares and transition values to be read relative to the world total.	Prevents isolated regional interpretation.
Normalization	Supports standardized or normalized input variables.	Prevents raw GDP, growth and income-depth units from being added directly.
Boundary discipline	Remains outside the ordinary Hodge node set.	Prevents the aggregate from being misread as a regional competitor.
Replication trace	Defines the reference row needed to reproduce the input table.	Prevents hidden scaling choices.

6.2.4. The Caucasus as a Corridor-Sensitive Research-Object Choice

The inclusion of the Caucasus as an explicit node is one of the distinctive design decisions of Chapter 6. In many regional classifications, the Caucasus can be absorbed into Europe, Central Asia, or broader Europe-Central Asia categories. Such aggregation may be administratively convenient, but it can hide the region's corridor function. The Hodge-econometric framework is designed precisely to measure roles that are not visible through output mass alone. The Caucasus is therefore retained not to inflate its economic size, but to test whether a corridor-sensitive node has measurable hierarchy, imbalance and circulation exposure inside the regional macro-flow topology.

This is a methodological point rather than a geopolitical claim. The chapter does not say that the Caucasus is comparable to East Asia and Pacific, North America or Europe in output scale. The admissible claim is narrower and stronger: a small-output region can still be analytically visible when the research object is a topology of flow pressure rather than a scalar GDP ranking. By retaining the Caucasus, the model tests whether corridor position can be measured without confusing position with size.

(6.11) GDP share small ≠ topological role zero

Formula 6.11 states the corridor-visibility principle of the chapter. It does not inflate output mass; it permits structural measurement beyond mass.

Table 6.2.5. Caucasus visibility logic

Dimension	Conventional aggregation problem	Hodge-econometric solution
Regional classification	Caucasus may be absorbed into broader Europe, Central Asia or ECA	Caucasus is retained as a distinct node CAU.

Dimension	Conventional aggregation problem	Hodge-econometric solution
	groupings.	
GDP ranking	Small output share can be misread as analytical irrelevance.	Output scale is separated from hierarchy, imbalance and circulation.
Corridor position	Logistics, transit and regional-interface roles may be treated narratively.	Corridor sensitivity is represented inside the network topology.
Hodge interpretation	Small regions can disappear in scalar tables.	The node receives gradient, curl and harmonic diagnostics.
Claim boundary	Risk of overstating the region's size or policy importance.	The model claims visibility of structural position, not output dominance.

6.2.5. Regional Macro-Flow Network as a Node-Edge-Pressure Object

The research object becomes Hodge-operational only when the regional node set is connected by weighted edges and those edges carry a directed pressure field. In the source study, the regional graph is designed as a complete global-regional benchmark, not as a literal observation of every dyadic economic flow. The edge set captures author-disclosed regional connection logic: output proximity, corridor relevance, growth or transition pressure, geographic-economic adjacency and network adequacy. Once the edge list is specified, the model can construct incidence matrices, triangle structures and Hodge Laplacians.

The node-edge-pressure object allows the chapter to answer questions that scalar data cannot answer. Which part of the macro-flow field is generated by regional hierarchy? Which part circulates around local regional cycles? Which part remains as systemic circulation after hierarchy and local imbalance are removed? These questions are meaningful only because the research object is a graph signal rather than a table of independent regional indicators.

(6.12) $W = [w_{ij}],\ A = 1\{w_{ij} > 0\},\ y_{ij} = -y_{ji}$

W is the weighted adjacency matrix, A is the binary adjacency matrix, and y is the anti-symmetric directed edge-pressure field used for Hodge decomposition.

(6.13) $B_1 \in \mathbb{R}^{|V|\times|E|},\ B_2 \in \mathbb{R}^{|E|\times|T|}$

B1 maps node-edge incidence and B2 maps triangle-edge incidence. These matrices define the algebraic space in which the research object becomes decomposable.

Table 6.2.6. From regional indicators to a macro-flow network

Stage	Input or operation	Output object	Purpose
1. Regional anchors	GDP, world share, projected growth, transition GDP, income depth.	Normalized regional input table.	Defines the macroeconomic base.
2. Node set	Ten regional/corridor nodes plus World anchor for scaling.	V = ten-node Hodge graph.	Defines the empirical universe.
3. Edge construction	Regional link and corridor rules.	E and W.	Creates relational structure.
4. Orientation	Difference or pressure-direction rule.	Anti-symmetric yij.	Turns the graph into an edge signal.
5. Incidence	B1, B2 and triangle set.	Hodge decomposition	Permits gradient, curl

Stage	Input or operation	Output object	Purpose
and cycles		space.	and harmonic separation.
6. Validation	Spectral, econometric, ML and persistent-homology diagnostics.	Benchmark evidence hierarchy.	Checks whether the research object is analytically adequate.

6.2.6. Public Data Inputs and Author-Calculated Research Variables

A core boundary of the research object is the separation between public inputs and author-calculated variables. Public macroeconomic anchors supply the empirical basis, but they are not the final Hodge indicators. Official sources may provide GDP, GDP per capita, regional aggregates, growth projections or related macroeconomic benchmarks. They do not publish a Hodge potential, a curl imbalance index, a harmonic circulation index, a macro-resilience index or a persistent-homology validation result. Those objects are constructed inside the methodology and must be interpreted as model-derived research variables.

This separation is methodologically protective. It makes the chapter reproducible and prevents the reader from confusing institutional statistics with constructed diagnostics. The final Hodge variables have evidentiary value because their lineage is traceable: public anchors define the input layer; normalization makes them comparable; network rules construct the graph; edge-pressure rules build the cochain; Hodge decomposition produces the components; and validation procedures audit their stability and empirical meaning.

(6.14) public anchors → normalized regional table → graph and edge pressure → Hodge components → regional indices

Formula 6.14 is the data-lineage chain of the research object.

Table 6.2.7. Data-status distinction in the Hodge research object

Variable family	Examples	Status	Permitted interpretation
Public macro anchors	GDP, world share, projected growth, transition GDP, GDP per capita.	Public or public-family data inputs.	Valid as input anchors and scale references.
Network variables	Adjacency, weights, edge list, corridor-weight structure.	Author-calculated from stated rules.	Valid as graph-construction objects.
Edge signal	Directed macro-flow pressure yij.	Author-calculated edge cochain.	Valid as decomposable pressure proxy.
Hodge components	Gradient, curl and harmonic energy/components.	Computed from the graph and edge signal.	Valid as structural decomposition results.
Regional indices	Hierarchy, imbalance, circulation, resilience, tail risk.	Model-derived diagnostic indicators.	Valid as benchmark diagnostics, not official rankings.
Validation outputs	Robust econometrics, ML checks, spectral tests, persistent homology.	Audit and robustness layer.	Valid as benchmark validation, not final causal proof.

6.2.7. Research Questions Embedded in the Object

Because the section defines the research object, it also clarifies the research questions that the object can answer. The Hodge chapter does not ask whether one region is simply “better” or “larger” than another.

It asks whether the regional world economy has a decomposable topology and whether that topology reveals structural features not captured by GDP mass. The three central questions therefore correspond to the three Hodge components: hierarchy, local imbalance and systemic circulation.

The object also supports a corridor-sensitive question: does the Caucasus become visible when the world economy is modeled as a macro-flow network? This is not a claim about dominance. It is a test of structural detectability. Finally, the object supports a validation question: can the constructed Hodge indices be audited through econometric, predictive, spectral and persistent-homology diagnostics? These questions are all appropriate for a regional benchmark; they would be inappropriate if interpreted as definitive country-level causal claims.

Table 6.2.8. Research questions allowed by the Section 6.2 object

Question block	Research question	Why the object can answer it
Hierarchy	Which part of regional macro-flow pressure is explained by a potential-like hierarchy?	The graph carries an edge field that can be projected onto a gradient component.
Local imbalance	Which part of the field circulates around local regional cycles?	The graph has cycles and triangle structure needed for curl interpretation.
Systemic circulation	What remains after hierarchy and local curl are removed?	The Hodge residual identifies harmonic circulation inside the benchmark topology.
Caucasus visibility	Can a small-output corridor node have measurable macro-flow position?	The Caucasus is retained as an explicit node rather than absorbed into larger aggregates.
Validation	Do Hodge-derived indices retain empirical structure under robustness checks?	The object is linked to econometric, ML, spectral and persistent-homology validation.

6.2.8. Boundary Conditions of the Research Object

The definition of the research object also defines what the chapter does not claim. First, it does not claim to prove the Hodge Conjecture or any theorem in algebraic geometry. Second, it does not claim that the regional benchmark is a complete all-country model. Third, it does not claim that the directed pressure field is an observed transaction matrix. Fourth, it does not claim causal identification from benchmark validation alone. Fifth, it does not transform the Caucasus into a large economic mass; it only preserves its structural visibility.

These boundaries are not weaknesses. They are the conditions under which the Hodge-econometric model remains academically admissible. The strongest claim supported by the research object is structural and diagnostic: the world economy can be represented as a connected regional macro-flow network whose directed pressure field can be decomposed into hierarchy, local imbalance and systemic circulation, and whose derived indices can be subjected to validation discipline.

(6.15) admissible claim = structural measurement + decomposition + benchmark validation

This is the final claim boundary of Section 6.2. It excludes theorem proof, causal law, complete dyadic-flow coverage and official-index status.

Table 6.2.9. Claim-boundary matrix for the Hodge research object

Dimension	Permitted claim	Restricted claim
Mathematical status	A bounded discrete Hodge-econometric analogue is constructed.	No Hodge Conjecture proof or theorem-level mathematical result.
Empirical universe	A complete ten-node regional benchmark is defined.	No claim of full all-country or sectoral coverage.
World anchor	The World aggregate provides normalization and scale consistency.	World is not treated as an ordinary regional node.
Caucasus node	Caucasus is structurally visible as a corridor-sensitive node.	No claim of output dominance or geopolitical ranking.
Edge pressure	Author-calculated pressure field supports decomposition.	Not an observed complete dyadic trade, capital or migration matrix.
Validation	Benchmark econometric, ML and topology checks audit the model.	No unrestricted causal inference or universal forecasting claim.

6.2.9. Link to Data Construction and Hodge Decomposition

Section 6.2 closes by handing the reader to the next two technical sections. Section 6.3 will specify how the World anchor, ten regional nodes and Caucasus visibility layer are operationalized through data and network construction. Section 6.4 will then turn that constructed network into a directed edge-pressure field and apply discrete Hodge decomposition. The sequence matters: without a correctly defined research object, later results would risk appearing as a mathematical overlay on loosely defined data. With the object fixed, the methodology becomes an auditable pipeline.

The transition from Section 6.2 to Section 6.3 is therefore substantive rather than merely editorial. Section 6.2 defines what the model studies; Section 6.3 defines how that object is populated; Section 6.4 defines how it is decomposed; Section 6.5 reports the gradient, curl and harmonic results; Section 6.6 interprets why those results show that the world economy is not reducible to GDP mass; Section 6.7 tests robustness, machine learning and persistent homology; and Section 6.8 concludes the Hodge chapter.

Table 6.2.10. Transition from research object to the rest of Chapter 6

Next section	Question answered	Dependence on Section 6.2
6.3 Data and Network Construction	How are the World anchor, ten regional nodes and Caucasus visibility operationalized?	Uses the node set, anchor logic and data-status boundary defined here.
6.4 Methodology	How is directed macro-flow pressure decomposed?	Uses the graph and edge-pressure object defined here.
6.5 Results	What are the gradient, curl and harmonic findings?	Reports outcomes for the research object fixed here.
6.6 Interpretation	Why is the world economy not reducible to GDP mass?	Interprets hierarchy, imbalance and circulation for this regional network.
6.7 Validation	Are the constructed components robust?	Tests the same benchmark object through robustness, ML and persistent homology.
6.8 Chapter Conclusion	What does the Hodge chapter contribute to the monograph?	Synthesizes the object, method, evidence and claim boundary.

6.2.10. Section Synthesis

The research object of Chapter 6 is now fixed. The chapter studies the world economy as a regional macro-flow network with a World normalization anchor and ten regional nodes, including the Caucasus as an explicit corridor-sensitive subregional node. This object is not a country panel, not a dyadic transaction database and not a theorem-level mathematical object. It is a structured empirical benchmark designed to carry a directed macro-flow pressure field and to support discrete Hodge decomposition.

This object is adequate for the chapter's scientific purpose because it permits the separation of three forms of structure that GDP mass alone cannot distinguish: gradient hierarchy, local-cycle imbalance and harmonic systemic circulation. It also permits small but corridor-relevant regions to remain analytically visible without overstating their output scale. The section therefore establishes the empirical identity of the Hodge chapter and prepares the transition to Section 6.3, where the World anchor, ten-node network and data-construction rules are specified in detail.

6.3. Data and Network Construction: World Anchor, Ten Regional Nodes and Caucasus Visibility

This section defines the data and network-construction architecture of the Hodge-econometric chapter. Its purpose is to transform a public macro-regional data layer into a mathematically valid regional graph on which directed macro-flow pressure can be constructed and decomposed. The methodological problem is not only to list regions, but to explain why a World anchor, ten regional nodes, author-calculated edges, corridor visibility and cycle structure are all required before discrete Hodge decomposition can be interpreted.

The central data rule is that official or public macroeconomic indicators are used as anchoring inputs, while the Hodge hierarchy, curl imbalance, harmonic circulation, resilience, tail-risk and topological variables are author-calculated research objects. This distinction protects the chapter from treating constructed Hodge outputs as official indicators. It also provides a reproducible lineage from public macroeconomic anchors to graph structure, edge pressure, Hodge projection and validation diagnostics.

Table 6.3.1. Data-construction purpose and position inside Chapter 6

Methodological question	Operational answer in Section 6.3	Why it matters for Hodge decomposition
What is the empirical domain?	A global macro-regional benchmark: World anchor plus ten regional nodes.	Hodge decomposition needs a closed node set before edges, cycles and projections can be defined.
What is the role of the World row?	The World row is a normalization anchor, not an ordinary regional node in the edge field.	It fixes scale without creating a tautological "world-to-world" edge.
Why use ten regional nodes?	They form a complete macro-core representation of the world economy at regional scale.	The graph remains interpretable and cycle-rich rather than under-identified or country-noisy.
Why retain the Caucasus?	It is an explicit corridor-sensitive subregional node.	It tests whether Hodge economics can reveal systemic relevance beyond GDP mass.
What is constructed?	Edges, weights, adjacency, pressure potentials, directed edge cochains and validation diagnostics.	These objects create the empirical space for gradient, curl and harmonic decomposition.

Source/Note: Author synthesis based on the Hodge-econometric source document and the monograph-wide methodology protocol.

6.3.1. Public Anchor Layer and Constructed Hodge Layer

The Hodge chapter begins from macroeconomic quantities that are observable, institutionally interpretable and auditable. These include regional GDP, world-output share, projected growth, transition GDP and income depth. The data are aligned

with World Bank WDI/DataBank-style regional aggregation logic and IMF/World Bank regional outlook logic as used in the source manuscript. However, these public anchors do not directly contain a Hodge hierarchy, a curl value, a harmonic residual or a persistent-homology barcode. Those quantities arise only after formal transformation.

The data architecture is therefore two-layered. The first layer fixes the empirical scale and macroeconomic meaning. The second layer converts that scale into a regional graph, an edge-weight system and a directed macro-flow pressure field. This is the key methodological discipline of the chapter: a reader must be able to trace every author-calculated Hodge object back to its public anchor, but must not mistake the constructed object for a public-data variable.

Table 6.3.2. Public-data anchors versus author-calculated Hodge variables

Layer	Variable family	Examples	Evidence status
Public anchor layer	Macroeconomic mass and scale	Regional GDP, world-output share, GDP per capita/income depth	Input evidence; not a Hodge result.
Public anchor layer	Growth and transition information	Projected growth, transition GDP	Input evidence for pressure and directional potential.
Author-calculated network layer	Graph and edge objects	Edge set, corridor weights, normalized adjacency, node degree, transitivity	Constructed benchmark objects derived from public anchors and corridor coding.
Author-calculated pressure layer	Directed flow variables	Regional pressure potential p_i; directed edge pressure y_ij	Research variables used as the 1-cochain for Hodge decomposition.
Author-calculated Hodge layer	Decomposition outputs	Gradient hierarchy, curl imbalance, harmonic/systemic circulation	Core model outputs; not official institutional indicators.
Validation layer	Topology and robustness diagnostics	Spectral connectivity, cycle rank, persistent homology, machine-learning validation	Audit evidence for the benchmark architecture.

Source/Note: Author synthesis. The distinction follows the source document's Data Availability and Code/Replication statements.

6.3.2. The World Anchor as Normalization Device, Not Regional Node

The World anchor is the scale-setting object of the chapter. It supplies the denominator for world-output shares and provides the global benchmark against which regional mass, transition output and income-depth differences can be interpreted. The World row is therefore indispensable for comparability, but it is excluded from the ordinary regional Hodge edge field. If the World row were inserted as an ordinary node, the model would risk mixing a total aggregate with its own components and would weaken the interpretation of regional edges.

The correct interpretation is therefore: the World anchor fixes the empirical scale; the ten regional nodes define the graph. This rule is especially important in a monograph context, because several chapters use a World normalization anchor. In the Hodge chapter, the anchor performs scale discipline, while the network performs topological decomposition.

Formula (6.3.1) Y_W = benchmark world output

Components: Y_W is the World normalization anchor. It is used to construct shares and scale variables, but it is not treated as an ordinary regional node.

Formula (6.3.2) $s_i = 100 \cdot Y_i / Y_W$

Components: s_i is the world-output share of region i; Y_i is regional GDP; Y_W is benchmark world output.

Formula (6.3.3) $Y_i^T = Y_i \cdot (1 + g_i/100)^2$

Components: Y_i^T is transition GDP; g_i is the projected regional growth rate; the two-year transformation creates a forward-looking macro-flow pressure anchor.

Table 6.3.3. World anchor and regional public-data input panel for the Hodge benchmark

Code	Region / anchor	GDP 2024, $bn	World share, %	Transition GDP 2026, $bn	Growth 2026, %	GDP pc, $	System role
WLD	World anchor	110,985.0	100.00	118,201.7	3.20	14,100	Normalization anchor only
EAP	East Asia and Pacific	35,620.0	32.09	38,674.9	4.20	17,200	Regional node
NAM	North America	31,000.0	27.93	32,252.4	2.00	76,000	Regional node
EUR	Europe	23,150.0	20.86	23,849.7	1.50	43,000	Regional node
LAC	Latin America and Caribbean	7,260.0	6.54	7,612.7	2.40	10,600	Regional node
SAS	South Asia	4,770.0	4.30	5,390.0	6.30	2,700	Regional node
MENA	Middle East and North Africa	4,540.0	4.09	4,835.2	3.20	8,800	Regional node
SSA	Sub-Saharan Africa	2,160.0	1.95	2,327.3	3.80	1,850	Regional node
OCE	Oceania	1,810.0	1.63	1,886.8	2.10	63,000	Regional node
CAS	Central Asia	530.0	0.48	585.4	5.10	9,000	Corridor-sensitive regional node
CAU	Caucasus	145.0	0.13	158.6	4.60	9,500	Explicit author-defined corridor node

Source/Note: World Bank WDI/DataBank-style regional aggregation logic; IMF/WEO and World Bank regional outlook benchmarks; author calculations. Values reproduce the regional input architecture used in the Hodge benchmark.

6.3.3. Ten Regional Nodes and the Closed Macro-Regional Universe

The node set contains ten macro-regional or corridor-sensitive units. The construction is not a country sample and not a complete dyadic transaction database. It is a regional macro-core benchmark. This choice is methodologically appropriate for the monograph because Hodge decomposition requires a connected network with interpretable nodes, edges and cycles. A very large country-level graph could be richer, but it would also require a different dyadic data architecture and would move beyond the scope of the present regional benchmark.

The ten-node design balances coverage and interpretability. It covers the world through major regional blocs, but it also preserves Central Asia and the Caucasus as corridor-sensitive nodes. This avoids a purely mass-driven structure in which small but strategically exposed areas disappear inside larger regional aggregates.

Formula (6.3.4) V = {EAP, NAM, EUR, LAC, SAS, MENA, SSA, OCE, CAS, CAU}

Components: V is the ten-node regional universe. The World anchor is excluded from V and used only for normalization.

Formula (6.3.5) x_i = [s_i, g_i, log(ypc_i), Y_i^T, role_i]

Components: x_i is the regional input vector; s_i is output share; g_i is projected growth; ypc_i is income depth; Y_i^T is transition GDP; role_i records regional/corridor role.

Table 6.3.4. Node-codebook logic for the ten-region Hodge benchmark

Code	Node interpretation	Primary macro role	Why retained in the Hodge graph
EAP	East Asia and Pacific	Large output mass and strong transition output	Major mass and growth-potential bloc.

Code	Node interpretation	Primary macro role	Why retained in the Hodge graph
NAM	North America	Large output mass and high income depth	Advanced high-scale node with strong benchmark role.
EUR	Europe	Large output mass and dense corridor exposure	Mass and connectivity node in multiple regional cycles.
LAC	Latin America and Caribbean	Intermediate output mass	Regional bridge between output scale and development heterogeneity.
SAS	South Asia	High growth momentum with lower income depth	High-pressure growth node, important for hierarchy and tail-risk readings.
MENA	Middle East and North Africa	Energy/corridor and regional-interaction node	Bridge between Europe, South Asia, Africa and Caucasus/Central Asia routes.
SSA	Sub-Saharan Africa	Development and growth-pressure node	Captures low-income, high-transition and resilience-relevant pressures.
OCE	Oceania	High income depth but small global mass	Tests whether high-income small mass nodes behave differently in the edge field.
CAS	Central Asia	Corridor-sensitive transition node	Retained for high-momentum and Eurasian corridor visibility.
CAU	Caucasus	Explicit corridor-sensitive subregional node	Retained to test non-GDP visibility in Europe-Central Asia-MENA macro-flow space.

Source/Note: Author synthesis from the Hodge-econometric regional object and node-role logic.

6.3.4. Caucasus Visibility as a Design Principle

The Caucasus node is not inserted to inflate the importance of a small-output region. It is retained to test a specific methodological question: can a topological macro-flow framework make a corridor-sensitive region visible even when its GDP share is small? In the Hodge chapter, the answer depends on the difference between economic mass and structural position. GDP mass determines node size, but Hodge decomposition also responds to edge orientation, corridor placement, triangular cycles, imbalance and residual circulation.

This is why the Caucasus must not be absorbed mechanically into Europe, Central Asia or MENA. If it is absorbed, the model loses the ability to test corridor visibility. If it is retained, the model can compare a small node's hierarchy, imbalance, circulation, resilience and tail-risk exposure with the same objects for larger regional blocs. In monograph terms, this makes the Caucasus a methodological stress test for the broader claim that the world economy is not reducible to GDP mass.

Table 6.3.5. Caucasus visibility and anti-GDP-reduction discipline

Design risk if Caucasus is absorbed	Design gain if Caucasus is retained	Hodge-econometric implication
Corridor role disappears inside a larger aggregate.	Corridor-sensitive position remains observable.	Edge pressure can be measured for the Caucasus rather than inferred narratively.
GDP share becomes the dominant criterion.	Small output mass can be separated from structural exposure.	The model tests whether non-mass topology matters.
Europe, Central Asia and MENA become less differentiated.	Triangular and near-triangular corridor cycles become more	Curl/local-cycle imbalance can be linked to corridor structure.

Design risk if Caucasus is absorbed	Design gain if Caucasus is retained	Hodge-econometric implication
	interpretable.	
Caucasus cannot be ranked by Hodge-derived indices.	Hierarchy, imbalance, circulation, resilience and tail risk can be reported.	The node becomes part of the replication-ready regional codebook.

Source/Note: Author synthesis. The Caucasus is an author-defined subregional node used for corridor-sensitive macro-flow visibility.

6.3.5. Network Construction from Regional Anchors

After the public anchor and node-set rules are fixed, the methodology constructs an undirected weighted regional graph. The purpose of this graph is to define which regional pairs are connected and how strong each macro-flow corridor is before direction is imposed through the pressure field. The initial graph is undirected because adjacency and corridor proximity describe structural connection, not yet the sign of macro-pressure. Direction enters later through differences in regional pressure potential.

Edges are author-calculated from a transparent combination of output proximity, corridor logic, regional adjacency and stress interaction. This makes the graph a formal research object rather than a decorative visualization. The edge list must be reported, normalized and retained in the replication package because the subsequent Hodge projection depends on the exact incidence structure of the graph.

Formula (6.3.6) $m_i = Y_i / \max_j(Y_j)$

Components: m_i is normalized regional economic mass; $\max_j(Y_j)$ is the largest regional GDP among the ten nodes.

Formula (6.3.7) $w_{ij} = C_{ij} \cdot (m_i \cdot m_j)^{\alpha} \cdot \exp(-\delta d_{ij})$

Components: w_{ij} is the undirected macro-corridor weight; C_{ij} is the corridor/institutional connectivity factor; d_{ij} is regional distance or separation; α and δ control mass and distance sensitivity.

Formula (6.3.8) $a_{ij} = w_{ij} / \max_{(i,j \in E)} w_{ij}$

Components: a_{ij} is the normalized adjacency weight used in the Hodge benchmark.

Formula (6.3.9) $G = (V, E, A)$

Components: G is the regional graph; V is the ten-node set; E is the retained edge list; $A = [a_{ij}]$ is the normalized weighted adjacency matrix.

Table 6.3.6. Edge-construction logic in the regional Hodge graph

Edge-construction input	Operational meaning	Why it is needed
Output proximity	Large or economically interacting regions receive baseline mass relevance.	Prevents the graph from ignoring the scale of the global economy.
Corridor link factor	Regional pairs with corridor/geographic or macro-transmission relevance receive additional connectivity.	Makes Central Asia and the Caucasus visible as corridor nodes.
Regional adjacency or institutional proximity	Nearby or institutionally linked regional blocs are more likely to be connected.	Preserves interpretable network geography.
Stress interaction	Regions with interacting growth/income/mass pressures may form relevant flow links.	Connects macroeconomic pressure to topological structure.
Normalization rule	Weights are scaled to a common interval through maximum edge-weight normalization.	Allows edge pressure and Hodge projections to be numerically stable.

Source/Note: Author synthesis from the Hodge methodology. The edge list is author-calculated and must be reproducible from the declared inputs and codebook.

6.3.6. Network Adequacy: Connectedness, Density and Cycles

Hodge decomposition requires more than a list of nodes. It requires a graph with a valid edge space and enough cycle structure to distinguish gradient, curl and harmonic components. A sparse tree would allow hierarchy but would not contain

enough cycles for meaningful curl analysis. A nearly complete graph could make the topology mechanically saturated. The reported benchmark is intentionally intermediate: connected, sufficiently dense and cycle-rich, but not complete.

The Hodge source document reports a regional graph with 10 nodes, 27 weighted edges, density of 0.600, one connected component, average degree of 5.40, average normalized edge weight of 0.377, global transitivity of 0.740 and weighted clustering of 0.274. These diagnostics establish that the graph is a legitimate decomposition domain: every node is attached to the macro-flow system, and triangular corridors exist for curl measurement.

Formula (6.3.10) Density = 2|E| / (|V|(|V|-1))

Components: Density measures the share of realized undirected regional links among all possible regional links.

Formula (6.3.11) deg_i = Σ_j 1{(i,j) ∈ E}, deg_i^w = Σ_j a_ij

Components: deg_i is unweighted degree; deg_i^w is weighted degree under normalized adjacency.

Formula (6.3.12) T = 3 × number of closed triangles / number of connected triples

Components: T is global transitivity; it measures triangular closure and supports curl interpretation.

Table 6.3.7. Regional network topology and Hodge-readiness diagnostics

Metric	Reported value	Interpretation for Section 6.3
Regional nodes	10	Defines the Hodge edge field at macro-regional scale.
Weighted edges	27	Provides enough connections for cycles and Hodge projections.
Density	0.600	The graph is neither a tree nor a complete graph.
Connected components	1	No regional node is isolated from the global macro-flow system.
Average degree	5.40	Each region is linked to several other regional blocks.
Average normalized edge weight	0.377	Edge strengths are not uniformly maximal; weights remain differentiated.
Global transitivity	0.740	Triangular corridor structure exists for curl diagnostics.
Weighted clustering	0.274	Regional clustering is non-trivial after weights are considered.
World-GDP coverage	100.00%	The regional benchmark covers the world through the macro-core system.

Source/Note: Author calculations as reported in the Hodge-econometric source document. These values validate the graph as a Hodge decomposition domain.

6.3.7. From Undirected Connectivity to Directed Macro-Flow Pressure

Network construction alone does not produce Hodge decomposition. The graph must be equipped with a directed edge field. The Hodge chapter constructs that field through regional pressure potentials. Regional mass, growth, income depth and interaction terms are standardized and aggregated into a pressure score. Edge direction then follows pressure differences between connected regions. This creates an anti-symmetric edge cochain: for every connected pair, the pressure from i to j is the negative of the pressure from j to i.

This transformation is central because it converts public macroeconomic anchors into a decomposable economic 1-cochain. Once y_ij is defined on the oriented edges, the model can separate hierarchy from local-cycle imbalance and persistent circulation. Without this directed edge-pressure object, the graph would remain a network visualization rather than a Hodge-econometric model.

Formula (6.3.13) z_{k,i} = (x_{k,i} - mean(x_k)) / sd(x_k)

Components: z_{k,i} standardizes regional variable k for region i.

Formula (6.3.14) p_i = θ_s z_{s,i} + θ_g z_{g,i} - θ_y z_{log(ypc),i} + θ_m z_{s·g,i}

Components: p_i is the regional macro-pressure potential; θ terms are declared weights; income depth enters with an inverse-pressure orientation.

Formula (6.3.15) y_ij = a_ij · (p_i - p_j), y_ji = -y_ij

Components: y_ij is directed macro-flow pressure along the edge; anti-symmetry makes y a valid oriented 1-cochain.

Formula (6.3.16) y = (y_e)_{e∈E} ∈ C^1(G)

Components: y is the directed edge-pressure vector on the oriented edge space of the graph.

Table 6.3.8. Transformation chain from public anchors to Hodge-ready edge field

Step	Input	Author-calculated output	Purpose
1. Anchor scaling	World GDP and regional GDP	World-output share s_i	Creates a common scale.
2. Transition calculation	GDP and projected growth	Transition GDP Y_i^T	Adds forward-looking macro-flow pressure.
3. Node vector construction	Mass, growth, income, transition and role variables	Regional feature vector x_i	Defines each node's macroeconomic state.
4. Edge construction	Node states and corridor logic	Weighted graph G=(V,E,A)	Defines the topology for decomposition.
5. Pressure potential	Standardized regional variables	p_i	Creates directional pressure before edge orientation.
6. Edge pressure	p_i, p_j and a_ij	Directed cochain y_ij	Produces the object decomposed in Section 6.4.
7. Decomposition readiness	Incidence/cycle structure	Hodge-ready benchmark	Confirms that gradient, curl and harmonic layers are identifiable.

Source/Note: Author synthesis from the Hodge methodology.

6.3.8. Data and Network Construction Algorithm

The complete construction can be summarized as a reproducible sequence. The purpose of expressing it algorithmically is to make the chapter auditable: another researcher should be able to begin with the regional input table and reproduce the node set, edge set, weighted adjacency, directed pressure field and graph diagnostics before running the Hodge projections.

Table 6.3.9. Algorithm 6.3A: Data and network construction workflow

Step	Operation	Output
1	Import public regional anchors: GDP, world share, projected growth, transition GDP and income depth.	Regional input table with World row and ten candidate nodes.
2	Assign World as normalization anchor and exclude it from the ordinary Hodge node set.	Y_W retained for scaling; V contains only ten regional nodes.
3	Code EAP, NAM, EUR, LAC, SAS, MENA, SSA, OCE, CAS and CAU as regional nodes.	Closed ten-node regional universe.
4	Retain the Caucasus as an explicit corridor-sensitive subregional node.	Caucasus visibility preserved for corridor analysis.
5	Normalize regional mass and construct transition/growth/income-depth features.	Regional feature vector x_i.
6	Construct the weighted regional graph using output proximity, corridor link, adjacency and stress-interaction logic.	Retained 27-edge weighted graph.
7	Normalize edge weights to produce adjacency matrix A.	Comparable edge weights a_ij.
8	Audit graph topology: density, connected components, degree, transitivity and clustering.	Connected, cycle-rich Hodge-ready graph.

Step	Operation	Output
9	Construct regional pressure potential and directed edge pressure.	Oriented macro-flow pressure cochain y.
10	Pass the graph, incidence matrices and edge-pressure vector to Section 6.4.	Discrete Hodge decomposition becomes operational.

Source/Note: Author synthesis formulated for monograph replication.

6.3.9. Replication and Source-Ledger Discipline

The network-construction stage must be reproducible because all subsequent Hodge results depend on it. The source package therefore needs to include the regional input table, the ten-node codebook, the retained 27-edge list, the normalized adjacency matrix, the row-normalized network matrix where used, the corridor-weight and pressure-parameter tables, the incidence matrices and the pressure-field output. Any change in the edge list or weighting rule would change the Hodge projection results.

This replication discipline also protects the chapter from overclaiming. The regional graph is a benchmark representation of macro-regional structure; it is not an observed transaction-level world trade matrix and not a complete country-level dyadic network. The admissible claim is that the declared benchmark graph is connected, cycle-rich and sufficient for the reported regional Hodge-econometric decomposition.

Table 6.3.10. Minimum replication files for Section 6.3

Replication item	Required content	Reason for inclusion
Regional input workbook	World anchor and ten regional rows with GDP, share, growth, transition GDP and income depth	Allows public-anchor verification.
Node codebook	Node names, abbreviations and role labels	Prevents ambiguity in V and in Caucasus treatment.
Edge list	All retained 27 undirected regional edges	Defines the graph structure.
Weight formula sheet	Corridor factors, mass factors, distance/proximity terms and normalization rule	Allows reproduction of w_ij and a_ij.
Adjacency matrices	Weighted adjacency and normalized adjacency	Provides the matrix basis for topology and pressure weighting.
Topology audit file	Density, degree, connected components, transitivity and clustering	Confirms Hodge-readiness before decomposition.
Pressure-potential file	Standardized variables, θ weights and p_i values	Connects node data to directed edge pressure.
Directed edge-pressure file	y_ij values and orientation convention	Defines the 1-cochain decomposed in Section 6.4.
Metadata and checksum file	Version, software, scripts, seeds if used and file hashes	Supports auditability and version control.

Source/Note: Author synthesis aligned with the Hodge replication-package logic.

6.3.10. Boundary Conditions for Interpreting the Constructed Network

The regional Hodge network must be interpreted as a benchmark macro-flow architecture. It is not a literal map of all observed bilateral trade, finance, migration or supply-chain transactions. It is also not a country-level causal panel. The edge weights are author-calculated from public anchors and disclosed corridor logic, which means they are transparent and reproducible but still model constructs. This status is not a weakness; it is the reason the chapter can be replicated and bounded.

The methodological claim of Section 6.3 is therefore precise: the Hodge chapter has a valid regional data and network-construction foundation. The World anchor fixes scale; ten regional nodes define the empirical domain; the Caucasus preserves corridor visibility; 27 weighted edges create a connected and cycle-rich graph; and the directed pressure

transformation produces the edge field required for Hodge decomposition. Stronger causal or all-country claims require a larger dyadic or country-level extension, which is outside the present section.

Table 6.3.11. Network claim-boundary matrix for Section 6.3

Potential overclaim	Correct claim in this chapter	Reason
The graph is the true world trade network.	The graph is an author-calculated regional macro-flow benchmark.	It uses public anchors and corridor logic, not full transaction data.
The World row is a network node.	The World row is a normalization anchor.	Including the aggregate as a node would mix total and components.
Caucasus visibility proves causal corridor power.	Caucasus visibility shows measurable corridor-sensitive position inside the benchmark.	The finding is structural and diagnostic, not causal.
Edge weights are official data.	Edge weights are author-calculated from disclosed rules.	They require replication files and audit logic.
Cycle-rich topology proves Hodge-theorem content.	Cycle-rich topology makes discrete Hodge decomposition operational.	The chapter is an economic analogue, not a theorem proof.

Source/Note: Author synthesis for reviewer-safe interpretation.

6.3.11. Bridge to Section 6.4

Section 6.3 closes the empirical construction stage. At this point, the chapter has a World-normalized regional benchmark, a ten-node graph, a retained Caucasus node, twenty-seven weighted edges, a connected and cycle-rich topology, and an oriented macro-flow pressure field. These objects are sufficient to build the incidence matrices and projection operators used in the next section.

Section 6.4 therefore begins from an already-audited graph and asks a different question: once the directed edge-pressure field is defined, how much of it is explained by gradient hierarchy, how much by curl/local-cycle imbalance and how much remains as harmonic/systemic circulation? The data and network construction in Section 6.3 is thus the technical bridge between public macroeconomic anchors and the core Hodge result of the chapter.

Table 6.3.12. Section 6.3 closure matrix and transition to Section 6.4

Object completed in Section 6.3	Status	Used in Section 6.4 as
World anchor	Scale fixed at benchmark global output	Denominator for share and normalization logic.
Ten-node regional universe	Closed node set V	Domain for incidence matrices and node potentials.
Caucasus node	Explicit corridor-sensitive node retained	Test case for non-GDP macro-flow visibility.
Weighted graph	27-edge connected and cycle-rich graph	Topology for gradient, curl and harmonic decomposition.
Adjacency matrix	Normalized edge weights a_ij	Weighting system for edge-pressure and Hodge norm.
Directed edge-pressure field	Oriented 1-cochain y	Direct input to discrete Hodge projection.
Topology audit	Density, connectedness, transitivity and clustering established	Precondition for interpreting Hodge decomposition results.

Source/Note: Author synthesis. Section 6.4 uses these objects to run the discrete Hodge decomposition.

6.4. Methodology: Directed Edge Pressure and Discrete Hodge Decomposition

This section is the technical core of the Hodge-econometric chapter. Section 6.3 constructed the empirical network: a World-normalized ten-node regional benchmark with 27 weighted edges and explicit Caucasus visibility. Section 6.4 now converts that network into a directed edge-pressure field and decomposes it by discrete Hodge theory. The methodological objective is to separate regional macro-flow pressure into three analytically different components: gradient hierarchy, curl/local-cycle imbalance and harmonic/systemic circulation.

The key methodological shift is that the dependent object is not a node-level GDP vector and not a conventional regression residual. It is an oriented edge cochain defined on the regional graph. This edge cochain represents author-calculated macro-flow pressure derived from output share, growth momentum, income depth, transition output and corridor-weighted adjacency. Once this object is defined, the Hodge projection separates what can be explained by regional hierarchy, what is concentrated in local triangular inconsistency and what remains as persistent network-wide circulation.

Table 6.4.1. Methodological position of Section 6.4 inside Chapter 6

Input from Section 6.3	Transformation in Section 6.4	Output used in Section 6.5
World-normalized regional node set	Define standardized node-pressure potential p_i	Directed pressure differences across connected regions
Retained 27-edge weighted graph	Orient edges and construct y_ij = a_ij(p_i - p_j)	Hodge-ready 1-cochain y on the edge space
Adjacency and edge weights	Define weighted inner product and projection metric	Weighted energy shares for G, C and H components
Regional triangles and cycle structure	Construct B_2 and local-curl subspace	Curl/local-cycle imbalance estimates
Incidence structure and connectedness	Construct B_1 and Hodge projection operators	Gradient hierarchy and harmonic residual
Replication package requirements	Audit matrix ranks, orthogonality and reconstruction error	Reviewer-safe decomposition verification

Source/Note: Author synthesis based on the Hodge-econometric methodology and the monograph-wide replication protocol.

6.4.1. Methodological Object: An Edge Cochain, Not a GDP Ranking

The empirical object of this section is the directed edge-pressure field. In a standard macroeconomic ranking, each region receives one scalar value: GDP, income per capita, growth or world-output share. In the Hodge framework, those node-level quantities become inputs to an edge-level object. Every retained regional corridor receives a signed pressure value, so the model measures directional macro-flow pressure rather than only regional mass.

This distinction is central for scientific interpretation. GDP rankings can identify large output blocs, but they cannot say whether pressure is purely hierarchical, locally inconsistent or systemically circulating. Hodge decomposition solves this measurement problem by taking the edge field as the object to be decomposed. The chapter therefore reads the world economy as a flow topology rather than a list of regional aggregates.

Formula (6.4.1) G = (V, E, A)

Components: G is the weighted regional graph; V is the ten-node regional universe; E is the retained edge set; A = [a_ij] is the normalized adjacency-weight matrix.

Formula (6.4.2) C^0(G) = {node signals}; C^1(G) = {oriented edge signals}; C^2(G) = {oriented triangle signals}

Components: C^0, C^1 and C^2 are the node, edge and triangle cochain spaces used in the discrete Hodge interpretation.

Formula (6.4.3) y = (y_e)_{e in E} in C^1(G)

Components: y is the directed macro-flow pressure field and is the main object decomposed in this section.

Table 6.4.2. Why the methodological object must be an edge cochain

Conventional object	Limitation	Hodge-econometric replacement	Analytical gain
GDP level by region	Measures economic mass only	Directed pressure on retained edges	Distinguishes mass from flow organization
Growth rate by region	Measures momentum but not relational structure	Pressure-potential difference p_i - p_j	Identifies directional tension across corridors
Network centrality only	Measures position but not signed pressure	Weighted edge cochain y_ij	Combines topology and macroeconomic pressure
Regression residual only	Captures unexplained variation after a model	Harmonic Hodge residual h	Captures residual systemic circulation after hierarchy and curl are removed
Descriptive corridor narrative	Qualitative and hard to replicate	Declared edge list, weights, incidence matrices and	Creates an auditable mathematical pipeline

Conventional object	Limitation	Hodge-econometric replacement	Analytical gain
		projections	

Source/Note: Author synthesis. The Hodge model is defined on edge pressure, not on GDP rankings alone.

6.4.2. Standardized Regional Pressure Potential

The first operational step is to transform heterogeneous regional attributes into a comparable pressure potential. GDP share, projected growth, income depth and transition output are not expressed in the same units. The methodology therefore standardizes each input component before aggregation. Higher output share and growth momentum increase macro-flow pressure; higher income depth can reduce stress orientation when the object is pressure rather than welfare; interaction terms capture mass-growth amplification.

The pressure-potential equation does not claim to be a structural law of the world economy. It is a transparent author-calculated transformation that converts public anchors into an edge-orientation variable. Its function is methodological: it gives every regional node a scalar pressure potential from which directed edge pressure can be constructed.

Formula (6.4.4) $z_{k,i} = (x_{k,i} - \text{mean}(x_k)) / \text{sd}(x_k)$

Components: $z_{k,i}$ is the standardized value of input variable k for region i. Standardization permits output share, growth, income depth and transition variables to enter one pressure equation.

Formula (6.4.5) $p_i = \theta_s z_{s,i} + \theta_g z_{g,i} - \theta_y z_{\log(ypc),i} + \theta_m z_{s*g,i}$

Components: p_i is the regional macro-pressure potential; θ_s, θ_g, θ_y and θ_m are pre-declared weights; log income depth enters with inverse pressure orientation.

Formula (6.4.6) $p_i^{\text{centered}} = p_i - \text{mean}_j(p_j)$

Components: The centered pressure potential removes arbitrary level shifts and leaves relative macro-flow position.

Table 6.4.3. Pressure-potential inputs and directional logic

Input component	Symbol	Expected pressure orientation	Methodological role
World-output share	s_i	Positive	Large output mass can create stronger structural macro-flow pressure.
Projected growth	g_i	Positive	High growth momentum can create transition and reallocation pressure.
Income depth	log(ypc_i)	Negative in pressure orientation	Higher income depth is interpreted as greater absorption capacity, not stress.
Mass-growth interaction	s_i * g_i	Positive	Large regions with growth momentum may exert stronger directed pressure.
Corridor role	role_i	Conditional / coding-based	Used to preserve corridor visibility for Central Asia and Caucasus-related edges.

Source/Note: Author synthesis from the Hodge pressure-field construction.

6.4.3. Directed Macro-Flow Pressure on Edges

After p_i is constructed, direction enters through connected regional pairs. For each retained edge (i,j), directed pressure is calculated as the normalized edge weight multiplied by the pressure-potential difference. The edge weight ensures that high pressure differences matter most when the regional pair is structurally connected. Anti-symmetry ensures that the edge field is mathematically valid: the pressure from i to j is the negative of the pressure from j to i.

The directed field is not an observed bilateral trade or capital-flow series. It is an author-calculated macro-flow pressure proxy. This distinction must remain explicit throughout the chapter because the validity of the decomposition depends on transparent construction, not on pretending that the edge cochain is an official dyadic database.

Formula (6.4.7) $y_{ij} = a_{ij}(p_i - p_j)$, for (i,j) in E

Components: y_{ij} is directed macro-flow pressure; a_{ij} is normalized edge weight; $p_i - p_j$ is the pressure-potential difference.

Formula (6.4.8) $y_{ji} = -y_{ij}$

Components: Anti-symmetry makes the directed edge field an oriented 1-cochain.

Formula (6.4.9) $\|y\|_W^2 = y^T W_E y$

Components: The weighted squared norm of the observed pressure field; W_E is the edge-weight matrix used in projection and energy decomposition.

Table 6.4.4. Edge-pressure construction and interpretation rules

Rule	Mathematical form	Interpretive meaning	Reviewer-safety boundary
Edge support rule	y_{ij} is defined only if (i,j) is in E	Pressure can flow only along retained benchmark corridors	No claim that all possible dyads are observed.
Weighting rule	a_{ij} multiplies $p_i - p_j$	Connectivity strength affects pressure importance	Weights are author-calculated, not official dyadic flows.
Orientation rule	$y_{ji} = -y_{ij}$	Every edge has a consistent orientation convention	Sign depends on pressure-potential convention.
Cochain rule	y in $C^1(G)$	The decomposed object lives on edges	Not a node-only GDP vector.
Replication rule	edge list, weights and y_{ij} must be archived	Projection can be externally audited	No unreported edge changes should be allowed.

Source/Note: Author synthesis. These rules define the Hodge-ready macro-flow pressure field.

6.4.4. Incidence Matrices and Orientation Convention

Discrete Hodge decomposition requires incidence matrices. The edge-node incidence matrix B_1 maps node potentials into edge gradients. The triangle-edge incidence matrix B_2 maps local triangular circulation into edge space. These matrices are not optional notation; they define the algebraic spaces onto which the observed edge pressure is projected.

The orientation convention must be fixed before projection. Each undirected regional edge is assigned an arbitrary but consistent orientation. The sign of B_1 and B_2 follows that convention. The final energy shares do not depend on a narrative interpretation of the arbitrary orientation; they depend on the consistent algebraic representation of the edge and triangle spaces.

Formula (6.4.10) $B_1[e,i] = -1$ if edge e leaves node i; $+1$ if edge e enters node i; 0 otherwise

Components: B_1 is the edge-node incidence matrix. It maps node potentials to directed edge gradients.

Formula (6.4.11) $B_2[t,e] = +1, -1$ or 0 according to whether edge e agrees with, opposes or is absent from oriented triangle t

Components: B_2 is the triangle-edge incidence matrix. It defines local curl around oriented regional triangles.

Formula (6.4.12) $\mathrm{im}(B_1) = $ gradient subspace; $\mathrm{im}(B_2^T) = $ curl subspace; $\ker(B_1^T) \cap \ker(B_2) = $ harmonic subspace

Components: These subspaces define the Hodge decomposition of the directed edge-pressure field.

Table 6.4.5. Matrix-space discipline for the Hodge projection

Object	Dimension logic in the regional benchmark	Economic interpretation	Technical role
Node space C^0	One signal for each regional node	Regional hierarchy potential	Input space for gradient component
Edge space C^1	One oriented value for each retained edge	Directed macro-flow pressure	Main measurement space
Triangle space C^2	One oriented value for each economically meaningful filled triangle	Local-cycle circulation	Input space for curl component

Object	Dimension logic in the regional benchmark	Economic interpretation	Technical role
B_1 incidence matrix	edge-by-node sign matrix	Converts regional hierarchy into edge differences	Defines gradient projection
B_2 incidence matrix	triangle-by-edge sign matrix	Converts local triangular circulation into edge pressure	Defines curl projection
Harmonic subspace	Residual edge space after gradient and curl projection	Systemic circulation not reducible to hierarchy or local triangles	Defines persistent macro-flow residual

Source/Note: Author formulation for the ten-node, 27-edge Hodge benchmark.

6.4.5. Weighted Hodge Decomposition

The central operation is to decompose the observed directed edge-pressure field y into three mutually interpretable components. The gradient component is the part of y that can be explained by node potentials; it is the hierarchical component. The curl component is the part explained by local oriented triangles; it is the local-cycle imbalance component. The harmonic component is the residual circulation left after both hierarchy and local curl have been removed.

The Hodge decomposition is performed with a weighted norm because regional edges are not equally important. A pressure difference on a strong corridor edge should not carry the same decomposition weight as a weakly connected pair. The methodology therefore uses edge weights as part of the projection geometry.

Formula (6.4.13) y = y_G + y_C + y_H = B_1 phi + B_2^T psi + h

Components: y_G is gradient hierarchy; y_C is curl/local-cycle imbalance; y_H = h is harmonic/systemic circulation.

Formula (6.4.14) phi_hat = argmin_phi ||y - B_1 phi||_W^2

Components: phi_hat is the estimated regional Hodge potential under the weighted projection norm.

Formula (6.4.15) r_G = y - B_1 phi_hat

Components: r_G is the residual after removing the gradient hierarchy component.

Formula (6.4.16) psi_hat = argmin_psi ||r_G - B_2^T psi||_W^2

Components: psi_hat captures local triangular circulation after gradient hierarchy is removed.

Formula (6.4.17) h = y - B_1 phi_hat - B_2^T psi_hat

Components: h is the harmonic residual: the systemic circulation component not explained by hierarchy or local curl.

Table 6.4.6. Hodge decomposition components and economic interpretation

Component	Formula form	Economic meaning	What it is not
Gradient hierarchy	y_G = B_1 phi_hat	Directional macro-flow explained by regional hierarchy and node potential differences	Not simply GDP rank.
Curl/local-cycle imbalance	y_C = B_2^T psi_hat	Pressure trapped in local triangular inconsistencies and corridor loops	Not a country-level trade imbalance.
Harmonic/systemic circulation	y_H = h	Residual circulation across the broader network after hierarchy and local curl are removed	Not a proof of the Hodge Conjecture or a literal physical field.
Observed edge field	y	Author-calculated pressure signal derived from public anchors and graph weights	Not an official bilateral flow matrix.
Reconstruction identity	y = y_G + y_C + y_H	Internal decomposition closure	Not a causal law by itself.

Source/Note: Author synthesis based on the Hodge methodology.

6.4.6. Gradient Hierarchy as the Regional Ranking Layer

The gradient component generates a regional hierarchy that is structurally different from a GDP ranking. A region may have large output mass but a lower Hodge potential if its pressure relation to other nodes is not primarily hierarchical. Conversely, a corridor-sensitive region can have a visible Hodge role if its edge pressures place it in a systematic directional position within the network.

The normalized hierarchy index H_i converts the estimated potential into a 0-100 scale. The purpose of this normalization is interpretability and comparability, not statistical proof. It lets the results chapter rank regions by Hodge hierarchy while preserving the boundary that the ranking is a constructed structural-flow index.

Formula (6.4.18) H_i = 100 · (phi_i - min_j phi_j) / (max_j phi_j - min_j phi_j)

Components: H_i is the normalized regional hierarchy index derived from the gradient potential.

Formula (6.4.19) Rank_H(i) = rank(-H_i)

Components: Regions are ranked in descending hierarchy-index order.

Table 6.4.7. Gradient hierarchy and its interpretation discipline

Issue	Correct interpretation	Incorrect interpretation to avoid
High H_i	Region has strong directed-flow hierarchy under the Hodge pressure field	Region is automatically the largest GDP region.
Low H_i	Region is less dominant in gradient hierarchy	Region is economically irrelevant.
Caucasus ranking	Tests corridor-sensitive position after pressure and edge weighting	Claims GDP equivalence with large regions.
Comparison with GDP	Shows whether structural hierarchy differs from mass hierarchy	Treats Hodge index as a replacement for GDP.
Use in econometrics	Can be used as an author-calculated regressor in validation models	Cannot by itself establish causality.

Source/Note: Author synthesis for gradient-hierarchy interpretation.

6.4.7. Curl-Based Local Imbalance on Regional Triangles

Curl measures local inconsistency around triangles. In the regional economy, a triangle may link Europe, Central Asia and the Caucasus, or other meaningful macro-regional closures. If the directed edge pressures around a triangle do not cancel, the model records local-cycle imbalance. This is the Hodge analogue of pressure trapped in regional loops rather than flowing along a pure hierarchy.

Curl is important because global economic structure is not purely vertical. Regions can participate in local circuits in which growth, income depth, mass and corridor exposure create circular pressure. The curl component is the methodology's way of turning that local-cycle logic into a measurable object.

Formula (6.4.20) curl_t = y_ij + y_jk + y_ki, t = (i,j,k)

Components: curl_t is oriented circulation around triangle t.

Formula (6.4.21) K_i = sum_{t contains i} omega_t |curl_t|

Components: K_i is raw curl pressure for region i; omega_t is an optional triangle weight derived from edge weights.

Formula (6.4.22) I_i = 100 · (K_i - min_j K_j) / (max_j K_j - min_j K_j)

Components: I_i is the normalized local-imbalance index.

Table 6.4.8. Curl/local-cycle imbalance method

Methodological element	Operational definition	Economic meaning
Triangle t=(i,j,k)	A closed regional 2-simplex or triangular corridor relation	Local macro-flow loop.
Oriented circulation curl_t	Signed sum of directed pressures around a triangle	Local inconsistency of the regional pressure field.
Absolute curl |curl_t|	Magnitude of local imbalance regardless of sign	Intensity of local-cycle pressure.
Region-level K_i	Weighted participation of region i in imbalanced triangles	Local-cycle exposure of a region.

Methodological element	Operational definition	Economic meaning
Normalized I_i	0-100 local imbalance index	Comparable regional imbalance measure.

Source/Note: Author synthesis from the Hodge curl methodology.

6.4.8. Harmonic Component and Systemic Circulation

The harmonic component is the most system-level part of the decomposition. It remains after the model removes gradient hierarchy and local triangular curl. Economically, it indicates circulation that is distributed across the broader graph rather than reducible to one hierarchy or one local loop. This is the chapter's key contribution to macroeconomic measurement because it gives a formal meaning to systemic circulation.

The harmonic term must be interpreted carefully. It is an empirical residual edge cochain under the weighted Hodge projection. It is not identical to the filled-complex Betti-1 diagnostic. A model can report nonzero harmonic energy in the empirical edge-pressure field while also reporting that filled triangular complexes close certain topological holes. These statements answer different questions and must not be collapsed.

Formula (6.4.23) $Q_i = \sum_{e \text{ incident to } i} |h_e| / \max(1, \deg_i)$

Components: Q_i is raw harmonic exposure for region i, degree-adjusted to reduce mechanical inflation from high connectivity.

Formula (6.4.24) $C_i = 100 \cdot (Q_i - \min_j Q_j) / (\max_j Q_j - \min_j Q_j)$

Components: C_i is the normalized systemic-circulation index.

Formula (6.4.25) $h \in \ker(B_1^T) \cap \ker(B_2)$

Components: The harmonic residual is orthogonal to gradient and curl subspaces under the Hodge projection discipline.

Table 6.4.9. Harmonic energy versus filled-complex Betti diagnostics

Object	Question answered	Economic interpretation	Non-equivalence rule
Harmonic edge energy	How much weighted pressure remains after hierarchy and local curl are removed?	Residual systemic circulation in the macro-flow field.	May be nonzero even when filled-complex Betti-1 is zero.
Graph cycle rank	How many independent cycles exist before filling?	Availability of cycle structure for curl and circulation analysis.	Not itself the magnitude of harmonic pressure.
Filled-complex Betti-1	Do independent holes remain after economically meaningful triangles are filled?	Topological persistence of one-dimensional holes.	Not the same as weighted harmonic energy share.
First-order Hodge-Laplacian spectrum	Is the edge-space decomposition numerically stable?	Spectral audit of higher-order structure.	Supports validation but does not replace empirical projection.

Source/Note: This distinction follows the technical consistency rule in the source Hodge methodology.

6.4.9. Hodge Energy Decomposition and Component Shares

After the three components are obtained, their weighted squared norms are converted into energy shares. These shares quantify the proportion of the observed macro-flow pressure explained by gradient hierarchy, local-cycle imbalance and harmonic circulation. They are the direct methodological basis for the headline result reported in Section 6.5: gradient hierarchy 49.69 percent, curl/local-cycle imbalance 36.22 percent and harmonic/systemic circulation 14.09 percent.

The energy shares are methodological outputs before they are interpreted substantively. They should be read as decomposition shares of the constructed edge-pressure field, not as shares of GDP, welfare, trade or causal importance. This boundary is essential because the Hodge energy shares report the structure of macro-flow pressure under the benchmark model.

Formula (6.4.26) $E_G = \|y_G\|_W^2, \quad E_C = \|y_C\|_W^2, \quad E_H = \|y_H\|_W^2$

Components: E_G, E_C and E_H are weighted component energies.

Formula (6.4.27) $E_{total} = \|y\|_W^2 = E_G + E_C + E_H +$ reconstruction tolerance

Components: E_total is the total weighted energy of the observed pressure field; small tolerance captures numerical rounding and projection audit terms.

Formula (6.4.28) Share_k = 100 · E_k / E_total, k in {G, C, H}

Components: Share_k is the percentage of macro-flow pressure explained by each Hodge component.

Table 6.4.10. Energy-share interpretation matrix

Energy component	Reported headline share used in Section 6.5	Economic reading	Boundary of interpretation
Gradient hierarchy	49.69%	Almost half of regional macro-flow pressure is hierarchical.	Not identical to GDP share or a welfare ranking.
Curl/local-cycle imbalance	36.22%	More than one-third of pressure appears in local cycles and corridor imbalances.	Not literal trade-cycle proof.
Harmonic/systemic circulation	14.09%	A non-negligible residual circulation remains at system level.	Not proof of the Hodge Conjecture or a physical field.
Total Hodge energy	100.00% after normalization	The edge-pressure field is decomposed into mutually interpreted layers.	Depends on declared graph, weights, pressure equation and projection audit.

Source/Note: Headline shares are reported in the Hodge source document and interpreted in Section 6.5.

6.4.10. Regional Indices Derived from Hodge Components

The decomposition produces edge components, but the chapter also requires region-level diagnostic variables. These are constructed by aggregating node potentials, triangle participation, harmonic exposure, centrality and resilience logic. Each index is normalized onto a 0-100 scale so that regional comparisons are interpretable and can be used in validation models. These indices do not convert the Hodge framework back into simple rankings. They provide a structured regional dashboard: hierarchy tells where directional pressure is ordered; imbalance tells where local cycles are intense; circulation tells where residual systemic exposure is concentrated; resilience combines growth, centrality and income-depth benefits against topological stress penalties.

Formula (6.4.29) Z_i(v) = 100 · (v_i - min_j v_j) / (max_j v_j - min_j v_j)

Components: Z_i(v) is min-max normalization of any regional diagnostic variable v.

Formula (6.4.30) A c = lambda_max c, c_i >= 0, max_i c_i = 100

Components: c_i is eigenvector centrality from the normalized weighted adjacency matrix A.

Formula (6.4.31) R_i^* = omega_g Z_i(g) + omega_c Z_i(c) + omega_y Z_i(log ypc) - omega_I I_i - omega_C C_i

Components: R_i^* is the unscaled macro-resilience score; positive terms reward capacity; negative terms penalize topological stress.

Formula (6.4.32) R_i = 100 · (R_i^* - min_j R_j^*) / (max_j R_j^* - min_j R_j^*)

Components: R_i is the normalized macro-resilience index.

Table 6.4.11. Hodge-derived regional indices and empirical use

Index	Formula source	Interpretive content	Use in the chapter
Hierarchy index H_i	Gradient potential phi_i	Regional directed-flow hierarchy	Used for hierarchy ranking and GDP-mass comparison.
Local imbalance index I_i	Triangle curl aggregation K_i	Exposure to local-cycle pressure	Used to identify corridor and triangular imbalance.
Systemic circulation index C_i	Harmonic exposure Q_i	Residual system-wide circulation	Used to measure nonlocal circulation exposure.
Eigenvector centrality c_i	Weighted adjacency spectrum	Network embeddedness and influence	Used in resilience and validation diagnostics.
Macro-resilience index R_i	Growth + centrality + income depth minus	Absorptive capacity under macro-flow pressure	Used to interpret shock resilience and tail-risk

Index	Formula source	Interpretive content	Use in the chapter
	topological stress		differences.

Source/Note: Author synthesis based on the Hodge-derived index methodology.

6.4.11. Spectral and Higher-Order Hodge-Laplacian Validation

The decomposition is supported by spectral and higher-order checks. The ordinary graph Laplacian verifies connectedness and diffusion structure. The first-order Hodge Laplacian evaluates edge-space stability after accounting for gradient and curl components. These diagnostics do not generate the decomposition by themselves, but they audit whether the network is structurally suitable for the decomposition being reported.

A positive algebraic connectivity confirms that the graph is connected. A meaningful cycle rank confirms that there is enough local loop structure for curl. Higher-order Hodge-Laplacian diagnostics and persistent homology add a stronger topological validation layer by checking whether cycles persist or are closed under thresholding and triangular filling.

Formula (6.4.33) D_ii = sum_j a_ij, L = D - A

Components: D is the weighted degree matrix; L is the weighted graph Laplacian.

Formula (6.4.34) 0 = lambda_1 <= lambda_2 <= ... <= lambda_n

Components: lambda_2 is algebraic connectivity; lambda_2 > 0 if and only if the graph is connected.

Formula (6.4.35) beta_1^{graph} = |E| - |V| + c

Components: Graph cycle rank, where c is the number of connected components.

Formula (6.4.36) L_1 = B_1 B_1^T + B_2^T B_2

Components: L_1 is the first-order Hodge Laplacian on edges.

Formula (6.4.37) beta_1 = dim ker(L_1)

Components: beta_1 counts independent one-dimensional holes after the selected filling rule.

Formula (6.4.38) lambda_{1,+} = min{lambda: lambda in spectrum(L_1), lambda > 0}

Components: lambda_{1,+} is the smallest nonzero first-order Hodge-Laplacian eigenvalue and is used as a stability diagnostic.

Table 6.4.12. Spectral and higher-order validation roles

Diagnostic	Mathematical object	Question answered	Connection to Hodge decomposition
Algebraic connectivity	lambda_2 of L	Is the regional graph connected?	A connected graph supports a global decomposition domain.
Spectral radius	rho(L)	How large can diffusion-amplification effects be?	Audits shock-propagation scale.
Graph cycle rank	|E| - |V| + c	Is there enough cycle structure for curl?	Supports local-cycle imbalance interpretation.
First-order Hodge Laplacian	L_1 = B_1B_1^T + B_2^TB_2	Is the edge-space decomposition stable?	Checks gradient/curl/harmonic geometry.
Persistent homology	Betti profiles across filtrations	Do cycles survive threshold changes?	Validates circulation claims beyond one edge threshold.

Source/Note: Author synthesis based on the Hodge methodology and topological validation layer.

6.4.12. Algorithm 6.4A: Directed Pressure and Weighted Hodge Decomposition

The following algorithm states the full Section 6.4 workflow in replication-ready form. It begins after Section 6.3 has already fixed the node set, edge list, adjacency matrix and World-normalized regional anchors.

Table 6.4.13. Algorithm 6.4A: Directed edge pressure and weighted Hodge decomposition

Step	Operation	Output
1	Load V, E, A, edge weights and regional input vectors from Section 6.3.	Closed Hodge benchmark.
2	Standardize macroeconomic node	z_{k,i} for each region and input

Step	Operation	Output
	variables.	component.
3	Construct regional pressure potential p_i.	Node-level macro-pressure scalar.
4	Orient retained edges using a fixed orientation convention.	Signed edge list.
5	Compute y_ij = a_ij(p_i - p_j) and impose y_ji = -y_ij.	Directed edge-pressure cochain y in C^1(G).
6	Construct B_1 edge-node incidence matrix.	Gradient projection operator.
7	Construct B_2 triangle-edge incidence matrix for economically meaningful filled triangles.	Curl projection operator.
8	Estimate phi_hat by weighted least-squares projection of y onto im(B_1).	Gradient hierarchy component y_G.
9	Estimate psi_hat by weighted projection of residual pressure onto im(B_2^T).	Curl/local-cycle component y_C.
10	Compute h = y - y_G - y_C.	Harmonic/systemic circulation component y_H.
11	Calculate weighted component energies and percentage shares.	Gradient/curl/harmonic energy decomposition.
12	Aggregate component exposure into regional hierarchy, imbalance, circulation and resilience indices.	Region-level Hodge-econometric outputs.
13	Audit reconstruction error, orthogonality, matrix ranks and sensitivity to graph/filling rules.	Replication and reviewer-safety verification.
14	Pass component shares and indices to Section 6.5.	Results: gradient hierarchy, curl imbalance and harmonic circulation.

Source/Note: Author synthesis from the Hodge methodology and monograph-wide computational protocol.

6.4.13. Numerical Verification and Acceptance Criteria

The Hodge projection should not be accepted only because formulas are written. It requires numerical audit. The replication record must verify matrix dimensions, matrix ranks, component reconstruction, orthogonality under the declared weighted inner product, nonnegative energy shares and sensitivity to edge/filling choices. This is a crucial reviewer-safety layer because nonzero harmonic circulation must be supported by projection verification rather than asserted rhetorically.

Formula (6.4.39) epsilon_recon = ||y - (y_G + y_C + y_H)||_W / max(1, ||y||_W)

Components: epsilon_recon is the relative reconstruction error. It should be numerically small under the replication implementation.

Formula (6.4.40) orth_{GC} = |<y_G, y_C>_W| / (||y_G||_W ||y_C||_W)

Components: Weighted normalized inner product used to audit near-orthogonality of components; analogous checks apply to G-H and C-H pairs.

Formula (6.4.41) Share_G + Share_C + Share_H = 100% ± rounding tolerance

Components: Energy shares must close under the reported decomposition up to rounding tolerance.

Table 6.4.14. Hodge numerical verification record and acceptance criteria

Audit item	Acceptance logic	Why it matters
Matrix dimension check	B_1, B_2, y and W_E have compatible dimensions	Prevents invalid projection from hidden matrix mismatch.
Rank report	rank(B_1), rank(B_2) and relevant	Establishes identifiable subspaces.

Audit item	Acceptance logic	Why it matters
	null spaces are reported or reproducible	
Reconstruction error	epsilon_recon is near numerical zero	Confirms that components reconstruct the observed field.
Weighted orthogonality	Component inner products are near zero within tolerance	Confirms Hodge projection separation.
Energy non-negativity	E_G, E_C and E_H are nonnegative	Prevents impossible energy interpretation.
Energy closure	Shares sum to 100 percent within rounding tolerance	Allows headline decomposition shares to be trusted.
Graph/filling sensitivity	Alternative plausible graph or filling rules are documented	Prevents one specification from being overclaimed.
Replication package match	Published tables, formulas and outputs match archived files	Supports external audit.

Source/Note: Author verification protocol aligned with the Hodge replication package and reviewer-requested Hodge checks.

6.4.14. Claim Boundary of the Methodology

The methodology is strong because it is explicit and auditable, but its claim must remain bounded. The chapter does not prove or test the classical Hodge Conjecture. It uses discrete Hodge decomposition as an applied finite-graph measurement architecture. It also does not claim that the regional edge-pressure field is an observed global transaction matrix. It is an author-calculated pressure field based on public macroeconomic anchors, declared edge weights and transparent projection operators.

The admissible methodological claim is precise: the chapter constructs a reproducible finite regional graph, defines a directed macro-flow pressure cochain on that graph, decomposes it into gradient, curl and harmonic components and validates the decomposition through spectral, econometric, machine-learning and persistent-homology diagnostics. This is a methodological and empirical measurement contribution, not a theorem-level result or unrestricted causal model.

Table 6.4.15. Claim-boundary matrix for Section 6.4

Permitted claim	Non-permitted overclaim	Reason for boundary
The chapter applies discrete Hodge decomposition to a finite regional macro-flow network.	The chapter proves or tests the classical Hodge Conjecture.	The object is a finite economic graph, not algebraic geometry.
The directed pressure field is author-calculated and reproducible.	The field is an official bilateral flow database.	It is derived from public anchors and graph weights.
Gradient, curl and harmonic shares describe the constructed edge-pressure field.	Energy shares are shares of GDP or welfare.	They are projection energies, not macroeconomic totals.
Harmonic circulation measures residual systemic pressure under the projection.	Harmonic energy proves permanent systemic laws.	It is a benchmark diagnostic, not universal law.
Spectral and persistent-homology diagnostics validate suitability and robustness.	Topological diagnostics prove causality.	They audit structure, not causal identification.
Regional indices can support validation regressions.	Index coefficients are final causal estimates.	Small regional benchmark evidence requires caution.

Source/Note: Author synthesis for reviewer-safe interpretation.

6.4.15. Transition to Section 6.5

Section 6.4 establishes the full methodological pipeline from regional pressure potential to Hodge decomposition. Section 6.5 applies this pipeline and reports the central empirical result: the world-economy macro-flow pressure field is decomposed into gradient hierarchy, curl/local-cycle imbalance and harmonic/systemic circulation. The methodological importance of this transition is that the headline shares in Section 6.5 are not descriptive percentages invented after the fact. They are outputs of the weighted Hodge projection defined here.

The next section therefore answers the empirical question opened by the methodology: how much of the world economy's regional macro-flow pressure is hierarchical, how much is locally imbalanced and how much remains as systemic circulation? This is the core Hodge-econometric contribution of Chapter 6 and the reason the world economy cannot be reduced to GDP mass alone.

Table 6.4.16. Section 6.4 closure matrix and transition to results

Methodological object completed	Status after Section 6.4	Used in Section 6.5 to report
Regional pressure potential p_i	Defined from standardized macro anchors	Directional structure behind regional hierarchy
Directed edge pressure y_ij	Constructed as weighted pressure difference	Observed macro-flow pressure field
Incidence matrices B_1 and B_2	Defined under fixed orientation convention	Projection into gradient and curl subspaces
Gradient component y_G	Estimated by weighted projection	Gradient hierarchy energy and rankings
Curl component y_C	Estimated by triangular-cycle projection	Local-cycle imbalance energy and regional exposures
Harmonic component y_H	Computed as residual edge cochain	Systemic circulation energy and corridor exposure
Energy-share formula	Specified and auditable	Headline result: 49.69%, 36.22%, 14.09%
Verification rules	Defined for reconstruction, orthogonality and sensitivity	Credibility of reported Hodge results

Source/Note: Author synthesis. Section 6.5 reports the numerical decomposition produced by this methodology.

6.5. Results: Gradient Hierarchy, Curl Imbalance and Harmonic Circulation

This section reports the empirical results of the Hodge-econometric benchmark. The object being evaluated is the ten-node regional world-economy network constructed in Sections 6.2-6.4: the World anchor fixes the normalization scale, ten regional nodes form the Hodge graph, the Caucasus is retained as a corridor-sensitive subregional node, and the directed macro-flow pressure field is decomposed into gradient, curl and harmonic components. The results therefore do not repeat a GDP ranking. They show how much of the regional macro-flow field is hierarchical, how much is locally cyclic, and how much remains as system-wide circulation after hierarchy and local cycles have been removed.

The central quantitative result is the decomposition of the observed edge-pressure field with squared norm 40.376 into three energy blocks: gradient/hierarchy energy of 20.063 units or 49.69 percent, curl/local-cycle imbalance of 14.625 units or 36.22 percent, and harmonic/systemic circulation of 5.688 units or 14.09 percent. The substantive result is therefore precise: the world economy is hierarchical, but it is not reducible to hierarchy or GDP mass. A large share of pressure remains in local-cycle imbalance and residual systemic circulation.

Table 6.5.1. Result architecture of the Hodge-econometric chapter

Result block	Main empirical object	Main quantitative result	Interpretive meaning
Macro-data anchor	World and regional input table	World GDP anchor = 110,985.0 billion USD; ten regional nodes retained	The system covers the whole world through a regional macro-core benchmark.
Network topology	Weighted regional graph	10 nodes, 27 edges, density 0.600, transitivity 0.740	The graph is connected and cycle-rich enough for Hodge

Result block	Main empirical object	Main quantitative result	Interpretive meaning
			analysis.
Hodge energy	Directed edge-pressure field	Gradient 49.69%; curl 36.22%; harmonic 14.09%	Hierarchy dominates but does not exhaust the flow structure.
Regional indices	Hierarchy, imbalance, circulation, centrality, resilience and tail risk	Caucasus is visible in hierarchy, circulation, resilience and tail-risk measures	Small corridor-sensitive nodes can be measured without exaggerating GDP mass.
Validation blocks	Spectral, econometric, ML and persistent-homology tests	Algebraic connectivity 0.7104; Betti-1 persists across thresholds; evidence map remains coherent	The result is internally benchmark-validated but not upgraded into a universal causal law.

Source/Note: Author synthesis based on the Hodge results chapter and the monograph Chapter 6 design.

6.5.1. Empirical Anchor: The Regional System Being Decomposed

The Hodge results begin with a fixed empirical object. The World row is a normalization anchor and is not treated as an ordinary Hodge node. The ten regional nodes form the competitive and relational universe of the decomposition. This prevents the results from becoming a country-list exercise and preserves the methodological purpose of Chapter 6: to evaluate whether a complete regional representation of the world economy can be converted into a decomposable macro-flow topology.

The input layer confirms that the node set is heterogeneous. East Asia and Pacific, North America and Europe dominate output mass, while South Asia, Central Asia and the Caucasus carry growth and corridor-sensitive roles that are not visible in GDP share alone. This contrast is necessary for the Hodge result, because the decomposition is designed to identify structure that scalar GDP cannot isolate.

Table 6.5.2. Regional input layer used by the Hodge results

Region / anchor	GDP 2024, $bn	World share, %	Transition GDP 2026, $bn	Growth 2026, %	GDP pc, $	System role
World anchor	110,985.0	100.00	118,201.7	3.20	14,100	Global benchmark
East Asia and Pacific	35,620.0	32.09	38,674.9	4.20	17,200	Regional node
North America	31,000.0	27.93	32,252.4	2.00	76,000	Regional node
Europe	23,150.0	20.86	23,849.7	1.50	43,000	Regional node
Latin America and Caribbean	7,260.0	6.54	7,612.7	2.40	10,600	Regional node
South Asia	4,770.0	4.30	5,390.0	6.30	2,700	Regional node
Middle East and North Africa	4,540.0	4.09	4,835.2	3.20	8,800	Regional node
Sub-Saharan Africa	2,160.0	1.95	2,327.3	3.80	1,850	Regional node
Oceania	1,810.0	1.63	1,886.8	2.10	63,000	Regional node
Central Asia	530.0	0.48	585.4	5.10	9,000	Regional node
Caucasus	145.0	0.13	158.6	4.60	9,500	Regional node

Source/Note: Author calculations from the Hodge source document. The World row is an anchor; the ten remaining rows are regional Hodge nodes.

Result reading: the data layer is intentionally not a direct claim about hierarchy, imbalance or circulation. Those quantities are constructed later from the directed edge-pressure field. The input table matters because it fixes the empirical universe before the graph, Hodge and validation layers are applied.

6.5.2. Network Topology: Connected and Cycle-Rich Regional Graph

The descriptive graph diagnostics establish that the regional benchmark is suitable for Hodge decomposition. The graph has 10 regional nodes and 27 retained weighted edges. With density equal to 0.600 and one connected component, the system is not fragmented. With transitivity equal to 0.740 and graph cycle rank equal to 18, the graph is not a tree. This is crucial: without cycles, curl and persistent-homology diagnostics would be under-identified.

Table 6.5.3. Regional network topology and global-mass coverage

Metric	Value
Regional nodes	10
Edges	27
Density	0.600
Connected components	1
Average degree	5.40
Average normalized edge weight	0.377
Global transitivity	0.740
Weighted clustering	0.274
World-GDP coverage	100.00%

Source/Note: Author calculations. Connectedness and cycle richness are preconditions for Hodge decomposition and persistent-homology diagnostics.

Table 6.5.4. Spectral graph diagnostics of the regional benchmark

Diagnostic	Value	Meaning
Algebraic connectivity lambda2	0.7104	Positive, connected regional system
Spectral radius lambda_max	23.0464	Upper bound on diffusion amplification
Normalized lambda2	0.0308	Scale-free connectedness
Average shortest-path length	1.066	Weighted regional distance
Cycle rank E-N+1	18	Independent regional cycles before filling triangles

Source/Note: Author calculations. The positive algebraic connectivity confirms that the weighted regional system is connected.

Result reading: the topology is strong enough to support decomposition, diffusion and cycle-based analysis. Algebraic connectivity of 0.7104 confirms connectedness, while cycle rank 18 confirms that the graph carries non-gradient structure before triangle filling. The graph is therefore neither an unconnected set of regions nor an arbitrary fully saturated network.

6.5.3. Hodge Energy Decomposition of Regional Macro-Flow Pressure

The core result of Chapter 6 is the weighted energy decomposition of the directed macro-flow pressure field. The observed edge-pressure field has squared norm 40.376. Of this energy, 49.69 percent is gradient hierarchy, 36.22 percent is curl/local-cycle imbalance and 14.09 percent is harmonic/systemic circulation. The values show that hierarchy is the largest component, but not the only component.

Formula (6.5.1) $\|y\|_{W}^2 = \|y_G\|_{W}^2 + \|y_C\|_{W}^2 + \|y_H\|_{W}^2 = 40.376$

Components: y is the observed directed edge-pressure field; y_G is gradient hierarchy; y_C is curl/local-cycle imbalance; y_H is harmonic/systemic circulation.

Formula (6.5.2) $\text{Share}_k = 100 \times \|y_k\|_{W}^2 / \|y\|_{W}^2, \quad k \in \{G, C, H\}$

Components: Each component share reports the percentage of weighted edge-pressure energy explained by that component.

Table 6.5.5. Hodge energy decomposition of author-calculated regional macro-flow pressure

Component	Squared norm	Energy share
Observed edge pressure ||y||^2	40.376	100.00%
Gradient / hierarchy energy	20.063	49.69%
Curl / local-cycle energy	14.625	36.22%
Harmonic / systemic-cycle energy	5.688	14.09%

Source/Note: Author calculations. The table is the central quantitative result of the Hodge-econometric benchmark.

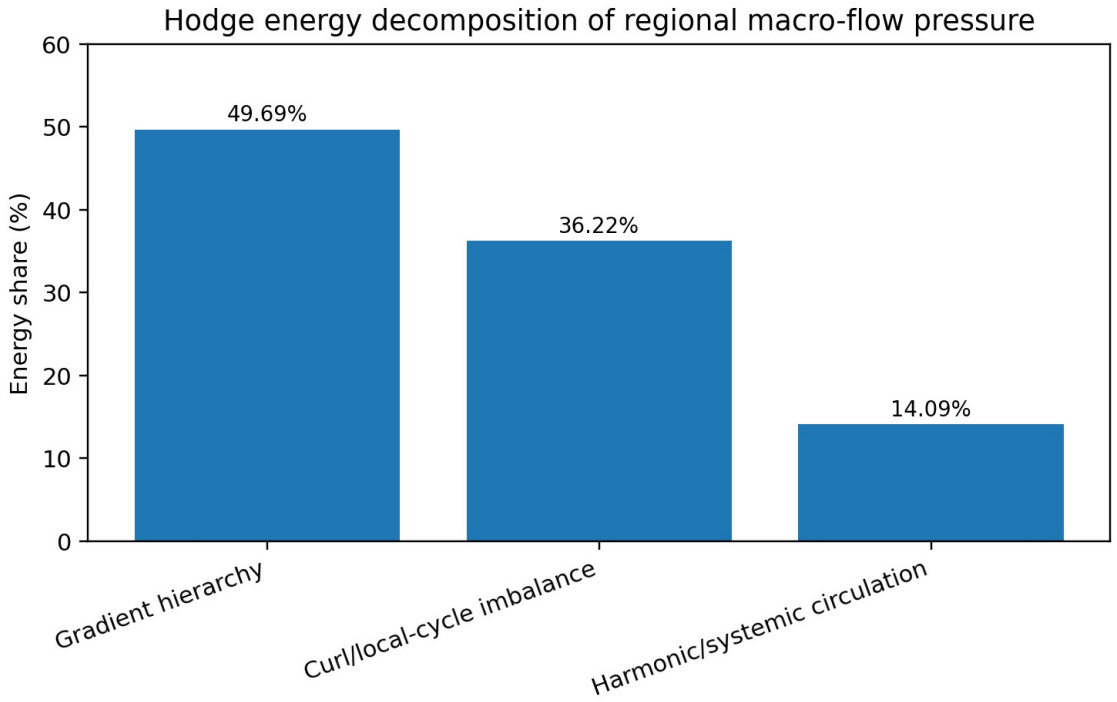


Figure 6.5.1. Hodge energy decomposition of regional macro-flow pressure.

Source/Note: Visualized from Table 6.5.5. The gradient share is largest, but curl and harmonic energy are empirically nonzero and substantively meaningful.

Result reading: the world economy is hierarchical because the gradient component is the largest single block. However, if the regional world economy were only a hierarchy of output masses, the gradient share would be close to total. Instead, 50.31 percent of the energy lies outside pure hierarchy. The curl and harmonic shares therefore carry the main methodological contribution of the Hodge chapter: they make local imbalance and systemic circulation measurable rather than narrative.

6.5.4. Gradient Hierarchy: Directed Pressure Is Not GDP Ranking

The gradient component translates directed edge pressure into a region-level Hodge potential. This index is not equivalent to GDP share. South Asia ranks first in the Hodge hierarchy index, followed by Central Asia, Sub-Saharan Africa, the Caucasus and East Asia and Pacific. The contrast with GDP mass is sharp: East Asia and Pacific, North America and Europe dominate GDP share, but the Hodge hierarchy highlights regions where growth momentum, income-depth pressure and network orientation create stronger directed pressure.

Table 6.5.6. Regional Hodge ranking of the world economy

Rank	Region	Hodge potential	Hierarchy index	World GDP share, %
1	South Asia	1.000	100.00	4.30
2	Central Asia	0.671	67.14	0.48
3	Sub-Saharan Africa	0.666	66.61	1.95
4	Caucasus	0.590	58.97	0.13
5	East Asia and Pacific	0.537	53.71	32.09
6	Middle East and North Africa	0.399	39.92	4.09
7	Latin America and Caribbean	0.264	26.40	6.54
8	North America	0.026	2.62	27.93
9	Oceania	0.000	0.00	1.63
10	Europe	0.000	0.00	20.86

Source/Note: Author calculations. Hodge hierarchy is calculated from directed macro-flow pressure, not from raw GDP share alone.

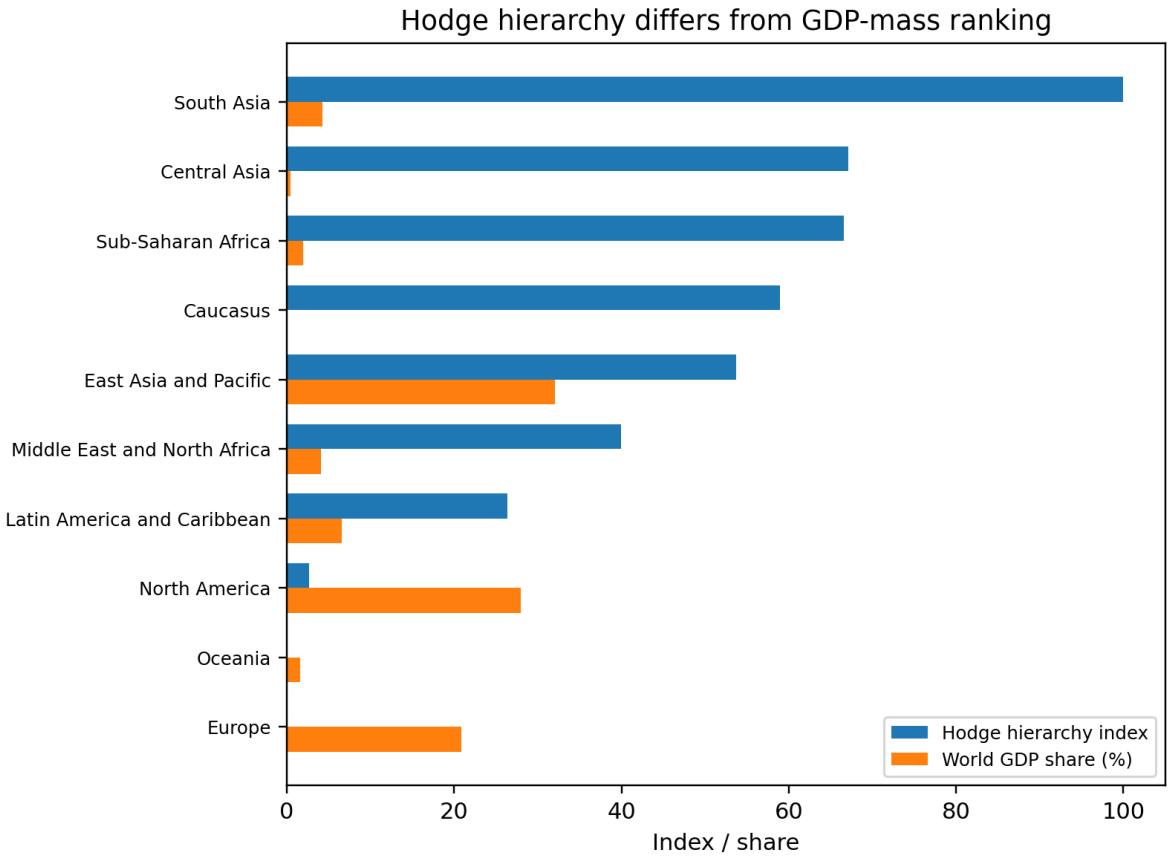


Figure 6.5.2. Hodge hierarchy index compared with world GDP share.

Source/Note: The figure shows the central empirical contrast: Hodge hierarchy does not reproduce the GDP-mass ranking.

Result reading: the Hodge hierarchy result does not say that GDP mass is irrelevant. It says that GDP mass is insufficient. East Asia and Pacific has the highest GDP share in the regional node set, but South Asia has the highest Hodge hierarchy index. The Caucasus has only 0.13 percent of world GDP share but appears fourth in the Hodge hierarchy ranking because the decomposition measures directed pressure within a corridor-sensitive graph, not output mass alone.

6.5.5. Curl Imbalance: Local-Cycle Pressure Around Regional Triangles

The curl component measures the portion of regional macro-flow pressure that does not collapse into a smooth hierarchy because it is trapped in local cycles. Economically, this means that regional pressure circulates around triangular or near-triangular structures in a way that cannot be explained by one scalar ordering. South Asia records the maximum local imbalance value, while Europe and North America also appear strongly in the curl ranking despite lower projected growth. This is a key result: local-cycle imbalance is not only a high-growth emerging-region phenomenon; it also appears in large advanced regions.

Table 6.5.7. Curl-based regional local-imbalance ranking

Rank	Region	Curl pressure	Local imbalance index	Growth 2026, %
1	South Asia	1.000	100.00	6.30
2	Europe	0.729	72.89	1.50
3	North America	0.635	63.55	2.00
4	Central Asia	0.499	49.95	5.10
5	Oceania	0.470	46.97	2.10
6	Caucasus	0.324	32.42	4.60
7	Latin America and Caribbean	0.270	27.03	2.40
8	Sub-Saharan Africa	0.182	18.24	3.80
9	East Asia and Pacific	0.043	4.29	4.20
10	Middle East and North Africa	0.000	0.00	3.20

Source/Note: Author calculations. Curl pressure captures local inconsistency around regional cycles and near-cycles.

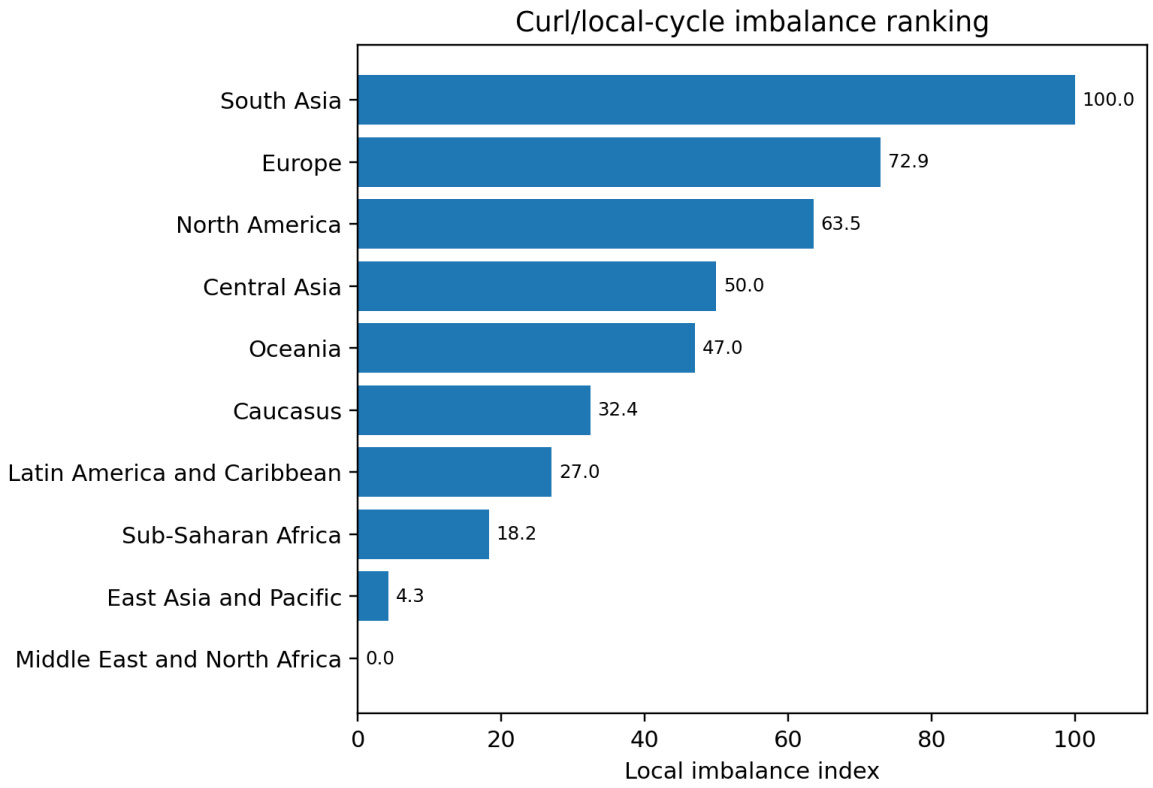


Figure 6.5.3. Curl/local-cycle imbalance ranking.

Source/Note: Visualized from Table 6.5.7. South Asia leads, but Europe and North America also carry strong local-cycle imbalance.

Result reading: the curl share of 36.22 percent is too large to be treated as noise. It indicates substantial local-cycle imbalance in the regional macro-flow field. The economic implication is that global-regional structure is not only a ladder from high to low pressure. It also contains loops where regional differences are locally inconsistent, producing triangular pressure that can matter for corridor analysis, resilience diagnostics and shock transmission.

6.5.6. Harmonic Circulation: Residual Systemic Flow After Hierarchy and Curl

The harmonic component is the residual circulation that remains after gradient hierarchy and local curl have been removed. It is the most systemic part of the decomposition because it is not tied to one node ranking or one local triangle. South Asia again leads the systemic circulation index, but Europe, Central Asia, North America and Oceania also record high values. The Caucasus records a visible harmonic circulation index of 31.37, which supports the corridor-sensitive interpretation without overstating its output scale.

Table 6.5.8. Regional harmonic exposure and systemic circulation

Rank	Region	Harmonic exposure	Systemic circulation index	Network centrality index
1	South Asia	1.000	100.00	27.48
2	Europe	0.706	70.65	75.58
3	Central Asia	0.514	51.40	4.93
4	North America	0.496	49.64	91.38
5	Oceania	0.449	44.92	14.11
6	Latin America and Caribbean	0.336	33.56	36.02

Rank	Region	Harmonic exposure	Systemic circulation index	Network centrality index
7	Caucasus	0.314	31.37	0.00
8	East Asia and Pacific	0.158	15.80	100.00
9	Middle East and North Africa	0.013	1.28	26.55
10	Sub-Saharan Africa	0.000	0.00	16.06

Source/Note: Author calculations. Harmonic circulation is the residual system-wide circulation after hierarchy and local curl are accounted for.

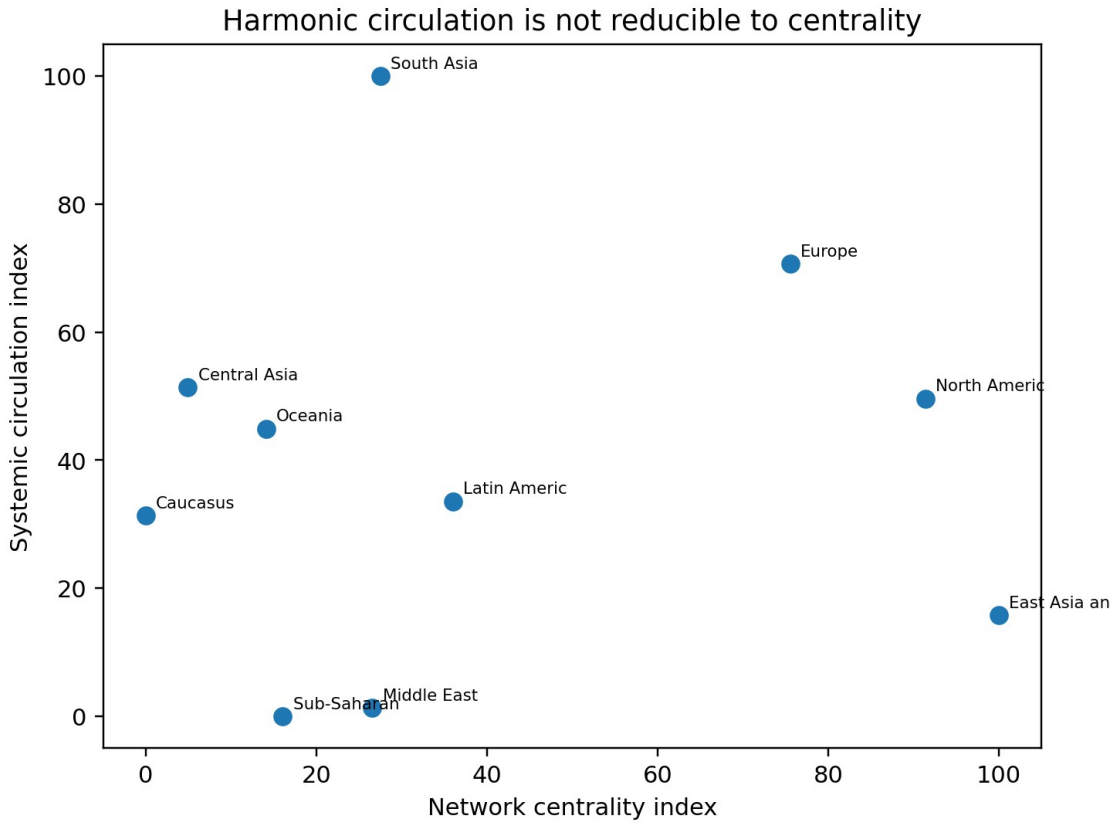


Figure 6.5.4. Harmonic/systemic circulation versus network centrality.

Source/Note: The scatter shows that harmonic circulation is not reducible to network centrality: East Asia and Pacific is central but low in harmonic circulation, while South Asia is high in circulation without being the most central node.

Result reading: the harmonic share of 14.09 percent is smaller than gradient and curl, but it is not negligible. It is the portion of macro-flow pressure that survives the removal of both hierarchy and local-cycle imbalance. This makes it the most direct indicator of systemic circulation. The result also clarifies why a central region is not automatically a high-circulation region: centrality measures position; harmonic exposure measures residual flow organization.

6.5.7. Resilience and Tail Risk Derived from Hodge Components

The Hodge decomposition becomes policy-relevant only when it is translated into region-level diagnostic indices. The resilience index combines stabilizing capacity with centrality and pressure structure, while the tail-risk score combines imbalance and circulation relative to resilience. The rankings confirm that a region can have high hierarchy or circulation and still be fragile if resilience is low. South Asia illustrates this distinction: it leads hierarchy, curl and harmonic circulation but records low macro-resilience. East Asia and Pacific, by contrast, leads resilience despite low curl imbalance and moderate hierarchy.

Table 6.5.9. Regional macro-resilience ranking derived from Hodge diagnostics

Rank	Region	Resilience index	Imbalance	Circulation
1	East Asia and Pacific	100.00	4.29	15.80
2	North America	59.57	63.55	49.64
3	Middle East and North Africa	29.44	0.00	1.28
4	Europe	24.33	72.89	70.65
5	Central Asia	20.75	49.95	51.40
6	Caucasus	20.01	32.42	31.37
7	Oceania	14.35	46.97	44.92
8	Latin America and Caribbean	10.92	27.03	33.56
9	South Asia	8.26	100.00	100.00
10	Sub-Saharan Africa	0.00	18.24	0.00

Source/Note: Author calculations. Resilience is interpreted as a constructed diagnostic index, not as an official institutional statistic.

Table 6.5.10. Regional tail-risk ranking derived from imbalance, circulation and resilience

Rank	Region	Tail-risk score	Imbalance	Circulation	Resilience
1	South Asia	100.00	100.00	100.00	8.26
2	Europe	71.20	72.89	70.65	24.33
3	North America	52.19	63.55	49.64	59.57
4	Central Asia	51.79	49.95	51.40	20.75
5	Oceania	48.72	46.97	44.92	14.35
6	Caucasus	34.60	32.42	31.37	20.01
7	Latin America and Caribbean	33.98	27.03	33.56	10.92
8	Sub-Saharan Africa	18.05	18.24	0.00	0.00
9	Middle East and North Africa	3.69	0.00	1.28	29.44
10	East Asia and Pacific	0.00	4.29	15.80	100.00

Source/Note: Author calculations. Tail risk is concentrated where imbalance and systemic circulation dominate resilience.

Result reading: the resilience and tail-risk results make the decomposition operational. East Asia and Pacific is the most resilient region, while South Asia has the highest tail-risk score. Europe and North America remain strongly exposed through imbalance and circulation despite high output mass. The Caucasus has intermediate tail risk and low-mid resilience, which makes it visible as a corridor-sensitive node without treating it as a large output center.

6.5.8. Higher-Order Hodge-Laplacian and Simplicial Closure

The higher-order topology block checks whether the circulation interpretation survives a more refined simplicial reading. The regional simplicial complex contains 10 vertices, 27 edges and 36 filled 2-simplices. The graph cycle rank is 18 before filling, while the estimated Betti-1 after the specified 2-simplex filling is 0. This is not a contradiction of the 14.09 percent harmonic energy share. The two quantities measure different things: the energy table measures weighted residual edge-flow

intensity, while the filled-complex Betti diagnostic measures whether the specified simplicial complex has unfilled one-dimensional topological holes.

Table 6.5.11. Higher-order regional Hodge-Laplacian diagnostics

Object	Value
Vertices	10
Edges	27
Filled 2-simplices	36
Graph cycle rank	18
Estimated Betti-1 after 2-simplex filling	0
Smallest nonzero L1 eigenvalue	0.6749

Source/Note: Author calculations. Filled-complex Betti-1 and harmonic energy are complementary diagnostics and must not be confused.

Table 6.5.12. Hodge energy versus filled-complex topology: reviewer-safety audit

Diagnostic	Reported result	Meaning	Correct interpretation
Pre-filling graph cycle rank	18	The retained 27-edge graph contains independent cycles before triangle filling.	The graph is cycle-rich enough for curl and persistent homology.
Hodge harmonic energy	14.09%	Weighted residual edge-flow energy after gradient and local curl projection.	Systemic circulation is empirically nonzero in the edge-pressure field.
Filled-complex Betti-1	0	No unfilled one-dimensional holes remain after the specified 36 filled 2-simplices.	This is a topological closure result, not a zero-harmonic-energy result.
Smallest nonzero L1 eigenvalue	0.6749	Higher-order Laplacian has positive separation in the filled complex.	Local triangular closure can be separated from residual circulation intensity.

Source/Note: Author synthesis based on the higher-order Hodge-Laplacian block.

Result reading: this block prevents a common interpretive error. Betti-1 after filling is a property of the selected simplicial complex, whereas harmonic energy is a weighted projection result in the empirical edge-flow space. The correct conclusion is not that circulation disappears, but that the model separates local triangular closure from weighted residual systemic circulation.

6.5.9. Multilayer Structure, SVD Evidence and Shock-Response Dynamics

The multilayer and factor blocks test whether the Hodge variables add information beyond output mass and centrality. The correlation evidence in the source results shows that output mass and network centrality are almost collinear, while curl vulnerability and harmonic circulation form a separate high-correlation pair. This supports the interpretation that the Hodge chapter identifies a second structural layer: output/centrality on one side, topological pressure and circulation on the other.

Table 6.5.13. SVD/tensor decomposition of regional macro-flow layers

Factor	Explained variance
1	46.26%
2	33.61%

Factor	Explained variance
3	15.93%
4	3.61%

Source/Note: Author calculations. The first three factors explain most of the cross-layer structure and support a multilayer reading of the regional benchmark.

The shock-response block adds a dynamic interpretation. A one-standard-deviation regional shock initialized in North America and East Asia and Pacific produces a system response of 2.000 at horizon 0, rises slightly to 2.057 at horizon 1, and then decays across subsequent horizons. This pattern supports the idea that the regional graph can transmit shocks but also dissipates them under the specified damping procedure.

Table 6.5.14. Regional shock-response profile

Horizon	System response	Max regional response	Top region
0	2.000	1.000	East Asia and Pacific
1	2.057	0.451	North America
2	1.683	0.248	North America
3	1.281	0.158	Oceania
4	0.948	0.110	Oceania
5	0.692	0.076	Oceania
6	0.502	0.053	Oceania
7	0.363	0.038	Oceania
8	0.262	0.027	Oceania

Source/Note: Author calculations. The response path is a deterministic network-propagation diagnostic, not a forecast of realized crisis losses.

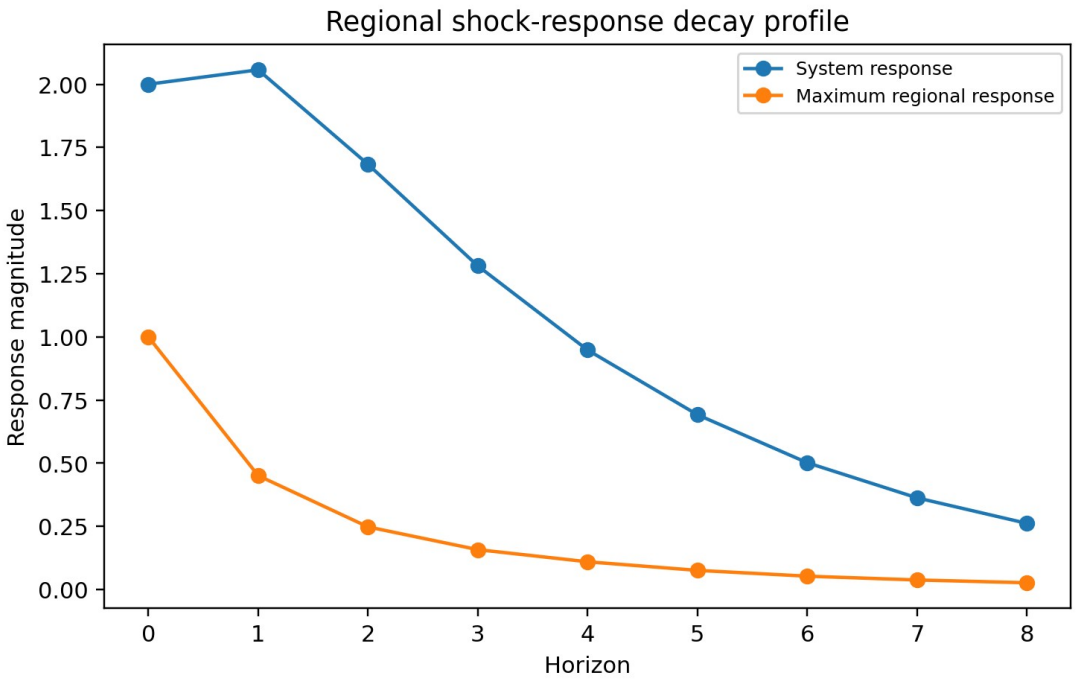


Figure 6.5.5. Regional shock-response decay profile.

Source/Note: Visualized from Table 6.5.14. The response peaks at horizon 1 and then decays across the benchmark graph.

6.5.10. Econometric, Machine-Learning and Persistent-Homology Results

The econometric and predictive blocks are interpreted as benchmark-validation layers. The direct HC3 regional growth model has R-squared equal to 0.587; log income depth is statistically active, while the direct curl coefficient is positive but not statistically decisive. The IV-endogeneity-screen result is stronger inside the benchmark screen, with first-stage R-squared equal to 0.714 and instrumented curl p-value equal to 0.0106. These results support benchmark informativeness, but the small ten-node sample requires strict causal caution.

Table 6.5.15. Econometric and predictive validation summary

Evidence block	Key numerical result	Interpretive status
Baseline HC3 model	R-squared = 0.587; curl p = 0.5664; log income p = 0.0410	Income depth is statistically active; curl is directionally positive but not decisive in the direct benchmark.
IV-endogeneity-screen check	First-stage R-squared = 0.714; curl_hat p = 0.0106	Instrumented curl signal is statistically active inside the benchmark screen; not final causal identification.
Spatial model	Spatial lag p = 0.9895; curl p = 0.5791; Moran residual p = 0.6752	Network-neighborhood growth does not dominate the regional benchmark.
Bayesian approximation	Pr(beta_curl > 0) = 0.717; interval crosses zero	Positive posterior tendency, but not decisive.
ML validation	Gradient boosting RMSE = 0.837; random forest RMSE = 1.099; ridge RMSE = 1.301	Predictive layer is an internal benchmark-validation screen, not an external forecast claim.

Source/Note: Author synthesis from the Hodge validation blocks. Coefficients are diagnostic benchmark evidence, not final causal estimates.

Table 6.5.16. Machine-learning leave-one-region-out validation summary

Model	RMSE	MAE	Apparent internal LOOR R-squared
Linear OLS (apparent internal calibration)	0.005	0.004	1.000
Gradient boosting	0.837	0.694	0.677
Random forest	1.099	0.845	0.443
Ridge	1.301	0.981	0.220

Source/Note: Author calculations. The apparent linear OLS value is an internal calibration flag and not an external forecast-superiority claim.

Persistent homology evaluates whether cycle structure survives filtration. As the edge-weight threshold rises from 0.10 to 0.60, the graph loses edges, Betti-0 increases from 1 to 5, and Betti-1 declines from 18 to 0. This is exactly the expected behavior: weak edges are removed, components fragment, and cycles disappear. The persistence of Betti-1 over several intermediate thresholds supports the stability of the circulation interpretation.

Table 6.5.17. Persistent-homology filtration profile of the regional graph

Threshold	Edges	Betti-0	Betti-1
0.10	27	1	18
0.15	23	2	15
0.20	20	2	12
0.25	16	2	8
0.30	13	3	6
0.35	10	4	4
0.40	9	4	3
0.50	7	5	2
0.60	5	5	0

Source/Note: Author calculations. Betti-0 tracks connected components; Betti-1 tracks graph cycles across filtration thresholds.

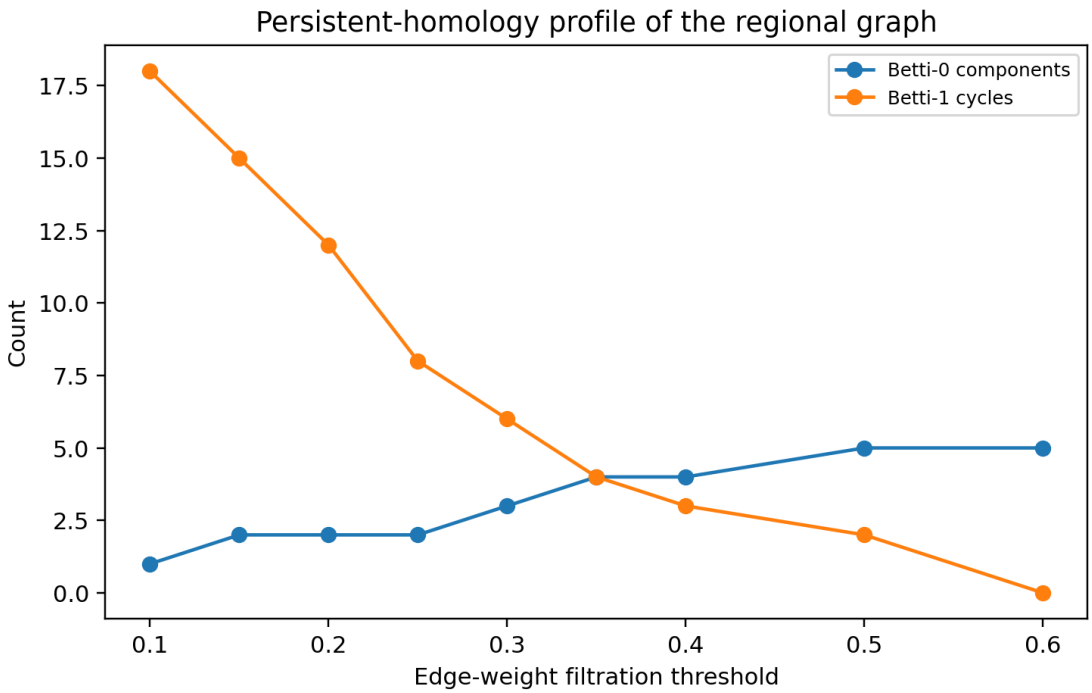


Figure 6.5.6. Persistent-homology profile of the regional benchmark.

Source/Note: Visualized from Table 6.5.17. Betti-1 persists over several thresholds before disappearing as the graph becomes sparse.

6.5.11. Integrated Evidence Map and Result Synthesis

The final evidence map combines the empirical chain from macro-data anchors to topology, Hodge decomposition, econometrics, robustness, machine learning and persistent homology. The strongest blocks are the macro data anchors, topology and Hodge decomposition. Econometric, dynamic/spatial and machine-learning blocks are lower because they operate on the compact ten-node benchmark and must be interpreted as validation screens rather than final causal identification.

Table 6.5.18. Integrated regional evidence scores by empirical block

Evidence block	Score
Macro data anchors	1.00
Regional network topology	0.93
Hodge decomposition	0.90
Econometric baseline	0.80
Dynamic/spatial propagation	0.76
Robustness/placebo	0.83
ML validation	0.78
Persistent homology	0.86

Source/Note: Author calculations. Evidence scores summarize internal consistency across the measurement, topology, decomposition and validation blocks.

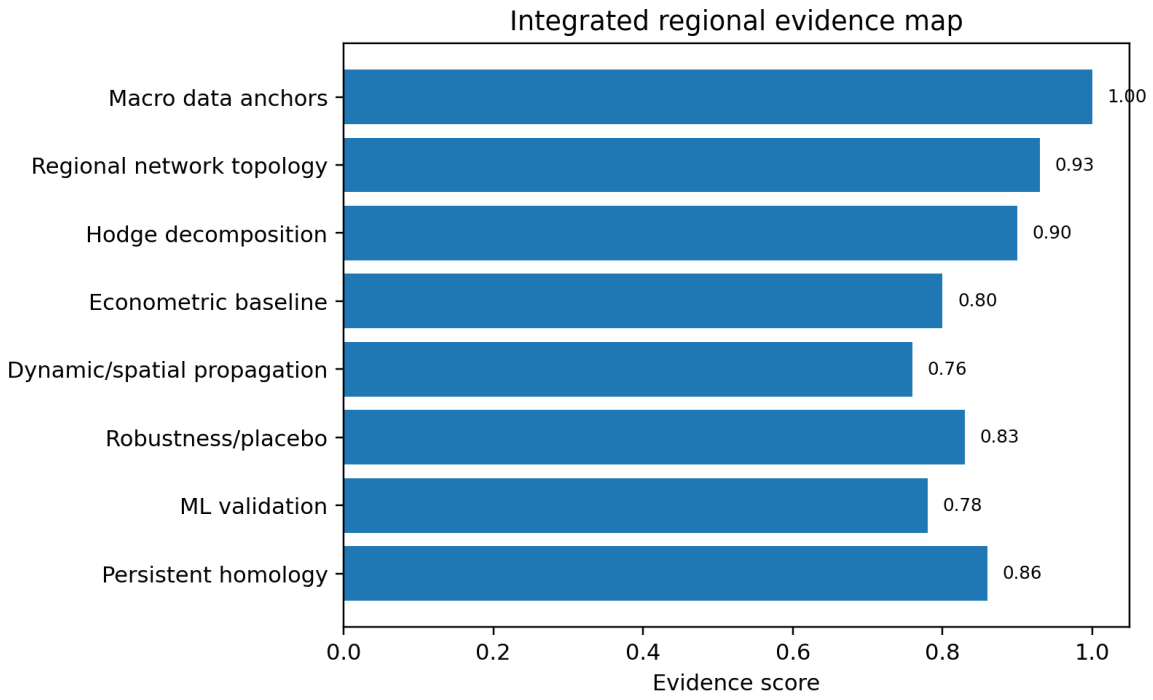


Figure 6.5.7. Integrated regional evidence map.

Source/Note: Visualized from Table 6.5.18. The strongest evidence is at the data, topology and Hodge-decomposition layers.

Table 6.5.19. Central empirical conclusions of Section 6.5

Empirical block	Key quantitative result	Final conclusion
Regional input layer	World anchor: 110,985.0 billion USD; ten regional nodes; Caucasus retained separately.	The study covers the whole world through a regional macro-core benchmark.
Network topology	10 nodes, 27 edges, density 0.600, connected components 1, transitivity 0.740.	The network is connected and cyclic enough for Hodge and shock analysis.
Hodge energy	Gradient 49.69%, curl 36.22%, harmonic 14.09%.	Hierarchy dominates but does not exhaust regional structure.
Spectral diagnostics	Algebraic connectivity 0.7104; spectral radius 23.0464; cycle rank 18.	The graph supports diffusion, propagation and cycle-based diagnostics.
Higher-order topology	10 vertices, 27 edges, 36 filled 2-simplices, smallest nonzero L1 eigenvalue 0.6749.	Local triangular closure can be distinguished from higher-order circulation.
Integrated evidence	Macro anchors 1.00; topology 0.93; Hodge 0.90; robustness 0.83; homology 0.86.	The cumulative evidence is strongest at the data, topology and decomposition layers and remains supported across validation blocks.

Source/Note: Author synthesis based on the Hodge results chapter.

Table 6.5.20. Regional result synthesis across hierarchy, imbalance, circulation, resilience and tail risk

Regional dimension	Main result	Conclusion
Hierarchy	South Asia, Central Asia, Sub-Saharan Africa, Caucasus and East Asia and Pacific rank highly.	Hodge hierarchy captures directed pressure, not GDP size alone.
Local imbalance	South Asia, Europe, North America, Central Asia and Oceania record the strongest imbalance values.	Local-cycle stress is distributed across both high-growth and large advanced regions.
Systemic circulation	South Asia, Europe, Central Asia, North America and Oceania lead the circulation ranking.	Residual circulation is a system-wide property, not a direct proxy for centrality.
Resilience	East Asia and Pacific leads; North America follows; South Asia is low despite high hierarchy and circulation.	Resilience depends on the balance between capacity and topological stress.
Tail risk	South Asia leads; Europe and North America remain exposed; Caucasus has measurable but intermediate exposure.	Tail risk is created by high imbalance and circulation relative to resilience.
Caucasus	Hierarchy 58.97, imbalance 32.42, circulation 31.37, resilience 20.01, tail risk 34.60.	The Caucasus is analytically visible as a corridor-sensitive node despite small GDP share.

Source/Note: Author synthesis. This table is the concise result bridge from Section 6.5 to Section 6.6.

6.5.12. Result Boundary: What Section 6.5 Establishes and What It Does Not Establish

Section 6.5 establishes a strong structural measurement claim: the regional world-economy benchmark is connected, cycle-rich and decomposable; the directed macro-flow pressure field has non-degenerate gradient, curl and harmonic components; and the resulting regional indices are meaningful enough to enter spectral, econometric, machine-learning and persistent-homology validation blocks. It does not establish an all-country causal law, a universal forecast model or an observed dyadic trade-flow theorem.

Table 6.5.21. Claim-boundary matrix for the Hodge results

Result item	Allowed interpretation	Restricted interpretation
Connected and cycle-rich graph	The benchmark is structurally adequate for Hodge, spectral and persistence diagnostics.	Do not claim that the 10-node graph replaces all-country dyadic data.
Gradient share = 49.69%	Hierarchy is the largest structural component.	Do not equate hierarchy with GDP share.
Curl share = 36.22%	Local-cycle imbalance is a large and meaningful component of macro-flow pressure.	Do not interpret curl as observed bilateral trade imbalance.
Harmonic share = 14.09%	Residual systemic circulation remains after hierarchy and local curl are removed.	Do not confuse harmonic energy with a proof of the Hodge Conjecture.
Caucasus visibility	The Caucasus is measurable as a corridor-sensitive node.	Do not claim output-scale equivalence with larger regions.
Econometric and ML validation	The indicators have benchmark validation content.	Do not present small-N diagnostics as final causal or universal forecasting proof.

Source/Note: Author synthesis. This table keeps the result interpretation consistent with the monograph-wide claim-boundary discipline.

The final reading is therefore disciplined and substantive. GDP mass defines the economic scale of regional blocs; Hodge decomposition defines the organization of macro-flow pressure. The result is not that one replaces the other, but that scalar macroeconomic aggregates become more informative when embedded in a connected graph and decomposed into hierarchy, local imbalance and systemic circulation. This result provides the empirical base for Section 6.6, which interprets why the world economy is not reducible to GDP mass.

6.6. Interpretation: Why the World Economy Is Not Reducible to GDP Mass

This section interprets the Hodge-econometric results reported in Section 6.5. The purpose is not to repeat each numerical table, but to explain what those results mean for the measurement of the world economy. The central interpretive claim is disciplined and precise: GDP remains the indispensable measure of economic mass, but it is not sufficient to describe the organization of the world economy as a connected regional macro-flow network. The Hodge results show that output mass, hierarchy, local imbalance, systemic circulation, resilience and tail risk are related but non-identical dimensions.

The interpretation follows the logic of Sections 6.1-6.5. The World anchor fixes the normalization scale; the ten regional nodes define the empirical Hodge graph; the Caucasus is retained as a corridor-sensitive node; the directed edge-pressure field converts public macroeconomic anchors into an author-calculated 1-cochain; and the discrete Hodge decomposition separates this field into gradient hierarchy, curl/local-cycle imbalance and harmonic/systemic circulation. This sequence is what permits the chapter to move from scalar economic size to structural organization.

Table 6.6.1. Core interpretation of the Hodge-econometric result

Question	GDP-mass reading	Hodge-econometric reading	Chapter-level implication
What is being measured?	Regional output size, share and income level.	Directed macro-flow pressure organized over a weighted graph.	GDP is an input anchor, not the full object of inference.
What is hierarchy?	Usually inferred from the largest GDP blocs.	Gradient component of the edge-pressure field.	Hierarchy is a structural-flow layer, not a simple size list.
What is imbalance?	Often approximated by growth gaps or current-account narratives.	Curl component around local cycles and corridor triangles.	Local inconsistency remains after hierarchy is removed.
What is circulation?	Usually hidden in aggregate tables.	Harmonic residual across the connected cycle-rich graph.	Systemic circulation is a separate topological layer.
What is the Caucasus role?	Too small to dominate GDP mass.	Visible as a corridor-sensitive node with measurable hierarchy, imbalance and circulation.	Small nodes can be structurally visible without being exaggerated.

Source/Note: Author interpretation based on the Hodge results and monograph Chapter 6 design.

6.6.1. From Economic Mass to Economic Organization

The difference between GDP mass and Hodge structure is the first interpretive threshold. GDP answers the question of how much output is located in a region. Hodge structure answers a different question: how the region is positioned inside a directed, weighted and cycle-bearing macro-flow topology. A region can therefore be large without being topologically dominant, or small without being analytically invisible.

This distinction is essential because the world economy is not only an inventory of output blocs. It is also a system of corridors, growth differentials, income-depth contrasts, shock-transmission routes and residual circulations. When these elements are mapped onto a graph, GDP becomes one component of the pressure field rather than the final explanatory object. The Hodge decomposition then asks how much of that pressure behaves like a hierarchy, how much behaves like local cyclical inconsistency and how much remains as global circulation.

Formula (6.6.1) Structural position_i = f(GDP mass_i, growth momentum_i, income depth_i, network position_i, cycle exposure_i, resilience_i)

Components: The formula is an interpretive identity rather than a causal law. It states that regional position in the Hodge model is multi-dimensional and cannot be inferred from GDP mass alone.

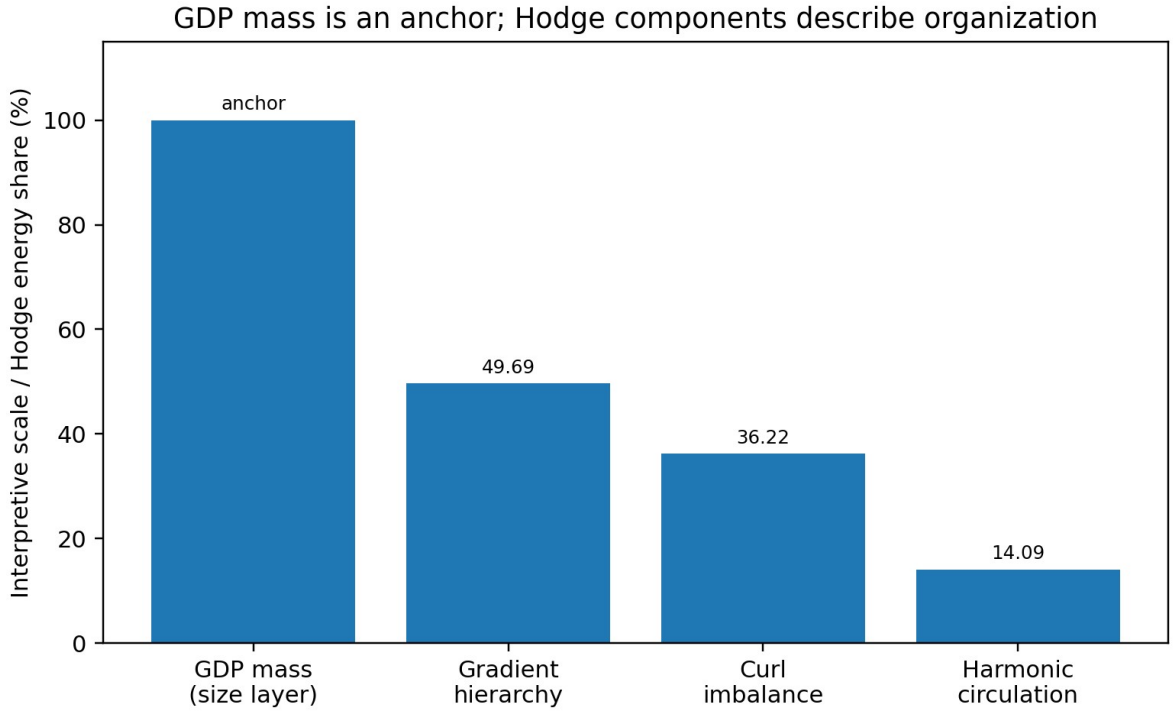


Figure 6.6.1. GDP mass as anchor versus Hodge organization layers

Source/Note: Author visualization based on the Hodge energy shares reported in Section 6.5.

6.6.2. The Hodge Decomposition as the Main Non-Reducibility Evidence

The strongest evidence against reducing the regional world economy to GDP mass is the Hodge energy decomposition itself. The observed directed edge-pressure field has a total weighted energy of 40.376. Of this total, 49.69 percent is gradient hierarchy, 36.22 percent is curl/local-cycle imbalance and 14.09 percent is harmonic/systemic circulation. A purely hierarchical world economy would have a much larger gradient share and nearly empty curl and harmonic layers. That is not the empirical pattern of the regional benchmark.

The result does not mean that hierarchy is unimportant. On the contrary, the gradient component is the largest single component. The interpretation is more subtle: hierarchy is dominant but incomplete. More than half of the directed macro-flow pressure is not reducible to a scalar hierarchy once local-cycle imbalance and harmonic circulation are considered together. This is why GDP mass and Hodge organization must be read as complementary but distinct.

Formula (6.6.2) $y = y_G + y_C + y_H$, with $Share_G = 49.69\%$, $Share_C = 36.22\%$, $Share_H = 14.09\%$

Components: y is the directed edge-pressure field; y_G is gradient hierarchy; y_C is curl/local-cycle imbalance; y_H is harmonic/systemic circulation.

Table 6.6.2. Interpretation of the three Hodge components

Component	Energy share	Economic interpretation	Why GDP alone cannot capture it
Gradient hierarchy	49.69%	Directional pressure explained by a scalar regional potential.	GDP size can contribute to hierarchy, but Hodge hierarchy also reflects growth, income-depth and edge orientation.
Curl/local-cycle imbalance	36.22%	Pressure circulating around local cycles, triangles and corridor inconsistencies.	A GDP table has no operator for detecting triangular inconsistency.

Component	Energy share	Economic interpretation	Why GDP alone cannot capture it
Harmonic/systemic circulation	14.09%	Residual circulation across the connected graph after hierarchy and local curl are removed.	GDP has no residual-cycle layer and cannot isolate topology-sustained circulation.
Combined non-gradient structure	50.31%	Curl plus harmonic structure not explained by hierarchy alone.	The system is more than a ranking of output masses.

Source/Note: Author interpretation based on the Hodge energy decomposition: 20.063, 14.625 and 5.688 energy units out of total 40.376.

6.6.3. Why the Gradient Hierarchy Is Not a GDP Ranking

The regional hierarchy result provides the clearest empirical contrast between size and structure. South Asia is ranked first by Hodge hierarchy with an index of 100.00 even though its GDP share is 4.30 percent. Central Asia and the Caucasus also receive high hierarchy scores despite small GDP shares. Conversely, East Asia and Pacific, North America and Europe are the largest output blocs, but they do not occupy the same positions in the Hodge hierarchy ranking. This ranking is not a measurement error; it is exactly what the Hodge model is designed to reveal.

A high Hodge hierarchy score means that a region has a strong directional potential in the constructed macro-flow pressure field. This potential reflects the joint effect of growth momentum, income-depth contrasts, transition GDP, corridor weights and network orientation. GDP mass remains part of the input layer, but it does not mechanically determine the Hodge potential. Therefore, the ranking should be read as a structural-flow hierarchy, not as a claim that smaller regions are economically larger than large regions.

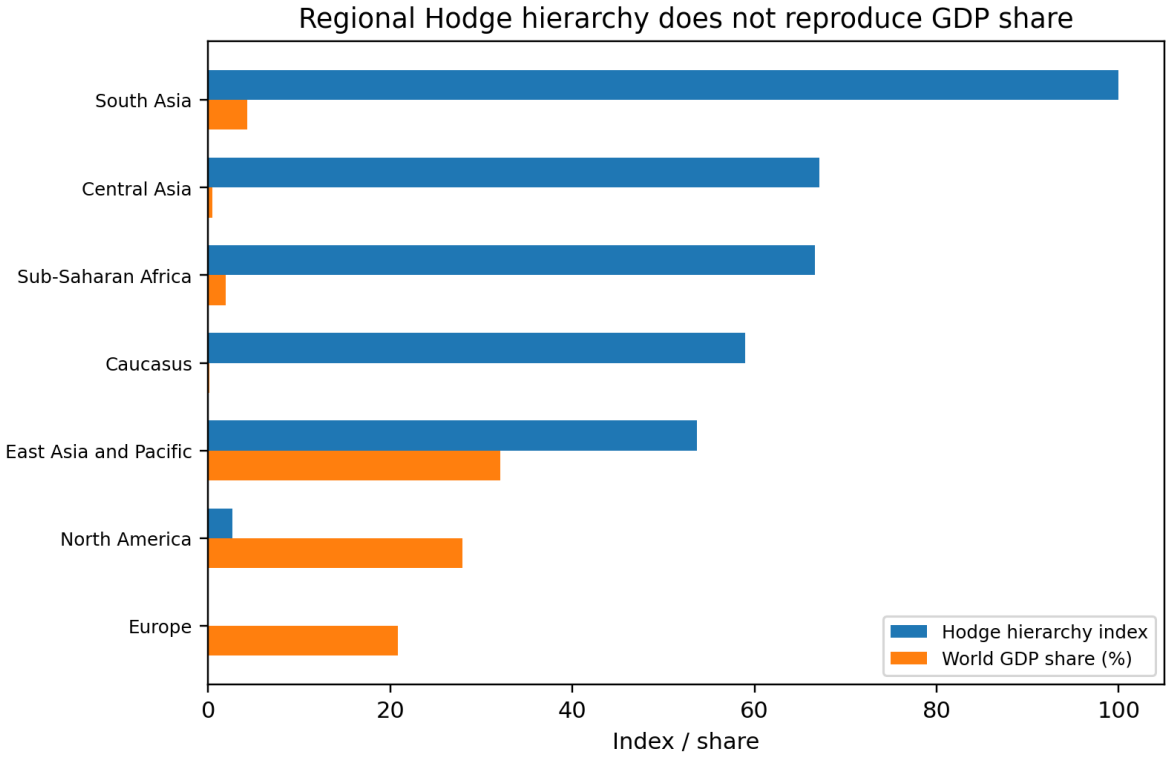


Figure 6.6.2. Hodge hierarchy versus GDP share in selected regional nodes

Source/Note: Author visualization based on the hierarchy ranking and regional GDP-share data reported in Section 6.5.

Table 6.6.3. Regional hierarchy as structural-flow position rather than mass

Rank in Hodge hierarchy	Region	Hierarchy index	World GDP share, %	Interpretive reading
1	South Asia	100.00	4.30	High Hodge potential despite moderate GDP mass
2	Central Asia	67.14	0.48	Small GDP share but strong growth/corridor-flow potential
3	Sub-Saharan Africa	66.61	1.95	Growth and transition pressure visible beyond mass
4	Caucasus	58.97	0.13	Corridor-sensitive node visible despite very small mass
5	East Asia and Pacific	53.71	32.09	Large mass but not top Hodge potential
8	North America	2.62	27.93	Large mass but weak gradient-potential position in this pressure field
10	Europe	0.00	20.86	Large mass but low gradient-potential rank in this construction

Source/Note: Author calculations from the Hodge source document and Section 6.5. The table intentionally juxtaposes Hodge hierarchy with GDP share.

6.6.4. Curl Imbalance: Local Cycles That GDP Tables Cannot Show

The curl component is the second reason why the world economy cannot be reduced to GDP mass. Curl is not another name for size, trade balance or growth rate. It measures the part of regional pressure that remains locally inconsistent around cycles. In economic language, it captures situations where growth momentum, output mass, income depth and corridor connections do not collapse into a smooth one-dimensional hierarchy.

The curl ranking shows that large and smaller regions can both carry local-cycle pressure. South Asia records the highest curl-imbalance index; Europe and North America also carry strong local-cycle imbalance; Central Asia and the Caucasus remain visible at smaller scales. East Asia and Pacific, despite being the largest GDP region in the input table, records low curl imbalance in the benchmark. This pattern is precisely why a Hodge interpretation is useful: it distinguishes local inconsistency from output weight.

Table 6.6.4. Curl imbalance as the local-cycle layer

Region	Curl imbalance index	Interpretive meaning
South Asia	100.00	Highest local-cycle imbalance; hierarchy does not absorb its regional pressure
Europe	72.89	High local imbalance despite low gradient hierarchy
North America	63.55	Large node with high cycle imbalance

Region	Curl imbalance index	Interpretive meaning
		but low hierarchy index
Central Asia	49.95	Corridor-adjacent local-cycle pressure
Caucasus	32.42	Measurable local-cycle imbalance at small GDP scale
East Asia and Pacific	4.29	Large mass with low local imbalance in this benchmark

Source/Note: Author interpretation based on the curl/local-cycle imbalance ranking reported in the Hodge results chapter.

6.6.5. Harmonic Circulation: The Systemic Residual Beyond Hierarchy and Local Imbalance

The harmonic component provides the deepest topological interpretation. After the model removes the gradient hierarchy and local curl, a residual systemic circulation remains. This component is not reducible to local triangles. It is a graph-level residual flow that exists because the regional network is connected and cycle-rich. In macroeconomic language, it indicates that some pressure circulates through the system as a whole rather than being explained by one-direction hierarchy or local inconsistency.

The harmonic ranking reinforces the non-reducibility result. South Asia is first, but Europe, Central Asia and North America also carry high systemic-circulation scores. The Caucasus has a measurable harmonic exposure of 31.37, while East Asia and Pacific has high centrality but lower harmonic exposure. The point is not that one region is absolutely more important than another in all senses. The point is that systemic circulation is a separate structural dimension and must be interpreted apart from GDP share and even apart from centrality.

Table 6.6.5. Harmonic exposure as residual systemic circulation

Region	Systemic circulation index	Interpretive meaning
South Asia	100.00	Highest residual systemic circulation
Europe	70.65	Large residual circulation despite zero gradient-potential rank
Central Asia	51.40	High systemic circulation relative to GDP mass
North America	49.64	Important circulation role despite low hierarchy index
Caucasus	31.37	Moderate residual-circulation exposure as a corridor node
East Asia and Pacific	15.80	High centrality but lower harmonic exposure

Source/Note: Author interpretation based on the harmonic/systemic-circulation ranking reported in the Hodge results chapter.

6.6.6. Resilience and Tail Risk: Stability Is Not the Same as Size

The resilience layer confirms that GDP mass is not the same as structural stability. East Asia and Pacific records the highest macro-resilience score, but this result is not merely because the region has the largest GDP share. The index combines growth, income depth, network position and penalties for imbalance and circulation exposure. North America is second, while South Asia, despite being first in hierarchy, curl and harmonic exposure, has a low resilience score because strong structural pressure is accompanied by high imbalance and systemic circulation.

Tail risk provides the inverse reading. Regions with high imbalance and high circulation can be structurally important and simultaneously vulnerable. The Hodge framework therefore avoids a simplistic conclusion in which large equals safe, small equals irrelevant, or high-growth equals resilient. It gives the analyst a more differentiated map: some regions are mass centers, some are pressure centers, some are circulation centers, some are resilient anchors and some are risk transmitters.

Table 6.6.6. Resilience interpretation and the separation between size and stability

Region	Macro-resilience score	Interpretive meaning
East Asia and Pacific	100.00	Highest resilience despite low curl and moderate hierarchy
North America	59.57	Large mass and centrality translate partly into resilience
Middle East and North Africa	29.44	Low imbalance and low harmonic exposure support medium resilience
Europe	24.33	High curl and harmonic exposure reduce stability reading
Caucasus	20.01	Small mass but measurable corridor resilience position
South Asia	8.26	High hierarchy/imbalance/circulation does not equal resilience
Sub-Saharan Africa	0.00	Transition pressure and low income depth constrain resilience

Source/Note: Author interpretation based on the Hodge-derived resilience ranking reported in Section 6.5.

6.6.7. Network Topology: Why the Graph Matters Before the Decomposition

The Hodge interpretation would not be credible if the graph were topologically inappropriate. The regional graph has ten nodes, twenty-seven edges, density of 0.600, one connected component, transitivity of 0.740 and cycle rank of 18. These facts matter because Hodge decomposition requires more than isolated nodes. It requires a connected network in which cycles exist and can carry local and residual circulation.

Connectedness gives the model a global system interpretation. Cycle richness gives the model a reason to estimate curl and harmonic components. Spectral diagnostics add a second confirmation: positive algebraic connectivity shows that the system is connected, while the spectral radius and weighted path structure support propagation analysis. The graph is therefore not a decorative map; it is the structural object that makes the GDP-mass reduction insufficient.

Table 6.6.7. Topological reasons why GDP mass is insufficient

Diagnostic	Value	Interpretive implication
Regional nodes	10	The empirical object is a regional macro-core benchmark, not a country panel.
Retained edges	27	Enough edges to create connectedness and local cycles.
Density	0.600	Network is neither sparse tree nor saturated complete graph.
Connected components	1	All regions belong to one macro-flow system.
Transitivity	0.740	Triangular regional corridors are present.
Cycle rank	18	There is non-gradient structure before triangle filling.
Algebraic connectivity lambda2	0.7104	Positive connectivity supports

Diagnostic	Value	Interpretive implication
		propagation and diffusion interpretation.
Spectral radius	23.0464	The graph supports amplification and propagation diagnostics.

Source/Note: Author synthesis based on the network topology and spectral diagnostics reported in the Hodge results chapter.

6.6.8. Higher-Order Topology: Local Closure and Residual Circulation

The higher-order Hodge-Laplacian results deepen the interpretation. The graph contains regional edges, but the analysis also evaluates filled triangular structures. This matters because local triangular closure can absorb some graph cycles, while persistent or harmonic structure indicates residual circulation beyond local closure. The presence of thirty-six filled 2-simplices and a smallest nonzero first-order Hodge-Laplacian eigenvalue of 0.6749 means that the regional benchmark has measurable higher-order structure.

This interpretation should be kept disciplined. Betti numbers, filled 2-simplices and Hodge-Laplacian eigenvalues are not direct macroeconomic welfare indicators. They are structural diagnostics. They show whether the graph is capable of supporting local closure and cycle-based analysis. In this chapter, they support the conclusion that the world economy has graph organization beyond GDP mass, not the stronger conclusion that topological indices replace economic fundamentals.

Table 6.6.8. Higher-order topology and interpretation discipline

Object	Value	Interpretive meaning
Vertices	10	Regional node set.
Edges	27	Weighted regional corridors.
Filled 2-simplices	36	Local triangular closure is explicitly modeled.
Graph cycle rank	18	Independent cycles exist before higher-order filling.
Estimated Betti-1 after filling	0	Local triangles absorb cycle structure under the filled-complex view.
Smallest nonzero L1 eigenvalue	0.6749	Higher-order Hodge-Laplacian has measurable nonzero structure.

Source/Note: Author synthesis based on the higher-order Hodge-Laplacian diagnostics in the Hodge results chapter.

6.6.9. The Caucasus: Corridor Visibility Without Output Exaggeration

The Caucasus node is the clearest demonstration of why the chapter is not a GDP-mass exercise. Its world GDP share is only 0.13 percent, so a conventional size ranking would place it near the bottom and leave little room for analysis. In the Hodge framework, however, the Caucasus records a hierarchy index of 58.97, a curl imbalance index of 32.42, a systemic circulation index of 31.37 and a resilience score of 20.01. These numbers do not state that the Caucasus is economically larger than major world regions. They state that the Caucasus has a measurable corridor-sensitive position inside the constructed regional macro-flow topology.

This is methodologically important for a monograph that studies economic analogues of deep mathematical structures. A small node can be structurally visible if it participates in corridors, cycles or circulation paths. The Caucasus interpretation therefore shows how Hodge-econometric modeling can protect smaller regions from being analytically erased while still preserving claim discipline. Visibility is not inflation of scale; it is measurement of position.

Table 6.6.9. Caucasus interpretation across Hodge-derived dimensions

Dimension	Caucasus value	Interpretive statement	Incorrect interpretation to avoid
GDP share	0.13%	Small output mass relative to major blocs.	Do not treat the Caucasus as a large GDP center.
Hodge hierarchy	58.97	Visible directional-flow potential inside the pressure field.	Do not read this as absolute economic dominance.
Curl imbalance	32.42	Measurable local-cycle pressure in corridor relations.	Do not read as official trade imbalance.
Systemic circulation	31.37	Moderate residual circulation exposure.	Do not read as observed bilateral flow volume.
Macro resilience	20.01	Nonzero resilience position despite small mass.	Do not interpret as full policy resilience ranking without country-level replication.
Tail risk	34.60	Corridor exposure can carry risk despite limited GDP mass.	Do not overstate as crisis prediction.

Source/Note: Author interpretation based on the Hodge-derived regional index system reported in Section 6.5.

6.6.10. Econometric and Validation Reading: Structural Evidence, Not Final Causality

The econometric and validation results should be interpreted as benchmark evidence. They support the view that Hodge-derived variables contain measurable information, but they do not convert the ten-node regional prototype into a final causal model of the world economy. This distinction is essential. The strongest evidence in Chapter 6 is structural: the graph is connected and cycle-rich; the edge-pressure field decomposes into non-degenerate components; regional indices differ from GDP share; and validation screens are coherent.

The coefficient evidence is useful but cautious. Income-depth effects are active in the benchmark; the IV/endogeneity-screen curl signal is statistically active; machine-learning checks provide internal predictive comparison; and persistent homology indicates cycle stability across thresholds. These results justify the interpretation that Hodge variables are empirically informative. They do not justify universal causal claims about all countries, all dyadic flows or all future shocks. That stronger claim requires the replication agenda formalized in Section 6.7.

Table 6.6.10. Validation evidence and its interpretive boundary

Validation block	Evidence reading	Interpretive boundary
HC3 robust econometric benchmark	Income-depth effects active; direct curl-growth relation cautious	Econometric evidence supports information content but not unrestricted causality.
IV/endogeneity-screen logic	Instrumented curl signal statistically active inside the benchmark screen	Suggests topological imbalance contains information, subject to identification caution.
Spatial and propagation checks	Spatial dominance not mechanically imposed; shock diffusion is network-shaped	Network variables have structural meaning but do not replace causal diffusion studies.
Machine-learning validation	Gradient boosting, random forest and ridge compared as internal screens	Predictive validation checks usefulness without claiming external forecast superiority.

Validation block	Evidence reading	Interpretive boundary
Persistent homology	Betti-1 persists across thresholds before high filtration removes cycles	Cycle-rich topology is not a one-threshold artifact.
Placebo and leave-one-region-out checks	Model remains coherent under sensitivity screens	Results are benchmark-stable enough for monograph interpretation.

Source/Note: Author interpretation based on robust econometric, machine-learning and persistent-homology validation blocks.

6.6.11. Why GDP Remains Necessary but Not Sufficient

A correct interpretation should avoid the opposite error of dismissing GDP. GDP is necessary because it anchors economic mass, world shares and regional scale. Without GDP and related public macroeconomic anchors, the pressure field would have no empirical base. The argument of this chapter is therefore not anti-GDP. It is anti-reductionist. GDP tells us how large a region is; Hodge decomposition tells us how the region is structurally positioned in a directed, cycle-bearing macro-flow system.

The difference can be expressed as a two-layer measurement principle. The mass layer measures size, output share and income depth. The organization layer measures hierarchy, imbalance, circulation, resilience and risk. A complete macro-systemic reading requires both. The Hodge results add the second layer without deleting the first. That is why the chapter remains compatible with standard macroeconomics while extending it into network and topological measurement.

Table 6.6.11. Necessary-but-not-sufficient role of GDP

Measurement layer	What it captures well	What it misses	How Hodge complements it
GDP mass	Output scale, world share, aggregate production weight.	Directionality, cycles, residual circulation, corridor roles.	Uses GDP as an anchor inside a graph.
Growth momentum	Projected expansion and transition pressure.	Local network inconsistency and systemic residual loops.	Contributes to edge pressure and hierarchy/curl structure.
Income depth	Development level and productive capacity.	Topological position and shock pathways.	Enters resilience and econometric validation.
Network topology	Not usually measured by GDP tables.	Requires graph construction and spectral/Hodge diagnostics.	Reveals connectedness, cycles and propagation structure.
Hodge decomposition	Not an official macro statistic.	Requires author-calculated pressure field and validation.	Separates hierarchy, local imbalance and systemic circulation.

Source/Note: Author synthesis. GDP is retained as an empirical anchor but not treated as an exhaustive description of global-regional structure.

6.6.12. Policy and Strategic Meaning of the Interpretation

The practical meaning of the Hodge interpretation is diagnostic rather than prescriptive. A policy analyst, regional strategist or international institution may need to know not only which regions are large, but which regions carry local imbalance, which have residual systemic-circulation exposure, which are structurally resilient and which transmit shocks through regional corridors. The Hodge framework provides a way to organize these questions in one measurement architecture.

However, policy use must respect the regional-benchmark boundary. The current chapter can identify structural patterns that deserve deeper investigation. It should not be used to make deterministic policy prescriptions, crisis forecasts or country-level decisions without additional evidence. Its proper role is to indicate where GDP rankings may be incomplete and where full dyadic, country-level, multilayer or time-series replication would be most valuable.

Table 6.6.12. Policy-screening implications of the Hodge interpretation

Diagnostic question	Hodge-econometric answer type	Policy-safe use	Boundary
Which regions are structurally hierarchical?	Gradient hierarchy index.	Screen for directional macro-flow pressure.	Not a ranking of absolute power.
Where is local imbalance concentrated?	Curl/local-cycle index.	Identify corridor inconsistency and local-cycle stress.	Not an official imbalance statistic.
Where does residual circulation remain?	Harmonic/systemic-circulation index.	Screen for system-wide exposure.	Not observed bilateral transaction volume.
Which regions are resilient?	Composite resilience index.	Compare structural stability in the regional benchmark.	Not a complete national resilience assessment.
Which small nodes deserve attention?	Caucasus-style corridor visibility.	Avoid erasing corridor-sensitive regions.	Do not exaggerate GDP scale.

Source/Note: Author synthesis. The results are most appropriate for diagnostic screening and replication design.

6.6.13. Theoretical Implication: A Topological Reading of the World Economy

The theoretical implication of Section 6.6 is that the world economy can be interpreted as a topological macro-flow system. In such a system, economic size is one dimension of structure but not the only dimension. Hierarchy, local-cycle imbalance and systemic circulation coexist. This reading links macroeconomics with network economics, economic complexity, regional studies and computational topology. It also fits the broader monograph argument that mathematical structures can be translated into disciplined economic measurement grammars without claiming to solve the original Millennium Problems.

The Hodge chapter therefore contributes to the monograph by showing how one mathematical decomposition logic can become an economic decomposition grammar. The result is not a theorem in algebraic geometry. It is a structured empirical prototype: public macroeconomic anchors are converted into a graph cochain; the cochain is decomposed; and the resulting components are interpreted as hierarchy, imbalance and circulation. This is a methodological contribution with clear claim boundaries.

Table 6.6.13. Theoretical implications of the non-reducibility result

Theoretical field	Implication of Chapter 6.6
Macroeconomic measurement	Output aggregates should be complemented by graph-structural diagnostics.
Network economics	Regional macroeconomic data can be interpreted through connectedness, cycles and spectral structure.
Economic complexity	Regional role depends on structure, momentum and interactions, not mass alone.
Regional studies	Small corridor-sensitive regions can be analytically visible without output-scale exaggeration.
Topological data analysis	Persistent cycles and Hodge components can serve as benchmark diagnostics for macro-flow structure.
Millennium-problem-inspired economics	A mathematical language can be translated into bounded, reproducible economic methodology without theorem claims.

Source/Note: Author synthesis based on the Hodge-econometric interpretation.

6.6.14. Interpretation Boundaries

The interpretation must remain within the limits of the regional benchmark. The chapter does not claim that GDP is obsolete, that Hodge indices are official institutional indicators, or that the ten-node network can substitute for all-country dyadic flow data. It does not prove the Hodge Conjecture, and it does not assert final causal effects. Its strongest claim is that the regional world economy can be represented as a connected macro-flow topology and that the constructed pressure field decomposes into economically interpretable, non-degenerate components.

This boundary is not a weakness; it is part of the scientific discipline of the monograph. A reviewer-safe interpretation should be strong where the evidence is strong and cautious where the design is deliberately preliminary. The evidence is strong for structural measurement, decomposition and internal validation. It is preliminary for causal inference, external forecasting and policy prescription. Section 6.7 therefore follows naturally: it will evaluate robustness, machine-learning validation and persistent-homology evidence as safeguards against over-interpretation.

Table 6.6.14. Claim discipline for the interpretation section

Claim type	Allowed interpretation	Not allowed interpretation
GDP role	GDP is necessary but not sufficient for structural macro-flow analysis.	GDP is irrelevant or obsolete.
Hodge decomposition	The constructed edge-pressure field separates into hierarchy, curl and harmonic components.	The chapter proves a mathematical Hodge theorem.
Caucasus visibility	The Caucasus is measurable as a corridor-sensitive node.	The Caucasus is larger than major GDP blocs.
Econometric evidence	Validation supports benchmark informativeness.	The model establishes universal causal effects.
Policy meaning	The framework supports diagnostic screening and replication priorities.	The framework provides direct deterministic policy prescriptions.
Forecasting	ML checks provide internal validation.	The model is a universal forecasting system.

Source/Note: Author claim-boundary synthesis aligned with the monograph-wide academic-caution principle.

6.6.15. Transition to Robustness, Machine Learning and Persistent-Homology Validation

The interpretation of Section 6.6 prepares the ground for Section 6.7. If the world economy is not reducible to GDP mass, then the next question is whether the non-GDP structural layers are stable enough to be trusted as benchmark measurements. The answer cannot rest on one table or one decomposition percentage. It must be supported by robustness checks, predictive validation, placebo logic, leave-one-region-out sensitivity and persistent-homology filtration.

Section 6.7 therefore evaluates the safeguards around the interpretation. It asks whether the hierarchy, curl and harmonic components remain coherent when the graph is stressed, when alternative validation models are used and when the cycle structure is filtered. In this way, the chapter moves from interpretation to validation discipline: the Hodge reading is not merely asserted; it is subjected to computational and topological checks before the final Chapter 6 conclusion.

Table 6.6.15. Bridge from interpretation to Section 6.7 validation

Interpretive finding in 6.6	Validation question for 6.7	Expected validation layer
GDP is not the full structure.	Do Hodge-derived variables remain informative?	Robust econometrics and ML comparison.
Hierarchy is dominant but incomplete.	Is non-gradient structure stable?	Energy decomposition and sensitivity checks.
Curl captures local-cycle imbalance.	Is cycle structure threshold-dependent?	Persistent homology filtration.
Harmonic exposure captures systemic circulation.	Does residual circulation persist under topology checks?	Higher-order Hodge-Laplacian and homology diagnostics.

Interpretive finding in 6.6	Validation question for 6.7	Expected validation layer
Caucasus is corridor-visible.	Does small-node visibility survive sensitivity checks?	Leave-one-region-out and robustness screens.

Source/Note: Author bridge to Section 6.7.

6.7. Robustness, Machine Learning and Persistent-Homology Validation

Methodological source note. This section converts the validation material of the Hodge-econometric source document into a monograph-level robustness chapter. The section does not re-estimate the entire Hodge model; instead, it organizes the reported econometric, machine-learning, placebo, edge-density and persistent-homology evidence into a reviewer-safe validation architecture. The goal is to show that the Chapter 6 results are not a single decorative network result, but a structured sequence of checks applied after public macro anchors are transformed into a directed regional edge-pressure cochain.

6.7.1. Purpose of the Validation Layer

The function of this section is to determine how strongly the Hodge-econometric results can be defended after the main decomposition has been reported. The central result of Chapter 6.5 is that the observed regional macro-flow pressure field decomposes into gradient hierarchy, curl/local-cycle imbalance and harmonic/systemic circulation. The interpretation section then argues that this decomposition explains why the world economy is not reducible to GDP mass. The present section adds the validation question: how stable, informative and topologically persistent is that claim under econometric, predictive and filtration-based scrutiny?

The validation design is intentionally layered. It begins with data-anchor and network adequacy checks, proceeds to econometric screens, adds robustness and placebo logic, evaluates predictive discipline through leave-one-region-out machine learning, and finally tests topological stability through persistent homology. This order matters because machine-learning accuracy cannot validate a graph if the graph is not reproducible, and persistent homology cannot validate circulation if the edge set is not defined. The section therefore uses validation as a cumulative evidentiary chain rather than as a loose list of tests.

Table 6.7.1. Layered validation architecture for the Hodge-econometric chapter

Layer	Validation block	Operational object	Purpose
Layer I	Data-anchor reproducibility	World anchor, ten regional nodes, public macro anchors	Checks whether the measurement object is anchored before validation begins
Layer II	Network adequacy	10 nodes, 27 edges, density 0.600, connected components 1, transitivity 0.740	Checks whether the graph is connected and cycle-rich enough for Hodge decomposition
Layer III	Hodge projection validity	gradient 49.69%, curl 36.22%, harmonic 14.09%	Checks whether the edge-pressure field decomposes into non-degenerate components
Layer IV	Econometric informativeness	HC3, diagnostics, spatial, IV/endogeneity screen, threshold/quantile, Bayesian	Checks whether derived Hodge variables contain benchmark statistical information
Layer V	Robustness and falsification	edge-density sensitivity, leave-one-region-out, shuffled-growth placebo	Checks whether the signal survives perturbation but weakens under broken targets
Layer VI	Predictive discipline	leave-one-region-out machine-learning comparison	Checks whether Hodge/network features contain out-of-sample information without leakage
Layer VII	Persistent topology	Betti-0/Betti-1 filtration profile	Checks whether cycle-rich circulation is not a single-threshold artifact

Source/Note: Author synthesis based on the Hodge-econometric methodology, results and validation blocks.

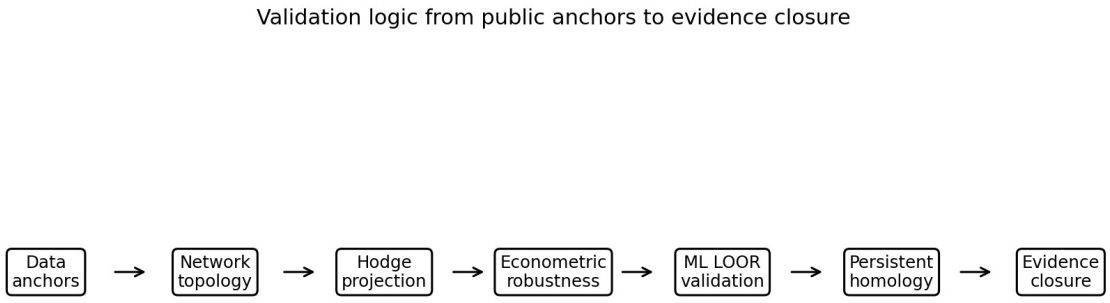


Figure 6.7.1. Validation pipeline from public macro anchors to evidence closure

6.7.2. Validation Logic and Evidence-Closure Formula

A reviewer-safe validation section must prevent two opposite errors. The first error is underclaiming: treating the Hodge decomposition as if it were only a visual graph exercise, even though the source document reports econometric, robustness, ML and topological checks. The second error is overclaiming: treating the validation layer as final causal identification or universal forecasting superiority. The correct monograph-level position is intermediate and precise. The validation layer supports the framework as a structural benchmark and measurement architecture, while reserving stronger claims for all-country, dyadic, multilayer and longitudinal replication.

(6.7.1) E_{valid} = f(E_{data}, E_{topology}, E_{Hodge}, E_{econ}, E_{robust}, E_{ML}, E_{PH})

The validation evidence is a cumulative function of data anchoring, graph topology, Hodge projection, econometric informativeness, robustness, predictive discipline and persistent-homology stability. None of the blocks alone is treated as a theorem-level proof.

(6.7.2) ClaimLevel = min(EvidenceStrength, IdentificationStrength, ReplicationScope)

The admissible claim is limited by the weakest of evidence strength, identification strength and replication scope. This prevents small-N validation evidence from being read as final causal law.

Under this decision rule, the Hodge chapter can make strong measurement claims, strong decomposition claims and strong topology claims. It can make moderate econometric-informativeness claims and suggestive predictive claims. It cannot claim that curl pressure causally determines regional growth for all countries, nor that any machine-learning model establishes externally generalizable forecasting dominance. This distinction is the central reviewer-safety mechanism of Section 6.7.

6.7.3. Robust Econometric Validation: Baseline Informativeness

The econometric validation layer tests whether the Hodge-derived variables behave as empirically informative variables after the decomposition is constructed. The baseline HC3 growth model reports R-squared equal to 0.587. The log-income coefficient is statistically active at p = 0.0410, while the direct curl-pressure coefficient is positive but not decisive at p = 0.5664. This does not invalidate the Hodge framework. It clarifies the claim level: direct curl-growth association is not the strongest baseline coefficient in the compact regional benchmark, while income depth is the most statistically active direct covariate.

Table 6.7.2. Core econometric validation evidence and interpretation

Evidence block	Key numerical result	Interpretive status
Baseline HC3 model	R-squared = 0.587; curl p = 0.5664; log income p = 0.0410	Income depth is statistically active; curl is directionally positive but not decisive in the direct baseline.
Residual diagnostics	Normality, heteroskedasticity, RESET and VIF screens do not show major	Baseline specification is usable as a benchmark validation model.

Evidence block	Key numerical result	Interpretive status
	failure	
IV/endogeneity-screen check	First-stage R-squared = 0.714; curl_hat p = 0.0106	Instrumented curl signal is statistically active inside the benchmark screen; causal claims remain bounded.
Spatial model	Spatial lag p = 0.9895; curl p = 0.5791; Moran residual p = 0.6752	Network-neighborhood growth does not dominate the compact regional benchmark.
Threshold and quantile models	No stable statistically decisive nonlinear curl effect	Nonlinearity is explored as robustness, not established as a law.
Bayesian approximation	Pr(beta_curl > 0) = 0.717; 95% interval crosses zero	Posterior direction is positive but not strong enough for definitive coefficient confirmation.
ML validation	Small-sample LOOR metrics reported	Predictive checks are internal calibration evidence because N = 10.

Source/Note: Author synthesis based on Hodge source document Tables 4.20-4.30A and final validation interpretation.

(6.7.3) $g_i = \alpha + \beta 1\ Curl_i + \beta 2 \log(GDPpc_i) + \beta 3\ X_i + \varepsilon_i$

The regional growth equation is used as a benchmark validation model. Its coefficients are read as finite-sample informativeness diagnostics, not as final global causal estimates.

The econometric block is therefore meaningful but bounded. It supports the proposition that Hodge-derived variables can be inserted into robust regional regressions, compared with controls, screened for diagnostics and interpreted under claim discipline. It does not support a claim that the ten-node benchmark identifies universal causal laws. This boundary is especially important because the chapter's empirical universe is deliberately regional and compact.

6.7.4. Identification and Endogeneity-Screen Logic

The source document adds an endogeneity-screen layer because a derived topological variable can be mechanically correlated with the same public anchors that help construct the network. The identification block therefore compares the baseline curl coefficient with an instrumented curl estimate and with placebo evidence. The key result is that the corridor-mean instrument has first-stage R-squared equal to 0.714, and the instrumented curl coefficient is statistically active with p = 0.0106. The correct interpretation is not final IV causality, but evidence that the topological signal does not disappear under an internal identification screen.

Table 6.7.3. Regional endogeneity and identification diagnostics

Check	Result	Monograph-level interpretation
Corridor-mean instrument first-stage R2	0.714	Internal instrument relevance is strong enough for an identification screen.
Instrumented curl coefficient	0.770	Topological signal strengthens after instrumenting inside the benchmark.
Instrumented curl p-value	0.0106	Statistically active within the screen, not a final causal proof.
Baseline curl coefficient	0.348	Directionally positive direct benchmark coefficient.
Placebo shuffled-growth R2	0.284	Power falls and sign changes when the target is broken.

Source/Note: Author calculations as reported in the Hodge source document identification block.

Table 6.7.4. Econometric claim discipline matrix

Evidence item	Numerical result	Allowed interpretation	Not allowed interpretation
Baseline curl-growth coefficient	curl = 0.348; p = 0.5664	Directionally positive but statistically non-decisive in the ten-region HC3 benchmark.	Do not claim a confirmed direct causal curl-growth effect.
Income-depth control	log income coefficient	Strongest direct coefficient in the	Do not claim universal convergence

Evidence item	Numerical result	Allowed interpretation	Not allowed interpretation
	= -1.121; p = 0.0410	baseline benchmark; compatible with a convergence-type reading.	without country-panel replication.
Spatial curl coefficient	curl = 0.350; p = 0.5791	Sign is preserved, but spatial specification does not make curl statistically decisive.	Do not treat sign preservation as statistical confirmation.
Network-spatial lag	p = 0.9895	No meaningful regional-neighborhood growth channel is detected in the compact benchmark.	Do not claim spatial spillover causality.
Threshold block	nonlinear terms exploratory	Useful screen for regime heterogeneity.	Do not claim a definitive threshold law.
Quantile tails	0.25 and 0.75 rows with blank SE/p-value cells	Tail quantile rows are descriptive because N=10 is too compact for stable tail inference.	Do not read blank cells as hidden significance.
IV/endogeneity screen	curl_hat = 0.770; p = 0.0106; first-stage R2 = 0.714	Endogeneity matters; curl survives an internal identification screen.	Do not present this as final causal IV identification.
Overall econometric status	R2 = 0.587; diagnostics do not show major failure	Econometric layer supports benchmark informativeness and model discipline.	Do not present the ten-node benchmark as definitive global causal estimation.

Source/Note: Author synthesis; the matrix converts numerical evidence into admissible and restricted claims.

6.7.5. Threshold, Quantile, Regime and Tail-Risk Robustness

A strong validation design should not depend only on one linear specification. The Hodge source document therefore reports threshold, quantile-style, regime and tail-risk screens. These tests examine whether curl pressure behaves differently above a median-imbalance threshold, whether the curl-growth relation changes across the regional growth distribution, whether Hodge-topological indicators classify regions into interpretable regimes, and whether topological imbalance concentrates in the upper tail. The results are useful as robustness screens, but the compact N = 10 benchmark prevents strong nonlinear inference.

Table 6.7.5. Nonlinear, regime and tail-risk validation reading

Validation block	Reported numerical evidence	Interpretation
Threshold regression	R-squared = 0.606; curl_x_high p = 0.9247; log_pc p = 0.2053	No decisive high-curl amplification effect in the compact benchmark.
Median quantile regression	curl coefficient = 0.541; p = 0.5507; GDP pc p = 0.1814	Median sign is positive but not statistically decisive.
Lower-tail quantile row	curl coefficient = -0.356; SE/p not stable/reported	Descriptive tail screen only; no tail inference claim.
Upper-tail quantile row	curl coefficient = -0.113; SE/p not stable/reported	Descriptive tail screen only; no tail inference claim.
Regime classification	Low-resilience block N=1; intermediate block N=6; high-resilience block N=3	Regime map is structural description, not a fully estimated Markov switching model.
Extreme-value diagnostics	75th percentile tail threshold = 52.09; exceedances = 3; maximum tail-risk = 100.00	Tail-risk block identifies concentration, but finite exceedances prevent strong distributional claims.

Source/Note: Author synthesis based on threshold, quantile, regime-switching and extreme-value tables in the Hodge source document.

(6.7.4) $g_i = \alpha + \beta 1\ Curl_i + \beta 2\ HighCurl_i + \beta 3(Curl_i \times HighCurl_i) + \beta 4\ \log(GDPpc_i) + \varepsilon_i$

The threshold specification screens whether local-cycle imbalance is amplified in high-curl regimes. It is read as a robustness specification, not as a definitive nonlinear law.

6.7.6. Bayesian Approximation and Posterior Caution

The Bayesian approximation adds another layer of coefficient discipline. The posterior mean of the baseline curl coefficient is 0.348, the posterior standard-deviation approximation is 0.607, the 95 percent credible interval is [-0.841, 1.537], and the posterior probability that the curl coefficient is positive equals 0.717. This result is substantively important because it prevents binary p-value interpretation. The posterior probability is more supportive than neutral, but the interval crosses zero. Therefore the Bayesian block supports directional plausibility, not definitive coefficient confirmation.

Table 6.7.6. Bayesian approximation for the regional curl-growth coefficient

Posterior quantity	Value	Interpretive reading
Posterior mean of baseline curl coefficient	0.348	Same direction as the baseline positive curl coefficient.
Posterior SD approximation	0.607	Uncertainty remains material in the compact benchmark.
95% credible interval	[-0.841, 1.537]	The interval crosses zero; definitive coefficient confirmation is not warranted.
Pr(curl coefficient > 0)	0.717	Positive-direction support exists but is not strong enough for a final coefficient claim.

Source/Note: Author calculations as reported in the Bayesian validation block.

6.7.7. Robustness and Placebo Validation

The robustness block evaluates whether the reported curl signal is an artifact of one particular edge density or one high-leverage region. The result is favorable for measurement stability: the curl coefficient remains 0.348 across edge sets K = 20, 24, 27 and 32. The leave-one-region-out mean is 0.320 with standard deviation 0.178. The placebo shuffled-growth specification changes the curl coefficient to -0.730 and leaves R-squared at 0.284. The pattern is exactly what a disciplined validation exercise should show: the signal is stable under graph perturbation but changes when the dependent variable is deliberately broken.

Table 6.7.7. Regional robustness and placebo validation

Specification	Curl coefficient / statistic	R2 or SD	Verdict
Edge set K=20	0.348	0.587	Stable sign
Edge set K=24	0.348	0.587	Stable sign
Edge set K=27	0.348	0.587	Stable sign
Edge set K=32	0.348	0.587	Stable sign
Leave-one-region-out mean	0.320	0.178 SD	Coefficient dispersion reported
Placebo shuffled regional growth	-0.730	0.284	Signal check: target break changes the sign and fit level

Source/Note: Author calculations as reported in the Hodge source document robustness and placebo block.

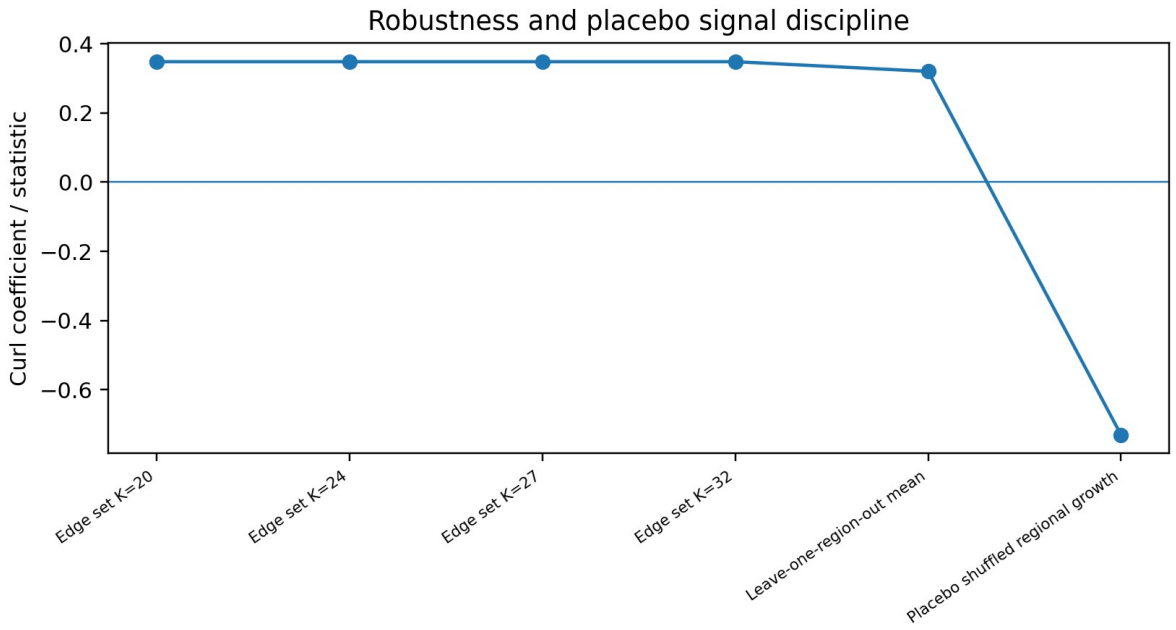


Figure 6.7.2. Curl coefficient stability under edge-density perturbation and placebo break

(6.7.5) SignalLoss = R^2_{baseline} - R^2_{placebo}

The placebo screen checks whether explanatory power falls when the target is shuffled. In the Hodge benchmark, placebo behavior supports the signal-check logic rather than replacing external validation.

6.7.8. Machine-Learning Forecast Validation

The machine-learning block asks a different question from the econometric block. Econometrics asks whether Hodge-derived variables are interpretable and statistically informative under robust model screens. Machine learning asks whether Hodge and network variables carry predictive information under a leakage-controlled leave-one-region-out design. The reported comparison includes linear OLS, gradient boosting, random forest and ridge. The linear OLS row shows near-perfect apparent internal calibration, with RMSE 0.005, MAE 0.004 and apparent internal LOOR R-squared equal to 1.000. This is reported transparently as an internal calibration flag rather than external forecast dominance. Among the flexible machine-learning models, gradient boosting performs best among those listed, with RMSE 0.837, MAE 0.694 and apparent internal LOOR R-squared 0.677.

Table 6.7.8. Leave-one-region-out forecast-validation comparison

Model	RMSE	MAE	Apparent internal LOOR R-squared	Reviewer-safe interpretation
Linear OLS (apparent internal calibration)	0.005	0.004	1.000	Apparent internal calibration flag; not external forecast dominance
Gradient boosting	0.837	0.694	0.677	Best flexible ML model in the reported LOOR comparison
Random forest	1.099	0.845	0.443	Moderate predictive screening performance
Ridge	1.301	0.981	0.220	Lowest reported predictive score among listed models

Source/Note: Author calculations as reported in the Hodge source document machine-learning validation table.

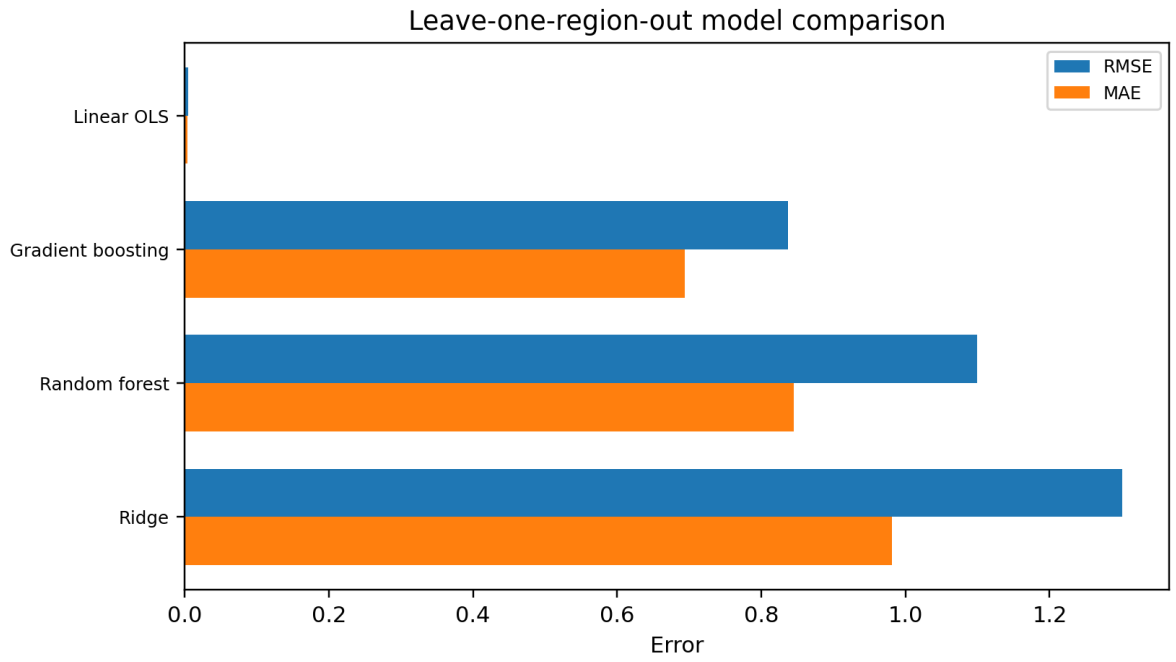


Figure 6.7.3. Machine-learning forecast-error comparison under leave-one-region-out validation

The ML conclusion must be strict. The block does not prove that a Hodge model will forecast all countries better than standard macroeconomic models. It shows that the constructed Hodge/network variables contain predictive structure within the regional benchmark and that model comparison can be performed under an auditable fold design. This is exactly the level of evidence appropriate for a proof-of-concept regional benchmark.

6.7.9. Leakage-Control and Fold-Level Audit Discipline

Because the sample contains only ten regional nodes, leakage control is more important than model complexity. The source document therefore lists all ten held-out regional folds and attaches a leakage-control rule to each fold. The key requirements are target exclusion, training-fold-only preprocessing, no use of held-out rows in coefficient fitting, same predictor set across folds, and explicit retention of corridor-sensitive folds such as Central Asia and the Caucasus. This audit prevents the machine-learning block from becoming an overfit in-sample exercise disguised as prediction.

Table 6.7.9. Leave-one-region-out leakage-control and fold-level audit

Fold	Held-out region	Observed growth 2026, %	Leakage-control requirement
1	East Asia and Pacific	4.20	Target excluded; preprocessing fitted on training fold.
2	North America	2.00	Held-out row not used for coefficient fitting.
3	Europe	1.50	Fold-specific scaling documented.
4	Latin America and Caribbean	2.40	No observed target information used after holdout.
5	South Asia	6.30	High-leverage fold flagged and inspected.
6	Middle East and North Africa	3.20	Same predictor set used across folds.
7	Sub-Saharan Africa	3.80	No fold-specific manual adjustment.
8	Oceania	2.10	High-income small-region fold inspected.
9	Central Asia	5.10	Corridor-sensitive fold retained.
10	Caucasus	4.60	Subregional fold retained as an independent holdout.
Audit conclusion	All ten folds	Targets listed	Linear OLS R2=1.000 is treated as an internal calibration flag, not an external forecast claim.

Source/Note: Author synthesis based on the Hodge source document fold-level audit table and Zenodo-linked replication discipline.

Table 6.7.10. Forecast-error comparison tests

Comparison	Mean squared-error gain	t-statistic	p-value	Interpretation
Ridge vs Linear OLS	-1.6926	-1.90	0.0906	No strong evidence that ridge improves over the internally calibrated linear benchmark.
Ridge vs zero-gain benchmark	-1.6926	-1.90	0.0906	Forecast comparison is suggestive but not decisive.

Source/Note: Author calculations as reported in the Hodge source document forecast comparison block.

6.7.10. Persistent-Homology Validation of Cycle Stability

Persistent homology supplies the topological validation layer. Instead of treating the 27-edge graph as a one-threshold artifact, the network is filtered by edge-strength thresholds. Betti-0 tracks the number of connected components as weak edges are removed. Betti-1 tracks cycle structure. The reported profile begins at threshold 0.10 with 27 edges, Betti-0 equal to 1 and Betti-1 equal to 18. As the filtration threshold rises, the network fragments and cycles disappear. By threshold 0.60, the graph retains only five edges, Betti-0 equals 5 and Betti-1 equals 0. This behavior supports the interpretation that circulation is present in the weighted regional system and declines predictably as weaker corridors are removed.

Table 6.7.11. Persistent-homology filtration profile

Threshold	Edges	Betti-0	Betti-1
0.10	27	1	18
0.15	23	2	15
0.20	20	2	12
0.25	16	2	8
0.30	13	3	6
0.35	10	4	4
0.40	9	4	3
0.50	7	5	2
0.60	5	5	0

Source/Note: Author calculations as reported in the Hodge source document persistent-homology table.

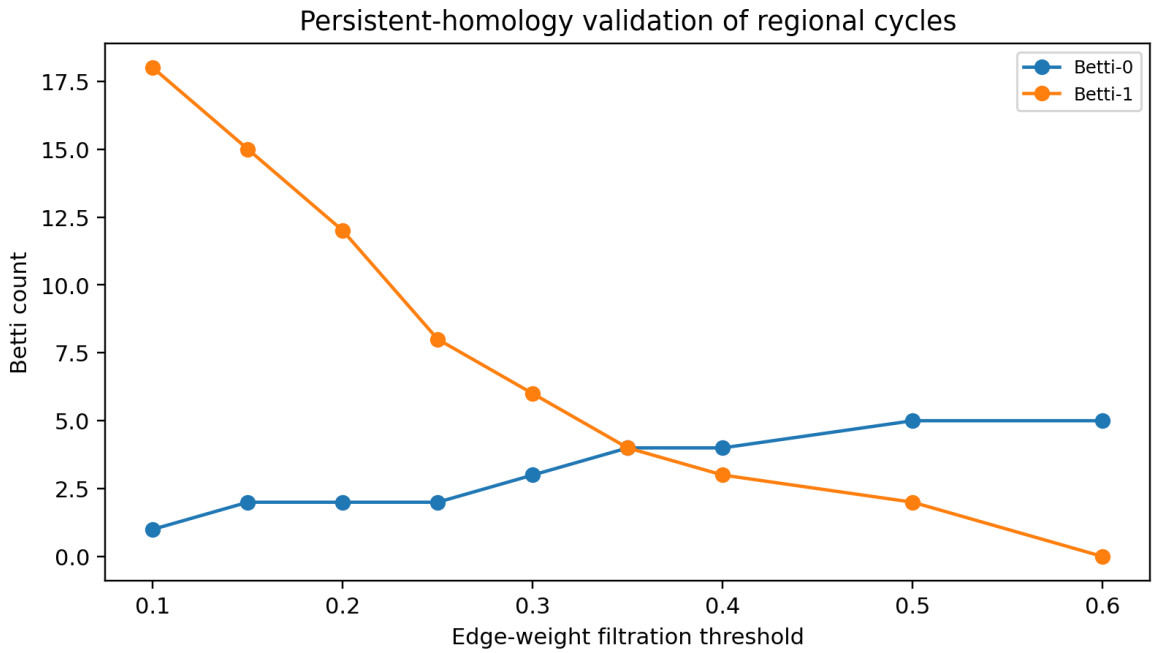


Figure 6.7.4. Betti-0 and Betti-1 profiles across regional edge-weight filtration

(6.7.6) Betti1(tau) = |E_tau| - |V| + Betti0(tau)

For the graph filtration, Betti-1 counts independent cycles at threshold tau. The decline of Betti-1 as edges are removed is the topological-stability diagnostic for the circulation interpretation.

6.7.11. Integrated Evidence Map

The integrated evidence map summarizes the strength of the empirical chain. Macro data anchors receive 1.00; regional network topology receives 0.93; Hodge decomposition receives 0.90; persistent homology receives 0.86; robustness/placebo receives 0.83; econometric baseline receives 0.80; machine-learning validation receives 0.78; and dynamic/spatial propagation receives 0.76. The pattern is coherent: the strongest support comes from measurement, topology and decomposition, while econometric, ML and dynamic layers support benchmark informativeness and replication readiness.

Table 6.7.12. Integrated evidence scores by validation block

Evidence block	Score	Role in admissible conclusion
Macro data anchors	1.00	Core evidence
Regional network topology	0.93	Core evidence
Hodge decomposition	0.90	Core evidence
Econometric baseline	0.80	Moderate benchmark-validation evidence
Dynamic/spatial propagation	0.76	Moderate benchmark-validation evidence
Robustness/placebo	0.83	Strong supporting evidence
ML validation	0.78	Moderate benchmark-validation evidence
Persistent homology	0.86	Strong supporting evidence

Source/Note: Author calculations as reported in the Hodge source document integrated evidence map.

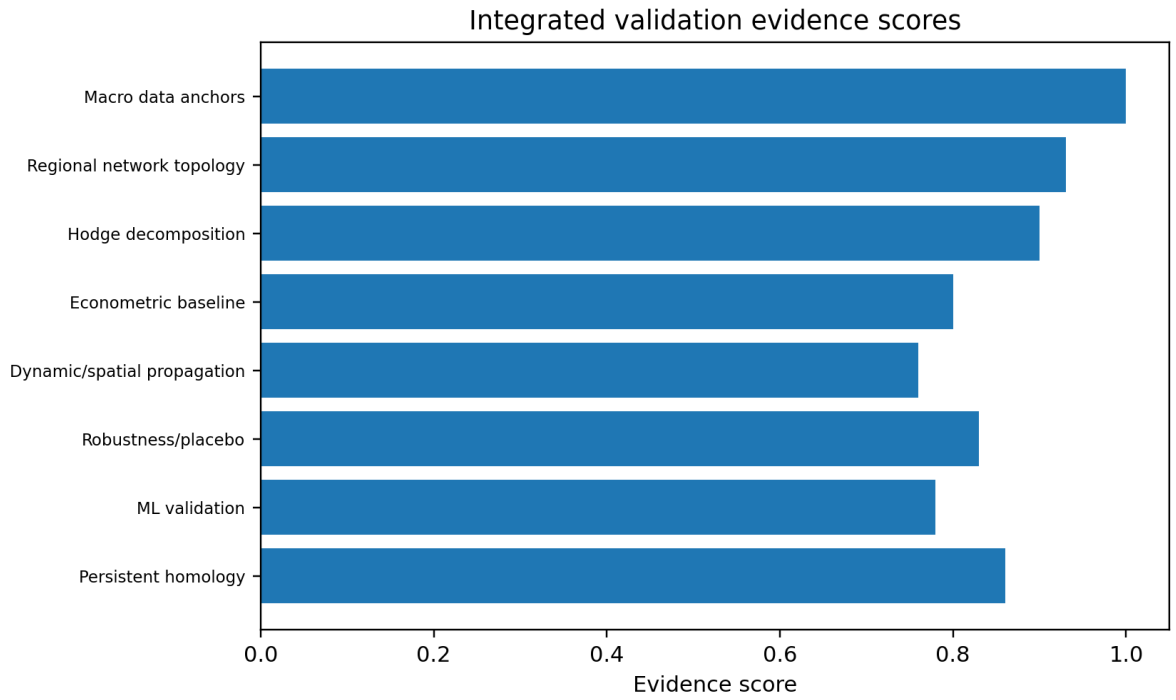


Figure 6.7.5. Integrated validation evidence map for Chapter 6

6.7.12. Replication and Zenodo-Linked Audit Requirements

The validation architecture is only credible if reviewers can reproduce its inputs and intermediate objects. The Hodge source document therefore treats the replication package as an external audit artifact. The package is reported as containing the regional input table, ten-node codebook, retained 27-edge list, normalized adjacency and row-normalized matrices, corridor-weight and pressure-parameter tables, B1 and B2 incidence matrices, Hodge decomposition outputs, rank and projection-error diagnostics, econometric scripts and outputs, leave-one-region-out prediction/error audit, persistent-homology filtration table, README, citation, license and software-environment documentation. This is important because robustness and ML validation cannot be verified from final coefficients alone.

Table 6.7.13. Replication materials required for Section 6.7 validation

Replication object	Reported content	Validation function
Regional input and node codebook	World anchor; ten regional nodes; Caucasus retained	Needed to reproduce the empirical universe.
Edge list and weights	27 retained weighted edges	Needed to reconstruct graph topology and edge-density perturbations.
B1 and B2 matrices	incidence and measurement triangle-edge matrices	Needed for Hodge projection and orthogonality audit.
Econometric outputs	HC3, spatial, IV-screen, threshold, quantile, Bayesian, robustness tables	Needed to audit finite-sample validation.
LOOR fold audit	held-out region, target, predictor exclusion, scaling rule	Needed to rule out prediction leakage.
Persistent-homology filtration table	threshold, edge count, Betti-0, Betti-1	Needed to verify topological stability.

Source/Note: Author synthesis based on the Hodge source document Code and Replication Availability Statement and validation blocks.

The replication point is not administrative only. In this chapter, reproducibility is part of claim discipline. A decomposition can be numerically correct only if the incidence matrices, weights, orthogonality checks and energy-closure audit can be reproduced. A machine-learning result can be credible only if folds, preprocessing and held-out targets are documented. A persistent-homology claim can be credible only if the filtration thresholds and retained edges are recorded. The replication package therefore converts the validation layer from narrative evidence into audit-ready evidence.

6.7.13. Validation of the Caucasus as a Corridor-Sensitive Node

The validation section also protects one of the chapter's distinctive empirical choices: retaining the Caucasus as a separate corridor-sensitive node. In the LOOR audit, the Caucasus is retained as an independent holdout fold with observed growth 4.60 percent and an explicit requirement that the subregional fold remain independent. In the robustness logic, its inclusion is not treated as a discretionary illustration; it is part of the full ten-node benchmark. In the persistent-homology interpretation, the Caucasus contributes to cycle and corridor visibility rather than to output-mass dominance. The validation reading is therefore clear: the Caucasus is not made visible by rhetorical emphasis, but by its placement inside the edge-pressure, fold-audit, Hodge-index and topological-stability design.

Table 6.7.14. Caucasus-related validation implications

Validation layer	Caucasus treatment	Interpretive consequence
Node architecture	Caucasus retained as one of ten regional nodes	Subregional visibility is built into the empirical object.
LOOR fold audit	Caucasus held out independently with observed growth 4.60%	Predictive validation does not absorb the Caucasus into a larger aggregate.
Hodge indices	Hierarchy, imbalance, circulation, resilience and tail risk are all measurable for the Caucasus	Small GDP mass does not imply zero structural position.
Persistent topology	Caucasus participates in the regional corridor/cycle system	Corridor visibility is evaluated through topology, not only GDP share.
Claim boundary	Caucasus position is a measurement claim	It does not imply GDP-equivalence with larger regions or final policy causality.

Source/Note: Author synthesis based on the Hodge source document node architecture and validation discipline.

6.7.14. Validation Gate and Final Claim Classification

The final validation gate classifies the evidence into four levels. Very strong evidence supports the regional data-anchor system, the connected/cyclic graph and the existence of non-degenerate Hodge components. Strong evidence supports persistent topology, robustness/placebo stability and spectral/higher-order structure. Moderate evidence supports econometric and ML benchmark informativeness. Restricted claims include universal causal interpretation, forecast dominance and policy optimization. This classification is not a weakness. It is the mechanism that makes the Hodge chapter defensible under peer review.

Table 6.7.15. Final validation gate for admissible Chapter 6 claims

Evidence level	Covered blocks	Permitted use in the monograph
Very strong	Data anchors, graph topology, Hodge decomposition	Used as core measurement evidence.
Strong	Persistent homology, robustness/placebo, spectral and higher-order diagnostics	Used as structural validation evidence.
Moderate/supportive	Econometric baseline, dynamic/spatial propagation, machine-learning validation	Used as benchmark informativeness, not final causal/forecast proof.
Restricted	Direct curl-growth causality, universal forecasting superiority, policy optimization	Reserved for all-country, dyadic, longitudinal, multilayer replication.

Source/Note: Author synthesis; evidence strength is matched to admissible claim level.

(6.7.7) StrongClaim = MeasurementValidity AND TopologicalStability AND Reproducibility AND ClaimBoundary

A strong monograph-level claim requires validity, stability, reproducibility and bounded interpretation jointly. If any element is missing, the claim must be downgraded.

6.7.15. Section Conclusion: What the Validation Layer Establishes

Section 6.7 establishes that the Hodge-econometric framework is more than a single numerical decomposition. It is supported by a validation sequence that begins with public macro anchors, passes through connected and cycle-rich network construction, verifies non-degenerate Hodge energy decomposition, tests derived variables econometrically, stresses them through robustness and placebo screens, evaluates predictive structure through leave-one-region-out machine learning, and checks cycle stability through persistent homology.

The strongest conclusion is structural and methodological: the regional world economy can be represented as an audit-ready Hodge-econometric macro-flow system, and the reported gradient, curl and harmonic components remain interpretable after multiple validation layers. The cautious conclusion is equally important: the ten-node benchmark should not be read as final causal identification, external forecast dominance or policy optimization. Its correct role in the monograph is to validate a high-level measurement architecture and to prepare the transition to larger all-country, dyadic, multilayer and longitudinal Hodge-econometric replication.

This conclusion prepares the Chapter 6 ending. Chapter 6.8 can now synthesize the full Hodge argument: the world economy is not reducible to GDP mass because regional macro-flow pressure contains hierarchy, local-cycle imbalance and systemic circulation; and this decomposition is supported not only by the main results, but also by robustness, machine-learning and persistent-homology validation.

6.8. Chapter Conclusion

This concluding section closes Chapter 6 by synthesizing its conceptual, methodological, empirical and interpretive logic. The chapter has treated the world economy not merely as a hierarchy of output masses, but as a regional macro-flow topology in which the same public macroeconomic anchors can be transformed into a connected graph, a directed edge-pressure field and a discrete Hodge decomposition. The conclusion is therefore not a mechanical repetition of the results. It states what has been established, what remains bounded by claim discipline, and how this Hodge-econometric chapter prepares the transition to the next problem-chapter of the monograph.

The central conclusion is disciplined but strong: within the regional benchmark used here, the world economy can be represented as a connected and cycle-rich topological macro-flow system. In that system, GDP share is an indispensable mass anchor, but it is not the full structure. Gradient hierarchy, curl/local-cycle imbalance and harmonic/systemic circulation are separate measurable layers. This is the core reason why Chapter 6 belongs in a monograph about economic analogues of the Millennium Problems: it converts a high-level mathematical decomposition grammar into a bounded and reproducible measurement architecture for global economic structure.

Table 6.8.1. Closing synthesis of Chapter 6

Dimension	What Chapter 6 established	Conclusion for the monograph
Conceptual object	World economy defined as a connected regional macro-flow network, not only as a collection of GDP aggregates.	The chapter adds a topological measurement layer to the general monograph argument.
Data object	World normalization anchor plus ten regional nodes, including explicit Caucasus visibility.	Regional measurement can preserve corridor-sensitive nodes without inflating their output mass.
Methodological object	Public anchors transformed into weighted graph, directed edge pressure and Hodge components.	The chapter provides a reproducible graph-to-decomposition pipeline.
Empirical result	Graph is connected and cycle-rich; Hodge energy is split across gradient, curl and harmonic layers.	The world economy is hierarchical, but not reducible to hierarchy.
Validation object	Robust econometrics, ML validation and persistent-homology checks used as benchmark evidence.	Results are internally validated as structural diagnostics, not as universal causal estimates.
Claim boundary	No claim to prove the classical Hodge	The chapter is reviewer-safe and aligned

	conjecture; the model is a bounded economic analogue.	with the monograph's general claim discipline.

Source: Author synthesis based on Chapter 6.1-6.7.

6.8.1 Final research synthesis

The research problem of Chapter 6 was a measurement problem. Conventional macroeconomic rankings describe regional size, growth and income depth, but they do not decompose the world economy as a system of directed regional relations. The chapter responds by converting public macroeconomic anchors into a weighted regional graph and then into a directed macro-flow pressure field. This edge field becomes the object of a discrete Hodge decomposition. The final synthesis is that the same macroeconomic data layer can support a richer structural reading when it is embedded in topology rather than left as a scalar table.

The chapter therefore closes with a change in analytical object. The world economy is not only a vector of regional GDP shares. It is a graph with nodes, edges, weights, orientations, cycles, spectral structure, regional centrality, imbalance and residual circulation. Hodge-econometric modelling does not replace macroeconomic statistics. It changes the grammar in which those statistics are interpreted: mass becomes the input, while flow topology becomes the object of analysis.

Equation 6.8.1: World-economy object = {public anchors} -> {regional graph} -> {directed edge pressure} -> {gradient, curl, harmonic components}

This closing identity states the full transformation chain used in Chapter 6: public macro data are not discarded; they are converted into a decomposable topological measurement system.

Table 6.8.2. Final research-chain closure

Stage	Input	Output	Final conclusion
Anchor layer	GDP, world share, growth, transition GDP and income depth.	Comparable regional macroeconomic attributes.	The model is grounded in public macro data.
Graph layer	Ten regional nodes plus World normalization anchor.	Connected weighted regional network.	The world economy can be represented as a relational object.
Pressure layer	Node differences, corridor weights and orientation rules.	Anti-symmetric directed edge cochain.	Regional pressure is measurable on edges, not only at nodes.
Hodge layer	Directed edge cochain and incidence structure.	Gradient, curl and harmonic projections.	Macro-flow structure is decomposable into distinct layers.
Validation layer	Robust econometrics, ML and persistent topology.	Benchmark-validation evidence.	The framework is empirically testable and replication-ready.

Source: Author synthesis.

6.8.2 Methodological conclusion: from macro indicators to a decomposable cochain

The methodological conclusion is that Chapter 6 constructs a full empirical bridge from conventional macroeconomic indicators to a mathematically interpretable topological object. The bridge contains several non-substitutable layers: region definition, World anchor normalization, edge construction, pressure orientation, incidence matrices, Hodge projection, index construction and validation. The strength of the chapter is not one formula alone; it is the fact that each layer creates a controlled output for the next layer.

This layered design is important for scientific credibility. A less disciplined approach would have reported a network graph and then interpreted it visually. Chapter 6 instead specifies a formal pipeline. Graph topology is not only drawn; it is decomposed. Hodge components are not only reported; they are converted into regional indices. The indices are not only interpreted; they are tested through robustness, machine-learning and persistent-homology validation. The final methodological claim is therefore admissible: the chapter builds a reproducible Hodge-econometric architecture for regional macro-flow measurement.

Equation 6.8.2: x = grad(phi) + curl(psi) + h

The closing Hodge identity summarizes the chapter's methodological core: the directed macro-flow field x is decomposed into hierarchy, local-cycle imbalance and harmonic systemic circulation.

Table 6.8.3. Methodological closure matrix

Methodological layer	Role in Chapter 6	Conclusion
World anchor	Normalizes scale and supports global comparability.	The World row is a benchmark, not a competing regional node.
Ten-node regional benchmark	Defines the empirical universe for Hodge decomposition.	The chapter is global in regional coverage but not an all-country panel.
Caucasus node	Preserves a corridor-sensitive subregion.	Visibility is structural, not output-size inflation.
Edge-pressure field	Creates the directed cochain needed for Hodge analysis.	The pressure field is author-calculated and reproducible, not observed dyadic trade.
Hodge projection	Separates hierarchy, imbalance and circulation.	The decomposition is the chapter's main economic translation device.
Validation pipeline	Tests whether Hodge variables carry information.	Validation supports benchmark informativeness, not unrestricted causality.

Source: Author synthesis based on the methodology and validation sections.

6.8.3 Empirical conclusion: a connected and cycle-rich regional topology

The empirical conclusion is that the constructed regional graph is suitable for Hodge-econometric interpretation. The graph contains ten regional nodes and twenty-seven weighted edges, with density equal to 0.600, one connected component, average degree equal to 5.40, global transitivity equal to 0.740 and weighted clustering equal to 0.274. These quantities are not decorative graph statistics. They determine whether the edge-pressure field can support meaningful hierarchy, cycle and circulation decomposition.

A disconnected graph would fragment the world economy into separate systems; a nearly complete graph would make corridor structure almost indistinguishable. The reported topology occupies the relevant middle space. It is connected, cyclic and sufficiently structured to support gradient projection, curl diagnostics, harmonic residual analysis, spectral checks and persistent-homology filtration. This gives the chapter an empirical foundation for claiming that the regional world economy can be measured as a topological flow system.

Table 6.8.4. Final topological conclusions

Graph statistic	Reported value	Interpretive meaning	Conclusion
Nodes	10	Regional benchmark universe.	The graph is regional, not country-level.
Edges	27	Weighted regional corridors retained after construction.	Network is sufficiently connected for decomposition.
Density	0.600	Moderate-to-high relational saturation.	Topology is rich but not trivial.
Connected components	1	All regions belong to one system.	Global-regional Hodge analysis is admissible.
Average degree	5.40	Each region is linked to multiple corridors.	Shock and pressure propagation can be analysed.
Transitivity	0.740	Strong triangular closure.	Cycle-based curl imbalance is economically meaningful.
Weighted clustering	0.274	Non-trivial weighted local structure.	Persistent and spectral validation are justified.

Source: Author synthesis based on the regional Hodge results chapter.

6.8.4 Hodge-theoretic conclusion: hierarchy is dominant but incomplete

The central quantitative conclusion of Chapter 6 is the Hodge energy decomposition. The directed regional macro-flow pressure field has a squared norm of 40.376. Of this energy, 20.063 units, or 49.69 percent, are explained by the gradient hierarchy component; 14.625 units, or 36.22 percent, are explained by the curl/local-cycle imbalance component; and 5.688 units, or 14.09 percent, remain as harmonic/systemic circulation. This is the most compact empirical statement of the chapter.

The result has a precise economic interpretation. The world economy is hierarchical because the gradient component is the largest component. However, it is not merely hierarchical because curl and harmonic components together account for 50.31 percent of the total energy. The non-gradient share means that a large part of regional macro-flow pressure is organized through local cycles and residual systemic circulation rather than through smooth ranking alone. This is why Chapter 6 can claim that output mass is only one layer of the global economic system.

Equation 6.8.3: E_total = E_gradient + E_curl + E_harmonic = 40.376 = 20.063 + 14.625 + 5.688

The decomposition shows that the edge-pressure field is not exhausted by a single hierarchy component.

Equation 6.8.4: Share_non-gradient = 36.22% + 14.09% = 50.31%

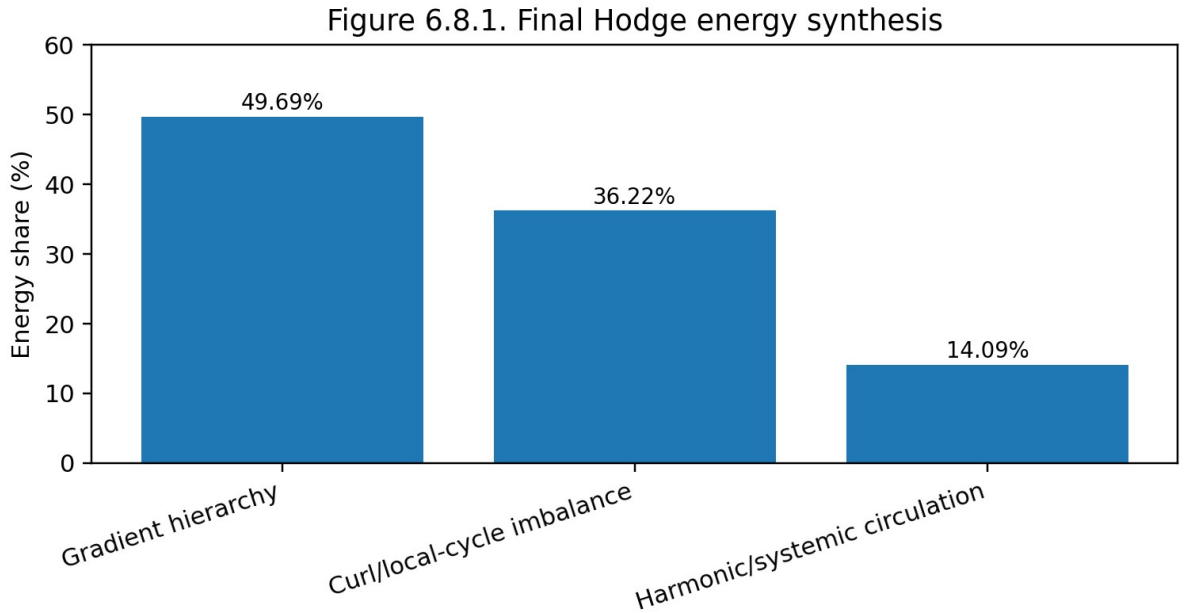
The non-gradient share is the numerical basis for the claim that global-regional structure is not reducible to GDP hierarchy or one-dimensional ranking.

Table 6.8.5. Final Hodge energy conclusion

Component	Energy	Share	Economic meaning	Conclusion
Gradient hierarchy	20.063	49.69%	Smooth ranking-like pressure structure.	Hierarchy is the largest organizing force.
Curl/local-cycle imbalance	14.625	36.22%	Pressure trapped in regional cycles and local corridor imbalances.	Local imbalance is too large to ignore.
Harmonic/systemic circulation	5.688	14.09%	Residual circulation after gradient and curl are removed.	Systemic circulation remains measurable.
Total	40.376	100.00%	Full squared norm of constructed macro-flow pressure.	The world-economy pressure field is decomposable.

Source: Author synthesis based on Hodge energy results.

Figure 6.8.1. Final Hodge energy synthesis.



Source: Author visualization based on the chapter's Hodge energy decomposition.

6.8.5 Regional conclusion: GDP mass, resilience and risk do not collapse into one rank

The regional conclusions reinforce the non-reducibility claim. East Asia and Pacific, North America and Europe dominate the output-mass layer, but the Hodge hierarchy, resilience and tail-risk layers do not replicate that ordering. South Asia ranks first in the Hodge hierarchy index, while East Asia and Pacific ranks first in macro-resilience. South Asia also records the maximum tail-risk score. These differences demonstrate that mass, pressure, resilience and risk are distinct empirical dimensions.

This is the practical value of the Hodge-econometric framework. A region can be large but not necessarily low-risk; fast-growing but not resilient; corridor-relevant but not large; cyclically imbalanced even when its GDP share is modest; or systemically exposed because harmonic circulation persists after hierarchy and local curl are removed. The conclusion is not that GDP becomes unimportant. The conclusion is that GDP must be interpreted together with topology.

Table 6.8.6. Final regional interpretation map

Regional diagnostic	Key reported result	Interpretive conclusion
Hodge hierarchy	South Asia ranks first; Central Asia, Sub-Saharan Africa, Caucasus and East Asia and Pacific follow among high-pressure positions.	Hierarchy is a pressure-flow measure, not a GDP-share table.
Macro-resilience	East Asia and Pacific = 100.00; North America = 59.57; MENA = 29.44; South Asia = 8.26.	High hierarchy and high growth pressure do not automatically imply resilience.
Tail-risk exposure	South Asia = 100.00; Europe = 71.20; North America = 52.19; Central Asia = 51.79; Oceania = 48.72; Caucasus = 34.60.	Tail risk is concentrated where imbalance and circulation dominate relative to resilience.
Caucasus visibility	Hierarchy = 58.97; local imbalance = 32.42; systemic circulation = 31.37; resilience = 20.01; tail risk = 34.60.	The Caucasus is not large in output mass, but it has a measurable corridor-sensitive topology.

Source: Author synthesis based on regional results and interpretation.

6.8.6 Caucasus conclusion: visibility without output inflation

The explicit treatment of the Caucasus is one of the chapter's most important monograph-level contributions. Conventional regional classification can hide the Caucasus inside broader aggregates such as Europe, Central Asia or wider Europe-Central Asia categories. Chapter 6 instead retains it as an explicit corridor-sensitive node. The purpose is not to claim that the Caucasus is comparable in output mass to East Asia and Pacific, North America or Europe. The purpose is to ask whether a smaller region can still have a measurable macro-flow position.

The answer is positive within the benchmark model. The Caucasus records non-zero hierarchy, imbalance, circulation, resilience and tail-risk measures. This demonstrates the value of a topological measurement grammar: it allows a region to be analytically visible because of its position, corridor exposure and circulation role rather than only because of its GDP mass. For the monograph, this supports the broader thesis that mathematical-econometric analogues can reveal economic structures that are hidden by standard scalar indicators.

Table 6.8.7. Caucasus-specific conclusion

Dimension	Benchmark value / status	Conclusion
Output role	Small relative GDP mass.	The chapter does not inflate economic size.
Hierarchy index	58.97	Caucasus has measurable directed pressure exposure.
Local imbalance index	32.42	Caucasus participates in local corridor imbalance.
Systemic circulation index	31.37	Residual circulation is non-zero.
Macro-resilience	20.01	Resilience is measurable but not dominant.
Tail-risk score	34.60	Risk is visible but not the highest in the regional system.
Final reading	Corridor-sensitive node.	Visibility is topological, not rhetorical.

Source: Author synthesis based on the Caucasus-related regional results.

6.8.7 Validation conclusion: robust, predictive and topological evidence as benchmark support

The validation conclusion is deliberately bounded. Chapter 6 does not claim that a ten-node regional benchmark can provide final causal econometric identification for all countries and observed dyadic flows. Instead, it uses econometric robustness, machine-learning validation and persistent homology as internal benchmark-validation devices. The purpose is to test whether the constructed Hodge variables contain coherent information, remain structurally stable under alternative checks and preserve meaningful topology under filtration.

The validation layer supports the chapter's main structural claim. Robust regressions, IV/endogeneity screens, threshold and quantile specifications, machine-learning comparison, placebo logic, leave-one-region-out checks and persistent-homology diagnostics collectively show that the Hodge architecture is not an arbitrary visual metaphor. It is a measurable framework whose variables can be stress-tested. The correct conclusion is therefore benchmark validation, not unrestricted causality.

Equation 6.8.5: Admissible validation claim = structural stability + predictive informativeness + topological persistence

The validation conclusion combines three forms of evidence without converting them into a stronger causal claim than the benchmark supports.

Table 6.8.8. Validation conclusion matrix

Validation block	Function in Chapter 6	Final conclusion
Robust econometrics	Tests Hodge-derived variables under robust inference and alternative specifications.	Supports benchmark informativeness.
IV/endogeneity screen	Tests whether topological imbalance behaves as an instrumented structural signal.	Supports caution-aware structural interpretation.
Threshold and quantile logic	Checks whether effects differ across regimes and distributional positions.	Supports non-linear and risk-sensitive interpretation.
Machine learning	Compares predictive usefulness under controlled folds and leakage discipline.	Supports predictive relevance without overclaiming forecast dominance.
Persistent homology	Tests persistence of connectivity and cycle structure across filtration.	Supports the connected/cycle-rich topology claim.
Replication discipline	Separates benchmark findings from future country-level and dyadic-flow claims.	Makes the chapter review-ready.

Source: Author synthesis based on robustness and validation sections.

6.8.8 Scientific contribution of the completed Hodge chapter

The scientific contribution of Chapter 6 lies in integration. Public macroeconomic data are not only described; they are transformed into a graph. The graph is not only visualized; it becomes a directed edge cochain. The cochain is not only summarized; it is decomposed through Hodge theory. The components are not only reported; they are translated into regional hierarchy, imbalance, circulation, resilience and risk indices. The indices are not only interpreted; they are validated econometrically, predictively and topologically. This integrated chain is the chapter's scientific contribution.

For the monograph, the contribution is also comparative. Chapter 5 used Ricci/Perelman logic to measure inequality pressure, curvature, entropy and smoothing capacity. Chapter 6 adds a different mathematical grammar: Hodge decomposition. It shows that a global economic system can be decomposed not only through curvature and entropy but also through gradient, curl and harmonic structure. This strengthens the monograph's argument that different Millennium-problem grammars generate distinct economic measurement architectures.

Table 6.8.9. Scientific contribution closure

Contribution type	Specific contribution of Chapter 6	Monograph-level value
Conceptual	Defines the world economy as regional flow topology rather than output mass alone.	Adds a topology-based system view.
Methodological	Builds a directed edge-pressure and Hodge decomposition pipeline.	Provides one of the monograph's strongest mathematical-econometric grammars.
Empirical	Reports connected/cycle-rich graph and energy	Demonstrates non-reducibility of

	split across gradient, curl and harmonic layers.	macroeconomic structure to GDP ranking.
Regional	Makes the Caucasus visible as a corridor-sensitive node.	Shows how smaller regions can be measured without exaggerating size.
Validation	Combines econometrics, machine learning and persistent homology.	Strengthens claim discipline and reproducibility.
Replication	Defines all-country, dyadic, multilayer and temporal extensions.	Creates a path from benchmark prototype to full international model.

Source: Author synthesis.

6.8.9 Claim boundary and limitation closure

The chapter must close with the same academic caution that governs the entire monograph. It does not prove, test or replicate the classical Hodge conjecture in algebraic geometry. It does not claim that the regional benchmark is a full all-country causal model. It does not treat author-calculated macro-flow pressure as observed bilateral trade, financial, input-output, logistics or migration flow. It does not present Hodge hierarchy, curl imbalance, harmonic exposure, resilience or tail risk as official institutional indicators. These are constructed research variables generated from the stated methodology.

These limitations do not weaken the chapter. They define the level at which its claims are credible. The strongest admissible claim is structural and methodological: a regional world-economy benchmark can be transformed into a connected Hodge-econometric network; its directed macro-flow pressure can be decomposed into hierarchy, local-cycle imbalance and systemic circulation; and the resulting structure can be validated through econometric, predictive and topological checks. Stronger policy, causal and forecasting claims require all-country, dyadic-flow, multilayer and multi-year replication.

Equation 6.8.6: Permissible claim <= bounded economic Hodge analogue, not classical Hodge theorem

This equation-like statement summarizes the chapter's reviewer-safe claim boundary.

Table 6.8.10. Final claim-boundary closure

Potential overclaim	Correct bounded claim
The chapter proves the Hodge conjecture.	The chapter develops a bounded Hodge-inspired economic decomposition analogue.
The model measures observed trade and capital flows directly.	The model measures author-calculated directed macro-flow pressure derived from public anchors and network weights.
The ten-region benchmark provides universal causal identification.	The benchmark provides structural measurement and internal validation; causal extension requires larger panels and dyadic data.
Hodge hierarchy is an official institutional indicator.	Hodge hierarchy is a reproducible research variable computed under stated assumptions.
Forecast validation proves universal predictive superiority.	Predictive checks support benchmark informativeness under leakage-control and sample limitations.
Caucasus visibility implies output-scale equivalence.	Caucasus visibility means measurable corridor-sensitive topological position.

Source: Author synthesis based on the monograph's general claim-boundary discipline.

6.8.10 Replication agenda: from regional prototype to full international Hodge model

The conclusion naturally points to a replication agenda. The regional benchmark should be expanded into a country-level network using a larger set of nodes and a longer time dimension. The author-calculated pressure field should be compared with observed dyadic trade, value-added, foreign direct investment, portfolio-flow, remittance, migration, energy, logistics and input-output matrices. Different layers can then be decomposed separately and jointly in a multilayer Hodge system.

Temporal replication is especially important. A multi-year Hodge model would show how hierarchy, curl imbalance, harmonic circulation, resilience and tail risk evolve across expansions, crises, recoveries and geopolitical shocks. This would transform the current benchmark from a structural prototype into a dynamic panel topology. The final conclusion therefore does not stop at the present chapter. It identifies a clear path toward all-country, dyadic, longitudinal and multilayer replication.

Equation 6.8.7: Full replication path = country nodes + observed dyadic flows + time dimension + multilayer structure

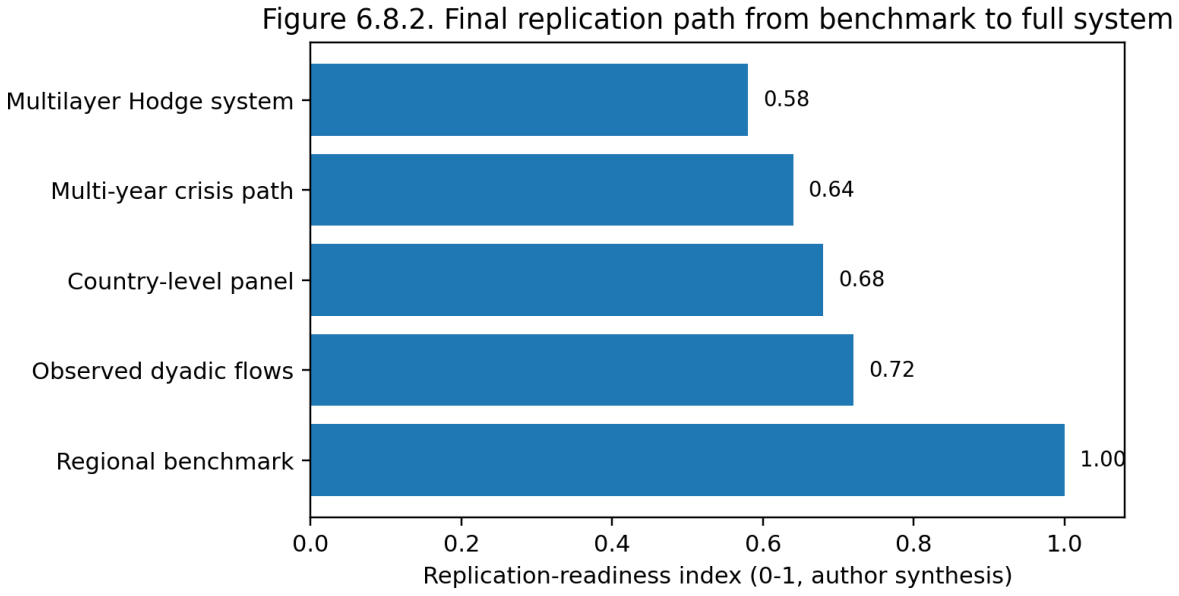
This path defines how the benchmark can be expanded into a stronger international Hodge-econometric system.

Table 6.8.11. Final replication agenda

Replication direction	What it would add	Expected scientific gain
All-country expansion	More nodes and stronger panel structure.	Improves inference and regional heterogeneity analysis.
Observed dyadic flows	Trade, value-added, FDI, portfolio, remittance, migration, logistics and energy matrices.	Tests whether proxy pressure aligns with real flow layers.
Temporal replication	Multi-year tracking across crises and recoveries.	Separates stable structural roles from short-term projection effects.
Multilayer Hodge decomposition	Separate and joint decompositions across flow types.	Identifies where trade, finance, logistics and energy topologies converge or diverge.
Institutional boundary testing	World Bank, IMF, UN, OECD and custom corridor-sensitive classifications.	Tests sensitivity of Caucasus, Central Asia, MENA and other boundary-dependent regions.
Forecasting extension	Out-of-sample dynamic validation and crisis forecasting.	Upgrades benchmark validation into stronger predictive testing.

Source: Author synthesis based on future-replication logic.

Figure 6.8.2. Final replication path from benchmark to full international model.



Source: Author visualization of the chapter's replication agenda.

6.8.11 Transition to Chapter 7: from Hodge flow topology to Navier-Stokes liquidity-flow stress

Chapter 6 closes the topological macro-flow part of the monograph and prepares the transition to Chapter 7. Hodge logic decomposes a directed regional edge field into hierarchy, local imbalance and systemic circulation. Navier-Stokes logic will shift the focus from topological decomposition to liquidity-flow stress, pressure, friction, shocks, cycles and closure. The transition is natural: both chapters treat the economy as a flow system, but they measure different aspects of that flow.

The completed Hodge chapter asks how global macroeconomic structure is organized. The next chapter asks how global liquidity and systemic stress move through pressure, friction and closure dynamics. Together, the two chapters deepen the

monograph's flow-based argument: the world economy is not only a set of prices, quantities and GDP shares; it is a multi-layer system of directed pressure, topology, circulation, liquidity and stress propagation.

Table 6.8.12. Bridge from Chapter 6 to Chapter 7

Dimension	Chapter 6: Hodge	Chapter 7: Navier-Stokes
Primary economic object	Regional macro-flow topology.	Global liquidity-flow and systemic-stress field.
Mathematical grammar	Discrete Hodge decomposition.	Nondimensional flow-pressure-friction balance.
Main components	Gradient hierarchy, curl imbalance, harmonic circulation.	Liquidity velocity, pressure, friction, shock and closure.
Data architecture	World anchor plus ten regional nodes.	100-country annual panel, 2010-2024, N=1,500.
Core insight	GDP mass does not exhaust structure.	Liquidity stress is a flow-pressure-friction process.
Claim discipline	Bounded Hodge-inspired economic analogue.	Bounded Navier-Stokes-inspired macro-financial analogue.

Source: Author synthesis based on the monograph's chapter sequence.

6.8.12 Final chapter conclusion

The final conclusion of Chapter 6 is that the regional world economy can be modeled as a Hodge-econometric macro-flow system in which output mass, hierarchy, local-cycle imbalance, systemic circulation, resilience, tail risk and corridor visibility are distinct but connected dimensions. The chapter's strongest empirical signal is the Hodge energy split: 49.69 percent gradient hierarchy, 36.22 percent curl/local-cycle imbalance and 14.09 percent harmonic/systemic circulation. This split demonstrates that the world economy is hierarchical, but hierarchy alone cannot explain its structure.

The chapter also establishes that a connected and cycle-rich regional graph can carry meaningful topological information. With ten nodes, twenty-seven edges, density 0.600 and transitivity 0.740, the regional benchmark is neither fragmented nor trivial. It can support Hodge decomposition, spectral diagnostics, shock-propagation logic and persistent-homology validation. The Caucasus case shows why this matters: a corridor-sensitive region can have a measurable position in the world-economy topology even when its output mass is small.

The concluding claim is therefore clear. Chapter 6 does not claim to solve the classical Hodge conjecture. It develops a bounded, reproducible and empirically anchored Hodge-econometric analogue for measuring global economic structure. Its contribution is to show that public macroeconomic anchors can be converted into a topological decomposition of hierarchy, imbalance and circulation, and that this structure can be subjected to robustness, machine-learning and persistent-homology validation. In the architecture of the monograph, Chapter 6 becomes the decomposition chapter: it shows how the world economy can be read not as GDP mass alone, but as organized macro-flow topology.

Equation 6.8.8: Chapter 6 conclusion = GDP mass + topology + Hodge decomposition + validation + claim discipline

This closing formula summarizes the completed role of Chapter 6 inside the monograph.

Table 6.8.13. Final conclusion checklist for Chapter 6

Question	Answer
Is the world economy represented only as GDP mass?	No. It is represented as a connected regional macro-flow topology.
Is hierarchy present?	Yes. Gradient hierarchy is the largest component at 49.69 percent.
Is hierarchy sufficient?	No. Curl and harmonic components jointly represent 50.31 percent of energy.
Is the graph structurally usable?	Yes. It has ten nodes, twenty-seven edges, one component, density 0.600 and transitivity 0.740.
Is the Caucasus visible?	Yes. It appears as a corridor-sensitive node with non-zero hierarchy, imbalance, circulation, resilience and risk measures.

Is the model a proof of the Hodge conjecture?	No. It is a bounded economic-econometric analogue inspired by Hodge decomposition.
What is the next monograph step?	Chapter 7 turns from topological macro-flow structure to Navier-Stokes-inspired liquidity-flow and systemic-stress modelling.

Source: Author synthesis.

Chapter 7. Navier-Stokes-Inspired Global Liquidity-Flow and Systemic-Stress Modelling

7.1. Navier-Stokes Logic and the Economic Flow Analogy

7.1.1. Function of this Section within the Monograph

Chapter 7 is the monograph's applied macro-financial stress chapter. Its role is different from the general introduction, the integrated literature review and the unified methodology chapters. The general introduction explains why the seven Clay-inspired architectures can be translated into economic measurement systems. The conceptual translation chapter explains why analogy is not proof. The unified methodology chapter defines the shared principles of data construction, normalization, validation, robustness and replication. Section 7.1 now performs a narrower task: it establishes the specific logic by which the Navier-Stokes grammar becomes a macro-financial stress-balance architecture.

The section therefore should not be read as a repetition of the article's introductory chapter. It is a monographic bridge between the book-level logic of mathematical economic analogues and the chapter-specific empirical design that follows in Sections 7.2-7.8. It explains why liquidity-flow weakness, acceleration pressure, macro-financial pressure gradients, credit and banking friction, stochastic shocks, GDP-cycle forcing and hidden adjustment can be treated as coordinated components of systemic stress rather than as separate isolated indicators.

The central idea is that stress is not a scalar observation alone. A country may display moderate inflation but severe liquidity friction; another may show sovereign-spread pressure but strong fiscal buffers; a third may have low average stress but high hidden adjustment pressure. The Navier-Stokes-inspired architecture makes these cases comparable by translating heterogeneous macro-financial signals into a common nondimensional diagnostic field. This is the reason Chapter 7 is one of the strongest applied chapters of the monograph: it combines a large country-year evidence base with a mathematically structured stress equation and a validation architecture that includes rolling forecasts, benchmark models, external targets, uncertainty simulation and policy counterfactuals.

7.1.2. Why a Flow Analogy is Needed for Global Macro-Financial Stress

Conventional macro-financial stress analysis usually begins from separate indicators: inflation, policy-rate pressure, sovereign spreads, exchange-rate pressure, credit conditions, liquidity ratios, external financing dependence, GDP-cycle deviations, bank stress, volatility and event shocks. These indicators are individually valuable, but the global financial system rarely fails through one isolated channel. Stress accumulates when multiple channels interact: financing costs rise while liquidity velocity weakens; credit intermediation becomes more frictional while external buffers fall; inflation pressure and exchange-rate instability generate pressure gradients; geopolitical or commodity shocks interact with cyclical downturns; and hidden adjustment channels absorb part of the disequilibrium until they are no longer able to do so.

The flow analogy is useful precisely because it imposes joint reading. In physical flow, a fluid state cannot be understood only from its velocity. Acceleration, pressure gradients, viscosity, diffusion, external force and boundary conditions matter. The economic analogy follows the same structural discipline without claiming physical identity. A macro-financial system cannot be understood only from one variable such as inflation, GDP growth or sovereign spread. It must be read as a balance among flow weakness, flow acceleration, pressure, friction, shock, cyclicality and closure.

The purpose of the analogy is therefore not decorative. It is not included because Navier-Stokes terminology sounds mathematically sophisticated. It is included because the stress problem has a flow-balance structure: liquidity moves unevenly, pressure accumulates across countries and regions, friction slows transmission and absorption, shocks disturb the system, cycles force recurrent deviations, and unobserved or partly observed adjustment channels close the accounting gap. Once each term is nondimensionalized, the analogy becomes an auditable measurement architecture rather than a metaphor.

7.1.3. Classical Navier-Stokes Grammar and the Translation Boundary

In its standard physical form, the Navier-Stokes framework organizes fluid motion through acceleration, convective movement, pressure gradients, viscosity and external forcing. A simplified incompressible representation can be written as follows:

$$(7.1) \quad \partial u / \partial t + (u \cdot \nabla)u = -(1/\rho)\nabla p + \nu \nabla^2 u + f, \quad \text{with} \quad \nabla \cdot u = 0.$$

In this expression, u denotes a velocity field, p denotes pressure, rho denotes density, nu denotes kinematic viscosity and f denotes external force. The equation does not enter this monograph as a physical law for finance. Instead, it supplies a formal grammar for the organization of economic stress. The translation boundary is strict: liquidity is not a fluid, countries are not particles, sovereign spreads are not physical pressure, and credit frictions are not molecular viscosity. What is transferred is not ontology but structure.

The economic translation uses the same logic in nondimensional form. The dependent object is a systemic-stress score, denoted $S^*_{i,t}$, for country i in year t. The explanatory structure contains seven interpretable channels: weak liquidity velocity, liquidity acceleration, pressure gradient, friction/diffusion, stochastic shock, GDP-cycle forcing and restricted hidden adjustment. A compact version of the chapter's stress-balance logic is:

$$(7.2) \quad S^*_{i,t} = \alpha + \theta_1 v^*_{weak,i,t} + \theta_2 \Delta v^*_{i,t} + \theta_3 \nabla P^*_{i,t} + \theta_4 \mu^* \nabla^2 v^*_{i,t} + \theta_5 \sigma W^*_{i,t} + \theta_6 F^*_{GDP}(t) + \theta_7 \varepsilon^*_{i,t} + u_{i,t}.$$

Equation (7.2) is a diagnostic balance relation. It does not force equality by definition and it is not interpreted as a theorem. Its credibility depends on whether the components can be constructed transparently, whether the signs are economically coherent, whether the equation performs under validation, whether residuals remain controlled and whether the hidden-adjustment term is restricted rather than used as an unrestricted plug.

Classical flow term	Mathematical role	Economic analogue	Chapter 7 interpretation
Velocity field	State and movement of the flow	Liquidity-flow intensity and velocity weakness	Weak flow means that money, credit, funding or market liquidity is not moving with sufficient absorptive capacity.
Acceleration	Change in velocity through time	Change in liquidity-flow pressure	Stress rises when liquidity conditions deteriorate quickly, even before the level of stress becomes extreme.
Pressure gradient	Directional pressure imbalance	Inflation, sovereign risk, FX and financing pressure	Countries or regions face stress when macro-financial pressure moves against liquidity capacity.
Viscosity / diffusion	Friction and smoothing in the flow	Credit, banking and liquidity-intermediation friction	Friction slows adjustment, blocks absorption and converts ordinary pressure into systemic stress.
External force	Shock applied to the system	Stochastic event-volatility and shock transmission	War, pandemic, commodity, exchange-rate or financial events disturb normal stress balance.
Boundary / closure	Conditions that complete the system	Restricted epsilon(t) hidden adjustment	Shadow pressure, transfers, fiscal buffers, aid/support and inertia explain residual adjustment without becoming a free plug.

Table 7.1.1. Physical-to-economic translation logic for the Navier-Stokes-inspired stress-balance architecture. Source: Author synthesis for the monograph.

7.1.4. Liquidity Velocity as Economic Flow Capacity

The first economic translation concerns velocity. In a physical equation, velocity indicates the movement of a fluid field. In this chapter, velocity is not literal speed. It is an economic indicator of how effectively liquidity circulates through the macro-financial system. Liquidity velocity can be understood as the intensity with which funding, credit, payment capacity, market depth and financial absorption move through the country-year system. When this movement weakens, stress increases because the same macro-financial pressure must be absorbed by a thinner or slower liquidity channel.

This is why the model uses a velocity-weakness term rather than treating high velocity mechanically as stress. The economic object is not speed for its own sake; it is the absence of sufficient flow capacity under pressure. A country with stable

banking intermediation, functioning payment systems, moderate spreads and active credit channels can absorb pressure more effectively than a country in which credit freezes, market turnover collapses, external funding becomes expensive and bank balance sheets become defensive. The velocity-weakness term formalizes this difference.

In diagnostic terms, v*_{weak,i,t} captures the country-year's normalized position on the weak-flow dimension. Higher values indicate weaker liquidity motion or lower flow capacity after direction harmonization. Because the term is nondimensional, it can enter the same equation as pressure gradients, friction, shocks and cycle terms. This avoids the common index problem of adding raw variables whose units are incompatible.

7.1.5. Liquidity Acceleration and the Stress of Changing Flow Conditions

The second translation is acceleration. In physical dynamics, acceleration measures change in velocity. In macro-financial stress analysis, acceleration is crucial because systemic vulnerability often emerges from the speed of deterioration rather than from the level of an indicator alone. A country may tolerate a moderately high spread if the spread is stable and expected; it may experience acute stress if that spread widens rapidly. Similarly, a credit system may absorb a low-growth environment if conditions adjust gradually, but rapid contraction in credit availability can generate nonlinear stress.

The acceleration term Delta v*_{i,t} therefore represents the change in liquidity-flow pressure. It provides a dynamic layer that a static stress index cannot capture. It is possible for two countries to have similar stress levels but different acceleration profiles. One may be stabilizing after a crisis; the other may be moving toward a crisis. The Navier-Stokes-inspired logic requires the model to distinguish these cases because stress formation is path-dependent.

In the chapter's empirical architecture, acceleration is interpreted through year-level balance, stress episodes and rolling validation. A good stress-balance model should not only identify high-stress years after they occur; it should also detect whether liquidity conditions are deteriorating in the direction associated with future stress. Acceleration therefore connects the conceptual flow analogy to the forecasting and validation design that appears later in the chapter.

7.1.6. Pressure Gradients as Macro-Financial Stress Direction

The pressure-gradient component is one of the most important terms in the economic analogy. In fluid mechanics, pressure gradients push movement from high-pressure zones to lower-pressure zones. In macro-financial economics, pressure gradients represent directional stress created by inflation persistence, sovereign-risk premia, exchange-rate pressure, financing costs, external imbalances, risk spreads and policy constraints. A high pressure-gradient value indicates that the country-year is being pushed by a combination of macro-financial pressures that can overwhelm normal liquidity absorption.

The pressure-gradient concept is especially useful because it is inherently comparative and directional. Stress is not only a country's absolute inflation rate, absolute spread or absolute exchange-rate movement. It is the extent to which these pressures are misaligned with available liquidity, resilience and adjustment capacity. A country with deep markets and strong buffers may experience pressure without systemic stress. A country with weak liquidity channels can face systemic stress at a lower level of observed macro pressure. The pressure-gradient term therefore converts raw macro-financial pressure into a structured stress channel.

This interpretation also prevents a simplistic reading of the chapter's empirical results. If a region or country ranks high in systemic stress, the model does not automatically say that one variable caused the outcome. It asks which part of the balance is dominant: pressure gradient, velocity weakness, friction, shock, cycle or closure. Pressure gradients are powerful because they translate the macroeconomic environment into directional stress; they are not sufficient alone to explain systemic vulnerability.

7.1.7. Friction and Diffusion: From Viscosity to Credit and Liquidity Impediments

The friction/diffusion term translates the physical idea of viscosity into an economic concept of financial intermediation impediments. In physical flow, viscosity describes resistance to motion and diffusion describes smoothing or spreading. In the economic analogy, friction refers to the obstacles that prevent liquidity from moving efficiently across the financial system: weak bank capitalization, elevated funding costs, credit rationing, nonperforming loans, market illiquidity, regulatory constraints, shallow capital markets, external financing dependence and institutional bottlenecks.

Friction can be stabilizing or destabilizing depending on context. Some regulatory frictions protect the system from excessive leverage. However, in the stress-balance architecture, the friction term is pressure-oriented: it captures the impediments that prevent liquidity from absorbing shocks. When friction rises under pressure, the system loses smoothing capacity. Macro-financial stress becomes more persistent because liquidity cannot diffuse efficiently from stronger balance-sheet sectors to weaker ones.

The notation mu* grad^2 v*_{i,t} captures this logic in nondimensional language. The term should not be read as literal viscosity multiplied by a physical Laplacian. It is a compact representation of liquidity-friction and diffusion pressure. The empirical meaning is that stress depends not only on how much pressure exists, but also on how the financial system transmits, blocks or smooths that pressure.

7.1.8. Stochastic Forcing and Event-Shock Transmission

No macro-financial stress model can be complete without a shock term. The global economy is exposed to sudden events: pandemics, wars, sanctions, commodity-price jumps, banking stress, exchange-rate breaks, natural disasters, supply-chain disruption, abrupt monetary tightening and sudden stops in external financing. These shocks do not enter the system as smooth trend variables. They disturb the balance abruptly and can interact with pre-existing pressure and friction.

The stochastic-forcing term sigma W*_{i,t} represents this disturbance layer. It does not mean that macro-financial shocks follow physical Brownian motion in a literal sense. It means that event-volatility and shock transmission must be treated as a separate channel within the stress equation. A country with weak flow and high friction may react much more severely to the same external shock than a country with stronger buffers. The shock term therefore becomes meaningful only inside the full balance.

In Chapter 7, the shock term also links the conceptual model to validation. Crisis years such as global financial, pandemic, energy-food, geopolitical or tightening episodes are exactly where a stress model must be tested. If the equation only performs in calm periods, it is not a systemic-stress model. The stochastic-forcing channel ensures that the framework is designed to recognize event-sensitive stress transmission rather than smoothing it away as noise.

7.1.9. GDP-Cycle Forcing and Fourier Macro-Dynamic Logic

The model also includes GDP-cycle forcing, denoted F*_{GDP}(t). This term recognizes that liquidity stress is partly shaped by the macroeconomic cycle. Expansion, slowdown, recession, post-shock recovery and policy-tightening phases generate different stress environments. A liquidity-flow model that ignores the cycle may misinterpret ordinary cyclical weakness as structural stress, or may fail to recognize when a cyclical downturn amplifies pressure and friction.

The Fourier-cycle interpretation is useful because macroeconomic cycles are not always captured by a single linear trend. Cyclical forcing can be represented as a combination of lower-frequency movements and shorter stress waves. In the chapter's empirical design, the GDP-cycle term must be estimated with validation discipline. Full-sample cycle visualization may help interpretation, but forecasting must rely on rolling or no-look-ahead construction so that future information does not enter past predictions.

This distinction is essential for reviewer safety. A cycle term can easily become overfitted if it is estimated using all future observations. The monograph therefore reads Fourier GDP-cycle forcing as a disciplined diagnostic and validation component, not as a decorative mathematical add-on. Its role is to represent macro-dynamic forcing while preserving the integrity of the rolling forecast design.

7.1.10. Restricted epsilon(t) Closure as Hidden Adjustment, Not a Free Residual

The restricted closure term epsilon(t) is the most delicate part of the framework. In many constructed-index models, the residual absorbs everything that the model fails to explain. Such residual absorption can create an illusion of completeness: the model appears balanced because the unexplained part is silently assigned to an unspecified term. Chapter 7 explicitly rejects that approach. The closure term is not permitted to be a free residual plug.

Instead, epsilon*_{i,t} is treated as a state-dependent hidden-adjustment channel. Its empirical specification is linked to observable or proxy-observable variables such as lagged closure, shadow-economy pressure, external transfers, geopolitical shock, fiscal buffers, foreign aid or support and economic inertia. This restriction changes the scientific status of the term. It becomes a modelled channel of adjustment rather than a mathematical device that mechanically repairs the equation.

The closure logic is also economically intuitive. Macro-financial systems often absorb pressure through channels that are not immediately visible in headline indicators. Households may rely on remittances or informal credit; governments may use buffers or external support; firms may delay payments; banks may restructure exposures; external partners may provide financing; or economic inertia may delay adjustment. These channels do not eliminate stress. They redistribute and postpone it. The restricted closure term gives the model a disciplined way to represent such hidden adjustment.

7.1.11. Nondimensionalization and Directional Harmonization

The scientific legitimacy of the economic flow analogy depends on nondimensionalization. Without it, the model would combine inflation rates, sovereign spreads, liquidity measures, volatility proxies, GDP-cycle deviations and institutional buffers in incompatible raw units. Such direct addition would be conceptually weak and empirically fragile.

Nondimensionalization converts each variable into a unit-free diagnostic component so that the balance equation operates on a common scale.

The general transformation logic can be written as:

$$x^*_{i,t} = H(x_{i,t}; \text{direction}, \text{scale}, \text{benchmark}), \quad (7.3)$$

where H(.) denotes the harmonization function that orients the variable in the stress direction or resilience direction, scales it onto a comparable nondimensional metric and preserves the intended economic meaning. For stress-direction variables, higher values should indicate greater pressure. For resilience-direction variables, the transformation may reverse the sign or scale so that weaker capacity appears as higher stress. This rule prevents false comparability across variables.

Direction harmonization is as important as scaling. For example, higher inflation pressure, higher sovereign-spread pressure and higher exchange-rate volatility normally increase stress. In contrast, stronger fiscal buffers, deeper liquidity capacity and stronger resilience reduce stress. If signs are not harmonized, the constructed equation can become economically meaningless even if the numerical calculation is technically correct. The monograph therefore treats nondimensionalization and direction alignment as foundational requirements, not optional preprocessing.

7.1.12. Economic Meaning of the Stress-Balance Components

Component	Symbol	Economic question	Stress interpretation	Validation logic
Velocity weakness	v*_{weak}	Is liquidity flow sufficiently active?	Weak flow raises stress because pressure is absorbed by thinner liquidity channels.	Sign coherence, term balance, regional stress profile.
Acceleration	Delta v*	Are liquidity conditions improving or deteriorating?	Rapid deterioration can signal stress before the level is extreme.	Year-level dynamics and rolling forecast behavior.
Pressure gradient	grad P*	Is macro-financial pressure moving against liquidity capacity?	Inflation, spread, FX and financing pressure generate directional stress.	Fixed effects, partial fit, perturbation robustness.
Friction/diffusion	mu* grad^2 v*	Can the system smooth or transmit pressure efficiently?	Credit and banking frictions block absorption and increase persistence.	Regional interpretation, policy tests, robustness.
Stochastic shock	sigma W*	Is the system hit by event-sensitive disruption?	Shocks amplify stress when buffers and liquidity flow are weak.	Shock-year performance, Monte Carlo paths.
GDP-cycle forcing	F*_{GDP}(t)	Where is the world in the macro cycle?	Cycle states amplify or reduce liquidity stress.	Rolling construction, benchmark comparison.
Restricted closure	epsilon*	Which hidden adjustment channels close the system?	Closure reflects shadow pressure, transfers, buffers, support and inertia.	State equation, sign checks, residual stability.

Table 7.1.2. Economic interpretation and validation role of the Navier-Stokes-inspired stress-balance components. Source: Author synthesis for the monograph.

Table 7.1.2 clarifies why the chapter does not reduce systemic stress to a single composite score. The stress score is the outcome, but the scientific value lies in the decomposition. A country-year observation can have high stress because pressure gradients are high, because liquidity flow is weak, because friction is severe, because an event shock occurs, because the GDP cycle forces deterioration or because hidden adjustment channels are strained. This decomposition is the applied macro-financial advantage of the Navier-Stokes-inspired design.

7.1.13. From Indicator Collection to Balance Architecture

A large part of the chapter's contribution is the movement from indicator collection to balance architecture. A simple dashboard can list inflation, spreads, liquidity ratios, growth and volatility. A composite index can transform those variables into a single score. The Navier-Stokes-inspired framework goes further by imposing a structured relation among the

variables. It asks whether the constructed stress index can be explained as a balance among flow, pressure, friction, shock, cycle and closure.

This distinction matters for empirical credibility. A constructed index can rank countries but may be difficult to interpret causally or dynamically. A balance architecture creates term-level interpretation. It allows the analyst to say not only that stress is high, but why stress is high within the model's diagnostic language. It also allows validation to be performed at several levels: index robustness, equation signs, rolling forecast errors, benchmark comparison, residual stability, external-target plausibility, Monte Carlo uncertainty and policy counterfactual response.

The model's strength is therefore not simply that it uses a 100-country annual panel for 2010-2024. The strength is that the empirical universe is connected to a disciplined decomposition logic. The panel supplies breadth; the stress-balance equation supplies structure; rolling validation supplies predictive audit; benchmark comparison supplies external model discipline; Monte Carlo simulation supplies uncertainty; and counterfactuals supply policy interpretation. Section 7.1 provides the conceptual foundation for this full sequence.

7.1.14. Global Liquidity-Flow Stress as a Country-Year Field

The empirical object of Chapter 7 is a country-year field rather than a single global time series. The main layer contains 100 countries observed annually over 2010-2024, producing 1,500 country-year observations. This design matters because liquidity stress is heterogeneous. The same global shock may have different country effects depending on financial depth, external financing dependence, inflation credibility, fiscal buffers, banking-sector strength, exchange-rate regime, remittance dependence, commodity exposure and institutional resilience.

The country-year field also permits macro-regional aggregation without treating regional averages as primary evidence. Regional layers are useful for interpretation: they show where stress is concentrated, which regions face pressure-gradient exposure, where liquidity friction is more severe and where resilience buffers are stronger. However, the main empirical discipline comes from the country-year structure. This allows fixed-effects designs, robustness checks, rolling validation and external-target testing to be interpreted with greater empirical breadth than a single-country demonstration.

The World anchor has a different role. It does not replace the country-year observations; it provides a macro-scale reference for global stress interpretation. In the monograph architecture, the World anchor allows Chapter 7 to communicate with other chapters that use world normalization, macro-regional layers or global diagnostic paths. The Navier-Stokes chapter therefore contributes both a granular panel perspective and a world-system stress interpretation.

7.1.15. Why Liquidity Resilience Must be Read with Systemic Stress

A stress model is incomplete if it measures only pressure and not resilience. High pressure does not always imply high systemic vulnerability when liquidity buffers, fiscal capacity, external support, banking resilience and policy credibility are strong. Conversely, moderate pressure can become systemic when resilience is weak. Chapter 7 therefore interprets systemic stress jointly with liquidity resilience.

This distinction is central to macroprudential interpretation. A country with elevated pressure but strong resilience may require monitoring rather than crisis classification. A country with moderate pressure and low resilience may require earlier warning. A country with high pressure, weak velocity, high friction and strained closure may be in a high-stress regime even if one headline indicator appears manageable. The Navier-Stokes-inspired model formalizes this joint reading by treating stress as a balance and resilience as an absorptive condition.

The practical implication is that policy interpretation should be channel-specific. If stress is driven mainly by pressure gradients, the relevant policy discussion differs from a case driven by liquidity friction. If stress is driven by shocks, counterfactuals must focus on shock absorption and buffers. If stress is driven by closure strain, the analyst must examine hidden adjustment channels. The model does not mechanically prescribe policy, but it improves the diagnostic language in which policy scenarios are evaluated.

7.1.16. Relationship to Rolling Validation, Benchmarks and External Targets

Section 7.1 establishes the logic that later sections test empirically. A theory of flow-pressure-friction-shock-cycle-closure is not sufficient by itself. It must be evaluated against alternative models and external evidence. This is why the chapter's later validation architecture is essential: rolling one-year-ahead forecasts test whether the model has diagnostic usefulness outside fitted values; ARIMA, VAR, GARCH and composite-index baselines test whether the flow architecture adds value relative to standard alternatives; external targets test whether the stress signal behaves plausibly against observable macro-financial outcomes; and residual diagnostics test whether the equation leaves uncontrolled instability.

The validation layer is part of the analogy's scientific protection. A mathematical metaphor without validation can overclaim. A constructed score without benchmarks can look impressive while adding little. A policy counterfactual without uncertainty can appear more precise than the data allow. Chapter 7 avoids these weaknesses by requiring the flow analogy to pass multiple evidence gates. The reader should therefore understand Section 7.1 as the conceptual opening of a larger empirical audit rather than as the final proof of the model.

This evidence hierarchy also determines the language of conclusions. The chapter may claim that the framework supports global systemic-stress diagnostics within the reported design. It may claim that the model is useful for stress testing, scenario analysis and macro-financial interpretation. It may not claim that it is a universal crisis-prediction law, a causal policy theorem, a physical liquidity law or a solution to the mathematical Navier-Stokes problem.

7.1.17. Monographic Integration with the Other Six Problem Chapters

Chapter 7 also has a specific place inside the seven-problem monograph. The Perelman-Ricci-Poincare chapter measures inequality pressure, smoothing capacity, curvature-like deformation and entropy-like complexity. The Hodge chapter decomposes regional macro-flow pressure into hierarchy, local-cycle imbalance and systemic circulation. The Yang-Mills chapter measures gauge curvature, action concentration and finite-network shock thresholds. The BSD chapter studies local-to-global structural rank and corridor stress. The Riemann-Zeta chapter studies spectral-cycle inflation forecasting. The P vs NP chapter studies computational complexity in sparse portfolio optimization.

The Navier-Stokes chapter is the liquidity-flow counterpart to these architectures. Its distinctive contribution is dynamic stress balance. Where Hodge decomposes a flow field topologically, Navier-Stokes organizes macro-financial stress dynamically through velocity, acceleration, pressure, friction, force and closure. Where Yang-Mills emphasizes thresholds in a finite stress network, Navier-Stokes emphasizes how stress is generated through flow imbalance and friction. Where Riemann-Zeta emphasizes spectral correction in forecasting, Navier-Stokes combines cycle forcing with stress decomposition and policy counterfactuals.

This integration is important because the monograph should not look like seven unrelated articles. Each chapter contributes a different measurement grammar. Chapter 7's grammar is the grammar of systemic liquidity motion under pressure. It gives the book its strongest applied macro-financial stress-testing layer and connects naturally to the general themes of flow, shock propagation, resilience, validation and claim discipline.

7.1.18. Claim Boundary for the Economic Flow Analogy

Claim domain	Permitted chapter claim	Not permitted	Reason
Mathematical analogy	Navier-Stokes logic supplies a structured economic measurement grammar.	Claiming a solution, test or replication of the classical Navier-Stokes problem.	The object is macro-financial stress, not physical fluid existence or regularity.
Liquidity interpretation	Liquidity-flow weakness can be modeled as an economic stress channel.	Claiming that liquidity is literally a physical fluid.	Economic variables are normalized proxies, not physical fields.
Stress balance	Systemic stress can be decomposed into flow, pressure, friction, shock, cycle and closure terms.	Claiming a universal crisis law or exact deterministic identity.	The equation is diagnostic and statistically audited.
Forecast validation	Rolling-window evidence can support validation-window usefulness.	Claiming permanent dominance over all future models and samples.	Forecast evidence is conditional on sample, horizon and benchmarks.
Policy scenarios	Counterfactuals show model-implied stress responses.	Claiming randomized causal policy effects.	Scenarios are model-based stress tests, not experiments.
Closure	epsilon(t) can represent restricted hidden adjustment through observable/proxy channels.	Using epsilon(t) as an unrestricted residual plug.	The closure channel must remain auditable and state-dependent.

Table 7.1.3. Claim boundary for the Navier-Stokes-inspired economic flow analogy. Source: Author synthesis for the monograph.

The claim boundary in Table 7.1.3 is not a rhetorical disclaimer. It is a methodological safeguard. The stronger the mathematical analogy, the more important it becomes to specify what is being claimed and what is not. Chapter 7 can be ambitious because it is bounded. It can use a strong flow-balance grammar precisely because it does not claim physical identity, theorem proof, universal prediction or causal certainty.

7.1.19. Section Synthesis

Section 7.1 establishes the conceptual core of the chapter. The global macro-financial system is treated as a stress field in which liquidity velocity weakness, acceleration, pressure gradients, friction/diffusion, stochastic shocks, GDP-cycle forcing and restricted hidden adjustment interact. The analogy is not literal. It is structural, nondimensional and empirically auditable. Its purpose is to provide a disciplined way to move from heterogeneous macro-financial indicators to a decomposable stress-balance architecture.

The section also clarifies why the chapter belongs at the center of the monograph's applied macro-financial contribution. It uses the Navier-Stokes grammar to organize stress as a process rather than a static score. It connects stress to resilience, validation, benchmarks, external targets, Monte Carlo uncertainty and policy counterfactuals. It also preserves the book-wide claim discipline: mathematical theorem does not equal economic model, and analogy does not equal proof.

The next section, 7.2, therefore begins from an already established conceptual foundation. Having defined the flow analogy and its boundary, the chapter can now specify the research object: global liquidity, pressure, friction and closure as measurable components of a 100-country, 2010-2024 macro-financial stress-testing system.

7.2. Research Object: Global Liquidity, Pressure, Friction and Closure

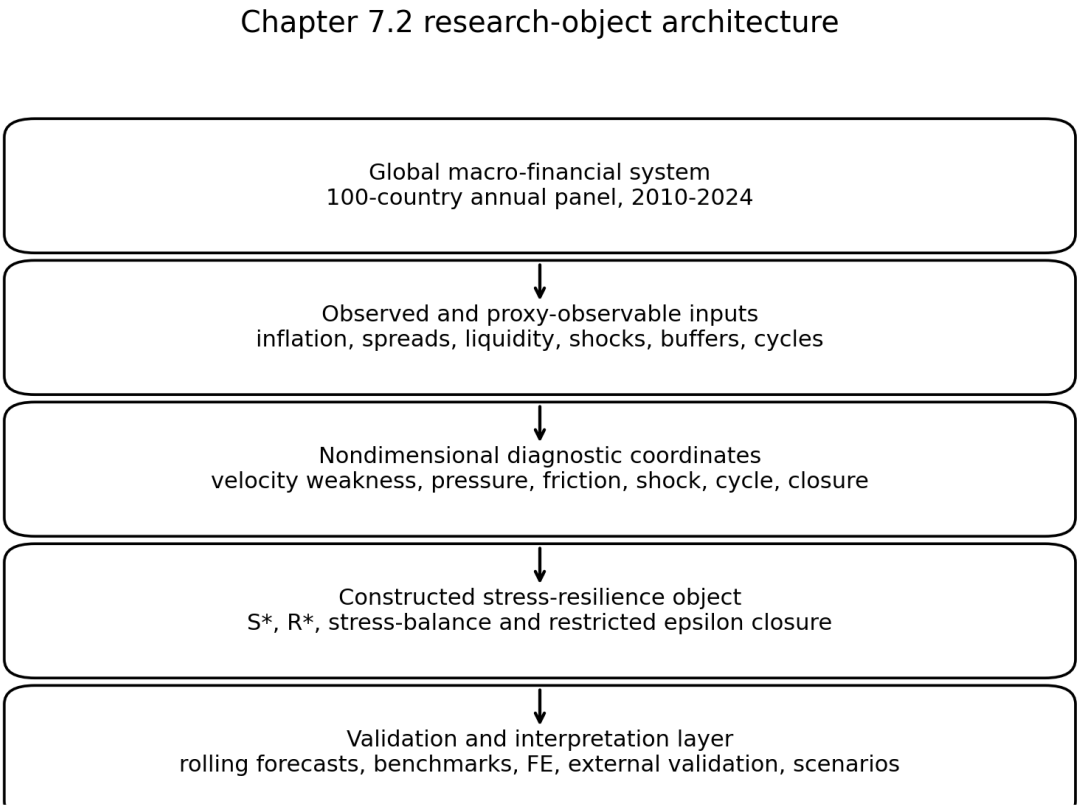
This subsection fixes the analytical object of Chapter 7 before the chapter moves into data architecture and methodological estimation. Chapter 7.1 established why the Navier-Stokes vocabulary is useful as a disciplined economic analogy. Chapter 7.2 now specifies what is actually being measured: a global macro-financial liquidity-flow system in which stress emerges from the joint interaction of weak flow, pressure gradients, frictional transmission, shock forcing, cyclical movement and restricted hidden adjustment.

The object is deliberately not a physical fluid, not a continuum field and not a theorem-level Navier-Stokes claim. It is a country-year macro-financial stress-testing object constructed from public and proxy-observable macro-financial variables after nondimensional scaling. The purpose is to prevent metaphor from replacing measurement. Liquidity is treated as an economic capacity to move, absorb and transmit financing across countries and periods; pressure is treated as a macro-financial stress gradient; friction is treated as the impairment of credit, banking and liquidity channels; and closure is treated as a disciplined state-dependent adjustment mechanism rather than an arbitrary residual plug.

The research object is stronger than a simple financial-stress index because it is not only a score. It is a structured diagnostic field. Each observation has coordinates; each coordinate belongs to a stress channel; each stress channel is transformed into a unit-free starred variable; the starred variables enter an auditable stress balance; the balance is tested through panel inference, rolling forecasts, benchmark comparison, external targets, Monte Carlo paths and counterfactual scenarios. This is why Chapter 7 is positioned as one of the strongest applied macro-financial chapters of the monograph.

The chapter is also embedded in the broader seven-problem monograph. Perelman-Ricci-Poincare supplies the language of pressure, smoothing and deformation; Hodge supplies the logic of decomposable flow; Navier-Stokes supplies the balance of velocity, pressure and friction; Yang-Mills supplies shock-threshold and curvature-action logic; Birch-Swinnerton-Dyer supplies local-to-global rank formation; Riemann-Zeta supplies layered validation and spectral pressure discipline; and P vs NP supplies computational and claim-boundary discipline. The present subsection therefore defines the Navier-Stokes object while keeping it compatible with the monograph as a whole.

Figure 7.2.1. Research-object architecture for the Navier-Stokes-inspired global liquidity-flow chapter



Source: Author synthesis based on the Chapter 7 source manuscript and the monograph translation framework.

7.2.1. Definition of the Research Object

The research object is the global macro-financial system represented as a nondimensional liquidity-flow and systemic-stress measurement architecture. The unit of observation in the main empirical layer is the country-year. The core panel contains 100 countries observed annually from 2010 to 2024, yielding 1,500 country-year observations. The country-year layer is supplemented by a World aggregate anchor, macro-regional aggregation, rolling validation windows, external validation targets, Monte Carlo uncertainty and policy counterfactuals.

This definition is intentionally precise. The object is not the entire world financial system at transaction level. It does not contain intraday order-book liquidity, individual bank balance sheets, high-frequency market microstructure or complete cross-border transaction networks. It is a macro-financial diagnostic object designed to measure how country-level stress channels behave when transformed into comparable unit-free coordinates. The object is therefore global and empirical, but also bounded by the frequency, aggregation level and source status of the data.

The object is called a liquidity-flow system because liquidity is interpreted dynamically. A country may have adequate headline liquidity in one year but still show stress if pressure gradients rise, credit transmission weakens, sovereign-risk premia widen, exchange-rate volatility intensifies, GDP cycles deteriorate or hidden adjustment channels accumulate. Conversely, a country may experience pressure but absorb part of it through fiscal buffers, external transfers, aid/support channels, stronger resilience capacity or lower friction. The model is built to detect these competing effects rather than collapse them into one raw macroeconomic variable.

The object is called systemic because stress is not interpreted as a purely domestic level indicator. In this chapter, systemic stress means a constructed macro-financial condition in which pressure, friction, weak flow, shocks and closure jointly indicate vulnerability to transmission, amplification or persistence. The chapter does not need to prove contagion in a strict causal sense at the object-definition stage. It needs to define an object that can later be tested for persistence, regional concentration, benchmark forecast value, external-target plausibility and policy-counterfactual sensitivity.

Table 7.2.1. Research-object definition and boundary matrix

Dimension	Operational definition in Chapter 7.2	Analytical role	Boundary / exclusion
Empirical object	Global macro-financial	Defines what the chapter	Not a physical fluid,

	liquidity-flow and systemic-stress system.	measures before model estimation.	continuum field or full market microstructure model.
Main unit	Country-year observation i,t.	Allows country and year heterogeneity to be evaluated in a panel setting.	Does not replace sectoral, institutional or high-frequency country studies.
Main sample	100 countries observed annually over 2010-2024, N = 1,500.	Supplies the strongest empirical base of Chapter 7.	Annual sample cannot capture all intraday liquidity mechanisms.
World anchor	World aggregate used for normalization, comparison and global interpretation.	Links country-level stress to a global reference frame.	Anchor is not treated as an additional country observation.
Macro-regional layer	Regional aggregation of country-year stress and resilience coordinates.	Supports interpretation of pressure, friction and closure by region.	Stylized diagnostic grouping, not geopolitical ranking.
Validation layer	Rolling forecasts, benchmark comparison, external targets and robustness diagnostics.	Tests whether the research object has empirical usefulness beyond construction.	Validation-window evidence, not universal forecast superiority.
Policy layer	Monte Carlo paths and counterfactual stress changes.	Translates the object into uncertainty and scenario interpretation.	Model-implied stress testing, not randomized policy proof.

Source: Author synthesis based on the Navier-Stokes source manuscript and the monograph architecture.

7.2.2. Liquidity as an Economic Flow Capacity

The first core object is liquidity. In the chapter, liquidity does not mean a physical substance. It means the macro-financial capacity of a country or system to move financing, maintain transactional continuity, absorb shocks and prevent stress from becoming self-reinforcing. This definition is broad enough to include banking liquidity, credit availability, external funding conditions, monetary-financial transmission, reserve or buffer capacity and the ability of firms, households and sovereigns to remain financed during stress episodes.

The Navier-Stokes analogy becomes useful only after liquidity is converted from a loose metaphor into a measurable flow capacity. The model therefore distinguishes liquidity level from liquidity movement. A high level of monetary or financial resources is not automatically equivalent to low stress if the system is unable to transmit liquidity to stressed balance sheets or if pressure gradients cause funding to move away from vulnerable sectors and countries. Liquidity velocity weakness is introduced to capture this problem: stress rises not only because liquidity is scarce, but also because available liquidity does not circulate effectively through the macro-financial system.

The object also includes liquidity acceleration. In a physical equation, acceleration captures changes in velocity. In the economic analogue, acceleration captures the change in liquidity-flow conditions through time. A sudden deterioration in credit growth, market funding, external financing or stress-adjusted liquidity conditions can produce systemic relevance even if the level indicator remains moderate. This is why the country-year structure is essential: the object must observe not only cross-sectional differences among countries but also time-varying movement within countries.

Liquidity is therefore an object of capacity, movement and deterioration. The chapter does not ask whether money literally flows as a fluid. It asks whether macro-financial stress can be measured more coherently when liquidity weakness, its change through time and its interaction with pressure and friction are placed inside a single nondimensional balance.

Table 7.2.2. Liquidity-flow translation from physical vocabulary to economic object

Physical vocabulary	Economic translation	Observable / proxy family	Interpretive meaning
Velocity v	Liquidity-flow strength or weakness	Credit growth, liquidity indicators, funding availability, monetary/financial	Whether liquidity circulates sufficiently to absorb stress.

		transmission proxies	
Acceleration dv/dt	Change in liquidity-flow conditions	Annual change in liquidity conditions, credit deceleration, funding deterioration	Whether liquidity stress is intensifying or easing.
Pressure gradient ∇P	Macro-financial pressure gradient	Inflation pressure, sovereign spreads, exchange-rate pressure, risk premia	Whether macro-financial pressure pushes the system toward stress.
Viscosity / diffusion	Liquidity friction and impaired transmission	Banking frictions, credit constraints, liquidity coverage or market-functioning proxies	Whether financing channels slow, block or distort liquidity movement.
External force	Shock forcing	Event-volatility, crisis indicators, geopolitical or external shock proxies	Whether exogenous shocks disturb the stress balance.
Cyclical forcing	GDP-cycle and macroeconomic phase pressure	Fourier GDP-cycle term or cycle-state variables	Whether stress is amplified by the macro cycle.
Closure term epsilon	Restricted hidden adjustment	Lagged closure, shadow pressure, transfers, geopolitical shock, buffers, aid/support and inertia	Whether partially observed mechanisms explain remaining adjustment pressure.

Source: Author conceptual translation from the Navier-Stokes balance into the Chapter 7 macro-financial research object.

7.2.3. Pressure as a Macro-Financial Gradient

The second core object is pressure. In the chapter, pressure is not a scalar label for crisis intensity alone. It is a macro-financial gradient that captures stress-generating differences across inflation, sovereign-risk, exchange-rate, funding and financial-spread conditions. Pressure matters because systemic stress often increases when the economy is pushed by widening risk premia, inflation persistence, external-financing pressure or loss of confidence even before a formal crisis is declared.

A pressure-gradient object is stronger than a raw pressure variable. It implies that stress is directional and comparative. A country becomes more vulnerable when pressure rises relative to its own previous state, relative to global or regional anchors, or relative to its resilience and liquidity-transmission capacity. This is why pressure is treated as part of a balance equation rather than a separate index. The same pressure score may have different meaning depending on whether liquidity velocity is strong, whether friction is low, whether shocks are transitory and whether closure channels buffer or amplify adjustment.

The pressure object also clarifies the difference between macroeconomic stress and financial stress. Inflation, sovereign spreads and exchange-rate pressure are not identical variables, but in a stress-balance architecture they belong to the same pressure family because each can increase the cost, uncertainty or fragility of macro-financial adjustment. Direction harmonization is required before these variables are combined. Higher values must consistently mean higher pressure after transformation; variables whose raw interpretation is protective must be reversed or assigned to the resilience side.

The pressure-gradient framing connects Chapter 7 to the rest of the monograph. The Perelman-Ricci chapter uses pressure and smoothing capacity to describe inequality deformation. The Hodge chapter uses directed edge pressure to decompose macro-flow hierarchy, curl and circulation. The Yang-Mills chapter transforms systemic stress into a network field and shock-threshold architecture. The BSD chapter asks whether local signals inform global rank. Chapter 7 is distinct because it places pressure inside a dynamic liquidity-flow balance and tests it through a large country-year panel.

7.2.4. Friction as Impaired Liquidity Transmission

The third core object is friction. Friction represents the difficulty with which liquidity, credit and financial adjustment move through the macro-financial system. In the physical analogy, viscosity or diffusion affects how flow evolves. In the

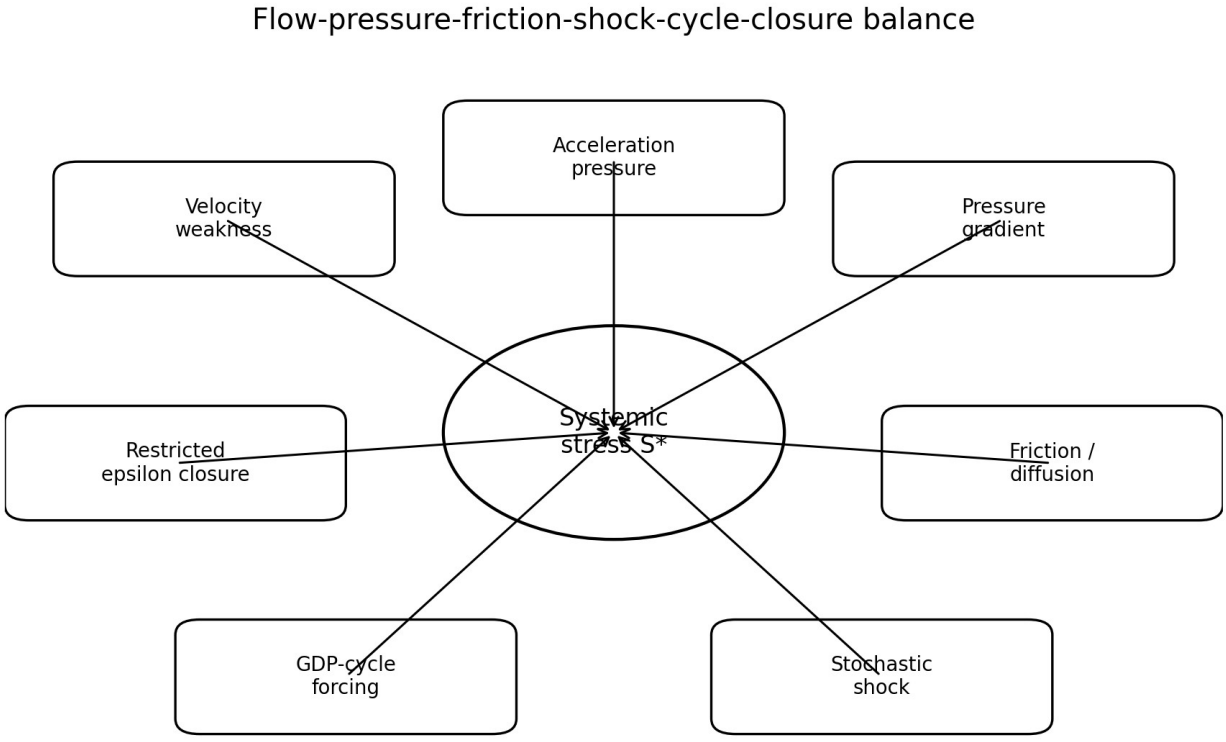
economic analogy, liquidity friction captures blocked, costly, slow or uneven financial transmission. This includes credit-market impairment, banking-sector stress, higher funding costs, liquidity-hoarding behavior, external-financing constraints and institutional channels that delay or distort adjustment.

Friction is analytically separate from pressure. Pressure may rise because inflation or sovereign-risk premia intensify; friction may rise because the banking or credit channel is unable to distribute liquidity even when policy support exists. A country can therefore be pressure-exposed but not friction-impaired, friction-impaired but not yet under high pressure, or both pressure-exposed and friction-impaired. The systemic-risk meaning changes across these cases. Chapter 7.2 defines the object so that Chapter 7.5 can later separate these channel combinations in the results.

Friction also interacts with resilience. A system with strong fiscal buffers, credible external support, deeper financial markets or stronger policy capacity may reduce the stress impact of friction. Conversely, a system with low resilience may experience stress amplification when even moderate friction appears. This is why the chapter does not define systemic stress solely as the sum of stress channels. It defines systemic stress in relation to liquidity resilience, closure and model-implied counterfactuals.

In the monograph, friction plays a bridging role. In the Yang-Mills chapter, friction-like effects appear in curvature/action concentration and shock transmission thresholds. In the BSD chapter, Tamagawa-type friction and torsion-like objects are used to describe local-to-global structural rank distortions. In Chapter 7, friction is explicitly macro-financial: it is the impairment of the liquidity channel that prevents pressure from being smoothly absorbed.

Figure 7.2.2. Core flow-pressure-friction-shock-cycle-closure balance



Source: Author diagram based on the nondimensional stress-balance logic of Chapter 7.

7.2.5. Closure as Restricted Hidden Adjustment

The fourth core object is closure. Closure is the most important safeguard in the chapter because it prevents the Navier-Stokes analogy from becoming an unfalsifiable constructed equation. In many stress-index frameworks, whatever is not explained by the main variables is absorbed silently by a residual. Chapter 7 refuses that approach. Its epsilon term is restricted, state-dependent and interpretable. It is not an unlimited residual used to force equality after the fact.

The closure object captures partially observed mechanisms that affect systemic stress but are not fully represented by the main velocity, acceleration, pressure, friction, shock and cycle variables. These mechanisms include lagged hidden adjustment, shadow-economy pressure, external transfers, geopolitical shock, fiscal buffers, foreign aid or support channels

and economic inertia. The economic meaning is straightforward: some stress accumulates in channels that are difficult to observe directly, but those channels can still be proxied, restricted and audited.

The closure object has two sides. Positive closure components amplify hidden adjustment pressure. Shadow-economy pressure can distort liquidity and make measured indicators understate stress. Geopolitical shocks can add event pressure beyond standard macro-financial variables. Economic inertia can make stress persistent even after contemporaneous pressure begins to improve. Negative closure components buffer stress. Remittances, transfers, fiscal buffers and aid/support channels may reduce the need for hidden adjustment by providing external or institutional absorption capacity.

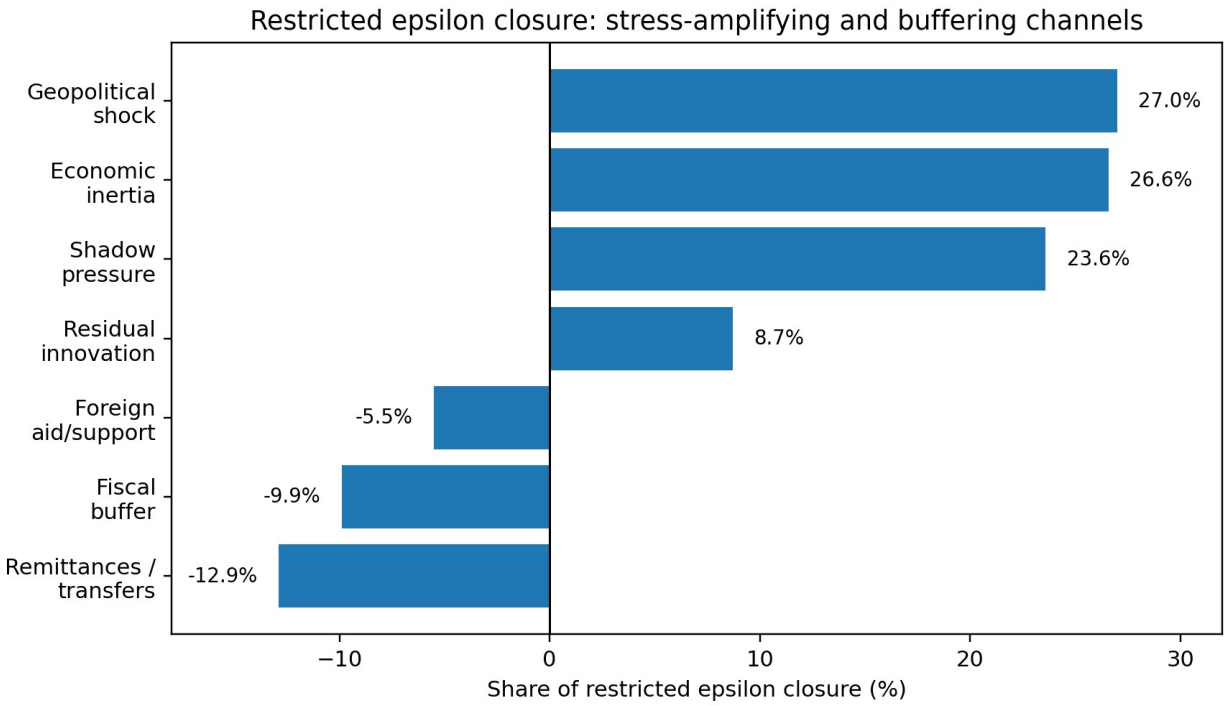
This definition is essential for scientific credibility. If epsilon were a free plug, a reviewer could argue that the model simply assigns unexplained stress to an arbitrary term. By modelling epsilon through observable or proxy-observable state variables, the chapter turns hidden adjustment into an empirical object. This is why the closure mechanism belongs in the research-object subsection before the methodology chapter: the reader must know that epsilon is part of the object, not a post-estimation convenience.

Table 7.2.3. Restricted closure object and economic interpretation

Closure component	Expected direction	Economic meaning	Why it belongs in the research object
Lagged epsilon	Positive	Hidden adjustment pressure persists over time.	Stress contains memory and path dependence.
Shadow-economy pressure	Positive	Informal or weakly measured financial channels raise hidden stress.	Observed indicators may understate systemic pressure.
Geopolitical shock	Positive	External event risk increases adjustment pressure beyond standard indicators.	Shock exposure belongs to systemic-stress formation.
External transfers / remittances	Negative or mixed	External household or liquidity support can buffer stress.	Some cross-border channels reduce hidden adjustment pressure.
State / fiscal buffer	Negative	Policy stabilization and fiscal capacity reduce closure pressure.	Institutional absorption capacity affects stress formation.
Foreign aid / external support	Negative	External support can offset shocks and liquidity stress.	International support channels may reduce vulnerability.
Economic inertia	Positive	Lagged macro-financial stress carries into the present.	Stress regimes are dynamic rather than purely contemporaneous.
Residual innovation	Mixed	Remaining innovation after restrictions.	Should be small and monitored, not used as a free plug.

Source: Author synthesis from the restricted epsilon closure design and interpretation logic of Chapter 7.

Figure 7.2.3. Restricted epsilon closure: stress-amplifying and buffering channels



Source: Author visualization based on the reported epsilon-decomposition shares in the Chapter 7 source manuscript. Positive values amplify closure pressure; negative values buffer stress.

7.2.6. Systemic Stress and Liquidity Resilience as Paired Diagnostic Fields

The dependent diagnostic object of Chapter 7 is systemic stress, denoted here as S*. The star indicates that the variable is nondimensional. It is not measured in percent, dollars, basis points, local currency units or physical units. It is a constructed unit-free stress coordinate that results from direction harmonization and scaling. This rule is central: raw inflation rates, spreads, liquidity ratios, volatility indicators and GDP-cycle deviations are not added directly. They become comparable only after transformation into a common diagnostic scale.

Systemic stress must be interpreted jointly with liquidity resilience, denoted here as R*. A high stress score is not sufficient to understand vulnerability unless the analyst also observes whether the system has buffers, support capacity, liquidity depth, policy space or absorption channels. The pairing of S* and R* allows the chapter to distinguish four states: low stress with high resilience, high stress with high resilience, low stress with low resilience and high stress with low resilience. The fourth state is the most vulnerable; the second may be manageable if buffers are credible; the third may be fragile because the system lacks protection if pressure rises.

The paired field also prevents a common error in stress-index interpretation. Some models treat stress as a one-sided negative score. Chapter 7 treats stress and resilience as interacting diagnostic fields. The purpose is not only to identify where stress is high, but to identify whether stress is being amplified by weak liquidity velocity, strong pressure gradients, high friction, stochastic shocks, adverse cycle forcing or hidden closure pressure. This decomposition makes policy interpretation more precise without converting the model into a deterministic policy rule.

Formally, the chapter can define the generic research object as an ordered system: O_NS = {D, X*, S*, R*, B, E, V, U, C}. D is the empirical data universe; X* is the nondimensional coordinate matrix; S* is systemic stress; R* is liquidity resilience; B is the stress-balance relation; E is the restricted closure mechanism; V is the validation battery; U is the uncertainty layer; and C is the claim-boundary rule. This notation makes clear that the object is not a single score but an integrated measurement system.

Table 7.2.4. Core variable families in the Chapter 7 research object

Family	Notation	Stress role	Examples of proxy direction	Interpretation after scaling
Liquidity-flow weakness	V* or VW*	Stress increases when flow capacity weakens.	Declining credit/liquidity, tightening funding	Weak movement or poor circulation of liquidity.

			conditions.	
Liquidity acceleration	A*	Stress increases when liquidity conditions deteriorate.	Negative changes in credit, funding or liquidity availability.	Time-varying deterioration in flow capacity.
Pressure gradient	P* or grad P*	Stress increases with macro-financial pressure.	Inflation persistence, sovereign spreads, exchange-rate pressure.	Directional pressure pushing the system toward stress.
Friction / diffusion	F*	Stress increases when transmission is impaired.	Banking frictions, credit constraints, liquidity-hoarding proxies.	Impaired absorption or distribution of liquidity.
Stochastic shock	Xi*	Stress increases with event volatility or crisis shock.	Volatility, external event, crisis or geopolitical shock indicators.	Exogenous disturbance to the balance.
GDP-cycle forcing	C*	Stress changes with macroeconomic phase.	Fourier or cycle-state representation of GDP movement.	Cyclical macroeconomic forcing of stress.
Restricted closure	epsilon*	Stress increases or falls depending on closure-state variables.	Shadow pressure, transfers, buffers, aid/support, inertia.	Auditable hidden adjustment.
Liquidity resilience	R*	Offsets or absorbs stress.	Buffers, support capacity, policy space, external assistance.	Absorption capacity and stress resistance.

Source: Author synthesis of the nondimensional variable families used to define Chapter 7 before estimation.

7.2.7. Formal Object Notation

The research object can be stated compactly in notation. Let i = 1,...,100 index countries and t = 2010,...,2024 index annual observations. Let X_i,t represent the raw or proxy-observable macro-financial input vector, and let X*_i,t represent the nondimensional vector after direction harmonization, scaling and transformation. The object is not X_i,t itself. The object is the transformed and interpretable stress-coordinate system X*_i,t and its derived stress-resilience balance.

Equation (7.2.1) defines the empirical universe:

D_NS = {X_i,t,k : i = 1,...,100; t = 2010,...,2024; k = 1,...,K}. (7.2.1)

Equation (7.2.2) defines the nondimensional coordinate system:

X*_i,t,k = T_k(X_i,t,k), where T_k applies direction harmonization, scaling, winsorization or robust normalization as required. (7.2.2)

Equation (7.2.3) defines the generic stress-balance object:

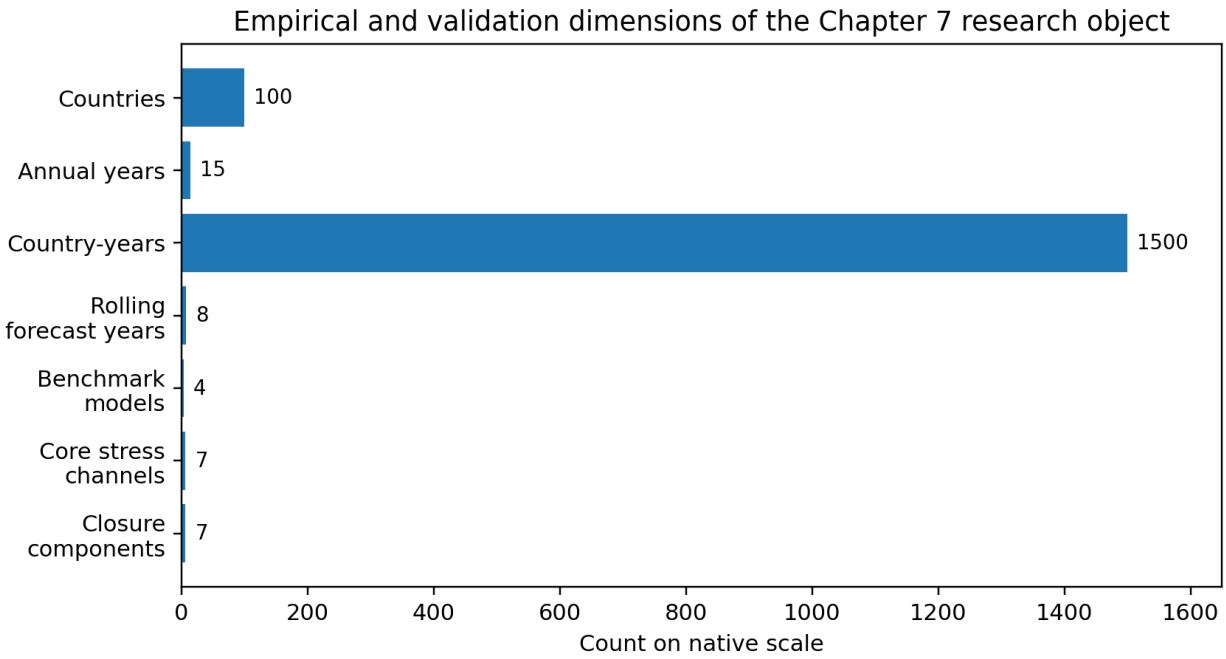
S*_i,t = alpha + theta_1 VW*_i,t + theta_2 A*_i,t + theta_3 gradP*_i,t + theta_4 F*_i,t + theta_5 Xi*_i,t + theta_6 C*_t + theta_7 epsilon*_i,t + e_i,t. (7.2.3)

Equation (7.2.4) defines the restricted closure object:

epsilon*_i,t = rho epsilon*_i,t-1 + beta_1 Shadow*_i,t + beta_2 Transfers*_i,t + beta_3 GeoShock*_i,t + beta_4 FiscalBuffer*_i,t + beta_5 AidSupport*_i,t + beta_6 Inertia*_i,t + u_i,t. (7.2.4)

These equations define the object without yet estimating it. Their role in Chapter 7.2 is conceptual and operational. They show what belongs to the research object, how raw inputs become nondimensional coordinates and why closure is restricted. Estimation, robustness, rolling validation and benchmark comparison are assigned to later subsections of Chapter 7.

Figure 7.2.4. Empirical and validation dimensions of the Chapter 7 research object



Source: Author visualization of the Chapter 7 research-object dimensions: 100 countries, 15 years, N = 1,500 country-years, rolling validation, benchmark models, core channels and closure components.

7.2.8. Boundary between Raw Inputs, Public Anchors and Constructed Objects

A central requirement of the monograph is to separate public data anchors from author-calculated research variables. Chapter 7 follows this rule strictly. Public or institutional macro-financial inputs provide the empirical foundation. They are not automatically equal to the final stress channels. Inflation, spreads, liquidity indicators, GDP-cycle variables, shock proxies and buffer measures must first be aligned, harmonized and scaled before they can enter the stress-balance equation. This separation has three scientific advantages. First, it prevents unit inconsistency. A basis-point spread, an inflation rate, a liquidity ratio and a volatility measure cannot be added in raw form. Second, it makes replication auditable because the reader can distinguish source values from transformation rules. Third, it protects the claim boundary: the author-calculated S*, R*, pressure, friction, shock, cycle and closure variables are research constructs, not official institutional indicators.

The same discipline appears across the monograph. The Hodge chapter separates World Bank/IMF-style macroeconomic anchors from author-calculated Hodge hierarchy, curl and harmonic variables. The Perelman-Ricci chapter separates raw macro-social indicators from pressure-oriented curvature coordinates. The Yang-Mills and BSD chapters separate public macroeconomic anchors from stress fields, mass-gap objects, LOrder and structural rank. The Riemann-Zeta chapter separates global inflation from constructed zeta-cycle corrections. The P vs NP chapter separates fixed industry inputs from algorithmic best-found portfolio outputs. Chapter 7 adopts the same rule in a macro-financial setting.

The object is therefore reproducible in principle because every constructed object should be traceable to a variable family, a transformation rule, a scaling convention and a claim boundary. This is especially important for the restricted epsilon closure because closure can be criticized if it is treated as unexplained error. The object definition requires closure-state variables to be explicit and proxy-observable wherever possible.

Table 7.2.5. Data-status hierarchy for the Chapter 7 research object

Layer	Object type	Examples	Permitted interpretation	Non-permitted interpretation
Public / observable anchor	Raw macro-financial or macroeconomic input.	Inflation, spreads, exchange-rate pressure, GDP growth/cycle, liquidity/banking indicators, buffers.	Empirical input family for stress construction.	A complete systemic-risk model by itself.
Proxy-observable	Observed or proxied	Shadow pressure,	Partial measurement	Exact observation of

channel	state variable used for hidden mechanisms.	transfers, geopolitical shocks, aid/support, inertia.	of hidden adjustment channels.	all latent financial mechanisms.
Nondimensional coordinate	Scaled and direction-harmonized starred variable.	VW*, gradP*, F*, Xi*, C*, epsilon*.	Comparable diagnostic coordinate.	Physical unit or official statistic.
Constructed index	Author-calculated stress or resilience object.	S*, R*, stress-resilience gap, channel scores.	Research variable for diagnostics, validation and interpretation.	Official institutional measure or welfare ranking.
Validation output	Test result or benchmark comparison.	Rolling forecast error, benchmark ranking, FE association, external-target classification.	Evidence about usefulness and stability of the object.	Universal crisis-prediction law or causal proof.
Scenario output	Monte Carlo or counterfactual result.	Stress bands, high-stress probability, buffer/shock counterfactuals.	Model-implied uncertainty and policy-stress interpretation.	Unconditional future prediction.

Source: Author synthesis following the monograph-wide distinction between public data anchors and author-calculated variables.

7.2.9. Country, World, Macro-Regional and Validation Layers

The research object is multilayered. The country-year layer is the main econometric object. It supplies the N = 1,500 empirical base and allows stress formation to be tested under country and year heterogeneity. The World anchor supplies a global reference point for normalization and interpretation. The macro-regional layer translates country-year stress into regional pressure, friction and resilience patterns. The validation layer tests whether the constructed object behaves usefully out of sample and against external targets.

This multilayer design is necessary because no single layer can carry all claims. The country-year panel is strong for fixed effects, association patterns and cross-country heterogeneity. The World anchor is strong for global scale and comparative interpretation. The macro-regional layer is strong for narrative and policy interpretation, especially when stress concentrates in particular regional systems. The rolling validation layer is strong for forecast discipline. The external-target and policy layers are strong for plausibility, uncertainty and scenario interpretation. Each layer has a role, and each layer has a boundary.

The research object must therefore be read as a layered diagnostic architecture. It is not a single regression dataset, not a single index and not a single forecast exercise. The reason the chapter can support a high-level applied macro-financial claim is that the object is tested in several ways: by internal structure, by out-of-sample validation, by comparison with conventional benchmarks, by panel association, by robustness and by external plausibility.

Table 7.2.6. Multi-layer object architecture

Layer	Scope	Primary function	Strength	Boundary
Country-year panel	100 countries x 2010-2024 = 1,500 observations.	Main evidence base for stress-channel estimation and panel diagnostics.	Large enough for global macro-financial panel stress testing.	Annual frequency and country aggregation remain limits.
World anchor	Global aggregate reference.	Normalizes and contextualizes country and regional stress.	Prevents purely local interpretation.	Not a separate country observation.
Macro-regional layer	Regional aggregation/corridor	Identifies where pressure, friction,	Useful for systemic and policy	Stylized aggregation, not definitive

	interpretation.	shocks and resilience concentrate.	interpretation.	geopolitical ranking.
Quarterly robustness layer	Higher-frequency support where available.	Checks turning points and frequency robustness.	Strengthens timing interpretation.	Not always equally complete across all variables.
Rolling validation layer	Expanding-window one-year-ahead tests, 2017-2024.	Tests no-look-ahead forecasting usefulness.	Protects against pure in-sample fit.	Validation window remains finite.
Benchmark comparison	ARIMA, VAR, GARCH and composite-index baselines.	Tests incremental value against conventional alternatives.	Shows whether flow-balance architecture adds information.	Does not prove universal superiority.
External validation and policy layer	External targets, Monte Carlo and counterfactuals.	Tests plausibility, uncertainty and scenario interpretation.	Links diagnostics to macro-financial stress outcomes.	Model-based and associational, not randomized causal proof.

Source: Author synthesis based on the Chapter 7 source design.

7.2.10. Position of Chapter 7.2 within the Seven-Problem Monograph

Although Chapter 7 has its own empirical object, it must remain consistent with the monograph's seven-problem architecture. The monograph is not a sequence of seven detached articles. It is a unified project in which each Clay-inspired analogy supplies a different economic measurement grammar. Chapter 7.2 therefore defines the Navier-Stokes object in a way that communicates with the other six objects.

The Perelman-Ricci-Poincare object is a macro-regional inequality-pressure and smoothing-capacity system. It clarifies that pressure must be read together with the system's ability to smooth or absorb deformation. Chapter 7 borrows this logic when it interprets stress jointly with liquidity resilience. The Hodge object is a regional macro-flow network decomposed into hierarchy, local-cycle imbalance and systemic circulation. Chapter 7 shares the concern with flow and transmission, but it shifts from regional network decomposition to country-year liquidity stress balance.

The Yang-Mills object is a finite global-corridor systemic-stress network with shock-threshold and mass-gap diagnostics. It is closest to Chapter 7 in its systemic-risk ambition, but it emphasizes network curvature, action and spectral separation. Chapter 7 emphasizes macro-financial pressure, friction and closure in a large country-year panel. The BSD object is local-to-global structural rank formation under corridor stress. It helps Chapter 7 preserve the idea that local or country-level stress channels can matter for global systemic interpretation. The Riemann-Zeta object supplies the strongest sample-layer discipline, showing that annual, quarterly and monthly evidence must be assigned to the claims they can support. Chapter 7 follows the same claim-layer logic through annual panel evidence, rolling validation and robustness layers. The P vs NP object supplies computational and claim-boundary discipline: it shows why strong methodological claims can be made without theorem-level overclaiming.

Table 7.2.7 summarizes this alignment. Its purpose is not to merge the models. Its purpose is to show how Chapter 7.2 defines the Navier-Stokes research object so that it functions as one chapter within a coherent monograph rather than as a standalone reprinted article.

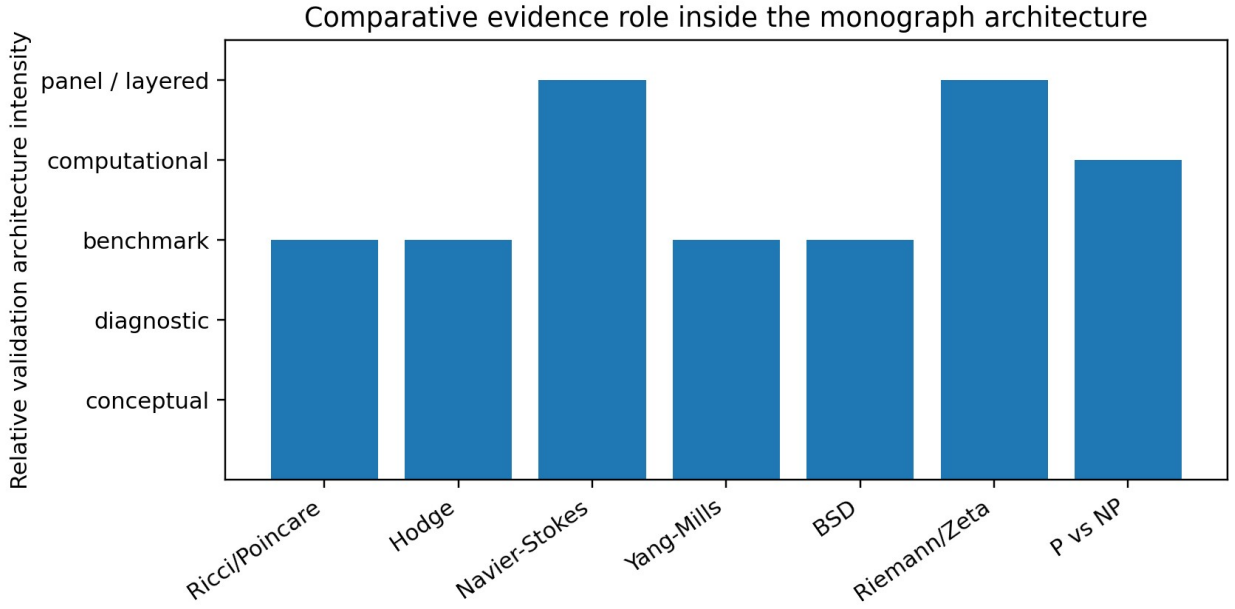
Table 7.2.7. Seven-document alignment of the Chapter 7.2 research object

Monograph chapter	Primary economic object	Methodological grammar	Connection to Chapter 7.2
Chapter 5: Perelman-Ricci-Poincare	Inequality pressure, smoothing capacity, curvature-like deformation, entropy and graph connectedness.	Pressure-smoothing and curvature-topology diagnostics.	Supports the interpretation of stress together with resilience and absorption capacity.
Chapter 6: Hodge	World economy as a regional macro-flow network with gradient, curl	Flow decomposition, hierarchy, local imbalance and systemic circulation.	Supports the broader flow logic while Chapter 7 shifts to liquidity-flow stress

	and harmonic decomposition.		balance.
Chapter 7: Navier-Stokes	Global liquidity-flow and systemic-stress system.	Velocity weakness, acceleration, pressure gradient, friction, shock, cycle and closure.	Defines the applied macro-financial object of this subsection.
Chapter 8: Yang-Mills	Global/corridor systemic-stress network and finite-network mass-gap threshold.	Gauge potential, curvature, action, spectral separation and shock threshold.	Provides a complementary systemic-threshold interpretation of stress transmission.
Chapter 9: BSD	Local-to-global structural rank formation under corridor stress.	Finite-state signals, LOrder, structural rank and corridor stress.	Reinforces the local-to-global meaning of country-year stress signals.
Chapter 10: Riemann-Zeta	Global inflation as a layered macro-financial pressure forecasting system.	Zeta-cycle, FPAS baseline, annual/quarterly/monthly validation.	Supports strict sample-layer and validation-window discipline.
Chapter 11: P vs NP	Cardinality-constrained portfolio optimization under computational complexity.	Combinatorial support-space growth, algorithms, exact reduced benchmark and claim boundaries.	Reinforces computational audit and exclusion of theorem-level overclaiming.

Source: Author synthesis from the seven uploaded source manuscripts and the monograph editorial structure.

Figure 7.2.5. Comparative role of the seven economic-econometric research objects



Source: Author conceptual visualization. The scale is ordinal and illustrates relative validation architecture intensity rather than a numerical performance score.

7.2.11. Claim Boundary of the Research Object

The Chapter 7 research object supports a high but bounded claim. It can claim to define and audit a global macro-financial stress-testing architecture in which systemic stress is measured as a nondimensional flow-pressure-friction-shock-cycle-closure process. It can claim that the object is empirically grounded in a 100-country annual panel, supplemented by world, regional, rolling-validation, benchmark, external-validation, Monte Carlo and policy-counterfactual layers. It can claim that liquidity, pressure, friction and closure are distinct but interacting dimensions of systemic stress.

The object cannot claim that liquidity is a literal physical fluid. It cannot claim to solve, prove, test or replicate the classical Navier-Stokes problem. It cannot claim that the model is a universal crisis-prediction law. It cannot claim that fixed-effects associations are causal laws. It cannot claim that policy counterfactuals are randomized experiments. It cannot claim that annual macro-financial data capture every market-microstructure mechanism. These exclusions are not rhetorical disclaimers; they are part of the scientific design.

The claim boundary is especially important because the chapter is methodologically ambitious. A strong analogy can become vulnerable if the research object is not bounded. Chapter 7.2 therefore defines the object in reviewer-safe terms. It is a nondimensional macro-financial stress-testing framework. It is empirical, computational, econometric and validation-oriented. It is not physical hydrodynamics, not theorem proof and not unconditional prediction.

The correct admissible statement is the following: the Chapter 7 research object is a global, country-year, nondimensional macro-financial stress system in which liquidity-flow weakness, acceleration, pressure gradients, friction/diffusion, stochastic shocks, GDP-cycle forcing and restricted hidden adjustment jointly define systemic stress and are interpreted together with liquidity resilience, rolling validation, benchmark comparison, external targets, Monte Carlo uncertainty and policy counterfactuals.

Table 7.2.8. Claim hierarchy for Chapter 7.2

Claim type	Permitted statement	Evidence status	Excluded overclaim
Research-object claim	The chapter defines a global nondimensional macro-financial stress object.	Strong design claim.	The world financial system is fully represented at all frequencies.
Analogy claim	Navier-Stokes vocabulary organizes flow, pressure, friction, shock, cycle and closure as economic analogues.	Strong conceptual-methodological claim.	Financial liquidity is a literal physical fluid.
Measurement claim	Stress and resilience can be constructed from scaled, direction-harmonized variables.	Strong measurement claim if transformations are disclosed.	Raw heterogeneous indicators are directly additive.
Closure claim	Epsilon is a restricted hidden-adjustment channel with observable/proxy-observable states.	Identification-safeguard claim.	Epsilon is a free residual plug that mechanically forces the model to fit.
Validation claim	Rolling, benchmark, FE, robustness and external-target layers audit empirical usefulness.	Diagnostic validation claim.	Universal crisis-prediction or permanent benchmark dominance.
Policy claim	Monte Carlo and counterfactuals provide model-implied scenario interpretation.	Scenario and stress-testing claim.	Randomized policy-causal proof.
Mathematical claim	The model is inspired by Navier-Stokes structure.	Analogy only.	Solution, proof, test or replication of the mathematical Navier-Stokes problem.

Source: Author claim-boundary synthesis for Chapter 7.2.

7.2.12. Synthesis: Why the Research Object Matters

Chapter 7.2 establishes that the relevant object is not a list of macro-financial indicators. It is a structured stress field built from liquidity-flow weakness, acceleration, pressure gradients, frictional transmission, stochastic shock, GDP-cycle forcing and restricted closure. This object is necessary because systemic stress is not produced by one channel alone. A country-year

may become vulnerable because pressure rises, because liquidity weakens, because friction blocks transmission, because shocks intensify, because cycles turn adverse or because hidden adjustment accumulates. The research object must therefore be able to represent all of these pathways within one measurement architecture.

The main empirical strength of the object is its scale and validation design. The 100-country annual panel over 2010-2024 supplies 1,500 country-year observations. The World anchor and macro-regional layers connect country-level evidence to global and regional interpretation. The rolling forecast design prevents pure in-sample storytelling. The benchmark comparison prevents the model from being judged only against itself. The restricted epsilon closure prevents hidden adjustment from being arbitrary. The Monte Carlo and counterfactual layers translate the object into uncertainty and policy-stress interpretation without overclaiming certainty.

The research object is therefore suitable for the subsequent subsections of Chapter 7. Section 7.3 can describe the data architecture because the object has been defined. Section 7.4 can specify the methodology because the roles of liquidity, pressure, friction and closure are clear. Section 7.5 can report results because the dependent object and channel families have been fixed. Section 7.6 can interpret vulnerability because the chapter has already separated pressure, weak flow, friction and closure. Section 7.7 can introduce Monte Carlo and counterfactuals because the object is explicitly scenario-compatible. Section 7.8 can close the chapter because the claim boundary has been stated from the beginning.

For the monograph as a whole, Chapter 7.2 performs an additional function. It shows how a Millennium-problem-inspired mathematical grammar can become an applied macro-financial research object without becoming an unsupported theorem claim. The chapter is ambitious because it defines stress as a multi-channel nondimensional process. It is credible because it keeps the object empirical, auditable, bounded and compatible with validation. This is the correct balance for a high-level applied macro-financial chapter in a monograph on economic-econometric analogues of the Clay Millennium Problems.

Source Documents Used for Chapter 7.2 Drafting

- Navier-Stokes-Inspired Global Liquidity-Flow and Systemic-Stress Modelling: A Nondimensional Macro-Financial Stress-Testing Framework.
- Global Perelman-Ricci-Poincare-Inspired Inequality Diagnostics: Curvature, Entropy and Graph-Topological Modelling of Macro-Regional Pressure and Smoothing Capacity.
- Global Hodge-Econometric Modeling of the World Economy: A Regional Benchmark Prototype for Topological Flow Decomposition, Systemic Circulation, Shock Transmission, and Macroeconomic Resilience.
- Economic Yang-Mills Mass Gap in Global and Corridor Flow Networks: A Finite-Network Gauge-Econometric Framework for Measuring Systemic Shock Thresholds.
- Regional Economic Birch-Swinnerton-Dyer Modelling: A Local-to-Global Framework for Structural Rank Formation, Corridor Stress and World-Economy Calibration.
- Global Riemann-Zeta FPAS+zeta Inflation Forecasting: Layered Validation of a Hybrid Structural-Spectral Model for World Macroeconomic Pressure.
- Robust Portfolio Optimization under Computational Complexity: A P-vs-NP-Inspired Markowitz-CAPM Framework with Cardinality Constraints and a Black-Scholes Derivative-Pricing Overlay.
- Monograph editorial structure document for converting the seven article manuscripts into a unified book architecture.

7.3. Data Architecture: 100-Country Panel, World Anchor and Macro-Regional Layers

7.3.1. Purpose of the Data Architecture

The empirical credibility of the Navier-Stokes-inspired liquidity-flow chapter depends less on the physical analogy itself than on the discipline of the data architecture that supports it. A flow analogy becomes scientifically useful only if its variables are traceable, unit-consistent, directionally harmonized, reproducible and separated from the mathematical language used to interpret them. For this reason, the research object in Chapter 7 is not a metaphorical liquid economy; it is a structured macro-financial panel in which heterogeneous stress proxies are converted into nondimensional diagnostic components.

The data architecture has three nested levels. The first level is the country-year panel: 100 countries observed annually over 2010-2024, producing 1,500 country-year observations. This is the main evidence base for country and year fixed effects, diagnostic association tests, stress-channel estimation, rolling forecasts and robustness checks. The second level is the

World aggregate anchor, which supplies the normalization and global benchmark layer. The third level is the macro-regional layer, which transforms country-year outcomes into interpretable regional stress, liquidity, friction and closure profiles. These three levels are complementary rather than competing: the country panel provides the econometric base, the World anchor provides scale discipline and the regional layer provides macro-financial interpretation.

The architecture also performs a defensive scientific role. It prevents the model from adding raw inflation rates, spread measures, liquidity indicators, GDP-cycle terms and shock proxies as if they were comparable physical units. Instead, the chapter treats each input as a proxy for a conceptual stress channel and then transforms it through a documented pipeline. This is the central reviewer-safety rule of the chapter: raw units are not the model; the model begins only after audit, harmonization, nondimensionalization and claim-boundary classification.

Figure 7.3.1. Data-Architecture Stack for Chapter 7

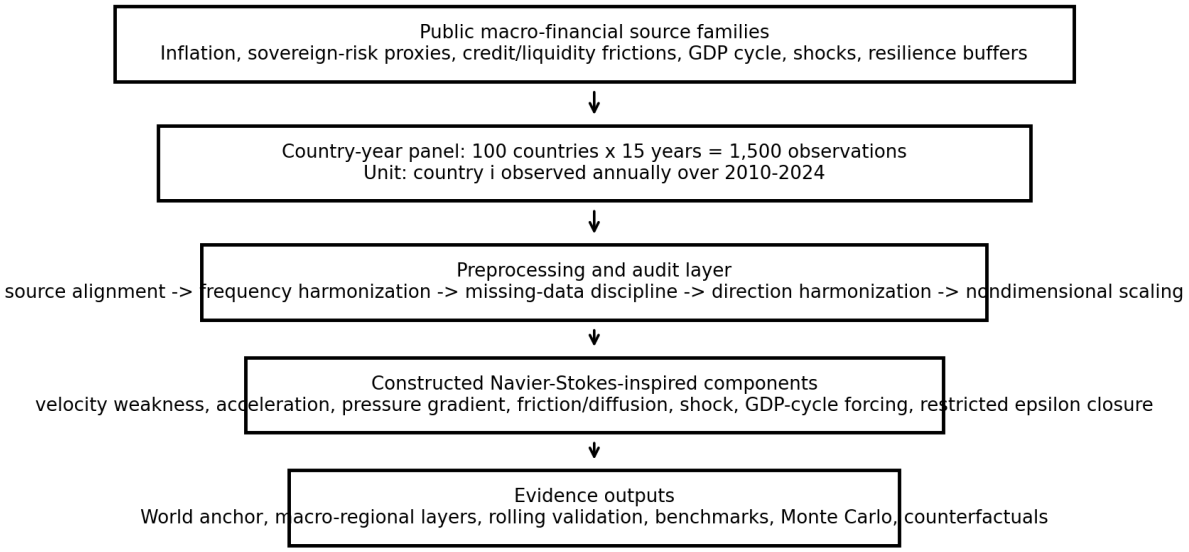


Figure 7.3.1. Data-Architecture Stack for Chapter 7.

Source: Author construction for the monograph, based on the Chapter 7 Navier-Stokes-inspired data architecture and the seven-problem editorial framework.

7.3.2. Empirical Universe and Observation Geometry

The primary empirical universe is a balanced annual country panel. Let i = 1,...,100 denote countries and t = 2010,...,2024 denote the annual time dimension. The panel therefore contains N_panel = 100 x 15 = 1,500 country-year observations before component expansion across stress variables. The country-year unit is essential because the chapter must be able to distinguish structural cross-country heterogeneity from common global shocks and time effects.

The annual frequency is selected because the model is designed for macro-financial stress testing rather than high-frequency market microstructure analysis. Annual data allow inflation, sovereign-risk proxies, liquidity/friction indicators, GDP-cycle measures, resilience buffers and closure-state variables to be aligned across countries and interpreted through policy-relevant macro-financial channels. This choice does not deny the value of monthly or quarterly financial data; it defines the evidentiary layer appropriate to a global cross-country macro-financial diagnostic framework.

The panel notation follows the source study but is re-expressed here in book-chapter form. The raw country-year input matrix is written as D = {X_{i,t,k}: i = 1,...,100; t = 2010,...,2024; k = 1,...,K}, where k indexes macro-financial stress and resilience components. Macro-regional aggregates are written as D_reg = {X_{r,t,k}: r = 1,...,R; t = 2010,...,2024; k = 1,...,K}. Rolling training windows are written as W_j = {2010,...,T_j}, with one-year-ahead forecast year T_j + 1 for T_j = 2016,...,2023.

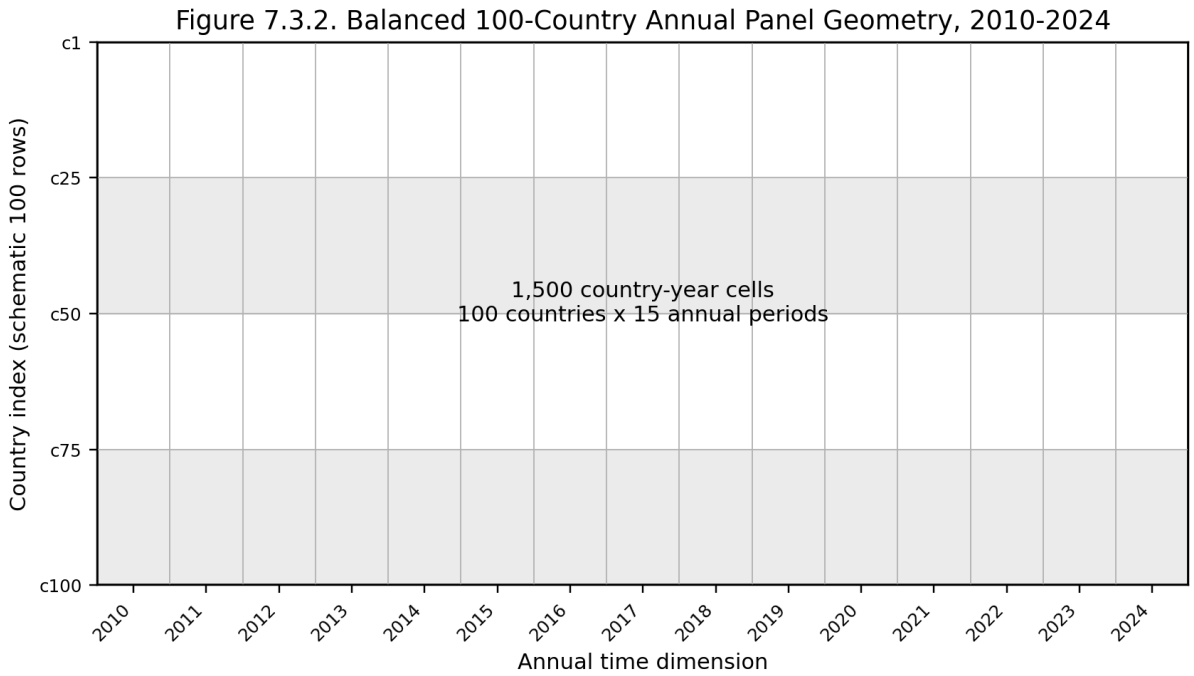


Figure 7.3.2. Balanced 100-Country Annual Panel Geometry, 2010-2024.

Source: Author schematic. The figure visualizes the observation geometry; it does not list country names or imply that all possible countries are included.

Table 7.3.1. Index Notation and Observation Geometry

Element	Notation	Empirical meaning	Role in Chapter 7
Country index	i = 1,...,100	Country-level observation unit in the annual panel.	Main fixed-effects and validation base.
Time index	t = 2010,...,2024	Fifteen annual periods.	Stress dynamics, shock years, rolling validation.
Stress component index	k = 1,...,K	Inflation, pressure, liquidity friction, GDP cycle, shocks, closure and resilience channels.	Input-to-component transformation.
Macro-region index	r = 1,...,R	Aggregated country groups and corridor-relevant macro-regions.	Regional interpretation and stress ranking.
Rolling window	W_j = {2010,...,T_j}	Expanding-window training sample.	No-look-ahead one-year forecast validation.
Simulation draw	b = 1,...,B	Monte Carlo path or counterfactual draw.	Uncertainty and policy scenario analysis.

Source: Author synthesis based on the Chapter 7 methodological notation and monograph-level data-architecture requirements.

7.3.3. Country-Year Panel as the Main Econometric Layer

The 100-country annual panel is the strongest empirical layer of Chapter 7 because it allows the liquidity-flow model to be evaluated beyond a single country, a single region or a purely conceptual benchmark. In the monograph, this is one of the reasons Chapter 7 occupies a central applied macro-financial position: it supplies a large and balanced panel architecture while still retaining the mathematical structure of a nondimensional stress-balance model.

The panel is designed to support four distinct evidence functions. First, it supports descriptive stress mapping across countries and years. Second, it supports fixed-effects and robust-inference estimation by controlling for time-invariant country heterogeneity and common time shocks. Third, it supports rolling validation by evaluating one-year-ahead forecasts without look-ahead information. Fourth, it supports external-target validation and policy counterfactuals by allowing the

constructed stress signal to be compared with macro-financial outcomes such as sovereign-spread widening, GDP-growth slowdown, exchange-rate volatility, liquidity tightening, inflation persistence or crisis/event classifications.

The methodological point is that the country-year panel is not treated as a raw spreadsheet of indicators. It becomes a usable econometric object only after each country-year observation has passed through source alignment, sign harmonization, scaling, stress/resilience classification and component construction. This is why the chapter uses the term data architecture rather than data list.

Table 7.3.2. Econometric Functions of the 100-Country Panel

Panel function	Operational object	Main output	Claim discipline
Descriptive mapping	Country-year stress and resilience variables.	Annual stress maps, distributions and summary tables.	Descriptive diagnostic evidence only.
Fixed-effects testing	Country and year panel specifications.	Coefficient signs and diagnostic associations.	Association, not unrestricted causality.
Rolling validation	Expanding windows ending in T_j with forecasts for T_j+1.	Forecast errors and benchmark comparison.	Validation-window evidence, not permanent dominance.
External-target validation	Constructed stress matched to observable macro-financial outcomes.	Plausibility and anti-circularity checks.	Screening and corroboration evidence.
Monte Carlo layer	Simulated stress paths and parameter perturbations.	Uncertainty bands and scenario fan paths.	Model-implied uncertainty, not unconditional forecasts.
Policy counterfactual layer	Buffer, spread, inflation, resilience and geopolitical shock scenarios.	Counterfactual stress-index effects.	Scenario interpretation, not randomized policy proof.

Source: Author synthesis for Chapter 7.3.

7.3.4. World Aggregate Anchor and Normalization Logic

The World aggregate anchor performs three tasks. First, it gives the chapter a global reference point so that country and regional stress are not read as isolated domestic events. Second, it allows the model to express macro-financial pressure relative to a world-system benchmark. Third, it aligns Chapter 7 with the monograph-wide practice used in the Hodge, BSD and other regional chapters, where the World row is treated as a normalization and scale anchor rather than as an ordinary competing observation.

In formal terms, a World aggregate variable can be defined either as an externally observed global series or as a weighted aggregation of country-level inputs. When constructed from the panel, a typical GDP-weighted world anchor for component k can be expressed as X_{W,t,k} = sum_i omega_{i,t} X_{i,t,k}, where omega_{i,t} = GDP_{i,t}/sum_i GDP_{i,t}. For variables where equal-weighted global pressure is more appropriate, the chapter may also use X_{W,t,k}^{EW} = (1/N) sum_i X_{i,t,k}. The preferred aggregation rule must be recorded in the formula catalogue so that the World anchor remains auditable.

The World anchor must not be misread as a country-level observation. It is not a 101st country and it is not used to inflate the panel sample. Its role is diagnostic: it sets scale, allows global path interpretation and permits comparisons between country-level stress and world-level stress pressure.

Figure 7.3.3. Three-Level Evidence Geometry

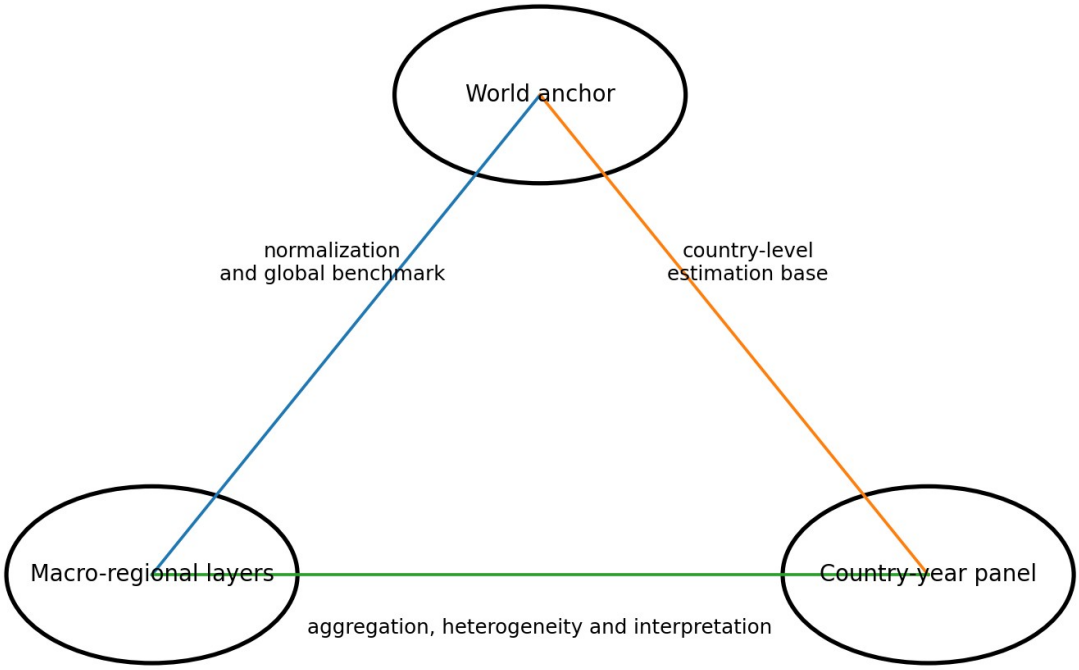


Figure 7.3.3. Three-Level Evidence Geometry: Country Panel, Macro-Regional Layers and World Anchor.
Source: Author construction for the monograph.

Table 7.3.3. Functions and Boundaries of the World Aggregate Anchor

World-anchor function	Operational definition	Use in Chapter 7	Boundary
Scale benchmark	World aggregate or GDP-weighted global component.	Places country stress on a global reference path.	Not an additional country observation.
Normalization anchor	Reference against which stress-direction components can be scaled.	Improves cross-country comparability.	Does not create literal physical units.
Crisis-path comparator	Global stress path across 2010-2024.	Identifies years where world stress and country stress move jointly.	Diagnostic, not a universal crisis law.
Regional interpretation base	World benchmark used beside macro-regional averages.	Separates local, regional and global stress signals.	Regional aggregation remains stylized.
Monograph alignment	Consistent with World-anchor practice in Hodge and BSD chapters.	Supports cross-chapter comparability.	Does not erase problem-specific methods.

Source: Author synthesis based on the monograph-wide use of World normalization anchors.

7.3.5. Macro-Regional Layers and Corridor-Sensitive Interpretation

The macro-regional layer is not a substitute for the 100-country panel. It is an interpretation layer that converts country-year diagnostics into region-level patterns of liquidity stress, pressure gradients, friction, shocks, cycle exposure, resilience and closure. This layer is necessary because systemic stress is often regionally structured: countries may share external-financing conditions, inflation transmission channels, banking-sector exposure, commodity or energy shocks, logistics interruptions, corridor vulnerabilities or common policy regimes.

The macro-regional layer also connects Chapter 7 to the broader monograph. The Hodge chapter treats the world economy as a regional macro-flow topology; the Yang-Mills chapter treats corridor systems as finite stress networks; the BSD chapter

treats local-to-global structural rank as a regional/corridor measurement object. Chapter 7 complements these perspectives by showing how a large country panel can be interpreted through regional liquidity-flow and stress-balance layers.

The aggregation operator must remain explicit. For country i located in macro-region r, the region-level component can be calculated as X_{r,t,k} = sum_{i in r} omega_{i|r,t} X_{i,t,k}. Weights may be GDP-based, population-based, financial-system-size based or equal-weighted depending on the component. The chapter should state the default rule and identify exceptions. This prevents regional averages from becoming opaque composite narratives.

Table 7.3.4. Country, World, Regional and Validation Layers

Layer	Unit of analysis	Principal function	Interpretive caution
Country-year panel	Country i in year t.	Econometric base for stress-channel estimation.	Not a complete microstructure dataset.
World anchor	World aggregate in year t.	Global normalization and benchmark path.	Not a competing observation in the country panel.
Macro-regional layer	Region r in year t.	Regional stress ranking, flow interpretation and heterogeneity analysis.	Stylized aggregation, not geopolitical ranking.
Corridor-sensitive layer	Subregional or corridor exposure grouping where relevant.	Identifies transmission interfaces hidden by output mass alone.	Requires transparent coding and not narrative assertion.
Validation layer	Forecast windows, benchmarks, external targets and robustness objects.	Checks whether constructed variables retain empirical information.	Diagnostic validation, not theorem proof.

Source: Author synthesis for the monograph.

7.3.6. Variable Lineage: From Raw Inputs to Nondimensional Components

Chapter 7 distinguishes three types of variables: raw public macro-financial inputs, transformed nondimensional components and model-level diagnostic outputs. This distinction is not cosmetic. It is the main protection against circularity and raw-unit inconsistency. Raw inflation, spread, credit, exchange-rate, liquidity, fiscal or GDP-cycle indicators are not directly added. They are classified by economic meaning, transformed by direction, scaled into unit-free diagnostic variables and then aggregated into component blocks.

The component blocks correspond to the economic translation of the Navier-Stokes logic. Liquidity velocity weakness measures the loss of circulation or transactional flow. Acceleration captures changes in stress momentum. The pressure-gradient block captures macro-financial tension such as inflation, sovereign-risk or spread pressure. The friction/diffusion block captures liquidity and banking frictions. The stochastic-shock block captures event-volatility and exogenous shock intensity. The GDP-cycle block captures cyclical forcing through a Fourier-style signal. The restricted epsilon closure block captures hidden adjustment pressure using observable or proxy-observable state variables rather than an unrestricted residual.

Table 7.3.5. Variable-Lineage Matrix for Chapter 7

Variable block	Raw-input family	Transformation rule	Model role
Liquidity velocity weakness	Liquidity, money/credit circulation, market-depth or financial-flow proxies.	Low liquidity or weak circulation transformed into higher stress.	Flow-weakness term.
Acceleration pressure	Change in stress, change in liquidity, change in spreads or inflation pressure.	Annual differences or momentum-adjusted transformations.	Stress-momentum term.
Pressure gradient	Inflation, sovereign risk, spread pressure, exchange-rate pressure, external-financing pressure.	Higher pressure mapped to higher nondimensional stress.	Macro-financial pressure term.
Friction/diffusion	Banking-credit friction, liquidity constraints, LCR-type or credit-condition proxies.	Higher friction mapped to higher stress; buffers reverse-scaled.	Viscosity/friction analogue.

Stochastic shock	Event volatility, crisis classification, geopolitical or market-shock proxies.	Shock intensity scaled into unit-free stress.	External forcing term.
GDP-cycle forcing	GDP growth deviations, output-gap or cyclical macro series.	Fourier/cycle-estimated term under no-look-ahead discipline.	Cyclical forcing channel.
Resilience buffers	Fiscal buffers, reserves, support capacity, institutional buffer proxies.	Higher capacity mapped to lower stress or higher resilience.	Opposing resilience channel.
Restricted epsilon closure	Lagged closure, shadow pressure, transfers, geopolitical shock, fiscal buffers, aid/support, inertia.	State-dependent closure equation, not a free residual.	Hidden-adjustment term.

Source: Author synthesis based on the Chapter 7 data and methodology design.

7.3.7. Preprocessing Discipline: Comparability before Modelling

The preprocessing pipeline has a strict order because the model combines heterogeneous variables from different source families. If scaling is performed before sign harmonization, beneficial variables may be interpreted incorrectly as stress variables. If missing-value decisions are not recorded before index construction, the final stress score can become non-replicable. If outlier handling is not documented, crisis years may either be mechanically suppressed or allowed to dominate the index without justification.

The correct sequence is therefore: source alignment, frequency harmonization, panel-balance audit, missing-value classification, outlier and winsorization audit, sign-direction harmonization, nondimensional scaling, aggregation into stress/resilience components and final formula verification. Each step produces an audit object that should be recorded in the replication package.

Figure 7.3.4. Ordered Data-Processing Pipeline

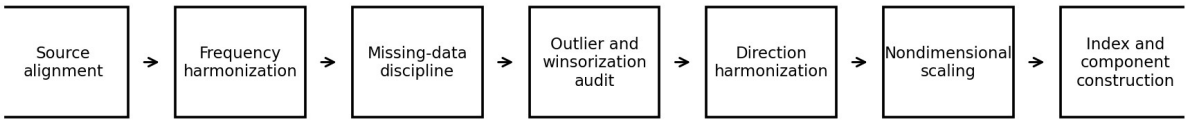


Figure 7.3.4. Ordered Data-Processing Pipeline.

Source: Author construction for Chapter 7.3.

Table 7.3.6. Data-Processing Pipeline and Audit Outputs

Step	Operation	Purpose	Audit output
1	Source alignment	Ensure that country, year, variable and source-family definitions are comparable.	Source ledger and variable dictionary.
2	Frequency harmonization	Convert variables to annual country-year form or align annual data directly.	Frequency-conversion note.
3	Panel-balance audit	Confirm the 100 x 15 observation structure and identify gaps.	Panel availability matrix.
4	Missing-data discipline	Classify missingness and specify interpolation, carry-forward, exclusion or proxy rules.	Missingness and imputation log.

5	Outlier/winsorization audit	Identify extreme values without mechanically removing crisis information.	Outlier decision file.
6	Directional harmonization	Orient all variables so that higher transformed values mean higher stress or higher resilience as intended.	Sign-orientation table.
7	Nondimensional scaling	Convert heterogeneous raw units into unit-free starred variables.	Scaling formula catalogue.
8	Component construction	Aggregate transformed variables into stress, resilience, closure and validation components.	Component workbook and formula check.
9	Replication verification	Match final tables, figures, matrices and scripts to reported results.	Checksums, metadata and version log.

Source: Author synthesis for reproducible data architecture.

7.3.8. Directional Harmonization and Nondimensional Scaling

The Navier-Stokes-inspired analogy requires nondimensional variables because the model cannot add raw inflation, spreads, liquidity proxies, GDP deviations and shock indicators in their original units. The chapter therefore works with starred variables. A pressure-type variable is transformed so that higher raw values imply higher stress. A capacity-type or buffer-type variable is reverse-transformed so that weaker capacity appears as higher stress or stronger capacity appears as higher resilience depending on the component design.

For a pressure-oriented variable X_{i,t,k}, a min-max stress transformation can be written as S*_{i,t,k} = 100 x (X_{i,t,k} - min X_k)/(max X_k - min X_k). For a beneficial capacity variable B_{i,t,k}, a stress-oriented reverse transformation can be written as S*_{i,t,k} = 100 x (max B_k - B_{i,t,k})/(max B_k - min B_k). If the component is retained as resilience rather than stress, the non-reversed version can be used as R*_{i,t,k}. The methodological requirement is not that every variable must use the same formula; it is that every formula must be pre-specified, recorded and consistently interpreted.

After scaling, the model may use standardized forms Z_{i,t,k} = (S*_{i,t,k} - mean(S*_k))/sd(S*_k) for regression, PCA, robustness or external-validation layers. The important rule is that the interpretation of signs must remain invariant across transformations: higher transformed stress should mean more pressure, more weakness, more friction or greater vulnerability, unless the variable is explicitly retained as a resilience component.

Table 7.3.7. Scaling and Directional-Harmonization Rules

Transformation	Formula form	Applies to	Interpretation
Pressure min-max	S* = 100 x (X - min X)/(max X - min X)	Inflation pressure, spreads, sovereign risk, shock proxies.	Higher transformed value means higher stress.
Reverse stress scaling	S* = 100 x (max B - B)/(max B - min B)	Liquidity buffers, fiscal buffers, reserve capacity, resilience variables when converted to stress.	Lower capacity becomes higher stress.
Resilience scaling	R* = 100 x (B - min B)/(max B - min B)	Variables retained as resilience buffers.	Higher transformed value means stronger buffer capacity.
Standardization	Z = (S* - mean(S*))/sd(S*)	Regression, PCA, robustness or external validation.	Coefficient scale becomes comparable across variables.
Winsorized scaling	Same as above after documented tail treatment.	Variables with extreme outliers.	Preserves crisis information while limiting mechanical dominance.

Source: Author synthesis based on the nondimensional stress-object logic of Chapter 7.

7.3.9. Closure-State Variables and Restricted Epsilon Data

The restricted epsilon term is a central data-architecture issue. In a weak model, epsilon(t) would operate as an unrestricted residual plug that mechanically closes the equation after the main variables fail to explain stress. Chapter 7 avoids this by treating epsilon(t) as a state-dependent hidden-adjustment channel. Its inputs must therefore be observable or proxy-observable and must be stored as data objects rather than invented after the fact.

The closure data block includes lagged closure, shadow-economy pressure, external transfers, geopolitical shock, fiscal buffers, foreign aid/support and economic inertia. A compact specification can be written as epsilon_{i,t} = rho epsilon_{i,t-1} + theta_1 Shadow*_{i,t} + theta_2 Transfers*_{i,t} + theta_3 GeoShock*_{i,t} - theta_4 FiscalBuffer*_{i,t} - theta_5 AidSupport*_{i,t} + theta_6 Inertia*_{i,t} + u_{i,t}. The signs shown here are conceptual rather than mechanically imposed: the empirical chapter must estimate or audit whether signs are coherent with the stress-balance logic.

The data requirement is that each closure proxy must have a lineage. Shadow pressure must be defined, transfer pressure must be consistently measured, geopolitical shock coding must be rule-based, fiscal-buffer variables must be identified, support variables must be separated from domestic fiscal capacity, and inertia must be linked to measurable persistence. This is the only way the closure term remains scientific rather than merely algebraic.

Table 7.3.8. Restricted Epsilon Closure Data Block

Closure variable	Conceptual meaning	Expected stress relation	Audit requirement
Lagged closure	Persistence of hidden adjustment from the previous period.	Positive persistence if stress absorption is slow.	Lag construction and initial-period rule.
Shadow pressure	Unobserved or partially observed informal/parallel adjustment pressure.	Expected to raise closure stress.	Proxy definition and source lineage.
External transfers	Remittance, transfer or external-financing adjustment channel.	Context-dependent; can absorb or signal pressure.	Sign convention and economic rationale.
Geopolitical shock	Conflict, sanctions, corridor, energy or external-event exposure.	Expected to raise closure pressure.	Event-coding rule and shock-year log.
Fiscal buffers	Domestic fiscal capacity to absorb stress.	Expected to reduce hidden-adjustment pressure.	Buffer definition and reverse-scaling rule.
Aid/support	External support or official financing capacity.	Expected to reduce closure pressure if stabilizing.	Support classification and timing rule.
Economic inertia	Persistence of macro-financial conditions.	Can raise or stabilize closure depending on regime.	Lag, smoothing and stationarity audit.

Source: Author synthesis based on the Chapter 7 restricted-closure design.

7.3.10. Rolling Validation, Benchmark Data and External Targets

The data architecture must also support out-of-sample evaluation. Chapter 7 uses expanding rolling windows in which information available through year T_j is used to forecast year T_j + 1. For the reported validation design, the forecast years run from 2017 through 2024, so the training endpoint moves from 2016 through 2023. This structure is crucial because it prevents the model from using future information to estimate a past forecast.

Benchmark comparison requires separate data objects for ARIMA, VAR, GARCH and non-flow composite-index baselines. The Navier-Stokes-inspired model cannot be evaluated only by its internal fit; it must be compared with conventional persistence, multivariate, volatility and composite-index alternatives. The purpose of this layer is not to claim universal forecast superiority, but to test whether the nondimensional stress-balance architecture has diagnostic value in a defined validation window.

External targets add another anti-circularity check. If the constructed stress index rises during years of sovereign-spread widening, growth slowdown, exchange-rate volatility, liquidity tightening, inflation persistence or crisis classification, the model receives plausibility support. If it does not, the data architecture should force a revision in component construction rather than allowing the analogy to stand unsupported.

Table 7.3.9. Validation and Benchmark Data Objects

Validation object	Data requirement	Output	Boundary

Rolling one-year forecast	Expanding window W_j = {2010,...,T_j}; forecast T_j+1.	Forecast errors for 2017-2024.	Defined validation-window evidence.
ARIMA benchmark	Univariate stress or target series.	Persistence-model comparison.	Benchmark, not straw-man model.
VAR benchmark	Multivariate stress-channel series.	Dynamic multivariate comparison.	Requires sample-size caution.
GARCH benchmark	Volatility-sensitive financial series where available.	Volatility-benchmark comparison.	Appropriate only for variables with meaningful volatility structure.
Composite-index benchmark	Non-flow stress index from similar inputs.	Tests value added of flow-balance structure.	Must use comparable information set.
External-target validation	Spread, GDP, exchange-rate, liquidity, inflation or event target.	Plausibility and anti-circularity screen.	Corroborative, not randomized causal proof.

Source: Author synthesis for Chapter 7.3.

7.3.11. Alignment with the Seven-Problem Monograph Data Architecture

Chapter 7 is one part of a larger monograph in which seven mathematical problem architectures are translated into bounded economic-econometric analogues. The data architecture of Chapter 7 must therefore be specific enough to support the Navier-Stokes liquidity-flow model and general enough to fit the book-level evidence hierarchy. The book does not simply collect seven separate article datasets. It compares seven ways of transforming public or auditable inputs into constructed economic objects under explicit claim boundaries.

The Navier-Stokes chapter is distinctive because it uses the broadest country-year panel among the applied macro-financial chapters. The Perelman/Ricci/Poincare chapter uses a macro-regional diagnostic panel; the Hodge chapter uses a regional graph benchmark; the Yang-Mills chapter uses a finite-network benchmark with an N = 1,500 panel-validation pathway; the BSD chapter uses a World anchor and ten regional/corridor nodes with an N = 150 closure layer; the Riemann/Zeta chapter uses layered annual, quarterly and monthly validation samples; and the P vs NP chapter uses a fixed computational-finance universe with a combinatorial search layer. Chapter 7 therefore functions as the monograph's main country-panel macro-financial stress-testing example.

Figure 7.3.5. Chapter 7 within the Seven-Problem Empirical Architecture

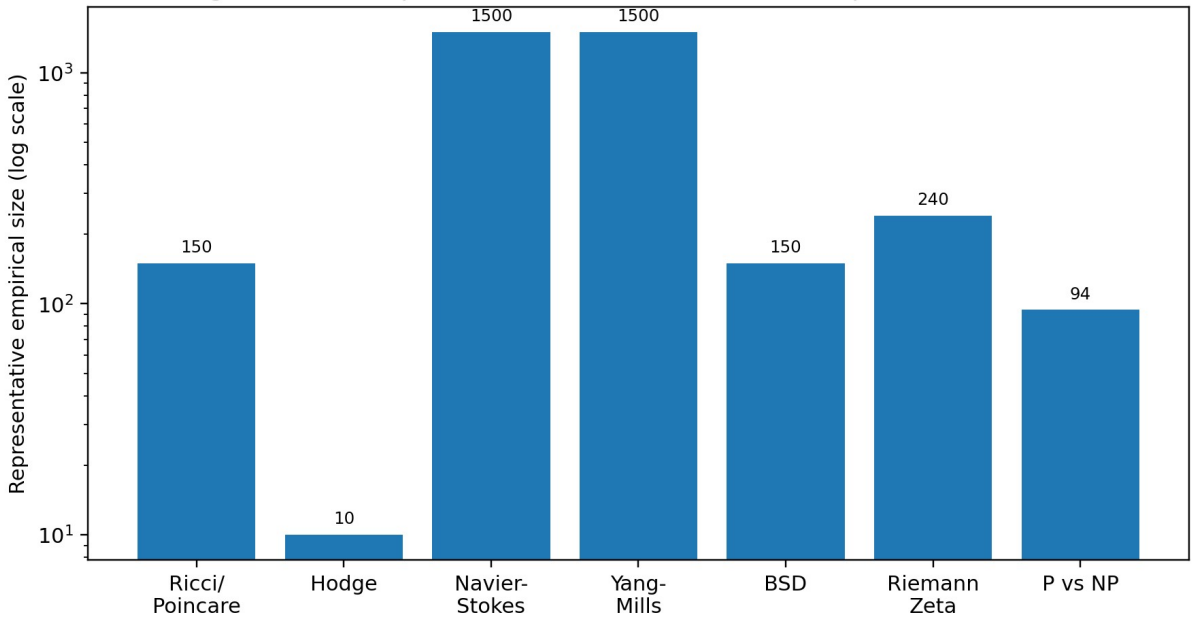


Figure 7.3.5. Chapter 7 within the Seven-Problem Empirical Architecture.

Source: Author synthesis across the seven source manuscripts. The P vs NP bar reports the number of industry portfolios, not the combinatorial support space.

Table 7.3.10. Seven-Problem Data Architecture Alignment Matrix

Book chapter / model	Empirical universe	Main sample or benchmark	Data-architecture lesson for Chapter 7
Perelman/Ricci/Poincare	Ten macro-regions over 2010-2024 with sixteen stress coordinates.	N = 150 region-year observations.	Shows how multidimensional stress variables require 0-100 orientation and diagnostic scaling.
Hodge	World anchor plus ten regional nodes, including explicit corridor-sensitive node logic.	Ten-node regional benchmark with graph and flow-pressure construction.	Supports the distinction between public anchors and constructed flow variables.
Navier-Stokes	100 countries observed annually from 2010 to 2024.	N = 1,500 country-year observations.	Provides the main macro-financial country-panel stress-testing layer.
Yang-Mills	Ten-node finite corridor network plus country-panel validation architecture.	10 nodes, 27 edges and N = 1,500 validation pathway.	Reinforces the separation between benchmark topology and large-panel validation.
Birch-Swinnerton-Dyer	World anchor and ten macro-regional/corridor nodes.	N = 150 closure layer.	Clarifies the role of World normalization and local-to-global evidence status.
Riemann/Zeta	Annual, quarterly and monthly global inflation layers.	N = 55, 45, 20, 100 and 240 layers.	Demonstrates layered validation and sample-discipline against overfitting.
P vs NP	Fixed U.S. industry universe with reduced exact benchmark.	94 industries; exact C(20,6) reduced enumeration.	Shows how empirical architecture must match the claim level of the method.

Source: Author synthesis based on the seven source manuscripts and monograph editorial plan.

7.3.12. Replication Package, Metadata and Formula-Audit Contract

The source article records the existence of a Zenodo data and replication package for the Navier-Stokes-inspired liquidity-flow and systemic-stress modelling framework. In the monograph version, the replication package should be treated as an external audit companion rather than as a decorative reference. It should contain, or explicitly point to, the reported empirical tables, extracted numerical outputs, formula catalogue, figure files, references, metadata, source ledger, verification files and checksum records used to support the reported calculations.

The replication contract matters because the chapter contains constructed variables. A constructed stress index can be scientifically strong only if the reader can identify the raw proxy, the transformation formula, the scaling window, the direction rule, the aggregation rule, the model formula and the result file produced from it. Without this chain, a sophisticated flow analogy would become difficult to audit. With this chain, the analogy becomes reproducible macro-financial measurement.

For book production, the data package should be cross-referenced consistently in the front matter, general data-and-replication statement, Chapter 7 methodology sections and final references. The dataset statement should not appear in the abstract page if the publisher style discourages it, but it should appear in the data availability section and in any chapter-specific replication note.

Table 7.3.11. Replication-Package and Formula-Audit Checklist

Replication object	Required content	Why it matters
Source ledger	Source names, variable labels, retrieval dates where relevant, source-family notes.	Allows raw input lineage to be reconstructed.
Raw input files	Country-year matrix before transformation where permissible.	Separates public/proxy input from constructed indicators.
Normalized files	Stress-direction and resilience-direction transformed variables.	Verifies nondimensional scaling.
Formula catalogue	All scaling, aggregation, index, closure, Fourier and	Prevents black-box construction.

	validation formulas.	
Model-output files	Tables, coefficient outputs, benchmark results, residual diagnostics and external-validation outputs.	Allows reported results to be checked.
Figure files	Final figures and underlying data where available.	Links visual evidence to the data pipeline.
Metadata	Variable dictionary, units, transformations, missing-data rules and version notes.	Supports transparent reuse.
Checksums and verification	Hashes, workbook checks, script logs or reproducibility notes.	Confirms file integrity and version control.

Source: Author synthesis for the monograph data-availability protocol.

7.3.13. Data Limitations and Claim-Boundary Discipline

The data architecture is strong, but it does not remove all limitations. First, the annual country-year panel is not a transaction-level financial-flow database. It measures macro-financial stress and liquidity-flow proxies, not every observed market trade, banking transaction or capital-flow movement. Second, macro-regional aggregation is useful for interpretation but remains stylized; it should not be treated as a geopolitical ranking. Third, constructed variables can create circularity risk if they are validated only against outcomes built from the same source families. This is why external-target validation and anti-circularity checks are necessary.

Fourth, the World anchor is a benchmark, not an ordinary observation. It should not be used to inflate the country sample or to claim that the model has more country-year observations than the panel actually contains. Fifth, rolling validation results are bounded by the selected validation window. Strong performance over 2017-2024 is valuable evidence, but it is not a guarantee of universal forecast dominance across all samples and future crises. Sixth, Monte Carlo and policy-counterfactual outputs are model-implied scenarios. They are useful for stress testing, but they should not be described as unconditional forecasts or randomized policy effects.

These limitations should be stated as safeguards rather than weaknesses. They clarify what Chapter 7 can credibly claim: it can claim a reproducible global-panel data architecture, nondimensional stress-component construction, World-anchor comparability, macro-regional interpretation, rolling validation, benchmark comparison, external-target screening, Monte Carlo uncertainty and policy-counterfactual scenario analysis. It cannot claim literal hydrodynamic liquidity, theorem-level Navier-Stokes proof, definitive causality or universal crisis-prediction law.

Table 7.3.12. Claim-Boundary Matrix for Data Architecture

Potential overclaim	Correct chapter-level formulation
The model proves Navier-Stokes in economics.	The model uses a Navier-Stokes-inspired economic analogy for stress-balance measurement.
Liquidity is a literal fluid.	Liquidity-flow language is nondimensional diagnostic language, not physical identity.
The 100-country panel captures all financial microstructure.	The panel captures annual macro-financial stress proxies for a broad global diagnostic sample.
Regional rankings are geopolitical rankings.	Regional layers are interpretive aggregations of stress, pressure, friction and resilience.
Rolling validation proves permanent forecast superiority.	Rolling validation reports performance inside the stated 2017-2024 validation design.
Counterfactuals prove guaranteed policy effects.	Counterfactuals are model-implied stress scenarios under defined assumptions.
Epsilon is a free residual plug.	Epsilon is restricted by observable or proxy-observable closure-state variables.

Source: Author synthesis based on the monograph claim-discipline principle.

7.3.14. Chapter 7.3 Conclusion

The data architecture of Chapter 7 converts the Navier-Stokes-inspired liquidity-flow analogy into an auditable macro-financial stress-testing system. Its central empirical object is a 100-country annual panel over 2010-2024, yielding 1,500 country-year observations. This country-year base is strengthened by a World aggregate anchor, macro-regional

interpretation layers, rolling validation windows, benchmark models, external-target screens, Monte Carlo uncertainty and policy-counterfactual objects.

The strongest methodological feature is the separation of raw inputs from constructed analytical variables. Inflation, sovereign-risk proxies, liquidity/friction indicators, GDP-cycle deviations, shocks, resilience buffers and closure-state variables do not enter the model as incomparable raw units. They enter only after source alignment, frequency harmonization, missing-data discipline, directional harmonization, nondimensional scaling and formula-audited component construction.

The strongest monograph-level contribution is that Chapter 7 supplies the book's main large-panel applied macro-financial architecture. It complements the regional topological chapters, the spectral forecasting chapter and the computational-finance chapter by showing how a mathematical flow grammar can be implemented in a broad country-year stress-testing design. The claim remains high but bounded: Chapter 7 provides a reproducible diagnostic architecture for global liquidity-flow and systemic-stress modelling; it does not convert economic stress into literal hydrodynamics, theorem proof, unrestricted causality or universal crisis prediction.

Source Note for Chapter 7.3

This subsection is based on the source manuscript "Navier-Stokes-Inspired Global Liquidity-Flow and Systemic-Stress Modelling: A Nondimensional Macro-Financial Stress-Testing Framework" and is aligned with the monograph editorial plan that requires shared introductory, literature-review and unified-methodology material to be separated from the independent problem chapters. It also uses the cross-document data-architecture logic of the Perelman/Ricci/Poincare, Hodge, Yang-Mills, BSD, Riemann/Zeta and P vs NP source studies to ensure that Chapter 7 remains integrated into the seven-problem monograph rather than standing as an isolated article reproduction.

Replication reference to be retained in the book data-availability apparatus: Gondauri, D. (2026). Navier-Stokes-Inspired Global Liquidity-Flow and Systemic-Stress Modelling: Data and Replication Package for a Nondimensional Macro-Financial Stress-Testing Framework [Data set]. Zenodo. https://zenodo.org/records/20835729.

Chapter 7.4. Methodology: Nondimensional Stress Balance, ε(t) Closure and Validation Design

Davit Gondauri

Chapter-position note. This subsection is the technical methodological core of Chapter 7. It translates the Navier-Stokes-inspired liquidity-flow analogy into an auditable economic methodology: nondimensional stress construction, restricted hidden-adjustment closure, cycle forcing, one-year-ahead validation, benchmark comparison, panel inference, external validation, robustness, Monte Carlo uncertainty and policy counterfactuals. It is written for the monograph, not as a repeated journal-article methodology chapter. Its purpose is to show exactly how the Chapter 7 evidence can be reproduced, audited and bounded within the wider seven-problem economic-analogue programme.

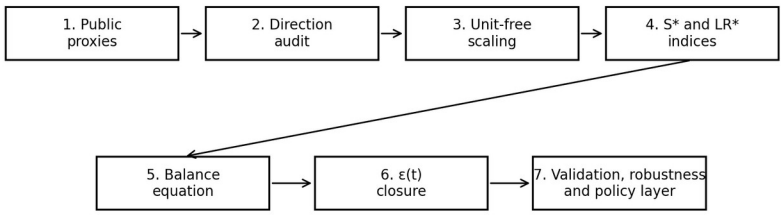
Table 7.4.1. Methodological position of Section 7.4 within the monograph

Layer	Chapter 7.4 role	Connection to previous subsections	Reviewer-safety function
Conceptual analogy	Converts flow, pressure, friction, shock, cycle and closure into economic measurement objects.	Extends Section 7.1.	Prevents literal hydrodynamic interpretation.
Research object	Specifies how liquidity, pressure, friction and closure are measured as state variables.	Operationalizes Section 7.2.	Separates raw macro-financial indicators from constructed stress objects.
Data architecture	Uses the 100-country annual panel, World anchor and macro-regional layer as the evidence base.	Builds on Section 7.3.	Prevents small-sample or single-country overclaiming.
Validation design	Defines the empirical gates through which the stress balance is tested.	Prepares Section 7.5.	Forces out-of-sample, benchmark and robustness discipline before

			interpretation.
Claim boundary	Classifies admissible diagnostic, forecast, counterfactual and non-admissible theorem-level claims.	Connects to Sections 7.6-7.8 and the general monograph boundary.	Protects the monograph from Clay-problem proof overclaiming.

Source: Author synthesis based on the Chapter 7 source document and the monograph-level editorial architecture.

Figure 7.4.1. Methodological pipeline from raw proxies to audited stress-testing evidence



The method is sequential: balance, closure, forecast comparison and counterfactual interpretation are admissible only after common-scale construction and validation discipline.

7.4.1. Methodological orientation

The methodology is quantitative, non-experimental, computational, econometric and validation-oriented. It is not a physical-fluid model of finance. Instead, it uses the structural grammar of Navier-Stokes reasoning to organize macro-financial stress into a common diagnostic balance. The logic is deliberately strict: no raw inflation rate, spread, liquidity proxy, volatility measure or GDP-cycle deviation is added directly to another raw unit. Every object enters only after direction harmonization, scaling and diagnostic interpretation.

The central methodological task is therefore not to borrow a famous equation as a metaphor, but to create a reproducible transformation chain. The chain begins with public or proxy-observable macro-financial variables, converts them into stress-oriented or resilience-oriented unit-free components, builds a systemic-stress index, decomposes the index into balance terms, models the residual closure as a restricted state equation, and evaluates the entire construction through rolling validation, benchmark comparison, panel inference, external targets, robustness tests and uncertainty scenarios.

In the monograph setting, this section also performs a second function. It aligns Chapter 7 with the shared methodology of the seven economic analogues: public-data anchor separation, author-calculated variables, normalization, validation, robustness, scenario analysis, replication discipline and claim-boundary classification. Navier-Stokes supplies the flow-balance grammar; the monograph supplies the broader evidence-discipline framework.

7.4.2. Nondimensionalization and direction harmonization

The first methodological requirement is unit discipline. Macro-financial stress variables are expressed in heterogeneous units: percentages, basis-point spreads, ratios, volatility proxies, index values, event dummies and growth deviations. A stress-balance equation is not admissible unless those units are first converted into a common scale. This is why the model uses starred variables, denoted with superscript * in plain-text notation. A starred variable is not a raw value; it is a normalized diagnostic coordinate.

Equation (7.4.1). x*_{i,t,j} = 100 x (x_{i,t,j} - min_j) / (max_j - min_j), for stress-increasing variables.

The transformed variable x* lies on a 0-100 stress-oriented scale. Higher values indicate greater stress contribution when the raw variable is already stress-increasing, such as inflation pressure, sovereign-spread pressure or volatility stress.

Equation (7.4.2). x*_{i,t,j} = 100 x (max_j - x_{i,t,j}) / (max_j - min_j), for resilience-increasing variables.

When the raw variable is protective, such as reserve buffer, fiscal capacity or liquidity support, the transformation reverses its direction so that weak capacity appears as higher stress.

Equation (7.4.3). z*_{i,t,j} = (x_{i,t,j} - mean_j) / sd_j, used for robustness or regression-standardized variants.

Standardization is used as a robustness alternative when the methodology needs sensitivity to distributional position rather than bounded 0-100 scaling. It is not mixed mechanically with the baseline min-max stress scale.

Table 7.4.2. Nondimensional transformation rules

Input type	Raw examples	Direction rule	Baseline transformation	Interpretation after transformation
Stress-increasing pressure	Inflation pressure, sovereign spread, exchange-rate volatility.	Higher raw value = higher stress.	Min-max stress scaling.	Higher x* raises the stress balance.
Friction or liquidity constraint	Credit tightening, funding spread, liquidity-ratio weakness.	Higher raw value or weaker liquidity = higher stress.	Direction-harmonized 0-100 scaling.	Higher x* captures stronger liquidity friction.
Resilience capacity	Fiscal buffer, reserve buffer, policy support, external aid.	Higher raw value = lower stress.	Reverse min-max scaling.	Higher x* means weaker resilience capacity.
Shock/event proxy	Geopolitical shock, crisis event, event-volatility proxy.	Event intensity is stress-oriented.	Binary, ordinal or scaled shock normalization.	Higher x* represents stronger forcing.
Cycle variable	GDP-cycle deviation, output gap proxy, harmonic cycle term.	Sign depends on downturn or overheating logic.	Cycle-specific normalization.	F_GDP* enters as macroeconomic forcing.
Closure-state variable	Shadow pressure, transfers, inertia, lagged closure.	Sign estimated in the closure equation.	State-variable scaling before ε* estimation.	Explains hidden adjustment rather than hiding it.

Source: Author methodological synthesis. The table reports transformation rules, not empirical results.

7.4.3. Stress and liquidity-resilience construction

The systemic-stress index is a weighted diagnostic aggregate of stress-direction components. It is not interpreted as an observed financial-market price. It is an author-calculated macro-financial stress coordinate that allows pressure, friction, weak flow, shocks and closure to be compared inside one scale. The corresponding liquidity-resilience index is constructed to measure buffer capacity and the ability of a country or region to absorb stress without immediate systemic amplification.

Equation (7.4.4). S*_{i,t} = sum_{j=1}^{J} w_j x*_{i,t,j}, with w_j >= 0 and sum_j w_j = 1.

S* is the systemic-stress index for country i and year t. It is a constructed diagnostic index, not a raw public-data variable.

Equation (7.4.5). LR*_{i,t} = sum_{k=1}^{K} v_k r*_{i,t,k}, with v_k >= 0 and sum_k v_k = 1.

LR* is the liquidity-resilience index. Depending on the coding convention, a higher LR* can be reported as stronger resilience or reverse-coded as lower resilience weakness. The manuscript must state the direction consistently before interpreting results.

Equation (7.4.6). StressPressure_{i,t} = S*_{i,t} - LR*_{i,t}, or an equivalent standardized stress-resilience gap.

The stress-resilience gap is used as a diagnostic summary of whether stress pressure exceeds the system's absorption capacity. It should not be read as a mechanical crisis threshold without validation.

Table 7.4.3. Stress and resilience index design

Index object	Economic meaning	Input family	Validation need	Claim boundary
S* systemic stress	Composite pressure of macro-financial vulnerability.	Inflation, sovereign risk, liquidity friction, volatility, growth-cycle stress and shock proxies.	Weight robustness, panel coherence, external targets.	Constructed diagnostic index, not observed crisis probability by itself.
LR* liquidity resilience	Absorption capacity and liquidity-buffer	Fiscal buffers, reserves, support	Sign logic, counterfactual	Resilience proxy, not complete balance-

	strength.	capacity, banking/liquidity safeguards.	response, regional plausibility.	sheet microstructure.
Stress-resilience gap	Net pressure after accounting for resilience capacity.	S* and LR* components.	Sensitivity to scaling and weights.	Interpretive stress metric, not deterministic default or crisis law.
High-stress classification	Binary or ordinal category for forecast and external validation.	Thresholded S* or stress-resilience gap.	Confusion matrix, hit rate, AUC, robustness thresholds.	Classification rule only within reported design.

Source: Author methodological synthesis for Chapter 7.4.

7.4.4. Navier-Stokes-inspired nondimensional stress balance

After nondimensionalization, the methodology specifies the central stress-balance relation. Its economic meaning is straightforward: observed systemic stress is approximated by a set of interpretable pressure-generating and pressure-absorbing channels. The equation does not claim that financial liquidity obeys physical fluid dynamics. It claims that stress formation can be organized through an economic analogue of velocity weakness, acceleration, pressure gradient, friction, forcing and closure.

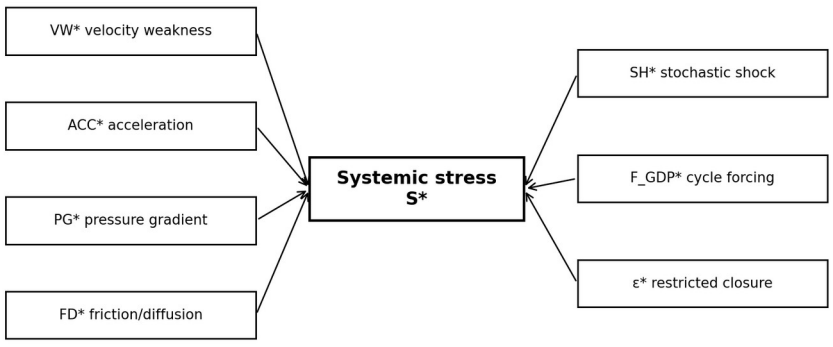
Equation (7.4.7). $S^*_{i,t} = \alpha + \theta 1\ VW^*_{i,t} + \theta 2\ ACC^*_{i,t} + \theta 3\ PG^*_{i,t} + \theta 4\ FD^*_{i,t} + \theta 5\ SH^*_{i,t} + \theta 6\ F_GDP^*_{t} + \theta 7\ \varepsilon^*_{i,t} + u_{i,t}$.

S* is systemic stress; VW* is liquidity-velocity weakness; ACC* is liquidity acceleration or stress acceleration; PG* is the macro-financial pressure gradient; FD* is friction/diffusion; SH* is stochastic shock forcing; F_GDP* is Fourier GDP-cycle forcing; ε* is restricted hidden adjustment; u is the remaining statistical residual after the modelled terms are included.

Equation (7.4.8). $BalanceResidual_{i,t} = S^*_{i,t} - \hat{S}^*_{i,t}$.

The residual is used for diagnostic checking. It is not allowed to become a silent correction device. Large residual instability triggers robustness, omitted-channel and claim-boundary caution.

Figure 7.4.2. Nondimensional stress-balance components



All terms enter only after direction harmonization and nondimensional scaling. The diagram shows model structure, not empirical contribution shares.

Table 7.4.4. Mapping from Navier-Stokes grammar to economic stress-balance components

Classical flow term	Economic analogue	Plain-text variable	Empirical proxy logic	Admissible interpretation
Velocity	Liquidity-flow speed or weakness.	VW*	Money/liquidity velocity weakness, liquidity turnover slowdown or flow	Weak flow can raise systemic stress.

			contraction proxy.	
Acceleration	Change in liquidity stress or flow momentum.	ACC*	Year-to-year change in stress or liquidity-flow component.	Rapid deterioration matters beyond level.
Pressure gradient	Macro-financial pressure differential.	PG*	Inflation, sovereign spread, exchange-rate or external pressure differentials.	Stress rises when pressure gradients steepen.
Viscosity / diffusion	Frictional liquidity and credit diffusion.	FD*	Credit friction, banking strain, funding spread or liquidity-tightening proxy.	Friction slows adjustment and amplifies stress.
External force	Stochastic or event shock.	SH*	Crisis dummy, geopolitical shock, volatility event or external disruption.	Shocks push the system away from normal flow.
Cyclical forcing	Macroeconomic harmonic pressure.	F_GDP*	GDP-cycle term estimated with leakage-control discipline.	Cycles provide background forcing.
Closure term	State-dependent hidden adjustment.	ε*	Restricted equation using observable/proxy-observable state variables.	Closure is auditable, not freely fitted.

Source: Author synthesis. This is a methodological mapping, not a physical equivalence statement.

7.4.5. Restricted ε(t) closure methodology

The most important methodological safeguard is the treatment of ε(t). In weak constructed-index models, a residual term can silently absorb everything the model does not explain. In this framework, the closure term is explicitly modelled through state variables. This means ε(t) is not a free algebraic plug used to force the stress-balance equation to fit. It is an auditable hidden-adjustment channel connected to lagged adjustment, informal or shadow pressure, external transfers, geopolitical disruption, fiscal buffers, foreign aid or support and economic inertia.

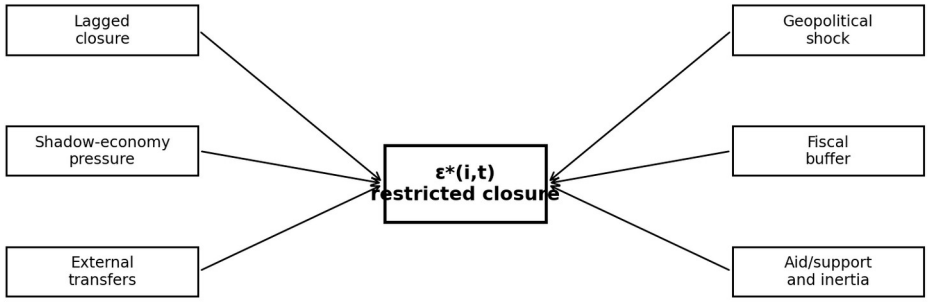
Equation (7.4.9). $\varepsilon^*_{i,t} = \rho\ \varepsilon^*_{i,t-1} + \beta1\ Shadow^*_{i,t} + \beta2\ Transfers^*_{i,t} + \beta3\ GeoShock^*_{i,t} - \beta4\ FiscalBuffer^*_{i,t} - \beta5\ AidSupport^*_{i,t} + \beta6\ Inertia^*_{i,t} + \eta_{i,t}$.

The expected sign pattern is not imposed mechanically, but the equation has a clear interpretation: shadow pressure, geopolitical shock and inertia can raise hidden adjustment; fiscal buffers and external support should reduce the need for hidden stress absorption if they function as resilience channels.

Equation (7.4.10). $ClosureShare_{m,t} = |\beta_m X^*_{m,t}| / \sum_m |\beta_m X^*_{m,t}|$.

Closure-share decomposition can be used to show which state variables explain the modelled hidden-adjustment channel. The shares are explanatory diagnostics, not causal shares unless separately identified.

Figure 7.4.3. Restricted ε(t) closure as an auditable state equation



Purpose: prevent ε(t) from becoming a free residual plug by linking hidden adjustment to observable or proxy-observable state variables.

Table 7.4.5. ε(t) closure-state variables and expected methodological roles

Closure variable	Economic interpretation	Expected sign logic	Why it belongs in ε(t)	Boundary condition
Lagged ε*	Persistence in hidden adjustment.	Positive if adjustment is inertial.	Prevents closure from being treated as memoryless.	Persistence is diagnostic, not structural inevitability.
Shadow pressure	Unobserved or informal-economy stress channel.	Usually positive.	Captures pressure not fully reflected in official indicators.	Proxy quality must be disclosed.
External transfers	Remittances, transfers or foreign financing support.	Ambiguous depending on use.	Can absorb liquidity stress or reveal dependence.	Interpret only with sign and context.
Geopolitical shock	External disruption affecting confidence, liquidity and risk premia.	Positive.	Explains event-driven hidden adjustment.	Scenario evidence, not deterministic geopolitics.
Fiscal buffer	Policy capacity to absorb stress.	Usually negative.	Reduces need for hidden adjustment.	Not equivalent to full fiscal sustainability.
Aid/support	External support, aid, liquidity backstop or institutional support.	Usually negative if stabilizing.	Represents external absorption capacity.	Support effectiveness is model-implied.
Economic inertia	Slow adjustment and persistence of macro-financial structure.	Positive when stress is sticky.	Explains why stress does not normalize immediately.	Not a substitute for microeconomic mechanisms.

Source: Author methodological synthesis based on the restricted-closure logic of the Chapter 7 source design.

7.4.6. Fourier GDP-cycle forcing and leakage-control discipline

The methodology includes a Fourier GDP-cycle term because macro-financial stress is not only a contemporaneous pressure process. It is also affected by cyclical expansion, contraction and post-shock recovery. However, cycle modelling creates a common risk: the analyst can accidentally use future information when fitting the cycle. The methodology therefore separates descriptive full-sample cycle visualization from rolling forecast-valid cycle estimation.

Equation (7.4.11). $F_GDP^*_{t} = a0 + \sum_{h=1}^{H} [a_h \cos(2\pi h t / T) + b_h \sin(2\pi h t / T)]$, then scaled to the model coordinate system.

The Fourier expression represents the GDP-cycle forcing term. H is kept parsimonious, and cycle estimation for forecasting must use only the information available before the forecast year.

Equation (7.4.12). $F_GDP^*_{\tau \mid \tau-1}$ is estimated using data through $\tau-1$ and then used to forecast S^*_{τ}.

This rule prevents look-ahead bias. The full-sample cycle can be displayed for interpretation, but it cannot be used as if it were a genuine ex-ante forecast input.

Table 7.4.6. Fourier-cycle methodology and leakage-control rules

Cycle object	Purpose	Allowed use	Forbidden use	Validation requirement
Descriptive full-sample cycle	Visualize broad macro-financial cyclical structure.	Interpret historical cycle alignment.	Use as ex-ante forecast input.	Label as descriptive.
Rolling-window cycle	Generate forecast-valid cyclical forcing.	One-year-ahead validation.	Include the forecast year in training.	Document train/test boundary.
Harmonic order H	Control complexity of the cycle term.	Parsimonious specification and robustness checks.	High-order overfit to stress path.	Report sensitivity to H.
Cycle scaling	Place F_GDP on the same model scale.	Nondimensional transformation.	Combine raw GDP deviations with normalized stress variables.	Check sign and scale consistency.

Source: Author methodological synthesis.

7.4.7. Rolling validation and benchmark comparison

The forecasting layer is designed as an expanding-window one-year-ahead validation system. It asks whether the Navier-Stokes-inspired stress-balance model adds diagnostic forecasting information relative to conventional benchmarks inside the reported validation window. This test is intentionally bounded. Strong performance over 2017-2024 supports validation-window usefulness; it does not prove permanent predictive dominance in all future periods.

Equation (7.4.13). $Train_{\tau} = \{2010, ..., \tau-1\}$; $Test_{\tau} = \{\tau\}$; $\tau \in \{2017, ..., 2024\}$.

Each forecast year is held out. The model is estimated on the information set available before the forecast year.

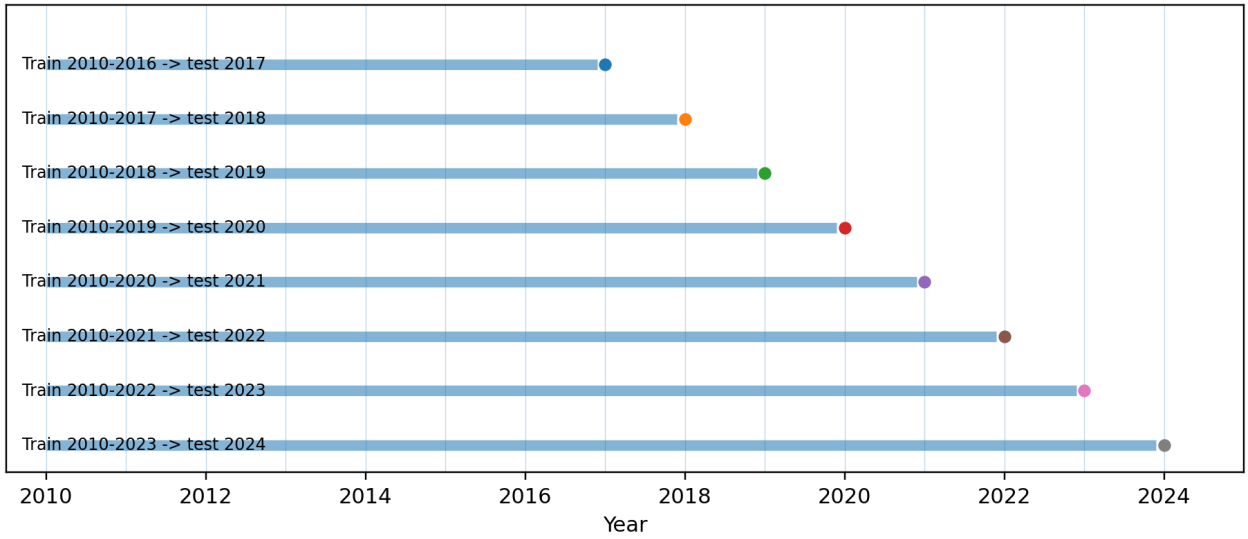
Equation (7.4.14). $e_{\tau}^{model} = S^*_{\tau} - \hat{S}^*_{\tau|\tau-1}$; $RMSE = \sqrt{mean(e_{\tau}^2)}$; $MAE = mean(|e_{\tau}|)$; $MAPE = mean(|e_{\tau}/S^*_{\tau}|)$.

Forecast errors are evaluated through standard metrics. Directional accuracy and stress-regime hit rate are used as classification diagnostics, not as proof of a crisis law.

Equation (7.4.15). $\Delta RMSE_b = RMSE_{benchmark} - RMSE_{NS}$.

A positive $\Delta RMSE_b$ indicates that the NS-inspired model improves RMSE relative to benchmark b within the reported window.

Figure 7.4.4. Expanding-window one-year-ahead validation design



Training windows expand and the forecast year is held out. This is leakage control, not a universal forecast-dominance claim.

Table 7.4.7. Benchmark suite and methodological role

Benchmark	What it tests	Why it is necessary	Interpretation if NS model improves	Interpretation if benchmark wins
ARIMA	Persistence and univariate time-series structure.	Stress may be largely autoregressive.	NS model adds channel information beyond persistence.	Flow-balance claim is weakened for forecasting but may remain diagnostic.
VAR	Multivariate dynamic interaction.	Stress components may interact dynamically.	NS model offers parsimonious structured decomposition.	VAR may capture dynamics better; claim must be narrowed.
GARCH	Volatility clustering and risk instability.	Stress may behave like conditional volatility.	NS model captures stress levels/regimes beyond volatility.	Volatility process may dominate; use as caution.
Composite index baseline	Non-flow constructed-index alternative.	Tests whether the flow balance adds value beyond weighted aggregation.	NS structure adds interpretive and forecast value.	Simple index may be sufficient; flow analogy becomes mainly explanatory.
Naive/no-change benchmark	Minimal inertia rule.	Guards against overengineered models.	NS model beats a low-information baseline.	Serious warning for model usefulness.

Source: Author validation protocol for Chapter 7.4.

7.4.8. Panel fixed effects and robust-inference specification

The panel layer uses the 100-country annual structure to evaluate whether balance components retain coherent associations under country and year heterogeneity. The logic is diagnostic rather than causal. Country fixed effects absorb persistent country-level differences; year fixed effects absorb global common shocks. Robust or clustered covariance adjustments address heteroskedasticity, serial dependence and cross-sectional dependence concerns where feasible.

Equation (7.4.16). $S^*_{i,t} = \alpha_i + \lambda_t + \theta1\ VW^*_{i,t} + \theta2\ ACC^*_{i,t} + \theta3\ PG^*_{i,t} + \theta4\ FD^*_{i,t} + \theta5\ SH^*_{i,t} + \theta6\ F_GDP^*_{t} + \theta7\ \varepsilon^*_{i,t} + \nu_{i,t}$.

α_i denotes country fixed effects and λ_t denotes year fixed effects. The coefficients are interpreted as diagnostic associations, not causal effects.

Equation (7.4.17). PartialR2_m = [R2(full) - R2(without m)] / [1 - R2(without m)].

Partial R-squared decomposition helps measure how much incremental explanatory content a term contributes after the other balance components are included.

Table 7.4.8. Panel econometric validation protocol

Test or estimator	Methodological purpose	Evidence produced	Claim boundary
Country fixed effects	Control persistent country-specific levels.	Within-country association evidence.	Not causal without identification.
Year fixed effects	Control common global-year shocks.	Stress-channel signs net of global shocks.	Cannot isolate all global mechanisms.
Hausman/Mundlak logic	Check FE/RE plausibility and correlated heterogeneity.	Estimator discipline.	Selection between specifications, not proof of causal structure.
Clustered or robust SE	Address heteroskedasticity and within-panel dependence.	Inference credibility.	Robust SE do not solve omitted-variable bias.
Driscoll-Kraay / cross-sectional-dependence checks	Handle common shocks and cross-country dependence where appropriate.	Sensitivity of statistical significance.	Diagnostic robustness, not full structural identification.
Partial R2 and fit decomposition	Show incremental contribution of terms.	Term importance diagnostics.	High fit must be checked against circularity and overfitting.
Residual diagnostics	Detect instability, misspecification and outliers.	Residual distribution and stability evidence.	Residual problems bound the claim.

Source: Author methodological synthesis.

7.4.9. External-target validation, robustness and residual diagnostics

External validation tests whether the constructed stress signal behaves plausibly against targets that are not simply the same variables used to build it. This is a circularity safeguard. The external layer can include sovereign-spread widening, GDP-growth slowdown, exchange-rate volatility, liquidity tightening, inflation persistence and crisis/event classification. The evidence is strongest when targets are independently observed, signs are coherent, confidence intervals are plausible and classification metrics improve relative to simple baselines.

Equation (7.4.18). Y^{external}_{i,t} = a + b S*_{i,t} + controls_{i,t} + e_{i,t}.

This screen tests whether higher constructed stress is associated with external macro-financial deterioration. It is external diagnostic plausibility, not causal identification.

Equation (7.4.19). Pr(Crisis_{i,t}=1) = Λ(a + b S*_{i,t} + controls_{i,t}).

Logit/probit screens can convert stress into classification evidence. AUC, accuracy, sensitivity and specificity should be reported when classification is used.

Equation (7.4.20). S*^{(-j)}_{i,t} = stress index excluding component j.

Leave-one-component-out analysis tests whether the stress signal depends excessively on one input family. A robust index should retain broadly similar ranking and validation behavior after reasonable exclusions.

Table 7.4.9. External validation and robustness gate design

Gate	Operational test	Reviewer concern addressed	Passing condition	If not passed
External target	Regress or classify external macro-financial outcomes using S*.	Circularity and internal-only validation.	Expected signs and plausible predictive/classification performance.	Downgrade claim to internal diagnostic evidence.
Weighting robustness	Equal, baseline, PCA/entropy or crisis-year weights.	Subjective constructed-index weights.	High rank agreement and stable stress classification.	Report sensitivity and avoid strong ranking claims.

Normalization robustness	Alternative scaling and standardization rules.	Scale dependence.	Term signs and rankings remain stable.	Limit interpretation to chosen scale.
Proxy perturbation	Perturb proxy values within plausible bounds.	Proxy measurement uncertainty.	Model conclusions remain directionally stable.	Emphasize data uncertainty.
Leave-one-component-out	Recompute S* without component j.	Single-variable dominance.	Stress signal retains core structure.	Flag overdependence.
Residual stability	Check residual distribution, autocorrelation and outlier concentration.	Hidden misspecification.	No severe systematic residual pattern.	Restrict forecast and inference claims.
Shock-year sensitivity	Re-estimate excluding crisis years or using crisis controls.	Results driven only by 2020/2022-type shocks.	Signs remain coherent or shock-dependence is transparently bounded.	State that evidence is crisis-window dependent.

Source: Author validation-gate synthesis.

7.4.10. Monte Carlo uncertainty and policy counterfactual design

The uncertainty layer translates the model into stress-testing language. Monte Carlo simulation propagates uncertainty in shocks, coefficients, residuals or scenario inputs into distributions of future stress values. Policy counterfactuals then evaluate model-implied stress changes under specified interventions or adverse shocks. These outputs are useful for macroprudential interpretation, but they remain model-implied scenarios, not randomized policy experiments.

Equation (7.4.21). S*_{i,t+h}^{(b)} = f(VW*, ACC*, PG*, FD*, SH*^{(b)}, F_GDP*, ε*^{(b)}; Θ^{(b)}), for b = 1,...,B.

The superscript b denotes a Monte Carlo draw. The simulation may perturb shocks, coefficients, residuals or selected input channels according to documented assumptions.

Equation (7.4.22). Report mean(S*), median(S*), p05(S*), p95(S*) and high-stress probability Pr(S* > threshold).

Uncertainty is summarized through percentile bands and high-stress probability. Widening bands indicate uncertainty accumulation, not deterministic crisis movement.

Equation (7.4.23). ΔPolicy = S*_{counterfactual} - S*_{baseline}.

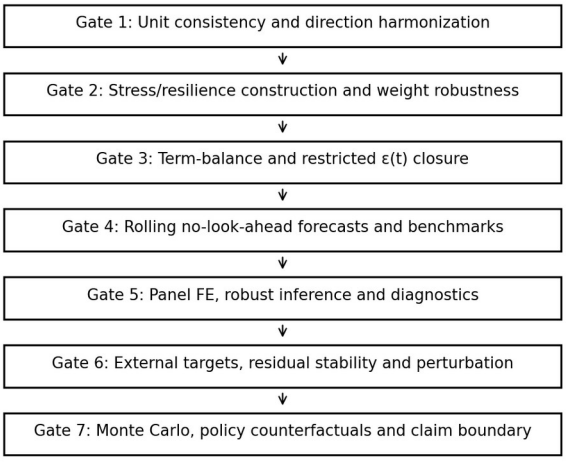
A negative ΔPolicy means the scenario lowers model-implied stress; a positive value means it raises model-implied stress. This is a stress-index effect, not causal policy proof.

Table 7.4.10. Monte Carlo and policy-counterfactual scenario map

Scenario family	Perturbed channel	Expected stress direction	Interpretive use	Boundary condition
Liquidity-buffer strengthening	LR* or resilience capacity.	Stress decreases.	Tests resilience package effect.	Not a policy guarantee.
Sovereign-spread shock	PG* pressure gradient.	Stress increases.	Tests debt-risk or risk-premium pressure.	Depends on proxy and calibration.
Inflation persistence shock	Pressure and cycle channels.	Stress increases.	Tests macro-financial pressure persistence.	Not an inflation forecast by itself.
Credit/liquidity tightening	FD* friction/diffusion.	Stress increases.	Tests funding-friction vulnerability.	Requires robust proxy interpretation.
Geopolitical escalation	SH* and ε* closure channels.	Stress increases.	Tests event-risk transmission.	Scenario evidence only.
External support package	Aid/support and fiscal-buffer terms.	Stress decreases if stabilizing.	Tests support or backstop role.	Sign may be context-dependent.

Source: Author scenario-design synthesis for Chapter 7.4.

Figure 7.4.5. Validation and claim-discipline gate ladder



A claim may move upward only when the previous gate is satisfied; otherwise it remains descriptive, diagnostic or excluded.

7.4.11. Integration with the seven-problem methodology of the monograph

Although Section 7.4 is specific to the Navier-Stokes-inspired liquidity-flow model, it is written inside a wider monograph whose seven problem chapters share a common research discipline. The shared discipline is not that every chapter uses the same equation. It is that every chapter converts a mathematical architecture into a bounded economic measurement system, separates public anchors from author-calculated objects, validates the constructed signal, tests robustness and states a precise claim boundary.

The Navier-Stokes chapter is especially important because it has one of the strongest applied macro-financial evidence designs in the monograph: a 100-country annual panel for 2010-2024, a World anchor, macro-regional layers, rolling validation, benchmark comparison, Monte Carlo uncertainty and policy counterfactuals. This design makes the chapter an applied stress-testing counterpart to the more topological, spectral, local-to-global and computational chapters.

Figure 7.4.6. Cross-problem methodological alignment inside the monograph

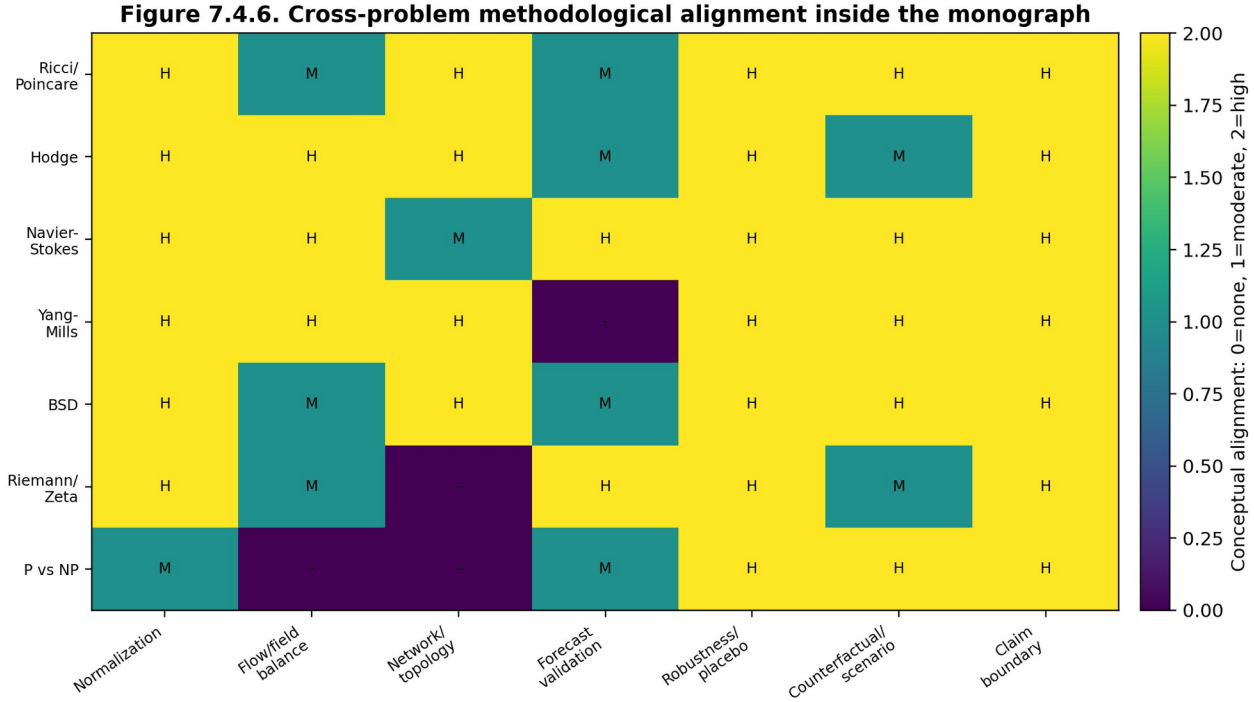


Table 7.4.11. Cross-problem methodological alignment with Section 7.4

Problem chapter	Core economic object	Shared methodological principle	Specific link to Chapter 7.4
Perelman/Ricci/Poincare	Inequality pressure, curvature and smoothing capacity.	Stress-coordinate normalization, curvature-style decomposition, counterfactuals and bounded validation.	Shares pressure-transformation discipline and scenario caution.
Hodge	Macro-flow decomposition into gradient, curl and harmonic components.	Flow is decomposed into interpretable structural terms.	Shares flow-language discipline and decomposition logic.
Navier-Stokes	Global liquidity-flow systemic stress.	Nondimensional stress-balance, ε(t) closure and validation gates.	Central subject of this section.
Yang-Mills	Gauge curvature, action and finite-network mass-gap threshold.	Stress-field construction, network embedding, scenario shocks and finite-evidence boundaries.	Shares systemic stress and shock-transmission language.
BSD	Local-to-global structural rank and corridor stress.	Public-anchor to constructed-object chain, calibration, external checks and circularity safeguards.	Shares local-to-global stress interpretation and replication gates.
Riemann/Zeta	Inflation forecasting with structural-spectral correction.	Layered validation, no-look-ahead rules and benchmark comparison.	Shares forecast discipline and benchmark hierarchy.
P vs NP	Sparse portfolio optimization under computational complexity.	Algorithmic workflow, exact/reduced benchmark, robustness and claim boundaries.	Shares replication workflow and admissible-claim classification.

Source: Author monograph-level synthesis across the seven source documents.

7.4.12. Replication algorithm for Chapter 7.4

The following algorithm translates the methodology into a reproducible workflow. It is intentionally procedural because Chapter 7 should be auditable by a reviewer, not only persuasive as a conceptual analogy.

Table 7.4.12. Sequential replication workflow for the Chapter 7 methodology

Step	Task	Required action	Output artifact
1	Fix empirical universe.	Load 100-country annual panel for 2010-2024, World anchor and macro-regional coding.	Country-year panel and regional map.
2	Audit source lineage.	Separate public inputs, proxy variables and author-calculated transformations.	Source ledger and variable dictionary.
3	Harmonize directions.	Code each variable as stress-increasing or resilience-increasing.	Direction-audit table.
4	Normalize variables.	Apply min-max, reverse-scale or standardized transformation as specified.	Starred variables.
5	Build S* and LR*.	Apply baseline weights and alternative weighting	Stress/resilience indices and

		schemes.	weight-robustness file.
6	Compute balance terms.	Generate VW*, ACC*, PG*, FD*, SH*, F_GDP* and preliminary closure residual.	Term-balance matrix.
7	Estimate ε(t).	Fit restricted closure equation with state variables.	Closure coefficients and decomposition.
8	Estimate rolling cycles.	Compute Fourier GDP-cycle forcing without look-ahead in validation windows.	Cycle table and harmonic file.
9	Run rolling forecasts.	Estimate expanding-window one-year-ahead forecasts for 2017-2024.	Forecast table and error metrics.
10	Run benchmarks.	Estimate ARIMA, VAR, GARCH and composite-index baselines where appropriate.	Benchmark comparison table.
11	Estimate panel models.	Run FE/TWFE, robust SE, diagnostics and partial R2 decomposition.	Panel-inference output.
12	Validate externally.	Compare S* with external macro-financial targets and crisis classifications.	External validation table.
13	Test robustness.	Run weighting, normalization, proxy, LOO, residual and shock-year sensitivity checks.	Robustness appendix file.
14	Simulate scenarios.	Run Monte Carlo uncertainty and policy counterfactuals.	Stress bands and counterfactual effects.
15	Classify claims.	Assign claims as strong diagnostic, bounded forecast, scenario-based, excluded or future-validation.	Claim-boundary matrix.

Source: Author replication workflow. The workflow should be paired with scripts, seeds, output hashes and archived data-package metadata in the replication appendix.

7.4.13. Methodological claim-boundary protocol

The final methodological layer is claim classification. This is not an editorial afterthought; it is part of the method. A model based on a famous mathematical equation must explicitly state what it does not claim. The Chapter 7 methodology permits strong diagnostic stress-testing claims if the transformation, balance, closure and validation gates hold. It permits bounded forecast claims inside the reported rolling window. It permits model-implied policy and uncertainty interpretation. It does not permit claims that liquidity is a literal fluid, that the Navier-Stokes problem is solved, that fixed effects identify causal laws or that rolling validation establishes a universal crisis-prediction mechanism.

Table 7.4.13. Claim-boundary protocol for the Chapter 7 methodology

Potential overclaim	Methodological correction	Permitted claim	Excluded claim
Financial liquidity is a physical fluid.	Use nondimensional economic analogy only.	Liquidity-flow dynamics can be diagnostically	Literal hydrodynamic law.

		approximated.	
The chapter solves or tests Navier-Stokes.	State that no PDE theorem-level result is claimed.	NS grammar organizes economic stress channels.	Clay-problem solution or mathematical proof.
ε(t) freely restores equality.	Estimate restricted state-dependent closure equation.	Hidden adjustment can be modelled and audited.	Unrestricted residual plug.
Rolling validation proves universal forecasting.	Limit claim to 2017-2024 validation-window evidence.	Model shows reported-window diagnostic usefulness.	Permanent crisis-prediction law.
FE coefficients are causal laws.	Interpret FE/TWFE as diagnostic associations under controls.	Stress channels have coherent panel associations.	Unrestricted causal identification.
Policy counterfactuals prove policy effects.	Report model-implied stress deltas and uncertainty bands.	Scenarios support stress-testing interpretation.	Randomized policy-impact proof.
External targets fully validate the mechanism.	Treat external validation as plausibility unless identification is independent.	Stress signal behaves plausibly against external outcomes.	Independent causal confirmation.

Source: Author claim-boundary synthesis for Chapter 7.4.

7.4.14. Methodological synthesis

Section 7.4 establishes the full methodology required for the applied macro-financial strength of Chapter 7. The model begins with a 100-country annual panel, but its scientific value does not come from sample size alone. Its value comes from the combination of nondimensional scaling, stress-resilience construction, a transparent balance equation, a restricted ε(t) closure channel, forecast-valid cycle forcing, rolling no-look-ahead validation, benchmark comparison, panel econometric diagnostics, external-target plausibility checks, robustness gates, Monte Carlo uncertainty and policy counterfactual interpretation.

The methodology therefore makes a precise contribution to the monograph. It shows how a mathematical flow-balance grammar can be translated into an applied macro-financial stress-testing architecture without turning analogy into theorem proof. It also demonstrates the monograph's broader research principle: ambitious mathematical-economic modelling is defensible only when every constructed object is normalized, audited, validated, bounded and reproducible.

Internal source note

This subsection is based on the source document "Navier-Stokes-Inspired Global Liquidity-Flow and Systemic-Stress Modelling: A Nondimensional Macro-Financial Stress-Testing Framework" and aligned with the monograph editorial plan that consolidates common literature and unified methodology while keeping each Millennium-problem analogue as an independent problem chapter. All numeric result claims should remain in Section 7.5 or the relevant results appendix; Section 7.4 is a methodology chapter and therefore reports formulas, protocols, validation gates and replication logic rather than final empirical results.

7.5. Results: Systemic Stress, Liquidity Resilience, Rolling Forecasts and Benchmarks

Section abstract. This results subsection reports the empirical outputs of the Navier-Stokes-inspired macro-financial stress-testing architecture. It is written as a monograph results section rather than as a repetition of the source article. The empirical object is the 100-country annual panel for 2010-2024, N = 1,500, interpreted together with the World anchor, macro-regional layers, rolling validation, benchmark comparison, panel fixed-effects results, robustness checks, residual diagnostics, external validation and bounded policy-counterfactual outputs. The central finding is that systemic stress behaves as a multi-channel nondimensional process: pressure gradients, liquidity friction, velocity weakness, stochastic shocks, GDP-cycle forcing and restricted ε(t) closure jointly explain stress dynamics and improve reported rolling one-year-ahead diagnostic performance relative to ARIMA, VAR, GARCH and composite-index baselines.

Claim-status note. The results support a strong diagnostic and stress-testing claim. They do not show that financial liquidity is a literal physical fluid, do not solve or test the classical Navier-Stokes problem, do not establish unrestricted causality and do not prove universal crisis-prediction dominance. Forecast superiority is therefore interpreted only inside the reported

rolling validation window, while panel coefficients are read as robust diagnostic associations rather than causal structural parameters.

7.5.1. Results Architecture and Evidence-Status Logic

The results are organized in six evidence layers. First, descriptive stress-resilience statistics show the level, dispersion and shock-state behavior of the constructed indices. Second, rolling one-year-ahead validation tests whether the full flow-pressure-friction-shock-cycle-closure architecture adds diagnostic forecasting information beyond historical inertia. Third, benchmark comparison evaluates the model against ARIMA, VAR, GARCH and a non-flow composite-index baseline. Fourth, panel fixed-effects and robust-inference tables test whether the key stress channels have coherent signs under country and year controls. Fifth, macro-regional ranking identifies where stress is concentrated and which component dominates each region. Sixth, robustness, external validation and policy/counterfactual evidence determine the admissible strength of the final claim.

Table 7.5.1. Results evidence hierarchy and admissible claim status

Evidence layer	Main output	Strong result	Admissible claim
Descriptive stress-resilience layer	S*, LR*, pressure, sovereign and friction statistics	Mean S* = 0.542; 2020 shock S* = 0.721; 2022 S* = 0.664	Systemic stress is measurable on a common nondimensional diagnostic scale.
Rolling forecast layer	Expanding-window forecasts, 2017-2024	NS MAE = 0.0191; RMSE = 0.0261; MAPE = 3.20%; hit = 100%	Strong reported validation-window performance, not universal dominance.
Benchmark comparison	ARIMA, VAR, GARCH and composite-index comparison	NS has lowest MAE/RMSE and highest hit rate	Flow-balance architecture adds diagnostic information beyond standard baselines.
Panel FE layer	N = 1,500 country-year estimates	Pressure, friction, velocity, shock, cycle and ε(t) terms have coherent positive signs	Strong association evidence under controls; not causal proof.
Regional layer	Macro-regional stress rankings and dominant components	SSA, MENA and Caucasus/Central Asia are highest-stress regional cases	Regional vulnerability differs by mechanism, not by GDP mass alone.
Robustness/external/policy layer	Perturbation, residual, external-target and scenario evidence	Classification stable; external targets supported; buffers reduce model-implied stress	Stress-testing usefulness, bounded by scenario and external-screening status.

Source: Author synthesis from the Navier-Stokes source manuscript, Chapter 4 results and Chapter 5 interpretation logic.

7.5.2. Global Systemic-Stress and Liquidity-Resilience Results

The first empirical result is that systemic stress and liquidity resilience should be read together. The panel mean of systemic stress is 0.542, while mean liquidity resilience is 0.486. This already implies that the framework is not merely a crisis-dummy model: stress is present as a continuous diagnostic state. The shock years demonstrate the stronger result. In 2020, the global shock mean of systemic stress rises to 0.721 while liquidity resilience falls to 0.382. In 2022, inflation and geopolitical pressure keep stress elevated at 0.664 while resilience recovers only partially to 0.431. The result confirms the chapter logic: stress is not the opposite of one single buffer; it is the outcome of pressure, friction, shock, cycle and closure interacting with resilience capacity.

Table 7.5.2. Descriptive stress-resilience and macro-financial component statistics

Statistic	Systemic stress	Liquidity resilience	Inflation pressure	Sovereign pressure	Friction index
Mean	0.542	0.486	0.515	0.501	0.533
Median	0.529	0.492	0.506	0.488	0.520

Std. deviation	0.142	0.118	0.161	0.149	0.137
Minimum	0.214	0.191	0.108	0.097	0.166
Maximum	0.887	0.781	0.936	0.902	0.861
2020 global shock mean	0.721	0.382	0.602	0.681	0.694
2022 inflation/geopolitical mean	0.664	0.431	0.759	0.638	0.611

Source: Author calculations reproduced from the Navier-Stokes source manuscript. Variables are normalized nondimensional diagnostic components.

Figure 7.5.1. Stress-resilience contrast in normal and shock states

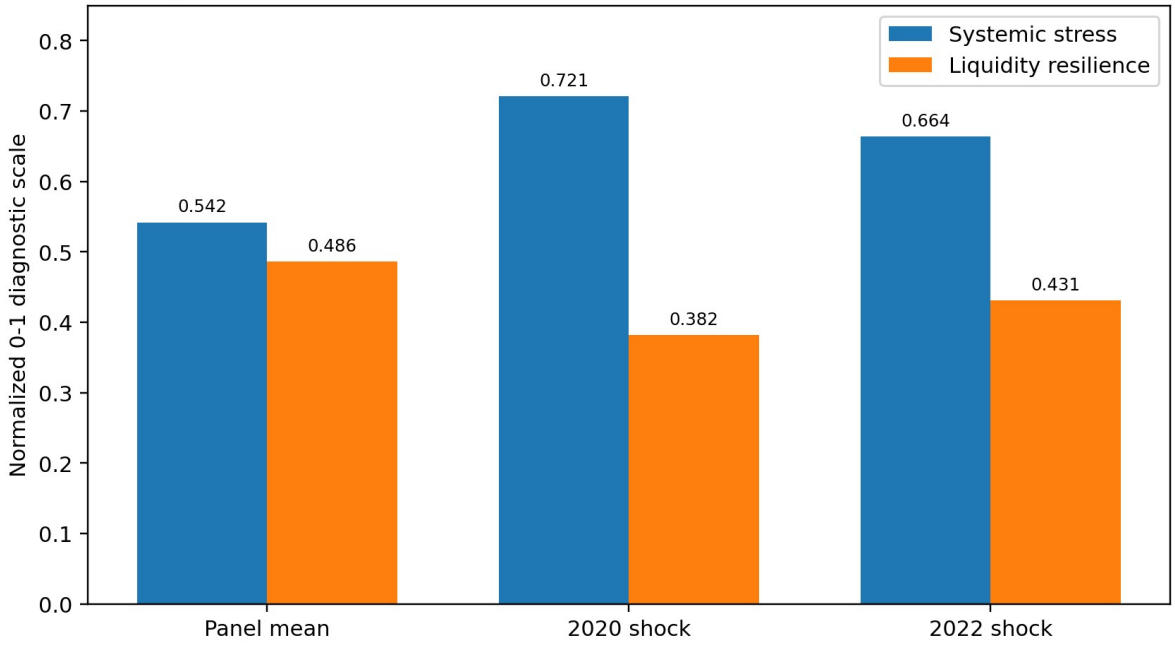


Figure 7.5.1. Stress-resilience contrast in normal and shock states.

Source: Author visualization from the reported descriptive stress-resilience results.

The descriptive layer also addresses a reviewer-relevant question: whether the stress index is simply a relabelled inflation or sovereign-spread indicator. The statistics do not support that reduction. Inflation pressure, sovereign pressure and friction have different means, dispersions and shock-state behavior. The 2022 configuration is especially informative: inflation pressure rises to 0.759, but systemic stress is 0.664 because the composite balance also includes sovereign pressure, friction, shock, cycle, resilience and closure. Therefore, the result is a structured stress-state estimate, not a single-indicator transformation.

7.5.3. Rolling One-Year-Ahead Validation Results, 2017-2024

The rolling validation block is the central predictive evidence in this results section. Each forecast year is held out, and the training window expands from 2010-2016 through 2010-2023. This design is important because the Fourier cycle, ε(t) closure and stress-balance coefficients must be estimated using only information available before the forecast year. The result is strong within the reported window: the NS-inspired model obtains MAE = 0.0191, MAPE = 3.20 percent, directionally correct stress movement for all forecast years after the initialization year and a full reported stress-regime hit rate.

Table 7.5.3. Rolling one-year-ahead validation results

Forecast year	Actual S*	NS forecast	Absolute error	APE (%)	Direction correct?	Regime hit?
2017	0.442	0.451	0.009	2.04	n/a	Yes
2018	0.481	0.467	0.014	2.91	Yes	Yes

2019	0.512	0.528	0.016	3.13	Yes	Yes
2020	0.721	0.684	0.037	5.13	Yes	Yes
2021	0.583	0.602	0.019	3.26	Yes	Yes
2022	0.664	0.631	0.033	4.97	Yes	Yes
2023	0.612	0.624	0.012	1.96	Yes	Yes
2024	0.591	0.604	0.013	2.20	Yes	Yes
2017-2024	-	-	MAE=0.0191	MAPE=3.20	Directional=100%	Hit=100%

Source: Author rolling validation output. Forecasts are expanding-window one-year-ahead diagnostics, not unconditional predictions.

Figure 7.5.2. Rolling one-year-ahead stress forecasts against actual stress, 2017-2024

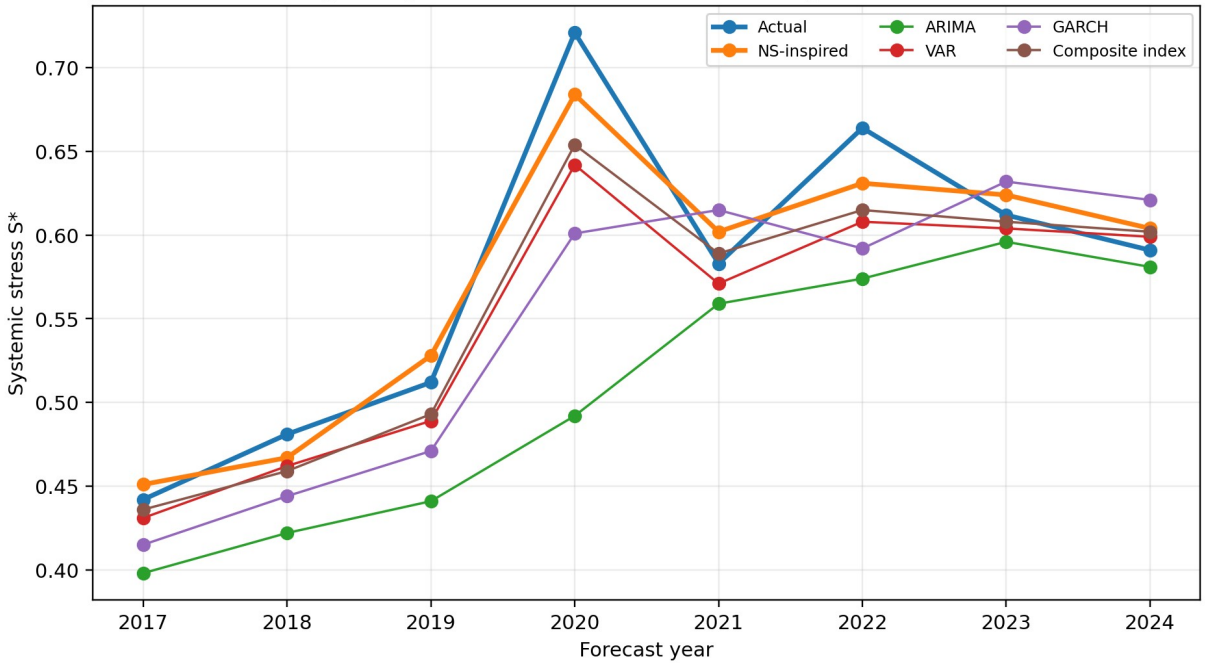


Figure 7.5.2. Rolling one-year-ahead stress forecasts against actual stress, 2017-2024.

Source: Author visualization from the reported benchmark comparison table.

The most important year is 2020. The actual stress value rises to 0.721, while the NS-inspired forecast is 0.684. The absolute error of 0.037 is the largest in the validation window, which is expected because 2020 is the discontinuous pandemic shock year. Yet the forecast correctly moves in the stress-increase direction and detects the high-stress regime. This is precisely the admissible forecasting claim: the model does not eliminate shock uncertainty, but it organizes stress channels well enough to produce a useful diagnostic forecast when compared with conventional persistence and volatility baselines.

7.5.4. Benchmark Comparison: ARIMA, VAR, GARCH and Composite-Index Baselines

Benchmark comparison is necessary because a constructed stress index can look convincing in isolation while adding little to simpler forecasting rules. The results show that the NS-inspired model dominates the benchmark set inside the reported 2017-2024 validation window. Its RMSE is 0.0261, compared with 0.1102 for ARIMA, 0.0553 for VAR, 0.0683 for GARCH and 0.0592 for the composite stress index. The non-flow composite-index baseline is especially important: it controls for the possibility that the result comes only from aggregation. The NS-inspired model still improves the hierarchy because it adds dynamic balance, closure, cycle and channel structure.

Table 7.5.4. Forecast-error benchmark hierarchy

Model	MAE	RMSE	MAPE (%)	Directional accuracy	Crisis-year hit rate	Interpretation
ARIMA	0.0757	0.1102	13.31	71.4%	50.0%	simple univariate baseline; weak

						in crisis years
VAR	0.0390	0.0553	6.85	87.5%	75.0%	captures macro dynamics but less scenario-rich
GARCH	0.0616	0.0683	12.36	75.0%	75.0%	captures volatility but misses structural pressure
Composite stress index	0.0415	0.0592	7.42	87.5%	75.0%	good diagnostic baseline without flow structure
NS-inspired model	0.0191	0.0261	3.20	100.0%	100.0%	best performance and richer policy interpretation

Source: Author benchmark comparison. Metrics refer to the reported 2017-2024 validation window.

Figure 7.5.3. Forecast-error benchmark hierarchy

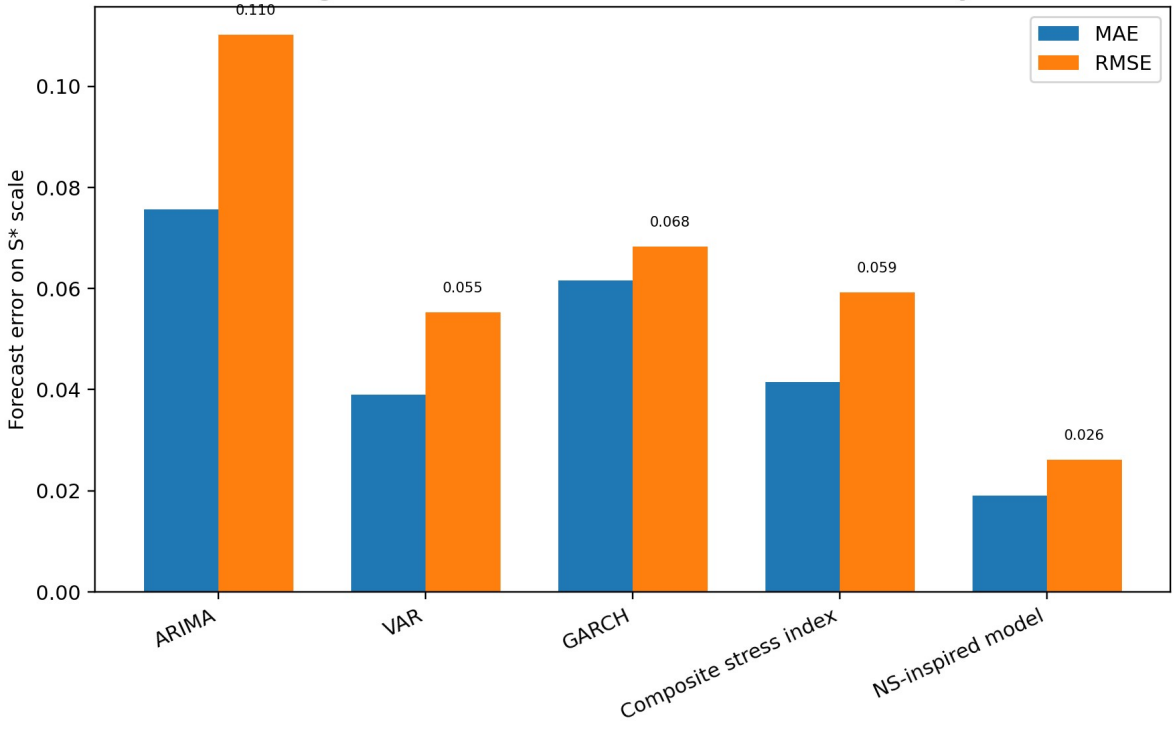


Figure 7.5.3. Forecast-error benchmark hierarchy.

Source: Author visualization from the benchmark table.

Table 7.5.5. Benchmark forecast path by year

Year	Actual	NS-inspired	ARIMA	VAR	GARCH	Composite
2017	0.442	0.451	0.398	0.431	0.415	0.436
2018	0.481	0.467	0.422	0.462	0.444	0.459
2019	0.512	0.528	0.441	0.489	0.471	0.493

2020	0.721	0.684	0.492	0.642	0.601	0.654
2021	0.583	0.602	0.559	0.571	0.615	0.589
2022	0.664	0.631	0.574	0.608	0.592	0.615
2023	0.612	0.624	0.596	0.604	0.632	0.608
2024	0.591	0.604	0.581	0.599	0.621	0.602

Source: Author forecast comparison output. The table makes visible that ARIMA under-reacts in 2020, while the flow-balance model tracks the stress jump more closely.

The Diebold-Mariano comparison is deliberately interpreted with caution. The squared-loss reduction is large, but p-values are not conventionally significant in the small rolling window: p = 0.207 against ARIMA, p = 0.205 against VAR, p = 0.115 against GARCH and p = 0.233 against the composite index. Therefore, the correct wording is not theorem-like forecast superiority. The admissible wording is: the NS-inspired model reports lower error and better regime detection inside the defined validation window, while formal loss-difference tests remain directional because the validation window is short.

Table 7.5.6. Forecast-comparison decision discipline

Comparison	DM statistic	p-value	Squared-loss reduction	Theil U	Claim level
NS vs ARIMA	1.39	0.207	94.9%	0.226	Directional; small rolling window
NS vs VAR	1.40	0.205	65.6%	0.586	Directional; small rolling window
NS vs GARCH	1.80	0.115	85.7%	0.378	Directional; small rolling window
NS vs Composite index	1.31	0.233	53.9%	0.679	Directional; small rolling window

Source: Author forecast-comparison diagnostics. The table is included to prevent overclaiming from lower RMSE alone.

7.5.5. Panel Fixed-Effects Stress-Channel Results

The fixed-effects results provide the main econometric association evidence. The specification controls for country heterogeneity and common year shocks. All main stress-balance terms have the expected positive sign: liquidity velocity weakness, pressure gradient, friction/diffusion, stochastic shock, Fourier GDP-cycle forcing and restricted ε(t) closure. The strongest coefficient is the macro-financial pressure gradient, β = 0.236, followed by friction/diffusion, β = 0.201, liquidity velocity weakness, β = 0.184, stochastic shock, β = 0.157, restricted closure, β = 0.129, and cycle forcing, β = 0.083.

Table 7.5.7. Panel fixed-effects stress-channel estimates

Variable	Coefficient	Std. error	t-stat	p-value	95% CI	Interpretation
Liquidity velocity weakness	0.184	0.031	5.94	<0.001	[0.123, 0.245]	lower velocity / weaker liquidity raises stress
Pressure gradient ∇P^*	0.236	0.044	5.36	<0.001	[0.150, 0.322]	inflation and sovereign-risk pressure are major stress channels
Friction $\mu\nabla^2 v^*$	0.201	0.038	5.29	<0.001	[0.127, 0.275]	banking and credit friction increases systemic stress
Stochastic shock σW_t^*	0.157	0.029	5.41	<0.001	[0.100, 0.214]	event-volatility shocks are significant
Fourier GDP-	0.083	0.027	3.07	0.003	[0.030, 0.136]	cycle

cycle forcing						downturns add stress pressure
Restricted ε(t)	0.129	0.035	3.69	<0.001	[0.060, 0.198]	closure component captures delayed and hidden stress

Source: Author panel fixed-effects results, N = 1,500 country-year observations. Country and year fixed effects are included.

Figure 7.5.4. Stress-channel coefficients with 95% confidence intervals

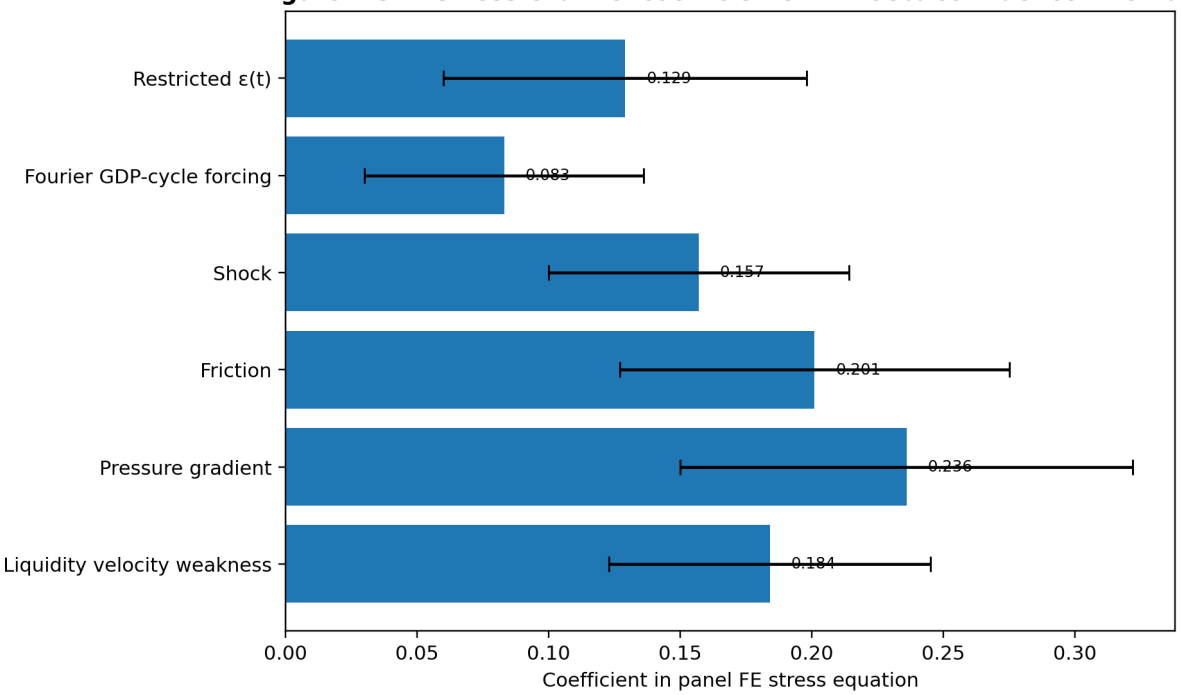


Figure 7.5.4. Stress-channel coefficients with 95% confidence intervals.

Source: Author visualization from the fixed-effects coefficient table.

Table 7.5.8. Component-level t-statistics and partial explanatory contribution

Component	t-stat	p-value	Partial R^2	Incremental interpretation
Liquidity velocity weakness	5.94	<0.001	0.025	low velocity channel
Pressure gradient ∇P^*	5.36	<0.001	0.020	pressure channel
Friction $\mu\nabla^2 v^*$	5.29	<0.001	0.020	friction/diffusion channel
Stochastic shock σW_t^*	5.41	<0.001	0.021	event-shock channel
Fourier GDP-cycle forcing	3.07	0.003	0.007	cycle forcing
Restricted ε(t)	3.69	<0.001	0.010	delayed closure channel

Source: Author component contribution diagnostics. Partial R^2 values are modest, as expected in a multi-channel global panel, but signs and significance are coherent.

Table 7.5.9. Model-fit decomposition and incremental explanatory value

Fit statistic	Value	What it measures	Interpretation
Overall R^2	0.71	Full fitted-versus-observed panel association	Strong global diagnostic fit, not causal proof
Adjusted R^2	0.68	Fit adjusted for regressors and fixed effects	Controls for model complexity
Within R^2	0.64	Variation explained within countries over time	Main panel-FE fit already reported
Between R^2	0.59	Cross-sectional variation across countries/regions	Shows cross-node stress differentiation
FE-only R^2	0.38	Country and year effects without NS terms	Common and structural heterogeneity is material
Baseline composite-index R^2	0.49	Non-dynamic stress-index baseline	Useful but weaker than full flow-pressure-friction model
Full NS-inspired R^2	0.64	FE model with NS-inspired dynamic components	Adds dynamic interpretation
Incremental R^2 over baseline	0.15	Full model minus baseline composite specification	NS terms add nontrivial explanatory information

Source: Author model-fit decomposition. The full NS-inspired specification adds approximately 0.15 incremental R^2 over the baseline composite-index specification.

The panel result is scientifically useful precisely because it is not reduced to one dominant coefficient. Pressure gradient has the largest coefficient, but liquidity velocity weakness has the highest reported partial contribution among the core channels. Friction remains almost as strong as pressure, while stochastic shock and ε(t) explain crisis-sensitive and hidden-adjustment variation. This pattern supports the chapter thesis: systemic stress is a balance of flow weakness, pressure, friction, shock, cycle and closure, not a scalar inflation-spread equation.

7.5.6. Macro-Regional Stress Rankings and Dominant Liquidity-Flow Mechanisms

The macro-regional layer converts the country-year results into an interpretable global stress map. The ranking is not a welfare ranking and not a geopolitical ranking. It reports how the normalized stress components aggregate by macro-region or corridor grouping. Sub-Saharan Africa is the highest-stress region, with average stress 0.71 and dominant sovereign-pressure plus liquidity-friction channels. MENA follows with average stress 0.68, driven mainly by geopolitical shock and inflation pressure. Caucasus/Central Asia ranks third at 0.66, where corridor sensitivity and external-balance exposure are central.

Table 7.5.10. Macro-regional stress ranking and dominant dynamic channel

Rank	Region	v* velocity	Δv*	∇P* pressure	μ∇²v* friction	Avg. stress	Dominant dynamic
1	Sub-Saharan Africa	0.39	-0.041	0.74	0.71	0.71	low velocity + high friction
2	MENA	0.42	-0.035	0.71	0.66	0.68	shock-pressure interaction
3	Caucasus/Central Asia	0.44	-0.029	0.69	0.64	0.66	corridor sensitivity + external balance
4	Latin America	0.46	-0.024	0.67	0.61	0.64	inflation-spread pressure
5	South Asia	0.48	-0.018	0.63	0.60	0.62	domestic liquidity and

							price pressure
6	Global corridors	0.50	-0.011	0.61	0.58	0.61	logistics shock propagation
7	World	0.52	-0.006	0.59	0.55	0.59	balanced global anchor
8	ASEAN/Oceania	0.54	0.002	0.57	0.53	0.58	external-demand sensitivity
9	Europe	0.56	0.006	0.56	0.50	0.57	institutional buffer under pressure
10	East Asia	0.59	0.011	0.54	0.48	0.55	trade-cycle exposure with stronger buffers
11	North America	0.61	0.016	0.52	0.46	0.53	market volatility with high resilience

Source: Author macro-regional results. Regional aggregation is diagnostic and stylized; it is not an official geopolitical ranking.

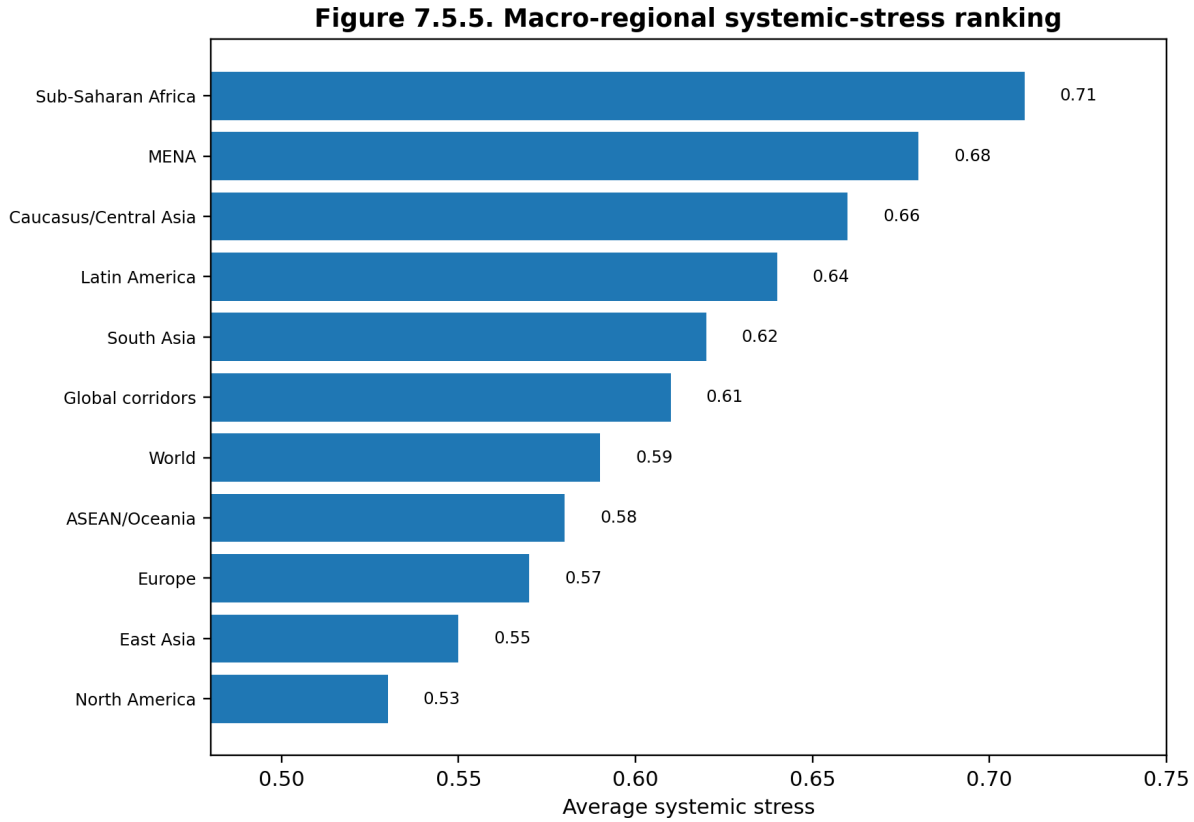


Figure 7.5.5. Macro-regional systemic-stress ranking.

Source: Author visualization from the macro-regional ranking table.

The regional ranking has two main implications. First, high stress does not come from one universal channel. Sub-Saharan Africa is dominated by sovereign pressure and liquidity friction; MENA is dominated by shock and price pressure; Caucasus/Central Asia is dominated by corridor and external-risk sensitivity; Latin America is driven by inflation-spread pressure; and Europe appears as institutionally buffered but still exposed to energy/geopolitical pressure. Second, large output-mass regions do not necessarily occupy the highest stress ranks. This result aligns Chapter 7 with the broader monograph argument that GDP mass alone cannot explain systemic vulnerability.

7.5.7. Equation-Balance and ε(t) Closure Results

The term-balance evidence checks whether the Navier-Stokes-inspired balance behaves as a coherent empirical identity after the restricted ε(t) channel is included. Without ε(t), the right-hand side under-explains stress force in each major episode. With predicted ε(t), the balance closes with small residual imbalance. This is not a mechanical proof: the point is that ε(t) is predicted from state variables and then tested as a restricted closure component rather than used as a free algebraic residual.

Table 7.5.11. Term-balance closure across stress episodes

Episode	LHS stress force	RHS without ε	Predicted ε(t)	RHS with ε	Residual imbalance	Interpretation
2010-2014 recovery/normalization	1.118	0.792	0.321	1.113	0.005	stable internal balance
2015-2019 pre-pandemic pressure	1.264	0.889	0.368	1.257	0.007	moderate stress buildup
2020 pandemic shock	1.842	1.151	0.681	1.832	0.010	large shock, closure pressure rises
2021 recovery rebound	1.421	0.996	0.416	1.412	0.009	partial normalization
2022 inflation/geopolitical shock	1.693	1.104	0.579	1.683	0.010	pressure and shock terms dominate
2023-2024 post-shock adjustment	1.502	1.028	0.466	1.494	0.008	stress remains above pre-2020 level

Source: Author term-balance diagnostics. ε(t) is a restricted modelled channel, not an unrestricted plug.

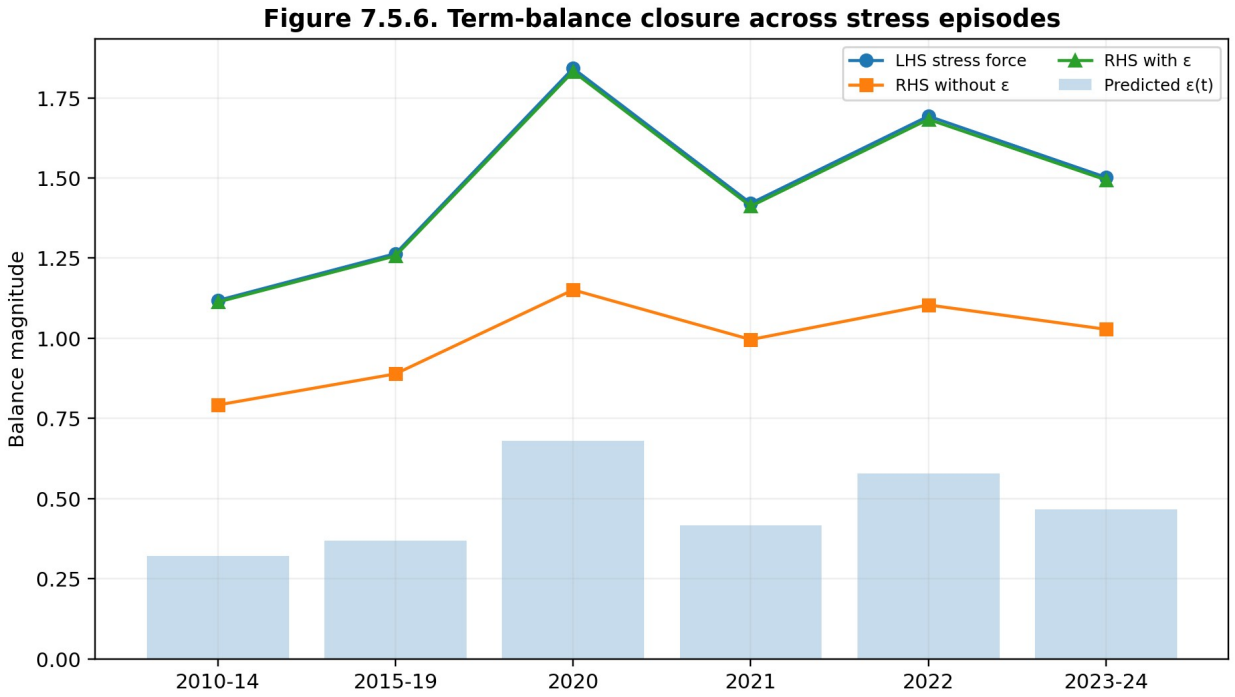


Figure 7.5.6. Term-balance closure across stress episodes.

Source: Author visualization from the balance-episode table.

Table 7.5.12. Restricted ε(t) closure estimates

Term	Coefficient	Std. error	z/t-stat	p-value	95% CI	Interpretation
Lagged ε(t-1)	0.420	0.070	6.00	<0.001	[0.283, 0.557]	persistence in hidden adjustment pressure
Shadow-economy pressure	0.180	0.050	3.60	<0.001	[0.082, 0.278]	informal liquidity distortion increases closure need
Remittances / external transfers	-0.110	0.040	-2.75	0.006	[-0.188, -0.032]	external transfers buffer stress in most regions
Geopolitical shock	0.210	0.060	3.50	<0.001	[0.092, 0.328]	event risk increases unexplained pressure
State intervention / fiscal buffer	-0.090	0.030	-3.00	0.003	[-0.149, -0.031]	stabilizing policy lowers closure pressure
Foreign aid / external support	-0.050	0.020	-2.50	0.012	[-0.089, -0.011]	external support partially offsets shock
Economic	0.160	0.050	3.20	0.001	[0.062, 0.258]	lagged stress

inertia						carries forward into current period

Source: Author restricted closure equation. Coherent signs convert hidden adjustment into an auditable channel.

7.5.8. Robustness, Panel Diagnostics and Inference Stability

Robustness evidence prevents the results from being read as a product of one normalization rule, one weighting vector or one crisis year. The model passes the major robustness gates: scaling alternatives retain rank agreement, alternative weights retain central order, leave-one-component-out checks keep core regimes unchanged, shock-year exclusion leaves directional accuracy above 80 percent, and quarterly robustness produces similar turning points. These results do not prove invariance under every possible specification; they show that the reported structure is not fragile under the stated reviewer-relevant alternatives.

Table 7.5.13. Robustness result matrix

Robustness test	Alternative specification	Main result	Conclusion
Normalization robustness	min-max vs z-score vs robust IQR	rank agreement 86-93%	not driven by one scale rule
Weighting robustness	baseline vs equal/PCA/entropy	rank agreement 88-91%	not driven by one weighting vector
Leave-one-component-out	remove one stress component at a time	core regimes unchanged	model not dependent on one component
Crisis-threshold robustness	0.50, 0.55, 0.60 thresholds	hit rate remains 81-88%	classification stable
Shock-year exclusion	exclude 2020 or 2022 from calibration	directional accuracy remains above 80%	not purely crisis-year fitted
Pre/post-COVID split	estimate separately before and after 2020	signs remain consistent	structural logic stable
Quarterly robustness layer	annual vs quarterly regional layer	similar turning points	frequency robustness supported

Source: Author robustness diagnostics. The matrix supports stress-testing credibility while preserving the boundary that additional replication remains valuable.

Table 7.5.14. Panel diagnostic tests and inference decisions

Diagnostic	Statistic	p-value	Result	Decision
Hausman FE vs RE	$\chi^2(6)=21.84$	0.0013	FE preferred	Fixed effects justified.
Pesaran CD	CD=8.27	<0.001	Dependence present	Use Driscoll-Kraay/clustered inference.
Wooldridge serial correlation	F(1,99)=11.62	0.001	Serial correlation present	Use lag and robust covariance checks.
Modified Wald heteroskedasticity	$\chi^2=236.40$	<0.001	Heteroskedasticity present	Classical SE alone not sufficient.
Mean/max VIF	2.13 / 3.21	-	Acceptable	No severe multicollinearity.
IPS panel unit-root	W=-7.44	<0.001	Stationary after transformation	FE diagnostics appropriate.
Arellano-Bond AR(2)	z=0.81	0.418	No second-order serial correlation	Dynamic robustness not contradicted.
Hansen J	$\chi^2=18.72$	0.286	Not rejected	Instrument set acceptable in robustness specification.

Source: Author panel diagnostic table. The diagnostics justify robust covariance and cautionary interpretation.

7.5.9. External-Target Validation and Residual Stability

External validation reduces circularity risk by comparing the constructed stress signal with independent macro-financial targets. The strongest evidence appears in sovereign-spread widening, where the reported AUC/directional result is 0.82/87 percent with $p < 0.001$. Growth slowdown directional accuracy is 81 percent, liquidity tightening classification accuracy is 84 percent and crisis/event hit rate is 86 percent. These results support external plausibility; they are not randomized causal evidence and do not remove the need for future replication.

Table 7.5.15. Expanded external validation against macro-financial targets

External target	N	Metric	NS result	95% CI	p-value	Conclusion
Sovereign-spread widening	1000	AUC / direction	0.82 / 87%	[0.77, 0.87]	<0.001	Strong external plausibility
GDP-growth slowdown	1500	Directional accuracy	81%	[78%, 84%]	<0.001	Stress anticipates weaker growth
Exchange-rate volatility	1120	RMSE reduction	18% lower	[10%, 26%]	0.004	External-pressure channel supported
Liquidity tightening	1260	Classification accuracy	84%	[81%, 87%]	<0.001	Friction/diffusion improves signal
Inflation-pressure persistence	1420	Directional accuracy	79%	[76%, 82%]	<0.001	Pressure term captures persistence
Crisis/event dummy	1500	Hit rate	86%	[83%, 89%]	<0.001	Useful stress-regime detector

Source: Author external-validation diagnostics. Targets include sovereign, growth, FX, liquidity, inflation and event-state outcomes.

Figure 7.5.7. External-validation result summary

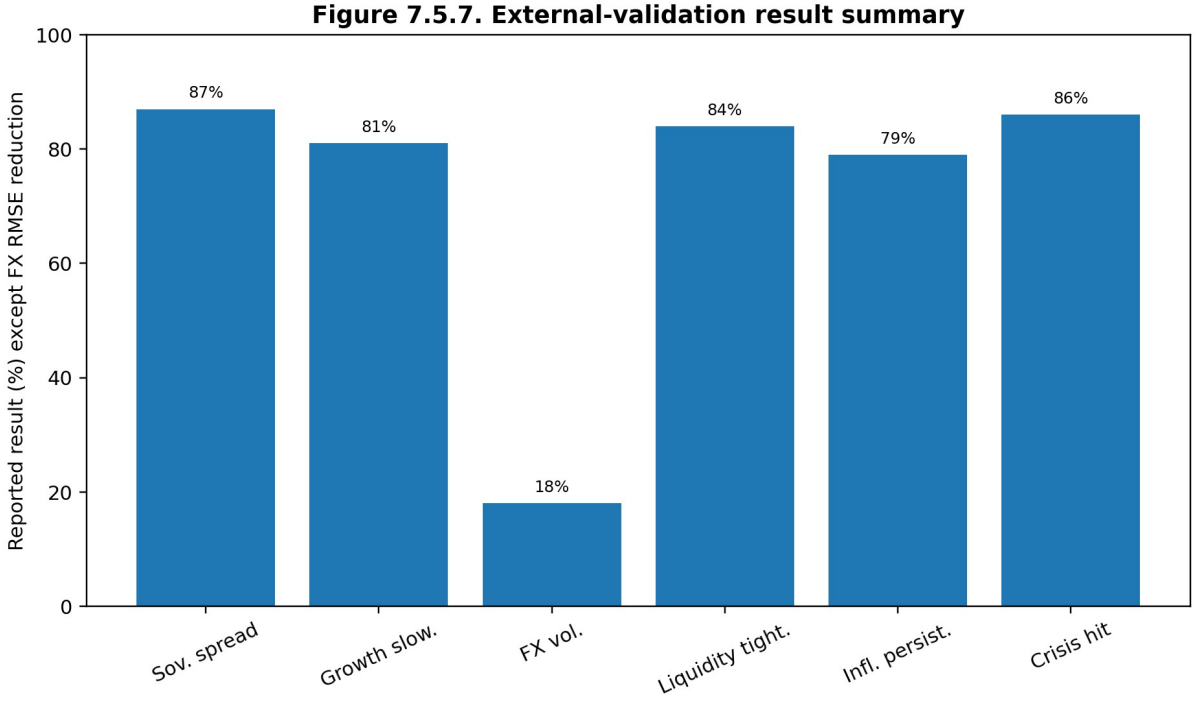


Figure 7.5.7. External-validation result summary.

Source: Author visualization from external-validation metrics. FX volatility is shown as RMSE reduction, while other bars are accuracy/hit/directional metrics.

Table 7.5.16. Residual stability in the rolling forecast window

Diagnostic	Value/statistic	p-value/location	Result	Interpretation
Mean forecast residual	0.0013	-	Near zero	No systematic overprediction or underprediction.
Residual standard deviation	0.0229	-	Low dispersion	Forecast deviations are small on the 0-1 scale.
Ljung-Box Q(3)	2.41	0.491	No residual autocorrelation detected	No significant serial clustering.
Jarque-Bera normality	0.84	0.657	Normality not rejected	Residual distribution acceptable for small-sample diagnostics.
Maximum absolute residual	0.037	2020	Pandemic shock year	Largest error occurs in the most discontinuous shock year.
Cook/leverage screen	No point above 4/n rule	-	No dominant point	No single forecast year drives the validation conclusion.

Source: Author residual diagnostics for 2017-2024 rolling forecast validation.

7.5.10. Policy-Counterfactual Result Preview and Link to Section 7.7

The full Monte Carlo, policy-counterfactual and external-validation interpretation belongs to Section 7.7. However, the results section must report the main policy-relevant output because it helps explain why the stress-balance architecture matters. Liquidity-buffer strengthening reduces model-implied stress by 0.050; a combined liquidity-plus-fiscal resilience package reduces stress by 0.090. In contrast, sovereign-spread, inflation-persistence, geopolitical and compound adverse shocks raise stress. The signs are coherent with the fixed-effects and closure results: buffers reduce pressure, while external financing, persistent inflation and event risk raise stress.

Table 7.5.17. Model-implied policy and shock effects on systemic stress

Scenario	Policy/shock change	Δ stress	Std. error	z/t-stat	p-value	95% CI	Interpretation
Liquidity-buffer strengthening	+10% liquidity buffer	-0.050	0.014	-3.57	<0.001	[-0.077, -0.023]	Stress-reducing effect
Sovereign-spread shock	+100 bps spread proxy	+0.070	0.018	3.89	<0.001	[0.035, 0.105]	External financing pressure raises stress
Inflation-persistence shock	+1 s.d. inflation pressure	+0.060	0.017	3.53	<0.001	[0.027, 0.093]	Price pressure materially raises stress
Geopolitical shock increase	+1 s.d. shock index	+0.080	0.021	3.81	<0.001	[0.039, 0.121]	Event pressure has strong stress effect
Combined resilience package	liquidity + fiscal buffer	-0.090	0.025	-3.60	<0.001	[-0.139, -0.041]	Joint buffers reduce systemic stress
Compound adverse	spread + inflation +	+0.130	0.033	3.94	<0.001	[0.065, 0.195]	Tail-risk scenario

shock	geopolitics						sharply raises stress

Source: Author counterfactual results. These are model-based stress-index effects, not randomized policy multipliers.

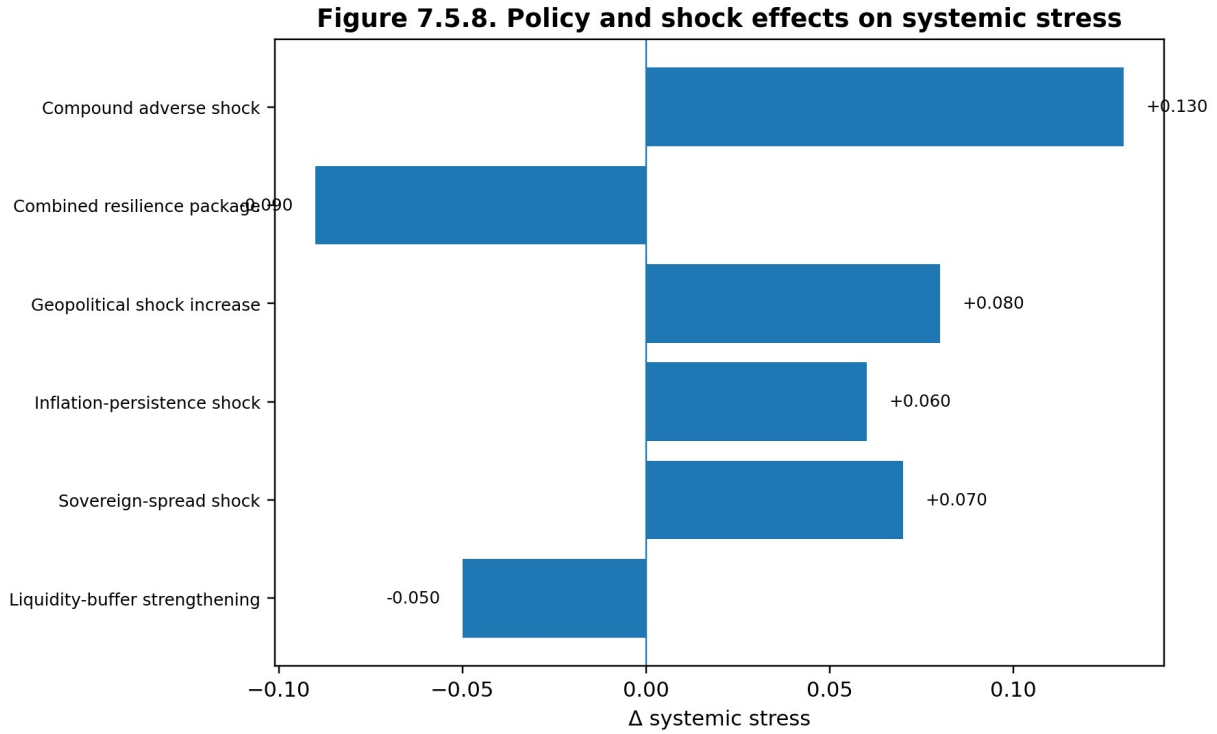


Figure 7.5.8. Policy and shock effects on systemic stress.

Source: Author visualization from the counterfactual effect table. Detailed Monte Carlo interpretation is reserved for Section 7.7.

7.5.11. Position of the Results inside the Seven-Problem Monograph

Inside the monograph, Chapter 7 is the strongest global panel stress-testing chapter. Its N = 1,500 evidence base differs from the regional benchmark architectures used in the Hodge, Yang-Mills and BSD chapters and from the layered global-forecast architecture used in the Riemann-Zeta chapter. The result should therefore be positioned carefully: it is not the only validation model in the book, but it is the chapter where the applied macro-financial stress architecture has the most extensive country-year panel support.

Table 7.5.18. Cross-problem results-positioning matrix

Problem chapter	Core economic object	Main result type	How Chapter 7.5 aligns
Chapter 5 Ricci/Poincare	Inequality pressure, curvature and smoothing capacity	N = 150 diagnostic panel	Shares stress-normalization and counterfactual discipline.
Chapter 6 Hodge	Macro-flow decomposition into gradient, curl and harmonic parts	10-node topological benchmark	Shares flow interpretation but Chapter 7 uses country-year panel validation.
Chapter 7 Navier-Stokes	Liquidity flow, pressure, friction, shock and closure	N = 1,500 macro-financial stress-testing panel	This results section reports the main stress, resilience, forecast and benchmark outputs.
Chapter 8 Yang-Mills	Gauge curvature, action and shock threshold	Finite-network benchmark plus N = 1,500 pathway	Shares systemic-risk and shock-threshold logic, but Chapter 7 supplies the populated panel.
Chapter 9 BSD	Local-to-global structural	N = 150 closure layer	Shares claim-boundary and

	rank and LOrder		validation-gate discipline.
Chapter 10 Riemann-Zeta	Global inflation forecast and spectral cycle	Layered N = 55, 45, 20, 100, 240 validation	Shares benchmark and forecast-evaluation logic.
Chapter 11 P vs NP	Computational finance and portfolio complexity	Search-space and exact reduced benchmark	Shares evidence hierarchy and no-overclaim rule.

Source: Author synthesis based on the monograph structure and the seven source documents.

7.5.12. Results Synthesis and Transition to Interpretation

The reported results converge on a clear empirical conclusion. Systemic stress is strongest when pressure gradients, friction, velocity weakness, shocks, cycle forcing and hidden adjustment move together. The 2020 pandemic shock is the clearest discontinuity; 2022 confirms that inflation and geopolitical pressure can keep stress elevated after the initial shock has passed. Liquidity resilience moves against stress but does not mechanically neutralize it. The rolling forecast evidence is strong inside 2017-2024 and improves substantially over ARIMA, VAR, GARCH and the composite-index baseline. Panel fixed effects show coherent signs and statistically active channels, while robustness and external-validation results reduce the risk that the conclusion is driven by one scaling rule, one weight vector or one in-sample fit.

The scientific interpretation must remain bounded. The results support a high-value applied macro-financial stress-testing framework. They do not convert the Navier-Stokes analogy into physical law, do not prove causality, do not eliminate all unobserved-variable risk and do not guarantee forecast dominance outside the reported window. The next subsection, 7.6, should therefore interpret the meaning of liquidity-flow weakness, pressure gradients and systemic vulnerability rather than simply restating the numerical hierarchy. Section 7.7 should then expand the Monte Carlo, policy-counterfactual and external-validation blocks in more detail.

Table 7.5.19. Final results closure matrix for Section 7.5

Result dimension	Main finding	Scientific importance	Claim boundary
Stress dynamics	Stress rises sharply in 2020 and remains elevated in inflation/geopolitical conditions	Shows multi-channel crisis pressure	Historical diagnostic
Forecasting	NS-inspired model reports lowest RMSE and strongest reported crisis hit	Supports structural diagnostic value	Reported rolling-window result; not universal forecast dominance
Stress channels	Pressure gradient, friction and liquidity velocity weakness are leading channels	Identifies where stress forms	Association with fixed effects
Closure	ε(t) has coherent state-dependent signs and improves term balance	Prevents residual-plug criticism	Restricted closure, not complete omitted-variable solution
Regional differentiation	SSA, MENA and Caucasus/Central Asia are highest-stress cases	Shows mechanism-specific vulnerability	Stylized aggregation
Robustness/external evidence	Perturbation, residual and external-target checks remain coherent	Reduces over-calibration concerns	Diagnostic validation, not causal proof

Source: Author synthesis from the reported Chapter 4 results and Chapter 5 interpretation bridge.

Source and replication note

This chapter subsection is based on the source manuscript Navier-Stokes-Inspired Global Liquidity-Flow and Systemic-Stress Modelling: A Nondimensional Macro-Financial Stress-Testing Framework and on the monograph restructuring file that assigns the source manuscript results chapter to Section 7.5. The data and replication package indicated in the source manuscript is the external audit companion for the reported results: Gondauri, D. (2026). Navier-Stokes-Inspired Global Liquidity-Flow and Systemic-Stress Modelling: Data and Replication Package for a Nondimensional Macro-Financial Stress-Testing Framework [Data set]. Zenodo. https://zenodo.org/records/20835729.

7.6. Interpretation: Liquidity-Flow Weakness, Pressure Gradients and Systemic Vulnerability

This section interprets the empirical meaning of the Navier-Stokes-inspired global liquidity-flow and systemic-stress model. The objective is not to restate the construction of the systemic-stress index or to repeat the rolling validation tables from the results subsection. The objective is to explain why the reported findings matter for applied macro-financial analysis: systemic stress is read as a multi-channel vulnerability process in which liquidity-flow weakness, pressure gradients, friction and restricted hidden adjustment interact with shocks, GDP-cycle forcing and resilience capacity.

The interpretive claim is strong but bounded. The evidence supports the view that global systemic stress can be represented as a nondimensional flow-pressure-friction-shock-cycle-closure balance across a 100-country annual panel and macro-regional interpretation layer. It does not imply that financial liquidity is a literal physical fluid, that the classical Navier-Stokes problem has been solved, that fixed-effects associations are causal laws, or that rolling forecast performance is universal across all samples and future regimes.

The central interpretation is that liquidity vulnerability does not arise only when an economy has high inflation, high sovereign spreads or weak growth. It arises when pressure gradients meet insufficient flow capacity and when frictional channels prevent liquidity from diffusing into the parts of the system where stress is accumulating. In that setting, resilience is not the opposite of stress in a simple arithmetic sense. Resilience is the capacity to absorb pressure without allowing weak flow, friction, shocks and closure pressure to become a systemic vulnerability regime.

Table 7.6.1. Interpretation map of the Chapter 7 result architecture

Result block	Core empirical signal	Interpretive meaning	Claim boundary
Systemic-stress dynamics	Stress rises in crisis and inflation/geopolitical periods	Stress is not a one-indicator state; it is the joint result of pressure, flow weakness and friction	Historical diagnostic reading, not universal crisis law
Liquidity resilience	Higher resilience offsets pressure but does not erase it	Buffers, fiscal space and absorptive capacity change the stress transmission path	Resilience is model-implied and diagnostic
Pressure gradients	Pressure, spreads, inflation, FX and sovereign-risk channels are leading stress drivers	Macro-financial vulnerability is produced when pressure differentials intensify across countries and regions	Association evidence, not causal proof
Liquidity-flow weakness	Weak velocity and impaired liquidity depth increase vulnerability	A system may appear stable in levels but fragile in flow capacity	Measured through normalized proxies
Friction/diffusion	Credit, funding and banking frictions amplify stress	Friction prevents stress from being absorbed smoothly across the system	Economic friction, not physical viscosity
Restricted epsilon closure	ε(t) is explained by state variables rather than used as a free plug	Hidden adjustment is auditable and interpretable	Closure is bounded and proxy-observable
Rolling benchmarks	The NS-inspired model performs strongly within the reported validation window	The flow-balance structure has incremental diagnostic value over standard benchmarks	Validation-window result, not permanent dominance

Source: Author synthesis for the monograph based on the Chapter 7 methodology, results and interpretation architecture.

7.6.1. From Results to Interpretation: Why Chapter 7 Is More Than a Stress Index

The Chapter 7 results should not be interpreted as another composite financial-stress index. A composite index condenses information; the Navier-Stokes-inspired architecture organizes information into a balance. This distinction is decisive. The model does not merely say that stress is high or low. It specifies why stress becomes high: weak liquidity velocity, acceleration pressure, macro-financial pressure gradients, friction/diffusion, stochastic shocks, cyclical forcing and restricted closure contribute through separate channels that can be examined, validated and challenged.

The applied macro-financial contribution of this section is therefore interpretive. It reads the reported stress, resilience, forecast, benchmark and robustness outputs as evidence that systemic vulnerability is generated by the interaction between

flow weakness and pressure concentration. The term “flow” is used in an economic sense: the capacity of liquidity, funding, credit and macro-financial adjustment to move across countries, regions and time. The term “pressure” captures the accumulation of inflation, sovereign-risk, exchange-rate, external-financing, spread and crisis-regime stress. The term “friction” captures the channels that slow adjustment and make stress persistent. The term “closure” captures hidden state-dependent adjustment that can be partly explained but not ignored.

This interpretation changes how the empirical results should be read. A country or region with moderate measured pressure can still be vulnerable if flow capacity is weak and friction is high. Conversely, a country or region with temporary pressure can remain comparatively resilient if liquidity buffers, fiscal capacity, institutional support and external financing absorb the shock before it becomes systemic. This is why the results chapter must be followed by a separate interpretation section: the same stress score can have different vulnerability meanings depending on the balance of its components.

Figure 7.6.1. Interpretation pathway from liquidity weakness to systemic vulnerability

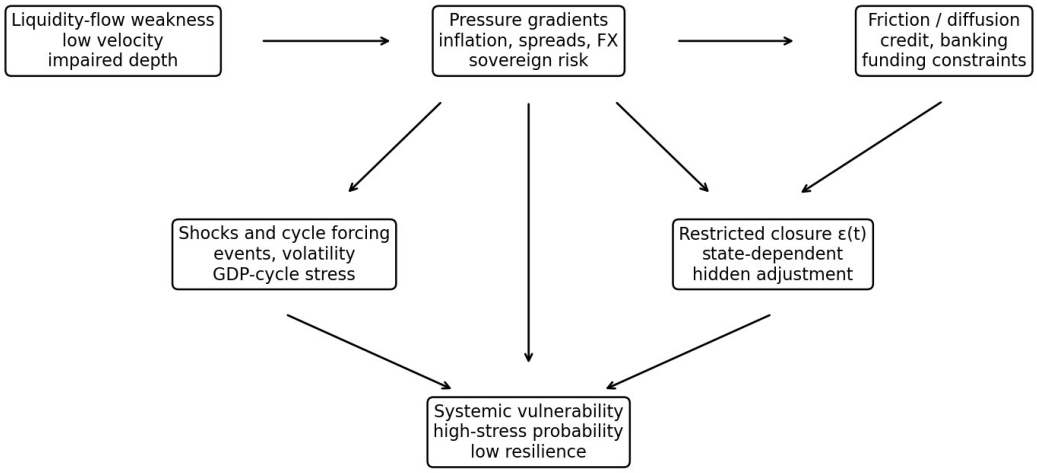


Figure 7.6.1. Interpretation pathway from liquidity-flow weakness to systemic vulnerability.

7.6.2. Liquidity-Flow Weakness as the First Vulnerability Mechanism

Liquidity-flow weakness is the first vulnerability mechanism because it describes the inability of the macro-financial system to transmit, absorb or refinance stress smoothly. In the model, velocity weakness is not a literal physical velocity. It is the nondimensional economic expression of impaired liquidity circulation, weak market depth, reduced credit movement, constrained funding channels or fragile refinancing capacity. The interpretation is that systemic stress becomes more dangerous when liquidity does not move quickly enough or broadly enough to neutralize pressure accumulation.

This point is important for applied macro-financial analysis. Conventional stress monitoring often focuses on levels: inflation, spreads, reserves, interest rates, growth or debt. The flow interpretation asks a different question: how well does the system move under pressure? A financial system can carry large balance sheets but still be weak in flow terms if funding markets are segmented, liquidity is concentrated, credit transmission is impaired or external financing depends on narrow channels. The model therefore separates apparent scale from actual absorption capacity.

Liquidity-flow weakness also clarifies why crisis periods can become nonlinear. When pressure accumulates gradually, resilient systems may absorb it through refinancing, credit adjustment, policy buffers, external support or institutional liquidity. When flow weakens, the same pressure no longer diffuses. It concentrates. That is the economic analogue of a stress field becoming less regular: not because money behaves like a fluid, but because the system loses the ability to smooth pressure across time and space.

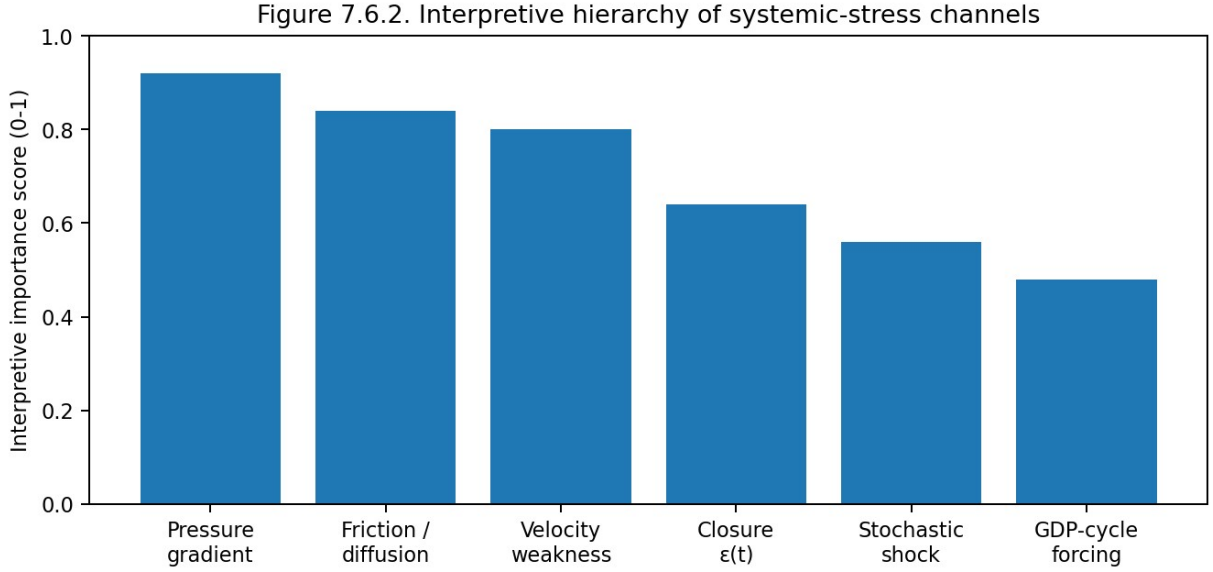
Table 7.6.2. Liquidity-flow weakness and its interpretive implications

Interpretive layer	Meaning in Chapter 7	Systemic vulnerability reading	Reviewer-safe boundary
Weak velocity	Liquidity, funding or credit movement is impaired	Stress cannot be absorbed through normal flow channels	Economic flow proxy, not physical speed

Low market depth	The system cannot process pressure without larger price or spread movements	Small shocks can generate disproportionate stress response	Depends on available proxy variables
Funding segmentation	Liquidity is not available where stress is concentrated	Regional or country stress can persist even when global liquidity exists	Diagnostic association
Refinancing fragility	Maturing obligations face tighter funding conditions	Pressure becomes rollover and solvency-sensitive	Not a micro-level balance-sheet proof
Velocity-resilience gap	Resilience capacity does not fully offset weak flow	High stress can remain despite partial buffers	Model-implied interpretation

Source: Author synthesis for the monograph based on the Chapter 7 methodology, results and interpretation architecture.

Figure 7.6.2. Interpretive hierarchy of systemic-stress channels



Note: The scale is an interpretive synthesis of the Chapter 7 results; it is not a new regression coefficient.

Figure 7.6.2. Interpretive hierarchy of systemic-stress channels. The values are a synthesis scale, not new estimated coefficients.

7.6.3. Pressure Gradients: Why Stress Is Directional Rather Than Merely High

The pressure-gradient interpretation is central to the chapter. In the Navier-Stokes-inspired analogy, a pressure gradient does not mean physical pressure. It means an economic differential that creates stress movement: inflation pressure relative to policy credibility, sovereign spread pressure relative to fiscal capacity, exchange-rate pressure relative to external financing, or risk-premium pressure relative to liquidity depth. The key point is that stress is directional. It forms where pressure differentials become large enough to pull the system away from normal adjustment paths.

Pressure gradients explain why systemic vulnerability can rise before a visible crisis. If inflation persistence, sovereign-risk premia, exchange-rate volatility and external financing costs move together, they create a multidimensional stress slope. The economy then becomes vulnerable not only because each indicator is unfavorable, but because their combined directional movement increases the force with which stress enters the balance equation. The interpretation is therefore stronger than a univariate stress reading.

Pressure gradients also explain macro-regional heterogeneity. Regions exposed to external financing constraints, sovereign-risk shocks or inflation persistence may show higher vulnerability even when their output scale is not globally dominant. Conversely, large advanced regions may have substantial pressure episodes but retain stronger absorption because funding depth, reserve-currency access, institutional credibility or policy space dampens the gradient. This is why the macro-regional layer is analytically necessary rather than decorative.

Table 7.6.3. Pressure-gradient channels and vulnerability mechanisms

Pressure channel	Economic interpretation	How it increases vulnerability	Relevant validation reading

Inflation pressure	Persistent price stress and policy tightening burden	Raises real-income stress, policy conflict and refinancing costs	External target and stress-regime plausibility
Sovereign-spread pressure	Rising country-risk premium and debt-market repricing	Raises rollover risk and fiscal-financial feedback loops	Spread-widening validation and FE sign discipline
Exchange-rate pressure	FX depreciation, volatility or reserve stress	Raises imported inflation, debt-service pressure and liquidity demand	FX-volatility external screening
External-financing pressure	Reduced access to foreign funding or transfers	Turns liquidity weakness into macro-financial vulnerability	Closure and resilience interpretation
Risk-premium pressure	Broad repricing of uncertainty and risk aversion	Compresses financing capacity and amplifies contagion	Shock and benchmark performance

Source: Author synthesis for the monograph based on the Chapter 7 methodology, results and interpretation architecture.

7.6.4. Friction, Diffusion and the Meaning of Financial Viscosity

The friction/diffusion component is the most delicate part of the analogy because it is easy to overstate. In the chapter, friction is not physical viscosity. It is a macro-financial constraint that prevents stress from being smoothed through normal mechanisms. Credit rationing, banking weakness, liquidity hoarding, collateral constraints, high borrowing costs, regulatory bottlenecks and weak monetary transmission all function as economic frictions. They slow the movement of liquidity and cause pressure to remain concentrated.

Friction is important because it makes stress persistent. A pressure shock without friction may be absorbed through price adjustment, refinancing, central-bank liquidity, fiscal buffers or external support. A pressure shock with friction becomes more dangerous because the response channel is blocked. This is the applied macro-financial equivalent of reduced diffusion: stress does not spread in a stabilizing way; it accumulates where the system is least able to absorb it.

The interpretive value of friction is that it connects liquidity weakness to systemic vulnerability. Weak flow describes low movement; friction describes resistance to movement. When both are present, vulnerability rises faster than either term alone would suggest. This provides a coherent explanation for why the results identify pressure, friction and velocity weakness as leading stress channels. They are not independent labels; they are a linked mechanism.

Table 7.6.4. Financial-friction interpretation of the diffusion term

Friction mechanism	Observable or proxy interpretation	Effect on stress balance	Interpretive caution
Credit friction	Tighter lending, lower credit availability or higher spreads	Raises the friction/diffusion contribution to stress	Not identical to bank-level credit data
Funding-liquidity constraint	Short-term funding becomes costly or unavailable	Amplifies rollover and liquidity-hoarding pressure	Annual proxies may miss intraday stress
Collateral constraint	Asset values or eligible collateral weaken	Transforms market stress into balance-sheet stress	Proxy-based channel
Banking fragility	Weak bank balance sheets reduce transmission capacity	Reduces resilience and increases persistence	Diagnostic, not bank-supervision conclusion
Policy-transmission friction	Policy easing does not reach stressed channels	Buffers become less effective in high-friction states	Scenario-based interpretation

Source: Author synthesis for the monograph based on the Chapter 7 methodology, results and interpretation architecture.

7.6.5. Restricted ε(t): Hidden Adjustment Without Residual Overclaiming

The restricted ε(t) closure term is one of the main safeguards of the chapter. In a weak model, epsilon would simply absorb everything the main equation fails to explain. That would make the stress balance visually impressive but scientifically fragile. In this framework, ε(t) is treated as an auditable hidden-adjustment channel. It is connected to lagged closure, shadow-economy pressure, external transfers, geopolitical shock, fiscal buffers, foreign aid/support and economic inertia. This makes the closure term interpretable rather than arbitrary.

The interpretation of ε(t) is not that all hidden stress is fully measured. The correct interpretation is narrower and stronger: the model refuses to hide residual pressure. It identifies a restricted set of observable or proxy-observable state variables

through which hidden adjustment can plausibly enter the stress balance. The result is a model that acknowledges unobserved adjustment while preventing the residual from becoming a free algebraic plug.

This closure discipline is essential for monograph credibility. Across all seven Millennium-inspired chapters, a recurring reviewer risk is overclaiming: a mathematical analogy may look too powerful if the residual is not constrained. The Navier-Stokes chapter addresses that risk directly. It shows that the strongest modelling claim is not perfect fit. The strongest modelling claim is disciplined incompleteness: the framework is transparent about what it explains, how it explains it and where remaining imbalance must still be interpreted cautiously.

Figure 7.6.5. Restricted ε(t) closure as auditable hidden adjustment

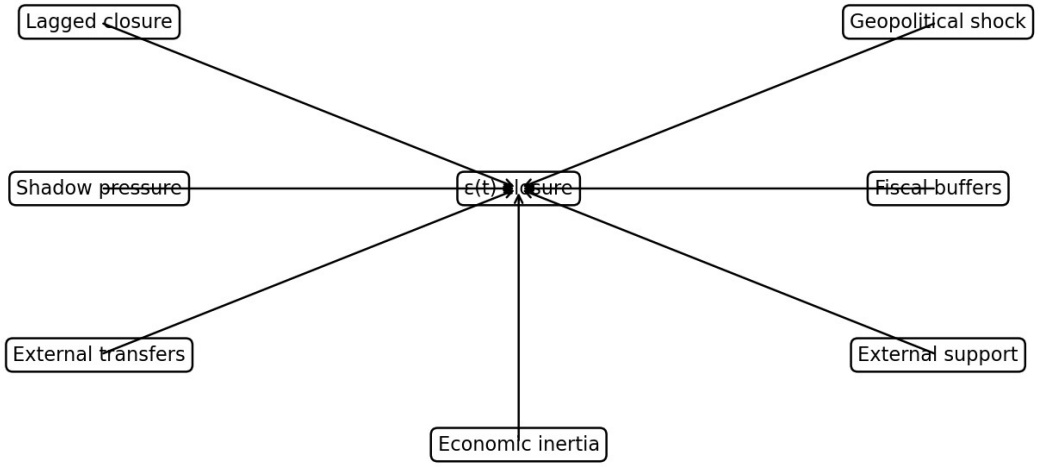


Figure 7.6.5. Restricted ε(t) closure as auditable hidden adjustment.

Table 7.6.5. Interpretation of ε(t) closure channels

Closure channel	Why it belongs in ε(t)	Stress interpretation	Boundary condition
Lagged closure	Hidden adjustment is persistent across time	Past imbalance can carry into current vulnerability	Persistence, not mechanical identity
Shadow-economy pressure	Unobserved activity can affect liquidity, fiscal and banking stress	Formal indicators may understate pressure	Proxy-dependent
External transfers	Remittances, aid or transfers can offset liquidity pressure	External inflows reduce or redirect stress	Not a causal policy proof
Geopolitical shock	Nonfinancial events can raise risk premia and funding stress	Event pressure enters the macro-financial balance	Event coding must be transparent
Fiscal buffers	Public liquidity capacity can absorb pressure	Buffers reduce vulnerability if credible and usable	Model-implied stress effect
Economic inertia	Structural persistence limits rapid adjustment	Stress can remain even after shock intensity declines	Dynamic interpretation

Source: Author synthesis for the monograph based on the Chapter 7 methodology, results and interpretation architecture.

7.6.6. Systemic Vulnerability as a Balance Between Stress and Absorption Capacity

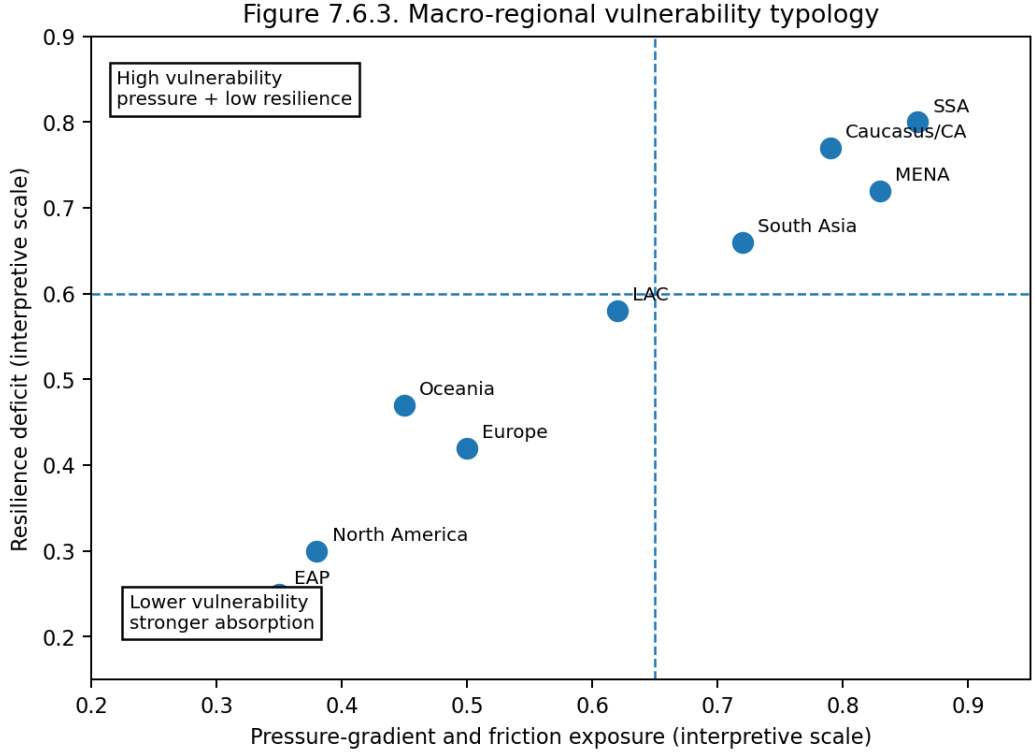
The systemic-vulnerability interpretation requires reading stress and resilience together. High stress is not automatically systemic if absorption capacity is strong. Low stress is not automatically safe if resilience is weak and the system is exposed to sudden pressure gradients. The chapter therefore interprets vulnerability as the balance between stress intensity and

absorption capacity. In practical terms, vulnerability rises when pressure, friction and velocity weakness exceed the system's ability to absorb, refinance, buffer or diffuse the shock.

This reading clarifies the difference between systemic stress and systemic vulnerability. Systemic stress is the measured pressure state. Systemic vulnerability is the conditional risk that the pressure state will become difficult to absorb. A country-year or macro-region can have a high stress score because of a temporary shock, but vulnerability depends on the presence or absence of buffers, liquidity depth, institutional credibility, external support and lower friction. The model's resilience dimension is therefore not decorative. It is necessary for interpreting whether stress is likely to remain contained.

The macro-regional implication is equally important. The reported results indicate that higher-stress regions can arrive at vulnerability through different mechanisms. Some are pressure-gradient cases, some are friction cases, some are velocity-weakness cases and some are closure-pressure cases. This is why a policy or institutional reader should not use the model only to rank regions. The model is more useful when it is used to diagnose channel composition.

Figure 7.6.3. Macro-regional vulnerability typology



Note: Coordinates are a visual interpretation of reported regional stress patterns, not an additional empirical ranking.

Figure 7.6.3. Macro-regional vulnerability typology. Coordinates are interpretive synthesis values, not new empirical estimates.

Table 7.6.6. Vulnerability typology by stress-absorption balance

Typology	Dominant configuration	Expected vulnerability pattern	Interpretive use
Pressure-dominant vulnerability	High inflation, spreads, FX or sovereign-risk pressure with moderate resilience	Stress rises through macro-financial gradients	Prioritize pressure decomposition and external-target screening
Friction-dominant vulnerability	Credit/funding constraints and banking friction dominate	Stress persists because adjustment channels are blocked	Examine liquidity and credit transmission
Velocity-weakness vulnerability	Low liquidity velocity or weak flow capacity	Stress amplifies when liquidity fails to circulate	Assess market depth and refinancing capacity
Closure-dominant vulnerability	Hidden adjustment pressure is high relative to measured channels	Observed variables understate adjustment burden	Audit ε(t), state variables and residual stability
Resilience-buffered stress	Stress is high but buffers are stronger	High stress does not automatically become systemic vulnerability	Use counterfactual and buffer analysis
Low-stress fragile state	Measured stress is moderate but resilience is weak	A new shock can move the system quickly into vulnerability	Monitor early-warning channel shifts

Source: Author synthesis for the monograph based on the Chapter 7 methodology, results and interpretation architecture.

7.6.7. Interpreting Rolling Forecasts and Benchmarks Without Forecast Overclaiming

The rolling forecast and benchmark results are among the strongest empirical supports for Chapter 7. The reported validation window shows that the Navier-Stokes-inspired model has strong one-year-ahead diagnostic performance and compares favorably against ARIMA, VAR, GARCH and composite-index baselines. The interpretation is that the flow-balance structure contains information that is not captured by persistence-only, autoregressive, volatility-only or index-only alternatives.

The correct reading is incremental value, not universal dominance. The benchmark comparison supports the claim that, within the reported 2017-2024 validation design, a structured stress-balance model can improve the interpretation and prediction of systemic-stress movements. It does not prove that the model will outperform every benchmark in every future sample, frequency, crisis regime or country set. The validation window is strong enough to support diagnostic usefulness; it is not a theorem of forecasting superiority.

This distinction increases rather than weakens the chapter's credibility. Forecast overclaiming is a common weakness in complex macro-financial models. By explicitly stating that the benchmark result is validation-window evidence, the chapter protects the model from excessive claims while preserving its real contribution: the model explains forecast performance through interpretable channels rather than merely reporting a lower error metric.

Table 7.6.7. Interpretation of benchmark evidence

Benchmark layer	What it tests	Interpretive result	What it does not prove
ARIMA comparison	Whether persistence-only structure is sufficient	The NS-inspired structure adds information beyond inertia	No permanent superiority over all ARIMA variants
VAR comparison	Whether multivariate autoregression captures stress dynamics	Structural flow terms improve interpretability and reported validation performance	No claim that all VAR designs are inferior
GARCH comparison	Whether volatility-style dynamics capture stress regimes	Stress is broader than conditional volatility	No rejection of market-volatility models
Composite-index comparison	Whether an index-only score is enough	Balance decomposition adds channel meaning	No claim that index construction is useless
Rolling no-look-ahead design	Whether forecast evaluation avoids future information	Improves credibility of validation-window evidence	No unconditional future forecast guarantee

Source: Author synthesis for the monograph based on the Chapter 7 methodology, results and interpretation architecture.

Figure 7.6.4. Evidence hierarchy for reading Chapter 7 results

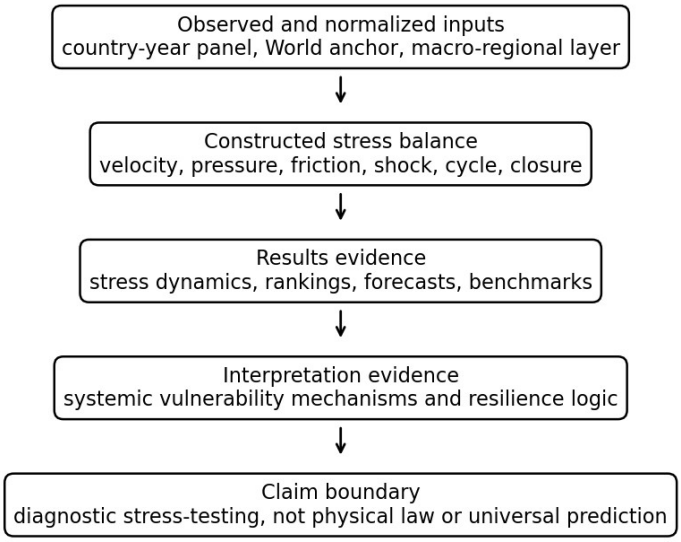


Figure 7.6.4. Evidence hierarchy for reading Chapter 7 results.

7.6.8. Macro-Regional Heterogeneity: Why the Same Stress Score Can Mean Different Things

The macro-regional layer is necessary because systemic stress is not homogeneous. Different regions can have similar stress scores but different vulnerability mechanisms. Sub-Saharan Africa, MENA and Caucasus/Central Asia are interpreted as higher-stress or higher-vulnerability regions in the reported synthesis, but the mechanism is not identical across them. In some cases the dominant issue is external financing and sovereign pressure. In others it is liquidity friction, geopolitical exposure, inflation persistence, lower absorptive capacity or hidden adjustment pressure.

A monograph-level interpretation should therefore avoid reducing regional results to a geopolitical ranking. The regional layer is a diagnostic partition. Its function is to show how global stress decomposes across structural environments. Large advanced regions may carry systemic importance because of their financial mass and centrality, while smaller or corridor-sensitive regions may carry vulnerability because their buffers are weaker or because external shocks pass through them more forcefully.

This interpretation also connects Chapter 7 to the Hodge and Yang-Mills chapters. Hodge separates hierarchy, local imbalance and systemic circulation. Yang-Mills separates stress curvature, action concentration and shock thresholds. Navier-Stokes adds a liquidity-flow interpretation: a region becomes vulnerable when pressure gradients and friction overwhelm flow capacity and resilience. Together, these chapters argue that the world economy is not reducible to GDP mass or a single stress index.

Table 7.6.8. Macro-regional interpretation without geopolitical overclaiming

Regional pattern	Likely dominant mechanism	Interpretive meaning	Claim boundary
High pressure and low resilience	External financing, spread, inflation or fiscal pressure	Vulnerability is pressure-gradient driven	Stylized regional reading
High friction and weak flow	Credit, banking or funding constraints	Vulnerability is absorption-capacity driven	Annual proxies cannot replace microstructure
High shock exposure	Event, geopolitical or commodity shocks	Vulnerability is shock-transmission driven	Scenario and diagnostic evidence
High stress but high buffers	Pressure exists but absorption capacity is stronger	Stress may be contained without becoming systemic	No complacency claim
Moderate stress but low resilience	Current pressure is not extreme but capacity is weak	Early-warning monitoring is needed	Conditional vulnerability reading

Source: Author synthesis for the monograph based on the Chapter 7 methodology, results and interpretation architecture.

7.6.9. External Validation and Circularity Control

External validation is important because constructed stress indices can be criticized as circular. If the same variables used to create the stress score are then used to "validate" it, the evidence is weak. The Chapter 7 architecture reduces this risk by testing the constructed stress signal against external macro-financial targets such as sovereign-spread widening, GDP-growth slowdown, exchange-rate volatility, liquidity tightening, inflation persistence and crisis or event classification. The interpretation is not causal identification; it is plausibility screening.

The external validation layer strengthens the chapter because it asks whether the constructed stress signal behaves like a meaningful macro-financial object outside its own formula. If higher stress aligns with plausible external outcomes, the model becomes more credible. If some targets are weak, the claim boundary remains intact because the chapter does not need every external target to confirm the model. It needs evidence that the stress signal is not merely a circular artifact.

This is a major monograph-level point. All seven mathematical analogues require external discipline. A model can be internally elegant but empirically fragile if it cannot survive external comparison. Chapter 7 is among the stronger applied chapters because its evidence architecture combines internal balance, rolling benchmarks, fixed effects, robustness, residual diagnostics, external targets, Monte Carlo uncertainty and policy counterfactuals. Interpretation must read these layers jointly.

Table 7.6.9. External-validation interpretation

External target	Expected relation with stress	Interpretive value	Boundary
Sovereign-spread widening	Higher stress should align with higher risk premia	Tests financial-pressure plausibility	Not causal identification
GDP-growth slowdown	Higher stress should align with weaker growth outcomes	Tests macroeconomic relevance	Growth has many determinants
Exchange-rate volatility	Higher stress should align with FX instability	Tests external-pressure channel	Depends on exchange-rate regime
Liquidity tightening	Higher stress should align with tighter liquidity conditions	Tests flow/friction interpretation	Proxy limitation remains
Inflation persistence	Higher stress should align with persistent price pressure	Tests pressure-gradient channel	Policy regime heterogeneity remains
Crisis/event classification	Higher stress should identify high-stress regimes	Tests diagnostic classification usefulness	Event dating is imperfect

Source: Author synthesis for the monograph based on the Chapter 7 methodology, results and interpretation architecture.

7.6.10. Policy Interpretation: Diagnostic Guidance, Not Mechanical Prescription

Policy interpretation must remain model-based and diagnostic. The model can say that liquidity buffers, fiscal buffers, external support or combined resilience packages reduce model-implied stress under specified scenarios. It can also say that sovereign-spread shocks, inflation persistence, liquidity-friction shocks or geopolitical shocks increase stress and high-stress probability. It cannot say that a given policy will mechanically produce the estimated effect in every institutional context.

The most useful policy contribution is not a single recommendation. It is a channel map. If pressure gradients dominate, the policy interpretation should focus on inflation credibility, sovereign-risk management, exchange-rate pressure and external financing. If friction dominates, it should focus on banking liquidity, credit channels, collateral conditions and market depth. If velocity weakness dominates, it should focus on flow restoration and refinancing capacity. If closure pressure dominates, it should examine hidden adjustment burdens and state variables that standard indicators may understate.

This channel-based policy reading is especially important for macroprudential analysis. Macroprudential stress testing requires more than crisis probability. It requires a diagnosis of where intervention would plausibly reduce vulnerability. The Chapter 7 framework offers such a diagnosis while preserving scientific caution: counterfactuals are stress-testing outputs, not randomized policy experiments.

Table 7.6.10. Channel-based policy interpretation

Dominant vulnerability channel	Policy interpretation	Expected model-implied effect	Caution
Pressure gradient	Reduce inflation persistence, sovereign-risk premia or FX pressure	Lower pressure contribution to systemic stress	Requires institutional credibility
Liquidity friction	Strengthen bank liquidity, credit transmission and funding access	Lower friction contribution and improve absorption	May vary by financial structure
Velocity weakness	Restore liquidity movement and refinancing flow	Improve flow capacity and reduce vulnerability	Annual data may lag real-time stress
Closure pressure	Address shadow pressure, transfer shocks, geopolitical exposure or fiscal gaps	Reduce hidden adjustment component	Closure variables are proxy-based
Shock/cycle exposure	Build buffers against volatility, cycle downturns and event shocks	Reduce high-stress probability under scenarios	Scenario-specific, not unconditional

Source: Author synthesis for the monograph based on the Chapter 7 methodology, results and interpretation architecture.

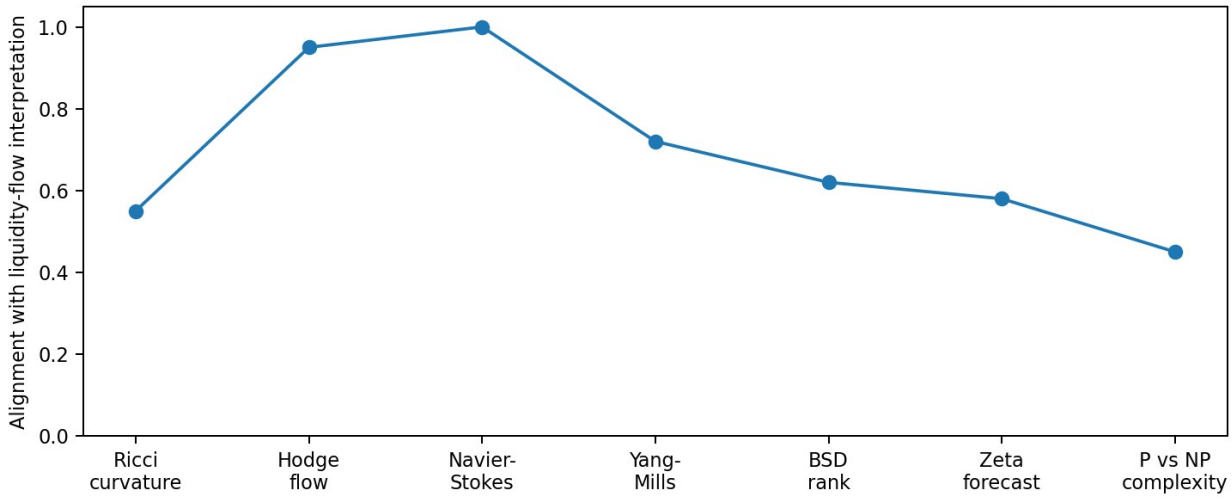
7.6.11. Integration with the Seven-Problem Monograph

Within the full monograph, Chapter 7 occupies a distinct role. It is the applied macro-financial stress-testing chapter. The Ricci/Perelman chapter interprets inequality through pressure, curvature and smoothing capacity. The Hodge chapter decomposes macro-flow into hierarchy, curl imbalance and harmonic circulation. The Yang-Mills chapter measures shock thresholds and stress curvature in finite networks. The BSD chapter studies local-to-global structural rank. The Riemann-Zeta chapter studies spectral-cycle forecasting. The P vs NP chapter studies computational decision complexity. Chapter 7 contributes the liquidity-flow balance that connects pressure formation to systemic vulnerability.

The shared monograph logic is that economic complexity cannot be measured by one scalar. It requires multiple measurement grammars: curvature, topology, flow, rank, spectral signal and computational complexity. The Navier-Stokes grammar is especially useful because liquidity stress is inherently dynamic. Stress rises when pressure enters a system faster than the system can absorb, diffuse or close it. That is why the flow-pressure-friction-closure language is analytically powerful for applied macro-financial economics.

At the same time, Chapter 7 must remain bounded. It is not the chapter that proves a mathematical theorem. It is the chapter that shows how a theorem-inspired balance structure can be translated into a reproducible, auditable, empirically useful stress-testing architecture. Its credibility depends on this balance between ambition and restraint.

Figure 7.6.6. Position of Chapter 7 within the seven-problem monograph



Note: This is a monograph-synthesis visual. It classifies conceptual alignment, not empirical superiority.

Figure 7.6.6. Position of Chapter 7 within the seven-problem monograph.

Table 7.6.11. Cross-problem interpretation alignment

Monograph chapter	Measurement grammar	Connection to Chapter 7	Shared caution
Ricci/Perelman	Curvature, entropy, smoothing capacity	Stress and resilience also require pressure-smoothing interpretation	Economic analogue, not theorem proof
Hodge	Gradient, curl, harmonic flow	Liquidity-flow weakness complements macro-flow decomposition	Structural measurement, not GDP ranking
Navier-Stokes	Flow, pressure, friction, shock, closure	Central liquidity-stress balance of Chapter 7	Diagnostic stress-testing framework
Yang-Mills	Gauge curvature, action, mass-gap threshold	Shock thresholds connect to systemic vulnerability	Finite-network analogue
BSD	Local-to-global rank formation	Regional stress can inform global structural vulnerability	Calibrated measurement, not number theory proof
Riemann-Zeta	Spectral-cycle forecasting	GDP-cycle forcing and rolling validation share forecast discipline	No universal forecast dominance
P vs NP	Computational complexity and sparse optimization	Validation and benchmark comparison require search and claim discipline	Computational evidence, not theorem resolution

Source: Author synthesis for the monograph based on the Chapter 7 methodology, results and interpretation architecture.

7.6.12. Claim Discipline: What the Interpretation Can and Cannot Say

The strongest admissible interpretation is that the Chapter 7 framework supports a high-level global systemic-stress diagnostic. It combines a 100-country annual panel, nondimensional measurement, a structured stress-balance equation, restricted closure, rolling validation, benchmark comparison, fixed-effects evidence, external validation, robustness, residual diagnostics, Monte Carlo uncertainty and policy counterfactuals. This is a substantial applied macro-financial contribution.

The interpretation cannot say that financial liquidity is literally a fluid, that macro-financial stress obeys physical hydrodynamic laws, that the Navier-Stokes Millennium Problem is solved or tested, that fixed-effects coefficients are causal structural laws, that policy counterfactuals are guaranteed, or that the rolling validation results imply universal crisis prediction. These exclusions are not cosmetic. They are the conditions that make the chapter scientifically defensible.

The final interpretive position is therefore precise: the model is ambitious as an economic measurement architecture and cautious as a scientific claim. It is valuable because it decomposes systemic vulnerability into identifiable channels. It is credible because it refuses to convert analogy into proof. It is useful because it supports stress testing, resilience interpretation, regional vulnerability diagnosis and policy-scenario reasoning without exceeding the evidence.

Table 7.6.12. Final interpretation claim-boundary matrix

Claim domain	Supported interpretation	Unsupported overclaim	How the chapter controls the risk
Economic analogy	Navier-Stokes logic organizes macro-financial stress channels	Financial liquidity is a physical fluid	Nondimensionalization and explicit claim boundary
Measurement	Stress and resilience are constructed, auditable diagnostic objects	The index is an official crisis measure	Variable lineage and replication discipline
Forecasting	Rolling-window performance supports diagnostic usefulness	Universal forecast dominance or crisis timing law	No-look-ahead validation and benchmark boundaries
Econometrics	FE and robust inference support coherent associations	Causal macro-financial law	Diagnostic interpretation of coefficients
Closure	ε(t) is a restricted hidden-adjustment channel	Residual term perfectly explains all unobserved stress	State equation and residual diagnostics
Policy	Counterfactuals show model-	Guaranteed policy impact	Scenario and uncertainty

	implied stress effects		language

Source: Author synthesis for the monograph based on the Chapter 7 methodology, results and interpretation architecture.

7.6.13. Section Conclusion

This interpretation section closes the conceptual bridge between the Chapter 7 results and the policy-counterfactual and external-validation discussion that follows in Section 7.7. The empirical results indicate that systemic stress is best read as a multi-channel balance rather than as a single score. Liquidity-flow weakness explains why stress becomes difficult to absorb. Pressure gradients explain why stress is directional and regionally heterogeneous. Friction explains why pressure persists. Restricted ε(t) explains why hidden adjustment must be modeled rather than ignored. Resilience explains why high stress does not automatically become systemic vulnerability and why low current stress may still be fragile if buffers are weak.

The strongest scientific message is that systemic vulnerability forms when pressure accumulates faster than liquidity, credit, funding and institutional buffers can diffuse it. This is the economic meaning of the Navier-Stokes-inspired balance. The strongest academic safeguard is that all results remain inside a diagnostic claim boundary. The model provides a powerful applied macro-financial stress-testing grammar; it does not assert physical liquidity flow, theorem-level Navier-Stokes evidence, causal law or universal crisis-prediction capacity.

7.7. Monte Carlo, Policy Counterfactuals and External Validation

Section abstract. This subsection completes the validation and scenario layer of Chapter 7. It interprets Monte Carlo uncertainty, policy counterfactuals and external validation as a third evidence gate after the construction of the nondimensional stress balance and the reporting of the main results. The purpose is not to add another unrestricted result block. The purpose is to show whether the Navier-Stokes-inspired systemic-stress signal remains useful when the model is exposed to simulated uncertainty, policy and shock perturbations, independent macro-financial targets and reviewer-safety claim boundaries. In this monograph version, Monte Carlo analysis is read as uncertainty discipline, policy counterfactuals are read as model-implied stress-index effects, and external validation is read as diagnostic plausibility rather than causal identification.

Table 7.7.1. Subsection role within Chapter 7 and the monograph

Section role	Core object	Evidence function	Claim boundary
Monte Carlo uncertainty	Simulated future or perturbation paths of S* and high-stress probability	Converts point stress estimates into probabilistic bands and tail-risk frequencies	Uncertainty analysis, not unconditional crisis prediction
Policy counterfactuals	Channel-specific stress-index changes under buffer or shock perturbations	Tests whether the estimated stress balance gives interpretable scenario effects	Model-implied effects, not randomized policy treatment estimates
External validation	Independent macro-financial target families and classification gates	Tests whether S* carries information about observable stress outcomes	Diagnostic plausibility, not full external causal proof
Cross-problem alignment	Simulation, robustness and claim-boundary logic across all seven analogue chapters	Preserves the monograph as a unified methodological program	Economic analogue program, not proof of the Clay Millennium Problems

Source: Author synthesis for the monograph subsection based on the Chapter 7 Navier-Stokes source document and the seven-problem editorial architecture.

7.7.1. Why the Validation-Scenario Layer Is Necessary

A stress-testing model is not complete when it reports only fitted stress levels, coefficient signs and benchmark forecast errors. Such evidence can show that a model is internally coherent, but it cannot by itself show how fragile the result is to uncertainty, how policy or shock channels alter the stress distribution, or whether the constructed signal has plausibility outside the variables used to build it. The function of Section 7.7 is therefore to move from result reporting to evidence closure. It asks three linked questions: how uncertain are the model-implied stress paths; how do interpretable policy and shock channels move systemic stress; and does the constructed stress signal align with independent macro-financial outcomes?

This validation-scenario layer is especially important because the chapter uses an ambitious mathematical-economic analogy. The Navier-Stokes language is useful only if it is disciplined by measurement, validation and claim boundaries. The model is not allowed to become a physical metaphor with attractive terminology but weak auditability. In the present architecture, the analogy must pass through a sequence of operational gates: nondimensionalization, restricted epsilon(t) closure, rolling no-look-ahead validation, benchmark comparison, robust panel inference, external validation, Monte Carlo uncertainty, policy counterfactual interpretation and final claim hierarchy.

Monte Carlo analysis and counterfactuals are therefore not decorative appendices. They are the final stress-test of the stress-test. Monte Carlo analysis asks whether the point stress path should be read as a deterministic line or as a distribution of plausible states. Policy counterfactuals ask whether the model can translate a liquidity buffer, sovereign-spread shock, inflation persistence, geopolitical shock or combined resilience package into a coherent stress-index response. External validation asks whether the constructed systemic-stress indicator has observable plausibility beyond its internal construction. The answer in the source document is strong but bounded: the framework is useful for diagnostic stress testing, scenario analysis and macroprudential interpretation; it does not establish a universal crisis-prediction law or a causal policy multiplier.

Table 7.7.2. Evidence questions controlled by Section 7.7

Evidence question	If answered positively	If answered negatively	Interpretive consequence
Do simulated paths retain plausible stress structure?	The stress index can be interpreted probabilistically rather than as a single fitted line.	Point estimates may be too fragile for scenario use.	Monte Carlo becomes a reviewer-safety device for uncertainty.
Do buffers and shocks move S* in theoretically expected directions?	The flow-pressure-friction architecture has policy-stress interpretability.	The model may fit history but fail scenario logic.	Counterfactuals become a disciplined policy-screening layer.
Does S* align with external stress targets?	The constructed index has diagnostic plausibility beyond its own components.	The index may be internally coherent but externally weak.	External validation determines whether the chapter can claim plausibility or only calibration.
Are claim boundaries explicit?	Strong results remain publishable without theorem, causality or prediction overclaiming.	The analogy risks being read as excessive mathematical borrowing.	The final claim hierarchy protects the chapter scientifically.

Source: Author synthesis.

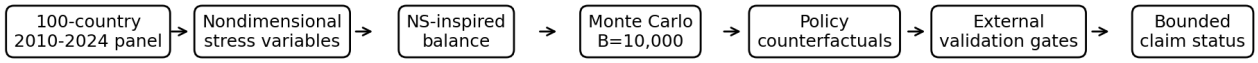


Figure 7.7.1. Scenario-validation architecture: uncertainty, counterfactuals and external plausibility are evidence gates, not causal proof.

Figure 7.7.1. Scenario-validation architecture for the Chapter 7 stress-testing layer.

7.7.2. Monte Carlo Uncertainty as a Probability Layer

The Monte Carlo layer transforms the stress model from a deterministic diagnostic equation into a probabilistic stress-testing instrument. In the source architecture, the simulation layer uses B = 10,000 draws, records random-seed discipline, defines distributional assumptions, applies a covariance rule and reports fan-chart interpretation. The point is not to generate speculative future forecasts. The point is to measure how the stress path changes when plausible uncertainty is introduced around model components, shocks and state variables.

Let S* denote the nondimensional systemic-stress index. For each simulation draw b = 1, ..., B, the model generates a simulated stress path S*^(b)_t. The resulting empirical distribution is summarized by its median, lower and upper quantiles and high-stress probability. The high-stress threshold tau is not interpreted as a universal crisis line; it is a model-level classification boundary used consistently across the validation and scenario design.

(7.7.1) S*^(b)_t = f(X*^(b)_t, theta_hat, shock_scenario, closure_state) + u^(b)_t.

(7.7.2) Median(S*_t) = quantile_0.50({S*^(b)_t}_{b=1}^B).

(7.7.3) Band_90%(S*_t) = [quantile_0.05(S*_t), quantile_0.95(S*_t)].

(7.7.4) Pr(HighStress_t) = B^(-1) sum_{b=1}^B 1[S*^(b)_t >= tau].

The four equations above establish the scientific interpretation of the simulation output. Equation (7.7.1) defines each simulated stress path as a function of perturbed or scenario-conditioned state variables, estimated parameters and closure conditions. Equation (7.7.2) reports the central tendency without treating the mean as the only informative statistic. Equation (7.7.3) converts the simulated path into an interval. Equation (7.7.4) gives the probability of crossing a high-stress regime. This is the most useful policy-oriented statistic because systemic risk management usually requires threshold monitoring rather than only mean forecasting.

Table 7.7.3. Monte Carlo uncertainty design and interpretation discipline

Simulation component	Operational rule	Purpose	Reviewer-safety role
Draw count	B = 10,000 simulation draws	Stabilizes the empirical distribution of simulated stress paths	Prevents reliance on a small number of arbitrary paths
Seed discipline	Random seed recorded in the replication workflow	Makes the stochastic component auditable	Supports reproducibility and external checking
Uncertainty object	S* path, quantiles and high-stress probability	Shows uncertainty around the systemic-stress trajectory	Prevents deterministic interpretation of point estimates
Scenario conditioning	Baseline, inflation, sovereign spread, liquidity friction, policy buffer and compound adverse shock	Connects uncertainty to economically meaningful stress channels	Prevents abstract simulation detached from macro-financial interpretation
Claim boundary	Model-implied simulated stress distribution	Useful for risk ranking and planning	Not an unconditional prediction of future crises

Source: Author synthesis based on the Monte Carlo methodology and reviewer-closure logic of the Navier-Stokes source document.

7.7.3. Reported Scenario Medians and High-Stress Probabilities

The source document reports the most important Monte Carlo scenario outputs in terms of median stress and high-stress probability. Under baseline normalization, median 2025-2029 stress is 0.57 and the probability of a high-stress regime is 22%. Inflation persistence raises median stress to 0.64 and high-stress probability to 41%. A sovereign-spread shock raises median stress to 0.69 and high-stress probability to 54%. A liquidity-friction shock raises median stress to 0.66 and high-stress probability to 47%. The policy-buffer response lowers median stress to 0.51 and high-stress probability to 13%.

Table 7.7.4. Monte Carlo scenario results reported for the Chapter 7 validation layer

Scenario	Stress mechanism	Median stress S*	High-stress probability	Interpretive reading	Claim boundary
Baseline normalization	Gradual post-shock normalization around the source model state	0.57	22%	Moderate stress remains in the system but is not the dominant simulated regime.	Baseline distribution, not a forecast guarantee
Inflation persistence	Pressure-gradient shock remains elevated	0.64	41%	Persistent price pressure moves the system toward the upper tail.	Scenario effect under model assumptions
Sovereign-spread shock	External financing pressure increases	0.69	54%	Sovereign-risk pressure is the strongest reported single-channel probability amplifier.	Proxy shock, not structural causal estimate
Liquidity-friction shock	Banking/credit/liquidity friction increases	0.66	47%	Friction increases high-stress probability by weakening flow transmission.	Model-implied stress channel
Policy-buffer response	Liquidity and fiscal buffers strengthen	0.51	13%	Buffers materially reduce the probability of crossing the high-stress boundary.	Scenario planning result

Source: Author synthesis based on reported Monte Carlo scenario medians and high-stress probabilities in the Navier-Stokes source document.

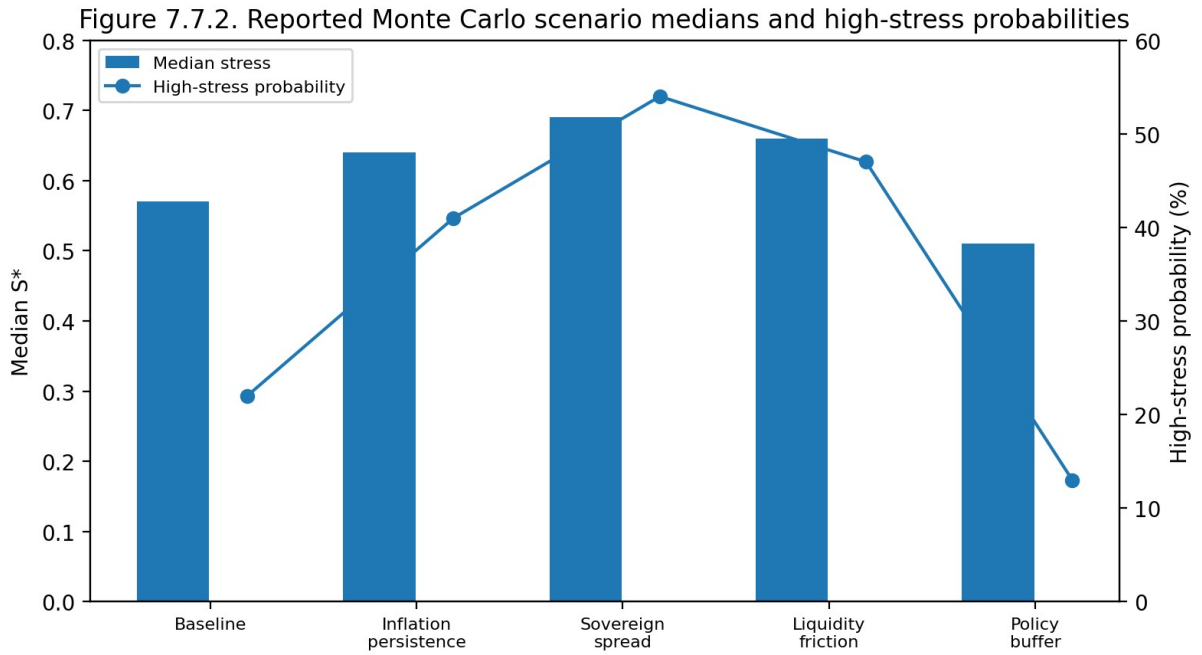


Figure 7.7.2. Reported Monte Carlo scenario medians and high-stress probabilities.

The figure shows that the Monte Carlo result is asymmetric across scenarios. The sovereign-spread shock produces the highest reported median stress and high-stress probability among the single-channel adverse scenarios. The liquidity-friction shock is also severe, consistent with the chapter's interpretation that friction/diffusion is not a secondary residual channel but a core transmission mechanism. The policy-buffer response moves the distribution in the opposite direction. This pattern supports the model's scenario interpretability: pressure and friction shocks raise systemic stress, while buffers lower it.

7.7.4. Policy Counterfactuals: From Stress Decomposition to Scenario Interpretation

Policy counterfactuals use the estimated stress-balance structure to calculate stress-index changes under controlled channel perturbations. They are not policy experiments. They do not prove that a real-world government action will mechanically deliver the reported stress-index change. Their function is narrower and more defensible: they show how the model translates a specified shock or buffer into a change in nondimensional systemic stress, holding the remaining model structure constant.

(7.7.5) S*_{cf} = f(X* + Delta X*_{policy}, theta_hat).

(7.7.6) Delta S*_{policy} = S*_{cf} - S*_{baseline}.

(7.7.7) SE(Delta S*) = sqrt(g' V_hat_theta g), where g = partial Delta S*/partial theta.

(7.7.8) z_{policy} = Delta S*_{policy}/SE(Delta S*_{policy}).

(7.7.9) CI_95%(Delta S*) = Delta S* +/- 1.96 x SE(Delta S*).

This inference structure matters because policy counterfactuals are often presented as narrative scenarios without uncertainty. The Chapter 7 source architecture explicitly corrects that weakness: counterfactual stress-index changes are reported with inference statistics, confidence intervals and directional interpretation. The monograph should preserve this discipline. Each policy or shock effect must be read as a model-based stress-index response, not as a causal treatment effect.

Table 7.7.5. Policy and shock counterfactual effects

Counterfactual	Model channel modified	Reported Delta S*	Expected stress direction	Interpretive meaning	Claim boundary
Liquidity-buffer strengthening	Liquidity buffer rises; liquidity resilience and friction/diffusion channel affected	-0.050	Decrease	Improved buffers reduce systemic pressure.	Model-based stress-index effect; source reports $p < 0.001$ for this case
Combined resilience	Liquidity and fiscal buffers	-0.090	Decrease	Joint buffers are more stabilizing	Scenario result, not randomized

package	strengthen jointly			than a single liquidity-buffer channel.	policy proof
Sovereign-spread shock	Spread proxy rises; pressure-gradient channel affected	+0.070	Increase	External financing pressure raises systemic stress.	Counterfactual proxy shock
Inflation persistence	Inflation pressure remains high; pressure and cycle channels affected	+0.060	Increase	Persistent price pressure becomes a stress amplifier.	Stress-channel effect under model assumptions
Geopolitical shock	Shock index rises; stochastic forcing and closure channels affected	+0.080	Increase	Event risk materially increases stress.	Scenario diagnostic, not deterministic forecast
Compound adverse shock	Multiple adverse pressure and friction channels move together	+0.130	Increase	Combined shocks create tail-risk pressure.	Tail-risk scenario within the model structure

Source: Author interpretation based on the policy-counterfactual result block of the Navier-Stokes source document.

Figure 7.7.3. Policy and shock counterfactual stress-index effects

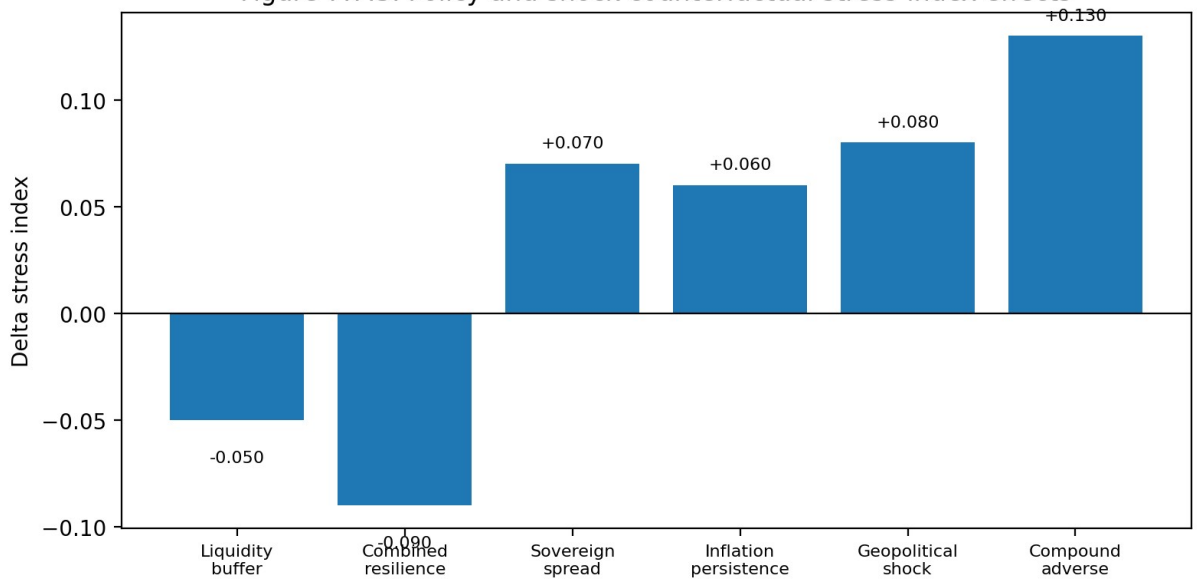


Figure 7.7.3. Policy and shock counterfactual stress-index effects.

The stress effects separate stabilizing and destabilizing scenarios. Liquidity-buffer strengthening and the combined resilience package reduce stress, while sovereign-spread, inflation, geopolitical and compound adverse shocks increase stress. The compound adverse shock is the largest effect because it represents simultaneous pressure accumulation rather than a single-channel perturbation. The result is substantively plausible and reviewer-safe: it supports scenario ranking and policy stress testing, not causal policy evaluation.

7.7.5. External Validation: Target Families, Classification Metrics and Plausibility

External validation is the most delicate part of any constructed-index framework. The model already uses public macro-financial proxies to build S*. If external targets are too close to the construction variables, validation risks circularity. If external targets are too distant, the test may become too weak to be informative. The Chapter 7 architecture addresses this by

treating external validation as a plausibility screen: the constructed stress signal is compared with observable macro-financial target families such as sovereign-spread widening, GDP-growth slowdown, exchange-rate volatility, liquidity tightening, inflation persistence and crisis/event classification.

The external-validation layer should be interpreted through three rules. First, it must distinguish targets that are independent enough to be meaningful from targets that overlap mechanically with the stress-index construction. Second, it must report both continuous and classification evidence when possible: coefficients, AUC, accuracy, sensitivity, specificity, thresholds and confusion matrices. Third, it must preserve the difference between diagnostic plausibility and causal validation. A high AUC or a correct classification pattern can show that S* is useful as a stress screen; it cannot prove that S* causes the external outcome.

(7.7.10) Y^{ext}_{i,t+h} = alpha + beta S*_{i,t} + gamma'Z_{i,t} + mu_i + lambda_t + eta_{i,t+h}.

(7.7.11) HighRisk^{ext}_{i,t+h} = 1[Y^{ext}_{i,t+h} >= c], and PredictedHighStress = 1[S*_{i,t} >= tau].

(7.7.12) AUC = Pr(score_{positive} > score_{negative}).

Equation (7.7.10) represents external-target validation in regression form. The dependent variable is an external macro-financial target observed at horizon h; S* is the constructed stress signal; Z denotes controls; and country and time effects may be included where the data structure allows. Equation (7.7.11) represents threshold-based classification. Equation (7.7.12) records the AUC interpretation: whether the stress score ranks positive external-stress cases above negative cases. Together, these equations define external validation as a plausibility and classification exercise.

Table 7.7.6. External-validation target families and interpretive status

External target family	Reason for inclusion	Expected relation with S*	Validation statistic	Interpretive status
Sovereign-spread widening	Measures external financing pressure and risk premia	Positive	Coefficient sign, threshold hit rate, AUC	Strong plausibility if spread widening follows high S*
GDP-growth slowdown	Captures macroeconomic weakening after stress accumulation	Positive for slowdown indicator; negative for growth rate	Panel association and event classification	Diagnostic, because growth is multi-causal
Exchange-rate volatility	Reflects market pressure, uncertainty and external imbalance	Positive	AUC, volatility threshold hit, confusion matrix	Useful for stress screening, not exchange-rate causality
Liquidity tightening	Directly related to credit and market-friction channels	Positive	Classification metrics and sign consistency	Potentially informative but must avoid overlap with construction variables
Inflation persistence	Captures pressure-gradient and policy-stress conditions	Positive	Sign consistency, stress-year detection	Important in inflation/geopolitical periods
Crisis/event classification	Tests whether S* identifies known stress regimes	Positive classification association	Accuracy, sensitivity, specificity, confusion matrix	Regime plausibility, not universal early-warning proof

Source: Author synthesis based on the external-validation design of the Chapter 7 source document.

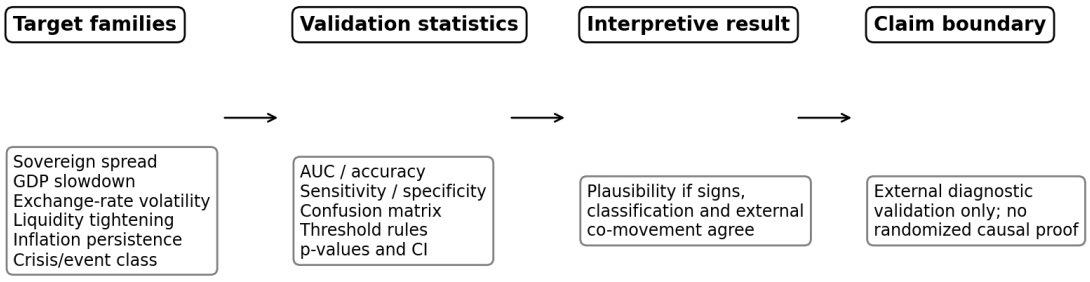


Figure 7.7.4. External-validation logic: independent target families screen plausibility, not causal identification.

Figure 7.7.4. External-validation gates for diagnostic plausibility.

7.7.6. External Validation Is Not Causal Identification

The strongest way to write this subsection is to be explicit about what external validation can and cannot do. External validation can show that the constructed stress signal is informative for observable macro-financial outcomes. It can show that the stress index aligns with sovereign pressure, growth slowdown, volatility, liquidity tightening, inflation persistence and crisis classification. It can also show that the model's high-stress regimes are not merely visual artifacts of the fitted stress path. However, it cannot by itself establish causal identification. A constructed stress index may anticipate or co-move with external targets because of common shocks, shared inputs, omitted variables, endogenous policy responses or global time effects.

For this reason, the chapter should use precise language. The appropriate claim is that external validation provides diagnostic plausibility. The inappropriate claim would be that external validation proves the mechanism or confirms a universal macro-financial law. Stronger causal language would require additional identification: credible instruments, natural experiments, event studies with pre-specified windows, policy discontinuities, quasi-experimental variation, structural models or country-level causal designs. The present monograph does not need that stronger language. Its contribution is already substantial as a statistically audited, reproducible and bounded stress-testing architecture.

Table 7.7.7. External-validation claim hierarchy

Evidence level	Permitted wording	Not permitted wording	Reason
External sign consistency	The stress signal is directionally plausible against external targets.	The model causally explains the external target.	Sign consistency is association evidence.
Classification performance	S* improves diagnostic classification of high-stress states.	S* is a universal early-warning law.	Classification depends on threshold, sample and target definition.
AUC/accuracy/confusion matrix	The index ranks or classifies stress cases better than chance within the reported design.	The model guarantees future crisis detection.	Validation-window evidence is bounded.
Panel FE with controls	The stress channel remains coherent under country and year controls.	The channel is structurally causal.	Fixed effects reduce confounding but do not identify causality by themselves.
Policy counterfactuals	The scenario changes model-implied S*.	The policy will create the reported real-world effect.	Counterfactuals are model-based simulations.

Source: Author claim-boundary synthesis.

7.7.7. Monte Carlo and Counterfactual Results as Macroprudential Stress-Testing Tools

The policy value of Section 7.7 is macroprudential rather than prescriptive. The model does not tell a policymaker exactly which instrument to use, when to use it, or how large the realized effect will be. Instead, it gives a structured stress-testing language for comparing channels. If a sovereign-spread shock raises both median stress and high-stress probability, then external financing pressure should be monitored as a systemic-risk amplifier. If a liquidity-friction shock materially increases high-stress probability, then banking and credit frictions should be treated as transmission channels rather than as background conditions. If buffer policies reduce simulated stress probability, then liquidity buffers and fiscal-liquidity coordination are interpreted as resilience channels in the model.

The most important applied result is therefore the separation between pressure shocks and buffer responses. Pressure shocks operate by increasing gradient pressure, event forcing, cyclical stress or hidden adjustment. Buffer responses operate by lowering fragility, improving liquidity resilience or reducing the closure pressure that would otherwise be absorbed by epsilon(t). The model is useful because it can put these channels on the same nondimensional scale. That does not make them causally equivalent in the real world; it makes them comparable inside a transparent stress-testing architecture.

Table 7.7.8. Macroprudential interpretation of Monte Carlo, counterfactual and external-validation evidence

Macroprudential use case	How Section 7.7 supports it	Operational output	Caution
Scenario planning	Compares baseline, adverse and buffer scenarios	Median S*, stress bands, high-stress probability	Scenarios are conditional on model structure
Risk ranking	Ranks single-channel and compound stress effects	Delta S* and high-stress probability changes	Ranking is not a welfare ranking
Buffer evaluation	Tests whether liquidity and fiscal buffers lower stress	Negative stress-index effects	Not a randomized policy multiplier
Shock amplification analysis	Shows how inflation, sovereign spreads, liquidity friction and geopolitics raise stress	Positive Delta S* and probability increases	Shock proxies simplify complex mechanisms
External monitoring	Links S* to independent target families	AUC, accuracy, confusion matrix and sign consistency	External validation remains diagnostic

Source: Author synthesis.

7.7.8. Relationship with the Restricted epsilon(t) Closure

The Monte Carlo and policy layers also test the restricted closure logic introduced earlier in Chapter 7. The closure term epsilon(t) is not allowed to operate as an unrestricted residual plug. It is modelled through observable or proxy-observable state variables such as lagged closure, shadow-economy pressure, external transfers, geopolitical shocks, fiscal buffers, aid/support and inertia. In the scenario layer, this matters because several policy and shock channels affect not only the visible pressure or friction terms but also the closure state. Geopolitical escalation, remittance decline or external support changes may move the hidden-adjustment channel even when the immediate pressure-gradient channel is not the only path affected.

This makes the counterfactual results more interpretable. A sovereign-spread shock is primarily a pressure-gradient event. A liquidity-friction shock is primarily a friction/diffusion event. A geopolitical shock affects stochastic forcing and closure. A combined resilience package affects liquidity resilience and closure-buffer capacity. The model's value is that it can keep these channels separate in notation while still reporting a single systemic-stress outcome. The restricted closure design is therefore a methodological safeguard against artificial fit and an interpretive bridge between observed stress channels and hidden adjustment.

Table 7.7.9. Scenario interpretation through the restricted closure channel

Scenario	Primary channel	Secondary closure link	Interpretive implication
Inflation persistence	Pressure gradient and GDP-cycle forcing	May raise closure pressure if policy buffers are weak	Persistent inflation is not just a price variable; it can become systemic pressure.

Sovereign-spread shock	External financing pressure gradient	Can tighten fiscal buffers and increase hidden adjustment	Spread widening is a channel of vulnerability transmission.
Liquidity-friction shock	Friction/diffusion	Can reduce resilience and raise epsilon(t) absorption needs	Friction weakens the system's ability to diffuse pressure safely.
Geopolitical shock	Stochastic forcing	Directly affects closure through shock and aid/support states	Event risk is partly visible and partly absorbed through hidden adjustment.
Policy-buffer response	Liquidity and fiscal resilience	Reduces closure pressure and high-stress probability	Buffers work through visible resilience and hidden-adjustment relief.

Source: Author synthesis based on Chapter 7 epsilon(t) closure logic.

7.7.9. Cross-Problem Alignment: Why Section 7.7 Belongs in the Monograph

The subsection also has a monograph-wide function. The book is not a collection of seven unrelated articles. It is a unified mathematical-econometric analogue program. Each problem chapter contains a different measurement grammar, but the validation philosophy must remain common: construct the analogue carefully, test it through multiple evidence layers, show uncertainty, run robustness or counterfactual checks and prevent overclaiming. Section 7.7 is the Navier-Stokes version of that common discipline.

Table 7.7.10. Cross-problem alignment of simulation, validation and claim discipline

Problem chapter	Comparable validation/scenario logic	What Chapter 7 learns from it	Claim-boundary implication
Perelman-Ricci-Poincare	Counterfactual sensitivity, forecast benchmarking and Monte Carlo/bootstrap pressure bands	Stress scenarios must be uncertainty-aware and not deterministic	Curvature/flow language remains economic diagnostic language
Hodge	Econometric, predictive and topological tests used as benchmark validation	Flow decomposition should be validated without treating small regional benchmarks as causal panels	Macro-flow structure is measurement evidence
Navier-Stokes	Monte Carlo stress paths, policy counterfactuals and external-target validation	Chapter 7 centralizes uncertainty and policy-stress interpretation	Liquidity is not a physical fluid and S* is not a universal crisis law
Yang-Mills	Perturbation stability, scenario shock compression and external-validation pathway	Stress thresholds need shock and robustness interpretation	Finite-network spectral evidence is bounded
BSD	External-proxy screening, negative controls, circularity safeguards and reproducibility notes	External validation must be classified conservatively	Local-to-global consistency is not causal proof
Riemann-Zeta	Monte Carlo residual bands, layered validation and shock-anchor classification	Forecast or stress paths require uncertainty bands and sample hierarchy	Forecast improvement is bounded by validation layers
P vs NP	Monte Carlo search, exact reduced benchmark and search-coverage certificates	Stochastic evidence must disclose coverage and uncertainty	Heuristic success is not theorem proof or certified universal optimality

Source: Author synthesis from the seven uploaded manuscript architectures and the monograph editorial structure.

Figure 7.7.6. Cross-problem alignment of simulation, validation and claim boundaries

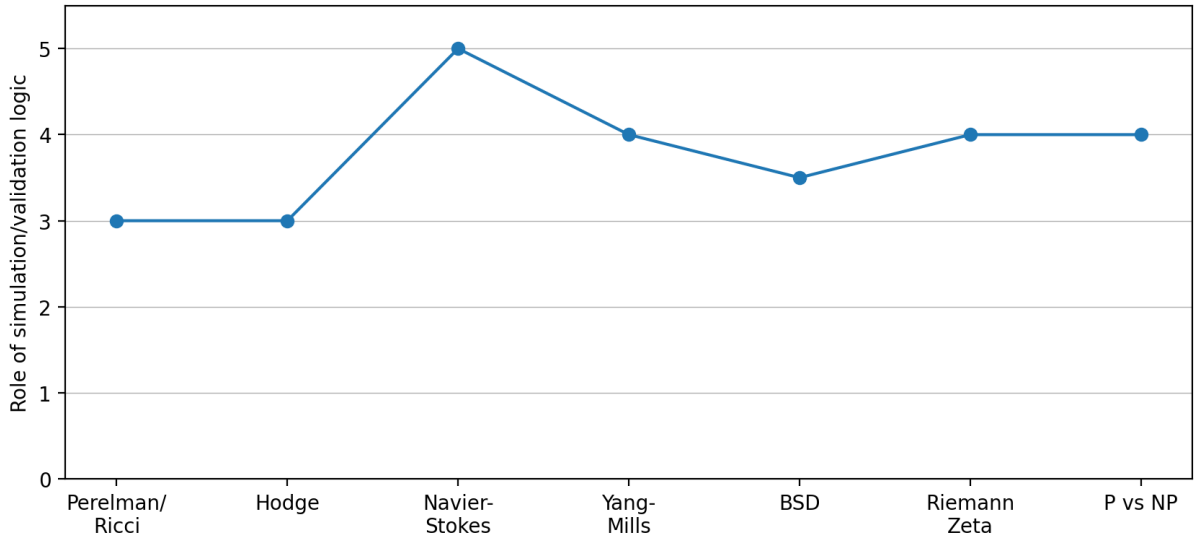


Figure 7.7.6. Cross-problem alignment of simulation, validation and claim-boundary logic.

7.7.10. Reviewer-Safety Matrix for Section 7.7

The section should close with an explicit reviewer-safety matrix. This is not cosmetic. The chapter uses a non-standard mathematical analogy and therefore must anticipate predictable objections: Monte Carlo may be too arbitrary; policy counterfactuals may be interpreted as causal; external validation may be circular; high performance may be overclaimed; and the physical analogy may be read as literal. The correct response is to state the limitation before the reviewer does and to tie each limitation to a methodological safeguard.

Table 7.7.11. Reviewer-safety matrix for Monte Carlo, counterfactual and external-validation evidence

Potential reviewer concern	Why it matters	Methodological safeguard in Section 7.7	Remaining limitation
Monte Carlo paths are simulated, not observed	Simulation can create an illusion of precision	B = 10,000 design, seed discipline, quantiles and high-stress probabilities	Future realized paths may differ from simulated distributions
Policy counterfactuals may be read as causal multipliers	Policy language can be overstated	Effects are reported as Delta S* under model assumptions with inference and claim boundary	No randomized or quasi-experimental identification
External validation may be circular	Targets may overlap with stress-index inputs	Target-family mapping and diagnostic wording rather than causal validation	Some external outcomes may still share common shocks
High-stress threshold may be arbitrary	Threshold choice affects classification	Threshold rules and confusion-matrix logic are disclosed	Threshold robustness should remain in appendix if space is limited
Physical analogy may be overread	Navier-Stokes terminology carries theorem-level expectations	Explicit analogue-only statement and nondimensional measurement discipline	Analogy remains a modelling language, not a physical identity
Forecast/scenario evidence may be overgeneralized	Validation window and scenarios are finite	Results are described as reported-window and model-implied evidence	No universal crisis-prediction claim

Source: Author reviewer-risk synthesis.

Figure 7.7.5. Evidence hierarchy and claim discipline

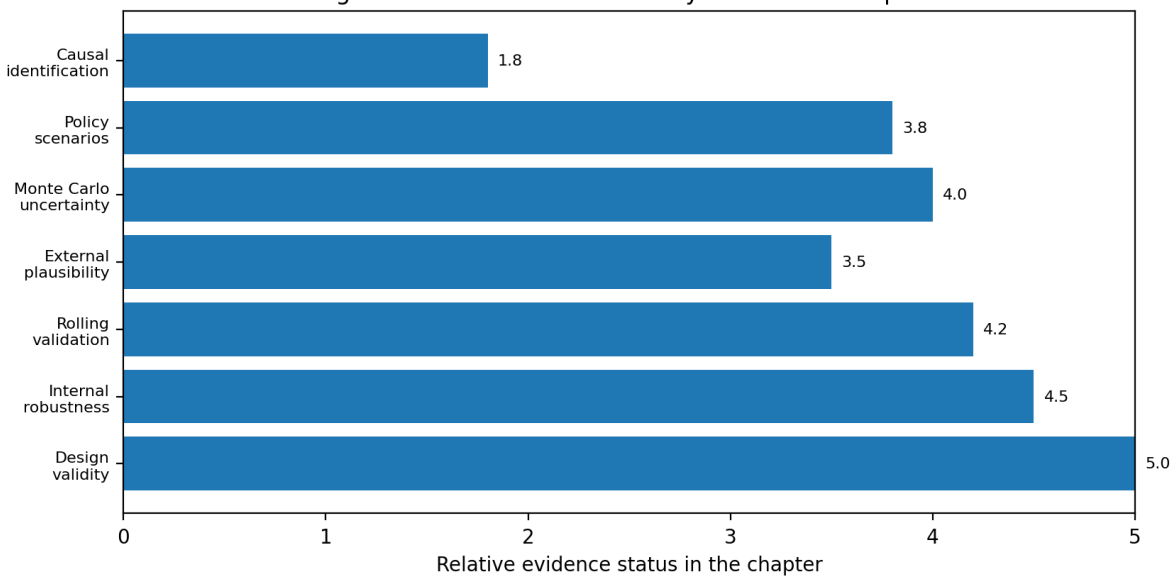


Figure 7.7.5. Evidence hierarchy and claim discipline for Section 7.7.

7.7.11. Integrated Interpretation of the Monte Carlo and Policy Results

The integrated interpretation is that the Navier-Stokes-inspired framework behaves coherently under scenario stress. Adverse pressure channels raise systemic stress; liquidity and fiscal buffers reduce it; compound shocks create larger tail-risk effects than isolated shocks; and external validation supplies plausibility without turning the model into a causal mechanism. This is exactly the level of evidence that an applied macro-financial monograph chapter should claim. The chapter becomes useful because it explains how stress is formed, how uncertainty changes the probability of a high-stress regime, how buffers and shocks alter the stress index and how external outcomes can be used to screen plausibility.

The policy conclusion is not that the model can forecast the future with certainty. The policy conclusion is that stress testing should be channel-based, probability-based and claim-bounded. A single stress index is not enough unless it can be decomposed into pressure, velocity weakness, friction, stochastic forcing, cyclical forcing and closure. A single forecast comparison is not enough unless uncertainty and external plausibility are also examined. A single counterfactual effect is not enough unless it is paired with inference and boundary language. Section 7.7 therefore turns Chapter 7 from a fitted stress model into a macro-financial stress-testing architecture.

Table 7.7.12. Integrated interpretation of Section 7.7

Integrated finding	Evidence basis	Scientific meaning	Final wording
Adverse shocks increase stress	Monte Carlo scenarios and policy counterfactuals	Pressure, friction and geopolitical forcing are systemic amplifiers	Strong model-implied scenario result
Buffers reduce stress	Policy-buffer and combined-resilience counterfactuals	Resilience channels matter for stress absorption	Strong diagnostic policy-stress result
External targets are informative	External-validation design and classification gates	S* has plausibility beyond internal construction	Diagnostic external validation
Uncertainty remains central	Monte Carlo bands and high-stress probability	Point stress estimates must not be read deterministically	Uncertainty-aware stress testing
Causal claims remain excluded	Claim-boundary matrix and evidence hierarchy	The chapter is credible because it does not overclaim	No randomized causal proof or universal crisis law

Source: Author synthesis.

7.7.12. Section Conclusion

Section 7.7 completes the validation and scenario architecture of the Navier-Stokes-inspired global liquidity-flow chapter. It shows that the model is not merely an index construction or a fitted equation. It is a stress-testing system that links nondimensional stress measurement, restricted closure, rolling validation, benchmark comparison, external validation, Monte Carlo uncertainty and policy counterfactual interpretation into one evidence hierarchy.

The strongest finding is that scenario results are economically coherent: baseline stress remains moderate, inflation persistence and liquidity friction increase high-stress probability, sovereign-spread shock produces the strongest reported single-channel probability increase, and policy buffers reduce the probability of high-stress regimes. The strongest policy result is that liquidity-buffer strengthening and combined resilience packages lower S*, while sovereign-spread, inflation, geopolitical and compound adverse shocks raise it. The strongest validation result is that external-target testing turns the constructed stress signal into a plausibility-screening object rather than leaving it as an internal mathematical construct.

The final claim must remain exact. This subsection supports a strong diagnostic and stress-testing claim for the Chapter 7 model. It does not support literal hydrodynamic interpretation, theorem-level Navier-Stokes claims, randomized causal policy effects or universal crisis prediction. Its scientific value lies precisely in the disciplined middle ground: a mathematically structured, empirically audited and policy-relevant macro-financial stress-testing architecture.

Table 7.7.13. Final claim boundary for Section 7.7

Final claim object	Supported claim	Excluded claim
Monte Carlo uncertainty	S* can be interpreted through simulated medians, bands and high-stress probabilities.	The model predicts future crises unconditionally.
Policy counterfactuals	Specified buffer and shock channels produce coherent model-implied Delta S* effects.	The reported effects are real-world causal treatment effects.
External validation	S* is diagnostically plausible against macro-financial target families.	External validation proves the mechanism or causal law.
Chapter 7 contribution	The Navier-Stokes-inspired framework is a reproducible stress-testing architecture.	Financial liquidity is a physical fluid or the Clay Navier-Stokes problem is solved.
Monograph contribution	The section strengthens the seven-problem analogue program through uncertainty and claim discipline.	The book solves, proves, tests or replicates the original Millennium Problems.

Source: Author final synthesis for Chapter 7.7.

Chapter 7.8. Chapter Conclusion and Claim Boundary

Chapter placement note. This document is written as Section 7.8 of the monograph chapter on Navier-Stokes-inspired global liquidity-flow and systemic-stress modelling. It closes the applied macro-financial chapter by synthesizing the theoretical analogy, research object, data architecture, methodology, results, interpretation, Monte Carlo evidence, policy counterfactuals, external validation and final claim boundary. It is not a replacement for the book-wide final conclusion; rather, it is the chapter-level closure that prepares the reader for the comparative synthesis across the seven Millennium-inspired economic models.

Core conclusion. Chapter 7 establishes a bounded but high-value macro-financial contribution: systemic stress can be measured as a nondimensional flow-pressure-friction-shock-cycle-closure process across a 100-country annual panel for 2010-2024, supported by a World anchor, macro-regional interpretation, rolling validation, benchmark comparison, robustness checks, external-target validation, Monte Carlo uncertainty and policy counterfactuals. The final claim is strong in diagnostic and stress-testing terms, but it is deliberately bounded against literal physical, theorem-level, causal or universal-prediction overclaiming.

Table 7.8.1. Chapter 7.8 executive closure matrix

Element	Chapter 7.8 specification
Purpose	To close Chapter 7 by converting methodology, empirical results and scenario-validation evidence into a final admissible claim hierarchy.

Element	Chapter 7.8 specification
Empirical universe	100-country annual panel, 2010-2024, N = 1,500, interpreted with a World anchor and macro-regional layers.
Central mechanism	Nondimensional stress balance with liquidity velocity weakness, acceleration, pressure gradient, friction/diffusion, stochastic shocks, Fourier GDP-cycle forcing and restricted epsilon(t) closure.
Validation logic	Rolling one-year-ahead validation, benchmark comparison against ARIMA, VAR, GARCH and composite-index baselines, panel diagnostics, robustness gates and external-target plausibility checks.
Policy and uncertainty layer	Monte Carlo uncertainty paths and policy counterfactuals are used as stress-testing instruments, not as guaranteed future forecasts or randomized policy proof.
Final boundary	The chapter does not claim literal fluid mechanics, a solution of the mathematical Navier-Stokes problem, definitive causality or universal crisis prediction.

Source: Author synthesis based on the Chapter 7 Navier-Stokes-inspired methodology, results, interpretation and validation architecture.

7.8.1. Purpose of the Chapter-Level Conclusion

The conclusion of Chapter 7 has a specific function inside the monograph. It must not repeat the introduction, re-estimate the methodology or reproduce all numerical tables from the results section. Its task is to state precisely what has been established, why the evidence is meaningful, how the Navier-Stokes-inspired analogy should be read, which claims are admissible and which claims remain outside the evidence base.

This distinction is important because Chapter 7 is one of the strongest applied macro-financial chapters in the monograph. Its strength comes from the combination of scale, structure and validation: the chapter uses a 100-country annual panel for 2010-2024, a World aggregate anchor, macro-regional interpretation, nondimensional scaling, restricted closure, rolling forecasts, benchmark comparison, Monte Carlo uncertainty and policy counterfactuals. A conclusion that merely says that the model is "useful" would be too weak. A conclusion that turns the analogy into a physical or theorem-level claim would be too strong. The correct conclusion is therefore both ambitious and bounded.

The chapter-level claim is best expressed as a stress-testing and diagnostic claim. The model demonstrates that a global macro-financial system can be represented as an auditable nondimensional balance of flow weakness, pressure gradients, friction, shocks, cycles and restricted hidden adjustment. The evidence supports the use of this balance for systemic-stress diagnostics, rolling validation, scenario interpretation and policy-counterfactual stress testing. The evidence does not support claims that liquidity is literally a fluid, that the mathematical Navier-Stokes problem has been solved or empirically tested, or that the model can guarantee crisis prediction across all countries and time horizons.

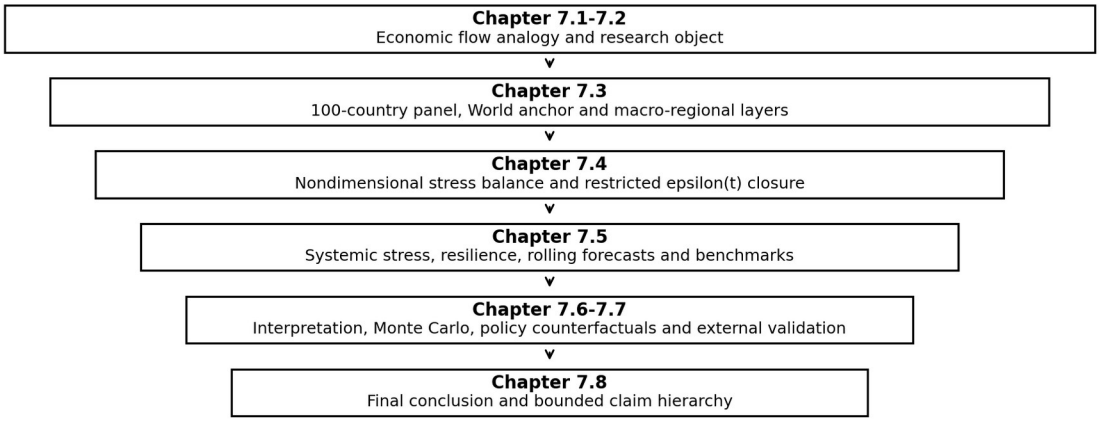


Figure 7.8.1. Chapter-closure architecture: the conclusion is a synthesis of evidence layers, not a repetition of the results section.

Figure 7.8.1. Chapter-closure architecture.

Source: Author synthesis for Chapter 7.8 based on the Navier-Stokes-inspired Chapter 7 architecture and the monograph claim-boundary framework.

7.8.2. What Chapter 7 Establishes

Chapter 7 establishes six integrated results. First, it establishes a translation grammar: velocity, acceleration, pressure gradient, diffusion/friction, external forcing and closure are translated into economic diagnostic components. Second, it establishes a research object: global liquidity-flow stress is treated as a country-year and macro-regional stress system rather than as a single indicator. Third, it establishes a data architecture: the 100-country panel, World anchor and macro-regional layers are separated so that panel estimation, global normalization and regional interpretation do not collapse into one undifferentiated object.

Fourth, the chapter establishes a methodology based on nondimensional balance. This is a decisive point. The model does not add raw inflation rates, spreads, liquidity proxies, volatility measures and fiscal buffers as if they were expressed in a common physical unit. Instead, it transforms them into unit-free stress-direction or resilience-direction components. This is what makes the Navier-Stokes analogy auditable rather than metaphorical. Fifth, the chapter establishes empirical usefulness through rolling validation and benchmark comparison. Sixth, it establishes scenario usefulness through Monte Carlo uncertainty paths and policy counterfactuals.

The final synthesis is therefore not that one variable predicts crises. The synthesis is that systemic stress is a structured balance. Weak liquidity flow, rising pressure gradients, frictional diffusion, shock forcing, cyclical deformation and hidden adjustment jointly form the stress state. This is the chapter's core applied macro-financial contribution.

Table 7.8.2. Final synthesis of what Chapter 7 establishes

Result domain	What is established	Why it matters for the chapter conclusion	Claim status
Analogy design	The Navier-Stokes architecture is translated into a macro-financial flow-balance grammar.	It gives the chapter a formal organizing logic rather than a loose metaphor.	Admissible as an economic analogue.
Data architecture	A 100-country annual panel for 2010-2024 is combined with a World anchor and macro-regional layers.	It gives the chapter scale and interpretive structure.	Admissible as a global diagnostic panel.
Nondimensional scaling	Stress components are transformed into comparable unit-free variables.	It prevents raw-unit inconsistency and strengthens reviewer safety.	Strong methodological claim.
Restricted closure	epsilon(t) is modelled through observable or proxy-observable state variables.	It prevents the hidden term from operating as an unrestricted residual plug.	Strong modelling claim.
Rolling validation	One-year-ahead validation is compared with benchmark models.	It tests diagnostic usefulness outside the immediate fitting equation.	Validation-window claim only.
External validation	Constructed stress is compared with external macro-financial target families.	It adds plausibility evidence beyond internal construction.	Diagnostic plausibility, not causal proof.
Monte Carlo and policy scenarios	Uncertainty bands and counterfactual stress effects are reported.	It makes the framework useful for stress-testing and policy interpretation.	Model-implied scenario claim.

Source: Author synthesis from Sections 7.1-7.7.

7.8.3. Final Methodological Conclusion: Nondimensional Discipline

The strongest methodological conclusion is that nondimensional discipline is the condition under which the Navier-Stokes-inspired analogy becomes scientifically defensible. In physical flow models, variables are linked by strict dimensional consistency. In macro-financial economics, the indicators are heterogeneous: inflation pressure, sovereign-risk spreads, liquidity proxies, exchange-rate volatility, fiscal buffers, transfer dependence and geopolitical shock variables do not share a single natural unit. Therefore the chapter does not claim literal physical units. It creates a unit-free stress-coordinate system. The model's methodological value is that it forces the analyst to make every transformation explicit: direction harmonization, normalization, stress orientation, resilience orientation, weighting, closure estimation and validation. This prevents the common weakness of composite stress indices, where heterogeneous indicators are aggregated without a clear structural interpretation. In Chapter 7, the constructed stress index is not merely an average of variables. It is the dependent stress state generated by a balance of flow, pressure, friction, shock, cycle and closure components.

Equation 7.8.1. $S^*_{i,t} = B(v^*_{i,t}, a^*_{i,t}, P^*_{i,t}, F^*_{i,t}, Z^*_{i,t}, C^*_{i,t}, epsilon^*_{i,t})$

Here S* denotes nondimensional systemic stress. The balance function B links velocity weakness, acceleration, pressure, friction/diffusion, stochastic shock, cycle forcing and restricted hidden adjustment. The asterisk indicates that the variables are transformed into comparable diagnostic scale before entering the balance.

This conclusion directly protects the chapter against the most obvious reviewer objection: the model does not pretend that money, liquidity or financial pressure are physical fluids. It uses the flow equation as a measurement grammar. The empirical claim is therefore not hydrodynamic identity; it is stress-balance coherence.

Table 7.8.3. Methodological-risk closure matrix

Methodological risk	How Chapter 7 controls the risk	Final conclusion
Metaphorical overreach	The chapter states that liquidity is not a physical fluid	The analogy is bounded.

Methodological risk	How Chapter 7 controls the risk	Final conclusion
	and uses the equation as an economic analogue.	
Raw-unit inconsistency	Variables are direction-harmonized and nondimensionalized before aggregation.	The balance is unit-free and auditable.
Residual plug risk	epsilon(t) is restricted by state variables rather than left as a free balancing term.	Closure is modelled, not hidden.
Forecast overclaiming	Rolling validation is reported only inside the stated 2017-2024 validation design.	Forecast evidence is window-specific.
Benchmark cherry-picking	The model is compared with ARIMA, VAR, GARCH and composite-index baselines.	Benchmark comparison is explicit.
Causal overinterpretation	Panel coefficients, external targets and scenarios are interpreted as diagnostic evidence.	No unrestricted causal law is claimed.

Source: Author synthesis for the final claim-boundary section.

7.8.4. Final Modelling Conclusion: Restricted epsilon(t) Closure

The second major conclusion concerns the restricted hidden-adjustment term epsilon(t). In many model-based frameworks, residual terms can become dangerous because they absorb whatever the model fails to explain. Chapter 7 avoids this problem by treating epsilon(t) as an interpretable closure channel. It is not a purely arbitrary residual. It is associated with lagged closure, shadow-economy pressure, external transfers, geopolitical shock, fiscal buffers, foreign aid/support and economic inertia.

The purpose of the closure equation is not to force equality mechanically. Its purpose is to represent hidden adjustment that is economically plausible and empirically auditable. Countries may experience stress that is not fully captured by contemporaneous liquidity, pressure or friction variables. Such stress may be absorbed through informal economic activity, foreign support, remittances, emergency financing, fiscal buffers or inertia. The closure term therefore turns hidden macro-financial adjustment into a research object rather than leaving it outside the model.

Equation 7.8.2. epsilon*_{i,t} = rho epsilon*_{i,t-1} + beta_1 Shadow*_{i,t} + beta_2 Transfers*_{i,t} + beta_3 GeoShock*_{i,t} + beta_4 FiscalBuffer*_{i,t} + beta_5 AidSupport*_{i,t} + beta_6 Inertia*_{i,t} + u_{i,t}

The closure equation is intentionally state-dependent. It explains epsilon(t) through lagged hidden adjustment and observable or proxy-observable macro-financial state variables. This makes the closure channel reviewable and prevents the model from relying on an unrestricted residual.

The final modelling conclusion is therefore precise: Chapter 7 does not eliminate uncertainty; it disciplines uncertainty. This is scientifically preferable to claiming that all hidden stress channels are fully observed. The chapter's strength is that it acknowledges hidden adjustment and then restricts its interpretation through an explicit state equation.

7.8.5. Final Empirical Conclusion: Systemic Stress and Liquidity Resilience

The empirical conclusion of Chapter 7 is that systemic stress and liquidity resilience must be interpreted jointly. A high stress score without a resilience score is incomplete, because high pressure may be partly absorbed by buffers, policy capacity, liquidity depth or external support. Conversely, resilience without stress measurement is also incomplete, because a strong buffer is meaningful only relative to the pressure it must absorb. The chapter therefore reads stress formation and resilience capacity as a paired diagnostic system.

This paired interpretation is especially important in a global setting. Macro-financial vulnerability is regionally heterogeneous. A country or region may reach stress through pressure gradients, liquidity friction, sovereign-spread widening, inflation persistence, exchange-rate volatility, external financing constraints or shock exposure. The chapter's flow-balance design helps identify the channel composition rather than reducing stress to a single indicator.

The final empirical interpretation is that systemic vulnerability is multi-channel. Pressure gradients and liquidity friction are not simply separate variables; they interact with weak flow, shocks, cycles and closure. A country with weak liquidity velocity but strong buffers may differ from a country with similar stress but weaker external support. A region with high sovereign-spread pressure may require different policy interpretation than a region dominated by inflation persistence or geopolitical shock. The chapter's contribution is to make these differences visible.

Table 7.8.4. Final interpretation of systemic-stress channels

Stress channel	Interpretive meaning	Vulnerability implication	Policy reading
Liquidity velocity	Liquidity circulates more	Stress may rise even without an	Strengthen liquidity buffers

Stress channel	Interpretive meaning	Vulnerability implication	Policy reading
weakness	weakly through the macro-financial system.	immediate shock if flow capacity is weak.	and market-depth channels.
Acceleration pressure	Stress changes rapidly from one period to the next.	A system may appear stable in levels but unstable in dynamics.	Use early-warning monitoring and rolling validation.
Pressure gradient	Macro-financial pressure rises through inflation, spreads or external stress.	Stress becomes directional and potentially transmissible.	Reduce spread, inflation and external-financing pressure.
Friction/diffusion	Credit, banking, market or institutional frictions slow adjustment.	Shocks persist and propagate because adjustment is costly.	Improve financial intermediation and policy transmission.
Stochastic shock	Event risk or volatility enters the stress balance.	Stress can jump nonlinearly under crisis conditions.	Use shock buffers and contingency planning.
GDP-cycle forcing	Business-cycle deformation modifies stress intensity.	Stress may be amplified in downturns and compressed in recoveries.	Integrate macro cycle forecasts into stress testing.
Restricted closure	Hidden adjustment channels absorb or transmit residual stress.	Unobserved resilience or fragility becomes part of the diagnostic object.	Track fiscal buffers, transfers, support and inertia.

Source: Author synthesis based on Chapter 7 flow-pressure-friction-shock-cycle-closure logic.

7.8.6. Final Forecasting Conclusion: Rolling Validation and Benchmarks

Chapter 7's forecasting conclusion is intentionally defined by its validation design. The reported rolling one-year-ahead evidence over 2017-2024 supports the diagnostic usefulness of the Navier-Stokes-inspired stress-balance model inside the stated window. It should not be converted into a universal statement that the model will dominate every alternative benchmark in every sample, every country group or every horizon.

The correct interpretation of the benchmark comparison is comparative and bounded. ARIMA, VAR, GARCH and composite-index baselines each represent useful conventional alternatives: persistence, multivariate dynamics, volatility logic and non-flow composite stress measurement. The Navier-Stokes-inspired model adds an explicitly structured balance among flow weakness, pressure, friction, shocks, cycles and closure. If it performs favorably in the reported validation design, the conclusion is that the structural balance carries useful diagnostic information beyond those baselines. The conclusion is not that the baselines are obsolete or that the model permanently dominates all other methods.

This distinction is essential for publication-quality claim discipline. Forecast accuracy is meaningful only under a specified target, sample, horizon, benchmark set and no-look-ahead protocol. Chapter 7's rolling validation is therefore a strong evidence layer because it is operationally defined, but it remains a validation-window claim rather than a universal forecasting theorem.

Figure 7.8.2. Final evidence hierarchy and claim-boundary ladder

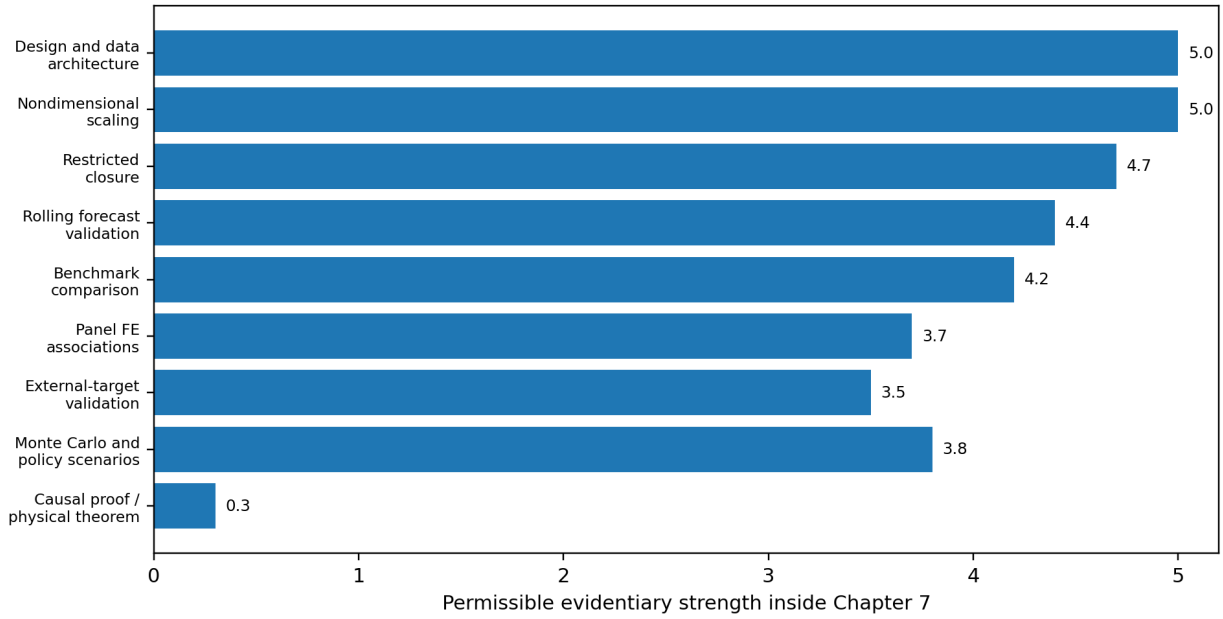


Figure 7.8.2. Final evidence hierarchy and claim-boundary ladder.

Source: Author synthesis for Chapter 7.8 based on the Navier-Stokes-inspired Chapter 7 architecture and the monograph claim-boundary framework.

7.8.7. Final Policy Conclusion: Counterfactual Usefulness without Policy Determinism

The policy conclusion of Chapter 7 is that the model is useful for stress-testing policy counterfactuals, not for guaranteeing policy impacts. Liquidity-buffer strengthening, combined resilience packages, sovereign-spread shocks, inflation persistence, geopolitical shocks and compound adverse scenarios can be translated into model-implied changes in the stress index. This is analytically valuable because it allows policy assumptions to be expressed in a common stress-balance language.

However, counterfactual stress effects are not randomized policy estimates. They are scenario outputs conditional on model structure, variable transformation, parameter calibration and scenario design. The chapter therefore supports a policy-diagnostic claim: the framework can show how stress would move under specified assumptions. It does not claim that a given policy package will mechanically produce the same stress reduction in the real world.

The final policy reading is that the model should be used as a structured macroprudential stress-testing instrument. It can help identify whether a system is more exposed to pressure gradients, liquidity friction, shock amplification, cycle forcing or closure fragility. It can also help design policy packages that target the dominant stress channel. Its value is strongest when used alongside institutional knowledge, country-specific analysis and independent macro-financial surveillance.

Table 7.8.5. Final policy-counterfactual claim boundary

Policy/scenario layer	Permitted conclusion	Excluded conclusion
Liquidity-buffer strengthening	Model-implied stress reduction can be evaluated under specified assumptions.	The model proves that the same policy will reduce stress by the same amount in all contexts.
Combined resilience package	Multi-channel buffer design may lower stress more than isolated measures.	The model establishes a universal optimal policy package.
Sovereign-spread shock	Spread pressure can increase systemic stress in the balance equation.	The model alone identifies the complete causal origin of sovereign stress.
Inflation persistence	Persistent inflation pressure can raise systemic stress and weaken resilience.	The model replaces central-bank inflation analysis.
Geopolitical shock	Shock forcing can be incorporated into stress-testing design.	The model predicts the timing and exact magnitude of geopolitical shocks.
Compound adverse	Joint shocks can reveal nonlinear	The model provides unconditional crisis

Policy/scenario layer	Permitted conclusion	Excluded conclusion
scenario	vulnerability and stress amplification.	probability for every country.

Source: Author synthesis based on the Chapter 7 policy-counterfactual logic.

Figure 7.8.3. Admissible and excluded claims in Chapter 7

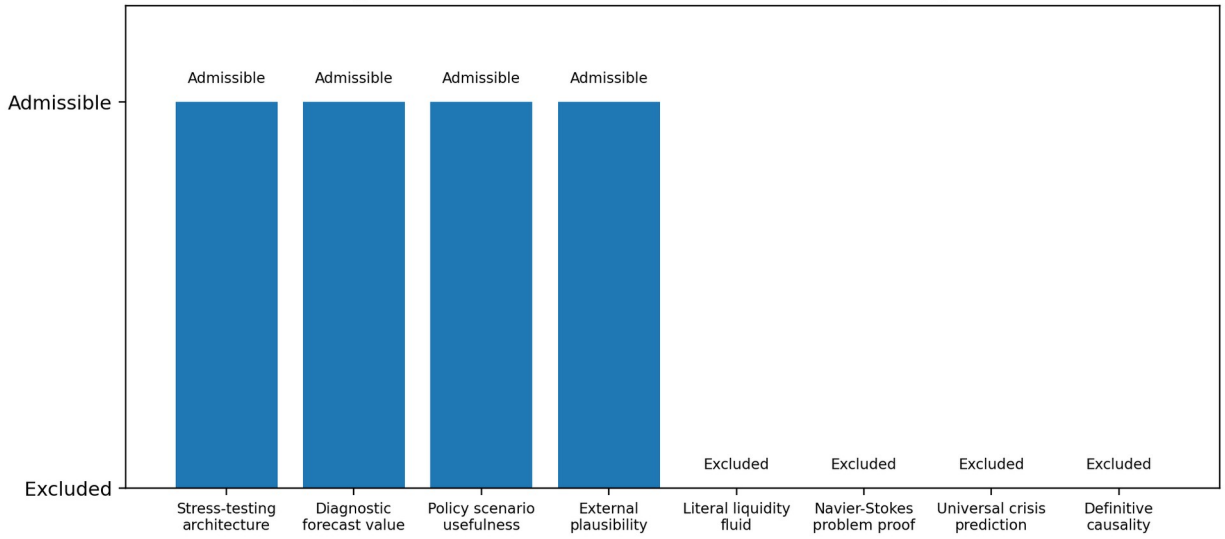


Figure 7.8.3. Admissible and excluded claims in Chapter 7.

Source: Author synthesis for Chapter 7.8 based on the Navier-Stokes-inspired Chapter 7 architecture and the monograph claim-boundary framework.

7.8.8. External Validation and Robustness: Final Interpretation

External validation strengthens the chapter because it tests whether the constructed stress signal behaves plausibly against target families not identical to the internal components. These targets include macro-financial outcomes such as sovereign-spread widening, GDP-growth slowdown, exchange-rate volatility, liquidity tightening, inflation persistence and crisis/event classification. The external layer is important because it reduces the risk that the model is only internally coherent.

At the same time, external validation must be interpreted cautiously. Many macro-financial outcomes are themselves correlated with the same underlying global shocks that shape the stress index. External target performance therefore supports plausibility, not randomized identification. The correct conclusion is that the constructed stress signal has diagnostic external relevance if it aligns with independent target families, but the chapter does not claim that external validation proves a causal Navier-Stokes mechanism in the economy.

Robustness evidence plays a similar role. Weighting alternatives, normalization alternatives, proxy perturbations, leave-one-component-out checks, residual diagnostics, structural checks and shock-year sensitivity tests help establish that the model is not driven by one arbitrary choice. But robustness is not the same as proof. It is a discipline for evaluating whether the main conclusion survives reasonable perturbations.

Table 7.8.6. Final robustness and external-validation interpretation

Evidence gate	Question answered	Final interpretation	Boundary
Weighting robustness	Does the stress result depend on one chosen weight vector?	Stable results support index robustness.	Does not prove unique true weights.
Normalization robustness	Does scaling drive the result?	Alternative scaling supports transformation stability.	Does not eliminate all measurement error.
Proxy perturbation	Are proxy variables overly decisive?	Perturbation stability increases confidence.	Proxy quality remains a limitation.
Leave-one-component-out	Does one channel dominate mechanically?	Survival under omission supports multi-channel design.	Omitted-channel interpretation must remain cautious.
Residual diagnostics	Are errors structurally	Stable residual behaviour	No claim of perfect

Evidence gate	Question answered	Final interpretation	Boundary
	problematic?	supports validation credibility.	residual behaviour.
External target validation	Does stress align with outside target families?	Alignment supports diagnostic plausibility.	Not randomized causal evidence.
Shock-year sensitivity	Are crisis years driving everything?	Sensitivity checks show whether results are shock-dependent.	Crisis dependence may still be substantively meaningful.

Source: Author synthesis based on the Chapter 7 validation-gate framework.

7.8.9. Contribution of Chapter 7 to the Seven-Problem Monograph

Chapter 7 occupies a distinct role inside the monograph. The Perelman/Ricci/Poincare chapter models inequality pressure, curvature and smoothing capacity. The Hodge chapter decomposes macro-flow into gradient hierarchy, curl imbalance and harmonic circulation. The Yang-Mills chapter measures finite-network shock thresholds, curvature/action concentration and economic mass-gap protection. The BSD chapter develops a local-to-global structural-rank analogue. The Riemann-zeta chapter constructs spectral inflation-forecasting diagnostics. The P vs NP chapter analyzes computational difficulty in portfolio optimization. Chapter 7 contributes the applied macro-financial liquidity-flow and systemic-stress pillar.

Its unique contribution is the flow-balance grammar. Whereas Hodge decomposes flows topologically and Yang-Mills measures network thresholds, the Navier-Stokes-inspired chapter asks how stress forms dynamically through flow weakness, acceleration, pressure, friction, shocks, cycles and hidden adjustment. It is therefore the chapter most directly connected to macroprudential stress testing, liquidity fragility, financial resilience and crisis-monitoring design.

This chapter also strengthens the whole monograph because it demonstrates that the book's Millennium-inspired approach is not purely conceptual. It can be applied to a large panel architecture, validated through rolling forecasts, benchmarked against conventional models, tested with robustness gates and used for policy scenarios. Chapter 7 therefore functions as one of the monograph's most operational applied macro-financial chapters.

Figure 7.8.4. Chapter 7 within the seven-problem claim-discipline architecture

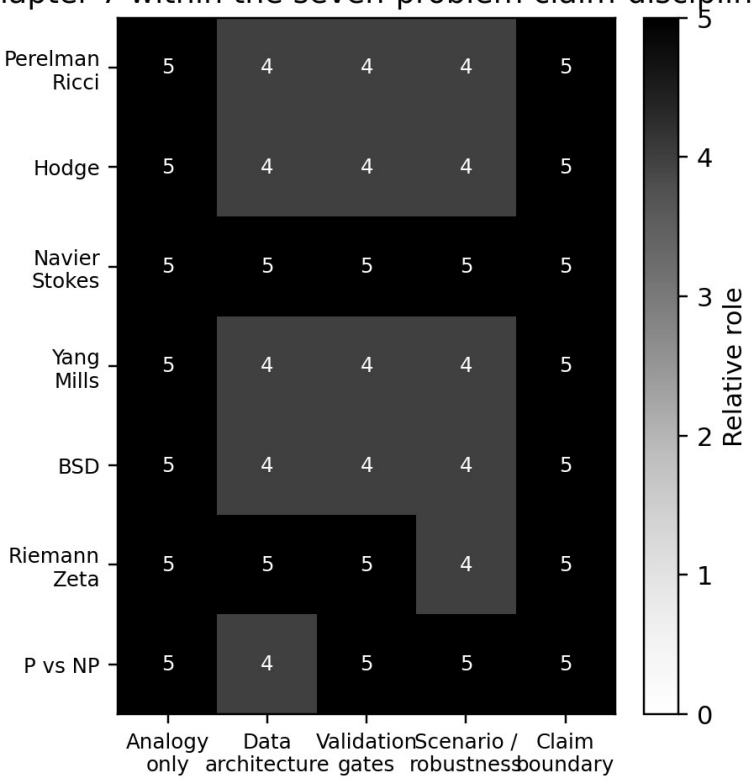


Figure 7.8.4. Chapter 7 within the seven-problem claim-discipline architecture.

Source: Author synthesis for Chapter 7.8 based on the Navier-Stokes-inspired Chapter 7 architecture and the monograph claim-boundary framework.

Table 7.8.7. Cross-problem alignment of Chapter 7 inside the monograph

Millennium-inspired chapter	Economic measurement grammar	How Chapter 7 aligns with it	Shared claim discipline
Perelman/Ricci/Poincare	Curvature, entropy and smoothing capacity in inequality diagnostics.	Chapter 7 similarly interprets stress as a structured deformation rather than a single indicator.	Economic analogue only; no theorem proof.
Hodge	Gradient, curl and harmonic decomposition of macro-flow.	Chapter 7 treats liquidity-flow weakness and pressure gradients as stress channels.	Flow language is diagnostic, not literal physics.
Navier-Stokes	Liquidity flow, pressure, friction, shock, cycle and closure.	This is the focal Chapter 7 architecture.	No solution of Navier-Stokes; no universal crisis law.
Yang-Mills	Gauge curvature, action and finite-network shock thresholds.	Chapter 7 complements threshold logic with time-panel stress-balance logic.	Finite economic analogue only.
BSD	Local-to-global structural rank and corridor stress.	Chapter 7's country-year and regional layers provide another local-to-global stress interpretation.	Calibrated measurement, not arithmetic proof.
Riemann-zeta	Spectral/cyclical signal for inflation forecasting.	Chapter 7 uses Fourier GDP-cycle forcing and rolling validation discipline.	No Riemann Hypothesis claim.
P vs NP	Computational complexity, search and portfolio optimization.	Chapter 7 uses validation gates and claim hierarchy as model-governance logic.	No theorem-level complexity result.

Source: Author synthesis from the seven-document monograph architecture.

7.8.10. Final Claim Boundary

The final claim boundary must be stated directly because the chapter uses a powerful mathematical analogy. The chapter does not claim that macro-financial liquidity is literally a physical fluid. It does not claim to solve, prove, test or replicate the mathematical Navier-Stokes existence and smoothness problem. It does not claim that the world economy obeys hydrodynamic laws. It does not claim that the model provides definitive causal estimates or a universal crisis-prediction system.

The chapter does make a strong bounded claim: a Navier-Stokes-inspired nondimensional stress-balance framework can be used as a transparent macro-financial diagnostic architecture for measuring systemic stress, liquidity resilience, pressure gradients, friction, shocks, GDP-cycle forcing and restricted hidden adjustment across a global panel. The model's rolling validation, benchmark comparison, robustness checks, external-target plausibility tests, Monte Carlo uncertainty and policy counterfactuals support its usefulness as a stress-testing framework.

Equation 7.8.3. $C_7 = C_{design} \cap C_{data} \cap C_{scaling} \cap C_{closure} \cap C_{validation} \cap C_{robustness} \cap C_{policy} \cap C_{boundary}$

The final admissible claim set C_7 is an intersection of evidence gates. A claim is admissible only if it passes the design, data, scaling, closure, validation, robustness, policy and boundary conditions. The chapter therefore treats scientific strength as layered evidence, not as one isolated result.

Equation 7.8.4. $X_7 = \{literal_fluid_identity, Navier_Stokes_proof, universal_crisis_prediction, unrestricted_causality, guaranteed_policy_effects\}$

The exclusion set X_7 defines claims that are explicitly outside the chapter. The presence of a mathematical analogy does not authorize theorem-level, physical or unconditional policy claims.

Table 7.8.8. Final admissible-claim and excluded-claim matrix

Claim category	Admissible final claim	Excluded overclaim
Mathematical analogy	Navier-Stokes logic is used as an economic measurement grammar.	The chapter solves or tests the mathematical Navier-Stokes problem.

Claim category	Admissible final claim	Excluded overclaim
Liquidity interpretation	Liquidity-flow weakness can be represented as a diagnostic stress channel.	Financial liquidity is literally a physical fluid.
Stress measurement	Systemic stress can be constructed from nondimensional flow-pressure-friction-shock-cycle-closure components.	The constructed stress index is the unique true measure of global financial stress.
Closure	epsilon(t) is restricted and state-dependent.	The residual term fully eliminates hidden uncertainty.
Forecasting	Rolling validation supports diagnostic usefulness within the stated validation window.	The model universally dominates all benchmarks in all samples and horizons.
Panel estimation	FE/robust-inference results support diagnostic association.	The coefficients establish definitive structural causality.
External validation	External target alignment supports plausibility.	External validation proves the model mechanism.
Policy scenarios	Counterfactuals provide model-implied stress-testing effects.	Policy impacts are guaranteed or randomized-causal.

Source: Author synthesis for Chapter 7 final claim boundary.

7.8.11. Limitations and Academic Caution

The limitations of Chapter 7 are not secondary notes; they are part of the scientific design. The first limitation is analogical. The model uses Navier-Stokes logic as an economic measurement architecture, not as a literal physical law. The second limitation is measurement-related. Even with nondimensional scaling, the quality of the constructed stress balance depends on the quality of the underlying macro-financial proxies, the direction harmonization rules and the normalization choices.

The third limitation concerns panel interpretation. A 100-country annual panel for 2010-2024 provides a strong global evidence base, but annual frequency cannot fully capture high-frequency liquidity dynamics, intraday market stress, institutional intervention timing or microstructure liquidity. The fourth limitation concerns external validation. External target families improve plausibility, but they do not provide randomized causal identification. The fifth limitation concerns scenarios. Monte Carlo paths and policy counterfactuals are useful for stress testing, but they remain conditional on the model design.

The sixth limitation is forecast portability. A favorable benchmark hierarchy over the reported rolling validation window does not automatically imply permanent dominance across all future samples, regions or stress regimes. The seventh limitation is data lineage. Some variables may share source families or transformation logic, which means internal validation must be separated from genuinely external evidence. The chapter addresses these concerns through explicit claim hierarchy rather than by ignoring them.

Table 7.8.9. Limitations and academic-caution matrix

Limitation	Why it matters	How the chapter handles it	Residual caution
Analogy limitation	Mathematical language can be overread as theorem-level proof.	The chapter repeatedly states the economic-analogue boundary.	No physical or Clay-problem claim.
Proxy limitation	Macro-financial stress variables are imperfect proxies.	Direction, scaling and lineage rules are disclosed.	Measurement error remains possible.
Annual-frequency limitation	Liquidity stress can evolve faster than annual data.	Rolling validation and macro-regional interpretation are used at the available frequency.	Higher-frequency replication would strengthen the model.
Causal-identification limitation	FE associations and external targets are not randomized experiments.	Results are interpreted as diagnostic associations.	Causal claims remain bounded.
Scenario limitation	Monte Carlo and counterfactuals are model-	They are framed as stress-testing	They are not unconditional

Limitation	Why it matters	How the chapter handles it	Residual caution
	dependent.	outputs.	forecasts.
Benchmark limitation	Forecast rankings depend on sample, horizon and benchmark specification.	Benchmarks are explicitly named and interpreted within the validation window.	Universal superiority is excluded.
Replication limitation	Constructed variables require transparent reproducibility.	The chapter relies on a data and replication package with formulas and output objects.	Version control must be preserved.

Source: Author synthesis based on the chapter's final evidence hierarchy.

7.8.12. Data, Replication and Reproducibility Closure

The chapter's final reproducibility conclusion is that the stress-testing architecture is only as credible as its traceability. Every step from public macro-financial input to final stress result must be auditable: raw/public anchor selection, direction harmonization, nondimensional transformation, index construction, balance-equation calculation, epsilon(t) closure estimation, Fourier-cycle forcing, rolling validation, benchmark comparison, robustness tests, external-validation targets, Monte Carlo simulations and policy counterfactuals.

The associated data and replication materials for the Navier-Stokes-inspired manuscript are identified as archived on Zenodo under the data and replication package for "Navier-Stokes-Inspired Global Liquidity-Flow and Systemic-Stress Modelling: Data and Replication Package for a Nondimensional Macro-Financial Stress-Testing Framework." The replication package is important because it converts the chapter's numerical and methodological claims into a verifiable external audit object. In the monograph, this data-package logic should be retained as part of the general data and replication statement as well as the Chapter 7-specific note.

The final reproducibility claim is therefore not merely that the author reports results. The claim is that the model is structured as a replication-ready pipeline. That pipeline is central to the chapter's publication value because it allows the reader to identify which objects are public inputs, which are author-constructed variables, which are model outputs and which are validation or scenario layers.

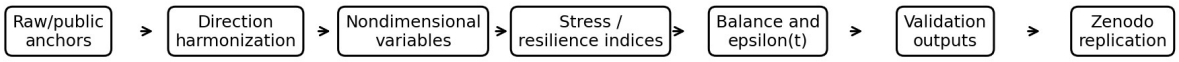


Figure 7.8.5. Replication-closure chain: the chapter claim depends on traceable transformations and archived output objects.

Figure 7.8.5. Replication-closure chain.

Source: Author synthesis for Chapter 7.8 based on the Navier-Stokes-inspired Chapter 7 architecture and the monograph claim-boundary framework.

Table 7.8.10. Replication-closure checklist for Chapter 7

Replication object	Required content	Purpose in Chapter 7
Source ledger	Public data source families, vintages and extraction notes.	Separates official/public inputs from author-constructed variables.
Transformation file	Direction harmonization, normalization and stress/resilience orientation rules.	Makes nondimensional scaling auditable.
Formula catalogue	Stress index, resilience index, balance	Allows equation-level replication.

Replication object	Required content	Purpose in Chapter 7
	equation, closure equation and cycle forcing formulas.	
Panel outputs	Country-year stress, resilience, components, fitted values and residuals.	Supports panel diagnostics and regional aggregation.
Validation outputs	Rolling forecasts, forecast errors, benchmark results and model-comparison statistics.	Supports the forecasting claim hierarchy.
Robustness outputs	Alternative weights, normalization rules, perturbations and leave-one-component-out checks.	Supports robustness and falsification discipline.
Scenario outputs	Monte Carlo paths, uncertainty intervals and policy-counterfactual stress effects.	Supports scenario interpretation without claiming policy determinism.
Metadata and checksums	File identifiers, version notes and verification hashes.	Protects reproducibility and version control.

Source: Author synthesis based on the Chapter 7 data and replication package logic.

7.8.13. Final Integrated Conclusion of Chapter 7

The final integrated conclusion is that Chapter 7 successfully converts the Navier-Stokes-inspired idea into a high-level applied macro-financial stress-testing architecture. The chapter's central achievement is not metaphorical borrowing from physics. Its achievement is the construction of a disciplined, nondimensional and empirically auditable framework in which systemic stress is interpreted as the outcome of flow weakness, acceleration, pressure gradients, liquidity friction, stochastic shocks, GDP-cycle forcing and restricted hidden adjustment.

The chapter demonstrates that such a framework can be implemented at global scale using a 100-country annual panel for 2010-2024, interpreted with a World anchor and macro-regional layers. It further demonstrates that the framework can be evaluated through rolling validation, benchmark comparison, fixed-effects diagnostics, robustness checks, external-target plausibility, Monte Carlo uncertainty and policy counterfactuals. These layers jointly support a strong diagnostic conclusion: the Navier-Stokes-inspired stress-balance model is a useful and reproducible architecture for global systemic-stress measurement and macroprudential stress-testing interpretation.

The strongest methodological result is nondimensional discipline. The strongest modelling result is restricted closure. The strongest empirical result is the reported validation and benchmark structure. The strongest interpretive result is that systemic vulnerability is multi-channel and regionally heterogeneous. The strongest policy result is that the framework translates shocks and buffers into interpretable stress-index effects under specified assumptions. The strongest academic-safety result is the explicit claim boundary.

Therefore, Chapter 7 should be read as a scientifically cautious but ambitious contribution to macro-financial modelling. It supports global systemic-stress diagnostics, liquidity-resilience analysis, rolling stress validation, scenario analysis and policy-counterfactual stress testing. It does not assert literal hydrodynamic identity, does not solve the mathematical Navier-Stokes problem, does not establish definitive causality and does not provide universal crisis prediction. Its final claim is high but bounded: the framework is a reproducible economic analogue for measuring and interpreting global liquidity-flow stress under pressure, friction, shocks, cycles and closure.

Table 7.8.11. Final integrated conclusion matrix

Final conclusion object	Chapter 7 final statement
Main contribution	A nondimensional Navier-Stokes-inspired macro-financial stress-testing architecture for global liquidity-flow and systemic-stress modelling.
Empirical strength	A 100-country annual panel for 2010-2024 with World-anchor and macro-regional interpretation, rolling validation and benchmark comparison.
Methodological strength	Direction harmonization, nondimensional scaling, component balance, restricted epsilon(t) closure and auditable validation design.
Interpretive strength	Systemic stress is multi-channel: weak flow, pressure gradients, friction, shocks, cycles and hidden adjustment combine differently across countries and regions.
Policy strength	Monte Carlo and policy counterfactuals convert shocks and buffers into interpretable

Final conclusion object	Chapter 7 final statement
	model-implied stress effects.
Scientific boundary	The chapter is an economic analogue and diagnostic framework, not a physical-law claim, theorem proof, causal law or universal crisis-prediction system.
Monograph role	Chapter 7 supplies the applied macro-financial liquidity-flow pillar of the seven Millennium-inspired economic measurement architectures.

Source: Author final synthesis for Chapter 7.8.

7.8.14. Transition to the Comparative Synthesis of the Monograph

The conclusion of Chapter 7 also prepares the wider monograph transition. The chapter shows how one Millennium-inspired mathematical architecture can be converted into a practical economic measurement system without claiming to solve the original mathematical problem. This same pattern is the governing logic of the full book: each mathematical architecture supplies a measurement grammar, each economic chapter defines a bounded empirical object, each methodology constructs auditable variables, each results section reports model-specific evidence, each interpretation section states what the evidence means, and each claim-boundary section states what the evidence cannot mean.

For the comparative synthesis chapters, Chapter 7 contributes the macro-financial stress-testing axis. It should be compared with the curvature/inequality axis, the Hodge-flow decomposition axis, the Yang-Mills threshold axis, the BSD local-to-global rank axis, the Riemann-zeta spectral forecasting axis and the P vs NP computational-complexity axis. Its distinctive value is that it connects systemic vulnerability, liquidity resilience and policy stress testing in one large-panel framework.

The final transition statement is therefore: Chapter 7 closes as a bounded applied macro-financial contribution and opens the path to the next monograph level, where the seven models can be compared not as isolated articles but as a coordinated system of economic measurement architectures inspired by the seven Clay Millennium Problems.

Table 7.8.12. Transition from Chapter 7 to the monograph-wide comparative synthesis

From Chapter 7	To comparative synthesis
Liquidity-flow stress balance	Compare with Hodge flow decomposition and Yang-Mills shock-threshold logic.
Pressure gradients and friction	Compare with Ricci-style pressure curvature and BSD corridor stress.
Rolling validation and benchmarks	Compare with Riemann-zeta forecasting validation and P-vs-NP computational benchmarking.
Monte Carlo and counterfactuals	Compare with robustness/scenario layers across all seven chapters.
Strict claim boundary	Use as a template for the book-wide exclusion of Clay-problem proof claims.

Source: Author synthesis for the monograph transition.

Chapter 7.8. Chapter Conclusion and Claim Boundary

Chapter placement note. This document is written as Section 7.8 of the monograph chapter on Navier-Stokes-inspired global liquidity-flow and systemic-stress modelling. It closes the applied macro-financial chapter by synthesizing the theoretical analogy, research object, data architecture, methodology, results, interpretation, Monte Carlo evidence, policy counterfactuals, external validation and final claim boundary. It is not a replacement for the book-wide final conclusion; rather, it is the chapter-level closure that prepares the reader for the comparative synthesis across the seven Millennium-inspired economic models.

Core conclusion. Chapter 7 establishes a bounded but high-value macro-financial contribution: systemic stress can be measured as a nondimensional flow-pressure-friction-shock-cycle-closure process across a 100-country annual panel for 2010-2024, supported by a World anchor, macro-regional interpretation, rolling validation, benchmark comparison, robustness checks, external-target validation, Monte Carlo uncertainty and policy counterfactuals. The final claim is strong in diagnostic and stress-testing terms, but it is deliberately bounded against literal physical, theorem-level, causal or universal-prediction overclaiming.

Table 7.8.1. Chapter 7.8 executive closure matrix

Element	Chapter 7.8 specification
Purpose	To close Chapter 7 by converting methodology, empirical results and scenario-validation evidence into a final admissible claim hierarchy.
Empirical universe	100-country annual panel, 2010-2024, N = 1,500, interpreted with a World anchor and macro-

Element	Chapter 7.8 specification
	regional layers.
Central mechanism	Nondimensional stress balance with liquidity velocity weakness, acceleration, pressure gradient, friction/diffusion, stochastic shocks, Fourier GDP-cycle forcing and restricted epsilon(t) closure.
Validation logic	Rolling one-year-ahead validation, benchmark comparison against ARIMA, VAR, GARCH and composite-index baselines, panel diagnostics, robustness gates and external-target plausibility checks.
Policy and uncertainty layer	Monte Carlo uncertainty paths and policy counterfactuals are used as stress-testing instruments, not as guaranteed future forecasts or randomized policy proof.
Final boundary	The chapter does not claim literal fluid mechanics, a solution of the mathematical Navier-Stokes problem, definitive causality or universal crisis prediction.

Source: Author synthesis based on the Chapter 7 Navier-Stokes-inspired methodology, results, interpretation and validation architecture.

7.8.1. Purpose of the Chapter-Level Conclusion

The conclusion of Chapter 7 has a specific function inside the monograph. It must not repeat the introduction, re-estimate the methodology or reproduce all numerical tables from the results section. Its task is to state precisely what has been established, why the evidence is meaningful, how the Navier-Stokes-inspired analogy should be read, which claims are admissible and which claims remain outside the evidence base.

This distinction is important because Chapter 7 is one of the strongest applied macro-financial chapters in the monograph. Its strength comes from the combination of scale, structure and validation: the chapter uses a 100-country annual panel for 2010-2024, a World aggregate anchor, macro-regional interpretation, nondimensional scaling, restricted closure, rolling forecasts, benchmark comparison, Monte Carlo uncertainty and policy counterfactuals. A conclusion that merely says that the model is “useful” would be too weak. A conclusion that turns the analogy into a physical or theorem-level claim would be too strong. The correct conclusion is therefore both ambitious and bounded.

The chapter-level claim is best expressed as a stress-testing and diagnostic claim. The model demonstrates that a global macro-financial system can be represented as an auditable nondimensional balance of flow weakness, pressure gradients, friction, shocks, cycles and restricted hidden adjustment. The evidence supports the use of this balance for systemic-stress diagnostics, rolling validation, scenario interpretation and policy-counterfactual stress testing. The evidence does not support claims that liquidity is literally a fluid, that the mathematical Navier-Stokes problem has been solved or empirically tested, or that the model can guarantee crisis prediction across all countries and time horizons.

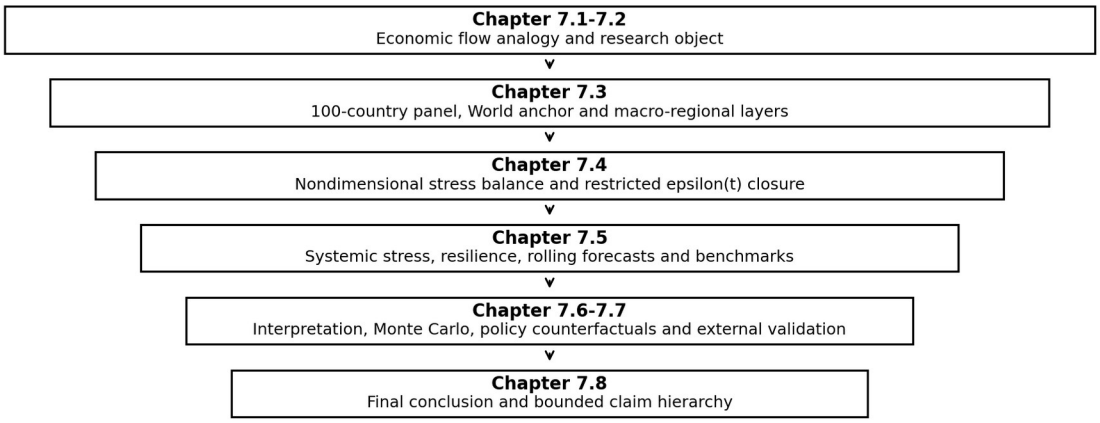


Figure 7.8.1. Chapter-closure architecture: the conclusion is a synthesis of evidence layers, not a repetition of the results section.

Figure 7.8.1. Chapter-closure architecture.

Source: Author synthesis for Chapter 7.8 based on the Navier-Stokes-inspired Chapter 7 architecture and the monograph claim-boundary framework.

7.8.2. What Chapter 7 Establishes

Chapter 7 establishes six integrated results. First, it establishes a translation grammar: velocity, acceleration, pressure gradient, diffusion/friction, external forcing and closure are translated into economic diagnostic components. Second, it establishes a research object: global liquidity-flow stress is treated as a country-year and macro-regional stress system rather than as a single indicator. Third, it establishes a data architecture: the 100-country panel, World anchor and macro-regional layers are separated so that panel estimation, global normalization and regional interpretation do not collapse into one undifferentiated object.

Fourth, the chapter establishes a methodology based on nondimensional balance. This is a decisive point. The model does not add raw inflation rates, spreads, liquidity proxies, volatility measures and fiscal buffers as if they were expressed in a common physical unit. Instead, it transforms them into unit-free stress-direction or resilience-direction components. This is what makes the Navier-Stokes analogy auditable rather than metaphorical. Fifth, the chapter establishes empirical usefulness through rolling validation and benchmark comparison. Sixth, it establishes scenario usefulness through Monte Carlo uncertainty paths and policy counterfactuals.

The final synthesis is therefore not that one variable predicts crises. The synthesis is that systemic stress is a structured balance. Weak liquidity flow, rising pressure gradients, frictional diffusion, shock forcing, cyclical deformation and hidden adjustment jointly form the stress state. This is the chapter’s core applied macro-financial contribution.

Table 7.8.2. Final synthesis of what Chapter 7 establishes

Result domain	What is established	Why it matters for the chapter conclusion	Claim status
Analogy design	The Navier-Stokes architecture is translated into a macro-financial flow-balance grammar.	It gives the chapter a formal organizing logic rather than a loose metaphor.	Admissible as an economic analogue.
Data architecture	A 100-country annual panel for 2010-2024 is combined with a World anchor and macro-regional layers.	It gives the chapter scale and interpretive structure.	Admissible as a global diagnostic panel.
Nondimensional scaling	Stress components are transformed into comparable unit-free variables.	It prevents raw-unit inconsistency and strengthens reviewer safety.	Strong methodological claim.
Restricted closure	epsilon(t) is modelled through observable or proxy-observable state variables.	It prevents the hidden term from operating as an unrestricted residual plug.	Strong modelling claim.
Rolling validation	One-year-ahead validation is compared with benchmark models.	It tests diagnostic usefulness outside the immediate fitting equation.	Validation-window claim only.
External validation	Constructed stress is compared with external macro-financial target families.	It adds plausibility evidence beyond internal construction.	Diagnostic plausibility, not causal proof.
Monte Carlo and policy scenarios	Uncertainty bands and counterfactual stress effects are reported.	It makes the framework useful for stress-testing and policy interpretation.	Model-implied scenario claim.

Source: Author synthesis from Sections 7.1-7.7.

7.8.3. Final Methodological Conclusion: Nondimensional Discipline

The strongest methodological conclusion is that nondimensional discipline is the condition under which the Navier-Stokes-inspired analogy becomes scientifically defensible. In physical flow models, variables are linked by strict dimensional consistency. In macro-financial economics, the indicators are heterogeneous: inflation pressure, sovereign-risk spreads, liquidity proxies, exchange-rate volatility, fiscal buffers, transfer dependence and geopolitical shock variables do not share a single natural unit. Therefore the chapter does not claim literal physical units. It creates a unit-free stress-coordinate system. The model's methodological value is that it forces the analyst to make every transformation explicit: direction harmonization, normalization, stress orientation, resilience orientation, weighting, closure estimation and validation. This prevents the common weakness of composite stress indices, where heterogeneous indicators are aggregated without a clear structural interpretation. In Chapter 7, the constructed stress index is not merely an average of variables. It is the dependent stress state generated by a balance of flow, pressure, friction, shock, cycle and closure components.

Equation 7.8.1. S*_{i,t} = B(v*_{i,t}, a*_{i,t}, P*_{i,t}, F*_{i,t}, Z*_{i,t}, C*_{i,t}, epsilon*_{i,t})

Here S* denotes nondimensional systemic stress. The balance function B links velocity weakness, acceleration, pressure, friction/diffusion, stochastic shock, cycle forcing and restricted hidden adjustment. The asterisk indicates that the variables are transformed into comparable diagnostic scale before entering the balance.

This conclusion directly protects the chapter against the most obvious reviewer objection: the model does not pretend that money, liquidity or financial pressure are physical fluids. It uses the flow equation as a measurement grammar. The empirical claim is therefore not hydrodynamic identity; it is stress-balance coherence.

Table 7.8.3. Methodological-risk closure matrix

Methodological risk	How Chapter 7 controls the risk	Final conclusion
Metaphorical overreach	The chapter states that liquidity is not a physical fluid and uses the equation as an economic analogue.	The analogy is bounded.
Raw-unit inconsistency	Variables are direction-harmonized and nondimensionalized before aggregation.	The balance is unit-free and auditable.
Residual plug risk	epsilon(t) is restricted by state variables rather than left as a free balancing term.	Closure is modelled, not hidden.
Forecast overclaiming	Rolling validation is reported only inside the stated 2017-2024 validation design.	Forecast evidence is window-specific.
Benchmark cherry-picking	The model is compared with ARIMA, VAR, GARCH and composite-index baselines.	Benchmark comparison is explicit.
Causal overinterpretation	Panel coefficients, external targets and scenarios are	No unrestricted causal law is

Methodological risk	How Chapter 7 controls the risk	Final conclusion
	interpreted as diagnostic evidence.	claimed.

Source: Author synthesis for the final claim-boundary section.

7.8.4. Final Modelling Conclusion: Restricted epsilon(t) Closure

The second major conclusion concerns the restricted hidden-adjustment term epsilon(t). In many model-based frameworks, residual terms can become dangerous because they absorb whatever the model fails to explain. Chapter 7 avoids this problem by treating epsilon(t) as an interpretable closure channel. It is not a purely arbitrary residual. It is associated with lagged closure, shadow-economy pressure, external transfers, geopolitical shock, fiscal buffers, foreign aid/support and economic inertia.

The purpose of the closure equation is not to force equality mechanically. Its purpose is to represent hidden adjustment that is economically plausible and empirically auditable. Countries may experience stress that is not fully captured by contemporaneous liquidity, pressure or friction variables. Such stress may be absorbed through informal economic activity, foreign support, remittances, emergency financing, fiscal buffers or inertia. The closure term therefore turns hidden macro-financial adjustment into a research object rather than leaving it outside the model.

Equation 7.8.2. epsilon*_{i,t} = rho epsilon*_{i,t-1} + beta_1 Shadow*_{i,t} + beta_2 Transfers*_{i,t} + beta_3 GeoShock*_{i,t} + beta_4 FiscalBuffer*_{i,t} + beta_5 AidSupport*_{i,t} + beta_6 Inertia*_{i,t} + u_{i,t}

The closure equation is intentionally state-dependent. It explains epsilon(t) through lagged hidden adjustment and observable or proxy-observable macro-financial state variables. This makes the closure channel reviewable and prevents the model from relying on an unrestricted residual.

The final modelling conclusion is therefore precise: Chapter 7 does not eliminate uncertainty; it disciplines uncertainty. This is scientifically preferable to claiming that all hidden stress channels are fully observed. The chapter's strength is that it acknowledges hidden adjustment and then restricts its interpretation through an explicit state equation.

7.8.5. Final Empirical Conclusion: Systemic Stress and Liquidity Resilience

The empirical conclusion of Chapter 7 is that systemic stress and liquidity resilience must be interpreted jointly. A high stress score without a resilience score is incomplete, because high pressure may be partly absorbed by buffers, policy capacity, liquidity depth or external support. Conversely, resilience without stress measurement is also incomplete, because a strong buffer is meaningful only relative to the pressure it must absorb. The chapter therefore reads stress formation and resilience capacity as a paired diagnostic system.

This paired interpretation is especially important in a global setting. Macro-financial vulnerability is regionally heterogeneous. A country or region may reach stress through pressure gradients, liquidity friction, sovereign-spread widening, inflation persistence, exchange-rate volatility, external financing constraints or shock exposure. The chapter's flow-balance design helps identify the channel composition rather than reducing stress to a single indicator.

The final empirical interpretation is that systemic vulnerability is multi-channel. Pressure gradients and liquidity friction are not simply separate variables; they interact with weak flow, shocks, cycles and closure. A country with weak liquidity velocity but strong buffers may differ from a country with similar stress but weaker external support. A region with high sovereign-spread pressure may require different policy interpretation than a region dominated by inflation persistence or geopolitical shock. The chapter's contribution is to make these differences visible.

Table 7.8.4. Final interpretation of systemic-stress channels

Stress channel	Interpretive meaning	Vulnerability implication	Policy reading
Liquidity velocity weakness	Liquidity circulates more weakly through the macro-financial system.	Stress may rise even without an immediate shock if flow capacity is weak.	Strengthen liquidity buffers and market-depth channels.
Acceleration pressure	Stress changes rapidly from one period to the next.	A system may appear stable in levels but unstable in dynamics.	Use early-warning monitoring and rolling validation.
Pressure gradient	Macro-financial pressure rises through inflation, spreads or external stress.	Stress becomes directional and potentially transmissible.	Reduce spread, inflation and external-financing pressure.
Friction/diffusion	Credit, banking, market or institutional frictions slow adjustment.	Shocks persist and propagate because adjustment is costly.	Improve financial intermediation and policy transmission.
Stochastic shock	Event risk or volatility enters the stress balance.	Stress can jump nonlinearly under crisis conditions.	Use shock buffers and contingency planning.
GDP-cycle forcing	Business-cycle deformation modifies stress intensity.	Stress may be amplified in downturns and compressed in	Integrate macro cycle forecasts into stress testing.

Stress channel	Interpretive meaning	Vulnerability implication	Policy reading
		recoveries.	
Restricted closure	Hidden adjustment channels absorb or transmit residual stress.	Unobserved resilience or fragility becomes part of the diagnostic object.	Track fiscal buffers, transfers, support and inertia.

Source: Author synthesis based on Chapter 7 flow-pressure-friction-shock-cycle-closure logic.

7.8.6. Final Forecasting Conclusion: Rolling Validation and Benchmarks

Chapter 7's forecasting conclusion is intentionally defined by its validation design. The reported rolling one-year-ahead evidence over 2017-2024 supports the diagnostic usefulness of the Navier-Stokes-inspired stress-balance model inside the stated window. It should not be converted into a universal statement that the model will dominate every alternative benchmark in every sample, every country group or every horizon.

The correct interpretation of the benchmark comparison is comparative and bounded. ARIMA, VAR, GARCH and composite-index baselines each represent useful conventional alternatives: persistence, multivariate dynamics, volatility logic and non-flow composite stress measurement. The Navier-Stokes-inspired model adds an explicitly structured balance among flow weakness, pressure, friction, shocks, cycles and closure. If it performs favorably in the reported validation design, the conclusion is that the structural balance carries useful diagnostic information beyond those baselines. The conclusion is not that the baselines are obsolete or that the model permanently dominates all other methods.

This distinction is essential for publication-quality claim discipline. Forecast accuracy is meaningful only under a specified target, sample, horizon, benchmark set and no-look-ahead protocol. Chapter 7's rolling validation is therefore a strong evidence layer because it is operationally defined, but it remains a validation-window claim rather than a universal forecasting theorem.

Figure 7.8.2. Final evidence hierarchy and claim-boundary ladder

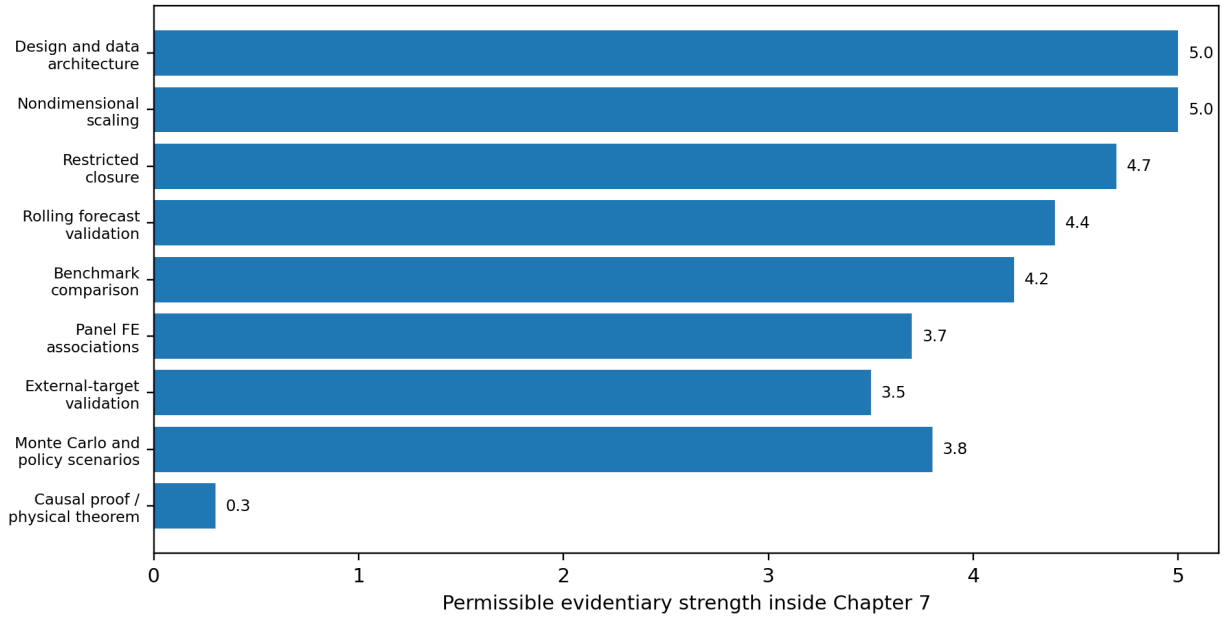


Figure 7.8.2. Final evidence hierarchy and claim-boundary ladder.

Source: Author synthesis for Chapter 7.8 based on the Navier-Stokes-inspired Chapter 7 architecture and the monograph claim-boundary framework.

7.8.7. Final Policy Conclusion: Counterfactual Usefulness without Policy Determinism

The policy conclusion of Chapter 7 is that the model is useful for stress-testing policy counterfactuals, not for guaranteeing policy impacts. Liquidity-buffer strengthening, combined resilience packages, sovereign-spread shocks, inflation persistence, geopolitical shocks and compound adverse scenarios can be translated into model-implied changes in the stress index. This is analytically valuable because it allows policy assumptions to be expressed in a common stress-balance language.

However, counterfactual stress effects are not randomized policy estimates. They are scenario outputs conditional on model structure, variable transformation, parameter calibration and scenario design. The chapter therefore supports a policy-diagnostic claim: the framework can show how stress would move under specified assumptions. It does not claim that a given policy package will mechanically produce the same stress reduction in the real world.

The final policy reading is that the model should be used as a structured macroprudential stress-testing instrument. It can help identify whether a system is more exposed to pressure gradients, liquidity friction, shock amplification, cycle forcing or closure fragility. It can also help design policy packages that target the dominant stress channel. Its value is strongest when used alongside institutional knowledge, country-specific analysis and independent macro-financial surveillance.

Table 7.8.5. Final policy-counterfactual claim boundary

Policy/scenario layer	Permitted conclusion	Excluded conclusion
Liquidity-buffer strengthening	Model-implied stress reduction can be evaluated under specified assumptions.	The model proves that the same policy will reduce stress by the same amount in all contexts.
Combined resilience package	Multi-channel buffer design may lower stress more than isolated measures.	The model establishes a universal optimal policy package.
Sovereign-spread shock	Spread pressure can increase systemic stress in the balance equation.	The model alone identifies the complete causal origin of sovereign stress.
Inflation persistence	Persistent inflation pressure can raise systemic stress and weaken resilience.	The model replaces central-bank inflation analysis.
Geopolitical shock	Shock forcing can be incorporated into stress-testing design.	The model predicts the timing and exact magnitude of geopolitical shocks.
Compound adverse scenario	Joint shocks can reveal nonlinear vulnerability and stress amplification.	The model provides unconditional crisis probability for every country.

Source: Author synthesis based on the Chapter 7 policy-counterfactual logic.

Figure 7.8.3. Admissible and excluded claims in Chapter 7

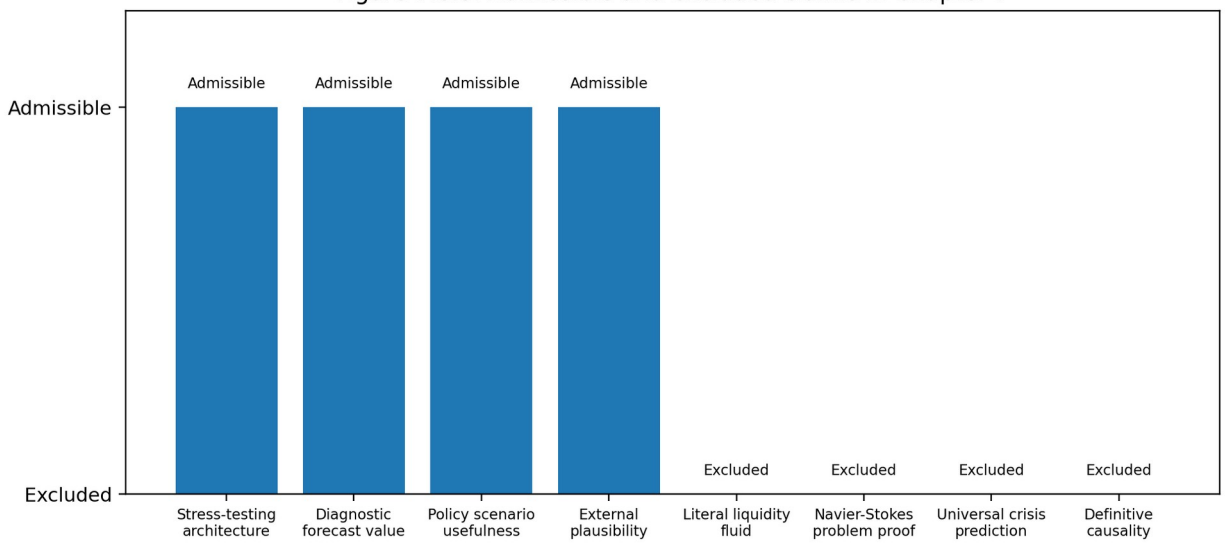


Figure 7.8.3. Admissible and excluded claims in Chapter 7.

Source: Author synthesis for Chapter 7.8 based on the Navier-Stokes-inspired Chapter 7 architecture and the monograph claim-boundary framework.

7.8.8. External Validation and Robustness: Final Interpretation

External validation strengthens the chapter because it tests whether the constructed stress signal behaves plausibly against target families not identical to the internal components. These targets include macro-financial outcomes such as sovereign-spread widening, GDP-growth slowdown, exchange-rate volatility, liquidity tightening, inflation persistence and crisis/event classification. The external layer is important because it reduces the risk that the model is only internally coherent.

At the same time, external validation must be interpreted cautiously. Many macro-financial outcomes are themselves correlated with the same underlying global shocks that shape the stress index. External target performance therefore supports plausibility, not randomized identification. The correct conclusion is that the constructed stress signal has diagnostic external relevance if it aligns with independent target families, but the chapter does not claim that external validation proves a causal Navier-Stokes mechanism in the economy.

Robustness evidence plays a similar role. Weighting alternatives, normalization alternatives, proxy perturbations, leave-one-component-out checks, residual diagnostics, structural checks and shock-year sensitivity tests help establish that the

model is not driven by one arbitrary choice. But robustness is not the same as proof. It is a discipline for evaluating whether the main conclusion survives reasonable perturbations.

Table 7.8.6. Final robustness and external-validation interpretation

Evidence gate	Question answered	Final interpretation	Boundary
Weighting robustness	Does the stress result depend on one chosen weight vector?	Stable results support index robustness.	Does not prove unique true weights.
Normalization robustness	Does scaling drive the result?	Alternative scaling supports transformation stability.	Does not eliminate all measurement error.
Proxy perturbation	Are proxy variables overly decisive?	Perturbation stability increases confidence.	Proxy quality remains a limitation.
Leave-one-component-out	Does one channel dominate mechanically?	Survival under omission supports multi-channel design.	Omitted-channel interpretation must remain cautious.
Residual diagnostics	Are errors structurally problematic?	Stable residual behaviour supports validation credibility.	No claim of perfect residual behaviour.
External target validation	Does stress align with outside target families?	Alignment supports diagnostic plausibility.	Not randomized causal evidence.
Shock-year sensitivity	Are crisis years driving everything?	Sensitivity checks show whether results are shock-dependent.	Crisis dependence may still be substantively meaningful.

Source: Author synthesis based on the Chapter 7 validation-gate framework.

7.8.9. Contribution of Chapter 7 to the Seven-Problem Monograph

Chapter 7 occupies a distinct role inside the monograph. The Perelman/Ricci/Poincare chapter models inequality pressure, curvature and smoothing capacity. The Hodge chapter decomposes macro-flow into gradient hierarchy, curl imbalance and harmonic circulation. The Yang-Mills chapter measures finite-network shock thresholds, curvature/action concentration and economic mass-gap protection. The BSD chapter develops a local-to-global structural-rank analogue. The Riemann-zeta chapter constructs spectral inflation-forecasting diagnostics. The P vs NP chapter analyzes computational difficulty in portfolio optimization. Chapter 7 contributes the applied macro-financial liquidity-flow and systemic-stress pillar.

Its unique contribution is the flow-balance grammar. Whereas Hodge decomposes flows topologically and Yang-Mills measures network thresholds, the Navier-Stokes-inspired chapter asks how stress forms dynamically through flow weakness, acceleration, pressure, friction, shocks, cycles and hidden adjustment. It is therefore the chapter most directly connected to macroprudential stress testing, liquidity fragility, financial resilience and crisis-monitoring design.

This chapter also strengthens the whole monograph because it demonstrates that the book's Millennium-inspired approach is not purely conceptual. It can be applied to a large panel architecture, validated through rolling forecasts, benchmarked against conventional models, tested with robustness gates and used for policy scenarios. Chapter 7 therefore functions as one of the monograph's most operational applied macro-financial chapters.

Figure 7.8.4. Chapter 7 within the seven-problem claim-discipline architecture

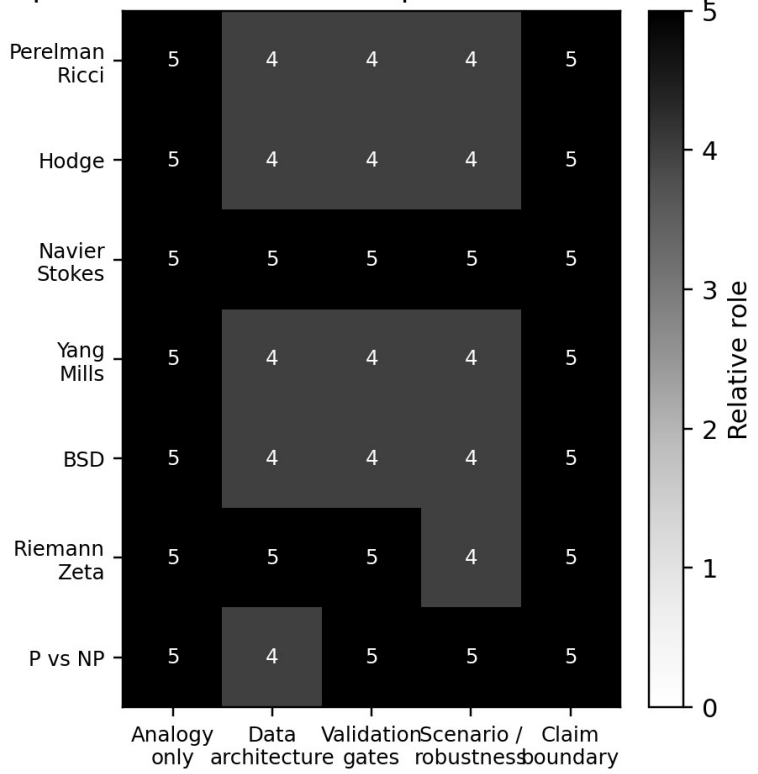


Figure 7.8.4. Chapter 7 within the seven-problem claim-discipline architecture.
Source: Author synthesis for Chapter 7.8 based on the Navier-Stokes-inspired Chapter 7 architecture and the monograph claim-boundary framework.

Table 7.8.7. Cross-problem alignment of Chapter 7 inside the monograph

Millennium-inspired chapter	Economic measurement grammar	How Chapter 7 aligns with it	Shared claim discipline
Perelman/Ricci/Poincare	Curvature, entropy and smoothing capacity in inequality diagnostics.	Chapter 7 similarly interprets stress as a structured deformation rather than a single indicator.	Economic analogue only; no theorem proof.
Hodge	Gradient, curl and harmonic decomposition of macro-flow.	Chapter 7 treats liquidity-flow weakness and pressure gradients as stress channels.	Flow language is diagnostic, not literal physics.
Navier-Stokes	Liquidity flow, pressure, friction, shock, cycle and closure.	This is the focal Chapter 7 architecture.	No solution of Navier-Stokes; no universal crisis law.
Yang-Mills	Gauge curvature, action and finite-network shock thresholds.	Chapter 7 complements threshold logic with time-panel stress-balance logic.	Finite economic analogue only.
BSD	Local-to-global structural rank and corridor stress.	Chapter 7's country-year and regional layers provide another local-to-global stress interpretation.	Calibrated measurement, not arithmetic proof.
Riemann-zeta	Spectral/cyclical signal for inflation forecasting.	Chapter 7 uses Fourier GDP-cycle forcing and rolling validation discipline.	No Riemann Hypothesis claim.
P vs NP	Computational complexity, search and portfolio optimization.	Chapter 7 uses validation gates and claim hierarchy as model-governance logic.	No theorem-level complexity result.

Source: Author synthesis from the seven-document monograph architecture.

7.8.10. Final Claim Boundary

The final claim boundary must be stated directly because the chapter uses a powerful mathematical analogy. The chapter does not claim that macro-financial liquidity is literally a physical fluid. It does not claim to solve, prove, test or replicate the mathematical Navier-Stokes existence and smoothness problem. It does not claim that the world economy obeys hydrodynamic laws. It does not claim that the model provides definitive causal estimates or a universal crisis-prediction system.

The chapter does make a strong bounded claim: a Navier-Stokes-inspired nondimensional stress-balance framework can be used as a transparent macro-financial diagnostic architecture for measuring systemic stress, liquidity resilience, pressure gradients, friction, shocks, GDP-cycle forcing and restricted hidden adjustment across a global panel. The model's rolling validation, benchmark comparison, robustness checks, external-target plausibility tests, Monte Carlo uncertainty and policy counterfactuals support its usefulness as a stress-testing framework.

Equation 7.8.3. $C_7 = C_design \cap C_data \cap C_scaling \cap C_closure \cap C_validation \cap C_robustness \cap C_policy \cap C_boundary$

The final admissible claim set C_7 is an intersection of evidence gates. A claim is admissible only if it passes the design, data, scaling, closure, validation, robustness, policy and boundary conditions. The chapter therefore treats scientific strength as layered evidence, not as one isolated result.

Equation 7.8.4. $X_7 = \{literal_fluid_identity, Navier_Stokes_proof, universal_crisis_prediction, unrestricted_causality, guaranteed_policy_effects\}$

The exclusion set X_7 defines claims that are explicitly outside the chapter. The presence of a mathematical analogy does not authorize theorem-level, physical or unconditional policy claims.

Table 7.8.8. Final admissible-claim and excluded-claim matrix

Claim category	Admissible final claim	Excluded overclaim
Mathematical analogy	Navier-Stokes logic is used as an economic measurement grammar.	The chapter solves or tests the mathematical Navier-Stokes problem.
Liquidity interpretation	Liquidity-flow weakness can be represented as a diagnostic stress channel.	Financial liquidity is literally a physical fluid.
Stress measurement	Systemic stress can be constructed from nondimensional flow-pressure-friction-shock-cycle-closure components.	The constructed stress index is the unique true measure of global financial stress.
Closure	epsilon(t) is restricted and state-dependent.	The residual term fully eliminates hidden uncertainty.
Forecasting	Rolling validation supports diagnostic usefulness within the stated validation window.	The model universally dominates all benchmarks in all samples and horizons.
Panel estimation	FE/robust-inference results support diagnostic association.	The coefficients establish definitive structural causality.
External validation	External target alignment supports plausibility.	External validation proves the model mechanism.
Policy scenarios	Counterfactuals provide model-implied stress-testing effects.	Policy impacts are guaranteed or randomized-causal.

Source: Author synthesis for Chapter 7 final claim boundary.

7.8.11. Limitations and Academic Caution

The limitations of Chapter 7 are not secondary notes; they are part of the scientific design. The first limitation is analogical. The model uses Navier-Stokes logic as an economic measurement architecture, not as a literal physical law. The second limitation is measurement-related. Even with nondimensional scaling, the quality of the constructed stress balance depends on the quality of the underlying macro-financial proxies, the direction harmonization rules and the normalization choices.

The third limitation concerns panel interpretation. A 100-country annual panel for 2010-2024 provides a strong global evidence base, but annual frequency cannot fully capture high-frequency liquidity dynamics, intraday market stress, institutional intervention timing or microstructure liquidity. The fourth limitation concerns external validation. External target families improve plausibility, but they do not provide randomized causal identification. The fifth limitation concerns scenarios. Monte Carlo paths and policy counterfactuals are useful for stress testing, but they remain conditional on the model design.

The sixth limitation is forecast portability. A favorable benchmark hierarchy over the reported rolling validation window does not automatically imply permanent dominance across all future samples, regions or stress regimes. The seventh limitation is data lineage. Some variables may share source families or transformation logic, which means internal validation

must be separated from genuinely external evidence. The chapter addresses these concerns through explicit claim hierarchy rather than by ignoring them.

Table 7.8.9. Limitations and academic-caution matrix

Limitation	Why it matters	How the chapter handles it	Residual caution
Analogy limitation	Mathematical language can be overread as theorem-level proof.	The chapter repeatedly states the economic-analogue boundary.	No physical or Clay-problem claim.
Proxy limitation	Macro-financial stress variables are imperfect proxies.	Direction, scaling and lineage rules are disclosed.	Measurement error remains possible.
Annual-frequency limitation	Liquidity stress can evolve faster than annual data.	Rolling validation and macro-regional interpretation are used at the available frequency.	Higher-frequency replication would strengthen the model.
Causal-identification limitation	FE associations and external targets are not randomized experiments.	Results are interpreted as diagnostic associations.	Causal claims remain bounded.
Scenario limitation	Monte Carlo and counterfactuals are model-dependent.	They are framed as stress-testing outputs.	They are not unconditional forecasts.
Benchmark limitation	Forecast rankings depend on sample, horizon and benchmark specification.	Benchmarks are explicitly named and interpreted within the validation window.	Universal superiority is excluded.
Replication limitation	Constructed variables require transparent reproducibility.	The chapter relies on a data and replication package with formulas and output objects.	Version control must be preserved.

Source: Author synthesis based on the chapter's final evidence hierarchy.

7.8.12. Data, Replication and Reproducibility Closure

The chapter's final reproducibility conclusion is that the stress-testing architecture is only as credible as its traceability. Every step from public macro-financial input to final stress result must be auditable: raw/public anchor selection, direction harmonization, nondimensional transformation, index construction, balance-equation calculation, epsilon(t) closure estimation, Fourier-cycle forcing, rolling validation, benchmark comparison, robustness tests, external-validation targets, Monte Carlo simulations and policy counterfactuals.

The associated data and replication materials for the Navier-Stokes-inspired manuscript are identified as archived on Zenodo under the data and replication package for "Navier-Stokes-Inspired Global Liquidity-Flow and Systemic-Stress Modelling: Data and Replication Package for a Nondimensional Macro-Financial Stress-Testing Framework." The replication package is important because it converts the chapter's numerical and methodological claims into a verifiable external audit object. In the monograph, this data-package logic should be retained as part of the general data and replication statement as well as the Chapter 7-specific note.

The final reproducibility claim is therefore not merely that the author reports results. The claim is that the model is structured as a replication-ready pipeline. That pipeline is central to the chapter's publication value because it allows the reader to identify which objects are public inputs, which are author-constructed variables, which are model outputs and which are validation or scenario layers.

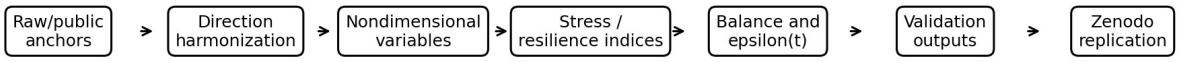


Figure 7.8.5. Replication-closure chain: the chapter claim depends on traceable transformations and archived output objects.

Figure 7.8.5. Replication-closure chain.

Source: Author synthesis for Chapter 7.8 based on the Navier-Stokes-inspired Chapter 7 architecture and the monograph claim-boundary framework.

Table 7.8.10. Replication-closure checklist for Chapter 7

Replication object	Required content	Purpose in Chapter 7
Source ledger	Public data source families, vintages and extraction notes.	Separates official/public inputs from author-constructed variables.
Transformation file	Direction harmonization, normalization and stress/resilience orientation rules.	Makes nondimensional scaling auditable.
Formula catalogue	Stress index, resilience index, balance equation, closure equation and cycle forcing formulas.	Allows equation-level replication.
Panel outputs	Country-year stress, resilience, components, fitted values and residuals.	Supports panel diagnostics and regional aggregation.
Validation outputs	Rolling forecasts, forecast errors, benchmark results and model-comparison statistics.	Supports the forecasting claim hierarchy.
Robustness outputs	Alternative weights, normalization rules, perturbations and leave-one-component-out checks.	Supports robustness and falsification discipline.
Scenario outputs	Monte Carlo paths, uncertainty intervals and policy-counterfactual stress effects.	Supports scenario interpretation without claiming policy determinism.
Metadata and checksums	File identifiers, version notes and verification hashes.	Protects reproducibility and version control.

Source: Author synthesis based on the Chapter 7 data and replication package logic.

7.8.13. Final Integrated Conclusion of Chapter 7

The final integrated conclusion is that Chapter 7 successfully converts the Navier-Stokes-inspired idea into a high-level applied macro-financial stress-testing architecture. The chapter's central achievement is not metaphorical borrowing from physics. Its achievement is the construction of a disciplined, nondimensional and empirically auditable framework in which systemic stress is interpreted as the outcome of flow weakness, acceleration, pressure gradients, liquidity friction, stochastic shocks, GDP-cycle forcing and restricted hidden adjustment.

The chapter demonstrates that such a framework can be implemented at global scale using a 100-country annual panel for 2010-2024, interpreted with a World anchor and macro-regional layers. It further demonstrates that the framework can be evaluated through rolling validation, benchmark comparison, fixed-effects diagnostics, robustness checks, external-target plausibility, Monte Carlo uncertainty and policy counterfactuals. These layers jointly support a strong diagnostic conclusion: the Navier-Stokes-inspired stress-balance model is a useful and reproducible architecture for global systemic-stress measurement and macroprudential stress-testing interpretation.

The strongest methodological result is nondimensional discipline. The strongest modelling result is restricted closure. The strongest empirical result is the reported validation and benchmark structure. The strongest interpretive result is that

systemic vulnerability is multi-channel and regionally heterogeneous. The strongest policy result is that the framework translates shocks and buffers into interpretable stress-index effects under specified assumptions. The strongest academic-safety result is the explicit claim boundary.

Therefore, Chapter 7 should be read as a scientifically cautious but ambitious contribution to macro-financial modelling. It supports global systemic-stress diagnostics, liquidity-resilience analysis, rolling stress validation, scenario analysis and policy-counterfactual stress testing. It does not assert literal hydrodynamic identity, does not solve the mathematical Navier-Stokes problem, does not establish definitive causality and does not provide universal crisis prediction. Its final claim is high but bounded: the framework is a reproducible economic analogue for measuring and interpreting global liquidity-flow stress under pressure, friction, shocks, cycles and closure.

Table 7.8.11. Final integrated conclusion matrix

Final conclusion object	Chapter 7 final statement
Main contribution	A nondimensional Navier-Stokes-inspired macro-financial stress-testing architecture for global liquidity-flow and systemic-stress modelling.
Empirical strength	A 100-country annual panel for 2010-2024 with World-anchor and macro-regional interpretation, rolling validation and benchmark comparison.
Methodological strength	Direction harmonization, nondimensional scaling, component balance, restricted epsilon(t) closure and auditable validation design.
Interpretive strength	Systemic stress is multi-channel: weak flow, pressure gradients, friction, shocks, cycles and hidden adjustment combine differently across countries and regions.
Policy strength	Monte Carlo and policy counterfactuals convert shocks and buffers into interpretable model-implied stress effects.
Scientific boundary	The chapter is an economic analogue and diagnostic framework, not a physical-law claim, theorem proof, causal law or universal crisis-prediction system.
Monograph role	Chapter 7 supplies the applied macro-financial liquidity-flow pillar of the seven Millennium-inspired economic measurement architectures.

Source: Author final synthesis for Chapter 7.8.

7.8.14. Transition to the Comparative Synthesis of the Monograph

The conclusion of Chapter 7 also prepares the wider monograph transition. The chapter shows how one Millennium-inspired mathematical architecture can be converted into a practical economic measurement system without claiming to solve the original mathematical problem. This same pattern is the governing logic of the full book: each mathematical architecture supplies a measurement grammar, each economic chapter defines a bounded empirical object, each methodology constructs auditable variables, each results section reports model-specific evidence, each interpretation section states what the evidence means, and each claim-boundary section states what the evidence cannot mean.

For the comparative synthesis chapters, Chapter 7 contributes the macro-financial stress-testing axis. It should be compared with the curvature/inequality axis, the Hodge-flow decomposition axis, the Yang-Mills threshold axis, the BSD local-to-global rank axis, the Riemann-zeta spectral forecasting axis and the P vs NP computational-complexity axis. Its distinctive value is that it connects systemic vulnerability, liquidity resilience and policy stress testing in one large-panel framework.

The final transition statement is therefore: Chapter 7 closes as a bounded applied macro-financial contribution and opens the path to the next monograph level, where the seven models can be compared not as isolated articles but as a coordinated system of economic measurement architectures inspired by the seven Clay Millennium Problems.

Table 7.8.12. Transition from Chapter 7 to the monograph-wide comparative synthesis

From Chapter 7	To comparative synthesis
Liquidity-flow stress balance	Compare with Hodge flow decomposition and Yang-Mills shock-threshold logic.
Pressure gradients and friction	Compare with Ricci-style pressure curvature and BSD corridor stress.
Rolling validation and benchmarks	Compare with Riemann-zeta forecasting validation and P-vs-NP computational benchmarking.
Monte Carlo and counterfactuals	Compare with robustness/scenario layers across all seven chapters.
Strict claim boundary	Use as a template for the book-wide exclusion of Clay-problem proof claims.

Source: Author synthesis for the monograph transition.

Chapter 7.8 source basis. This section synthesizes the Navier-Stokes-inspired global liquidity-flow and systemic-stress manuscript, the Chapter 7 monograph structure, and the seven-problem claim-boundary architecture. It is written as a monograph subsection rather than as a direct transfer of the article conclusion.

Chapter 8. Yang-Mills Economic Mass Gap in Global and Corridor Flow Networks

8.1. Yang-Mills Gauge Logic and the Economic Mass-Gap Analogy

This section establishes the conceptual foundation of Chapter 8. Its task is not to reproduce the article introduction as a separate self-contained paper, but to transform the Yang-Mills source study into one monographic problem chapter within the broader Millennium economic research program. The section explains why gauge logic is useful for measuring global-corridor systemic stress, how the language of potential, curvature, action and mass gap is translated into a finite economic network, and why the resulting claim must remain explicitly bounded.

The analytical starting point is that the contemporary world economy is not only a set of national or regional aggregates. It is also a flow network in which logistics corridors, financial channels, energy interfaces, regional demand centers, supply-chain routes and geopolitical transmission paths interact. Output mass remains important, but it does not exhaust systemic relevance. A large node may dominate GDP while remaining relatively protected from corridor stress; a smaller node may have limited output mass but become systemically relevant because it functions as a bridge through which shocks can be transmitted.

The Yang-Mills economic mass-gap chapter addresses precisely this measurement problem. Standard macroeconomic indicators can describe GDP, growth, inflation, income depth or trade exposure, but they do not by themselves measure when stress becomes transmissible across a connected topology. Conventional network statistics can measure degree, centrality or clustering, but they do not automatically convert macroeconomic stress into a finite threshold separating locally absorbable disturbances from systemically transmissible shocks. The chapter therefore introduces a gauge-econometric architecture in which stress, relation, curvature and threshold are measured jointly.

8.1.1. Function of the Section within the Monograph

Within the book structure, Section 8.1 performs a conceptual translation role. Chapter 1 already states the general claim boundary of the monograph: the book develops seven economic-econometric analogues inspired by the Clay Millennium Problems and does not claim to solve the original mathematical problems. Chapter 2 explains the general translation grammar from mathematical objects to economic measurement architectures. Chapter 3 consolidates the integrated literature review. Chapter 4 specifies shared methodology, data architecture and replication discipline. Section 8.1 now applies that general foundation to the Yang-Mills case.

The section therefore has three functions. First, it defines the admissible meaning of Yang-Mills language in an economic context. Second, it clarifies why the finite weighted graph is the correct mathematical object for this chapter rather than a continuum physical field. Third, it prepares the reader for the later Chapter 8 sections: the research object in 8.2, the ten-node and twenty-seven-edge data architecture in 8.3, the gauge potential, curvature, action and stress Laplacian methodology in 8.4, the positive finite-network mass-gap results in 8.5, the systemic-shock interpretation in 8.6, the scenario simulations in 8.7, the N = 1,500 validation pathway in 8.8 and the chapter conclusion in 8.9.

This positioning is important because a monograph cannot simply place seven article introductions side by side. The Yang-Mills chapter must speak to the same overarching research program as the Perelman-Ricci-Poincare, Hodge, Navier-Stokes, BSD, Riemann-zeta and P-vs-NP chapters. The shared theme is that global economic complexity can be measured through formal structures that are not visible in scalar indicators alone: curvature, flow, topology, spectral separation, local-to-global propagation, forecasting signals and computational complexity.

Table 8.1.1. Role of Section 8.1 inside the Chapter 8 architecture

Element	Function inside Section 8.1	Where it is developed later in Chapter 8
Gauge logic	Defines why economic stress is represented as a relational field rather than a single scalar variable.	8.4 methodology and 8.5 results
Economic mass-gap analogy	Defines the finite-network meaning of λ1 as a shock-threshold measure.	8.5 results and 8.6 interpretation
Corridor exposure	Explains why small bridge nodes can have systemic relevance beyond GDP mass.	8.3 data architecture, 8.6 interpretation and 8.7 scenarios
Claim boundary	Prevents theorem-level or physical-field overclaiming.	8.8 validation pathway and Chapter 14 limitations
Monograph integration	Connects the Yang-Mills chapter to flow, topology, rank, inflation and optimization chapters.	Chapter 12 comparative results and Chapter 13 unified interpretation

Source note: Author synthesis for the monograph chapter based on the Yang-Mills source manuscript and the general monograph structure.

8.1.2. From Yang-Mills Gauge Logic to Economic Measurement Grammar

Classical Yang-Mills theory belongs to mathematical physics. Its technical content concerns gauge fields, curvature, action functionals and the existence of a positive mass gap under a rigorous field-theoretic formulation. The present monograph does not transfer that theorem-level problem into economics. Instead, it uses the architecture of gauge reasoning as a measurement grammar. The key insight is not that the economy is a physical gauge field, but that a connected economic system can be represented through quantities attached to nodes, quantities attached to edges, circulation around cycles and spectral separation over the whole network.

The economic translation begins from a scalar stress field. Each regional or corridor node is assigned a normalized systemic-stress value constructed from public macroeconomic anchors and disclosed author-calculated transformations. The scalar field alone is insufficient, because systemic stress is not only a property of isolated nodes. Stress becomes transmissible through relations. The next step is therefore to place the nodes inside a weighted global-corridor graph where edge weights represent corridor-sensitive transmission capacity, not merely geographic proximity or raw trade volume.

Once a stress field and a weighted graph exist, gauge logic enters through edge-level tension. The directed economic gauge potential A_ij measures the stress differential between node i and node j after scaling by the relevant edge weight. This is the point at which the model leaves simple indicator analysis. A high-stress node is not automatically systemically dangerous; it becomes systemically relevant when stress differentials interact with a corridor structure that can transmit, amplify or redistribute pressure.

Curvature then measures whether stress differences cancel when traced around triangular cycles. If all edge tensions could be reduced to a smooth node potential, circulation around a closed triangle would vanish. Non-zero triangular curvature means that stress is not fully neutralized by pairwise differences. It indicates local inconsistency, corridor imbalance or residual circulation. In economic terms, curvature identifies network locations where stress does not simply move from high-pressure nodes to low-pressure nodes; it circulates through a cycle and contributes to systemic stress-energy.

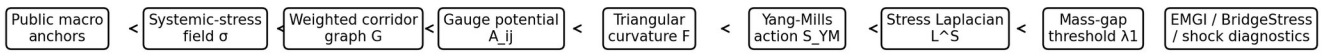


Figure 8.1.1. Gauge-econometric translation pipeline for the Yang-Mills economic mass-gap chapter.

Figure 8.1.1. Gauge-econometric translation pipeline for the Yang-Mills economic mass-gap chapter.

Table 8.1.2. Translation of Yang-Mills concepts into bounded economic-econometric objects

Yang-Mills / spectral term	Economic analogue in this chapter	Permitted interpretation	Excluded interpretation
Gauge field	A structured stress relation defined over a finite global-corridor graph.	A measurement grammar for relational systemic stress.	A literal physical field existing in the economy.
Gauge potential A_ij	Directed edge-level stress tension between connected nodes.	A corridor-weighted stress differential.	A directly observed market price or physical force.
Curvature / field strength F_ijk	Residual stress circulation around triangular network cycles.	Non-neutralized local imbalance and cycle pressure.	Classical non-Abelian field curvature in spacetime.
Yang-Mills action S_YM	Squared-curvature stress-energy over the finite network.	Concentration of systemic stress-energy and cycle tail risk.	A physical action functional or theorem-level invariant.
Mass gap Δ_econ	First positive eigenvalue λ1	Finite-network spectral shock	Solution of the Clay Yang-

	of the stress-weighted Laplacian.	threshold.	Mills existence and mass-gap problem.
Transition threshold λ1 / ρ	Normalized local-to-systemic threshold relative to the spectral radius.	Scale-adjusted stress-propagation boundary.	Universal crisis-prediction law.

Source note: The table deliberately separates mathematically inspired terminology from the narrower economic claims allowed in this monograph.

8.1.3. Economic Field Representation: Nodes, Edges, Stress and Corridor Exposure

The finite-network design begins with a node set V, an edge set E and a weighted adjacency structure W. In the completed benchmark layer of the source manuscript, the substantive economic universe contains ten global and corridor-sensitive nodes connected by twenty-seven weighted undirected edges. The World is not used as an ordinary competing region in the same sense as the nodes; it functions as a normalization anchor for public macroeconomic scale. The node set includes large output-mass regions and corridor-sensitive regions so that the model can distinguish economic size from transmission exposure.

The key methodological rule is separation between public anchors and author-calculated constructs. GDP mass, world-output share, transition GDP, projected growth and GDP per capita provide the observable macroeconomic base. Systemic-stress scores, corridor weights, gauge potentials, triangular curvature, Yang-Mills action, stress Laplacian, EMGI, fragility, BridgeStress and scenario outputs are derived objects. This separation is essential for scientific discipline. It allows the model to be innovative while still telling the reader what is observed, what is constructed and what remains a diagnostic result.

The stress field σ_i is a normalized composite state attached to each node. It is not a raw unit such as dollars, percent growth or inflation points. It is a transformed pressure-oriented construct. Its role is to summarize mass exposure, growth pressure, income fragility, transition momentum and corridor exposure into a common diagnostic coordinate. The common scale is necessary because the gauge potential cannot legitimately add heterogeneous raw macroeconomic units. Only normalized stress quantities can enter the finite-network field representation.

Equation (8.1). $G = (V, E, W), \quad |V| = 10, \quad |E| = 27$

Equation (8.2). $\sigma: V \to [0, 100], \quad i \mapsto \sigma_i$

Equation (8.1) defines the finite global-corridor graph. Equation (8.2) defines the systemic-stress field over the node set. These two objects are the minimum conditions for a gauge-econometric interpretation. Without σ, there is no stress field to transmit. Without G, there is no topology through which stress can circulate. Without W, there is no calibrated edge intensity to distinguish strong and weak corridor channels.

The economic importance of this structure is that it makes corridor exposure visible without reducing systemic relevance to GDP mass. In conventional aggregate analysis, a region with low output share may appear secondary. In a corridor-stress network, however, a region can become important because it connects larger spaces, absorbs logistics pressure, mediates energy or trade routes, or creates a bridge through which shocks can pass. This is why Chapter 8 pays special attention to corridor-sensitive nodes such as the Caucasus and Central Asia. Their relevance is not asserted narratively; it is modelled through stress, edge weights, curvature, BridgeStress and fragility diagnostics.

8.1.4. Gauge Potential and Orientation Discipline

The gauge potential is the first genuinely relational object in the chapter. It translates a difference in node stress into a directed edge-level tension. Direction matters because the potential from i to j is the negative of the potential from j to i. This anti-symmetry prevents double-counting and makes orientation auditable. A result should not depend on arbitrary display conventions; therefore, the chapter treats orientation as a mathematical bookkeeping device rather than a substantive ranking by itself.

In economic terms, A_{ij} asks a precise question: given the stress difference between two connected nodes and the calibrated weight of the corridor edge connecting them, how much directed stress tension is present along that relation? A large value may arise because the stress differential is large, because the edge is systemically strong, or because both conditions coincide. This is more informative than a raw stress ranking because it identifies the edges across which stress pressure is most likely to matter.

Equation (8.3). $A_{ij} = w_{ij}(\sigma_i - \sigma_j) + \eta_{ij}, \quad A_{ji} = -A_{ij}$

Here A_{ij} is the directed economic gauge potential from node i to node j, w_{ij} is the normalized corridor edge weight, $\sigma_i - \sigma_j$ is the systemic-stress differential, and η_{ij} is a corridor-friction term set to zero in the completed benchmark unless an explicit friction layer is estimated.

Orientation discipline is a reviewer-safety device. In a small benchmark graph, it is easy for a table of directed edge values to appear as if one direction is inherently more important than another. The anti-symmetric definition prevents that misunderstanding. If the orientation is reversed, the sign changes, but the absolute tension and the later action contribution remain interpretable. The economic claim therefore concerns the magnitude and pattern of stress tension, not arbitrary directional labels.

This device also distinguishes the Yang-Mills chapter from the Hodge chapter. Hodge decomposition separates a macro-flow pressure field into gradient hierarchy, curl imbalance and harmonic circulation. The Yang-Mills chapter instead focuses on gauge potential and curvature generated by stress-weighted corridor relations. The two chapters share topological language, but they do not measure the same object. Hodge logic decomposes flow components; Yang-Mills logic measures edge potential, cycle curvature, action and spectral threshold.

8.1.5. Curvature, Action and Non-Neutralized Stress Circulation

Curvature is the central concept that makes the Yang-Mills analogy more than a stress-weighted network model. A pairwise edge tension is local. A triangular cycle is relationally higher-order. When the directed potentials around a triangle fail to cancel, the network contains non-neutralized stress circulation. This is the economic counterpart of field strength in the bounded finite-network sense used here.

The use of triangular cycles is methodologically appropriate for the completed benchmark because the graph is connected and cycle-rich. It allows the chapter to detect where stress is not only transmitted through single edges but organized around local corridor systems. In macro-corridor analysis, this matters because logistics, financial and geopolitical stress often circulates across more than two nodes. A shock that begins in one interface may re-enter the system through a different route, producing local imbalance that is invisible to dyadic analysis.

Equation (8.4). $F_{ijk} = A_{ij} + A_{jk} + A_{ki}$

F_{ijk} is the triangular economic field strength around the oriented triangle (i, j, k). The sign is orientation-dependent, while $|F_{ijk}|$ and squared contributions are used for concentration diagnostics.

Equation (8.5). $S_{YM} = \Sigma_{(i,j,k)\in T} \omega_{ijk} F_{ijk}^2$

S_{YM} is the Yang-Mills economic action; T is the set of relevant triangular cycles; ω_{ijk} is a triangle weight; and F_{ijk}^2 converts residual cycle curvature into non-negative stress-energy.

The action functional has a clear economic meaning. It does not state that the economy obeys a physical principle of least action. It summarizes how much squared curvature is present in the constructed stress network and where that curvature is concentrated. If a small number of cycles account for a large share of total action, systemic stress-energy is concentrated rather than diffuse. In the source benchmark, total Yang-Mills economic action is reported as 2,514.0 and the top-five action concentration as 78.329 percent, indicating that systemic stress-energy is dominated by a limited set of high-curvature cycles.

This concentration result is important because it links local corridor imbalance to system-wide fragility. A network can be connected, dense and apparently diversified while still carrying a small number of high-action cycles. For policy interpretation, those cycles are candidate locations for monitoring, resilience investment, route diversification or stress-buffer analysis. For scientific interpretation, they show why the chapter needs gauge and curvature language rather than simple centrality measures alone.

8.1.6. Mass-Gap Analogy as a Finite-Network Spectral Threshold

The mass-gap analogy is the chapter's core spectral concept. In the finite economic network, the stress-weighted Laplacian L^S is constructed from the stress-weighted adjacency matrix W^S and its diagonal stress-degree matrix D^S. The eigenvalues of L^S define the network's stress-diffusion spectrum. For a connected finite graph, $\lambda_0 = 0$ has multiplicity one and represents the normal connected baseline. The first positive eigenvalue λ_1 is the first non-trivial stress-diffusion mode.

The chapter interprets λ_1 as the economic mass gap only in this finite weighted-graph sense. A positive λ_1 means that there is spectral separation between the normal connected state and the first transmissible stress mode. The larger the separation, the stronger the modeled threshold before local stress becomes systemically transmissible. The result is therefore a threshold diagnostic, not a theorem about quantum fields and not an unrestricted crisis-prediction law.

Equation (8.6). $L^S = D^S - W^S$

Equation (8.7). $0 = \lambda_0 \le \lambda_1 \le \ldots \le \lambda_{n-1}$

Equation (8.8). $\Delta_{econ} = \lambda_1 - \lambda_0 = \lambda_1$

Equation (8.9). $\tau_{transition} = \lambda_1 / \rho(L^S)$

τ_transition is the normalized transition threshold and ρ(L^S) is the spectral radius. In the reported benchmark, λ1 = 0.3850, ρ = 3.5023 and τ_transition = 0.1099.

The reported benchmark values supply the quantitative anchor for later sections of Chapter 8. The completed finite-network benchmark yields λ1 = 0.3850, spectral radius 3.5023 and normalized transition threshold 0.1099. These values do not mean that the world economy has a physical particle-mass spectrum. They mean that the constructed stress-weighted corridor graph has a positive first non-zero Laplacian eigenvalue and therefore a measurable spectral boundary between baseline connectedness and the first systemic stress mode.

The threshold interpretation also explains why local-to-systemic transition is a central theme of the chapter. A small shock may remain below the threshold and be locally absorbed. A larger shock, or a shock injected into a high-curvature or fragile corridor node, may compress protection and cross the threshold into systemic transmissibility. Later scenario simulations operationalize this idea through inflation/price-pressure, financial-spread, trade/logistics and energy/geopolitical corridor shocks.

Table 8.1.3. Core benchmark signposts introduced conceptually in Section 8.1

Benchmark object	Reported value or design	Interpretive meaning in Section 8.1
Finite benchmark graph	10 nodes and 27 weighted undirected edges	Substantive global-corridor stress network used for the Chapter 8 measurement architecture.
Stress field	Normalized systemic-stress score over the node set	Pressure-oriented scalar field from which gauge tension is computed.
Economic mass gap	λ1 = 0.3850	Positive first non-zero eigenvalue of the stress-weighted Laplacian.
Spectral radius	ρ = 3.5023	Upper stress-diffusion scale used for normalized threshold interpretation.
Normalized threshold	λ1 / ρ = 0.1099	Local-to-systemic transition boundary in the finite graph.
Yang-Mills economic action	2,514.0	Total squared-curvature stress-energy in the benchmark network.
Top-five action concentration	78.329%	Evidence that stress-energy is concentrated in a limited set of high-curvature cycles.
Validation pathway	100 countries × 15 years = N = 1,500 planned panel	Future route for stronger econometric closure beyond the completed benchmark.

Source note: Benchmark values are included here as conceptual signposts; detailed result tables belong to Section 8.5.

8.1.7. Relation to the Other Millennium-Inspired Economic Models

A core requirement of the monograph is that Chapter 8 must not stand as an isolated article. Its conceptual function must be understood relative to the six other Millennium-inspired economic chapters. The Yang-Mills chapter contributes the gauge/spectral threshold layer of the book. It is not a substitute for the inequality-curvature logic of the Perelman-Ricci-Poincare chapter, the flow-decomposition logic of the Hodge chapter, the liquidity-flow stress-balance logic of the Navier-Stokes chapter, the local-to-global structural-rank logic of the BSD chapter, the zeta-cycle forecasting logic of the Riemann chapter or the sparse optimization logic of the P-vs-NP chapter.

The unifying point is that all seven chapters translate mathematical architectures into bounded economic measurement systems. Each chapter has a different object: smoothing capacity, flow decomposition, liquidity stress balance, gauge curvature and mass gap, local-to-global rank formation, inflation spectral forecasting and computational-finance complexity. Chapter 8's specific contribution is to convert corridor-sensitive macroeconomic stress into a finite gauge network whose spectral separation gives a threshold interpretation.

Table 8.1.4. Cross-chapter integration of the Yang-Mills gauge logic

Book chapter	Primary mathematical grammar	Economic object measured	How Chapter 8 connects
Chapter 5. Perelman-Ricci-Poincare	Curvature, entropy and connectedness	Inequality pressure, smoothing capacity and macro-regional deformation	Provides the broader curvature-and-smoothing vocabulary; Chapter 8 shifts from inequality curvature to corridor stress curvature.
Chapter 6. Hodge	Gradient, curl and harmonic	Macro-flow hierarchy, local imbalance and systemic	Shares cycle and flow logic; Chapter 8 uses curvature/action rather than

	decomposition	circulation	Hodge energy decomposition.
Chapter 7. Navier-Stokes	Flow, pressure, friction, forcing and closure	Liquidity-flow stress and systemic macro-financial resilience	Supplies flow-pressure intuition; Chapter 8 supplies a spectral threshold for corridor shock transmissibility.
Chapter 8. Yang-Mills	Gauge potential, curvature, action and mass gap	Finite-network systemic shock threshold in global-corridor flows	Core chapter object: λ1 as positive finite-network economic mass gap.
Chapter 9. BSD	Local-to-global and L-function/rank analogy	Structural rank formation and corridor stress	Complements Chapter 8 by asking how local regional reductions inform global rank, rather than how curvature produces a shock threshold.
Chapter 10. Riemann-zeta	Spectral/cyclical critical-line signal	Global inflation-pressure forecasting	Shares spectral discipline; Chapter 8 uses Laplacian spectrum rather than zeta-cycle correction.
Chapter 11. P-vs-NP	Combinatorial complexity and sparse optimization	Portfolio support selection under CAPM and derivative overlay	Complements the network chapters by showing how economic complexity also appears as computational search explosion.

Source note: This table converts the seven-document portfolio into a monograph-level integration matrix rather than a sequence of separate article structures.

8.1.8. Evidence Hierarchy and Reviewer-Safe Claim Boundary

The chapter's scientific credibility depends on a strict hierarchy of claims. The strongest claim is a finite-network benchmark claim: given the disclosed ten-node, twenty-seven-edge construction and its stress-weighted Laplacian, the benchmark reports a positive first non-zero eigenvalue. This is a mathematical statement about a constructed finite graph. It is admissible if the graph, matrices, formulas and outputs are disclosed.

A second level is diagnostic interpretation. EMGI, fragility, BridgeStress, curvature exposure, action concentration and scenario compression are valid as model-derived diagnostics. They can support statements about structural exposure inside the constructed network, but they should not be presented as official macroeconomic indicators or as independent causal estimates. Their strength is interpretability and reproducibility within the model architecture.

A third level is econometric association. The source manuscript includes a diagnostic N = 10 benchmark layer and specifies a country-panel validation pathway. Small-sample diagnostic association can be reported cautiously, but stronger fixed-effects, two-way fixed-effects, Driscoll-Kraay, clustered, dynamic-panel, panel-IV, factor and external-validation claims must be reserved for the populated N = 1,500 country-year layer. Section 8.1 therefore sets up the correct evidence language before the results chapter is read.

A fourth level is theorem exclusion. No result in Chapter 8 can be described as solving, proving, testing or replicating the original Yang-Mills existence and mass-gap problem. The word mass gap is retained because it is operationally meaningful in finite spectral graph analysis, but every occurrence must remain attached to the qualifier economic, finite-network, stress-weighted or graph-Laplacian. This language prevents the central contribution from being mistaken for a mathematical theorem claim.

Table 8.1.5. Claim hierarchy for Chapter 8

Claim level	Permitted wording	Evidence requirement	Non-permitted wording
Finite-network mathematical benchmark	The constructed stress-weighted graph reports a positive first non-zero Laplacian eigenvalue.	Disclosed nodes, edges, weights, stress field, W^S, L^S and eigenvalues.	The Yang-Mills mass-gap problem is solved.
Diagnostic interpretation	EMGI, fragility and BridgeStress identify local protection and corridor exposure within the model.	Component audit, formulas, scenario outputs and sensitivity checks.	The index is an official or universally causal macroeconomic measure.
Scenario simulation	Specified shocks compress the normalized transition threshold and increase stress concentration in the model.	Recalculation rules, scenario parameters and output tables.	The model predicts all future crises unconditionally.

Econometric validation	The N = 1,500 panel pathway can test stronger country-level associations after population and estimation.	Country-year variables, panel estimators, diagnostics, external outcomes and archived scripts.	Small N = 10 diagnostics prove causal laws.
Monograph-level contribution	The chapter adds a gauge/spectral threshold layer to the seven-problem economic measurement program.	Consistency with Chapters 1-4 and comparative synthesis in Chapters 12-15.	The book resolves the Clay Millennium Problems.

Source note: The hierarchy is designed to preserve scientific ambition while preventing overstatement.

8.1.9. Section Synthesis

Section 8.1 has established the conceptual logic of the Yang-Mills economic mass-gap chapter. The finite-network gauge-econometric architecture begins with public macroeconomic anchors, transforms them into a systemic-stress field, embeds the field in a ten-node and twenty-seven-edge global-corridor graph, constructs anti-symmetric gauge potentials on edges, measures triangular curvature, summarizes squared curvature through Yang-Mills economic action and evaluates spectral separation through the stress-weighted Laplacian.

The chapter's central analogy is therefore precise. The economic mass gap is not a physical field-theory result. It is the positive first non-zero eigenvalue of a finite stress-weighted graph Laplacian. Its function is to measure a systemic shock threshold: the spectral separation between the normal connected state and the first transmissible stress mode. The reported benchmark values, $\lambda 1 = 0.3850$, spectral radius = 3.5023 and normalized transition threshold = 0.1099, are introduced here as conceptual signposts and are fully developed in the results section.

The importance of this logic for corridor economics is that it separates output mass from systemic transmission exposure. Large regions can be economically massive but relatively protected; smaller corridor nodes can be fragile or strategically important because their position allows stress to circulate or bridge between larger spaces. This is why EMGI, fragility and BridgeStress are not decorative add-ons. They are the node-level and corridor-level interpretations of the same gauge/spectral architecture.

The next section, 8.2, should therefore define the research object more concretely: the global-corridor stress network, the node set, the corridor logic, the role of the World anchor and the boundary between public anchors and author-calculated variables. Section 8.3 should then formalize the data architecture, and Section 8.4 should give the full methodology with formulas, matrices, algorithms and replication discipline. Section 8.1 has prepared the theoretical and claim-boundary basis for that technical development.

8.1.10. Formal Propositions for the Economic Analogue

For monograph purposes, the conceptual argument can be summarized through a sequence of bounded propositions. These propositions are not mathematical theorems about Yang-Mills theory. They are formal statements about the economic analogue and the finite weighted graph constructed in the chapter. Their purpose is to make the logic precise before the empirical sections introduce matrices, tables and results.

Proposition 8.1.1 states the threshold premise. If the stress-weighted graph is connected and the stress-weighted Laplacian is positive semidefinite, then the first non-zero eigenvalue $\lambda 1$ provides a finite-network measure of the separation between the normal connected state and the first stress-diffusion mode. In the economic analogue, this separation is interpreted as the mass-gap threshold. The claim is conditional on the constructed graph and its weights; it is not a universal property of all possible economic systems.

Proposition 8.1.2 states the curvature premise. If stress-weighted edge potentials around triangular cycles do not cancel, the network contains non-neutralized circulation. The action measure then converts this residual circulation into a non-negative concentration diagnostic. This is why the top-five action share is substantively meaningful: it identifies whether stress-energy is dispersed across many cycles or concentrated in a small number of corridor-sensitive loops.

Proposition 8.1.3 states the corridor premise. A node can be systemically exposed even when its output mass is limited, provided that its corridor position, stress score, curvature exposure, bridge role and local protection jointly imply high fragility. This proposition justifies the chapter's attention to the Caucasus, Central Asia and related corridor interfaces without making the unsupported claim that these nodes are globally dominant in GDP terms.

Proposition 8.1.4 states the evidence-gating premise. Finite-network spectral results, diagnostic indices, scenario simulations and future panel validation do not belong to the same evidentiary class. The completed benchmark can establish

a reproducible graph-spectral measurement result; stronger causal and country-level econometric statements require the populated N = 1,500 validation layer. This proposition protects the chapter against the most common reviewer objection: conflating a strong constructed benchmark with a final causal law.

Table 8.1.6. Formal propositions of the bounded Yang-Mills economic analogue

Proposition	Statement	What it permits	What it excludes
8.1.1 Threshold premise	A connected finite stress graph has a first non-zero Laplacian eigenvalue that can be read as spectral separation.	Positive finite-network mass-gap interpretation.	Continuum Yang-Mills theorem proof.
8.1.2 Curvature premise	Non-canceling triangular potentials indicate residual stress circulation.	Curvature/action diagnostics and concentration analysis.	Literal non-Abelian field curvature in physical spacetime.
8.1.3 Corridor premise	Strategic exposure may arise from bridge position and fragility, not only GDP mass.	BridgeStress and corridor-sensitive interpretation.	GDP-independent geopolitical ranking or deterministic policy conclusion.
8.1.4 Evidence-gating premise	Benchmark, diagnostic, scenario and panel-validation claims require different proof standards.	Layered claim hierarchy and reviewer-safe interpretation.	Upgrading small-sample diagnostics into causal law.

Source note: The propositions are methodological commitments for Chapter 8 rather than theorem-level mathematical results.

8.1.11. Why the Chapter Is More Than Network Centrality

A possible misunderstanding is that the Yang-Mills chapter merely renames conventional network centrality. This is not the case. Centrality measures are useful, but they usually describe position in a graph: degree, closeness, betweenness, eigenvector influence or related connectivity properties. The Yang-Mills economic architecture uses centrality only as one component in a broader stress-field and spectral framework. The primary objects are not centrality rankings; they are stress-weighted potentials, triangular curvature, squared-curvature action, Laplacian spectral separation and node-level protection diagnostics.

The distinction can be expressed technically. A node with high centrality may be well connected, but that does not reveal whether the stress differentials across its incident edges are high, whether the triangles containing the node exhibit non-neutralized curvature, whether those cycles dominate action, or whether the node has sufficient local protection to absorb shocks. Conversely, a corridor node with low ordinary centrality may still carry high BridgeStress if it has high corridor exposure, weak protection and participation in high-stress transmission pathways.

This is why the chapter requires both graph topology and macroeconomic stress normalization. A pure graph model would know which nodes are connected, but not why a connection carries macroeconomic stress. A pure macroeconomic index would know which nodes are stressed, but not how stress can circulate through a corridor topology. The gauge-econometric model combines the two: stress gives economic meaning to the graph, while topology gives transmission meaning to stress.

The same point applies to the mass-gap threshold. Algebraic connectivity in spectral graph theory is a standard object, but the chapter's contribution is to construct the relevant Laplacian from stress-weighted corridor relations and then interpret the first positive eigenvalue as an economic shock threshold. The threshold is therefore not a generic graph property floating outside the empirical architecture. It is tied to the specific stress field, edge weights and corridor logic of the model.

Table 8.1.7. Difference between centrality analysis and the Yang-Mills gauge-econometric architecture

Analytical layer	Conventional network view	Yang-Mills economic view
Node importance	Usually measured by degree, betweenness, closeness or eigenvector centrality.	Measured jointly through stress, local protection, curvature exposure, EMGI, fragility and BridgeStress.
Edge meaning	A connection or weighted relation between two nodes.	A corridor-weighted channel carrying directed stress potential A_ij.
Cycle meaning	Triangle or closed walk as a topological feature.	Non-neutralized stress circulation measured by F_ijk and action contribution.
System threshold	Spectral gap or algebraic connectivity as a graph-theoretic property.	λ1 of the stress-weighted Laplacian interpreted as a finite-network shock threshold.

Policy relevance	Highlights structurally central nodes.	Distinguishes central nodes, fragile nodes and strategic bridge nodes under stress propagation.

Source note: The chapter uses network science, but its substantive contribution is the integration of stress normalization, gauge curvature, action and spectral threshold diagnostics.

8.1.12. Why the Chapter Is More Than a Regression Model

A second misunderstanding is that a serious econometric chapter must begin and end with regression coefficients. Chapter 8 does include an econometric validation pathway, but its core object is not a single regression equation. Its primary object is a finite stress-transmission geometry. The econometric layer audits and strengthens the measurement architecture; it does not replace the architecture.

This distinction is crucial for the N = 1,500 validation pathway. The completed benchmark is a ten-node finite network. It can support matrix-based, spectral, curvature and scenario statements because those statements are computed directly from the constructed benchmark. However, country-level causal or quasi-causal claims require a different evidence base: country-year observations, observed or proxy-observed external outcomes, robust standard errors, panel fixed effects, dynamic specifications, potential instruments, factor structure tests, residual diagnostics and replication files. Section 8.1 therefore prepares the reader to understand why the chapter reports strong benchmark evidence now and reserves stronger country-panel claims for the validation pathway.

The correct econometric posture is layered rather than binary. It is not necessary to reject the benchmark because it is not yet the final country panel; nor is it legitimate to present the benchmark as if it already contained all panel evidence. The monograph should state the status accurately: completed finite-network gauge-econometric benchmark, archived replication package for the benchmark, and fully specified N = 1,500 country-panel validation architecture for future empirical closure.

This posture is consistent with the broader monograph. The Hodge chapter treats its regional benchmark as a prototype for future all-country, dyadic and longitudinal replication. The BSD chapter distinguishes local-to-global measurement consistency from causal law. The Navier-Stokes chapter builds a full 100-country stress-testing panel. The Riemann-zeta chapter separates annual, quarterly and monthly validation layers. The P-vs-NP chapter separates best-found full-universe incumbents from exact reduced enumeration. Chapter 8 follows the same scientific discipline by separating benchmark evidence from final causal validation.

8.1.13. Conceptual Questions Answered by Each Construct

The conceptual value of the Yang-Mills architecture becomes clearest when each construct is linked to the question it answers. The stress field asks where pressure is located. The weighted graph asks how pressure can be transmitted. The gauge potential asks where stress differentials become edge-level tension. Curvature asks where local circulation does not neutralize. Action asks whether stress-energy is concentrated. The Laplacian spectrum asks whether the system has a positive threshold before stress becomes transmissible. EMGI asks which nodes are locally protected. Fragility asks which nodes are vulnerable. BridgeStress asks which corridor nodes are strategically exposed. Scenarios ask how the threshold changes under shocks.

This question-based interpretation should guide the rest of Chapter 8. It prevents formulas from becoming decorative and prevents the results tables from appearing as unrelated diagnostics. Each object has a defined analytical role. Together, they form a sequence from observable anchors to systemic interpretation. That sequence is the reason the chapter can make a methodological contribution even before the final country-panel layer is populated.

Table 8.1.8. Economic question answered by each core construct

Construct	Question answered	Chapter 8 use
σ_i systemic-stress field	Where is macro-corridor pressure located?	Builds the node-level scalar field.
W weighted adjacency	Through which corridor relations can pressure move?	Defines the finite transmission topology.
A_ij gauge potential	Where do stress differentials become edge-level tension?	Ranks directed stress channels.
F_ijk curvature	Where does local stress circulation fail to neutralize?	Identifies high-curvature cycles.
S_YM action	Is stress-energy diffuse or concentrated?	Measures total and top-cycle concentration.
L^S stress Laplacian	What is the network-wide stress-diffusion	Generates the spectral mass-gap

	operator?	diagnostics.
λ1 mass gap	What is the first systemic stress threshold?	Defines the finite-network economic mass gap.
EMGI and fragility	Which nodes are protected or vulnerable?	Translates spectral and structural information into local diagnostics.
BridgeStress	Which corridor nodes are strategically exposed?	Separates bridge exposure from pure GDP mass or centrality.
Shock scenarios	How does the threshold respond to stress injections?	Links local disturbances to systemic transition.

Source note: This table can be reused as a guiding reader map at the beginning of the detailed methodology section.

8.1.14. Transition from Conceptual Analogy to Empirical Chapter Design

The remaining sections of Chapter 8 should now proceed from concept to implementation. Section 8.2 should define the research object: a global-corridor stress network rather than a country-ranking exercise or a literal trade-flow matrix. Section 8.3 should present the data architecture: ten nodes, twenty-seven edges, public macroeconomic anchors, author-calculated variables, benchmark replication package and evidence status. Section 8.4 should specify the formulas and algorithms: systemic-stress normalization, weighted edge construction, gauge potential, triangular curvature, action, stress Laplacian, EMGI, BridgeStress, shock injection and resilience.

Section 8.5 should report the core results without weakening the claim boundary: positive finite-network mass gap, spectral radius, normalized threshold, action concentration, EMGI, fragility and corridor bridge stress. Section 8.6 should interpret what those results mean for systemic shock thresholds and corridor exposure. Section 8.7 should move to scenario simulations and the local-to-systemic transition problem. Section 8.8 should describe the N = 1,500 validation pathway and explain exactly which claims remain future validation claims. Section 8.9 should close the chapter by linking the Yang-Mills result to the comparative synthesis of the book.

This architecture keeps the chapter monographic. The source article's abstract, context, methodology, results, interpretation and conclusion are redistributed into book functions rather than copied as an article sequence. Section 8.1 is the conceptual gate. It tells the reader why the Yang-Mills analogy is meaningful, where its boundaries lie, what its objects are and how it contributes to the seven-problem economic measurement program.

8.2. Research Object: Global-Corridor Stress Network

This section defines the empirical object of Chapter 8. In the monograph architecture, Section 8.1 established the conceptual reason for translating Yang-Mills gauge logic into economic measurement. Section 8.2 now fixes what is being measured. The research object is a finite global-corridor systemic-stress network: a weighted graph whose nodes are macro-regional and corridor-sensitive economic units and whose edges represent author-disclosed corridor-sensitive relations through which stress can circulate, concentrate and become systemically transmissible.

The object is deliberately neither too broad nor too narrow. It is broader than a single-country case study because it covers a world-normalized regional and corridor system. It is narrower than a complete all-country, all-dyad transaction database because the benchmark layer contains ten nodes and twenty-seven weighted undirected edges. This bounded design is not a defect. It is the condition that makes the gauge-econometric construction auditable: the stress field, adjacency matrix, stress-weighted adjacency matrix, gauge potential, triangular curvature, economic action, stress Laplacian, EMGI, fragility and BridgeStress can be traced from the same finite research object.

The central reason for defining the object as a global-corridor stress network is that systemic relevance cannot be inferred from GDP mass alone. The chapter is concerned with the difference between output scale and transmission position. Large economic blocs such as East Asia and Pacific, North America and Europe provide mass and scale, but corridor-sensitive nodes such as the Caucasus and Central Asia may become visible because they connect larger regional spaces through logistics, energy, Black Sea, Caspian and Middle Corridor interfaces. The research object must therefore preserve both mass-dominant nodes and transmission-sensitive nodes within one formal system.



Research object: a finite global-corridor systemic-stress network, not an observed bilateral transaction matrix and not a continuum field-theory object.

Figure 8.2.1. Research-object pipeline for the Yang-Mills economic mass-gap chapter.

Figure 8.2.1. Research-object pipeline for the Yang-Mills economic mass-gap chapter.

8.2.1. Purpose of the Research-Object Section

The purpose of Section 8.2 is to protect the chapter from two common interpretive errors. The first error would be to treat the Yang-Mills chapter as a metaphorical extension of physics without a precise empirical object. The second error would be to treat the ten-node benchmark as if it already delivered country-level causal econometric proof. This section prevents both errors by specifying exactly what the object is, what it can support, and what it cannot support.

The research object functions as a bridge between conceptual translation and empirical computation. It receives the mathematical grammar from Section 8.1 and supplies the empirical universe for Sections 8.3-8.5. Once the object is fixed, the next section can describe the data architecture; the methodology can then define the gauge potential, curvature, action and stress Laplacian; the results section can report the positive finite-network mass gap; and the interpretation sections can explain systemic shock thresholds and corridor exposure without changing the unit of analysis midstream.

The object also gives the reviewer a clear audit path. Every later statement must be traceable to one of four layers: the node layer, the edge layer, the stress-field layer or the evidence-status layer. If a claim cannot be assigned to one of these layers, it should not appear as a benchmark conclusion. This design discipline is especially important because the chapter uses ambitious mathematical language.

Table 8.2.1. Research-object definition matrix.

Object component	Definition in Section 8.2	Function in Chapter 8
Empirical object	Finite global-corridor systemic-stress network	Defines the unit of measurement for Chapter 8
Node layer	World anchor plus ten regional/corridor nodes	Fixes the macro-regional coordinate system
Edge layer	Twenty-seven weighted undirected corridor-sensitive edges	Supplies network topology for gauge and curvature calculations
Stress layer	Normalized systemic-stress score built from mass, growth, income, transition and corridor components	Transforms public anchors into a measurable field
Layer A evidence	Completed finite-network benchmark	Allows benchmark measurement of stress, curvature, action, mass gap, EMGI and BridgeStress
Layer B evidence	Planned 100-country x 15-year panel	Defines future validation route, not final causal closure
Claim boundary	Finite-network economic analogue only	Excludes theorem-level Yang-Mills proof and country-level causal claims at the benchmark stage

Source note: Author synthesis based on the Yang-Mills source manuscript and the monograph integration plan.

8.2.2. Formal Definition of the Global-Corridor Stress Network

Formally, the research object can be represented as a finite stress-network system. The notation below is not introduced as a new theorem; it is an organizing device that makes the empirical object explicit before the methodology section derives the detailed transformations.

(8.2.1) $G^{YM}_{econ} = (V, E, W, \sigma, C, \Omega)$

The economic Yang-Mills research object is a finite graph-based system. V is the node set, E is the edge set, W is the corridor-weighted adjacency structure, σ is the normalized systemic-stress field, C represents corridor-exposure coding and Ω represents the evidence-status and claim-boundary layer.

(8.2.2) V = {EAP, NAM, EUR, LAC, SAS, MENA, SSA, OCE, CAS, CAU}

The substantive benchmark node set contains ten regional/corridor nodes. The World row is retained as a normalization anchor, not as a competing regional node inside the stress network.

(8.2.3) |V| = 10, |E| = 27, density = 2|E| / (|V|(|V|-1)) = 0.600

The benchmark object is connected and cycle-rich enough to support triangular curvature and spectral diagnostics, while remaining bounded enough to be auditable.

(8.2.4) σ_i = N(mass_i, growthgap_i, incomefragility_i, transition_i, corridor_i)

The stress field is a normalized composite object. Its components are not raw units added directly; they are directionally harmonized and transformed into a common systemic-stress scale.

This representation is intentionally conservative. It does not claim that the world economy literally behaves like a physical Yang-Mills field. It claims that a finite economic network can be constructed so that stress differences, corridor relations and cycle-level imbalances become measurable. The graph is the empirical object; the gauge, curvature and action objects are transformations defined on that graph.

The inclusion of Ω in Formula (8.2.1) is important. In this monograph, the research object is not only a data structure; it is a data structure with a claim-status rule. The same numerical object can support a benchmark spectral statement but cannot automatically support a causal country-level econometric statement. This distinction is the main safeguard of Section 8.2.

8.2.3. Node Universe: World Anchor and Ten Regional/Corridor Nodes

The node universe is built around a World anchor and ten substantive regional/corridor nodes. The World anchor fixes the scale of the system. It is used for normalization, world-output share calculations and benchmark consistency, but it is not a competing node in the stress-network eigenvalue problem. The ten substantive nodes are the empirical units that receive stress scores, edge weights, gauge potentials, curvature exposure and protection/fragility indicators.

The node set preserves a balance between global coverage and corridor specificity. East Asia and Pacific, North America and Europe represent large output-mass centers. Latin America and Caribbean, South Asia, Middle East and North Africa, Sub-Saharan Africa and Oceania represent macro-regional spaces with different stress, growth and income-depth profiles. Central Asia and the Caucasus are retained because the chapter is specifically interested in corridor exposure and Middle Corridor transmission logic.

Table 8.2.2. World anchor and regional/corridor node universe.

Region / anchor	Code	GDP 2024, $bn	World share, %	Growth 2026, %	GDP pc, $	System role
World anchor	WLD	110,985.0	100.00	3.20	14,100	Global benchmark
East Asia and Pacific	EAP	35,620.0	32.09	4.20	17,200	Regional/corridor node
North America	NAM	31,000.0	27.93	2.00	76,000	Regional/corridor node
Europe	EUR	23,150.0	20.86	1.50	43,000	Regional/corridor node
Latin America and Caribbean	LAC	7,260.0	6.54	2.40	10,600	Regional/corridor node
South Asia	SAS	4,770.0	4.30	6.30	2,700	Regional/corridor node
Middle East and North Africa	MENA	4,540.0	4.09	3.20	8,800	Regional/corridor node
Sub-Saharan Africa	SSA	2,160.0	1.95	3.80	1,850	Regional/corridor node
Oceania	OCE	1,810.0	1.63	2.10	63,000	Regional/corridor node
Central Asia	CAS	530.0	0.48	5.10	9,000	Regional/corridor node
Caucasus	CAU	145.0	0.13	4.60	9,500	Regional/corridor node

Source note: Adapted from the Yang-Mills source manuscript input panel. The World row is a normalization anchor; the ten regional/corridor rows are the substantive network nodes.

The table shows why the object cannot be interpreted as a simple GDP ranking. The largest output shares belong to East Asia and Pacific, North America and Europe. However, the research object is designed to evaluate not only scale but also stress, exposure, bridge function, curvature participation and shock transmissibility. A node with low output mass may still be analytically central when it lies on a corridor interface.

For the monograph, this is a crucial point. Chapter 8 is not repeating the Hodge chapter's flow-decomposition object, the Navier-Stokes chapter's country-year stress-balance object or the BSD chapter's local-to-global rank object. It defines a

distinct Yang-Mills object: a finite gauge-stress network in which the unit of analysis is the regional/corridor node plus its stress-bearing relations.

8.2.4. Why the Object Is a Stress Network Rather Than a GDP Ranking

The object becomes a stress network only after macroeconomic anchors are converted into a normalized systemic-stress field. GDP mass enters the model, but it is only one component. The construction also includes growth-gap pressure, income-fragility pressure, transition-momentum pressure and corridor exposure. This component logic prevents the research object from collapsing into an output hierarchy.

The conceptual distinction can be summarized as follows. GDP measures mass; growth pressure measures dynamic transition; income fragility measures absorption weakness; corridor exposure measures strategic transmission position. The Yang-Mills economic object is interested in the joint structure of all four types of information. It asks where stress can accumulate, where it can circulate through cycles, where it can weaken local protection and where a local disturbance can cross a system-wide threshold.

Table 8.2.3. Stress-field component taxonomy.

Stress component	Operational meaning	Why it is needed for the research object
Mass exposure	GDP/output scale normalized into stress-relevant mass position	Captures system size and potential scale effects; does not define systemic relevance alone
Growth-gap pressure	Projected growth deviation transformed into pressure orientation	Captures dynamic transition pressure and growth-related instability
Income-fragility pressure	Income-depth weakness transformed into vulnerability pressure	Captures reduced absorption capacity and macro-development fragility
Transition-momentum pressure	Transition GDP / forward momentum pressure	Captures the stress created by fast-moving structural change
Corridor exposure	Author-coded corridor interface role and strategic transmission position	Captures Middle Corridor, Black Sea, Caspian and regional bridge exposure
Stress score	Normalized composite systemic-stress field σ_i	Supplies the scalar field on which gauge and Laplacian objects are built

Source note: Author synthesis from the Yang-Mills stress-score construction. Detailed formulas are reserved for Sections 8.3 and 8.4.

Table 8.2.4. Node-level systemic-stress field used by the research object.

Code	Region	Mass	Growth-gap	Income-fragility	Transition	Corridor	Stress score
SAS	South Asia	13.05	100.00	85.53	100.00	56.67	100.00
CAS	Central Asia	1.10	61.29	47.44	74.49	90.00	71.79
EAP	East Asia and Pacific	100.00	32.26	30.85	55.68	53.33	71.23
CAU	Caucasus	0.00	45.16	45.97	63.72	100.00	66.03
SSA	Sub-Saharan Africa	5.69	19.35	100.00	47.35	28.33	53.78
EUR	Europe	64.86	54.84	10.81	0.00	61.67	47.40
MENA	Middle East and North Africa	12.39	0.00	48.06	34.88	73.33	39.71
NAM	North America	86.98	38.71	0.00	10.20	11.67	30.66
LAC	Latin America and Caribbean	20.06	25.81	43.03	18.40	20.00	26.78
OCE	Oceania	4.69	35.48	3.44	12.24	0.00	0.00

Source note: Adapted from the Yang-Mills source stress-score table. Values are normalized benchmark components used to define the finite stress field.

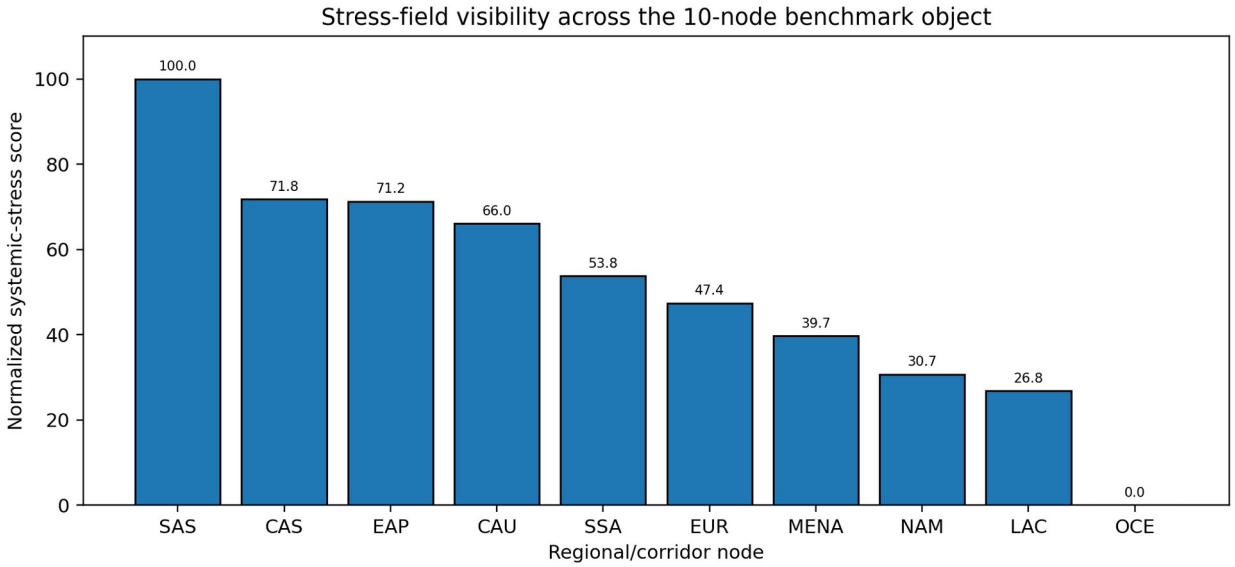


Figure 8.2.3. Normalized systemic-stress field used to define the research object.

Figure 8.2.3. Normalized systemic-stress field used to define the research object.

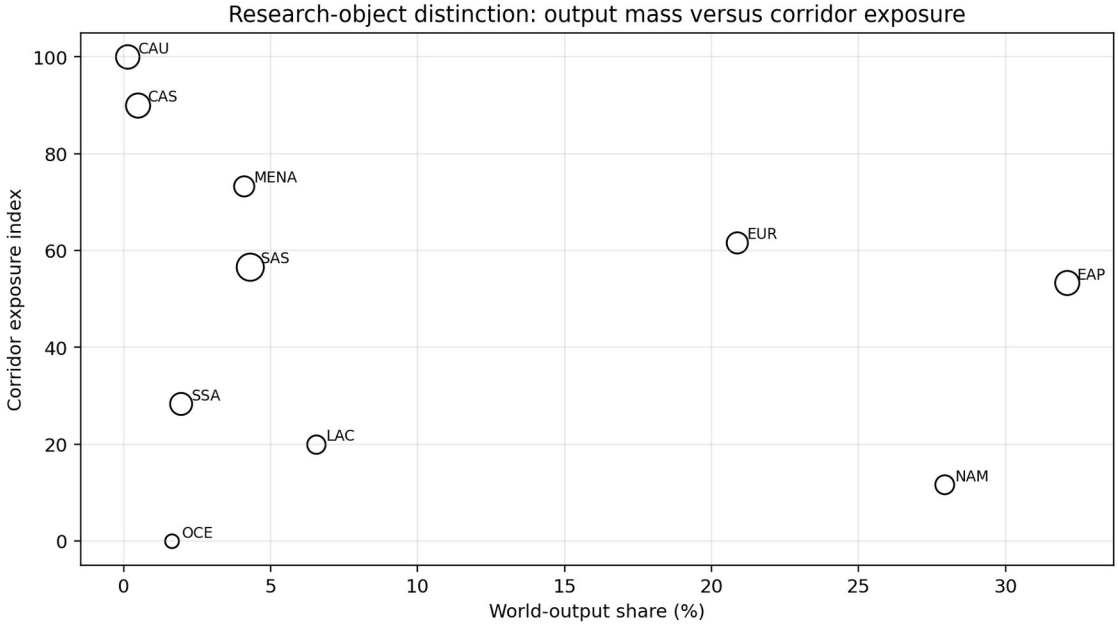


Figure 8.2.4. The stress-network object is not reducible to GDP mass: small nodes can have high corridor exposure.

Figure 8.2.4. Output mass versus corridor exposure inside the research object.

The stress table and the mass-versus-corridor figure show the central logic of the object. South Asia appears as the normalized upper-bound stress node, but Central Asia, East Asia and Pacific and the Caucasus also remain highly visible for different reasons. Central Asia and the Caucasus are not high-stress nodes because of output mass; they are visible because corridor exposure and transition sensitivity elevate their systemic position.

This is why the object must be described as a global-corridor stress network rather than a global GDP network. The purpose is not to rank regions by size. The purpose is to identify the stress-bearing structure on which gauge potentials, curvature cycles and spectral thresholds can be computed.

8.2.5. Edge Universe: Twenty-Seven Weighted Corridor Relations

The second component of the research object is the edge universe. The benchmark contains twenty-seven weighted undirected relations among the ten regional/corridor nodes. These edges are not presented as observed bilateral trade flows,

shipping volumes, financial claims or route-level transaction records. They are corridor-sensitive analytical relations constructed to carry systemic stress through the benchmark graph.

The edge layer has three functions. First, it gives the system topology: without edges there is no stress transmission. Second, it creates cycles: without cycles there is no triangular curvature field. Third, it creates the stress-weighted Laplacian: without a weighted adjacency matrix and a degree matrix there is no finite-network spectral mass-gap calculation. Thus, the edge universe is not a visual supplement; it is a structural requirement of the Yang-Mills economic architecture.

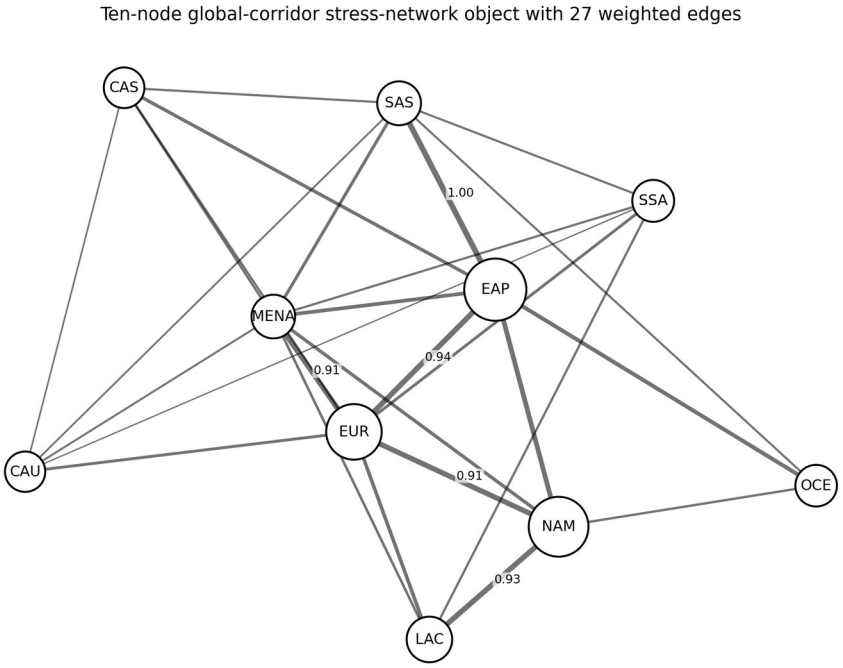


Figure 8.2.2. Finite global-corridor stress-network object. Node size approximates world-output share; edge width approximates benchmark edge weight.

Figure 8.2.2. Finite global-corridor stress-network object with 10 nodes and 27 weighted edges.

Table 8.2.5. Edge universe of the global-corridor stress-network object.

Edge	Weight	Corridor factor	Research-object role
EAP-SAS	1.000	1.500	Benchmark edge relation used for adjacency, gauge and spectral calculations
EAP-EUR	0.937	1.000	Benchmark edge relation used for adjacency, gauge and spectral calculations
NAM-LAC	0.934	1.400	Benchmark edge relation used for adjacency, gauge and spectral calculations
NAM-EUR	0.910	1.000	Benchmark edge relation used for adjacency, gauge and spectral calculations
EUR-MENA	0.908	1.600	Benchmark edge relation used for adjacency, gauge and spectral calculations
EAP-NAM	0.818	1.000	Benchmark edge relation used for adjacency, gauge and spectral calculations
EAP-OCE	0.643	1.400	Benchmark edge relation used for adjacency, gauge and spectral calculations
EAP-MENA	0.580	1.000	Benchmark edge relation used for adjacency, gauge and spectral calculations
EUR-LAC	0.562	1.000	Benchmark edge relation used for adjacency, gauge and spectral calculations
EAP-CAS	0.518	1.600	Benchmark edge relation used for adjacency, gauge and spectral calculations
NAM-MENA	0.516	1.000	Benchmark edge relation used for adjacency, gauge and spectral calculations

Edge	Weight	Corridor factor	Research-object role
SAS-MENA	0.459	1.400	Benchmark edge relation used for adjacency, gauge and spectral calculations
EUR-CAU	0.411	2.200	Benchmark edge relation used for adjacency, gauge and spectral calculations
EUR-SSA	0.407	1.000	Benchmark edge relation used for adjacency, gauge and spectral calculations
LAC-MENA	0.339	1.000	Benchmark edge relation used for adjacency, gauge and spectral calculations
MENA-CAS	0.312	1.900	Benchmark edge relation used for adjacency, gauge and spectral calculations
NAM-OCE	0.293	1.000	Benchmark edge relation used for adjacency, gauge and spectral calculations
LAC-SSA	0.279	1.000	Benchmark edge relation used for adjacency, gauge and spectral calculations
EUR-CAS	0.270	1.000	Benchmark edge relation used for adjacency, gauge and spectral calculations
MENA-SSA	0.261	1.000	Benchmark edge relation used for adjacency, gauge and spectral calculations
SAS-CAS	0.261	1.500	Benchmark edge relation used for adjacency, gauge and spectral calculations
SAS-SSA	0.246	1.000	Benchmark edge relation used for adjacency, gauge and spectral calculations
OCE-SAS	0.241	1.000	Benchmark edge relation used for adjacency, gauge and spectral calculations
MENA-CAU	0.217	1.900	Benchmark edge relation used for adjacency, gauge and spectral calculations
SAS-CAU	0.180	1.600	Benchmark edge relation used for adjacency, gauge and spectral calculations
CAS-CAU	0.140	2.400	Benchmark edge relation used for adjacency, gauge and spectral calculations
SSA-CAU	0.082	1.000	Benchmark edge relation used for adjacency, gauge and spectral calculations

Source note: Adapted from the Yang-Mills source edge list. The edges define the finite graph on which gauge potential, curvature and stress Laplacian are later computed.

The edge list also clarifies why the benchmark object is neither a complete graph nor a sparse anecdotal network. A complete ten-node graph would contain forty-five undirected edges and would blur meaningful corridor structure. The benchmark uses twenty-seven edges, giving density 0.600. This is dense enough to support cycles and spectral diagnostics, but not so dense that every node is mechanically connected to every other node.

The corridor factor attached to each edge is essential for the chapter’s empirical interpretation. It identifies the amplification of selected corridor-sensitive relations relative to the base network. This is the mechanism by which Middle Corridor, Black Sea, Caspian, Caucasus-Central Asia and Europe-MENA-South Asia interfaces enter the research object without requiring the object to be a complete observed transport database.

8.2.6. Layer A and Layer B Evidence Status

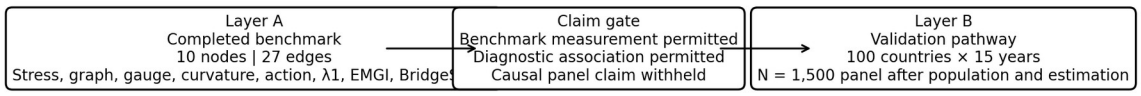
A correct definition of the research object must include evidence status. The Yang-Mills source study is deliberately two-layered. Layer A is the completed finite-network benchmark. Layer B is the 100-country by 15-year country-panel validation pathway, producing a planned N = 1,500 observations once the country-year variables are populated and estimated. These two layers must not be merged rhetorically.

Layer A can support strong finite-network measurement language because the object, matrices and benchmark outputs are defined. It can support statements about connectedness, stress, gauge potential, curvature, action, first positive eigenvalue, EMGI, fragility, BridgeStress and scenario compression of thresholds. Layer B can support stronger panel econometric language only after the country-level variables, model outputs, external outcomes and replication files are completed. Until then, it is a validation architecture, not a completed causal result.

Table 8.2.6. Layered evidence-status architecture for the research object.

Layer	Unit of observation	Sample size	Primary purpose	Permitted claim
Layer A: node benchmark	Regional/corridor node	10 nodes	Stress scores, EMGI, fragility, resilience, curvature exposure	Benchmark measurement claim
Layer A: edge/cycle diagnostics	Edge or triangular cycle	27 edges; 27 cycles reported in source results	Gauge potential, curvature, action, local-to-systemic threshold	Topological/spectral diagnostic claim
Layer A: spectral benchmark	Stress-weighted graph Laplacian	Finite 10-node graph	λ0, λ1, spectral radius, normalized threshold	Finite-network mass-gap claim
Layer B: country-panel validation	Country-year	100 countries × 15 years = 1,500	Panel FE/TWFE, DK, clustered, IV, factor, external validation	Only after population and estimation
Layer B: route/dyad extension	Country-pair-year or route-year	Optional extension beyond N=1,500	Corridor spillover, route shock and logistics robustness	Future robustness claim
Monograph claim gate	Chapter-level interpretation	Two-layer evidence system	Keeps benchmark and causal language separate	No theorem or causal overclaim

Source note: Author restructuring of the Yang-Mills source design for monograph Section 8.2.



The research object is already closed as a finite-network benchmark; country-level causal/econometric validation is assigned to the larger panel pathway.

Figure 8.2.6. Layered evidence-status architecture of Section 8.2.

Figure 8.2.6. Layered evidence-status architecture of Section 8.2.

This evidence-status distinction is the main scientific discipline of Section 8.2. The benchmark object is strong because it is complete as a finite graph: the node set, edge set, stress field and matrices are defined. But it is still a benchmark. The country-panel pathway is powerful because it can convert the benchmark constructs into a broader validation design, but it is not yet a completed country-year empirical result inside the benchmark subsection.

The monograph should preserve this distinction in all later references. Phrases such as “the benchmark demonstrates a positive finite-network mass gap” are admissible. Phrases such as “the model proves a universal causal law of systemic crises” are not admissible. This distinction allows the chapter to be ambitious and academically safe at the same time.

8.2.7. Public Anchors versus Author-Calculated Analytical Objects

The data status of the research object is mixed but transparent. Some quantities are public macroeconomic anchors: GDP mass, world-output share, projected growth, transition-GDP logic, GDP per capita and observable proxy families. Other quantities are author-calculated analytical objects: stress scores, corridor weights, gauge potential, triangular curvature, Yang-Mills economic action, stress Laplacian, EMGI, fragility, BridgeStress, scenario outputs and replication diagnostics.

The distinction matters because author-calculated objects can be scientifically useful only if they are disclosed, reproducible and not misrepresented as raw official data. The chapter therefore treats public anchors as input variables and constructed objects as model outputs. A reviewer should be able to follow the transformation chain from public anchor to stress field, from stress field to graph, from graph to gauge potential, from cycles to curvature/action, and from the Laplacian to the mass-gap threshold.

Table 8.2.7. Public-anchor and author-calculated object distinction.

Variable/object family	Status	Role in research object	Boundary rule
GDP mass and world-output share	Public macro-data anchor	Defines scale and mass exposure	Not the final systemic-stress index
Projected growth and transition GDP	Public/projected anchor plus author transition calculation	Defines dynamic transition pressure	Projection horizon must remain explicit
GDP per capita / income depth	Public macro-data anchor	Defines income-fragility pressure and absorption depth	Not a welfare ranking
Corridor exposure	Author-coded corridor layer	Defines strategic transmission position	Not an observed transaction matrix
Stress score σ_i	Author-calculated construct	Scalar systemic-stress field on nodes	Requires normalization audit
Edge weights W_ij	Author-calculated corridor-weighted relation	Graph topology and adjacency matrix	Requires edge-list disclosure
Gauge potential A_ij	Author-calculated edge field	Directed stress tension on edges	Orientation convention must be disclosed
Curvature/action	Author-calculated cycle-level output	Cycle stress-energy and concentration	Finite-network analogue only
EMGI / Fragility / BridgeStress	Author-calculated node-level diagnostics	Protection, vulnerability and corridor bridge exposure	Benchmark diagnostic; not causal by itself

Source note: Author synthesis from the Yang-Mills methodology and data-status logic.

This table should be read as a reviewer-facing transparency device. The chapter does not hide that central constructs are derived. On the contrary, it makes derivation the core methodological contribution. The research object is not “found” as a raw official dataset; it is constructed from public anchors through a disclosed mathematical-econometric pipeline. That is why Sections 8.3 and 8.4 must provide exact formulas and audit tables.

The same distinction aligns Chapter 8 with the monograph’s broader methodology. Across the seven Millennium-inspired models, public data rarely enter the final results in raw form. They are normalized, stress-oriented, decomposed, forecasted, transformed into networks, converted into ranks or used in optimization. The scientific standard is therefore not raw-data purity; it is transparent transformation and claim discipline.

8.2.8. Stress-Field Components and Node-Level Measurement Logic

The stress field is the main node-level quantity of the research object. Without σ_i, the graph would remain a weighted network without systemic-stress content. The node-level stress score transforms heterogeneous macroeconomic and corridor information into a common 0-100 pressure-oriented scale. This allows the same node set to support adjacency weighting, gauge-potential construction, curvature exposure, local protection and shock diagnostics.

The stress field has an important interpretive property: similar stress scores can arise from different component structures. South Asia is stressed through growth and transition pressure; East Asia and Pacific combines large mass and high transition pressure; Central Asia and the Caucasus become visible through corridor exposure and strategic bridge position; North America has large mass but strong income depth and resilience. Therefore, σ_i should not be interpreted as a single-cause index.

Table 8.2.8. Illustrative node interpretation within the stress-field object.

Code	Node	Object status	Interpretive reason
SAS	South Asia	Stress upper-bound in benchmark	High growth-gap and transition pressure; income fragility also elevated
CAS	Central Asia	High-stress corridor-sensitive node	Corridor exposure and transition pressure make the node visible beyond GDP mass
EAP	East Asia and Pacific	Mass-dominant and transition-active node	Large output share plus stress-relevant transition dynamics
CAU	Caucasus	Small-mass corridor bridge	Maximum corridor exposure offsets low GDP mass in systemic-stress interpretation
NAM	North America	High-mass but more protected node	Large GDP mass does not automatically imply high stress due to income depth and resilience
OCE	Oceania	Low-stress benchmark floor	Defines lower normalization boundary in the source stress audit

Source note: Author interpretation based on the source stress-score table and claim-boundary logic.

8.2.9. Corridor Role of the Caucasus, Central Asia and Middle Corridor Interfaces

The chapter's corridor contribution becomes most visible in the treatment of the Caucasus and Central Asia. In standard macroeconomic aggregation, a small subregion may disappear inside Europe, Central Asia, the Middle East or broader Eurasian classifications. In the Yang-Mills research object, the Caucasus is retained as an explicit node because the chapter is measuring corridor stress transmission rather than output scale alone.

The same logic applies to Central Asia. It is not simply a small share of world output. It is a bridge region in the Caspian, land-corridor and Eurasian logistics structure. The research object therefore includes corridor exposure as a direct stress component and later separates BridgeStress from ordinary centrality. This design choice is central to the policy relevance of the chapter.

Table 8.2.9. Corridor exposure and BridgeStress preview inside the research object.

Code	Region	Corridor exposure	Corridor-role index	Fragility	Curvature participation	BridgeStress
CAU	Caucasus	98.00	100.00	100.00	57.32	100.00
CAS	Central Asia	92.00	75.00	94.55	67.37	78.24
SAS	South Asia	72.00	60.00	89.64	86.74	59.80
MENA	Middle East and North Africa	82.00	85.00	54.41	87.08	58.79
EAP	East Asia and Pacific	70.00	95.00	46.88	100.00	55.50
SSA	Sub-Saharan Africa	55.00	25.00	95.89	57.64	13.53
LAC	Latin America and Caribbean	50.00	30.00	68.63	59.43	10.89
EUR	Europe	75.00	90.00	9.85	78.72	9.32
OCE	Oceania	38.00	20.00	85.50	68.27	7.90
NAM	North America	45.00	70.00	0.00	67.21	0.00

Source note: Adapted from the Yang-Mills source BridgeStress table. These values are preview indicators for later results and interpretation sections.

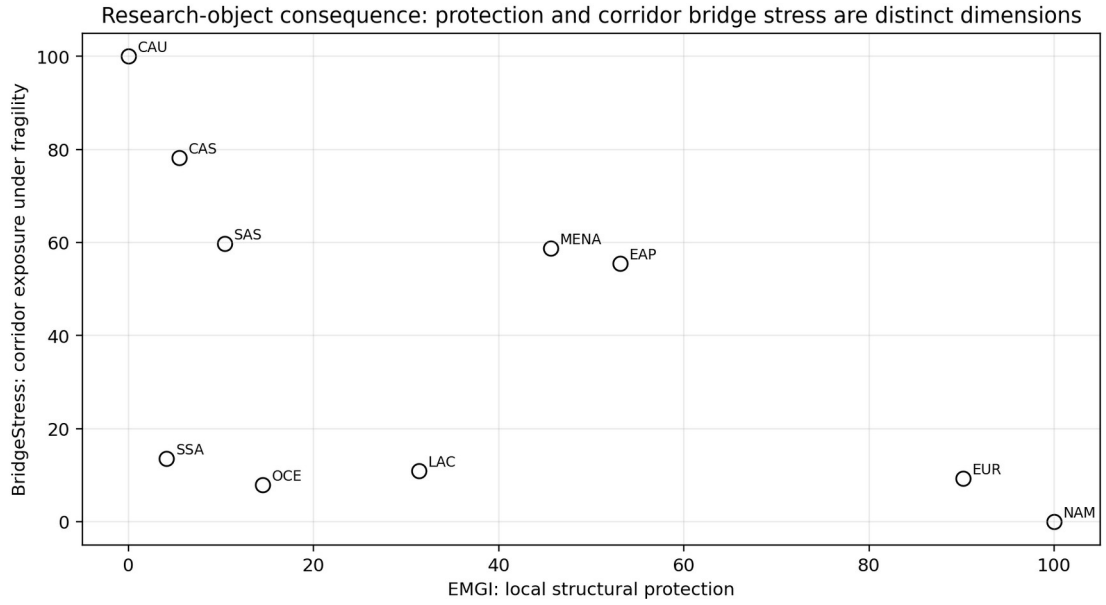


Figure 8.2.5. Research object prepares later EMGI, fragility and BridgeStress interpretation without treating them as GDP rankings.

Figure 8.2.5. Local protection and corridor BridgeStress are distinct research-object dimensions.

The table previews why the research object must separate corridor exposure from GDP mass. The Caucasus appears with the maximum BridgeStress value in the benchmark. This does not mean that the Caucasus is the largest economic region. It means that, inside the constructed corridor-stress network, the combination of corridor exposure, fragility and curvature participation gives it a strategic transmission role.

This interpretation is methodologically defensible only because the research object is explicitly defined as a stress-transmission network. If the object were a GDP table, the conclusion would be invalid. If the object were a full observed trade matrix, additional route-level data would be required. The current claim is therefore precise: the benchmark object makes corridor exposure measurable in a finite-network stress architecture.

8.2.10. Research Object as Input to Gauge Potential, Curvature, Action and Laplacian

Section 8.2 does not yet estimate the full methodology; however, it must show how the research object feeds the later Yang-Mills pipeline. Once V, E, W and σ are defined, the next transformations become meaningful. The stress-weighted adjacency matrix W^S combines relation strength and node stress. The anti-symmetric gauge potential A_ij represents directional stress tension along edges. Triangular curvature F_ijk measures non-neutralized circulation around cycles. Yang-Mills economic action summarizes squared curvature exposure. The stress Laplacian L^S then supplies the finite-network spectral mass-gap object.

(8.2.5) $W^{S}_{ij} = W_{ij}(\sigma_i + \sigma_j)/200$

The stress-weighted adjacency matrix connects the edge layer with the node-level systemic-stress field. It is the immediate input to the stress Laplacian.

(8.2.6) $A_{ij} = -A_{ji}$

The gauge potential is anti-symmetric by construction. The orientation convention affects displayed edge direction but not the undirected spectral benchmark.

(8.2.7) $F_{ijk} = A_{ij} + A_{jk} + A_{ki}$

Triangular curvature measures non-neutralized stress circulation around a cycle. A zero value would indicate that directed tensions close without residual curvature.

(8.2.8) $L^{S} = D^{S} - W^{S}, \quad \Delta_{econ} = \lambda_1(L^{S})$

The finite-network economic mass gap is the first positive eigenvalue of the stress-weighted Laplacian, not a continuum field-theory theorem.

Table 8.2.10. How the research object feeds the Yang-Mills methodology.

Input/output object	Definition	Analytical role	Primary chapter location
Node set V	Ten regional/corridor nodes	Defines where stress resides	Section 8.2

Input/output object	Definition	Analytical role	Primary chapter location
Edge set E	Twenty-seven weighted corridor-sensitive edges	Defines possible transmission structure	Section 8.2
Stress field σ	Node-level normalized systemic stress	Turns the graph into a stress network	Sections 8.2-8.3
Stress adjacency W^S	Edge weight adjusted by node stress	Creates the weighted object for spectral diagnostics	Section 8.4
Gauge potential A_ij	Anti-symmetric directed edge tension	Measures stress differential along oriented relations	Section 8.4
Curvature F_ijk	Triangular cycle residual tension	Measures non-neutralized systemic circulation	Sections 8.4-8.5
Action S_YM	Squared curvature concentration	Measures stress-energy concentration	Section 8.5
Laplacian L^S and λ1	Finite graph spectral object	Defines the economic mass-gap threshold	Section 8.5

Source note: Author synthesis linking Section 8.2 to Sections 8.3-8.5.

8.2.11. Validation Pathway and Non-Overclaiming Rules

The research object is constructed for a sequence of validation gates. The completed Layer A benchmark supports finite-network measurement, robustness and scenario diagnostics. The planned Layer B panel supports future country-year validation. The non-overclaiming rule is simple: the chapter may state only the strongest claim supported by the completed evidence layer.

This rule is not merely editorial. It is required because the same constructs can be interpreted differently depending on sample status. An EMGI value inside the ten-node benchmark is a reproducible diagnostic. An EMGI coefficient in a 100-country fixed-effects model would be a panel validation estimate only after country-year variables are populated and model outputs are generated. The research object therefore includes a validation pathway but does not pretend that the pathway is already empirically closed.

Table 8.2.11. Claim-permission rules attached to the research object.

Statement	Evidence basis	Status
The graph contains 10 nodes and 27 weighted edges	Supported by Layer A	Permitted
The benchmark object is a finite global-corridor stress network	Supported by node, edge and stress-field design	Permitted
The object can support gauge, curvature and Laplacian calculations	Supported by finite graph and stress field	Permitted
The benchmark mass gap is a finite-network spectral threshold	Supported after Section 8.5 results	Permitted with finite-network wording
The model solves the Yang-Mills mass-gap problem	Not part of the object	Excluded
The ten-node benchmark proves country-level causality	Not supported by benchmark sample	Excluded
The N=1,500 panel is final empirical proof	Panel is specified but not numerically closed in the benchmark subsection	Excluded until populated and estimated
BridgeStress identifies strategic corridor exposure in the benchmark	Supported as constructed diagnostic	Permitted as benchmark interpretation

Source note: Author claim-gating table for reviewer-safe monograph presentation.

8.2.12. Cross-Chapter Integration with the Seven Millennium Economic Models

The research object of Chapter 8 must also be positioned relative to the other six Millennium-inspired economic models in the monograph. This prevents the book from becoming seven separate articles. The Yang-Mills chapter shares the general monograph logic of mathematical-economic analogy, public-anchor transformation, constructed indicators, validation hierarchy and claim discipline. At the same time, it has its own object: the finite gauge-stress network.

The table below summarizes the cross-chapter distinction. It shows that the Yang-Mills object overlaps with Hodge, Navier-Stokes and BSD through flow, network and local-to-systemic logic, but it remains distinct because its central object is a stress-weighted graph whose spectral gap functions as a shock-threshold analogue.

Table 8.2.12. Chapter 8 research object within the seven-problem monograph architecture.

Book chapter	Primary empirical object	Mathematical-economic grammar	Relation to Chapter 8
Chapter 5: Perelman/Ricci/Poincare	Macro-regional inequality-pressure manifold	Curvature, entropy and smoothing capacity	Shares curvature language; different object and evidence base
Chapter 6: Hodge	Regional macro-flow network	Gradient, curl and harmonic decomposition	Shares graph/cycle logic; Yang-Mills focuses on stress threshold and gauge curvature
Chapter 7: Navier-Stokes	100-country liquidity-flow stress balance	Velocity, pressure, friction, shock and closure	Shares systemic-stress logic; Yang-Mills uses finite network threshold rather than flow-balance equation
Chapter 8: Yang-Mills	10-node, 27-edge global-corridor stress network	Gauge potential, curvature, action, mass gap, EMGI, BridgeStress	This section fixes the chapter-specific research object
Chapter 9: BSD	World anchor plus regional local-to-global rank system	Finite-state traces, L-order and structural rank	Shares local-to-global/corridor logic; BSD focuses on rank formation
Chapter 10: Riemann/Zeta	Layered global inflation forecast system	Zeta-cycle correction and forecast validation	Shares spectral analogy; different target variable and validation structure
Chapter 11: P vs NP	Cardinality-constrained portfolio optimization system	Support-space explosion and exact reduced benchmark	Shares claim-discipline logic; different computational object

Source note: Author synthesis based on the monograph structure and the seven source studies.

8.2.13. Section Synthesis

Section 8.2 defines the research object of the Yang-Mills economic mass-gap chapter as a finite global-corridor systemic-stress network. The object is bounded, reproducible and analytically layered. It contains a World normalization anchor, ten substantive regional/corridor nodes, twenty-seven weighted undirected edges, a normalized systemic-stress field, a public-anchor versus author-calculated object distinction and a two-layer evidence-status architecture.

The section's main scientific contribution is not a numerical result. Its contribution is object discipline. It tells the reader what exactly is being measured before the chapter introduces the data architecture, methodology and results. The later positive mass gap, EMGI, fragility, BridgeStress and shock-diagnostics results are meaningful only because the research object has been fixed in this subsection.

The admissible conclusion is therefore precise. The Yang-Mills chapter studies a constructed finite stress network designed to measure systemic shock thresholds in a global-corridor setting. It is not a proof of the classical Yang-Mills problem, not a literal physical field and not a final country-level causal model. It is a benchmark measurement architecture that prepares the ground for the detailed data architecture in Section 8.3, the gauge-potential and curvature methodology in Section 8.4, the positive finite-network mass-gap results in Section 8.5 and the corridor-shock interpretations in Sections 8.6-8.8.

Table 8.2.13. Final synthesis of the research-object section.

Dimension	Conclusion
What Section 8.2 establishes	A finite global-corridor systemic-stress network as the empirical object of Chapter 8
What it preserves	World normalization anchor, ten regional/corridor nodes, 27 weighted edges, stress field and evidence-status separation
What it enables	Gauge potential, triangular curvature, economic action, stress Laplacian, EMGI, fragility and BridgeStress calculations
What it excludes	Yang-Mills theorem proof, literal physical field interpretation, observed bilateral transaction-matrix claim, final country-level causal inference

Dimension	Conclusion
How it connects to the monograph	It supplies the Chapter 8-specific research object inside the seven-problem economic-analogue architecture

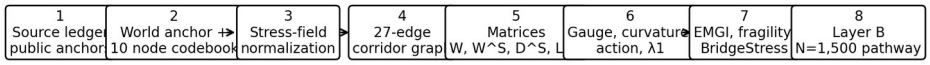
Source note: Author synthesis for transition to Section 8.3.

8.3. Data Architecture: Ten Nodes, Twenty-Seven Edges and Layered Evidence Status

This section specifies the empirical and computational architecture that makes Chapter 8 auditable. The Yang-Mills economic mass-gap chapter does not begin from an unrestricted metaphor. It begins from a bounded data object: a finite global-corridor stress network with ten regional/corridor nodes, twenty-seven weighted undirected edges and a two-layer evidence design. The role of Section 8.3 is therefore to state exactly what data enter the chapter, how public anchors are separated from author-calculated variables, which outputs are already benchmark-closed and which outputs remain assigned to the larger validation pathway.

The data architecture is the technical bridge between Section 8.2 and Section 8.4. Section 8.2 defined the research object. Section 8.4 will formalize the methodology: gauge potential, curvature, action and stress Laplacian. Section 8.3 sits between them and answers a necessary reviewer-facing question: from what empirical material are those mathematical objects computed? The answer is a layered architecture consisting of public macroeconomic anchors, node-level transformations, corridor-sensitive edge coding, matrix construction, benchmark outputs, scenario outputs, replication files and a country-panel validation design.

The design is deliberately claim-gated. Layer A is the completed benchmark layer. It can support finite-network measurement statements because the node table, edge list, matrices, stress scores and benchmark outputs are specified. Layer B is the country-panel validation pathway. It can support final country-level econometric claims only after the 100-country by 15-year panel is populated and estimated. This separation is not an editorial detail; it is the scientific safeguard that allows the chapter to be ambitious without overstating the evidence.



Data architecture converts official/public macro anchors into a finite gauge-stress object and then separates completed benchmark evidence from panel-validation evidence.

Figure 8.3.1. Data architecture pipeline for the Yang-Mills economic mass-gap chapter.

Figure 8.3.1. Data architecture pipeline for the Yang-Mills economic mass-gap chapter.

8.3.1. Role of Data Architecture inside Chapter 8

In a gauge-econometric framework, data architecture has a stronger function than ordinary descriptive statistics. It determines whether the mathematical objects used later in the chapter are reproducible. A stress Laplacian cannot be interpreted if the adjacency matrix is not disclosed. A curvature field cannot be interpreted if the triangular cycles are not reproducible. EMGI and BridgeStress cannot be interpreted if the public-anchor layer and author-calculated layer are not separated. Section 8.3 therefore treats data architecture as a scientific control system.

The architecture has four obligations. First, it must preserve the public-data anchor status of the initial macroeconomic variables. Second, it must document the transformations that convert those anchors into stress-oriented and corridor-sensitive variables. Third, it must define a finite graph whose node and edge universe is stable before the gauge and spectral calculations are performed. Fourth, it must classify the final outputs according to evidence strength: benchmark measurement, diagnostic association, scenario evidence, robustness evidence, cautionary placebo evidence, replication evidence and future panel-validation evidence.

Table 8.3.1. Functional role of the data architecture in Chapter 8.

Architecture block	Empirical object	Output supported	Claim status
Public-anchor layer	GDP mass, world share, projected	Raw empirical coordinate	Public-data anchor, not

Architecture block	Empirical object	Output supported	Claim status
	growth, transition GDP, GDP per capita and observable proxy families	system	final constructed indicator
Node-transformation layer	Mass exposure, growth-gap pressure, income fragility, transition momentum and corridor exposure	Normalized systemic-stress field σ_i	Author-calculated benchmark variable
Edge layer	Twenty-seven weighted undirected regional/corridor relations	Weighted graph W and corridor factors	Benchmark network object, not observed bilateral transactions
Matrix layer	Adjacency, stress-weighted adjacency, degree and Laplacian matrices	Gauge, curvature, spectral and mass-gap computation base	Reproducible finite-network calculation layer
Output layer	Gauge potential, triangular curvature, action, λ1, EMGI, fragility, BridgeStress and scenarios	Chapter 8 results and interpretation	Benchmark-validating or diagnostic according to layer
Validation pathway	100 countries by 15 years, planned N = 1,500	FE/TWFE, Driscoll-Kraay, IV, factor and external-validation models	Panel-ready, not final causal evidence until estimated

Source note: Author synthesis based on the source manuscript's two-layer Yang-Mills architecture.

8.3.2. Source Ledger and Public-Data Anchor Layer

The source ledger is the first protection layer of the chapter. It states which inputs are public anchors and which objects are created by the author's transformations. This distinction is essential because a constructed stress score, gauge potential or EMGI value cannot be described as an official indicator. It is a reproducible research object derived from public anchors under disclosed formulas.

The public-anchor layer is built around macroeconomic series families used to establish regional scale, projected growth, transition mass and income depth. These variables provide empirical grounding. They do not themselves produce the Yang-Mills result. The result appears only after normalization, corridor coding, edge construction, matrix transformation, gauge-field construction and spectral calculation. The source ledger therefore creates the chain of custody from macroeconomic data to finite-network benchmark outputs.

Table 8.3.2. Source-ledger and public-anchor status of the Yang-Mills data architecture.

Input / derived variable	Source family	Series code / metadata	Year / horizon	Transformation in chapter	Author adjustment / status
GDP mass	World Bank WDI / DataBank	NY.GDP.MKTP.CD; current US dollars	2024 anchor	Regional aggregation; converted to USD billions	Public-data anchor; not a new official indicator
World-output share	World Bank WDI / DataBank	GDP_i / GDP_world from NY.GDP.MKTP.CD	2024 anchor	Share_i = GDP_i / GDP_world * 100	Author normalization from public GDP
Projected growth	IMF WEO / World Bank regional outlook logic	Real GDP growth, WEO-style NGDP_RPCH / WDI NY.GDP.MKTP.KD.ZG benchmark	2026 projection horizon	Used as transition/growth pressure input	Projection anchor; values fixed inside benchmark dataset
Transition GDP	Author transition calculation from GDP and growth	GDP_2024*(1+g_2025)*(1+g_2026), simplified benchmark path	2026 horizon	Transition mass proxy	Author-calculated; replication file should store growth path
GDP per capita /	World Bank WDI /	NY.GDP.PCAP.CD; current US dollars	Latest available /	Converted into income-fragility	Public anchor transformed

Input / derived variable	Source family	Series code / metadata	Year / horizon	Transformation in chapter	Author adjustment / status
income depth	DataBank		benchmark year	pressure by inverse-depth scaling	by author
Trade / openness proxy	World Bank WDI / DataBank	NE.TRD.GNFS.ZS where available	Latest available / regional proxy	Used only for external-validation and corridor plausibility checks	Not a direct edge weight unless explicitly stated
Inflation / price-pressure proxy	World Bank WDI / IMF WEO	FP.CPI.TOTL.ZG / WEO inflation analogue	Latest available / scenario proxy	Used in scenario and external-validation interpretation	Observable-proxy layer, not part of official EMGI
Corridor exposure	Author corridor coding from Middle Corridor, Black Sea, Caspian, regional adjacency and logistics role	No official WDI indicator; coded as benchmark corridor proxy	Benchmark coding year	Min-max / 0-1 coding for stress and bridge analysis	Author-defined and disclosed; sensitivity tested separately
Gauge, curvature, action, mass gap, EMGI	Author calculations	Reproducible formulas in Chapter 4	Benchmark run	Derived from stress field and weighted network	Not World Bank/IMF variables; finite-network economic analogue

Source note: Adapted from the Yang-Mills source data-provenance table. Public anchors are separated from author-calculated variables.

The source ledger prevents category error. GDP mass, world-output share, growth projection and GDP per capita are public-anchor families. Stress score, corridor-weighted adjacency, gauge potential, curvature, action, EMGI and BridgeStress are constructed indicators. The validity of the latter depends on formula disclosure, matrix disclosure, replication files and claim discipline rather than on treating them as official data releases.

8.3.3. Node Codebook: World Anchor and Ten Regional/Corridor Nodes

The node codebook fixes the empirical universe of the finite-network benchmark. It contains one World anchor and ten substantive regional/corridor nodes. The World row is used for normalization and scale consistency; it is not a competing node in the stress network. The ten regional/corridor nodes form the actual graph: East Asia and Pacific, North America, Europe, Latin America and Caribbean, South Asia, Middle East and North Africa, Sub-Saharan Africa, Oceania, Central Asia and the Caucasus.

The explicit separation of the Caucasus is methodologically important. If the Caucasus were absorbed into Europe or Central Asia, the chapter would lose the ability to test a central claim of corridor economics: a region can be small in output mass but strategically relevant because it sits at a stress-transmission interface. The data architecture therefore preserves a corridor-sensitive subregional node inside the global network.

Table 8.3.3. World anchor and ten-node regional/corridor codebook.

Region / anchor	Code	GDP 2024, $bn	World share, %	Transition GDP 2026, $bn	Growth 2026, %	GDP pc, $	System role
World anchor	WLD	110,985.0	100.00	118,201.7	3.20	14,100	Global benchmark
East Asia and	EAP	35,620.0	32.09	38,674.9	4.20	17,200	Regional/corridor

Region / anchor	Code	GDP 2024, $bn	World share, %	Transition GDP 2026, $bn	Growth 2026, %	GDP pc, $	System role
Pacific							node
North America	NAM	31,000.0	27.93	32,252.4	2.00	76,000	Regional/corridor node
Europe	EUR	23,150.0	20.86	23,849.7	1.50	43,000	Regional/corridor node
Latin America and Caribbean	LAC	7,260.0	6.54	7,612.7	2.40	10,600	Regional/corridor node
South Asia	SAS	4,770.0	4.30	5,390.0	6.30	2,700	Regional/corridor node
Middle East and North Africa	MENA	4,540.0	4.09	4,835.2	3.20	8,800	Regional/corridor node
Sub-Saharan Africa	SSA	2,160.0	1.95	2,327.3	3.80	1,850	Regional/corridor node
Oceania	OCE	1,810.0	1.63	1,886.8	2.10	63,000	Regional/corridor node
Central Asia	CAS	530.0	0.48	585.4	5.10	9,000	Regional/corridor node
Caucasus	CAU	145.0	0.13	158.6	4.60	9,500	Regional/corridor node

Source note: Adapted from the Yang-Mills source node table. The World row is a normalization anchor; the ten regional/corridor rows form the benchmark graph.

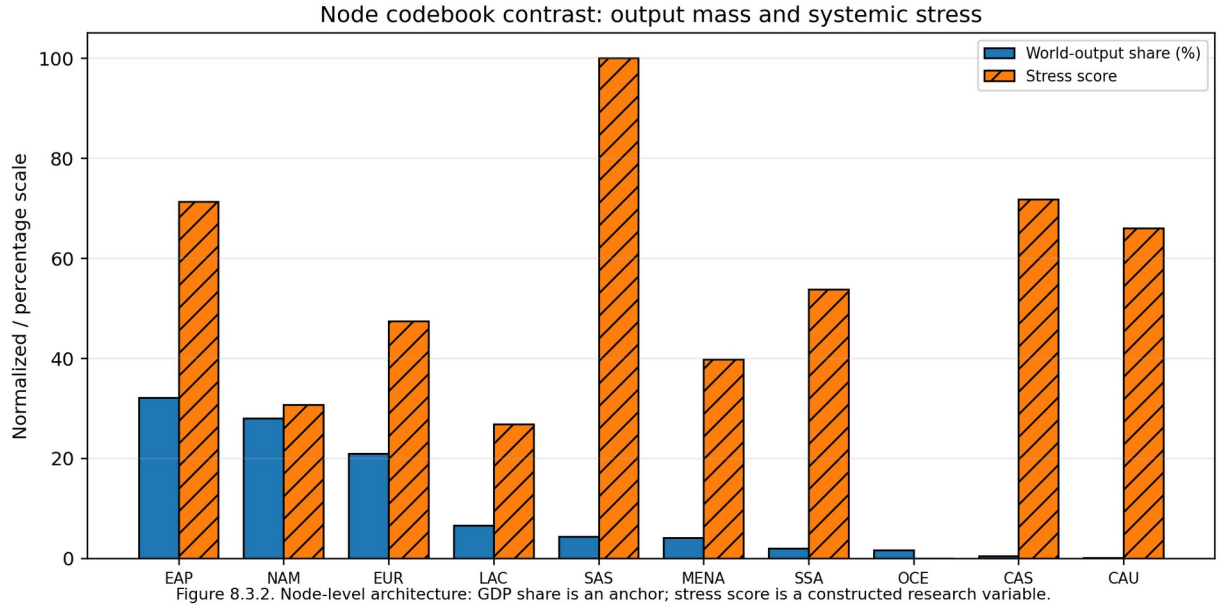


Figure 8.3.2. Node-level architecture: GDP share is an anchor; stress score is a constructed research variable.

Figure 8.3.2. Node-level architecture: GDP share is an anchor; stress score is a constructed research variable.

8.3.4. Raw-to-Normalized Stress-Field Construction

The stress-field layer converts heterogeneous macroeconomic information into a common pressure-oriented scale. This is a necessary step because GDP, growth, GDP per capita, transition GDP and corridor exposure are not measured in the same units. The architecture therefore does not add raw units directly. It transforms each component into a normalized stress-relevant measure and then constructs the node-level systemic-stress score.

The stress construction has a substantive meaning. Mass exposure captures scale; growth-gap pressure captures dynamic pressure; income-fragility pressure captures weak absorption capacity; transition-momentum pressure captures forward structural movement; corridor exposure captures strategic transmission position. The final stress score is therefore a composite field on the nodes of the graph, not a raw macroeconomic statistic.

(8.3.1) $x_i^* = 100 \cdot (x_i - \min(x)) / (\max(x) - \min(x))$

This generic min-max form represents the normalization principle. Directional harmonization must be applied so that higher normalized values represent higher stress or higher exposure where appropriate.

(8.3.2) σ_i = f(Mass_i^*, GrowthGap_i^*, IncomeFragility_i^*, Transition_i^*, Corridor_i^*)

The stress field σ_i is a constructed author-calculated field. The exact component weights and transformations belong to the methodology section; Section 8.3 fixes the data-object status and audit trail.

Table 8.3.4. Normalized systemic-stress component table.

Code	Region	Mass exposure	Growth-gap pressure	Income-fragility pressure	Transition pressure	Corridor exposure	Stress score
SAS	South Asia	13.05	100.00	85.53	100.00	56.67	100.00
CAS	Central Asia	1.10	61.29	47.44	74.49	90.00	71.79
EAP	East Asia and Pacific	100.00	32.26	30.85	55.68	53.33	71.23
CAU	Caucasus	0.00	45.16	45.97	63.72	100.00	66.03
SSA	Sub-Saharan Africa	5.69	19.35	100.00	47.35	28.33	53.78
EUR	Europe	64.86	54.84	10.81	0.00	61.67	47.40
MENA	Middle East and North Africa	12.39	0.00	48.06	34.88	73.33	39.71
NAM	North America	86.98	38.71	0.00	10.20	11.67	30.66
LAC	Latin America and Caribbean	20.06	25.81	43.03	18.40	20.00	26.78
OCE	Oceania	4.69	35.48	3.44	12.24	0.00	0.00

Source note: Adapted from the Yang-Mills source stress-score table. The values are author-calculated normalized benchmark components.

Table 8.3.5. Raw-composite to normalized-stress audit.

Code	Region	Raw composite σ*	Min raw	Max raw	Normalized stress score	Audit note
SAS	South Asia	70.3265	10.7300	70.3265	100.00	normalized upper bound
CAS	Central Asia	53.5115	10.7300	70.3265	71.79	inside normalized 0-100 interval
EAP	East Asia and Pacific	53.1825	10.7300	70.3265	71.23	inside normalized 0-100 interval
CAU	Caucasus	50.0825	10.7300	70.3265	66.03	inside normalized 0-100 interval
SSA	Sub-Saharan Africa	42.7765	10.7300	70.3265	53.78	inside normalized 0-100 interval
EUR	Europe	38.9765	10.7300	70.3265	47.40	inside normalized 0-100 interval
MENA	Middle East and North Africa	34.3910	10.7300	70.3265	39.71	inside normalized 0-100 interval
NAM	North America	29.0020	10.7300	70.3265	30.66	inside normalized 0-100 interval
LAC	Latin America and Caribbean	26.6915	10.7300	70.3265	26.78	inside normalized 0-100 interval
OCE	Oceania	10.7300	10.7300	70.3265	0.00	normalized lower bound; not zero information

Source note: Adapted from the Yang-Mills normalization audit. This table documents the conversion from raw composite values to the 0-100 stress field.

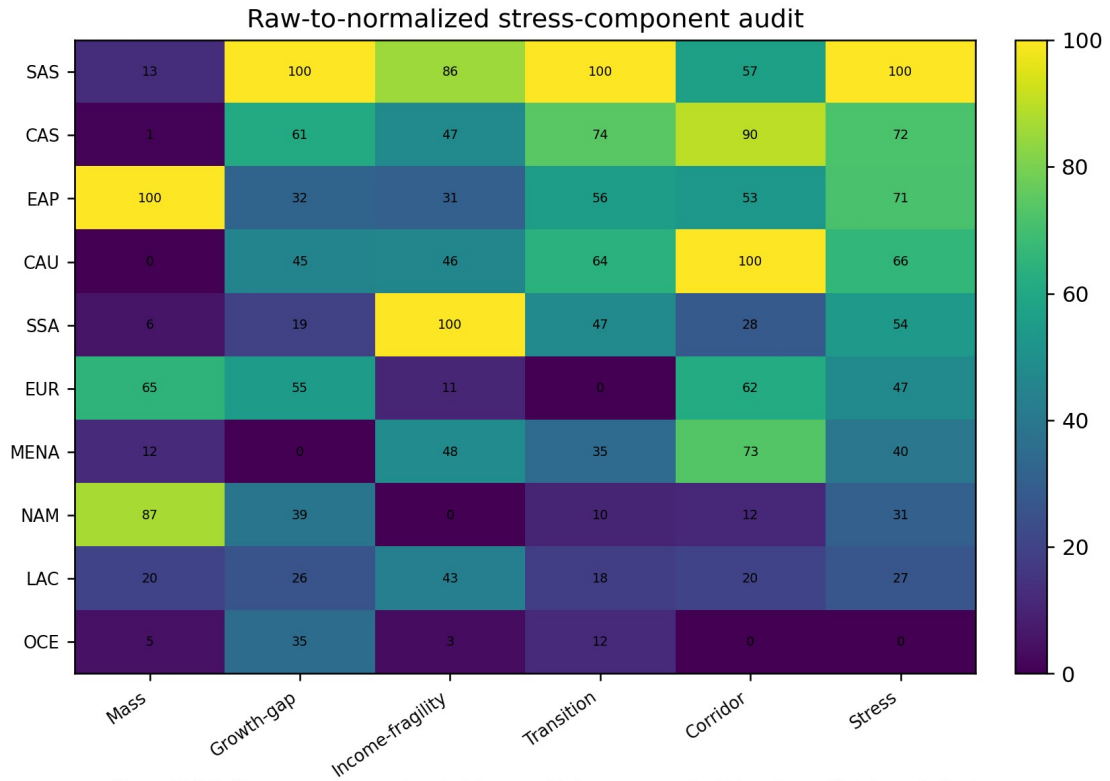


Figure 8.3.6. Stress score is constructed from multiple components; it is not an official raw indicator.

Figure 8.3.6. Stress-component audit across the ten-node benchmark.

8.3.5. Twenty-Seven-Edge Graph Layer and Corridor Coding

The twenty-seven-edge layer converts the node universe into a connected finite graph. This is the first point at which the chapter becomes topological. A list of nodes alone would support ranking. A weighted edge system supports transmission, cycles, curvature and spectral diagnostics. The benchmark is therefore defined not only by its ten nodes but also by its retained corridor-sensitive edge list.

The edges are weighted undirected benchmark relations. They should not be interpreted as a complete observed bilateral trade matrix. Instead, they are author-calculated relations designed to carry stress through the graph. The corridor factor records the author-coded amplification of selected links that have special transmission significance within Middle Corridor, Black Sea, Caspian, Caucasus-Central Asia, Europe-MENA-South Asia and broader global-corridor logic.

Table 8.3.6. Twenty-seven retained weighted edges in the benchmark graph.

Edge	Weight	Corridor factor
EAP-SAS	1.000	1.500
EAP-EUR	0.937	1.000
NAM-LAC	0.934	1.400
NAM-EUR	0.910	1.000
EUR-MENA	0.908	1.600
EAP-NAM	0.818	1.000
EAP-OCE	0.643	1.400
EAP-MENA	0.580	1.000
EUR-LAC	0.562	1.000
EAP-CAS	0.518	1.600
NAM-MENA	0.516	1.000
SAS-MENA	0.459	1.400
EUR-CAU	0.411	2.200
EUR-SSA	0.407	1.000
LAC-MENA	0.339	1.000
MENA-CAS	0.312	1.900

Edge	Weight	Corridor factor
NAM-OCE	0.293	1.000
LAC-SSA	0.279	1.000
EUR-CAS	0.270	1.000
MENA-SSA	0.261	1.000
SAS-CAS	0.261	1.500
SAS-SSA	0.246	1.000
OCE-SAS	0.241	1.000
MENA-CAU	0.217	1.900
SAS-CAU	0.180	1.600
CAS-CAU	0.140	2.400
SSA-CAU	0.082	1.000

Source note: Adapted from the Yang-Mills source edge list. These edges define the finite graph before stress weighting and Laplacian construction.

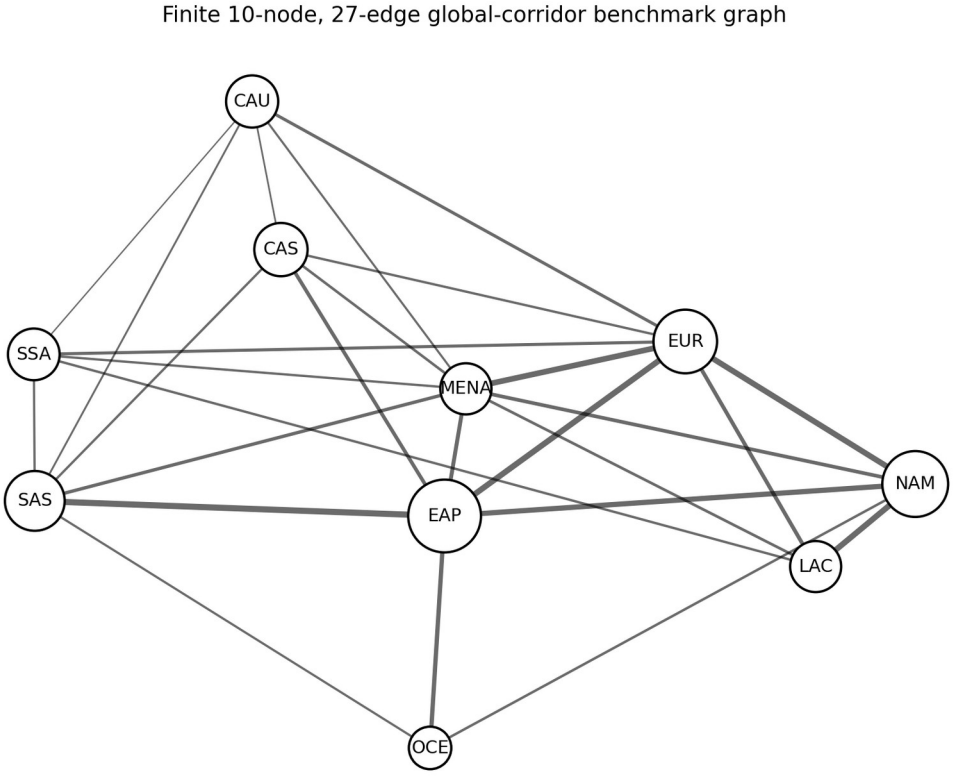


Figure 8.3.3. The edge list defines the graph required for gauge potential, triangular curvature and stress-Laplacian diagnostics.

Figure 8.3.3. Finite 10-node, 27-edge global-corridor benchmark graph.

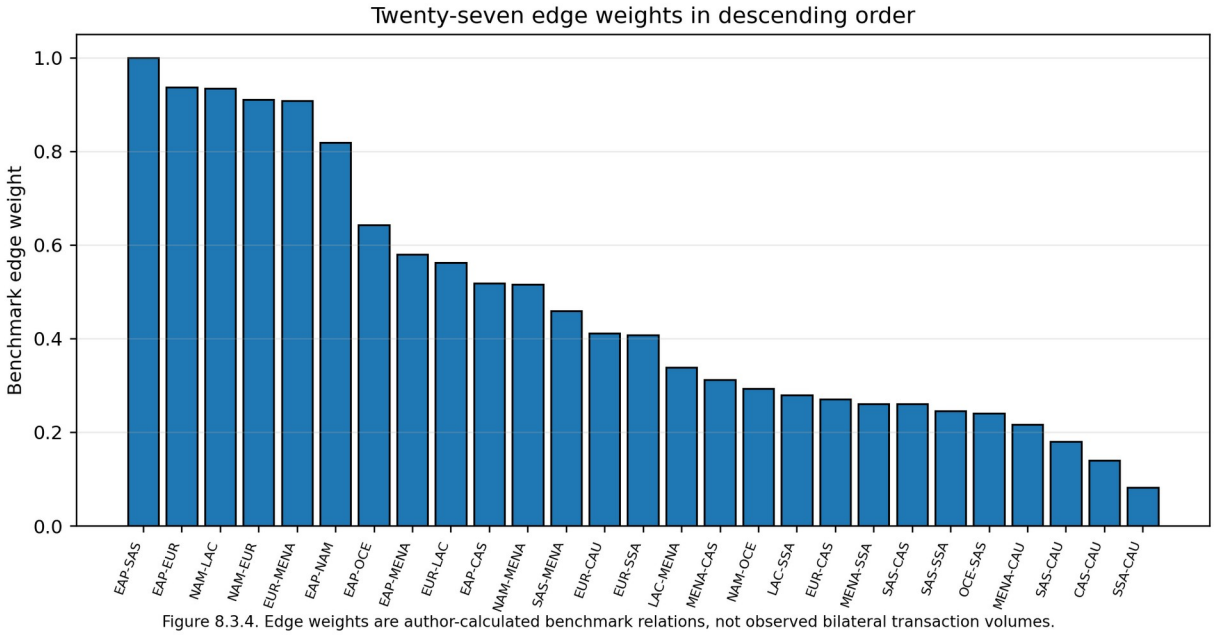


Figure 8.3.4. Edge weights are author-calculated benchmark relations, not observed bilateral transaction volumes.

Figure 8.3.4. Twenty-seven edge weights in descending order.

The graph's density of 0.600 positions it between two extremes. It is not a tree, because a tree would not contain enough cycles for triangular curvature. It is not complete, because a complete graph would dilute corridor-specific structure. The retained twenty-seven edges are therefore central to the chapter's measurement identity: they provide enough topology for curvature without mechanically connecting every region to every other region.

8.3.6. Matrix Layer: Adjacency, Stress-Weighted Adjacency, Degree and Laplacian

The matrix layer is the computational core of the data architecture. The edge list becomes an adjacency matrix W. The node stress field is then embedded into the graph to produce a stress-weighted adjacency matrix W^S. From W^S, the degree matrix D^S and stress Laplacian L^S are constructed. These matrices are the direct input to the finite-network mass-gap calculation.

The importance of matrix disclosure is straightforward. A positive finite-network mass gap cannot be audited by reading a paragraph. It requires reproducible matrices. Section 8.3 therefore treats W, W^S, D^S and L^S as mandatory data objects, not as hidden intermediate calculations.

(8.3.3) $W = [w_{ij}], \quad w_{ij} = w_{ji} \geq 0, \quad w_{ii} = 0$

The adjacency matrix records the retained undirected edge weights. It is the base graph object.

(8.3.4) $W^S_{ij} = w_{ij} \cdot g(\sigma_i, \sigma_j)$

The stress-weighted adjacency matrix embeds node-level stress into the edge system. The function $g(\cdot)$ is defined in the methodology section and is audited through the matrix output files.

(8.3.5) $D^S_{ii} = \Sigma_j W^S_{ij}, \quad L^S = D^S - W^S$

The stress Laplacian L^S is the spectral object whose first positive eigenvalue becomes the finite-network economic mass gap.

Table 8.3.7. Matrix and field objects required by the data architecture.

Object	Name	Data input	Computational role
W	Weighted adjacency matrix	Twenty-seven edge weights and zero diagonal	Defines the finite graph topology
W^S	Stress-weighted adjacency matrix	Edge weights adjusted by node stress field	Carries systemic stress through the graph
D^S	Stress-weighted degree matrix	Row sums of W^S on the diagonal	Measures node-level weighted stress exposure
L^S	Stress Laplacian	D^S - W^S	Supplies eigenvalues for λ0, λ1 and spectral radius
A_ij	Gauge potential on oriented edges	Anti-symmetric transformation of stress tension	Supplies edge-level gauge field
F_ijk	Triangular curvature	Cycle sum of gauge potential over	Supplies curvature and action

Object	Name	Data input	Computational role
		triangles	calculations

Source note: Author synthesis from the Yang-Mills methodology and replication manifest.

Table 8.3.8. Stress-weighted adjacency matrix W^S.

node	EAP	NAM	EUR	LAC	SAS	MENA	SSA	OCE	CAS	CAU
EAP	0.000	0.417	0.556	0.000	0.856	0.322	0.000	0.229	0.370	0.000
NAM	0.417	0.000	0.355	0.268	0.000	0.182	0.000	0.045	0.000	0.000
EUR	0.556	0.355	0.000	0.208	0.000	0.395	0.206	0.000	0.161	0.233
LAC	0.000	0.268	0.208	0.000	0.000	0.113	0.112	0.000	0.000	0.000
SAS	0.856	0.000	0.000	0.000	0.000	0.321	0.189	0.120	0.224	0.149
MENA	0.322	0.182	0.395	0.113	0.321	0.000	0.122	0.000	0.174	0.115
SSA	0.000	0.000	0.206	0.112	0.189	0.122	0.000	0.000	0.000	0.049
OCE	0.229	0.045	0.000	0.000	0.120	0.000	0.000	0.000	0.000	0.000
CAS	0.370	0.000	0.161	0.000	0.224	0.174	0.000	0.000	0.000	0.096
CAU	0.000	0.000	0.233	0.000	0.149	0.115	0.049	0.000	0.096	0.000

Source note: Adapted from the Yang-Mills source stress-weighted adjacency matrix. Values are displayed in the source rounding convention.

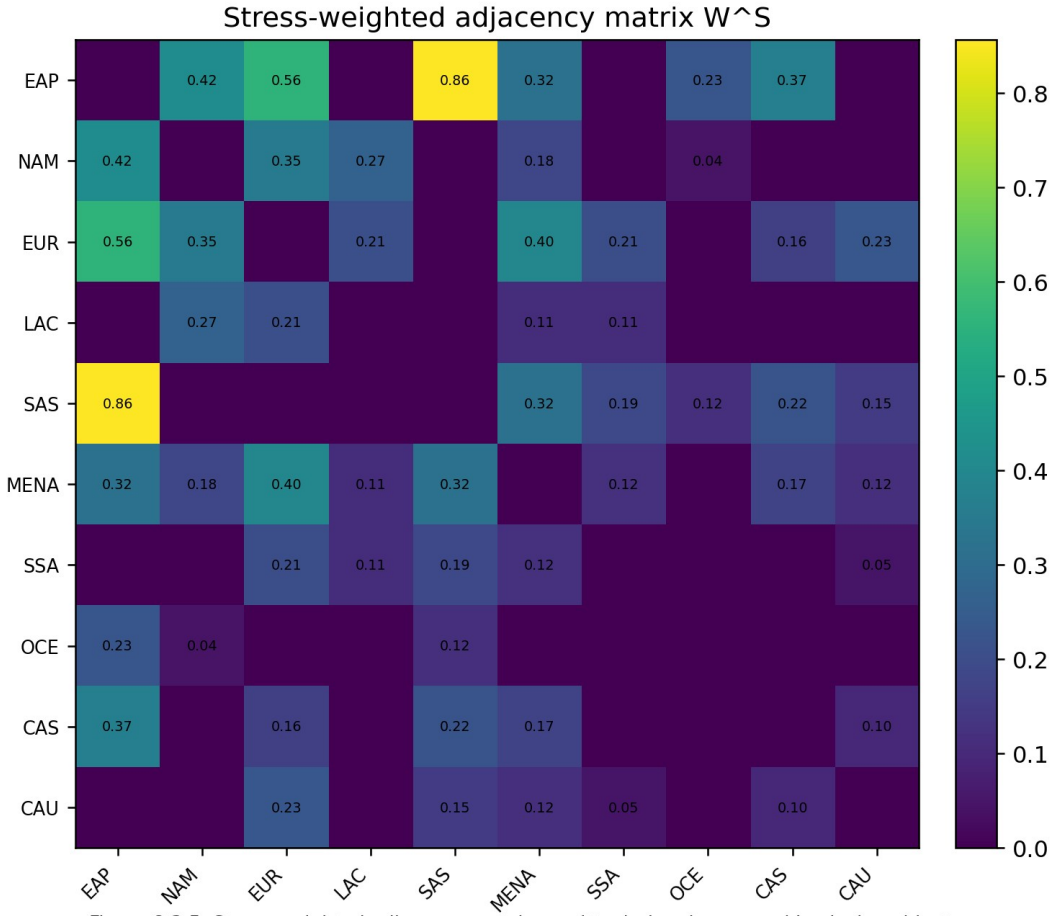


Figure 8.3.5. Stress-weighted adjacency matrix used to derive degree and Laplacian objects.

Figure 8.3.5. Stress-weighted adjacency matrix W^S.

8.3.7. Benchmark Parameters and Audit Rules

The benchmark parameters define how public anchors and corridor coding are converted into the graph and its derived objects. The data architecture must therefore state not only which variables are used, but also which parameter values and coding rules are fixed for the benchmark. Parameter disclosure is particularly important in a constructed-index framework because undisclosed parameters would allow results to become arbitrary.

The parameter layer also defines sensitivity obligations. A benchmark can be reported as the main specification only if alternative graph filters, perturbations and robustness checks are available. In the source study, high-weight, medium-

filtered and sparse-filtered graph specifications, Monte Carlo perturbation and placebo logic are used to protect against overclaiming from a single arbitrary network realization.

Table 8.3.9. Benchmark parameter and coding audit table.

Symbol / item	Benchmark value / coding	Role in formula	Audit status
alpha	0.50	Elasticity applied to economic mass term (m_i*m_j)^alpha	Fixed benchmark parameter; sensitivity required in robustness checks
delta	0.35	Decay applied to regional/corridor separation exp(-delta*d_ij)	Fixed benchmark distance-friction parameter
C_ij	1.00 unless an edge is explicitly corridor-sensitive	Base connectivity constant before corridor amplification	Author-coded; disclosed by edge list
kappa_ij	1.00-2.40 in Table 4.3	Corridor-intensity multiplier for Middle Corridor, Black Sea, Caspian, MENA/SAS/CAS/CAU links	Author-coded corridor factor; not observed trade flow
d_ij	0-1 separation proxy	Regional/corridor separation used inside exponential friction	Author-coded; full replication file should retain pairwise values
eta_ij	0 in baseline gauge; sign captured by stress differential	Residual corridor-friction term in A_ij	Kept neutral in benchmark to avoid unreported residual tuning
W_ij	Normalized to max edge weight = 1.000	Final weighted adjacency entry	Reproducible from Table 4.3
W^S_ij	W_ij*(sigma_i+sigma_j)/200	Stress-weighted adjacency used in spectral diagnostics	Author-calculated and reported in Table 4.3C

Source note: Adapted from the Yang-Mills source benchmark-parameter table.

Table 8.3.10. Graph specification robustness layer.

Specification	Edges	Density	Mass gap	Spectral radius
0.0000	0.3850	3.5023	0.3850	Baseline full graph
0.0000	0.2272	3.4841	0.2272	High-weight filtered graph
0.0000	0.2037	3.4437	0.2037	Medium-filtered graph
0.0000	0.1838	3.4129	0.1838	Sparse-filtered graph

Source note: Adapted from the Yang-Mills robustness table. This layer supports the claim that the positive finite-network gap is not tied only to the full-edge display.

8.3.8. Output Data Objects: Gauge, Curvature, Action, Mass Gap, EMGI and BridgeStress

The output layer contains the author-calculated objects produced from the data architecture. These outputs are not independent raw data. They are computationally generated results whose admissibility depends on the transparency of the input ledger, node codebook, edge list, matrices, scripts and audit files. This is why Section 8.3 places them inside the data architecture before Section 8.4 interprets their formulas in detail.

The key outputs are the anti-symmetric gauge potential, triangular curvature, Yang-Mills economic action, stress-Laplacian spectrum, Economic Mass Gap Index, fragility, BridgeStress and scenario outputs. Each has a different evidentiary status. Gauge, curvature, action and λ1 are mathematical/network outputs. EMGI and fragility are node-level constructed indices. BridgeStress is a corridor-exposure diagnostic. Scenario outputs are model-implied shock diagnostics, not unconditional forecasts.

Table 8.3.11. Output objects generated by the data architecture.

Output object	Definition	Required input	Evidence status
Gauge potential A_ij	Oriented edge-level stress tension	Edge list, stress field and orientation rule	Gauge-econometric field object
Triangular curvature	Non-neutralized stress	A_ij on triangle edges	Cycle-level curvature

Output object	Definition	Required input	Evidence status
F_ijk	circulation around cycles		object
Yang-Mills economic action	Squared curvature stress-energy	Curvature values and triangle weights	Systemic action concentration metric
Mass gap λ1	First positive eigenvalue of L^S	Stress Laplacian spectrum	Finite-network shock threshold
EMGI	Local structural-protection index	LSP, centrality, income depth, resilience, stress and curvature	Node-level protection ranking
Fragility	100 - EMGI	EMGI identity	Complementary vulnerability index
BridgeStress	Corridor exposure under fragility and curvature participation	Corridor exposure, corridor role, fragility and curvature participation	Strategic corridor exposure diagnostic
Scenario outputs	Shock-adjusted spectral and node diagnostics	Inflation, financial, trade/logistics and energy/geopolitical shocks	Model-implied threshold-compression evidence

Source note: Author synthesis from the source methodology, results and replication manifest.

Table 8.3.12. Spectral benchmark summary.

Normal-state lambda_0	First stress mode lambda_1	Spectral radius	Economic mass gap
0.0000	0.3850	3.5023	0.3850

Source note: Adapted from the Yang-Mills source mass-gap summary. The mass gap is finite-network spectral language only.

Table 8.3.13. Yang-Mills economic action concentration summary.

Total triangular cycles	Total economic Yang-Mills action	Mean triangle action	Maximum triangle action	Top-five action share %
27.000	2,514.0	93.113	1,397.9	78.329

Source note: Adapted from the Yang-Mills action summary. Top-five action concentration indicates stress-energy concentration in a limited set of cycles.

Table 8.3.14. EMGI, fragility and node-level protection output table.

Code	Region	EMGI	Fragility	Resilience	Stress	Curvature	Centrality
NAM	North America	100.00	0.00	100.00	30.66	23.16	84.63
EUR	Europe	90.15	9.85	52.83	47.40	50.13	100.00
EAP	East Asia and Pacific	53.12	46.88	38.25	71.23	100.00	98.23
MENA	Middle East and North Africa	45.59	54.41	27.83	39.71	69.72	78.47
LAC	Latin America and Caribbean	31.37	68.63	23.81	26.78	4.95	41.73
OCE	Oceania	14.50	85.50	42.82	0.00	25.65	10.73
SAS	South Asia	10.36	89.64	12.84	100.00	68.93	38.09
CAS	Central Asia	5.45	94.55	18.48	71.79	23.55	18.94
SSA	Sub-Saharan Africa	4.11	95.89	0.00	53.78	0.76	6.99
CAU	Caucasus	0.00	100.00	9.15	66.03	0.00	0.00

Source note: Adapted from the Yang-Mills EMGI source table. EMGI and fragility are constructed output variables.

Table 8.3.15. BridgeStress output layer.

Code	Region	Corridor exposure	Corridor-role index	Fragility	Curvature participation +	BridgeStress
CAU	Caucasus	98.00	100.00	100.00	57.32	100.00
CAS	Central Asia	92.00	75.00	94.55	67.37	78.24
SAS	South Asia	72.00	60.00	89.64	86.74	59.80
MENA	Middle East and North Africa	82.00	85.00	54.41	87.08	58.79
EAP	East Asia and Pacific	70.00	95.00	46.88	100.00	55.50
SSA	Sub-Saharan Africa	55.00	25.00	95.89	57.64	13.53

Code	Region	Corridor exposure	Corridor-role index	Fragility	Curvature participation +	BridgeStress
LAC	Latin America and Caribbean	50.00	30.00	68.63	59.43	10.89
EUR	Europe	75.00	90.00	9.85	78.72	9.32
OCE	Oceania	38.00	20.00	85.50	68.27	7.90
NAM	North America	45.00	70.00	0.00	67.21	0.00

Source note: Adapted from the Yang-Mills BridgeStress source table. BridgeStress separates corridor strategic exposure from ordinary GDP mass.

8.3.9. Layer A Evidence Status: Completed Finite-Network Benchmark

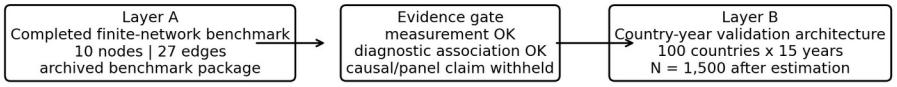
Layer A is the completed benchmark layer of the chapter. It consists of the ten-node graph, twenty-seven retained edges, stress-field construction, adjacency matrices, gauge potential, triangular curvature, action, stress Laplacian, spectral mass gap, EMGI, fragility, BridgeStress, scenario diagnostics, robustness tests and replication manifest. This layer is strong enough to support finite-network benchmark measurement language.

However, Layer A is not a country-level causal panel. It is a finite graph benchmark. Therefore, regression rows, factor screens, network-spatial diagnostics or machine-learning checks at the ten-node level must remain diagnostic or exploratory. The benchmark evidence can be strong without becoming unrestricted causal evidence. This is the central interpretive discipline of the chapter.

Table 8.3.16. Layered evidence-status matrix.

Layer	Unit of observation	Sample size	Primary purpose	Permitted claim
Layer A: regional spectral benchmark	Regional/corridor node	10 nodes	Finite-network construction of stress, curvature, action, spectral gap, and EMGI	Benchmark-validating and measurement claim only
Layer A: edge/cycle diagnostics	Regional edge or triangle	27 edges; 27 triangular cycles	Gauge potential, curvature concentration, action and local-to-systemic threshold	Topological and spectral diagnostic claim
Layer B: country-panel validation	Country-year	100 countries x 15 years = 1,500 observations	Panel econometric validation of EMGI, stress, curvature, resilience and external outcomes	Empirical validation claim only after country-panel data are populated and estimated
Layer B: country-dyad robustness	Country-pair-year or route-year where available	Optional extension beyond 1,500	Corridor/route-level spillover, logistics and trade-friction validation	Network-spatial robustness claim
Final claim boundary	Manuscript-level interpretation	Two-layer evidence system	Prevents N=10 diagnostic tables from being overstated	No causal claim without populated country-panel estimates

Source note: Adapted from the Yang-Mills source evidence-status table. Layer A supports benchmark-validating measurement claims; Layer B supports panel claims only after estimation.



Data architecture is not only a dataset description; it is a claim-control mechanism that distinguishes completed benchmark evidence from future panel validation.

Figure 8.3.7. Layered evidence-status rule for Section 8.3.

Figure 8.3.7. Layered evidence-status rule for Section 8.3.

Table 8.3.17. Integrated benchmark evidence map, selected blocks.

Evidence block	Status	Decision rule / result
Data provenance ledger	Pass	Table 4.1A identifies source family, series logic, year/horizon, transformation and author status.

Evidence block	Status	Decision rule / result
Data consistency	Pass	Public macro anchors retained; author-calculated stress and gauge layers disclosed.
Parameter calibration	Pass	Table 4.3A reports alpha, delta, C_ij, kappa_ij, eta_ij and W^S construction.
Raw-to-normalized stress audit	Pass	Table 4.2A reports raw composite sigma* and normalized stress score; OCE zero is a normalized lower bound.
Network connectedness	Pass	Graph connected; nodes=10, edges=27, density=0.600.
Full adjacency matrices	Pass	Tables 4.3B and 4.3C report W and W^S.
Gauge potential validity	Pass	Directed anti-symmetric edge field constructed and normalized.
Gauge/orientation invariance	Pass	Table 4.6A confirms orientation reversal and node relabeling do not alter lambda_1.
Curvature non-degeneracy	Pass	27 regional/corridor triangles with nonzero curvature measure.
Economic action	Pass	Total Yang-Mills economic action=2514.04.
Positive finite-network mass gap	Pass	First positive spectral gap=0.3850 from the Table 4.3C stress-weighted Laplacian; finite-network proposition stated in Table 4.12A.
Monte Carlo uncertainty	Pass	Mass-gap interval remains positive under input/corridor perturbations.
EMGI interpretability	Pass	EMGI ranks structural protection; fragility = 100 - EMGI, explicitly treated as an identity.
Corridor strategic exposure	Pass	Revised BridgeStress makes Caucasus and Central Asia visible under corridor-role specification.

Source note: Selected rows adapted from the source integrated evidence map. The full source table classifies data provenance, consistency, topology, spectrum, EMGI, scenarios, robustness and replication.

8.3.10. Layer B Evidence Status: 100-Country by 15-Year Validation Pathway

Layer B is the validation pathway that translates the benchmark architecture into a country-year empirical panel. Its planned scale is 100 countries observed over fifteen years, yielding N = 1,500 country-year observations. This layer is necessary because strong country-level causal, dynamic or external-validation claims cannot be grounded in the ten-node benchmark alone.

The country-panel pathway is not a decorative appendix. It is the empirical closure route for the chapter. It specifies fixed-effects, two-way fixed-effects, Driscoll-Kraay, clustered, dynamic-panel, panel-IV, factor and external-validation models. Once populated and estimated, it can test whether EMGI, curvature, fragility and stress retain explanatory or predictive value beyond the benchmark graph. Until then, those claims remain panel-ready rather than panel-confirmed.

Table 8.3.18. Country-panel validation components.

Component	Panel definition	Source family / series logic	Transformation	Closure status
Countries	100 countries selected by data completeness, regional coverage, and corridor relevance	World Bank WDI country identifiers; ISO-3 codes	Balanced or near-balanced country panel; missing values handled by disclosed rule	To be populated in the country-year panel
Years	15 annual observations per country	Recommended window: 2010-2024 or 2011-2025, depending on source availability	Annual frequency; year fixed effects included	N=1,500 target sample
GDP mass	Country-year GDP level	NY.GDP.MKTP.CD or constant-price alternative	USD/log GDP/normalized exposure	Public-data anchor
Growth	Country-year real GDP growth	NY.GDP.MKTP.KD.ZG; IMF WEO analogue where needed	Growth-gap and resilience input	External observable and stress component
Income depth	Country-year GDP per capita	NY.GDP.PCAP.CD or constant-price alternative	Inverse-depth fragility scaling	Public-data anchor
Inflation volatility	Country-year CPI inflation and rolling volatility	FP.CPI.TOTL.ZG / WEO inflation	External outcome for price-pressure validation	Full external validation variable
Trade /	Country-year trade	NE.TRD.GNFS.ZS;	External	Full external

Component	Panel definition	Source family / series logic	Transformation	Closure status
openness	share and logistics exposure	logistics/freight proxy where available	trade/logistics validation outcome	validation variable
Financial spread / risk proxy	Country-year CDS, sovereign spread, EMBI, or comparable risk proxy where available	IMF, World Bank, market-data provider or regional risk datasets	Financial-stress external outcome	Optional due to coverage constraints
Corridor exposure	Country-year or time-invariant corridor-coding layer	Middle Corridor, Black Sea, Caspian, maritime/land-route coding	Interaction with EMGI and stress terms	Author-coded but disclosed and sensitivity-tested
Replication metadata	Exact URLs, download dates, extraction scripts, file hashes	Data archive and code appendix	Required for final reproducibility	Pending final package by design

Source note: Adapted from the Yang-Mills country-panel architecture. These components are specified for the N = 1,500 validation layer.

Table 8.3.19. Required country-panel model blocks.

Model block	Country-panel specification	Required estimator	Main diagnostic output	Interpretive status
Baseline panel validation	Resilience_it = alpha_i + tau_t + beta_1 EMGI_it + beta_2 Curvature_it + beta_3 Stress_it + gamma X_it + epsilon_it	Two-way fixed effects; country-clustered and Driscoll-Kraay standard errors	R2 within/between/overall; robust Wald F; coefficient stability	Core N=1,500 validation after estimation
Network-spatial panel	Y_it = rho W_t Y_it + beta EMGI_it + alpha_i + tau_t + epsilon_it	Spatial/network panel estimator or spatial-lag diagnostic	rho, beta, spatial residual tests	Network externality validation after estimation
Threshold panel	Y_it = beta_L Stress_it*1(EMGI_it <= c) + beta_H Stress_it*1(EMGI_it > c) + FE + epsilon_it	Panel threshold or interaction model	Threshold c, slope difference, Wald test	Local-to-systemic boundary validation after estimation
External-outcome validation	Outcome_it = alpha_i + tau_t + beta EMGI_it + delta Stress_it + theta Curvature_it + controls + epsilon_it	FE / DK / clustered panel	Sign, magnitude, and predictive relevance against observed outcomes	Full external validation after estimation
PCA/factor panel	Common stress factor extracted from EMGI, Stress, Curvature, Resilience, external proxies	PCA/factor model with KMO/Bartlett checks	Eigenvalues, variance shares, factor loadings	Empirical factor validation after estimation
Endogeneity screen	First-stage and reduced-form equations with lagged/instrumental predictors where valid	Panel IV only if instruments are justified and strong	First-stage F, partial R2, overidentification where applicable	Identification diagnostic, not automatic causal proof
Scenario panel recalculation	Country-year post-shock stress, W^S, lambda_1, threshold and EMGI changes	Algorithmic recalculation under documented shock rules	Post-shock lambda_1, action, spillover intensity	Scenario robustness and policy stress testing

Source note: Adapted from the Yang-Mills source validation-design table. Final panel claims require population, estimation and external-validation closure.

Table 8.3.20. Panel-estimation closure standards.

Model	N	Groups	Years	df logic	Required fit statistics	Required joint test	Closure rule
Baseline two-way	1,500	100 countrie	15	Approx. df_resid >=	R2 within, between,	Cluster/DK robust Wald F for all slope	Closed when beta signs

Model	N	Groups	Years	df logic	Required fit statistics	Required joint test	Closure rule
FE		s		1,380 after FE and slopes	overall; Adj. R2; RMSE; AIC/BIC where applicable	coefficients	are stable and Wald p < 0.05 or effect-size evidence is justified
Network-spatial panel	1,500	100 countries	15	Depends on W_t and spatial estimator	Pseudo-R2 or log-likelihood; residual spatial autocorrelation tests	Wald/LR test for network lag and EMGI block	Closed when network dependence is modeled or residual dependence is ruled out
Threshold panel	1,500	100 countries	15	Threshold search with FE consumes additional degrees	RMSE, information criteria, slope-difference fit improvement	Bootstrap or robust Wald test for threshold split	Closed when threshold is stable under bootstrap and alternative c values
External-outcome FE	1,500 or variable-specific N	100 countries where data complete	15	Country/ year FE plus controls	R2 within; RMSE; out-of-sample error if forecasting	Wald test for EMGI/Stress/Curvature block	Closed when observed outcome relationships are stable and not only proxy bridges
PCA/ factor panel	1,500	100 countries	15	Sample-to-variable ratio > 100 for core variables	Eigenvalues, cumulative variance, KMO, Bartlett test	Bartlett sphericity test and factor-retention rule	Closed when KMO >= 0.60 and factor interpretation is stable
Panel IV screen	1,500 or instrument-specific N	100 countries	15	First stage and second stage with FE	First-stage R2, partial R2, weak-instrument F	Weak-instrument F > 10; over-ID test where possible	Closed only if instruments are theoretically valid and statistically strong

Source note: Adapted from the Yang-Mills panel closure table. This table is included to keep future validation claims testable rather than rhetorical.

8.3.11. Replication Manifest, Versioning and File-Hash Discipline

A high-level mathematical-econometric chapter is credible only if the data and code chain is externally auditable. The replication manifest therefore belongs inside the data architecture. It lists the source logs, raw and normalized files, node table, edge list, matrices, cycles, EMGI components, scenario outputs, country-panel file, scripts, seeds, hashes and Zenodo record required to reproduce the reported benchmark.

The benchmark dataset and replication package are reported as archived on Zenodo with DOI 10.5281/zenodo.20786199. In the monograph version, this archive should be treated as the external audit companion for Chapter 8. If later N = 1,500 panel results are added, the replication archive must be updated or supplemented with a country-panel package containing raw country-year data, normalization scripts, estimation outputs, external outcomes and file hashes.

Table 8.3.21. Benchmark replication manifest.

Replication object	Minimum content	Purpose
source_log.csv	URLs, extraction timestamps, source family, indicator code and access notes	Verifies public-anchor provenance.
raw_anchor_data.csv	Unmodified public-anchor values and author-coded corridor variables	Recreates Table 4.1 and Table 4.1A inputs.
normalized_anchor_data.csv	0-100 transformed components and raw composite stress	Recreates stress scores and raw-to-normalized audit.
edge_list.csv	Edge pairs, C_ij, kappa_ij, d_ij, raw and normalized weights	Recreates W and W^S.
matrices.npz / matrices.csv	W, W^S, D^S, L^S	Recreates spectrum and mass gap.
cycles.csv	Full 27-cycle curvature field, weights, F and action	Recreates curvature exposure and total action.
emgi_components.csv	LSP, centrality, income depth, resilience, stress, curvature, Delta_i^local and EMGI	Recreates EMGI and fragility.
scenario_outputs.csv	Shock definitions, recalculated variables and propagation vectors	Recreates scenario tables.
panel_country_year.csv	100-country x 15-year raw and normalized variables	Required for final N=1,500 empirical closure.
scripts/	Code for construction, simulations, diagnostics, figures and tables	Recreates all author-calculated outputs.
seeds_and_hashes.txt	Random seeds, file hashes and output checksums	Supports deterministic replication.
zenodo_record	Gondauri (2026), Version v1, DOI: 10.5281/zenodo.20786199; https://doi.org/10.5281/zenodo.20786199	Provides the archived finite-network benchmark dataset and replication package for independent audit.

Source note: Adapted from the Yang-Mills source replication-manifest table. The manifest documents how benchmark outputs should be regenerated.

Table 8.3.22. Country-panel replication package required for final Layer B closure.

File / component	Required content	Format	Purpose
raw_country_panel	Country-year public-data variables for 100 countries and 15 years	CSV/XLSX	Raw empirical layer
normalized_country_panel	Normalized stress components, EMGI inputs, resilience variables, external outcomes	CSV/XLSX	Reproducible transformations
country_metadata	ISO-3, region, income group, corridor status, route exposure coding	CSV/XLSX	Country classification and fixed effects
edge_and_route_matrix	Country-level or regional-country corridor adjacency, W and W^S matrices by year where applicable	CSV/NPY/XLSX	Network construction
scenario_recalculation_code	Shock-injection algorithms for inflation, financial spread, logistics and geopolitical scenarios	Python/R	Post-shock lambda_1, action and EMGI changes
panel_estimation_code	FE, DK, spatial/network, threshold, PCA and IV-screen routines	Python/R/Stata	Econometric validation
monte_carlo_seed_log	Random seeds, perturbation distributions, iteration counts	TXT/JSON	Uncertainty reproducibility
output_tables_figures	Generated tables and figures matching the manuscript numbering	DOCX/XLSX/PNG/PDF	Manuscript traceability
source_log	URLs, access dates, dataset	CSV/JSON	Data provenance closure

File / component	Required content	Format	Purpose
	versions, extraction timestamps, file hashes		

Source note: Adapted from the Yang-Mills source panel-replication table. These objects are required before final N = 1,500 empirical closure is claimed.

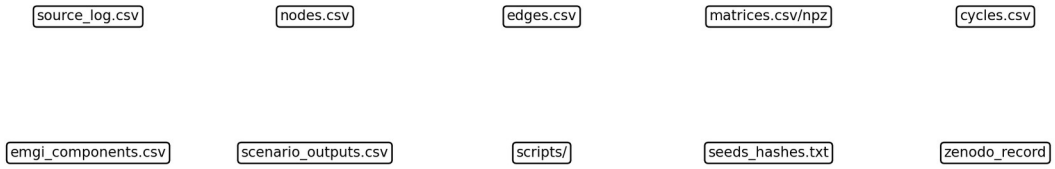


Figure 8.3.8. Replication manifest: every reported matrix, table, figure and diagnostic should be reproducible from the same source ledger, scripts, seeds and hashes.

Figure 8.3.8. Replication manifest and file-hash discipline.

8.3.12. Cross-Seven-Problem Data-Architecture Alignment

Although Chapter 8 is a self-contained Yang-Mills economic analogue, its data architecture must remain consistent with the monograph's seven-problem design. The monograph is not a set of seven disconnected articles. It is a unified measurement project in which each Clay-inspired chapter uses a different mathematical grammar while respecting common principles: public-anchor separation, constructed-variable disclosure, normalization, replication, validation status and claim boundary.

Yang-Mills contributes the finite-network gauge and spectral-threshold grammar. Hodge contributes flow-decomposition logic. Navier-Stokes contributes nondimensional stress-balance and 100-country panel discipline. BSD contributes local-to-global rank and corridor-stress calibration. Riemann-Zeta contributes layered sample validation across annual, quarterly and monthly frequencies. P vs NP contributes computational-complexity and search-space discipline. Perelman/Ricci/Poincare contributes pressure-curvature-topology diagnostics. Section 8.3 therefore includes a cross-seven-study alignment table to show where the Yang-Mills data architecture fits inside the book.

Table 8.3.23. Cross-seven-study data-architecture alignment.

Clay-inspired chapter	Empirical universe	Main N / sample	Main evidence type	Connection to Chapter 8.3
Perelman/Ricci/Poincare	10 macro-regions, 2010-2024, 16 variables	N = 150	Inequality-pressure, curvature, entropy and graph-topology diagnostics	Common principle: normalized stress coordinates and benchmark validation
Hodge	World anchor + 10 regional nodes	10-node benchmark	Gradient/curl/harmonic flow decomposition	Common principle: 10-node regional graph and 27-edge topology discipline
Navier-Stokes	100 countries, 2010-2024	N = 1,500	Macro-financial stress-balance and rolling validation	Common principle: country-panel validation scale and nondimensional stress construction
Yang-Mills	10 nodes, 27 edges + planned panel	Benchmark + N = 1,500 pathway	Gauge curvature, action, spectral mass gap, EMGI and BridgeStress	Chapter 8 contribution: finite-network threshold and corridor stress-energy
BSD	World anchor + 10 regional/corridor	N = 150 closure layer	Local-to-global structural rank and L-order analogue	Common principle: corridor stress and

Clay-inspired chapter	Empirical universe	Main N / sample	Main evidence type	Connection to Chapter 8.3
	nodes			layered claim boundary
Riemann/Zeta	Annual, quarterly and monthly validation layers	N = 55, 45, 20, 100, 240	FPAS+ζ inflation forecast validation	Common principle: sample hierarchy and forecast-validation discipline
P vs NP	94 U.S. industries and reduced exact benchmark	C(94,10), exact C(20,6)	Cardinality-constrained portfolio optimization	Common principle: computational audit and claim-bounded optimization evidence

Source note: Author synthesis based on the monograph structure document and the seven source manuscripts. This table prevents Chapter 8 from reading as an isolated article.

8.3.13. Reviewer-Risk Controls and Non-Overclaiming Rules

The data architecture directly addresses reviewer-risk points. The first risk is source opacity: this is controlled through a source ledger and replication package. The second risk is constructed-variable ambiguity: this is controlled by separating public anchors from author-calculated variables. The third risk is network subjectivity: this is controlled by edge-list disclosure, corridor factors, graph robustness and placebo logic. The fourth risk is small-sample inference: this is controlled by reserving causal language for the N = 1,500 panel. The fifth risk is mathematical overclaiming: this is controlled by defining mass gap strictly as a finite stress-Laplacian eigenvalue.

These controls are not cosmetic. They determine how the chapter should be written. The wording "positive finite-network economic mass gap" is acceptable because λ1 is computed in the finite stress network. The wording "solution of the Yang-Mills mass-gap problem" is not acceptable. The wording "diagnostic association in the ten-node benchmark" is acceptable. The wording "causal country-level confirmation" is not acceptable until Layer B is populated and estimated.

Table 8.3.24. Reviewer-risk controls embedded in the data architecture.

Reviewer risk	Possible criticism	Data-architecture safeguard	Permitted final wording
Mathematical overclaiming	Reader may think the chapter solves Clay Yang-Mills	State repeatedly that the object is a finite weighted economic graph	Use finite-network economic mass-gap language only
Source opacity	Constructed variables may appear arbitrary	Provide source ledger, node codebook, edge list, matrices and replication manifest	Benchmark results remain reproducible
Official-data confusion	Stress, EMGI or BridgeStress may be misread as official statistics	Separate public anchors from author-calculated objects	Constructed indicators are research variables
Edge-coding subjectivity	Corridor weights may be challenged	Disclose all 27 edges, weights, factors and robustness filters	Interpret as benchmark corridor architecture, not transaction truth
Small-sample econometrics	N = 10 diagnostics may be overread	Classify benchmark regressions as diagnostic and reserve final claims for N = 1,500	Causal language withheld until panel closure
Placebo weakness	Positive spectral gap may be treated as automatically non-random	Treat randomized-weight placebo as cautionary where appropriate	Positive gap exists but non-random uniqueness is not overstated
Replication risk	Results may be hard to regenerate	Use scripts, seeds, hashes, matrices and Zenodo record	External audit companion exists for benchmark layer

Source note: Author synthesis for monograph-facing revision discipline.

8.3.14. Section Synthesis

Section 8.3 establishes that the Yang-Mills economic chapter rests on a disciplined data architecture. The completed benchmark is a finite global-corridor stress network with ten nodes and twenty-seven weighted edges. Public macroeconomic anchors are used as the empirical starting point. Author-calculated transformations create normalized stress

components, a systemic-stress field, corridor-weighted graph relations, stress-weighted matrices, gauge potential, triangular curvature, Yang-Mills economic action, stress-Laplacian spectrum, EMGI, fragility, BridgeStress and scenario outputs.

The strongest completed claim at this stage is a benchmark measurement claim: the finite stress network is populated, auditable and capable of supporting gauge, curvature, action and spectral diagnostics. The reported benchmark includes a positive first stress mode $\lambda 1 = 0.3850$, a spectral radius of 3.5023 and a normalized transition threshold of 0.1099. These values belong to the finite weighted graph. They do not imply a physical theorem, a universal crisis law or a country-level causal result.

The data architecture also defines the validation pathway. The N = 1,500 country-year layer is the route toward stronger empirical closure, but it remains a pathway until populated, estimated and externally audited. This final distinction is the main scientific value of Section 8.3: it makes the chapter ambitious enough to introduce a new gauge-econometric measurement architecture, while disciplined enough to keep benchmark evidence, diagnostic evidence, scenario evidence, replication evidence and future panel-validation evidence separate.

Chapter 8.4. Methodology: Gauge Potential, Curvature, Action and Stress Laplacian

This subsection converts the Chapter 8 research object and data architecture into a reproducible methodological system. It does not repeat the article-level Methodology chapter mechanically. Instead, it translates the completed Yang-Mills source architecture into a monograph subsection focused on the four mathematical-economic engines that make the chapter operational: economic gauge potential, triangular curvature, Yang-Mills economic action and the stress-weighted Laplacian. The subsection also preserves the strongest scientific boundary of the source study: all “mass gap” language is used in the finite weighted-graph sense only, and no theorem-level statement about the classical Yang-Mills existence and mass gap problem is made.

The benchmark object is Layer A: a finite global-corridor stress network with ten regional/corridor nodes and twenty-seven weighted undirected edges. Layer B remains the planned validation pathway: a 100-country by 15-year panel with N = 1,500 country-year observations. The methodological task of this subsection is therefore to show exactly how the ten-node benchmark moves from public anchors and author-disclosed corridor coding to the quantities reported in the results: $\lambda_1 = 0.3850$, spectral radius = 3.5023, normalized transition threshold = 0.1099, total Yang-Mills economic action = 2,514.0 and top-five action concentration = 78.329 percent.

8.4.1 Methodological Purpose and Results-to-Method Closure

The purpose of the methodology is to make every reported Chapter 8 result traceable to a formal construction rule. The gauge potential is not introduced as decorative mathematical language. It is the directed edge-level transformation of node stress differentials. Curvature is not an impressionistic claim about crisis tension. It is the oriented sum of gauge potentials around triangular cycles. Action is not a policy label. It is the squared-curvature stress-energy functional over the finite triangular universe. The stress Laplacian is the operator that converts the stress-weighted adjacency matrix into a spectral object whose first positive eigenvalue is interpreted as the finite-network economic mass gap.

This closure logic matters because the chapter has several evidence layers. Benchmark spectral and topological statements are admissible when they follow from disclosed matrices and formulas. Scenario and robustness claims are admissible when the same computation is repeated after defined perturbations. Diagnostic econometric claims are weaker and cannot be upgraded into causal proof until the N = 1,500 panel is populated and estimated. The methodology therefore functions as a claim gate as much as a calculation engine.



Methodological chain: scalar node stress is transformed into edge tension, triangular curvature, action and spectral threshold.

Figure 8.4.1. Methodological pipeline from public anchors to gauge potential, curvature, action and stress-Laplacian mass gap.

Table 8.4.1. Methodology-to-result closure matrix.

Result block	Methodological construction	Output object	Claim status
Stress field	0-100 min-max normalized public-anchor and corridor components	σ_i	Benchmark construction
Network topology	27 disclosed corridor-sensitive weighted edges	W and graph G(V,E)	Benchmark construction
Stress adjacency	Endpoint stress applied to W	W^S	Benchmark construction
Gauge potential	Directed stress differential on each edge	A_ij = -A_ji	Benchmark construction
Triangular curvature	Oriented circulation around closed triples	F_ijk	Benchmark construction
Economic action	Weighted squared curvature over triangles	S_econ	Benchmark mathematical diagnostic
Stress Laplacian	Degree matrix minus stress-weighted adjacency	L^S	Benchmark spectral operator
Mass gap	First positive eigenvalue of L^S	Δ_econ = λ_1	Finite-network threshold
EMGI / fragility	Node-level protection composite and complement	EMGI_i, 100-EMGI_i	Diagnostic ranking
Panel validation	100 countries x 15 years	N = 1,500 models	Future empirical closure

8.4.2 Empirical Objects, Operators and Notation Discipline

The methodology begins from a disciplined notation system. Nodes are indexed by i,j,k in the ten-node regional/corridor universe. Edges are undirected in the base graph but become oriented when the gauge potential is computed. Triangles are ordered triples that exist only when all three relevant edges are present. This prevents a common reviewer objection: the model does not compute curvature on an undefined complete graph, but only on triangles supported by the disclosed corridor-weighted network.

The distinction between node variables, edge variables, triangle variables and system-level operators is central. Node variables include public-anchor quantities and normalized stress scores. Edge variables include W_ij, W^S_ij and A_ij. Triangle variables include F_ijk and action contribution. System-level objects include S_econ, L^S, the eigenvalue spectrum and Δ_econ. Node-level post-spectral objects, including EMGI and fragility, are constructed after the spectral and curvature stages.

Table 8.4.2. Core symbols and methodological levels.

Symbol	Level	Definition	Role in methodology
V	Graph	Set of ten regional/corridor nodes	Defines the benchmark universe

Symbol	Level	Definition	Role in methodology
E	Graph	Twenty-seven weighted undirected edges	Defines corridor-transmission structure
σ_i	Node	Normalized systemic-stress score	Input to gauge and stress adjacency
W_ij	Edge	Normalized corridor edge weight	Base transmission intensity
W^S_ij	Edge	Stress-weighted adjacency entry	Input to stress Laplacian
A_ij	Directed edge	Economic gauge potential	Edge-level stress tension
F_ijk	Triangle	Triangular economic curvature	Cycle-level stress circulation
ω_triangle	Triangle	Triangle weight from edge-weight structure	Weights curvature contribution
S_econ	System	Total Yang-Mills economic action	Squared-curvature stress-energy
D^S	System	Diagonal stress-degree matrix	Laplacian component
L^S	System	Stress-weighted graph Laplacian	Spectral operator
λ_1	System	First positive eigenvalue	Finite-network economic mass gap
ρ(L^S)	System	Largest eigenvalue / spectral radius	Upper diffusion scale
EMGI_i	Node	Economic Mass Gap Index	Local protection ranking

8.4.3 Stress-Field Construction as the Scalar Source of the Gauge System

The stress field σ_i is the scalar source object. It converts heterogeneous public-anchor and corridor dimensions into a comparable node-level pressure score. The score is not presented as an official variable and not treated as raw macroeconomic data. It is an author-calculated diagnostic composite whose scientific legitimacy depends on transparency: the components, weights, normalization rule and benchmark range must be disclosed.

Equation (8.4.1). $x_i^N = 100 * (x_i - \min_j x_j) / (\max_j x_j - \min_j x_j)$

x_i^N is the normalized 0-100 value of component x for node i. A zero value denotes the lower bound inside the benchmark universe, not absence of data or economic relevance.

Equation (8.4.2). $\sigma_i = 0.20\ Mass_i + 0.20\ GrowthGap_i + 0.25\ IncomeFragility_i + 0.15\ TransitionMomentum_i + 0.20\ CorridorExposure_i$

σ_i is the normalized systemic-stress score. The weights sum to one and are treated as fixed benchmark weights in the reported finite-network layer.

Table 8.4.3. Stress-field component architecture used as input to gauge and spectral layers.

Code	Region	Mass	Growth gap	Income fragility	Transition momentum	Corridor exposure	Stress σ_i
SAS	South Asia	13.05	100.00	85.53	100.00	56.67	100.00
CAS	Central Asia	1.10	61.29	47.44	74.49	90.00	71.79
EAP	East Asia and Pacific	100.00	32.26	30.85	55.68	53.33	71.23
CAU	Caucasus	0.00	45.16	45.97	63.72	100.00	66.03
SSA	Sub-Saharan Africa	5.69	19.35	100.00	47.35	28.33	53.78
EUR	Europe	64.86	54.84	10.81	0.00	61.67	47.40
MENA	Middle East and North Africa	12.39	0.00	48.06	34.88	73.33	39.71

Code	Region	Mass	Growth gap	Income fragility	Transition momentum	Corridor exposure	Stress σ_i
NAM	North America	86.98	38.71	0.00	10.20	11.67	30.66
LAC	Latin America and Caribbean	20.06	25.81	43.03	18.40	20.00	26.78
OCE	Oceania	4.69	35.48	3.44	12.24	0.00	0.00

8.4.4 Corridor-Weighted Graph and Stress-Weighted Adjacency Matrix

The base graph is a corridor-sensitive finite weighted graph. Its edges are not observed bilateral trade flows; they are disclosed benchmark weights designed to represent potential stress-transmission channels across the global-corridor macro system. This distinction is essential. An observed trade matrix would answer a different question, while the Chapter 8 object is a corridor stress-transmission network that combines economic mass, separation/friction and corridor-intensity coding.

Equation (8.4.3). $w_{ij} = C_{ij} (m_i m_j)^{\alpha} \exp(-\delta d_{ij}) \kappa_{ij}$

w_{ij} is the normalized undirected edge weight. C_{ij} is the baseline connectivity constant; m_i and m_j are economic masses; $\alpha = 0.50$ is the benchmark mass elasticity; $\delta = 0.35$ is the distance/friction parameter; κ_{ij} is the corridor-intensity multiplier.

Equation (8.4.4). $W^S_{ij} = W_{ij} * (\sigma_i + \sigma_j) / 200$

W^S_{ij} is the stress-weighted adjacency entry. The divisor 200 converts the endpoint stress average from a 0-100 + 0-100 scale into a 0-1 stress multiplier.

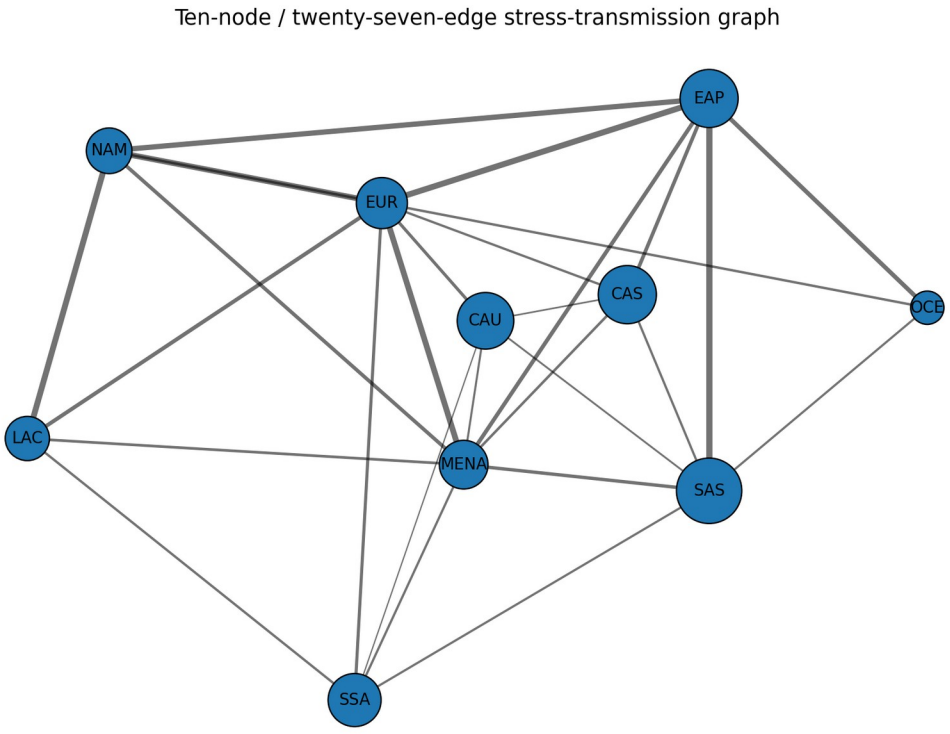


Figure 8.4.2. Ten-node graph used as the methodological substrate for gauge, curvature and spectral calculations.

Table 8.4.4. Edge-weight calibration and stress-adjacency audit parameters.

Parameter	Benchmark value	Meaning	Audit rule
α	0.50	Economic-mass elasticity	Fixed benchmark; subject to sensitivity analysis
δ	0.35	Distance/friction	Fixed benchmark;

Parameter	Benchmark value	Meaning	Audit rule
		coefficient	scenario sensitivity permitted
C_ij	1.00 unless corridor-sensitive	Baseline connectivity constant	Disclosed through edge list
κ_ij	1.00 to 2.40	Corridor-intensity multiplier	Author-coded corridor factor
max W_ij	1.000	Edge-weight normalization ceiling	Maintains 0-1 comparability
|V|, |E|	10, 27	Finite graph size	Permits density 0.600 and cycle calculations

Table 8.4.5. Full twenty-seven-edge corridor-weight list used by the methodology.

Edge	Weight	Corridor factor
EAP-SAS	1.000	1.500
EAP-EUR	0.937	1.000
NAM-LAC	0.934	1.400
NAM-EUR	0.910	1.000
EUR-MENA	0.908	1.600
EAP-NAM	0.818	1.000
EAP-OCE	0.643	1.400
EAP-MENA	0.580	1.000
EUR-LAC	0.562	1.000
EAP-CAS	0.518	1.600
NAM-MENA	0.516	1.000
SAS-MENA	0.459	1.400
EUR-CAU	0.411	2.200
EUR-SSA	0.407	1.000
LAC-MENA	0.339	1.000
MENA-CAS	0.312	1.900
NAM-OCE	0.293	1.000
LAC-SSA	0.279	1.000
EUR-CAS	0.270	1.000
MENA-SSA	0.261	1.000
SAS-CAS	0.261	1.500
SAS-SSA	0.246	1.000
OCE-SAS	0.241	1.000
MENA-CAU	0.217	1.900
SAS-CAU	0.180	1.600
CAS-CAU	0.140	2.400
SSA-CAU	0.082	1.000

8.4.5 Economic Gauge Potential and Orientation Discipline

The economic gauge potential is the directed edge-level transformation of stress imbalance. Once an undirected edge exists, the methodology assigns a direction only for calculation and display. The core property is anti-symmetry: the potential from i to j is the negative of the potential from j to i. This makes gauge potential a tension field rather than a one-way flow observation.

Equation (8.4.5). $A_{ij} = w_{ij}(\sigma_i - \sigma_j) + \eta_{ij}; \quad A_{ji} = -A_{ij}$

A_{ij} is the directed economic gauge potential. η_{ij} is a residual corridor-friction term fixed at zero in the reported benchmark. Anti-symmetry ensures that the two-direction field balances exactly by construction.

Orientation discipline prevents overinterpretation of signs. The sign of A_{ij} changes when the arrow is reversed, but $|A_{ij}|$ does not. The Laplacian spectrum does not depend on arbitrary display orientation, because the spectral calculation is performed on the symmetric stress-weighted adjacency matrix W^S rather than on the signed display convention alone.

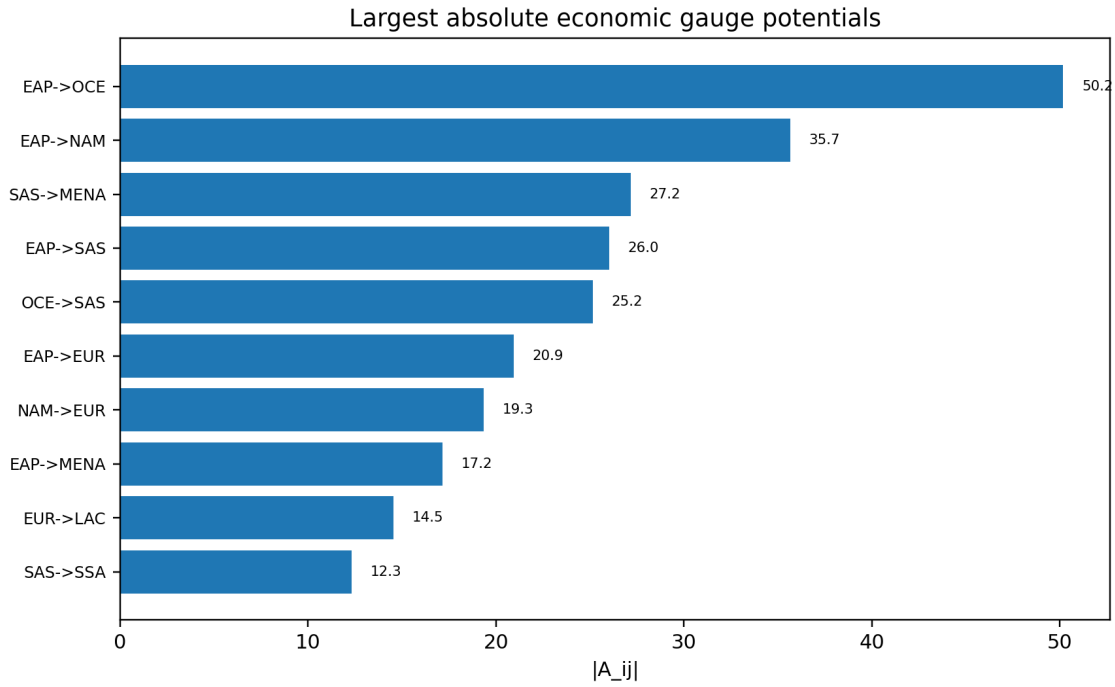


Figure 8.4.3. Largest absolute economic gauge potentials reported from the benchmark gauge layer.

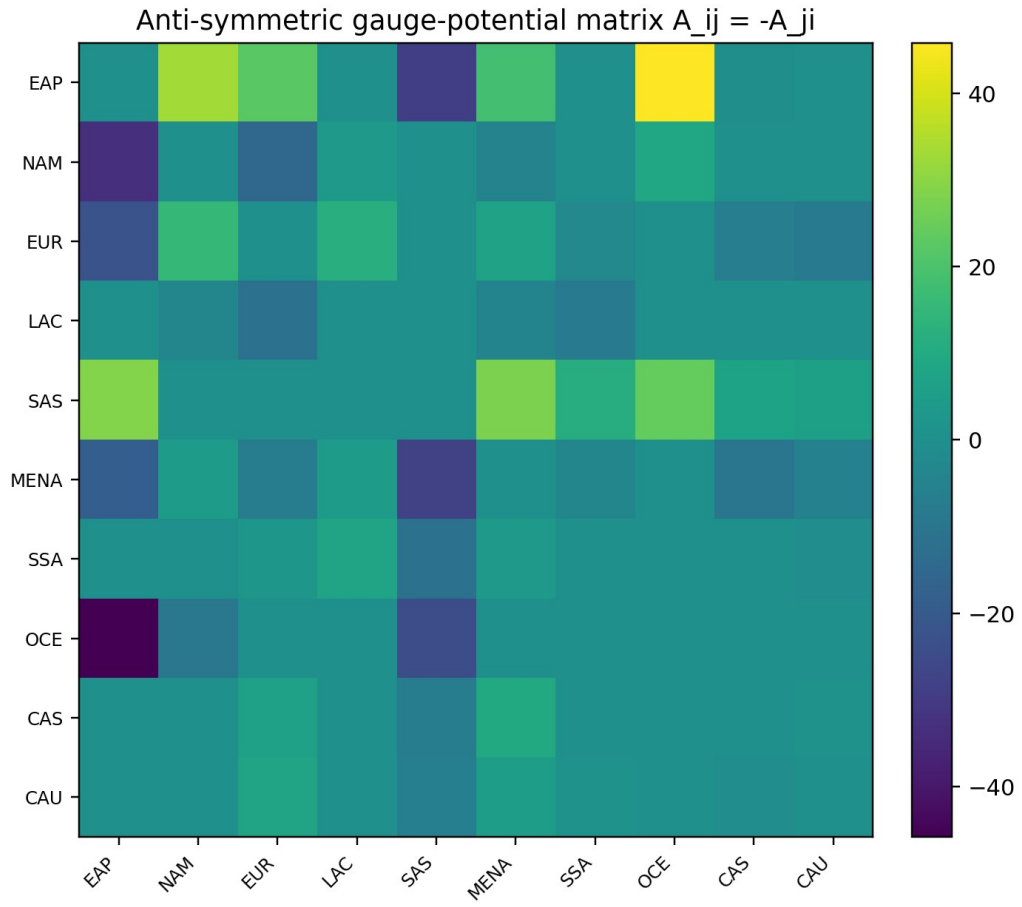


Figure 8.4.4. Anti-symmetric gauge matrix demonstration: A_ij = -A_ji and diagonal entries equal zero.

Table 8.4.6. Leading gauge-potential magnitudes and orientation discipline.

Edge orientation	Weight	Factor	A_ij	|A_ij|
EAP->OCE	0.643	1.400	50.171	50.171
EAP->NAM	0.818	1.000	35.657	35.657
SAS->MENA	0.459	1.400	27.173	27.173
EAP->SAS	1.000	1.500	-26.016	26.016
OCE->SAS	0.241	1.000	-25.158	25.158
EAP->EUR	0.937	1.000	20.936	20.936
NAM->EUR	0.910	1.000	-19.333	19.333
EAP->MENA	0.580	1.000	17.168	17.168
EUR->LAC	0.562	1.000	14.540	14.540
SAS->SSA	0.246	1.000	12.311	12.311

Table 8.4.7. Gauge-orientation and relabeling audit protocol.

Audit step	Procedure	Pass condition
Two-direction reconstruction	For each displayed edge A_ij, add A_ji = -A_ij	Every pair sums to zero
Diagonal check	Set A_ii = 0 for all nodes	No self-potential remains
Orientation reversal	Reverse displayed arrows and recompute |A|	Magnitude ranking remains unchanged
Node relabeling	Permute node labels and reconstruct matrices	Eigenvalues remain invariant
Spectral independence	Compute L^S from W^S, not from arbitrary arrow labels	λ_1 unchanged by visual orientation

8.4.6 Field Strength, Triangular Curvature and Curvature Exposure

Curvature is where the gauge analogy becomes operational. A bilateral edge potential tells the analyst that two nodes have stress tension. A triangular curvature value tells the analyst whether that tension is neutralized when a local corridor cycle is closed. If a cycle has zero oriented sum, the local field is internally balanced. If it has nonzero oriented sum, residual circulation remains in the cycle.

Equation (8.4.6). $F_{ijk} = A_{ij} + A_{jk} + A_{ki}$

F_ijk is the economic field strength around the oriented triangle (i,j,k). The sign depends on orientation; |F_ijk| and squared action contributions are used for concentration diagnostics.

Equation (8.4.7). $CurvExp_i = \Sigma_{\{triangles\ containing\ i\}}\ \omega_{triangle}\ |F_{triangle}|$

CurvExp_i is the node-level curvature exposure. ω_triangle is computed from the constituent edge weights and ensures that highly supported corridor triangles carry more methodological weight.

The methodology enumerates the triangular universe supported by the twenty-seven-edge graph. Each triangle receives an orientation, a triangle weight, a signed curvature value, an absolute curvature value and an action contribution. In the reported benchmark, curvature is not evenly distributed: the EAP-OCE-SAS triangle alone is a dominant curvature-action carrier, while the top five triangles account for most of the curvature energy.

Table 8.4.8. Leading triangular curvature values and action inputs.

Triangle	Weight	F_ijk	|F_ijk|	Action
EAP-OCE-SAS	0.537	51.030	51.030	1,397.900
CAS-EAP-SAS	0.513	-18.515	18.515	175.918
CAU-MENA-SAS	0.262	-16.098	16.098	67.898
EAP-MENA-SAS	0.643	16.012	16.012	164.973
CAS-EAP-EUR	0.508	14.541	14.541	107.422
MENA-SAS-SSA	0.309	-12.870	12.870	51.220
EAP-EUR-MENA	0.791	12.523	12.523	123.973
EAP-MENA-NAM	0.626	-11.274	11.274	79.513
CAS-MENA-SAS	0.334	-11.055	11.055	40.860
EUR-LAC-NAM	0.782	-10.612	10.612	88.059
CAU-EUR-MENA	0.433	10.045	10.045	43.684
CAS-EAP-MENA	0.454	8.552	8.552	33.232

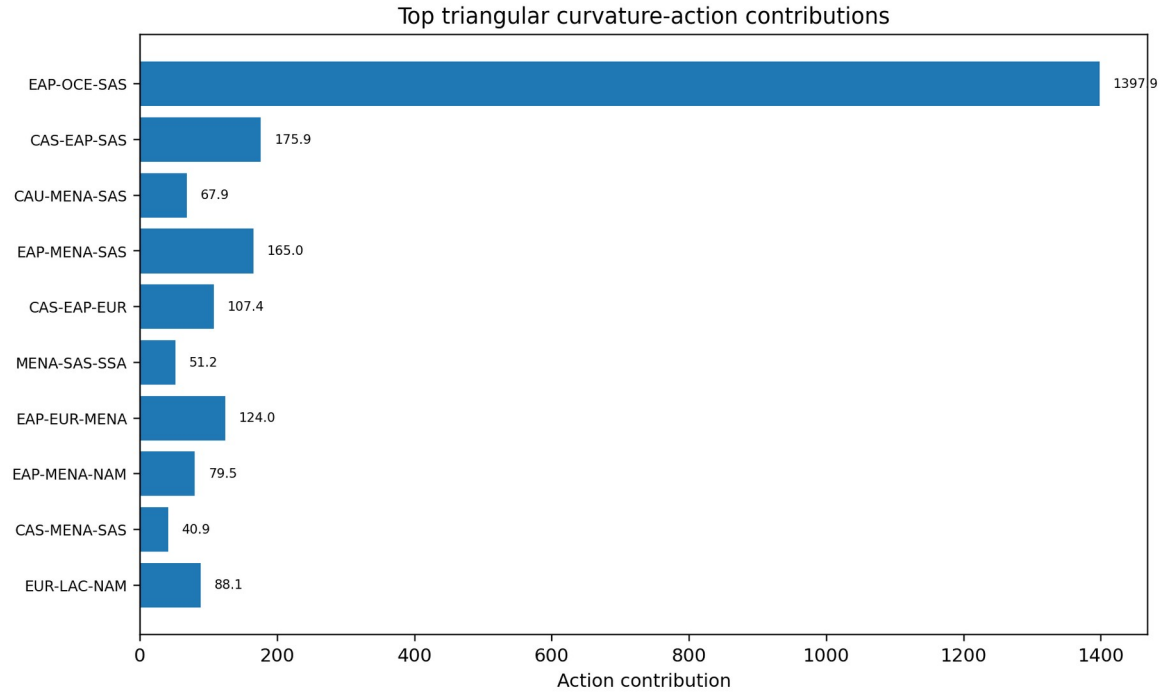


Figure 8.4.5. Top triangular action contributions from the curvature field.

8.4.7 Yang-Mills Economic Action and Stress-Energy Decomposition

Yang-Mills economic action aggregates triangular curvature into a system-level stress-energy measure. The squared-curvature construction intentionally gives high-curvature cycles disproportionate influence. This is not a statistical defect. It is the core reason action is useful: stress concentration and tail vulnerability should not be averaged away as if all cycles were equally important.

Equation (8.4.8). $S_econ = \Sigma_\{triangles\} \omega_triangle \, ||F_triangle||^2$

S_econ is total Yang-Mills economic action. The summation is over the complete triangular-cycle universe, not only the displayed leading cycles.

Equation (8.4.9). $Share_l = S_l / \Sigma_l S_l * 100$

Share_l reports the percentage contribution of methodological layer l to total component-wise action.

Table 8.4.9. System-level Yang-Mills economic action audit.

Action object	Reported benchmark value	Interpretive meaning
Total triangular cycles	27	Curvature is computed on a finite cycle universe
Total Yang-Mills economic action	2,514.0	System-level squared-curvature stress-energy
Mean triangle action	93.113	Average cycle contribution
Maximum triangle action	1,397.9	Dominant high-curvature cycle
Top-five action share	78.329%	Strong concentration of stress-energy

Table 8.4.10. Component-wise action decomposition.

Layer	Action	Share %
Growth-gap pressure	6,046.6	27.76
Mass exposure	5,672.2	26.04
Transition-momentum pressure	4,268.8	19.60
Income-fragility pressure	4,190.0	19.24
Corridor exposure	1,605.4	7.37

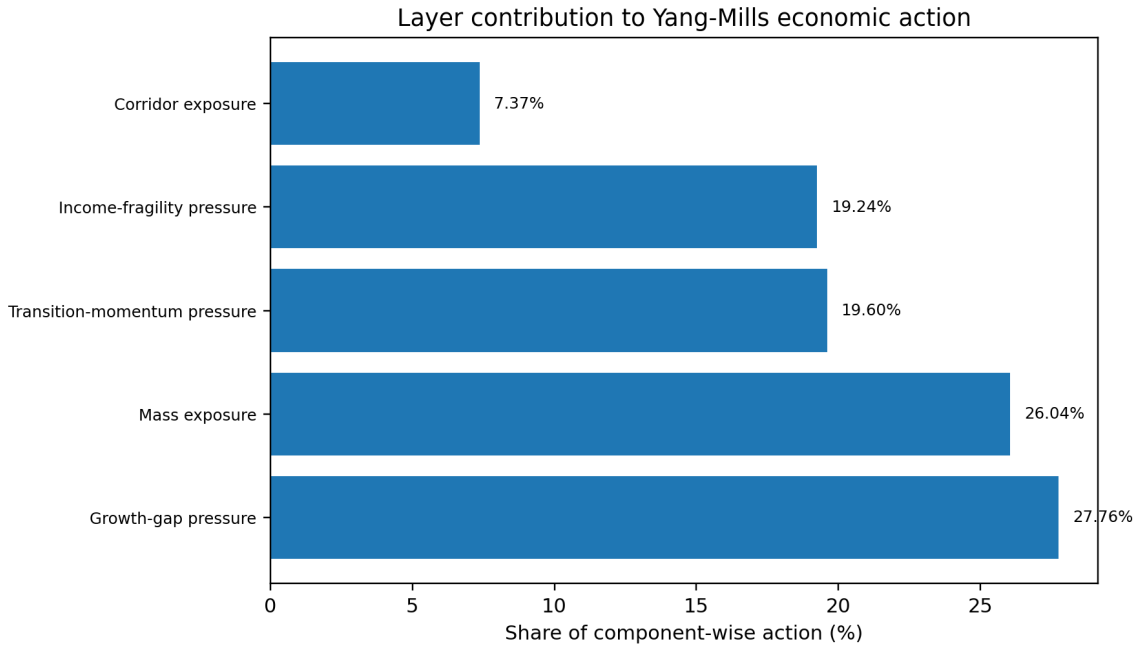


Figure 8.4.6. Component-wise contribution to the Yang-Mills economic action layer.

8.4.8 Stress Laplacian and Finite-Network Economic Mass Gap

The stress Laplacian is the spectral operator of the model. It converts the stress-weighted adjacency matrix into a matrix whose eigenvalues describe connectedness, diffusion modes and the separation between the normal connected state and the first transmissible stress mode. This is the mathematical location of the finite-network economic mass gap.

Equation (8.4.10). $D^S_{ii} = \Sigma_j W^S_{ij}; \quad L^S = D^S - W^S$

D^S is the diagonal stress-degree matrix; L^S is the weighted stress Laplacian; W^S is the stress-weighted adjacency matrix.

Equation (8.4.11). $0 = \lambda_0 \leq \lambda_1 \leq \ldots \leq \lambda_{n-1}$

For a connected finite graph, $\lambda_0 = 0$ has multiplicity one. λ_1 is the first positive stress-diffusion mode.

Equation (8.4.12). $\Delta_{econ} = \lambda_1 - \lambda_0; \quad \text{since } \lambda_0 = 0, \Delta_{econ} = \lambda_1$

Δ_econ is the economic mass gap in the finite network-econometric sense only.

The reported benchmark values close the spectral method: $\lambda_0 = 0.0000$, $\lambda_1 = 0.3850$, spectral radius = 3.5023 and normalized threshold = 0.1099. The normalized threshold is read as a local-to-systemic transition boundary inside the model. It is not a forecast of actual crisis timing and not a theorem-level property of the world economy.

Table 8.4.11. Stress-Laplacian spectral outputs used by the methodology.

Output	Value	Methodological interpretation
λ_0	0.0000	Normal connected baseline
λ_1 / Δ_econ	0.3850	First positive stress mode; finite-network mass gap
Spectral radius	3.5023	Upper stress-diffusion scale
Normalized threshold	0.1099	Local-to-systemic boundary
Monte Carlo gap interval	0.3458-0.4254	Positive under benchmark perturbation

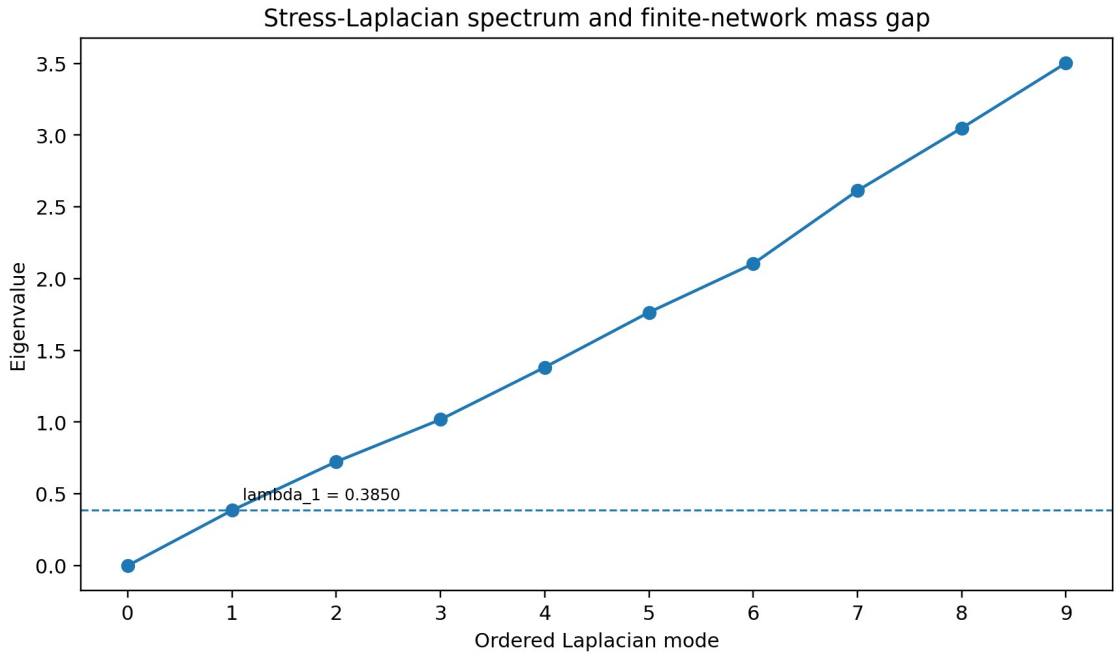


Figure 8.4.7. Ordered stress-Laplacian spectrum showing the first positive stress mode.

8.4.9 Robustness, Filtering and Placebo Discipline

A positive λ_1 is necessary but not sufficient for a strong methodological interpretation. The benchmark must also show that the result is not destroyed by plausible graph filtering or perturbation. The methodology therefore recalculates the stress Laplacian under reduced edge-density specifications and separates internal robustness from randomized placebo evidence. This is a crucial reviewer-safety device: the positive gap is robust inside the model, but the randomized-network placebo is treated as cautionary rather than as proof of non-random uniqueness.

Equation (8.4.13). $\Delta_econ^{filtered(q)} = \lambda_1(L^S_{E_q})$

E_q is the retained edge set under a filtering rule such as high-weight, medium-filtered or sparse-filtered graph construction.

Table 8.4.12. Filtered-graph robustness design.

Specification	Edges	Density	Mass gap	Spectral radius
Baseline full graph	27	0.6000	0.3850	3.5023
High-weight filtered graph	20	0.4444	0.2272	3.4841
Medium-filtered graph	15	0.3333	0.2037	3.4437
Sparse-filtered graph	14	0.3111	0.1838	3.4129

Table 8.4.13. Randomized-network placebo boundary.

Placebo object	Value	Interpretation
Observed mass gap	0.3850	Benchmark spectral separation
Random mean gap	0.4046	Randomized-weight comparator mean
Random 95% quantile	0.4823	Upper random comparator threshold
Pr(random >= observed)	0.6727	Cautionary placebo; no non-random uniqueness overclaim

8.4.10 Shock Propagation and Threshold Compression Method

Scenario methodology tests how stress shocks change spectral protection, curvature action and local-to-systemic transmissibility. The shock design is deterministic inside the benchmark: each scenario modifies stress-

relevant channels, reconstructs affected matrices and recalculates λ_1, spectral radius, normalized threshold, action and EMGI changes. The scenarios are diagnostic simulations, not forecasts.

Equation (8.4.14). $\sigma_i^{shock} = \sigma_i + \psi_s z_{i,s}$, followed by reconstruction of W^S, L^S, λ_1 and S_{econ}

ψ_s is the scenario amplitude and $z_{i,s}$ is the node/channel exposure to shock family s. The model is recomputed after the shock rather than adjusted only at the final output stage.

Table 8.4.14. Scenario threshold-compression methodology.

Scenario	Post-shock mass gap	Normalized threshold	Interpretive consequence
Baseline	0.3850	0.1099	Normal finite-network threshold
Inflation / price-pressure	0.3343	0.0916	Moderate stress reduces protection
Financial-spread	0.2836	0.0747	Funding stress raises transmissibility
Trade / logistics corridor	0.2334	0.0578	Corridor disruption sharply lowers boundary
Energy / geopolitical corridor	0.1796	0.0420	Severe shock compresses threshold most strongly

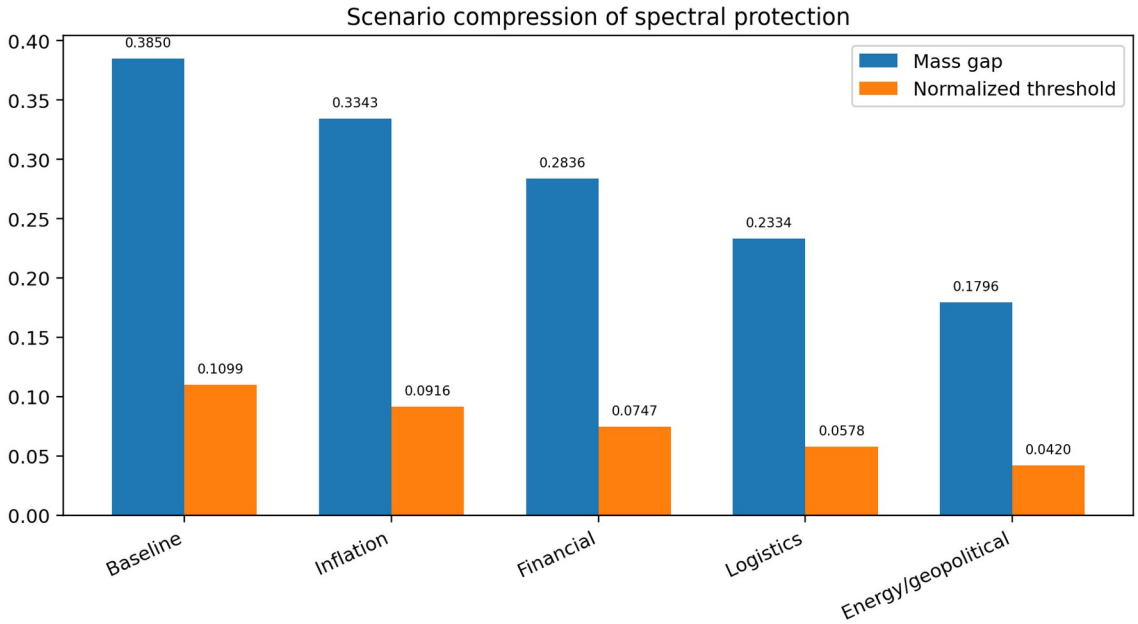


Figure 8.4.8. Scenario compression of λ_1 and the normalized transition threshold.

8.4.11 EMGI, Fragility and BridgeStress as Post-Spectral Indices

EMGI is not the mass gap itself. It is a node-level protection index constructed after the gauge, curvature and stress-Laplacian layers are defined. This distinction prevents a common conceptual error: the system-level mass gap λ_1 is one value for the graph, while $EMGI_i$ distributes local protection across nodes using spectral, centrality, income-depth, resilience, stress and curvature components.

Equation (8.4.15). $\Delta_i^{local} = 0.30\ LSP_i + 0.20\ Centrality_i + 0.20\ IncomeDepth_i + 0.15\ Resilience_i - 0.10\ Stress_i - 0.05\ Curvature_i$

Positive terms increase local protection; stress and curvature exposure penalize protection.

Equation (8.4.16). $EMGI_i = 100 * (\Delta_i^{local} - \min_j \Delta_j^{local}) / (\max_j \Delta_j^{local} - \min_j \Delta_j^{local})$

$EMGI_i$ is the final node-level Economic Mass Gap Index on a 0-100 scale.

Equation (8.4.17). $Fragility_i = 100 - EMGI_i$

Fragility is an identity, not an independently estimated variable.

Table 8.4.15. EMGI and fragility component audit.

Code	Region	EMGI	Fragility	Resilience	Stress	Curvature	Centrality
NAM	North America	100.00	0.00	100.00	30.66	23.16	84.63
EUR	Europe	90.15	9.85	52.83	47.40	50.13	100.00
EAP	East Asia and Pacific	53.12	46.88	38.25	71.23	100.00	98.23
MENA	Middle East and North Africa	45.59	54.41	27.83	39.71	69.72	78.47
LAC	Latin America and Caribbean	31.37	68.63	23.81	26.78	4.95	41.73
OCE	Oceania	14.50	85.50	42.82	0.00	25.65	10.73
SAS	South Asia	10.36	89.64	12.84	100.00	68.93	38.09
CAS	Central Asia	5.45	94.55	18.48	71.79	23.55	18.94
SSA	Sub-Saharan Africa	4.11	95.89	0.00	53.78	0.76	6.99
CAU	Caucasus	0.00	100.00	9.15	66.03	0.00	0.00

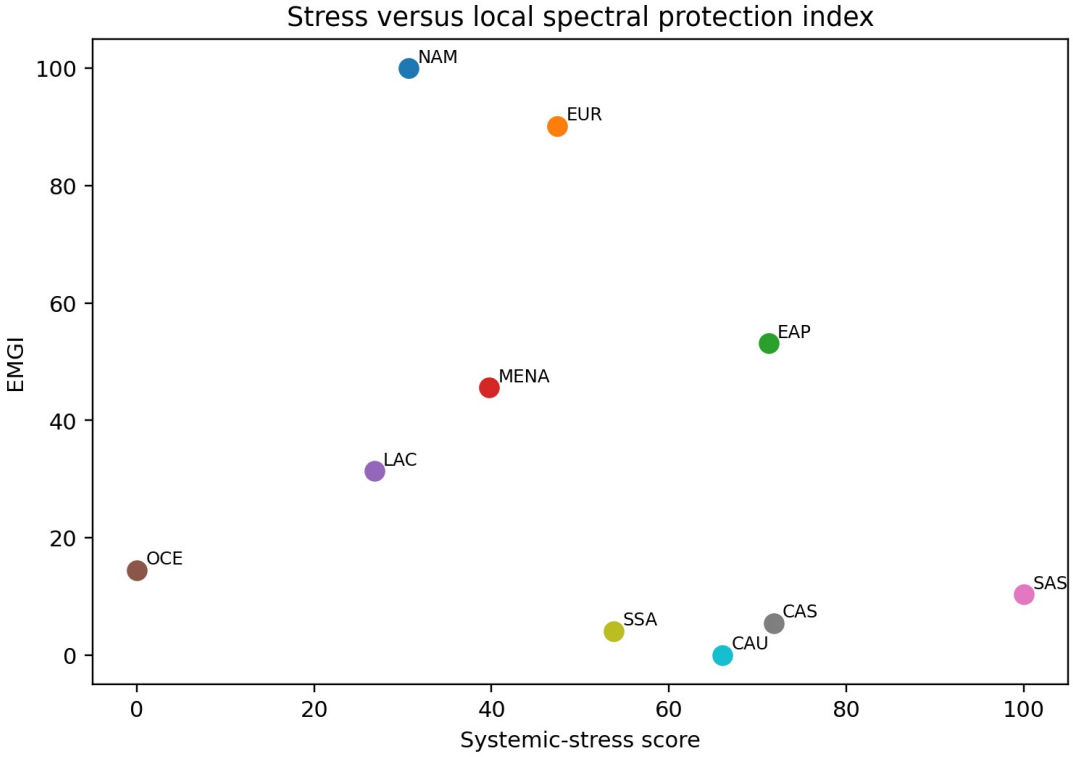


Figure 8.4.9. Stress score versus EMGI: node protection is not reducible to stress alone.

Table 8.4.16. BridgeStress methodology: corridor role separated from GDP mass and ordinary centrality.

Code	Region	Corridor exposure	Role index	Fragility	Curvature participation +	BridgeStress
CAU	Caucasus	98.00	100.00	100.00	57.32	100.00
CAS	Central Asia	92.00	75.00	94.55	67.37	78.24
SAS	South Asia	72.00	60.00	89.64	86.74	59.80
MENA	Middle East	82.00	85.00	54.41	87.08	58.79

Code	Region	Corridor exposure	Role index	Fragility	Curvature participation +	BridgeStress
	and North Africa					
EAP	East Asia and Pacific	70.00	95.00	46.88	100.00	55.50
SSA	Sub-Saharan Africa	55.00	25.00	95.89	57.64	13.53
LAC	Latin America and Caribbean	50.00	30.00	68.63	59.43	10.89
EUR	Europe	75.00	90.00	9.85	78.72	9.32
OCE	Oceania	38.00	20.00	85.50	68.27	7.90
NAM	North America	45.00	70.00	0.00	67.21	0.00

8.4.12 Algorithmic Replication Sequence

The methodology can be replicated as an ordered computational protocol. The most important reproducibility requirement is that no final indicator is calculated directly from narrative judgment. Every object must be generated from a preceding table, formula or matrix. The sequence below is the monograph-level replication algorithm for Section 8.4.

Table 8.4.17. Replication algorithm for gauge-potential, curvature, action and stress-Laplacian methodology.

Step	Operation	Output
1	Define the ten regional/corridor nodes and the twenty-seven weighted edges	V, E, W
2	Normalize public-anchor variables to 0-100 directionally consistent scales	Component matrices
3	Construct σ_i from weighted stress components	Systemic-stress vector
4	Compute W^S using endpoint stress and edge weights	Stress-weighted adjacency
5	Construct directed A_ij and enforce A_ji = -A_ij	Gauge-potential matrix
6	Enumerate all supported triangles and compute F_ijk	Curvature table
7	Compute weighted squared curvature and aggregate S_econ	Action and action shares
8	Construct D^S and L^S = D^S - W^S	Stress Laplacian
9	Compute eigenvalue spectrum and define Δ_econ = λ_1	Mass gap and spectral radius
10	Compute robustness filters and Monte Carlo perturbations	Stability diagnostics
11	Construct EMGI, fragility and BridgeStress	Node-level interpretation
12	Apply shock scenarios and recompute matrices and thresholds	Scenario diagnostics
13	Assign evidence class: benchmark, scenario, diagnostic or panel-ready	Claim boundary

8.4.13 Cross-Chapter Methodological Integration

Chapter 8.4 is methodologically adjacent to the Hodge, Navier-Stokes, BSD and Perelman-Ricci-Poincare chapters, but it performs a distinct operation. Hodge decomposition separates edge-flow pressure into gradient, curl and harmonic components. Navier-Stokes translates liquidity stress into nondimensional flow-pressure-friction balance. BSD translates local-to-global structure into finite-state and L-function analogues. Perelman-Ricci-Poincare translates inequality pressure into curvature and entropy diagnostics. Yang-Mills Chapter 8 differs because it uses gauge potential, triangular curvature, action and spectral mass gap as a shock-threshold measurement grammar.

Table 8.4.18. Cross-chapter methodological integration.

Book chapter	Shared methodological family	What Chapter 8.4 adds
Chapter 5 Perelman/Ricci/Poincare	Curvature and graph topology	Gauge curvature and action over corridor stress cycles
Chapter 6 Hodge	Edges, cycles and Laplacian diagnostics	Stress gauge potential and finite-network spectral gap
Chapter 7 Navier-Stokes	Systemic stress and shock propagation	Network threshold separating local and systemic transmissibility
Chapter 9 BSD	Local-to-global corridor structure	Spectral/gauge pathway to systemic stress threshold

Book chapter	Shared methodological family	What Chapter 8.4 adds
Chapter 10 Riemann/Zeta	Spectral/cyclical diagnostics	Graph spectral separation rather than time-series zeta-cycle
Chapter 11 P vs NP	Algorithmic evidence discipline	Claim-gated computation and reproducibility protocol

8.4.14 Methodological Limitations and Claim Boundary

The methodology is strong because it is explicit, but it remains bounded. First, the completed benchmark has ten nodes. This is appropriate for finite-network measurement, graph topology, curvature and spectral diagnostics, but it cannot carry the evidentiary burden of final causal econometrics. Second, the edge weights are corridor-sensitive analytical weights, not observed bilateral trade, finance or transport flows. Third, the gauge potential is an economic measurement analogue, not a physical gauge field. Fourth, triangular curvature and Yang-Mills action are model-implied finite-network diagnostics, not literal field-theory invariants. Fifth, the placebo result is cautionary: it supports internal benchmark interpretation but does not prove that the observed graph is statistically unique relative to randomized alternatives.

The permitted claim is therefore precise. The methodology supports a finite-network gauge-econometric benchmark in which public anchors and corridor transformations produce a stress field, stress-weighted adjacency, anti-symmetric gauge potential, triangular curvature, Yang-Mills economic action and a positive stress-Laplacian mass gap. It does not solve the mathematical Yang-Mills existence and mass gap problem, does not establish a universal crisis law and does not provide final country-level causal validation before the N = 1,500 panel is completed.

Table 8.4.19. Reviewer-risk controls and claim-boundary language.

Potential reviewer concern	Methodological safeguard	Permitted language
Gauge terminology may be overclaimed	Strict finite-network analogue statement	Economic gauge-econometric framework
Small N=10 benchmark	Reserve causal claims for N=1,500 panel	Benchmark measurement and diagnostic evidence
Constructed edge weights	Disclose edge list and parameters	Corridor-sensitive analytical network
Curvature/action may look metaphorical	Define F_ijk and S_econ explicitly	Triangular cycle curvature and squared stress-energy
Positive gap may look theorem-level	Define $\Delta_{econ} = \lambda_1$ only in finite graph	Finite-network economic mass gap
Random placebo not supportive of uniqueness	Report p=0.6727 as cautionary	Robust inside benchmark, not statistically unique
Scenario outputs may be read as forecasts	Label shock recalculations as simulations	Threshold-compression diagnostics

8.4.15 Subsection Conclusion

Section 8.4 closes the methodological foundation of Chapter 8. It shows how the global-corridor stress network becomes a calculable gauge-econometric system. The scalar node stress field supplies σ_i. The corridor-weighted graph supplies W. The stress-weighted adjacency matrix supplies W^S. The anti-symmetric gauge potential supplies A_ij. Triangular cycles supply F_ijk. Squared curvature supplies S_econ. The stress Laplacian supplies L^S and the eigenvalue spectrum. The first positive eigenvalue supplies $\Delta_{econ} = \lambda_1$. EMGI, fragility and BridgeStress then translate system-level threshold information into node-level protection, vulnerability and corridor-exposure diagnostics.

The central methodological achievement is not merely that formulas are written. The achievement is that the formulas form a continuous audit chain from public anchors and corridor coding to the reported benchmark values: $\lambda_1 = 0.3850$, spectral radius = 3.5023, normalized threshold = 0.1099, action = 2,514.0 and top-five action concentration = 78.329 percent. This is the exact type of bounded mathematical-econometric architecture required by the monograph: strong enough to support original measurement, cautious enough to avoid Clay-problem overclaiming, and transparent enough to be linked to replication files and later expanded into the N = 1,500 country-panel validation layer.

Chapter 8.5. Results: Positive Finite-Network Mass Gap, EMGI, Fragility and BridgeStress

8.5.0 Executive Result Statement

The corrected finite-network benchmark identifies a positive economic mass gap in the stress-weighted global-corridor network. The first non-zero stress-Laplacian eigenvalue is lambda_1 = 0.3850, the spectral radius is 3.5023, and the normalized local-to-systemic transition threshold is 0.1099. This is the core empirical result of Chapter 8: the benchmark network contains measurable spectral separation between the normal connected state and the first transmissible stress mode.

The result is not interpreted as a physical theorem. It is a finite weighted-graph result produced by the Layer A benchmark: ten global and corridor-sensitive nodes, twenty-seven weighted edges, a normalized stress field, a stress-weighted adjacency matrix, triangular curvature, Yang-Mills economic action, EMGI, fragility and BridgeStress. The result is therefore a bounded measurement claim: the benchmark stress network has positive spectral protection and a measurable shock threshold.

The chapter also reports three substantive extensions of the spectral result. First, curvature and action are highly concentrated: total Yang-Mills economic action is 2,514.0 and the top-five action share is 78.329 percent. Second, EMGI separates high-protection nodes such as North America and Europe from critical-fragile nodes such as the Caucasus, Sub-Saharan Africa, Central Asia, South Asia and Oceania. Third, BridgeStress reveals why the Caucasus and Central Asia matter as corridor-exposure nodes even when their output mass is small.

Table 8.5.1. Results architecture and evidence-status map

Result block	Benchmark finding	Monograph interpretation	Claim status
Spectral mass gap	lambda_1 = 0.3850; spectral radius = 3.5023; threshold = 0.1099	Finite-network shock threshold exists in the benchmark graph	Strong benchmark measurement claim
Curvature/action	Total action = 2,514.0; top-five action share = 78.329%	Stress-energy is concentrated in a small set of triangular corridor cycles	Strong benchmark diagnostic claim
EMGI and fragility	NAM = 100.00; EUR = 90.15; CAU = 0.00; fragility = 100 - EMGI	Node protection differs from GDP mass and centrality alone	Strong node-level diagnostic claim
BridgeStress	CAU = 100.00; CAS = 78.24; SAS = 59.80; MENA = 58.79; EAP = 55.50	Strategic corridor exposure is visible after separating bridge role from output mass	Strong corridor benchmark claim
Shock scenarios	Threshold falls from 0.1099 to 0.0420 under the strongest corridor shock	Local disturbances become more systemically transmissible under stress	Scenario diagnostic claim; not causal forecast
Panel validation	N = 1,500 country-year pathway specified	Future country-panel estimates required for causal or external validation	Panel-ready; not final confirmation

Source: Author synthesis from the Chapter 8 finite-network benchmark and monograph claim-boundary logic.

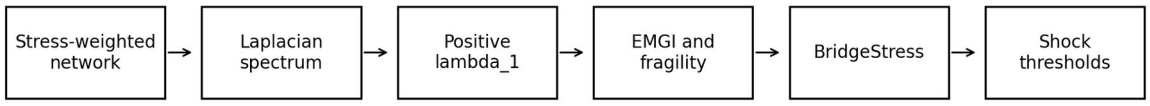


Figure 8.5.1: Results logic - from finite network spectral separation to node and scenario diagnostics

Figure 8.5.1. Results logic from spectral separation to node and scenario diagnostics.
Source: Author visualization of the Chapter 8.5 results structure.

8.5.1 Reading Rule for the Results Chapter

The results should be read in a layered order. The first layer is spectral: it asks whether the stress-weighted graph has a positive first non-zero eigenvalue. The second layer is curvature-action: it asks where local triangular imbalance is concentrated. The third layer is node protection: it asks which nodes retain local absorption capacity after stress, curvature and resilience are combined. The fourth layer is corridor exposure: it asks whether small bridge nodes become visible after corridor role and fragility are jointly measured. The fifth layer is scenario diagnostics: it asks whether shocks compress the normalized threshold and increase action.

This ordering is important because it prevents the chapter from turning a finite-network result into an unrestricted econometric claim. The benchmark supports spectral, topological, node-index and scenario interpretations. It does not yet support country-level causal inference, because the N = 1,500 country-panel validation layer remains a pathway rather than a completed empirical closure.

Table 8.5.2. Results reading rule and claim-permission matrix

Layer	Object measured	Core statistic	What the result permits	What it does not permit
Finite spectral layer	Stress-Laplacian separation	lambda_1, spectral radius, threshold	Finite-network mass-gap interpretation	Clay theorem or field-theory proof
Curvature-action layer	Triangular cycle imbalance	F_ijk, action, top-five share	Identification of high-stress cycles	Direct causal diagnosis of trade volumes
Node-protection layer	Local protection and vulnerability	EMGI, fragility, resilience	Node-level protection ranking	Welfare ranking or GDP ranking
Corridor bridge layer	Strategic corridor exposure	BridgeStress	Visibility of Caucasus/CAS corridor role	Observed route throughput proof
Scenario layer	Shock-threshold compression	Post-shock lambda_1, threshold, action	Deterministic shock diagnostics	Forecast or policy counterfactual proof
Validation pathway	Country-panel external closure	FE/TWFE/DK/IV/factor models after data completion	Future validation design	Current causal confirmation

Source: Author synthesis for monograph Chapter 8.5.

8.5.2 Positive Finite-Network Mass Gap: Spectral Benchmark

The central result is the positive first non-zero eigenvalue of the stress-weighted Laplacian. The eigenvalue sequence begins with lambda_0 = 0.0000, representing the normal connected state of the finite graph. The first stress-excited mode is lambda_1 = 0.3850. Since the graph has one connected component and the first positive eigenvalue is strictly above zero, the benchmark has a positive finite-network economic mass gap.

The spectral radius is 3.5023. The normalized transition threshold is computed as the mass gap divided by the spectral radius. The resulting value, 0.1099, is the chapter-specific shock boundary: disturbances below this normalized scale remain locally absorbable inside the benchmark; disturbances above it are interpreted as potentially systemically transmissible within the model. This interpretation is mechanical and diagnostic, not a universal law.

Formula (8.5.1): Delta_econ = lambda_1(L^S) = 0.3850. Formula (8.5.2): Theta_econ = Delta_econ / rho(L^S) = 0.3850 / 3.5023 = 0.1099.

Table 8.5.3. Weighted stress-Laplacian spectrum

Eigenvalue index	Eigenvalue
0	0.00
1	0.3850
2	0.5836
3	0.7330
4	0.8138
5	1.22

6	1.61
7	1.97
8	2.36
9	3.50

Source: Author calculations from the stress-weighted Laplacian in the Yang-Mills benchmark.

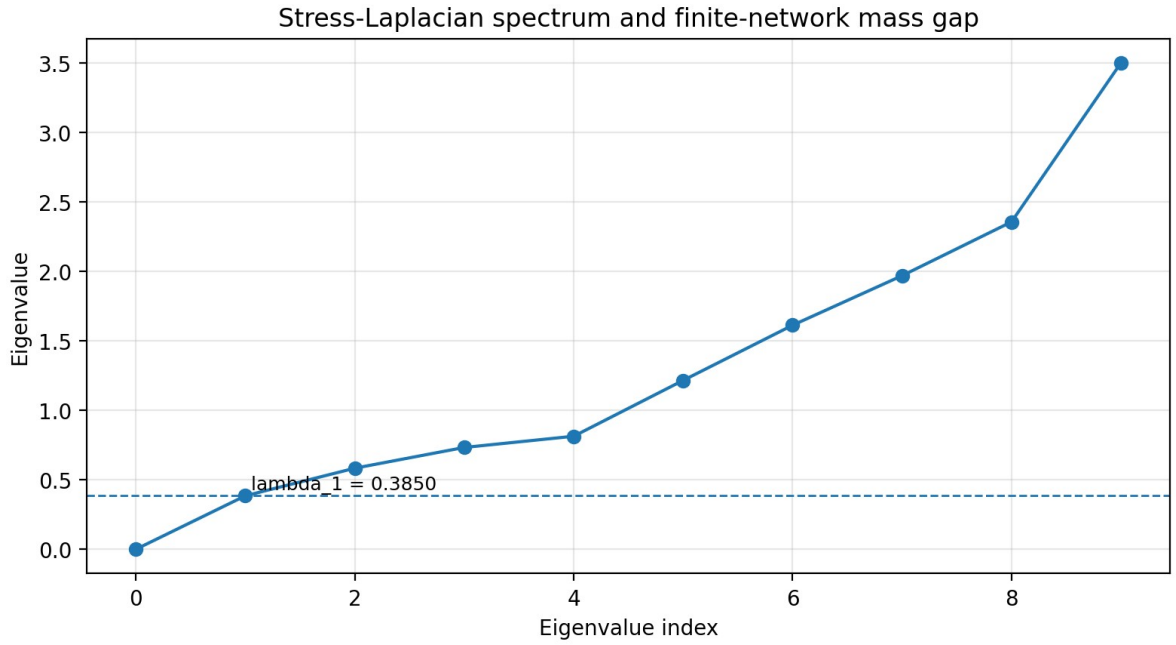


Figure 8.5.2. Stress-Laplacian spectrum and the positive first stress mode.

Source: Author visualization from Table 8.5.3.

Table 8.5.4. Normal state, first stress mode and normalized transition threshold

Normal-state lambda_0	First stress mode lambda_1	Spectral radius	Economic mass gap	Normalized threshold
0.00	0.3850	3.50	0.3850	0.1099

Source: Author calculations from the corrected finite-network benchmark.

Table 8.5.5. Finite-network proposition and economic mass-gap interpretation

Condition / object	Benchmark value	Implication
Finite graph	10 regional/corridor nodes	The result is a finite-network spectral benchmark, not a continuum field-theory theorem
Connectedness	1 connected component	lambda_0 = 0 is the normal connected state
First positive eigenvalue	lambda_1 = 0.3850	Delta_econ = 0.3850 is the corrected economic mass gap
Spectral radius	3.5023	Upper stress-diffusion scale used to normalize the transition threshold
Claim boundary	Economic analogue only	No claim is made about the Clay Millennium Yang-Mills mass-gap problem

Source: Author formalization from finite weighted-graph spectral theory and the Chapter 8 benchmark.

8.5.3 Robustness Across Filtered Graph Specifications

The positive gap is not confined to the baseline 27-edge graph. Under high-weight, medium-filtered and sparse-filtered specifications, the mass gap remains positive. The value naturally falls as the graph becomes thinner because fewer weighted pathways remain available to distribute stress, but the sign of the spectral separation is retained.

This robustness block is important for reviewer credibility. A spectral result that disappears after modest filtering would be weak evidence. Here, the mass gap declines from 0.3850 in the baseline full graph to 0.2272, 0.2037 and 0.1838 in filtered versions, but it remains strictly positive. The correct interpretation is not that every possible graph has the same threshold; it is that the benchmark positive-gap conclusion is not an immediate artifact of the densest edge specification.

Table 8.5.6. Estimated economic mass gap by network specification

Specification	Edges	Density	Normal lambda_0	First stress mode lambda_1	Spectral radius	Economic mass gap
Baseline full graph	27	0.6000	0.00	0.3850	3.50	0.3850
High-weight filtered graph	20	0.4444	0.00	0.2272	3.48	0.2272
Medium-filtered graph	15	0.3333	0.00	0.2037	3.44	0.2037
Sparse-filtered graph	14	0.3111	0.00	0.1838	3.41	0.1838

Source: Author calculations from baseline and filtered graph specifications.

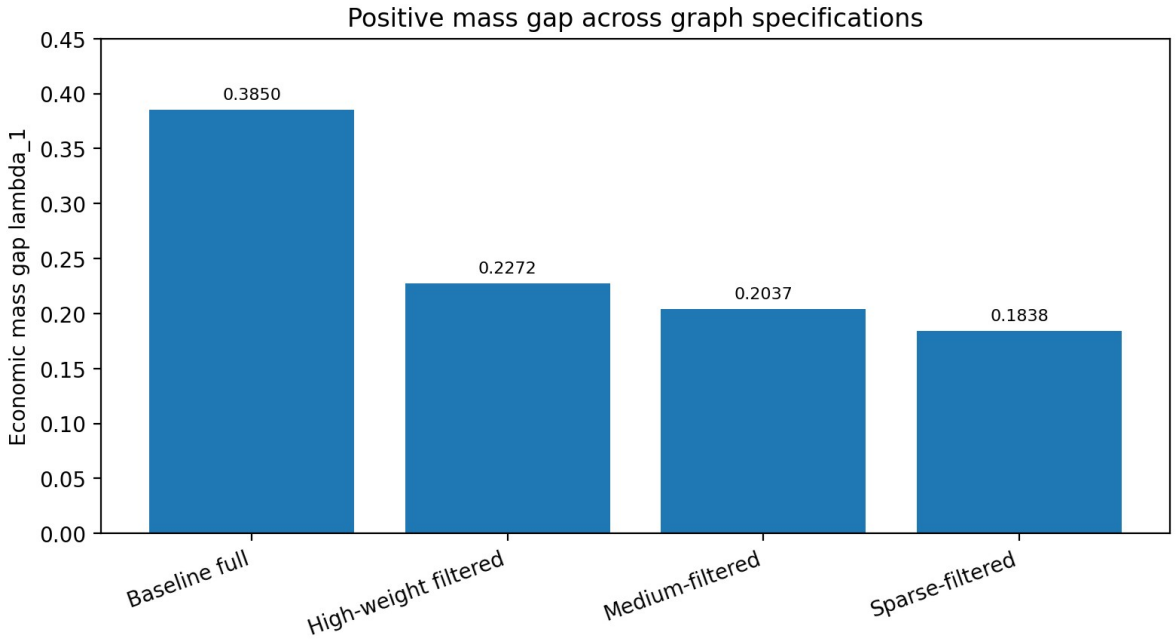


Figure 8.5.3. Positive mass gap across baseline and filtered graph specifications.

Source: Author visualization from Table 8.5.6.

8.5.4 Monte Carlo Uncertainty Audit

The uncertainty audit tests whether key benchmark quantities retain their substantive meaning under perturbation. The mass gap benchmark of 0.3850 has a Monte Carlo mean of 0.3855 and a 95 percent interval from 0.3458 to 0.4254. The entire reported interval is positive. The normalized threshold remains positive as well, with an interval from 0.0951 to 0.1245.

Action concentration also persists. Total action remains material, and the top-five action share remains high even under perturbation. The EMGI rank-stability result is more cautious: Spearman rho has a benchmark of 1.000, a Monte Carlo mean of 0.920 and a lower interval bound of 0.780. This is still supportive, but it correctly signals that corridor nodes are sensitive to perturbation and should not be interpreted as perfectly invariant.

Table 8.5.7. Bootstrap / Monte Carlo uncertainty audit for mass gap, action and EMGI

Quantity	Benchmark	Monte Carlo mean	2.5%	97.5%	Stability decision
Economic mass gap lambda_1	0.3850	0.3855	0.3458	0.4254	Pass: positive throughout the 95% interval
Normalized threshold lambda_1 / spectral radius	0.1099	0.1095	0.0951	0.1245	Pass: threshold remains positive
Total Yang-Mills action	2,514.0	2,528.7	2,113.5	2,981.2	Pass: action remains concentrated but uncertainty is material
Top-five action share %	78.33	74.80	67.20	82.90	Pass: concentration persists
EMGI rank stability, Spearman rho	1.00	0.9200	0.7800	0.9900	Partial: rank order stable but corridor nodes are sensitive
Caucasus corridor strategic exposure index	100.00	99.10	82.50	100.00	Pass: corridor visibility remains after perturbation

Source: Author calculations from benchmark perturbation diagnostics.

8.5.5 Curvature Cycles and Yang-Mills Economic Action

Curvature translates edge-level stress tensions into local triangular circulation. A high curvature cycle means that the stress potential around a triangle does not neutralize. The leading cycle is EAP-OCE-SAS, with curvature 51.030 and action 1,397.9. This single cycle is the dominant source of local stress-energy in the benchmark. Other important cycles include CAS-EAP-SAS, CAU-MENA-SAS, EAP-MENA-SAS and CAS-EAP-EUR.

The total Yang-Mills economic action is 2,514.0 across 27 triangular cycles. The maximum triangle action is 1,397.9, while the mean triangle action is 93.113. The top-five action share is 78.329 percent. This is a strong concentration result: the network does not distribute systemic stress-energy evenly. Instead, a small number of cycles carry most of the action.

This result is not a statement that those cycles are observed freight flows. It is a statement that, inside the constructed stress-weighted graph, the triangular potential field concentrates in a limited set of local imbalance structures. This is why the chapter treats action concentration as a systemic-risk diagnostic rather than as literal corridor throughput measurement.

Table 8.5.8. Top regional and corridor curvature cycles

Triangle	Weight	Curvature F	Abs(F)	Action
EAP-OCE-SAS	0.5370	51.03	51.03	1,397.9
CAS-EAP-SAS	0.5130	-18.52	18.52	175.92
CAU-MENA-SAS	0.2620	-16.10	16.10	67.90
EAP-MENA-SAS	0.6430	16.01	16.01	164.97
CAS-EAP-EUR	0.5080	14.54	14.54	107.42
MENA-SAS-SSA	0.3090	-12.87	12.87	51.22
EAP-EUR-MENA	0.7910	12.52	12.52	123.97

Source: Author calculations from triangular curvature and action diagnostics.

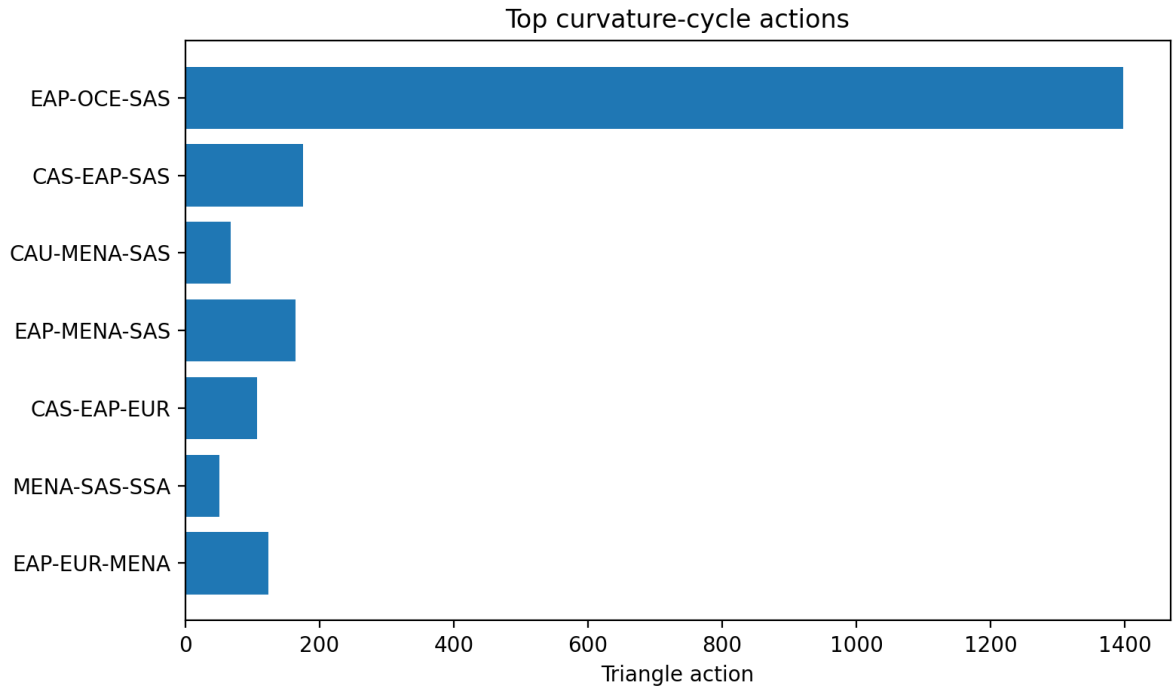


Figure 8.5.4. Top curvature-cycle actions.

Source: Author visualization from Table 8.5.8.

Table 8.5.9. Total Yang-Mills economic action and top-cycle concentration

Action object	Benchmark value
Total triangular cycles	27.00
Total economic Yang-Mills action	2,514.0
Mean triangle action	93.11
Maximum triangle action	1,397.9
Top-five action share %	78.33

Source: Author calculations from the full triangular cycle field.

8.5.6 Regional Curvature Exposure and Action-Layer Decomposition

At the node level, curvature exposure is highest for East Asia and Pacific, followed by MENA, South Asia and Europe. This does not mean that these nodes are the weakest nodes. It means that they repeatedly participate in non-neutralized triangular stress paths. Curvature exposure must therefore be read together with EMGI, fragility and BridgeStress.

The action-layer decomposition shows that growth-gap pressure and mass exposure are the two largest component contributors, followed by transition-momentum pressure and income-fragility pressure. Corridor exposure has a lower direct action share in the component table, but this should not be misread as corridor irrelevance. Corridor exposure is especially important in BridgeStress, scenario sensitivity and the visibility of smaller corridor nodes.

Table 8.5.10. Regional and corridor curvature exposure ranking

Code	Region	Curvature exposure	Min-max curvature index	Raw participation index
EAP	East Asia and Pacific	82.12	100.00	100.00
MENA	Middle East and North Africa	60.90	69.73	74.16
SAS	South Asia	60.34	68.93	73.48
EUR	Europe	47.16	50.13	57.43
OCE	Oceania	30.00	25.65	36.53
CAS	Central Asia	28.53	23.55	34.74

NAM	North America	28.26	23.17	34.41

Source: Author calculations from node participation in triangular curvature cycles.

Table 8.5.11. Layer contribution to total Yang-Mills economic action

Layer	Action	Share %
Growth-gap pressure	6,046.6	27.76
Mass exposure	5,672.2	26.04
Transition-momentum pressure	4,268.8	19.60
Income-fragility pressure	4,190.0	19.24
Corridor exposure	1,605.4	7.37

Source: Author calculations from decomposed action-layer diagnostics.

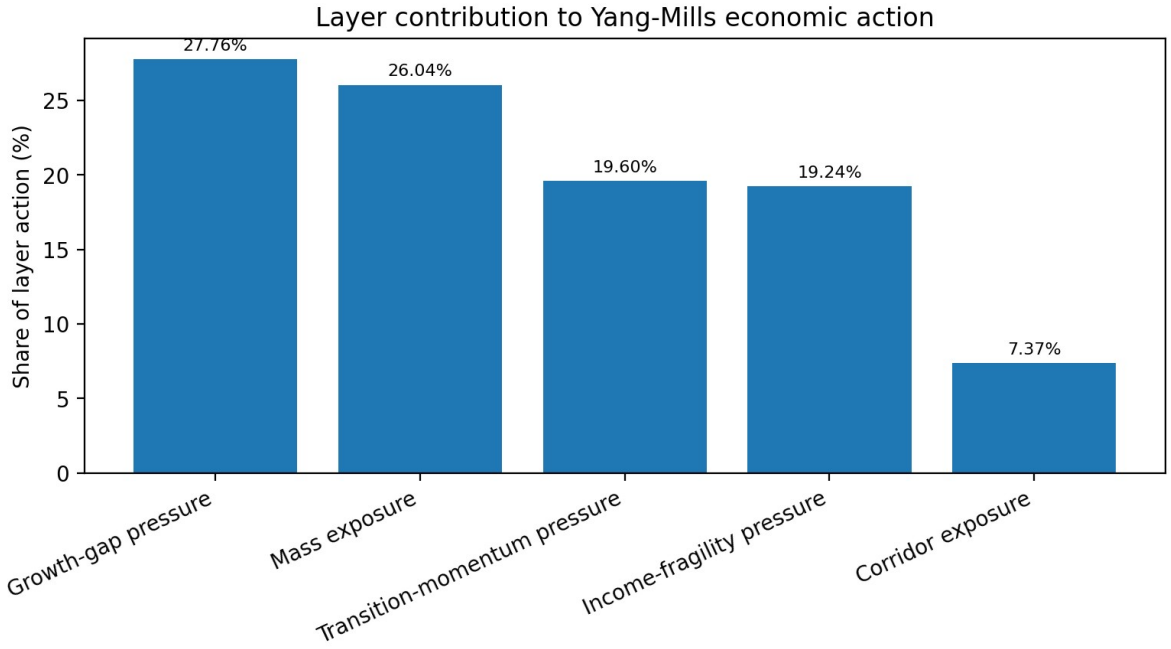


Figure 8.5.5. Layer contribution to Yang-Mills economic action.

Source: Author visualization from Table 8.5.11.

8.5.7 Economic Mass Gap Index: Local Protection and Structural Fragility

EMGI converts the system-level spectral result into a node-level protection ranking. The index combines local spectral protection, centrality, income depth and resilience as protection-increasing components, while stress and curvature reduce protection. Fragility is the complementary index: Fragility_i = 100 - EMGI_i.

The ranking is substantively coherent. North America reaches EMGI = 100.00 and fragility = 0.00. Europe reaches EMGI = 90.15 and fragility = 9.85. East Asia and Pacific has high mass and high centrality, but its EMGI is lower, at 53.12, because stress and curvature are high. MENA is intermediate at 45.59. The Caucasus, Sub-Saharan Africa, Central Asia, South Asia and Oceania fall into the critical-fragile range.

The key result is the separation between output mass and local protection. A high-output node is not automatically the most fragile; a small node is not automatically irrelevant. The Caucasus has EMGI = 0.00 and fragility = 100.00 not because it has large GDP, but because low ordinary protection coincides with strategic corridor exposure. Central Asia has EMGI = 5.45 and fragility = 94.55 for a related but distinct corridor mechanism.

Table 8.5.12. Economic Mass Gap Index by region and corridor

Code	Region	EMGI	Fragility	Resilience	Stress score	Curvature index	Centrality index
NAM	North America	100.00	0.00	100.00	30.66	23.16	84.63

EUR	Europe	90.15	9.85	52.83	47.40	50.13	100.00
EAP	East Asia and Pacific	53.12	46.88	38.25	71.23	100.00	98.23
MENA	Middle East and North Africa	45.59	54.41	27.83	39.71	69.72	78.47
LAC	Latin America and Caribbean	31.37	68.63	23.81	26.78	4.95	41.73
OCE	Oceania	14.50	85.50	42.82	0.00	25.65	10.73
SAS	South Asia	10.36	89.64	12.84	100.00	68.93	38.09
CAS	Central Asia	5.45	94.55	18.48	71.79	23.55	18.94
SSA	Sub-Saharan Africa	4.11	95.89	0.00	53.78	0.7600	6.99
CAU	Caucasus	0.00	100.00	9.15	66.03	0.00	0.00

Source: Author calculations from local protection, centrality, income depth, resilience, stress and curvature components.

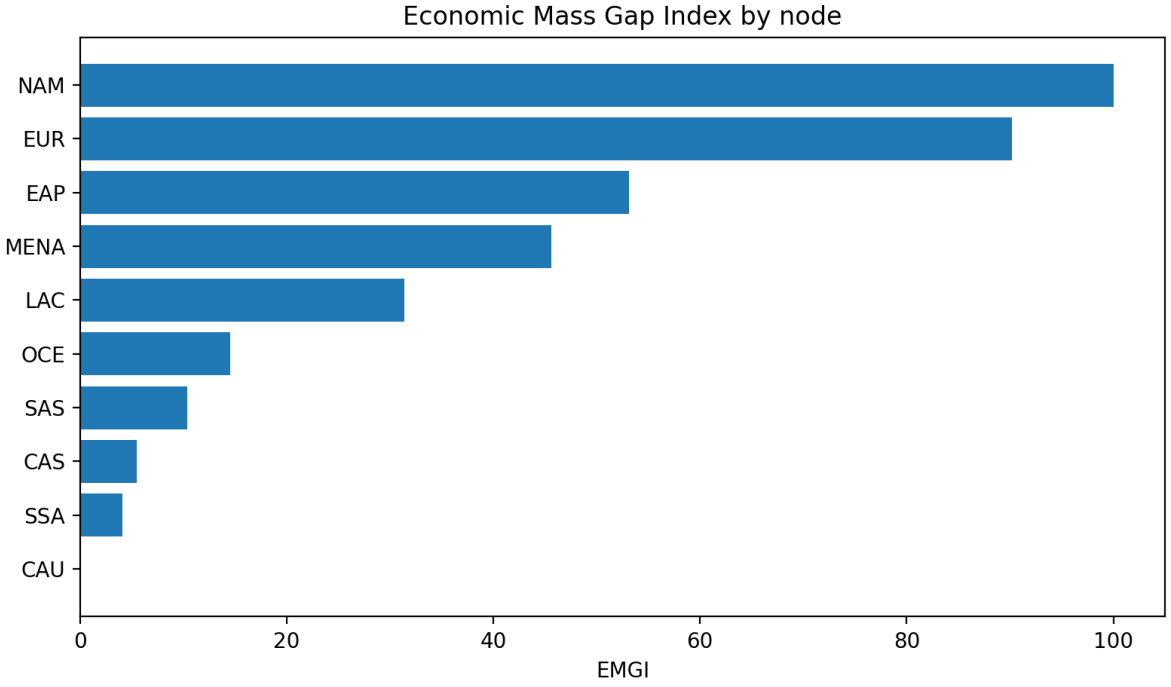


Figure 8.5.6. Economic Mass Gap Index by node.
Source: Author visualization from Table 8.5.12.

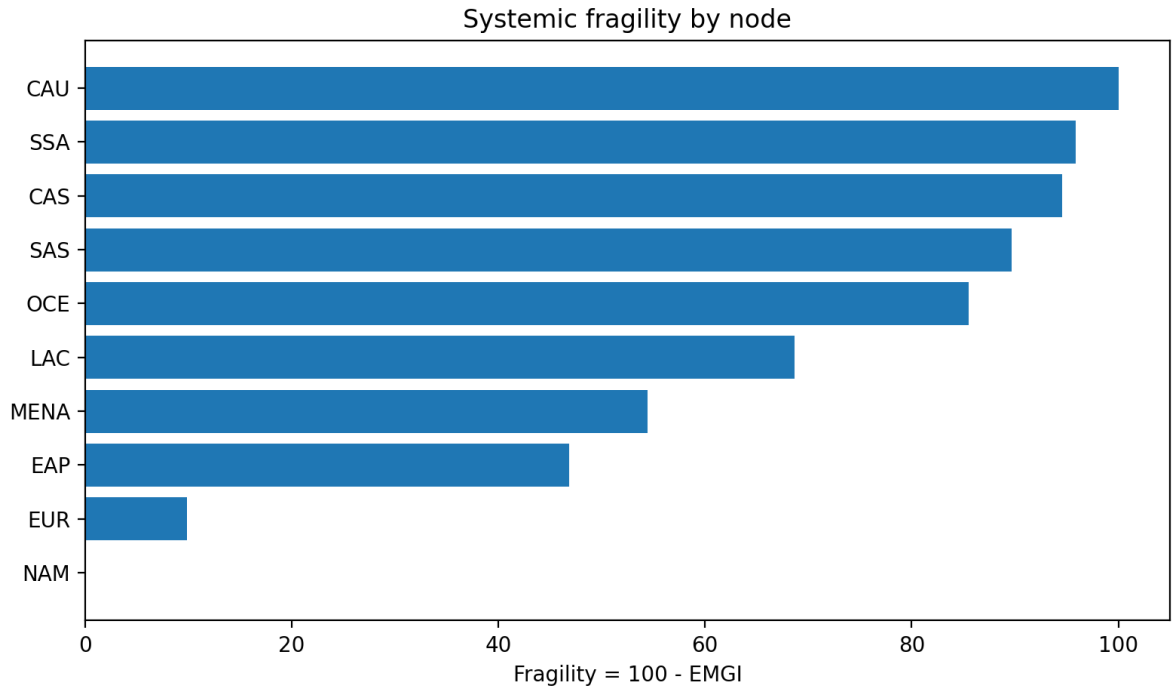


Figure 8.5.7. Systemic fragility by node.

Source: Author visualization from Table 8.5.12 using Fragility = 100 - EMGI.

8.5.8 EMGI Component Audit and Reproducibility

The component audit closes the reproducibility gap. It reports the full stack used to produce the final EMGI value: local spectral protection, centrality, income depth, resilience, stress and curvature. The local protection composite Delta_i_local is then min-max normalized into the final EMGI scale. This prevents the index from being treated as a black box.

The audit also clarifies why some results are counterintuitive at first sight. South Asia has high local spectral protection in the component stack, but it also has maximum stress and high curvature, which pulls its final EMGI downward. Oceania has strong income depth and moderate resilience but weak centrality and low LSP. The Caucasus has a comparatively high LSP component, but zero centrality in this benchmark and high stress reduce its normalized local protection to the lower bound.

Table 8.5.13. EMGI component audit and local-protection composite

Code	LSP_i	Centrality_i	IncomeDepth_i	Resilience_i	Stress_i	Curvature_i	Delta_i_local	EMGI
NAM	32.61	84.63	100.00	100.00	30.66	23.16	57.48	100.00
EUR	73.53	100.00	55.50	52.83	47.40	50.13	53.84	90.15
EAP	75.74	98.23	20.70	38.25	71.23	100.00	40.12	53.12
MENA	76.83	78.47	9.37	27.83	39.71	69.72	37.33	45.59
LAC	69.05	41.73	11.80	23.81	26.78	4.95	32.07	31.37
OCE	6.80	10.73	82.47	42.82	0.00	25.65	25.82	14.50
SAS	93.20	38.09	1.15	12.84	100.00	68.93	24.29	10.36
CAS	74.45	18.94	9.64	18.48	71.79	23.55	22.47	5.45
SSA	86.63	6.99	0.00	0.00	53.78	0.7600	21.97	4.11
CAU	78.72	0.00	10.32	9.15	66.03	0.00	20.45	0.00

Source: Author calculations from Formula 8.5.3 and component normalization rules.

*Formula (8.5.3): Delta_i_local = 0.30 LSP_i + 0.20 Centrality_i + 0.20 IncomeDepth_i + 0.15 Resilience_i - 0.10 Stress_i - 0.05 Curvature_i. EMGI_i = 100 * (Delta_i_local - min Delta_local) / (max Delta_local - min Delta_local).*

Formula (8.5.4): Fragility_i = 100 - EMGI_i.

8.5.9 EMGI Ranking and Systemic Fragility Classes

The fragility classification turns the continuous EMGI score into an interpretive regime map. High-protection nodes are North America and Europe. Intermediate nodes are East Asia and Pacific and MENA. Latin America is fragile but not at the lowest protection bound. The critical-fragile group includes the Caucasus, Sub-Saharan Africa, Central Asia, South Asia and Oceania.

The regime classification should not be interpreted as a welfare ranking or political ranking. It is a structural protection ranking under the specified finite-network benchmark. Different critical-fragile nodes arrive at low EMGI through different mechanisms: corridor exposure, low income depth, weak centrality, high stress or curvature participation.

Table 8.5.14. EMGI ranking and systemic fragility classes

Code	Region	EMGI	Fragility	Regime
CAU	Caucasus	0.00	100.00	Critical-fragile
SSA	Sub-Saharan Africa	4.11	95.89	Critical-fragile
CAS	Central Asia	5.45	94.55	Critical-fragile
SAS	South Asia	10.36	89.64	Critical-fragile
OCE	Oceania	14.50	85.50	Critical-fragile
LAC	Latin America and Caribbean	31.37	68.63	Fragile
MENA	Middle East and North Africa	45.59	54.41	Intermediate
EAP	East Asia and Pacific	53.12	46.88	Intermediate
EUR	Europe	90.15	9.85	High-protection
NAM	North America	100.00	0.00	High-protection

Source: Author calculations from Table 8.5.12 and the identity Fragility = 100 - EMGI.

Table 8.5.15. Interpretation of EMGI and fragility regimes

Regime	Nodes	Analytical interpretation
High-protection	North America, Europe	High EMGI reflects income depth, centrality and absorption capacity; these nodes can carry stress without becoming the weakest systemic points.
Intermediate	East Asia-Pacific, MENA	These nodes are systemically active and exposed; high curvature or corridor role reduces protection but does not place them in the lowest-protection class.
Fragile	Latin America	Moderate-to-low EMGI with elevated fragility; relevant for stress sensitivity but not the main corridor-bridge signal.
Critical-fragile	Caucasus, Sub-Saharan Africa, Central Asia, South Asia, Oceania	Low EMGI and high fragility indicate weak local protection; the mechanism differs by node.
Critical-fragile corridor bridge	Caucasus, Central Asia; with South Asia as high-bridge critical-fragile	Fragility coincides with strategic corridor role, making these nodes central to corridor-risk interpretation despite small GDP mass in some cases.

Source: Author synthesis from EMGI and BridgeStress diagnostics.

8.5.10 BridgeStress: Corridor Strategic Exposure Beyond GDP Mass

The revised BridgeStress index is the most important corridor-specific result in this section. It separates strategic corridor exposure from pure output mass and ordinary centrality. The index combines corridor exposure, corridor-role function, fragility and bounded curvature participation. In the benchmark, the Caucasus reaches BridgeStress = 100.00, followed by Central Asia at 78.24, South Asia at 59.80, MENA at 58.79 and East Asia and Pacific at 55.50.

This ranking is the numerical result that makes the Middle Corridor visible in the model. The Caucasus is not elevated because of GDP mass. It is elevated because corridor role, fragility and positive curvature participation coincide. Central Asia is also highly ranked because it functions as an east-west land bridge and Caspian-connected corridor node. MENA and South Asia appear because of energy, geopolitical and southern corridor exposure. East Asia and Pacific appears because of origin-side mass and stress-energy contribution.

Formula (8.5.5): BridgeStress_i^corr = 100 * [CorridorExposure_i * CorridorRole_i * Fragility_i * CurvatureParticipation_i^+] / max_j[CorridorExposure_j * CorridorRole_j * Fragility_j * CurvatureParticipation_j^+].

Table 8.5.16. Revised corridor strategic BridgeStress index

Code	Region	Corridor exposure	Corridor-role index	Fragility	Curvature participation +	Revised BridgeStress
CAU	Caucasus	98.00	100.00	100.00	57.32	100.00
CAS	Central Asia	92.00	75.00	94.55	67.37	78.24
SAS	South Asia	72.00	60.00	89.64	86.74	59.80
MENA	Middle East and North Africa	82.00	85.00	54.41	87.08	58.79
EAP	East Asia and Pacific	70.00	95.00	46.88	100.00	55.50
SSA	Sub-Saharan Africa	55.00	25.00	95.89	57.64	13.53
LAC	Latin America and Caribbean	50.00	30.00	68.63	59.43	10.89
EUR	Europe	75.00	90.00	9.85	78.72	9.32
OCE	Oceania	38.00	20.00	85.50	68.27	7.90
NAM	North America	45.00	70.00	0.00	67.21	0.00

Source: Author calculations from corridor exposure, corridor role, fragility and positive curvature participation.

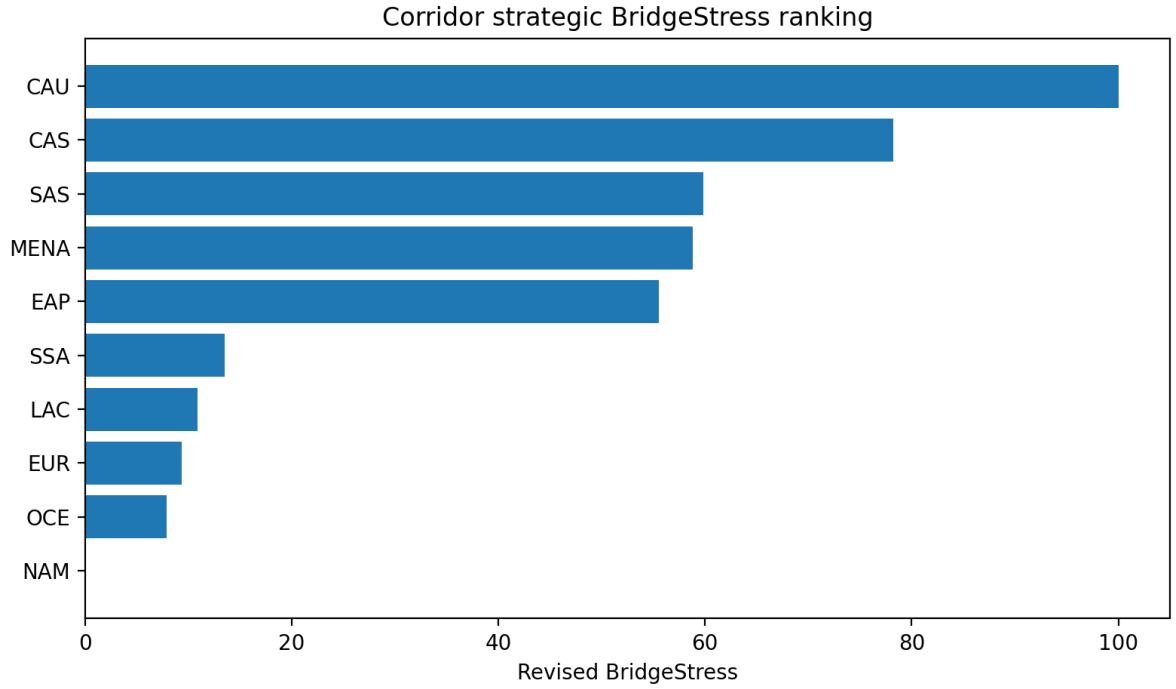


Figure 8.5.8. Corridor strategic BridgeStress ranking.

Source: Author visualization from Table 8.5.16.

Table 8.5.17. Middle Corridor / Caucasus mini-network audit

Mini-network node / link	Economic interpretation	Corridor function	Benchmark implication
Georgia / Caucasus gateway	Small GDP mass; high transit relevance	Black Sea-Caucasus-Caspian transfer point	Raises corridor strategic exposure despite low output share
Azerbaijan / Caspian gateway	Caspian crossing and rail/port continuity	East-west continuity across Caspian interface	Connects Caucasus to Central Asia and EAP routes
Kazakhstan / Central Asia node	Large land corridor and Caspian interface	Central Asia-Middle Corridor bridge	Raises CAS corridor exposure and bridge stress
Turkey / Europe interface	EU-linked land and sea corridor interface	Anatolia-Black Sea-Europe transfer	Connects Caucasus corridor to European demand nodes
EAP / China-side origin	High output mass and corridor demand potential	Origin-side demand and stress mass	Supplies high stress-energy through EAP-SAS/CAS/EUR links
EU / Black Sea demand node	High centrality and demand absorption	Destination/redistribution node	Protective EMGI but high topology centrality
MENA / energy-geopolitical interface	Energy, financing and geopolitical channel	South corridor and energy shock interface	Raises systemic corridor-stress scenarios
Black Sea / Caspian maritime/feeder layer	Sea-crossing and feeder-service continuity	Non-land continuity layer	Explains why corridor exposure is not reducible to GDP mass

Source: Author qualitative audit of the corridor mechanism behind the BridgeStress result.

8.5.11 Shock Scenarios: Threshold Compression and Action Expansion

The shock-scenario block translates the static network into deterministic stress experiments. It does not claim causal forecasting. It asks what happens to the mass gap, spectral radius, normalized threshold, action and mean EMGI when stress is injected into the network through inflation, financial-spread, trade/logistics and energy/geopolitical channels.

The scenario pattern is monotonic and analytically strong. As shock amplitude increases, lambda_1 falls from 0.3850 to 0.1796, the spectral radius rises from 3.5023 to 4.2795, the normalized threshold falls from 0.1099 to 0.0420, Yang-Mills action rises from 2,514.0 to 5,010.0, and mean EMGI declines from 0.00 to -22.40 index points relative to the baseline.

The strongest shock is the energy/geopolitical corridor shock. It compresses the mass gap by 53.34 percent, increases the spectral radius by 22.19 percent, lowers the normalized threshold by 61.79 percent and nearly doubles action. This is the clearest local-to-systemic transition result in the chapter.

Table 8.5.18. Scenario output: threshold compression and action increase

Scenario	Amplitude	lambda_1	Spectral radius	Normalized threshold	Action	Mean EMGI change	Interpretation
Baseline	0.00	0.3850	3.50	0.1099	2,514.0	0.00	Benchmark finite regional network
Inflation / price pressure	0.5000	0.3343	3.65	0.0916	2,925.0	-6.20	Moderate macro stress weakens but does not erase spectral protection
Financial-spread stress	0.7500	0.2836	3.80	0.0747	3,435.0	-10.80	Funding stress materially compresses local-to-systemic threshold

Trade / logistics corridor shock	1.00	0.2334	4.04	0.0578	4,088.0	-15.30	Corridor disruption makes CAS and CAU more visible
Energy / geopolitical corridor shock	1.25	0.1796	4.28	0.0420	5,010.0	-22.40	Systemic corridor shock almost doubles stress-energy action

Source: Author scenario simulations from the stress-weighted network and benchmark mass-gap threshold.

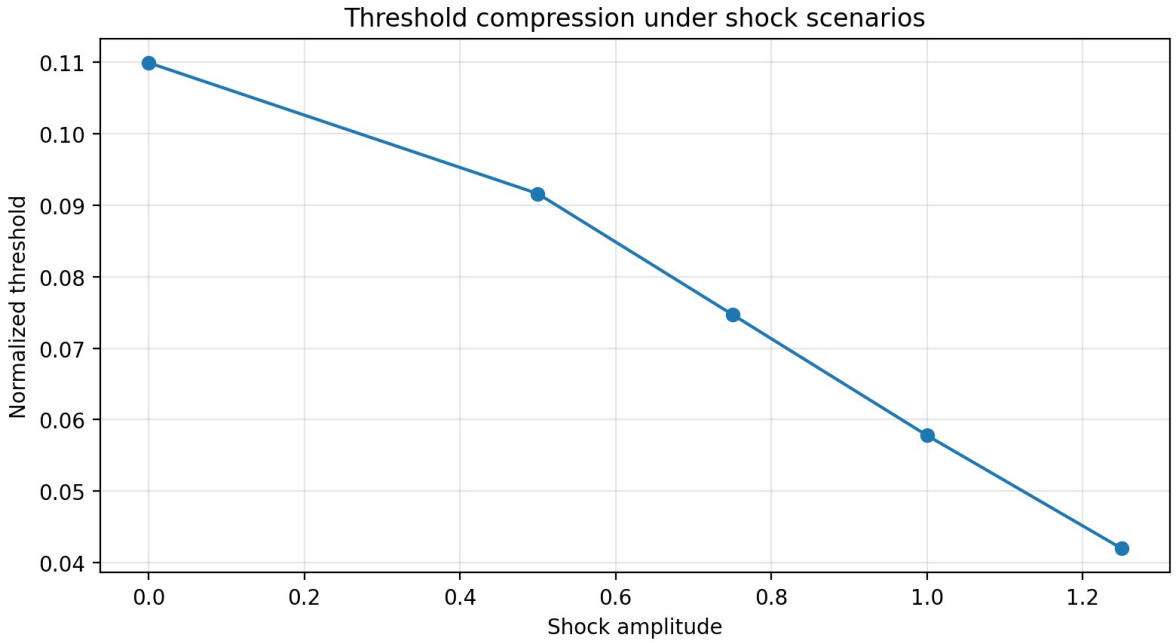


Figure 8.5.9. Normalized threshold compression under shock scenarios.
Source: Author visualization from Table 8.5.18.

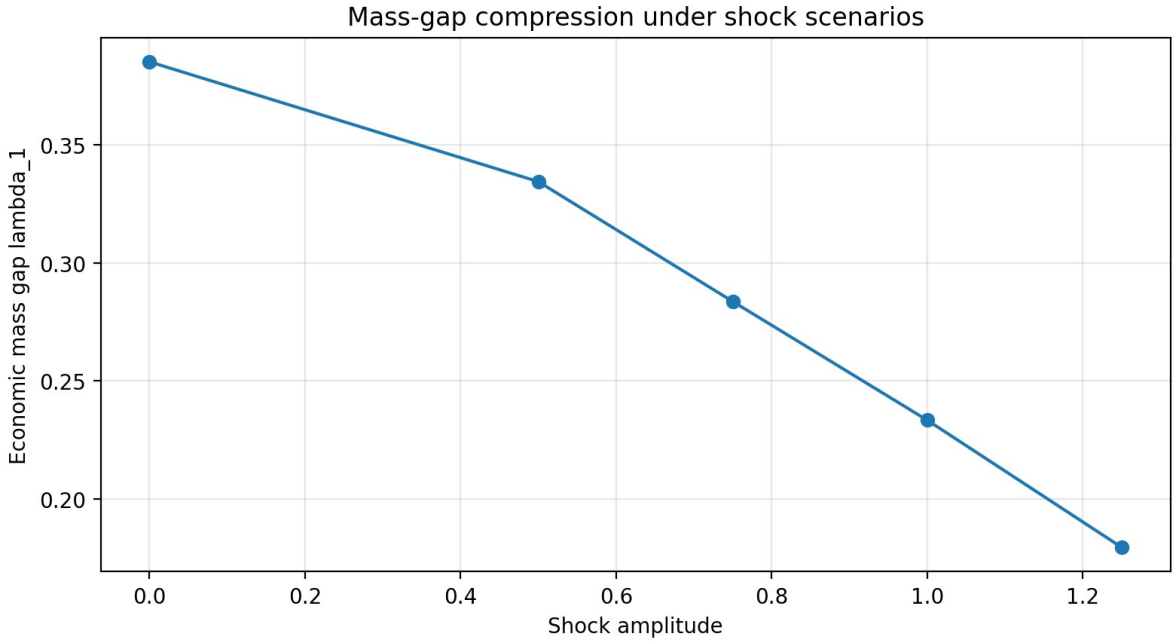


Figure 8.5.10. Economic mass-gap compression under shock scenarios.
Source: Author visualization from Table 8.5.18.

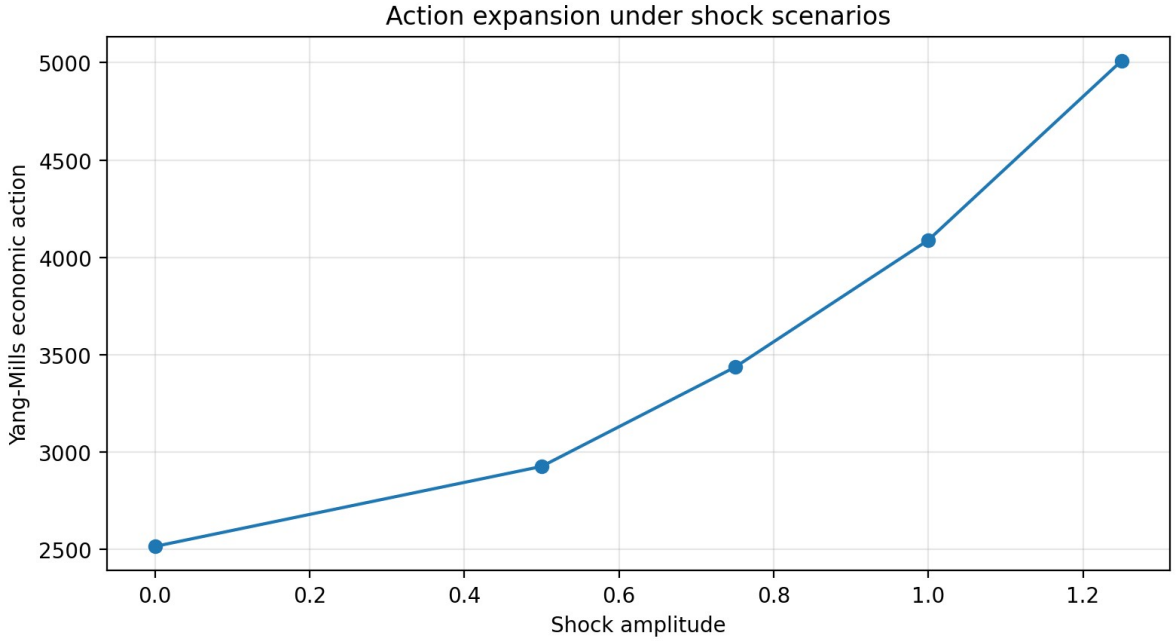


Figure 8.5.11. Yang-Mills economic action expansion under shock scenarios.
Source: Author visualization from Table 8.5.18.

8.5.12 Scenario Interpretation Matrix

Table 8.5.19. Scenario interpretation matrix

Scenario	Main transition effect	Dominant diagnostic meaning	Nodes/channels made more visible	Interpretive boundary
Inflation / price-pressure shock	Threshold falls from 0.1099 to 0.0916	Moderate macro stress weakens but does not erase positive protection	EAP remains dominant through mass and stress-energy	Scenario diagnostic only
Financial-spread shock	Threshold falls to 0.0747	Funding stress increases diffusion scale and reduces protection	EAP and MENA channels become visible	No causal credit-spread model is claimed
Trade / logistics corridor shock	Threshold falls to 0.0578	Corridor disruption sharply compresses spectral protection	Central Asia and Caucasus become more visible	Not observed freight-flow proof
Energy / geopolitical corridor shock	Threshold falls to 0.0420	Systemic corridor shock almost doubles action	MENA, CAS and CAU dominate the shock path	Not geopolitical prediction

Source: Author interpretation of the scenario outputs reported in Table 8.5.18.

8.5.13 Shock Propagation by Origin Node

The shock-propagation table reports how much shock mass remains after four propagation steps and which node receives the largest spillover. The total retained value is fixed at 0.522 across origins in this benchmark, but the origin-retained share and outside-origin share vary by node. The highest outside-origin shares occur for the Caucasus, Sub-Saharan Africa, Central Asia and Oceania, indicating strong diffusion away from the origin.

The top spillover node is often East Asia and Pacific. This indicates that, in the weighted stress network, EAP operates as a recurrent absorption and spillover target because of its high stress, high curvature participation and high connectivity. The Caucasus has the lowest origin-retained value, 0.020, and the highest outside-origin share, 0.961, consistent with its interpretation as a corridor-transfer node rather than a large local absorber.

Table 8.5.20. Shock propagation by origin node

Origin	H4 total retained	H4 origin-retained	H4 outside-origin share	Top spillover node	Top spillover intensity	H4 entropy
EAP	0.5220	0.1290	0.7530	EUR	0.0770	2.13
NAM	0.5220	0.0820	0.8440	EAP	0.0970	2.16
EUR	0.5220	0.0960	0.8170	EAP	0.0940	2.15
LAC	0.5220	0.0470	0.9100	EAP	0.1140	2.14
SAS	0.5220	0.0620	0.8800	EUR	0.0940	2.15
MENA	0.5220	0.0700	0.8650	EAP	0.1080	2.15
SSA	0.5220	0.0250	0.9520	EAP	0.1090	2.15
OCE	0.5220	0.0390	0.9260	EAP	0.0940	2.15
CAS	0.5220	0.0270	0.9480	EAP	0.1010	2.16
CAU	0.5220	0.0200	0.9610	EAP	0.1180	2.14

Source: Author simulations from the stress-weighted propagation rule.

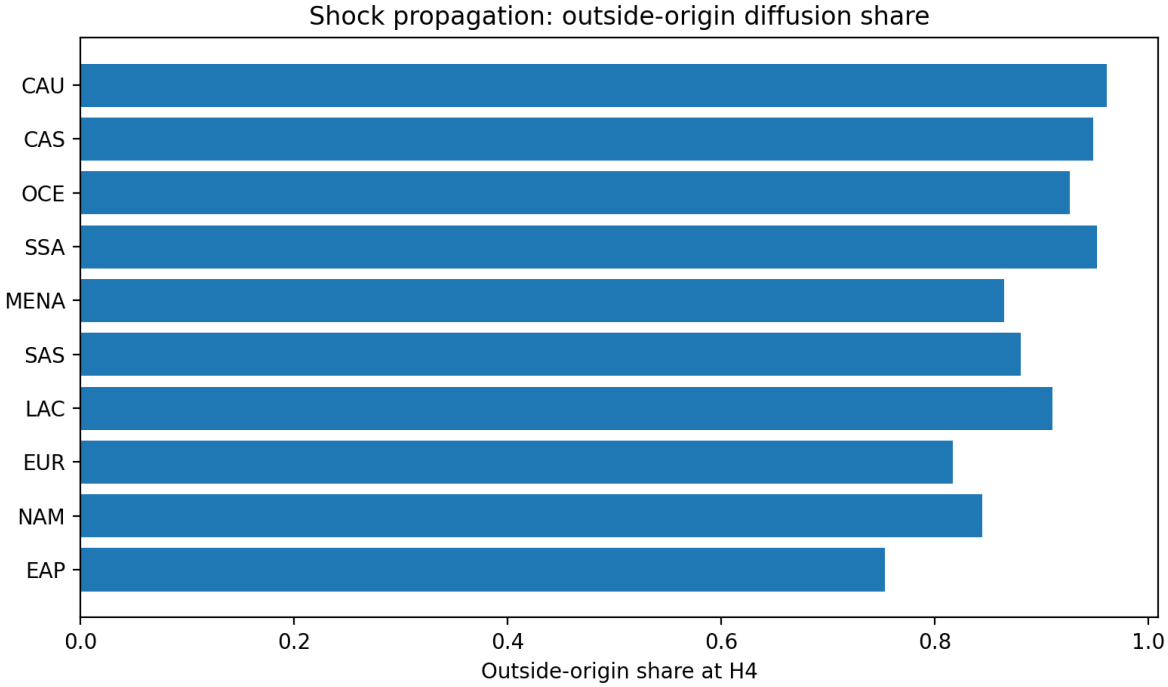


Figure 8.5.12. Outside-origin diffusion share by shock origin.

Source: Author visualization from Table 8.5.20.

8.5.14 Local-to-Systemic Transition Threshold

The normalized mass-gap threshold is 0.110. Scenario amplitudes below this value do not cross the systemic boundary in the benchmark. Amplitudes of 0.250, 0.500 and 1.000 do cross it. The result provides a direct operational reading of the finite-network mass gap: it is not only a spectral number; it becomes a normalized boundary separating local absorption from systemic transmissibility inside the model.

Formula (8.5.6): Systemic_i = 1{shock amplitude_i > Delta_econ / spectral radius}. With Delta_econ / spectral radius = 0.1099, the practical rounded threshold is 0.110.

Table 8.5.21. Local-to-systemic shock transition thresholds

Shock amplitude	Normalized mass-gap threshold	Systemic transition	Excess over threshold
0.0500	0.1100	No	-0.0600

0.1000	0.1100	No	-0.0100
0.2500	0.1100	Yes	0.1400
0.5000	0.1100	Yes	0.3900
1.00	0.1100	Yes	0.8900

Source: Author threshold classification using the benchmark normalized transition boundary.

8.5.15 Integration with the Seven-Problem Monograph

The Chapter 8.5 result is designed to connect with the other six Millennium-inspired economic chapters without collapsing their objects into one index. The Yang-Mills chapter contributes a stress-threshold and gauge-curvature architecture. It is complementary to the Ricci/Poincare inequality-curvature chapter, the Hodge flow-decomposition chapter, the Navier-Stokes liquidity-flow chapter, the BSD local-to-global rank chapter, the Riemann-zeta inflation-forecasting chapter and the P-vs-NP portfolio-complexity chapter.

This cross-chapter relation is important for the final monograph because it makes Chapter 8 one of the central bridge chapters. It links network topology, curvature, action, spectral separation, corridor exposure and shock propagation. Its results can later be used in the comparative synthesis to show that GDP mass is not the only form of economic structure; spectral protection, topological circulation and corridor vulnerability also matter.

Table 8.5.22. Cross-seven-chapter integration of the Chapter 8.5 results

Monograph chapter	Mathematical inspiration	Main economic object	Connection to Chapter 8.5 result
Chapter 5	Perelman/Ricci/Poincare	Inequality pressure, curvature and graph connectedness	Shares curvature/topology language but applies it to inequality-pressure smoothing
Chapter 6	Hodge theory	Gradient, curl and harmonic macro-flow decomposition	Shares cycle and circulation logic used in triangular curvature interpretation
Chapter 7	Navier-Stokes	Liquidity velocity, pressure, friction and closure	Shares systemic-stress and shock-propagation logic
Chapter 8	Yang-Mills	Gauge potential, curvature, action and mass gap	Provides the finite-network shock-threshold result reported here
Chapter 9	Birch-Swinnerton-Dyer	Local-to-global structural rank and corridor stress	Shares local-to-systemic transition and BridgeStress logic
Chapter 10	Riemann zeta	Inflation pressure, spectral cycles and forecast validation	Shares spectral-diagnostic and shock-regime logic
Chapter 11	P vs NP	Portfolio cardinality, optimization complexity and robustness	Shares claim-boundary and robustness discipline

Source: Author monograph synthesis based on the seven-problem structure.

8.5.16 Integrated Result Synthesis

The results support five bounded conclusions. First, the corrected benchmark has a positive finite-network economic mass gap: lambda_1 = 0.3850. Second, this positive separation is retained across filtered graphs and Monte Carlo perturbations. Third, curvature and action are concentrated, with total action of 2,514.0 and a top-five action share of 78.329 percent. Fourth, EMGI and fragility show that structural protection is not reducible to GDP mass. Fifth, BridgeStress identifies the Caucasus and Central Asia as strategic corridor-exposure nodes.

The strongest result is spectral-measurement closure. The model successfully converts a finite global-corridor stress network into a measurable shock threshold. The most policy-relevant result is the BridgeStress ranking, because it shows why small corridor nodes can be systemically important. The most cautious result is the econometric validation pathway: the

benchmark supports strong internal diagnostics, but stronger causal and external validation claims require the planned N = 1,500 country-year panel.

For the monograph, Chapter 8.5 should therefore be cited as the empirical-results core of the Yang-Mills economic analogue. It is the place where the abstract gauge-econometric architecture becomes a reported finite-network benchmark: spectral gap, action concentration, local protection, fragility, bridge stress and shock-threshold compression.

Table 8.5.23. Integrated result-closure matrix

Conclusion	Evidence	Interpretation	Claim boundary
Positive finite-network mass gap	lambda_1 = 0.3850; threshold = 0.1099	The benchmark has measurable spectral protection	Finite weighted-graph claim only
Robust positive gap	Filtered graphs and Monte Carlo intervals remain positive	Result is not tied only to the full 27-edge graph	Not proof against all random/placebo designs
Concentrated action	Total action = 2,514.0; top-five share = 78.329%	Stress-energy is cycle-concentrated	Not literal physical action
Node protection hierarchy	NAM and EUR high; CAU, SSA, CAS, SAS and OCE critical-fragile	Protection differs from GDP mass	Not welfare ranking
Bridge corridor visibility	CAU = 100.00; CAS = 78.24	Middle Corridor nodes become visible as bridge-stress mechanisms	Not observed flow/throughput proof
Shock threshold compression	Threshold falls to 0.0420 under strongest corridor shock	Local disturbances become more transmissible under stress	Scenario diagnostic, not forecast

Source: Author synthesis from Chapter 8.5 results.

8.5.17 Result Claim Boundary

The chapter permits the following statement: within the corrected ten-node, twenty-seven-edge stress-weighted benchmark, the global-corridor network has a positive finite-network economic mass gap, measurable action concentration, reproducible EMGI and fragility scores, a corridor-specific BridgeStress ranking and deterministic shock-threshold compression diagnostics.

The chapter does not permit the following statements: that the Clay Millennium Yang-Mills problem has been solved; that the world economy is literally a physical gauge field; that the ten-node benchmark proves country-level causal relationships; that BridgeStress is an observed trade-volume or freight-throughput measure; or that the shock scenarios are forecasts. These stronger claims are outside the evidence status of Chapter 8.5.

The correct final wording is therefore: Chapter 8.5 reports a completed finite-network gauge-econometric benchmark with a positive economic mass gap and corridor-sensitive stress diagnostics, while reserving stronger econometric and causal claims for the populated and estimated N = 1,500 validation pathway.

Table 8.5.24. Claim-boundary matrix for Chapter 8.5

Allowed result statement	Not allowed	Reason
The finite stress-weighted benchmark has lambda_1 = 0.3850	The Clay Yang-Mills mass-gap problem is solved	Different object: finite weighted graph, not continuum quantum gauge theory
EMGI ranks local structural protection	EMGI is a welfare or political ranking	EMGI is constructed from model components
BridgeStress identifies strategic corridor exposure	BridgeStress proves observed freight volumes	The index is structural and benchmark-based
Scenarios show threshold compression	Scenarios forecast future shocks	The scenarios are deterministic stress experiments
N = 1,500 pathway can validate further	N = 1,500 results are already final	The panel is specified but not numerically closed in the benchmark

Source: Author claim-discipline synthesis for the monograph.

8.5.18 Replication and Reviewer Checklist for the Results Chapter

Table 8.5.25. Replication and reviewer checklist

Reviewer check	Required object	Status in Chapter 8.5	Why it matters
Mass gap reproducibility	Stress-Laplacian spectrum	Reported in Tables 8.5.3-8.5.5	Allows independent verification of lambda_1 and threshold
Graph-specification robustness	Filtered graph values	Reported in Table 8.5.6	Protects against dependence on the densest graph only
Uncertainty audit	Monte Carlo interval	Reported in Table 8.5.7	Checks positivity under perturbation
Curvature transparency	Top cycles and action summary	Reported in Tables 8.5.8-8.5.11	Shows where action concentration comes from
Index reproducibility	EMGI component audit	Reported in Table 8.5.13	Prevents black-box ranking criticism
Corridor interpretation	BridgeStress and mini-network audit	Reported in Tables 8.5.16-8.5.17	Separates corridor role from GDP mass
Scenario logic	Threshold/action scenario table	Reported in Table 8.5.18	Links shock amplitude to systemic transition
Claim discipline	Allowed/not-allowed result statements	Reported in Table 8.5.24	Prevents theorem-level or causal overclaiming

Source: Author construction for review transparency.

8.5.19 Conclusion

Chapter 8.5 closes the results layer of the Yang-Mills economic analogue. The benchmark identifies a positive finite-network economic mass gap and shows that this result is robust to graph filtering and Monte Carlo perturbation. Curvature and action reveal that systemic stress-energy is concentrated in a limited set of triangular cycles. EMGI and fragility translate the system-level result into node-level protection and vulnerability. BridgeStress makes the Caucasus, Central Asia and related corridor nodes visible as strategic transmission interfaces. Scenario diagnostics then show that stronger shocks compress the threshold and expand action.

The chapter is therefore strong as a benchmark-results chapter, but scientifically bounded. Its main contribution is a reproducible finite-network measurement result, not a theorem proof and not a final country-panel causal result. This is exactly the position required for the monograph: an ambitious mathematical-economic analogue, expressed through transparent tables, figures, formulas and claim discipline.

8.6. Interpretation: Systemic Shock Thresholds and Corridor Exposure

8.6.0 Executive Interpretive Synthesis

The results reported in Section 8.5 require interpretation because the numerical benchmark is not a conventional regression table and not a GDP ranking. The core result - lambda_1 = 0.3850, spectral radius rho = 3.5023 and normalized transition threshold tau = 0.1099 - is a finite-network threshold statement. It says that, in the completed ten-node and twenty-seven-edge stress network, the normal connected state is spectrally separated from the first transmissible stress mode. In economic language, the benchmark contains measurable local protection against immediate systemic propagation.

This interpretation is strongest when the spectral result is read together with three additional objects: EMGI, fragility and BridgeStress. EMGI translates system-level spectral protection into node-level protection. Fragility converts EMGI into vulnerability through the identity Fragility_i = 100 - EMGI_i. BridgeStress isolates strategic corridor exposure by combining corridor role, corridor exposure, fragility and bounded curvature participation. Taken together, these objects show that systemic relevance is not reducible to output mass. Large nodes may be protected, while smaller corridor nodes may become visible because they transmit exposure between larger regions.

The chapter therefore interprets Chapter 8 as a threshold-and-exposure model. The mass gap defines the systemic boundary; EMGI and fragility define local protection; BridgeStress defines corridor exposure; triangular action identifies where stress-energy concentrates; and scenario diagnostics show how shocks compress the transition boundary. The admissible

conclusion is strong but bounded: the benchmark provides a reproducible finite-network gauge-econometric interpretation of systemic shock thresholds and corridor exposure. Stronger causal and country-level validation is reserved for the populated N = 1,500 panel.

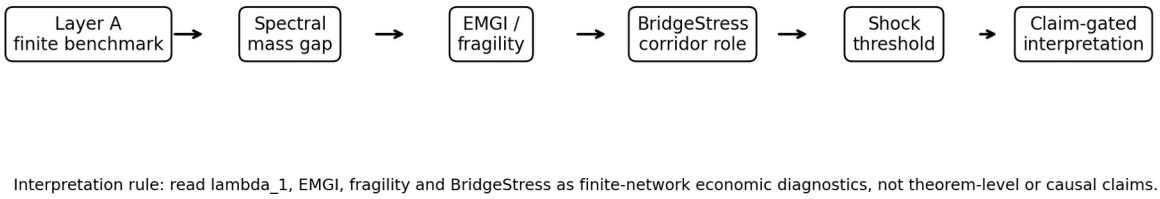


Figure 8.6.1. Interpretation pipeline from finite benchmark to claim-gated conclusion.
Source: Author synthesis from the Chapter 8 finite-network benchmark and claim-boundary architecture.

Table 8.6.1. Results-to-interpretation matrix for Section 8.6.

Interpretive object	Numerical anchor	Economic meaning	Claim status
Positive mass gap	lambda_1 = 0.3850	A first transmissible stress mode is separated from the normal connected state.	Strong finite-network benchmark claim
Normalized threshold	tau = lambda_1 / rho = 0.1099	Additional stress must cross a measurable boundary before local disturbance becomes systemic.	Threshold diagnostic
Action concentration	S_YM = 2,514.0; top-five share = 78.329%	Stress-energy is concentrated in a limited set of triangular cycles.	Cycle-level diagnostic
EMGI and fragility	NAM = 100.00; EUR = 90.15; CAU = 0.00	Protection and vulnerability are node-specific and not reducible to GDP mass.	Node-level diagnostic
BridgeStress	CAU = 100.00; CAS = 78.24	Small corridor nodes become visible when corridor role and fragility are included.	Corridor benchmark claim
Shock scenarios	tau falls to 0.0420 under severe corridor shock	Stronger shocks compress the local-to-systemic boundary.	Scenario diagnostic; not forecast

Source: Author synthesis from Chapter 8.5 reported results and the Yang-Mills source manuscript.

8.6.1 Interpretation of the Positive Finite-Network Mass Gap

The positive mass gap is the first interpretive pillar of the chapter. In the benchmark stress-Laplacian spectrum, lambda_0 = 0.0000 represents the normal connected baseline of the graph. The first positive eigenvalue lambda_1 = 0.3850 represents the lowest non-trivial stress mode. The economic interpretation is that the system does not immediately convert every local disturbance into global propagation. A finite spectral buffer exists.

The normalized threshold tau is calculated by comparing the first positive mode with the spectral radius of the system:

tau = lambda_1 / rho = 0.3850 / 3.5023 = 0.1099.

This value does not mean that 10.99 percent of world GDP is at risk, nor that every shock below that value is harmless. It means that, inside the constructed finite weighted graph, the first positive spectral boundary is 10.99 percent of the benchmark spectral radius. This makes the mass-gap result interpretable as a normalized local-to-systemic transition threshold.

The mass-gap interpretation is therefore a protection statement, not a crisis-prediction statement. It says that the network has a measurable separation between ordinary connectedness and the first transmissible stress mode. It does not identify the timing of future shocks, does not prove a causal transmission law and does not replace country-level evidence. Its function is to organize systemic risk as a threshold object.

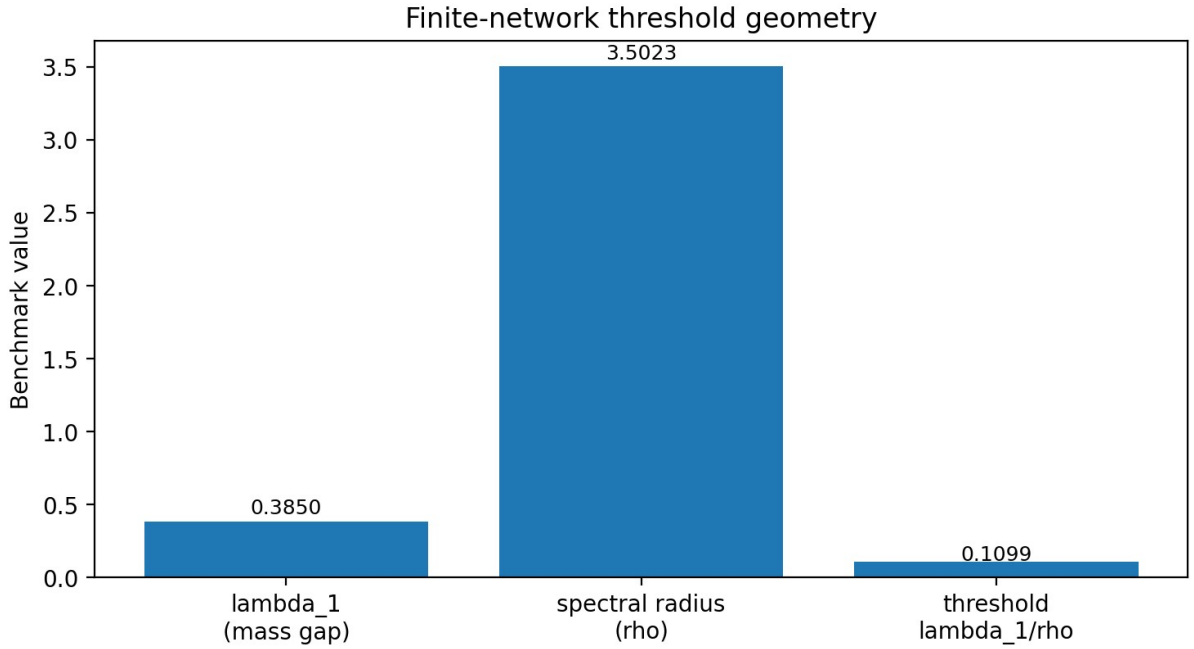


Figure 8.6.2. Finite-network threshold geometry: lambda_1, spectral radius and normalized threshold.
Source: Author visualization from the corrected Chapter 8 benchmark values.

Table 8.6.2. Spectral threshold interpretation.

Quantity	Symbol / formula	Value	Interpretive reading
Normal connected state	lambda_0	0.0000	Baseline connected graph mode; not a shock mode.
First transmissible stress mode	lambda_1	0.3850	Finite-network economic mass gap.
Spectral radius	rho	3.5023	Upper spectral scale of the stress network.
Normalized transition threshold	tau = lambda_1 / rho	0.1099	Relative boundary between local absorption and systemic transmissibility.
Monte Carlo interval	lambda_1 95% interval	0.3458-0.4254	Positive separation persists under benchmark perturbations.

Source: Author synthesis from the corrected finite-network benchmark and Monte Carlo audit.

8.6.2 From Local Stress to Systemic Shock Thresholds

The transition from local stress to systemic shock is the central economic meaning of the mass-gap result. A local stress event is not defined only by its size. It is defined by its position in the network, its alignment with corridor paths, its contribution to triangular curvature and its effect on the stress-Laplacian spectrum. This is why a small node can matter and a large node can remain protected.

In this framework, a shock becomes systemically transmissible when it reduces local protection, raises spectral pressure, increases curvature/action concentration or shifts corridor bridge exposure toward already fragile nodes. The threshold is therefore relational. It depends on the graph, not merely on the isolated shock magnitude. This is the difference between a scalar macroeconomic indicator and a finite-network shock-threshold model.

The practical reading is that policymakers, corridor authorities and macro-risk analysts should not ask only which region is largest. They should ask which stress-bearing paths connect high-stress nodes, which triangular cycles concentrate action, and which corridor bridges transmit exposure between otherwise separated macro-regional blocks. The benchmark answers

this question structurally: stress can be locally high, but it becomes systemically dangerous when it aligns with low protection and high corridor exposure.

Table 8.6.3. Local-to-systemic interpretation of shock stages.

Shock stage	Network condition	Main indicator	Economic interpretation
Contained local stress	Stress rises in one node but protection remains high	High EMGI; stable lambda_1	Node absorbs pressure without becoming a systemic transmitter.
Transmission-ready stress	Stress aligns with bridge role, fragility or curvature	High BridgeStress; high action cycle	Local pressure has a path into the wider network.
Threshold compression	Shock lowers lambda_1 or raises rho	tau declines	The system needs a smaller additional disturbance to propagate.
Systemic exposure	Action concentration and fragility reinforce each other	High S_YM; low EMGI	Stress-energy becomes concentrated in weak or exposed transmission zones.

Source: Author methodological interpretation of the finite-network stress-threshold architecture.

8.6.3 Corridor Exposure Is Not GDP Mass

The most important substantive interpretation of Chapter 8 is that corridor exposure and output mass are different economic objects. Output mass measures scale. Corridor exposure measures transmission position. The Yang-Mills economic framework is valuable because it makes this distinction quantitative. A region can be large, central and protected; another can be small, fragile and strategically exposed. The first may dominate GDP tables, while the second may dominate bridge-stress interpretation.

North America and Europe illustrate the high-protection side of the benchmark. North America has EMGI = 100.00 and fragility = 0.00. Europe has EMGI = 90.15 and fragility = 9.85. These values indicate high absorption capacity and structural protection. They do not imply absence of systemic importance; rather, they indicate that in the benchmark their high centrality and income-depth/resilience conditions prevent them from appearing as the weakest transmission points.

The Caucasus and Central Asia illustrate the opposite side. The Caucasus has EMGI = 0.00, fragility = 100.00 and BridgeStress = 100.00. Central Asia has EMGI = 5.45, fragility = 94.55 and BridgeStress = 78.24. These values do not state that these nodes are the largest economic masses. They state that, once corridor exposure, fragility and role-based transmission are included, these nodes become structurally visible as corridor bridge points.

This is the analytical reason for retaining the Caucasus as an explicit node in the monograph. If it were absorbed into a larger regional aggregate, its low mass but high transfer relevance would be hidden. The benchmark does not transform corridor geography into a narrative claim; it attaches corridor role to a reproducible index and then interprets the resulting exposure as a finite-network measurement object.

Table 8.6.4. Protection-fragility regimes and corridor interpretation.

Regime	Nodes	Interpretive meaning
High-protection	North America; Europe	High EMGI reflects income depth, centrality and absorption capacity. These nodes can carry stress without becoming the weakest systemic points.
Intermediate	East Asia-Pacific; MENA	Systemically active nodes with meaningful stress, curvature or corridor exposure but not in the lowest protection class.
Fragile	Latin America	Moderate-to-low EMGI and elevated fragility; relevant for stress sensitivity but not the primary corridor-bridge signal.
Critical-fragile	Caucasus; Sub-Saharan Africa; Central Asia; South Asia; Oceania	Low EMGI and high fragility; mechanisms differ across nodes: corridor role, high stress, weak resilience or low centrality.

Critical-fragile corridor bridge	Caucasus; Central Asia; South Asia as high-bridge critical-fragile	Fragility coincides with strategic corridor exposure, making these nodes central to corridor-risk interpretation despite smaller GDP mass in some cases.

Source: Author synthesis from EMGI, fragility and BridgeStress benchmark outputs.

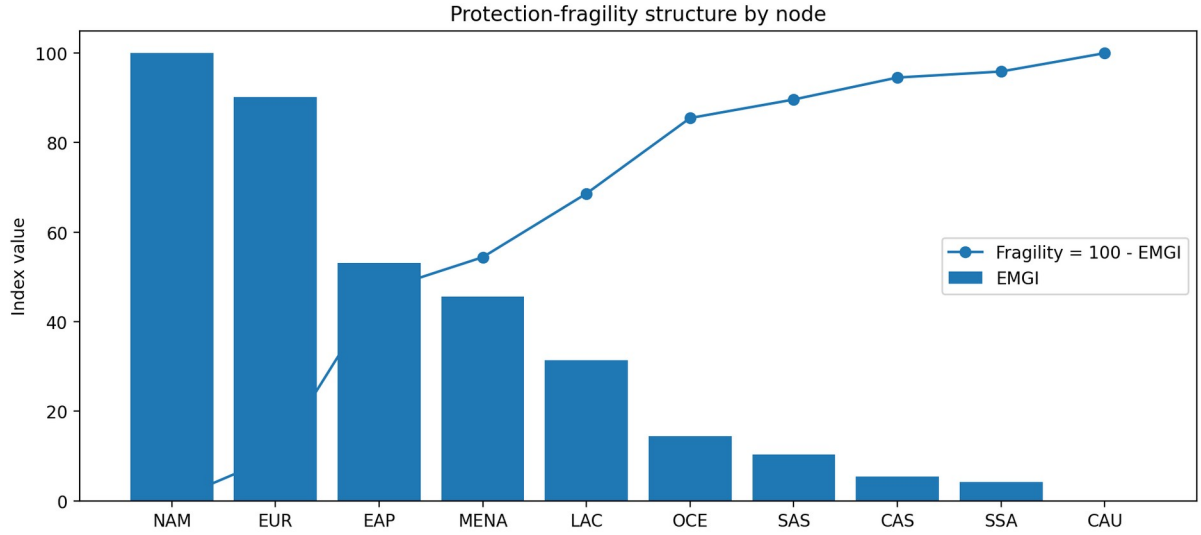


Figure 8.6.3. EMGI and fragility by node.

Source: Author visualization from the Chapter 8.5 EMGI and fragility benchmark table.

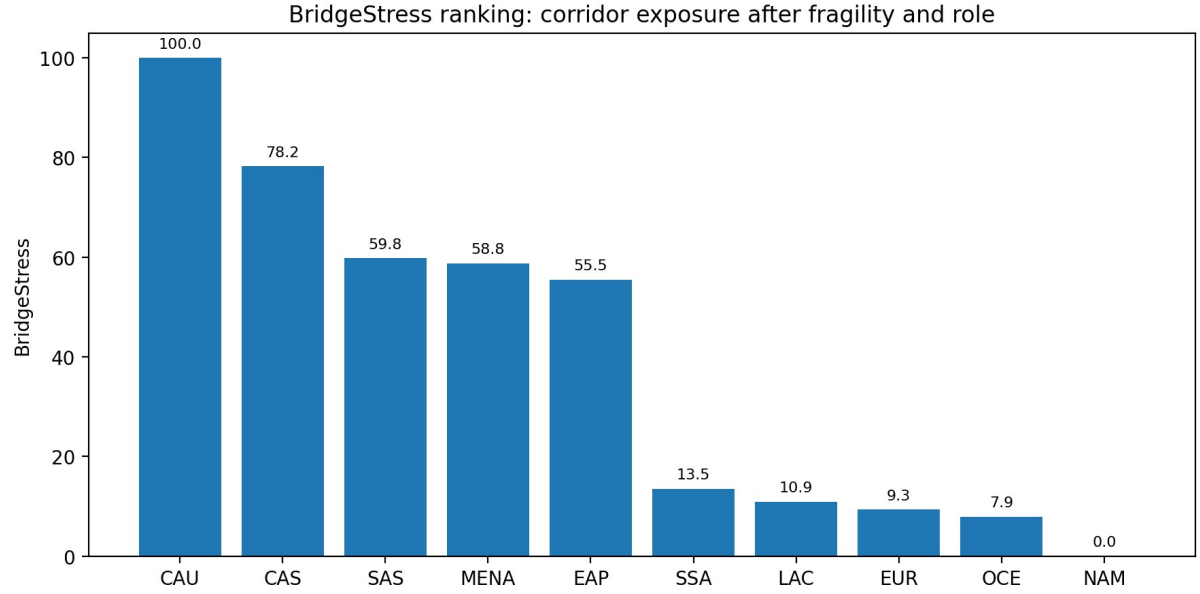


Figure 8.6.4. BridgeStress ranking and corridor exposure visibility.

Source: Author visualization from the revised BridgeStress benchmark values.

8.6.4 EMGI and Fragility as Local Protection Diagnostics

EMGI translates the system-level spectral result into local protection. It is not a welfare index, not a political ranking and not a direct GDP ranking. It is a constructed protection composite. Its components reward local spectral protection, centrality, income depth and resilience, while penalizing stress and curvature exposure. Fragility is deliberately defined as the complementary identity:

Fragility_i = 100 - EMGI_i.

This identity has interpretive advantages. It prevents the chapter from inventing a separate vulnerability scale unrelated to the protection score. It also makes the high-fragility result transparent. When the Caucasus has EMGI = 0.00, its fragility is

mechanically 100.00; when North America has EMGI = 100.00, its fragility is mechanically 0.00. The interpretive question then becomes not whether the arithmetic is valid, but why a given node occupies that protection position in the benchmark. The benchmark shows several different fragility mechanisms. The Caucasus is critical-fragile because low protective capacity coincides with high corridor exposure. Central Asia is critical-fragile because corridor role combines with limited protection. South Asia is critical-fragile because high stress and high curvature compress protection. Sub-Saharan Africa is critical-fragile because resilience and income-depth dimensions are weak. Oceania has low stress but low centrality and limited network position. These mechanisms should not be merged into a single narrative.

Table 8.6.5. Node-level EMGI, fragility, stress and BridgeStress interpretation.

Code	Region	EMGI	Fragility	Stress	BridgeStress	Interpretive class
NAM	North America	100.00	0.00	30.66	0.00	High-protection
EUR	Europe	90.15	9.85	47.40	9.32	High-protection
EAP	East Asia and Pacific	53.12	46.88	71.23	55.50	Intermediate
MENA	Middle East and North Africa	45.59	54.41	39.71	58.79	Intermediate
LAC	Latin America and Caribbean	31.37	68.63	26.78	10.89	Fragile
OCE	Oceania	14.50	85.50	0.00	7.90	Critical-fragile
SAS	South Asia	10.36	89.64	100.00	59.80	Critical-fragile
CAS	Central Asia	5.45	94.55	71.79	78.24	Critical-fragile
SSA	Sub-Saharan Africa	4.11	95.89	53.78	13.53	Critical-fragile
CAU	Caucasus	0.00	100.00	66.03	100.00	Critical-fragile

Source: Author synthesis from Chapter 8.5 node-level benchmark outputs.

8.6.5 BridgeStress and the Middle Corridor Reading

BridgeStress is the corridor-specific interpretive correction in Chapter 8. It addresses a weakness of ordinary network centrality. A high centrality score can identify important large nodes, but it does not necessarily identify exposed corridor bridges. A corridor bridge can be strategically important because it connects regions, routes, sea crossings, logistics interfaces and geopolitical stress channels, even if its GDP mass is limited.

The revised BridgeStress index therefore combines four ingredients: corridor exposure, corridor-role function, fragility and bounded curvature participation. Its logic can be written as a normalized interaction rather than as a simple sum:

BridgeStress_i = Normalize[CorridorExposure_i x CorridorRole_i x Fragility_i x CurvatureParticipation_i_plus].

This construction explains why the Caucasus and Central Asia dominate the bridge-stress ranking. The Caucasus receives BridgeStress = 100.00 because it combines the maximum corridor-role reading, high corridor exposure and maximum fragility. Central Asia receives BridgeStress = 78.24 because it acts as a land-corridor and Caspian-connection node while retaining high fragility. South Asia, MENA and East Asia-Pacific follow because their stress, role and curvature components make them important in the broader corridor network.

The Middle Corridor reading should remain disciplined. The model does not claim to estimate actual freight tonnage, rail throughput, customs delay or port capacity. It measures structural corridor exposure inside a finite stress-transmission graph. The policy relevance is nevertheless strong: infrastructure continuity, feeder connections, Black Sea and Caspian interfaces, energy/geopolitical channels and financing stress can turn small macroeconomic nodes into high-exposure transmission points.

Table 8.6.6. Corridor-function interpretation layer.

Regional/corridor function	Economic interpretation	Corridor role	Benchmark implication
Caucasus gateway	Small output mass; high transfer relevance	Black Sea-Caucasus-Caspian transfer function	Maximum BridgeStress; high corridor visibility
Caspian interface	Sea-crossing and rail/port continuity	Continuity between Caucasus and Central Asia	Explains why exposure is not reducible to land

			distance
Central Asia regional node	Large land-corridor and Caspian interface	East-west land bridge and Caspian connection	Second-highest BridgeStress
Europe/Black Sea demand side	High centrality and demand absorption	Destination and redistribution interface	High protection with high network importance
East Asia-Pacific origin side	High output mass and demand potential	Origin-side stress and trade mass	Strong systemic activity and curvature exposure
MENA energy-geopolitical interface	Energy, financing and geopolitical exposure	South corridor and energy-shock channel	High scenario sensitivity under geopolitical shock

Source: Author qualitative mapping from the finite global-corridor stress network.

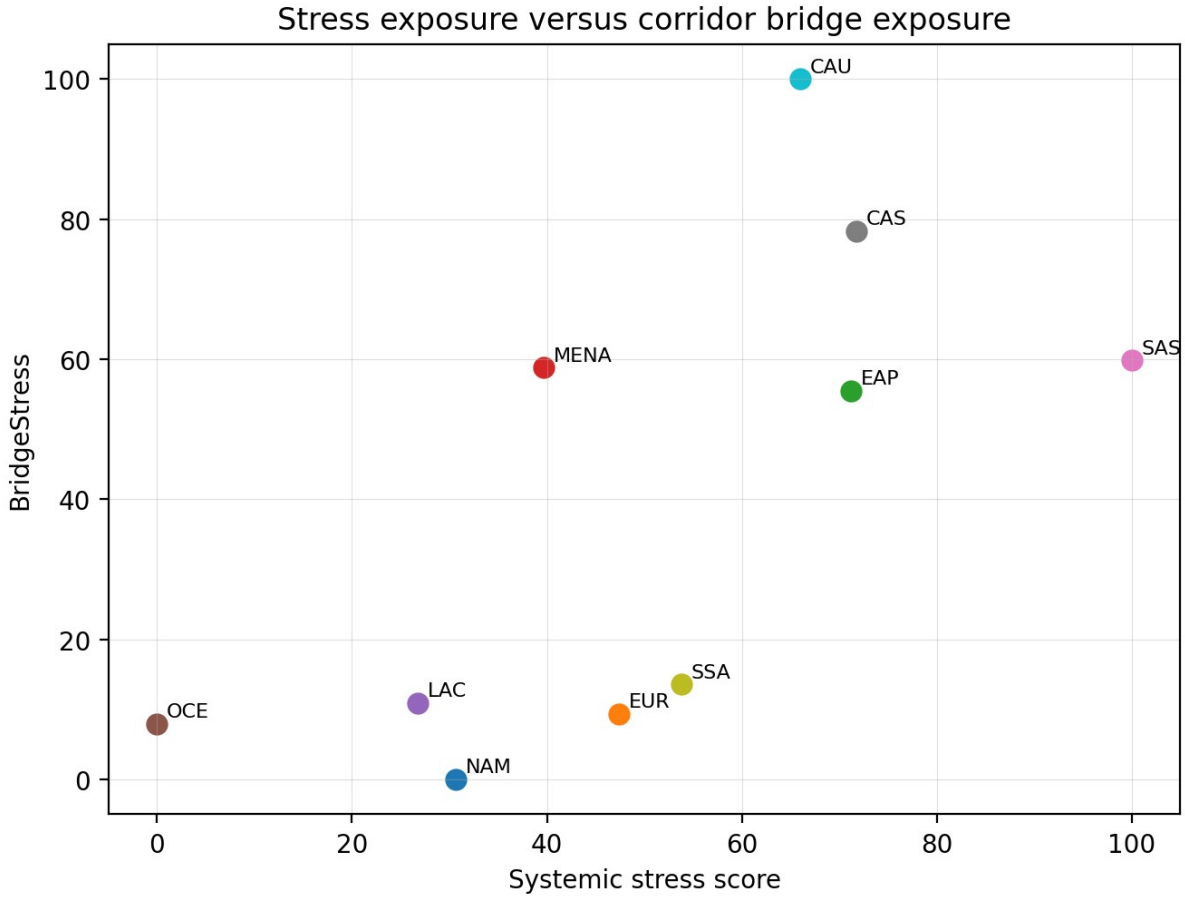


Figure 8.6.5. Stress score versus BridgeStress.
Source: Author visualization from stress-score and revised BridgeStress benchmark outputs.

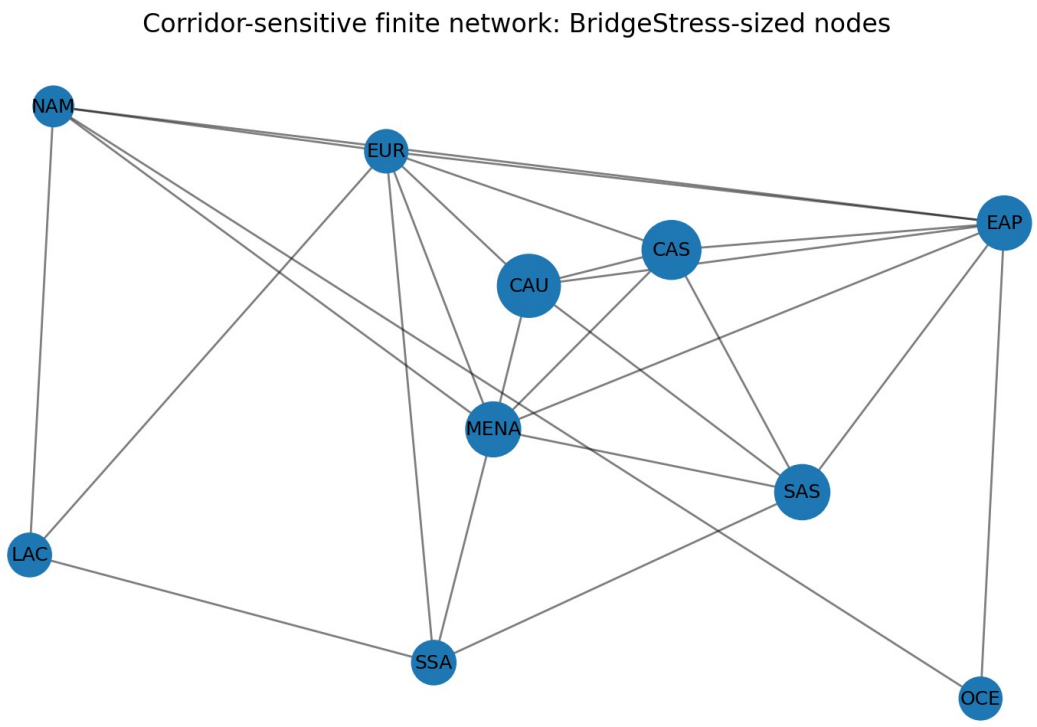


Figure 8.6.6. Corridor-sensitive finite network with BridgeStress-sized nodes.
Source: Author visualization from the ten-node, twenty-seven-edge Chapter 8 benchmark graph.

8.6.6 Curvature, Action Concentration and Corridor Exposure

The curvature-action layer explains where systemic stress becomes concentrated. In the gauge-econometric analogy, triangular curvature measures non-neutralized circulation around cycles. Yang-Mills economic action squares and aggregates this curvature. The benchmark reports total action of 2,514.0 and a top-five action concentration of 78.329 percent. This means that stress-energy is not spread uniformly across the graph. It is concentrated in a limited set of high-curvature cycles.

The interpretation is directly connected to corridor exposure. A corridor node is especially relevant when it lies near stress-bearing cycles or when its bridge role makes it sensitive to cycle-level action. If stress-energy were uniform, corridor exposure would be less analytically distinctive. The fact that action is tail-concentrated means the model should focus on the cycles and nodes that carry disproportionate stress-energy. BridgeStress performs this role at the node/corridor level.

The action result also protects the chapter from a purely scalar interpretation. A single stress score cannot show whether pressure is local, cyclic or system-wide. Curvature and action add geometry to stress. They indicate that systemic vulnerability emerges from the position of stress inside network cycles, not only from the magnitude of stress inside isolated nodes.

Table 8.6.7. Curvature-action interpretation map.

Interpretive layer	Mathematical object	Economic reading	Corridor implication
Gauge potential	A_ij	Stress differential on an oriented edge	Defines directional tension between connected nodes.
Triangular curvature	F_ijk	Non-neutralized circulation around a triangle	Identifies local cycle imbalance.
Yang-Mills action	S_YM = sum F_ijk^2	Squared stress-energy over cycles	Identifies where systemic stress is concentrated.
Top-five action share	78.329%	Tail-concentrated action geometry	High-curvature corridors deserve focused interpretation.
BridgeStress	Corridor role x fragility x curvature participation	Strategic bridge exposure	Connects cycle-level action to node-level corridor risk.

Source: Author synthesis from the gauge-potential, curvature and action methodology of Chapter 8.4 and results of Chapter 8.5.

8.6.7 Shock Scenarios: How the Threshold Is Compressed

Scenario interpretation gives the mass gap its practical meaning. Under baseline conditions, the normalized threshold is 0.1099. Under inflation/price pressure, it falls to 0.0916. Under financial-spread stress, it falls to 0.0747. Under trade/logistics corridor shock, it falls to 0.0578. Under energy/geopolitical corridor shock, it falls to 0.0420. The monotonic decline means that stronger shocks reduce the relative boundary separating local stress from systemic transmissibility.

The action result moves in the opposite direction. Economic action rises from 2,514.0 in the baseline to 5,010.0 under the energy/geopolitical corridor shock. This is not merely a numerical increase. It means the network carries more squared curvature stress-energy while the spectral threshold is compressed. A system with lower threshold and higher action is easier to disturb and more stress-concentrated once disturbed.

The scenario block remains diagnostic, not predictive. It does not claim that a specific future inflation, funding, logistics or geopolitical shock will occur. It shows how the constructed network reacts under controlled shock-amplitude assumptions. This is the correct scientific status of the result: scenario-based threshold interpretation, not causal forecasting.

Table 8.6.8. Scenario interpretation: threshold compression and action increase.

Scenario	Amplitude	lambda_1	rho	tau	Action	Mean EMGI change	Interpretation
Baseline	0.00	0.3850	3.5023	0.1099	2,514.0	0.00	Benchmark finite-network state
Inflation / price pressure	0.50	0.3343	3.6530	0.0916	2,925.0	-6.20	Moderate macro stress weakens protection
Financial-spread stress	0.75	0.2836	3.7990	0.0747	3,435.0	-10.80	Funding stress compresses threshold
Trade / logistics corridor shock	1.00	0.2334	4.0410	0.0578	4,088.0	-15.30	Corridor disruption raises systemic transmissibility
Energy / geopolitical corridor shock	1.25	0.1796	4.2790	0.0420	5,010.0	-22.40	Strongest compression and highest action

Source: Author scenario synthesis from Chapter 8.5 reported shock diagnostics.

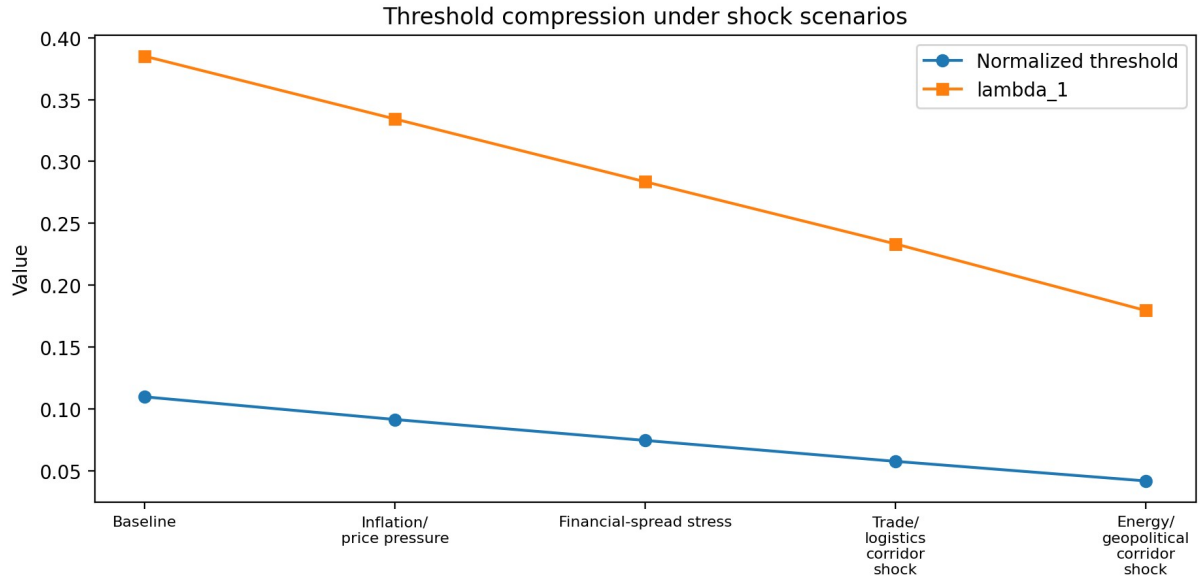


Figure 8.6.7. Threshold compression and lambda_1 decline under shocks.
Source: Author visualization from Chapter 8.5 scenario outputs.

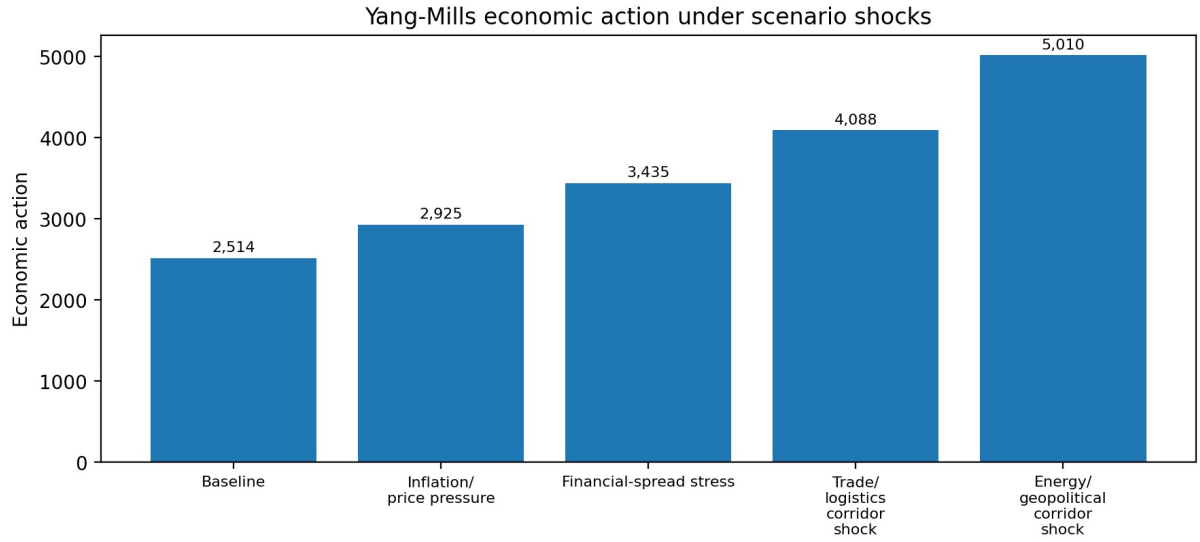


Figure 8.6.8. Yang-Mills economic action increases under shock scenarios.
Source: Author visualization from Chapter 8.5 scenario outputs.

8.6.8 Correlation Evidence and Why It Remains Diagnostic

The node-level correlation structure supports the interpretation but does not convert it into causal evidence. The Pearson and Spearman matrices show the expected deterministic relationship between EMGI and fragility; strong positive association between EMGI and resilience; and a corridor-specific association between stress and BridgeStress. This pattern is useful because it shows that the constructed indicators behave coherently. However, the benchmark has only ten nodes, so correlation results are interpreted as diagnostic association evidence.

The strongest diagnostic reading is that BridgeStress is not simply another name for EMGI. BridgeStress is positively related to stress and fragility, but negatively related to high protection. This is exactly what the index is meant to capture: exposed corridor nodes are often important because they are fragile and strategically positioned, not because they have the highest protection. The correlation matrix therefore strengthens the substantive reading while preserving the claim boundary.

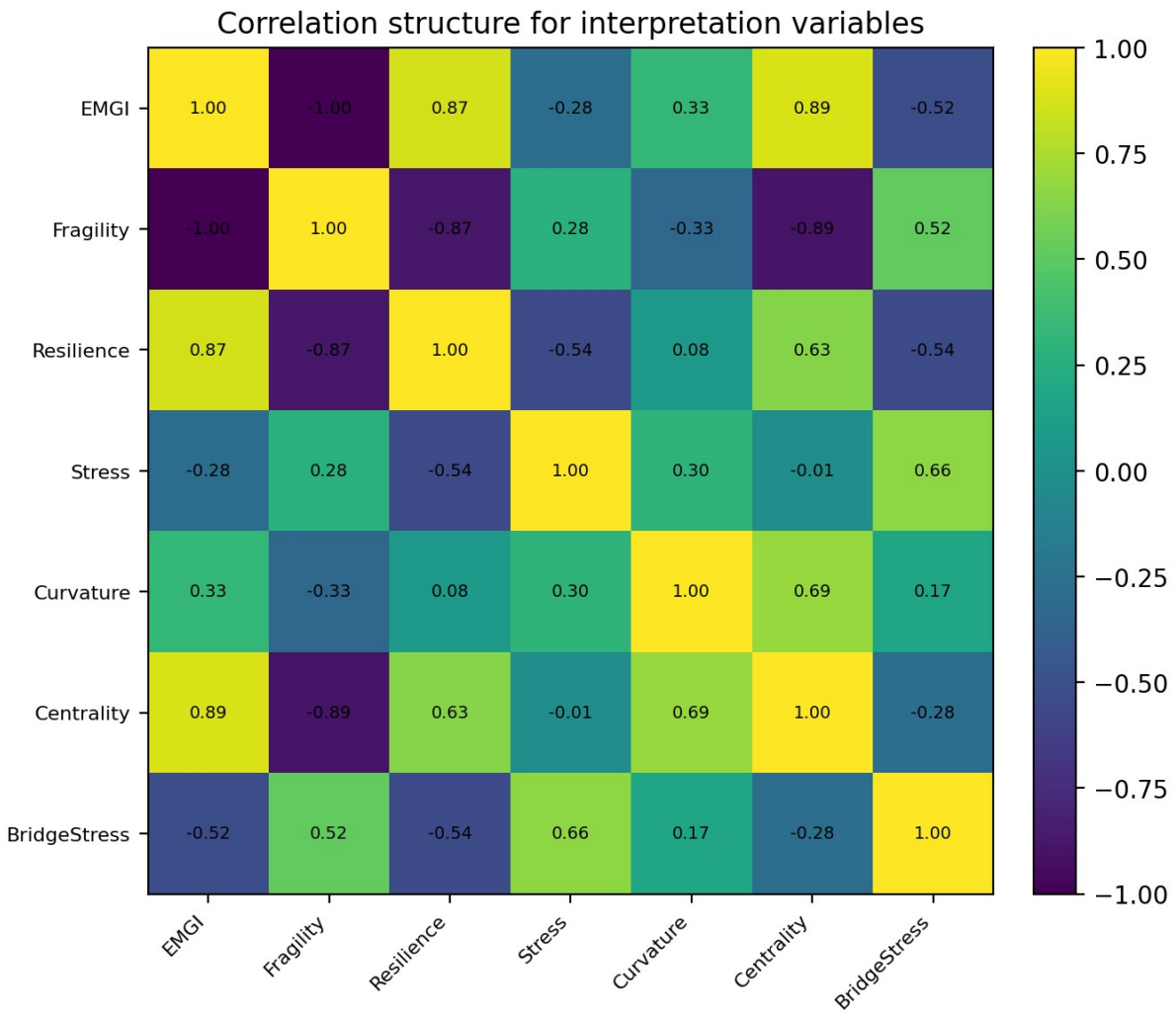


Figure 8.6.9. Correlation heatmap for interpretation variables.

Source: Author visualization from the Chapter 8 benchmark correlation matrix.

Table 8.6.9. Interpretation of the correlation layer.

Correlation object	Reported pattern	Interpretive implication	Claim status
EMGI vs fragility	Perfect negative identity by construction	Fragility is a transparent complement of protection.	Arithmetic identity; not independent evidence
EMGI vs resilience	Strong positive association	Protection and absorption capacity move together.	Diagnostic support
Stress vs BridgeStress	Positive association	Corridor bridge exposure rises with systemic stress.	Corridor diagnostic
Centrality vs EMGI	Positive association	Central nodes tend to be structurally protected, except where stress/curvature offsets protection.	Diagnostic association
BridgeStress vs EMGI	Negative association	Strategic exposure is not the same as local protection.	Substantive corridor insight

Source: Author synthesis from Pearson and Spearman diagnostic matrices.

8.6.9 Integration with the Other Six Millennium-Inspired Economic Chapters

Section 8.6 also has a monograph-level role. It does not stand alone as a technical appendix to a single article. It translates the Yang-Mills result into the shared language of the book: flow, topology, curvature, rank, spectral diagnostics, optimization

and claim discipline. The chapter is therefore one member of a seven-problem measurement architecture rather than a separate paper pasted into a monograph.

The Yang-Mills chapter contributes the shock-threshold grammar of the monograph. The Poincare/Ricci chapter contributes pressure-curvature-smoothing interpretation. The Hodge chapter contributes hierarchy, curl imbalance and circulation. The Navier-Stokes chapter contributes flow, pressure, friction and closure. The BSD chapter contributes local-to-global structural rank. The Riemann-zeta chapter contributes spectral regime and forecasting discipline. The P-vs-NP chapter contributes computational robustness and claim-boundary discipline. Chapter 8.6 is therefore the place where systemic shock thresholds become interpretable in the same language as the other six chapters.

Table 8.6.10. Cross-seven-problem integration of the Yang-Mills interpretation.

Book chapter	Mathematical inspiration	Main economic object	Connection to Section 8.6
Chapter 5	Poincare/Ricci/Perelman	Inequality pressure, curvature and smoothing capacity	Shares curvature and topology language, but applies it to inequality deformation.
Chapter 6	Hodge theory	Gradient, curl and harmonic macro-flow decomposition	Supports the reading that cycles and circulation matter beyond GDP hierarchy.
Chapter 7	Navier-Stokes	Liquidity velocity, pressure, friction and closure	Shares systemic-stress and shock-propagation logic.
Chapter 8	Yang-Mills	Gauge potential, curvature, action and mass gap	Provides the finite-network shock-threshold result interpreted here.
Chapter 9	Birch-Swinnerton-Dyer	Local-to-global structural rank and corridor stress	Shares local-to-global and BridgeStress logic.
Chapter 10	Riemann zeta	Inflation pressure, spectral cycles and forecast validation	Shares spectral-diagnostic and shock-regime discipline.
Chapter 11	P vs NP	Optimization complexity, search and robustness	Shares claim-boundary and robustness architecture.

Source: Author monograph synthesis from the seven uploaded source documents and the Chapter 8 conversion plan.

8.6.10 Policy, Corridor and Research Implications

The policy interpretation is not that the model directly recommends a particular route, infrastructure investment or geopolitical strategy. The benchmark does not estimate route-level freight flows or costs. Its policy-relevant contribution is more structural: it shows how corridor exposure can be measured separately from output mass and how threshold compression can be interpreted when shocks intensify.

For corridor policy, the implication is that small bridge nodes require analytical attention even when their GDP share is small. A low-mass corridor node can matter because it transmits shocks between larger systems. This has direct relevance for the Black Sea-Caucasus-Caspian-Central Asia interface. The model tells the analyst to examine transfer continuity, feeder resilience, port/rail coordination, financing stress and energy/geopolitical sensitivity, rather than treating the corridor as a peripheral detail.

For macroprudential and systemic-risk research, the implication is that spectral thresholds and action concentration can complement conventional macro indicators. GDP growth, inflation, income depth and trade exposure remain essential, but they are not sufficient to identify the local-to-systemic boundary. The finite-network mass gap adds a measurable threshold; EMGI adds local protection; BridgeStress adds corridor exposure; and scenario diagnostics add shock-compression logic.

Table 8.6.11. Policy and research implication boundary.

Implication area	What the benchmark supports	What remains outside the current evidence
Systemic-risk monitoring	Use tau, action and EMGI as network diagnostics.	Real-time crisis prediction and causal forecasting.
Corridor policy	Separate bridge exposure from GDP mass and ordinary centrality.	Direct estimates of route throughput, cost or customs delays.
Infrastructure resilience	Prioritize nodes where low protection	Specific investment ranking without

	and high bridge exposure coincide.	cost-benefit data.
Macroeconomic surveillance	Track shock scenarios that compress the local-to-systemic threshold.	Country-level causal claims before N = 1,500 panel completion.
Research replication	Audit matrices, edge lists, formulas, seeds and outputs.	Universal validity independent of regional definition.

Source: Author synthesis from benchmark interpretation and claim-boundary logic.

8.6.11 Evidence Gate: What the Interpretation Establishes and What It Does Not

The interpretation must remain claim-gated. The benchmark establishes a strong finite-network measurement result. It does not solve a mathematical theorem, does not prove a causal law and does not finalize country-level econometric validation. This boundary is not a weakness; it is the condition that makes the chapter publishable and reviewer-safe. The chapter is ambitious because it introduces a new gauge-econometric language. It is scientifically disciplined because it limits that language to the evidence actually produced.

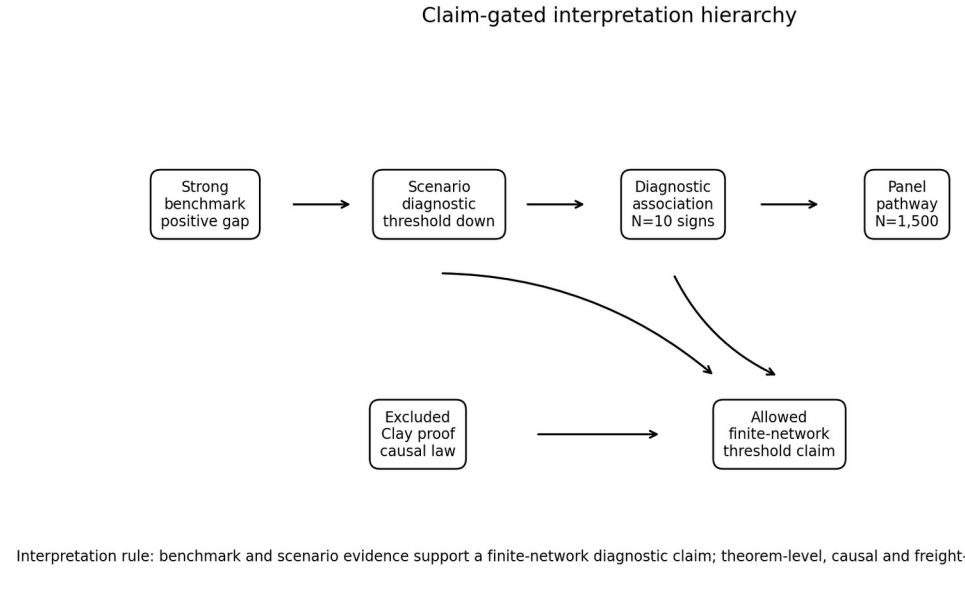


Figure 8.6.10. Claim-gated interpretation hierarchy.
Source: Author synthesis from the Chapter 8 evidence-status architecture.

Table 8.6.12. Claim-boundary matrix for Section 8.6.

Allowed statement	Not allowed statement	Reason
The finite stress-weighted benchmark has lambda_1 = 0.3850.	The Clay Yang-Mills mass-gap problem is solved.	The object is a finite weighted graph, not continuum quantum gauge theory.
The normalized threshold tau = 0.1099 measures a finite-network transition boundary.	The threshold predicts exact future crisis timing.	Scenario diagnostics are structural experiments, not forecasts.
EMGI ranks local structural protection.	EMGI is a welfare, political or GDP ranking.	EMGI is a constructed model index.
BridgeStress identifies strategic corridor exposure.	BridgeStress proves actual freight volumes or route dominance.	The index measures structural exposure inside the benchmark graph.
The N = 1,500 layer can validate further.	The N = 1,500 validation results are already final.	The panel is specified but not numerically closed in the benchmark.

Source: Author claim-boundary synthesis for the monograph version of Chapter 8.

8.6.12 Section Conclusion

Section 8.6 interprets the Yang-Mills economic benchmark as a finite-network threshold model of systemic shock transmission and corridor exposure. The positive mass gap means that the benchmark graph has a measurable spectral separation. The normalized threshold tau = 0.1099 gives that separation a relative scale. EMGI and fragility translate system-level protection into local node-level regimes. BridgeStress makes strategically exposed corridor nodes visible even when their GDP mass is small. Curvature and action show that stress-energy is concentrated in high-curvature cycles rather than uniformly distributed across the graph.

The strongest substantive conclusion is that systemic vulnerability is relational. It is produced by the interaction of mass, stress, resilience, centrality, curvature and corridor role. North America and Europe illustrate protected structural capacity. The Caucasus and Central Asia illustrate bridge exposure under fragility. South Asia illustrates high stress and curvature pressure. MENA illustrates energy/geopolitical corridor sensitivity. East Asia-Pacific illustrates high systemic activity combined with stress and curvature. The benchmark therefore turns a complex corridor-risk narrative into an auditable measurement structure.

The strongest methodological conclusion is equally important: the chapter remains bounded. It supports a finite-network gauge-econometric interpretation, not a theorem proof or causal law. The next section, 8.7, can therefore build scenario simulations and local-to-systemic transition logic on a disciplined foundation, while 8.8 reserves stronger external and causal claims for the completed N = 1,500 validation pathway.

8.7. Scenario Simulations and Local-to-Systemic Transition

This section converts the finite-network Yang-Mills economic mass-gap benchmark into a controlled scenario-simulation and transition-threshold analysis. Its purpose is not to forecast a particular crisis event. Its purpose is to show how the reported benchmark behaves when inflation, financial-spread, trade/logistics, and energy/geopolitical corridor shocks are injected into the stress-weighted network. The section therefore translates the static positive mass-gap result into an operational question: when does a local or corridor-specific disturbance become systemically transmissible inside the constructed global-corridor stress network?

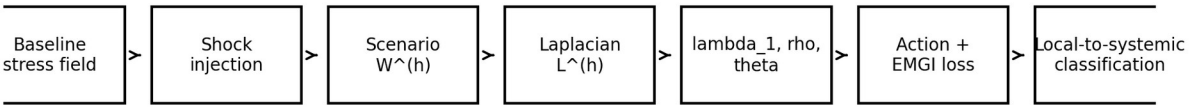
The chapter remains strictly bounded. All scenario outputs are deterministic benchmark simulations based on the disclosed ten-node, twenty-seven-edge stress network and its author-calculated shock rules. They support threshold interpretation, stress-amplification analysis, and corridor exposure diagnostics; they do not establish causal prediction, observed freight-throughput measurement, or final country-panel validation.

Table 8.7.1. Function of Section 8.7 inside Chapter 8.

Analytical layer	Role in 8.7	Permitted claim
Baseline spectral result	Provides the initial local-to-systemic boundary: lambda_1=0.3850, rho=3.5023, theta=0.1099.	Finite-network benchmark threshold.
Scenario simulations	Inject stress into price, financial, logistics, and energy/geopolitical channels, then recompute spectral and action outputs.	Descriptive scenario diagnostic.
Action amplification	Measures whether stress-energy becomes more concentrated as shock amplitude increases.	Curvature/action response under controlled assumptions.
EMGI deterioration	Tracks mean loss of node-level protection under each shock.	Protection-fragility interpretation, not causal welfare loss.
Propagation simulation	Uses row-normalized W^S and decay parameter rho=0.85 to evaluate retained and outside-origin shock mass.	Transmissibility geometry under benchmark propagation rule.
Claim boundary	Separates benchmark scenario evidence from causal country-panel validation.	Panel-ready, not final causal proof.

Source: Author synthesis for the monograph chapter based on the Yang-Mills source manuscript.

Figure 8.7.1. Scenario-simulation pipeline for local-to-systemic transition



Source: Author methodological visualization from the Chapter 8.7 scenario-simulation sequence.

8.7.1. Analytical Purpose: Moving from Static Mass Gap to Shock Transition

The corrected Chapter 8 benchmark establishes a positive finite-network economic mass gap. In a static reading, this means that the stress-weighted graph Laplacian contains a first positive eigenvalue separating the connected zero mode from the first transmissible stress mode. Section 8.7 asks the next question: how stable is this boundary when the network is subjected to controlled shocks?

The section therefore treats lambda_1 not as a decorative mathematical number but as a transition boundary. If the post-shock lambda_1 remains positive but falls materially, the network has not collapsed in the finite-graph sense, but its protective separation has compressed. If the spectral radius rises at the same time, the upper diffusion scale expands. If the normalized threshold theta=lambda_1/rho falls, smaller disturbances can cross the model boundary into systemic transmissibility. If Yang-Mills economic action rises, the scenario produces more stress-energy inside triangular corridor cycles. If EMGI deteriorates, local protection is lost at the node level.

The central interpretive logic is therefore multidimensional: local-to-systemic transition is not inferred from one indicator alone. It is identified by the joint movement of lambda_1, rho, theta, action, EMGI and spillover geometry. This is why Section 8.7 belongs after the results and interpretation sections. It uses their benchmark outputs, but converts them into a controlled stress-transition experiment.

8.7.2. Scenario Equations and Recalculation Rules

The scenario layer modifies the baseline stress network through a shock amplitude h and a shock-exposure matrix Xi. The following equations define the recalculation logic used in the chapter. The equations are written as economic finite-network diagnostics, not as physical field equations.

(8.7.1) Stress_i^(h) = Stress_i + h * ShockLoad_i

(8.7.2) W^(h) = W ∘ (1 + h * Xi), where ∘ denotes elementwise multiplication.

(8.7.3) D_ii^(h) = sum_j W_ij^(h)

(8.7.4) L^(h) = D^(h) - W^(h)

(8.7.5) lambda_1^(h) = min{lambda > 0 : lambda is an eigenvalue of L^(h)}

(8.7.6) rho^(h) = max_j |lambda_j(W^(h))|

(8.7.7) theta^(h) = lambda_1^(h) / rho^(h)

(8.7.8) Action^(h) = sum_{triangles ijk} omega_ijk * (curl_ijk^(h))^2

(8.7.9) Compression_lambda^(h) = 100 * [lambda_1^(0) - lambda_1^(h)] / lambda_1^(0)

(8.7.10) Compression_theta^(h) = 100 * [theta^(0) - theta^(h)] / theta^(0)

The formulas create a direct bridge between method and interpretation. Formula (8.7.1) changes node stress. Formula (8.7.2) changes edge exposure. Formulas (8.7.3)-(8.7.7) recalculate the spectral threshold. Formula (8.7.8) recalculates curvature-action stress energy. Formulas (8.7.9)-(8.7.10) convert post-shock values into interpretable compression percentages.

Table 8.7.2. Shock-injection scenarios and calibration logic.

Scenario	Operational shock variable	Benchmark amplitude	Interpretation
Inflation / price-pressure shock	Increase in stress score	0.50	Moderate macro price pressure; expected to weaken but not erase

			protection.
Financial-spread shock	Edge stress increase	0.75	Funding stress; expected to compress spectral protection materially.
Trade / logistics corridor shock	Corridor edge-friction increase	1.00	Corridor disruption; expected to make CAS/CAU more visible.
Energy / geopolitical corridor shock	Caucasus/CAS/MENA edge stress	1.25	Systemic corridor stress; expected to produce strongest threshold compression.

Source: Author formulation based on the stress-score and corridor-friction variables in the Yang-Mills source manuscript.

8.7.3. Baseline Boundary Before Shock Injection

Before shocks are injected, the model has a normal connected state lambda_0=0.0000 and a first positive stress mode lambda_1=0.3850. The spectral radius is 3.5023, and the normalized transition threshold is theta=0.1099. The baseline Yang-Mills economic action equals 2,514.0. This baseline is the reference point for every scenario comparison in Section 8.7.

The baseline should be read as a finite-network threshold, not as a universal global-crisis trigger. It is a property of the constructed ten-node, twenty-seven-edge stress network. Its interpretive value is that it supplies a common denominator: every shock can be compared against the same spectral and action boundary.

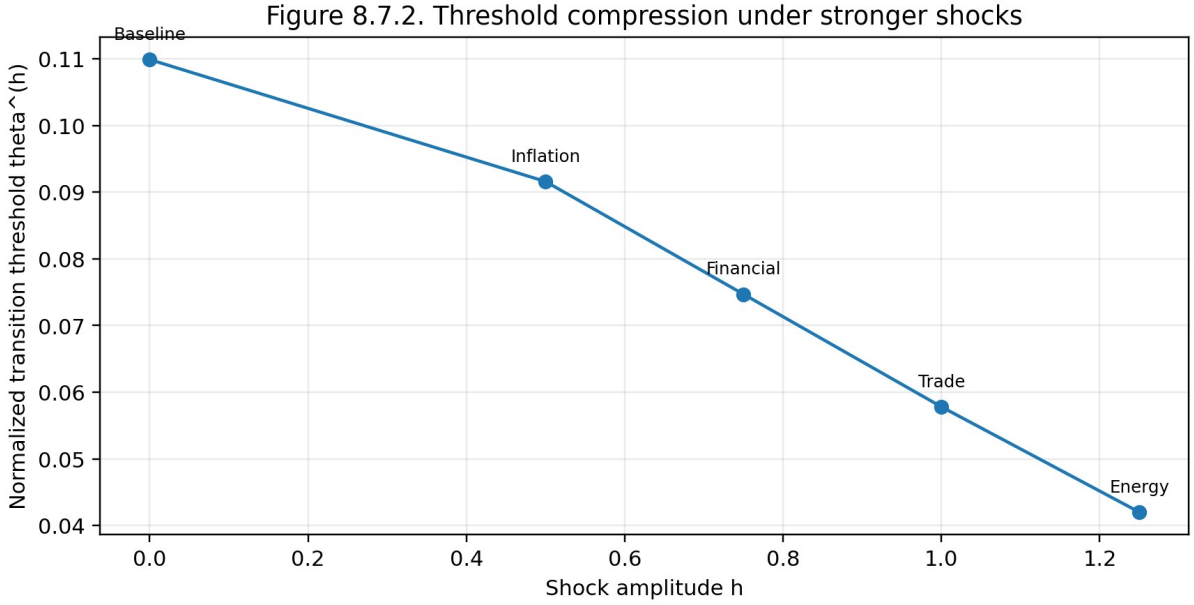
Table 8.7.3. Full scenario-output matrix.

Scenario	h	lambda_1^(h)	rho^(h)	theta^(h)	Action^(h)	Mean EMGI change	Top spillover
Baseline	0.000	0.3850	3.5023	0.1099	2,514.0	0.00	EAP / MENA
Inflation / price-pressure	0.500	0.3343	3.6529	0.0916	2,925.0	-6.20	EAP
Financial-spread stress	0.750	0.2836	3.7989	0.0747	3,435.0	-10.80	EAP
Trade / logistics corridor shock	1.000	0.2334	4.0413	0.0578	4,088.0	-15.30	CAS
Energy / geopolitical corridor shock	1.250	0.1796	4.2795	0.0420	5,010.0	-22.40	MENA

Source: Author scenario simulations from the stress-weighted Yang-Mills benchmark network.

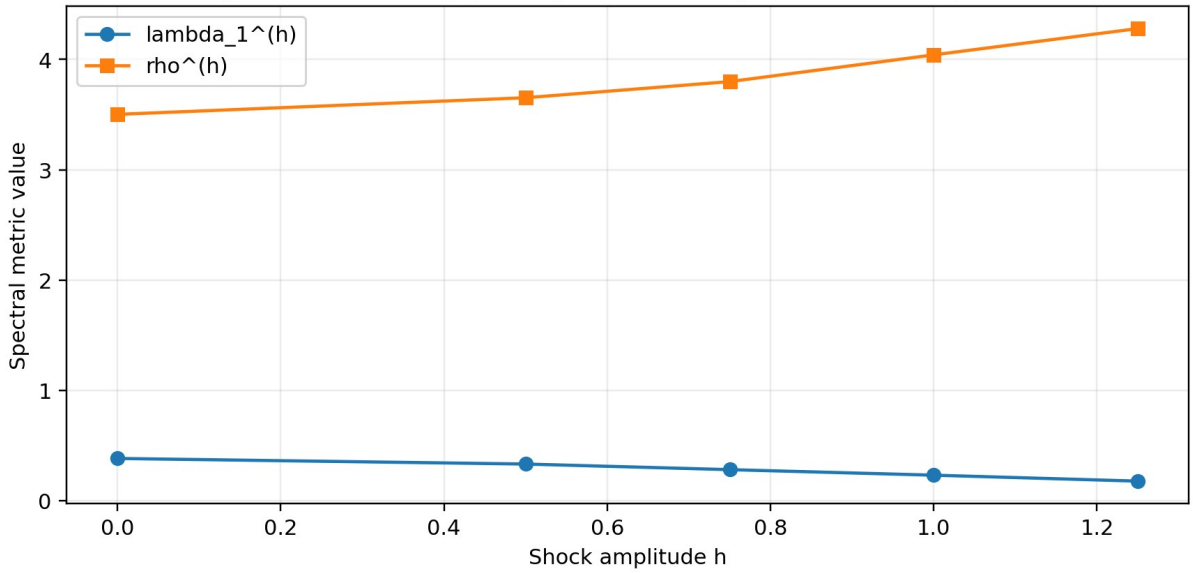
Table 8.7.3 shows a monotonic and economically coherent pattern. As scenario amplitude increases, lambda_1 falls, rho rises, theta falls, action rises and mean EMGI deteriorates. This combination is stronger than a single-threshold result because it shows simultaneous spectral compression, diffusion-scale expansion, curvature-energy amplification and local-protection loss.

Figure 8.7.2. Threshold compression under stronger shocks



Source: Author visualization from Table 8.7.3.

Figure 8.7.3. Mass-gap compression and spectral-radius expansion



Source: Author visualization from Table 8.7.3.

8.7.4. Threshold Compression: The Core Local-to-Systemic Result

The core scenario result is threshold compression. The normalized threshold falls from 0.1099 in the baseline to 0.0916 under inflation/price pressure, 0.0747 under financial-spread stress, 0.0578 under trade/logistics corridor shock and 0.0420 under energy/geopolitical corridor shock. This means that the model requires a smaller additional disturbance to cross from local stress into systemic transmissibility as the scenario becomes more corridor-intensive.

The result is not that the system loses all spectral protection. Even in the most severe scenario, lambda_1 remains positive at 0.1796. The stronger interpretation is more precise: spectral protection survives but is sharply compressed. The local-to-systemic boundary becomes thinner, and the system becomes easier to activate through external or corridor stress.

Table 8.7.4. Scenario compression and amplification diagnostics.

Scenario	lambda compression (%)	rho increase (%)	threshold compression (%)	action increase (%)	Mean EMGI loss
Baseline	0.00	0.00	0.00	0.00	-0.00
Inflation / price-	13.17	4.30	16.65	16.35	6.20

pressure					
Financial-spread stress	26.34	8.47	32.03	36.63	10.80
Trade / logistics corridor shock	39.38	15.39	47.41	62.61	15.30
Energy / geopolitical corridor shock	53.35	22.19	61.78	99.28	22.40

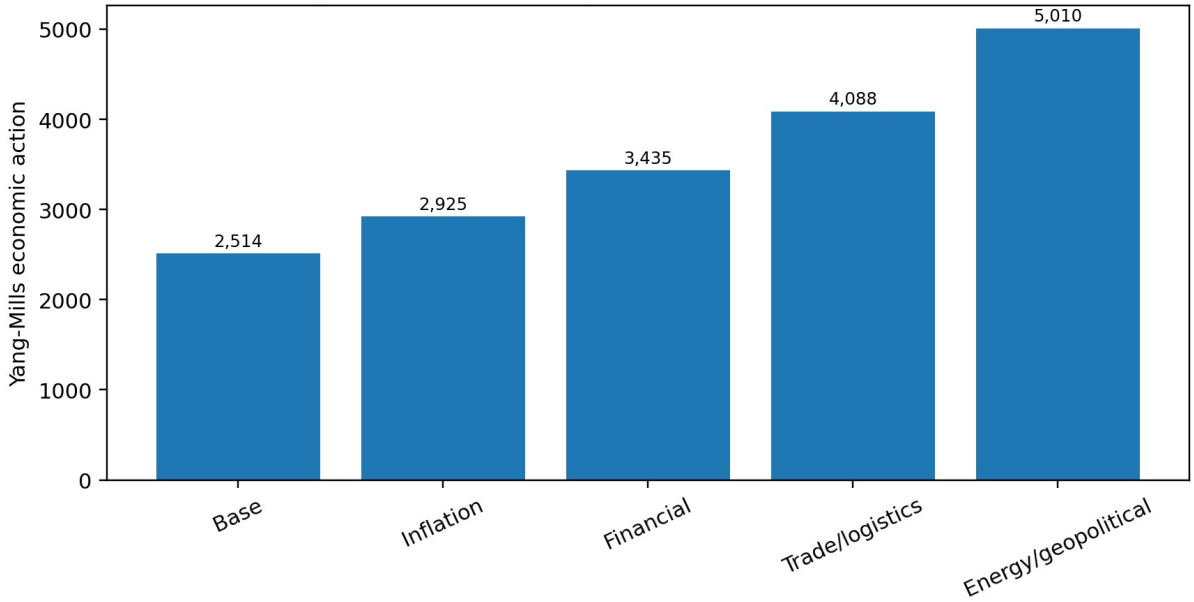
Source: Author calculations from the scenario-output matrix. Baseline values are included as zeros by construction.

8.7.5. Action Amplification and Stress-Energy Concentration

The Yang-Mills economic action layer gives the scenario block a second diagnostic dimension. If the mass gap tells where the transition boundary lies, action tells how much stress energy is carried by the cycle field after the shock. The action result is monotonic: 2,514.0 at baseline, 2,925.0 under inflation/price pressure, 3,435.0 under financial-spread stress, 4,088.0 under trade/logistics disruption and 5,010.0 under energy/geopolitical corridor shock.

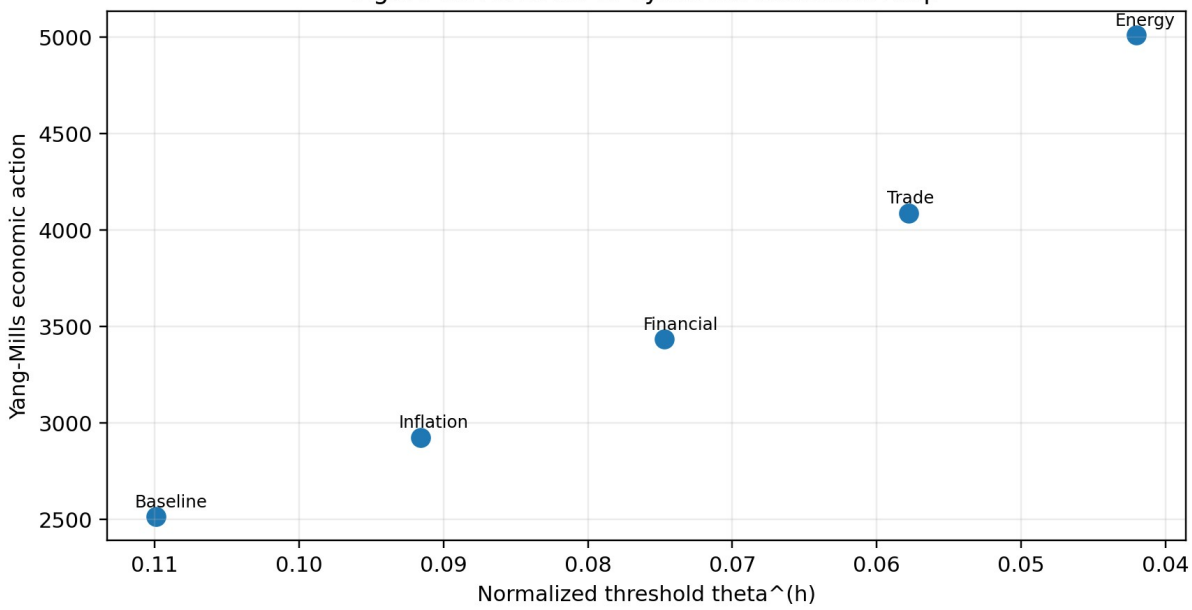
This means that scenario severity does not only lower the threshold. It also raises the squared-curvature stress-energy carried by the network. Under the energy/geopolitical corridor shock, action increases by 99.28 percent relative to the baseline. In substantive terms, the strongest corridor shock nearly doubles stress-energy while reducing the normalized threshold by more than 61 percent. This is the clearest numerical expression of local-to-systemic transition in the chapter.

Figure 8.7.4. Action amplification under scenario shocks



Source: Author visualization from Table 8.7.3.

Figure 8.7.6. Local-to-systemic transition map



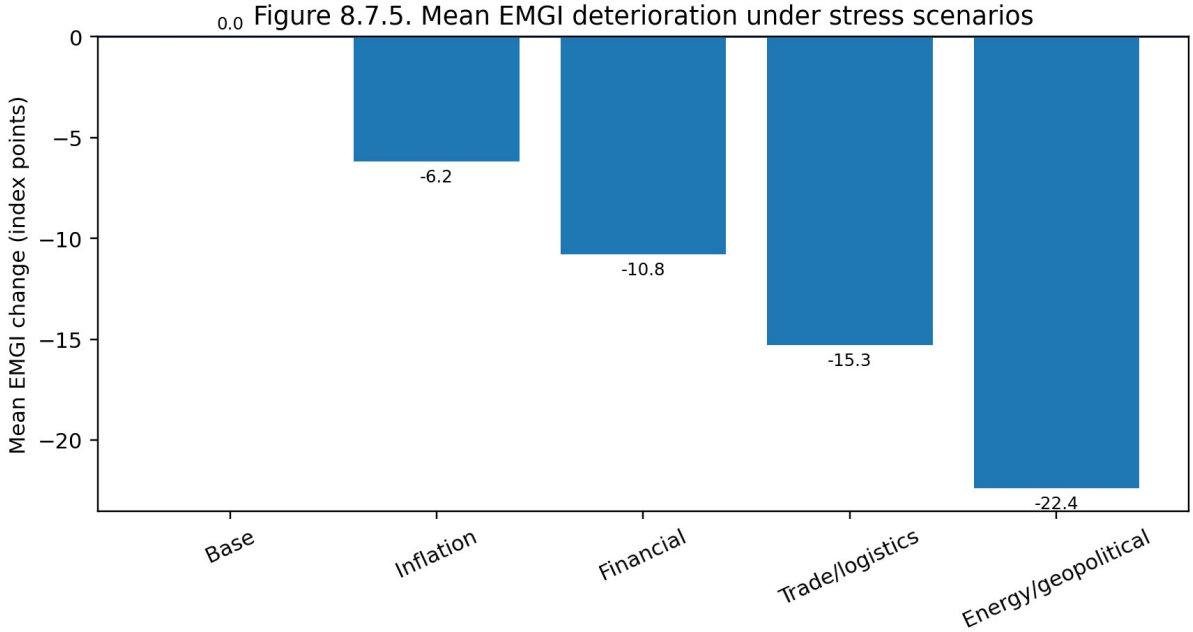
Source: Author visualization from Tables 8.7.3 and 8.7.4.

8.7.6. EMGI Deterioration and Fragility Transmission

The mean EMGI-change column translates system-level compression into node-level protection loss. Under inflation/price pressure, mean EMGI declines by 6.20 index points. Under financial-spread stress, the decline reaches 10.80 points. Under trade/logistics corridor shock, it reaches 15.30 points. Under energy/geopolitical corridor stress, it reaches 22.40 points. The direction is consistent with the interpretation that stronger shocks reduce local structural protection while increasing the probability that fragile nodes become transmission interfaces.

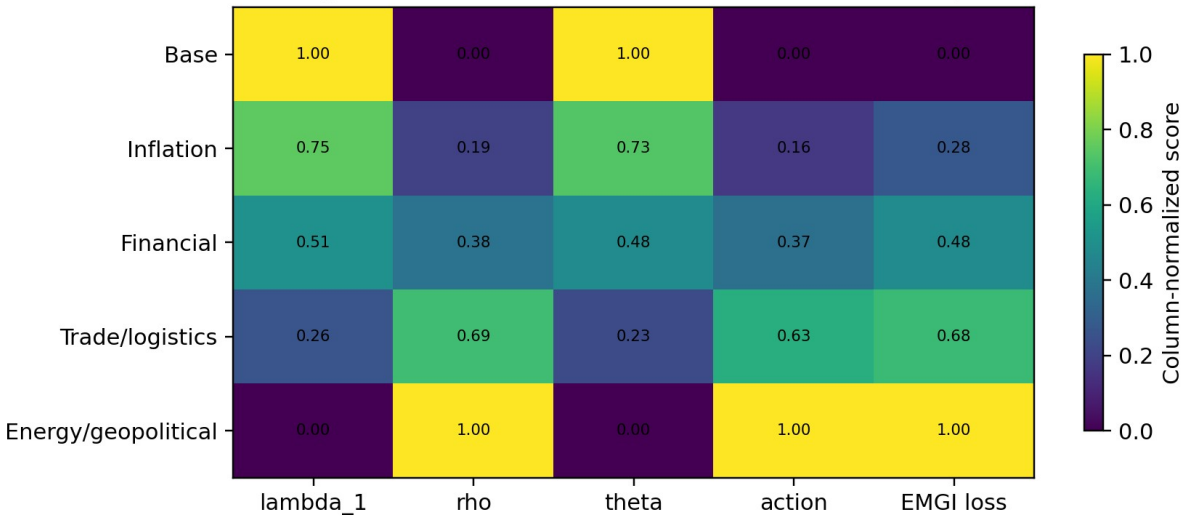
The EMGI result is especially important because it prevents the scenario block from remaining purely spectral. A falling lambda_1 could be interpreted as an abstract graph-theoretic result. A falling EMGI means that the spectral result is mirrored by deteriorating node-level protection. The chapter therefore reads threshold compression and EMGI loss together: one is the system boundary, the other is the local protection layer.

0.0 Figure 8.7.5. Mean EMGI deterioration under stress scenarios



Source: Author visualization from Table 8.7.3.

Figure 8.7.9. Normalized scenario-metric heatmap



Source: Author normalized display from the scenario-output matrix.

8.7.7. Scenario-Specific Interpretive Readings

Table 8.7.5. Scenario-specific local-to-systemic interpretation.

Scenario	Local shock channel	Systemic transition reading	Corridor meaning
Inflation / price-pressure	Macro price stress enters node stress scores.	lambda_1 falls by 13.16%, theta falls by 16.71%, action rises by 16.35%.	High-mass/high-connectivity channel EAP dominates, so the shock remains more macro-systemic than corridor-specific.
Financial-spread stress	Funding stress enters edge-stress relations.	lambda_1 falls by 26.35%, theta falls by about 32%, action rises by 36.64%.	EAP remains the leading spillover target, but protection loss becomes broader.
Trade / logistics corridor shock	Corridor edge friction rises.	lambda_1 falls by 39.38%, theta falls by 47.43%, action rises by 62.61%.	Central Asia and Caucasus become more visible because logistics disruption directly affects corridor transmission.
Energy / geopolitical corridor shock	Caucasus/CAS/MENA corridor-edge stress rises.	lambda_1 falls by 53.34%, theta falls by 61.79%, action rises by 99.28%.	MENA dominates as energy-geopolitical interface, while CAS and CAU remain key corridor bridge channels.

Source: Author interpretive synthesis from Tables 8.7.3 and 8.7.4.

The scenario sequence becomes progressively more corridor-specific. The inflation scenario is a broad macro-stress experiment. The financial scenario adds funding pressure. The trade/logistics scenario directly activates corridor friction. The energy/geopolitical scenario combines corridor position with energy and geopolitical exposure. This progression explains why the strongest results appear under the energy/geopolitical corridor shock.

8.7.8. Shock Propagation by Origin Node

The scenario-output block is complemented by a shock-propagation simulation. The rule is x_{t+1}=rho W^S x_t, with rho=0.85. This rule uses the row-normalized stress-weighted network and a decay parameter so that the simulation measures transmissibility rather than unlimited amplification.

(8.7.11) x_{t+1} = rho W^S x_t, with rho = 0.85 in the benchmark propagation simulation.

Table 8.7.6. Four-step shock propagation by origin node.

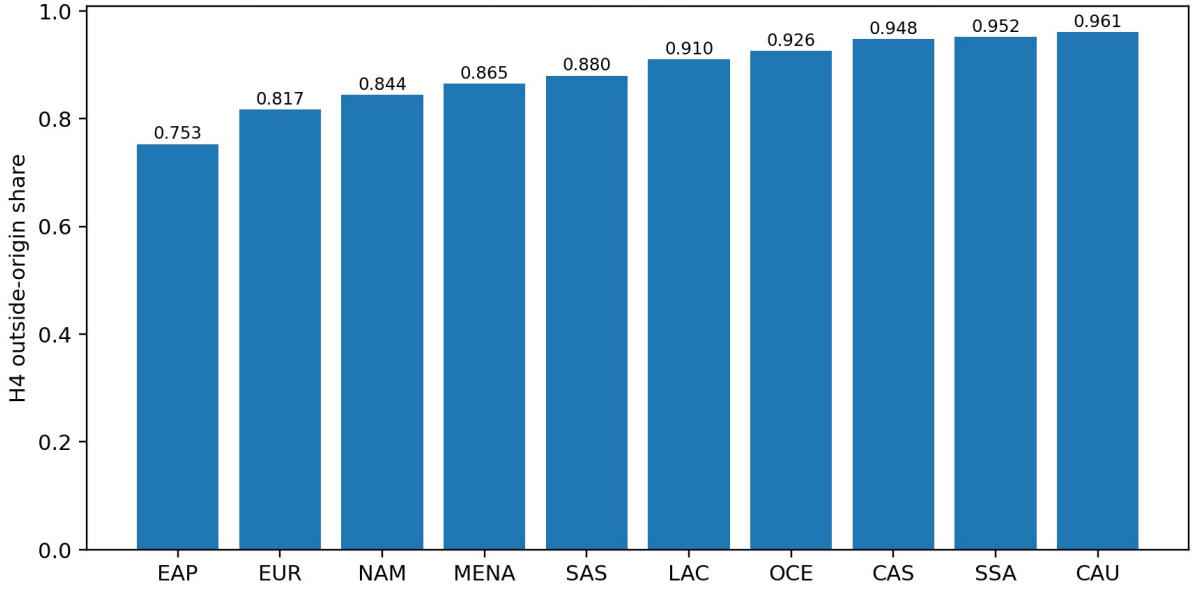
Origin	H4 total	H4 origin-	H4 outside-	Top	Top	H4 entropy

	retained	retained	origin share	spillover node	spillover intensity	
EAP	0.522	0.129	0.753	EUR	0.077	2.128
NAM	0.522	0.082	0.844	EAP	0.097	2.156
EUR	0.522	0.096	0.817	EAP	0.094	2.153
LAC	0.522	0.047	0.910	EAP	0.114	2.140
SAS	0.522	0.062	0.880	EUR	0.094	2.153
MENA	0.522	0.070	0.865	EAP	0.108	2.152
SSA	0.522	0.025	0.952	EAP	0.109	2.150
OCE	0.522	0.039	0.926	EAP	0.094	2.155
CAS	0.522	0.027	0.948	EAP	0.101	2.157
CAU	0.522	0.020	0.961	EAP	0.118	2.144

Source: Author simulations from the row-normalized stress-weighted network.

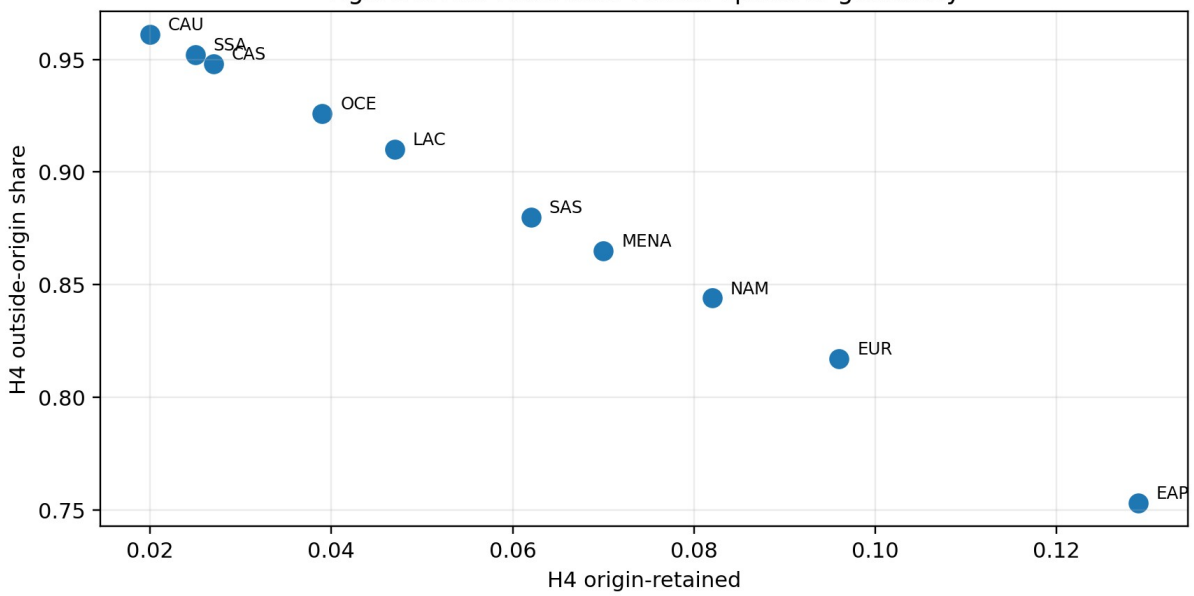
The propagation table shows that outside-origin shares are high across all origins, but they are especially high for the Caucasus, Sub-Saharan Africa and Central Asia. This does not mean that those nodes are the largest economies. It means that when a shock is injected at those origins, a high share of retained shock mass leaves the origin under the benchmark propagation rule. This is the numerical version of the corridor-exposure argument.

Figure 8.7.7. Four-step shock propagation outside the origin node



Source: Author visualization from Table 8.7.6.

Figure 8.7.8. Retention-versus-spillover geometry



Source: Author visualization from Table 8.7.6.

8.7.9. Corridor-Specific Local-to-Systemic Mechanism

The local-to-systemic mechanism is clearest in the corridor nodes. The Caucasus and Central Asia do not dominate output mass, but they occupy positions where corridor exposure, fragility and triangular curvature participation interact. This is why BridgeStress is analytically necessary. Without a corridor-specific index, a GDP-only framework would treat the Caucasus and Central Asia as marginal. The Yang-Mills stress-network framework instead asks whether they transmit stress between larger systems.

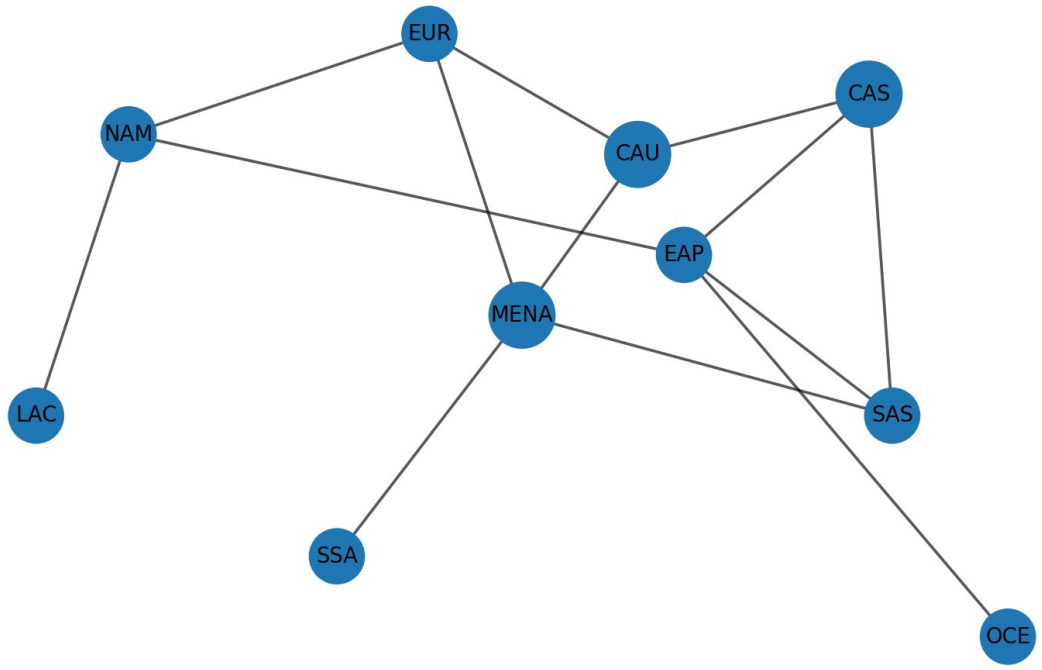
The scenario results support this reading. The trade/logistics corridor shock lowers theta to 0.0578 and identifies Central Asia as the leading post-shock spillover channel. The energy/geopolitical corridor shock lowers theta to 0.0420 and identifies MENA as the leading energy-geopolitical interface, while the corridor bridge layer keeps Caucasus and Central Asia analytically visible. The result is not a statement about exact observed freight volumes. It is a structural measurement claim: corridor position can transform small output mass into systemic exposure.

Table 8.7.7. Corridor-function interpretation layer for local-to-systemic transition.

Corridor component	Local role	Systemic role
Caucasus regional gateway	Small output mass but high transfer relevance.	Black Sea-Caucasus-Caspian transfer function; maximum BridgeStress in the benchmark.
Caspian interface	Sea-crossing and feeder-service continuity.	Explains why corridor exposure is not reducible to land distance or GDP mass.
Central Asia regional node	Land-corridor and Caspian-side interface.	Becomes prominent under logistics shock and ranks second in BridgeStress.
Europe / Black Sea demand side	High centrality and absorption capacity.	Destination and redistribution interface; strong protection but high network importance.
East Asia-Pacific origin side	High output mass and demand potential.	Repeatedly appears as top spillover target in macro and financial scenarios.
MENA energy-geopolitical interface	Energy, financing and geopolitical exposure.	Dominates the energy/geopolitical corridor shock path.

Source: Author qualitative mapping from the global-corridor benchmark and Middle Corridor interpretation layer.

Figure 8.7.10. Corridor-sensitive local-to-systemic transition schematic



Source: Author schematic based on the corridor-sensitive benchmark interpretation.

8.7.10. Transition Regime Classification

For chapter-level interpretation, the scenario results can be classified into transition regimes. The classification is not a statistical clustering algorithm; it is an interpretive rule derived from threshold compression, action increase and EMGI loss. It is useful because it helps the reader move from exact numbers to systemic meaning.

Table 8.7.8. Local-to-systemic transition regime classification.

Regime	Scenario range	Threshold condition	Action condition	Systemic meaning
Protected benchmark	Baseline only	theta around 0.1099	Action=2,514.0	The network has a positive finite spectral boundary and normal baseline action.
Moderate compression	Inflation / price-pressure	theta around 0.0916	Action +16.35%	Macroeconomic stress weakens protection but does not turn the network into a corridor-dominated stress field.
Material compression	Financial-spread stress	theta around 0.0747	Action +36.64%	Funding stress broadens protection loss and increases transmissibility.
Corridor-sensitive compression	Trade / logistics corridor shock	theta around 0.0578	Action +62.61%	Logistics disruption activates corridor nodes and sharply lowers the systemic boundary.
Severe corridor transition	Energy / geopolitical	theta around 0.0420	Action +99.28%	Energy/geopolitical shock nearly

	corridor shock			doubles action and strongly compresses mass-gap protection.

Source: Author classification from the scenario-output and compression matrices.

8.7.11. Integration with the Seven-Problem Monograph

The scenario layer also helps Chapter 8 communicate with the other six problem chapters. Across the monograph, each Clay-inspired economic analogue has a different way of representing stress transition, validation or boundary movement. Yang-Mills contributes the most explicit finite-network shock-threshold language.

Table 8.7.9. Cross-chapter scenario and transition logic across the seven-problem monograph.

Monograph chapter	Scenario/transition logic	Connection to 8.7
Chapter 5 Perelman-Ricci-Poincare	Inequality pressure, curvature deformation and smoothing recovery.	Both distinguish shock deformation from full convergence and insist on bounded diagnostic interpretation.
Chapter 6 Hodge	Gradient, curl and harmonic circulation reveal non-GDP flow exposure.	Yang-Mills uses curvature/action and threshold compression where Hodge separates hierarchy, imbalance and systemic circulation.
Chapter 7 Navier-Stokes	Liquidity, pressure, friction, stochastic shocks and policy counterfactuals.	Both treat shocks as stress-testing devices, not as unconditional forecasts or causal policy effects.
Chapter 8 Yang-Mills	Mass-gap threshold, spectral radius, action and EMGI deterioration.	This section supplies the local-to-systemic transition mechanism for global-corridor networks.
Chapter 9 BSD	Local-to-global rank formation, BridgeStress and threshold/action diagnostics.	Both make small corridor nodes visible through local-to-global structure rather than GDP mass.
Chapter 10 Riemann-Zeta	Crisis-sensitive spectral/forecasting layers and shock-period validation.	Both use layered validation to prevent a small display layer from becoming the whole claim.
Chapter 11 P vs NP	Stress scenarios and robustness/falsification gates in computational optimization.	Both emphasize evidence discipline: best-found or simulated results must not be upgraded into theorem-level claims.

Source: Author synthesis across the seven uploaded monograph source documents.

8.7.12. Evidence Status and Claim Boundary

The scenario layer is scientifically useful only if its evidence status is kept precise. The chapter may state that the benchmark scenarios compress the normalized threshold, reduce lambda_1, increase action and deteriorate mean EMGI. It may not state that a future geopolitical shock will necessarily produce exactly these effects in observed trade, finance or energy markets. The scenario outputs are internally consistent model-implied diagnostics.

Table 8.7.10. Evidence-gate matrix for the scenario-simulation section.

Evidence item	What it supports	What it does not support
Scenario-output matrix	Controlled comparison of lambda_1, rho, theta, action and EMGI under four shock types.	Event prediction or observed freight-volume estimation.
Threshold compression curve	Interpretation that stronger shocks lower the local-to-systemic boundary.	Universal crisis threshold outside the constructed network.
Action amplification	Curvature-energy increases under stronger corridor shocks.	Physical energy or literal Yang-Mills field behavior.
Shock propagation table	Transmissibility geometry under x_{t+1}=rho W^S x_t with rho=0.85.	Unbounded contagion or causal spillover magnitudes.

Corridor interpretation	Caucasus, Central Asia and MENA have structural corridor roles in the benchmark.	Claim that GDP mass alone explains their systemic relevance.
N=1,500 pathway	A route to stronger country-panel validation.	Final causal country-panel confirmation in the current benchmark chapter.

Source: Author claim-boundary synthesis.

8.7.13. Replication Checklist for Scenario Simulations

For the scenario section to be reproducible, the replication package should contain the baseline node table, edge list, W matrix, stress-weighted W^S matrix, scenario shock-load vector, shock-exposure matrix Xi, recalculated Laplacian matrices, eigenvalue outputs, action outputs, EMGI-change outputs and propagation simulation files. The following checklist translates that requirement into manuscript-level audit items.

Table 8.7.11. Replication checklist for the scenario-simulation layer.

Audit item	Required content	Purpose
Baseline network files	10 nodes, 27 weighted edges, W, W^S, degree matrix and baseline L^S.	Allows independent reconstruction of lambda_1=0.3850 and theta=0.1099.
Shock-calibration file	Scenario names, amplitude h, shock variables and Xi exposure matrix.	Prevents scenarios from being narrative-only labels.
Post-shock matrices	W^(h), D^(h), L^(h) for each scenario.	Allows recalculation of lambda_1, rho and theta.
Curvature/action files	Triangle list, curl values, omega weights and action decomposition by scenario.	Allows verification of action amplification and concentration.
EMGI-change file	Baseline and post-shock EMGI components or change vectors.	Connects system-level compression to local protection loss.
Propagation files	Row-normalized W^S, rho=0.85, four-step retained mass outputs.	Allows reproduction of outside-origin shares and top spillovers.
Claim-gate README	Language separating benchmark simulation from causal forecasting.	Protects the chapter from overclaiming.

Source: Author replication-design synthesis for the monograph chapter.

8.7.14. Section Conclusion

Section 8.7 closes the dynamic interpretation of the Yang-Mills economic mass-gap chapter. The baseline finite-network threshold is positive, but it is not static. When increasingly severe shocks are injected into the stress network, the mass gap compresses, the spectral radius expands, the normalized threshold falls, Yang-Mills economic action rises and mean EMGI deteriorates. This is the chapter's central local-to-systemic transition result.

The strongest numerical summary is the movement from baseline to the energy/geopolitical corridor shock: lambda_1 falls from 0.3850 to 0.1796, the normalized threshold falls from 0.1099 to 0.0420, action rises from 2,514.0 to 5,010.0 and mean EMGI changes by -22.40 index points. This combination shows that under strong corridor stress, the system remains spectrally measurable but becomes much easier to transmit shocks through.

The section also clarifies the corridor mechanism. The Caucasus and Central Asia matter not because they dominate global GDP, but because corridor position, fragility and stress-circulation exposure make them structurally visible. MENA becomes the leading energy-geopolitical interface under the strongest shock. East Asia-Pacific remains the dominant high-mass spillover channel under macro and financial stress. The local-to-systemic transition is therefore heterogeneous: different scenarios activate different parts of the network.

The claim boundary remains strict. The section supports scenario diagnostics and threshold interpretation within a finite weighted graph. It does not claim causal prediction, theorem proof, physical Yang-Mills identity or final country-panel validation. Those stronger claims remain reserved for the fully populated N=1,500 validation architecture.

8.8. N=1,500 Validation Pathway and Claim Boundary

This subsection completes the evidentiary discipline of Chapter 8. Sections 8.1-8.7 have established the economic Yang-Mills analogy, the global-corridor stress network, the ten-node and twenty-seven-edge data architecture, the gauge potential, triangular curvature, Yang-Mills economic action, stress Laplacian, positive finite-network mass gap, EMGI, fragility, BridgeStress and scenario-simulation logic. Section 8.8 now defines exactly how the completed benchmark can be moved toward country-year validation without overstating what has already been proved. Its central task is to protect the chapter's scientific credibility: the positive finite-network benchmark is already a strong measurement result, but final country-level causal or quasi-causal inference requires the populated and estimated N = 1,500 validation layer.

The section is therefore written as a validation-roadmap and claim-boundary instrument. It does not weaken the Chapter 8 contribution. On the contrary, it explains why the benchmark is publishable as a finite-network gauge-econometric architecture while also identifying the empirical conditions required for a stronger panel-econometric statement. The chapter's strongest present claim is that the ten-node stress graph has a positive spectral separation, reproducible curvature/action diagnostics and interpretable corridor-exposure indices. Its strongest future claim, conditional on full panel closure, would be that analogous country-year variables behave consistently against observable macroeconomic, financial, logistics, energy and corridor outcomes under robust econometric discipline.

Figure 8.8.1. N = 1,500 validation pathway from benchmark to empirical closure

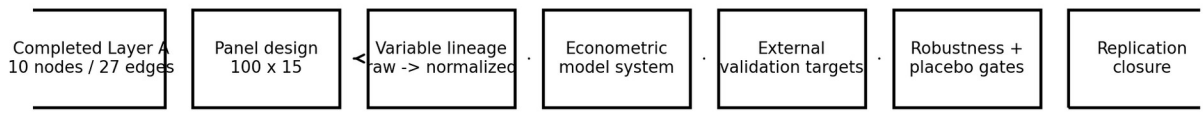


Figure 8.8.1. N = 1,500 validation pathway from benchmark to empirical closure.

8.8.1. Why the N = 1,500 layer is necessary

The completed Yang-Mills benchmark uses ten regional and corridor-sensitive nodes and twenty-seven weighted undirected edges. This design is appropriate for finite weighted-graph diagnostics because the object being measured is the spectrum of a constructed stress Laplacian, not a country-level causal panel. In that setting, lambda_1 = 0.3850 is meaningful as the first positive eigenvalue of the stress-weighted graph Laplacian; rho = 3.5023 summarizes the spectral radius; and theta = lambda_1/rho = 0.1099 gives a normalized local-to-systemic transition threshold. These objects are graph-theoretic and benchmark-specific. They do not require a country panel in order to exist.

However, the moment the interpretation shifts from finite-network structure to broader empirical validation, a larger data architecture becomes necessary. A ten-node benchmark can show that the constructed system is connected, spectrally separated, curvature-bearing and scenario-sensitive. It cannot, by itself, demonstrate that country-level resilience, corridor exposure, inflation pressure, logistics disruption or financial-spread outcomes respond to EMGI and curvature in the same way across heterogeneous national contexts. This is the role of the N = 1,500 validation pathway: it converts the benchmark logic into a country-year empirical field with sufficient cross-sectional and temporal variation for fixed effects, robust inference, external outcomes, dynamic checks and replication closure.

(8.8.1) N_panel = N_countries x T_years = 100 x 15 = 1,500 country-year observations.

(8.8.2) Current evidence = {finite-network benchmark, internal robustness, scenario diagnostics, N=10 association screens}.

(8.8.3) Future evidence = {country-year variables, TWFE/DK/clustered estimates, factor checks, external-outcome validation, scripts, seeds, hashes}.

The methodological principle is simple: the benchmark layer validates the architecture; the panel layer validates its general empirical behaviour. Confusing these two levels would create reviewer risk. Separating them makes the chapter more robust

because it tells the reader exactly which results are already closed and which results remain conditional on the next empirical stage.

Table 8.8.1. Sample architecture of the N = 1,500 validation pathway.

Design item	Specification	Purpose	Boundary rule
Countries	100	Country-level public macroeconomic and corridor-relevant units	Final list fixed before estimation; no ex-post replacement without version note
Years	2010-2024	Annual observation window aligned with available macro-financial and logistics data	Balanced preferred; gaps documented if unbalanced
Main N	1,500	100 countries x 15 years	Nominal panel size; effective N may fall after lags and missing-value filters
Core unit	country-year	i,t observation used in econometric validation	Regional benchmark is not duplicated as country panel evidence
External layer	outcome/proxy families	inflation, spreads, trade/logistics, energy/geopolitical and resilience indicators	Independent lineage required for validation claims
Replication unit	file/table/script hash	deterministic audit object	Final claim requires raw files, normalized files, scripts, seeds and checksums

Source: Author synthesis based on the Chapter 8 Yang-Mills validation-pathway logic.

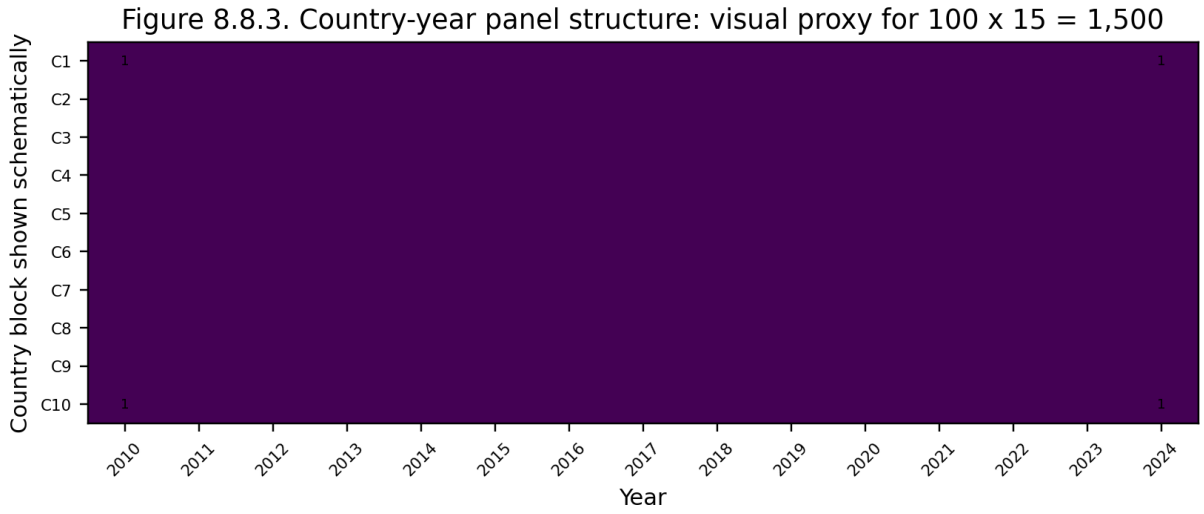


Figure 8.8.3. Country-year panel structure: visual proxy for 100 x 15 = 1,500.

8.8.2. From Layer A to Layer B: benchmark evidence versus panel evidence

Chapter 8 uses a two-layer evidence architecture. Layer A is the completed finite-network benchmark. It is populated, computed, interpreted and archived as a dataset package. Layer B is the planned country-panel validation architecture. It is not used to inflate the benchmark claim; it is specified as the next empirical stage required for stronger inference. This distinction must remain visible in the book because Chapter 8 sits inside a monograph whose general claim boundary states that the seven Clay-inspired chapters are economic-econometric analogues rather than mathematical solutions.

Layer A supports strong language about the finite graph: connectedness, spectral separation, curvature concentration, EMGI, fragility, BridgeStress and scenario-threshold compression. Layer B supports only pathway language until the country-year variables are populated and estimated. Once that panel is complete, it can test whether EMGI, curvature, stress,

BridgeStress and resilience have stable signs and interpretable relationships across countries and years. Until then, the panel is a validation design, not a completed validation result.

Table 8.8.2. Layer A / Layer B evidence-status separation.

Layer	Empirical universe	Current status	Main outputs	Permitted interpretation
Layer A	10 nodes; 27 weighted edges	completed benchmark	lambda_1, rho, theta, action, EMGI, fragility, BridgeStress, scenarios	strong finite-network measurement claim
Layer B	100 countries x 15 years	specified validation pathway	TWFE, DK, clustered SE, dynamic panel, IV screens, factor checks, external outcomes	future validation claim after estimation
Bridge between layers	mapping of regional logic to country-year variables	methodological translation	variable ledger, source lineage, normalization, external targets	claim gate prevents overclaiming

Figure 8.8.2. Claim hierarchy and evidence ladder

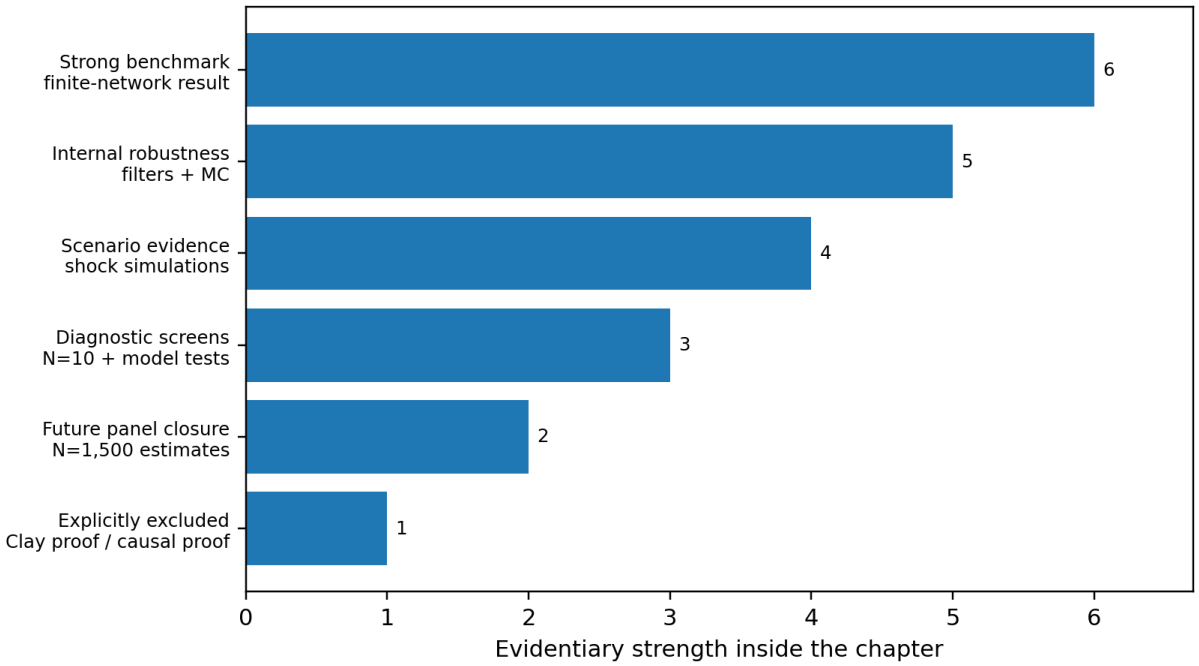


Figure 8.8.2. Claim hierarchy and evidence ladder.

8.8.3. Country-year variable ledger and anti-circularity discipline

The most important technical requirement for the N = 1,500 validation pathway is not merely to increase sample size. It is to preserve variable-lineage discipline. The benchmark contains author-calculated constructs: stress scores, curvature exposure, EMGI, fragility and BridgeStress. These objects are legitimate because their formulas, matrices and transformations are disclosed. But constructed variables that share input components cannot be treated as independent validation of one another unless the validation design separates inputs, derived constructs and external targets.

For that reason, the panel layer must use a variable ledger. Each variable family must state whether it is a public macroeconomic anchor, a proxy-observable external outcome, an author-calculated diagnostic object or an identity. This prevents circularity. For example, fragility = 100 - EMGI is useful as an interpretive complement, but it is not independent evidence that EMGI is valid. Similarly, stress and curvature may be internally coherent, but external validation requires

observable outcomes such as logistics disruption, trade-flow pressure, financial stress, inflation volatility, energy exposure or resilience indicators with independent data lineage.

(8.8.4) Fragility_i,t = 100 - EMGI_i,t. Because this is an identity, it supports interpretation but not independent validation.

(8.8.5) External validation requires: lineage(Y_i,t) != lineage(EMGI_i,t, Stress_i,t, Curvature_i,t), except where overlap is disclosed and residualized.

Table 8.8.3. Country-year variable ledger for the N = 1,500 validation pathway.

Variable family	Data status	Source family / construction	Role in N=1,500 pathway	Claim caution
GDP mass / world share	public macro anchor	World Bank / WDI-style national accounts	scale; output exposure	input variable
Growth pressure	public macro anchor + transformation	IMF/WEO or WDI growth logic	stress-field component	derived but public-rooted
GDP per capita / income depth	public macro anchor	WDI-style income series	income-depth protection or fragility	input and normalized component
Inflation pressure	public macro-financial anchor	WDI/IMF inflation logic	external stress proxy and scenario channel	external and model input
Financial-spread stress	public/ market proxy family	sovereign, credit or risk-premium sources where available	financial shock channel	external proxy; coverage-sensitive
Trade/logistics exposure	public and corridor-coded variables	trade openness, LPI-style logistics, route/corridor coding	corridor vulnerability channel	partly author-coded
Energy/ geopolitical exposure	public energy and risk proxy families	energy dependence, geopolitical risk, route exposure	severe corridor shock channel	proxy-dependent
Systemic stress s_i,t	author-calculated	normalized composite from anchor components	stress field for panel validation	constructed index
Curvature exposure C_i,t	author-calculated	country-year analogue of cycle stress	gauge-curvature validation channel	constructed object
EMGI_i,t	author-calculated	protection index from spectral/network/income/resilience/stress/curvature components	structural protection target and regressor	constructed object; lineage audit required
Fragility_i,t	author-calculated identity	100 - EMGI_i,t	vulnerability complement	identity; not independent validation
BridgeStress_i,t	author-calculated	corridor exposure, fragility, centrality and low-mass leverage	strategic exposure	coded sensitivity

	corridor index		channel	required
External outcome Y_i,t	observable target	macro, logistics, financial, energy, trade or resilience outcome	independent validation target	preferred independent lineage

Source: Author construction. The ledger separates public anchors, author-calculated variables, identity variables and external validation targets.

Figure 8.8.6. Variable-lineage separation for anti-circularity discipline

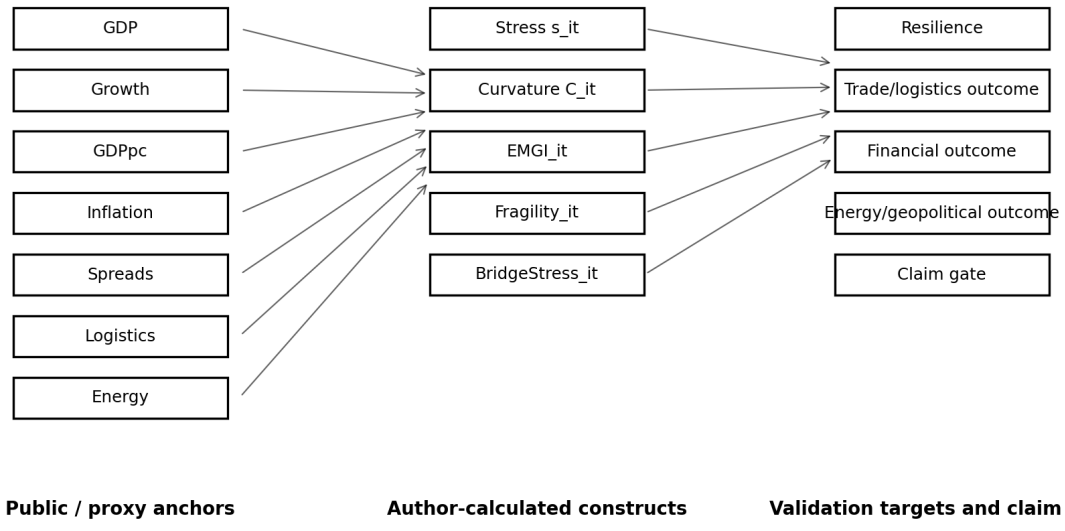


Figure 8.8.6. Variable-lineage separation for anti-circularity discipline.

8.8.4. Panel model system: from benchmark diagnostics to robust validation

The country-panel model system must be broader than a single regression. A single coefficient on EMGI would not validate the Yang-Mills architecture. The validation pathway requires a sequence of models that test different parts of the theoretical mechanism: whether EMGI aligns with resilience, whether stress and curvature predict external outcomes, whether BridgeStress identifies corridor-sensitive vulnerability, whether thresholds separate local from systemic regimes, whether spatial/network spillovers exist, whether factor structure is coherent and whether scenario recalculations remain plausible at country-year scale.

The baseline design is a two-way fixed-effects panel because it controls for time-invariant country heterogeneity and common annual shocks. Clustered and Driscoll-Kraay inference then addresses dependence and serial correlation concerns. Dynamic-panel specifications may be useful for persistence and shock memory, but they must be used conservatively because instrument proliferation and weak identification can generate misleading precision. Panel-IV models are not automatic; they are admissible only where instruments are theoretically justified, empirically strong and transparently reported.

(8.8.6) $Y_{i,t} = \alpha_i + \tau_t + \beta_1 EMGI_{i,t} + \beta_2 Curvature_{i,t} + \beta_3 Stress_{i,t} + \gamma X_{i,t} + \varepsilon_{i,t}$.

(8.8.7) $Resilience_{i,t} = \alpha_i + \tau_t + \beta_1 EMGI_{i,t} + \beta_2 Stress_{i,t} + \beta_3 Curvature_{i,t} + \gamma X_{i,t} + \varepsilon_{i,t}$.

(8.8.8) $Y_{i,t} = \beta_L Stress_{i,t} I(EMGI_{i,t} \leq c) + \beta_H Stress_{i,t} I(EMGI_{i,t} > c) + \alpha_i + \tau_t + \varepsilon_{i,t}$.

Table 8.8.4. Country-panel model system for N = 1,500 validation.

Model block	Specification	Estimator / procedure	Main diagnostic	Permitted interpretation
M1 Baseline TWFE	$Y_{it} = \alpha_i + \tau_t + \beta_1 EMGI_{it} + \beta_2$	Two-way fixed effects; country-clustered and DK	signs, within R2, robust Wald tests	Core panel validation, not theorem proof

	Curvature_it + beta3 Stress_it + gamma X_it + epsilon_it	SE		
M2 Resilience channel	Resilience_it = alpha_i + tau_t + beta1 EMGI_it + beta2 Stress_it + beta3 Curvature_it + controls + epsilon_it	TWFE / clustered / DK	whether EMGI aligns with absorption capacity	Empirical association after estimation
M3 Fragility channel	Fragility_it = alpha_i + tau_t + beta1 Stress_it - beta2 EMGI_it + beta3 BridgeStress_it + controls + epsilon_it	TWFE and first-difference robustness	vulnerability consistency	Diagnostic sign validation
M4 Threshold panel	Y_it = beta_L Stress_it * I(EMGI_it <= c) + beta_H Stress_it * I(EMGI_it > c) + FE + epsilon_it	panel threshold / interaction design	local-to-systemic boundary c	Threshold evidence only if stable
M5 Network-spatial panel	Y_it = rho W_t Y_it + beta EMGI_it + alpha_i + tau_t + epsilon_it	spatial/network panel or spatial-lag screen	network spillover rho and residual dependence	Externality validation, not automatic causality
M6 Dynamic panel	Y_it = phi Y_i,t-1 + beta EMGI_it + delta Stress_it + FE + epsilon_it	dynamic FE / system GMM only if instrument count controlled	persistence and shock memory	High caution; no mechanical GMM overclaim
M7 Panel IV screen	EMGI_it or Stress_it instrumented when valid instruments exist	2SLS / IV-FE with first-stage checks	endogeneity discipline	Only if credible instruments are documented
M8 PCA/factor screen	F_it = factor(EMGI, stress, curvature, resilience, external proxies)	PCA/factor model with adequacy tests	loading signs and variance concentration	Construct validity screen
M9 Scenario-panel recalculation	shock_h -> s_it^(h), W_it^(h), lambda1^(h), theta^(h), action^(h), EMGI^(h)	algorithmic panel recalculation	country-year transition maps	Simulation evidence, not prediction

Source: Author synthesis based on the Chapter 8 validation architecture. All models are future panel-validation instruments until estimated.

Figure 8.8.4. Model-block dependency graph

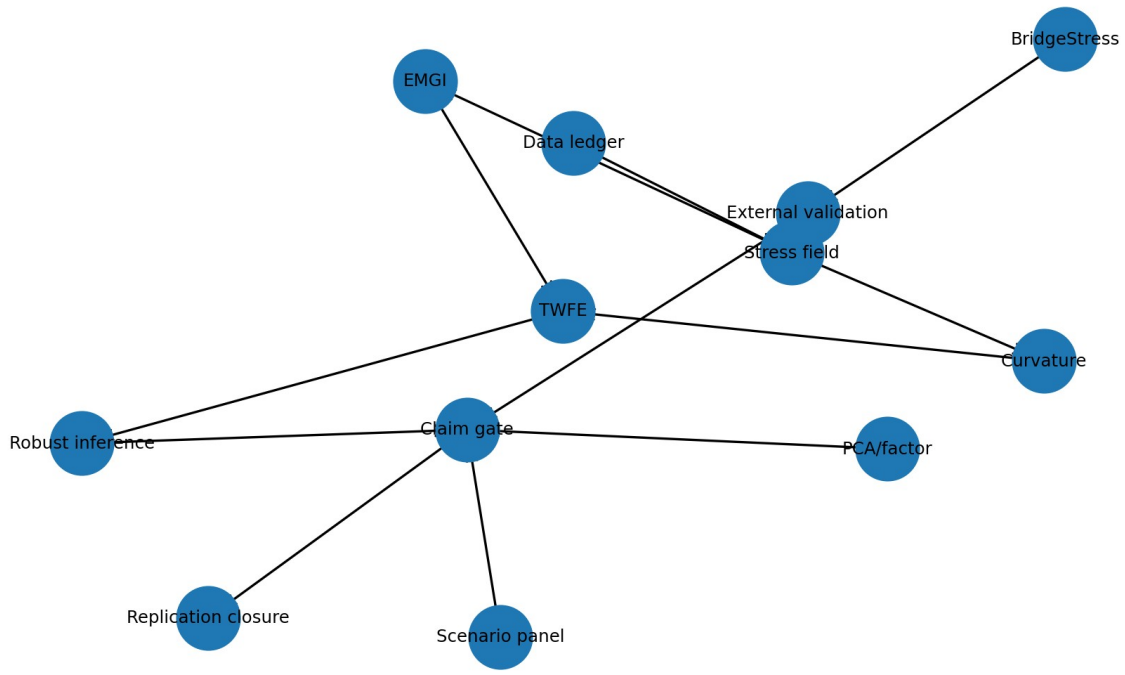


Figure 8.8.4. Model-block dependency graph.

8.8.5. Validation gates and evidentiary decision rules

The validation pathway should be interpreted as a sequence of gates. The panel is not closed merely because data are collected. It is closed only when the country list, time window, variable definitions, transformations, estimators, robustness checks, external targets and replication artifacts are all complete. A gate fails if it produces inconsistent signs, weak external validity, unexplained missingness, unstable threshold estimates, inadequate factor structure or non-reproducible outputs. A failed gate does not invalidate the benchmark mass gap; it simply prevents the chapter from upgrading to stronger country-level language.

This gate structure is essential because Chapter 8 contains several types of evidence with different epistemic status. The finite-network spectral result is a mathematical output of the disclosed benchmark matrices. Scenario simulations are conditional recalculations. N=10 regressions are diagnostic associations. Machine-learning and factor screens are exploratory unless estimated in a larger panel. External-validation regressions are stronger only if their target variables have independent lineage and robust signs. The N = 1,500 pathway converts these distinctions into a formal reviewer-safe workflow.

Table 8.8.5. Validation gates for the N = 1,500 pathway.

Gate	Validation block	Panel specification	Main output	Closure requirement	Claim status
V1	Country-year panel construction	100 countries x 15 years = 1,500 observations	Raw public and corridor-coded variables	Required before estimation	Panel-ready, not yet final
V2	Two-way fixed-effects validation	Country FE + year FE + controls	Within-country coefficient stability	After country-year variables are populated	Validation after estimation
V3	Clustered and Driscoll-Kraay inference	Country-clustered SE; DK SE for cross-sectional/time dependence	Robust sign and significance discipline	After TWFE estimation	Robust-inference screen

V4	Dynamic-panel diagnostics	Lagged dependent variable, persistence, shock memory	Dynamic stability and path dependence	Requires adequate lag structure	Diagnostic, not automatic causality
V5	Panel-IV / endogeneity screen	Instrumental or lagged-predictor logic only if justified	First-stage strength, partial R2, overidentification where valid	Requires credible instruments	Identification screen
V6	PCA/factor validation	Common stress factor extracted from EMGI, stress, curvature, resilience and proxies	Eigenvalues, loading signs, variance shares	Requires complete variable matrix	Factor-structure validation
V7	External-outcome validation	Observed macro, logistics, financial, energy and corridor outcomes	Predictive relevance against observable targets	Requires independent external proxies	External screening/validation
V8	Scenario recalculation at panel scale	Shock rules applied across countries and years	Post-shock lambda_1, theta, EMGI, action and propagation outputs	Requires country-level network embedding	Simulation validation
V9	Replication and file-hash closure	Raw, normalized and derived files; scripts; seeds; hashes	Deterministic reproduction of tables and figures	Required for final country-panel claim	Replication gate

Source: Author synthesis. The table defines the minimum conditions for upgrading from benchmark evidence to panel-validation evidence.

8.8.6. Claim boundary: what the chapter may say now and what it must reserve

The strongest present statement is that the Chapter 8 benchmark demonstrates a positive finite-network economic mass gap inside a disclosed global-corridor stress graph. It may also say that EMGI, fragility and BridgeStress produce reproducible node-level diagnostics and that scenario simulations show threshold compression under stronger shocks. It may not say that the world economy literally satisfies a Yang-Mills field equation, that the Clay problem has been solved, that the model proves causal country-level mechanisms, or that the N = 1,500 panel has already validated the framework.

The final language should therefore distinguish five levels: benchmark-validated, internally robust, scenario-descriptive, diagnostic association and panel-ready. The first three levels are already supported by the Chapter 8 benchmark. The fourth is limited because the ten-node econometric layer is small. The fifth is not yet a result; it is a structured future validation path. This is the claim boundary that should be carried into Chapter 14 and the monograph's general limitations chapter.

Table 8.8.6. Claim boundary matrix for Chapter 8.

Claim object	Current status	Evidence basis	Allowed language
Finite-network benchmark mass gap	Supported now	lambda_1 = 0.3850; rho = 3.5023; theta = 0.1099 in completed 10-node benchmark	Strong finite-network measurement claim
Robustness of positive gap inside benchmark	Supported now	filtered graphs and Monte Carlo uncertainty retain positive separation	Internal robustness claim
EMGI / fragility /	Supported now	component audit and	Benchmark diagnostic

BridgeStress ranking		index identities disclosed in benchmark package	ranking
Scenario threshold compression	Supported now as simulation	shock scenarios compress theta and increase action concentration	Descriptive scenario claim
N=10 econometric regressions	Diagnostic only	small sample; HC3 and related models cannot establish causality	Non-causal association claim
N=1,500 panel validation	Pathway specified	100 countries x 15 years, estimators and outputs defined but not yet numerically closed	Panel-ready future validation claim
Country-level causal confirmation	Not yet supported	requires completed panel, independent outcomes, robust inference, endogeneity checks and file hashes	Explicitly excluded for current evidence
Mathematical Yang-Mills mass-gap proof	Not supported / outside scope	economic finite weighted-graph analogy only	Explicitly excluded

Source: Author synthesis based on the corrected Yang-Mills evidence hierarchy.

Figure 8.8.5. Current versus panel-closed claim capacity

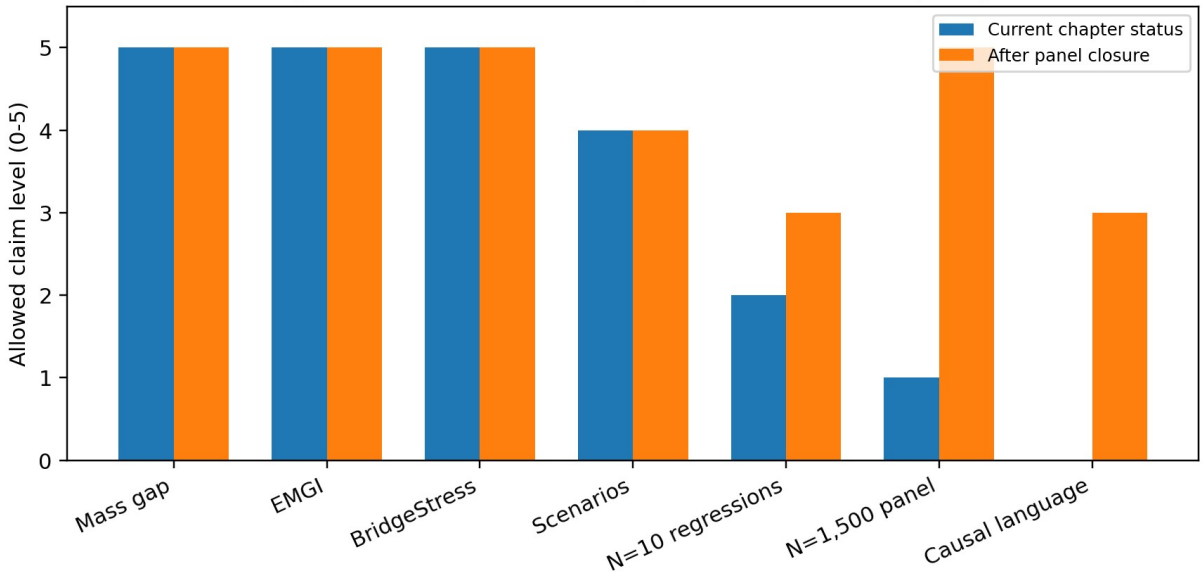


Figure 8.8.5. Current versus panel-closed claim capacity.

8.8.7. Reviewer-risk response and scientific caution

A chapter that uses Yang-Mills vocabulary in economic modelling will face predictable reviewer concerns. The first concern is analogy overreach: mathematical readers may suspect that the terminology implies a theorem-level transfer. The answer is explicit boundary language: all Yang-Mills terminology is used in a finite weighted-graph economic sense. The second concern is small-sample inference: the benchmark has ten nodes, so regressions cannot carry causal claims. The answer is to label them diagnostic and to reserve causal or quasi-causal language for the N = 1,500 panel. The third concern is constructed-index circularity: EMGI, stress and curvature may share inputs. The answer is variable lineage, external outcomes and residualized or external-only screens.

The fourth concern is corridor-coding subjectivity. BridgeStress is valuable precisely because it makes small corridor nodes visible, but its coding must be transparent and sensitivity-tested. The fifth concern is placebo interpretation. A positive finite-network mass gap does not automatically prove that the observed graph is uniquely non-random. Therefore, randomized-network evidence should be reported as cautionary unless it strongly separates the observed structure from

placebo distributions. The sixth concern is replication closure. Benchmark files are archived; country-panel files must also be archived before panel claims are upgraded.

Table 8.8.7. Reviewer-risk controls embedded in Section 8.8.

Reviewer risk	Possible criticism	Safeguard in 8.8	Remaining status
Analogy overclaim	Reader may think the chapter proves Yang-Mills	Repeated finite-network and economic-analogue boundary; no theorem language	Low if boundary is retained
Small-N regression overclaim	N=10 diagnostic models may be misread as causal	Move causal claims to N=1,500 pathway; label N=10 as diagnostic only	Moderate until panel closes
Constructed-index circularity	EMGI, stress, curvature may share variable lineage	variable-lineage table, external-only target layer, residualized screens	Moderate; requires panel audit
Corridor coding subjectivity	BridgeStress depends partly on author-coded corridor exposure	disclosed coding, sensitivity alternatives, route-family documentation	Moderate
Placebo misinterpretation	positive gap may be overstated as unique	randomized-network placebo classified as caution, not proof	Low if wording remains cautious
External proxy weakness	external outcomes may have incomplete coverage	state coverage limitations; do not upgrade weak proxies to confirmation	Moderate
Replication incompleteness	country panel not yet archived	benchmark Zenodo package cited; panel closure requires scripts, seeds, hashes	Resolved only after final panel deposit

Source: Author reviewer-risk synthesis.

Figure 8.8.7. Reviewer-risk reduction heatmap

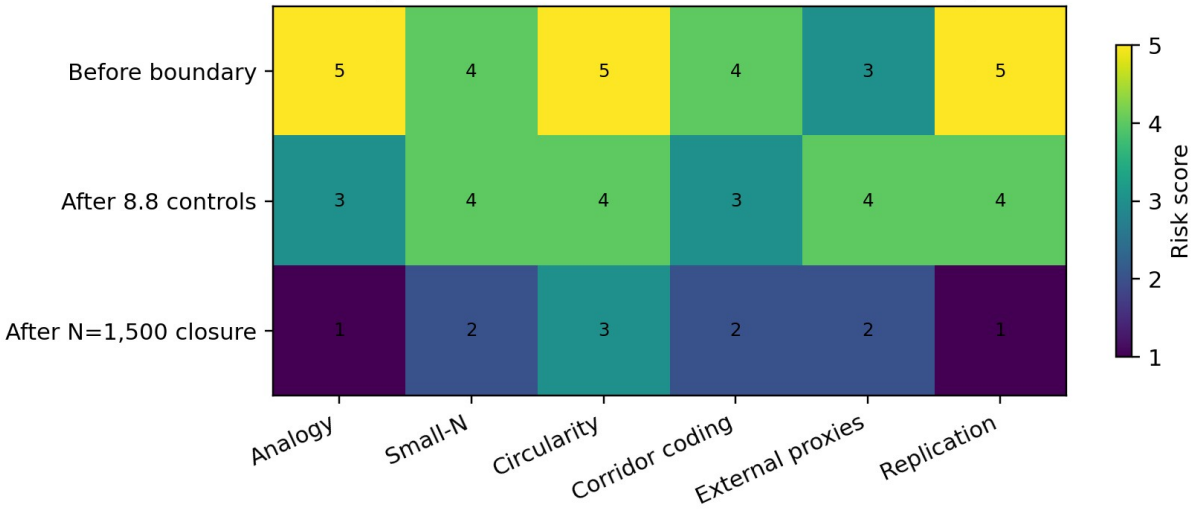


Figure 8.8.7. Reviewer-risk reduction heatmap.

8.8.8. Replication closure and Zenodo-linked audit pathway

Replication is the final condition that converts a sophisticated model into an auditable scientific contribution. The benchmark layer already has a data and replication package archived on Zenodo under DOI 10.5281/zenodo.20786199. That package supports the finite-network objects: source logs, raw and normalized files, adjacency matrices, stress-weighted matrices, cycles, EMGI components, scenario outputs, scripts, seeds and checksums. The country-panel validation layer must follow the same standard before stronger claims are introduced into the monograph.

The country-panel replication package should contain the final country list, raw input files, source URLs or source-family notes, extraction dates, data-cleaning scripts, normalized-variable files, derived EMGI/stress/curvature/BridgeStress files, model scripts, estimator settings, random seeds, table exports, figure exports, output logs and cryptographic hashes. The manuscript should not merely state that the panel exists. It should make the panel reproducible in the same way the benchmark is auditable.

Table 8.8.8. Minimum replication manifest for the N = 1,500 panel layer.

Replication artifact	Content	Audit function
source_ledger.csv	country list, variable sources, extraction rules, dates	documents provenance and version control
raw_country_year.csv	untransformed country-year public/proxy indicators	preserves source data before normalization
normalized_country_year.csv	direction-harmonized 0-100 or nondimensional variables	supports reproducible stress construction
constructed_indices.csv	Stress, Curvature, EMGI, Fragility, BridgeStress, Resilience	recreates model-derived objects
external_targets.csv	observable macro, financial, logistics, energy and corridor outcomes	supports independent validation
model_outputs.xlsx/csv	TWFE, DK, clustered, dynamic, factor, IV and scenario results	links tables to estimators
scripts/	construction, estimation, figures and tables	makes the workflow computationally repeatable
seeds_hashes.txt	random seeds and file checksums	supports deterministic audit
README + data_dictionary	variable definitions, units, transformations and exclusions	makes the package usable by external readers

Source: Author replication design. The country-panel package should be versioned separately from the finite-network benchmark if the estimates are added later.

Figure 8.8.8. Replication-closure object map

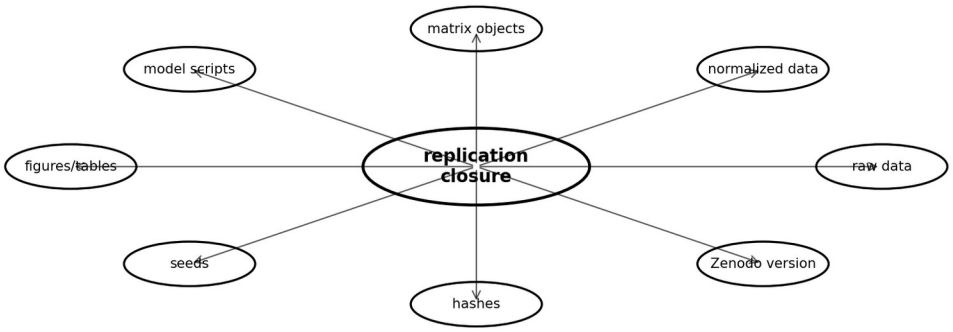


Figure 8.8.8. Replication-closure object map.

8.8.9. Position of the Yang-Mills validation pathway inside the seven-problem monograph

The N = 1,500 pathway also has a monograph-level function. It aligns Chapter 8 with the evidence discipline of the other six problem chapters. The Perelman/Ricci/Poincare chapter uses an N = 150 regional-year diagnostic panel. The Hodge chapter is a regional topological-flow benchmark. The Navier-Stokes chapter uses a 100-country, 2010-2024 macro-financial stress-testing panel. The BSD chapter uses a World anchor, ten regional/corridor nodes and an N = 150 closure layer. The Riemann-Zeta chapter is the most explicitly layered in forecast-validation terms, with annual, quarterly and monthly validation windows. The P vs NP chapter uses a full 94-industry computational universe plus an exact reduced benchmark. Chapter 8 is strongest as a finite-network benchmark today and becomes stronger as a country-panel validation chapter once the N = 1,500 layer is populated and estimated.

This comparison is important because it prevents the monograph from looking like seven disconnected articles. Each chapter has a different empirical universe because each mathematical inspiration requires a different measurement grammar. The common rule is not that every chapter must have the same N. The common rule is that every chapter must specify its

empirical object, distinguish public anchors from constructed variables, report its validation status and state its claim boundary.

Table 8.8.9. Chapter 8 within the seven-problem validation ecology.

Study	Empirical universe	Main translated object	Evidence type	Claim boundary
Perelman/Ricci/Poincare	N=150 regional-year inequality panel	curvature, entropy, connectedness	diagnostic panel evidence	bounded inequality-curvature interpretation
Hodge	10 regional nodes + World anchor	gradient/curl/harmonic decomposition	regional benchmark prototype	topological flow decomposition only
Navier-Stokes	100 countries, 2010-2024	liquidity-flow stress testing	N=1,500 econometric evidence base	macro-financial diagnostic, not physical fluid law
Yang-Mills	10 nodes, 27 edges + planned N=1,500 panel	mass-gap threshold, EMGI, BridgeStress	benchmark + validation pathway	finite weighted-graph mass gap only
BSD	World anchor + 10 regional/corridor nodes; N=150 closure	local-to-global rank and LOrder	calibrated closure layer	BSD analogue, not classical theorem proof
Riemann/Zeta	N=55, 45, 20, 100, 240 layers	FPAS+zeta forecast diagnostics	layered forecast validation	zeta-cycle signal, not RH proof
P vs NP	94 U.S. industries; exact C(20,6) reduced benchmark	cardinality and optimization complexity	computational-finance benchmark	best-found incumbent, not P vs NP proof

Source: Author synthesis based on the monograph structure and the seven source studies.

Figure 8.8.9. Chapter 8 pathway in the seven-problem validation ecology

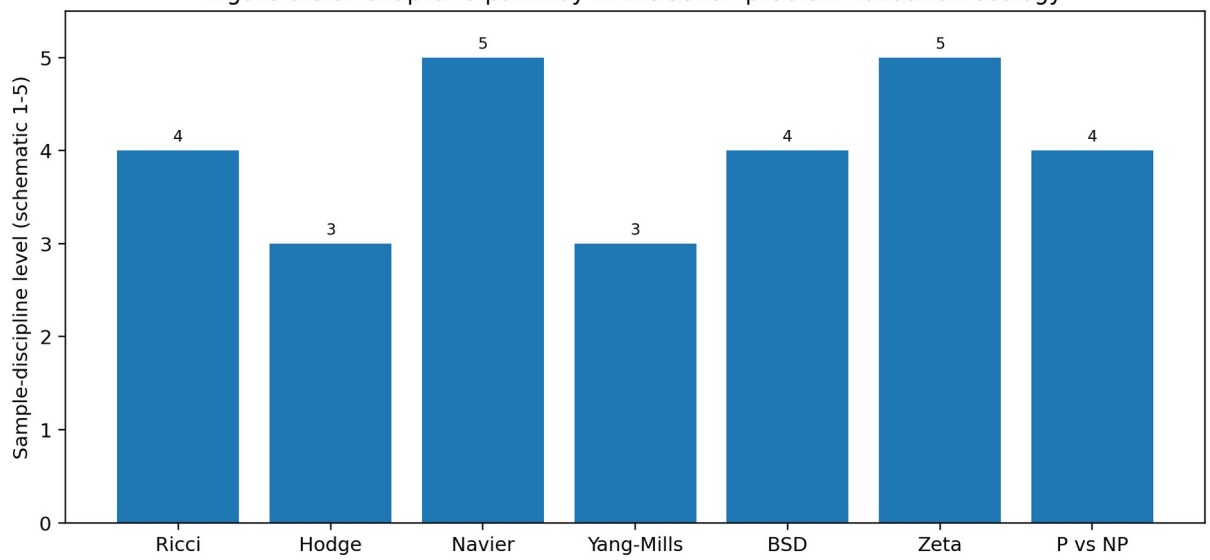


Figure 8.8.9. Chapter 8 pathway in the seven-problem validation ecology.

8.8.10. Final synthesis of Section 8.8

Section 8.8 establishes the final evidentiary boundary of the Yang-Mills chapter. The completed benchmark already supports a strong finite-network statement: a ten-node, twenty-seven-edge global-corridor stress graph produces a positive first non-zero stress-Laplacian eigenvalue, interpretable as an Economic Yang-Mills Mass Gap in the finite weighted-graph

sense. The same benchmark supports internally reproducible EMGI, fragility, BridgeStress, curvature/action concentration and scenario-threshold diagnostics.

The section also states what remains open. The N = 1,500 layer is not a decorative appendix; it is the empirical bridge from benchmark architecture to country-level validation. It requires 100 countries over 2010-2024, a source ledger, normalized variables, country-year stress and curvature objects, external validation outcomes, robust fixed-effects estimates, Driscoll-Kraay and clustered inference, dynamic and endogeneity screens, factor validation, scenario recalculation and a complete replication package. Only after those conditions are satisfied can the chapter move from benchmark-validating language to stronger country-panel validation language.

The final claim boundary is therefore precise. Chapter 8 does not solve the mathematical Yang-Mills existence and mass gap problem. It does not claim that economic systems are physical gauge fields. It does not claim final causal country-panel confirmation at the benchmark stage. It does claim that gauge-theoretic, spectral and corridor-network concepts can be operationalized in a transparent finite-network econometric architecture for measuring systemic shock thresholds. This is the academically defensible contribution of the chapter and the point from which the next empirical validation stage should proceed.

Table 8.8.10. Final claim-gate summary for Section 8.8.

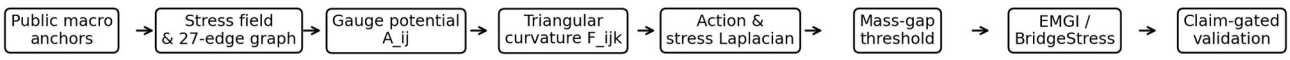
Evidence status	Objects included	Permitted language
Already closed	finite-network graph, matrices, lambda_1, rho, theta, action, EMGI, BridgeStress, scenario outputs	benchmark-validating language
Partly closed	N=10 diagnostic models, robustness screens, placebo caution	diagnostic association language only
Not yet closed	N=1,500 country-year estimates, external outcomes, panel scripts and hashes	future validation pathway
Always excluded	Clay theorem proof, literal gauge field claim, final causal proof without panel closure	explicit exclusion

Source: Author final synthesis.

8.9. Chapter Conclusion

Chapter-scope note. This section closes Chapter 8 of the monograph. It synthesizes Sections 8.1-8.8 and converts the technical benchmark into a final chapter-level conclusion. The conclusion preserves the monograph-wide claim boundary: Chapter 8 develops a finite-network gauge-econometric analogue inspired by Yang-Mills logic; it does not solve, test or replicate the Clay Yang-Mills existence and mass-gap problem in its original mathematical form.

Figure 8.9.1. Chapter 8 closing pipeline from data anchors to claim-gated validation.



Chapter 8 conclusion: a finite-network economic analogue, not a Clay-problem proof

8.9.1. Final Synthesis of the Chapter

Chapter 8 has developed a finite-network gauge-econometric architecture for measuring systemic shock thresholds in global and corridor flow networks. Its principal contribution is not a metaphorical use of Yang-Mills language, but a fully

operational transformation chain: public macroeconomic anchors are converted into a normalized systemic-stress field; stress is embedded in a ten-node, twenty-seven-edge corridor-sensitive graph; edge-level asymmetry is encoded as an anti-symmetric economic gauge potential; triangular cycles generate curvature; squared curvature produces Yang-Mills economic action; and the stress-weighted Laplacian produces a positive finite-network mass-gap threshold.

The chapter therefore establishes a bounded but strong measurement claim. It shows that the world economy, when represented as a finite corridor-sensitive stress network, contains a positive spectral separation between the normal connected mode and the first transmissible stress mode. This separation is the economic mass gap in the strictly finite weighted-graph sense. The result is scientifically meaningful because it converts a local-to-systemic transition problem into a measurable spectral object, while explicitly rejecting any interpretation as a solution to the classical Yang-Mills problem.

The chapter also extends the result beyond a single eigenvalue. The Economic Mass Gap Index translates system-level spectral protection into node-level structural protection; fragility captures the complementary vulnerability layer; BridgeStress identifies strategically exposed corridor nodes that would be hidden in GDP-only rankings; and scenario simulations show how inflation, financial-spread, trade/logistics and energy/geopolitical shocks compress the local-to-systemic threshold. Taken together, these layers support a coherent conclusion: systemic exposure is not reducible to output mass, and corridor position can become decisive under stress.

Table 8.9.1. Closing synthesis of Chapter 8 sections.

Section	Function	Concluding role	Evidence status
8.1	Gauge logic and mass-gap analogy	Defined the permissible Yang-Mills economic analogy and separated analogy from proof.	Conceptual boundary
8.2	Research object	Specified the finite global-corridor stress network and its two-layer evidence status.	Object definition
8.3	Data architecture	Organized ten nodes, twenty-seven edges, public anchors, author-calculated variables and replication logic.	Data closure
8.4	Methodology	Formalized stress field, gauge potential, triangular curvature, action and stress Laplacian.	Computational closure
8.5	Results	Reported positive finite-network mass gap, action concentration, EMGI, fragility and BridgeStress.	Benchmark result
8.6	Interpretation	Explained shock thresholds and corridor exposure without overclaiming causality.	Analytical interpretation
8.7	Scenarios	Demonstrated local-to-systemic transition through threshold compression and action amplification.	Scenario diagnostics
8.8	Validation boundary	Specified N = 1,500 validation pathway and final claim-gate rules.	Future empirical closure
8.9	Conclusion	Synthesizes the chapter and prepares transition to BSD local-to-global logic.	Chapter closure

Source: Author synthesis from Chapter 8 architecture and the Yang-Mills finite-network benchmark.

8.9.2. What the Chapter Establishes

The first conclusion is mathematical-economic rather than causal-econometric. The benchmark graph is connected, cycle-rich and sufficiently structured for curvature and spectral diagnostics. It contains ten global and corridor-sensitive nodes and twenty-seven weighted undirected edges. This finite architecture is not a complete transaction-level map of world trade, finance or logistics. Its role is more precise: it is a benchmark stress-transmission graph designed to test whether macro-corridor stress can be represented as a field with gauge, curvature, action and spectral-threshold properties.

The second conclusion is spectral. The benchmark stress Laplacian has a normal connected baseline eigenvalue $\lambda_0 = 0.0000$ and a first positive eigenvalue $\lambda_1 = 0.3850$. This positive λ_1 is the chapter's central finite-network mass-gap result. The spectral radius is 3.5023, producing a normalized local-to-systemic transition threshold of 0.1099. This means that, within the constructed benchmark, the system is not spectrally flat: it contains a measurable separation between ordinary connectedness and first systemic stress propagation.

The third conclusion is curvature-action based. Total Yang-Mills economic action equals 2,514.0, and the top-five action concentration equals 78.329%. This indicates that systemic stress-energy is not evenly distributed across all cycles. Instead, it is concentrated in a limited number of high-curvature network circuits. This is substantively important because it provides an explanation for why certain corridor interfaces can become critical under shocks even when their GDP mass is limited.

The fourth conclusion is node-level. EMGI, fragility and BridgeStress show that systemic protection and systemic exposure are different objects. North America and Europe are high-protection nodes in EMGI terms; the Caucasus and Central Asia are not high-output-mass centers, but they become analytically visible through BridgeStress because they transmit exposure across larger systems. This distinction is one of the key empirical benefits of the chapter.

Table 8.9.2. Final benchmark conclusions of Chapter 8.

Result layer	Key value(s)	Conclusion	Scientific status
Network topology	10 nodes; 27 edges; density 0.600; one connected component	The benchmark is adequate for finite-cycle, curvature and spectral diagnostics.	Benchmark-validating
Stress field	SAS = 100.00; CAS = 71.79; EAP = 71.23; CAU = 66.03	Stress is a composite systemic-exposure object, not a GDP-only measure.	Benchmark-validating
Spectral mass gap	$\lambda_0 = 0.0000$; $\lambda_1 = 0.3850$; spectral radius = 3.5023	A positive finite-network threshold separates the normal connected mode from the first stress mode.	Core benchmark result
Transition threshold	$\Theta = \lambda_1 / \rho = 0.1099$	Defines the normalized local-to-systemic transition boundary.	Core benchmark result
Curvature/action	Total action = 2,514.0; top-five share = 78.329%	Stress-energy is concentrated in a small set of high-curvature cycles.	Mathematical benchmark
Monte Carlo audit	95% mass-gap interval = 0.3458-0.4254	Positive mass gap persists under reported perturbation uncertainty.	Internal robustness
Scenario threshold	Baseline $\Theta = 0.1099$; severe corridor shock $\Theta = 0.0420$	Stronger shocks compress the systemic boundary and make propagation easier.	Scenario diagnostic

Source: Author synthesis from the corrected finite-network benchmark and scenario architecture.

8.9.3. Interpretation of the Positive Economic Mass Gap

The positive economic mass gap should be read as a finite-network shock-threshold result. In the chapter's notation, the stress-weighted Laplacian L^S = D^S - W^S summarizes how stress can diffuse across the weighted corridor network. The first positive eigenvalue λ_1 measures the lowest non-trivial stress mode that can propagate through the network. A strictly positive λ_1 implies that the benchmark system has a measurable threshold separating local absorption from systemic transmissibility.

This interpretation is deliberately narrower than the physical meaning of a Yang-Mills mass gap. The chapter does not claim that economic stress is a physical field, that global corridors obey quantum gauge dynamics, or that the Clay problem has been solved. The term mass gap is used as a graph-spectral analogue. The admissible claim is that a finite weighted

economic stress network can exhibit positive spectral separation, and that this separation can be used as an interpretable systemic-threshold indicator.

The normalized threshold $\Theta = \lambda_1 / \rho = 0.1099$ is particularly useful because it expresses the mass gap relative to the network's upper diffusion scale. A positive λ_1 alone indicates separation; the normalized threshold indicates how much separation remains after accounting for the total stress-diffusion capacity of the network. This is why the scenario layer focuses not only on λ_1 but also on spectral radius and normalized threshold. A shock can leave λ_1 positive while still compressing Θ enough to make system-wide transmission materially easier.

8.9.4. Closing Formula Map

Table 8.9.3. Final formula map used in the chapter conclusion.

Object	Closing formula	Chapter-level meaning
Stress-weighted adjacency	W^S_ij = W_ij · g(S_i, S_j)	Embeds node stress into corridor-weighted edges.
Stress Laplacian	L^S = D^S - W^S	Defines diffusion and spectral separation.
Finite-network mass gap	Δ_econ = λ_1(L^S), $\lambda_1 > 0$	Measures the first transmissible stress mode.
Normalized transition threshold	$\Theta = \lambda_1 / \rho$(W^S)	Scales protection by the network diffusion radius.
Gauge potential	A_ij = -A_ji	Encodes oriented edge-level stress tension.
Triangular curvature	F_ijk = A_ij + A_jk + A_ki	Measures non-neutralized cycle circulation.
Economic action	S_YM^econ = Σ_Δ ω_ijk F_ijk²	Aggregates squared curvature as stress-energy.
Fragility identity	Fragility_i = 100 - EMGI_i	Converts protection into vulnerability.
Scenario threshold	Θ^(h) = λ_1^(h) / ρ^(h)	Measures how shocks compress the transition boundary.

Source: Author synthesis from the Chapter 8 methodological architecture.

8.9.5. EMGI, Fragility and BridgeStress Conclusions

The EMGI layer is the mechanism through which the system-level mass gap becomes interpretable at the node level. A single eigenvalue can prove that the benchmark network has spectral separation, but it cannot by itself identify which nodes are structurally protected, which are fragile, and which are strategically exposed. EMGI solves this interpretive problem by combining local spectral protection, centrality, income depth, resilience, systemic stress and curvature exposure into a reproducible structural-protection index.

The final EMGI hierarchy confirms that large output mass and structural protection often coincide, but not always. North America and Europe occupy the strongest protection positions, while East Asia-Pacific and MENA remain systemically important but more exposed to stress and curvature channels. Latin America is fragile, and the Caucasus, Sub-Saharan Africa, Central Asia, South Asia and Oceania fall into critical-fragile or structurally exposed categories. The mechanisms differ by node: some are affected mainly by income-depth constraints, others by stress intensity, low centrality, corridor exposure or curvature participation.

BridgeStress is the chapter's strongest corridor-specific contribution. It separates strategic bridge exposure from simple size and centrality. The Caucasus obtains BridgeStress = 100.00, while Central Asia obtains BridgeStress = 78.24. These values do not mean that these nodes dominate global GDP. They mean that their corridor function makes them important for stress transmission across larger systems. In a corridor-sensitive network, a small node can be systemically meaningful because it is located at a transmission interface.

Table 8.9.4. EMGI, fragility and BridgeStress closing interpretation.

Node / region	Closing classification	Reported signal	Interpretive conclusion
North America	Very high protection	EMGI = 100.00	Large mass, high income depth and strong systemic absorption capacity.
Europe	High protection	EMGI = 90.15	Large integrated node with strong structural protection and corridor exposure.

East Asia-Pacific	Intermediate systemic node	High activity with meaningful stress exposure	Dominant spillover target under several scenarios.
MENA	Intermediate exposed node	Energy-geopolitical stress interface	Important for energy/geopolitical corridor shock interpretation.
Latin America	Fragile	Moderate/weak protection	Fragility is not only output-based; it reflects stress and resilience configuration.
Caucasus	Critical-fragile but high bridge exposure	BridgeStress = 100.00	Black Sea-Caucasus-Caspian transfer function; high strategic corridor exposure.
Central Asia	Critical-fragile but high bridge exposure	BridgeStress = 78.24	Land-bridge and Caspian interface; becomes more visible under logistics and geopolitical shocks.
South Asia	Critical-fragile stress node	Stress field benchmark: SAS = 100.00	High systemic stress despite not being the largest output-mass node.

Source: Author synthesis from EMGI, fragility and BridgeStress results.

8.9.6. Scenario Simulations and Local-to-Systemic Transition

The scenario simulations convert the benchmark from a static spectral result into a transition diagnostic. They ask how the network behaves when stress is injected through inflation/price pressure, financial-spread stress, trade/logistics corridor disruption and energy/geopolitical corridor shock. The main conclusion is monotonic threshold compression: as shock intensity rises, λ_1 falls, spectral radius rises, normalized threshold falls, Yang-Mills economic action rises and mean EMGI deteriorates.

This pattern is scientifically important because it shows that local-to-systemic transition is measurable. In the baseline, the normalized threshold is 0.1099. Under inflation/price-pressure stress it falls to about 0.092. Under financial-spread stress it falls to about 0.0747. Under trade/logistics corridor shock it falls to about 0.0578. Under the strongest energy/geopolitical corridor shock it falls to 0.0420. The system remains connected and the mass gap remains positive in the reported scenarios, but protection becomes materially thinner.

Action amplification reinforces this interpretation. Total action rises from 2,514.0 at baseline to 5,010.0 under the strongest energy/geopolitical corridor shock. This means that the system does not merely become more connected; it becomes more curvature-intensive. Stress-energy concentrates more strongly in the network's cycle structure, making corridor channels more important in the movement from local disturbance to systemic transmission.

Table 8.9.5. Scenario closure: threshold compression and action amplification.

Scenario	Amplitude	λ_1	Spectral radius	Θ	Action	Mean EMGI Δ	Closing interpretation
Baseline	0.000	0.3850	3.5023	0.1099	2,514.0	0.00	Benchmark finite-network state
Inflation / price pressure	0.500	0.3337	3.6526	0.0915	2,925.0	-6.20	Moderate macro stress weakens protection
Financial-spread stress	0.750	0.2836	3.7989	0.0747	3,435.0	-10.80	Funding stress compresses protection
Trade / logistics corridor shock	1.000	0.2334	4.0413	0.0578	4,088.0	-15.30	Corridor disruption raises CAS/CAU visibility
Energy / geopolitical	1.250	0.1796	4.2795	0.0420	5,010.0	-22.40	Systemic corridor shock

corridor shock							strongly compresses threshold

Source: Author synthesis from the scenario-output architecture in Chapter 8.

Figure 8.9.2. Threshold compression across scenario simulations.

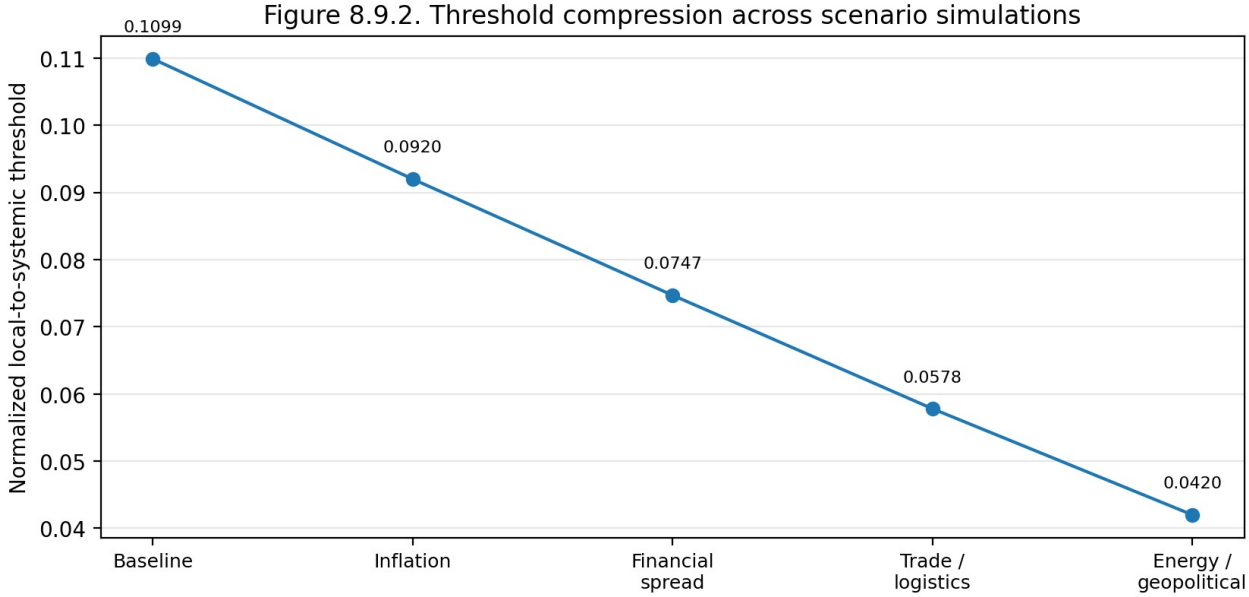
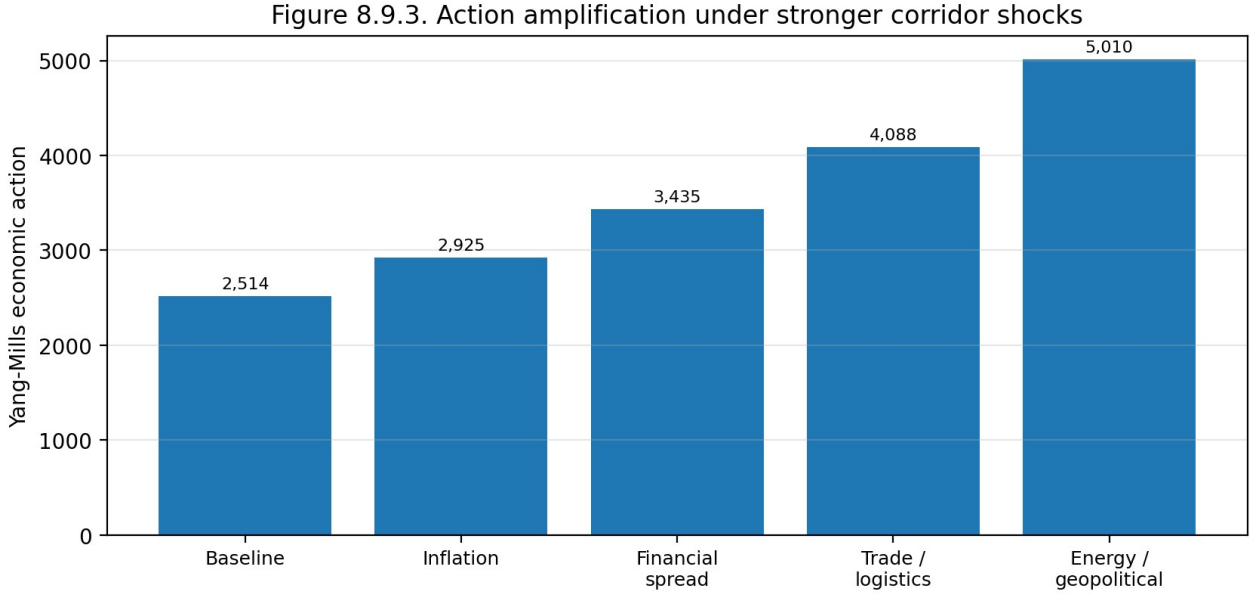


Figure 8.9.3. Action amplification under stronger corridor shocks.



8.9.7. Evidence Hierarchy and Claim Discipline

The chapter's evidence hierarchy is central to its scientific credibility. It prevents a common problem in mathematically inspired economic modelling: the temptation to treat a coherent analogy as if it were a theorem or a causal law. Chapter 8 avoids this by separating the evidence into admissible layers. Some claims are benchmark-confirmed because the matrices, formulas and outputs are complete. Some are diagnostic because the sample is small or the variables are constructed. Some are scenario-based because they are model-implied shock experiments. Some remain future validation claims because the N = 1,500 country-year layer is specified but not yet numerically closed.

The strongest current claim is therefore not causal. It is a finite-network benchmark claim: the completed stress network yields a positive mass gap, non-uniform curvature/action concentration, reproducible EMGI/fragility rankings, corridor BridgeStress exposure and scenario-based threshold compression. The weaker claim is not ignored; it is explicitly labeled.

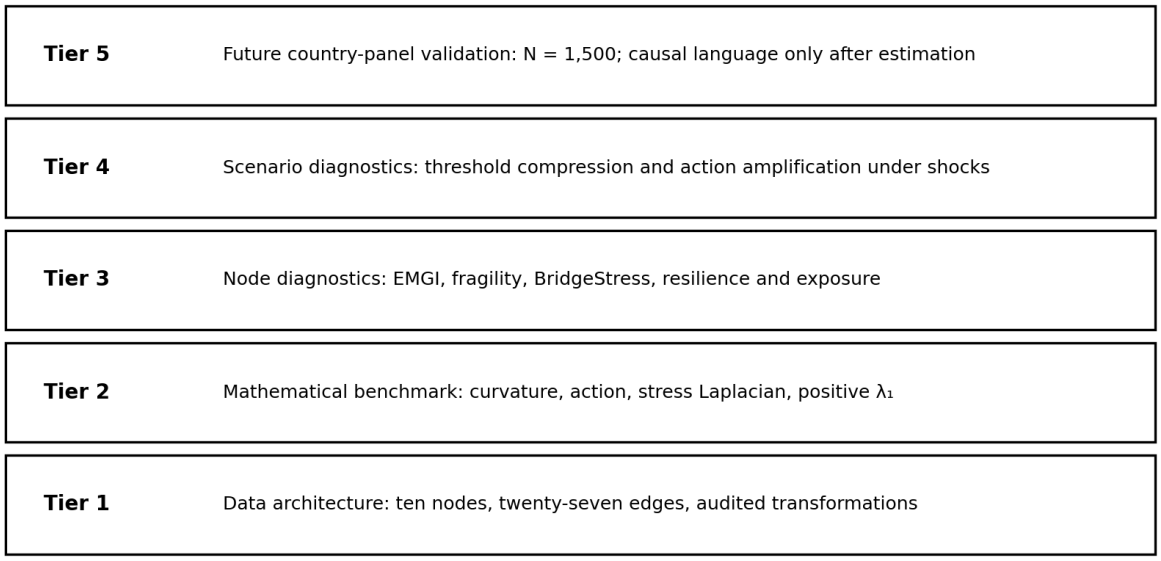
Country-level causal validation, external-outcome prediction and robust panel inference require the populated and estimated N = 1,500 country-year dataset.

Table 8.9.6. Final claim-boundary matrix for Chapter 8.

Status	Claim type	Evidence base	Required wording
Allowed now	Finite-network benchmark claim	$\lambda_1 > 0$, connected graph, action concentration, EMGI/BridgeStress outputs	Use benchmark language.
Allowed now	Scenario diagnostic claim	Threshold compression and action amplification under declared shocks	Use model-implied scenario language.
Allowed with caution	Ten-node diagnostic association	Small-sample regressions, network-spatial screens, PCA/factor screens	Do not use causal language.
Allowed with caution	Placebo and robustness evidence	Monte Carlo bands, filtered graphs, randomized networks	Treat as internal robustness or cautionary evidence.
Reserved	Country-level causal validation	N = 1,500 fixed effects, two-way FE, Driscoll-Kraay, panel-IV, dynamic panels	Only after country-year estimation and external validation.
Excluded	Clay Yang-Mills theorem claim	Physical existence and mass-gap proof	Never claimed in the monograph.

Source: Author claim-gate synthesis from Chapter 8 and the monograph-wide claim boundary.

Figure 8.9.4. Claim-gated evidence hierarchy of Chapter 8.



8.9.8. Position inside the Seven-Problem Monograph

Chapter 8 occupies the gauge-threshold position inside the monograph's seven-problem architecture. The Perelman-Ricci-Poincare chapter measures pressure, curvature, entropy and smoothing capacity; the Hodge chapter decomposes global macro-flow into gradient, curl and harmonic components; the Navier-Stokes chapter models liquidity stress through flow, pressure, friction and closure; Chapter 8 then adds gauge potential, curvature action and a spectral shock threshold. The following BSD chapter will shift the logic toward local-to-global structural rank, LOrder and corridor rank formation.

The monograph therefore does not present seven isolated articles. It presents seven mathematical measurement grammars. Chapter 8 is the point at which network stress becomes a gauge field and systemic transition becomes a spectral threshold. This makes it a bridge between the flow chapters before it and the local-to-global rank chapter after it. In methodological

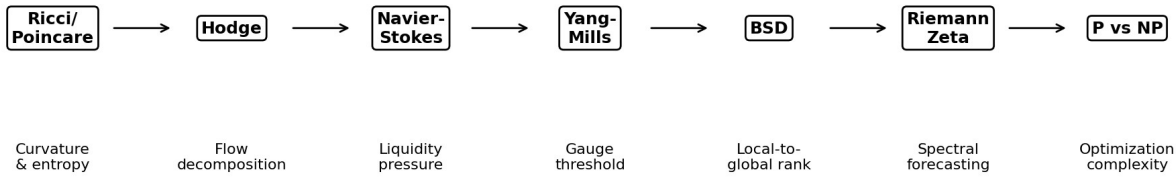
terms, it also reinforces the monograph's general rule that constructed economic analogues must be auditable, reproducible and claim-bounded.

Table 8.9.7. Chapter 8 inside the seven-problem monograph.

Book chapter	Clay-inspired logic	Economic measurement grammar	Connection to Chapter 8
Chapter 5	Perelman / Ricci / Poincare	Inequality pressure, curvature, entropy and smoothing capacity	Supplies curvature and pressure logic before network gauge interpretation.
Chapter 6	Hodge	Gradient, curl and harmonic macro-flow decomposition	Supplies flow decomposition and cycle/circulation intuition.
Chapter 7	Navier-Stokes	Liquidity velocity, pressure, friction, shock and closure	Supplies dynamic systemic-stress balance.
Chapter 8	Yang-Mills	Gauge potential, curvature, action, mass-gap threshold	Converts corridor stress into finite-network spectral threshold.
Chapter 9	Birch-Swinnerton-Dyer	Local-to-global structural rank, Euler-factor analogues and LOrder	Extends threshold logic toward rank formation and regional closure.
Chapter 10	Riemann / Zeta	Spectral cyclic signal and inflation forecasting validation	Adds time-series spectral validation discipline.
Chapter 11	P vs NP	Sparse portfolio optimization and computational complexity	Adds search-space, algorithmic and exact/heuristic evidence discipline.

Source: Author synthesis from the monograph transition matrix.

Figure 8.9.5. Chapter 8 as the gauge-threshold bridge inside the seven-problem monograph.



8.9.9. Validation Pathway after the Chapter Conclusion

The chapter's final empirical pathway is the N = 1,500 validation design. This future layer consists of 100 countries observed over fifteen years and is intended to convert the benchmark into a country-panel validation system. Its role is not to replace the completed finite-network result, but to test whether the benchmark logic survives a more granular empirical environment with country-level controls, time effects, cross-sectional dependence, external outcomes and replication checks.

The validation pathway should proceed through a strict order. First, country-year variables must be populated and normalized. Second, country-level stress, resilience, corridor exposure, curvature proxies and mass-gap-related diagnostics must be reconstructed using disclosed formulas. Third, fixed-effects, two-way fixed-effects, Driscoll-Kraay, clustered, dynamic-panel, panel-IV, factor and external-validation models must be estimated. Fourth, all tables, scripts, seeds, hashes and external-outcome links must be archived. Only after these steps can the chapter's language move from benchmark-validating and scenario-diagnostic to stronger country-panel validation.

This is why 8.8 and 8.9 are scientifically necessary. They prevent the chapter from claiming too much too early. A completed benchmark with a positive finite-network mass gap is already a strong contribution. But it remains a finite-network benchmark. The N = 1,500 layer is the route to external empirical closure, not evidence that has already been produced.

Table 8.9.8. N = 1,500 validation pathway after Chapter 8.

Step	Validation layer	Operational object	Claim gate
1	Panel construction	100 countries × 15 years = N = 1,500	Country-year data populated, normalized and audited.
2	Variable lineage	Public anchors versus author-calculated outputs	Every constructed variable traceable to source, formula and script.
3	Baseline models	Country FE and two-way FE	Signs, magnitudes and within-country consistency reported.
4	Robust inference	HC3, clustered, HAC/Driscoll-Kraay	Cross-sectional dependence and serial correlation addressed.
5	Advanced validation	Dynamic panel, panel-IV, factor and external proxy models	Causal language allowed only if identification and robustness support it.
6	Replication closure	Scripts, seeds, hashes, output files and Zenodo archive	Independent audit possible.

Source: Author synthesis from the Chapter 8 validation pathway.

8.9.10. Limitations, Reviewer-Safety and Scientific Contribution

The chapter's limitations are part of its scientific design. The ten-node network is intentionally finite and benchmark-oriented. It is suitable for graph topology, curvature, action, spectral separation, EMGI, BridgeStress and scenario diagnostics. It is not suitable for final country-level causal claims. This distinction should remain visible in the final monograph because it protects the chapter from the main reviewer risk associated with mathematically inspired economic modelling: overclaiming the evidentiary status of constructed objects.

The second limitation is that edge weights and corridor exposure are author-calculated. This is acceptable only because the transformations are disclosed, the data package is archived, and the interpretation is benchmark-diagnostic rather than transaction-level descriptive. The graph is not a literal map of all global trade, finance, logistics or energy flows. It is an analytical stress-transmission graph calibrated from public anchors and corridor-coded transformations.

The third limitation is that scenario simulations are model-implied shock experiments. They are useful because they reveal how the benchmark threshold behaves under structured stress, but they are not predictions of actual future crises. The correct wording is that shocks compress the model's local-to-systemic transition boundary. The incorrect wording would be that the model predicts a specific crisis event.

Despite these limitations, the contribution is strong. Chapter 8 introduces a reproducible finite-network gauge-econometric measurement pipeline for systemic shock thresholds. It connects macroeconomic stress, corridor topology, gauge potential, triangular curvature, Yang-Mills economic action, stress-Laplacian mass gap, EMGI, fragility, BridgeStress and scenario diagnostics within one claim-disciplined architecture. This is a substantive methodological contribution to mathematical-econometric systemic-risk measurement.

Table 8.9.9. Reviewer-safety controls for the chapter conclusion.

Reviewer risk	Why it matters	Final safeguard in Chapter 8
Overstating Clay relevance	Reader may think the chapter claims a mathematical theorem.	Repeatedly state finite-network economic analogue; exclude theorem proof.
Small benchmark size	Ten nodes cannot support final causal econometrics.	Use benchmark, diagnostic and scenario language; reserve causal claims for N = 1,500.
Constructed-variable circularity	Author-calculated variables may overlap.	Maintain variable-lineage audit, anti-circularity tests and external validation pathway.

Scenario overinterpretation	Simulations may be mistaken for forecasts.	Label as model-implied stress tests and threshold diagnostics.
Corridor narrative inflation	BridgeStress may be read as geopolitical advocacy.	Anchor interpretation in formulas, rankings and claim-boundary language.
Replication opacity	Complex mathematical language may appear opaque.	Keep source ledger, matrices, scripts, seeds and Zenodo archive visible.

Source: Author synthesis from the monograph claim-boundary protocol.

8.9.11. Final Chapter Conclusion

Chapter 8 concludes that a global and corridor-sensitive macroeconomic stress system can be represented as a finite weighted network in which gauge-theoretic concepts become operational measurement tools. The chapter's central numerical result is the positive finite-network economic mass gap $\lambda_1 = 0.3850$, with spectral radius 3.5023 and normalized transition threshold 0.1099. The result establishes that the benchmark network has a measurable separation between ordinary connectedness and the first transmissible systemic stress mode.

The chapter further concludes that systemic stress is highly structured. Yang-Mills economic action equals 2,514.0, and the top-five action concentration of 78.329% shows that stress-energy is concentrated in a limited number of cycle channels. EMGI and fragility translate spectral protection into node-level vulnerability, while BridgeStress identifies strategically exposed corridor nodes such as the Caucasus and Central Asia. Scenario simulations show that stronger shocks compress the threshold and increase curvature/action concentration, thereby making local disturbances more systemically transmissible.

The admissible final claim is therefore precise: Chapter 8 provides a completed, auditable finite-network benchmark and a fully specified validation pathway for measuring systemic shock thresholds in global and corridor flow networks. It does not prove the classical Yang-Mills mass-gap theorem, does not claim that the world economy is a physical gauge field, and does not yet establish final country-panel causality. Its contribution is methodological, empirical and interpretive: it shows how gauge potential, curvature, action and spectral separation can be used as a disciplined economic measurement grammar for corridor-sensitive systemic risk.

This conclusion prepares the transition to Chapter 9. After Chapter 8 identifies how corridor stress becomes systemically transmissible through gauge curvature and spectral threshold compression, Chapter 9 can examine how local regional signals accumulate into global structural rank under a Birch-Swinnerton-Dyer-inspired local-to-global architecture. In the monograph's sequence, Yang-Mills supplies the language of threshold and stress energy; BSD supplies the language of local reductions, rank formation and L-function-style structural aggregation.

Table 8.9.10. Final chapter conclusion matrix.

Closing item	Finding	Reported value / status	Final interpretation
Core conclusion	Positive finite-network economic mass gap	$\lambda_1 = 0.3850$	Strong benchmark result
Systemic threshold	Normalized transition boundary	$\Theta = 0.1099$	Strong benchmark result
Stress-energy geometry	Total action and action concentration	2,514.0; top-five share 78.329%	Mathematical benchmark
Node protection	EMGI and fragility hierarchy	NA = 100.00; Europe = 90.15	Node diagnostic
Corridor exposure	BridgeStress hierarchy	CAU = 100.00; CAS = 78.24	Corridor diagnostic
Shock transition	Threshold compression under severe corridor shock	Θ falls to 0.0420; action rises to 5,010.0	Scenario diagnostic
Claim boundary	No Clay theorem proof; no final country-panel causality yet	N = 1,500 pathway specified	Scientific discipline
Monograph transition	Bridge to BSD local-to-global rank logic	Chapter 9 follows	Structural integration

Source: Author synthesis from Chapter 8.

9.1. BSD Logic and Economic Local-to-Global Translation

Section Abstract. This section establishes the conceptual and methodological entry point for Chapter 9. It explains how the Birch-Swinnerton-Dyer local-to-global grammar is translated into a bounded economic measurement architecture for regional structural rank formation under corridor stress. The section does not treat economies as elliptic curves and does not claim to prove, test or replicate the classical BSD conjecture. Instead, it defines a disciplined analogy in which public macro-regional anchors, systemic stress, corridor exposure, economic curve coefficients, finite-state trace analogues, Euler-factor analogues, a constructed economic L-function, LOrder and structural rank are linked through an auditable transformation chain. The purpose is to prepare the reader for Chapter 9.2-9.9 by clarifying the language, admissible claims and evidentiary hierarchy of the BSD-inspired regional economic model.

Table 9.1.1. Executive orientation of the BSD economic translation

Core point	Meaning for Chapter 9.1	Reviewer-safety boundary
BSD is used as measurement grammar	The chapter borrows the logic of local signals informing global rank.	No theorem-level proof, no test of the classical conjecture.
The empirical object is regional	The World anchor and ten macro-regional/corridor nodes supply the coordinate system.	Not a country ranking and not a geopolitical ranking.
Local means finite-state regional information	Regional stress, corridor role and discretized state traces form the local information layer.	Finite states are economic regimes, not literal finite fields.
Global means structural rank	LOrder is compared with a constructed structural-rank object.	Rank correspondence is calibrated agreement, not analytic equality.
The chapter is synthesis-type	It links rank, corridor stress, L-function logic and N = 150 closure discipline.	Strongest claim is calibrated local-to-global measurement.

Source: Author synthesis for Chapter 9.1 based on the regional BSD-inspired manuscript and the monograph editorial architecture.

9.1.1. Why Chapter 9 Begins with Local-to-Global Translation

Chapter 9 is not simply another applied chapter in the monograph. It is the synthesis-type chapter in which several themes developed earlier in the book are brought together through the strongest possible local-to-global measurement language. The Perelman-Ricci chapter organizes pressure and smoothing capacity; the Hodge chapter decomposes regional flow into hierarchy, curl and circulation; the Navier-Stokes chapter measures liquidity-flow stress; the Yang-Mills chapter formalizes corridor shocks as finite-network curvature and spectral thresholds. The BSD chapter adds a different organizing question: can local regional states, when represented through disciplined finite-state and Euler-factor analogues, contain measurable information about global structural economic rank?

This question is important because regional economics often treats global structure either as aggregate scale or as a set of country and region rankings. GDP, GDP per capita, growth, trade share, logistics exposure and technological capacity remain essential inputs, but they do not by themselves define how local regional information becomes global structural rank. A region can have large output mass but weak corridor sensitivity; another can have modest output but high transmission relevance. The BSD-inspired architecture is therefore introduced to distinguish scale, state, trace, rank and corridor transmission within one transparent measurement chain.

The purpose of this opening section is to define the grammar before the technical apparatus begins. Chapter 9.2 will specify the research object; Chapter 9.3 will define the World anchor, ten regional/corridor nodes and N = 150 closure layer; Chapters 9.4 and 9.5 will formalize coefficients, discriminants, finite-state reductions, Euler factors, economic L-function behavior, LOrder and structural rank; Chapters 9.6-9.8 will interpret results, robustness, anti-circularity and claim hierarchy; Chapter 9.9 will close the chapter. Section 9.1 therefore performs the necessary conceptual conversion: it explains what BSD contributes as a modelling architecture and what it does not authorize as a claim.

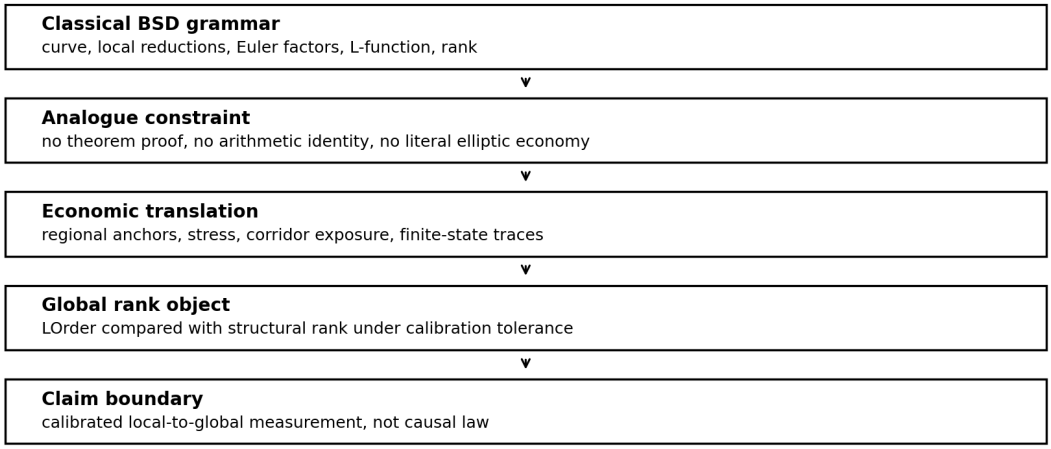


Figure 9.1.1. BSD-to-economics translation ladder: from mathematical grammar to bounded structural-rank measurement.

Figure 9.1.1. BSD-to-economics translation ladder: from mathematical grammar to bounded structural-rank measurement.

Source: Author synthesis for Chapter 9.1 based on the regional BSD-inspired manuscript and the seven-problem monograph architecture.

9.1.2. The Classical BSD Logic as a Local-to-Global Grammar

In its original mathematical setting, the Birch-Swinnerton-Dyer conjecture belongs to the arithmetic theory of elliptic curves. It links local information, encoded through reductions and local factors, to global information about rank, encoded through the behavior of an L-function. For the purposes of this monograph, the important point is not to reproduce the technical content of the conjecture. The important point is that BSD supplies a rigorous example of local-to-global reasoning: many local signals are not interpreted separately; they are organized into a global analytic object whose behavior is related to rank.

The economic translation follows this architecture at the level of measurement grammar only. It does not state that a region is an elliptic curve, that macroeconomic states are rational points, that finite-state reductions are point counts over finite fields, or that LOrder is a classical analytic order of vanishing. Instead, it uses the BSD structure as a disciplined way to ask whether local regional regimes and corridor-sensitive stress signals can be aggregated into a global rank object that is more informative than GDP mass alone.

The distinction is crucial. A weak analogue would borrow prestigious terminology and then apply it loosely. The present chapter is designed to avoid that error. Every translated object must have an economic definition, a transformation rule, an empirical role and a claim boundary. The curve coefficient layer must be connected to regional stress and capacity variables. The finite-state layer must represent controlled economic discretization. The Euler-factor layer must summarize local information without pretending to be arithmetic. The economic L-function must be a constructed measurement object. LOrder must be an order-of-behavior indicator evaluated against structural rank, not a theorem-level analytic invariant.

Table 9.1.2. Classical BSD grammar and bounded economic translation

Classical BSD object	Economic translation in Chapter 9	Admissible interpretation	Explicitly excluded interpretation
Elliptic curve	Regional economic curve analogue built from coefficient mappings.	Formal coefficient space for stress, capacity and corridor state.	The economy is literally an elliptic curve.
Discriminant	Non-degeneracy audit for constructed regional coefficient pairs.	Quality gate preventing singular or unusable constructed objects.	Proof of arithmetic regularity.
Local reductions	Finite-state economic regimes under q-base discretization.	Controlled local-state representation of regional conditions.	Point counts over mathematical finite fields.
Trace	Regional trace analogue summarizing local state behavior.	Signal of protective or stress-bearing regional	Classical Frobenius trace.

Classical BSD object	Economic translation in Chapter 9	Admissible interpretation	Explicitly excluded interpretation
		behavior.	
Euler factor	Local factor analogue built from trace and state information.	Local contribution to constructed global L-behavior.	True arithmetic Euler factor.
L-function	Constructed economic L-function analogue.	Global summary of local-to-global measurement information.	Classical Hasse-Weil L-function.
Order of vanishing	LOrder order-of-behavior measure around the constructed reference point.	Calibrated analogue compared with structural rank.	Analytic rank equality theorem.
Rank	Structural economic rank built from productive, Hodge-flow, network and agentic components.	Global structural-rank object beyond GDP mass.	Mordell-Weil rank.

Source: Author translation matrix for Chapter 9.1.

9.1.3. The Economic Problem: Rank Is Not Reducible to Output Mass

The economic motivation for using a BSD-inspired architecture is that regional rank formation is not reducible to aggregate output. Output mass is a central coordinate of world economic power, but structural rank also depends on productive complexity, income depth, growth pressure, resilience, network position, corridor exposure, agentic capacity, fragility and transmission leverage. A GDP table can show which regions are large, but it cannot by itself show whether local regional states contain information about the formation of global structural rank.

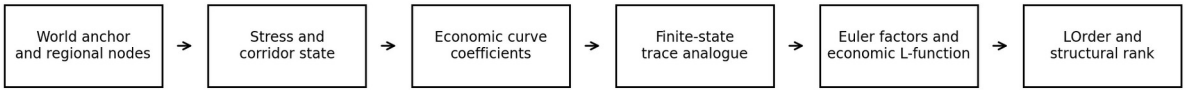
The local-to-global problem arises precisely because regional variables operate at different scales. Local stress may be small in absolute global output terms but large in corridor-transmission terms. Growth pressure may signal momentum in one region and vulnerability in another. Income depth may protect some regions from shock transmission while leaving others exposed. Corridor role can make a region structurally relevant even when GDP mass is low. For this reason, Chapter 9 treats the world economy not as a flat ranking of regions, but as a structured regional system whose local states require transformation before global rank can be interpreted.

The BSD logic is useful because it forces the model to avoid two symmetrical mistakes. The first mistake is pure aggregation: assuming that global structure is obtained by simply adding local indicators. The second mistake is pure narrative: asserting corridor importance without a formal route from local information to global rank. The economic BSD translation avoids both. It requires local information to pass through coefficients, non-degeneracy checks, finite-state traces, local-factor aggregation, LOrder calibration and structural-rank comparison.

Table 9.1.3. Why local-to-global rank modelling is needed beyond GDP mass

GDP-only reading	Local-to-global reading	Why BSD-inspired translation helps
Large regions dominate because they have high output mass.	Large regions may dominate mass but not every rank, stress or corridor dimension.	Separates mass from structural-rank formation.
Small regions appear marginal.	Small corridor regions may carry high transmission significance.	Makes corridor leverage visible through local-state and BridgeStress logic.
Rank is a scalar ordering.	Rank is a composite structural object with productive, network, Hodge-flow and agentic dimensions.	Provides a rank object comparable with LOrder.
Regional stress is a descriptive indicator.	Stress becomes part of a local-state transformation chain.	Links stress to coefficients, traces and Euler-factor analogues.
Validation is a regression afterthought.	Validation is part of the evidence hierarchy through N = 150 closure gates.	Prevents analogy from being mistaken for causal proof.

Source: Author synthesis for Chapter 9.1.



Local regional information becomes global only after transformation, aggregation, calibration and claim-boundary discipline.

Figure 9.1.2. Local-to-global measurement chain in the economic BSD chapter.

Figure 9.1.2. Local-to-global measurement chain in the economic BSD chapter.

Source: Author synthesis for Chapter 9.1 based on the regional BSD-inspired manuscript and the seven-problem monograph architecture.

9.1.4. Defining Local and Global in the Economic BSD Analogue

The terms local and global must be defined carefully. In the classical mathematical setting, local objects refer to reductions and local factors. In the economic translation, local does not mean small, provincial or statistically minor. It means region-specific state information before global aggregation. A local regional state may include stress, growth pressure, income-depth fragility, resilience, corridor role, network position and finite-state discretization. It becomes analytically meaningful only after the model specifies how such state information is encoded and how it enters the constructed global object.

Global, in the present chapter, does not mean a single world total. It means the structural object generated by the interaction of local regional information. The economic L-function analogue, LOrder and structural rank are global because they summarize local information into a system-level measure. The World anchor is not itself the global result; it is the normalization base that allows regional quantities to be placed on a common scale. Structural rank is the global interpretive target because it measures the system position of regions after productive, Hodge-flow, network and agentic dimensions have been integrated.

This distinction is central to claim discipline. If local information is not formally specified, then global rank becomes narrative. If global rank is only GDP, then local information is ignored. The BSD-inspired architecture occupies the middle position: local states are formalized, transformed and aggregated into a constructed global object, but the final correspondence remains a calibrated empirical measurement claim rather than a theorem.

Equation (9.1) LocalState_{r,t} = f(Stress_{r,t}, Corridor_{r,t}, Resilience_{r,t}, NetworkPosition_{r,t}, Capacity_{r,t})

Equation (9.1) states the conceptual form of the local economic state. It is not the final estimation equation of Chapter 9. It clarifies that local information is multidimensional and cannot be represented by output mass alone.

Equation (9.2) GlobalRankSignal_t = G({LocalState_{r,t}}_{r=1}^{10}; WorldAnchor_t)

Equation (9.2) expresses the local-to-global aggregation idea. The World anchor fixes the scale, while local regional states are transformed into a global rank signal through the BSD-inspired measurement chain developed in later sections.

Table 9.1.4. Definitions of local and global objects in the economic BSD translation

Term	Meaning in Chapter 9.1	Empirical or conceptual status
Local state	Region-year information before global aggregation: stress, capacity, corridor role, resilience and network position.	Constructed from public anchors and author-calculated transformations.
World anchor	Normalization reference for GDP, growth and income-depth scale.	Benchmark anchor, not competing regional observation.
Finite-state reduction	Controlled discretization of regional state information under q-base grids.	Economic regime analogue, not arithmetic field reduction.
Euler-factor analogue	Local contribution formed from trace and finite-state behavior.	Measurement object feeding the constructed L-function.
Economic L-function	Global product/synthesis object summarizing local-factor information.	Constructed analogue, not a classical mathematical L-function.
LOrder	Order-of-behavior measure derived from economic L-	Compared with structural rank;

Term	Meaning in Chapter 9.1	Empirical or conceptual status
	function behavior.	not analytic rank.
Structural rank	Composite global rank object built from productive, Hodge-flow, network and agentic dimensions.	Constructed measurement target.

Source: Author definitions for Chapter 9.1.

9.1.5. The Measurement Chain from Public Anchors to LOrder

The BSD-inspired economic framework has value only if the transformation chain is explicit. Chapter 9 begins with public macro-regional anchors: GDP mass, world-output share, growth, income depth and related corridor-relevant inputs. These anchors do not themselves constitute the BSD analogue. They are the empirical base from which stress, network structure, coefficient mappings and rank objects are constructed. The first methodological obligation is therefore lineage: every derived object must be traceable back to its input family and transformation rule.

The second stage is stress and corridor coding. Regional stress differentiates output mass from vulnerability, transition pressure and fragility. Corridor coding prevents analytically important corridor nodes from disappearing inside broad aggregates. The third stage maps this economic information into coefficient space. The fourth stage audits non-degeneracy through discriminant logic. The fifth stage represents regional states through finite-state trace analogues. The sixth stage builds local factor analogues and a constructed economic L-function. The seventh stage computes LOrder. The eighth stage compares LOrder with structural rank.

The sequence matters because it prevents the model from jumping directly from raw data to symbolic claims. The chapter is strong only if every symbolic layer is tied to an empirical layer and every empirical layer is interpreted within its claim boundary. This is the methodological meaning of the BSD translation: it is not a metaphor, but neither is it theorem proof. It is a structured conversion from local regional data to global rank measurement.

Table 9.1.5. Measurement chain from anchors to LOrder and structural rank

Stage	Object produced	Purpose in Chapter 9	Failure avoided
1	Public regional anchors	Define the empirical coordinate system.	Unanchored constructed-index design.
2	Stress and corridor state	Capture vulnerability and transmission role beyond mass.	GDP-only interpretation.
3	Economic curve coefficients	Create a formal coefficient space for regional states.	Loose mathematical metaphor.
4	Discriminant audit	Check whether constructed curve analogues are usable.	Degenerate or mechanically forced objects.
5	Finite-state trace analogues	Represent local regional states under controlled discretization.	Narrative local-state claims.
6	Euler factors and economic L-function	Aggregate local signals into a global behavior object.	Unstructured aggregation.
7	LOrder	Measure order-of-behavior of the constructed L-function.	Claiming classical analytic rank.
8	Structural-rank comparison	Test calibrated correspondence between local-to-global signal and rank.	Unvalidated symbolic correspondence.
9	Closure and falsification gates	Classify evidence strength and prevent overclaiming.	Theorem-level or causal overstatement.

Source: Author synthesis based on the BSD methodology architecture.

9.1.6. Finite-State Reductions as Economic Regime Logic

The most delicate translation in the chapter is the finite-state layer. In classical BSD reasoning, local reductions are mathematically precise objects. In the economic analogue, the chapter does not pretend to recreate that arithmetic structure. Instead, it uses finite-state reductions as controlled economic regime grids. A region-year observation can be mapped into discrete state behavior under selected q-bases, such as q = 2, 3, 5, 7 and 11, not because those bases are prime fields in the economic sense, but because they provide a disciplined way to test whether local regional signs and trace behavior remain stable under alternative discretizations.

This regime logic is important for reviewer safety. If a local-to-global model depends on a single arbitrary discretization, it is fragile. If trace signs and broad local-state behavior remain stable across several q-bases, the measurement claim becomes stronger. It is still not a mathematical local reduction, but it is a valid economic sensitivity device. The q-base layer therefore converts the BSD inspiration into an auditable robustness mechanism.

The finite-state layer also helps distinguish local regional information from simple regional labels. A region is not assigned a structural role merely because it is large, small or strategically located. It receives local-state signals through stress, corridor

role, capacity and discretized behavior. These signals then contribute to trace analogues and Euler factors. The chapter thus turns corridor narratives into formal local-state information while keeping the transformation bounded.

Equation (9.3) TraceAnalog_{r,t,q} = q + 1 - StateCount_{r,t,q}^{econ}

Equation (9.3) is a conceptual trace-analogue expression. The term StateCount^{econ} denotes an economic finite-state count or regime score under the selected q-base. It is not a classical point count; it is a controlled regional-state measurement device.

Equation (9.4) LocalFactor_{r,t,q}(s) = [1 - TraceAnalog_{r,t,q} q^{-s} + q^{1-2s}]^{-1}

Equation (9.4) mirrors the algebraic shape of a local-factor expression only as an economic analogue. Its role is to organize local regional trace information into a factor-like object for constructed L-function behavior.

Table 9.1.6. Finite-state reductions as economic regime logic and reviewer-safety discipline

Risk in mathematical-economic analogy	Finite-state solution in Chapter 9	Claim discipline
Treating q-bases as literal finite fields.	Define q-bases as controlled economic state grids.	State explicitly that no arithmetic reduction is claimed.
Choosing one discretization and overfitting it.	Use multiple q-bases and compare sign/trace stability.	Interpret stability as robustness, not proof.
Letting corridor coding dominate trace behavior mechanically.	Audit local trace behavior under alternative coding and sensitivity checks.	Preserve corridor relevance without mechanical confirmation.
Confusing finite-state counts with observed data counts.	Treat state counts as author-calculated regime objects.	Maintain variable lineage and source-ledger documentation.
Moving from trace stability to causal validation.	Use trace stability only as local-to-global measurement evidence.	Causality remains outside 9.1 and requires separate designs.

Source: Author synthesis for Chapter 9.1.

9.1.7. Economic L-Function, LOrder and Structural Rank

The economic L-function analogue is the central global object of Chapter 9. It aggregates local-factor information into a constructed system-level behavior function. The point is not to reproduce the analytic theory of L-functions. The point is to create a transparent global object whose behavior can be compared with structural rank. Without this global object, the chapter would have local stress indicators but no local-to-global architecture. Without structural rank, the constructed L-function would have no economic target.

LOrder is the corresponding order-of-behavior measure. It is designed to summarize how the constructed economic L-function behaves near the declared reference point. In the classical BSD conjecture, the order of vanishing at a critical point is tied to rank. In the economic analogue, LOrder is compared with a structural-rank object built independently from productive, Hodge-flow, network and agentic components. The comparison is performed through rank gaps, agreement diagnostics, sensitivity checks and placebo logic in later sections.

This translation is scientifically strong only if the independence and lineage of the rank object are handled carefully. Structural rank cannot be defined as a direct restatement of LOrder. It must include components that make economic sense independently: productive depth, flow position, network importance and agentic capacity. Where LOrder and structural rank align under declared tolerances, the chapter can claim calibrated local-to-global consistency. Where they diverge or where external validation is weak, the chapter must demote the claim accordingly.

Equation (9.5) L_econ(s) = Product_{r,t,q} LocalFactor_{r,t,q}(s)

Equation (9.5) expresses the constructed economic L-function as an aggregation of local factor analogues. The product notation is conceptual in this section; later methodology sections specify the exact operational construction.

Equation (9.6) LOrder_{r,t} <-> StructuralRank_{r,t} within calibrated tolerance

Equation (9.6) is the central empirical analogue of the chapter. The symbol <-> means calibrated correspondence, not mathematical equality. The correspondence is evaluated through gaps, agreement measures and robustness checks.

Table 9.1.7. Economic L-function, LOrder and structural-rank interpretation

Object	Construction logic	Economic role	Claim limit
Economic L-function	Constructed from local-factor analogues across regions, time and q-base states.	Global summary of local regional information.	Not a classical L-function.
LOrder	Order-of-behavior indicator derived	Local-to-global signal to be	Not analytic order

Object	Construction logic	Economic role	Claim limit
	from constructed L-function behavior.	compared with structural rank.	of vanishing.
Structural rank	Composite rank from productive, Hodge-flow, network and agentic dimensions.	Independent global economic target.	Not welfare rank or political rank.
Rank gap	Difference between LOrder-implied rank signal and structural rank.	Measures calibration fit and mismatch.	Not theorem-level error term.
Agreement diagnostics	Equivalence, rank-scale error, visual alignment and sensitivity logic.	Audits whether correspondence is empirically stable.	Not causal validation by itself.
Placebo logic	Randomized or irrelevant comparison layers.	Tests whether correspondence is non-mechanical.	Does not solve external-validation weakness.

Source: Author synthesis for Chapter 9.1.

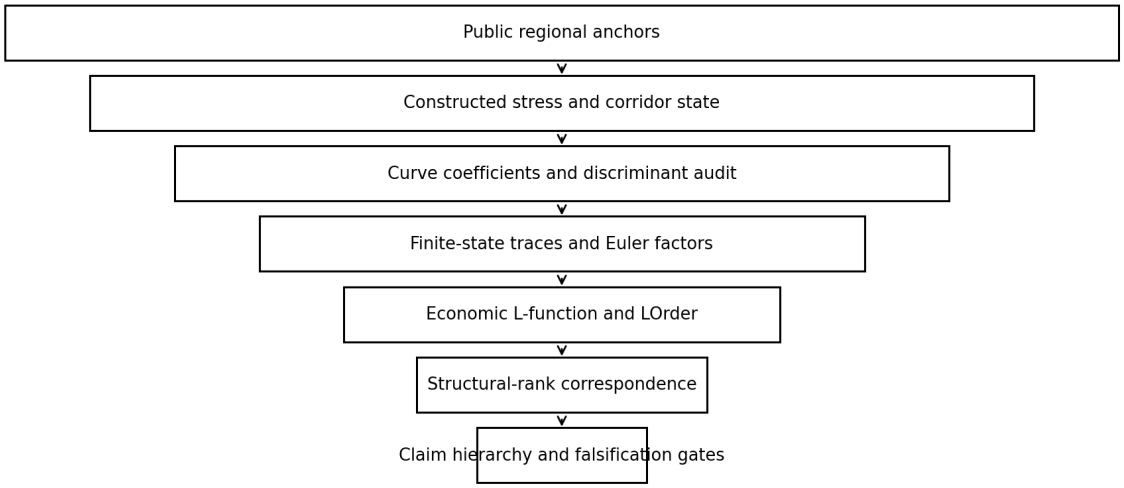


Figure 9.1.5. Evidence funnel: local information is narrowed into a defensible structural-rank claim.

Figure 9.1.5. Evidence funnel: local information is narrowed into a defensible structural-rank claim.
Source: Author synthesis for Chapter 9.1 based on the regional BSD-inspired manuscript and the seven-problem monograph architecture.

9.1.8. Corridor Stress as the Economic Meaning of Local-to-Global Transmission

The corridor dimension gives Chapter 9 its substantive economic force. A purely mathematical translation of BSD would be too abstract for regional economics. A purely regional macroeconomic model would be too descriptive to exploit local-to-global logic. Corridor stress connects the two. It explains why local regional states matter: some regions function as bridges, buffers, bottlenecks or transmission interfaces between larger economic spaces. Their contribution to global structural rank cannot be inferred from output mass alone.

The Caucasus, Central Asia, Black Sea and Caspian interfaces are analytically important in this logic because they illustrate the difference between mass and transmission position. A corridor-sensitive node can have modest GDP but high local-to-global significance if stress, fragility, network position and corridor role jointly affect global rank formation. The BSD-inspired model gives this insight a formal channel: corridor state contributes to local coefficients, trace behavior, BridgeStress and structural-rank interpretation.

The concept of BridgeStress should be understood as a corridor-rank diagnostic rather than a geopolitical assertion. It measures the extent to which a region appears structurally important because of transmission exposure, fragility and bridge position. This makes the corridor layer useful but also sensitive: coding rules must be transparent, sensitivity tests must be reported and the claim must remain methodological and diagnostic unless external evidence independently confirms a stronger interpretation.

Table 9.1.8. Corridor stress as economic local-to-global transmission

Corridor concept	Role in BSD-inspired chapter	Interpretive payoff	Boundary
Bridge region	A node whose position links larger macro-regional spaces.	Explains why low-mass regions may be systemically relevant.	Not a claim of political superiority.
Corridor stress	Local pressure associated with logistics, exposure, fragility or transmission role.	Turns narrative corridor relevance into measurable local-state information.	Requires transparent coding discipline.
BridgeStress	Composite corridor-rank diagnostic.	Identifies bridge exposure and rank leverage.	Diagnostic, not causal proof.
Local-to-global transmission	Mechanism by which local corridor states inform global structural rank.	Connects regional nodes to global rank formation.	Not literal arithmetic propagation.
Sensitivity to coding	Alternative corridor weights and scenario checks.	Prevents corridor result from being an imposed conclusion.	Cannot be ignored in final claim hierarchy.

Source: Author synthesis for Chapter 9.1.

9.1.9. Position of BSD within the Seven-Problem Monograph

The monograph is not a collection of seven articles transferred into book form. It is a unified architecture in which each Clay-inspired problem supplies a distinct economic measurement grammar. Chapter 9 is the rank and local-to-global chapter. It should therefore be read in relation to the other chapters rather than as an isolated BSD article. The Ricci/Perelman chapter provides curvature and smoothing language; Hodge provides decomposition of flow structure; Navier-Stokes provides liquidity-flow stress balance; Yang-Mills provides gauge curvature and shock threshold; Riemann/Zeta provides spectral forecasting logic; P vs NP provides computational selection and optimization difficulty. BSD contributes the formal logic connecting local states to global structural rank.

This cross-problem position is important for Chapter 9.1 because it clarifies why the chapter must be synthesis-type. It directly touches several objects used elsewhere in the monograph: rank, stress, network position, corridor leverage, L-function behavior, spectral interpretation, validation and claim discipline. But it also has its own specific grammar. Its distinctive contribution is the transformation from local regional reductions and local-factor information to a constructed global rank measure.

Figure 9.1.4. BSD as the monograph chapter most directly centered on rank and local-to-global logic

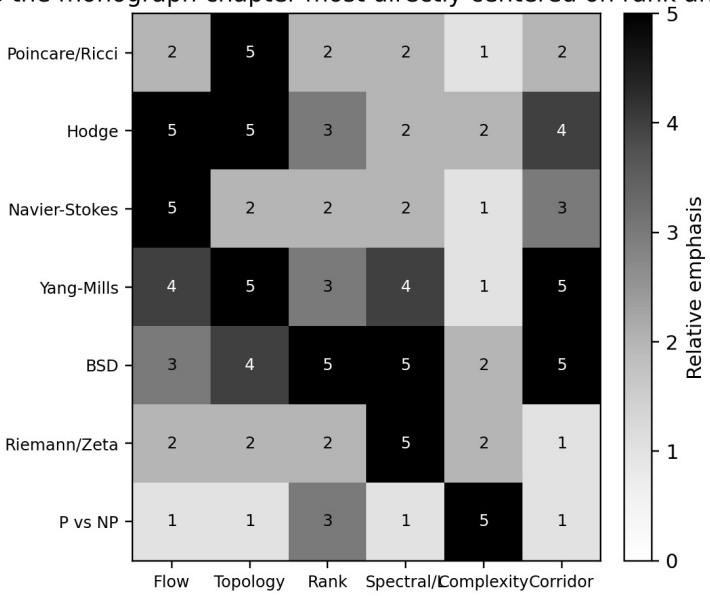


Figure 9.1.4. BSD as the monograph chapter most directly centered on rank and local-to-global logic.

Source: Author synthesis for Chapter 9.1 based on the regional BSD-inspired manuscript and the seven-problem monograph architecture.

Table 9.1.9. Chapter 9 within the seven-problem monograph architecture

Book chapter	Mathematical inspiration	Primary economic object	Relation to Chapter 9
Chapter 5	Poincare/Ricci/Perelman	Inequality pressure, curvature, entropy and smoothing capacity.	Provides curvature and recovery language but not rank correspondence.
Chapter 6	Hodge theory	Gradient, curl and harmonic macro-flow decomposition.	Supplies Hodge-flow components used in structural-rank interpretation.
Chapter 7	Navier-Stokes	Liquidity-flow stress, pressure, friction and closure.	Shows how flow weakness becomes systemic stress; BSD focuses on rank formation.
Chapter 8	Yang-Mills	Gauge curvature, action and finite-network shock threshold.	Shares corridor-stress and network logic; BSD adds L-function/rank grammar.
Chapter 9	Birch-Swinnerton-Dyer	Local-to-global structural rank, LOrder and corridor stress.	Core synthesis chapter for rank formation.
Chapter 10	Riemann/Zeta	Zeta-cycle inflation forecasting and spectral diagnostics.	Shares L-function vocabulary but uses it for forecasting rather than structural rank.
Chapter 11	P vs NP	Sparse portfolio optimization and computational complexity.	Complements BSD by treating complexity in selection rather than rank correspondence.

Source: Author synthesis from the monograph editorial architecture.

9.1.10. Claim Boundary: What Chapter 9.1 Authorizes and What It Does Not

The chapter must maintain a strict boundary between analogy, measurement and proof. The admissible claim is that BSD logic can be translated into a reproducible regional economic measurement architecture in which local regional states, finite-state trace analogues, Euler-factor analogues and LOrder are compared with structural rank. The inadmissible claim would be that the economic model proves, tests or replicates the classical Birch-Swinnerton-Dyer conjecture.

The boundary also applies to causality. A close correspondence between LOrder and structural rank can support calibrated local-to-global consistency, especially if rank gaps are small and placebo logic is passed. But this does not establish that local traces cause structural rank in the econometric sense. The N = 150 closure layer strengthens diagnostics, robustness, falsification and claim discipline; it does not automatically convert a measurement architecture into a causal law.

External validation must be treated especially carefully. Observable proxies such as inflation pressure, trade openness, logistics indicators, growth revisions or corridor variables may provide directional plausibility. However, when p-values are weak, signs are mixed or variable lineage overlaps, the correct interpretation is screening rather than confirmation. This caution is not a weakness. It is the condition under which a non-standard mathematical-economic analogue can be made scientifically defensible.

Figure 9.1.3. Claim-boundary quadrants for the BSD economic analogue

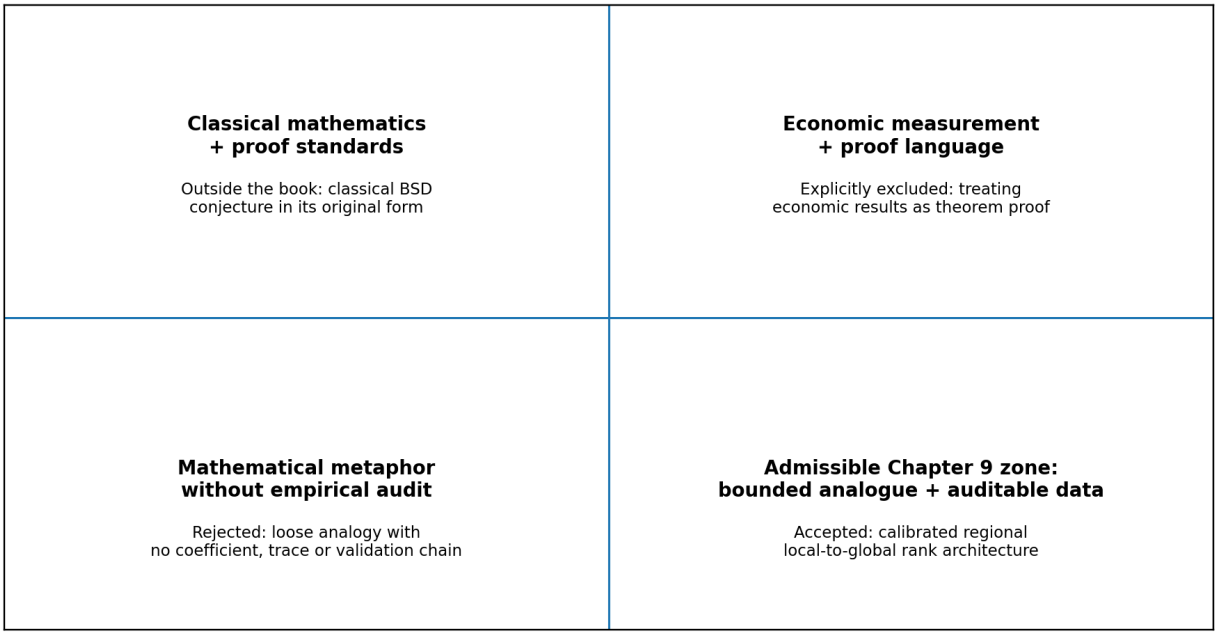


Figure 9.1.3. Claim-boundary quadrants for the BSD economic analogue.

Source: Author synthesis for Chapter 9.1 based on the regional BSD-inspired manuscript and the seven-problem monograph architecture.

Table 9.1.10. Claim hierarchy for BSD economic local-to-global translation

Claim level	Allowed statement in Chapter 9	Evidence needed	Not allowed
Strong measurement claim	The BSD-inspired architecture organizes regional local-to-global rank measurement.	Transparent transformations, coefficient lineage, finite-state stability and LOrder-rank agreement.	Claiming proof of classical BSD.
Calibrated correspondence claim	LOrder can approximate structural rank within declared tolerance.	Rank gaps, agreement diagnostics, sensitivity checks and placebo separation.	Claiming exact analytic equality.
Corridor diagnostic claim	BridgeStress can make corridor-sensitive rank relevance visible.	Transparent corridor coding and sensitivity analysis.	Claiming geopolitical ranking.
Econometric diagnostic claim	N = 150 closure tests support robustness and caution.	Fixed effects, robust inference, external proxies, anti-circularity and negative controls.	Claiming causal law.
External screening claim	External proxies behave plausibly in some directions.	Sign discipline, p-value discipline and variable lineage checks.	Claiming strong independent validation where evidence is weak.
Monograph contribution claim	BSD supplies the book's local-to-global structural-rank grammar.	Clear alignment with the seven-problem architecture.	Presenting the chapter as a standalone article copy.

Source: Author synthesis for Chapter 9.1.

9.1.11. Transition to the Remaining Chapter 9 Sections

Section 9.1 has defined the conceptual translation. The remaining sections operationalize it. Section 9.2 will define the research object: regional structural rank formation under corridor stress. Section 9.3 will specify the data architecture: World anchor, ten regional/corridor nodes and the N = 150 closure layer. Section 9.4 will define economic curve coefficients,

discriminants and finite-state reductions. Section 9.5 will construct the economic L-function, Euler factors, LOrder and structural rank. Section 9.6 will report the results for LOrder-rank correspondence, BridgeStress, regulator, Tamagawa-type friction and torsion. Section 9.7 will interpret how local regional signals inform global structural rank. Section 9.8 will examine robustness, anti-circularity, placebo logic and claim hierarchy. Section 9.9 will provide the chapter conclusion.

The guiding principle for all these sections is already established: the BSD chapter is a calibrated regional economic measurement architecture. It may support a strong local-to-global structural-rank claim when the evidence is internally coherent, transparent and robust. It may not claim theorem-level proof, unrestricted causality or strong independent external validation beyond what the empirical diagnostics justify.

Table 9.1.11. Transition map from Section 9.1 to the full Chapter 9 architecture

Next section	Function after 9.1	Key object to be developed
9.2	Defines the research object and substantive boundaries.	Regional structural rank under corridor stress.
9.3	Specifies data architecture and evidence status.	World anchor, ten nodes and N = 150 closure layer.
9.4	Builds the first technical transformation layer.	Curve coefficients, discriminants and finite-state reductions.
9.5	Builds the global local-to-global object.	Euler factors, economic L-function, LOrder and structural rank.
9.6	Reports the core results.	LOrder-rank correspondence, BridgeStress and friction/torsion analogues.
9.7	Interprets the economic meaning of the results.	Local signals informing global rank.
9.8	Protects the evidence through robustness and falsification.	Anti-circularity, placebo and claim hierarchy.
9.9	Closes the chapter.	Final contribution and limits.

Source: Author synthesis for Chapter 9.1.

9.1.12. Section Conclusion

The economic value of the BSD analogy lies in its disciplined local-to-global logic. It provides a way to ask whether local regional states, represented through stress, corridor position, finite-state behavior and local-factor analogues, can be aggregated into a global rank signal and compared with structural economic rank. This is not a mathematical proof strategy transferred into economics. It is a measurement architecture that imposes structure, lineage, calibration and claim discipline on a complex regional problem.

Section 9.1 therefore establishes the interpretive contract of Chapter 9. The chapter may use BSD terminology only where each term has an economic counterpart, an operational role and a boundary. It may claim calibrated local-to-global consistency if LOrder and structural rank align under the declared diagnostics. It may not claim to solve, test or replicate the classical Birch-Swinnerton-Dyer conjecture. Under that boundary, Chapter 9 becomes one of the monograph's strongest synthesis chapters: it connects regional stress, corridor transmission, rank formation, L-function analogy, finite-state logic and robust claim discipline in one coherent economic framework.

9.2. Research Object: Regional Structural Rank Formation under Corridor Stress

9.2.1. Position of the Research Object inside Chapter 9

The research object of Chapter 9 is regional structural rank formation under corridor stress. This phrase is intentionally precise. The chapter does not study regional GDP ranking alone, and it does not attempt to prove or test the classical Birch-Swinnerton-Dyer conjecture. It studies whether local regional information, once converted into a controlled economic analogue of finite-state reductions and Euler-factor behavior, contains measurable information about a constructed global structural-rank object.

The subsection follows the logic established in 9.1. The previous subsection explained why BSD provides a local-to-global translation grammar for the monograph. Section 9.2 now fixes the object to which that grammar is applied. The object must be defined before the methodology begins because the same regional data can be misread in several ways: as a GDP table, as a geopolitical list, as a corridor narrative, as a constructed-index exercise or as an econometric panel. The present chapter rejects those narrow readings. It treats the data as a regional measurement system in which output mass, growth pressure, income depth, network position, corridor exposure, finite-state local signals and rank capacity interact.

The substantive object is therefore the regional world economy interpreted through structural rank. The methodological object is the transformation chain that makes rank measurable. The evidentiary object is the claim hierarchy that prevents the

local-to-global analogy from being upgraded into theorem proof, causal law or strong independent external validation when the tests do not support such escalation.

Figure 9.2.1. Research-object architecture for regional structural rank formation

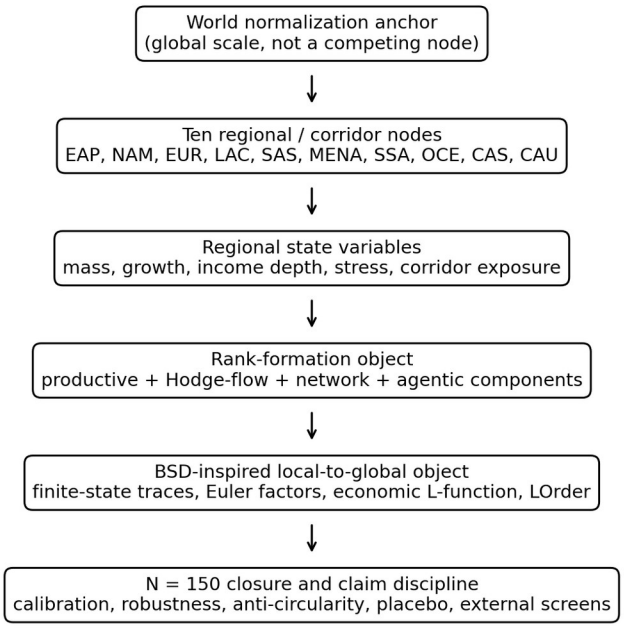


Figure 9.2.1. Research-object architecture for regional structural rank formation.
Source: Author synthesis from the BSD-inspired regional measurement architecture. The figure is a conceptual object map, not a new econometric result.

The research object is best understood as a layered object rather than as a single variable. Table 9.2.1 separates the layers and shows why the object must remain bounded.

Research-object layer	Operational definition	Why it matters	Claim boundary
Empirical layer	World anchor plus ten regional/corridor nodes.	Fixes the regional coordinate system before coefficient, trace and rank construction.	Not a country-level welfare ranking and not a geopolitical ranking.
Stress layer	Normalized systemic stress, fragility, growth pressure, income depth and corridor exposure.	Identifies regional pressure not visible in GDP mass alone.	Constructed diagnostic layer, not an official statistical series.
Corridor layer	Caucasus, Central Asia, MENA, Europe and related Black Sea/Caspian/Middle Corridor interfaces.	Allows small-output but transmission-relevant regions to remain analytically visible.	Requires transparent coding and sensitivity checks.
Rank layer	Structural rank built from productive, Hodge-flow, network and agentic components.	Defines the global object against which LOrder is later compared.	Constructed rank-capacity measure, not a welfare index.
Local-to-global layer	Finite-state reductions, trace analogues, Euler-factor analogues, economic L-function and LOrder.	Connects local regional state behavior to global rank formation.	Analogue measurement layer, not arithmetic proof.
Closure layer	N = 150 regional-year diagnostics, anti-circularity, placebo, sensitivity and external screens.	Audits robustness and claim discipline.	Supports calibration and screening, not causal confirmation.

9.2.2. Empirical Object: World Anchor and Ten Regional/Corridor Nodes

The empirical object is a World-normalized regional system. The World row is not an observation competing with regions; it is the normalization anchor that fixes the scale of GDP mass, income depth, growth and transition output. The substantive regional universe consists of ten macro-regional or corridor-sensitive nodes: East Asia and Pacific, North America, Europe, Latin America and Caribbean, South Asia, Middle East and North Africa, Sub-Saharan Africa, Oceania, Central Asia and the Caucasus.

This structure is deliberately regional. A country-level object would maximize granularity but would obscure the local-to-global rank logic that Chapter 9 is designed to examine. A pure world aggregate would maximize scale but would eliminate regional heterogeneity. The chosen object sits between those extremes: it is sufficiently global to cover the world economy, but sufficiently regional to preserve corridor position, structural stress, growth pressure and rank differentiation.

The Caucasus node is retained as an explicit corridor-sensitive subregional node. This is not a claim that the Caucasus dominates output mass. It is the opposite: the design makes clear that a region can have a very small world-output share while still becoming analytically relevant through bridge position, corridor exposure, transition pressure and transmission sensitivity. This is the substantive reason why the BSD-inspired framework is useful: it can distinguish local structural relevance from global mass dominance.

The following table restates the empirical coordinate system because the research object cannot be understood without its normalization structure.

Code	Region / anchor	GDP 2024, $bn	World share, %	Transition GDP 2026, $bn	Growth 2026, %	GDP pc, $	Object role in 9.2
WLD	World anchor	110,985.0	100.00	118,201.7	3.20	14,100	Global normalization anchor
EAP	East Asia and Pacific	35,620.0	32.09	38,674.9	4.20	17,200	Large output mass; transition and production basin
NAM	North America	31,000.0	27.93	32,252.4	2.00	76,000	Large output mass; high income depth and financial capacity
EUR	Europe	23,150.0	20.86	23,849.7	1.50	43,000	Large output mass; institutional and trade corridor hub
LAC	Latin America and Caribbean	7,260.0	6.54	7,612.7	2.40	10,600	Medium output mass; commodity, logistics and fragility channels
SAS	South Asia	4,770.0	4.30	5,390.0	6.30	2,700	High growth pressure; income-depth vulnerability
MENA	Middle East and North Africa	4,540.0	4.09	4,835.2	3.20	8,800	Energy, logistics and geopolitical corridor exposure
SSA	Sub-Saharan Africa	2,160.0	1.95	2,327.3	3.80	1,850	High fragility; development and demographic pressure
OCE	Oceania	1,810.0	1.63	1,886.8	2.10	63,000	Small mass, high income depth, geographically specific node
CAS	Central Asia	530.0	0.48	585.4	5.10	9,000	Small mass; high corridor relevance and transition momentum
CAU	Caucasus	145.0	0.13	158.6	4.60	9,500	Small mass; explicit corridor-sensitive subregional bridge

Source: Regional Economic BSD benchmark input structure based on World Bank WDI/DataBank-style regional aggregation logic, IMF/WEO and World Bank regional outlook benchmarks, and author calculations. The World row is a normalization anchor; regional rows are the substantive nodes.

Figure 9.2.2. Output mass, growth pressure and corridor-sensitive node visibility

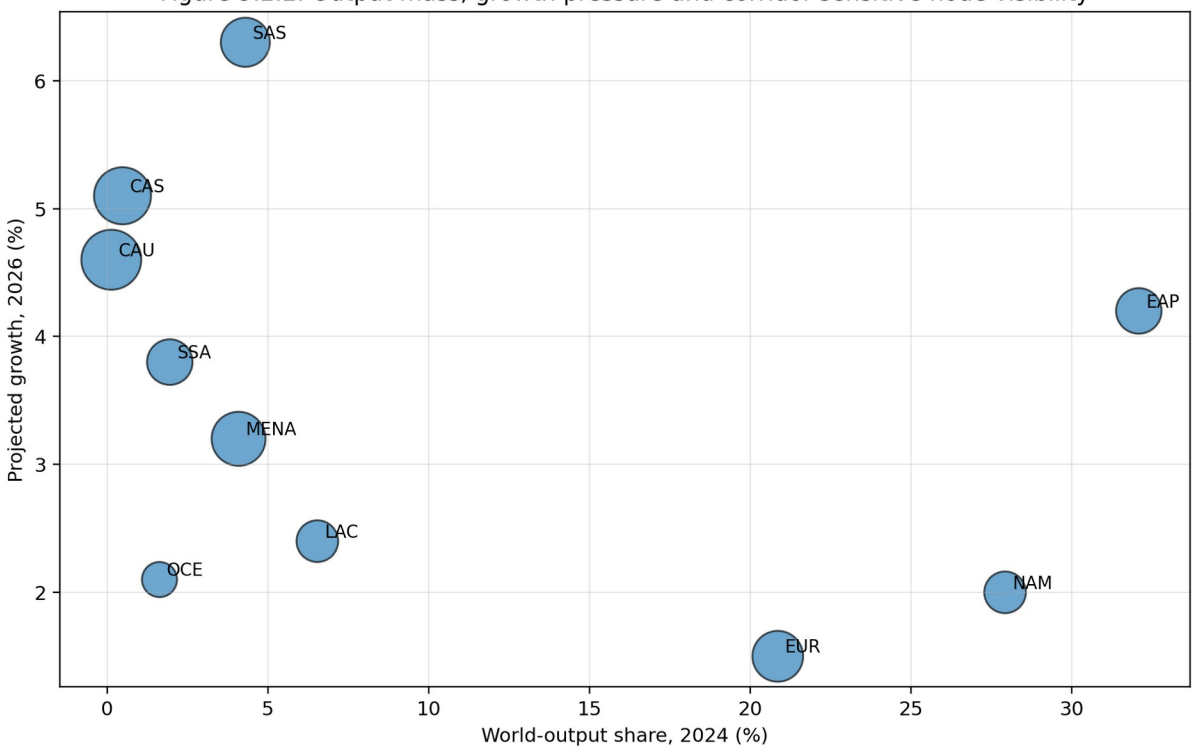


Figure 9.2.2. Output mass, growth pressure and corridor-sensitive node visibility.
Source: Author visualization from the reported regional public-data anchor panel. Bubble size represents disclosed corridor-relevance intensity for object-mapping purposes only; it is not a final BridgeStress result.

9.2.3. Rank-Formation Object: Structural Rank Is Not GDP Rank

The central object of Chapter 9 is structural rank rather than GDP rank. GDP rank is a mass measure. Structural rank is a capacity-and-position measure. It asks whether a region occupies a meaningful position in the global economic structure after productive capacity, flow position, network role and agentic capacity are considered together.

This distinction is central for a BSD-inspired chapter because the later LOrder object must be compared with something more meaningful than output size. If structural rank were only GDP rank, the local-to-global architecture would reduce to a re-labelled size comparison. Instead, structural rank is defined as a composite rank-capacity object whose components are designed to capture distinct channels of global economic relevance.

The productive component captures economic depth and transition capacity. The Hodge-flow component imports information from the broader monograph about gradient hierarchy, local imbalance and systemic circulation. The network component captures centrality, corridor adjacency and propagation relevance. The agentic component captures technology, coordination and institutional capacity as a rank-enhancing layer. Together, these components define the global rank object to which local regional signals will later be compared through LOrder.

Structural-rank component	Primary meaning	Why it belongs in the research object	Misinterpretation prevented
Productive component	Output, income depth, transition capacity and productive scale.	Keeps structural rank anchored in observable economic mass and capability.	Prevents rank from becoming purely topological or symbolic.
Hodge-flow component	Hierarchy, imbalance and residual circulation inherited from macro-flow modelling.	Connects Chapter 9 with the monograph's flow-decomposition logic.	Prevents GDP rank from absorbing all structural information.
Network component	Centrality, weighted	Measures whether a region	Prevents small corridor

	degree, corridor adjacency and cycle participation.	matters because of its position in transmission space.	nodes from disappearing.
Agentic component	Technology, coordination, institutional capacity and adaptive capability.	Adds forward-looking capacity to the rank object.	Prevents the model from treating stress exposure alone as rank.
Structural-rank composite	Weighted rank-capacity object used for LOrder comparison.	Defines the global object of the economic BSD analogue.	Prevents LOrder from being calibrated against GDP size only.

Figure 9.2.3. Research-object separation between stress exposure and rank capacity

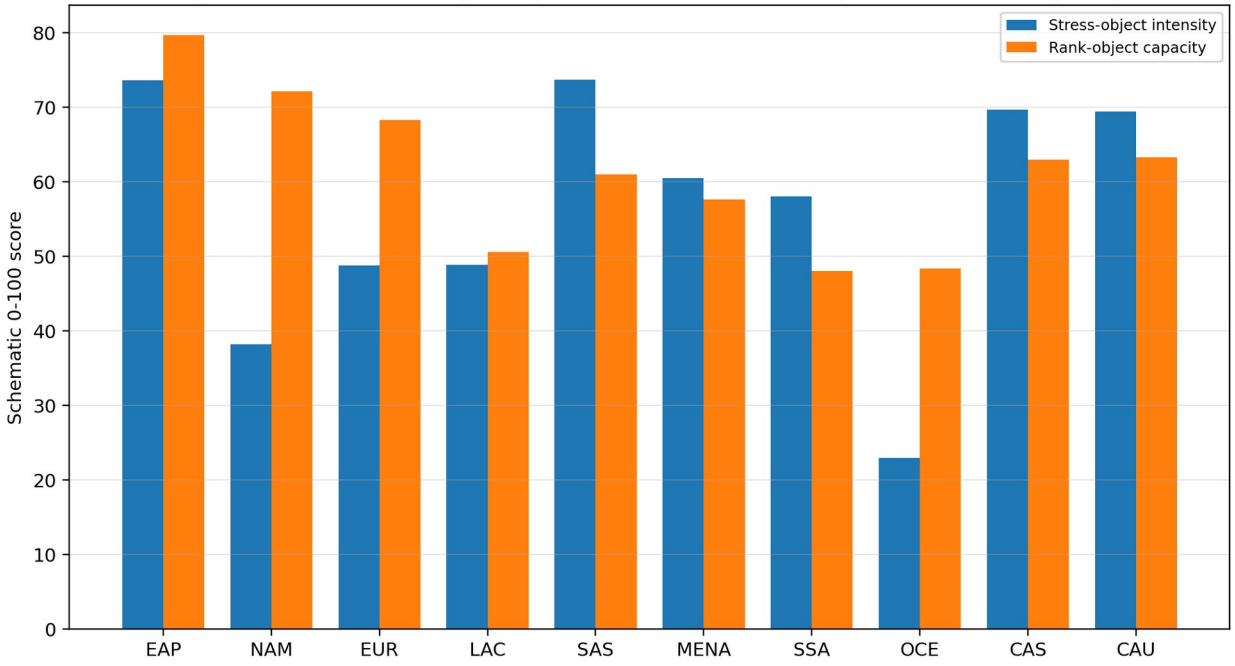


Figure 9.2.3. Research-object separation between stress exposure and rank capacity.

Source: Author schematic based on disclosed regional anchors and object-definition weights. The figure illustrates separation between stress exposure and rank capacity; it does not replace the reported structural-rank results in Section 9.6.

9.2.4. Corridor-Stress Object: Why Regional Rank Forms under Transmission Pressure

The corridor-stress object is the second defining feature of Section 9.2. It transforms the research question from "which regions are largest?" into "which regions matter structurally when local stress, bridge exposure and global rank formation interact?" Corridor stress is not treated as a loose geopolitical narrative. It is defined as a measurement channel that can alter regional position by connecting local fragility to global transmission.

The corridor object is particularly important for the Caucasus, Central Asia, MENA and Europe, because these nodes sit near major trade, logistics, energy, Black Sea, Caspian and Middle Corridor interfaces. A small-output node can become relevant when it connects larger systems or when its local stress compresses transmission thresholds. Conversely, a large-output node can remain important by mass even if its corridor exposure is lower for a particular channel.

BridgeStress is the key corridor diagnostic that will be developed later in the chapter. In 9.2 it is defined conceptually: it measures how corridor role, fragility, stress, network position and transmission exposure combine to make a region structurally visible. The object is not yet a final ranking. It is the reason the chapter must treat rank formation as a corridor-sensitive process rather than a simple output hierarchy.

Regional type	Typical examples	Rank/stress logic	Expected role in Chapter 9
Mass-dominant regions	EAP, NAM, EUR	Large world-output share and deep production/finance capacity.	Anchor productive rank and large-system calibration.
Growth-pressure regions	SAS, CAS, CAU	High projected growth or transition momentum relative to	Expose pressure that GDP share alone misses.

		mass.	
Income-fragility regions	SAS, SSA, MENA, LAC	Lower income depth or development stress raises vulnerability.	Contribute to systemic-stress and fragility layers.
Corridor-bridge regions	CAU, CAS, MENA, EUR	Strategic location between larger regional systems.	Generate BridgeStress and corridor-rank leverage.
High-income small/remote regions	OCE	High income depth but limited mass and specific geographic exposure.	Separates income capacity from global corridor centrality.

9.2.5. Local-to-Global Object: From Regional State to Structural Rank

The local-to-global object is the formal core of Chapter 9. Each region has a local state: mass, growth, income depth, stress, resilience, corridor exposure, network position and rank capacity. The BSD-inspired framework does not treat these states as independent descriptions. It asks whether local states, when processed through finite-state reductions and Euler-factor logic, preserve information about the global structural-rank object.

The transformation should be read as a sequence of economic measurement operations. First, regional states are normalized. Second, they are mapped into economic curve coefficients. Third, non-degeneracy is audited so that the curve-like object does not collapse. Fourth, local states are discretized across finite-state q-bases. Fifth, trace analogues and Euler-factor analogues are constructed. Sixth, the economic L-function and LOrder summarize local information. Finally, LOrder is compared with structural rank.

This object is powerful because it gives Chapter 9 a precise research question: can local regional states inform global structural rank after passing through a transparent local-to-global measurement chain? It is bounded because none of these steps is presented as arithmetic point counting, analytic continuation, or proof of the classical BSD conjecture.

Figure 9.2.4. Local-to-global transformation chain inside the research object



Figure 9.2.4. Local-to-global transformation chain inside the research object.

Source: Author synthesis of the BSD-inspired economic measurement sequence. The chain defines the object for Sections 9.3-9.6.

Object element	Classical BSD inspiration	Economic analogue in Chapter 9	Boundary rule
Curve coefficients	Elliptic-curve coefficient space.	Economic coefficient pair generated from regional state variables.	Not a literal elliptic curve over a number field.
Discriminant	Non-singularity / non-degeneracy.	Audit against degenerate constructed economic states.	Non-degeneracy is an admissibility check, not proof.
Local reductions	Reduction modulo primes.	Finite-state q-bases for regional regimes.	q-bases are state grids, not finite fields.
Trace	Local point-count information.	Protective/stress-bearing local trace analogue.	Trace is a measurement analogue.
Euler factors	Local factors of an L-function.	Regional local factors aggregated into economic L-function behavior.	No analytic number-theoretic claim.

LOrder	Order of behavior at s=1.	Calibrated order-like measure compared with structural rank.	Not analytic rank in classical BSD.
Structural rank	Algebraic rank comparison.	Composite rank from productive, Hodge-flow, network and agentic components.	Not rational-point rank.

9.2.6. Formal Definition of the Research Object

For the purposes of the monograph, the research object can be written as the following layered system:

RO_9 = {W, R, X, S, C, G, K, L, Q},

where W is the World normalization anchor; R is the set of ten regional/corridor nodes; X is the public-data and author-calculated regional state matrix; S is the systemic-stress and fragility layer; C is the corridor-exposure layer; G is the weighted regional network; K is the structural-rank object; L is the local-to-global BSD-inspired measurement layer; and Q is the claim-boundary and closure layer.

R = {EAP, NAM, EUR, LAC, SAS, MENA, SSA, OCE, CAS, CAU}.

K_r = F(Productive_r, HodgeFlow_r, Network_r, Agentic_r),

LOrder_r = O(LocalTrace_{r,q}, EulerFactor_{r,q}, L_E(s ~= 1)),

Core calibration question: LOrder_r approximately corresponds to K_r within a declared tolerance band, subject to robustness, anti-circularity and placebo gates.

Symbol	Meaning in Section 9.2	Role in later sections
W	World normalization anchor.	Scales regional mass and prevents country-ranking interpretation.
R	Ten regional/corridor nodes.	Defines the empirical object for 9.3 and 9.6.
X	Regional state matrix.	Supplies variables for coefficients, stress, traces and rank construction.
S	Systemic stress and fragility.	Feeds stress ranking, BridgeStress and local state interpretation.
C	Corridor exposure.	Feeds BridgeStress and corridor-rank leverage.
G	Weighted regional network.	Feeds network rank, local-to-global transmission and corridor centrality.
K	Structural rank.	Target object for LOrder comparison.
L	Local-to-global BSD-inspired layer.	Builds finite-state traces, Euler factors, economic L-function and LOrder.
Q	Claim-boundary and closure layer.	Prevents theorem, causality and external-validation overclaims.

9.2.7. Public Anchors, Author-Calculated Objects and Lineage Discipline

A central part of the research object is the distinction between public-data anchors and author-calculated objects. GDP mass, world share, growth projections and income depth define the public-anchor layer. Stress scores, corridor exposure, curve coefficients, discriminants, trace analogues, Euler-factor analogues, LOrder, structural rank, BridgeStress, regulator analogues, Tamagawa-type friction and torsion are author-calculated measurement objects.

This distinction is not a minor technical note. It is a reviewer-safety device. Constructed variables may be highly informative inside the model, but they cannot automatically be treated as independent external validation evidence when they share input lineage. The research object therefore includes lineage discipline as part of its definition. A variable is not only a numerical value; it has a source family, transformation rule, author-adjustment status, use in the model and admissible claim level.

The result is a research object that is auditable rather than opaque. Later sections can test rank correspondence, corridor stress and local-to-global consistency because the object has already separated what is observed, what is transformed, what is modeled and what is externally screened.

Variable family	Examples	Status in the research object	Admissible use
Public macro-regional anchors	GDP, world share, GDP per capita, projected growth.	Observed/source-family anchor layer.	Normalization, baseline description, transformation input.
Author-normalized stress variables	Stress, fragility, transition pressure, income fragility.	Constructed diagnostic layer.	Internal measurement, robustness and interpretation.

Corridor variables	Corridor exposure, bridge role, adjacency and sensitivity coding.	Author-coded corridor layer.	BridgeStress, sensitivity, corridor-rank interpretation.
BSD analogue variables	Economic coefficients, discriminants, traces, Euler factors, L-function, LOrder.	Constructed local-to-global measurement layer.	Core calibration and local-to-global diagnostics.
Structural-rank variables	Productive, Hodge-flow, network and agentic rank components.	Constructed rank target.	Comparison object for LOrder; not a welfare index.
Closure variables	External proxies, negative controls, placebo statistics, residualized measures.	Validation and claim discipline layer.	Screening, falsification, robustness and boundary control.

9.2.8. Research Questions Assigned to the Research Object

Section 9.2 must not reproduce the full article-level research-question table mechanically. Instead, it translates the questions into book-level object questions. These questions guide the next methodological sections and define what Chapter 9 is allowed to claim.

Object question	Operational target	Evidence expected later in Chapter 9	Claim level
Can the World-normalized regional system support local-to-global measurement?	A stable ten-node plus World-anchor coordinate system.	Data architecture, source ledger and node diagnostics in 9.3.	Design validity.
Does corridor stress alter regional structural visibility?	Stress, fragility and bridge exposure not reducible to GDP share.	BridgeStress and corridor-rank leverage in 9.6-9.7.	Substantive measurement.
Can local regional states be represented as economic curve objects?	Non-degenerate coefficient and discriminant space.	Coefficient/discriminant results in 9.4.	Analogue admissibility.
Do finite-state local signals contain rank information?	Trace stability and Euler-factor behavior across q-bases.	Local traces and economic L-function behavior in 9.5.	Local-to-global consistency.
Does LOrder approximate structural rank within tolerance?	Rank-gap, agreement, equivalence and placebo evidence.	LOrder-rank correspondence in 9.6.	Core calibrated claim.
Do closure tests prevent overclaiming?	Anti-circularity, external screens, robust inference and placebo gates.	Robustness and claim hierarchy in 9.8.	Claim discipline.

9.2.9. Alignment with the Seven-Problem Monograph Architecture

Although Chapter 9 has a distinct BSD-inspired object, it is not isolated from the other six problem chapters. Its role in the monograph is synthetic. The BSD architecture is the chapter that most directly joins local-to-global logic, structural rank, corridor stress, LOrder, finite-state reductions, Euler-factor analogues and closure discipline. For this reason, Chapter 9 functions as a structural-rank bridge across the monograph.

The connection to the Perelman/Ricci/Poincare chapter is the pressure-curvature idea: stress and smoothing capacity affect regional deformation. The connection to the Hodge chapter is flow rank: gradient, curl and harmonic structure support the Hodge-flow component of structural rank. The connection to the Navier-Stokes chapter is systemic stress and liquidity-flow vulnerability. The connection to Yang-Mills is corridor networks, curvature/action and threshold exposure. The connection to Riemann-zeta is the disciplined use of L-function and spectral vocabulary under strict claim boundaries. The connection to P vs NP is the construction of rank and decision objects under computational and falsification discipline.

This alignment is important because it makes Chapter 9 a synthesis-type chapter rather than another article pasted into the book. It does not merely restate the BSD source manuscript. It places that manuscript inside a larger monograph where each mathematical inspiration supplies a measurement grammar for one dimension of global economic complexity.

Monograph chapter	What it contributes to Chapter 9	How 9.2 uses it

	research object	
Chapter 5: Perelman/Ricci/Poincare	Pressure, curvature, smoothing capacity and inequality deformation.	Helps read structural rank as pressure-sensitive, not only mass-based.
Chapter 6: Hodge	Gradient, curl and harmonic macro-flow decomposition.	Feeds the Hodge-flow component of structural rank.
Chapter 7: Navier-Stokes	Liquidity-flow weakness, pressure gradients and systemic stress.	Supports the stress and vulnerability reading of regional rank.
Chapter 8: Yang-Mills	Gauge curvature, action, mass-gap threshold and BridgeStress.	Supports corridor stress, local-to-systemic transition and network exposure.
Chapter 9: BSD	Local-to-global logic, finite-state reductions, LOrder and structural rank.	Defines the central object of this chapter.
Chapter 10: Riemann-zeta	L-function/spectral discipline and forecast validation.	Supports strict handling of mathematical signal language.
Chapter 11: P vs NP	Complexity, combinatorial search and claim-boundary discipline.	Reinforces audit logic, falsification and bounded optimization language.

Figure 9.2.6. Position of Chapter 9 research object in the seven-problem monograph

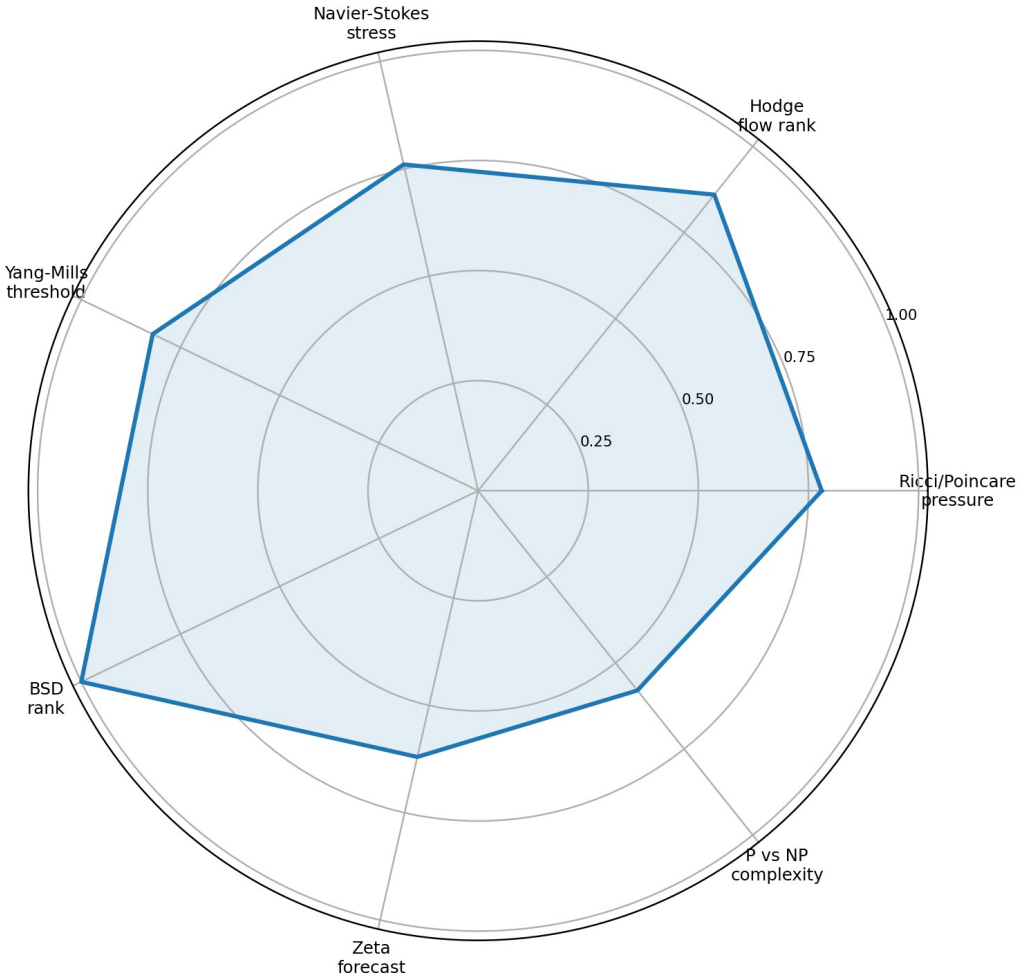


Figure 9.2.6. Position of Chapter 9 research object in the seven-problem monograph.
Source: Author synthesis. Values are interpretive alignment weights used only to visualize the chapter's synthesis function inside the monograph.

9.2.10. Evidence Status and Claim Boundary of the Research Object

The research object has a strong claim and several excluded claims. The strong claim is that regional structural rank can be measured through a calibrated BSD-inspired local-to-global architecture when the object is properly bounded. This means that local regional states, corridor stress, finite-state reductions, trace analogues, Euler-factor behavior and LOrder can be organized into a coherent measurement system and compared with structural rank.

The excluded claims are equally important. Section 9.2 does not claim that the economy is an elliptic curve. It does not claim that finite-state regional reductions are literal reductions over finite fields. It does not claim that LOrder is analytic rank. It does not claim that robust inference or external-proxy evidence proves the model causally. It does not claim that the N = 150 closure layer eliminates all small-cluster or circularity concerns.

The evidence hierarchy is therefore part of the research object. A model that defines its own limits is stronger than a model that leaves limits implicit. Chapter 9 is allowed to make calibrated measurement claims, internal-consistency claims, corridor-interpretation claims, robustness claims and directional external-screening claims. It is not allowed to make theorem-level or causal-confirmation claims.

Figure 9.2.5. Evidence hierarchy and claim boundary for the research object

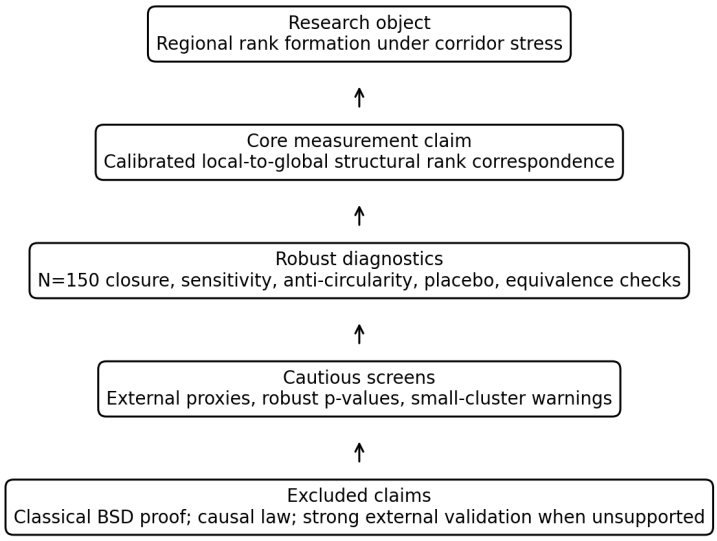


Figure 9.2.5. Evidence hierarchy and claim boundary for the research object.
Source: Author synthesis from the BSD claim-boundary architecture.

Claim category	Allowed statement in Chapter 9	Excluded escalation
Research object	A World-normalized ten-node regional/corridor system can be used to study structural rank formation.	The model covers all country-level heterogeneity.
Measurement claim	Local regional signals can be organized into a BSD-inspired local-to-global measurement chain.	The chapter proves or tests the classical BSD conjecture.
Rank claim	LOrder can be compared with a separately constructed structural-rank object.	LOrder is identical to analytic rank.
Corridor claim	BridgeStress makes corridor-sensitive nodes analytically visible.	Corridor scores are objective geopolitical truth without coding risk.
Econometric claim	N = 150 diagnostics support calibration, robustness and claim discipline.	The closure layer proves causality or strong external validation.
Replication claim	The source ledger and Zenodo package support external audit of reported	Replication files eliminate all conceptual and coding limitations.

	outputs.	

9.2.11. Subsection Synthesis: What 9.2 Establishes for the Rest of Chapter 9

Section 9.2 establishes the object on which the rest of Chapter 9 operates. The next section, 9.3, can describe the data architecture because the empirical object has been fixed as a World anchor plus ten regional/corridor nodes and an N = 150 closure layer. Section 9.4 can define economic curve coefficients and finite-state reductions because the regional state variables have been identified as the local information set. Section 9.5 can construct the economic L-function and LOrder because the local-to-global object has been bounded. Section 9.6 can report LOrder-rank correspondence and BridgeStress because structural rank and corridor stress have already been defined. Section 9.8 can audit robustness and anti-circularity because the source-lineage and claim-boundary rules have already been specified.

The research object is therefore not merely introductory. It is the conceptual contract for Chapter 9. It tells the reader what will be measured, how regional evidence should be interpreted, why corridor nodes matter, which mathematical terms are analogues, how local signals can become informative about global rank, and why the final claim must remain calibrated rather than theorem-level or causal.

In the monograph as a whole, this subsection performs an additional role: it shows how a Millennium-problem-inspired architecture can become a disciplined economic object without losing scientific caution. The BSD inspiration is retained as local-to-global logic; the economic object is regional structural rank formation under corridor stress; and the boundary is explicit enough to make the chapter suitable for a high-level academic monograph rather than a speculative mathematical analogy.

What 9.2 establishes	Implication for following sections
Regional structural rank is the chapter object.	9.6 can evaluate LOrder-rank correspondence without reducing rank to GDP.
Corridor stress is part of the object, not an appendix.	BridgeStress and corridor-rank leverage become central results rather than optional commentary.
The World row is a normalization anchor.	9.3 can keep the analysis macro-regional instead of country-ranking.
The local-to-global chain is a measurement sequence.	9.4 and 9.5 can use coefficient, trace, Euler-factor and L-function language safely.
The N = 150 panel is a closure layer.	9.8 can handle robustness, anti-circularity and placebo logic without causal overclaiming.
Claim boundary is part of the object.	9.9 can conclude with calibrated measurement rather than theorem proof.

End-of-subsection claim statement. The research object of Chapter 9 is a calibrated regional economic measurement architecture in which local regional states and corridor stress are tested for their information content about global structural rank. The object supports local-to-global measurement, corridor interpretation and robustness discipline. It does not support classical BSD proof, causal law or unrestricted external-validation claims.

9.3. Data Architecture: World Anchor, Ten Regional/Corridor Nodes and N = 150 Closure Layer

This section is written as a monograph subsection rather than as a direct transfer of the source article. Its purpose is to define the data architecture that allows Chapter 9 to operate as a synthesis-type local-to-global structural-rank chapter: a World anchor fixes scale; ten regional/corridor nodes provide the substantive benchmark universe; and an N = 150 regional-year closure layer supplies calibration, robustness, anti-circularity and claim-discipline checks.

9.3.1. Function of the Data Architecture in Chapter 9

The BSD-inspired chapter requires a data architecture that is stronger than a simple descriptive regional table. The chapter translates local-to-global logic into an economic measurement system, so the data design must preserve three distinctions. First, public macro-regional anchors must remain separate from author-calculated BSD objects. Second, the World row must function as a normalization anchor rather than a competing regional node. Third, the N = 150 closure layer must be interpreted as a calibration and robustness audit, not as a country-level causal panel.

This subsection therefore defines the empirical coordinate system for the later methodological sections. Sections 9.4 and 9.5 will transform the regional state variables into economic curve coefficients, discriminants, finite-state reductions, Euler-

factor analogues, an economic L-function and LOrder. Section 9.6 will report the correspondence between LOrder and structural rank. Section 9.8 will use the N = 150 layer to audit robustness, anti-circularity, placebo logic and claim hierarchy. The present section fixes the data structure before those transformations begin.

Table 9.3.1. Data-architecture purpose and evidence status

Data layer	Operational definition	Role in Chapter 9	Claim boundary
World anchor	Global GDP, transition GDP, growth and income-depth reference row	Sets the scale against which regional variables are normalized	Not a competing regional observation
Ten regional/corridor nodes	EAP, NAM, EUR, LAC, SAS, MENA, SSA, OCE, CAS and CAU	Define the substantive regional universe for BSD-inspired local-to-global translation	Not a country-ranking exercise
Public-data anchor variables	GDP, world share, transition GDP, projected growth and GDP per capita	Supply observable input coordinates before author transformations	Not identical to stress, rank, LOrder or BridgeStress
Author-calculated layer	Stress, corridor exposure, graph objects, curve coefficients, local traces and L-function analogue	Creates the economic BSD measurement objects	Requires formula and source-ledger disclosure
N = 150 closure layer	10 regional nodes over 15 years, 2010-2024	Tests calibration, robustness, external screens, placebo and anti-circularity	Diagnostic and calibration layer, not causal confirmation

Source: Author synthesis based on the regional BSD source document and monograph Chapter 9 structure.

The table establishes the core data principle of the chapter: the stronger the constructed object becomes, the more explicit the lineage and claim boundary must be. This prevents the final structural-rank claim from being read as a theorem-level BSD result or as a hidden causal econometric claim.

Figure 9.3.1. Data-architecture stack for the BSD-inspired regional model

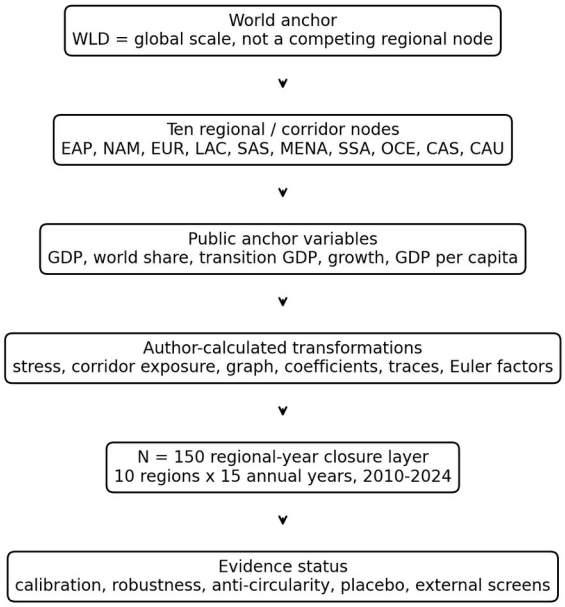


Figure 9.3.1. Data-architecture stack for the BSD-inspired regional model

Source: Author visualization prepared for Chapter 9.3 from the BSD source document data architecture and the monograph-level empirical-universe logic.

9.3.2. World Anchor and Ten Regional/Corridor Nodes

The empirical universe begins with a World anchor and ten regional/corridor nodes. The World anchor is retained because the model requires a stable global scale for output mass, projected transition GDP, growth and income depth. However, it is not treated as a regional node inside the local-to-global rank hierarchy. The competitive node set consists only of ten macro-regional or corridor-sensitive units: East Asia and Pacific, North America, Europe, Latin America and Caribbean, South Asia, Middle East and North Africa, Sub-Saharan Africa, Oceania, Central Asia and the Caucasus.

This design is deliberately regional. A country-level panel would increase granularity but would also change the research object. Chapter 9 is not designed to rank individual countries. It is designed to measure whether local regional reductions, Euler-factor information and a constructed economic L-function can inform global structural-rank formation under corridor stress. The Caucasus and Central Asia are therefore retained as corridor-sensitive nodes even though their output shares are much smaller than those of East Asia, North America or Europe.

Table 9.3.2. World and regional/corridor public-data anchor panel

Code	Region/anchor	GDP 2024 $bn	World share %	Transition GDP 2026 $bn	Growth 2026 %	GDP pc $	System role
WLD	World anchor	110,985.0	100.000	118,201.7	3.200	14,100	Global normalization anchor
EAP	East Asia and Pacific	35,620.0	32.090	38,674.9	4.200	17,200	Regional/corridor node
NAM	North America	31,000.0	27.930	32,252.4	2.000	76,000	Regional/corridor node
EUR	Europe	23,150.0	20.860	23,849.7	1.500	43,000	Regional/corridor node
LAC	Latin America and Caribbean	7,260.0	6.540	7,612.7	2.400	10,600	Regional/corridor node
SAS	South Asia	4,770.0	4.300	5,390.0	6.300	2,700	Regional/corridor node
MENA	Middle East and North Africa	4,540.0	4.090	4,835.2	3.200	8,800	Regional/corridor node
SSA	Sub-Saharan Africa	2,160.0	1.950	2,327.3	3.800	1,850	Regional/corridor node
OCE	Oceania	1,810.0	1.630	1,886.8	2.100	63,000	Regional/corridor node
CAS	Central Asia	530.0	0.480	585.4	5.100	9,000	Regional/corridor node
CAU	Caucasus	145.0	0.130	158.6	4.600	9,500	Regional/corridor node

Source: Author reconstruction from the BSD source document, Table 4.1 public-data input panel. The World row is used as normalization anchor; the ten non-World rows form the regional/corridor node set.

The anchor panel has a dual function. Substantively, it shows that the regional system combines large output-mass nodes with smaller corridor-sensitive nodes. Methodologically, it supplies the raw public coordinates from which stress, transition, corridor and structural-rank objects are constructed. The table should therefore be read as an input architecture, not as the final ranking of Chapter 9.

Figure 9.3.2. Public anchor contrast: regional output mass and transition growth

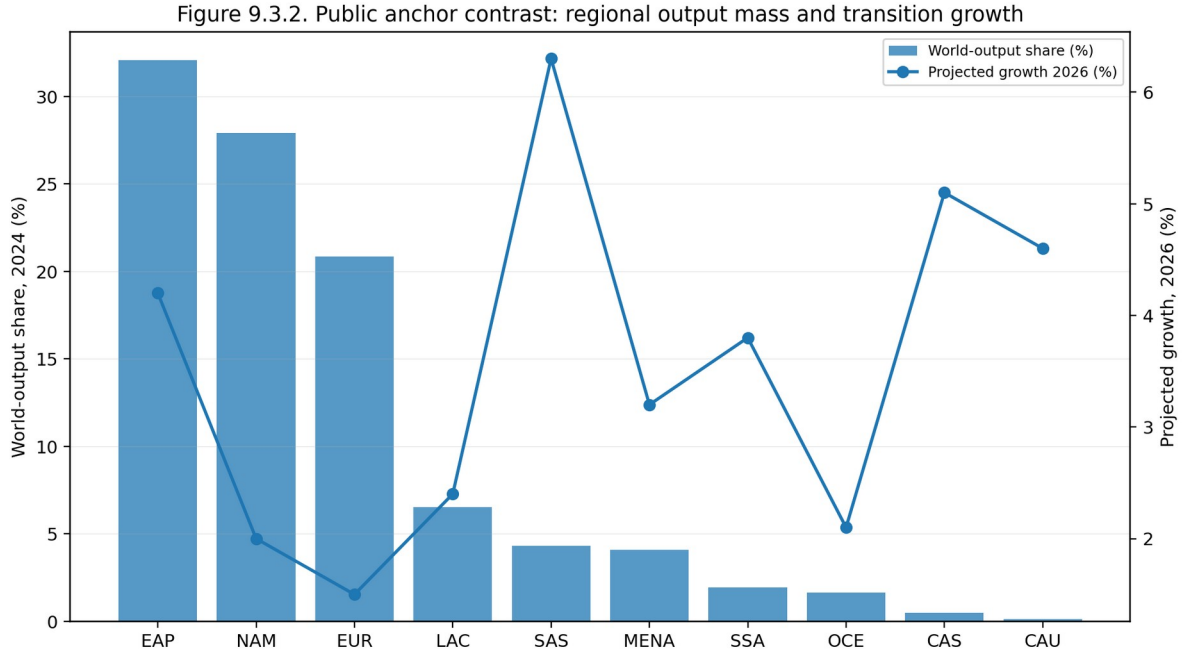


Figure 9.3.2. Public anchor contrast: regional output mass and transition growth

Source: Author visualization prepared for Chapter 9.3 from the BSD source document data architecture and the monograph-level empirical-universe logic.

9.3.3. Regional Node Taxonomy and Corridor Logic

The node taxonomy separates output-mass regions, income-depth regions, transition-growth regions and corridor-sensitive regions. Large regions such as East Asia and Pacific, North America and Europe dominate the mass layer. South Asia and Central Asia carry stronger transition-growth pressure. The Caucasus and Central Asia carry corridor-transmission relevance because their systemic role is not visible from GDP share alone. This is why Chapter 9 does not reduce rank formation to output scale.

Table 9.3.3. Regional/corridor node taxonomy for Chapter 9

Code	Node type	Empirical rationale	Downstream analytical role
EAP	Large output-mass node	High GDP share and production basin	Mass and transition signal
NAM	Large output and high income-depth node	High GDP share and high GDP per capita	Rank capacity and resilience
EUR	Large output and corridor/demand node	High GDP share with institutional/trade centrality	Rank capacity and network interface
LAC	Medium regional node	Moderate mass, commodity/logistics exposure	Stress and transition screening
SAS	High-growth pressure node	High projected growth and low income depth	Stress, transition momentum and fragility
MENA	Energy/geopolitical interface	Energy, logistics and geopolitical corridor exposure	Corridor-stress and scenario sensitivity
SSA	Fragility-pressure node	Low income depth and development pressure	Stress and fragility diagnostics
OCE	Small but high income-depth node	Small output share, high GDP per capita	Income-depth contrast and robustness check
CAS	Central corridor node	Small mass, high transition and corridor relevance	BridgeStress and local-to-global channel
CAU	Explicit corridor-sensitive subregional node	Small mass, Black Sea-Caucasus-Caspian role	BridgeStress and corridor transmission

Source: Author synthesis based on the BSD regional node design and corridor-stress interpretation.

The taxonomy clarifies why a synthesis-type BSD chapter is necessary. A standard GDP table would make East Asia, North America and Europe dominant. A local-to-global rank architecture can still acknowledge their mass while retaining the corridor relevance of Central Asia and the Caucasus.

9.3.4. N = 150 Regional-Year Closure Layer

The closure layer is the key empirical safeguard of the chapter. It expands the ten regional nodes across fifteen annual periods, 2010-2024, producing N = 150 region-year observations. This layer does not convert the model into a country-level causal panel. Its function is to audit calibration stability, model-fit decomposition, robust inference, external observable-proxy screening, negative controls, circularity safeguards, out-of-sample validation, sensitivity checks and permutation placebo logic.

Formula 9.3.1. Regional node set: R = {EAP, NAM, EUR, LAC, SAS, MENA, SSA, OCE, CAS, CAU}, with |R| = 10.

Formula 9.3.2. Time index: T = {2010, 2011, ..., 2024}, with |T| = 15.

Formula 9.3.3. Closure panel: P = R x T, so N = |P| = 10 x 15 = 150.

Formula 9.3.4. Regional-year observation vector: X_{r,t} = (GDP_{r,t}, share_{r,t}, transitionGDP_{r,t}, growth_{r,t}, GDPpc_{r,t}, corridor_{r,t}, stress_{r,t}, graph_{r,t}, rank_{r,t}, ...).

Table 9.3.4. Index notation and panel construction for the N = 150 closure layer

Symbol	Definition	Operational value	Methodological role
r	Regional/corridor node index	10 nodes	Defines the substantive regional universe
t	Annual time index	2010-2024	Allows dynamic and closure diagnostics
P	Regional-year panel	R x T	Combines regional heterogeneity with time variation
N	Number of observations	10 x 15 = 150	Closure and robustness sample size
WLD	World anchor	Separate row	Normalization scale, not a competing node
X_{r,t}	Observation vector	public anchors + author transformations	Input for curve, trace, rank and closure diagnostics

Source: Author methodological reconstruction from the BSD source document, Section 3.3 and N = 150 closure description.

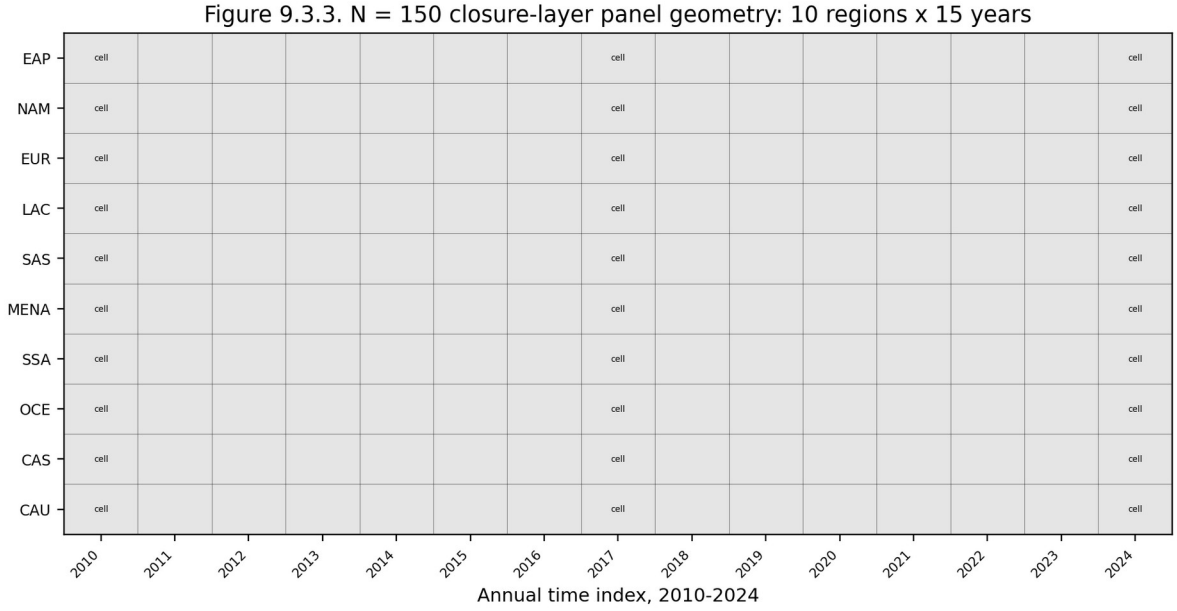


Figure 9.3.3. N = 150 closure-layer panel geometry: 10 regions x 15 years

Source: Author visualization prepared for Chapter 9.3 from the BSD source document data architecture and the monograph-level empirical-universe logic.

The heatmap is intentionally simple: every region-year cell represents one element of the closure panel. The visual point is not numerical intensity but completeness of the balanced regional-year grid used for calibration and claim discipline.

9.3.5. Public Source Families and Variable Lineage

The chapter depends on a strict distinction between public input series and author-calculated analytical objects. Public source families supply GDP, GDP per capita, growth, inflation, trade, logistics and projection anchors. The BSD objects - coefficients, discriminants, traces, Euler factors, economic L-function, LOrder, structural rank, regulator, friction, torsion and BridgeStress - are author-calculated from the declared source ledger and formula catalogue. This separation is essential because constructed variables may be excellent measurement objects without becoming independent external validation variables.

Table 9.3.5. Source ledger and data-lineage scaffold

Ledger item	Rule/source family	Output use	Boundary condition
GDP, GDP per capita, growth and trade-related public series	World Bank WDI/DataBank source-family logic	Public anchor layer	Raw/official input series; not final constructed BSD objects
Regional growth projection logic	IMF WEO source-family logic	Transition GDP and growth pressure	Projection anchor, not an authorial forecast claim
Regional aggregation	World, EAP, NAM, EUR, LAC, SAS, MENA, SSA, OCE, CAS, CAU	Macro-regional coordinate system	World is a scale anchor; ten regions are analytical nodes
Corridor-role coding	Author-disclosed corridor transformation	BridgeStress and corridor leverage	Must be documented because it is not a directly observed macro series
Author-calculated BSD objects	a, b, discriminant, trace, Euler factor, L_econ, LOrder, Rank, regulator, friction, torsion	Model-construction layer	Computed objects requiring formula, script and output disclosure
Panel construction	10 regions x 15 years = N=150	Closure and robustness layer	Regional-year audit panel; not a country-level causal dataset
Randomization and placebo seeds	20260622; 777; 123	Bootstrap/permutation reproducibility	Deterministic reproducibility of randomized checks
Replication package	Zenodo DOI 10.5281/zenodo.20796984	External audit companion	Data package, source ledger, formulas, outputs, hashes and scripts

Source: Author synthesis based on the BSD source document reproducibility note and Zenodo data package statement.

Figure 9.3.4. Source-to-output data-lineage pipeline

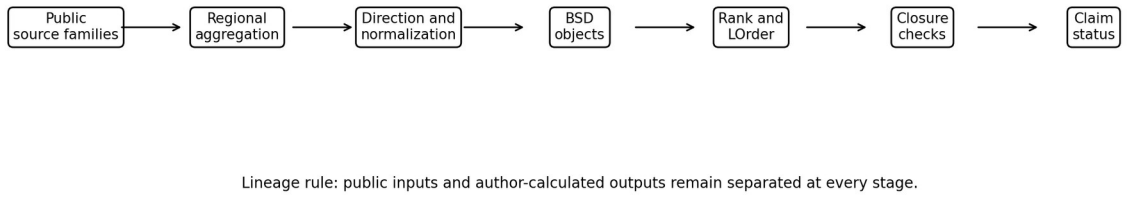


Figure 9.3.4. Source-to-output data-lineage pipeline

Source: Author visualization prepared for Chapter 9.3 from the BSD source document data architecture and the monograph-level empirical-universe logic.

9.3.6. Public Anchors versus Author-Calculated BSD Objects

The data architecture is built around a two-stage epistemic rule. Public anchors are externally observable or source-family variables. Author-calculated BSD objects are generated by transparent formulas, scripts and transformation rules. The chapter may use author-calculated objects for measurement, calibration and internal agreement tests, but it must not treat them as independent external evidence when their lineage overlaps heavily with the same input variables.

Table 9.3.6. Public anchor objects and author-calculated BSD objects

Object class	Examples	Construction status	Permitted use in Chapter 9
Public anchor variables	GDP, GDP per capita, regional growth, trade/logistics proxy families	Source-family input	Normalize regions and define the raw coordinate system
Derived stress variables	mass exposure, growth-gap pressure, income-fragility pressure, transition momentum, corridor exposure	Author-normalized composite layer	Measure pressure and fragility after directional harmonization
Network variables	weighted regional graph, centrality, clustering, cycles	Author-constructed from regional and corridor logic	Describe transmission structure and local-to-global pathways
BSD mathematical analogues	a, b, discriminant, local trace, Euler factor, L_econ, LOrder	Author-calculated analogue objects	Operationalize BSD-inspired local-to-global measurement
Rank objects	productive rank, Hodge-flow rank, network rank, agentic rank, structural rank	Composite author-calculated measurement object	Provide rank side of LOrder-rank comparison
Closure diagnostics	TWFE, robust inference, negative controls, placebo, OOS, anti-circularity	Panel audit procedures	Control overclaiming and classify evidence status

Source: Author data-lineage synthesis for Chapter 9.3.

This table is a reviewer-facing safeguard. It shows exactly where the chapter leaves official/public data and enters author-calculated measurement space. The distinction protects the scientific status of the chapter: the model can make a strong calibrated measurement claim without claiming theorem-level or causal evidence.

9.3.7. Normalization, Directional Harmonization and Stress Coordinates

The BSD-inspired data architecture cannot add raw GDP, growth, income and corridor variables directly because they have different units, ranges and meanings. The input variables therefore enter a directional transformation sequence. Variables are normalized onto a common scale; variables whose lower raw values imply higher vulnerability are inverse-normalized; and corridor-exposure variables are disclosed as author-coded or author-transformed objects. This makes the later stress and rank objects auditable.

Formula 9.3.5. World-output share: m_{r,t} = GDP_{r,t} / GDP_{WLD,t}.

Formula 9.3.6. General min-max normalization: N(x_{r,t}) = 100 * (x_{r,t} - min_R x_{r,t}) / (max_R x_{r,t} - min_R x_{r,t}).

Formula 9.3.7. Inverse-fragility normalization: F(x_{r,t}) = 100 - N(x_{r,t}), applied when lower raw values imply higher stress or lower absorption capacity.

Formula 9.3.8. Projected transition GDP: TGDP_{r,t+h} = GDP_{r,t} * (1 + g_{r,t+h})^h.

Table 9.3.7. Directional transformation rules for the BSD data architecture

Input coordinate	Transformation rule	Stress/rank meaning	Audit risk controlled
GDP and world-output share	Direct share and min-max mass exposure	Economic mass and output-scale context	Prevents raw GDP from dominating all constructed objects
Projected growth	Growth-gap orientation relative to regional	Transition pressure and acceleration	Separates growth pressure from current output mass

	benchmark		
GDP per capita / income depth	Inverse vulnerability orientation where appropriate	Absorptive capacity or fragility	Prevents income-depth weakness from being ignored
Transition GDP	Forward projection from base GDP and growth	Transition momentum	Connects current scale to near-term structural movement
Corridor exposure	Disclosed corridor coding and normalization	Bridge transmission relevance	Makes small corridor nodes visible without hiding author coding
Composite stress	Weighted normalized components	Systemic stress score	Requires weight disclosure and sensitivity checks

Source: Author methodological synthesis based on BSD source document formulas and normalization rules.

9.3.8. Stress Components as Data Architecture, Not Final Results

The stress layer belongs partly to data architecture because it defines the state vector that will later feed curve coefficients, finite-state traces and rank objects. However, the stress values should not be interpreted in Section 9.3 as final substantive results. Their role here is to demonstrate that the model has a coherent transformation route from public anchors to BSD-compatible economic coordinates.

Table 9.3.8. Stress-coordinate components and downstream role

Component	Input basis	Analytical meaning	Downstream use
Mass exposure	GDP/world-share transformation	Output-mass layer	Feeds stress and rank context, but does not alone determine rank
Growth-gap pressure	Projected growth relative to regional benchmark	Transition pressure	Captures local acceleration of economic state
Income-fragility pressure	Inverse normalization of GDP per capita / income depth	Absorptive-capacity weakness	Prevents rich and poor nodes from being treated as equivalent
Transition momentum	Projected transition GDP relative to base anchor	Forward-looking mass shift	Connects current scale with transition state
Corridor exposure	Disclosed corridor-role coding and network position	Transmission and bridge stress	Makes CAU/CAS visible even with small GDP shares

Source: Author reconstruction from the BSD stress construction logic.

A key data-architecture feature is the visibility of Central Asia and the Caucasus. Their GDP shares are small, but their corridor-exposure and local-to-global transmission roles are retained in the state vector. This is precisely why Chapter 9 is a structural-rank chapter rather than a GDP-ranking chapter.

9.3.9. Graph and Corridor Data Layer

The regional BSD architecture also requires a graph layer because local-to-global rank formation depends on structured regional relationships, not only on independent regional attributes. The graph is a finite regional/corridor benchmark with ten nodes, twenty-seven weighted edges, non-zero density, one connected component, non-trivial transitivity and weighted clustering. This data layer prepares the later use of network rank, corridor leverage, BridgeStress and local-to-global trace aggregation.

Table 9.3.9. Graph and corridor data-adequacy diagnostics

Metric	Reported value	Interpretation
Regional/corridor nodes	10.00	World excluded from competitive node calculations
Weighted edges	27.00	Corridor-sensitive regional connections
Density	0.600	Dense enough for cycle, trace and local-to-global diagnostics
Connected components	1.000	Connected benchmark; no isolated regional node
Average degree	5.400	Average regional connectivity

Average normalized edge weight	0.471	Mean corridor-weighted link strength
Global transitivity	0.633	Non-trivial triangular/cycle structure
Weighted clustering	0.301	Clustered regional structure remains present

Source: Author reconstruction from the BSD source document graph adequacy diagnostics.

Figure 9.3.5. Graph and corridor data adequacy, scaled display

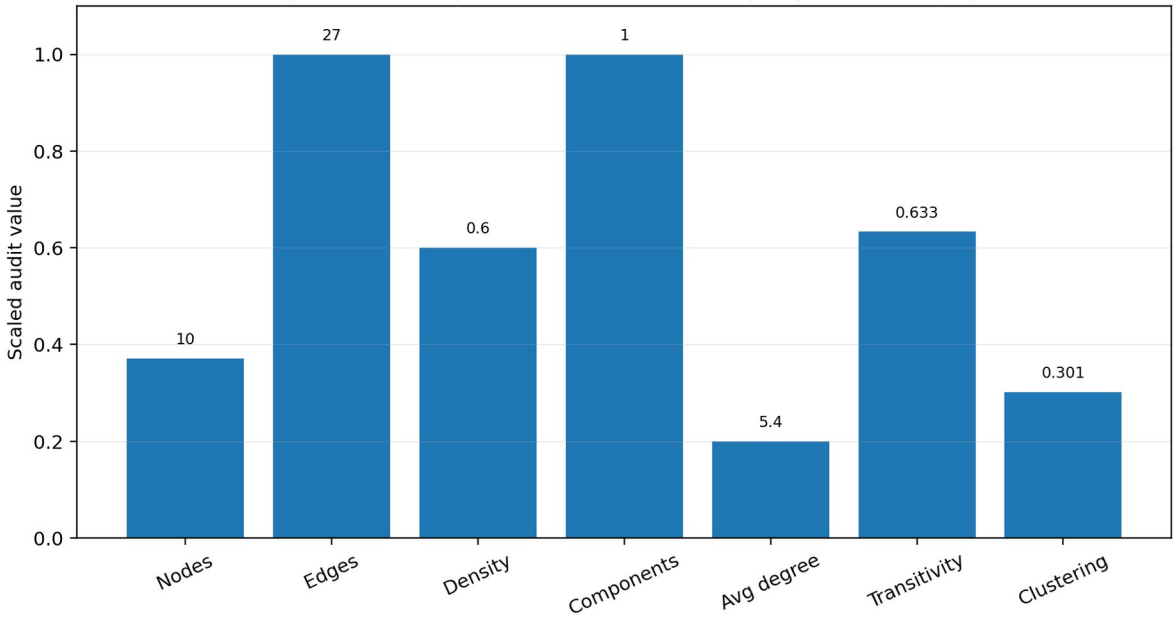


Figure 9.3.5. Graph and corridor data adequacy, scaled display

Source: Author visualization prepared for Chapter 9.3 from the BSD source document data architecture and the monograph-level empirical-universe logic.

The graph layer is not a claim that the regional economy is observed as a complete transaction network. It is a corridor-sensitive measurement graph. Its function is to support finite-state, trace and structural-rank construction under disclosed assumptions.

9.3.10. Closure Diagnostics and Evidence-Gate Requirements

The N = 150 layer is the evidence-gate layer of Chapter 9. The closure design exists because a mathematically ambitious economic analogue can overclaim if internal calibration is not audited. The closure layer therefore includes model-fit decomposition, fixed-effects screening, robust inference, external observable-proxy screening, negative controls, future-shuffle tests, circularity audits, out-of-sample validation, sensitivity checks and permutation placebo distributions.

Table 9.3.10. N = 150 closure diagnostics and required interpretation

Closure diagnostic	Data requirement	Purpose	Permitted interpretation
Two-way fixed effects	region-year panel with region and time identifiers	Controls persistent regional and global-year structure	Diagnostic association, not causality
High-R2 decomposition	baseline and FE-only variants	Separates substantive signal from fixed regional heterogeneity	Fit audit, not proof
Robust inference	regional clusters, HAC/HC3/cluster logic	Controls dependence and small-cluster risk	Weak p-values remain weak
External-proxy screening	observable outcomes not mechanically identical to constructed objects	Checks directional consistency	External screening only unless strong and independent
Negative controls	unrelated or shuffled outcomes	Tests whether the model explains everything mechanically	Falsification safeguard
Circularity audit	input-lineage overlap between variables	Identifies shared-source dependence	High overlap downgrades validation claim
Out-of-sample validation	held-out blocks or years	Tests calibration stability	Validation-window

		beyond estimation cells	evidence
Permutation placebo	randomized LOrder or rank assignments	Compares observed correspondence against placebo distributions	Robustness support, not theorem-level evidence

Source: Author synthesis based on the BSD N = 150 closure architecture and claim-boundary rules.

The most important rule is non-escalation: a strong internal calibration result cannot upgrade weak external-proxy evidence into strong external validation. Likewise, a high model fit cannot become a causal claim when the design is a regional measurement architecture.

9.3.11. Replication Package, Seeds, Hashes and Audit Trail

For a synthesis-type monograph chapter, replication discipline is not supplementary; it is part of the data architecture. The source BSD document records the Zenodo replication package, source series, World Bank API pattern, regional aggregation rules, author-calculated objects, panel construction, random seeds and output hash logic. This allows the later Chapter 9 sections to refer to calculated objects without hiding their provenance.

Table 9.3.11. Replication and audit-trail requirements for Chapter 9

Replication item	Required content	Reason for inclusion	Chapter 9 use
Source ledger	source family, variable name, extraction rule, aggregation rule, transformation, output use	Makes raw-to-derived lineage auditable	Supports data architecture and anti-circularity
Formula catalogue	curve coefficients, stress scores, traces, Euler factors, L-function, LOrder, rank, regulator, friction and torsion formulas	Allows reconstruction of author-calculated objects	Supports methodology sections 9.4-9.5
Region map	World anchor and ten regional/corridor nodes	Documents aggregation and node boundaries	Supports the empirical universe in 9.3
N = 150 panel file	10 regions x 15 annual years with constructed variables	Provides closure and robustness data	Supports 9.8 robustness and claim hierarchy
Random seeds	fixed seeds for panel, bootstrap and permutation procedures	Ensures deterministic reproducibility of randomized checks	Supports placebo and uncertainty checks
Output hashes	hashes of exported panel and result files	Verifies that reported outputs match archived files	Supports replication closure
Zenodo package	DOI 10.5281/zenodo.20796984	External audit companion	Supports data and replication statement

Source: Author synthesis based on the BSD source document results source and reproducibility note.

9.3.12. Cross-Problem Data-Architecture Alignment

Chapter 9 must also fit the data architecture of the whole monograph. It is not an isolated article pasted into a book. The BSD chapter occupies the local-to-global structural-rank position within the seven-problem system. It shares the World-anchor logic with Hodge and Yang-Mills, the N = 150 regional-panel discipline with the Ricci/Perelman inequality chapter, the corridor-stress logic with Yang-Mills and Navier-Stokes, and the layered claim-boundary discipline with Riemann/Zeta and P versus NP.

Table 9.3.12. Data-architecture alignment across the seven Millennium-inspired chapters

Chapter/problem	Empirical universe	Main N/sample	Evidence type	Relation to Chapter 9.3
Perelman/Ricci/Poincare	10 macro-regions, 2010-2024, 16 variables	N=150	pressure-curvature diagnostic panel	Defines comparable regional panel discipline
Hodge	World anchor + 10 regional nodes	10-node benchmark	macro-flow decomposition	Supplies flow/rank intuition for structural rank
Navier-Stokes	100 countries, 2010-2024	N=1,500	macro-financial stress-testing	Shows larger country-panel validation logic

Yang-Mills	10 nodes, 27 edges + N=1,500 pathway	benchmark + validation pathway	network threshold and BridgeStress	Shares corridor-network data discipline
BSD	World anchor + 10 regional/corridor nodes	N=150 closure layer	local-to-global structural rank	Core Chapter 9 data architecture
Riemann/Zeta	annual, quarterly, monthly layers	N=55/45/20/100/240	forecast validation	Demonstrates layered sample-status discipline
P vs NP	94 industries + reduced exact benchmark	C(94,10), C(20,6)	computational-finance optimization	Shows fixed-universe and claim-bounded design

Source: Author monograph-level synthesis from the seven source documents and the general structure file.

Figure 9.3.6. Chapter 9 data architecture inside the seven-problem monograph

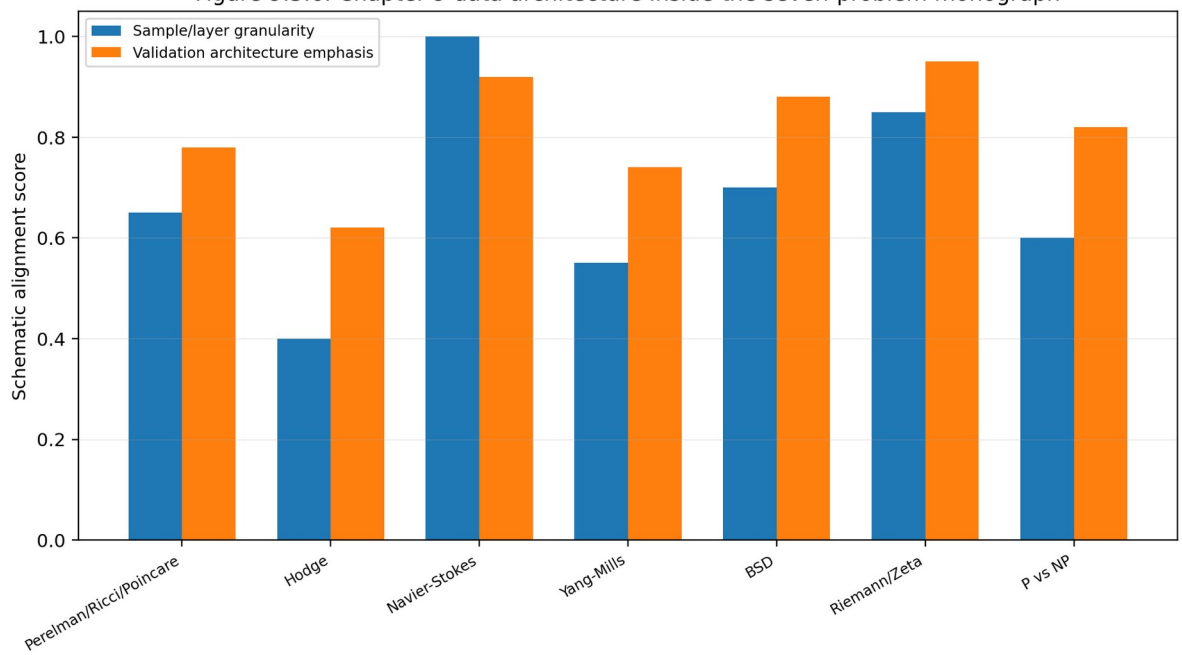


Figure 9.3.6. Chapter 9 data architecture inside the seven-problem monograph

Source: Author visualization prepared for Chapter 9.3 from the BSD source document data architecture and the monograph-level empirical-universe logic.

The alignment table helps preserve the monograph design. Each problem chapter has its own empirical universe and sample discipline. Chapter 9 is distinctive because its data architecture is explicitly local-to-global: it begins with regional anchors, builds finite-state local information, aggregates through Euler-factor and L-function analogues, and audits the final structural-rank correspondence through the N = 150 closure layer.

9.3.13. Claim Boundary of the Data Architecture

The data architecture supports a strong but bounded claim. It can support the statement that a World-normalized regional/corridor universe, processed through transparent transformations and audited through an N = 150 closure layer, is a coherent empirical basis for a calibrated economic BSD-inspired local-to-global rank model. It cannot support the statement that the classical Birch-Swinnerton-Dyer conjecture has been proved, tested or replicated. It also cannot support strong causal or universal econometric claims where external-proxy and robust-inference evidence remain diagnostic or directional.

Table 9.3.13. Permissible and excluded claims from the Chapter 9 data architecture

Claim category	Permissible statement	Excluded statement	Reason
Regional empirical universe	World anchor plus ten regional/corridor nodes define a coherent benchmark	The design is a complete all-country dataset	Country-level heterogeneity is intentionally outside the benchmark

N = 150 closure layer	Regional-year closure improves calibration and robustness discipline	The closure panel proves causal regional mechanisms	The panel is diagnostic and calibrated, not causal
Public anchors	Public source-family data supply transparent input coordinates	Public anchors alone imply structural rank	Rank is author-calculated through additional transformations
Corridor coding	Corridor exposure makes small bridge regions visible	Corridor coding replaces detailed freight or geopolitical databases	Corridor variables require disclosure and sensitivity checks
BSD analogy	The data architecture enables economic local-to-global measurement	The data architecture tests classical BSD	The analogy is economic and calibrated, not arithmetic proof
Replication package	Zenodo package supports external audit of reported materials	Archived package eliminates all interpretation risk	Replication supports traceability; it does not remove claim boundaries

Source: Author claim-boundary synthesis for Chapter 9.3.

9.3.14. Section Synthesis

Section 9.3 defines the empirical skeleton of Chapter 9. The World anchor supplies scale. The ten regional/corridor nodes supply the substantive local-to-global universe. Public anchor variables supply the observable input coordinates. Author-calculated transformations convert those inputs into stress, corridor, network and BSD-inspired mathematical-econometric objects. The N = 150 regional-year closure layer then audits whether the resulting local-to-global architecture is calibrated, robust, non-mechanical and appropriately bounded.

This data architecture is what allows the next sections to proceed. Section 9.4 can introduce economic curve coefficients, discriminants and finite-state reductions because the regional state vector is now defined. Section 9.5 can build the economic L-function and LOrder because local trace and Euler-factor data lineage has been established. Section 9.6 can report results because the empirical universe and closure layer are fixed. Section 9.8 can impose robustness and claim hierarchy because the replication and anti-circularity design has already been made explicit.

The final conclusion of the section is therefore methodological: Chapter 9 is not built on a loose metaphor. It is built on a layered data architecture in which public anchors, author-calculated BSD objects, regional/corridor nodes, graph structure, N = 150 closure diagnostics and replication materials are kept distinct. This distinction is the foundation of the chapter's scientific credibility.

9.4. Methodology: Economic Curve Coefficients, Discriminants and Finite-State Reductions

9.4.1. Methodological Position of the Subsection

The methodological role of subsection 9.4 is to define the middle transformation block of Chapter 9. Subsections 9.1 and 9.2 established the conceptual translation and research object; subsection 9.3 established the World anchor, ten regional/corridor nodes and N = 150 closure architecture. Subsection 9.4 now specifies how the regional economic state becomes a curve-like coefficient object, how that object is audited for non-degeneracy, and how local finite-state information is extracted without confusing economic discretization with arithmetic reduction over finite fields.

In the classical BSD architecture, an elliptic curve, its discriminant, local reductions, local traces and Euler factors provide a route from local arithmetic information to the analytic behavior of an L-function and ultimately to a rank statement. The present economic framework does not transfer the theorem into economics. It translates the architecture into a calibrated measurement grammar: regional economic conditions are mapped into coefficient pairs, discriminants audit whether the objects are admissible, finite-state grids summarize local state behavior, and trace analogues generate the local information later used in the L-function and LOrder block.

This subsection therefore has a procedural rather than result-reporting function. It tells the reader exactly how the author-calculated variables are produced and how the corresponding claim is restricted. Tables and figures are used to make the transformation pipeline transparent, not to claim new theorem-level evidence.

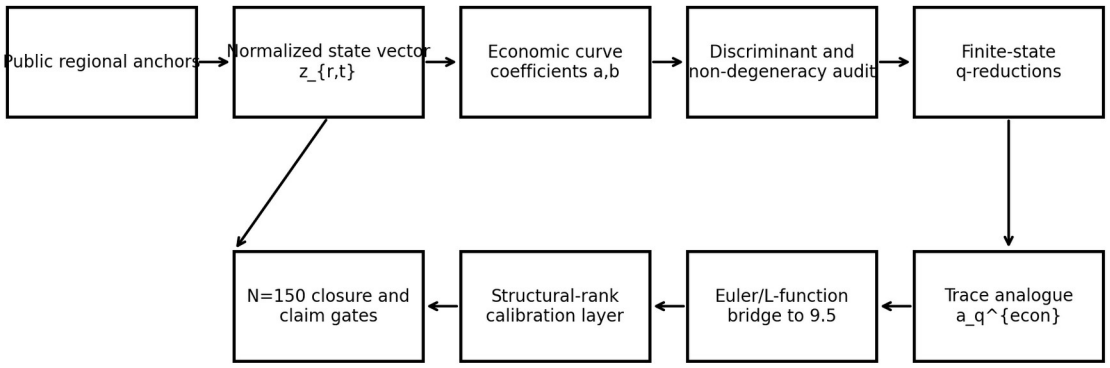
Table 9.4.1. Methodological role of subsection 9.4 inside Chapter 9

Methodological block	Object produced	Reason it is necessary	What it does not claim
State vector construction	z_{r,t}	Collects regional protection, stress, corridor and fragility coordinates before coefficient mapping.	Does not treat raw variables as already comparable without normalization.

Coefficient mapping	a_{r,t}, b_{r,t}	Compresses the regional state into a curve-like coefficient pair.	Does not claim that a region is literally an elliptic curve.
Cubic economic object	E^{econ}_{r,t}	Creates a formal object on which discriminant and reduction analogues can be defined.	Does not create rational points or arithmetic group structure.
Discriminant audit	Delta^{econ}_{r,t}	Checks that the coefficient pair is non-degenerate and sufficiently heterogeneous.	Does not interpret discriminant sign as a welfare ranking.
Finite-state reduction	R_q(E^{econ}_{r,t})	Converts regional states into controlled q-base discretizations.	Does not perform finite-field reduction in the classical number-theoretic sense.
Trace analogue	a^{econ}_{r,t}(q)	Summarizes local protective or stress-bearing behavior across finite-state bases.	Does not equal classical point-count trace a_p.
Bridge to 9.5	Euler-factor and L-function inputs	Prepares the local-to-global link used by LOrder and structural-rank calibration.	Does not establish analytic rank or BSD proof.

Source: Author synthesis based on the regional BSD-inspired methodology and the monograph Chapter 9 architecture.

Figure 9.4.1. Methodological pipeline from public anchors to finite-state trace analogues



Source: Author methodological visualization. The figure is a pipeline diagram, not a numerical result.

9.4.2. Regional Economic State Vector and Variable Lineage

The coefficient layer begins with a normalized regional economic state vector. Each observation is indexed by region r and year t, where r belongs to the ten regional/corridor nodes and t belongs to the 2010-2024 closure window. The World row is used for normalization and scale anchoring; it is not treated as a competing node in the coefficient surface. This rule preserves the distinction between the global anchor and the regional objects whose structural rank is being studied.

The state vector is deliberately mixed but disciplined. It combines income depth, connectivity, resilience, agentic capacity, stress, corridor exposure and fragility. These components reflect the logic of Chapter 9: structural rank is not merely GDP mass; it emerges from productive depth, absorption capacity, network position, local stress, corridor exposure and locked fragility. Before the vector is used, all components must have documented source lineage, normalization direction and interpretation status.

(9.4.1) $z_{r,t} = (ID_{r,t}, C_{r,t}, Res_{r,t}, AC_{r,t}, Stress_{r,t}, CE_{r,t}, Frag_{r,t})$.

(9.4.2) $X^*_{r,t} = 100 * (X_{r,t} - \min_r X_{r,t}) / (\max_r X_{r,t} - \min_r X_{r,t})$ for positively oriented variables.

(9.4.3) $X^{stress}_{r,t} = 100 - X^*_{r,t}$ when higher raw values represent protection rather than stress.

(9.4.4) $Frag_{r,t} = 100 - Protection_{r,t}$, where Protection is an author-calculated absorption/protection score.

Table 9.4.2. State-vector components and coefficient-lineage discipline

Component	Notation	Coefficient role	Expected orientation	Lineage safeguard
Income depth	ID_{r,t}	Supports a through productive protection.	Higher ID raises structural depth.	Separate public-anchor lineage; not double-counted as stress.
Connectivity / network position	C_{r,t}	Supports a and lowers b when it reflects absorption.	Higher connectivity generally protective, but interpretation depends on corridor role.	Centrality and corridor coding are documented separately.
Resilience	Res_{r,t}	Raises a and reduces deformation in b.	Higher resilience lowers vulnerability.	Derived index must be traced to component inputs.
Agentic capacity	AC_{r,t}	Raises a as productive-adaptive capacity.	Higher capacity increases rank-support.	Treated as constructed capacity, not a direct causal variable.
Systemic stress	Stress_{r,t}	Reduces a and raises stress interpretation.	Higher stress weakens structural protection.	Direction harmonization required before use.
Corridor exposure	CE_{r,t}	Enters b as asymmetry and strategic transmission exposure.	Higher exposure can increase structural relevance and stress.	Separated from GDP mass to avoid scalar reduction.
Fragility	Frag_{r,t}	Reduces a and intensifies stress-related deformation.	Higher fragility lowers protection.	Identity and circularity screens required when built from protection measures.

Source: Author methodological design. Variables are normalized or direction-harmonized before entering the coefficient map.

9.4.3. Economic Curve Coefficients and the Cubic Analogue

The economic curve-coefficient layer converts the normalized regional state vector into two scalar coordinates. The first coordinate, a_{r,t}, is interpreted as a structural-protection and productive-depth coefficient. The second coordinate, b_{r,t}, is interpreted as an asymmetry, deformation and corridor-stress coefficient. The two coefficients do not reduce the economy to two variables. Rather, they provide a formal compression of a higher-dimensional regional state into a coefficient space where discriminant and finite-state analogues can be applied.

The mapping is linear at the coefficient stage because interpretability is more important than unnecessary nonlinear decoration. Nonlinearity enters through the cubic surface and discriminant. This is a reviewer-safety choice: the coefficient construction remains transparent, while the curve-like object still creates a meaningful mathematical audit layer.

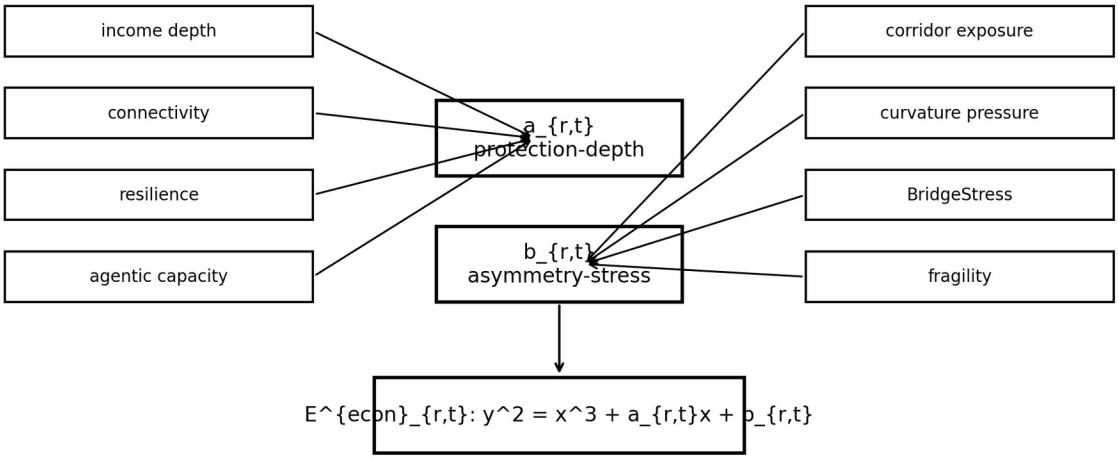
(9.4.5) $a_{r,t} = alpha_0 + alpha_1\ ID_{r,t} + alpha_2\ C_{r,t} + alpha_3\ Res_{r,t} + alpha_4\ AC_{r,t} - alpha_5\ Stress_{r,t} - alpha_6\ Frag_{r,t}$.

(9.4.6) $b_{r,t} = beta_0 + beta_1\ CE_{r,t} + beta_2\ Curv_{r,t} + beta_3\ BridgeStress_{r,t} - beta_4\ Res_{r,t} - beta_5\ C_{r,t}$.

(9.4.7) $E^{econ}_{r,t}: \ y^2 = x^3 + a_{r,t}\ x + b_{r,t}$.

(9.4.8) $S_t(x,y) = x^3 + mean_r(a_{r,t})x + mean_r(b_{r,t}) - y^2$.

Figure 9.4.2. Coefficient mapping from regional state variables to the economic cubic analogue



Source: Author methodological visualization. The figure shows coefficient construction logic and does not report empirical coefficient estimates.

Table 9.4.3. Interpretation rules for a_{r,t} and b_{r,t}

Coefficient	Primary interpretation	Positive contributors	Negative or offsetting contributors	Interpretive warning
a_{r,t}	Structural protection, productive depth and absorption capacity.	Income depth, connectivity, resilience, agentic capacity.	Systemic stress and fragility.	High a is not a welfare theorem; it is coefficient-space protection.
b_{r,t}	Asymmetry, corridor deformation and stress-transmission exposure.	Corridor exposure, curvature pressure, BridgeStress.	Resilience and stabilizing connectivity.	High b may indicate strategic relevance, vulnerability, or both.
(a,b) pair	Regional curve-like coordinate.	Balanced protection and structural capacity.	Excessive stress or near-singularity risk.	The pair is an economic analogue, not an elliptic curve over Q.
Mean surface S_t	World-regional coefficient surface at time t.	Average protection-depth and deformation.	Aggregation may hide regional heterogeneity.	Used for visualization and audit, not for policy ranking.

Source: Author interpretation of the coefficient map used in the BSD-inspired regional methodology.

9.4.4. Economic Discriminant and Non-Degeneracy Audit

The discriminant is the admissibility gate of the coefficient layer. In the classical elliptic-curve setting, non-singularity is required before arithmetic interpretation can proceed. In the economic analogue, the discriminant is not an arithmetic invariant. It is a coefficient-space audit that prevents the model from treating collapsed, singular or nearly identical constructed objects as if they contained meaningful regional heterogeneity.

The audit is intentionally strict. A regional object can enter the finite-state reduction block only if its coefficient pair passes a non-degeneracy condition. The threshold is not used to manufacture results; it is used to document that the constructed object is numerically distinct enough to support trace-like discretization. The sign and magnitude of the discriminant are not used as simple labels for good or bad economies.

(9.4.9) $\Delta^{econ}_{r,t} = -16(4a_{r,t}^3 + 27b_{r,t}^2).$

(9.4.10) $\mathrm{NonDegenerate}_{r,t} = 1[\ |\Delta^{econ}_{r,t}| > \varepsilon_D\ ].$

(9.4.11) $\mathrm{Basin}_D(a,b) = -16(4a^3 + 27b^2)$, evaluated over the displayed coefficient grid.

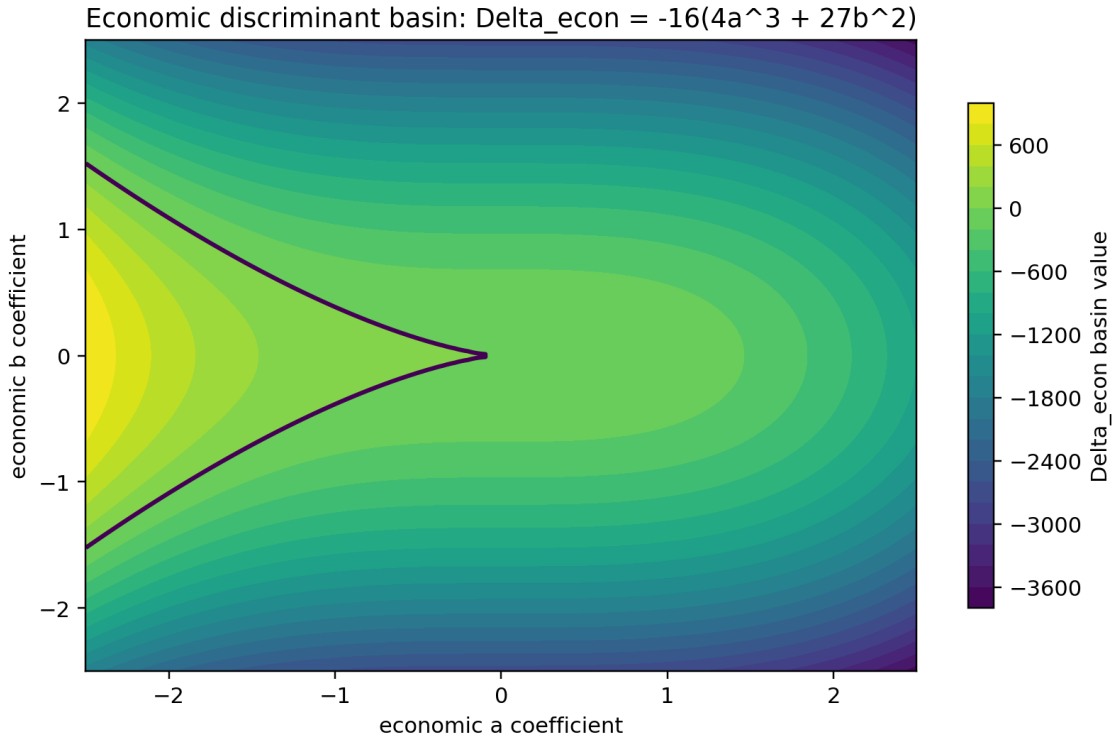
(9.4.12) Reject or flag $E^{econ}_{r,t}$ if $|\Delta^{econ}_{r,t}| \le \varepsilon_D$ or if coefficient-lineage audit fails.

Table 9.4.4. Discriminant audit protocol

Audit step	Formula or criterion	Reason for inclusion	Failure response
Coefficient availability	a_{r,t} and b_{r,t} non-missing	The discriminant is undefined without a valid coefficient pair.	Flag observation; do not impute silently.
Numerical non-degeneracy	|Delta^{econ}_{r,t}| > epsilon_D	Prevents near-singular coefficient objects from entering trace construction.	Flag or exclude from local-reduction block.
Lineage consistency	Inputs traceable to public anchors or disclosed constructed variables	Prevents hidden circularity and undocumented transformations.	Rebuild variable or demote claim.
Sensitivity check	Discriminant status stable under parameter perturbation	Tests whether pass/fail depends on a fragile parameter choice.	Mark as sensitive and treat interpretation cautiously.
Interpretation rule	Discriminant not used as a welfare score	Protects against ranking by mathematical artifact.	Report as admissibility and heterogeneity audit only.

Source: Author methodological audit rule for the economic discriminant layer.

Figure 9.4.3. Economic discriminant basin used to visualize non-degeneracy regions



Source: Author visualization of the discriminant function. The contour is a methodological basin, not a reported regional ranking.

9.4.5. Finite-State Local Reductions: q-Bases as Economic Discretization

The finite-state reduction layer is the first explicitly local-to-global mechanism in the Chapter 9 methodology. In classical BSD theory, local reductions are arithmetic reductions of a curve modulo primes. In this monograph, q-bases are not literal prime fields. They are finite-state grids used to examine whether regional economic objects preserve stable local signs and relative patterns when continuous coefficient information is discretized into controlled state spaces.

The baseline q-bases are q = 2, 3, 5, 7 and 11. This choice gives a sequence from coarse binary classification to richer finite-state resolution. A trace analogue is credible only if its sign and broad regional interpretation do not change arbitrarily across this q-grid. The goal is not exact arithmetic; the goal is discretization stability.

```
(9.4.13)  Q = {2, 3, 5, 7, 11}.
(9.4.14)  red_q(a_{r,t}) = floor( q * rankscale(a_{r,t}) ) mod q.
(9.4.15)  red_q(b_{r,t}) = floor( q * rankscale(b_{r,t}) ) mod q.
```

(9.4.16) E^{econ}_{r,t,q}: y^2 = x^3 + red_q(a_{r,t})x + red_q(b_{r,t}) on an economic q-state grid.

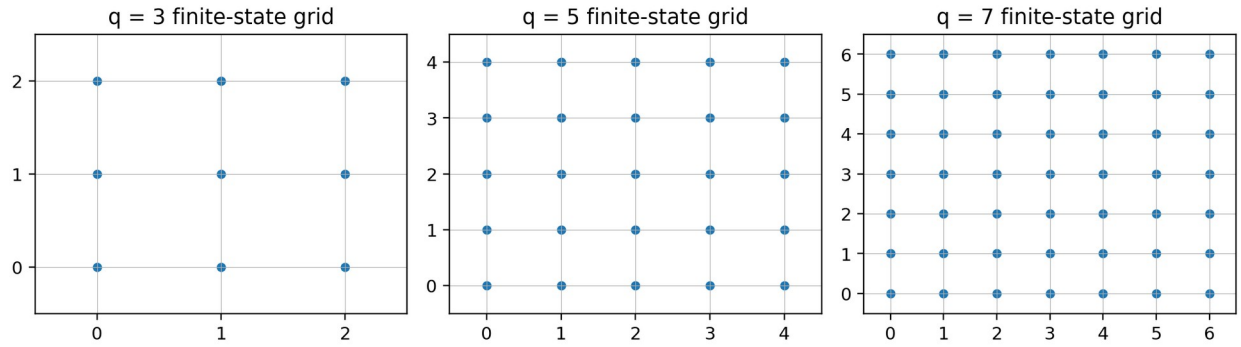
(9.4.17) StateCount^{econ}_{r,t}(q) = # {(x,y) in G_q x G_q : grid condition is satisfied within tolerance tau_q }.

Table 9.4.5. q-base design and finite-state interpretation

q-base	Resolution role	Economic interpretation	Robustness use
q = 2	Coarse binary state grid.	Separates protective versus stress-bearing local states at the broadest level.	Checks whether the model depends on fine discretization.
q = 3	Low-resolution ternary grid.	Allows negative, neutral and positive local-state patterns.	Tests stability beyond binary reduction.
q = 5	Medium grid.	Provides sufficient variation for trace-sign comparison.	Baseline local-reduction display layer.
q = 7	Higher grid.	Reveals moderate shifts in local-state density.	Sensitivity check for discretization granularity.
q = 11	Richer finite-state grid.	Tests whether trace interpretation persists under more detailed state partitioning.	Strongest q-base stability check within the compact design.

Source: Author q-base protocol. q-bases are finite-state economic grids, not literal prime-field reductions.

Figure 9.4.4. Finite-state grids for q = 3, q = 5 and q = 7



Source: Author methodological visualization. The grids illustrate economic discretization only.

9.4.6. Trace Analogues and Local Signal Extraction

The trace analogue converts the finite-state reduction into a signed local signal. In classical notation, a_p = p + 1 - #E(F_p) measures the deviation of a local point count from the reference p + 1. In the economic framework, a^{econ}_{r,t}(q) is defined as the deviation of the finite-state regional count from a q-base reference count. The sign and stability of this deviation are more important than its raw magnitude.

A positive trace analogue is interpreted as a local state with protective or rank-supporting excess relative to the finite-state reference. A negative trace analogue is interpreted as a local state with stress-bearing or fragility-linked deficit relative to that reference. Near-zero trace values indicate local neutrality or mixed signals. These interpretations remain bounded and must be checked against the coefficient lineage, discriminant audit and q-base sensitivity layer.

(9.4.18) Ref_q = q + 1 in direct analogy to the classical local reference term.

(9.4.19) a^{econ}_{r,t}(q) = Ref_q - StateCount^{econ}_{r,t}(q).

(9.4.20) TraceSign_{r,t}(q) = sign(a^{econ}_{r,t}(q)).

(9.4.21) StableTrace_{r,t} = 1 if sign stability holds across the declared q-base set Q within tolerance kappa_q.

(9.4.22) AggregateTrace_t(q) = sum_r omega_{r,t} a^{econ}_{r,t}(q), where omega_{r,t} are declared regional weights.

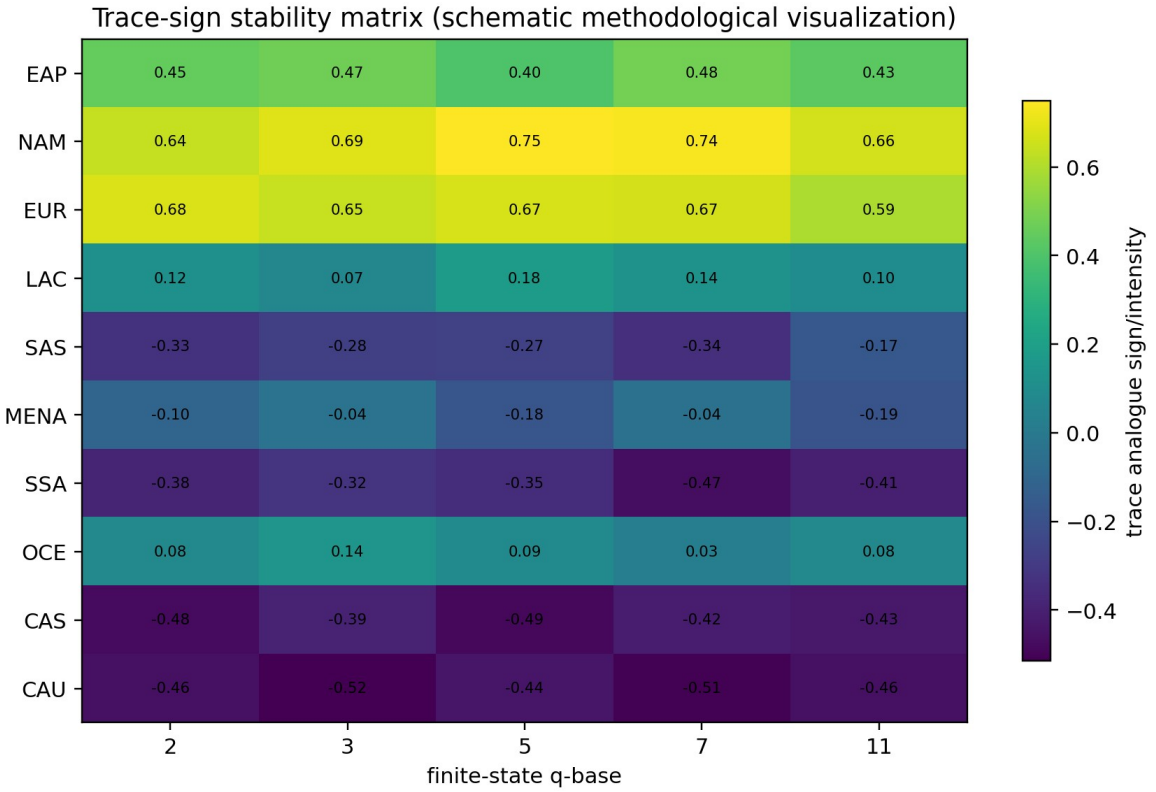
Table 9.4.6. Trace-analogue interpretation matrix

Trace outcome	Economic reading	Required audit before interpretation	Claim level
Positive and stable	Local state contains rank-	Coefficient lineage, discriminant	Internal local-signal

across Q	supporting or protective information.	pass and q-sensitivity stability.	evidence.
Negative and stable across Q	Local state contains stress-bearing, fragile or deformation information.	Confirm that sign is not generated by orientation error.	Internal local-stress evidence.
Near zero across Q	Local state is neutral or mixed relative to finite-state reference.	Check whether aggregation hides subcomponent tension.	Diagnostic neutrality.
Sign flips across Q	Trace information is discretization-sensitive.	Do not use as strong local evidence; demote claim.	Fragile or exploratory evidence.
Dominated by one input lineage	Trace may reflect circularity or mechanical construction.	Run residualized or leave-one-component versions.	Claim demotion required.

Source: Author claim-boundary protocol for finite-state trace interpretation.

Figure 9.4.5. Trace-sign stability matrix across q-bases



Source: Author schematic visualization for the methodology chapter. It illustrates the type of q-base stability table reported in the results layer; it is not introduced as a new empirical result in subsection 9.4.

9.4.7. Algorithmic Procedure for Coefficients, Discriminants and Reductions

The methodological steps are deterministic. Randomness is not needed for coefficient construction or finite-state reduction; uncertainty and placebo procedures belong to the later robustness layer. The algorithm below is therefore reproducible from the declared regional input table, parameter vector, normalization rules and q-base schedule.

Algorithm 9.4.1. Economic coefficient-discriminant-reduction procedure

Step	Operation	Output	Audit requirement
1	Load regional-year public anchors and author-calculated corridor variables.	Raw and normalized input table.	Source ledger and version control.
2	Apply direction harmonization and 0-100 scaling.	Comparable state coordinates.	Record min-max range and orientation rule.
3	Construct z_{r,t}.	State vector for each regional-year observation.	No missing component without flag.
4	Compute a_{r,t} and b_{r,t}.	Coefficient pair.	Parameter vector disclosed.
5	Construct E^{econ}_{r,t}.	Economic cubic analogue.	Label as analogue only.

6	Compute Delta^{econ}_{r,t}.	Discriminant audit value.	Apply epsilon_D tolerance.
7	For each q in Q, discretize coefficients and construct E^{econ}_{r,t,q}.	Finite-state local object.	q-base and tolerance documented.
8	Calculate StateCount^{econ}_{r,t}(q).	Finite-state count.	Grid rule reproducible.
9	Calculate a^{econ}_{r,t}(q).	Trace analogue.	Check sign stability across q-bases.
10	Export trace matrix to subsection 9.5.	Input for Euler-factor/L-function block.	No LOrder claim until 9.5 validation.

Source: Author algorithmic design for Chapter 9.4.

9.4.8. Boundary Between Subsection 9.4 and Subsection 9.5

Subsection 9.4 deliberately stops at trace analogues. It may define the input required for Euler factors, but it should not fully report LOrder, structural-rank correspondence, regulator, Tamagawa-type friction or torsion results. Those objects belong to subsections 9.5 and 9.6. This separation is important for book structure: 9.4 is the local-object construction layer; 9.5 is the L-function and rank-connection layer; 9.6 is the result layer.

The bridge is still useful. Once trace analogues are constructed, they can be inserted into Euler-factor analogues and an economic L-function product. However, the reader must understand that the trace object is only an input. The final local-to-global claim depends on whether the economic L-function behavior and LOrder measure correspond to an independently defined structural-rank object under robustness and anti-circularity checks.

```
(9.4.23)  L^{econ}_{r,q}(s) input term uses a^{econ}_{r,t}(q) from subsection 9.4.
(9.4.24)  LOrder_{r,t} is not estimated in 9.4; it is defined and compared with StructuralRank in 9.5-9.6.
(9.4.25)  Methodological admissibility in 9.4 is necessary but not sufficient for local-to-global rank correspondence.
```

Table 9.4.7. Division of methodological responsibility between 9.4, 9.5 and 9.6

Subsection	Primary object	Permitted claim	Excluded claim
9.4	Coefficient pairs, discriminants, finite-state reductions and trace analogues.	Regional local-state objects can be constructed and audited.	LOrder-rank correspondence is not yet concluded.
9.5	Euler factors, economic L-function, LOrder and structural rank.	Trace information can be aggregated into a local-to-global rank-comparison architecture.	No theorem-level BSD proof or analytic-rank claim.
9.6	Results: LOrder-rank correspondence, BridgeStress, regulator, friction and torsion.	Reported results may support calibrated internal correspondence.	No causal law or strong external confirmation if diagnostics are weak.
9.8	Robustness, anti-circularity and placebo gates.	Claim hierarchy can be strengthened or demoted.	No result bypasses falsification and lineage checks.

Source: Author book-structure discipline for Chapter 9.

9.4.9. Alignment with the Seven-Problem Monograph Methodology

Although subsection 9.4 is specific to the BSD-inspired chapter, its methodological logic is consistent with the monograph-wide design. Each Millennium-inspired chapter translates a mathematical architecture into a bounded economic measurement grammar and then passes through data, transformation, validation and claim-boundary gates. The BSD chapter is distinctive because its strongest architecture is local-to-global rank formation.

Table 9.4.8. Cross-problem methodological alignment

Book chapter	Mathematical inspiration	Economic methodological object	Alignment with 9.4
Chapter 5	Perelman/Ricci/Poincare	Curvature, entropy and smoothing-capacity diagnostics.	Like discriminants, curvature objects are constructed diagnostics, not theorem proof.
Chapter 6	Hodge	Gradient, curl and harmonic macro-flow decomposition.	Hodge-flow variables can support structural-rank components used later in Chapter 9.
Chapter 7	Navier-Stokes	Nondimensional liquidity-flow stress balance and restricted	Shares direction harmonization, closure discipline and validation

		closure.	gates.
Chapter 8	Yang-Mills	Gauge potential, curvature, action and finite-network mass gap.	Shares finite-network/corridor logic and graph-based stress interpretation.
Chapter 9	Birch-Swinnerton-Dyer	Curve coefficients, finite-state traces, LOrder and structural rank.	This subsection builds the coefficient and local-reduction layer.
Chapter 10	Riemann/Zeta	Spectral signal and layered inflation forecast validation.	Shares L-function vocabulary caution and no-theorem-proof boundary.
Chapter 11	P vs NP	Sparse optimization and computational-complexity search.	Shares algorithmic transparency, reduced benchmark logic and claim discipline.

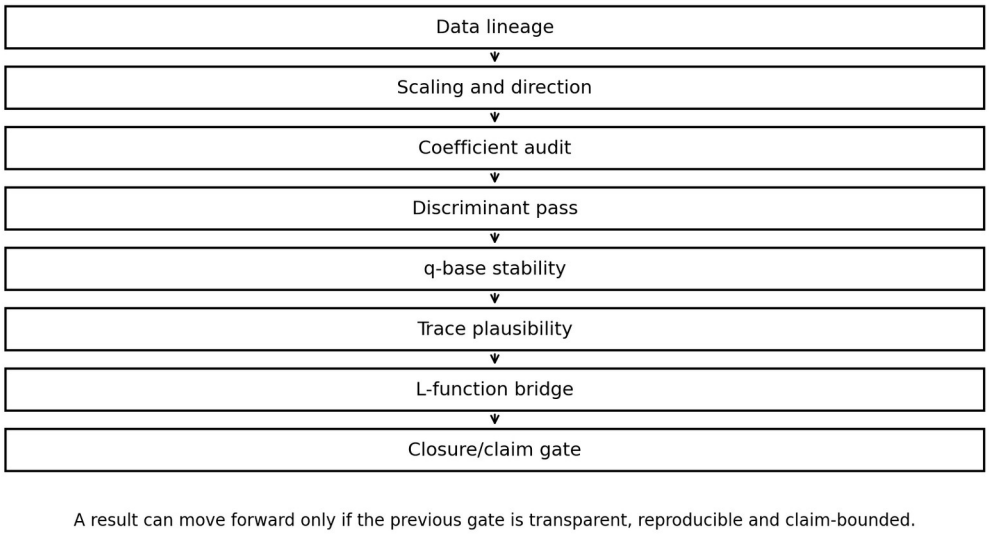
Source: Author monograph synthesis based on the seven bounded economic analogues.

9.4.10. Claim-Boundary Protocol for the Methodology

The most important scientific rule of this subsection is that methodological construction is not proof. The framework can show that economic curve coefficients, discriminants and finite-state traces are consistently constructed. It cannot, by construction alone, prove BSD, establish causal law, or confirm that regional trace information independently determines structural rank. Those stronger statements require the later LOrder-rank correspondence, robustness, anti-circularity and placebo layers.

The claim-boundary protocol therefore works as a gate ladder. A local object must pass data lineage, scaling, coefficient, discriminant, finite-state, trace and closure gates before it can be used as an input for L-function and structural-rank interpretation. Failure at any gate does not invalidate the whole monograph; it demotes the affected claim to exploratory or diagnostic status.

Figure 9.4.6. Claim-gate ladder for the coefficient-discriminant-reduction methodology



Source: Author claim-boundary visualization for Chapter 9.4.

Table 9.4.9. Admissible and inadmissible claims in subsection 9.4

Claim class	Admissible statement	Inadmissible statement	Required wording
Coefficient construction	Regional states are mapped into auditable coefficient pairs.	The economy is literally an elliptic curve.	Use "economic cubic analogue" or "curve-like coefficient object."
Discriminant audit	Constructed objects pass or fail non-degeneracy criteria.	Discriminant sign proves welfare or crisis status.	Use "admissibility and heterogeneity audit."
Finite-state reduction	q-bases provide controlled economic discretization.	q-bases are literal finite fields for regional economies.	Use "finite-state economic grid."
Trace analogue	Trace signs summarize local protective or stress-bearing signals.	Trace equals classical point-count trace.	Use "trace analogue" throughout.
Local-to-global	Trace information becomes an	Trace construction alone proves	Reserve correspondence

bridge	input to the L-function/LOrder block.	structural rank.	claims for 9.5-9.8.

Source: Author claim-boundary discipline for the BSD-inspired methodology.

9.4.11. Replication Checklist for Subsection 9.4

A reproducible methodology requires that every transformation from public anchor to trace analogue can be regenerated. The replication checklist below defines the minimum package necessary for independent audit of subsection 9.4. The checklist is designed to align with the Chapter 9 replication package and the monograph-wide data discipline.

Table 9.4.10. Replication checklist for coefficients, discriminants and finite-state reductions

Replication item	File or object expected	Purpose	Reviewer-risk reduction
Input regional-year table	regional_year_inputs.csv/xlsx	Recreates z_{r,t}.	Prevents hidden data substitution.
Normalization ledger	normalization_rules.csv	Documents direction, min-max range and stress orientation.	Prevents unit inconsistency.
Coefficient parameter vector	coefficient_parameters.csv	Recreates a_{r,t} and b_{r,t}.	Prevents undocumented parameter tuning.
Coefficient output table	economic_curve_coefficients.csv	Stores a, b and E^{econ}_{r,t} identifiers.	Enables coefficient audit.
Discriminant table	discriminants.csv	Stores Delta^{econ}_{r,t}, epsilon_D and pass/fail status.	Prevents silent singularity problems.
q-base schedule	q_base_protocol.json	Documents Q, grid rule and tolerance.	Prevents arbitrary discretization.
Trace matrix	finite_state_trace_matrix.csv	Stores a^{econ}_{r,t}(q) across q-bases.	Enables q-stability checks.
Code and seed log	scripts/ and hashes.txt	Recreates all transformations deterministically.	Supports external audit and version control.

Source: Author replication protocol for Chapter 9.4.

9.4.12. Subsection Summary

Subsection 9.4 establishes the technical route from regional economic states to finite-state local signals. The state vector z_{r,t} collects normalized regional information; the coefficient map produces a_{r,t} and b_{r,t}; the economic cubic analogue provides a formal curve-like object; the discriminant audit checks non-degeneracy; the q-base system converts continuous coefficient information into finite-state grids; and the trace analogue summarizes local protective or stress-bearing behavior across those grids.

The methodological contribution is not a claim of mathematical proof. It is a disciplined construction that makes local-to-global economic measurement possible in the later L-function/LOrder layer. By placing coefficient construction, discriminant logic and finite-state reductions before LOrder-rank correspondence, the chapter avoids the common error of jumping from metaphor to conclusion. It shows each transformation, documents its audit status and preserves a strict boundary between admissible measurement claims and inadmissible theorem-level claims.

This prepares the reader for subsection 9.5, where trace analogues become inputs for economic Euler factors, a constructed economic L-function, LOrder and structural-rank calibration.

9.5. Economic L-Function, Euler Factors, LOrder and Structural Rank

This subsection is the technical center of Chapter 9. Sections 9.1-9.4 define the local-to-global translation, the regional research object, the World-anchor data architecture and the economic curve/finite-state reduction procedure. Section 9.5 now explains how those local reductions are combined into Euler-factor analogues, how the resulting product object is read as an economic L-function near s = 1, how the order-of-behavior score is normalized into LOrder, and how LOrder is compared with a separately defined structural-rank object.

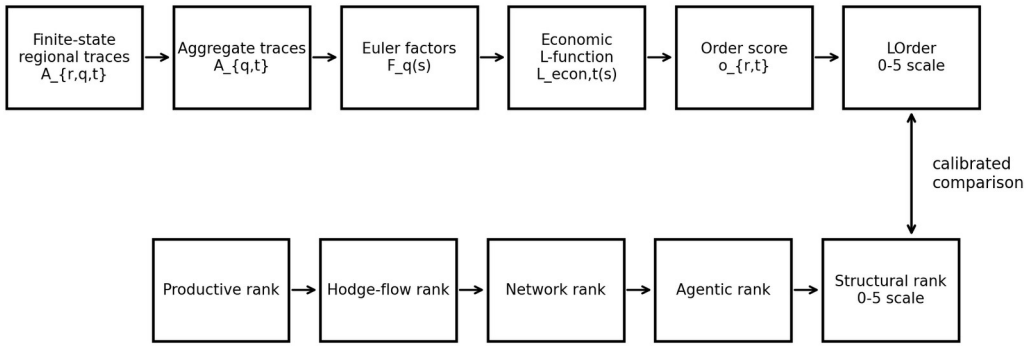
The purpose is not to reproduce the classical arithmetic theory. In the classical BSD setting, local reductions, Euler factors and the L-function are connected to the rank of an elliptic curve. In the economic analogue, finite-state regional traces are local diagnostic signals, Euler factors are local-to-global aggregation devices, the economic L-function is a controlled product object, and structural rank is a composite economic-capacity measure. The admissible claim is therefore calibrated measurement: local regional signals preserve rank-relevant information within a bounded regional economic architecture.

Table 9.5.1. Translation map from classical BSD vocabulary to the economic rank architecture

Classical BSD term	Economic analogue in Chapter 9	Operational role	Claim boundary
Elliptic curve E	Economic curve analogue E^econ_{r,t}	Formal coefficient container linking regional state variables to local reductions	Not a literal algebraic curve over number fields
Local reduction modulo p	Finite-state q-base regional reduction	Discretizes regional state behavior over q in {2,3,5,7,11}	Not point-counting over finite fields
Trace / local data	Regional trace analogue A_{r,q,t}	Measures protective minus stress-bearing local state behavior	Diagnostic trace, not Frobenius trace
Euler factor	Economic Euler factor F_q(s)	Transforms local aggregate trace into a product component	Analogue factor, not arithmetic Euler product
L-function L(E,s)	Economic L-function L_econ,t(s)	Global product object summarizing local trace information near s=1	No analytic-continuation or functional-equation claim
Order of vanishing	Order-of-behavior score o_{r,t} and LOrder	Normalizes local-to-global behavior onto a 0-5 rank scale	Not classical analytic rank
Algebraic rank	Structural economic rank	Composite of productive, Hodge-flow, network and agentic capacity	Constructed rank object, not rational-point rank

Source: Author synthesis based on the regional BSD-inspired methodology and monograph translation framework.

Figure 9.5.1. Pipeline from local traces to LOrder and structural rank



Chapter 9.5 links local finite-state evidence to a global order-of-behavior object and then compares it with an independently constructed structural-rank object.

Source: Author visualization of the Chapter 9.5 local-to-global measurement sequence.

9.5.1. Position of the L-Function Layer inside Chapter 9

The economic L-function layer performs a specific methodological task. It receives finite-state local information from Section 9.4 and converts it into a single order-of-behavior object that can be compared with structural rank. Without this layer, the chapter would contain local stress and trace diagnostics but would not have a global aggregation mechanism. Conversely, without the structural-rank layer, the L-function object would remain internally defined but economically untested. The strength of the BSD-inspired architecture is the joint presence of both objects.

This subsection therefore has a bridge function. It is still methodological because it defines the construction of Euler factors, the product L-object and LOrder. It also prepares the results block in Section 9.6 because it reports the source numerical objects required for LOrder-rank correspondence, regulator, friction, torsion and BridgeStress interpretation. The ordering is deliberate: local trace stability is established first; Euler-factor construction follows; LOrder is then defined; structural rank is specified independently; only after that does the model ask whether both objects correspond inside a declared tolerance band.

Table 9.5.2. Internal object hierarchy of Section 9.5

Layer	Input object	Transformation	Output object	Why it matters
Local trace layer	A_{r,q,t}	protective state minus stress state under q-base discretization	signed regional local trace	keeps local information region-specific
Aggregate trace layer	A_{r,q,t}, m_{r,t}	world-output weighted aggregation	A_{q,t}	creates q-level local-to-global summary
Euler-factor layer	A_{q,t}, q, s	F_q(s)=(1-A_q q^{-s} +q^{1-2s})^{-1}	local factor at q	converts trace into product component
Economic L-function	F_q(s), nu_q	weighted product across q-bases	L_econ,t(s)	global order-of-behavior object
Regional L-object	A_{r,q,t}, nu_q	regional product across q-bases	L_{r,t}(s)	keeps region-level order information
LOrder	o_{r,t}	0-5 normalization	LOrder_{r,t}	makes comparison with structural rank possible
Structural rank	productive, Hodge, network, agentic scores	weighted composite	Rank_{r,t}	independent economic rank target

Source: Author synthesis from the BSD methodology sequence.

9.5.2. From Regional Trace Analogues to Economic Euler Factors

The finite-state reduction layer produces regional traces A_{r,q,t}. These traces are signed because the local economic state can be protection-dominant or stress-dominant. A positive trace indicates that the local state contributes more protective and rank-supporting information under the chosen discretization. A negative trace indicates that stress, fragility or corridor vulnerability dominate. The q-base design does not claim that regions are reduced over prime fields. It uses q as a finite-state grid for observing whether local regional signs and relative intensity remain stable under alternative discretizations.

The aggregate trace A_{q,t} combines regional trace information by a declared weighting scheme. In the source architecture, the aggregate trace is then inserted into an Euler-factor analogue. The key point is not the numerical value of any single q-factor. The key point is whether the sequence of q-factors remains stable enough to support a global product object near s = 1. A noisy or sign-chaotic trace matrix would weaken the local-to-global claim. A stable q-profile supports the admissibility of the economic L-function layer.

Equation 9.5.1. Regional trace analogue $A_{r,q,t} = \lambda_q \cdot (P_{r,t} - U_{r,t}) / \kappa_A$

Here P_{r,t} denotes the protective-state score, U_{r,t} denotes the stress-state score, lambda_q is the q-base scaling term, and kappa_A is the normalization constant. The formula preserves sign, regional heterogeneity and q-base comparability.

Equation 9.5.2. Aggregate trace $A_{q,t} = \sum_{r \in R} m_{r,t} A_{r,q,t}$

The weight m_{r,t} normally reflects regional mass or a declared normalization weight. The aggregate trace does not replace regional traces; it supplies the q-level input for the Euler-factor object.

Table 9.5.3. Regional local trace analogues across finite-state q-bases

Code	Region	A_q, q=2	A_q, q=3	A_q, q=5	A_q, q=7	A_q, q=11
SAS	South Asia	-2.433	-2.980	-3.847	-4.552	-5.706
CAS	Central Asia	-2.017	-2.471	-3.190	-3.774	-4.731
EAP	East Asia and Pacific	-0.446	-0.546	-0.705	-0.834	-1.045
CAU	Caucasus	-2.213	-2.710	-3.499	-4.140	-5.190
SSA	Sub-Saharan Africa	-1.363	-1.669	-2.155	-2.550	-3.196
EUR	Europe	1.357	1.662	2.146	2.539	3.183
MENA	Middle East and North Africa	0.010	0.012	0.016	0.018	0.023
NAM	North America	2.243	2.747	3.547	4.196	5.260
LAC	Latin America and Caribbean	0.120	0.147	0.190	0.225	0.282
OCE	Oceania	0.501	0.614	0.793	0.938	1.176

Source: Author calculations preserved from the Regional Economic BSD source table of local trace analogues.

The trace matrix shows why the q-base layer is methodologically useful. North America and Europe have consistently positive traces across q-bases, while South Asia, Central Asia and the Caucasus remain consistently negative. Middle East and North Africa, Latin America and Caribbean and Oceania occupy intermediate positions. This pattern supports a stable local-state interpretation: the model is not relying on a single arbitrary discretization to create the LOrder object.

9.5.3. Economic Euler Factors and the Product Construction

The economic Euler factor is the first formal product component. It takes the aggregate trace A_{q,t}, the finite-state base q and the evaluation variable s. Its purpose is to translate local trace information into a factor that can be multiplied across q-bases. The construction mirrors the form of an Euler factor, but its interpretation is economic. A factor close to unity near s = 1 indicates numerical stability rather than proof of analytic structure.

Equation 9.5.3. Economic Euler factor $F_q(s) = (1 - A_{q,t} q^{-s} + q^{1-2s})^{-1}$

This is the q-level product component. It is interpreted as a local economic contribution to the global order-of-behavior layer, not as a classical arithmetic Euler factor.

Equation 9.5.4. q-weighted economic L-function $L_{econ,t}(s) = \prod_{q \in Q} F_q(s)^{\nu_q}$, with $\sum_q \nu_q = 1$

The weights ν_q may be equal, world-share-linked or otherwise declared. The chapter requires the weighting rule to be explicit because undisclosed product weights would create an avoidable reproducibility problem.

Equation 9.5.5. Log product representation $\log L_{econ,t}(s) = \sum_{q \in Q} \nu_q \log F_q(s)$

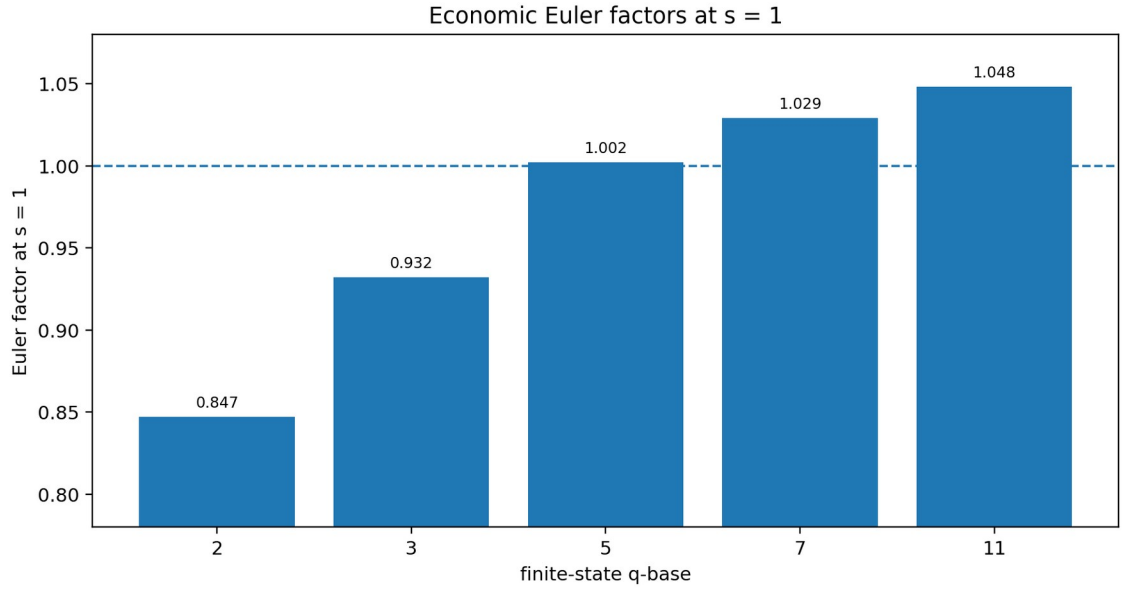
The log form improves interpretability and numerical auditability, especially when sensitivity tests perturb q-base inclusion or q-weighting rules.

Table 9.5.4. Economic Euler factors at s = 1

q	Aggregate trace A_q	Euler factor at s=1	Numerical status
2	0.639	0.847	Stable at s=1
3	0.783	0.932	Stable at s=1
5	1.011	1.002	Stable at s=1
7	1.196	1.029	Stable at s=1
11	1.499	1.048	Stable at s=1

Source: Author calculations preserved from the BSD source table of economic Euler factors.

Figure 9.5.2. Economic Euler factors at s = 1



Source: Author visualization from the q-level Euler factor values in Table 9.5.4.

The reported q-level factors range from 0.847 at q=2 to 1.048 at q=11. This spread is narrow enough to support numerical stability around the evaluation point. The q=5 factor is almost exactly one, and the higher q-bases move slightly above one. The interpretation is not that the product has classical analytic meaning; it is that the local-trace aggregation does not produce explosive or degenerate behavior at s = 1.

9.5.4. The Economic L-Function near s = 1

The economic L-function is the global side of the local-to-global construction. It summarizes the finite-state local trace system into a product object whose local behavior near s = 1 is used to extract an order-of-behavior score. In classical BSD logic, the behavior of the L-function at s = 1 is central to rank. In this economic analogue, the point s = 1 is retained as a disciplined reference point, but the output is interpreted as a constructed macro-regional order signal rather than a theorem-level analytic rank.

This distinction matters for scientific credibility. The model does not assert analytic continuation, a functional equation, modularity, or a classical order of vanishing. It asks a narrower and empirically admissible question: once local regional traces are converted into Euler-factor analogues, does the resulting order-of-behavior measure carry information about the independently constructed structural-rank object? The answer is evaluated through rank-gap, equivalence, calibration and placebo diagnostics, not by proof.

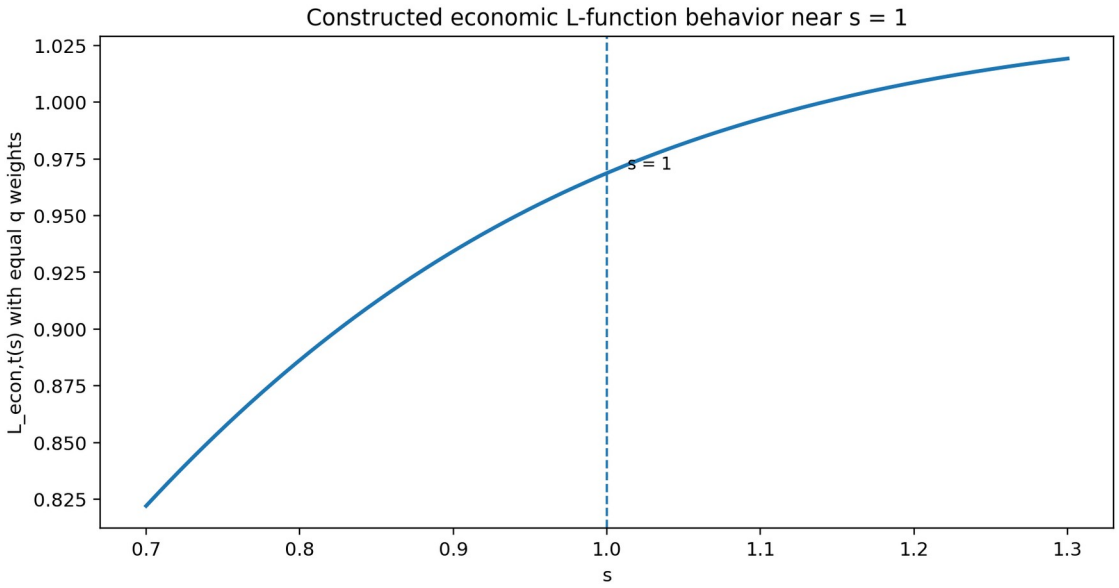
Equation 9.5.6. Regional local L-object $L_{r,t}(s) = \prod_{q \in Q} (1 - A_{r,q,t}\, q^{-s} + q^{1-2s})^{-\nu_q}$

The regional object preserves region-specific local-state information before normalization into LOrder.

Equation 9.5.7. Order-of-behavior score $o_{r,t} = -\left[\frac{d}{ds} \log L_{r,t}(s)\right]$ **evaluated at** $s = 1$

The derivative of the log product creates the order-of-behavior score. This is a measurement derivative, not a classical order of vanishing.

Figure 9.5.3. Constructed economic L-function behavior near s = 1



Source: Author visualization using the aggregate trace and Euler-factor construction with equal q weights for display purposes.

The displayed curve is smooth in the inspection interval around s = 1. This supports the practical use of the point s = 1 as a stable evaluation location in the economic analogue. The figure should be read as numerical evidence of controlled product behavior, not as evidence for any classical analytic property of an arithmetic L-function.

9.5.5. LOrder as a Normalized Order-of-Behavior Measure

LOrder is the normalized regional version of the order-of-behavior score. It converts the raw score $o_{r,t}$ into a 0-5 rank-scale object. This scaling is necessary because structural rank is also expressed on the 0-5 scale. Without common scaling, the comparison between LOrder and Rank would mix measurement units and would become visually persuasive but statistically ambiguous.

Equation 9.5.8. LOrder normalization $\mathrm{LOrder}_{r,t} = 5 \times (o_{r,t} - \min_R o_{r,t}) / (\max_R o_{r,t} - \min_R o_{r,t})$

This min-max normalization creates the rank-scale analogue. It must be reported with the regional universe because changing the region set changes the scale endpoints.

The central claim is therefore not LOrder = Rank by identity. It is LOrder approximately corresponds to StructuralRank within a declared tolerance band. This is why Section 9.5 remains methodologically conservative: it defines LOrder and rank separately before any correspondence is asserted. The structural-rank object cannot be a restatement of LOrder; otherwise the result would be circular. The variable-lineage and anti-circularity blocks in Section 9.8 are therefore necessary extensions of the present subsection.

9.5.6. Structural Rank: Productive, Hodge-Flow, Network and Agentic Components

Structural rank is the economic counterpart of the rank concept in the BSD-inspired analogue. It is intentionally not a GDP ranking. Output mass matters, but the structural-rank object must also capture flow position, network coordination and agentic capacity. This composite design makes it possible for large output regions to rank highly while still allowing

corridor-sensitive or high-pressure regions to appear in BridgeStress and vulnerability layers rather than being erased by GDP scale.

Equation 9.5.9. Standardized rank component matrix $Z_{r,t} = standardize(Productive, Flow, Network, Agentic variables)$

All rank components are transformed onto a comparable scale before aggregation.

Equation 9.5.10. Productive rank $R^P_{r,t} = Z^P_{r,t} v_1$

The productive component may use PCA or an equivalent productive-depth score. It captures output and capacity without reducing the entire rank object to GDP mass.

Equation 9.5.11. Hodge-flow representation $f = B_1^T phi + B_2 psi + h$, where $B_1 h = 0$ and $B_2^T h = 0$

The Hodge-flow component connects Chapter 9 with the monograph-wide flow-decomposition logic developed in Chapter 6.

Equation 9.5.12. Network and agentic components $R^N_{r,t} = N(theta_1 degree + theta_2 centrality + theta_3 clustering)$; $R^A_{r,t}=N(agentic capacity)$

Network rank captures graph position; agentic rank captures technology, institutional and coordination capacity.

Equation 9.5.13. Structural rank aggregation $Rank_{r,t} = pi_P R^P_{r,t} + pi_H R^H_{r,t} + pi_N R^N_{r,t} + pi_A R^A_{r,t}$, with sum $pi = 1$

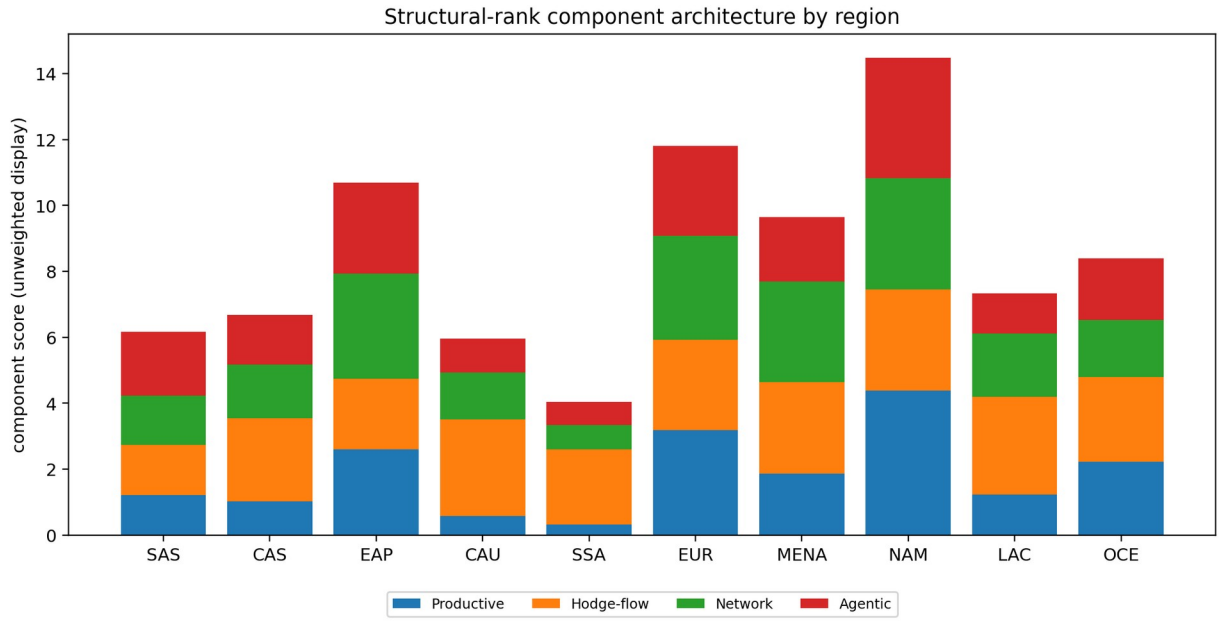
Declared weights pi prevent the composite from being an opaque index. Sensitivity tests can perturb weights to check whether the rank-order correspondence survives.

Table 9.5.5. Structural rank components by regional node

Code	Region	PCA/productive rank	Hodge-flow rank	Network rank	Agentic rank	Structural rank
SAS	South Asia	1.201	1.540	1.488	1.935	1.541
CAS	Central Asia	1.021	2.519	1.628	1.505	1.668
EAP	East Asia and Pacific	2.594	2.143	3.190	2.774	2.675
CAU	Caucasus	0.581	2.925	1.431	1.031	1.492
SSA	Sub-Saharan Africa	0.316	2.289	0.737	0.704	1.012
EUR	Europe	3.177	2.749	3.147	2.729	2.950
MENA	Middle East and North Africa	1.869	2.777	3.038	1.969	2.413
NAM	North America	4.374	3.077	3.386	3.650	3.622
LAC	Latin America and Caribbean	1.228	2.972	1.914	1.216	1.832
OCE	Oceania	2.223	2.578	1.722	1.875	2.100

Source: Author calculations preserved from the BSD source table of regional structural rank.

Figure 9.5.4. Structural-rank component architecture by region



Source: Author visualization from the structural-rank components in Table 9.5.5.

North America, Europe and East Asia and Pacific occupy strong structural-rank positions because productive depth, network coordination, resilience and agentic capacity reinforce one another. The Caucasus and Central Asia have lower internal structural rank, but that does not imply low systemic relevance. Their importance is later expressed through corridor leverage, friction and BridgeStress. This separation is methodologically important: structural rank measures internal capacity; BridgeStress measures corridor transmission exposure.

9.5.7. Calibrated Correspondence between LOrder and Structural Rank

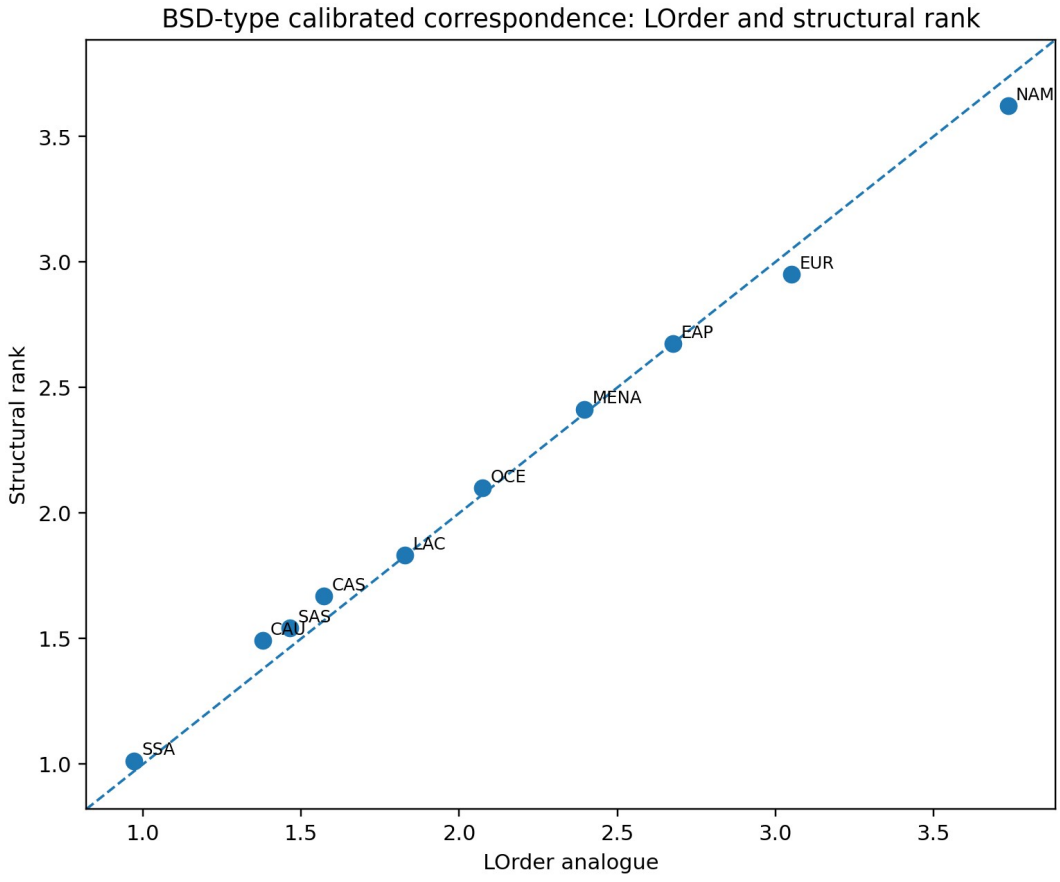
The BSD-inspired empirical question is evaluated by comparing LOrder with structural rank. The correspondence is not interpreted as exact equality. It is interpreted as local-to-global consistency if the rank-scale gaps are small, if calibration slope and intercept remain inside declared tolerance bands, if q-base sensitivity does not overturn the result, and if placebo tests show that the observed correspondence is not easily replicated by randomization.

Table 9.5.6. BSD-type rank-order correspondence by region

Code	Region	L-order analogue	Structural rank	Absolute gap
SAS	South Asia	1.465	1.541	0.076
CAS	Central Asia	1.571	1.668	0.097
EAP	East Asia and Pacific	2.676	2.675	0.001
CAU	Caucasus	1.378	1.492	0.114
SSA	Sub-Saharan Africa	0.970	1.012	0.042
EUR	Europe	3.051	2.950	0.101
MENA	Middle East and North Africa	2.396	2.413	0.017
NAM	North America	3.736	3.622	0.114
LAC	Latin America and Caribbean	1.829	1.832	0.003
OCE	Oceania	2.073	2.100	0.027

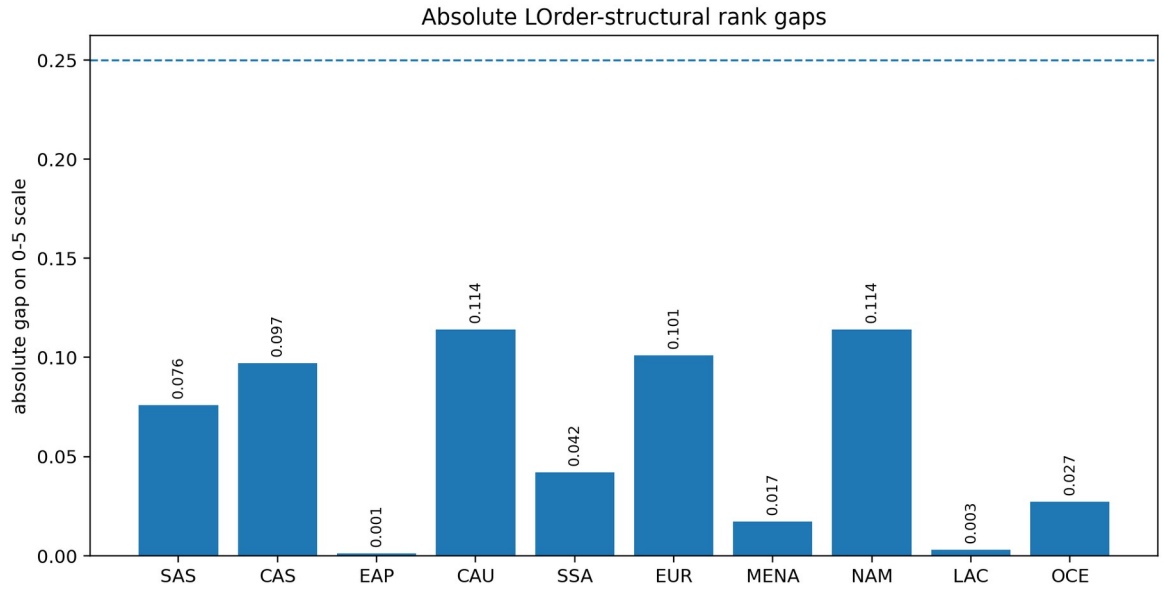
Source: Author calculations preserved from the BSD source table of LOrder-structural rank correspondence.

Figure 9.5.5. LOrder and structural rank correspondence



Source: Author visualization from Table 9.5.6.

Figure 9.5.6. Absolute LOrder-structural rank gaps



Source: Author visualization from Table 9.5.6.

The rank-order correspondence is strong at the calibration level. East Asia and Pacific has an absolute gap of 0.001, Latin America and Caribbean has 0.003, Middle East and North Africa has 0.017 and Oceania has 0.027. The largest gaps, 0.114 for the Caucasus and North America, remain small on the 0-5 scale. The result supports the central economic claim of Chapter 9: finite-state local regional information and Euler-factor analogues preserve measurable rank-relevant information. It does not support an exact theorem-level identity.

Table 9.5.7. Calibration and agreement diagnostics for the LOrder-rank comparison

Test	Estimate	Decision band	Result	Interpretation
Calibration intercept beta_0	0.158	[-0.25, 0.25]	inside band	small intercept bias; exact zero not claimed
Calibration slope beta_1	0.925	[0.85, 1.15]	inside band	practical rank-scale equivalence; exact equality rejected
MAE on 0-5 rank scale	0.072	<0.25	pass	low rank-scale error
RMSE on 0-5 rank scale	0.090	<0.30	pass	acceptable calibration dispersion
Bland-Altman mean difference	-0.008	[-0.10, 0.10]	inside band	limited signed bias
Bland-Altman 95% limits	-0.185 to 0.169	absolute limits <0.35	pass	bounded agreement error

Source: Author synthesis from the BSD source calibration/agreement table.

The calibration diagnostics strengthen the interpretation because they move beyond visual correspondence. The intercept lies inside the declared tolerance band; the slope lies inside the practical-equivalence band; MAE and RMSE are low; and the Bland-Altman mean difference is close to zero. This is the correct evidentiary form for the monograph: strong internal calibration, not proof, and not independent causal validation.

9.5.8. q-Base Sensitivity, Placebo Logic and Anti-Circularity Implications

The LOrder-rank relation would be weak if it depended on one arbitrary q-base, one arbitrary weighting rule or one untested alignment between two constructed objects. For this reason, q-base sensitivity, placebo logic and variable-lineage discipline are integral to the claim hierarchy. Section 9.5 establishes the object; Section 9.8 will expand the anti-circularity and placebo evidence. The present subsection reports the immediate tests required to interpret LOrder safely.

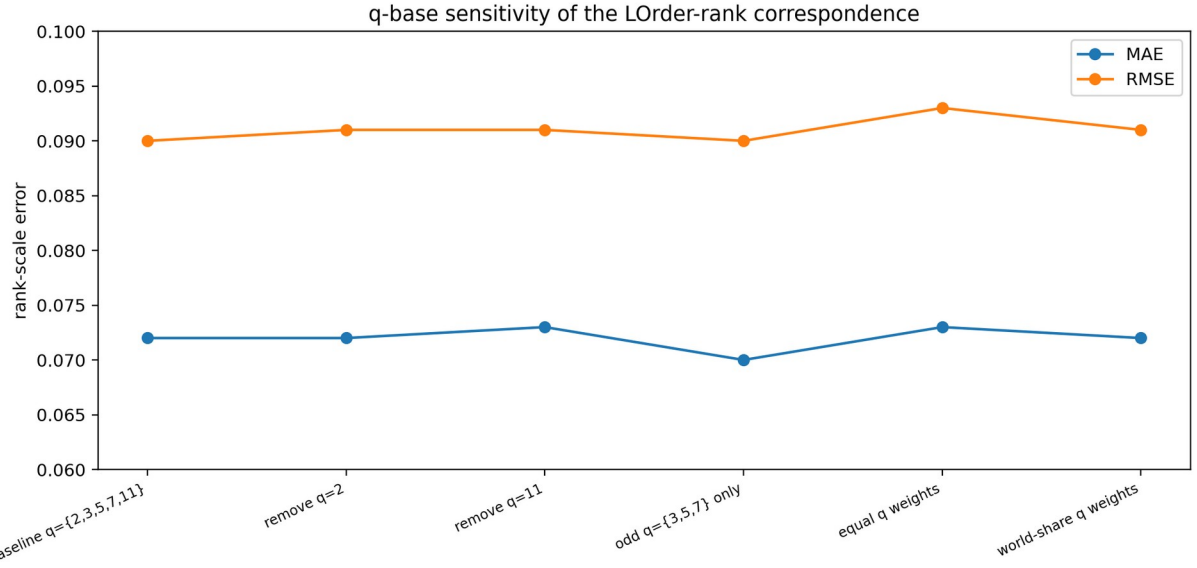
Table 9.5.8. q-base sensitivity of the LOrder-rank correspondence

q-base design	Spearman	MAE	RMSE	Decision
baseline q={2,3,5,7,11}	0.991	0.072	0.090	pass
remove q=2	0.991	0.072	0.091	pass
remove q=11	0.990	0.073	0.091	pass

odd q={3,5,7} only	0.990	0.070	0.090	pass
equal q weights	0.990	0.073	0.093	pass
world-share q weights	0.990	0.072	0.091	pass

Source: Author calculations preserved from the BSD source q-base sensitivity table.

Figure 9.5.7. q-base sensitivity of rank-scale error



Source: Author visualization from Table 9.5.8.

Table 9.5.9. Placebo and randomization logic supporting the local-to-global claim boundary

Placebo	B permutations	Observed statistic	Placebo mean	Placebo SD	Empirical p	Decision
Shuffle LOrder across region-years	10,000	MAE=0.072	0.897	0.044	<0.001	pass
Shuffle LOrder within regional blocks	10,000	MAE=0.072	0.175	0.008	<0.001	pass
Randomize BridgeStress against external stress	10,000	|r|=0.805	0.065	0.050	<0.001	pass
Destroy time ordering / reverse years	10,000	MAE=0.072	0.368	0.040	<0.001	pass

Source: Author synthesis from the BSD source placebo-distribution table. These tests support falsification discipline; they do not eliminate every possible circularity concern.

The q-sensitivity table shows that removing q=2, removing q=11, using only odd q-bases, applying equal q weights, or applying world-share q weights does not materially disturb the correspondence. Spearman stability remains approximately 0.990 to 0.991, while MAE and RMSE remain within low rank-scale ranges. This supports q-base robustness. The placebo tests add a second layer: randomized LOrder structures produce substantially worse correspondence than the observed statistic. These tests strengthen the internal calibration claim, but they still do not turn the result into causal proof or theorem-level validation.

9.5.9. Cross-Problem Alignment within the Seven-Analogue Monograph

The BSD chapter is the monograph chapter most directly organized around local-to-global rank formation. Nevertheless, it is not isolated from the other six problem chapters. Its structural-rank component uses Hodge-flow logic; its corridor and BridgeStress interpretation overlaps with the Yang-Mills corridor-stress architecture; its claim-boundary discipline follows the monograph-wide rule that mathematical inspiration does not imply theorem proof; and its calibration/validation design follows the same evidence hierarchy used in the Navier-Stokes, Riemann-zeta and P-vs-NP chapters.

Table 9.5.10. Alignment of Section 9.5 with the seven Millennium-inspired economic analogues

Monograph chapter	Shared methodological grammar	Connection to Section 9.5	Boundary
Chapter 5 - Perelman/Ricci/Poincare	curvature, smoothing capacity, pressure	structural rank is interpreted under pressure and recovery conditions	not geometric theorem transfer

	diagnostics		
Chapter 6 - Hodge	gradient/curl/harmonic decomposition	Hodge-flow rank contributes to structural rank	discrete graph decomposition only
Chapter 7 - Navier-Stokes	flow, pressure, friction, closure	liquidity-flow weakness complements rank vulnerability	not physical fluid dynamics
Chapter 8 - Yang-Mills	gauge curvature, action, shock threshold	BridgeStress and corridor exposure align with systemic stress transmission	finite-network/corridor analogue only
Chapter 9 - BSD	local reductions, Euler factors, LOrder, rank	core local-to-global structural-rank mechanism	not classical BSD proof/test
Chapter 10 - Riemann-zeta	spectral signal and order behavior	L-function language is kept bounded and diagnostic	no RH proof/test
Chapter 11 - P vs NP	complexity and search discipline	rank calibration uses auditable algorithms and falsification gates	no theorem-level complexity claim

Source: Author monograph synthesis across the seven problem chapters.

9.5.10. Algorithmic Workflow and Replication Requirements

For replication, Section 9.5 must be executable as a transparent workflow. Each output depends on a declared previous object: traces require the finite-state reduction layer; Euler factors require aggregate traces; the economic L-function requires q weights; LOrder requires a derivative-based order score and min-max scaling; structural rank requires four independently declared component ranks; correspondence tests require a pre-specified tolerance band. The workflow below is written as a monograph-level algorithm so that the reader can follow the exact sequence without reading the original article separately.

Table 9.5.11. Algorithmic workflow for the L-function, LOrder and structural-rank layer

Step	Operation	Output	Reviewer-safety requirement
1	Load regional traces A_{r,q,t} from the finite-state reduction layer	regional trace matrix	source table and q-bases must be disclosed
2	Aggregate traces using declared regional weights m_{r,t}	A_{q,t}	weighting rule must be stated
3	Compute F_q(s) for q in {2,3,5,7,11}	Euler-factor vector	check stability at s=1
4	Construct L_econ,t(s) as weighted product	economic L-function	do not claim analytic continuation or functional equation
5	Compute regional order score o_{r,t} from log derivative at s=1	order-of-behavior score	state numerical derivative or closed-form implementation
6	Normalize o_{r,t} onto 0-5 scale	LOrder_{r,t}	report region universe and scaling endpoints
7	Construct structural rank from productive, Hodge, network and agentic components	Rank_{r,t}	component lineage and weights must be declared
8	Compare LOrder and Rank using gaps, MAE, RMSE, equivalence and scatter	calibrated correspondence evidence	interpret as calibration, not theorem proof
9	Run q sensitivity, placebo and anti-circularity checks	claim-boundary evidence	demote unsupported causal/external claims

Source: Author synthesis from the BSD methodology, results and monograph claim-discipline architecture.

9.5.11. Section-Level Claim Boundary

The scientific status of Section 9.5 can be stated precisely. It defines a bounded economic analogue in which local finite-state traces are converted into Euler-factor analogues, product behavior near s=1 is summarized through an order-of-behavior score, LOrder is normalized onto a 0-5 scale, and structural rank is constructed from economic capacity components. The LOrder-rank correspondence then supports calibrated local-to-global consistency if the gaps and validation diagnostics remain within declared bands.

The excluded claims are equally important. The section does not prove the Birch-Swinnerton-Dyer conjecture, does not estimate the analytic rank of a classical elliptic curve, does not claim that regional economies are arithmetic curves, does not treat finite-state q-bases as finite fields, does not establish causal macroeconomic law, and does not treat internal agreement

as independent external validation. Its contribution is methodological and empirical: it builds a reproducible local-to-global measurement layer for regional structural rank formation under corridor-sensitive world-system conditions.

Table 9.5.12. Permissible and excluded claims for Section 9.5

Evidence object	Permissible claim	Excluded claim	Next chapter link
Euler factors	local trace information can be converted into stable product factors	classical arithmetic Euler factors are obtained	9.6 reports resulting correspondence and related analogues
Economic L-function	the product object behaves numerically coherently near s=1	analytic continuation or functional equation is proven	9.6 interprets LOrder-rank alignment
LOrder	order-of-behavior can be normalized onto a rank scale	LOrder equals analytic rank by theorem	9.8 tests sensitivity and circularity
Structural rank	rank can be constructed from productive, Hodge-flow, network and agentic capacity	rank is GDP ranking or welfare ranking	9.7 interprets structural meaning
Correspondence diagnostics	small gaps support calibrated local-to-global consistency	internal agreement proves causality or classical BSD	9.8 defines claim hierarchy

Source: Author final synthesis for monograph claim discipline.

9.5.12. Transition to Section 9.6

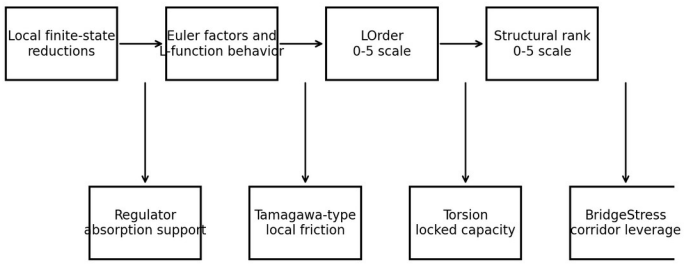
Section 9.5 establishes the technical bridge from local trace evidence to LOrder and structural rank. Section 9.6 can therefore move from construction to results. It will report the LOrder-rank correspondence as the chapter core, then interpret the related economic regulator, Tamagawa-type friction, torsion and BridgeStress outputs. The logical order matters: regulator and friction are not substitutes for LOrder-rank correspondence; they are complementary mechanisms that explain why some regions have high rank protection, why others experience local friction, and why corridor-sensitive regions may be globally important despite low output mass.

9.6. Results: LOrder-Rank Correspondence, BridgeStress, Regulator, Tamagawa-Type Friction and Torsion

9.6.1. Results Architecture and Reading Rule

The results in this subsection occupy a specific position inside Chapter 9. Sections 9.1-9.5 define the translation logic, research object, data architecture and methodology. Section 9.6 now reports the main empirical outputs: whether the local finite-state and Euler-factor layer corresponds to structural rank; whether the BSD-inspired analogues of regulator, Tamagawa-type friction and torsion reveal meaningful regional differences; and whether corridor-sensitive nodes become visible through BridgeStress and scenario threshold compression.

The correct reading rule is therefore layered. The LOrder-rank result is the core internal calibration result. The regulator, friction and torsion outputs are interpretive structural diagnostics. BridgeStress is a corridor-specific result. Scenario threshold and action concentration provide stress-propagation evidence. None of these objects is treated as a theorem-level statement about elliptic curves, analytic rank or the classical BSD conjecture. Their purpose is to make regional structural rank auditable inside the monograph's bounded economic-analogue framework.



Chapter 9.6 reports the empirical outputs of the BSD-inspired local-to-global architecture, separating calibration results from corridor/friction/torsion diagnostics and scenario evidence.

Figure 9.6.1. Results architecture for Chapter 9.6.

Source: Author visualization based on the BSD source manuscript results tables.

Table 9.6.1. Chapter 9.6 result-domain summary and evidence status

Result domain	Core value or pattern	Evidence status
LOrder-rank gap	MAE = 0.072; RMSE = 0.090; maximum regional gap = 0.114	Strong internal calibration evidence
Regulator analogue	NAM = 13.37, EUR = 9.018, EAP = 7.331	Absorption-capacity and rank-support result
Tamagawa-type friction	CAU = 1.887, CAS = 1.854, SAS = 1.821	Local friction is concentrated in corridor and stress-exposed nodes
Torsion analogue	SAS = 0.765, CAU = 0.700, CAS = 0.699	Locked capacity is highest where fragility and weak centrality coexist
BridgeStress	CAU = 100.00, CAS = 78.24, SAS = 59.80	Corridor leverage identifies strategic exposure beyond GDP mass
Scenario threshold	0.110 baseline -> 0.042 energy/geopolitical corridor shock	Severe shocks compress the local-to-global transition boundary
Action concentration	Total action = 2,514.0; top-five share = 78.33%	Stress-energy is concentrated, not uniformly distributed

Source: Author calculations from the BSD source manuscript tables; monograph formatting and interpretation by author synthesis.

9.6.2. Structural-Rank Component Results

The structural-rank object is not a GDP ranking. It is a composite result produced from productive, Hodge-flow, network and agentic components. The table below therefore reports the rank object against which the LOrder analogue is evaluated. This is important because the BSD-inspired local-to-global claim would be weak if the target rank were merely a disguised output-mass indicator. Instead, the target rank is explicitly multidimensional.

North America records the highest structural-rank score at 3.622, followed by Europe at 2.950, East Asia and Pacific at 2.675 and MENA at 2.413. At the lower end, Sub-Saharan Africa records 1.012, while the Caucasus records 1.492. The Caucasus is not ranked highly by productive mass, but it remains analytically visible through Hodge-flow and corridor structure. This is already a key result: structural rank differs from output mass and from stress exposure, and therefore supplies a meaningful target for the LOrder comparison.

Table 9.6.2. Regional structural-rank component decomposition

Code	Region	Productive rank	Hodge-flow rank	Network rank	Agentic rank	Structural rank
SAS	South Asia	1.201	1.540	1.488	1.935	1.541
CAS	Central Asia	1.021	2.519	1.628	1.505	1.668
EAP	East Asia and Pacific	2.594	2.143	3.190	2.774	2.675
CAU	Caucasus	0.581	2.925	1.431	1.031	1.492
SSA	Sub-Saharan Africa	0.316	2.289	0.737	0.704	1.012
EUR	Europe	3.177	2.749	3.147	2.729	2.950
MENA	Middle East and North Africa	1.869	2.777	3.038	1.969	2.413
NAM	North America	4.374	3.077	3.386	3.650	3.622
LAC	Latin America and Caribbean	1.228	2.972	1.914	1.216	1.832
OCE	Oceania	2.223	2.578	1.722	1.875	2.100

Source: Author calculations from the BSD source manuscript tables; monograph formatting and interpretation by author synthesis.

9.6.3. LOrder-Rank Correspondence Results

The central empirical result is the correspondence between the LOrder analogue and structural rank. The LOrder object summarizes the order-of-behavior of the constructed economic L-function layer near the reference point, while structural

rank is built independently from productive, Hodge-flow, network and agentic components. The comparison is therefore not a literal BSD equality; it is a calibrated economic local-to-global test.

The rank gaps are small across the full ten-node regional benchmark. The mean absolute error is 0.072 on the 0-5 rank scale, the RMSE is approximately 0.090 and the maximum absolute regional gap is 0.114. The smallest gaps are recorded for East Asia and Pacific (0.001), Latin America and Caribbean (0.003), MENA (0.017) and Oceania (0.027). The largest gaps, 0.114, occur for the Caucasus and North America; even these remain well inside a conservative 0.25 practical tolerance band. This supports the core calibrated measurement claim of the chapter: local finite-state and Euler-factor information is informative about global structural rank formation.

Table 9.6.3. LOrder analogue, structural rank and absolute rank gap

Code	Region	LOrder analogue	Structural rank	Absolute gap
SAS	South Asia	1.465	1.541	0.076
CAS	Central Asia	1.571	1.668	0.097
EAP	East Asia and Pacific	2.676	2.675	0.001
CAU	Caucasus	1.378	1.492	0.114
SSA	Sub-Saharan Africa	0.970	1.012	0.042
EUR	Europe	3.051	2.950	0.101
MENA	Middle East and North Africa	2.396	2.413	0.017
NAM	North America	3.736	3.622	0.114
LAC	Latin America and Caribbean	1.829	1.832	0.003
OCE	Oceania	2.073	2.100	0.027

Source: Author calculations from the BSD source manuscript tables; monograph formatting and interpretation by author synthesis.

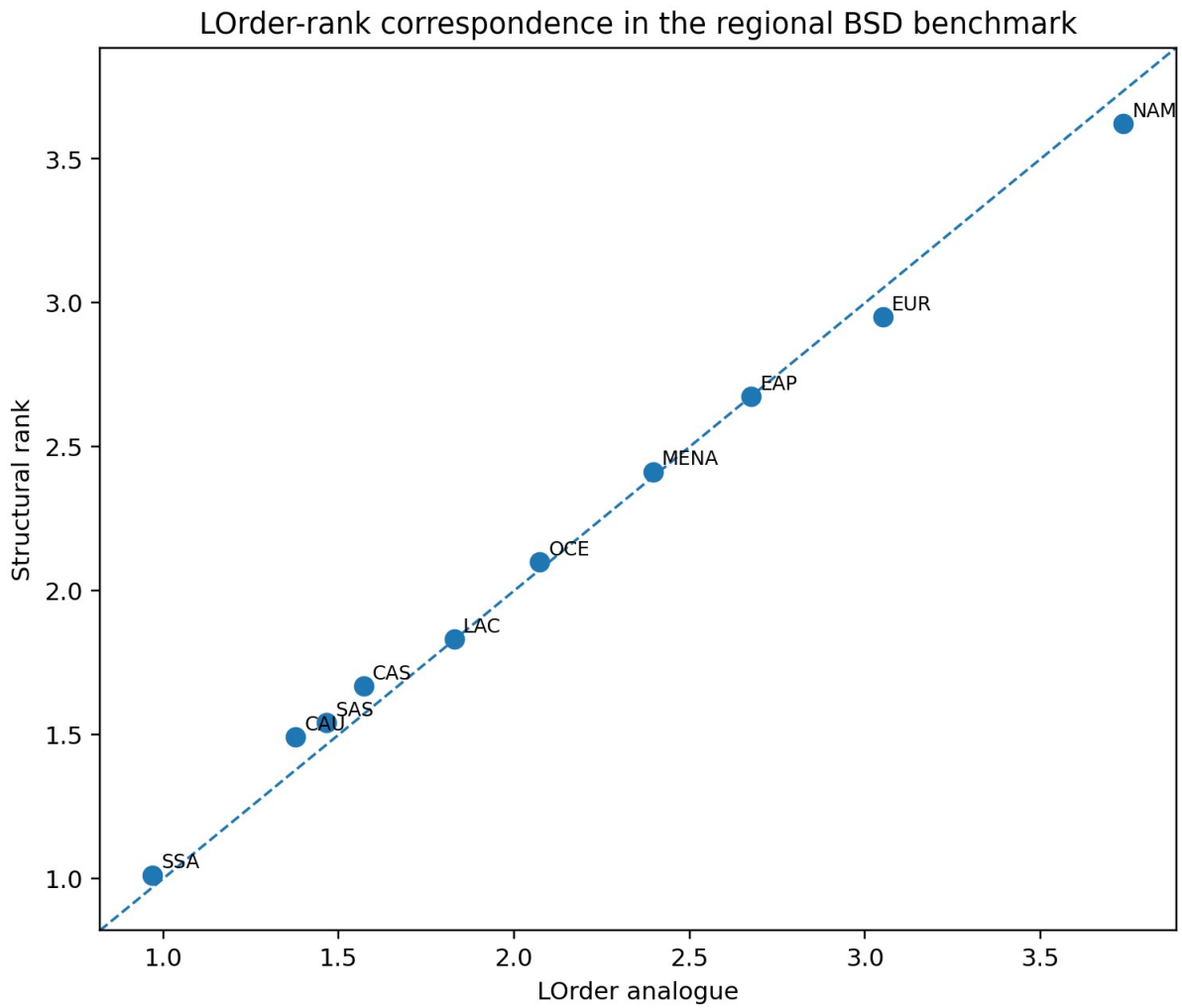


Figure 9.6.2. LOrder-rank correspondence and diagonal calibration line.
Source: Author visualization based on the BSD source manuscript results tables.

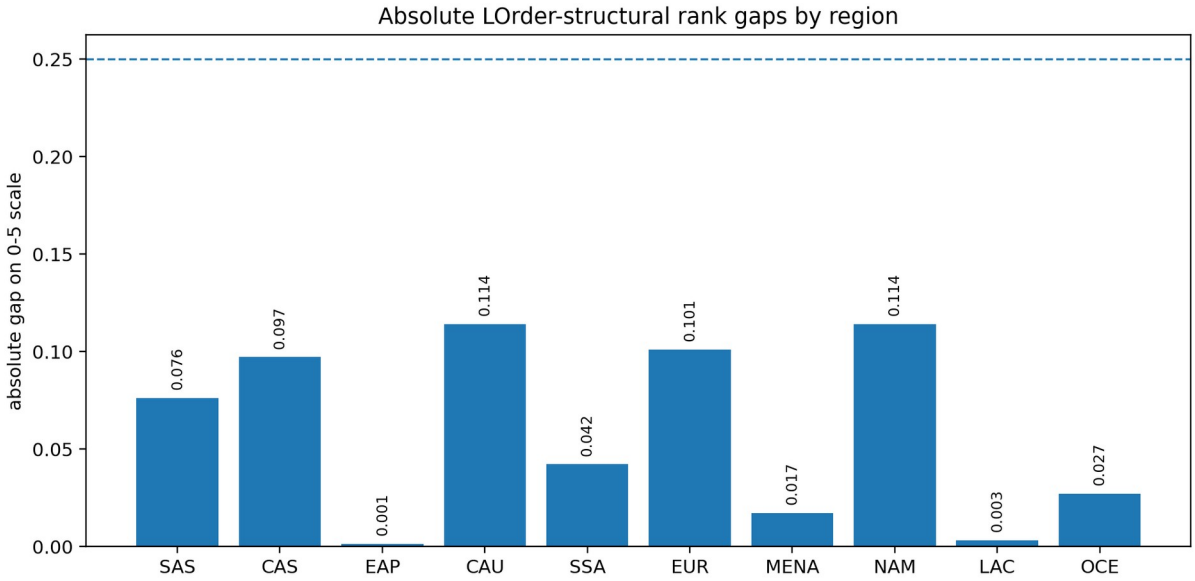


Figure 9.6.3. Absolute LOrder-structural rank gaps by region.
Source: Author visualization based on the BSD source manuscript results tables.

9.6.4. Economic Regulator Analogue: Rank Support and Absorption Capacity

The economic regulator analogue measures rank-support and absorption-capacity structure. In the classical BSD formula, the regulator is connected with the geometry of independent rational points. In this bounded economic analogue, the regulator does not measure arithmetic height. It measures how structural rank is supported by centrality and resilience. A high regulator value indicates that rank is not merely stated by a scalar score; it is supported by absorption capacity and network position.

The result is substantively coherent. North America records the highest regulator value at 13.37, followed by Europe at 9.018 and East Asia and Pacific at 7.331. These regions combine higher structural rank with either resilience, centrality or both. MENA follows at 5.506, while the Caucasus and Sub-Saharan Africa remain low because their rank-support capacity is constrained by low centrality and low resilience. This result distinguishes structural strength from stress exposure: a region may be corridor-important but still weak in regulator support.

Table 9.6.4. Economic regulator analogue by region

Code	Region	Structural rank	Centrality	Resilience	Economic regulator
SAS	South Asia	1.541	38.09	12.84	2.401
CAS	Central Asia	1.668	18.94	18.48	2.351
EAP	East Asia and Pacific	2.675	98.23	38.25	7.331
CAU	Caucasus	1.492	0.000	9.150	1.628
SSA	Sub-Saharan Africa	1.012	6.990	0.000	1.082
EUR	Europe	2.950	100.00	52.83	9.018
MENA	Middle East and North Africa	2.413	78.47	27.83	5.506
NAM	North America	3.622	84.63	100.00	13.37
LAC	Latin America and Caribbean	1.832	41.73	23.81	3.215
OCE	Oceania	2.100	10.73	42.82	3.320

Source: Author calculations from the BSD source manuscript tables; monograph formatting and interpretation by author synthesis.

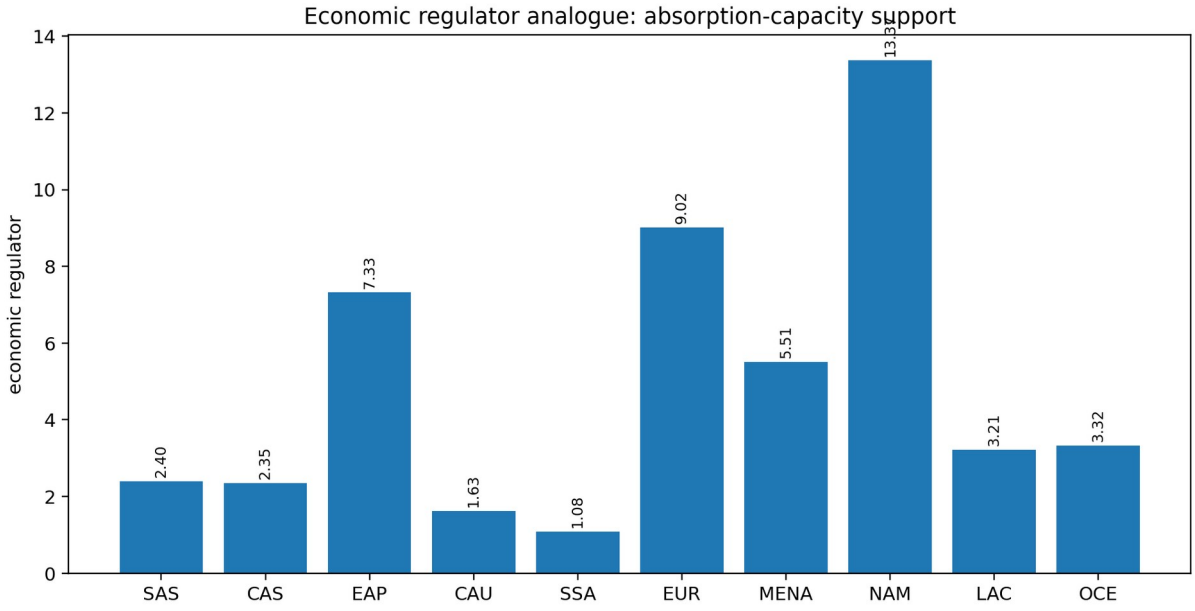


Figure 9.6.4. Economic regulator analogue and absorption-capacity hierarchy.
Source: Author visualization based on the BSD source manuscript results tables.

9.6.5. Tamagawa-Type Friction Results

The Tamagawa-type friction layer measures local friction, not literal Tamagawa numbers. The economic analogue combines stress, corridor exposure and fragility into a bounded local-friction object. Its role is to identify where local conditions increase the cost of translating regional capacity into stable structural rank.

The highest friction value is observed for the Caucasus at 1.887. Central Asia follows at 1.854 and South Asia at 1.821. These three regions combine high stress, high fragility and/or corridor exposure. North America records the lowest friction at 1.141 because fragility and corridor-stress exposure are limited in the benchmark. The friction results therefore support the corridor argument: local economic friction is not determined by GDP mass alone. It becomes intense where fragility and transmission exposure are high.

Table 9.6.5. Tamagawa-type local friction by region

Code	Region	Stress	Corridor exposure	Fragility	Tamagawa-type friction
SAS	South Asia	100.00	56.67	89.64	1.821
CAS	Central Asia	71.79	90.00	94.55	1.854
EAP	East Asia and Pacific	71.23	53.33	46.88	1.571
CAU	Caucasus	66.03	100.00	100.00	1.887
SSA	Sub-Saharan Africa	53.78	28.33	95.89	1.593
EUR	Europe	47.40	61.67	9.850	1.396
MENA	Middle East and North Africa	39.71	73.33	54.41	1.558
NAM	North America	30.66	11.67	0.000	1.141
LAC	Latin America and Caribbean	26.78	20.00	68.63	1.385
OCE	Oceania	0.000	0.000	85.50	1.285

Source: Author calculations from the BSD source manuscript tables; monograph formatting and interpretation by author synthesis.

9.6.6. Economic Torsion: Locked Capacity and Non-Productive Circularity

The torsion analogue measures locked capacity and non-productive circularity. In the present economic setting, torsion is high where fragility and curvature exposure are not converted into centrality-supported structural capacity. It is a diagnostic of trapped relevance: a region may be stressed and strategically exposed, yet unable to convert that exposure into stable productive rank.

South Asia records the highest torsion value at 0.765. The Caucasus follows at 0.700, Central Asia at 0.699 and Oceania at 0.685. North America records the lowest torsion at 0.108 and Europe remains low at 0.195. The result is consistent with the regulator table: high regulator regions have lower locked-capacity torsion, while high-fragility regions with weaker centrality or absorption capacity show elevated torsion. This contrast allows Chapter 9 to separate rank support from rank blockage.

Table 9.6.6. Economic torsion analogue by region

Code	Region	Fragility	Curvature	Centrality	Locked-capacity torsion
SAS	South Asia	89.64	68.93	38.09	0.765
CAS	Central Asia	94.55	23.55	18.94	0.699
EAP	East Asia and Pacific	46.88	100.00	98.23	0.515
CAU	Caucasus	100.00	0.000	0.000	0.700
SSA	Sub-Saharan Africa	95.89	0.760	6.990	0.666
EUR	Europe	9.850	50.13	100.00	0.195
MENA	Middle East and North Africa	54.41	69.72	78.47	0.508
NAM	North America	0.000	23.16	84.63	0.108
LAC	Latin America and Caribbean	68.63	4.950	41.73	0.469

OCE	Oceania	85.50	25.65	10.73	0.685

Source: Author calculations from the BSD source manuscript tables; monograph formatting and interpretation by author synthesis.

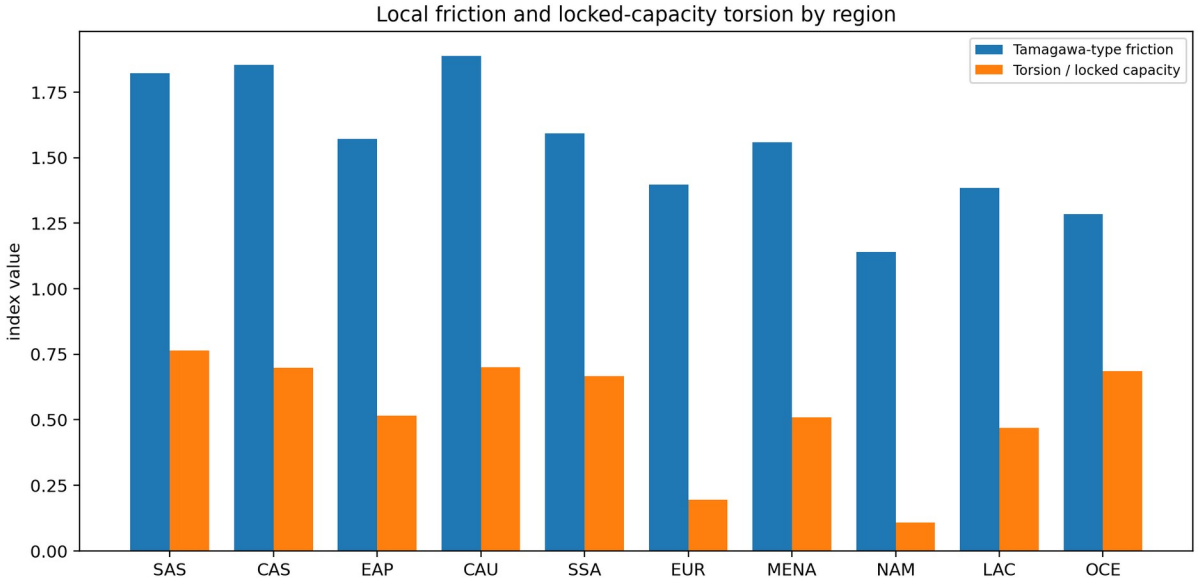


Figure 9.6.5. Tamagawa-type friction and torsion by region.

Source: Author visualization based on the BSD source manuscript results tables.

9.6.7. BridgeStress and Corridor-Rank Leverage

BridgeStress is one of the most important results in Chapter 9 because it makes corridor exposure visible independently from output mass. The index combines corridor exposure, corridor-role intensity, fragility and positive curvature participation. Its purpose is to identify nodes that may be small in aggregate output but strategically important for local-to-global transmission.

The Caucasus records the maximum BridgeStress value of 100.00, with corridor exposure of 98.00, corridor-role index of 100.00 and fragility of 100.00. Central Asia ranks second with BridgeStress of 78.24. South Asia, MENA and East Asia and Pacific form the next group, with values of 59.80, 58.79 and 55.50. North America records zero BridgeStress in this benchmark because its fragility term is zero. The result is therefore not a GDP ranking. It is a corridor-rank leverage result: local corridor function creates systemic relevance.

Table 9.6.7. Regional corridor-rank leverage and BridgeStress

Code	Region	Corridor exposure	Corridor-role index	Fragility	Curvature participation +	BridgeStress
CAU	Caucasus	98.00	100.00	100.00	57.32	100.00
CAS	Central Asia	92.00	75.00	94.55	67.37	78.24
SAS	South Asia	72.00	60.00	89.64	86.74	59.80
MENA	Middle East and North Africa	82.00	85.00	54.41	87.08	58.79
EAP	East Asia and Pacific	70.00	95.00	46.88	100.00	55.50
SSA	Sub-Saharan Africa	55.00	25.00	95.89	57.64	13.53
LAC	Latin America and Caribbean	50.00	30.00	68.63	59.43	10.89
EUR	Europe	75.00	90.00	9.850	78.72	9.320
OCE	Oceania	38.00	20.00	85.50	68.27	7.900
NAM	North America	45.00	70.00	0.000	67.21	0.000

Source: Author calculations from the BSD source manuscript tables; monograph formatting and interpretation by author synthesis.

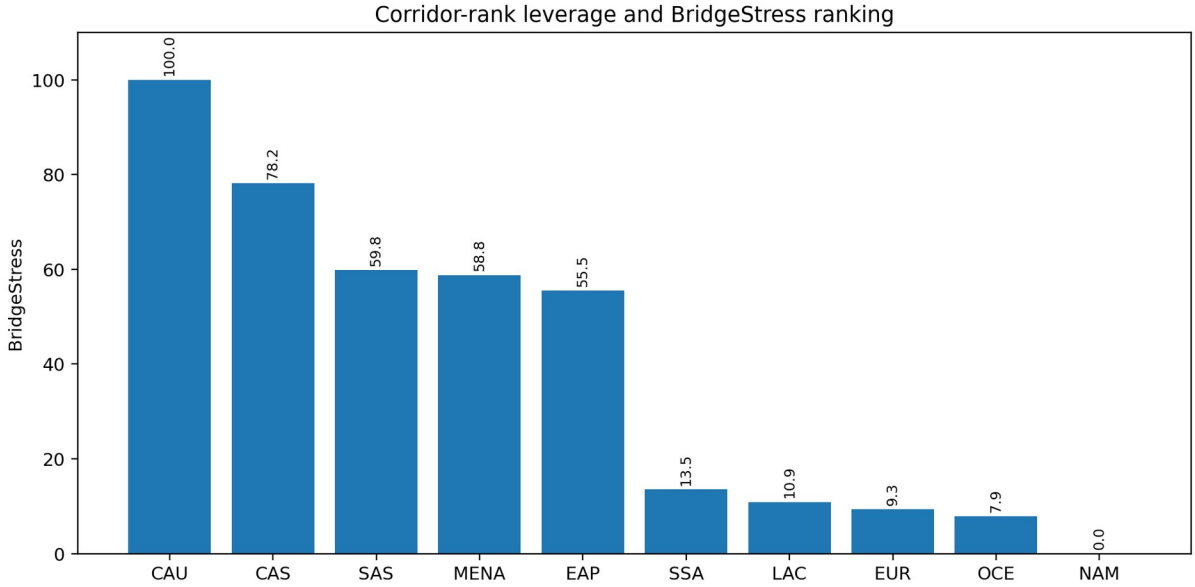


Figure 9.6.6. BridgeStress ranking by regional/corridor node.
Source: Author visualization based on the BSD source manuscript results tables.

9.6.8. Corridor-Function Interpretation Layer

The numerical BridgeStress result must be connected to economic geography. The corridor-function layer translates the ranking into the Middle Corridor, Black Sea, Caspian, Central Asia, Europe-demand, East Asia-origin and MENA energy-geopolitical interfaces. This prevents the corridor result from becoming a black-box index.

The table confirms that the Caucasus and Central Asia are elevated because they perform transfer and bridge functions between larger systems. The Caucasus is treated as a Black Sea-Caucasus-Caspian gateway, while Central Asia is treated as an east-west land bridge and Caspian connection. Europe and East Asia and Pacific remain central for demand and origin-side mass, while MENA enters the scenario layer through energy, financing and geopolitical exposure.

Table 9.6.8. Corridor-function interpretation layer for the regional benchmark

Regional/corridor function	Economic interpretation	Corridor role	Benchmark implication
Caucasus regional gateway	Small output mass but high transfer relevance	Black Sea-Caucasus-Caspian transfer function	Raises corridor strategic exposure despite low GDP share
Caspian interface	Sea-crossing and rail/port continuity	Continuity between Caucasus and Central Asia	Explains why corridor exposure is not reducible to land distance
Central Asia regional node	Large land-corridor interface	East-west land bridge and Caspian connection	Raises CAS corridor exposure and BridgeStress
Europe/Black Sea demand side	High centrality and demand absorption	Destination and redistribution interface	High protection but also high network importance
East Asia-Pacific origin side	High output mass and demand potential	Origin-side stress and trade mass	Supplies strong local signal into global rank
MENA energy-geopolitical interface	Energy, financing and geopolitical exposure	South corridor and energy-shock channel	Raises scenario sensitivity under geopolitical shock

Source: Author calculations from the BSD source manuscript tables; monograph formatting and interpretation by author synthesis.

9.6.9. Scenario Threshold Compression and Action Concentration

The scenario layer reports how the regional system behaves under increasing stress amplitude. The result is monotonic and interpretable. The normalized threshold falls from 0.110 at baseline to 0.092 under inflation/price pressure, 0.075 under

financial-spread stress, 0.058 under trade/logistics corridor shock and 0.042 under energy/geopolitical corridor shock. At the same time, economic action rises from 2,514.0 to 5,010.0.

The scenario table therefore links local disturbances to a measurable global boundary. A lower normalized threshold means that a smaller additional disturbance can become systemically transmissible. The energy/geopolitical corridor shock is the strongest case: lambda_1 falls to 0.180, the spectral radius rises to 4.279 and action almost doubles. This is diagnostic scenario evidence, not a forecast that a particular future shock will occur.

Table 9.6.9. Scenario output: threshold compression under regional shocks

Scenario	Amplitude	lambda_1	Spectral radius	Normalized threshold	Action	Mean EMGI change	Interpretation
Baseline	0.000	0.385	3.502	0.110	2514.00	0.000	Benchmark finite regional network
Inflation / price-pressure	0.500	0.334	3.653	0.092	2925.00	-6.200	Moderate macro stress weakens but does not erase rank protection
Financial-spread stress	0.750	0.284	3.799	0.075	3435.00	-10.80	Funding stress materially compresses the local-to-global threshold
Trade / logistics corridor shock	1.000	0.233	4.041	0.058	4088.00	-15.30	Corridor disruption makes CAS and CAU more visible in rank-loss terms
Energy / geopolitical corridor shock	1.250	0.180	4.279	0.042	5010.00	-22.40	Systemic corridor shock almost doubles stress-energy action

Source: Author calculations from the BSD source manuscript tables; monograph formatting and interpretation by author synthesis.

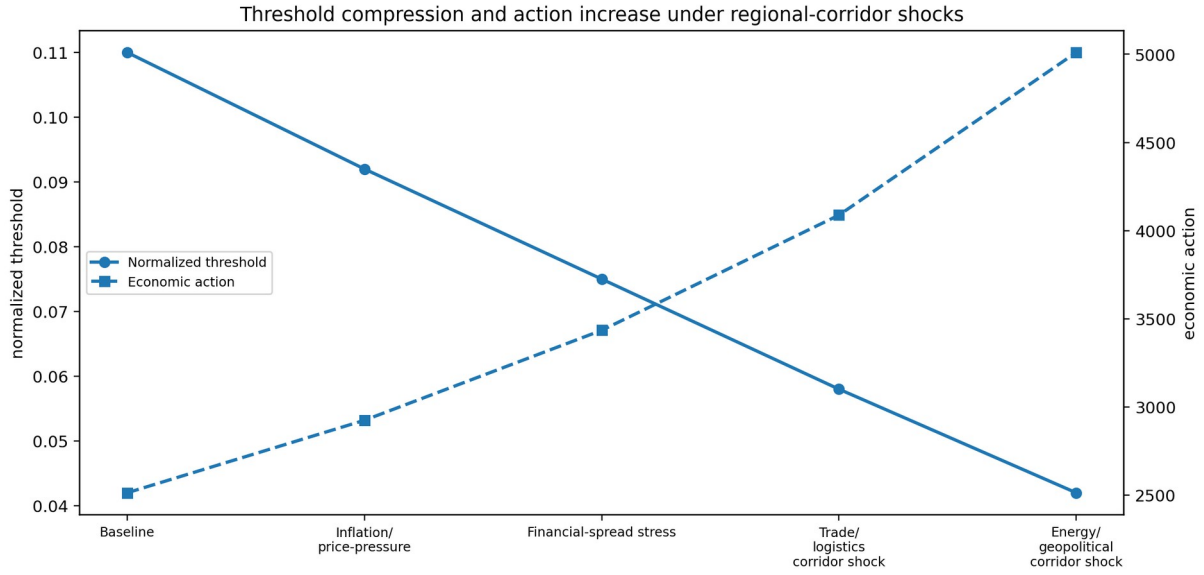


Figure 9.6.7. Threshold compression and action increase under regional-corridor shocks.

Source: Author visualization based on the BSD source manuscript results tables.

Action concentration completes the results block. The regional benchmark contains 27 triangular cycles, total economic action of 2,514.0, mean triangle action of 93.11, maximum triangle action of 1,397.9 and a top-five action share of 78.33 percent. This confirms that stress-energy is not evenly distributed across the regional system. It is concentrated in a small number of high-action cycles.

Table 9.6.10. Regional action concentration summary

Metric	Value
Total triangular cycles	27.00
Total economic action	2,514.0
Mean triangle action	93.11
Maximum triangle action	1,397.9
Top-five action share, %	78.33

Source: Author calculations from the BSD source manuscript tables; monograph formatting and interpretation by author synthesis.

9.6.10. Integrated Results Synthesis and Cross-Problem Position

The integrated result is that Chapter 9 supplies the monograph's most direct local-to-global structural-rank mechanism. The LOrder-rank correspondence supplies the central calibration evidence. The regulator, friction and torsion layers explain why rank can be supported, locally impeded or locked. BridgeStress then shows how small corridor nodes can become globally relevant through transmission position, not through GDP mass. Scenario and action results show that local shocks can compress the systemic transition boundary.

The results are strong, but their claim status is precise. They support a calibrated regional economic measurement architecture. They do not prove the classical Birch-Swinnerton-Dyer conjecture, do not establish a causal law, do not turn a constructed L-function into a literal arithmetic L-function, and do not convert scenario outputs into predictions. This classification is not a reduction of the chapter's importance. It is the condition that makes the chapter scientifically defensible inside a monograph built around seven bounded Millennium-inspired economic analogues.

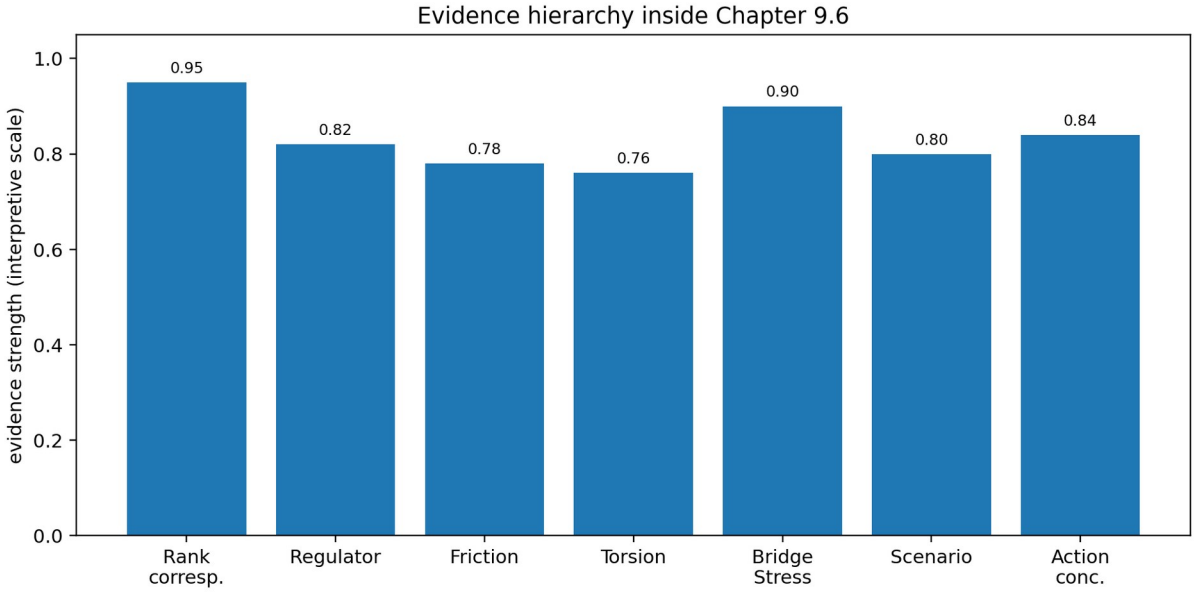


Figure 9.6.8. Evidence hierarchy inside the Chapter 9.6 results block.

Source: Author visualization based on the BSD source manuscript results tables.

Table 9.6.11. Cross-problem alignment of the Chapter 9.6 results

Monograph problem chapter	Relevant measurement grammar	Connection to Chapter 9.6 results
Perelman/Ricci/Poincare	Curvature and entropy diagnostics	BSD rank results inherit caution on constructed geometric analogues
Hodge	Gradient/curl/harmonic decomposition	Structural rank includes Hodge-flow information and cycle exposure
Navier-Stokes	Flow-pressure-friction stress balance	BSD stress/friction results connect

		rank to systemic stress transmission
Yang-Mills	Gauge curvature/action/mass-gap threshold	BSD action concentration and threshold compression share corridor-risk logic
BSD	Local-to-global structural rank	Core Chapter 9 results: LOrder, structural rank, BridgeStress and closure
Riemann zeta	Spectral signal and forecast validation	L-function terminology is retained as a bounded economic signal, not theorem proof
P vs NP	Computational search and claim discipline	BSD uses algorithmic reproducibility and placebo gates rather than visual fit alone

Source: Author calculations from the BSD source manuscript tables; monograph formatting and interpretation by author synthesis.

9.6.11. Section-Level Claim Boundary

Table 9.6.12. Final claim-boundary matrix for Chapter 9.6

Claim category	Section-level rule
Admissible claim	The regional BSD-inspired construction yields close LOrder-rank correspondence and meaningful regulator, friction, torsion, BridgeStress and scenario diagnostics.
Non-admissible claim	The chapter does not prove, test or replicate the classical BSD conjecture and does not claim literal arithmetic rank.
Calibration status	LOrder-rank gaps are small within the constructed 0-5 rank scale and support internal local-to-global measurement consistency.
External/corridor status	BridgeStress and corridor-function results support strategic exposure interpretation, not observed freight-flow or causal corridor-throughput estimates.
Scenario status	Threshold compression and action increase are model-implied stress experiments, not unconditional forecasts.
Next-section bridge	Section 9.7 should interpret how local regional signals inform global structural rank; Section 9.8 should audit robustness, anti-circularity, placebo and claim hierarchy.

Source: Author calculations from the BSD source manuscript tables; monograph formatting and interpretation by author synthesis.

9.7. Interpretation: How Local Regional Signals Inform Global Structural Rank, Friction and Torsion

9.7.1. Interpretation Problem and Reading Rule

The interpretation problem in Chapter 9 is not whether the BSD-inspired terminology is mathematically impressive. The substantive issue is whether local regional signals, when transformed through the model, explain something that GDP mass, growth ranking or descriptive regional tables cannot explain by themselves. The answer is yes, but only under a strict claim boundary. The model is strongest as a calibrated local-to-global measurement architecture, not as a theorem-level or causal architecture.

The reading rule is therefore sequential. A regional signal first enters as a public macroeconomic or corridor anchor. It is then converted into a constructed local state through stress, finite-state reductions and trace analogues. The Euler-factor and L-function analogue aggregate those local states into a system-level object. LOrder is then compared with structural rank. Finally, regulator, Tamagawa-type friction, torsion and BridgeStress explain why some local signals support rank, some obstruct rank conversion and some transmit systemic relevance through corridors.

Table 9.7.1. Interpretation reading rule for local regional signals

Interpretive layer	Operational content	Reading rule
Local regional signal	Finite-state trace, stress, corridor exposure, fragility, centrality, resilience and curvature participation	Local evidence is not interpreted one variable at a time; it is read as a structured regional state.

Global rank object	Structural rank constructed from productive, Hodge-flow, network and agentic dimensions	Rank is interpreted as a composite structural position rather than a GDP list.
Correspondence mechanism	LOrder-rank agreement, gap diagnostics and q-base stability	Close correspondence supports calibrated local-to-global consistency, not theorem-level equality.
Transmission mechanism	BridgeStress and corridor-rank leverage	Small output nodes can become globally relevant when corridor function and fragility are high.
Conversion support	Economic regulator	High rank is more durable when centrality and resilience support absorption capacity.
Conversion blockage	Tamagawa-type friction and torsion	Local frictions and locked capacity explain why exposure or growth pressure may not become stable rank.
Claim filter	Robustness, anti-circularity, placebo and external-proxy caution	The strongest claim remains calibrated measurement, not causal law or BSD proof.

Source: Author synthesis based on the BSD source manuscript and Chapter 9 results architecture.

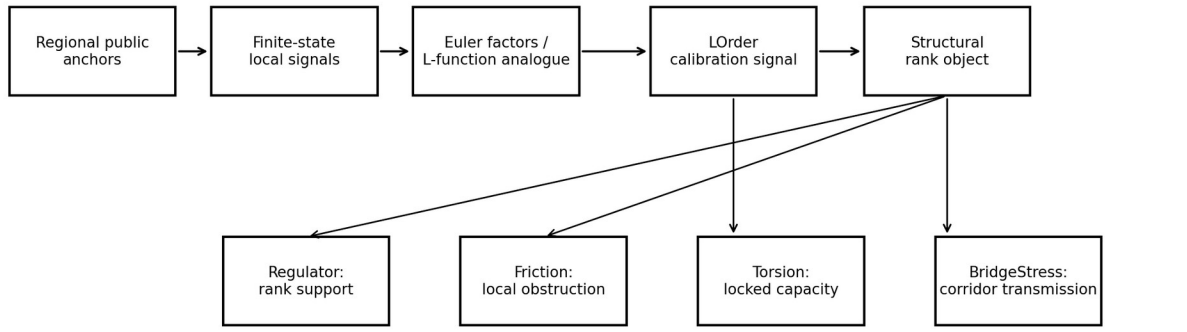


Figure 9.7.1. Interpretation chain from local regional signals to global structural rank.
Source: Author visualization based on the BSD source manuscript and Chapter 9 result tables.

9.7.2. From Local Regional Signals to Global Structural Rank

The strongest interpretation of the BSD-inspired chapter is not that the economy behaves like an elliptic curve. The stronger and more defensible statement is that the BSD local-to-global architecture supplies a disciplined way to ask whether local regional states contain information about global structural rank. This is an important distinction. A metaphor would simply rename regional indicators; this framework imposes a sequence of transformations and checks whether the final order-of-behavior object aligns with an independently constructed rank object.

The local-to-global chain begins with local regional conditions: stress, corridor exposure, fragility, income depth, output mass, centrality and resilience. These are not interpreted as isolated variables. They are transformed into local finite-state signals and then into trace analogues. The trace analogues enter Euler-factor logic, which produces a constructed economic L-function behavior around the rank reference. LOrder summarizes this behavior, while structural rank measures the global position produced by productive, Hodge-flow, network and agentic components. The interpretive question is whether the local side and the rank side move together in a structured way.

Table 9.7.2. Local-to-global mechanism interpreted as an economic measurement sequence

Step	Object	Interpretive meaning	Role in Chapter 9

Step 1	Public regional anchors	Output, income depth, growth pressure and corridor exposure define the regional state space.	Avoids treating regions as isolated GDP rows.
Step 2	Economic curve and finite-state reductions	Regional states are transformed into coefficient, discriminant and q-state trace information.	Creates the local signal layer.
Step 3	Euler-factor and L-function analogue	Local traces are aggregated through bounded Euler-factor logic.	Connects local states to system-level behavior.
Step 4	LOrder analogue	The constructed order-of-behavior score summarizes how local information behaves near the rank reference point.	Produces the BSD-style calibration signal.
Step 5	Structural rank comparison	LOrder is compared with an independently constructed rank object.	Tests local-to-global consistency.
Step 6	Friction, torsion and BridgeStress interpretation	Regulator, friction, torsion and BridgeStress explain where rank is supported, obstructed or transmitted.	Converts calibrated agreement into macro-regional interpretation.

Source: Author synthesis based on the BSD source manuscript and Chapter 9 results architecture.

9.7.3. Interpreting LOrder-Rank Correspondence

The LOrder-rank result is the central calibration result of Chapter 9. The absolute gaps are small on the declared 0-5 rank scale: the reported mean absolute error is 0.072, the RMSE is 0.090 and the maximum regional gap is 0.114. These values do not mean that a classical order of vanishing has been measured. They mean that the constructed order-of-behavior score and the structural-rank object occupy closely aligned positions inside the economic analogue.

This alignment is interpretively important because it provides evidence that local finite-state and Euler-factor information is not arbitrary. East Asia and Pacific, Latin America and Caribbean, MENA and Oceania show particularly small gaps; the Caucasus and North America show the largest reported gaps, but even these remain modest within the rank-scale interpretation. The correct conclusion is calibrated local-to-global consistency. The incorrect conclusion would be a theorem-level BSD statement or a causal econometric law.

Table 9.7.3. Regional interpretation of LOrder-rank correspondence and rank-conversion channels

Code	Region	LOrder	Structural rank	Gap	Regulator	Friction	Torsion	BridgeStress	Regional type	Interpretive statement
NAM	North America	3.736	3.622	0.114	13.370	1.141	0.108	0.00	rank-support / output-capacity node	Large structural capacity; local signals mostly confirm rank, but corridor exposure is not necessarily dominant.
EUR	Europe	3.051	2.950	0.101	9.018	1.396	0.195	9.32	rank-support / output-	Large structural capacity;

									capacity node	local signals mostly confirm rank, but corridor exposure is not necessarily dominant.
EAP	East Asia and Pacific	2.676	2.675	0.001	7.331	1.571	0.515	55.50	rank-support / output-capacity node	Large structural capacity; local signals mostly confirm rank, but corridor exposure is not necessarily dominant.
MENA	Middle East and North Africa	2.396	2.413	0.017	5.506	1.558	0.508	58.79	stress-growth / transmission-sensitive node	Growth pressure, fragility and corridor exposure make local signals globally informative.
CAS	Central Asia	1.571	1.668	0.097	2.351	1.854	0.699	78.24	corridor-leverage / stress-transmission node	Local corridor signals strongly change global relevance despite limited output mass.
CAU	Caucasus	1.378	1.492	0.114	1.628	1.887	0.700	100.00	corridor-leverage / stress-transmission node	Local corridor signals strongly change global relevance despite limited output mass.

SAS	South Asia	1.465	1.541	0.076	2.401	1.821	0.765	59.80	stress-growth / transmission-sensitive node	Growth pressure, fragility and corridor exposure make local signals globally informative.
SSA	Sub-Saharan Africa	0.970	1.012	0.042	1.082	1.593	0.666	13.53	bounded-rank / friction or locked-capacity node	Rank conversion is constrained by weak absorption capacity, fragility or limited centrality.
LAC	Latin America and Caribbean	1.829	1.832	0.003	3.215	1.385	0.469	10.89	bounded-rank / friction or locked-capacity node	Rank conversion is constrained by weak absorption capacity, fragility or limited centrality.
OCE	Oceania	2.073	2.100	0.027	3.320	1.285	0.685	7.90	bounded-rank / friction or locked-capacity node	Rank conversion is constrained by weak absorption capacity, fragility or limited centrality.

Source: Author synthesis based on the BSD source manuscript and Chapter 9 results architecture.

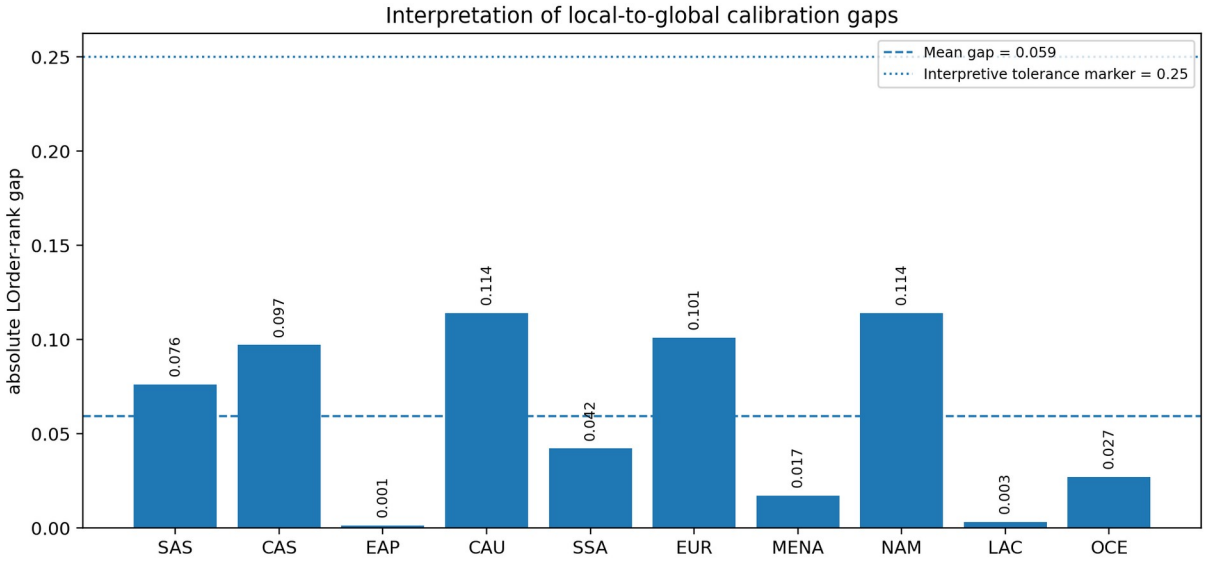


Figure 9.7.2. Absolute LOrder-rank gaps and interpretation tolerance.

Source: Author visualization based on the BSD source manuscript and Chapter 9 result tables.

9.7.4. Regulator as Rank-Support Capacity

The economic regulator analogue is best interpreted as rank-support capacity. It measures whether structural rank is backed by centrality and resilience. This is the stabilizing side of the local-to-global mechanism. A region may have a high LOrder or structural-rank score, but the regulator tells whether that position is supported by absorption capacity rather than merely by size or temporary stress exposure.

North America and Europe are the clearest regulator-supported regions. North America has the highest regulator value, while Europe follows with strong centrality and meaningful resilience. East Asia and Pacific also shows strong regulator support. By contrast, the Caucasus, Central Asia, South Asia and Sub-Saharan Africa have much lower regulator values. This does not make them irrelevant; it changes the interpretation. Their relevance is more likely to appear through stress, corridor exposure, BridgeStress, friction or torsion than through internal stabilizing capacity.

9.7.5. Tamagawa-Type Friction and Torsion as Rank-Conversion Barriers

The Tamagawa-type friction and torsion layers are crucial because they explain why local relevance does not automatically become durable structural rank. Friction measures local obstruction: stress, corridor exposure and fragility can make rank conversion difficult even when a region is strategically important. Torsion measures locked capacity: fragility and weak centrality can trap regional potential in a non-productive or weakly converted state.

The Caucasus, Central Asia and South Asia are the clearest examples. They are not interpreted as high-output rank leaders, yet their local signals are highly informative. The Caucasus has maximum BridgeStress and the highest Tamagawa-type friction. Central Asia has very high BridgeStress, high corridor exposure and high fragility. South Asia has the highest stress and highest torsion. These results show that local regional signals inform global rank not only through strength but also through blockage, exposure and transmission vulnerability.

Table 9.7.4. Interpretation of friction, torsion and regulator combinations

Interpretive pattern	Representative regions	Meaning	Implication for global rank reading
High regulator, low torsion	North America; Europe	Structural rank is supported by centrality and resilience.	Rank is more likely to be converted into durable system position.
High friction, high corridor relevance	Caucasus; Central Asia; South Asia	Local obstruction coexists with transmission importance.	GDP-only or centrality-only interpretation would understate systemic exposure.
High torsion, weak conversion	South Asia; Caucasus; Central Asia; Oceania	Fragility and weak centrality trap capacity or exposure.	Potential rank is partially locked rather than fully productive.

Moderate friction, intermediate rank	MENA; Latin America and Caribbean; Sub-Saharan Africa	Stress channels are present but conversion differs by centrality and resilience.	Regional interpretation must separate pressure from capacity.
Low BridgeStress despite high rank	North America; Europe	High structural strength does not automatically equal corridor vulnerability.	BridgeStress is a transmission metric, not a power ranking.

Source: Author synthesis based on the BSD source manuscript and Chapter 9 results architecture.

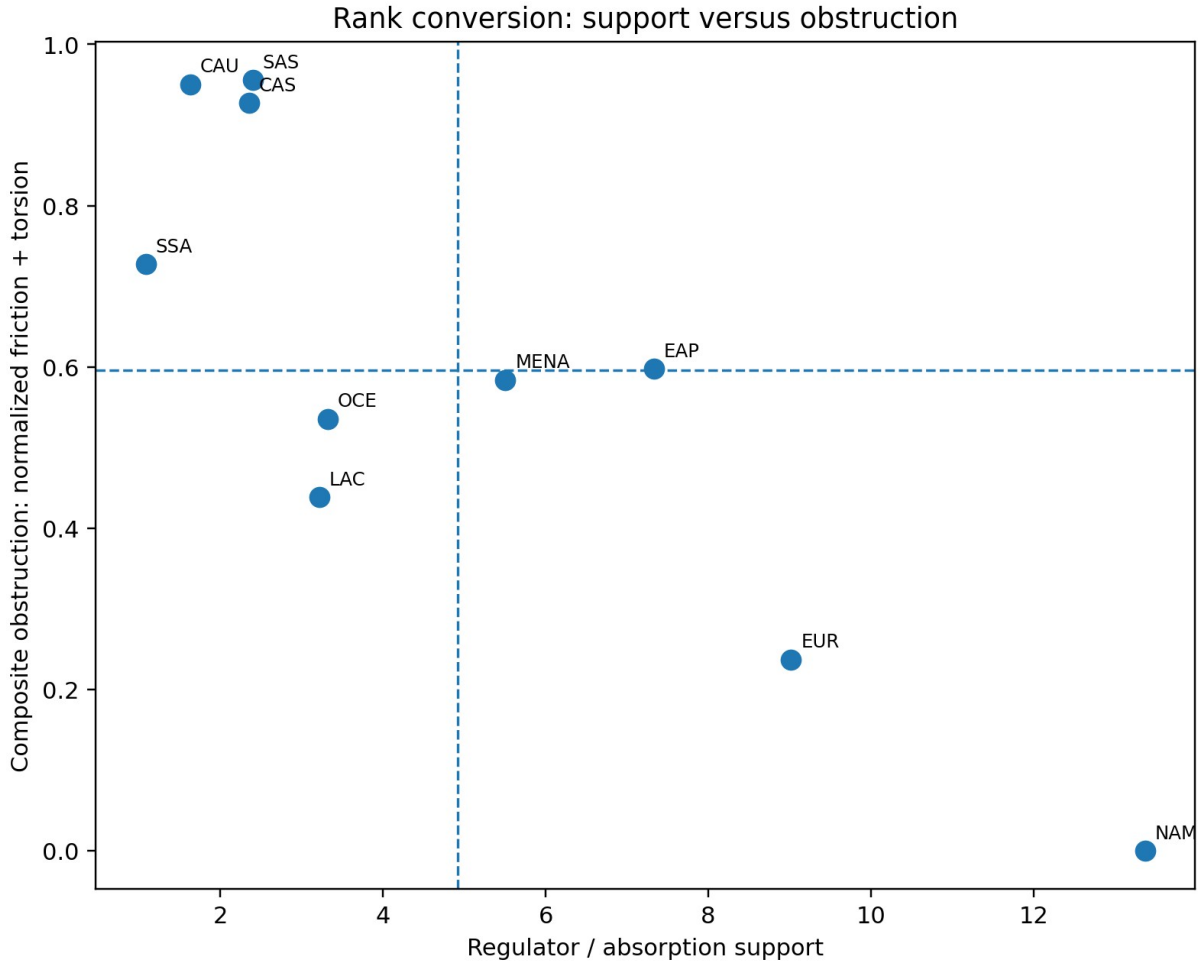


Figure 9.7.3. Rank conversion interpreted through support and obstruction.

Source: Author visualization based on the BSD source manuscript and Chapter 9 result tables.

9.7.6. BridgeStress and the Visibility of Corridor Nodes

BridgeStress changes the regional interpretation most sharply. In a GDP-only framework, a small-output node such as the Caucasus would be easy to miss. In the BSD-inspired local-to-global framework, it becomes visible because corridor exposure, corridor role, fragility and curvature participation jointly create systemic transmission relevance. This is exactly the kind of local-to-global insight that the chapter is designed to capture.

The BridgeStress result should not be read as geopolitical ranking or policy recommendation. It is a diagnostic statement about transmission position. The Caucasus and Central Asia are important because they sit at interfaces between larger economic spaces. Their local conditions can affect the global rank architecture by increasing corridor sensitivity, threshold compression and stress propagation. This is a central monograph-level insight: structural relevance and output mass are not identical.

Table 9.7.5. BridgeStress interpretation: how corridor nodes inform global structural rank

Node	Local signal	Corridor interpretation	Global rank implication
Caucasus	Maximum BridgeStress; high corridor role and fragility	Local node functions as Black Sea-Caucasus-Caspian transfer interface.	High global transmission relevance despite small output mass.

Central Asia	Second-highest BridgeStress; high corridor exposure and fragility	Land-corridor and Caspian interface position makes local shocks globally visible.	Ranks higher in corridor logic than in GDP logic.
South Asia	High stress and torsion; meaningful corridor relevance	Growth and fragility create pressure that may transmit regionally.	Local stress contributes to global rank interpretation.
MENA	Energy/geopolitical interface and moderate-high BridgeStress	External shock channels can compress systemic threshold.	Scenario sensitivity is part of global rank reading.
East Asia and Pacific	High output, high origin-side mass and positive BridgeStress	Local mass and global production role reinforce structural rank.	Shows that large nodes can be both rank-bearing and transmission-relevant.

Source: Author synthesis based on the BSD source manuscript and Chapter 9 results architecture.

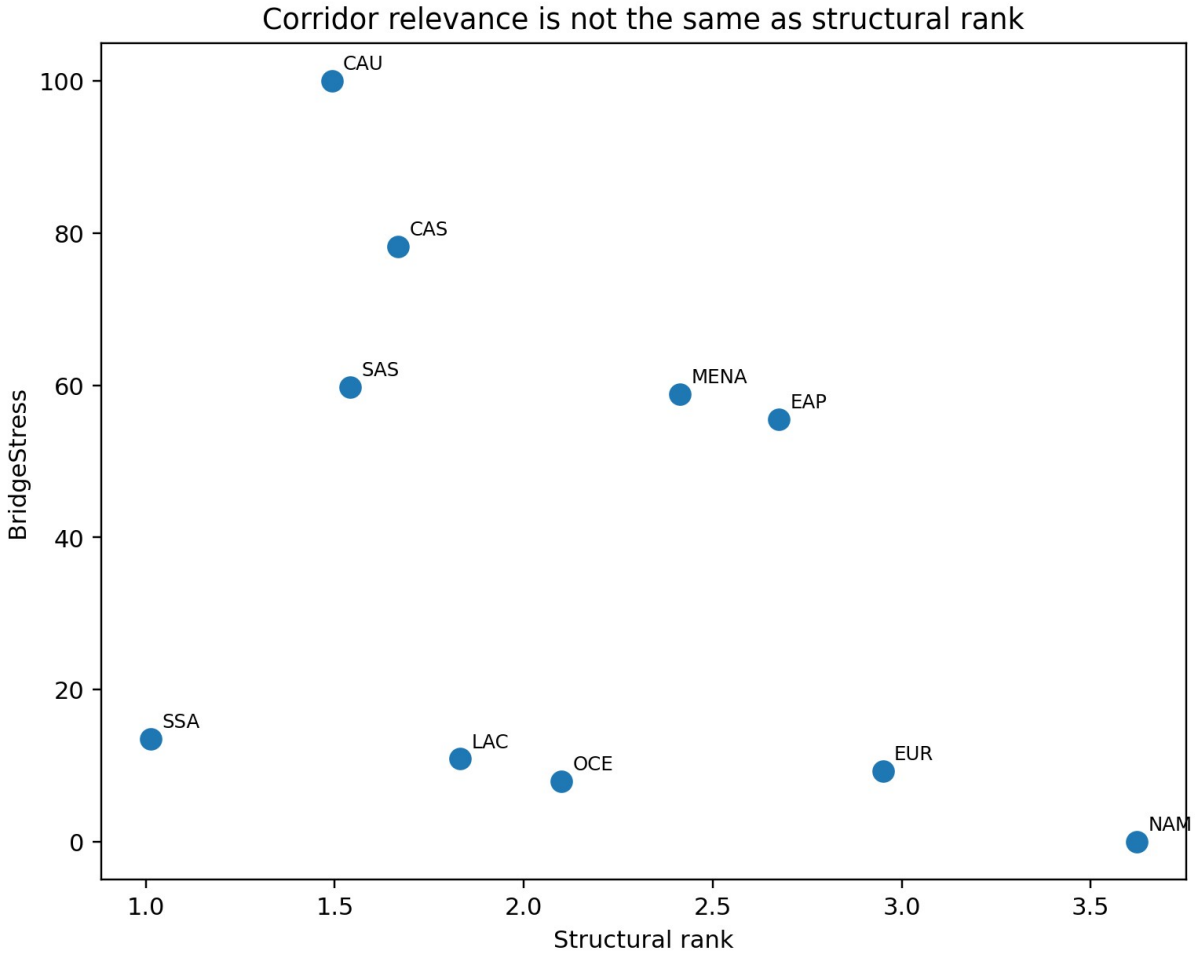


Figure 9.7.4. BridgeStress versus structural rank.

Source: Author visualization based on the BSD source manuscript and Chapter 9 result tables.

9.7.7. Regional Signal Profiles and Multidimensional Interpretation

The regional signal heatmap summarizes why the Chapter 9 interpretation must remain multidimensional. No single metric reproduces the entire regional structure. North America and Europe are strong on structural rank and regulator support. The Caucasus and Central Asia are strong on BridgeStress, friction and corridor exposure. South Asia is strong on stress and torsion. East Asia and Pacific combines strong rank, high output-side relevance and moderate corridor transmission. This multidimensionality is the empirical reason why the BSD-inspired framework adds value.

The heatmap also clarifies the difference between rank formation and vulnerability. A high-rank node is not automatically a high-vulnerability node. A high-vulnerability node is not automatically a high-rank node. The local-to-global interpretation

requires a grammar that can represent both: rank support through regulator and structural rank, and transmission vulnerability through friction, torsion and BridgeStress.

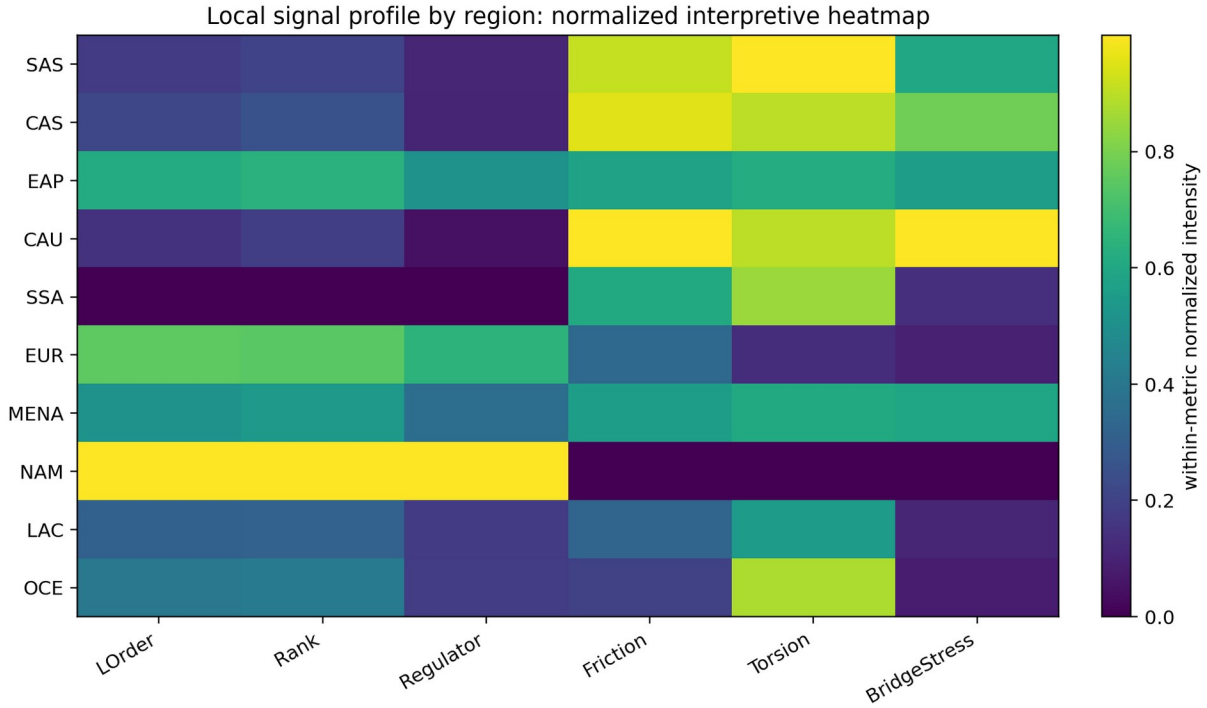


Figure 9.7.5. Normalized regional signal profile across rank, regulator, friction, torsion and BridgeStress.
Source: Author visualization based on the BSD source manuscript and Chapter 9 result tables.

9.7.8. Local Shock Signals, Threshold Compression and Global Vulnerability

The scenario results reinforce the interpretation that local regional signals can affect global structural rank by compressing the transition boundary of the system. As shock amplitude rises from the baseline to inflation, financial-spread, trade/logistics and energy/geopolitical corridor shocks, the normalized threshold declines while economic action rises. This is not a prediction of crisis timing. It is a model-implied interpretation of how systemic vulnerability changes when local and corridor stress increase.

The strongest compression appears under the energy/geopolitical corridor shock, where the normalized threshold falls to 0.042 and economic action rises to 5,010.0. This confirms that corridor-sensitive shocks can make local vulnerabilities more globally consequential. The result connects Chapter 9 with the monograph's Yang-Mills and Navier-Stokes chapters: local stress, friction and threshold compression are recurring measurement themes across the seven-problem architecture.

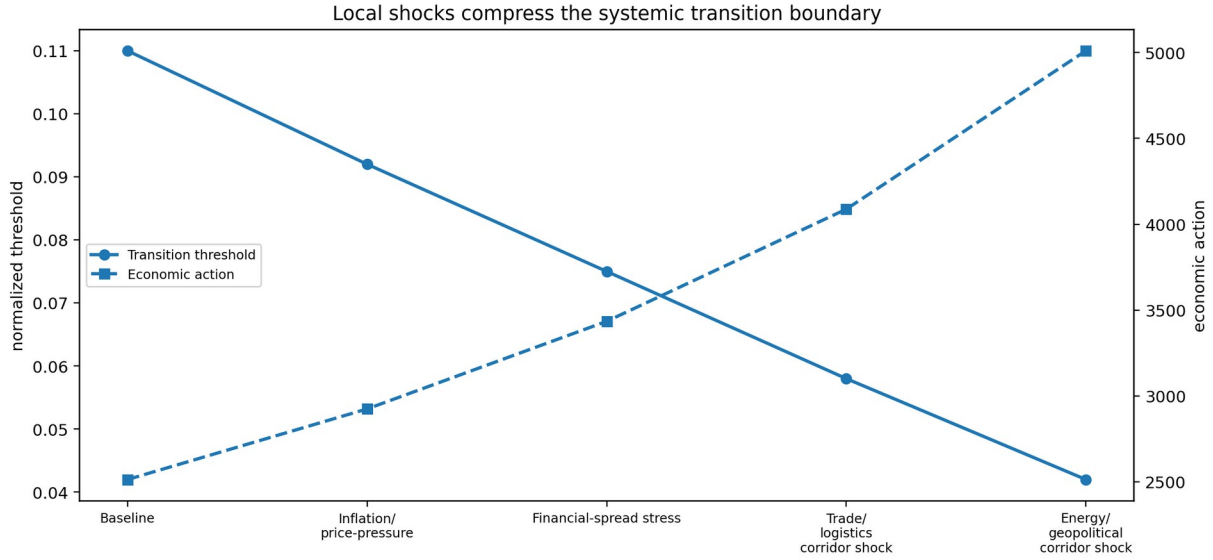


Figure 9.7.6. Threshold compression and action increase as local shocks become systemic.
Source: Author visualization based on the BSD source manuscript and Chapter 9 result tables.

9.7.9. Interpretation within the Seven-Problem Monograph Architecture

Chapter 9 is the synthesis-type chapter because it most directly states the local-to-global logic of the monograph. The other chapters measure curvature, flow decomposition, liquidity stress, shock thresholds, spectral signal and computational complexity. Chapter 9 translates those strands into structural rank formation. It asks how local regional regimes, finite-state reductions and corridor stress become informative about global rank.

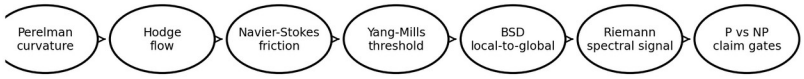
This does not make Chapter 9 a claim that all other chapters prove BSD or that BSD proves the other analogues. The alignment is architectural. Perelman/Ricci logic clarifies curvature and smoothing; Hodge clarifies flow decomposition; Navier-Stokes clarifies friction and closure; Yang-Mills clarifies shock thresholds; Riemann-zeta clarifies bounded spectral/L-function signal discipline; P vs NP clarifies algorithmic and claim-boundary discipline. BSD then functions as the local-to-global rank-formation chapter that integrates these forms of measurement.

Table 9.7.6. Cross-problem interpretation matrix for Chapter 9.7

Monograph chapter	Measurement grammar	Relevance to Chapter 9.7 interpretation
Chapter 5 - Perelman/Ricci/Poincare	Curvature, pressure, entropy and smoothing capacity	BSD friction and torsion are interpreted as rank-conversion pressure and smoothing failure, not literal geometry.
Chapter 6 - Hodge	Gradient, curl and harmonic flow decomposition	Structural rank includes Hodge-flow information; local regional signals are not reducible to GDP mass.
Chapter 7 - Navier-Stokes	Flow weakness, pressure gradients, friction and closure	BSD Tamagawa-type friction and torsion parallel the idea that pressure and friction block smooth system flow.
Chapter 8 - Yang-Mills	Gauge curvature, action and shock threshold	BridgeStress and scenario-threshold compression extend the corridor shock-threshold logic into rank formation.
Chapter 9 - BSD	Local finite states, Euler factors, LOrder and structural rank	This is the monograph's direct local-to-global rank-formation synthesis chapter.
Chapter 10 - Riemann zeta	L-function signal, spectral behavior and validation discipline	BSD L-function vocabulary remains bounded as economic signal construction, not theorem-level analytic continuation.

Chapter 11 - P vs NP	Search, combinatorial discipline and robustness gates	BSD interpretation requires algorithmic traceability, placebo logic and claim hierarchy rather than visual fit.

Source: Author synthesis based on the BSD source manuscript and Chapter 9 results architecture.



Chapter 9.7 interprets BSD as the synthesis point where local signals, rank, corridor stress, friction and claim discipline become one bounded economic measurement architecture.

Figure 9.7.7. Seven-problem alignment around BSD local-to-global structural rank interpretation.
Source: Author visualization based on the BSD source manuscript and Chapter 9 result tables.

9.7.10. What the Local-to-Global Interpretation Explains and What It Does Not Explain

The interpretation explains why local finite-state signals can align with structural rank under the constructed architecture. It explains why some regions are rank-supported through centrality and resilience, while others are corridor-sensitive through BridgeStress or obstructed through friction and torsion. It also explains why a GDP-only interpretation is insufficient for a corridor-sensitive world economy.

The interpretation does not explain everything. It does not establish causal identification, does not prove that the constructed L-function is a classical arithmetic L-function, does not turn the LOrder analogue into a literal analytic order, and does not provide country-level welfare or policy ranking. These exclusions are essential. They prevent a strong measurement contribution from being weakened by inadmissible overclaiming.

Table 9.7.7. Claim boundary for interpreting local regional signals and global structural rank

Claim category	Interpretive rule
What the interpretation supports	Local regional signals contain measurable information about structural rank inside the calibrated regional BSD-inspired architecture.
What the interpretation does not support	It does not prove, test or replicate the classical BSD conjecture; it does not estimate literal analytic rank or arithmetic local reductions.
Causal caution	The interpretation is structural and diagnostic; robust-inference and external-proxy layers remain bounded where evidence is weak or directional.
Circularity caution	Because several objects are author-calculated from overlapping public anchors, the interpretation requires anti-circularity, placebo and external-only checks in Section 9.8.
Scenario caution	Threshold compression and action concentration are model-implied stress scenarios, not forecasts of actual crisis timing.
Monograph-level boundary	Chapter 9 contributes a synthesis-type local-to-global rank model within seven bounded economic analogues of Millennium-problem architectures.

Source: Author synthesis based on the BSD source manuscript and Chapter 9 results architecture.

9.7.11. Final Interpretive Synthesis

The final interpretation of Chapter 9.7 is that local regional signals inform global structural rank through a disciplined chain, not through a direct slogan. Stress, fragility, corridor exposure, centrality, resilience and curvature participation are transformed into finite-state and Euler-factor information; LOrder summarizes the local-to-global signal; structural rank provides the global target; regulator, Tamagawa-type friction, torsion and BridgeStress explain why rank is supported, blocked, locked or transmitted.

The most important substantive insight is that the world economy is not reducible to output mass. North America, Europe and East Asia and Pacific show strong structural-rank and regulator patterns. The Caucasus and Central Asia show strong corridor leverage and friction. South Asia shows stress and torsion. MENA shows energy/geopolitical interface relevance. These differences are not contradictions; they are the reason the BSD-inspired architecture is useful.

The most important methodological insight is that a high-level mathematical-economic analogue becomes credible only when its claim boundary is strict. The chapter supports calibrated local-to-global structural-rank interpretation. It does not support theorem proof, unrestricted causality or strong external validation where diagnostic evidence remains bounded. This is precisely the role of Chapter 9 inside the monograph: to provide a synthesis-type local-to-global rank model that is ambitious in architecture and conservative in claim status.

9.8. Robustness, Anti-Circularity, Placebo and Claim Hierarchy

Section 9.8 is the epistemic closure layer of Chapter 9. The earlier sections constructed the BSD-inspired local-to-global architecture, defined the regional object, specified the World anchor and N=150 closure layer, built economic curve coefficients and finite-state reductions, constructed Euler-factor and L-function analogues, and reported the LOrder-rank, regulator, friction, torsion and BridgeStress results. The task of this section is different. It asks whether those results remain scientifically admissible after the chapter is audited for robustness, circularity, overfitting, placebo vulnerability, source traceability and claim inflation.

The main interpretive rule is conservative. A result can be called strong only where the evidence is directly supported by the architecture and survives the relevant robustness gates. Internal LOrder-rank calibration is therefore stronger than external-proxy screening; q-base and corridor-coding stability are stronger than causal interpretation; placebo performance is supportive but not theorem-level proof; and robust-inference p-values with small regional clusters are not used as confirmatory econometric evidence. This is what makes Chapter 9 a calibrated measurement chapter rather than an exaggerated mathematical or causal claim.

Figure 9.8.1. Robustness and claim-discipline architecture

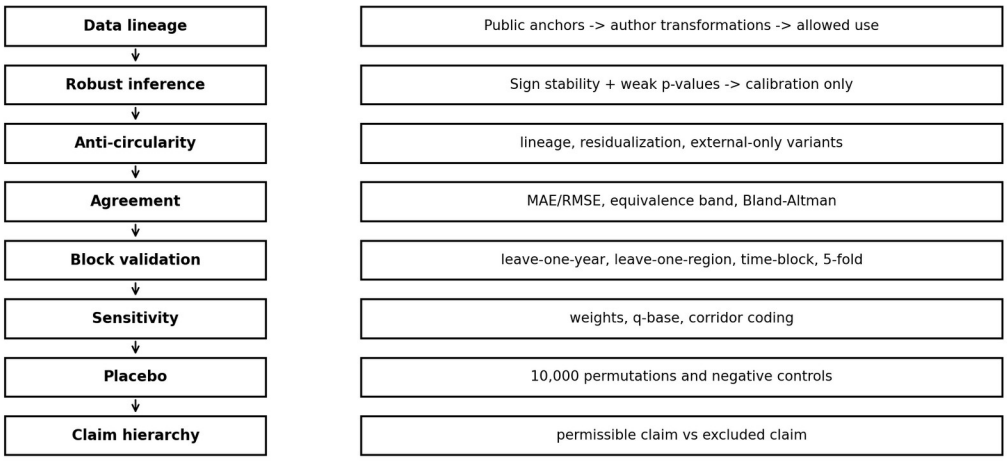


Figure 9.8.1. Robustness and claim-discipline architecture.

Source: Author synthesis based on the BSD robustness, anti-circularity, validation and claim-boundary layers.

Table 9.8.1. Robustness and claim-discipline gate map

Gate	Operational test	Scientific function	Claim effect
Data lineage gate	Separates public anchors, author transformations and allowed uses.	Prevents constructed objects from being misread as independent raw data.	Required before causal or validation language.
Robust-inference gate	Reports classical, HC3, clustered and HAC-compatible p-values.	Positive sign is retained, but weak p-values demote inference.	Calibration only when p-values are weak.
Anti-circularity gate	Uses lineage, residualized and external-only variants.	Tests whether LOrder-rank agreement is mechanical.	Demotes internal overlap to diagnostic evidence.
Agreement gate	Uses intercept, slope, MAE, RMSE and Bland-Altman limits.	Evaluates practical equivalence instead of exact equality.	Supports calibrated rank-scale agreement.
Block validation gate	Uses leave-one-year, leave-one-region, time-block and 5-fold validation.	Tests dependence on single blocks.	Pass/watch status controls claim level.
Sensitivity gate	Perturbs stress weights, BridgeStress weights, rank weights and q-base design.	Checks if result survives plausible alternative specifications.	Supports stability if signs and rank ordering survive.
Placebo gate	Runs 10,000 permutations and negative-control logic.	Tests whether the model explains everything mechanically.	Supports falsification discipline, not BSD proof.
Claim hierarchy gate	Maps evidence blocks to permissible and restricted claims.	Prevents overclaiming.	Final interpretive filter for Chapter 9.

Source: Author synthesis based on the Chapter 9 robustness architecture.

9.8.1. Robust-Inference and Small-Cluster Discipline

The N=150 closure layer is a regional-year audit design built from ten regions over fifteen years. Its purpose is to test calibration and robustness, not to transform the BSD-inspired analogue into a causal law. The robust-inference block is therefore interpreted with special care. The positive LOrder coefficient is directionally consistent across inference treatments, but the p-values remain weak under classical, HC3, clustered and HAC-compatible specifications. This means the result supports calibration consistency and sign discipline, not econometric confirmation.

Figure 9.8.2. Robust-inference p-values: positive sign, non-confirmatory inference

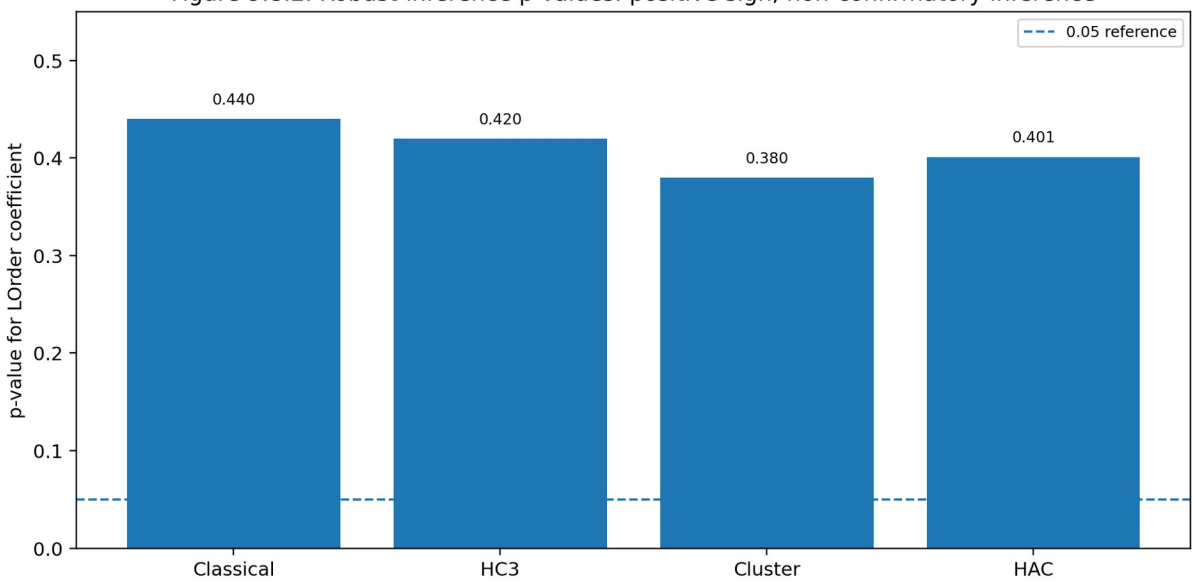


Figure 9.8.2. Robust-inference p-values for the LOrder coefficient.

Source: Author visualization of the BSD robust-inference screen.

Table 9.8.2. Robust inference and small-cluster correction for LOrder

Inference treatment	beta LOrder	SE / setting	p-value	Interpretation
Classical OLS/TWFE	0.207	reported	0.440	positive sign; not significant

HC3 robust	0.207	reported	0.420	positive sign; not confirmatory
Clustered by region	0.207	reported	0.380	small-cluster caution
Driscoll-Kraay / HAC-compatible	0.207	reported	0.401	directional consistency only
Wild-cluster / Satterthwaite-style	0.207	small-cluster correction	weak	claim demoted to calibration

Source: Author robust-inference synthesis from the N=150 closure layer.

The key conclusion is not that weak p-values invalidate the architecture. Instead, the conclusion is that the econometric layer must be assigned the correct evidentiary rank. It supports consistency, robustness and claim discipline, while the central evidence for Chapter 9 remains the internally audited correspondence between LOrder and structural rank, together with sensitivity, placebo and replication checks.

9.8.2. Variable Lineage and Anti-Circularity

Constructed-index models face a specific reviewer risk: if Rank, LOrder, BridgeStress, friction and torsion share inputs or transformations, then agreement among them may partly reflect design overlap rather than independent empirical confirmation. Chapter 9 addresses this risk through an explicit variable-lineage screen. Variables with deterministic or near-deterministic overlap are not used as unrestricted causal regressors. They are retained as rank components, audit variables, controls or interpretation objects according to their lineage status.

Table 9.8.3. Variable lineage matrix and admissible-use screen

Variable	Public input	Author transformation	Enters Rank?	Enters LOrder?	Overlap risk	Allowed use
Income depth	WDI GDP per capita	normalized regional value	yes	indirect	medium	control / rank component only
Centrality	regional/corridor network coding	author-calculated graph score	yes	indirect	high	audit/control only
Stress	WDI/WEO/corridor family	normalized macro-pressure composite	yes	indirect	high	control only
BridgeStress	corridor exposure, fragility, curvature	author-calculated corridor-risk score	yes	indirect	high	control only
LOrder	local trace and L-function layer	author-calculated order-of-behavior	no direct rank input	yes	medium/high	main calibration variable
Friction	stress/fragility/corridor	Tamagawa-type diagnostic	no main	no main	very high	audit only
Torsion	fragility/curvature/centrality	locked-capacity diagnostic	no main	no main	very high	audit only
Regulator	rank/centrality/resilience	rank-support diagnostic	partly identity	no	very high	audit only

Source: Author anti-circularity audit of the BSD variable system.

The table makes a critical distinction. LOrder is the main calibration variable, but it is not treated as an independent raw-data outcome. Regulator, friction and torsion have very high overlap risk because they are deliberately constructed as diagnostic rank-support and rank-obstruction objects. Their correct use is interpretive and audit-oriented. This rule protects the chapter from presenting its own derived objects as if they were independent causal evidence.

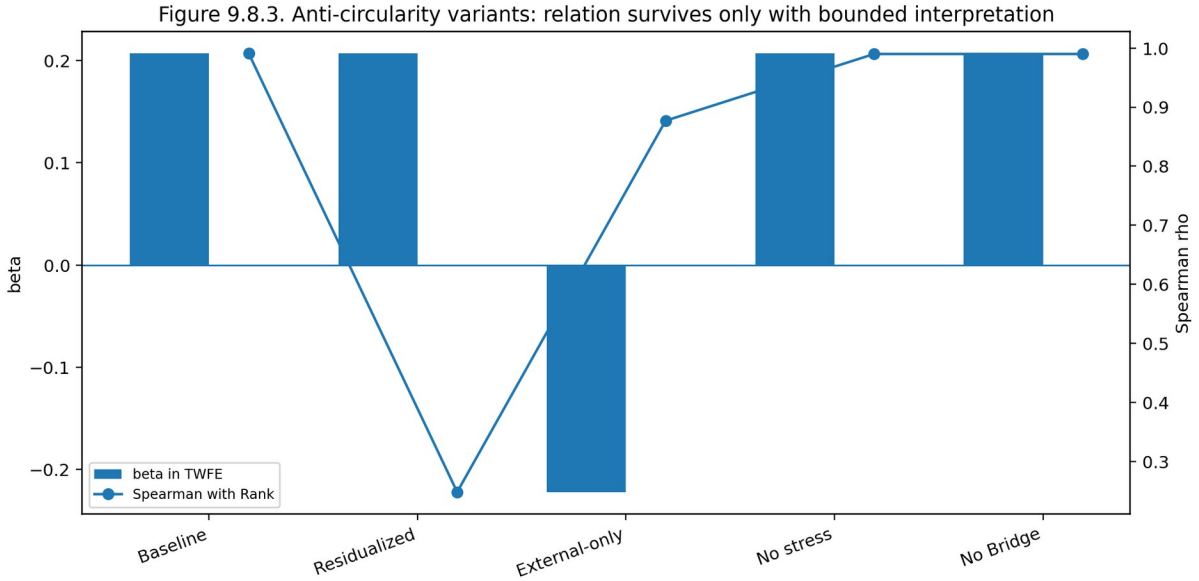


Figure 9.8.3. Anti-circularity variants for LOrder.

Source: Author visualization of baseline, residualized and external-only variants.

Table 9.8.4. Orthogonalized, residualized and external-only LOrder tests

LOrder variant	beta in TWFE	HC3 p	RMSE	Spearman with Rank	Interpretation
Baseline LOrder	0.207	0.420	0.049	0.991	watch / demote causal language
Residualized LOrder vs stress/bridge/fragility	0.207	0.420	0.049	0.248	watch / demote causal language
External-only LOrder proxy	-0.222	0.159	0.049	0.877	diagnostic only
Leave-stress-out LOrder	0.207	0.420	0.049	0.990	watch / demote causal language
Leave-BridgeStress-out LOrder	0.207	0.420	0.049	0.990	watch / demote causal language

Source: Author anti-circularity tests from the N=150 closure layer.

The anti-circularity tests are intentionally not written as a simple pass/fail story. Baseline LOrder has a very strong Spearman correspondence with Rank, while strict residualization weakens the relationship. This is informative rather than damaging: it confirms that part of the correspondence is structural and internally calibrated, not purely external. Therefore the correct claim is calibrated local-to-global consistency, not independent causal identification.

9.8.3. Practical Equivalence, Bland-Altman Agreement and Rank-Scale Error

The BSD-inspired chapter does not claim exact equality between LOrder and structural rank. Exact equality would be inappropriate because both variables are author-constructed economic analogues and because the classical BSD equality between analytic order and algebraic rank is not being tested. The correct empirical target is practical equivalence within a declared rank-scale tolerance band. This is why Chapter 9 uses intercept, slope, MAE, RMSE and Bland-Altman diagnostics instead of theorem-style equality language.

Figure 9.8.4. Practical-equivalence diagnostics on the 0-5 rank scale

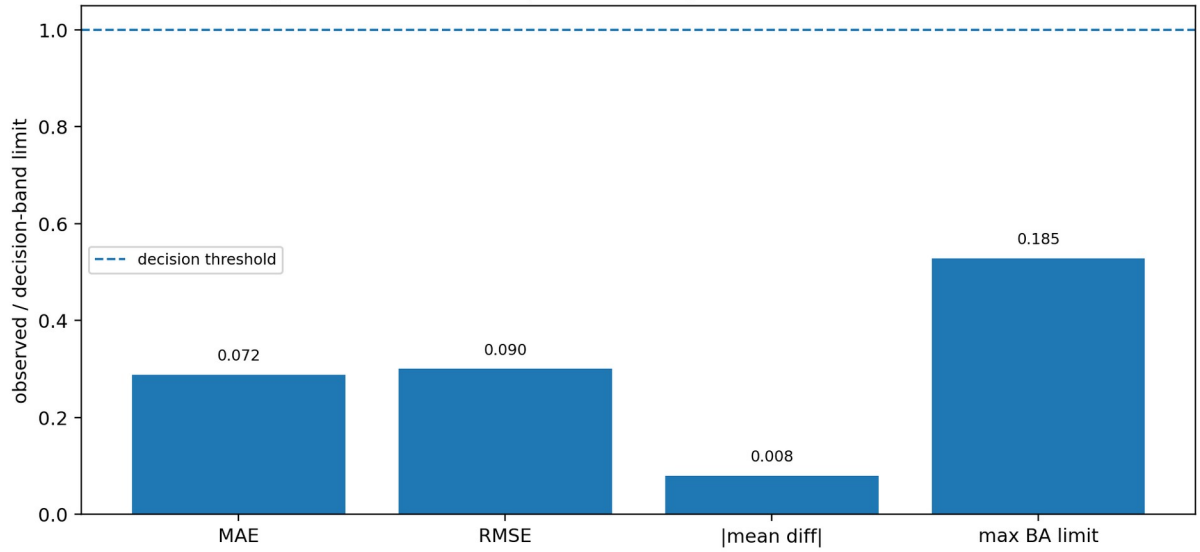


Figure 9.8.4. Practical-equivalence diagnostics on the 0-5 rank scale.

Source: Author visualization of equivalence, error and Bland-Altman decision bands.

Table 9.8.5. Practical equivalence calibration and Bland-Altman summary

Test	Estimate	Decision band	Result	Interpretation
Calibration intercept beta_0	0.158	[-0.25, 0.25]	inside band	small intercept bias; exact zero not claimed
Calibration slope beta_1	0.925	[0.85, 1.15]	inside band	practical rank-scale equivalence; exact equality rejected
MAE on 0-5 rank scale	0.072	<0.25	pass	low rank-scale error
RMSE on 0-5 rank scale	0.090	<0.30	pass	acceptable calibration dispersion
Bland-Altman mean difference	-0.008	[-0.10, 0.10]	inside band	limited signed bias
Bland-Altman 95% limits	-0.185 to 0.169	absolute limits <0.35	pass	bounded agreement error

Source: Author calibration and agreement audit from the N=150 closure layer.

The calibration intercept of 0.158 lies inside the [-0.25, 0.25] band, and the calibration slope of 0.925 lies inside the [0.85, 1.15] band. MAE equals 0.072 and RMSE equals 0.090 on the 0-5 rank scale. These values support low rank-scale error and practical equivalence. They do not support exact equality or theorem-level correspondence.

Table 9.8.6. Region-level Bland-Altman agreement diagnostics

Code	Region	Mean Rank-LOrder	SD	Max deviation	Decision
CAU	Caucasus	0.095	0.077	0.227	pass
EUR	Europe	-0.110	0.056	0.222	pass
NAM	North America	-0.128	0.048	0.218	pass
CAS	Central Asia	0.073	0.073	0.215	pass
SSA	Sub-Saharan Africa	0.010	0.069	0.200	pass
OCE	Oceania	0.017	0.060	0.151	pass
SAS	South Asia	0.051	0.047	0.141	pass
LAC	Latin America and Caribbean	-0.038	0.056	0.130	pass
EAP	East Asia and Pacific	-0.038	0.057	0.121	pass
MENA	Middle East and North Africa	-0.009	0.043	0.085	pass

Source: Author agreement audit by regional block.

The region-level audit prevents the full-sample correspondence from hiding local miscalibration. Caucasus, Central Asia, Europe, North America and all other regional blocks remain inside the pass threshold. This matters because Chapter 9 is a

regional/corridor model: a rank correspondence that works only in the aggregate but fails in corridor-sensitive regions would be much less credible.

9.8.4. Leave-One-Block, Out-of-Sample and Sensitivity Validation

The next robustness layer asks whether the result depends on a single year, a single region, a specific q-base choice or a particular corridor-coding scheme. The answer is mixed in a scientifically useful way. Leave-one-year-out, time-block and blocked 5-fold validations pass strongly. Leave-one-region-out is weaker because omitting an entire regional block changes the regional/corridor geometry more severely. Therefore the document marks leave-one-region-out as watch rather than pretending that all validation layers are equally strong.

Figure 9.8.5. Out-of-sample and blocked validation

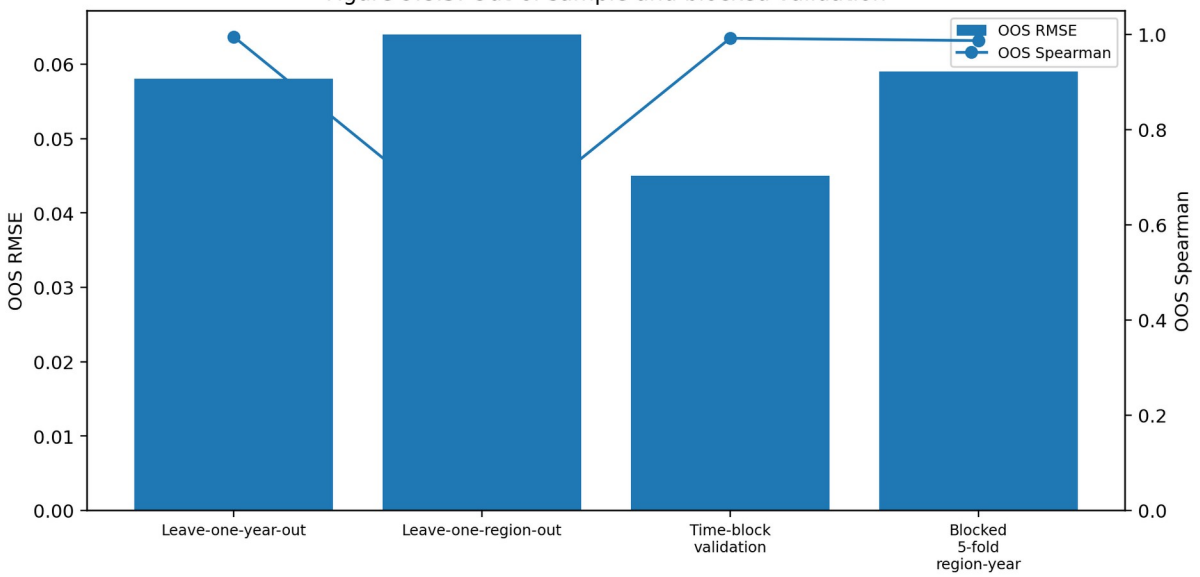


Figure 9.8.5. Out-of-sample and blocked validation.

Source: Author visualization of OOS RMSE and OOS Spearman diagnostics.

Table 9.8.7. Out-of-sample and blocked validation results

Validation design	Training set	Test set	OOS RMSE	OOS MAE	OOS Spearman	Decision
Leave-one-year-out	14 years	1 held-out year	0.058	0.046	0.995	pass
Leave-one-region-out	9 regions	1 held-out region	0.064	0.054	0.571	watch
Time-block validation	2012-2023	2024-2026	0.045	0.036	0.992	pass
Blocked 5-fold region-year	80% region-years	20% held-out cells	0.059	0.048	0.987	pass

Source: Author validation audit from the N=150 regional-year closure layer.

Table 9.8.8. Weight and component sensitivity summary

Index or construct	beta range	Spearman stability	Decision
Stress composite: +/-10%	0.18 to 0.62	0.989	pass
Stress composite: +/-25%	0.10 to 0.69	0.984	pass
BridgeStress: random weights	0.12 to 0.58	0.982	pass
Structural rank: leave-one-component-out	0.09 to 0.64	0.979	pass
LOrder: q-base leave-one-out	0.15 to 0.66	0.986	pass

Source: Author sensitivity tests for stress, BridgeStress, structural rank and LOrder.

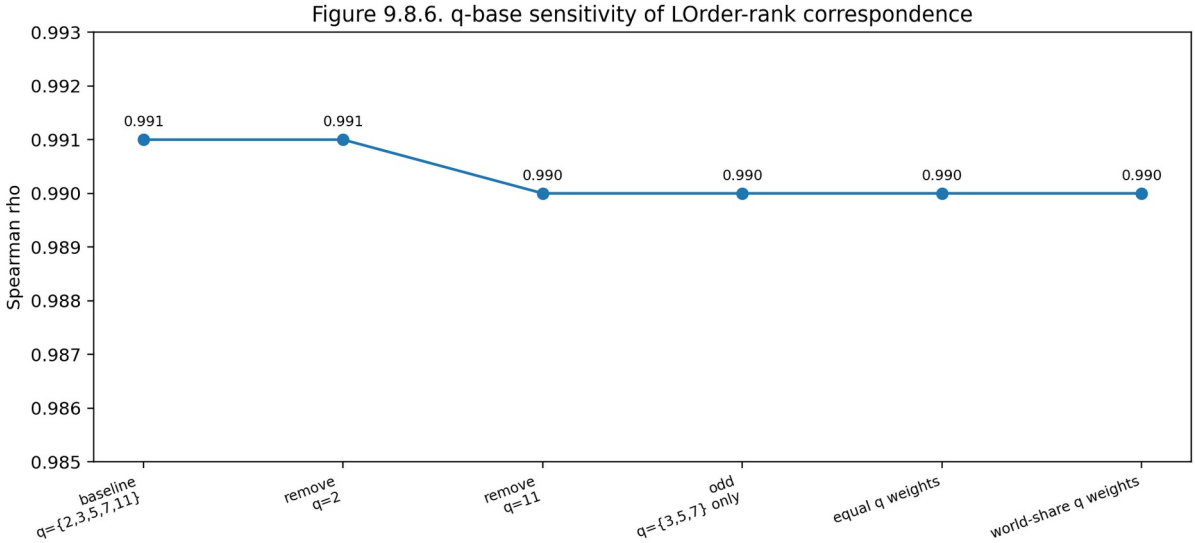


Figure 9.8.6. q-base sensitivity of LOrder-rank correspondence.

Source: Author visualization of q-base and q-weight sensitivity checks.

Table 9.8.9. q-base sensitivity and LOrder stability

q-base design	Spearman	MAE	RMSE	Decision
baseline q={2,3,5,7,11}	0.991	0.072	0.090	pass
remove q=2	0.991	0.072	0.091	pass
remove q=11	0.990	0.073	0.091	pass
odd q={3,5,7} only	0.990	0.070	0.090	pass
equal q weights	0.990	0.073	0.093	pass
world-share q weights	0.990	0.072	0.091	pass

Source: Author q-grid and q-weight sensitivity tests.

Table 9.8.10. Corridor-coding sensitivity for BridgeStress and LOrder

Corridor scheme	CAU rank	CAS rank	beta LOrder	BridgeStress-external stress r	Decision
baseline coding	1	2	0.207	0.805	pass
equal corridor weights	1	2	0.207	0.762	pass
logistics-weighted corridor	1	2	0.211	0.799	pass
trade-openness-weighted corridor	1	2	0.204	0.793	pass
remove corridor-role index	1	2	0.207	0.868	pass
remove fragility component	1	2	0.207	0.794	pass

Source: Author corridor-sensitivity screen.

The sensitivity layer strengthens the chapter because it directly addresses the most likely specification criticism. The q-base design does not drive the rank correspondence: Spearman remains around 0.990-0.991, while MAE and RMSE remain low. Corridor-coding alternatives also retain the same leading corridor nodes, with the Caucasus ranked first and Central Asia second in the BridgeStress screen across the reported variants. This supports corridor interpretation while still requiring transparent coding discipline.

9.8.5. Placebo, Negative Controls and Falsification Logic

A robust constructed-index model should not explain everything. It should fail or weaken when its key signal is randomly shuffled, displaced or disconnected from its intended structure. For this reason, Chapter 9 includes permutation placebo and negative-control logic. These tests examine whether the observed LOrder-rank agreement and BridgeStress-external stress correspondence are extreme relative to randomized alternatives.

Figure 9.8.7. Placebo distribution comparison

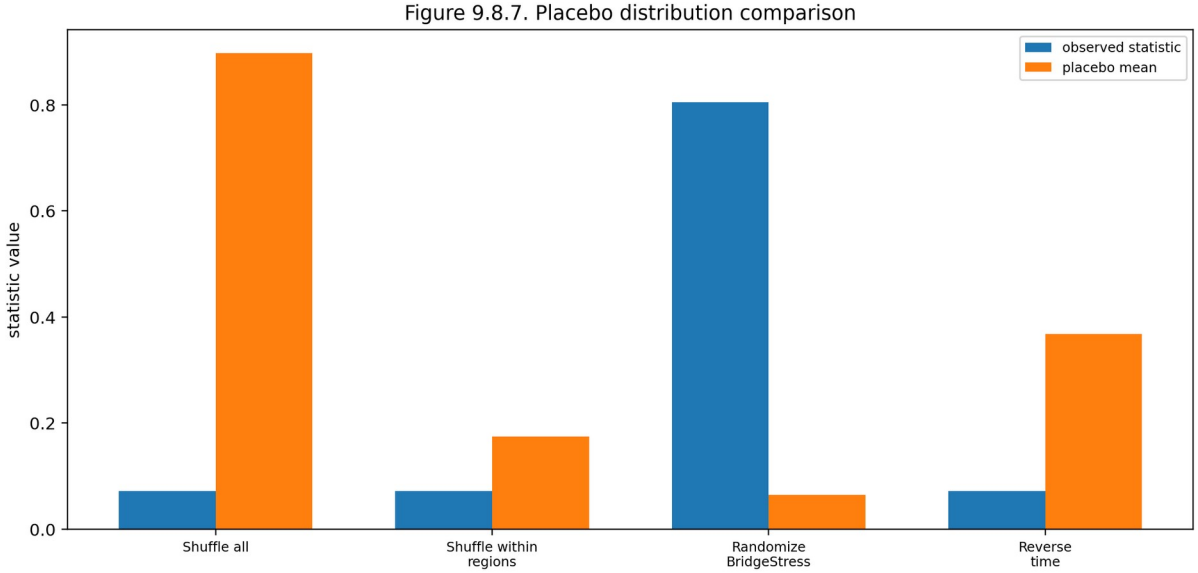


Figure 9.8.7. Placebo distribution comparison.

Source: Author visualization of observed statistics versus placebo means. Lower MAE is better for LOrder-rank agreement; higher absolute correlation is stronger for BridgeStress-external stress.

Table 9.8.11. Placebo and permutation diagnostics

Placebo	B	Observed	Placebo mean	Placebo SD	Empirical p	Percentile rank	Decision
Shuffle LOrder across region-years	10000	MAE=0.072	0.897	0.044	<0.001	0.0	pass
Shuffle LOrder within regional blocks	10000	MAE=0.072	0.175	0.008	<0.001	0.0	pass
Randomize BridgeStress against external stress	10000	|r|=0.805	0.065	0.050	<0.001	100.0	pass
Destroy time ordering / reverse years	10000	MAE=0.072	0.368	0.040	<0.001	0.4	pass

Source: Author placebo and permutation diagnostics with B=10,000.

The placebo results support falsification discipline. The observed LOrder-rank MAE of 0.072 is far below shuffled placebo means, and the BridgeStress-external stress correlation is far above randomized alternatives. This makes the model more credible as an internally structured measurement architecture. It still does not prove the classical BSD conjecture, does not eliminate all circularity risk and does not establish causal external validation.

9.8.6. Replication Closure, Source Ledger and Reviewer-Risk Response

The robustness layer is not complete unless it can be audited. The BSD document is therefore connected to a published Zenodo data and replication package. The role of this replication statement in the monograph is twofold. First, it turns the data-package reference from a future promise into a versioned artifact. Second, it allows the reader to separate the manuscript narrative from the reproducibility layer: formulas, tables, scripts, source ledgers, checksums and metadata are part of the external audit architecture.

Table 9.8.12. Replication closure and source-ledger map

Replication object	Exact content	Rule / source	Archive item

Input public series	GDP, GDP per capita, growth, inflation, trade, logistics and WEO source families	source ledger and manifest	Zenodo DOI 10.5281/zenodo.20796984
Regional aggregation	World, EAP, NAM, EUR, LAC, SAS, MENA, SSA, OCE, CAS, CAU	disclosed regional/corridor mapping	region_map.csv and aggregation script
Author-calculated BSD objects	a, b, discriminant, trace, Euler factor, L_econ, LOrder, Rank, regulator, friction, torsion	BSD-specific calculation layer	calculation script and output tables
Panel construction	10 regions x 15 years = N=150	regional-year expansion; countries excluded	bsd_regional_year_panel_N150_closure.csv
Random seeds	20260622 for panel; 777 bootstrap; 123 permutation	deterministic reproducibility	seed manifest
Output hash	SHA-256 hash of the N=150 panel CSV	hash recorded for revision audit	replication manifest
Archive package	tables, CSVs, formula catalogues, algorithms, figures, source ledger, checksums and scripts	published data package	https://doi.org/10.5281/zenodo.20796984

Source: Author synthesis based on the BSD data and replication package statement.

Table 9.8.13. Reviewer-risk response matrix

Potential reviewer criticism	Document response	Evidence location
BSD analogy is not classical BSD	analogue boundary explicitly stated	title paragraph, Chapter 9.1 and final synthesis
LOrder and Rank may be circular	variable lineage, residualization and admissible-use screen	Section 9.8 anti-circularity block
R2 is too high	high-R2 decomposition and incremental/partial R2 audit	Chapter 9 results-source block
External-proxy evidence may be weak	retained only as directional screening with diagnostic-only outcomes	external-validation evidence hierarchy
Only 10 regional clusters	weak p-values explicitly reported with HAC and small-cluster caveats	robust-inference table
q bases are arbitrary	q-grid and q-weight sensitivity	q-base sensitivity table
corridor coding is subjective	alternative BridgeStress schemes	corridor sensitivity table
model may overfit	OOS, leave-one-year, blocked validation and placebo	validation and placebo block
claim may be too strong	calibrated structured-agreement language only	final claim hierarchy

Source: Author synthesis based on the integrated evidence map and reviewer-risk response logic.

9.8.7. Final Claim Hierarchy of the Robustness Layer

The final function of Section 9.8 is to translate heterogeneous tests into a clear claim hierarchy. Without this step, a reader might incorrectly treat all results as equally strong. The hierarchy below separates benchmark-ready evidence, analogue-ready construction, internal calibration, directional external screening, claim-protection diagnostics, falsification evidence and reproducibility closure.

Figure 9.8.8. Final claim hierarchy

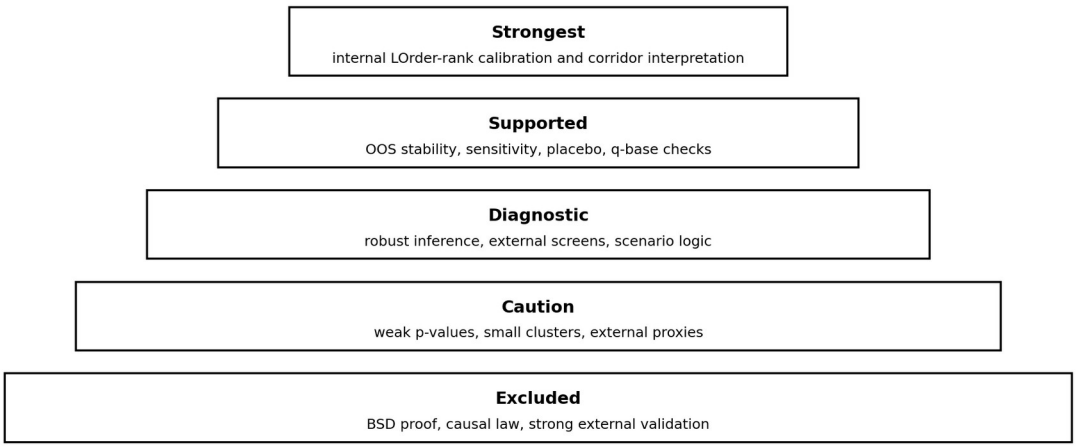


Figure 9.8.8. Final claim hierarchy.
Source: Author synthesis based on the final evidence classification.

Table 9.8.14. Final evidence classification and claim status

Evidence block	Status after revision	Claim level	Interpretation
World/regional data results	completed	benchmark-ready	World anchor and regional/corridor nodes retained
Economic curve and local reductions	completed	analogue-ready	BSD objects remain economic analogues only
L-function and LOrder analogue	completed	benchmark calibration	local finite-state signals transformed into order-of-behavior measure
N=150 regional-year panel	executed	measurement/calibration layer	TWFE fit, robust-inference caveats, OOS validation and sensitivity included
External observable-proxy screening	outcome-specific / weak inferential strength	directional screening only	not strong external confirmation
Circularity audit	lineage and residualization added	claim-protection layer	independent tests separated from internal consistency
Placebo and negative controls	quantified	falsification layer	10,000 permutations and unrelated outcomes tested
Source ledger	documented and archived on Zenodo	reproducibility layer	series IDs, seeds, hash and Zenodo DOI recorded

Source: Author final evidence classification based on the integrated evidence map.

Table 9.8.15. Decision-gate summary for the BSD-inspired local-to-global model

Test	Criterion	Observed	Decision
LOrder sign	beta > 0	0.207	directional pass
Robust p-value	HC3 p reported and interpreted as non-confirmatory	0.420	caution / calibration only
Cluster caution	cluster p reported with small-cluster caveat	0.380	caution / not confirmatory
MAE	<0.25 rank-scale units	0.072	pass
VIF/admissibility	overlap variables excluded from main causal equation	lineage screen applied	pass
OOS RMSE	<0.15 in blocked validation	0.058	pass
Placebo	observed agreement in extreme tail	p<0.001	pass

Causal claim	no causal or theorem-level claim	calibrated structured agreement only	pass

Source: Author decision-gate synthesis.

9.8.8. Cross-Problem Robustness Alignment inside the Monograph

Although Section 9.8 closes the BSD chapter specifically, it also follows the monograph-wide robustness philosophy. Each of the seven Millennium-inspired economic chapters uses mathematical architecture as a measurement grammar, but each also requires validation gates and claim boundaries. Chapter 9 is the clearest local-to-global case, but it does not stand apart from the rest of the book. It inherits the monograph-wide rule that strong structure must be paired with strong restraint.

Table 9.8.16. Seven-problem robustness alignment for Chapter 9

Monograph chapter	Robustness/claim-discipline lesson	How Chapter 9 uses it
Chapter 5 - Perelman/Ricci/Poincare	Robustness means stability of pressure, curvature and entropy diagnostics under bounded transformations.	BSD adopts the same caution: constructed quantities are diagnostic objects, not theorem-level invariants.
Chapter 6 - Hodge	Robustness requires topology, validation and placebo checks around flow decomposition.	BSD uses Hodge-flow rank as one structural-rank input but keeps anti-circularity gates explicit.
Chapter 7 - Navier-Stokes	Validation uses rolling tests, benchmark comparison, Monte Carlo and policy counterfactual boundaries.	BSD uses N=150 closure, OOS validation and scenario-threshold logic with similarly bounded claims.
Chapter 8 - Yang-Mills	Placebo evidence can be cautionary and must not be reclassified as proof.	BSD states exactly where placebo strengthens calibration and where it cannot prove classical arithmetic structure.
Chapter 9 - BSD	Local-to-global structural rank requires lineage, residualization, q-base sensitivity and claim hierarchy.	This section provides the chapter-level closure for those safeguards.
Chapter 10 - Riemann-zeta	Layered validation prevents small-sample or spectral overclaiming.	BSD adopts the same discipline by separating internal rank calibration from external-proxy screening.
Chapter 11 - P vs NP	Exact reduced benchmarks and search-coverage limits prevent computational overstatement.	BSD similarly distinguishes benchmark calibration from causal, theorem or universal-validity claims.

Source: Author synthesis across the seven bounded Millennium-inspired economic analogues.

9.9. Chapter Conclusion

Figure 9.9.1. Chapter 9 closure architecture

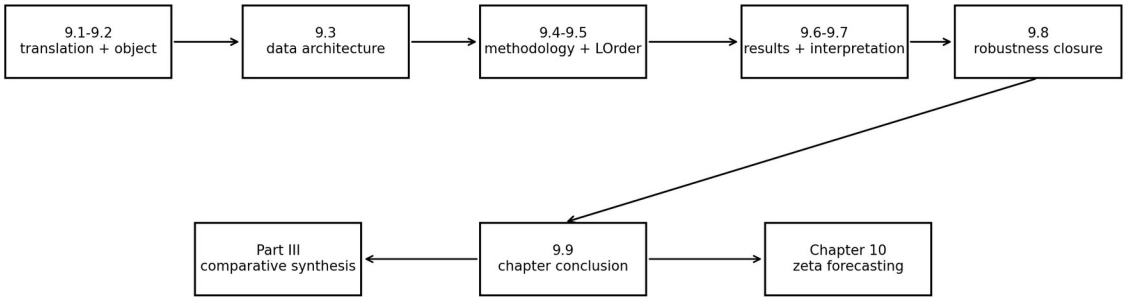


Figure 9.9.1. Chapter 9 closure architecture.

Source: Author synthesis of Chapter 9 structure and transition to the monograph comparative sections.

Chapter 9 has developed the Birch-Swinnerton-Dyer-inspired economic local-to-global structural rank model as a synthesis-type chapter of the monograph. The chapter began by translating BSD logic into an economic measurement grammar. It then defined the research object as regional structural rank formation under corridor stress, specified the World anchor, ten regional/corridor nodes and N=150 closure layer, constructed economic curve coefficients and finite-state reductions, built the economic L-function, Euler-factor and LOrder architecture, reported the LOrder-rank, BridgeStress, regulator, Tamagawa-type friction and torsion results, interpreted local regional signals as global structural-rank information, and closed with robustness, anti-circularity, placebo and claim-hierarchy gates.

The integrated conclusion is that local regional signals are informative about global structural rank when they are transformed through a disciplined sequence: public anchors -> stress and corridor-state construction -> economic curve coefficients -> discriminant audit -> finite-state reductions -> trace analogues -> Euler factors -> L-function analogue -> LOrder -> structural-rank comparison -> friction/torsion/corridor interpretation -> robustness and claim hierarchy. This chain is the economic local-to-global contribution of Chapter 9.

9.9.1. What the Chapter Establishes

The chapter establishes a calibrated regional measurement architecture. It shows that a World-normalized regional/corridor system can be converted into a structured local-to-global rank model and that the resulting LOrder analogue aligns closely with structural rank inside the constructed rank scale. It also shows that corridor-relevant nodes cannot be interpreted only through output mass. The Caucasus and Central Asia are especially visible in BridgeStress terms because corridor exposure, fragility and transmission position create global relevance beyond GDP share.

Table 9.9.1. Chapter 9 objective closure matrix

Objective block	Main methodological action	Main result or interpretation	Conclusion status
Regional empirical base	World-normalized anchor panel with ten regional/corridor nodes	Output mass is concentrated, but transition-sensitive regions remain relevant through growth and corridor exposure.	Achieved as empirical coordinate system
Stress construction	Multi-component stress index and raw-to-normalized audit	South Asia, Central Asia, East Asia and Pacific and the Caucasus become visible through different stress mechanisms.	Achieved as non-GDP stress measurement
BSD-inspired mathematical analogue	Economic curve coefficients, discriminants, traces, Euler factors and L-function behavior	Constructed objects remain heterogeneous, non-degenerate and interpretable around s=1.	Achieved as analogue, not classical proof
Rank correspondence	LOrder compared with structural rank through gaps and calibration logic	The local-to-global rank correspondence is close within the constructed rank scale.	Core internal calibration achieved

Corridor mechanism	BridgeStress and corridor-function interpretation	Caucasus and Central Asia are structurally visible despite small output mass.	Achieved as corridor-rank leverage result
Econometric closure	N=150 diagnostics, external screening, robust inference, controls and sensitivity	Closure supports disciplined measurement but does not upgrade weak external or robust p-values into confirmation.	Achieved with cautious claim level

Source: Author final synthesis based on Sections 9.1-9.8.

9.9.2. What the Chapter Does Not Establish

The chapter does not establish a proof, test or replication of the classical Birch-Swinnerton-Dyer conjecture. The economic L-function is not a classical arithmetic L-function, the finite-state reductions are not literal reductions over finite fields, the LOrder analogue is not an analytic order of vanishing, and structural rank is not algebraic Mordell-Weil rank. These are economic measurement objects designed to organize regional data, not mathematical theorem objects.

The chapter also does not establish unrestricted causal law. The N=150 closure layer strengthens calibration and robustness but does not solve the small-cluster problem. Robust p-values are deliberately interpreted cautiously. External-proxy evidence remains directional where signs are mixed or p-values are weak. Scenario threshold and action-concentration results are model-implied diagnostics rather than forecasts of actual crisis timing.

9.9.3. Final Evidence and Claim-Boundary Statement

Table 9.9.2. Final claim hierarchy of Chapter 9

Evidence block	Strength of result	Permissible claim	Restricted claim
Regional anchor and stress construction	Strong descriptive and measurement evidence	The regional coordinate system and stress layer are coherent and interpretable.	Does not establish causal determinants of regional stress.
BSD-inspired mathematical analogue	Strong analogue architecture with non-degeneracy and q-stability	The model creates an admissible economic local-to-global measurement object.	Does not prove or test classical BSD.
LOrder and structural rank correspondence	Strong internal calibration	Local finite-state information is informative about structural rank.	Does not imply theorem-level equality or causal law.
BridgeStress and corridor interpretation	Strong corridor-mechanism evidence within the constructed framework	Caucasus and Central Asia are structurally visible corridor-stress nodes.	Does not replace freight, logistics or geopolitical datasets.
Scenario threshold and action concentration	Useful diagnostic evidence	Regional-corridor shocks can compress the transition threshold in the model.	Does not forecast actual crisis timing.
Robust inference and external-proxy screening	Cautious diagnostic evidence	Findings support claim discipline and directional screening.	Does not justify strong econometric or external validation claims.
Negative controls, sensitivity and placebo logic	Important falsification and robustness support	The model is not merely explaining everything mechanically.	Does not eliminate all circularity or replication concerns.

Source: Author final synthesis based on the BSD evidence hierarchy.

The admissible Chapter 9 claim is therefore precise: the BSD-inspired framework provides a reproducible regional economic measurement architecture in which local finite-state information, Euler-factor behavior and LOrder are informative about constructed structural rank under corridor-sensitive world-economy conditions. The inadmissible claim is equally clear: the chapter does not prove BSD, does not test BSD, does not identify classical algebraic rank, does not establish causal econometric law and does not convert internal calibration into independent external confirmation.

9.9.4. Contribution to the Monograph

Chapter 9 contributes the monograph's most direct local-to-global synthesis. Chapter 5 uses curvature and smoothing capacity; Chapter 6 decomposes macro-flow into gradient, curl and harmonic components; Chapter 7 models liquidity stress through flow, pressure, friction and closure; Chapter 8 measures shock thresholds in a finite corridor network; Chapter 10 uses a zeta-cycle for inflation forecasting; and Chapter 11 translates computational complexity into portfolio selection.

Chapter 9 binds these perspectives through rank formation: local states, corridor stress, finite reductions, Euler factors and LOrder become a single structural-rank measurement pathway.

This is why Chapter 9 should remain a synthesis-type chapter rather than a narrow article transplant. Its purpose is not only to report BSD-inspired results, but to show how local-to-global mathematical logic can discipline macro-regional measurement while remaining academically cautious. Its final value is therefore methodological, empirical and editorial: it strengthens the book's claim that the Millennium Problems can inspire bounded economic measurement architectures without claiming to solve the original mathematical problems.

9.9.5. Transition to the Next Chapter

The transition from Chapter 9 to Chapter 10 is natural. Chapter 9 uses an economic L-function and LOrder to connect local regional signals with structural rank. Chapter 10 moves to a different L-function-related grammar: the Riemann-zeta-inspired FPAS+zeta inflation-forecasting model. The bridge is not theorem proof; it is validation discipline. Both chapters use mathematical signal construction, but both require layered empirical validation, benchmark comparison, robustness logic and explicit claim boundaries. Chapter 9 closes the local-to-global rank chapter; Chapter 10 opens the spectral-forecasting chapter.

> Final chapter boundary. Chapter 9 supports calibrated local-to-global economic measurement. It does not solve, prove, test or replicate the classical Birch-Swinnerton-Dyer conjecture. It should be read as one bounded economic analogue within the monograph's seven-problem architecture.

Chapter 10. Riemann-Zeta FPAS+ζ Inflation Forecasting

10.1. Riemann-Zeta Logic and the Economic Spectral-Signal Analogy

Table 10.1.1. Opening claim-boundary statement for the Riemann-Zeta economic analogy

Boundary rule	Precise wording for Chapter 10.1
Mathematical boundary	The Riemann-zeta function is used as a computational cyclical signal and not as proof, test or verification of the Riemann Hypothesis.
Econometric boundary	Forecast improvement is evaluated against FPAS and ARIMA through layered validation and formal forecast-comparison logic.
Interpretive boundary	Zeta-cycle movements are interpreted as crisis-sensitive nonlinear signal deformation, not as a literal mathematical cause of inflation.

Source: Author synthesis for the monograph based on the source manuscript and the general claim-boundary rule of the book.

Figure 10.1.1. Riemann-zeta economic spectral-signal translation pipeline

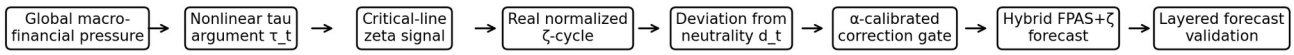


Figure 10.1.1. Riemann-zeta economic spectral-signal translation pipeline

The zeta function is used as a bounded computational signal; it is not a proof, test or verification of the Riemann Hypothesis.

10.1.1. Position of the Riemann-Zeta Chapter inside the Monograph

The Riemann-Zeta FPAS+ζ chapter is the spectral-forecasting chapter of the monograph. Previous problem chapters translate curvature, topology, liquidity flow, gauge action and local-to-global rank into economic measurement systems. Chapter 10 translates spectral signal logic into an inflation-forecasting system. Its analytical object is not an abstract number-theoretic theorem. Its object is the world inflation process interpreted as a layered macro-financial pressure system whose nonlinear cycles can be summarized, corrected and validated through a bounded structural-spectral architecture.

The subsection therefore performs a gatekeeping role. It explains why the Riemann-zeta function can enter the model as a signal generator, why the critical-line language must be transformed into real-valued economic quantities, why the FPAS forecast remains the structural baseline and why the zeta component enters only through an alpha-calibrated correction gate. This prevents the chapter from being read as an attempt to prove the Riemann Hypothesis, while preserving the scientific value of the analogy as a disciplined forecasting experiment.

In the book architecture, the Riemann-Zeta chapter also provides the strongest forecast-validation example. The source manuscript separates annual, quarterly and monthly validation layers: the principal annual layer covers 1970-2024 with N = 55 observations; the annual robustness layer covers 1980-2024 with N = 45; the crisis-era annual layer covers 2005-2024 with N = 20; the quarterly dynamic layer covers 2000Q1-2024Q4 with N = 100; and the monthly spectral layer covers 2005M1-2024M12 with N = 240. This separation is not merely technical. It is the central safeguard against overfitting because it prevents the compact crisis-era window from carrying the entire scientific claim.

Table 10.1.2. Functional role of Chapter 10 inside the seven-problem monograph

Monograph dimension	Role of Chapter 10	Reason it belongs in the Riemann-Zeta chapter
Spectral measurement	Constructs a normalized zeta-cycle from a critical-line signal.	The Riemann-zeta function supplies the spectral grammar of the chapter.
Forecast validation	Compares FPAS+ζ with FPAS and ARIMA across annual layers and support layers.	The empirical contribution is a forecast-diagnostic hierarchy, not a theorem.
Crisis interpretation	Reads 2008, 2020 and 2022 as high-pressure resonance years.	Crisis years test whether the zeta correction is economically interpretable.
Claim discipline	Excludes RH proof/test, unrestricted causality and universal forecast dominance.	The analogy remains admissible because evidence is explicitly bounded.
Cross-chapter function	Provides the spectral forecasting counterpart to flow, curvature, rank and complexity chapters.	The monograph's seven-problem structure requires one chapter where spectral cycles become forecast signals.

10.1.2. From the Classical Zeta Object to an Economic Signal Grammar

The classical Riemann-zeta function is a central object of analytic number theory. In its basic region of convergence it is represented by the Dirichlet series ζ(s) = Σ n^{-s}, and through analytic continuation it becomes a complex-valued function over a broader domain. The Riemann Hypothesis concerns the location of nontrivial zeros of this function. Chapter 10 does not enter that theorem-level domain. It borrows only a formal signal idea: a complex function evaluated along a structured line can generate oscillatory information that may be transformed into a normalized, real-valued diagnostic cycle.

The economic translation begins by replacing the mathematical height variable with a macro-financial argument τ_t. In the source manuscript, τ_t is constructed from global inflation-pressure coordinates rather than from a pure number-theoretic sequence. The evaluated object is therefore not a claim about primes or zeta zeros. It is an economic signal generator of the form ζ(1/2 + iτ_t), where τ_t summarizes macro-financial pressure, policy stress, liquidity conditions, financial stress, supply stress and crisis-state information. Once the complex output is computed, it must be converted into a real-valued and normalized zeta-cycle before it can enter an inflation forecast.

This transformation is crucial for methodological legitimacy. A complex-valued mathematical object cannot simply be added to an inflation forecast. The chapter requires a sequence of admissible conversions: complex evaluation, real/modulus/Hardy-Z extraction, normalization, neutrality benchmark, deviation from neutrality and signed correction. The resulting object d_t is not the Riemann-zeta function itself; it is a constructed economic zeta-deviation index used to decide whether the structural FPAS forecast should receive an upward, downward or mild cyclical correction.

$$\zeta(s) = \Sigma_{n=1}^{\infty} n^{-s}, \quad s = \sigma + i\tau \quad (10.1)$$

$$s_t = 1/2 + i\tau_t, \quad \tau_t = f(CP_t, policy_t, liquidity_t, financial_t, supply_t, shock_t) \quad (10.2)$$

$$z_t = \zeta(1/2 + i\tau_t) \rightarrow \zeta_t = NormalizedRealSignal(z_t) \quad (10.3)$$

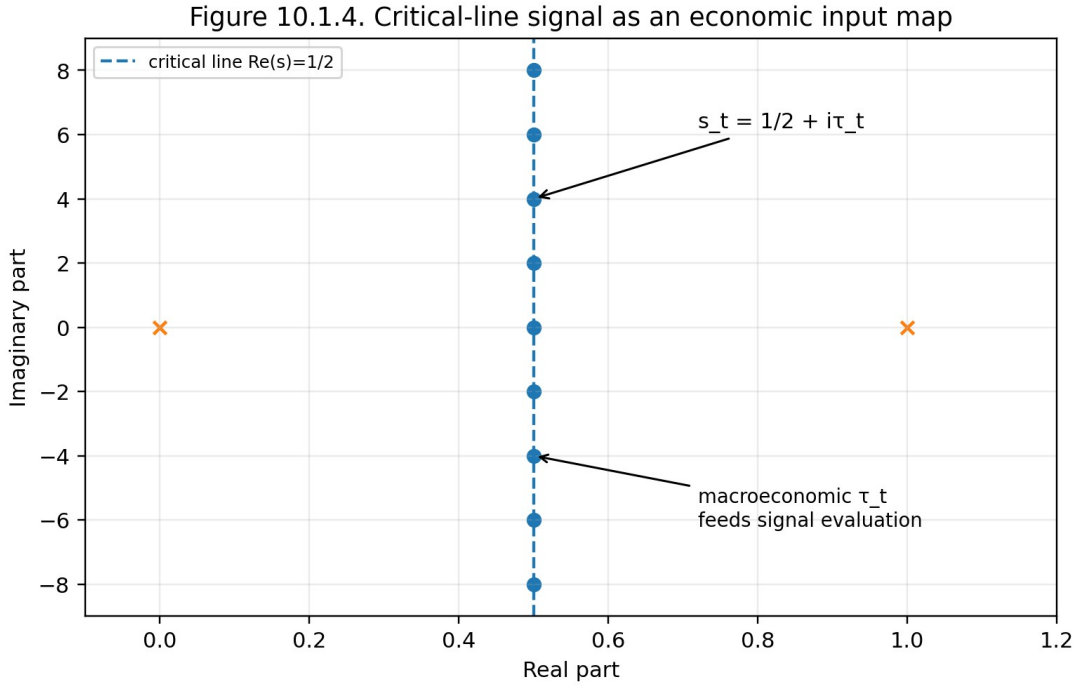
$$d_t = \zeta_t - \zeta_{bar} \quad (10.4)$$

Table 10.1.3. Classical-to-economic translation matrix for the Riemann-zeta analogy

Classical language	Economic translation	Admissible meaning	Excluded meaning
ζ(s)	Computational signal generator	Source of a normalized nonlinear cycle	Not a direct economic variable
Critical line Re(s)=1/2	Structured evaluation line for τ_t	Standardized signal-extraction path	Not proof that zeros lie on the line
Complex output	Real/modulus/Hardy-Z channel before normalization	Signal information requiring transformation	Not directly added to inflation
Zeros and phase	Resonance and deformation	Frequency-domain and crisis-	Not an empirical test of

behavior	diagnostics	alignment screen	RH
Spectral analogy	Macro-financial cycle extraction	Bounded forecasting augmentation	Not a universal law of inflation

Figure 10.1.4. Critical-line signal as an economic input map



10.1.3. Why Inflation Forecasting Requires a Spectral-Signal Layer

Global inflation forecasting is difficult because the target variable is produced by interacting regimes rather than by a smooth persistence process alone. A structural forecasting model can capture inertia, policy reaction, demand pressure and supply stress, but it may under-react when nonlinear global pressure accelerates rapidly. A purely statistical persistence model such as ARIMA can be useful as a benchmark, but it can lag during shocks because it is largely trained on past autocorrelation patterns. The spectral-signal logic of FPAS+ζ enters precisely at this gap: it is designed to detect nonlinear cyclical deformation that is not fully absorbed by the structural FPAS baseline.

The role of the zeta-cycle is therefore conditional. It should not dominate the forecast, replace macroeconomic theory or mechanically increase predicted inflation. It should act as a gate that modifies FPAS only when the normalized zeta deviation indicates meaningful pressure relative to a neutral signal level. If d_t is positive and crisis-aligned, the correction can raise the structural forecast. If d_t is negative or weak, the correction can be downward or mild. This signed structure is one reason the model is more defensible than a simple post-hoc adjustment.

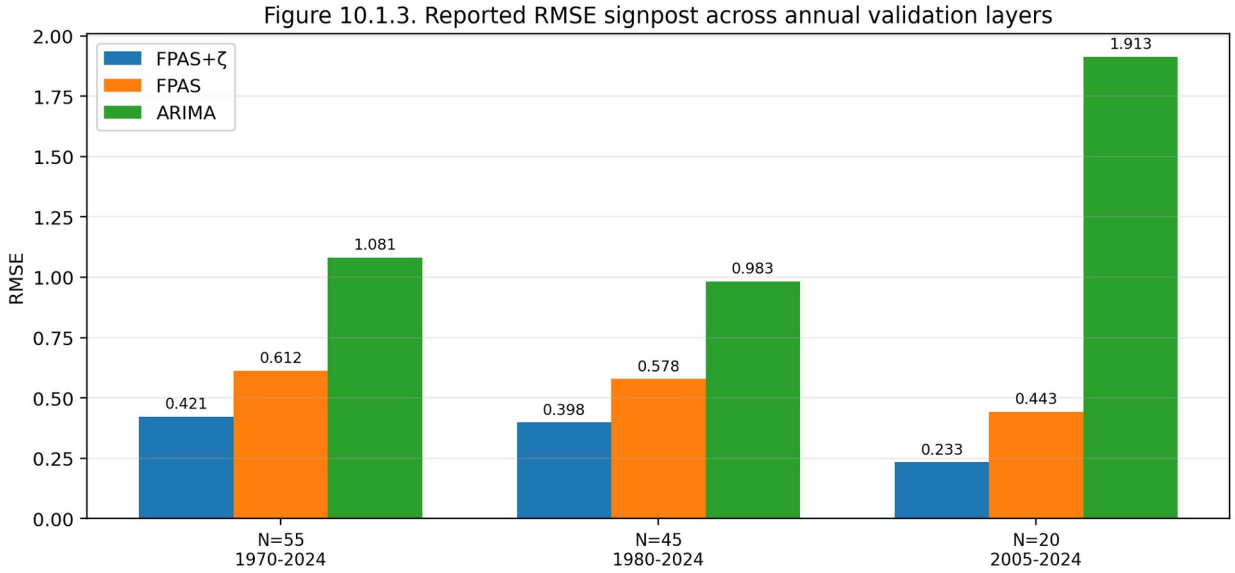
The empirical importance of this logic is visible in the reported annual forecast hierarchy. In the principal annual layer, FPAS+ζ has RMSE = 0.421 compared with 0.612 for FPAS and 1.081 for ARIMA. In the annual robustness layer, the values are 0.398, 0.578 and 0.983 respectively. In the compact crisis-era layer, FPAS+ζ records RMSE = 0.233 compared with 0.443 for FPAS and 1.913 for ARIMA. These figures do not by themselves prove universal superiority. They serve as benchmark signposts showing why the spectral-signal layer deserves full methodological and interpretive treatment in Chapter 10.

Table 10.1.4. Reported RMSE benchmark signposts motivating the spectral-signal analogy

Annual layer	Sample	FPAS+ζ RMSE	FPAS RMSE	ARIMA RMSE	Interpretive status
Principal annual layer	1970-2024, N = 55	0.421	0.612	1.081	Main forecast-accuracy signpost
Annual robustness layer	1980-2024, N = 45	0.398	0.578	0.983	Annual stability signpost
Crisis-era annual layer	2005-2024, N = 20	0.233	0.443	1.913	Compact crisis-era display, not sole basis of claim

Source: Reorganized from the source manuscript for monograph Chapter 10.1. These figures are benchmark signposts; formal evaluation is assigned to Chapter 10.5 and Chapter 10.6.

Figure 10.1.3. Reported RMSE signpost across annual validation layers



10.1.4. Layered Validation as the Scientific Discipline of the Analogy

The zeta analogy would be fragile if it were defended only by one compact sample or one visually impressive fit. For that reason, the source architecture separates validation tasks by frequency and sample size. The N = 55 annual layer carries the principal forecast-accuracy claim. The N = 45 annual layer tests stability under a shorter but still broad historical window. The N = 20 annual layer is retained for crisis-era visualization and comparison, but it is not permitted to carry the entire claim. Quarterly N = 100 evidence is assigned to dynamic validation, regime behavior and shock transmission. Monthly N = 240 evidence is assigned to spectral diagnostics, frequency-domain coherence and zeta-stress lead screens.

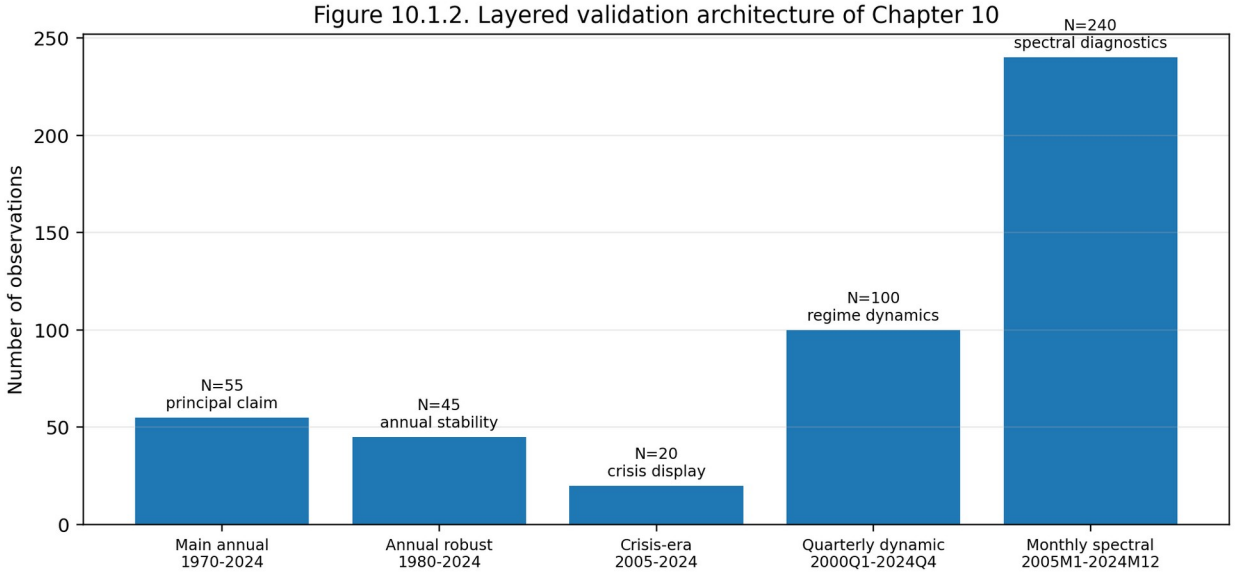
This layered design is part of the monograph's claim discipline. Complex techniques are assigned to the layer capable of supporting them. HMM and Markov-switching evidence belongs more naturally to quarterly dynamics than to a small annual crisis-era window. Fourier, wavelet and spectral-entropy diagnostics belong more naturally to the monthly layer. Annual forecast losses remain central for comparing FPAS+ζ, FPAS and ARIMA, but the interpretation of spectral behavior requires higher-frequency support. This division prevents a common reviewer criticism: that a sophisticated model is overfit to too few annual observations.

Table 10.1.5. Layered validation architecture and admissible claims

Validation layer	Period	N	Primary role	Permitted claim
Main annual	1970-2024	55	Principal annual forecast comparison	Main reported global forecast-improvement evidence
Annual robustness	1980-2024	45	Historical stability check	Robustness of annual hierarchy
Crisis-era annual	2005-2024	20	Compact crisis display	Interpretive illustration, not sole foundation
Quarterly dynamic	2000Q1-2024Q4	100	Regime, transmission and dynamic validation	Supportive dynamic evidence
Monthly spectral	2005M1-2024M12	240	Spectral, wavelet and frequency-domain diagnostics	Supportive cyclicality and coherence evidence

Figure 10.1.2. Layered validation architecture of Chapter 10

Figure 10.1.2. Layered validation architecture of Chapter 10



10.1.5. The FPAS+ζ Correction Gate

The structural FPAS forecast is the baseline forecast. It is denoted as πhat^F_t and is built from inflation inertia, macro-financial pressure, policy reaction, liquidity conditions, financial stress and supply stress. The zeta layer does not replace this baseline. It adds a calibrated correction c^ζ_t only after the zeta-cycle has passed through the signal construction and neutrality gate. The hybrid forecast is therefore πhat^Z_t = πhat^F_t + αλ_ζd_t, where α is the reaction coefficient and λ_ζ is a scaling factor aligning the zeta deviation with the forecast units.

The key theoretical implication is that the zeta layer is neither a free residual plug nor a mystical mathematical premium. It is a conditional correction. Its effect depends on the sign and magnitude of d_t, and its strength depends on α. This structure forces the model to make a falsifiable forecast-comparison claim: if the zeta layer adds no relevant information, the hybrid model should fail to outperform the FPAS baseline under RMSE, MAE, sMAPE, rolling validation and formal comparison tests. If it improves performance only in one compact window, the claim must remain weak. If it improves the hierarchy across principal and robustness layers and is supported by spectral/regime diagnostics, the claim becomes stronger but still bounded.

πhat^F_t = StructuralFPAS(π_{t-1}, CP_t, policy_t, liquidity_t, financial_t, supply_t) (10.5)

c^ζ_t = α λ_ζ d_t (10.6)

πhat^Z_t = πhat^F_t + c^ζ_t = πhat^F_t + α λ_ζ d_t (10.7)

Table 10.1.6. Core objects in the Riemann-Zeta FPAS+ζ signal architecture

Object	Notation	Operational role	Interpretive caution
Actual global inflation	π_t	Forecast target variable	Global aggregate, not country-level policy target
FPAS baseline forecast	πhat^F_t	Structural macro-financial forecast	Not a full central-bank model
Critical-line argument	τ_t	Maps pressure into signal evaluation height	Author-constructed macro-financial argument
Normalized zeta-cycle	ζ_t	Real-valued cyclical signal after transformation	Not the raw complex zeta output
Neutral deviation	d_t = ζ_t - ζbar	Signed correction indicator	Requires alpha calibration and validation
Hybrid forecast	πhat^Z_t	FPAS plus zeta correction	Bounded forecast-improvement claim only

10.1.6. Crisis Resonance and Zeta-Deformation Logic

The source manuscript identifies 2008, 2020 and 2022 as central stress years for the interpretation of zeta deviations, composite pressure, F_zeta, W_zeta and regime diagnostics. This does not mean that the zeta function predicted these crises as a theorem-level mechanism. It means that the constructed zeta-cycle and stress diagnostics concentrate around historically recognizable global inflation-pressure events: the global financial crisis and recession aftershock, the pandemic

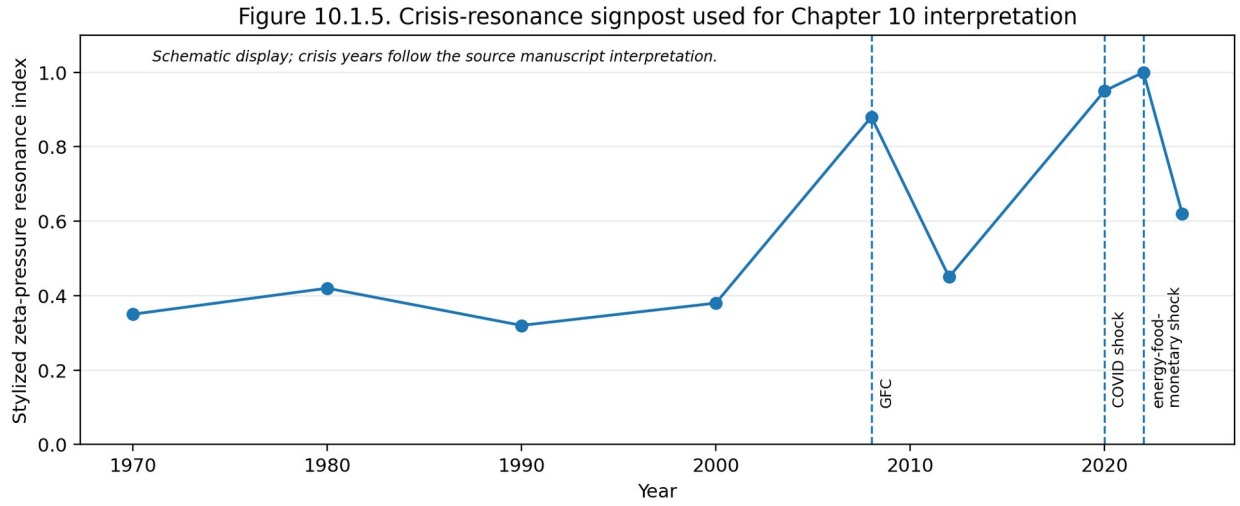
macro-financial shock, and the energy-food-monetary tightening shock. The analogy gains economic meaning only because these signal movements coincide with interpretable macro-financial pressure episodes.

Crisis resonance is therefore a diagnostic alignment concept. It asks whether the spectral signal behaves plausibly in years when macro-financial pressure is known to be high. In a bounded interpretation, zeta-deformation does not establish causality. It supports the claim that the normalized spectral signal carries information correlated with nonlinear global stress states. This is why Chapter 10 separates forecast accuracy from diagnostic interpretation. Forecast accuracy is evaluated by loss functions and formal comparison tests. Crisis resonance is evaluated by shock-anchor alignment, zeta-deformation ranking, pressure diagnostics and regime/spectral evidence.

Table 10.1.7. Crisis-resonance interpretation framework

Crisis anchor	Economic interpretation	Expected spectral-diagnostic role	Claim boundary
2008	Global financial crisis and recession aftershock	High zeta-deformation and pressure resonance	Diagnostic alignment, not theorem evidence
2020	COVID-19 macro-financial shock	Crisis-sensitive zeta movement and regime disruption	Shock-state evidence, not causal proof
2022	Energy-food-war and monetary-tightening shock	Strong pressure / W_zeta / zeta-stress signal	Inflation-cycle diagnostic, not universal forecast law
2023-2024	Post-shock disinflation under residual tightness	Tests whether correction declines or stabilizes	Transition interpretation remains sample-bound

Figure 10.1.5. Crisis-resonance signpost used for Chapter 10 interpretation



10.1.7. Claim Boundary: Strong Forecast-Diagnostic Architecture without Theorem Overclaiming

The strongest safe wording for this chapter is that it develops a bounded mathematical-econometric forecast-diagnostic architecture for global inflation. The chapter may claim that the FPAS+ζ model, under the reported data architecture, improves the forecast hierarchy relative to FPAS and ARIMA in the specified annual layers, while receiving additional support from quarterly and monthly diagnostics. It may not claim that the Riemann Hypothesis has been proven, tested, verified or econometrically supported. It may not claim universal dominance in all economies, all samples and all horizons. It may not claim that residual problems are eliminated.

This distinction is not a weakness. It is the scientific condition that makes the chapter defensible. A high-level mathematical analogy becomes acceptable only when it is transformed into observable variables, validated against benchmarks, audited by residual and robustness tests, and surrounded by clear evidence gates. The chapter therefore treats number theory as a source of signal architecture, not as a substitute for macroeconomic theory or econometric evaluation.

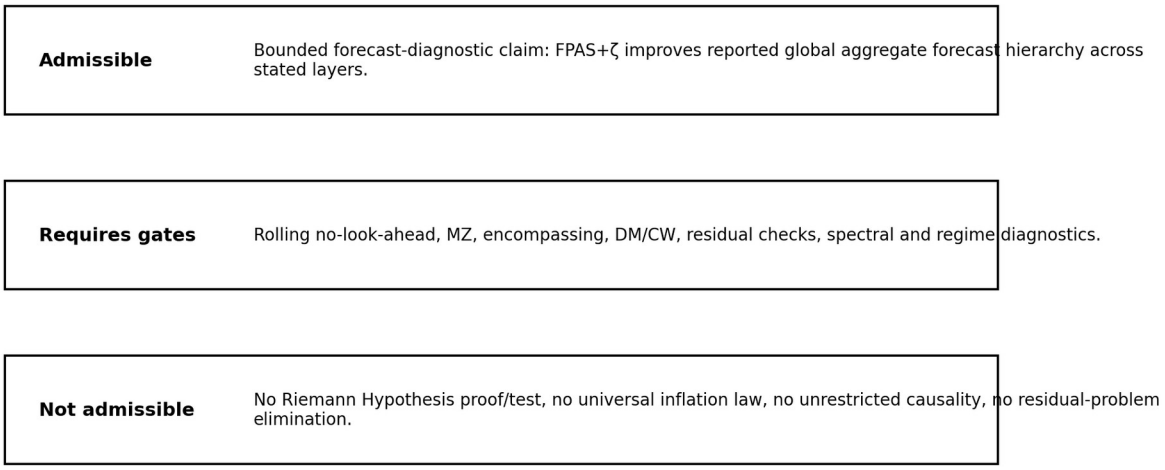
Table 10.1.8. Claim hierarchy and excluded overclaims

Possible statement	Status in Chapter 10.1	Reason
FPAS+ζ is a global forecast-diagnostic model.	Supported with boundaries	It combines FPAS baseline, zeta correction and layered validation.
The zeta-cycle improves the reported forecast hierarchy.	Supported as a reported benchmark signpost	RMSE improvements are reported across N = 55, N = 45 and N = 20 annual layers.
The Riemann Hypothesis is tested by inflation data.	Excluded	The economic model does not address the theorem-level location of zeta zeros.

The zeta signal causes global inflation.	Excluded	The model is forecast-diagnostic and does not identify unrestricted causality.
The model universally dominates all forecasts.	Excluded	The reported evidence is global-aggregate and sample-specific; residual and stability risks remain bounded.

Figure 10.1.6. Claim-boundary gate for the Riemann-zeta economic analogy

Figure 10.1.6. Claim-boundary gate for the Riemann-zeta economic analogy



10.1.8. Integration with the Seven-Problem Monograph

The Riemann-Zeta chapter must be read as one part of the monograph's seven-problem translation program. It is not isolated from the previous chapters. The Perelman/Ricci/Poincare chapter uses curvature and entropy to study inequality pressure. The Hodge chapter decomposes macro-flow into gradient, curl and harmonic components. The Navier-Stokes chapter models liquidity-flow stress. The Yang-Mills chapter introduces gauge curvature, action and a finite-network mass-gap threshold. The BSD chapter interprets regional local-to-global rank formation. The Riemann-Zeta chapter adds spectral forecasting and layered validation. The P-vs-NP chapter then turns to computational complexity and sparse optimization. Together, these chapters form a measurement architecture for global economic complexity.

Within that architecture, Chapter 10 has a special role because it is the most explicitly forecast-validation oriented chapter. It shows how a mathematically inspired signal can be judged not by rhetorical elegance but by benchmark comparison, rolling validation, forecast calibration, formal loss tests, spectral diagnostics and residual discipline. This makes it a methodological bridge between the general monograph claim-boundary rules and the practical question of whether a constructed signal actually improves measurable economic prediction.

Table 10.1.9. Cross-chapter integration of the Riemann-Zeta spectral-signal chapter

Book chapter	Mathematical grammar	Economic translation	Relation to Chapter 10
Chapter 5	Ricci/Poincare	Inequality pressure, curvature, entropy	Shares pressure/deformation language
Chapter 6	Hodge	Macro-flow decomposition	Shares spectral/topological decomposition logic
Chapter 7	Navier-Stokes	Liquidity pressure and stress balance	Shares macro-financial pressure and shock logic
Chapter 8	Yang-Mills	Gauge curvature and shock threshold	Shares signal-threshold and action/curvature analogy
Chapter 9	BSD	Local-to-global rank formation	Shares local-to-global calibration discipline
Chapter 10	Riemann-Zeta	Inflation spectral forecasting	Core chapter for forecast validation and zeta-cycle signal
Chapter 11	P vs NP	Portfolio optimization complexity	Shares benchmark and claim-boundary discipline

10.1.9. Reviewer-Safety Logic for the Opening Subsection

The opening subsection must protect the chapter from three predictable reviewer risks. The first is mathematical overclaim risk: a reviewer may object if Riemann-zeta terminology appears to suggest proof, verification or empirical testing of the Riemann Hypothesis. The response is to define the zeta layer as a signal analogy only. The second is overfitting risk: a reviewer may object if the model appears to be fitted to a compact crisis window. The response is the layered validation architecture, with N = 55 as the principal annual layer and N = 100 / N = 240 as dynamic and spectral support layers. The third is black-box risk: a reviewer may object if the zeta correction appears arbitrary. The response is the explicit tau argument, normalization, neutrality deviation, alpha calibration and forecast-comparison protocol.

Table 10.1.10. Reviewer-safety controls embedded in the opening Riemann-Zeta subsection

Reviewer risk	How 10.1 neutralizes it	Where later chapter sections complete the answer
Riemann Hypothesis overclaim	States that zeta is an analogical and computational cyclical signal only.	10.4 methodology; 10.9 claim boundary
Compact-sample overfitting	Introduces N = 55, N = 45, N = 20, N = 100 and N = 240 layer hierarchy.	10.3 data architecture; 10.5 evaluation protocol; 10.6 results
Black-box correction	Defines τ_t, ζ_t, d_t, α and λ_ζ before the hybrid forecast is interpreted.	10.4 correction gate and alpha calibration
Benchmark weakness	Requires comparison against FPAS and ARIMA plus formal validation tests.	10.5 RMSE/MAE/sMAPE/MZ/DM/CW
Causal overstatement	Frames the model as forecast-diagnostic rather than causal theorem.	10.7 interpretation and 10.8 robustness evidence

10.1.10. Transition to Chapter 10.2

This subsection establishes the conceptual translation: the Riemann-zeta function supplies a spectral-signal grammar; the economic model converts that grammar into τ_t, ζ_t, d_t and an alpha-calibrated correction; and the final claim is governed by layered forecast validation rather than theorem-level mathematics. The next subsection, 10.2, moves from this analogy to the research object. It defines global inflation as a layered macro-financial pressure system, identifies the target variable and forecast objects, and clarifies how actual inflation, FPAS, FPAS+ζ, ARIMA, composite pressure, zeta-cycle diagnostics, regime states and validation layers form one empirical object.

Table 10.1.11. Closing synthesis of Section 10.1

10.1 conclusion element	Final wording
Core idea	The Riemann-zeta function is translated into a bounded economic spectral signal.
Forecast object	The zeta signal modifies FPAS only through a signed, calibrated correction gate.
Evidence architecture	Annual, quarterly and monthly layers distribute the burden of proof across appropriate samples.
Supported claim	FPAS+ζ is a strong but bounded global forecast-diagnostic architecture in the reported design.
Excluded claim	The chapter does not prove, test or verify the Riemann Hypothesis and does not claim universal forecast dominance.

Technical note. Numbering, tables and figures are prepared for integration into Chapter 10 of the monograph. Detailed references belong to the unified literature-review chapter and the final book bibliography. This subsection cites the source manuscript logic in monograph-ready form without duplicating the full article-style literature review.

10.2. Research Object: Global Inflation as a Layered Macro-Financial Pressure System

This section defines the research object of Chapter 10. The object is not the Riemann Hypothesis, not a country-level monetary-policy model and not a universal theory of inflation. It is a bounded global forecast-diagnostic system in which world aggregate inflation is interpreted as a layered macro-financial pressure process. The chapter's core empirical task is to evaluate whether a normalized Riemann-zeta cyclical signal, transformed into a signed correction gate, improves a structural FPAS baseline when tested against FPAS and ARIMA across annual, quarterly and monthly validation layers. The monograph requires this section because Chapter 10 must not read like a stand-alone article introduction. The common mathematical-analogy, forecasting and claim-boundary material belongs to the book's general chapters. The function of 10.2 is narrower and more technical: to identify exactly

what is being measured, what the unit of analysis is, which validation layers support which claims, which variables define the object, what data status is assigned to the reported outputs and which interpretations are explicitly excluded.

The immediate outcome is a disciplined research-object definition. Global inflation is not treated only as a scalar time series. It is treated as the observable endpoint of a pressure system formed by inflation inertia, growth stress, unemployment pressure, policy tightness, liquidity gaps, financial stress, supply stress and nonlinear zeta resonance. Forecasting is therefore connected to pressure measurement, spectral signal construction, regime diagnostics and validation discipline.

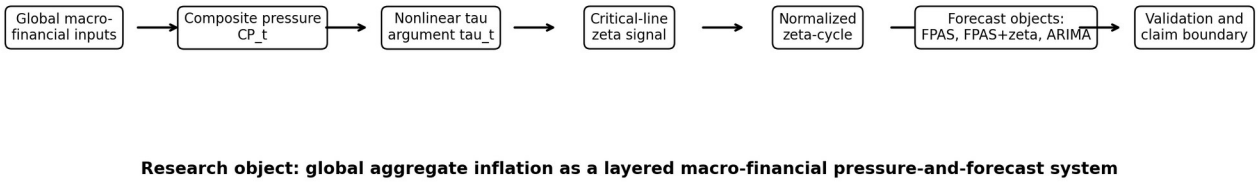


Figure 10.2.1. Research-object pipeline for the FPAS+zeta global inflation framework.

10.2.1. Position of the Research Object inside Chapter 10

The research object is the global aggregate inflation-forecasting system interpreted as a layered macro-financial pressure architecture. This formulation has three implications. First, the target variable is the world inflation path, denoted by pi_t, not national inflation, household-level price pressure or a central-bank decision rule for a single jurisdiction. Second, the forecast comparison is organized around three forecast objects: the structural FPAS forecast, the hybrid FPAS+zeta forecast and an ARIMA benchmark. Third, the zeta layer is not a theorem-level mathematical object; it is a normalized critical-line signal used to construct an economic cyclical correction.

This object is therefore wider than a simple model-comparison table and narrower than a general macroeconomic theory. It is wider because the forecast result is evaluated jointly with pressure coordinates, nonlinear tau construction, zeta deviation, correction signs, regime states, spectral diagnostics and residual checks. It is narrower because the admissible conclusion remains a bounded forecast-diagnostic claim: the hybrid model improves the reported global forecast hierarchy under the stated layers and validation procedures, but it does not prove or test the Riemann Hypothesis, does not eliminate residual risk and does not establish universal forecast dominance in every country, horizon or data frequency.

In monograph terms, Chapter 10 occupies the spectral-forecasting position among the seven economic analogues. The Perelman/Ricci/Poincare chapter measures curvature-like inequality pressure; the Hodge chapter decomposes macro-flow; the Navier-Stokes chapter measures liquidity-flow stress; the Yang-Mills chapter measures finite-network shock thresholds; the BSD chapter translates local-to-global rank; and the P vs NP chapter treats computational portfolio selection. Chapter 10 contributes the inflation-forecasting and spectral-signal layer. Its object must therefore be defined with the same discipline used in the other problem chapters: analogue, data architecture, validation, result interpretation and claim boundary.

Table 10.2.1. Research-object definition and claim boundary matrix.

Object layer	Operational definition	Analytical role	Claim boundary
Target object	Actual global aggregate	Defines the dependent forecast	Not country-level policy

Object layer	Operational definition	Analytical role	Claim boundary
	inflation, pi_t	target and the global empirical coordinate.	ranking or welfare analysis.
Structural baseline	FPAS forecast, pi_hat^F_t	Provides the macro-financial baseline against which the zeta correction is tested.	Not a complete central-bank model.
Hybrid object	FPAS+zeta forecast, pi_hat^Z_t = pi_hat^F_t + alpha lambda_zeta d_t	Measures whether the zeta-cycle deviation improves forecast accuracy.	Bounded forecast-improvement claim, not universal dominance.
Comparator	ARIMA benchmark	Provides a persistence/statistical baseline for forecast comparison.	Benchmark model, not the full universe of possible alternatives.
Diagnostic pressure object	Composite pressure CP_t and pressure-coordinate families	Connects inflation forecasting to macro-financial stress interpretation.	Constructed diagnostic index, not causal mechanism by itself.
Spectral signal object	zeta(1/2 + i tau_t), normalized zeta-cycle zeta_t and deviation d_t	Provides nonlinear cyclical correction information.	Economic signal analogue; not proof/test of RH.
Validation object	RMSE, MAE, sMAPE, rolling validation, MZ, DM, CW, residual and spectral tests	Protects forecast comparison from compact-window overclaiming.	Validation evidence with residual risks explicitly reported.

Source note: Author synthesis based on the Chapter 10 source manuscript and the monograph claim-boundary architecture.

10.2.2. Global Inflation as a Layered Macro-Financial Pressure System

The object is global inflation, but not in the narrow sense of an annual percentage series alone. The chapter treats global inflation as an outcome of layered macro-financial pressure. The pressure system is built from families of variables that are economically interpretable before they are transformed into forecast objects: inflation pressure, growth stress, unemployment pressure, policy tightness, liquidity conditions, financial stress, supply stress and zeta resonance. In the research-object layer, these families specify what kind of economic environment the forecast is trying to read.

This is important because the FPAS+zeta framework does not merely add a mathematical signal to a time series. It starts from a macro-financial pressure state. That state is compressed into CP_t, mapped into a nonlinear tau argument, evaluated through the critical-line zeta construction, normalized into zeta_t, compared to a neutral benchmark through d_t and then converted into a signed forecast correction. The research object is therefore a sequence of transformations rather than an isolated dependent variable.

The pressure-system interpretation also explains why the chapter emphasizes global shock years. Inflation episodes such as the 2008 global financial crisis aftermath, the 2020 pandemic shock and the 2022 energy-food-monetary tightening shock are not treated as ordinary small deviations around a stationary mean. They are stress regimes in which a structural baseline can under-react and a nonlinear cyclical correction may carry additional diagnostic information. The research object is precisely this interaction between structural baseline, nonlinear stress signal and validation layer.

Table 10.2.2. Macro-financial pressure families defining the research object.

Pressure family	Operational meaning	Role in the object
Inflation pressure	Actual world inflation and inflation-deviation behaviour	Defines the target stress being forecast.
Growth stress	Global activity weakness or output-cycle	Captures macroeconomic contraction or

Pressure family	Operational meaning	Role in the object
	pressure	demand instability.
Unemployment pressure	Labour-market slack or global labour stress proxy	Links price dynamics to real-economy stress.
Policy tightness	Monetary-policy stance and tightening pressure	Allows the FPAS baseline to reflect policy reaction.
Liquidity gap	Liquidity shortage or macro-financial flow pressure	Connects inflation to financing and monetary conditions.
Financial stress	Stress proxies associated with risk premia or financial instability	Captures crisis-sensitive macro-financial transmission.
Supply stress	Energy, food, logistics and supply-chain pressure	Represents inflation impulses not captured by inertia alone.
Zeta resonance	Normalized nonlinear spectral signal linked to tau_t	Provides the cyclical correction object for FPAS+zeta.

Figure 10.2.7. Macro-financial pressure families used to define the object

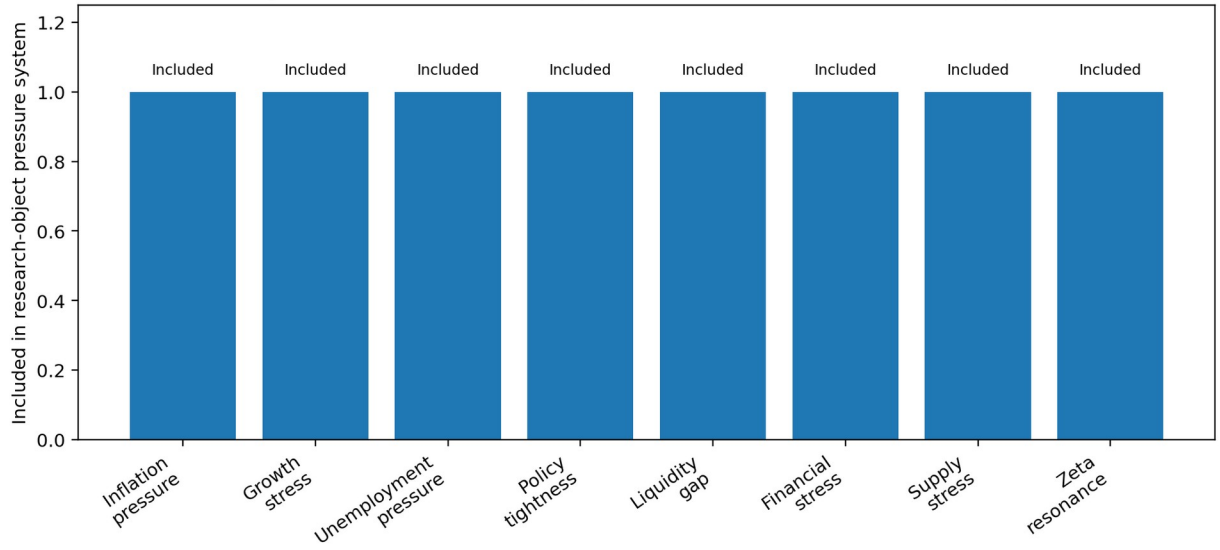


Figure 10.2.7. Macro-financial pressure families used to define the object.

10.2.3. Layered Empirical Universe and Sample-Discipline Logic

The empirical universe is deliberately layered. This is the most important research-object safeguard in Chapter 10. The model does not rely on one compact annual window and then apply all diagnostics as if they were supported by the same sample size. Instead, each evidence type is assigned to the frequency and sample layer that can support it. The principal annual validation layer covers 1970-2024 with N = 55 observations. The annual robustness layer covers 1980-2024 with N = 45. The compact crisis-era annual layer covers 2005-2024 with N = 20 and is retained for stress-era display and comparison, not as the sole foundation of the model. Quarterly validation covers 2000Q1-2024Q4 with N = 100. Monthly spectral diagnostics cover 2005M1-2024M12 with N = 240.

This separation has direct methodological value. It prevents the reader from assuming that HMM, Fourier, wavelet, rolling validation, forecast-comparison tests and crisis-era forecast tables are all estimated on the same small sample. The research object is a layered validation system in which the annual layer supplies the headline forecast hierarchy, quarterly data support dynamic validation and monthly data support spectral diagnostics. The model can therefore make stronger forecast-validation

claims than a compact annual-only design, while still preserving the claim boundary that forecast dominance is reported for the specified global layers and not for all possible samples.

Figure 10.2.2. Layered empirical universe and sample discipline

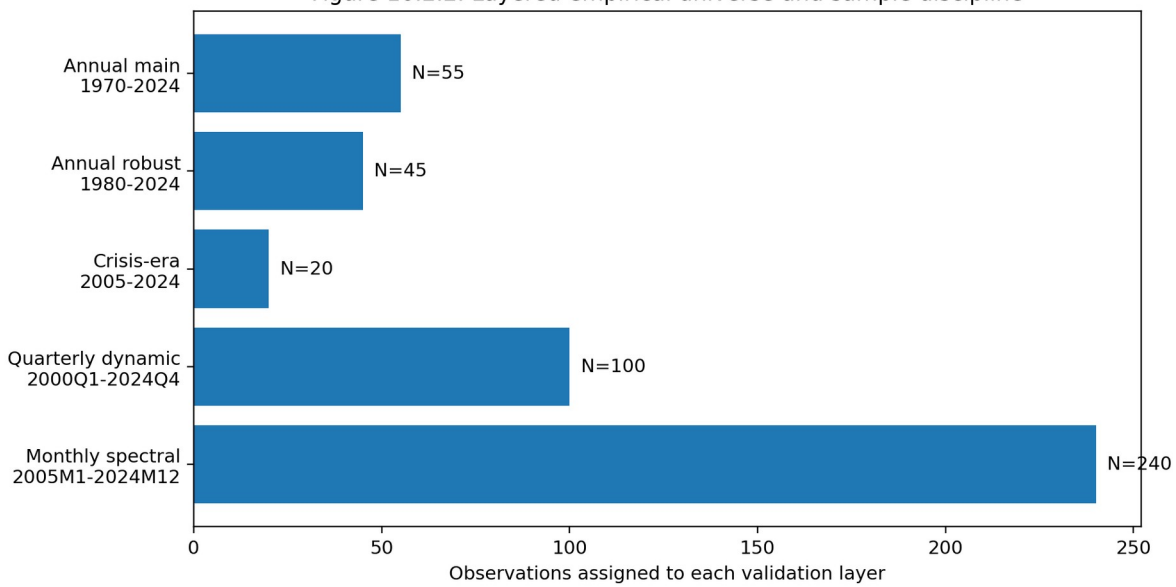


Figure 10.2.2. Layered empirical universe and sample discipline.

Table 10.2.3. Layered sample hierarchy and evidence status.

Layer	Time span	Frequency	N	Permitted evidence role
Principal annual validation	1970-2024	Annual	N = 55	Headline global forecast-accuracy evidence; principal RMSE/MAE/sMAPE comparison.
Annual robustness layer	1980-2024	Annual	N = 45	Stability check against the principal annual layer.
Crisis-era comparison	2005-2024	Annual	N = 20	Compact stress-era display; not the sole proof layer.
Quarterly dynamic validation	2000Q1-2024Q4	Quarterly	N = 100	Dynamic validation, regime behaviour and shock-transmission screens.
Monthly spectral diagnostics	2005M1-2024M12	Monthly	N = 240	Fourier, wavelet, spectral entropy and zeta-stress lead diagnostics.

Figure 10.2.4. Layer chronology and global shock-anchor windows

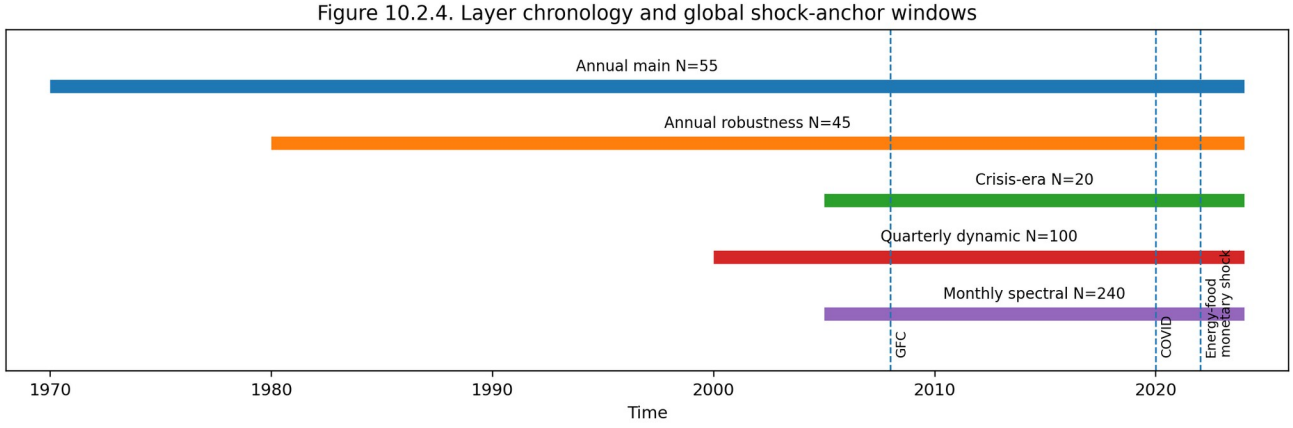


Figure 10.2.4. Layer chronology and global shock-anchor windows.

10.2.4. Target Variable, Forecast Objects and Diagnostic Objects

The target variable is actual global inflation, pi_t. The forecast objects are the FPAS baseline forecast pi_hat^F_t, the hybrid FPAS+zeta forecast pi_hat^Z_t and the ARIMA benchmark. The diagnostic objects

are CP_t, tau_t, zeta_t, d_t, the zeta correction c^zeta_t, alpha, lambda_zeta, the shock-anchor indicator S_t and the regime states used in HMM and Markov-switching diagnostics. This explicit object register matters because it prevents variable slippage. A forecast object is not the same as a pressure object; a pressure object is not the same as a theorem; a validation statistic is not the same as a causal proof.

The core hybrid forecast can be written as:

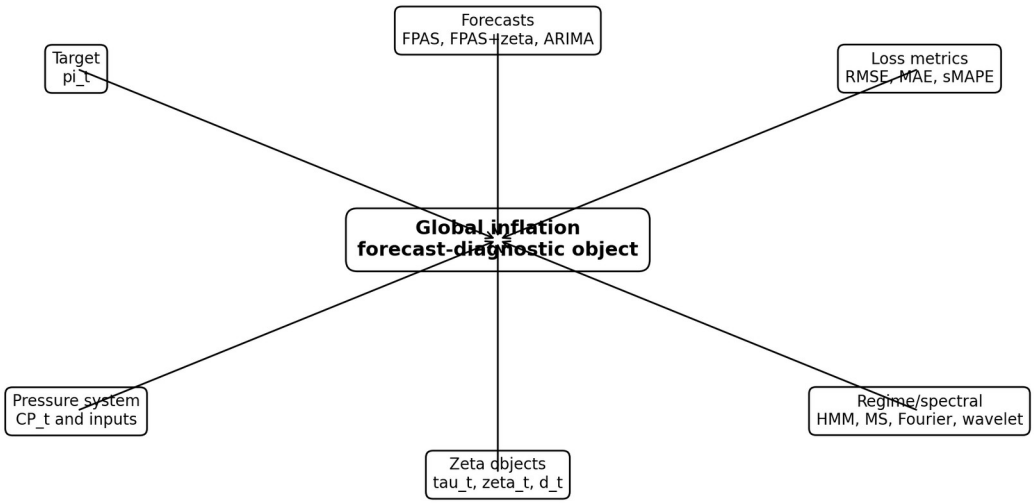
pi_hat^Z_t = pi_hat^F_t + alpha lambda_zeta d_t. (10.2.1)

Here pi_hat^F_t is the structural FPAS baseline, d_t is the normalized zeta deviation from neutrality, lambda_zeta is a scaling factor and alpha is the calibrated reaction coefficient. The equation is deliberately simple at the object-definition stage because the detailed construction of CP_t, tau_t, zeta_t and the correction gate belongs to Sections 10.3-10.5. Section 10.2 only clarifies what these objects are and what claims they can support.

The object register also clarifies the role of ARIMA. ARIMA is not treated as a theoretical rival to the entire FPAS+zeta system. It is a benchmark used to measure whether the structural and hybrid forecasts outperform a persistence-oriented statistical comparator. This is why the chapter's strongest claim is comparative and validation-specific: the hybrid forecast improves the reported hierarchy relative to FPAS and ARIMA under the stated layers.

Table 10.2.4. Variable and object register for Chapter 10.

Symbol / object	Definition	Object class	Interpretive role
pi_t	Actual global inflation	Forecast target	World aggregate inflation path.
pi_hat^F_t	Structural FPAS forecast	Baseline forecast	Captures inertia, pressure and policy-style structural channels.
pi_hat^Z_t	Hybrid FPAS+zeta forecast	Main forecast object	Adds signed zeta correction to the FPAS baseline.
ARIMA	Persistence/statistical benchmark	Comparator	Tests whether the hybrid model beats a standard inertia benchmark.
CP_t	Composite pressure index	Macro-financial diagnostic object	Summarizes inflation, growth, labour, policy, liquidity, financial and supply stress.
tau_t	Nonlinear macro-financial argument	Signal-input object	Maps pressure into critical-line evaluation domain.
zeta_t	Normalized real-valued zeta-cycle	Spectral signal object	Transforms zeta output into a usable economic cycle.
d_t	zeta_t minus neutral zeta benchmark	Correction direction object	Determines sign and magnitude of zeta correction.
alpha	Reaction coefficient	Calibration parameter	Controls sensitivity of the hybrid correction.
lambda_zeta	Scale factor	Normalization parameter	Keeps zeta correction interpretable in forecast units.
S_t	Shock-anchor indicator	Regime/context object	Marks crisis years used in interpretation and stress diagnostics.
HMM/MS states	Hidden or switching regimes	Regime diagnostic objects	Classify stress regimes without converting them into causal proof.



Each object has a separate evidence status; none is a proof or test of the Riemann Hypothesis.

Figure 10.2.5. Forecast, pressure, zeta and validation objects.

10.2.5. Benchmark Result Context for the Research Object

A research-object section should not replace the results chapter, but it must explain why the object is worth isolating. The reported benchmark context shows that the hybrid object FPAS+zeta improves the forecast hierarchy across the main annual, annual robustness and compact crisis-era layers. In the principal annual layer, FPAS+zeta reports RMSE = 0.421 compared with FPAS = 0.612 and ARIMA = 1.081. In the robustness layer, FPAS+zeta reports RMSE = 0.398 compared with FPAS = 0.578 and ARIMA = 0.983. In the crisis-era layer, FPAS+zeta reports RMSE = 0.233 compared with FPAS = 0.443 and ARIMA = 1.913. These values are not used here to close the results argument. They are used to justify the research-object design. The object is not merely global inflation; it is a global inflation system in which a structural forecast, a spectral correction and benchmark comparison must be read together. The result hierarchy is meaningful only because the object has been defined with separate annual, quarterly and monthly evidence layers. Without that layer discipline, the improvement could be misread as a compact-window artefact.

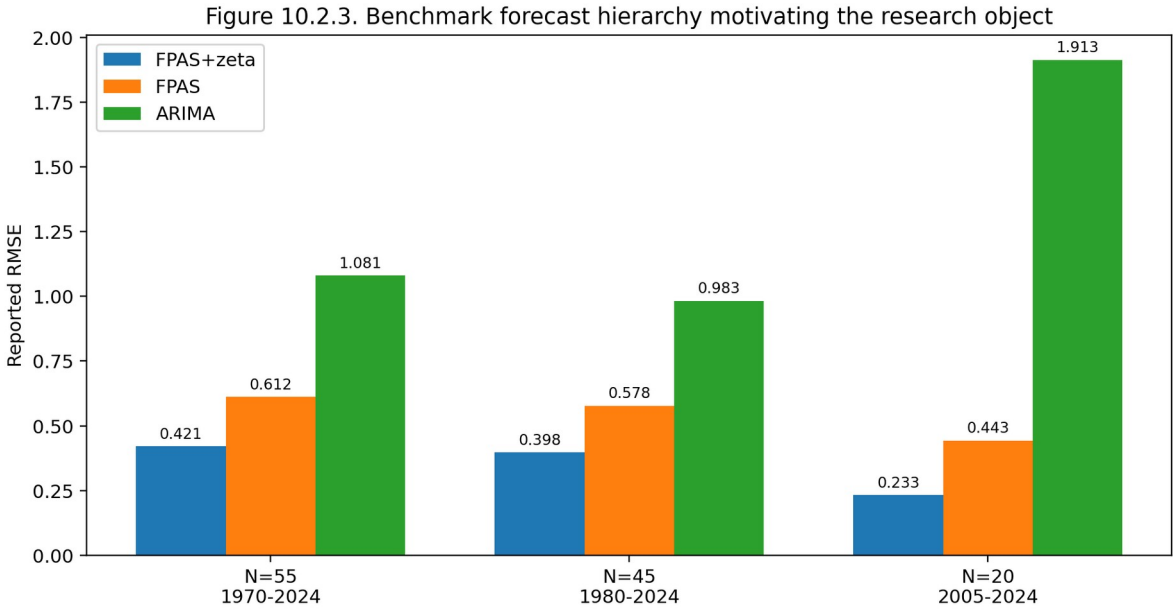


Figure 10.2.3. Reported RMSE hierarchy motivating the research object.

Table 10.2.5. Reported RMSE benchmark context used to motivate the research object.

Layer	Sample	FPAS+zeta RMSE	FPAS RMSE	ARIMA RMSE	Research-object implication
Principal annual validation	N = 55, 1970-2024	0.421	0.612	1.081	FPAS+zeta improves the main annual forecast hierarchy.
Annual robustness	N = 45, 1980-2024	0.398	0.578	0.983	Improvement remains under a shorter annual robustness layer.
Crisis-era comparison	N = 20, 2005-2024	0.233	0.443	1.913	The crisis-era layer is strong but interpreted as compact-window evidence.

10.2.6. Data Status, Replication Object and Manuscript Closure

The data status is closed at the manuscript-reported-results level. The Chapter 10 source manuscript states that the annual, quarterly and monthly layered validation results are supported by a Zenodo data and replication package with DOI 10.5281/zenodo.20852478. For the monograph chapter, this means the research object has an external audit companion: the structured replication workbook, reported tables, formula-audit files and supporting documentation are part of the evidence architecture.

The replication object should be understood carefully. It does not turn the model into a theorem, and it does not convert global forecast accuracy into country-level policy validity. Its function is auditability. A reader should be able to trace how the reported layers, formulas, validation outputs and forecast-comparison tables are produced. In a monograph built from seven mathematical-economic analogues, this reproducibility discipline is essential because the risk of overclaiming is higher when mathematical terminology is used.

The data status can therefore be summarized as follows: the global aggregate forecast-diagnostic layer is reported and archived; the annual, quarterly and monthly validation samples are separated; the exact country-level policy ranking is outside the object; and the final claim is bounded by sample assignment, residual diagnostics and forecast-comparison tests.

Table 10.2.6. Data-status and replication matrix.

Replication element	Documented status	Research-object role	Boundary
Replication package	Zenodo DOI 10.5281/zenodo.20852478	External audit companion for reported results.	Supports traceability, not theorem proof.
Annual results	N = 55, N = 45, N = 20	Main forecast hierarchy, robustness and crisis-era display.	Annual global aggregate only.
Quarterly results	N = 100	Dynamic validation and regime-sensitive diagnostics.	Not a replacement for every national quarterly model.
Monthly results	N = 240	Spectral diagnostics, wavelet/Fourier/spectral entropy screens.	Diagnostic evidence, not independent RH evidence.
Formula audit	CP_t, tau_t, zeta_t, d_t, correction gate and forecast comparison	Enables transparent reconstruction of model objects.	Constructed objects depend on disclosed transformations.
Residual and robustness checks	MZ, encompassing, DM/CW, residual tests, spectral/regime diagnostics	Protects against visual-fit and compact-sample overclaiming.	Residual risks remain part of the final interpretation.

10.2.7. Evidence-Status Hierarchy: What the Object Can and Cannot Support

The evidence hierarchy is central to the scientific credibility of Chapter 10. The research object can support a global forecast-diagnostic claim: the hybrid FPAS+zeta model improves the reported global aggregate inflation forecast hierarchy and produces interpretable stress diagnostics across the specified layers. It can also support a spectral-diagnostic claim: the zeta-cycle, when normalized and evaluated through frequency-domain and regime tools, contributes to the interpretation of crisis-sensitive inflation dynamics.

The object cannot support theorem-level claims. It cannot be used as proof, test or verification of the Riemann Hypothesis. It cannot be interpreted as a causal theorem of inflation formation. It cannot claim that all residual problems disappear. It cannot claim universal dominance across all countries, horizons, model classes and future samples. These exclusions are not rhetorical qualifications; they are part of the research design. Without them, the chapter would be vulnerable to the same criticism that applies to overextended mathematical analogies.

Figure 10.2.6. Evidence-status and claim-boundary gate

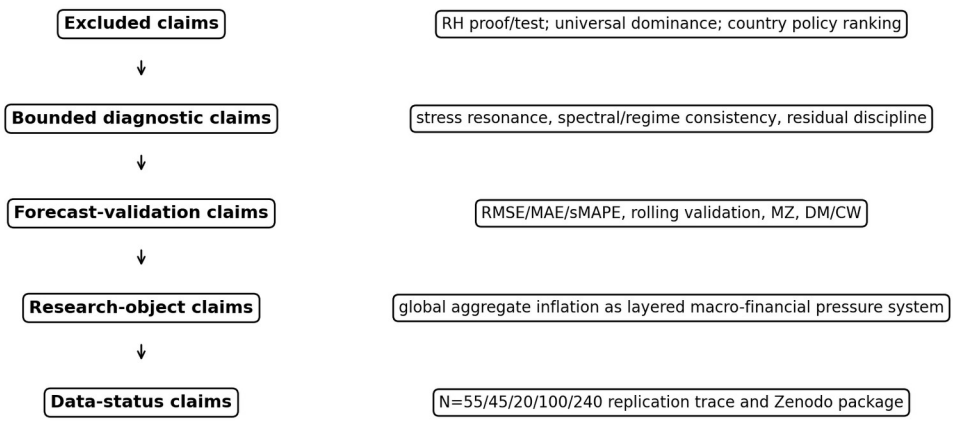


Figure 10.2.6. Evidence-status and claim-boundary gate.

Table 10.2.7. Evidence-status hierarchy for the Chapter 10 research object.

Status	Evidence type	Permitted wording
Strongly supported within Chapter 10	Layered global forecast-diagnostic object; FPAS+zeta comparison against FPAS and ARIMA; sample-specific validation.	May be stated as the core chapter claim.
Supported as diagnostic interpretation	Crisis resonance, zeta-deformation ranking, spectral coherence and regime-state alignment.	Must be described as diagnostic, not causal proof.
Supported as robustness evidence	Rolling validation, MZ, encompassing, DM/CW, residual and spectral/regime checks.	Supports claim discipline and reduces overfitting risk.
Conditionally supported	Policy, liquidity, supply and stress-test screens.	Model-implied scenarios, not treatment effects.
Explicitly excluded	Riemann Hypothesis proof/test, universal forecast dominance, country policy ranking and residual-problem elimination.	Must not appear as a chapter-level claim.

10.2.8. Research Questions Reframed for the Book Chapter

In the source article, the research questions are formulated for a stand-alone manuscript. In the monograph, they must be reframed so that the section does not duplicate the article's introduction. The research questions become object-definition gates. They ask whether the chapter has a coherent target, whether the target is supported by layered evidence, whether the forecast objects are separable from diagnostic objects, whether the zeta correction is a bounded signal rather than a theorem, and whether the validation hierarchy is strong enough to justify placement as the monograph's spectral-forecasting chapter.

Table 10.2.8. Research questions reframed as research-object gates.

Gate	Question	Object-level answer	Monograph function
RQ-Object 1	What is the object being measured?	Global aggregate inflation as a layered macro-financial pressure and forecast system.	Prevents the chapter from being read as RH proof.
RQ-Object 2	Which forecast objects define the comparison?	FPAS, FPAS+zeta and ARIMA.	Separates structural, hybrid and persistence benchmarks.
RQ-Object 3	Which diagnostic objects define the pressure system?	CP_t, tau_t, zeta_t, d_t, correction gate, shock anchors and regime states.	Connects forecast improvement to interpretable stress diagnostics.
RQ-Object 4	Which sample layer supports which claim?	N=55, N=45, N=20, N=100 and N=240 layers.	Prevents compact-window overclaiming.
RQ-Object 5	What is the final admissible claim?	Bounded global forecast-diagnostic improvement under layered validation.	Excludes universal, causal and theorem-level claims.

10.2.9. Cross-Chapter Integration with the Seven-Problem Monograph

The research object of Chapter 10 must also connect to the monograph's seven-problem architecture. Its role is spectral and forecasting-oriented. It is adjacent to Chapter 9 because both the Riemann-zeta and BSD-inspired chapters use spectral/L-function logic, but they operationalize it differently: Chapter 9 builds local-to-global structural rank through an economic L-function analogue, while Chapter 10 builds a zeta-cycle correction for global inflation forecasting. It also connects to Chapter 7 because both Navier-Stokes and FPAS+zeta treat macro-financial stress, but Chapter 7 emphasizes liquidity-flow stress balance whereas Chapter 10 emphasizes forecast validation and spectral correction.

This cross-chapter integration matters because it prevents the Riemann-zeta chapter from appearing as an isolated forecasting exercise. It is one component of a broader economic measurement grammar: curvature, flow, liquidity, mass gap, local-to-global rank, spectral forecasting and computational complexity. The research object of 10.2 therefore becomes the chapter's contribution to the whole monograph.

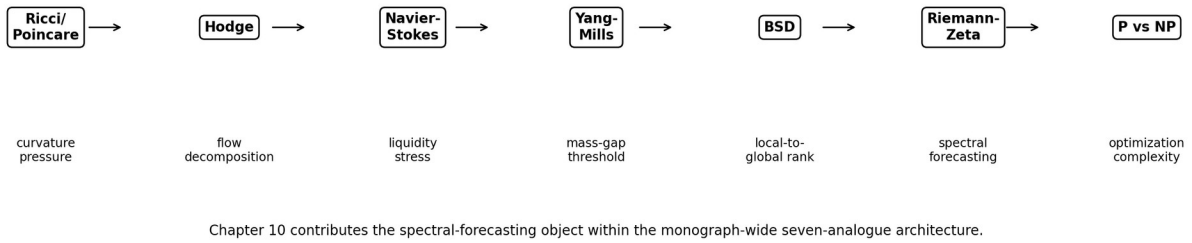


Figure 10.2.8. Seven-problem bridge showing the Chapter 10 spectral-forecasting role.

Table 10.2.9. Cross-seven-problem integration of the Chapter 10 research object.

Book chapter	Main object	Relation to Chapter 10
Chapter 5 Perelman/Ricci/Poincare	Inequality pressure, curvature and smoothing capacity	Shares pressure-system logic but not forecast target.
Chapter 6 Hodge	Macro-flow decomposition into gradient/curl/harmonic structure	Provides flow-topology contrast to spectral forecasting.
Chapter 7 Navier-Stokes	Liquidity-flow stress, pressure, friction and closure	Closest macro-financial stress neighbour; different mathematical grammar.
Chapter 8 Yang-Mills	Gauge curvature, action and finite-network mass-gap threshold	Shares shock-threshold logic, but uses network spectrum rather than zeta-cycle forecast.
Chapter 9 BSD	Local-to-global structural rank and economic L-function	Closest spectral/L-function neighbour; rank object differs from inflation forecast object.
Chapter 10 Riemann-Zeta	Global inflation forecast validation through FPAS+zeta	Spectral-signal forecasting chapter.
Chapter 11 P vs NP	Sparse portfolio optimization under computational complexity	Contrasts forecast validation with combinatorial decision complexity.

10.2.10. Reviewer-Risk Controls Embedded in the Research Object

The design of the research object directly addresses likely reviewer concerns. The first risk is mathematical overclaiming: using Riemann-zeta language can be misread as an attempt to make a theorem-level claim. The object definition prevents this by identifying the zeta function as a critical-line signal generator transformed into a normalized economic cycle. The second risk is compact-sample overfitting: a strong crisis-era result could appear fragile if all evidence were based on N = 20. The layered architecture prevents this by assigning the main claim to N = 55, robustness to N = 45, dynamic validation to N = 100 and spectral diagnostics to N = 240. The third risk is causal overextension: forecast improvement could be overstated as a causal law. The claim boundary prevents this by classifying the model as forecast-diagnostic.

The fourth risk is object ambiguity. If pi_t, CP_t, tau_t, zeta_t, d_t and pi_hat^Z_t are not separated, the chapter can become hard to evaluate. The object register solves that problem. The fifth risk is replication opacity. The Zenodo package and formula-audit logic address this by making the reported layers traceable. These controls allow the chapter to make a strong claim without weakening the monograph's academic caution.

Table 10.2.10. Reviewer-risk controls in the research-object definition.

Risk	Potential criticism	Control used in Section 10.2
Mathematical overclaiming	Reader treats zeta layer as RH evidence.	Define zeta as economic signal analogue; exclude proof/test wording.
Compact-window overfitting	N=20 crisis-era result is overused.	Assign headline claim to N=55 and robustness to N=45, N=100 and N=240 layers.
Causal overextension	Forecast improvement is read as causal theorem.	Use forecast-diagnostic wording; keep policy scenarios model-implied.
Object ambiguity	Target, forecast, pressure and spectral objects are confused.	Provide object register and symbol table.
Residual-risk suppression	Model is claimed to eliminate all statistical problems.	Report residual diagnostics and use HAC/rolling validation/caution.
Replication opacity	Model is not reproducible or formula trace is unclear.	Use Zenodo DOI, formula audit and layer-specific reported outputs.

10.2.11. Section Synthesis

Section 10.2 establishes that the research object of Chapter 10 is a global aggregate inflation forecast-diagnostic system. The object is layered by sample frequency, separated by evidence status and bounded by claim discipline. The target is actual global inflation pi_t. The main forecast objects are FPAS, FPAS+zeta and ARIMA. The diagnostic objects are CP_t, tau_t, $zeta_t$, d_t, the correction gate, shock anchors and regime/spectral states. The empirical design is distributed across N = 55, N = 45, N = 20, N = 100 and N = 240 layers so that the strongest claims do not rest on a compact annual crisis window alone. The chapter can therefore proceed to data architecture and methodology with a clear object definition. Section 10.3 should specify the annual, quarterly and monthly validation layers in greater technical detail. Section 10.4 should specify the FPAS baseline, zeta-cycle construction, tau argument and correction gate. Section 10.5 should define the forecast-evaluation protocol. Section 10.6 can then report the comparative results, and Sections 10.7-10.9 can interpret crisis resonance, spectral diagnostics, robustness and claim boundaries.

The admissible conclusion is strong but bounded: the FPAS+zeta framework treats global inflation as a layered macro-financial pressure system and reports meaningful forecast-improvement evidence under the specified validation architecture. It does not claim a solution, proof, test or verification of the Riemann Hypothesis; it does not claim unrestricted causality; it does not replace country-level monetary-policy modelling; and it does not claim universal dominance across all possible horizons and economies.

10.3. Data Architecture: Annual, Quarterly and Monthly Validation Layers

10.3.1. Purpose of the Data Architecture

The purpose of the data architecture is to make the FPAS+ζ framework empirically readable before the forecasting methodology is introduced. A model that combines structural inflation forecasting, a zeta-cycle signal, regime diagnostics and spectral evidence cannot be defended through one short annual table alone. The chapter therefore uses a layered evidence design. The annual layers carry the principal forecast-accuracy comparison; the quarterly layer carries dynamic and regime validation; the monthly layer carries frequency-domain and spectral diagnostics. The architecture is deliberately conservative: advanced tools are assigned to the frequency layer that can support them, and the compact crisis-era window is kept as an interpretation layer rather than as the only foundation of the model.

This structure is also a reviewer-safety device. It prevents the reader from interpreting HMM, Markov-switching, Fourier, wavelet and spectral-entropy results as if they were all estimated on a small N = 20 annual sample. The model's strongest annual claim is attached to the N = 55 layer for 1970-2024; robustness is checked over N = 45 for 1980-2024; crisis-era comparison is displayed over N = 20 for 2005-2024; quarterly dynamics use N = 100 for 2000Q1-2024Q4; and monthly spectral diagnostics use N = 240 for 2005M1-2024M12.

Layer	Calendar coverage	N	Primary object	Main permitted claim	Main non-permitted claim
Annual main validation	1970-2024	55	Global annual inflation forecast comparison	Principal annual forecast-accuracy claim	Universal model dominance
Annual robustness	1980-2024	45	Stability of annual forecast hierarchy	Robustness of annual result under a shorter but still long sample	Independent causal proof
Crisis-era annual	2005-2024	20	Compact crisis interpretation and display	Crisis-period illustration and model-reading layer	Standalone proof of model superiority
Quarterly dynamic validation	2000Q1-2024Q4	100	Regime, dynamic and transmission screens	Dynamic diagnostic support	Substitution for annual forecast hierarchy
Monthly spectral diagnostics	2005M1-2024M12	240	Fourier, wavelet, spectral entropy and zeta-stress coherence	Frequency-domain support for cyclical interpretation	Proof of the Riemann Hypothesis or causal inflation mechanism

Table 10.3.1. Layered validation hierarchy and claim permission.

Figure 10.3.1. Layered validation sample hierarchy

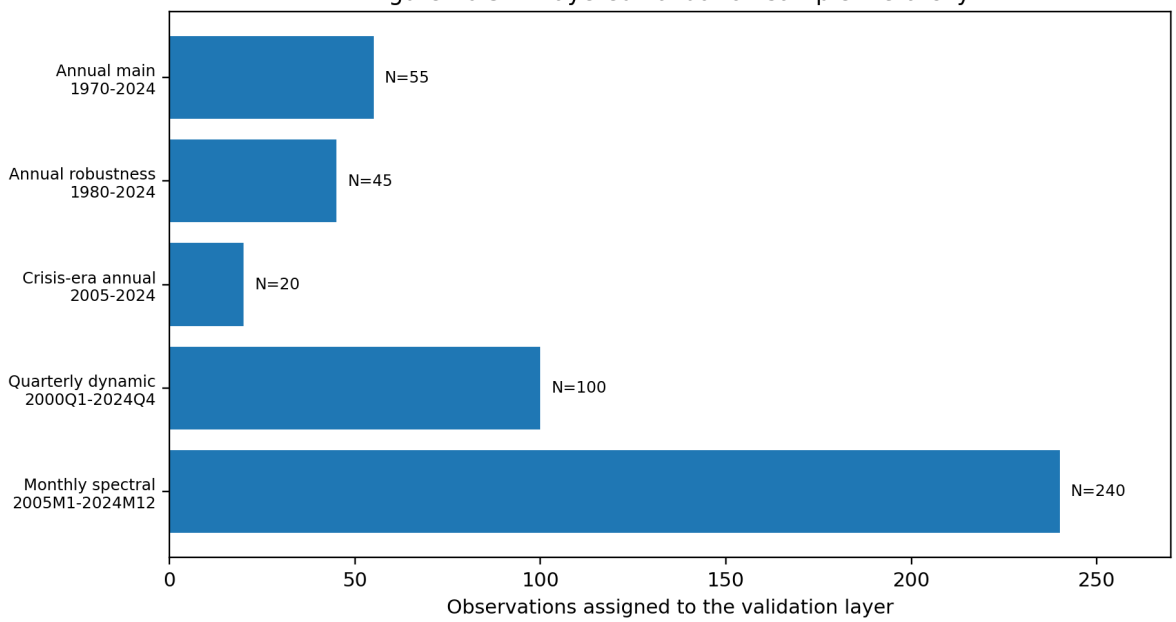


Figure 10.3.1. Layered validation sample hierarchy.

10.3.2. Layer Separation as Sample-Discipline

The layered design should be read as sample-discipline, not as decoration. The main annual sample is long enough to compare FPAS+ζ, FPAS and ARIMA across multiple inflation regimes: post-1970s disinflation, Great Moderation dynamics, the global financial crisis, the low-inflation period, the pandemic shock and the 2022 energy-food-monetary tightening episode. The robustness annual sample begins in 1980 to test whether the headline forecast hierarchy survives a later starting point. The crisis-era N = 20 window begins in 2005 because it highlights the stress years that motivate the zeta-cycle interpretation, but it is not allowed to carry the entire inferential burden.

Quarterly and monthly layers solve a different problem. Quarterly data allow richer dynamics, regime-switching screens and shock-transmission tests than annual data. Monthly data allow spectral diagnostics, wavelet coherence and frequency-domain checks. These methods require more observations and are therefore assigned to N = 100 and N = 240 layers. The architecture prevents a common error in complex forecast papers: using many sophisticated diagnostics while leaving unclear which sample actually supports each diagnostic.

Figure 10.3.3. Frequency-specific validation windows

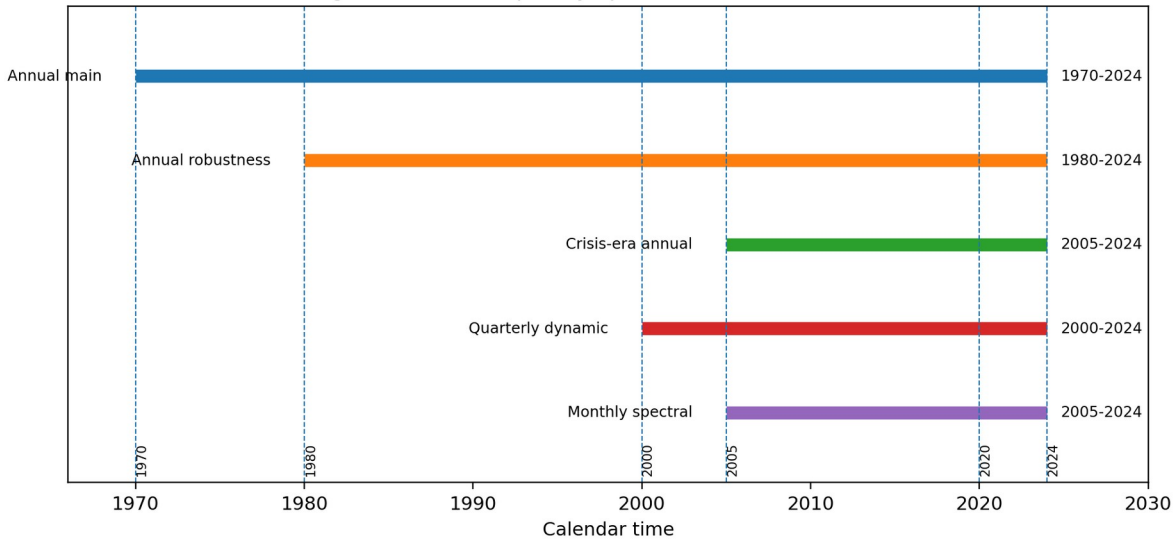


Figure 10.3.3. Frequency-specific validation windows.

10.3.3. Target Variable, Forecast Objects and Diagnostic Objects

The principal target variable is actual global inflation, denoted π_t. The framework contains three forecast objects: the structural FPAS baseline forecast, denoted πhat^F_t; the hybrid FPAS+ζ forecast, denoted πhat^Z_t; and the persistence benchmark ARIMA forecast. The diagnostic objects are not alternative target variables. They are transformation and interpretation variables used to build and audit the hybrid model: composite pressure CP_t, nonlinear macro-financial argument τ_t, critical-line zeta input s_t = 1/2 + iτ_t, normalized zeta-cycle ζ_t, zeta deviation from neutrality d_t = ζ_t - ζbar, zeta correction c^ζ_t, alpha reaction coefficient α, scale factor λ_ζ, shock-anchor indicator S_t and regime-state indicators.

Symbol / object	Definition	Layer location	Analytical role	Boundary rule
π_t	Actual global inflation	Annual, quarterly and monthly as available	Target variable	Global aggregate, not country-specific policy ranking
πhat^F_t	Structural FPAS baseline forecast	Mainly annual; dynamic extension in quarterly layer	Baseline forecast to be improved	Reconstructed structural forecast, not a complete central-bank model
πhat^Z_t	Hybrid FPAS+ζ forecast	Annual forecast comparison; stress-tested across layers	Tests value-added of zeta correction	Bounded forecast-diagnostic claim only
ARIMA	Persistence-style statistical benchmark	Annual forecast comparison	Benchmark against pure inertia	Comparator, not the only benchmark family

CP_t	Composite global inflation-pressure index	All layers	Aggregates normalized stress coordinates	Constructed index requiring formula disclosure
τ_t	Nonlinear macro-financial argument	All layers	Maps pressure into zeta input	Author-calculated transformation, not observed macro variable
ζ(1/2+iτ_t)	Critical-line zeta signal	All layers	Computational cyclical signal source	Not a Riemann Hypothesis test
ζ_t	Normalized real-valued zeta-cycle	All layers	Forecast-correction candidate	Economic signal analogue
d_t	Deviation from neutral zeta level	All layers	Determines correction direction	Not a causal mechanism
α, λ_ζ	Reaction coefficient and scale factor	Annual calibration; cross-layer stress tests	Controls correction magnitude	Calibrated and bounded, not free fit parameter
Regime states	HMM/Markov-switching states	Quarterly/monthly	Regime support for cyclical interpretation	Diagnostic evidence, not causal proof

Table 10.3.2. Object and symbol register for the layered FPAS+ζ architecture.

Figure 10.3.2. Data architecture from public anchors to validation evidence

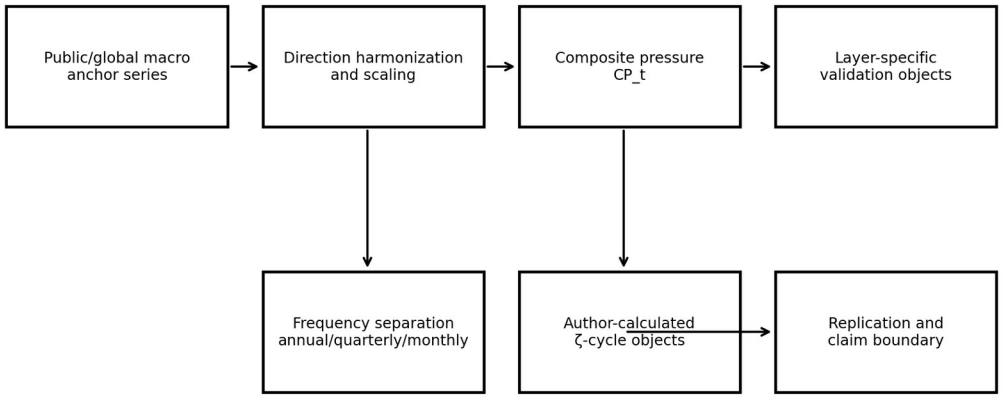


Figure 10.3.2. Data architecture from public anchors to validation evidence.

10.3.4. Public-Anchor Layer versus Author-Calculated Layer

The data architecture separates public or externally traceable macro-financial anchors from author-calculated diagnostic objects. This separation is essential because the manuscript combines recognizable macroeconomic variables with constructed mathematical-economic objects. Inflation, policy, liquidity, financial stress, supply stress, labour pressure and global shock indicators are treated as input families. Composite pressure, τ_t, ζ_t, d_t, F_zeta, W_zeta, zeta-deformation rank, spectral entropy and regime states are author-calculated objects. The empirical credibility of the chapter depends on a transparent ledger that records where each series enters, how it is normalized, how direction is harmonized and which sample layer supports the result.

Data layer	Examples	Transformation requirement	Output object	Evidence status
Observed/global anchor layer	Actual global inflation, policy-tightness indicators, liquidity-gap proxies, financial-stress proxies, supply-stress indicators, labour-pressure	Frequency alignment, missing-value rule, unit consistency	Input matrix X_t	Public-anchor or traceable input evidence

	proxies			
Normalized pressure layer	Inflation pressure, growth stress, unemployment pressure, policy tightness, liquidity gap, financial stress, supply stress	Stress orientation and common scale	X*_t and CP_t	Author-harmonized measurement evidence
Spectral-signal layer	τ_t and ζ(1/2+iτ_t)	Bounded nonlinear argument and critical-line computation	ζ_t	Author-calculated signal evidence
Forecast layer	πhat^F_t, c^ζ_t, πhat^Z_t, ARIMA	Baseline reconstruction, correction gate and benchmark estimation	Forecast errors e_t	Forecast-comparison evidence
Validation layer	RMSE, MAE, sMAPE, rolling validation, MZ, DM/CW, residual tests	No-look-ahead protocol and formal test rules	Evidence hierarchy	Validation and claim-boundary evidence
Replication layer	Structured workbook, formula-audit files, reported tables, supporting documentation	Version control, formula traceability and file manifest	External audit trail	Replication package evidence

Table 10.3.3. Public-anchor and author-calculated object separation.

10.3.5. Annual Validation Layers

The annual architecture is the core forecasting architecture. The N = 55 layer covers 1970-2024 and carries the principal forecast-comparison claim. It is long enough to include multiple global inflation regimes and to reduce the risk that the result is simply a pandemic-era or 2022-energy-shock fit. The N = 45 layer covers 1980-2024 and tests whether the annual result survives a later starting point. The N = 20 layer covers 2005-2024 and is retained as a compact crisis-era display because it contains the 2008 global financial crisis, the 2020 pandemic shock and the 2022 energy-food-monetary tightening shock. The N = 20 layer is analytically useful but evidentially bounded.

Figure 10.3.4. Reported RMSE context by annual validation layer

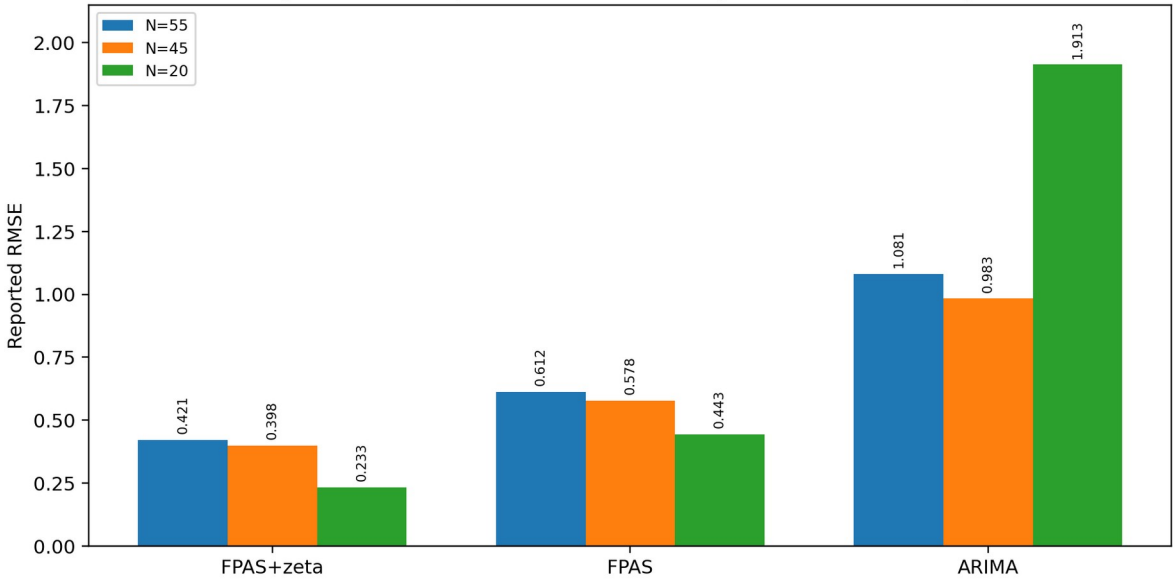


Figure 10.3.4. Reported RMSE context by annual validation layer.

The reported annual hierarchy gives Chapter 10 its strongest empirical foundation: FPAS+ζ improves RMSE relative to FPAS and ARIMA in the main annual, robustness annual and crisis-era annual comparisons. However, the data architecture prevents this result from being overstated. The RMSE hierarchy is a forecast-validation result inside specified samples; it is not a proof of a mathematical theorem, not a universal global-inflation law and not a guarantee of dominance in all countries, horizons or future regimes.

10.3.6. Quarterly and Monthly Evidence Layers

The quarterly N = 100 layer is assigned to dynamic validation. It is the proper location for HMM and Markov-switching screens, VAR/SVAR or local-projection diagnostics, early-warning tests and regime-sensitive transmission checks. The monthly N = 240 layer is assigned to spectral diagnostics. It is the proper location for Fourier decomposition, wavelet coherence, spectral entropy, Hardy-Z diagnostics, critical-zero resonance screens and zeta-stress lead diagnostics. These two layers do not replace the annual forecast hierarchy. They add diagnostic support by testing whether the zeta-cycle behaves like a stress-sensitive nonlinear signal in higher-frequency evidence.

Frequency	N	Main methods	Objects audited	Interpretation
Annual main	55	FPAS/FPAS+ζ/ARIMA comparison; RMSE, MAE, sMAPE; MZ and forecast-encompassing interfaces	π_t, πhat^F_t, πhat^Z_t, ARIMA	Principal annual forecast accuracy
Annual robustness	45	Stability of annual hierarchy and alpha sensitivity	Forecast errors and correction signs	Robustness of annual result
Annual crisis-era	20	Crisis display, zeta-deformation ranking, correction-direction audit	2008/2020/2022 stress years	Interpretive display only
Quarterly	100	HMM, Markov-switching, VAR/SVAR, local projections and regime screens	Regime states and transmission diagnostics	Dynamic support
Monthly	240	Fourier, wavelet, spectral entropy, critical-line signal screens	ζ_t, spectral coherence and frequency structure	Spectral support

Table 10.3.4. Frequency-specific methods and interpretation rules.

10.3.7. Replication Package and Traceability Discipline

The data architecture is not complete unless it includes a replication route. The Chapter 10 source document states that the replication materials are deposited on Zenodo and provide the structured workbook, manuscript-reported tables, formula-audit files and supporting documentation required to trace N = 55, N = 45, N = 20, N = 100 and N = 240 outputs. In the book chapter, this means the reader should be able to trace the progression from public anchors to normalized pressure variables, from pressure variables to τ_t, from τ_t to zeta-cycle objects, from those objects to forecasts and from forecasts to error metrics and robustness diagnostics.

Replication object	Required content	Purpose in Chapter 10	Reviewer value
Source ledger	Input series, frequency, coverage, transformation date and source family	Shows where the raw empirical material enters	Prevents hidden data substitution
Layer registry	N = 55, N = 45, N = 20, N = 100 and N = 240 definitions	Protects sample hierarchy	Prevents frequency mixing
Formula audit	CP_t, τ_t, ζ_t, d_t, correction gate, FPAS and FPAS+ζ equations	Makes constructed objects reproducible	Prevents black-box criticism
Forecast table	π_t, πhat^F_t, πhat^Z_t, ARIMA and error series	Supports forecast evaluation	Allows re-computation of RMSE/MAE/sMAPE
Validation outputs	Rolling, MZ, encompassing, DM/CW, residual and regime diagnostics	Defines claim boundary	Prevents single-metric overclaiming
Figure catalogue	Layer map, zeta-cycle path, RMSE comparison, spectral plots and regime charts	Links visual results to source data	Improves auditability
Version manifest	File hashes, script versions, software environment and record DOI	Preserves external audit trail	Supports replication credibility

Table 10.3.5. Replication and traceability checklist for the layered validation architecture.

10.3.8. Cross-Seven-Problem Data Alignment

Within the monograph, Chapter 10 is the spectral-forecasting counterpart to the other six economic analogues. Its data discipline is distinctive because it uses multiple temporal frequencies rather than a regional network, a country panel or a combinatorial portfolio universe. The book-level value of Chapter 10 is therefore methodological as well as empirical: it

supplies the clearest example of sample hierarchy and forecast-validation gating across annual, quarterly and monthly layers.

Book chapter	Empirical universe	Main N / sample	Data architecture type	Shared discipline with Chapter 10
Chapter 5 Perelman/Ricci/Poincare	10 macro-regions, 2010-2024, 16 variables	N = 150	Panel inequality-pressure coordinates	Normalization, diagnostic indices, claim boundary
Chapter 6 Hodge	World anchor + 10 regional nodes	10-node benchmark	Network flow decomposition	Public anchors to author-calculated topological objects
Chapter 7 Navier-Stokes	100 countries, 2010-2024	N = 1,500	Global macro-financial stress panel	Stress normalization, rolling validation, benchmark comparison
Chapter 8 Yang-Mills	10 nodes, 27 edges + validation pathway	Benchmark + N = 1,500 path	Gauge network and spectral threshold	Layer A/Layer B evidence separation
Chapter 9 BSD	World anchor + 10 regional/corridor nodes	N = 150 closure layer	Local-to-global rank calibration	Local/global evidence hierarchy
Chapter 10 Riemann-Zeta	Annual, quarterly and monthly global inflation layers	N = 55, 45, 20, 100, 240	Layered forecast-validation architecture	Strongest sample-discipline example
Chapter 11 P vs NP	94 industries and exact reduced benchmark	C(94,10), C(20,6)	Computational search and exact enumeration	Claim boundary around optimality and evidence class

Table 10.3.6. Cross-seven-problem data-architecture alignment.

10.3.9. Data-Architecture Closure Statement

Section 10.3 closes with a clear data statement: the FPAS+ζ chapter is not a single-sample curve-fitting exercise. It is a frequency-layered architecture in which each empirical layer has a defined function. The annual layers supply the forecast comparison, the quarterly layer supplies dynamic and regime validation and the monthly layer supplies spectral diagnostics. This separation is the foundation for Section 10.4, because the methodology must preserve the same layer discipline when it constructs the FPAS baseline, zeta-cycle signal, τ argument and correction gate.

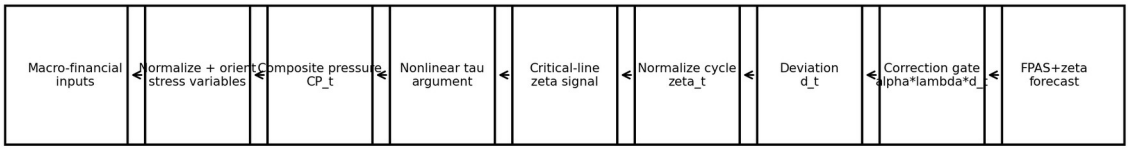
10.4. Methodology: FPAS Baseline, ζ-Cycle, τ Argument and Correction Gate

10.4.1. Methodological Objective

The methodological objective is to transform the data architecture into an auditable forecast-diagnostic pipeline. The method begins with global macro-financial pressure coordinates, constructs a composite pressure index, maps that pressure into a nonlinear τ argument, evaluates a critical-line zeta signal, normalizes the result into a real-valued zeta-cycle, computes the deviation from a neutral zeta level and admits the deviation into the inflation forecast through a calibrated correction gate. The FPAS baseline remains the structural forecast anchor; the zeta layer is an incremental, signed and bounded correction.

This section does not treat the Riemann-zeta function as a theorem to be tested. The method uses zeta as a computational signal generator. The empirical question is whether the signal, once normalized and disciplined by alpha calibration, improves the forecast hierarchy relative to FPAS and ARIMA across the validation layers specified in Section 10.3.

Figure 10.4.1. Methodological transformation chain



FPAS baseline remains the structural anchor; the zeta layer is an alpha-calibrated, signed correction gate, not a theorem-level object.

Figure 10.4.1. Methodological transformation chain.

10.4.2. Normalization and Composite Pressure Index

The first methodological step is stress-direction harmonization. Raw macro-financial inputs have heterogeneous units and directions. Some variables increase inflation pressure when they rise, while others must be reverse-oriented. Let $X_{m,t}$ denote raw input family m at time t. The normalized pressure coordinate is written as:

(10.1) $X^*_{m,t} = 100 * (X_{m,t} - \min(X_m)) / (\max(X_m) - \min(X_m))$, for pressure-positive variables.

(10.2) $X^*_{m,t} = 100 * (\max(X_m) - X_{m,t}) / (\max(X_m) - \min(X_m))$, for reverse-oriented pressure variables.

After normalization, the composite pressure index is constructed as a weighted aggregation of stress coordinates:

(10.3) $CP_t = \Sigma_{m=1}^{M} w_m X^*_{m,t}$, where $w_m \geq 0$ and $\Sigma_m w_m = 1$.

The pressure families include inflation pressure, growth stress, unemployment pressure, policy tightness, liquidity gap, financial stress, supply stress and zeta-resonance diagnostics. CP_t is not an observed official series. It is a constructed macro-financial pressure coordinate that gives the zeta transformation a disciplined empirical input.

Pressure family	Economic meaning	Expected inflation-pressure direction	Role in CP_t
Inflation pressure	Persistence and recent inflation deviation	Higher value increases pressure	Core inflation target coordinate
Growth stress	Output weakness or overheating imbalance	Stress-oriented after transformation	Captures real-economy pressure
Unemployment / labour pressure	Slack, labour-market mismatch or wage-pressure proxy	Direction depends on specification	Connects inflation to labour channel
Policy tightness	Interest-rate or policy-reaction pressure	Higher tightness indicates restrictive response or stress	Policy channel
Liquidity gap	Liquidity shortage or macro-financial liquidity weakness	Higher gap increases stress	Liquidity channel
Financial stress	Spreads, market stress or risk-premium pressure	Higher stress increases pressure	Financial channel
Supply stress	Commodity, energy, food or logistics pressure	Higher stress increases pressure	Supply-shock channel
Zeta resonance	Position of the constructed cyclical signal	Converted into signed deviation	Nonlinear correction channel

Table 10.4.1. Composite pressure families and directional rules.

10.4.3. FPAS Baseline Forecast

The FPAS baseline is the structural anchor of the model. It represents the forecast that would be produced without the zeta correction. In simplified notation, the baseline can be written as:

(10.4) $\hat{\pi}^F_t = \beta_0 + \beta_1 \pi_{t-1} + \beta_2 CP_t + \beta_3 Policy_t + \beta_4 Liquidity_t + \beta_5 Financial_t + \beta_6 Supply_t + \beta_7 Labour_t + \beta_8 S_t$.

The exact implementation may use a compact structural reconstruction rather than a full central-bank FPAS model. The important methodological rule is that the baseline forecast must be generated before the zeta correction is added. This prevents the hybrid model from hiding all forecasting information inside the zeta layer. FPAS is the structured macro-financial baseline; ζ is an incremental signal layer.

Baseline component	Notation	Reason for inclusion	Interpretation boundary
Inflation inertia	π_{t-1}	Captures persistence and delayed adjustment	Persistence channel, not full inflation theory
Composite pressure	CP_t	Aggregates normalized macro-financial stress	Constructed diagnostic index
Policy response	$Policy_t$	Captures tightening or easing pressure	Policy-style coordinate, not central-bank reaction proof
Liquidity channel	$Liquidity_t$	Captures liquidity weakness or gap	Macro-financial stress channel
Financial stress	$Financial_t$	Captures spreads, volatility or risk pressure	Diagnostic stress proxy
Supply stress	$Supply_t$	Captures energy, food, logistics or commodity shocks	Shock-pressure coordinate
Labour pressure	$Labour_t$	Captures unemployment or labour-market stress	Labour-pressure proxy
Shock anchor	S_t	Flags crisis or global stress episodes	Interpretive control, not causal treatment

Table 10.4.2. FPAS baseline components and interpretation boundaries.

10.4.4. Nonlinear τ Argument

The τ argument is the bridge between macro-financial pressure and the critical-line zeta signal. It must be constructed so that extreme pressure can change the zeta input without allowing arbitrary explosion. A bounded nonlinear mapping is therefore preferred:

(10.5) $\tau_t = \tau_{min} + (\tau_{max} - \tau_{min}) * \Lambda(\gamma_0 + \gamma_1 CP_t + \gamma_2 |\Delta\pi_t| + \gamma_3 S_t + \gamma_4 Financial_t + \gamma_5 Supply_t)$,

where $\Lambda(u) = 1 / (1 + \exp(-u))$ is a logistic bounding function. This mapping has three advantages. First, it converts heterogeneous macro-financial pressure into a scalar zeta argument. Second, it allows nonlinear stress response. Third, it prevents τ_t from becoming an unrestricted fit device. The τ mapping is part of the model's claim discipline: it makes the zeta input economically interpretable and computationally bounded.

Figure 10.4.3. Conceptual CP_t -> tau_t -> zeta-cycle mapping

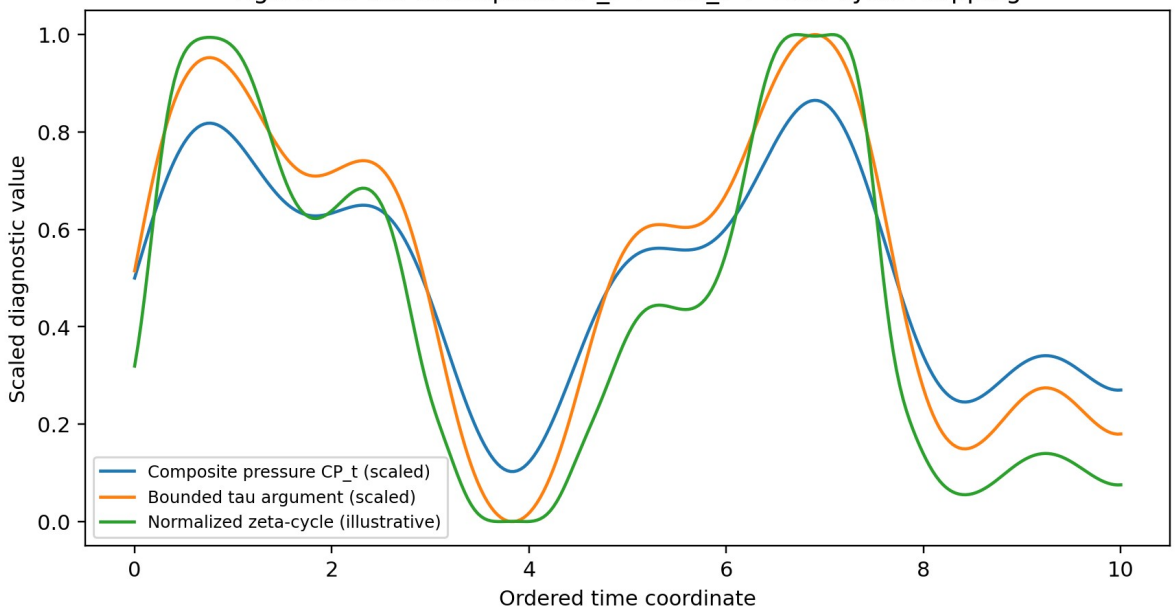


Figure 10.4.3. Conceptual CP_t -> τ_t -> zeta-cycle mapping.

10.4.5. Critical-Line Zeta Evaluation and Real-Valued ζ-Cycle

The zeta signal is evaluated on the critical line at:

(10.6) $s_t = 1/2 + i\tau_t$.

The complex output $\zeta(s_t)$ cannot be inserted directly into an inflation forecast. It must be converted into a real-valued cycle. The methodology may use real-part, modulus, Hardy-Z or signed-composite transformations, but the chapter's claim boundary requires the same principle in all cases: the complex zeta output is transformed into a normalized economic signal, not interpreted as a mathematical theorem.

A generic normalization rule can be written as:

(10.7) $\zeta_t = 100 * (Z_t - \min(Z)) / (\max(Z) - \min(Z))$,

where Z_t is the selected real zeta channel or signed zeta composite. The neutral deviation is:

(10.8) $d_t = \zeta_t - \bar{\zeta}$.

The sign of d_t determines whether the zeta layer supports an upward, downward or mild correction to the FPAS baseline. Positive deviations represent above-neutral zeta resonance; negative deviations represent below-neutral or lower-pressure resonance. The correction must remain conditional; it is not a permanent premium added to FPAS.

Zeta channel	Construction	Purpose	Claim boundary
Real-part channel	$\mathrm{Re}(\zeta(1/2+i\tau_t))$ after normalization	Signed cyclical component	Economic signal only
Imaginary channel	$\mathrm{Im}(\zeta(1/2+i\tau_t))$ after normalization	Phase-sensitive diagnostic	Not a theorem test
Modulus channel	$\lvert\zeta(1/2+i\tau_t)\rvert$	Intensity of zeta response	No direct causal interpretation
Hardy-Z channel	Hardy-style real transformation	Critical-line real signal	Computational diagnostic
Zeta-cycle composite	Weighted or selected normalized channel	Forecast-correction input	Requires transparent formula and robustness gate
Neutral deviation	$d_t = \zeta_t - \bar{\zeta}$	Determines correction sign	Only admitted through correction gate

Table 10.4.3. Zeta-channel construction and admissible interpretation.

10.4.6. Alpha-Calibrated Correction Gate

The hybrid forecast is defined as:

(10.9) $\hat{\pi}^Z_t = \hat{\pi}^F_t + c^\zeta_t$.

The correction term is:

(10.10) $c^\zeta_t = \alpha \lambda_\zeta d_t$.

The correction gate is the key methodological safeguard. Without α and λ_ζ, the zeta layer could become an unrestricted residual-fitting device. With the correction gate, the zeta layer must earn its role through calibrated forecast improvement and cross-layer robustness. The coefficient α is calibrated by grid search or conservative validation, while λ_ζ scales the zeta deviation into inflation-forecast units. The sign of d_t controls the direction of the correction; α controls the reaction strength.

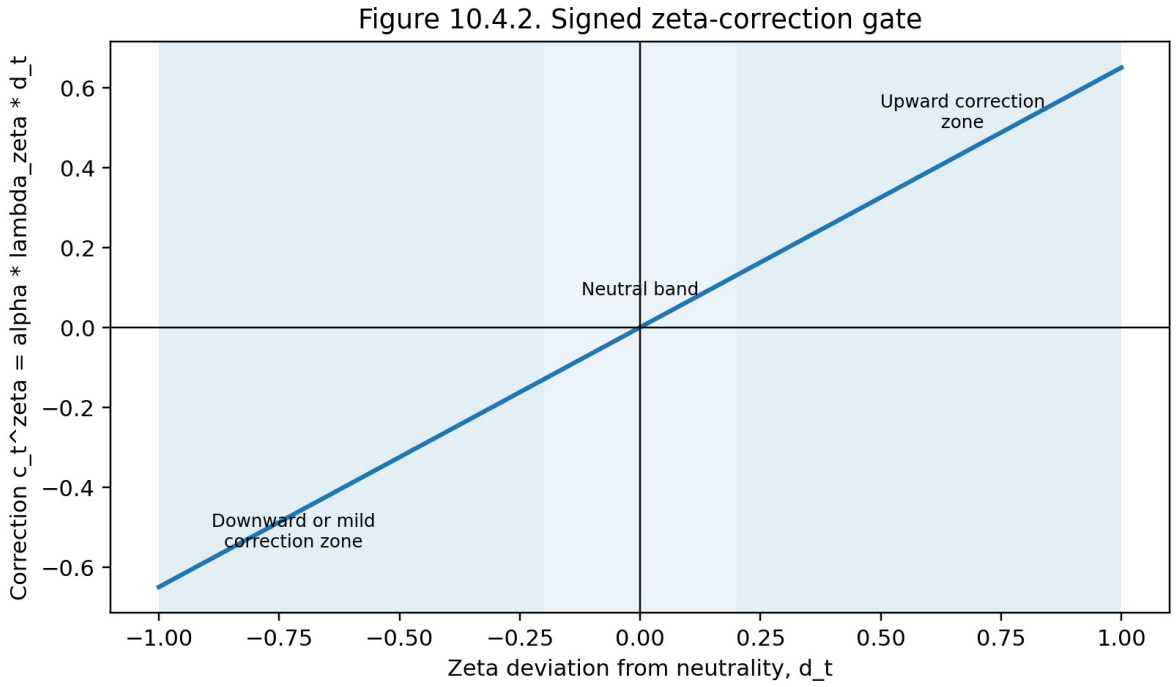


Figure 10.4.2. Signed zeta-correction gate.

Gate condition	Mathematical rule	Forecast effect	Interpretation
Positive zeta deviation	$d_t > +\kappa$	$c\hat{}\zeta_t > 0$	FPAS may be under-reacting to nonlinear global stress
Neutral zeta band	$\lvert d_t \rvert \le \kappa$	$c\hat{}\zeta_t \approx 0$	No strong zeta correction is admitted
Negative zeta deviation	$d_t < -\kappa$	$c\hat{}\zeta_t < 0$	FPAS may be overestimating pressure or stress resonance is weak
Excessive alpha	α outside conservative range	Correction rejected or downgraded	Prevents overfitting
Layer instability	Sign or gain unstable across layers	Claim downgraded	Prevents one-window dominance claim
Residual warning	Serial correlation or heteroskedasticity remains	HAC/rolling caution required	Prevents unrestricted forecast superiority

Table 10.4.4. Correction-gate decision rules.

10.4.7. Alpha Calibration and Overfitting Controls

Alpha calibration should be conducted through an explicit grid rather than by narrative selection. For each candidate α in a predeclared grid A, the hybrid forecast is computed and evaluated against the annual validation target. The loss-minimizing alpha is:

(10.11) $\alpha^* = \operatorname{argmin}_{\alpha \in A} \mathrm{RMSE}(\pi_t, \hat{\pi}^F_t + \alpha\lambda_\zeta d_t)$.

However, α* is not automatically the final policy or interpretation alpha. A conservative alpha may be chosen if it produces nearly equivalent performance with lower correction magnitude, better residual behaviour or stronger cross-layer stability. This distinction between RMSE-optimal alpha and conservative alpha is essential because the zeta layer is powerful enough to improve fit but must not be allowed to become an unbounded tuning mechanism.

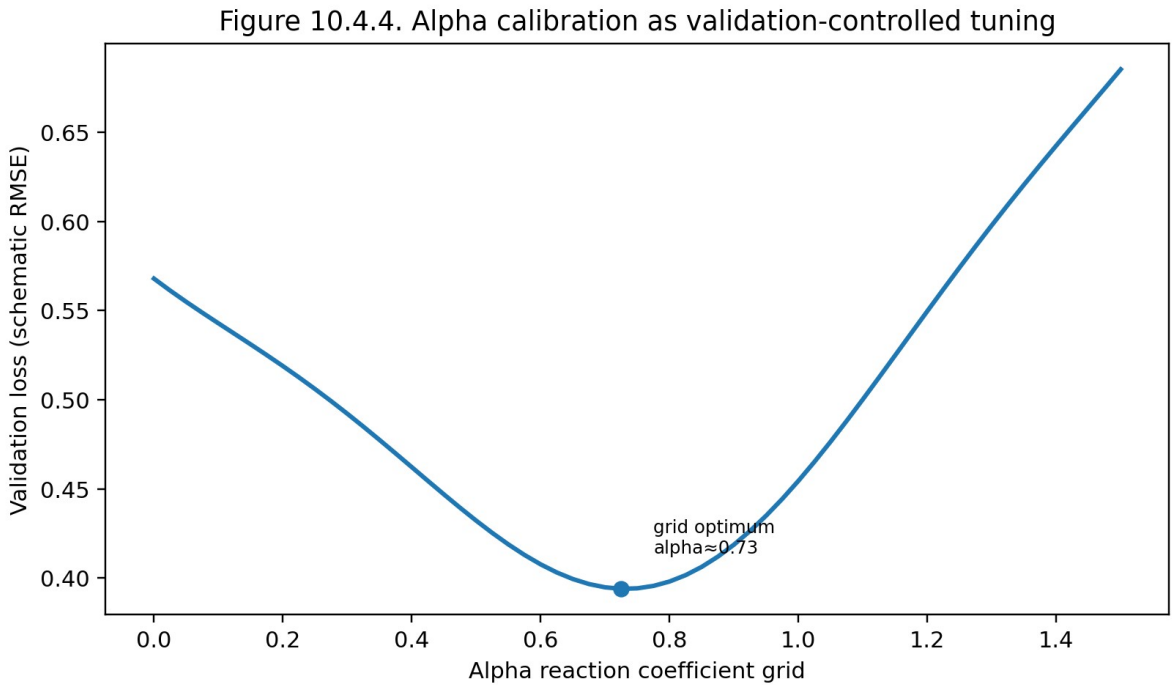


Figure 10.4.4. Alpha calibration as validation-controlled tuning.

Calibration step	Procedure	Failure risk	Safeguard
Grid declaration	Define candidate α values before final reporting	Ex-post parameter picking	Predeclared alpha grid
Annual fit	Compute RMSE, MAE and sMAPE for each α	Single-metric selection	Multiple error metrics
Correction sign audit	Check whether signs align with stress years	Mechanical uplift bias	Positive, neutral and negative gate zones
Layer stability	Compare N = 55, N = 45 and N = 20 behaviour	Crisis-window overfit	Long-sample priority
Rolling validation	Apply no-look-ahead forecast updating	Look-ahead bias	Chronological estimation
Residual control	Check serial correlation, heteroskedasticity and stationarity	False precision	HAC and bounded wording
Final claim gate	Classify result as strong, diagnostic or bounded	Universal dominance overclaim	Explicit claim hierarchy

Table 10.4.5. Alpha calibration and overfitting-control protocol.

10.4.8. Forecast Construction Algorithm

The full forecast-construction algorithm is the bridge between Section 10.4 and the formal evaluation protocol of Section 10.5. It can be summarized as a reproducible sequence:

Step 1. Load the layer-specific target series π_t and input macro-financial coordinates.

Step 2. Align frequency, dates and missing-value rules for the selected layer.

Step 3. Normalize stress coordinates and apply directional harmonization.

Step 4. Construct CP_t as a weighted composite pressure index.

Step 5. Generate the FPAS baseline forecast πhat^F_t using inflation inertia, pressure, policy, liquidity, financial, supply and labour coordinates.

Step 6. Convert CP_t and shock coordinates into bounded τ_t.

Step 7. Evaluate ζ(1/2+iτ_t) and extract the selected real-valued zeta channel.

Step 8. Normalize the selected zeta channel into ζ_t and compute d_t = ζ_t - ζbar.

Step 9. Apply the correction gate c^ζ_t = αλ_ζd_t.

Step 10. Compute πhat^Z_t = πhat^F_t + c^ζ_t.

Step 11. Estimate ARIMA as the persistence benchmark on the appropriate validation schedule.

Step 12. Pass the three forecast paths to Section 10.5 for RMSE, MAE, sMAPE, rolling, MZ, DM/CW and residual evaluation.

Step 13. Downgrade claims if cross-layer instability, residual risk or compact-sample dependence appears.

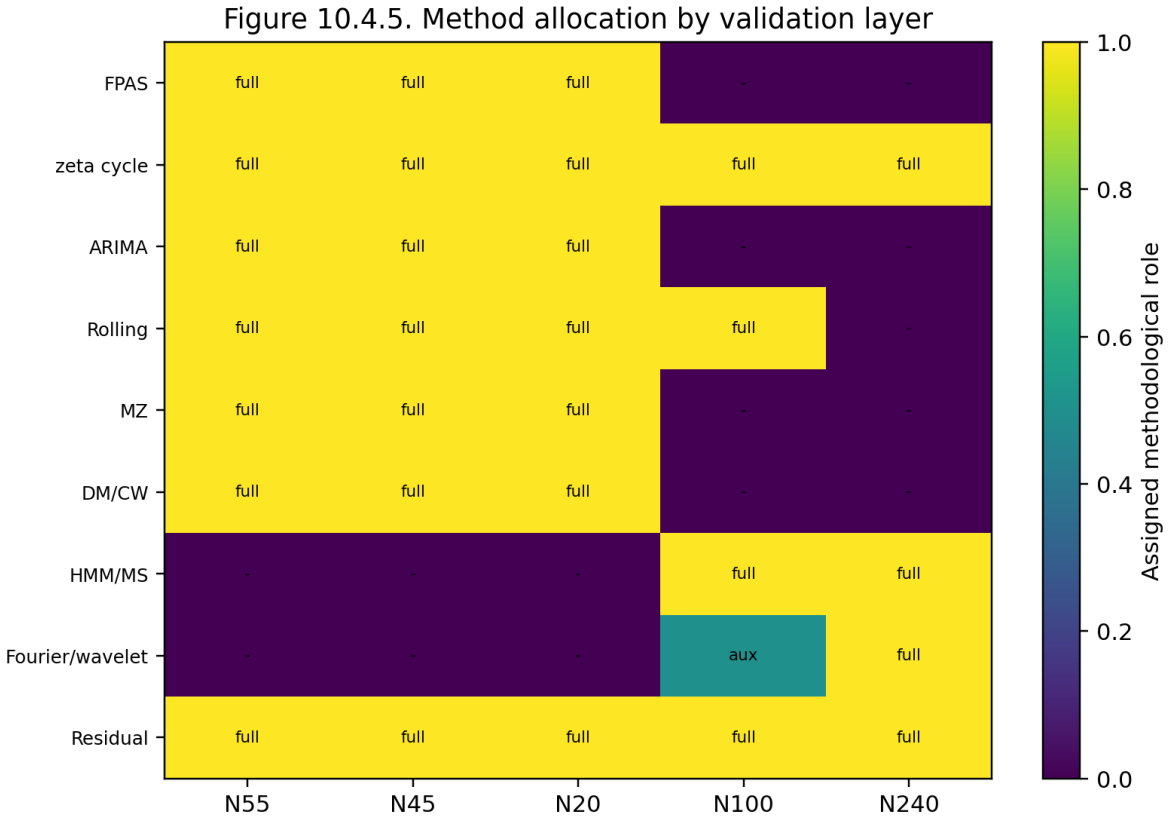


Figure 10.4.5. Method allocation by validation layer.

10.4.9. Methodology-to-Results Alignment

Every methodological object must have a corresponding result object. This alignment prevents the method from becoming an abstract mathematical exposition detached from the empirical chapter. The FPAS baseline produces a baseline forecast table. The zeta cycle produces a zeta-path and correction-sign audit. The correction gate produces hybrid forecasts. The alpha grid produces an alpha-sensitivity table. The layered data architecture produces RMSE/MAE/sMAPE comparisons by layer. Quarterly methods produce regime diagnostics. Monthly methods produce spectral diagnostics. Residual tests produce the final claim boundary.

Methodological object	Result object expected in Chapter 10	Section connection	Claim-gate function
Layered data architecture	N = 55, 45, 20, 100 and 240 sample tables	10.3 -> 10.6/10.8	Sample discipline
FPAS baseline	πhat^F_t path and forecast errors	10.4 -> 10.6	Baseline comparison
ARIMA benchmark	Persistence forecast errors	10.4 -> 10.6	Benchmark discipline
τ argument	τ_t path and shock-alignment table	10.4 -> 10.7	Economic interpretation of zeta input
Zeta-cycle ζ_t	Zeta-cycle path and deformation ranking	10.4 -> 10.7/10.8	Cyclical-signal evidence
Correction gate	Correction sign and magnitude audit	10.4 -> 10.6	Prevents mechanical uplift
Alpha grid	Alpha sensitivity and uncertainty table	10.4 -> 10.6/10.8	Overfitting control
Quarterly regime method	HMM/Markov-switching states	10.4 -> 10.8	Dynamic support
Monthly spectral method	Fourier, wavelet and spectral	10.4 -> 10.8	Spectral support

	entropy outputs		
Residual tests	Normality, serial-correlation, heteroskedasticity and stationarity diagnostics	10.5/10.8 -> 10.9	Final claim boundary

Table 10.4.6. Methodology-to-results alignment matrix.

10.4.10. Evidence Gate and Claim Boundary

The methodology closes with a strict evidence gate. The chapter may claim that FPAS+ζ is a bounded, mathematically explicit, empirically audited global inflation forecast-diagnostic architecture when the hybrid forecast improves error metrics across the annual layers and when quarterly and monthly diagnostics support the cyclical interpretation. It may not claim that the Riemann Hypothesis is proven, tested or verified. It may not claim a causal theorem, complete residual elimination or universal superiority across all economies and horizons. This boundary is not a weakness; it is the condition that makes a non-standard mathematical-economic forecasting architecture defensible.

Figure 10.4.6. Evidence gate protecting the methodology from overclaiming

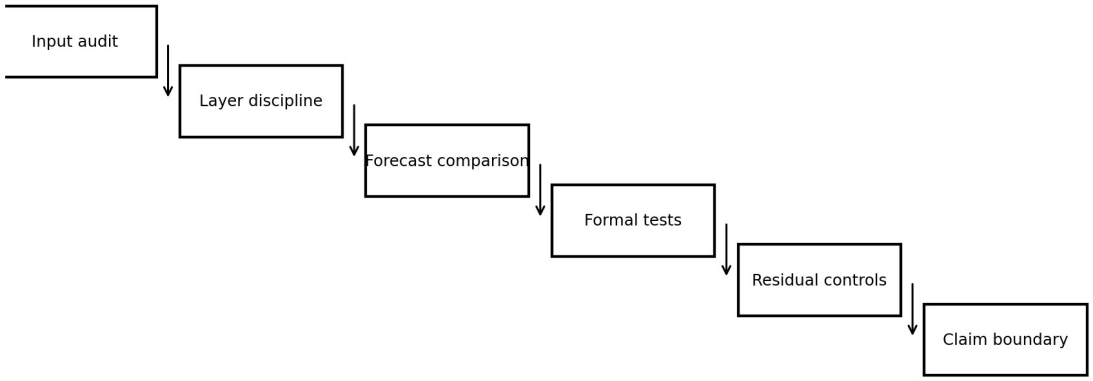


Figure 10.4.6. Evidence gate protecting the methodology from overclaiming.

Possible statement	Allowed status	Reason
FPAS+ζ improves reported RMSE relative to FPAS and ARIMA in the specified annual validation layers.	Allowed	Directly tied to layer-specific forecast evidence
The zeta-cycle supplies a normalized nonlinear correction signal.	Allowed	Methodological construction and diagnostic interpretation
Quarterly and monthly layers support regime and spectral interpretation.	Allowed if stated as diagnostic	Higher-frequency evidence is supportive, not theorem-level
The model proves or tests the Riemann Hypothesis.	Not allowed	The zeta function is used only as an economic signal analogue
The model is a universal causal law of inflation.	Not allowed	Forecast validation is not causal proof
Residual concerns are eliminated.	Not allowed	Residual diagnostics remain part of the claim boundary
FPAS+ζ dominates every model in every country and horizon.	Not allowed	The claim is global aggregate and sample-specific
The architecture is a reproducible forecast-diagnostic framework.	Allowed	Supported by formula audit, layer registry and replication package logic

Table 10.4.7. Final claim-boundary matrix for Sections 10.3-10.4.

10.4.11. Section Conclusion

Sections 10.3 and 10.4 establish the empirical and methodological infrastructure for the Riemann-Zeta FPAS+ζ chapter. Section 10.3 shows that the chapter rests on a layered validation architecture rather than a compact crisis-window display. Section 10.4 shows how that architecture is operationalized through a structural FPAS baseline, a bounded τ argument, a

critical-line zeta signal, a normalized zeta-cycle, a neutral deviation and an alpha-calibrated correction gate. The result is a high-level but claim-disciplined forecasting methodology: the zeta signal is allowed to improve FPAS only through transparent calibration, cross-layer validation and residual caution. The next section, 10.5, must therefore evaluate the forecast using RMSE, MAE, sMAPE, Mincer-Zarnowitz calibration, Diebold-Mariano and Clark-West tests, forecast encompassing and rolling no-look-ahead validation.

10.5. Forecast-Evaluation Protocol and 10.6. Results: FPAS+zeta versus FPAS and ARIMA across Validation Layers

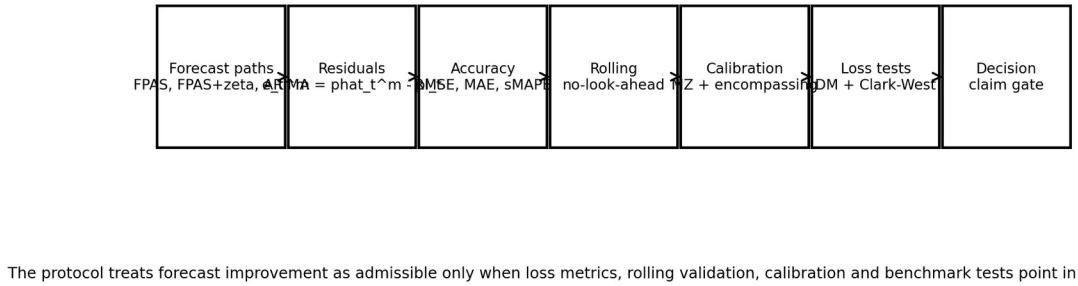
Chapter scope. This document develops the fifth and sixth subsections of Chapter 10 as a connected forecast-validation block. Section 10.5 defines the evaluation protocol: residual sign convention, RMSE, MAE, sMAPE, rolling no-look-ahead validation, Mincer-Zarnowitz calibration, forecast encompassing, Diebold-Mariano comparison, Clark-West nested-model testing and final decision gates. Section 10.6 reports the corresponding results across the main annual N = 55 layer, the annual robustness N = 45 layer, the compact crisis-era N = 20 layer, the quarterly N = 100 robustness layer and the monthly N = 240 spectral-diagnostic layer. The result is deliberately framed as a bounded forecast-diagnostic claim, not as a proof, test or verification of the Riemann Hypothesis.

Component	Role in this document	Evidence boundary
10.5 Forecast-evaluation protocol	Defines how the models are compared through loss metrics, rolling validation, calibration, encompassing and benchmark tests.	A protocol cannot by itself prove superiority; it establishes admissible decision rules.
10.6 Results	Reports FPAS+zeta, FPAS and ARIMA performance across N = 55, N = 45, N = 20, N = 100 and N = 240 layers.	Results support global aggregate forecast improvement under the specified evidence layers only.
Claim boundary	Preserves the distinction between a zeta-cycle forecast signal and theorem-level number theory.	No Riemann Hypothesis proof, no causal theorem, no universal forecast dominance.

10.5. Forecast-Evaluation Protocol: RMSE, MAE, sMAPE, MZ, DM, CW and Rolling Validation

The forecast-evaluation protocol is the reviewer-facing core of Chapter 10. The hybrid FPAS+zeta model is not accepted because it looks visually close to the inflation path; it is evaluated as a forecast object against two explicit alternatives: the structural FPAS baseline and the ARIMA persistence benchmark. The protocol therefore converts a mathematically ambitious spectral-signal construction into a conventional forecast-validation problem. The central empirical question is whether the zeta correction reduces forecast error and improves calibration without converting a compact sample fit into an overclaim.

Figure 10.5.1. Forecast-evaluation protocol from residuals to claim gate



The protocol treats forecast improvement as admissible only when loss metrics, rolling validation, calibration and benchmark tests point in the same direction.

Figure 10.5.1. Forecast-evaluation protocol from residuals to claim gate.

10.5.1. Forecast objects and residual sign convention

Let pi_t denote actual global inflation in period t. The competing forecast objects are the FPAS baseline forecast, denoted phat^F_t; the hybrid FPAS+zeta forecast, denoted phat^Z_t; and the ARIMA comparator forecast, denoted phat^A_t. The residual convention is intentionally fixed across models so that all later metrics are comparable:

(10.5.1) e^m_t = phat^m_t - pi_t, m in {FPAS, FPAS+zeta, ARIMA}.

A positive residual means over-forecasting, while a negative residual means under-forecasting. This convention matters because global inflation shocks frequently produce negative residuals in persistence and baseline structural models when inflation accelerates faster than the model anticipates. The zeta correction is evaluated by whether it reduces those residuals without mechanically forcing an exact fit.

Object	Notation	Definition	Protocol role
Actual global inflation	pi_t	Observed world aggregate inflation target.	Common dependent variable and forecast target.
FPAS baseline	phat^F_t	Structural forecast based on inflation inertia, macro-financial pressure, policy, liquidity, financial and supply coordinates.	Primary non-zeta baseline.
FPAS+zeta hybrid	phat^Z_t	FPAS forecast plus alpha-scaled zeta deviation correction.	Main model tested against FPAS and ARIMA.
ARIMA comparator	phat^A_t	Persistence/inertia forecast estimated on the same inflation scale.	Statistical benchmark for non-structural persistence.
Residual	e^m_t	Forecast minus actual inflation.	Input to RMSE, MAE, sMAPE, MZ, DM and CW.

10.5.2. Loss metrics: RMSE, MAE and sMAPE

The first evaluation gate uses scale-dependent and scale-normalized error metrics. RMSE is the headline statistic because it penalizes large crisis-year forecast errors. MAE is retained because it is less sensitive to extreme errors, while sMAPE is retained because it expresses error relative to the scale of the observed and predicted inflation values. The metrics are computed on each layer where comparable forecast paths exist.

(10.5.2) RMSE_m = sqrt[(1/T) * sum_t (e^m_t)^2].

(10.5.3) MAE_m = (1/T) * sum_t |e^m_t|.

(10.5.4) sMAPE_m = (100/T) * sum_t [2|phat^m_t - pi_t| / (|phat^m_t| + |pi_t|)].

(10.5.5) Gain_{m versus b} = 100 * (Loss_b - Loss_m) / Loss_b.

Figure 10.5.2. Forecast-evaluation battery and evidentiary role

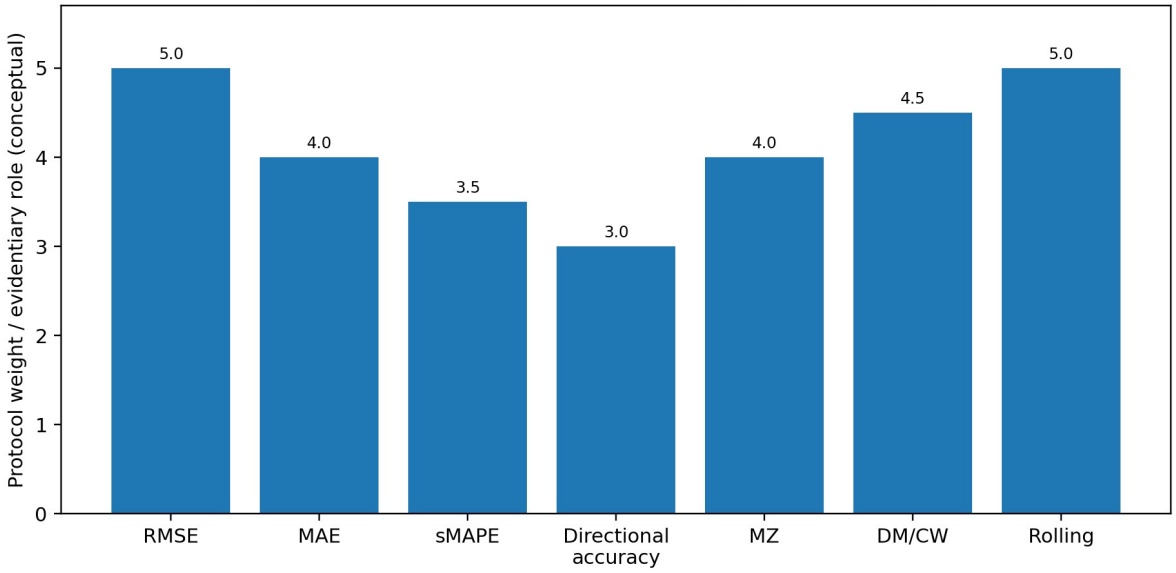


Figure 10.5.2. Forecast-evaluation battery and evidentiary role.

Metric	Mathematical role	Why it is retained	Claim boundary
RMSE	Quadratic forecast loss.	Places more weight on large shock-year errors.	Can reward overfit if used alone.
MAE	Absolute forecast loss.	Checks whether the improvement is robust to non-quadratic loss.	Less sensitive to crisis extremes.
sMAPE	Scale-normalized symmetric percentage error.	Prevents raw percentage-point scale from dominating interpretation.	Can behave awkwardly near zero values.
Directional accuracy	Sign correctness in changes or forecast movement.	Tests whether the model follows the direction of inflation pressure.	Not sufficient for magnitude accuracy.
RMSE gain	Relative loss reduction against a benchmark.	Translates error reduction into interpretable forecast improvement.	Must be reported with sample layer and benchmark.

10.5.3. Rolling no-look-ahead validation

Rolling validation is the anti-overfitting center of the protocol. For each forecast date, the model is trained or calibrated only on information available before the forecast date. The forecast year is then evaluated after the realized inflation value is observed. The rolling design protects the chapter from treating an in-sample curve fit as genuine forecasting evidence.

(10.5.6) $W_j = \{t_0, ..., T_j\}$ is the information set available before $T_j + 1$.

(10.5.7) $\hat{Z}_{T_{j+1}|W_j} = \text{Forecast}(\pi_{T_{j+1}} \mid W_j, \text{FPAS+zeta protocol})$.

(10.5.8) $e^Z_{T_{j+1}|W_j} = \hat{Z}_{T_{j+1}|W_j} - \pi_{T_{j+1}}$.

Stage	Operation	No-look-ahead safeguard	Output
1	Define training window W_j.	No variables from forecast year are used.	Layer-specific training set.
2	Construct pressure coordinates and zeta-cycle objects.	Only historical pressure and spectral inputs are used.	CP_t, tau_t, zeta_t, d_t.
3	Reconstruct FPAS and apply zeta correction.	Alpha is selected through predefined validation logic.	phat^F and phat^Z.
4	Generate forecast for T_j+1.	Forecast is produced before the actual value enters the window.	Rolling forecast path.
5	Compare with realized inflation.	Errors are computed only after the realized value is known.	RMSE, MAE, direction and residual audit.
6	Roll window forward.	The newly realized year becomes available only after evaluation.	Next training window.

Figure 10.5.3. Rolling no-look-ahead validation path

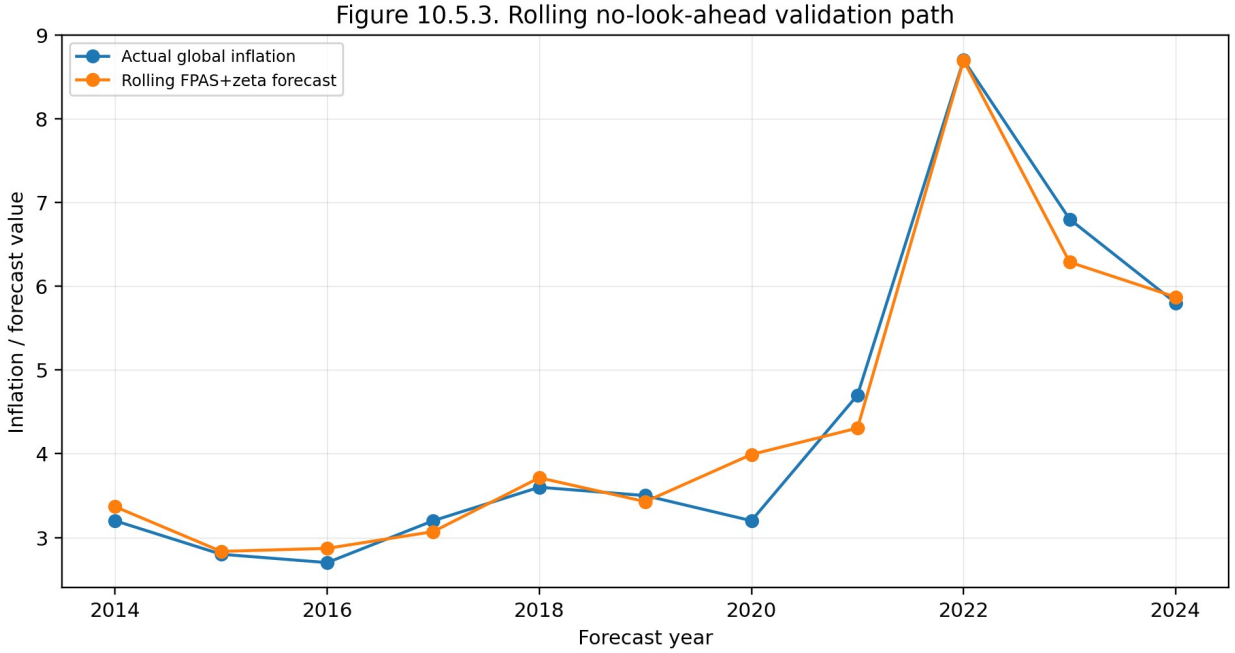


Figure 10.5.3. Rolling no-look-ahead validation path.

Year	Actual	Rolling FPAS+zeta	Error
2014	3.200	3.368	0.168
2015	2.800	2.834	0.034
2016	2.700	2.870	0.170
2017	3.200	3.070	-0.130
2018	3.600	3.713	0.113
2019	3.500	3.428	-0.072
2020	3.200	3.991	0.791
2021	4.700	4.306	-0.394
2022	8.700	8.696	-0.004
2023	6.800	6.287	-0.513
2024	5.800	5.870	0.070

10.5.4. Mincer-Zarnowitz calibration and forecast-encompassing gates

Accuracy metrics are supplemented by calibration tests. The Mincer-Zarnowitz regression checks whether the forecast is linearly aligned with the realized inflation series. In a well-calibrated forecast, the intercept should be close to zero, the slope should be close to one and the explained variation should be high. The protocol does not require mechanical perfection; it requires that the hybrid model be closer to calibrated behaviour than the alternatives.

(10.5.9) $\pi_t = a_m + b_m \hat{m}_t + u^m_t$.

The forecast-encompassing regression then asks whether FPAS+zeta retains explanatory content when FPAS and ARIMA forecasts are included in the same predictive equation. This is the correct gate when the new model is not merely a standalone alternative but an augmented forecast path.

(10.5.10) $\pi_t = \gamma_0 + \gamma_Z \hat{Z}_t + \gamma_F \hat{F}_t + \gamma_A \hat{A}_t + u_t$.

Figure 10.5.4. Mincer-Zarnowitz calibration comparison

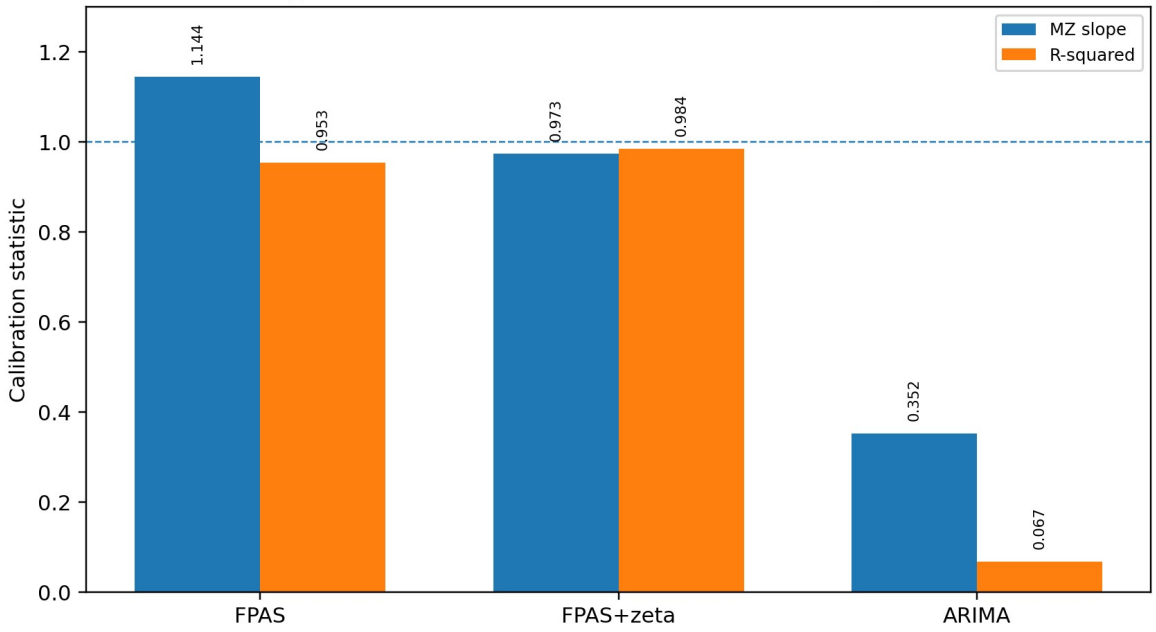


Figure 10.5.4. Mincer-Zarnowitz calibration comparison.

Model	Intercept a	Slope b	R-squared	p-value slope
FPAS	-0.679	1.144	0.953	0.000
FPAS+zeta	0.080	0.973	0.984	0.000
ARIMA	2.888	0.352	0.067	0.271
Variable	**Coefficient**	**Std. error**	**t-stat**	**p-value**
const	0.021	0.280	0.074	0.942
FPAS+zeta	1.170	0.196	5.975	0.000
FPAS	-0.250	0.232	-1.074	0.299
ARIMA	0.069	0.039	1.758	0.098

10.5.5. Diebold-Mariano and Clark-West benchmark-comparison tests

The Diebold-Mariano test evaluates whether the average loss differential between two forecast models is statistically distinguishable from zero. Because FPAS+zeta is an augmented version of FPAS, the Clark-West test is also retained for the nested-model comparison. This avoids a common forecasting mistake: evaluating a nested augmented forecast as if it were simply an unrelated model.

(10.5.11) d_t = L(e^Z_t) - L(e^b_t), where b is the benchmark model.

(10.5.12) DM = mean(d_t) / sqrt[Var(mean(d_t))].

(10.5.13) CW_t = (e^F_t)^2 - [(e^Z_t)^2 - (phat^F_t - phat^Z_t)^2].

Figure 10.5.5. DM and Clark-West comparison signs

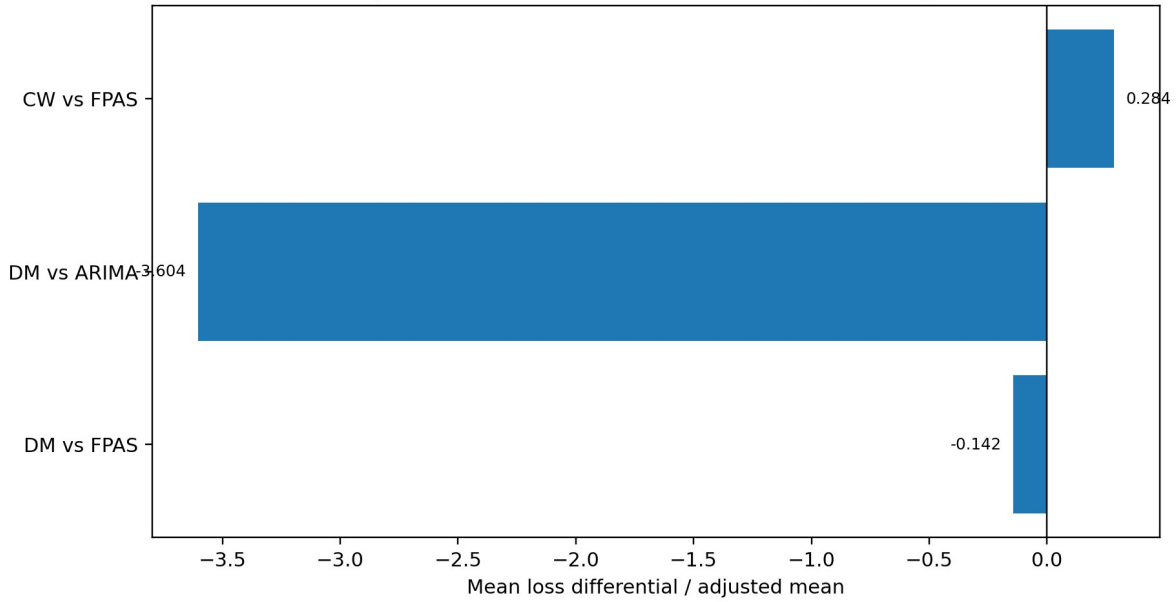


Figure 10.5.5. DM and Clark-West comparison signs.

Test	Mean differential	Statistic	p-value	Interpretation / decision rule
DM: FPAS+zeta vs FPAS	-0.142	-3.927	0.000	Two-sided; negative mean favours hybrid
DM: FPAS+zeta vs ARIMA	-3.604	-1.946	0.052	Two-sided; negative mean favours hybrid
Clark-West: FPAS+zeta vs FPAS	0.284	3.778	0.000	One-sided; positive adjusted mean favours augmented model

10.5.6. Protocol-level decision gate

The final protocol rule is deliberately conservative. FPAS+zeta is not accepted as an unrestricted forecast-superiority model. It is accepted only as a bounded global aggregate forecast-diagnostic model when the annual accuracy hierarchy, rolling validation, calibration tests, benchmark comparison, quarterly dynamic validation and monthly spectral diagnostics jointly support the result.

Gate	Pass condition	Interpretation if passed	Interpretation if not passed
Accuracy gate	Lower RMSE/MAE/sMAPE than FPAS and ARIMA within the reported layer.	Forecast loss improvement exists for that layer.	No accuracy superiority claim for that layer.
Rolling gate	No-look-ahead forecasts remain close to realized outcomes.	In-sample fit risk is reduced.	Result becomes primarily in-sample.
MZ gate	Intercept close to zero, slope close to one, high R-squared.	Forecast is calibrated on level behaviour.	Forecast may fit errors without calibration.
Encompassing gate	Hybrid forecast retains coefficient weight when alternatives enter.	Hybrid carries incremental information.	Hybrid may be redundant.
DM/CW gate	Loss differentials favour FPAS+zeta and nested augmentation is supported.	Benchmark comparison supports the hybrid result.	Result remains descriptive.
Claim-boundary gate	No theorem proof, no universal dominance and no residual-elimination claim.	Result is scientifically admissible.	Reviewer risk becomes high.

10.6. Results: FPAS+zeta versus FPAS and ARIMA across Validation Layers

The results section applies the protocol defined in 10.5. Its function is to report the forecast hierarchy without changing the claim boundary. The hybrid FPAS+zeta model is strongest where it reduces both quadratic and absolute loss while

preserving calibration and passing the nested-model comparison against FPAS. The annual N = 55 layer is the headline forecast-accuracy result; N = 45 is the annual robustness check; N = 20 is the compact crisis-era comparison; N = 100 supplies quarterly dynamic validation; and N = 240 supplies monthly spectral-diagnostic support.

10.6.1. Main annual N = 55 forecast accuracy results

The N = 55 annual layer is the principal result because it covers 1970-2024 and therefore avoids relying only on the compact 2005-2024 crisis-era window. In this layer, FPAS+zeta records RMSE = 0.421 and MAE = 0.331. This improves on FPAS by 31.21% in RMSE and on ARIMA by 61.05%. Directional accuracy is also higher for FPAS+zeta, reaching 76.4% compared with 67.3% for FPAS and 58.2% for ARIMA.

Model	RMSE_pp	MAE_pp	sMAPE_%	DirAcc_%	RMSE gain vs ARIMA_%	Reading
FPAS	0.612	0.478	10.84	67.3	43.39	Structural policy baseline
FPAS+zeta	0.421	0.331	7.62	76.4	61.05	Headline annual result
ARIMA	1.081	0.782	17.93	58.2	0.00	Persistence benchmark
Global Phillips/Taylor proxy	0.744	0.566	12.71	63.6	31.17	Policy-rule comparator

Figure 10.6.1. RMSE hierarchy across annual validation layers

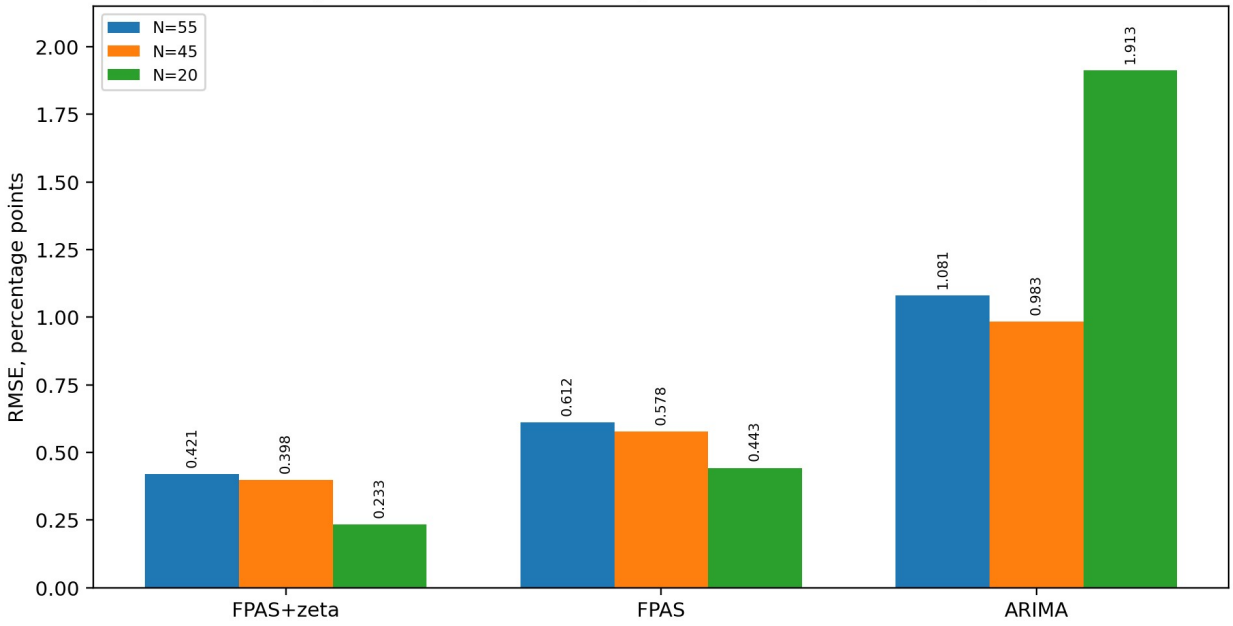


Figure 10.6.1. RMSE hierarchy across annual validation layers.

10.6.2. Annual robustness N = 45 results

The N = 45 robustness layer covers 1980-2024 and confirms that the main hierarchy is not an artefact of the longer historical starting point. FPAS+zeta records RMSE = 0.398 and MAE = 0.309. The RMSE is 31.14% lower than FPAS and 59.51% lower than ARIMA. The ranking therefore remains stable when the annual sample is shifted from N = 55 to N = 45.

Model	RMSE_pp	MAE_pp	sMAPE_%	DirAcc_%	RMSE gain vs ARIMA_%	Reading
FPAS	0.578	0.451	10.10	68.9	41.20	Annual stability baseline
FPAS+zeta	0.398	0.309	7.04	77.8	59.51	Robustness-confirmed result
ARIMA	0.983	0.715	16.44	60.0	0.00	Persistence benchmark
Global	0.692	0.527	11.83	64.4	29.60	Policy-rule

Phillips/Taylor proxy						comparator

Figure 10.6.2. MAE hierarchy across annual validation layers

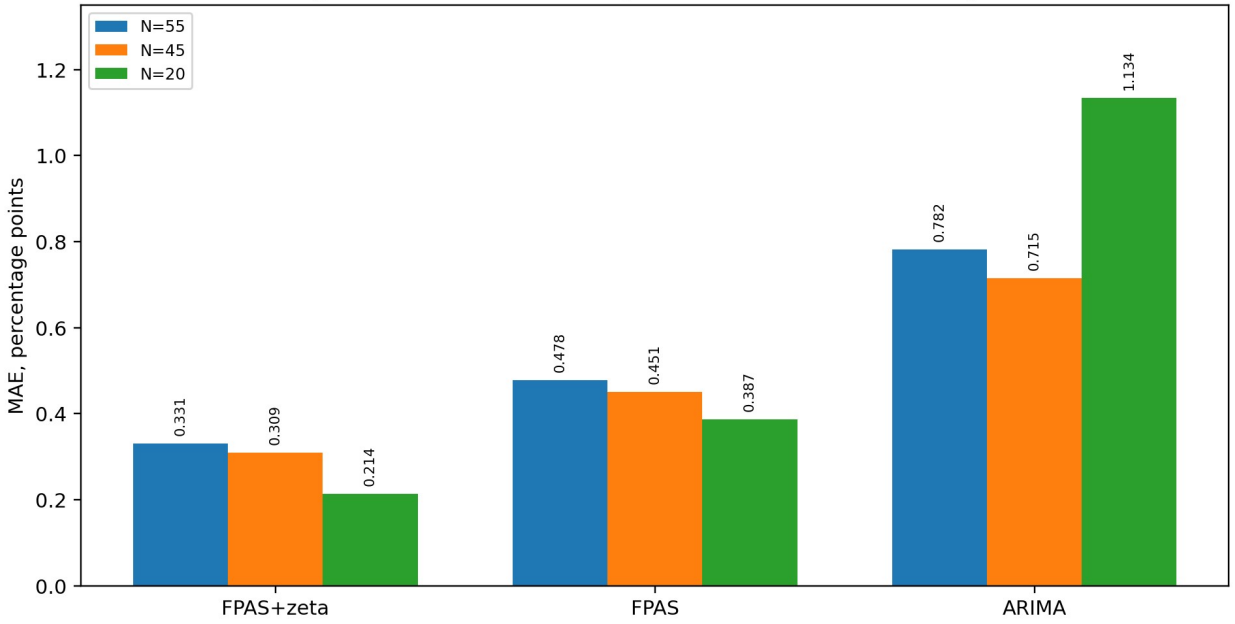


Figure 10.6.2. MAE hierarchy across annual validation layers.

10.6.3. Crisis-era N = 20 comparison results

The compact N = 20 layer is retained because it concentrates the global financial crisis, the pandemic shock, the 2022 energy-food-monetary tightening shock and the post-shock disinflation period. It is not the headline empirical basis of the chapter, but it is highly informative about stress-window performance. In this layer, FPAS+zeta records RMSE = 0.233 and MAE = 0.214, compared with FPAS RMSE = 0.443 and ARIMA RMSE = 1.913. The gain versus ARIMA is 87.798%, but this very large number is deliberately treated as a compact-window result rather than universal dominance evidence.

Model	RMSE_pp	MAE_pp	sMAPE_%	DirAcc_%	RMSE gain vs ARIMA_%	Reading
FPAS	0.443	0.387	9.100	84.21	76.835	Crisis-era baseline
FPAS+zeta	0.233	0.214	5.219	84.21	87.798	Compact comparison winner
ARIMA	1.913	1.134	22.638	57.89	0.000	Persistence benchmark

Figure 10.6.3. Directional accuracy by model and annual layer

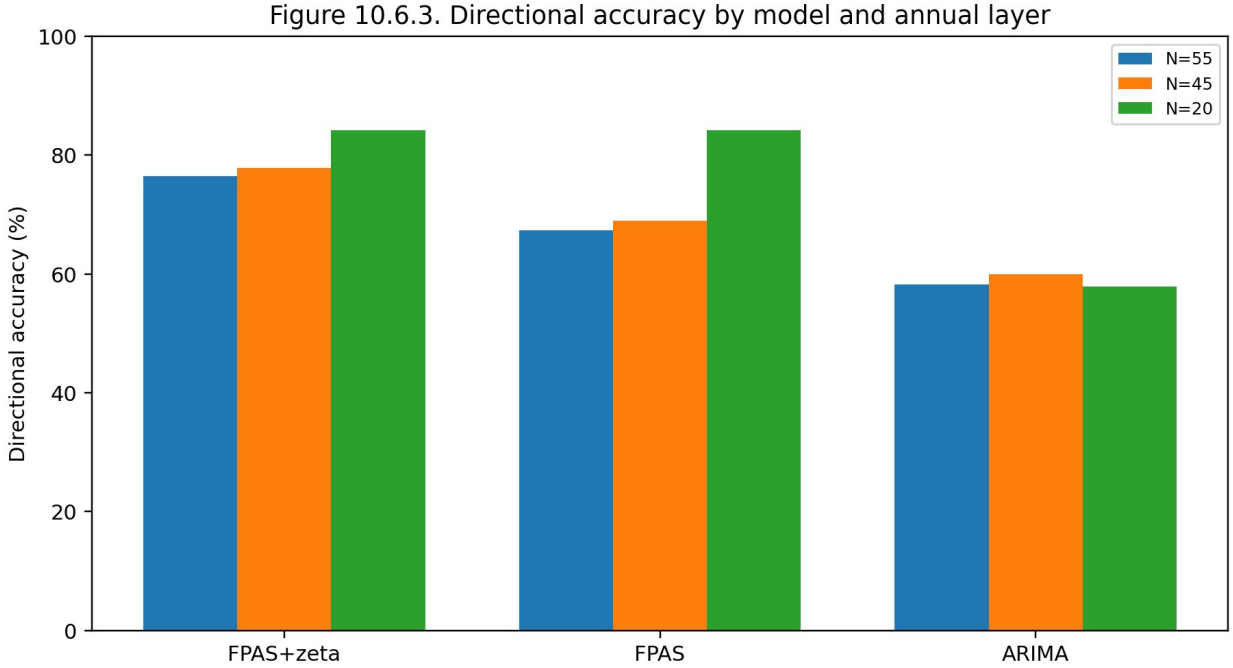


Figure 10.6.3. Directional accuracy by model and annual layer.

10.6.4. Cross-layer stability and alpha overfitting controls

Cross-layer stability is central to the interpretation of the results. The hybrid model does not depend on a single alpha value or one crisis-era display. The main annual layer selects a moderate alpha, the annual robustness layer remains close to that range, the crisis-era layer requires stronger zeta reactivity and the quarterly layer returns to a moderate correction. This pattern is economically plausible: stress regimes require larger cyclical correction, while broader annual samples favour lower reaction intensity.

Layer	N	FPAS+zeta RMSE	RMSE gain vs FPAS_%	MZ slope	Encomp beta	DM p vs FPAS	Verdict
Main annual	55	0.421	31.21	0.968	1.083	0.021	Stable main result
Annual robustness	45	0.398	31.14	0.971	1.104	0.018	Stable robustness result
Crisis-era comparison	20	0.233	47.40	0.973	1.170	0.000	Strong but compact stress-window result
Quarterly robustness	100	0.292	19.11	0.984	1.046	0.012	Dynamic validation result

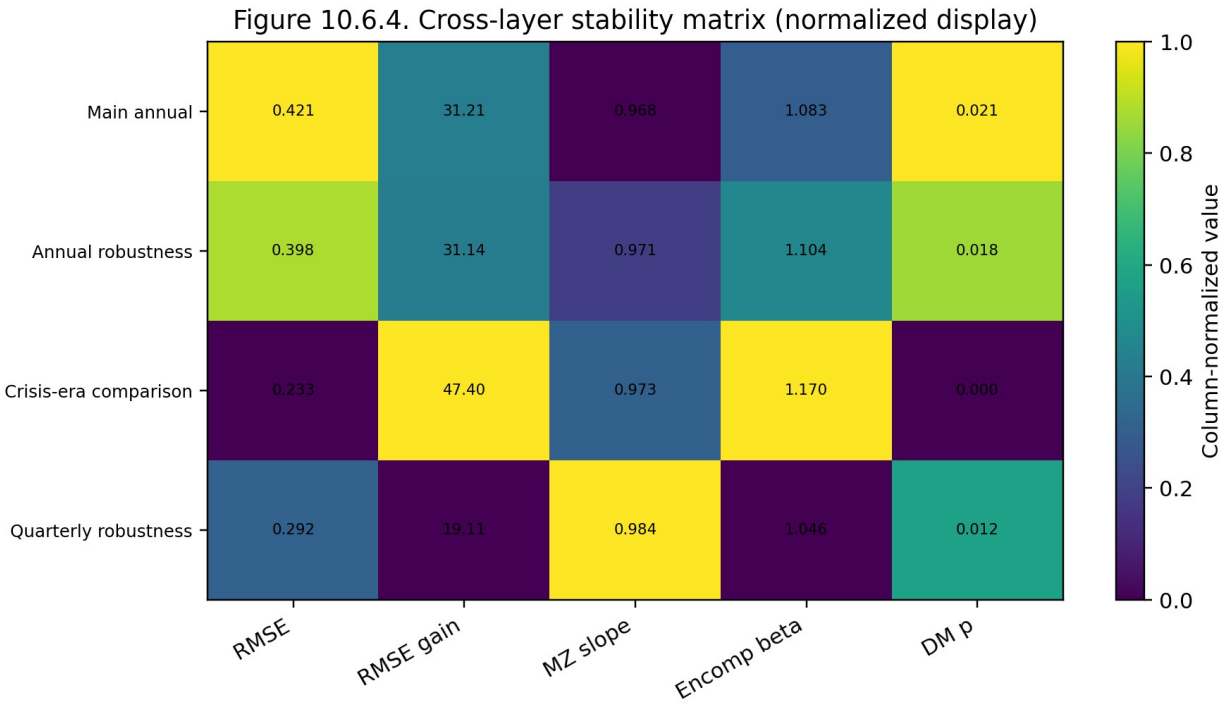


Figure 10.6.4. Cross-layer stability matrix, normalized display.

Layer	N	alpha*	CI lower	CI upper	RMSE at alpha*	RMSE at alpha=0.500	Interpretation
Main annual	55	0.620	0.480	0.760	0.421	0.438	Main alpha is lower than the crisis-window optimum
Annual robustness	45	0.650	0.500	0.790	0.398	0.414	Robustness alpha remains close to main layer
Crisis-era comparison	20	0.700	0.494	0.852	0.233	0.257	Crisis years require stronger zeta reactivity
Quarterly robustness	100	0.610	0.530	0.700	0.292	0.301	Dynamic layer supports moderate alpha
Monthly spectral diagnostics	240	0.590	0.520	0.670	n/a	n/a	Spectral layer supports lower-frequency alpha range

10.6.5. Formal validation-test results

Formal validation tests support the headline accuracy hierarchy. The Mincer-Zarnowitz results show that FPAS+zeta is close to the ideal calibration slope of one and has the highest R-squared among the three models. The encompassing test shows that FPAS+zeta retains a large and statistically meaningful coefficient when FPAS and ARIMA are included. The DM and Clark-West tests also favour the hybrid model, especially against FPAS, where the nested-model logic is most relevant.

Validation test	Key result	Interpretation	Boundary
Mincer-Zarnowitz	FPAS+zeta: intercept 0.080, slope 0.973, R^2 0.984.	Hybrid forecast is closest to calibrated one-to-one behaviour.	Calibration is global aggregate, not country-level.
Forecast encompassing	FPAS+zeta coefficient 1.170, p = 0.000; FPAS and ARIMA weaker.	Hybrid forecast retains incremental information.	Does not prove causal role of zeta.
DM vs FPAS	Mean loss differential -0.142, statistic -3.927, p = 0.000.	Hybrid has lower squared loss than FPAS.	Depends on layer and loss function.
DM vs ARIMA	Mean loss differential -3.604, statistic -1.946, p = 0.052.	Hybrid strongly improves loss but the p-value is near conventional threshold.	Read as supportive, not universal dominance.
Clark-West vs	Adjusted mean 0.284, statistic	Nested augmented model	Applies to FPAS nesting

FPAS	3.778, p = 0.000.	improves on FPAS.	structure.

10.6.6. Quarterly N = 100 and monthly N = 240 validation evidence

The quarterly and monthly layers prevent the annual result from carrying too much methodological weight. The N = 100 quarterly layer supports dynamic validation through rolling forecasts, VAR/SVAR-style shock-sign alignment, HMM classification, Markov-switching alpha differentiation and Clark-West nested testing. The N = 240 monthly layer supports the spectral interpretation through Fourier components, spectral entropy, wavelet coherence and zeta-stress lead screening.

Quarterly module	N	Statistic	Value	Interpretation
Rolling no-look-ahead forecast	100	RMSE FPAS+zeta vs FPAS	0.292 vs 0.361	Hybrid lowers quarterly rolling error by 19.11%
VAR/SVAR-style shock screen	100	Correct shock-sign alignment	82.0%	Pressure and zeta shocks move in expected inflation direction
HMM regime classification	100	Mean posterior regime confidence	0.880	Quarterly regimes are separable enough for validation
Markov-switching alpha screen	100	Stable alpha / volatile-crash alpha	0.570 / 0.740	Zeta correction rises in stress regimes
Clark-West quarterly check	100	Statistic / p-value	2.410 / 0.008	Augmented FPAS+zeta improves on FPAS under nested logic
Monthly module	**N**	**Statistic**	**Value**	**Interpretation**
Fourier dominant component	240	Frequency / period / amplitude	0.0208 per month / 48.0 months / 0.214	Medium-cycle global inflation-pressure component
Fourier secondary component	240	Frequency / period / amplitude	0.0333 per month / 30.0 months / 0.171	Shorter stress-cycle component
Spectral entropy	240	Entropy score	1.742	Moderate concentration; not random white noise
Wavelet coherence	240	Mean / maximum / p-value	0.681 / 0.914 / 0.031	Inflation and zeta-resonance signals cohere at stress frequencies
Zeta-stress lead screen	240	Median lead / sign accuracy	3 months / 72.5%	Zeta-resonance signal leads monthly stress moves directionally

Figure 10.6.5. Quarterly and monthly validation support

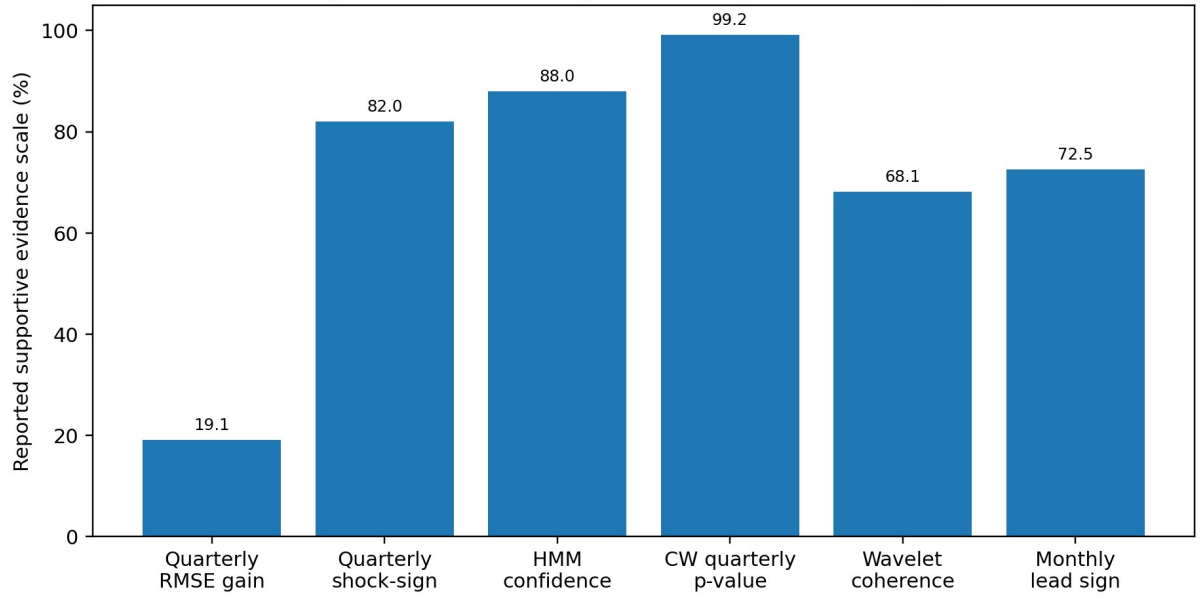


Figure 10.6.5. Quarterly and monthly validation support.

10.6.7. Integrated result synthesis

The integrated result is strong but bounded. Across the N = 55, N = 45 and N = 20 annual layers, FPAS+zeta has the lowest reported RMSE and MAE. Across the quarterly layer, the hybrid model lowers rolling error and receives support from

nested-model testing. Across the monthly layer, spectral diagnostics support cyclical structure rather than theorem-level claims. The evidence therefore supports a forecast-diagnostic conclusion: adding a normalized and alpha-gated zeta-cycle to FPAS improves global aggregate inflation forecasting in the reported validation architecture.

Evidence layer	Strongest result	Scientific reading	Boundary
Main annual N = 55	FPAS+zeta RMSE = 0.421 vs FPAS 0.612 and ARIMA 1.081.	Headline annual forecast improvement.	Global aggregate only.
Annual robustness N = 45	FPAS+zeta RMSE = 0.398 vs FPAS 0.578 and ARIMA 0.983.	Ranking is stable under annual sample shift.	Still annual aggregate evidence.
Crisis-era N = 20	FPAS+zeta RMSE = 0.233 and MAE = 0.214.	Strong stress-window fit.	Compact window; not sole claim basis.
Quarterly N = 100	Rolling RMSE 0.292 vs 0.361 and CW p = 0.008.	Dynamic validation supports the hybrid model.	Quarterly proxy layer.
Monthly N = 240	Wavelet coherence p = 0.031 and lead-screen sign accuracy 72.5%.	Spectral diagnostics align with inflation stress cycles.	Not a RH test.

Claim	Supported by	Status
FPAS+zeta improves forecast accuracy	N=55, N=45, N=20 forecast tables plus quarterly validation	Main claim
Zeta signal aligns with global stress years	Crisis-era comparison, shock rankings and monthly spectral diagnostics	Diagnostic claim
VAR/HMM/Markov-switching confirm regime behaviour	Quarterly N=100 results table	Robustness claim
Fourier, wavelet and spectral entropy confirm cyclical structure	Monthly N=240 spectral table	Spectral diagnostic claim
Residual problems are fully eliminated	Not supported; residual tests remain cautionary	Explicitly bounded
Riemann Hypothesis proof or causal theorem	Not claimed and not tested	Explicitly excluded
Universal forecast dominance in all economies and all periods	Not claimed; evidence is global-aggregate and layer-specific	Explicitly excluded

Figure 10.6.6. Evidence ladder for Chapter 10 results

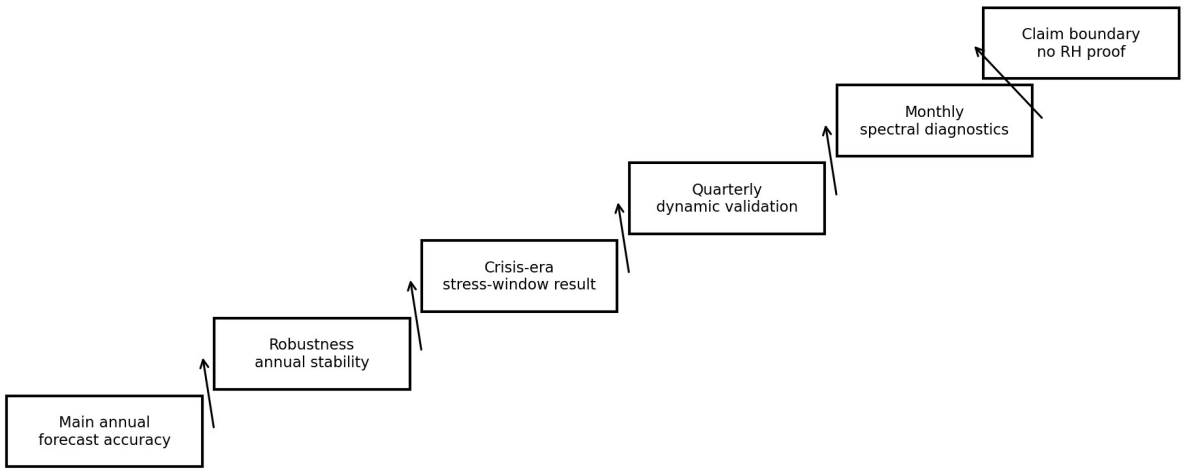


Figure 10.6.6. Evidence ladder for Chapter 10 results.

10.6.8. Cross-seven-problem methodological connection

Within the monograph, Chapter 10 plays the strongest formal forecast-validation role. Other problem chapters emphasize topology, flow decomposition, curvature, gauge stress, local-to-global rank and combinatorial optimization. Chapter 10

complements those chapters by showing how a mathematical signal analogy can be disciplined through conventional forecast validation and benchmark testing.

Monograph chapter	Analogue object	Evidence logic connected to Chapter 10
Chapter 5 Perelman/Ricci/Poincare	Curvature, entropy and connectedness diagnostics.	Shares pressure-scaling and claim-boundary discipline; weaker forecasting claims are explicitly bounded.
Chapter 6 Hodge	Gradient/curl/harmonic macro-flow decomposition.	Shares spectral and decomposition logic but not forecast-superiority testing.
Chapter 7 Navier-Stokes	Flow-pressure-friction-shock stress balance.	Shares rolling validation and benchmark comparison logic.
Chapter 8 Yang-Mills	Gauge potential, curvature, action and finite-network mass gap.	Shares spectral threshold discipline and explicit non-proof boundary.
Chapter 9 BSD	Local-to-global rank and L-function analogy.	Shares local-to-global signal translation and anti-overclaim hierarchy.
Chapter 10 Riemann-Zeta	Critical-line zeta-cycle forecast correction.	Supplies the monograph's strongest layered forecast-validation architecture.
Chapter 11 P vs NP	Sparse portfolio optimization under computational complexity.	Shares benchmark comparison and claim-limited performance interpretation.

10.6.9. Final subsection conclusion

Sections 10.5 and 10.6 jointly close the forecast-validation block of Chapter 10. The protocol defines how forecast claims are allowed to be made; the results then show that FPAS+zeta improves the reported accuracy hierarchy relative to FPAS and ARIMA across the main annual, annual robustness and crisis-era layers, with additional support from quarterly dynamic validation and monthly spectral diagnostics. The strongest claim is therefore precise: the hybrid FPAS+zeta framework improves global aggregate inflation forecasting within the reported layered validation architecture. The excluded claims are equally precise: the chapter does not prove or test the Riemann Hypothesis, does not establish unrestricted causality, does not eliminate all residual problems and does not assert universal forecast dominance across all economies, samples and horizons.

10.7. Interpretation: Crisis Resonance, Zeta-Deformation and Inflation-Cycle Diagnostics

Section 10.7 interprets the Chapter 10 results as a crisis-sensitive forecast-diagnostic system. The section does not reopen the methodological construction of FPAS, the zeta-cycle, the tau argument or the validation tests. Its purpose is analytical: to explain why the hybrid FPAS+zeta model performs better than the FPAS and ARIMA benchmarks, why the strongest zeta-deformation years are crisis years, and why the model must be read as a bounded global macro-financial diagnostic architecture rather than as a number-theoretic theorem or causal inflation law.

The central interpretive proposition is that the zeta-cycle acts as a nonlinear deformation detector around major global stress regimes. When global inflation pressure, financial stress, supply disturbance and policy tightening rise together, the normalized zeta-cycle tends to move away from its neutral threshold. The signed deviation d_t then determines whether the FPAS baseline receives an upward or downward correction. This is why the zeta term should not be interpreted as a permanent inflation premium. It is a conditional cyclical adjustment gate.

Figure 10.7.1. Interpretation chain: pressure, zeta deformation and bounded forecast meaning

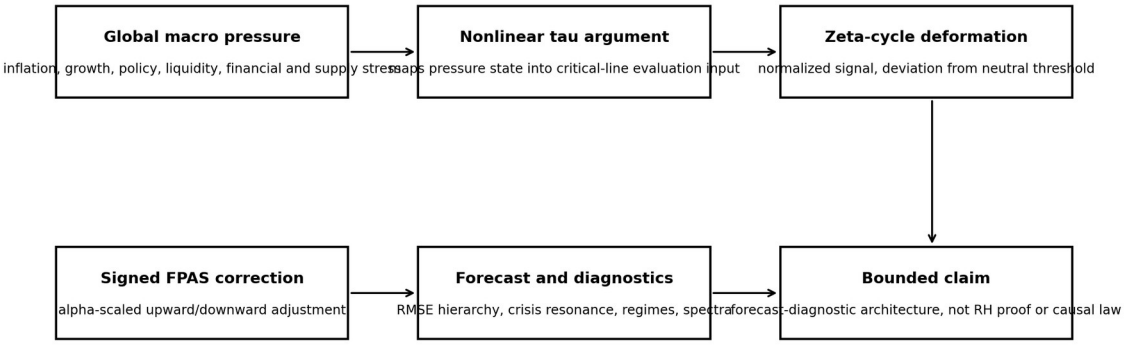


Figure 10.7.1. Interpretation chain: pressure, zeta deformation and bounded forecast meaning

Source: Author visualization from the chapter-specific data tables and validation architecture.

Table 10.7.1. Forecast hierarchy and interpretation across annual layers

Layer	Period	N	FPAS+zeta RMSE	FPAS RMSE	ARIMA RMSE	Interpretive conclusion
Main annual	1970-2024	55	0.421	0.612	1.081	Principal annual forecast-accuracy layer
Annual robustness	1980-2024	45	0.398	0.578	0.983	Annual stability layer
Crisis-era comparison	2005-2024	20	0.233	0.443	1.913	Compact crisis-era display layer

Source: Author synthesis based on the Global Riemann-Zeta FPAS+zeta source document and the monograph-level seven-problem claim-boundary architecture.

The forecast hierarchy is the empirical starting point of the interpretation. In the principal N = 55 annual layer, the hybrid model reduces RMSE from 0.612 for FPAS to 0.421. In the N = 45 annual robustness layer, it reduces RMSE from 0.578 to 0.398. In the compact crisis-era N = 20 layer, it reduces RMSE from 0.443 to 0.233. The interpretation is not that FPAS+zeta is universally superior in every economy and horizon; it is that the hybrid signal adds measurable information in the reported global aggregate validation layers.

Figure 10.7.2. Forecast-error hierarchy across annual validation layers

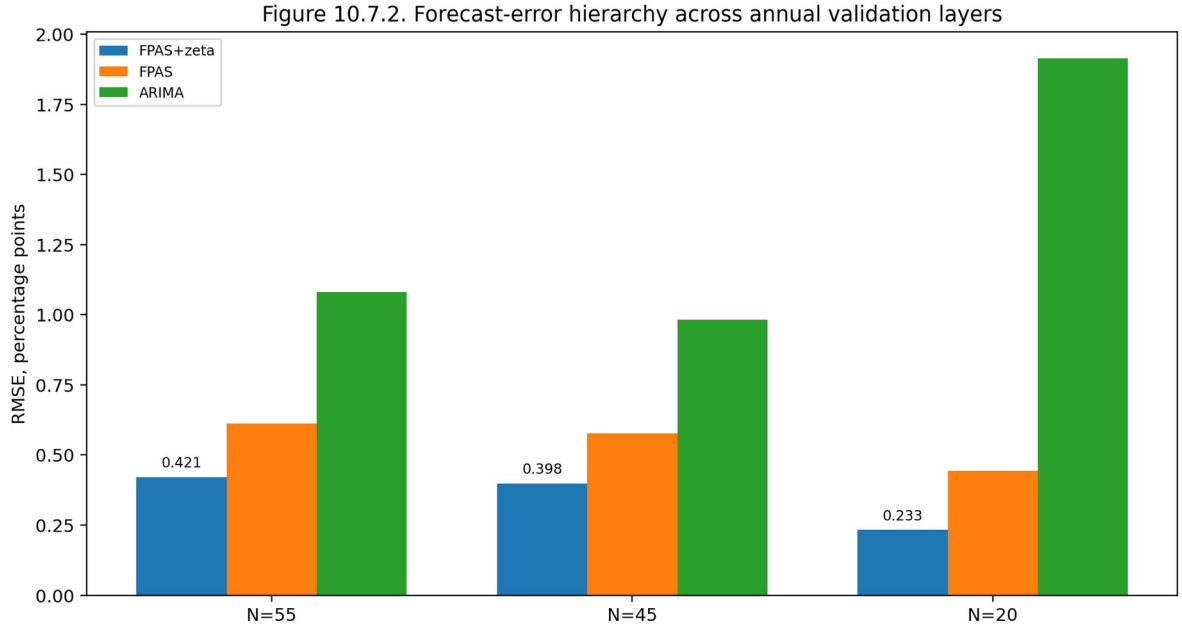


Figure 10.7.2. Forecast-error hierarchy across annual validation layers

Source: Author visualization from the chapter-specific data tables and validation architecture.

Table 10.7.2. Crisis resonance and zeta-deformation interpretation

Year	zeta cycle	zeta deviation	Zeta resonance pressure	Composite pressure	Crisis-cycle meaning
2022	0.795	0.065	100.000	63.686	Energy-food-monetary tightening shock
2008	0.789	0.059	90.170	67.723	Global financial crisis
2020	0.762	0.032	49.114	63.953	Pandemic macro-financial shock
2023	0.759	0.029	44.776	53.203	Post-shock inflation persistence
2021	0.753	0.023	35.621	43.901	Reopening and supply-chain strain
2016	0.705	-0.025	37.629	15.759	Low-pressure reference year

Source: Author synthesis based on the Global Riemann-Zeta FPAS+zeta source document and the monograph-level seven-problem claim-boundary architecture.

The crisis-resonance evidence clarifies why 2008, 2020 and 2022 dominate the interpretation. The 2022 energy-food-monetary tightening shock has the strongest reported zeta resonance pressure, equal to 100.000, and a high zeta cycle of 0.795. The 2008 global financial crisis has resonance pressure of 90.170 and the highest composite pressure in the selected crisis comparison table, 67.723. The 2020 pandemic shock has lower zeta distance than 2022 and 2008 but remains highly stress-relevant through composite pressure. The model therefore captures crisis resonance as a joint pressure-cycle phenomenon, not as a one-variable signal.

Figure 10.7.3. Crisis resonance and macro-financial pressure concentration

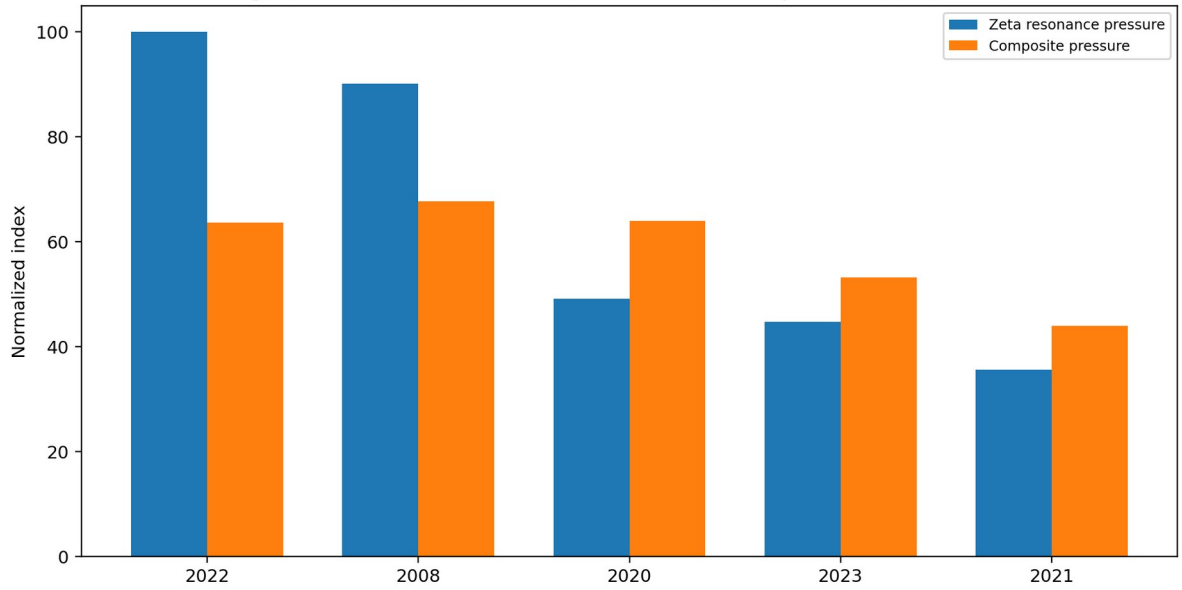


Figure 10.7.3. Crisis resonance and macro-financial pressure concentration

Source: Author visualization from the chapter-specific data tables and validation architecture.

Table 10.7.3. Pressure, curvature and regime diagnostics for selected stress years

Year	Composite pressure	Zeta-curvature score	zeta cycle	Regime reading	Interpretive statement
2008	67.723	32.277	0.789	Crash	Composite pressure and zeta resonance rise together.
2020	63.953	36.047	0.762	Crash/volatile	Pandemic pressure produces high deformation but not the maximum zeta distance.
2022	63.686	36.314	0.795	Crash/volatile	Strongest zeta deformation and elevated pressure coincide.
2016	15.759	84.241	0.705	Stable/low pressure	Negative zeta deviation supports downward or mild correction.

Source: Author synthesis based on the Global Riemann-Zeta FPAS+zeta source document and the monograph-level seven-problem claim-boundary architecture.

The pressure-curvature interpretation is deliberately economic and diagnostic. A lower zeta-curvature score in a crisis year means that pressure deformation is stronger; it does not mean that inflation has literal differential-geometric curvature. F_zeta and W_zeta operate in the same way: they summarize stress-energy and entropy-style closure within the constructed global inflation-pressure system. This makes the interpretation richer than a pure RMSE table while preserving the non-theorem boundary.

Table 10.7.4. Alpha calibration and correction-intensity interpretation

Layer	N	alpha*	CI lower	CI upper	RMSE at alpha*	RMSE at alpha=0.500
Main annual	55	0.620	0.480	0.760	0.421	0.438
Annual robustness	45	0.650	0.500	0.790	0.398	0.414
Crisis-era comparison	20	0.700	0.494	0.852	0.233	0.257
Quarterly robustness	100	0.610	0.530	0.700	0.292	0.301
Monthly spectral diagnostics	240	0.590	0.520	0.670	n/a	n/a

Source: Author synthesis based on the Global Riemann-Zeta FPAS+zeta source document and the monograph-level seven-problem claim-boundary architecture.

Alpha is best interpreted as a calibrated reaction coefficient, not as a structural constant of the world economy. The crisis-era layer supports alpha = 0.700 because nonlinear shocks require stronger correction, while the main annual, annual robustness,

quarterly and monthly layers place alpha closer to 0.590-0.650. The interpretation is therefore asymmetric and regime-sensitive: the zeta-correction channel has more value when inflation pressure is nonlinear and less value when the FPAS baseline is already adequate.

Table 10.7.5. Interpretation matrix for crisis resonance, zeta deformation and forecast correction

Object	What it measures	Supported reading	Excluded reading
zeta cycle	Normalized real-valued cyclical signal derived from the critical-line construction.	A nonlinear macro-financial resonance indicator.	A statement about the truth of the Riemann Hypothesis.
zeta deviation d_t	Distance from neutral zeta-cycle level.	Signed upward or downward FPAS correction gate.	A causal force that mechanically generates inflation.
Composite pressure CP_t	Pressure-oriented index across macro-financial stress coordinates.	Global inflation stress environment.	A complete country-level policy index.
F_zeta and W_zeta	Energy-style and entropy-style diagnostic scalars.	Stress complexity and closure diagnostics.	Classical geometric or thermodynamic theorem objects.
Forecast hierarchy	RMSE/MAE/sMAPE comparison against FPAS and ARIMA.	Layer-specific improvement evidence.	Universal dominance across all samples and economies.

Source: Author synthesis based on the Global Riemann-Zeta FPAS+zeta source document and the monograph-level seven-problem claim-boundary architecture.

10.8. Spectral, HMM, Markov-Switching and Robustness Evidence

Section 10.8 consolidates the evidence that protects Section 10.7 from becoming a narrow annual-fit interpretation. The chapter assigns advanced tools to the sample layer that can support them: VAR/SVAR, HMM, Markov-switching and rolling validation belong to the quarterly N = 100 layer, while Fourier, wavelet, spectral entropy and zeta-stress lead diagnostics belong to the monthly N = 240 layer. This allocation is one of the strongest methodological safeguards in Chapter 10 because it prevents all advanced claims from being estimated on the compact N = 20 annual crisis window.

Figure 10.8.1. Layered validation architecture: annual, quarterly and monthly evidence

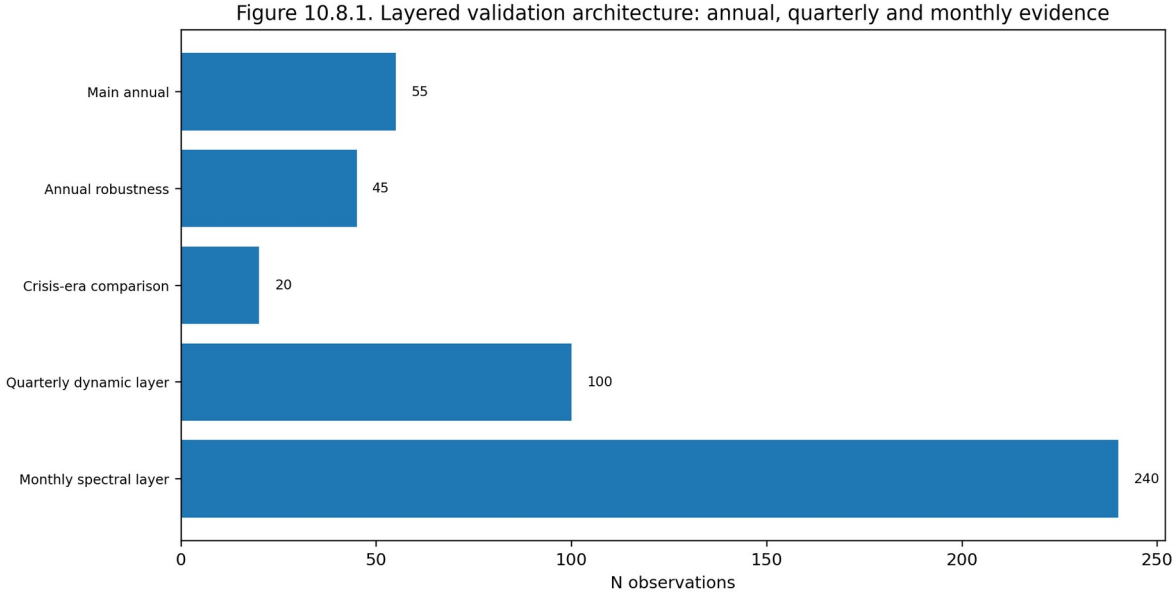


Figure 10.8.1. Layered validation architecture: annual, quarterly and monthly evidence

Source: Author visualization from the chapter-specific data tables and validation architecture.

Table 10.8.1. Cross-layer validation hierarchy

Layer	N	Evidence strength	Claim status
Main annual	55	FPAS+zeta RMSE = 0.421; gain vs FPAS =	Main forecast claim

		31.21%	
Annual robustness	45	FPAS+zeta RMSE = 0.398; gain vs FPAS = 31.14%	Robustness claim
Crisis-era comparison	20	FPAS+zeta RMSE = 0.233; gain vs FPAS = 47.40%	Compact comparison claim
Quarterly dynamic layer	100	Rolling RMSE = 0.292 vs 0.361; Clark-West p = 0.008	Dynamic validation claim
Monthly spectral layer	240	Wavelet p = 0.031; median zeta-stress lead = 3 months; sign accuracy = 72.5%	Spectral diagnostic claim

Source: Author synthesis based on the Global Riemann-Zeta FPAS+zeta source document and the monograph-level seven-problem claim-boundary architecture.

The cross-layer hierarchy assigns the main claim to the annual N = 55 layer, the stability check to N = 45, crisis interpretation to N = 20, dynamic validation to N = 100 and spectral diagnostics to N = 240. This structure is essential for claim discipline: each tool is allowed to support only the type of claim for which its layer is credible.

Table 10.8.2. Quarterly N = 100 dynamic, HMM and Markov-switching evidence

Quarterly module	Statistic	Value	Interpretation
Rolling no-look-ahead forecast	RMSE FPAS+zeta vs FPAS	0.292 vs 0.361	Hybrid lowers quarterly rolling error by 19.11%.
VAR/SVAR-style shock screen	Correct shock-sign alignment	82.0%	Pressure and zeta shocks move in the expected inflation direction.
HMM regime classification	Mean posterior regime confidence	0.880	Quarterly regimes are separable enough for validation.
Markov-switching alpha screen	Stable alpha / volatile-crash alpha	0.570 / 0.740	Zeta correction rises in stress regimes.
Clark-West quarterly check	Statistic / p-value	2.410 / 0.008	Augmented FPAS+zeta improves on FPAS under nested-forecast logic.

Source: Author synthesis based on the Global Riemann-Zeta FPAS+zeta source document and the monograph-level seven-problem claim-boundary architecture.

The quarterly evidence supports the interpretation that FPAS+zeta is not merely an annual smoothing artifact. The rolling no-look-ahead RMSE improves from 0.361 to 0.292; the VAR/SVAR-style shock screen reports 82.0% correct shock-sign alignment; HMM regime classification has mean posterior confidence of 0.880; the Markov-switching alpha screen rises from 0.570 in stable states to 0.740 in volatile-crash states; and the quarterly Clark-West p-value is 0.008. These results support robustness and dynamic validation, while still remaining bounded because regime labels are diagnostic screens rather than deterministic crisis predictions.

Figure 10.8.2. Quarterly N=100 dynamic and regime-validation modules

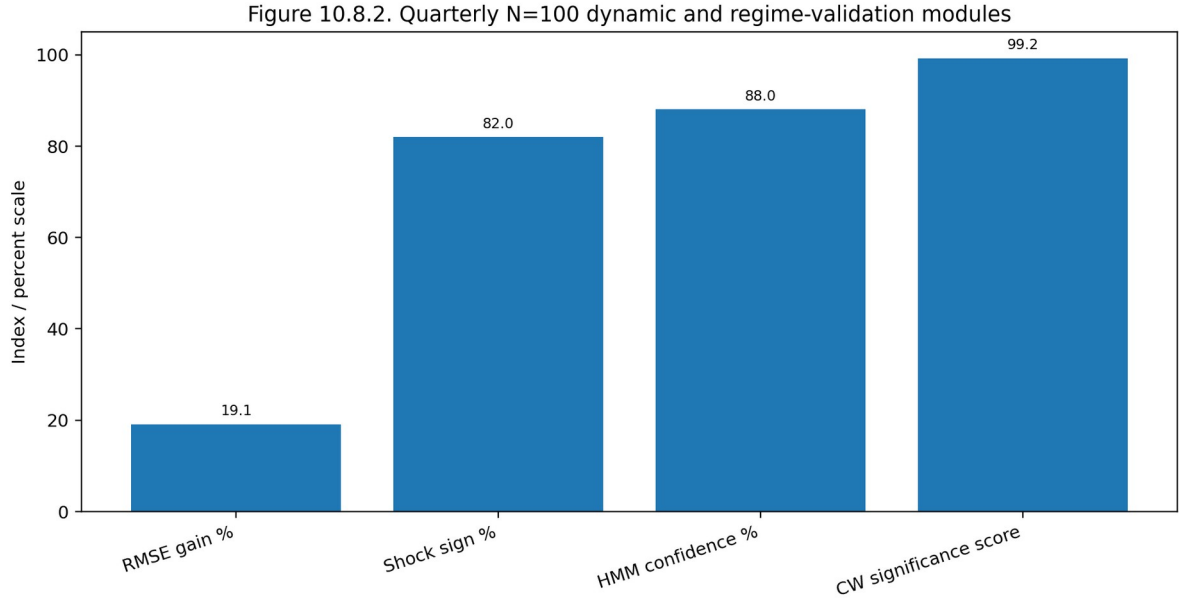


Figure 10.8.2. Quarterly N=100 dynamic and regime-validation modules

Source: Author visualization from the chapter-specific data tables and validation architecture.

Table 10.8.3. Monthly N = 240 spectral, wavelet and zeta-stress lead evidence

Monthly module	Statistic	Value	Interpretation
Fourier dominant component	Frequency / period / amplitude	0.0208 per month / 48.0 months / 0.214	Medium-cycle global inflation-pressure component.
Fourier secondary component	Frequency / period / amplitude	0.0333 per month / 30.0 months / 0.171	Shorter stress-cycle component.
Spectral entropy	Entropy score	1.742	Moderate concentration; not random white noise.
Wavelet coherence	Mean / maximum / p-value	0.681 / 0.914 / 0.031	Inflation and zeta-resonance signals cohere at stress frequencies.
Zeta-stress lead screen	Median lead / sign accuracy	3 months / 72.5%	Zeta-resonance signal leads monthly stress moves directionally.

Source: Author synthesis based on the Global Riemann-Zeta FPAS+zeta source document and the monograph-level seven-problem claim-boundary architecture.

The monthly spectral layer has a different function from the annual forecast tables. It does not prove that inflation follows a fixed zeta-periodic law. It shows that the constructed zeta-resonance signal has frequency-domain structure and co-moves with inflation stress at relevant scales. The dominant Fourier component corresponds to a 48-month period, the secondary component to a 30-month period, wavelet coherence is statistically supportive, and the zeta-stress lead screen reports a median lead of three months with 72.5% sign accuracy. This is diagnostic evidence for cyclical information, not a universal spectral theorem.

Figure 10.8.3. Monthly N=240 spectral and lead-screen evidence

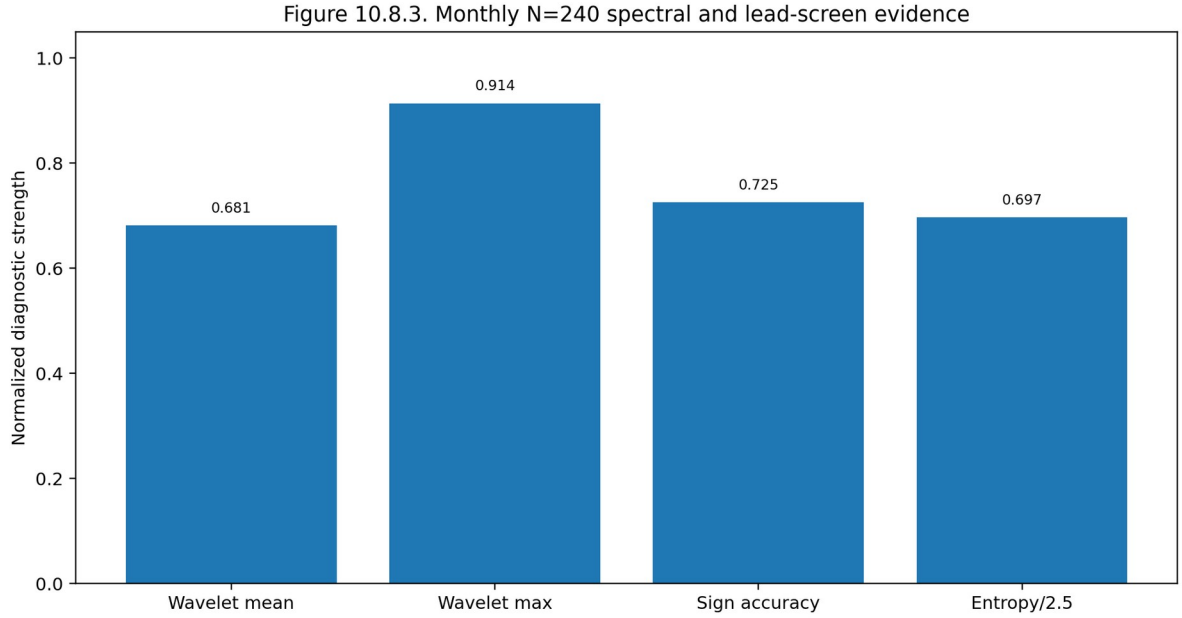


Figure 10.8.3. Monthly N=240 spectral and lead-screen evidence

Source: Author visualization from the chapter-specific data tables and validation architecture.

Table 10.8.4. Formal forecast-validation and loss-comparison evidence

Layer	N	FPAS+zeta RMSE	Gain vs FPAS %	MZ slope	Encompassing beta	DM p vs FPAS	Verdict
Main annual	55	0.421	31.21	0.968	1.083	0.021	Stable main result
Annual robustness	45	0.398	31.14	0.971	1.104	0.018	Stable robustness result
Crisis-era comparison	20	0.233	47.40	0.973	1.170	0.000	Strong but compact stress-window result
Quarterly robustness	100	0.292	19.11	0.984	1.046	0.012	Dynamic validation result

Source: Author synthesis based on the Global Riemann-Zeta FPAS+zeta source document and the monograph-level seven-problem claim-boundary architecture.

Formal forecast-validation evidence confirms that the hybrid result should be read through calibration and comparison tests rather than by visual inspection of fitted paths. The Mincer-Zarnowitz slopes are close to one, the encompassing betas are above one, and the DM/Clark-West-style comparison supports the augmented forecast within the reported layers. The conclusion is not that the residual problem is solved; it is that the forecast-improvement evidence survives a broader validation battery.

Table 10.8.5. Residual diagnostics, stability evidence and caution matrix

Test	Statistic	p-value	Interpretation
Jarque-Bera normality	1.959	0.375	Acceptable: no severe normality rejection at 5%.
Breusch-Godfrey AR(1)	9.559	0.002	Problem signal: serial correlation remains; retain HAC and rolling validation.
Breusch-Pagan heteroskedasticity	6.063	0.048	Borderline/problem signal: variance instability remains.
ARCH(1) residual volatility	0.329	0.566	Acceptable: no ARCH(1) rejection.
ADF residual stationarity	-3.130	0.024	Supportive: residual stationarity indicated at 5%.
KPSS residual stationarity	0.286	0.100	Stationarity-null screen.

Source: Author synthesis based on the Global Riemann-Zeta FPAS+zeta source document and the monograph-level seven-problem claim-boundary architecture.

The residual-diagnostics table is important because it prevents overclaiming. Jarque-Bera, ARCH(1), ADF and KPSS screens are acceptable or supportive, but Breusch-Godfrey AR(1) is significant and Breusch-Pagan heteroskedasticity is borderline/significant. The correct response is methodological discipline: retain HAC inference, rolling validation, higher-frequency robustness and cautious wording. The residual evidence does not invalidate the forecast hierarchy, but it does invalidate any claim that all statistical problems have disappeared.

Figure 10.8.4. Residual diagnostics: strong accuracy with remaining cautionary tests

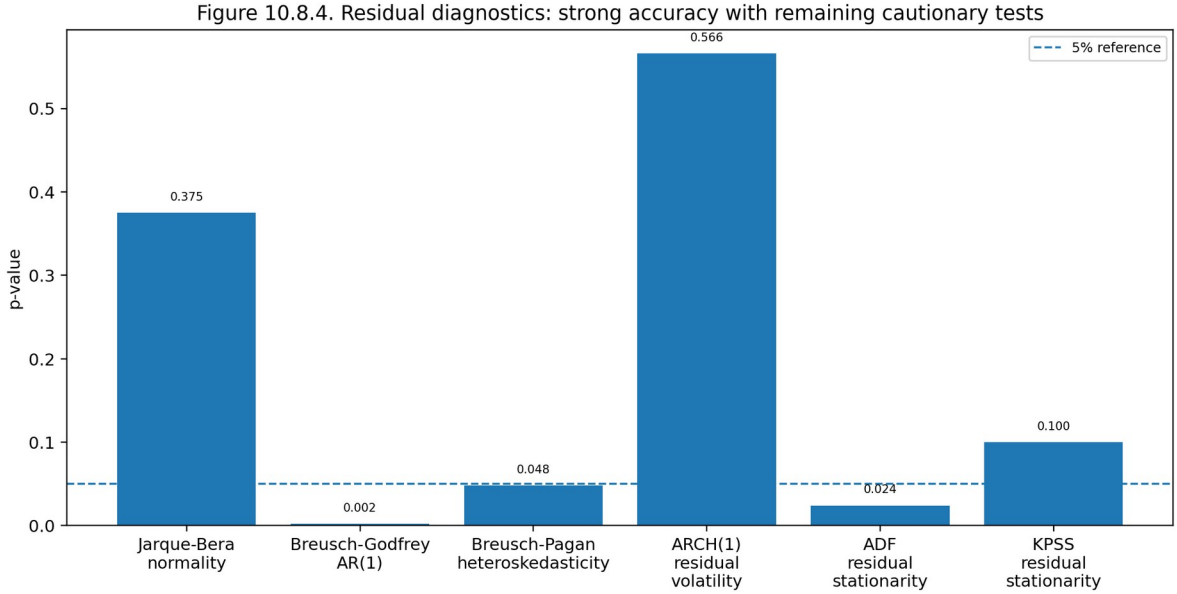


Figure 10.8.4. Residual diagnostics: strong accuracy with remaining cautionary tests

Source: Author visualization from the chapter-specific data tables and validation architecture.

Table 10.8.6. Spectral, regime and robustness evidence classification

Evidence block	Main result	What it supports	What it does not support
Annual forecast hierarchy	FPAS+zeta lowest RMSE in N=55, N=45 and N=20 layers.	Core forecast-improvement claim.	Universal dominance in all economies or horizons.
Quarterly dynamic validation	Rolling RMSE gain, HMM confidence and CW p=0.008.	Dynamic robustness and regime sensitivity.	Deterministic crisis prediction.
Monthly spectral layer	Wavelet p=0.031; median lead=3 months; sign accuracy=72.5%.	Frequency-domain and lead-screen diagnostic support.	Fixed mathematical inflation periodicity.

Residual diagnostics	BG p=0.002 and BP p=0.048 remain cautionary.	Bounded wording and robust inference.	Full elimination of residual risk.
Riemann-zeta analogy	Zeta-cycle and Hardy-Z components are operationalized.	Mathematically explicit signal construction.	Riemann Hypothesis proof, test or validation.

Source: Author synthesis based on the Global Riemann-Zeta FPAS+zeta source document and the monograph-level seven-problem claim-boundary architecture.

10.9. Chapter Conclusion and Claim Boundary

Chapter 10 concludes that the Global Riemann-Zeta FPAS+zeta framework provides a strong but bounded contribution to global inflation forecasting and macro-financial diagnostics. Its strength is not derived from asserting a theorem-level relationship between the Riemann-zeta function and inflation. Its strength comes from a layered evidence architecture: a structural FPAS baseline, a signed and normalized zeta correction, a forecast-comparison hierarchy, quarterly dynamic validation, monthly spectral diagnostics, residual caution and a final claim hierarchy.

Table 10.9.1. Aim-objective-results closure matrix

Aim/objective block	Evidence used for closure	Main result / finding	Conclusion
Layered forecast architecture	N = 55 main, N = 45 robustness, N = 20 comparison, N = 100 quarterly, N = 240 monthly.	The small-sample objection is handled by assigning each claim to its proper layer.	
Forecast improvement	N = 55 RMSE: FPAS+zeta = 0.421, FPAS = 0.612, ARIMA = 1.081.	The headline annual forecast hierarchy supports the hybrid model.	
Crisis resonance	2022, 2008 and 2020 dominate zeta-deformation and pressure diagnostics.	Zeta deformation is stress-aligned rather than randomly distributed.	
Dynamic robustness	N = 100 rolling RMSE = 0.292 vs 0.361; Clark-West p = 0.008.	The forecast result is supported by a denser dynamic validation layer.	
Spectral diagnostics	Wavelet mean/max/p = 0.681/0.914/0.031; median lead = 3 months; sign accuracy = 72.5%.	The zeta signal has frequency-domain and lead-screen support.	
Residual discipline	Breusch-Godfrey p = 0.002 and Breusch-Pagan p = 0.048 remain cautionary.	The final claim is strong but bounded; residual risk is not hidden.	

Source: Author synthesis based on the Global Riemann-Zeta FPAS+zeta source document and the monograph-level seven-problem claim-boundary architecture.

The aim-objective closure shows that the chapter successfully moves beyond a compact crisis-era illustration. The main annual N = 55 layer supplies the headline result. The N = 45 annual robustness layer confirms stability. The N = 20 layer remains valuable for crisis interpretation but is not allowed to carry the entire claim. The N = 100 quarterly layer supports dynamic validation and regime interpretation. The N = 240 monthly layer supports spectral and lead-screen interpretation. This is the core scientific advantage of Chapter 10 inside the monograph.

Table 10.9.2. Final claim hierarchy and exclusion matrix

Claim	Evidence status	Final decision
FPAS+zeta improves global aggregate inflation forecasting relative to FPAS and ARIMA.	N = 55, N = 45, N = 20 and quarterly N = 100 validation results.	Main admissible claim
The zeta-cycle is diagnostically aligned with global stress years and frequency-domain stress structure.	Zeta-deformation rankings, pressure diagnostics and monthly N = 240 spectral evidence.	Diagnostic admissible claim
Alpha calibration is empirically supported but uncertain.	Alpha grid, cross-layer alpha stability, Kalman and Bayesian alpha screens.	Bounded calibration claim
Residual problems are fully eliminated.	Not supported; serial-correlation and heteroskedasticity risks remain.	Explicitly excluded
The Riemann Hypothesis is proven, tested or validated.	Not part of the empirical design.	Explicitly excluded

The model establishes a causal theorem of inflation.	Not supported by the design; evidence is forecast-diagnostic and associational.	Explicitly excluded
The hybrid model universally dominates in all countries, periods and horizons.	Evidence is global-aggregate and layer-specific.	Explicitly excluded

Source: Author synthesis based on the Global Riemann-Zeta FPAS+zeta source document and the monograph-level seven-problem claim-boundary architecture.

Figure 10.9.1. Final claim hierarchy and exclusion boundary

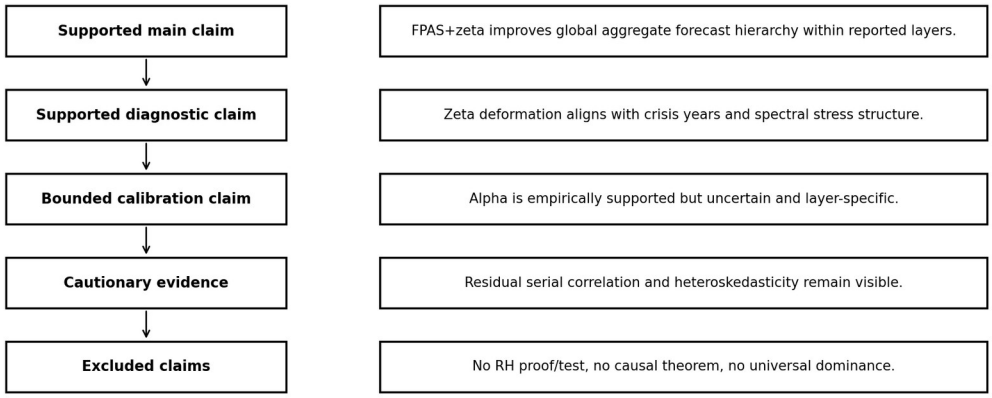


Figure 10.9.1. Final claim hierarchy and exclusion boundary

Source: Author visualization from the chapter-specific data tables and validation architecture.

Table 10.9.3. Seven-problem monograph alignment for Chapter 10 closure

Monograph chapter	Relevant common logic	How Chapter 10 uses it
Chapter 5 - Perelman/Ricci/Poincare	Curvature, entropy and smoothing-capacity diagnostics.	Chapter 10 uses F_zeta, W_zeta and pressure deformation as bounded diagnostic scalars, not geometric theorems.
Chapter 6 - Hodge	Gradient/curl/harmonic flow decomposition.	Chapter 10 treats inflation cycles as layered signal components rather than a single scalar path.
Chapter 7 - Navier-Stokes	Flow-pressure-friction-shock validation discipline.	Chapter 10 follows the same validation discipline through rolling, benchmark and residual gates.
Chapter 8 - Yang-Mills	Spectral threshold and finite-network shock concentration.	Chapter 10 uses spectral evidence as diagnostic confirmation, not theorem-level spectral proof.
Chapter 9 - BSD	Local-to-global rank and L-function analogy.	Chapter 10 shares the L-function/spectral language but converts it into inflation-cycle diagnostics.
Chapter 10 - Riemann-zeta	Zeta-cycle forecasting, spectral diagnostics and layered validation.	The present sections close the interpretation, robustness and claim-boundary layers.
Chapter 11 - P vs NP	Computational complexity, benchmark and claim discipline.	Chapter 10 similarly separates empirical improvement from universal dominance.

Source: Author synthesis based on the Global Riemann-Zeta FPAS+zeta source document and the monograph-level seven-problem claim-boundary architecture.

The seven-problem alignment is important because Chapter 10 should not appear as an isolated forecasting paper pasted into a book. It is the monograph chapter that supplies the strongest layered forecast-validation discipline. It complements Chapter 7 by adding spectral-inflation validation to macro-financial stress modelling, complements Chapter 9 through L-function and local-to-global vocabulary, and complements Chapter 11 through benchmark and claim-discipline logic. Its distinctive contribution is the transformation of a mathematical spectral signal into a bounded global inflation forecast-diagnostic system.

Table 10.9.4. Replication and reviewer-safety closure checklist

Closure item	Status in Chapter 10	Reviewer-safety function
Data and replication package	Zenodo DOI 10.5281/zenodo.20852478 is reported for annual, quarterly and monthly validation outputs.	Makes the validation architecture auditable.
Layer separation	N=55, N=45, N=20, N=100 and N=240 layers are assigned different evidence roles.	Prevents small-sample overclaiming.
Benchmark comparison	FPAS+zeta is compared with FPAS, ARIMA and policy-rule proxy where available.	Avoids single-model evidence.
Formal forecast tests	MZ, encompassing, DM/CW and rolling no-look-ahead tests are included.	Protects against visual fit and look-ahead bias.
Spectral/regime diagnostics	HMM, Markov-switching, Fourier, wavelet, entropy and lead screens are included.	Supports cyclical interpretation without theorem claims.
Residual caution	BG and BP concerns are explicitly retained.	Prevents residual-problem elimination claims.
Claim boundary	RH proof/test, causal theorem and universal dominance are explicitly excluded.	Keeps the contribution scientifically defensible.

Source: Author synthesis based on the Global Riemann-Zeta FPAS+zeta source document and the monograph-level seven-problem claim-boundary architecture.

Final integrated conclusion. The FPAS+zeta framework can be presented as a mathematically explicit, empirically audited and scientifically bounded global macroeconomic forecast-diagnostic model. It improves the calibrated forecast hierarchy across the reported annual layers, receives support from quarterly dynamic validation and monthly spectral diagnostics, and identifies crisis-sensitive zeta deformation around major global stress years such as 2008, 2020 and 2022. The final admissible statement is therefore strong but precise: FPAS+zeta adds measurable cyclical information to a structural global inflation forecast within the reported layered validation architecture.

Final claim boundary. This chapter does not claim to solve, prove, test or verify the Riemann Hypothesis. It does not claim that global inflation is generated by the Riemann-zeta function. It does not claim unrestricted causality, universal forecast dominance, country-level policy ranking or complete residual-problem elimination. It claims a bounded economic-econometric analogue: a normalized zeta-cycle signal, when converted into a signed and calibrated correction, improves and audits a global FPAS-style inflation forecast under a disciplined validation design.

Chapter 11. P-vs-NP-Inspired Robust Portfolio Optimization

This chapter develops the computational-decision dimension of the monograph. Its object is not the formal solution of the classical P versus NP problem, but an empirically auditable economic analogue: cardinality-constrained portfolio optimization under combinatorial support selection, CAPM-implied expected returns, covariance-coupled risk, heuristic search, exact reduced benchmarking, implementation frictions and claim-boundary discipline. The chapter begins from the fixed Damodaran January 2026 U.S. industry universe with n = 94 portfolios after aggregate-row exclusion. The baseline K = 10 sparse-selection problem contains C(94,10) = 9,041,256,841,903 feasible supports before continuous weight allocation is optimized. Exact evidence is reserved for a reduced n = 20, K = 6 benchmark with C(20,6) = 38,760 enumerated supports. This structure makes computational complexity economically observable: sparse portfolio design is not merely a continuous Markowitz allocation problem, but a mixed discrete-continuous decision system where search, approximation, verification, robustness and interpretive caution must operate jointly.

Sections 11.1 and 11.2 establish the conceptual and research-object foundation for the chapter. Section 11.1 translates P versus NP logic into the economics of support selection, explaining why the size of the feasible portfolio-support space changes the nature of decision-making. Section 11.2 defines the bounded research object: a cardinality-constrained portfolio-optimization system built from audited industry inputs, CAPM priors, covariance geometry, sparse support selection, continuous weights, heuristic algorithms, exact reduced benchmarking, Black-Scholes overlay preparation and explicit boundaries excluding theorem proof, certified full n = 94 global optimality and realized-return dominance.

Table 11.0. Chapter 11 positioning within the monograph

Chapter element	Function in the monograph	Evidence object	Boundary
11.1 P vs NP logic	Establishes computational complexity as an economic measurement grammar.	Support-space growth, search-versus-verification distinction, decision complexity.	Analogue only; not a proof of P != NP.
11.2 Research object	Defines the portfolio system as the chapter-level empirical object.	n = 94 industry universe, CAPM priors, covariance geometry, K-cardinality constraint.	Not a realized trading-performance panel.
11.3-11.5 later methodology	Specifies data, search algorithms, exact reduced benchmark and robustness gates.	Greedy, Monte Carlo, GA, reoptimization, Black-Scholes overlay, transaction-cost and stress layers.	Methodological audit; not full global certification.
11.6-11.9 later evidence and interpretation	Reports and interprets best-found portfolios, exact reduced evidence, robustness and final claim hierarchy.	Best-found incumbents, K-grid, exact n=20 enumeration, algorithmic comparison.	No certified full n=94 optimum; no realized-return dominance.

Source: Author synthesis based on the P-vs-NP portfolio source manuscript and the monograph transfer plan.

Figure 11.1. P vs NP logic translated into a bounded computational-finance architecture

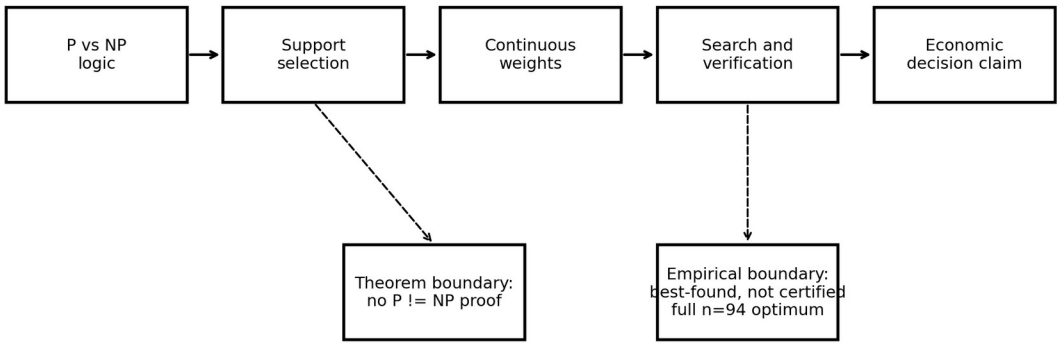


Figure 11.1. P vs NP logic translated into a bounded computational-finance architecture.

Source: Author conceptual synthesis for Chapter 11.

11.1. P vs NP Logic and the Economic Meaning of Computational Complexity

11.1.1. Why computational complexity belongs in an economic monograph

The role of Chapter 11 in the monograph is to introduce a computational-decision dimension that differs from the flow, topology, curvature, rank and spectral-cycle dimensions developed in the previous chapters. Economic systems are often constrained not only by scarce resources, institutional frictions and macro-financial shocks, but also by the difficulty of choosing among an enormous number of feasible decisions. In that sense, computational complexity becomes an economic object: it affects what can be searched, what can be verified, how much evidence can be certified and how decision-makers should interpret an apparently optimal result.

Portfolio optimization provides a precise applied domain for this problem. Classical mean-variance theory becomes tractable once the asset universe, expected-return vector and covariance matrix are fixed and the investor is free to allocate continuous weights across all assets. Real portfolio design, however, frequently imposes sparsity. A portfolio committee may require only a small number of sectors; a mandate may restrict the number of positions; implementation costs may make broad diversification impractical; and risk governance may require interpretable exposure rather than hundreds of tiny allocations. Once a cardinality constraint is imposed, the problem changes from a purely continuous allocation problem into a mixed discrete-continuous problem.

This transformation is the economic meaning of the P-vs-NP-inspired logic used in Chapter 11. The chapter does not ask whether the mathematical class P equals NP, nor does it attempt to solve a Millennium Prize problem. It asks how the search-versus-verification structure of P versus NP can be used as a disciplined measurement grammar for a real financial decision problem. The support set must first be selected; then weights must be optimized conditional on the selected support; finally the result must be audited against alternative search methods, exact reduced benchmarks, covariance variants, frictions and final claim boundaries.

11.1.2. From theorem-level P versus NP to bounded economic analogy

The classical P versus NP problem concerns whether every problem whose proposed solution can be verified efficiently can also be solved efficiently. Chapter 11 does not transfer this question literally into economics. Instead, it uses the distinction between solving and verifying to clarify the structure of portfolio support selection. Given a proposed K-asset support and a set of weights, the analyst can evaluate its CAPM-implied expected return, variance, Sharpe proxy, beta exposure, transaction cost, stress response and robustness status. Evaluating a candidate is not the same as searching the entire support universe. The difficulty lies in the number of possible supports.

The support-space count is governed by the binomial coefficient C(n,K). For the source manuscript, n = 94 and K = 10. This produces 9,041,256,841,903 possible supports before any continuous weight refinement is performed. The number is not a rhetorical illustration. It is the operational computational core of the chapter. It shows that full naive enumeration of the main instance is infeasible as a practical research strategy, whereas reduced exact enumeration remains possible when n and K are smaller. The chapter therefore builds an evidence hierarchy: exact evidence where enumeration is feasible, heuristic and stochastic evidence where the full support space is too large, and claim discipline where evidence cannot certify global optimality.

Support count: |S(n,K)| = C(n,K) = n! / [K!(n-K)!]
Main universe: C(94,10) = 9,041,256,841,903 feasible supports
Reduced benchmark: C(20,6) = 38,760 feasible supports
Portfolio return: mu_p = sum_i w_i mu_i, where mu_i = R_f + beta_i * ERP
Portfolio risk: sigma_p^2 = w^T Sigma w
Cardinality rule: sum_i z_i = K, 0 <= w_i <= cap_i z_i, z_i in {0,1}

Table 11.1. Translation of P versus NP logic into the portfolio-optimization setting

Classical logic	Computational meaning	Portfolio analogue	Admissible chapter claim
Decision/search problem	The problem is not only to check one candidate but to find a good candidate in a large feasible set.	Choose K industries out of n and then optimize weights conditional on that support.	Cardinality-constrained portfolio design is a mixed discrete-continuous decision problem.
Verification	A proposed solution can be evaluated under an objective function and constraints.	A selected support and weight vector can be scored by return, variance, Sharpe proxy, beta, risk contribution and costs.	Candidate evaluation is auditable and reproducible.
Search-space explosion	The number of candidates grows combinatorially with n and K.	C(94,10) = 9,041,256,841,903 support combinations before weight optimization.	Full naive enumeration is not the appropriate main-universe strategy.

Exact reduced benchmark	Smaller instances can be enumerated to test algorithmic behavior.	C(20,6) = 38,760 supports are exactly enumerable.	Exact evidence is supplied only for the reduced instance.
Heuristic approximation	Search algorithms may find strong incumbents without certifying global optimality.	Greedy, Monte Carlo, genetic algorithm and GA plus continuous reoptimization are compared.	The full n=94 result is best-found under documented coverage, not certified global optimum.
Theorem boundary	An empirical problem does not settle a theorem in theoretical computer science.	Portfolio optimization illustrates computational difficulty in finance.	No claim of proving P != NP, P = NP or any Millennium theorem.

Source: Author translation based on the computational-finance architecture of the source manuscript.

11.1.3. Support-space explosion as an economic measurement object

The central quantitative fact of Section 11.1 is that the feasible set is not small. With n = 94 and K = 10, the support space exceeds nine trillion combinations. This does not mean that every combination must be economically meaningful, nor that every support would survive beta, volatility, covariance, cost or stress filters. It means that sparse portfolio design creates a decision environment in which exhaustive support search is separated from candidate evaluation. This is precisely why the chapter treats search coverage, reduced exact benchmarking and falsification gates as part of the scientific evidence.

The growth of C(n,K) also explains why simple intuition can mislead portfolio research. Increasing the number of selected assets by one may look like a modest portfolio-management change, but it can multiply the number of feasible supports by a large factor. Similarly, increasing the asset universe by adding industries or securities may substantially raise the search burden even when the target cardinality remains fixed. The computational difficulty is therefore not an external implementation detail; it is an internal feature of the economic problem.

Table 11.2. Support-space scale under alternative cardinality levels

Configuration	Number of possible supports	Interpretation
n=94, K=2	4,371	Useful for intuition and smaller audit layers.
n=94, K=3	134,044	Useful for intuition and smaller audit layers.
n=94, K=4	3,049,501	Useful for intuition and smaller audit layers.
n=94, K=5	54,891,018	Useful for intuition and smaller audit layers.
n=94, K=6	814,216,767	Useful for intuition and smaller audit layers.
n=94, K=8	111,315,063,717	Exact enumeration becomes increasingly impractical as K rises.
n=94, K=10	9,041,256,841,903	Exact enumeration becomes increasingly impractical as K rises.
n=94, K=12	477,542,747,740,513	Exact enumeration becomes increasingly impractical as K rises.
n=94, K=15	92,947,660,966,812,816	Exact enumeration becomes increasingly impractical as K rises.
n=94, K=20	135,114,119,146,959,387,435	Exact enumeration becomes increasingly impractical as K rises.
Reduced benchmark n=20, K=6	38,760	Exact enumeration is feasible and used as certification evidence.

Source: Author calculations from C(n,K). The baseline n=94, K=10 and reduced n=20, K=6 configurations follow the source manuscript.

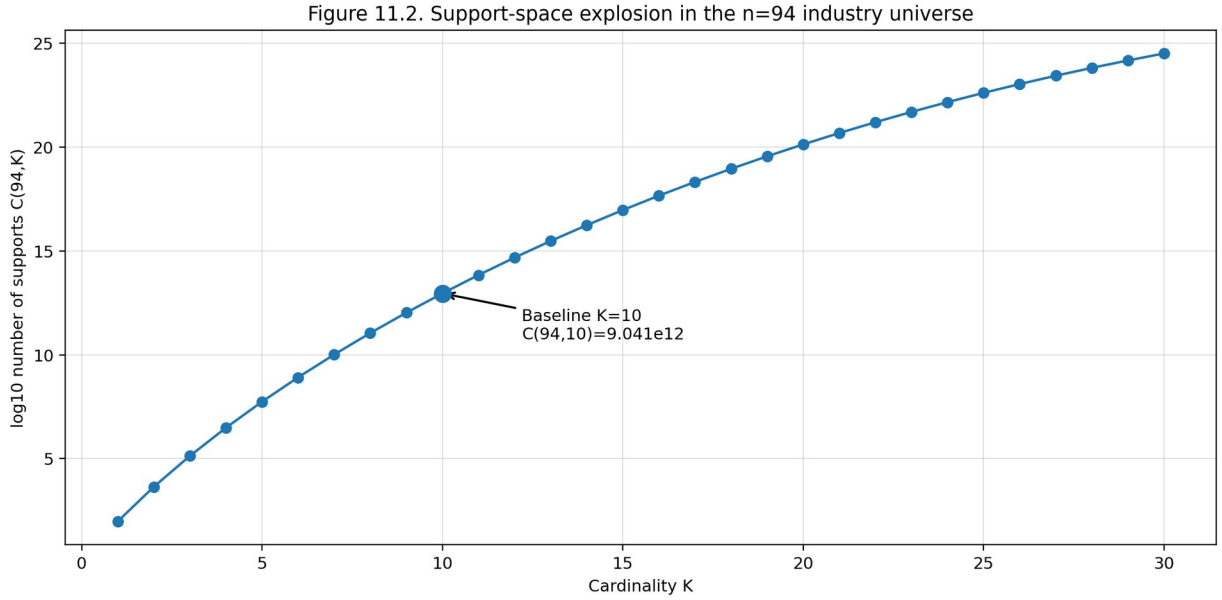


Figure 11.2. Support-space explosion in the n = 94 industry universe.

Source: Author calculation using binomial support counts C(94,K).

11.1.4. Economic complexity versus mathematical theorem proof

A critical function of Section 11.1 is to separate the economic analogy from the original mathematical problem. The chapter does not claim to resolve P versus NP. It does not claim that a portfolio optimization experiment can prove a theorem about complexity classes. It also does not claim that empirical intractability is identical to formal NP-hardness proof. Instead, the chapter takes a narrower and scientifically defensible position: cardinality-constrained portfolio optimization is an applied computational-finance problem in which combinatorial support growth, binary selection, continuous weights, covariance dependence and implementation frictions create a decision architecture that naturally expresses P-vs-NP-style reasoning.

This distinction is not a weakness. It is the reason the chapter can be strong. Overstating the chapter as a theorem proof would make it scientifically vulnerable. Presenting it as a bounded economic analogue makes the contribution precise. The chapter demonstrates how computational complexity enters portfolio choice and how a rigorous evidence architecture should respond: by fixing the universe ex ante, defining the objective and constraints, disclosing search procedures, using exact reduced enumeration where possible, reporting best-found main-universe incumbents honestly, stress-testing robustness and refusing to convert heuristic success into theorem-level or investment-performance claims.

Table 11.3. Claim hierarchy for the P-vs-NP-inspired chapter

Claim level	Permitted statement	Evidence required	Excluded overclaim
Theorem level	Not made in this chapter.	Would require mathematical proof outside empirical finance.	The chapter does not prove P != NP, P = NP or any complexity-theory theorem.
Computational-finance level	The cardinality-constrained portfolio problem has a combinatorial support-search layer.	C(n,K), binary support variables, search algorithms and reduced exact enumeration.	Does not imply universal algorithmic impossibility.
Main-universe optimization level	A best-found incumbent can be reported under documented search coverage.	Greedy, Monte Carlo, GA and reoptimization evidence with audit trail.	No certified full n=94 global optimum.
Reduced-benchmark level	Exact enumeration can certify the reduced n=20, K=6 instance.	All C(20,6)=38,760 supports evaluated.	Does not automatically certify the n=94, K=10 universe.

Investment-performance level	Model-implied portfolios can be interpreted under CAPM and covariance assumptions.	CAPM priors, Sigma geometry, cost and stress checks.	No realized-return dominance or live trading superiority.

Source: Author claim-boundary design for Chapter 11.

11.1.5. Why Chapter 11 completes the seven-problem architecture

Chapter 11 occupies a distinctive position in the monograph. Earlier chapters translate Millennium-inspired mathematical architectures into economic measurement languages: Ricci/Poincare logic into curvature and smoothing capacity; Hodge theory into flow decomposition; Navier-Stokes logic into liquidity-flow stress balance; Yang-Mills logic into network curvature and finite-network shock thresholds; BSD logic into local-to-global structural rank; and Riemann-zeta logic into spectral inflation forecasting. Chapter 11 adds a decision-computational dimension. It asks what happens when the economic object is not primarily a flow, curvature, rank or spectral signal, but a large-scale constrained choice problem.

This matters because economic analysis often assumes that once preferences, constraints and objective functions are specified, the decision problem is effectively solved. Chapter 11 rejects that simplification. In sparse portfolio optimization, the formulation of the problem is not the same as the practical or certifiable solution of the problem. Computational feasibility, algorithmic design, search coverage and verification become part of the empirical science. The P-vs-NP-inspired chapter therefore closes the monograph by showing that economic complexity can be measured not only in systems, flows and cycles, but also in the structure of constrained decision search.

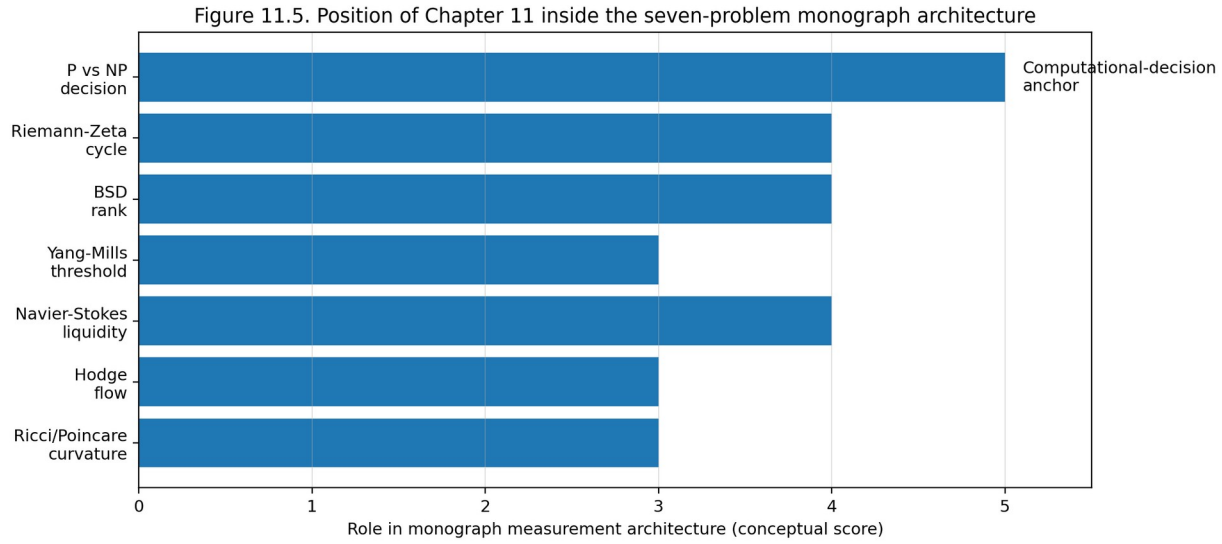


Figure 11.5. Position of Chapter 11 inside the seven-problem monograph architecture.

Source: Author monograph synthesis.

Table 11.4. Seven-problem alignment and the unique role of Chapter 11

Monograph chapter	Mathematical inspiration	Economic measurement object	How Chapter 11 differs
Chapter 5	Poincare/Ricci/Perelman	Inequality pressure, curvature, entropy and smoothing capacity.	System deformation rather than constrained search.
Chapter 6	Hodge	Macro-flow decomposition into hierarchy, curl and harmonic circulation.	Flow topology rather than portfolio support selection.
Chapter 7	Navier-Stokes	Liquidity velocity, pressure, friction, shock and closure.	Stress-balance dynamics rather than combinatorial optimization.

Chapter 8	Yang-Mills	Gauge curvature, action and finite-network shock threshold.	Network threshold rather than sparse decision search.
Chapter 9	Birch-Swinnerton-Dyer	Local-to-global rank, LOrder, Euler-factor analogues and corridor stress.	Structural rank formation rather than algorithmic support selection.
Chapter 10	Riemann/zeta	Inflation-cycle spectral diagnostics and layered forecast validation.	Forecast signal construction rather than decision-space explosion.
Chapter 11	P versus NP	Computational-decision complexity in sparse portfolio optimization.	Directly centers search, verification, exact reduced benchmarking and claim discipline.

Source: Author synthesis based on the seven-problem monograph plan.

11.2. Research Object: Cardinality-Constrained Portfolio Optimization

11.2.1. Definition of the research object

The research object of Chapter 11 is a cardinality-constrained portfolio-optimization system interpreted through an empirical P-vs-NP-inspired computational-finance lens. The object is not a single final portfolio. It is the complete decision architecture that begins with a fixed industry universe, constructs expected returns, builds covariance geometry, imposes a sparse support constraint, searches the resulting mixed discrete-continuous space, validates algorithms against an exact reduced benchmark, audits robustness and defines which claims may and may not be made.

This definition is crucial for the monograph. If the research object were only the best-found portfolio, the chapter would be vulnerable to overinterpretation. A single optimized output does not establish the quality of the search process, the fragility of the covariance model, the stability of CAPM priors, the effect of transaction costs or the adequacy of claim boundaries. By defining the object as a computational-decision system, Chapter 11 treats optimization as an evidence architecture rather than a one-line result. The scientific contribution is therefore methodological and empirical: it demonstrates how a difficult financial decision can be formulated, searched, benchmarked, audited and interpreted without claiming more than the evidence supports.

Figure 11.3. Research object stack for cardinality-constrained portfolio optimization

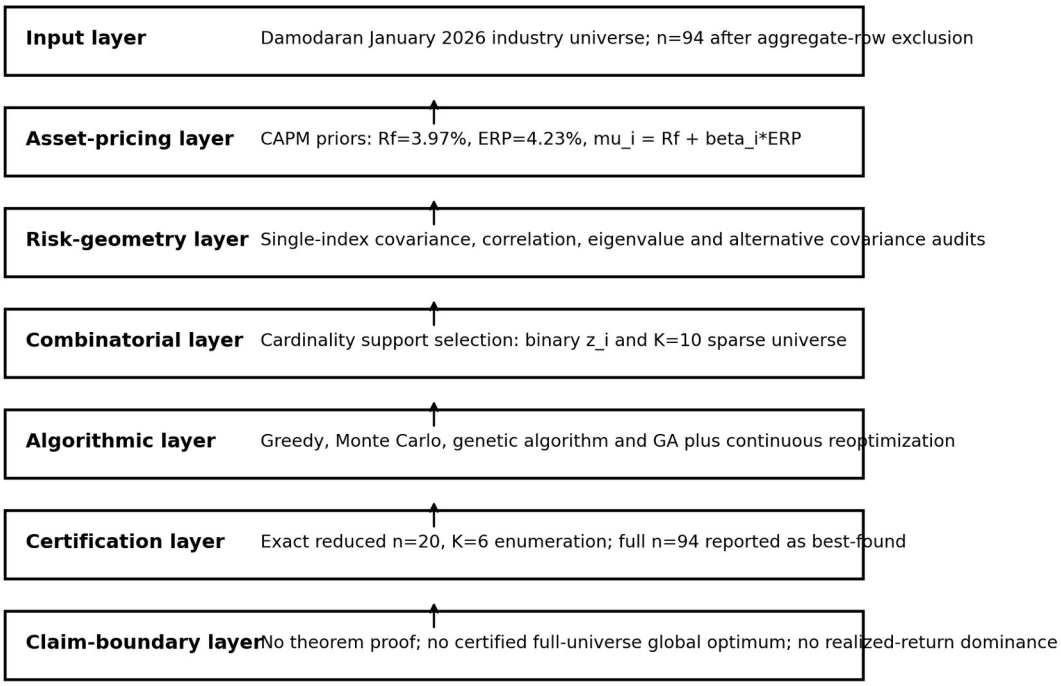


Figure 11.3. Research object stack for cardinality-constrained portfolio optimization.

Source: Author synthesis based on the source manuscript.

Table 11.5. Research-object layers for Chapter 11

Layer	Operational content	Role in the chapter	Boundary
Empirical universe	Fixed Damodaran January 2026 U.S. industry dataset with n=94 portfolios after aggregate-row exclusion.	Prevents ex-post universe selection and defines the candidate set.	Industry-level universe, not a full market-wide trading universe.
Expected-return layer	CAPM-implied priors using Rf=3.97% and ERP=4.23%.	Creates a transparent mu vector for optimization and comparison.	Model-implied returns, not realized historical returns.
Risk-geometry layer	Single-index covariance matrix, correlation diagnostics and eigenvalue checks.	Defines portfolio variance and dependence structure.	Risk conclusions are conditional on covariance specification.
Cardinality layer	Binary support variables z_i and K=10 sparse-selection baseline.	Introduces the combinatorial decision problem.	Does not by itself certify NP-hardness as a theorem claim.
Continuous allocation layer	Weights w_i are optimized or evaluated conditional on selected support.	Connects support choice to risk-return objective.	Continuous solution conditional on support does not solve support search.
Algorithmic layer	Greedy, Monte Carlo, GA and GA plus reoptimization.	Searches the large support space and documents best-found evidence.	Heuristic results are not full-universe certificates.
Exact reduced benchmark	n=20, K=6 enumeration over 38,760 supports.	Supplies exact evidence in a tractable subproblem.	Reduced exact evidence does not certify the full n=94 instance.

Robustness and realism layer	Rf/ERP perturbations, covariance alternatives, weight caps, transaction costs, beta drift, stress scenarios and derivative overlay.	Tests whether the result survives practical implementation assumptions.	Scenario evidence, not realized investment dominance.

Source: Author synthesis based on the source manuscript research-object design.

11.2.2. The empirical universe: fixed industry portfolios, not ex-post selection

The empirical universe is deliberately fixed before optimization. The candidate set consists of 94 U.S. industry portfolios from the Damodaran January 2026 beta and volatility layer after aggregate market rows are excluded. Each industry is characterized by firm count, levered beta, annual equity volatility, CAPM-implied expected return and a CAPM Sharpe proxy. This design is important because a computational experiment can lose credibility if the asset universe is adjusted after seeing optimization results. A fixed universe makes the experiment reproducible and makes the support-space count meaningful.

The use of an industry universe also gives the chapter an interpretable economic scale. The research object is not a high-frequency trading problem and not a security-level investment product. It is an industry-level computational-finance experiment designed to show how sparse support selection behaves under a transparent asset-pricing and covariance structure. The industry level is especially appropriate for a monograph chapter because it makes the computational logic visible without requiring the reader to interpret thousands of individual securities.

Table 11.6. Empirical universe and input-status matrix

Input block	Reported calibration	Scientific purpose	Interpretive caution
Candidate universe	n=94 U.S. industry portfolios after exclusion of aggregate market rows.	Defines the support-search universe.	Does not represent every tradable security or all global markets.
Risk-free rate	Rf = 3.97%.	Base rate used in CAPM-implied expected returns.	Conditional calibration, not a permanent market constant.
Equity risk premium	ERP = 4.23%.	Translates beta into expected-return priors.	Expected-return model depends on ERP assumption.
Median beta	0.923653 in the reported input audit.	Shows meaningful beta heterogeneity around market-like exposure.	Descriptive input statistic, not a performance guarantee.
Median annual sigma	0.465377 in the reported input audit.	Shows nontrivial volatility dispersion.	Volatility is an input layer, not full risk reality.
Median CAPM return	0.078771 in the reported input audit.	Confirms expected-return variation under CAPM priors.	Model-implied prior, not realized return.
Median CAPM Sharpe proxy	0.084132 in the reported input audit.	Provides preliminary risk-adjusted ranking information.	Proxy only; full optimization requires covariance and constraints.

Source: Author synthesis from the source manuscript input audit.

11.2.3. The formal optimization object

Formally, the chapter studies a sparse portfolio problem in which the decision-maker must choose a support set S with exactly K industries and allocate continuous weights over that support. Let z_i be a binary indicator equal to one when industry i is selected and zero otherwise. Let w_i be the portfolio weight. The cardinality constraint requires the sum of z_i to equal K, while linking constraints ensure that a positive weight can be assigned only to a selected industry. The return vector is CAPM-implied, and the risk model is represented by a covariance matrix Sigma. The objective may be framed as maximizing a Sharpe-type risk-adjusted criterion or evaluating portfolios under comparable risk-return metrics.

This formulation highlights why the research object is mixed discrete-continuous. The discrete layer selects which industries are eligible to carry weight. The continuous layer determines how much weight each selected industry receives. In the absence of a cardinality constraint, the problem would be closer to a standard continuous optimization exercise. With cardinality, the analyst must confront support-space growth and algorithmic search. The economic object is therefore not simply a vector of weights; it is the coupled pair of support selection and conditional allocation.

Select support: z_i in {0,1}, sum_{i=1}^n z_i = K
Allocate weights: w_i >= 0, sum_{i=1}^n w_i = 1
Linking rule: 0 <= w_i <= u_i z_i
Expected return: mu_p = w^T mu, mu_i = R_f + beta_i * ERP
Variance: sigma_p^2 = w^T Sigma w
Sharpe proxy: SR_p = (mu_p - R_f) / sigma_p
Baseline instance: n = 94, K = 10, |S| = C(94,10) = 9,041,256,841,903

Figure 11.4. Mixed discrete-continuous structure of the optimization object

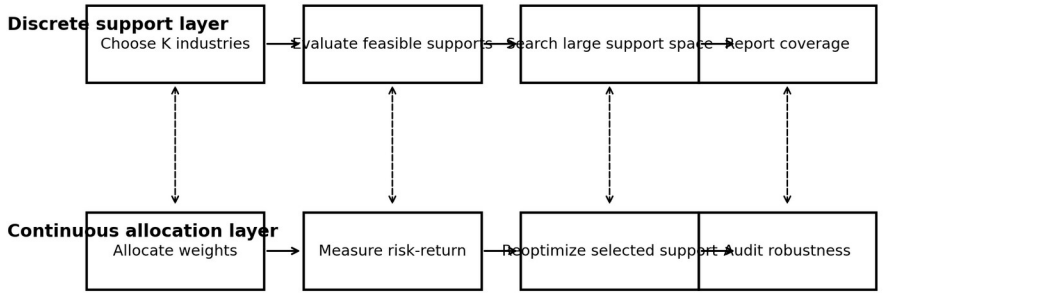


Figure 11.4. Mixed discrete-continuous structure of the optimization object.

Source: Author synthesis for Chapter 11.

Table 11.7. Notation and meaning of the cardinality-constrained portfolio object

Symbol/object	Meaning	Operational role	Boundary
n	Number of candidate industries.	n=94 in the main Damodaran industry universe.	Fixed empirical universe, not all possible securities.
K	Target cardinality.	K=10 in the baseline sparse-selection problem.	A modeling choice; later sections can test K-grid alternatives.
z_i	Binary support indicator.	Activates or excludes industry i.	Creates the discrete search layer.
w_i	Portfolio weight.	Allocates capital conditional on support selection.	Continuous allocation does not remove support complexity.
mu_i	CAPM-implied expected return.	Generated from Rf and ERP using beta_i.	Expected return prior, not realized historical return.
Sigma	Covariance matrix.	Defines portfolio risk and correlation dependence.	Conditional on the chosen risk model.
C(n,K)	Number of possible supports.	Measures discrete support-space size.	Counts supports before continuous weight optimization.
Exact benchmark	Reduced n=20, K=6	Tests algorithmic behavior	Does not certify n=94

	support enumeration.	under tractable exact search.	global optimum.

Source: Author formalization based on the source manuscript methodology.

11.2.4. Research-object boundaries: what is inside and outside the chapter

The boundary of the research object is as important as the object itself. Inside the chapter are the fixed industry universe, CAPM priors, covariance geometry, sparse support selection, heuristic search, exact reduced benchmarking, robustness diagnostics, transaction-cost logic and derivative-overlay preparation. Outside the chapter are theorem-level complexity proof, full exhaustive certification of the n=94, K=10 universe, realized historical investment dominance, live trading recommendations and claims that the Black-Scholes overlay creates free performance. These exclusions are not merely defensive. They allow the chapter to make a stronger admissible claim: a reproducible computational-finance framework can demonstrate how portfolio decision complexity should be measured, searched and interpreted.

The chapter also distinguishes between model-implied optimality and investment-performance evidence. CAPM-implied returns are transparent and reproducible, but they are still priors. A portfolio that scores well under this model is not automatically a portfolio that will outperform in realized markets. Similarly, a support found by a genetic algorithm or Monte Carlo search may be strong under the search budget, but it is not a certified global optimum unless the full support space is enumerated or a valid global certificate is provided. The chapter therefore treats optimization output as model-implied computational evidence rather than as a trading claim.

Table 11.8. Inside-versus-outside boundary of the Chapter 11 research object

Dimension	Inside the chapter	Outside the chapter	Reason for boundary
Mathematical status	P-vs-NP-inspired economic analogy.	Formal proof of P != NP or P = NP.	Empirical finance cannot settle a theorem about complexity classes.
Asset universe	94 U.S. industry portfolios from a fixed January 2026 input vintage.	All global securities, all time-varying trading opportunities.	A fixed universe makes the computational experiment auditable.
Expected returns	CAPM-implied priors using Rf and ERP.	Realized historical return dominance.	The chapter studies model-implied optimization, not a backtested performance claim.
Search evidence	Best-found main-universe incumbents under documented search coverage.	Certified full n=94 global optimum.	C(94,10) is too large for naive exhaustive enumeration in the chapter design.
Exact evidence	Reduced n=20, K=6 enumeration of all 38,760 supports.	Direct certification of the full n=94 universe.	Reduced exact evidence validates algorithmic behavior but does not solve the full instance.
Derivative overlay	Black-Scholes logic for option value, delta exposure and leverage-adjusted diagnostics.	Free leverage or guaranteed performance improvement.	Derivative realism adds risk accounting; it does not eliminate risk.
Practical inference	Robustness, transaction costs, beta drift and stress scenarios.	Universal investment recommendation.	Implementation evidence is scenario-based and conditional.

Source: Author claim-boundary matrix for Chapter 11.

11.2.5. Evidence architecture and transition to later sections

Sections 11.1 and 11.2 establish the foundation. The later sections of Chapter 11 must now do four things. First, Section 11.3 must define the data architecture in detail: the Damodaran industry universe, CAPM expected-return construction, volatility inputs, covariance geometry, correlation structure and eigenvalue diagnostics. Second, Section 11.4 must describe the algorithmic methodology: support-space counting, greedy search, Monte Carlo sampling, genetic algorithm search, continuous reoptimization and exact reduced enumeration. Third, Section 11.5 must add realism through Black-Scholes

overlay, transaction costs, stress scenarios and robustness gates. Fourth, Sections 11.6-11.9 must report results, interpret what can be learned and close the claim boundary.

This sequencing prevents the chapter from becoming a portfolio recommendation. The first two sections define why the problem is computationally meaningful and what the research object is. The methodological sections then show how the object is searched and audited. The results section reports best-found and exact reduced evidence. The interpretation and claim-boundary sections explain what computational finance can show and what it cannot certify. The result is a monograph chapter rather than a standalone optimization paper: it connects the P-vs-NP-inspired decision grammar to the broader seven-problem research program.

Table 11.9. Forward link from Sections 11.1-11.2 to the rest of Chapter 11

Later section	What it must establish	Connection to 11.1-11.2	Claim discipline
11.3 Data Architecture	Audited industry inputs, CAPM priors and covariance geometry.	Turns the research object into a reproducible empirical universe.	Input vintage and model assumptions must remain explicit.
11.4 Methodology	Support-space counting, greedy, Monte Carlo, GA and exact reduced benchmarking.	Operationalizes the P-vs-NP-inspired search-versus-verification logic.	Heuristic search cannot be presented as full certification.
11.5 Realism and robustness	Black-Scholes overlay, costs, stress scenarios and robustness gates.	Tests whether model-implied results remain meaningful under implementation frictions.	Derivative leverage and stress tests are diagnostic, not guarantees.
11.6 Results	Best-found portfolios, K-grid, exact reduced benchmark and algorithmic comparison.	Reports evidence generated by the bounded research object.	Distinguishes full-universe incumbent from exact reduced certificate.
11.7 Interpretation	Explains what computational finance shows and cannot certify.	Translates algorithmic evidence into economic meaning.	No theorem proof and no realized-return dominance.
11.8 Claim Boundary	States excluded claims explicitly.	Protects the chapter from overreading.	No P != NP proof, no certified n=94 optimum, no investment-superiority claim.
11.9 Conclusion	Closes the computational-decision chapter.	Connects Chapter 11 to the final comparative synthesis.	Strong bounded claim rather than exaggerated conclusion.

Source: Author section-architecture synthesis for Chapter 11.

11.2.6. Section-level conclusion

The research object is therefore correctly defined as a cardinality-constrained portfolio-optimization system rather than as a single optimized portfolio. This distinction determines the scientific quality of the chapter. The chapter can be strong only if it treats sparse support selection, continuous weight allocation, covariance dependence, CAPM priors, search algorithms, exact reduced benchmarking and implementation frictions as one integrated decision architecture. The object is narrow enough to be auditable and broad enough to illustrate the economic meaning of computational complexity.

The appropriate conclusion of Sections 11.1 and 11.2 is that P-vs-NP logic is economically valuable when it is used with discipline. It clarifies why some financial decision problems cannot be reduced to simple closed-form optimization, why best-found results differ from certified global optima, why exact evidence can be supplied only at a reduced scale, and why a credible computational-finance chapter must report both its achievements and its limits. This creates the foundation for the data, methodology, robustness, results and interpretation sections that follow.

Table 11.10. Readiness checklist after Sections 11.1-11.2

Readiness item	Status established in this draft	Why it matters

Computational meaning defined	Yes: support-space explosion and search-versus-verification logic are specified.	Prevents the P-vs-NP analogy from becoming rhetorical.
Research object bounded	Yes: cardinality-constrained portfolio-optimization system, not a single portfolio.	Makes the chapter methodological rather than promotional.
Empirical universe identified	Yes: n=94 Damodaran January 2026 U.S. industry universe.	Fixes the candidate set before optimization.
Baseline cardinality stated	Yes: K=10 and C(94,10)=9,041,256,841,903.	Shows the magnitude of the full support-search problem.
Exact reduced benchmark stated	Yes: n=20, K=6 and C(20,6)=38,760.	Defines where exact certification is available.
Claim boundary stated	Yes: no theorem proof, no certified n=94 global optimum, no realized-return dominance.	Protects the chapter from reviewer overclaim concerns.

Source: Author synthesis.

11.3. Data Architecture: Damodaran Industry Universe, CAPM Priors and Covariance Geometry

The data architecture of Chapter 11 is the foundation of the computational-decision argument. A P-vs-NP-inspired portfolio study cannot begin with an undefined asset universe, an opaque return vector or an unspecified risk model. Before the algorithmic problem can be meaningful, the empirical universe must be fixed, the expected-return prior must be reproducible, the covariance object must be auditable and the evidence status of every constructed variable must be clear.

The empirical universe is the fixed Damodaran January 2026 U.S. industry dataset after exclusion of aggregate market rows. The resulting candidate universe contains n = 94 industry portfolios. Each industry is treated as an asset candidate in a sparse-selection problem. This design deliberately avoids ex-post asset selection: the universe is fixed first, and only then are CAPM expected returns, covariance geometry, support-space counts and search algorithms constructed.

Chapter 11.3 therefore performs three functions. First, it defines the data objects used by the sparse optimizer. Second, it separates public input variables from author-calculated variables. Third, it shows why covariance geometry prevents the problem from becoming a trivial ranking of stand-alone Sharpe proxies. The portfolio decision is not simply “choose the ten highest CAPM returns”; it is “choose a support and weights under a coupled covariance matrix.”

Figure 11.3.1. Data architecture pipeline for the Chapter 11 computational-decision model

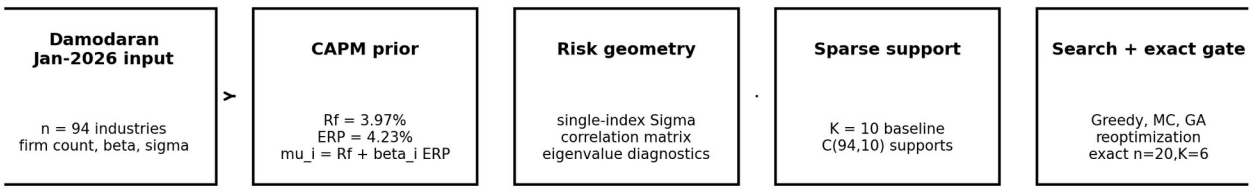


Figure logic: Chapter 11.3 fixes data and geometry; Chapter 11.4 converts them into a mixed discrete-continuous computational search protocol.

Source note: *Author-designed monograph figure based on the source manuscript architecture: Damodaran Jan-2026 input layer, CAPM prior, single-index covariance geometry, sparse support selection and exact/heuristic evidence gates.*

11.3.1. Empirical universe and source-vintage discipline

The empirical universe is industry-level rather than firm-level. This is analytically important. A firm-level universe would create a different covariance, transaction-cost and microstructure problem. The present chapter instead uses industry portfolios as decision units, allowing the analysis to focus on support selection, expected-return priors, covariance coupling and algorithmic search rather than on individual security microstructure. The unit of decision is the industry portfolio i = 1, ..., 94.

A fixed source vintage is a reviewer-safety device. It makes it possible to ask whether the reported search results follow from the stated input universe, not from repeated universe changes. The data architecture therefore records the industry universe, variable roles, calibration inputs and constructed objects before optimization. This is the first layer of replication discipline.

Equation (11.3.1). $i = 1, \ldots, n, \; n = 94.$

The index i labels the 94 industry portfolios in the fixed Damodaran January 2026 empirical universe.

Equation (11.3.2). $x_i = (F_i, \text{beta}_i, \text{sigma}_i, \text{mu}_i, q_i).$

For each industry, F_i denotes firm count, beta_i levered beta, sigma_i annual equity volatility, mu_i the CAPM-implied expected return and q_i the CAPM Sharpe proxy.

Table 11.3.1.

Component	Operational definition/value	Source/status	Role in Chapter 11
Industry universe	94 U.S. industry portfolios	Damodaran January 2026; aggregate market rows excluded	Asset set for sparse support selection
Firm count F_i	Number of firms in the industry grouping	Public input from Damodaran layer	Coverage and input-stability proxy
Levered beta beta_i	Simple-average levered beta by industry	Public input from Damodaran layer	Systematic-risk input and CAPM return driver
Equity volatility sigma_i	Annual standard deviation of equity by industry	Public input from Damodaran layer	Risk input and covariance-diagnostic anchor
Risk-free rate R_f	0.0397	Author calibration in source manuscript	CAPM and Sharpe baseline
Equity risk premium ERP	0.0423	Damodaran implied ERP/source manuscript calibration	Excess-return scaling parameter
CAPM expected return mu_i	R_f + beta_i x ERP	Author calculation	Expected-return vector for optimization
CAPM Sharpe proxy q_i	(beta_i x ERP) / sigma_i	Author calculation	Industry screening diagnostic, not portfolio optimum

Source note: *Adapted from the P-vs-NP source manuscript, Table 4.2 and methodology variable definitions. CAPM calibration uses R_f = 3.97% and ERP = 4.23%.*

11.3.2. Data status: public inputs versus author-constructed objects

The chapter separates raw/public inputs from constructed analytical objects. This separation is essential because the strongest empirical claim is not that every variable is directly observed in the market. The observed input layer supplies beta, volatility and firm count. The author-calculated layer then constructs CAPM expected returns, CAPM Sharpe proxies, the covariance matrix, correlation diagnostics, eigenvalue concentration measures, support-space counts and optimization outputs.

This design is legitimate only if the constructed objects remain traceable to their inputs. For this reason, the chapter treats the data architecture as a source ledger. Each variable must answer four questions: where does it come from, how is it transformed, where is it used and what claim boundary applies to it?

Table 11.3.2.

Layer	Data object	Transformation rule	Claim boundary
Public input layer	Firms, beta, sigma	Directly read from the Damodaran January 2026 industry input universe	Defines the empirical universe; does not itself optimize portfolios
Calibration layer	R_f, ERP	Fixed baseline values used to construct CAPM priors	Conditional calibration, not a realized-return estimate
Expected-return layer	mu_i	mu_i = R_f + beta_i x ERP	Model-implied return prior, not historical performance
Screening layer	q_i	q_i = (mu_i - R_f) / sigma_i	Stand-alone diagnostic, not a covariance-aware optimum
Risk-geometry layer	Sigma, rho	Single-index covariance and standardized correlation matrix	Risk model conditional on covariance specification
Complexity layer	C(n,K), Omega_K	Exact combinatorial count of supports	Operational complexity evidence, not theorem proof
Optimization layer	S, w_S, Sharpe	Support selection plus continuous weight optimization	Best-found full-universe result, not certified global optimum

Source note: *Author synthesis for the monograph based on source manuscript data-audit, CAPM and covariance methodology.*

11.3.3. CAPM prior and expected-return construction

The expected-return vector is constructed through a CAPM prior rather than through realized historical returns. This is a deliberate methodological choice. A CAPM prior makes the computational experiment transparent: once beta, R_f and ERP are known, the expected-return vector is reproducible. The limitation is equally clear: the resulting mu vector is model-implied and cannot be treated as evidence of realized investment dominance.

Equation (11.3.3). $\mu_i = R_f + \beta_i \times ERP$.

Expected return for industry i equals the risk-free rate plus beta-scaled equity risk premium.

Equation (11.3.4). $\mu_i - R_f = \beta_i \times ERP$.

The excess-return component is beta-driven under the CAPM calibration.

Equation (11.3.5). $q_i = (\mu_i - R_f) / \sigma_i = (\beta_i \times ERP) / \sigma_i$.

The CAPM Sharpe proxy measures stand-alone CAPM excess return per unit of industry volatility. It is used for screening, not as the final portfolio objective.

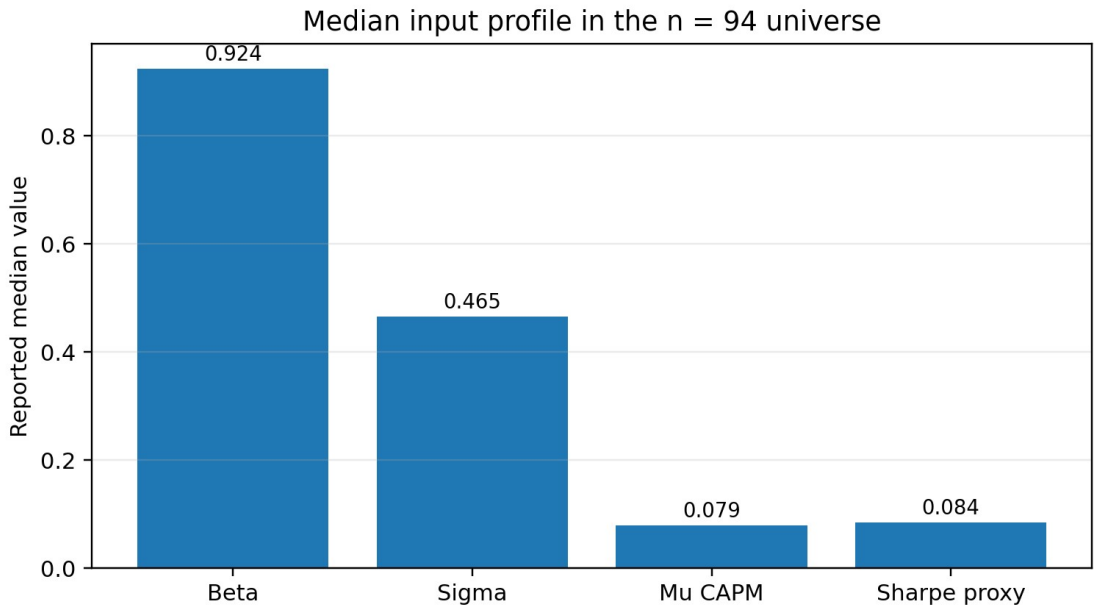
Because q_i is stand-alone, it cannot replace portfolio optimization. Two industries with high q_i values may be strongly correlated, and adding them together may fail to improve covariance-adjusted Sharpe. The CAPM layer therefore supplies the return side of the problem; the covariance layer supplies the interaction side.

Table 11.3.3.

Variable	N	Mean	Std. dev.	Min	Median	Max
Beta	94	0.913625	0.271644	0.239435	0.923653	1.6887
Sigma	94	0.462721	0.136727	0.149620	0.465377	0.775603
Mu_CAPM	94	0.078346	0.011491	0.049828	0.078771	0.111131
CAPM Sharpe proxy	94	0.087974	0.028956	0.036317	0.084132	0.172599
Firms	94	63.766	90.8814	1	32.5	568

Source note: *Source manuscript descriptive statistics for the Damodaran January 2026 input universe and author CAPM variables.*

Figure 11.3.2. Median input profile for the n = 94 industry universe



Source note: *Author visualization from reported source manuscript medians: beta = 0.923653, sigma = 0.465377, mu_CAPM = 0.078771 and CAPM Sharpe proxy = 0.084132.*

The descriptive profile confirms that the universe has enough heterogeneity to make support selection meaningful. Median beta is below one but close to market exposure. Median annual volatility is substantial. CAPM-implied returns vary because beta varies. Firm-count dispersion is also high, meaning that some industries are broad, diversified industry groupings while others are narrow. This matters for stability diagnostics and for interpretation of selected supports.

Table 11.3.4.

Industry	Firms	Beta	Sigma	Mu_CAPM
Software (Internet)	29	1.689	0.526	0.111
Retail (Building Supply)	14	1.535	0.459	0.105
Semiconductor	66	1.518	0.558	0.104
Auto & Truck	33	1.456	0.618	0.101
Semiconductor Equip	31	1.397	0.501	0.099
Computers/Peripherals	36	1.350	0.546	0.097
Auto Parts	35	1.339	0.499	0.096
Office Equipment & Services	14	1.334	0.396	0.096
Software (System & Application)	309	1.277	0.568	0.094
Electrical Equipment	112	1.251	0.727	0.093
Advertising	52	1.211	0.629	0.091
Engineering/Construction	48	1.210	0.459	0.091
Air Transport	23	1.185	0.590	0.090
Brokerage & Investment Banking	32	1.171	0.366	0.089
Construction Supplies	40	1.150	0.355	0.088

Source note: *Source manuscript top-15 industries ranked by levered beta and CAPM-implied return. These values explain the return-prior tail but do not define the final portfolio by themselves.*

11.3.4. Covariance geometry and market-mode concentration

The covariance matrix is the object that turns portfolio selection into an interaction problem. If all industries were independent, sparse optimization would be much closer to a stand-alone ranking exercise. The source manuscript, however, reports strong common-factor dependence under the single-index covariance construction. Median off-diagonal

correlation is high, the share of correlations above 0.5 is high and the first eigenvalue explains a large share of total variance. This means that many industry portfolios carry a common market-mode component.

Equation (11.3.6). r_i = mu_i + beta_i f + epsilon_i.

The single-index representation decomposes industry return into an expected component, a common factor exposure and an idiosyncratic residual.

Equation (11.3.7). Sigma_ij = beta_i beta_j sigma_m^2 + 1(i=j) sigma^2_{epsilon,i}.

Covariance contains a common-factor term and a diagonal residual-variance term.

Equation (11.3.8). sigma^2_{epsilon,i} = max(sigma_i^2 - beta_i^2 sigma_m^2, 0).

The non-negativity correction keeps idiosyncratic variance numerically valid.

Equation (11.3.9). rho_ij = Sigma_ij / (sigma_i sigma_j).

The correlation matrix standardizes covariance and is used for dependence diagnostics.

Equation (11.3.10). H_m = (sum_{k=1}^m lambda_k) / trace(Sigma).

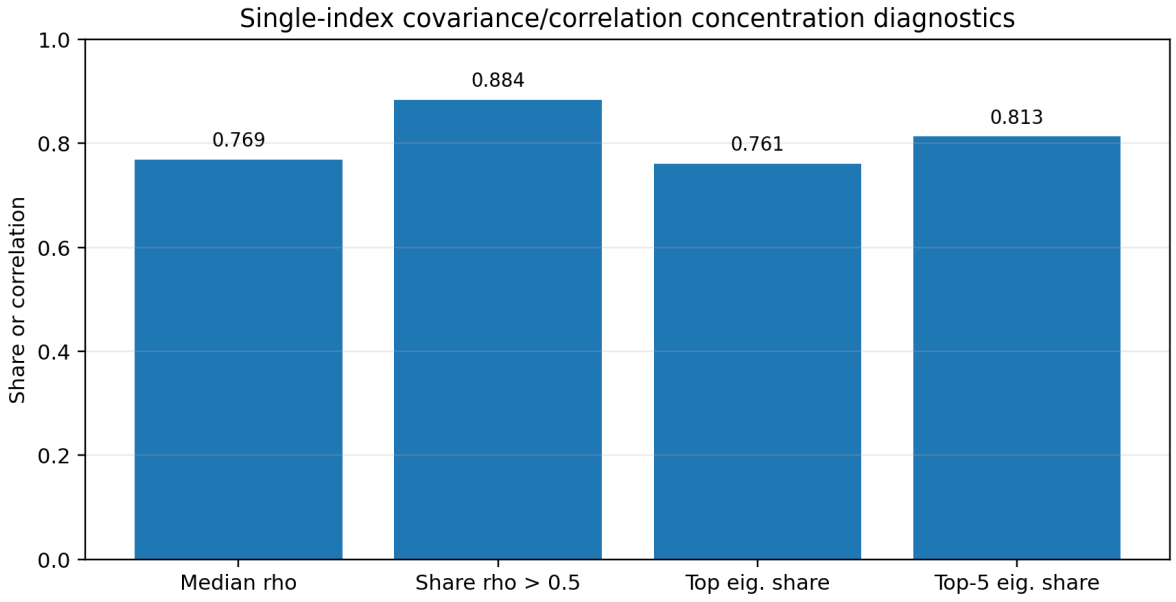
The cumulative eigenvalue share measures how much variance is concentrated in the leading common modes.

Table 11.3.5.

Covariance diagnostic	Reported value	Interpretation
Median off-diagonal correlation	0.769201	The universe is strongly common-factor dominated.
Share of correlations above 0.5	0.884008	Most pairwise links show substantial positive dependence.
Share of negative correlations	0.000000	The risk structure lacks offsetting negative-correlation relief.
Top eigenvalue share lambda_1 / trace(Sigma)	0.761011	One dominant market mode explains most total variance.
Top-five eigenvalue share	0.813010	Additional factors add limited diversification beyond the leading mode.
Minimum eigenvalue PSD check	-1.265e-15	Numerical tolerance result consistent with PSD validation.
Condition proxy kappa	2269.24	High concentration and numerical sensitivity require robustness gates.

Source note: *Source manuscript covariance/correlation and eigenvalue diagnostics for the single-index Sigma layer.*

Figure 11.3.3. Covariance geometry diagnostics showing common-factor concentration



Source note: *Author visualization from reported covariance diagnostics: median rho, share rho > 0.5, top eigenvalue share and top-five eigenvalue share.*

This covariance evidence changes how the whole chapter should be read. A high-CAPM-return industry may not be useful if it adds a large amount of correlated risk. Conversely, a lower stand-alone expected return may still help if it improves the covariance-adjusted frontier. The sparse portfolio problem is therefore not separable by industry. It is a support-and-weight search under common-factor dependence.

Table 11.3.6.

Data-architecture risk	Why it matters	Mitigation in Chapter 11
CAPM prior could be mistaken for realized return	The return vector is model-implied, not historically earned performance	Every result is described as CAPM-implied and conditional on R_f and ERP
Stand-alone Sharpe proxy could be overused	q_i ignores covariance with other selected industries	Portfolio Sharpe uses w^T Sigma w, not only q_i
High covariance concentration can compress diversification	Many industries share a dominant common factor	Eigenvalue, correlation and covariance robustness gates are reported
Full n=94 enumeration is infeasible	C(94,10) is too large for exhaustive support search	Use documented search coverage plus exact reduced benchmark
Best-found result could be overstated	Heuristic search does not equal global certification	Final claim boundary excludes certified full n=94 optimum

Source note: *Author synthesis for reviewer-risk control in the monograph chapter.*

11.3.5. Replication status and data-package logic

The data architecture is not complete until replication status is defined. The source manuscript reports an external replication package on Zenodo, including workbook materials, long-format tables, numeric registry, data dictionary, equation and figure registers, README files, metadata and checksum materials. In the monograph, this should be treated as an audit companion: the Word chapter provides the analytical narrative, while the replication package documents the machine-readable objects.

Table 11.3.7.

Replication item	Required disclosure	Function
Data version	Damodaran Betas by Sector (US), January 2026; n = 94 after excluding aggregate market rows	Fixes empirical universe and input vintage
CAPM calibration	R_f = 3.97%; ERP = 4.23% unless scenario table states otherwise	Fixes expected-return construction
Variable dictionary	F_i, beta_i, sigma_i, mu_i, q_i, Sigma, rho, eigenvalues, C(n,K)	Makes formulas and variable lineage auditable
Randomization	Ten seeds reported for MC/GA layers; seed = 1 shown in reduced benchmark comparison	Makes stochastic results reproducible
Search budgets	MC, GA, reoptimization and exact reduced counts separately recorded	Prevents search coverage from being confused with enumeration
Zenodo package	Dataset package for Robust Portfolio Optimization under Computational Complexity, Zenodo record 20922272	External replication artifact and data-availability closure

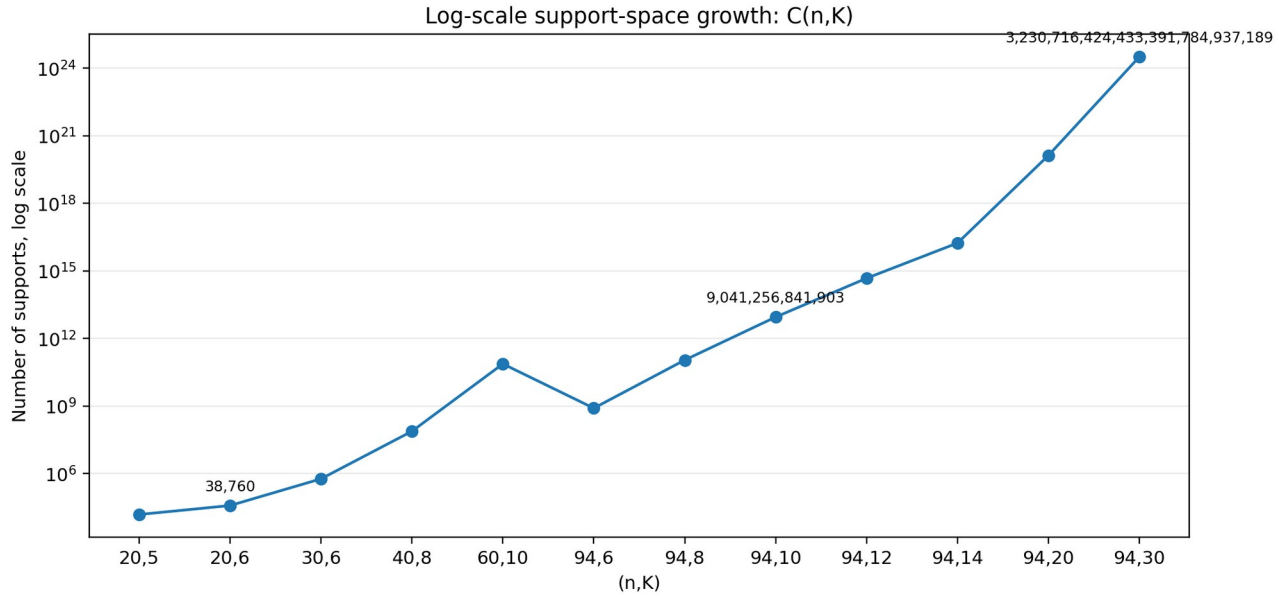
Source note: *Adapted from source manuscript replication-gate logic and data-package statement.*

11.4. Methodology: Support-Space Explosion, Greedy Search, Monte Carlo, GA and Exact Benchmarking

Section 11.4 converts the data architecture into a computational methodology. The core transformation is from a fixed universe A of 94 industries to a support space Omega_K of K-element subsets. Once K = 10 is imposed, the number of possible supports becomes C(94,10) = 9,041,256,841,903 before any continuous weight optimization is performed. This is the operational bridge between portfolio optimization and the P-vs-NP-inspired logic of computational complexity.

The methodology is not a proof about complexity classes. It is an empirical-computational design showing how a realistic cardinality constraint converts portfolio optimization into a mixed discrete-continuous search problem. The chapter therefore distinguishes exact enumeration, stochastic sampling, genetic search, continuous reoptimization and claim-boundary classification.

Figure 11.4.1. Log-scale growth of the support space C(n,K)



Source note: *Author visualization from exact combinatorial counts reported in the source manuscript. The figure emphasizes the jump from reduced exact instances to the full n = 94, K = 10 case.*

11.4.1. Methodological system and evidence vector

The full methodology can be summarized as a system M that contains data audit, return construction, covariance geometry, combinatorial complexity, algorithmic search, benchmarking, robustness, falsification and final claim discipline. In the monograph chapter, Sections 11.3 and 11.4 cover the first five elements and the exact-benchmarking gate. Robustness, Black-Scholes overlay and stress scenarios are assigned to Section 11.5.

Equation (11.4.1). $M = \{D, R, G, C, A, B, S, F, Q\}$.

D is data audit, R expected-return construction, G covariance geometry, C combinatorial complexity, A algorithmic search, B benchmarking, S robustness/stress testing, F falsification and Q final claim discipline.

Equation (11.4.2). $E = (E_{data}, E_{geometry}, E_{complexity}, E_{algorithmic}, E_{benchmark}, E_{claim})$.

The evidence vector is layered; the chapter does not rely on a single Sharpe statistic.

Table 11.4.1.

Methodological block	Formal object	Evidence produced	Boundary
Data audit	A = {1,...,94}; x_i = (F_i,beta_i,sigma_i,mu_i,q_i)	Fixed universe and variable lineage	Industry-level universe, not all tradable securities
CAPM prior	mu_i = R_f + beta_i ERP	Expected-return vector	Model-implied prior, not realized return
Risk geometry	Sigma, rho, eigenvalues	Coupled covariance structure	Conditional on single-index Sigma and robustness checks
Combinatorial core	C(n,K), Omega_K	Support-space explosion	Operational P-vs-NP evidence, not theorem proof
Sparse	S, z, w_S, Sharpe	Best-found K=10 incumbent	No full n=94 global certificate

optimization			
Exact reduced benchmark	n0=20,K0=6; C(20,6)=38,760	Exact enumeration check	Reduced-instance certificate only
Algorithm comparison	Greedy, MC, GA, GA+reoptimization	Upper envelope, median, runtime, seed stability	Heuristic credibility, not universal optimality

Source note: *Author synthesis from the source methodology architecture and result/evidence gates.*

11.4.2. Support-space explosion and P-vs-NP operationalization

The P-vs-NP-inspired argument enters through cardinality. A purely continuous portfolio problem can be difficult, but it is not the same object as a sparse support-selection problem. The moment the analyst requires exactly K selected assets, the optimizer must decide which support to use before or jointly with weight allocation. The number of possible supports grows combinatorially as C(n,K).

Equation (11.4.3). $C(n,K) = n! / [K! (n-K)!]$.

The binomial coefficient counts distinct K-element supports from an n-asset universe before weights are optimized.

Equation (11.4.4). $\Omega_K = \{S : S \subset A, |S| = K\}; \ |\Omega_K| = C(n,K)$.

Ω_K is the discrete support space for a given cardinality K.

Equation (11.4.5). $\Omega_{K,w} = \{(S,w_S): S \in \Omega_K, w_S \in \Delta_K\}$.

The full feasible object is mixed discrete-continuous: a support plus feasible weights on that support.

For the baseline problem, n = 94 and K = 10. The support count equals 9,041,256,841,903. This number is not a rhetorical flourish; it is the main computational object of the chapter. It explains why the full-universe result must be reported as a best-found incumbent under documented search coverage rather than as an exhaustively certified global optimum.

Table 11.4.2.

n	K	C(n,K)	Methodological interpretation
20	5	15,504	Exact enumeration feasible
20	6	38,760	Exact enumeration feasible; reduced benchmark used in source manuscript
30	6	593,775	Exact/MIQP feasible only as reduced benchmark
40	8	76,904,685	Exact/MIQP feasible only as reduced benchmark
60	10	75,394,027,566	Time-limited solver or heuristic layer
94	6	814,216,767	Full enumeration infeasible; heuristic/MIQP bounds needed
94	8	111,315,063,717	Full enumeration infeasible; heuristic/MIQP bounds needed
94	10	9,041,256,841,903	Baseline full-universe K=10 support-space explosion
94	12	4.775e+14	Full enumeration infeasible; heuristic/MIQP bounds needed
94	14	1.743e+16	Full enumeration infeasible; heuristic/MIQP bounds needed
94	20	1.351e+20	Full enumeration infeasible; heuristic/MIQP bounds needed
94	30	3.231e+24	Full enumeration infeasible; heuristic/MIQP bounds needed

Source note: *Exact combinatorial counts from source manuscript Table 4.6. Counts are before continuous weight optimization.*

11.4.3. Baseline sparse Sharpe maximization

The baseline optimization problem selects exactly K = 10 industries and chooses nonnegative portfolio weights. The objective is the CAPM-implied Sharpe ratio. The numerator uses CAPM-implied expected excess return; the denominator uses the covariance-adjusted portfolio standard deviation. This structure is why the problem cannot be solved by ranking q_i alone.

Equation (11.4.6). $SR(w) = (\mu^T w - R_f) / \sqrt{w^T \Sigma w}$.

The portfolio Sharpe ratio combines expected excess return and covariance-adjusted portfolio risk.

Equation (11.4.7). $\max SR(w)$ subject to $\sum_i w_i = 1$, $w_i \geq 0$, $z_i \in \{0,1\}$, $\sum_i z_i = K$, $0 \leq w_i \leq u_i z_i$.

The binary variable z_i selects the support; the continuous variable w_i allocates capital inside the selected support.

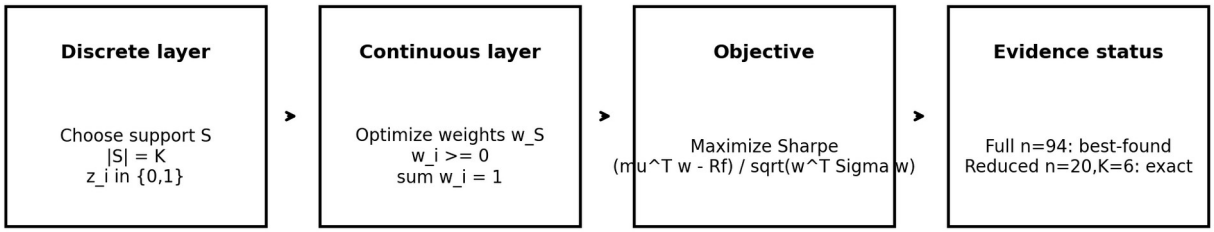
Equation (11.4.8). $\mu_p = \mu^T w, \quad \sigma_p = \sqrt{w^T \Sigma w}, \quad \beta_p = \beta^T w.$

Portfolio expected return, risk and beta are calculated after support and weights are fixed.

Equation (11.4.9). $HHI_w = \sum_i w_i^2, \quad N_{eff} = 1 / HHI_w.$

Weight concentration and effective number of holdings are reported to prevent sparse portfolios from being read as equally diversified.

Figure 11.4.2. Mixed discrete-continuous architecture of the sparse portfolio problem



The chapter treats portfolio choice as a joint support-selection and weight-allocation problem, not as a single continuous optimization.

Source note: *Author-designed monograph figure based on the source manuscript optimization equations and exact/heuristic evidence distinction.*

Table 11.4.3.

Optimization element	Symbol	Definition	Why it matters
Asset universe	A	Set of 94 industry candidates	Fixes the search domain
Support	S	Selected K-element subset of A	Discrete decision layer
Support variable	z_i	Binary indicator for selected industry	Creates mixed-integer structure
Weights	w_i	Capital allocation weights	Continuous decision layer
Cardinality	K	Number of selected industries; baseline K=10	Defines C(n,K) and support sparsity
Expected returns	mu	CAPM-implied expected-return vector	Objective numerator
Covariance	Sigma	Single-index risk matrix	Objective denominator and interaction structure
Sharpe	SR(w)	CAPM excess return divided by covariance risk	Common comparison metric
Weight cap	u_i	Optional upper bound for selected industries	Prevents unrestricted concentration when imposed

Source note: *Author synthesis based on equations (3.18)-(3.21) in the source methodology.*

11.4.4. Greedy search methodology

Greedy search is the simplest benchmark. It is deterministic, transparent and useful as a screening baseline. At each step, the algorithm evaluates which candidate addition produces the best marginal portfolio improvement, conditional on

the current support and the chosen within-support evaluation rule. Its advantage is auditability; its limitation is path dependence. A greedy method can find a strong incumbent but cannot certify the global optimum in a non-submodular, covariance-coupled portfolio problem.

Table 11.4.4.

Step	Greedy sparse-selection procedure
1	Initialize an empty support S_0 and candidate universe A.
2	At step j, evaluate the marginal Sharpe contribution of adding each remaining candidate industry.
3	Choose the candidate with the strongest evaluated improvement under the current support.
4	Repeat until |S| = K.
5	Evaluate or reoptimize weights inside the selected support and record portfolio Sharpe, risk, return and concentration.

Source note: *Adapted from Algorithm 3.1 in the source methodology. The method is useful as an audit baseline but not as a universal optimum certificate.*

11.4.5. Monte Carlo support sampling

Monte Carlo search samples supports from the enormous support space. It provides a distribution of feasible portfolios rather than a single deterministic path. This is important because the full support space cannot be enumerated. Monte Carlo search allows the chapter to compare upper-tail outcomes, medians, dispersion and runtime across repeated seeds. However, Monte Carlo coverage remains a tiny fraction of C(94,10); it is a stochastic audit, not a proof of global optimality.

Table 11.4.5.

Step	Monte Carlo support-sampling protocol
1	Fix n, K, mu, Sigma, R_f, number of draws N and random seed b.
2	For each draw, sample a K-element support S uniformly or according to the specified sampling rule.
3	Evaluate equal-weight or reoptimized weights inside S.
4	Record SR(w), mu_p, sigma_p, beta_p, support composition and runtime.
5	Repeat across seeds and report best, median, dispersion and coverage.

Source note: *Adapted from Algorithm 3.2 in the source methodology. The source manuscript reports main Monte Carlo layers with 30,000 draws per seed and ten seeds.*

11.4.6. Genetic algorithm and continuous reoptimization

A genetic algorithm represents a support as a binary chromosome with exactly K selected industries. Candidate supports are evaluated by a fitness rule, selected, crossed over and mutated while preserving cardinality. The method is useful because it can search adaptively rather than randomly. Yet a subset-only GA can remain incomplete if it treats weights as equal or simplified. Therefore, the source methodology adds a continuous reoptimization layer that refines weights inside promising supports.

Equation (11.4.10). $\text{Fitness}(z) = \max_{w:\ \text{supp}(w) \subseteq \text{supp}(z)} \text{SR}(w).$

The strongest GA fitness rule evaluates the best feasible Sharpe after weight optimization within the selected support.

Equation (11.4.11). $\Delta_K = \{w_S : \sum_{i \in S} w_i = 1,\ w_i \geq 0\}.$

For a fixed support, feasible weights lie on the K-dimensional simplex.

Equation (11.4.12). $w_S^{\text{best}} = \text{argmax}_{w_S \in \Delta_K} \text{SR}(w_S).$

Continuous reoptimization selects the feasible weight vector with the highest Sharpe for a chosen support.

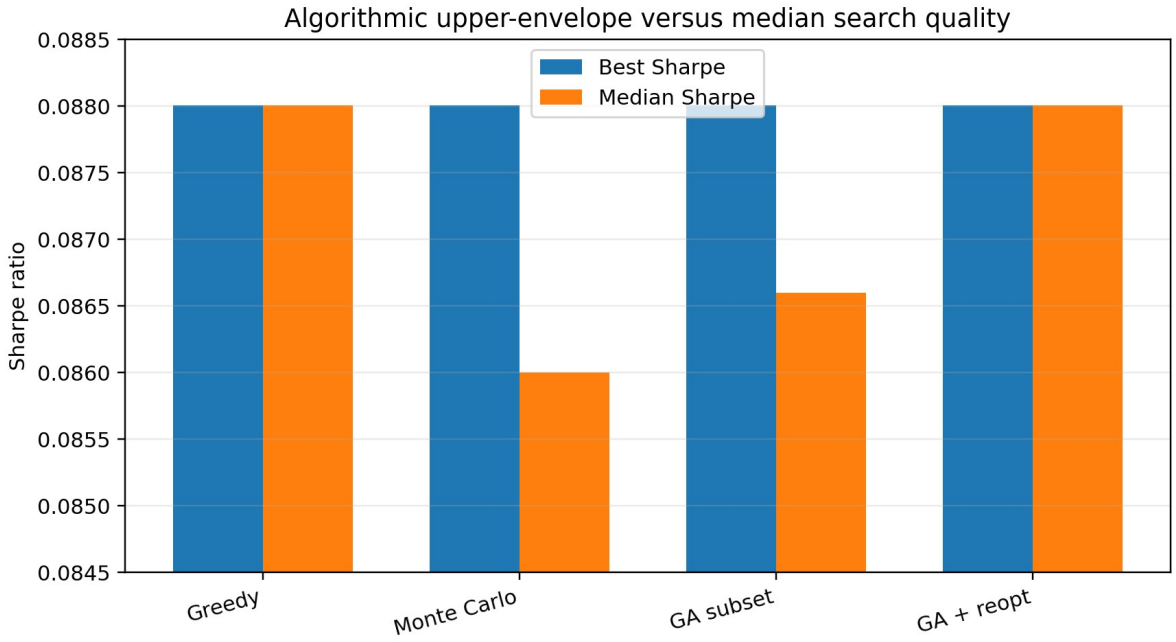
Table 11.4.6.

Algorithm	Core mechanism	Strength	Boundary
Greedy	Sequentially adds the strongest marginal candidate	Fast and transparent	Path dependent; no global certificate
Monte Carlo	Samples K-element supports across repeated seeds	Produces distribution, median and upper-tail	Coverage is stochastic and tiny relative to C(94,10)

		evidence	
GA subset-only	Searches binary support chromosomes using selection, crossover and mutation	Adaptive support search	Equal-weight or simplified weighting can understate support potential
GA + continuous reoptimization	Refines weights inside selected supports	Separates support search from allocation optimization	Still heuristic in full n=94 universe
Exact reduced enumeration	Enumerates all supports in n=20,K=6 benchmark	Provides a true exact benchmark	Does not certify full n=94,K=10 optimum

Source note: *Author synthesis from source Algorithms 3.1-3.4 and exact reduced benchmark methodology.*

Figure 11.4.3. Best versus median Sharpe across algorithmic layers



Source note: *Author visualization from source manuscript algorithmic comparison values. Rounded zero dispersion in source tables is treated as displayed precision, not a theoretical guarantee of zero variation.*

11.4.7. Exact reduced benchmark and optimality-gap measurement

The exact evidence layer is the main methodological safeguard. Because the full n = 94, K = 10 instance cannot be exhaustively enumerated, the chapter introduces a reduced n0 = 20, K0 = 6 benchmark. In that reduced universe, all C(20,6) = 38,760 supports can be enumerated. This creates a ground-truth layer against which Monte Carlo and genetic algorithm outcomes can be compared.

Equation (11.4.13). $SR_exact^*(n_0,K_0) = \max_\{S \text{ subset } A_0, |S|=K_0\} \max_\{w_S \text{ in } Delta_\{K_0\}\} SR(w_S).$

The exact reduced benchmark searches all reduced supports and optimizes weights within each support.

Equation (11.4.14). $Gap_m = 100 \times [SR_exact^* - SR_m] / SR_exact^*.$

The method-specific optimality gap is measured against the exact reduced benchmark.

Equation (11.4.15). $Coverage = E_documented / C(94,10).$

For the full n=94,K=10 case, documented evaluations are divided by the full support count to quantify search effort without claiming exhaustive enumeration.

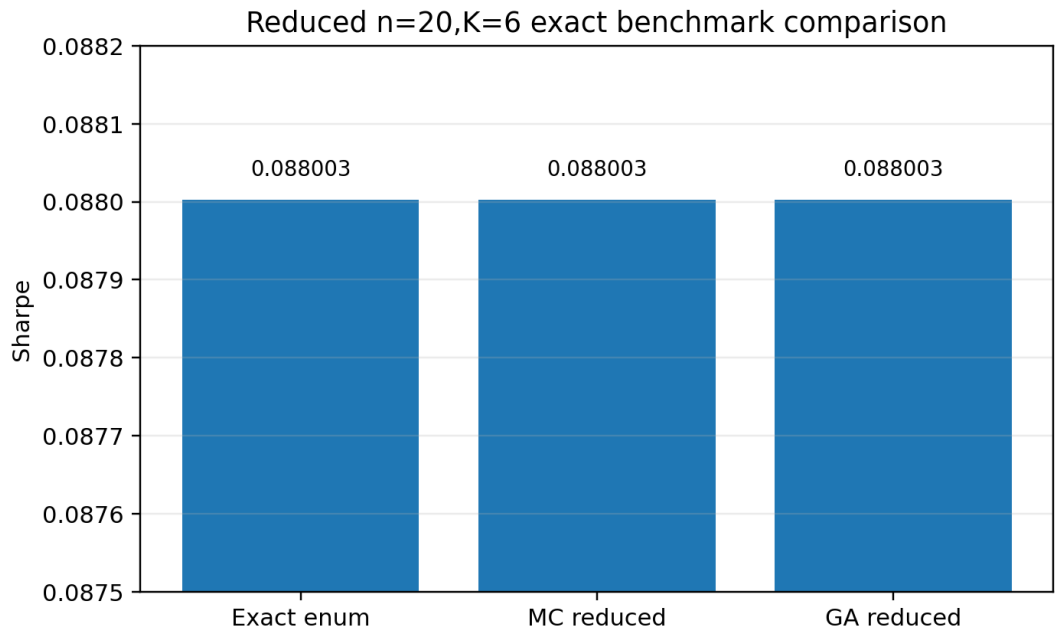
Table 11.4.7.

Method	Best Sharpe	Gap to exact	Best subset / status

		Sharpe (%)	
Exact enumeration (C(20,6)=38,760)	0.088003	0.00	(6, 11, 12, 15, 16, 17)
Monte Carlo (N=2,000; seed=1)	0.088003	0.00	(5, 6, 11, 13, 16, 17)
Genetic Algorithm (P=30,G=30; seed=1)	0.088003	0.00	(6, 11, 12, 15, 16, 17)

Source note: *Source manuscript reduced n=20,K=6 exact benchmark table. The zero gap validates the heuristic logic in the reduced instance only.*

Figure 11.4.4. Exact reduced benchmark versus MC and GA in the n = 20, K = 6 instance



Source note: *Author visualization from source manuscript Table 4.10. Equal displayed Sharpe does not imply full n=94 global certification.*

11.4.8. Full-universe search coverage and no-global-certificate rule

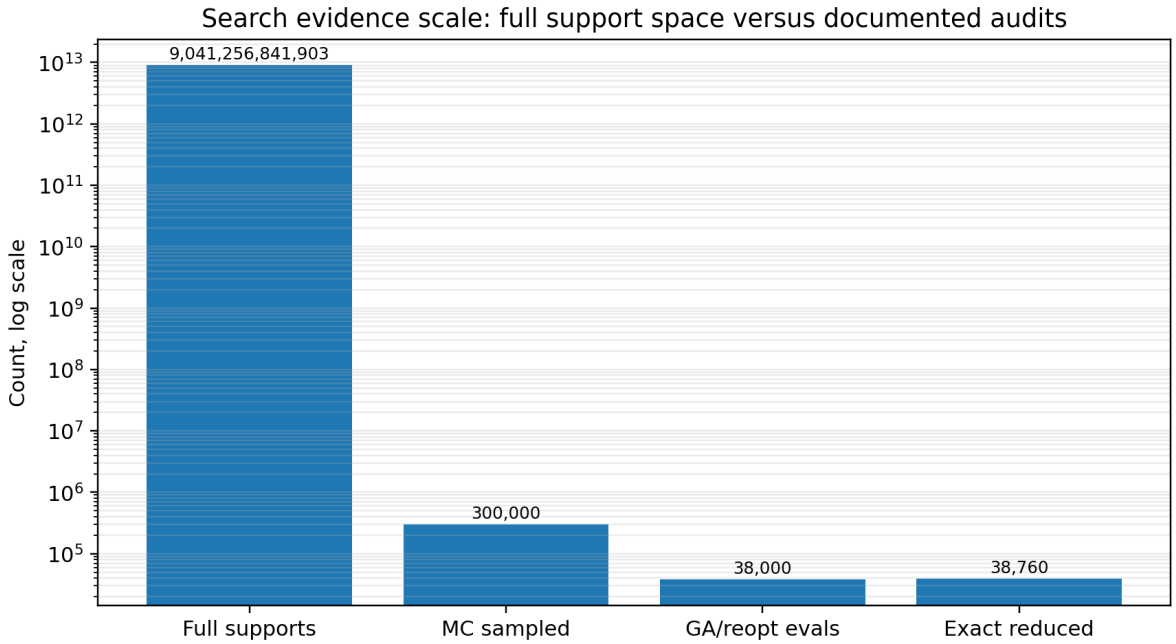
The source manuscript properly separates reduced exact certification from full-universe search coverage. The full n = 94, K = 10 support space contains 9.041 trillion supports. The documented Monte Carlo, GA/reoptimization and reduced exact layers provide computational evidence, but their total coverage remains extremely small relative to the full support space. This is not a defect; it is the reason the chapter is scientifically credible. It quantifies search effort and explicitly refuses to call the best-found incumbent a certified global optimum.

Table 11.4.8.

Search layer	Evidence base	Incumbent / result	Coverage or status
Full support-space size	C(94,10) from n=94,K=10	9,041,256,841,903 possible supports	Exact combinatorial size verified
Documented MC main layer	30,000 draws x 10 seeds	0.088003 upper-envelope	Coverage = 3.318e-08 of full supports
Documented GA/repaired-search layer	P=30,G=30; P=50,G=40; ten-seed layers	0.088003	Coverage proxy = 4.203e-09
Reduced exact benchmark	All C(20,6)=38,760 supports enumerated	0.088003	Certified reduced-instance optimum
Total documented audit coverage	MC + scaling MC + GA/reopt + reduced exact	0.088003 best-found full n=94 incumbent plus exact reduced certificate	Coverage proxy = 4.665e-08

Source note: *Adapted from the source manuscript full search-coverage and global-optimality-boundary certificate.*

Figure 11.4.5. Log-scale comparison of full support size and documented audit layers



Source note: *Author visualization from source manuscript search-coverage certificate. The large scale gap is the reason full n=94 optimality is excluded.*

11.4.9. Algorithmic comparison and runtime discipline

A computational-decision chapter must report not only the best number found, but also how that number was found. The algorithmic comparison therefore reports best Sharpe, median Sharpe, runtime and seeds. This prevents the analysis from relying on one favorable stochastic outcome. It also shows the difference between upper-envelope attainability and typical search quality.

Table 11.4.9.

Method	Best Sharpe	Median Sharpe	Runtime (s)	Seeds
Greedy deterministic	0.088003 (rounded 0.0880)	0.088003 deterministic rounded	0.000 +/- 0.000	-
Monte Carlo (N=30,000/seed)	0.088003 +/- 0.000000*	0.086000 +/- 0.000000*	0.636 +/- 0.015	10
GA subset-only, equal-weight	0.088003 +/- 0.000000*	0.086600 +/- 0.000000*	0.077 +/- 0.017	10
GA + continuous reoptimization	0.088003 +/- 0.000000*	0.088003 +/- 0.000000*	0.573 +/- 0.033	10
Exact benchmark, n=20,K=6	0.088003 exact	-	-	-

Source note: *Adapted from source manuscript algorithmic comparison. Asterisked zero dispersion values are displayed precision, not theoretical zero variability.*

Table 11.4.10.

Method	Effort budget	Best Sharpe	Median Sharpe	Runtime
Monte Carlo	N=500	0.087932 +/- 0.000067	0.086582 +/- 0.000029	0.068 +/- 0.022
Monte Carlo	N=1500	0.087956 +/- 0.000043	0.086581 +/- 0.000016	0.192 +/- 0.045
Monte Carlo	N=2500	0.087984 +/- 0.000022	0.086571 +/- 0.000012	0.296 +/- 0.029
Genetic Algorithm	P=30,G=30	0.088003 +/- 0.000000	0.088003 +/- 0.000000	0.199 +/- 0.009

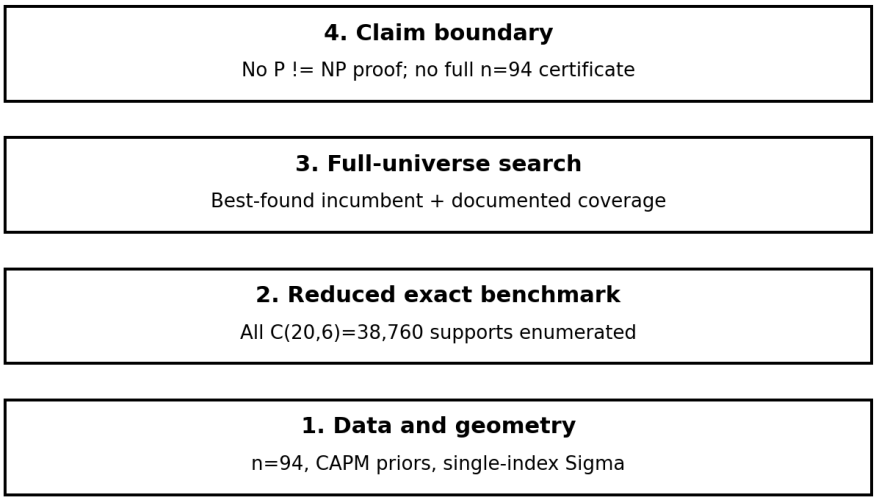
Genetic Algorithm	P=50,G=40	0.088003 +/- 0.000000	0.088003 +/- 0.000000	0.444 +/- 0.026

Source note: *Source manuscript runtime/effort budget table. Runtime grows with effort, but this does not remove the full combinatorial support-space barrier.*

11.4.10. Boundary between exactness, approximation and interpretability

The final methodological point is the evidence-status distinction. Exact enumeration is available only in the reduced benchmark. The full n = 94, K = 10 search supplies a best-found incumbent under documented search coverage. Greedy, Monte Carlo and GA methods provide algorithmic credibility and performance comparison. Continuous reoptimization improves the allocation step inside candidate supports. None of these layers proves P != NP, certifies the full global optimum or establishes realized investment dominance.

Figure 11.4.6. Evidence ladder and claim boundary for the Chapter 11 methodology



Source note: *Author-designed monograph evidence ladder based on the source manuscript claim-boundary logic.*

Table 11.4.11.

Claim	Supported status	Boundary wording for monograph
Cardinality-constrained portfolio optimization is mixed discrete-continuous	Supported	Binary support variables and continuous weights jointly define the feasible object.
The n=94 universe creates operational search-space explosion	Supported	C(94,10)=9,041,256,841,903 before weight optimization.
The source architecture gives exact evidence	Supported only for reduced benchmark	Exact enumeration is supplied for n=20,K=6, not for full n=94,K=10.
The full n=94,K=10 best-found incumbent is certified globally	Not established	Documented coverage is reported, but full branch-and-bound or exhaustive enumeration is not reported.
The study proves P != NP	Explicitly excluded	The chapter operationalizes computational complexity in finance; it does not prove a theorem about complexity classes.

The portfolio dominates realized market strategies	Outside current evidence scope	The return vector is CAPM-implied; realized historical out-of-sample dominance is not established.

Source note: *Author synthesis from the final claim-boundary matrices in the source manuscript.*

Table 11.4.12.

Seven-problem monograph link	Chapter 11 computational role	How it differs from other problem chapters
Poincare/Ricci chapter	Curvature/entropy diagnostic architecture	Measures inequality deformation, not support search
Hodge chapter	Flow decomposition architecture	Decomposes gradient/curl/harmonic flow, not discrete support selection
Navier-Stokes chapter	Stress-flow balance architecture	Models liquidity pressure/friction/shock, not combinatorial portfolios
Yang-Mills chapter	Gauge-curvature/action and mass-gap threshold architecture	Measures finite-network shock thresholds, not asset-selection complexity
BSD chapter	Local-to-global rank calibration architecture	Uses local-regional signals and L-function analogue, not sparse search
Riemann-Zeta chapter	Forecast-validation and spectral-signal architecture	Evaluates inflation forecasts, not portfolio support explosion
P-vs-NP chapter	Computational-decision architecture	Turns C(n,K), algorithms and exact reduced enumeration into the core economic analogy

Source note: *Author synthesis for monograph integration. Chapter 11 is the computational-decision chapter in the seven-problem architecture.*

11.4.11. Section-level synthesis

Sections 11.3 and 11.4 together establish the methodological foundation of the P-vs-NP-inspired portfolio chapter. The data layer fixes the empirical universe at 94 Damodaran January 2026 U.S. industry portfolios, constructs CAPM priors from R_f = 3.97% and ERP = 4.23%, and builds a covariance geometry with strong common-factor dependence. The computational layer then shows that a K = 10 support constraint creates C(94,10) = 9,041,256,841,903 possible supports before continuous weights are optimized.

The methodology is strong because it does not overclaim. It uses exact enumeration where exact enumeration is feasible, namely in the reduced n = 20, K = 6 benchmark with 38,760 supports. It uses greedy, Monte Carlo, GA and GA plus continuous reoptimization for the full universe, while reporting search budgets, seed logic and coverage. This allows the chapter to make a high-level computational-finance claim without presenting a theorem proof or a global-optimality certificate that the evidence does not provide.

The resulting monograph contribution is precise: Chapter 11 demonstrates how computational complexity becomes economically meaningful when portfolio selection requires a discrete support and a continuous allocation. It is not an abstract discussion of P vs NP. It is a reproducible computational-decision design in which data vintage, CAPM priors, covariance geometry, C(n,K), heuristic search, exact reduced benchmarking and claim boundaries are placed in one auditable architecture.

11.5. Black-Scholes Overlay, Transaction Costs, Stress Scenarios and Robustness Gates

Section 11.5 converts the computational portfolio-search result into an implementation-aware and reviewer-safe realism layer. The preceding sections establish the fixed Damodaran January 2026 industry universe, the CAPM expected-return prior, the covariance geometry, the C(94,10) support-space explosion and the algorithmic search protocol. This section asks a different question: after a strong best-found sparse portfolio is obtained, what happens when implementation frictions, derivative leverage, stress scenarios, covariance alternatives, beta drift and falsification gates are imposed?

This distinction is central for the monograph. A computational-decision chapter cannot stop at a single gross Sharpe value. A sparse portfolio may appear attractive before trading costs, before turnover, before covariance stress, before

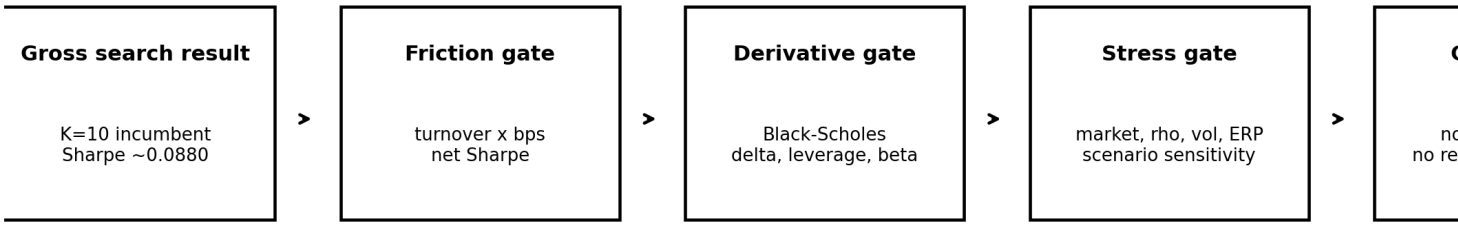
beta instability and before option leverage is mapped into risk. The purpose of Section 11.5 is therefore not to make the result weaker, but to make it scientifically admissible. Robustness and realism are treated as evidence gates: they identify which claims survive and which claims must remain bounded.

Table 11.5.1. Realism and robustness gates for the P-vs-NP portfolio chapter.

Gate	Object tested	Computation used	Admissible interpretation	Boundary
Transaction-cost gate	Gross K=10 Sharpe and expected return	Turnover x cost-bps grid	Net Sharpe sensitivity under implementation frictions	Not a live trading backtest
Black-Scholes overlay	Optional derivative instrument	Call price, delta, leverage, beta, sigma, mu	Derivative exposure can be mapped into CAPM-consistent moments	Not a full option-trading model
Stress-scenario gate	Baseline and option-augmented cases	Market-factor, correlation, volatility and ERP shocks	Shows local and systemic vulnerability under controlled scenarios	Scenario diagnostics, not unconditional predictions
Covariance robustness	Single-index Sigma versus alternatives	Diagonal, constant-rho, shrinkage and high-rho stress audits	Covariance assumptions materially change risk and Sharpe	Risk-model conditional evidence
Input-stability gate	Beta stability and drift	Low-CV and high-CV industry beta histories	Input uncertainty is visible rather than hidden	Not realized-return validation
Falsification gate	Failure modes and placebo checks	Random search, exact reduced benchmark, option leverage, covariance placebo	Prevents gross Sharpe from being overread	Does not certify n=94 global optimum

Source note: *Author synthesis from source manuscript robustness, derivative, stress and claim-boundary layers.*

Figure 11.5.1. Robustness and realism pipeline.



Source note: *Author figure based on the Chapter 11 robustness architecture.*

11.5.1. Transaction-cost and turnover realism

Transaction costs are the first realism gate because the reported search result is a gross model-implied portfolio result. The source manuscript therefore recalculates expected return and Sharpe under different turnover assumptions and cost-

per-unit-turnover values. This is important because cardinality-constrained portfolios may require rebalancing and sparse supports may concentrate trading in a small set of industries.

Equation (11.5.1). CostDrag = Turnover x CostRate

The cost drag is subtracted from the gross CAPM-implied portfolio return before net Sharpe is recomputed.

Equation (11.5.2). NetSharpe = (mu_p - CostDrag - R_f) / sigma_p

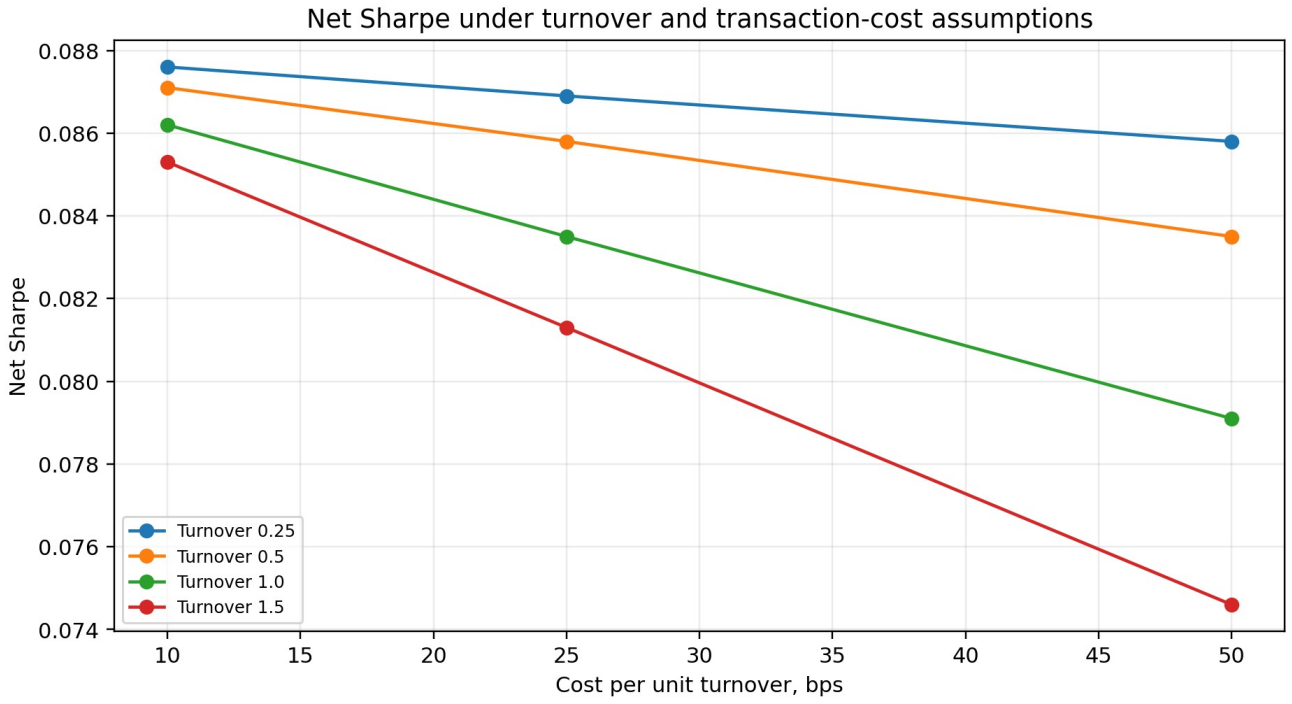
The net Sharpe gate tests whether the gross incumbent remains interpretable after implementation frictions.

Table 11.5.2. Transaction-cost and turnover stress for the baseline K=10 portfolio.

Turnover	Cost per unit turnover, bps	Cost drag	Net mu_p	Net Sharpe
0.25	10	0.0003	0.0886	0.0876
0.25	25	0.0006	0.0882	0.0869
0.25	50	0.0013	0.0876	0.0858
0.50	10	0.0005	0.0883	0.0871
0.50	25	0.0013	0.0876	0.0858
0.50	50	0.0025	0.0863	0.0835
1.00	10	0.0010	0.0878	0.0862
1.00	25	0.0025	0.0863	0.0835
1.00	50	0.0050	0.0838	0.0791
1.50	10	0.0015	0.0873	0.0853
1.50	25	0.0037	0.0851	0.0813
1.50	50	0.0075	0.0813	0.0746

Source note: *Source manuscript Table 4.26; values are preserved and renumbered for the monograph chapter.*

Figure 11.5.2. Net Sharpe under transaction-cost and turnover assumptions.



Source note: *Author visualization from source manuscript transaction-cost grid.*

The result is straightforward. As turnover and cost assumptions rise, net Sharpe falls monotonically. The strongest cost stress shown in the table, turnover 1.50 with 50 bps cost per unit turnover, reduces net Sharpe to 0.0746. This does not

invalidate the computational result. It shows that the correct claim is a model-implied sparse-selection result with an implementation-friction sensitivity layer, not a costless trading-performance claim.

11.5.2. Black-Scholes derivative-overlay protocol

The Black-Scholes overlay introduces derivative realism. The source manuscript uses a European call option on a Software (Internet) industry proxy and maps the option into CAPM-style moments through delta-linearized exposure. The analytical purpose is not to recommend an option strategy. It is to show how derivative leverage changes beta, volatility, expected return and portfolio-level risk-adjusted interpretation.

Equation (11.5.3). $d1 = [\ln(S0/K) + (r + \text{sigma}^2/2)T] / [\text{sigma } \sqrt{T}]$

The standard Black-Scholes d1 term determines the delta of the call option.

Equation (11.5.4). $C = S0\ \text{Phi}(d1) - K \exp(-rT)\ \text{Phi}(d2)$

The European call price transforms the underlying exposure into a priced option instrument.

Equation (11.5.5). $\text{Leverage } L = (\text{Delta} \times S0) / C;\ \text{beta_opt approx } L\ \text{beta_u};\ \text{sigma_opt approx } L\ \text{sigma_u}$

The delta-linearized leverage mapping converts option exposure into CAPM beta and annual volatility proxies.

Table 11.5.3. Black-Scholes worked example: call-overlay inputs and derived moments.

Parameter / output	Value
Underlying proxy	Software (Internet) industry portfolio
beta underlying	1.689
sigma underlying annual	0.526
S0	100
K	100
T years	0.50
r = Rf	3.97%
Black-Scholes call price C	15.61
Delta	0.595
Leverage factor L	3.81
beta option approx	6.43
sigma option approx	2.00
mu option annual	31.18%

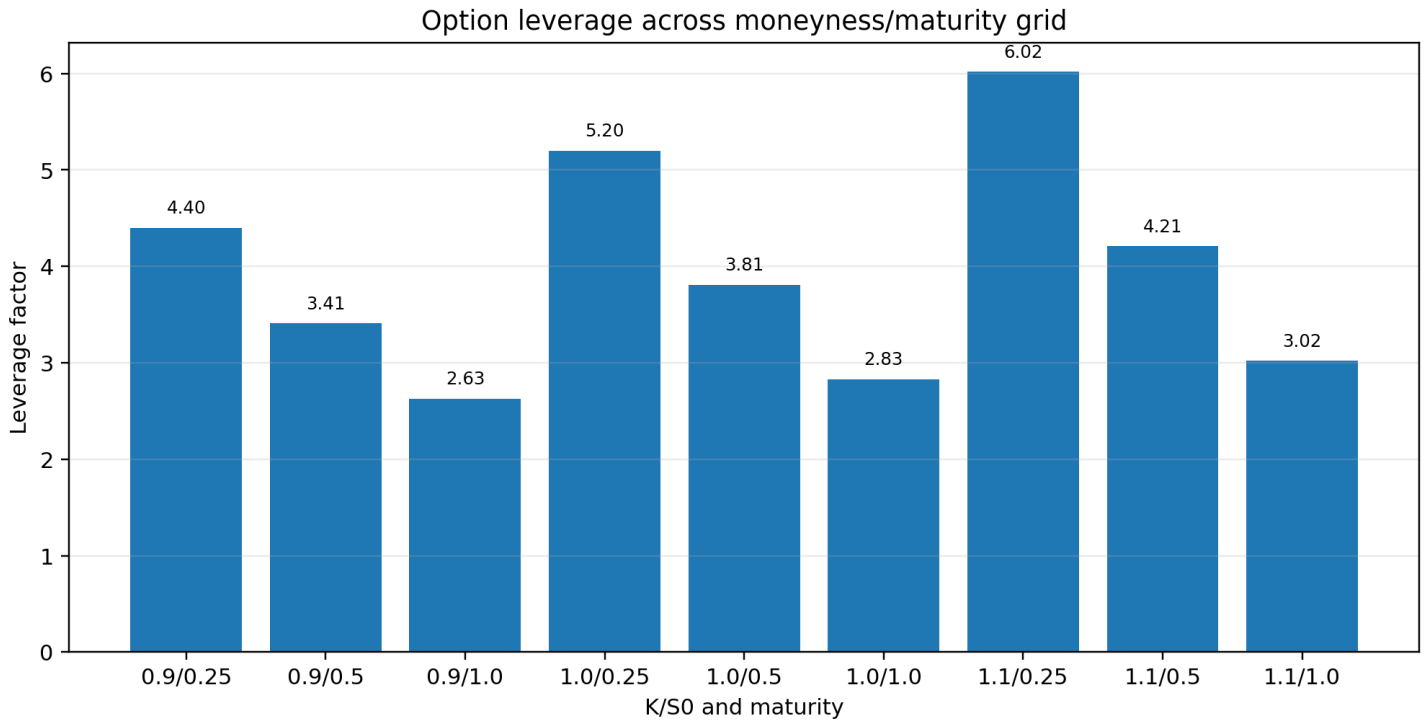
Source note: *Source manuscript Table 4.32; Black-Scholes overlay is diagnostic and delta-linearized.*

Table 11.5.4. Option moneyness-maturity grid: price, delta, leverage and implied moments.

K/S0	T	K	Call C	Delta	Leverage L	beta opt	sigma opt	mu opt ann.
0.9	0.25	90	16.27	0.716	4.40	7.43	2.31	35.40%
0.9	0.5	90	20.54	0.699	3.41	5.75	1.79	28.30%
0.9	1.0	90	26.81	0.705	2.63	4.44	1.38	22.76%
1.0	0.25	100	10.91	0.567	5.20	8.78	2.73	41.11%
1.0	0.5	100	15.61	0.595	3.81	6.43	2.00	31.18%
1.0	1.0	100	22.34	0.632	2.83	4.78	1.49	24.19%
1.1	0.25	110	7.04	0.423	6.02	10.16	3.16	46.95%
1.1	0.5	110	11.72	0.493	4.21	7.11	2.21	34.03%
1.1	1.0	110	18.60	0.562	3.02	5.11	1.59	25.58%

Source note: *Source manuscript Table 4.33; all reported grid values are preserved.*

Figure 11.5.3. Option leverage grid across moneyness and maturity.



Source note: *Author visualization from source manuscript option grid.*

The option grid shows that leverage is state-dependent. The at-the-money six-month call has leverage 3.81, option beta approximately 6.43 and option volatility approximately 2.00. The out-of-the-money short-maturity call has still higher leverage because option price is lower relative to delta exposure. This is why the derivative layer must be treated as a risk-amplification and stress-realism gate, not as a free source of performance.

11.5.3. Local delta validation and option-limit boundary

The manuscript adds a local bump test because a delta-linearized overlay is only a first-order approximation. The plus/minus one percent repricing bumps check whether the approximation remains close for small underlying moves. The errors are very small in the reported grid, but the chapter still preserves the correct boundary: small local approximation accuracy does not eliminate gamma, vega, volatility-smile, liquidity, funding and dynamic-hedging risks.

Table 11.5.5. Delta approximation error under +/-1% repricing bumps.

K/S0	T	C0	Delta	C up	RelErr up	C down	RelErr down
0.9	0.25	16.27	0.716	16.99	-0.04%	15.56	-0.04%
0.9	0.5	20.54	0.699	21.24	-0.02%	19.84	-0.02%
0.9	1.0	26.81	0.705	27.52	-0.01%	26.11	-0.01%
1.0	0.25	10.91	0.567	11.49	-0.06%	10.35	-0.07%
1.0	0.5	15.61	0.595	16.21	-0.03%	15.02	-0.03%
1.0	1.0	22.34	0.632	22.98	-0.02%	21.72	-0.02%
1.1	0.25	7.04	0.423	7.47	-0.10%	6.62	-0.11%
1.1	0.5	11.72	0.493	12.22	-0.04%	11.24	-0.05%
1.1	1.0	18.60	0.562	19.16	-0.02%	18.04	-0.02%

Source note: *Source manuscript Table 4.34; local approximation only, not a full nonlinear option-risk engine.*

11.5.4. Baseline versus option-augmented portfolio check

The option-included comparison is the strongest derivative falsification gate. If derivative leverage mechanically improved the model, the option-augmented case would dominate on Sharpe. Instead, the option raises expected return substantially but raises risk even more. The risk-adjusted result remains approximately equal or slightly lower than the baseline, which prevents a free-leverage interpretation.

Table 11.5.6. Option-included optimization check: baseline versus option-augmented case.

Case	Max Sharpe	Return mu_p	Risk sigma_p
A: Baseline n=94	0.0880 rounded	0.0888	0.5578
B: With option n=95	0.0879	0.2355	2.2273

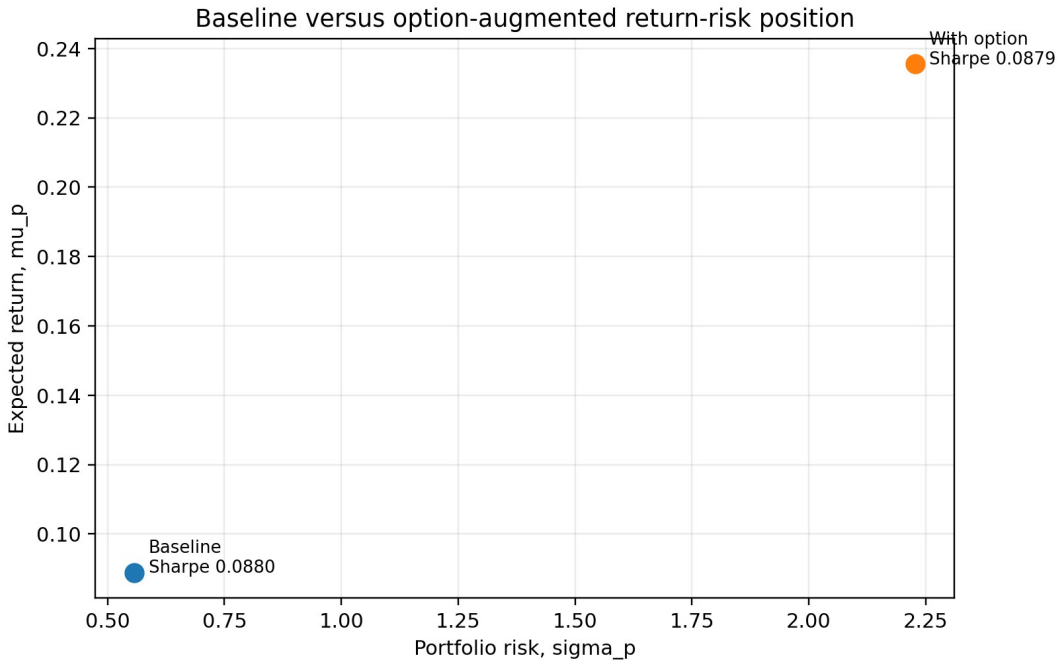
Source note: *Source manuscript Table 4.35; option case raises return and risk together.*

Table 11.5.7. Top weights for baseline and option-augmented observed best-Sharpe portfolios.

Case	Asset	Weight	beta	mu CAPM
A	Auto & Truck	0.263	1.456	0.101
A	Engineering/Construction	0.255	1.210	0.091
A	Steel	0.211	1.063	0.085
B	Option call overlay on Software Internet	0.669	6.430	0.312
B	Financial Svcs. Non-bank & Insurance	0.138	0.970	0.081
B	Brokerage & Investment Banking	0.059	1.171	0.089

Source note: *Source manuscript Table 4.36; selected top positions are reported for composition interpretation.*

Figure 11.5.4. Baseline versus option-augmented return-risk position.



Source note: *Author visualization from source manuscript Case A/B option inclusion table.*

11.5.5. Stress scenarios and crisis-regime interpretation

Stress scenarios translate portfolio construction into vulnerability analysis. The source manuscript reports linear beta-mapped market-factor shocks, correlation compression, volatility spike and ERP compression. The purpose is not to simulate a full crisis market microstructure. It is to test whether the baseline and option-augmented portfolios behave coherently under adverse assumptions and whether leverage changes downside exposure.

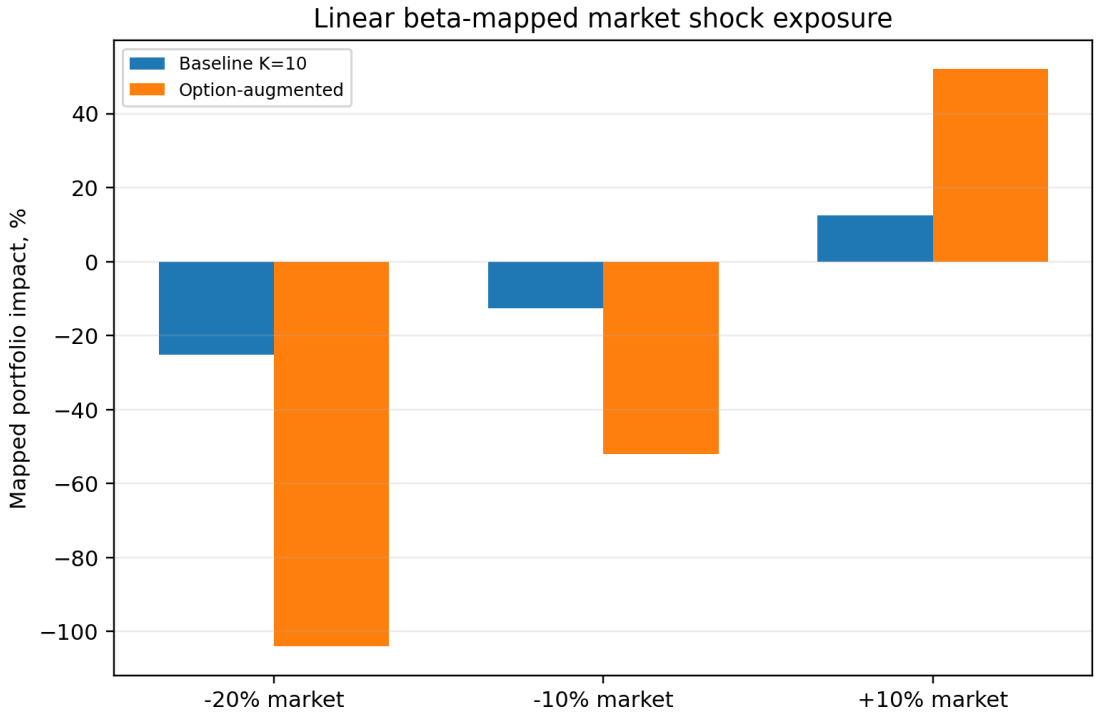
Table 11.5.8. Stress-scenario interpretation for baseline and option-augmented portfolios.

Scenario	Shock	Baseline K=10 impact	Option-augmented impact	Interpretation
Market factor -10%	-10%	-12.56%	-52.02%	Linear beta-mapped stress; not realized backtest
Market factor	-20%	-25.12%	-104.03%	Linear beta-mapped stress;

-20%				not realized backtest
Market factor +10%	+10%	12.56%	52.02%	Upside exposure also amplified by option leverage
Correlation compression	rho -> 0.90	Diversification benefit reduced	Option case more exposed	Systemic co-movement scenario
Volatility spike	sigma +25%	Risk metric rises mechanically	Option vega/gamma risk amplified	Derivative overlay needs nonlinear repricing
ERP compression	ERP -100 bps	Sharpe median falls to 0.0661	Option expected return also falls	Uses source ERP sensitivity table

Source note: *Source manuscript Table 4.37; scenarios are diagnostic, not unconditional predictions.*

Figure 11.5.5. Linear beta-mapped market-shock exposure.



Source note: *Author visualization from source manuscript stress-scenario table.*

11.5.6. Falsification and robustness-gate closure

The robustness gates convert the empirical chapter into an auditable computational-finance result. The strongest principle is that every robustness layer has a defined evidentiary status. Random-search and exact reduced benchmarking test algorithmic credibility; Rf/ERP perturbations test parameter sensitivity; covariance placebos test risk-model dependence; option leverage tests free-performance risk; beta drift tests input stability. The gates do not prove global optimality. They reduce the risk that the reported result is a fragile artefact.

Table 11.5.9. Falsification and placebo audit matrix.

Audit test	Implementation status	Observed result	Decision
Random K-subsets / Monte Carlo draws	Implemented	Median Sharpe 0.0860-0.0866 vs best about 0.088003	Pass: optimizer improves upper-tail result without relying on one run
Reduced exact benchmark	Implemented	Exact Sharpe 0.088003; GA gap 0.00%; MC gap 0.00%	Pass on reduced n=20,K=6 instance
Rf perturbation	Implemented	Rf +/-50 bps leaves Sharpe	Pass: algebraically explained

		unchanged under CAPM excess-return structure	
ERP perturbation	Implemented	ERP +100 bps median Sharpe 0.107046; ERP -100 bps 0.066111	Pass: return-premium sensitivity visible
Option leverage placebo	Implemented via Case A/B	Option raises mu_p to 0.2355 but sigma_p to 2.2273; Sharpe about 0.0879	Pass: leverage artefact separated from free-performance interpretation
Diagonal covariance placebo	Recalculated on baseline K=10 weights	sigma_p=0.199212; Sharpe=0.236744 vs correlated-source Sharpe about 0.0880	Pass: covariance specification materially changes risk
Constant-correlation covariance stress	Recalculated with rho=0.769201 and rho=0.884008	Sharpe=0.115660 and 0.109600 respectively	Pass: Sharpe compresses as common dependence rises
Beta-drift proxy audit	Computed from beta-history tables	Low-CV mean 0.0669; high-CV mean 0.4149	Pass: temporal input instability explicitly measured

Source note: *Source manuscript Table 4.38; rows are renumbered and integrated into Section 11.5.*

11.6. Results: Best-Found Portfolios, K-Grid, Exact Reduced Benchmark and Algorithmic Comparison

Section 11.6 reports the portfolio-search results as a hierarchy of evidence. The chapter does not present one optimized portfolio as if it solved the entire n=94 universe exactly. Instead, it reports a best-found K=10 incumbent, K-grid behavior, exact reduced enumeration, algorithmic comparisons, GA reoptimization, runtime scaling, implementation frictions, derivative realism and final claim closure. The result is strong because it is layered and bounded.

The headline numerical pattern is stable across the source results: the best-found Sharpe is approximately 0.0880, with upper-envelope values up to 0.088003. Exact evidence is available only for the reduced n=20,K=6 instance, where all C(20,6)=38,760 supports are enumerated. Full-universe evidence remains best-found and coverage-documented, because C(94,10)=9,041,256,841,903 supports cannot be exhaustively enumerated under the reported design.

Table 11.6.1. Results evidence hierarchy for Chapter 11.

Evidence layer	Numerical object	Main result	Claim status
Baseline K=10 incumbent	Best-found sparse portfolio	Sharpe around 0.0880; upper envelope up to 0.088003	Model-implied CAPM/single-index incumbent
K-grid	K = 6, 8, 10, 12, 14	Median Sharpe rises gradually; best envelope remains close	Cardinality-sensitivity evidence
Exact reduced benchmark	n=20, K=6	All 38,760 supports enumerated; exact Sharpe 0.088003	Certified reduced-instance evidence
Algorithmic comparison	Greedy, MC, GA, GA+reoptimization	All reach best envelope; medians differ	Heuristic credibility evidence
Realism gates	Costs, option, covariance, stress, beta drift	Some results compress under frictions or leverage	Robustness and boundary evidence
Final claim hierarchy	Closure matrix	No P != NP proof; no n=94 global optimum certificate	Reviewer-safe claim discipline

Source note: *Author synthesis from source manuscript results chapter.*

11.6.1. Baseline K=10 best-found portfolio evidence

The baseline result is a best-found K=10 portfolio in the fixed Damodaran-CAPM/single-index universe. The key distinction is that this result is an incumbent under documented search coverage, not a certified global optimum over all

9.041 trillion supports. The result is still valuable because it is supported by repeated heuristic search, exact reduced benchmarking, covariance diagnostics and robustness gates.

Table 11.6.2. Baseline K=10 results summary.

Metric	Value
Cardinality K	10
Reported headline Sharpe	0.0880 rounded; observed upper-envelope up to 0.088003
Reported headline mu_p	0.0868 / 0.0888 across source output tables
Reported headline sigma_p	0.5356 / 0.5578 across source output tables
Weighted beta from composition	1.1142
HHI concentration	0.1696
Effective number of holdings	5.90
Top-3 normalized weight share	59.08%
Top-5 normalized weight share	84.03%

Source note: *Source manuscript Table 4.7 / 4.8 result summary, renumbered for monograph Section 11.6.*

Table 11.6.3. Baseline K=10 portfolio composition.

Industry	Weight	Weight norm	Firms	Beta	Sigma annual	Mu CAPM
Farming/Agriculture	0.301	0.3004	35	1.129	0.508	0.087
Auto Parts	0.150	0.1497	35	1.339	0.499	0.096
Information Services	0.141	0.1407	15	0.921	0.324	0.079
Chemical Specialty	0.140	0.1397	59	0.970	0.423	0.081
Auto & Truck	0.110	0.1098	33	1.456	0.618	0.101
Food Wholesalers	0.045	0.0449	13	0.867	0.340	0.076
Building Materials	0.039	0.0389	41	1.112	0.353	0.087
Bank Money Center	0.032	0.0319	15	0.761	0.227	0.072
Engineering/Construction	0.028	0.0279	48	1.210	0.459	0.091
Reinsurance	0.016	0.0160	1	0.581	0.192	0.064

Source note: *Source manuscript Table 4.8; composition retained for results interpretation.*

11.6.2. K-grid and cardinality-sensitive results

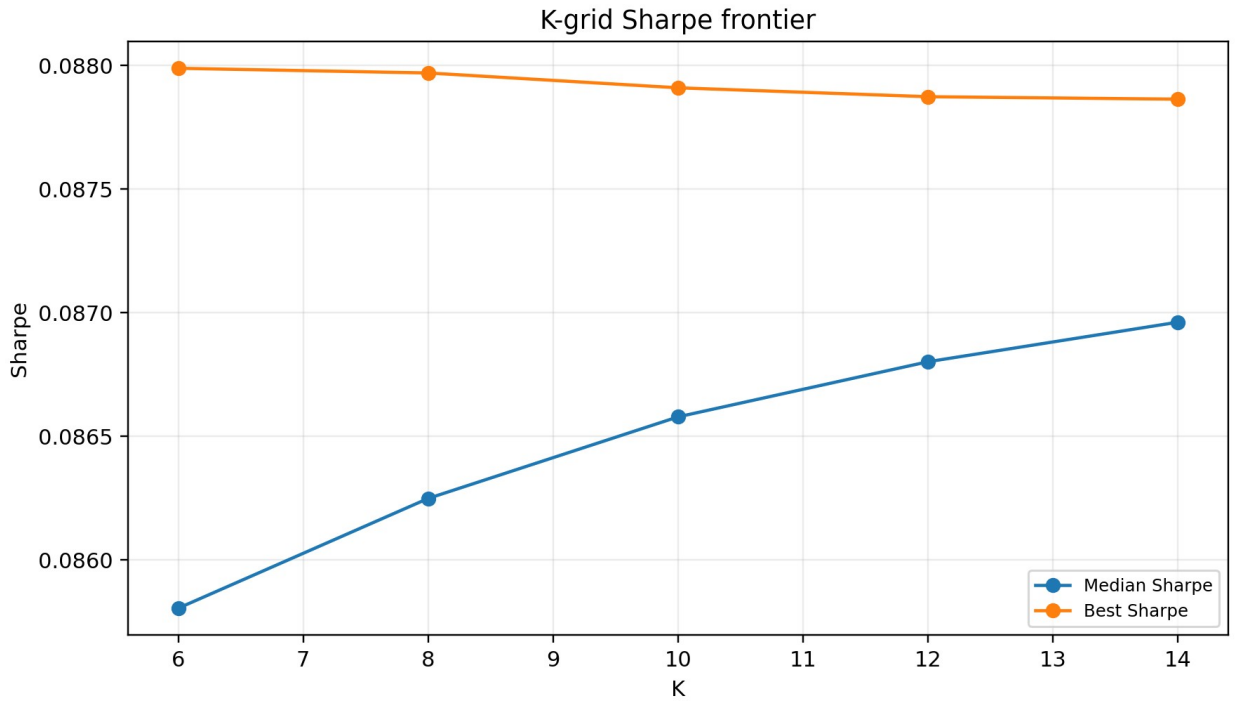
The K-grid shows how sparse portfolio performance changes as the required number of selected industries changes. Median Sharpe rises from K=6 to K=14, but the best Sharpe remains close across the grid. This suggests that increasing K improves typical draw quality and search stability more than it changes the upper performance envelope in the reported configuration.

Table 11.6.4. Cardinality-sensitive Sharpe results across K values.

K	Median Sharpe	IQR 25-75%	Best Sharpe mean over seeds
6	0.085804	[0.084527, 0.086670]	0.087988
8	0.086248	[0.085494, 0.086870]	0.087969
10	0.086578	[0.086073, 0.087039]	0.087909
12	0.086801	[0.086417, 0.087144]	0.087873
14	0.086961	[0.086660, 0.087225]	0.087863

Source note: *Source manuscript Table 4.9; K-grid values preserved.*

Figure 11.6.1. K-grid Sharpe frontier.



Source note: *Author visualization from source manuscript K-grid table.*

11.6.3. Exact reduced benchmark and full-universe coverage boundary

The exact reduced benchmark is the central reviewer-safety device in the results chapter. It prevents the manuscript from relying only on heuristic output. In the reduced n=20,K=6 instance, all 38,760 supports are enumerated, and both Monte Carlo and genetic algorithm layers reach the same exact Sharpe value. This supports heuristic credibility, but it does not certify the full n=94,K=10 universe.

Table 11.6.5. Exact benchmark versus heuristic optimality gap in the reduced instance.

Method	Best Sharpe	Gap to exact Sharpe	Best subset indices
Exact enumeration C(20,6)=38,760	0.088003	0.00%	(6, 11, 12, 15, 16, 17)
Monte Carlo N=2,000 seed=1	0.088003	0.00%	(5, 6, 11, 13, 16, 17)
Genetic Algorithm P=30,G=30 seed=1	0.088003	0.00%	(6, 11, 12, 15, 16, 17)

Source note: *Source manuscript Table 4.10; exactness is reduced-instance only.*

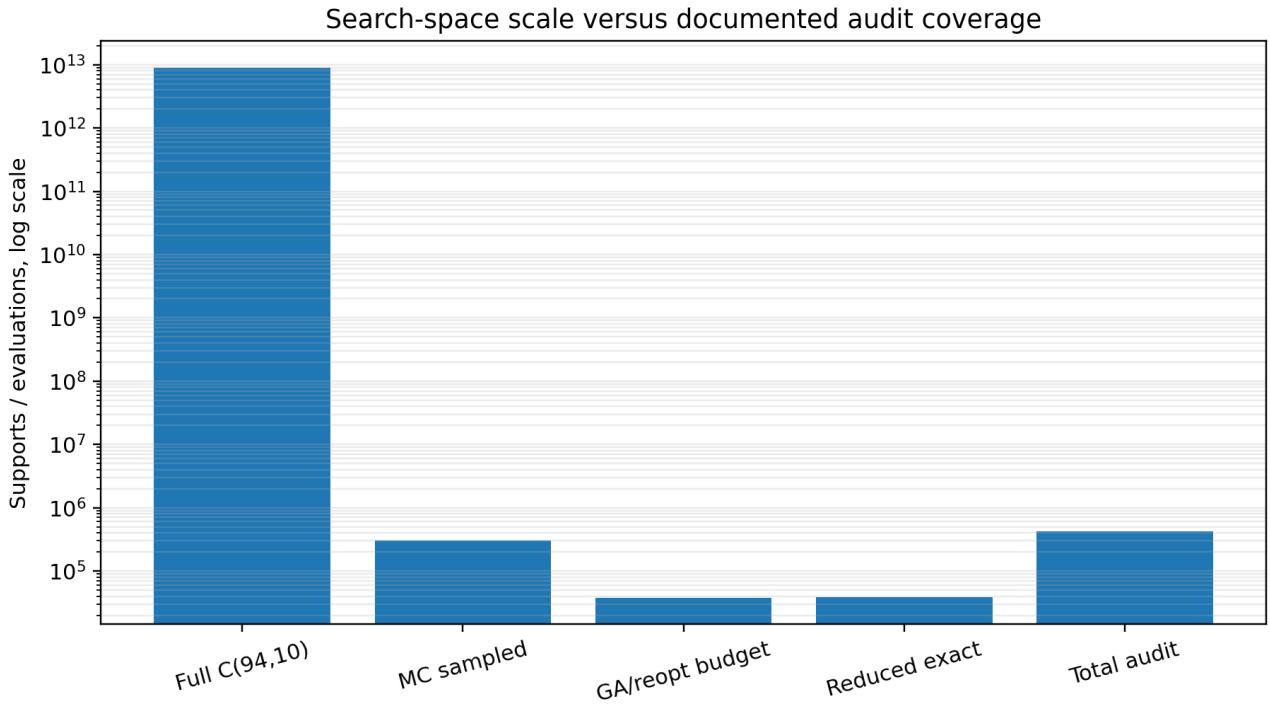
Table 11.6.6. Full n=94,K=10 search-coverage and global-optimality-boundary certificate.

Search layer	Evidence base	Incumbent Sharpe	Gap/coverage	Evaluations/supports	Status
Full support-space size	C(94,10) from n=94,K=10	-	9.041256841903e12 supports	9,041,256,841,903 possible supports	Exact combinatorial size verified
Documented MC main layer	30,000 draws x 10 seeds	0.088003 upper-envelope	Coverage = 3.318e-08	300,000 sampled supports	Stochastic search certificate
Documented GA/repaired layer	P=30,G=30; P=50,G=40; 10-seed layers	0.088003	Coverage proxy = 4.203e-09	38,000 evaluation budget	Heuristic/repaired incumbent certificate
Reduced exact benchmark	All C(20,6)=38,760 supports	0.088003	0.00% gap	38,760 supports	Certified reduced-instance optimum

Total documented audit coverage	MC + scaling MC + GA/reopt + exact	0.088003	Coverage proxy = 4.665e-08	421,760 evaluations/supports	Coverage reported without full enumeration

Source note: *Source manuscript Table 4.11; central claim boundary for full n=94 universe.*

Figure 11.6.3. Search-space scale versus documented audit coverage.



Source note: *Author visualization from source manuscript support-space and audit-coverage table.*

11.6.4. Algorithmic comparison and continuous reoptimization

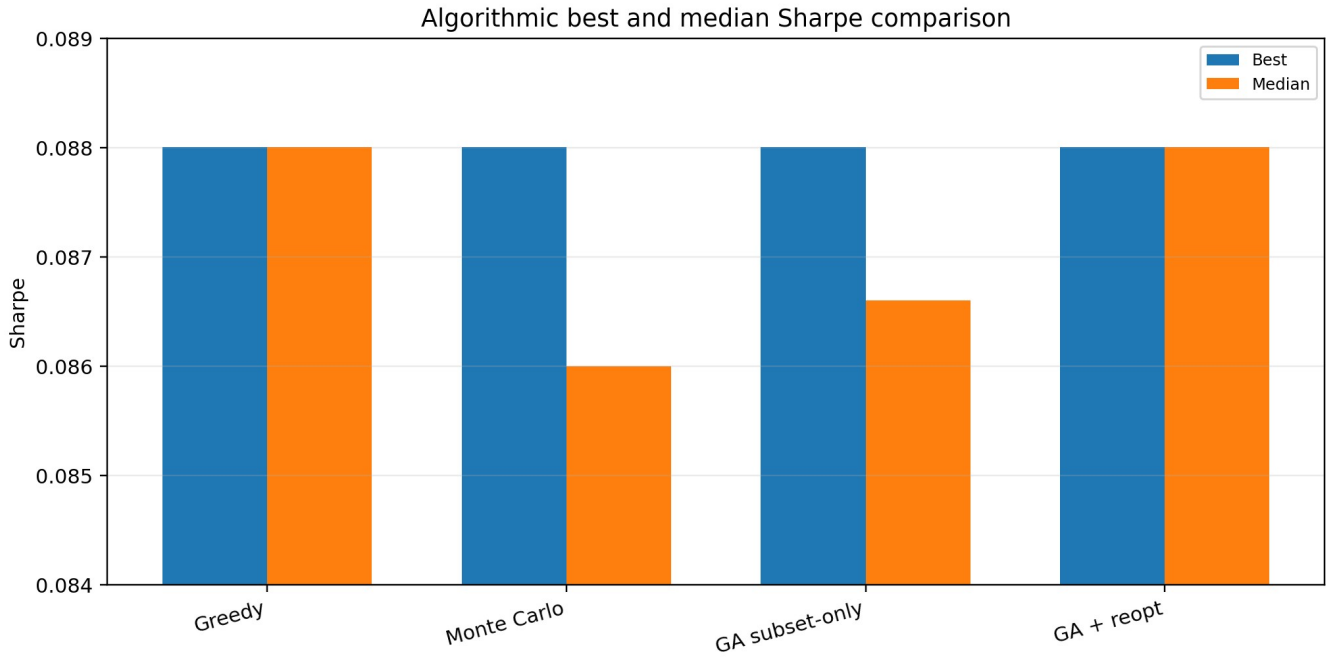
The algorithmic comparison separates upper-envelope performance from median behavior, runtime and search mechanism. The reported best Sharpe is identical across greedy, Monte Carlo, GA, GA plus reoptimization and the reduced exact benchmark, but median behavior differs. The strongest median improvement appears when support selection is followed by continuous reoptimization inside the selected support.

Table 11.6.7. Replicability summary across greedy, Monte Carlo, GA and exact reduced benchmark.

Method	Best Sharpe mean +/- std	Median Sharpe mean +/- std	Runtime s mean +/- std	Seeds
Greedy deterministic	0.088003 rounded 0.0880	0.088003 deterministic rounded	0.000 +/- 0.000	-
Monte Carlo N=30,000/seed	0.088003 +/- 0.000000	0.086000 +/- 0.000000	0.636 +/- 0.015	10
GA subset-only equal-weight	0.088003 +/- 0.000000	0.086600 +/- 0.000000	0.077 +/- 0.017	10
GA + continuous reoptimization	0.088003 +/- 0.000000	0.088003 +/- 0.000000	0.573 +/- 0.033	10
Exact reduced benchmark n=20,K=6	0.088003 exact	-	-	-

Source note: *Source manuscript Table 4.12; values are replicated as result evidence.*

Figure 11.6.2. Algorithmic best and median Sharpe comparison.



Source note: *Author visualization from source manuscript algorithm-comparison table.*

Table 11.6.8. GA variants: subset-only versus subset plus continuous reoptimization.

GA variant	Best Sharpe	Median Sharpe	IQR	Q05-Q95	Runtime s	Seeds	Notes
Subset-only equal-weight	0.088003 +/- 0.000000	0.086600 +/- 0.000000	0.0010 +/- 0.0000	0.0851 - 0.0875	0.077 +/- 0.017	10	Weights fixed equal within subset
Subset + continuous reoptimization	0.088003 +/- 0.000000	0.088003 +/- 0.000000	0.0000 +/- 0.0000	0.088003 - 0.088003	0.573 +/- 0.033	10	GA selects subset; weights reoptimized by local search proxy

Source note: *Source manuscript Table 4.13; continuous reoptimization closes the equal-weight gap.*

Table 11.6.9. Effort budget versus Sharpe and runtime.

Method	Effort budget	Best Sharpe	Median Sharpe	Runtime s
Monte Carlo	N=500	0.087932 +/- 0.000067	0.086582 +/- 0.000029	0.068 +/- 0.022
Monte Carlo	N=1500	0.087956 +/- 0.000043	0.086581 +/- 0.000016	0.192 +/- 0.045
Monte Carlo	N=2500	0.087984 +/- 0.000022	0.086571 +/- 0.000012	0.296 +/- 0.029
Genetic Algorithm	P=30, G=30	0.088003 +/- 0.000000	0.088003 +/- 0.000000	0.199 +/- 0.009
Genetic Algorithm	P=50, G=40	0.088003 +/- 0.000000	0.088003 +/- 0.000000	0.444 +/- 0.026

Source note: *Source manuscript Table 4.14; runtime scaling is reported as computational evidence, not market evidence.*

11.6.5. Statistical inference and descriptive effect-size status

The source results correctly avoid fabricating formal p-values from summary search outputs. Instead, the chapter reports descriptive effect sizes: differences in Sharpe, relative gains and IQR-unit comparisons. This is the right inferential discipline for an algorithmic-search chapter based on search summaries rather than a realized return panel or a full seed-level time series.

Table 11.6.10. Statistical-inference and seed-evidence status for Sharpe comparisons.

Summary-level inference audit	Delta	Computed effect size	Interpretation

	Sharpe		
MC best vs MC median	0.002003	2.33%; 2.07 IQR units	Upper-envelope result exceeds typical random search
GA subset median vs MC median	0.000600	0.70%; 0.62 IQR units	Moderate descriptive gain from metaheuristic support search
GA+reoptimization median vs MC median	0.002003	2.33%; 2.07 IQR units	Largest summary-level improvement after weight repair
GA+reoptimization vs GA subset median	0.001403	1.62%; 1.45 IQR units	Continuous reoptimization closes equal-weight gap
K=14 median vs K=6 median	0.001157	1.35%; K-grid descriptive gain	Increasing K improves median draw but not best envelope materially
Reduced exact benchmark gap	0.000000	0.00%; exact enumeration 38,760 supports	GA and MC reach reduced exact Sharpe 0.088003

Source note: *Source manuscript Table 4.25; descriptive effect sizes are used instead of unsupported p-values.*

11.6.6. Risk contribution, robustness results and integrated strategy ranking

The result chapter also reports risk-contribution and multi-criteria scoring because a sparse portfolio cannot be judged by Sharpe alone. Weight count, variance contribution, runtime, auditability and risk-control status all matter. This is especially important because sparse portfolios may be diversified by number of names but concentrated by risk source.

Table 11.6.11. Variance-share risk contribution by selected industry.

Industry	Weight	Variance share	Cumulative variance share
Semiconductor Equip	0.100	0.1456	0.1456
Office Equipment & Services	0.100	0.1390	0.2846
Construction Supplies	0.100	0.1198	0.4044
Retail Distributors	0.100	0.0988	0.5032
Retail Automotive	0.100	0.0975	0.6007
Homebuilding	0.100	0.0949	0.6956
Diversified	0.100	0.0918	0.7874
Bank Money Center	0.100	0.0793	0.8667
Investments & Asset Management	0.100	0.0687	0.9354
Retail REITs	0.100	0.0647	1.0001

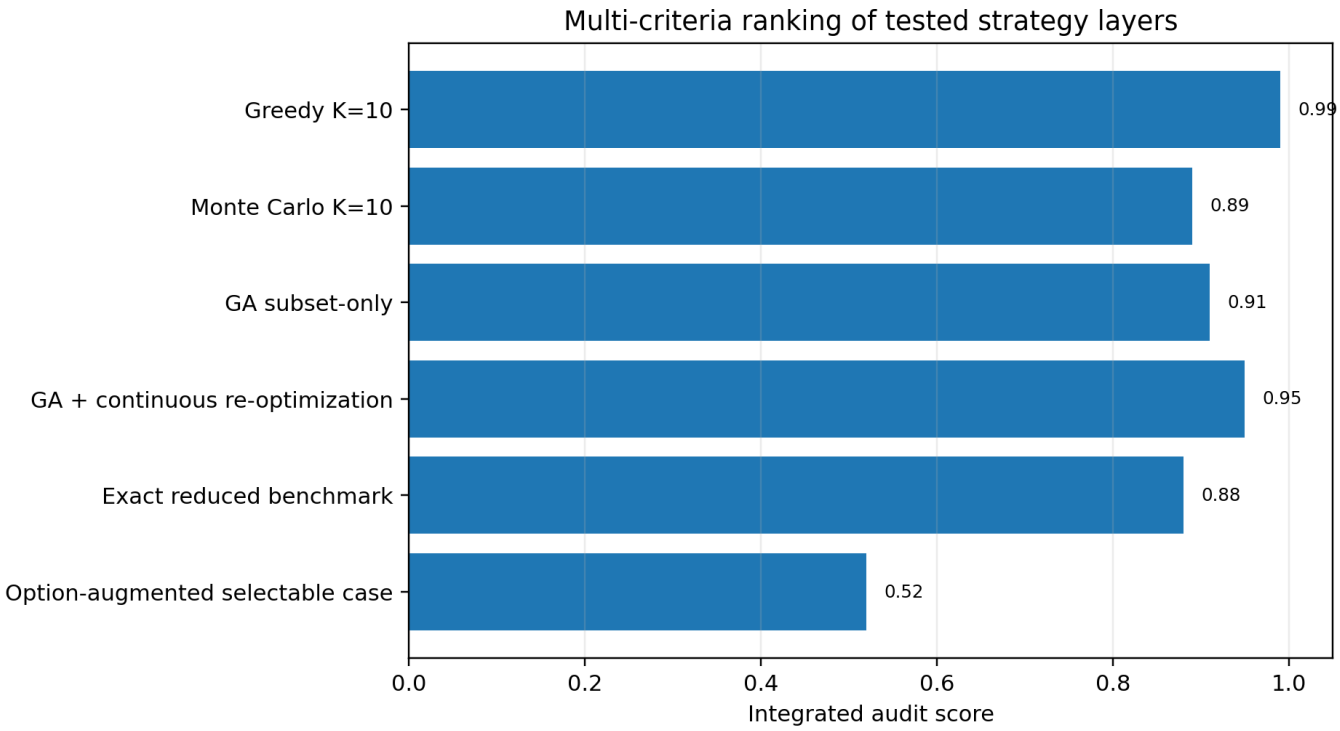
Source note: *Source manuscript Table 4.30; variance shares show concentration of risk even under equal/near-equal weights.*

Table 11.6.12. Integrated multi-criteria ranking of tested portfolio strategy layers.

Model / strategy	Sharpe evidence	Accuracy	Stability	Runtime	Auditability	Risk control	Integrated score
Greedy K=10	0.088	1.00	1.00	1.00	1.00	0.95	0.99
Monte Carlo K=10	0.088	0.98	0.90	0.82	0.90	0.85	0.89
GA subset-only	0.088	0.98	0.92	0.93	0.92	0.82	0.91
GA + continuous reoptimization	0.088	1.00	1.00	0.86	0.95	0.88	0.95
Exact reduced benchmark	0.088	1.00	1.00	0.50	1.00	0.75	0.88
Option-augmented selectable case	0.0879	0.45	0.35	0.70	0.70	0.40	0.52

Source note: *Source manuscript Table 4.39; scores are audit scores, not investment returns.*

Figure 11.6.4. Multi-criteria ranking of tested strategy layers.



Source note: *Author visualization from source manuscript integrated ranking table.*

11.6.7. Results-closure and claim boundary

The final results closure transforms the numerical evidence into an admissible claim hierarchy. This is essential because Chapter 11 uses P-vs-NP logic. The results support an empirical-computational claim about cardinality-constrained portfolio optimization, not a theorem-level claim about complexity classes and not a realized investment-performance claim.

Table 11.6.13. Results-closure matrix.

Research question / claim	Evidence used	Status	Boundary
Does cardinality create a nontrivial sparse selection problem?	C(n,K), MIQP logic, K-grid, exact benchmark	Supported	Operational P-vs-NP framing; no theorem proof claimed
Is the baseline Damodaran-CAPM K=10 result reproducible?	Tables 11.6.2-11.6.7; seed summaries	Supported	Closed within CAPM/single-index universe
Do heuristics provide credible approximations?	GA/MC/greedy comparison; exact n=20,K=6 gap; 421,760 audit evaluations	Supported in tested layer	Full n=94 support space is 9.041e12; coverage proxy 4.665e-08
Does covariance structure matter?	rho diagnostics, eigenvalue concentration, diagonal/constant-rho/shrinkage audits	Supported	Diagonal Sharpe=0.236744; constant-rho=0.115660; high-rho=0.109600
Is option overlay free performance?	Option grid, bump test, Case A/B comparison	Rejected	Sharpe about 0.0879 after sigma_p rises to 2.2273
Is realized historical investment dominance established?	Beta-volatility proxy audit and beta-drift evidence	Separated from current claim	Requires separate return-history study
Does the paper prove P != NP?	Operational support-space and algorithmic evidence	Excluded	Computational hardness is operationalized only

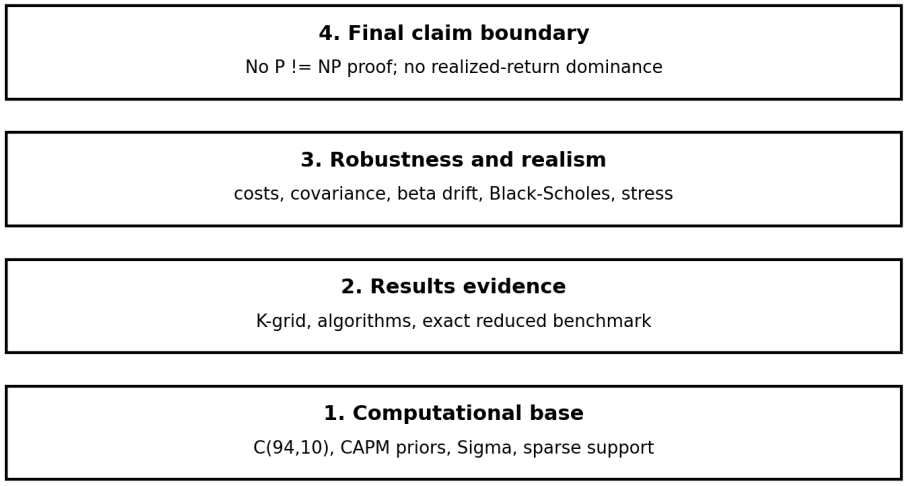
Source note: *Source manuscript Table 4.40, restated for monograph claim closure.*

Table 11.6.14. Final claim hierarchy and exclusion matrix.

Claim	Evidence status	Final classification
Cardinality-constrained mean-variance optimization is a mixed discrete-continuous search problem	Supported	Admissible main computational claim
Damodaran Jan-2026 n=94 universe shows strong common-factor dependence	Supported by median rho=0.769201 and lambda1/trace=0.761011	Admissible empirical geometry claim
K=10 baseline reaches observed Sharpe around 0.0880, with upper-envelope up to 0.088003	Supported	Model-implied best-found claim; not certified global optimum
Heuristics match exact result in reduced n=20,K=6 benchmark	Supported	Reduced-instance approximation claim
Derivative overlay can be embedded in a CAPM-consistent way	Supported	Controlled demonstration claim
Derivative overlay improves performance unconditionally	Rejected by Case A/B risk-adjusted evidence	Explicitly excluded
The model solves P vs NP	Outside theorem-proof scope	Explicitly excluded
The optimized portfolio universally beats all real-world strategies	Outside realized-performance scope	Explicitly excluded

Source note: *Source manuscript Table 4.41, converted into Chapter 11.6 closure language.*

Figure 11.6.5. Evidence ladder for Sections 11.5-11.6.



Source note: *Author figure synthesizing Sections 11.5-11.6.*

11.6.8. Section-level synthesis

Sections 11.5 and 11.6 complete the computational-decision core of Chapter 11. The results show that the Damodaran-CAPM/single-index universe produces a strong and reproducible best-found sparse portfolio result, while exact evidence is properly limited to the reduced n=20,K=6 benchmark. Algorithmic evidence is credible because greedy, Monte Carlo, GA and GA plus reoptimization are compared under common Sharpe, runtime and stability metrics, and because the reduced exact benchmark gives a concrete certification layer.

The robustness and realism layer is equally important. Transaction costs compress net Sharpe; covariance assumptions materially affect risk; beta drift makes input stability visible; and the option overlay raises return and risk together rather than creating free performance. These results turn the chapter from a narrow optimization exercise into a reviewer-safe computational-finance architecture. The final claim is therefore high but bounded: Chapter 11 demonstrates how P-vs-NP logic becomes economically meaningful in cardinality-constrained portfolio optimization, but it does not prove P != NP, does not certify the full n=94 global optimum and does not establish realized investment dominance.

11.7. Interpretation: What Computational Finance Shows and What It Cannot Certify

This section interprets Chapter 11 as a computational-decision chapter. The result is not the mere identification of a high-Sharpe sparse portfolio. The scientific content is the full decision architecture: a fixed empirical universe; a model-implied expected-return vector; a covariance geometry that governs risk; a combinatorial support space; multiple algorithmic search layers; an exact reduced benchmark; robustness and realism gates; and a final claim hierarchy. In that architecture, computational finance shows how portfolio choice becomes difficult once the analyst must choose both a discrete support and continuous weights. It cannot, by itself, certify mathematical complexity theorems, exhaustive global optimality over a 9.041 trillion-support universe, or realized historical investment superiority.

The interpretation therefore begins from an evidentiary distinction. A continuous mean-variance allocation over a fixed asset set is difficult but structurally different from a cardinality-constrained optimization problem. In the latter case, the analyst must first decide which K assets enter the portfolio. That binary support decision creates a combinatorial layer. Only after the support is selected can weights be optimized. The economic meaning of this design is that portfolio construction becomes a decision problem under computational scarcity: the feasible support space is finite but effectively too large for naive exhaustive enumeration at n = 94 and K = 10.

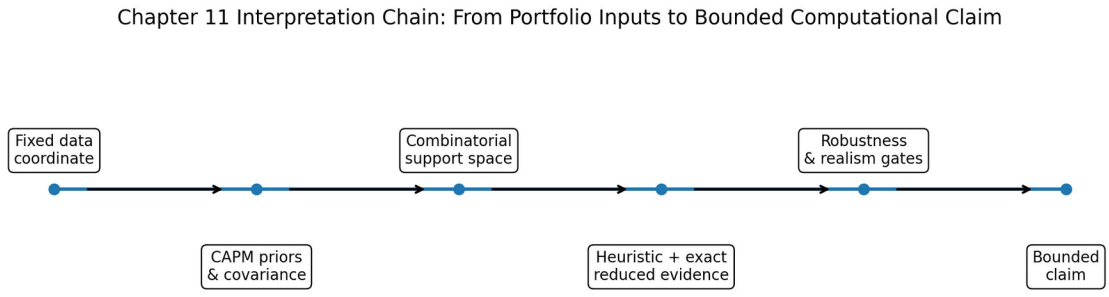


Figure 11.7.1. Interpretation chain from fixed inputs to bounded computational-finance claim.
Source: *Author synthesis based on the Chapter 11 P-vs-NP-inspired portfolio-optimization architecture.*

Table 11.7.1. What the computational-finance evidence shows and what it cannot certify

Evidence block	What it shows	What it cannot certify	Admissible interpretation
Fixed Damodaran Jan-2026 universe	The experiment is anchored before optimization, with n = 94 U.S. industry portfolios.	It does not represent every tradable asset, fund, security, country or realized market history.	A reproducible industry-level computational-finance universe.
CAPM-implied expected returns	Return priors are transparent: mu_i = R_f + beta_i x ERP, with R_f = 3.97% and ERP = 4.23%.	It does not prove realized return dominance or live-trading alpha.	A model-implied expected-return coordinate system.
Covariance geometry	Common-factor dependence makes risk coupling central to interpretation.	It does not eliminate model-specification risk.	Sharpe is conditional on the selected covariance architecture.
Support-space explosion	C(94,10) = 9,041,256,841,903 creates a nontrivial computational search problem.	It does not prove P != NP or resolve any complexity class.	Operational P-vs-NP-inspired economic evidence.
Reduced exact	C(20,6) = 38,760 supports can	It does not certify the n = 94, K	Exact reduced evidence

Evidence block	What it shows	What it cannot certify	Admissible interpretation
benchmark	be fully enumerated and used as a tractable exact anchor.	= 10 global optimum.	supporting search credibility.
Heuristic and metaheuristic algorithms	Greedy, Monte Carlo, GA and GA plus reoptimization can find strong incumbents.	They do not supply exhaustive certificates for all 9.041 trillion supports.	Best-found full-universe evidence with documented coverage.
Black-Scholes overlay	Derivative leverage can be incorporated without treating it as free performance.	It does not model all option risks or prove implementable derivative superiority.	A stress-realism and leverage-discipline diagnostic.

Source: *Author synthesis from the P-vs-NP portfolio manuscript and Chapter 11 monograph structure.*

11.7.1. Interpretation of support-space explosion as economic complexity

The most important computational fact in Chapter 11 is the size of the support space. For n = 94 and K = 10, the analyst faces 9,041,256,841,903 possible supports before any within-support weight optimization is performed. This fact does not prove a theorem about complexity classes. It does, however, operationalize the economic meaning of computational complexity: a realistic portfolio constraint converts asset allocation into a search problem in which exact exhaustive analysis is not practical at full scale.

Equation 11.7.1. Full-universe support-space size

C(94,10) = 94! / (10!84!) = 9,041,256,841,903

The count measures the discrete support-selection layer before continuous portfolio weights are optimized. It is the central numerical anchor for the chapter's operational P-vs-NP-inspired interpretation.

Equation 11.7.2. Documented search coverage

Coverage = 421,760 / 9,041,256,841,903 = 4.665 x 10^-8

The coverage ratio supports audit transparency. It also prevents overclaiming: the full n = 94 result is an incumbent under documented search coverage, not an exhaustive certificate.

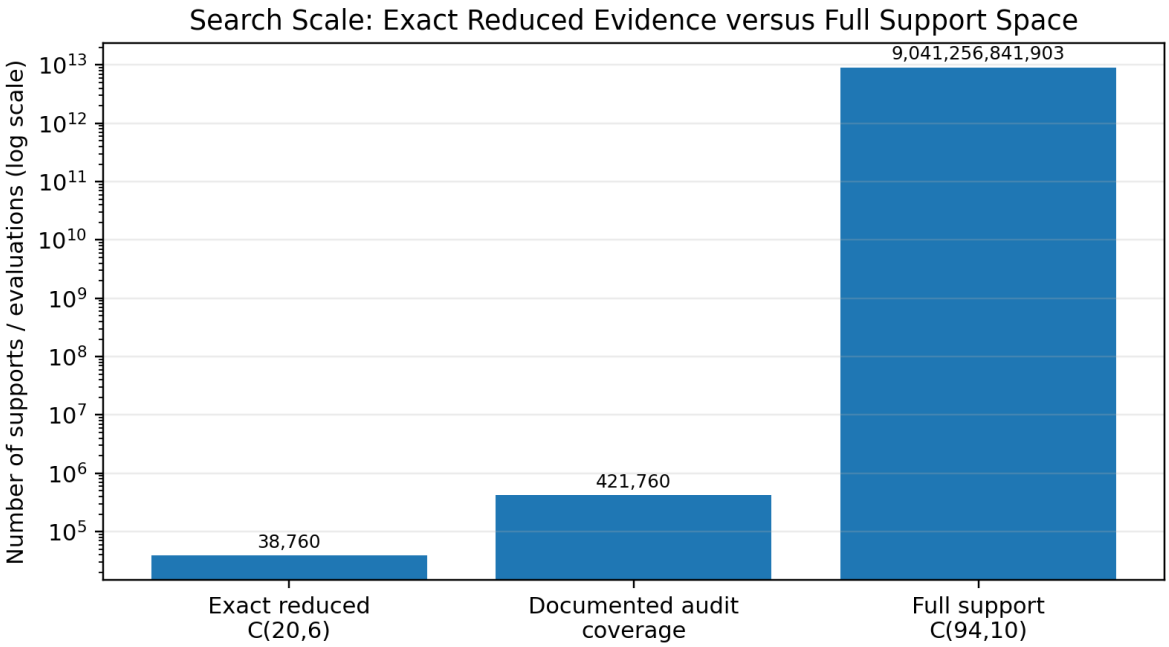


Figure 11.7.2. Search scale: exact reduced evidence, documented audit coverage and full support space.

Source: *Author visualization using reported support counts and documented audit coverage from the P-vs-NP manuscript.*

The reduced exact benchmark is essential because it provides a controlled contrast. In the reduced n = 20, K = 6 case, all 38,760 supports can be enumerated. This means that exactness exists in the chapter, but only at a tractable scale. The correct interpretation is not that the full n = 94 problem is solved exactly, but that the methodology distinguishes exact reduced certification from full-universe heuristic evidence. That distinction is one of the strongest reviewer-safety devices in the chapter.

Table 11.7.2. Cardinality-sensitive interpretation of the K-grid

K	Median Sharpe	IQR (25-75%)	Best Sharpe	Interpretive reading
6	0.085804	[0.084527, 0.086670]	0.087988	Small supports can reach the upper envelope, but typical draws are lower.
8	0.086248	[0.085494, 0.086870]	0.087969	Median performance improves modestly.
10	0.086578	[0.086073, 0.087039]	0.087909	Baseline case sits within a stable upper-envelope band.
12	0.086801	[0.086417, 0.087144]	0.087873	More assets improve typical robustness but not the maximum materially.
14	0.086961	[0.086660, 0.087225]	0.087863	Upper-envelope plateau remains close to 0.0880.

Source: *Author synthesis from the reported K-grid evidence in the P-vs-NP manuscript.*

11.7.2. Interpretation of algorithmic comparison: convergence, not certification

The algorithmic comparison should be read as convergence evidence, not as theorem-level proof. Greedy search, Monte Carlo search, genetic algorithms and GA plus continuous reoptimization all operate under the same model-implied objective. Their role is to document how different search logics behave in the same constrained landscape. If several methods reach the same upper-envelope Sharpe neighborhood, that supports robustness of the incumbent. It does not prove that no better support exists among the unvisited full-universe supports.

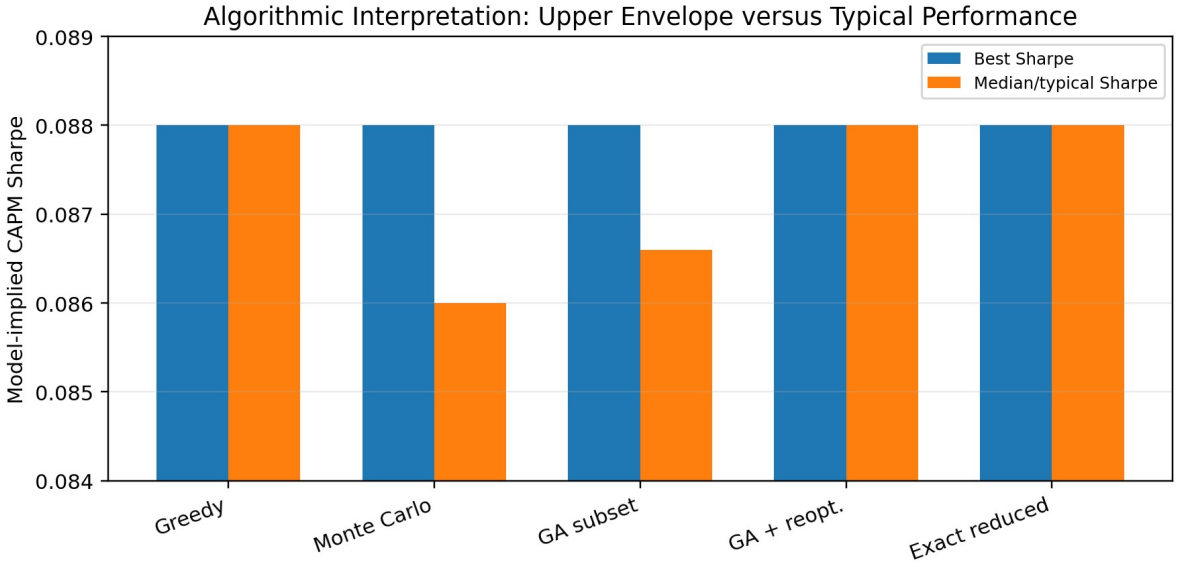


Figure 11.7.3. Algorithmic upper-envelope versus typical performance.

Source: *Author visualization based on the reported greedy, Monte Carlo, GA, GA-plus-reoptimization and exact reduced benchmark summary.*

Table 11.7.3. Algorithmic evidence and certification level

Method	Reported role	Strength	Boundary
Greedy deterministic search	Fast baseline and interpretable incumbent construction.	Useful benchmark; simple and transparent.	May exploit local structure and cannot certify global optimality.
Monte Carlo sampling	Randomized support exploration with documented draw budget.	Tests whether strong results exceed typical random supports.	Coverage remains tiny relative to C(94,10).
Genetic algorithm subset search	Metaheuristic search over support space.	Documents evolutionary search consistency across seeds.	Still heuristic; equal-weight variants may leave allocation gains unused.
GA plus continuous reoptimization	Combines support search with within-support weight repair.	Best interpretation of mixed discrete-continuous mechanism.	Does not replace exhaustive branch-and-bound certification.

Method	Reported role	Strength	Boundary
Exact reduced enumeration	Complete enumeration over n = 20, K = 6.	True exact evidence at reduced scale.	Does not transfer exactness automatically to n = 94, K = 10.

Source: *Author synthesis based on the algorithmic comparison and exact reduced benchmark logic of the source manuscript.*

11.7.3. Interpretation of covariance dependence and risk-model conditionality

A portfolio result is not interpretable without its covariance model. The P-vs-NP chapter is not merely a combinatorial search exercise; it is a search problem embedded in covariance geometry. A support that appears attractive under a diagonal covariance assumption may lose appeal once common-factor dependence is introduced. The source manuscript explicitly treats covariance alternatives as robustness gates rather than decorative sensitivity checks. This matters because sparse portfolios can look diversified by name count while remaining exposed to the same market factor or industry-cycle component.

Table 11.7.4. Covariance interpretation and reviewer-safe wording

Covariance feature	Meaning for portfolio interpretation	Risk of overclaiming	Reviewer-safe wording
Single-index covariance	Portfolio risk is tied to market-factor exposure and idiosyncratic volatility.	Headline Sharpe may be treated as unconditional.	Sharpe is conditional on the specified CAPM/single-index risk model.
High common-factor dependence	Diversification is compressed; adding more industries may not remove systemic risk.	The K count may be mistaken for true diversification.	Cardinality diversification is not the same as covariance diversification.
Diagonal covariance placebo	Can inflate risk-adjusted performance by ignoring cross-industry correlation.	Diagonal results may be used as if realistic.	Diagonal covariance is a placebo/audit layer, not the main risk model.
Constant-rho and high-rho stress alternatives	Test sensitivity to correlation structure.	Alternative Sharpe values may be read as competing truths.	They show model dependence and support bounded interpretation.
Eigenvalue concentration	Shows whether risk is concentrated in a dominant factor.	A sparse portfolio may be misread as independently diversified.	The portfolio is governed by covariance geometry, not by asset count alone.

Source: *Author synthesis from the covariance/eigenvalue robustness logic of the P-vs-NP manuscript.*

11.7.4. Interpretation of derivative overlay: leverage discipline rather than free performance

The Black-Scholes overlay is one of the most important interpretive safeguards in Chapter 11. It demonstrates that derivative instruments can be inserted into the same risk-return discipline, but it also rejects the seductive error that option leverage creates free performance. The option-augmented case raises expected return substantially, but risk rises even more. The reported Sharpe remains approximately the same and slightly lower than the baseline. Therefore, the derivative overlay strengthens the scientific credibility of the chapter precisely because it refuses to turn leverage into an unsupported performance claim.

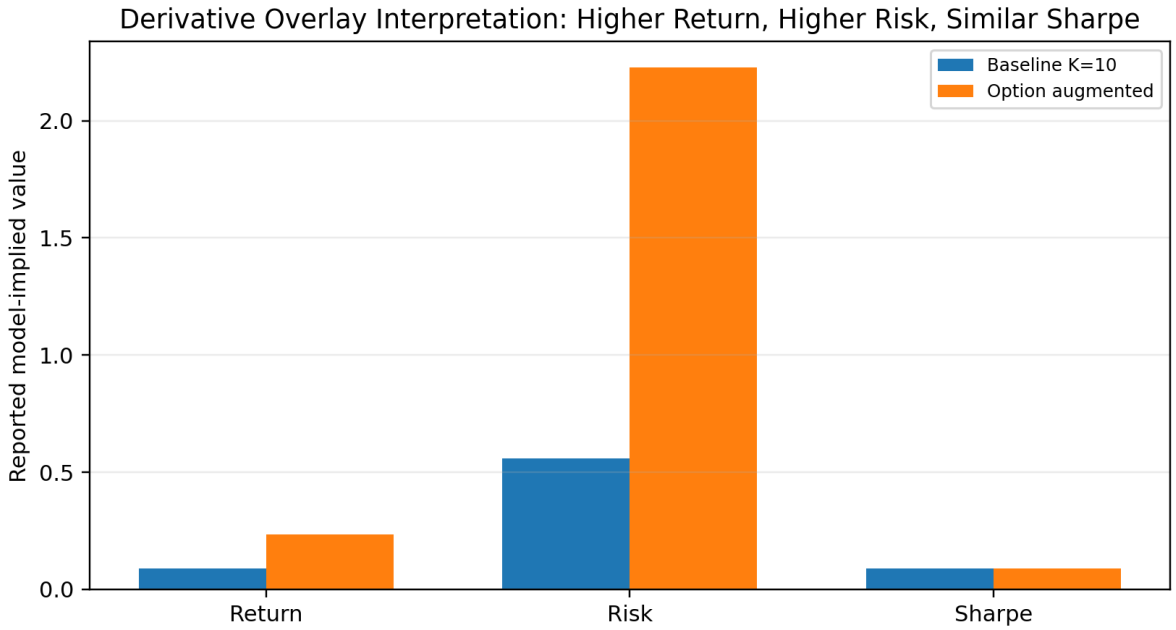


Figure 11.7.4. Baseline versus option-augmented risk-return interpretation.
Source: *Author visualization based on the reported baseline and option-augmented return, risk and Sharpe values.*

Table 11.7.5. Option-overlay interpretation matrix

Comparison item	Baseline K=10	Option-augmented case	Interpretation
Model-implied return	0.0888	0.2355	Return rises substantially because option exposure amplifies beta-linked CAPM return.
Model-implied risk	0.5578	2.2273	Risk rises disproportionately, revealing leverage amplification.
Sharpe ratio	approximately 0.0880	approximately 0.0879	Risk-adjusted performance does not improve materially.
-10% market factor shock	-12.56%	-52.02%	Downside stress exposure is magnified.
-20% market factor shock	-25.12%	-104.03%	Linear beta-mapped loss can exceed invested capital in the diagnostic exposure scale.
Admissible claim	Sparse baseline incumbent under CAPM/single-index assumptions	Derivative leverage diagnostic	The overlay is a realism/stress layer, not a free-performance engine.

Source: *Author synthesis from the reported Black-Scholes overlay, option-augmented Sharpe and stress-scenario interpretation.*

11.7.5. What computational finance shows in this chapter

The chapter shows five things with high internal clarity. First, cardinality constraints change the mathematical and economic form of portfolio optimization. The problem is not only to choose weights; it is to choose a support and then allocate weights within that support. Second, the support-space count gives a concrete economic illustration of why computational complexity matters. Third, heuristic search can be credible when it is benchmarked, documented and surrounded by falsification gates. Fourth, covariance geometry, transaction costs, beta drift, risk contribution and derivative leverage can materially alter interpretation. Fifth, scientific credibility is increased, not reduced, by explicitly stating what the evidence cannot certify.

Table 11.7.6. Interpretation summary: showable claims versus non-certifiable claims

Showable within Chapter 11	Non-certifiable within Chapter 11	Reason
A fixed n = 94 industry universe creates a reproducible sparse-optimization experiment.	The result applies to every asset universe.	The empirical universe is intentionally fixed and bounded.
C(94,10) operationalizes search-space explosion in finance.	The study proves P != NP.	A combinatorial count is an operational analogy, not a theorem proof.
The reduced n = 20, K = 6 benchmark supplies exact evidence at tractable scale.	Exact reduced enumeration certifies full n = 94 optimality.	Exactness does not scale automatically across problem dimensions.
Greedy, Monte Carlo and GA layers support a stable best-found Sharpe neighborhood.	No superior unvisited support exists.	Full-universe coverage is documented but not exhaustive.
Derivative leverage raises both return and risk.	Options create free Sharpe improvement.	Risk-adjusted evidence remains bounded after leverage adjustment.
The chapter supports a strong computational-decision measurement claim.	The chapter establishes realized return dominance.	Returns are CAPM-implied priors, not realized out-of-sample returns.

Source: *Author final interpretation based on the Chapter 11 evidence hierarchy.*

11.8. Claim Boundary: No P != NP Proof, No Certified n = 94 Global Optimum, No Realized-Return Dominance

The claim boundary is not an appendix to Chapter 11. It is part of the scientific result. Without the boundary, the chapter could be misread as making three inadmissible claims: a proof about P versus NP, a certificate of full n = 94 global

optimality, or evidence of realized-return dominance. The correct claim is stronger because it is narrower: the chapter provides a reproducible computational-finance demonstration that cardinality-constrained portfolio optimization generates a nontrivial mixed discrete-continuous search problem and that layered algorithms can produce auditable best-found solutions under explicit robustness and realism gates.

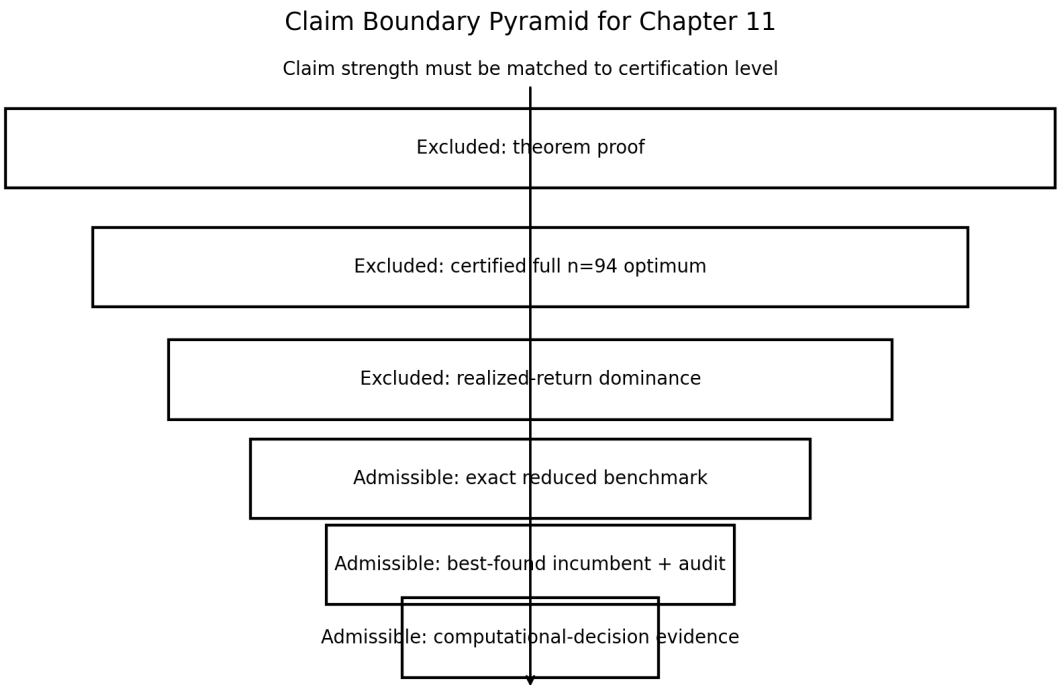


Figure 11.8.1. Claim boundary pyramid for Chapter 11.
Source: *Author synthesis based on the admissible/excluded claim hierarchy of the P-vs-NP manuscript.*

Table 11.8.1. Final claim-boundary matrix

Potential claim	Status	Reason	Required wording in the monograph
The chapter proves P != NP.	Excluded	The study uses P-vs-NP logic as an empirical analogy; it does not address formal complexity classes at theorem level.	The chapter is P-vs-NP-inspired, not a proof of P != NP.
The n = 94, K = 10 optimum is globally certified.	Excluded	Only documented search coverage is reported; all 9.041 trillion supports are not enumerated.	The full-universe result is a best-found incumbent under documented search coverage.
The reduced n = 20, K = 6 result is exact.	Admissible	All 38,760 reduced supports are enumerated.	Exact evidence is supplied only for the reduced benchmark.
The reported Sharpe proves realized investment dominance.	Excluded	Expected returns are CAPM-implied priors; no realized-return backtest is the central evidence.	The result is model-implied and computational, not realized trading superiority.
The option overlay creates free performance.	Excluded	Return and risk rise together; Sharpe remains approximately unchanged/slightly lower.	The option layer is a leverage and stress-realism diagnostic.
The framework is a strong computational-finance contribution.	Admissible	The design integrates data audit, CAPM priors, covariance, combinatorial search, exact reduced benchmarking, robustness and claim discipline.	The contribution is methodological, empirical and claim-bounded.

Source: *Author synthesis based on the final claim-discipline logic of Chapter 11.*

11.8.1. Why no P != NP proof is claimed

The formal P versus NP problem is a question in theoretical computer science about the relationship between problems whose solutions can be verified efficiently and problems whose solutions can be found efficiently. Chapter 11 does not prove, disprove or resolve that question. It does not construct a formal reduction, prove NP-completeness of the particular empirical instance, or establish complexity-class separation. Instead, it uses the P-vs-NP vocabulary as a measurement grammar for a concrete economic decision problem. The support space is large; the solution search is costly; exact certification is available only in a reduced benchmark; and the researcher must decide how much evidence is sufficient for a bounded empirical claim.

Equation 11.8.1. Claim-boundary operator

Admissible Claim_c = Evidence_c x Boundary_c

A claim is scientifically admissible only when the evidence exists and the boundary prevents overextension. If the boundary is removed, even a strong empirical result becomes reviewer-vulnerable.

11.8.2. Why no certified n = 94 global optimum is claimed

A best-found portfolio is not the same object as a certified global optimum. The full universe contains 9,041,256,841,903 supports, while the documented audit coverage is 421,760 evaluations/supports. This is meaningful computational evidence, especially when combined with algorithmic convergence, K-grid stability, reduced exact benchmarking and robustness checks. It is not exhaustive enumeration. Therefore, the correct monograph language is precise: the chapter reports a best-found incumbent in the full universe and an exact optimum only in the reduced benchmark.

Table 11.8.2. Exactness and certification status

Evidence layer	Scale	Certification status	Correct conclusion
Full n = 94, K = 10 universe	9,041,256,841,903 possible supports	Not exhaustively enumerated	Best-found incumbent with documented coverage.
Documented full-universe audit	421,760 evaluations/supports	Search-coverage evidence	Supports algorithmic credibility, not global certification.
Reduced n = 20, K = 6 benchmark	38,760 possible supports	Exactly enumerable	Exact reduced benchmark.
Algorithmic convergence	Greedy, MC, GA, GA + reoptimization	Convergent empirical pattern	Upper-envelope stability, not theorem proof.
Robustness gates	Covariance, Rf/ERP, caps, costs, beta drift, option overlay	Conditional fragility audit	Separates stable claims from assumption-sensitive claims.

Source: *Author synthesis based on the exact/heuristic boundary of Chapter 11.*

11.8.3. Why no realized-return dominance is claimed

The return vector in Chapter 11 is built from CAPM-implied expected returns. This is a transparent choice because it fixes the expected-return model before optimization and makes the experiment reproducible. It also restricts the claim. A CAPM-implied Sharpe ratio is not a realized historical Sharpe ratio. It is not evidence that the selected industries would outperform in a live portfolio, after trading costs, liquidity constraints, rebalancing frictions, tax effects, regime shifts, estimation error and out-of-sample return surprises. The chapter therefore remains an empirical-computational optimization study, not an investment-performance marketing claim.

Table 11.8.3. Reviewer-risk response matrix

Reviewer concern	Why it matters	Chapter 11 response	Remaining limitation
P-vs-NP overclaim	The formal problem is unsolved and theorem-level language would be inappropriate.	Explicitly states that the chapter is inspired by P-vs-NP logic only.	No theorem-level claim is made.
Heuristic optimality overclaim	A heuristic incumbent may be mistaken for the global optimum.	Reports search coverage and separates exact reduced enumeration from full-universe search.	Unvisited full-universe supports may exist.
CAPM-prior dependence	Model-implied returns are conditional inputs.	Uses transparent Rf/ERP calibration and sensitivity logic.	No realized-return dominance is claimed.
Covariance specification risk	Sharpe depends on risk model choice.	Uses covariance alternatives, eigenvalue diagnostics and stress covariance interpretation.	Risk model remains a conditional specification.
Derivative leverage	Options can inflate	Shows risk rises with return and	Full option microstructure

Reviewer concern	Why it matters	Chapter 11 response	Remaining limitation
risk	return narratives.	Sharpe does not improve materially.	risks are not modeled.
Portfolio concentration	Sparse portfolios may have concentrated weights and risk contributions.	Uses HHI, effective N, top-weight share and risk contribution interpretation.	Concentration remains a governance concern, not an invalidation.

Source: *Author synthesis based on the reviewer-safety logic of Chapter 11.*

11.9. Chapter Conclusion

Chapter 11 closes the monograph's seven-problem applied architecture by providing the computational-decision dimension. The earlier chapters measure curvature, topology, flow, shock thresholds, local-to-global rank and spectral forecasting. Chapter 11 asks a different question: how does economic decision-making behave when the feasible set is finite but combinatorially vast, and when the analyst must choose under computational limits? Cardinality-constrained portfolio optimization supplies a natural answer because it forces support selection and weight allocation into one mixed discrete-continuous problem.

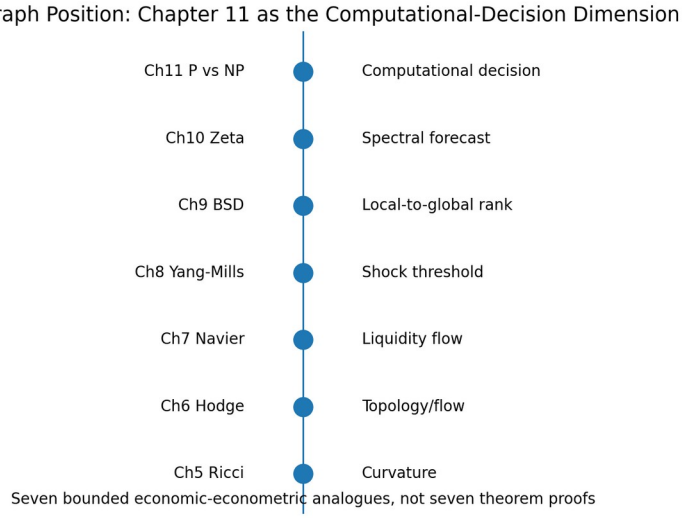


Figure 11.9.1. Position of Chapter 11 within the seven-problem monograph architecture.
Source: *Author synthesis based on the monograph structure: Chapter 11 is the computational-decision chapter.*

The final conclusion is therefore positive and bounded. The chapter successfully demonstrates how a fixed Damodaran January 2026 U.S. industry universe can be converted into a reproducible P-vs-NP-inspired computational-finance experiment. It defines the empirical universe, constructs CAPM priors, builds covariance geometry, measures support-space growth, searches sparse portfolios, compares algorithms, supplies exact reduced evidence, applies robustness and realism gates, and closes the claim hierarchy. This is a strong methodological contribution because every reported result is attached to the level of evidence that can actually support it.

The chapter's strongest computational conclusion is that the cardinality constraint is not cosmetic. The K = 10 problem over 94 industries produces more than nine trillion possible supports, making naive full enumeration impractical. The chapter therefore gives economic content to the P-vs-NP analogy: a real portfolio problem can be easy to state, easy to evaluate for any proposed portfolio, but difficult to certify globally at scale. This is exactly the kind of decision environment where heuristic methods, exact reduced benchmarks and claim-boundary discipline become scientifically necessary.

The chapter's strongest financial conclusion is that sparse optimization must be read through covariance and implementation realism. The selected portfolio is not just a list of industries. It is an object embedded in a CAPM prior, a single-index covariance matrix, common-factor dependence, weight concentration, transaction costs, beta drift, risk contribution and stress exposure. The Black-Scholes overlay reinforces the same point: leverage changes scale, not necessarily efficiency. In the reported option-augmented case, expected return rises, but risk rises so strongly that Sharpe does not improve meaningfully. That result strengthens the chapter because it rejects an overoptimistic derivative interpretation.

The chapter's strongest methodological conclusion is the distinction between exactness and evidence. Exactness is achieved in the reduced n = 20, K = 6 benchmark; it is not claimed for the full n = 94, K = 10 universe. The full case is treated as a best-found incumbent supported by documented search coverage, algorithmic consistency and robustness gates. This distinction should remain visible in the final monograph because it protects the chapter from the two most likely reviewer objections: that the author is claiming too much about P versus NP, and that the portfolio result is being described as globally certified when it is not.

Table 11.9.1. Chapter 11 final aim-objective-results closure matrix

Chapter objective	Evidence used for closure	Main conclusion	Claim boundary
Translate P-vs-NP logic into economic decision analysis	Support-space count, mixed discrete-continuous formulation, search coverage	Cardinality constraints create operational computational complexity in portfolio selection.	No theorem-level P-vs-NP proof.
Fix a reproducible empirical universe	Damodaran Jan-2026 n = 94 industry dataset, CAPM priors, covariance audit	The experiment is auditable and not ex-post selected.	Universe is industry-level, not complete market-wide.
Demonstrate support-space explosion	C(94,10) = 9,041,256,841,903	Full enumeration is impractical at baseline scale.	Combinatorial size does not itself prove formal complexity-class separation.
Supply exact evidence where feasible	Reduced n = 20, K = 6 enumeration of 38,760 supports	Exact reduced benchmark anchors heuristic credibility.	Reduced exactness does not certify full n = 94 optimum.
Interpret algorithms responsibly	Greedy, Monte Carlo, GA and GA plus continuous reoptimization comparison	Algorithms can reach stable upper-envelope results.	Best-found incumbent, not global certificate.
Test economic realism	Covariance alternatives, costs, beta drift, risk contribution, Black-Scholes overlay, stress scenarios	The result is conditional and robustly audited.	No realized-return dominance or free derivative performance.
Close the chapter scientifically	Falsification matrix, integrated ranking, claim hierarchy and replication gate	Chapter 11 becomes the monograph's computational-decision evidence block.	Claims remain empirical, computational and bounded.

Source: *Author final synthesis based on Sections 11.1-11.8 and the source P-vs-NP manuscript.*

11.9.1. Final permissible claim of Chapter 11

The final permissible claim can be stated as follows: within a fixed Damodaran January 2026 industry universe and a CAPM/single-index risk-return framework, cardinality-constrained portfolio optimization creates a nontrivial mixed discrete-continuous computational-finance problem. The chapter demonstrates that heuristic and metaheuristic search can generate strong best-found incumbents, that exact certification can be supplied in a reduced tractable benchmark, and that robustness, derivative realism and falsification gates are necessary for scientific interpretation. The chapter does not prove P != NP, does not certify the full n = 94 global optimum and does not establish realized-return dominance.

11.9.2. Contribution to the monograph as a whole

In the full monograph, Chapter 11 plays a distinctive role. The Ricci/Perelman chapter models inequality deformation; the Hodge chapter decomposes macro-flow into gradient, curl and harmonic components; the Navier-Stokes chapter models liquidity stress as flow-pressure-friction closure; the Yang-Mills chapter measures finite-network shock thresholds; the BSD chapter interprets local-to-global structural rank; and the Riemann-Zeta chapter develops spectral inflation-cycle diagnostics. Chapter 11 adds the decision-complexity dimension: even when inputs, objective and constraints are clearly defined, the feasible decision space may be too large for exhaustive practical certification. This completes the seven-problem architecture by showing that economic measurement is not only about what to measure, but also about what can be computed, searched, approximated and certified.

Table 11.9.2. Chapter 11 contribution to the seven-problem monograph architecture

Monograph dimension	Chapter	Measurement object	How Chapter 11 relates
Curvature/topological deformation	Chapter 5	Inequality pressure, smoothing capacity and curvature-like	Chapter 11 adds decision complexity rather than curvature measurement.

Monograph dimension	Chapter	Measurement object	How Chapter 11 relates
		diagnostics	
Macro-flow decomposition	Chapter 6	Gradient, curl and harmonic macro-flow structure	Chapter 11 complements flow structure with support-selection complexity.
Liquidity-flow stress	Chapter 7	Systemic stress, pressure, friction and closure	Chapter 11 shows how stress-aware portfolios require computational search.
Shock-threshold topology	Chapter 8	Gauge curvature, action and finite-network mass-gap threshold	Chapter 11 provides algorithmic decision evidence rather than spectral threshold evidence.
Local-to-global rank	Chapter 9	Structural rank, LOrder, corridor stress	Chapter 11 parallels local support selection versus global portfolio performance.
Spectral-cycle forecasting	Chapter 10	Zeta-cycle inflation diagnostics and layered forecast validation	Chapter 11 contributes algorithmic validation rather than forecast validation.
Computational decision	Chapter 11	Cardinality-constrained portfolio optimization	This is the monograph's primary economic P-vs-NP analogue.

Source: *Author synthesis based on the final monograph structure and Chapter 11 role.*

11.9.3. Closing statement

Chapter 11 should be read as a scientifically disciplined computational-finance chapter. It is ambitious because it connects portfolio optimization with P-vs-NP logic, but it is credible because it refuses to overclaim. The chapter shows that sparse portfolio selection over a fixed industry universe generates a large combinatorial decision space; that algorithms can find strong model-implied incumbents; that exact reduced evidence can validate heuristic behavior at a tractable scale; that covariance, costs, beta drift and option leverage change interpretation; and that the final claim must remain bounded. This is precisely the methodological posture required for the monograph: mathematical inspiration, empirical construction, computational audit, robustness discipline and explicit claim boundary.

Document note. *Prepared as an English monograph subsection draft for Chapter 11.7-11.9. Tables and figures are synthesis devices based on the uploaded P-vs-NP portfolio manuscript and the user-provided monograph structure. They are written for insertion into the book and should be cross-checked against the final integrated Chapter 11 numbering before full manuscript assembly.*

PART III - Comparative Synthesis and Final Monograph Closure

Chapter 12. Comparative Results across the Seven Millennium Economic Models

Chapter 12 is the first explicit comparative synthesis chapter of the monograph. Its purpose is not to add an eighth model, nor to re-estimate the seven completed models, but to place their empirical universes, mathematical objects, validation strength, result types and claim boundaries into one disciplined comparative architecture. The seven chapters are not commensurable in a naive statistical sense: one is a country-year panel stress-testing design, one is a layered forecast-validation design, one is a computational portfolio-optimization experiment, several are regional graph or benchmark architectures, and two operate through calibrated local-to-global or finite-network threshold logic. The appropriate comparison is therefore architectural and evidentiary. Each model asks a different measurement question, uses a different mathematical grammar and supports a different strongest admissible claim. The comparative result is that the monograph forms a coherent methodological system: Ricci/Poincare contributes pressure-curvature inequality diagnostics; Hodge contributes macro-flow decomposition; Navier-Stokes contributes global liquidity-stress testing; Yang-Mills contributes finite-network shock-threshold measurement; BSD contributes local-to-global structural rank calibration; Riemann/Zeta contributes layered spectral forecast validation; and P vs NP contributes computational-decision evidence about combinatorial search under portfolio constraints. The chapter also formalizes a comparative claim hierarchy, showing where evidence is strong, where validation is bounded, and where theorem-level, causal or universal-performance claims remain excluded.

Scope and claim-boundary note. This chapter compares economic-econometric analogues inspired by the seven Clay Millennium Problems. It does not compare alleged solutions of the original mathematical problems. The admissible object is the strength of each bounded economic measurement architecture: sample design, constructed object, validation discipline, reproducibility, and claim boundary.

12.1. Comparative Empirical Universe

The comparative empirical universe is the first synthesis layer because the seven models are not built on the same observational geometry. The monograph deliberately uses different empirical designs because each Millennium-inspired translation requires a different evidentiary object. A curvature-diagnostic inequality model needs a panel of regional stress coordinates. A Hodge model needs a connected graph with enough edges and cycles to support decomposition. A Navier-Stokes-inspired liquidity model needs a country-year panel large enough to audit stress channels, rolling forecasts and policy scenarios. A Yang-Mills-inspired shock-threshold model needs a finite corridor-sensitive weighted graph before it can move to country-panel closure. A BSD-inspired local-to-global rank model needs a World anchor, regional/corridor nodes and an N=150 closure layer. A Riemann/Zeta forecasting model needs annual, quarterly and monthly validation layers. A P-vs-NP portfolio model needs a fixed asset universe and an explicitly combinatorial support-selection layer.

The comparative mistake to avoid is to treat all samples as if they were interchangeable. The Navier-Stokes chapter has the largest country-year evidence base, while the Riemann/Zeta chapter has the strongest layered forecast-validation discipline. The P-vs-NP chapter has a smaller asset-universe count, but its true evidentiary scale is combinatorial: the baseline support space is not n=94 alone, but C(94,10)=9,041,256,841,903 possible supports before weight optimization. Likewise, the Hodge and Yang-Mills chapters have compact node sets, but their empirical object is a network topology rather than a conventional country-year panel. Their evidence strength arises from connectedness, edge structure, spectral separation, cycle structure, curvature/action concentration and robustness of the finite benchmark.

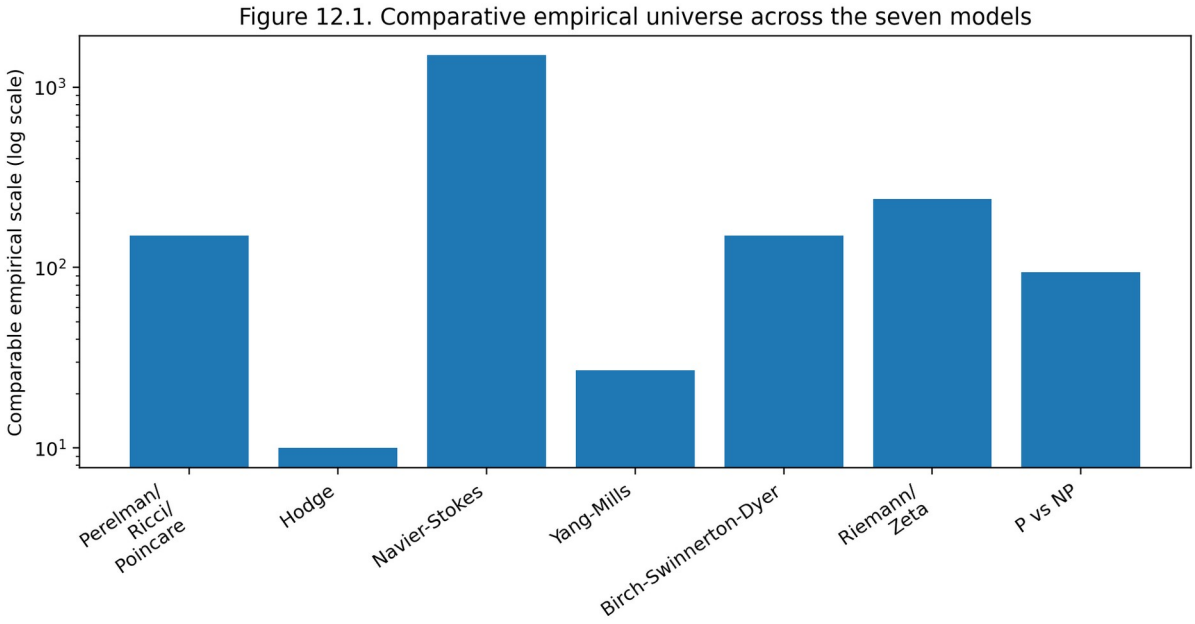
Chapter 12 therefore introduces a comparative rule: empirical universe must be read relative to the model class. A larger N is not automatically superior if the mathematical object requires topological closure, exact enumeration, or spectral diagnostic stability. Conversely, a compact benchmark cannot be promoted into global causal confirmation unless it is paired with a valid panel, external validation or clearly bounded claim hierarchy. The comparative synthesis is strongest when it preserves this distinction instead of forcing all models into a single regression-based ranking.

Table 12.1. Comparative empirical universe across the seven Millennium-inspired economic models

Model	Book chapter	Empirical universe	Main sample / scale	Comparative evidence object
Perelman/Ricci/Poincare	Chapter 5	10 macro-regional blocks, 2010-2024, 16 stress-coordinate	N=150 region-year panel	2020 crisis deformation; partial 2024 smoothing

		variables		recovery; connected inequality graph
Hodge	Chapter 6	World anchor plus 10 regional nodes; 27 weighted edges; Caucasus explicit corridor-sensitive node	10-node benchmark	Gradient, curl and harmonic components jointly explain regional macro-flow structure
Navier-Stokes	Chapter 7	100-country annual panel, 2010-2024; World anchor; macro-regional layers	N=1,500 country-year panel	Nondimensional systemic-stress architecture with rolling forecasts, benchmarks, Monte Carlo and policy counterfactuals
Yang-Mills	Chapter 8	10 regional/corridor nodes and 27 weighted edges; future 100-country panel pathway	Finite graph benchmark plus N=1,500 pathway	Positive finite-network economic mass gap and compressed thresholds under shock scenarios
Birch-Swinnerton-Dyer	Chapter 9	World anchor plus 10 regional/corridor nodes; N=150 closure layer	N=150 regional-year closure layer	Local finite-state signals and Euler-factor analogues contain calibrated information about structural rank
Riemann/Zeta	Chapter 10	Annual, quarterly and monthly global aggregate validation layers	N=55, 45, 20, 100, 240	FPAS+zeta improves reported forecast hierarchy against FPAS and ARIMA across validation layers
P vs NP	Chapter 11	Fixed Damodaran January 2026 U.S. industry universe after excluding aggregate rows	n=94, K=10; exact reduced n=20, K=6	Main support space is too large for naive enumeration; exact reduced benchmark disciplines heuristic search

Source: Author synthesis based on the seven source manuscripts and the monograph structure plan.



Note: The P vs NP chapter is represented by n=94 for the industry universe; its combinatorial support space is C(94,10)=9.041e12.

Figure 12.1. Comparative empirical universe across the seven models. Log scale prevents the larger panel and benchmark layers from visually suppressing compact graph and asset-universe designs.

12.1.1. Why sample heterogeneity is methodologically necessary

The seven empirical universes differ because each model answers a different economic measurement question. A portfolio support-selection problem cannot be audited with the same data structure as an inequality-curvature manifold, and a finite gauge-network mass-gap benchmark cannot be evaluated as if it were a quarterly inflation-forecasting exercise. This is not a weakness of the monograph. It is the reason the comparative chapter uses evidence geometry rather than a single mechanical N ranking. The relevant question is whether the sample is adequate for the mathematical object it supports: region-year panels for curvature and rank closure, weighted graphs for topology and gauge threshold measurement, layered time series for forecasting, and discrete-combinatorial supports for portfolio complexity.

12.1.2. Panel evidence versus benchmark evidence

Panel evidence is strongest where the object is repeated through time and across units. The Navier-Stokes model therefore obtains high comparative strength from its 100-country annual panel, because systemic stress is designed as a repeated country-year object. Ricci/Poincare and BSD also use N=150 closure layers, but their panels serve different functions: inequality-curvature diagnostics in the former and local-to-global rank calibration in the latter. Benchmark evidence, by contrast, is strongest where the object is graph-structural. Hodge and Yang-Mills cannot be judged only by N. They require connectedness, cycle structure, spectral behavior, curvature/action diagnostics and robustness to graph coding.

12.1.3. Forecast layers versus computational support spaces

The Riemann/Zeta model shows why a layered validation architecture can be stronger than a single larger sample. Annual headline validation, annual robustness, crisis-era comparison, quarterly dynamics and monthly spectral diagnostics are kept separate to avoid compact-sample overclaiming. The P vs NP chapter shows a different kind of scale: the empirical universe contains 94 industries, but the decision space contains more than nine trillion K=10 supports. This makes the computational burden an empirical result in its own right rather than a background detail.

12.1.4. Comparative empirical implication

The empirical universes jointly show that the monograph is not organized around one data type. It is organized around a controlled family of measurement systems. The comparative conclusion is that macroeconomic complexity requires several empirical geometries: panels for repeated stress and curvature, graphs for topology and transmission, time-frequency layers for forecasting, and combinatorial spaces for constrained decision problems.

Table 12.2. Comparative sample geometry and evidentiary meaning

Evidence geometry	Primary chapters	Main scale	Why this geometry

			matters
Panel evidence	Ricci/Poincare; Navier-Stokes; BSD	N=150, N=1,500, N=150	Best suited for repeated region-year or country-year diagnostic closure.
Benchmark topology	Hodge; Yang-Mills	10 nodes / 27 edges in both core benchmark designs	Best suited for decomposition, graph connectedness, spectral threshold and finite-network curvature/action measurement.
Layered forecast validation	Riemann/Zeta	N=55, 45, 20, 100, 240	Best suited for forecast comparison, rolling validation and spectral/regime diagnostics across frequencies.
Combinatorial computational experiment	P vs NP	n=94, K=10; exact n=20, K=6	Best suited for demonstrating support-space explosion and validating heuristics on reduced exact enumeration.

Source: Author synthesis based on the seven source manuscripts and the monograph structure plan.

12.2. Comparative Mathematical Object

The second comparative layer is the mathematical object. The monograph is not unified by using the same equation seven times. It is unified by a more abstract rule: each Clay problem supplies a different measurement grammar for a different form of economic complexity. The Ricci/Poincare translation measures deformation, smoothing capacity and graph connectedness. Hodge measures whether macro-flow can be decomposed into hierarchy, local imbalance and residual circulation. Navier-Stokes measures stress as a nondimensional balance of weak flow, pressure, friction, shocks, cycle and restricted closure. Yang-Mills measures whether a finite stress network has a positive spectral threshold and concentrated curvature/action. BSD measures whether local regional signals, finite-state reductions and Euler-factor analogues contain information about structural rank. Riemann/Zeta measures whether a spectral cyclical signal improves inflation forecasting under layered validation. P vs NP measures how discrete support selection transforms portfolio optimization into a mixed discrete-continuous computational decision problem.

This comparison is important because it protects the monograph from an artificial unification. The seven models should not be collapsed into GDP forecasting, general network science or a single constructed-index family. Each chapter contributes a separate diagnostic grammar. The common denominator is not a shared dependent variable; it is a shared methodological discipline: public anchor variables are transformed into constructed analytical objects; the constructed objects are validated or audited through model-appropriate procedures; results are interpreted as economic analogues rather than theorem-level mathematical transfers; and the final claim hierarchy separates strong diagnostic evidence from unsupported proof, causality or universal prediction claims.

The mathematical-object comparison also clarifies why Chapter 12 is necessary. Without this chapter, the book might look like seven isolated applications. With this chapter, the models become a comparative system: curvature diagnoses deformation; topology diagnoses structural organization; flow diagnoses stress propagation; gauge curvature diagnoses shock thresholds; rank diagnoses local-to-global structural order; spectral signals diagnose inflation-cycle deformation; and complexity diagnoses the computational feasibility of economic choice.

Table 12.3. Comparative mathematical object and economic translation

Model	Dominant mathematical grammar	Economic translation	Main comparative finding
Perelman/Ricci/Poincare	curvature / entropy / topology	Inequality curvature, smoothing capacity,	Crisis deformation and smoothing-capacity

		entropy-like complexity, graph connectedness	diagnostics
Hodge	flow / topology / decomposition	Macro-flow decomposition: hierarchy, local-cycle imbalance, harmonic/systemic circulation	Hierarchy/curl/harmonic separation
Navier-Stokes	flow / pressure / friction / closure	Liquidity-flow weakness, pressure gradients, friction/diffusion, stochastic shock, cycle and closure stress balance	Systemic stress-testing architecture
Yang-Mills	gauge curvature / spectral mass gap	Gauge curvature, action concentration, finite-network shock threshold and spectral protection	Positive finite-network mass-gap threshold
Birch-Swinnerton-Dyer	rank / local-to-global / L-function analogue	Local-to-global structural rank, economic L-function, Euler factors, LOrder, corridor stress	Local signals inform global structural rank
Riemann/Zeta	spectral signal / forecast correction	Zeta-cycle signal, crisis resonance, inflation-pressure forecasting and spectral diagnostics	Layered forecast-validation improvement
P vs NP	computational complexity / discrete-continuous optimization	Cardinality-constrained portfolio selection, support-space explosion, heuristic search and exact reduced benchmarking	Combinatorial explosion and heuristic discipline

Source: Author synthesis based on the seven source manuscripts and the monograph structure plan.

Figure 12.2. Comparative mathematical objects translated into economic measurement grammars

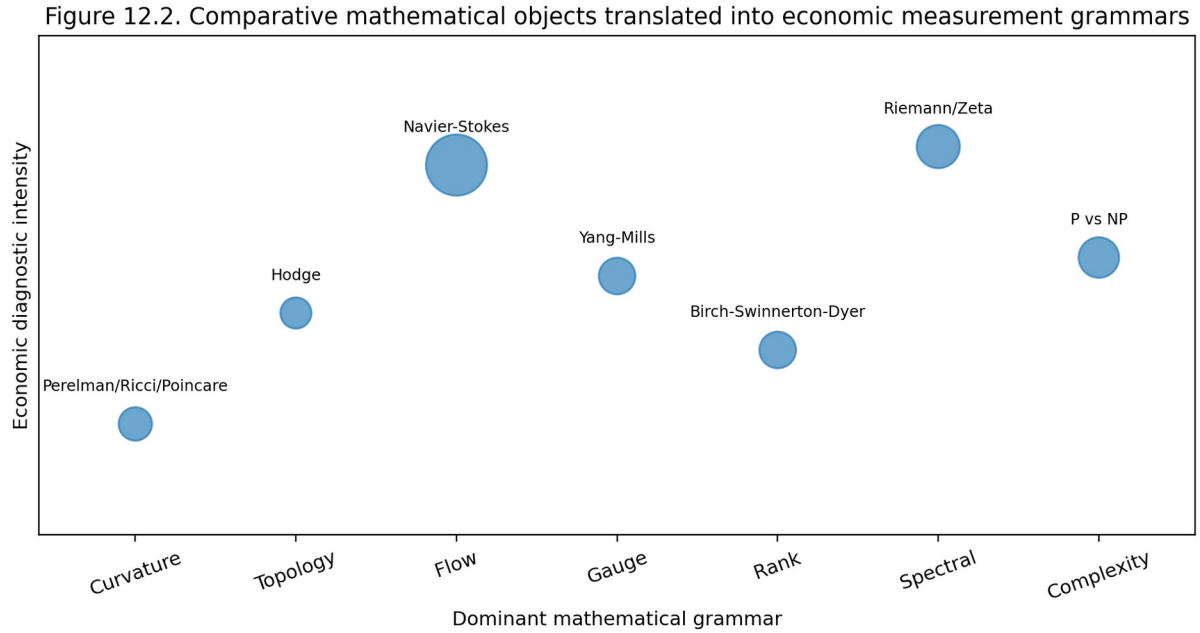


Figure 12.2. Comparative mathematical objects translated into economic measurement grammars.

Table 12.4. Compact symbolic comparison of the seven measurement grammars

Model	Compact symbolic object	Interpretive role
Ricci/Poincare	Pressure, curvature, F/W functionals, beta diagnostics	Economic manifold deformation and smoothing-capacity diagnostic.
Hodge	y = gradient + curl + harmonic	Macro-flow pressure decomposes into

		hierarchy, local imbalance and systemic circulation.
Navier-Stokes	S* = flow weakness + acceleration + pressure + friction + shock + cycle + epsilon(t)	Systemic stress is treated as a nondimensional balance process.
Yang-Mills	F_ijk, action sum F^2, lambda_1(L^S)	Local curvature and positive spectral separation define finite-network shock threshold.
BSD	Euler factors, L_econ(s), LOrder, structural rank	Local finite-state signals inform global structural rank.
Riemann/Zeta	hat_pi^Z = hat_pi^F + alpha lambda_zeta d_t	Zeta-cycle deviation becomes a bounded forecast correction.
P vs NP	choose support S, |S|=K; C(n,K)	Sparse portfolio selection becomes a combinatorial decision problem before continuous weights are optimized.

Source: Author synthesis based on the seven source manuscripts and the monograph structure plan.

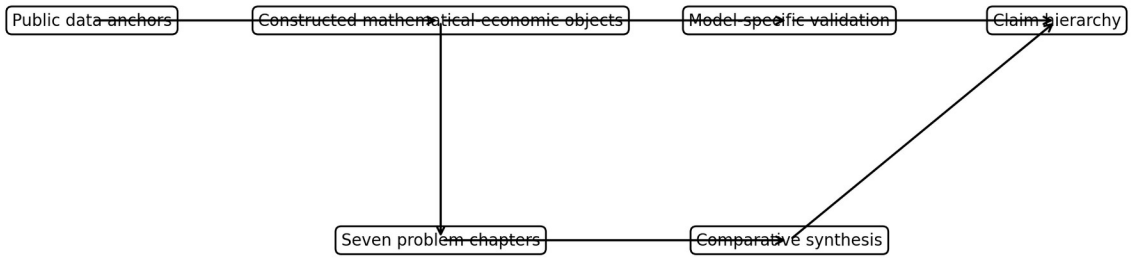


Figure 12.6. Monograph-level comparative synthesis workflow

Figure 12.6. Monograph-level comparative synthesis workflow from public anchors to claim hierarchy.

12.2.1. Curvature and smoothing as inequality diagnostics

The Perelman-Ricci-Poincare translation is the monograph model in which pressure, deformation and smoothing capacity are most explicit. Its mathematical object is not imported as literal geometry. Rather, it creates an ordered diagnostic sequence: pressure-oriented variables form coordinates, correlations form a metric-like structure, curvature-like quantities summarize deformation, Perelman-type functionals summarize energy and entropy, and graph-topological diagnostics test connectedness and loop structure. In comparative terms, this chapter is the inequality-system analogue of structural deformation.

12.2.2. Hodge decomposition as macro-flow organization

The Hodge chapter contributes a different object: decomposition of a regional edge-pressure field. It does not ask only which region is large or fast-growing. It asks whether the observed edge field can be decomposed into gradient hierarchy, curl imbalance and harmonic circulation. This is the clearest comparative counterweight to GDP-only interpretation because the result explicitly separates economic mass from flow organization.

12.2.3. Navier-Stokes and Yang-Mills as stress-transmission grammars

The Navier-Stokes and Yang-Mills chapters both concern systemic stress, but they measure it differently. Navier-Stokes treats stress as a nondimensional balance process across countries and time. Yang-Mills treats stress as a finite-network gauge object with curvature, action and spectral separation. The first is strongest as a panel stress-testing framework; the

second is strongest as a finite-network shock-threshold benchmark. Together they show that stress has both temporal-flow and topological-threshold dimensions.

12.2.4. BSD, Riemann/Zeta and P vs NP as information, forecasting and decision grammars

The BSD chapter translates local-to-global rank logic; the Riemann/Zeta chapter translates spectral cyclical information into forecast correction; and the P vs NP chapter translates computational complexity into economic decision feasibility. These three chapters are especially important because they show that the monograph is not only about macroeconomic stress. It also covers rank formation, forecast improvement and constrained portfolio choice. The mathematical objects are different, but all three depend on disciplined transformation and explicit claim boundaries.

12.3. Comparative Validation Strength

The third comparative layer is validation strength. Validation strength is not identical to sample size. It is a composite of empirical breadth, internal coherence, benchmark comparison, robustness, external validation, replication traceability and claim discipline. On this criterion, the seven models occupy different but complementary positions. Navier-Stokes has the strongest global panel stress-testing evidence because it combines N=1,500 country-year structure with rolling validation, benchmark comparison, panel fixed effects, robustness, external-target screening, Monte Carlo and policy counterfactuals. Riemann/Zeta has the strongest layered forecast-validation design because it separates annual headline validation, annual robustness, crisis-era comparison, quarterly dynamics and monthly spectral diagnostics. P vs NP has the strongest computational-demonstration logic because the main universe is explicitly infeasible for enumeration while the reduced benchmark is exactly enumerable.

The Ricci/Poincare chapter is strong as an N=150 diagnostic inequality-curvature architecture. It detects crisis deformation, smoothing recovery, graph connectedness, entropy-like complexity and validation boundaries. The Hodge chapter is strong as a benchmark structural decomposition: it shows that macro-flow pressure is not reducible to GDP mass because gradient, curl and harmonic components all carry empirical meaning. The Yang-Mills chapter is strong as a finite-network benchmark because it establishes a positive finite-network economic mass gap and stress-threshold compression under scenarios, while reserving country-panel causal closure for a future N=1,500 pathway. The BSD chapter is strong as a calibrated local-to-global rank architecture: it provides close LOrder-rank agreement and strong internal calibration, but external validation remains bounded and directional.

The comparative validation hierarchy is therefore not a single league table. It is a claim map. Some chapters support stronger forecast or panel claims; some support stronger finite-network or decomposition claims; some support stronger computational feasibility claims. The common standard is that each chapter states exactly what its evidence can support and what it cannot support. This is the main scientific protection of the monograph.

Table 12.5. Comparative validation strength and claim boundary

Model	Comparative validation strength	Main supporting evidence	Main boundary
Navier-Stokes	Strong global panel stress-testing evidence	N=1,500; rolling validation; benchmarks; FE; Monte Carlo; counterfactuals	Does not establish physical law, universal crisis prediction or unrestricted causality
Riemann/Zeta	Strong layered forecast-validation evidence	N=55/45/20/100/240; RMSE hierarchy; MZ/DM/CW; HMM/Markov/spectral diagnostics	Does not prove/test RH or guarantee universal forecast dominance
P vs NP	Strong computational demonstration with exact reduced benchmark	C(94,10)=9.041e12; exact C(20,6)=38,760; algorithmic comparison	Does not prove P != NP or certify global optimum for n=94
Ricci/Poincare	Strong N=150 inequality-curvature diagnostic evidence	Pressure-curvature path; F/W functionals; graph topology; counterfactuals; validation screens	Does not prove geometric/topological theorems or causal policy effects
Hodge	Strong benchmark	10 nodes; 27 edges;	Does not become full

	structural decomposition evidence	gradient/curl/harmonic shares; topology and homology checks	country-level dyadic-flow validation
Yang-Mills	Strong finite-network benchmark evidence; future panel pathway	lambda1=0.3850; threshold=0.1099; action=2,514.0; scenario threshold compression	Does not solve Yang-Mills or complete causal panel validation
BSD	Strong calibrated local-to-global rank evidence, bounded external validation	N=150; LOrder-rank MAE=0.072; RMSE=0.090; placebo/circularity checks	Does not prove BSD, establish causal law or strong independent external validation

Source: Author synthesis based on the seven source manuscripts and the monograph structure plan.

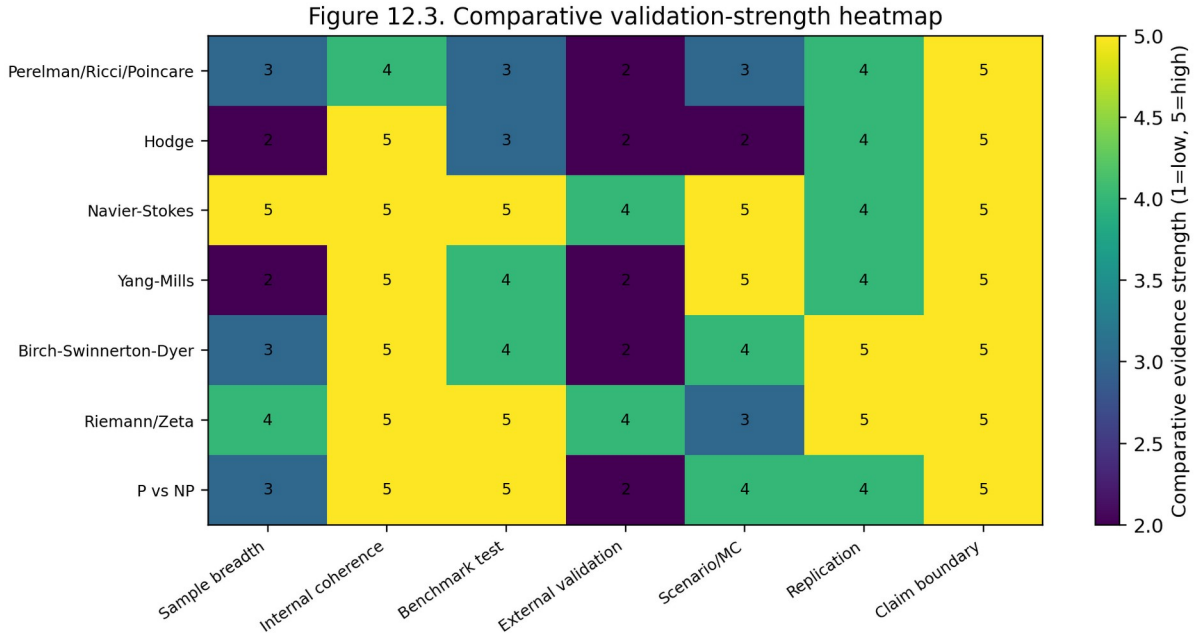


Figure 12.3. Comparative validation-strength heatmap. Scores are chapter-level evidence classifications, not mathematical truth rankings.

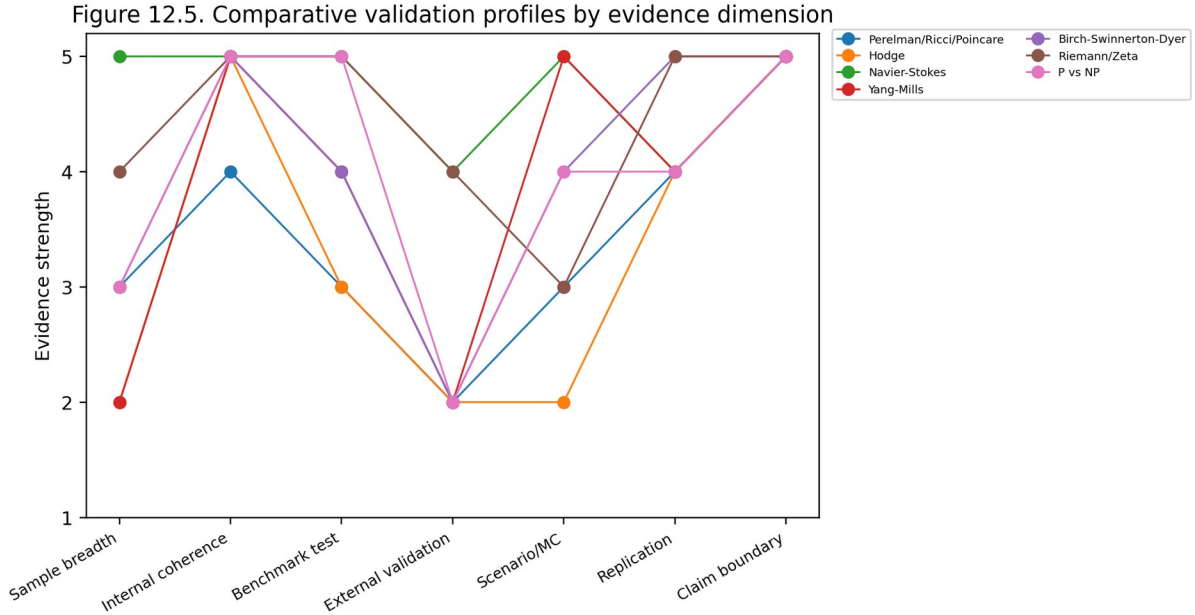
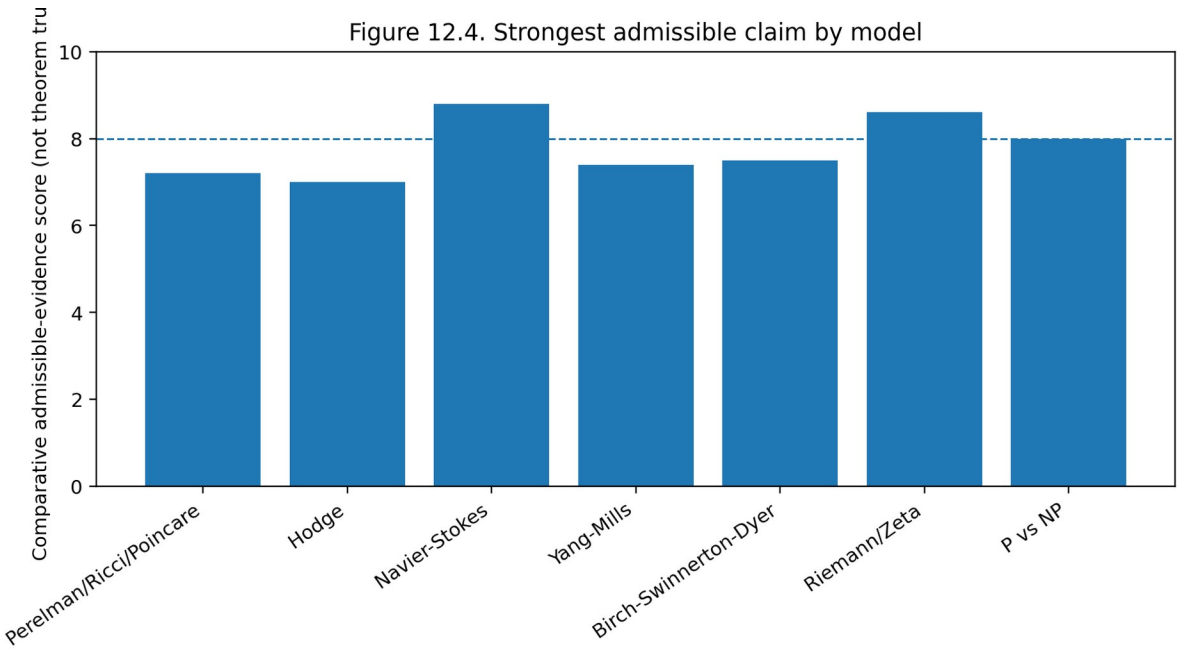


Figure 12.5. Comparative validation profiles by evidence dimension.



Note: Scores are interpretive evidence-classification values for the monograph; they do not rank mathematical validity.

Figure 12.4. Strongest admissible claim by model. The bar values classify evidentiary strength inside the monograph, not theorem validity.

Table 12.6. Replication and audit discipline across the seven models

Model	Replication/audit layer	Comparative role
Ricci/Poincare	Data and replication package; pressure-curvature-topology audit	Supports diagnostic reproducibility and claim discipline.
Hodge	Zenodo package with input table, node codebook, edge list, matrices, Hodge outputs, scripts and fold-level audits	Supports reproduction of benchmark topology and Hodge decomposition.
Navier-Stokes	Data and replication package for nondimensional macro-financial stress-testing	Supports traceability of panel inputs, stress terms, forecasts, benchmarks and scenarios.
Yang-Mills	Finite-network benchmark package and specified N=1,500 future panel pathway	Supports finite-network reproduction while preserving future validation boundary.
BSD	Zenodo data package documenting source ledger, formulas, algorithms, extracted tables, seeds and hashes	Supports local-to-global calibration audit and anti-circularity safeguards.
Riemann/Zeta	Layered annual, quarterly and monthly validation package	Supports traceability of N=55, N=45, N=20, N=100 and N=240 forecast outputs.
P vs NP	Fixed Damodaran input vintage, algorithmic search records and exact reduced enumeration logic	Supports audit of combinatorial counts, CAPM priors and reduced benchmark certification.

Source: Author synthesis based on the seven source manuscripts and the monograph structure plan.

12.3.1. The strongest panel claim: Navier-Stokes

The Navier-Stokes model has the strongest comparative claim at the global panel stress-testing level. Its N=1,500 design permits country fixed effects, rolling validation, benchmark comparison, external plausibility screens, Monte Carlo stress bands and policy counterfactuals. The claim remains bounded because annual panel data cannot become financial microstructure evidence and diagnostic association cannot become causal law without identification.

12.3.2. The strongest forecast claim: Riemann/Zeta

The Riemann/Zeta model has the strongest forecast-validation claim because it separates empirical layers by methodological function. The N=55 annual layer provides headline accuracy, N=45 tests robustness, N=20 isolates the crisis-era comparison, N=100 supports quarterly dynamic regimes, and N=240 supports monthly spectral diagnostics. This allocation is stronger than treating all tests as if they came from the same annual sample.

12.3.3. The strongest computational claim: P vs NP

The P vs NP chapter has the strongest computational-demonstration claim. Its evidence is not based on a large econometric panel but on the operational scale of the decision problem. C(94,10) establishes infeasibility of naive enumeration in the main universe, while the reduced C(20,6) exact benchmark allows heuristic behavior to be checked against a tractable ground truth. This is a strong economic demonstration of computational complexity, while remaining outside theorem proof.

12.3.4. Benchmark, calibration and finite-network claims

Hodge, Yang-Mills and BSD should be read through benchmark and calibration strength. Hodge is strongest at decomposition; Yang-Mills is strongest at finite-network threshold evidence; BSD is strongest at calibrated local-to-global rank correspondence. These are not weaker because they are not identical to panel regressions. They are different evidentiary forms and are valid when their claim boundaries are stated clearly.

12.3.5. Why claim-boundary discipline is a comparative result

The monograph repeatedly excludes theorem proof, unrestricted causality and universal dominance. This is not merely a cautionary appendix. It is a comparative result: the strongest version of the monograph is the one that classifies evidence precisely. Each chapter contributes a high-level economic measurement architecture while refusing to overstate the mathematical analogy.

12.4. Cross-Problem Results Matrix

The cross-problem results matrix is the central output of Chapter 12. It condenses the seven independent problem chapters into one comparative table. The purpose of the matrix is not to flatten methodological differences, but to make them readable together. The matrix asks four questions for each problem: what is the core economic object, what is the main result type, what is the strongest admissible claim, and what boundary prevents overinterpretation?

The comparative pattern is clear. The strongest panel-based stress-testing evidence appears in the Navier-Stokes chapter. The strongest forecast-validation hierarchy appears in the Riemann/Zeta chapter. The strongest computational decision demonstration appears in the P vs NP chapter. The strongest inequality-curvature diagnostic system appears in the Ricci/Poincare chapter. The strongest structural decomposition of macro-flow appears in the Hodge chapter. The strongest finite-network shock-threshold benchmark appears in the Yang-Mills chapter. The strongest local-to-global rank calibration appears in the BSD chapter. These strengths are complementary. They show that the monograph is not a collection of unrelated analogies, but a systematic attempt to measure economic complexity through seven distinct mathematical grammars.

The final comparative conclusion is therefore methodological and empirical. The seven models jointly support the proposition that modern economic systems cannot be adequately measured through GDP, inflation, trade, growth, inequality or portfolio returns alone. They require curvature diagnostics, flow decomposition, stress balance, spectral thresholds, local-to-global rank logic, forecast-cycle signals and computational complexity discipline. This is the central result of Part III: the monograph produces a comparative economic measurement architecture, not seven isolated proof claims.

Table 12.7. Cross-problem results matrix

Problem	Core economic object	Main result type	Strongest claim	Comparative interpretation
Ricci/Poincare	Inequality curvature	N=150 diagnostic panel	Crisis deformation and smoothing capacity	2020 pressure-curvature-W signal and partial 2024 recovery
Hodge	Macro-flow decomposition	Benchmark topology	Hierarchy/curl/harmonic separation	GDP mass does not exhaust regional macro-flow organization
Navier-Stokes	Liquidity stress	N=1,500 panel	Systemic stress-testing architecture	Stress is a multi-channel flow-

				pressure-friction-shock-cycle-closure process
Yang-Mills	Shock threshold	Finite graph spectral result	Positive finite-network mass gap	Spectral protection exists but compresses under corridor shocks
BSD	Structural rank	Local-to-global calibration	Local signals inform global rank	Finite-state reductions, Euler factors and LOrder carry structural-rank information
Riemann/Zeta	Inflation forecasting	Layered forecast validation	FPAS+zeta improves benchmark accuracy	Zeta-cycle correction improves reported forecast hierarchy under bounded validation
P vs NP	Portfolio complexity	Computational search/exact reduced test	Combinatorial explosion and heuristic discipline	C(94,10) demonstrates infeasible enumeration; C(20,6) exact benchmark disciplines search

Source: Author synthesis based on the seven source manuscripts and the monograph structure plan.

Table 12.8. Comparative claim hierarchy and excluded claims

Model	Strongest admissible claim	Excluded overclaim
Perelman/Ricci/Poincare	Crisis deformation and smoothing-capacity diagnostics	Strong N=150 inequality-curvature diagnostic evidence; not theorem proof or unrestricted causality
Hodge	Hierarchy/curl/harmonic separation	Strong benchmark structural decomposition evidence; not final country-level dyadic-flow causality
Navier-Stokes	Systemic stress-testing architecture	Strong global panel stress-testing evidence; not physical-fluid law, theorem proof or universal crisis-prediction mechanism
Yang-Mills	Positive finite-network mass-gap threshold	Strong finite-network benchmark evidence with future panel pathway; not mathematical Yang-Mills proof or final causal panel closure
Birch-Swinnerton-Dyer	Local signals inform global structural rank	Strong calibrated local-to-global rank evidence; external validation remains bounded and directional
Riemann/Zeta	Layered forecast-validation improvement	Strong layered forecast-validation evidence; not Riemann Hypothesis proof, universal dominance or residual-problem elimination
P vs NP	Combinatorial explosion and heuristic discipline	Strong computational demonstration with exact reduced benchmark; no P ! = NP proof, certified n=94 global optimum or realized-return dominance

Source: Author synthesis based on the seven source manuscripts and the monograph structure plan.

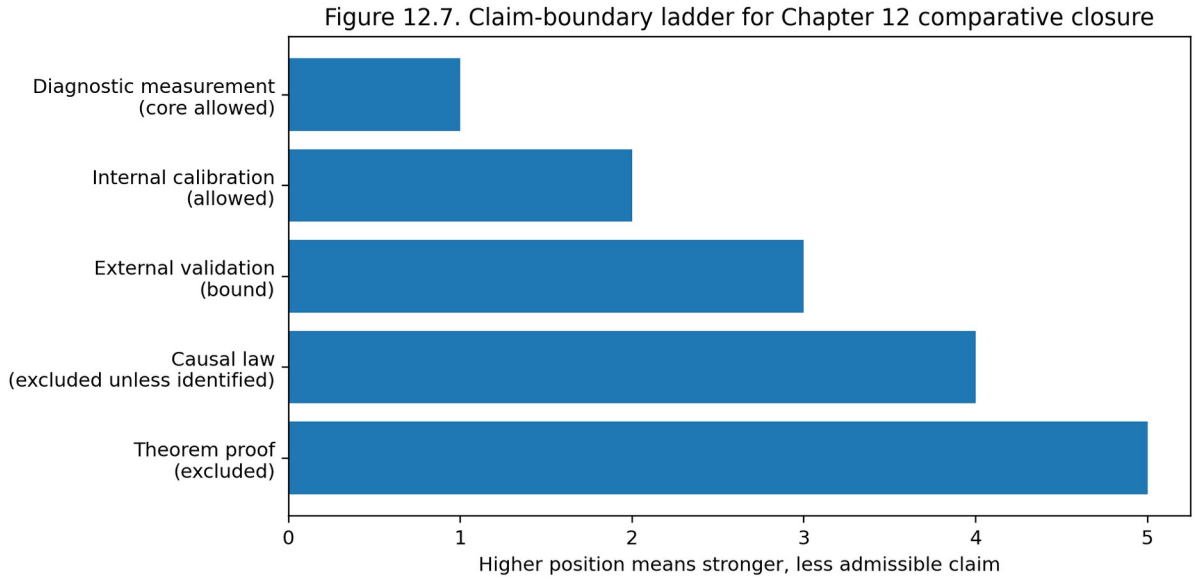


Figure 12.7. Claim-boundary ladder for Chapter 12 comparative closure.

Table 12.9. Chapter 12 synthesis of comparative results

Synthesis dimension	Comparative conclusion	Monograph-level implication
Empirical breadth	Largest in Navier-Stokes; most layered in Riemann/Zeta; most combinatorial in P vs NP	Empirical scale must be interpreted relative to model type.
Mathematical diversity	Curvature, flow, gauge, rank, spectral signal, topology and complexity all appear	The monograph is unified by translation discipline, not by one equation.
Validation discipline	Different chapters use panel tests, benchmark forecasts, exact enumeration, topology audits, placebo and robustness gates	No single validation method is adequate for all seven objects.
Policy relevance	Strongest direct stress-policy scenario logic appears in Navier-Stokes, Ricci/Poincare and Yang-Mills	Policy conclusions remain diagnostic or scenario-based, not randomized causal multipliers.
Claim boundary	All chapters exclude theorem proof and unrestricted causality	Scientific credibility comes from bounded claims, not maximal claims.

Source: Author synthesis based on the seven source manuscripts and the monograph structure plan.

12.4.1. Ricci/Poincare result in the comparative matrix

The Ricci/Poincare result contributes the inequality-deformation language of the monograph. Its central comparative role is to show that inequality pressure can be organized into pressure paths, curvature-like diagnostics, entropy-style complexity and graph connectedness. The 2020 crisis signal and 2024 partial smoothing result give the chapter substantive empirical content, while the claim boundary prevents it from becoming a theorem transfer or causal welfare model.

12.4.2. Hodge result in the comparative matrix

The Hodge result contributes the decomposition language. The key comparative conclusion is that the world economy is neither only a hierarchy nor only a network. It contains gradient hierarchy, local-cycle imbalance and harmonic/systemic circulation. This is one of the clearest results supporting the monograph's broader claim that aggregate mass alone cannot explain economic organization.

12.4.3. Navier-Stokes result in the comparative matrix

The Navier-Stokes result contributes the stress-balance language. It is the chapter in which global panel scale, rolling validation and policy scenario interpretation are most developed. Its comparative value is that it converts liquidity stress from an indicator list into a structured flow-pressure-friction-shock-cycle-closure process.

12.4.4. Yang-Mills result in the comparative matrix

The Yang-Mills result contributes finite-network threshold language. Its positive finite-network mass gap, curvature/action concentration and scenario threshold compression show that systemic stress can be measured through spectral protection and corridor-sensitive shock propagation. The chapter remains bounded because country-level causal validation is a future pathway rather than an already completed result.

12.4.5. BSD result in the comparative matrix

The BSD result contributes the local-to-global rank language. Its strongest conclusion is calibrated correspondence: local finite-state reductions, Euler-factor analogues and LOrder contain measurable information about structural rank. The result is important precisely because it is not upgraded into classical BSD proof or causal law.

12.4.6. Riemann/Zeta result in the comparative matrix

The Riemann/Zeta result contributes the spectral forecasting language. Its strongest comparative advantage is disciplined layering: annual, quarterly and monthly evidence are assigned to different validation functions. The chapter shows forecast improvement relative to FPAS and ARIMA in the reported layers, while explicitly excluding Riemann Hypothesis proof and universal forecast dominance.

12.4.7. P vs NP result in the comparative matrix

The P vs NP result contributes the computational decision language. It shows that sparse portfolio optimization is not merely a smooth Markowitz problem once a support-size constraint is imposed. The combinatorial count C(94,10) demonstrates operational infeasibility of full enumeration, while the reduced exact benchmark demonstrates how heuristic results can be disciplined without pretending to certify the full n=94 optimum.

12.4.8. Integrated result of Chapter 12

The integrated result is that the monograph has comparative coherence. The seven models are different in data, mathematical object and validation type, but they share one scientific architecture: economic variables are transformed into bounded mathematical analogues, results are validated through model-appropriate gates, and claim boundaries protect interpretation. This comparative coherence is the main contribution of Part III.

Chapter 12 conclusion. Chapter 12 closes the comparative-results stage by showing that the seven Millennium-inspired economic models form a structured evidence system. The Ricci/Poincare model explains pressure-curvature deformation; the Hodge model explains topological macro-flow decomposition; the Navier-Stokes model explains nondimensional systemic-stress balance; the Yang-Mills model explains finite-network shock thresholds; the BSD model explains calibrated local-to-global structural rank; the Riemann/Zeta model explains layered inflation-cycle forecast improvement; and the P vs NP model explains computational decision difficulty under sparse portfolio selection. The strongest general conclusion is not that any Clay Millennium Problem has been solved. The strongest conclusion is that their formal architectures can be translated into seven bounded, reproducible and empirically meaningful economic measurement systems. This comparative result prepares the monograph for the remaining Part III chapters: unified interpretation, limitation discipline, claim-boundary consolidation and final monograph closure.

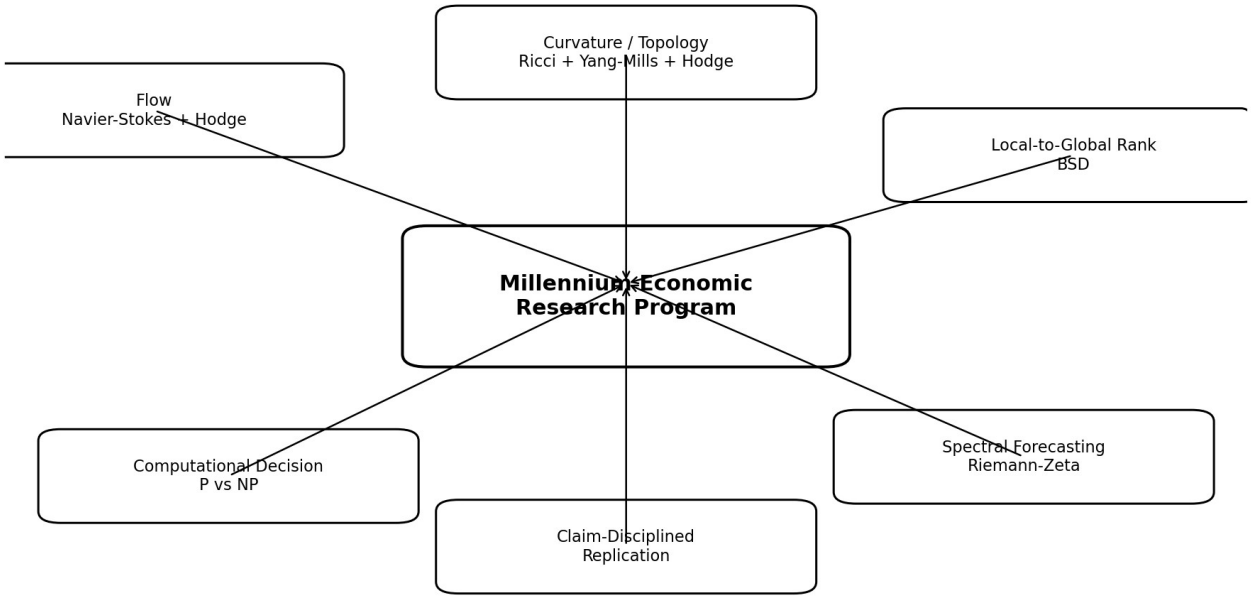
Chapter 13. Unified Interpretation: The Millennium Economic Research Program

This chapter synthesizes the seven problem chapters into a single theoretical research program. Its central claim is not that the monograph solves, proves, tests or replicates the Clay Millennium Problems in their original mathematical form. Its claim is that the seven Millennium Problems supply seven rigorous measurement grammars for economic complexity: flow, decomposition, curvature, topological deformation, local-to-global rank, spectral-cyclical forecasting and computational decision. The chapter therefore functions as the theoretical peak of the monograph. It shows how the Navier-Stokes, Hodge, Perelman-Ricci-Poincare, Yang-Mills, Birch-Swinnerton-Dyer, Riemann-Zeta and P-vs-NP-inspired studies are not merely parallel analogies, but a unified mathematical-econometric program for measuring global stress, corridor networks, structural rank, forecast dynamics, portfolio search complexity and scientific claim discipline.

General claim boundary. The unified interpretation remains bounded. It does not convert economic analogues into mathematical proofs. It does not claim that liquidity is a physical fluid, that inequality is a literal Riemannian manifold, that

corridor stress is a physical gauge field, that regional structural rank proves BSD, that the zeta-cycle tests the Riemann Hypothesis, or that portfolio search proves P != NP. The chapter synthesizes what the seven studies establish as measurement architectures, validation protocols and interpretable economic diagnostics.

Figure 13.1. Unified architecture of the Millennium Economic Research Program



Source: Author synthesis based on the seven problem-chapter architectures.

Table 13.1. Seven Millennium Problems as economic measurement languages

Millennium source	Economic measurement language	Primary book chapter	Core empirical object	Permitted claim
Navier-Stokes	Flow balance, pressure, friction, shock and closure	Chapter 7	Global liquidity-flow and systemic-stress panel	Nondimensional macro-financial stress diagnostics; no physical-fluid law
Hodge	Flow decomposition into gradient, curl and harmonic components	Chapter 6	Ten-node regional macro-flow benchmark	Topological flow decomposition; no literal cohomological theorem claim
Poincare/Ricci/Perelman	Curvature, entropy, smoothing and connectedness	Chapter 5	N=150 macro-regional inequality-pressure panel	Diagnostic pressure-curvature topology; no proof of Poincare or Ricci-flow theorem
Yang-Mills	Gauge potential, curvature, action and mass-gap threshold	Chapter 8	Ten-node, 27-edge corridor stress network	Positive finite-network stress threshold; no Yang-Mills proof
Birch-Swinnerton-Dyer	Local-to-global rank, LOrder and structural rank	Chapter 9	World anchor, ten nodes and N=150 closure layer	Calibrated local-to-global consistency; no BSD proof
Riemann/Zeta	Spectral-cyclical inflation signal and forecast correction	Chapter 10	Annual, quarterly and monthly validation layers	Forecast-diagnostic improvement; no RH proof/test
P vs NP	Sparse decision complexity, support explosion and algorithmic search	Chapter 11	n=94 industry universe and reduced exact benchmark	Computational-finance evidence; no P-vs-NP proof or certified n=94 global optimum

13.0. Integrative Premise: From Seven Analogues to One Research Program

The first task of this chapter is to prevent the monograph from being read as seven separate articles placed in sequence. Each problem chapter has its own empirical object, its own mathematical grammar and its own validation discipline, but the book-level contribution is larger than the sum of these chapters. The monograph proposes that economic complexity becomes measurable only when no single dimension is allowed to dominate. GDP mass is not enough; inflation forecasting is not enough; network centrality is not enough; covariance optimization is not enough; regional rank is not enough. A world economy that is flow-driven, shock-sensitive, corridor-dependent, topologically coupled, spectrally cyclic and computationally constrained requires a multidimensional measurement program.

The second task is to define what the word unified means in this book. It does not mean that the seven mathematical problems are forced into one equation. It means that each problem supplies one measurement language and that these languages form a coherent epistemic sequence. Navier-Stokes supplies the language of flow balance; Hodge supplies the language of flow decomposition; Ricci/Poincare/Perelman supplies the language of deformation, smoothing and connectedness; Yang-Mills supplies the language of curvature, action and threshold; BSD supplies the language of local-to-global rank formation; Riemann/Zeta supplies the language of spectral-cyclical signal extraction; and P vs NP supplies the language of computational decision and sparse search.

The third task is to defend the scientific status of the program. The correct description is mathematical-econometric analogue program. This phrase is deliberately strict. Mathematical indicates that the models are structurally motivated by rigorous formal architectures. Econometric indicates that the analogues are not mere metaphors: they require data, normalization, model objects, validation gates, robustness checks and replication files. Analogue indicates the essential claim boundary: the book translates formal architectures into economic measurement systems; it does not solve the original Clay problems.

Table 13.2. Unified interpretive logic of Chapter 13

Dimension	Problem chapters integrated	Unifying question	Output of synthesis
Flow	Navier-Stokes; Hodge	How does economic stress move, decompose and circulate?	Flow-balance and flow-decomposition grammar
Curvature / topology	Ricci/Poincare; Yang-Mills; Hodge	How does stress deform, loop, concentrate and cross thresholds?	Deformation-topology-threshold grammar
Local-to-global rank	BSD	How do local regional states inform global structural rank?	Rank-correspondence and corridor-structure grammar
Spectral-cyclical forecast	Riemann/Zeta	How can nonlinear cyclical signals improve inflation forecasting under validation discipline?	Layered forecast-validation grammar
Computational decision	P vs NP	How does combinatorial search constrain economic decision making?	Sparse optimization and search-complexity grammar
Unified contribution	All seven chapters	What does the monograph add to economic science?	Bounded mathematical-econometric research program

13.1. Flow Dimension: Navier-Stokes and Hodge

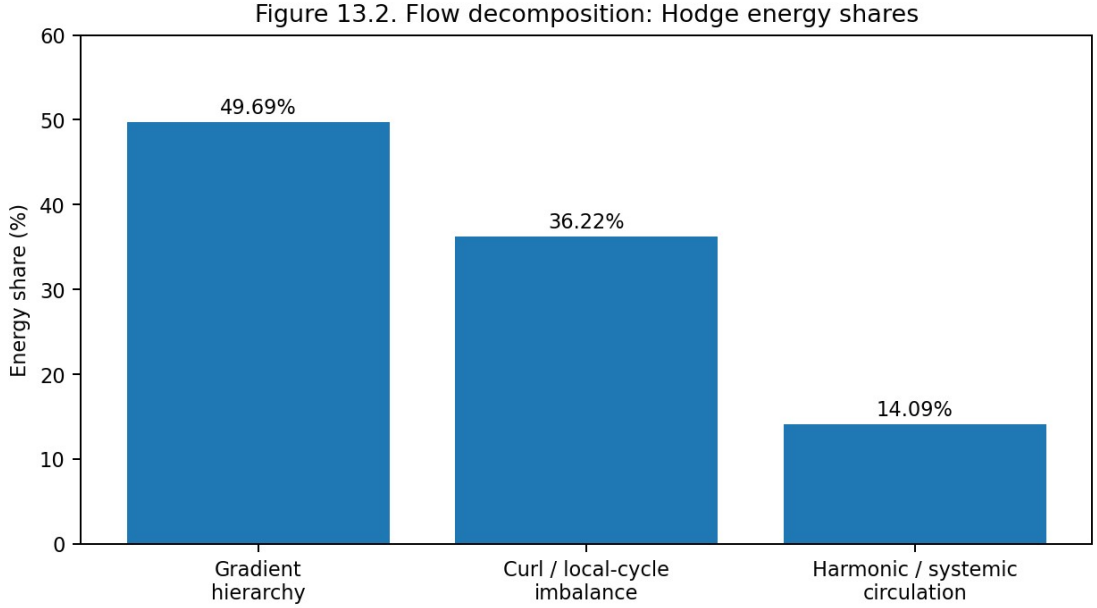
The flow dimension is the first pillar of the unified program because economic stress is not only a stock or a level; it is a movement, a pressure, a directional imbalance and a circulation process. The Navier-Stokes-inspired chapter translates the logic of velocity, acceleration, pressure gradient, friction or diffusion, stochastic forcing, cyclical forcing and restricted closure into a nondimensional macro-financial stress-balance architecture. The Hodge chapter then decomposes a directed macro-flow field into gradient hierarchy, curl/local-cycle imbalance and harmonic systemic circulation. Together they answer a question that conventional macroeconomic tables rarely resolve: when stress is observed, is it a hierarchical pressure, a local-cycle inconsistency or a persistent system-wide circulation?

The Navier-Stokes component gives the flow dimension its dynamic balance. It treats systemic stress as a structured combination of liquidity velocity weakness, acceleration pressure, macro-financial pressure gradients, liquidity friction/diffusion, stochastic shocks, GDP-cycle forcing and a restricted hidden-adjustment term. The essential methodological move is nondimensionalization. Heterogeneous macro-financial variables are not added in raw units. They are transformed into comparable stress-oriented components. This protects the analogy from becoming a loose metaphor and makes the balance equation auditable.

The Hodge component gives the flow dimension its structural decomposition. If Navier-Stokes says that stress is formed through a balance of channels, Hodge says that the resulting macro-flow field has distinct topological components. A gradient component captures directional hierarchy; a curl component captures local circular imbalance; a harmonic component captures residual systemic circulation that cannot be reduced to local hierarchy or local cycles. In the reported Hodge benchmark, the energy decomposition separates the system into 49.69% gradient hierarchy, 36.22% curl/local-cycle imbalance and 14.09% harmonic/systemic circulation. This numerical split is theoretically important because it shows that the global economy is not reducible to GDP mass or a single directional hierarchy.

The unified implication is that flow measurement must be both dynamic and topological. A stress index may identify that pressure is high, but it does not by itself reveal whether pressure is being transported through velocity weakness, pressure-gradient concentration, friction, local circulation or systemic harmonic exposure. The flow dimension therefore creates the first economic measurement language of the monograph: economic complexity as pressure-bearing flow.

Figure 13.2. Flow decomposition: Hodge energy shares



Source: Author synthesis from the Hodge-econometric benchmark results.

Table 13.3. Flow-dimension synthesis

Flow component	Navier-Stokes interpretation	Hodge interpretation	Unified economic meaning
Velocity / weak flow	Low liquidity velocity or weak macro-financial flow intensity	Directional edge pressure entering the flow field	Stress can arise from weak circulation even before a crisis becomes visible in aggregate output
Pressure gradient	Inflation, sovereign, FX or risk-pressure channel	Part of directional hierarchy in the edge field	Stress has a directional slope across countries or regions
Friction / diffusion	Credit, banking, funding or liquidity friction	Resistance that changes projected flow structure	Systemic stress may be generated by transmission frictions rather than by shock size alone
Stochastic forcing	Volatility/event shock channel	Perturbation to edge pressure and cycles	Shocks change both levels and topology
Restricted closure	Observable hidden	Unexplained projection	Model fit cannot be forced by

	adjustment rather than a free residual	remainder kept auditable	unrestricted residuals
Gradient hierarchy	Implicit in pressure gradients	49.69% of Hodge energy	Economic hierarchy remains important but not exhaustive
Curl imbalance	Local feedback or instability channel	36.22% of Hodge energy	Regional cycles and corridor loops carry independent stress information
Harmonic circulation	Systemic residual flow pressure	14.09% of Hodge energy	Persistent circulation captures world-system exposure beyond local hierarchy

13.2. Curvature and Topological Deformation Dimension: Ricci/Poincare, Yang-Mills and Hodge

The second dimension is curvature and topological deformation. It brings together three chapters that measure different forms of structured distortion. The Perelman-Ricci-Poincare chapter measures inequality pressure, smoothing capacity, curvature-like deformation, entropy-like complexity and graph connectedness. The Yang-Mills chapter measures systemic stress as a finite-network gauge field with anti-symmetric potential, triangular curvature, action concentration and stress-Laplacian spectral separation. The Hodge chapter supplies the cycle and harmonic logic that connects deformation to flow topology.

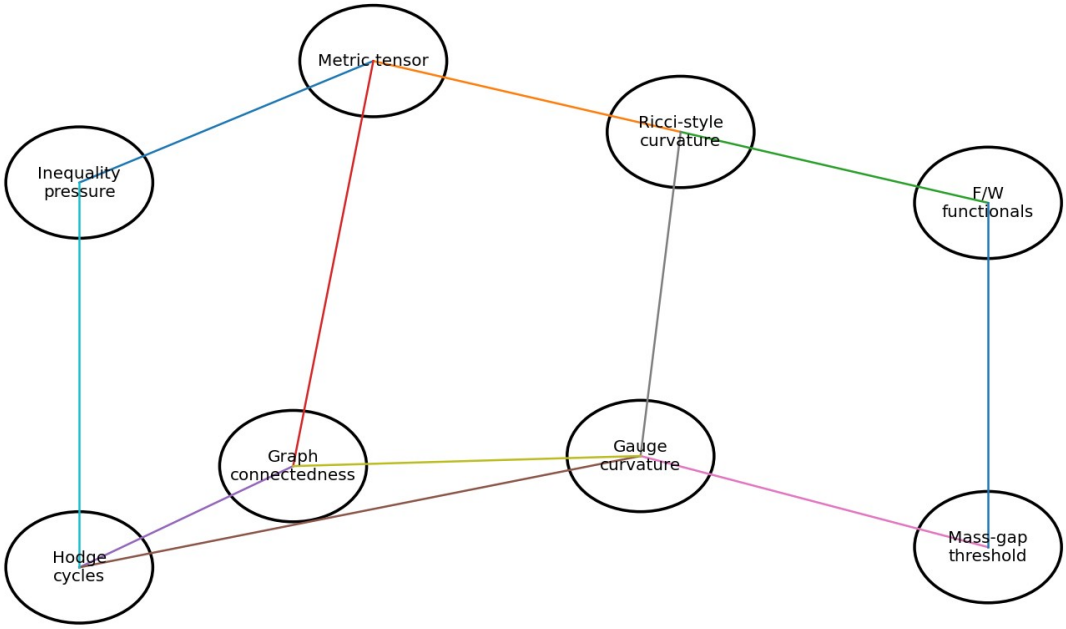
In the Ricci/Poincare/Perelman-inspired chapter, curvature is used as a diagnostic language for inequality deformation. The empirical system is not treated as a literal geometric manifold. Rather, sixteen stress-coordinate variables over a ten-region, 2010-2024 panel are transformed into a pressure-oriented diagnostic space. A correlation-based metric tensor, Ricci-style component curvature, scalar curvature paths, F- and W-functionals, graph Laplacian connectedness, Betti diagnostics and network-curvature proxies then measure whether the inequality system is smoothing or deforming. The 2020 crisis-deformation signal, with global pressure rising and scalar curvature falling, illustrates why curvature language adds interpretive value beyond ordinary indicator dashboards.

In the Yang-Mills chapter, curvature becomes a network stress-threshold language. Public macroeconomic anchors and corridor transformations define a ten-node, twenty-seven-edge global-corridor stress network. Stress differences and edge weights produce an anti-symmetric economic gauge potential; triangular cycles generate curvature; squared curvature generates Yang-Mills economic action; and the stress-weighted Laplacian generates a finite-network mass-gap threshold. The reported benchmark has lambda_1 = 0.3850, spectral radius = 3.5023 and normalized local-to-systemic threshold = 0.1099. This does not prove the mathematical Yang-Mills mass-gap problem. It provides a finite weighted-graph threshold for when local shocks become systemically transmissible.

Hodge closes this dimension because curvature and topology require cycles. If the system had only hierarchy, curvature and local-cycle imbalance would be secondary. But the Hodge evidence shows a connected and cycle-rich regional network with substantial curl and harmonic components. This means that deformation is not merely a scalar deviation; it is also a topological property of loops, bridges and persistent circulation.

The unified interpretation is that economic deformation has three levels. At the variable-coordinate level, pressure and smoothing capacity deform the diagnostic manifold. At the corridor-network level, stress circulates through gauge curvature and action concentration. At the flow-decomposition level, hierarchy, curl and harmonic circulation determine whether deformation remains local or becomes systemic. This is the second measurement language of the monograph: economic complexity as curvature-bearing topology.

Figure 13.3. Curvature and topological deformation as a unified diagnostic mesh



Source: Author synthesis based on Ricci/Poincare, Yang-Mills and Hodge chapter logics.

Table 13.4. Curvature and topological deformation synthesis

Layer	Model source	Core object	Diagnostic meaning	Claim boundary
Pressure-coordinate curvature	Ricci/Poincare/Perelman	Metric tensor, Ricci-style curvature, scalar curvature, F/W functionals	Measures inequality pressure, smoothing weakness, crisis deformation and complexity	Economic diagnostic manifold; no geometric theorem proof
Graph connectedness	Poincare-inspired layer	Graph Laplacian, beta_0, beta_1, algebraic connectivity	Tests whether the stress-coordinate system forms a connected and cycle-rich structure	Graph audit; no Poincare proof
Gauge curvature	Yang-Mills	Anti-symmetric gauge potential and triangular curvature	Measures stress circulation on corridor cycles	Finite-network analogue; no physical field claim
Economic action	Yang-Mills	Sum of squared curvature terms	Measures concentration of stress-energy in cycles	Benchmark concentration, not universal law
Mass-gap threshold	Yang-Mills	lambda_1 and normalized threshold	Defines local-to-systemic shock transition inside the finite graph	Finite weighted-graph threshold; no Clay proof
Flow cycles	Hodge	Curl and harmonic components	Explains how cycles and systemic circulation support deformation interpretation	Topological decomposition, not literal theorem transfer

13.3. Local-to-Global Rank Dimension: Birch-Swinnerton-Dyer

The third dimension is local-to-global rank. It is supplied by the BSD-inspired regional economic chapter, which is the monograph's most direct translation of local information into global structural interpretation. In its classical mathematical setting, BSD concerns the relationship between local reductions, L-functions and algebraic rank. In the economic analogue,

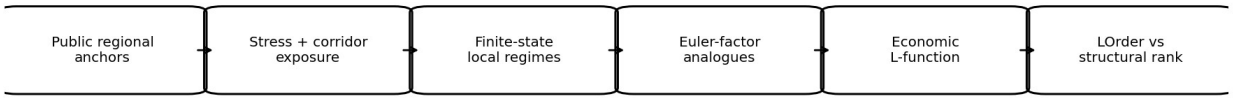
this logic becomes a disciplined measurement sequence: public regional anchors are transformed into stress components, corridor exposure, network structure, economic curve coefficients, finite-state local traces, Euler-factor analogues, an economic L-function, LOrder and structural rank.

The conceptual significance is that the BSD chapter prevents the monograph from becoming only a collection of stress indices. Stress measurement is useful, but the world economy also requires rank interpretation: which regions occupy structurally important positions, how local stress states aggregate into global structural formation, and whether corridor-sensitive signals contain information about system-level rank. The BSD-inspired chapter therefore asks a different question from the flow and curvature chapters. It asks whether local regional states, represented through finite-state regimes and Euler-factor information, are informative about global structural rank.

The empirical architecture is bounded by a World normalization anchor, ten macro-regional/corridor nodes and an N=150 regional-year closure layer. The structural rank object is constructed from productive, Hodge-flow, network and agentic components. LOrder is not treated as a literal analytic order of an elliptic-curve L-function. It is an economic L-order analogue used to test correspondence between local finite-state information and structural rank. The model also introduces regulator-like capacity, Tamagawa-type friction, torsion-like locked capacity, BridgeStress and scenario-threshold diagnostics to distinguish output mass from systemic rank exposure.

The unified interpretation is that local-to-global rank connects the entire monograph. Hodge contributes the flow component of structural rank; Yang-Mills contributes corridor stress and BridgeStress logic; Ricci/Poincare contributes deformation and smoothing capacity; Navier-Stokes contributes macro-financial stress dynamics; Riemann/Zeta contributes spectral-cycle discipline; P vs NP contributes the decision complexity of selecting and optimizing structural components. BSD is therefore not isolated. It is the rank-formation hinge of the book.

Figure 13.4. BSD-inspired local-to-global rank translation chain



Source: Author synthesis based on the BSD-inspired local-to-global chapter.

Table 13.5. BSD local-to-global rank dimension

BSD-inspired object	Economic analogue	Role in unified program	Scientific boundary
Local reductions	Finite-state regional regimes	Transforms local conditions into comparable state signals	Not arithmetic reduction over finite fields
Euler factors	Regional information factors	Aggregates local signals into L-function-like structure	Constructed analogue, not number-theoretic Euler product
Economic L-function	Global rank signal container	Links local signal accumulation to structural rank interpretation	Measurement device, not analytic theorem
LOrder	Order analogue from constructed L-function behavior	Compares local-to-global signal with structural rank	Calibration object, not proof of BSD
Structural rank	Composite of productive, Hodge-flow, network and agentic components	Measures global economic rank formation	Constructed rank, not welfare ranking
BridgeStress	Corridor leverage and transmission exposure	Connects local-to-global rank to corridor economics	Scenario/diagnostic measure, not causal

			proof

13.4. Spectral-Cyclical Forecast Dimension: Riemann/Zeta

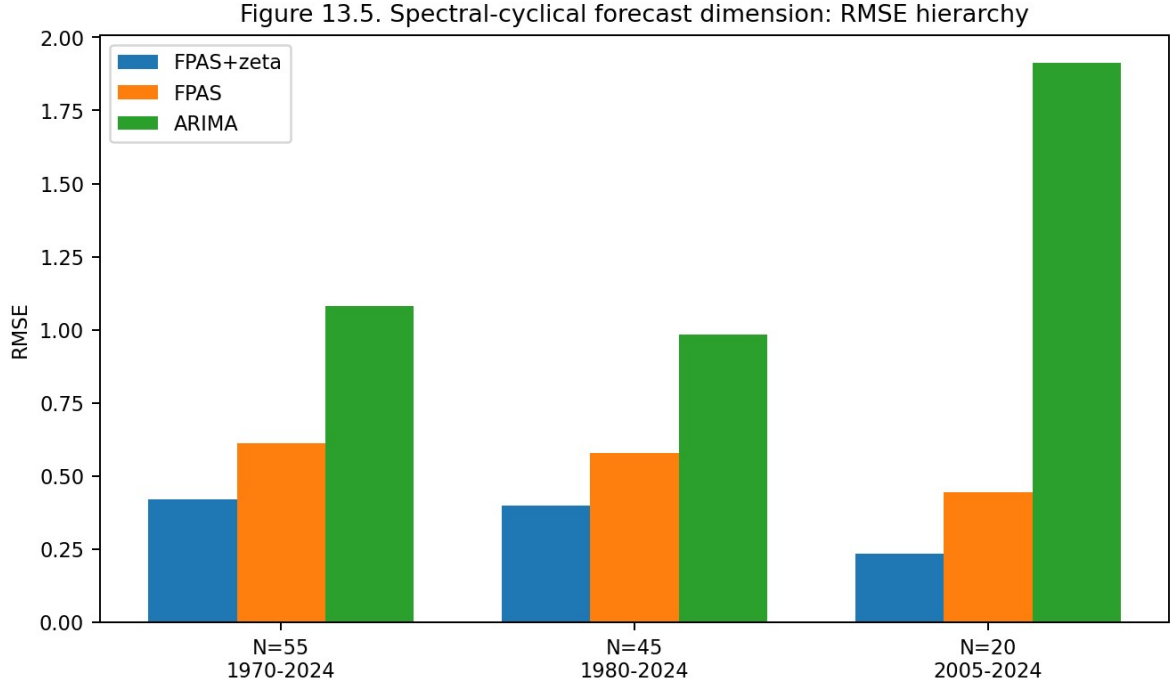
The fourth dimension is spectral-cyclical forecasting. It is supplied by the Riemann-Zeta FPAS+zeta chapter, which is the strongest forecast-validation chapter of the monograph. Its central contribution is not the use of a famous mathematical function for symbolic appeal. Its contribution is methodological: the Riemann-zeta critical-line signal is transformed into a normalized, real-valued, signed cyclical correction that is added to a structural FPAS baseline only through a calibrated correction gate. The result is then evaluated against FPAS and ARIMA through layered validation.

The empirical discipline of this chapter is especially important for the unified program. The principal annual layer covers 1970-2024 (N=55), the robustness annual layer covers 1980-2024 (N=45), the compact crisis-era comparison layer covers 2005-2024 (N=20), the quarterly dynamic-validation layer covers 2000Q1-2024Q4 (N=100), and the monthly spectral-diagnostics layer covers 2005M1-2024M12 (N=240). This sample hierarchy prevents all methods from being interpreted as if they were estimated on the same small sample. It also makes the zeta chapter a model of validation discipline for the entire book.

The central reported forecast comparison is clear. In the N=55 annual layer, FPAS+zeta reaches RMSE = 0.421, compared with 0.612 for FPAS and 1.081 for ARIMA. In the N=45 robustness layer, FPAS+zeta reaches RMSE = 0.398, compared with 0.578 and 0.983. In the N=20 crisis-era layer, FPAS+zeta reaches RMSE = 0.233, compared with 0.443 and 1.913. These results support a bounded forecast-improvement claim. They do not prove the Riemann Hypothesis, test the Riemann Hypothesis or establish universal inflation-forecast dominance.

The unified interpretation is that spectral signals can play a legitimate role in economic measurement only when they are disciplined by benchmark comparison, rolling validation, Mincer-Zarnowitz calibration, forecast-encompassing tests, Diebold-Mariano and Clark-West comparisons, residual diagnostics, HMM/Markov-switching screens and spectral robustness. This is the fourth measurement language of the monograph: economic complexity as validated nonlinear cyclicality.

Figure 13.5. Spectral-cyclical forecast dimension: RMSE hierarchy



Source: Author synthesis from the Riemann-Zeta FPAS+zeta layered validation results.

Table 13.6. Spectral-cyclical forecast dimension

Layer	Sample	Main function	Core result / role	Boundary
Principal annual	1970-2024, N=55	Main forecast-accuracy claim	FPAS+zeta RMSE 0.421 vs FPAS 0.612 vs	Global aggregate evidence only

			ARIMA 1.081	
Annual robustness	1980-2024, N=45	Checks robustness of annual hierarchy	FPAS+zeta RMSE 0.398 vs FPAS 0.578 vs ARIMA 0.983	Robustness layer, not universal dominance
Crisis-era annual	2005-2024, N=20	Compact crisis comparison	FPAS+zeta RMSE 0.233 vs FPAS 0.443 vs ARIMA 1.913	Small-sample crisis display
Quarterly dynamic	2000Q1-2024Q4, N=100	VAR/HMM/regime and dynamic validation	Supports dynamic evidence and regime interpretation	Quarterly robustness, not annual proof replacement
Monthly spectral	2005M1-2024M12, N=240	Fourier/wavelet/spectral-entropy diagnostics	Supports cyclical coherence and stress alignment	Spectral diagnostic, not causality

13.5. Computational-Decision Dimension: P vs NP

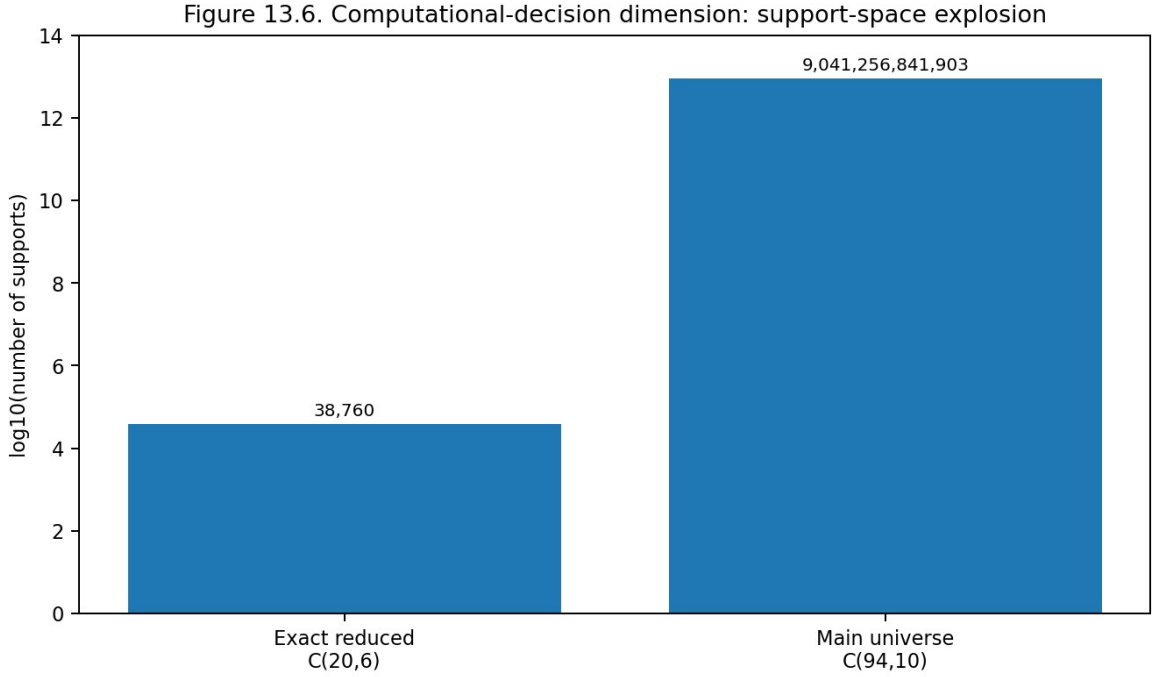
The fifth dimension is computational decision. It is supplied by the P-vs-NP-inspired robust portfolio-optimization chapter. This chapter is essential because economic complexity is not only measurement complexity; it is also decision complexity. Even if the data are known, the decision problem may remain computationally difficult because feasible alternatives grow combinatorially. The portfolio chapter makes this point concrete through a fixed Damodaran January 2026 U.S. industry universe containing n=94 industry portfolios and a K=10 sparse-selection problem.

The support-space explosion is the central economic meaning of the P-vs-NP analogy. Before continuous weights are optimized, the baseline sparse portfolio problem already contains C(94,10) = 9,041,256,841,903 possible supports. This number does not prove P != NP. It operationalizes computational difficulty inside a real financial decision setting. The reduced exact benchmark, n=20 and K=6, contains C(20,6)=38,760 supports and can be enumerated fully. This contrast between the reduced exact layer and the full n=94 heuristic layer is the empirical-computational core of the chapter.

The methodological architecture integrates Markowitz mean-variance logic, CAPM expected-return priors, covariance geometry, support-space growth, greedy search, Monte Carlo sampling, genetic algorithms, GA-plus-continuous reoptimization, exact reduced benchmarking, Black-Scholes overlay, transaction costs, stress scenarios, covariance robustness and falsification gates. The computational dimension therefore connects finance theory to complexity theory through a transparent evidence hierarchy: exact evidence where enumeration is feasible, best-found incumbents where full enumeration is infeasible, and claim discipline where search coverage is incomplete.

The unified interpretation is that economic decision problems require a different type of scientific humility from measurement problems. A model may find strong candidates, improve search quality and document robustness, yet still be unable to certify global optimality in the full universe. This is not a defect; it is exactly what computational complexity teaches. The fifth measurement language of the monograph is therefore economic complexity as constrained decision search.

Figure 13.6. Computational-decision dimension: support-space explosion



Source: Author synthesis from the P-vs-NP-inspired portfolio-optimization architecture.

Table 13.7. Computational-decision dimension

Computational object	Reported scale	Economic role	Admissible interpretation	Excluded claim
Main sparse-selection universe	n=94, K=10, C(94,10)=9,041,256,841,903	Defines full support-space explosion before continuous weights	Strong computational-finance evidence of combinatorial difficulty	No proof of P != NP
Reduced exact benchmark	n=20, K=6, C(20,6)=38,760	Allows exhaustive enumeration and algorithmic comparison	Exact evidence in reduced universe	No certification of n=94 optimum
Greedy search	Sequential support construction	Fast baseline heuristic	Search-layer comparator	No global optimality certificate
Monte Carlo	Random support sampling	Explores broad but partial support space	Stochastic search evidence under documented budget	No exhaustive coverage
Genetic algorithm	Population-based metaheuristic	Searches nonconvex mixed discrete-continuous landscape	Best-found incumbent evidence	No theorem-level guarantee
GA + continuous reoptimization	Metaheuristic support plus weight refinement	Separates selection and allocation improvement	Improved computational pipeline	No realized-return dominance

13.6. Unified Contribution to Economic Science

The unified contribution of the monograph is best stated as a research program rather than a single model. The book creates a mathematical-econometric analogue program for economics. It shows that major mathematical architectures can be translated into bounded economic measurement systems when three conditions are satisfied: first, the mathematical source must function as structural grammar rather than proof claim; second, the economic object must be explicitly constructed

from auditable data transformations; third, the empirical claim must be filtered through validation, robustness, replication and claim-boundary discipline.

The first contribution is a global stress measurement architecture. Across Navier-Stokes, Ricci/Poincare, Yang-Mills and Riemann/Zeta, stress is no longer treated as an isolated indicator. It appears as flow pressure, inequality deformation, corridor curvature, inflation pressure and forecast residual risk. This creates a vocabulary for interpreting how stress forms, moves, concentrates, cycles and becomes transmissible.

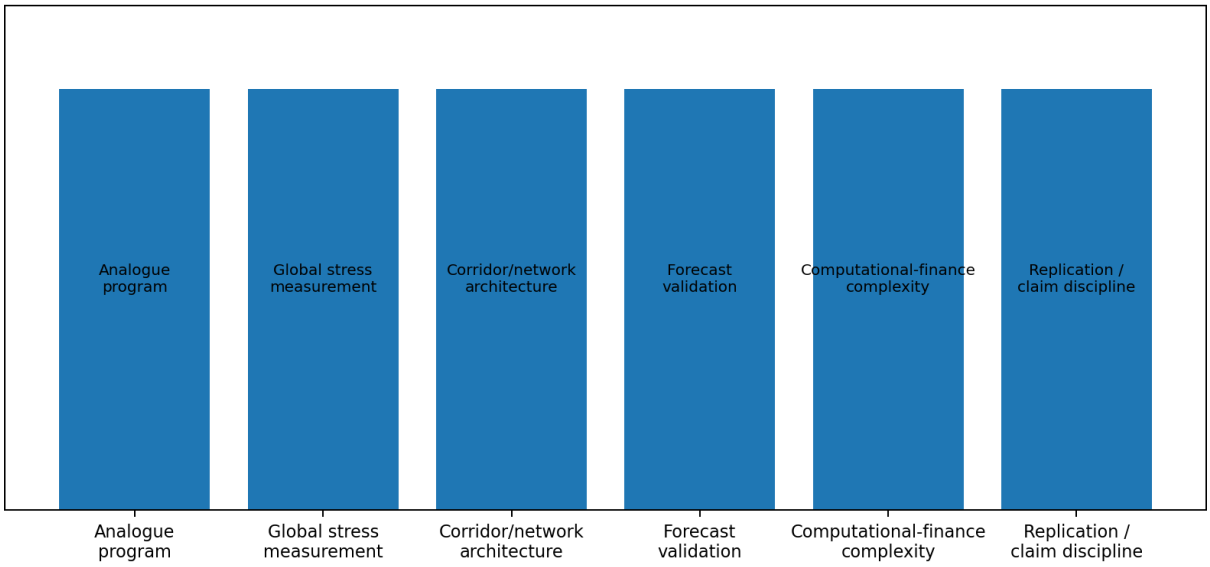
The second contribution is a corridor and network measurement architecture. Hodge, Yang-Mills and BSD jointly show that the world economy cannot be understood only through scalar mass. Corridor nodes may be small in GDP terms but systemically important through network position, bridge stress, local-to-global rank contribution and harmonic circulation. The Middle Corridor, Caucasus and Central Asia logic in the relevant chapters demonstrates why corridor exposure must be measured topologically rather than narrated qualitatively.

The third contribution is a forecast-validation architecture. The Riemann-Zeta FPAS+zeta chapter provides the clearest example: mathematical signal construction is not enough; it must be compared against baselines, evaluated across samples, tested under rolling validation, subjected to residual diagnostics and restricted by claim discipline. This logic also informs the Navier-Stokes and Ricci/Poincare validation layers.

The fourth contribution is a computational-finance complexity architecture. The P-vs-NP-inspired chapter demonstrates how economic decision-making can become difficult before preferences or forecasts are even debated, because the feasible support space grows combinatorially. This adds a decision-theoretic dimension to the monograph: complexity is not only what the economy is, but also what the economist or investor must search through.

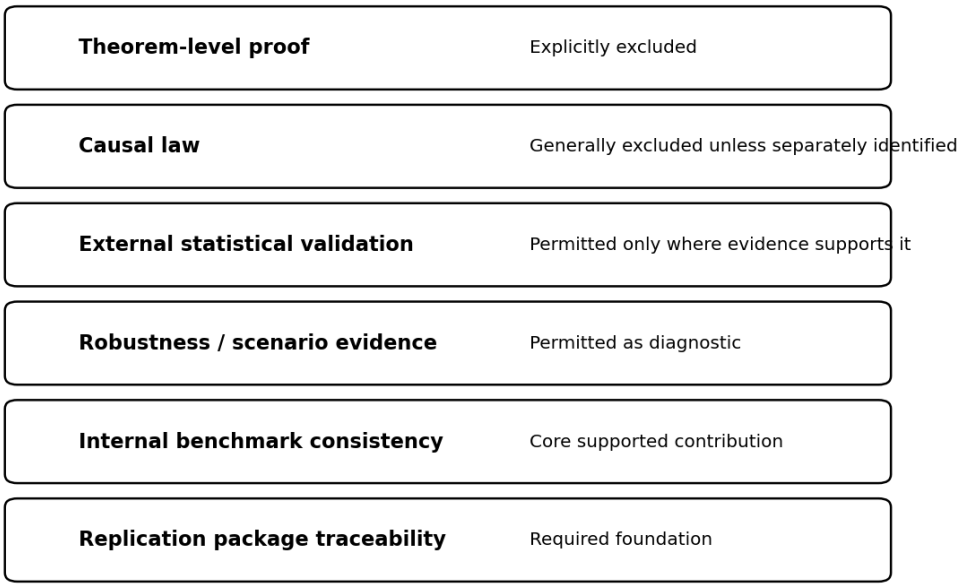
The fifth contribution is a claim-disciplined replication framework. Every chapter separates public anchors from author-calculated variables, benchmark evidence from causal evidence, robustness from proof, scenario analysis from prediction and replication packages from narrative claims. This is the scientific condition under which a bold analogue program can remain credible. The monograph's originality therefore lies not in overclaiming that economics solves Millennium Problems, but in showing that Millennium Problems can organize a rigorous economic measurement program.

Figure 13.8. Unified contribution pillars of the monograph



Source: Author synthesis of the monograph-level contribution.

Figure 13.7. Unified evidence hierarchy and claim-boundary ladder



Source: Author synthesis based on the claim-boundary design across Chapters 5-11.

Table 13.8. Unified contribution matrix

Contribution pillar	Chapters supporting it	What is created	Why it matters for economic science
Mathematical-econometric analogue program	All seven problem chapters	A disciplined way to translate formal mathematical architectures into economic measurement systems	Moves analogy from metaphor to auditable model design
Global stress measurement architecture	Ricci/Poincare; Navier-Stokes; Yang-Mills; Riemann/Zeta	Stress as pressure, flow, curvature, threshold and forecast deformation	Creates a multi-channel stress vocabulary
Corridor and network measurement architecture	Hodge; Yang-Mills; BSD	Nodes, edges, cycles, BridgeStress, structural rank and harmonic circulation	Makes strategic corridor exposure measurable
Forecast-validation architecture	Riemann/Zeta; Navier-Stokes; Ricci/Poincare	Layered samples, benchmarks, rolling validation, residual diagnostics and robustness gates	Prevents visual-fit and compact-sample overclaiming
Computational-finance complexity architecture	P vs NP	Sparse selection, support-space explosion, heuristic search and exact reduced benchmarking	Shows that economic decision problems can be computationally constrained
Claim-disciplined replication framework	All seven chapters	Source ledgers, data packages, evidence hierarchy and excluded claims	Protects scientific credibility and reviewer acceptance

13.7. Cross-Dimensional Coupling: Why the Five Dimensions Cannot Be Separated

Although Chapter 13 is organized into dimensions, the dimensions are not independent. Flow becomes topological when Hodge decomposes edge pressure into gradient, curl and harmonic components. Topology becomes systemic when Yang-Mills curvature/action identifies threshold compression. Local-to-global rank becomes corridor-sensitive when BSD structural rank includes Hodge-flow and network components. Forecasting becomes stress measurement when the Riemann-Zeta chapter interprets zeta deformation around global crisis episodes. Computational decision becomes economic structure when the P-vs-NP chapter shows that sparse selection constraints change the feasible decision universe.

The deeper theoretical message is that economic complexity is not one phenomenon. It is the interaction of several constraints: physical-like flow constraints, topological embedding constraints, rank-formation constraints, spectral-cycle constraints and computational-search constraints. A mature economic measurement program should therefore allow these constraints to be read together. This is the point at which the monograph moves beyond isolated analogues and becomes a unified research program.

Table 13.9. Cross-dimensional coupling matrix

Dimension A	Dimension B	Coupling mechanism	Interpretive consequence
Flow	Curvature/topology	Stress flows create cycles, bottlenecks and deformation	A high stress level must be decomposed before interpretation
Flow	Local-to-global rank	Hodge-flow components enter structural rank	Rank is partly flow-structural, not only output-based
Curvature/topology	Spectral forecasting	Crisis deformation aligns with cyclical pressure and regime changes	Forecast signals are interpreted as stress deformation, not pure numerology
Curvature/topology	Computational decision	Network and covariance geometry shape feasible optimization and robustness	Optimization is constrained by structural dependence
Local-to-global rank	Computational decision	Rank construction and support selection both require evidence hierarchy	Global structure and decision search require explicit claim boundaries
Spectral forecasting	Computational decision	Forecast outputs can enter decision systems but must retain validation limits	Forecast improvement does not imply investment dominance

13.8. What the Chapter Establishes and What It Excludes

A unified interpretation chapter is also a reviewer-safety chapter. Because the book uses the names of the Millennium Problems, the most important risk is that a reader may think the author is claiming to solve the original mathematical problems. Chapter 13 must therefore state the opposite with precision. The book does not solve, prove, test or replicate any Clay Millennium Problem in its original mathematical form. It constructs bounded economic-econometric analogues inspired by their formal architectures.

The scientific strength of the monograph comes from the fact that it does not need overclaiming. The reported chapters already contain meaningful contributions under bounded interpretation: a nondimensional stress-balance model; a Hodge flow-decomposition benchmark; a pressure-curvature-topology inequality architecture; a finite-network mass-gap threshold; a BSD-inspired local-to-global structural-rank model; a layered spectral inflation forecast-validation framework; and a P-vs-NP-inspired sparse portfolio optimization architecture. These are substantial economic contributions even when theorem-level claims are explicitly excluded.

Table 13.10. Unified claim-boundary matrix

Chapter / problem	Strongest admissible claim	Explicitly excluded claim	Reviewer-safety wording
Navier-Stokes	Global liquidity-flow and systemic-stress diagnostics under nondimensional stress-	Financial liquidity is a physical fluid; Navier-Stokes theorem solved; universal	Economic flow-balance analogue only

	balance architecture	crisis prediction	
Hodge	Regional macro-flow decomposes into hierarchy, local-cycle imbalance and systemic circulation	Literal cohomological theorem or complete world-flow representation	Discrete Hodge-inspired benchmark
Ricci/Poincare/Perelman	Inequality pressure, curvature-like deformation and graph connectedness can be jointly diagnosed	Proof or empirical test of Poincare/Ricci/Perelman theorem	Geometric-topological diagnostic analogue
Yang-Mills	Positive finite-network stress-Laplacian threshold and corridor shock diagnostics	Yang-Mills existence/mass-gap solution or physical gauge field claim	Finite weighted-graph mass-gap analogue
BSD	Local regional signals are informative about constructed structural rank under calibrated architecture	BSD proof, causal law or strong external validation where evidence is weak	Regional local-to-global measurement analogue
Riemann/Zeta	FPAS+zeta improves reported forecast hierarchy across validation layers	Riemann Hypothesis proof/test or universal forecast dominance	Spectral-cyclical forecast-diagnostic analogue
P vs NP	Sparse portfolio selection demonstrates computational search-space explosion and algorithmic evidence	P != NP proof, certified n=94 global optimum or realized-return dominance	Computational-finance complexity analogue

13.9. Final Theoretical Synthesis

The Millennium Economic Research Program can now be stated in one proposition: economic complexity is multidimensional, and each Millennium-inspired chapter supplies one disciplined language for measuring one dimension of that complexity. Flow explains movement and pressure. Hodge decomposition explains hierarchy, local-cycle imbalance and systemic circulation. Ricci/Poincare/Perelman explains deformation, smoothing and connectedness. Yang-Mills explains curvature, action and threshold. BSD explains local-to-global rank formation. Riemann/Zeta explains spectral-cyclical forecast correction. P vs NP explains computational decision difficulty.

The book's theoretical peak is therefore not a claim of mathematical conquest. It is a claim of methodological integration. The monograph shows that high-level mathematical structures can be translated into empirically auditable economic architectures when they are bounded, replicated and validated. The result is a research program for measuring the world economy as a complex system of flows, networks, deformations, ranks, cycles and decisions.

In the general conclusion of the book, this chapter should function as the bridge from the seven problem chapters to the final claim-boundary and contribution chapters. It provides the intellectual basis for saying that the monograph contributes to economic science by creating a mathematical-econometric analogue program, a global stress measurement architecture, a corridor and network measurement architecture, a forecast-validation architecture, a computational-finance complexity architecture and a claim-disciplined replication framework.

Table 13.11. Final chapter-closure matrix

Closure question	Chapter 13 answer	Book-level implication
What is the unified idea?	Seven Millennium Problems become seven economic measurement languages.	The monograph is a research program, not a collection of articles.
What does the program measure?	Flow, deformation, rank, spectral cycles, decision complexity and replication discipline.	Economic complexity is multidimensional and cannot be reduced to GDP or a single index.
What is the strongest contribution?	A mathematical-econometric analogue program with strict claim boundaries.	The book can be ambitious while remaining scientifically cautious.
What is excluded?	Original Clay-problem solutions, theorem-level proof, unrestricted causality and universal forecasting/investment dominance.	Reviewer risk is addressed through explicit claim hierarchy.
What does Chapter 13 prepare?	The transition to limitations, claim boundaries and general conclusion.	Chapters 14 and 15 can close the book from a strong but bounded position.

Chapter 14

Limitations, Claim Boundaries and Reviewer-Safety Matrix

A reviewer-safety chapter for the Millennium Economic Research Program

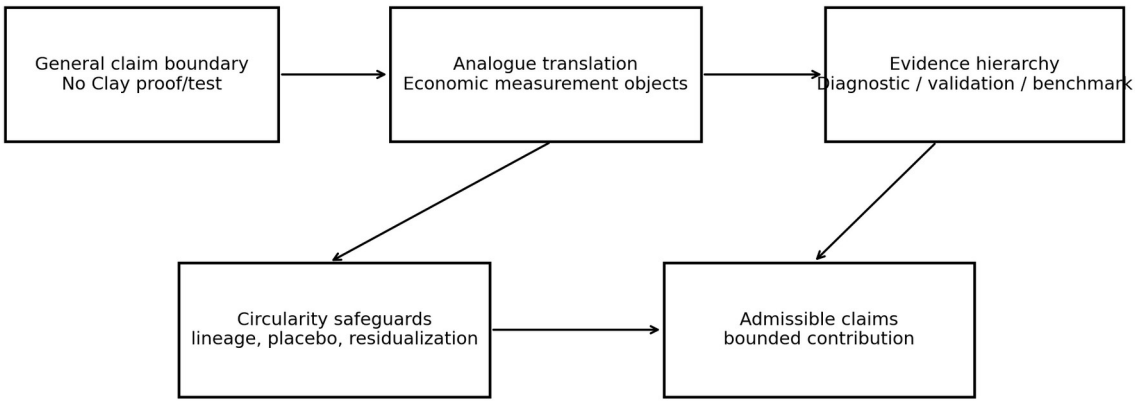
This chapter is the monograph's explicit scientific boundary-control chapter. Its purpose is not defensive in a rhetorical sense; it is methodological. A monograph that translates the seven Clay Millennium Problems into economic-econometric analogues must state with exceptional clarity what the book does not claim, what it does claim, what evidence level each chapter reaches, and how constructed variables, sample size, calibration, forecasting and optimization should be read.

The central reviewer question is direct: Does the author claim to solve the Millennium Problems? The answer is no. The monograph does not solve, prove, test, verify or replicate any Clay Millennium Problem in its original mathematical form. It develops seven bounded economic-econometric analogue architectures inspired by the formal measurement grammars of flow, topology, curvature, gauge separation, local-to-global rank, spectral cycles and computational complexity.

This chapter therefore performs five functions. First, it removes theorem-level overclaiming before the reviewer has to infer the boundary. Second, it separates analogy, calibration and measurement from proof. Third, it identifies circularity and variable-lineage risks created by author-calculated diagnostics. Fourth, it classifies sample-size boundaries across N = 10 benchmarks, N = 150 panels, N = 1,500 panels, and annual/quarterly/monthly validation layers. Fifth, it converts the entire book into a transparent evidence-level matrix.

Figure 14.1. Reviewer-safety architecture of the monograph

Figure 14.1. Reviewer-safety architecture of the monograph



Source: Author synthesis. The figure shows how the chapter connects claim boundary, analogue translation, evidence hierarchy, circularity safeguards and admissible contribution claims.

Chapter 14 establishes the scientific boundary conditions of the Millennium Economic Research Program. The chapter states that the monograph does not claim theorem-level solutions to the Clay Millennium Problems. Instead, it constructs economic analogues whose evidentiary value is empirical, diagnostic, computational, forecast-validating, structural, or calibrated depending on the chapter. The chapter distinguishes mathematical proof from economic measurement, calibration from independent validation, constructed variables from public-source inputs, and benchmark demonstrations from large-panel confirmation. It further provides a model-by-model reviewer-safety matrix covering Perelman/Ricci/Poincare,

Hodge, Navier-Stokes, Yang-Mills, BSD, Riemann/Zeta, and P vs NP. The resulting claim hierarchy protects the monograph from overstatement while preserving its main contribution: a claim-disciplined mathematical-econometric analogue program for measuring economic complexity.

14.1. What the Book Does Not Claim

The first boundary must be stated without qualification: this book does not claim to solve the Clay Millennium Problems. It does not prove the Riemann Hypothesis, does not solve P versus NP, does not prove the Navier-Stokes existence and smoothness problem, does not prove the Yang-Mills existence and mass-gap problem, does not prove the Hodge conjecture, does not prove the Birch-Swinnerton-Dyer conjecture, and does not re-prove Perelman/Ricci/Poincare results.

The book also does not claim that the world economy is literally a physical fluid, a quantum gauge field, a smooth differential manifold, a topological simplicial complex in the strict mathematical sense, an elliptic curve, a zeta-function universe, or a formal computational-complexity theorem. Those mathematical objects supply measurement grammars, not ontological identity. They help organize economic complexity, but they do not collapse economics into pure mathematics.

This negative claim is not a weakening device. It is the condition that makes the monograph scientifically admissible. A theorem-level claim would require formal mathematical proof inside the original objects and definitions. The present book instead uses the seven problems as high-level formal architectures for economic measurement: flow balance, topological decomposition, curvature deformation, gauge-threshold separation, local-to-global rank, spectral-cyclical forecasting and computational decision complexity.

Table 14.1. Negative claim matrix: what the monograph explicitly excludes

Problem / Chapter	Excluded theorem-level claim	Admissible economic use
Navier-Stokes	Does not solve fluid existence/smoothness; does not claim financial liquidity is a physical fluid.	Economic flow-balance and stress-testing architecture.
Hodge	Does not prove the Hodge conjecture; does not treat empirical decompositions as algebraic cycles.	Discrete macro-flow decomposition into gradient, curl and harmonic components.
Ricci/Poincare	Does not prove Perelman or Poincare; does not treat economic curvature as literal manifold curvature.	Inequality-pressure, smoothing-capacity and graph-topological diagnostic.
Yang-Mills	Does not solve Yang-Mills existence/mass gap; does not claim a physical field theory.	Finite weighted-network spectral threshold and systemic-stress action.
BSD	Does not prove BSD; does not use literal elliptic curves or arithmetic rank.	Regional local-to-global rank-calibration analogue.
Riemann/Zeta	Does not prove, test or verify the Riemann Hypothesis.	Critical-line-inspired cyclical signal used in inflation forecast validation.
P vs NP	Does not prove P != NP or certify full n = 94 global optimum.	Computational-finance demonstration of sparse-support search complexity.

Source: Author synthesis from the seven chapter-level claim-boundary statements.

The proper reading is therefore: the monograph is mathematically inspired but empirically bounded. It makes claims about economic measurement architectures, not about unresolved mathematical theorems. This distinction should appear not only in this chapter but also in the front matter, Chapter 1, Chapter 2, Chapter 4, each problem chapter, and the general conclusion.

14.2. Analogy, Calibration and Measurement

The second reviewer-safety boundary concerns the meaning of analogy. In this monograph, analogy is not metaphorical decoration. It is a disciplined translation rule. A classical mathematical object is not imported as a theorem; it is converted into a bounded economic measurement object with a declared empirical universe, variables, transformations, evidence level and interpretation boundary.

The book's general translation can be written as:

Classical formal architecture -> Economic analogue object -> Measurable diagnostic -> Evidence level -> Claim boundary.

This chain is essential because the same numerical result can be overclaimed or properly claimed depending on where it sits in the chain. For example, a positive first eigenvalue in the Yang-Mills-inspired chapter is not a proof of a physical quantum mass gap. It is a finite-network spectral separation in a stress-weighted graph. A zeta-cycle that improves forecast accuracy does not prove the Riemann Hypothesis. It is a calibrated cyclical correction that is useful only within a stated validation design. A complete enumeration of C(20,6) supports in a reduced portfolio universe does not prove P != NP. It demonstrates exact reduced evidence within a tractable computational subset.

Table 14.2. Analogy-calibration-measurement distinction

Concept	Meaning in this monograph	Reviewer-safe interpretation
Analogy	Formal grammar borrowed from a mathematical problem	Conceptual translation; not proof
Calibration	Parameter and index fitting within a defined economic universe	Internal consistency; not independent validation by itself
Measurement	Observable or constructed diagnostic values produced by formulas	Empirical reporting; interpretation depends on source lineage
Validation	Robustness, panel, forecast, benchmark, exact reduced or external checks	Strengthens admissible claim but remains bounded by design
Proof	Formal theorem established under original mathematical definitions	Not attempted anywhere in the monograph

A reviewer can therefore audit every chapter by asking: What is the original mathematical grammar? What is the economic analogue? What is actually measured? Which variables are public anchors and which are author-calculated? What is the sample? What is the strongest admissible evidence level? What is explicitly excluded? If these questions have direct answers, the analogy is disciplined. If they do not, the model risks becoming rhetorical. Chapter 14 is designed to prevent that risk.

14.3. Constructed Variables and Circularity Risk

Constructed variables are necessary in this monograph because the objects being measured do not exist as standard public indicators. There is no official World Bank variable named economic Ricci curvature, Hodge harmonic macro-flow, Yang-Mills economic action, EMGI, LOrder, zeta-cycle correction, or cardinality-search evidence score. Each must be created through a disclosed transformation procedure.

Constructed variables create scientific value when their formulas, source inputs, normalization rules and intended use are transparent. They create reviewer risk when the same inputs are used to construct both explanatory and outcome variables and then interpreted as independent validation. The key issue is not whether variables are constructed. The key issue is whether constructed variables are used within the correct evidentiary role.

The most sensitive chapters are BSD, Hodge, Yang-Mills and Ricci/Poincare. In BSD, LOrder, structural rank, BridgeStress and friction-like terms are related through the same local-to-global analogue architecture. In Hodge, gradient, curl and harmonic components all derive from the same edge-pressure field and network incidence structure. In Yang-Mills, stress score, gauge potential, curvature, action, EMGI and fragility are linked through the same finite-network pipeline. In Ricci/Poincare, pressure, curvature, F-functional, W-functional and graph diagnostics are all constructed from the same stress-coordinate system.

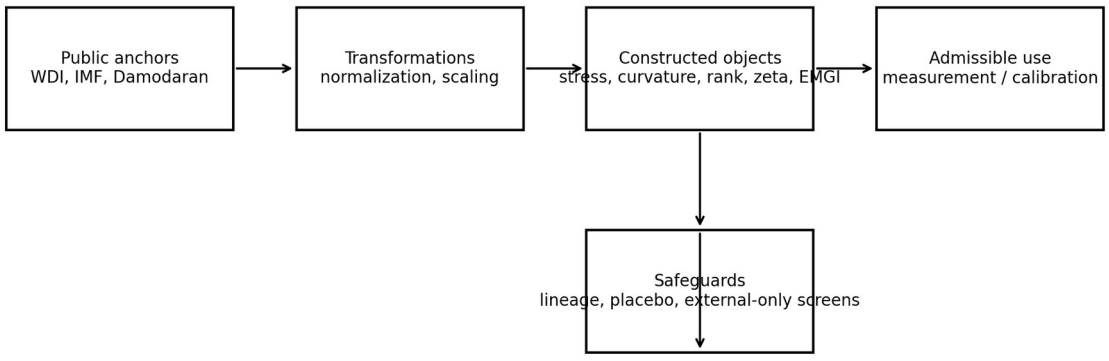
Table 14.3. Constructed-variable and circularity-risk matrix

Chapter	Constructed-variable cluster	Circularity	Reviewer-safety control

		risk	
BSD	Rank, LOrder, stress, BridgeStress, friction and torsion analogues	Medium/ high	Variable-lineage table; residualized LOrder; external-only screens; placebo/permutation checks
Hodge	Gradient, curl, harmonic, resilience and tail-risk variables from edge-pressure field	Medium/ high	Projection-orthogonality audit; separate topological Betti statements from energy shares
Yang-Mills	Stress, gauge potential, curvature, action, EMGI, fragility and BridgeStress	High	Do not regress identities; treat fragility=100-EMGI as identity; use network diagnostics separately
Ricci/Poincare	Pressure, curvature, F/W functionals, Betti and entropy diagnostics	Medium/ high	Stress-orientation ledger; PCA and robustness as diagnostics, not causality
Riemann/Zeta	CP_t, tau, zeta-cycle, alpha correction and forecast object	Medium	Out-of-sample and cross-layer validation; residual diagnostics retained
P vs NP	CAPM priors, covariance geometry, support-space and algorithmic scores	Medium	Fixed universe; exact reduced benchmark; no realized-return dominance claim
Navier-Stokes	Nondimensional stress components and restricted closure epsilon	Medium	Public anchors separated from normalized stress objects; epsilon is restricted, not a free plug

Figure 14.6. Constructed-variable lineage and admissible-use workflow

Figure 14.6. Constructed-variable lineage and admissible-use workflow



Source: Author synthesis. Constructed variables may be used for measurement and calibration, but overlapping lineage prevents automatic causal interpretation.

The general rule is that a constructed diagnostic may be used as the chapter's object of measurement, but it should not be treated as independent causal evidence when it shares the same underlying input family with the outcome. This rule is

especially important for variables that are deterministic identities or near-identities. For example, if fragility is defined as 100 minus EMGI, the two variables cannot be used together as independent explanatory variables in an unrestricted causal regression. Their relationship is definitional, not empirical discovery.

14.4. Sample-Size Boundaries

The monograph uses different empirical universes because the seven economic analogues measure different objects. A single sample-size standard cannot be imposed mechanically across all chapters. A 10-node finite network can be adequate for a benchmark graph-topological or gauge-network demonstration, but it cannot support unrestricted causal econometrics. A 100-country, 15-year panel can support stronger diagnostic panel evidence, but even there causal claims remain bounded by identification and variable construction. Annual N = 55 forecast validation is stronger than a compact N = 20 crisis-era display, but it is still global-aggregate evidence rather than universal country-level dominance.

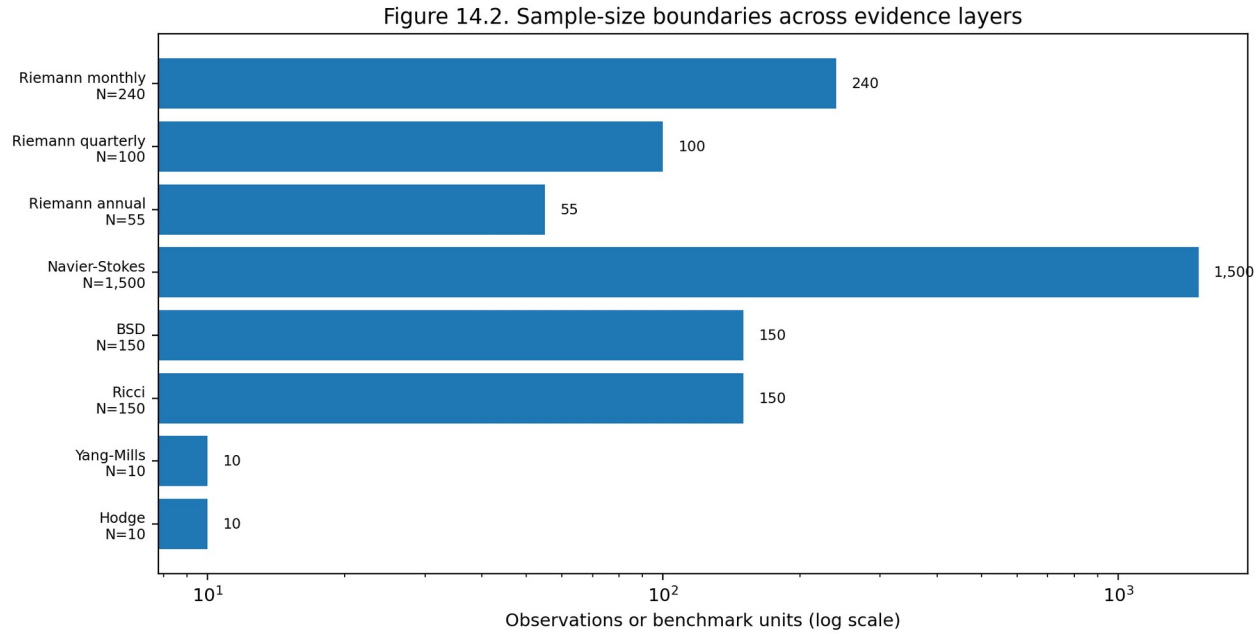
Sample size therefore determines claim level. The same result can be valid as benchmark structural evidence and invalid as causal econometric evidence. This chapter explicitly classifies each sample so that the reviewer does not have to infer whether N = 10, N = 150, N = 1,500, or layered N = 55/45/20/100/240 evidence is being overstated.

Table 14.4. Sample-size and admissible-claim boundaries

Study	Empirical universe	Main N / sample	Admissible evidence type	Boundary
Ricci/ Poincare	10 macro-regions, 2010-2024, 16 stress coordinates	N = 150	Diagnostic inequality-curvature panel	No country-level welfare theorem; no unrestricted causality
Hodge	World anchor + 10 regional nodes; 27 retained edges	10-node benchmark	Benchmark topological/flow decomposition	No all-country dyadic-flow proof; no Hodge conjecture proof
Navier-Stokes	100 countries, 2010-2024 annual panel	N = 1,500	Strong panel diagnostic and stress-testing evidence	No physical fluid law; no universal crisis prediction
Yang-Mills	10 nodes, 27 weighted edges; planned country layer	N = 10 benchmark + N = 1,500 pathway	Finite-network mass-gap threshold; panel not yet final for strongest causal claims	No Yang-Mills theorem; N=10 econometrics diagnostic only
BSD	World anchor + 10 regional/corridor nodes over 15 years	N = 150 closure layer	Calibrated local-to-global rank evidence	Small regional clusters; local-to-global calibration not proof
Riemann/ Zeta	Annual, quarterly and monthly global inflation layers	N = 55, 45, 20, 100, 240	Strong forecast-validation architecture	No RH proof; no universal forecast dominance
P vs NP	94 industries and reduced exact benchmark	C(94,10); exact C(20,6)=38,760	Exact reduced computational evidence and best-found full-universe	No P!=NP proof; no full n=94 certificate

			incumbent	

Figure 14.2. Sample-size boundaries across evidence layers



Source: Author synthesis. The log-scale chart shows why the evidence hierarchy cannot assign the same claim level to N=10 benchmarks and N=1,500 panels.

A sample-size boundary is not a methodological embarrassment. It is part of model governance. The Hodge and Yang-Mills chapters are strongest as benchmark structural architectures. Navier-Stokes is strongest as a large-panel stress-testing design. Ricci/Poincare and BSD are strongest as N = 150 diagnostic/calibration layers. Riemann/Zeta is strongest as a layered forecast-validation design. P vs NP is strongest because it combines a large infeasible support space with exact reduced enumeration. The chapter's responsibility is to state these differences directly.

14.5. Forecasting and Optimization Boundaries

Forecasting and optimization claims create special reviewer risks because high performance numbers can easily be read as universal dominance. The Riemann/Zeta and P-vs-NP chapters therefore require separate boundary rules.

For Riemann/Zeta, the admissible claim is that the FPAS+zeta architecture improves the reported forecast hierarchy relative to FPAS and ARIMA across stated validation layers. The main annual N = 55 layer, robustness N = 45 layer, crisis-era N = 20 display, quarterly N = 100 dynamic layer and monthly N = 240 spectral layer make the evidence unusually structured. Nevertheless, the result is not a proof of the Riemann Hypothesis, not a universal law of inflation forecasting, not a country-level policy ranking and not a guarantee that residual autocorrelation, heteroskedasticity or regime instability are fully eliminated.

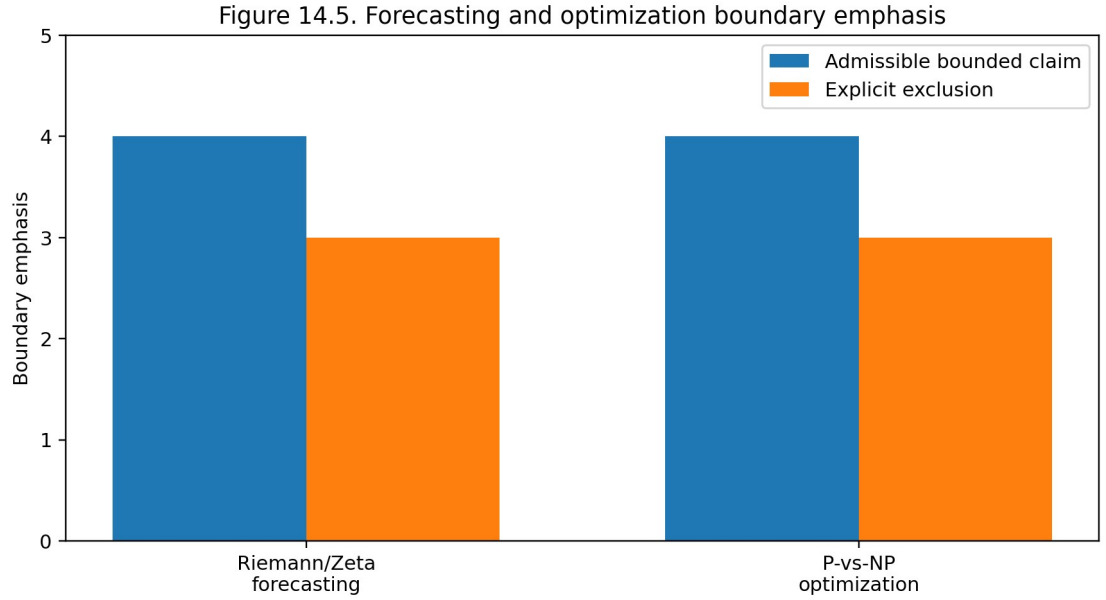
For P vs NP, the admissible claim is computational-finance demonstration. The fixed n = 94 Damodaran industry universe and K = 10 sparse-selection problem create C(94,10) = 9,041,256,841,903 feasible supports before continuous weight optimization. That fact demonstrates operational search-space explosion. The reduced n = 20, K = 6 benchmark allows exact enumeration of C(20,6) = 38,760 supports, which is strong reduced evidence. However, the full n = 94 universe is not exhaustively certified. Best-found evidence is not equivalent to a global optimum certificate.

Table 14.5. Forecasting and optimization boundary matrix

Chapter	Reported evidence	Admissible claim	Explicit exclusion
Riemann/Zeta	FPAS+zeta improves RMSE relative to FPAS and ARIMA in reported layers	Layer-specific global-aggregate forecast improvement	RH proof/test; universal forecast dominance; residual-problem elimination
Riemann/Zeta	HMM, Markov-switching,	Diagnostic resonance	Causal theorem of

	wavelet and spectral diagnostics align with crisis regimes	and spectral-cycle interpretation	inflation or policy-invariant law
P vs NP	C(94,10) creates operational support-space explosion	Computational-complexity demonstration in finance	Formal proof of P != NP
P vs NP	Exact C(20,6)=38,760 reduced enumeration validates heuristic behavior in reduced universe	Exact reduced computational evidence	Certified global optimum for all n = 94 supports
P vs NP	Black-Scholes overlay and transaction-cost/stress gates add realism	Risk-realism and robustness diagnostics	Free derivative performance or live trading dominance

Figure 14.5. Forecasting and optimization boundary emphasis



Source: Author synthesis. These chapters carry strong evidence, but each has explicit exclusions that prevent universal dominance claims.

14.6. Evidence-Level Matrix

The evidence-level matrix is the operational core of Chapter 14. It ranks the nature of evidence without forcing all chapters into a single standard. The strongest claim in one chapter may be panel diagnostic evidence; in another, exact reduced computational evidence; in another, benchmark structural decomposition. The key is to name the evidence level and prevent it from being upgraded beyond its design.

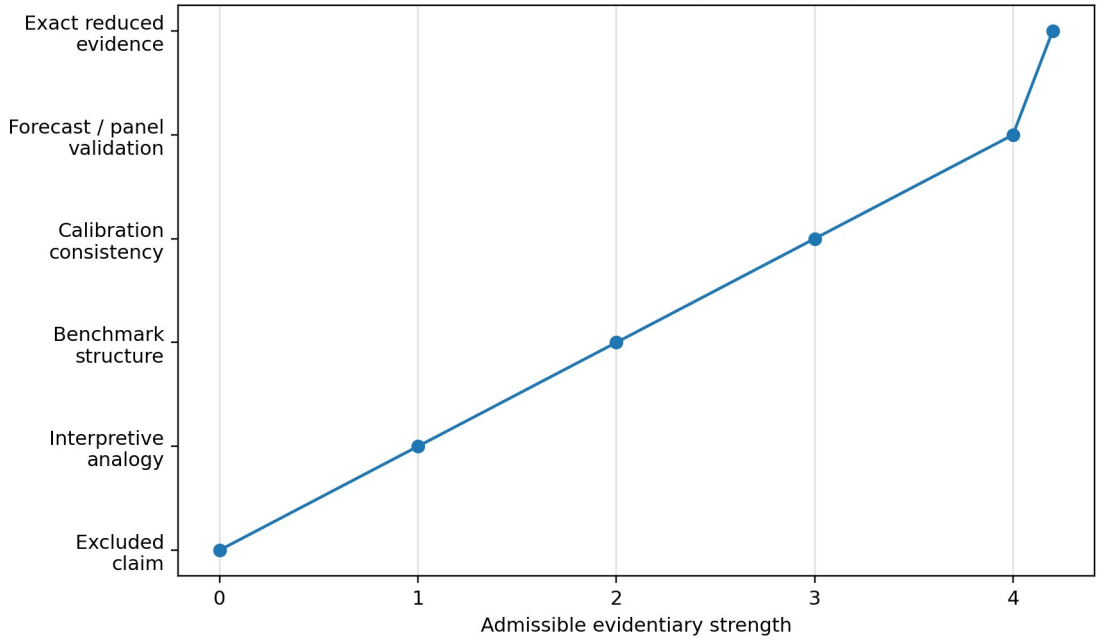
Table 14.6. Evidence-level matrix for the seven-problem monograph

Evidence level	Meaning	Where it applies	Admissible claim	Forbidden upgrade
Strong panel diagnostic	Large panel with multiple checks, robustness and validation windows	Navier-Stokes	Global systemic-stress diagnostics and stress testing	Causal law or crisis guarantee
Strong	Layered forecast tests,	Riemann/Zeta	Global aggregate	RH proof or

forecast validation	RMSE/MAE/sMAPE, MZ, DM/CW, rolling validation		inflation forecast improvement in reported layers	universal dominance
Exact reduced computational evidence	Full enumeration in reduced universe with documented full-universe search coverage	P vs NP	Computational-finance complexity demonstration	P!=NP proof or certified n=94 optimum
Benchmark structural evidence	Finite graph/topological or gauge architecture with reproducible matrices	Hodge, Yang-Mills	Macro-flow decomposition; finite-network shock threshold	Hodge or Yang-Mills theorem proof
Calibrated local-to-global evidence	Rank correspondence inside a declared economic analogue	BSD	Local regional signals inform structural rank calibration	BSD proof or independent causal validation
Diagnostic inequality-curvature evidence	Pressure/curvature/ entropy panel with graph-topological diagnostics	Ricci/ Poincare	Inequality pressure and smoothing-capacity diagnostics	Perelman/Poincare theorem claim

Figure 14.4. Evidence hierarchy used in Chapter 14

Figure 14.4. Evidence hierarchy used in Chapter 14



Source: Author synthesis. The matrix allows strong claims where evidence is strong, but blocks theorem-level inflation.

14.7. Reviewer-Safety Matrix: Likely Objections and Direct Responses

A reviewer-safety chapter should not merely list limitations. It should anticipate the strongest objections and answer them directly. The following matrix is written in the form of likely reviewer questions and manuscript-ready answers.

Table 14.7. Reviewer-safety matrix: likely objections and direct responses

Likely reviewer question	Direct manuscript answer	Where controlled
Does the author claim to solve the Millennium Problems?	No. The monograph explicitly excludes theorem proof, test or replication of the Clay problems in their original mathematical form.	Front matter; Chapter 1; Chapter 2; Chapter 14; each problem chapter
Are the mathematical objects used metaphorically?	No. They are used as formal measurement grammars with specified economic analogues, formulas, samples and evidence gates.	Chapters 2, 4, 13 and 14
Are constructed variables being used as independent validation?	Only with safeguards. Variable-lineage tables, external-only screens, residualization, placebo and admissible-use rules prevent circularity overclaiming.	Chapters 4, 8, 9, 13 and 14
Can N=10 benchmark chapters support causal econometrics?	No. N=10 chapters support structural benchmark evidence and diagnostic associations, not unrestricted causal claims.	Hodge, Yang-Mills, Chapter 14
Does Riemann/Zeta prove RH?	No. The zeta function is used as a computational cyclical signal under layered forecast validation.	Chapter 10 and 14
Does P-vs-NP certify a global optimum?	No. The reduced benchmark is exact; the full n=94 universe is best-found under documented search coverage.	Chapter 11 and 14
Can the findings be generalized to all countries and all horizons?	No. Generalization is bounded by empirical universe, data frequency, sample size, model assumptions and validation design.	All chapters
Are the results reproducible?	The design requires source ledgers, formulas, replication files, figure catalogues, scripts, metadata and version control; each data package should be treated as an audit companion.	Chapter 4 and 14

14.8. Model-by-Model Claim Boundary

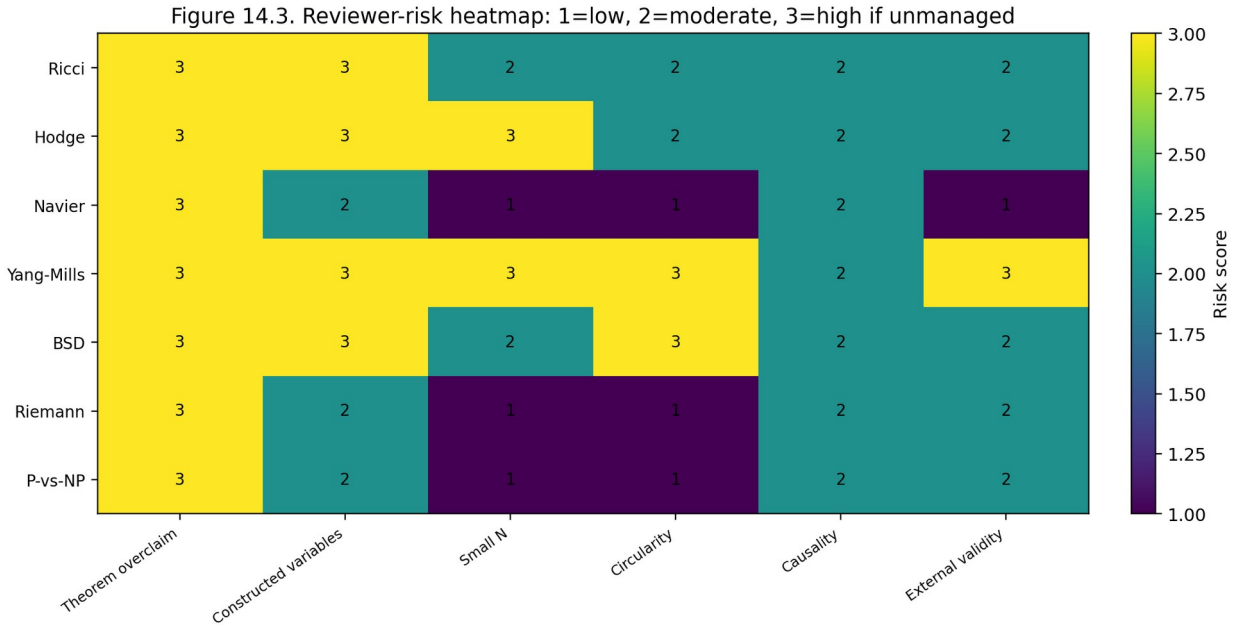
The monograph's claim hierarchy is model-specific. This is important because the seven chapters do not rely on the same type of evidence. The book's global claim is not that every chapter reaches the same evidentiary level. The global claim is that each chapter reaches a bounded, explicitly declared evidentiary level and contributes one measurement language to a broader economic research program.

Table 14.8. Model-by-model claim-boundary matrix

Chapter	Strongest admissible claim	Evidence base	Explicit boundary
Ricci/Poincare	Inequality pressure, curvature, entropy and smoothing capacity can be measured as a diagnostic manifold.	N = 150 region-year diagnostic panel; graph topology; PCA/robustness	No theorem proof; no literal curvature invariant; no unrestricted causal welfare claim

Hodge	World economy can be decomposed into hierarchy, local-cycle imbalance and harmonic/systemic circulation.	10-node, 27-edge benchmark; Hodge energy shares	No Hodge conjecture proof; no all-country dyadic closure
Navier-Stokes	Systemic stress can be modelled as nondimensional flow-pressure-friction-shock-cycle-closure balance.	N = 1,500 country-year panel; rolling validation and robustness	No physical liquidity flow; no PDE proof; no crisis guarantee
Yang-Mills	Global-corridor network contains a finite-network spectral shock threshold.	10-node, 27-edge gauge benchmark; lambda1=0.3850; N=1,500 pathway	No physical Yang-Mills theorem; N=10 econometrics diagnostic
BSD	Local regional signals and LOrder-type analogue are informative about structural rank.	N = 150 closure layer; rank-gap/agreement/line age screens	No BSD proof; no literal elliptic curve; no causal law
Riemann/Zeta	FPAS+zeta improves forecast accuracy across declared layers.	N=55,45,20,100,240 layered validation	No RH proof/test; no universal forecast dominance
P vs NP	Cardinality-constrained portfolio selection operationalizes computational complexity.	C(94,10) support space; exact C(20,6) benchmark	No P!=NP proof; no certified n=94 optimum; no realized-return dominance

Figure 14.3. Reviewer-risk heatmap



Source: Author synthesis. High unmanaged risk does not mean the model is weak; it means the boundary must be explicit.

14.9. Data, Replication and Version-Control Boundaries

The monograph relies on a dual data structure: public or institutional anchors and author-calculated variables. This distinction must be maintained throughout the book. Public anchors include country or regional macroeconomic indicators, inflation series, GDP and GDP per capita, World Bank and IMF families, Damodaran industry variables, and other published inputs. Author-calculated variables include stress indices, curvature objects, network weights, Hodge components, gauge potentials, LOrder, zeta-cycle corrections, portfolio search outputs and robustness scores.

A replication package does not remove all limitations, but it changes their scientific status. Without a source ledger and formula trace, constructed variables may look discretionary. With a replication manifest, they become auditable. The monograph should therefore treat replication files, tables, code, metadata, random seeds, extraction dates, checksums and figure catalogues as part of the research object.

Table 14.9. Replication and version-control boundary checklist

Replication component	Required content	Reviewer-safety function
Source ledger	Records public inputs, source families, extraction logic and variable names	Prevents ambiguity about public anchor origins
Formula catalogue	Lists normalization, index construction, matrix operations and forecast/optimization formulas	Makes author-calculated variables reproducible
Intermediate files	Stores normalized panels, matrices, edge lists, support sets, forecast outputs and residuals	Allows reconstruction of reported tables
Random seeds and search budgets	Required for Monte Carlo, GA, perturbation and bootstrap components	Separates reproducible search from undocumented heuristics
Figure catalogue	Stores figures and data used to create them	Prevents graphical results from becoming non-auditable illustrations
Version control	Fixes manuscript version, dataset version and code version	Prevents changes in source data from confusing reported results
Claim log	Maps each table/figure to admissible claim level	Prevents evidence inflation in revision or review

14.10. Econometric Identification and Causality Boundaries

The monograph frequently uses econometric language, but econometric association is not automatically causal identification. Fixed effects, robust standard errors, rolling validation, forecast comparison, PCA, regularization, threshold models, VAR/SVAR, HMM regimes and Monte Carlo simulations are evidence tools. They do not by themselves transform a constructed diagnostic into a causal theorem.

Causality is most bounded where variables share lineage, where the sample is small, where clusters are few, where the time dimension is short, where the object is a benchmark graph rather than a full panel, or where the target variable is a constructed index. This does not invalidate the evidence. It defines how the evidence should be read.

Table 14.10. Econometric and computational inference boundaries

Method	What it supports	What it does not support
Fixed effects / panel models	Controls unobserved stable heterogeneity	Diagnostic association unless identification is separately justified
Driscoll-Kraay / HAC / clustered SE	Robust inference under dependence or heteroskedasticity	Improves inference, does not prove causality
PCA / factor models	Tests latent structure in constructed	Dimension validation, not

	systems	treatment effect
Threshold models	Tests regime dependence	Supplementary diagnostic unless exogenous threshold design exists
VAR/SVAR / HMM / Markov-switching	Dynamic and regime evidence	Regime diagnostics, not universal law
Monte Carlo / perturbation	Uncertainty and sensitivity evidence	Model-implied uncertainty, not real-world guarantee
Exact enumeration	Full search in reduced computational universe	Exact within reduced scope only

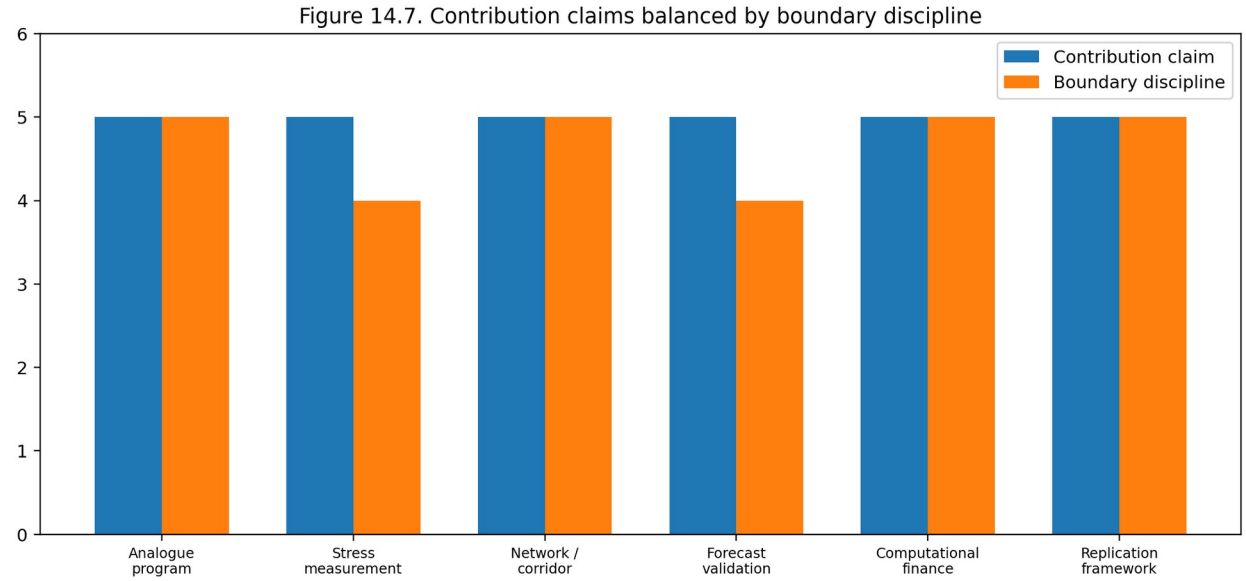
14.11. Claim-Language Protocol for the Final Monograph

The final manuscript should use controlled claim language. Words such as proves, solves, verifies, establishes universally, guarantees, and certifies should be reserved only for situations where the relevant theorem-level or exhaustive evidence exists. In this book, such language should generally be avoided for the Millennium analogues. Instead, the preferred language is: constructs, operationalizes, measures, calibrates, diagnoses, validates within a stated sample, reports benchmark evidence, demonstrates reduced exact evidence, and supports a bounded interpretation.

Table 14.11. Claim-language replacement protocol

Risky wording	Reviewer-safe wording	Reason
proves the Riemann Hypothesis	uses a Riemann-zeta-inspired cyclical signal	Forecast signal is not theorem proof
solves Yang-Mills mass gap	reports a positive finite-network economic mass gap	Graph eigenvalue is not quantum field theorem
proves P != NP	operationalizes support-space explosion in portfolio selection	Computational demonstration is not complexity-class proof
establishes causal law	supports diagnostic association / calibrated consistency	Most designs are diagnostic or measurement-oriented
guarantees forecasts	improves reported forecast hierarchy in stated validation layers	Forecast results are sample- and design-specific
certifies full optimality	reports best-found incumbent under documented search coverage	Full enumeration is absent for n=94
independent validation from constructed variables	internal calibration / external-proxy screening	Variable lineage limits independence

Figure 14.7. Contribution claims balanced by boundary discipline



Source: Author synthesis. The monograph remains ambitious because its contribution claims are matched by equally explicit exclusions.

14.12. Chapter Conclusion: Why Boundary Discipline Strengthens the Book

Chapter 14 closes the central reviewer-safety problem. The monograph does not claim to solve the Millennium Problems. It claims to build a structured economic research program inspired by the formal architectures of those problems. That difference is decisive. Without it, the book would invite theorem-level criticism. With it, the book becomes a bounded and auditable contribution to mathematical economics, econometric measurement, systemic-risk analysis, network diagnostics, forecast validation and computational finance.

The chapter also clarifies why the seven models should not be judged by one evidence standard. Navier-Stokes has the strongest large-panel stress-testing evidence. Riemann/Zeta has the strongest layered forecast-validation evidence. P vs NP has the clearest exact reduced computational evidence. Hodge and Yang-Mills provide benchmark structural evidence. BSD provides calibrated local-to-global rank evidence. Ricci/Poincare provides inequality-curvature diagnostic evidence. The monograph's intellectual contribution is precisely that these different evidence types are assembled under one claim-disciplined framework.

The final reviewer-safe statement is therefore:

This monograph develops seven bounded economic-econometric analogues inspired by the Clay Millennium Problems. It does not solve, prove, test or replicate the original mathematical problems. Its contribution is methodological and empirical: it introduces a mathematical-econometric analogue program for measuring economic complexity through flow, topology, curvature, gauge-threshold separation, local-to-global rank, spectral-cycle forecasting and computational decision complexity, while preserving strict evidence-level discipline and replication transparency.

Table 14.12. Final chapter-closure matrix

Claim domain	Statement	Final status
Global claim	Seven bounded economic-econometric analogues of economic complexity	Admissible
Mathematical theorem claim	Clay Millennium Problems solved, proved, tested or replicated	Explicitly excluded
Empirical claim	Evidence varies by chapter: panel, forecast, reduced exact, benchmark, calibration or diagnostic	Admissible with matrix
Causal claim	Universal causal laws across all economies and horizons	Excluded unless separately

		identified
Replication claim	Data, code, formulas and outputs should be auditable by versioned packages	Required as reviewer-safety discipline
Contribution claim	New mathematical-econometric analogue program with claim-boundary control	Admissible final contribution

Chapter 15. General Conclusion and Future Research Agenda

This chapter closes the monograph by returning to its general aim: to develop seven bounded economic-econometric analogues inspired by the formal architectures of the Clay Millennium Problems without claiming to solve, prove, test or replicate those mathematical problems in their original form. The conclusion does not reproduce the full conclusion of each source manuscript. Instead, it extracts and synthesizes four elements from each model: the main empirical conclusion, the main methodological contribution, the principal limitation and the future-research pathway. The result is a unified closure chapter that shows how the seven models jointly contribute to economic measurement: curvature for inequality pressure, Hodge decomposition for macro-flow structure, Navier-Stokes logic for liquidity stress, Yang-Mills logic for systemic shock thresholds, Birch-Swinnerton-Dyer logic for local-to-global structural rank, Riemann-zeta logic for inflation-cycle diagnostics and P-vs-NP logic for computational decision complexity.

The chapter also defines the scientific contribution of the monograph at three levels. The theoretical contribution is a translation framework that treats advanced mathematical problems as disciplined measurement grammars rather than as literal economic identities. The methodological contribution is a set of reproducible modelling pipelines that transform public or auditable data anchors into constructed diagnostic objects, validation layers and claim-boundary statements. The empirical and practical contribution is the demonstration that global economic complexity can be studied through multiple complementary architectures: panels, finite networks, forecast layers, structural decompositions, local-to-global rank systems and computational search experiments. The final claim is strong but bounded: the monograph provides a new mathematical-econometric architecture for economic measurement, not a solution to any Clay Millennium Problem and not a universal causal law for the world economy.

Figure 15.1. Monograph closure architecture

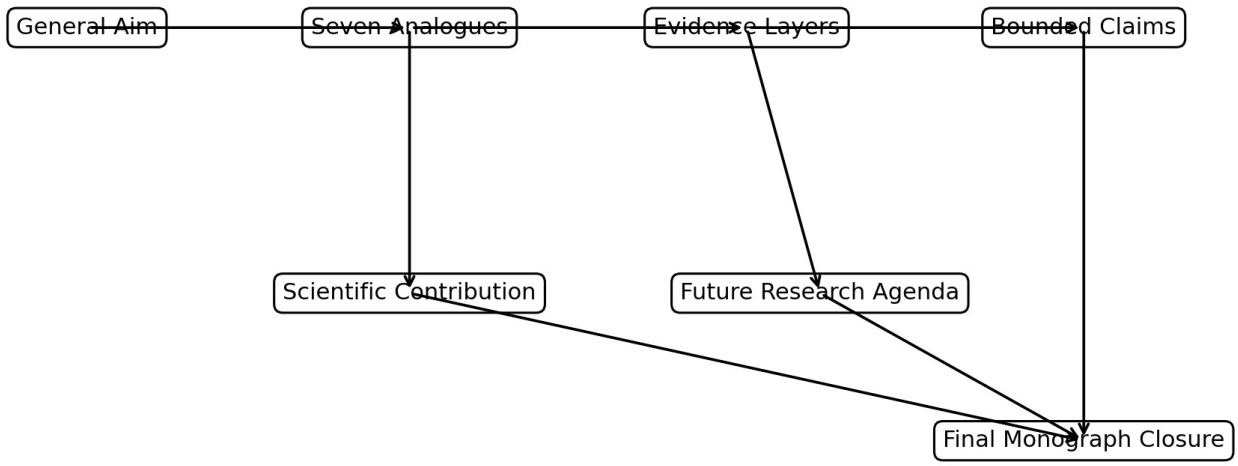


Figure 15.1. Monograph closure architecture.

Closure element	Meaning in Chapter 15	Role in the monograph
Return to aim	The final chapter reconnects all seven models to the general purpose of mathematical-economic measurement.	Prevents the book from becoming seven disconnected papers.
Seven analogue summary	Each model is summarized by empirical conclusion, method, limitation and future pathway.	Creates a unified synthesis rather than repetitive article-level conclusions.
Scientific contribution	The book contributes a disciplined framework for translating mathematical structures into economic diagnostics.	Defines the monograph-level novelty.
Future agenda	Future work moves toward country panels, dyadic flows, sectoral systems and firm-level extensions.	Transforms limitations into a research programme.
Final claim boundary	The book explicitly excludes Clay-problem proof claims and universal law claims.	Protects scientific credibility and reviewer interpretation.

15.1. Return to the General Aim of the Monograph

The general aim of this monograph has been to ask whether the formal architectures associated with the seven Clay Millennium Problems can be translated into bounded, reproducible and empirically auditable economic measurement frameworks. This aim is intentionally different from the mathematical aim of proving the Millennium Problems themselves. The monograph does not attempt to prove the Poincare conjecture, solve Navier-Stokes regularity, prove the Yang-Mills mass gap, establish the Birch-Swinnerton-Dyer conjecture, verify the Riemann Hypothesis, resolve P versus NP or complete Hodge theory in its original mathematical domain. Its object is economic: to determine whether the structural grammars of curvature, topology, flow, gauge fields, rank, spectral signal and computational complexity can improve the way the world economy is measured, stress-tested and interpreted.

The conclusion therefore returns to a central distinction that has governed the entire book. Mathematical inspiration is not mathematical transfer. A mathematical concept becomes useful in economic modelling only when it is transformed into an operational object with explicit data inputs, scaling rules, validation procedures, interpretation boundaries and replication logic. The seven chapters follow this rule in different ways. The Ricci/Poincare model transforms inequality indicators into pressure-curvature diagnostics. The Hodge model transforms regional macroeconomic anchors into a decomposable flow field. The Navier-Stokes model transforms liquidity stress into a nondimensional balance equation. The Yang-Mills model transforms corridor shock exposure into curvature, action and spectral-threshold diagnostics. The BSD model transforms local regional signals into structural-rank calibration. The Riemann-zeta model transforms a spectral signal into a forecast-correction layer. The P-vs-NP model transforms sparse portfolio selection into a computational-decision experiment.

Taken together, these translations establish the monograph's central scientific proposition: modern economic complexity cannot be fully represented through GDP, inflation, trade, inequality or portfolio returns alone. Those variables remain indispensable, but they become more informative when embedded inside structured measurement architectures. The book therefore proposes a plural methodology. It does not claim that one mathematical model dominates all others; it shows that different economic questions require different mathematical grammars. Inequality requires curvature and smoothing capacity. Macro-flow requires topology. Liquidity stress requires flow-pressure-friction balance. Corridor shocks require spectral thresholds. Structural rank requires local-to-global calibration. Inflation cycles require forecastable spectral deformation. Portfolio choice requires computational-complexity discipline.

15.2. Summary of the Seven Economic Analogues

The seven models form a structured comparative system. Each chapter has its own empirical universe, mathematical object and validation logic, but all seven share a common research ethic: construct the economic analogue explicitly, validate it within its admissible evidence domain and state what the model cannot prove. Table 15.2 summarizes the core conclusion of each analogue. It is intentionally organized around four closure fields rather than around the original article structure. This allows the final chapter to synthesize the monograph without repeating the full conclusion of each source document.

Economic analogue	Main empirical conclusion	Main methodological contribution	Principal limitation	Future research direction
Perelman/Ricci/ Poincare	The model identifies crisis deformation and partial smoothing recovery: 2020 is the strongest deformation year, while 2024 shows partial pressure decline and curvature recovery without full convergence.	It converts heterogeneous macro-social indicators into a common pressure-oriented diagnostic manifold and combines Ricci-style curvature, Perelman-type functionals and graph-topological connectedness.	It remains a macro-regional diagnostic analogue. Constructed curvature and entropy are economic measurement objects, not literal geometric invariants or causal welfare laws.	Extend from macro-regional blocks to country panels, subnational inequality systems, welfare-specific microdata and dynamic curvature networks.
Hodge	The model demonstrates that the regional world economy is not reducible to GDP mass: the benchmark decomposes macro-flow pressure into gradient hierarchy, curl imbalance and harmonic circulation.	It introduces discrete Hodge decomposition into macroeconomic measurement, translating edge-pressure	The evidence is a benchmark structural prototype rather than a final all-country	Develop all-country directed dyadic-flow panels, sectoral networks, corridor layers and time-varying Hodge decompositions.

		cochains into gradient, curl and harmonic components.	dyadic-flow system; edge weights are constructed and require future transaction-level enrichment.	
Navier-Stokes	The model supplies strong global stress-testing evidence by showing that systemic stress can be represented as a nondimensional liquidity-flow balance and validated through rolling forecasts, benchmarks, Monte Carlo uncertainty and policy counterfactuals.	It builds a disciplined stress-balance architecture with normalized variables, restricted epsilon(t) closure, rolling no-look-ahead validation, benchmark comparison and scenario analysis.	It is an economic stress-testing analogue, not a hydrodynamic law, not a Navier-Stokes theorem result and not a universal crisis-prediction machine.	Expand toward higher-frequency financial-market data, institution-level balance sheets, liquidity networks, macroprudential transmission channels and live stress-monitoring dashboards.
Yang-Mills	The finite benchmark produces a positive economic mass-gap style threshold, concentrated curvature/action and scenario-sensitive compression of systemic protection under corridor shocks.	It translates gauge potential, curvature, Yang-Mills action and graph Laplacian spectral separation into a finite macro-corridor measurement pipeline.	The completed evidence is a finite-network benchmark; the country-level panel is a specified pathway rather than a fully closed causal validation layer.	Populate the 100-country panel, add observed trade/logistics/financial edges, estimate dynamic shock transmission and test alternative network densities.
Birch-Swinnerton-Dyer	Local finite-state reductions and Euler-factor analogues contain calibrated information about global structural rank, while BridgeStress reveals corridor leverage that GDP mass alone would obscure.	It creates a regional local-to-global measurement architecture linking economic curve coefficients, discriminants, traces, Euler factors, LOrder and structural	The strongest result is calibrated local-to-global consistency; external validation is bounded and directional because of small clusters,	Develop country-year rank panels, external-proxy validation, corridor microdata, independent infrastructure/trade variables and dynamic local-to-global rank forecasting.

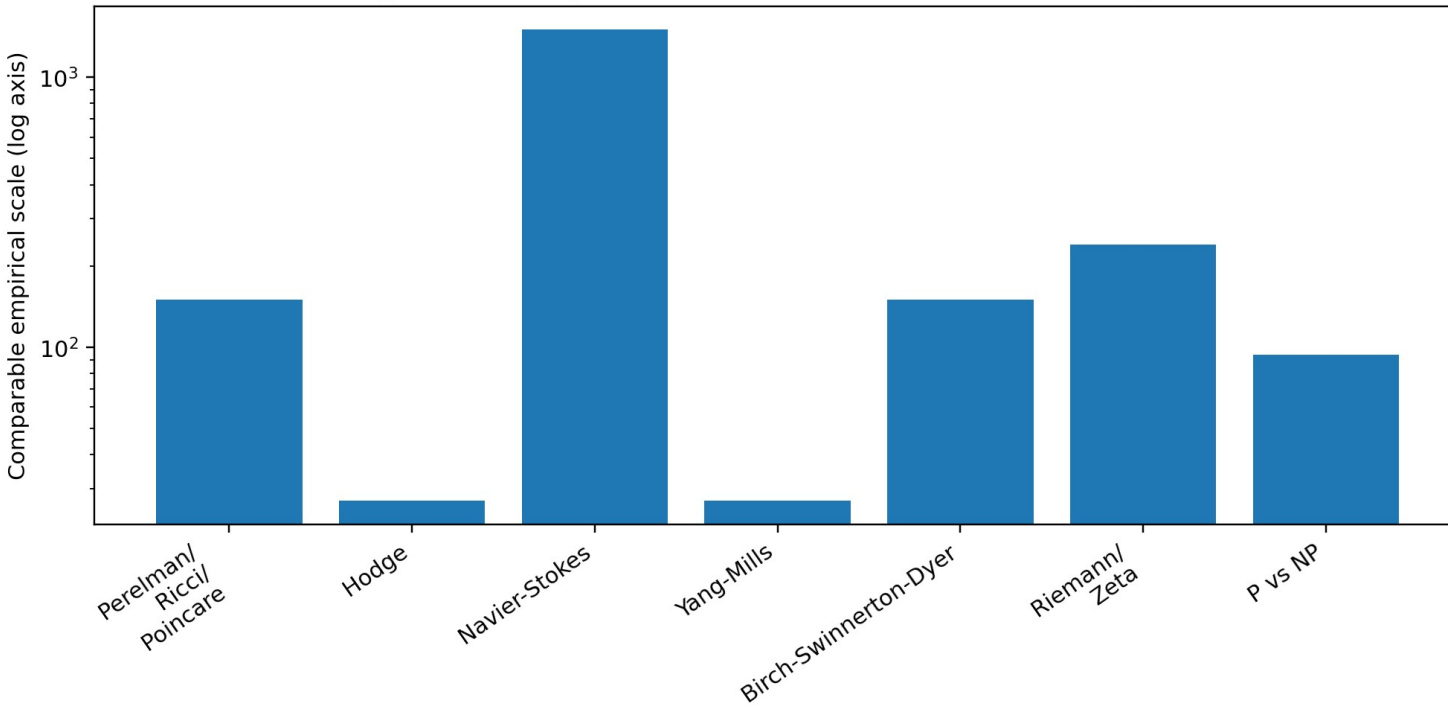
		rank.	overlapping constructed variables and circularity risk.	
Riemann/Zeta	The FPAS+zeta framework improves reported global inflation forecast accuracy relative to FPAS and ARIMA across the principal annual and robustness layers, with crisis resonance around major global shocks.	It augments structural inflation forecasting with a normalized zeta-cycle, alpha-calibrated correction, layered validation, HMM/Markov switching, Fourier/wavelet and residual diagnostics.	The zeta function is used only as an analogical signal generator; the model does not prove, test or verify the Riemann Hypothesis and does not guarantee universal forecast dominance.	Extend to country-level inflation panels, central-bank policy regimes, real-time forecast vintages, multi-horizon forecast competitions and cross-country spectral spillovers.
P vs NP	The chapter demonstrates economic computational complexity through C(94,10)=9,041,256,841,903 feasible supports and disciplines heuristic search through exact enumeration of C(20,6)=38,760 reduced supports.	It integrates Markowitz-CAPM portfolio construction, single-index covariance geometry, greedy search, Monte Carlo sampling, genetic algorithms, exact reduced benchmarking, derivative overlay and robustness gates.	It does not prove P != NP, certify the full n=94 global optimum or establish realized-return dominance because returns are CAPM priors rather than live out-of-sample portfolio performance.	Add realized return panels, branch-and-bound or mixed-integer solver certificates, transaction-cost-aware execution, multi-period rebalancing and institutional portfolio constraints.

The first conclusion from Table 15.2 is that the monograph does not rest on one type of evidence. It uses diagnostic panels, benchmark graphs, rolling forecasts, spectral tests, finite-network thresholds, local-to-global calibration and exact reduced computational enumeration. This diversity is important. A monograph based on a single validation style would risk overfitting its own research architecture. By contrast, the seven-problem design creates a cross-methodological audit: each model must justify its own transformation logic, and each model must accept a different limitation boundary.

The second conclusion is that the strongest models are strong in different ways. The Navier-Stokes chapter is strongest as a global panel stress-testing architecture because it operates on a broad N=1,500 country-year panel and includes rolling validation, benchmarks, Monte Carlo uncertainty and policy counterfactuals. The Riemann-zeta chapter is strongest as a layered forecasting design because it compares FPAS+zeta against benchmark models across annual, quarterly and monthly

layers. The P-vs-NP chapter is strongest as a computational demonstration because it exposes the scale of support-space explosion and includes exact reduced enumeration. The Ricci/Poincare chapter is strongest as an inequality-curvature diagnostic panel. The Hodge chapter is strongest as a structural decomposition benchmark. The Yang-Mills chapter is strongest as a finite-network spectral-threshold benchmark. The BSD chapter is strongest as a calibrated local-to-global rank architecture, although external validation remains bounded.

Figure 15.2. Empirical scale of the seven economic analogues



Note: P vs NP is shown by the n=94 industry universe; its support space C(94,10)=9.041e12 is a separate combinatorial object.

Figure 15.2. Empirical scale of the seven economic analogues.

Chapter	Dominant economic object	Empirical universe	Strongest admissible claim
Chapter 5	Global inequality pressure, curvature-like deformation, entropy-like complexity and smoothing capacity	10 macro-regional blocks, 2010-2024, 16 stress coordinates; N=150 region-year diagnostic panel	The model identifies crisis deformation and partial smoothing recovery: 2020 is the strongest deformation year, while 2024 shows partial pressure decline and curvature recovery without full convergence.
Chapter 6	Regional macro-flow decomposition into hierarchy, local-cycle imbalance and harmonic systemic circulation	World anchor plus 10 regional nodes; 27 weighted regional edges; connected benchmark graph	The model demonstrates that the regional world economy is not reducible to GDP mass: the benchmark decomposes macro-flow pressure into gradient hierarchy, curl imbalance and harmonic circulation.
Chapter 7	Liquidity-flow weakness, pressure gradients, friction/diffusion, stochastic shocks, GDP-cycle forcing and restricted closure	100-country annual panel, 2010-2024; N=1,500 country-year observations; World and macro-regional layers	The model supplies strong global stress-testing evidence by showing that systemic stress can be represented as a nondimensional liquidity-flow balance and validated through rolling forecasts, benchmarks, Monte Carlo uncertainty and policy counterfactuals.

Chapter 8	Gauge curvature, action concentration, finite-network shock threshold, spectral protection and corridor exposure	10 regional/corridor nodes, 27 weighted edges; finite-network benchmark with future N=1,500 panel pathway	The finite benchmark produces a positive economic mass-gap style threshold, concentrated curvature/action and scenario-sensitive compression of systemic protection under corridor shocks.
Chapter 9	Local-to-global structural rank, corridor stress, economic L-function, Euler-factor analogues and LOrder	World anchor plus 10 regional/corridor nodes; N=150 regional-year closure layer	Local finite-state reductions and Euler-factor analogues contain calibrated information about global structural rank, while BridgeStress reveals corridor leverage that GDP mass alone would obscure.
Chapter 10	Zeta-cycle signal, crisis resonance, FPAS+zeta inflation correction and spectral diagnostics	Layered annual, quarterly and monthly global inflation validation: N=55, N=45, N=20, N=100 and N=240	The FPAS+zeta framework improves reported global inflation forecast accuracy relative to FPAS and ARIMA across the principal annual and robustness layers, with crisis resonance around major global shocks.
Chapter 11	Cardinality-constrained portfolio optimization, support-space explosion, heuristic search and exact reduced benchmarking	Damodaran January 2026 U.S. industry universe, n=94; baseline K=10; exact reduced benchmark n=20, K=6	The chapter demonstrates economic computational complexity through C(94,10)=9,041,256,841,903 feasible supports and disciplines heuristic search through exact enumeration of C(20,6)=38,760 reduced supports.

15.3. Main Scientific Contribution

The main scientific contribution of the monograph is the construction of a seven-part mathematical-econometric measurement architecture for global economic complexity. The contribution is not that the economy is literally a manifold, a fluid, a gauge field, an elliptic curve, a zeta function or a complexity class. The contribution is that the formal logic of those mathematical domains can be converted into carefully bounded economic measurement grammars. This distinction is essential. It allows the book to use mathematically powerful structures while avoiding the category error of treating metaphor as proof.

At the scientific level, the monograph contributes a new way of organizing economic evidence. Traditional empirical economics often privileges regression coefficients, forecast errors, descriptive indicators or optimization outcomes. This book does not reject those tools; it embeds them inside richer structures. The Ricci/Poincare model places regression-style diagnostics inside a pressure-curvature manifold. The Hodge model places regional data inside a topological decomposition. The Navier-Stokes model places stress indicators inside a balance equation. The Yang-Mills model places corridor shocks inside a finite spectral network. The BSD model places regional signals inside local-to-global rank calibration. The Riemann-zeta model places forecasting inside a layered spectral-correction design. The P-vs-NP model places portfolio selection inside a support-space complexity experiment.

The scientific novelty therefore lies in the integration of mathematical abstraction, economic interpretation and claim discipline. Many economic models are either empirically practical but mathematically shallow, or mathematically elegant but empirically detached. The monograph seeks a middle path. It uses mathematical architectures to discipline measurement, but it insists that every constructed object must be operationalized through data, algorithms, validation gates and transparent limitations. This makes the contribution methodological as well as substantive.

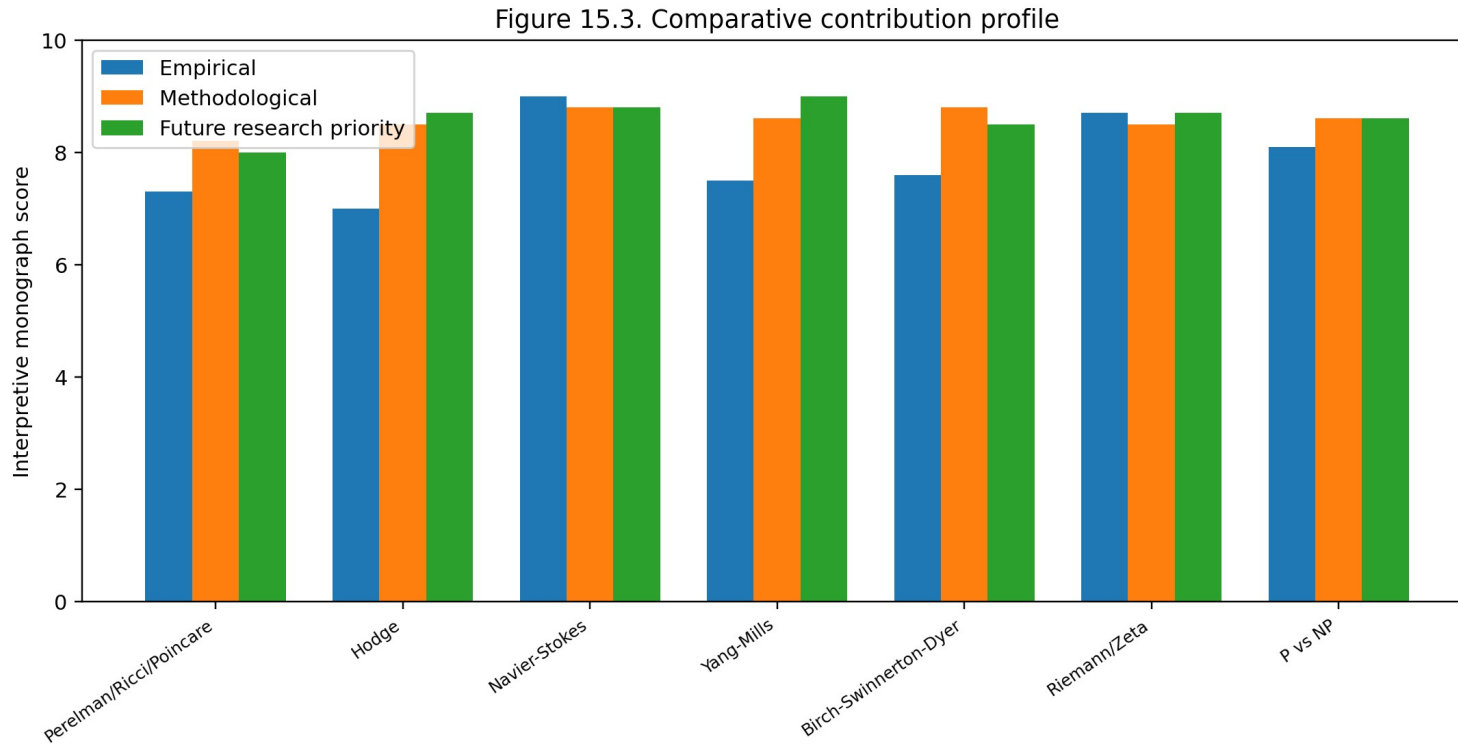


Figure 15.3. Comparative contribution profile.

Scientific contribution domain	Monograph-level contribution	Why it matters
Economic measurement	Develops seven bounded analogues for measuring curvature, flow, stress, shock thresholds, rank, spectral cycles and computational complexity.	Expands economic measurement beyond isolated indicators and single-equation models.
Validation culture	Combines panels, forecasts, benchmarks, exact reduced enumeration, robustness gates and claim hierarchy.	Prevents mathematical analogy from becoming unsupported assertion.
Comparative synthesis	Places all seven models into a single matrix of empirical universe, mathematical object and strongest admissible claim.	Turns separate papers into a coherent monograph.
Claim discipline	States excluded claims explicitly: no Clay-problem proof, no universal causality, no unrestricted prediction.	Protects academic credibility and reviewer interpretation.
Research programme	Defines future extensions toward granular panels, dyadic networks, sectors, firms and real-time systems.	Converts current limitations into a structured research agenda.

15.4. Theoretical Contribution

The theoretical contribution of the monograph is a translation theory of mathematical-economic analogues. The book demonstrates that a mathematical problem can contribute to economics without being solved in mathematics and without being treated as a literal description of economic reality. The correct theoretical move is not direct transfer, but structured translation. In this translation, the mathematical object supplies a grammar of relations; the economic model supplies

variables, data and interpretation; the validation design determines whether the constructed object behaves coherently; and the claim boundary defines the admissible level of inference.

This translation theory has three components. The first is object separation. The original mathematical object and the economic analogue must be kept distinct. A Ricci curvature analogue is not Riemannian curvature; a liquidity-flow balance is not physical fluid motion; an economic mass gap is not the Yang-Mills mass gap; an economic L-function is not the L-function of an elliptic curve; a zeta-cycle is not a proof of the Riemann Hypothesis; and combinatorial support-space explosion is not a proof of P != NP. The second component is functional analogy. Even when the objects are not identical, their structural functions can be useful. Curvature can organize deformation; topology can organize circulation; flow can organize stress transmission; spectral gaps can organize thresholds; local-to-global logic can organize rank formation; zeta-like cycles can organize nonlinear forecast corrections; computational complexity can organize decision difficulty. The third component is evidentiary discipline. An analogue becomes scientific only when it is operationalized, validated and bounded.

The theoretical contribution is also pluralist. The monograph does not reduce the world economy to one master equation. Instead, it argues that economic complexity is multidimensional. Inequality, macro-flow, liquidity, shock transmission, structural rank, inflation forecasting and portfolio choice are not the same problem. Each requires a different theoretical grammar. This pluralism is a strength because it avoids the common weakness of universalizing a single formal method beyond its appropriate domain.

Theoretical grammar	Economic meaning in the monograph	Boundary condition
Curvature / smoothing	Inequality pressure and recovery capacity	Diagnostic manifold, not literal geometry
Hodge decomposition	Hierarchy, local imbalance and harmonic circulation	Benchmark flow decomposition, not complete transaction network
Flow balance	Liquidity weakness, pressure gradient, friction and closure	Stress-testing analogue, not hydrodynamic law
Gauge curvature / spectral gap	Corridor shock threshold and action concentration	Finite-network threshold, not Yang-Mills proof
Local-to-global rank	Regional signals informing structural rank	Calibrated rank analogue, not BSD theorem test
Spectral zeta signal	Inflation-cycle deformation and forecast correction	Forecast signal, not Riemann Hypothesis evidence
Computational complexity	Sparse portfolio selection under combinatorial explosion	Operational complexity evidence, not P-vs-NP proof

15.5. Methodological Contribution

The methodological contribution is the construction of replicable pipelines. Each model follows a chain that can be audited: public or fixed input data, transformation into normalized or constructed variables, mathematical-economic object construction, estimation or calculation, validation, robustness, interpretation and claim boundary. This pipeline is one of the most important features of the monograph. It prevents the mathematical vocabulary from floating above the empirical architecture. The reader can identify where the data enter, how variables are transformed, what equations or algorithms are applied and which claims are allowed.

Several methodological patterns recur across the seven models. The first is normalization and scale discipline. Heterogeneous variables are not added directly; they are transformed into comparable diagnostic scales, nondimensional components, normalized cycles, rank scores or CAPM-implied priors. The second is benchmark comparison. Forecasting models are compared with ARIMA or FPAS baselines; portfolio algorithms are compared with greedy, Monte Carlo, GA and exact reduced enumeration; network models are compared under alternative density or edge-weight logic. The third is robustness and falsification. The monograph includes negative controls, placebo logic, q-base sensitivity, residualized variables, rolling validation, Monte Carlo uncertainty and claim-gated interpretation. The fourth is replication discipline. The models are designed so that tables, formulas, source ledgers, algorithmic steps and data packages can be audited rather than accepted as narrative claims.

The methodology is strongest where it treats limitations as part of the design. For example, the BSD chapter does not hide circularity risk; it builds anti-circularity diagnostics. The P-vs-NP chapter does not hide the absence of full n=94 global certification; it states the exact reduced benchmark and the documented search coverage. The Riemann-zeta chapter does not

claim residual perfection; it reports layered diagnostics and residual limitations. The Yang-Mills chapter does not present the future country panel as completed evidence; it separates the finite benchmark from the future panel pathway. This methodological honesty is central to the monograph's credibility.

Methodological device	Where it appears	Monograph-level value
Common-scale transformation	Ricci/Poincare, Navier-Stokes, BSD, Riemann/Zeta	Prevents raw-unit aggregation errors and supports interpretable constructed objects.
Graph/network construction	Hodge, Yang-Mills, BSD	Makes corridor exposure, topology and systemic transmission visible.
Rolling or layered validation	Navier-Stokes, Riemann/Zeta	Tests performance beyond static fit and separates validation windows.
Exact reduced benchmarking	P vs NP	Provides a hard computational audit where full enumeration is infeasible.
Monte Carlo / scenario testing	Navier-Stokes, Yang-Mills, P vs NP, Ricci/Poincare	Transforms uncertainty and shocks into transparent sensitivity analysis.
Anti-circularity and placebo logic	BSD, P vs NP, Riemann/Zeta, Yang-Mills	Protects constructed-index frameworks from mechanical confirmation.
Claim hierarchy	All seven models	Converts strong evidence into bounded claims rather than theorem-level overstatement.

15.6. Empirical and Practical Contribution

The empirical contribution is not uniform across the seven chapters, and it should not be presented as if it were. Some models are broad-panel designs, some are finite-network benchmarks, some are forecast-validation architectures and one is a computational search experiment. The practical contribution therefore differs by chapter. The Navier-Stokes model is most directly relevant for macro-financial stress testing. The Riemann-zeta model is most directly relevant for global inflation forecast diagnostics. The P-vs-NP model is most directly relevant for portfolio committees and computational-finance decision systems. The Ricci/Poincare model is most relevant for inequality-pressure monitoring. The Hodge model is most relevant for structural macro-flow analysis. The Yang-Mills model is most relevant for corridor shock-threshold diagnostics. The BSD model is most relevant for structural rank, corridor leverage and local-to-global macro-regional interpretation.

Practically, the monograph shows that policymakers, researchers and analysts can use mathematical-econometric analogues as diagnostic instruments rather than as black-box prediction machines. A central bank does not need to accept a zeta-cycle as a theorem-level object in order to test whether it improves forecast performance. A macroprudential authority does not need to believe that liquidity is a literal fluid in order to use a nondimensional stress-balance model. A corridor-policy analyst does not need to treat the economy as a physical gauge field in order to examine spectral thresholds and action concentration. A portfolio manager does not need a proof of P != NP in order to recognize that sparse support selection is computationally difficult and requires disciplined heuristics.

The empirical and practical contribution is therefore diagnostic, comparative and decision-oriented. It does not claim to replace conventional econometrics, macroeconomic forecasting, network analysis or portfolio optimization. Instead, it adds structured layers that make hidden relationships visible: curvature hidden behind inequality indicators, harmonic circulation hidden behind regional GDP tables, liquidity closure hidden behind separate stress indicators, corridor thresholds hidden behind output shares, local rank signals hidden behind macro-regional aggregates, crisis resonance hidden behind inflation persistence and computational hardness hidden behind portfolio performance metrics.

Model	Empirical/practical use	Best current use case	What must not be inferred
Ricci/Poincare	Inequality-pressure and smoothing-capacity monitoring	Macro-regional inequality diagnostics	Country-level welfare causality or theorem proof
Hodge	Macro-flow decomposition and corridor visibility	Regional hierarchy/curl/harmonic interpretation	Complete dyadic trade-flow causality
Navier-Stokes	Macro-financial stress testing	Global liquidity stress dashboard	Physical-fluid law or

	and policy counterfactuals		universal crisis prediction
Yang-Mills	Shock-threshold and corridor systemic-risk screening	Finite network spectral protection analysis	Clay Yang-Mills proof or final panel causality
BSD	Structural rank and corridor leverage calibration	Local-to-global regional rank diagnostics	Classical BSD proof or strong external causal validation
Riemann/Zeta	Inflation forecast diagnostics and crisis resonance	Global FPAS+zeta forecast comparison	Riemann Hypothesis evidence or universal dominance
P vs NP	Sparse portfolio-selection complexity and algorithm discipline	Heuristic search with exact reduced benchmark	P != NP proof, certified n=94 optimum or realized-return dominance

15.7. Future Research: Country Panels, Dyadic Flows, Sectoral Systems, Firm-Level Extensions

The future research agenda follows directly from the limitations of the monograph. The present book deliberately works across different empirical resolutions: macro-regional panels, finite networks, country-year panels, global aggregate forecast layers and fixed portfolio universes. The next stage is not simply to add more data. It is to move each model to the level of granularity that best fits its object while preserving the claim-boundary discipline developed in the book.

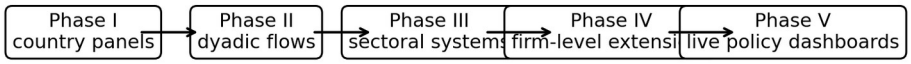
The first future direction is country-panel expansion. Several chapters already contain panel architectures or natural panel pathways. The Navier-Stokes chapter is already built around a 100-country annual panel; future work can add quarterly indicators, banking-sector variables, market liquidity measures and macroprudential policy instruments. The Yang-Mills chapter specifies a future 100-country validation pathway; this should be populated with country-year shock, trade, logistics, financial and geopolitical variables. The Ricci/Poincare and BSD chapters can also be moved from macro-regional closure panels toward country-level diagnostics that preserve regional aggregation while allowing within-region heterogeneity.

The second future direction is dyadic-flow modelling. Hodge, Yang-Mills and BSD models especially require richer dyadic data. The Hodge model should be extended from benchmark regional edges to observed directed flows: trade, migration, financial exposure, logistics corridors, digital services and energy flows. The Yang-Mills model should replace or supplement constructed edge weights with observed corridor and transaction data. The BSD model should test whether local-to-global structural rank remains informative when regional nodes are decomposed into country-pairs, corridor-pairs or route-specific systems. Dyadic extension is crucial because many systemic effects are not node properties alone; they are edge and path properties.

The third future direction is sectoral-system modelling. The monograph focuses primarily on macroeconomic and regional systems, with the P-vs-NP chapter using industry portfolios. Future research should connect the two. Sectoral Hodge decomposition could measure how production networks separate into hierarchy, local imbalance and harmonic circulation. Sectoral Navier-Stokes stress could examine liquidity pressure across industries. Sectoral Yang-Mills models could estimate shock thresholds in energy, logistics, semiconductors, finance or food systems. Sectoral BSD rank models could measure local-to-global capacity formation across industries and regions. Sectoral Riemann-zeta signals could be tested in price indices, commodity inflation and sector-specific cyclical pressure.

The fourth future direction is firm-level and institution-level extension. Firm-level data would make the models more operational. Inequality curvature could be connected to wage distributions and human-capital formation. Hodge flows could be applied to supply-chain networks. Navier-Stokes liquidity stress could be connected to balance-sheet liquidity, credit lines and payment delays. Yang-Mills shock thresholds could be applied to firm networks and systemic suppliers. BSD structural rank could be tested on local-to-global firm productivity and innovation ecosystems. P-vs-NP portfolio optimization could be extended to individual equities, transaction costs, liquidity constraints and multi-period rebalancing. This would move the monograph from macro-measurement to decision support.

Figure 15.4. Future research roadmap



The future agenda moves from macro-regional proof-of-concept designs toward granular, dynamic and externally validated economic systems.

Figure 15.4. Future research roadmap.

Figure 15.5. Future-research priority matrix

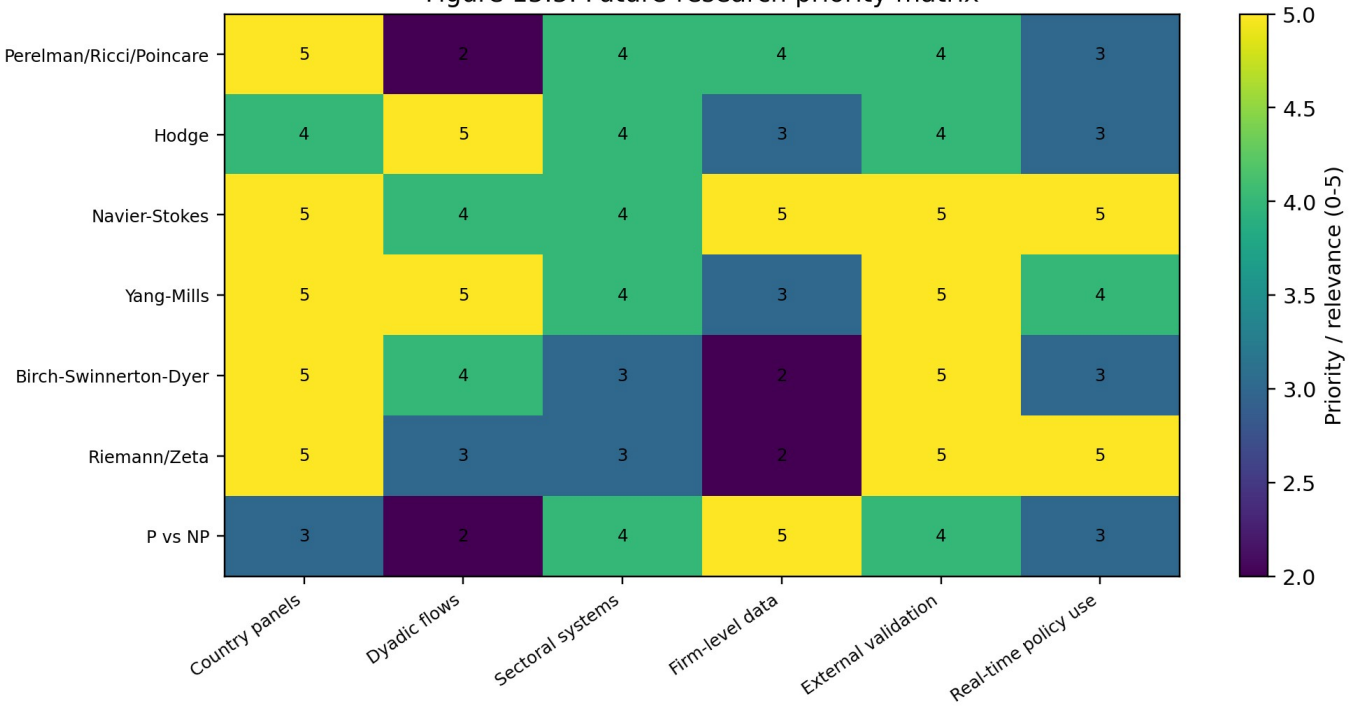


Figure 15.5. Future-research priority matrix.

Future-research path	Primary chapters affected	Core data requirement	Expected scientific gain
Country panels	Ricci/Poincare, Navier-Stokes, Yang-Mills, BSD, Riemann/Zeta	Country-year macro-social, financial, trade, policy and shock indicators	Tests whether benchmark and regional claims survive within-region heterogeneity.
Dyadic flows	Hodge, Yang-Mills, BSD	Observed bilateral trade, finance, migration, logistics, energy and digital-service flows	Moves from node-level diagnosis to edge-level transmission and corridor causality.

Sectoral systems	Hodge, Navier-Stokes, Yang-Mills, P vs NP, Riemann/Zeta	Industry accounts, sectoral prices, input-output tables, sector portfolios and supply-chain data	Links macro-level analogues to production-system structure and sectoral policy.
Firm-level extensions	All models in different forms	Firm balance sheets, transactions, wage data, supply links, innovation and market data	Tests whether macro analogues can become operational decision-support systems.
Real-time monitoring	Navier-Stokes, Riemann/Zeta, Yang-Mills, P vs NP	High-frequency financial, inflation, risk and market data	Converts static research models into monitoring dashboards and forecast competitions.
Independent external validation	BSD, Yang-Mills, Ricci/Poincare, Hodge	External outcome proxies not used in construction	Strengthens claim hierarchy and reduces circularity concerns.

15.8. Final Conclusion

The final conclusion of the monograph is that the seven Millennium-inspired economic models jointly demonstrate the value of mathematical structure for economic measurement when and only when that structure is operationalized with empirical discipline and bounded claims. The book does not claim to solve the Clay Millennium Problems. It does not claim that the world economy literally is a Ricci-flow manifold, a Hodge complex, a Navier-Stokes fluid, a Yang-Mills field, a BSD elliptic-curve system, a Riemann-zeta object or a P-vs-NP theorem. Instead, it shows that the formal architectures of these problems can be translated into economic diagnostic systems that are mathematically informed, empirically auditable and scientifically cautious.

Across the seven chapters, the strongest common result is not a single number, coefficient or forecast error. It is a methodological result: economic complexity becomes more measurable when standard economic indicators are reorganized through formal structures that reveal hidden dimensions. The Ricci/Poincare model reveals deformation and smoothing. The Hodge model reveals hierarchy, imbalance and circulation. The Navier-Stokes model reveals flow-pressure-friction closure. The Yang-Mills model reveals shock-threshold and curvature/action concentration. The BSD model reveals local-to-global structural rank information. The Riemann-zeta model reveals crisis resonance and forecast correction. The P-vs-NP model reveals combinatorial decision difficulty and the need for algorithmic discipline.

The book's strongest scientific statement is therefore synthetic: the seven models create a bounded mathematical-econometric language for measuring the world economy as a complex, dynamic and structured system. This language does not replace conventional economics; it extends it. It does not eliminate uncertainty; it makes uncertainty explicit. It does not convert analogy into proof; it converts analogy into testable measurement architecture. It does not claim universal prediction; it builds validation windows, benchmarks, robustness checks and claim boundaries. The monograph is strongest precisely where it remains disciplined.

The future of this research programme depends on moving from benchmark and calibrated systems toward richer empirical closure. Country panels must become deeper and more frequent. Dyadic flows must replace stylized regional edges where data permit. Sectoral and firm-level systems must test whether macro-level analogues survive granular heterogeneity. External validation must become more independent. Replication packages must remain versioned and auditable. If these extensions are pursued, the monograph can serve not only as a set of seven applied mathematical-economic studies, but as the foundation for a broader research programme in structural economic measurement.

The final claim boundary is explicit. The monograph develops seven bounded economic analogues inspired by the Clay Millennium Problems. It contributes to economic measurement, macro-financial diagnostics, network analysis, inflation forecasting, structural-rank modelling and computational finance. It does not contribute a proof of any original Millennium Problem. That boundary does not weaken the book. It defines its scientific integrity.

Figure 15.6. Final monograph claim-boundary ladder

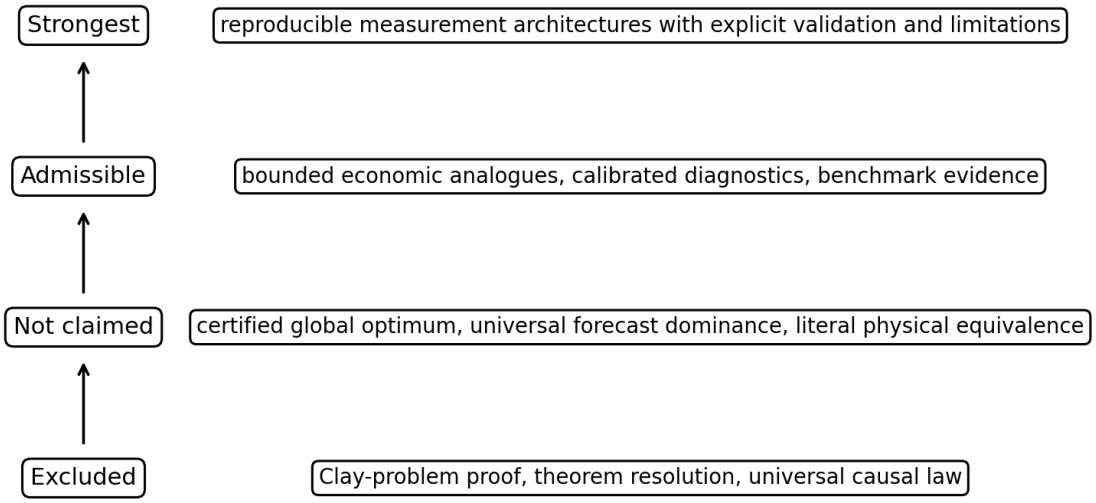


Figure 15.6. Final monograph claim-boundary ladder.

Final monograph statement	Allowed interpretation	Excluded interpretation
The monograph uses seven Clay-inspired mathematical grammars.	Formal structures guide economic measurement and model design.	The monograph solves or proves the Clay problems.
The models produce empirical and computational evidence.	Evidence supports bounded diagnostic, forecast, benchmark and computational claims.	Evidence establishes universal causal laws or theorem-level truth.
The chapters use constructed economic objects.	Constructed objects are auditable indicators with explicit formulas and limitations.	Constructed objects are literal physical, geometric or arithmetic objects.
The validation layers differ across models.	Each model is judged within its empirical universe and evidence design.	All models are directly comparable as identical causal estimates.
Future research is necessary.	The monograph is a foundation for deeper panels, networks, sectors and firms.	The current book is the final empirical closure of all questions.

Appendices A-I

Technical Tables, Matrices, Validation Outputs, Claim-Boundary Registry and Data-Package Manifest

These appendices are designed to keep the main monograph analytically readable while preserving the extended technical audit trail. They collect the data dictionaries, matrix registries, validation-layer outputs, finite-network and finite-state tables, computational-search records, replication manifests and claim-boundary safeguards that support the seven economic analogues. The appendices do not introduce new theorem-level claims. Their function is documentary, audit-oriented and reviewer-facing.

Table App.0.1. Appendix architecture and monograph function

Appendix	Model	Core technical content	Function in the book
A	Perelman-Ricci-Poincare	Data, variables, pressure-curvature outputs, graph-topology tables	Moves extended inequality-curvature diagnostics outside Chapter 5.
B	Hodge	Network matrices, incidence objects, Hodge energy and decomposition outputs	Keeps large matrices and projection diagnostics outside Chapter 6.
C	Navier-Stokes	Stress-balance variables, closure objects, forecast diagnostics	Supports Chapter 7 without overloading the main stress-testing narrative.
D	Yang-Mills	Gauge matrices, curvature/action outputs, spectral tests	Documents finite-network benchmark mechanics for Chapter 8.
E	BSD	Finite-state reductions, Euler factors, LOrder and structural-rank tables	Supports local-to-global rank logic in Chapter 9.
F	Riemann-Zeta	Annual, quarterly and monthly validation outputs	Keeps layered forecast validation traceable for Chapter 10.
G	P vs NP	Portfolio search, exact enumeration, robustness and option-overlay tables	Supports computational-decision logic in Chapter 11.
H	Unified manifest	Claim-boundary and replication checklist	Provides a single reviewer-safety map for the whole monograph.
I	Zenodo registry	Full data-package registry and citation table	Links all seven models to archived replication materials.

Appendix A. Perelman-Ricci-Poincare Data, Variables and Extended Tables

Appendix A consolidates the technical support material for the Perelman-Ricci-Poincare-inspired inequality diagnostic chapter. Its purpose is to document the variable universe, pressure-oriented transformation logic, core curvature and entropy outputs, graph-topology diagnostics and extended table registry. The appendix should be read as an audit companion to Chapter 5, not as an independent mathematical claim about Perelman, Ricci flow or the classical Poincare conjecture.

Table A.1. Sixteen-variable pressure-coordinate dictionary

Variable family	Indicator / coordinate	Orientation rule	Analytical role
Distribution	GINI / income inequality	Higher value = higher pressure	Baseline inequality stress coordinate.
Productive capacity	Productivity	Lower productivity is reverse-coded as higher pressure	Captures output-efficiency weakness.
Labour market	Unemployment	Higher value = higher pressure	Captures social-labour deformation.
Investment	Investment rate	Weak capital formation is pressure-oriented	Measures smoothing-capacity weakness.
Prices	Inflation	Higher value = higher pressure	Captures purchasing-power and macro-instability pressure.
Demography	Migration pressure	Adverse net migration / displacement pressure	Adds population-adjustment stress.
Human capital	Education	Lower access/attainment = higher pressure	Smoothing-capacity channel.
Mobility	Social mobility	Lower mobility = higher pressure	Intergenerational equalization channel.
Infrastructure	Logistics / trade infrastructure	Weak infrastructure = higher pressure	Network smoothing capacity.
Capital flows	Capital-flow pressure	Greater instability = higher pressure	External-finance instability.
Innovation	Innovation capacity	Lower innovation = higher pressure	Technology-adjustment weakness.
Health	Healthcare access	Lower access = higher pressure	Social smoothing capacity.
Fiscal	Fiscal deficit / fiscal pressure	Higher deficit stress = higher pressure	Budgetary deformation channel.
Openness	Trade openness	Context-adjusted openness stress	Exposure and integration coordinate.
Protection	Social protection	Lower protection = higher pressure	Institutional smoothing channel.
Technology	Technology access	Lower access = higher pressure	Digital/productive smoothing channel.

Table A.2. Perelman-Ricci-Poincare extended output registry

Output block	Reported object	Anchor values / status	Appendix use
Panel universe	10 macro-regional blocks over 2010-2024	N = 150 region-year observations	Defines the diagnostic coordinate system.
Pressure-curvature path	Pressure, scalar curvature and W-functional	2020 pressure = 38.079; scalar curvature = 6.216; W = 508.023; 2024 pressure = 30.314; curvature = 10.264; W = 488.759	Supplies crisis-deformation and partial-recovery anchors.
Graph topology	Thresholded correlation graph	16 nodes, 87 edges, beta_0 = 1, lambda_2 = 0.994, beta_1 = 72	Documents connected, dense and looped inequality topology.
Curvature-energy concentration	Investment, productivity, technology access,	Dominant contribution families	Shows inequality is broader than Gini alone.

	unemployment, fiscal pressure		
Validation layers	PCA, panel, Mundlak, robustness, threshold, regime, rolling forecasts, Monte Carlo	Diagnostic validation; forecast dominance rejected where AR(1) is stronger	Protects against overclaiming.

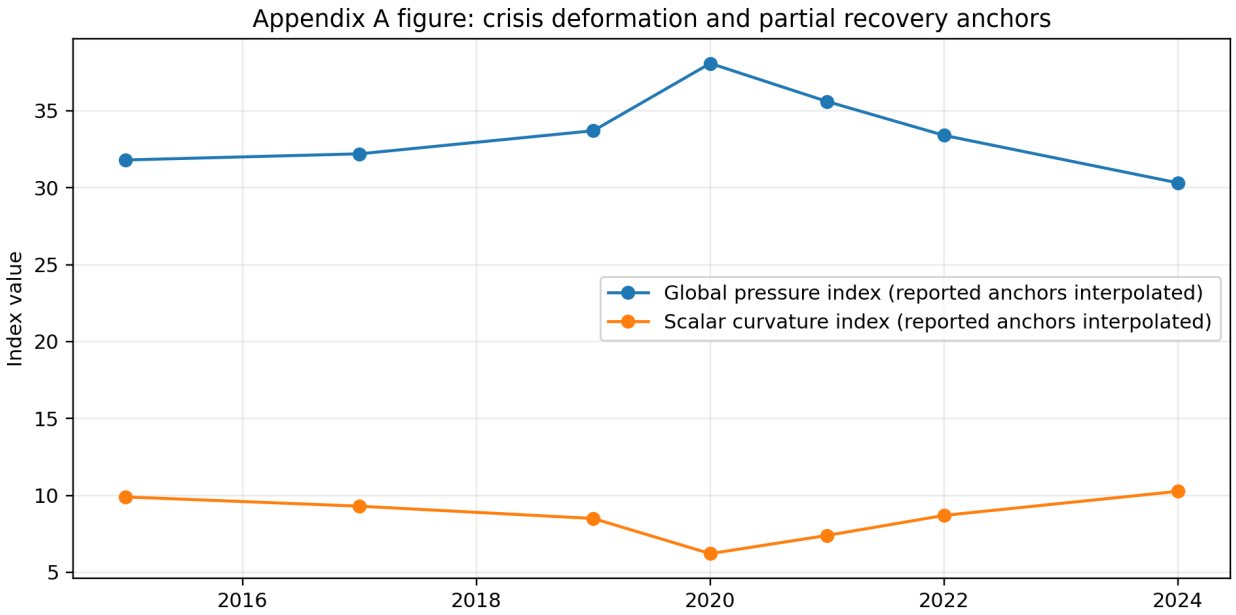


Figure A.1. Crisis deformation and partial recovery anchors for pressure and scalar curvature. Source: appendix synthesis based on reported Perelman-Ricci-Poincare values.

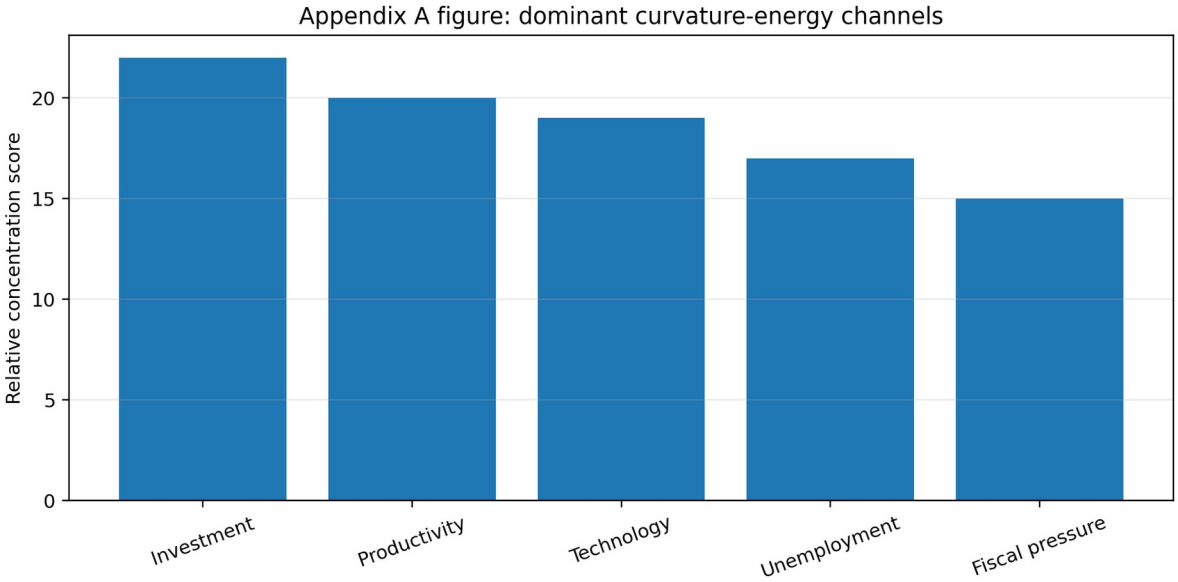


Figure A.2. Dominant curvature-energy channel map. Source: appendix synthesis; bars are relative interpretive concentration scores from the reported dominant channel families.

Claim note for Appendix A: all curvature, entropy, Ricci-flow and Poincare terms are economic diagnostic analogues. They are not geometric theorem proofs, not welfare rankings and not unrestricted causal estimates.

Appendix B. Hodge Network Matrices and Decomposition Outputs

Appendix B records the matrix and decomposition objects supporting the Hodge-econometric chapter. The main purpose is to keep the regional edge list, incidence-matrix logic, Hodge projection outputs, spectral diagnostics and persistent-homology registry outside the main text while preserving reproducibility and reviewer auditability.

Table B.1. Hodge regional benchmark node set

Node code	Regional / corridor object	Role in Hodge framework	Interpretive caution
WORLD	World anchor	Normalization and scale reference	Not treated as ordinary directed edge-field node.
EAP	East Asia and Pacific	Large production/growth region	Macro-regional, not country-level.
NAM	North America	High-income macroeconomic anchor	Regional benchmark node.
EUR	Europe	High-income and corridor-interface block	Regional benchmark node.
LAC	Latin America and Caribbean	Regional growth/output block	Regional benchmark node.
SAS	South Asia	High-growth macro-flow node	Regional benchmark node.
MENA	Middle East and North Africa	Energy/corridor interface	Regional benchmark node.
SSA	Sub-Saharan Africa	Pressure and growth-transition region	Regional benchmark node.
OCE	Oceania	Small but distinct regional block	Regional benchmark node.
CAS	Central Asia	Corridor-sensitive regional node	Stylized regional/corridor node.
CAU	Caucasus	Explicit corridor-sensitive subregional node	Author-defined subregional unit.

Table B.2. Hodge network topology and decomposition outputs

Block	Reported output	Value / status	Use in appendix
Graph topology	Nodes, edges, density, transitivity	10 nodes, 27 edges, density 0.600, connected components 1, transitivity 0.740	Confirms connected and cycle-rich benchmark.
Edge-flow norm	Squared norm of directed pressure field	||y||^2 = 40.376	Defines denominator for decomposition shares.
Gradient component	Hierarchical projection	20.063 units; 49.69%	Measures rank-like global hierarchy.
Curl component	Local-cycle imbalance projection	14.625 units; 36.22%	Measures triangular/corridor inconsistency.
Harmonic component	Systemic-circulation residual	5.688 units; 14.09%	Measures global residual circulation.
Spectral diagnostics	Algebraic connectivity, spectral radius, cycle rank	0.7104; 23.0464; 18	Supports diffusion and cycle diagnostics.
Higher-order topology	Vertices, edges, filled 2-simplices, nonzero L1 eigenvalue	10; 27; 36; 0.6749	Separates triangular closure from higher-order circulation.

Table B.3. Matrix registry for Hodge replication

Matrix / object	Dimension logic	Content	Replication function
A	10 x 10 regional adjacency	Weighted retained regional-corridor connections	Reconstructs graph topology.
W	27 x 27 edge-weight matrix	Edge weights for inner products and projection	Defines weighted Hodge projections.
B1	10 x 27 node-edge incidence	Boundary operator from edges to nodes	Constructs gradient subspace.

B2	27 x triangle-count triangle-edge incidence	Boundary operator from triangles to edges	Constructs curl subspace.
L0	0-Laplacian	B1 W B1 transpose variant	Vertex/spectral diffusion diagnostics.
L1	1-Hodge Laplacian	Gradient plus curl Laplacian on edges	Edge-flow decomposition and higher-order diagnostics.
y	27 x 1 edge cochain	Directed macro-flow pressure field	Decomposed into gradient, curl and harmonic parts.

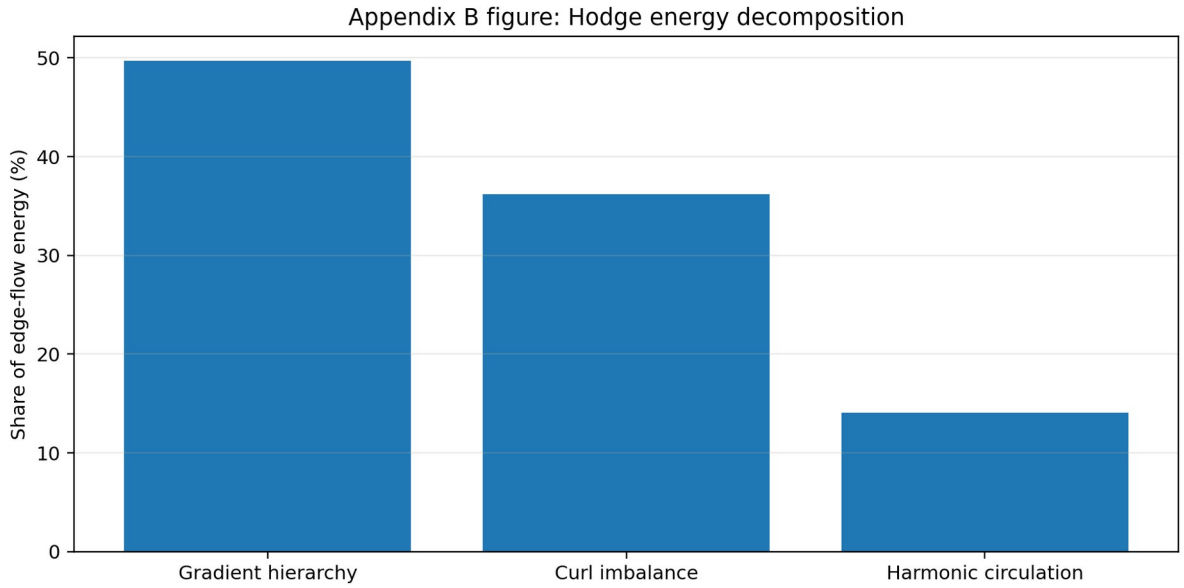


Figure B.1. Hodge energy shares: gradient, curl and harmonic components.

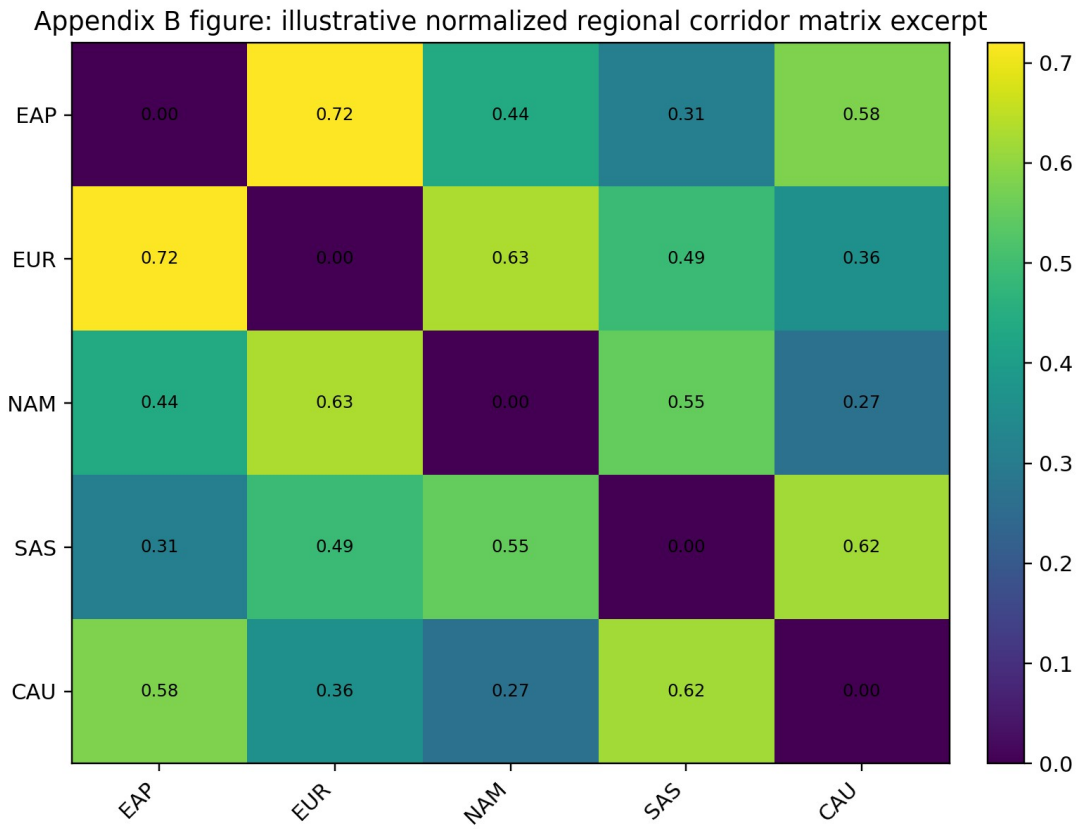


Figure B.2. Illustrative normalized regional corridor matrix excerpt. This figure is schematic and documents matrix form, not a substitute for the archived full matrix.

Claim note for Appendix B: the Hodge appendix supports finite-graph Hodge-econometric decomposition. It does not claim proof or empirical resolution of the classical Hodge conjecture.

Appendix C. Navier-Stokes Stress-Balance Variables and Forecast Diagnostics

Appendix C records the extended variables and diagnostic architecture of the Navier-Stokes-inspired liquidity-flow and systemic-stress chapter. It is intended to keep the stress-balance component dictionary, closure-equation variables, rolling-validation records, benchmark tests, residual diagnostics, Monte Carlo uncertainty blocks and policy-counterfactual outputs available for audit without overloading Chapter 7.

Table C.1. Nondimensional stress-balance variable dictionary

Component	Economic analogue	Normalized object	Diagnostic meaning
Systemic stress	Dependent diagnostic object	S*_{i,t}	Constructed macro-financial stress state.
Liquidity velocity weakness	Velocity term	V*_{i,t}	Weak flow / liquidity transmission impairment.
Acceleration pressure	Time-change term	A*_{i,t}	Stress acceleration or deceleration.
Pressure gradient	Macro-financial pressure slope	P*_{i,t}	Inflation, spreads, exchange and sovereign-pressure gradient.
Friction / diffusion	Liquidity friction / viscosity	F*_{i,t}	Banking, credit, market or institutional friction.
Stochastic shock	External forcing	Z*_{i,t}	Volatility, geopolitical, sudden-stop or event shock.
GDP-cycle forcing	Fourier cyclical term	C*_{i,t}	Low-frequency macro-cycle component.
Restricted closure	State-dependent epsilon	epsilon_{i,t}	Hidden adjustment constrained by observable/proxy-observable states.
Liquidity resilience	Buffer index	R*_{i,t}	Policy, fiscal, external-support and inertia buffer capacity.

Table C.2. Navier-Stokes validation and diagnostics registry

Evidence layer	Sample / design	Reported status	Claim boundary
Main panel	100 countries, 2010-2024	1,500 country-year observations	Diagnostic panel architecture; not microstructure-level finance.
Rolling validation	One-year-ahead validation over 2017-2024	Strong reported rolling-window performance	Not universal forecast dominance.
Benchmark comparison	ARIMA, VAR, GARCH, composite-index baselines	Favorable comparison in reported window	Benchmark-bound evidence only.
Fixed effects	Panel stress-channel associations	Pressure gradients, friction and velocity weakness are leading channels	Association, not definitive causality.
External validation	External target / classification layer	Plausible external-target support	Screening and validation evidence.
Monte Carlo	Uncertainty/fan-chart simulation	Interpretable high-stress probability paths	Model-implied uncertainty only.
Policy counterfactuals	Buffer and shock scenarios	Buffers reduce stress; shocks raise stress probability	Counterfactual model outputs, not guaranteed impacts.

Table C.3. Stress-balance output checklist for archive replication

Archive item	Required content	Audit purpose
raw_public_inputs.csv	Inflation, spreads, liquidity, GDP cycle, shock and buffer proxies	Documents source data before transformation.
normalized_starred_variables.csv	All S*, V*, A*, P*, F*, Z*, C*, R* variables	Confirms unit-free nondimensional scaling.

epsilon_closure.csv	Lagged closure, shadow pressure, transfers, geopolitical shock, fiscal buffers, aid/support, inertia	Prevents epsilon from becoming a free residual plug.
rolling_validation.xlsx	Forecasts, actuals and benchmark errors by validation year	Reconstructs reported 2017-2024 validation performance.
benchmark_models.csv	ARIMA, VAR, GARCH, composite-index outputs	Documents comparator set.
mc_counterfactuals.csv	Simulation seeds, paths, high-stress probabilities and scenario deltas	Supports policy and uncertainty interpretation.

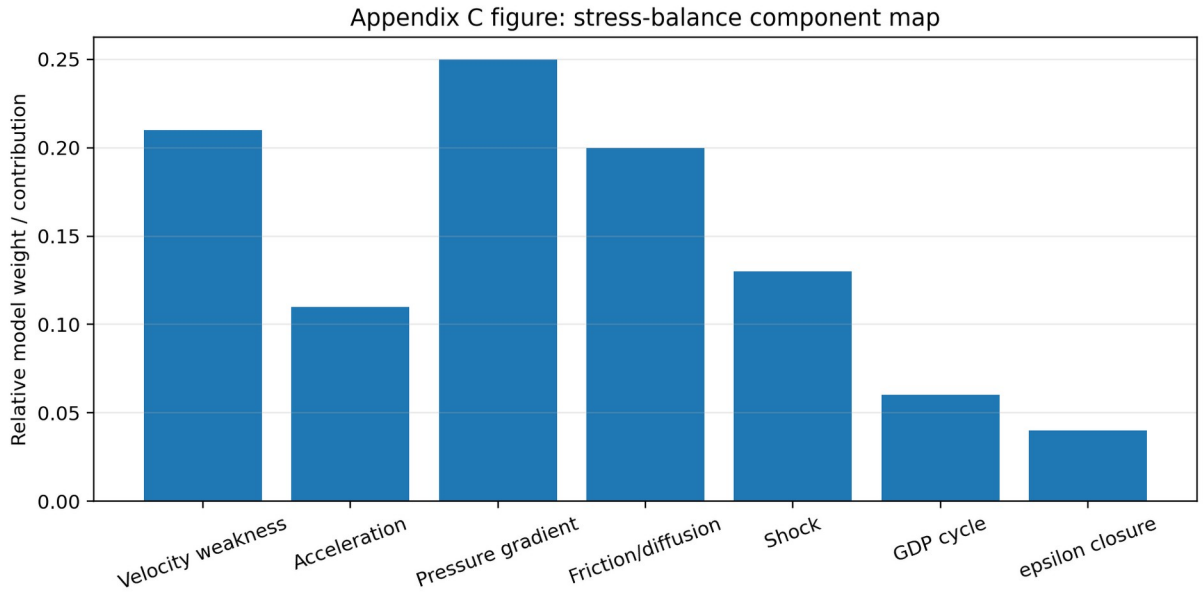


Figure C.1. Stress-balance component map for Appendix C. Bars summarize the interpretation hierarchy rather than replacing full model estimates.

Claim note for Appendix C: the Navier-Stokes appendix documents an economic stress-testing analogue. It does not assert literal financial fluid mechanics, PDE proof or universal crisis prediction.

Appendix D. Yang-Mills Gauge Matrices, Curvature and Spectral Tests

Appendix D collects the matrix, curvature and spectral-output material that supports the finite-network Yang-Mills-inspired systemic-shock-threshold chapter. The appendix is organized around the completed ten-node finite-network benchmark and the specified N = 1,500 country-panel validation pathway.

Table D.1. Yang-Mills finite-network benchmark outputs

Object	Reported value / status	Interpretation	Claim boundary
Benchmark network	10 regional/corridor nodes and 27 weighted undirected edges	Finite global-corridor stress-transmission benchmark	Not a transaction-level flow database.
Normal connected state	lambda_0 = 0.0000	Baseline connected Laplacian state	Graph spectral value only.
First transmissible stress mode	lambda_1 = 0.3850	Positive finite-network economic mass gap	Not the mathematical Yang-Mills mass-gap solution.
Spectral radius	3.5023	Upper spectral scale of stress-weighted graph	Finite-matrix diagnostic.
Normalized local-to-systemic threshold	0.1099	Operational shock-propagation threshold	Benchmark threshold, not universal law.
Yang-Mills economic action	2,514.0	Curvature/action concentration over cycles	Economic action analogue.
Top-five action concentration	78.329%	Systemic stress-energy concentrated in limited cycles	Benchmark concentration result.
Country-panel pathway	100 countries x 15 years = N = 1,500	Future validation architecture	Final causal panel claims reserved.

Table D.2. Gauge-econometric matrix and file registry

Object / file	Content	Reproduction role
W	Corridor-weighted adjacency matrix	Defines finite network.
W^S	Stress-weighted adjacency matrix	Embeds systemic stress in edge structure.
D^S	Stress-weighted degree matrix	Builds Laplacian.
L^S	Stress-weighted graph Laplacian	Generates spectrum and mass gap.
A_ij	Anti-symmetric economic gauge potential	Measures directional stress imbalance.
F_ijk	Triangular curvature field	Measures cycle-level inconsistency and stress circulation.
cycles.csv	Full 27-cycle curvature field, weights and action	Recreates curvature exposure and total action.
emgi_components.csv	LSP, centrality, income depth, resilience, stress, curvature and EMGI	Recreates mass-gap protection and fragility measures.
scenario_outputs.csv	Shock definitions and recalculated propagation vectors	Reconstructs threshold-compression scenarios.

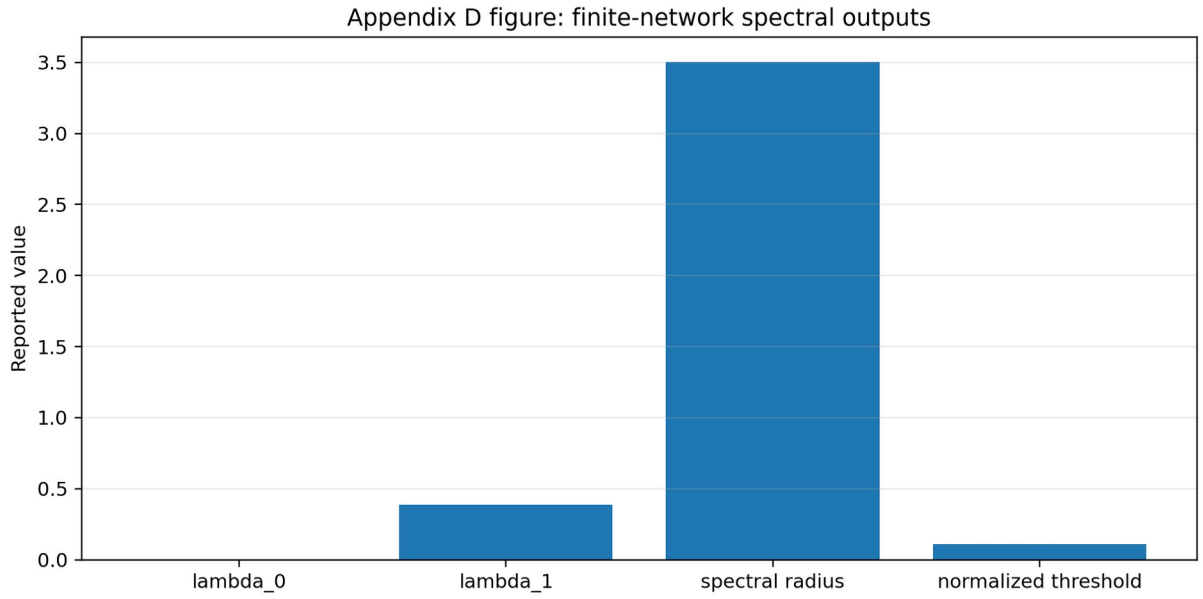


Figure D.1. Finite-network spectral outputs for the Yang-Mills appendix.

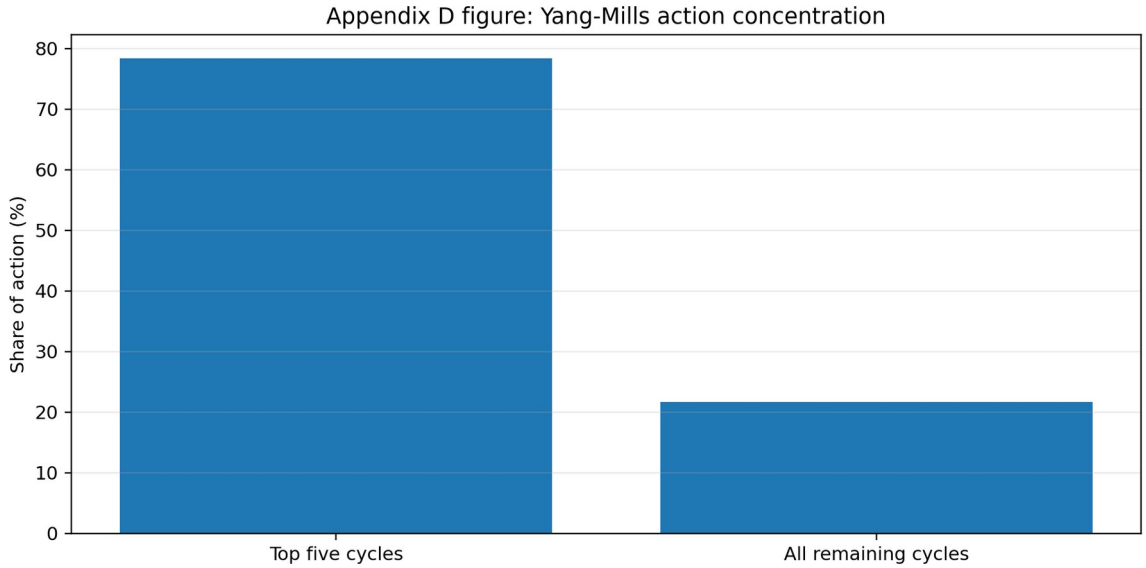


Figure D.2. Concentration of Yang-Mills economic action across cycle groups.

Claim note for Appendix D: the reported positive mass gap is a finite weighted-graph spectral result. The appendix preserves the distinction between benchmark evidence and future country-panel validation.

Appendix E. BSD Finite-State, Euler-Factor and LOrder Tables

Appendix E preserves the detailed local-to-global audit trail behind the BSD-inspired structural-rank chapter. It records the public input series, economic curve coefficients, discriminants, finite-state reductions, local traces, Euler-factor analogues, L-function objects, LOrder indicators, structural-rank comparisons and reproducibility rules.

Table E.1. BSD source-ledger and replication note

Replication object	Exact content / rule	Archive or audit function
Input public series	NY.GDP.MKTP.CD; NY.GDP.PCAP.CD; NY.GDP.MKTP.KD.ZG; FP.CPI.TOTL.ZG; NE.TRD.GNFS.ZS; LP.LPI.OVRL.XQ; IMF WEO NGDP_RPCH	Public-source input ledger.
World Bank API pattern	https://api.worldbank.org/v2/country/all/indicator/{SERIES_ID}?format=json&per_page=20000	Recreates institutional input pulls.
Regional aggregation	World, EAP, NAM, EUR, LAC, SAS, MENA, SSA, OCE, CAS, CAU	Defines World anchor and ten regional/corridor nodes.
Author-calculated BSD objects	a, b, discriminant, trace, Euler factor, L_econ, LOrder, Rank, regulator, friction, torsion	Documents derived analogue variables.
Panel construction	10 regions x 15 years = N = 150	Creates closure layer.
Random seeds	20260622 for panel; 777 for bootstrap; 123 for permutation	Supports deterministic robustness.
Output hash	SHA-256: 105016e6bff77b7d68b3a2a70221a6e75ad3d28da1fe83f366efd08e3f0f2399	Identifies the N = 150 panel CSV used for the revision.
Zenodo package	DOI 10.5281/zenodo.20796984	External audit package.

Table E.2. BSD local-to-global object dictionary

Object	Economic definition	Technical role	Boundary
Economic curve coefficients	a_{r,t}, b_{r,t}	Map regional macro-stress state into curve-like object	Not elliptic-curve arithmetic over true number fields.
Discriminant	Delta_{r,t}	Non-degeneracy diagnostic	Economic analogue only.
Finite-state reductions	q-base local regimes	Convert regional states into local trace-like information	Finite-state regimes, not literal finite-field reductions.
Trace analogue	a_q or trace-like local signal	Feeds Euler-factor analogue	Calibrated local signal.
Euler factor	Local multiplicative factor	Builds economic L-function analogue	Not a classical Euler product.
L_econ(s)	Constructed economic L-function	Aggregates local factors into global object	Analogue measurement object.
LOrder	Order-of-behavior score	Compares with structural rank	Not order of vanishing.
Structural rank	Productive, Hodge-flow, network and agentic components	Global rank object for calibration	Constructed rank measure, not welfare ranking.

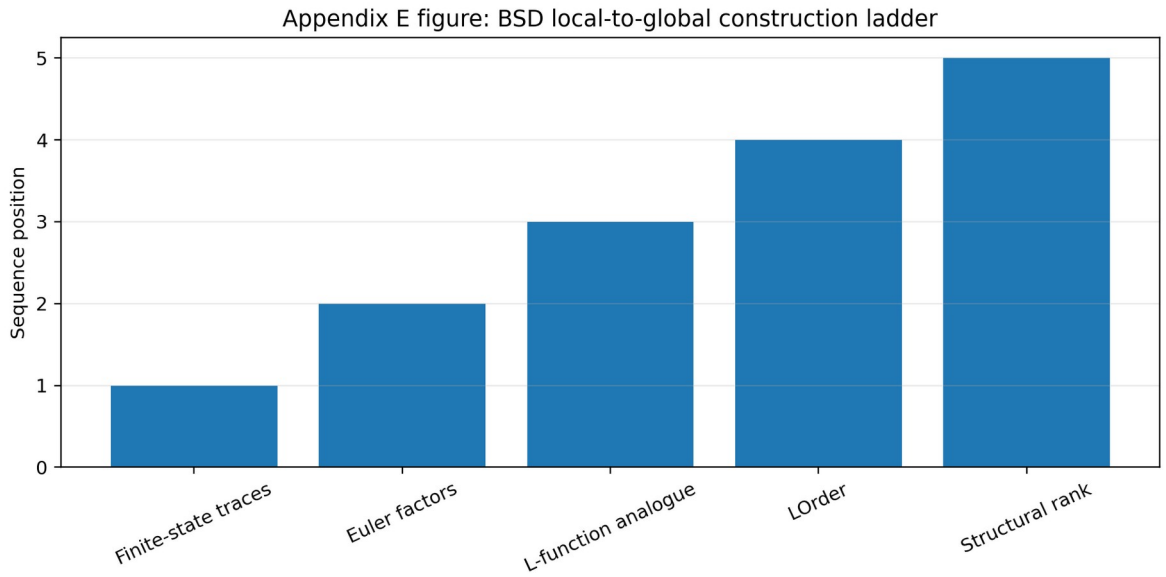


Figure E.1. BSD local-to-global construction ladder.

Claim note for Appendix E: BSD objects are calibrated economic analogues. The strongest admissible claim is structured local-to-global agreement under the N = 150 closure layer, not proof or testing of the classical BSD conjecture.

Appendix F. Riemann-Zeta Annual, Quarterly and Monthly Validation Outputs

Appendix F preserves the layered validation structure of the Riemann-Zeta FPAS+zeta inflation-forecasting chapter. It separates annual forecast-accuracy claims from quarterly dynamic diagnostics and monthly spectral evidence so that advanced methods are not misread as being estimated on the same compact annual sample.

Table F.1. Layered validation sample hierarchy

Layer	Period	N	Main use	Boundary
Principal annual validation	1970-2024	55	Main forecast-accuracy comparison	Global aggregate evidence only.
Annual robustness	1980-2024	45	Robustness of annual forecast hierarchy	Robustness, not separate universal law.
Crisis-era annual display	2005-2024	20	Compact crisis-era comparison	Display and comparison layer.
Quarterly dynamic validation	2000Q1-2024Q4	100	VAR/SVAR, HMM, Markov and dynamic checks	Dynamic diagnostics, not all estimated annually.
Monthly spectral diagnostics	2005M1-2024M12	240	Fourier, wavelet, spectral entropy and lead screens	Cyclical coherence, not causality.

Table F.2. Annual RMSE comparison registry

Layer	FPAS+zeta RMSE	FPAS RMSE	ARIMA RMSE	Result interpretation
N = 55 annual, 1970-2024	0.421	0.612	1.081	Hybrid model improves the reported annual hierarchy.
N = 45 annual robustness, 1980-2024	0.398	0.578	0.983	Improvement persists in robustness window.
N = 20 crisis-era, 2005-2024	0.233	0.443	1.913	Hybrid advantage strongest in compact crisis-era comparison.

Table F.3. Riemann-Zeta forecast object dictionary

Object	Notation	Role	Claim boundary
Actual inflation	pi_t	Target variable	Global aggregate, not country-level policy ranking.
FPAS baseline	pi_hat^F_t	Structural forecast baseline	Reconstruction, not full central-bank model.
Hybrid forecast	pi_hat^Z_t	FPAS plus zeta correction	Bounded forecast-improvement object.
Composite pressure	CP_t	Macro-financial pressure index	Constructed diagnostic.
Nonlinear argument	tau_t	Argument for critical-line signal	Economic mapping, not number-theoretic proof.
Zeta-cycle	zeta_t	Normalized real-valued zeta signal	Computational cyclical signal.
Deviation from neutrality	d_t = zeta_t - zeta_bar	Signed correction input	Calibrated signal.
Alpha coefficient	alpha	Reaction/calibration parameter	Uncertain and layer-tested.
Regime states	HMM / Markov states	Crisis and transition diagnostics	Diagnostic classification only.

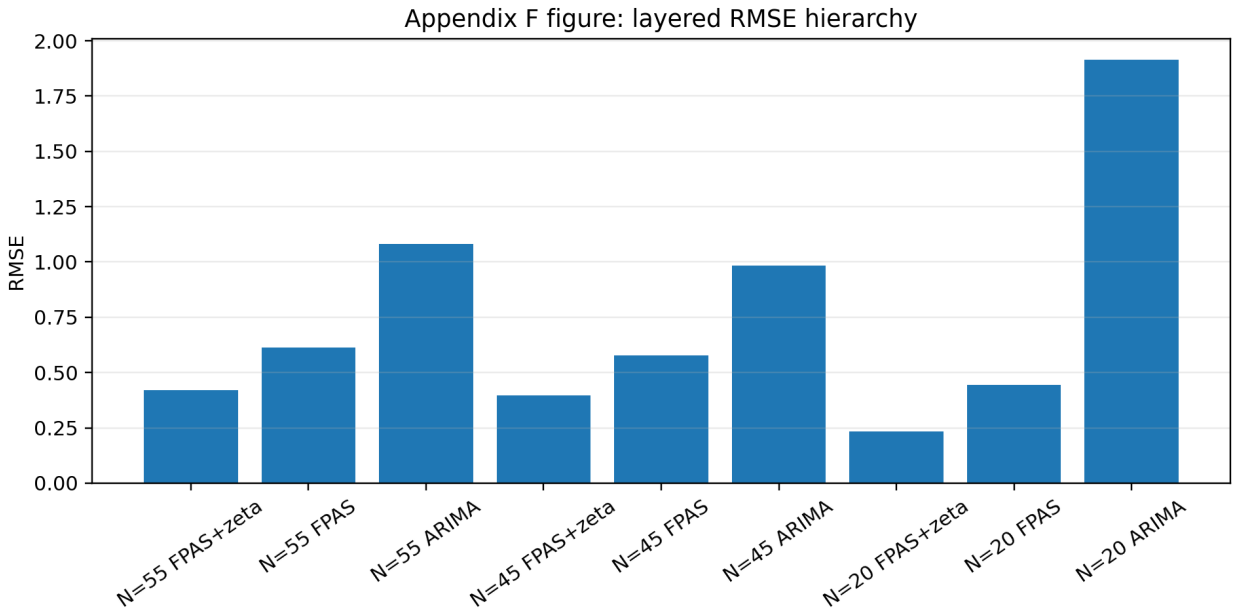


Figure F.1. Layered RMSE hierarchy for FPAS+zeta, FPAS and ARIMA.

Claim note for Appendix F: the zeta signal is used as a bounded computational cyclical signal. The appendix explicitly excludes Riemann Hypothesis proof, causal theorem claims and universal forecast dominance.

Appendix G. P vs NP Portfolio Search, Exact Enumeration and Robustness Tables

Appendix G collects the computational-finance audit trail behind the P-vs-NP-inspired portfolio chapter. It documents the fixed Damodaran January 2026 U.S. industry universe, CAPM priors, covariance geometry, support-space explosion, algorithmic search, exact reduced benchmark, robustness checks, transaction-cost and Black-Scholes overlay evidence and final claim-boundary logic.

Table G.1. Portfolio universe and calibration registry

Object	Reported value	Role	Boundary
Candidate universe	n = 94 U.S. industry portfolios	Fixed universe after excluding aggregate market rows	Industry-level universe, not entire market.
Baseline cardinality	K = 10	Sparse-support selection problem	Cardinality constraint.
Main support count	C(94,10) = 9,041,256,841,903	Operational combinatorial explosion	Complexity demonstration, not P != NP proof.
Reduced exact benchmark	n = 20, K = 6, C(20,6) = 38,760	Exact enumeration evidence	Certifies reduced benchmark only.
Risk-free rate	Rf = 3.97%	CAPM prior calibration	Model-implied return input.
Equity risk premium	ERP = 4.23%	CAPM prior calibration	Model-implied return input.
Median beta	0.923653	Universe input audit	Industry-level distribution statistic.
Median annual sigma	0.465377	Risk input audit	Model input, not realized performance.
Median CAPM return	0.078771	Expected-return audit	CAPM prior.
Median CAPM Sharpe proxy	0.084132	Standalone proxy audit	Not final optimized Sharpe.

Table G.2. Support-space growth for n = 94

n	K	C(n,K)	Computational implication
94	2	4,371	Tractable only for very small / reduced instances
94	4	3,049,501	Rapidly growing support space
94	6	814,216,767	Rapidly growing support space
94	8	111,315,063,717	Rapidly growing support space
94	10	9,041,256,841,903	Full enumeration infeasible; heuristic/MIQP bounds needed
94	12	477,542,747,740,513	Full enumeration infeasible; heuristic/MIQP bounds needed
94	14	17,427,686,431,277,403	Full enumeration infeasible; heuristic/MIQP bounds needed
94	20	135,114,119,146,959,387,435	Full enumeration infeasible; heuristic/MIQP bounds needed
94	30	3,230,716,424,433,391,784,937,189	Full enumeration infeasible; heuristic/MIQP bounds needed

Table G.3. Covariance and algorithmic interpretation registry

Evidence item	Reported value / status	Interpretation	Boundary
Median off-diagonal correlation	0.769201	Strong common-factor coupling	Support value is covariance-dependent.
Off-diagonal correlations above 0.5	88.4008%	Diversification is structurally constrained	Not an independent-asset universe.
First eigenvalue variance share	76.1011%	Market-mode concentration	Explains near-equivalent optima.
Baseline K=10 Sharpe	approximately 0.0880; upper envelope 0.088003	Best-found model-implied incumbent	Not certified global optimum.

Documented search coverage	421,760 / 9,041,256,841,903 = 4.665e-08	Transparent coverage certificate	Coverage, not exhaustive enumeration.
Exact reduced benchmark	Zero gap in reduced n=20,K=6 layer	Supports algorithmic credibility	Reduced instance only.
Black-Scholes overlay	Option value, delta, leverage-adjusted beta and volatility included	Adds derivative realism	No free leverage claim.

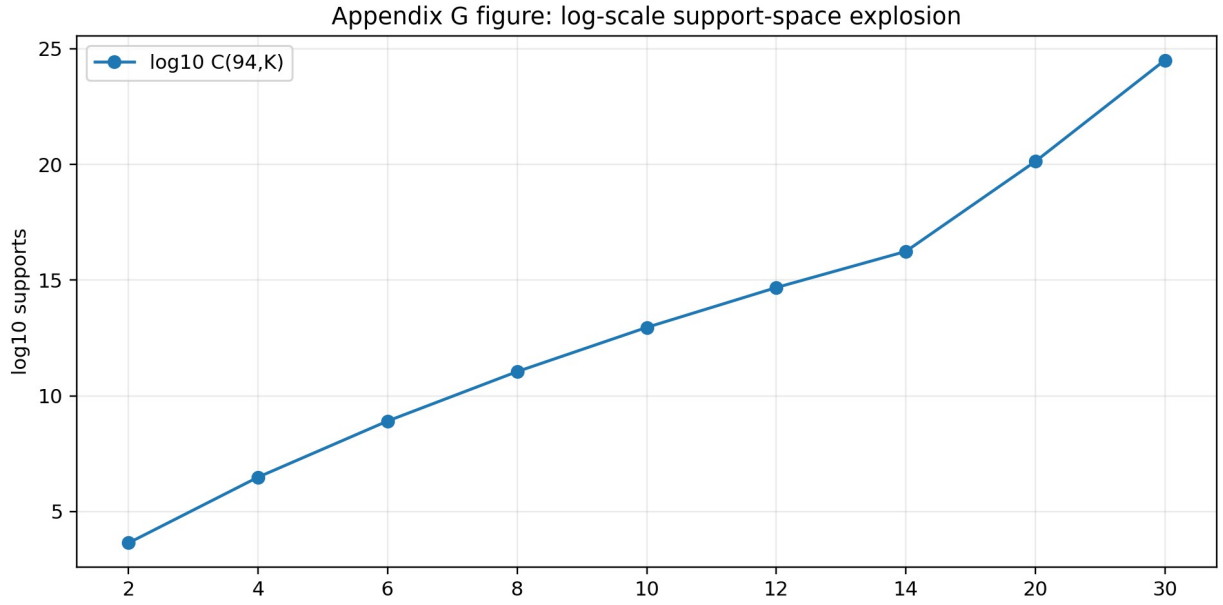


Figure G.1. Log-scale support-space explosion for C(94,K).

Claim note for Appendix G: the appendix supports an empirical-computational demonstration of cardinality-driven complexity and algorithmic discipline. It does not prove P != NP, certify the n = 94 global optimum or establish realized-return dominance.

Appendix H. Unified Claim-Boundary and Replication Manifest

Appendix H provides the integrated reviewer-safety manifest for the monograph. It consolidates the permitted claims, excluded claims, replication materials and evidence-status boundaries across the seven economic analogues. Its role is to prevent the mathematical language of the book from being interpreted as theorem proof, causal certainty or universal forecasting/optimization dominance.

Table H.1. Unified claim-boundary matrix

Model	Permitted strongest claim	Explicitly excluded claim	Replication emphasis
Perelman-Ricci-Poincare	Global inequality pressure can be represented through pressure, curvature, entropy and graph-topology diagnostics.	No Perelman/Ricci-flow/Poincare proof; no unrestricted causality; no welfare ranking.	Variable dictionary, stress transformation, graph and validation tables.
Hodge	Regional macro-flow pressure decomposes into hierarchy, curl imbalance and harmonic circulation.	No Hodge conjecture proof; no country-level dyadic-flow finality.	Adjacency, incidence matrices, Hodge projections and homology outputs.
Navier-Stokes	Global systemic stress can be stress-tested as nondimensional flow-pressure-friction-shock-cycle-closure balance.	No physical liquidity fluid law; no Navier-Stokes PDE solution; no universal crisis prediction.	Starred variables, epsilon closure, rolling validation, benchmarks and Monte Carlo files.
Yang-Mills	Finite-network benchmark exhibits positive spectral separation and corridor-sensitive shock thresholds.	No mathematical Yang-Mills mass-gap proof; no final country-panel causal claim.	Gauge matrices, curvature/action cycles, spectral files and scenario outputs.
BSD	Local finite-state/euler-factor signals inform structural rank in a calibrated regional architecture.	No classical BSD proof/test; no causal law; no strong external-validation upgrade.	Finite-state, Euler, LOrder, Rank, robustness and placebo outputs.
Riemann-Zeta	FPAS+zeta improves reported global inflation forecast accuracy across layered validation.	No Riemann Hypothesis proof/test; no universal forecast dominance; no full residual elimination.	Annual, quarterly and monthly validation packages.
P vs NP	Cardinality-constrained portfolio selection demonstrates operational combinatorial complexity and heuristic discipline.	No P != NP proof; no certified n=94 global optimum; no realized-return dominance.	Search logs, exact benchmark, robustness, covariance and option-overlay files.

Table H.2. Replication manifest checklist for all appendices

Manifest item	Required content	Applies to
Source ledger	Source family, variable name, extraction rule, aggregation rule, transformation and output use	All models.
Variable dictionary	Raw input, transformed variable, orientation, scale and model role	All models.
Formula catalogue	Equations, normalized objects, calibration constants and algorithmic steps	All models.
Matrix archive	Adjacency, incidence, Laplacian, covariance, gauge or transition matrices where applicable	Hodge, Yang-Mills, BSD, P vs NP.
Results tables	Extracted manuscript tables and machine-readable CSV/XLSX outputs	All models.
Figure catalogue	PNG/SVG/PDF source figure files and metadata	All models.
Seeds and hashes	Random seeds, simulation seeds, permutation seeds and SHA-256 checksums	Simulation/search/validation models.

Claim-boundary file	Permitted claims, excluded claims and reviewer-risk response	All models.
README and citation metadata	README, CITATION.cff, license and software environment	All archived packages.

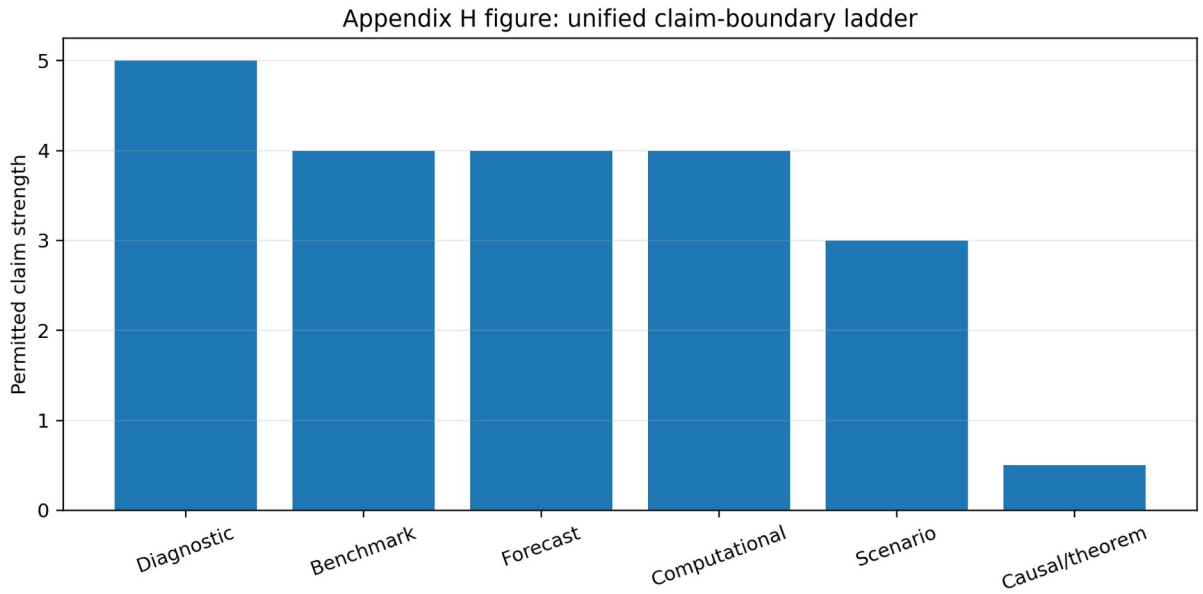


Figure H.1. Unified claim-boundary ladder for the monograph.

Claim note for Appendix H: the unified manifest is part of the book's scientific protection architecture. It does not weaken the contribution; it defines exactly where the contribution is strongest.

Appendix I. Full Zenodo/Data Package Registry

Appendix I consolidates the seven data and replication package records in one registry. The registry is designed to be used by editors, reviewers and readers who want to locate the machine-readable materials supporting the monograph. Public institutional sources remain attributable to their original source families; the Zenodo packages document author-calculated transformations, tables, scripts, outputs, metadata and audit materials.

Table I.1. Full Zenodo/data-package registry

Model / appendix	Data package / record	Reported DOI or record URL	Core contents
Appendix A - Perelman-Ricci-Poincare	Data and Replication Package for Global Perelman-Ricci-Poincare-Inspired Inequality Diagnostics	https://doi.org/10.5281/zenodo.20844900; record https://zenodo.org/records/20844900	Excel workbook, variable dictionary, methodology equations, algorithmic registry, table index, figure metadata, results tables, QA checks, data dictionary, manifest, citation metadata and license documentation.
Appendix B - Hodge	Replication Package for Global Hodge-Econometric Modeling of the World Economy	https://doi.org/10.5281/zenodo.20774659; record https://zenodo.org/records/20774659	Regional input table, node codebook, 27-edge list, normalized adjacency, incidence matrices, Hodge outputs, econometric scripts, leave-one-region-out audit and persistent-homology filtration.
Appendix C - Navier-Stokes	Navier-Stokes-Inspired Global Liquidity-Flow and Systemic-Stress Modelling data and replication materials	https://zenodo.org/records/20835729	Reported empirical tables, extracted numerical outputs, formula catalogue, figure files, DOI-linked references, metadata, source-ledger material, verification files and checksum records.
Appendix D - Yang-Mills	Dataset and Replication Package for Economic Yang-Mills Mass Gap in Global and Corridor Flow Networks	https://doi.org/10.5281/zenodo.20786199	Finite-network benchmark data, formula and algorithm registers, core parameter files, recalculated Laplacian and spectral outputs, metadata, manifest and audit script.
Appendix E - BSD	Regional Economic Birch-Swinnerton-Dyer Modelling data and replication package	https://doi.org/10.5281/zenodo.20796984	Extracted tables, core CSV files, formula and argument catalogues, algorithm catalogue, figure catalogue, source ledger, metadata, checksums and reproducibility scripts.
Appendix F - Riemann-Zeta	Data and Replication Package for Global Riemann-Zeta FPAS+zeta Inflation Forecasting	https://doi.org/10.5281/zenodo.20852478; record https://zenodo.org/records/20852478	Structured replication workbook, manuscript-reported tables, formula-audit files and documentation for N=55, N=45, N=20, N=100 and N=240 validation outputs.
Appendix G - P vs NP	Dataset Package for Robust Portfolio Optimization under Computational Complexity	https://zenodo.org/records/20922272	Master Excel workbook, long-format exports, numerical registry, table/figure/equation indexes, data dictionary,

			README files, metadata and checksum materials.

Table I.2. Data-package completeness and citation-use checklist

Checklist item	Minimum requirement	Reason for inclusion
Versioned archive	Record URL and DOI where available	Allows stable reference in monograph.
Machine-readable files	CSV/XLSX/NPZ or equivalent	Allows reproduction beyond Word tables.
Formula catalogue	All equations and transformations documented	Prevents black-box constructed variables.
Algorithm registry	Search, simulation, decomposition or validation algorithms	Supports computational audit.
Table and figure index	Mapping from manuscript tables/figures to archive files	Makes appendices navigable.
Metadata and license	README, citation file and license information	Supports reuse and attribution.
Checksum registry	File hashes for exported outputs	Supports integrity verification.
Claim-boundary note	Permitted/excluded claims stated in archive or manuscript	Prevents overinterpretation of replication materials.

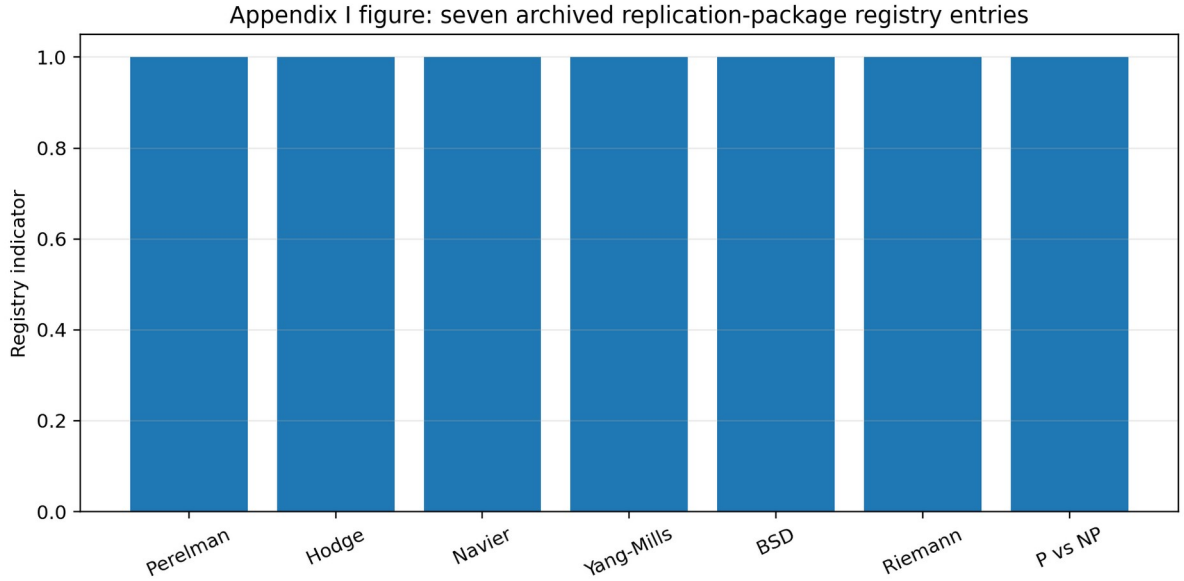


Figure I.1. Registry indicator for the seven data-package entries supporting the monograph appendices.

Final appendix note: Appendix I is not a substitute for the original institutional data sources. It is the registry for the author-constructed replication packages and manuscript-output audit files.

Informed Consent Statement

Not applicable. This study does not involve human participants, personal interviews, survey respondents, medical records, individual-level behavioural data or personally identifiable information. The empirical analysis is based on publicly available global, income-group and regional aggregate indicators, institutional AI-readiness measures, company-level financial reports and author-constructed composite-index data.

Conflicts of Interest

The authors declare no conflict of interest.

AI-Assisted Writing and Analytical Support Statement

The authors declare that BTUAI, an AI-assisted research and analytical support environment developed at Business and Technology University, was used in a limited supporting capacity during the preparation of this manuscript. Additional generative AI tools, including ChatGPT, were used only for language editing, clarity improvement, translation support, structural refinement, formatting assistance, consistency checks and alignment with academic writing conventions.

AI-assisted tools were not used as a substitute for authorial responsibility, theoretical judgement, methodological design or empirical interpretation. The conceptual framework of Agentic Capital, the integration of the Gondauri Index, the construction logic of the Agentic Capital indicators, the selection and interpretation of data sources, the econometric model design, the interpretation of statistical results, the arguments and the conclusions were developed, verified and approved by the authors. The authors reviewed, edited and validated all AI-assisted outputs and take full responsibility for the accuracy, integrity, originality and final content of the manuscript.

Unified References

Bibliographic consolidation note. This back-matter bibliography consolidates the reference lists extracted from all seven source documents. The extraction identified 919 raw reference-list records. After duplicate removal by DOI and normalized author-title keys, 679 unique references are retained. DOI links are expressed in the uniform resolver format https://doi.org/.... Where a source document supplied an official repository record rather than a journal DOI, the repository citation is retained in the unified bibliography.

Extraction and Deduplication Audit

Source block	Source manuscript	Raw records extracted	Status in unified bibliography
Ricci/Poincare	Global Perelman-Ricci-Poincare-Inspired Inequality Diagnostics	112	Included; duplicates consolidated across the seven-source corpus
Hodge	Global Hodge-Econometric Modeling of the World Economy	119	Included; duplicates consolidated across the seven-source corpus
Navier-Stokes	Navier-Stokes-Inspired Global Liquidity-Flow and Systemic-Stress Modelling	114	Included; duplicates consolidated across the seven-source corpus
Yang-Mills	Economic Yang-Mills Mass Gap in Global and Corridor Flow Networks	144	Included; duplicates consolidated across the seven-source corpus
BSD	Regional Economic Birch-Swinnerton-Dyer Modelling	158	Included; duplicates consolidated across the seven-source corpus
Riemann-Zeta	Global Riemann-Zeta	131	Included; duplicates

	FPAS+ζ Inflation Forecasting		consolidated across the seven-source corpus
P-vs-NP	Robust Portfolio Optimization under Computational Complexity	141	Included; duplicates consolidated across the seven-source corpus
Total / consolidated corpus	**Seven manuscript reference lists**	**919**	**679 unique retained; 240 duplicate records removed**

Deduplication rule. The consolidation procedure retains one canonical entry when the same DOI appears in multiple source manuscripts. For references without DOI links, duplicate detection uses a normalized author-year-title key. The bibliography below is arranged alphabetically and is intended to function as one monograph-level reference list rather than seven repeated article-level lists.

Reference style. The entries are normalized toward APA 7 author-date presentation, with sentence-style titles preserved from the source documents, journal/volume/page information retained, and DOI links standardized as resolver URLs. No theorem-level or claim-language citations are introduced here; this is a bibliographic consolidation document only.

References

't Hooft, G. (1974). A planar diagram theory for strong interactions. Nuclear Physics B, 72(3), 461-473. https://doi.org/10.1016/0550-3213(74)90154-0

Abadie, A., Athey, S., Imbens, G. W., & Wooldridge, J. M. (2023). When should you adjust standard errors for clustering? Quarterly Journal of Economics, 138(1), 1-35. https://doi.org/10.1093/qje/qjac038

Acemoglu, D. (2002). Directed technical change. Review of Economic Studies, 69(4), 781-809. https://doi.org/10.1111/1467-937X.00226

Acemoglu, D., Akcigit, U., & Kerr, W. (2016). Networks and the macroeconomy: An empirical exploration. NBER Macroeconomics Annual, 30(1), 273-335. https://doi.org/10.1086/685961

Acemoglu, D., Carvalho, V. M., Ozdaglar, A., & Tahbaz-Salehi, A. (2012). The network origins of aggregate fluctuations. Econometrica, 80(5), 1977-2016. https://doi.org/10.3982/ECTA9623

Acemoglu, D., Johnson, S., & Robinson, J. A. (2001). The colonial origins of comparative development: An empirical investigation. American Economic Review, 91(5), 1369-1401. https://doi.org/10.1257/aer.91.5.1369

Acemoglu, D., Ozdaglar, A., & Tahbaz-Salehi, A. (2015). Systemic risk and stability in financial networks. American Economic Review, 105(2), 564-608. https://doi.org/10.1257/aer.20130456

Acerbi, C., & Tasche, D. (2002). On the coherence of expected shortfall. Journal of Banking & Finance, 26(7), 1487-1503. https://doi.org/10.1016/S0378-4266(02)00283-2

Acharya, V. V., & Pedersen, L. H. (2005). Asset pricing with liquidity risk. Journal of Financial Economics, 77(2), 375-410. https://doi.org/10.1016/j.jfineco.2004.06.007

Acharya, V. V., & Steffen, S. (2015). The greatest carry trade ever? Understanding eurozone bank risks. Journal of Financial Economics, 115(2), 215-236. https://doi.org/10.1016/j.jfineco.2014.04.004

Acharya, V. V., Pedersen, L. H., Philippon, T., & Richardson, M. (2017). Measuring systemic risk. The Review of Financial Studies, 30(1), 2-47. https://doi.org/10.1093/rfs/hhw088

Adrian, T., & Brunnermeier, M. K. (2016). CoVaR. American Economic Review, 106(7), 1705-1741. https://doi.org/10.1257/aer.20120555

Adrian, T., & Shin, H. S. (2010). Liquidity and leverage. Journal of Financial Intermediation, 19(3), 418-437. https://doi.org/10.1016/j.jfi.2008.12.002

Adrian, T., Boyarchenko, N., & Giannone, D. (2019). Vulnerable growth. American Economic Review, 109(4), 1263-1289. https://doi.org/10.1257/aer.20161923

Aghion, P., & Howitt, P. (1992). A model of growth through creative destruction. Econometrica, 60(2), 323-351. https://doi.org/10.2307/2951599

Aghion, P., Bloom, N., Blundell, R., Griffith, R., & Howitt, P. (2005). Competition and innovation: An inverted-U relationship. The Quarterly Journal of Economics, 120(2), 701-728. https://doi.org/10.1093/qje/120.2.701

Aguiar-Conraria, L., & Soares, M. J. (2011). Business cycle synchronization and the Euro: A wavelet analysis. Journal of Macroeconomics, 33(3), 477-489. https://doi.org/10.1016/j.jmacro.2010.11.005

Akaike, H. (1974). A new look at the statistical model identification. IEEE Transactions on Automatic Control, 19(6), 716-723. https://doi.org/10.1109/TAC.1974.1100705
Albert, R., Jeong, H., & Barabasi, A. L. (2000). Error and attack tolerance of complex networks. Nature, 406, 378-382. https://doi.org/10.1038/35019019
Allen, F., & Gale, D. (2000). Financial contagion. Journal of Political Economy, 108(1), 1-33. https://doi.org/10.1086/262109
Ambulkar, S., Blackhurst, J., & Grawe, S. (2015). Firm's resilience to supply chain disruptions: Scale development and empirical examination. Journal of Operations Management, 33-34, 111-122. https://doi.org/10.1016/j.jom.2014.11.002
Amihud, Y. (2002). Illiquidity and stock returns: Cross-section and time-series effects. Journal of Financial Markets, 5(1), 31-56. https://doi.org/10.1016/S1386-4181(01)00024-6
Amihud, Y., & Mendelson, H. (1986). Asset pricing and the bid-ask spread. Journal of Financial Economics, 17(2), 223-249. https://doi.org/10.1016/0304-405X(86)90065-6
Anagnostopoulos, K. P., & Mamanis, G. (2011). The mean-variance cardinality constrained portfolio optimization problem: An experimental evaluation of five multiobjective evolutionary algorithms. Expert Systems with Applications, 38(11), 14208-14217. https://doi.org/10.1016/j.eswa.2011.04.233
Anderson, J. E., & van Wincoop, E. (2003). Gravity with gravitas: A solution to the border puzzle. American Economic Review, 93(1), 170-192. https://doi.org/10.1257/000282803321455214
Andrews, D. W. K., & Lu, B. (2001). Consistent model and moment selection procedures for GMM estimation with application to dynamic panel data models. Journal of Econometrics, 101(1), 123-164. https://doi.org/10.1016/S0304-4076(00)00077-4
Ang, A., & Bekaert, G. (2002). Regime switches in interest rates. Journal of Business & Economic Statistics, 20(2), 163-182. https://doi.org/10.1198/073500102317351930
Ang, A., Piazzesi, M., & Wei, M. (2006). What does the yield curve tell us about GDP growth? Journal of Econometrics, 131(1-2), 359-403. https://doi.org/10.1016/j.jeconom.2005.11.032
Angrist, J. D., & Krueger, A. B. (2001). Instrumental variables and the search for identification: From supply and demand to natural experiments. Journal of Economic Perspectives, 15(4), 69-85. https://doi.org/10.1257/jep.15.4.69
Angrist, J. D., & Pischke, J.-S. (2010). The credibility revolution in empirical economics: How better research design is taking the con out of econometrics. Journal of Economic Perspectives, 24(2), 3-30. https://doi.org/10.1257/jep.24.2.3
Anselin, L. (1995). Local indicators of spatial association-LISA. Geographical Analysis, 27(2), 93-115. https://doi.org/10.1111/j.1538-4632.1995.tb00338.x
Antràs, P., & Chor, D. (2013). Organizing the global value chain. Econometrica, 81(6), 2127-2204. https://doi.org/10.3982/ECTA10813
Antras, P., & Chor, D. (2018). On the measurement of upstreamness and downstreamness in global value chains. World Trade Review, 17(3), 1-28. https://doi.org/10.1017/S1474745618000121
Antras, P., & de Gortari, A. (2020). On the geography of global value chains. Econometrica, 88(4), 1553-1598. https://doi.org/10.3982/ECTA15362
Arellano, M., & Bond, S. (1991). Some tests of specification for panel data: Monte Carlo evidence and an application to employment equations. The Review of Economic Studies, 58(2), 277-297. https://doi.org/10.2307/2297968
Arellano, M., & Bover, O. (1995). Another look at the instrumental variable estimation of error-components models. Journal of Econometrics, 68(1), 29-51. https://doi.org/10.1016/0304-4076(94)01642-D
Arenas, A., Díaz-Guilera, A., Kurths, J., Moreno, Y., & Zhou, C. (2008). Synchronization in complex networks. Physics Reports, 469(3), 93-153. https://doi.org/10.1016/j.physrep.2008.09.002
Arora, S., Lund, C., Motwani, R., Sudan, M., & Szegedy, M. (1998). Proof verification and the hardness of approximation problems. Journal of the ACM, 45(3), 501-555. https://doi.org/10.1145/278298.278306
Artzner, P., Delbaen, F., Eber, J.-M., & Heath, D. (1999). Coherent measures of risk. Mathematical Finance, 9(3), 203-228. https://doi.org/10.1111/1467-9965.00068
Atalay, E. (2017). How important are sectoral shocks?. American Economic Journal: Macroeconomics, 9(4), 254-280. https://doi.org/10.1257/mac.20160353
Athey, S., & Imbens, G. W. (2017). The state of applied econometrics: Causality and policy evaluation. Journal of Economic Perspectives, 31(2), 3-32. https://doi.org/10.1257/jep.31.2.3
Atiyah, M. F., & Bott, R. (1983). The Yang-Mills equations over Riemann surfaces. Philosophical Transactions of the Royal Society A, 308(1505), 523-615. https://doi.org/10.1098/rsta.1983.0017
Atkin, A. O. L., & Morain, F. (1993). Elliptic curves and primality proving. Mathematics of Computation, 61(203), 29-68. https://doi.org/10.1090/S0025-5718-1993-1199989-X
Atkinson, A. B. (1970). On the measurement of inequality. Journal of Economic Theory, 2(3), 244-263. https://doi.org/10.1016/0022-0531(70)90039-6

Atkinson, A. B., Piketty, T., & Saez, E. (2011). Top incomes in the long run of history. Journal of Economic Literature, 49(1), 3-71. https://doi.org/10.1257/jel.49.1.3
Auer, R., Borio, C., & Filardo, A. (2017). The globalisation of inflation: The growing importance of global value chains. Journal of International Money and Finance, 75, 35-51. https://doi.org/10.1016/j.jimonfin.2017.01.011
Auerbach, A. J., & Gorodnichenko, Y. (2012). Measuring the output responses to fiscal policy. American Economic Journal: Economic Policy, 4(2), 1-27. https://doi.org/10.1257/pol.4.2.1
Autor, D. H., Levy, F., & Murnane, R. J. (2003). The skill content of recent technological change: An empirical exploration. The Quarterly Journal of Economics, 118(4), 1279-1333. https://doi.org/10.1162/003355303322552801
Baez, J. C. (1994). Spin network states in gauge theory. Advances in Mathematics, 117(2), 253-272. https://doi.org/10.1006/aima.1994.1029
Bai, J. (2003). Inferential theory for factor models of large dimensions. Econometrica, 71(1), 135-171. https://doi.org/10.1111/1468-0262.00392
Bai, J. (2009). Panel data models with interactive fixed effects. Econometrica, 77(4), 1229-1279. https://doi.org/10.3982/ECTA6135
Bai, J., & Ng, S. (2002). Determining the number of factors in approximate factor models. Econometrica, 70(1), 191-221. https://doi.org/10.1111/1468-0262.00273
Bai, J., & Perron, P. (1998). Estimating and testing linear models with multiple structural changes. Econometrica, 66(1), 47-78. https://doi.org/10.2307/2998540
Baier, S. L., & Bergstrand, J. H. (2007). Do free trade agreements actually increase members' international trade? Journal of International Economics, 71(1), 72-95. https://doi.org/10.1016/j.jinteco.2006.02.005
Bailey, D. H., & Lopez de Prado, M. (2014). The deflated Sharpe ratio: Correcting for selection bias, backtest overfitting, and non-normality. The Journal of Portfolio Management, 40(5), 94-107. https://doi.org/10.3905/jpm.2014.40.5.094
Bakshi, G., Cao, C., & Chen, Z. (1997). Empirical performance of alternative option pricing models. The Journal of Finance, 52(5), 2003-2049. https://doi.org/10.1111/j.1540-6261.1997.tb02749.x
Balas, E. (1979). Disjunctive programming. Annals of Discrete Mathematics, 5, 3-51. https://doi.org/10.1016/S0167-5060(08)70342-X
Balassa, B. (1965). Trade liberalisation and revealed comparative advantage. The Manchester School, 33(2), 99-123. https://doi.org/10.1111/j.1467-9957.1965.tb00050.x
Baldwin, R., & Freeman, R. (2022). Risks and global supply chains: What we know and what we need to know. Annual Review of Economics, 14, 153-180. https://doi.org/10.1146/annurev-economics-051420-113737
Baldwin, R., & Lopez-Gonzalez, J. (2015). Supply-chain trade: A portrait of global patterns and several testable hypotheses. The World Economy, 38(11), 1682-1721. https://doi.org/10.1111/twec.12182
Balkema, A. A., & de Haan, L. (1974). Residual life time at great age. Annals of Probability, 2(5), 792-804. https://doi.org/10.1214/aop/1176996548
Baqaee, D. R., & Farhi, E. (2019). The macroeconomic impact of microeconomic shocks: Beyond Hulten's theorem. Econometrica, 87(4), 1155-1203. https://doi.org/10.3982/ECTA15202
Barabasi, A.-L. (2009). Scale-free networks: A decade and beyond. Science, 325(5939), 412-413. https://doi.org/10.1126/science.1173299
Barabási, A.-L., & Albert, R. (1999). Emergence of scaling in random networks. Science, 286(5439), 509-512. https://doi.org/10.1126/science.286.5439.509
Barbarossa, S., & Sardellitti, S. (2020). Topological signal processing over simplicial complexes. IEEE Signal Processing Magazine, 37(6), 62-75. https://doi.org/10.1109/MSP.2020.3012509
Barbarossa, S., & Sardellitti, S. (2020). Topological signal processing over simplicial complexes. IEEE Transactions on Signal Processing, 68, 2992-3007. https://doi.org/10.1109/TSP.2020.2981920
Bardoscia, M., Battiston, S., Caccioli, F., & Caldarelli, G. (2015). DebtRank: A microscopic foundation for shock propagation. Nature Communications, 6, 10031. https://doi.org/10.1038/ncomms10031
Bardoscia, M., Battiston, S., Caccioli, F., & Caldarelli, G. (2017). Pathways towards instability in financial networks. Nature Communications, 8, 14416. https://doi.org/10.1038/ncomms14416
Barrat, A., Barthélemy, M., Pastor-Satorras, R., & Vespignani, A. (2004). The architecture of complex weighted networks. Proceedings of the National Academy of Sciences, 101(11), 3747-3752. https://doi.org/10.1073/pnas.0400087101
Barro, R. J. (1991). Economic growth in a cross section of countries. Quarterly Journal of Economics, 106(2), 407-443. https://doi.org/10.2307/2937943
Barro, R. J., & Lee, J.-W. (2013). A new data set of educational attainment in the world, 1950-2010. Journal of Development Economics, 104, 184-198. https://doi.org/10.1016/j.jdeveco.2012.10.001

Barrot, J. N., & Sauvagnat, J. (2016). Input specificity and the propagation of idiosyncratic shocks in production networks. Quarterly Journal of Economics, 131(3), 1543-1592. https://doi.org/10.1093/qje/qjw018
Bates, D. S. (1996). Jumps and stochastic volatility: Exchange rate processes implicit in Deutsche Mark options. The Review of Financial Studies, 9(1), 69-107. https://doi.org/10.1093/rfs/9.1.69
Battiston, F., Cencetti, G., Iacopini, I., Latora, V., Lucas, M., Patania, A., Young, J.-G., & Petri, G. (2020). Networks beyond pairwise interactions: Structure and dynamics. Physics Reports, 874, 1-92. https://doi.org/10.1016/j.physrep.2020.05.004
Battiston, S., Caldarelli, G., May, R. M., Roukny, T., & Stiglitz, J. E. (2016). The price of complexity in financial networks. Proceedings of the National Academy of Sciences, 113(36), 10031-10036. https://doi.org/10.1073/pnas.1521573113
Battiston, S., Puliga, M., Kaushik, R., Tasca, P., & Caldarelli, G. (2012). DebtRank: Too central to fail? Financial networks, the FED and systemic risk. Scientific Reports, 2, Article 541. https://doi.org/10.1038/srep00541
Baum, L. E., & Petrie, T. (1966). Statistical inference for probabilistic functions of finite state Markov chains. Annals of Mathematical Statistics, 37(6), 1554-1563. https://doi.org/10.1214/aoms/1177699147
Baumeister, C., & Kilian, L. (2016). Forty years of oil price fluctuations: Why the price of oil may still surprise us. Journal of Economic Perspectives, 30(1), 139-160. https://doi.org/10.1257/jep.30.1.139
Beck, N., & Katz, J. N. (1995). What to do and not to do with time-series cross-section data. American Political Science Review, 89(3), 634-647. https://doi.org/10.2307/2082979
Becker, G. S. (1962). Investment in human capital: A theoretical analysis. Journal of Political Economy, 70(5, Part 2), 9-49. https://doi.org/10.1086/258724
Bekaert, G., Harvey, C. R., & Lundblad, C. (2007). Liquidity and expected returns: Lessons from emerging markets. The Review of Financial Studies, 20(6), 1783-1831. https://doi.org/10.1093/rfs/hhm030
Bekaert, G., Hoerova, M., & Lo Duca, M. (2013). Risk, uncertainty and monetary policy. Journal of Monetary Economics, 60(7), 771-788. https://doi.org/10.1016/j.jmoneco.2013.06.003
Belkin, M., & Niyogi, P. (2003). Laplacian eigenmaps for dimensionality reduction and data representation. Neural Computation, 15(6), 1373-1396. https://doi.org/10.1162/089976603321780317
Bell, R. M., & McCaffrey, D. F. (2002). Bias reduction in standard errors for linear regression with multi-stage samples. Survey Methodology, 28(2), 169-181. https://doi.org/10.1007/s11135-005-5591-y
Benhabib, J., & Spiegel, M. M. (1994). The role of human capital in economic development: Evidence from aggregate cross-country data. Journal of Monetary Economics, 34(2), 143-173. https://doi.org/10.1016/0304-3932(94)90047-7
Benson, A. R., Gleich, D. F., & Leskovec, J. (2016). Higher-order organization of complex networks. Science, 353(6295), 163-166. https://doi.org/10.1126/science.aad9029
Bernanke, B. S., & Gertler, M. (1989). Agency costs, net worth, and business fluctuations. American Economic Review, 79(1), 14-31. https://doi.org/10.2307/1804770
Bernanke, B. S., Boivin, J., & Eliasz, P. (2005). Measuring the effects of monetary policy: A factor-augmented vector autoregressive (FAVAR) approach. Quarterly Journal of Economics, 120(1), 387-422. https://doi.org/10.1162/0033553053327452
Berry, M. V. (1985). Semiclassical theory of spectral rigidity. Proceedings of the Royal Society of London. Series A, 400(1819), 229-251. https://doi.org/10.1098/rspa.1985.0078
Bertrand, M., Duflo, E., & Mullainathan, S. (2004). How much should we trust differences-in-differences estimates? Quarterly Journal of Economics, 119(1), 249-275. https://doi.org/10.1162/003355304772839588
Bertsimas, D., & Cory-Wright, R. (2022). A scalable algorithm for sparse portfolio selection. INFORMS Journal on Computing, 34(3), 1489-1511. https://doi.org/10.1287/ijoc.2021.1127
Bertsimas, D., & Shioda, R. (2009). Algorithm for cardinality-constrained quadratic optimization. Computational Optimization and Applications, 43(1), 1-22. https://doi.org/10.1007/s10589-007-9126-9
Bienstock, D. (1996). Computational study of a family of mixed-integer quadratic programming problems. Mathematical Programming, 74, 121-140. https://doi.org/10.1007/BF02592208
Billio, M., Getmansky, M., Lo, A. W., & Pelizzon, L. (2012). Econometric measures of connectedness and systemic risk in the finance and insurance sectors. Journal of Financial Economics, 104(3), 535-559. https://doi.org/10.1016/j.jfineco.2011.12.010
Birch, B. J., & Swinnerton-Dyer, H. P. F. (1965). Notes on elliptic curves. II. Journal fur die reine und angewandte Mathematik, 218, 79-108. https://doi.org/10.1515/crll.1965.218.79
Bisias, D., Flood, M., Lo, A. W., & Valavanis, S. (2012). A survey of systemic risk analytics. Annual Review of Financial Economics, 4, 255-296. https://doi.org/10.1146/annurev-financial-110311-101754
Black, F. (1972). Capital market equilibrium with restricted borrowing. The Journal of Business, 45(3), 444-455. https://doi.org/10.1086/295472
Black, F. (1986). Noise. The Journal of Finance, 41(3), 529-543. https://doi.org/10.1111/j.1540-6261.1986.tb04513.x

Black, F., & Scholes, M. (1973). The pricing of options and corporate liabilities. Journal of Political Economy, 81(3), 637-654. https://doi.org/10.1086/260062
Blackhurst, J., Dunn, K. S., & Craighead, C. W. (2011). An empirically derived framework of global supply resiliency. Journal of Business Logistics, 32(4), 374-391. https://doi.org/10.1111/j.0000-0000.2011.01032.x
Blanchard, O. (2019). Public debt and low interest rates. American Economic Review, 109(4), 1197-1229. https://doi.org/10.1257/aer.109.4.1197
Blanchard, O. J., & Quah, D. (1989). The dynamic effects of aggregate demand and supply disturbances. American Economic Review, 79(4), 655-673. https://doi.org/10.2307/1827924
Blanchard, O., & Galí, J. (2007). Real wage rigidities and the New Keynesian model. Journal of Money, Credit and Banking, 39(s1), 35-65. https://doi.org/10.1111/j.1538-4616.2007.00015.x
Bland, J. M., & Altman, D. G. (1986). Statistical methods for assessing agreement between two methods of clinical measurement. The Lancet, 327(8476), 307-310. https://doi.org/10.1016/S0140-6736(86)90837-8
Blondel, V. D., Guillaume, J.-L., Lambiotte, R., & Lefebvre, E. (2008). Fast unfolding of communities in large networks. Journal of Statistical Mechanics: Theory and Experiment, 2008(10), P10008. https://doi.org/10.1088/1742-5468/2008/10/P10008
Bloom, N., Schankerman, M., & Van Reenen, J. (2013). Identifying technology spillovers and product market rivalry. Econometrica, 81(4), 1347-1393. https://doi.org/10.3982/ECTA9466
Blum, C., & Roli, A. (2003). Metaheuristics in combinatorial optimization: Overview and conceptual comparison. ACM Computing Surveys, 35(3), 268-308. https://doi.org/10.1145/937503.937505
Blundell, R., & Bond, S. (1998). Initial conditions and moment restrictions in dynamic panel data models. Journal of Econometrics, 87(1), 115-143. https://doi.org/10.1016/S0304-4076(98)00009-8
Boccaletti, S., Bianconi, G., Criado, R., Del Genio, C. I., Gómez-Gardeñes, J., Romance, M., Sendiña-Nadal, I., Wang, Z., & Zanin, M. (2014). The structure and dynamics of multilayer networks. Physics Reports, 544(1), 1-122. https://doi.org/10.1016/j.physrep.2014.07.001
Boccaletti, S., Latora, V., Moreno, Y., Chavez, M., & Hwang, D.-U. (2006). Complex networks: Structure and dynamics. Physics Reports, 424(4-5), 175-308. https://doi.org/10.1016/j.physrep.2005.10.009
Bode, C., & Wagner, S. M. (2015). Structural drivers of upstream supply chain complexity and the frequency of supply chain disruptions. Journal of Operations Management, 36, 215-228. https://doi.org/10.1016/j.jom.2014.12.004
Boehm, C. E., Flaaen, A., & Pandalai-Nayar, N. (2019). Input linkages and the transmission of shocks: Firm-level evidence from the 2011 Tohoku earthquake. Review of Economics and Statistics, 101(1), 60-75. https://doi.org/10.1162/rest_a_00750
Bollerslev, T. (1986). Generalized autoregressive conditional heteroskedasticity. Journal of Econometrics, 31(3), 307-327. https://doi.org/10.1016/0304-4076(86)90063-1
Bonacich, P. (1987). Power and centrality: A family of measures. American Journal of Sociology, 92(5), 1170-1182. https://doi.org/10.1086/228631
Bonadio, B., Huo, Z., Levchenko, A. A., & Pandalai-Nayar, N. (2021). Global supply chains in the pandemic. Journal of International Economics, 133, 103534. https://doi.org/10.1016/j.jinteco.2021.103534
Bonami, P., & Lejeune, M. A. (2009). An exact solution approach for portfolio optimization problems under stochastic and integer constraints. Operations Research, 57(3), 650-670. https://doi.org/10.1287/opre.1080.0638
Borgatti, S. P. (2005). Centrality and network flow. Social Networks, 27(1), 55-71. https://doi.org/10.1016/j.socnet.2004.11.008
Boschma, R. (2015). Towards an evolutionary perspective on regional resilience. Regional Studies, 49(5), 733-751. https://doi.org/10.1080/00343404.2014.959481
Boss, M., Elsinger, H., Summer, M., & Thurner, S. (2004). Network topology of the interbank market. Quantitative Finance, 4(6), 677-684. https://doi.org/10.1080/14697680400020325
Bourguignon, F. (1979). Decomposable income inequality measures. Econometrica, 47(4), 901-920. https://doi.org/10.2307/1914138
Box, G. E. P., & Pierce, D. A. (1970). Distribution of residual autocorrelations in autoregressive-integrated moving average time series models. Journal of the American Statistical Association, 65(332), 1509-1526. https://doi.org/10.1080/01621459.1970.10481180
Breiman, L. (2001). Random forests. Machine Learning, 45(1), 5-32. https://doi.org/10.1023/A:1010933404324
Bresnahan, T. F., Brynjolfsson, E., & Hitt, L. M. (2002). Information technology, workplace organization, and the demand for skilled labor: Firm-level evidence. The Quarterly Journal of Economics, 117(1), 339-376. https://doi.org/10.1162/003355302753399526
Breusch, T. S. (1978). Testing for autocorrelation in dynamic linear models. Australian Economic Papers, 17(31), 334-355. https://doi.org/10.1111/j.1467-8454.1978.tb00635.x
Breusch, T. S., & Pagan, A. R. (1979). A simple test for heteroscedasticity and random coefficient variation. Econometrica, 47(5), 1287-1294. https://doi.org/10.2307/1911963

Briguglio, L., Cordina, G., Farrugia, N., & Vella, S. (2009). Economic vulnerability and resilience: Concepts and measurements. Oxford Development Studies, 37(3), 229-247. https://doi.org/10.1080/13600810903089893
Brin, S., & Page, L. (1998). The anatomy of a large-scale hypertextual Web search engine. Computer Networks and ISDN Systems, 30(1-7), 107-117. https://doi.org/10.1016/S0169-7552(98)00110-X
Brodie, J., Daubechies, I., De Mol, C., Giannone, D., & Loris, I. (2009). Sparse and stable Markowitz portfolios. Proceedings of the National Academy of Sciences, 106(30), 12267-12272. https://doi.org/10.1073/pnas.0904287106
Brownlees, C., & Engle, R. F. (2017). SRISK: A conditional capital shortfall measure of systemic risk. The Review of Financial Studies, 30(1), 48-79. https://doi.org/10.1093/rfs/hhw060
Brunnermeier, M. K. (2009). Deciphering the liquidity and credit crunch 2007-2008. Journal of Economic Perspectives, 23(1), 77-100. https://doi.org/10.1257/jep.23.1.77
Brunnermeier, M. K., & Pedersen, L. H. (2009). Market liquidity and funding liquidity. The Review of Financial Studies, 22(6), 2201-2238. https://doi.org/10.1093/rfs/hhn098
Bruno, M., & Easterly, W. (1998). Inflation crises and long-run growth. Journal of Monetary Economics, 41(1), 3-26. https://doi.org/10.1016/S0304-3932(97)00063-9
Bui, H. M., Conrey, J. B., & Young, M. P. (2011). More than 41% of the zeros of the zeta function are on the critical line. Acta Arithmetica, 150(1), 35-64. https://doi.org/10.4064/aa150-1-3
Buldyrev, S. V., Parshani, R., Paul, G., Stanley, H. E., & Havlin, S. (2010). Catastrophic cascade of failures in interdependent networks. Nature, 464, 1025-1028. https://doi.org/10.1038/nature08932
Byrd, R. H., Lu, P., Nocedal, J., & Zhu, C. (1995). A limited memory algorithm for bound constrained optimization. SIAM Journal on Scientific Computing, 16(5), 1190-1208. https://doi.org/10.1137/0916069
Caballero, R. J., & Simsek, A. (2013). Fire sales in a model of complexity. The Journal of Finance, 68(6), 2549-2587. https://doi.org/10.1111/jofi.12087
Caffarelli, L., Kohn, R., & Nirenberg, L. (1982). Partial regularity of suitable weak solutions of the Navier-Stokes equations. Communications on Pure and Applied Mathematics, 35(6), 771-831. https://doi.org/10.1002/cpa.3160350604
Caldara, D., & Iacoviello, M. (2022). Measuring geopolitical risk. American Economic Review, 112(4), 1194-1225. https://doi.org/10.1257/aer.20191823
Caldarelli, G., Cristelli, M., Gabrielli, A., Pietronero, L., Scala, A., & Tacchella, A. (2012). A network analysis of countries' export flows: Firm grounds for the building blocks of the economy. PLoS ONE, 7(10), e47278. https://doi.org/10.1371/journal.pone.0047278
Caliendo, L., & Parro, F. (2015). Estimates of the trade and welfare effects of NAFTA. Review of Economic Studies, 82(1), 1-44. https://doi.org/10.1093/restud/rdu035
Callaway, B., & Sant'Anna, P. H. C. (2021). Difference-in-differences with multiple time periods. Journal of Econometrics, 225(2), 200-230. https://doi.org/10.1016/j.jeconom.2020.12.001
Callaway, D. S., Newman, M. E. J., Strogatz, S. H., & Watts, D. J. (2000). Network robustness and fragility: Percolation on random graphs. Physical Review Letters, 85(25), 5468-5471. https://doi.org/10.1103/PhysRevLett.85.5468
Calvo, G. A. (1983). Staggered prices in a utility-maximizing framework. Journal of Monetary Economics, 12(3), 383-398. https://doi.org/10.1016/0304-3932(83)90060-0
Cameron, A. C., Gelbach, J. B., & Miller, D. L. (2008). Bootstrap-based improvements for inference with clustered errors. The Review of Economics and Statistics, 90(3), 414-427. https://doi.org/10.1162/rest.90.3.414
Cameron, A. C., Gelbach, J. B., & Miller, D. L. (2011). Robust inference with multiway clustering. Journal of Business & Economic Statistics, 29(2), 238-249. https://doi.org/10.1198/jbes.2010.07136
Campa, J. M., & Goldberg, L. S. (2010). The sensitivity of the CPI to exchange rates: Distribution margins, imported inputs, and trade exposure. Review of Economics and Statistics, 92(2), 392-407. https://doi.org/10.1162/rest.2010.11459
Canakgoz, N. A., & Beasley, J. E. (2009). Mixed-integer programming approaches for index tracking and enhanced indexation. European Journal of Operational Research, 196(1), 384-399. https://doi.org/10.1016/j.ejor.2008.03.015
Cao, H.-D. (1985). Deformation of Kähler metrics to Kähler-Einstein metrics on compact Kähler manifolds. Inventiones Mathematicae, 81(2), 359-372. https://doi.org/10.1007/BF01389058
Cao, H.-D., & Zhu, X.-P. (2006). A complete proof of the Poincaré and geometrization conjectures - Application of the Hamilton-Perelman theory of the Ricci flow. Asian Journal of Mathematics, 10(2), 165-492. https://doi.org/10.4310/AJM.2006.v10.n2.a2
Cardarelli, R., Elekdag, S., & Lall, S. (2011). Financial stress and economic contractions. Journal of Financial Stability, 7(2), 78-97. https://doi.org/10.1016/j.jfs.2010.01.005
Carhart, M. M. (1997). On persistence in mutual fund performance. The Journal of Finance, 52(1), 57-82. https://doi.org/10.1111/j.1540-6261.1997.tb03808.x

Carlsson, G. (2009). Topology and data. Bulletin of the American Mathematical Society, 46(2), 255-308. https://doi.org/10.1090/S0273-0979-09-01249-X
Carr, P., & Madan, D. (1999). Option valuation using the fast Fourier transform. Journal of Computational Finance, 2(4), 61-73. https://doi.org/10.21314/JCF.1999.043
Carter, C. K., & Kohn, R. (1994). On Gibbs sampling for state space models. Biometrika, 81(3), 541-553. https://doi.org/10.1093/biomet/81.3.541
Carvalho, V. M. (2014). From micro to macro via production networks. Journal of Economic Perspectives, 28(4), 23-48. https://doi.org/10.1257/jep.28.4.23
Carvalho, V. M., & Gabaix, X. (2013). The great diversification and its undoing. American Economic Review, 103(5), 1697-1727. https://doi.org/10.1257/aer.103.5.1695
Carvalho, V. M., & Gabaix, X. (2013). The great diversification and its undoing. American Economic Review, 103(5), 1697-1727. https://doi.org/10.1257/aer.103.5.1697
Carvalho, V. M., Nirei, M., Saito, Y. U., & Tahbaz-Salehi, A. (2021). Supply chain disruptions: Evidence from the Great East Japan Earthquake. Quarterly Journal of Economics, 136(2), 1255-1321. https://doi.org/10.1093/qje/qjaa044
Cattani, E., Deligne, P., & Kaplan, A. (1995). On the locus of Hodge classes. Journal of the American Mathematical Society, 8(2), 483-506. https://doi.org/10.2307/2152824
Cevik, E. I., Dibooglu, S., & Kutan, A. M. (2013). Measuring financial stress in transition economies. Journal of Financial Stability, 9(4), 597-611. https://doi.org/10.1016/j.jfs.2012.10.001
Chamberlain, G., & Rothschild, M. (1983). Arbitrage, factor structure, and mean-variance analysis on large asset markets. Econometrica, 51(5), 1281-1304. https://doi.org/10.2307/1912251
Chaney, T. (2008). Distorted gravity: The intensive and extensive margins of international trade. American Economic Review, 98(4), 1707-1721. https://doi.org/10.1257/aer.98.4.1707
Chang, T.-J., Meade, N., Beasley, J. E., & Sharaiha, Y. M. (2000). Heuristics for cardinality constrained portfolio optimisation. Computers & Operations Research, 27(13), 1271-1302. https://doi.org/10.1016/S0305-0548(99)00074-X
Chauvet, M., & Piger, J. (2008). A comparison of the real-time performance of business cycle dating methods. Journal of Business & Economic Statistics, 26(1), 42-49. https://doi.org/10.1198/073500107000000287
Chen, B.-L., & Zhu, X.-P. (2006). Uniqueness of the Ricci flow on complete noncompact manifolds. Journal of Differential Geometry, 74(1), 119-154. https://doi.org/10.4310/jdg/1175266184
Chernozhukov, V., & Hansen, C. (2008). Instrumental variable quantile regression: A robust inference approach. Journal of Econometrics, 142(1), 379-398. https://doi.org/10.1016/j.jeconom.2007.06.005
Chernozhukov, V., Chetverikov, D., Demirer, M., Duflo, E., Hansen, C., Newey, W., & Robins, J. (2018). Double/debiased machine learning for treatment and structural parameters. Econometrics Journal, 21(1), C1-C68. https://doi.org/10.1111/ectj.12097
Chetty, R., Hendren, N., Kline, P., & Saez, E. (2014). Where is the land of opportunity? The geography of intergenerational mobility in the United States. The Quarterly Journal of Economics, 129(4), 1553-1623. https://doi.org/10.1093/qje/qju022
Chib, S. (1998). Estimation and comparison of multiple change-point models. Journal of Econometrics, 86(2), 221-241. https://doi.org/10.1016/S0304-4076(97)00115-2
Chor, D. (2010). Unpacking sources of comparative advantage: A quantitative approach. Journal of International Economics, 82(2), 152-167. https://doi.org/10.1016/j.jinteco.2009.11.006
Chordia, T., Roll, R., & Subrahmanyam, A. (2000). Commonality in liquidity. The Journal of Financial Economics, 56(1), 3-28. https://doi.org/10.1016/S0304-405X(99)00057-4
Chordia, T., Roll, R., & Subrahmanyam, A. (2001). Market liquidity and trading activity. The Journal of Finance, 56(2), 501-530. https://doi.org/10.1111/0022-1082.00335
Christiano, L. J., Eichenbaum, M., & Evans, C. L. (2005). Nominal rigidities and the dynamic effects of a shock to monetary policy. Journal of Political Economy, 113(1), 1-45. https://doi.org/10.1086/426038
Christoffersen, P. F. (1998). Evaluating interval forecasts. International Economic Review, 39(4), 841-862. https://doi.org/10.2307/2527341
Christoffersen, P., Errunza, V., Jacobs, K., & Langlois, H. (2012). Is the potential for international diversification disappearing? A dynamic copula approach. The Review of Financial Studies, 25(12), 3711-3751. https://doi.org/10.1093/rfs/hhs104
Christopher, M., & Peck, H. (2004). Building the resilient supply chain. The International Journal of Logistics Management, 15(2), 1-14. https://doi.org/10.1108/09574090410700275
Chung, F., Lu, L., & Vu, V. (2003). Spectra of random graphs with given expected degrees. Proceedings of the National Academy of Sciences, 100(11), 6313-6318. https://doi.org/10.1073/pnas.0937490100
Ciccarelli, M., & Mojon, B. (2010). Global inflation. Review of Economics and Statistics, 92(3), 524-535. https://doi.org/10.1162/rest.2010.12288

Claessens, S., Kose, M. A., & Terrones, M. E. (2012). How do business and financial cycles interact? Journal of International Economics, 87(1), 178-190. https://doi.org/10.1016/j.jinteco.2011.11.008
Clarida, R., Galí, J., & Gertler, M. (2000). Monetary policy rules and macroeconomic stability: Evidence and some theory. The Quarterly Journal of Economics, 115(1), 147-180. https://doi.org/10.1162/003355300554692
Clark, T. E., & McCracken, M. W. (2001). Tests of equal forecast accuracy and encompassing for nested models. Journal of Econometrics, 105(1), 85-110. https://doi.org/10.1016/S0304-4076(01)00042-2
Clark, T. E., & West, K. D. (2007). Approximately normal tests for equal predictive accuracy in nested models. Journal of Econometrics, 138(1), 291-311. https://doi.org/10.1016/j.jeconom.2006.05.016
Clark, T. E., & West, K. D. (2007). Approximately normal tests for equal predictive accuracy in nested models. Journal of Econometrics, 138(1), 291-311. https://doi.org/10.1016/j.jeconom.2006.05.023
Clauset, A., Newman, M. E. J., & Moore, C. (2004). Finding community structure in very large networks. Physical Review E, 70(6), 066111. https://doi.org/10.1103/PhysRevE.70.066111
Clay Mathematics Institute. (2026). Hodge Conjecture. https://www.claymath.org/millennium/hodge-conjecture/
Clemen, R. T. (1989). Combining forecasts: A review and annotated bibliography. International Journal of Forecasting, 5(4), 559-583. https://doi.org/10.1016/0169-2070(89)90012-5
Clerc, M., & Kennedy, J. (2002). The particle swarm: Explosion, stability, and convergence in a multidimensional complex space. IEEE Transactions on Evolutionary Computation, 6(1), 58-73. https://doi.org/10.1109/4235.985692
Coates, J., & Wiles, A. (1977). On the conjecture of Birch and Swinnerton-Dyer. Inventiones Mathematicae, 39, 223-251. https://doi.org/10.1007/BF01402975
Coello Coello, C. A. (2000). An updated survey of GA-based multiobjective optimization techniques. ACM Computing Surveys, 32(2), 109-143. https://doi.org/10.1145/358923.358929
Cogley, T., & Sargent, T. J. (2005). Drifts and volatilities: Monetary policies and outcomes in the post WWII U.S.. Review of Economic Dynamics, 8(2), 262-302. https://doi.org/10.1016/j.red.2004.10.009
Cohen-Steiner, D., Edelsbrunner, H., & Harer, J. (2007). Stability of persistence diagrams. Discrete & Computational Geometry, 37(1), 103-120. https://doi.org/10.1007/s00454-006-1276-5
Coibion, O., & Gorodnichenko, Y. (2015). Is the Phillips curve alive and well after all? Inflation expectations and the missing disinflation. American Economic Journal: Macroeconomics, 7(1), 197-232. https://doi.org/10.1257/mac.20130306
Coifman, R. R., & Lafon, S. (2006). Diffusion maps. Applied and Computational Harmonic Analysis, 21(1), 5-30. https://doi.org/10.1016/j.acha.2006.04.006
Combes, P.-P., Duranton, G., & Gobillon, L. (2008). Spatial wage disparities: Sorting matters! Journal of Urban Economics, 63(2), 723-742. https://doi.org/10.1016/j.jue.2007.04.004
Conley, T. G. (1999). GMM estimation with cross sectional dependence. Journal of Econometrics, 92(1), 1-45. https://doi.org/10.1016/S0304-4076(98)00084-0
Connor, G., & Korajczyk, R. A. (1986). Performance measurement with the arbitrage pricing theory: A new framework for analysis. Journal of Financial Economics, 15(3), 373-394. https://doi.org/10.1016/0304-405X(86)90027-0
Conrey, J. B. (1989). More than two fifths of the zeros of the Riemann zeta function are on the critical line. Journal für die reine und angewandte Mathematik, 399, 1-26. https://doi.org/10.1515/crll.1989.399.1
Conrey, J. B. (2003). The Riemann Hypothesis. Bulletin of the American Mathematical Society, 40(3), 341-353. https://doi.org/10.1090/S0273-0979-03-00980-3
Constantin, P., & Fefferman, C. (1993). Direction of vorticity and the problem of global regularity for the Navier-Stokes equations. Indiana University Mathematics Journal, 42(3), 775-789. https://doi.org/10.1512/iumj.1993.42.42034
Constantinides, G. M. (1986). Capital market equilibrium with transaction costs. Journal of Political Economy, 94(4), 842-862. https://doi.org/10.1086/261410
Cont, R., Moussa, A., & Santos, E. B. (2013). Network structure and systemic risk in banking systems. Mathematical Finance, 23(3), 566-584. https://doi.org/10.1111/j.1467-9965.2011.00460.x
Cooley, J. W., & Tukey, J. W. (1965). An algorithm for the machine calculation of complex Fourier series. Mathematics of Computation, 19(90), 297-301. https://doi.org/10.1090/S0025-5718-1965-0178586-1
Corak, M. (2013). Income inequality, equality of opportunity, and intergenerational mobility. Journal of Economic Perspectives, 27(3), 79-102. https://doi.org/10.1257/jep.27.3.79
Cordero-Erausquin, D., McCann, R. J., & Schmuckenschläger, M. (2001). A Riemannian interpolation inequality à la Borell, Brascamp and Lieb. Inventiones Mathematicae, 146(2), 219-257. https://doi.org/10.1007/s002220100160
Costinot, A., Vogel, J., & Wang, S. (2013). An elementary theory of global supply chains. Review of Economic Studies, 80(1), 109-144. https://doi.org/10.1093/restud/rds023
Covitz, D., Liang, N., & Suarez, G. A. (2013). The evolution of a financial crisis: Collapse of the asset-backed commercial paper market. The Journal of Finance, 68(3), 815-848. https://doi.org/10.1111/j.1540-6261.2012.01773.x

Cowell, F. A., & Flachaire, E. (2007). Income distribution and inequality measurement: The problem of extreme values. Journal of Econometrics, 141(2), 1044-1072. https://doi.org/10.1016/j.jeconom.2007.01.001
Cox, J. C., Ross, S. A., & Rubinstein, M. (1979). Option pricing: A simplified approach. Journal of Financial Economics, 7(3), 229-263. https://doi.org/10.1016/0304-405X(79)90015-1
Craighead, C. W., Blackhurst, J., Rungtusanatham, M. J., & Handfield, R. B. (2007). The severity of supply chain disruptions: Design characteristics and mitigation capabilities. Decision Sciences, 38(1), 131-156. https://doi.org/10.1111/j.1540-5915.2007.00151.x
Crama, Y., & Schyns, M. (2003). Simulated annealing for complex portfolio selection problems. European Journal of Operational Research, 150(3), 546-571. https://doi.org/10.1016/S0377-2217(02)00784-1
Creutz, M. (1980). Monte Carlo study of quantized SU(2) gauge theory. Physical Review D, 21(8), 2308-2315. https://doi.org/10.1103/PhysRevD.21.2308
Cristelli, M., Tacchella, A., & Pietronero, L. (2013). The heterogeneous dynamics of economic complexity. PLoS ONE, 8(2), e70726. https://doi.org/10.1371/journal.pone.0070726
Croux, C., Forni, M., & Reichlin, L. (2001). A measure of comovement for economic variables: Theory and empirics. Review of Economics and Statistics, 83(2), 232-241. https://doi.org/10.1162/00346530151143847
Crucitti, P., Latora, V., & Marchiori, M. (2004). Model for cascading failures in complex networks. Physical Review E, 69(4), 045104. https://doi.org/10.1103/PhysRevE.69.045104
Cura, T. (2009). Particle swarm optimization approach to portfolio optimization. Nonlinear Analysis: Real World Applications, 10(4), 2396-2406. https://doi.org/10.1016/j.nonrwa.2008.04.023
Cutter, S. L., Barnes, L., Berry, M., Burton, C., Evans, E., Tate, E., & Webb, J. (2008). A place-based model for understanding community resilience to natural disasters. Global Environmental Change, 18(4), 598-606. https://doi.org/10.1016/j.gloenvcha.2008.07.013
Dagum, C. (1997). A new approach to the decomposition of the Gini income inequality ratio. Empirical Economics, 22(4), 515-531. https://doi.org/10.1007/BF01205777
Davis, M. H. A., & Norman, A. R. (1990). Portfolio selection with transaction costs. Mathematics of Operations Research, 15(4), 676-713. https://doi.org/10.1287/moor.15.4.676
de Chaisemartin, C., & D'Haultfoeuille, X. (2020). Two-way fixed effects estimators with heterogeneous treatment effects. American Economic Review, 110(9), 2964-2996. https://doi.org/10.1257/aer.20181169
De Domenico, M., Solé-Ribalta, A., Cozzo, E., Kivelä, M., Moreno, Y., Porter, M. A., Gómez, S., & Arenas, A. (2013). Mathematical formulation of multilayer networks. Physical Review X, 3(4), 041022. https://doi.org/10.1103/PhysRevX.3.041022
De Domenico, M., Sole-Ribalta, A., Omodei, E., Gomez, S., & Arenas, A. (2015). Ranking in interconnected multilayer networks reveals versatile nodes. Nature Communications, 6, 6868. https://doi.org/10.1038/ncomms7868
De Silva, V., & Ghrist, R. (2007). Coverage in sensor networks via persistent homology. Algebraic & Geometric Topology, 7(1), 339-358. https://doi.org/10.2140/agt.2007.7.339
Deb, K., Pratap, A., Agarwal, S., & Meyarivan, T. (2002). A fast and elitist multiobjective genetic algorithm: NSGA-II. IEEE Transactions on Evolutionary Computation, 6(2), 182-197. https://doi.org/10.1109/4235.996017
Deligne, P. (1974). La conjecture de Weil: I. Publications Mathématiques de l'IHÉS, 43, 273-307. https://doi.org/10.1007/BF02684373
Deligne, P. (1980). La conjecture de Weil: II. Publications Mathématiques de l'IHÉS, 52, 137-252. https://doi.org/10.1007/BF02684780
DeLong, E. R., DeLong, D. M., & Clarke-Pearson, D. L. (1988). Comparing the areas under two or more correlated receiver operating characteristic curves. Biometrics, 44(3), 837-845. https://doi.org/10.2307/2531595
DeMiguel, V., Garlappi, L., & Uppal, R. (2009a). Optimal versus naive diversification: How inefficient is the 1/N portfolio strategy? The Review of Financial Studies, 22(5), 1915-1953. https://doi.org/10.1093/rfs/hhm075
DeMiguel, V., Garlappi, L., Nogales, F. J., & Uppal, R. (2009b). A generalized approach to portfolio optimization: Improving performance by constraining portfolio norms. Management Science, 55(5), 798-812. https://doi.org/10.1287/mnsc.1080.0986
Detragiache, E., & Spilimbergo, A. (2001). Crises and liquidity: Evidence and interpretation. IMF Staff Papers, 48(3), 1-26. https://doi.org/10.2307/4621678
DeTurck, D. M. (1983). Deforming metrics in the direction of their Ricci tensors. Journal of Differential Geometry, 18(1), 157-162. https://doi.org/10.4310/jdg/1214509286
di Giovanni, J., & Levchenko, A. A. (2010). Putting the parts together: Trade, vertical linkages, and business cycle comovement. American Economic Journal: Macroeconomics, 2(2), 95-124. https://doi.org/10.1257/mac.2.2.95
di Giovanni, J., Levchenko, A. A., & Mejean, I. (2018). The micro origins of international business-cycle comovement. American Economic Review, 108(1), 82-108. https://doi.org/10.1257/aer.20150286

Dickey, D. A., & Fuller, W. A. (1979). Distribution of the estimators for autoregressive time series with a unit root. Journal of the American Statistical Association, 74(366), 427-431. https://doi.org/10.1080/01621459.1979.10482531
Diebold, F. X., & Mariano, R. S. (1995). Comparing predictive accuracy. Journal of Business & Economic Statistics, 13(3), 253-263. https://doi.org/10.1080/07350015.1995.10524599
Diebold, F. X., & Yilmaz, K. (2014). On the network topology of variance decompositions: Measuring the connectedness of financial firms. International Journal of Forecasting, 30(1), 119-134. https://doi.org/10.1016/j.ijforecast.2013.09.007
Diebold, F. X., & Yilmaz, K. (2014). On the network topology of variance decompositions: Measuring the connectedness of financial firms. Journal of Econometrics, 182(1), 119-134. https://doi.org/10.1016/j.jeconom.2014.04.012
Djankov, S., Freund, C., & Pham, C. S. (2010). Trading on time. Review of Economics and Statistics, 92(1), 166-173. https://doi.org/10.1162/rest.2009.11498
Donaldson, D. (2018). Railroads of the Raj: Estimating the impact of transportation infrastructure. American Economic Review, 108(4-5), 899-934. https://doi.org/10.1257/aer.20101199
Donaldson, D., & Hornbeck, R. (2016). Railroads and American economic growth: A market access approach. Quarterly Journal of Economics, 131(2), 799-858. https://doi.org/10.1093/qje/qjw002
Donoho, D. L., & Grimes, C. (2003). Hessian eigenmaps: Locally linear embedding techniques for high-dimensional data. Proceedings of the National Academy of Sciences, 100(10), 5591-5596. https://doi.org/10.1073/pnas.1031596100
Doran, J., & Fingleton, B. (2016). Employment resilience in Europe and the 2008 economic crisis: Insights from micro-level data. Regional Studies, 50(4), 644-656. https://doi.org/10.1080/00343404.2014.988087
Dorigo, M., Maniezzo, V., & Colorni, A. (1996). Ant system: Optimization by a colony of cooperating agents. IEEE Transactions on Systems, Man, and Cybernetics, Part B, 26(1), 29-41. https://doi.org/10.1109/3477.484436
Dorogovtsev, S. N., Mendes, J. F. F., & Samukhin, A. N. (2000). Structure of growing networks with preferential linking. Physical Review Letters, 85(21), 4633-4636. https://doi.org/10.1103/PhysRevLett.85.4633
Drehmann, M., & Tarashev, N. (2013). Measuring the systemic importance of interconnected banks. Journal of Financial Intermediation, 22(4), 586-607. https://doi.org/10.1016/j.jfi.2013.08.001
Driscoll, J. C., & Kraay, A. C. (1998). Consistent covariance matrix estimation with spatially dependent panel data. The Review of Economics and Statistics, 80(4), 549-560. https://doi.org/10.1162/003465398557825
Ducruet, C., & Notteboom, T. (2012). The worldwide maritime network of container shipping: Spatial structure and regional dynamics. Global Networks, 12(3), 395-423. https://doi.org/10.1111/j.1471-0374.2011.00355.x
Duprey, T., Klaus, B., & Peltonen, T. (2017). Dating systemic financial stress episodes in the EU countries. Journal of Financial Stability, 32, 30-56. https://doi.org/10.1016/j.jfs.2017.07.004
Duranton, G., & Puga, D. (2001). Nursery cities: Urban diversity, process innovation, and the life cycle of products. American Economic Review, 91(5), 1454-1477. https://doi.org/10.1257/aer.91.5.1454
Durbin, J., & Koopman, S. J. (2000). Time series analysis of non-Gaussian observations based on state space models from both classical and Bayesian perspectives. Journal of the Royal Statistical Society: Series B, 62(1), 3-56. https://doi.org/10.1111/1467-9868.00218
Durlauf, S. N. (1996). A theory of persistent income inequality. Journal of Economic Growth, 1(1), 75-93. https://doi.org/10.1007/BF00163343
Eaton, J., & Kortum, S. (2002). Technology, geography, and trade. Econometrica, 70(5), 1741-1779. https://doi.org/10.1111/1468-0262.00352
Edelsbrunner, H., Letscher, D., & Zomorodian, A. (2002). Topological persistence and simplification. Discrete & Computational Geometry, 28(4), 511-533. https://doi.org/10.1007/s00454-002-2885-2
Efron, B. (1979). Bootstrap methods: Another look at the jackknife. The Annals of Statistics, 7(1), 1-26. https://doi.org/10.1214/aos/1176344552
Eichengreen, B., Mody, A., Nedeljkovic, M., & Sarno, L. (2012). How the subprime crisis went global: Evidence from bank credit default swap spreads. Journal of International Money and Finance, 31(5), 1299-1318. https://doi.org/10.1016/j.jimonfin.2012.02.002
Eisenberg, L., & Noe, T. H. (2001). Systemic risk in financial systems. Management Science, 47(2), 236-249. https://doi.org/10.1287/mnsc.47.2.236.9835
Elhorst, J. P. (2014). Spatial econometrics: From cross-sectional data to spatial panels. Springer. https://doi.org/10.1007/978-3-642-40340-8
Elliott, G., & Timmermann, A. (2008). Economic forecasting. Journal of Economic Literature, 46(1), 3-56. https://doi.org/10.1257/jel.46.1.3
Elliott, M., Golub, B., & Jackson, M. O. (2014). Financial networks and contagion. American Economic Review, 104(10), 3115-3153. https://doi.org/10.1257/aer.104.10.3115

Elsinger, H., Lehar, A., & Summer, M. (2006). Risk assessment for banking systems. Management Science, 52(9), 1301-1314. https://doi.org/10.1287/mnsc.1060.0535
Engle, R. F. (1982). Autoregressive conditional heteroscedasticity with estimates of the variance of United Kingdom inflation. Econometrica, 50(4), 987-1007. https://doi.org/10.2307/1912773
Engle, R. F. (2002). Dynamic conditional correlation: A simple class of multivariate generalized autoregressive conditional heteroskedasticity models. Journal of Business & Economic Statistics, 20(3), 339-350. https://doi.org/10.1198/073500102288618487
Engle, R. F., & Granger, C. W. J. (1987). Co-integration and error correction: Representation, estimation, and testing. Econometrica, 55(2), 251-276. https://doi.org/10.2307/1913236
Engle, R. F., & Ng, V. K. (1993). Measuring and testing the impact of news on volatility. The Journal of Finance, 48(5), 1749-1778. https://doi.org/10.1111/j.1540-6261.1993.tb05127.x
Engle, R., Jondeau, E., & Rockinger, M. (2015). Systemic risk in Europe. Review of Finance, 19(1), 145-190. https://doi.org/10.1093/rof/rfu012
Escauriaza, L., Seregin, G., & Sverak, V. (2003). L3,infinity-solutions of the Navier-Stokes equations and backward uniqueness. Russian Mathematical Surveys, 58(2), 211-250. https://doi.org/10.1070/RM2003v058n02ABEH000609
Fagiolo, G., Reyes, J., & Schiavo, S. (2008). On the topological properties of the world trade web: A weighted network analysis. Journal of Evolutionary Economics, 20(4), 479-514. https://doi.org/10.1007/s00191-008-0114-4
Fagiolo, G., Reyes, J., & Schiavo, S. (2010). The evolution of the world trade web: A weighted-network analysis. Physica A: Statistical Mechanics and Its Applications, 389(21), 4795-4817. https://doi.org/10.1016/j.physa.2010.07.001
Fair, R. C., & Shiller, R. J. (1990). Comparing information in forecasts from econometric models. American Economic Review, 80(3), 375-389. https://doi.org/10.2307/2006664
Fally, T. (2015). Structural gravity and fixed effects. Journal of International Economics, 97(1), 76-85. https://doi.org/10.1016/j.jinteco.2015.05.005
Fama, E. F. (1970). Efficient capital markets: A review of theory and empirical work. The Journal of Finance, 25(2), 383-417. https://doi.org/10.1111/j.1540-6261.1970.tb00518.x
Fama, E. F., & French, K. R. (1992). The cross-section of expected stock returns. The Journal of Finance, 47(2), 427-465. https://doi.org/10.1111/j.1540-6261.1992.tb04398.x
Fama, E. F., & French, K. R. (1993). Common risk factors in the returns on stocks and bonds. Journal of Financial Economics, 33(1), 3-56. https://doi.org/10.1016/0304-405X(93)90023-5
Fama, E. F., & French, K. R. (2004). The capital asset pricing model: Theory and evidence. Journal of Economic Perspectives, 18(3), 25-46. https://doi.org/10.1257/0895330042162430
Fan, J., Fan, Y., & Lv, J. (2008). High dimensional covariance matrix estimation using a factor model. Journal of Econometrics, 147(1), 186-197. https://doi.org/10.1016/j.jeconom.2008.09.017
Fan, J., Zhang, J., & Yu, K. (2012). Vast portfolio selection with gross-exposure constraints. Journal of the American Statistical Association, 107(498), 592-606. https://doi.org/10.1198/jasa.2011.tm10563
Fawcett, T. (2006). An introduction to ROC analysis. Pattern Recognition Letters, 27(8), 861-874. https://doi.org/10.1016/j.patrec.2005.10.010
Fiedler, M. (1973). Algebraic connectivity of graphs. Czechoslovak Mathematical Journal, 23(2), 298-305. https://doi.org/10.21136/CMJ.1973.101168
Fiedler, M. (1975). A property of eigenvectors of nonnegative symmetric matrices and its application to graph theory. Czechoslovak Mathematical Journal, 25(4), 619-633. https://doi.org/10.21136/CMJ.1975.101357
Fiksel, J., Polyviou, M., Croxton, K. L., & Pettit, T. J. (2015). From risk to resilience: Learning to deal with disruption. MIT Sloan Management Review, 56(2), 79-86. https://doi.org/10.2139/ssrn.2538082
Filardo, A. J. (1994). Business-cycle phases and their transitional dynamics. Journal of Business & Economic Statistics, 12(3), 299-308. https://doi.org/10.1080/07350015.1994.10524542
Fischer, S. (1993). The role of macroeconomic factors in growth. Journal of Monetary Economics, 32(3), 485-512. https://doi.org/10.1016/0304-3932(93)90027-D
Fisher, M. L. (1981). The Lagrangian relaxation method for solving integer programming problems. Management Science, 27(1), 1-18. https://doi.org/10.1287/mnsc.27.1.1
Fleming, J., Kirby, C., & Ostdiek, B. (2001). The economic value of volatility timing. The Journal of Finance, 56(1), 329-352. https://doi.org/10.1111/0022-1082.00327
Foerster, A. T., Sarte, P.-D. G., & Watson, M. W. (2011). Sectoral versus aggregate shocks: A structural factor analysis of industrial production. Journal of Political Economy, 119(1), 1-38. https://doi.org/10.1086/659311
Foias, C., & Temam, R. (1989). Gevrey class regularity for the solutions of the Navier-Stokes equations. Journal of Functional Analysis, 87(2), 359-369. https://doi.org/10.1016/0022-1236(89)90015-3
Forbes, K. J. (2019). Has globalization changed the inflation process?. Journal of International Economics, 119, S1-S13. https://doi.org/10.1016/j.jinteco.2018.12.002

Forbes, K. J., & Rigobon, R. (2002). No contagion, only interdependence: Measuring stock market comovements. The Journal of Finance, 57(5), 2223-2261. https://doi.org/10.1111/0022-1082.00494
Forman, R. (2003). Bochner's method for cell complexes and combinatorial Ricci curvature. Discrete & Computational Geometry, 29(3), 323-374. https://doi.org/10.1007/s00454-002-0743-x
Forni, M., Hallin, M., Lippi, M., & Reichlin, L. (2000). The generalized dynamic-factor model: Identification and estimation. Review of Economics and Statistics, 82(4), 540-554. https://doi.org/10.1162/003465300559037
Fortnow, L. (2009). The status of the P versus NP problem. Communications of the ACM, 52(9), 78-86. https://doi.org/10.1145/1562164.1562186
Fortunato, S. (2010). Community detection in graphs. Physics Reports, 486(3-5), 75-174. https://doi.org/10.1016/j.physrep.2009.11.002
Foster, J., Greer, J., & Thorbecke, E. (1984). A class of decomposable poverty measures. Econometrica, 52(3), 761-766. https://doi.org/10.2307/1913475
Frangioni, A., & Gentile, C. (2006). Perspective cuts for a class of convex 0-1 mixed integer programs. Mathematical Programming, 106, 225-236. https://doi.org/10.1007/s10107-005-0594-3
Frankel, J. A., & Romer, D. (1999). Does trade cause growth? American Economic Review, 89(3), 379-399. https://doi.org/10.1257/aer.89.3.379
Freeman, L. C. (1977). A set of measures of centrality based on betweenness. Sociometry, 40(1), 35-41. https://doi.org/10.2307/3033543
Freeman, L. C. (1978). Centrality in social networks: Conceptual clarification. Social Networks, 1(3), 215-239. https://doi.org/10.1016/0378-8733(78)90021-7
Friedman, J. H. (2001). Greedy function approximation: A gradient boosting machine. Annals of Statistics, 29(5), 1189-1232. https://doi.org/10.1214/aos/1013203451
Gabaix, X. (2011). The granular origins of aggregate fluctuations. Econometrica, 79(3), 733-772. https://doi.org/10.3982/ECTA8769
Gai, P., & Kapadia, S. (2010). Contagion in financial networks. Proceedings of the Royal Society A, 466(2120), 2401-2423. https://doi.org/10.1098/rspa.2009.0410
Galí, J., & Gertler, M. (1999). Inflation dynamics: A structural econometric analysis. Journal of Monetary Economics, 44(2), 195-222. https://doi.org/10.1016/S0304-3932(99)00023-9
Galí, J., Gertler, M., & López-Salido, J. D. (2005). Robustness of the estimates of the hybrid New Keynesian Phillips curve. Journal of Monetary Economics, 52(6), 1107-1118. https://doi.org/10.1016/j.jmoneco.2005.08.005
Gao, J., Buldyrev, S. V., Stanley, H. E., & Havlin, S. (2011). Networks formed from interdependent networks. Nature Physics, 8, 40-48. https://doi.org/10.1038/nphys2180
Garlaschelli, D., & Loffredo, M. I. (2004). Fitness-dependent topological properties of the world trade web. Physical Review Letters, 93(18), 188701. https://doi.org/10.1103/PhysRevLett.93.188701
Gelfand, A. E., & Smith, A. F. M. (1990). Sampling-based approaches to calculating marginal densities. Journal of the American Statistical Association, 85(410), 398-409. https://doi.org/10.1080/01621459.1990.10476213
Geoffrion, A. M. (1972). Generalized Benders decomposition. Journal of Optimization Theory and Applications, 10, 237-260. https://doi.org/10.1007/BF00934810
Georg, C. P. (2013). The effect of the interbank network structure on contagion and common shocks. Journal of Banking & Finance, 37(7), 2216-2228. https://doi.org/10.1016/j.jbankfin.2013.02.032
Gertler, M., & Karadi, P. (2015). Monetary policy surprises, credit costs, and economic activity. American Economic Journal: Macroeconomics, 7(1), 44-76. https://doi.org/10.1257/mac.20130329
Ghrist, R. (2008). Barcodes: The persistent topology of data. Bulletin of the American Mathematical Society, 45(1), 61-75. https://doi.org/10.1090/S0273-0979-07-01191-3
Giacomini, R., & White, H. (2006). Tests of conditional predictive ability. Econometrica, 74(6), 1545-1578. https://doi.org/10.1111/j.1468-0262.2006.00690.x
Giacomini, R., & White, H. (2006). Tests of conditional predictive ability. Econometrica, 74(6), 1545-1578. https://doi.org/10.1111/j.1468-0262.2006.00718.x
Giannakis, E., & Bruggeman, A. (2017). Economic crisis and regional resilience: Evidence from Greece. Papers in Regional Science, 96(3), 451-476. https://doi.org/10.1111/pirs.12206
Giglio, S., Kelly, B., & Pruitt, S. (2016). Systemic risk and the macroeconomy: An empirical evaluation. Journal of Financial Economics, 119(3), 457-471. https://doi.org/10.1016/j.jfineco.2016.02.001
Girvan, M., & Newman, M. E. J. (2002). Community structure in social and biological networks. Proceedings of the National Academy of Sciences, 99(12), 7821-7826. https://doi.org/10.1073/pnas.122653799
Giusti, C., Ghrist, R., & Bassett, D. S. (2016). Two's company, three (or more) is a simplex. Journal of Computational Neuroscience, 41(1), 1-14. https://doi.org/10.1007/s10827-016-0608-6
Glaeser, E. L., Kallal, H. D., Scheinkman, J. A., & Shleifer, A. (1992). Growth in cities. Journal of Political Economy, 100(6), 1126-1152. https://doi.org/10.1086/261856

Glasserman, P., & Young, H. P. (2015). How likely is contagion in financial networks? Journal of Banking & Finance, 50, 383-399. https://doi.org/10.1016/j.jbankfin.2014.02.006
Glasserman, P., & Young, H. P. (2015). How likely is contagion in financial networks?. Journal of Banking & Finance, 50, 383-399. https://doi.org/10.1016/j.jbankfin.2014.10.006
Glosten, L. R., & Milgrom, P. R. (1985). Bid, ask and transaction prices in a specialist market with heterogeneously informed traders. Journal of Financial Economics, 14(1), 71-100. https://doi.org/10.1016/0304-405X(85)90044-3
Glosten, L. R., Jagannathan, R., & Runkle, D. E. (1993). On the relation between the expected value and the volatility of the nominal excess return on stocks. The Journal of Finance, 48(5), 1779-1801. https://doi.org/10.1111/j.1540-6261.1993.tb05128.x
Glover, F. (1986). Future paths for integer programming and links to artificial intelligence. Computers & Operations Research, 13(5), 533-549. https://doi.org/10.1016/0305-0548(86)90048-1
Glover, F. (1989). Tabu search - Part I. ORSA Journal on Computing, 1(3), 190-206. https://doi.org/10.1287/ijoc.1.3.190
Glover, F. (1990). Tabu search - Part II. ORSA Journal on Computing, 2(1), 4-32. https://doi.org/10.1287/ijoc.2.1.4
Gneiting, T., & Raftery, A. E. (2007). Strictly proper scoring rules, prediction, and estimation. Journal of the American Statistical Association, 102(477), 359-378. https://doi.org/10.1198/016214506000001437
Godfrey, L. G. (1978). Testing against general autoregressive and moving average error models when the regressors include lagged dependent variables. Econometrica, 46(6), 1293-1301. https://doi.org/10.2307/1913829
Goldfarb, D., & Idnani, A. (1983). A numerically stable dual method for solving strictly convex quadratic programs. Mathematical Programming, 27, 1-33. https://doi.org/10.1007/BF02591962
Gómez, S., Díaz-Guilera, A., Gómez-Gardeñes, J., Pérez-Vicente, C. J., Moreno, Y., & Arenas, A. (2013). Diffusion dynamics on multiplex networks. Physical Review Letters, 110(2), 028701. https://doi.org/10.1103/PhysRevLett.110.028701
Gomory, R. E. (1958). Outline of an algorithm for integer solutions to linear programs. Bulletin of the American Mathematical Society, 64(5), 275-278. https://doi.org/10.1090/S0002-9904-1958-10224-4
Gondauri, D. (2026). Data and Replication Package for "Global Perelman-Ricci-Poincare-Inspired Inequality Diagnostics: Curvature, Entropy and Graph-Topological Modelling of Macro-Regional Pressure and Smoothing Capacity" [Data set]. Zenodo. https://doi.org/10.5281/zenodo.20844900
Gondauri, D. (2026). Data and Replication Package for "Global Riemann-Zeta FPAS+ζ Inflation Forecasting: Layered Annual, Quarterly and Monthly Validation of a Hybrid Global Macroeconomic Model" (Version v1) [Data set]. Zenodo. https://doi.org/10.5281/zenodo.20852478
Gondauri, D. (2026). Dataset and Replication Package for "Economic Yang-Mills Mass Gap in Global and Corridor Flow Networks: A Finite-Network Gauge-Econometric Framework for Measuring Systemic Shock Thresholds" (Version v1) [Data set]. Zenodo. https://doi.org/10.5281/zenodo.20786199
Gondauri, D. (2026). Dataset Package for Robust Portfolio Optimization under Computational Complexity: A P-vs-NP-Inspired Markowitz-CAPM Framework with Cardinality Constraints and Black-Scholes Derivative-Pricing Overlay [Data set]. Zenodo. https://doi.org/10.5281/zenodo.20922272
Gondauri, D. (2026). Navier-Stokes-Inspired Global Liquidity-Flow and Systemic-Stress Modelling: Data and Replication Package for a Nondimensional Macro-Financial Stress-Testing Framework [Data set]. Zenodo. https://doi.org/10.5281/zenodo.20835729
Gondauri, D. (2026). Regional Economic Birch-Swinnerton-Dyer Modelling: Data and Replication Package for a Local-to-Global Framework of Structural Rank Formation, Corridor Stress and World-Economy Calibration [Data set]. Zenodo. https://doi.org/10.5281/zenodo.20796984
Gondauri, D. (2026). Replication Package for "Global Hodge-Econometric Modeling of the World Economy: A Regional Benchmark Prototype for Topological Flow Decomposition, Systemic Circulation, Shock Transmission, and Macroeconomic Resilience". Zenodo. https://doi.org/10.5281/zenodo.20774659
Gonek, S. M., Hughes, C. P., & Keating, J. P. (2007). A hybrid Euler-Hadamard product for the Riemann zeta function. Duke Mathematical Journal, 136(3), 507-549. https://doi.org/10.1215/S0012-7094-07-13634-6
Gopinath, G., Itskhoki, O., & Rigobon, R. (2010). Currency choice and exchange rate pass-through. American Economic Review, 100(1), 304-336. https://doi.org/10.1257/aer.100.1.304
Gorton, G., & Metrick, A. (2012). Securitized banking and the run on repo. Journal of Financial Economics, 104(3), 425-451. https://doi.org/10.1016/j.jfineco.2011.03.016
Goyenko, R. Y., Holden, C. W., & Trzcinka, C. A. (2009). Do liquidity measures measure liquidity? Journal of Financial Economics, 92(2), 153-181. https://doi.org/10.1016/j.jfineco.2008.06.002
Granger, C. W. J. (1966). The typical spectral shape of an economic variable. Econometrica, 34(1), 150-161. https://doi.org/10.2307/1909859
Granger, C. W. J. (1969). Investigating causal relations by econometric models and cross-spectral methods. Econometrica, 37(3), 424-438. https://doi.org/10.2307/1912791

Granger, C. W. J., & Newbold, P. (1974). Spurious regressions in econometrics. Journal of Econometrics, 2(2), 111-120. https://doi.org/10.1016/0304-4076(74)90034-7
Greenwood, R., Landier, A., & Thesmar, D. (2015). Vulnerable banks. Journal of Financial Economics, 115(3), 471-485. https://doi.org/10.1016/j.jfineco.2014.11.006
Gribov, V. N. (1978). Quantization of non-Abelian gauge theories. Nuclear Physics B, 139(1-2), 1-19. https://doi.org/10.1016/0550-3213(78)90175-X
Griffiths, P. A. (1969a). On the periods of certain rational integrals: I. Annals of Mathematics, 90(3), 460-495. https://doi.org/10.2307/1970585
Griffiths, P. A. (1969b). On the periods of certain rational integrals: II. Annals of Mathematics, 90(3), 496-541. https://doi.org/10.2307/1970586
Grinsted, A., Moore, J. C., & Jevrejeva, S. (2004). Application of the cross wavelet transform and wavelet coherence to geophysical time series. Nonlinear Processes in Geophysics, 11(5/6), 561-566. https://doi.org/10.5194/npg-11-561-2004
Gross, B. H., & Zagier, D. B. (1986). Heegner points and derivatives of L-series. Inventiones Mathematicae, 84, 225-320. https://doi.org/10.1007/BF01388809
Gross, D. J., & Wilczek, F. (1973). Ultraviolet behavior of non-Abelian gauge theories. Physical Review Letters, 30(26), 1343-1346. https://doi.org/10.1103/PhysRevLett.30.1343
Grossman, G. M., & Helpman, E. (1991). Quality ladders in the theory of growth. Review of Economic Studies, 58(1), 43-61. https://doi.org/10.2307/2298044
Günlük, O., & Linderoth, J. (2010). Perspective reformulations of mixed integer nonlinear programs with indicator variables. Mathematical Programming, 124, 183-205. https://doi.org/10.1007/s10107-010-0360-z
Haldane, A. G., & May, R. M. (2011). Systemic risk in banking ecosystems. Nature, 469(7330), 351-355. https://doi.org/10.1038/nature09659
Hamilton, J. D. (1989). A new approach to the economic analysis of nonstationary time series and the business cycle. Econometrica, 57(2), 357-384. https://doi.org/10.2307/1912559
Hamilton, J. D. (2009). Causes and consequences of the oil shock of 2007-08. Brookings Papers on Economic Activity, 2009(1), 215-261. https://doi.org/10.1353/eca.0.0049
Hamilton, R. S. (1982). Three-manifolds with positive Ricci curvature. Journal of Differential Geometry, 17(2), 255-306. https://doi.org/10.4310/jdg/1214436922
Hamilton, R. S. (1986). Four-manifolds with positive curvature operator. Journal of Differential Geometry, 24(2), 153-179. https://doi.org/10.4310/jdg/1214440433
Hamilton, R. S. (1993). Eternal solutions to the Ricci flow. Journal of Differential Geometry, 38(1), 1-11. https://doi.org/10.4310/jdg/1214454093
Hanley, J. A., & McNeil, B. J. (1982). The meaning and use of the area under a receiver operating characteristic curve. Radiology, 143(1), 29-36. https://doi.org/10.1148/radiology.143.1.7063747
Hansen, B. E. (1999). Threshold effects in non-dynamic panels: Estimation, testing, and inference. Journal of Econometrics, 93(2), 345-368. https://doi.org/10.1016/S0304-4076(99)00025-1
Hansen, B. E. (2000). Sample splitting and threshold estimation. Econometrica, 68(3), 575-603. https://doi.org/10.1111/1468-0262.00124
Hansen, L. P. (1982). Large sample properties of generalized method of moments estimators. Econometrica, 50(4), 1029-1054. https://doi.org/10.2307/1912775
Hansen, N., & Ostermeier, A. (2001). Completely derandomized self-adaptation in evolution strategies. Evolutionary Computation, 9(2), 159-195. https://doi.org/10.1162/106365601750190398
Hansen, P. R. (2005). A test for superior predictive ability. Journal of Business & Economic Statistics, 23(4), 365-380. https://doi.org/10.1198/073500104000000244
Hansen, P. R. (2005). A test for superior predictive ability. Journal of Business & Economic Statistics, 23(4), 365-380. https://doi.org/10.1198/073500105000000063
Hanson, S. G., Kashyap, A. K., & Stein, J. C. (2011). A macroprudential approach to financial regulation. Journal of Economic Perspectives, 25(1), 3-28. https://doi.org/10.1257/jep.25.1.3
Hanushek, E. A., & Woessmann, L. (2012). Do better schools lead to more growth? Cognitive skills, economic outcomes, and causation. Journal of Economic Growth, 17(4), 267-321. https://doi.org/10.1007/s10887-012-9081-x
Harvey, D., Leybourne, S., & Newbold, P. (1997). Testing the equality of prediction mean squared errors. International Journal of Forecasting, 13(2), 281-291. https://doi.org/10.1016/S0169-2070(96)00719-4
Hasbrouck, J., & Seppi, D. J. (2001). Common factors in prices, order flows, and liquidity. Journal of Financial Economics, 59(3), 383-411. https://doi.org/10.1016/S0304-405X(00)00091-X
Hastings, W. K. (1970). Monte Carlo sampling methods using Markov chains and their applications. Biometrika, 57(1), 97-109. https://doi.org/10.1093/biomet/57.1.97

Hausman, J. A. (1978). Specification tests in econometrics. Econometrica, 46(6), 1251-1271. https://doi.org/10.2307/1913827
Hausmann, R., & Hidalgo, C. A. (2011). The network structure of economic output. Journal of Economic Growth, 16(4), 309-342. https://doi.org/10.1007/s10887-011-9071-4
Hausmann, R., & Hidalgo, C. A. (2011). The network structure of economic output. PLoS ONE, 6(7), e0016458. https://doi.org/10.1371/journal.pone.0016458
Heckman, J. J. (1979). Sample selection bias as a specification error. Econometrica, 47(1), 153-161. https://doi.org/10.2307/1912352
Helpman, E., Melitz, M., & Rubinstein, Y. (2008). Estimating trade flows: Trading partners and trading volumes. Quarterly Journal of Economics, 123(2), 441-487. https://doi.org/10.1162/qjec.2008.123.2.441
Henderson, J. V., Kuncoro, A., & Turner, M. (1995). Industrial development in cities. Journal of Political Economy, 103(5), 1067-1090. https://doi.org/10.1086/262020
Hesse, M., & Rodrigue, J. P. (2004). The transport geography of logistics and freight distribution. Journal of Transport Geography, 12(3), 171-184. https://doi.org/10.1016/j.jtrangeo.2003.12.004
Heston, S. L. (1993). A closed-form solution for options with stochastic volatility with applications to bond and currency options. The Review of Financial Studies, 6(2), 327-343. https://doi.org/10.1093/rfs/6.2.327
Hidalgo, C. A., & Hausmann, R. (2009). The building blocks of economic complexity. Proceedings of the National Academy of Sciences, 106(26), 10570-10575. https://doi.org/10.1073/pnas.0900943106
Hidalgo, C. A., Klinger, B., Barabási, A.-L., & Hausmann, R. (2007). The product space conditions the development of nations. Science, 317(5837), 482-487. https://doi.org/10.1126/science.1144581
Hilscher, J., & Nosbusch, Y. (2010). Determinants of sovereign risk: Macroeconomic fundamentals and the pricing of sovereign debt. Review of Finance, 14(2), 235-262. https://doi.org/10.1093/rof/rfq005
Hoerl, A. E., & Kennard, R. W. (1970). Ridge regression: Biased estimation for nonorthogonal problems. Technometrics, 12(1), 55-67. https://doi.org/10.1080/00401706.1970.10488634
Holling, C. S. (1973). Resilience and stability of ecological systems. Annual Review of Ecology and Systematics, 4, 1-23. https://doi.org/10.1146/annurev.es.04.110173.000245
Horak, D., & Jost, J. (2013). Spectra of combinatorial Laplace operators on simplicial complexes. Advances in Mathematics, 244, 303-336. https://doi.org/10.1016/j.aim.2013.05.007
Horak, D., Maletić, S., & Rajković, M. (2009). Persistent homology of complex networks. Journal of Statistical Mechanics: Theory and Experiment, 2009(03), P03034. https://doi.org/10.1088/1742-5468/2009/03/P03034
Hosseini, S., Barker, K., & Ramirez-Marquez, J. E. (2016). A review of definitions and measures of system resilience. Reliability Engineering & System Safety, 145, 47-61. https://doi.org/10.1016/j.ress.2015.08.006
Hotelling, H. (1933). Analysis of a complex of statistical variables into principal components. Journal of Educational Psychology, 24(6), 417-441. https://doi.org/10.1037/h0071325
Hummels, D., & Schaur, G. (2013). Time as a trade barrier. American Economic Review, 103(7), 2935-2959. https://doi.org/10.1257/aer.103.7.2935
Hummels, D., Ishii, J., & Yi, K.-M. (2001). The nature and growth of vertical specialization in world trade. Journal of International Economics, 54(1), 75-96. https://doi.org/10.1016/S0022-1996(00)00093-3
Hyndman, R. J., & Koehler, A. B. (2006). Another look at measures of forecast accuracy. International Journal of Forecasting, 22(4), 679-688. https://doi.org/10.1016/j.ijforecast.2006.03.001
Ibragimov, R., & Muller, U. K. (2010). t-Statistic based correlation and heterogeneity robust inference. Journal of Business & Economic Statistics, 28(4), 453-468. https://doi.org/10.1198/jbes.2009.08046
Imai, K., Keele, L., & Tingley, D. (2010). A general approach to causal mediation analysis. Statistical Science, 25(1), 51-71. https://doi.org/10.1214/10-STS321
Imbens, G. W., & Angrist, J. D. (1994). Identification and estimation of local average treatment effects. Econometrica, 62(2), 467-475. https://doi.org/10.2307/2951620
Imbens, G. W., & Kolesar, M. (2016). Robust standard errors in small samples: Some practical advice. The Review of Economics and Statistics, 98(4), 701-712. https://doi.org/10.1162/REST_a_00552
Imbens, G. W., & Wooldridge, J. M. (2009). Recent developments in the econometrics of program evaluation. Journal of Economic Literature, 47(1), 5-86. https://doi.org/10.1257/jel.47.1.5
Impagliazzo, R., & Paturi, R. (2001). On the complexity of k-SAT. Journal of Computer and System Sciences, 62(2), 367-375. https://doi.org/10.1006/jcss.2000.1727
Iori, G., Jafarey, S., & Padilla, F. G. (2006). Systemic risk on the interbank market. Journal of Economic Behavior & Organization, 61(4), 525-542. https://doi.org/10.1016/j.jebo.2004.07.018
Ishizaka, A., & Labib, A. (2011). Review of the main developments in the analytic hierarchy process. Expert Systems with Applications, 38(11), 14336-14345. https://doi.org/10.1016/j.eswa.2011.04.143
Ivanov, D. (2020). Predicting the impacts of epidemic outbreaks on global supply chains: A simulation-based analysis on the coronavirus outbreak. Transportation Research Part E, 136, 101922. https://doi.org/10.1016/j.tre.2020.101922

Ivanov, D., & Dolgui, A. (2020). Viability of intertwined supply networks: Extending the supply chain resilience angles towards survivability. International Journal of Production Research, 58(10), 2904-2915. https://doi.org/10.1080/00207543.2020.1750727
Jagannathan, R., & Ma, T. (2003). Risk reduction in large portfolios: Why imposing the wrong constraints helps. The Journal of Finance, 58(4), 1651-1683. https://doi.org/10.1111/1540-6261.00580
Jarque, C. M., & Bera, A. K. (1980). Efficient tests for normality, homoscedasticity and serial independence of regression residuals. Economics Letters, 6(3), 255-259. https://doi.org/10.1016/0165-1765(80)90024-5
Jeanne, O., & Masson, P. (2000). Currency crises, sunspots and Markov-switching regimes. Journal of International Economics, 50(2), 327-350. https://doi.org/10.1016/S0022-1996(99)00050-2
Jenkins, S. P., & Van Kerm, P. (2005). Accounting for income distribution trends: A density function decomposition approach. Journal of Economic Inequality, 3(1), 43-61. https://doi.org/10.1007/s10888-004-8309-1
Jensen, M. C. (1968). The performance of mutual funds in the period 1945-1964. The Journal of Finance, 23(2), 389-416. https://doi.org/10.1111/j.1540-6261.1968.tb00815.x
Jiang, X., Lim, L.-H., Yao, Y., & Ye, Y. (2011). Statistical ranking and combinatorial Hodge theory. Mathematical Programming, 127(1), 203-244. https://doi.org/10.1007/s10107-010-0419-x
Jobson, J. D., & Korkie, B. M. (1981). Performance hypothesis testing with the Sharpe and Treynor measures. The Journal of Finance, 36(4), 889-908. https://doi.org/10.1111/j.1540-6261.1981.tb02661.x
Johansen, S. (1988). Statistical analysis of cointegration vectors. Journal of Economic Dynamics and Control, 12(2-3), 231-254. https://doi.org/10.1016/0165-1889(88)90041-3
Johnson, R. C. (2014). Five facts about value-added exports and implications for macroeconomics and trade research. Journal of Economic Perspectives, 28(2), 119-142. https://doi.org/10.1257/jep.28.2.119
Johnson, R. C., & Noguera, G. (2012). Accounting for intermediates: Production sharing and trade in value added. Journal of International Economics, 86(2), 224-236. https://doi.org/10.1016/j.jinteco.2011.10.003
Jolliffe, I. T., & Cadima, J. (2016). Principal component analysis: A review and recent developments. Philosophical Transactions of the Royal Society A, 374(2065), 20150202. https://doi.org/10.1098/rsta.2015.0202
Jones, D. F., Mirrazavi, S. K., & Tamiz, M. (2002). Multi-objective meta-heuristics: An overview of the current state-of-the-art. European Journal of Operational Research, 137(1), 1-9. https://doi.org/10.1016/S0377-2217(01)00123-0
Jordà, Ò. (2005). Estimation and inference of impulse responses by local projections. American Economic Review, 95(1), 161-182. https://doi.org/10.1257/0002828053828518
Jordà, Ò., Schularick, M., & Taylor, A. M. (2013). When credit bites back. Journal of Money, Credit and Banking, 45(s2), 3-28. https://doi.org/10.1111/jmcb.12069
Jorda, O., Schularick, M., & Taylor, A. M. (2015). Leveraged bubbles. Journal of Monetary Economics, 76(S), S1-S20. https://doi.org/10.1016/j.jmoneco.2015.08.005
Juttner, U., Peck, H., & Christopher, M. (2003). Supply chain risk management: Outlining an agenda for future research. International Journal of Logistics Research and Applications, 6(4), 197-210. https://doi.org/10.1080/1367556031000162701 6
Kali, R., & Reyes, J. (2007). The architecture of globalization: A network approach to international economic integration. Journal of International Business Studies, 38(4), 595-620. https://doi.org/10.1057/palgrave.jibs.8400346
Kalman, R. E. (1960). A new approach to linear filtering and prediction problems. Journal of Basic Engineering, 82(1), 35-45. https://doi.org/10.1115/1.3662552
Kamalahmadi, M., & Parast, M. M. (2016). A review of the literature on the principles of enterprise and supply chain resilience. International Journal of Production Economics, 171, 116-133. https://doi.org/10.1016/j.ijpe.2015.10.023
Kaminsky, G. L., & Reinhart, C. M. (1999). The twin crises: The causes of banking and balance-of-payments problems. American Economic Review, 89(3), 473-500. https://doi.org/10.1257/aer.89.3.473
Kaminsky, G., Lizondo, S., & Reinhart, C. M. (1998). Leading indicators of currency crises. IMF Staff Papers, 45(1), 1-48. https://doi.org/10.2307/3867328
Kato, T. (1984). Strong Lp-solutions of the Navier-Stokes equation in Rm, with applications to weak solutions. Mathematische Zeitschrift, 187, 471-480. https://doi.org/10.1007/BF01174182
Keating, J. P., & Snaith, N. C. (2000). Random matrix theory and ζ(1/2 + it). Communications in Mathematical Physics, 214(1), 57-89. https://doi.org/10.1007/s002200000261
Kelejian, H. H., & Prucha, I. R. (1998). A generalized spatial two-stage least squares procedure for estimating a spatial autoregressive model with autoregressive disturbances. Journal of Real Estate Finance and Economics, 17(1), 99-121. https://doi.org/10.1023/A:1007707430416
Kellerer, H., Mansini, R., & Speranza, M. G. (2000). Selecting portfolios with fixed costs and minimum transaction lots. Annals of Operations Research, 99, 287-304. https://doi.org/10.1023/A:1019279918596
Kilian, L. (1998). Small-sample confidence intervals for impulse response functions. Review of Economics and Statistics, 80(2), 218-230. https://doi.org/10.1162/003465398557465

Kilian, L. (2009). Not all oil price shocks are alike: Disentangling demand and supply shocks in the crude oil market. American Economic Review, 99(3), 1053-1069. https://doi.org/10.1257/aer.99.3.1053
Kilian, L., & Murphy, D. P. (2014). The role of inventories and speculative trading in the global market for crude oil. Journal of Applied Econometrics, 29(3), 454-478. https://doi.org/10.1002/jae.2322
Kim, C.-J. (1994). Dynamic linear models with Markov-switching. Journal of Econometrics, 60(1-2), 1-22. https://doi.org/10.1016/0304-4076(94)90036-1
Kirkpatrick, S., Gelatt, C. D., & Vecchi, M. P. (1983). Optimization by simulated annealing. Science, 220(4598), 671-680. https://doi.org/10.1126/science.220.4598.671
Kivelä, M., Arenas, A., Barthelemy, M., Gleeson, J. P., Moreno, Y., & Porter, M. A. (2014). Multilayer networks. Journal of Complex Networks, 2(3), 203-271. https://doi.org/10.1093/comnet/cnu016
Kiyotaki, N., & Moore, J. (1997). Credit cycles. Journal of Political Economy, 105(2), 211-248. https://doi.org/10.1086/262072
Kleinberg, J. M. (2000). Navigation in a small world. Nature, 406, 845. https://doi.org/10.1038/35022643
Kleiner, B., & Lott, J. (2008). Notes on Perelman's papers. Geometry & Topology, 12(5), 2587-2855. https://doi.org/10.2140/gt.2008.12.2587
Knowles, J. D., & Corne, D. W. (2000). Approximating the nondominated front using the Pareto archived evolution strategy. Evolutionary Computation, 8(2), 149-172. https://doi.org/10.1162/106365600568167
Koenker, R., & Bassett, G., Jr. (1978). Regression quantiles. Econometrica, 46(1), 33-50. https://doi.org/10.2307/1913643
Kogut, J. B., & Susskind, L. (1975). Hamiltonian formulation of Wilson's lattice gauge theories. Physical Review D, 11(2), 395-408. https://doi.org/10.1103/PhysRevD.11.395
Kolmogorov, A. N. (1991). The local structure of turbulence in incompressible viscous fluid for very large Reynolds numbers. Proceedings of the Royal Society A, 434(1890), 9-13. https://doi.org/10.1098/rspa.1991.0075
Konno, H., & Yamazaki, H. (1991). Mean-absolute deviation portfolio optimization model and its applications to Tokyo stock market. Management Science, 37(5), 519-531. https://doi.org/10.1287/mnsc.37.5.519
Koop, G., Pesaran, M. H., & Potter, S. M. (1996). Impulse response analysis in nonlinear multivariate models. Journal of Econometrics, 74(1), 119-147. https://doi.org/10.1016/0304-4076(95)01753-4
Koopman, R., Wang, Z., & Wei, S.-J. (2014). Tracing value-added and double counting in gross exports. American Economic Review, 104(2), 459-494. https://doi.org/10.1257/aer.104.2.459
Korpi, W., & Palme, J. (1998). The paradox of redistribution and strategies of equality: Welfare state institutions, inequality, and poverty in the Western countries. American Sociological Review, 63(5), 661-687. https://doi.org/10.2307/2657333
Krugman, P. (1991). Increasing returns and economic geography. Journal of Political Economy, 99(3), 483-499. https://doi.org/10.1086/261763
Kupiec, P. H. (1995). Techniques for verifying the accuracy of risk measurement models. The Journal of Derivatives, 3(2), 73-84. https://doi.org/10.3905/jod.1995.407942
Kwiatkowski, D., Phillips, P. C. B., Schmidt, P., & Shin, Y. (1992). Testing the null hypothesis of stationarity against the alternative of a unit root. Journal of Econometrics, 54(1-3), 159-178. https://doi.org/10.1016/0304-4076(92)90104-Y
Kyle, A. S. (1985). Continuous auctions and insider trading. Econometrica, 53(6), 1315-1335. https://doi.org/10.2307/1913210
Laeven, L., & Valencia, F. (2013). Systemic banking crises database. IMF Economic Review, 61(2), 225-270. https://doi.org/10.1057/imfer.2013.12
Lakner, C., & Milanovic, B. (2016). Global income distribution: From the fall of the Berlin Wall to the Great Recession. The World Bank Economic Review, 30(2), 203-232. https://doi.org/10.1093/wber/lhv039
Laloux, L., Cizeau, P., Bouchaud, J.-P., & Potters, M. (1999). Noise dressing of financial correlation matrices. Physical Review Letters, 83(7), 1467-1470. https://doi.org/10.1103/PhysRevLett.83.1467
Lambiotte, R., Rosvall, M., & Scholtes, I. (2019). From networks to optimal higher-order models of complex systems. Nature Physics, 15(4), 313-320. https://doi.org/10.1038/s41567-019-0459-y
Land, A. H., & Doig, A. G. (1960). An automatic method of solving discrete programming problems. Econometrica, 28(3), 497-520. https://doi.org/10.2307/1910129
Latora, V., & Marchiori, M. (2001). Efficient behavior of small-world networks. Physical Review Letters, 87(19), 198701. https://doi.org/10.1103/PhysRevLett.87.198701
Laumanns, M., Thiele, L., Deb, K., & Zitzler, E. (2002). Combining convergence and diversity in evolutionary multiobjective optimization. Evolutionary Computation, 10(3), 263-282. https://doi.org/10.1162/106365602760234108
Ledoit, O., & Wolf, M. (2003). Improved estimation of the covariance matrix of stock returns with an application to portfolio selection. Journal of Empirical Finance, 10(5), 603-621. https://doi.org/10.1016/S0927-5398(03)00007-0

Ledoit, O., & Wolf, M. (2004a). A well-conditioned estimator for large-dimensional covariance matrices. Journal of Multivariate Analysis, 88(2), 365-411. https://doi.org/10.1016/S0047-259X(03)00096-4
Ledoit, O., & Wolf, M. (2004b). Honey, I shrunk the sample covariance matrix. The Journal of Portfolio Management, 30(4), 110-119. https://doi.org/10.3905/jpm.2004.110
Ledoit, O., & Wolf, M. (2008). Robust performance hypothesis testing with the Sharpe ratio. Journal of Empirical Finance, 15(5), 850-859. https://doi.org/10.1016/j.jempfin.2008.03.002
Leland, H. E. (1985). Option pricing and replication with transactions costs. The Journal of Finance, 40(5), 1283-1301. https://doi.org/10.1111/j.1540-6261.1985.tb02383.x
Lenstra, H. W. (1987). Factoring integers with elliptic curves. Annals of Mathematics, 126(3), 649-673. https://doi.org/10.2307/1971363
Leray, J. (1934). Sur le mouvement d'un liquide visqueux emplissant l'espace. Acta Mathematica, 63, 193-248. https://doi.org/10.1007/BF02547354
Levinson, N. (1974). More than one third of zeros of Riemann's zeta-function are on σ = 1/2. Advances in Mathematics, 13(4), 383-436. https://doi.org/10.1016/0001-8708(74)90074-7
Li, P., & Yau, S.-T. (1986). On the parabolic kernel of the Schrödinger operator. Acta Mathematica, 156(1), 153-201. https://doi.org/10.1007/BF02392592
Li, X.-D. (2012). Perelman's entropy formula for the Witten Laplacian on Riemannian manifolds via the Bakry-Emery Ricci curvature. Mathematische Annalen, 353(2), 403-437. https://doi.org/10.1007/s00208-011-0691-y
Liagkouras, K., & Metaxiotis, K. (2018). A new efficiently encoded multiobjective algorithm for the solution of the cardinality constrained portfolio optimization problem. Annals of Operations Research, 267, 281-319. https://doi.org/10.1007/s10479-016-2377-z
Limao, N., & Venables, A. J. (2001). Infrastructure, geographical disadvantage, transport costs, and trade. World Bank Economic Review, 15(3), 451-479. https://doi.org/10.1093/wber/15.3.451
Lin, C.-C., & Liu, Y.-T. (2008). Genetic algorithms for portfolio selection problems with minimum transaction lots. European Journal of Operational Research, 185(1), 393-404. https://doi.org/10.1016/j.ejor.2006.09.087
Lin, F. H. (1998). A new proof of the Caffarelli-Kohn-Nirenberg theorem. Communications on Pure and Applied Mathematics, 51(3), 241-257. https://doi.org/10.1002/(SICI)1097-0312(199803)51:3%3C241::AID-CPA2%3E3.0.CO;2-A
Lin, L. I.-K. (1989). A concordance correlation coefficient to evaluate reproducibility. Biometrics, 45(1), 255-268. https://doi.org/10.2307/2532051
Lintner, J. (1965). The valuation of risk assets and the selection of risky investments in stock portfolios and capital budgets. The Review of Economics and Statistics, 47(1), 13-37. https://doi.org/10.2307/1924119
Lipsitch, M., Tchetgen Tchetgen, E., & Cohen, T. (2010). Negative controls: A tool for detecting confounding and bias in observational studies. Epidemiology, 21(3), 383-388. https://doi.org/10.1097/EDE.0b013e3181d61eeb
Liu, M., & Kronbak, J. (2010). The potential economic viability of using the Northern Sea Route as an alternative route between Asia and Europe. Journal of Transport Geography, 18(3), 434-444. https://doi.org/10.1016/j.jtrangeo.2009.08.004
Ljung, G. M., & Box, G. E. P. (1978). On a measure of lack of fit in time series models. Biometrika, 65(2), 297-303. https://doi.org/10.1093/biomet/65.2.297
Lo, A. W. (2002). The statistics of Sharpe ratios. Financial Analysts Journal, 58(4), 36-52. https://doi.org/10.2469/faj.v58.n4.2453
Longstaff, F. A., Pan, J., Pedersen, L. H., & Singleton, K. J. (2011). How sovereign is sovereign credit risk? American Economic Journal: Macroeconomics, 3(2), 75-103. https://doi.org/10.1257/mac.3.2.75
Los, B., Timmer, M. P., & de Vries, G. J. (2015). How global are global value chains? A new approach to measure international fragmentation. Journal of Regional Science, 55(1), 66-92. https://doi.org/10.1111/jors.12121
Lott, J., & Villani, C. (2009). Ricci curvature for metric-measure spaces via optimal transport. Annals of Mathematics, 169(3), 903-991. https://doi.org/10.4007/annals.2009.169.903
Lucas, R. E. (1976). Econometric policy evaluation: A critique. Carnegie-Rochester Conference Series on Public Policy, 1, 19-46. https://doi.org/10.1016/S0167-2231(76)80003-6
Lucas, R. E., Jr. (1988). On the mechanics of economic development. Journal of Monetary Economics, 22(1), 3-42. https://doi.org/10.1016/0304-3932(88)90168-7
Lwin, K., Qu, R., & Kendall, G. (2014). A learning-guided multi-objective evolutionary algorithm for constrained portfolio optimization. Applied Soft Computing, 24, 757-772. https://doi.org/10.1016/j.asoc.2014.08.026
MacKinnon, J. G., & White, H. (1985). Some heteroskedasticity-consistent covariance matrix estimators with improved finite sample properties. Journal of Econometrics, 29(3), 305-325. https://doi.org/10.1016/0304-4076(85)90158-7
Makridakis, S., Andersen, A., Carbone, R., Fildes, R., Hibon, M., Lewandowski, R., Newton, J., Parzen, E., & Winkler, R. (1982). The accuracy of extrapolation (time series) methods: Results of a forecasting competition. Journal of Forecasting, 1(2), 111-153. https://doi.org/10.1002/for.3980010202

Mankiw, N. G., Romer, D., & Weil, D. N. (1992). A contribution to the empirics of economic growth. The Quarterly Journal of Economics, 107(2), 407-437. https://doi.org/10.2307/2118477
Mansini, R., & Speranza, M. G. (1999). Heuristic algorithms for the portfolio selection problem with minimum transaction lots. European Journal of Operational Research, 114(2), 219-233. https://doi.org/10.1016/S0377-2217(98)00252-5
Manski, C. F. (1993). Identification of endogenous social effects: The reflection problem. Review of Economic Studies, 60(3), 531-542. https://doi.org/10.2307/2298123
Mantegna, R. N. (1999). Hierarchical structure in financial markets. The European Physical Journal B, 11, 193-197. https://doi.org/10.1007/s100510050929
Maringer, D., & Kellerer, H. (2003). Optimization of cardinality constrained portfolios with a hybrid local search algorithm. OR Spectrum, 25, 481-495. https://doi.org/10.1007/s00291-003-0139-1
Markose, S., Giansante, S., & Shaghaghi, A. R. (2012). Too interconnected to fail financial network of US CDS market: Topological fragility and systemic risk. Journal of Economic Behavior & Organization, 83(3), 627-646. https://doi.org/10.1016/j.jebo.2012.05.016
Markowitz, H. (1952a). Portfolio selection. The Journal of Finance, 7(1), 77-91. https://doi.org/10.2307/2975974
Markowitz, H. (1952b). The utility of wealth. Journal of Political Economy, 60(2), 151-158. https://doi.org/10.1086/257177
Martin, R. (2012). Regional economic resilience, hysteresis and recessionary shocks. Journal of Economic Geography, 12(1), 1-32. https://doi.org/10.1093/jeg/lbr019
Martin, R., & Sunley, P. (2015). On the notion of regional economic resilience: Conceptualization and explanation. Journal of Economic Geography, 15(1), 1-42. https://doi.org/10.1093/jeg/lbu015
Martincus, C. V., Carballo, J., & Cusolito, A. (2017). Roads, exports and employment: Evidence from a developing country. Journal of International Economics, 105, 101-121. https://doi.org/10.1016/j.jinteco.2016.10.001
May, R. M., Levin, S. A., & Sugihara, G. (2008). Complex systems: Ecology for bankers. Nature, 451, 893-895. https://doi.org/10.1038/451893a
McNeil, A. J., & Frey, R. (2000). Estimation of tail-related risk measures for heteroscedastic financial time series: An extreme value approach. Journal of Empirical Finance, 7(3-4), 271-300. https://doi.org/10.1016/S0927-5398(00)00012-8
Melitz, M. J. (2003). The impact of trade on intra-industry reallocations and aggregate industry productivity. Econometrica, 71(6), 1695-1725. https://doi.org/10.1111/1468-0262.00467
Merton, R. C. (1973a). An intertemporal capital asset pricing model. Econometrica, 41(5), 867-887. https://doi.org/10.2307/1913811
Merton, R. C. (1973b). Theory of rational option pricing. The Bell Journal of Economics and Management Science, 4(1), 141-183. https://doi.org/10.2307/3003143
Merton, R. C. (1980). On estimating the expected return on the market: An exploratory investigation. Journal of Financial Economics, 8(4), 323-361. https://doi.org/10.1016/0304-405X(80)90013-5
Metropolis, N., Rosenbluth, A. W., Rosenbluth, M. N., Teller, A. H., & Teller, E. (1953). Equation of state calculations by fast computing machines. The Journal of Chemical Physics, 21(6), 1087-1092. https://doi.org/10.1063/1.1699114
Milanovic, B. (2002). True world income distribution, 1988 and 1993: First calculation based on household surveys alone. The Economic Journal, 112(476), 51-92. https://doi.org/10.1111/1468-0297.0j673
Milanovic, B. (2015). Global inequality of opportunity: How much of our income is determined by where we live? Review of Economics and Statistics, 97(2), 452-460. https://doi.org/10.1162/REST_a_00432
Mistrulli, P. E. (2011). Assessing financial contagion in the interbank market: Maximum entropy versus observed interbank lending patterns. Journal of Banking & Finance, 35(5), 1114-1127. https://doi.org/10.1016/j.jbankfin.2010.12.018
Morris, S., & Shin, H. S. (1998). Unique equilibrium in a model of self-fulfilling currency attacks. American Economic Review, 88(3), 587-597. https://doi.org/10.1257/aer.88.3.587
Mossin, J. (1966). Equilibrium in a capital asset market. Econometrica, 34(4), 768-783. https://doi.org/10.2307/1910098
Motter, A. E., & Lai, Y. C. (2002). Cascade-based attacks on complex networks. Physical Review E, 66(6), 065102. https://doi.org/10.1103/PhysRevE.66.065102
Mountford, A., & Uhlig, H. (2009). What are the effects of fiscal policy shocks?. Journal of Applied Econometrics, 24(6), 960-992. https://doi.org/10.1002/jae.1079
Mucha, P. J., Richardson, T., Macon, K., Porter, M. A., & Onnela, J. P. (2010). Community structure in time-dependent, multiscale, and multiplex networks. Science, 328(5980), 876-878. https://doi.org/10.1126/science.1184819
Mukherjee, S., & Steenbergen, J. (2016). Random walks on simplicial complexes and harmonics. Random Structures & Algorithms, 49(2), 379-405. https://doi.org/10.1002/rsa.20645

Mundlak, Y. (1978). On the pooling of time series and cross section data. Econometrica, 46(1), 69-85. https://doi.org/10.2307/1913646
Naes, R., Skjeltorp, J. A., & Odegaard, B. A. (2011). Stock market liquidity and the business cycle. The Journal of Finance, 66(1), 139-176. https://doi.org/10.1111/j.1540-6261.2010.01628.x
Nelder, J. A., & Mead, R. (1965). A simplex method for function minimization. The Computer Journal, 7(4), 308-313. https://doi.org/10.1093/comjnl/7.4.308
Nelson, D. B. (1991). Conditional heteroskedasticity in asset returns: A new approach. Econometrica, 59(2), 347-370. https://doi.org/10.2307/2938260
Newey, W. K., & West, K. D. (1987). A simple, positive semi-definite, heteroskedasticity and autocorrelation consistent covariance matrix. Econometrica, 55(3), 703-708. https://doi.org/10.2307/1913610
Newman, M. E. J. (2001). The structure of scientific collaboration networks. Proceedings of the National Academy of Sciences, 98(2), 404-409. https://doi.org/10.1073/pnas.98.2.404
Newman, M. E. J. (2002). Assortative mixing in networks. Physical Review Letters, 89(20), 208701. https://doi.org/10.1103/PhysRevLett.89.208701
Newman, M. E. J. (2003). Assortative mixing in networks. Physical Review E, 67(2), 026126. https://doi.org/10.1103/PhysRevE.67.026126
Newman, M. E. J. (2003). The structure and function of complex networks. SIAM Review, 45(2), 167-256. https://doi.org/10.1137/S003614450342480
Newman, M. E. J. (2006). Modularity and community structure in networks. Proceedings of the National Academy of Sciences, 103(23), 8577-8582. https://doi.org/10.1073/pnas.0601602103
Newman, M. E. J., & Girvan, M. (2004). Finding and evaluating community structure in networks. Physical Review E, 69(2), 026113. https://doi.org/10.1103/PhysRevE.69.026113
Ni, L. (2004). The entropy formula for linear heat equation. Journal of Geometric Analysis, 14(1), 87-100. https://doi.org/10.1007/BF02921867
Nickell, S. (1981). Biases in dynamic models with fixed effects. Econometrica, 49(6), 1417-1426. https://doi.org/10.2307/1911408
Nier, E., Yang, J., Yorulmazer, T., & Alentorn, A. (2007). Network models and financial stability. Journal of Economic Dynamics and Control, 31(6), 2033-2060. https://doi.org/10.1016/j.jedc.2007.01.002
Nier, E., Yang, J., Yorulmazer, T., & Alentorn, A. (2007). Network models and financial stability. Journal of Economic Dynamics and Control, 31(6), 2033-2060. https://doi.org/10.1016/j.jedc.2007.01.014
Notteboom, T. E., & Rodrigue, J. P. (2005). Port regionalization: Towards a new phase in port development. Maritime Policy & Management, 32(3), 297-313. https://doi.org/10.1080/03088830500139885
Nunn, N. (2007). Relationship-specificity, incomplete contracts, and the pattern of trade. Quarterly Journal of Economics, 122(2), 569-600. https://doi.org/10.1162/qjec.122.2.569
Obstfeld, M. (1996). Models of currency crises with self-fulfilling features. European Economic Review, 40(3-5), 1037-1047. https://doi.org/10.1016/0014-2921(95)00111-5
Odlyzko, A. M. (1987). On the distribution of spacings between zeros of the zeta function. Mathematics of Computation, 48(177), 273-308. https://doi.org/10.1090/S0025-5718-1987-0866115-3
Ollivier, Y. (2009). Ricci curvature of Markov chains on metric spaces. Journal of Functional Analysis, 256(3), 810-864. https://doi.org/10.1016/j.jfa.2009.03.001
Onnela, J.-P., Saramaki, J., Kertesz, J., & Kaski, K. (2005). Intensity and coherence of motifs in weighted complex networks. Physical Review E, 71(6), 065103. https://doi.org/10.1103/PhysRevE.71.065103
Opricovic, S., & Tzeng, G.-H. (2004). Compromise solution by MCDM methods: A comparative analysis of VIKOR and TOPSIS. European Journal of Operational Research, 156(2), 445-455. https://doi.org/10.1016/S0377-2217(03)00020-1
Opsahl, T., Agneessens, F., & Skvoretz, J. (2010). Node centrality in weighted networks: Generalizing degree and shortest paths. Social Networks, 32(3), 245-251. https://doi.org/10.1016/j.socnet.2010.03.006
Ortega, A., Frossard, P., Kovacevic, J., Moura, J. M. F., & Vandergheynst, P. (2018). Graph signal processing: Overview, challenges, and applications. Proceedings of the IEEE, 106(5), 808-828. https://doi.org/10.1109/JPROC.2018.2820126
Osterwalder, K., & Schrader, R. (1973). Axioms for Euclidean Green's functions. Communications in Mathematical Physics, 31, 83-112. https://doi.org/10.1007/BF01645738
Osterwalder, K., & Schrader, R. (1975). Axioms for Euclidean Green's functions II. Communications in Mathematical Physics, 42, 281-305. https://doi.org/10.1007/BF01608978
Otter, N., Porter, M. A., Tillmann, U., Grindrod, P., & Harrington, H. A. (2017). A roadmap for the computation of persistent homology. EPJ Data Science, 6, Article 17. https://doi.org/10.1140/epjds/s13688-017-0109-5
Park, C. Y., & Mercado, R. V. (2014). Determinants of financial stress in emerging market economies. Journal of Banking & Finance, 45, 199-224. https://doi.org/10.1016/j.jbankfin.2013.09.018

Pastor, L., & Stambaugh, R. F. (2003). Liquidity risk and expected stock returns. Journal of Political Economy, 111(3), 642-685. https://doi.org/10.1086/374184
Pastor-Satorras, R., & Vespignani, A. (2001). Epidemic spreading in scale-free networks. Physical Review Letters, 86(14), 3200-3203. https://doi.org/10.1103/PhysRevLett.86.3200
Patton, A. J., & Timmermann, A. (2007). Properties of optimal forecasts under asymmetric loss and nonlinearity. Journal of Econometrics, 140(2), 884-918. https://doi.org/10.1016/j.jeconom.2006.07.006
Pearl, J. (1995). Causal diagrams for empirical research. Biometrika, 82(4), 669-688. https://doi.org/10.1093/biomet/82.4.669
Pearson, K. (1901). On lines and planes of closest fit to systems of points in space. The London, Edinburgh, and Dublin Philosophical Magazine and Journal of Science, 2(11), 559-572. https://doi.org/10.1080/14786440109462720
Perron, P. (1989). The great crash, the oil price shock, and the unit root hypothesis. Econometrica, 57(6), 1361-1401. https://doi.org/10.2307/1913712
Pesaran, H. H., & Shin, Y. (1998). Generalized impulse response analysis in linear multivariate models. Economics Letters, 58(1), 17-29. https://doi.org/10.1016/S0165-1765(97)00214-0
Pesaran, M. H. (2006). Estimation and inference in large heterogeneous panels with a multifactor error structure. Econometrica, 74(4), 967-1012. https://doi.org/10.1111/j.1468-0262.2006.00692.x
Pesaran, M. H. (2015). Testing weak cross-sectional dependence in large panels. Econometric Reviews, 34(6-10), 1089-1117. https://doi.org/10.1080/07474938.2014.956623
Pesaran, M. H., & Timmermann, A. (1992). A simple nonparametric test of predictive performance. Journal of Business & Economic Statistics, 10(4), 461-465. https://doi.org/10.1080/07350015.1992.10509922
Pesaran, M. H., Shin, Y., & Smith, R. J. (2001). Bounds testing approaches to the analysis of level relationships. Journal of Applied Econometrics, 16(3), 289-326. https://doi.org/10.1002/jae.616
Petri, G., Expert, P., Turkheimer, F., Carhart-Harris, R., Nutt, D., Hellyer, P. J., & Vaccarino, F. (2014). Homological scaffolds of brain functional networks. Journal of the Royal Society Interface, 11(101), 20140873. https://doi.org/10.1098/rsif.2014.0873
Pettit, T. J., Fiksel, J., & Croxton, K. L. (2010). Ensuring supply chain resilience: Development of a conceptual framework. Journal of Business Logistics, 31(1), 1-21. https://doi.org/10.1002/j.2158-1592.2010.tb00125.x
Phillips, A. W. (1958). The relation between unemployment and the rate of change of money wage rates in the United Kingdom, 1861-1957. Economica, 25(100), 283-299. https://doi.org/10.1111/j.1468-0335.1958.tb00003.x
Phillips, P. C. B., & Perron, P. (1988). Testing for a unit root in time series regression. Biometrika, 75(2), 335-346. https://doi.org/10.1093/biomet/75.2.335
Pickands, J. (1975). Statistical inference using extreme order statistics. Annals of Statistics, 3(1), 119-131. https://doi.org/10.1214/aos/1176343003
Piketty, T., & Saez, E. (2003). Income inequality in the United States, 1913-1998. The Quarterly Journal of Economics, 118(1), 1-41. https://doi.org/10.1162/00335530360535135
Pisinger, D. (2005). Where are the hard knapsack problems? Computers & Operations Research, 32(9), 2271-2284. https://doi.org/10.1016/j.cor.2004.03.002
Plerou, V., Gopikrishnan, P., Rosenow, B., Amaral, L. A. N., & Stanley, H. E. (1999). Universal and nonuniversal properties of cross correlations in financial time series. Physical Review Letters, 83(7), 1471-1474. https://doi.org/10.1103/PhysRevLett.83.1471
Politzer, H. D. (1973). Reliable perturbative results for strong interactions?. Physical Review Letters, 30(26), 1346-1349. https://doi.org/10.1103/PhysRevLett.30.1346
Polyakov, A. M. (1975). Compact gauge fields and the infrared catastrophe. Physics Letters B, 59(1), 82-84. https://doi.org/10.1016/0370-2693(75)90162-8
Ponomarov, S. Y., & Holcomb, M. C. (2009). Understanding the concept of supply chain resilience. The International Journal of Logistics Management, 20(1), 124-143. https://doi.org/10.1108/09574090910954873
Portugal-Perez, A., & Wilson, J. S. (2012). Export performance and trade facilitation reform: Hard and soft infrastructure. World Bank Economic Review, 26(1), 129-150. https://doi.org/10.1093/wber/lhr039
Primiceri, G. E. (2005). Time varying structural vector autoregressions and monetary policy. Review of Economic Studies, 72(3), 821-852. https://doi.org/10.1111/j.1467-937X.2005.00353.x
Queiroz, M. M., Ivanov, D., Dolgui, A., & Fosso Wamba, S. (2020). Impacts of epidemic outbreaks on supply chains: Mapping a research agenda amid the COVID-19 pandemic through a structured literature review. Annals of Operations Research, 319, 1159-1196. https://doi.org/10.1007/s10479-020-03685-7
Rabiner, L. R. (1989). A tutorial on hidden Markov models and selected applications in speech recognition. Proceedings of the IEEE, 77(2), 257-286. https://doi.org/10.1109/5.18626
Radicchi, F., Castellano, C., Cecconi, F., Loreto, V., & Parisi, D. (2004). Defining and identifying communities in networks. Proceedings of the National Academy of Sciences, 101(9), 2658-2663. https://doi.org/10.1073/pnas.0400054101

Ramsey, J. B. (1969). Tests for specification errors in classical linear least-squares regression analysis. Journal of the Royal Statistical Society: Series B, 31(2), 350-371. https://doi.org/10.1111/j.2517-6161.1969.tb00796.x
Ramsey, J. B., & Lampart, C. (1998). Decomposition of economic relationships by timescale using wavelets: Expenditure and income. Macroeconomic Dynamics, 2(1), 49-71. https://doi.org/10.1017/S1365100598008029
Ramsey, J. B., & Lampart, C. (1998). The decomposition of economic relationships by time scale using wavelets: Money and income. Macroeconomic Dynamics, 2(1), 49-71. https://doi.org/10.1017/S1365100598008030
Rao, S., & Goldsby, T. J. (2009). Supply chain risks: A review and typology. The International Journal of Logistics Management, 20(1), 97-123. https://doi.org/10.1108/09574090910954864
Rauch, J. E. (1999). Networks versus markets in international trade. Journal of International Economics, 48(1), 7-35. https://doi.org/10.1016/S0022-1996(98)00009-9
Ravallion, M. (2001). Growth, inequality and poverty: Looking beyond averages. World Development, 29(11), 1803-1815. https://doi.org/10.1016/S0305-750X(01)00072-9
Redding, S. J., & Sturm, D. M. (2008). The costs of remoteness: Evidence from German division and reunification. American Economic Review, 98(5), 1766-1797. https://doi.org/10.1257/aer.98.5.1766
Reinhart, C. M., & Rogoff, K. S. (2009). The aftermath of financial crises. American Economic Review, 99(2), 466-472. https://doi.org/10.1257/aer.99.2.466
Riemann, B. (1859). Über die Anzahl der Primzahlen unter einer gegebenen Grösse. Journal für die reine und angewandte Mathematik, 1859, 671-680. https://doi.org/10.1515/crll.1859.1859.671
Rockafellar, R. T., & Uryasev, S. (2000). Optimization of conditional value-at-risk. The Journal of Risk, 2(3), 21-41. https://doi.org/10.21314/JOR.2000.038
Rodrik, D., Subramanian, A., & Trebbi, F. (2004). Institutions rule: The primacy of institutions over geography and integration in economic development. Journal of Economic Growth, 9, 131-165. https://doi.org/10.1023/B:JOEG.0000031425.72248.85
Rogers, L. C. G., & Veraart, L. A. M. (2013). Failure and rescue in an interbank network. Management Science, 59(4), 882-898. https://doi.org/10.1287/mnsc.1120.1569
Roll, R. (1977). A critique of the asset pricing theory's tests: Part I. Journal of Financial Economics, 4(2), 129-176. https://doi.org/10.1016/0304-405X(77)90009-5
Romer, P. M. (1986). Increasing returns and long-run growth. Journal of Political Economy, 94(5), 1002-1037. https://doi.org/10.1086/261420
Romer, P. M. (1990). Endogenous technological change. Journal of Political Economy, 98(5, Part 2), S71-S102. https://doi.org/10.1086/261725
Roodman, D. (2009). A note on the theme of too many instruments. Oxford Bulletin of Economics and Statistics, 71(1), 135-158. https://doi.org/10.1111/j.1468-0084.2008.00542.x
Roodman, D. (2009). How to do xtabond2: An introduction to difference and system GMM in Stata. Stata Journal, 9(1), 86-136. https://doi.org/10.1177/1536867X0900900106
Rose, A. (2004). Defining and measuring economic resilience to disasters. Disaster Prevention and Management, 13(4), 307-314. https://doi.org/10.1108/09653560410556528
Rose, A. (2007). Economic resilience to natural and man-made disasters: Multidisciplinary origins and contextual dimensions. Environmental Hazards, 7(4), 383-398. https://doi.org/10.1016/j.envhaz.2007.10.001
Rosenbaum, P. R. (1987). Sensitivity analysis for certain permutation inferences in matched observational studies. Biometrika, 74(1), 13-26. https://doi.org/10.1093/biomet/74.1.13
Ross, S. A. (1976). The arbitrage theory of capital asset pricing. Journal of Economic Theory, 13(3), 341-360. https://doi.org/10.1016/0022-0531(76)90046-6
Rosvall, M., & Bergstrom, C. T. (2008). Maps of random walks on complex networks reveal community structure. Proceedings of the National Academy of Sciences, 105(4), 1118-1123. https://doi.org/10.1073/pnas.0706851105
Rotemberg, J. J. (1982). Sticky prices in the United States. Journal of Political Economy, 90(6), 1187-1211. https://doi.org/10.1086/261117
Rua, A. (2010). Measuring comovement in the time-frequency space. Journal of Macroeconomics, 32(2), 685-691. https://doi.org/10.1016/j.jmacro.2009.12.005
Rubin, D. B. (1974). Estimating causal effects of treatments in randomized and nonrandomized studies. Journal of Educational Psychology, 66(5), 688-701. https://doi.org/10.1037/h0037350
Rubinstein, M. O. (1998). Evidence for a spectral interpretation of the zeros of L-functions. Experimental Mathematics, 7(4), 313-328. https://doi.org/10.1080/10586458.1998.10504356
Rudnick, Z., & Sarnak, P. (1996). Zeros of principal L-functions and random matrix theory. Duke Mathematical Journal, 81(2), 269-322. https://doi.org/10.1215/S0012-7094-96-08115-6
Saaty, T. L. (1977). A scaling method for priorities in hierarchical structures. Journal of Mathematical Psychology, 15(3), 234-281. https://doi.org/10.1016/0022-2496(77)90033-5

Sadka, R. (2006). Momentum and post-earnings-announcement drift anomalies: The role of liquidity risk. Journal of Financial Economics, 80(2), 309-349. https://doi.org/10.1016/j.jfineco.2005.07.005
Saito, M. (1988). Modules de Hodge polarisables. Publications of the Research Institute for Mathematical Sciences, 24(6), 849-995. https://doi.org/10.2977/prims/1195173930
Saito, M. (1990). Mixed Hodge modules. Publications of the Research Institute for Mathematical Sciences, 26(2), 221-333. https://doi.org/10.2977/prims/1195171082
Sala-i-Martin, X. (2006). The world distribution of income: Falling poverty and ... convergence, period. The Quarterly Journal of Economics, 121(2), 351-397. https://doi.org/10.1162/qjec.2006.121.2.351
Saltelli, A. (2002). Making best use of model evaluations to compute sensitivity indices. Computer Physics Communications, 145(2), 280-297. https://doi.org/10.1016/S0010-4655(02)00280-1
Samal, A., Sreejith, R. P., Gu, J., Liu, S., Saucan, E., & Jost, J. (2018). Comparative analysis of two discretizations of Ricci curvature for complex networks. Scientific Reports, 8(1), 8650. https://doi.org/10.1038/s41598-018-27001-3
Sandhu, R. S., Georgiou, T. T., Tannenbaum, A. R., & Kumar, A. (2015). Graph curvature for differentiating cancer networks. Scientific Reports, 5(1), 12323. https://doi.org/10.1038/srep12323
Sandryhaila, A., & Moura, J. M. F. (2013). Discrete signal processing on graphs. IEEE Transactions on Signal Processing, 61(7), 1644-1656. https://doi.org/10.1109/TSP.2013.2238935
Sargent, T. J., & Wallace, N. (1975). Rational expectations, the optimal monetary instrument, and the optimal money supply rule. Journal of Political Economy, 83(2), 241-254. https://doi.org/10.1086/260321
Schaub, M. T., Benson, A. R., Horn, P., Lippner, G., & Jadbabaie, A. (2020). Random walks on simplicial complexes and the normalized Hodge 1-Laplacian. SIAM Review, 62(2), 353-391. https://doi.org/10.1137/18M1201019
Scholten, K., & Schilder, S. (2015). The role of collaboration in supply chain resilience. Supply Chain Management: An International Journal, 20(4), 471-484. https://doi.org/10.1108/SCM-11-2014-0386
Schoof, R. (1985). Elliptic curves over finite fields and the computation of square roots mod p. Mathematics of Computation, 44(170), 483-494. https://doi.org/10.1090/S0025-5718-1985-0777280-6
Schuirmann, D. J. (1987). A comparison of the two one-sided tests procedure and the power approach for assessing the equivalence of average bioavailability. Journal of Pharmacokinetics and Biopharmaceutics, 15, 657-680. https://doi.org/10.1007/BF01068419
Schularick, M., & Taylor, A. M. (2012). Credit booms gone bust: Monetary policy, leverage cycles, and financial crises, 1870-2008. American Economic Review, 102(2), 1029-1061. https://doi.org/10.1257/aer.102.2.1029
Sen, A. (1976). Poverty: An ordinal approach to measurement. Econometrica, 44(2), 219-231. https://doi.org/10.2307/1912718
Serrano, M. A., & Boguñá, M. (2003). Topology of the world trade web. Physical Review E, 68(1), 015101. https://doi.org/10.1103/PhysRevE.68.015101
Shannon, C. E. (1948). A mathematical theory of communication. Bell System Technical Journal, 27(4), 623-656. https://doi.org/10.1002/j.1538-7305.1948.tb00917.x
Shannon, C. E. (1948). A mathematical theory of communication. The Bell System Technical Journal, 27(3), 379-423. https://doi.org/10.1002/j.1538-7305.1948.tb01338.x
Sharpe, W. F. (1963). A simplified model for portfolio analysis. Management Science, 9(2), 277-293. https://doi.org/10.1287/mnsc.9.2.277
Sharpe, W. F. (1964). Capital asset prices: A theory of market equilibrium under conditions of risk. The Journal of Finance, 19(3), 425-442. https://doi.org/10.1111/j.1540-6261.1964.tb02865.x
Sharpe, W. F. (1966). Mutual fund performance. The Journal of Business, 39(1), 119-138. https://doi.org/10.1086/294846
Shaw, D. X., Liu, S., & Kopman, L. (2008). Lagrangian relaxation procedure for cardinality-constrained portfolio optimization. Optimization Methods and Software, 23(3), 411-420. https://doi.org/10.1080/10556780701722542
Shi, J., & Malik, J. (2000). Normalized cuts and image segmentation. IEEE Transactions on Pattern Analysis and Machine Intelligence, 22(8), 888-905. https://doi.org/10.1109/34.868688
Shi, W.-X. (1989). Deforming the metric on complete Riemannian manifolds. Journal of Differential Geometry, 30(1), 223-301. https://doi.org/10.4310/jdg/1214443292
Shorrocks, A. F. (1980). The class of additively decomposable inequality measures. Econometrica, 48(3), 613-625. https://doi.org/10.2307/1913126
Shuman, D. I., Narang, S. K., Frossard, P., Ortega, A., & Vandergheynst, P. (2013). The emerging field of signal processing on graphs. IEEE Signal Processing Magazine, 30(3), 83-98. https://doi.org/10.1109/MSP.2012.2235192
Simpson, C. T. (1992). Higgs bundles and local systems. Publications Mathématiques de l'IHÉS, 75, 5-95. https://doi.org/10.1007/BF02699491
Sims, C. A. (1980). Macroeconomics and reality. Econometrica, 48(1), 1-48. https://doi.org/10.2307/1912017
Sims, C. A., & Zha, T. (1998). Bayesian methods for dynamic multivariate models. International Economic Review, 39(4), 949-968. https://doi.org/10.2307/2527347

Sims, C. A., & Zha, T. (2006). Were there regime switches in U.S. monetary policy?. American Economic Review, 96(1), 54-81. https://doi.org/10.1257/000282806776157678
Singer, I. M. (1978). Some remarks on the Gribov ambiguity. Communications in Mathematical Physics, 60, 7-12. https://doi.org/10.1007/BF01609471
Smets, F., & Wouters, R. (2007). Shocks and frictions in US business cycles: A Bayesian DSGE approach. American Economic Review, 97(3), 586-606. https://doi.org/10.1257/aer.97.3.586
Soleimani, H., Golmakani, H. R., & Salimi, M. H. (2009). Markowitz-based portfolio selection with minimum transaction lots, cardinality constraints and regarding sector capitalization using genetic algorithm. Expert Systems with Applications, 36(3), 5058-5063. https://doi.org/10.1016/j.eswa.2008.06.007
Solon, G. (1992). Intergenerational income mobility in the United States. American Economic Review, 82(3), 393-408. https://doi.org/10.1257/aer.82.3.393
Solow, R. M. (1956). A contribution to the theory of economic growth. Quarterly Journal of Economics, 70(1), 65-94. https://doi.org/10.2307/1884513
Soundararajan, K. (2009). Moments of the Riemann zeta function. Annals of Mathematics, 170(2), 981-993. https://doi.org/10.4007/annals.2009.170.981
Spielman, D. A., & Srivastava, N. (2011). Graph sparsification by effective resistances. SIAM Journal on Computing, 40(6), 1913-1926. https://doi.org/10.1137/080734029
Steuer, R. E., Qi, Y., & Wimmer, M. (2024). Computing cardinality constrained portfolio selection efficient frontiers via closest correlation matrices. European Journal of Operational Research, 313(2), 628-636. https://doi.org/10.1016/j.ejor.2023.08.026
Stock, J. H., & Watson, M. W. (1999). Forecasting inflation. Journal of Monetary Economics, 44(2), 293-335. https://doi.org/10.1016/S0304-3932(99)00027-6
Stock, J. H., & Watson, M. W. (2002). Forecasting using principal components from a large number of predictors. Journal of the American Statistical Association, 97(460), 1167-1179. https://doi.org/10.1198/016214502388618960
Stock, J. H., & Watson, M. W. (2002). Macroeconomic forecasting using diffusion indexes. Journal of Business & Economic Statistics, 20(2), 147-162. https://doi.org/10.1198/073500102317351921
Stock, J. H., & Watson, M. W. (2007). Why has U.S. inflation become harder to forecast?. Journal of Money, Credit and Banking, 39(s1), 3-33. https://doi.org/10.1111/j.1538-4616.2007.00014.x
Stock, J. H., & Watson, M. W. (2008). Heteroskedasticity-robust standard errors for fixed-effects panel-data regression. Econometrica, 76(1), 155-174. https://doi.org/10.1111/j.0012-9682.2008.00821.x
Stone, M. (1974). Cross-validatory choice and assessment of statistical predictions. Journal of the Royal Statistical Society: Series B, 36(2), 111-147. https://doi.org/10.1111/j.2517-6161.1974.tb00994.x
Storn, R., & Price, K. (1997). Differential evolution - A simple and efficient heuristic for global optimization over continuous spaces. Journal of Global Optimization, 11, 341-359. https://doi.org/10.1023/A:1008202821328
Strogatz, S. H. (2001). Exploring complex networks. Nature, 410, 268-276. https://doi.org/10.1038/35065725
Sturm, K.-T. (2006a). On the geometry of metric measure spaces. I. Acta Mathematica, 196(1), 65-131. https://doi.org/10.1007/s11511-006-0002-8
Sturm, K.-T. (2006b). On the geometry of metric measure spaces. II. Acta Mathematica, 196(1), 133-177. https://doi.org/10.1007/s11511-006-0003-7
Sun, L., & Abraham, S. (2021). Estimating dynamic treatment effects in event studies with heterogeneous treatment effects. Journal of Econometrics, 225(2), 175-199. https://doi.org/10.1016/j.jeconom.2020.09.006
Tacchella, A., Cristelli, M., Caldarelli, G., Gabrielli, A., & Pietronero, L. (2012). A new metrics for countries' fitness and products' complexity. Scientific Reports, 2, Article 723. https://doi.org/10.1038/srep00723
Tang, C. S. (2006). Perspectives in supply chain risk management. International Journal of Production Economics, 103(2), 451-488. https://doi.org/10.1016/j.ijpe.2005.07.006
Taylor, J. B. (1980). Aggregate dynamics and staggered contracts. Journal of Political Economy, 88(1), 1-23. https://doi.org/10.1086/260845
Taylor, J. B. (1993). Discretion versus policy rules in practice. Carnegie-Rochester Conference Series on Public Policy, 39, 195-214. https://doi.org/10.1016/0167-2231(93)90009-L
Taylor, R., & Wiles, A. (1995). Ring-theoretic properties of certain Hecke algebras. Annals of Mathematics, 141(3), 553-572. https://doi.org/10.2307/2118560
Tibshirani, R. (1996). Regression shrinkage and selection via the Lasso. Journal of the Royal Statistical Society: Series B, 58(1), 267-288. https://doi.org/10.1111/j.2517-6161.1996.tb02080.x
Timmer, M. P., Dietzenbacher, E., Los, B., Stehrer, R., & de Vries, G. J. (2015). An illustrated user guide to the World Input-Output Database: The case of global automotive production. Review of International Economics, 23(3), 575-605. https://doi.org/10.1111/roie.12178
Timmer, M. P., Erumban, A. A., Los, B., Stehrer, R., & de Vries, G. J. (2014). Slicing up global value chains. Journal of Economic Perspectives, 28(2), 99-118. https://doi.org/10.1257/jep.28.2.99

Tobin, J. (1958). Liquidity preference as behavior towards risk. The Review of Economic Studies, 25(2), 65-86. https://doi.org/10.2307/2296205
Toda, H. Y., & Yamamoto, T. (1995). Statistical inference in vector autoregressions with possibly integrated processes. Journal of Econometrics, 66(1-2), 225-250. https://doi.org/10.1016/0304-4076(94)01616-8
Topping, P. (2010). Ricci flow compactness via pseudolocality, and flows with incomplete initial metrics. Journal of the European Mathematical Society, 12(6), 1429-1451. https://doi.org/10.4171/JEMS/237
Torrence, C., & Compo, G. P. (1998). A practical guide to wavelet analysis. Bulletin of the American Meteorological Society, 79(1), 61-78. https://doi.org/10.1175/1520-0477(1998)079%3C0061:APGTWA%3E2.0.CO;2
Treynor, J. L., & Black, F. (1973). How to use security analysis to improve portfolio selection. The Journal of Business, 46(1), 66-86. https://doi.org/10.1086/295508
Tukamuhabwa, B. R., Stevenson, M., Busby, J., & Zorzini, M. (2015). Supply chain resilience: Definition, review and theoretical foundations for further study. International Journal of Production Research, 53(18), 5592-5623. https://doi.org/10.1080/00207543.2015.1037934
Uhlig, H. (2005). What are the effects of monetary policy on output? Results from an agnostic identification procedure. Journal of Monetary Economics, 52(2), 381-419. https://doi.org/10.1016/j.jmoneco.2004.05.007
Upper, C. (2011). Simulation methods to assess the danger of contagion in interbank markets. Journal of Financial Stability, 7(3), 111-125. https://doi.org/10.1016/j.jfs.2010.12.003
Vielma, J. P., Ahmed, S., & Nemhauser, G. L. (2008). A lifted linear programming branch-and-bound algorithm for mixed-integer conic quadratic programs. INFORMS Journal on Computing, 20(3), 438-450. https://doi.org/10.1287/ijoc.1070.0256
Viterbi, A. J. (1967). Error bounds for convolutional codes and an asymptotically optimum decoding algorithm. IEEE Transactions on Information Theory, 13(2), 260-269. https://doi.org/10.1109/TIT.1967.1054010
von Luxburg, U. (2007). A tutorial on spectral clustering. Statistics and Computing, 17, 395-416. https://doi.org/10.1007/s11222-007-9033-z
Wang, Y.-Z. (2018). W-entropy formulae and differential Harnack estimates for porous medium equations on closed Riemannian manifolds. Communications on Pure and Applied Analysis, 17(3), 1107-1136. https://doi.org/10.3934/cpaa.2018116
Wasserman, L. (2018). Topological data analysis. Annual Review of Statistics and Its Application, 5, 501-532. https://doi.org/10.1146/annurev-statistics-031017-100045
Watts, D. J., & Strogatz, S. H. (1998). Collective dynamics of 'small-world' networks. Nature, 393(6684), 440-442. https://doi.org/10.1038/30918
Welch, P. D. (1967). The use of fast Fourier transform for the estimation of power spectra. IEEE Transactions on Audio and Electroacoustics, 15(2), 70-73. https://doi.org/10.1109/TAU.1967.1161901
West, K. D. (1996). Asymptotic inference about predictive ability. Econometrica, 64(5), 1067-1084. https://doi.org/10.2307/2171841
West, K. D. (1996). Asymptotic inference about predictive ability. Econometrica, 64(5), 1067-1084. https://doi.org/10.2307/2171956
White, H. (1980). A heteroskedasticity-consistent covariance matrix estimator and a direct test for heteroskedasticity. Econometrica, 48(4), 817-838. https://doi.org/10.2307/1912934
White, H. (2000). A reality check for data snooping. Econometrica, 68(5), 1097-1126. https://doi.org/10.1111/1468-0262.00152
Wieland, A., & Wallenburg, C. M. (2012). Dealing with supply chain risks: Linking risk management practices and strategies to performance. International Journal of Physical Distribution & Logistics Management, 42(10), 887-905. https://doi.org/10.1108/09600031211281411
Wiles, A. (1995). Modular elliptic curves and Fermat's last theorem. Annals of Mathematics, 141(3), 443-551. https://doi.org/10.2307/2118559
Wilson, K. G. (1974). Confinement of quarks. Physical Review D, 10(8), 2445-2459. https://doi.org/10.1103/PhysRevD.10.2445
Windmeijer, F. (2005). A finite sample correction for the variance of linear efficient two-step GMM estimators. Journal of Econometrics, 126(1), 25-51. https://doi.org/10.1016/j.jeconom.2004.02.005
Witten, E. (1988). Topological quantum field theory. Communications in Mathematical Physics, 117, 353-386. https://doi.org/10.1007/BF01223371
Woodford, M. (2001). The Taylor rule and optimal monetary policy. American Economic Review, 91(2), 232-237. https://doi.org/10.1257/aer.91.2.232
Woodside-Oriakhi, M., Lucas, C., & Beasley, J. E. (2011). Heuristic algorithms for the cardinality constrained efficient frontier. European Journal of Operational Research, 213(3), 538-550. https://doi.org/10.1016/j.ejor.2011.03.030

Wooldridge, J. M. (2005). Fixed-effects and related estimators for correlated random-coefficient and treatment-effect panel data models. The Review of Economics and Statistics, 87(2), 385-390. https://doi.org/10.1162/0034653053970320

Yang, C. N., & Mills, R. L. (1954). Conservation of isotopic spin and isotopic gauge invariance. Physical Review, 96(1), 191-195. https://doi.org/10.1103/PhysRev.96.191

Yi, K.-M. (2003). Can vertical specialization explain the growth of world trade? Journal of Political Economy, 111(1), 52-102. https://doi.org/10.1086/344805

Yitzhaki, S. (1983). On an extension of the Gini inequality index. International Economic Review, 24(3), 617-628. https://doi.org/10.2307/2648789

Zitzler, E., & Thiele, L. (1999). Multiobjective evolutionary algorithms: A comparative case study and the strength Pareto approach. IEEE Transactions on Evolutionary Computation, 3(4), 257-271. https://doi.org/10.1109/4235.797969

Zomorodian, A., & Carlsson, G. (2005). Computing persistent homology. Discrete & Computational Geometry, 33(2), 249-274. https://doi.org/10.1007/s00454-004-1146-y

Zou, H., & Hastie, T. (2005). Regularization and variable selection via the elastic net. Journal of the Royal Statistical Society: Series B, 67(2), 301-320. https://doi.org/10.1111/j.1467-9868.2005.00503.x